



Precast/Prestressed Concrete Institute

BRIDGE DESIGN MANUAL

3rd Edition, Second Release, August 2014

Version Compressed for ePub

MNL-133-14

1st Edition, First Printing, 1997

2nd Edition, First Printing, 2003

3rd Edition, First Release, First Printing, November 2011

Precast Prestressed Concrete

BRIDGE DESIGN MANUAL

Third Edition, Second Release, August 2014

MNL-133-14



200 W. Adams Street, Suite 2100
Phone: (312) 786-0300
<http://www.pci.org>

Chicago, IL 60606-5230
Fax: (312) 786-0353
e-mail: PCIBridgeManual@pci.org

MNL-133-14

Copyright© 2014

Precast/Prestressed Concrete Institute

First Edition, First Printing, 1997

Second Edition, First Printing, 2003

Third Edition, First Release, November 2011

Third Edition, Second Release, August 2014

All rights reserved.

No part of this printed or electronic document may be reproduced
in any form without the written permission of
the Precast/Prestressed Concrete Institute

ISBN 978-0-9797042-4-6

Substantial effort has been made to ensure that all data and information in this Manual are accurate. However, PCI cannot accept responsibility for any errors or oversights or for the use of material. The user must recognize that no publication can substitute for experienced judgment. This document is intended for use by personnel competent to evaluate the significance and limitations of its contents and able to accept responsibility for the application of the material it contains.

Printed in U.S.A.

Third Edition, Second Release, August 2014

Like the previous releases, the additions comprising this release underwent rigorous reviews by specialized teams and ultimately the PCI Committee on Bridges followed by the Technical Activities Council. The Transportation Activities Council was responsible for the conduct of the process with the direction of William N. Nickas, PCI Managing Director, Transportation Systems.

The principal chapter authors were: new Chapter 15–Seismic Design: the PCI Committee on Bridges, Subcommittee on Seismic Design; new Chapter 19–Repair and Rehabilitation: Henry G. Russell, and new Chapter 21–Pedestrian Bridges: John S. Dick.

Third Edition, First Release, November 2011

The PCI Bridge Design Manual is sponsored by the PCI Committee on Bridges and the PCI Bridge Producers Committee under the purview of the Technical and Transportation Activities Councils. The project required the special talent and expertise of many individuals. While it is not possible to properly and completely recognize and acknowledge the contributions of all, a partial listing includes the following persons:

Bridge Design Manual Steering Committee, part of the Transportation Activities Council

Chuck Prussack, Chairman	Kevin R. Eisenbeis
Andrew J. Keenan, Vice Chairman	Roy L. Eriksson
Heinrich O. Bonstedt	R. Jon Grafton
Reid W. Castrodale	Michael L. McCool
Vijay Chandra	Mary Lou Ralls

Serving as Technical Activities Council liaison, Stephen J. Seguirant

Third Edition Principal Chapter Authors and Quality Control Persons:

Mantu C. Baishya	Emily Lorenz	Mohsen A. Shahawy
Steve C.S. Cai	Dennis R. Mertz	John Stanton
John A. Corven	William N. Nickas	Chuanbing Sun
John S. Dick	Henry G. Russell	Wallace N. Turner
Kevin R. Eisenbeis	Francesco M. Russo	

Blue Ribbon Panel Reviewers:

Sameh S. Badie	Ralph Dorsife	Chuck Prussack
Shrinivas B. Bhide	Roy L. Eriksson	Hugh D. Ronald
Richard Brice	Amgad Fawzy Girgis	Thomas K. Saad
Heinrich O. Bonstedt	R. Jon Grafton	Stephen J. Seguirant
Reid W. Castrodale	Benjamin Graybeal	Bala Shivakumar
Vijay Chandra	Bijan Khaleghi	PCI Sustainability Council
David Chapman	Andrew J. Keenan	Maher K. Tadros
W. Randy Cox	Richard A. Miller	Edward P. Wasserman
Dennis Drews	Carin Roberts-Wollmann	Stephen Zendegui
	Andre V. Pavlov	Toorak Zokaie

Document Assembly Contractor:
Michael W. Robertson

Cover Design:
Paul Grigonis

Project Manager and Editor-In-Chief
William N. Nickas

First Edition, 1997
Second Edition, 2003

Under the direction of the **Bridge Design Manual Steering Committee**

Chuck Prussack, Co-Chairman

Reid W. Castrodale, Co-Chairman

Heinrich O. Bonstedt

Scott E. Olson

Roy L. Eriksson

Joe Roche

Richard R. Imper

Harold E. Wescott, Jr.

Principal Second Edition Chapter Authors:

Alex Aswad

Henry G. Russell

Maher K. Tadros (Principal Author)

Hussein Khalil

Stephen J. Seguirant

Stephen Zendegui

Mary Lou Ralls

Contributing Second Edition Chapter Authors:

Sameh S. Badie

Steve L. Cheney

Manouchehr Karshenas

Mohsen A. Saleh

Karen A. Bexten

Deborah Derrick (editing)

M. Keith Kaufman

Eric J. Schindler

Kris G. Bassi

James G. Gallt

Robert F. Mast

Mohsen A. Shahawy

Heinrich O. Bonstedt

Richard J. Golec

Dennis Merwood

Q. D. Spruill, Jr

Reid W. Castrodale

James S. Guarre

Mary Lou Ralls

Maher K. Tadros

Blue Ribbon Panel:

Heinrich O. Bonstedt

Ned M. Cleland

Daniel P. Jenny

Reid W. Castrodale

Greg Force

C. Douglas Sutton

Manual Review Panel:

Ernie Acree

Jeffrey Davis

John B. Kelly

Chuck Prussack

James M. Barker

Jeffrey Ehler

Sudhakar R. Kulkarni

Omar Qudus

Robert M. Barnoff

Roy L. Eriksson

Gordon Nagle

Joe Roche

Heinrich O. Bonstedt

Larry G. Fischer

Scott E. Olson

Steve Sabra

Reid W. Castrodale

Jack J. Gabriel

S. K. Pal

Rita L. Seraderian

Vijay Chandra

James R. Hoblitzell

Rick Phillips

Lynden VanderVeen

William Clawson

Richard R. Imper

Phillip C. Pierce

Edward P. Wasserman

William Gene Corley

Mostafa Jamshidi

Kent Preston

Harold E. Wescott, Jr.

Project Manager and Editor-In-Chief

John S. Dick

This page left blank intentionally

FOREWORD

BACKGROUND AND REVISIONS

Beginning in the mid-1980s, the PCI Bridge Producers Committee and the PCI Committee on Bridges created plans for the development of this comprehensive bridge design manual. It was the consensus of bridge designers and producers alike that the 1980 publication, *Precast/Prestressed Concrete Short Span Bridges—Spans to 100 Feet* and the 1985 *Design Supplement to Short Span Bridges* had served their original purposes. The first and second editions of this manual incorporated information needed to reflect the extensive changes occurring at the time in the *AASHTO Standard Specifications*, and coverage of the requirements of the then new *AASHTO LRFD Specifications*. It also included such timely topics as continuity considerations, seismic requirements, and spliced-beam innovations. It was and is intended for multiple users including: owner agencies, practicing consulting bridge engineers, contractors, industry material suppliers and fabricators, and university professors and students. This third edition is focused entirely on the *LRFD Specifications*. Almost all references to the *Standard Specifications* have been deleted. An exception is Chapter 18—Load Rating Procedures that provides methods for bridges originally designed by the *AASHTO Standard Specifications*.

In preparation for development of the contents of the original manual, several surveys of design professionals, owner agencies, regional associations, and precast concrete producers were conducted over a span of 10 years, the latest of which was in June 1994. The contents of this revised manual include the most important topics identified by these surveys plus several new subjects.

Based on the results of the surveys, a planning report was prepared for PCI in August 1994 by Richard R. Imper, Maher K. Tadros, and Stephen Zendegui. The information from the report was further refined by the PCI Bridge Design Manual Steering Committee and became the outline and plan for the first edition. Preparation of the manual began in June 1995 by a team of 26 authors, under the direction of Maher K. Tadros. It should be emphasized that the manual is intended to be expanded and updated as needed, especially as the *AASHTO Specifications* are revised and the state-of-the-art advanced.

Much of the material included in this manual did not exist in other publications. For example, hand calculation examples using the *LRFD Specifications*, fabrication and erection of precast, prestressed concrete products, and preliminary design aids appear here in a PCI publication for the first time. There are new examples and charts given for concrete strengths representative of the state-of-the-art, rather than conventional values.

The manual is intended to be a national document reflecting the latest knowledge and successful practices. During the nearly 50 years that precast, prestressed concrete bridges had been in existence when this work was begun, designers resorted to a variety of resources, including company brochures, state highway agency manuals, reference books, and computer software. These resources were fully utilized in the development of this manual. The authors, however, avoided making recommendations based on individual local practices, or on ideas or concepts that have not been implemented in actual field conditions. It is hoped that state highway agencies will use this manual as their principal design guide, and supplement it with local criteria and details as needed.

There are a number of computer programs for design of precast concrete bridges. Neither the authors nor PCI certify or endorse any of these programs. Rather, this manual is intended to explain the theories and practices of bridge design, regardless of software tools used in design. Some of the work presented in the manual is based on computer runs using several programs for verification purposes. However, the manual's use by designers does not require the use of any of these programs. A popular method of utilizing personal computers in design is spreadsheet software and Mathcad. The Mathcad-like examples provided throughout the manual are documented in step-by-step detail to allow designers to develop their own spreadsheet programs for similar design tasks.

The Third Edition, First Release included examples using various precast, prestressed concrete bridge beams and products. These examples illustrate several alternate *LRFD Specifications* provisions including prestress losses, shear design, and transformed sections. The original Chapter 1 was moved to an introduction and a new topic—Sustainability—became chapter 1. There were many revisions to most chapters to keep the information and methods current with the *LRFD Specifications* and developments in practice.

The Third Edition, Second Release adds three new chapters: 15–Seismic Design; 19–Repair and Rehabilitation; and 21–Pedestrian Bridges. Important—this fully searchable electronic publication allows the user to search on any word, by code equation, or to find the source of a calculation value anywhere in the text.

OBJECTIVES

This manual is intended to provide a comprehensive document for the design, fabrication, and construction of bridges using precast or precast, prestressed concrete components, including precast, post-tensioned products. The document addresses precast concrete products produced in PCI-Certified manufacturing plants. It presents recommendations recognizing all the best current industry practices available for use by designers. Its flexible format allows for changes that occur in the industry. It is intended to provide both advanced information for experienced designers and basic information to designers, students, and educators who are not familiar with bridge design. It explains the application of the AASHTO *LRFD Specifications* provisions pertaining to prestressed concrete beams in addition to the AASHTO *Standard Specifications* criteria still in use for load rating. In addition, it provides preliminary design aids to help in selecting cost-effective bridge systems and for sizing precast concrete members.

CONTENTS

Introduction, Prestressed Concrete Bridges—The High Performance Solution

This is a general promotional section with numerous illustrations. It includes the benefits of precast concrete bridges for both new construction and rehabilitation. It gives examples of successful projects. This chapter includes an introduction of various types of precast concrete products made nationally for bridge construction, and examples of bridge beam shapes.

Chapter 1, Sustainability

This new chapter introduces bridge engineers to sustainability concepts and provides new approaches and considerations for bridge design and construction.

Chapter 2, Material Properties

Key properties of all major materials currently used for precast, prestressed concrete bridge structures are explained in this chapter. It also reviews concrete constituent materials and mix requirements for strength and durability, hardened concrete properties, prestressing and post-tensioning reinforcement, nonprestressing reinforcement, and concrete grouts. High performance concrete is discussed. The chapter features a reference list of more than 120 relevant standards and publications by AASHTO, ACI, and ASTM. A useful chart cross-references identical AASHTO and ASTM standards.

Chapter 3, Fabrication and Construction

This chapter describes the complete fabrication process and the implications of fabrication for design. It will help to inform the design professional about general precast industry practices and explains product components and details. It explains the impact different materials have on production. Quality and fabrication control are described. Also covered are product evaluation and repair, camber, sweep, and accelerated curing. Transportation and erection are covered including the use of cranes, launching trusses, and temporary support towers. Field-placed concrete for decks and diaphragms is discussed.

Chapter 4, Strategies for Economy

The chapter discusses the options that designers have to further improve the cost-effectiveness of precast, prestressed concrete bridges. Six sections outline and describe topics such as: geometry (span–depth, vertical and horizontal curves, skewed ends and flared spans); designer options (structural system selection, diaphragms, strand profiles, reinforcing details, bearing systems, high strength concrete); fabrication systems; shipping and erection methods; and, the use of additional economical precast products.

Chapter 5, Aesthetics

Provides guidelines by which aesthetics can become a part of an engineer’s design technique, including geometry, superstructure type, pier shape, abutment shape, surface treatment, signing, lighting, and landscaping.

Chapter 6, Preliminary Design

The criteria that must be considered early in bridge planning are discussed. Provides numerous charts and design graphs to assist in the selection of common bridge beams. Issues discussed include structure-type, hydraulics, construction, utilities, safety, and aesthetics. Piers, abutments, and foundations are discussed. Beam design charts are included for voided and solid slab beams, box beams, AASHTO I-beams, AASHTO-PCI bulb-tee beams, deck bulb-tee beams, double-stemmed beams, and a selection of U beam shapes.

Chapter 7, Loads and Load Distribution

This chapter addresses the AASHTO *LRFD Specifications*. Live load effects are emphasized and moments and shear forces discussed. Live load distribution factors are listed and described for common types of precast concrete superstructures. Findings and recommendations are presented concerning refined methods of analysis.

Chapter 8, Design Theory and Procedure

This chapter is an extensive review of design procedures that include: introduction to prestressed concrete fundamentals; critical section and fiber locations; estimation of number of strands; cracking moment; ultimate flexure; and maximum and minimum reinforcement limits. Also included is: bond, transfer, and development lengths; shear; loss of prestress; deflection; slab design and analysis, and detailing for creep effects at pier joints.

Chapter 9, Design Examples

Eleven problems are included that illustrate the step-by-step process for design. Each design case is solved by the AASHTO *LRFD Specifications*. Bridge types included are a simple-span adjacent box beam bridge, typical simple-span AASHTO-PCI bulb-tee beam bridge, a three-span bulb-tee beam bridge made continuous for live load and impact, a simple-span deck bulb-tee beam bridge, a U-beam bridge, double-tee beam bridge, and a stay-in-place deck panel system. Each example solution provides details, explanation, and precise reference to the applicable specification section.

Chapter 10, Bearings

The chapter includes selection and detailing guides for elastomeric bearings and an introduction to other types of bearings. Newly updated examples illustrate AASHTO Method A and B according to the *LRFD Specifications* procedures.

Chapter 11, Extending Spans

This chapter describes the effectiveness of various methods for extending span capacity such as the use of high-strength concrete, continuity, spliced beams, and post-tensioned beams. It discusses effects on substructure geometry and provides numerical design examples and successful details of constructed bridges.

Chapter 12, Curved and Skewed Bridges

This covers ordinary highway and specialty bridges. It emphasizes stringer bridge systems. The chapter describes the effects of skew and curvature on design and detailing of both superstructures and substructures. The issues related to handling and transportation are also covered.

Chapter 13, Integral Bridges

This chapter is based on a PCI state-of-the-art report and discusses analysis, design techniques, and current practices plus a review of several case studies.

Chapter 14, Precast Segmental Bridges

This chapter is a work in progress. It describes the two most common methods of precast concrete segmental bridge construction: balanced cantilever and span-by-span. These solutions are discussed in detail. A few sections of the chapter such as methods of construction and geometry control will be completed and available in a future release.

Chapter 15, Seismic Design

Considerations for the selection of structural systems for precast concrete bridges in seismic regions are addressed in depth. The objective of this report is to present state-of-the-practice information on the seismic design of ordinary highway bridges containing precast components. The chapter is based on a PCI state-of-the-art report published in 2014.

Chapter 16, Additional Bridge Products

The chapter will discuss design and detailing of precast concrete bridge products including piers, abutments, full-depth deck panels, stay-in-place composite deck panels, piles, pile caps, railings, culverts, and earth retaining systems. The chapter will be completed and available in a future release.

Chapter 17, Railroad Bridges

Included in this chapter are the specific requirements for railroad bridges, and the benefits of precast concrete for these structures. It provides typical product details and construction considerations as well as detailed examples.

Chapter 18, Load Rating Procedures

The chapter describes strength evaluation including rating factors and load testing. It covers analysis and load distribution methods according to both AASHTO *Standard* and *LRFD Specifications*. It includes lessons learned and the tools to consider when load rating older structures using the *LRFD* methods.

Chapter 19, Repair and Rehabilitation

This chapter includes the following topics: repair of new products prior to shipment; repair of deterioration or damage during construction and during service life; and strengthening techniques. It is based on a PCI publication with a similar name.

Chapter 20, Piling and Substructures

The chapter will be completed and available in a future release.

Chapter 21, Pedestrian Bridges

The chapter includes pedestrian bridges and other similar bridges that may be used for purposes such as equestrian or wildlife crossings and snowmobile bridges. It is a guide for the use of precast concrete in these structures. It provides the unique considerations for pedestrian facilities including the Americans with Disabilities Act requirements for design.

Appendix A, Notation**Appendix B, AASHTO/PCI Standard Products****Appendix C, Local/Regional Products****Appendix D, Sample Specifications****Appendix F, PCI Certification Programs****THE REVIEW PROCESS**

This manual has undergone extensive reviews during its original preparation and through recent revisions. The process was under the direction of the PCI Managing Director of Transportation Systems who in turn worked with the guidance of the PCI Transportation Activities Council. Formal reviews were performed by a quality control engineer and an editor. This was followed by detailed reviews by a specially appointed Blue Ribbon Panel or by the PCI Committee on Bridges. These reviews culminated with formal ballots. Valid comments were incorporated and the changes re-reviewed by the same groups. The resulting drafts were given formal reviews by the PCI Technical Activities Council. Final changes were approved by a liaison appointed by TAC, then released for printing. Future changes to the Manual will undergo a similar review procedure. The process was developed to ensure that the manual meets the quality standards of the Precast/Prestressed Concrete Institute, that it includes state-of-the-art information, and is representative of industry practices and procedures.

USER INSTRUCTIONS

UI 1.0 USING THIS MANUAL

The PCI Bridge Design Manual has been designed for complete flexibility and ease of updating. The electronic version and optional loose-leaf format makes it easy to revise and insert material. You may wish to add, for example, pages of notes or additional material of your choosing.

UI 1.1 LOCATION IN THE MANUAL

The electronic version contains links to sections within the manual and to websites. The user may use a page number or section number to jump to a topic. On the top of each page is a section number indicating the topic shown on the page and most paragraphs are not only numbered, but also titled. The paragraph titles quickly identify the subject of the text.

UI 1.1.1 Paragraph Numbers

Each main paragraph in the text is identified with a decimal numbering system similar to the familiar system in the *AASHTO LRFD Specifications*. This is the system that is used here to organize this page you are reading. The outline organization of these numbers can be easily scanned in the Table of Contents at the beginning of each chapter. The hierarchy of the system is also apparent by the type size and font used in the text. All of the design examples include an identical section numbering system so that a specific topic of design will have the same number in every example.

UI 1.1.2 Page Header

Each page contains a header that identifies:

- Name of the Manual
- Chapter number
- Chapter Title
- Number and title of the sub-section(s) of text that begin and end each page
- Chapters 8 and 9 also show the primary Section number in the header

By referring to this header, you can quickly locate a general area of a chapter. Then, by looking at the paragraph number and title, you can locate specific topics and text.

UI 1.1.3 Page Footer

The lower right corner of each page shows the month and year of publication. There is a section number and page number on each page. Revised sheets will contain “a, b, . . .” after the page number with a new date. This will prove useful in keeping your manual current with revised pages. Hint: If you maintain a paper copy, you may wish to print these downloaded pages on colored paper for easy identification.

UI 1.1.4 Figures and Tables

All Figures and Tables contained in the manual are numbered to the Section where they first appear. Example: **Figure 3.2.4.3-1** is found in Section 3.2.4.3 and **Figure 3.2.4.3-2** is the second figure to appear in that same Section. Figures and Tables referenced in the text are in **bold type**.

UI 1.1.5 Equations

Equations from the *AASHTO LRFD Specifications* are identified by [LRFD] with exception being Chapter 18—Load Rating Procedures and Appendix A—Notations that references both *LRFD* and *Standard Specifications* to help create a cross reference for terminology. Other equations are numbered to the Section where they first appear as for Figures and Tables described above.

UI 1.1.6 Electronic Document Navigation Help

Instructions for using and navigating the electronic version of this document are available by pressing the “F1” key or at: <http://www.adobe.com/products/digitaleditions/help/>

UI 1.2 REVISIONS

Regular revisions to this manual are to be expected. The AASHTO specifications on which this manual is based, are revised annually. To receive revisions, or notices of revisions, it is necessary to register your copy of the manual as described elsewhere. There is no cost or obligation for you to do so. Use the web links and portal provided to you when you received this manual or call or write PCI at the address and number on the inside title page. You will receive a notice at your registered email when you need to download the updated releases.

UI 1.2.1 Errors and Omissions

UI 1.2.1.1 Your Help Needed

Your help will be very much appreciated in locating errors and identifying omissions. Please contact PCI with your observations and suggestions. Email your input to PCIBridgeManual@pci.org

UI 1.2.1.2 Dissemination of Corrections

Errors corrected will be assembled and emailed to registered manual-holders at regular intervals. The replacement pages will readily identify the revision and the page will be identified as revised in the footer. Revisions will be emailed free of charge. Those that have a paper copy will need to print and insert the revised page.

UI 1.2.2 Revisions Due to Specifications Changes

Revisions to the AASHTO specifications may require more significant revisions to the manual. Major revisions may require the payment of a fee. Registered manual-holders will be notified of these opportunities to update their books.

UI 1.2.3 Additions

Periodically, new material will be compiled for this manual. Additional chapters are being developed on such topics as:

- Additional Bridge Products chapter
- Completion of the Precast Segmental Bridges chapter
- Piling and Substructures chapter

Divider tabs have already been prepared and included for these additions. Also, at least one more design example is expected to be made available as an electronic download with the next release of this edition.

UI 1.3 SUGGESTIONS

UI 1.3.1 Your Suggestion

Your suggestions and comments concerning this Manual will be greatly appreciated. Please e-mail to PCIBridgeManual@pci.org.

UI 1.3.2 Our Suggestion

We strongly urge the designer, in the early stages of a project, to contact one or more PCI Plant Certified precast concrete manufacturers. The manufacturer can advise about locally available precast sections, spans, prestressing capabilities, locally accepted methods of construction, etc. The producer can often help with framing solutions and cost estimates. They can provide specific design information about special local, state, or regional precast sections. Some have prepared inserts for Appendix C—Local/Regional Products for this manual. PCI can supply a current list of quality-certified producers. A current list is also readily available on the PCI website at the address on the inside cover page of this manual.

TABLE OF CONTENTS

Introduction

Chapter 1 – Sustainability

- 1.1 Scope
- 1.2 Life Cycle
- 1.3 General Sustainability Concepts
- 1.4 Sustainability and Precast Concrete Bridges
- 1.5 Sustainable Features of Precast Concrete
- 1.6 Simplified Tools and Rating Systems
- 1.7 State-of-the-Art and Best Practices
- 1.8 Keywords
- 1.9 References

Chapter 2 – Material Properties

Notation

- 2.1 Scope
- 2.2 Plant Products
- 2.3 Concrete Materials
- 2.4 Selection of Concrete Mix Requirements
- 2.5 Concrete Properties
- 2.6 Grout Materials
- 2.7 Prestressing Strand
- 2.8 Nonprestressed Reinforcement
- 2.9 Post-Tensioning Materials
- 2.10 Fiber Reinforced Polymer Reinforcement
- 2.11 Reinforcement Sizes and Properties
- 2.12 Relevant Standards and Publications

Chapter 3 – Fabrication & Construction

Notation

- 3.1 Scope
- 3.2 Product Components and Details
- 3.3 Fabrication
- 3.4 Plant Quality Control and Quality Assurance
- 3.5 Transportation

- 3.6 Installation
- 3.7 Diaphragms
- 3.8 Precast Deck Panels
- 3.9 Precast Full-Depth Bridge Deck Panels
- 3.10 References

Chapter 4 – Strategies for Economy

- 4.0 Introduction
- 4.1 Geometry
- 4.2 Design
- 4.3 Production
- 4.4 Delivery and Erection
- 4.5 Other Products
- 4.6 Additional Consideration
- 4.7 Summary and References

Chapter 5 – Aesthetics

- 5.1 Introduction
- 5.2 Aesthetics Design Concept
- 5.3 Project Aesthetics
- 5.4 Component Aesthetics
- 5.5 Appurtenance Aesthetics
- 5.6 Maintenance of Aesthetic Features
- 5.7 Cost of Aesthetics
- 5.8 Summary
- 5.9 Publications for Further Study

Chapter 6 – Preliminary Design

- Notation
- 6.0 Scope
- 6.1 Preliminary Plan
- 6.2 Superstructure
- 6.3 Substructure
- 6.4 Foundations
- 6.5 Preliminary Member Selection
- 6.6 Description of Design Charts
- 6.7 Preliminary Design Examples

- 6.8 References
- 6.9 Preliminary Design Charts
- 6.10 Preliminary Design Data

Chapter 7 – Loads & Load Distribution

Notation

- 7.1 Scope
- 7.2 Load Types
- 7.3 Load Combinations and Design Methods
- 7.4 Simplified Distribution Methods
- 7.5 Refined Analysis Methods
- 7.6 References

Chapter 8 – Design Theory & Procedure

Notation

- 8.0 AASHTO Specification References
- 8.1 Principles and Advantages of Prestressing
- 8.2 Flexure
- 8.3 Strand Transfer and Development Lengths
- 8.4 Shear
- 8.5 Horizontal Interface Shear
- 8.6 Loss of Prestress
- 8.7 Camber and Deflection
- 8.8 Deck Slab Design
- 8.9 Transverse Design of Adjacent Box Beam Bridges
- 8.10 Lateral Stability of Slender Members
- 8.11 Bending Moments and Shear Forces Due to Vehicular Live Loads
- 8.12 Strut-and-Tie Modeling of Disturbed Regions
- 8.13 Detailed Methods of Time-Dependent Analysis
- 8.14 References

Chapter 9 – Design Examples

Notation

- 9.0 Introduction
- 9.1a Design Example – Bulb-Tee (BT-72), Single Span with Composite Deck. Designed using Transformed Section Properties, General Shear Procedure, and Refined Estimates of Prestress Losses

- 9.1b Design Example – Bulb-Tee (BT-72), Single Span with Composite Deck. Designed using Gross Section Properties, Appendix B5 Shear Procedure, and Refined Estimates of Prestress Losses
- 9.1c Design Example – Bulb-Tee (BT-72), Single Span with Composite Deck. Designed using Transformed Section Properties, Simplified Shear, and Approximate Prestress Losses
- 9.2 Design Example – Bulb-Tee (BT-72), Three Spans with Composite Deck. Designed using Transformed Section Properties, General Shear Procedure, and Refined Estimates of Prestress Losses
- 9.3 Design Example – Deck Bulb-Tee (DBT-53), Single Span with Noncomposite Surface. Designed using Transformed Section Properties, General Shear Procedure, and Refined Estimates of Prestress Losses
- 9.4 Design Example – Box Beam (BIII-48), Single Span with Noncomposite Surface. Designed using Transformed Section Properties, General Shear Procedure, and Refined Estimates of Prestress Losses
- 9.5 Design Example – Box Beam (BIII-48), Single Span with Composite Deck. Designed using Transformed Section Properties, General Shear Procedure, and Refined Estimates of Prestress Losses
- 9.6 Design Example – U-Beam (TX-U54), Single Span with Precast Panels and Composite Deck. Designed using Transformed Section Properties, General Shear Procedure, and Refined Estimates of Prestress Losses
- 9.7 Design Example – Double-Tee Beam (NEXT 36 D), Single Span with Noncomposite Surface. Designed using Transformed Section Properties, General Shear Procedure, and Refined Estimates of Prestress Losses
- 9.8 Design Example – Double-Tee Beam (NEXT 36 F), Single Span with Composite Deck. Designed using Transformed Section Properties, General Shear Procedure, and Refined Estimates of Prestress Losses
- 9.9 Design Example – Precast Composite Slab System. To be included in the next edition.
- 9.10 Design Example – Precast Concrete Stay-in-Place Deck Panel System. Designed using Transformed Section Properties and Refined Estimates of Prestress Losses

Chapter 10 – Bearings

Notation

- 10.1 Introduction
- 10.2 History of Elastomeric Bearings
- 10.3 Specifications
- 10.4 Loads and Movements for Design
- 10.5 Planning the Bearing Layout
- 10.6 Types of Elastomeric Bearings

- 10.7 Behavior of Elastomeric Bearings
- 10.8 Design of Elastomeric Bearings
- 10.9 Bearing Selection Guide
- 10.10 References

Chapter 11 – Extending Spans

Notation

- 11.1 Introduction
- 11.2 High-Performance Concrete
- 11.3 Continuity
- 11.4 Spliced-Beam Structural Systems
- 11.5 Examples of Spliced-Beam Bridges
- 11.6 Post-Tensioning Analysis
- 11.7 Post-Tensioning Anchorages in I-Beams
- 11.8 Design Example: Two-Span Beam Spliced Over Pier
- 11.9 Design Example: Single Span, Three Segment Beam
- 11.10 References

Chapter 12 – Curved & Skewed Bridges

Notation

- 12.1 Scope
- 12.2 Skew and Grade Effects
- 12.3 Curved Bridge Configurations
- 12.4 Useful Geometric Approximations
- 12.5 Structural Behavior of Curved Bridges
- 12.6 Design Considerations
- 12.7 Fabrication
- 12.8 Handling, Transportation, and Erection
- 12.9 Design Example
- 12.10 Detailed Final Design
- 12.11 References

Chapter 13 – Integral Bridges

- 13.1 Introduction
- 13.2 Integral (Jointless) Bridges
- 13.3 Superstructure Design
- 13.4 Abutment Design

- 13.5 Pier Design
- 13.6 Analysis Considerations
- 13.7 Survey of Current Practice
- 13.8 Case Studios
- 13.9 Conclusions
- 13.1 Cited References
- 13.11 Bibliography

Chapter 14 – Segmental Bridges

- 14.1 Introduction
- 14.2 Precast Segments
- 14.3 Transverse Analysis
- 14.4 Balanced Cantilever Construction
- 14.5 Span-by-Span Construction
- 14.6 Diaphragms, Anchor Blocks and Deviation Details
- 14.7 Geometry Control
- 14.8 Prestressing with Post-Tensioning
- 14.9 Cited References
- 14.10 PCI Journal Segmental Bridge Bibliography

Chapter 15 – Seismic Design

- 15.1 Introduction
- 15.2 Structural System Considerations
- 15.3 Seismic Design Criteria
- 15.4 Seismic Analysis
- 15.5 Connection Details
- 15.6 Design Examples
- 15.7 Cited References

Chapter 16 – Additional Bridge Products

Under Development

Chapter 17 – Railroad Bridges

Notation

- 17.0 Introduction
- 17.1 Typical Products and Details
- 17.2 Construction Considerations

- 17.3 The American Railway Engineering and Maintenance-of-Way Association Load Provisions
- 17.4 Current Design Practice
- 17.5 Case Study No. 1 – Truss Bridge Replacement
- 17.6 Case Study No. 2 – Timber Trestle Replacement
- 17.7 Case Study No. 3 – Through Plate Girder Replacement
- 17.8 DESIGN EXAMPLE - DOUBLE-CELL BOX BEAM, SINGLE SPAN, NONCOMPOSITE, DESIGNED IN ACCORDANCE WITH AREMA SPECIFICATIONS
- 17.9 References

Chapter 18 – Load Rating Procedures

Notation

- 18.1 Overview of Bridge Load Rating
- 18.2 Loads and Distribution
- 18.3 Rating Methodology
- 18.4 Rating by Load Testing
- 18.5 Load Rating Report
- 18.6 Rating Example
- 18.7 References

Chapter 19 – Repair & Rehabilitation

- 19.1 Scope
- 19.2 Repair of New Products
- 19.3 Repair of Products Damaged During Construction and Service Life
- 19.4 Strengthening Techniques
- 19.5 Specification and Manuals
- 19.6 Reference

Chapter 20 – Piles

Under Development

Chapter 21 – Recreational Bridges

- 21.1 Introduction
- 21.2 Description, Guidelines, and Examples
- 21.3 Special Use Pedestrian Bridges
- 21.4 Cited References

Appendix A - Notation

Appendix B – AASHTO/PCI Standard Products

Appendix C – PCI Regional Products

Appendix D – Sample Specification

Appendix E – Glossary (under development)

Appendix F – PCI Certification Programs

BRIDGE DESIGN

Precast, Prestressed Concrete Bridges – The High Performance Solution



Since its introduction in the United States in 1949, precast, prestressed concrete has rapidly become the preferred composite material for bridge design and construction. Today, it remains the solution of choice for transportation agencies and their bridge designers across the country. This growth came, and will continue to come, from the commitment of precasters to develop, improve, and implement advanced materials, products and technology all aimed at enhancing the performance of these bridges and the options available to the designer.

This publication is intended to provide the designer with an understanding of the precast, prestressed concrete industry and an introduction to the application of this material to bridge design and construction.

Growth of the Industry

The combination of prestressed high strength steel to counteract tensile stresses, and high performance concrete to provide compressive strength, makes this unique composite material adaptable to many situations, especially to the design and construction of bridges.

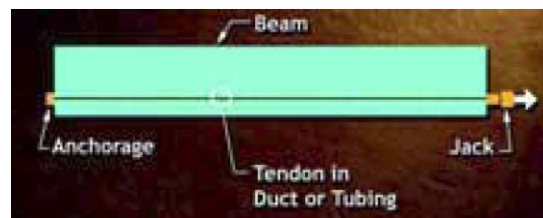


Professor Gustav Magnel, one of the pioneers of prestressed concrete, explained it very simply to his students by using a stack of books. When concrete is precompressed, as the lower row of books are, it can carry not only its own weight but also a significant amount of superimposed loads, represented by the books on top.



There are two ways of introducing prestress into a concrete member:

- Post-tensioning applies to concrete where steel strands or bars are tensioned against the concrete after the concrete has hardened. Cement grout is usually pumped to fill the duct.



- Pretensioning applies to concrete where steel strands are tensioned between abutments before the concrete is placed in the forms. After the concrete has hardened, force in the strands is transferred to the concrete by releasing anchors at the abutments. The transfer of force occurs through the bond between concrete and steel.



Walnut Lane Memorial Bridge
 Photo: © Lawrence S. Williams, Inc.

The single most important event leading to the founding of the precast, prestressed concrete industry in North America was the construction, in 1949 and '50, of the famed Walnut Lane Memorial Bridge in Fairmont Park, Philadelphia, Pennsylvania. From a technical perspective it is innovative, and from an historical perspective, it is fascinating that the Walnut Lane Memorial Bridge was constructed with prestressed concrete. Consider that there was very little published information on the subject and no experience with linear prestressing in this country. The bridge became a reality through a fortunate sequence of events, and the vision, courage and persistence of a few extraordinary individuals.



The 1950s was the decade that saw the introduction of 7-wire prestressing strand, plant pretensioning, long-line steel casting beds, chemical admixtures, high early-strength concrete, steam curing and many other innovations. These developments coupled with the technical and logistical support provided by the Precast/Prestressed Concrete Institute (PCI), chartered in 1954, fostered the rapid growth of the industry. Applications of precast and prestressed concrete designs quickly began to appear in a wide variety of impressive structures. By 1958, there were more than 200 prestressing plants in the United States.

Precast and prestressed concrete products, while designed in accordance with evolving engineering standards, gained an excellent reputation because the industry, early on, recognized the need for quality above all else. PCI's Plant Certification program quickly became an integral part of plant production. PCI Plant Certification assures specifiers that each manufacturing plant has been audited for its processes and its capability to consistently produce quality products.

Performance of Prestressed Concrete Bridges

The National Bridge Inventory, maintained by the Federal Highway Administration (FHWA), reveals that of about 475,000 bridges with spans of 20 feet and more, 173,000 are rated as substandard.

The fact that a bridge is "deficient" does not imply that it is unsafe or is likely to collapse. It may be either structurally or functionally deficient. A deficient bridge may need significant maintenance, rehabilitation or sometimes, even replacement. Proper load posting, restricted use and various other methods of traffic control can allow these bridges to continue to be used.



What is causing the nation's bridge problem? One contributing factor is age – the average age of all bridges is now about 45 years. Another factor is increasing vehicle sizes and weights, as well as traffic volumes, that are well beyond what many structures were designed for when they were put into service. A third major factor was limited corrosion resistance in coastal regions and the increasing use of de-icing salts in cold climates. These salts seep through and under the bridge decks, corroding reinforcing bars in decks, in beams and in substructures. Salts readily attack exposed steel members.

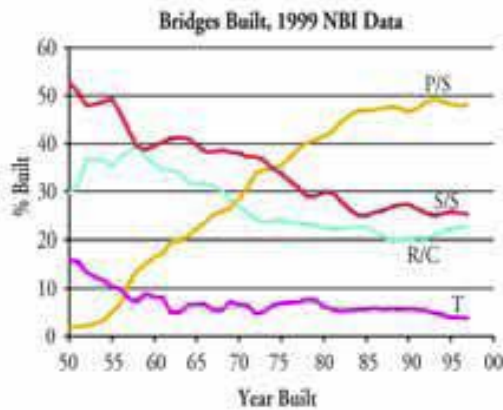
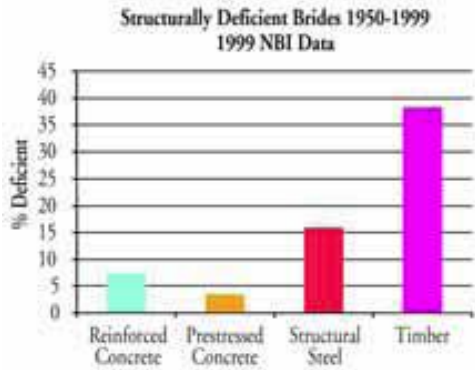
Studies of the National Bridge Inventory data clearly indicate the superior performance of prestressed concrete bridges when compared to the performance of other materials of an equal age.

In addition, owners and designers have long recognized the low initial cost, low maintenance requirements and extended life expectancy of prestressed concrete bridges. This is reflected in the increasing market share of prestressed concrete, which has grown from zero percent in 1950 to about 50 percent now. It's the only structural material to have experienced continuous growth during this period.

This growth is not only reflected in short-span bridges, but is also now occurring for spans over 150 feet. These spans have been the exclusive domain of structural steel for many years.



Precast concrete bridges have also been shown to be highly durable and fire resistant, and they have excellent riding characteristics. Precast concrete bridges can be installed during all seasons and opened to traffic more rapidly than any other permanent type of bridge. In addition, very slender bridges can be achieved with solid slabs, box beams, multi stemmed units and I-beams. The clean, attractive lines of concrete beams help bridge designers meet the most demanding aesthetic requirements.



Since 1950, tens of thousands of prestressed bridges have been built and many are under construction in all parts of the United States.

They range in size from short spans...



to medium spans...



to some of the largest projects in the world

There are several good reasons why precast, prestressed concrete bridges have gained such wide acceptance. Some bridge designers are surprised to learn that precast, prestressed concrete bridges are usually lower in first cost than other types of bridges. Coupled with savings in maintenance, precast bridges offer maximum economy. Case-after-case can be cited at locations throughout the United States, and these bridges are attractive as well as economical.

The overall economy of a structure is measured in terms of its life-cycle costs. This includes the initial cost of the structure plus the total operating costs. For stationary bridges, the operating cost is the maintenance cost. Precast, prestressed concrete bridges designed and built in accordance with AASHTO or AREMA specifications should require little, if any, maintenance. Because of the high quality of materials used, prestressed members are particularly durable. Fatigue problems are nonexistent because traffic loads induce only minor net stresses.

Advantages of Prestressed Concrete Bridges

Low Initial Cost



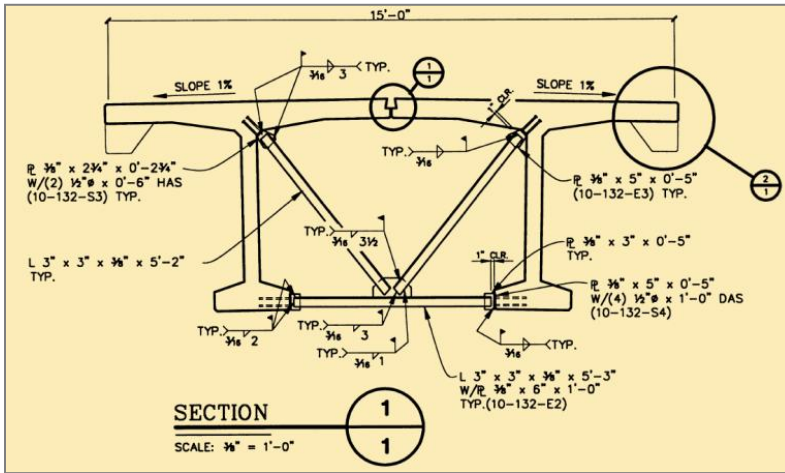
The state of Minnesota saved more than 16% – half a million dollars – by planning for a prestressed alternate to a steel bridge. The 700-foot-long bridge is jointless up to the abutments and is the longest continuous bridge in the state. It also contained the state’s longest single concrete span. A Minnesota transportation official stated, “Originally, we didn’t think concrete was suited to this...bridge. However, the fabricator showed us it was a viable alternative. Everything went smoothly...we’re well satisfied...”

Minimal Maintenance



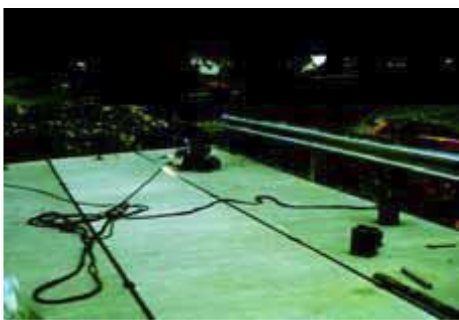
On the Illinois Toll Highway System, during 1957 and 1958, the superstructures of more than 250 bridges were built with precast prestressed concrete I-beams. They span up to 90 feet and some of them have precast stay-in-place deck panels, precast diaphragms, and 94 use spun-cast, hollow cylinder pile column bents. They have withstood heavy traffic, severe weathering and very high salt applications. Yet, these bridges have required very little maintenance. Other projects in all parts of North America have exhibited similar experience – little or no maintenance has been required on precast prestressed concrete bridges.

Of course, no painting is needed. Some bridge engineers estimate the lifecycle cost of re-painting steel bridges to be 15 to 25% of the initial cost. Painting bridges is environmentally unfriendly and can be especially expensive when accomplished over busy highways, streams and railroad rights-of-way, or in rugged terrain.



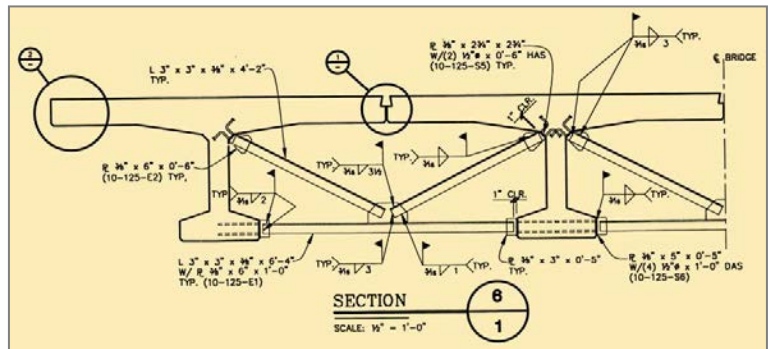
Durable Concrete

One of the reasons for selecting prestressed concrete beams with integral precast decks for this bridge was the durability of prestressed concrete and the resulting low maintenance requirements. As a result of a winter flood, the single lane bridge on a major forest road was washed out, cutting access to a U.S. highway for a half dozen homes...including one with an elderly resident needing continuing medical care. After only 15 days of receiving plans, the precaster had fabricated the two, 135-foot-long spans with 7'-6"-wide integral decks, and the bridge was opened to traffic 3 days later - 18 days in all. The U.S. Forest Service stated that the bridge was least expensive, fastest and the best solution.



Precast, prestressed concrete bridge components are easy to erect, particularly when the tops of the units form the entire deck slab - called an integral deck bridge. Formwork and site-cast concrete are eliminated. Connections between these adjacent units often consist of welding adjoining plates and grouting a continuous keyway. Carefully planned details speed the construction process and result in overall economy.

Simple Solution



Replacing this bridge on US Route 95 in Idaho illustrates another example of the advantages of very fast, yet simple construction:

New Year’s Day: Rains and melting snow washed out this bridge over the Little Salmon River linking the northern and southern parts of the state.

January 4: The Idaho Department of Transportation contacted the precaster to investigate solutions. They determined that the fastest way to replace the three spans was to use a single 80-foot span comprised of bulb-tees with an integral deck. The top flange would be 8-inches thick and 8’-6” wide. The diaphragms would also be precast onto the ends of the girders.

January 8: Engineers in the Bridge Section approved shop drawings and tensioning calculations.

January 18: Bulb-tees were shipped 240 miles and set in place...just 17 days after the flood! Included in the shipment were intermediate steel diaphragms, guardrail posts and guardrail...all the components to complete the structure.

January 25: The project was completed. The bridge was in service just 24 days after the flood!

Integral deck bridges can be set on precast or other abutments and erected through practically any weather. They can be opened to traffic very rapidly.

All Weather Construction



In Ketchikan, Alaska, a bridge on the only highway to the north was washed out when an old dam gave way on October 26. Integral deck girders were selected for the 85-ft span. The 12 girders were designed and precast in the state of Washington, then shipped by rail and barge to Alaska. The girders were installed and the bridge was completed and opened to traffic on December 19 - only 54 days after the washout - despite the problems of design, remote location, great distances, and adverse weather conditions during the onset of an Alaskan winter!

The planned replacement of substandard bridges can be accomplished easily with precast prestressed sections. In some cases, existing abutments can be used, but in others, it is easier and more economical to build new ones, or to utilize precast abutments and wing walls supported on cast-in-place footings.

Fast Construction



Mitchell Gulch Bridge, southeast of Denver, was scheduled for replacement with three, 10 ft by 6 ft cast-in-place box culverts. This would require three months of traffic detour on a key commuter route carrying 12,000 vehicles per day. A contractor-suggested alternate resulted in the replacement of the bridge in less than 48 hours – requiring traffic interruption only from Friday night until Sunday.

The project required driving H-piles in advance of closure, dismantling the old bridge, then installing a precast wingwall and abutment system. Next, prestressed voided slabs were installed and grouted along the joints. Fill was placed over the slabs and compacted. Finally, asphalt paving was laid and the bridge opened to traffic. Commuters on Monday morning weren't any the wiser – exactly as planned!

The replacement of bridges may not always be easy to plan in advance. Fires, floods and accidents are but a few reasons for emergency replacements or repairs. Precast concrete and industry manufacturers have consistently demonstrated response to disasters large and small.

Emergency Response



In 1996, the bridge over Salt Creek on I-75 near Venice, Florida, was damaged beyond repair when a tanker loaded with diesel fuel crashed and rolled underneath. The five-span, 330-foot-long bridge required 25 AASHTO beams, 65 ft, 3-1/2 in. long. Exposed precast piles were salvaged by cutting them just below ground line, then splicing on precast extensions. The extensions arrived on-site just two days after they were ordered. The first five beams were delivered and erected four days after production began, and all 25 beams arrived within seven days. The new bridge was reopened to traffic just 18 days after the accident.



In May 2002, two barges hit and collapsed four spans of the I-40 bridge over the Arkansas River near Webber Falls, Oklahoma. Fourteen people were lost. Originally steel, three spans were replaced with 36, 72-in.-deep precast bulb-tee beams, 130-foot long. After a spectacular effort by the entire design and construction team, the bridge was opened to traffic in just 65 days. State officials stated that, "...precast concrete offered us a speed advantage over replacing the entire bridge with steel."



Interstate 65 in Birmingham, Alabama was brought to a standstill on a Saturday morning in January 2002, when a tanker load of gasoline crashed and burned under a steel bridge. The state quickly designed a replacement bridge and construction began only 16 days after the accident. Prestressed concrete bulb-tee beams, 54-in. deep and 140-ft long, were used in the new bridge, which was both wider and some 20-ft longer to provide for additional future lanes. Using high strength concrete that achieved 8,500 psi in 14 days, the span-to-depth ratio is an impressive 31:1. Fabrication of the beams required only 15 days. The new bridge was opened to traffic just 65 days after the accident and 36 days after construction began. A state designer said that precast concrete "...could be cast and delivered to the jobsite before steel fabricators could even procure material and start fabrication." The general contractor said, "There was no way we could have gone with steel girders because the lead time was prohibitive. The precast was on site within a very short period of time."

A common requirement of bridges is that the superstructure be as shallow as possible in order to provide maximum clearance with minimum approach grades. Through the technique of prestressing, the designer is able to utilize the maximum possible span-to-depth ratio. Span-to-depth ratios as high as 35:1, or even more, can be achieved with solid slabs, voided slabs, box beams, multi-stemmed units, I-beams or bulb-tee sections, each within their respective span ranges. Even though deeper sections will require less prestressing steel, the overall economy of a project may dictate the shallowest available section.

Slender Bridges

The Sedley Bridge provides a crossing for county Rt. 475W over the Norfolk Southern/CSX Railroad tracks in Porter County, Indiana. Faced with severe clearance and approach embankment constraints, the designer chose a unique through-girder solution that resulted in a 112-foot span having an effective structure depth of just 14 inches.



The Yale Avenue Bridge carries Interstate 25 over Yale Avenue, a busy urban arterial in Denver, Colorado. The structure was Colorado’s entry in the Federal Highway Administration’s High Performance Concrete Showcase program. It is designed for traditional Interstate highway loading. The adjacent, single-cell box beams measure 67 in. wide by 30 inches deep and use 10,000 psi concrete (at 56 days). The bridge has two continuous spans (for live load) of 100 and 114 ft and is 138-ft wide. Composite topping has a minimum thickness of 5 in. for a total structure depth of 35 in. and a span-to-depth ratio of 39:1.



The San Angelo (Texas) Bridges, carrying U.S. 87 over the North Concho River and South Orient Railroad, are parallel, eight- and nine-span structures. One bridge used primarily conventional concrete and the other, high performance concrete as part of the Federal Highway Administration’s HPC Showcase program. Designed as simple spans, one used 0.6-in.- diameter strands with 13,500 psi concrete to achieve a length of 157-ft with 54-in.-deep beams plus 3-1/2-in.-thick precast concrete deck panels plus 4-1/2-in. cast-in-place composite concrete topping to achieve a 30.4:1 span-to-depth ratio.



The Clarks Viaduct located in Omaha, is a four-span bridge over U.S. Highway 30 and the Union Pacific Railroad. It has a 52-degree skew and spans of 100, 151, 148 and 128.5 ft. The superstructure is a modified Nebraska 1100 beam, 50-in. deep, using 8,500 psi concrete. The beams sit on unique, individual cast-in-place pier tables to extend their spans. The beams are made fully continuous for superimposed dead loads and live load by splicing high-strength reinforcement extended from the ends of the beams through the cast-in-place tables between the ends of the beams. Including the 7-1/2-in. deck, the span-to-depth ratio is 31.5:1.

Beams that include integral decks, such as this one, can achieve exceptionally high span-to-depth ratios. In addition, they can be installed very quickly while requiring little site-cast concrete.

Aesthetic Bridges



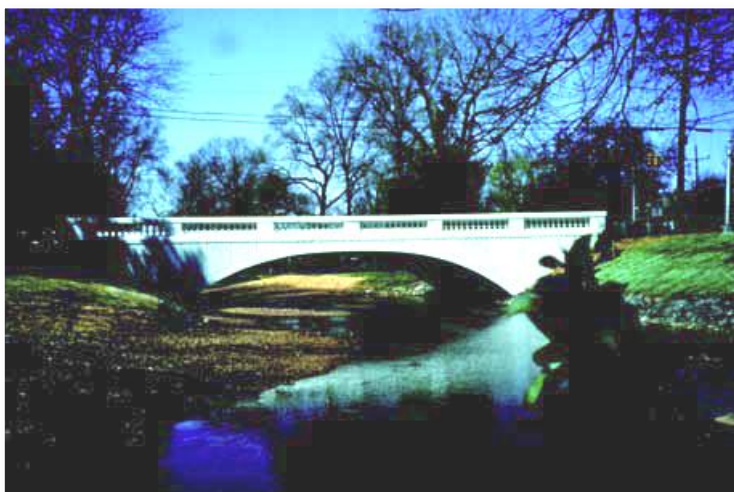
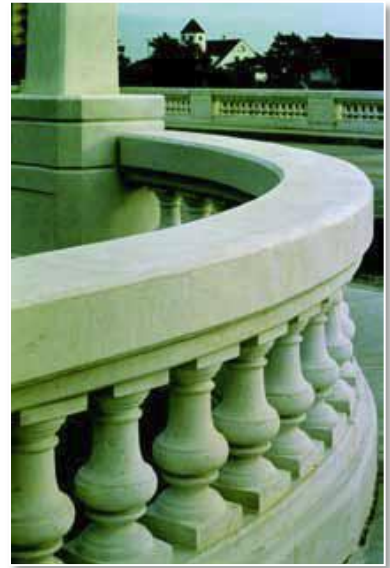
Two very different parks use precast concrete in special ways. The Bridge over Clear Creek, Zion National Park, Utah, uses colored aggregate, sandblasting and pigments to match the bridge to the surrounding native stone. Costing just \$60/SF, the project was considerably less than either steel or cast-in-place.

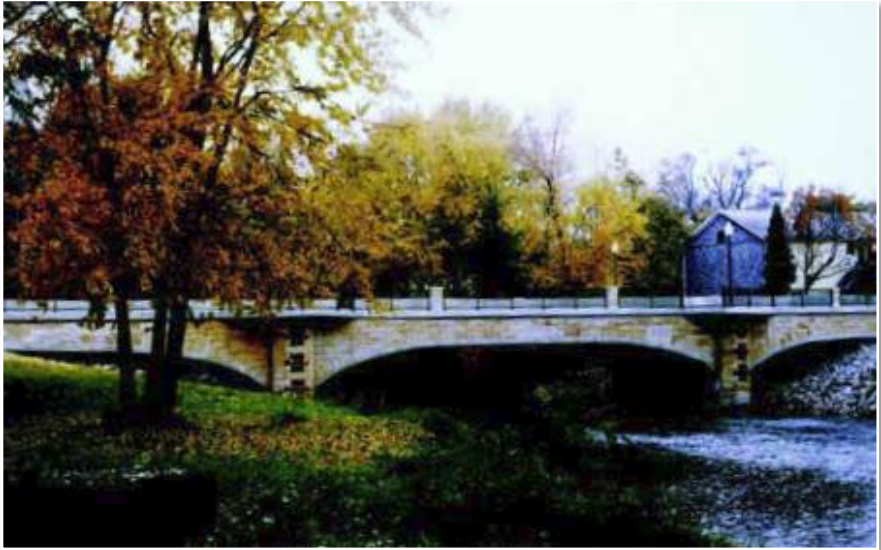
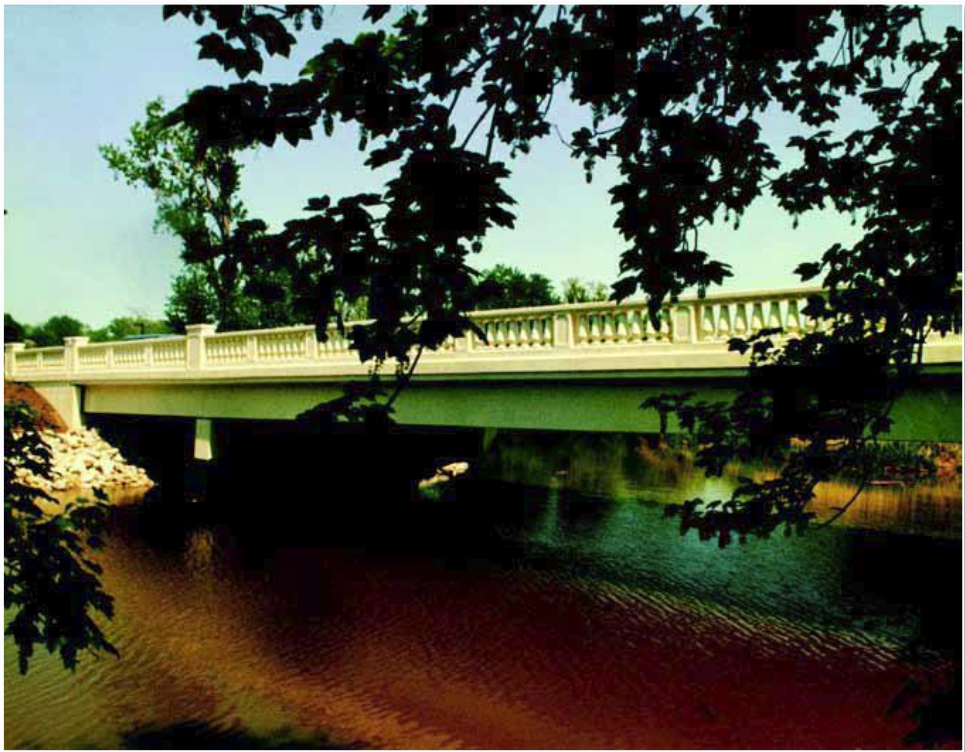
Two bridges in Kil-Cona Park in Winnipeg provide an attractive compliment to these family recreational surroundings



Attractive Bridges

More and more often, designers are adding architectural and aesthetic treatments to precast bridges. These include panels that create an arch appearance or decorative railings. Some solutions are shown in the accompanying photos.





Bridges are subjected to a hostile environment as well as repeated impact loadings. Some must endure intense sun, high temperatures and brackish water. Others must withstand not only the freezing and thawing provided by nature but also the potential for damage induced with the use of de-icing chemicals. High strength prestressed concrete has excellent freeze-thaw and chemical resistance. Also, prestressed concrete bridges are not easily damaged by fire.

Fire Performance



The Washington State Route 509 Bridge over the Puyallup River near Tacoma was damaged in December, 2002, when a railroad car containing 30,000 gallons of methanol burned beneath span number 8. The span is 146 ft in length and uses 15 lines of 74-in.-deep bulb-tee beams. An investigation revealed that the fire reached temperatures of 3,000 degrees F. The study showed that no significant amount of prestress was lost. A plan was immediately developed for repairs that would permit the bridge to remain in service.



After this timber deck truss bridge burned, an extremely busy 2-lane link was severed between two major population areas.



It was replaced by a safe, low maintenance, prestressed concrete bridge with a record span for this area of 141 ft. It was erected without falsework over an environmentally sensitive, salmon-bearing river. It opened seven months after bid.

Steel girder bridges frequently exhibit disturbing vibrations. The natural frequency of vibration of these bridges can coincide with the frequencies of traffic and then resonance occurs. There are documented cases that show that light bulbs in fixtures installed on steel bridges burn out more rapidly because of such vibrations. There are indications that concrete decks on steel bridges need replacement significantly sooner than concrete decks cast on concrete girders. The natural frequency of vibration of prestressed girder bridges, because of their mass and stiffness, does not coincide with vehicle frequencies. The public will feel safe, secure and comfortable when riding on prestressed concrete bridges. Owners report that decks are less likely to crack prematurely when built on stiff concrete bridges.

Excellent Riding Characteristics



The public will not only be safe but they will feel more secure and comfortable on a concrete bridge that holds traffic vibrations to an absolute minimum. Long continuous spans and integral abutments eliminate or reduce expansion joints for a smoother ride and reduced maintenance.



Quality Assurance

Prestressed concrete is economical because it is an efficient composite of high-strength steel and high performance concrete. To take advantage of this efficiency, precasting plants have developed sophisticated quality control programs that assure the customer that products meet exacting specifications.



Precast prestressed concrete products are rigorously inspected and quality is controlled at the precasting plant. In fact, each operation in the manufacturing process provides for a point of scheduled inspection and control.



During fabrication and handling, portions of prestressed concrete beams are subjected to some of the highest stresses they will ever encounter as structural members. So, in a sense, prestressed members are load-tested during fabrication, handling and installation.



Engineers put their professional reputation on the line whenever they specify a structural material. This requires that they work with the most reputable and qualified sources.

A plant that is PCI Certified tells the engineer several important things:

- The facility has demonstrated production and quality control procedures that meet national industry standards.
- A nationally recognized, independent consulting engineering firm conducts at least two unannounced annual audits. The auditors are accredited engineers. The firm is engaged by PCI for all audits nation-wide.
- Each plant must maintain a comprehensive Quality System Manual (QSM) based on national standards and approved by PCI. The QSM is available for review by owner agencies.

The rigid audits cover more than 150 items. Standards are based on the Manual for Quality Control for Plants and Production of Structural Precast Concrete, PCI manual MNL-116. The audits evaluate concrete materials and stockpiles, concrete mixing, transporting, placing, consolidation and finishing. Procedures are inspected for tensioning of strands and transfer of prestress; concrete curing and temperature controls; product stripping, handling and storage. In-house QC procedures are reviewed thoroughly. In addition, engineering, shop drawings, record keeping and many other practices related to quality production are examined.

- QC personnel must be PCI-Certified, attained by passing written and practical examinations.
- The designer will know that the producer has PCI confirmed capabilities and that the producer stands behind their products.

Failure to maintain acceptable standards makes loss of certification mandatory.

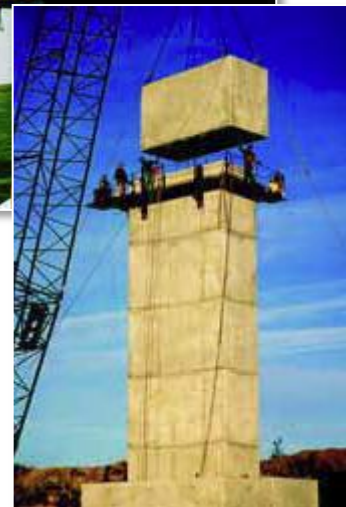


Totally Precast Concrete Bridges

Work zones and detours are difficult problems faced by highway agencies. Using precast concrete and with techniques such as integral deck bridges, traffic interruptions can be minimized because of the availability of plant produced sections and the speed of erecting and completing the bridge.

The versatility of the precast, prestressed concrete industry provides the designer with many options. Can one use precast bridge components to build an “Instant Bridge”? Almost! There are many ways to put a bridge together with precast concrete products.

In addition to the well known superstructure elements – girders and deck slabs – substructure components can be precast.



Precast concrete piles are quite popular in many parts of the country. They come in different sizes and shapes, ranging from 10-inch-square piles to 66-inch-diameter cylindrical piles such as this 172-ft-long unit.

In addition, pile caps can be precast.



Piers and abutments can also be made of precast concrete pieces quickly assembled in the field.



There are many benefits to using precast concrete elements to construct prefabricated bridges. They include:

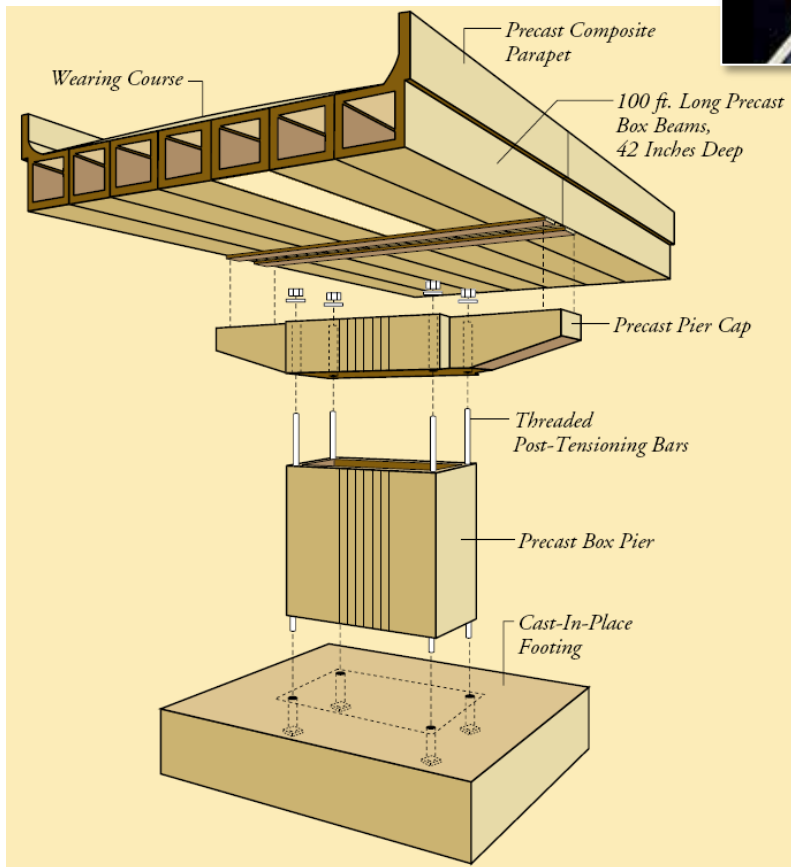
- A single contractor working with only one familiar material can control the schedule for erection of the entire bridge.
- Precast concrete structural elements are made in manufacturing plants under controlled conditions in advance of need and stockpiled for “just-in-time” delivery and erection.
- No need for curing cast-in-place concrete: precast bridge piers can be erected in one working day and beams can be erected immediately following the piers.
- Corrosion resistance and excellent concrete quality is provided through in-plant manufacture of all of the structural elements.
- Fully cured precast concrete structural elements can be delivered to the site. These elements contain little potential for additional shrinkage or creep.
- Owner agencies complete more work in a shorter period of time, resulting in:
 - Reduced cost of handling traffic
 - Reduced accident exposure
 - Reduced inconvenience to the traveling public
 - Fewer motorist complaints
- Contractors benefit from:
 - Reduced exposure of personnel to traffic hazards
 - Greater dollar volume of work accomplished in a shorter period
 - Fewer delays due to weather conditions
 - Less dependence on remote delivery of ready-mixed concrete
- Lower costs for:
 - Forms
 - Cranes
 - Skilled field labor
 - Scaffolding and shoring
- The same crane already needed on the job site for erecting beams and girders may be used for erecting bridge piers and other elements.
- Reduction of motorist delays, complaints and accidents. According to a report by the Texas Transportation Institute, costs incurred by drivers passing through a work zone, along with engineering costs, can be \$10,000 to \$20,000 per day. In urban areas, a federal report states that the cost of work zones can reach \$50,000 per day.

Minimal Traffic Disruption



In San Juan, Puerto Rico, the four, totally precast concrete Baldorioty de Castro Avenue bridges were built in record setting time, attractively and economically.

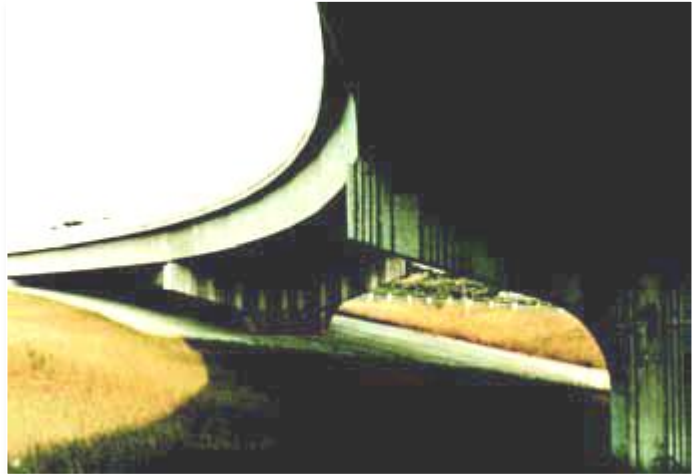
Each of four bridges, ranging in length from 700 to 900 feet, was erected in less than 36 hours – that’s from the time traffic was re-routed on Friday night until traffic resumed over the new bridge on Saturday or Sunday! This included the piers, the superstructure, the overlay and lighting. It was well within the owner’s construction allowance of 72 hours per bridge; a condition established to minimize disruption to one of the city’s most highly traveled corridors.



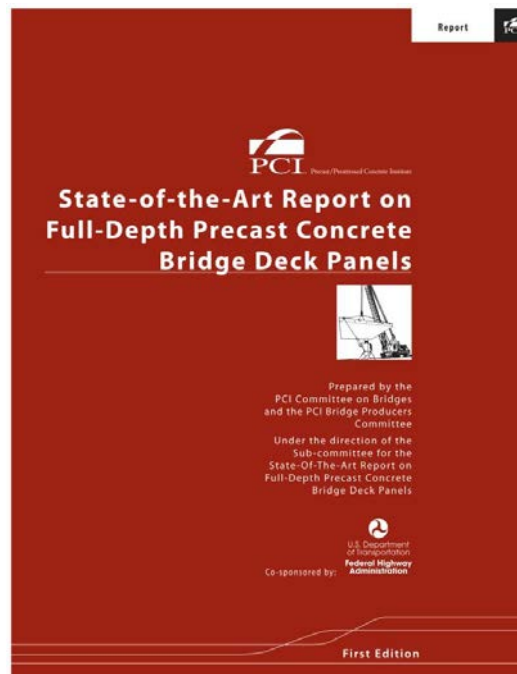
In addition to speed, the bridges also met the city’s budgetary needs. The four box beam bridges were constructed for \$2 million less than the next lowest bid for another material. In addition, the bridges will prove durable and maintenance-free, adding value to this investment.

The Future

Innovation in bridge construction has been, and will continue to be the ongoing focus in the precast concrete industry. The development of horizontally curved precast concrete bridges is one such example out of the past.

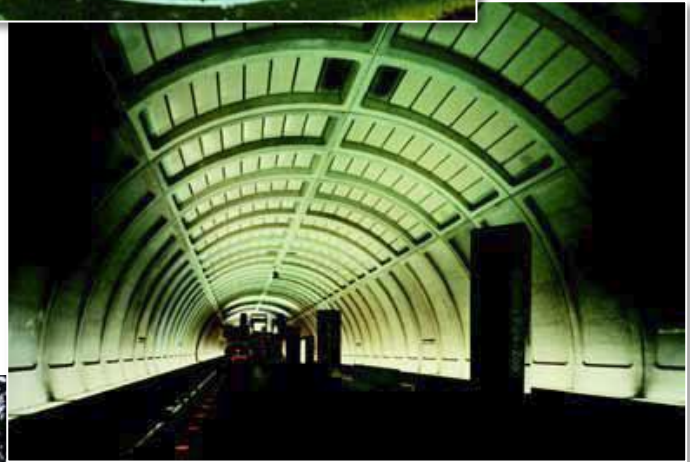


Another development was the use of precast deck panels. Used as stay-in-place forms, the panels improve safety on the jobsite, reduce field placement of reinforcing steel and concrete for bridge decks, resulting in considerable savings. The panels become composite for live loads with the field-placed concrete and are now common in many states.

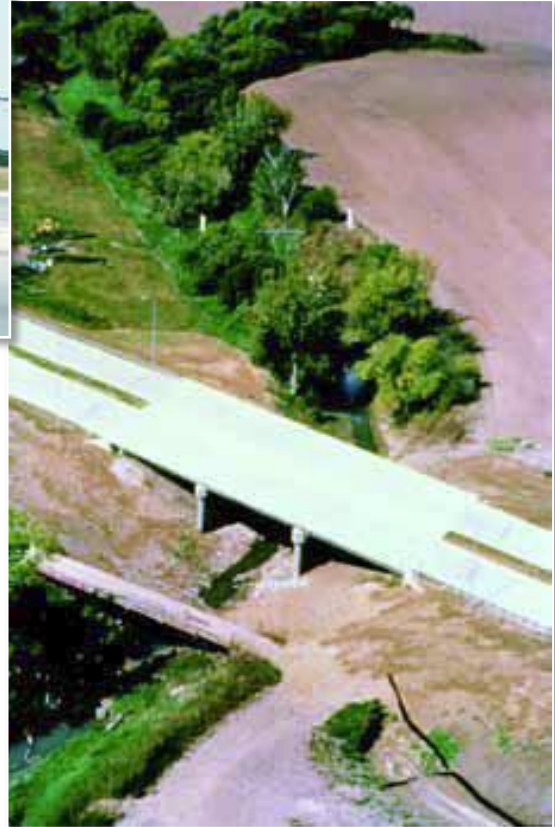


Shown above, PCI with a co-sponsorship from FHWA has issued a State-of-the-Art Report on Full-Depth Precast Concrete Bridge Deck Panels (SOA-01-1911). This effort hopes to familiarize bridge owners with a new solution as a practical alternative to cast-in-place concrete decks.

Material properties, such as corrosion resistance, fire resistance and durability have been improved in a process of continuous evolution. These inherent qualities of precast, prestressed concrete together with a high degree of design flexibility also make it ideal for a wide variety of other applications such as poles, storage tanks, retaining walls, railroad sleepers and sound barriers. All have benefited from plant standardization and the production repetitions achieved from it.



Concrete in the 12,000 to 14,000 psi range is already commercially available. The Louetta Road Bridge in Houston, Texas and the 120th Street and Giles Road Bridge in Sarpy County, Nebraska, both completed in 1996, are examples of bridges with 12,000 to 14,000 psi concrete girders and 5,000 to 8,000 psi concrete decks. Further, the Louetta Road Bridge utilizes high strength precast concrete hollow segmental piers. The Federal Highway Administration, jointly with PCI and numerous states, has consistently promoted the use of High Performance Concrete in bridge applications. High Performance Concrete often involves higher than average compressive strength. But other factors, such as stiffness, permeability and abrasion resistance, in addition to strength, may be requirements of High Performance Concrete. This often depends on the geographic location of the bridge and the component for which it is used.



The benefits of High Performance Concrete include:

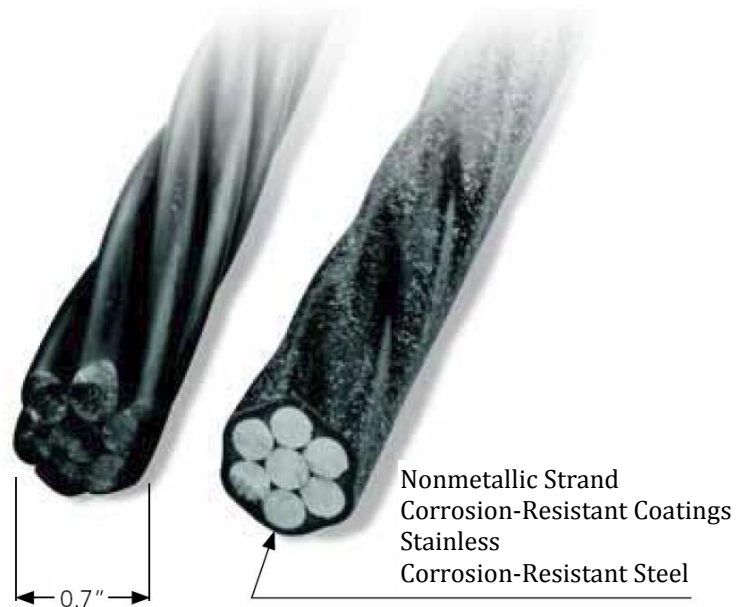
- 1) reduced initial construction costs resulting from wider beam spacing and,
- 2) longer spans and reduced long-term costs that result because of fewer replacements and fewer repairs.
- 3) enhanced durability.



Lightweight aggregate concrete with strengths in the 7,000 to 10,000 psi range is possible. Lightweight concrete reduces dead loads and results in lower seismic forces.

Synthetic, organic and steel fibers have been shown to improve toughness and shrinkage cracking. Recent developments in high performance fiber-reinforced concrete hold promise in terms of performance and cost effectiveness.

Strands of larger diameters and higher strengths will become more common as higher strength concretes are used and the demand for higher prestress force increases. When 0.6-inch diameter strands are used in conjunction with high strength concrete, in the 10,000 to 12,000 psi range, standard I-beams and other products have significantly increased span and spacing capabilities. Strands of 0.7-inch diameter are available in the marketplace but have yet to see significant use (see below). Epoxy-coated (see below) and stainless steel strands will further enhance product durability.



Nonmetallic reinforcement such as glass, carbon and aramid fiber composites will be increasingly used for special applications. A recent demonstration project has shown the compatibility of carbon fiber strands for prestressing a double-tee bridge. Both internally bonded pretensioning and external unbonded prestressing systems were used.

Prestressed concrete got its start as a unique composite material. Further developments by the industry and its suppliers have continued to refine the performance of the product for a wide range of bridge applications.

Today, it gives the public extraordinarily good value for their money.

The reputation of the precast, prestressed concrete industry has been built on the strength, imagination, consistency and integrity of its people and products alike. These attributes will continue to make prestressed concrete the solution of choice for the nation's bridges... not only today, but far into the future.

This page intentionally left blank

1.1 SCOPE.....	1 - 3
1.2 LIFE CYCLE.....	1 - 3
1.2.1 LIFE-CYCLE COST AND SERVICE LIFE.....	1 - 3
1.2.2 ENVIRONMENTAL LIFE-CYCLE INVENTORY AND LIFE-CYCLE ASSESSMENT.....	1 - 4
1.2.2.1 LCI Boundary.....	1 - 4
1.2.2.2 Concrete and Concrete Products LCI.....	1 - 5
1.2.2.2.1 Raw Materials.....	1 - 5
1.2.2.2.2 Fuel and Energy.....	1 - 5
1.2.2.2.3 Emissions to Air.....	1 - 6
1.2.2.3 Life-cycle impact assessment (LCIA).....	1 - 6
1.3 GENERAL SUSTAINABILITY CONCEPTS.....	1 - 7
1.3.1 TRIPLE BOTTOM LINE.....	1 - 7
1.3.2 COST OF GREEN.....	1 - 8
1.3.3 HOLISTIC/INTEGRATED DESIGN.....	1 - 8
1.3.4 REDUCE, REUSE, RECYCLE.....	1 - 8
1.3.4.1 Reduce the amount of material used and the toxicity of waste materials.....	1 - 8
1.3.4.2 Reuse products and containers; repair what can be reused.....	1 - 9
1.3.4.3 Recycle as much as possible, which includes buying products with recycled content.....	1 - 9
1.3.5 TERMINOLOGY.....	1 - 9
1.4 SUSTAINABILITY AND PRECAST CONCRETE BRIDGES.....	1 - 10
1.4.1 DURABILITY.....	1 - 10
1.4.1.1 Corrosion resistance.....	1 - 10
1.4.1.2 Inedible.....	1 - 11
1.4.1.3 Ultraviolet resistance.....	1 - 11
1.4.2 RESISTANCE TO NATURAL DISASTERS.....	1 - 11
1.4.2.1 Tornado, hurricane, and wind resistance.....	1 - 11
1.4.2.2 Flood resistance.....	1 - 11
1.4.2.3 Earthquake resistance.....	1 - 11
1.4.3 AESTHETICS.....	1 - 11
1.4.3.1 Section shapes, sizes, color and texture.....	1 - 11
1.4.3.2 Lighting.....	1 - 11
1.4.4 MITIGATING THE URBAN HEAT ISLAND EFFECT.....	1 - 11
1.4.4.1 Smog.....	1 - 12
1.4.4.2 Albedo (solar reflectance).....	1 - 12
1.4.4.3 Emittance.....	1 - 12
1.4.4.4 Mitigation approaches.....	1 - 13
1.4.5 ENVIRONMENTAL PROTECTION.....	1 - 13
1.4.5.1 Context sensitive solutions.....	1 - 13
1.4.5.2 Protection of waterways.....	1 - 13

1.4.5.3 Reduced site disturbance..... 1 - 13

1.4.6 USER CONSIDERATIONS..... 1 - 13

 1.4.6.1 Construction delays..... 1 - 13

 1.4.6.2 Radiation and toxicity 1 - 13

 1.4.6.3 Resistance to noise (sound barriers)..... 1 - 13

1.5 SUSTAINABLE FEATURES OF PRECAST CONCRETE..... 1 - 14

 1.5.1 CONSTITUENT MATERIALS 1 - 14

 1.5.1.1 Concrete..... 1 - 14

 1.5.1.2 Portland Cement..... 1 - 14

 1.5.1.3 Fly Ash, Slag Cement, and Silica Fume 1 - 15

 1.5.1.4 Recycled Aggregates 1 - 15

 1.5.1.5 Admixtures 1 - 16

 1.5.1.6 Color Pigments 1 - 16

 1.5.2 ABUNDANT MATERIALS..... 1 - 16

 1.5.3 LOCAL MATERIALS..... 1 - 16

 1.5.4 FACTORY CONTROL..... 1 - 16

 1.5.4.1 Reduced Waste, Site Disturbance..... 1 - 16

1.6 SIMPLIFIED TOOLS AND RATING SYSTEMS 1 - 17

 1.6.1 GREENROADS 1 - 17

 1.6.2 GREENLITES 1 - 17

 1.6.3 CEEQUAL..... 1 - 17

 1.6.4 ENVISION 1 - 18

1.7 STATE-OF-THE-ART AND BEST PRACTICES 1 - 18

 1.7.1 PCI SUSTAINABLE PLANTS PROGRAM 1 - 18

1.8 KEYWORDS 1 - 18

1.9 REFERENCES..... 1 - 19

SUSTAINABILITY

1.1 SCOPE

There isn't one universally agreed upon definition of sustainability. Most often, sustainability is explained in terms of sustainable development, which the World Commission on Environment and Development defined as "development that meets the needs of the present without compromising the ability of future generations to meet their own needs."¹ Sustainability is a developing, dynamic and fundamental concept for all engineering applications. This process generates a variety of acronyms; section 1.3.5 "Terminology" is presented for reference and to assist with reading this chapter.

Materials can have a significant effect on the environmental impact of the construction, maintenance, rehabilitation, and operation of a bridge. Some materials may have to be used in special configurations, or employ different combinations, to achieve sustainability; the inherent properties of precast concrete, however, make it a natural choice for achieving sustainability in bridges. Precast concrete contributes to sustainable practices by incorporating integrated design, using materials efficiently, and reducing construction waste, site disturbance, and noise.

Although most consumers are concerned with the present and future health of the natural environment, few are willing to pay more for a product, process, or innovation that minimizes environmental burdens. The concept of sustainability, however, balances sustainable design with cost-effectiveness (see section on Triple Bottom Line). Using integrated design (also called holistic design), a bridge's materials and systems are examined from the perspective of all project team members and users. AASHTO and FHWA have always encouraged a life-cycle cost analysis (LCCA) approach in bridge-type selection studies. Items like cost, durability (or service life), environmental impact, constructability, work zone impact, and quality of user experience are also considered when decisions are made regarding the selection of a bridge's design.

1.2 LIFE CYCLE

A life-cycle analysis is a tool that can be used in terms of the economy (life-cycle cost analysis or LCCA) or environment (life-cycle assessment or LCA). When designing for the triple bottom line—environment, society, and economy—there is not a single tool that can assess economic, environmental, and equity (societal) impacts concurrently. Although the two approaches are different, they each consider the impacts of the design over the entire life of the bridge—from extraction to disposal—which is an essential part of sustainable design. When the resource impacts of sustainable design are considered over the life of the structure, a more cost-effective sustainable design often becomes apparent.

Looking at single environmental criterion, such as carbon dioxide emissions, is similar to choosing designs based on first-cost alone. A full set of environmental impacts includes land use, resource use, climate change, health effects, acidification, and toxicity. To get the whole picture, the entire structure (all components and systems) must be evaluated for a full range of environmental impacts for the full service life.

Practitioners of sustainable design believe that the key to sustainability is adaptable, durable bridges designed to minimize the use of materials. The material efficiency, durability, and longevity of precast concrete makes it an ideal choice for sustainable bridge design.

1.2.1 LIFE-CYCLE COST AND SERVICE LIFE

A life-cycle-cost analysis (LCCA) is a tool used to make economic decisions for selection of materials and systems. This analysis is the practice of accounting for all expenditures incurred over the lifetime of a particular structure. Costs at any given time are discounted back to a fixed date, based on assumed rates of inflation and the time-value of money. An LCCA is performed in terms of dollars and is equal to the construction cost plus the present value of future utility, maintenance, and replacement costs over the life of the facility.

Using this widely accepted method, it is possible to compare the economics of different bridge alternatives that may have different cash flow factors but that provide a similar standard of service. The result is financial information for decision making, which can be used to balance capital costs and future operation, repair, or maintenance costs. Quite often, designs with the lowest first costs will require greater repair and maintenance costs during the service life. So, even with their low initial cost, these designs may have a greater life-cycle cost. Conversely, durable materials, such as precast concrete, often have a lower life-cycle cost. Transportation-industry owners and design professionals are familiar with the benefits of a lesser life-cycle cost.

1.2.2 ENVIRONMENTAL LIFE-CYCLE INVENTORY AND LIFE-CYCLE ASSESSMENT

A life-cycle assessment (LCA) is an environmental assessment of the life cycle of a product, process, or structure. An LCA considers all aspects of a product life cycle — from the first stages of harvesting and extracting raw materials from nature, to transforming and processing these raw materials into a product, to using the product, and ultimately recycling it or disposing of it back into nature. When performing an LCA, financial impacts are not considered and monetary units are not part of the analysis. Instead, an LCA accounts for environmental impacts in terms of mass or energy use (inputs) and emissions to air, water, and land (outputs).

The LCA of a bridge project is necessary to evaluate its full environmental impact over its entire service life. Green rating systems that focus only on a single criterion, such as recycled content or carbon dioxide emissions, or a portion of the service life provide only a partial snapshot of the environmental impact a structure can leave. An LCA of a bridge project includes environmental effects due to:

- Extraction of materials and fuel used for energy.
- Manufacture of bridge components.
- Transportation of materials and components.
- Assembly and construction.
- Operation including energy consumption, maintenance, and repair as well as user vehicle fuel use and emissions during repair.
- Demolition, disposal, recycling, and reuse of the bridge at the end of its functional or useful life.

The four primary steps in an LCA are:³

- Goal and scope definition
- Life-cycle inventory (LCI) analysis
- Life-cycle impact assessment (LCIA)
- Interpretation and conclusions

An LCI is the second stage of an LCA (after goal and scope definition). An LCI accounts for all the individual environmental flows to and from a product, process, or system throughout its life cycle. It consists of the materials and energy needed to make and use a product, process, or system and the emissions to air, land, and water associated with making and using that product, process, or system.

An LCA involves a time consuming manipulation of large quantities of data. A model such as SimaPro* provides data for common materials and options for selecting LCA impacts. The Portland Cement Association (PCA) publishes reports with life-cycle inventory (LCI) data on cement and concrete.^{4,5} This data is also in the U.S. LCI database.[†]

Organizations such as the International Organization for Standardization[‡] have documented standard procedures for conducting an LCA. These procedures are generally consistent with each other: they are all scientific, transparent, and repeatable.

1.2.2.1 LCI Boundary

The usefulness of an LCA or LCI depends on where the boundaries of a product are drawn. If two LCA analyses will be compared, the boundaries of the compared studies must be the same. A common approach is to consider all the environmental flows from extraction to deconstruction (including reuse, recycling, and disposal, if

* www.pre.nl

† www.nrel.gov/lci/

‡ www.ISO.org

SUSTAINABILITY**1.2.2.1 LCI Boundary/1.2.2.2 Fuel and Energy**

necessary). For example, the system boundary for precast concrete operations should include most of the inputs and outputs associated with producing concrete — from extracting raw material to producing mixed concrete ready for placement in forms.

The system boundary should also include the upstream profile of manufacturing cement, as well as quarrying and processing aggregates, and transporting cement, fly ash, and aggregates to the precast concrete manufacturing facility. Energy and emissions associated with transporting the primary materials from their source to the manufacturing plant are also included in the boundary.

A complete precast concrete LCI would also include upstream profiles of fuel, electricity, water, or supplementary cementitious materials, form preparation, placing the concrete in the formwork, curing, and stripping. An upstream profile can be thought of as a separate LCI that is itself an ingredient to a product. For example, the upstream profile of cement is essentially an LCI of cement, which can be imported into an LCI of precast concrete. The LCI of precast concrete itself can then be imported into an LCI of a product, such as a bridge.

The LCI of materials generally do not consider embodied energy and emissions associated with construction of manufacturing plant equipment and buildings, nor the heating and cooling of such buildings. This is generally acceptable if their materials, embodied energy and associated emissions account for less than 1% of those in the process being studied. For example, the Society of Environmental Toxicology and Chemistry[§] guidelines indicate that inputs to a process do not need to be included in an LCI if they:

- are less than 1% of the total mass of the processed materials or product,
- do not contribute significantly to a toxic emission, and
- do not have a significant associated energy consumption.

Similarly, ISO 14044³ requires that these “cut-off criteria” be based on mass, energy, and environmental significance.

1.2.2.2 Concrete and Concrete Products LCI

During the LCI phase of an LCA, all the individual environmental flows to and from a product throughout its life cycle are quantified. The data gathered in an LCI is voluminous by nature and does not lend itself well to comparisons and concise summaries; that is the function of the LCA. The data in typical LCI reports are often grouped into three broad categories: materials, energy, and emissions.

1.2.2.2.1 Raw Materials

Approximately 1.6 lb of raw materials, excluding water, are required to make 1 lb of cement.^{4,5} This is primarily due to the calcination of limestone. In addition to the mixture water, the LCI assumes that precast concrete consumes 17.5 gal./yd³ of water for washout of the mixer and equipment used to transfer concrete to molds.

Solid waste from precast concrete plants is insignificant. Waste is about 2.5% of the mass of concrete used in production. About 95% of this waste is further beneficially reused through crushing and recycling at the plant, resulting in about 0.2 lb/ft³ (about 0.1%) of actual waste.

1.2.2.2.2 Fuel and Energy.

The amount of energy required to manufacture or produce a product can be shown in units of energy, such as joules or BTUs, or as amounts of fuel or electricity. Embodied energy per unit volume of concrete is primarily a function of the cement content of the mixture. For example, cement manufacturing accounts for about 75 to 80% of total energy in a 5000 psi concrete. Energy used in operations at the concrete plant contributes 10 to 20%, while aggregate processing and transportation each contribute about 5%.

The embodied energy of a concrete mixture increases in direct proportion to its cement content. Therefore, the embodied energy of concrete is sensitive to the cement content of the mixture and to the assumptions about LCI energy data in cement manufacturing.

Replacing cement with supplementary cementitious materials, such as fly ash, slag cement, or silica fume, has the effect of lowering the embodied energy of the concrete. Fly ash, slag cement, and silica fume do not contribute to the energy and emissions embodied in the concrete (except for the small energy contributions due to slag

[§] www.SETAC.org

SUSTAINABILITY**1.2.2.2 Fuel and Energy/1.2.2.3 Life-cycle impact assessment (LCIA)**

granulation/grinding, which is included).⁶ These products are recovered materials from industrial processes (also called post-industrial recycled materials) and if not used in precast concrete would use up valuable landfill space. When supplementary cementitious materials are used, the proportioned concrete mixture using the project materials should be tested to demonstrate that it meets the required concrete properties for the project. The optimum amounts of SCMs used with portland or blended cement are determined by testing, the relative cost and availability of the materials, and the specified properties of the concrete.

With a 50% slag cement replacement for portland cement in a 5000 psi mixture, embodied energy changes from 1.7 to 1.1 MBTU/yd³, a 34% reduction. Fly ash or slag cement replacement of portland cement can also significantly reduce embodied emissions. For instance, a 45% carbon dioxide emissions reduction is achievable with 50% substitution of slag for portland cement in a 7500 psi mixture. Certain aesthetic (color) and early compressive strength restrictions apply when using supplementary cementitious materials.

Embodied energy of reinforcing steel used in concrete is relatively small because it represents only about a 1% of the weight in a unit of concrete and it is manufactured mostly from recycled scrap metal. Reinforcing steel has over 90% recycled content according to the Concrete Reinforcing Steel Institute (www.crsi.org). The process for manufacturing reinforcing bars from recycled steel uses significant energy and should be considered if the reinforcing bar content is more than 1% of the weight of the concrete. The effects of other metal in bridges such as fasteners and tendons should also be considered.

It is assumed that at a typical site and in a precast concrete plant, concrete production formwork is reused a number of times through the repetitious nature of work, so its contribution to an LCI or LCA is negligible. Steel and wood formwork is generally recycled at the end of its useful life.

1.2.2.2.3 Emissions to Air.

The greatest amount of particulate matter (dust) in the precast concrete manufacturing process comes from cement manufacturing and aggregate production. The single largest contributor to particulate emissions in both cement manufacturing and aggregate production is quarry operations (quarry operations include blasting, haul roads, unloading, and stockpiling).

In cement manufacturing, quarry operations account for approximately 60% of total particulate emissions. In aggregate production, quarry operations are responsible for approximately 90% of particulate emissions. Approximately 30% of the particulate emissions associated with concrete production are from aggregate production and approximately 60% are embodied in the cement. However, particulate emissions from quarries are highly variable and sensitive to how dust is managed on haul roads and in other quarry operations.

The amounts of carbon dioxide (CO₂) and other combustion gases associated with concrete production are primarily a function of the cement content. Emissions of CO₂ increase in approximately a one-to-one ratio with the cement content of concrete. That is, for every additional pound of cement per cu yd of concrete, there will be an increase in CO₂ emissions by approximately 1 lb. Because of the CO₂ emissions from calcination and from fuel combustion in cement manufacturing, the cement content of the concrete accounts for about 90% of the CO₂ emissions associated with concrete production. Thus, concrete LCI results are significantly influenced by the cement content of the concrete and the basis of the CO₂ data in the cement LCI.

The fact that cement manufacturing accounts for approximately 70% of fuel consumption per unit volume of concrete indicates that the amounts of combustion gases, sulfur dioxide (SO₂), and nitrous oxides (NO_x), are sensitive to cement content of the mixture.

Cement kiln dust is a waste product of the cement manufacturing process and can be used to help maintain soil fertility. An industry-weighted average of 94 lb of cement kiln dust is generated per ton of cement. Of this about 75 lb are land-filled and about 19 lb are recycled in other operations.

1.2.2.3 Life-cycle impact assessment (LCIA)

During this phase of LCA, the LCI data (mass and energy flowing through the system boundary) is assigned to environmental impact categories and the relative effect of the inventory data within each impact category is weighted. Among LCA practitioners, this phase is called life-cycle impact assessment (LCIA), and it consists of category definition, classification, and characterization. Category definition consists of identifying which impact categories are relevant to the product being studied.

SUSTAINABILITY**1.2.2.3 Life-cycle impact assessment (LCIA)/1.3.1 Triple Bottom Line**

Classification consists of grouping related substances into environmental impact categories. For example, the gases carbon dioxide (CO₂), methane (CH₄), and nitrous oxide (N₂O) are considered greenhouse gases; therefore, they can be grouped together in an impact category called climate change. There are many environmental impact categories to choose from. The categories chosen depend on the goal and scope of the LCA. According to ASHRAE/USGBC/IES Standard 189.1, an LCA should include the following environmental impact indicators:⁷

- acidification
- climate change
- ecotoxicity
- eutrophication
- human-health effects
- land use (or habitat alteration)
- ozone layer depletion
- resource use
- smog

According to ISO 14044,³ the only mandatory step in life-cycle impact assessment phase is characterization. In characterization, weighting factors are assigned according to a substance's relative contribution to the impact category. In terms of global warming potential, one pound of CH₄ is 20 times more potent than one pound of CO₂, and one pound of N₂O is 320 times more potent than one pound of CO₂. Therefore, CO₂ is assigned a weighting factor of 1, CH₄ a factor of 20, and N₂O a factor of 320.

It is important to consider that there is no scientific basis for comparing across environmental impact categories. For example, global warming potential cannot be compared with potential ozone depletion. A well-referenced standard states that weighting of impact categories "shall not be used in LCA studies intended to be used in comparative assertions intended to be disclosed to the public."³

At the end of the LCA, the role of the practitioner is to present the results and interpret their meanings. The practitioner also evaluates the quality of the LCA by considering sensitivity and checking consistency, as well as identifying any significant issues from the LCI and LCIA phase. Most LCAs are also peer reviewed by a third party (usually called a critical review).

1.3 GENERAL SUSTAINABILITY CONCEPTS

1.3.1 TRIPLE BOTTOM LINE

The triple bottom line — environment, society, and economy — emphasizes that economic design decisions are related to environmental and social consequences. Consequences to society include impacts on users, communities, and developing countries, as well as ethics, population growth, and security. Reducing material, energy, and emissions used to design, build, maintain, and dispose of bridges reduces environmental impacts far beyond those of the bridges themselves, such as:

- Using less materials means fewer new quarries are needed.
- Using less energy means fewer new power plants need to be constructed, less pollution is emitted into the air, and dependence on foreign energy sources is reduced.
- Less emissions to atmosphere means cleaner air and a reduction in respiratory conditions, such as asthma.
- Using less water means a reduction in demands on the infrastructure to find and deliver new sources of water as well as less energy to process, treat, and transport water.

All of these examples indicate how choices we make during the construction of bridges can affect the local community. These are especially important since most communities do not want new power plants, quarries, or landfills built near them.

The community can also be considered globally. Carbon dioxide (CO₂) emissions in the U.S. were reduced in 2002 for the first time and in 2005, emissions were 5.9 ktons. This slow down in growth was due to a decrease in manufacturing and a stagnant economy. China's most rapid phase of growth has been in this decade, with an emissions increase of 63% to 5.6 ktons, between 2001 and 2005 alone. In four years, China's emissions grew four

SUSTAINABILITY**1.3.1 Triple Bottom Line/1.3.4.1 Reduce the amount of material used and the toxicity of waste materials**

times more rapidly than the global average.² This growth in emissions is reflective of a dependency on industry. Global CO₂ emissions did not decrease in 2002, they merely shifted to other countries.

1.3.2 COST OF GREEN

A sustainable design can result in reduced project costs and a bridge that is resource efficient. Reusing materials, such as demolished concrete for base or fill material, can reduce costs associated with hauling and disposing of materials. When sustainability is an objective at the outset of the design process, the cost of a sustainable bridge is competitive. Typical state highway procedures for bridge and transportation facility designs must consider many sustainable attributes such as context sensitive solutions, durability, reduced construction-related user delays, environmental impact, and noise during construction, among others.

1.3.3 HOLISTIC/INTEGRATED DESIGN

A key tenet of sustainable design is the holistic or integrated design approach. This approach requires coordinating the structural, site, and other requirements early in the schematic design phases to discern possible system interactions, and then deciding which beneficial interactions are essential for project success. For example, deck drainage can be incorporated into the pedestrian sidewalk or shoulder design. This could impact the drainage design by requiring fewer pipes and perhaps allow for quicker construction.

A holistic viewpoint will also take into account the surrounding site environment:

- Can bike paths be incorporated for those who live in the community?
- Can native landscaping be used to reduce the need for irrigation?
- Does placing plantings on a bridge add to future durability concerns?
- Can using concrete as a road surface reduce the number of light fixtures required on a bridge?

Some elements of integrated design include:

- Emphasize the integrated process.
- Consider the structure as a whole — often interactive, often multi-functional.
- Focus on the life cycle.
- Have disciplines work together as a team from the start.
- Conduct relevant assessments to help determine requirements and set goals.
- Develop tailored solutions that yield multiple benefits while meeting requirements and goals.
- Evaluate solutions.
- Ensure requirements and goals are met.

Contracts and requests for proposals (RFPs) should clearly describe sustainability requirements and project documentation required.⁸

1.3.4 REDUCE, REUSE, RECYCLE

One of the most-well-recognized slogans of the environmental movement is reduce, reuse, recycle. This common slogan can also be applied to the bridge industry.

1.3.4.1 Reduce the amount of material used and the toxicity of waste materials.

Precast and prestressed concrete can be designed to optimize (or lessen) the amount of concrete used. Closer tolerances can be met when elements are made in a production environment and this also decreases material use. Industrial wastes such as fly ash, slag cement, and silica fume can be used as partial replacements for cement—with certain aesthetic (color) and early compressive strength considerations—thereby reducing the amount of cement used in concrete. Precast concrete generates a low amount of waste with a low toxicity. It is generally assumed that 2.5% of the concrete at a plant is waste, but because it is generated at the plant, 95% of the waste is used beneficially. For more information on how PCI plants reduce waste, see Section 1.7.1 on the PCI Sustainable Plant Program.

1.3.4.2 Reuse products and containers; repair what can be reused.

Precast concrete bridge girders can be reused for pedestrian crossings or for other applications. According to a presentation by Burnell, more-sustainable bridge projects will incorporate simplified deconstruction as a design criterion.⁹ To reuse components effectively, engineers need to be able to determine the residual service life of the components. Long emphasized the need for testing equipment that could be used to determine the durability or remaining life of bridges in place.¹⁰

Other ways that the concept of reuse is facilitated with precast concrete components are:

- Concrete pieces from demolished structures can be reused to protect shorelines and create fisheries.
- Because the precast process is self-contained, formwork and finishing materials are reused.
- Wood forms can generally be used 25 to 30 times without major maintenance while fiberglass, concrete, and steel forms have significantly longer service lives.

1.3.4.3 Recycle as much as possible, which includes buying products with recycled content.

Concrete in most urban areas is recycled as fill or road base. In mild climates where recycled concrete is not contaminated with road salts, recycled concrete can be used as coarse aggregate in new concrete. Wood and steel forms are recycled when they become worn or obsolete. Virtually all reinforcing steel is made from recycled steel. Many cement plants burn waste-derived fuels such as spent solvents, used oils, and tires in the manufacture of cement.

1.3.5 TERMINOLOGY

Admixture: material, other than water, aggregate, and hydraulic cement, used as an ingredient of concrete, mortar, grout, or plaster and added to the batch immediately before or during mixing. Chemical admixtures are most commonly used for freeze-thaw protection, to retard or accelerate the concrete setting time, or to allow less water to be used in the concrete.

Albedo: solar reflectance; see reflectance.

Calcination: process of heating a source of calcium carbonate, such as limestone, to high temperatures, thereby causing a chemical reaction that releases CO₂. This CO₂ is not related to the fuel used to heat the calcium carbonate.

Cement: see portland cement.

Cementitious material (cementing material): any material having cementing properties or contributing to the formation of hydrated calcium silicate compounds. When proportioning concrete, the following are considered cementitious materials: portland cement, blended hydraulic cement, fly ash, ground granulated blast-furnace slag (also called slag cement), silica fume, calcined clay, metakaolin, calcined shale, and rice husk ash.

Concrete: mixture of binding materials and coarse and fine aggregates. Portland cement and water are commonly used as the binding medium for normal concrete, but may also contain pozzolans, slag cement, and/or chemical admixtures.

Embodied energy: The total amount of primary energy required to manufacture or produce a product.

Emittance: the ability of the material to emit, or let go of, heat.

Greenhouse gas emissions: emissions that have the potential to increase air temperatures at the earth's surface, including carbon dioxide, methane, nitrous oxide, chlorofluorocarbons, water vapor, and aerosols (particles of 0.001 to 10 µm diameter).

GreenLites: a program developed by the New York State Department of Transportation to evaluate the sustainability of project designs before the designs go to bid.

Greenroads: a performance metric developed by the University of Washington and CH2M HILL to quantify the sustainable attributes of a roadway project

LEED (Leadership in Energy and Environmental Design): a voluntary green building rating system that is a consensus-based national standard for developing high-performance, sustainable buildings. LEED is both a standard for certification and a design guide for sustainable construction and operation. As a standard, it is

SUSTAINABILITY**1.3.5 Terminology/1.4.1.1 Corrosion resistance**

predominantly performance-based, and as a design guide, it takes a whole-building approach that encourages a collaborative, integrated design and construction process. LEED is administered by the U.S. Green Building Council (USGBC).

Portland cement: Calcium silicate hydraulic cement produced by pulverizing portland cement clinker, and usually containing calcium sulfate and other compounds.

Pozzolan: siliceous or siliceous and aluminous materials, like fly ash or silica fume, which in itself possess little or no cementitious value but which will, in finely divided form and in the presence of moisture, chemically react in the presence of portland cement to form compounds possessing cementitious properties.

Reflectance: the ratio of the amount of light or solar energy reflected from a material surface to the amount shining on the surface. Solar reflectance includes light in the visible, infrared, and ultraviolet range. For artificial lighting, the reflectance refers to the particular type of lighting used in the visible spectrum.

Silica fume: very fine non-crystalline silica which is a byproduct from the production of silicon and ferrosilicon alloys in an electric arc furnace; used as a pozzolan in concrete.

Slag cement (Ground granulated blast-furnace slag): a nonmetallic hydraulic cement consisting essentially of silicates and aluminosilicates of calcium developed in a molten condition simultaneously with iron in a blast furnace. This slag is cooled and ground in a manner to produce slag cement. Slag cement can be used as a partial replacement or addition to portland cement in concrete.

Supplementary cementitious materials: materials that when used in conjunction with portland cement contribute to the properties of hardened concrete through hydraulic or pozzolanic activity or both.

Sustainable development: development that meets the needs of the present without compromising the ability of future generations to meet their own needs.¹ In more tangible terms, sustainability refers to the following: not compromising future quality of life; remediating environmental damage done in the past; and recognizing that our economy, environment, and social well-being are interdependent.

Sustainability rating systems: a set of criteria used to quantify that a bridge, building, or other item in the built environment is sustainable, green, or energy-conserving.

Urban heat island: microclimates near urban or suburban areas that are warmer than surrounding areas due to the replacement of vegetation with hardscape, bridges, pavements, and other structures.

1.4 SUSTAINABILITY AND PRECAST CONCRETE BRIDGES

1.4.1 DURABILITY

A key factor in reuse of components is the durability of the original structure. Precast concrete components provide a long service life due to their durable and low-maintenance concrete surfaces. Annual maintenance does not require painting, which can be costly and harmful to the environment as well as dangerous for workers who are suspended at a height over busy highways and other types of crossings.

Precast concrete construction provides the opportunity to disassemble the bridge should its use or function change, and the components can be reused in a different application. These characteristics of precast concrete make it sustainable in two ways: it avoids contributing solid waste to landfills and it reduces the depletion of natural resources and production of air and water pollution caused by new construction.

1.4.1.1 Corrosion resistance

The inherent alkalinity of concrete results in a system of concrete and reinforcing steel that does not corrode in most environments. A common reason for spalling of concrete is corrosion of reinforcing steel due to inadequate concrete cover. Precast concrete offers increased resistance to this type of spalling due to its denser concrete and because reinforcement and concrete are placed in a plant, with more quality control than site-cast or cast-in-place concrete construction. This reduces variations in concrete cover over reinforcing steel and reduces the likelihood of inadequate cover.

SUSTAINABILITY**1.4.1.1 Corrosion resistance/1.4.4 Mitigating the Urban Heat Island Effect****1.4.1.2 Inedible**

Vermin and insects cannot destroy concrete because it is inedible. Some softer construction materials are inedible but still provide pathways for insects. Due to its hardness, vermin and insects will not bore through concrete.

1.4.1.3 Ultraviolet resistance

The ultraviolet (UV) range of solar radiation does not harm concrete. Using non-fading colored pigments in concrete retains the color in concrete long after paints have faded due to the sun's effects. Precast concrete is ideal for using pigments because the controlled production allows for replication of color for all components for a project.

1.4.2 RESISTANCE TO NATURAL DISASTERS

Concrete is resistant to tornados, hurricanes, wind, floods, and earthquakes.

1.4.2.1 Tornado, hurricane, and wind resistance

Precast concrete can be economically designed to resist tornadoes, hurricanes, and wind. Hurricanes are prevalent in coastal regions. Tornadoes are particularly prevalent in the path of hurricanes and in the central plains of the U.S.

1.4.2.2 Flood resistance

In general, concrete is not damaged by water; concrete that does not dry out continues to gain strength in the presence of moisture. Concrete submerged in water absorbs very small amounts of water even over long periods of time, and typically this water does not damage the concrete.

1.4.2.3 Earthquake resistance

Precast concrete can be designed to be resistant to earthquakes. Earthquakes in Guam, United States (Richter Scale 8.1); Manila, Philippines (Richter Scale 7.2); and Kobe, Japan (Richter Scale 6.9), have subjected precast concrete structures to some of nature's deadliest forces. Appropriately designed precast concrete systems have a proven capacity to withstand these major earthquakes.

1.4.3 AESTHETICS**1.4.3.1 Section shapes, sizes, color and texture**

Precast concrete can be manufactured in a variety of shapes, sizes, colors, and textures to blend in with the environment. Many different colors of precast concrete are possible with different combinations of cement, pigments, and aggregate. Form-liners, sand blasting, acid etching, tooling, polishing, or embedment of clay or stone products are just some of the ways to change the texture of precast concrete.

Non-fading color pigments are used to provide the decorative colors in precast concrete. They are insoluble and generally nontoxic, although some may contain trace amounts of heavy metals. Many iron oxide pigments are primarily the byproduct of material recycling (manufactured by precipitating scrap steel). See Section 3.5.2 for more information on surface treatments of precast concrete components, and Section 4.1 on geometric possibilities.

1.4.3.2 Lighting

Light-colored precast concrete and other surfaces will reduce energy costs associated with outdoor lighting. The more reflective surfaces will reduce the amount of fixtures and lighting required. Light-colored precast concrete can reduce outdoor lighting requirements.

1.4.4 MITIGATING THE URBAN HEAT ISLAND EFFECT

Precast concrete provides reflective surfaces that minimize the urban heat island effect. Cities and urban areas are 3°F to 8°F warmer than surrounding areas due to the urban heat island effect. This difference is attributed to heat absorption of building materials and pavements that have taken the place of vegetation. Urban heat islands are primarily attributed to horizontal surfaces, such as roofs and hardscape, which absorb solar radiation. In this

SUSTAINABILITY**1.4.4 Mitigating the Urban Heat Island Effect/1.4.4.3 Emittance**

context, hardscape includes roads, decks, and walkways. Research has shown the average temperature of Los Angeles has risen steadily over the past half century, and is now 6°F to 7°F warmer than 50 years ago.¹¹

Two methods of mitigating heat islands are providing shade and increasing albedo. Trees provide shade that reduces temperatures at the surface. Trees and plants provide transpiration and evaporation that cool the surfaces and air surrounding them. Shade can also be provided by geological features (hills, mountains) or structures that shade themselves. Using materials with higher albedos (solar reflectance values), such as precast concrete, will reduce the heat island effect, save energy, and improve air quality.

Studies indicate people will avoid using air-conditioning at night if temperatures are less than 75°F. Mitigating the urban heat island effect to keep summer temperatures in cities less than 75°F at night has the potential to save large amounts of energy in the urban areas by reducing the demand for air conditioning in buildings.

1.4.4.1 Smog

Smog levels have also been correlated to temperature rise. Thus, as the temperature of urban areas increases, so does the probability of smog and pollution. In Los Angeles, the probability of smog increases by 3% with every degree Fahrenheit of temperature rise. Studies for Los Angeles and 13 cities in Texas have found that there are almost never any smog episodes when the temperature is below 70°F. The probability of episodes begins at about 73°F and, for Los Angeles, exceeds 50% by 90°F. Reducing the daily high in Los Angeles by 7°F is estimated to eliminate two-thirds of the smog episodes.

Smog and air pollution are the main reasons EPA mandates expensive, clean fuels for vehicles and reduced particulate emissions from industrial facilities such as cement and asphalt production plants. The EPA now recognizes that air temperature is as much a contributor to smog as nitrogen oxide (NO_x) and volatile organic compounds (VOCs). The effort to reduce particulates in the industrial sector alone costs billions of dollars per year, whereas reduction in smog may be directly related to the reflectance and colors of the infrastructure that surround us. Installing high-albedo decks and pavements is a cost-effective way to reduce smog.

1.4.4.2 Albedo (solar reflectance)

Albedo, which in this case is synonymous with solar reflectance, is the ratio of the amount of solar radiation reflected from a material surface to the amount shining on the surface. Solar radiation includes the ultraviolet and infrared as well as the visible spectrum. Albedo is measured on a scale not reflective (0.0) to 100% reflective (1.0). Generally, materials that appear to be light-colored in the visible spectrum have high albedo and those that appear dark-colored have low albedo. However, because reflectivity in the solar radiation spectrum determines albedo, color in the visible spectrum is not always a true indicator of albedo.

Surfaces with lower albedos absorb more solar radiation. The ability to reflect infrared light is of great importance because infrared light is most responsible for heating. On a sunny day when the air temperature is 55°F, surfaces with dark acrylic paint will heat up to 90°F more than air temperatures, to 145°F. Light surfaces, such as white acrylic, will heat up to 20°F more, to a temperature of 75°F. The color, composition, and surface texture of the materials greatly affect the surface temperature and the amount of absorbed solar radiation. The effect of albedo and solar radiation on surface temperatures is referred to as the sol-air temperature and can be calculated.

Traditional portland cement concrete generally has an albedo or solar reflectance of approximately 0.4, although values can vary; measured values are reported in the range of 0.4 to 0.5. The solar reflectance of new concrete is greater when the surface reflectance of the sand and cementitious materials in the concrete are greater. Surface finishing techniques also have an effect, with smoother surfaces generally having a higher albedo. For concrete elements with white portland cement, values are reported in the range of 0.7 to 0.8. Albedo is most commonly measured using a solar-spectrum reflectometer (ASTM C1549)¹² or a pyranometer (ASTM E1918).¹³

1.4.4.3 Emittance

In addition to albedo, the material's surface emittance affects surface temperature. While albedo is a measure of the solar radiation reflected away from the surface, surface emittance is the ability of the material to emit, or let go of, heat. A white surface exposed to the sun is relatively cool because it has a high reflectivity and a high emittance. A shiny metal surface is relatively warm because it has a low emittance, even though it has a high albedo. The emittance of most non-reflecting (non-metal) surfaces such as concrete is in the range of 0.85 to 0.95.

SUSTAINABILITY**1.4.4.3 Emittance/1.4.6.3 Resistance to noise (sound barriers)**

The emittance of aluminum foil, aluminum sheet, and galvanized steel, all dry and bright, are 0.05, 0.12, and 0.25, respectively.

1.4.4.4 Mitigation approaches

One method to reduce the urban heat island effect is to change the albedo of the urban area. This is accomplished by replacing low albedo surfaces with materials of higher albedo. This change is most cost effective when done in the initial design or during renovation or replacement due to other needs.

1.4.5 ENVIRONMENTAL PROTECTION**1.4.5.1 Context sensitive solutions**

With the seemingly unlimited combinations of color and texture possible with precast concrete, bridges can easily be designed to blend into their surroundings. They can also be design to replicate indigenous or historical colors or features.

1.4.5.2 Protection of waterways

Because precast concrete is manufactured off site in a controlled environment, there is less chance of formwork, falsework, and construction-related debris to fall into waterways that bridges are spanning.

1.4.5.3 Reduced site disturbance

Less dust and waste is created at the construction site because only needed precast concrete elements are delivered and there is no debris from formwork and associated fasteners—construction sites are cleaner and neater. Fewer trucks and less time are required for construction because concrete is made offsite; this is particularly beneficial in urban areas where minimal traffic disruption is critical. There is also less noise at the construction site because concrete is made offsite.

1.4.6 USER CONSIDERATIONS**1.4.6.1 Construction delays**

There are synergies between reducing environmental impacts and reducing construction-related user delays. During initial construction, minimizing on-site construction lessens the amount of time that drivers are inconvenienced. Likewise, by choosing a bridge with greater durability and fewer maintenance requirements, delays during the service life of the bridge can also be reduced. This in turn reduces energy consumption of user vehicles and the resultant emissions to air.

1.4.6.2 Radiation and toxicity

Concrete is resistant to most natural environments; it is sometimes exposed to substances that can attack and cause deterioration. The resistance of concrete to chlorides is good, and using less permeable concrete can increase the resistance even more. This is achieved by using a low water-cementitious materials ratio (around 0.40), adequate curing, and supplementary cementitious materials such as slag cement or silica fume. The best defense against sulfate attack, where this is an issue, are the measures suggested previously; in addition, one can use cement specially formulated for sulfate environments.

1.4.6.3 Resistance to noise (sound barriers)

Precast concrete walls provide a buffer between outdoor noise and the indoor environment. Because land is becoming scarcer, buildings are being constructed closer together and near noise sources such as highways, railways, and airports. Precast concrete panels also provide effective sound barriers separating buildings from highways or industrial areas from residential areas. The greater mass of concrete walls can reduce sound penetrating through a wall. An 8-in.-thick flat wall panel (95 psf) has a sound transmission coefficient (STC) of 58 and outdoor-indoor transmission class (OITC) of 50.

1.5 SUSTAINABLE FEATURES OF PRECAST CONCRETE

The production of precast concrete has many environmental benefits, including:

- Less material is required because precise mixture proportions and tighter tolerances are achievable.
- Less concrete waste is created because of tight control of quantities of constituent materials.
- Excess concrete is often used for other uses such as plant improvement projects or is recycled at the plant in the production process.
- Waste materials are more likely to be recycled because concrete production is in one location.
- Gray water often recycled into future mixtures, or used for plant dust-control.
- Hardened concrete recycled (presently about 5% to 20% of aggregate in precast concrete can be recycled concrete; in the future this could be higher.)
- Steel forms and other materials are reused.
- Less dust and waste is created at the construction site because only needed precast concrete elements are delivered and there is no debris from formwork and associated fasteners—construction sites are cleaner and neater.
- Fewer trucks and less time are required for construction because concrete is made offsite; this is particularly beneficial in urban areas where minimal traffic disruption is critical.
- Precast concrete units are normally large components, so greater portions of the bridge are completed with each activity.
- Less noise at construction site because concrete is made offsite.

Less concrete is generally used in precast/prestressed concrete bridges than in other concrete bridges because of the optimization of materials. A properly designed precast concrete system will result in smaller structural members, longer spans, and less material used on-site; this translates directly into economic savings, which can also result in environmental savings. Using less material means using fewer natural resources and less manufacturing and transportation energy—not to mention the avoided emissions from mining, processing, and transporting raw and finished material.

1.5.1 CONSTITUENT MATERIALS

1.5.1.1 Concrete

Concrete is basically a mixture of two components: aggregates and paste. The paste, comprised of portland cement and water, binds the aggregates (usually sand and gravel or crushed stone) into a rocklike mass. The paste hardens because of the chemical reaction of the cement and water. Supplementary cementitious materials and chemical admixtures may also be included in the paste. The absolute volume of cement is usually between 7% and 15% and the water between 14% and 21%.

1.5.1.2 Portland Cement

Portland cement (hereafter called cement) is made by heating common minerals, primarily crushed limestone, clay, iron ore, and sand, to a white-hot mixture to form clinker. This intermediate product is ground, with a small amount of gypsum, to form a fine gray powder called cement. To trigger the necessary chemical reactions in the kiln, these raw materials must reach about 2700°F—the temperature of molten iron. Although the portland cement industry is energy intensive, the U.S. cement industry has reduced energy usage per ton of cement by 35% since 1972.^{14,15}

Carbon dioxide emissions from a cement plant are divided into two source categories: combustion and calcination. Combustion accounts for approximately 35% and calcination 65% of the total CO₂ emissions from a cement manufacturing facility. The combustion-generated CO₂ emissions are related to fuel use. The calcination CO₂ emissions are formed when the raw material is heated and CO₂ is liberated from the calcium carbonate. As concrete is exposed to the air and carbonates, it reabsorbs some of the CO₂ released during calcination. When ground to small particles at the end of its useful life, concrete will reabsorb the CO₂ emitted during calcination. Calcination is a necessary key to cement production. Therefore, the focus of reductions in CO₂ emissions during cement manufacturing is on reducing fuel and energy use.

Although cement production increased 53% from 1990 to 2006, net CO₂ emissions increased only 35%, proving a decoupling of production and related emissions.⁸

White portland cement is a true portland cement that differs from gray cement chiefly in color. The manufacturing process is controlled so that the finished product will be white. White portland cement is made of selected raw materials containing negligible amounts of iron and magnesium oxides– the substances that give cement its gray color. White cement is used primarily for architectural purposes in precast concrete and glass-fiber-reinforced concrete (GFRC) components. Using white cement with pigments provides more consistency in the final color of the concrete. White portland cement should be specified as white portland cement meeting the specifications of ASTM C150, Type I, II, III, or V.¹⁶

1.5.1.3 Fly Ash, Slag Cement, and Silica Fume

Fly ash, slag cement, and silica fume are industrial byproducts; their use as a replacement for portland cement does not contribute to the energy and CO₂ effects of cement in concrete. If not used in concrete, these supplementary cementitious materials (SCMs) would use valuable landfill space.

Fly ash is a by-product of the combustion of pulverized coal in electric power generating plants. Slag cement is made from iron blast-furnace slag.¹⁷ Silica fume is a by-product from the electric arc furnace used in the production of silicon or ferrosilicon alloy. These types of industrial by-products are considered post-industrial or pre-consumer recycled materials. Fly ash is commonly used at cement replacement levels up to 35%, slag cement up to 60%, and silica fume up to 7%. When slag cement replaces 50% of the portland cement in a 7500 psi concrete mixture, greenhouse gas emissions per cubic yard of concrete are reduced by 45%.

SCMs may slightly alter the color of hardened concrete. Color effects are related to the color and amount of the material used in concrete. Many SCMs resemble the color of portland cement and therefore have little effect on color of the hardened concrete. Some silica fumes may give concrete a slightly bluish or dark gray tint and tan fly ash may impart a tan color to concrete when used in large quantities. Slag cement and metakaolin (a clay SCM without recycled content) can make concrete lighter. Slag cement can initially impart a bluish or greenish undertone that disappears over time as concrete is allowed to dry.

The optimum amounts of supplementary cementitious materials used with portland or blended cement are determined by testing, the relative cost and availability of the materials, and the specified properties of the concrete. When supplementary cementitious materials are used, the proportioned concrete mixture (using the project materials) should be tested to demonstrate that it meets the required concrete properties for the project. Some pozzolans increase curing times, which can be a concern on projects where construction schedule has a greater impact.

The durability of products with recycled content materials should be carefully researched during the design process to ensure comparable life-cycle performance. There would obviously be a net negative impact if a product offering a 20% to 30% recycled content had only half the expected service life of a product with a lower or no recycled content.

1.5.1.4 Recycled Aggregates

The environmental attributes of concrete can be improved by using aggregates derived from industrial waste or using recycled concrete as aggregates. Blast furnace slag is a lightweight aggregate with a long history of use in the concrete industry.

Recycled concrete can be used as aggregate in new concrete, particularly the coarse portion. When using the recycled concrete as aggregate, the following should be taken into consideration:

- Recycled concrete as aggregate will typically have higher absorption and lower specific gravity than natural aggregate and will produce concrete with slightly higher drying shrinkage and creep. These differences become greater with increasing amounts of recycled fine aggregates.
- Too many recycled fines can also produce a harsh and unworkable mixture. Many transportation departments have found that using 100% coarse recycled aggregate, but only about 10% to 20% recycled fines, works well.¹⁸ The remaining percentage of fines is natural sand.
- When crushing the concrete, it is difficult to control particle size distribution, meaning that the “aggregate” may fail to meet grading requirements of ASTM C33.²²
- The chloride content of recycled aggregates is of concern if the material will be used in reinforced concrete. This is particularly an issue if the recycled concrete is from pavements in northern climates where road salt is freely spread in the winter.

SUSTAINABILITY**1.5.1.4 Recycled Aggregates/1.5.4.1 Reduced Waste, Site Disturbance**

- The alkali content and type of aggregate in the system is probably unknown, and therefore if mixed with unsuitable materials, a risk of alkali-silica reaction (ASR) is possible.
- There is no standard method for assessing the durability of recycled concrete aggregate in a similar way to how natural aggregate is assessed.

1.5.1.5 Admixtures

The freshly mixed (plastic) and hardened properties of concrete may be changed by adding chemical admixtures to the concrete, usually in liquid form, during batching. Chemical admixtures are commonly used to:

- adjust setting time or hardening,
- reduce water demand,
- increase workability,
- intentionally entrain air,
- inhibit corrosion, and
- adjust other fresh or hardened concrete properties.

Admixtures provide enhancing qualities in concrete but are used in such small quantities that they do not adversely affect the environment. Their dosages are usually in the range of 0.005 to 0.2% of the concrete mass.

1.5.1.6 Color Pigments

Non-fading color pigments are used to provide the decorative colors in precast concrete. They are insoluble and generally nontoxic, although some may contain trace amounts of heavy metals. Many iron oxide pigments are primarily the byproduct of material recycling (manufactured by precipitating scrap steel).

1.5.2 ABUNDANT MATERIALS

Concrete is used in almost every country of the world as a basic building material. Aggregates, about 85% of concrete, are generally low-energy, local, naturally occurring sand and stone. Limestone and clay needed to manufacture cement are prevalent in most countries. Concrete contributes to a sustainable environment because it does not use scarce resources.

Limestone and aggregate quarries are easily reused. While quarrying is intense, it is closely contained and temporary. When closed, aggregate quarries are generally converted to their natural state or into recreational areas or agricultural uses. In contrast, other material mining operations can be extensive and damaging to the environment as well as involve deep pits that are rarely restored.

1.5.3 LOCAL MATERIALS

Using local materials reduces the transportation required to ship heavy building materials, and the associated energy and emissions. Most precast concrete plants are within 200 miles of a site. The cement, aggregates, and reinforcing steel used to make the concrete and the raw materials to manufacture cement are usually obtained or extracted from sources within 200 miles of the precast concrete plant.

Precast concrete elements are usually shipped efficiently because of their large, often repetitive sizes and the ability to plan their shipment during the normal course of the project.

1.5.4 FACTORY CONTROL**1.5.4.1 Reduced Waste, Site Disturbance**

Precast concrete girders can be reused when bridges are expanded and precast concrete can be recycled as road base, fill, or aggregate in new concrete at the end of its useful life. Concrete pieces from demolished structures can be reused to protect shorelines. Most concrete from demolition in urban areas is recycled and not placed in landfills.

Precast concrete minimizes the total waste generated on a construction site by fabricating and optimizing components off site. Less dust and waste is created at the construction site because only needed precast concrete elements are delivered; there is no debris from formwork and associated fasteners. Fewer trucks and less time are required for construction because concrete is made offsite; particularly beneficial in urban areas where

minimal traffic disruption is critical. Precast concrete units are normally large components, so greater portions of the bridge are completed with each activity, creating less disruption overall. Less noise is generated at construction sites because concrete is made offsite.

1.6 SIMPLIFIED TOOLS AND RATING SYSTEMS

1.6.1 GREENROADS

Greenroads²⁰ is a performance metric developed by the University of Washington and CH2M HILL to quantify the sustainable attributes of a roadway project. Metrics are tracked in two separate best-practice categories: mandatory and voluntary. Minimum levels of sustainable activities are provided in the mandatory best-practices project requirements. Optional attributes, which show how the project has moved toward a truly sustainable endeavor, are included in the voluntary credits. For a given project, the Greenroads team verifies the application and the point totals and assigns a level.

Some of the limitations of the Greenroads program include:

- Exclusion, by omission, of roadway structures such as bridges, tunnels, and soundwalls.
- Lack of evaluation of long-term maintenance, except for that which is required by other credits.
- Evaluation criteria, such as a long-life pavement credit, which focuses only on pavement thickness.

1.6.2 GREENLITES

GreenLITES²¹ is a program developed by the New York State Department of Transportation to evaluate the sustainability of project designs before the designs go to bid. Project designs are evaluated based on environmental impact in five categories:

- Sustainable sites
- Water quality
- Materials and resources
- Energy and atmosphere
- Innovation/unlisted

There is a lack of quantification of improvement needed to receive points, and many of the credits do not have clear submission requirements.

1.6.3 CEEQUAL

Civil Engineering Environmental Quality Assessment and Awards Scheme (CEEQUAL)²² was developed by a team led by the United Kingdom (UK) Institution of Civil Engineers (ICE) with financial support from UK governmental agencies and from the ICE's Research & Development Enabling Fund. CEEQUAL also received support and participation from UK professional and industry associations and civil engineering consultants and contractors. It is managed jointly by Construction Industry Research and Information Association (CIRIA) and Crane Environmental.

The objectives of CEEQUAL are:

- To recognize good, very good, or excellent environmental and social practice in civil engineering and public work projects,
- To promote improved sustainability performance in project specification, design, and construction, and
- To create a climate of environmental awareness and continuous improvement in the industry.

CEEQUAL is an environmental and sustainability rating system with twelve categories that are reviewed and scored including:

- Project Management,
- Land Use,
- Landscape,
- Ecology & Biodiversity,
- Historic Environment,

- Water Resources and the Water Environment,
- Energy and Carbon,
- Material Use,
- Waste Management,
- Transport,
- Effects on Neighbors, and
- Relations with Local Community and Other Stakeholders

The categories require evidence to be collected by the Assessor and reviewed by the Verifier. It would be difficult to secure a Whole Project Award without detailed documentation. Because of the lack of specificity in many of the categories, the objectivity of the Assessor and Verifier will play an important role in collection of evidence for each category and scoring of the results.

1.6.4 ENVISION

Envision²³ is a sustainable infrastructure rating system developed by the Institute for Sustainable Infrastructure (ISI), a non-profit collaboration of the American Society of Civil Engineers, the American Council of Engineering Companies, and the American Public Works Association. Through the use of Envision, ISI intends to encourage the use of more sustainable technologies and methods, which will ultimately improve the performance of infrastructure. The rating system will evaluate, grade, and give recognition to projects that:

- Conserve and regenerate resources
- Restore and maintain ecological systems
- Protect human health and the environment
- Improve the quality of life for communities

According to the preliminary guidance manual, released for public review in August of 2011, Envision can be applied to roads, bridges, pipelines, railways, airports, dams, levees, landfills, water treatment systems, and other components of public infrastructure. As of August 2011, the rating system had four stages, with Stage 1 and Stage 2 ready for roll-out. The four stages are:

- Stage 1: users can access resources and a project sustainability checklist;
- Stage 2: users can rate projects versus sustainability measures. With verification of a certain number of objectives met, projects may receive Envision awards.
- Stage 3: users can rate projects versus sustainability measures; awards given for set achievements in key areas.
- Stage 4: users can access industry-recognized decision support tools to compare alternatives, performance trade-offs, and cost.

1.7 STATE-OF-THE-ART AND BEST PRACTICES

1.7.1 PCI SUSTAINABLE PLANTS PROGRAM

In recognition of the critical nature of sustainability in the built environment, PCI is developing a Sustainable Plants Program (SPP). The goal of the program is to give PCI-certified precast concrete plant operators the tools and resources needed to measurably improve their environmental and economic performance. This benchmarking of environmental data will allow for the measurement of ongoing performance and will allow PCI producer members to better manage metrics implemented with the SPP.

As part of the SPP, PCI producer members will track data in categories of energy, waste, recycling, transportation, and materials. Initially, plants will be encouraged to collect data and implement improvement strategies. Data will be tracked separately for architectural and structural precast concrete products.

1.8 KEYWORDS

albedo, bridges, calcination, cementitious material (cementing material), emittance, greenhouse gas emissions, life cycle, LCA, LCI, pozzolan, precast concrete, reflectance, silica fume, slag cement (ground granulated blast-furnace slag), supplementary cementitious materials, sustainability, sustainability rating systems, urban heat island.

1.9 REFERENCES

1. World Commission on Environment and Development. 1987. "Report on Our Common Future," Oxford University Press, New, York, NY.
<http://www.un.org/documents/ga/res/42/ares42-187.htm>
2. World Resources Institute. Energy and Resources Searchable Database.
http://earthtrends.wri.org/searchable_db/index.php?action=select_variable&theme=6 <Accessed November 3, 2011>
3. International Organization for Standardization (ISO). 2006., Environmental Management—Life Cycle Assessment—Requirements and Guidelines. ISO 14044. Geneva, Switzerland, www.iso.org <Accessed November 3, 2011>.
http://www.iso.org/iso/catalogue_detail?csnumber=38498 (Fee)
4. Marceau, M.L. M.A. Nisbet, and M.G. VanGeem. 2006. Life Cycle Inventory of Portland Cement Manufacture, R&D Serial No. 2095b, Portland Cement Association, Skokie, IL. www.cement.org <Accessed November 3, 2011>.
<http://www.cement.org/bookstore/profile.asp?store=&pagenum=1&pos=0&catID=&id=11004> (Fee)
5. Marceau, M.L. M.A. Nisbet, and M.G. VanGeem. Life Cycle Inventory of Portland Cement Concrete, R&D Serial No. 3011, Portland Cement Association, 2007, www.cement.org <Accessed November 3, 2011>.
<http://www.cement.org/bookstore/profile.asp?store=&pagenum=1&pos=0&catID=&id=15222> (Fee)
6. Marceau, M.L., Gajda, J., and VanGeem, M.G. 2002. "Use of Fly Ash in Concrete: Normal and High Volume Ranges," PCA R&D Serial No. 2604, PCA, Skokie, IL, www.cement.org <Accessed November 3, 2011>.
<http://members.cement.org/ebiz50/ProductCatalog/Product.aspx?ID=81> (Fee)
7. ASHRAE/USGBC/IES Standard 189.1-2009, *Standard for the Design of High Performance Green Buildings*, ASHRAE, Atlanta, GA, www.ashrae.org <Accessed November 3, 2011>.
<http://members.cement.org/ebiz50/ProductCatalog/Product.aspx?ID=81> (Fee)
8. Portland Cement Association (PCA), website for sustainable solutions using concrete,
<http://www.concretethinker.com> <Accessed November 3, 2011>.
9. Burnell, Kelly. Sustainable Bridge Design: *What Does a More Sustainable Bridge Project Look Like?* Presentation at the APWA Spring 2009 Conference.
<http://www.docstoc.com/docs/34381820/Sustainable-Bridge-Design>
10. Long, Adrian E. *Sustainable Bridges through Innovative Advances*. Presentation at the Joint ICE and TRF Fellows Lecture, May 2, 2007.
<http://www.transportresearchfoundation.co.uk/PDF/lectures/Adrian%20Long%20paper.pdf>
11. Heat Island Group Home Page, <http://heatisland.lbl.gov> <Accessed November 3, 2011>.
12. ASTM Subcommittee C16.30. 2009 *Standard Test Method for Determination of Solar Reflectance Near Ambient Temperature Using a Portable Solar Reflectometer*. ASTM C1549-09. ASTM International, West Conshohocken, PA, www.astm.org <Accessed November 3, 2011>.
<http://www.astm.org/Standards/C1549.htm> (Fee)
13. ASTM Subcommittee D08.18. 2006. *Standard Test Method for Measuring Solar Reflectance of Horizontal and Low-Sloped Surfaces in the Field*. ASTM E1918-06. ASTM International, West Conshohocken, PA, www.astm.org <Accessed November 3, 2011>.
<http://www.astm.org/Standards/E1918.htm> (Fee)
14. PCA. *U.S. and Canadian Labor-Energy Input Survey*, Skokie, IL, www.cement.org <Accessed November 3, 2011>.
<http://members.cement.org/ebiz50/ProductCatalog/Product.aspx?ID=324> (Fee)
15. PCA. 2006. Report on Sustainable Manufacturing. PCA, Skokie, IL, www.cement.org <Accessed November 3, 2011>.
http://www.cement.org/smreport09/images/shared_images/SustainReport08.pdf

16. ASTM Subcommittee C01.10. 2009. *Standard Specification for Portland Cement*. ASTM C150/C150M-09. ASTM International, West Conshohocken, PA, www.astm.org <Accessed November 3, 2011>. <http://www.astm.org/Standards/C150.htm> (Fee)
17. Slag Cement Association, "Slag Cement and the Environment," Slag Cement in Concrete No. 22, 2003, www.slagcement.org <Accessed November 3, 2011>. http://www.slagcement.org/Sustainability/pdf/No22_Environmental_Benefits.pdf
18. PCA. 2011. *Design and Control of Concrete Mixes*, EB001, 15th Ed., PCA, Skokie, IL, www.cement.org <Accessed November 3, 2011>. <http://members.cement.org/ebiz50/ProductCatalog/Product.aspx?ID=245> (Fee)
19. PCI. 2008. Acoustics. Designers Notebook (DN) 18. PCI, Chicago, IL, www.pci.org <Accessed November 3, 2011>. http://www.pci.org/view_file.cfm?file=AS-08WI-2.pdf
20. Muench, S.T., Anderson, J.L., Hatfield, J.P., Koester, J.R., & Söderlund, M. et al. 2011. *Greenroads Manual v1.5*. Seattle, WA: University of Washington. <http://www.greenroads.us/1/home.html> <Accessed November 3, 2011>.
21. New York State Department of Transportation (NYDOT). 2010. GreenLITES Project Design Certification Program, April, <http://www.dot.ny.gov/programs/greenlites?nd=nysdot> <Accessed November 3, 2011>.
22. CEEQUAL. *CEEQUAL Assessment Manual for Projects Version 4*, CIRIA, London, United Kingdom, December 2008. <http://www.ceequal.com> <Accessed November 3, 2011>.
23. Institute for Sustainable Infrastructure (ISI). 2011. Envision Rating System. <http://www.sustainableinfrastructure.org/rating/index.cfm> <Accessed November 3, 2011>.

MATERIAL PROPERTIES

Table of Contents

NOTATION..... 2 - 5

2.1 SCOPE..... 2 - 7

2.2 PLANT PRODUCTS 2 - 7

 2.2.1 Advantages..... 2 - 7

2.3 CONCRETE MATERIALS 2 - 7

 2.3.1 Cement..... 2 - 7

 2.3.1.1 AASHTO M85 2 - 7

 2.3.1.2 AASHTO M240 2 - 8

 2.3.1.3 ASTM C1157 2 - 8

 2.3.1.4 Restrictions 2 - 8

 2.3.2 Aggregates..... 2 - 8

 2.3.3 Chemical Admixtures 2 - 9

 2.3.3.1 Purpose 2 - 9

 2.3.3.2 Calcium Chloride..... 2 - 9

 2.3.3.3 Corrosion Inhibitors..... 2 - 9

 2.3.3.4 Air-Entraining Admixtures..... 2 - 9

 2.3.3.5 Shrinkage-Reducing Admixtures..... 2 - 9

 2.3.4 Supplementary Cementitious Materials 2 - 9

 2.3.4.1 Fly Ash and Natural Pozzolans 2 - 10

 2.3.4.2 Silica Fume..... 2 - 10

 2.3.4.3 Ground Granulated Blast-Furnace Slag 2 - 10

 2.3.5 Water 2 - 10

2.4 SELECTION OF CONCRETE MIX REQUIREMENTS..... 2 - 10

 2.4.1 Concrete Strength at Transfer..... 2 - 11

 2.4.2 Concrete Strength at Service Loads 2 - 11

 2.4.3 High-Performance Concrete..... 2 - 11

 2.4.3.1 High-Strength Concrete 2 - 11

 2.4.3.2 Low-Permeability Concrete 2 - 11

 2.4.3.3 Self-Consolidating Concrete..... 2 - 11

 2.4.3.4 Ultra-High-Performance Concrete..... 2 - 12

 2.4.4 Durability..... 2 - 12

 2.4.4.1 Freeze-Thaw Damage 2 - 12

 2.4.5 Workability 2 - 13

 2.4.6 Water-Cementitious Materials Ratio..... 2 - 13

 2.4.6.1 Based on Strength 2 - 13

 2.4.6.2 Based on Durability 2 - 14

 2.4.7 Density 2 - 14

 2.4.7.1 Normal Weight Concrete..... 2 - 14

 2.4.7.2 Lightweight Concrete..... 2 - 14

MATERIAL PROPERTIES

Table of Contents

2.4.7.3 Blended Aggregates..... 2 - 14

2.4.7.4 Unit Weight 2 - 14

2.4.8 Effect of Heat Curing..... 2 - 14

2.4.9 Sample Mixes 2 - 16

2.5 CONCRETE PROPERTIES 2 - 16

2.5.1 Introduction 2 - 16

2.5.2 Compressive Strength..... 2 - 16

 2.5.2.1 Variation with Time 2 - 17

 2.5.2.2 Effect of Accelerated Curing 2 - 17

2.5.3 Modulus of Elasticity 2 - 17

 2.5.3.1 Calculations (E_c)..... 2 - 18

 2.5.3.2 Variations (E_c)..... 2 - 18

2.5.4 Modulus of Rupture 2 - 18

2.5.5 Heat of Hydration..... 2 - 18

2.5.6 Durability..... 2 - 19

 2.5.6.1 Test Methods 2 - 19

 2.5.6.2 Alkali-Aggregate Reactivity 2 - 19

 2.5.6.3 Delayed Ettringite Formation 2 - 19

2.5.7 Shrinkage..... 2 - 19

 2.5.7.1 Calculation of Shrinkage..... 2 - 20

2.5.8 Creep..... 2 - 22

 2.5.8.1 Calculation of Creep 2 - 22

2.5.9 Coefficient of Thermal Expansion..... 2 - 22

2.6 GROUT MATERIALS..... 2 - 23

2.6.1 Definitions and Applications..... 2 - 23

2.6.2 Types and Characteristics 2 - 23

 2.6.2.1 Performance Requirements..... 2 - 23

 2.6.2.2 Materials..... 2 - 23

2.6.3 ASTM Tests 2 - 24

2.6.4 Grout Bed Materials 2 - 24

2.6.5 Epoxy Resins 2 - 24

2.6.6 Overlays..... 2 - 24

2.6.7 Post-Tensioned Members..... 2 - 24

2.7 PRESTRESSING STRAND 2 - 24

2.7.1 Strand Types 2 - 25

 2.7.1.1 Epoxy-Coated Strand 2 - 25

 2.7.1.1.1 Effect of Heat..... 2 - 25

2.7.2 Material Properties 2 - 25

2.7.3 Relaxation..... 2 - 25

MATERIAL PROPERTIES

Table of Contents

2.7.3.1 Epoxy-Coated Strand	2 - 26
2.7.4 Fatigue Strength	2 - 26
2.7.4.1 Stress Range.....	2 - 27
2.7.5 Surface Condition.....	2 - 27
2.7.6 Splicing.....	2 - 27
2.8 NONPRESTRESSED REINFORCEMENT.....	2 - 27
2.8.1 Deformed Bars.....	2 - 27
2.8.1.1 Specifications.....	2 - 27
2.8.1.2 Corrosion Protection.....	2 - 28
2.8.2 Mechanical Splices.....	2 - 28
2.8.2.1 Types.....	2 - 28
2.8.3 Welded Wire Reinforcement.....	2 - 28
2.8.4 Fatigue Strength of Nonprestressed Reinforcement.....	2 - 29
2.9 POST-TENSIONING MATERIALS.....	2 - 29
2.9.1 Strand Systems.....	2 - 29
2.9.2 Bar Systems	2 - 29
2.9.3 Splicing.....	2 - 29
2.9.4 Ducts	2 - 29
2.10 FIBER REINFORCED POLYMER REINFORCEMENT.....	2 - 30
2.10.1 Introduction.....	2 - 30
2.10.2 Mechanical Properties.....	2 - 30
2.10.3 Prestressed Concrete Bridge Applications.....	2 - 30
2.10.4 Specifications	2 - 30
2.11 REINFORCEMENT SIZES AND PROPERTIES	2 - 30
2.12 RELEVANT STANDARDS AND PUBLICATIONS	2 - 33
2.12.1 AASHTO Standard Specifications	2 - 33
2.12.2 AASHTO Standard Methods of Test.....	2 - 34
2.12.3 ACI Publications	2 - 34
2.12.4 ASTM Standard Specifications.....	2 - 35
2.12.5 ASTM Standard Test Methods and Practices	2 - 36
2.12.6 Cross References ASTM-AASHTO	2 - 38
2.12.7 Cited References	2 - 38

This page intentionally left blank

NOTATION

A	=	constant
A_s^*	=	nominal area of prestressing steel
B	=	constant
$\psi(t, t_0)$	=	creep coefficient at t days after loading
$(E_c)_t$	=	modulus of elasticity of concrete at an age of t days
f'_c	=	specified concrete compressive strength
f'_{ci}	=	concrete compressive strength at time of transfer
$(f'_c)_t$	=	concrete compressive strength at an age of t days
$(f'_c)_{28}$	=	concrete compressive strength at an age of 28 days
f_{min}	=	minimum stress level in reinforcement
f_{ps}	=	stress in prestressing strand
f_{pt}	=	stress in prestressing strands immediately after transfer
f_{py}	=	yield strength of prestressing steel
f_r	=	modulus of rupture
f'_s	=	ultimate strength of prestressing steel
H	=	annual average ambient relative humidity
k_f	=	factor for the effect of concrete strength
k_{hs}	=	humidity factor for shrinkage
k_{hc}	=	humidity factor for creep
k_s	=	factor for the effect of volume-to-surface ratio
k_{td}	=	time development factor
K	=	constant
K_1	=	constant
K_L	=	constant
S	=	surface area of concrete exposed to drying
ϵ_{sh}	=	shrinkage strain at a concrete age of t days
t	=	age of concrete from time of casting or age of concrete from end of curing to the time being considered
t_i	=	age of concrete at time of load application
V	=	volume of concrete
w_c	=	density of concrete
Δf_{pR1}	=	relaxation loss between time of transfer and deck placement
Δf_{pR2}	=	relaxation loss between time of deck placement and final time
$(\Delta F)_{TH}$	=	constant amplitude fatigue threshold
ϵ_{ps}	=	strain in prestressing strand

This page intentionally left blank

Material Properties

2.1 SCOPE

This chapter contains a description of the properties of all major materials currently used for precast, prestressed concrete bridge structures. It includes a discussion of concrete constituent materials, mix requirements, hardened concrete properties, pretensioning and post-tensioning reinforcement, nonprestressed reinforcement, and grouts used between precast members and other components. Recent developments in high-performance concrete and nonmetallic reinforcement are also introduced. Discussion of the materials specifically used in fabrication and construction is included in Chapter 3.

2.2 PLANT PRODUCTS

The production of precast concrete components in a plant environment offers several advantages compared to on-site production. Many of these advantages occur because one company is responsible for quality control throughout production. This results in closer monitoring of raw materials, steel placement, concrete production and delivery, concrete curing, and shipment. The overall effect is to produce a product with more consistent material properties than can be achieved with site-cast concrete.

2.2.1 Advantages

In many aspects, the material properties of precast components are superior to those of cast-in-place members. Precast concrete components are required to achieve a minimum concrete strength for prestress transfer and removal from their precasting beds at an early age (12 to 18 hours). This often results in concrete that has a 28- or 56-day compressive strength in excess of the specified strength. Consequently, the concrete has a higher modulus of elasticity and less creep than would occur if the actual strength were equal to the specified strength. The use of accelerated curing to achieve the transfer strength also results in less shrinkage and creep. From a durability aspect, precast concrete members have a low permeability and, therefore, are better suited for use in aggressive environments such as coastal areas and locations where deicing salts are used.

2.3 CONCRETE MATERIALS

The five major component materials of concrete are cement, aggregates, chemical admixtures, supplementary cementitious materials, and water.

2.3.1 Cement

Cement for use in bridge construction generally conforms to one of the following specifications:

- AASHTO M85 Portland Cement
- AASHTO M240 Blended Hydraulic Cement
- ASTM C1157 Hydraulic Cement

2.3.1.1 AASHTO M85

The AASHTO Specification M85 lists ten types of portland cement as follows:

- Type I Normal
- Type IA Normal, air-entraining
- Type II Moderate sulfate resistance
- Type IIA Moderate sulfate resistance, air-entraining
- Type II(MH) Moderate heat of hydration, moderate sulfate resistance
- Type II(MH)A Moderate heat of hydration, moderate sulfate resistance, air-entraining
- Type III High early strength
- Type IIIA High early strength, air-entraining
- Type IV Low heat of hydration
- Type V High sulfate resistance

MATERIAL PROPERTIES**2.3.1.1 AASHTO M85/2.3.2 Aggregates**

Type I portland cement is a general purpose cement suitable for all uses where the special properties of other types of cement are not required. Type II portland cement is used where precaution against moderate sulfate attack is important or to reduce the heat of hydration. Type III portland cement provides high strengths at an early age and is particularly appropriate for obtaining high strengths for prestress transfer. Type IV portland cement is used to reduce the heat of hydration and is particularly beneficial in mass concrete structures. Type V portland cement is used in concrete exposed to severe sulfate attack. Types IA, IIA, II(MH)A, and IIIA, correspond in composition to Types I, II, II(MH), and III, respectively, except that small quantities of air-entraining material are included in the cement. Some cements are designated with a combined type classification, such as Type I/II, indicating that the cement meets the requirements of the indicated types.

2.3.1.2 AASHTO M240

The AASHTO Specification M240 lists two types of blended hydraulic cements for general concrete construction as follows:

- Type IS(X) Portland blast-furnace slag cement
- Type IP(X) Portland-pozzolan cement

The suffix (X) denotes the targeted percentage of slag or pozzolan expressed by mass of the total product. Special properties may be specified by adding the following suffixes:

- (A) Air entraining
- (MS) Moderate sulfate resistance
- (MH) Moderate heat of hydration
- (HS) High sulfate resistance
- (LH) Low heat of hydration

Blended hydraulic cements are produced by intergrinding and/or blending various combinations of portland cement, ground granulated blast-furnace slag, fly ash, and other pozzolans. These cements can be used to produce different properties in the hardened concretes.

2.3.1.3 ASTM C1157

The ASTM Specification C1157 is a performance specification listing physical test requirements as opposed to prescriptive restrictions on ingredients or cement chemistry. ASTM C1157 lists six types of cement as follows:

- Type GU General use
- Type HE High early strength
- Type MS Moderate sulfate resistance
- Type HS High sulfate resistance
- Type MH Moderate heat of hydration
- Type LH Low heat of hydration

2.3.1.4 Restrictions

The *LRFD Construction Specifications* generally restrict cement usage to portland cement Types I, II, or III; air-entrained portland cement Types IA, IIA, or IIIA; or blended hydraulic cements Types IP or IS. For Type IP, the pozzolan constituent shall not exceed 20% of the total mass. It should also be noted that not all types of cement are readily available and that the use of some types is not permitted by some states.

2.3.2 Aggregates

Aggregates for concrete consist of fine and coarse materials. Fine aggregate for normal weight concrete should conform to the requirements of AASHTO M6. Coarse aggregate for normal weight concrete should conform to the requirements of AASHTO M80. Some states specify a combined grading for fine and coarse aggregates. Lightweight aggregate for use in lightweight or sand-lightweight concrete should conform to the requirements of AASHTO M195. The maximum size of aggregate should be selected based on mix-requirements and the minimum clear spacing between reinforcing steel, clear cover to reinforcing steel, and thickness of the member in accordance with AASHTO specifications. If aggregates susceptible to alkali-aggregate reactivity are used in prestressed concrete members, special precautions must be observed. These include the use of low alkali cements, blended cements, or pozzolans.

MATERIAL PROPERTIES**2.3.4 1 Fly Ash and Natural Pozzolans/2.4 Selection of Concrete Mix Requirements****2.3.3 Chemical Admixtures**

Chemical admixtures are used in precast, prestressed concrete to provide air entrainment, reduce water content, improve workability, retard setting times, and accelerate strength development. Chemical admixtures, except air-entraining admixtures, should conform to the requirements of AASHTO M194. This specification lists the following types of admixtures:

- Type A Water-reducing
- Type B Retarding
- Type C Accelerating
- Type D Water-reducing and retarding
- Type E Water-reducing and accelerating
- Type F Water-reducing, high range
- Type G Water-reducing, high range and retarding

2.3.3.1 Purpose

Water-reducing admixtures and high-range water-reducing admixtures are used to allow for a reduction in the water-cementitious materials ratio while maintaining or improving workability. Accelerating admixtures are used to decrease the setting time and increase the early strength development. They are particularly beneficial in precast concrete construction to facilitate early form removal and transfer of prestressing force. Since admixtures can produce different results with different cements, and at different temperatures, selection of admixtures should be based on the plant materials and conditions that will be utilized in production. Compatibility between admixtures is also important and should be specifically addressed when using combinations of admixtures produced by different companies.

2.3.3.2 Calcium Chloride

Calcium chloride has been used in the past as an accelerator since it is very effective and economical. The use of calcium chloride in concrete promotes corrosion of metals due to the presence of chloride ions. Consequently, calcium chloride should not be permitted in prestressed concrete members. Accelerators without chlorides may be used.

2.3.3.3 Corrosion Inhibitors

Corrosion-inhibiting admixtures are also available for use in concrete to protect reinforcement from corrosion. These admixtures block the passage of chloride ions to the steel reinforcement and, thereby, reduce or eliminate corrosion of the reinforcement. Corrosion-inhibiting admixtures are more likely to be effective in cast-in-place bridge components that are directly exposed to chloride ions than in precast concrete bridge members that exhibit lower permeability.

2.3.3.4 Air-Entraining Admixtures

Air-entraining admixtures are used in concrete primarily to increase the resistance of the concrete to freeze-thaw damage when exposed to water and deicing chemicals. They may also be used to increase workability and facilitate handling and finishing. Air-entraining admixtures should conform to AASHTO M154. The air content of fresh concrete is generally determined using the pressure method (AASHTO T152) or the volumetric method (AASHTO T196). The pressure method should not be used with lightweight concrete. A pocket-size air indicator (AASHTO T199) can be used for quick checks but is not a substitute for the other more accurate methods.

2.3.3.5 Shrinkage-Reducing Admixtures

Shrinkage-reducing admixtures have the potential to reduce shrinkage by 25 to 50%. These admixtures have negligible effect on slump and air content but can delay setting and early strength gain.

2.3.4 Supplementary Cementitious Materials

Supplementary cementitious materials, also called mineral admixtures, consist of fly ash, ground granulated blast-furnace slag, silica fume, and natural pozzolans. They are added to concrete to improve or change the properties of hardened hydraulic cement concrete such as earlier strength development or less heat of hydration. They may also be used to improve the resistance of concrete to reactive aggregates and to replace cement. They have also been used in high-strength concrete to produce higher strengths at early or later ages. The use of supplementary cementitious materials may affect the workability and finishing characteristics of fresh concrete.

MATERIAL PROPERTIES**2.3.4 1 Fly Ash and Natural Pozzolans/2.4 Selection of Concrete Mix Requirements****2.3.4.1 Fly Ash and Natural Pozzolans**

AASHTO M295 lists three classes of fly ash and natural pozzolans as follows:

- Class N Raw or calcined natural pozzolans
- Class F Fly ash
- Class C Fly ash

High-Reactive Metakaolin (HRM) is a manufactured white powder that meets the requirements of a Class N pozzolan. HRM has a particle size significantly smaller than that of cement particles, but not as fine as silica fume. Fly ash is a finely divided residue that results from the combustion of pulverized coal in power generation plants. Class F fly ash has pozzolanic properties; Class C has some cementitious properties in addition to pozzolanic properties. Some fly ashes meet both Class F and Class C classifications. Selection of these materials will depend on their local availability and their effect on concrete properties.

2.3.4.2 Silica Fume

Silica fume meeting the requirements of AASHTO M307 may also be used as a supplementary cementitious material in concrete. Silica fume is a very fine pozzolanic material produced as a by-product in electric arc furnaces used for the production of elemental silicon or ferro-silicon alloys. Silica fume is also known as condensed silica fume and microsilica. The use of silica fume can improve the early age strength development of concrete and is particularly beneficial in achieving high transfer strengths in high-strength concrete beams. The use of silica fume in concrete generally results in concrete that has low permeability. The use of silica fume increases the water demand in concrete. Consequently, it is generally used in combination with a water-reducing admixture or a high-range water-reducing admixture. Concrete containing silica fume has significantly less bleeding and the potential for plastic shrinkage is increased. Therefore, early moisture loss should be prevented under conditions that promote rapid surface drying such as low humidity and high temperatures.

2.3.4.3 Ground Granulated Blast-Furnace Slag

Ground granulated blast-furnace slag, also called slag cement, meeting the requirements of AASHTO M302 may be used in concrete to provide higher strengths and lower permeability, reduce heat of hydration, and increase resistance to alkali-silica reaction and sulfate attack. Slag cement is produced from molten slag tapped from an iron blast furnace, then rapidly quenched with water in a granulator. The resulting glassy granules are then dried and either ground to a fine powder to make slag cement or interground with portland cement to produce a blended cement.

2.3.5 Water

Water used in mixing concrete must be clean and free of oil, salt, acid, alkali, sugar, vegetable, or other injurious substances. Water known to be of potable quality may be used without testing. However, if there is doubt, water should meet the requirements of AASHTO T26. Mixing water for concrete should not contain a chloride ion concentration in excess of 1,000 ppm or sulfates as SO_4 in excess of 1,300 ppm per the *LRFD Construction Specifications*.

2.4 SELECTION OF CONCRETE MIX REQUIREMENTS

This section discusses various aspects of concrete mix requirements that need to be considered by the owner or the owner's engineer. Selection of concrete ingredients and proportions to meet the minimum requirements stated in the specifications and contract documents should be the responsibility of the precast concrete producer. Wherever possible, the mix requirements should be stated on the basis of the required performance and not be over-restrictive to the producer. The producer should be allowed to show through trial batches or mix history that a proposed mix design will meet or exceed the specified performance criteria. Consequently, prescriptive requirements such as minimum cement content should be avoided.

MATERIAL PROPERTIES**2.4.1 Concrete Strength at Transfer/2.4.3.3 Self-Consolidating Concrete****2.4.1 Concrete Strength at Transfer**

For prestressed concrete bridge beams, the Engineer generally specifies minimum strengths at time of transfer of the prestressing strand force and at 28 days, although ages other than 28 days may be used. The Engineer may also specify a minimum compressive strength at time of beam erection, or a minimum compressive strength at time of post-tensioning if a combination of pretensioning and post-tensioning is utilized. For most prestressed concrete bridge beams, the specified strength at time of transfer will control the concrete mix proportions. Based on the *LRFD Specifications*, the transfer strength is selected so that the temporary concrete stresses in the beam, before losses due to creep and shrinkage, do not exceed 60% of the concrete compressive strength at time of transfer in pretensioned members and at time of stressing of post-tensioned members. In addition, the strength is selected so that, in tension areas with no bonded reinforcement, the tensile stress will not exceed 0.2 ksi or $0.0948\sqrt{f'_{ci}}$ where f'_{ci} is the compressive strength of concrete at time of transfer in ksi. In areas with a specified amount of bonded reinforcement, the maximum tensile stress cannot exceed $0.24\sqrt{f'_{ci}}$.

2.4.2 Concrete Strength at Service Loads

The design of most precast, prestressed concrete members is generally based on a concrete compressive strength at 28 days of 5.0 to 6.0 ksi. However, because the mix proportions are generally dictated by transfer strengths, concrete strengths at 28 days are frequently in excess of the specified 28-day value and actual strengths of 8.0 ksi or more are often achieved. Consequently, mix requirements are generally based on the transfer strengths and the precaster only has to ensure that the mix will provide concrete with a compressive strength in excess of that specified for 28 days.

The minimum compressive strength, in some cases, may be controlled by the need to meet a minimum requirement for special exposure conditions as discussed in Section 2.4.6.2.

2.4.3 High-Performance Concrete

High-performance concrete is defined by the American Concrete Institute as concrete meeting special combinations of performance and uniformity requirements that cannot always be achieved routinely using conventional constituents and normal mixing, placing, and curing practices (Russell, 1999). For precast, prestressed concrete bridge beams, this usually means higher concrete compressive strength, lower permeability, or easier placement. For some projects, modulus of elasticity, creep, and shrinkage values may be specified.

2.4.3.1 High-Strength Concrete

Concrete with specified strengths in excess of 8.0 ksi is being specified by some states to achieve longer span lengths, wider beam spacing, or the use of shallower sections. In such cases, the concrete strength is typically specified at 56 days because of the strength gain that is possible in higher strength concrete between 28 and 56 days. The higher strengths are generally achieved through the use of higher cementitious materials content, lower water-cementitious materials ratio, and supplementary cementitious materials.

2.4.3.2 Low-Permeability Concrete

Low-permeability concrete is beneficial in reducing the rate of penetration of chlorides into the concrete. It is frequently specified with reference to AASHTO T277, which is a rapid test to determine the penetration of chloride ions into concrete. Alternatively, it may be specified using ponding procedures such as those described in AASHTO T259. Low-permeability concrete can be achieved using the same approaches to achieve high-strength concrete; higher cementitious materials content, lower water-cementitious materials ratio, and supplementary cementitious materials. Consequently, most high-strength concretes have a low permeability but not all low-permeability concretes have high strength.

2.4.3.3 Self-Consolidating Concrete

Self-consolidating concrete (SCC) is a highly flowable, nonsegregating concrete that can spread into place, fill the formwork, and encapsulate the reinforcement without any mechanical consolidation (ACI 237R). The use of SCC results in smooth concrete surfaces with less "bugholes," requires less labor to place, and results in a quieter work environment. SCC is generally more expensive than regular concrete and requires more stringent quality control.

MATERIAL PROPERTIES**2.4.3.3 Self-Consolidating Concrete/2.4.4.1 Freeze-Thaw Damage**

The flowing characteristics of SCC are achieved by increasing the amount of fine material, using a high-range water-reducing admixture, and, in some cases, including a viscosity-modifying admixture. Further information about the use of SCC in precast, prestressed concrete is provided in PCI Guidelines (PCI, forthcoming) and NCHRP Report 628 (Khayat and Mitchell, 2009).

The following test methods are available for use with SCC:

- ASTM C1610 Test Method for Static Segregation of Self-Consolidating Concrete Using Column Technique
- ASTM C1611 Test Method for Slump Flow of Self-Consolidating Concrete
- ASTM C1621 Test Method for Passing Ability of Self-Consolidating Concrete by J-Ring
- ASTM C1712 Test Method for Rapid Assessment of Static Segregation Resistance of Self-Consolidating Concrete Using Penetration Test

2.4.3.4 Ultra-High-Performance Concrete

Ultra-high-performance concrete (UHPC) is a cementitious composite material that contains cement, fine sand, silica fume, ground quartz, superplasticizer, steel or plastic fibers, and water. Compared to conventional concretes, hardened UHPC has exceptional durability, high compressive strength, usable tensile strength, and long-term stability. In addition, fresh UHPC has the flowability characteristics of SCC (Graybeal, 2006A, 2006B). UHPC has been used for the beams of several bridge structures in the United States and as a field-cast joint material to create splice connections between deck components. (Graybeal and Lwin, 2010).

2.4.4 Durability

Durability is a concern when bridges are exposed to aggressive environments. This generally occurs where deicing salts are utilized on highways during winter or in coastal regions where structures are exposed to salt from sea water. The Engineer must be concerned about the deleterious effects of freezing and thawing, chemical attack, and corrosion of embedded or exposed metals. The ideal approach is to make the concrete as impermeable as possible. In this respect, precast, prestressed concrete has inherent advantages over cast-in-place concrete since it is produced in a controlled environment that results in high quality concrete. In addition, the mix proportions needed to achieve a relatively high-strength concrete tend to produce lower permeability concretes. As a result, precast, prestressed concrete bridge beams have an excellent record of performance in aggressive environments.

2.4.4.1 Freeze-Thaw Damage

Freeze-thaw damage generally manifests itself by scaling of the concrete surface. This occurs as a result of temperature fluctuations that cause freezing and thawing when the concrete is saturated. Freeze-thaw damage is magnified when deicing chemicals are present. To minimize freeze-thaw damage, a minimum air content is generally specified. The presence of entrained air provides space for ice to expand without developing high pressures that would otherwise damage the concrete. **Table 2.4.4.1-1**, based on ACI 211.1, provides the required air content for severe and moderate exposure conditions for various maximum aggregate sizes. Severe exposure is defined as a climate where the concrete may be in almost continuous contact with moisture prior to freezing, or where deicing salts come in contact with the concrete. This includes bridge decks. Salt laden air, as found in coastal areas, is also considered a severe exposure. A moderate exposure is one where deicing salts are not used or where concrete will only occasionally be exposed to moisture prior to freezing. This is generally the case for bridge beams. It should be noted that some state highway departments specify air contents that are slightly different from those shown in **Table 2.4.4.1-1**. In addition, many states do not require air entrainment in prestressed concrete beams because beams are sheltered by the deck or other conditions exist such that air entrainment is not required for good performance.

MATERIAL PROPERTIES**2.4.4.1 Freeze-Thaw Damage/2.4.6.1 Based on Strength**

Table 2.4.4.1-1
Total Air Content for Frost-Resistant Concrete

Nominal Maximum Aggregate Size, in.	Minimum Air Content*, percent	
	Severe Exposure	Moderate Exposure
3/8	7-1/2	6
1/2	7	5-1/2
3/4	6	5
1	6	4-1/2
1-1/2	5-1/2	4-1/2

*The usual tolerance on air content as delivered is $\pm 1.5\%$

2.4.5 Workability

The ease of mixing, placing, consolidating, and finishing freshly mixed concrete is called workability. Concrete should be workable but should not segregate or bleed excessively. Excessive bleeding increases the water-cementitious materials ratio near the top surface and a weak top layer of concrete with poor durability may result. For prestressed concrete bridge beams, particular attention should be paid to ensure that concrete has adequate workability so that it will consolidate around the prestressing strands, particularly at end regions of beams where a high percentage of nonprestressed reinforcement is present. It is also important that concrete can be placed in the webs of beams without segregation. Workability can be enhanced through the use of water-reducing admixtures, high-range water-reducing admixtures, and air-entraining agents. No standard test exists for the measurement of workability. The concrete slump test is the most generally accepted method used to measure consistency of concrete but it should not be used as a means to control workability.

2.4.6 Water-Cementitious Materials Ratio

The water-cementitious materials ratio is the ratio of the amount of water, exclusive of that absorbed by the aggregate, to the amount of cementitious materials in a concrete or mortar mixture. As such, the amount of water includes that within the admixtures and that in the aggregate in excess of the saturated surface-dry condition. The amount of cementitious material includes cement and other cementitious materials, such as fly ash, silica fume, and slag cement. The total cementitious materials content for compressive strengths from 4.0 to 10.0 ksi can vary from 600 to 1,000 lb/yd³ and will also vary on a regional basis.

2.4.6.1 Based on Strength

When strength, not durability, controls the mix design, the water-cementitious materials ratio and mixture proportions required to achieve specified strength should be determined from field data or the results of trial batch strength tests. The trial batches should be made from actual job materials. When no other data are available, **Table 2.4.6.1-1**, which is based on ACI 211.1, may be used as a starting point for mix design procedures for normal weight concrete.

Table 2.4.6.1-1
Approximate Ratios for Trial Batches

Compressive Strength at 28 days, ksi	Water-Cementitious Materials Ratio by Weight	
	Non-Air-Entrained Concrete	Air-Entrained Concrete
6.0	0.41	—
5.0	0.48	0.40
4.0	0.57	0.48

MATERIAL PROPERTIES**2.4.6.2 Based on Durability/2.4.8 Effect of Heat Curing****2.4.6.2 Based on Durability**

When durability is a major consideration in the concrete mix design, the maximum water-cementitious materials ratio should be limited. For precast, prestressed concrete members exposed to deicing chemicals, salt, brackish water, seawater, or spray from these sources, the maximum ratio will generally be 0.40.

2.4.7 Density**2.4.7.1 Normal Weight Concrete**

The density of plain normal weight concrete is generally in the range of 0.140 to 0.150 kip/ft³. The density varies depending on the amount and density of the aggregate and the air, water, and cement contents. The *LRFD Specifications* provides the following densities for plain concrete:

Table 2.4.7.1-
Plain Concrete Densities [LRFD Table 3.5.1-1]

Concrete	Density, kip/ft ³
Lightweight	0.110
Sand-Lightweight	0.120
Normal Weight with $f'_c < 5.0$ ksi	0.145
Normal Weight with $5.0 \text{ ksi} \leq f'_c \leq 15.0$ ksi	$0.140 + 0.001 f'_c$

where f'_c = specified concrete compressive strength

2.4.7.2 Lightweight Concrete

Lightweight concrete, sand-lightweight concrete (also called semi-lightweight concrete), and specified density concrete may also be utilized in precast, prestressed concrete bridge construction with the use of suitable lightweight aggregates. Lightweight aggregate concretes generally have a density of 0.090 to 0.105 kip/ft³. Sand-lightweight concretes have a density of 0.105 to 0.130 kip/ft³ with a common range of 0.110 to 0.115 kip/ft³. When lightweight concrete is used in prestressed concrete members, special consideration must be given to using mix design procedures for lightweight concrete as given in ACI 211.2.

2.4.7.3 Blended Aggregates

Where suitable lightweight aggregates are available, a common practice is to blend lightweight with normal weight aggregates to achieve a desired concrete density. This is done to control beam (or other product) weights to satisfy shipping limitations, jobsite conditions such as crane size or reach limits, or plant or erection equipment capacities.

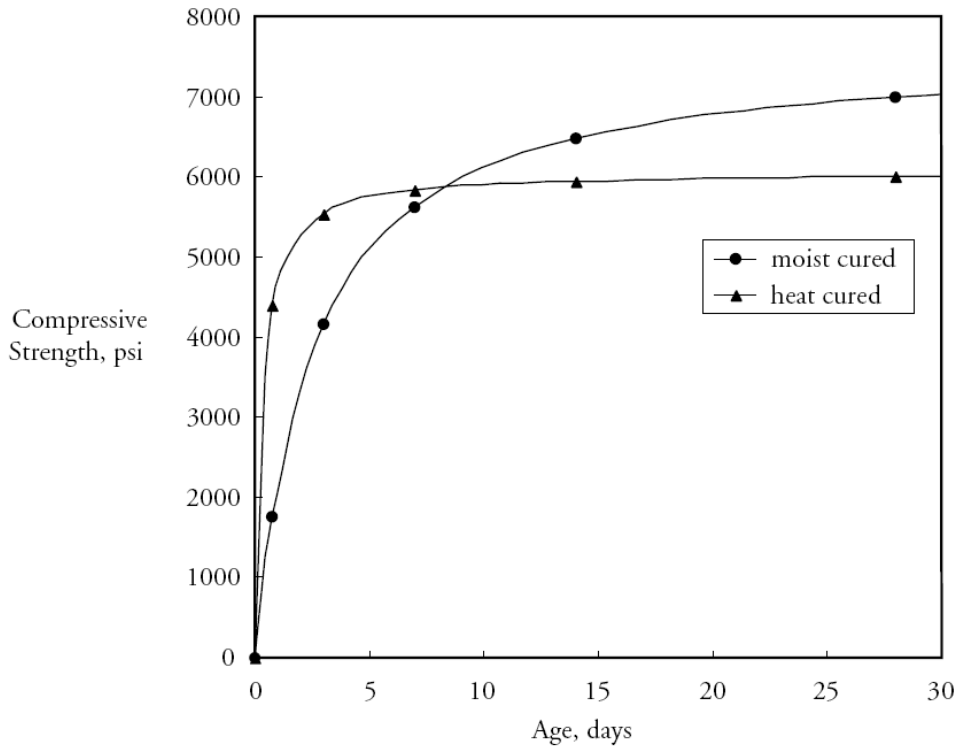
2.4.7.4 Unit Weight

In the design of reinforced or prestressed concrete structures, the unit weight for design purposes is generally taken as 0.005 kip/ft³ greater than the density of plain concrete. However, for members with large quantities of prestressing strand, a higher amount may be more appropriate.

2.4.8 Effect of Heat Curing

Because of the need for early strength gain, Type III cement is often used in precast concrete so that formwork may be reused on a daily basis. This generally requires that the transfer strength be achieved no later than 18 hours after the concrete is placed and may be achieved at 12 hours or less. To accelerate the strength gain, it is often necessary to raise the temperature of the concrete. In some situations, such as with high-strength concrete, the increase in temperature can be provided by the internal heat of hydration. However, in most situations, it is necessary to utilize an external source of heat, such as steam or radiant heat, to reach the necessary release strengths. The use of external heat causes the concrete temperature to be higher at an earlier age than would be achieved from the natural heat of hydration. A consequence of achieving high transfer strength is a reduction in the later age strengths compared to strengths that would have been obtained if the concrete had not been heat cured. This is illustrated in **Figure 2.4.8-1**. The effect of heat curing on the concrete compressive strength development must be taken into account in the selection of mix requirements and in the preparation of trial mixes.

Figure 2.4.8-1
Effect of Curing on Concrete Compressive Strength Gain



MATERIAL PROPERTIES
2.4.9 Sample Mixes/2.5.2 Compressive Strength

2.4.9 Sample Mixes

Sample concrete mixes for seven different concrete compressive strengths are shown in **Table 2.4.9-1**. These are concrete mixes from different precasting plants. It should not be assumed that these mixture proportions will always produce the same concrete compressive strengths when used with different materials.

Table 2.4.9-1
Sample Production Concrete Mixes

Mix	A	B	C	D	E	F	G
Specified Strength, ksi							
Transfer	3.5	4.0	5.0	6.0	4.50	6.0	8.8
28 Days	5.0	6.0	7.5	7.5	8.00	10.0	13.1
Quantities per yd³							
Cement, lb	705	705	850	750	451	750	671
Fly Ash, lb	0	0	0	140	0	0	316
Silica Fume, lb	0	0	0	0	0	95	0
Slag, lb	0	0	0	0	301	0	0
Normal Weight Sand, lb	1,055	1,085	935	1,085	541	1,030	1,029
Lightweight Sand, lb	0	0	0	0	390	0	0
Normal Weight Coarse Aggregate, lb	1,790	1,920	1,770	1,980	605	1,870	1,918
Lightweight Coarse Aggregate, lb	0	0	0	0	696	0	0
Water, lb	270	285	300	230	255	230	247
Air Entrainment, fl. oz.	5	0	17	0	UNKN	3	0
Water-Reducer, fl. oz.	25	53	29	0	22	10	0
High Range Water-Reducer, fl. oz.	125	0	145	160	56	85	200
Concrete Properties							
Water-Cementitious Materials Ratio	0.38	0.40	0.36	0.26	0.34	0.31	0.25
Slump, in.	3-1/2	4-3/4	4	6	UNKN	5	9
Density, kip/ft ³	0.142	0.148	0.140	0.145	0.120	0.147	UNKN
Air Content, %	6.0	N/A	6.0	N/A	5.5 to 7.0	5.0	N/A
Transfer Strength, ksi (Actual)	3.8	4.4	5.3	6.7	4.7	9.1	8.8
28-day Strength, ksi (Actual)	5.7	6.4	8.0	9.4	8.1	10.5	13.9
56-day Strength, ksi (Actual)	UNKN	UNKN	UNKN	UNKN	UNKN	UNKN	15.2

UNKN – Unknown; NA – Not Applicable

2.5 CONCRETE PROPERTIES

2.5.1 Introduction

Concrete properties such as modulus of elasticity, tensile strength, shear strength, and bond strength are frequently expressed in terms of the compressive strength. Generally, expressions for these quantities have been empirically established based on data for concretes having compressive strengths up to 6.0 ksi. Through research, these empirical relationships have been reevaluated for higher concrete compressive strengths up to 10 ksi. Unless indicated otherwise, the relationships in this section may be assumed applicable for concrete with compressive strengths up to 10 ksi. Where alternative expressions are available for higher strength concretes, they are discussed in each section.

2.5.2 Compressive Strength

Compressive strength is generally measured by testing 6 x 12-in. cylinders in accordance with standard AASHTO or ASTM procedures. The precast concrete industry also uses 4 x 8-in. cylinders. Some state highway departments permit the use of either 6 x 12-in. or 4 x 8-in. cylinders for quality control. For high-strength concretes, the use of smaller size cylinders may be necessary because of limitations on testing machine capacities. For precast, prestressed concrete members it is particularly important that the concrete cylinders used to determine transfer

MATERIAL PROPERTIES**2.5.2 Compressive Strength/2.5.3 Modulus of Elasticity**

strengths be cured in an identical manner to the bridge members. In general, this is accomplished by curing the concrete cylinders alongside the prestressed concrete member until transfer of the prestressing strands. A more advanced technique of match curing is also available. In this procedure, the cylinders are enclosed in a container in which the temperature is controlled to match the temperature of the concrete member. The test cylinders then undergo the same time-temperature history as the concrete member.

2.5.2.1 Variation with Time

The variation of concrete compressive strength with time may be approximated by the following general calculation:

$$(f'_c)_t = \frac{t}{A + Bt} (f'_c)_{28} \quad (\text{Eq. 2.5.2.1-1})$$

where:

$(f'_c)_t$ = concrete compressive strength at an age of t days

$(f'_c)_{28}$ = concrete compressive strength at an age of 28 days

A and B = constant

t = age of concrete, days

The constants A and B are functions of both the type of cementitious material used and the type of curing employed. The use of normal weight, sand-lightweight or all lightweight aggregate does not appear to affect these constants significantly. Typical values recommended by ACI 209 are given in **Table 2.5.2.1-1**. The constants for current practice shown in **Table 2.5.2.1-1** are based on the sample mixes shown in **Table 2.4.9-1**. These mixes have release strengths that vary from 63 to 87% of the 28-day strength.

**Table 2.5.2.1-
Values of Constants A and B**

Source	Curing	Cement	A	B
ACI 209	Moist	I	4.00	0.85
ACI 209	Moist	III	2.30	0.92
ACI 209	Steam	I	1.00	0.95
ACI 209	Steam	III	0.70	0.98
Current Practice	Heat	III	0.28	0.99

2.5.2.2 Effect of Accelerated Curing

As shown in **Figure 2.4.8-1**, a concrete that is heat cured will have higher initial strengths but lower strength at later ages when compared to the same concrete that is moist cured. It should be emphasized that these are general relationships and variations will occur for different concretes and curing procedures. When fly ash is used as a supplementary cementitious material, it may be appropriate to determine the compressive strength at 56 days to take advantage of the later strength gain. Therefore, it is important that the strength gain relationship be established through trial mixes or previous experience using local producer data. This is particularly important for release strengths that can occur as early as 12 hours. If the relationship is unknown, the values listed in **Table 2.5.2.1-1** for current practice will give an approximate relationship.

2.5.3 Modulus of Elasticity

The modulus of elasticity is the ratio of uniaxial normal stress to corresponding strain up to the proportional limit for both tensile and compressive stresses. It is the material property that determines the amount of deformation under load. It is used to calculate camber at release, elastic deflections caused by dead and live loads, axial shortening and elongation, prestress losses, buckling, and relative distribution of applied forces in composite and non-homogeneous structural members. Modulus of elasticity is determined in accordance with ASTM C469.

MATERIAL PROPERTIES**2.5.3.1 Calculations (E_c)/2.5.5. Heat of Hydration****2.5.3.1 Calculations (E_c)**

For concrete compressive strengths less than 15.0 ksi, the following equation from the *LRFD Specifications* may be used to predict the modulus of elasticity:

$$(E_c)_t = 33,000K_1(w_c)^{1.5}\sqrt{(f'_c)_t} \quad [\text{LRFD Eq. 5.4.2.4-1}]$$

where

- $(E_c)_t$ = modulus of elasticity of concrete at an age of t days, ksi
- K_1 = correction factor for source of aggregate to be taken as 1.0 unless determined by physical test
- w_c = density of concrete, kip/ft³
- $(f'_c)_t$ = compressive strength of concrete at an age of t days, ksi

Based on the analysis of over 4400 data points, Rizkalla, et al. (2007) proposed the following equation for use with concrete compressive strengths up to 18 ksi:

$$(E_c)_t = 310,000 K_1 (w_c)^{2.5} (f'_c)^{0.33} \quad (\text{Eq. 2.5.3.1-1})$$

Equation 2.5.3.1-1 provides a mean of the ratio of predicted to measured values closer to 1 than LRFD Eq. 5.4.2.1-1. For normal weight concrete, Eq. 2.5.3.1-1 results in a higher modulus of elasticity for compressive strengths below 7.5 ksi and a lower modulus above 7.5 ksi. For lightweight concrete, Eq. 2.5.3.1-1 results in a lower modulus of elasticity for all compressive strengths.

2.5.3.2 Variations (E_c)

Deviations from predicted values are highly dependent on the properties and proportions of the coarse aggregate used in the concrete. Consequently, where local producer data are available, they should be utilized in place of the values determined from these standard equations. This is particularly important in computing the camber at release as these modulus of elasticity equations have not been developed specifically for determination of the modulus of heat cured concrete at an early age.

2.5.4 Modulus of Rupture

The modulus of rupture is a measure of the flexural tensile strength of the concrete. It can be determined by testing, but the modulus of rupture for structural design is generally assumed to be a function of the concrete compressive strength. It may be predicted by the following equation for compressive strengths up to 15.0 ksi.

$$f_r = K\sqrt{f'_c} \quad (\text{Eq. 2.5.4-1})$$

where

- f_r = modulus of rupture, ksi
- K = a constant, taken as follows:
 - 0.20 to 0.37 for normal weight concrete depending on the requirement for a lower or upper bound value
 - 0.20 for sand-lightweight concrete
 - 0.17 for all-lightweight concrete

Rizkalla, et al. (2007) has suggested that the lower bound value of K should be revised to 0.19 for concrete compressive strengths up to 18 ksi.

2.5.5 Heat of Hydration

Heat of hydration is the heat generated when cement and water react. The amount of heat generated is largely dependent on the chemical composition of the cement but an increase in cement content, fineness or curing temperature will increase the heat of hydration. Heat of hydration is particularly important in heat-cured concretes where the heat generated by the chemical reaction of the cement in conjunction with heat curing can be used to accelerate the development of compressive strength. The heat of hydration can be measured using ASTM C186. When prestressed concrete beams are heat cured, the heat generated by hydration cannot escape from the surface of the member. Consequently, under this condition, the beams may be considered as mass concrete. Procedures for determining the temperature rise in mass concrete are described in ACI 207.1. However, as an

MATERIAL PROPERTIES**2.5.5. Heat of Hydration/2.5.7 Shrinkage**

approximate calculation, it can be assumed that a temperature rise of 10 to 15 °F will occur for each 100 lb of cement used in the concrete. More precise calculations can be made using the actual concrete mix proportions, specific heat of the concrete, and heat generated per unit mass of cement.

2.5.6 Durability

Durability refers to the ability of concrete to resist deterioration from the environment or service conditions in which it is placed. Properly designed concrete should survive throughout its service life without significant distress.

2.5.6.1 Test Methods

The following test procedures may be used to check the durability of concrete made with a specific mix:

Freeze-thaw resistance	AASHTO T161
Deicer scaling resistance	ASTM C672
Abrasion resistance	ASTM C418, C779 and C944
Chloride permeability	AASHTO T277, T259, and ASTM C1543
Alkali-aggregate reactivity	ASTM C227, C289, C295, C441, C586, C1260, and C1567
Sulfate resistance ASTM	C452 and C1012

It is not necessary to perform all the above tests to prove that a concrete will be durable. In general, a concrete that has a low permeability will also have a high resistance to freeze-thaw cycles and surface scaling. It should also be noted that a concrete that does not perform very well in the above tests will not necessarily perform poorly in the field. Concrete that performs well in the above tests will nearly always perform well in an actual structure. This is the case for precast concrete members that are produced under controlled factory conditions.

2.5.6.2 Alkali-Aggregate Reactivity

Aggregates containing certain constituents can react with alkali hydroxides in concrete and produce potentially harmful expansion. The reactivity has two forms—alkali-silica reaction (ASR) and alkali-carbonate reaction (ACR). ASR is the more important concern because the presence of silica in aggregate is more common. Methods for determining reactivity and dealing with ASR are reported by Thomas, et al. (2008) and Fournier, et al. (2010).

2.5.6.3 Delayed Ettringite Formation

Delayed ettringite formation (DEF) is defined by ACI as a form of sulfate attack by which mature hardened concrete is damaged by internal expansion during exposure to cyclic wetting and drying in service. The internal expansion is caused by the late formation of ettringite. It is unlikely to occur unless the concrete has been exposed to temperatures during curing greater than 160 °F. The formation of DEF is also dependent on the chemistry of the cementitious materials and is less likely to occur in concrete made with pozzolan or slag cement. The *LRFD Construction Specifications* limit the maximum concrete temperature during the curing of precast components to 160 °F. The same limit should also be considered applicable to cast-in-place concrete. For precast members, PCI recommends that the maximum concrete temperature during curing be limited to 150 °F for products exposed to damp or continuously wet environmental conditions. An increase to 170 °F is allowed if a mitigation concrete mix design is employed. (PCI 2011).

2.5.7 Shrinkage

Precast concrete members are subjected to air drying as soon as they are removed from the forms. During this exposure to the atmosphere, the concrete slowly loses some of its original water, causing shrinkage to occur. The amount and rate of shrinkage vary with the relative humidity, temperature, size of member, and amount of nonprestressed reinforcement.

MATERIAL PROPERTIES

2.5.7.1 Calculation of Shrinkage

2.5.7.1 Calculation of Shrinkage

Procedures to calculate the amount of shrinkage and creep have been published in the *LRFD Specifications*. For concretes with specified compressive strengths up to 15 ksi and devoid of shrinkage-prone aggregates, shrinkage strain, ϵ_{sh} may be taken as

$$\epsilon_{sh} = k_s k_{hs} k_f k_{td} (0.48 \times 10^{-3}) \quad \text{[LRFD Eq. 5.4.2.3.3-1]}$$

where

- k_s = factor for the effect of the volume-to-surface ratio of the component from **Table 2.5.7.1-1**
- k_{hs} = humidity factor for shrinkage from **Table 2.5.7.1-2**
- k_f = factor for the effect of concrete strength from **Table 2.5.7.1-3**
- k_{td} = time development factor from **Table 2.5.7.1-4**

Table 2.5.7.1-1
Factor k_s for Volume-to-Surface Ratio

Beam Section	Volume/Surface in.	k_s
AASHTO Type I	3.05	1.05
AASHTO Type II	3.37	1.01
AASHTO Type III	4.06	1.00
AASHTO Type IV	4.74	1.00
AASHTO Type V	4.44	1.00
AASHTO Type VI	4.41	1.00
AASHTO-PCI BT-54	3.01	1.06
AASHTO-PCI BT-63	3.01	1.06
AASHTO-PCI BT-72	3.01	1.06

The above factors are based on the following equation:

$$\text{Shrinkage: } k_s = 1.45 - 0.13(V/S) \geq 1.0 \quad \text{[LRFD Eq. 5.4.2.3.2-2]}$$

where

- V = volume of concrete, in.³
- S = surface area of concrete exposed to drying, in.²

The volume to surface area ratio for long members such as beams may be computed as the ratio of cross-sectional area to section perimeter. For pretensioned I-beams, T-beams, and box beams, with an average thickness of 6 to 8 in., the value of k_s may be taken as 1.00.

Table 2.5.7.1-2 Correction Factors k_{hs} and k_{hc} for Relative Humidity

Average Ambient Relative Humidity %	Shrinkage Factor, k_{hs}	Creep Factor, k_{hc}
40	1.44	1.24
50	1.30	1.16
60	1.16	1.08
70	1.02	1.00
80	0.88	0.92

The above factors are based on the following equations:

$$\text{Shrinkage: } k_{hs} = 2.00 - 0.014H \text{ for } 30 \leq H \leq 81 \quad \text{[LRFD Eq. 5.4.2.3.3-2]}$$

$$\text{Creep: } k_{hc} = 1.56 - 0.008H \text{ for } 30 \leq H \leq 100 \quad \text{[LRFD Eq. 5.4.2.3.2-3]}$$

where H = annual average ambient relative humidity in percent. A relative humidity map taken from the *LRFD Specifications* is shown in **Figure 2.5.7.1-1**.

MATERIAL PROPERTIES

2.5.7.1 Calculation of Shrinkage

Table 2.5.7.1-3
Factor k_f for Concrete Strength

Concrete Strength f'_{ci} , ksi	Strength Factor, k_f
4	1.00
5	0.83
6	0.71
7	0.63
8	0.56
9	0.50
10	0.45

The above factors are based on the following equation:

$$k_f = \frac{5}{1 + f'_{ci}} \quad \text{[LRFD Eq. 5.4.2.3.2-4]}$$

where f'_{ci} = specified concrete strength at transfer, ksi

Table 2.5.7.1-4
Time-Development Factor, k_{td}

Time, t , days	Specified Concrete Strength at Transfer, ksi				
	4.0	5.0	6.0	7.0	8.0
0	0.000	0.000	0.000	0.000	0.000
7	0.135	0.146	0.159	0.175	0.194
14	0.237	0.255	0.275	0.298	0.326
28	0.384	0.406	0.431	0.459	0.491
56	0.554	0.577	0.602	0.629	0.659
90	0.667	0.687	0.709	0.732	0.756
180	0.800	0.814	0.809	0.845	0.861
365	0.890	0.899	0.908	0.917	0.926
730	0.942	0.947	0.952	0.957	0.962
1,000	0.957	0.961	0.964	0.968	0.972
5,000	0.991	0.992	0.993	0.993	0.994
10,000	0.996	0.996	0.996	0.997	0.997
20,000	0.998	0.998	0.998	0.998	0.999

The above factors are based on the following equation

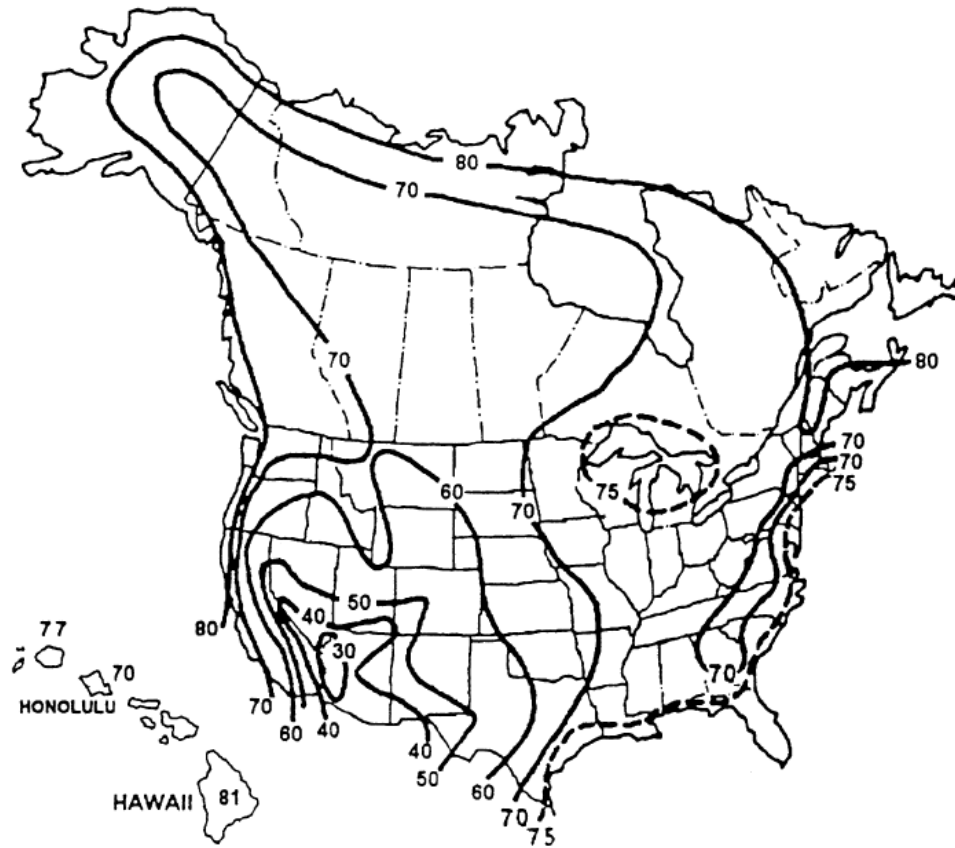
$$k_{td} = \frac{t}{61 - 4f'_{ci} + t} \quad \text{[LRFD Eq. 5.4.2.3.2-5]}$$

where t = age of concrete from the end of curing to the time being considered, days

MATERIAL PROPERTIES

2.5.7.1 Calculation of Shrinkage/2.5.9 Coefficient of Thermal Expansion

Figure 2.5.7.1-1
Average Annual Ambient Relative Humidity



2.5.8 Creep

Prestressed concrete beams are subjected to the effects of creep as soon as the prestressing force is transferred to the concrete in the plant. Creep of concrete results in time-dependent changes in camber and prestress forces. The amount and rate of creep vary with the concrete age at loading, stress level, relative humidity, temperature, size of member and amount of nonprestressed reinforcement. The following calculations are based on the *LRFD Specifications*.

2.5.8.1 Calculation of Creep

Creep strains may be calculated by multiplying the elastic strains by a creep coefficient, $\psi(t, t_i)$.

$$\Psi(t, t_i) = 1.9k_s k_{hc} k_f k_{td} t_i^{-0.118} \quad \text{[LRFD Eq. 5.4.2.3.2-1]}$$

where

- t = time from age of loading to the time being considered, days
- t_i = age of concrete at time of load application, days
- k_{hc} = humidity factor for creep from **Table 2.5.7.1-2**

The size factor, k_s , may be taken from **Table 2.5.7.1-1**, and the time-development factor, k_{td} , from **Table 2.5.7.1-4**.

2.5.9 Coefficient of Thermal Expansion

The coefficient of thermal expansion of concrete varies with the aggregate type as shown in **Table 2.5.9-1**, which is based on ACI 209. The range for normal weight concrete is generally 5 to 7×10^{-6} per $^{\circ}\text{F}$ when made with siliceous aggregates and 3.5 to 5×10^{-6} per $^{\circ}\text{F}$ when made with calcareous aggregates. The range for structural lightweight concrete is 3.6 to 6.0×10^{-6} per $^{\circ}\text{F}$ depending on the type of aggregate and the amount of natural sand.

MATERIAL PROPERTIES**2.5.9 Coefficient of Thermal Expansion/2.6.2.2 Materials**

For design, coefficients of 6×10^{-6} per °F for normal weight concrete and 5×10^{-6} per °F for lightweight concrete are frequently used. If greater accuracy is needed, tests should be made on the specific concrete. Because the coefficient of thermal expansion for steel is also about 6×10^{-6} per °F, the thermal effects on precast, prestressed concrete members are evaluated by treating them as plain concrete and utilizing the coefficient of thermal expansion for concrete.

Table 2.5.9-1 Format revised
Coefficients of Thermal Expansion of Concrete

Rock Type	millionths/°F
Chert	6.6
Quartzite	5.7
Quartz	6.2
Sandstone	5.2
Marble	4.6
Siliceous Limestone	4.6
Granite	3.8
Dolerite	3.8
Basalt	3.6
Limestone	3.1

2.6 GROUT MATERIALS

2.6.1 Definitions and Applications

When precast, prestressed concrete members are placed adjacent to each other, load transfer between adjacent members is often achieved through a grouted keyway. The keyway may or may not extend for the full depth of the member. The keyway is grouted with one of several different grouting materials, which are described in this section. In some bridges, no additional deck work is performed after grouting. In other bridges, a composite concrete deck may be cast on the members or the top surface of the members may be coated with a waterproofing membrane and overlaid with an asphaltic wearing course.

2.6.2 Types and Characteristics

ASTM Specification C1107 covers three consistencies of packaged dry hydraulic-cement grouts (non-shrink) intended for use under applied load. These grouts are composed of hydraulic cement, fine aggregate, and other ingredients and generally only require the addition of mixing water for use. Three consistencies of grout are classified as follows:

Flowable – a flow of 125 to 145 when tested in accordance with ASTM C1437

Fluid – a time of efflux of 10 to 30 sec. when tested in accordance with ASTM C939

Plastic – a flow of 100 to 125 when tested in accordance with ASTM C1437

2.6.2.1 Performance Requirements

Performance requirements for compressive strengths and maximum and minimum expansion levels are given in ASTM C1107. Although these grouts are termed nonshrink, the intent is to provide a final length that is not shorter than the original length at placement. This is achieved through an expansion mechanism prior to any shrinkage occurring.

2.6.2.2 Materials

Different cementitious materials may be used to produce grout. These include portland cement, shrinkage-compensating cement, expansive portland cement made with special additives, epoxy-cement resins, and magnesium ammonium phosphate cement (Gulyas, et al., 1995).

MATERIAL PROPERTIES**2.6.3 ASTM Tests/2.7 Prestressing Strand****2.6.3 ASTM Tests**

C109	Test Method for Compressive Strength of Hydraulic Cement Mortars (Using 2-in. or [50-mm] Cube Specimens)
C138	Test Method for Density (Unit Weight), Yield, and Air Content (Gravimetric) of Concrete
C157	Test Method for Length Change for Hardened Hydraulic-Cement Mortar and Concrete
C185	Test Method for Air Content of Hydraulic Cement Mortar
C827	Test Method for Change in Height at Early Ages of Cylindrical Specimens from Cementitious Mixtures
C939	Test Method for Flow of Grout for Preplaced-Aggregate Concrete (Flow Cone Method)
C1090	Test Method for Measuring Changes in Height of Cylindrical Specimens from Hydraulic-Cement Grout
C1437	Test Method for Flow of Hydraulic Cement Mortar

2.6.4 Grout Bed Materials

The same materials that are used for grouting keyways between precast concrete members may be used for grout beds to support structural and non-structural members. In some cases, the grout will be very stiff and is referred to as dry pack. Dry pack will often have a very high compressive strength because of the low water-cementitious materials ratio. It is often compacted by hand tamping.

2.6.5 Epoxy Resins

Epoxy-resin grouts can be used between precast concrete members where increased bonding and tensile capacity are required. When these are used, consideration should be given to the higher coefficient of thermal expansion and the larger creep properties of epoxy grouts. Requirements for epoxy-resin based bonding systems are given in ASTM C881.

2.6.6 Overlays

When concrete overlays are placed on precast concrete members, a preparation technique involving a $\frac{1}{16}$ to $\frac{1}{8}$ -in.-thick layer of cementitious grout is brushed onto the concrete surface. The grout is placed a short distance ahead of the overlay concrete. The grout should not be allowed to dry prior to the overlay placement. Otherwise, the dry grout may act as a poor surface for bonding. It is particularly important that the concrete surface be clean and sound and that the grout be well brushed into the concrete surface.

2.6.7 Post-Tensioned Members

Grouting of post-tensioned members is described in the *PTI Post-Tensioning Manual* (2006). Requirements for grout and grouting procedures are given in Section 10 of the *LRFD Construction Specifications*. Training and certification on implementing grouting specifications for post-tensioned structures is available from the American Segmental Bridge Institute (www.asbi-assoc.org).

2.7 PRESTRESSING STRAND

Although prestressed concrete may be produced with strands, wires, or bars, precast, prestressed concrete bridge members are generally produced using seven-wire strand conforming to AASHTO M203. Seven-wire strand consists of a straight center wire that is wrapped by six wires in a helical pattern. Strand sizes range from $\frac{3}{8}$ -in. to 0.6-in. diameter, as shown in **Table 2.11.1**. The larger size strands are used in prestressed concrete beams because this results in fewer strands. The use of 0.6-in. diameter strand is essential to take full advantage of high strength concrete. Strand with a diameter of 0.7 in. has been used on an experimental basis.

MATERIAL PROPERTIES**2.7.1 Strand Type/2.7.3 Relaxation****2.7.1 Strand Types**

Two types of strands are covered in AASHTO M203: “low-relaxation” and “stress-relieved” (normal-relaxation). However, in recent years, the use of low-relaxation strand has progressively increased to a point that normal-relaxation strand is seldom used. Two grades of strand are generally used in prestressed concrete construction. These are Grades 250 and 270, which have minimum ultimate strengths of 250 and 270 ksi, respectively. In general, Grade 270 is used in prestressed concrete bridge beams. Grade 250 strand may be used where lower levels of precompression are required. In addition to smooth, uncoated strands, epoxy-coated strands are available.

2.7.1.1 Epoxy-Coated Strand

Epoxy-coated strand is seven-wire prestressing strand with an organic, fusion-bonded epoxy coating that can vary in thickness from 15 to 45 mils. Two types of coatings are available. A smooth type has low bond characteristics and is intended for use in unbonded, post-tensioned systems, external post-tensioned systems, and stay cables. An epoxy-coated strand with particles of grit embedded in the surface is used in bonded pretensioned and post-tensioned systems.

In addition to the strand having an external coating, it can also be manufactured with the interstices between the individual wires filled with epoxy. This prevents the entry of corrosive chemicals, either by capillary action, or other hydrostatic forces. This type of strand should be specified when there is risk of contaminants or moisture entering at the ends of tendons. Epoxy-coated strand should comply with ASTM A882. This specification requires that all prestressing steel strand to be coated shall meet the requirements of AASHTO M203.

2.7.1.1.1 Effect of Heat

For pretensioned applications with epoxy-coated strands where accelerated curing techniques are employed, the temperature of the concrete surrounding the strand at the time of prestress transfer should be limited to a maximum of 150 °F and the concrete temperature should be falling. The epoxy-coating will not be damaged if this recommended temperature is not exceeded during the curing cycle. Concrete temperatures under sustained fire exposure conditions will most likely be considerably higher than the epoxy can withstand. This could result in a complete loss of bond between the strand and the concrete. Although bridge structures may not require a specific fire resistance rating, the likelihood of vehicle fires and subsequent effects of elevated temperatures should be evaluated. More specific information on the use of epoxy-coated strand is given in the report by the PCI Committee on Epoxy-Coated Strand (1993).

2.7.2 Material Properties

Cross-sectional properties, design strengths, and idealized stress-strain curves of Grade 250 and 270 low-relaxation seven-wire strands are given in Section 2.11. Also, see Chapter 8, Section 8.2.2.6.

2.7.3 Relaxation

Relaxation is the time-dependent reduction of stress in a prestressing tendon. When a strand is stressed and held at a constant length, the stress in the strand decreases with time, as illustrated in **Figure 2.7.3-1**. Relaxation losses increase with stress level and temperature. The relaxation losses of low-relaxation strand are considerably less than the losses in normal-relaxation strand. Relaxation of a prestressing strand depends on the stress level in the strand. However, because of other prestress losses, there is a continuous reduction of the strand stress, which causes a reduction in relaxation. Therefore, several complex and empirical relationships have been proposed for the determination of relaxation losses. Several of these methods are based on the loss that would occur if the strand were under constant strain. This loss is then reduced by the effects of elastic shortening, creep, and shrinkage. Early research work on relaxation was performed by Magura (1964). Subsequently, many other design recommendations have been made. The most recent recommendation from the *LRFD Specifications* is as follows:

$$\Delta f_{pR1} = \frac{f_{pt}}{K_L} \left(\frac{f_{pt}}{f_{py}} - 0.55 \right) \quad [\text{LRFD Eq. 5.9.5.4.2c-1}]$$

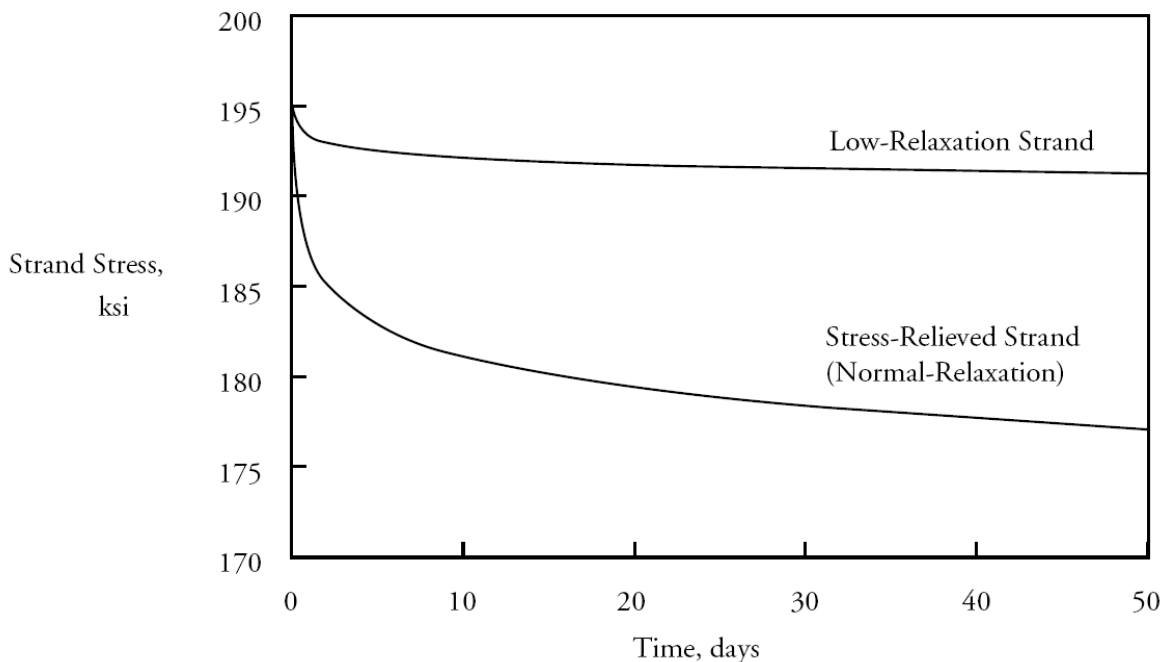
and

$$\Delta f_{pR2} = \Delta f_{pR1} \quad [\text{LRFD Eq. 5.9.5.4.3c-1}]$$

where

- Δf_{pR1} = relaxation loss between time of transfer and deck placement, ksi
- Δf_{pR2} = relaxation loss between time of deck placement and final time, ksi
- f_{pt} = stress in prestressing strands immediately after transfer $\geq 0.55 f_{py}$, ksi
- K_L = 30 for low-relaxation strands
= 7 for other prestressing steel
- f_{py} = yield strength of prestressing steel, ksi

Figure 2.7.3-1
Comparison of Relaxation Losses



2.7.3.1 Epoxy-Coated Strand

Tests of epoxy-coated, low-relaxation strands have shown the relaxation to be significantly higher than that of uncoated strand. The use of relaxation losses equal to double the relaxation loss calculated for uncoated strand has been recommended by manufacturers. Individual manufacturers of epoxy-coated strand should be consulted for suitable relaxation loss values.

2.7.4 Fatigue Strength

If the precompression in a prestressed concrete member is sufficient to ensure an uncracked section at service loads, the stress range in the strands is not likely to be high enough for fatigue of the strand to be a critical design factor. Fatigue considerations have not been a major factor in the specification of prestressing strand for bridges because bridge beams are designed to be uncracked. The actual and allowable fatigue life of prestressing strand depend on the stress range and the minimum stress level. The stress range may be affected by the strand radius of curvature, particularly in harped strand.

MATERIAL PROPERTIES**2.7.4.1 Stress Range/2.8.1.1 Specifications****2.7.4.1 Stress Range**

The following design provisions for fatigue are provided in the *LRFD Specifications*: [LRFD Art. 5.3.3.3]

The stress range in prestressing tendons shall not exceed:

- 18.0 ksi for radii of curvature in excess of 30 ft and
- 10.0 ksi for radii of curvature not exceeding 12 ft

A linear interpolation may be used for radii between 12 and 30 ft

2.7.5 Surface Condition

In a pretensioned member, the prestressing force in a strand is transferred from the strand to the concrete by bond. Strand surface condition has long been recognized as a primary factor affecting bonding of concrete to prestressing strand. An increase in the surface roughness, such as light surface rust, increases the bond between the concrete and the strand and results in a shorter development length. However, researchers have found it difficult to consistently quantify the effects of surface characteristics (Buckner 1994). This means that the increase in bond strength can possibly provide an extra margin of safety, but is not always consistent and should not be counted on to provide a shorter development length unless tests are conducted with specific strand. Chemicals on the strand surface can result in a reduction in bond between the concrete and strand and longer development lengths. Consequently, PCI recommends that "Prestressing strand shall conform to the requirements of ASTM A416 and shall be certified by its manufacturer to bond to concrete of a normal strength and consistency in conformance with the prediction equations for transfer and development lengths given in both ACI and AASHTO specifications."

2.7.6 Splicing

Lengths of prestressing strand can be connected using specialized strand connectors. Generally, this is not necessary in precast, prestressed concrete bridges. In situations where splicing of strands is necessary, consult the specific manufacturer's literature for details. The use of splice chucks in plant production is described in Chapter 3.

2.8 NONPRESTRESSED REINFORCEMENT

Nonprestressed reinforcement generally consists of deformed bars or welded wire reinforcement. Material properties and sizes of nonprestressed reinforcement are given in **Tables 2.11-2** and **2.11-3**.

2.8.1 Deformed Bars

Reinforcing bars should be deformed except plain bars may be used for spirals or for dowels at expansion or contraction joints. Reinforcing bars are generally specified to have yield strengths of 60.0 ksi (Grade 60). In some situations, a yield strength of 75.0 ksi (Grade 75) may be specified, although this would be unusual in bridges.

2.8.1.1 Specifications

Reinforcing bars should conform to one of the following specifications:

AASHTO M31	Specification for Deformed and Plain Carbon-Steel Bars for Concrete Reinforcement
AASHTO M322	Specification for Rail-Steel and Axle-Steel Deformed Bars for Concrete Reinforcement
ASTM A706	Specification for Low-Alloy Deformed and Plain Bars for Concrete Reinforcement
ASTM A767	Specification for Zinc-Coated (Galvanized) Steel Bars for Concrete Reinforcement
AASHTO M284	Specification for Epoxy-Coated Reinforcing Bars: Materials and Coating Requirements
ASTM A955	Specification for Deformed and Plain Stainless Steel Bars for Concrete Reinforcement
ASTM A1035	Specification for Deformed and Plain, Low-carbon, Chromium, Steel Bars for Concrete Reinforcement

MATERIAL PROPERTIES**2.8.1.1 Specifications/2.8.3 Welded Wire Reinforcement**

The most widely used type and grade of bars conform to ASTM A615 Grade 60 and include bars with sizes from No. 3 through No. 11, No. 14, and No. 18. When welding is required or when more bendability and controlled ductility are required, as in seismic-resistant design, low-alloy reinforcing bars conforming to ASTM A706 should be considered.

Deformed bars may be assembled into mats consisting of two layers of bars at right angles to each other with welds at the intersections in accordance with the following:

AASHTO M54 Specification for Welded Deformed Steel Bar Mats for Concrete Reinforcement

2.8.1.2 Corrosion Protection

When coated reinforcing bars are required as a corrosion protection system, the bars may be either zinc-coated or epoxy-coated and conform to ASTM A767 or AASHTO M284, respectively. Epoxy-coated reinforcing bars are generally used in bridge decks exposed to a salt environment.

When uncoated, corrosion-resistant reinforcing bars are required, the bars may be either stainless steel or low-carbon steel and conform to ASTM A955 or ASTM A1035, respectively.

2.8.2 Mechanical Splices

The most common method for splicing reinforcing bars is the lap splice. However, when lap splices are undesirable or impractical, mechanical or welded connections may be used. In general, a mechanical connection should develop, in tension or compression, at least 125% of the specified yield strength of the bars being connected. This is to ensure that yielding of the bars will occur before failure in the mechanical connection.

2.8.2.1 Types

Mechanical connections can be categorized as compression-only, tension-only and tension-compression. In most compression-only mechanical connections, the compressive stress is transferred by concentric bearing from one bar to the other. The mechanical connection then serves to hold the bars in concentric contact. Various types of mechanical connections are available that will handle both tension and compression forces. These connectors use a variety of couplers that may be cold swaged, cold extruded, hot forged, grout filled, steel filled or threaded. Tension-only mechanical connections generally use a steel coupling sleeve with a wedge. This is only effective when the reinforcing bar is pulled in tension. Most mechanical connection devices are proprietary and further information is available from individual manufacturers. Descriptions of the physical features and installation procedures for selected mechanical splices are described in ACI 439.3R.

2.8.3 Welded Wire Reinforcement

Welded wire reinforcement (WWR) is a prefabricated reinforcement consisting of cold-drawn wires welded together in square or rectangular grids. Each wire intersection is electrically resistance-welded by a continuous automatic welder. Pressure and heat fuse the intersecting wires into a homogeneous section and fix all wires in their proper position. WWR may consist of plain wires, deformed wires or a combination of both. WWR can also be galvanized or epoxy coated. WWR conforms to one of the following specifications:

AASHTO M55 Specification for Steel Welded Wire Reinforcement, Plain, for Concrete

AASHTO M221 Specification for Steel Welded Wire Reinforcement, Deformed, for Concrete

ASTM A884 Specification for Epoxy-Coated Steel Wire and Welded Wire Fabric for Reinforcement

ASTM A1064 Specification for Steel Wire and Welded Wire Reinforcement, Plain and Deformed for Concrete

Wire sizes are specified by a letter, W or D, followed by a number indicating the cross-sectional area of the wire in hundredths of a square inch. Plain wire sizes use the letter W; deformed wire sizes use the letter D. Wire sizes from W2 to W45 and D2 to D45 may be specified. Wire spacings generally vary from 2 to 12 in. The Engineer should check on availability of styles before specifying because all sizes may not be locally available.

MATERIAL PROPERTIES**2.8.4 Fatigue Strength of Nonprestressed Reinforcement/2.9.4 Ducts****2.8.4 Fatigue Strength of Nonprestressed Reinforcement**

The *LRFD Specifications* limits the allowable stress range caused by live load plus impact at service load to:

$$(\Delta F)_{TH} = 24 - 0.33f_{min} \quad \text{for straight reinforcement and WWR without a cross weld in the high stress region} \quad [\text{LRFD Eq. 5.5.3.2-1}]$$

$$(\Delta F)_{TH} = 16 - 0.33f_{min} \quad \text{for straight WWR reinforcement with a cross weld in the high stress region} \quad [\text{LRFD Eq. 5.5.3.2-2}]$$

where

$$(\Delta F)_{TH} = \text{constant-amplitude fatigue threshold, ksi}$$

$$f_{min} = \text{minimum stress level, tensile stress is positive, compressive stress is negative, ksi}$$

2.9 POST-TENSIONING MATERIALS

Post-tensioning systems may be conveniently divided into three categories depending on whether the stressing tendon is wire, strand, or bar. For bridge construction, wire systems are generally not used. Further information on post-tensioning systems has been published by the Post-Tensioning Institute (PTI, 2006). For details of proprietary systems, the manufacturers' literature should be consulted.

2.9.1 Strand Systems

Strand systems utilize the same strand and strand types that are used for pretensioned concrete members. In post-tensioning systems, the strands are generally combined to form a complete tendon and may consist of any quantity from a single strand to 55 strands. Anchorages for strand systems utilize the wedge principle in which the individual strands are anchored with wedges into a single tendon anchorage. In a post-tensioned multi-strand system, all strands are tensioned at the same time. Strand tendons may be tensioned in the plant, on the construction site, or in the finished structure.

2.9.2 Bar Systems

Bar systems generally utilize a single bar in a post-tensioning duct. The surface of the bar may be smooth with rolled threads of the required length at both ends, or the thread deformation may be rolled-on over the entire length of the bar during manufacturing. This permits the bar to be cut at any point and threaded fittings added. The bars are anchored using a threaded nut. Different types of anchorages are used at the tensioning and dead end anchorages. Bars for use in post-tensioning systems should conform to AASHTO M275. This specification covers both plain and deformed bars.

2.9.3 Splicing

Various proprietary systems are available for splicing both strand and bar systems. Couplers are required to develop at least 95% of the minimum specified ultimate strength of the tendon without exceeding the specified anchorage set (PTI, 2006).

2.9.4 Ducts

Ducts for post-tensioning systems may be either rigid or semi-rigid and made of ferrous metal, polyethylene, or polypropylene. They may also be formed in the concrete with removable cores. The use of polyethylene or polypropylene ducts is generally recommended for corrosive environments. Polyethylene ducts should not be used on radii less than 30 ft because of the polyethylene's lack of resistance to abrasion during pulling and tensioning the tendons. The inside diameter of ducts should be at least $\frac{1}{4}$ in. larger than the nominal diameter of single bar or strand tendons. For multiple bar or strand tendons, the inside cross-sectional area of the duct should be at least twice the net area of the prestressing steel. Where tendons are to be placed by the pull-through method, the duct area should be at least 2.5 times the net area of the prestressing steel. The size of the duct shall not exceed 0.4 times the least gross concrete thickness at the duct. Specific details about the placement of duct are provided in Section 10 of the *LRFD Construction Specifications*.

MATERIAL PROPERTIES

2.10 Fiber Reinforced Polymer Reinforcement/2.11 Reinforcement Sizes and Properties

2.10 FIBER REINFORCED POLYMER REINFORCEMENT

2.10.1 Introduction

An emerging technology, with potential application in prestressed concrete, consists of prestressing bars and tendons made from fiber reinforced polymer (FRP) composites. This class of material consists of a polymer matrix such as polyester, vinylester, epoxy, or phenolic resin, which is reinforced with fibers such as aramid, carbon, glass or steel. These composites have tensile strengths similar to conventional strand and bar systems and are particularly suitable for applications where weight, durability, corrosion resistance, and resistance to electromagnetic currents are relevant. Details of FRP composites are given in ACI 440.

2.10.2 Mechanical Properties

The mechanical properties of FRP vary significantly from one product to another. Factors such as type and volume of fiber and resin play a major role in establishing the characteristics of the product. The mechanical properties of all composites are affected by loading history, loading duration, temperature, and moisture. Model test methods for the short-term and long-term mechanical, thermo-mechanical, and durability testing of FRP bars and laminates are available (ACI 440.3R). It is anticipated that these methods may be adopted by ASTM or AASHTO. Material properties of FRPs are highly directionally dependent. The properties usually quoted are those in the longitudinal direction of the reinforcement (ACI 440). Specific properties of available products should always be obtained from the supplier.

2.10.3 Prestressed Concrete Bridge Applications

According to ACI Committee 440 (ACI 440.4), three prestressed concrete bridges have been built in North America using FRP tendons. Two bridges are located in Canada, and one in Southfield, Mich. In addition, four demonstration projects with FRP pretensioned concrete piles have been conducted in the United States.

Because FRP tendons have different stress-strain relationships compared to steel strand, design criteria have been developed for use with aramid and carbon fiber tendons. Glass fiber tendons were excluded because of poor resistance to creep under sustained loads and they are more susceptible to alkaline degradation (ACI 440.4). The design criteria take into account the linear stress-strain relationship and the sudden rupture of FRP tendons.

2.10.4 Specifications

The following specifications may be used with FRP reinforcement:

ACI 440.5 Specification for Construction with Fiber-Reinforced Polymer Reinforcing Bars

ACI 440.6 Specification for Carbon and Glass Fiber-Reinforced Polymer Bar Materials for Concrete Reinforcement.

2.11 REINFORCEMENT SIZES AND PROPERTIES

Table 2.11-1

Properties and Design Strengths of Prestressing Steel

Seven-Wire Low Relaxation based on AASHTO M203 Strand Grade 270 ($f_s' = 270$ ksi)

Nominal Diameter, in.	3/8	7/16	1/2	1/2 Special	9/16	0.6	0.7
Nominal Area, A_s^* , in. ²	0.085	0.115	0.153	0.167	0.192	0.217	0.294
Nominal Weight, plf	0.29	0.39	0.52	0.53	0.65	0.74	1.00
Minimum Tensile Strength, kip	23.0	31.0	41.3	45.0	51.7	58.6	79.4
Minimum Yield Strength, kip	20.7	27.9	37.2	40.5	46.5	52.7	71.5
0.70 $f_s' A_s^*$ kip	16.1	21.7	28.9	31.6	36.3	41.0	55.6
0.75 $f_s' A_s^*$ kip	17.2	23.3	31.0	33.8	38.9	44.0	59.5
0.80 $f_s' A_s^*$ kip	18.4	24.8	33.0	36.1	41.4	46.9	63.5

MATERIAL PROPERTIES

2.11 Reinforcement Sizes and Properties

Table 2.11-1 (cont.)

Properties and Design Strengths of Prestressing Steel

Seven-Wire Low Relaxation Strand based on AASHTO M203 Grade 250 ($f_s' = 250$ ksi)

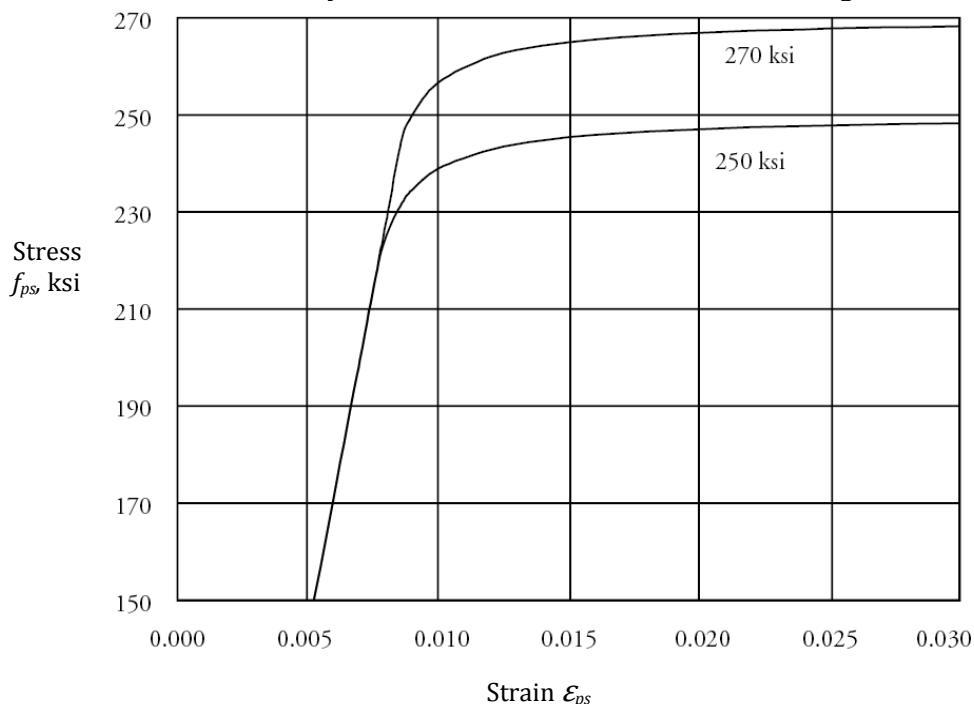
Nominal Diameter, (in.)	3/8	7/16	1/2	0.6
Nominal Area, A_s^* , in. ²	0.080	0.108	0.144	0.216
Nominal Weight, plf	0.27	0.37	0.49	0.74
Minimum Tensile Strength, kip	20.0	27.0	36.0	54.0
Minimum Yield Strength, kip	18.0	24.3	32.4	48.6
0.70 $f_s' A_s^*$, kip	14.0	18.9	25.2	37.8
0.75 $f_s' A_s^*$, kip	15.0	20.3	27.0	40.5
0.80 $f_s' A_s^*$, kip	16.0	21.6	28.8	43.2

Deformed Prestressing Bars based on AASHTO M275 Grade 150 ($f_s' = 150$ ksi)

Nominal Diameter, (in.)	5/8	3/4	1	1-1/4	1-3/8	1-3/4	2-1/2
Nominal Area, A_s^* , in. ²	0.28	0.42	0.85	1.25	1.58	2.58	5.16
Nominal Weight, plf	0.98	1.49	3.01	4.39	5.56	9.10	18.20
Minimum Tensile Strength, kip	42.0	6.30	127.5	187.5	237.0	387.0	774.0
Minimum Yield Strength, kip	33.6	50.4	102.0	150.0	189.6	309.6	619.2
0.70 $f_s' A_s^*$, kip	29.4	44.1	89.3	131.3	165.9	270.9	541.8
0.75 $f_s' A_s^*$, kip	31.5	47.3	95.6	140.6	177.8	290.3	580.5
0.80 $f_s' A_s^*$, kip	33.6	50.4	102.0	150.0	189.6	309.6	619.2

Figure 2.11-1

Idealized Stress-Strain Curve for Seven-Wire Low-Relaxation Prestressing Strand



These curves can be approximated by the following equations:

250 ksi strand

For $\epsilon_{ps} \leq 0.0076$: $f_{ps} = 28,500 \epsilon_{ps}$ (ksi)

For $\epsilon_{ps} > 0.0076$: $f_{ps} = 250 - 0.04/(\epsilon_{ps} - 0.0064)$ (ksi)

270 ksi strand

For $\epsilon_{ps} \leq 0.0086$: $f_{ps} = 28,500 \epsilon_{ps}$ (ksi)

For $\epsilon_{ps} > 0.0086$: $f_{ps} = 270 - 0.04/(\epsilon_{ps} - 0.007)$ (ksi)

MATERIAL PROPERTIES

2.11 Reinforcement Sizes and Properties

Table 2.11-2
Reinforcing Bar Sizes based on AASHTO M31

Bar Size Designation No.	Weight plf	Nominal Dimensions		
		Diameter in.	Area in. ²	Perimeter in.
3	0.376	0.375	0.11	1.178
4	0.668	0.500	0.20	1.571
5	1.043	0.625	0.31	1.963
6	1.052	0.750	0.44	2.356
7	20.44	0.875	0.60	2.749
8	2.670	1.000	0.79	3.142
9	3.400	1.128	1.00	3.544
10	4.303	1.270	1.27	3.990
11	5.313	1.410	1.56	4.430
14	7.650	1.693	2.25	5.320
18	13.600	2.257	4.00	7.090

Table 2.11-3
Sizes of Wires used in Welded Wire Reinforcement based on AASHTO M32 and M225

Wire Size Number*		Nominal Diameter in.	Nominal Weight plf	Area, in. ² /ft of width						
Plain	Deformed			Center-to-Center Spacing, in.						
				2	3	4	6	8	10	12
W45	D45	0.757	1.530	2.700	1.800	1.350	0.900	0.675	0.540	0.450
W31	D31	0.628	1.054	1.860	1.240	0.930	0.620	0.465	0.372	0.310
W30	D30	0.618	1.020	1.800	1.200	0.900	0.600	0.450	0.360	0.300
W28	D28	0.597	0.952	1.680	1.120	0.840	0.560	0.420	0.336	0.280
W26	D28	0.575	0.884	1.560	1.040	0.780	0.520	0.390	0.312	0.260
W24	D24	0.553	0.816	1.440	0.960	0.720	0.480	0.360	0.288	0.240
W22	D22	0.529	0.748	1.320	0.880	0.660	0.440	0.330	0.264	0.220
W20	D20	0.505	0.680	1.200	0.800	0.600	0.400	0.300	0.240	0.200
W18	D18	0.479	0.612	1.080	0.720	0.540	0.360	0.270	0.216	0.180
W16	D16	0.451	0.544	0.960	0.640	0.480	0.320	0.240	0.192	0.160
W14	D14	0.422	0.476	0.840	0.560	0.420	0.280	0.210	0.168	0.140
W12	D12	0.391	0.408	0.720	0.480	0.360	0.240	0.180	0.144	0.120
W11	D11	0.374	0.374	0.660	0.440	0.330	0.220	0.165	0.132	0.110
W10	D10	0.357	0.340	0.600	0.400	0.300	0.200	0.150	0.120	0.100
	D9	0.339	0.306	0.540	0.360	0.270	0.180	0.132	0.108	0.090
W8	D8	0.319	0.272	0.480	0.320	0.240	0.160	0.120	0.096	0.080
	D7	0.299	0.238	0.420	0.280	0.210	0.140	0.105	0.084	0.070
W6	D6	0.276	0.204	0.360	0.240	0.180	0.120	0.090	0.072	0.060
W5.5		0.265	0.187	0.330	0.220	0.165	0.110	0.083	0.066	0.055
W5	D5	0.252	0.170	0.300	0.200	0.150	0.100	0.075	0.60	0.050
W4.5		0.238	0.153	0.270	0.180	0.135	0.090	0.068	0.054	0.045
W4	D4	0.226	0.136	0.240	0.160	0.120	0.080	0.060	0.048	0.040
W3.5		0.211	0.119	0.210	0.140	0.105	0.070	0.057	0.042	0.035
	D3	0.195	0.102	0.180	0.120	0.090	0.060	0.045	0.036	0.030
W2.9		0.192	0.098	0.174	0.116	0.087	0.058	0.044	0.035	0.029
W2.5		0.178	0.085	0.150	0.100	0.075	0.050	0.038	0.030	0.025
W2	D2	0.159	0.068	0.120	0.080	0.060	0.040	0.030	0.024	0.020

* Other wire sizes may be available from local producers

2.12 RELEVANT STANDARDS AND PUBLICATIONS

The following list of selected standards and manuals is provided for the convenience of the reader because not all documents are referenced in the text of this chapter. The complete serial designation of each document includes a year of adoption. However, since these documents are updated on a frequent basis, the year has been omitted. The reader is referred to the respective organizations for the latest revisions and year of adoption.

2.12.1 AASHTO Standard Specifications

AASHTO LRFD Bridge Design Specifications

Standard Specifications for Transportation Materials and Methods of Sampling and Testing

- M6 Fine Aggregate for Hydraulic Cement Concrete*
- M31 Deformed and Plain Carbon Steel Bars for Concrete Reinforcement*
- M32 Steel Wire, Plain, for Concrete Reinforcement*
- M43 Sizes of Aggregate for Road and Bridge Construction*
- M54 Welded Deformed Steel Bar Mats for Concrete Reinforcement*
- M55 Steel Welded Wire Reinforcement, Plain, for Concrete*
- M80 Coarse Aggregate for Hydraulic Cement Concrete*
- M85 Portland Cement*
- M144 Calcium Chloride*
- M154 Air-Entraining Admixtures for Concrete*
- M194 Chemical Admixtures for Concrete*
- M195 Lightweight Aggregates for Structural Concrete*
- M203 Steel Strand, Uncoated Seven-Wire for Concrete Reinforcement*
- M204 Uncoated Stress-Relieved Steel Wire for Prestressed Concrete*
- M205 Molds for Forming Concrete Test Cylinders Vertically*
- M221 Steel Welded Wire Reinforcement, Deformed, for Concrete*
- M225 Steel Wire, Deformed, for Concrete Reinforcement*
- M235 Epoxy Resin Adhesives*
- M240 Blended Hydraulic Cement*
- M275 Uncoated High Strength Steel Bars for Prestressing Concrete*
- M284 Epoxy-Coated Reinforcing Bars: Materials and Coating Requirements*
- M295 Coal Fly Ash and Raw or Calcined Natural Pozzolan for Use in Concrete*
- M302 Ground Granulated Blast-Furnace Slag for Use in Concrete and Mortars*
- M307 Silica Fume Used in Cementitious Mixtures*
- M317 Epoxy-Coated Reinforcing Bars: Handling Requirements for Fabrication and Job Site*
- M321 High-Reactivity Pozzolans for Use in Hydraulic-Cement Concrete, Mortar, and Grout*
- M322 Rail-Steel and Axle-Steel Deformed Bars for Concrete Reinforcement*
- M327 Processing Additions for Use in the Manufacture of Hydraulic Cements*

MATERIAL PROPERTIES**2.12.2 AASHTO Standards Methods of Test/2.12.3 ACI Publications****2.12.2 AASHTO Standard Methods of Test**

- T22 *Compressive Strength of Cylindrical Concrete Specimens*
- T23 *Making and Curing Concrete Test Specimens in the Field*
- T24 *Obtaining and Testing Drilled Cores and Sawed Beams of Concrete*
- T26 *Quality of Water to Be Used in Concrete*
- T106 *Compressive Strength of Hydraulic Cement Mortar (Using 50 mm or 2 in. Cube Specimens)*
- T121 *Density (Unit Weight), Yield, and Air Content (Gravimetric) of Concrete*
- T131 *Time of Setting of Hydraulic Cement by Vicat Needle*
- T137 *Air Content of Hydraulic Cement Mortar*
- T152 *Air Content of Freshly Mixed Concrete by the Pressure Method*
- T160 *Length Change of Hardened Hydraulic Cement Mortar and Concrete*
- T161 *Resistance of Concrete to Rapid Freezing and Thawing*
- T196 *Air Content of Freshly Mixed Concrete by the Volumetric Method*
- T199 *Air Content of Freshly Mixed Concrete by the Chace Indicator*
- T259 *Resistance of Concrete to Chloride Ion Penetration*
- T277 *Electrical Indication of Concrete's Ability to Resist Chloride Ion Penetration*
- T299 *Rapid Identification of Alkali-Silica Reaction Products in Concrete*
- T303 *Accelerated Detection of Potentially Deleterious Expansion of Mortar Bars Due to Alkali-Silica Reaction*
- T318 *Water Content of Freshly Mixed Concrete Using Microwave Oven Drying*
- T325 *Estimating the Strength of Concrete in Transportation Construction by Maturity Tests*
- T334 *Estimating the Cracking Tendency of Concrete*
- T336 *Coefficient of Thermal Expansion of Hydraulic Cement Concrete*

2.12.3 ACI Publications

- 207.1 *Guide to Mass Concrete*
- 209R *Prediction of Creep, Shrinkage, and Temperature Effects in Concrete Structures*
- 211.1 *Standard Practice for Selecting Proportions for Normal, Heavyweight, and Mass Concrete*
- 211.2 *Standard Practice for Selecting Proportions for Structural Lightweight Concrete*
- 212.3R *Chemical Admixtures for Concrete*
- 213R *Guide for Structural Lightweight-Aggregate Concrete*
- 221R *Guide for Use of Normal Weight and Heavyweight Aggregates in Concrete*
- 223 *Standard Practice for the Use of Shrinkage-Compensating Concrete*
- 232.2R *Use of Fly Ash in Concrete*
- 233R *Slag Cement in Concrete and Mortar*
- 234R *Guide for the Use of Silica Fume in Concrete*
- 237R *Self-Consolidating Concrete*
- 308R *Guide to Curing Concrete*

MATERIAL PROPERTIES**2.12.3 ACI Publications/2.12.4 ASTM Standard Specifications**

- 315 *Details and Detailing of Concrete Reinforcement*
- 318 *Building Code Requirements for Structural Concrete and Commentary*
- 343R *Analysis and Design of Reinforced Concrete Bridge Structures*
- 345R *Guide for Concrete Highway Bridge Deck Construction*
- 363R *Report on High-Strength Concrete*
- 363.2 *Guide to Quality Control and Testing of High-Strength Concrete*
- 423.3R *Recommendations for Concrete Members Prestressed with Unbonded Tendons*
- 439.3R *Types of Mechanical Splices for Reinforcing Bars*
- 440R *Report on Fiber-Reinforced Polymer (FRP) Reinforcement for Concrete Structures*
- 440.1R *Guide for the Design and Construction of Structural Concrete Reinforced with FRP Bars*
- 440.3R *Guide Test Methods for Fiber-Reinforced Polymers (FRPs) for Reinforcing or Strengthening Concrete Structures*
- 440.4R *Prestressing Concrete Structures with FRP Tendons*
- 440.5 *Specification for Construction with Fiber-Reinforced Polymer Reinforcing Bars*
- 440.6 *Specification for Carbon and Glass Fiber-Reinforced Polymer Bar Materials for Concrete Reinforcement*

2.12.4 ASTM Standard Specifications

- A82 *Specification for Steel Wire, Plain, for Concrete Reinforcement*
- A184 *Specification for Welded Deformed Steel Bar Mats for Concrete Reinforcement*
- A185 *Specification for Steel Welded Wire Reinforcement, Plain, for Concrete Reinforcement*
- A416 *Specification for Steel Strand, Uncoated Seven-Wire for Prestressed Concrete*
- A421 *Specification for Uncoated Stress-Relieved Steel Wire for Prestressed Concrete*
- A496 *Specification for Steel Wire, Deformed, for Concrete Reinforcement*
- A497 *Specification for Steel Welded Wire Reinforcement, Deformed, for Concrete*
- A615 *Specification for Deformed and Plain Carbon-Steel Bars for Concrete Reinforcement*
- A706 *Specification for Low-Alloy Steel Deformed and Plain Bars for Concrete Reinforcement*
- A722 *Specification for Uncoated High-Strength Steel Bars for Prestressing Concrete*
- A767 *Specification for Zinc-Coated (Galvanized) Steel Bars for Concrete Reinforcement*
- A775 *Specification for Epoxy-Coated Steel Reinforcing Bars*
- A882 *Specification for Filled Epoxy-Coated Seven-Wire Prestressing Steel Strand*
- A884 *Specification for Epoxy-Coated Steel Wire and Welded Wire Reinforcement*
- A955 *Specification for Deformed and Plain Stainless-Steel Bars for Concrete Reinforcement*
- A996 *Specification for Rail-Steel and Axle-Steel Deformed Bars for Concrete Reinforcement*
- A1022 *Specification for Deformed and Plain Stainless Steel Wire and Welded Wire for Concrete Reinforcement*
- A1035 *Specification for Deformed and Plain, Low-carbon, Chromium, Steel Bars for Concrete Reinforcement*
- A1064 *Specification for Steel Wire and Welded Wire Reinforcement, Plain and Deformed, for Concrete*
- C33 *Specification for Concrete Aggregates*
- C94 *Specification for Ready-Mixed Concrete*

MATERIAL PROPERTIES**2.12.4 ASTM Standard Specifications/2.12.5 ASTM Standard Test Methods and Practices**

- C150 Specification for Portland Cement*
- C260 Specification for Air-Entraining Admixtures for Concrete*
- C330 Specification for Lightweight Aggregates for Structural Concrete*
- C465 Specification for Processing Additions for Use in the Manufacture of Hydraulic Cements*
- C470 Specification for Molds for Forming Concrete Test Cylinders Vertically*
- C494 Specification for Chemical Admixtures for Concrete*
- C595 Specification for Blended Hydraulic Cements*
- C618 Specification for Coal Fly Ash and Raw or Calcined Natural Pozzolan for Use in Concrete*
- C845 Specification for Expansive Hydraulic Cement*
- C881 Specification for Epoxy-Resin-Base Bonding Systems for Concrete*
- C989 Specification for Slag Cement for Use in Concrete and Mortars*
- C1107 Specification for Package Dry, Hydraulic-Cement Grout (Nonshrink)*
- C1157 Performance Specification for Hydraulic Cement*
- C1240 Specification for Silica Fume Used in Cementitious Mixtures*
- D98 Specification for Calcium Chloride*
- D448 Standard Classification for Sizes of Aggregate for Road and Bridge Construction*
- D3963 Specification for Fabrication and Jobsite Handling of Epoxy-Coated Steel Reinforcing Bars*

2.12.5 ASTM Standard Test Methods and Practices

- C31 Practice for Making and Curing Concrete Test Specimens in the Field*
- C39 Test Method for Compressive Strength of Cylindrical Concrete Specimens*
- C42 Test Method for Obtaining and Testing Drilled Cores and Sawed Beams of Concrete*
- C109 Test Method for Compressive Strength of Hydraulic Cement Mortars (Using 2-in. or 50-mm Cube Specimens)*
- C138 Test Method for Density (Unit Weight), Yield, and Air Content (Gravimetric) of Concrete*
- C157 Test Method for Length Change of Hardened Hydraulic-Cement Mortar and Concrete*
- C173 Test Method for Air Content of Freshly Mixed Concrete by the Volumetric Method*
- C185 Test Method for Air Content of Hydraulic Cement Mortar*
- C186 Test Method for Heat of Hydration of Hydraulic Cement*
- C191 Test Method for Time of Setting of Hydraulic Cement by Vicat Needle*
- C227 Test Method for Potential Alkali Reactivity of Cement-Aggregate Combinations (Mortar-Bar Method)*
- C231 Test Method for Air Content of Freshly Mixed Concrete by the Pressure Method*
- C289 Test Method for Potential Alkali-Silica Reactivity of Aggregates (Chemical Method)*
- C295 Guide for Petrographic Examination of Aggregates for Concrete*
- C418 Test Method for Abrasion Resistance of Concrete by Sandblasting*
- C441 Test Method for Effectiveness of Pozzolans or Ground Blast-Furnace Slag in Preventing Excessive Expansion of Concrete Due to the Alkali-Silica Reaction*
- C452 Test Method for Potential Expansion of Portland-Cement Mortars Exposed to Sulfate*
- C469 Test Method for Static Modulus of Elasticity and Poisson's Ratio of Concrete in Compression*

MATERIAL PROPERTIES**2.12.6 Cross References ASTM-AASHTO/2.12.7**

- C512 *Test Method for Creep of Concrete in Compression*
- C586 *Test Method for Potential Alkali Reactivity of Carbonate Rocks as Concrete Aggregates (Rock-Cylinder Method)*
- C597 *Test Method for Pulse Velocity Through Concrete*
- C666 *Test Method for Resistance of Concrete to Rapid Freezing and Thawing*
- C672 *Test Method for Scaling Resistance of Concrete Surfaces Exposed to Deicing Chemicals*
- C779 *Test Method for Abrasion Resistance of Horizontal Concrete Surfaces*
- C803 *Test Method for Penetration Resistance of Hardened Concrete*
- C805 *Test Method for Rebound Number of Hardened Concrete*
- C827 *Test Method for Change in Height at Early Ages of Cylindrical Specimens of Cementitious Mixtures*
- C881 *Epoxy-Resin-Base Bonding Systems for Concrete*
- C900 *Test Method for Pullout Strength of Hardened Concrete*
- C939 *Test Method for Flow of Grout for Preplaced-Aggregate Concrete (Flow Cone Method)*
- C944 *Test Method for Abrasion Resistance of Concrete or Mortar Surfaces by the Rotating-Cutter Method*
- C1012 *Test Method for Length Change of Hydraulic-Cement Mortars Exposed to a Sulfate Solution*
- C1090 *Test Method for Measuring Changes in Height of Cylindrical Specimens of Hydraulic-Cement Grout*
- C1202 *Test Method for Electrical Indication of Concrete's Ability to Resist Chloride Ion Penetration*
- C1260 *Test Method for Potential Alkali-Reactivity of Aggregates (Mortar-Bar Method)*
- C1293 *Test Method for Determination of Length Change of Concrete Due to Alkali-Silica Reaction*
- C1362 *Test Method for Flow of Freshly Mixed Hydraulic-Cement Concrete*
- C1437 *Test Method for Flow of Hydraulic Cement Mortar*
- C1543 *Test Method for Determining the Penetration of Chloride Ion into Concrete by Ponding*
- C1567 *Test Method for Determining the Potential Alkali-Silica Reactivity of Combinations of Cementitious Materials and Aggregates (Accelerated Mortar-Bar Method)*
- C1581 *Test Method for Determining Age at Cracking and Induced Tensile Stress Characteristics of Mortar and Concrete under Restrained Shrinkage*
- C1610 *Test Method for Static Segregation of Self-Consolidating Concrete Using Column Technique*
- C1611 *Test Method for Slump Flow of Self-Consolidating Concrete*
- C1621 *Test Method for Passing Ability of Self-Consolidating Concrete by J-Ring*
- C1712 *Test Method for Rapid Assessment of Static Segregation Resistance of Self-Consolidating Concrete Using Penetration Test*

2.12.6 Cross References ASTM-AASHTO

This list of cross references is provided for ease of comparing two similar documents. In many cases, the two documents are not identical and should not be interchanged without review of their content.

ASTM	AASHTO	ASTM	AASHTO	ASTM	AASHTO	ASTM	AASHTO
A82	M32	A996	M322	C191	T131	C881	M235
A184	M54	C31	T23	C231	T152	C989	M302
A185	M55	C39	T22	C260	M154	C1202	T277
A416	M203	C42	T24	C330	M195	C1240	M307
A421	M204	C109	T106	C465	M327	D98	M144
A496	M225	C138	T121	C470	M205	D448	M43
A497	M221	C150	M85	C494	M194	D3963	M317
A615	M31	C157	T160	C595	M240		
A722	M275	C173	T196	C618	M295		
A775	M284	C185	T137	C666	T161		

2.12.7 Cited References

The following cited references are in addition to any cited references included in the previous sections.

- 1 AASHTO. 2010. *AASHTO LRFD Bridge Construction Specifications*, 3rd ed. American Association of State Highway and Transportation Officials, Washington, DC, https://bookstore.transportation.org/Item_details.aspx?id=1583 (Fee)
- 2 AASHTO. 2010. *AASHTO LRFD Bridge Design Specifications*, 5th ed. American Association of State Highway and Transportation Officials, Washington, DC. https://bookstore.transportation.org/Item_details.aspx?id=1560 (Fee)
- 3 Buckner, D. C. 1994. *An Analysis of Transfer and Development Lengths for Pretensioned Concrete Structures*, Report No. FHWA-RD-94-049, Federal Highway Administration, U.S. Department of Transportation, Washington, DC. 108 pp.
- 4 Fornier, B., M. A. Berube, K. Folliard, and M. Thomas. 2010. "Report on the Diagnosis, Prognosis and Mitigation of Alkali-Silica Reaction (ASR) in Transportation Structures," Report No. FHWA-HIF-09-004, Federal Highway Administration, U. S. Department of Transportation, Washington, DC. 147 pp. <http://www.fhwa.dot.gov/pavement/concrete/pubs/hif09004/hif09004.pdf>
- 5 Graybeal, B. A., 2006A. *Material Property Characterization of Ultra-High Performance Concrete*, Report No. FHWA-HRT-06-103, Federal Highway Administration, U. S. Department of Transportation, McLean, VA. 186 pp. <http://www.fhwa.dot.gov/publications/research/infrastructure/structures/06103/index.cfm>
- 6 Graybeal, B. A., 2006B. *Structural Behavior of Ultra-High Performance Concrete Prestressed I-Girders*, Report No. FHWA-HRT-06-115, Federal Highway Administration, U. S. Department of Transportation, McLean, VA. 104 pp. <http://www.fhwa.dot.gov/publications/research/infrastructure/structures/06115/index.cfm>
- 7 Graybeal, B. A. and M. M. Lwin. 2010. "Deployment of Ultra-High-Performance Concrete Technology." *ASPIRE*, Precast/Prestressed Concrete Institute, Summer, pp 50-51. http://www.aspirebridge.com/pdfs/magazine/issue_15/FHWA.pdf
- 8 Gulyas, R. J., G. J. Wirthlin, and J. T. Champa. 1995. "Evaluation of Keyway Grout Test Methods for Precast Concrete Bridges," *PCI Journal*, Precast/Prestressed Concrete Institute, Chicago, IL. V. 40, No. 1 (January-February), pp. 44-57. http://www.pci.org/view_file.cfm?file=JL-95-JANUARY-FEBRUARY-5.pdf
http://www.pci.org/view_file.cfm?file=JL-95-JANUARY-FEBRUARY-6.pdf
- 9 Khayat, K. H. and D. Mitchell. 2009. *Self-Consolidating Concrete for Precast, Prestressed Concrete Bridge Elements*," NCHRP Report 628, Transportation Research Board, Washington, DC. 31 pp. + Appendices. http://onlinepubs.trb.org/Onlinepubs/nchrp/nchrp_rpt_628.pdf

- 10 Magura, D. D., M. A. Sozen, and C. P. Seiss. 1964. "A Study of Stress Relaxation in Prestressing Reinforcement," *PCI Journal*, Precast/Prestressed Concrete Institute, Chicago, IL. V. 9, No. 2 (April), pp. 13-57.
http://www.pci.org/pdf/find/knowledge_bank/active/MNL-133-97_ch2.pdf
- 11 PCI Committee on Epoxy-Coated Strand. 1993. "Guidelines for the Use of Epoxy-Coated Strand," *PCI Journal*, Precast/Prestressed Concrete Institute, Chicago, IL. V. 38, No. 4 (July-August), pp. 26-32.
http://www.pci.org/view_file.cfm?file=JL-93-JULY-AUGUST-6.pdf
http://www.pci.org/view_file.cfm?file=JL-93-JULY-AUGUST-7.pdf
http://www.pci.org/view_file.cfm?file=JL-93-JULY-AUGUST-8.pdf
- 12 PCI Committee on Concrete Materials Technology, forthcoming. *Guidelines for the Use of Self-Consolidating Concrete in Precast/Prestressed Concrete*. Precast/Prestressed Concrete Institute, Chicago, IL.
http://www.pci.org/view_file.cfm?file=TR-6-03_PCI_SCC_GUIDELINES.PDF
- 13 PCI Plant Certification Committee and the Precast Architectural Committee. 2011. *Manual for Quality Control for Plants and Production of Architectural Precast Concrete Products*, (MNL 117-11). Precast/Prestressed Concrete Institute, Chicago, IL.
http://www.pci.org/view_file.cfm?file=JL-97-JULY-AUGUST-13.pdf
- 14 PTI. 2006. *Post-Tensioning Manual*, 6th ed. Post-Tensioning Institute, Farmington Hills, MI. 356 pp.
http://post-tensioning.org/Uploads/2011_forWeb.pdf (Fee)
- 15 Rizkalla, S., A. Mirmiran, P. Zia, et al. 2007. *Application of the LRFD Bridge Design Specifications to High-Strength Structural Concrete: Flexure and Compression Provisions*, NCHRP Report 595. Transportation Research Board, Washington, DC. 28 pp.
http://onlinepubs.trb.org/onlinepubs/nchrp/nchrp_rpt_595.pdf
- 16 Russell, H. G. 1999. "ACI Defines High-Performance Concrete." *Concrete International*, American Concrete Institute, Farmington, MI. V. 21, No. 2 (February), pp. 56-57.
http://www.concreteinternational.com/pages/featured_article.asp?ID=217
- 17 Thomas, M. D. A., B. Fornier, and K. J. Folliard. 2008. "Report on Determining the Reactivity of Concrete Aggregates and Selecting Appropriate Measures for Preventing Deleterious Expansion in New Concrete Construction," Report No. FHWA-HIF-09-001, Federal Highway Administration, U. S. Department of Transportation, Washington, DC. 20 pp.
<http://www.fhwa.dot.gov/pavement/concrete/asr/hif09001/index.cfm>

This page intentionally left blank

FABRICATION AND CONSTRUCTION**Table of Contents**

NOTATION.....	3 - 9
Fabrication and Construction.....	3 - 11
3.1 SCOPE.....	3 - 11
3.2 PRODUCT COMPONENTS AND DETAILS	3 - 11
3.2.1 Concrete.....	3 - 11
3.2.1.1 Cement.....	3 - 12
3.2.1.2 Aggregates	3 - 12
3.2.1.3 Admixtures	3 - 12
3.2.1.3.1 Water-Reducing Admixtures.....	3 - 12
3.2.1.3.2 Retarders and Accelerators	3 - 12
3.2.1.3.3 Air-Entraining Admixtures	3 - 13
3.2.1.3.4 Corrosion Inhibitors.....	3 - 13
3.2.1.3.5 Mineral Admixtures.....	3 - 13
3.2.2 Prestressing Steel	3 - 13
3.2.2.1 Pretensioning.....	3 - 14
3.2.2.2 Post-Tensioning	3 - 14
3.2.2.3 Strand Size and Spacing.....	3 - 14
3.2.2.4 Strand Anchors and Couplers for Pretensioning.....	3 - 15
3.2.2.5 Strand Anchors and Couplers for Post-Tensioning.....	3 - 15
3.2.2.6 Epoxy-Coated Strand	3 - 16
3.2.2.6.1 Types of Epoxy Coating.....	3 - 17
3.2.2.6.2 Anchorage of Epoxy-Coated Strand	3 - 17
3.2.2.6.3 Protection of the Epoxy Coating	3 - 17
3.2.2.6.4 Epoxy Coating and Elevated Temperatures	3 - 17
3.2.2.7 Indented Strand.....	3 - 18
3.2.2.8 Prestressing Bars.....	3 - 18
3.2.3 Nonprestressed Reinforcement.....	3 - 20
3.2.3.1 Reinforcement Detailing	3 - 21
3.2.3.2 Developing Continuity.....	3 - 22
3.2.3.2.1 Continuity with Post-Tensioning.....	3 - 22
3.2.3.2.2 Continuity with Nonprestressed Reinforcement	3 - 23
3.2.3.2.3 Continuity in Full-Depth Members	3 - 24
3.2.3.3 Coated Nonprestressed Reinforcement	3 - 25
3.2.3.3.1 Epoxy-Coated Nonprestressed Reinforcement.....	3 - 25
3.2.3.3.2 Galvanized Nonprestressed Reinforcement.....	3 - 25

FABRICATION AND CONSTRUCTION

Table of Contents

3.2.3.4 Welded Wire Reinforcement..... 3 - 25

3.2.3.5 Suggested Reinforcement Details 3 - 26

3.2.4 Embedments and Blockouts..... 3 - 28

3.2.4.1 Embedments and Blockouts for Attachments 3 - 28

3.2.4.2 Embedments and Blockouts for Diaphragms 3 - 29

3.2.4.3 Embedments and Blockouts for Deck Construction 3 - 29

3.2.4.4 Lifting Devices 3 - 31

 3.2.4.4.1 Strand Lift Loops 3 - 32

 3.2.4.4.2 Other Lifting Embedments..... 3 - 33

3.2.4.5 Blockouts for Shipping..... 3 - 33

3.2.5 Surface Treatments 3 - 33

3.2.5.1 Protecting Product Ends 3 - 33

 3.2.5.1.1 Ends Cast into Concrete..... 3 - 33

 3.2.5.1.2 Exposed Ends 3 - 34

 3.2.5.1.3 Epoxy Mortar End Patches..... 3 - 34

 3.2.5.1.4 Portland Cement Mortar End Patches 3 - 34

 3.2.5.1.5 Patching Ends with Proprietary Products..... 3 - 34

3.2.5.2 Intentionally Roughened Surfaces..... 3 - 35

3.2.5.3 Cosmetic Surface Treatments 3 - 35

3.2.5.4 Architectural Finishes 3 - 35

3.2.5.5 Durability-Related Treatments 3 - 36

3.2.5.6 Protection of Exposed Steel 3 - 36

3.3 FABRICATION 3 - 37

3.3.1 Forms and Headers..... 3 - 37

3.3.1.1 Self-Stressing Forms 3 - 38

 3.3.1.1.1 Applications of Self-Stressing Forms..... 3 - 38

3.3.1.2 Non-Self-Stressing Forms 3 - 39

 3.3.1.2.1 Design of Non-Self-Stressing Forms 3 - 39

3.3.1.3 Adjustable Forms 3 - 39

3.3.1.4 Advantages of Precast Concrete Formwork..... 3 - 42

3.3.1.5 Other Form Considerations 3 - 42

3.3.1.6 Headers..... 3 - 42

 3.3.1.6.1 Header Configuration 3 - 43

3.3.1.7 Internal Void Forms 3 - 43

 3.3.1.7.1 Mandrel Systems 3 - 43

FABRICATION AND CONSTRUCTION

Table of Contents

3.3.1.7.2 Retractable Inner Forms	3 - 44
3.3.1.7.3 Sacrificial Inner Forms	3 - 45
3.3.2 Prestressing	3 - 45
3.3.2.1 Types of Pretensioning Beds	3 - 45
3.3.2.1.1 Abutment Beds	3 - 45
3.3.2.1.2 Strutted Beds	3 - 46
3.3.2.2 Strand Profile	3 - 47
3.3.2.2.1 Straight Strands	3 - 47
3.3.2.2.2 Harped Strands	3 - 48
3.3.2.2.3 Harping Devices	3 - 48
3.3.2.2.4 Anchorage of Harping Devices	3 - 49
3.3.2.3 Tensioning	3 - 50
3.3.2.4 Pretensioning Configuration	3 - 50
3.3.2.5 Tensioning Prestressing Steel	3 - 50
3.3.2.5.1 Tensioning Individual Strands	3 - 51
3.3.2.5.2 Tensioning Strands as a Group	3 - 51
3.3.2.6 Prestressing Strand Elongation	3 - 51
3.3.2.7 Variables Affecting Strand Elongation	3 - 51
3.3.2.7.1 Dead End and Splice Chuck Seating	3 - 52
3.3.2.7.2 Elongation of Abutment Anchor Rods	3 - 52
3.3.2.7.3 Prestressing Bed Deformations	3 - 52
3.3.2.7.4 Live End Chuck Seating	3 - 52
3.3.2.7.5 Temperature Corrections	3 - 52
3.3.2.7.6 Friction	3 - 53
3.3.2.8 Transfer	3 - 54
3.3.2.8.1 Hydraulic Transfer	3 - 54
3.3.2.8.2 Transfer by Flame Cutting	3 - 54
3.3.2.8.3 Transfer at Bulkheads	3 - 54
3.3.2.8.4 Harped Strand Considerations at Transfer	3 - 54
3.3.2.9 Strand Debonding	3 - 55
3.3.3 Nonprestressed Reinforcement and Embedments	3 - 55
3.3.3.1 Placement and Attachment	3 - 55
3.3.3.2 Installation of Lifting Devices	3 - 56
3.3.3.3 Concrete Cover	3 - 56
3.3.3.4 Steel Spacing Design	3 - 56

FABRICATION AND CONSTRUCTION

Table of Contents

3.3.4 Concrete Batching, Mixing, Delivery, and Placement 3 - 57

 3.3.4.1 Delivery Systems 3 - 57

 3.3.4.2 Consolidation Techniques 3 - 57

 3.3.4.3 Normal Weight Concrete..... 3 - 57

 3.3.4.4 Lightweight Concrete 3 - 57

 3.3.4.5 High-Performance Concrete 3 - 58

3.3.5 Concrete Curing..... 3 - 58

 3.3.5.1 Benefits of Accelerated Curing 3 - 59

 3.3.5.2 Preventing Moisture Loss 3 - 59

 3.3.5.3 Methods of Accelerated Curing 3 - 59

 3.3.5.3.1 Accelerated Curing by Convection..... 3 - 60

 3.3.5.3.2 Accelerated Curing with Radiant Heat..... 3 - 61

 3.3.5.3.3 Accelerated Curing with Steam..... 3 - 61

 3.3.5.3.4 Accelerated Curing with Electric Heating Elements..... 3 - 61

 3.3.5.4 Curing Following Stripping 3 - 62

 3.3.5.5 Optimizing Concrete Curing 3 - 62

 3.3.5.5.1 Determination of Preset Time 3 - 62

 3.3.5.5.2 Rate of Heat Application 3 - 63

3.3.6 Removing Products from Forms 3 - 64

 3.3.6.1 Form Suction 3 - 64

3.3.7 In-Plant Handling 3 - 64

 3.3.7.1 Handling Equipment 3 - 65

 3.3.7.2 Rigging..... 3 - 66

 3.3.7.3 Handling Stresses 3 - 66

 3.3.7.4 Lateral Stability during Handling 3 - 67

3.3.8 In-Plant Storage..... 3 - 67

 3.3.8.1 Storage of Eccentrically Prestressed Products..... 3 - 67

 3.3.8.2 Storage of Concentrically Prestressed or Conventionally Reinforced Products 3 - 67

 3.3.8.3 Stacking..... 3 - 68

 3.3.8.4 Weathering..... 3 - 69

3.3.9 Roughened Surfaces..... 3 - 69

 3.3.9.1 Roughening Exposed Surfaces..... 3 - 70

 3.3.9.2 Roughening Formed Surfaces..... 3 - 70

3.3.10 Match-Cast Members 3 - 71

 3.3.10.1 Match Casting Techniques 3 - 71

FABRICATION AND CONSTRUCTION

Table of Contents

3.3.10.2 Joining Match-Cast Members with Epoxy	3 - 72
3.4 PLANT QUALITY CONTROL AND QUALITY ASSURANCE	3 - 72
3.4.1 Plant and Inspection Agency Interaction	3 - 72
3.4.2 Product Evaluation and Repair	3 - 73
3.4.2.1 Surface Voids	3 - 73
3.4.2.2 Honeycomb and Spalls	3 - 73
3.4.2.3 Repairing Large Voids	3 - 74
3.4.2.4 Cracks	3 - 74
3.4.2.4.1 Plastic Shrinkage Cracks	3 - 74
3.4.2.4.2 Cracks Due to Restraint of Volume Change	3 - 75
3.4.2.4.3 Differential Curing Cracks	3 - 75
3.4.2.4.4 Accidental Impact Cracks.....	3 - 76
3.4.2.5 Crack Repair.....	3 - 76
3.4.2.5.1 Autogenous Healing	3 - 76
3.4.2.5.2 Crack Repair by Epoxy Injection.....	3 - 76
3.4.2.5.3 Crack Repair by Concrete Replacement.....	3 - 76
3.4.2.6 Camber	3 - 76
3.4.2.6.1 Measuring Camber	3 - 77
3.4.2.6.2 Thermal Influences on Camber	3 - 77
3.4.2.6.3 Mitigation of Camber Growth	3 - 77
3.4.2.7 Sweep.....	3 - 78
3.4.2.7.1 Mitigation of Sweep.....	3 - 78
3.4.3 Water-Cementitious Materials Ratio	3 - 78
3.4.3.1 Mineral Admixtures and Workability.....	3 - 78
3.4.3.2 Water-Cementitious Materials Ratio and Durability.....	3 - 78
3.4.3.3 Water-Cementitious Materials Ratio without Water-Reducing Admixtures.....	3 - 79
3.4.3.4 Water-Cementitious Materials Ratio with Water-Reducing Admixtures.....	3 - 79
3.4.3.5 Controlling Water-Cementitious Materials Ratio.....	3 - 79
3.4.3.6 Testing Water-Cementitious Materials Ratio.....	3 - 79
3.4.4 Strand Condition	3 - 79
3.4.5 Concrete Strength Testing	3 - 80
3.4.5.1 Number of Cylinders	3 - 80
3.4.5.2 Test Cylinder Size	3 - 81
3.4.5.3 Alternate Cylinder Capping Methods.....	3 - 81
3.4.5.4 Cylinder Curing Systems and Procedures	3 - 81

FABRICATION AND CONSTRUCTION

Table of Contents

3.4.5.4.1 Cylinder Curing Cabinets 3 - 81

3.4.5.4.2 Self-Insulated Cylinder Molds..... 3 - 82

3.4.5.4.3 Long-Term Cylinder Curing..... 3 - 82

3.4.5.5 Concrete Cores..... 3 - 82

3.4.5.6 Non-Destructive Testing 3 - 82

3.4.6 Tolerances 3 - 83

3.5 TRANSPORTATION 3 - 83

3.5.1 Weight Limitations 3 - 83

3.5.2 Size Limitations 3 - 84

3.5.3 Trucking..... 3 - 84

3.5.3.1 Flat-Bed Trailers 3 - 85

3.5.3.2 “Low-Boy” Trailers 3 - 85

3.5.3.3 “Pole” Trailers 3 - 85

3.5.3.4 Steerable Trailers 3 - 86

3.5.3.5 Truck Loading Considerations 3 - 87

3.5.4 Rail Transportation 3 - 88

3.5.5 Barge Transportation 3 - 88

3.5.6 Lateral Stability during Shipping..... 3 - 89

3.6 INSTALLATION 3 - 89

3.6.1 Jobsite Handling..... 3 - 90

3.6.1.1 Single-Crane Lifts 3 - 90

3.6.1.2 Dual-Crane Lifts 3 - 90

3.6.1.3 Passing from Crane to Crane 3 - 90

3.6.1.4 Launching Trusses 3 - 91

3.6.1.4.1 Launching Trusses for Single-Piece Construction 3 - 91

3.6.1.4.2 Launching Trusses for Segmental Construction..... 3 - 92

3.6.2 Support Surfaces..... 3 - 92

3.6.2.1 Inspection of Support Surfaces 3 - 92

3.6.2.2 Temporary Support Towers..... 3 - 92

3.6.3 Abutted Members..... 3 - 93

3.6.3.1 Vertical Alignment 3 - 94

3.6.3.2 Shear Keys 3 - 94

3.6.3.2.1 Grout or Concrete in Shear Keys 3 - 95

3.6.3.2.2 Grouting Procedures for Shear Keys 3 - 95

3.6.3.3 Welded Connectors 3 - 95

FABRICATION AND CONSTRUCTION

Table of Contents

3.6.3.4 Lateral Post-Tensioning 3 - 95

3.6.3.5 Skewed Bridges 3 - 96

3.7 DIAPHRAGMS 3 - 96

3.7.1 Cast-In-Place Concrete Diaphragms 3 - 96

3.7.2 Precast Concrete Diaphragms 3 - 97

 3.7.2.1 Individual Precast Concrete Diaphragms 3 - 97

 3.7.2.2 Secondary-Cast Precast Concrete Diaphragms 3 - 97

3.7.3 Steel Diaphragms 3 - 98

3.7.4 Temporary Diaphragms for Construction 3 - 99

3.7.5 Diaphragms in Skewed Bridges 3 - 99

3.8 PRECAST DECK PANELS 3 - 99

3.8.1 Deck Panel Systems 3 - 99

3.8.2 Handling Deck Panels 3 - 100

3.8.3 Installation of Deck Panels 3 - 100

3.9 PRECAST FULL-DEPTH BRIDGE DECK PANELS 3 - 101

3.9.1 System Description 3 - 101

 3.9.1.1 Panels with Post-Tensioning 3 - 101

 3.9.1.2 Panels without Post-Tensioning 3 - 101

3.9.2 Details and Considerations 3 - 101

3.10 REFERENCES 3 - 102

FABRICATION AND CONSTRUCTION

This page intentionally left blank

NOTATION

A_s	= area of a prestressing strand, in. ²
A_s^*	= total prestressing steel area, in. ²
D	= prestressing steel elongation, in.
E_s	= modulus of elasticity of prestressing steel, ksi
f'_c	= specified compressive strength of concrete, ksi
f_{pu}	= specified tensile strength of prestressing steel, ksi
L	= total length of prestressing steel from anchorage to anchorage, in.; length of member, ft
P_s	= design jacking force, kips

FABRICATION AND CONSTRUCTION

3.1 Scope/3.2.1 Concrete

This page intentionally left blank

Fabrication and Construction

3.1 SCOPE

This chapter describes materials and techniques used in the fabrication, handling, transportation and erection of precast, prestressed concrete bridge components. It also discusses how the components are integrated into the completed structure. Familiarity with this chapter will enable bridge designers to take advantage of the flexibility and economy of precast, prestressed concrete products. It will help to avoid the pitfalls that can make precast systems less cost-effective. In addition to fabrication, quality control procedures are described that maximize product quality, making products cast in industry-certified plants, a superior solution.

Manufacturers certified by the Precast/Prestressed Concrete Institute (PCI), accomplish quality control and improvement in accordance with the industry's quality manual MNL-116 that defines the standards for structural bridge products. PCI standards for quality precast concrete production and erection are difficult to achieve. Once attained and practiced consistently, these standards contribute to improved and continued customer satisfaction—not only by ensuring that the manufacturing and installation processes are high quality, but by making the construction process faster and smoother for all parties involved.

The standards ensure that plants maintain high-quality operations and output through daily internal-control processes and inspections of operations, materials, equipment, products and processes. This is a dynamic improvement process that is constantly being revised to meet the ever-changing challenges of this industry.

3.2 PRODUCT COMPONENTS AND DETAILS

Precast, prestressed concrete bridge products generally consist of concrete, reinforcement and various embedments used for temporary or structural connections. Variations in these components affecting cost and constructability are summarized in this chapter. These descriptions are not intended to be all-inclusive, and the reader is directed to the references for more information.

3.2.1 Concrete

Plant-cast concrete bridge products are structurally efficient sections that are relatively thin and congested with reinforcement and embedments. It is therefore imperative that fresh concrete (portland cement, fine aggregate, coarse aggregate, water, and admixtures) have sufficient workability to fill all spaces without voids, honeycombing or segregation. The following sections describe variations in individual concrete constituents that can be beneficial or detrimental to concrete placement, consolidation, and finishing, but discounting the influence of other components in the mixture. In reality, the behavior of fresh concrete will depend on the interaction of all constituents. Both fresh and hardened concrete properties vary widely due to the availability and nature of local materials. PCI-Certified plants have standard in-house mixtures with proven histories of placeability, strength, and durability. Bridge designers should consult their local producers for information on their experience with local materials and concretes, including:

- High-performance concrete (HPC)
- Flowing concrete mixes
- Ultra-high-performance concrete (UHPC)
- Self-consolidating concrete (SCC) mixes

FABRICATION AND CONSTRUCTION**3.2.1 Concrete/3.2.1.3.2 Retarders and Accelerators****3.2.1.1 Cement**

The quantity and fineness of cement play important roles in the behavior of fresh concrete, as described in ACI 225R. Lean mixtures (those using less cement) with coarsely ground cement are generally harsh and difficult to consolidate and finish. As the quantity or fineness of the cement increases, the mixture becomes more cohesive. Very rich mixtures with finely ground cement can be overly cohesive or sticky. AASHTO M85 Type III cement, normally used in precast products for its high-early strength characteristics, is the finest grind of portland cement available. As the fineness of the cement increases, the cement content which produces optimum workability with minimum water, is reduced.

3.2.1.2 Aggregates

The behavior of fresh concrete can be significantly affected by the physical properties of the aggregates, as described in ACI 221R. The maximum size and gradation of the fine aggregate, as well as the shape and texture of both the fine and coarse aggregates, affect the water content required to produce workable concrete. Rough, angular aggregates require more cement and water for workability than smooth, rounded aggregates. Too many flat or elongated pieces of coarse aggregate can result in a harsh mixture. Porous aggregates will affect the water demand if not sufficiently saturated at the time of batching.

The maximum coarse aggregate size should be smaller than the tightest space the concrete is expected to fill. ACI 318 limits the maximum coarse aggregate size to one-fifth the narrowest dimension between form sides, one-third the depth of slabs, or three-quarters the minimum clear dimension between reinforcement. The smallest practical maximum coarse aggregate size is $\frac{3}{8}$ in., however, this should not be interpreted as permitting a $\frac{1}{2}$ -in. minimum clear dimension between reinforcement. Other restrictions apply. See **Section 3.3.3.4** for discussion on steel spacing.

3.2.1.3 Admixtures

All admixtures in a given concrete mix must be compatible with each other as well as with the cement. Combinations of admixtures can exacerbate or mitigate placement and finishing problems. The admixture manufacturer should be consulted before combinations are used.

3.2.1.3.1 Water-Reducing Admixtures

In precast plants, fresh concrete mixes are augmented with one or more admixtures. The purpose of an admixture is to produce a desired property of concrete, either in its fresh or hardened form. ACI 212.3R provides a detailed description of commonly available chemical admixtures.

Strength and durability considerations of hardened concrete for bridge applications normally dictate concrete mixtures with low water-cementitious materials ratios. Without chemical admixtures, these mixtures can exhibit poor workability. Normal water-reducing admixtures decrease water demand from 5 to 12% for the same workability, or increase workability for the same water content. High-range water-reducing admixtures (superplasticizers) decrease water demand from 12% to more than 30%. Under most conditions, water reducers are used for both purposes; to reduce water demand and provide optimum workability. The ability to produce workable concrete while maintaining low water-cementitious materials ratios aids in the early strength gain necessary for a daily production cycle. Concretes using water-reducing admixtures are also less likely to segregate during placement.

3.2.1.3.2 Retarders and Accelerators

Water-reducing admixtures normally do not increase the working life of fresh concrete, and frequently decrease it, particularly with high-range water-reducers. Rapid loss of workability can often be controlled by the addition of a retarding admixture. Water-reducing admixtures have also been known to retard the set of concrete. This can be controlled by the introduction of a non-chloride accelerating admixture.

FABRICATION AND CONSTRUCTION**3.2.1.3.3 Entraining Admixtures/3.2.2 Prestressing Steel****3.2.1.3.3 Air-Entraining Admixtures**

In some cases, high-range water-reducers make finishing more difficult because of the lower water content and the resulting lack of bleed water which normally rises to the surface. This can also be true of air-entraining admixtures. At low and moderate cement contents, air-entraining admixtures make fresh concrete more workable and cohesive, reducing segregation and bleed water. However, at high cement contents, the mixture can become overly cohesive or sticky. Air-entrainment also reduces concrete strength in approximate proportion to the amount entrained, unless the mix proportions are readjusted. Excessive air contents can affect both early- and long-term concrete strengths, and should be avoided.

3.2.1.3.4 Corrosion Inhibitors

Corrosion inhibitors are occasionally specified for the protection of embedded steel, and have various effects on the behavior of fresh concrete. Calcium nitrite, for example, accelerates the set of the concrete, reduces the amount of entrained air, and increases the likelihood of plastic and drying shrinkage cracking. When these chemical admixtures are used, proper mix adjustments and curing techniques should be specified in accordance with the manufacturer's recommendations.

3.2.1.3.5 Mineral Admixtures

Mineral admixtures are sometimes used to improve economy, strength or durability. Fly ash can be an economical alternative if used to replace cement, and will usually increase the workability of concrete. However, its properties include retarding initial set so it needs to be used cautiously in a daily production cycle. ACI 226.3R provides guidance on the use of fly ash.

Fresh concrete with slag cement or silica fume up to 5% by weight of cement will normally behave much like conventional concrete. However, higher dosages can result in overly cohesive mixtures, difficult finishing due to lack of bleed water, longer setting times and increased shrinkage. As with all concrete constituents, this detrimental behavior can be controlled with good mix design, batching, placing and curing practices. The report by the PCI Committee on Durability (1994), provides helpful information on the use of silica fume.

3.2.2 Prestressing Steel

Most precast concrete bridge components are prestressed for added strength and serviceability. Prestressing is achieved by one of two methods: pretensioning or post-tensioning. The primary difference between the two methods is the point in production at which the prestressing tendons are tensioned.

Pretensioning is most economical for plant-cast products, since much of the necessary material used in post-tensioning is eliminated. Post-tensioning may be required in the plant if pretensioning equipment or facilities are inadequate or not suited for the project. Bridge designers should consult their local producers for information on plant capabilities.

Combinations of pretensioning and post-tensioning within the same member have proven to be cost-effective. For example, combinations of pre- and post-tensioning may reduce the concrete strength required at transfer of prestress. In other cases, pretensioned strands have been designed to carry a predetermined percentage of the dead load in a simple span (e.g., its own weight plus that of the cast-in-place deck without shoring). Then, post-tensioned tendons continuous over several spans are added for strength for subsequent dead and live loads.

Figure 3.2.2-1a and **b** shows several types and sizes of prestressing tendons (0.7-in.-diameter strand is also available but not shown). For pretensioning, the common tendon material is a 7-wire strand, whereas in post-tensioning, single- or multi-strand tendons or high strength bars are commonly used.

FABRICATION AND CONSTRUCTION

3.2.2 Prestressing Steel/3.2.2.3 Strand Size and Spacing

*Figure 3.2.2-1
Prestressing Steel*



a) Post-Tensioning Bars

b) 7-Wire Prestressing Strands

From the left: $\frac{3}{8}$ in.; $\frac{3}{8}$ in. surface indented; $\frac{1}{2}$ in.; $\frac{9}{16}$ in.; 0.6 in.; 0.6 in. epoxy-coated with embedded surface grit

3.2.2.1 Pretensioning

In pretensioning, strands are first jacked to a specified force in a predetermined profile. Concrete is placed in direct contact with the tensioned strands and then cured. When the concrete achieves the specified transfer strength, forms are stripped and the tension in the strands is transferred to the concrete. For some products, tension in the strands is first released, and then the product is removed from fixed forms. See **Section 3.3.6** for more information on removing forms from products and products from their forms. The force in the strands is transferred to the product by the bond which develops between the concrete and surface of the strands.

3.2.2.2 Post-Tensioning

Post-tensioning is a method where the prestressing force is introduced into the concrete after it has been cast and cured. The tendons are then jacked between anchorages embedded in the concrete. Post-tensioning tendons may be internal or external to the concrete cross section.

For internal tendons, ducts or sleeves are provided in the concrete into which the prestressing tendons are inserted. Internal tendons may remain unbonded after stressing, or may be bonded by pressure grouting the ducts. Another type of internal tendon is a single strand that has had a factory application of grease followed by insertion into a plastic hose-like sleeve. These remain unbonded and the grease protects against corrosion.

External tendons, although outside of the concrete cross section, are normally contained within the structure. For example, tendons within the voids of box beams are considered external. External tendons are normally draped between anchorage points to achieve the desired profile. By definition, external tendons are unbonded, even though they may be encased in metal or plastic ducts and pressure grouted. All unbonded tendons, whether internal or external, should be permanently protected against corrosion.

3.2.2.3 Strand Size and Spacing

Seven-wire prestressing strand meets the requirements of AASHTO M203 and is used for both pretensioned and post-tensioned applications. It is available in the sizes and grades shown in **Chapter 2, Table 2.11-1**. The predominant size and grade used for pretensioning is $\frac{1}{2}$ in. diameter, uncoated, 270 ksi, although 0.6-in.-diameter is becoming the preferred size for bridge beams and certain other products. Most proprietary post-tensioning systems accommodate either $\frac{1}{2}$ in. or 0.6 in. diameter, 270 ksi strands. Two- and three-wire strands are also available, but their use, along with the other sizes and grades of seven-wire strand, is much less common for bridge applications.

FABRICATION AND CONSTRUCTION**3.2.2.3 Strand Size and Spacing/3.2.2.5 Strand Anchors and Couplers for Post-Tensioning**

The minimum clear distance between pretensioned strands, as required by LRFD Article 5.10.3.3.1 is 1.33 times the maximum aggregate size with center-to-center distance not less than those shown in LRFD Table 5.10.3.3.1-1. This spacing is:

- 1.5 in. for $\frac{3}{8}$ -in.-diameter strand
- 1.75 in. for $\frac{7}{16}$ -, $\frac{1}{2}$ -, and $\frac{1}{2}$ -in.-special-diameter strand
- 2.0 in. for $\frac{9}{16}$ -, $\frac{9}{16}$ -special-, and 0.6-in.-diameter strand

Post-tensioned tendons, which are mechanically anchored and do not rely on bond to the concrete at transfer, are exempt from these requirements. In 2011, there were ongoing studies to review the requirements for spacing of 0.7-in.-diameter strand.

3.2.2.4 Strand Anchors and Couplers for Pretensioning

A typical anchor for pretensioned strand is shown in **Figure 3.2.2.4-1**. Normally referred to as a “strand chuck,” the device consists of a hardened steel barrel with a machined conical core. This barrel receives the jaw or wedge assembly. Wedges are used in sets of 2 or 3 pieces. They are held in alignment by a rubber “O-ring” and are tapered to match the conical shape of the barrel. The wedges have machined serrations or “teeth” that bite into and grip the strand, distributing the radial load to the barrel. The cap is spring loaded to keep the wedges in place during jacking or tensioning.

Figure 3.2.2.4-1
Strand Chuck Showing Internal Components



Figure 3.2.2.4-2
Strand Splice Chuck Showing Internal Components



A coupler, or “splice chuck,” as the name suggests, is used to splice two lengths of strand together. As shown in **Figure 3.2.2.4-2**, they are essentially the same as strand chucks, with the exception that in place of the spring loaded head, they are furnished with male and female threads, enabling them to screw onto each other back-to-back. Couplers are not used within precast members, but rather are used to connect strand between members or strand passing through the member with “bridle” strand. See **Sections 3.2.2.6.2** and **3.3.2.4** for a description of “bridle” strand and its use.

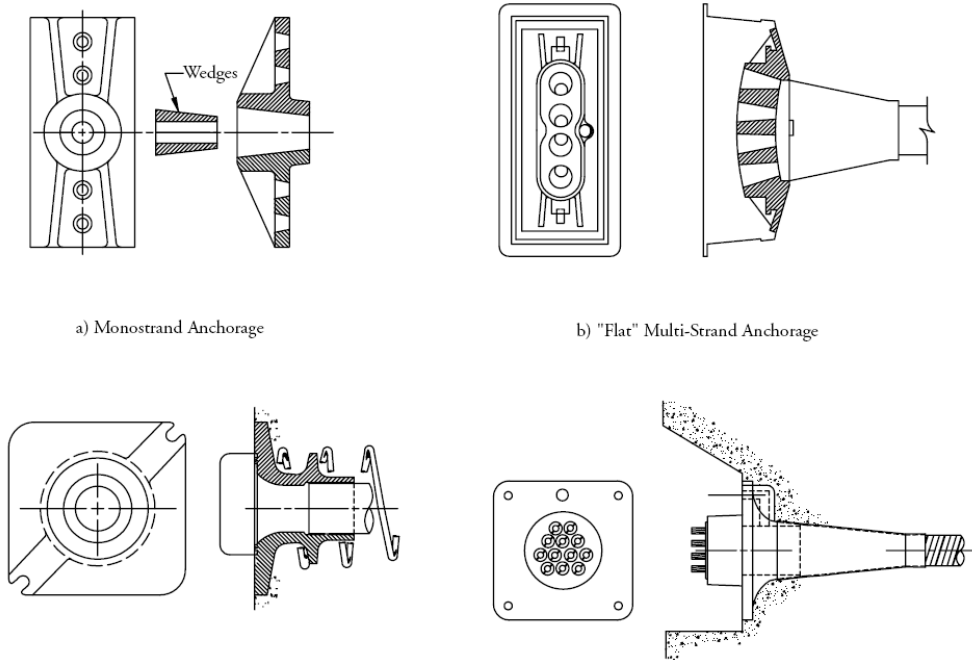
3.2.2.5 Strand Anchors and Couplers for Post-Tensioning

Most anchors for post-tensioned strand are proprietary, but generally use wedges similar to pretensioning anchors. These anchorages are embedded in the concrete prior to stressing, and are reinforced to resist the bursting stresses associated with high localized concentrated loads. In many cases, the wedges are hydraulically pressed into conical holes in the anchor head to reduce seating losses after jacking. Post-tensioning tendons vary from single strand tendons to multiple strand tendons which occupy the same duct and anchorage device. **Figure 3.2.2.5-1a-1d** shows typical post-tensioning anchorages.

FABRICATION AND CONSTRUCTION

3.2.2.5 Strand Anchors and Couplers for Post-Tensioning/3.2.2.6 Epoxy-Coated Strand

Figure 3.2.2.5-1a-1d
Types of Post-Tensioning Anchorages

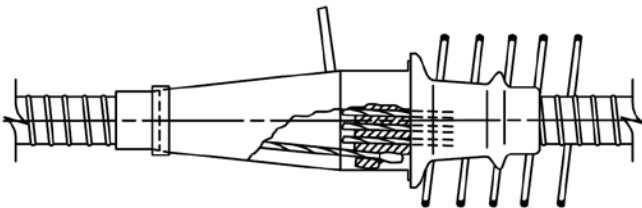


a) Monostrand Anchorage

b) "Flar" Multi-Strand Anchorage

Proprietary post-tensioning couplers are also available to join a new tendon to one which has already been placed and stressed. One such coupler is shown in **Figure 3.2.2.5-2**. These are not generally permitted for use in the U.S.

Figure 3.2.2.5-2
Post-Tensioning Coupler



3.2.2.6 Epoxy-Coated Strand

Seven-wire prestressing strand with an organic coating meeting the requirements of ASTM A882 is available for conditions that require a higher degree of corrosion protection. In pretensioned and bonded post-tensioned applications, this normally applies to exposure conditions that are particularly harsh, such as direct exposure to seawater. For unbonded post-tensioned applications, unless an alternate system of corrosion protection is employed, the epoxy coating provides the only barrier between the uncoated strand and the environment. The following sections present information and procedures for the use of epoxy-coated strand that are different from, or in addition to, those for uncoated strand. These sections are not intended to be all inclusive. A report by the PCI Ad Hoc Committee on Epoxy-Coated Strand (1993) provides excellent guidance on the use of epoxy-coated strand.

It should be emphasized that the use of epoxy-coated strand has significant cost implications. The cost of coated strand can be three times the cost of uncoated strand, and the set-up labor costs can increase by as much as 30%. For most bridge applications where the prestressing tendons are bonded, the plant-cast quality of the concrete, the concrete cover, and the limits on tensile stresses under service loads, provide excellent corrosion protection without coated strand.

FABRICATION AND CONSTRUCTION**3.2.2.6.1 Types of Epoxy Coating/3.2.2.6.4 Epoxy Coating and Elevated Temperatures****3.2.2.6.1 Types of Epoxy Coating**

Two types of epoxy coatings are available. For pretensioned or bonded post-tensioned applications, the epoxy surface is embedded with aluminum oxide grit to aid in the bond of the concrete to the surface. Coating without the grit is smooth and will not accept concrete bond. It is intended for unbonded post-tensioned, external post-tensioned or cable stay applications. The thickness of the coating for strand meeting ASTM A882 may vary from 25 to 45 mils. Strand with less variable coating thickness is also available, and may be necessary for compatibility with stressing hardware. Manufacturers of epoxy-coated strand should be consulted. For pretensioned applications, holes in the stressing abutments will usually need to be enlarged to accommodate the additional coating thickness.

Coatings with grit are extremely abrasive and appropriate precautions must be taken during handling. All workers should wear heavy protective gloves when handling the strand. Dragging the strand over steel form soffits or through holes in stressing abutments can abrade forms and elongate holes. This can result in out-of-tolerance strand positioning. Holes should be checked periodically. Dragging the strand over inappropriate surfaces or through unchamfered holes can cause damage to the coating or erosion of the grit. Any coating damage should be repaired in accordance with the manufacturer's recommendations. Loss of the grit will reduce effectiveness of the concrete bond.

3.2.2.6.2 Anchorage of Epoxy-Coated Strand

Special anchors with "bite-through" wedges designed specifically for epoxy-coated strand must be used for tensioning and seating. Once seated, wedges should not be allowed to unseat during tensioning, since the serrations can become filled with epoxy coating. Therefore, final tensioning of epoxy-coated strand should be accomplished with a single stroke of the jack. Anchorage seating losses are typically higher for epoxy-coated strand than for uncoated strand (see **Sects. 3.3.2.7.1** and **3.3.2.7.4**). This should be considered in the tensioning and elongation calculations. Wedge assemblies must be thoroughly inspected and cleaned prior to reuse. Epoxy-coated strand should not be gripped by the wedges in locations where it was damaged, heated or previously gripped.

When the length of the concrete member is substantially shorter than the length of the stressing bed between abutments, a technique is used to save material costs. Uncoated "bridle" strand is often coupled to the epoxy-coated strand for the stressing bed length outside the member. See Section 3.3.2.4 for more discussion on "bridle" strand. This coupling can be done by one of two methods. The epoxy coating can be stripped from the end of the strand using a device specifically designed for this purpose. The strands can then be joined using a standard splice chuck. Alternatively, a special splice chuck can be manufactured to grip epoxy-coated strand on one side, and uncoated strand on the other.

3.2.2.6.3 Protection of the Epoxy Coating

Sharp deflection of the strand profile, such as harping in pretensioned or external post-tensioned applications, should be minimized. Friction at the deflection point during tensioning can cause damage to the coating. Tensioning the strands in a straight profile, then pulling or pushing them into the deflected position, minimizes damage. Cushioning materials can also help alleviate such damage. In internal post-tensioned applications, galvanized spiral-wound metal duct is not recommended, as damage to the coating can result from abrasion at the duct seams. Smooth polyethylene duct will minimize damage.

3.2.2.6.4 Epoxy Coating and Elevated Temperatures

At elevated temperatures like those sometimes used during accelerated curing of the concrete, the stability of the coating may be reduced, which can lead to a partial or total loss of prestress at transfer. ASTM A882 requires the epoxy coating to be capable of withstanding temperatures up to 150 °F without reduction of bond. Accordingly, the temperature of the concrete surrounding the strand must be below 150 °F and falling prior to transfer of prestress. The potential of exposure of the members to fire, and the possible loss of prestress, should be evaluated when specifying epoxy-coated strands.

FABRICATION AND CONSTRUCTION

3.2.2.7 Indented Strand/3.2.2.8 Prestressing Bars

3.2.2.7 Indented Strand

Seven-wire prestressing strand with small indentations in the outer wires conforming to ASTM A886 is available in the sizes and grades shown in **Table 3.2.2.7-1**. This material is identical to normal prestressing strand meeting the requirements of AASHTO M203 with the exception of the indentations. The purpose of the indentations is to increase bond between concrete and strand and decrease the transfer and development length of pretensioned strand.

Indented strand is only used in short members where short transfer of the prestress force is critical. One common application is in precast, prestressed concrete railroad ties. Nearly all bridge products are of sufficient length to accommodate the transfer and development length provided by normal strand. However, some short span prestressed bridge members (e.g., stay-in-place deck forms) may benefit from the use of indented strand. Due to the decreased transfer length of indented strand, splitting and bursting forces at the ends of pretensioned members will increase compared to members using normal strand.

Table 3.2.2.7-1
Properties of Indented Strand

Nominal Diameter		Tensile Strength	Normal Area	Nominal Weight
in.	in.	lb	in. ²	lb/1,000ft
Grade 250				
1/4	(0.250)	9,000	0.036	122
5/16	(0.313)	14,500	0.058	197
3/8	(0.375)	20,000	0.080	272
7/16	(0.438)	27,000	0.108	367
1/2	(0.500)	36,000	0.144	490
	(0.600)	54,000	0.216	737
Grade 270				
5/16	(0.313)	16,500	0.061	210
3/8	(0.375)	23,000	0.085	290
7/16	(0.438)	31,000	0.115	390
1/2	(0.500)	41,300	0.153	520
	(0.600)	58,600	0.217	740

3.2.2.8 Prestressing Bars

Prestressing bars conforming to AASHTO M275 are fabricated from high-strength steel with a minimum ultimate tensile strength of 150 ksi. The bars are either plain or deformed. Available sizes of deformed prestressing bars are shown in **Chapter 2, Table 2.11-1**. Plain bars are not commonly used in prestressing.

Figure 3.2.2.8-1
Prestressing Bar Anchor and Coupler



FABRICATION AND CONSTRUCTION

3.2.2.8 Prestressing Bars

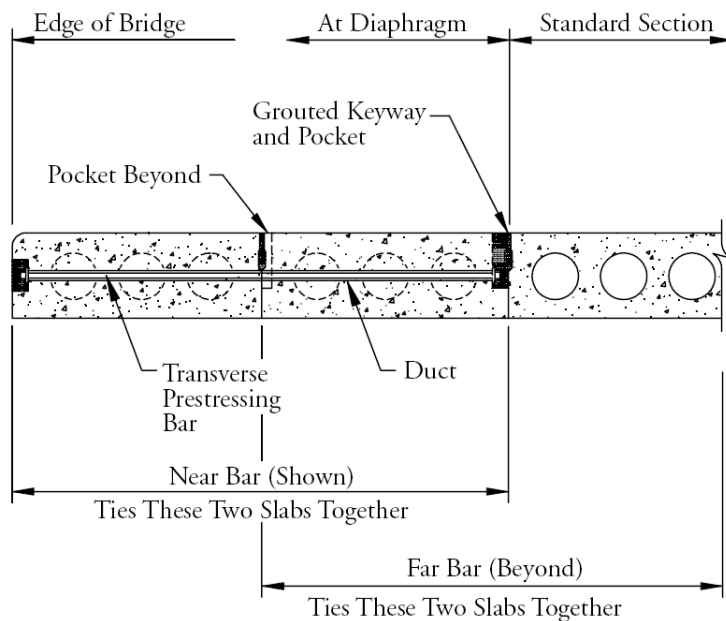
Deformed bars are generally used for post-tensioned applications where the tendon profile is straight and relatively short. In this application, the deformations are not specifically intended to provide bond with the concrete, as with mild reinforcement, but rather to allow the bars to be anchored or coupled with screw-on devices specifically designed for this purpose. Anchorage devices are normally of the plate variety, and are installed prior to casting the concrete to distribute the post-tensioning force during tensioning. **Figure 3.2.2.8-1** shows a typical anchorage device and coupler. Prestressing bars are normally not used in pretensioned applications.

Due to the relatively short lengths and large bar areas, the tensioning operation is characterized by short elongations, which at times are difficult to measure and compare to theoretical values. Accurate ram calibrations are important for proper stress application. Prestressing bars are normally bonded by grouting, or may be left unbonded with appropriate corrosion protection measures.

The uses of prestressing bars include transverse post-tensioning of bridge decks, diaphragms, and precast multi-beam decks (flat slabs, slab beams, box beams, etc.), as well as the connection of precast members to other precast members or to cast-in-place construction. **Figures 3.2.2.8-2** through **4** illustrate some of these applications.

Note that in **Figure 3.2.2.8-2**, the detail shown is often used for skewed bridges with skew angle greater than 20 degrees. For bridges with skew angle less than 20 degrees, or zero, lateral post-tensioning extends from edge-to-edge of bridge. (See Sects. 3.6.3.4 and 3.6.3.5).

Figure 3.2.2.8-2
Voided Slab Beams Connected through Diaphragms with Threaded Post-Tensioning Bars



FABRICATION AND CONSTRUCTION**3.2.3 Nonprestressed Reinforcement/3.2.3.1 Reinforcement Detailing**

Figure 3.2.2.8-3
Box Beams Connected through Diaphragms with Threaded Post-Tensioning Bars

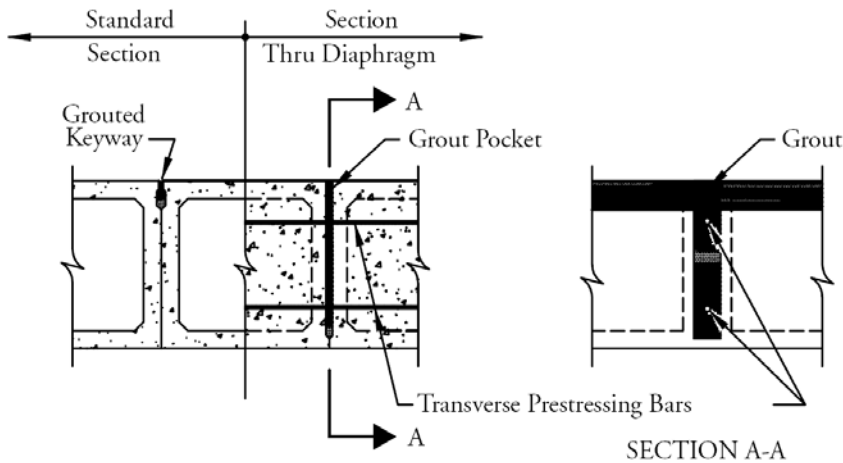
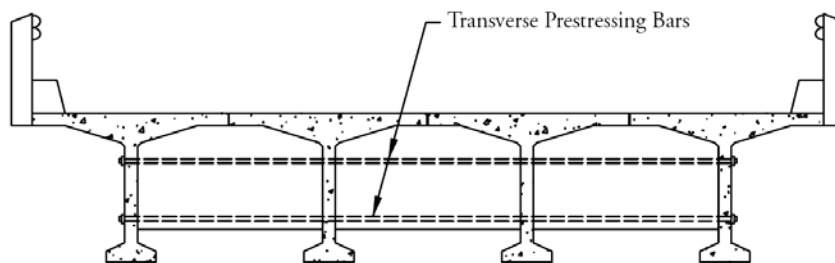


Figure 3.2.2.8-4
Deck Bulb-Tees Connected through Diaphragms with Threaded Post-Tensioning Bars



3.2.3 Nonprestressed Reinforcement

Precast, prestressed concrete bridge products are nearly always supplemented with nonprestressed reinforcement, generally referred to as “mild steel,” “mild reinforcement,” or “conventional reinforcement.” This material conforms to AASHTO M32, AASHTO M225, AASHTO M31 or ASTM A706. AASHTO M32 and AASHTO M225 address cold-worked steel wires that are smooth and deformed, respectively, and used primarily as spiral reinforcement for piles and columns. They are also used in the fabrication of welded wire reinforcement. AASHTO M31 is the most common type of deformed reinforcing bar (although this specification also includes plain bars, they are rarely used as concrete reinforcement). ASTM A706 applies to low-alloy steel deformed bars which are intended for circumstances where embrittlement, sometimes associated with AASHTO M31 bars, must be avoided. This can apply to field bent bars, or to bars to be welded. However, in some parts of the country, the availability of ASTM A706 bars is limited, particularly in small quantities. Procedures for field bending of AASHTO M31 bars, as well as proper preheating to permit welding are widely used. Consideration should be given to availability when specifying ASTM A706 reinforcement.

Prestressing steel is usually provided for all positive moments in flexural members, but may be supplemented with nonprestressed reinforcement. In many cases, negative moments at the supports of continuous spans are resisted entirely by mild steel, either in the cast-in-place deck, or in connections between precast members. Axial loads can be resisted entirely by prestressing steel, nonprestressed reinforcement, or a combination of both. Shear and torsion effects generally require the use of nonprestressed reinforcement. Flexural stresses transverse

FABRICATION AND CONSTRUCTION

3.2.3 Nonprestressed Reinforcement/3.2.3.1 Reinforcement Detailing

to the prestressing steel, bursting forces due to development of the prestressing forces, tensile stresses in the top flange of eccentrically prestressed members during handling, and confinement of the core of concrete piles and columns are all resisted by mild reinforcement. The following sections suggest configurations of nonprestressed reinforcement that are compatible with prestressed concrete members, and are considered standards in the industry.

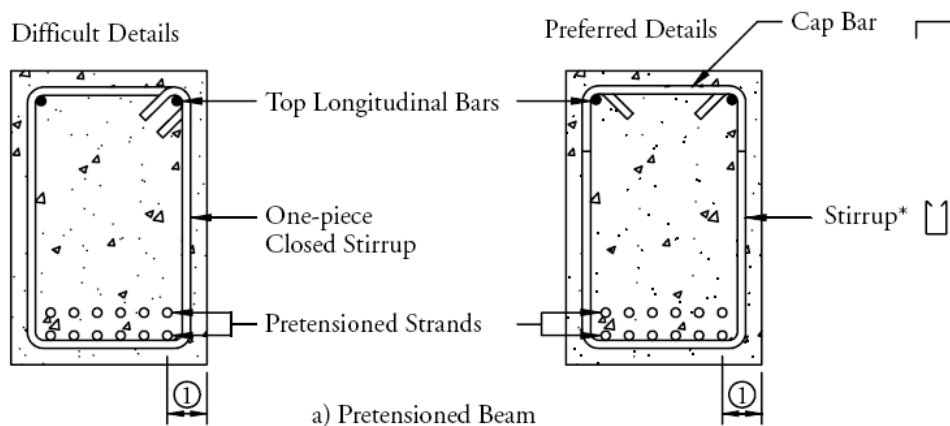
3.2.3.1 Reinforcement Detailing

In pretensioned applications, prestressing strand must be pulled from reels through one stressing abutment, over the casting bed, and into the opposite stressing abutment (or coupled into “bridle” strand already anchored to the opposite abutment). This is done either by hand, or using a winch system that can pull several strands at a time. In either case, threading the strand through closed mild steel configurations, such as shown in **Figure 3.2.3.1-1a**, becomes labor intensive, particularly when the reinforcement cannot be bundled into compact groups and spread out after tensioning (such as with heavy spiral reinforcement or some welded wire reinforcement cages). Whenever possible, mild reinforcement should be detailed for placement after the prestressing strand has been strung in the bed and tensioned. If this is not feasible, the bars should be open at the top to allow the strands to be pulled over them. The bars may be capped after tensioning if necessary. Only where mild reinforcement is required for torsion or confinement should closed bars or spirals be considered.

Care must also be taken when specifying single bar ties with bends at both ends, such as used in compression members (shown in **Figure 3.2.3.1-1b**) and in the anchorage zones of prestressed concrete flexural members. These bars should be detailed with the assumption that they are the last ones placed in the assembly, and that the prestressing strands cannot move to accommodate them. Bars with 90-degree bends at one end, and 135-degree bends at the other, with the bends alternating from side to side of the member, are generally satisfactory for placing after tensioning. **Section 3.2.3.5** offers suggestions for nonprestressed reinforcement for common prestressed concrete bridge products. Note that 135-degree hooks are required in the AASHTO specifications in regions requiring seismic resistance or for members resisting torsion.

When detailing bars that enclose prestressing strands, proper consideration should be given to the bend radius. The dimension from the edge of the member to the strand must be sufficient to allow for both the bend radius and the required concrete cover.

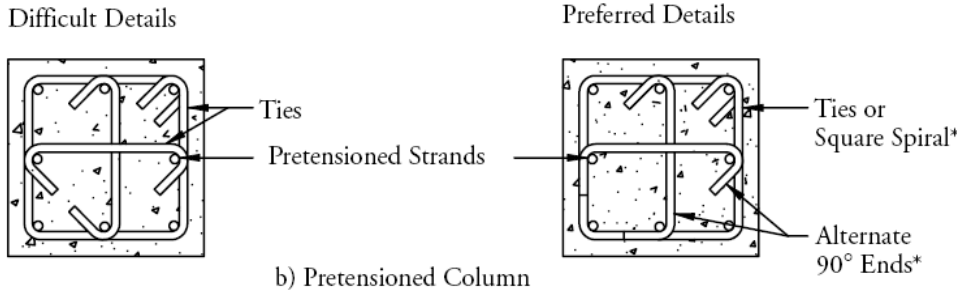
Figure 3.2.3.1-1a
Reinforcement Details Showing Fabrication Considerations
(Pretensioned Beam)



FABRICATION AND CONSTRUCTION

3.2.3.1 Reinforcement Detailing/3.2.3.2.1 Continuity with Post-Tensioning

Figure 3.2.3.1-1b
Reinforcement Details Showing Fabrication Considerations
(Pretensioned Column)



- ① Minimum Dimension = Concrete Cover + Stirrup Bar Diameter + Stirrup Bend Radius
- * See text regarding 135-degree hooks

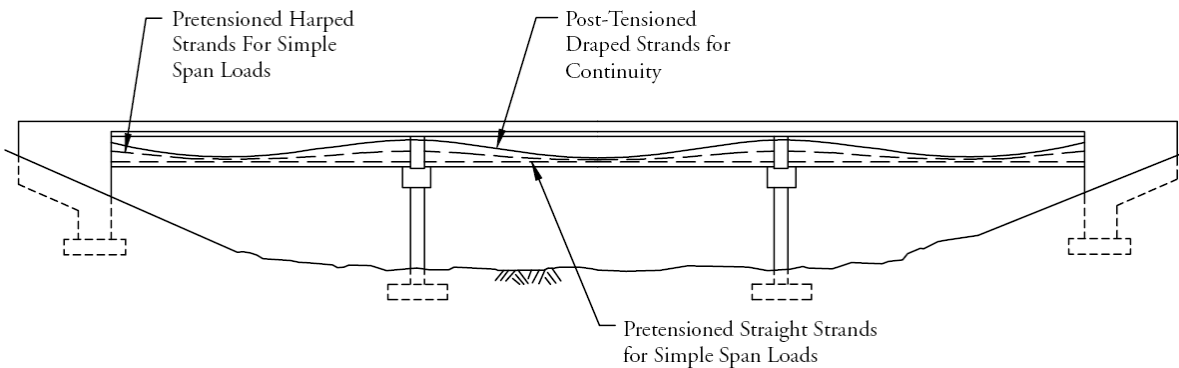
3.2.3.2 Developing Continuity

Several methods are available for developing continuity in adjacent spans with precast concrete bridge members. These are discussed in Sections 3.2.3.2.1 through 3.2.3.2.3 and specifically address development of negative moments over interior piers. Often, positive moments must also be considered over the piers. The most economical means of developing positive moments over the piers is by extending the necessary number of strands from the bottom flange of the precast member, and anchoring them into the pier by bending them up to provide sufficient development length. These strands may also be anchored by mechanical means, but this option is more expensive.

3.2.3.2.1 Continuity with Post-Tensioning

Continuity of precast, prestressed concrete spans can be achieved in several ways. The solution shown in **Figure 3.2.3.2.1-1a** could be considered the most structurally efficient. The precast members are pretensioned for the portion of the dead load imposed prior to developing continuity, and post-tensioning is added for all subsequent loads, with the tendon profile following the continuous span moment envelope. However, considering that only a limited number of standard section depths are readily available, that site conditions usually limit the range of span lengths, and that post-tensioning carries a higher cost than pretensioning, this may not be the most cost-effective alternative.

Figure 3.2.3.2.1-1a
Continuity Developed with Post-Tensioning

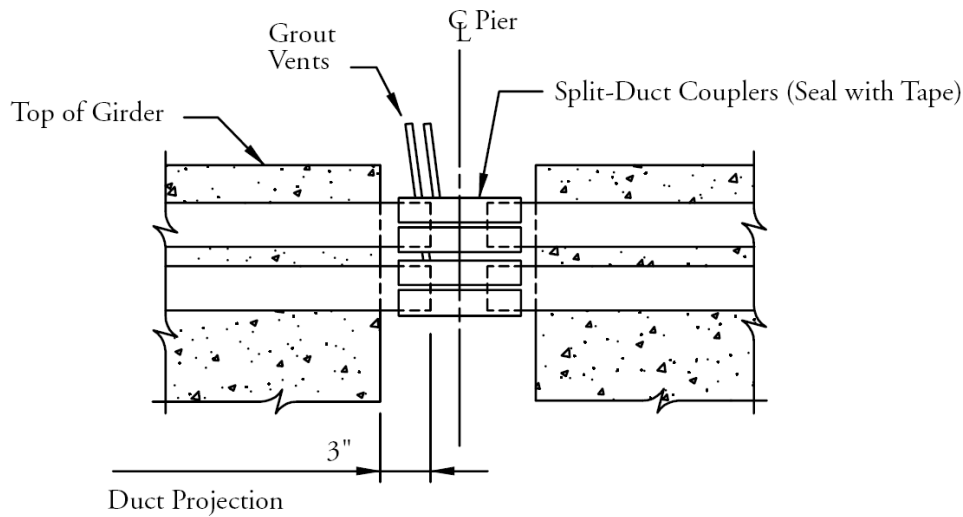


a) Bridge Elevation Showing Tendon Profiles

FABRICATION AND CONSTRUCTION

3.2.3.2.1 Continuity with Post-Tensioning/3.2.3.2.2 Continuity with Nonprestressed Reinforcement

Figure 3.2.3.2.1-1b
Continuity Developed with Post-Tensioning

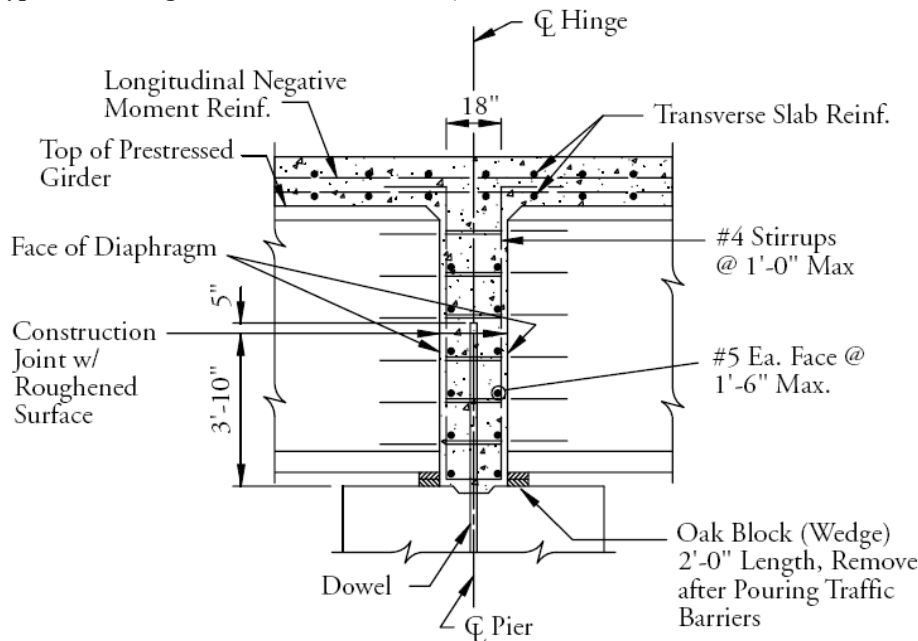


b) Duct Spliced Over Pier

3.2.3.2.2 Continuity with Nonprestressed Reinforcement

A simple solution for bridges with cast-in-place decks is to proportion the longitudinal nonprestressed reinforcement in the deck over the piers to resist the negative moments. This is a very common and cost-effective method of developing continuity because it involves only straight reinforcing bars that are easily placed and spliced. A typical detail used in the State of Washington is shown in **Figure 3.2.3.2.2-1**. The detail is not typical of most agencies in the method used to transfer end reactions.

Figure 3.2.3.2.2-1
Example of Continuity Developed with Conventional Deck Reinforcement
(typical Washington State Detail—see text)



FABRICATION AND CONSTRUCTION

3.2.3.2.3 Continuity in Full-Depth Members

3.2.3.2.3 Continuity in Full-Depth Members

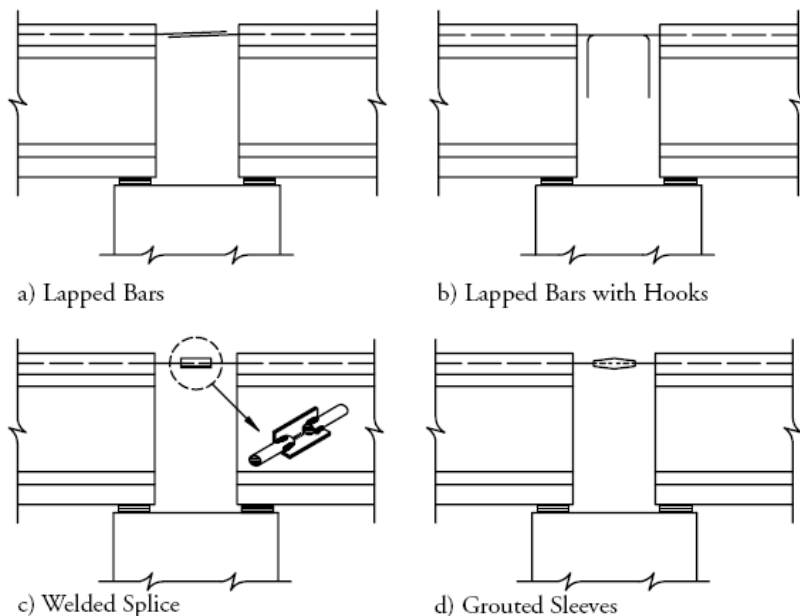
Precast members which are full depth, or are topped only with a non-structural wearing surface, must be post-tensioned over the piers as described earlier, or must have projecting reinforcement spliced in some manner to provide negative moment capacity. Several methods have been successfully employed in splicing the projecting reinforcement, some of which are illustrated in **Figure 3.2.3.2.3-1**.

If the pier is of sufficient width, the simplest and least expensive method is to provide a non-contact lap splice of mild reinforcement extending from the top of the precast members (**Fig. 3.2.3.2.3-1a**). These bars may also be hooked to aid with development (**Fig. 3.2.3.2.3-1b**). In this case, the bars should be allowed to be field bent, since the form normally extends past the end of the member, and may interfere with the placement of pre-bent bars. In both cases, the bars should be staggered horizontally to avoid interference with bars from the facing member, and with reinforcement projecting from the pier.

When the pier does not provide sufficient width for lapped or hooked bars, nonprestressed reinforcement projecting from the top of the precast members may be spliced mechanically by welding, with grouted splice sleeves, or with mechanical splices. Some of the more common splice details are shown in **Figures 3.2.3.2.3-1c through 1e**. A wide variety of generic and proprietary splicing details are available. Each detail has advantages and disadvantages with respect to material cost, labor cost, tolerances for fabrication and erection, and the degree of quality control required to properly execute the splice. Bridge designers should consult local producers for information on the splice details favored by builders in the local area.

Yet another solution involves coupling prestressing strands that extend from the top of the precast members. After coupling the strands, the members are jacked apart at the pier to induce required tensile forces in the coupled strands. This is shown in **Figure 3.2.3.2.3-1f** and reported by Tadros, et al. (1993) and Ficenec, et al. (1993). With the members held apart, the cast-in-place closure is made. Once the closure concrete attains design strength, the jack is released to apply compression across the joint. The resulting continuous spans behave much the same as with the post-tensioned solution, without the expense of the post-tensioning hardware.

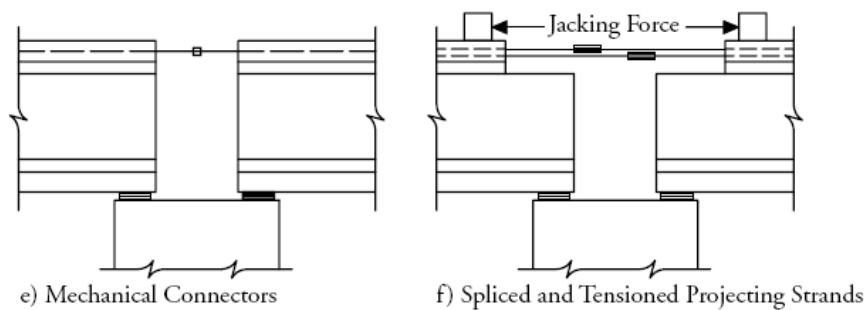
Figure 3.2.3.2.3-1a-1f
Methods to Establish Continuity



Figures 3.2.3.2.3-1e and 1f on following page

FABRICATION AND CONSTRUCTION

3.2.3.2.3 Continuity in Full-Depth Members/3.2.3.4 Welded Wire Reinforcement

**3.2.3.3 Coated Nonprestressed Reinforcement**

Reinforcing bars coated for corrosion protection are naturally more expensive than uncoated bars, both in material and labor costs. Epoxy coating conforms to AASHTO M284 or ASTM A934 and galvanizing conforms to ASTM A767. Special epoxy coatings, such as designed for the protection of steel pipe, raises material costs when specified for use on reinforcing bars. Increased development lengths of epoxy-coated bars will slightly increase the amount of material required.

The quality of plant-cast concrete, the control of concrete cover, and the limits on tensile stresses for prestressed concrete members under service loads provide excellent corrosion protection for uncoated reinforcement under normal exposure conditions. Coated reinforcement should only be considered for severe exposure conditions.

3.2.3.3.1 Epoxy-Coated Nonprestressed Reinforcement

The effectiveness of epoxy coatings in preventing corrosion is only as good as the integrity of the coating, as summarized by D'Arcy, et al. (1996). Consequently, specifications for the bars for shipping, handling, placing, and protection during concrete placement are increasingly restrictive. Labor costs are increased for these types of bars due to the special handling required to prevent damage to the coating, and to repairing areas damaged due to cutting, bending or handling. When specifying bars to be cut and bent prior to coating, consideration should be given to constructability. For example, hooked bars projecting from the ends of precast members may interfere with the formwork at the member ends. In many cases, field bending of bars is the best option for constructability.

3.2.3.3.2 Galvanized Nonprestressed Reinforcement

When specifying reinforcement to be bent prior to hot-dip galvanizing, the specifications should direct the fabricator to ASTM A767, which dictates larger finished bend diameters for No. 7 bars and larger than is standard for uncoated bars. This is important in preventing embrittlement of the steel during the hot galvanizing process.

3.2.3.4 Welded Wire Reinforcement

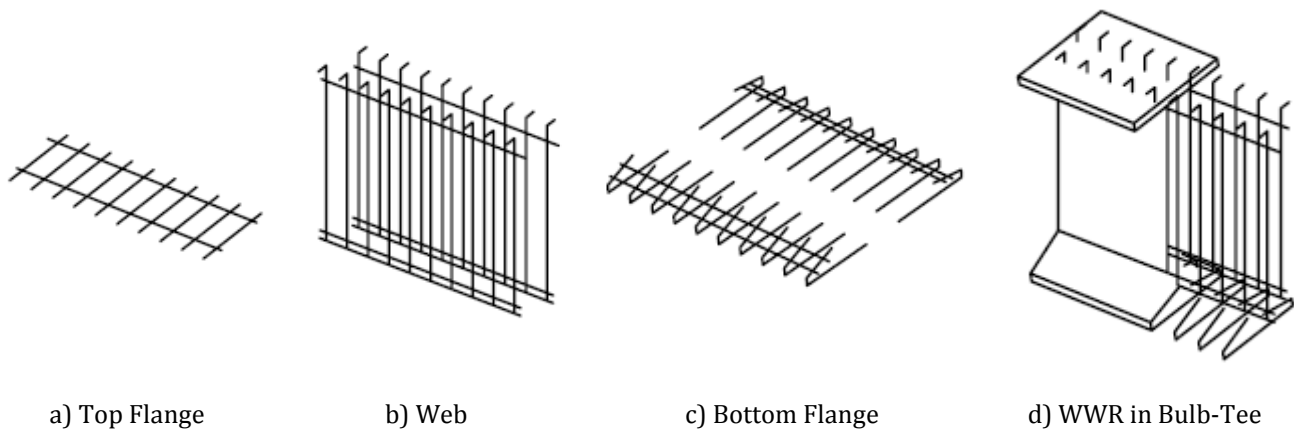
Welded wire reinforcement (WWR) has long been the standard for reinforcing floor slabs, wall panels and other flat-cast products. The material has gained popularity as an alternate for nonprestressed reinforcing bars in precast concrete bridge products. WWR configurations for typical bulb-tees are shown in **Figure 3.2.3.4-1**. Note that the web reinforcement shown in **Figure 3.2.3.4-1b** is developed by a pair of welded cross-wires in the bottom flange and a hook at the top (the top cross-wire is used to maintain the stirrup spacing). It is important to keep cross-wires out of the mid-height portion of the web where high shear stresses generally develop, as the cross-wires can produce stress concentrations in the reinforcement in areas of cracking. Single sheets of similar WWR web reinforcement are commonly used in each web of stemmed members.

Depending on the configuration of the WWR sheets, the cost of this material can be from 50 to 100% higher than mild reinforcing bars. However, savings in labor and inspection costs, as well as use of the increased strength of the material as permitted by the *LRFD Specifications*, can more than offset the increased material cost. The price and availability of WWR suitable for precast bridge products varies in different geographical regions. Local producers should be consulted for information on the cost effectiveness of WWR in their area. Alternate details for WWR and bars will allow the precaster to proceed with production if supply of either material is limited or interrupted.

FABRICATION AND CONSTRUCTION

3.2.3.4 Welded Wire Reinforcement/3.2.3.5 Suggested Reinforcement Details

Figure 3.2.3.4-1
Welded Wire Reinforcement in a Bulb-Tee



Sheets of WWR can be made in virtually any configuration up to approximately 14.5 ft wide, with smooth (AASHTO M55) or deformed (AASHTO M221) wires up to 5/8 in. diameter (W31 or D31, the equivalent of a No. 5 reinforcing bar). The sheets are normally shipped flat and bent at the precast plant, since shipping pre-bent sheets can result in a large amount of “ghost” freight. The sheet lengths are limited by the length of available benders, which is currently a maximum of about 30 ft.

Figure 3.2.3.4-1 shows the end reinforcement of a typical prestressed concrete bridge beam using WWR. The labor savings results from eliminating the need to tie individual bars into the required configuration. Improvement in quality can also be expected, since the bar spacing of WWR is much more precise than can be expected from bending and tying individual bars.

The key to efficient use of WWR is standardization. Purchasing is most economical when ordering in truckload quantities. Therefore, unless the project is large, the precast producer must be reasonably assured that any WWR that ends up in inventory will be usable on future projects. WWR configurations should also be detailed to allow installation after the prestressing strands have been placed and tensioned. Much of the savings attributed to the use of WWR will be lost if the strands must be pulled through long runs of enclosed reinforcement.

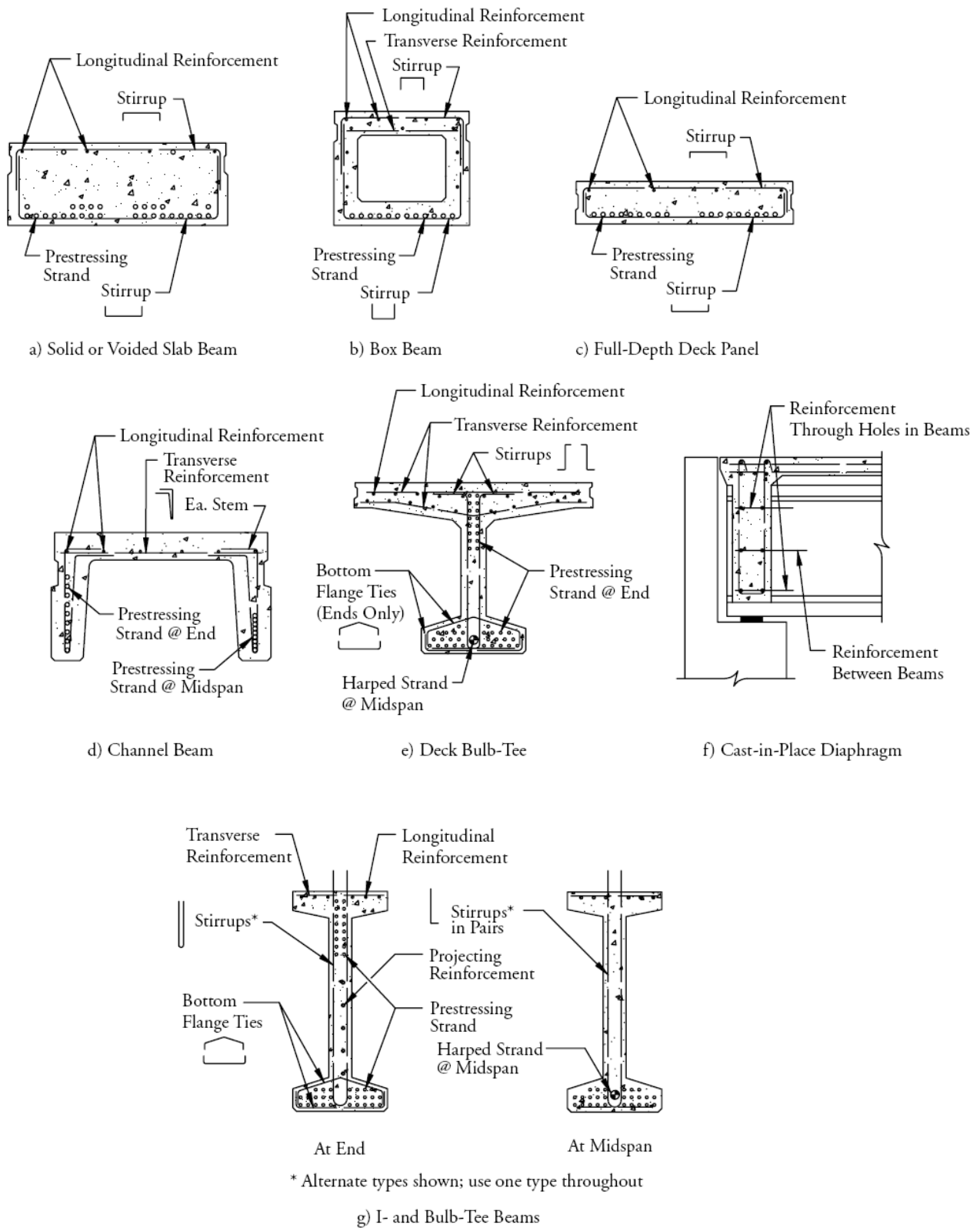
3.2.3.5 Suggested Reinforcement Details

Figure 3.2.3.5-1 shows suggested nonprestressed reinforcement configurations for various types of standard precast concrete bridge products. WWR cages can be patterned after these configurations.

FABRICATION AND CONSTRUCTION

3.2.3.5 Suggested Reinforcement Details

Figure 3.2.3.5-1a-1g
Recommended Reinforcement Configurations for Standard Products



FABRICATION AND CONSTRUCTION

3.2.4 Embedments and Blockouts/3.2.4.1 Embedments and Blockouts for Attachments

3.2.4 Embedments and Blockouts

Embedments and blockouts in precast concrete bridge products are used typically for the following:

- Hanging utilities
- Connecting the members to other members of the structural system
- Attaching cast-in-place concrete formwork
- Handling and shipping the members

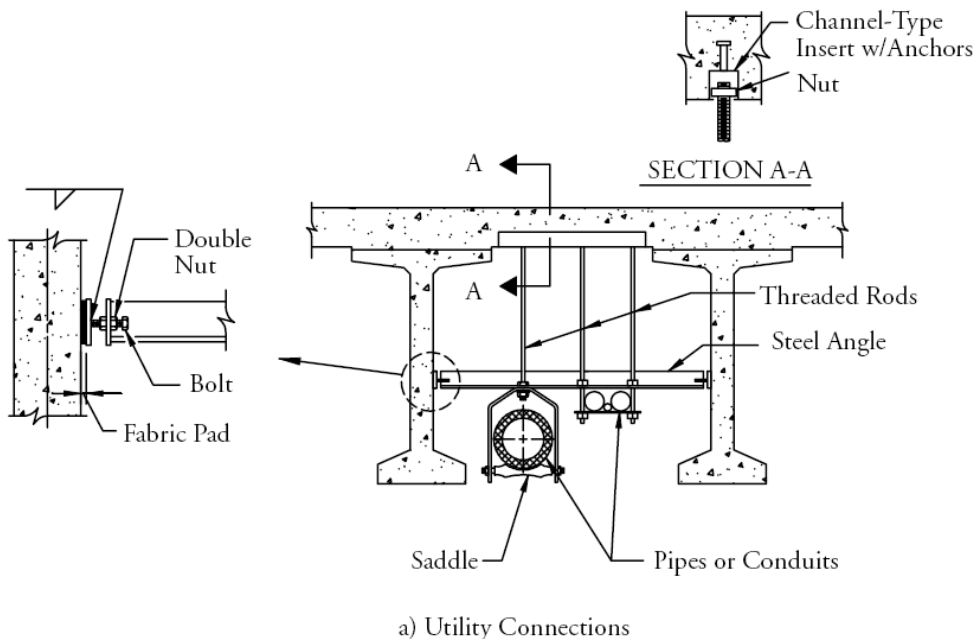
The following sections describe common embedments and blockouts used for these purposes. A wide range of details are used throughout the country. Bridge designers should consult with local producers for preferred details.

3.2.4.1 Embedments and Blockouts for Attachments

Numerous types of embedments are available for connecting miscellaneous items, such as utilities and guardrails, to precast concrete members. These embedments range from simple threaded inserts to complex welded assemblies. Depending upon the anticipated exposure, the embedments can consist of uncoated steel, coated steel, stainless steel, plastics or any other material which is both suitable for the intended purpose and compatible with both the concrete and reinforcing steel as such not to detract from meeting the intended service life. Examples of common connections are shown in Figure 3.2.4.1-1a and 1b.

The combined tolerances for all parts of the system should be considered when detailing attachments to inserts that are embedded in precast members. Slotted or oversized holes are highly recommended wherever possible. **Section 3.4.6** provides information on industry standard tolerances. A simple and durable solution is a hole cast through the member that will allow bolting with standard galvanized fasteners.

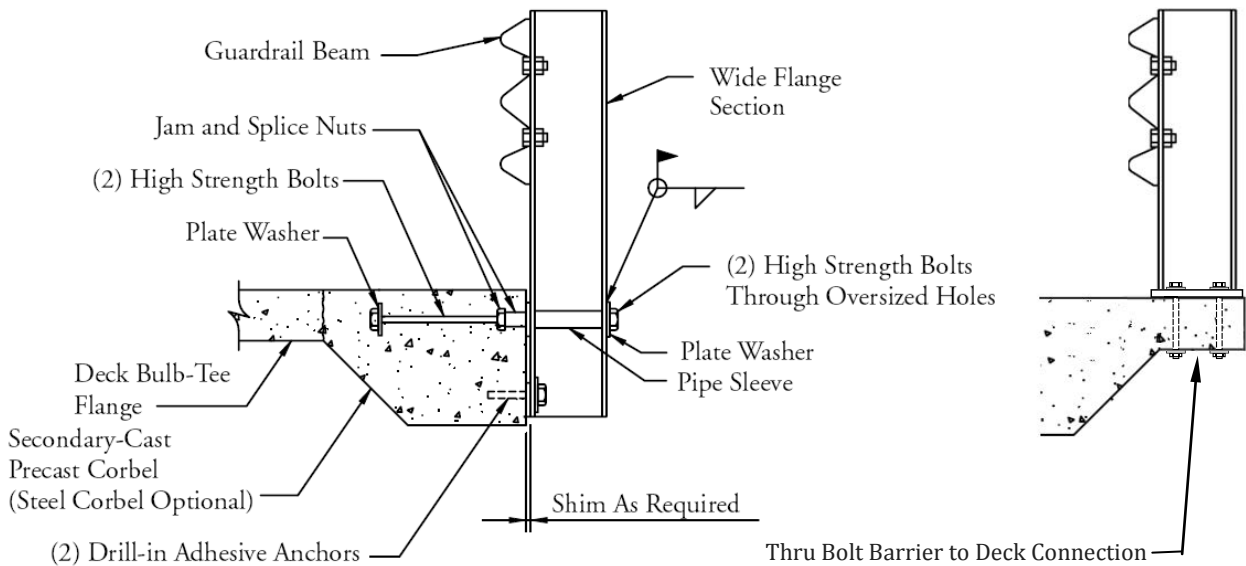
*Figure 3.2.4.1-1a
Common Attachments*



FABRICATION AND CONSTRUCTION

3.2.4.1 Embedments and Blockouts for Attachements/3.2.4.3 Embedments and Blockouts for Deck Construction

Figure 3.2.4.1-1b
Common Attachments



b) Alternate Guardrail/Barrier Connections

3.2.4.2 Embedments and Blockouts for Diaphragms

Embedments for diaphragms depend on the type of diaphragm used, ranging from threaded inserts and through holes for reinforcement for cast-in-place concrete and attachment of temporary diaphragms, to welded assemblies for precast concrete and steel diaphragms. A detailed discussion and examples of typical diaphragms are included in **Section 3.7**.

3.2.4.3 Embedments and Blockouts for Deck Construction

Deck construction usually falls into one of three methods:

- Cast-in-place concrete over bulb-tees or I-beams
- Cast-in-place concrete over composite stay-in-place deck panel forms
- No cast-in-place concrete but simply connecting together, totally precast concrete members (normally referred to as adjacent precast multi-beam decks)

Embedments and blockouts required for decks vary for each type of construction.

Placing cast-in-place concrete over bulb-tees or I-beams requires supplementary formwork, which is normally hung from the beams. This can be done economically with a series of holes and bolts, through either the beam flange or web, as shown in **Figure 3.2.4.3-1**. Form attachment can also be accomplished with proprietary systems, such as that shown in **Figure 3.2.4.3-2**. Other methods can also be employed to attach the formwork.

FABRICATION AND CONSTRUCTION

3.2.4.3 Embedments and Blockouts for Deck Construction

Figure 3.2.4.3-1
Typical Cast-In-Place Deck Forming Methods

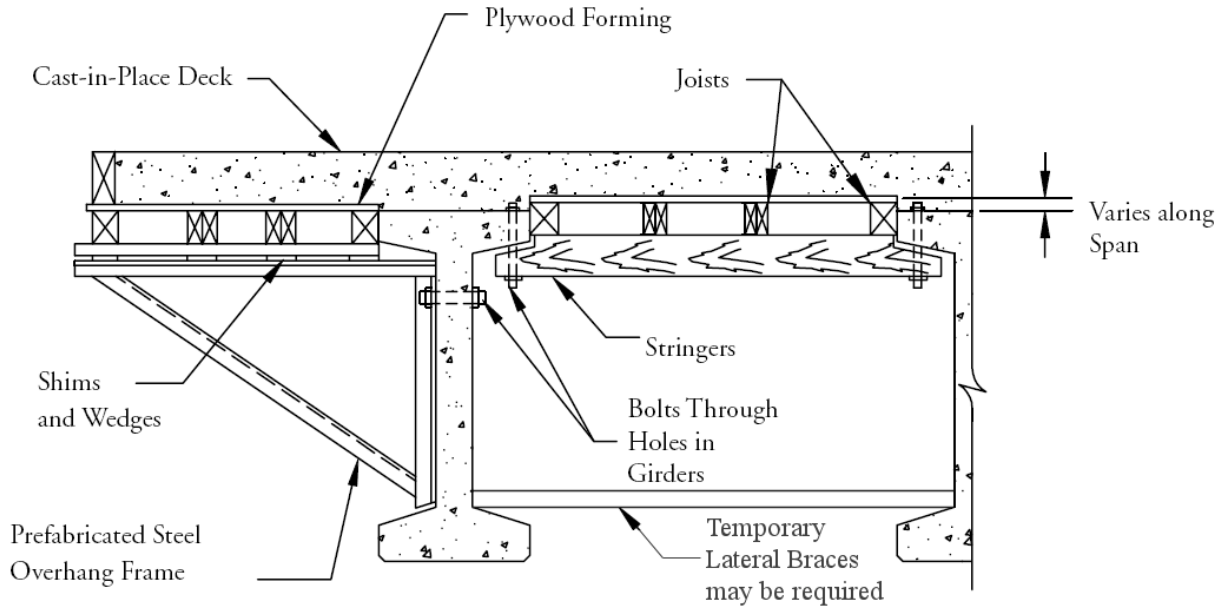
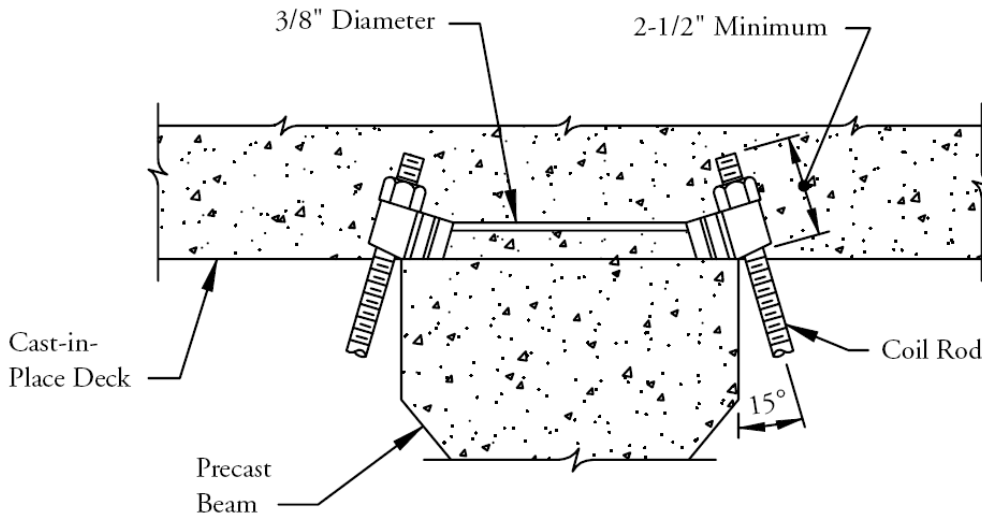
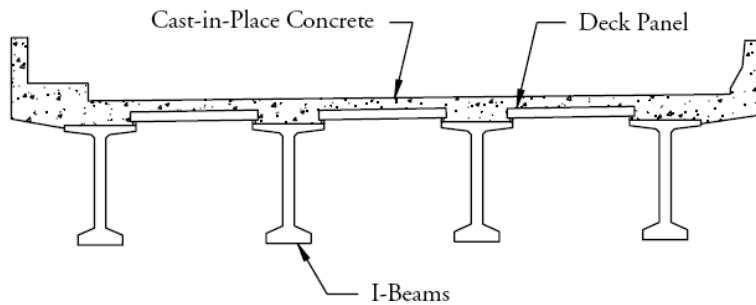


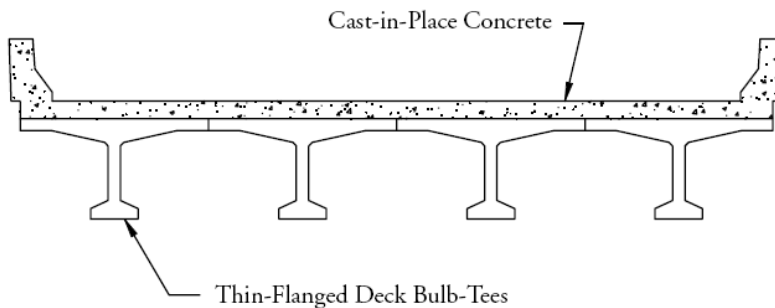
Figure 3.2.4.3-2
Proprietary Cast-In-Place Deck Forming Method



Composite concrete stay-in-place deck forms fall into two general categories. The first is thin prestressed concrete deck panels designed to span between spread box beams or the flanges of bulb-tees, I-beams or steel beams. The second is thin, wide flanges cast integrally with bulb-tees in the plant. The bulb-tees (or similar wide-flanged products) are abutted in the field. These are shown in **Figure 3.2.4.3-3a-3b**. Neither system requires embedments or blockouts in the beams, except for forming the edge overhang slab in deck panel systems. Typical embedments in deck panels are discussed in **Section 3.8**. Thin-flange deck bulb-tees require no embedments or blockouts for deck construction, except perhaps inserts for attachment of the formwork at the edge of the cast-in-place deck.

FABRICATION AND CONSTRUCTION**3.2.4.3 Embedments and Blockouts for Deck Construction/3.2.4.4 Lifting Devices****Figure 3.2.4.3-3a-3b****Composite Bridge Deck Systems**

a) Precast Concrete Composite Deck Panels



b) Thin-Flange Deck Bulb-Tee Deck System

Methods to connect multi-beam decks vary depending on the type of members being joined. Connections are normally welded or post-tensioned. **Section 3.6.3** discusses typical details and considerations.

3.2.4.4 Lifting Devices

Lifting devices embedded in precast concrete bridge members normally consist of strand lift loops, bolts or proprietary metal inserts. For very heavy lifts, prestressing bars have also been used. The type of lifting device employed depends upon several considerations:

- Configuration of the member
- Load on each device
- Angle of the lifting line
- Distance between the embedment and the edge of the concrete
- Preference of the precast plant

The strength of the embedded lifting device is governed by the weakest link in its load path. This can be the strength of the device itself, the bond between the device and the concrete, or for shallow embedments, the strength of the shear cone that can be pulled from the concrete. Most precast plants and vendors of proprietary lifting devices have extensive experience in the design and use of lifting devices.

Bent reinforcing bars should not be used as lifting devices. Bending a bar decreases the ductility of the material in the region of the bend. Highly concentrated loads from a shackle or crane hook have been known to fracture bent bars in a brittle manner. In addition, bent reinforcing bars do not have the flexibility of strand lift loops. When picking with angled cables, which is very common in both plant handling and field erection, flexibility is critical in distributing the load uniformly to all strands and both legs of the loop.

3.2.4.4.1 Strand Lift Loops

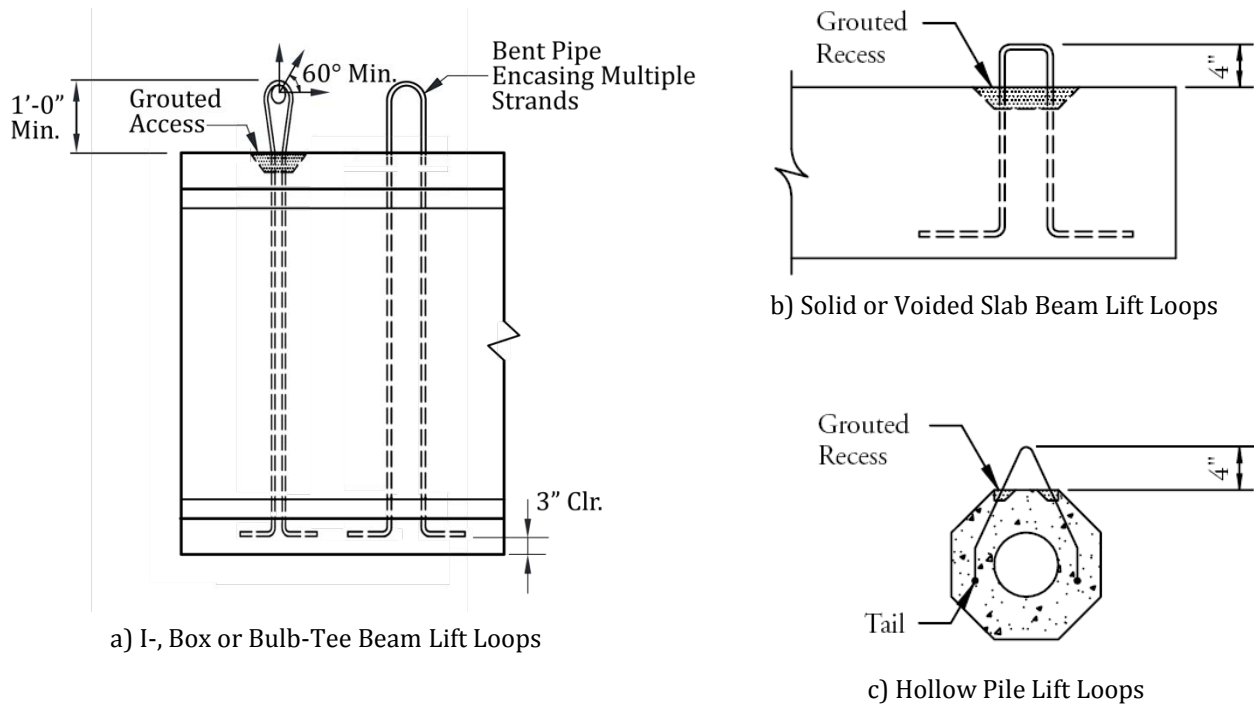
Prestressing strand lift loops are widely used due to their high strength and flexibility. Loops can be bent into nearly any configuration suited to the intended application. They are also economical since in many cases they are made from what would otherwise be “waste” strand, such as the tail end of a strand pack, or tails cut from a production run. Strand that has been damaged by gripping jaws or pitted with rust should not be used for lift loops.

The capacity of strand lift loops is governed by the following:

- Size and grade of the strand
- Configuration of the loop
- Length of embedment into the concrete
- Diameter of the pin used through the loops during lifting

Typical lift loop configurations are shown in **Figure 3.2.4.4.1-1**. The capacity of lift loops embedded with angled legs, as shown in **Figure 3.2.4.4.1-1c**, are reduced due to the increased resultant force in each leg. Loops lifted with angled cables are similarly reduced, particularly when their projection from the concrete is insufficient to allow the loops to flex to the same angle as the cable. Strand embedment must be of sufficient length to avoid bond failure. Tails can be added to the ends of the loops to increase embedment, such as shown in **Figures 3.2.4.4.1-1b and 3.2.4.4.1-1c**. The surrounding concrete should be adequately reinforced to prevent splitting and loss of bond. Small diameter shackle pins or hooks, when used through strand lift loops, can significantly decrease the capacity of the loop. Schedule 40 or 80 bent pipe has been used to load a bundle of strands.

*Figure 3.2.4.4.1-1a-1c
Typical Lift Loop Configurations*



FABRICATION AND CONSTRUCTION**3.2.4.4.2 Other Lifting Embedments/3.2.5.1.1 Ends Cast into Concrete****3.2.4.4.2 Other Lifting Embedments**

Bolts used for lifting perform much the same as headed studs. Embedment must be sufficient to prevent concrete shear cone failure, and edge distance must be considered when it encroaches on the shear cone.

A wide range of common proprietary lifting devices also are available. For bridge applications, these are normally limited to precast products that are relatively thin and light such as precast wing walls, barriers and soundwalls. When the lift location is exposed in the structure, the selection of the device can be influenced by the assurance that the “patch” over the device will be durable considering the demands of bridge applications.

3.2.4.5 Blockouts for Shipping

Precast members are normally secured to the truck, railcar or barge with chains or straps (tie-downs), which are draped over the top of the member and tightened. Wide, thin top flanges can sustain damage if the tension in the chain or strap is applied to the tip of the flange. Some producers provide blockouts in the flange adjacent to a web for tie-downs to pass through. **Section 3.5.3.5** discusses these blockouts in further detail.

3.2.5 Surface Treatments

Since most bridge products are cast in precision-made steel forms, it makes sense to design and fabricate the form so that the precast member requires minimum additional surface treatment. In most cases, this finishing needs to be performed by hand, so the most obvious savings are economic. Finishing operations such as removing lips or fins at form joints, patching voids due to paste bleed at form joints, and sacking bugholes, add time to the production cycle and increase the production cost of the product. Leaving small air holes untreated has become common practice for piling and elements where surface finish does not detract from the product.

Theoretically it is possible, using rigid steel forms and compaction of the concrete by vibration, to produce members that are uniform in appearance and with a “glass-like” form finish. This finish will not only be aesthetically pleasing, but it will produce a surface with optimum durability. A densely compacted cement-paste surface finish produced against steel forms results in a surface with minimum porosity and permeability, and maximum long-term durability. Any additional surface treatments or patching are unlikely to improve, or even match, the durability of densely compacted concrete. In reality, however, some areas on pretensioned products will require surface treatment in spite of the best possible form design.

This section does not cover patching of major “honeycomb” areas or large voids. It also does not cover the repair of structural cracks or large spalls caused by form removal. These subjects are discussed in **Section 3.4.2**.

3.2.5.1 Protecting Product Ends

The parts of a prestressed product that typically require surface treatment are the ends where the prestressing strands exit and have been trimmed off after transfer. Usually for production expediency, and because of the physical constraints of the bulkheads, the projecting strands are initially cut off during stripping about 6 in. from the concrete surface. During the finishing stage, depending on the exposure of the product ends in the finished structure, the strand ends are treated in one of two ways as described in **3.2.5.1.1** or **3.2.5.1.2**.

3.2.5.1.1 Ends Cast into Concrete

If the ends of the member are incorporated into the pier or abutment with cast-in-place concrete, the treatment of the strand ends is not critical. The producer only needs to protect them from corrosion during storage. In this case, after the strands are cut off flush, it is satisfactory to simply paint them with a two-component epoxy. A thin coat, approximately $\frac{1}{8}$ in. thick, will suffice and only in a 2 in. square area over each strand. In applying the epoxy, it is important that the strand and surrounding concrete be relatively clean. Often, if the strands are burned off with a poorly adjusted oxy-acetylene torch, the surrounding area is blackened with acetylene soot and melted slag, which should be removed prior to epoxy application. It is for this reason that many producers prefer to grind off the projecting strand with a hand-held high speed disc grinder. This method leaves a clean area for the epoxy coating.

FABRICATION AND CONSTRUCTION**3.2.5.1.2 Exposed Ends/3.2.5.1.5 Patching Ends with Proprietary Products****3.2.5.1.2 Exposed Ends**

Strand ends that are to be exposed for the service life of the structure are normally recessed and patched. Various methods are used. A common procedure is to provide a recess with a proprietary expanded foam cube placed around each strand, directly against the inside of the bulkhead. This recess-forming device, sometimes called a "doughnut," is approximately 1½ in. square and ¾ in. thick, with a hole through the center to accommodate the strand. The doughnut is split on one edge and can be placed over the strand at any location before or after tensioning. During the finishing process, the expanded foam and projecting strand are burned out using an oxy-acetylene torch. The recess is first cleaned-out to remove any remains of the expanded foam and strand slag, then patched flush with the concrete surface.

For maximum durability, the material used to patch the recess should be appropriate. A poorly selected material applied in the recess will soon shrink, deteriorate, or even fall out. This will leave the strands exposed to the environment, promoting corrosion by the capillary action of liquid through the interstices of the seven-wire strand.

3.2.5.1.3 Epoxy Mortar End Patches

Epoxy mortar is often used to patch strand recesses, since it is widely assumed to be less permeable and more durable than portland cement mortar. This is generally true, assuming the epoxy has been appropriately selected and mixed, and the correct epoxy binder-to-sand ratio has been used. However, field experience has shown that the use of incorrect procedures to prepare epoxy mortars, particularly in selection of the sand type, gradation, and mixing procedures, can result in a porous patch that provides inadequate protection of the strand end.

Epoxy mortar sands should be angular in shape, since sands with rounded particles tend to roll under the trowel, making placement difficult. The sand should also be dry. Two good sand gradations are blends by volume of two parts 12 mesh to one part 80 mesh, or three parts 16 mesh to one part 90 mesh. When graded sands are not available, 30-mesh silica sand works reasonably well. Most epoxy resin suppliers can furnish these sands.

Another disadvantage of epoxy mortar patches is that pure epoxies generally have a higher coefficient of thermal expansion than concrete. Larger patches, particularly those using pure epoxy, can fail due to differential expansion and contraction of the patch and the parent concrete. More than cost reduction, this is the primary reason that a silica sand "extender" is used in epoxy mortar. The incorporation of sand reduces the coefficient of thermal expansion of the epoxy mortar mixture.

3.2.5.1.4 Portland Cement Mortar End Patches

Considering the high demand for quality control and the cost of epoxy mortars, some producers patch the strand recesses with portland cement mortar. This mortar is considerably less expensive, and also has a coefficient of thermal expansion similar to that of the parent concrete. It is easier to work with, and can be matched to the member finish. A patch made with gray portland cement and sand will generally be darker than the surrounding concrete. This outcome can be mitigated by using 25 to 40% white portland cement in the patch mix. The usual cement-to-sand ratio is 1:2, and an epoxy bonding compound is applied to the recess before the mortar is troweled in. The "dry-pack" method of placement is also common. Properly executed, these portland cement patches perform as well or better than epoxy mortar patches, and are more economical.

3.2.5.1.5 Patching Ends with Proprietary Products

Proprietary patching compounds can also be used to fill recesses. In general, these are about the same cost as epoxy mortar. The majority of these materials are Portland cement based and contain combinations of accelerators, bonding agents, fillers, and workability, curing, and shrinkage-compensating aids. The performance of such material should be carefully evaluated by the producer. In some cases, long-term durability could be sacrificed in favor of ease of initial application. Other proprietary patching compounds are available that are not portland cement based. Examples are: polyester resin-based materials, high alumina cement-based material, and magnesium phosphate cement-based materials. These materials are often promoted as providing a solution to

FABRICATION AND CONSTRUCTION**3.2.5.1.5 Patching Ends with Proprietary Products/3.2.5.4 Architectural Finishes**

patching in temperatures below 40 °F, where portland cement and epoxy-based mortars are not recommended. However, in practice this is rarely necessary because in cold weather climates, precast members are usually cured with heat. With careful timing, the producer can take advantage of the elevated temperature of the member immediately after stripping to perform the patch and cure the patching material. Use of these proprietary non-portland cement-based patching materials should be carefully evaluated on a case-by-case basis by an accredited concrete laboratory.

3.2.5.2 Intentionally Roughened Surfaces

Another bridge product surface that often requires non-cosmetic treatment is one which is intentionally roughened to promote mechanical bond of cast-in-place concrete to the member. This is usually specified when the member is to be made composite with cast-in-place concrete. Most I-beams and bulb-tees are designed to act compositely with a cast-in-place concrete deck. **Section 3.3.9** covers the preparation of these surfaces in detail.

3.2.5.3 Cosmetic Surface Treatments

Surface finishes resulting from good daily production practices will not be entirely “glass-like.” Some of the most common imperfections are:

- Small surface “bugholes” formed by entrapped water and air bubbles at the form surface, particularly on vertical surfaces
- Dark lines and areas denoting high cement paste concentrations
- “Pour-lines” due to the overlapping of individual concrete placements
- Granular surface areas where the paste has bled out of form joints
- Imperfections and offsets at form joints

There are as many theories about the cause of these aesthetic surface blemishes as there are suggested methods to avoid them. The best methods of placement and compaction do not consistently eliminate their occurrence. For this reason, many producers “rub” or “sack” the surface of the member immediately after it is stripped. This involves wetting the member with water, hand-applying a 1:1 fine sand and Portland cement mortar to the surface using a sponge-faced trowel to fill any bugholes, then curing the application. Often, this surface is then rubbed with a burlap sack and cement powder. This procedure, which is more art than science, benefits greatly from the care, knowledge and diligence of an experienced concrete finisher. In general, unless the bridge is in a high visibility zone, this additional finishing needs only to be done on the exterior surface of the fascia beams. For high visibility zones where a uniform appearance is required, pigmented sealers can be applied.

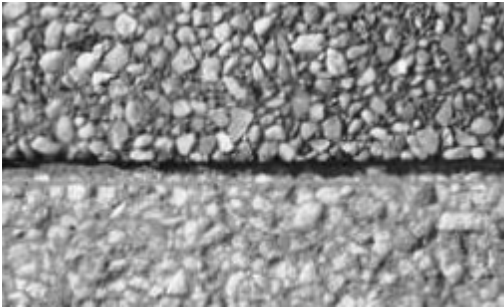
3.2.5.4 Architectural Finishes

A wide variety of architectural concrete finishes, normally used for building cladding applications, could be used in the production of precast concrete bridge members. These include colored concrete using integral dyes, the use of white cement, exposed aggregate finishes, ribs or other textured surfaces, and the application of stains. Practically, however, except for the application of stains, these treatments are rarely employed for large structural members, such as I-beams or bulb-tees. The need to optimize the concrete’s early strength gain normally precludes the use of white cement, which is usually ground to AASHTO M85 Type I specifications. The other processes may also prove difficult to control under large-scale production runs typical of large bridge members. The same is not true of other types of bridge products, such as median barriers or soundwalls, where architectural treatments are standard practice. **Figures 3.2.5.4-1** and **2** show some typical architectural finishes. Local producers should be consulted for economically available architectural treatments.

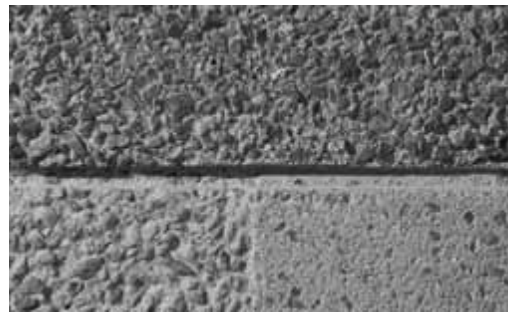
FABRICATION AND CONSTRUCTION

3.2.5.4 Architectural Finishes/3.2.5.5 Durability –Related Treatments

*Figure 3.2.5.4-1a-1b
Architectural Finishes with Exposed Aggregate*

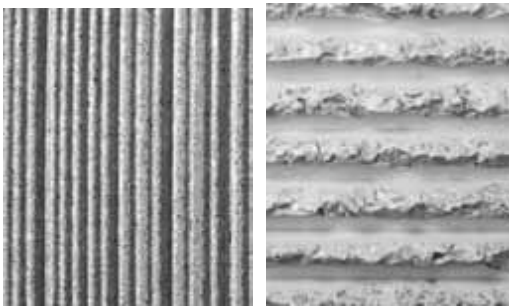


*a) Top: Surface Retarded & Exposed
Bottom: Medium Sandblast*

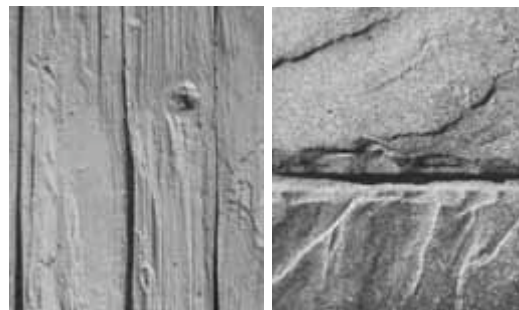


*b) Top: Surface Retarded & Exposed
Bottom Left: Deep Sandblast
Bottom Right: Light Sandblast*

*Figure 3.2.5.4-2a-2b
Architectural Finishes Made with Formliners*



*a) Left: Striated
Right: Hammered Rib*



*b) Left: Cedar Stake
Right: Ashlar Stone*

3.2.5.5 Durability-Related Treatments

Some specifications require a final surface treatment be applied to precast concrete bridge members as added assurance of long-term durability. The most common treatment employed is the application of a penetrating sealer, such as a silane or siloxane coating. Various studies conclude that, assuming the material is properly selected and applied, these materials enhance the long-term durability of concrete, as summarized by D’Arcy, et al (1996). From a producer’s perspective, one of the difficulties associated with the application of silanes is that the members must be kept dry for a minimum period before application. In rainy climates, this requires the members to be stored and the work performed under cover. Considering the size and number of the products involved, most precast plants do not have facilities appropriate for this operation. The most economical application of these sealers is usually accomplished in the field, since delivery schedules are no longer an issue, and the application can wait for good weather, or can be done under the cover of the completed bridge deck. Epoxy coatings have also been specified to provide surface protection, long-term durability, and wear resistance. Most surface treatments have limited life and need periodic renewal to achieve continued protection.

3.2.5.6 Protection of Exposed Steel

Another issue that should not be overlooked is protection of projecting reinforcing bars, strand and metal hardware embedded in the member. If the products are expected to be stored for a significant length of time, projecting reinforcing bars and strand are normally coated with zinc-rich paint for protection against corrosion

FABRICATION AND CONSTRUCTION**3.2.5.5 Durability –Related Treatments/3.3.1 Forms and Headers**

prior to incorporation into the structure. If this is not done, the projecting steel quickly develops a surface coating of rust. Although this is usually not detrimental over short storage periods, and can be cleaned off immediately before delivery, wet weather will cause this rust to run down the faces of the member, causing unsightly stains that are difficult to remove and may create a future inspection concern.

The most common protection for metal embedments is hot-dip galvanizing before they are cast into the concrete (AASHTO M111). This results in the optimum long-term protection of the embedments. When welding galvanized embedments, it is important to first remove the zinc coating from the area of the weld. Toxic fumes are produced from welding on galvanizing, and the zinc may contaminate the weld metal, which can result in a structurally deficient weld. After the welding has been performed, the damaged coating should be restored, either by “soldering” over the area with zinc rod, or by painting the area with a zinc-rich paint.

For this reason, zinc-rich paints are sometimes specified in lieu of galvanizing. The embedments are given an initial coat of paint before being cast into the concrete, and are given subsequent coats after the welding has been completed. Epoxy-based and other volatile solvent zinc-rich paints were once popular for this application. However, with increasing hazardous waste disposal regulations, the recent tendency has been towards water-based zinc-rich paints.

3.3 FABRICATION

Precast, prestressed concrete bridge products are fabricated under strictly controlled plant manufacturing conditions to assure the highest level of quality possible in concrete construction. Industry standards demand uniform quality of finished products nation-wide. This section will discuss standard methods of concrete forming, batching, placing and curing, as well as tensioning of the prestressing steel and placement of nonprestressed reinforcement. Fabrication methods and production capabilities differ from plant to plant, with varying consequences for the design of precast concrete bridge members. Bridge designers should consult with local producers for specific information on plant capabilities.

3.3.1 Forms and Headers

Forms used in the precast, prestressed concrete industry are unique to the standard product they are intended to produce, though most forms have three common characteristics. First, forms are fabricated with a constant cross section. Second, they are long and slender, with overall lengths ranging from 20 ft to more than 600 ft. Finally, they must be capable of producing the same concrete shape repeatedly to very accurate dimensional tolerances. For example, the PCI manual, MNL-116, allows a casting tolerance for the width of an I-beam web of only $+\frac{3}{8}$ in., $-\frac{1}{4}$ in. Therefore, most bridge product forms use steel construction. **Figure 3.3.1-1** shows typical forms used in the industry.

Figure 3.3.1-1a-1b
Common Precasting Forms



a) AASHTO I-Beam



b) Stemmed Channel Section

FABRICATION AND CONSTRUCTION

3.3.1 Forms and Headers/3.3.1.1.1 Applications of Self-Stressing Forms

*Figure 3.3.1-1c-1d
Common Precasting Forms*



c) AASHTO-PCI Bulb-Tee



d) Beam/Pile

3.3.1.1 Self-Stressing Forms

A self-stressing form is used not only to produce the concrete product, but also to resist the initial prestressing force. The form’s longitudinal stiffeners and skin are used as the compression member against which the prestressing strands are jacked. This method is often cost-effective, since it eliminates the need for a traditional prestressing bed (see Sect. 3.3.2.1). Figure 3.3.1.1-1 shows a typical self-stressing form and its associated stressing hardware.

*Figure 3.3.1.1-1
Self-Stressing Form for a Stemmed Section*



Members of different cross sections can be cast in the same self-stressing form, as long as the form is designed for the largest and most highly pretensioned section. For example, it is quite common to cast 24-in.-deep stemmed members in a 36-in.-deep self-stressing form by using 12-in.-tall “false bottoms” in the stems. Likewise, 8-ft-wide stemmed members can be cast in a 10-ft-wide self-stressing form by using “false sides.” The prestressing force is still distributed over the original form configuration. This can also be done with other member types.

3.3.1.1.1 Applications of Self-Stressing Forms

Self-stressing forms have become a popular solution for precast members where the location of the prestressing force is not excessively high or eccentric. For bridges, they are used for stemmed members, prismatic or trapezoidal beams, box beams and voided slab beams. There are two basic considerations that limit the use of self-stressing forms. First, the eccentricity of the prestressing force must be small enough to allow the load to be

FABRICATION AND CONSTRUCTION**3.3.1.1.1 Applications of Self-Stressing Forms/3.3.1.3 Adjustable Forms**

distributed to the form in a reasonably uniform manner. Second, this type of form requires the strands to be jacked against the entire cross-section of the form, including the sides, which must be in place during stressing. Set-up crews must be able to assemble the reinforcement cage and install embedments from the top only. If the form is deeper than the length of a person's arm, it is difficult to place material in the bottom of the form.

Self-stressing forms can also be designed to accommodate harped or draped strands. The vertical reaction from deflected strands can be transferred through the form into the foundation. For this reason, among others, it is usually necessary to mount the form on a reinforced concrete slab. These slabs run full length, and are slightly wider than the form. The self-stressing form is attached to this slab to maintain alignment, to provide intermediate bracing for the compressive force, and to provide anchorage to prevent the form from being lifted off the ground during stripping.

If a product cast in a self-stressing form is to be heat cured, it is essential to recognize that the form will expand as the concrete temperature is elevated. For a 600-ft-long form, it is not uncommon for the form to expand up to 6 in. during the curing cycle. Also, the form will shorten due to the prestressing force imparted during jacking. For these reasons, the form attachment to the slab must not restrain the form in the longitudinal direction. The usual approach is to weld or bolt a 20 to 40 ft section of the form to the slab, either at one end or in the center, and design all the other connections to allow longitudinal movement.

3.3.1.2 Non-Self-Stressing Forms

Tall, slender bridge members such as I-beams, bulb-tees, deck bulb-tees and large stemmed members are usually cast in forms that are not self-stressing. The primary reason for this is that the prestressing strands, nonprestressed reinforcement, and embedments are, by necessity due to accessibility, placed in the form with the sides removed. Also, these types of members usually have a relatively high location (eccentricity) of prestress. Since the bulk of the prestressing force would need to be distributed to in-place form sides, self-stressing forms are not appropriate for these applications.

However, with the use of only straight strands and control of concrete stresses through strand debonding, a few self-stressing forms have been used. This requires relatively large reaction beams along the edges of the form.

Most often, the prestressing force and deflected strand vertical reactions are resisted by an independent prestressing bed. These beds are discussed in detail in **Section 3.3.2.1**.

3.3.1.2.1 Design of Non-Self-Stressing Forms

The design and fabrication of side forms for casting prestressed concrete bridge members are not governed solely by the equivalent fluid pressures induced during concrete placement, but also by the need to minimize temporary and permanent deformations, and to account for the effects of external form vibration, repeated heating and cooling cycles, and repeated use.

In practice, this requires the forms to be fabricated from steel. When using ¼-in.-thick form skins, continuous vertical and horizontal stiffeners are usually required at no more than 2 ft 6 in. on center in each direction. Some manufacturers fabricate forms with 3/16-in.-thick steel skin and the same stiffener spacing. During repeated use, this steel tends to "oil-can" between bulkheads, or suffer premature damage due to fatigue induced by external form vibration. Vertical stiffeners are usually fabricated from ¼-in.-thick plate with folded flanges. Horizontal stiffeners can be standard steel shapes, or can be fabricated by the form manufacturer. Each form supplier has a preference and usually provides the form design to accommodate the specified casting procedure.

3.3.1.3 Adjustable Forms

Innovative form design not only facilitates rapid daily assembly and disassembly, but also provides long form life. Most producers purchase forms that are easily modified to accommodate various member sizes with similar cross sections. For example, I-beam and bulb-tee forms are commonly designed with a standard shape for top and

FABRICATION AND CONSTRUCTION

3.3.1.3 Adjustable Forms

bottom flanges, and a variable web height. This allows the same flange forms to be used for shallow and deep members with varying span lengths. The forms are split horizontally, usually near mid-height, and bolt-in “fillers” are used to vary the beam depth. **Figure 3.3.1.3-1** illustrates a typical adjustable form. Beam flange and web widths can also vary by adjusting the width between form sides. However, since the shape of the form sides is normally fixed, other horizontal beam dimensions are affected incrementally. Some manufacturers have forms that can accommodate wider top flanges. Producers should be consulted for dimensions of forms that vary from the local standard.

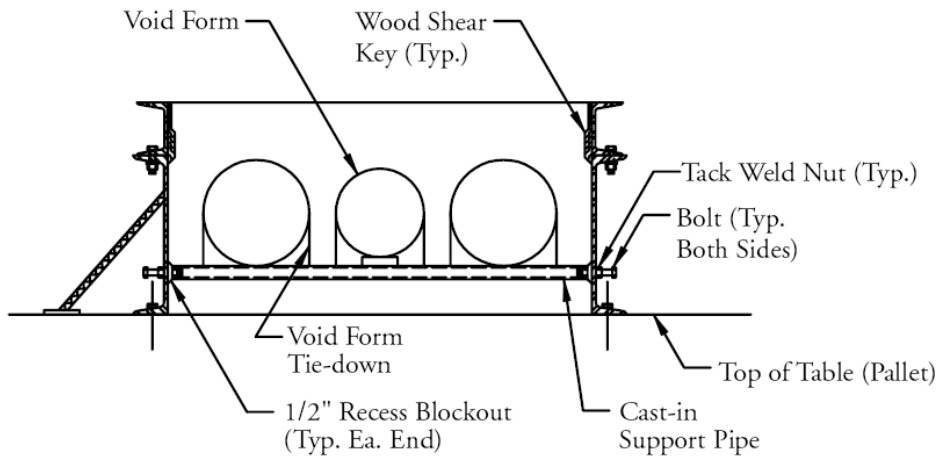
I-beam and bulb-tee bottom flanges are formed in two ways. Some producers use flat steel pallets, with the sides and top of the bottom flange form being part of the side form. This allows for easy adjustment of width. Other producers use “pans” that form the bottom and sides of the bottom flange. The top of the bottom flange form is part of the side form. In this case, varying beam widths require different pan widths. Minor variations to the form shape should be acceptable to the specifier in order to maximize competition.

Figure 3.3.1.3-1
Bulb-Tee Form Used to Fabricate a Florida DOT Section. Horizontal Joint is where the Form can be Separated for Installation of Fillers to Increase the Depth of the Section

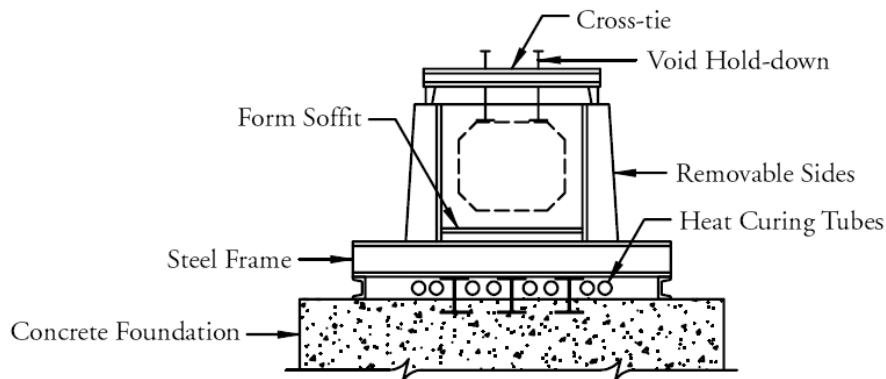


Voided slab beams and box beams are normally cast on horizontal steel pallets with removable side forms. Pallets are usually sized to accommodate the widest member normally specified. Narrower members can be cast with relative ease. Concrete slabs can be used in lieu of steel pallets, although the uniformity of heat for curing the bottom flange of the member becomes less reliable and some state specifications preclude the use of casting in a concrete form. **Figure 3.3.1.3-2** illustrates typical prismatic form configurations. The depth is not as easily varied because most producers do not have a variety of side forms on hand. Bridge designers should consult with local producers for available form depths. Small increases in depth using standard side forms are accommodated by “adding” to the side form, most commonly with steel angles. Decreases in depth can be achieved by manually screeding the concrete down below the top of the form. Special “drop” screeds are used for this purpose. Members with mild reinforcement projecting from the top complicate the use of drop screeds.

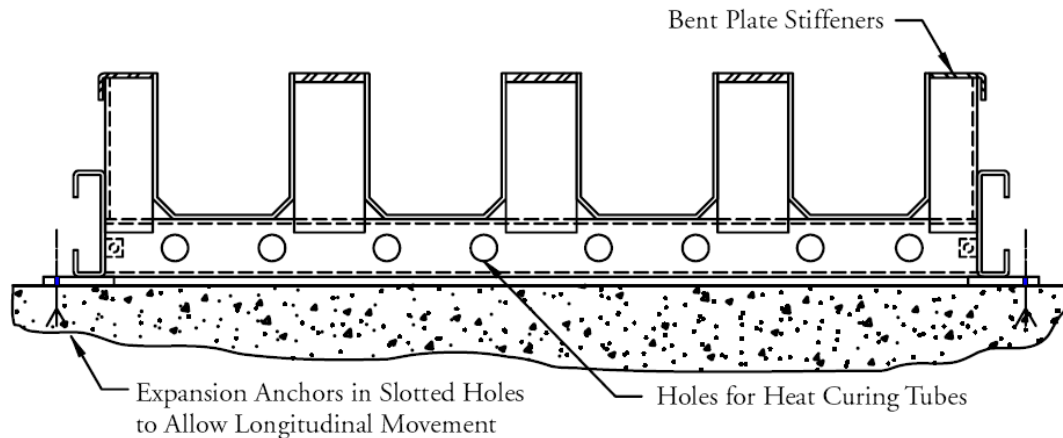
Figure 3.3.1.3-2a-2c
Various Form Configurations



a) Voided Slab Formed on a Steel Pallet



b) Box Beam Form on a Concrete Bed



c) Square Piling Quad Form on a Concrete Bed

FABRICATION AND CONSTRUCTION**3.3.1.4 Advantages of Precast Concrete Formwork/3.3.1.6 Headers****3.3.1.4 Advantages of Precast Concrete Formwork**

A unique and attractive feature of plant-cast bridge members, in contrast to typical jobsite construction, is the elimination of “through-bolts,” “she-bolts,” or “snap-ties.” Such devices are laborious to place, inhibit placement of reinforcement and embedments, and require patching of the resulting recesses. Most forms used in the precast industry are held together only at the top and bottom, resulting in increased productivity, and patch-free vertical surfaces. Also, precast formwork joints are designed to minimize paste bleed during concrete placement.

3.3.1.5 Other Form Considerations

Side forms for deep, thin bridge members tend to be heavy and usually require stripping by crane or some other mechanical device. Since side forms are relatively slender, cranes usually cannot remove them in one piece for the full length of a long member. Side forms are normally bolted together in 20 or 40 ft sections. To reduce the equipment and labor required to strip the forms, some producers install “rollaway” form sides. This system uses side forms mounted on trolleys and transverse rails that allow them to be rolled away laterally from the member during stripping. Long side forms can then stay in one piece for subsequent production. A disadvantage of this system is that the sides need to be retracted far enough to allow the work crews access for production. Many plants do not have sufficient space for this system, particularly those with parallel prestressing beds. Some plants are equipped with rolling trollies to facilitate both form roll back and longitudinal movement to the next form when the casting beds are oriented end to end.

Side forms that are mounted vertical, or that form shear keys in the sides of members, must be removed daily to strip the product. This increases both labor costs and wear and tear on the forms. Where possible, the sides of products should have a minimum draft of $\frac{1}{8}$ in./ft ($\frac{1}{4}$ in./ft is preferable) so that the side forms may stay in place during stripping. Concrete members formed in rigid, single-piece forms, always require adequate draft on surfaces that could otherwise meet at right angles.

3.3.1.6 Headers

The terms “header,” “endplate,” “bucket” and “bulkhead” are used interchangeably in the precast concrete industry to describe devices used to form the ends of precast members. In this manual, the word “endplate” is used to describe a device that forms the end of a single member, or the last member in a series of members cast end-to-end in a prestressing bed. The word “bulkhead” is used to describe a device that forms the adjacent ends of two members cast in series. “Header” can refer to either an endplate or bulkhead. **Figure 3.3.1.6-1** illustrates typical endplates and bulkheads. They can also be seen in **Figure 3.3.1-1c**.

Figure 3.3.1.6-1a-1b
Forms for Ends of Sections



a) I-Beam End Plate



b) Stem Bulkheads or Buckets for a Triple-Stemmed Section

FABRICATION AND CONSTRUCTION**3.3.1.6.1 Header Configuration/3.3.1.7.1 Mandrel System****3.3.1.6.1 Header Configuration**

A requirement common to both endplates and bulkheads is the penetration by the prestressing strands. The hole that each individual strand passes through not only controls the strand location, but also may be subject to forces from intentional or unintentional deflection of the strand. Some headers are designed with slots at edges to accommodate placement after some or all of the strands have been tensioned. Holes should be oversized a minimum of $1/16$ in. and the edges should be rounded. Sharp edges can damage a strand during tensioning, with potentially catastrophic results. Both endplates and bulkheads must be restrained longitudinally to resist movement during concrete placement, as well as being dragged by elongation of the strands during tensioning. Most producers are reluctant to drill side forms for attaching endplates, due to damage to the forms caused by the penetrations. Various alternate methods are used to secure the endplates, such as cable clamps to fix the bulkheads on the strands already tensioned.

Forms designed to cast several members in series can present problems with the extended projection of strands or reinforcing bars. Header configurations that can present problems are normally limited to shallow members, such as stemmed members or slab beams. These standard bulkheads are just wide enough to allow cutting of the strands between members, and cannot accommodate longer projections. Extended projections can also create problems during stripping of the members. In some cases, it is more economical to use threaded reinforcing bar couplers to provide extended projections.

3.3.1.7 Internal Void Forms

Members such as voided slab beams, hollow box beams and hollow piling require internal voids. Forming can be achieved in one of three ways:

- A retractable “mandrel” system
- A collapsible form, which is retracted after the concrete has hardened
- Casting around sacrificial forming material

All internal forms must be accurately located and held in place during concrete placement. In monolithic pours, the inner forms will have a tendency to float. The force required to hold the inner form in place can be calculated assuming the concrete to be completely liquefied. Hold-down systems usually consist of vertical compression struts that react against crossbeams that span the top of the form. These vertical struts are normally tapered, coated with a debonding agent, and withdrawn after the concrete has hardened. In designing such systems, the inner form must be analyzed to determine the spacing of the restraining struts, both for the span of the form material between struts, and for the local stresses imposed by the struts. When expanded polystyrene blocks are used, appropriately sized pads are placed on top of the block under each strut to prevent localized compression failure of the block.

Flotation forces during concrete placement can be controlled to some extent by casting procedures and timing. If the concrete initially placed directly under the void form is allowed to approach initial set prior to further concrete placement around the vertical form sides, the flotation forces are substantially reduced. In the fabrication of box beams, some producers place the bottom slab as a first stage. After the concrete hardens—normally the next day—the void form is placed, an epoxy bond coat is applied to the cold joint, and the webs and top flange are placed. For void forms with vertical sides, this results in very little uplift.

3.3.1.7.1 Mandrel Systems

A system of forming internal voids employs a vibrating steel slip-form, normally referred to as a mandrel, which is pulled through the concrete during placement. The concrete used with this technique must be designed with a low slump, so that it does not collapse after the mandrel passes. Mandrels must have a constant cross-section throughout their length, and are not easily modified to produce shapes with varying dimensions. Together with the necessary winches and tooling required for their operation, mandrels represent a significant investment for the precast producer. Consequently, their use is normally limited to standard cross sections. **Figure 3.3.1.7.1-1**

FABRICATION AND CONSTRUCTION

3.3.1.7.1 Mandrel System/3.3.1.7.2 Retractable Inner Forms

shows a typical mandrel used for casting hollow prestressed concrete piles. The design of endplates and bulkheads is complicated by the need for the mandrel to pass. Solid sections or diaphragms within a precast member, if required, are usually added later with a secondary cast.

Figure 3.3.1.7.1-1

Cylindrical Slip-Form for “Mandrel” Hollow Piling



3.3.1.7.2 Retractable Inner Forms

Retractable inner void forms are stationary, and the concrete is cast around them to create the void. These forms must be designed to collapse for removal after the concrete has hardened. Articulating forms of this nature, as well as their retraction tooling, are expensive, and are normally reserved for standard shapes with large voids (such as box beams), or for large projects that can tolerate high initial tooling costs. **Figure 3.3.1.7.2-1a-1b** illustrates a typical retractable form.

Figure 3.3.1.7.2-1a-1b

Removable Void Form



a) Void Form Expanded for Casting



b) Void Form Retracted for Removal

FABRICATION AND CONSTRUCTION**3.3.1.7.3 Sacrificial Inner Forms/3.3.2.1.1 Abutment Beds****3.3.1.7.3 Sacrificial Inner Forms**

Sacrificial inner forms can be made from wax-coated cardboard tubes or boxes, prefabricated plywood boxes, or blocks of expanded polystyrene. The choice of material depends on the size and shape of the voids. For example, voids in a typical 4-ft-wide- by 2-ft-deep slab beam are usually formed with cardboard tubes plugged with plywood endplates. However, to create the inner void of a large box beam, the choice may be between blocks of expanded polystyrene cut to size with hot wires, or boxes constructed from plywood. Expanded polystyrene is the most common choice because it is relatively inexpensive and eliminates the risk of collapse that can occur with hollow void forms. All internal void forms need to be vented to the surface to avoid entrapped gas and moisture that could expand and damage the fresh concrete. **Figures 3.3.1.7.3-1a** and **1b** illustrate typical applications of sacrificial inner forms

Figure 3.3.1.7.3-1a-1b
Stay-In-Place Inner Forms



a) Waxed Cardboard Tube



b) Polystyrene Foam Billet

3.3.2 Prestressing

Careful control of the prestressing operation is critical to the quality of prestressed concrete products. The following sections describe common types of beds used for pretensioning, typical procedures, and controls employed to ensure that the proper level of prestress is delivered to the concrete. Pretensioning procedures apply only to strand, since prestressing bars are not used in pretensioned applications. An article by Preston (1990) describes the manufacture of strand and its corrosion characteristics; precautions during use and for handling; and special considerations during concrete curing and transfer of prestress.

3.3.2.1 Types of Pretensioning Beds

In addition to the self-stressing forms described in **Section 3.3.1.1**, two basic types of prestressing beds are commonly used in precasting plants. These are generally referred to as “abutment-type” beds, and “strutted” beds. In contrast to self-stressing forms, both types are independent of the formwork used to cast the member.

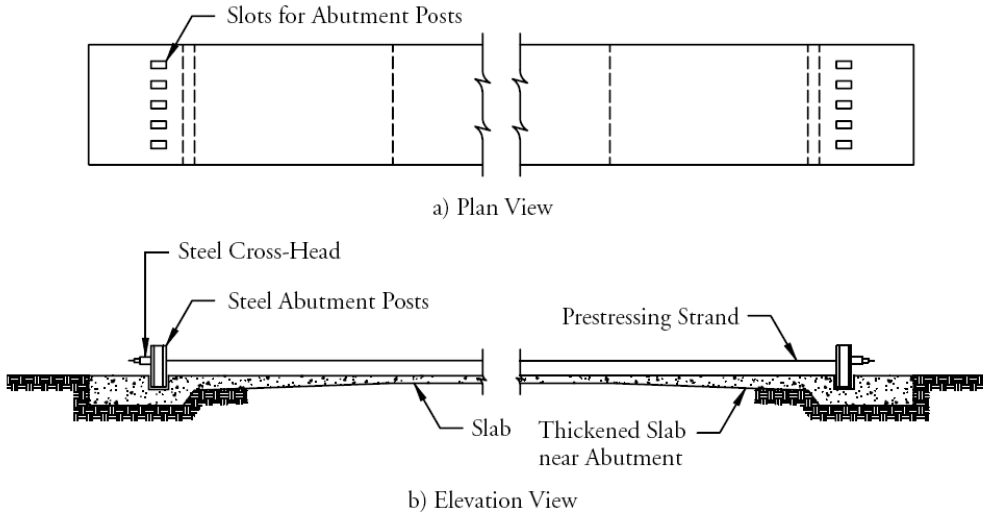
3.3.2.1.1 Abutment Beds

A bed employing abutments normally consists of a full length concrete slab, which is substantially thickened at each end to provide foundations for the support of vertical steel or concrete “uprights” (abutments). A typical profile is shown in **Figure 3.3.2.1.1-1**. The center portion of the slab is designed to carry the highest design axial force from the prestressing operation, as well as vertical forces created by deflected strands. The thickened ends are designed to transfer concentrated loads from the abutments into the body of the slab, and to resist overturning moments from the eccentricity of the prestress force. Global overturning is usually countered by the inertial resistance of the concrete foundation’s mass. Although abutment beds have the highest capacity among available types, all pretensioning beds are limited in the number of strands that can be accommodated, either due to the total prestressing force, or strand eccentricity from the bed’s center of resistance. Bridge designers should check with local producers for pretensioning capabilities.

FABRICATION AND CONSTRUCTION

3.3.2.1.1 Abutment Beds/3.3.2.1.2 Struttred Beds

Figure 3.3.2.1.1-1
Permanent Prestressing Bed with Fixed Abutments

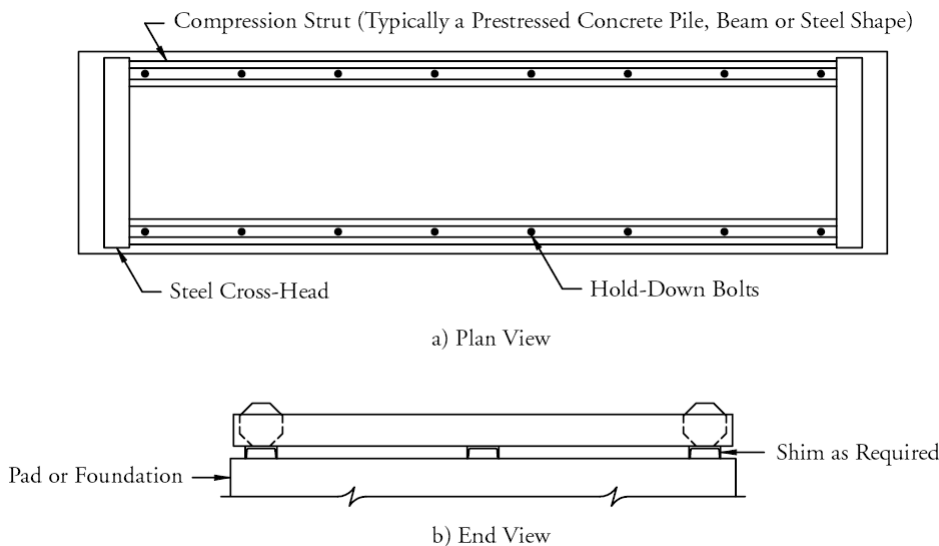


Steel abutments are usually inserted into “slots” or “trenches” cast into the foundation. Though slots limit the transverse adjustment capability of the abutments, they are more economically incorporated into the foundation design. Trenches provide a large degree of flexibility, but are more expensive to accommodate. The type chosen depends upon the anticipated use of the facility. When necessary, strands are distributed transversely by “cross-heads” spanning horizontally between uprights. “Distributions,” or templates, which are independent of the stressing hardware, are also employed to deflect strands vertically or horizontally from the configuration of the holes in the standard stressing hardware, to the configuration required for the precast member.

3.3.2.1.2 Struttred Beds

Struttred beds employ independent compression struts running from end-to-end. **Figure 3.3.2.1.2-1** schematically shows a struttred bed. The strands are stressed between cross-heads, which span from strut-to-strut. These set-ups are normally reserved for strand patterns in a few horizontal planes, such as with prestressed slab beams or wall panels.

Figure 3.3.2.1.2-1a-1b
“Struttred” Prestressing Bed



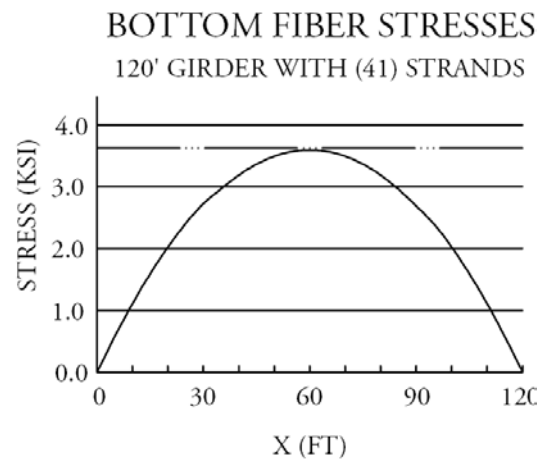
FABRICATION AND CONSTRUCTION

3.3.2.2 Strand Profile/3.3.2.2.1 Straight Strands

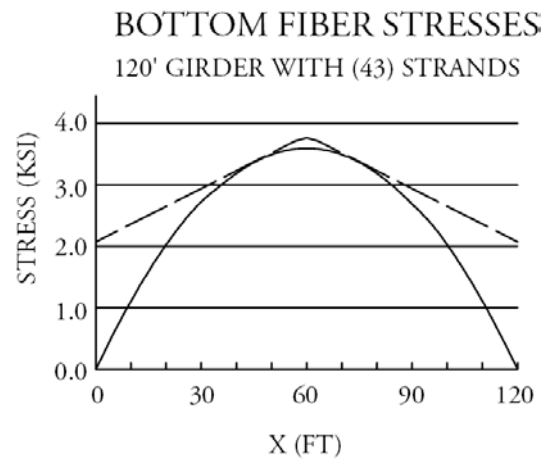
3.3.2.2 Strand Profile

Pretensioning strands can project straight through the length of a member, can be deflected in straight segments to a desired profile, or can be a combination of both. Straight strands are the simplest to install and tension, while deflected strands, normally referred to as “harped” or “draped” strands, more closely follow the moment envelope of flexural members. **Figure 3.3.2.2-1** illustrates how varying strand profiles correlate with typical moment envelopes. Post-tensioned strands can be straight, or can be draped in a curved profile to best fit the moment envelope. Post-tensioned bars are normally used for straight profiles only.

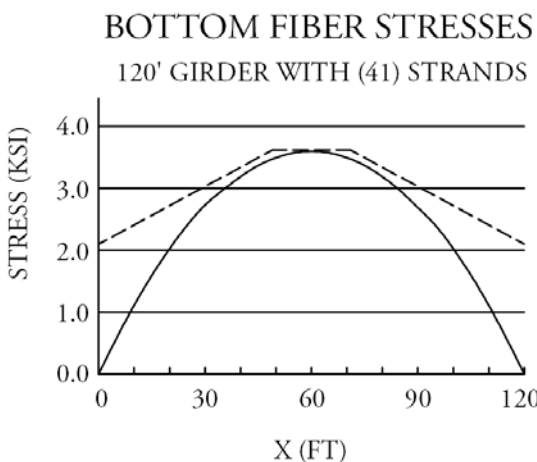
Figure 3.3.2.2-1a-1c
Bottom Fiber Stresses for Three Strand Profiles



a) Straight Strands



b) Single Harp at Midspan



c) Double Harp at 0.4L

Note: These Graphs Represent Simple Span I-Beams with a 6-Ft Spacing Designed for Zero Tension.

3.3.2.2.1 Straight Strands

Historically, pretensioned members containing straight strands only, were normally wide and relatively shallow, such as voided slab beams and some box beams. In recent years, advancements in design, testing, and codification have fostered the use of straight strands in deep bridge beams such as I-beams and bulb-tees. In shallow

FABRICATION AND CONSTRUCTION

3.3.2.2.1 Straight Strands/3.3.2.2.3 Harping Devices

members, the strands are distributed horizontally across the width of the member as uniformly and symmetrically as possible, although they can be offset to some degree to avoid openings or other obstructions. By necessity, the eccentricity of the prestressing force would be relatively small. Otherwise, excessive tensile and compressive stresses can develop at the ends of the member, where these stresses are not offset by the member dead load moment. Straight strands in the top of the member can compensate for this to some degree, but often result in design inefficiencies. The most common approach to control end stresses is to debond some of the strands at the member ends. Harping strands that are distributed across a wide, shallow member is very difficult and should be avoided. In deep sections, large eccentricities are needed and the resulting concrete stresses at the ends are controlled through debonding. Debonding is an effective tool and the method is discussed in **Section 3.3.2.9**.

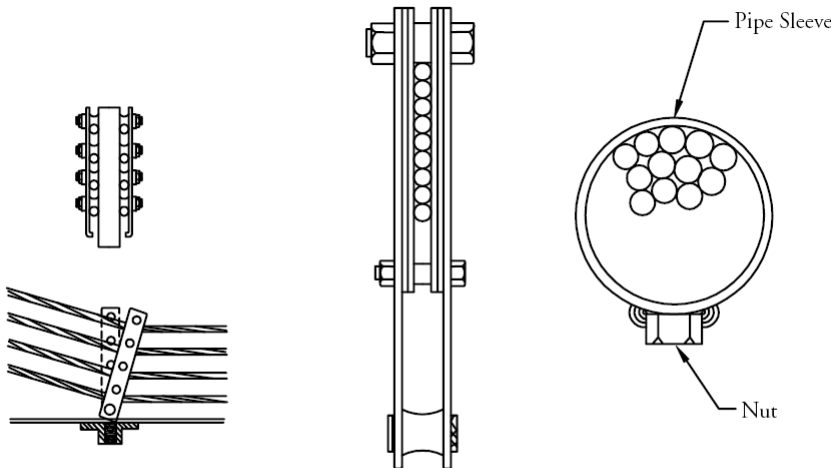
3.3.2.2.2 Harped Strands

Harped strands are most commonly used in the webs of relatively deep members, such as I-beams, bulb-tees, stemmed sections and deep box beams. The resulting reduction of the eccentricity of the prestressing force at the member ends reduces or eliminates the need for debonding. Harped strands can be deflected in one or more locations along the length of the member. As **Figure 3.3.2.2-1** shows, a single midspan harp provides better correlation to the moment envelope than straight strands, but not as good as multiple harp locations in a concrete member. For negative moments created by cantilevers, the strands can be lifted at the location of the support and held at the top of the member for the length of the cantilever. For safety reasons, the slope of deflected strands should not exceed about 9 degrees.

3.3.2.2.3 Harping Devices

Devices used to deflect pretensioned strands at the point of the harp vary from plant-to-plant. **Figure 3.3.2.2.3-1** illustrates common types. Some devices maintain the same strand spacing throughout the length of the member, others bundle the strands into one or more vertical rows, and still others bundle the strands at one or more discrete locations. Maintaining constant strand spacing throughout the member is normally not necessary unless the member is unusually short. In fact, it limits the maximum strand eccentricity that could otherwise be achieved. Bundling strands at discrete locations provides optimum eccentricity, though the strands must be splayed between the harp point and the member ends to assure bond development of each individual strand. Different harping devices are used with different products and with different harping methods.

*Figure 3.3.2.2.3-1a-1c
Harping Devices*



a) Two Columns with Uniformly Spaced Rows

b) Single-Stacked Column

c) Strand Bundle

FABRICATION AND CONSTRUCTION

3.3.2.3 Pretensioning/3.3.2.5 Tensioning Prestressing Steel

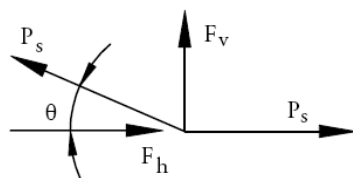
3.3.2.2.4 Anchorage of Harping Devices

Some forms are designed to accommodate deflected strands, and therefore provide for the attachment of harping devices to the form. This is common with “one-piece” forms without removable sides, such as used to cast stemmed members. With this type, the endplates and bulkheads are designed to hold the strands in position at the ends of products (Fig. 3.3.2.2.3-1b). The strands are first stressed straight, and then are subsequently pushed down from the top of the form at midspan with “fork” type harping devices by greased, tapered steel pins. The harping hardware can normally be anchored anywhere along the length of the form. After the concrete has cured, the tapered pins are pulled from the top of the members, and the holes are filled with approved durable material. Strands can also be pulled down and anchored from beneath some forms.

For other types of bridge members, such as I-beams, bulb-tees and box beams, most plants anchor harping devices to the concrete floor of the prestressing bed with embedments provided at a constant spacing. Normally, the member design is not especially sensitive to the harp location, and generous tolerances on the longitudinal location of the harp point (on the order of 18 to 20 in.) should be specified to allow the use of established anchor locations. At the ends of the member, the harped strands are usually not held in position by the endplates, but rather by steel “horses” and blocks that are placed beyond the endplates of the form. When the harped strands are held at a location away from the endplate, it is difficult to maintain small tolerances on their vertical position at the point they enter the member. Therefore, if the member design is not sensitive to vertical location of the harped strands at the member ends, generous tolerances (on the order of ± 1 in.) should be specified.

The vertical and horizontal forces developed by the harping operation are shown in Figure 3.3.2.2.4-1. Both must be considered when selecting the type and number of harping devices. Local producers should be consulted for harping capabilities on specific products. Vertical harp forces that exceed the capacity of the harping devices can usually be split into two or more locations that straddle the intended location. Horizontal forces occur when the angle of the harped strands differs on each side of the harping device and can be a problem for the “push-down” harping method described above. The tapered pins used in this procedure are relatively long and slender, and are normally not designed for combined flexure and axial loads. For this reason, unless the tapered pins are designed for combined flexure and axial loads, stemmed members manufactured with this method should be designed with straight strands, or a single harp at midspan only. Devices holding harped strands from beneath the form are generally not subject to this limitation.

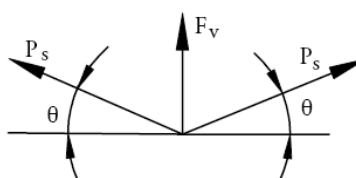
Figure 3.3.2.2.4-1a-1c
Calculating Harping Forces



$$F_v = P_s(\sin \theta)$$

$$F_h = P_s - P_s(\cos \theta)$$

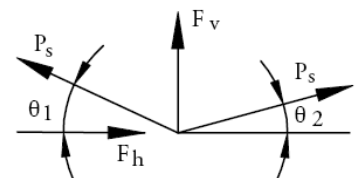
a) Each Point of a Double Harp



$$F_v = 2P_s(\sin \theta)$$

$$F_h = 0$$

b) Single-Point Harp



$$F_v = P_s(\sin \theta_1) + P_s(\sin \theta_2)$$

$$F_h = P_s(\cos \theta_2) - P_s(\cos \theta_1)$$

c) Harp with Asymmetrical Strand Trajectories

FABRICATION AND CONSTRUCTION

3.3.2.3 Pretensioning/3.3.2.5 Tensioning Prestressing Steel

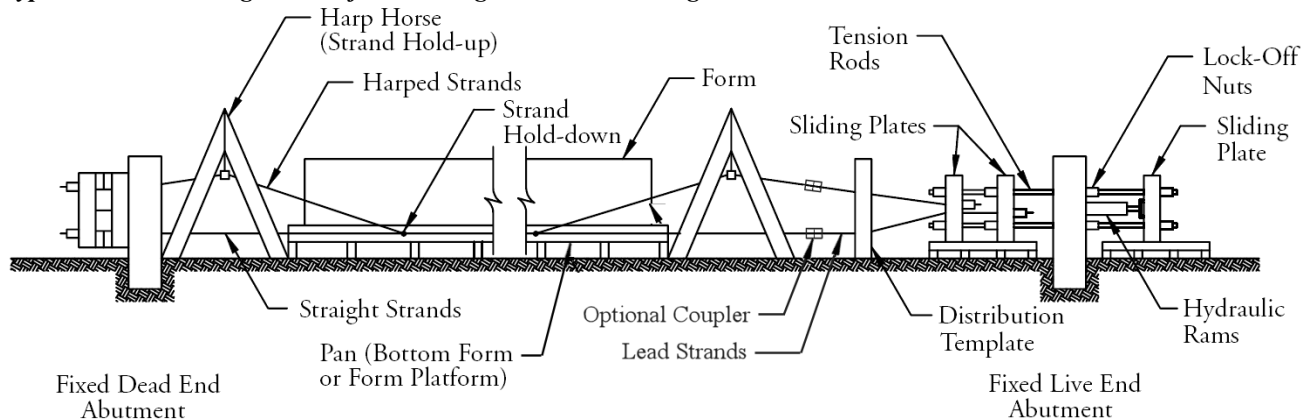
3.3.2.3 Tensioning

Procedures used to tension prestressing steel vary widely, but all share the results of imparting the intended amount of precompression to the concrete at a given location. The following sections describe the procedures and controls used in the tensioning operation, as well as corrections for the influence of external variables. Precast plants compensate for the effects of external influences in each casting line, and should be consulted for specific information. Though the discussion below chiefly addresses pretensioning with strand, many aspects are also applicable to post-tensioning with strand or bars.

3.3.2.4 Pretensioning Configuration

A typical pretensioning set-up is shown in **Figure 3.3.2.4-1**. The end of the bed from which the strands are tensioned or jacked is referred to as the “live” end, while the opposite end is called the “dead” end. In most cases, the precast member is shorter than the prestressing bed. In order to reduce the amount of strand that is cut off and wasted daily, the member is positioned in the line as close as possible to the dead end. This also reduces the amount of stressed “free” strand that must be dealt with during transfer (as discussed in Sect. 3.3.2.8). This minimum dimension is normally dictated by the need to deflect the strands from standard holes in the abutments into the endplate at the end of the precast member, while maintaining a shallow slope on the strands (see Sect. 3.3.2.2.2). Positioning the member in this manner normally leaves free strand at the live end. In order to reduce strand waste, most producers use “lead” or “bridle” strands at the live end, which are spliced onto the production strands, and then reused each day of casting.

Figure 3.3.2.4-1
Typical Prestensioning Bed Profile Showing Strand Tensioning and Deviation Devices

**3.3.2.5 Tensioning Prestressing Steel**

Prestressing steel is tensioned to the intended force with hydraulic pumps and rams. The tensioning system is calibrated to correlate the force delivered to the prestressing steel with a gage pressure read by the operator. The single most important control over this operation is a check of the calculated value of strand elongation compared to the actual elongation measured during the tensioning process. These values must agree (within 5% for pretensioning according to the PCI Manual 116 and 7% according to the AASHTO *LRFD Construction Specifications* for post-tensioning) to validate the procedure. This correlation provides assurances that equipment malfunction would be detected if it were to occur during tensioning operations. In addition, many variables enter into elongation calculations, all of which must be considered to properly compare the results. PCI-certified plant processes capture this fundamental quality control information. Strands may be tensioned individually, or as a group. In pretensioning, procedures differ for these two methods. A plant’s quality system manual will address its specific method for tensioning.

FABRICATION AND CONSTRUCTION**3.3.2.5.1 Tensioning Individual Strands/3.3.2.7 Variables Affecting Strand Elongations****3.3.2.5.1 Tensioning Individual Strands**

A strand tensioned individually is first jacked to an initial force, or “index” load, somewhere between 5 to 25% of its final tensioning force. The reason for this is to take up any slack in the system, which can hamper the reliability of elongation measurements. An initial measurement of the ram extension is taken, and the strand is then tensioned to 100% of its design force. The ram extension is again measured, and the difference between the measured extensions should reasonably match the calculated incremental elongation. This same procedure is also used for post-tensioning single strands or bars. Post-tensioned bars are normally tensioned individually. In this case, the concrete element is elastically shortening as the load is applied.

3.3.2.5.2 Tensioning Strands as a Group

For strands tensioned as a group (this is sometimes called “gang tensioning” or “multiple strand tensioning”), the pretensioning procedure is slightly different than that for strands tensioned individually. Prior to jacking the strands to their initial load, each individual strand is “preloaded” to an initial force smaller than the index load (usually about 2,000 lbs). This is done to assure that all strands begin the tensioning process with the same amount of force. The tensioning then proceeds in the same manner as for individual strands. Preloading is normally not required in stressing multiple-strand post-tensioning systems, since the strands are confined within a duct, and have about the same amount of slack.

3.3.2.6 Prestressing Strand Elongation

The basic equation for the elongation of prestressing steel is:

$$D = \frac{P_s L}{A_s E} \quad (\text{Eq. 3.3.2.6-1})$$

Variations in the steel area and modulus of elasticity are common, though usually quite small. The areas of prestressing strands shown in **Table 2.11-1** are reliable average values, as are the areas for prestressing bars. Average values for the modulus of elasticity are 28,600 ksi for prestressing strand, and 29,000 ksi for prestressing bars. The use of average values for area and modulus of elasticity are normally satisfactory for elongation calculations. If a higher-than-normal degree of precision is necessary, mill certificates available from the steel manufacturers provide the actual area and modulus of elasticity for each heat of steel.

Equation 3.3.2.6-1 is based on several idealized assumptions. The prestressing steel:

- has a uniform modulus of elasticity and cross section of constant area,
- is held by infinitely stiff supports at each end, and
- is maintained at a constant temperature.

In reality, strand often has factory splices within its length; prestressing bed components deform to varying degrees under compressive load; and some movement or “seating” occurs at the anchorage devices. Steel temperatures are rarely constant, particularly when the temperature of the fresh concrete differs substantially from the ambient temperature. Consequently, the basic equation **must** be modified to account for these unavoidable factors.

3.3.2.7 Variables Affecting Strand Elongation

External variables fall into two categories: 1) those requiring adjustments to the jacking force and 2) those that merely result in additional elongation. Since the operator is jacking to a predetermined gage pressure, irrespective of the ram extension, the definitive point in time separating the two categories is when the jacks reach 100% of their intended load, just prior to seating the live end chucks. For multiple-strand jacking, all external influences occurring before live end seating show up as additional elongation. Live end seating, and the effects of any subsequent external influences, are corrected by adjustments to the jacking force, subject to the limitations on the maximum stress in the strand given in **LRFD Table 5.9.3-1**. *PCI's Quality Control Technician/Inspector Level I & II Training Manual* and PCI manual, MNL-116 provide further discussion on influences external to the prestressing process, as well as examples of elongation calculations.

FABRICATION AND CONSTRUCTION**3.3.2.7.1 Dead End and Splice Chuck Seating/3.3.2.7.5 Temperature Corrections****3.3.2.7.1 Dead End and Splice Chuck Seating**

As the strands are tensioned, they move through the chucks as the wedges seat into the chuck barrels. The additional elongation from this source is the incremental movement that occurs between the index load and final load. This is normally small (on the order of $\frac{1}{8}$ in. per chuck), since most of the movement occurs while jacking to the index load. Dead end and splice chuck seating are independent of whether the strands are jacked individually, or as a group. However, where bridles are used with multiple-strand tensioning, the same number of splice chucks should be used on each strand in the system to assure uniform elongation values.

3.3.2.7.2 Elongation of Abutment Anchor Rods

Some multiple-strand tensioning systems employ steel blocks and anchor rods for jacking purposes. **Figure 3.3.2.4-1** illustrates this system. The stretching of these rods may add to the elongation of the system, and the apparent elongation of the strands, depending on where the measurements are taken.

3.3.2.7.3 Prestressing Bed Deformations

Prestressing beds are heavily loaded, and will shorten axially during jacking. For abutment-type beds, this is usually minimal. For strutted beds and self-stressing forms, the relatively small area of the compression members can result in significant shortening. Uprights and cross-heads will also deflect under load. For multiple-strand tensioning, these deformations are of no consequence, other than to add elongation to the system. However, prestressing bed deformations will influence the final load on strands stressed individually. Theoretically, the bed shortens incrementally as each strand is jacked. Strands tensioned early in the sequence will lose force as subsequent strands are tensioned. This is normally corrected by over-tensioning strands jacked early in the sequence. Depending on the number of strands, one or more groups can be over-tensioned to average values. If the earliest strands cannot be jacked high enough to compensate for the total bed shortening (due to specification limits), then re-tensioning is required. Post-tensioning is comparable to pretensioning with self-stressing forms, with the obvious difference being that the "form" is the concrete member itself, which undergoes elastic shortening as the load from the strand jacking is applied.

3.3.2.7.4 Live End Chuck Seating

When strand is pretensioned individually, it is normally pulled through the live end chuck by a center-hole ram that bears directly on the chuck. The direction of the pull is opposite that which seats the wedges. Therefore, when the force in the strand is released, the strand will move through the chuck significantly more than dead end or splice chucks (on the order of $\frac{3}{8}$ in.). This is corrected by increasing the jacking load to compensate for the expected seating value.

Multiple-strand pretensioning systems normally are locked-off with abutment anchor rods as described in **Section 3.3.2.7.2**. Therefore, the live end chucks seat much the same as dead end or splice chucks, with the result being a small net gain in elongation. With most systems, seating of abutment anchor rods is relatively small (about $\frac{1}{8}$ in.). Some multiple-strand post-tensioning rams have secondary pistons that seat the live end wedges prior to releasing the load, thereby reducing the amount of seating loss at the live end.

3.3.2.7.5 Temperature Corrections

Strands tensioned at cold temperatures, then exposed to relatively warm concrete (or grout for post-tensioning), will undergo thermal expansion and lose some of the force applied during jacking. The opposite is true of warm temperatures and cooler concrete. **Table 3.3.2.7.5-1** shows the percentage of prestress change as a function of the temperature differential and the percentage of the bed used.

FABRICATION AND CONSTRUCTION

3.3.2.7.5 Temperature Corrections/3.3.2.7.6 Friction

Table 3.3.2.7.5-1

Percentage of Strand Stress Change due to Temperature Differentials

		Temperature Variation (Degrees Fahrenheit)									
		5	10	15	20	25	30	35	40	45	50
% of Bed In Use	5	0.0	0.0	0.1	0.1	0.1	0.1	0.2	0.2	0.2	0.2
	10	0.0	0.1	0.1	0.2	0.2	0.3	0.3	0.4	0.4	0.5
	15	0.1	0.1	0.2	0.3	0.4	0.4	0.5	0.6	0.7	0.7
	20	0.1	0.2	0.3	0.4	0.5	0.6	0.7	0.8	0.9	1.0
	25	0.1	0.2	0.4	0.5	0.6	0.7	0.9	1.0	1.1	1.2
	30	0.1	0.3	0.4	0.6	0.7	0.9	1.0	1.2	1.3	1.5
	35	0.2	0.3	0.5	0.7	0.9	1.0	1.2	1.4	1.5	1.7
	40	0.2	0.4	0.6	0.8	1.0	1.2	1.4	1.6	1.8	2.0
	45	0.2	0.4	0.7	0.9	1.1	1.3	1.5	1.8	2.0	2.2
	50	0.2	0.5	0.7	1.0	1.2	1.5	1.7	2.0	2.2	2.5
	55	0.3	0.5	0.8	1.1	1.4	1.6	1.9	2.2	2.4	2.7
	60	0.3	0.6	0.9	1.2	1.5	1.8	2.1	2.4	2.7	3.0
	65	0.3	0.7	1.0	1.3	1.6	1.9	2.2	2.6	2.9	3.2
	70	0.3	0.7	1.0	1.4	1.7	2.1	2.4	2.8	3.1	3.4
	75	0.4	0.7	1.1	1.5	1.8	2.2	2.6	3.0	3.3	3.7
	80	0.4	0.8	1.2	1.6	2.0	2.4	2.8	3.1	3.5	3.9
	85	0.4	0.8	1.3	1.7	2.1	2.5	2.9	3.3	3.8	4.2
	90	0.4	0.9	1.3	1.8	2.2	2.7	3.1	3.5	4.0	4.4
	95	0.5	0.9	1.4	1.9	2.3	2.8	3.3	3.7	4.2	4.7
	100	0.5	1.0	1.5	2.0	2.5	3.0	3.5	4.0	4.5	5.0

Again, corrections for anticipated temperature differentials can be made by adjusting the jacking force. This correction is not applicable to self-stressing forms because the form changes length with temperature change, countering changes in strand force.

3.3.2.7.6 Friction

Friction is another external variable that must be addressed in the prestressing operation. In pretensioning, friction is normally not a issue with straight strands, but can significantly reduce the force in the strands at the dead end if the strands are deflected at several points along the bed. If this is a problem with a particular bed setup, it will be indicated by a reduction in the measured elongations.

Rather than compensating for friction in the jacking load or elongation calculations, most plants have developed tensioning or harping procedures that diminish the effects of friction. For example, some proprietary harping devices feature rollers to decrease friction losses when the strands are tensioned in the harped position (**Fig. 3.3.2.2.3-1a**). These devices are usually expensive and limit the eccentricity that can otherwise be achieved with harped strands. Some plants tension the strands in a straight, or partially deflected profile, then complete harping after the strands are tensioned. The resulting change in geometry will increase the force in the strand. With multiple-strand pretensioning systems, the strands can either be under-tensioned to compensate for the expected increase in force, or the rams can be relaxed concurrent with the harping operation to maintain the same force level in the strands. Strands that are jacked individually can be tensioned to lower forces to compensate for the added force due to the change in geometry.

Friction during post-tensioning is unavoidable, and is therefore inherent in elongation calculations. In curved tendons, the strands are in contact with the duct for most of their length, and consequently develop a significant amount of friction. The *PTI Post-Tensioning Manual and LRFD Specifications* provide guidance and example calculations for the amount of friction that can be expected when post-tensioning tendons.

FABRICATION AND CONSTRUCTION**3.3.2.8 Transfer/3.3.2.8.4 Harped Strand Considerations at Transfer****3.3.2.8 Transfer**

Once the concrete has achieved its specified transfer strength (as determined by cylinder tests or other non-destructive testing methods), the force (tension) in the strands is transferred from the prestressing bed into the product. This is often referred to as detensioning or releasing the strands. If the concrete cure has been accelerated by heat, the product should still be near its maximum temperature at the time of transfer. Otherwise, the unstressed concrete will cool and contract, sometimes resulting in vertical, transverse cracking along the length of the member.

Force in the strands can be released hydraulically, by flame cutting, or a combination of both. Hydraulic transfer is normally used with multiple-strand tensioning systems, while heat from a cutting torch is used with both multiple- and single-strand systems. The sequence of transfer is very important for safety reasons, as well as for avoiding damage to the product. Strands should always be transferred symmetrically.

It has been shown that abrupt, single-strand transfer resulting from rapid cutting with oxy-acetylene torches, can result in small spider web-like cracking from bursting or splitting stressing at or near the beam end. Gang transfer results in a more gradual release of force with often less end cracking.

3.3.2.8.1 Hydraulic Transfer

With hydraulic transfer of force, the strands are usually relaxed (jacked down) from the live end with the same tensioning system used to jack them. Because the strand is bonded with the concrete, the free strand at the dead end will tend to pull the product toward the dead end as the live end force is released. The lesser the amount of free strand, the less the tendency to slide. If the member slides, it can bind in the form. Items projecting through the formwork, such as harping device hold-downs, can damage both the product and the formwork. Sliding can be prevented in two ways:

1. Let the live end down in increments, while heat cutting the appropriate number of strands at the dead end. For example, in a line with eight strands, the live end force can be released in 25% increments, with two strands being cut at the dead end after each increment.
2. Use short stroke "let-down" rams at the dead end. These rams are released proportionally to the live end rams, allowing the force in the strands to remain the same at either end of the member.

3.3.2.8.2 Transfer by Flame Cutting

When flame cutting is used without hydraulic transfer, individual strands must be cut simultaneously at both ends of the member. When strands are cut at one end only, the force in each remaining strand will increase, possibly to the breaking point. The prestressing forces must be kept as equal as possible at each end throughout the entire procedure. For safety reasons, flame cutting should only be applied to relatively short lengths of tensioned free strand, and then only after applying initial detempering heat to allow the strands to yield and relax prior to cutting. This process not only results in improved safety, but also reduces the abrupt shock to the precast member.

3.3.2.8.3 Transfer at Bulkheads

When several members are cast end-to-end in a line, it may be necessary to cut the strands between members simultaneously with the ends, depending on the type of bulkheads used. Bulkheads can be designed to resist the compressive forces developed between members as the ends of the line are transferred. In this case, the strands between members can be cut after the line has been transferred. However, "soft" bulkheads, such as those made from wood, will crush and allow the precast members to slide if the strands between members are not cut simultaneously with the ends.

3.3.2.8.4 Harped Strand Considerations at Transfer

The vertical forces developed by harped strands can cause cracking in the tops of members if the harp hold-downs are released prior to transfer. These forces can sometimes exceed the weight of the member, and cause the

FABRICATION AND CONSTRUCTION**3.3.2.8.4 Harped Strand Considerations at Transfer/3.3.3.1 Placement and Attachment**

member to lift from the bed. In these cases, enough prestress must be transferred prior to releasing the hold-down devices to reduce the uplift. This partial transfer must be done symmetrically at both ends of the bed to prevent overstressing the remaining strands.

3.3.2.9 Strand Debonding

In pretensioned members, strands can be debonded for all or part of the member length for three reasons:

- Reduce excessive concrete stresses at the member ends
- Allow the casting of members in the same bed having different numbers of strand
- Prevent concrete bond to strands used for temporary handling and shipping purposes

Various methods are used for debonding, including encapsulating the strand in sheaths (also referred to as “blanketing” or “sleeving”), or applying a bond breaker to the surface of the strand. The effectiveness of these methods varies.

The bond of concrete to tensioned strand develops from several mechanisms as described by Gerwick (1993). These include:

- Chemical adhesion
- Shrinkage of the concrete surrounding the strand
- Mechanical interlock on the deformations between the intertwined wires
- Swelling of the strand after transfer due to Poisson’s ratio, commonly referred to as the “Hoyer” effect.

Bond breakers on strand generally serve to reduce only the chemical adhesion, and therefore, are not as effective as strand encapsulation.

Debonded strands can be encapsulated with different materials, some more effective than others. The key properties of encapsulating materials are watertightness, strength, and durability to withstand concrete placement, and nonreactivity with concrete or steel. The material must provide enough space between the concrete and strand to mitigate the effects of concrete shrinkage and strand swelling. The sheaths must be properly sealed to avoid intrusion of cement paste during concrete placement and consolidation.

3.3.3 Nonprestressed Reinforcement and Embedments

In precast concrete fabrication, the placement of mild reinforcement and embedments is generally simpler than in cast-in-place construction, which further improves the quality of plant-cast products. This section describes methods used by precast concrete manufacturers to secure embedments, and provides detailing hints that take full advantage of plant-cast products.

3.3.3.1 Placement and Attachment

Precast products are normally cast in an orientation providing the easiest access for placement of embedded items. Although most methods of securing embedments do not differ between precast and cast-in-place construction, the ease of access is critical to the quality of the finished product. For example, vertical members, such as piles, piers and abutment walls, are cast and shipped horizontally by precast plants, and are only tipped to vertical for erection purposes. In members that are not pretensioned, mild steel reinforcement cages are typically set into forms, rather than the forms being placed around them, facilitating the inspection of concrete cover and embedment locations. Placing, tying and inspecting mild reinforcing bars are much more efficient when the member is cast horizontally at ground level, rather than high in the air or below grade.

Tensioned prestressing strands provide an excellent platform for supporting mild reinforcement. Whenever possible, mild reinforcement transverse to the member should be detailed to be tied directly to the strands. This provides excellent control of the bar location, and minimizes the need for “chairs” or “bolsters.” Chairs can be used to support the strands if they sag under the weight of the bars. Whenever possible, mild steel reinforcement should be detailed for installation after strands are tensioned. **Sections 3.2.3.1 and 3.2.3.4** provide suggestions for efficient reinforcement configurations.

FABRICATION AND CONSTRUCTION**3.3.3.2 Installation of Lifting Devices/3.3.3.4 Steel Spacing Design****3.3.3.2 Installation of Lifting Devices**

The installation of lifting devices is critical to the safe handling of precast concrete products. Improperly designed or installed devices could fail, with potentially catastrophic consequences. **Section 3.2.4.4** describes common configurations. Proprietary devices should be installed in accordance with the manufacturer's recommendations. Generic devices must be properly designed and installed. For any type of lifting device, a very important consideration is proper consolidation of concrete around the device and its anchorage.

The most common type of generic lifting device for large bridge products is prestressing strand lift loops. In many cases, multiple loops are required at each location. When using multiple loops, each must be held at the same height above the concrete surface, and must be engaged by the straight pin of a shackle. It is very important that each strand in the group carry its proportionate share of the load. Also, inserting multiple strands into metal pipes or conduits, then bending to the desired loop shape, does not ensure that each strand will carry its proportionate share of the load. Curved engagement surfaces, such as a hook or the curved end of a shackle, will load the loops unevenly, potentially creating a progressive failure of individual loops. The legs of each loop should be splayed to allow concrete to envelop them individually. Bundled loop legs can exhibit significantly reduced capacity.

3.3.3.3 Concrete Cover

The amount of concrete cover surrounding reinforcement is important for providing protection of the steel from corrosion. Cover must be sufficient to allow the largest aggregate particles to pass between the reinforcement and the form. Due to superior control of form dimensions, reinforcement placement, concrete quality, curing, and inspection procedures, ACI 318 allows the concrete cover requirements for precast products to be reduced when compared to cast-in-place construction. Concrete cover in precast fabrication is normally assured by the use of "chairs" or "bolsters," by the rigidity of pretensioned strands, or by a combination of both.

3.3.3.4 Steel Spacing Design

The spacing of prestressing steel and mild reinforcement must be sufficient to allow the largest aggregate particles to pass freely between strands or bars. **Section 3.2.2.3** discusses the minimum spacing of prestressing strand. For precast concrete, the *LRFD Specifications* requires the minimum clear distance between parallel mild steel reinforcing bars in a layer to be not less than one bar diameter, 1.33 times the maximum aggregate size, or 1 in. These restrictions are intended to allow concrete to fully envelope the reinforcement. At closer spacings, the reinforcement can act much like a sieve, segregating the larger coarse aggregate particles from the cement paste and smaller aggregate.

Most precast plants use coarse aggregate gradations with a maximum particle size of $\frac{3}{4}$ in. For members with reinforcing bar sizes of No. 8 or less, this means a minimum clear distance between bars of 1 in. At this spacing, it is not practical to effectively use even the smallest of internal vibrators (normally called "stingers," the smallest of which are 1 in. in diameter) to consolidate the concrete, making external vibration the only reliable method available for consolidation. Limiting possible consolidation methods can increase production costs, particularly if the standard side forms are not stiff enough to withstand external vibration, or have not been previously equipped with external vibrator tracks. When possible, reinforcement spacing should be maximized to allow concrete to be consolidated with either internal or external vibration, to reduce cost and improve the quality of the finished product.

Other embedments can also create congestion. Post-tensioning ducts in thin beam webs can obstruct a substantial percentage of the web, making internal vibration of the concrete below the level of the duct very difficult. While the *AASHTO Specifications* have historically limited the maximum duct size to 40% of the web width, some states have used ratios as high as 55%. Forcing internal stingers past ducts can dent and possibly puncture the ducts, creating blockages that are difficult to clear. In this case, the webs should be detailed thick enough for easy passage of the stinger, or external vibration should be used to consolidate the concrete below the level of the ducts. Bridge designers should consult local producers for advice on embedment configurations and clearances.

FABRICATION AND CONSTRUCTION**3.3.4 Concrete Batching, Mixing, Delivery, and Placement/3.3.4.1 Lightweight Concrete****3.3.4 Concrete Batching, Mixing, Delivery, and Placement**

Procedures used to batch and mix concrete for precast concrete bridge products do not differ substantially from those used in cast-in-place concrete construction. Concrete is normally batched and mixed in a central stationary mixer, though shrink mixing (partial central and partial truck mixing) can also be used. However, in plants that mix their own concrete, the proximity of the mixer and final destination allows a wider range of delivery and placement options.

The general requirements for equipment and procedures used for batching, mixing, delivering, and placing concrete are covered in detail in PCI manual, MNL-116. The required result of all processes, from mixer to final placement, is to provide concrete of a uniform, consolidated consistency without segregation of aggregates and paste.

3.3.4.1 Delivery Systems

A wide range of methods are used by precast plants to deliver concrete from the mixer to the forms, including pumps, conveyors, "sidewinders," truck mixers, and short-haul buggies carrying buckets or hoppers. Typically, delivery systems are designed to ensure a continuous supply of freshly mixed concrete for the duration of the placement. By necessity, precast concrete products are limited in weight, and do not require placement of large volumes of concrete. Concrete can be batched, mixed, delivered, and placed by the plant in relatively small quantities, resulting in excellent control of the concrete consistency.

3.3.4.2 Consolidation Techniques

As discussed in **Section 3.3.1.2.1**, forms for standard precast concrete bridge products are normally of steel construction, and are usually much stiffer than the typical forms used in cast-in-place construction. Part of the reason for this is to allow the use of external form vibration. Areas of the cross section that are difficult to reach with internal vibrators, such as the bottom flange of deep I-beams, are easily consolidated with external vibration. Concrete consolidated with properly executed external vibration is extremely dense and durable. In many cases, combinations of internal and external vibration are used to further enhance consolidation.

3.3.4.3 Normal Weight Concrete

The term "normal weight" concrete is conventionally used to describe mixtures containing naturally occurring igneous, sedimentary, or metamorphic mineral aggregates. Such aggregates are predominantly siliceous or calcareous in composition, with a specific gravity between 2.25 and 2.65. The resulting concrete unit weights are normally between 145 and 160 pcf, with 28-day compressive strengths ranging from 5.0 ksi to in excess of 10.0 ksi in some parts of the country.

The use of normal weight concrete is predominant in the production of precast concrete bridge products. For most types of bridge members, normal weight concrete provides the best performance for the lowest cost. Efficient, state-of-the-art precast bridge products generally require relatively high concrete strengths in slender sections that are congested with reinforcement. The resulting need for low water-cementitious materials ratios and high workability has led to the widespread use of water-reducing admixtures. As discussed in **Section 3.2.1.3.1**, water-reducing admixtures can also reduce the working life of concrete. However, since the interval between mixing and placing is short when precast plants mix and deliver their own concrete, optimum workability is usually maintained throughout the duration of the placement.

3.3.4.4 Lightweight Concrete

Lightweight and semi-lightweight concretes can be produced with unit weights ranging from approximately 100 pcf up to the unit weight of normal weight concrete. This is done by replacing varying quantities of normal weight aggregate with lightweight aggregate. For example, replacement of normal weight coarse aggregates with all ESCS (expanded shale, clay and slate) lightweight coarse aggregates can result in structural concretes with unit weights

FABRICATION AND CONSTRUCTION**3.3.5 Concrete Curing/3.3.5.3 Methods of Accelerated Curing**

as low as 110 pcf. Further reduction of the concrete unit weight is achieved by also replacing the normal weight sand with lightweight sand. Additional information about structural lightweight concrete is found in ACI 213R. (Also, see **Sects. 2.4.7.2** and **2.4.7.3**.)

Members made with lightweight concrete are easier to handle and ship, and reduce the superstructure weight, with resulting economies in substructure and seismic design. However, depending on the type of aggregate, lightweight concrete can exhibit lower compressive strength and always has a lower modulus of elasticity than comparable normal weight concrete. This results in increased deformations (camber, deflections, and elastic shortening). Creep deformation is independent of modulus of elasticity and, with some lightweight aggregates, can be less than comparable normal weight concrete. The ultimate shrinkage of lightweight concrete is also generally higher than normal weight concrete. Creep, shrinkage, and splitting tensile strength (which affects shear strength) values should be provided by the aggregate supplier.

The 2011 annual business meeting of the AASHTO Subcommittee on Bridges and Structures resulted in more *LRFD Specifications* provisions that addressed the growing use of lightweight aggregate concrete. Additional information can be found in Russell, 2007, and Cousins, 2011. Procedures for batching, mixing, transporting, and placing lightweight concrete are essentially the same as for normal weight concrete, although special handling of the lightweight aggregate concrete must be considered. The aggregates must be saturated surface dry prior to batching. Lightweight aggregate suppliers should be consulted for recommendations. For the “softer” lightweight aggregates, overmixing should be avoided to prevent grinding of the aggregate. When using a lightweight mixture for the first time, verification should be provided that standard handling and placing techniques will result in concrete of uniform consistency.

3.3.4.5 High-Performance Concrete

High-performance concrete is a mixture exhibiting one or more specific properties in its hardened form, such as high strength, low permeability, low shrinkage or abrasion resistance. Some of these properties occur naturally when striving to achieve others. For example, the density needed for concrete to exhibit low permeability normally also results in high strength. There are those who believe that to achieve high-performance concrete, mineral admixtures must be added to conventional, normal weight concrete. This is not necessarily the case. As reported by Pfeifer, et al. (1996), the low water-cementitious materials ratio and accelerated curing required to achieve overnight transfer strength results in concrete of comparable durability to moist-cured concrete with silica fume. In some parts of the country, materials and fabrication procedures are of such high quality that precast plants routinely produce high-performance concrete with standard normal weight mixes.

Batching and mixing procedures for high-performance concretes containing chemical or mineral admixtures are essentially the same as for standard concretes, with the exception of the addition of the admixture. Admixtures should be charged into the mixer in accordance with the manufacturer’s recommendations. Water-reducing admixtures usually provide better performance if added after the cement and water have reacted for several minutes. Depending on the type of high-performance concrete, some delivery systems are better than others. For example, concretes with relatively high dosages of silica fume tend to be overly cohesive, and are difficult to pump. **Section 3.2.1.3** discusses the effects that different types of admixtures have on concrete placement and consolidation. Sophisticated techniques, such as external form vibration, are generally required to successfully place high-performance concrete in typical precast concrete bridge members.

3.3.5 Concrete Curing

The economic viability of precast concrete depends on the ability of the plant to fabricate precast products on a daily basis. In special circumstances, forms can be used—“turned over”—twice each day. For some precast products, the required concrete strength at stripping may be low enough to allow normal curing practices for the relatively short duration between casting and stripping. However, most pretensioned products require relatively high concrete strengths at the transfer of prestress, which cannot be achieved without accelerating the strength

FABRICATION AND CONSTRUCTION**3.3.5 Concrete Curing/3.3.5.3 Methods of Accelerated Curing**

gain of the concrete. This section describes methods used by precast plants to accelerate concrete curing, and the beneficial effects these techniques have on the properties of the concrete. **Section 3.3.5.5** addresses both the quality control aspects and optimization of accelerated curing.

Apart from the use of Type III cement and accelerating admixtures, the primary method of accelerating the strength gain of concrete is with the application of heat. This process, along with prevention of moisture loss from the hardening concrete, is called accelerated curing.

3.3.5.1 Benefits of Accelerated Curing

In a typical precast plant, stripping of the prior day's casting and set-up of a new member are normally scheduled to be accomplished in a standard 8-hour shift. Assuming concrete placement occurs during the subsequent 4 hours, that leaves 12 to 16 hours to cure the concrete and achieve the required stripping or transfer strength prior to the start of the next cycle. For most bridge products, accelerated curing is the only way to achieve these strengths in the available curing period. Optimum application of modern cements, admixtures, and accelerated curing systems can result in concrete strengths at transfer of prestress of 6.5 ksi and higher, facilitating a wide variety of sophisticated, long-span products. The ability to achieve high overnight strength is not uniform throughout the country, nor is it consistent from plant to plant. Bridge designers should consult with local producers. For economy, the specified transfer and stripping strengths should always be the minimum required by design, subject to the *LRFD Specifications* minimum values of 4.0 ksi for pretensioned members (except piles), or 3.5 ksi for post-tensioned members and pretensioned piles.

Accelerated curing is also beneficial to concrete durability. Studies by Klieger (1960) and Pfeifer, et al., (1987, 1996) have shown that accelerating the early strength development of concrete by heat curing improves freeze-thaw durability and reduces chloride permeability, as well as decreasing absorption and the volume of permeable voids within the concrete. This is particularly important in areas where de-icing chemicals are common, and in coastal areas.

3.3.5.2 Preventing Moisture Loss

Moisture loss from exposed surfaces must be prevented during the entire curing cycle. Several methods are used to achieve this:

- Covering the exposed surface with wet burlap
- Covering with a polyethylene sheet vapor barrier
- Covering with impermeable curing blankets
- Applying a curing compound

Moisture loss varies with the geographic location of the plant, the ambient conditions, and whether the bed is inside or outdoors. In cool climates with relatively high humidity, covering the product with an impervious sheet during the curing cycle is generally all that is necessary. In hot climates with low humidity, additional means of moisture retention, such as wet burlap or other absorbent material, may be necessary. Failure to take precautions can allow rapid evaporation of mix water from the concrete, resulting in plastic shrinkage cracking and, in severe cases, a loss of strength development in the affected area. Bridge designers should consult with local manufacturers for applicable moisture loss prevention techniques employed.

3.3.5.3 Methods of Accelerated Curing

Accelerated curing begins only after the concrete achieves its initial set, which is generally 3 to 5 hours after batching. Once heat is applied, the temperature of the concrete is permitted to increase at a rate of up to 36 °F per hour to a maximum concrete temperature of 150 °F, where it is held for the remainder of the curing period. The maximum temperature may be exceeded in some circumstances by 5 °F for up to 2 hours. When the concrete is appropriately modified with fly ash, ground-granulated blast-furnace slag, or Metakaolin, the curing temperature may be increased to 170 °F. If the precast members are installed in a location that is dry or subject to infrequent

FABRICATION AND CONSTRUCTION**3.3.5.3 Methods of Accelerated Curing/3.3.5.3.1 Accelerated Curing by Convection**

wetting in service, they may be cured at temperatures up to 180 °F. There are additional provisions that apply to temperature. The preceding limitations and temperature controls are presently PCI standard practices and are implemented in the PCI Plant Certification program but are awaiting publication by PCI. Similar provisions have been published in ACI 301. This standard allows a maximum temperature of 158 °F comparable to the 150 °F limitation above. **Section 3.3.5.5** provides further discussion on optimizing the accelerated curing cycle.

When heating the air surrounding the forms, uniform concrete curing temperatures are sometimes difficult to control in members of variable or complex shape. Differential expansion between portions of a member with varying volume-to-surface ratios can create thermal stresses at the interface, possibly causing cracks.

Thermostatic control is also difficult in some cases, since many heaters are not adjustable (they are either on or off), and the temperature of the air in the enclosure will not be the same as the temperature of the concrete. For these reasons, it is important to monitor the internal temperature of the concrete and not the temperature of the enclosure.

All accelerated curing methods perform substantially better when used with metal forms as compared to wooden forms. Wooden forms have inherent insulating properties that restrict heat from reaching the concrete. Steel forms and concrete have similar thermal expansion properties, but the coefficient of thermal expansion for wood is only about half of that for concrete, resulting in increased wear on wooden forms during repeated heating cycles. Care must be taken when placing heaters around wooden forms, which have been known to catch fire during the curing process.

With accelerated curing, the heat of hydration of the cementitious materials in the concrete must be considered when determining the amount of heat to apply to the member. Massive members with large volume-to-surface ratios generate large amounts of heat during hydration. High-performance concrete combining portland cement with mineral admixtures exhibits increased heat of hydration. Internal concrete temperatures of the first members cast under these circumstances should be closely monitored to assure they remain below the maximum allowable temperature and allowable rate of temperature rise.

3.3.5.3.1 Accelerated Curing by Convection

The most common method of increasing the temperature of the concrete to accelerate curing is by elevating the temperature of the air surrounding the form. A typical convection process involves “tenting” the form with a frame and a polyethylene sheet or insulated tarp, and placing gas-fired forced air heaters under the tent. **Figure 3.3.5.3.1-1** shows an insulated tarpaulin on a track-mounted reel. Depending upon the member size, heaters from 50,000 to 500,000 Btu/hr are common. A rule of thumb is that one cubic yard of concrete will require about 2,000,000 to 4,000,000 Btu-hrs to raise the concrete temperature approximately 100 °F in a 12-hour curing period. In order to most accurately determine the concrete strength, producers use “match curing” cylinder devices. These tools replicate conditions in the concrete while the product is curing.

FABRICATION AND CONSTRUCTION**3.3.5.3.1 Accelerated Curing by Convection/3.3.5.3.4 Accelerated Curing with Electric Heating Elements****Figure 3.3.5.3.1-1****Track-Mounted Insulated Tarpaulin Reel****3.3.5.3.2 Accelerated Curing with Radiant Heat**

Heat can also be provided by electric or gas radiant heaters. Producers have successfully cured small products by using common hardware-store-variety heaters under the enclosure. For larger products, such as stemmed members or box beams, finned tubes installed under the form can be used to circulate hot water or hot oil from either a localized or central boiler. In the case of hot water, a typical 2-in.-diameter finned tube operating at 200 °F will produce about 1,200 Btu/ft/hr. Elaborate piping schemes are employed in an attempt to maintain uniform heat throughout the concrete cross section. Antifreeze is added to the water to prevent the line from freezing when the system is inactive.

3.3.5.3.3 Accelerated Curing with Steam

Another method used to provide heat for accelerated curing is steam. Steam may be provided in a closed circulating system or as “live” steam which is allowed to enter the enclosure, or a combination of both. Live steam exhibits the same thermal characteristics as convection or radiant heat, with the added benefit of providing a moisture-saturated environment. This largely eliminates the potential for moisture loss from exposed concrete surfaces. The ability to pipe the steam to the most advantageous locations, and to control the boiler temperature and flow, allows good uniformity during curing. Advancements in today’s steam generators have proven to be effective and efficient.

Two significant disadvantages of live steam curing are the high cost of energy required to generate the steam, and the deleterious effect steam and condensed hot water have on the plant, tooling and forms. Even the best curing covers and energy-efficient boilers result in relatively high curing costs. In addition, collection of the condensate runoff is costly and messy, and steam causes metal tooling and forms to corrode at an accelerated rate. This can be particularly detrimental to strand anchorage devices and harping hardware.

3.3.5.3.4 Accelerated Curing with Electric Heating Elements

The heat for accelerated curing can also be provided by electrical heating elements attached to the skin of metal forms. These elements are firmly secured to the form skin, which is then covered with 2 to 3 in. of sprayed-on foam insulation. The heat is provided by conduction through the metal form to the concrete.

Several advantages exist with this technology. First, the time-temperature curve can be programmed precisely to deliver the optimum curing cycle. This can also be done with other curing systems, but with less direct control of the concrete temperature. Further discussion of the optimum curing cycle can be found in **Section 3.3.5.5**.

The second advantage is that electric curing is energy efficient. The forms are heated directly, rather than energy being wasted by heating the surrounding environment. Exposed areas of concrete are covered with impervious curing blankets that are relatively light and easily removed. Typical installations demonstrate energy consumption significantly less than with other systems. Though there are initial costs associated with the elements, power distribution, and computer controls, the long-term energy savings and superior curing control can provide a rapid pay-back when compared to other systems.

FABRICATION AND CONSTRUCTION**3.3.5.3.4 Accelerated Curing with Electric Heating Elements/3.3.5.5.1 Determination of Preset Time**

A third advantage of electric curing is that by planning the spacing and control of the electric heating elements, different parts of a member can be cured with varying energy outputs. Thin flanges can be treated differently than bulky webs, resulting in a more uniform cure of the entire cross section, with less potential for cracking due to thermal stresses. This degree of control is not available with any other curing system. Besides the relatively high initial cost, one disadvantage of electric curing is that it can only be used with metal forms.

3.3.5.4 Curing Following Stripping

Specifications sometimes require an additional period of moist curing following the accelerated curing cycle. Studies by Klieger (1960) have shown that this additional moist curing period is not necessary, and may in fact be detrimental to the freeze-thaw durability of the concrete. Accelerated curing by the application of heat is equivalent or superior to the moist cure period specified for cast-in-place concrete. Further hydration of the cement under moist conditions is not necessary after the accelerated cycle.

PCI Manual 116 limits the cooling rate for heat-cured members to 50 °F per hour. In general, many decades of industry experience with accelerated curing have not revealed any distress due to thermal shock. Additional discussions of extended moist curing and stripping to storage in cold temperatures can be found in PCI Publication, TR-1, 1981.

3.3.5.5 Optimizing Concrete Curing

The methods used to accelerate the early strength gain of concrete in precast bridge members, as well as the benefits of accelerated curing, are discussed in **Section 3.3.5**. **Section 3.3.5.3** introduces the concept of an optimum curing cycle, which is made up of three critical stages:

- Stage 1 – Preset or initial set period
- Stage 2 – Rapid strength gain, during which the temperature gain of the concrete is accelerated
- Stage 3 – Moderate strength gain, during which the maximum curing temperature is maintained

Regardless of curing method, plants monitor concrete temperature with thermocouples embedded in the product. Because of heat gain from hydration of the cementitious materials, it is important that the temperature of the concrete, not the air under the enclosure, be monitored during this process. This is discussed in **Section 3.3.5.3**. In more sophisticated systems, a computer monitors the thermocouples and automatically adjusts the heat applied to the product by activating switches or valves. Some plants use night watchmen to control the heat application. In either case, the goal is to add heat energy to augment the heat of hydration and achieve a temperature that follows a predetermined optimum cycle.

The following sections describe the quality control aspects of this process.

3.3.5.5.1 Determination of Preset Time

As introduced in **Section 3.3.5.3**, application of heat should begin only after the concrete has taken its initial set. Temperatures as low as 125 °F have been shown by Hanson (1963) to significantly decrease the 28-day strength of the concrete when applied with an insufficient preset period. Concrete placed in warm or cold temperatures should be maintained at the placement temperature until the preset period is complete. This preset period is currently established by AASHTO T197 (ASTM C403) for each mix design in use. Unfortunately, this test procedure is difficult and time consuming to perform in the plant.

In recent years, an alternate test method has been developed that is easier to perform. In lieu of initial set, it is now recognized that the optimum time to start the application of heat may correspond more closely to the initial development of the cement's heat of hydration. This point can be determined by a hydration chamber, which is an enclosure in which freshly mixed concrete is placed and maintained in nearly adiabatic conditions. Using commercially available chambers, it is possible to determine the onset of hydration, and hence determine the optimum preset period. Electric curing equipment suppliers offer curing systems in which the computer controller, with the aid of a hydration chamber, automatically determines the optimum preset time and programs

FABRICATION AND CONSTRUCTION

3.3.5.5.1 Determination of Preset Time/3.3.5.5.2 Rate of Heat Application

the curing cycle. Thermocouples in the precast members drive heated cylinder molds that provide test cylinders with an identical time-temperature history as the members in the forms.

If too much time elapses before heat is introduced, the effectiveness of accelerated curing is reduced.

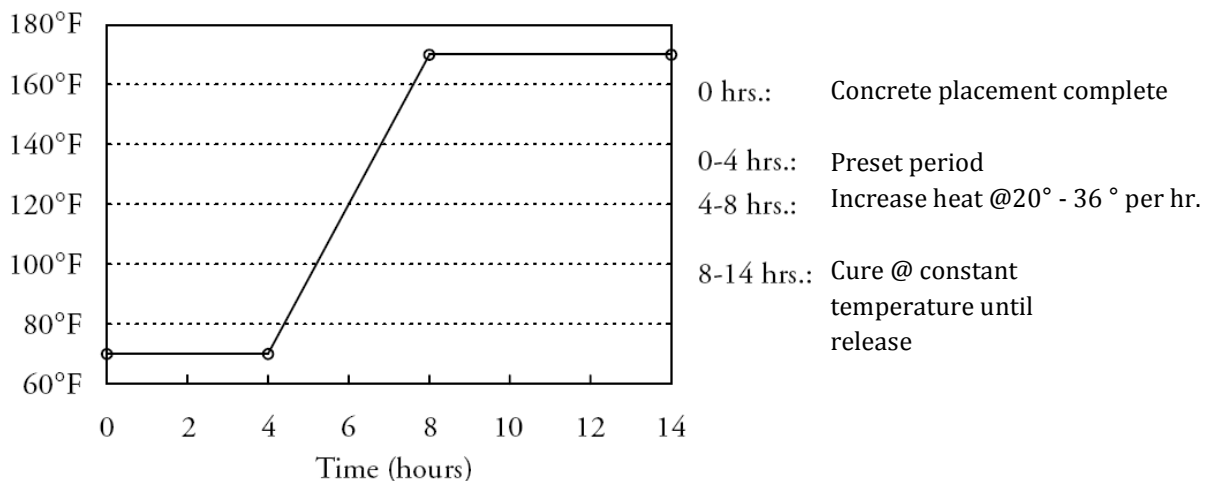
3.3.5.5.2 Rate of Heat Application

Once heat is applied, the rate of heat gain must be controlled to prevent damage to the concrete. The *LRFD Bridge Construction Specifications* (Article 8.11.3.5) and PCI industry standards limit the temperature rise to a maximum of 40 °F and 36 °F per hour, respectively.

The optimum rate of heat application can be determined by balancing the concepts of concrete “maturity,” the thermodynamic law of heat exchange, and the power requirements of the curing system. Maturity is defined as the area under the time-temperature curve. A typical time-temperature curve is illustrated in **Figure 3.3.5.5.2-1**. For a given concrete mix, equal maturities theoretically result in equal concrete strengths, and can be obtained with different rates of heat application by varying the length of time the heat is applied. The desirability of long preset periods, combined with the need for a minimum level of maturity to achieve the required concrete transfer strength, can lead to the conclusion that the concrete temperature should be raised rapidly. However, the law of heat exchange requires a larger amount of heat energy for rapid increases in temperature than for more gradual increases.

Figure 3.3.5.5.2-1
Typical Time-Temperature Curing Cycle Graph

These considerations have implications for both the initial and operating cost of the curing system. For example,



with an electric curing system, the watt density of the heating elements on the form would need to be high, resulting in a close spacing of the elements. The system would also require greater peak power capacity. The high initial cost of the elements, as well as a larger power supply, is usually not justified when the peak power demand will be required for less than 25% of the curing cycle. Economic analysis of the installation and operating costs show that the optimum solution is to install a system that under 100% power raises the concrete temperature at a slower rate, usually between 15 °F to 20 °F per hour. Curing system equipment suppliers can assist with this determination.

FABRICATION AND CONSTRUCTION**3.3.6 Removing Products from Forms/3.3.7 In-Plant Handling****3.3.6 Removing Products from Forms**

Regardless of whether a product is cured normally or with accelerated methods, common procedures and precautions must be followed to safely remove the member from the form without damage. This procedure is referred to as “stripping” the products or, sometimes, “stripping the beds.” The sequence of tasks is generally performed in the following order:

1. Verify that the strength of the concrete in the product is at or above the specified stripping or transfer strength. Concrete strength testing is discussed in **Section 3.4.5**.
2. For accelerated curing systems, cease heating. In some of the more sophisticated systems, the heat can be stopped before Step 1 based on the “maturity” calculated from the time-temperature curve. See **Section 3.3.5.2**.
3. Remove curing blankets, tarpaulins, and where necessary, side forms. For pretensioned products that have been heat cured, the members must still be warm and moist at the time of transfer. If not, the unstressed concrete, still restrained by the tensioned strands, will cool and contract, possibly resulting in transverse cracking through the member. See **Section 3.3.1.5** for a discussion on the removal of side forms.
4. Remove all remaining ties, inserts and other devices that will prevent lifting the product free of the form, with the exception of the strand hold-down devices. Strand hold-downs are to be released at the appropriate time in the transfer sequence. **Section 3.3.2.8.4** provides discussion on releasing strand hold-downs.
5. For pretensioned products, transfer the prestressing force using the procedures and precautions outlined in **Section 3.3.2.8**. Cut all strands at both ends of a member if the force is transferred hydraulically.
6. Connect proper rigging to the lifting devices embedded in the member, and install lateral stability hardware, if required. See **Sections 3.2.4.4** and **3.3.3.2** for information on lifting devices. **Section 3.3.7.4** discusses lateral stability issues for long slender members.

3.3.6.1 Form Suction

After performing the steps listed in the previous section, the member is now ready to be stripped from the form and transported to the yard for storage. When lifting the product from the form, the cranes, rigging, and lifting devices should be sized considering factors including the amount of suction expected from the specific form. Concrete stresses should also be determined considering such effects. Suction on pretensioned members whose side forms have been removed is normally minimal, since elastic shortening and camber that result at the transfer of prestress will usually break the bond between the concrete and the remaining forms. Pretensioned members should not have transverse monolithic ribs or diaphragms unless provisions are made in the formwork to prevent the member from locking itself into the form as it undergoes shrinkage and elastic shortening. Conventionally reinforced members removed from fixed forms with numerous drafted vertical surfaces can experience significant suction. For purposes of analysis, increasing the member dead load by 50% is normally sufficient to account for form suction.

3.3.7 In-Plant Handling

Precast plants are normally designed in “linear” fashion in order to facilitate the most efficient movement of products from the casting bed to yard storage. **Figure 3.3.7-1** shows the linear pattern of a typical precast plant. Usually, products just stripped are first moved from the casting bed to a designated finishing area. The finish area is set up to provide ready access to all portions of the member that need post-stripping finish work. For deep members, this area may include scaffolding or platforms with railings that meet OSHA fall protection standards. Many of the finishing tasks described in **Section 3.2.5** are performed in this area. Once the member is moved into storage, access is normally limited due to stacking and adjacent stored members.

FABRICATION AND CONSTRUCTION

3.3.7 In-Plant Handling/3.3.7.1 Handling Equipment

Figure 3.3.7-1
Typical Precasting Plant Aerial Photo Showing “Linear” Layout



Precast products should be handled only with properly designed and installed lifting devices. The lifting devices used in the plant may or may not be the same as those used for erection in the field, since the product orientation in the completed structure may not be the same as that in which it is cast, stored and shipped. Erection considerations are sometimes significantly different than handling and storage considerations in the plant.

3.3.7.1 Handling Equipment

Precast products are moved around the yard by a variety of equipment, ranging from large forklifts to large gantry cranes on tracks. Rubber-tired gantry cranes, normally referred to as travel lifts, or straddle-carriers, are probably the most common choice by precast producers. See **Figure 3.3.7.1-1**. This equipment is designed to lift and transport heavy loads without the need for shuttle trucks or other equipment, and are not confined to movement on tracks. Travel lifts can use relatively narrow aisles to pass between stored products, allowing the producer to maximize yard storage. Travel lifts are widely available in capacities that accommodate the heaviest practical precast members. Maximum piece weights can be limited by lifting equipment available in the plant, or by the maximum weight that can be shipped by truck. Bridge designers should consult local producers for plant handling capability.

Figure 3.3.7.1-1
Straddle-Carrier



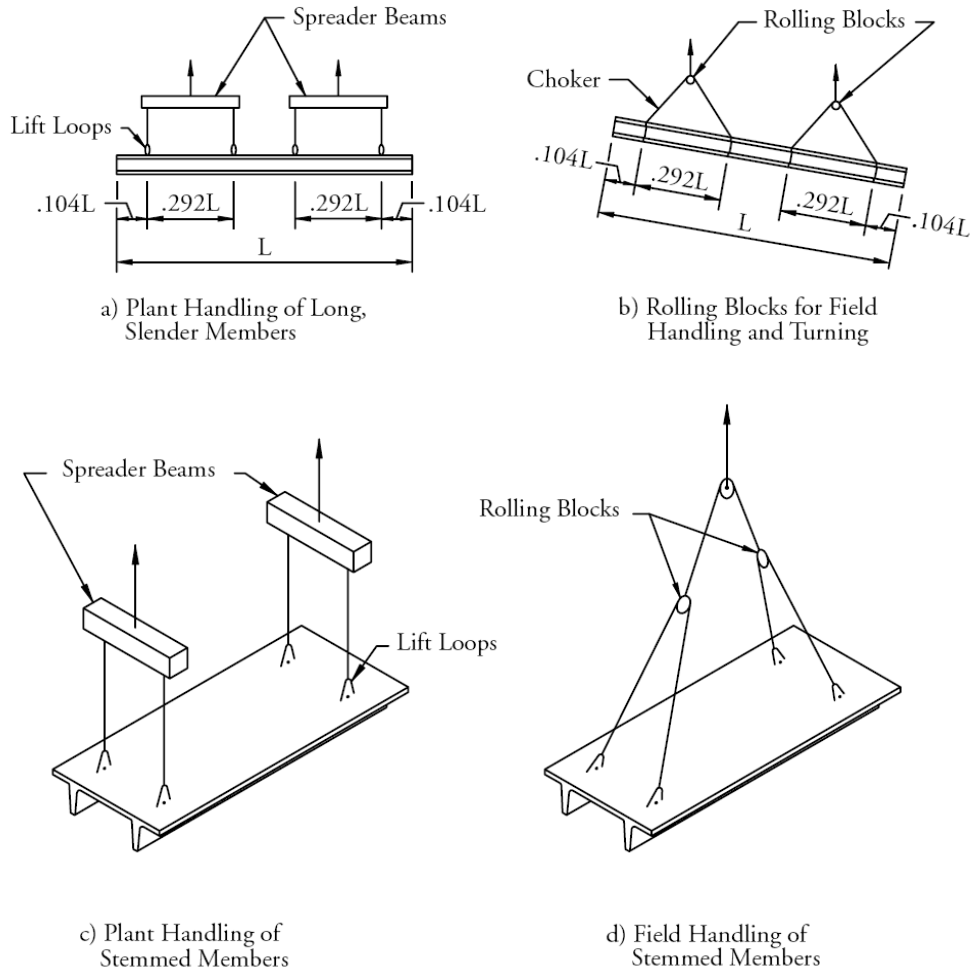
FABRICATION AND CONSTRUCTION

3.3.7.2 Rigging/3.3.7.3 Handling Stresses

3.3.7.2 Rigging

When multiple lifting points are used, techniques for equalizing the load on each lifting device are necessary to assure that the rigging is statically determinate. This is usually done with rolling blocks, spreader beams or lifting trusses. **Figure 3.3.7.2-1** shows typical rigging arrangements for multiple point lifts.

Figure 3.3.7.2-1a-1d
Rigging for Multiple Point Lifting



3.3.7.3 Handling Stresses

The most critical time in handling a precast member in the plant is when it is initially lifted from the form. The concrete strength is lower and, in pretensioned members, the prestressing force is higher than at any other time in the life of the member. To minimize concrete stresses due to the eccentricity of prestress, pretensioned flexural members are handled with lifting devices as close as practical to the location where the member will be supported in the structure. With the exception of members with pretensioned cantilevers, lifting devices are located near the ends.

Centrically pretensioned or conventionally reinforced members are handled at two or more points in order to restrict the concrete tensile stresses below the cracking limit. Normally, a capacity-to-load ratio of 1.5 is applied to the concrete modulus of rupture (see **Section 2.5.4**), resulting in an allowable tensile stress of $5\sqrt{f'_c}$ for normal weight concrete. In addition, an impact factor is applied to the dead weight of the member if form suction is expected to be significant, as discussed in **Section 3.3.6.1**. Optimum lifting locations equalize positive and

FABRICATION AND CONSTRUCTION**3.3.7.3 Handling Stresses/3.3.8.2 Storage of Concentrically Prestressed or Conventionally Reinforced Products**

negative moments in members of constant cross section where the section modulus is the same at the top and bottom. For example, members lifted at two points will have equal positive and negative moments if the lifting points are located 0.207 times the member length from the ends. The use of optimum lifting locations is not always necessary, as long as the concrete stresses are within allowable limits. In many cases, available plant equipment determines the lifting locations. Phillips and Sheppard (1980) and the PCI Design Handbook provide useful information on handling precast concrete products.

3.3.7.4 Lateral Stability during Handling

Long, slender sections can become unstable when handled with lifting devices located near the ends. Studies by Mast (1989 and 1993) conclude that the most important parameter for lateral stability during handling is the lateral bending stiffness of the member. The simplest method to improve lateral stiffness is to move the lifting devices in from the ends. However, doing so normally increases the concrete stresses at the lifting points and, sometimes, the required concrete transfer strength. Other methods of improving lateral stiffness are available, as discussed by Imper and Laszlo (1987), but add to the cost of the product. See **Section 8.10** for a more in-depth discussion of lateral stability considerations during handling and shipping.

3.3.8 In-Plant Storage

Precast products must be stored so they do not touch the ground and in a manner that minimizes the potential for damage. Storage foundations should be of sufficient size and strength to resist crushing or excessive settlement. Properly designed storage is normally governed by consideration of the control of permanent concrete deformations rather than control of concrete stresses. Although improper storage can lead to cracking, spalling, or other damage, supports that cause no apparent initial damage can result in undesirable permanent deformations caused by creep of the concrete. Storage techniques depend on the product type, and whether the members are eccentrically prestressed, concentrically prestressed, or conventionally reinforced.

3.3.8.1 Storage of Eccentrically Prestressed Products

Eccentrically prestressed flexural members (without pretensioned cantilevers) should be supported as close to the ends as possible. Storing members on supports a significant distance from the ends may result in undesirable camber growth. Deep members, such as I-beams or bulb-tees, should always be stored plumb. The dead load of an out-of-plumb member induces moments about its weak axis, which can lead to a permanent horizontal sweep. Long, slender members may require temporary bracing for stability during long-term storage.

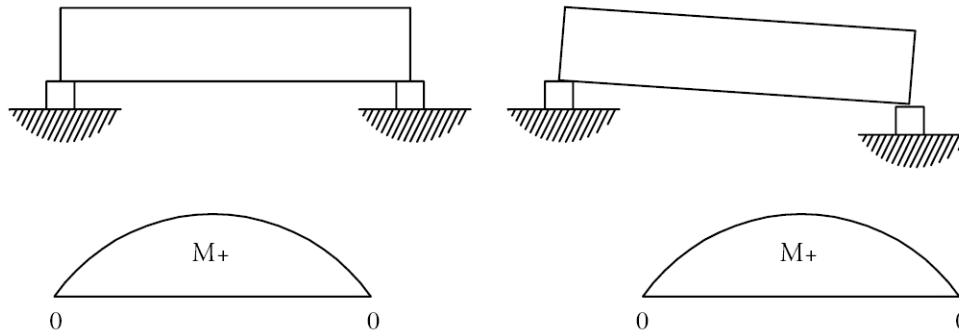
3.3.8.2 Storage of Concentrically Prestressed or Conventionally Reinforced Products

Concentrically prestressed piles are supported in storage at relatively short intervals along their length (approximately 20 ft). Piles are normally long and slender, with a relatively high level of prestress. Although they can be handled and shipped with relatively large spaces between supports, storing them in this manner for more than a few days can result in permanent deformations. Conventionally reinforced beams and columns are normally stored with supports under the lifting locations. Wall panels, which are usually cast flat, can be stored in this orientation for a short period, but generally are turned on edge for long-term storage to prevent permanent bowing or warping.

FABRICATION AND CONSTRUCTION

3.3.8.2 Storage of Concentrically Prestressed or Conventionally Reinforced Products/3.3.8.3 Stacking

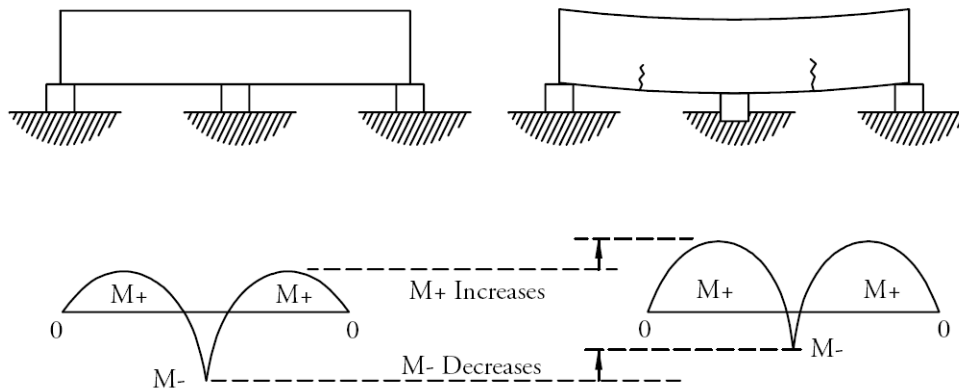
Figure 3.3.8.2-1a-1b
Product Storage Points



M Diagram

No Change in Moments Due to Settlement
Settlement in a Two-Point Support System: No Redistribution of Moment

a) Two-Point Supports



M Diagram

Change in Moment Due to Settlement

b) Multiple Supports

Multiple supports must be set and maintained at the proper elevation to provide uniform support to the member. This is not as critical for two-point supports, because differential settlement between supports has no detrimental effect on concrete stresses. However, misplaced or differential settlement of multiple supports can have a substantial effect on both concrete stresses and permanent deformations. **Figure 3.3.8.2-1** illustrates this condition.

3.3.8.3 Stacking

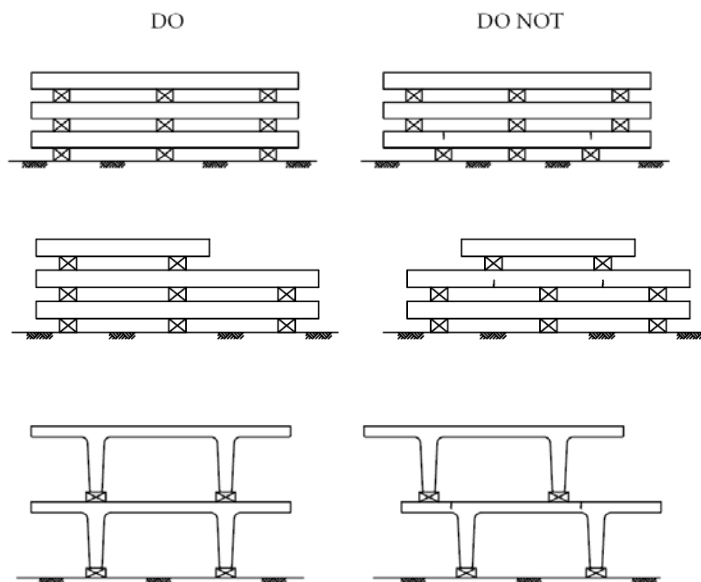
In most precast plants, yard storage is limited. Deep flexural members, such as I-beams or some box beams, are generally placed close to one another to conserve space. Shallow members, such as deck panels, stemmed members, or piles, are normally stacked. When stacking products, foundations and supports between levels, must be of sufficient size and strength to support the increased weight. Foundations and intermediate supports must

FABRICATION AND CONSTRUCTION

3.3.8.3 Stacking/3.3.9 Roughened Surfaces

align vertically, providing a direct load path to the foundation. Short members should not be stacked on longer members, unless the supports can be aligned vertically, or analysis shows that the lower members will not be damaged or otherwise compromised. **Figure 3.3.8.3-1** illustrates some “dos and don’ts” for stacking. Steel projecting from the tops of members, such as stirrups or lifting devices, can hamper stacking. Supports between levels must be of sufficient height to prevent damage to the projecting steel, or marring of the upper-level concrete soffits.

Figure 3.3.8.3-1
Some “Dos” and “Do Nots” When Stacking Precast Products



3.3.8.4 Weathering

For long-term storage, consideration should be given to the effects of weathering. It is not practical to expect precast concrete products to be stored indoors, or to be effectively protected from the environment. **Section 3.2.5.6** discusses measures that may be taken to prevent corrosion of exposed steel, and the resulting unsightly staining of the concrete surface. When a “like new” appearance is desired in the finished structure, the most cost-effective choice is to clean the concrete surfaces at completion of construction.

3.3.9 Roughened Surfaces

Many precast concrete bridge products are designed to behave compositely with cast-in-place concrete. That is, the two separate concrete placements are intended to act as a unit when resisting externally applied loads. In order for this to occur, shear must be transferred across the interface between the two concrete layers. Typical designs use the “shear-friction” concept at the interface. Design advantages are realized when the surface of the precast member which will interface with cast-in-place concrete is intentionally roughened to a full amplitude of approximately $\frac{1}{4}$ in., although the shear-friction concept does not require roughening. See LRFD Article 5.8.4.3. Roughening of surfaces is very common in the precast industry. Methods used depend upon whether the surface to be roughened is exposed or formed.

A requirement common to both exposed and formed roughened surfaces is that they must be clean and free of laitance prior to placing the cast-in-place concrete. It is also generally desirable to moisten the precast surface prior to the second placement.

FABRICATION AND CONSTRUCTION**3.3.9.1 Roughening Exposed Surfaces/3.3.9.2 Roughening Formed Surfaces****3.3.9.1 Roughening Exposed Surfaces**

The standard method of roughening exposed surfaces is to “rake” or “broom” the concrete while it is still in its plastic state. After the concrete has been struck level, a workman rakes the surface with a tool that creates grooves at a specified spacing and depth. These grooves normally run transverse to the direction of the anticipated shear force, and must be deep enough to produce the desired roughness, but not so deep so as to dislodge individual aggregate particles near the surface. **Figure 3.3.9.1-1** shows a typical raked surface.

This type of surface is common on the tops of I-beams, bulb-tees, and box beams that are subsequently made composite with a cast-in-place concrete bridge deck.

Figure 3.3.9.1-1
Roughened Composite Surface

**3.3.9.2 Roughening Formed Surfaces**

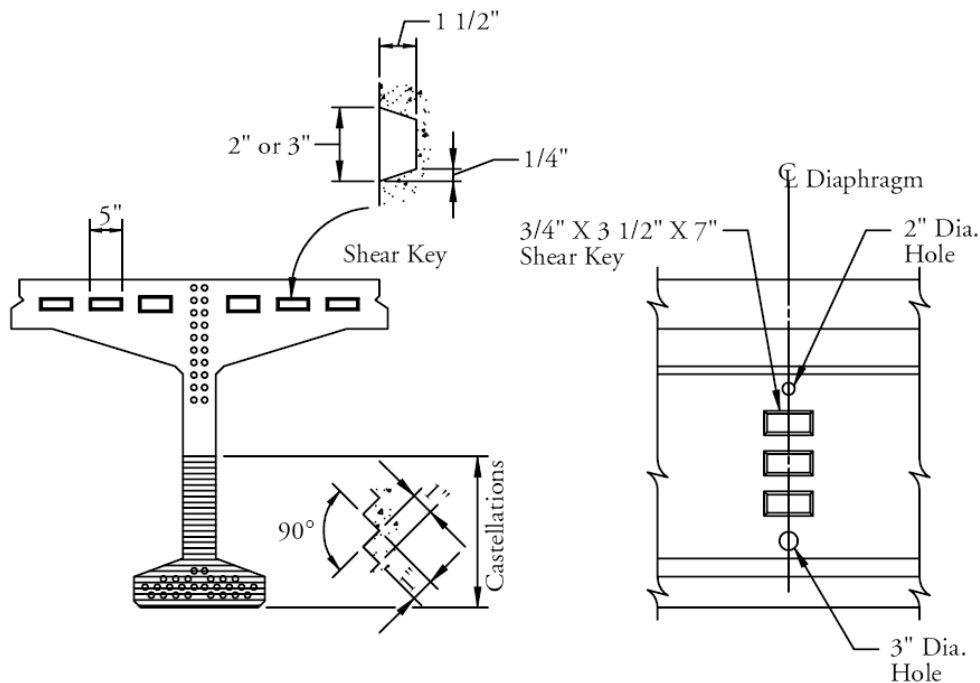
Obviously, formed surfaces cannot be roughened in the same manner as exposed surfaces. Several methods are used to roughen formed surfaces:

- chemical surface set retarders
- deep sandblasting
- textured form liner
- bush-hammering
- shear keys
- castellations
- multiple sawings of parallel grooves

Surface set retarders, which locally retard the setting of cement, are painted onto the form in the desired location prior to casting the concrete. After form removal, the retarder is pressure washed from the concrete surface, resulting in a roughened, exposed-aggregate finish. Set retarders are formulated with different strengths to result in varying depths of retardation. Normally, the strongest formulation is required to achieve the roughness desired for composite action. Both sandblasting and bush-hammering are done manually after the product is stripped. They are labor intensive. Shear keys and castellations are formed into the concrete surface. **Figure 3.3.9.2-1** shows typical shear key and castellation configurations. Roughened formed surfaces are normally used at the interface with cast-in-place concrete diaphragms, or at beam ends that frame into cast-in-place piers.

FABRICATION AND CONSTRUCTION**3.3.9.2 Roughening Formed Surfaces/3.3.10.1 Match Casting Techniques**

Figure 3.3.9.2-1a-1b
Typical Castellations and Shear Keys in Formed Surfaces



a) Beam End for End Diaphragm Cast

b) Beam Web for Intermediate Diaphragm Cast

3.3.10 Match-Cast Members

Match-cast precast products are typically used in segmental construction to ensure the proper fit-up of mating surfaces between precast segments while providing for the profile grade and horizontal alignment required by design. Segment sizes are most often determined by available handling and shipping equipment capacities, but may also be dictated by the amount of form the manufacturer has on hand. Although practically any type of precast product can be match cast, this construction method applies primarily to long-span construction using flanged box beam or deep I-beam segments. There are many exceptions. A major truss bridge was recently redecked using full-depth, match-cast slabs that were prestressed both longitudinally and transversely.

3.3.10.1 Match Casting Techniques

Two basic techniques are used to match cast precast bridge segments, one employing a stationary form, the other involving a form that is moved for every casting. With the stationary form, the first segment is cast with endplates at both ends of the form. After this segment has been cured to a concrete strength adequate for stripping, it is lifted out of the form and positioned adjacent to the form so that one of its ends serves as the endplate for the match-cast end of the second segment. The other end of the second segment is formed with one of the original endplates.

The positioning of the first segment relative to the form is critical, since it dictates the precise alignment of the two segments in the completed structure. Sophisticated surveying techniques, together with adjustable screw jacks and stops, are normally used to accurately position the segment. Prior to casting, the match-cast end of this segment is coated with a debonding agent to allow separation of the segments after casting.

After the second segment achieves stripping strength, both segments can be stripped from the form. The first segment is moved to storage, while the conventionally formed end of second segment assumes the role of the endplate for the third segment to be cast. This process continues until all segments are cast.

FABRICATION AND CONSTRUCTION**3.3.10.1 Match Casting Techniques/3.4.1 Plant and Inspection Agency Interaction**

The “moving form” technique begins in a similar manner; however, after the first segment is cast and cured, it is left stationary on the form pallet. The form is stripped, moved longitudinally, and positioned at the end of the first segment. The second segment is then match-cast against the first in the same manner as described above. This approach has the advantage of decreasing segment handling, but requires multiple form pallets and significantly more space.

3.3.10.2 Joining Match-Cast Members with Epoxy

A common method of joining match-cast segments is by “cementing” them together with a thin (approximately 0.02- to 0.04-in.-thick) layer of epoxy bonder. Because the epoxy coat is thin, it is essential that the member ends be properly mated. The normal construction sequence begins with the application of a slow-setting epoxy to the mating ends. The epoxy should be applied in accordance with the manufacturer’s recommendations. The ends are then assembled, and an initial post-tensioning force is applied across the interface. Gerwick (1993) notes that the best results are obtained when the epoxy cures under a stress of about 40 psi. This is done progressively for each pair of match-cast segments. Once a predetermined number of segments have been joined, and the epoxy in all joints has cured, a final post-tensioning force is applied to the superstructure (or portion of the superstructure). In segmental I-beam bridges, final post-tensioning is usually done after the cast-in-place deck has been placed.

3.4 PLANT QUALITY CONTROL AND QUALITY ASSURANCE

Plant-cast concrete bridge products benefit substantially from the controlled conditions under which they are fabricated. **Section 3.3** offers many examples of fabrication procedures that are easier to control and inspect than is the case with field construction. PCI-Certified plants are required to maintain rigorous quality control programs that satisfy the requirements of the project specifications, or PCI Manual 116, whichever are more stringent. At least twice each year, certified plants receive unannounced audits for compliance with these requirements by an independent engineering firm that is employed and accredited by PCI. The following section discusses plant quality control procedures, and the resulting benefits to the purchaser.

In 2009, the AASHTO Subcommittee on Bridges and Structures, during their general business meeting, passed a resolution officially recognizing “National industry certification programs for personnel, production, and quality control related to prefabricated structural bridge components and processes”. The committee cited a number of reasons that technical institutes are the best source to ensure that standards and certification procedures fully engage current research results and state-of-the-art techniques. Following this meeting a number of activities took place to further emphasize the value that continuous quality feedback has on the overall relevance of industry-accredited plant quality. Further, without a direct chain of custody to the body of knowledge related to the industry in question, those that are performing plant audits may or may not have full understanding of documents and standards related to the process. PCI joined with the American Institute of Steel Construction and published a white paper titled “Quality Systems in the Construction Industry”. See references AASHTO Resolution, 2009 and AISC-PCI, 2009.

3.4.1 Plant and Inspection Agency Interaction

The production process for precast, prestressed concrete differs substantially from common field construction. Consequently, it is important that quality control personnel be qualified to inspect all phases of fabrication. PCI currently offers three levels of training and certification for quality control personnel, with a fourth for accreditation of the auditors themselves. Since the evaluation criteria for plant certification includes personnel qualifications, PCI-Certified plants must employ in-house quality control personnel who have been suitably trained in the inspection of precast, prestressed concrete products. This is not necessarily the case with outside inspection sources. However, some agencies have taken advantage of PCI training seminars, and require that their agency personnel are appropriately certified.* In addition, the production process frequently begins before

FABRICATION AND CONSTRUCTION**3.4.1 Plant and Inspection Agency Interaction/3.4.2.2 Honeycomb and Spalls**

sunrise with the testing of transfer strength cylinders, and ends after sunset with the covering of the product for accelerated curing. This time span complicates the inspection of all phases of fabrication by an individual inspector. Precast plants efficiently schedule their team of in-house inspectors to cover all phases of production.

**For further details contact the PCI Director of Certification Programs*

In order to make the best use of available personnel, several agencies have developed Quality Control/Quality Assurance programs that shift the accountability and responsibility for product quality to the manufacturer. Under these programs, the manufacturer is responsible for performing day-to-day quality control functions, while the agency assumes the role of review and acceptance. PCI Plant Certification provides the basis for these programs, which are then expanded to cover any specific needs of the agency. These industry/agency partnerships are part of the National Quality Initiative (NQI), which has been endorsed by the American Association of State Highway and Transportation Officials (AASHTO), Federal Highway Administration (FHWA), American Road and Transportation Builders Association (ARTBA), American Consulting Engineers Council (ACEC), Associated General Contractors of America (AGCA), American Public Works Association (APWA), and the concrete and asphalt industries. For more information on these programs, consult the AASHTO reports titled *Quality Assurance Guide Specifications (1996)* and *Implementation Manual For Quality Assurance (1996)*.

3.4.2 Product Evaluation and Repair

As with any manufacturing process, non-conformances can occur in precast concrete bridge products. Examples may include voids or cracks in the concrete, missing or improperly located inserts or holes, and incorrect projection of reinforcement. Nonconformances fall into one of three categories:

- Those that can be accepted in spite of the non-conformance
- Those that can be repaired satisfactorily
- Those that require rejection of the member

The following topics are covered in greater detail in PCI Manual 137, *Manual for the Evaluation and Repair of Precast, Prestressed Concrete Bridge Products*. This manual was developed by a group representing owner agencies, designers, and industry for the purpose of promoting a greater degree of uniformity with respect to the evaluation and repair procedures for precast, prestressed concrete bridge beams, deck panels, and similar precast products.

3.4.2.1 Surface Voids

In spite of the finest placing and consolidation techniques, surface voids or “bugholes” resulting from water and air bubbles trapped against the side forms should be anticipated in hardened concrete surfaces. These minor imperfections are usually not structurally detrimental. Additional finishing requirements should be based on the end use of the product, and should be established in the contract documents. It is generally not practical to specify an acceptable level of imperfections, such as an allowable percentage of void area within a given square foot of concrete surface, since these judgments are highly subjective. Maximum acceptable void sizes (diameter and depth) can be specified, although the evaluation of these criteria is tedious. The most cost-effective choice is to accept the surface “as-is.” Beyond this, it is questionable which is more economical: to identify and patch individual voids larger than specified; or to simply finish the entire surface as described in **Section 3.2.5.3**. PCI Manual 116 also provides a description of various grades of surface finishes.

3.4.2.2 Honeycomb and Spalls

Larger imperfections, such as honeycombed surfaces or spalls, require mortar patching. This type of repair, while being relatively simple to execute, is difficult to control from the perspective of long-term durability. The relatively shallow nature of the patch creates differential shrinkage between the patching and parent materials,

FABRICATION AND CONSTRUCTION**3.4.2.2 Honeycomb and Spalls/3.4.2.4.1 Plastic Shrinkage Cracks**

potentially resulting in cracking or failure of the patch. The following techniques are recommended and will mitigate problems with durability:

- Proper preparation of the void
- Application of a bonding agent *
- Patching mortar that exhibits low shrinkage properties
- Careful curing of the patch

*Some prepackaged mortars do not need additional bonding agents.

Most producers have proven patching materials and established procedures with proven performance histories. For honeycombed areas, it is important to remove all loose material to expose sound concrete prior to applying the patch. See **Section 3.2.5** for further information on patching materials and procedures.

Like conventional structural concrete, it is important that patches be properly cured after application, because their durability depends on the ultimate strength of the material and control of shrinkage. Application of a non-weathering, non-staining curing compound to a patch surface is recommended.

3.4.2.3 Repairing Large Voids

Very large voids, including those in pretensioned bridge products, can often be repaired by the concrete replacement method. By necessity, this repair procedure is performed prior to transferring the prestressing force to the member. First, the defective concrete is carefully chipped out to expose sound concrete. Care must be taken to avoid damaging reinforcing bars or strands. An epoxy-bond coat is then applied to all surfaces, and new concrete is consolidated into the void using internal vibration. This new concrete is specified to be the same or better than the concrete used in the original placement. The cure of the patch is carefully controlled and accelerated until it reaches the strength required for transfer of the prestressing force.

The key to the quality of concrete replacement is the ability to fully consolidate the new concrete into all portions of the void. From this perspective, the orientation of the void is important. For example, replacement of concrete in the top of an I-beam bottom flange is relatively easy to achieve. It is more difficult on vertical surfaces, such as I-beam webs.

3.4.2.4 Cracks

Cracks develop in conventionally reinforced precast members when the tensile stresses exceed the tensile strength of the concrete. In prestressed members, cracks occur when the tensile stresses exceed the tensile strength of the concrete combined with the internal stresses imparted by the prestressing. Tensile stresses develop in several ways:

- Restraint of volume changes
- Internal forces from prestressing
- Externally applied loads

Precast concrete bridge products are designed to be furnished crack-free. However, cracks should not be considered a reason for rejection unless the product is structurally or aesthetically impaired beyond repair. The following sections discuss cracks related to fabrication, common fabrication procedures used to minimize such cracking, and methods of repairing cracks that occur. **Section 3.3.7.3** discusses control of cracks during plant handling. Gerwick (1993) provides a comprehensive discussion of cracking. Also, see *PCI Fabrication and Shipment Cracks in Precast or Prestressed Beams and Columns* (1985).

3.4.2.4.1 Plastic Shrinkage Cracks

A common cause of cracking is shrinkage of the cement paste while the concrete is in its plastic state. During this period, the concrete has developed little or no tensile strength. Excessive evaporation of moisture from the surface will cause the paste to shrink, resulting in cracks that are jagged, discontinuous, and multidirectional in appearance, not unlike a crack pattern observed in a dried mud puddle. The shallow nature of these cracks

FABRICATION AND CONSTRUCTION**3.4.2.4.1 Plastic Shrinkage Cracks/3.4.2.4.3 Differential Curing Cracks**

(usually less than ½ in.) means they normally are not of structural concern, and can easily be repaired by rubbing full with mortar. However, they are unsightly, and often raise questions about the acceptability of the product. The best solution is to prevent these cracks from occurring altogether by providing a saturated atmosphere over all exposed surfaces during the curing process.

3.4.2.4.2 Cracks Due to Restraint of Volume Change

Volume changes are most pronounced along the longitudinal axis of a member, and can result from several sources, including:

- Temperature changes
- Drying shrinkage
- Elastic shortening upon transfer of prestress
- Creep of the concrete

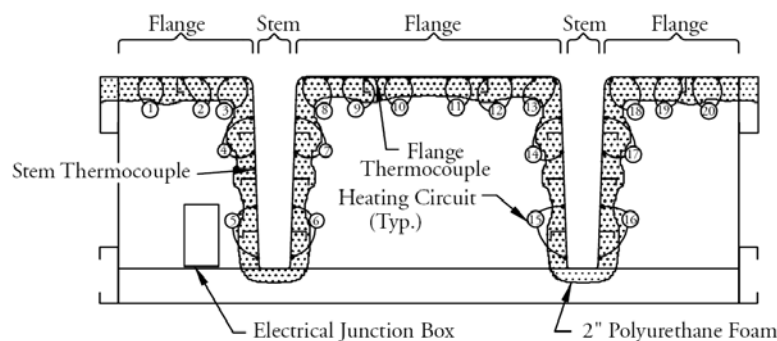
If these movements occur before the member is stripped, certain forms or attachments may restrain the change in volume, possibly resulting in tensile stresses and cracking. Cracks of this nature are normally continuous, narrow and relatively straight. To mitigate this potential for cracking, forms should be of a constant cross section, with no appreciable offset at joints, and attachments restraining the longitudinal movement of the member should be removed as soon as possible after accelerated curing is discontinued. Attachments transverse to the longitudinal axis of the member, such as monolithically cast diaphragms, should not be used unless provisions are made in the formwork to accommodate the anticipated volume changes.

Prestressing strands can also restrain longitudinal volume changes. It is not uncommon for an I-beam to develop vertical cracks at intervals along its length when it is allowed to cool with the strands still tensioned. One way to prevent this is to keep the member warm until transfer, although this is not always practical for beams that remain in forms over a weekend. Zia and Caner (1993) found this potential for cracking to diminish with increased length of free strand in the casting bed.

3.4.2.4.3 Differential Curing Cracks

Differential curing can also contribute to volume change cracking. Some products, such as stemmed members, have cross-sectional regions with varying volume-to-surface ratios. Depending upon the type of accelerated curing used, some regions can be warmer than others, causing a thermal differential that can result in cracking. This phenomenon contributes to a relatively common crack at the interface between the web and flange of stemmed members. One advantage of electric curing is that by varying the spacing and control of the heating elements for areas of different volume-to-surface ratios, relative heat gain can be better balanced. **Figure 3.4.2.4.3-1** shows a common electric curing configuration for stemmed members. The elements are more closely spaced in the flange than in the web, since the large open top results in significant heat loss from the flange with less heat of hydration. The flange and web elements are controlled separately by flange and web thermocouples to provide uniform heat gain in the different segments.

Figure 3.4.2.4.3-1
Form Cross Section Showing Electric Heat Element Layout and Insulation



FABRICATION AND CONSTRUCTION**3.4.2.4.4 Accidental Impact Cracks/3.4.2.6 Camber****3.4.2.4.4 Accidental Impact Cracks**

Another source of cracks during fabrication is from accidental impact. This type of cracking comes in all shapes and forms, and must be evaluated on an individual basis. A common example is cracking of the top flange of I-beams or bulb-tees during form removal. These cracks are not considered structurally significant unless they show signs that the reinforcement crossing the crack has yielded, such as for large crack widths or displacement of the adjacent surfaces.

3.4.2.5 Crack Repair**3.4.2.5.1 Autogenous Healing**

Under certain conditions, cracks in precast concrete members can literally repair themselves by autogenous healing. This process can be best described as unhydrated portland cement crystals growing together across the crack in the presence of moisture and under a clamping force. Zia and Caner (1993) recommends the region of the crack be kept moist a minimum of 7 days.

3.4.2.5.2 Crack Repair by Epoxy Injection

The most common method of repairing relatively narrow structural cracks is by epoxy injection. Modern epoxy injection methods using equipment that automatically meters, mixes and injects the two-component epoxy are very convenient and give excellent results. Follow manufacturer recommendations to seal cracks and install epoxy injection ports. Cracks as small as 0.002 in. have been successfully injected in the field with full penetration. Cracks, however, should be evaluated with regard to location and effect on serviceability. Small cracks in compression zones in service and not exposed to severe environments, may be best left alone. The ACI Committee 224 report, *Control of Cracking in Concrete Structures*, states that tolerable crack widths are 0.006 in. for concrete exposed to seawater and seawater spray, wetting and drying; 0.007 in. for concrete exposed to deicing chemicals; and 0.012 in. for concrete exposed to humidity, moist air or soil. It is recommended that the agency and precast producers establish limits for acceptable crack widths as well as repair procedures for those cracks that are determined to need repair. This type of repair is not always aesthetically acceptable, but most producers have developed cosmetic procedures to improve the appearance of the repair.

3.4.2.5.3 Crack Repair by Concrete Replacement

Large cracks which suggest yielding of the reinforcement generally are not repaired by epoxy injection. If the damage is localized, an appropriate repair procedure is to remove the damaged concrete and replace it in the manner described in **Section 3.4.2.3**. In cases where this repair is not applicable, judgment must be exercised as to the structural severity of the crack.

3.4.2.6 Camber

Camber is defined as the net upward deflection of an eccentrically prestressed member due to the combined member dead load moment and eccentricity of the prestress force. Camber can increase or decrease with time, depending on the level of prestress and sustained loads. A typical camber versus time graph is shown in **Figure 3.4.2.6-1**. Camber can be predicted with relative accuracy at the time of initial prestress, but the prediction of long-term camber should be considered an approximation.

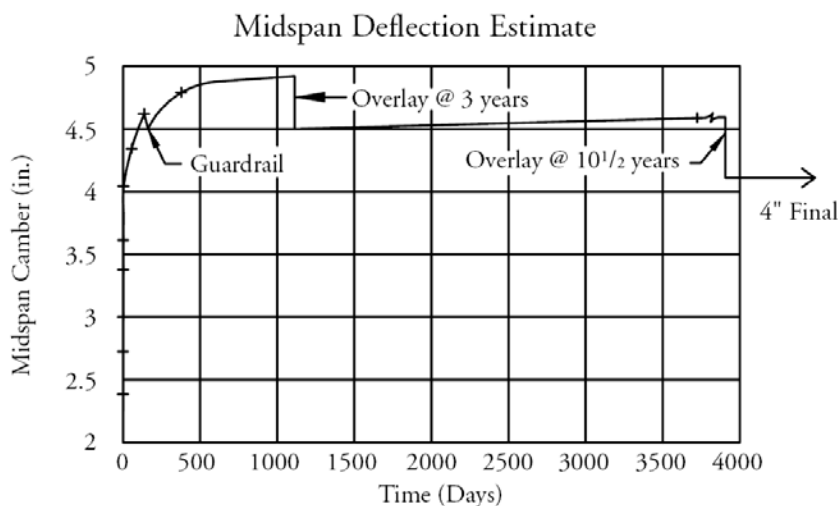
Measuring and recording actual initial camber, and comparing results to the theoretically computed value, is valuable in quantifying the consistency of production, assumed material properties as compared to actual, and quality control. Small variations in initial camber indicate good consistency in tensioning and concreting procedures, while large camber variations may represent poor consistency. Camber that is significantly lower than expected can indicate inadequate tensioning, improper quantity or placement of strands, or loss of bond between concrete and strand (excessive strand slip). Low camber can also result from concrete transfer strength that is higher than anticipated, such as in members that remain in the form over a weekend prior to initial prestress. Camber significantly higher than expected can result from low concrete strength, excessive force in the strands, or improper quantity or placement of strands.

FABRICATION AND CONSTRUCTION

3.4.2.6 Camber/3.4.2.6.3 Mitigation of Camber Growth

Predicting camber variability should be a mean (average) value, preferably with an indication of the range of variability but it is highly influenced by the modulus of elasticity. The variations in camber become more significant as the use of high-strength concrete, longer spans, and more heavily prestressed concrete beams continues to increase. The variability from the calculated value can be assumed to be $\pm 50\%$. See Tadros, et al., 2011.

Figure 3.4.2.6-1
Typical Time-Camber Graph (Deck Bulb-Tee)



3.4.2.6.1 Measuring Camber

The PCI Manual 116 requires measurement of camber to be taken on all members produced from the first cast on a new or unusual bed layout, and on no less than 25% of all other members produced each day. This measurement is to be taken as soon as possible after initial prestress, but not to exceed 72 hours after transfer of the prestressing force. The elapsed time to measurement of camber after transfer should remain consistent for a plant.

Several methods are used to measure initial camber. The simplest is to measure the upward deflection at midspan immediately after transfer, but before the member is lifted from the form, using the form soffit as the point of reference. Some products, such as stemmed members, are not easily accessible for this measurement. Once a product is stripped and moved to the yard, camber can be measured with a stringline, laser level, or a surveying level and rod. Camber measurements should be taken to a well defined point on the member, such as the top corner of a bottom flange, and not to an inconsistent surface, such as an intentionally roughened top flange.

3.4.2.6.2 Thermal Influences on Camber

Camber measurements should not be taken when the member is influenced by temporary differences in surface temperature. On a sunny day, the top of the top flange can be significantly warmer than the rest of the member, leading to a temporary increase in camber. Camber readings under these conditions will be misleading.

3.4.2.6.3 Mitigation of Camber Growth

Practical methods for mitigating camber growth are limited. As discussed in **Section 3.3.8.1**, eccentrically pretensioned flexural members should be stored on dunnage located as close to the ends as possible (or final support locations for members with cantilevers). Moving the dunnage away from the ends toward midspan reduces the dead load deflection, and can lead to increased permanent upward deflection. Adding a load to a member in storage to reduce long-term creep and camber is generally not feasible. Control is best accomplished

FABRICATION AND CONSTRUCTION**3.4.2.6.3 Mitigation of Camber Growth/3.4.3.2 Water-Cementitious Materials Ratio and Durability**

by scheduling production closer to erection or, if not possible, by allowing for increased camber in the design and detailing of the structure. In an unusual situation where camber is not adequate, it can be increased by moving the dunnage in from the ends during storage.

3.4.2.7 Sweep

Sweep is defined as horizontal bowing of a member, and can result from one of the following:

- Misaligned forms
- Lateral offset of the pretensioning strands
- Improper tensioning
- Thermal effects (sun on one surface)
- Improper storage

3.4.2.7.1 Mitigation of Sweep

Sweep is usually measured with a string line after the first day of production in a new form set-up. Once the initial casting is found to be acceptable, it is generally satisfactory to estimate the straightness of subsequent members, measuring only when the eye indicates a potential problem. As with camber, sweep should not be measured when the member is influenced by temporary differences in surface temperature from face-to-face.

The most obvious methods to control straightness are to assure that the forms are installed straight and true and that the prestressing strands are properly located. Also, as discussed in **Section 3.3.8.1**, precast members that are within tolerance for sweep must be stored plumb. Excessive sweep can sometimes be corrected by leaning the member in the direction opposite the sweep during storage. In this case, the effects of creep will work to straighten the member. In other cases, long slender members can be pulled laterally into alignment prior to final attachment in the structure

3.4.3 Water-Cementitious Materials Ratio

The definition of water-cementitious materials ratio and its relationship to mix design is discussed in **Chapter 2 Section 2.4.6**. In addition to portland cement, certain mineral admixtures are cementitious or pozzolanic and contribute to the strength of concrete. These are discussed in **Section 2.3.4**. Additional information may be found in the PCI manual, TM-103.

3.4.3.1 Mineral Admixtures and Workability

The high water demand of mineral admixtures has a significant impact on concrete workability. The influence of water-cementitious materials ratio on workability depends on the proportions of the different cementitious materials. For example, if a mix uses 225 pcy of water, 500 pcy of AASHTO M85 Type III cement, and 50 pcy of silica fume, its water-cementitious materials ratio is 0.41 ($225/500+50$). Assume this mix has a slump of 4 in. with a certain dosage of a water-reducing admixture. If the silica fume content is increased to 100 lb, and the cement content is reduced to 450 lb, the water-cementitious materials ratio is still 0.41, but the concrete will have a slump less than 4 in. if the same dosage of admixture is used. Trial mixes that investigate the relationship between mix constituents, plastic concrete properties, and hardened properties are essential in effective use of these admixtures and various mix designs. A discussion on calculating the relative equivalency of cementitious materials in mix designs is given in ACI 211.1.

3.4.3.2 Water-Cementitious Materials Ratio and Durability

It has been well documented that the primary variable affecting concrete durability is the water-cementitious materials ratio. Studies by Pfeifer, et al. (1987, 1996) have shown that lowering the water-cementitious materials ratio of a given mix reduces the chloride permeability of the concrete. Neville (1996) provides extensive discussion on the benefits of low water-cementitious materials ratios in improving concrete's resistance to abrasion, freeze-thaw deterioration, chemical attack, and deterioration in sea water.

FABRICATION AND CONSTRUCTION**3.4.3.2 Water-Cementitious Materials Ratio and Durability/3.4.4 Strand Condition**

A basic tenet is that the strength of concrete, be it compressive, tensile, or flexural, is inversely proportional to the water-cementitious materials ratio. Furthermore, the values of modulus of elasticity, shrinkage, creep, and permeability also have inverse relationships to the water-cementitious materials ratio. Hence, in producing high quality concrete, the goal is to keep the water-cementitious materials ratio to a minimum, and to maintain consistency throughout the concrete placement.

3.4.3.3 Water-Cementitious Materials Ratio without Water-Reducing Admixtures

Before the advent of water-reducing admixtures, the only means of obtaining a low water-cementitious materials ratio was to use minimal water in the mix. In order to achieve the strength necessary to make precast concrete bridge products feasible, concretes used high cement contents, very low slumps, and water-cementitious materials ratios in the range of 0.45 to 0.50. Good placement and consolidation were difficult to achieve with the relatively unsophisticated equipment available at the time.

3.4.3.4 Water-Cementitious Materials Ratio with Water-Reducing Admixtures

Water-reducing admixtures have made it possible to produce workable concrete while simultaneously decreasing the water content. The effects of water-reducing admixtures on the workability of concrete are discussed in **Section 3.2.1.3.1**. Normal water-reducing admixtures can generally produce workable concrete with water-cementitious ratios as low as 0.40. High-range water-reducing admixtures can further reduce the ratio to about 0.30 or slightly lower. Water-cementitious materials ratios at this low level can be handled in precast plants because of the short duration between mixing and placing, as well as the use of sophisticated consolidation techniques. This is generally not true of cast-in-place concrete construction.

Water-reducing admixtures can also be viewed as “cement-reducers.” Because the strength of concrete increases as the water-cementitious materials ratio decreases, in many cases the cement content can be reduced while maintaining concrete strength.

3.4.3.5 Controlling Water-Cementitious Materials Ratio

The PCI Manual 116 requires water to be added to the mixer within a tolerance of $\pm 1.5\%$ or one gallon, whichever is greater, from that which is specified in the mix design. This quantity of water includes free moisture in the aggregates, as discussed in **Section 2.4.6**. Most plants use some form of moisture meter that allows for continuous adjustment of water, based on the free moisture contained in the aggregates. Batching scales are accurately calibrated to assure that materials delivered to the mixer are within the specified tolerances.

3.4.3.6 Testing Water-Cementitious Materials Ratio

Concrete slump measured in accordance with AASHTO T119 provides a good measure of batching consistency for all types of concrete. For concretes without water-reducing admixtures, it can also provide an indication of water-cementitious materials ratios. However, this is generally not true of concretes with water-reducing admixtures. Concretes with very low water-cementitious materials ratios can exhibit high slumps when dosed with high-range water-reducers, yet are superior for use with precast products. As discussed in **Section 3.2.1.3**, concrete with water-reducing admixtures is less likely to segregate during placement than conventional concrete. Consequently, slump is not an appropriate indicator of water-cementitious materials ratio, and hence long-term performance, in mixes using water-reducing admixtures. The actual water-cementitious materials ratio of water-reduced concrete is best determined by calculation using the recorded quantity of each constituent added to the mixer, plus the free moisture in the aggregates.

3.4.4 Strand Condition

Prestressing strand must be protected from corrosion prior to use. Most strand suppliers provide protective wrappings for this purpose. Once this wrapping is removed, the strand pack should still be protected from extended exposure to the elements. The high tensile strength of strand makes it more susceptible to corrosion

FABRICATION AND CONSTRUCTION**3.4.4 Strand Condition/3.4.5.1 Number of Cylinders**

than lower strength steels. Storage under cover is preferred as a means of minimizing corrosion, but is not always practical.

Strand in which corrosion has pitted the surface should not be used. However, the presence of light rust on strand is not detrimental to bond, and in fact light rust can increase bond. If no pitting has developed on the strand surface, then there has been no loss of effective strand area. The rule of thumb is that if rust can be removed with a pencil eraser, and the strand shows no pits, then the rust level is not detrimental and the strand is acceptable for use. An article by Sason (1992) provides suggestions and photographs to assist in strand surface evaluation.

Special care must be used to prevent contamination of strand from form release agents, mud, grease or other contaminants. Form release agents should be applied to the form before stringing the strands in the bed. After stringing and tensioning, the strand should be inspected for contamination, and cleaned with an effective solvent if necessary before concrete placement.

Packing bands on strand packs should not be cut with a torch flame as doing so may damage the strand. In addition, welding in the vicinity of strands must be strictly prohibited.

3.4.5 Concrete Strength Testing

There are generally three intervals when it is important to evaluate the compressive strength of the concrete in a prestressed bridge member:

- At the time of transfer of the prestressing force
- At the time of transportation and erection
- At 28 days

If the member is shipped and erected after 28 days from casting, strength tests are normally not required for shipping. Cylinder ages other than 28 days may be specified for members that will receive loads at ages appreciably different from 28 days. Also, recent, higher strength concrete mixes have been used that specify strength testing at 56 days. By far, the most common method of evaluating concrete compressive strength is by making and testing cylinders of the production concrete. This testing is done in accordance with the relevant specifications. PCI Manual 116 provides guidelines used by the industry for concrete strength testing. It includes further discussion on the compressive strength of concrete.

Molds used for forming concrete test cylinders must meet the requirements of AASHTO M205, which describes both reusable and single-use molds. In general, reusable molds are used in precast plant production. When very high-strength concretes are being produced, it may be necessary to use very rigid molds, such as reusable steel molds, to ensure that dimensional tolerances of the test cylinders are maintained. Otherwise, precision grinding of the ends or casting end caps may be necessary. See **Section 3.4.5.3**.

3.4.5.1 Number of Cylinders

PCI Manual 116 requires the strength at any given age to be determined by the average of at least two cylinder tests, with the exception of the transfer strength or predictive strengths less than 28 days, which can be determined by one cylinder test. Many specifications for bridge products require an average of two cylinder tests each time the concrete strength is to be determined, and still others require three cylinder tests for any age. Testing two cylinders at three separate ages requires a minimum of six cylinders for each product or production line of products cast in a continuous pour. From a producer's perspective, there is a certain level of risk in casting only the minimum number of test specimens. If the first cylinder broken falls below the specified transfer strength, too few specimens remain for the required testing. Many plants cast extra cylinders to account for this possibility. When sophisticated curing systems are used, the concrete maturity can give a good indication of when the first cylinder should be tested, as discussed in **Section 3.3.5.5.2**. When the number of cylinders made is not adequate, alternate methods of determining the concrete compressive strength are necessary, as discussed in **Sections 3.4.5.5** and **3.4.5.6**.

FABRICATION AND CONSTRUCTION**3.4.5.2 Test Cylinder Size/3.4.5.4.1 Cylinder Curing Cabinets****3.4.5.2 Test Cylinder Size**

Test cylinders made in a plant are cast in accordance with AASHTO T23 and PCI Manual 116. Both allow the use of 6 x 12 in. and 4 x 8 in. cylinders. Because of the high strength of concrete commonly associated with precast bridge products, the smaller cylinders are more compatible with the limitations of more common and less costly testing machines.

Studies by Neville (1966) indicate that 4 x 8 in. test cylinders can result in a slightly higher compressive strength than 6 x 12 in. cylinders. This becomes more pronounced with increasing concrete strength. Accordingly, PCI Manual 116 requires that side-by-side 4 x 8 in. and 6 x 12 in. samples be made and tested to develop a correlation between the two sizes. **Table 3.4.5.2-1** shows a sample correlation of concrete strength for the two cylinder sizes.

Table 3.4.5.2-1
Sample Correlation of Cylinder Compressive Strengths for 4 x 8 in. versus 6 x 12 in. Cylinders

Concrete Strength Range (ksi)	$\frac{f'_c(4" \times 8")}{f'_c(6" \times 12")}$
2.0 – 3.0	1.00
3.5 – 5.5	1.05
5.5 – 7.5	1.07
7.5 – 11.0	1.12

3.4.5.3 Alternate Cylinder Capping Methods

The ends of cast cylinders or drilled cores are usually not plane, flat, and at right angles to the side of the cylinder. PCI Manual 116 requires cylinders to be capped unless their ends are cast or ground to within 0.002 in. of a plane surface.

The capping material used historically has been a fast setting sulfur compound applied in accordance with ASTM C617. This method generates toxic sulfur fumes and involves the hazard of handling very hot molten sulfur. Though this method served the industry well for many years, it is now used much less often. In 1985, AASHTO adopted a method of compression strength testing (AASHTO T22 Annex) using neoprene pads and steel retainer caps. This reusable capping system reduces the cost of sample preparation, since neoprene pads are less expensive than sulfur capping compound and the labor required to prepare a cylinder for testing is reduced. This capping system also produces more consistent test results, and diminishes the effect of the human element in the capping operation. The average compressive strengths obtained are equivalent to, or slightly higher than, cylinders capped with molten sulfur.

3.4.5.4 Cylinder Curing Systems and Procedures

The strength of concrete test cylinders made to evaluate the strength of the concrete in a precast bridge member is only meaningful if the cylinders and the member have been cured under similar time-temperature conditions. The common practice of placing cylinder molds on top, along side, or under product forms may not produce representative test specimens. Cylinders cured in this manner generally do not gain strength as rapidly as the product, and sometimes the reverse can be true. This method is unreliable and can provide misleading results.

3.4.5.4.1 Cylinder Curing Cabinets

Cylinder curing cabinets are essentially insulated enclosures into which standard cylinder molds are placed. There are two basic types of cabinets: a wet system where water is used as the heat transfer medium, and a dry system where air in the cabinet is the heat transfer medium. Both systems usually incorporate an electric heating

FABRICATION AND CONSTRUCTION**3.4.5.4.1 Cylinder Curing Cabinets/3.4.5.6 Non-Destructive Testing**

system with a thermostat that senses the product temperature and in turn controls the heating system to closely approximate the product temperature.

The water-filled cabinet provides more uniform heat to the test specimen and is easier to control. The test specimen temperature will slightly lag that of the product during the warm-up period, since the water must be heated before the heat can get to the cylinder mold. Temperatures of cylinders in water-filled cabinets will not follow the member if the product temperature begins to fall significantly. The insulated cabinet is incapable of dissipating the heat energy unless the cabinet is opened to the surrounding air.

The dry cabinet consumes less energy than the wet cabinet and is easier to maintain. However, it is susceptible to creating slightly variable temperatures in the cylinders, as temperature is difficult to control with precision. The dry cabinet is easier to cool. Neither cabinet is readily portable and therefore must be set up permanently in one location. Either cabinet is a better solution than placing test specimens with the product.

3.4.5.4.2 Self-Insulated Cylinder Molds

This state-of-the-art method of curing concrete test specimens utilizes metal molds that are self-insulated and have a built-in heater and temperature sensor that work in conjunction with a solid-state temperature controller. A thermocouple located to sense the internal temperature of the precast concrete member being cured is plugged into the controller, along with the thermocouple from the cylinder mold. The controller continuously compares the temperature of the member with the temperature of the test specimen, and toggles the test mold heater on or off depending on whether the temperature of the test specimen is above or below the product temperature. This system is capable of maintaining the temperature of the test specimen within 5 °F of the product temperature, regardless of whether the temperature of the product is rising or falling.

3.4.5.4.3 Long-Term Cylinder Curing

Typically, all cylinders are initially cured under conditions similar to those of the product. After the transfer cylinders are tested and the member is stripped, the later-age cylinders are removed from their molds, and placed in moist storage at 73.4 °F (± 3 °F) in accordance with AASHTO T23.

Some specifications require that the cylinders be stored with the product. Most precast concrete bridge members have much larger volume-to-surface ratios than the cylinders. Consequently, storage under the same conditions would cause the cylinders to both dry and cool much faster than the product they are intended to represent. Experience has shown that cylinders stored in this manner, particularly during the cold winter months, suffer reduced strength development and do not accurately represent the strength of the product. They should never be used for acceptance testing of the concrete mix or ultimate strength of the concrete in the product.

3.4.5.5 Concrete Cores

As mentioned in **Section 3.4.5.1**, when the number of cast cylinders is inadequate, an alternate means of determining concrete strength is necessary. One of the most common procedures involves drilling and testing cores from the precast member in accordance with AASHTO T24. Cores are usually removed from a “neutral” location in the product, such as near the neutral axis of a flexural member, and must also be located to avoid reinforcement and other embedments. These cores are not evaluated by the same criteria as cast cylinders, since the aggregates are cut at the sides and cannot be compared to a molded specimen. ACI 318 states that concrete in an area represented by core tests shall be considered structurally adequate if the average of three cores is equal to at least 85% of f'_c and if no single core is less than 75% of f'_c . Campbell and Tobin (1967) provides further information on core strengths. Further, the size and shape of the core must be considered when evaluating its strength, as described by Neville (1966). All holes resulting from cores must be filled with a low shrinkage concrete having a compressive strength at least equal to that of the precast member.

3.4.5.6 Non-Destructive Testing

Several alternate procedures can be used to test the concrete strength of products without destroying the product or the area tested. PCI Manual 116 lists the methods currently available. These procedures are normally

FABRICATION AND CONSTRUCTION**3.4.5.6 Non-Destructive Testing/3.5.1 Weight Limitations**

employed for comparative or qualitative purposes, and are not intended to replace cylinder testing.

Nondestructive test methods are acceptable provided the following conditions are met:

- A correlation curve is established for each combination of concrete mix design, curing procedure, and age of test
- A minimum of 30 tests is used for each correlation curve
- Test results fall within the 95% confidence limits of the correlation curve
- Correlation curves are established for each test instrument, even of the same type

If properly correlated with cylinder tests, nondestructive tests may be used to evaluate the transfer strength of products if the number of available cylinders is insufficient. Rebound hammer testing is commonly used to determine concrete strength at all ages for dry-cast products, such as hollow-core slabs.

3.4.6 Tolerances

Good design and detailing practices for precast components and connections always consider allowable tolerances for fabrication, erection, and interfacing field construction. PCI Manual 116 lists industry standard tolerances for typical precast concrete bridge members. Details allowing generous tolerances usually result in economies during construction, while extremely stringent tolerances can be very expensive and in some cases, may not be achievable. Designers should consult local producers when considering tolerances that are tighter than the industry standards.

3.5 TRANSPORTATION

One of the most important aspects of precast component design is the ability to move the member from the precast plant to the jobsite. Three modes of transportation are used in the industry: truck, rail, and barge. The following sections describe issues involved in selecting a mode of transportation. The availability of transportation modes, and limitations on member weights and sizes, vary widely depending on the geographical location of the plant and jobsite. Bridge designers should consult with local producers on transportation considerations in their area.

3.5.1 Weight Limitations

The maximum shipping weight of a precast member depends upon the mode of transportation and geographical proximity of the plant and jobsite. For shipping by truck, restrictions vary from 50 to 220 kips, depending on state regulations and available equipment. Unique haul rigs have become available that are able to extend their axles to expand their footprint in width to occupy more than one travel lane. See **Figure 3.5.1-1**. The largest have a capacity of 340 kips. Normally, the maximum weight is determined by the number and minimum spacing of axles that distribute the load to the roadway surface. The minimum spacing requirement is more difficult to achieve with short heavy members than with long heavy members. Single axle loads of 12 to 16 kips generally do not require "overload" permits, as long as the axle spacing exceeds the specified minimum spacing. Special permits may allow an increase in load per axle, but may require escorts, engineering evaluation costs, or an indirect routing of the load. Maximum axle loads permitted vary from state to state. Some states further limit axle loads after a period of freezing temperatures. Other jurisdictions may allow higher tire pressures when the ground is frozen.

FABRICATION AND CONSTRUCTION

3.5.1 Weight Limitations/3.5.3 Trucking

Figure 3.5.1-1**Hauling Rig with Axles that Extend Laterally to Spread Load Over Multiple Lanes**

Standard rail cars can usually accommodate larger loads than a standard truck. Rail cars range in capacity from approximately 120 to 200 kips. However, unless the rail system runs directly from the precast plant to the jobsite, members must be trucked for at least some portion of the route and the weight of the member may be restricted by the trucking limitations. Double handling increases transportation costs.

The same trucking limitations can be true of barge transportation. However, for marine construction accessible by barge, the weight is only limited by the rated capacity of the loading equipment or barge. Very large precast concrete floating pontoons for bridges (in excess of 5,500 tons) have been successfully delivered by barge.

3.5.2 Size Limitations

The ability to ship a precast member can be limited by its overall dimensions. Dimensional restrictions depend on state regulations, equipment limitations, and physical constraints along the route to the jobsite. Physical constraints include height and width clearances, and required turning radii. Alternate routes can often be selected to alleviate these constraints.

For trucking with an “over-dimension” permit, state regulations generally restrict the height of a loaded member to 14 ft above the roadway surface. Without a permit, this may be restricted to 12 ft. For width, either with or without permits, the ranges are 12 to 16 ft and 8 to 10 ft, respectively. Most states do not restrict the length of a load, though many require permits for loads over a specified length. Permitted loads may or may not require escort vehicles. Maximum lengths are normally dictated by the smallest turning radius enroute.

Delivery by rail can be significantly more restrictive. Clearances limited by tunnels and other obstructions are often very restrictive. Long precast members, which may span several rail cars, require at least one end support to articulate to accommodate the turning radius of each car. This can further exacerbate clearances at the midpoint of the member. Dimensional limitations for rail delivery are heavily route dependent, and must be closely coordinated with the railroad.

Product dimensions are usually not limited by barge delivery. In most cases, if a product can be made and handled in the plant, it can be shipped by barge. As with weight restrictions, this usually applies only if both the precast plant and jobsite are accessible by barge.

3.5.3 Trucking

The most common mode of transporting precast concrete products is by truck, since most precast plants do not have easy access to rail spurs or waterways. Trucking is accommodated with four basic configurations of trailers:

- Standard flat-bed trailers
- “Low-boy” trailers
- “Pole” trailers
- Steerable trailers

FABRICATION AND CONSTRUCTION

3.5.3 Trucking/3.5.3.3 “Pole” Trailers

Each truck configuration is pulled by a standard tractor, with the differences provided by the trailer arrangement. The following sections describe in general terms the characteristics of the various trailers. As trailer dimensions and hauling capacities vary throughout the country, the dimensions and capacities given in the following sections should be considered approximate.

3.5.3.1 Flat-Bed Trailers

Relatively small precast concrete products are shipped on standard flat-bed trailers, as shown in **Figure 3.5.3.1-1**. The trailers are 8 ft wide and 40 to 53 ft long, with the top of the bed approximately 4.5 ft above the roadway surface. The beds are typically supported on dual axles at the back of the trailer and on dual axles at the rear of the tractor—a total of four axles. For loads without special permits, hauling capacity is limited to approximately 50 to 60 kips. This type of trailer is normally used to transport short-span flexural members, such as stemmed members or voided slab beams, and other miscellaneous bridge products, such as substructure components or stay-in-place deck panels.

*Figure 3.5.3.1-1
Typical Flat-Bed Trailer*



*Figure 3.5.3.2-1
Low-Boy Trailer*

**3.5.3.2 “Low-Boy” Trailers**

“Low-boy” trailers are used when height restrictions become a problem for flat-bed trailers. Approximately 35 ft of the center section of the trailer is lowered to reduce the top of the bed to within 2 ft of the roadway surface. These trailers are used to haul tall loads, such as wall panels shipped on edge or large segments as shown in **Figure 3.5.3.2-1**. The overall dimensions and hauling capacity of these trailers are similar to standard flat-bed trailers because they are usually supported by four axles.

3.5.3.3 “Pole” Trailers

“Pole” trailers are configurations where the front and rear axle-sets (or “jeeps”) are connected with a telescoping pole, as shown in **Figure 3.5.3.3-1**. Therefore, the distance between the front and rear axles is adjustable. Typical pole trailers can extend to approximately 60 ft between supports, and are used to carry precast members longer than can be handled with standard flat-bed trailers. Their hauling capacity depends on the number and spacing of axles, as discussed in **Section 3.5.1**.

FABRICATION AND CONSTRUCTION

3.5.3.3 "Pole" Trailers 3.5.3.4 Steerable Trailers

*Figure 3.5.3.3-1
Typical "Pole" Trailer with Additional
Pole Extending Beyond Rear Axle-Sets*



*Figure 3.5.3.4-1
Steerable Trailer*



3.5.3.4 Steerable Trailers

The trailing end of a very long precast member is usually supported by a detached steerable trailer. Members as long as 185 ft have been delivered with this equipment. There are two basic types of steerable trailers.

One type of trailer is outfitted with a cab and steering wheel, as shown in **Figure 3.5.3.4-1**. The steerable trailer is secured to the member, which in turn is secured to the tractor or front jeep. During delivery, the steerable trailer is operated by a driver who, in conjunction with the tractor driver, maneuvers the member to the jobsite.

Another type of steerable trailer is remotely steered by the tractor driver. The driver's controls activate hydraulic cylinders that off-set the rear dollies. This trailer is efficient and highly maneuverable. Examples are shown in **Figures 3.5.3.4-2 and 3.5.1-1**.

*Figure 3.5.3.4-2
Remotely-Steered Trailer*



FABRICATION AND CONSTRUCTION**3.5.3.5 Truck Loading Considerations****3.5.3.5 Truck Loading Considerations**

Precast products should be loaded on trucks with supports located as close as possible to the lifting devices. Previous codes stated concrete stresses should be checked considering impact during transportation (generally, an addition or reduction of 20% of the member weight is adequate for calculation for impact during truck delivery). The LRFD Articles 5.14.1.2.1 and C5.14.1.2.1, places the responsibility on the contractor to provide adequate devices and methods for safe hauling of precast products. In addition, the contractor is responsible for storage, loading, handling, erection, and temporary bracing of precast elements.

For members with multiple lift points, “rocker” assemblies are used to equalize the load at each support location, as shown in **Figure 3.5.3.5-1**.

*Figure 3.5.3.5-1
Rocker Support Assembly on Pole Trailer*



Chains, wire rope or nylon straps are used to secure the load to the trailer or jeep. As mentioned in **Section 3.2.4.5**, some producers provide blockouts in the top flange to prevent damage from the chains, as shown in **Figure 3.5.3.4-1**. When using “pole” or steerable trailers, the front and rear supports are generally designed to swivel to allow for the relative rotation between the front and rear jeeps during turns. Chains must be secured to the top of the swivel assembly to allow the jeep to turn relative to the member, as shown in **Figure 3.5.3.5-2**.

*Figure 3.5.3.5-2
Swivel Support on “Jeep”*



FABRICATION AND CONSTRUCTION

3.5.4 Rail Transportation/3.5.5 Barge Transportation

3.5.4 Rail Transportation

Economically, rail transportation is usually only viable for transporting precast members over relatively long distances, or for projects on railroad rights-of-way. Rail cars are constrained to travel on tracks, which normally necessitates moving the member from storage to the rail siding by truck or travel crane. Also, rail cars endure considerably more impact than trucks, and require substantially more longitudinal and transverse lashing and restraint, as shown in **Figure 3.5.4-1**. As mentioned in **Section 3.5.2**, long precast members must straddle several cars, and require swivel supports to accommodate relative rotation, much like “pole” or steerable truck trailers. A rail car swivel support is shown in **Figure 3.5.4-2**. Compared to trucks, rail cars are more difficult to obtain and schedule on a consistent and reliable basis.

*Figure 3.5.4-1
Railcar Lashing Example*



*Figure 3.5.4-2
Railcar Swivel Support*



3.5.5 Barge Transportation

Where available, barge transportation is the most economical mode of transportation for precast concrete products. In local areas, barging is generally limited to marine construction, as shown in **Figure 3.5.5-1**. However, barges are also used to transport precast products over very long distances for land-based projects, with either truck or rail being used from the dock to the jobsite. The large hauling capacity and dimensional flexibility of barge transportation make it the most attractive, and in some cases, the only feasible mode of transportation.

*Figure 3.5.5-1
Barge Loaded with Piles*



FABRICATION AND CONSTRUCTION**3.5.5 Barge Transportation/3.6 Installation**

Figure 3.5.5-2
Barge Loaded with Beams



The large hauling capacity of a barge with respect to its deck area, usually requires the members to be stacked one on another on the deck. In this case, the stacking considerations discussed in **Section 3.3.8.3** must be observed. The wood dunnage between the stack and the deck generally must align with the internal barge bulkheads. To conserve deck space, wide-flanged members can be nested, as shown in **Figure 3.5.5-2**. The members are blocked and lashed together, and secured to the deck as a unit. This process improves the stability of each individual member during the journey.

For open ocean tows, a significant amount of lashing is required to secure the load. In many cases, vertical uprights, or “stanchions,” are used to prevent the load from shifting. Under storm conditions, impact can be significant, sometimes as high as 100%, and members must be supported with this in mind.

3.5.6 Lateral Stability during Shipping

Long, slender members can become unstable when supported near the ends, as discussed in **Section 3.3.7.4**. Studies by Mast (1993) conclude that, unlike handling, the most important parameter for lateral stability during shipping is the roll stiffness of the trailer or jeep. Methods used for improving the lateral stiffness of long, slender members for handling, as discussed by Imper and Laszlo (1987), do nothing to improve the roll stiffness of the support during transportation. Most producers have extensive experience with shipping long members, and should be consulted on maximum practical shipping lengths. In lieu of experience, the roll stiffness of transportation vehicles should be evaluated according to the method proposed by Mast (1993), particularly when roadway superelevations and cross slopes will be encountered on the delivery route. In some areas, there is available, sophisticated, heavy hauling equipment that feature self-leveling trailers that pivot on rocker supports controlled hydraulically. Some have axles that extend laterally for better stability against overturning on cross slopes. This capability also is used to distribute loads on bridges over a larger area.

3.6 INSTALLATION

When a bridge member arrives at the jobsite, it must be erected into position for final integration into the structure. The following sections describe the methods used to install typical precast concrete bridge components, and the materials and procedures used in the integration process.

FABRICATION AND CONSTRUCTION**3.6.1 Onsite Handling/3.6.1.3 passing from Crane to Crane****3.6.1 Jobsite Handling**

A variety of methods are employed to erect precast concrete bridge members, ranging from single mobile cranes to sophisticated launching trusses. The method chosen depends primarily on member weights and lengths, available crane capacities and access conditions at the site. Erection costs are strongly influenced by the number of cranes required, the crane capacity, and the desired speed of erection. Additional information can be found in the PCI publication, *“Erectors’ Manual: Standards and Guidelines for the Erection of Precast Concrete Products”* (1999).

3.6.1.1 Single-Crane Lifts

The preferred method of erecting long beams is with a single crane located at either bridge beam support or somewhere between supports. Single cranes located at a support are generally limited to short spans of 60 ft or less. I-beams as long as 120 ft have been erected with a single crane placed at midspan. This requires open access for both the crane and the delivery vehicle near midspan to reduce the reach the crane must make to lift the beam.

Figure 3.6.1.1-1 shows a single-crane lift.

Single-crane lifts require a sufficient length of boom to keep the cables at a specified minimum angle from horizontal, generally 60 degrees or more. Spreader bars or struts can also be used to maintain this minimum angle.

Figure 3.6.1.1-1
One-Crane Lift



Figure 3.6.1.2-1
Two-Crane Lift

**3.6.1.2 Dual-Crane Lifts**

Erection utilizing two cranes is usually faster than with one crane, but also more expensive. This method requires close coordination between cranes and is normally used when long beams can be delivered along the bridge span. Each crane is positioned near the supports and swing the beams from the delivery vehicle directly to their final position. **Figure 3.6.1.2-1** shows a dual-crane lift. Dual-crane lifts do not require the very long boom lengths of single-crane lifts. This is important in situations where headroom is limited, such as erection under a bridge overpass or near or under power transmission lines.

3.6.1.3 Passing from Crane to Crane

Passing beams from crane to crane is normally required when erecting long beams over waterways and railways, where neither the cranes nor the delivery vehicles have access between supports. Using this process, a crane is

FABRICATION AND CONSTRUCTION**3.6.1.3 passing from Crane to Crane/3.6.1.4.1 Launching Trusses for Single Piece Construction**

placed at each of the near and far supports. A truck with steerable trailer, backs the beam to the near crane, which lifts the end of the beam from the steerable trailer. As the tractor, supporting the other end of the beam, backs up, the near crane moves the beam end as far out into the span as allowed by its lifting capacity. The far crane is then hooked onto a separate lifting device at the end out into the span and, provided it has the capacity, picks up the load until the near crane can be released. If neither crane has sufficient load capacity at the transfer point, a triangular load transfer plate is used to spread the load between cranes until the beam is close enough to be carried by the far crane alone. The far crane and tractor continue to move the beam out into the span until the near crane can lift the end of the beam off the tractor. Erection then proceeds in the same manner as for dual crane lifts.

3.6.1.4 Launching Trusses

Launching trusses are used when, due to ecological or practical considerations, the methods described in **Sections 3.6.1.1** through **3.6.1.3** are not feasible. This generally occurs with long spans in the range of 135 to 200 ft. Launching trusses eliminate the need for cranes, delivery vehicle or temporary support towers to be placed near midspan, and can be used for both single-piece or segmental construction. Launching trusses are usually shipped in pieces and assembled at the jobsite. Methods of installing the trusses vary depending on the type of construction. A unique truss was deployed in an environmentally sensitive area minimizing the associated construction impacts by using overhead pile driving and bridge beam launching techniques. See Homsy, 2010.

3.6.1.4.1 Launching Trusses for Single-Piece Construction

The use of launching trusses for single-piece construction is usually reserved for long, single-span crossings where access is possible only at the ends. In this scenario, a crane is positioned at both the near and far abutments, and the truss is assembled on a runway behind the near abutment. Due to its relatively light weight and strength, the locations where the truss may be picked are flexible, and the crane at the near abutment is able to “pass” the truss to the crane at the far end. **Figure 3.6.1.4.1-1** shows a launching truss in position.

The long, precast beams are shipped from the plant either as single pieces, or in segments that are assembled into full-length beams in a staging area at the jobsite. A truck with steerable trailer backs the beam to the near crane, which lifts the end of the beam from the steerable trailer, and places it on a trolley on top of the truss. The tractor then backs the beam across the span until the crane at the far end can reach the end on the trolley. The crane at the near end picks the beam from the tractor, and both cranes swing the beam to its final position.

Figure 3.6.1.4.1-1
Setting Precast Beam with Launching Truss



Figure 3.6.1.4.2-1
Assembling Precast Segments with Launching Truss



FABRICATION AND CONSTRUCTION

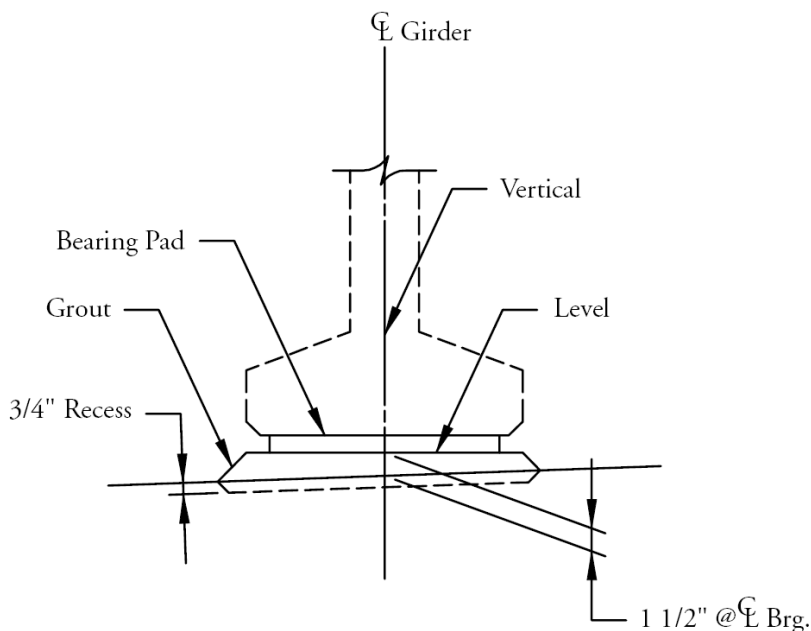
3.6.1.4.2 Launching Trusses for Segmental Construction/3.6.2.2 Temporary Support Towers

3.6.1.4.2 Launching Trusses for Segmental Construction

Launching trusses for segmental construction are very sophisticated equipment, and are generally reserved for large, multi-span, segmental box beam construction. These trusses are designed to launch themselves from pier to pier, and to lift and hold large box sections in place until the segment is post-tensioned to the structure. **Figure 3.6.1.4.2-1** shows a launching truss used for segmental construction.

3.6.2 Support Surfaces

The construction of supports for precast flexural members is important to provide uniform bearing for the generally high concentrated forces at the beam ends. Elastomeric bearing pads are used predominantly as beam supports. Therefore, the as-cast condition of both the support surface and the beam soffit are critical in providing good bearing. Many designers specify a rectangular grout pad, approximately 1.5 in. thick, to be accurately placed on the pier or abutment as a second stage placement, as shown in **Figure 3.6.2-1**. Support surfaces may be level or sloped to match the roadway profile. When level support surfaces are used with sloped beams, a beveled recess in the beam soffit is used to assure proper slope. For members with two or more support stems, the relative elevation of the multiple support surfaces is critical to prevent warping of the section.

*Figure 3.6.2-1**Elastomeric Pad and Grout Pedestal Bearing Detail***3.6.2.1 Inspection of Support Surfaces**

Prior to mobilizing erection equipment, the support surfaces should be checked for horizontal and vertical control, as well as flatness and level or slope. This can be done with standard surveying equipment and a carpenter's level. Flatness is normally limited to $1/16$ in. tolerance, and is checked by passing a straightedge over the surface. Any "dishing" of the surface can be detected by light under the straightedge. The same type of check is performed on the beam soffit or bearing recess. Support surfaces and beam soffits that are out of tolerance, normally are corrected by grinding.

3.6.2.2 Temporary Support Towers

When precast concrete beams are too long or too heavy to be shipped as a single piece, they can be cast in segments, erected on temporary support towers, and spliced together in their final position. Support towers usually extend the full width of the bridge to accommodate continuous erection and splicing operations. A solid

FABRICATION AND CONSTRUCTION**3.6.2.2 Temporary Support Towers/3.6.3 Abutted Members**

foundation, usually a compacted crushed gravel base, must be provided for the towers, since very little settlement can be tolerated between the time the splice is completed and the post-tensioning is applied across the joint. Two or more timber mats, placed in perpendicular directions, support the towers and distribute the loads to the base.

The towers themselves are typically heavy-duty aluminum scaffold frames, cross-braced for lateral stability and to reduce the unsupported length of the posts. **Figure 3.6.2.2-1** shows a typical temporary support tower. The top of each post of the frame is fitted with a screw jack, which supports a continuous steel beam across the full width of the bridge. A series of headframes, or interconnected steel beam platforms, are supported on the continuous steel beams and support the beam segments at the splice. Normally, provisions are made for hydraulic jacks to be placed under the beams for final adjustments prior to completing the splice. Abdel-Karim (1992) provides further information on the use of temporary support towers. Also, see **Chapter 11**.

Figure 3.6.2.2-1
Temporary Support Tower

**3.6.3 Abutted Members**

Precast members are abutted by placing them side by side on the supports, and connecting them together so that loads on the bridge deck are shared by adjacent members. The *LRFD Specifications* refers to abutted deck members as precast concrete multi-beam decks. Members that are commonly abutted include solid and voided slab beams, deck bulb-tees, stemmed members and box beams. Connection details include welding, bolting, grouted shear keys, cast-in-place overlays and transverse post-tensioning. The following sections describe materials and procedures used to connect abutted members. Previous practices have been revisited, focusing on extending service life beyond 50 years. The *LRFD Specifications* seeks to extend service life beyond 75 years. Current FHWA initiatives place emphasis on accelerated bridge construction utilizing prefabricated bridge elements and systems. This approach requires greater attention and focus to be placed upon connections and construction details. To further the technology, FHWA initiated a report titled, "Connection Details for Prefabricated Bridge Elements and Systems" (See Culmo, 2009). The article by Hanna, et al., 2011, proposes two non post-tensioned connection solutions.

Box beams have been used extensively for rapid construction. Russell, 2009, and the PCI State of the Art report on Precast, Prestressed Adjacent Box Beam Bridges (2011b) offer current concepts for this product application.

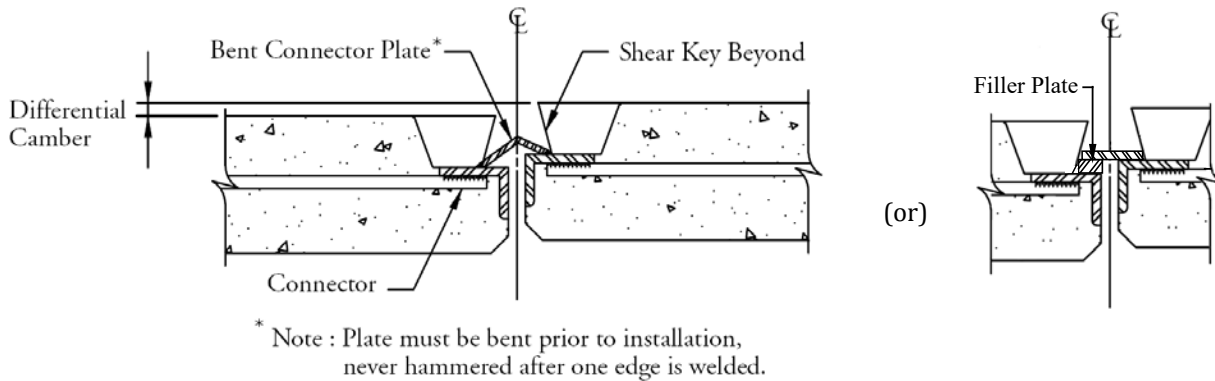
FABRICATION AND CONSTRUCTION

3.6.3.1 Vertical Alignment/3.6.3.2 Shear Keys

3.6.3.1 Vertical Alignment

The allowable differential camber between abutted deck members is usually limited to 1/2 in. This is an important consideration since there is often no concrete overlay to compensate for the vertical offset at the joints. However, the stiffer nature of abutted deck members leads to less total camber, and consequently less differential camber, than members that receive a cast-in-place deck. Small amounts of offset between abutted deck members are normally mitigated by feathering grout across the shear key joint. Larger offsets can be minimized by shimming the beam ends to split the offset difference between the ends and midspan, or by leveling the members at midspan with a jack/lever arrangement prior to making the connection between members. Caution must be exercised when leveling thin-flanged abutted members, since weld plates can spall out of the thin flange under the loads imposed by the leveling. Connections should be detailed to accommodate the allowable differential camber, as shown in **Figure 3.6.3.1-1**.

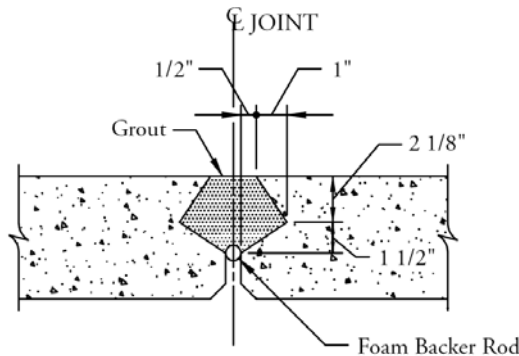
Figure 3.6.3.1-1
Welded Flange Connection Showing Condition with Differential Camber



3.6.3.2 Shear Keys

Load sharing between abutted members is normally achieved through shear keys, as shown in **Figure 3.6.3.2-1**, which are filled with grout or concrete. The clamping force required to confine the joint is typically provided by lateral ties consisting of welded connections or transverse post-tensioning. The shear key configuration and joint width vary depending on the type of member and joint filler to be used. Most producers have preferred configurations of shear keys for each standard product, and Stanton and Mattock (1986) provides recommendations for the design and configuration of shear keys. Abutted members that subsequently receive a composite cast-in-place overlay may not require shear keys or lateral ties.

Figure 3.6.3.2-1
Typical Shear Key Connection



FABRICATION AND CONSTRUCTION**3.6.3.2.1 Grout or Concrete in Shear Keys/3.6.3.4 Lateral Post-Tensioning****3.6.3.2.1 Grout or Concrete in Shear Keys**

The choice of grout or concrete to fill shear keys depends primarily on the minimum width of the joint. Concrete can only be used with joint widths approximately 2 in. or greater for two reasons: the joint must accommodate a pencil vibrator (1 in. dia.) for consolidation of the concrete, and the aggregate must be sized 1/5 the minimum joint dimension. Narrower joints are filled with a flowable grout composed primarily of portland cement and fine aggregate, as described in **Section 2.6**. Both grout and concrete joint fillers must be non-shrink.

3.6.3.2.2 Grouting Procedures for Shear Keys

Thirty minutes prior to grouting shear keys, the joint surfaces must be wetted to achieve a saturated, surface dry condition. The temperature of both the air and concrete should be a minimum of 40 °F. A volume of grout adequate to fill one or more joints is mixed and placed, preferably with a rolling trough that directs the grout into the joint. The grout is sometimes placed over the joint on the deck, and scraped into the joint with a squeegee, but this tends to stain the deck surface. Consolidation of the grout is accomplished by rodding. The quality control of this operation is important to ensure the soundness and durability of the joint.

3.6.3.3 Welded Connectors

Welded connectors generally consist of plates or angles embedded in the sides of the top flange, and anchored to the concrete with welded reinforcing bars, studs or deformed bar anchors. In some plants, connectors consist of full-flange-width reinforcing bars welded to plates on both edges of the flange. These connectors are recessed from the top surface of abutted deck members to provide the required cover from the roadway surface, as shown in **Figure 3.6.3.1-1**. This recess is sized to assure adequate access for field welding the connecting plate. Stanton and Mattock (1986) recommends the maximum spacing of welded connectors be the width of the top flange, or 5 ft, whichever is less. Welded connections are most commonly used with deck bulb-tees and stemmed members.

3.6.3.4 Lateral Post-Tensioning

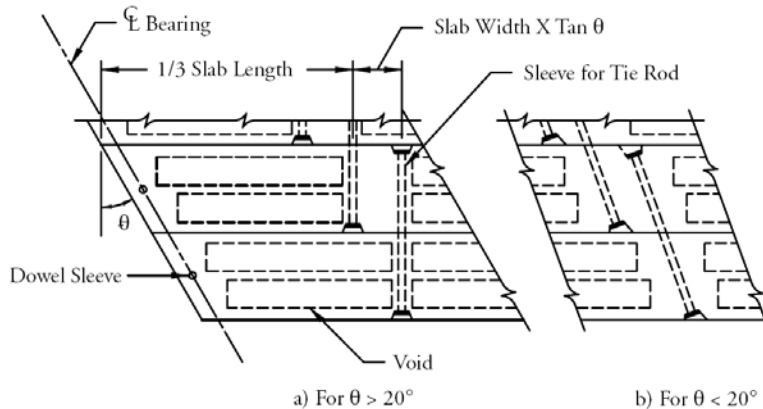
Lateral post-tensioning, located at or above the section's mid-depth, is most often used as the lateral tie system for voided slab beams and box beams, although it can also be used in the flange or concrete diaphragms of stemmed members. Typically, the longitudinal spacing corresponds with diaphragm locations, at the ends and at approximately 40-ft centers. Prestressing bars are most common, although strand systems can also be used. Lateral post-tensioning requires no field welding, and the prestressing steel is fully protected in the completed structure.

One application of lateral post-tensioning for slab beams is shown in **Figure 3.6.3.4-1**. Staggered prestressing bars are placed in ducts normal to the longitudinal axis of the slabs, tying them together two at a time. The bars are placed as erection proceeds, and are stressed using a torque wrench or jack. Enlarged pockets are provided in the shear keys to provide clearance from the bar end to the adjacent slab. This procedure minimizes increase in the bridge width due to dimensional creep, and problems due to misaligned ducts when post-tensioning the full deck width.

FABRICATION AND CONSTRUCTION

3.6.3.4 Lateral Post-Tensioning/3.7.1 Cast-In-Place Concrete Diaphragms

Figure 3.6.3.4-1
Lateral Post-Tensioning Connection of Skewed Voided Slab Beams



3.6.3.5 Skewed Bridges

Welded and post-tensioned connections for members abutted on skewed bridges can either follow the skew, or be normal to the longitudinal axis of the member. Connections that follow the skew are normally limited to skews of 20 degrees or less. For skewed, post-tensioned connections, a wedge-shaped pocket is required in the shear key to ensure uniform bearing of the prestressing force on the concrete surface, as shown in **Figure 3.6.3.4-1**.

New systems utilizing nonmetallic prestressed carbon fiber composite cables are being investigated and constructed on a trial basis in Michigan. See Grace, 2011.

3.7 DIAPHRAGMS

Diaphragms are “stiffeners” that are normal to the longitudinal axis of the bridge and connect precast flexural members to one another. They are generally specified at the bridge ends, and in most regions of the country, at a maximum of 40-ft intervals along the length of the bridge. Rabbat et al. (1982) concludes that end diaphragms ensure uniform reactions at the span ends and provide a smoother ride over the support. In other locations, however, studies by Lin and VanHorn (1969), McCarthy, et al. (1979), Sengupta and Breen (1973), Sithichaikasem and Gamble (1972), and Wong and Gamble (1973) conclude that intermediate diaphragms are not necessary for load distribution and, are in fact, in most cases, detrimental. These studies were performed on bridges with cast-in-place decks, and their conclusions may not be applicable to fully-decked, abutted members. Intermediate diaphragms may also be added above traffic lanes to provide additional strength in the event of impact from overheight vehicles.

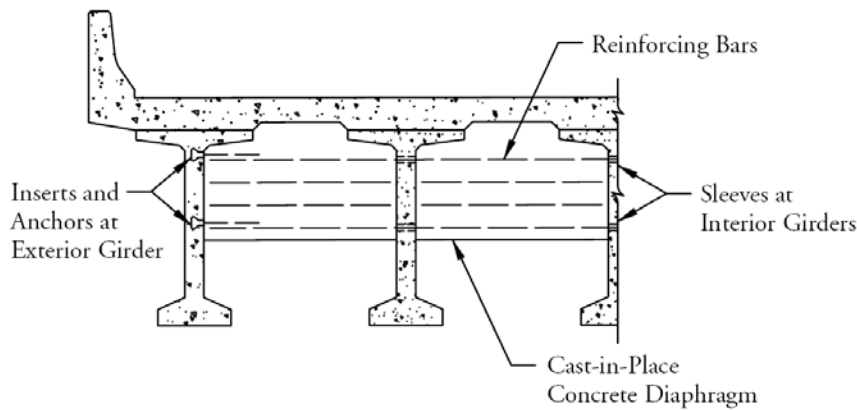
3.7.1 Cast-In-Place Concrete Diaphragms

The most common type of diaphragm is cast-in-place, as shown in **Figure 3.7.1-1**. Interior beams are fabricated with holes through the web to allow the top and bottom diaphragm reinforcement to pass through. Exterior beams have threaded inserts embedded in the interior face to accommodate threaded reinforcing steel, bolts or other types of anchors. In lieu of threaded inserts, some exterior beams are cast with holes through the web and a recessed pocket in the exterior face. Threaded reinforcement is passed through the hole, and secured with hand-tightened nut and washer. After the diaphragm concrete has gained some strength, the nut is tightened firmly, and the recess is coated with epoxy and patched with grout. Fully-decked, abutted members, such as deck bulb-tees, are provided with “casting slots,” or holes, in the deck to facilitate concrete placement.

FABRICATION AND CONSTRUCTION

3.7.1 Cast-In-Place Concrete Diaphragms/3.7.2.2 Secondary-Cast Precast Concrete Diaphragms

Figure 3.7.1-1
Cast-in-Place Concrete Diaphragm Details

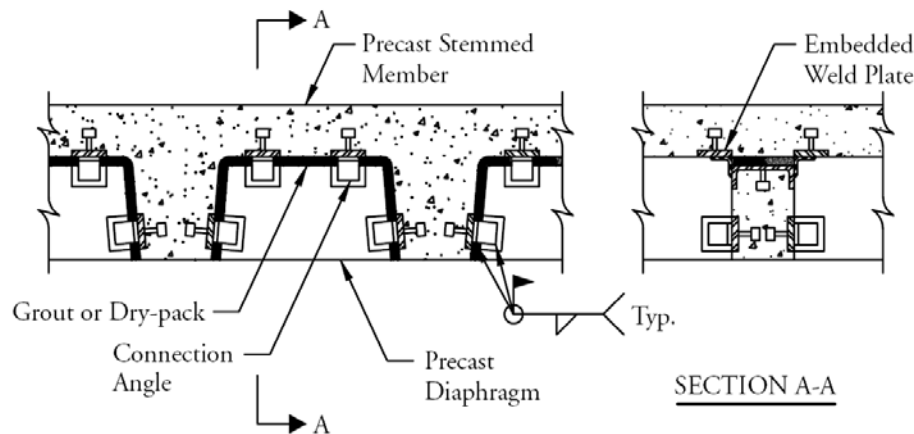


3.7.2 Precast Concrete Diaphragms

3.7.2.1 Individual Precast Concrete Diaphragms

Diaphragms can be fabricated as separate precast pieces and shipped loose to the jobsite for installation into the structure. **Figure 3.7.2.1-1** shows a precast diaphragm detail. These diaphragms must be cast to the shape of the webs and flanges of adjacent beams, and are sensitive to fabrication and erection tolerances. Connections to adjacent beams are usually made by welding. This method can be tedious during erection. In some cases, tie rods through sleeves in the diaphragms have also been used. The geometry of the structure generally determines the feasibility of precast diaphragms. Among the available diaphragm types, they are the most difficult to properly execute.

Figure 3.7.2.1-1
Individual, Separate, Precast Concrete Diaphragms



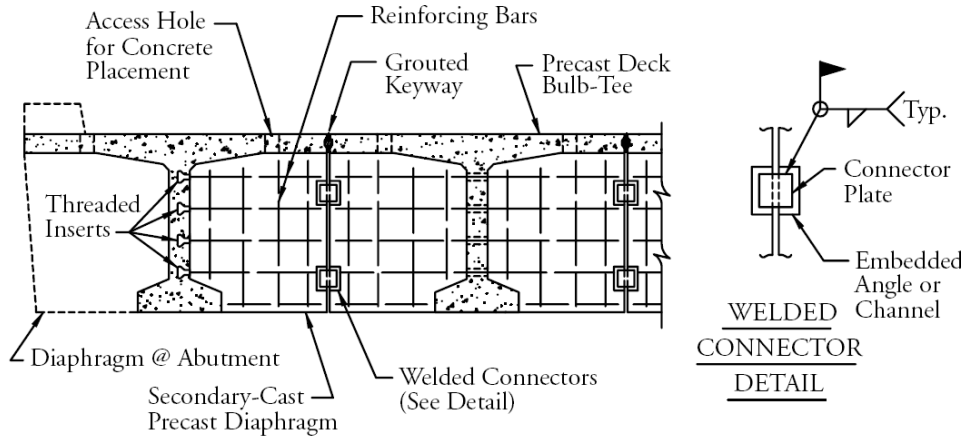
3.7.2.2 Secondary-Cast Precast Concrete Diaphragms

Another option for providing precast diaphragms is to cast the diaphragm directly onto the individual beams in the precast yard, as shown in **Figure 3.7.2.2-1**. The diaphragm reinforcement and connections to the beams are similar to cast-in-place diaphragms. The joint occurs at midpoint between beams, and the connection between diaphragms is usually accomplished by welding or mechanical splicing of exposed reinforcement. The most important aspect of this type of diaphragm is alignment in the field. Proper execution sometimes requires match-casting of the diaphragms in the precast yard.

FABRICATION AND CONSTRUCTION

3.7.2.2 Secondary-Cast Precast Concrete Diaphragms/3.7.3 Steel Diaphragms

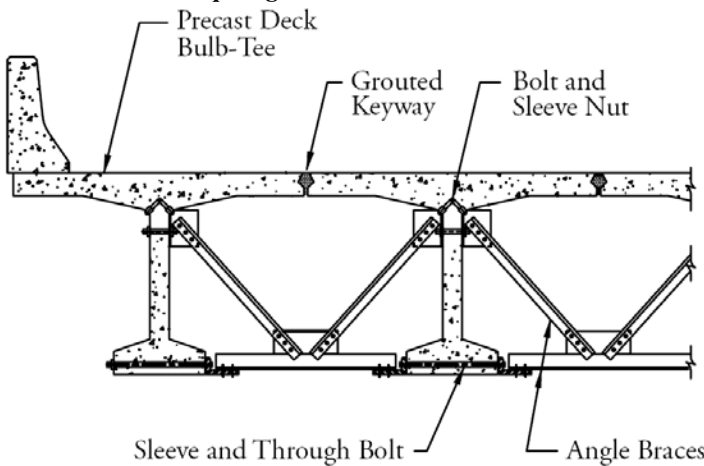
Figure 3.7.2.2-1
Secondary-Cast, Precast Concrete Diaphragms



3.7.3 Steel Diaphragms

Steel braces have proven to be an efficient and cost-effective means of providing diaphragms, particularly in remote locations where cast-in-place concrete is not readily available. **Figures 3.7.3-1 and 3.7.3-2** show two types of steel diaphragms used in the industry. The first is normally referred to as a “K” brace. This configuration is not as stiff as most other types of diaphragms, and consequently is used at shorter intervals of approximately 25 ft maximum. The second type is often called a “delta” brace, and has been successfully used at 40-ft intervals. Both types are normally hot-dip galvanized, and connected to the beams by welding. The precautions discussed in **Section 3.2.5.6** should be observed when welding galvanized steel. The “K” brace has also been detailed with bolted connections. Due to cumulative fabrication and erection tolerances, predrilled bolt holes are difficult to line-up, so the holes in one of the connecting elements are normally field-drilled.

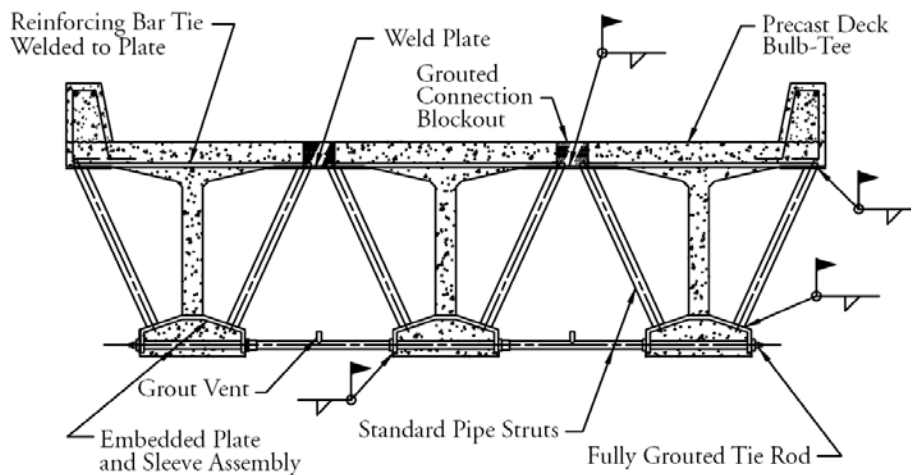
Figure 3.7.3-1
Steel “K” Brace Diaphragms



FABRICATION AND CONSTRUCTION

3.7.3 Steel Diaphragms/3.8.1 Deck Panel Systems

Figure 3.7.3-2
Steel “Delta” Brace Diaphragms



3.7.4 Temporary Diaphragms for Construction

After the beams have been erected, and before they are permanently connected into the structure, they can be subjected to forces of nature that could cause them to topple off the supports. Forces include wind, earthquake or thermally-induced sweep. Temporary braces consisting of steel or timber are used to stabilize the beams. Braces are removed after the final connections are made.

3.7.5 Diaphragms in Skewed Bridges

Diaphragms in skewed bridges can either follow the skew angle or frame normal to the longitudinal axis of the beams. In general, diaphragms perpendicular to the beams are easier to detail and execute, particularly with precast or steel diaphragms. Bridge designers should consult with local manufacturers for the most cost-effective means of providing diaphragms on skewed bridges.

3.8 PRECAST DECK PANELS

Precast, prestressed composite bridge deck panels, combined with a cast-in-place overlay, provide an efficient and cost-effective method of constructing bridge decks. The following sections describe key facets of the fabrication and installation of these panels. Extensive coverage of this subject may be found in PCI's Recommended Practice for Precast Prestressed Concrete Composite Bridge Deck Panels (1988).

3.8.1 Deck Panel Systems

Precast composite bridge deck panels are 3 to 4 in. thick concrete slabs that span between the top flanges of concrete or steel beams. These panels provide a working platform for deck reinforcement placement, and a stay-in-place form for the cast-in-place concrete overlay. **Figure 3.8.1-1** shows panels in place. The panels are fabricated using the materials and procedures discussed in **Sections 3.2** and **3.3**. Prestressing strands in the panels are oriented perpendicular to the longitudinal axis of the beams and provide all of the positive reinforcement required for the span of the deck between beams. The panels become composite with the cast-in-place overlay to resist superimposed dead and live loads. The interface shear connection is typically achieved only by roughening the top surface of the precast slabs. Projecting mild reinforcement across the interface is not normally required (see LRFD Article 9.7.4.3.3).

Both proprietary and generic panel systems are available to the construction industry. Proprietary systems employ patented methods of erection, temporary support, adjustments, and forming of the gap between the bottom of the panel and the top of the beam. Generic systems use conventional methods to achieve the same results.

FABRICATION AND CONSTRUCTION

3.8.1 Deck Panel Systems/3.8.3 Installation of Deck Panels

Figure 3.8.1-1
Installation of Precast Concrete Deck Panels



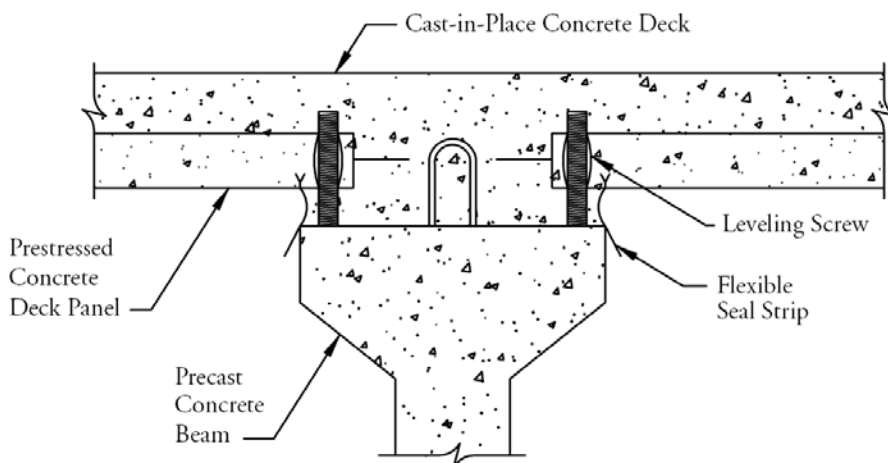
3.8.2 Handling Deck Panels

Precast composite bridge deck panels can be handled with the conventional techniques described in **Section 3.3.7**, or with proprietary lifting equipment. Proprietary lifting equipment is normally designed to lift the panels along the edge, eliminating the need for embedded lifting devices. This equipment is also designed for quick release to speed erection of the panels.

3.8.3 Installation of Deck Panels

After the panels are erected, they must be temporarily supported until placement of the cast-in-place overlay which also provides concrete under the panel for support. Most systems incorporate a minimum of four screw-jack embedments near the panel corners, which are provided for two purposes. The first is to frame a gap between the bottom of the panel and the top of the beam flange large enough to allow grout or concrete to fully fill the gap, providing uniform bearing for the panel. The minimum gap is nominally 1 in. for grout and 1½ in. for concrete. The screw jacks also allow the panel elevations to be adjusted for the desired profile grade, drainage slope or superelevation, while correcting for beam camber and dead load deflections, maintaining a relatively constant overall deck thickness. **Figure 3.8.3-1** shows a typical detail at the top of the beam. Some proprietary systems offer cast-in baffles to retain grout or concrete in the gap.

Figure 3.8.3-1
Stay-In-Place Composite Deck Panels Bearing Detail (Proprietary System)



FABRICATION AND CONSTRUCTION**3.9 Precast Full Depth Bridge Deck Panels/3.9.2 Details and Considerations****3.9 PRECAST FULL-DEPTH BRIDGE DECK PANELS**

Full-depth precast concrete bridge deck panels provide another method to reduce construction time and lesson the impact to the travelling public. This innovative, practical, and economic solution is a viable alternative to cast-in-place concrete bridge decks. The precast panels are characterized by consistent, high quality materials and fabrication. The system becomes more cost effective with an increase in bridge length and the number of required panels. The capability to rapidly place these panels and reopen the bridge to traffic makes this a creative design alternative.

3.9.1 System Description

A full-depth precast concrete deck consists of a series of precast concrete panels, cast to full depth in thickness. To be viable, the panels must meet and enhance the structural design and geometric requirements for a project. The panels connect to the beams with a grouted detail that connects anchors from the beam to the precast panel so that the structure acts compositely. Panels are often as wide as the bridge, up to handling and shipping limitations of about 40 ft. They are pretensioned in this direction. For wider bridges, two panels may be joined end to end to create a longitudinal joint in the deck. Panels are about 10 ft long in the direction of travel.

3.9.1.1 Panels with Post-Tensioning

One method of construction is to post-tension numerous panels together longitudinally (in the direction of travel) to achieve load transfer between panels. Post-tensioning ducts cast into the panels are spliced at transverse joints and the joints are filled with high-strength concrete or grout. Because the panels are prestressed in both directions, long-term performance is expected to be superior. Panels in service for 30 years have demonstrated such performance.

3.9.1.2 Panels without Post-Tensioning

Full-depth deck panels may also be connected at transverse joints without post-tensioning. Reinforcement projecting from both adjacent faces are spliced together with ultra-high-performance concrete fill in the joint. This system has undergone research at the FHWA Turner-Fairbank Highway Research Center and has been demonstrated in several projects by the New York State DOT and the Iowa DOT as well as several projects in Canada. The research has shown that No. 5 epoxy-coated bars can be developed when lapped inside a 6-in.-wide joint. The FHWA research is summarized in Technical Bulletin FHWA-HRT-11-022. See Graybeal, 2010.

3.9.2 Details and Considerations

The proper design and specifications for these systems enhance constructability and successful installation. Attention must be given to the joints between adjacent panels and the connections between the deck and supporting systems, along with post-tensioning methods, if used.

PCI, with the sponsorship of the FHWA, has published a *State-of-the-Art Report on Full-Depth Precast Concrete Bridge Deck Panels* (2011a). The report will assist owner agencies, designers, precasters, and contractors with design methodology, connection details, fabrication suggestions, and construction guidelines.

A reference for owners and engineers considering waterproofing membranes and overlays is, NCHRP Synthesis 20-05, Topic 42-07, "Water Proofing Membranes for Concrete Bridge Decks" (see Russell, 2012).

3.10 REFERENCES

The following AASHTO standard specifications for materials and standard test methods are by the American Association of State Highway and Transportation Officials, Washington, DC.

1. AASHTO. 2010. *AASHTO LRFD Bridge Construction Specifications*, 3rd Edition. American Association of State Highway and Transportation Officials, Washington, DC.
https://bookstore.transportation.org/Item_details.aspx?id=1583 (Fee)
2. AASHTO M31 Standard Specification for Deformed and Plain Billet-Steel Bars for Concrete Reinforcement
https://bookstore.transportation.org/item_details.aspx?ID=1623 (Fee)
3. AASHTO M32 Standard Specification for Cold-Drawn Steel Wire for Concrete Reinforcement
https://bookstore.transportation.org/item_details.aspx?ID=1438 (Fee)
4. AASHTO M55 Standard Specification for Steel Welded Wire Fabric, Plain, for Concrete Reinforcement
https://bookstore.transportation.org/item_details.aspx?ID=1439 (Fee)
5. AASHTO M85 Standard Specification for Portland Cement
https://bookstore.transportation.org/item_details.aspx?ID=1814 (Fee)
6. AASHTO M111 Standard Specification for Zinc (Hot-Dip Galvanized) Coatings on Iron and Steel Products
https://bookstore.transportation.org/item_details.aspx?ID=1816 (Fee)
7. AASHTO M203 Standard Specification for Steel Strand, Uncoated Seven-Wire Stress-Relieved for Prestressed Concrete
https://bookstore.transportation.org/item_details.aspx?ID=1085 (Fee)
8. AASHTO M205 Standard Specification for Molds for Forming Concrete Test Cylinders Vertically
https://bookstore.transportation.org/item_details.aspx?ID=1822 (Fee)
9. AASHTO M221 Standard Specification for Welded Deformed Steel Wire Fabric for Concrete Reinforcement
https://bookstore.transportation.org/item_details.aspx?ID=1455 (Fee)
10. AASHTO M225 Standard Specification for Steel Wire, Deformed, for Concrete Reinforcement
https://bookstore.transportation.org/item_details.aspx?ID=1456 (Fee)
11. AASHTO M275 Standard Specification for Uncoated High-Strength Steel Bar for Prestressing Concrete
https://bookstore.transportation.org/item_details.aspx?ID=1263 (Fee)
12. AASHTO M284 Standard Specification for Epoxy Coated Reinforcing Bars
https://bookstore.transportation.org/item_details.aspx?ID=1464 (Fee)
13. AASHTO T22 Compressive Strength of Cylindrical Concrete Specimens
https://bookstore.transportation.org/item_details.aspx?ID=1676 (Fee)
14. AASHTO T23 Standard Method of Test for Making and Curing Concrete Test Specimens in the Field
https://bookstore.transportation.org/item_details.aspx?ID=1278 (Fee)
15. AASHTO T24 Standard Method for Obtaining and Testing Drilled Cores and Sawed Beams of Concrete
https://bookstore.transportation.org/item_details.aspx?ID=1120 (Fee)

FABRICATION AND CONSTRUCTION

3.10 References

16. AASHTO T119 Standard Method of Test for Slump of Portland Cement Concrete
https://bookstore.transportation.org/item_details.aspx?ID=1853 (Fee)
17. AASHTO T197 Standard Method of Test for Time of Setting of Concrete Mixtures by Penetration Resistance
https://bookstore.transportation.org/item_details.aspx?ID=1872 (Fee)
18. AASHTO Resolution. 2009. *A Resolution of the AASHTO Highway Subcommittee on Bridges and Structures*.
<http://www.pci.org> and click on the “Quality Systems” icon.
19. Abdel-Karim, A. M. and M. K. Tadros. 1992. *State-of-the-Art of Precast/Prestressed Concrete Spliced-Girder Bridges*. (SG-92). PCI Committee on Bridges Report, Precast/Prestressed Concrete Institute, Chicago, IL, (October).
http://www.pci.org/view_file.cfm?file=SG_92.PDF
20. ACI Committee 211, “Standard Practice for Selecting Proportions for Normal, Heavyweight, and Mass Concrete,” (ACI 211.1), American Concrete Institute, Farmington Hills, MI.
<http://www.concrete.org/PUBS/JOURNALS/AbstractDetails.asp?srctype=ALL&keywords=ACI+211.1&ID=5092> (Fee)
21. ACI Committee 212, “Chemical Admixtures for Concrete,” (ACI 212.3R), American Concrete Institute, Farmington Hills, MI.
<http://www.concrete.org/PUBS/JOURNALS/AbstractDetails.asp?srctype=ALL&keywords=ACI+212.3R&ID=13402> (Fee)
22. ACI Committee 213, “Guide for Structural Lightweight Aggregate Concrete,” (ACI 213R), American Concrete Institute, Farmington Hills, MI.
<http://www.concrete.org/PUBS/JOURNALS/AbstractDetails.asp?srctype=ALL&keywords=ACI+213R&ID=12965> (Fee)
23. ACI Committee 221, “Guide to Use of Normal Weight Aggregates in Concrete,” (ACI 221R), American Concrete Institute, Farmington Hills, MI.
<http://www.concrete.org/PUBS/JOURNALS/AbstractDetails.asp?srctype=ALL&keywords=ACI+221R&ID=5107> (Fee)
24. ACI Committee 224, “Control of Cracking in Concrete Structures,” (ACI 224R), American Concrete Institute, Farmington Hills, MI.
<http://www.concrete.org/PUBS/JOURNALS/AbstractDetails.asp?srctype=ALL&keywords=ACI+224R&ID=10632> (Fee)
25. ACI Committee 225, “Guide to the Selection and Use of Hydraulic Cements,” (ACI 225R), American Concrete Institute, Farmington Hills, MI.
<http://www.concrete.org/PUBS/JOURNALS/AbstractDetails.asp?srctype=ALL&keywords=ACI+225R&ID=5117> (Fee)
26. ACI Committee 226, “Use of Fly Ash in Concrete” (ACI 226.3R), American Concrete Institute, Farmington Hills, MI.
<http://www.concrete.org/PUBS/JOURNALS/AbstractDetails.asp?srctype=ALL&keywords=ACI+Committee+226&ID=1612> (Fee)

FABRICATION AND CONSTRUCTION

3.10 References

27. ACI Committee 301, "Specifications for Structural Concrete" (ACI301-10), American Concrete Institute, Farmington Hills, MI.
<http://www.concrete.org/PUBS/JOURNALS/AbstractDetails.asp?srctype=ALL&keywords=ACI+Committee+301&ID=51664148> (Fee)
28. ACI Committee 318, "Building Code Requirements for Structural Concrete," (ACI 318), American Concrete Institute, Farmington Hills, MI.
http://www.concrete.org/COMMITTEES/committeehome.asp?committee_code=0000318-00 (Fee)
29. AASHTO Highway Subcommittee on Construction. 1996. *Implementation Manual for Quality Assurance*, (AASHTO IMQA), American Association of State Highway and Transportation Officials, Washington, DC.
https://bookstore.transportation.org/Item_details.aspx?id=1162 (Fee)
30. AASHTO Highway Subcommittee on Construction. 1996. *Quality Assurance Guide Specifications*, (AASHTO QA), American Association of State Highway and Transportation Officials, Washington, DC.
https://bookstore.transportation.org/Item_details.aspx?id=1162 (Fee)
31. AISC-PCI. 2009. White paper on "Quality Systems in the Construction Industry." Visit <http://www.pci.org> and click on the "Quality Systems" icon.

The following ASTM standard specifications for materials and test methods are from ASTM International, West Conshohocken, PA.

32. ASTM A706 Standard Specification for Low-Alloy Steel Deformed Bars for Concrete Reinforcement
<http://www.astm.org/DATABASE.CART/HISTORICAL/A706A706M-05.htm> (Fee)
33. ASTM A767 Standard Specification for Zinc-Coated (Galvanized) Steel Bars for Concrete Reinforcement
<http://www.astm.org/Standards/A767.htm> (Fee)
34. ASTM A882 Standard Specification for Epoxy-Coated Seven-Wire Prestressing Steel Strand
<http://www.astm.org/Standards/A882.htm> (Fee)
35. ASTM A886 Standard Specification for Steel Strand, Indented, Seven-Wire Stress-Relieved for Prestressed Concrete
<http://www.astm.org/Standards/A886.htm> (Fee)
36. ASTM A934 Standard Specification for Epoxy-Coated Prefabricated Steel Reinforcing Bars
<http://www.astm.org/Standards/A934.htm> (Fee)
37. ASTM C403 Standard Test Method for Time of Setting of Concrete Mixtures by Penetration Resistance
<http://www.astm.org/Standards/C403.htm> (Fee)
38. ASTM C617 Standard Practice for Capping Cylindrical Concrete Specimens
<http://www.astm.org/Standards/C617.htm> (Fee)
39. Campbell, R. R. and R. E. Tobin. 1967. "Core and Cylinder Strengths of Natural and Lightweight Concrete." *ACI Journal*, Proceedings, American Concrete Institute, Farmington Hills, MI. V. 64, No. 4, (April), pp.190-195.
<http://www.concrete.org/PUBS/JOURNALS/OLJDetails.asp?Home=JP&ID=7555> (Fee)

FABRICATION AND CONSTRUCTION

3.10 References

40. Cousins, T. 2012. *High-Performance/High-Strength Lightweight Concrete for Bridge Girders and Decks*. NCHRP Project 18-15. Transportation Research Board, Washington, DC. (To be published in 2012).
<http://apps.trb.org/cmsfeed/TRBNetProjectDisplay.asp?ProjectID=481>
41. Culmo. 2009. *Connection Details for Prefabricated Bridge Elements and Systems*. FHWA-IF-09-010. Federal Highway Administration, Washington, DC.
<http://www.fhwa.dot.gov/bridge/prefab/if09010/report.pdf>.
42. D'Arcy, T. J., W. J. Korkosz, and L. Sennour. 1996. *Durability of Precast, Prestressed Concrete Structures*. (R&D 10), PCI Research Report. Precast/Prestressed Concrete Institute, Chicago, IL. 164 pp.
https://netforum.pci.org/eweb/dynamicpage.aspx?webcode=category&ptc_key=0507c294-2971-4f91-9306-e93441879240&ptc_code=R&D%20Report (Fee)
43. Homsy, E., M. Mallet, and P. LeFave. 2010. The New Top Down Construction Method For the Washington Bypass in North Carolina. In Proceedings of the PCI Annual Convention and National Bridge Conference, May 29-June 2, Washington, DC. Precast/Prestressed Concrete Institute, Chicago, IL.
<http://pci.org> Go to bookstore
44. Ficenec, J. A., S. D. Kneip, M. K. Tadros, and L. G. Fischer. 1993 "Prestressed Spliced IGirders: Tenth Street Viaduct Project, Lincoln, Nebraska." *PCI Journal*, Precast/Prestressed Concrete Institute, Chicago, IL. V. 38, No. 5, (September-October), pp. 38-48.
http://www.pci.org/view_file.cfm?file=JL-93-SEPTEMBER-OCTOBER-11.pdf
45. Gerwick, B. C. 1993. *Construction of Prestressed Concrete Structures*. Second Edition, John Wiley & Sons, Inc., New York, NY., 591 pp.
http://books.google.com/books?id=SPia1SEzJWMC&pg=PR4&lpg=PR4&dq=John+Wiley+%26+Sons,+Inc.,+1993+Construction+of+Prestressed+concrete+Structures&source=bl&ots=7PUsna9_Yg&sig=X-Q1g-I7mVqLWUDyCWEIRW-rrdl&hl=en&ei=TEu5Tvy3Io_82gX6r4zCBw&sa=X&oi=book_result&ct=
46. Grace, N. F., K. D. Patki, E. M. Soliman, and J. Q. Hanson. 2011. "Flexural Behavior of Side-by-Side Box Beam Bridges: A Comparative Study." *PCI Journal*, Precast/Prestressed Concrete Institute, Chicago, IL. V. 56, No. 3 (Summer), pp. 94-112.
http://www.pci.org/view_file.cfm?file=JL-11-SUMMER-9.PDF
47. Graybeal, B. A. 2010. *Field-Cast UHPC Connections for Modular Bridge Deck Elements*. FHWA Tech Brief FHWA-HRT-11-022, Federal Highway Administration, Washington, DC.
<http://www.fhwa.dot.gov/publications/research/infrastructure/structures/11022/11022.pdf>.
48. Hanna, K., G. Marcous, and M. K. Tadros. 2011. "Adjacent Box Girders without Integral Diaphragms or Post-Tensioned Joints" *PCI Journal*, Precast/Prestressed Concrete Institute, Chicago, IL. V. 56, No. 4 (Fall), pp. 51-64.
http://www.pci.org/view_file.cfm?file=JL-11-FALL-8.pdf
49. Hanson, J. A. 1963. "Optimum Steam-Curing Procedures in Precasting Plants." *ACI Journal*, American Concrete Institute, Farmington Hills, MI. V. 60, No. 1, (January).
<http://www.concrete.org/PUBS/JOURNALS/AbstractDetails.asp?SearchID=791188&date=betweendate&anywords=Hanson&aftermonth=1&afterday=1&afteryear=1963&beforemonth=1&beforeday=1&beforeyear=1963&searchmonth=1&searchday=1&searchyear=2011&ID=7843> (Fee)

FABRICATION AND CONSTRUCTION

3.10 References

50. Imper, R. R., and G. Laszlo. 1987. "Handling and Shipping of Long Span Bridge Beams." *PCI Journal*, Precast/Prestressed Concrete Institute, Chicago, IL. V. 32, No. 6, (November-December), pp. 86-101.
http://www.pci.org/view_file.cfm?file=JL-87-NOVEMBER-DECEMBER-6.pdf
51. Klieger, P. 1960. "Some Aspects of Durability and Volume Change of Concrete for Prestressing." *Journal*, PCA Research and Development Laboratories, Portland Cement Association, Skokie, IL. V. 2, No. 3, (September), pp. 2-12.
52. Lin, C. and D. A. VanHorn. 1969. "The Effect of Midspan Diaphragms on Load Distribution in a Prestressed Concrete Box-Beam Bridge." Report No. 315.6. Fritz Engineering Laboratory, Lehigh University Institute of Research, Bethlehem, PA., (March).
http://digital.lib.lehigh.edu/fritz/pdf/315_6.pdf
53. Mast, R. F. 1989. "Lateral Stability of Long Prestressed Concrete Beams—Part 1." *PCI Journal*, Precast/Prestressed Concrete Institute, Chicago, IL. V. 34, No. 1, (January-February), pp. 34-53.
http://www.pci.org/view_file.cfm?file=JL-89-JANUARY-FEBRUARY-3.pdf
54. Mast, R. F. 1993. "Lateral Stability of Long Prestressed Concrete Beams—Part 2." *PCI Journal*, Precast/Prestressed Concrete Institute, Chicago, IL. V. 38, No. 1, (January-February), pp. 70-88.
http://www.pci.org/view_file.cfm?file=JL-93-JANUARY-FEBRUARY-30.pdf
55. McCarthy, W., K. R. White, and J. Minor. 1979. "Interior Diaphragms Omitted on the Gallup East Interchange Bridge—Interstate 40." *Journal of Civil Engineering Design*, pp. 95-112.
56. Miller, B. D. and Frank, D. A. 2011. "Certification Programs Creating the Right Environment for Quality and Safety." *The Construction Specifier Magazine*, 7 pp.
<http://www.pci.org> and click on the "Quality Systems" icon.
57. Neville, A. M. 1966. "A General Relation for Strength of Concrete Specimens of Different Shapes and Sizes." *ACI Journal*, American Concrete Institute, Farmington Hills, MI. Proceedings. V. 63, No. 10, (October), pp. 1095-1109.
<http://www.concrete.org/PUBS/JOURNALS/AbstractDetails.asp?SearchID=791198&date=betweendate&anywords=Neville&aftermonth=10&afterday=1&afteryear=1966&beforemonth=10&beforeday=1&beforeyear=1966&searchmonth=1&searchday=1&searchyear=2011&ID=7664> (Fee)
58. Neville, A. M. 1996. *Properties of Concrete*. Fourth and Final Edition, John Wiley & Sons, Inc., New York, NY.
http://books.google.com/books/about/Properties_of_concrete.html?id=mKEeAQAAIAAJ
59. Nickas, W. N. and Frank, D. A. 2009. "Certification Relies on a Body of Knowledge and Continuous Improvement." *ASPIRE, The Concrete Bridge Magazine*, 4 pp.
<http://www.pci.org> and click on the "Quality Systems" icon.
60. PCI Technical Report No. 1. 1981. *Energy-Efficient Accelerated Curing of Concrete*. TR-1-82, Precast/Prestressed Concrete Institute, Chicago, IL.
https://netforum.pci.org/eweb/dynamicpage.aspx?webcode=category&ptc_key=a7a370b7-172a-44f1-893f-95fc13d86b58&ptc_code=Technical%20Report (Fee)
61. PCI Committee on Quality Control Performance Criteria. 1985. "Fabrication and Shipment Cracks in Precast or Prestressed Beams and Columns." *PCI Journal*, Precast/Prestressed Concrete Institute, Chicago, IL. V. 30, No.

FABRICATION AND CONSTRUCTION

3.10 References

- 3, (May-June), pp. 24-49.
http://www.pci.org/view_file.cfm?file=W1815_IR271.PDF
62. PCI Bridge Producers Committee. 1988. "Recommended Practice for Precast Prestressed Concrete Composite Bridge Deck Panels." *PCI Journal*, Precast/Prestressed Concrete Institute, Chicago, IL. V. 33, No. 2, (March-April), pp. 67-109.
http://www.pci.org/view_file.cfm?file=JL-88-MARCH-APRIL-6.pdf
http://www.pci.org/view_file.cfm?file=JL-88-MARCH-APRIL-7.pdf
63. PCI Ad Hoc Committee on Epoxy-Coated Strand. 1993. "Guidelines for the Use of Epoxy-Coated Strand." *PCI Journal*, Precast/Prestressed Concrete Institute, Chicago, IL. V. 38, No. 4, (July-August), pp. 26-32.
http://www.pci.org/view_file.cfm?file=JL-93-JULY-AUGUST-6.pdf
http://www.pci.org/view_file.cfm?file=JL-93-JULY-AUGUST-7.pdf
http://www.pci.org/view_file.cfm?file=JL-93-JULY-AUGUST-8.pdf
64. PCI Committee on Durability. 1994. "Guide to Using Silica Fume in Precast/Prestressed Concrete Products." *PCI Journal*, Precast/Prestressed Concrete Institute, Chicago, IL. V. 39, No. 5, (September-October), pp. 36-45.
http://www.pci.org/view_file.cfm?file=JL-94-SEPTEMBER-OCTOBER-5.pdf
65. PCI Erectors Committee. 1999. *Erectors' Manual: Standards and Guidelines for the Erection of Precast Concrete Products*. (MNL-127-99), Precast/Prestressed Concrete Institute, Chicago, IL., 96 pp.
http://www.pci.org/view_file.cfm?file=W1734_MNL-127-99.PDF
66. PCI Manual 116. 1999. *Manual for Quality Control for Plants and Production of Structural Precast Concrete Products*. Fourth Edition. (MNL-116-99). Precast/Prestressed Concrete Institute, Chicago, IL., 340 pp.
http://www.pci.org/view_file.cfm?file=W1728_MNL_116-99.PDF
67. PCI Manual 137. 2006. *Manual for the Evaluation and Repair of Precast, Prestressed Concrete Bridge Products*. (MNL-137-06), Precast/Prestressed Concrete Institute, Chicago, IL., 72 pp.
http://netforum.pci.org/eweb/dynamicpage.aspx?webcode=category&ptc_key=5d967c30-b4c7-4993-bab8-f3cd6142e004&ptc_code=Bridges (Fee)
68. *PCI Design Handbook—Precast and Prestressed Concrete*. 2010. Seventh Edition. Precast/Prestressed Concrete Institute, Chicago, IL. 828 pp.
<http://www.pci.org/cms/index.cfm/DHSeventhEdition>
69. PCI. 2011a. *State of the Art Report on Full-Depth Precast Concrete Bridge Deck Panels*. (SOA-01-1911), Precast/Prestressed Concrete Institute, Chicago, IL., 150 pp.
http://netforum.pci.org/eweb/dynamicpage.aspx?webcode=category&ptc_key=5d967c30-b4c7-4993-bab8-f3cd6142e004&ptc_code=Bridges (Fee)
70. PCI. 2011b. *State of the Art report on Precast, Prestressed Adjacent Box Beam Bridges*. (SOA-02-2011), Precast/Prestressed Concrete Institute, Chicago, IL., 99 pp.
<http://pci.org> Go to bookstore
71. Pfeifer, D. W., J. R. Landgren, and A. Zoob. 1987. "Protective Systems for New Prestressed and Substructure Concrete." (FHWA/RD-86/193), Federal Highway Administration, Washington, DC., (April), 126 pp.
<http://www.icpi.org/node/2268> (Fee)

FABRICATION AND CONSTRUCTION

3.10 References

72. Pfeifer, D. W., M. R. Sherman, and D. B. McDonald. 1996. "Durability of Precast Concrete, Part II—Chloride Permeability Study." PCI Research Program Report, Precast/Prestressed Concrete Institute, Chicago, IL. (January).
https://pci.org/view_file.cfm?file=JL-96-JULY-AUGUST-9.pdf
73. Phillips, W. R. and D. A. Sheppard. 1980. *Plant Cast Precast and Prestressed Concrete—A Design Guide*. Second Edition, Prestressed Concrete Manufacturers Association of California.
<http://www.amazon.com/Plant-Cast-Precast-Prestressed-Concrete-Design/dp/0070567603> (Fee)
74. *Post-Tensioning Manual*. 2006. Sixth Edition (TAB.1-06), Post-Tensioning Institute, Farmington Hills, MI, 354 pp.
http://post-tensioning.org/product/x_YTPk14GcmUY2lkPT/General (Fee)
75. Preston, H. K. 1990. "Handling Prestressed Concrete Strand." *PCI Journal*, Precast/Prestressed Concrete Institute, Chicago, IL. V. 35, No. 6, (November-December), pp. 68-71.
http://www.pci.org/view_file.cfm?file=JL-90-NOVEMBER-DECEMBER-6.pdf
76. *Quality Control Technician/Inspector Level I & II Training Manual*. 2009. Second Edition, (TM-101), Precast/Prestressed Concrete Institute, Chicago, IL., 168 pp.
https://netforum.pci.org/eweb/dynamicpage.aspx?webcode=category&ptc_key=a7ba327a-0cc2-48cc-bc3e-1c8f49f2168e&ptc_code=Quality%20Control%20&%20Quality%20Assurance (Fee)
77. *Quality Control Personnel Certification Level III Training Manual*. 1996. (TM-103), Precast/Prestressed Concrete Institute, Chicago, IL., 243 pp.
https://netforum.pci.org/eweb/dynamicpage.aspx?webcode=category&ptc_key=a7ba327a-0cc2-48cc-bc3e-1c8f49f2168e&ptc_code=Quality%20Control%20&%20Quality%20Assurance (Fee)
78. Rabbat, B. G., T. Takayanagi, and H. G. Russell. 1982. "Optimized Sections for Major Prestressed Concrete Bridge Girders." (FHWA/RD-82/005), Federal Highway Administration, Washington, DC., (February), 178 pp.
<http://www.fhwa.dot.gov/publications/research/infrastructure/structures/05058/05.cfm>
79. Russell, H. G. 2007. *Synthesis of Research and Provisions Regarding the Use of Lightweight Concrete in Highway Bridges*. (FHWA-HRT-07-053), Federal Highway Administration, Washington, DC., 114 pp.
<http://www.fhwa.dot.gov/publications/research/infrastructure/bridge/07051/index.cfm>
80. Russell, H. G. 2009. *Adjacent Precast Concrete Box Beam Bridges: Connection Details*. NCHRP Synthesis 393, Transportation Research Board of the National Academies, Washington, DC., 86 pp.
<http://www.trb.org/Publications/Blurbs/160850.aspx> (Fee)
81. Russell, H. G. 2012. *Waterproofing Membranes for Concrete Bridge Decks*. NCHRP Synthesis 20-05, Topic 42-07. (To be published in 2012).
<http://apps.trb.org/cmsfeed/TRBNetProjectDisplay.asp?ProjectID=2943>
82. Sason, Augusto S. 1992. "Evaluation of Degree of Rusting on Prestressed Concrete Strand." *PCI Journal*, Precast/Prestressed Concrete Institute, Chicago, IL. V. 37, No. 3, (May-June), pp. 25-30.
http://www.pci.org/view_file.cfm?file=JL-92-MAY-JUNE-4.pdf
http://www.pci.org/view_file.cfm?file=JL-92-MAY-JUNE-5.pdf

FABRICATION AND CONSTRUCTION

3.10 References

83. Sengupta, S. and J. E. Breen. 1973. "The Effect of Diaphragms in Prestressed Concrete Girders and Slab Bridges." Research Report 158-1F, Center of Highway Research, University of Texas at Austin, TX.
<http://www.amazon.com/s?ie=UTF8&rh=n%3A283155%2Ck%3Aeffect%20diaphragms%20prestressed%20concrete%20girder%20slab%20bridges&page=1> (Fee)
84. Sithichai kasem, S. and W. L. Gamble. 1972. "Effects of Diaphragms in Bridges with Prestressed Concrete I-Section Girders." Civil Engineering Studies, Structural Research Series No. 383, Department of Civil Engineering, University of Illinois, Urbana, IL., (February).
<http://www.google.com/search?client=safari&rls=en&q=NCHRP+Synthesis+393&ie=UTF-8&oe=UTF-8#sclient=psy->
85. Stanton, J. F. and A. H. Mattock. 1986. "Load Distribution and Connection Design for Precast Stemmed Multibeam Bridge Superstructures." National Cooperative Highway Research Program Report No. 287, Transportation Research Board, National Research Council, Washington, DC., (November).
<http://pubsindex.trb.org/view/1986/m/277795>
86. Tadros, M. K., J. A. Ficenec, A. Einea, and S. Holdsworth. 1993. "A New Technique to Create Continuity in Prestressed Concrete Members." *PCI Journal*, Precast/Prestressed Concrete Institute, Chicago, IL. V. 38, No. 5, (September-October), pp. 30-37.
http://www.pci.org/view_file.cfm?file=JL-93-SEPTEMBER-OCTOBER-8.pdf
http://www.pci.org/view_file.cfm?file=JL-93-SEPTEMBER-OCTOBER-9.pdf
http://www.pci.org/view_file.cfm?file=JL-93-SEPTEMBER-OCTOBER-10.pdf
87. Tadros, M. K., F. Fawzy, and K. E. Hanna. 2011. "Precast, Prestressed Girder Camber Variability." *PCI Journal*, Precast/Prestressed Concrete Institute, Chicago, IL. V. 56, No. 1, (Winter), pp. 135-154.
http://www.pci.org/view_file.cfm?file=JL-11-WINTER-11.pdf
88. Wong, A. Y. C. and W. L. Gamble. 1973. "Effects of Diaphragms in Continuous Slab and Girder Highway Bridges." Department of Civil Engineering, Structural Research Series No. 391, Department of Civil Engineering, University of Illinois, Urbana, IL., (May), 123 pp.
<http://www.ideals.illinois.edu/bitstream/handle/2142/13804/SRS-391.pdf?sequence=2>
89. Zia, P. and A. Caner. 1993. "Cracking in Large-Sized Long-Span Prestressed Concrete AASHTO Girders." Final Report, (FHWA/NC/94-003), Research Project 23241-93-3, Center for Transportation Engineering Studies, Department of Civil Engineering, North Carolina State University, Raleigh, NC., (October), 98 pp.
<http://trid.trb.org/view.aspx?id=404767>

This page intentionally left blank

4.0 INTRODUCTION 4 - 5

4.1 GEOMETRY 4 - 5

 4.1.1 Span Length vs. Structure Depth 4 - 5

 4.1.1.1 Shallow Sections 4 - 5

 4.1.1.2 Deeper Sections 4 - 6

 4.1.1.3 Water Crossings 4 - 6

 4.1.1.3.1 Vertical Profile at Water Crossings 4 - 6

 4.1.1.4 Grade Crossings 4 - 6

 4.1.1.5 Wearing Surface 4 - 6

 4.1.2 Member Spacing 4 - 6

 4.1.2.1 Wider Spacings 4 - 6

 4.1.3 Maximizing Span Lengths 4 - 7

 4.1.3.1 Advantages of Maximum Spans 4 - 7

 4.1.3.2 Limitations of Maximum Spans 4 - 7

 4.1.4 Splicing Beams to Increase Spans 4 - 7

 4.1.5 Special Geometry Conditions 4 - 7

 4.1.5.1 Horizontal Curves 4 - 7

 4.1.5.2 Vertical Curves 4 - 7

 4.1.5.3 Skews 4 - 8

 4.1.5.4 Flared Structures 4 - 8

 4.1.5.5 Varying Span Lengths 4 - 9

 4.1.6 Product Availability 4 - 9

 4.1.6.1 Economy of Scale 4 - 9

4.2 DESIGN 4 - 10

 4.2.1 Advantages of Simple Spans 4 - 10

 4.2.2 Limitations of Simple Spans 4 - 10

 4.2.3 Continuity 4 - 10

 4.2.3.1 Achieving Continuity 4 - 11

 4.2.3.2 Limitations of Continuity 4 - 11

 4.2.4 Integral Caps and Abutments 4 - 11

 4.2.4.1 Advantages 4 - 11

 4.2.4.2 Disadvantages 4 - 11

 4.2.5 Intermediate Diaphragms 4 - 11

 4.2.5.1 Need for Intermediate Diaphragms 4 - 11

 4.2.5.2 Steel Diaphragms 4 - 11

 4.2.5.3 Precast Concrete Diaphragms 4 - 11

 4.2.5.4 Temporary Diaphragms 4 - 12

 4.2.6 Prestressing 4 - 12

 4.2.6.1 Strand Considerations 4 - 12

STRATEGIES FOR ECONOMY

Table of Contents

4.2.6.2 Harped Strands..... 4 - 12

 4.2.6.2.1 Harped Profiles 4 - 12

 4.2.6.2.2 Harping Methods 4 - 12

4.2.6.3 Straight Strands..... 4 - 13

 4.2.6.3.1 Advantages of Straight Strands..... 4 - 13

 4.2.6.3.2 Debonding Strands 4 - 13

 4.2.6.3.3 Limitations of Straight Strands 4 - 13

4.2.6.4 Strand Spacing..... 4 - 14

4.2.7 Nonprestressed Reinforcement..... 4 - 14

 4.2.7.1 Detailing for Ease of Fabrication 4 - 14

 4.2.7.2 Excessive Reinforcement..... 4 - 14

 4.2.7.3 Welded Wire Reinforcement..... 4 - 14

4.2.8 Durability 4 - 16

 4.2.8.1 Benefits of the Fabrication Process..... 4 - 16

 4.2.8.2 Additional Protection 4 - 16

4.2.9 Bearing Systems..... 4 - 16

 4.2.9.1 Embedded Bearing Plates..... 4 - 17

 4.2.9.2 Bearing Devices..... 4 - 17

 4.2.9.3 Bearing Replacement..... 4 - 17

4.2.10 Concrete Compressive Strengths..... 4 - 17

4.2.11 Lightweight Concrete..... 4 - 17

 4.2.11.1 Material Properties..... 4 - 17

 4.2.11.2 Major Bridges with Lightweight Concrete..... 4 - 17

4.2.12 Touch Shoring 4 - 18

 4.2.12.1 Example Project..... 4 - 18

 4.2.12.2 Limitations..... 4 - 18

4.2.13 Spliced Beams..... 4 - 18

4.3 PRODUCTION 4 - 18

 4.3.1 Beam Top Finish 4 - 18

 4.3.2 Side and Bottom Finishes 4 - 19

 4.3.3 Appurtenances..... 4 - 19

4.4 DELIVERY AND ERECTION 4 - 19

 4.4.1 Transportation 4 - 19

 4.4.1.1 Water Delivery..... 4 - 19

 4.4.1.2 Truck Delivery 4 - 19

 4.4.1.3 Rail Delivery 4 - 19

 4.4.2 Handling and Erection..... 4 - 20

 4.4.2.1 Lifting Devices 4 - 20

 4.4.2.2 Support and Lift Locations..... 4 - 20

STRATEGIES FOR ECONOMY

Table of Contents

4.5 OTHER PRODUCTS..... 4 - 20

 4.5.1 Stay-in-Place Deck Panels..... 4 - 20

 4.5.2 Full Depth Precast Decks..... 4 - 21

 4.5.3 Precast Substructures..... 4 - 21

 4.5.3.1 Advantages of Precast Substructures 4 - 21

 4.5.3.2 Components 4 - 21

 4.5.3.3 Connections..... 4 - 22

 4.5.4 Barriers 4 - 22

4.6 ADDITIONAL CONSIDERATIONS..... 4 - 22

 4.6.1 Wide Beams..... 4 - 22

 4.6.2 Adjacent Members 4 - 22

 4.6.3 High Strength Concrete..... 4 - 23

 4.6.4 Contract Considerations..... 4 - 23

4.7 SUMMARY AND REFERENCES..... 4 - 23

 4.7.1 Summary 4 - 23

 4.7.2 Cited References 4 - 23

This page intentionally left blank

Strategies for Economy

4.0 INTRODUCTION

The use of precast, prestressed concrete products for the construction of bridges results in very economical, high quality structures. This is due to several factors:

- Mass production of standardized, low maintenance sections
- A factory environment that requires stringent quality control validated by the Precast/Prestressed Concrete Institute
- Rapid erection and construction
- The use of high quality, inexpensive and locally available materials for production

This chapter discusses issues for the designer to consider that will improve the cost effectiveness of precast, prestressed concrete bridge construction.

4.1 GEOMETRY

All bridges must meet the specific geometric constraints for each unique site. The length of the bridge must be sufficient to cross the obstruction beneath it. This can be accomplished by providing a lesser number of long spans or a larger number of shorter spans. The locations of piers and bents may be restricted by roads or rail lines and their necessary horizontal clearances. Likewise, specific requirements for ships or barges may dictate the placement of piers on either side of a main channel. Existing utilities may limit the locations of foundations. At other locations, such as stream and creek crossings, the designer may have more control over placement of the substructure. The choice of span length can also be affected by the cost of substructure units. Where the foundation conditions are poor or the piers are tall, it could be more economical to use longer spans. The choice of span length should result from the lowest combined cost of the superstructure and substructure. Each site must be evaluated to determine the most appropriate span arrangement to accommodate the necessary horizontal and vertical clearances of the system below the bridge.

4.1.1 Span Length vs. Structure Depth

The depth of the bridge superstructure increases incrementally based on the span length. As a general rule, this is also true for precast, prestressed concrete. However, the structural efficiency of deeper sections may not always result in cost efficiency.

Raw bridge cost is not the only basis for selecting structure type. Hydraulics or profile grades may require shallow superstructures. Structures that can be constructed rapidly might be justified if the time to travel a detour, and therefore user costs, can be minimized. Environmental considerations could justify the extra cost of special aesthetic structural designs.

Superstructure depth is frequently controlled by minimum vertical clearance requirements. These are typically established by the functional classification of the highway and the construction classification of the project. A common requirement is that the bridge superstructure be as shallow as possible to satisfy both minimum vertical clearance requirements and to minimize approach grades. Therefore, a high span-to-depth ratio is often desirable.

4.1.1.1 Shallow Sections

Shallower beams may require more prestressing strands and higher concrete transfer strength, but, as a rule, are less expensive, since less concrete is required. In addition to the reduced direct material cost, reduced costs can be realized by lower shipping and handling weights. Spans of up to 40 ft can be achieved using solid slabs, voided slab beams or stemmed members that are placed side by side. For a given span length, voided slab beams or stemmed members may use less material and be relatively lightweight. However, solid slabs may be less expensive, since the forms are relatively inexpensive and the fabrication of the solid slab is less complicated.

STRATEGIES FOR ECONOMY

4.1.1.2 Deeper Sections/4.1.2.1 Wider Spacings

4.1.1.2 Deeper Sections

As span length increases, there is the need to increase section properties of the superstructure components, while reducing their weight. Deeper sections such as box beams and deeper stemmed sections, placed side by side, become advantageous. The greater depth contributes to an increased moment of inertia, while the reduction of the concrete in the voided portion of the beam helps to keep the weight of the section to a minimum. As span length continues to increase, the use of superstructure components not placed side by side become a more cost-effective solution. These types of systems, such as spread box beams and I-beams, require the use of a cast-in-place concrete deck or full depth concrete panels to span between beams.

4.1.1.3 Water Crossings

For typical stream or creek crossings where the foundation conditions are good, it may be more economical to use a larger number of shorter spans. The cost of additional substructure units must be evaluated against savings from the use of smaller cranes which can be used with shorter, lighter beams. Physical constraints on the location of substructures generally are few and are probably restricted only to hydraulic considerations. The balance between the number and costs of substructure units and the size of the superstructure members becomes the primary factor in minimizing construction costs.

4.1.1.3.1 Vertical Profile at Water Crossings

Superstructure depth must be balanced between maintaining freeboard of the stream and reducing the impact on the vertical profile of the bridge and cost of approach roadways. Increased structure depth may increase the volume of fill for the approach roadways and have an effect on right-of-way requirements to accommodate roadway fill.

4.1.1.4 Grade Crossings

At grade crossings, span lengths are generally dictated by horizontal clearance requirements and other safety considerations. The span lengths usually are such that the use of spread box beams or I-beams is effective. Depth of structure becomes a consideration in establishing the bridge profile while maintaining the required vertical clearance for the transportation system below. As with water crossings, the structure depth will have a direct impact on the volume of approach roadway fill and the measures necessary to accommodate that fill.

4.1.1.5 Wearing Surface

The use of a wearing surface may be desirable to improve durability and enhance the quality of the ride. A cast-in-place concrete composite topping is a superior wearing surface for high traffic volumes and can also increase the load carrying capacity of the superstructure. On rural bridges with low traffic volumes, especially when deicing salt is not used, the untopped precast concrete surface provides outstanding durability and lowest possible construction cost. In other cases, a waterproofing membrane and asphalt surface can be used effectively.

4.1.2 Member Spacing

As span length increases, it becomes necessary to evaluate the use of various beam types, and the depth of beams versus the number of beams required. For a given span length, a 54-in.-deep beam and a 63-in.-deep beam may both be acceptable. The number of 54-in.-deep beams required in the bridge cross section will likely be more than 63-in.-deep beams.

4.1.2.1 Wider Spacings

Generally, the use of fewer beams at a greater spacing will prove to be the more economical superstructure than more beams at a lesser spacing. The use of fewer members means reduced volume of beam concrete and fewer beams to fabricate, ship and erect. Other savings result from the reduction in the number of bearing devices, fewer end diaphragms to form and cast, fewer bays between the beams in which to install and remove deck forms and fewer hours needed to inspect. Very wide beam spacings (in excess of 12 ft) must be carefully considered, since the cost of the deck and its forming may override the savings of the reduced number of beams. Future deck replacement and staged construction should also be considered in selecting beam spacing. Today, designers recognize that the time to construct a cast-in-place concrete deck generally adds time to the bridge construction schedule. This adds to user delays and is a topic for early designer evaluation and should be discussed with the owner.

STRATEGIES FOR ECONOMY**4.1.3 Maximizing Span Lengths/4.1.5.2 Vertical Curves****4.1.3 Maximizing Span Lengths**

For a given beam depth, it is often advantageous to use the beam at its maximum span length, even if closer spacings are required.

4.1.3.1 Advantages of Maximum Spans

By using a beam at its maximum span capability, the designer can achieve a longer span without increasing the depth of the structure. This can provide for better horizontal and vertical clearances for the roadway, railway, or waterway below. Additionally, for longer bridges, the use of extended spans means fewer substructures must be constructed. Often, longer spans are necessary and consideration of superstructure cost versus substructure cost must be evaluated. For example, when very expensive substructures are required, such as those designed to resist ship impact or that require deep or massive foundations, the cost of the superstructure with longer spans usually becomes more economical.

4.1.3.2 Limitations of Maximum Spans

Designers must be cognizant of the limitations of production facilities and handling, shipping, and erection equipment due to longer beams. The use of beam sections that are not available through local producers will usually be more expensive if forms must be purchased to manufacture a small number of beams. Local producers may not have prestressing beds capable of withstanding large prestressing forces. Longer beams are heavier and may require larger cranes for handling and erection. Special trucks and trailers may be required to transport the beams to the job site. Generally, increased weights are not an issue for erection over water provided the beams can be transported to the site by barge.

4.1.4 Splicing Beams to Increase Spans

To increase the span capabilities of precast, prestressed concrete beams, designers should consider the technique of splicing. Through the use of post-tensioning or other splicing methods, continuity and its inherent benefits relative to moment reduction in the superstructure and a reduction in the number of expansion joints can be achieved. Splicing beams also reduces the size and weight of individual segments, allowing easier handling and erection, and lighter weights for shipping. Splicing does, however, have additional costs associated with the time to splice the sections, often the need for temporary supports, and the splicing system itself. For more detailed information on the use of spliced beams, see **Chapter 11**.

4.1.5 Special Geometry Conditions

Overall bridge geometry is very often dictated by the roadway designers. The bridge location within a roadway system frequently establishes the bridge within a horizontal curve, a vertical curve, with skewed substructures, or with flared spans to accommodate ramps.

4.1.5.1 Horizontal Curves

Straight precast, prestressed concrete beams can usually be used for horizontally curved bridges. The beam placement must take into account the degree of curvature and the span length. The primary impact of the curve is to the location of the exterior beams. The overhang of the deck must be evaluated at the beam ends and at midspan to ensure that proper consideration is given to the loading of the beam under both dead and live loads.

4.1.5.2 Vertical Curves

The profile of the deck may include crest or sag vertical curves. The designer must consider the camber of the beam relative to the deck profile to establish the proper buildup of concrete or haunch over the beam (**Figure 4.1.5.2-1**). The volume of concrete in the build-up is larger in wider beams such as bulb-tees (**Figure 4.1.5.2-2**). Horizontal curves also affect the volume of concrete in the build-up due to the superelevation of the roadway. However, this build-up concrete is inexpensive since costs are almost exclusively a function of the concrete material cost. No additional forming, placement or curing costs result from the build-up. In some locations, producers have successfully fabricated beams with a specified top profile and cross slope (within reasonable limits) to accommodate a certain vertical profile and superelevation. This is often done with deck bulb-tees, which are wide, erected with their top flanges touching, and using no cast-in-place concrete topping or asphalt wearing surface.

STRATEGIES FOR ECONOMY

4.1.5.2 Vertical Curves/4.1.5.4 Flared Structures

Figure 4.1.5.2-1
Beam Camber/Deck Relationship

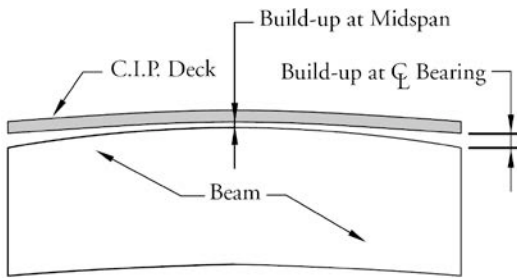
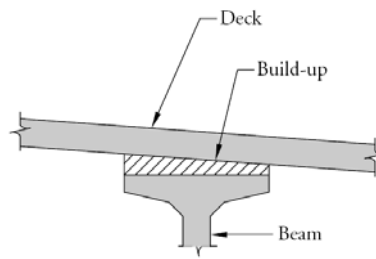


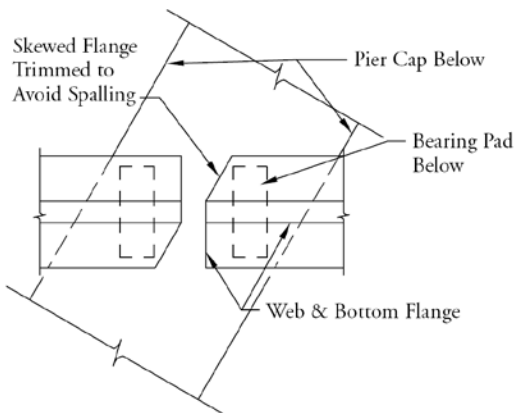
Figure 4.1.5.2-2
Build-up over Beam



4.1.5.3 Skews

Substructures that are skewed to the beam require some consideration. If possible, avoid skewed supports. The *LRFD Specifications* modify the live load distribution factor for skewed superstructures. Additionally, beam ends are usually skewed so that the ends of the beams are parallel to the substructure. Small skews normally will not affect the cost of precast, prestressed concrete beams. Extreme skews usually require the producer to take measures to reduce spalling of the beam end during the strand transfer operation. Otherwise, the “point” on the beam end must support the dead weight of the beam when in the prestressing bed. This, combined with elastic shortening, usually results in spalls. One method to reduce spalls is to trim the point of the skew from the beam as depicted in **Figure 4.1.5.3-1**. If a spall does occur, it is generally minor and can be easily repaired or embedded in to the diaphragm without affecting the integrity of the bearing area. Some state DOTs have standards details that include embedded galvanized bearing plates to strengthen beam ends.

Figure 4.1.5.3-1
Beam Ends at Support with Large Skew



4.1.5.4 Flared Structures

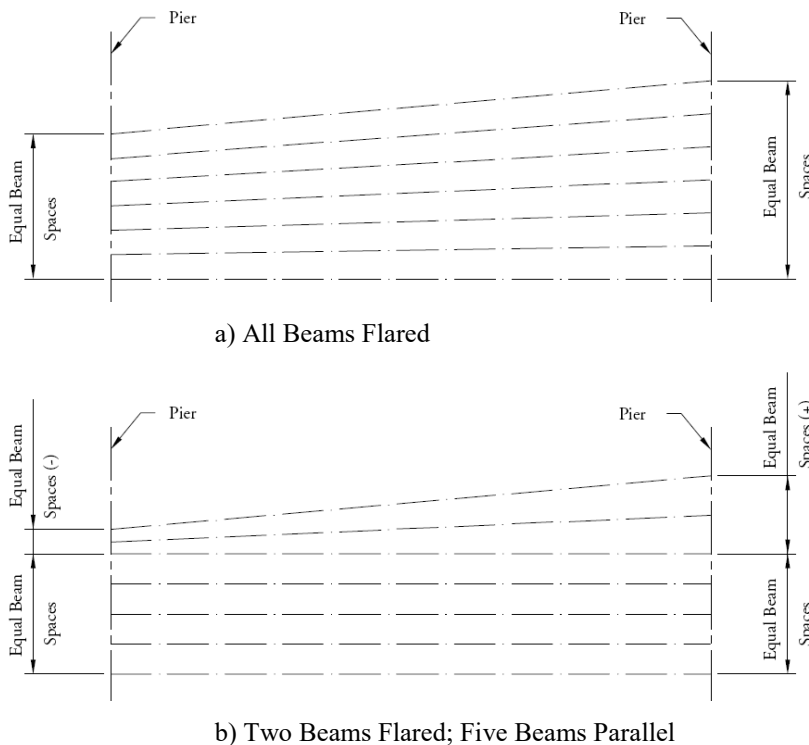
Flared spans are those that have one end wider than the other. By using as many parallel beams within the span as possible, the designer can reduce the fabrication and construction costs of the superstructure. This results from maintaining more uniform beam lengths, typical beam end skews and reduced deck forming costs. **Figure 4.1.5.4-1** shows two beam layouts that could be used for a flared span. Note that with all beams flared, each of the beams is unique. The alternate with five parallel beams has three unique beams and the deck forming will be more uniform.

Flared spans generate girder lengths that vary only slightly, but can lead to designs with varying strand patterns. It is typically more economical to specify a common strand pattern for all girders in the span based on the most severe design, or no more than two groupings of strand patterns for the same span. This affords the manufacturer the most flexibility in scheduling production when more than one girder is produced on the same prestressing line.

STRATEGIES FOR ECONOMY

4.1.5.4 Flared Structures 4.1.6.1 Economy of Scale

Figure 4.1.5.4-1
Span Configurations For a Flared

**4.1.5.5 Varying Span Lengths**

When possible, design precast beams with the same cross section and strand pattern. Optimum economy from precasting results from repetition and the production of identical sections. If a bridge consists of different span lengths, it may be better to design all of the precast units with the same cross section rather than to design each span for the minimum depth-to-span ratio.

4.1.6 Product Availability

Designers must determine the availability of precast products in the local area. If the product selected for the project is not available within 200 to 500 miles, depending on the geographic region, a cost premium for shipping from a distant location or for local form purchase may be added to the project. Designs using local and readily available member types will result in lower prices.

4.1.6.1 Economy of Scale

If a single project uses a large quantity of a specific product, or if a new product will be used as a standard for future bridges, the cost of new forms, when amortized over a large volume, becomes far less significant. Designers should consult local producers early in the study phase of a bridge project to determine the available precast products or the costs associated with new products for a specific application. Many times it is possible to create a new section by making small, inexpensive modifications to existing forms, such as casting a 3-ft 6-in.-deep box beam in a 4-ft 0-in.-deep form, or placing AASHTO Type II I-beam side forms on a wider Type IV I-beam bottom form.

4.2 DESIGN

Many decisions made during the design of precast, prestressed concrete bridges have a direct economic impact on the bridge construction cost and time needed for construction. Some of these bridge design decisions are:

- Structural system (simple spans versus continuity)
- Integral caps and/or abutments
- Use of intermediate diaphragms
- Prestressing systems
- Durability systems
- Bearing systems
- Use of lightweight aggregate concrete
- Special construction techniques (i.e. accelerated bridge construction and project accelerated construction technologies)

4.2.1 Advantages of Simple Spans

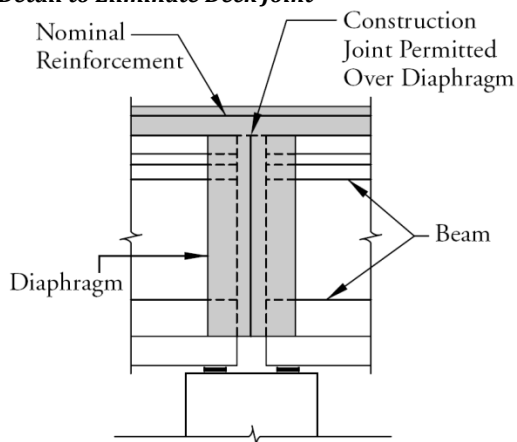
Simple span prestressed concrete superstructures can result in very economical bridges. Many designers rely almost exclusively on simple spans for this very reason. With simple spans, end diaphragms and end connections are greatly simplified. There is a significant reduction in the volume of reinforcement required over interior supports. There are also substantially reduced structural effects of short and long term volume changes due to temperature variations, creep, and shrinkage.

4.2.2 Limitations of Simple Spans

Use of simple spans may, however, limit the span length for a product or require more beams for a span. The use of more prestressing strands may allow for an increased span length, but may create a need for increased concrete strength at transfer of the prestress force. This may force the cycle time of the prestressed bed to be increased, reducing the efficiency of the plant. There may also be more joints over substructures which can affect deck ride quality. Also, joints must be maintained to reduce premature deterioration of the substructure and bearing devices caused by road salts and deicers. Some designers have successfully eliminated this problem by casting the deck continuous over supports and placing additional reinforcing steel in the deck to reduce deck cracking (**Figure 4.2.2-1**).

Figure 4.2.2-1

Detail to Eliminate Deck Joint



4.2.3 Continuity

In designing continuous superstructures, designers can take advantage of increased span lengths or reduce the number of beams required for a span. The smaller positive moments that occur in continuous systems will reduce the required number of prestressing strands. Continuity will reduce the number of joints in the superstructure and enhance redundancy of the structure.

A continuous superstructure also increases the resistance of the structure to horizontal forces, particularly seismic loads and ship impact forces.

STRATEGIES FOR ECONOMY**4.2.3.1 Achieving Continuity/4.2.5.3 Precast Concrete Diaphragms****4.2.3.1 Achieving Continuity**

Continuity is usually achieved with the use of enhanced, positive beam connections over supports and by reinforcing the deck over the supports to withstand the negative moments due to composite dead and live loads. Longitudinal post-tensioning of the beams adds cost, but can also be used to achieve continuity. Refer to **Chapter 11** for a full discussion of these issues.

4.2.3.2 Limitations of Continuity

Proper detailing of continuous superstructures over the supports should be provided to avoid diaphragm cracking. Some end diaphragms with improper details have resulted in cracks from volumetric changes in the concrete. Use of continuity without post-tensioning requires a significant increase in the amount of mild steel reinforcement in the deck. Some states design beams as simple spans but use continuous slabs over the supports to eliminate joints and reduce the negative effects of the volumetric changes.

4.2.4 Integral Caps and Abutments

Integral pier caps and abutments have been used successfully in several areas. By creating proper connections between the superstructure and substructure, moments from the superstructure are distributed to the substructure components. More information on integral bridges is found in **Chapter 13** and the PCI Bridges Committee Report on Integral Bridges (2001).

4.2.4.1 Advantages

In addition to the benefits of reduced positive moments in the span, there is also a significant increase in the resistance to horizontal forces and redundancy of the structure. Transverse joints and bearing devices are virtually eliminated. Integral abutments are flexible and tolerate a wide range of temperature movements. Integral abutments can be used for precast concrete bridges with lengths up to 1,000 ft. There is also strong potential to reduce the overall construction cost of the substructure.

4.2.4.2 Disadvantages

Design for this type of system is somewhat more difficult than for a continuous superstructure since substructure stiffness must be considered in the distribution of forces. Very stiff substructures make the system sensitive to volumetric changes. Also, connection design and construction requires more attention.

4.2.5 Intermediate Diaphragms

Intermediate diaphragms are a significant cost in the construction of prestressed concrete bridges. When used, intermediate diaphragms may be constructed of either concrete or structural steel. If concrete is used for these diaphragms, it will probably be permanent and its weight must be considered in the design of the beams.

4.2.5.1 Need for Intermediate Diaphragms

Although AASHTO implies that intermediate diaphragms are necessary, several research papers have concluded they are not required. References are cited in **Chapter 3, Section 3.7**. The cost to construct and install forms and reinforcement for diaphragms is very high, as is the connection to the beams. Several states have eliminated the use of intermediate diaphragms without negative impact on the performance of their prestressed concrete bridges.

4.2.5.2 Steel Diaphragms

Galvanized structural steel diaphragms are usually bolted to inserts in the beams, eliminating the field forming and casting expense. However, accurate detailing of the steel and placement of the inserts are necessary to ensure proper fit in the field. Connections must allow for fabrication and construction tolerances. Steel diaphragms may also be more susceptible to corrosion, resulting in higher maintenance costs.

4.2.5.3 Precast Concrete Diaphragms

Precast concrete diaphragms have been successfully used. Precast diaphragms reduce the field labor costs associated with the forming and placing of cast-in-place concrete. However, as with steel diaphragms, care must be taken in the detailing and fabrication of the precast diaphragms to accommodate fabrication and construction tolerances. Connection schemes for precast diaphragms must also be carefully considered. Development of details and tests in Pennsylvania has resulted in PennDOT acceptance of a standard for precast diaphragms (PennDOT, 1996).

STRATEGIES FOR ECONOMY

4.2.5.4 Temporary Diaphragms/4.2.6.2.2 Harping Methods

4.2.5.4 Temporary Diaphragms

For some longer spans and deeper beams, temporary intermediate diaphragms may be desirable to increase the stability of the beams prior to and during placement of the concrete deck. Typically, these temporary diaphragms are steel.

4.2.6 Prestressing

The selection of either stress-relieved (normal-relaxation) or low-relaxation strands and the size of prestressing strand has a direct impact on the cost of prestressed concrete products. **Section 7 of Chapter 2** discusses the various types of prestressing strand materials that are available. Currently, the most common strand used in beams is seven-wire, low-relaxation, Grade 270 strand. The steel used in this strand can be pulled to a higher initial stress and exhibits lower losses than normal-relaxation strand.

4.2.6.1 Strand Considerations

The use of fewer strands with larger diameter is generally more cost effective than the use of a larger number of smaller diameter strands. The cost of the strand is usually not directly proportional to the area of the strand (larger strands are proportionately slightly less expensive). But even if it were, the labor to install the larger number of smaller diameter strands will almost always make the use of the larger size strands more cost effective. As concrete design strength increases, the use of larger strands and their associated larger forces becomes more desirable. The use of larger strand enables the designer to place a larger prestressing force almost at the same eccentricity as the same number of smaller strands. This will increase the capacity of the beam. Using a lesser number of larger strands may also reduce congestion and facilitate concrete placement.

Designers are urged to avoid using more strands or prestressing force than required by design. Excessive strand is costly and can significantly increase camber.

Beams may be designed with strands having either a straight or harped trajectory.

4.2.6.2 Harped Strands

Very often, some of the prestressing strands are placed in a harped (deflected or sometimes draped) profile along the length of the beam. By harping the strands, designers are able to place the strands at the lowest position at midspan where the positive moment is largest, but raise the center of gravity of the prestress force near the end of the beam where the moments are reduced (see **Figure 3.3.2.4-1**). Raising the strands reduces the eccentricity and therefore the negative moment associated with the prestress force. The reduced negative moment results in lower compressive stresses in the bottom of the beam and lower tensile stresses in the top of the beam near its ends. In **Chapter 3**, detailed information on harping strands is contained in **Section 3.3.2**.

4.2.6.2.1 Harped Profiles

The method of achieving a harped strand profile requires the use of hold-down devices and either hold-up or pick-up devices. The location of the hold-down should be approximately 0.4 to 0.45 of the beam length from the ends. Some designers have located the hold-down points as close to the ends as 0.3L; others have used a single point at midspan. Based on the shape of the typical positive moment envelope, the use of the 0.4L to 0.45L location may be the most appropriate choice. Use of a location closer to the end does not appear to provide increased capacity, and increases the forces in the hold-up and hold-down devices. When using a single hold down at the center of the beam, the load transmitted to the anchorage for the hold down sometimes becomes excessive.

4.2.6.2.2 Harping Methods

A hold-down device normally consists of rollers attached to a vertical rod, which passes through the bottom form and is anchored to the form substructure or foundation to resist the vertical component of the prestress force. The force that must be resisted by the hold-down device, and therefore its size, depends on the number of harped strands and the trajectory angle of the strands. There is a cost associated with the hold-down devices since they remain in the beam and are not reused. Additionally, when the hold-down locations along the length of the prestress bed are moved to accommodate different beam lengths, the bottom form must be patched.

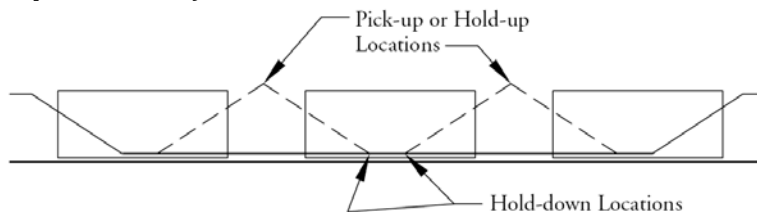
Frequently, precast concrete producers use hold-up devices to raise the profile of the strand at the ends of beams and then tension the strands in their already harped profile. Others lift the harped strand to the proper elevation after tensioning the strands. Again, the number of harped strands and their angle directly influence the size and

STRATEGIES FOR ECONOMY

4.2.6.2.2 Harping Methods/4.2.6.3.3 Limitations of Straight Strands

cost of the hold-up/pick-up device. **Figure 4.2.6.2.2-1** shows a typical harped strand profile in a prestressing bed. The designer can reduce the cost of the prestressed product by minimizing both the number of harped strands and the heights of the holdup points.

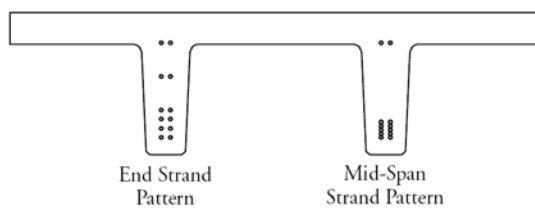
Figure 4.2.6.2.2-1
Harped Strand Profile



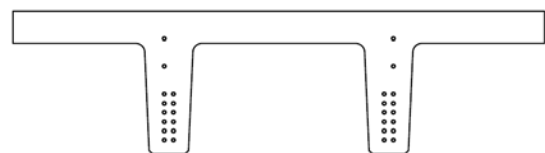
4.2.6.3 Straight Strands

The use of straight strand offers some advantages in the fabrication of prestressed concrete products. There are instances when the addition of a few straight strands can eliminate the need for harped strands. This option should be seriously evaluated, since the straight strand option, while using more strands, results in easier fabrication. **Figure 4.2.6.3-1** depicts a harped strand pattern and an alternate straight strand pattern. The increase in stresses due to more strands may be reduced by debonding some of the strands in the ends of the beams (see also **Chapter 3, Section 3.3.2.9**).

Figure 4.2.6.3-1a-1b
Straight vs. Harped Strands



a) Harped Strand Pattern – 24 strands required



b) Alternate Straight Strand Pattern – 28 strands required

4.2.6.3.1 Advantages of Straight Strands

The use of straight strands is generally less expensive than harped strands for several reasons:

- Hold-down/hold-up devices are not required
- Placement of beams within the bed is less restricted
- The stressing operation is made simpler and safer
- Transfer operations are also simplified (hold-down and hold-up devices do not have to be released)
- Varying beam lengths will not require moving hold-down locations
- The cost of repairing the bottom form is eliminated

4.2.6.3.2 Debonding Strands

The effect of harping on stresses can be approximated by using straight strands located as required for the maximum positive moment and debonding some of the strands near the ends of the beam. Debonding is achieved by sheathing the strand in plastic tubing. By selectively debonding strands, the designer can effectively control the prestress force and eccentricity, achieving results similar to harping strands.

4.2.6.3.3 Limitations of Straight Strands

When increasing the number of strands, it may become necessary to increase the transfer compressive strength and/or the final design compressive strength of the concrete in order to resist the larger compressive force. Disadvantages of using debonded strands include the elimination of the vertical components of the prestressing force, which may result in a slight increase in shear reinforcement. Design effort may be increased to determine proper debonding patterns, shear reinforcement, and camber. Designers should consult precast producers in the project area to determine strand harping capability and debonding preference.

STRATEGIES FOR ECONOMY

4.2.6.4 Strand Spacing/4.2.7.3 Welded Wire Reinforcement

4.2.6.4 Strand Spacing

The *AASHTO LRFD Specifications* currently requires that strands be spaced, center-to-center, not less than 1.75 in. for ½-in.-diameter strand and 2.0 in. for 0.6-in.-diameter strand. Most plants have fabricated stressing headers and bulk heads that provide for a particular spacing. Before designing with unique strand spacing, it should be determined whether the change will require the producer to modify plant equipment. Designers should consult producers in the geographic area of the project to determine strand patterns and configurations being used (see **Chapter 3, Section 3.2.2.3**).

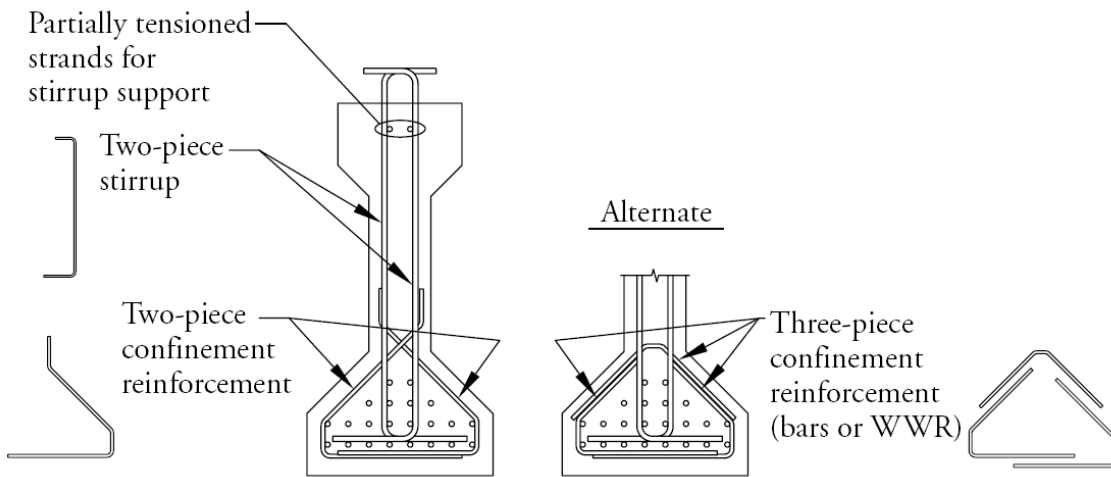
4.2.7 Nonprestressed Reinforcement

Proper detailing of mild steel reinforcement offers the designer an important opportunity to contribute to cost savings. As discussed in **Chapter 3**, the reinforcement is generally placed within the beam after the strands have been tensioned.

4.2.7.1 Detailing for Ease of Fabrication

If the reinforcement is detailed closed around the strands, it requires that the strands be threaded through the closed bars. By using two-piece bars that can be placed after the strand is tensioned, the fabrication process is simplified. **Figure 4.2.7.1-1** illustrates two-piece stirrups and two-piece confinement reinforcement in an I-beam. When specifying concrete cover and spacing of strands and bars, the designer must consider reinforcing bar diameters and bend radii to avoid conflicts. In order to support reinforcing steel located in the tops of some beams and the stirrups in all beams, some producers may prefer to locate one or two strands near the top of the beams (see **Figure 4.2.6.3-1**). Some support could be provided by longitudinal reinforcing bars, but strand is slightly less expensive than mild steel reinforcement and is readily available at precast plants. This strand may be fully tensioned (if considered in the design), or tensioned to a force of 5,000 to 10,000 lbs. The producer can then tie the reinforcement to the strand, which will provide firm support.

Figure 4.2.7.1-1
Multi-Piece Reinforcement



4.2.7.2 Excessive Reinforcement

Minimize the amount of reinforcing steel in prestressed concrete members. There appears to be a tendency to add more reinforcement than is needed “just to be safe.” Often, the added reinforcement merely creates congestion making consolidation of the concrete difficult without contributing significantly to the structural strength or behavior.

4.2.7.3 Welded Wire Reinforcement

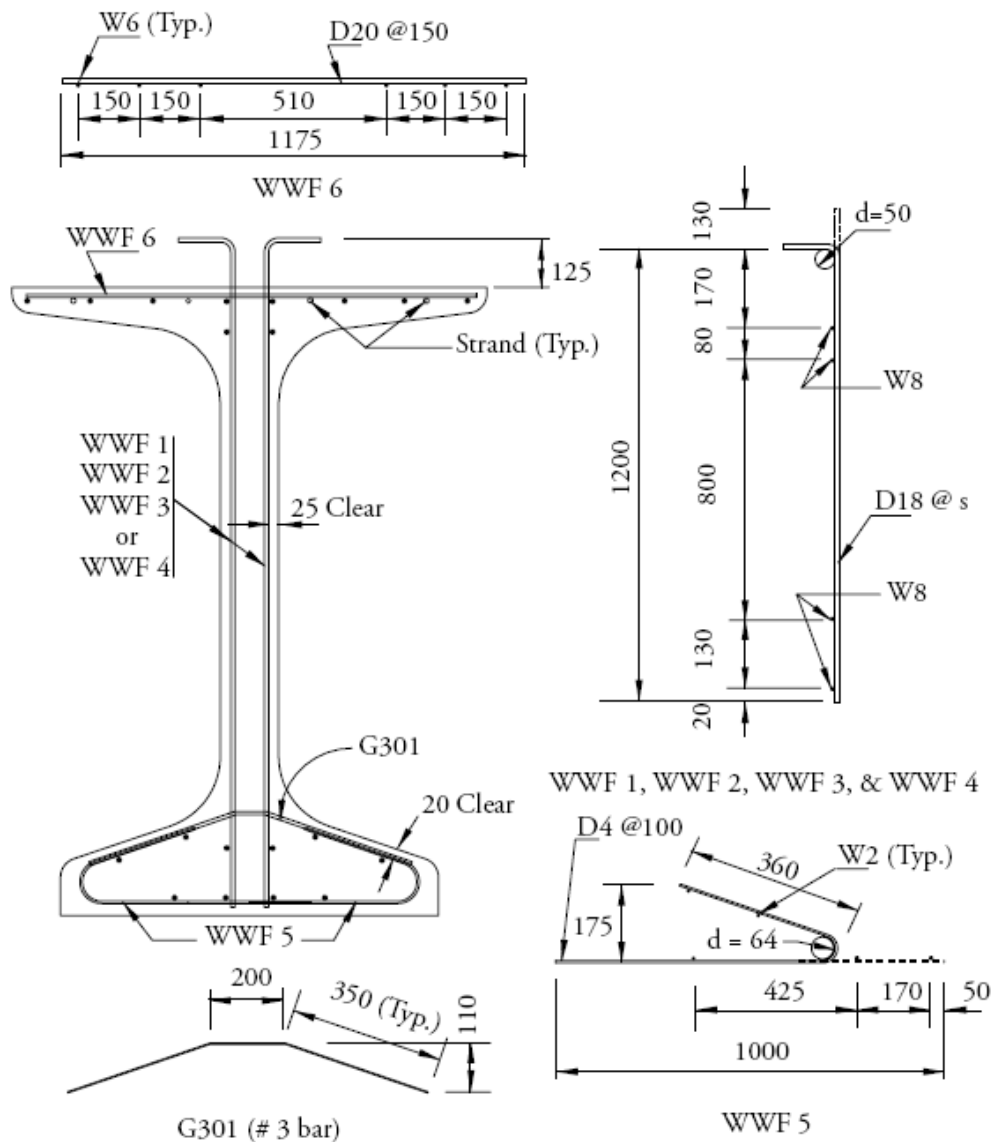
Welded wire reinforcement (WWR) can be a very cost-effective way to place mild steel reinforcing in precast, prestressed concrete members. WWR is a prefabricated reinforcement consisting of parallel, cold-drawn wires welded together in square or rectangular grids. Each wire intersection is electrically resistance-welded by a

STRATEGIES FOR ECONOMY

4.2.7.3 Welded Wire Reinforcement

continuous automatic welder. The use of WWR is particularly advantageous where large areas have uniform reinforcing spacings, such as flanges of double tees and web shear steel in beams. Although the material cost of the WWR is normally more than that of reinforcing bars, cost of installation will normally be substantially less. An example of WWR details for a precast concrete I-beam is shown in **Figure 4.2.7.3-1** for the Nebraska University (NU) metric-dimensioned beam section.

Figure 4.2.7.3-1
Welded Wire Reinforcement Details used by the Nebraska Department of Roads



Fabric Designation	WWF1	WWF2	WWF3	WWF4
Spacing, s (mm)	50	100	200	300

- Notes:
- Dimensions in mm
 - 1 inch = 25.4 mm
 - D18 designates a deformed wire whose area is 0.18 in.²
 - W designates a smooth wire

STRATEGIES FOR ECONOMY

4.2.8 Durability/4.2.9 Bearing Systems

4.2.8 Durability

Prestressed concrete products have an excellent durability record. Review of data in the National Bridge Inventory compiled by the Federal Highway Administration has confirmed the performance of precast, prestressed bridges in all regions of the country. There are several reasons for this excellent record.

4.2.8.1 Benefits of the Fabrication Process

Most prestressed concrete products are fabricated in certified manufacturing plants where strict quality control is maintained. The quality of the concrete is exceptional, and it generally has a higher density and strength than field-placed concrete. Curing procedures, especially those during the first several hours after the concrete is cast, contribute to higher concrete quality. The concrete is almost always maintained in compression due to prestressing, and is therefore essentially crack free. These factors reduce the penetration of water and chloride ions into the concrete, increasing its life. In addition, many precast plants use heat to accelerate curing of the concrete. Recent tests have shown that this further increases the concrete's ability to resist chloride penetration (Pfeifer et al., 1987 and Sherman et al., 1996).

4.2.8.2 Additional Protection

Additional measures can be taken to further enhance the durability of prestressed concrete. **Chapter 2** discusses several measures that can be taken to enhance the material properties of the concrete, e.g., using low water/cementitious materials ratios and certain concrete additives. Providing the proper concrete cover around the reinforcement is essential, but excessive cover does little to enhance durability of the product. If the ends of the precast product are not encased in cast-in-place concrete, it is important to seal or coat exposed prestressing strands and mild steel reinforcing with an appropriate coating. See **Chapter 3, Section 3.2.5.1**.

4.2.9 Bearing Systems

Bearing systems for precast, prestressed concrete products can be very simple. The bearings need to be designed to transfer the design vertical and horizontal forces to the substructure. Discussion of the role of and requirements for bearing plates is given in **Chapter 10**.

The photo in **Figure 4.2.9-1** is an example of poor design and detailing of the bearing area. It can result in instability of the beam and may have been driven in part by provisions of the current *LRFD Specifications*. A much better detail would be to make the pad as wide as the sole plate and to weld the sole plate to the shoe plate embedded in the beam (see **Chapter 10**).

Figure 4.2.9-1

Illustration of a reinforced bearing designed without regard for system performance during construction.



STRATEGIES FOR ECONOMY**4.2.9.1 Embedded Bearing Plates/4.2.11.2 Major Bridges with Lightweight Concrete****4.2.9.1 Embedded Bearing Plates**

In most cases, embedded bearing plates are not needed. If large horizontal forces, such as seismic loads, must be transmitted from the superstructure to the substructure, bearing plates may be necessary on some beams. Beams erected on a steep grade may also need embedded bearing plates with additional beveled or tapered plates to avoid “walking” down the grade. In lieu of costly tapered bearing plates, elastomeric bearing pads placed directly between the precast product and the substructure are commonly used unless longitudinal grades exceed 2%.

4.2.9.2 Bearing Devices

Elastomeric bearing pads are very economical. The bearing pad must be properly designed to accommodate the bearing pressure and the volumetric changes in the superstructure. If necessary, laminated pads can be used, but they cost substantially more than plain pads. Tapered bearing pads have been used in several places to accommodate roadway grades of up to 5%. These pads are more expensive to manufacture than flat pads, but much less expensive than tapered plates. For shallow grades, many states slope the concrete cap at the bearing to provide full contact between the bearing pad and the cap/beam. Pot bearings have been used in conjunction with bearing plates on precast products, but their expense must be carefully considered. They are normally not recommended.

4.2.9.3 Bearing Replacement

Provision for future replacement of bearing devices may be required in some locations. This requires the designer to provide a suitable and practical means for raising the superstructure for removal and replacement of the bearing device. End diaphragms, when used on bridges, can often be designed and detailed to serve this purpose.

4.2.10 Concrete Compressive Strengths

Concrete compressive strength requirements can significantly affect costs. Strength required at transfer of prestress force is likely to be a predominant concern to the producer. Precast concrete plants rely on the daily use of prestressing beds. Therefore, the concrete strength at transfer of prestress should be kept to the minimum required to stay within allowable temporary stresses. Local fabricators are the best source of information on details related to optimum concrete strength.

4.2.11 Lightweight Concrete

Lightweight concrete has been successfully used on many bridges in the United States since the early 1950s. Its earliest applications were in lightweight concrete deck slabs. Lighter weight beams will allow longer spans or greater beam spacings for the same strand and concrete strength. Lightweight concrete use has become more popular in seismic areas where reductions in weight will reduce seismic forces transmitted to the substructure elements, resulting in substantial savings.

4.2.11.1 Material Properties

Concrete strengths of structural-grade expanded shale, clay and slate produced by the rotary kiln method) (ESCS) lightweight aggregate concrete are in the same range as those for normal weight concrete with the same cementitious materials content. Contact a local producer of ESCS aggregate for assistance with mix designs. The modulus of elasticity for a lightweight concrete will be significantly less than that of a normal weight concrete with the same strength. For detailed material properties, refer to ASTM STP 169C (1994). Obtaining concrete strengths in lightweight concrete comparable to the commonly used strengths of normal weight concrete is not difficult. Greater creep, shrinkage, and deflections must be appropriately evaluated and accounted for when lightweight concrete is used.

4.2.11.2 Major Bridges with Lightweight Concrete

There are many notable bridges constructed with lightweight concrete. Some of these include:

- Suwanee River Bridge on U.S. Route 19 at Fanning Springs, Fla. Built in 1964 with Type IV AASHTO I-beams, it uses 5 ksi lightweight concrete at 120 pcf to achieve six, 121-ft spans. These were constructed in three, 2-span continuous units.
- Chesapeake Bay Bridges near Annapolis, Md.
- Napa River Bridge on State Route 29 near Napa, Calif. This is a segmental, prestressed concrete bridge 2,230 ft long with 250 ft spans. It was constructed in 1978.

STRATEGIES FOR ECONOMY**4.2.11.2 Major Bridges with Lightweight Concrete/4.3.1 Beam Top Finish**

- Sebastian Inlet Bridge over the Indian River, Fla. Approach spans are 73 ft long and main spans are 100, 180, and 100 ft long. A drop-in I-beam of lightweight concrete, 72 in. deep, is supported by 2 cantilevered pier beams. Built in 1964, the cast-in-place deck, curbs and parapets are also lightweight concrete.
- Full-depth deck panels of lightweight concrete were used on the Woodrow Wilson Bridge in Washington, D.C., and the Governor Nice Bridge on Maryland Route 301 over the Potomac River.

4.2.12 Touch Shoring

Touch shoring is a technique that has been used to extend the capacity of precast, prestressed concrete beams. The process is to provide proper temporary supports during construction to carry a predetermined portion of the weight of the cast-in-place concrete deck when it is cast. After curing of the deck slab concrete, the temporary shoring is removed and the slab weight is transferred to the composite system rather than the prestressed beam alone. The additional capacity of the beams provides for wider beam spacing or longer spans compared to a similar unshored system.

4.2.12.1 Example Project

In 1988, touch shoring was used for the main span carrying twin structures of the Florida Turnpike over I-595 in Ft. Lauderdale. For this project, a Type V I-beam, which normally is limited to simple spans of approximately 135 ft, was used for a 150-ft span. This scheme was used in lieu of a spliced beam system and saved over \$100,000.

4.2.12.2 Limitations

The drawbacks of the touch shoring system are additional cost of the temporary support and the sensitivity of the system to possible shoring settlements during construction. Touch shoring should be utilized cautiously, with proper attention given to the temporary support design and construction. Subsequent deck replacement will also require specific design and construction provisions; this may be a deterrent to the use of touch shoring in some applications.

4.2.13 Spliced Beams

Concrete structure span ranges have continued to increase with advancements in materials, equipment, and techniques. Spliced beam technology that utilizes post-tensioning can extend span ranges. These beams can be post-tensioned after field-cast concrete closures are made. Some owners have placed the deck and post-tensioned a second stage on the composite section. See Chapter 11 for much more information on spliced beams.

One perceived disadvantage of a two-stage post-tensioned bridge is the concern about complete deck removal and replacement. Solutions for this concern in some areas include durability strategies such as managing chlorides with a membrane or a sacrificial bonded concrete overlay on the deck.

4.3 PRODUCTION

Several decisions made by designers can affect production costs adversely. Specific topics include concrete finishes, aesthetic requirements and elements projecting from beams. Refer to **Chapter 3** for detailed discussion of precast, prestressed concrete product manufacture.

4.3.1 Beam Top Finish

If the precast product is to be covered with a concrete topping, the top surface of the precast member should be intentionally roughened to provide mechanical interlock with the topping. This can be done by using a rough float, heavy broom or raked finish to provide a proper bonding surface for the cast-in-place concrete. If this concrete topping is to act compositely with the beam, the designer should provide for the proper volume of mild steel reinforcement extending from the top of the beam into the deck. However, the projection of this steel should be kept to the minimum required since it interferes with the leveling and finishing of the top of the beam. If stay-in-place (SIP) concrete panels are to be used for deck forms, a smooth edge of an appropriate width should be provided as a bearing surface for the SIP panels.

STRATEGIES FOR ECONOMY**4.3.2 Side and Bottom Finishes/4.4.1.3 Rail Delivery****4.3.2 Side and Bottom Finishes**

Precast, prestressed concrete products used as bridge components are normally cast in steel forms. The resulting finish is typically excellent. However, as with all concrete products, there can be minor blemishes or voids which are generally not considered to be defects. Major flaws in the finish may need to be repaired. Since bridges are usually viewed from some distance, minor surface flaws cannot easily be seen, especially on interior beams. A requirement to eliminate all minor blemishes in these surfaces adds unnecessary cost to the products. It may be desirable to provide special treatment only to products on the exteriors of bridges. Although costly, the aesthetic qualities of bridges have been enhanced through the use of exposed aggregate concrete and special form liners to create distinctive designs or finishes.

4.3.3 Appurtenances

It is sometimes necessary to connect appurtenances to the surfaces of precast units. To reduce the cost, it is necessary to eliminate projections from the beams. Most precast, prestressed concrete members are cast in precision-made steel forms. Projections can be accommodated only by modifying the forms. It is better practice to utilize details that permit attachment through use of threaded inserts, embedded weld plates, or through bolts, as shown in **Chapter 3, Section 3.2.4**.

4.4 DELIVERY AND ERECTION

Transportation of precast, prestressed concrete bridge products to the bridge site can represent a significant portion of the construction cost. The transportation system from the plant to the site and the means for erecting the product at the bridge must be considered in the design. When a substantial amount of precast members is required on the project, industry-certified producers are able to establish jobsite precasting plants.

4.4.1 Transportation

Construction of bridges over navigable waterways normally makes product delivery by barge possible. Inland bridges will necessitate delivery of components by truck or rail.

4.4.1.1 Water Delivery

Manufacturing plants located on waterways that are also accessible to the project site can load products directly on barges for delivery. When direct delivery by barge from plant to jobsite is possible, product weight is a relatively minor concern, since it will be limited only by barge capacity and plant and erection handling equipment capacity. Direct delivery by barge will usually be more economical than overland delivery.

4.4.1.2 Truck Delivery

When shipping overland, several issues will affect the cost. The most dominant consideration is product weight. Smaller products (up to 45 tons) will normally not require special equipment or permits for shipping. Larger components may require special trailers with additional axles, dual steering systems, and load distribution systems to reduce and equalize the loads to the axles. These larger components may also require the shipping agency to obtain special permits for hauling over highways and bridges. Arrangements for lead and following vehicles and coordination with local traffic control agencies may be required. Evaluation of the highway between the bridge site and precast plant should include horizontal and vertical geometry limitations and capacity of bridges that must be crossed. Additionally, the contractor must provide adequate access to the bridge site by furnishing a suitable haul road. The haul road must be sufficient to support the loaded weight of the truck and be relatively smooth and level so as not to induce excessive twisting or tilting of the precast members.

4.4.1.3 Rail Delivery

Another mode of transportation for finished products is rail. Rail transport may be especially advantageous for heavy products where rail access is available at both the precast plant and jobsite. Placement limitations of loads on the rail cars, as well as load capacities of the cars themselves may also determine the feasibility of rail shipment.

Short products may be accommodated on one car. Long products may require several cars to be attached into a "set" that will carry a single product. If more than one car is used to carry a product, special attention must be

STRATEGIES FOR ECONOMY**4.4.1.3 Rail Delivery/4.5.1 Stay-in-Place Deck Panels**

given to the support bolsters on the cars to provide for horizontal rotation. The products must be tied down well in all directions to overcome significant transportation-induced loads. During design, anticipated rail shipment should always be coordinated with precast producers and the railroad.

4.4.2 Handling and Erection

Generally, precast plants have cranes and other equipment for handling products in the plant. At the bridge site, the contractor must have crane(s) to provide adequate lifting capability at the required working radius. Unstable soil conditions may necessitate the use of mats for crane stability. Longer beams may require special handling or a supplemental bracing system to provide proper lateral stability during lifting and shipping. Environmental constraints may require that special techniques be used for erection of precast components. For long or heavy precast products, the designer should discuss shipping and erection methods with both producers and contractors during the design phase.

4.4.2.1 Lifting Devices

For most precast products, the producer will provide means for attaching the precast component to the crane. Usually, the producer will use loops of prestressing strands embedded in the concrete. This is often the most cost-effective lifting device. Other specialty lifting devices may be required, but the producer should be allowed to select the means of handling the product.

4.4.2.2 Support and Lift Locations

When prestressed concrete products are resting on supports, it is usually desirable for the supports to be located near the ends of the product. Long prestressed piles may require several points of support and lifting. The location of the lifting points must consider the stability of the product. It may be desirable to locate the lifting device some distance from the ends of long slender members. The bending stresses associated with the resulting cantilevers must be considered when locating lifting points more than several feet from the ends. **Chapter 3** and **Chapter 8** discuss this topic in detail. Designers should consult local fabricators to determine the preferred method of providing stability while maintaining stresses within acceptable limits.

4.5 OTHER PRODUCTS

In addition to using precast, prestressed concrete beams, designers can further increase the cost effectiveness of their designs by considering the use of other manufactured concrete components for bridges. **Chapter 16** contains more detailed descriptions of these products and their applications.

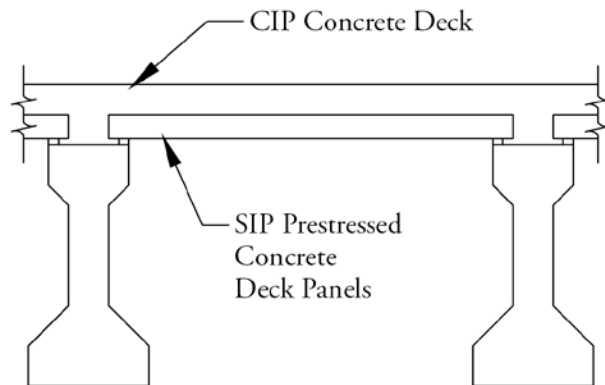
4.5.1 Stay-in-Place Deck Panels

Cast-in-place (CIP) concrete bridge decks are used on most bridge superstructures and usually require temporary forms. Stay-in-place (SIP), partial-depth, composite concrete deck panels, schematically shown in **Figure 4.5.1-1**, offer several advantages over the use of traditional removable form systems or SIP metal forms. Since the lower portion of the deck (SIP panel) is pretensioned, all of the advantages associated with plant-cast concrete are incorporated in the deck. The deck durability is enhanced since the SIP panel is virtually crack free. The SIP concrete panel is not subject to the corrosion susceptibility of a metal SIP form. Cost advantages result from the elimination of the bottom mat of reinforcement in the deck and a reduction in the volume of concrete that must be field cast. Field labor is not required to remove the forms after the deck cures. For further information, refer to "Precast Prestressed Concrete Bridge Deck Panels" (1988) published by PCI.

STRATEGIES FOR ECONOMY

4.5.1 Stay-in-Place Deck Panels/4.5.3.2 Components

Figure 4.5.1-1
Typical Deck Configuration with SIP Concrete Panels



4.5.2 Full Depth Precast Decks

In addition to using precast concrete as deck forms, full-depth precast bridge decks have been used successfully on many projects. The main advantages associated with this type of construction are the speed with which the deck is placed, and the previously enumerated benefits that are associated with plant-cast concrete. Connection of this type of deck to the beams and connections between the individual deck units must be properly designed to include bearing of the slab on the beams as well as proper shear transfer, since composite action is usually desired. The publication, “State-of-the-Art Report on Full-Depth Precast Concrete Bridge Deck Panels,” (2011) discusses the use of this product in detail.

4.5.3 Precast Substructures

Economic designs of bridge substructures can be achieved using precast components, especially when there is the possibility of form reuse. The precast components are generally simple to form and fabricate. Precast substructures have been successfully used on both large and small bridges.

4.5.3.1 Advantages of Precast Substructures

Increased speed of construction can decrease costs through reduced traffic maintenance requirements, enhanced safety and reduced overhead for the contractor. For construction over water, using smaller crews working less time not only reduces labor costs, but can significantly decrease workman’s compensation expenses. Plant-cast concrete will exhibit high quality in materials and production and provide long-term durability.

4.5.3.2 Components

Precast substructure components include prestressed concrete piles, abutment walls, caps for pile bents, pier columns and caps. Precast piles are precompressed to resist the stresses that result from driving. The other components listed are normally reinforced with mild steel. Pile bents with prestressed piles and concrete caps have been used in lieu of piers, especially for short-span bridges. Precast bent caps are very simple to fabricate and have been used widely. For grade crossings, precast pier caps eliminate the need for erecting and removing expensive form work, installing the reinforcing cage and curing the cap at an elevation above grade. Bridges successfully built using precast columns and caps include the Sunshine Skyway Bridge in Tampa Bay, Fla., and the Edison Bridge in Ft. Myers, Fla., shown in **Figure 4.5.3.2-1**.

STRATEGIES FOR ECONOMY

4.5.3.2 Components/4.6.2 Adjacent Members

Figure 4.5.3.2-1
*Edison Bridge, Ft. Meyers, Fla.,
showing precast concrete columns and caps*

**4.5.3.3 Connections**

A primary concern for designers of economical precast substructures is to provide effective and durable, yet reasonably simple means of connecting precast components to other precast and CIP components. The connections between precast elements must be designed and detailed for full transfer of all applicable forces. Bent caps normally provide a socket in the cap into which the piles are set and subsequently grouted. Other connection schemes use reinforcing bar splices such as mechanical splices, or grouted sleeves, and post-tensioning. The report, Culmo, 2009, provides a compendium of connections used by agencies across the country.

4.5.4 Barriers

Precast concrete railings or barriers are being used more frequently. Cast-in-place railings are normally cast independent of the bridge deck requiring separate delivery of concrete. Precasting the railing or barrier eliminates this requirement and speeds the construction process. Barriers have been attached to bridges by bolted connections or with the use of bar splicing devices and mechanical anchors.

4.6 ADDITIONAL CONSIDERATIONS

When compared to other bridge systems, the direct cost of precast concrete components alone can be significantly less. There are other benefits that can be achieved with the use of specific products or materials.

4.6.1 Wide Beams

Over the past several years, the use of precast, prestressed concrete beams with wide top flanges has grown in use. The increased width provides a smaller area requiring deck forming, probable reduction in the amount of deck reinforcement, improved lateral stability for handling, and shipping, and a wider work surface for construction crews prior to installation of deck forms. Excessive width may, however, increase the volume of haunch concrete over the beam and, for very thin flanges, increase the difficulty of deck removal and replacement.

4.6.2 Adjacent Members

By placing precast concrete beams side-by-side, the need for a CIP concrete deck may be eliminated, further reducing the cost and increasing the speed of construction. This is especially beneficial at remote construction sites where transporting concrete to the site is difficult or too time consuming. Cost savings related to the deck include forming, placing, finishing, curing, form stripping, and the material and delivery expense. By eliminating the deck through the use of properly designed connections, total construction can be completed in significantly less time.

STRATEGIES FOR ECONOMY

4.6.3 High Strength Concrete/4.7.2 Cited References

4.6.3 High Strength Concrete

The use of higher strength concrete has been increasing. With higher strength, comes the ability to increase the span length for given beam depths and the associated economy of longer spans. These longer spans are accompanied by increases in the amount of prestressing force in the products. Designers must take into account the potential increase in beam camber and also increased concrete transfer concrete strengths that could preclude casting on a daily cycle. The ability of prestressing beds to withstand the larger prestress force should also be investigated. The stability of long, slender members during handling and shipping must be considered as part of the member design. Certified precast producers in most areas are familiar with these parameters and can provide assistance.

4.6.4 Contract Considerations

During the planning phase of projects, agencies should evaluate contract procedures and use one that gives the best opportunity to save money. When a number of small bridges are to be constructed or replaced in one area, significant savings can be realized by grouping several bridges into one contract.

4.7 SUMMARY AND REFERENCES**4.7.1 Summary**

There are several keys to the economical use of precast, prestressed concrete for bridges. These include proper design and detailing, local availability of products, repetitive use of products, and open communications between designers, contractors, and manufacturers starting with the concept of the design through final construction. As noted several times in this chapter, designers should contact local precast, prestressed concrete fabricators to obtain information vital to the design of a cost-effective structure.

4.7.2 Cited References

1. AASHTO. 2010. *AASHTO LRFD Bridge Design Specifications*, Fifth Edition with 2011 Interim Revisions. American Association of State Highway and Transportation Officials, First Edition, Washington, DC. <https://bookstore.transportation.org> (Fee)
2. ASTM STP 169C. 1995. *Significance of Tests and Properties of Concrete and Concrete-Making Materials*. Chapter 48, Lightweight Concrete and Aggregates. ASTM International, West Conshohocken, PA., p. 522. http://www.astm.org/DIGITAL_LIBRARY/STP/SOURCE_PAGES/STP169C_foreword.pdf
3. ATC/MCEER Joint Venture. 2002. *Comprehensive Specification for the Seismic Design of Bridges*. NCHRP, No. 472. Transportation Research Board, Washington, DC., 55 pp. http://onlinepubs.trb.org/onlinepubs/nchrp/nchrp_rpt_472.pdf
4. Castrodale, R. W. and C. D. White. 2004. *Extending Span Ranges of Precast Prestressed Concrete Girders*, NCHRP Report 517, Transportation Research Board, Washington, DC, 2004, 552 pp. http://www.trb.org/Main/Blurbs/Extending_Span_Ranges_of_Precast_Prestressed_Concr_154330.aspx (Fee)
5. Culmo, M. P. 2009. *Connection Details for Prefabricated Bridge Elements and Systems*, Publication FHWA-IF-09-010. Federal Highway Administration, Washington, DC. 568 pp. <http://www.fhwa.dot.gov/bridge/prefab/if09010/report.pdf>.
6. Eberhand, M. 2011. System Performance of Accelerated Bridge Construction (ABC) Connections in Moderate-to-High Seismic Regions, Quake Summit 2011—Earthquake & Multi-Hazards Resilience: Progress and Challenges. Network for Earthquake Engineering Simulation (NEES) and MCEER. June 9-11. Buffalo, NY.
7. Marsh, M. L., M. Wernli, B. E. Garrett, J. E. Stanton, M. O. Eberhard, and M. D. Weinert. 2011. *Application of Accelerated Bridge Construction Connections in Moderate-to-High Seismic Regions*. NCHRP Report 698. Transportation Research Board, Washington, DC. 55 pp. http://onlinepubs.trb.org/onlinepubs/nchrp/nchrp_rpt_698.pdf

STRATEGIES FOR ECONOMY

4.6.3 High Strength Concrete/4.7.2 Cited References

8. PCI Bridge Producers Committee. 1988. "Recommended Practice for Precast Prestressed Concrete Composite Bridge Deck Panels," *PCI Journal*, Precast/Prestressed Concrete Institute, Chicago, IL. V. 33, No. 2 (March-April), pp. 67-109.
http://www.pci.org/view_file.cfm?file=JL-88-MARCH-APRIL-6.pdf
http://www.pci.org/view_file.cfm?file=JL-88-MARCH-APRIL-7.pdf
9. PCI Committee on Bridges. 2001. *State-of-the-Art of Precast/Prestressed Integral Bridges*. (IB-01). Precast/Prestressed Concrete Institute, Chicago, IL. 100 pp.
http://netforum.pci.org/eweb/dynamicpage.aspx?webcode=category&ptc_key=5d967c30-b4c7-4993-bab8-f3cd6142e004&ptc_code=Bridges (Fee)
10. PennDOT. 1996. Pennsylvania Department of Transportation, Strike-Off Letter 431-96-51, Drawing 95-406-BQAD, for proprietary precast concrete diaphragms for use with I-beams, December 9.
Refer to Chapter 13 of the PCI Bridge Design Manual
11. Pfeifer, D. W., J. R. Landgren, and A. B. Zosb. 1987. *Protective Systems for New Prestressed and Substructure Concrete*. FHWA Report No. FHWA/RD-86/193, National Technical Information Service, Springfield, VA., April.
12. Sherman, M. R., D. B. McDonald, and D. W. Pfeifer. 1996. "Durability Aspects of Precast Prestressed Concrete—Part 1: Historical Review," and "Part 2: Chloride Permeability Study." *PCI Journal*, Precast/Prestressed Concrete Institute, Chicago, IL. V. 41, No. 4 (July-August), pp. 62-74 and 76-95.
http://www.pci.org/view_file.cfm?file=JL-96-JULY-AUGUST-7.pdf
http://www.pci.org/view_file.cfm?file=JL-96-JULY-AUGUST-8.pdf
http://www.pci.org/view_file.cfm?file=JL-96-JULY-AUGUST-9.pdf

5.1 INTRODUCTION	5 - 3
5.1.1 Public Involvement.....	5 - 3
5.1.2 Team Approach	5 - 3
5.1.2.1 Early Involvement.....	5 - 3
5.1.2.2 Team Composition	5 - 3
5.1.3 Collaborative Effort	5 - 3
5.2 AESTHETICS DESIGN CONCEPTS.....	5 - 4
5.2.1 Definitions.....	5 - 4
5.3 PROJECT AESTHETICS.....	5 - 5
5.3.1 Alignment.....	5 - 5
5.3.2 Span Arrangement	5 - 5
5.3.2.1 Superstructure.....	5 - 5
5.3.2.2 Substructure	5 - 6
5.3.3 Surface Treatments.....	5 - 6
5.3.4 Standard Designs and Details.....	5 - 8
5.3.5 Sketches and Study Models.....	5 - 8
5.4 COMPONENT AESTHETICS	5 - 8
5.4.1 Abutments.....	5 - 9
5.4.2 Piers	5 - 9
5.4.3 Pier Caps and Crossbeams.....	5 - 10
5.4.4 Beams.....	5 - 13
5.4.5 Traffic Barriers and Pedestrian Railings	5 - 14
5.5 APPURTENANCE AESTHETICS.....	5 - 14
5.5.1 Signs.....	5 - 14
5.5.2 Light Standards.....	5 - 15
5.5.3 Utilities	5 - 15
5.5.4 Slope Protection	5 - 16
5.5.5 Noise Walls	5 - 16
5.6 MAINTENANCE OF AESTHETIC FEATURES	5 - 16
5.6.1 Drainage.....	5 - 16
5.6.2 Maintenance Manual	5 - 17
5.7 COST OF AESTHETICS	5 - 17
5.8 SUMMARY	5 - 17
5.9 PUBLICATIONS FOR FURTHER STUDY.....	5 - 18

This page intentionally left blank

AESTHETICS

5.1 INTRODUCTION

This chapter is a discussion intended to help engineers incorporate aesthetics into bridge design. The primary focus of the chapter is on typical concrete overpass and underpass bridges, although much of this information is applicable to all bridges. Designers are encouraged to reflect on past personal experience and independently broaden their study of aesthetics, particularly for larger structures.

This information is intentionally presented in a general, abstract way to encourage designers to apply it as appropriate for local conditions and preferences. The suggestions can be combined in numerous ways to arrive at a solution that is uniquely suited to a particular structure. Strict imitation of the guidelines given here will not necessarily lead to success.

Pleasing appearance should be considered in all bridge designs, although it must be achieved in a reasonable way. Consequently, design considerations such as site location, cost, environmental impact, constructability, and future maintenance must be balanced against aesthetic objectives as the project progresses. The most cost-efficient way to do this is by considering aesthetics at the onset of the design process.

5.1.1 Public Involvement

The incorporation of aesthetics in public projects must begin with the premise that success with aesthetics is in the eye of the beholder. Engineers must accept that people living near and using a structure should be given the opportunity to express their concerns for appearance before the design process begins. Conversely, public meetings provide engineers with an opportunity to explain to the public those project constraints that may influence aesthetic treatments.

5.1.2 Team Approach

Engineering efforts to incorporate aesthetics in bridge design must include all of the many professional disciplines involved in the design of public transportation facilities. Participation of these disciplines on a design team from the beginning of a project facilitates the best integration of a range of aesthetic design possibilities.

5.1.2.1 Early Involvement

An important step to aesthetic enhancement is team building and participation in the conceptual development of the project. Typically, the greatest aesthetic impact is made in the selection of the primary structural elements, including shapes, spans, and proportions. Consequently, the bridge designer must have input from all members of the design team prior to this selection. If aesthetics are not considered until after the primary structural elements are selected and designed, it is practically impossible to make the resulting structure attractive by adding superficial ornamentation. Simply put, early selection of attractive primary structural elements and proportions can produce pleasing aesthetic results, usually without adding significant cost.

5.1.2.2 Team Composition

The makeup of the team will depend on the size and complexity of the project. A project can include disciplines for structural design, lighting, geotechnical engineering, acoustics, landscaping, civil-environmental engineering, and maintenance. Inclusion of an architect or aesthetics consultant on the team is desirable. If there is a lead architect, that individual must have past bridge design experience. Proper composition of the team will save a substantial amount of time during the initial phases of design when the basic structural systems are being suggested and evaluated.

5.1.3 Collaborative Effort

A genuine collaboration between the public and members of the design team can yield significant structural and aesthetic improvements in bridge design. The collaborative effort will be most successful if a multi-disciplinary team works in consultation with the public through the conceptual development of a project. This approach is also the best method for obtaining a balance of structural efficiency, economy, and the highest overall aesthetic quality.

5.2 AESTHETICS DESIGN CONCEPTS

There are no generic formulas for achieving good aesthetic bridge design. Art in any form is highly subjective and personal. However, there are some forms of architecture that have a universal and timeless appeal due to their aesthetic quality, such as the civic structures of the Greek and Roman periods. Their appeal is embodied in the aesthetic design concepts these ancient societies developed over many hundreds of years, including order, balance, rhythm, line, mass, scale, unity, proportion, clarity of function, form, simplicity, color, texture, harmony, and craftsmanship.

Understanding and correctly applying these concepts enhances the opportunities for providing the public with a structure of high visual quality without compromising structural integrity or substantially increasing cost. The objective is to make bridge designs more attractive through the application of these concepts.

5.2.1 Definitions

The following is a brief description of universal aesthetic concepts as they apply to bridge design. They are provided as a reference for evaluation of the effects of proposed solutions by the multi-disciplinary design team.

Order – the presence of only those edges and lines necessary to establish the characteristic form and function of the bridge. Application of the concept should lead the designer to a refined design to which nothing can be added or removed without disturbing the harmony of the whole.

Balance – repetition of the various elements of the bridge, and localized details, so as to establish harmony without monotony. Application of the concept should leave observers of the bridge with a sense of the structure in its entirety as opposed to a sense of any one of its component parts.

Rhythm – a characteristic order in the repetition of individual bridge elements. Application of the concept is evidenced by the spacing of superstructure elements; the arrangement of substructure units and the elements within them; the spacing of expansion and construction joints in walls, spans, parapets, or curbs; the spacing and appearance of lighting fixtures; and any other details repeated throughout the bridge.

Line – the sight lines voluntarily or involuntarily followed by the eye when viewing a bridge. Application of the concept establishes smooth, flowing lines in the profiles of spans, piers, abutments, wing walls, parapets, railings, and junctures of different elements and materials.

Mass – the visual heaviness or lightness of the individual parts of the bridge.

Scale – the size of individual bridge elements as they relate to each other, the bridge as a whole, and the bridge site.

Unity – a collective arrangement of elements and materials to elicit a sense of singular form and function.

Proportion – relative size, visual mass, and spatial relation of individual components throughout the bridge and of the individual components to the scale of the entire bridge and its surroundings. Application of the concept should establish favorable dimensional relations between various elements; between height, width, and breadth; between closed surfaces and openings; and between the light and dark areas caused by sunlight and shadow. The proportions of elements should give an impression of balance.

Clarity of function – the necessity that each element serves its intended function and visually conveys to the viewer that it is appropriate and sufficient to perform its intended function. Application of the concept should produce simplicity in arrangement of elements reflecting by size and distribution the flow of forces through the structure.

Form – the distinctive appearance of the bridge as defined by the geometric arrangement of its elements and the individual geometry of each element. Application of the concept expresses both the overall stability of the structural form and the function of each component element in sustaining overall stability.

Simplicity – limiting the elements employed in a bridge to only those essential in establishing a form sufficient to serve the intended function. Application of the concept should produce clean lines, a minimum number of elements, an absence of clutter, and avoid disruptive details; a form's lack of complication.

Color – primarily utilized in bridges to either blend the bridge with its natural setting or to establish a clear contrast with its natural setting. Application of the concept should be understood to not simply be cosmetic, but rather a means of defining, clarifying, modifying, accentuating, or subduing the visual effect of the individual bridge elements or the bridge as a whole.

Texture – surface characteristics of component materials or the treatments applied to component surfaces to alter the visual details of the surface. Application of the concept is effective in reducing the visual mass of abutments and piers with large uninterrupted surfaces. Provided the texture is of appropriate scale, when viewed from a distance, texturing can establish a sense of balance, harmony, rhythm, and line.

Harmony – the collective embodiment of each of the aesthetic design concepts within a bridge unified with its surrounding environment. This is evidenced as an independent aesthetic design concept by the fact that bridges of equivalence in every other facet must satisfy unique aesthetic design requirements merely by virtue of whether they are to function in an urban setting or a rural setting. Application of the concept should blend the individual elements of the bridge into its whole, blend the bridge with its environment, and establish its relationship to nearby structures through structural form, function, surface finishes, color, and landscaping.

Craftsmanship – all aspects of construction, from carpentry work to concrete placement to the application of surface finishes, require specialized skills or special construction procedures. The aforementioned aesthetic concepts cannot be successful if their application is predicated on a standard of craftsmanship that cannot be achieved.

5.3 PROJECT AESTHETICS

5.3.1 Alignment

The compatibility of bridge alignment with overall site geometry contributes substantially to the aesthetic quality of a project. Traffic clearance, waterway opening, terrain, geotechnical conditions, right-of-way, and utilities are typical engineering constraints that influence horizontal and vertical alignment. Such constraints are interdisciplinary concerns that can create major aesthetic challenges.

Bridge designers are often given roadway geometry as a predetermined feature of the project. This can result in challenges such as oddly shaped piers or straddle bents in urban interchanges.

Vertical profile is often the dominant aesthetic feature of a structure. Predetermined roadway geometry associated with roadway design criteria, such as sight distance and design speed, is often the governing criterion.

Designers should exercise judgment in evaluating alignment and request plausible changes by the design team that retain or improve overall project quality and improve the appearance of the structure. Alternatives should be sought that provide an appropriate solution for the bridge without compromising the requirements of the other engineering disciplines. Graceful horizontal and vertical alignments provide a sound beginning for a successful bridge.

5.3.2 Span Arrangement

Generally, an aesthetic goal in design is to make the superstructure appear as slender as possible without appearing to lack necessary strength. The superstructure of a tall bridge will look thin in comparison to the space below the bridge. A beam of constant depth in a long bridge will look thin because the eye judges depth in relation to length. The reverse is also true. The superstructure of a short span bridge with low underclearance will have a tendency to look much deeper.

5.3.2.1 Superstructure

In the effort to economize, engineers generally strive to reduce the number of beam lines by increasing the girder spacing. To achieve cost efficiency and aesthetic quality, the designer should utilize the most structurally efficient beam cross sections that are available. However, consideration should be given to the use of high-strength concrete as necessary to minimize girder depth. Another tool is to employ continuity over interior supports to facilitate use of shallower girders, at the same time eliminating problematic joints in the superstructure.

Figure 5.3.2.2-1

Balance occurs when the span lengths and height of the bridge become proportional, as in the Folsom Lake Crossing, Folsom, Calif. (Photo: CH2M HILL)



5.3.2.2 Substructure

The very nature of a bridge is to span obstructions, such as roads, rivers, deep valleys, railroads, and the like. Substructure units supporting these spans must have the apparent visual strength necessary to support applied loads without themselves becoming a visual detriment to the aesthetics of the bridge. It is highly desirable to maintain the same geometry for piers and for abutments within a bridge. Repetition of substructure geometry creates an inherent visual symmetry that, when coupled with physical symmetry in the position of substructure units under the bridge, produces unity in appearance, form, function, and strength. In spite of this, a unique balance occurs when span lengths and the height of the structure become proportional. This can be illustrated simply by the three-span bridge shown in **Figure 5.3.2.2-1**.

Certainly there are occasions when site constraints preclude locating the substructure units where desired. The designer should pursue alternatives that provide a degree of symmetry, or whose form most closely follows the natural topography of the site. Furthermore, the designer should convey to the design team the potential benefits of increasing bridge length when such an increase accommodates a more adventurous structural and aesthetic substructure layout.

5.3.3 Surface Treatments

Structural materials have a characteristic color and texture in their natural state. With respect to each of the structure's surfaces, a decision must be made whether to leave the structural material natural or to add color, texture, pattern, or surfacing material. Such additions often provide economical opportunities to enhance the visual interest of the structure and establish harmony with its surroundings.

Textured concrete is sometimes used on portions of abutments and wide piers to reduce their visual mass as shown in **Figure 5.3.3-1**. A texture can be used effectively on the exterior face of a concrete traffic barrier to accentuate the horizontal lines of the barrier (**Fig. 5.3.3-2**). Color can play a significant role in the overall aesthetic effect but should be used with full awareness that harmonious color composition is difficult to achieve. External

coatings are the most promising approach to coloring concrete and can be quite durable when correctly applied. Textured or pigmented concrete provides the additional advantage of not requiring extensive finishing labor because the finish is largely present when the concrete forms are removed. This option is being used more frequently. **Figure 5.3.3-3** shows examples of how color was used to help bridges establish harmony with their surroundings.

Figure 5.3.3-1

Textures are incorporated into the concrete surfaces to reduce visual mass.



**a) Portland and Western
L Street Bridge, Columbia City, Oregon.
(Photo: OBEC Consulting Engineers)**



**b) Minnesota Crosstown Project,
Crosstown Commons, Minnesota.
(Photo: Minnesota Department of Transportation)**

Figure 5.3.3-2

Texture and color were used to accentuate the horizontal barrier.



Main Street Bridge in Pueblo, Colorado.

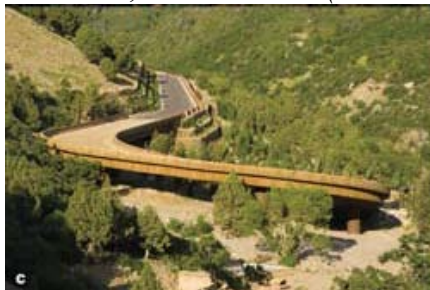
Contract documents should specify the quality of the surface finish desired with regard to issues such as bug holes, wood grain and form impressions, and surface blemishes and discoloration. If it is deemed necessary, the contractor should prepare sample panels of representative concrete textures or colors for approval. When required, a high-quality concrete stain will even out variations in the color of surfaces. In addition, graffiti may be more easily removed from sealed surfaces.

Figure 5.3.3-3 Surface Treatments

a) Black iron oxide integral color was used in both the piers and superstructure of the Blue Ridge Parkway Viaduct, Grandfather Mountain, North Carolina. (Photo: FIGG)



b) Integral color was used in both the cast-in-place concrete and precast concrete in Zion National Park, Utah. (Photo: Federal Lands Highways)



c) Stain and fractured-fin texture were used in the Big Cottonwood Canyon Loop Road Bridge near Salt Lake City, Utah. (Photo: Michael Baker Jr. Inc.)



d) The Sycamore Creek Bridge on Arizona State Road 87 northeast of Phoenix harmonizes with its surroundings through the application of surface applied stain. (Photo: Arizona DOT)

5.3.4 Standard Designs and Details

Many owner agencies and consultants facilitate the design of repetitious structures with libraries of standard designs and details. Consequently, the design of short- and medium-span bridges may be a process of selecting and combining standard details. Precast concrete bridges, based on assemblies of standardized components, lend themselves particularly well to this method. There is obvious economy in this approach, but bridge designers should not neglect responsibility for the appearance of the structure.

Standard designs and standard details can be both aesthetic challenges and aesthetic opportunities. Often, the biggest impediments to enhanced appearance are inappropriate standard details. Custom designs and details are sometimes rejected on the notion that costs will automatically increase. However, the benefits of standardization are based on repetition, so attractive standard details can be repeated as readily as unattractive ones.

Standard pier shapes, parapet profiles, and standard abutments essentially establish the appearance of a typical bridge regardless of other efforts by the designer. The solution is to develop attractive standard designs and details and allow bridge designers the flexibility to apply them appropriately.

5.3.5 Sketches and Study Models

Sketches drawn to scale are helpful for visualizing the aesthetic qualities of proposed designs and details. Scale models can be very helpful for demonstrating the aesthetic features of individual elements and overall bridge concepts in three dimensions. Vehicle and pedestrian objects should be included to provide perspective and scale. This is particularly true for sketches or models used as visual aids at public presentations.

5.4 COMPONENT AESTHETICS

Discussion of the appearance of individual elements within a bridge is not meant to imply that aesthetic bridges can be designed in pieces. All elements of the structure need to be consistent with each other and contribute to the visual impact of the whole structure.

5.4.1 Abutments

Abutments visually anchor the ends of the bridge. The abutment location and geometry substantially define the shape of the opening under the end spans. In general, for highway overpasses, the bridge will appear more open and less obtrusive, and the abutment will seem less massive the farther up the slope it is moved away from the traveled way. Specifically, the visual mass of an abutment must be in proportion to the span and depth of the superstructure. Reducing the size of the abutment by lengthening the span is not necessarily a cost issue, as savings in abutment walls and foundations may offset the cost of additional structure length.

For shorter structures and from viewpoints near the ends of longer structures, the shape and detail of the abutment will make a major impression. For structures passing over pedestrian or vehicular traffic, the most memorable aspect of the structure could be the provisions employed at the ends of the bridge. Such provisions may include surface treatments of color and texture, the transitional geometry afforded by a sloping front face on the abutment, or simply eliminating the presence of expansion joints that sometimes result in unsightly water staining. To that end, the use of integral abutments is strongly encouraged because they eliminate water leaks and the structural deterioration that frequently occurs as a result.

5.4.2 Piers

From any viewpoint, particularly at oblique angles to the structure, the shape of the piers will have a major visual impact. Given the standardized nature of many precast concrete superstructure elements, the piers and abutments are major opportunities to give the bridge a memorable appearance. In fact, for bridges on tall piers, the supporting elements are often the defining visual components.

Pier placement establishes not only the points at which the structure contacts the topography but also the shape of the openings framed by the piers and superstructure. The success of the visual relationship between the structure and its surrounding topography will depend heavily on the apparent logic of pier placement.

Piers can be designed in many different shapes and sizes depending on the style, width, length, and height of the bridge. Flared or tapered piers are generally more pleasing than those of uniform plan geometry (**Fig. 5.4.2-1**). The cost of formwork is often cited as an obstacle to tapered or flared piers. However, if the taper or flare is done consistently from pier to pier and in only one direction at a time, a single form can be reused repeatedly to achieve a cost-effective improvement in appearance. On one bridge, all piers should have the same general appearance.

Figure 5.4.2-1

These piers offer pleasing geometries.



*a) Brainerd Bypass Bridge, Brainerd, Minn.
(Photo: Neil Kveberg, Minnesota DOT)*



*b) Sanibel Island Bridge A, Lee County, Fla.
(Photo: Lee County)*

Fly-over ramps should generally be supported by single-shaft rectangular or oblong columns, rather than by pier lines with numerous round or square columns. Minimizing the number of individual supporting elements reduces visual clutter under the bridge. Architectural precast concrete panels can be placed around or between columns as one method of transforming a cluttered multi-column pier into a single aesthetic unit.

5.4.3 Pier Caps and Crossbeams

Bridges composed of multiple precast concrete beams usually require the use of a crossbeam to transfer loads from the superstructure to the columns. In general, crossbeams interrupt the flow of the bridge's horizontal lines and add visual mass to both the superstructure and piers.

Generally, a recessed (raised) crossbeam (**Fig. 5.4.3-1**) is preferable. A semi-recessed crossbeam (**Fig. 5.4.3-4**) is the next-best solution. With imagination, a lowered crossbeam will also work if the crossbeam is incorporated into the shape of the pier as shown in **Figures 5.4.2-1a** and **5.4.3-3**.

The ends of pier caps and lowered crossbeams frequently present an abrupt, visually undesirable projection, borne of functional necessity but absent of any aesthetic value. Tapering the bottom of the projecting end upward so that the end of the projection is shallower than it is wide neutralizes the abrupt disruption of the bridge's horizontal lines while also visually characterizing the flow of forces (**Fig. 5.4.3-2** and **5.4.5-1**). Moreover, pier cap and crossbeam projections of semi-circular plan geometry are effective in merging form and function (**Fig. 5.4.3-5**).

*Figure 5.4.3-1
Piers, Caps, and Railings*



*a) This bridge uses raised crossbeams and open railings to reduce its perceived depth.
La Center Bridge over the East Fork Lewis River, La Center, Washington.
(Photo: Berger/ABAM Engineers Inc.)*

*Figure 5.4.3-1 (cont.)
Piers, Caps, and Railings*



b) and c) The use of a raised crossbeam and color accentuate slenderness as the motorist approaches this bridge located on a curve. (State Route 456 over the Norfolk Southern Railroad, Oneida, Scott County, Tenn. (Photo: Tennessee Department of Transportation)



*Figure 5.4.3-2
Cross Beams*



*Tapering the depth of the crossbeam to become a shallow projection in the profile of the bridge avoids abrupt disruption of the horizontal lines. State Route 18 Bridge at Covington, Wash.
(Photo: Washington State DOT)*

*Figure 5.4.3-3
Cross Beam*



*This urban bridge incorporates the crossbeam into the pier. 27th Street Bridge, Kansas City, Mo.
(Photo: Harrington & Cortelyou Inc.)*

*Figure 5.4.3-4
Cross Beam*



*A semi-raised crossbeam or inverted tee beam reduces the perceived depth at the pier.
(Photo: Dan Dorgan)*

Figure 5.4.3-5
Cross Beam



A semicircular projection of the precast concrete crossbeams minimizes disruption of the bridge's horizontal lines. Route 70 over Manasquan River Bridge, New Jersey. (Photo: Arora and Associates)

5.4.4 Beams

The selection of a precast concrete beam depends on structural requirements, cost, and aesthetics (for example, U-beams, adjacent or spread box beams, bulb tees, and I-beams). However, for any beam type, it is visually imperative that either the same depth beam is maintained for the entire length of the bridge or depth changes be accomplished through gradual transitions rather than abrupt changes. Properly proportioned haunched beams of any type satisfy the structural objective of achieving longer spans with the aesthetic benefit of a graceful shape. The haunch conveys to the viewer a sense of the flow of forces within the structure.

Continuity of the structure over piers provides structural efficiency and substantially enhances the aesthetic quality of the bridge. Continuity may enable the use of a shallower superstructure and eliminates problematic joints, which can leak and produce unsightly staining and deterioration. The aesthetics of the bridge can be further improved by framing continuous girder lines through a raised, recessed pier crossbeam to emphasize the horizontal lines in the bridge.

The underside of the superstructure is in view more often than most designers anticipate, particularly when there are pedestrians or non-vehicular traffic under the bridge. This means that the underside should be as uncluttered and simple as possible. When a series of precast beams is used, it is important to maintain an orderly arrangement to avoid visual confusion. Precast concrete box beams and U-beams improve aesthetics because fewer visible elements are needed. Box sections can also offer the opportunity to enclose certain types of utility lines that otherwise would be visible and unattractive.

For structural and cost efficiencies, deck overhangs should be dimensioned to transfer loads to the exterior beams that are comparable to loads on interior beams. Doing so will have a secondary aesthetic effect of causing a portion of the exterior beam to be in shadow with the illusion of being shallower. It is unfortunate that regional preferences and construction practices that evolve over time can result in adoption of specified maximum overhang dimensions. Bridge designers should recognize the reluctance of contractors to move toward increased overhang dimensions, given that many already own overhang brackets for the smaller overhangs they are accustomed to constructing. However, designers must also recognize their responsibility for creating cost-effective, aesthetically pleasing bridges.

While it would be imprudent to attempt to establish any universal rule for what the overhang dimension should be, the benefits are numerous for establishing a superstructure cross section within which all girder lines support comparable loads. These benefits can include cost savings by:

- reducing the number of beam line
- possibly reducing the number of pier columns
- reducing pier cap lengths
- reducing the overall substructure footprint
- increasing the number of viable pier types

All of these improve the aesthetics of the bridge by reducing visual clutter and increasing open space under the bridge.

5.4.5 Traffic Barriers and Pedestrian Railings

These are bridge elements that can be varied a great deal depending on the desired appearance and structural design requirements. The shape and proportions of the parapet or traffic barrier at the roadway level also influence the way the superstructure is perceived. The shape and combined depth of the barrier and girder determine the visual span/depth ratio of the superstructure. Accenting the horizontal line of the barrier improves the overall visual appearance.

If the bridge has a pedestrian sidewalk, consider placing a concrete traffic barrier between the traffic lane and sidewalk to make the sidewalk more pedestrian friendly. Open railings can be positive features on a bridge, particularly if they substitute for all or part of a solid parapet. Keep the sight lines (view) from the bridge as open as possible. Heavy horizontal pedestrian railings tend to obstruct the view, whereas a vertical baluster-style railing (**Fig. 5.4.5-1**) is less obtrusive.

A pedestrian screen can make the parapet appear massive with comparable negative effects on the proportions of the entire structure. Screens should be avoided if at all possible. When they are required, designers should carefully consider specific details. For instance, the use of simplified connections can limit visual clutter and additional visual mass. Also, partial pedestrian cages composed of lightweight elements can achieve a measure of transparency by virtue of their contrast with the heavy elements of the superstructure. In some cases, the use of colored coatings such as vinyl on galvanized chain-link fencing provides color contrast and prevents staining of the concrete.

*Figure 5.4.5-1
Pedestrian Railings*



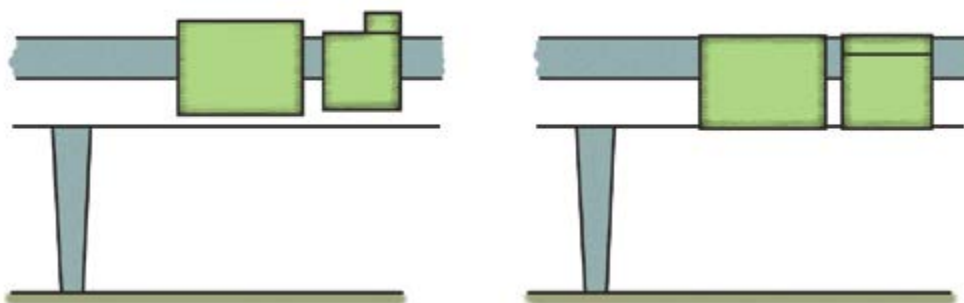
*The open baluster railing is less obtrusive for pedestrians and the tapered crossbeam avoids a more abrupt disruption of the bridge's horizontal lines. Route 52 Bridge over the Wallkill River, Walden, N.Y.
(Photo: J&R Slaw Inc.)*

5.5 APPURTENANCE AESTHETICS

5.5.1 Signs

Signs placed on a bridge for bridge traffic should be of the same height, if not the same size, when placed side by side. As with the bridge itself, sign supports should have the appearance of adequate visual strength to support the sign. Furthermore, the location and attachment of the sign supports on the bridge become critical and should be carefully evaluated to least disturb the visual lines. Placement of the sign supports at the pier line is appropriate for both structural and aesthetic reasons.

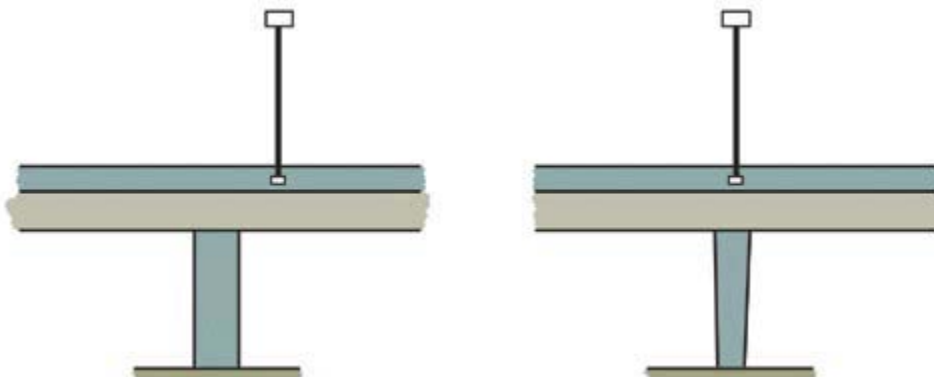
Figure 5.5.1-1
Signs (right) are mounted within the silhouette of the bridge.



5.5.2 Light Standards

When highway lighting is required on a bridge, the types of luminaries and supports should be given careful consideration since these elements make a significant visual impact that is well within the control of the bridge designer. Typically, light standards extending above the bridge (**Fig. 5.5.2-1**) should align with the substructures. Their color and style should be coordinated with other elements of the bridge, particularly other lighting and metal elements within the highway corridor.

Figure 5.5.2-1
Light standard (right) aligns with the substructure.



5.5.3 Utilities

The primary objective must be to accommodate present and future utilities with as little visual exposure as possible. Construction and accessibility requirements often lead designers to carelessly attach utilities in exposed areas and thereby significantly degrade the appearance of the bridge. Hiding them from view or incorporating them into the architectural design is very important. The contractor should not be expected to resolve the detailing of these elements in the field. Their location should be detailed on the construction drawings. For bridges with multiple precast beams, utility lines can be concealed from view if they are located between the interior beams rather than along the outside face of the bridge as depicted in **Figure 5.5.3-1**.

Figure 5.5.3-1

Two examples of utilities hidden within spaces between beams.



5.5.4 Slope Protection

Embankments at the ends of bridges commonly require some form of slope protection. Materials typically used include precast concrete blocks, semi-open-face masonry units, cast-in-place concrete, crushed rock, or stones. The particular material selected for a specific bridge should relate either to the bridge or to the surrounding landscape.

5.5.5 Noise Walls

As with pedestrian screens, noise walls on bridges should be avoided if at all possible. When used, they are best kept as clearly distinct elements apart from the bridge with favorable aesthetic characteristics of their own that harmonize with the bridge and the surrounding landscape.

5.6 MAINTENANCE OF AESTHETIC FEATURES

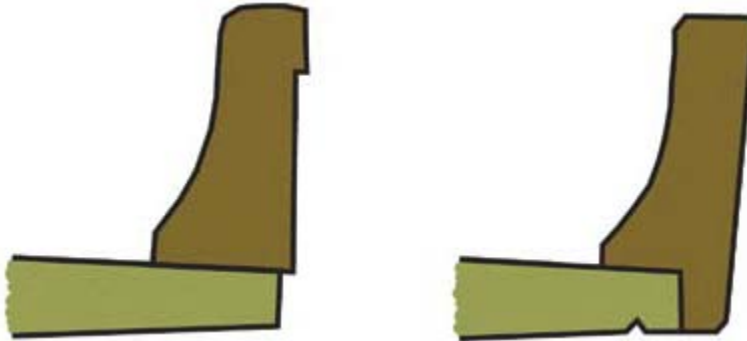
5.6.1 Drainage

Sustaining the aesthetic quality of an in-service bridge is itself a challenge, considering the many environmental factors to which a bridge is subjected. Although many environmental factors are beyond the control of engineers, the deleterious effects of water are typically the most severe and yet are largely within the control of the design team and in particular the bridge designer. Drainage details must be critically evaluated since concrete will eventually stain if exposed to rainwater runoff. All concrete surfaces should be detailed to prevent the ponding of water. To the extent possible, drainage should be sufficient to wash away debris that tends to pond water and cause surface discoloration and deterioration. Additionally, a drip groove on the underside of the deck slab just inside the fascia line (**Fig. 5.6.1-1**) will control discoloration and deterioration of the outside face of the slab and the exterior girder at virtually no additional cost.

As long as drip grooves are provided, through-barrier drains (open slots at the base of the barrier) are preferred for deck drainage. If drainpipes are required, there should be as few of them as possible. Consideration should be given to vehicular and pedestrian traffic below in determining the location of drains.

Figure 5.6.1-1

Illustration of drip groove under deck. Note the smooth face of the barrier on the right, reducing the number of shadow lines.



5.6.2 Maintenance Manual

Bridge weathering characteristics and maintenance requirements must be considered during the design phase. A maintenance manual should show where and how future utilities can be installed, manufacturer information, equipment warranties, concrete stain color, graffiti removal information, and any other information of use in preserving the aesthetics of the bridge. A manual should be provided for each type of bridge to those who will be responsible for maintenance.

5.7 COST OF AESTHETICS

Specific aesthetic treatments are rarely cost free. However, coordination of simple details by the design team early in the design process can produce dramatic aesthetic improvement without significant cost. Furthermore, attention to details such as amount of deck slab overhang, jointless, superstructure continuity, and elimination of deck drains can substantially enhance the aesthetic quality of a bridge in both the short term and the long term while actually reducing costs.

5.8 SUMMARY

Bridge aesthetics must be addressed in all stages of a project: conceptualization, evolution, and final design. A collaborative effort between the engineering community and the public should be undertaken to satisfy the utilitarian need to move vehicles and people by means of a bridge conceived as a harmonious union of form and function that is admired and appreciated by users and observers. Thoughtful application of aesthetic design principles transforms precast concrete bridge elements into durable, unified structures that serve as cultural landmarks in both urban and rural environments.

Fundamental to aesthetic bridge design success is the achievement of function through the use of well-proportioned, simple forms composed of continuous straight or smoothly curved lines and a minimum number of elements. Careful consideration must be given to the aesthetic impact made by each element as well as the collective harmony of all elements.

Aesthetic bridge design requires not only harmony in the integration of component parts, but also the integration of the entire structure into its environment. Bridge designers must be able to envision a structural system of proper proportion and scale in relation to its surroundings. A designer has perhaps no greater responsibility than to communicate to others the importance of integrating bridge geometry with overall project geometry.

5.9 PUBLICATIONS FOR FURTHER STUDY

1. *Bridges*, Fritz Leonhardt, The MIT Press, 55 Hayward Street, Cambridge, MA 02142, 1984, 308 pp.
http://www.amazon.com/Bridges-Aesthetics-Design-Fritz-Leonhardt/dp/0262121050/ref=ntt_at_ep_dpt_1
(Fee)
2. *Bridge Aesthetics Around the World*, Transportation Research Board Publications Office, 500 Fifth Street NW, Washington, DC 20001, 1991, 308 pp.
<http://books.trbbookstore.org/baatsc.aspx> (Fee)
3. *Bridgescape, The Art of Designing Bridges*, Second Edition, Frederick Gottemoeller, John Wiley & Sons, Inc., Hoboken, NJ 07030, 2004, 316 pp.
<http://www.wiley.com/WileyCDA/WileyTitle/productCd-0471267732.html> (Fee)

PRELIMINARY DESIGN

Table of Contents

NOTATION..... 6 - 3

6.0 SCOPE..... 6 - 5

6.1 PRELIMINARY PLAN 6 - 5

 6.1.1 General 6 - 5

 6.1.2 Development..... 6 - 5

 6.1.3 Factors for Consideration 6 - 5

 6.1.3.1 General 6 - 5

 6.1.3.2 Site..... 6 - 5

 6.1.3.3 Structure..... 6 - 5

 6.1.3.4 Hydraulics..... 6 - 6

 6.1.3.5 Construction 6 - 6

 6.1.3.6 Utilities 6 - 6

 6.1.4 Required Details..... 6 - 7

6.2 SUPERSTRUCTURE 6 - 10

 6.2.1 Beam Layout 6 - 10

 6.2.2 Jointless Bridges..... 6 - 10

6.3 SUBSTRUCTURES 6 - 10

 6.3.1 Piers 6 - 10

 6.3.1.1 Open Pile Bents..... 6 - 10

 6.3.1.2 Encased Pile Bents 6 - 10

 6.3.1.3 Hammerhead Piers 6 - 10

 6.3.1.4 Multi-Column Bents..... 6 - 12

 6.3.1.5 Wall Piers 6 - 12

 6.3.1.6 Segmental Precast Piers 6 - 12

 6.3.2 Abutments..... 6 - 12

 6.3.3 Hydraulics..... 6 - 13

 6.3.4 Safety..... 6 - 13

 6.3.5 Aesthetics 6 - 13

6.4 FOUNDATIONS..... 6 - 13

6.5 PRELIMINARY MEMBER SELECTION..... 6 - 13

 6.5.1 Product Types 6 - 13

 6.5.2 Design Criteria 6 - 14

 6.5.2.1 Live Loads 6 - 15

 6.5.2.2 Dead Loads 6 - 15

 6.5.2.3 Composite Deck..... 6 - 16

 6.5.2.4 Concrete Strength and Allowable Stresses 6 - 16

 6.5.2.5 Strands and Spacing 6 - 17

 6.5.2.6 Design Limits..... 6 - 17

 6.5.3 High Strength Concrete..... 6 - 17

PRELIMINARY DESIGN

Table of Contents

6.5.3.1 Attainable Strengths 6 - 17

6.5.3.2 Limiting Stresses 6 - 17

6.6 DESCRIPTION OF DESIGN CHARTS..... 6 - 18

6.6.1 Product Groups..... 6 - 18

6.6.2 Maximum Spans Versus Spacings 6 - 18

6.6.3 Number of Strands 6 - 18

6.6.4 Controls..... 6 - 18

6.7 PRELIMINARY DESIGN EXAMPLES 6 - 19

6.7.1 Preliminary Design Example No. 1 6 - 19

6.7.2 Preliminary Design Example No. 2 6 - 19

6.8 REFERENCES 6 - 20

6.9 PRELIMINARY DESIGN CHARTS..... 6 - 21

6.10 PRELIMINARY DESIGN DATA 6 - 39

NOTATION

f_b = calculated concrete stress at the bottom fiber of the beam

f'_c = compressive strength of concrete for use in design

f'_{ci} = minimum concrete compressive strength required at transfer

f_t = calculated concrete stress at the top fiber of the beam

L = span length

M_u = factored moment at the section

M_r = nominal factored flexural resistance of the section

This page intentionally left blank

Preliminary Design

6.0 SCOPE

Preliminary design is usually the first step in designing an economical precast, prestressed concrete bridge. This chapter discusses the preliminary plan, superstructure and substructure considerations, foundations, and member selection criteria with design aids and examples. Additional information is given in Chapter 4, "Strategies for Economy."

6.1 PRELIMINARY PLAN

6.1.1 General

The preliminary planning process consists of collecting and analyzing site information, applying established policies and practices, and considering alternatives including cost evaluations, for the purpose of providing the bridge that is the most cost effective and the most functionally, structurally, and aesthetically appropriate. The preliminary plan lays the groundwork for the final bridge design. It specifies the structure type and is the basis for the design schedule estimate and construction cost estimate.

6.1.2 Development

The preliminary planning process begins with bridge site data. Preliminary studies such as type, size, and location (TS&L) studies, geometric data, foundation data, and hydraulic data are reviewed. Preliminary geometric approval is received. Structure alternatives are evaluated considering such details as length, type, geometric constraints such as vertical and horizontal clearances, span arrangement, staging, falsework, substructure requirements, environmental and community issues, and costs. Plan, elevation, and section views are developed and approved. Cost estimates are prepared. The preliminary plan and cost estimate are approved prior to beginning final design.

6.1.3 Factors for Consideration

A number of factors should be addressed at the preliminary design stage.

6.1.3.1 General

Funding classification (for example, state funds, federal and state funds, or local funds) and available funding level should be determined. Environmental concerns include site conditions (for example, wetlands or environmentally sensitive areas) and mitigating measures.

6.1.3.2 Site

Site requirements that should be determined include topography, horizontal alignment (curves and skews), required clearances, vertical alignment and limits, superelevation, and existing and proposed utilities. Safety considerations include sight distances, horizontal clearance to piers, and hazards to pedestrians.

End slopes are controlled by soil conditions and stability, right-of-way availability, fill height or depth of cut, roadway alignment and functional classification, and existing site conditions.

6.1.3.3 Structure

Structural considerations include foundation and groundwater conditions, requirements for future widening, and anticipated settlement. Aesthetics, including general appearance, level of visibility, and compatibility with surroundings and adjacent structures should be evaluated. Railroad separations may require negotiations with the railroad company concerning clearances, geometry, utilities, drainage, and provision for maintenance roads.

The total length of the bridge can be based on horizontal and vertical clearances to roadway(s) or rail(s) below or above, or hydraulic studies if over water, and/or environmental concerns such as wildlife crossings or other restrictions as set by the owner

PRELIMINARY DESIGN**6.1.3.3 Structure/6.1.4 Required Details**

agency. The bridge width is typically controlled by the width of the approaching roadway. The span arrangement is controlled by such factors as:

- Allowable beam depth due to clearance requirements
- Placement of piers in waterways
- Horizontal clearance between supports and rights-of-way below
- Economic ratio of end span to interior span

Considering the ratios of spans, the following have been found to produce a balanced design, where the reinforcement requirements for end spans are comparable to those for interior spans:

End span/interior span	Condition
0.95	Simple span for beam and deck weight, continuous span for all other loads
0.80	Simple span for beam weight, continuous span for all other loads

As previously discussed, bridge details are largely dictated by obstructions above and below ground, maximum span limitations, and required abutment locations. However, to the extent possible, large skews, steep profile grades, sharp horizontal curves, and differing span lengths should be avoided. Slightly lengthening the bridge may be preferable to using an extreme skew angle that tightly fits the bridge site.

6.1.3.4 Hydraulics

Hydraulic considerations include bridge deck drainage, stream flow conditions and channel drift, passage of flood debris, scour, and the effect of the pier as an obstruction (for example, the pier's shape, width, skew, number of columns), banks and pier protection, permit requirements for navigation, and stream work limitations. After piers have been located, specific information on scour and backwater is obtained.

Vertical clearances for water crossings should satisfy floodway clearance requirements. In accordance with the flood history, nature of the site, character of drift, and other factors, the minimum vertical clearance (for the 100-year flood, for example) is determined. The roadway profile and the bridge superstructure depth should accommodate this clearance requirement. Bridges over navigable waters should also comply with any clearance requirements of the U.S. Coast Guard.

6.1.3.5 Construction

Construction considerations include falsework and other construction clearances, working space requirements, hauling and erection details, access to the site, construction season, and construction scheduling limitations. Safety considerations such as traffic flow, staging, detours, and falsework requirements should be addressed.

Access routes should be checked and sites reviewed to ensure that the precast concrete beams can be transported to the site. Possible routes to the site should be adequate to handle the truck and trailer that will be hauling the beams. Generally, the designer is not responsible for construction of the bridge. However, prudent designers always consider constructability issues. Therefore, it is recommended that both size and weight of the beams be checked and hauling permit requirements determined. The details related to erecting the beams once they reach the site also need to be assessed. The site should be reviewed for adequate space for the contractor to position the cranes and equipment necessary to lift and place the beams.

6.1.3.6 Utilities

Often, electric, water, telephone, and other utility conduits are required to be supported by the bridge. Most loads imposed by these utilities, except perhaps those of large water pipes, do not have significant impact on structural design. However, aesthetics and accessibility to utility lines, as well as relocation of existing utilities, may affect the selection of the superstructure system.

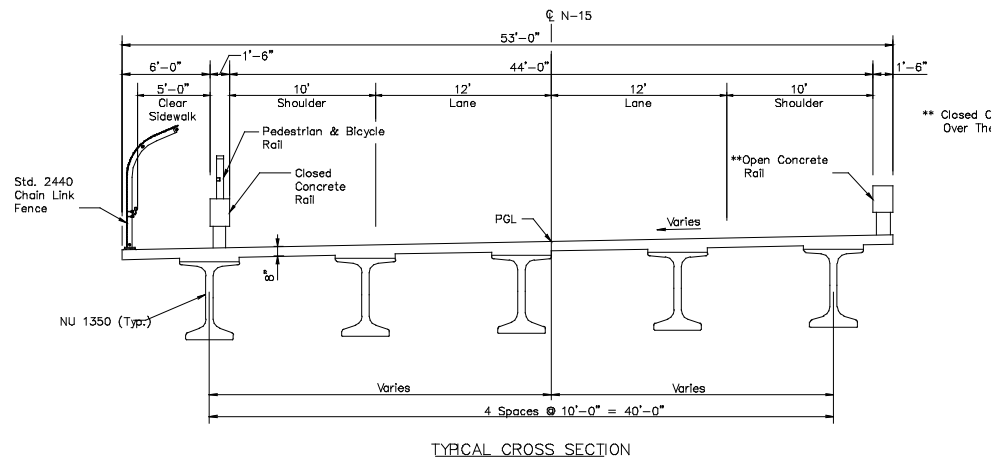
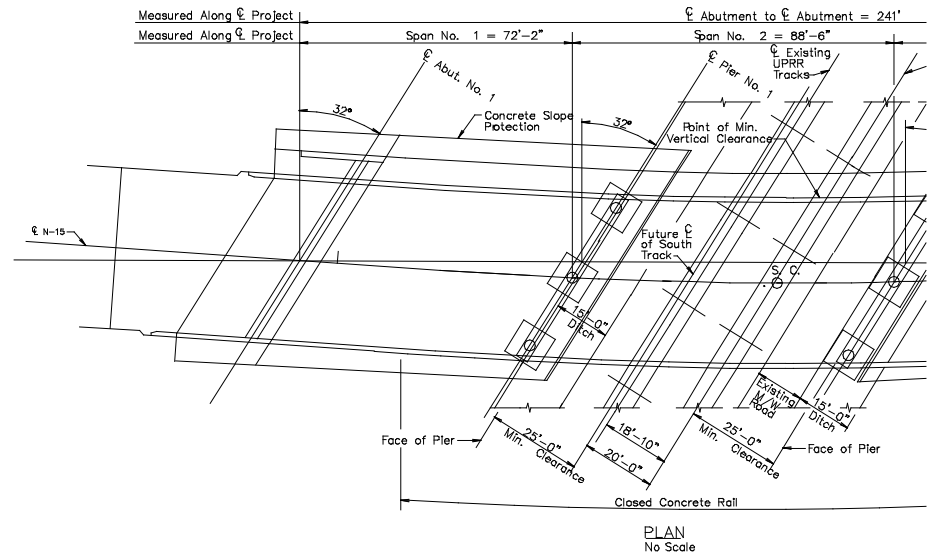
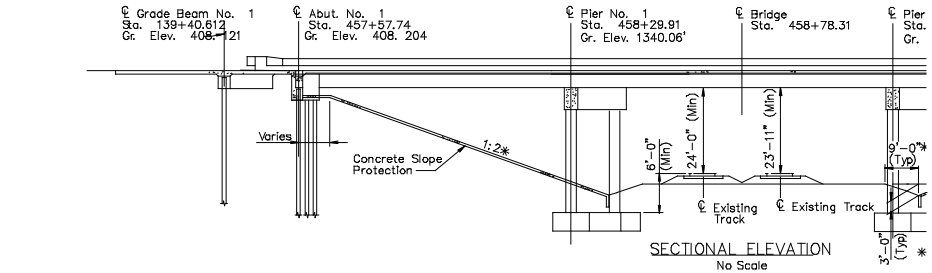
6.1.4 Required Details

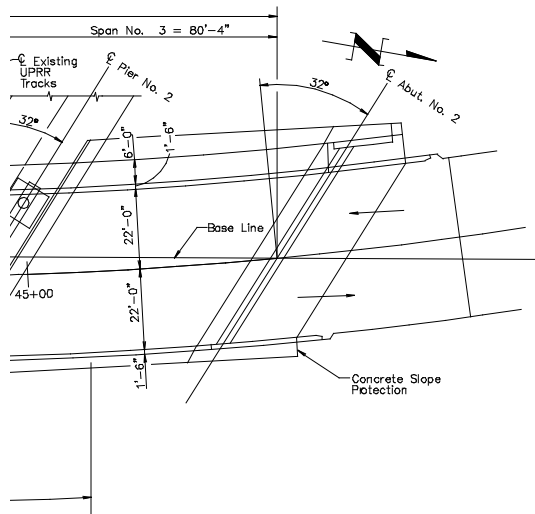
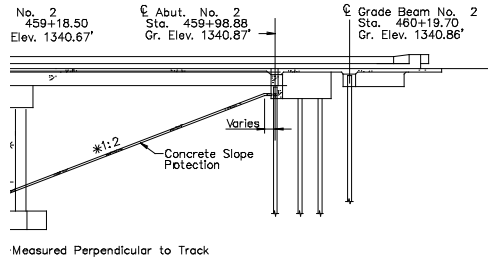
The preliminary plan should include, as a minimum, the following details (see **Figure 6.1.4-1**)

- Location, including highway identification, name of city or county, and major features crossed
- Total length
- Total width
- Span arrangement with expansion joint locations
- Abutment and pier type with dimensions
- Foundation type with dimensions
- End slopes, with type and rate
- Profile grade and superelevation diagram
- Horizontal alignment
- Hydraulic data
- Cross-section, including barrier type and wearing surface type
- Beam type, number and spacing
- Deck thickness and build-up dimensions, if applicable
- Minimum vertical and horizontal clearances, with dimensions
- Utilities
- Borings
- Superstructure bearing types (expansion, fixed, guided, etc.)
- Design method (or specification)
- Design loads

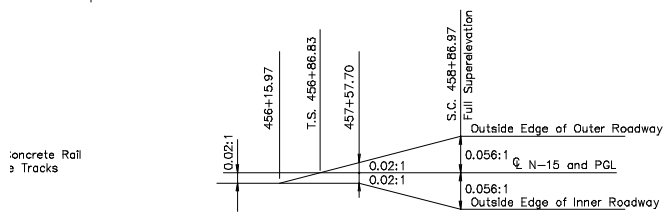
:

Figure 6.1.4-1
Example Preliminary Plan

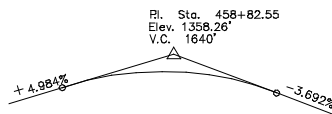




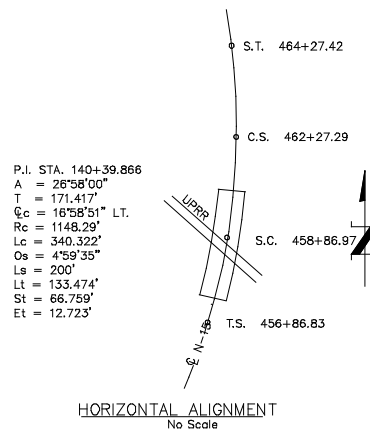
Horizontal Alignment and Vertical Profile shown are at Profile Grade Line.
Top of slab elevations are at Profile Grade Line.
File size, type and capacity shall be provided in final design by the Nebraska Department of Roads.



SUPERELEVATION DIAGRAM
No Scale



VERTICAL PROFILE - N-15
No Scale



PRELIMINARY DESIGN**6.3.1.2 Encased Pile Bents/6.3.1.3 Hammerhead Piers****6.2 SUPERSTRUCTURE****6.2.1 Beam Layout**

Redundant supporting elements minimize the risk of catastrophic collapse. A typical guideline would recommend a minimum of four beams or webs. This number allows the bridge to be repaired in phases under traffic. For roadways less than 30 ft wide, a minimum of three beams or webs may sometimes be justified.

When establishing beam layout, deck overhangs should be limited to 0.50 times the beam spacing. In some cases, this ratio has been increased to 0.625. However, large overhangs may require more costly form erection brackets and provisions to prevent overturning of the exterior beams.

Design aids are provided at the end of this chapter to assist with superstructure system selection for preliminary design.

6.2.2 Jointless Bridges

By using integral abutments at bridge ends, long continuous jointless bridge construction is possible with prestressed concrete beams. Some proponents believe that lengths on the order of 1,000 ft are realistic with this construction method. The elimination of joints minimizes beam end deterioration from inadequate protection from leaking joints and deleterious materials, such as deicing chemicals applied to the deck. Chapter 13 has more information on integral bridges.

6.3 SUBSTRUCTURES**6.3.1 Piers**

In selecting the pier type, preliminary designs should be made for various configurations to evaluate costs. The most economical pier may not be the one with the least material, but instead, the one that is easiest to form and that maximizes repetitive use of forms. This is especially true on large bridge projects. Structures crossing bodies of water may require consideration of vessel collision. These structures may also incorporate dolphins or fender systems

The most commonly used pier types are illustrated in **Figure 6.3.1-1** and discussed below.

6.3.1.1 Open Pile Bents

Open pile bents are used on low-volume roads and stream crossings where the possibility of debris entrapment between piles is not likely. Open pile bents are extremely economical. This type can be readily combined with precast concrete pile caps to permit rapid construction.

6.3.1.2 Encased Pile Bents

Encased pile bents are used in water crossings where the channel carries debris or where protection against ice is desired. This pier type is usually preferred when scour is a concern and spans are of medium length.

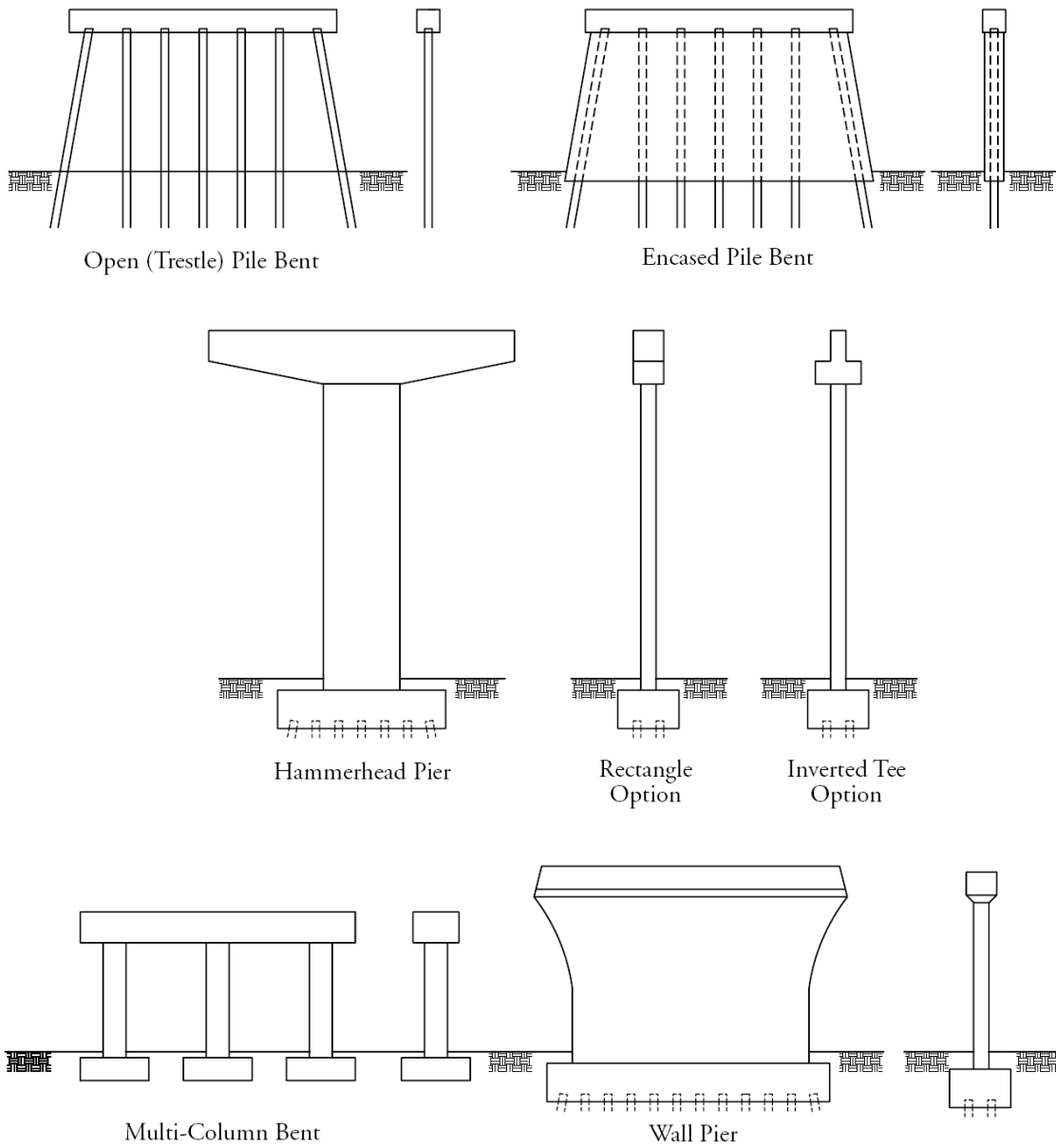
6.3.1.3 Hammerhead Piers

With increasing pier height, the hammerhead pier becomes more economical, since this type offers a reduction in material and forming. Hammerhead piers are sometimes used as crash walls when constructed adjacent to railroad tracks. Other types of piers may also be used next to railroads as long as sufficient crash wall requirements are provided.

PRELIMINARY DESIGN

6.3.1.2 Encased Pile Bents/6.3.1.3 Hammerhead Piers

Figure 6.3.1-1
Types of Commonly Used Piers



PRELIMINARY DESIGN**6.3.1.4 Multi-Column Bents/6.3.2 Abutments****6.3.1.4 Multi-Column Bents**

Multi-column bents are sometimes referred to as rigid frame piers. Basically, this pier type is a concrete beam supported on at least two columns. It is used for wide superstructures and longer spans. Generally, a round column is the simplest and the most economical shape since forms are commercially available and require no form ties. This reduces labor considerably. Forms for this type of pier are most likely found in a typical contractor's inventory. Columns may be extensions of piles or drilled shafts.

In situations where vertical clearance is a concern, a cap shaped like an inverted tee may be used to reduce the depth of cap beneath the superstructure.

6.3.1.5 Wall Piers

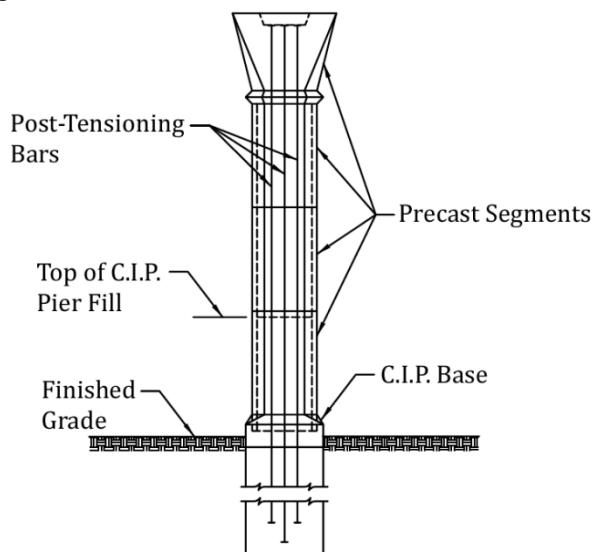
Traditionally used for river crossings, a wall pier is typically constructed as a combination of a solid shaft and hammerhead pier to resist lateral loads. Some states now use wall piers for bridges over divided highways. These types of piers can be precast with simple forming systems. The decreased forming costs and increased labor efficiency generally compensate for added material. This pier configuration also helps resist the 400 kip collision load specified by the *LRFD Specifications*.

6.3.1.6 Segmental Precast Piers

Precast concrete segmental piers can be thin-walled hollow segments, match-cast or mass-produced with a thin mortar or epoxy joint between segments. Shims can be used to maintain proper vertical alignment. The joint should be designed to resist the anticipated loads, provide a thorough closure of the joint, and be designed considering permissible creep and shrinkage characteristics.

Post-tensioned threaded bars are generally inserted in ducts cast in the segments and stressed. Later, ducts are grouted solid. Another alternative is the use of splice sleeves that couple reinforcing bars to provide full bar capacity. **Figure 6.3.1.6-1** shows a drawing of a column designed with precast segments.

Figure 6.3.1.6-1
Segmental Concrete Pier Column

**6.3.2 Abutments**

Unlike piers, abutment types do not vary widely. The most common types of abutments are the backwall type and the integral type. For more information on integral abutments, see Chapter 13. Among the advantages of the integral type is the elimination of the deck joint, which often leaks and causes deterioration, and is therefore a maintenance item. Integral abutments are flexible and tolerate movement caused by expansion and contraction of the superstructure due to temperature changes. It may be necessary, however, to use a backwall abutment if bridge length or skew dictate.

PRELIMINARY DESIGN**6.3.2 Abutments/6.5.1 Product Types**

For precast abutment walls, full capacity may be accomplished by means of field welding of connecting steel plates, followed by corrosion protection of exposed steel.

Location of the abutments is a function of the profile grade of the bridge, the minimum vertical and horizontal clearances required, and the type and rate of end slope.

6.3.3 Hydraulics

Pier shapes that streamline flow and reduce scour are recommended. Consideration is based on the anticipated depth of scour at the bridge piers. Measures to protect the piers from scour activity (for example, riprap and pier alignment to stream flow) are recommended.

For bridges over navigable channels, piers adjacent to the channel may require pier protection as determined by the U.S. Coast Guard. The requirement is based on the horizontal clearance provided for the navigation channel and the type of navigation traffic using the channel. In many cases, piers in navigable waterways should be designed to resist vessel impact in accordance with AASHTO requirements.

6.3.4 Safety

Due to safety concerns, fixed objects should be placed as far from the edge of the roadway as economically feasible, maintaining minimum horizontal clearances to bridge piers and retaining walls.

Redundant supporting elements minimize the risk of catastrophic collapse. A typical guideline would recommend a minimum of two columns for roadways from 30 to 40 ft wide and three columns for roadways 40 to 60 ft wide. Also recommended is collision protection or design for collision loads in accordance with *LRFD Specifications* on piers with one or two columns.

6.3.5 Aesthetics

The principal direction of view of the piers should be considered when determining their size, shape, and spacing. The piers should be correctly sized to handle the structural loads required by the design and shaped to enhance the aesthetics of the overall structure. Column spacing should not be so small as to create the appearance of a "forest of columns." Chapter 5 discusses aesthetics in greater detail.

6.4 FOUNDATIONS

Typical foundation types include:

- Spread footings
- Drilled shafts
- Steel pipe piles
- Prestressed concrete piles
- Steel H-piles
- Timber piles

Round or square columns of multi-column bents, usually rest on single drilled shafts or on footings that cap multiple piles. Single columns usually rest on footings that cap multiple piles or drilled shafts.

Prestressed concrete piles are used extensively in the coastal regions, as well as other locations. For short bents on stream crossings, a line of piles may be extended into the cap, forming a trestle pile bent. These are economically competitive even when the soil is suitable for drilled shafts.

Prestressed piles can double as foundations and piers, thus reducing the amount of on-site forming and concreting. Precast, prestressed concrete piles come in different sizes and shapes, ranging from 10 x 10-in.-square piles to 66-in.-diameter hollow cylinder piles.

6.5 PRELIMINARY MEMBER SELECTION**6.5.1 Product Types**

The preliminary design charts in **Section 6.9** are based on a blend of "national" and regional products. Data used to generate the design charts and basic information resulting from computer runs is provided in tables in **Section**

PRELIMINARY DESIGN**6.5.1 Product Types/6.5.2 Design Criteria**

6.10. Traditional sections such as rectangular box beams, AASHTO I-beams and AASHTO-PCI Bulb-Tee sections are included because these are still commonly used for bridges with a wide range of configurations. Several other beam types are also included because they represent innovative design approaches and newer concepts gaining more widespread use. These include a non-composite deck bulb-tee family of shapes, various composite U-beams and a variation on traditional double-tee stemmed beams known as the NEXT beam.

The design charts are not an exhaustive summary of available products since many regional standards exist beyond those presented herein. There are dozens of additional beam types that have not been covered, yet are used successfully by individual states or regionally. States such as Washington, Utah, Texas, Nebraska, Florida, Pennsylvania, the New England states, and others have all produced many variations on traditional I-beams, wide-flange concrete beams, multi-web stemmed beams, solid and hollow plank sections, and others. Many of the states have design charts similar to those presented in this chapter indicating the span capability of local products. As with most design and construction decisions, knowledge of the local marketplace is important in determining the optimal configuration for a bridge.

6.5.2 Design Criteria

The design charts and graphs provided in this chapter were developed to satisfy flexure at the Strength I and Service III limit states according to the AASHTO *LRFD Specifications* Fifth Edition 2010, and the 2011 Interim Revisions. The following criteria were used to develop the various design data points used to make up the families of curves.

- Prestressed beam concrete design strength, f'_c up to 8 ksi and concrete strength at transfer of prestress f'_{ci} up to 6.8 ksi
- Allowable tension at transfer = $0.24\sqrt{f'_{ci}}$ considering bonded auxiliary reinforcement is present to permit the use of the higher allowable stress
- Transformed section properties are used for all stress calculations
- The AASHTO LRFD Approximate Method is used for long-term prestress loss computations with an assumed relative humidity of 70%.
- Strands are 0.6-in.-diameter, Grade 270, low-relaxation type
- A standard single slope 42-in.-high barrier rail is assumed on each side of the bridge. The estimated weight of 0.500 kips/ft is shared equally by the exterior and first interior beams for all preliminary beam calculations.
- A 0.035 ksf future wearing surface allowance is included with the load effect distributed evenly to all beams.
- For bridges with a cast-in-place concrete deck, the concrete strength is 4.0 ksi. A minimum thickness of 8 in. is used with ½-in. deducted for long-term wear when determining structural properties. For larger beam spacings, an increased slab thickness is provided consistent with usual engineering practice. See Section 6.5.2.3.
- Shear design was checked for an assumed stirrup layout using the AASHTO LRFD general procedure.

Various trial designs were performed considering both an exterior and the first interior beam. For spread closed box, I-beam, and bulb-tee type cross sections, a standard overhang of 3.5 ft measured from the centerline of the exterior beam was used for all variations of the typical section. This is in the range of standard overhangs for closed box and I-beam bridges.

Beam spacings of 6, 8, 10, and 12 ft were chosen to represent a reasonable upper and lower bound of spacings in use today. Within that range of spacings, it is generally found that for the narrower beam spacings, the exterior beam governs—that is it requires more strands for a given span length than an interior beam or has a slightly shorter maximum span length. For wider beam spacings, the interior beam begins to control. This is a reflection of the LRFD live load distribution factor variations between exterior and interior beams.

Generally for the range of parameters studied, the controlling beam (interior or exterior) was found to require several more strands and only reduced the maximum possible span length on the order of 5 to 10 ft. Therefore, it is not unnecessarily conservative to make all the beams of equal configuration. Due to the sensitivity of the exterior beam design to the weight of railing, method of distribution, actual overhang distance, and other assumptions that vary from state to state, the preliminary design charts presented herein are for a typical first

PRELIMINARY DESIGN**6.5.2 Design Criteria/6.5.2.2 Dead Loads**

interior beam. The engineer is cautioned to use these charts accordingly and also to check an exterior beam design for the specific bridge conditions to make sure that the governing member is identified.

For composite U-beams, the overhang measured from the centerline of the exterior beam was selected as 6 ft. With precast section widths of 6 to 8 ft for common U-beams, this results in a physical overhang beyond the exterior web on the order of 2 to 3 ft, a reasonable dimension. The spacing of U-beams was chosen to vary from 10 to 18 ft. The minimum spacing of 10 ft reflects a reasonable minimum spacing given that the precast section will be 6 to 8 ft wide typically at its top. This is a near practical minimum beam spacing. At the upper end, a beam spacing of 18 ft was selected. This is the upper end of the limit of the empirical AASHTO live load distribution factors and results in a clear deck span between boxes of about 10 to 12 ft, still a reasonable slab span for conventionally reinforced decks and easily accommodated by traditional deck forming systems including stay-in-place precast deck panels.

Two NEXT beam types were chosen for evaluation, Type D and Type F. The Type D section has a thick top flange (8 in.) that can serve directly as the structural slab for the bridge. The design considers that a 3-in.-thick asphalt wearing surface is used. The other beam type, Type F, has a 4-in.-thick top flange that primarily serves as a continuous stay-in-place form for a traditional 8-in.-thick composite cast-in-place deck with a future overlay allowance.

6.5.2.1 Live Loads

The live load considered for the charts is the HL-93 loading with all designs based on a single span bridge. A random check of selected designs for the Type 3, 3S2 and 3-3 rating loads indicated that the HL-93 designs governed the design and resulted in designs with inventory and operating rating factors greater than 1.0 for the various notional rating vehicles. Live load moment and shear are distributed to the beams in accordance with the AASHTO empirical equations for live load distribution found in LRFD Section 4.6.2.2 with the exception that the rigid rotation model for exterior beams is not considered. The rigid rotation model is only stipulated for bridges with diaphragms and cross frames that are sufficient to induce a load distribution mechanism analogous to the rigid body distribution usually assumed for elements like pile groups or footings. For a prestressed concrete I-beam or bulb-tee section such as cross-section (k) in LRFD Table 4.6.2.2.1-1, the designer should consider whether the exterior diaphragms required by the specifications or agency policy are sufficient in number and stiffness to produce such behavior. If so, the design charts may prove to be unconservative for exterior beams in some instances and the designer should be aware that three potential exterior beam distribution factors might apply—the simple beam, AASHTO empirical, and rigid rotation model.

Since various types of beams and cross sections have been studied, a unique approach to live load distribution is required for each solution. The following load distribution models from LRFD Table 4.6.2.2.1-1 were considered in the development of the design graphs.

- For AASHTO I-beam and bulb-tee sections, cross-section Type (k) was used.
- For spread box beams, cross-section Type (b) was used.
- For U-beams, cross-section Type (c) was used.
- For adjacent box beams with a cast-in-place concrete overlay, Type (f) was used. All adjacent box beams were assumed to have a composite, cast-in-place concrete slab. Charts for non-composite box beams with an asphalt overlay were not developed.
- For deck bulb-tee bridges without transverse post-tensioning in the flanges, cross-section Type (j) was used.
- For double-tee NEXT Type D and F beams, cross-section (k) was used to be consistent with the PCI Northeast Chapter assumptions in developing the section and details. (see **Appendix C**)

6.5.2.2 Dead Loads

The design of the first interior beam was performed assuming that the beam carries 50% of the weight of the barrier rail. A 42-in.-high single slope barrier rail was assumed, weighing approximately 0.500 kips/ft, with half of this load carried by the exterior beam and half by the first interior beam. The practice of distributing the parapet load to exterior and interior beams varies widely amongst engineers and agencies from even distribution to all beams to rules requiring a larger share of this load be carried by the exterior beam(s). For purposes of developing the design charts, it was assumed that the exterior beam carries 50% of the barrier rail and the first interior beam

PRELIMINARY DESIGN

6.5.2.2 Dead Loads/6.5.2.4 Concrete Strength and Allowable Stresses

carries the remaining 50%. With heavy parapet loads, stiff beams, and relatively short overhangs, this approach is considered a reasonable approximation. Cast-in-place slab loads are assigned on a tributary basis. An allowance of 0.035 ksf is provided between gutter lines, uniformly carried by all beams, to provide for an additional wearing surface (*DW*) loading.

6.5.2.3 Composite Deck

For all spread beam designs (box, I-beam, U-beam, etc.), a composite deck section is used with the thickness as shown in Table 6.5.2.3-1.

**Table 6.5.2.3-1
Assumed Deck Thickness**

Beam Type	Beam Spacing ft	C.I.P Deck Thickness in.
Box Beams 48 in. wide	Adjacent	6.0
	6, 8, 10, 12	8.0
Box Beams 36 in. wide	Adjacent	6.0
	6, 8, 10	8.0
	12	8.5
Bulb-Tees BT-54, BT-63, BT-72	6, 8, 10	8.0
	12	9.0
Deck Bulb-Tees	Adjacent	None
I-Beams Types II, III, IV	6, 8	8.0
	10	8.5
	12	9.5
I-Beams Types V, VI	6, 8, 10	8.0
	12	9.0
NEXT Beams Type D	Adjacent	None
NEXT Beams Type F	Adjacent	8.0
U-Beams	10, 14	8.0
	18	10

See **Appendix C** for spliced U-Beams and curved spliced U-Beams from PCI Zone 6.

The deck comprises 4.0 ksi compressive strength concrete in all cases. A haunch thickness of 2 in. was typically used to provide additional dead load on the section as well as to slightly offset the deck from the top of the precast section. The use of the haunch to offset the composite slab is a practice that varies throughout the country. Some agencies consider the slab to sit on top of the precast section while still providing for a haunch load. Others use the minimum haunch as typical for the entire span length (approach taken herein). There are other approaches as well.

For all design cases, a ½ in. reduction in slab thickness is included for wear.

For adjacent sections that are considered to have a composite topping, the topping thickness is assumed equal to 6 in. for box beams and 8 in. for NEXT Type F beams. The topping weight is based on the indicated thickness. However, composite section properties were determined with the assumption that long-term wear and/or longitudinal profiling (deck grinding) reduces the thickness by ½ in.

6.5.2.4 Concrete Strength and Allowable Stresses

The precast concrete products are assumed to have $f'_{ci} = 6.8$ ksi and $f'_c = 8.0$ ksi, and the cast-in-place topping is assumed to have $f'_c = 4.0$ ksi. These material properties are in keeping with readily available concrete mixes around the country. Substantially higher precast concrete transfer strengths have been achieved and are available on a regional basis.

PRELIMINARY DESIGN**6.5.2.4 Concrete Strength and Allowable Stresses/6.5.3.2 Limiting Stresses**

The allowable concrete tensile stresses are taken as $0.24\sqrt{f'_{ci}}$ ksi at transfer and $0.19\sqrt{f'_c}$ ksi at service. The allowable compression is taken as $0.6f'_{ci}$ ksi at transfer and $0.6f'_c$ ksi at service.

6.5.2.5 Strands and Spacing

The use of 0.6-in., seven-wire, 270 ksi low-relaxation strands is assumed in all applications. The center-to-center strand spacing is assumed to be 2 in. These larger strands, as compared to traditional ½-in.-diameter strands provide about 40% higher tensile capacity at only about 20% increase in diameter.

All strands are assumed to have an initial tension of 202.5 ksi prior to transfer. Member end stresses are assumed to be controlled through debonding (shielding) and/or harping of some of the strands as needed. Prestress losses are calculated using the AASHTO approximate method for long-term losses in lieu of the detailed time-dependent estimates. Losses are based on an assumed 70% relative humidity.

Strand patterns used by producers vary. For the box beams in the charts in Section 6.9, two layers of strands are assumed in the bottom flanges.

6.5.2.6 Design Limits

The charts depict the maximum span length achievable for a certain beam spacing given the materials and allowable stresses described herein. The selection of a unique number of strands, transfer strength, beam spacing, and span length is an interaction of various checks. For each design data point a check of initial stresses at transfer, final stresses at service load, and factored moment capacity was considered. The concrete strength was stipulated as 8.0 ksi at 28 days and not to exceed 6.8 ksi at transfer (though it could be lower if all checks are satisfied otherwise). Most owners or precasters use a 3 ksi minimum concrete strength for initial handling as recommended in PCI MNL-116 Section C5.3.17. At times, any of the stress or strength criteria can control and the chart simply indicates a specific combination of span length, number of strands, and beam spacing where all checks were satisfied.

For the longer spans, camber growth and stability of the beams during handling and shipping should also be evaluated.

6.5.3 High Strength Concrete

In analyzing current practice, little difficulty is encountered anywhere in the country in obtaining 8.0 ksi concrete on a consistent basis and is the strength used for the development of the design charts.

6.5.3.1 Attainable Strengths

In recent years, higher strength concretes have been commercially achieved. The strength ranges from 10 to 15 ksi. Use of such strengths is expected to increase in the future. The use of higher strength concrete permits the use of longer span lengths, wider beam spacings, or shallower sections. The increased span capacity should be weighed against the possible cost increase associated with producing higher strength concrete. Chapter 4 discusses many of these considerations.

6.5.3.2 Limiting Stresses

The *LRFD Specifications* allows the use of design concrete strengths above 10.0 ksi for normal weight concrete when allowed by specific articles or when physical tests are made to establish the relationships between the concrete strength and other properties. Appendix C5 of the *LRFD Specifications* contains a table showing the articles for which strengths above 10.0 ksi are currently permitted. These include Articles 5.4.2.3—Shrinkage and Creep; 5.4.2.4—Modulus of Elasticity; 5.4.2.6—Modulus of Rupture; and 5.9.5—Loss of Prestress.

Three NCHRP research projects have been completed to address design provisions for shear, transfer and development length of strand, splice length of non-prestressed deformed reinforcement, flexure, and compression for specified compressive strengths up to 15 and 18 ksi (Hawkins and Kuchma, 2007; Rizkalla et al., 2007; and Ramirez and Russell, 2008). The three research projects provide revisions to allow more provisions to be extended to specified concrete compressive strengths above 10.0 ksi for normal weight concrete. Implementation of these provisions will support greater use of concrete with specified compressive strengths greater than 10.0 ksi.

6.6 DESCRIPTION OF DESIGN CHARTS

6.6.1 Product Groups

The design charts in **Section 6.9** provide preliminary design information for different products grouped into several types. These include:

CHARTS	PRODUCTS
Charts BB-1 through BB-10	AASHTO box beams
BT-1 through BT-4	AASHTO-PCI bulb-tees
DBT-1 through DBT-2	Deck bulb-tees
IB-1 through IB-6	AASHTO I-beams
NEXT-1 and NEXT-6	NEXT Double-tee beams
U-1 through U-5	U-Beams

(Geometric properties for products are given in Appendix B.)

6.6.2 Maximum Spans Versus Spacings

Within each group, the first chart, e.g. BB-1, BT-1,... etc., depicts the maximum attainable span versus member spacing for all member depths within the group. This type of chart is convenient to use in the early stages of design to identify product types, spacings, and approximate depths for the span length being considered.

6.6.3 Number of Strands

The remainder of the charts within each group give the number of strands needed for specified span lengths and beam spacings. This type of information is needed to: (1) develop an estimate of the final design requirements, and (2) to determine if the number of strands needed is within the prestressing bed capacity of local producers. Otherwise, the member depth, or spacing if applicable, must be adjusted.

In developing the charts, no attempt was made to judge whether or not the number of strands given is feasible for local production. The number of strands was strictly based on flexural stress or strength requirements. In some cases, e.g., shallow I-beams at wide spacing, shear capacity may require an unreasonable stirrup arrangement. A complete check should be made during final design.

It should be noted that all charts were based on providing the lowest possible center of gravity of strands in the midspan section. This is accomplished by filling the first (bottom) row to capacity before any strands can be placed in the second row, and so on.

6.6.4 Controls

For each scenario, various potential controls were checked. In general, the maximum span was first established by satisfying the Strength I and Service III limit states. When strands could no longer be added to the section, or doing so did not increase span capacity, the practical maximum span was established. However this was usually a large number of strands for a particular beam section. Checks of stress at transfer were also performed. To mitigate the high stresses in the transfer region, the use of harping (with a hold down at $0.4L$) or debonding was used to control the beam end stresses. Maximum debonding limits of 40% of the strands in a row and 25% of the total number of strands were enforced with the exception that if the number of debonded strands was only one strand over the maximum due to rounding, that was considered an acceptable solution. The charts do not indicate the nature of the control but generally for narrower beam spacings the trend was for Service III to govern and for wider spacing, longer spans, Strength I was a common control. Most of the intermediate to longer spans required some debonding or harping to control the end zone stresses.

PRELIMINARY DESIGN

6.7 Preliminary Design Examples/6.7.2 Preliminary Design Example No. 2

6.7 PRELIMINARY DESIGN EXAMPLES

6.7.1 Preliminary Design Example No. 1

Design a simple span for HL-93 loading with a 95 ft design span. The total width of the bridge is 36 ft 0 in. The conditions do not allow for field forming of the concrete deck.

Referring to the preliminary design charts, the only applicable products would be adjacent box beams or deck bulb-tees in order to avoid deck forming. Using the charts, possible solutions are summarized in **Table 6.7.1-1**.

Table 6.7.1-1
Product Options for Example No. 1¹

Product		Depth in.	Spacing in.	Topping (Deck)	Number of Strands	Design Chart
Deck Bulb-Tees 6-ft-Wide Flange		41	72	No	26	DBT-2
		53	72	No	20	DBT-2
		65	72	No	18	DBT-2
AASHTO Box Beams	BII-36	33	36	Yes	22	BB-7
	BIII-36	39	36	Yes	18	BB-7
	BIV-36	42	36	Yes	16	BB-7
	BII-48	33	48	Yes	27	BB-2
	BIII-48	39	48	Yes	23	BB-2
	BIV-48	42	48	Yes	19	BB-2

Note 1. Refer to **Section 6.5** for design assumptions.

From the table above, the deck bulb-tee generally requires more depth, but fewer beams and, therefore, fewer total strands. Please note that the product may not be available in all regions. Further, unless weight of a single beam is a factor, wider units allow casting, transporting, and installing fewer pieces. This usually results in lower cost.

Detailed Design Examples 9.3, 9.4, and 9.5, Chapter 9, have similar spans and loading requirements. In those examples, AASHTO BIII-48 box beams and DBT-53s are used. Considering **Table 6.7.1-1**, it is clear that a shallower section could be used.

6.7.2 Preliminary Design Example No. 2

Design a simple span for HL-93 loading with 120 ft design span. The total width of the bridge is 51 ft 0 in. with a cast-in-place deck slab 8 in. thick. **Table 6.7.2-1** shows the product options and the number of strands required for each product.

PRELIMINARY DESIGN

6.7.2 Preliminary Design Example No. 2/6.8 References

Table 6.7.2-1
Product Options for Example No. 2¹

Products		Depth in.	Spacing ft	Deck Thickness in.	Number of Strands	Design Chart
AASHTO I-Beams	IV	54	8	8.0	42	IB-4
		54	6	8.0	36	IB-4
	V	63	12	9.0	46	IB-5
		63	10	8.0	48	IB-5
	VI	63	8	8.0	42	IB-5
		63	6	8.0	32	IB-5
		72	12	9.0	40	IB-6
		72	10	8.0	42	IB-6
		72	8	8.0	36	IB-6
		72	6	8.0	26	IB-6
AASHTO- PCI Bulb-Tees	BT-54	54	6	8.0	34	BT-2
	BT-63	63	6	8.0	28	BT-3
	BT-72	72	6	8.0	24	BT-4
		72	8	8.0	34	BT-4
		72	10	8.0	38	BT-4
		72	12	9.0	36	BT-4
Deck Bulb-Tees 6-ft-Wide Flange		53	6	None	30	DBT-2
		65	6	None	23	DBT-2
AASHTO Box Beams	BIV-36	39	3	6.0	27	BB-7
	BIV-48	42	4	6.0	31	BB-5
Washington U-Beams	U66G5	66	10	8.0	47	U-4
	U78G5	78	14	8.0	49	U-5
		78	10	8.0	43	U-5

Note 1. Refer to **Section 6.5** for design assumptions.

It is generally most beneficial to use the widest possible spacing to minimize the number of beam lines. Clearance requirements may dictate the structure depth. Assuming no maximum depth limitations, the most economical products will be the deepest in order to minimize the number of strands required. Accordingly, an AASHTO Type VI I-beam or 72-in.-deep bulb-tee (BT-72) at 12 ft spacing are recommended. However, since the bulb-tee is a lighter section and the number of strands required (36 strands) is less, a BT-72 at 12 ft spacing is a more efficient solution.

A deck bulb-tee can be utilized for this bridge if the product is locally available. An AASHTO box beam is also suitable if the superstructure depth needs to be relatively shallow.

Detailed Design Example 9.3, Chapter 9, has a 120-ft simple span, concrete strength of 6.5 ksi and HL-93 loading conditions. Referring to the above table, the BT-72 was chosen with 9 ft spacing.

6.8 REFERENCES

1. AASHTO. 2010. *AASHTO LRFD Bridge Design Specifications*, Fifth Edition with 2011 Interim Revisions. American Association of State Highway and Transportation Officials, First Edition, Washington, DC. <https://bookstore.transportation.org> (Fee)
2. Hawkins, N. M. and D. A., Kuchma, 2007. *Application of LRFD Bridge Design Specifications to High-Strength Concrete: Shear Provisions*. NCHRP Report 579. Transportation Research Board. Washington, DC. 197 pp. http://onlinepubs.trb.org/onlinepubs/nchrp/nchrp_rpt_579.pdf
3. Rizkalla, S., A. Mirmiran, P. Zia, et al. 2007. *Application of the LRFD Bridge Design Specifications to High-Strength Structural Concrete: Flexure and Compression Provisions*. NCHRP Report 595. Transportation Research Board. Washington, DC. 28 pp. http://onlinepubs.trb.org/onlinepubs/nchrp/nchrp_rpt_595.pdf

PRELIMINARY DESIGN

6.8 References/6.9 Preliminary Design Charts

4. Ramirez, J. A. and B. W. Russell. 2008. *Transfer, Development, and Splice Length for Strand/Reinforcement in High-Strength Concrete*. NCHRP Report 603. Transportation Research Board. Washington, DC. 122 pp.
http://onlinepubs.trb.org/onlinepubs/nchrp/nchrp_rpt_603.pdf

6.9 PRELIMINARY DESIGN CHARTS

The design charts listed in Table 6.9-1 are included in this section, Section 6.10 provides tables that correspond to each of these charts that show input and output data from which the charts were developed.

Table 6.9-1
Design Charts

Chart No.	Beam Type	Chart Type
BB-1	AASHTO Box Beams 48 in. Wide	Maximum span versus beam spacing
BB-2	AASHTO Adjacent Box Beams 48 in. Wide	No. of strands versus span length
BB-3	AASHTO Spread Box Beams BII-48	No. of strands versus span length
BB-4	AASHTO Spread Box Beams BIII-48	No. of strands versus span length
BB-5	AASHTO Spread Box Beams BIV-48	No. of strands versus span length
BB-6	AASHTO Box Beams 36 in. Wide	Maximum span versus beam spacing
BB-7	AASHTO Adjacent Box Beams 36 in. Wide	No. of strands versus span length
BB-8	AASHTO Spread Box Beams BII-36	No. of strands versus span length
BB-9	AASHTO Spread Box Beams BIII-36	No. of strands versus span length
BB-10	AASHTO Spread Box Beams BIV-36	No. of strands versus span length
BT-1	AASHTO-PCI Bulb-Tees	Maximum span versus beam spacing
BT-2	AASHTO-PCI Bulb-Tees BT-54	No. of strands versus span length
BT-3	AASHTO-PCI Bulb-Tees BT-63	No. of strands versus span length
BT-4	AASHTO-PCI Bulb-Tees BT-72	No. of strands versus span length
DBT-1	Deck Bulb-Tees	Maximum span versus section depth
DBT-2	Deck Bulb-Tees	No. of strands versus span length
IB-1	AASHTO I-Beams	Maximum span versus beam spacing
IB-2	AASHTO I-Beams Type II	No. of strands versus span length
IB-3	AASHTO I-Beams Type III	No. of strands versus span length
IB-4	AASHTO I-Beams Type IV	No. of strands versus span length
IB-5	AASHTO I-Beams Type V	No. of strands versus span length
IB-6	AASHTO I-Beams Type VI	No. of strands versus span length
NEXT-1	NEXT Type D Beams	Maximum span versus section depth
NEXT-2	NEXT Type D x 96 Beams	No. of strands versus span length
NEXT-3	NEXT Type D x 120 Beams	No. of strands versus span length
NEXT-4	NEXT Type F Beams	Maximum span versus section depth
NEXT-5	Next Type F x 96 Beams	No. of strands versus span length
NEXT-6	Next Type F x 144 Beams	No. of strands versus span length
U-1	U-Beams	Maximum span versus beam spacing
U-2	Texas U-40 Beams	No. of strands versus span length
U-3	Texas U-54 Beams	No. of strands versus span length
U-4	Washington U66G5 Beams	No. of strands versus span length
U-5	Washington U78G5 Beams	No. of strands versus span length

PRELIMINARY DESIGN

6.9 Preliminary Design Charts

Chart BB-1
AASHTO Box Beams 48 in. Wide

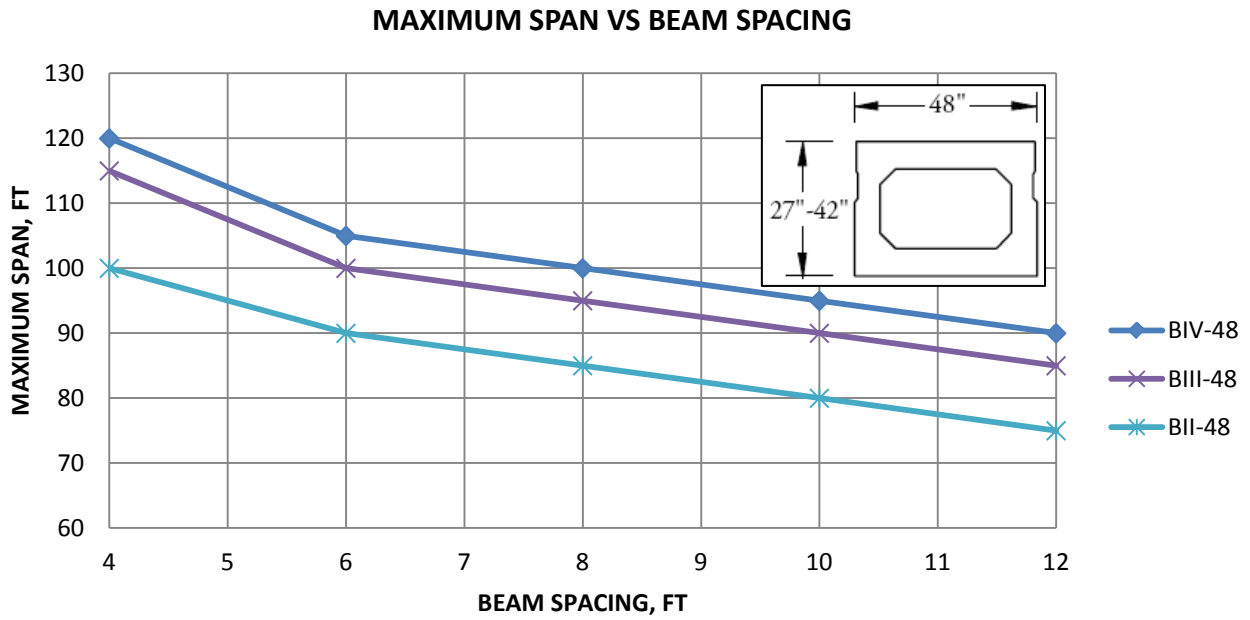
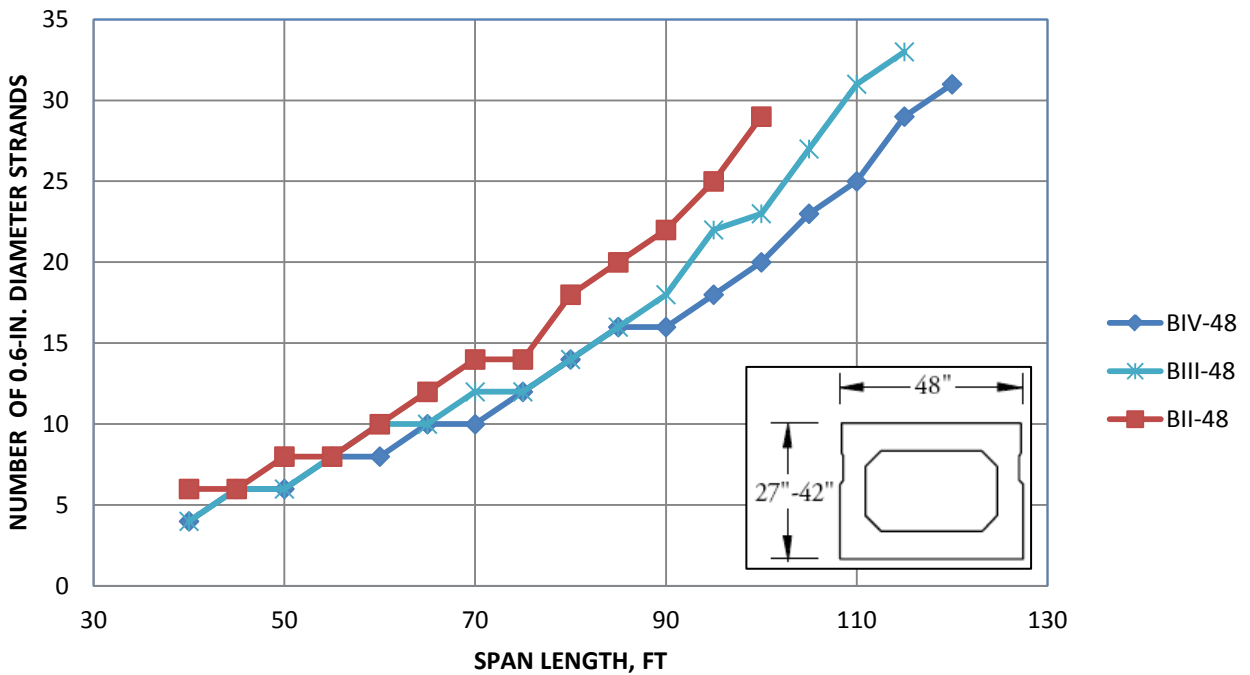


Chart BB-2
AASHTO Adjacent Box Beams 48 in. Wide



PRELIMINARY DESIGN

6.9 Preliminary Design Charts

Chart BB-3
AASHTO Spread Box Beams BII-48

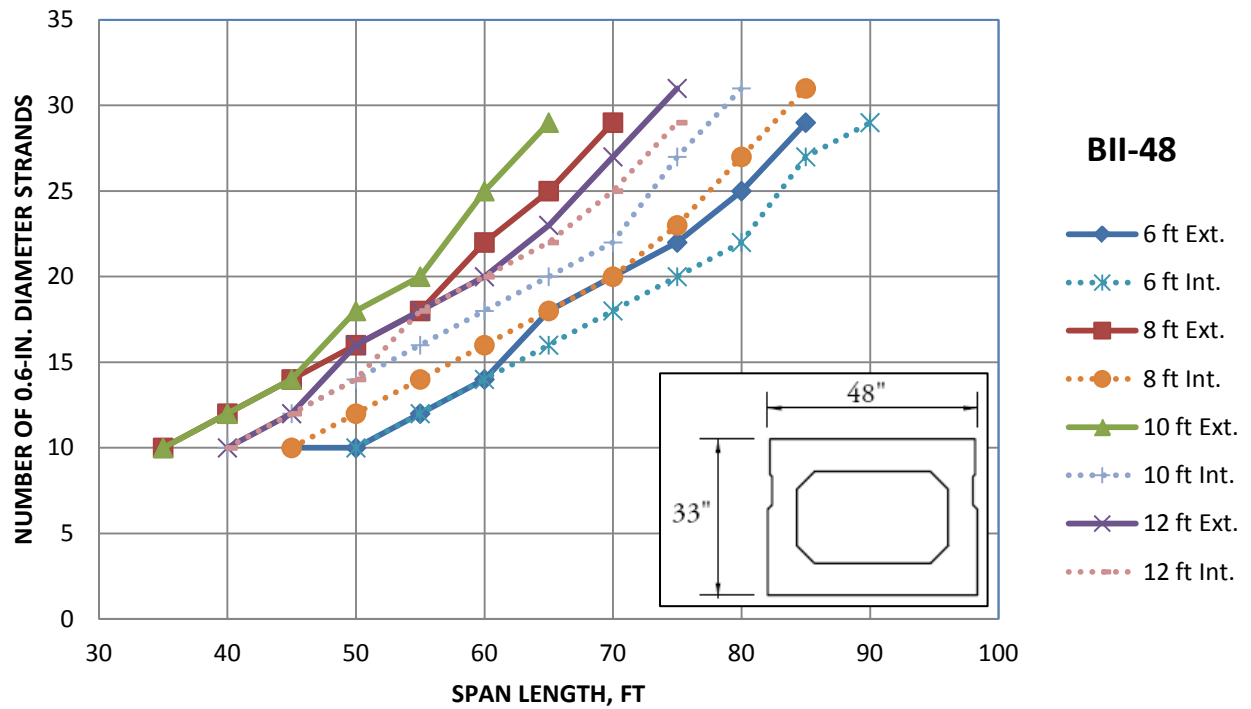
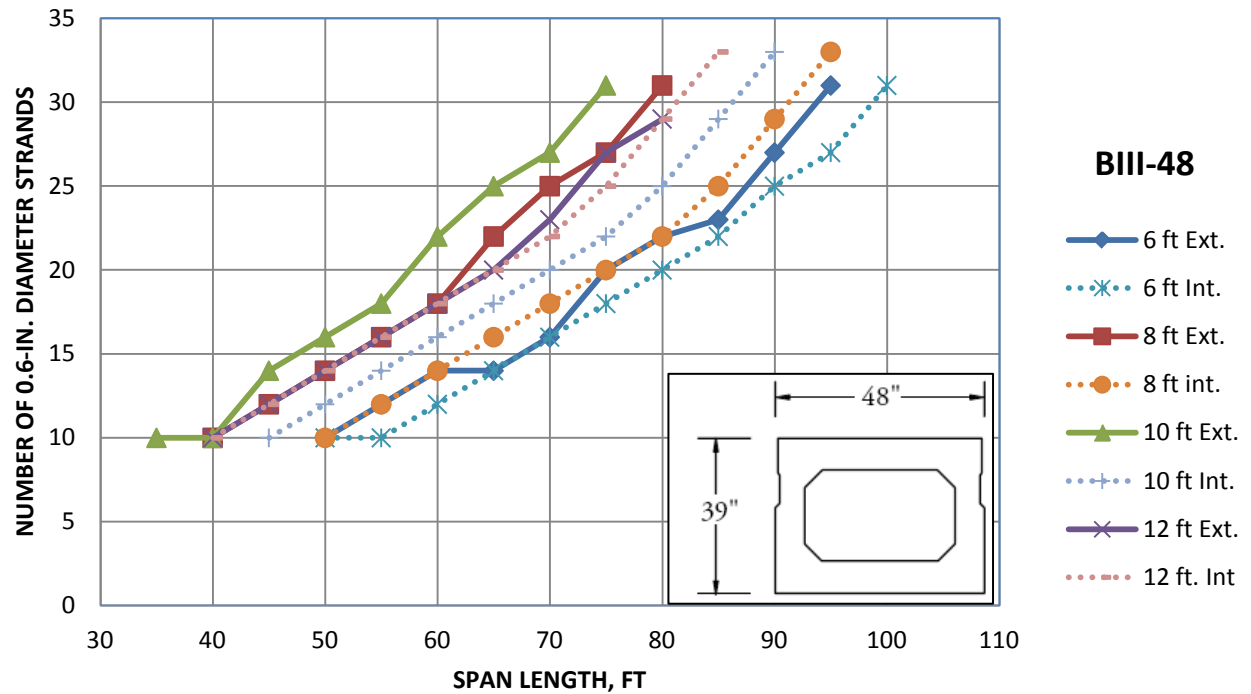


Chart BB-4
AASHTO Spread Box Beams BIII-48



PRELIMINARY DESIGN

6.9 Preliminary Design Charts

Chart BB-5
AASHTO Spread Box Beams BIV-48

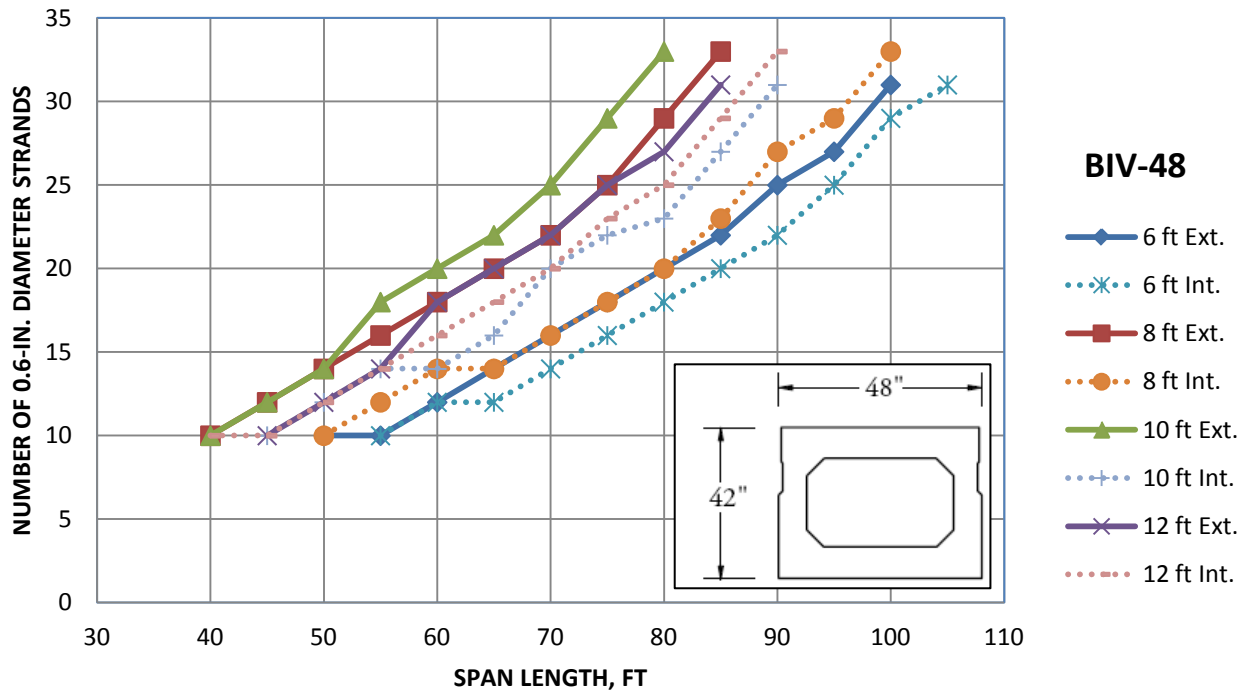
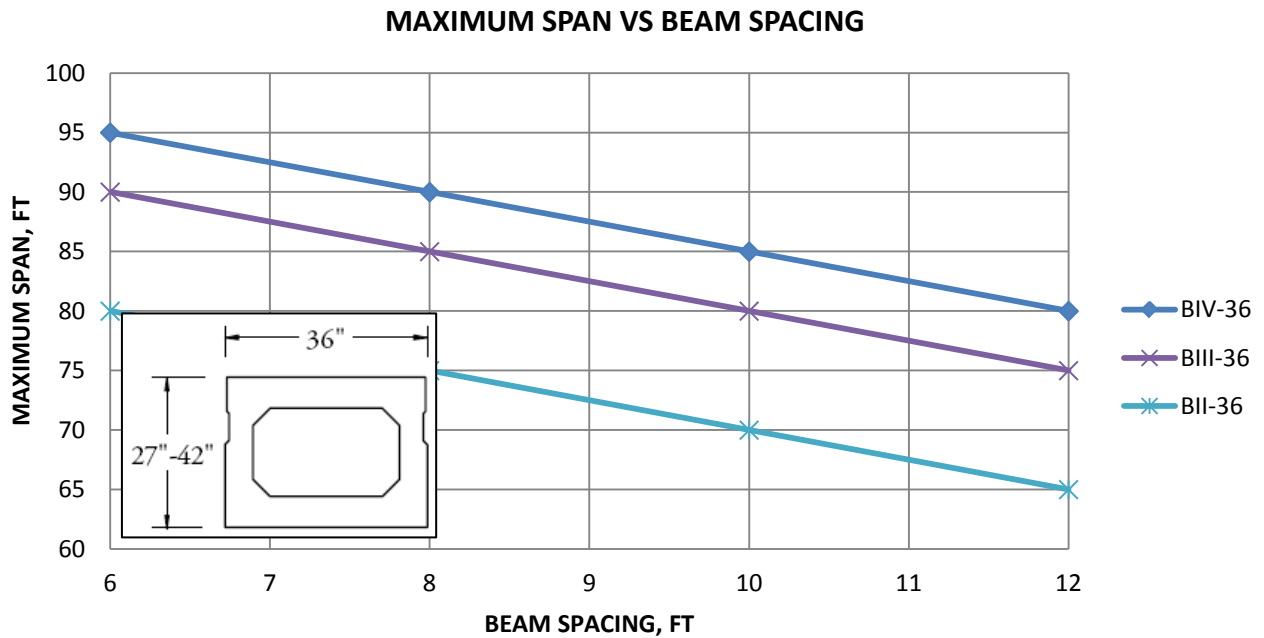


Chart BB-6
AASHTO Box Beams 36 in. Wide



PRELIMINARY DESIGN

6.9 Preliminary Design Charts

Chart BB-7
AASHTO Adjacent Box Beams 36 in. Wide

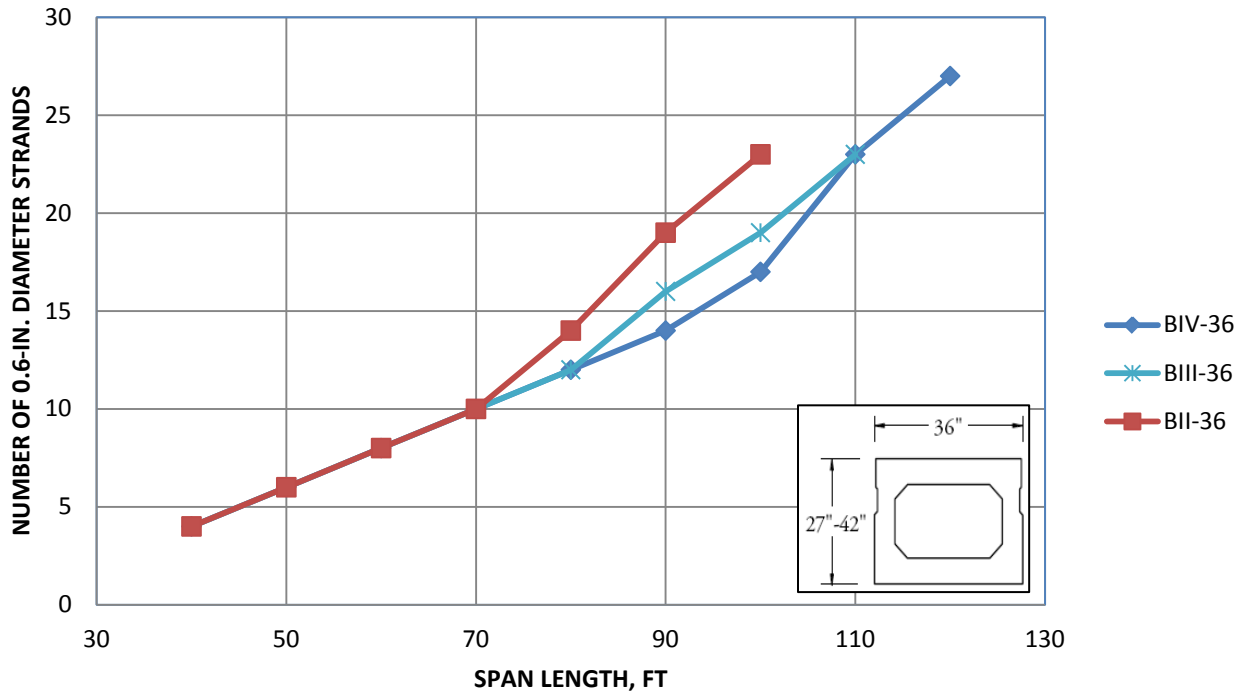


Chart BB-8
AASHTO Spread Box Beams BII-36

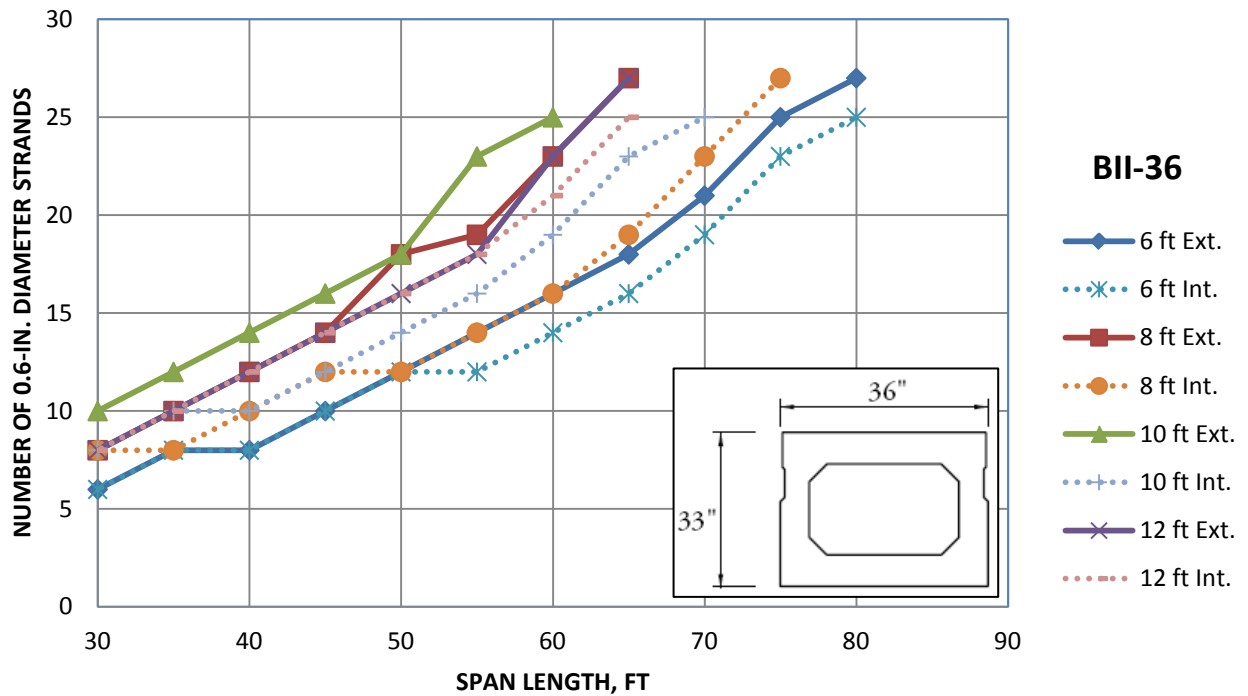


Chart BB-9
AASHTO Spread Box Beams BIII-36

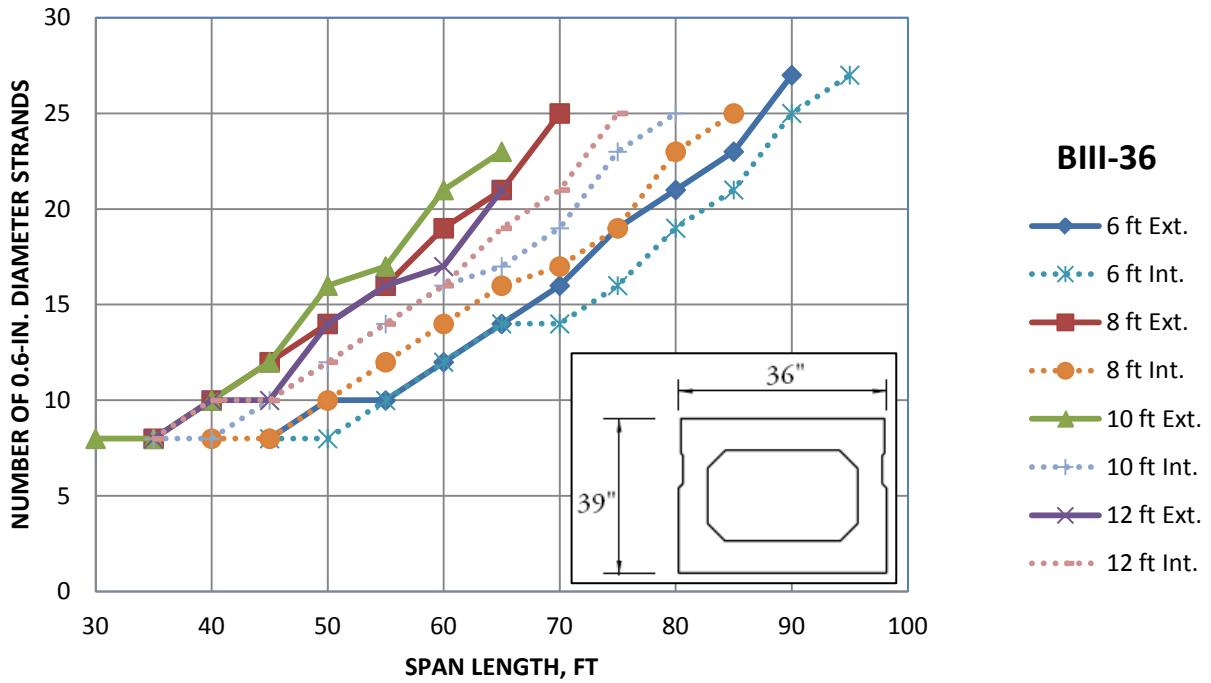


Chart BB-10
AASHTO Spread Box Beams BIV-36

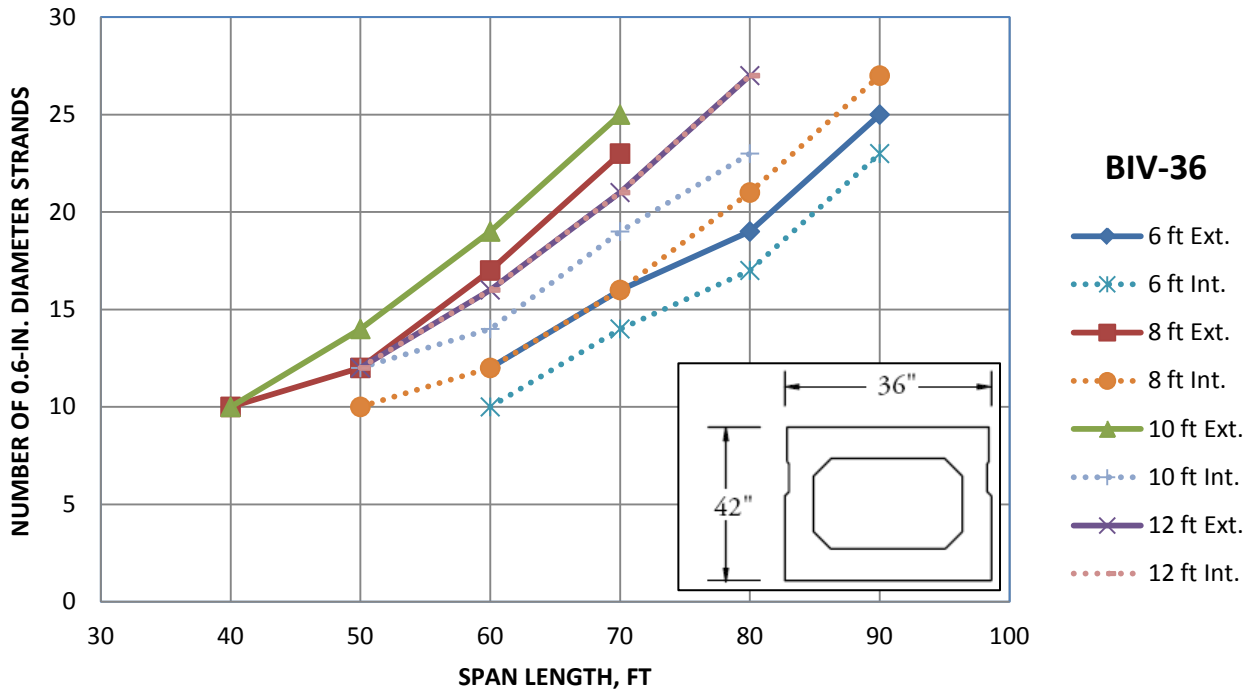


Chart BT-1

AASHTO-PCI Bulb-Tees

MAXIMUM SPAN VS BEAM SPACING

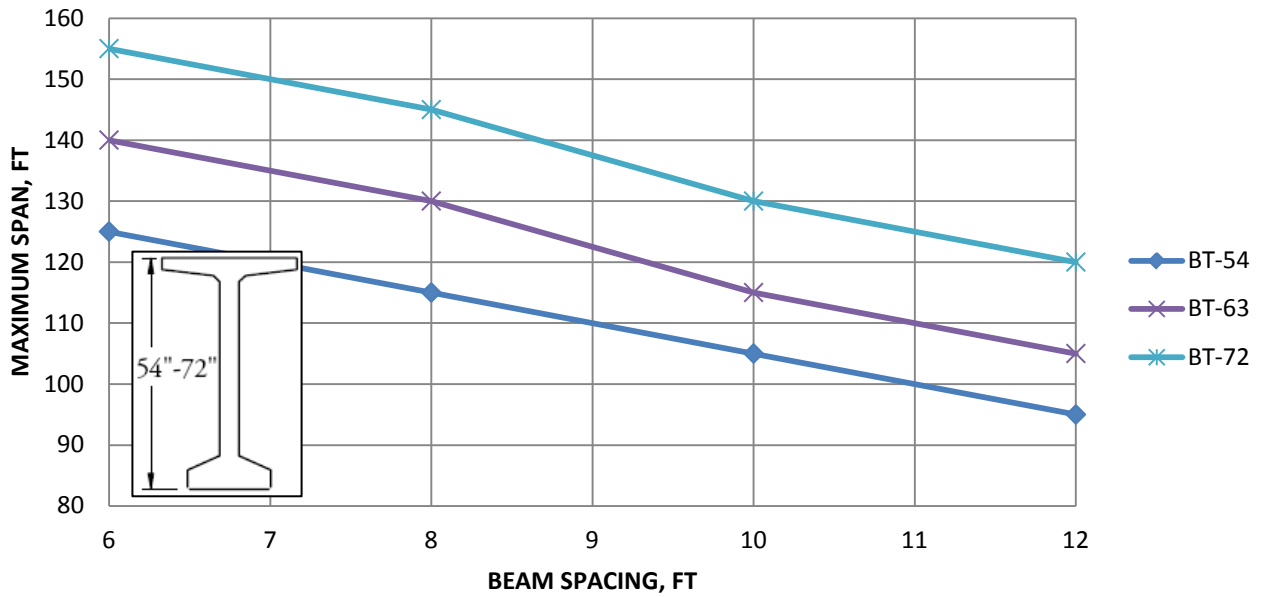
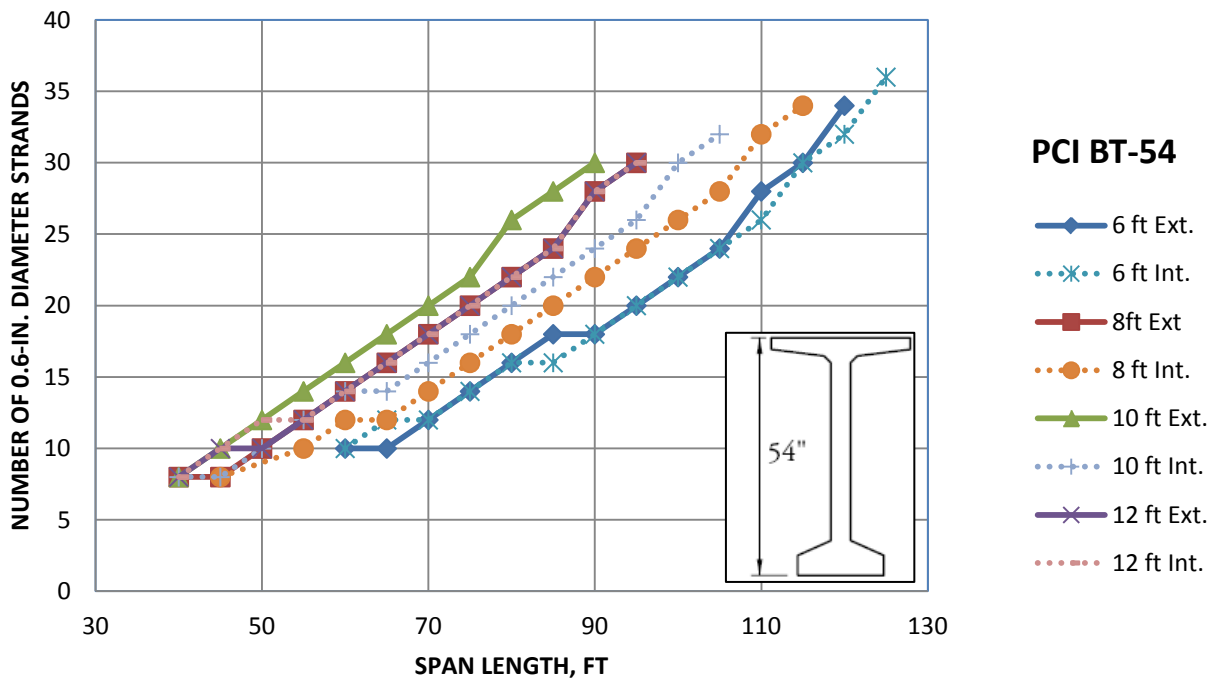


Chart BT-2
AASHTO-PCI Bulb-Tees BT-54



PRELIMINARY DESIGN

6.9 Preliminary Design Charts

Chart BT-3
AASHTO-PCI Bulb-Tees BT-63

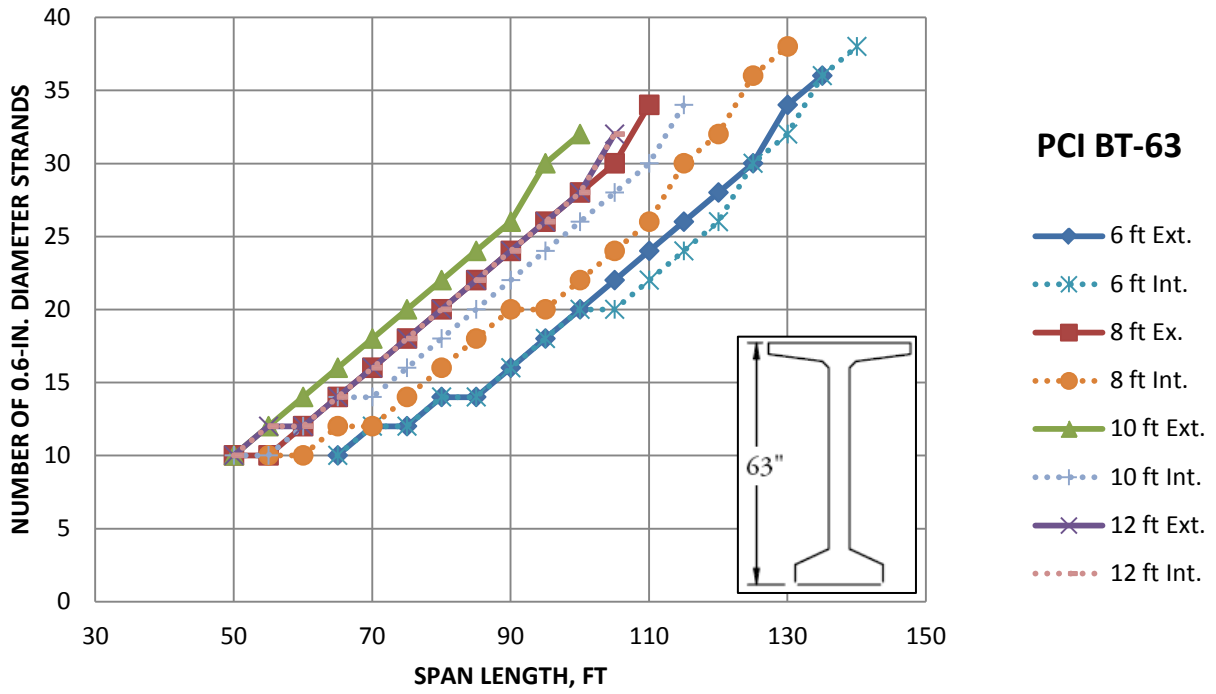


Chart BT-4
AASHTO-PCI Bulb-Tees BT-72

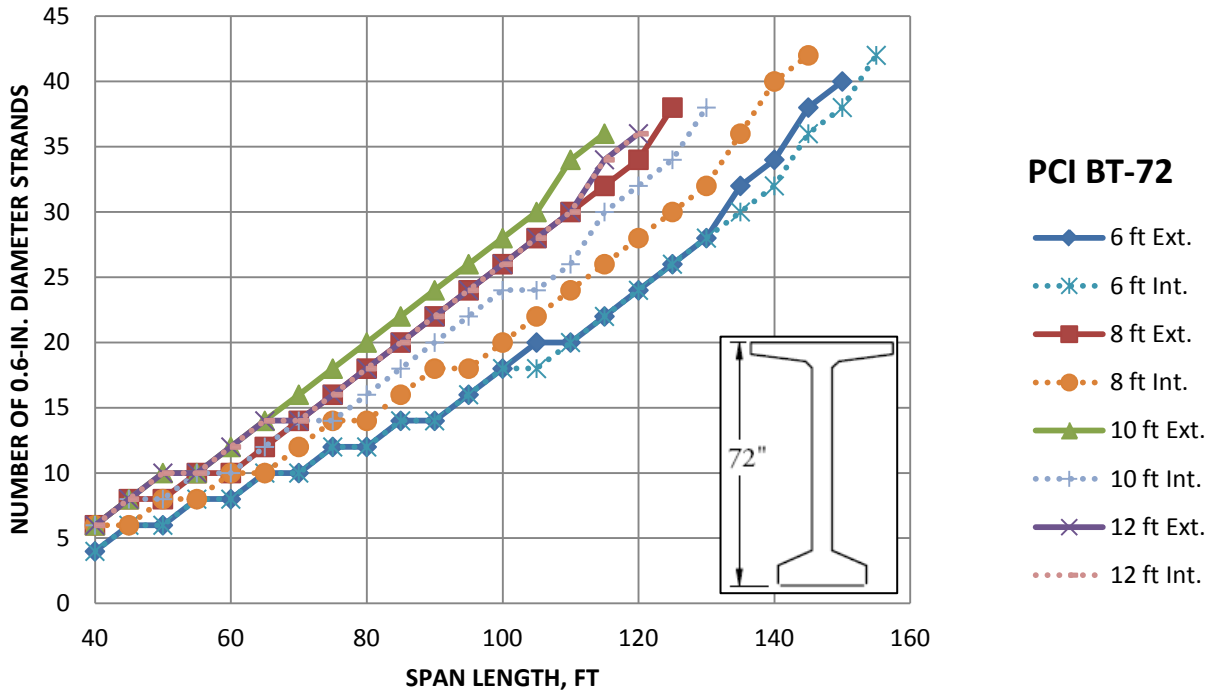


Chart DBT-1
Deck Bulb-Tees

MAXIMUM SPAN VS SECTION DEPTH FOR 6-FT-WIDE TOP FLANGE

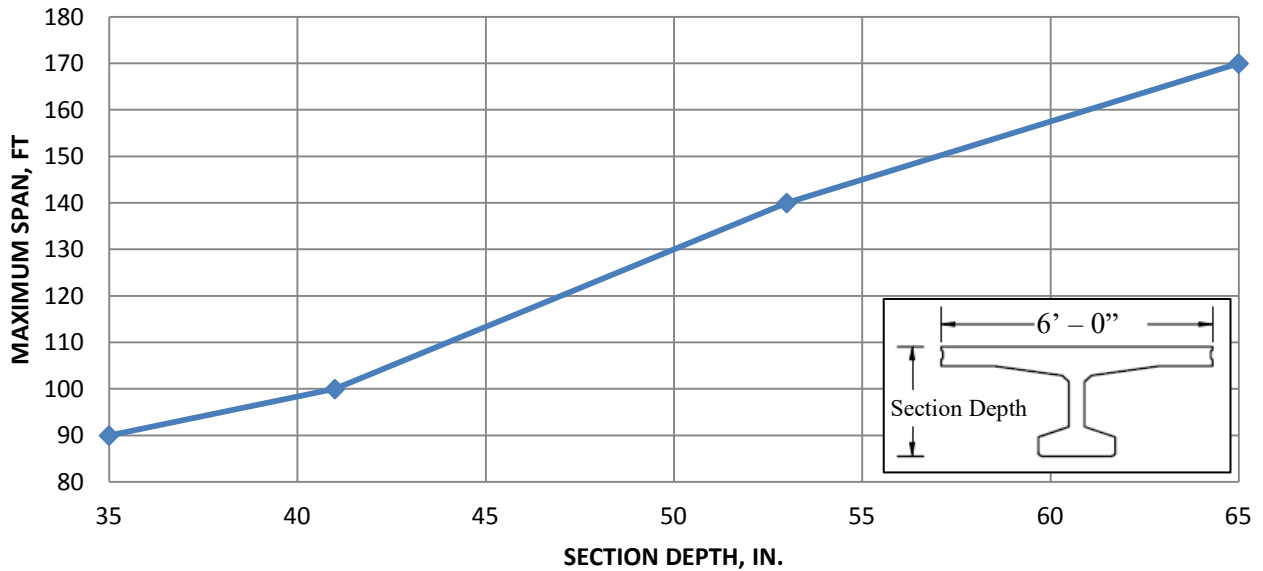


Chart DBT-2
Deck Bulb-Tees

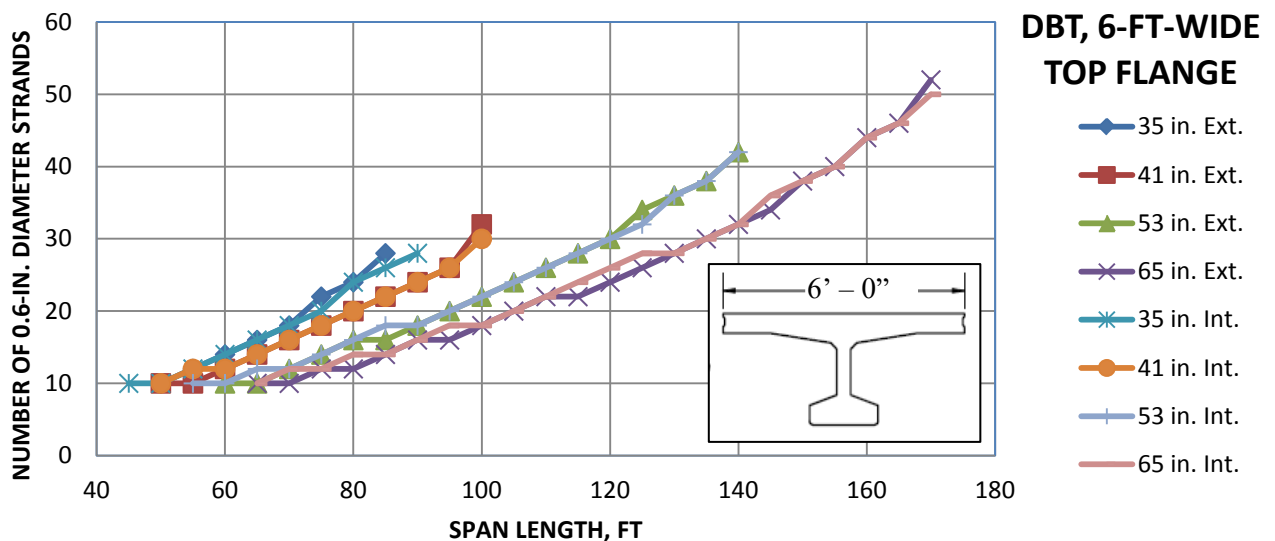


Chart IB-1
AASHTO I-Beams

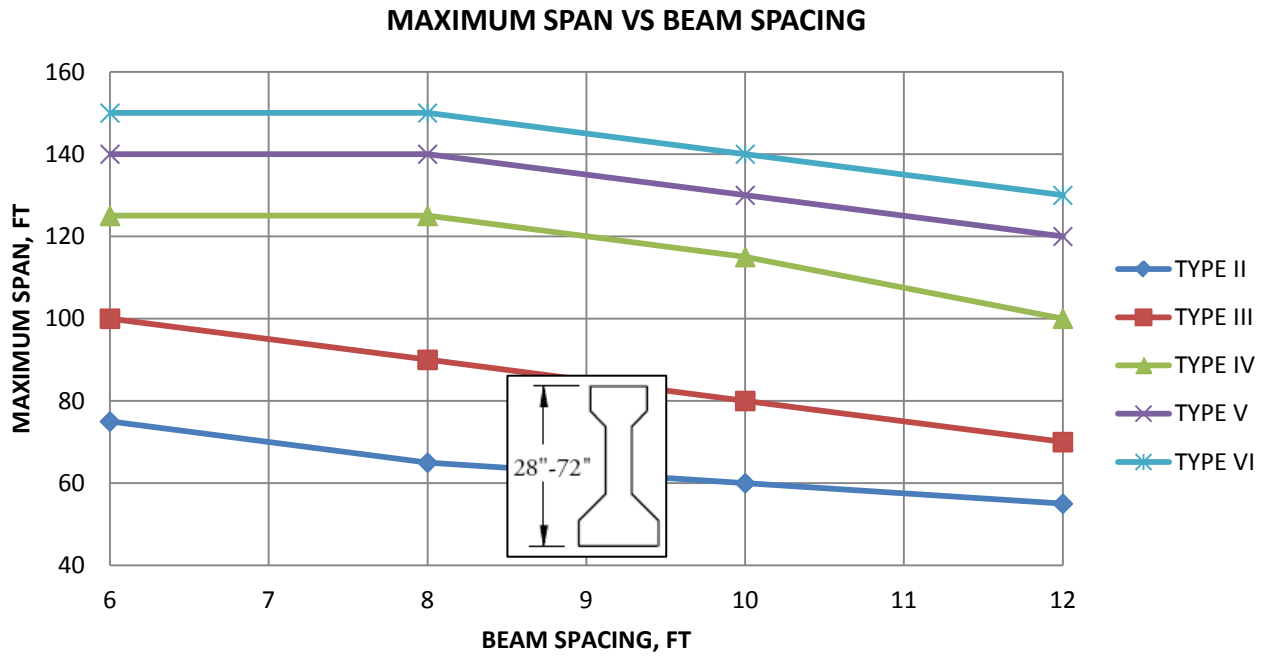


Chart IB-2
AASHTO I-Beams Type II

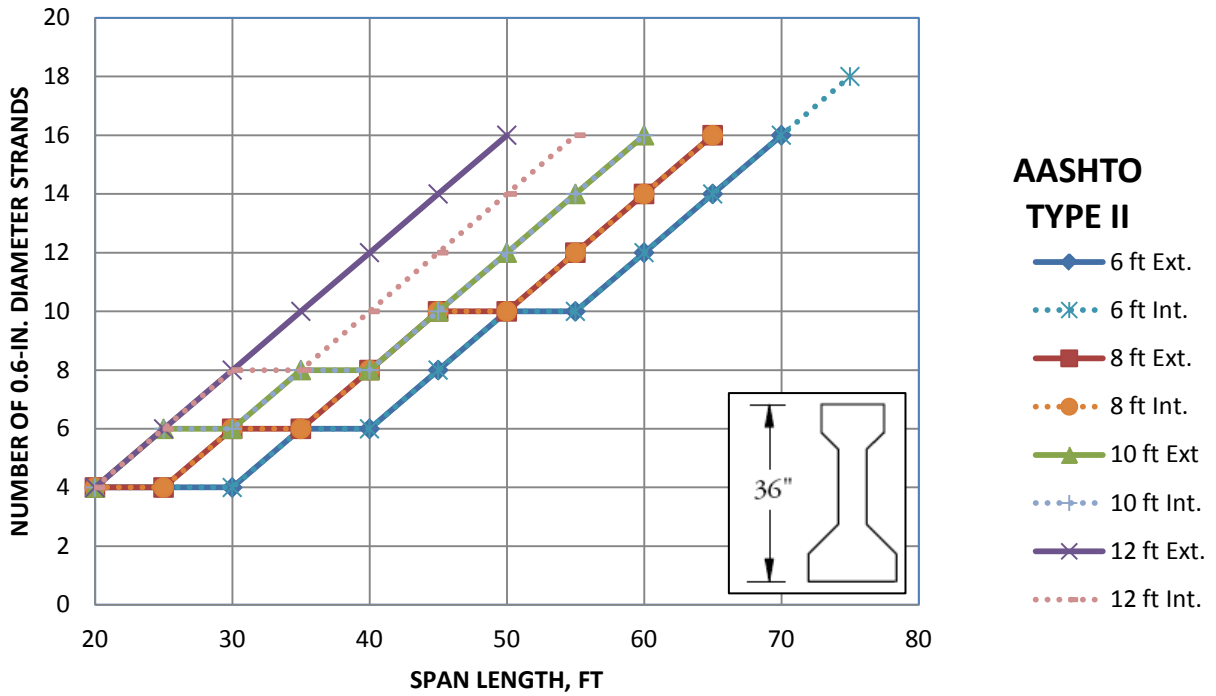


Chart IB-3
AASHTO I-Beams Type III

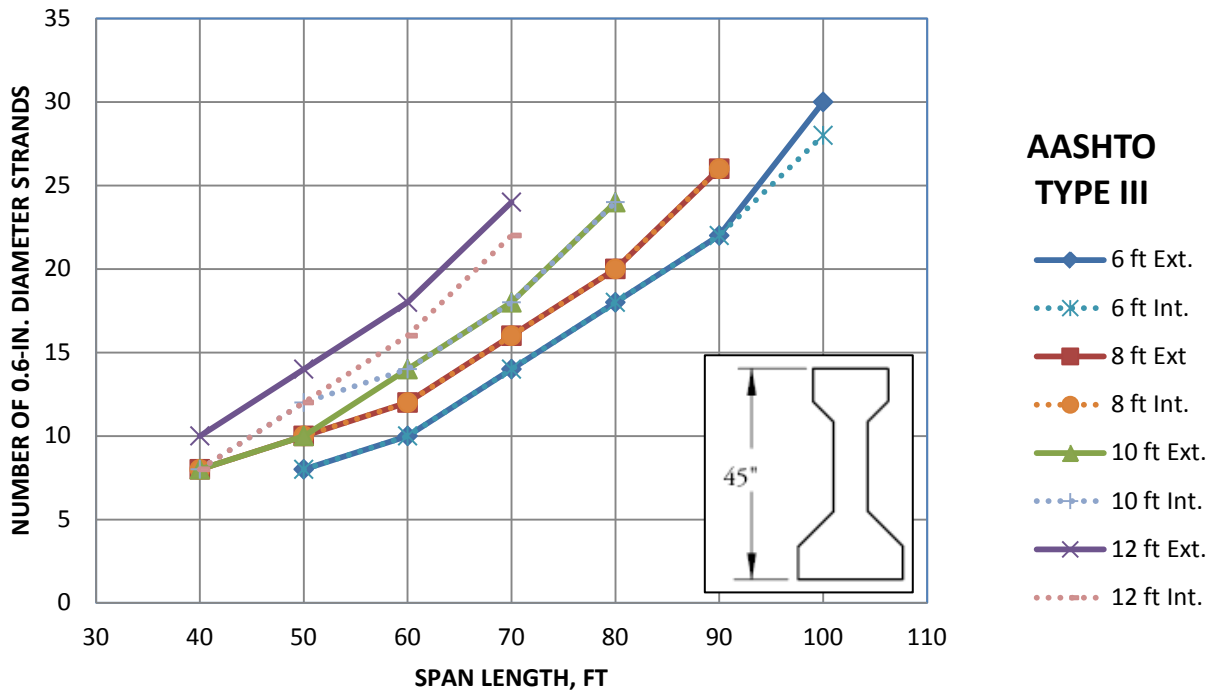
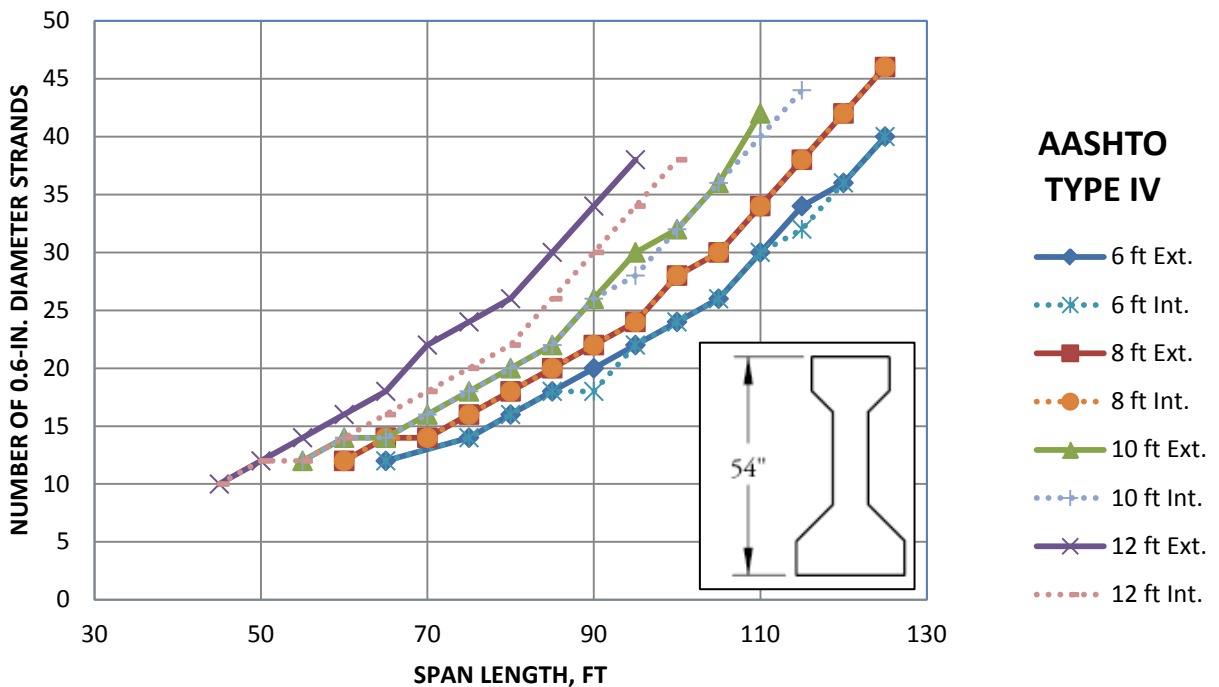


Chart IB-4
AASHTO I-Beams Type IV



PRELIMINARY DESIGN

6.9 Preliminary Design Charts

Chart IB-5
AASHTO I-Beams Type V

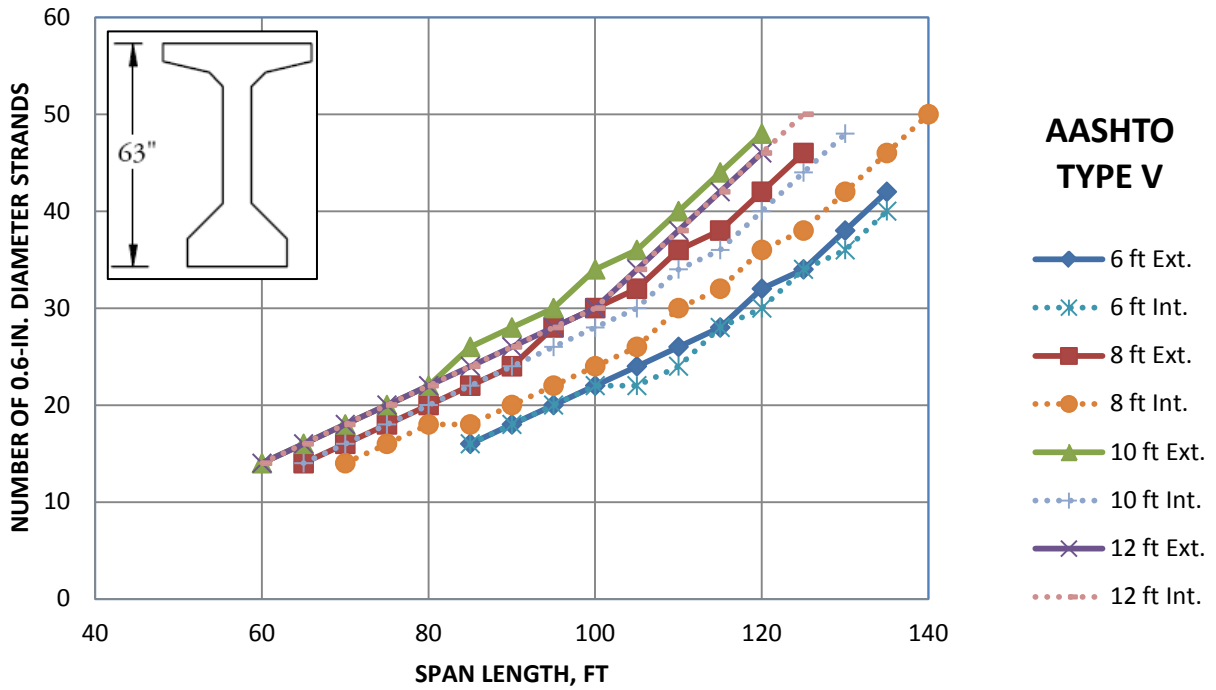


Chart IB-6
AASHTO I-Beams Type VI

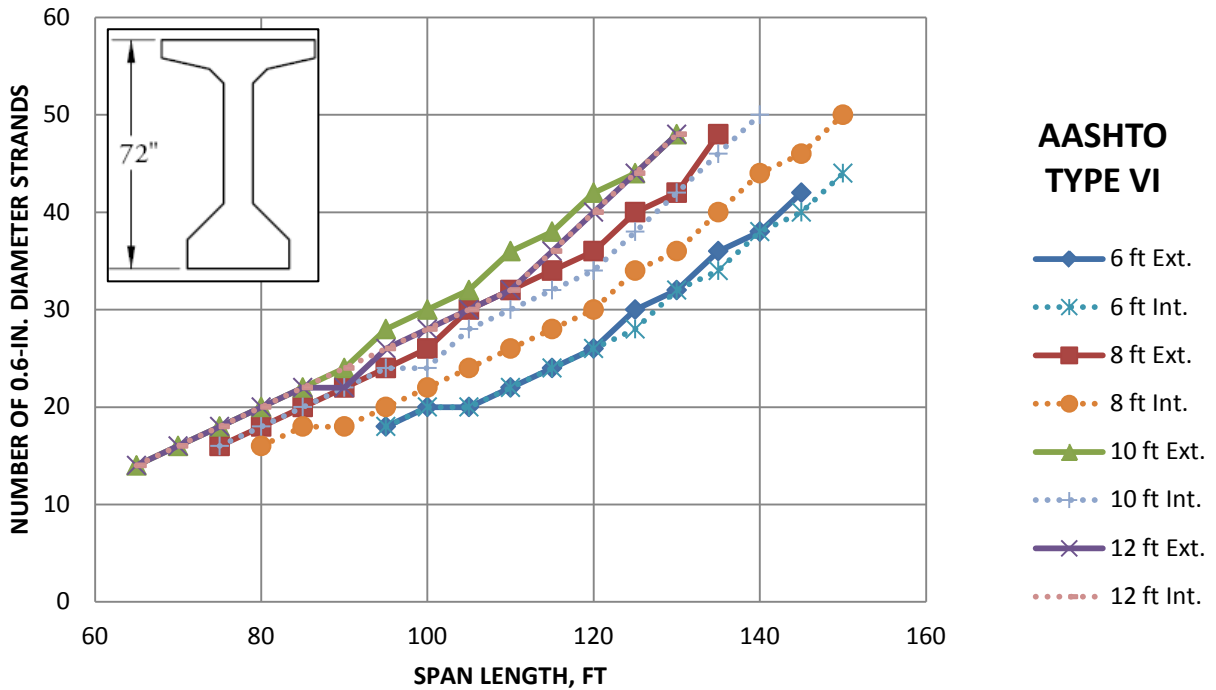


Chart NEXT-1
NEXT Type D Beams

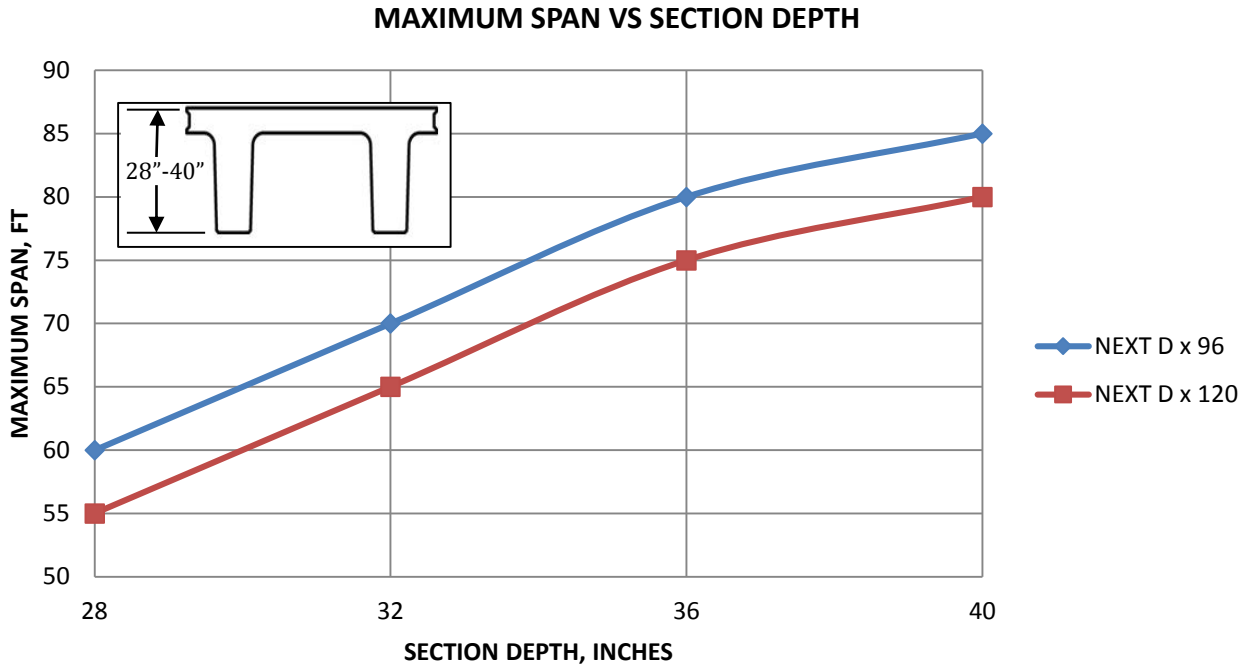


Chart NEXT-2
NEXT Type D x 96 Beams

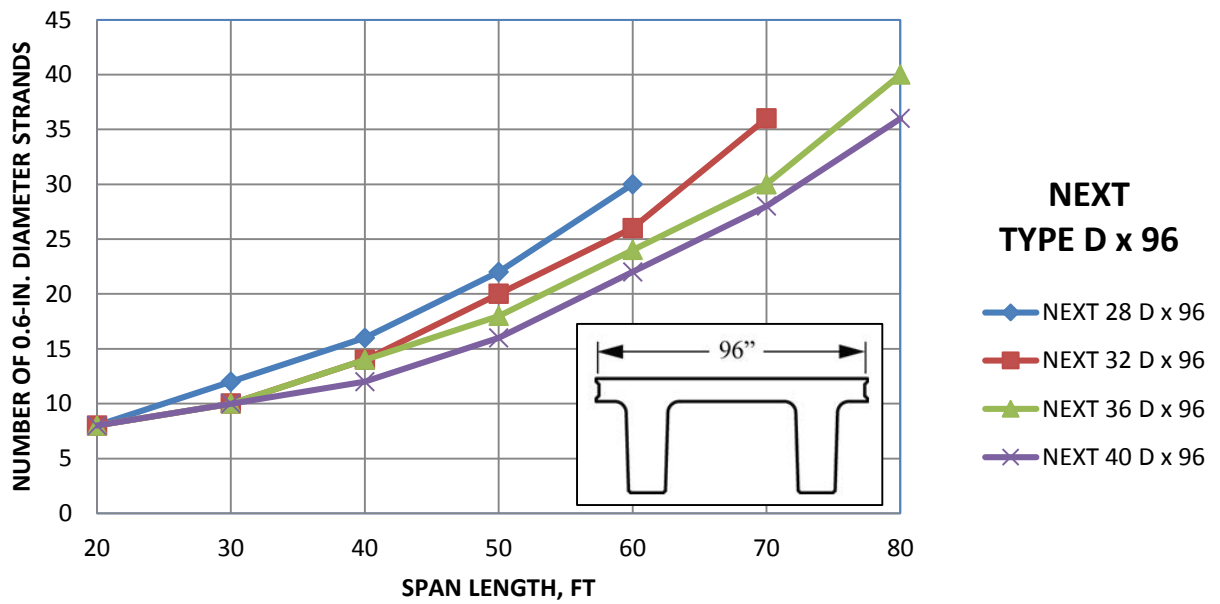


Chart NEXT-3
NEXT Type D x 120 Beams

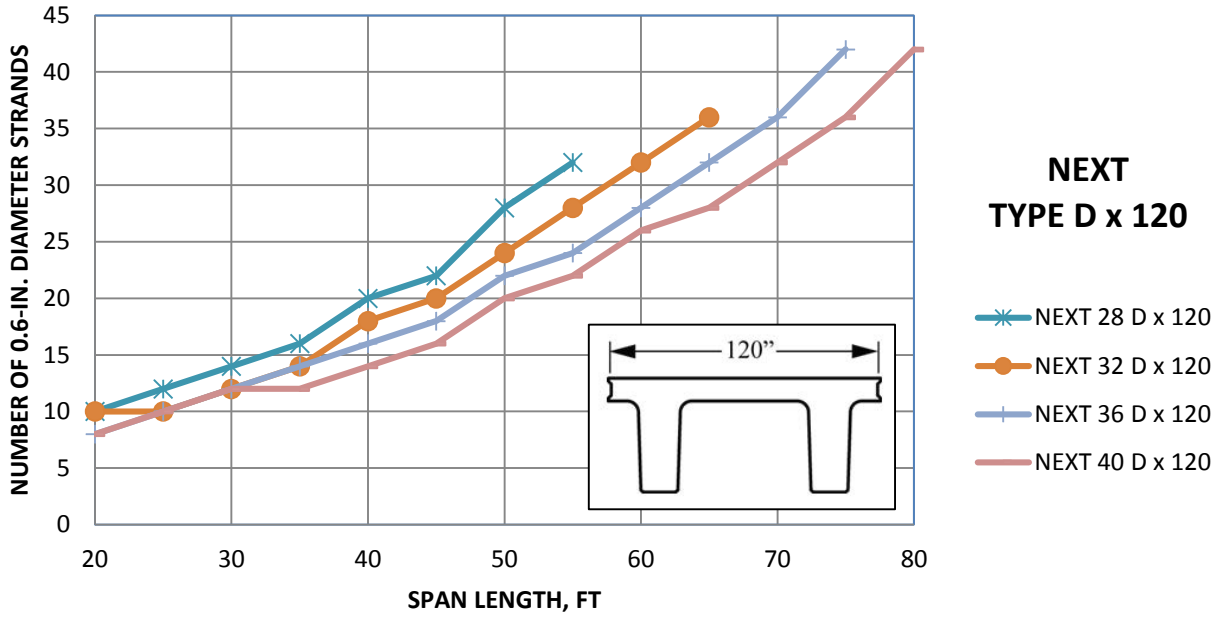


Chart NEXT-4
NEXT Type F Beams

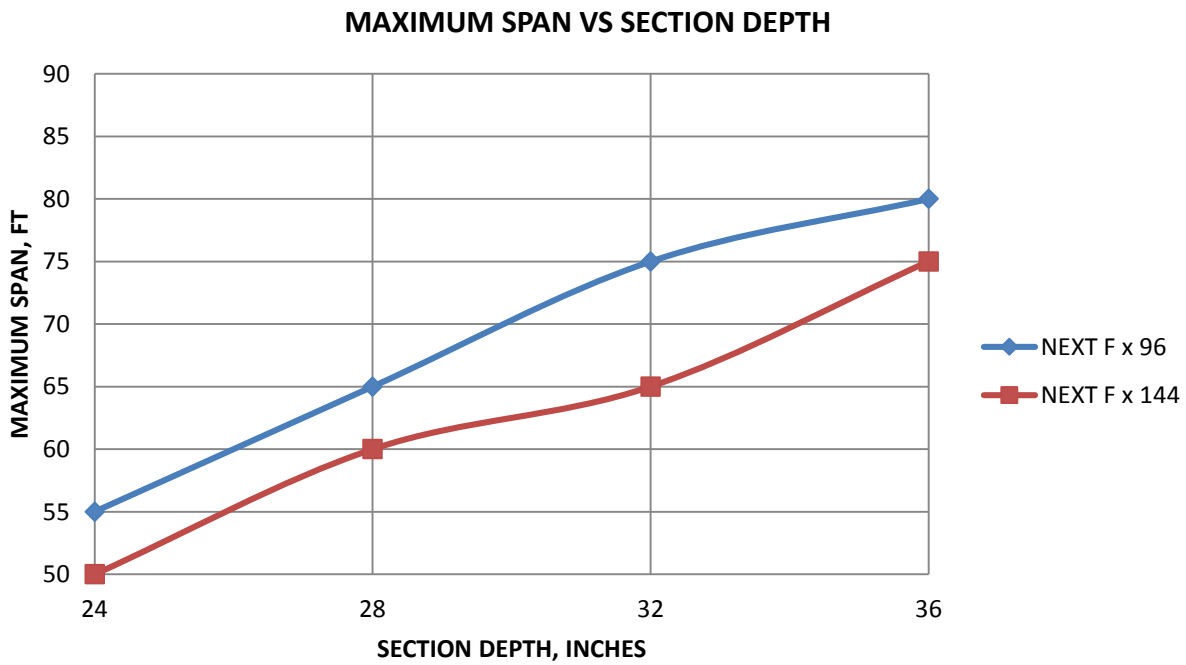


Chart NEXT-5
NEXT Type F x 96 Beams

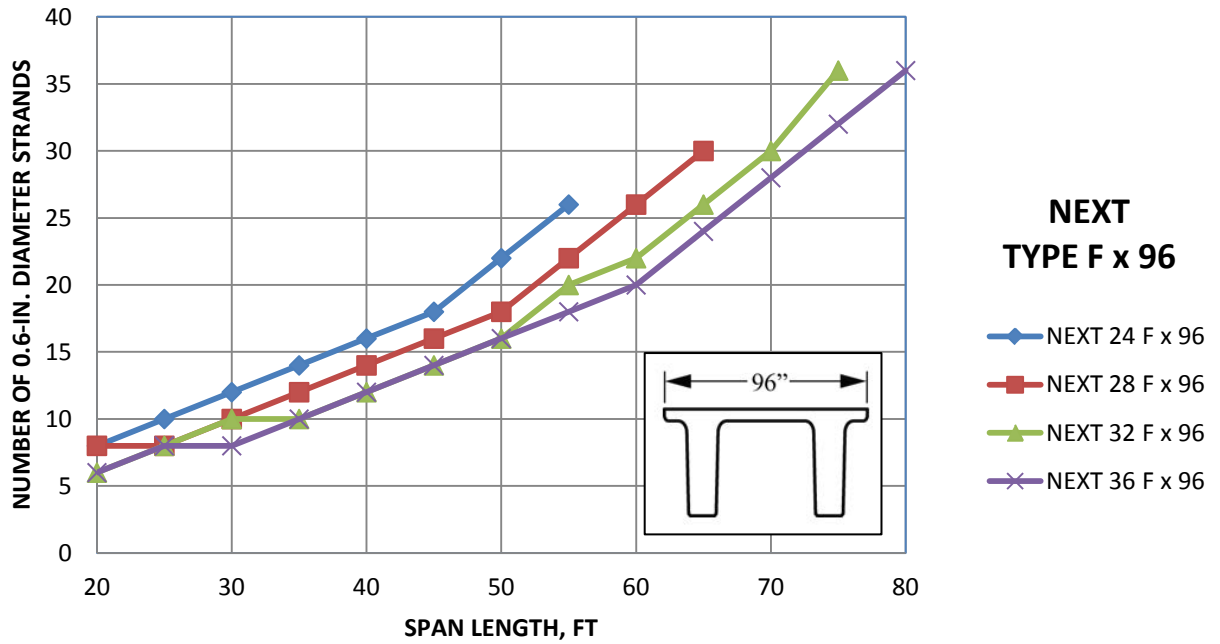


Chart NEXT-6
NEXT Type F x 144 Beams

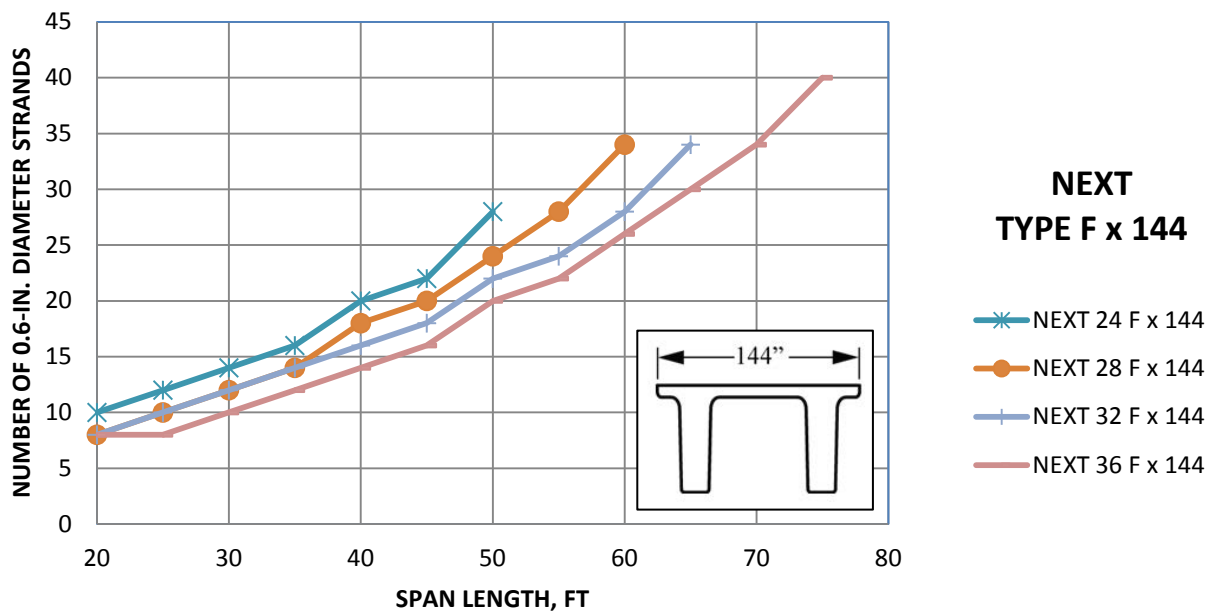


Chart U-1
U-Beams

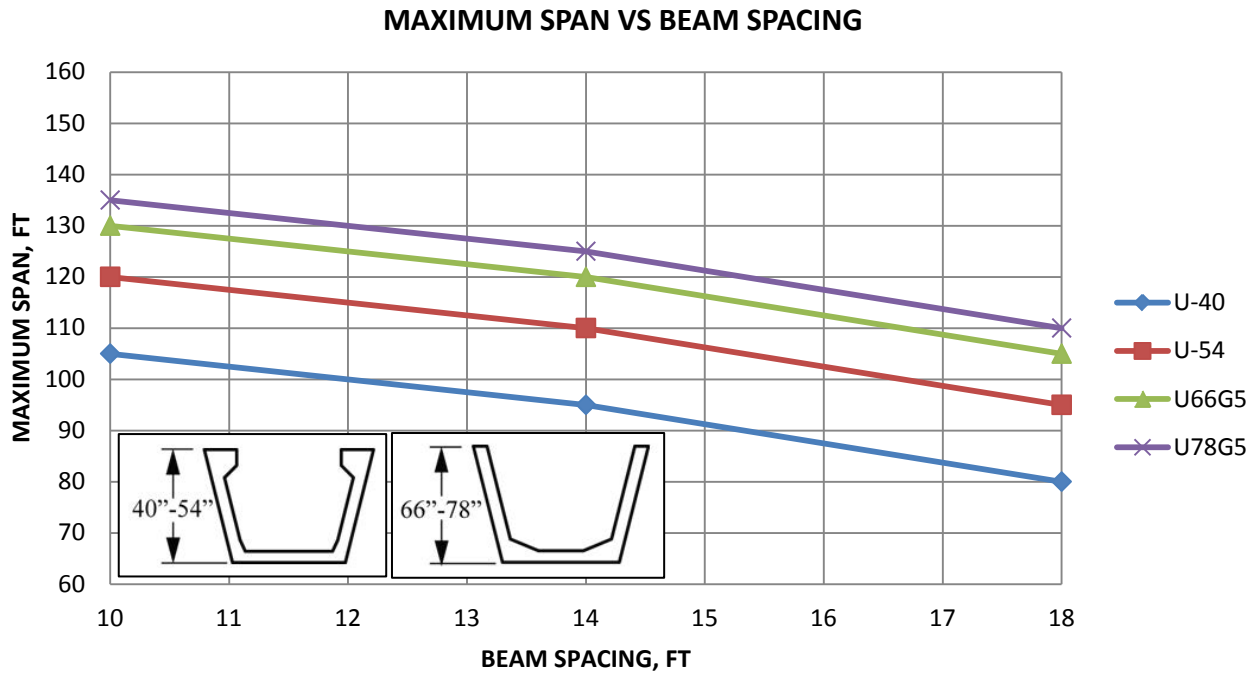


Chart U-2
Texas U-40 Beams

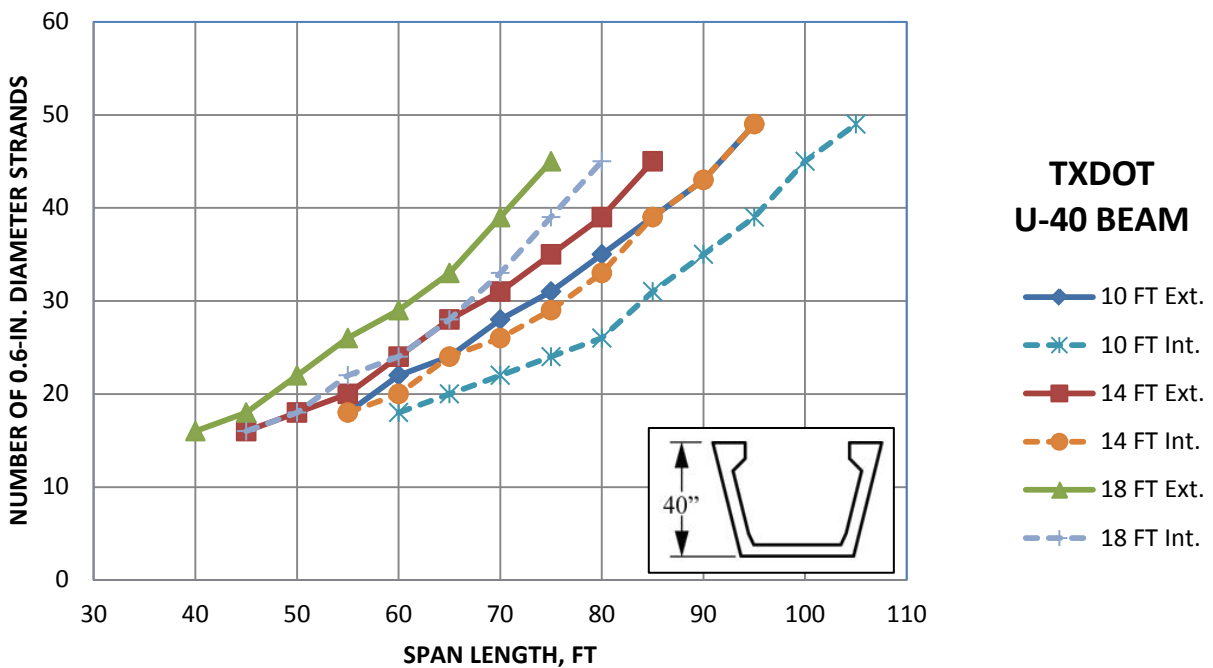


Chart U-3
Texas U-54 Beams

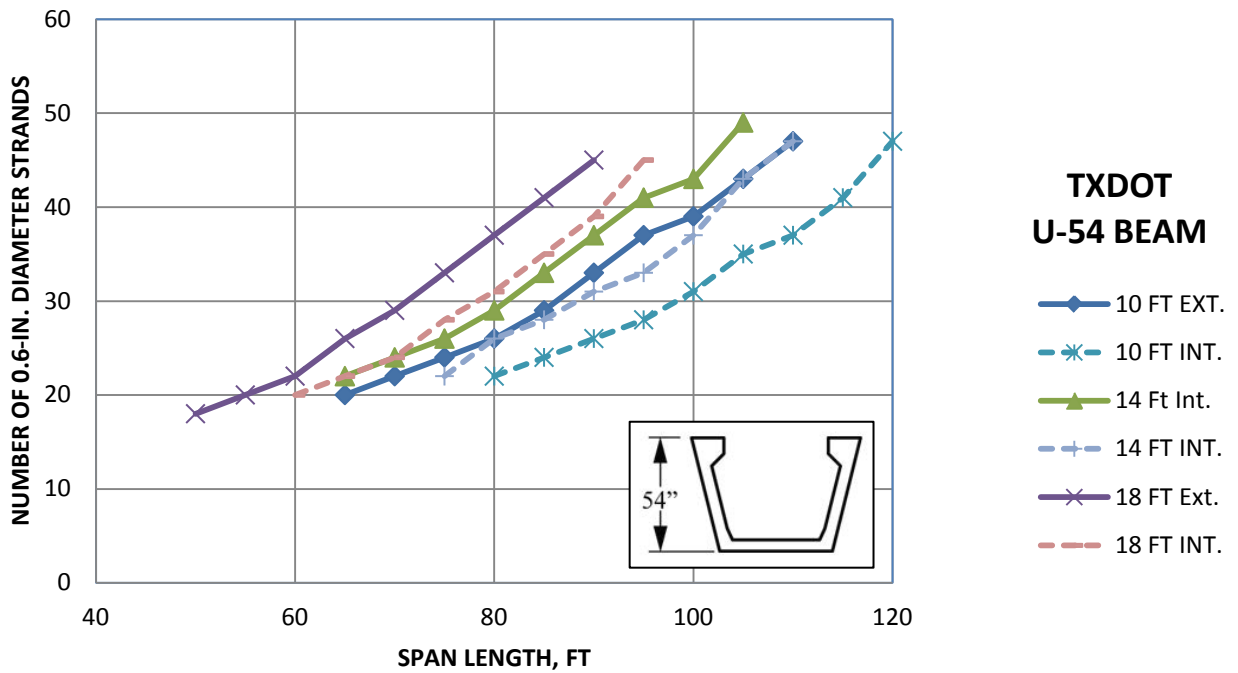
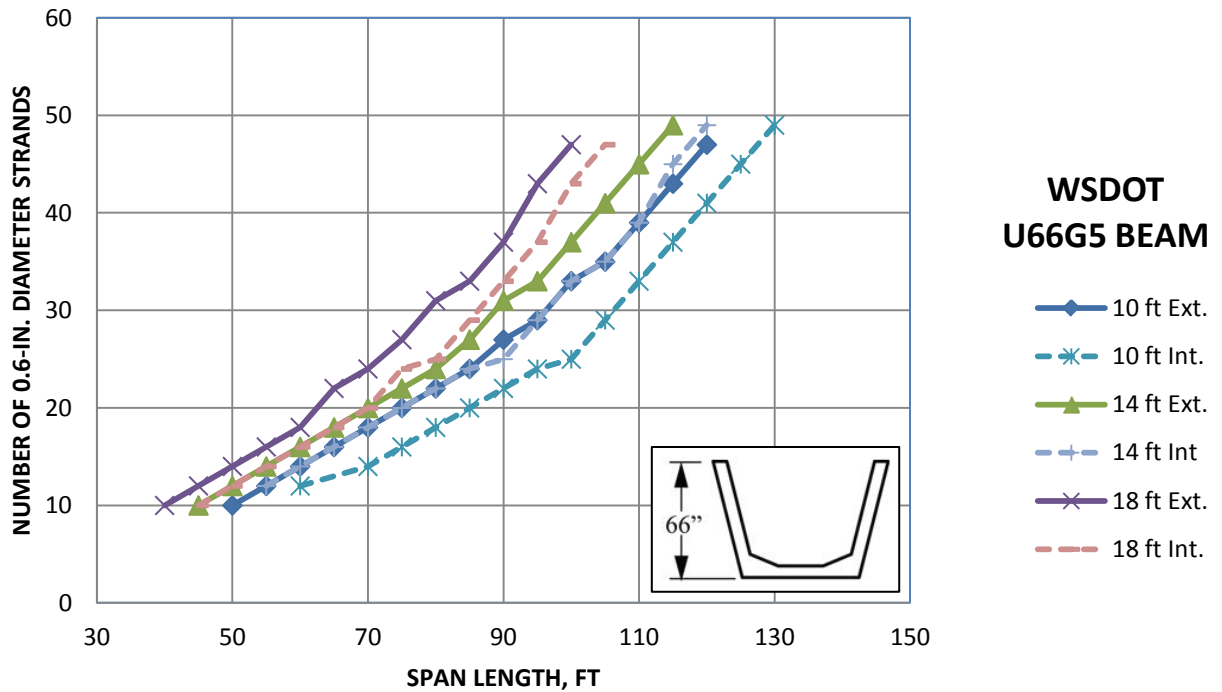


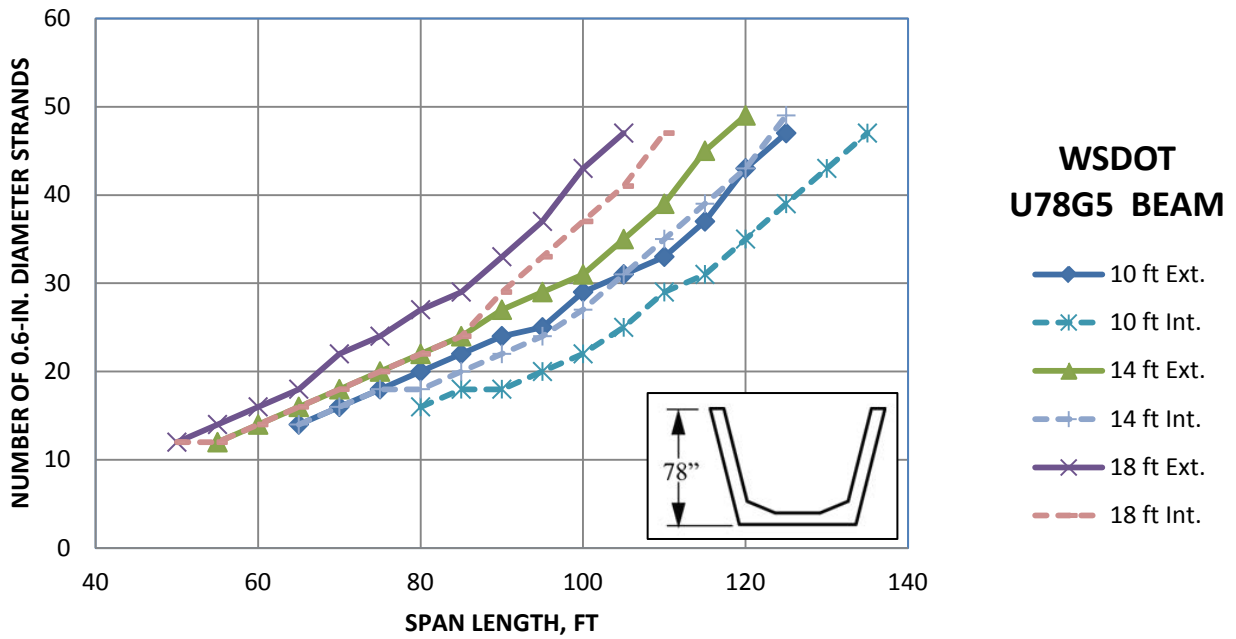
Chart U-4
Washington U66G5 Beams



PRELIMINARY DESIGN

6.9 Preliminary Design Charts

Chart U-5
Washington U78G5 Beams



PRELIMINARY DESIGN

6.10 Preliminary Design Data

6.10 PRELIMINARY DESIGN DATA

This section contains input data and results from computer runs to generate the preliminary design charts presented in **Section 6.9**. These table numbers correspond to the chart numbers in **Section 6.9**.

*Table BB-1**AASHTO Box Beams 48 in. Wide – Maximum Span (ft) vs. Beam Spacing*

Spacing Beam	4 ft	6 ft	8 ft	10 ft	12ft
BIV-48	120	105	100	95	90
BIII-48	115	100	95	90	85
BII-48	100	90	85	80	75

PRELIMINARY DESIGN

6.10 Preliminary Design Data

*A minimum concrete transfer strength of 3.0 ksi is recommended by PCI MNL-116 section 5.3.17.

**Final camber is net deflection after all losses and noncomposite and composite dead loads are applied.

Table BB-2

AASHTO Adjacent Box Beams 48 in. Wide

Spacing ft	Span ft	Slab Thickness in.	f'_{ci} ksi	No. of Strands	Final Camber in.**	f_b @ L/2 ksi	f_t @ L/2 ksi	M_u @ L/2 ft-kips	M_r @ L/2 ft-kips	Control
AASHTO BII Adjacent 48-in.-Wide Exterior Box Beam										
BII	40	6	1.358*	6	0.08	0.059	0.454	817	1,077	Strength
BII	45	6	1.344*	6	-0.02	-0.121	0.610	992	1,077	Strength
BII	50	6	1.813*	8	0.03	-0.053	0.720	1,186	1,414	Strength
BII	55	6	1.800*	8	-0.18	-0.269	0.910	1,393	1,414	Strength
BII	60	6	2.266*	10	-0.18	-0.238	1.051	1,612	1,741	Strength
BII	65	6	2.727*	12	-0.21	-0.229	1.208	1,843	2,058	Strength
BII	70	6	3.185	14	-0.27	-0.240	1.382	2,088	2,365	Strength
BII	75	6	3.178	14	-0.87	-0.517	1.631	2,345	2,365	Stress
BII	80	6	4.091	18	-0.58	-0.326	1.779	2,615	2,951	Stress
BII	85	6	4.540	20	-0.87	-0.399	2.001	2,898	3,231	Stress
BII	90	6	4.986	22	-1.26	-0.493	2.240	3,194	3,502	Stress
BII	95	6	5.612	25	-1.54	-0.517	2.490	3,503	3,873	Stress
BII	100	6	6.409	29	-1.65	-0.479	2.754	3,825	4,327	Stress
AASHTO BIII Adjacent 48-in.-Wide Exterior Box Beam										
BIII	40	6	0.822*	4	-0.02	-0.105	0.414	836	846	Strength
BIII	45	6	1.266*	6	0.04	0.005	0.481	1,015	1,253	Strength
BIII	50	6	1.254*	6	-0.06	-0.158	0.625	1,214	1,253	Strength
BIII	55	6	1.694*	8	-0.02	-0.083	0.720	1,427	1,648	Strength
BIII	60	6	2.130*	10	0.04	-0.025	0.828	1,652	2,033	Strength
BIII	65	6	2.121*	10	-0.21	-0.226	1.009	1,890	2,033	Strength
BIII	70	6	2.554*	12	-0.22	-0.198	1.143	2,142	2,408	Strength
BIII	75	6	2.547*	12	-0.64	-0.424	1.349	2,406	2,408	Stress
BIII	80	6	2.979*	14	-0.75	-0.427	1.508	2,685	2,773	Stress
BIII	85	6	3.407	16	-0.92	-0.447	1.682	2,976	3,128	Stress
BIII	90	6	3.833	18	-1.16	-0.484	1.868	3,281	3,474	Stress
BIII	95	6	4.675	22	-0.88	-0.321	2.015	3,600	4,137	Stress
BIII	100	6	4.885	23	-1.56	-0.502	2.256	3,932	4,298	Stress
BIII	105	6	5.653	27	-1.53	-0.416	2.467	4,277	4,879	Stress
BIII	110	6	6.409	31	-1.54	-0.359	2.693	4,637	5,427	Stress
BIII	115	6	6.789	33	-2.33	-0.503	2.965	5,009	5,690	Stress
AASHTO BIV Adjacent 48-in.-Wide Exterior Box Beam										
BIV	40	6	0.799*	4	0.00	-0.061	0.373	845	905	Strength
BIV	45	6	1.228*	6	0.06	0.059	0.429	1,027	1,340	Strength
BIV	50	6	1.215*	6	-0.02	-0.088	0.561	1,229	1,340	Strength
BIV	55	6	1.639*	8	0.04	0.002	0.643	1,444	1,765	Strength
BIV	60	6	1.626*	8	-0.12	-0.168	0.798	1,672	1,765	Strength
BIV	65	6	2.046*	10	-0.09	-0.104	0.903	1,914	2,179	Strength
BIV	70	6	2.033*	10	-0.37	-0.297	1.080	2,169	2,179	Stress
BIV	75	6	2.447*	12	-0.40	-0.258	1.209	2,437	2,583	Strength
BIV	80	6	2.857*	14	-0.45	-0.233	1.349	2,719	2,977	Strength
BIV	85	6	3.263	16	-0.53	-0.222	1.502	3,015	3,361	Strength
BIV	90	6	3.250	16	-1.17	-0.459	1.724	3,325	3,361	Stress
BIV	95	6	3.651	18	-1.40	-0.473	1.900	3,648	3,735	Stress
BIV	100	6	4.047	20	-1.71	-0.499	2.087	3,985	4,100	Stress
BIV	105	6	4.640	23	-1.77	-0.426	2.259	4,336	4,630	Stress
BIV	110	6	5.001	25	-2.32	-0.497	2.487	4,701	4,954	Stress
BIV	115	6	5.724	29	-2.28	-0.376	2.689	5,079	5,574	Stress
BIV	120	6	6.075	31	-3.06	-0.474	2.942	5,472	5,872	Stress

PRELIMINARY DESIGN

*A minimum concrete transfer strength of 3.0 ksi is recommended by PCI MNL-116 section 5.3.17.

6.10 Preliminary Design Data

**Final camber is net deflection after all losses and noncomposite and composite dead loads are applied.

Table BB-3
AASHTO Spread Box Beams BII-48

Spacing ft	Span ft	Slab Thickness in.	f'_{ci} ksi	No. of Strands	Camber in.	f_b @ L/2 ksi	f_t @ L/2 ksi	M_u @ L/2 ft-kips	M_r @ L/2 ft-kips	Control
AASHTO BII 48-in.-Wide Exterior Beam										
6	45	8	2.300*	10	0.21	0.072	0.651	1,556	1,883	Strength
6	50	8	2.283*	10	0.05	-0.207	0.871	1,873	1,883	Strength
6	55	8	2.738*	12	0.06	-0.241	1.046	2,210	2,238	Strength
6	60	8	3.187	14	0.03	-0.299	1.242	2,567	2,586	Stress
6	65	8	4.085	18	0.33	-0.124	1.398	2,944	3,262	Strength
6	70	8	4.518	20	0.24	-0.232	1.636	3,342	3,590	Strength
6	75	8	4.945	22	0.06	-0.363	1.894	3,760	3,912	Stress
6	80	8	5.550	25	-0.03	-0.417	2.168	4,197	4,363	Stress
6	85	8	6.324	29	0.00	-0.400	2.457	4,655	4,930	Stress
8	35	8	2.334*	10	0.28	0.240	0.39	1,572	1,906	Strength
8	40	8	2.788*	12	0.39	0.229	0.523	1,916	2,271	Strength
8	45	8	3.237	14	0.51	0.169	0.687	2,328	2,630	Strength
8	50	8	3.680	16	0.62	0.068	0.878	2,790	2,985	Strength
8	55	8	4.118	18	0.71	-0.060	1.093	3,277	3,333	Strength
8	60	8	4.994	22	1.08	0.034	1.272	3,791	4,016	Strength
8	65	8	5.598	25	1.25	-0.051	1.529	4,329	4,495	Strength
8	70	8	6.372	29	1.54	-0.069	1.804	4,893	5,104	Strength
10	35	8	2.334*	10	0.25	0.116	0.422	1,785	1,920	Strength
10	40	8	2.788*	12	0.34	0.076	0.567	2,174	2,291	Strength
10	45	8	3.237	14	0.43	-0.019	0.744	2,641	2,657	Strength
10	50	8	4.134	18	0.73	0.097	0.890	3,165	3,377	Strength
10	55	8	4.567	20	0.81	-0.075	1.123	3,717	3,731	Strength
10	60	8	5.614	25	1.27	0.068	1.318	4,298	4,577	Strength
10	65	8	6.388	29	1.56	0.028	1.592	4,908	5,212	Strength
12	40	8	2.317*	10	0.15	-0.055	0.608	1,843	1,930	Strength
12	45	8	2.771*	12	0.18	-0.127	0.785	2,249	2,304	Strength
12	50	8	3.680	16	0.40	0.020	0.929	2,705	3,043	Strength
12	55	8	4.118	18	0.39	-0.127	1.163	3,189	3,407	Strength
12	60	8	4.550	20	0.31	-0.304	1.423	3,701	3,767	Stress
12	65	8	5.197	23	0.32	-0.387	1.680	4,241	4,301	Strength
12	70	8	5.979	27	0.35	-0.428	1.983	4,810	4,961	Stress
12	75	8	6.745	31	0.31	-0.506	2.314	5,406	5,608	Stress

PRELIMINARY DESIGN

6.10 Preliminary Design Data

*A minimum concrete transfer strength of 3.0 ksi is recommended by PCI MNL-116 section 5.3.17.

**Final camber is net deflection after all losses and noncomposite and composite dead loads are applied.

Table BB-3 (continued)

Spacing ft	Span ft	Slab Thickness in.	f'_{ci} ksi	No. of Strands	Final Camber in.**	f_b @ L/2 ksi	f_t @ L/2 ksi	M_u @ L/2 ft-kips	M_r @ L/2 ft-kips	Control
AASHTO BII 48-in.-Wide Interior Beam										
6	50	8	2.283*	10	0.05	-0.13	0.836	1,726	1,883	Strength
6	55	8	2.738*	12	0.06	-0.138	0.999	2,015	2,238	Strength
6	60	8	3.187	14	0.03	-0.168	1.183	2,319	2,586	Strength
6	65	8	3.630	16	-0.04	-0.221	1.386	2,640	2,928	Strength
6	70	8	4.069	18	-0.19	-0.294	1.608	2,976	3,262	Stress
6	75	8	4.501	20	-0.43	-0.390	1.850	3,328	3,590	Stress
6	80	8	4.929	22	-0.79	-0.506	2.111	3,697	3,912	Stress
6	85	8	5.931	27	-0.53	-0.325	2.353	4,083	4,649	Stress
6	90	8	6.308	29	-1.23	-0.509	2.678	4,485	4,930	Stress
8	45	8	2.300*	10	0.14	-0.055	0.703	1,730	1,906	Strength
8	50	8	2.754*	12	0.16	-0.080	0.866	2,052	2,271	Strength
8	55	8	3.204	14	0.16	-0.129	1.052	2,392	2,630	Strength
8	60	8	3.647	16	0.12	-0.202	1.259	2,750	2,985	Strength
8	65	8	4.085	18	0.00	-0.298	1.488	3,126	3,333	Stress
8	70	8	4.518	20	-0.2	-0.418	1.738	3,520	3,677	Stress
8	75	8	5.165	23	-0.28	-0.438	1.981	3,933	4,183	Stress
8	80	8	5.947	27	-0.32	-0.409	2.264	4,364	4,802	Stress
8	85	8	6.713	31	-0.44	-0.411	2.571	4,815	5,402	Stress
10	40	8	2.317*	10	0.2	0.066	0.555	1,658	1,920	Strength
10	45	8	2.771*	12	0.25	0.039	0.712	1,990	2,291	Strength
10	50	8	3.220	14	0.28	-0.022	0.895	2,360	2,657	Strength
10	55	8	3.664	16	0.27	-0.110	1.102	2,748	3,019	Strength
10	60	8	4.101	18	0.2	-0.223	1.332	3,157	3,377	Strength
10	65	8	4.534	20	0.05	-0.362	1.586	3,585	3,731	Stress
10	70	8	4.961	22	-0.21	-0.527	1.864	4,034	4,080	Stress
10	75	8	5.963	27	-0.02	-0.397	2.127	4,504	4,897	Stress
10	80	8	6.729	31	-0.12	-0.424	2.443	4,995	5,524	Stress
12	40	8	2.317*	10	0.15	-0.059	0.609	1,851	1,930	Strength
12	45	8	2.771*	12	0.18	-0.112	0.781	2,219	2,304	Strength
12	50	8	3.220	14	0.18	-0.202	0.982	2,628	2,675	Strength
12	55	8	4.118	18	0.39	-0.065	1.148	3,058	3,407	Strength
12	60	8	4.550	20	0.31	-0.213	1.400	3,509	3,767	Strength
12	65	8	4.978	22	0.14	-0.389	1.679	3,982	4,124	Stress
12	70	8	5.582	25	-0.01	-0.492	1.978	4,477	4,633	Stress
12	75	8	6.356	29	-0.11	-0.528	2.298	4,994	5,286	Stress

PRELIMINARY DESIGN

*A minimum concrete transfer strength of 3.0 ksi is recommended by PCI MNL-116 section 5.3.17.

6.10 Preliminary Design Data

**Final camber is net deflection after all losses and noncomposite and composite dead loads are applied.

Table BB-4
AASHTO Spread Box Beams BIII-48

Spacing ft	Span ft	Slab Thickness in.	f'_{ci} ksi	No. of Strands	Final Camber in.**	f_b @ L/2 ksi	f_t @ L/2 ksi	M_u @ L/2 ft-kips	M_r @ L/2 ft-kips	Control
AASHTO BIII 48-in.-Wide Exterior Beam										
6	50	8	2.147*	10	0.16	0.004	0.681	1,897	2,176	Strength
6	55	8	2.573*	12	0.22	0.010	0.818	2,239	2,589	Strength
6	60	8	2.995*	14	0.27	-0.004	0.972	2,602	2,996	Strength
6	65	8	2.981*	14	0.00	-0.282	1.201	2,986	2,996	Strength
6	70	8	3.399	16	-0.05	-0.332	1.388	3,390	3,395	Stress
6	75	8	4.232	20	0.24	-0.164	1.533	3,814	4,173	Strength
6	80	8	4.635	22	0.13	-0.255	1.754	4,260	4,552	Strength
6	85	8	4.827	23	-0.31	-0.480	2.019	4,726	4,740	Stress
6	90	8	5.574	27	-0.20	-0.414	2.254	5,212	5,433	Stress
6	95	8	6.307	31	-0.13	-0.374	2.507	5,720	6,102	Stress
8	40	8	2.175*	10	0.25	0.142	0.453	1,931	2,199	Strength
8	45	8	2.602*	12	0.34	0.129	0.581	2,347	2,622	Strength
8	50	8	3.023	14	0.44	0.083	0.731	2,814	3,040	Strength
8	55	8	3.440	16	0.54	0.014	0.901	3,307	3,452	Strength
8	60	8	3.852	18	0.62	-0.077	1.089	3,826	3,860	Strength
8	65	8	4.676	22	0.97	0.044	1.241	4,370	4,658	Strength
8	70	8	5.250	25	1.16	0.004	1.458	4,941	5,224	Strength
8	75	8	5.615	27	1.13	-0.173	1.722	5,538	5,589	Strength
8	80	8	6.347	31	1.41	-0.166	1.969	6,160	6,304	Strength
10	35	8	2.189*	10	0.23	0.265	0.317	1,797	2,213	Strength
10	40	8	2.175*	10	0.21	0.018	0.489	2,190	2,213	Strength
10	45	8	3.037	14	0.44	0.223	0.568	2,661	3,067	Strength
10	50	8	3.454	16	0.55	0.143	0.732	3,189	3,488	Strength
10	55	8	3.866	18	0.64	0.038	0.916	3,747	3,904	Strength
10	60	8	4.689	22	0.97	0.143	1.064	4,334	4,723	Strength
10	65	8	5.264	25	1.16	0.085	1.281	4,949	5,307	Strength
10	70	8	5.628	27	1.17	-0.110	1.545	5,594	5,685	Strength
10	75	8	6.360	31	1.43	-0.125	1.794	6,269	6,429	Strength
12	40	8	2.175*	10	0.19	0.128	0.461	1,864	2,223	Strength
12	45	8	2.602*	12	0.25	0.107	0.597	2,269	2,656	Strength
12	50	8	3.023	14	0.30	0.049	0.758	2,730	3,085	Strength
12	55	8	3.440	16	0.33	-0.034	0.940	3,219	3,511	Strength
12	60	8	3.852	18	0.33	-0.141	1.143	3,736	3,933	Strength
12	65	8	4.259	20	0.27	-0.274	1.369	4,283	4,352	Strength
12	70	8	4.868	23	0.32	-0.315	1.587	4,857	4,973	Strength
12	75	8	5.615	27	0.42	-0.304	1.837	5,461	5,750	Strength
12	80	8	5.976	29	0.10	-0.529	2.145	6,093	6,134	Stress

PRELIMINARY DESIGN

6.10 Preliminary Design Data

*A minimum concrete transfer strength of 3.0 ksi is recommended by PCI MNL-116 section 5.3.17.

**Final camber is net deflection after all losses and noncomposite and composite dead loads are applied.

Table BB-4 (continued)

Spacing ft	Span ft	Slab Thickness in.	f'_{ci} ksi	No. of Strands	Final Camber in.**	f_b @ L/2 ksi	f_t @ L/2 ksi	M_u @ L/2 ft-kips	M_r @ L/2 ft-kips	Control
AASHTO BIII 48-in.-Wide Interior Beam										
6	50	8	2.147*	10	0.16	0.058	0.654	1,770	2,176	Strength
6	55	8	2.132*	10	0.00	-0.166	0.842	2,067	2,176	Strength
6	60	8	2.559*	12	0.01	-0.156	0.984	2,379	2,589	Strength
6	65	8	2.981*	14	0.00	-0.163	1.142	2,708	2,996	Strength
6	70	8	3.399	16	-0.05	-0.189	1.316	3,054	3,395	Strength
6	75	8	3.811	18	-0.15	-0.233	1.506	3,416	3,787	Strength
6	80	8	4.218	20	-0.31	-0.294	1.711	3,795	4,173	Strength
6	85	8	4.621	22	-0.56	-0.373	1.933	4,191	4,552	Stress
6	90	8	5.196	25	-0.70	-0.371	2.161	4,604	5,090	Stress
6	95	8	5.561	27	-1.22	-0.503	2.433	5,035	5,433	Stress
6	100	8	6.293	31	-1.30	-0.446	2.685	5,483	6,102	Stress
8	50	8	2.147*	10	0.08	-0.117	0.731	2,101	2,199	Strength
8	55	8	2.573*	12	0.10	-0.122	0.875	2,449	2,622	Strength
8	60	8	2.995*	14	0.11	-0.146	1.036	2,816	3,040	Strength
8	65	8	3.412	16	0.08	-0.190	1.215	3,201	3,452	Strength
8	70	8	3.825	18	0.00	-0.254	1.411	3,605	3,860	Strength
8	75	8	4.232	20	-0.14	-0.337	1.625	4,028	4,261	Stress
8	80	8	4.635	22	-0.37	-0.439	1.856	4,470	4,658	Stress
8	85	8	5.210	25	-0.51	-0.462	2.095	4,931	5,224	Stress
8	90	8	5.949	29	-0.52	-0.413	2.344	5,413	5,949	Stress
8	95	8	6.674	33	-0.59	-0.389	2.611	5,913	6,654	Stress
10	45	8	2.161*	10	0.15	-0.019	0.603	2,035	2,213	Strength
10	50	8	2.588*	12	0.19	-0.034	0.744	2,413	2,642	Strength
10	55	8	3.009	14	0.21	-0.070	0.904	2,810	3,067	Strength
10	60	8	3.426	16	0.21	-0.127	1.084	3,228	3,488	Strength
10	65	8	3.838	18	0.16	-0.206	1.283	3,666	3,904	Strength
10	70	8	4.246	20	0.05	-0.306	1.501	4,125	4,315	Stress
10	75	8	4.648	22	-0.13	-0.426	1.738	4,606	4,723	Stress
10	80	8	5.223	25	-0.25	-0.469	1.985	5,108	5,307	Stress
10	85	8	5.963	29	-0.27	-0.442	2.242	5,632	6,059	Stress
10	90	8	6.688	33	-0.34	-0.441	2.521	6,177	6,794	Stress
12	40	8	2.175*	10	0.19	0.118	0.464	1,891	2,223	Strength
12	45	8	2.602*	12	0.25	0.108	0.597	2,267	2,656	Strength
12	50	8	3.023	14	0.3	0.067	0.753	2,685	3,085	Strength
12	55	8	3.440	16	0.33	0.003	0.929	3,124	3,511	Strength
12	60	8	3.852	18	0.33	-0.083	1.126	3,585	3,933	Strength
12	65	8	4.259	20	0.27	-0.191	1.344	4,068	4,352	Strength
12	70	8	4.662	22	0.14	-0.322	1.583	4,574	4,767	Stress
12	75	8	5.237	25	0.08	-0.377	1.833	5,103	5,364	Stress
12	80	8	5.976	29	0.10	-0.362	2.095	5,654	6,134	Stress
12	85	8	6.701	33	0.06	-0.376	2.380	6,230	6,890	Stress

PRELIMINARY DESIGN

*A minimum concrete transfer strength of 3.0 ksi is recommended by PCI MNL-116 section 5.3.17.

6.10 Preliminary Design Data

**Final camber is net deflection after all losses and noncomposite and composite dead loads are applied.

Table BB-5
AASHTO Spread Box Beams BIV-48

Spacing ft	Span ft	Slab Thickness in.	f'_{ci} ksi	No. of Strands	Final Camber in.**	f_b @ L/2 ksi	f_t @ L/2 ksi	M_u @ L/2 ft-kips	M_r @ L/2 ft-kips	Control
AASHTO BIV 48-in.-Wide Exterior Beam										
6	50	8	2.085*	10	0.18	0.079	0.608	1,909	2,322	Strength
6	55	8	2.072*	10	0.06	-0.143	0.790	2,254	2,322	Strength
6	60	8	2.486*	12	0.09	-0.138	0.926	2,620	2,765	Strength
6	65	8	2.896*	14	0.11	-0.152	1.078	3,006	3,200	Strength
6	70	8	3.302	16	0.11	-0.184	1.245	3,414	3,629	Strength
6	75	8	3.702	18	0.07	-0.233	1.428	3,842	4,050	Strength
6	80	8	4.098	20	-0.02	-0.299	1.626	4,291	4,465	Strength
6	85	8	4.490	22	-0.17	-0.383	1.839	4,761	4,873	Stress
6	90	8	5.051	25	-0.20	-0.388	2.057	5,252	5,454	Stress
6	95	8	5.408	27	-0.56	-0.523	2.317	5,764	5,826	Stress
6	100	8	6.124	31	-0.50	-0.472	2.555	6,296	6,552	Stress
8	40	8	2.111*	10	0.24	0.206	0.401	1,939	2,346	Strength
8	45	8	2.526*	12	0.34	0.208	0.515	2,357	2,798	Strength
8	50	8	2.935*	14	0.44	0.181	0.65	2,826	3,245	Strength
8	55	8	3.340	16	0.55	0.133	0.803	3,322	3,686	Strength
8	60	8	3.741	18	0.65	0.064	0.973	3,843	4,123	Strength
8	65	8	4.136	20	0.74	-0.025	1.160	4,391	4,554	Strength
8	70	8	4.528	22	0.80	-0.133	1.364	4,965	4,980	Strength
8	75	8	5.089	25	0.95	-0.165	1.574	5,565	5,589	Strength
8	80	8	5.812	29	1.23	-0.127	1.792	6,192	6,372	Strength
8	85	8	6.521	33	1.52	-0.114	2.029	6,844	7,134	Strength
10	40	8	2.111*	10	0.21	0.093	0.434	2,198	2,360	Strength
10	45	8	2.526*	12	0.30	0.071	0.558	2,671	2,818	Strength
10	50	8	2.935*	14	0.38	0.015	0.704	3,202	3,272	Strength
10	55	8	3.753	18	0.65	0.170	0.813	3,762	4,167	Strength
10	60	8	4.149	20	0.75	0.067	0.997	4,351	4,608	Strength
10	65	8	4.540	22	0.83	-0.057	1.200	4,970	5,045	Strength
10	70	8	5.101	25	0.98	-0.107	1.411	5,618	5,673	Strength
10	75	8	5.824	29	1.25	-0.088	1.630	6,296	6,482	Strength
10	80	8	6.533	33	1.52	-0.096	1.869	7,003	7,276	Strength
12	45	8	2.098*	10	0.13	-0.052	0.585	2,279	2,369	Strength
12	50	8	2.513*	12	0.17	-0.086	0.727	2,742	2,831	Strength
12	55	8	2.922*	14	0.19	-0.144	0.889	3,233	3,290	Strength
12	60	8	3.741	18	0.41	0.008	1.014	3,754	4,197	Strength
12	65	8	4.136	20	0.40	-0.098	1.216	4,303	4,645	Strength
12	70	8	4.528	22	0.35	-0.226	1.438	4,881	5,089	Strength
12	75	8	5.089	25	0.36	-0.281	1.668	5,488	5,729	Strength
12	80	8	5.446	27	0.11	-0.469	1.945	6,124	6,145	Stress
12	85	8	6.162	31	0.15	-0.478	2.204	6,789	6,966	Stress

PRELIMINARY DESIGN

6.10 Preliminary Design Data

*A minimum concrete transfer strength of 3.0 ksi is recommended by PCI MNL-116 section 5.3.17.

**Final camber is net deflection after all losses and noncomposite and composite dead loads are applied.

Table BB-5 (continued)

Spacing ft	Span ft	Slab Thickness in.	f'_{ci} ksi	No. of Strands	Final Camber in.**	f_b @ L/2 ksi	f_t @ L/2 ksi	M_u @ L/2 ft-kips	M_r @ L/2 ft-kips	Control
AASHTO BIV 48-in.-Wide Interior Beam										
6	55	8	2.072*	10	0.06	-0.079	0.757	2,092	2,322	Strength
6	60	8	2.486*	12	0.09	-0.056	0.883	2,408	2,765	Strength
6	65	8	2.473*	12	-0.16	-0.289	1.083	2,741	2,765	Strength
6	70	8	2.883*	14	-0.21	-0.295	1.238	3,091	3,200	Strength
6	75	8	3.289	16	-0.29	-0.319	1.408	3,458	3,629	Stress
6	80	8	3.689	18	-0.42	-0.358	1.592	3,842	4,050	Stress
6	85	8	4.085	20	-0.62	-0.414	1.790	4,243	4,465	Stress
6	90	8	4.477	22	-0.90	-0.486	2.004	4,662	4,873	Stress
6	95	8	5.038	25	-1.06	-0.477	2.220	5,098	5,454	Stress
6	100	8	5.762	29	-1.05	-0.394	2.442	5,552	6,192	Stress
6	105	8	6.112	31	-1.69	-0.531	2.715	6,024	6,552	Stress
8	50	8	2.085*	10	0.12	-0.034	0.655	2,124	2,346	Strength
8	55	8	2.499*	12	0.16	-0.024	0.783	2,476	2,798	Strength
8	60	8	2.909*	14	0.19	-0.032	0.927	2,847	3,245	Strength
8	65	8	2.896*	14	-0.07	-0.295	1.145	3,236	3,245	Strength
8	70	8	3.302	16	-0.14	-0.336	1.320	3,645	3,686	Stress
8	75	8	3.702	18	-0.25	-0.396	1.511	4,073	4,123	Stress
8	80	8	4.098	20	-0.44	-0.472	1.718	4,520	4,554	Stress
8	85	8	4.690	23	-0.47	-0.453	1.914	4,988	5,191	Stress
8	90	8	5.421	27	-0.42	-0.376	2.132	5,474	5,983	Stress
8	95	8	5.774	29	-0.90	-0.524	2.404	5,981	6,372	Stress
8	100	8	6.484	33	-0.98	-0.489	2.656	6,508	7,134	Stress
10	45	8	2.098*	10	0.16	0.055	0.536	2,056	2,360	Strength
10	50	8	2.513*	12	0.22	0.056	0.662	2,438	2,818	Strength
10	55	8	2.922*	14	0.27	0.038	0.805	2,839	3,272	Strength
10	60	8	2.909*	14	0.06	-0.237	1.024	3,261	3,272	Strength
10	65	8	3.314	16	0.02	-0.292	1.201	3,704	3,722	Strength
10	70	8	4.124	20	0.24	-0.135	1.340	4,169	4,608	Strength
10	75	8	4.515	22	0.14	-0.231	1.553	4,654	5,045	Strength
10	80	8	4.703	23	-0.25	-0.458	1.811	5,162	5,262	Stress
10	85	8	5.433	27	-0.2	-0.400	2.037	5,692	6,079	Stress
10	90	8	6.149	31	-0.19	-0.368	2.282	6,243	6,881	Stress
12	40	8	2.111*	10	0.19	0.181	0.409	1,909	2,369	Strength
12	45	8	2.098*	10	0.13	-0.055	0.586	2,289	2,369	Strength
12	50	8	2.513*	12	0.17	-0.075	0.724	2,712	2,831	Strength
12	55	8	2.922*	14	0.19	-0.116	0.881	3,155	3,290	Strength
12	60	8	3.327	16	0.18	-0.178	1.056	3,621	3,745	Strength
12	65	8	3.728	18	0.14	-0.260	1.251	4,109	4,197	Strength
12	70	8	4.124	20	0.04	-0.362	1.464	4,620	4,645	Stress
12	75	8	4.716	23	0.04	-0.372	1.669	5,154	5,310	Strength
12	80	8	5.076	25	-0.24	-0.532	1.937	5,712	5,729	Stress
12	85	8	5.799	29	-0.25	-0.507	2.186	6,293	6,557	Stress
12	90	8	6.508	33	-0.31	-0.509	2.455	6,898	7,372	Stress

PRELIMINARY DESIGN

6.10 Preliminary Design Data

*A minimum concrete transfer strength of 3.0 ksi is recommended by PCI MNL-116 section 5.3.17.

**Final camber is net deflection after all losses and noncomposite and composite dead loads are applied.

Table BB-6

AASHTO Box Beams 36 in. Wide – Maximum Span (ft) vs. Beam Spacing

Spacing Beam	4 ft	6 ft	8 ft	10 ft	12 ft
BIV-36	120	95	90	85	80
BIII-36	110	90	85	80	75
BII-36	100	80	75	70	65

Table BB-7

AASHTO Adjacent Box Beams 36 in. Wide

Spacing ft	Span ft	Slab Thickness in.	f'_{ci} ksi	No. of Strands	Final Camber in.**	f_b @ L/2 ksi	f_t @ L/2 ksi	M_u @ L/2 ft-kips	M_r @ L/2 ft-kips	Control
AASHTO BII Adjacent 36-in.-Wide Exterior Box Beam										
BII-36	40	6	1.114*	4	0.00	-0.094	0.499	660	722	Strength
BII-36	50	6	1.690*	6	-0.04	-0.140	0.754	959	1,061	Strength
BII-36	60	6	2.257*	8	-0.23	-0.260	1.078	1,305	1,386	Stress
BII-36	70	6	2.815*	10	-0.68	-0.450	1.465	1,692	1,698	Stress
BII-36	80	6	3.940	14	-0.82	-0.380	1.829	2,121	2,284	Stress
BII-36	90	6	5.262	19	-0.89	-0.266	2.251	2,594	2,931	Stress
BII-36	100	6	6.227	23	-1.97	-0.421	2.814	3,109	3,378	Stress
AASHTO BIII Adjacent 36-in.-Wide Exterior Box Beam										
BIII-36	40	6	1.038*	4	0.03	0.001	0.394	684	839	Strength
BIII-36	50	6	1.572*	6	0.05	0.006	0.59	987	1,236	Strength
BIII-36	60	6	2.099*	8	0.00	-0.053	0.846	1,344	1,620	Strength
BIII-36	70	6	2.618*	10	-0.20	-0.170	1.155	1,745	1,989	Strength
BIII-36	80	6	3.130	12	-0.67	-0.343	1.517	2,190	2,346	Stress
BIII-36	90	6	4.160	16	-0.78	-0.272	1.849	2,680	3,022	Stress
BIII-36	100	6	4.871	19	-1.67	-0.435	2.302	3,215	3,478	Stress
BIII-36	110	6	5.784	23	-2.72	-0.537	2.793	3,794	4,035	Stress
AASHTO BIV Adjacent 36-in.-Wide Exterior Box Beam										
BIV-36	40	6	1.004*	4	0.04	0.032	0.354	698	897	Strength
BIV-36	50	6	1.521*	6	0.08	0.056	0.528	1,001	1,324	Strength
BIV-36	60	6	2.030*	8	0.06	0.018	0.757	1,364	1,736	Strength
BIV-36	70	6	2.532*	10	-0.07	-0.072	1.036	1,772	2,135	Strength
BIV-36	80	6	3.027	12	-0.40	-0.215	1.364	2,225	2,521	Strength
BIV-36	90	6	3.515	14	-1.05	-0.408	1.741	2,723	2,894	Stress
BIV-36	100	6	4.248	17	-1.73	-0.508	2.126	3,268	3,429	Stress
BIV-36	110	6	5.604	23	-1.71	-0.309	2.508	3,858	4,365	Stress
BIV-36	120	6	6.473	27	-2.89	-0.429	2.999	4,494	4,874	Stress

PRELIMINARY DESIGN

6.10 Preliminary Design Data

*A minimum concrete transfer strength of 3.0 ksi is recommended by PCI MNL-116 section 5.3.17.

**Final camber is net deflection after all losses and noncomposite and composite dead loads are applied.

Table BB-8

AASHTO Spread Box Beams BII-36

Spacing ft	Span ft	Slab Thickness in.	f'_{ci} ksi	No. of Strands	Final Camber in.**	f_b @ L/2 ksi	f_t @ L/2 ksi	M_u @ L/2 ft-kips	M_r @ L/2 ft-kips	Control
AASHTO BII 36-in.-Wide Exterior Beam										
6	20	8	0.419*	4	-0.03	-0.142	0.517	456	491	Stress
6	25	8	1.027*	6	0.00	0.044	0.540	612	879	Strength
6	30	8	1.009*	6	-0.06	-0.154	0.687	794	879	Strength
6	35	8	1.609*	8	-0.01	-0.037	0.762	1,003	1,248	Strength
6	40	8	1.591*	8	-0.13	-0.294	0.957	1,232	1,248	Stress
6	45	8	2.182*	10	-0.10	-0.248	1.086	1,504	1,610	Stress
6	50	8	2.764*	12	-0.08	-0.243	1.243	1,809	1,966	Stress
6	55	8	3.337	14	-0.06	-0.267	1.424	2,133	2,314	Stress
6	60	8	3.902	16	-0.08	-0.321	1.630	2,476	2,655	Stress
6	65	8	4.457	18	-0.14	-0.403	1.861	2,837	2,990	Stress
6	70	8	5.236	21	-0.07	-0.387	2.102	3,218	3,461	Stress
6	75	8	6.225	25	0.18	-0.282	2.357	3,617	4,053	Stress
6	80	8	6.702	27	-0.18	-0.483	2.691	4,035	4,340	Stress
8	20	8	1.046*	6	0.01	0.062	0.457	683	865	Strength
8	25	8	1.646*	8	0.07	0.171	0.506	944	1,263	Strength
8	30	8	1.627*	8	0.04	-0.100	0.678	1,230	1,263	Strength
8	35	8	2.219*	10	0.10	-0.059	0.782	1,541	1,633	Strength
8	40	8	2.800*	12	0.19	-0.053	0.913	1,875	1,998	Strength
8	45	8	3.373	14	0.28	-0.109	1.080	2,276	2,358	Strength
8	50	8	4.510	18	0.65	0.106	1.190	2,727	3,061	Strength
8	55	8	4.776	19	0.60	-0.193	1.462	3,201	3,233	Strength
8	60	8	5.778	23	0.94	-0.117	1.692	3,699	3,872	Strength
8	65	8	6.754	27	1.32	-0.085	1.953	4,222	4,491	Strength
10	20	8	1.046*	6	0.01	-0.001	0.465	778	868	Strength
10	25	8	1.646*	8	0.06	0.080	0.522	1,076	1,272	Strength
10	30	8	2.237*	10	0.13	0.121	0.610	1,401	1,647	Strength
10	35	8	2.819*	12	0.21	0.123	0.728	1,754	2,018	Strength
10	40	8	3.391	14	0.32	0.085	0.877	2,134	2,384	Strength
10	45	8	3.955	16	0.42	-0.019	1.063	2,590	2,746	Strength
10	50	8	4.510	18	0.50	-0.176	1.284	3,102	3,104	Strength
10	55	8	5.795	23	0.97	0.035	1.467	3,641	3,942	Strength
10	60	8	6.278	25	0.98	-0.228	1.779	4,207	4,266	Strength
12	20	8.5	1.046*	6	0.01	0.023	0.459	728	884	Strength
12	25	8.5	1.646*	8	0.04	0.130	0.517	973	1,297	Strength
12	30	8.5	1.627*	8	-0.01	-0.144	0.703	1,236	1,297	Strength
12	35	8.5	2.219*	10	0.03	-0.107	0.825	1,519	1,681	Strength
12	40	8.5	2.800*	12	0.05	-0.108	0.980	1,823	2,060	Strength
12	45	8.5	3.373	14	0.06	-0.188	1.174	2,222	2,436	Strength
12	50	8.5	3.937	16	0.03	-0.321	1.404	2,671	2,809	Stress
12	55	8.5	4.493	18	-0.05	-0.493	1.667	3,148	3,177	Stress
12	60	8.5	5.778	23	0.27	-0.296	1.896	3,652	4,045	Stress
12	65	8.5	6.754	27	0.39	-0.308	2.204	4,184	4,715	Stress

PRELIMINARY DESIGN

*A minimum concrete transfer strength of 3.0 ksi is recommended by PCI MNL-116 section 5.3.17.

6.10 Preliminary Design Data

**Final camber is net deflection after all losses and noncomposite and composite dead loads are applied.

Table BB-8 (continued)

Spacing ft	Span ft	Slab Thickness in.	f'_{ci} ksi	No. of Strands	Final Camber in.**	f_b @ L/2 ksi	f_t @ L/2 ksi	M_u @ L/2 ft-kips	M_r @ L/2 ft-kips	Control
AASHTO BII 36-in.-Wide Interior Beam										
6	20	8	0.419*	4	-0.03	-0.143	0.517	457	491	Stress
6	25	8	1.027*	6	0.00	0.043	0.541	614	879	Strength
6	30	8	1.009*	6	-0.06	-0.148	0.685	784	879	Strength
6	35	8	1.609*	8	-0.01	-0.014	0.753	968	1,248	Strength
6	40	8	1.591*	8	-0.13	-0.251	0.941	1,166	1,248	Stress
6	45	8	2.182*	10	-0.10	-0.182	1.060	1,402	1,610	Strength
6	50	8	2.764*	12	-0.08	-0.149	1.206	1,663	1,966	Strength
6	55	8	2.746*	12	-0.42	-0.475	1.468	1,939	1,966	Stress
6	60	8	3.319	14	-0.49	-0.490	1.659	2,228	2,314	Stress
6	65	8	3.884	16	-0.62	-0.532	1.873	2,533	2,655	Stress
6	70	8	4.723	19	-0.55	-0.441	2.066	2,852	3,155	Stress
6	75	8	5.725	23	-0.36	-0.288	2.302	3,186	3,760	Stress
6	80	8	6.208	25	-0.80	-0.444	2.617	3,535	4,053	Stress
8	20	8	1.046*	6	0.01	0.143	0.433	554	865	Strength
8	25	8	1.027*	6	-0.01	-0.050	0.565	741	887	Strength
8	30	8	1.627*	8	0.04	0.079	0.625	944	1,263	Strength
8	35	8	1.609*	8	-0.04	-0.166	0.807	1,163	1,263	Strength
8	40	8	2.200*	10	0.00	-0.095	0.918	1,399	1,633	Strength
8	45	8	2.782*	12	0.04	-0.072	1.060	1,678	1,998	Strength
8	50	8	2.764*	12	-0.22	-0.420	1.324	1,989	1,998	Stress
8	55	8	3.337	14	-0.28	-0.460	1.519	2,316	2,358	Stress
8	60	8	3.902	16	-0.38	-0.530	1.741	2,659	2,712	Stress
8	65	8	4.740	19	-0.32	-0.469	1.944	3,019	3,233	Stress
8	70	8	5.743	23	-0.17	-0.349	2.193	3,396	3,872	Stress
8	75	8	6.719	27	-0.03	-0.271	2.471	3,790	4,491	Stress
10	20	8	1.046*	6	0.01	0.080	0.447	644	868	Strength
10	25	8	1.027*	6	-0.02	-0.138	0.590	861	892	Strength
10	30	8	1.627*	8	0.02	-0.036	0.662	1,095	1,272	Strength
10	35	8	2.219*	10	0.07	0.031	0.764	1,347	1,647	Strength
10	40	8	2.200*	10	-0.06	-0.273	0.990	1,617	1,647	Stress
10	45	8	2.782*	12	-0.06	-0.288	1.153	1,939	2,018	Stress
10	50	8	3.355	14	-0.08	-0.346	1.348	2,296	2,384	Stress
10	55	8	3.919	16	-0.14	-0.436	1.571	2,672	2,746	Stress
10	60	8	4.758	19	-0.07	-0.398	1.779	3,065	3,282	Stress
10	65	8	5.760	23	0.08	-0.304	2.036	3,478	3,942	Stress
10	70	8	6.243	25	-0.26	-0.523	2.377	3,910	4,266	Stress
12	20	8.5	1.046*	6	0.01	0.021	0.459	731	884	Strength
12	25	8.5	1.646*	8	0.04	0.127	0.517	976	1,297	Strength
12	30	8.5	1.627*	8	-0.01	-0.146	0.704	1,240	1,297	Strength
12	35	8.5	2.219*	10	0.03	-0.110	0.825	1,524	1,681	Strength
12	40	8.5	2.800*	12	0.05	-0.111	0.980	1,829	2,060	Strength
12	45	8.5	3.373	14	0.06	-0.171	1.171	2,191	2,436	Strength
12	50	8.5	3.937	16	0.03	-0.277	1.397	2,594	2,809	Stress
12	55	8.5	4.493	18	-0.05	-0.419	1.655	3,017	3,177	Stress
12	60	8.5	5.271	21	-0.08	-0.468	1.932	3,460	3,704	Stress
12	65	8.5	6.260	25	-0.02	-0.434	2.231	3,924	4,382	Stress

PRELIMINARY DESIGN

6.10 Preliminary Design Data

*A minimum concrete transfer strength of 3.0 ksi is recommended by PCI MNL-116 section 5.3.17.

**Final camber is net deflection after all losses and noncomposite and composite dead loads are applied.

Table BB-9

AASHTO Spread Box Beams BIII-36

Spacing ft	Span ft	Slab Thickness in.	f'_{ci} ksi	No. of Strands	Final Camber in.**	f_b @ L/2 ksi	f_t @ L/2 ksi	M_u @ L/2 ft-kips	M_r @ L/2 ft-kips	Control
AASHTO BIII 36-in.-Wide Exterior Beam										
6	45	8	2.145*	8	0.19	0.040	0.567	1,524	1,756	Strength
6	50	8	2.678*	10	0.30	0.085	0.687	1,834	2,176	Strength
6	55	8	2.663*	10	0.14	-0.200	0.912	2,162	2,176	Strength
6	60	8	3.189	12	0.21	-0.198	1.070	2,511	2,589	Strength
6	65	8	3.708	14	0.26	-0.219	1.248	2,878	2,996	Strength
6	70	8	4.219	16	0.29	-0.264	1.445	3,265	3,395	Stress
6	75	8	4.944	19	0.46	-0.210	1.646	3,672	3,962	Strength
6	80	8	5.403	21	0.34	-0.325	1.907	4,097	4,325	Stress
6	85	8	5.856	23	0.13	-0.462	2.187	4,542	4,681	Stress
6	90	8	6.761	27	0.42	-0.367	2.433	5,007	5,375	Stress
8	35	8	2.175*	8	0.23	0.190	0.325	1,552	1,771	Strength
8	40	8	2.709*	10	0.35	0.236	0.424	1,891	2,199	Strength
8	45	8	3.234	12	0.50	0.232	0.554	2,296	2,622	Strength
8	50	8	3.752	14	0.66	0.189	0.710	2,751	3,040	Strength
8	55	8	4.263	16	0.82	0.118	0.889	3,230	3,452	Strength
8	60	8	4.988	19	1.11	0.143	1.073	3,734	4,042	Strength
8	65	8	5.446	21	1.22	-0.004	1.319	4,263	4,421	Strength
8	70	8	6.362	25	1.67	0.078	1.534	4,817	5,166	Strength
10	30	8	2.190*	8	0.20	0.334	0.182	1,410	1,780	Strength
10	35	8	2.175*	8	0.21	0.068	0.357	1,766	1,780	Strength
10	40	8	2.709*	10	0.31	0.084	0.469	2,149	2,213	Strength
10	45	8	3.234	12	0.44	0.046	0.612	2,610	2,642	Strength
10	50	8	4.278	16	0.79	0.260	0.702	3,126	3,488	Strength
10	55	8	4.523	17	0.82	0.001	0.939	3,670	3,696	Strength
10	60	8	5.461	21	1.19	0.100	1.128	4,242	4,481	Strength
10	65	8	5.914	23	1.28	-0.095	1.396	4,842	4,867	Strength
12	35	8.5	2.175*	8	0.18	0.147	0.349	1,552	1,805	Strength
12	40	8.5	2.709*	10	0.27	0.187	0.463	1,863	2,247	Strength
12	45	8.5	2.693*	10	0.17	-0.129	0.693	2,242	2,247	Strength
12	50	8.5	3.752	14	0.45	0.113	0.785	2,695	3,119	Strength
12	55	8.5	4.263	16	0.51	0.017	0.988	3,177	3,550	Strength
12	60	8.5	4.508	17	0.38	-0.254	1.257	3,687	3,764	Strength
12	65	8.5	5.446	21	0.62	-0.167	1.480	4,225	4,572	Strength

PRELIMINARY DESIGN

*A minimum concrete transfer strength of 3.0 ksi is recommended by PCI MNL-116 section 5.3.17.

6.10 Preliminary Design Data

**Final camber is net deflection after all losses and noncomposite and composite dead loads are applied.

Table BB-9 (continued)

Spacing ft	Span ft	Slab Thickness in.	f'_{ci} ksi	No. of Strands	Final Camber in.**	f_b @ L/2 ksi	f_t @ L/2 ksi	M_u @ L/2 ft-kips	M_r @ L/2 ft-kips	Control
AASHTO BIII 36-in.-Wide Interior Beam										
6	45	8	2.145*	8	0.19	0.084	0.547	1,438	1,756	Strength
6	50	8	2.130*	8	0.07	-0.160	0.744	1,707	1,756	Strength
6	55	8	2.663*	10	0.14	-0.111	0.872	1,990	2,176	Strength
6	60	8	3.189	12	0.21	-0.083	1.018	2,288	2,589	Strength
6	65	8	3.708	14	0.26	-0.078	1.184	2,601	2,996	Strength
6	70	8	3.693	14	-0.16	-0.391	1.450	2,929	2,996	Stress
6	75	8	4.204	16	-0.23	-0.424	1.652	3,273	3,395	Stress
6	80	8	4.929	19	-0.16	-0.356	1.855	3,632	3,962	Stress
6	85	8	5.388	21	-0.43	-0.455	2.118	4,008	4,325	Stress
6	90	8	6.304	25	-0.20	-0.318	2.345	4,399	5,031	Stress
6	95	8	6.747	27	-0.68	-0.461	2.645	4,806	5,375	Stress
8	40	8	2.160*	8	0.20	0.155	0.429	1,432	1,771	Strength
8	45	8	2.145*	8	0.12	-0.096	0.622	1,719	1,771	Strength
8	50	8	2.678*	10	0.20	-0.065	0.751	2,037	2,199	Strength
8	55	8	3.204	12	0.27	-0.057	0.901	2,372	2,622	Strength
8	60	8	3.723	14	0.33	-0.073	1.072	2,724	3,040	Strength
8	65	8	4.234	16	0.36	-0.113	1.263	3,093	3,452	Strength
8	70	8	4.479	17	0.13	-0.321	1.516	3,480	3,657	Strength
8	75	8	4.944	19	-0.03	-0.428	1.772	3,885	4,042	Stress
8	80	8	5.871	23	0.20	-0.297	1.994	4,307	4,796	Stress
8	85	8	6.318	25	-0.13	-0.452	2.291	4,748	5,166	Stress
10	35	8	2.175*	8	0.21	0.256	0.303	1,377	1,780	Strength
10	40	8	2.160*	8	0.17	0.014	0.486	1,654	1,780	Strength
10	45	8	2.693*	10	0.25	0.043	0.609	1,983	2,213	Strength
10	50	8	3.219	12	0.33	0.037	0.758	2,349	2,642	Strength
10	55	8	3.738	14	0.41	0.005	0.929	2,733	3,067	Strength
10	60	8	4.248	16	0.46	-0.053	1.124	3,136	3,488	Strength
10	65	8	4.494	17	0.28	-0.281	1.382	3,559	3,696	Strength
10	70	8	4.958	19	0.15	-0.410	1.644	4,001	4,091	Stress
10	75	8	5.885	23	0.36	-0.303	1.875	4,463	4,867	Stress
10	80	8	6.333	25	0.07	-0.484	2.184	4,946	5,249	Stress
12	35	8.5	2.175*	8	0.18	0.144	0.349	1,557	1,805	Strength
12	40	8.5	2.709*	10	0.27	0.185	0.464	1,869	2,247	Strength
12	45	8.5	2.693*	10	0.17	-0.128	0.693	2,239	2,247	Strength
12	50	8.5	3.219	12	0.22	-0.168	0.864	2,651	2,685	Strength
12	55	8.5	3.738	14	0.24	-0.236	1.060	3,083	3,119	Stress
12	60	8.5	4.248	16	0.22	-0.332	1.283	3,536	3,550	Stress
12	65	8.5	4.973	19	0.28	-0.334	1.514	4,010	4,170	Stress
12	70	8.5	5.432	21	0.09	-0.509	1.811	4,507	4,572	Stress
12	75	8.5	6.347	25	0.21	-0.454	2.080	5,026	5,366	Stress

PRELIMINARY DESIGN

6.10 Preliminary Design Data

*A minimum concrete transfer strength of 3.0 ksi is recommended by PCI MNL-116 section 5.3.17.

**Final camber is net deflection after all losses and noncomposite and composite dead loads are applied.

Table BB-10

AASHTO Spread Box Beams BIV-36

Spacing ft	Span ft	Slab Thickness in.	f'_{ci} ksi	No. of Strands	Final Camber in.**	f_b @ L/2 ksi	f_t @ L/2 ksi	M_u @ L/2 ft-kips	M_r @ L/2 ft-kips	Control
AASHTO BIV 36-in.-Wide Exterior Beam										
6	60	8	3.083	12	0.28	-0.073	0.953	2,528	2,765	Strength
6	70	8	4.079	16	0.43	-0.100	1.287	3,289	3,629	Strength
6	80	8	4.769	19	0.16	-0.371	1.754	4,129	4,239	Stress
6	90	8	6.108	25	0.31	-0.349	2.216	5,046	5,395	Stress
8	40	8	2.616*	10	0.34	0.305	0.368	1,898	2,346	Strength
8	50	8	3.111	12	0.44	0.007	0.703	2,763	2,798	Strength
8	60	8	4.357	17	0.85	0.039	0.999	3,752	3,905	Strength
8	70	8	5.712	23	1.37	0.041	1.404	4,841	5,132	Strength
10	40	8	2.616*	10	0.31	0.168	0.409	2,157	2,360	Strength
10	50	8	3.626	14	0.56	0.096	0.688	3,138	3,272	Strength
10	60	8	4.823	19	0.94	0.023	1.041	4,260	4,369	Strength
10	70	8	6.162	25	1.41	-0.067	1.488	5,494	5,614	Strength
12	50	8	3.111	12	0.29	-0.037	0.747	2,678	2,831	Strength
12	60	8	4.106	16	0.39	-0.184	1.119	3,662	3,745	Strength
12	70	8	5.257	21	0.44	-0.342	1.588	4,757	4,828	Stress
12	80	8	6.579	27	0.46	-0.498	2.134	5,962	6,087	Stress
AASHTO BIV 36-in.-Wide Interior Beam										
6	60	8	2.560*	10	-0.02	-0.271	0.990	2,317	2,322	Stress
6	70	8	3.570	14	0.03	-0.239	1.297	2,967	3,200	Strength
6	80	8	4.303	17	-0.30	-0.427	1.713	3,679	3,840	Stress
6	90	8	5.658	23	-0.26	-0.333	2.141	4,456	5,016	Stress
8	50	8	2.588*	10	0.23	0.028	0.666	2,061	2,346	Strength
8	60	8	3.083	12	0.11	-0.238	1.031	2,756	2,798	Strength
8	70	8	4.079	16	0.12	-0.290	1.387	3,521	3,686	Stress
8	80	8	5.230	21	0.08	-0.330	1.822	4,358	4,728	Stress
8	90	8	6.553	27	0.03	-0.347	2.318	5,269	5,924	Stress
10	50	8	3.111	12	0.36	0.138	0.665	2,374	2,818	Strength
10	60	8	3.598	14	0.24	-0.197	1.069	3,170	3,272	Strength
10	70	8	4.796	19	0.36	-0.210	1.456	4,044	4,369	Strength
10	80	8	5.685	23	0.01	-0.477	1.986	5,000	5,203	Stress
12	50	8	3.111	12	0.29	-0.024	0.743	2,648	2,831	Strength
12	60	8	4.106	16	0.39	-0.128	1.104	3,530	3,745	Strength
12	70	8	5.257	21	0.44	-0.233	1.558	4,496	4,828	Strength
12	80	8	6.579	27	0.46	-0.328	2.087	5,549	6,087	Stress

PRELIMINARY DESIGN

6.10 Preliminary Design Data

Table BT-1
AASHTO-PCI Bulb-Tees – Maximum Span vs. Beam Spacing

Spacing Beam	6 ft	8 ft	10 ft	12 ft
PCI BT54	125	115	105	95
PCI BT63	140	130	115	105
PCI BT72	155	145	130	120

PRELIMINARY DESIGN

6.10 Preliminary Design Data

*A minimum concrete transfer strength of 3.0 ksi is recommended by PCI MNL-116 section 5.3.17.

**Final camber is net deflection after all losses and noncomposite and composite dead loads are applied.

Table BT-2

AASHTO-PCI Bulb-Tee BT-54

Spacing ft	Span ft	Slab Thickness in.	f'_{ci} ksi	No. of Strands	Final Camber in.**	f_b @ L/2 ksi	f_t @ L/2 ksi	M_u @ L/2 ft-kips	M_r @ L/2 ft-kips	Control
AASHTO-PCI Bulb-Tee, 54-in.-Deep Exterior Beam										
6	60	8	2.300*	10	0.33	0.087	0.700	2,562	2,908	Strength
6	65	8	2.193*	10	0.20	-0.140	0.872	2,901	2,908	Strength
6	70	8	2.643*	12	0.33	-0.062	0.980	3,258	3,467	Strength
6	75	8	3.050	14	0.45	-0.032	1.122	3,663	4,000	Strength
6	80	8	3.444	16	0.55	-0.019	1.277	4,087	4,525	Strength
6	85	8	3.824	18	0.65	-0.025	1.446	4,531	5,044	Strength
6	90	8	3.679	18	0.25	-0.330	1.683	4,994	5,044	Stress
6	95	8	4.038	20	0.22	-0.366	1.877	5,477	5,555	Stress
6	100	8	4.384	22	0.13	-0.418	2.083	5,978	6,060	Stress
6	105	8	4.717	24	-0.04	-0.488	2.303	6,499	6,558	Stress
6	110	8	5.478	28	0.16	-0.338	2.514	7,039	7,495	Stress
6	115	8	5.758	30	-0.50	-0.459	2.775	7,599	7,954	Stress
6	120	8	6.454	34	-0.99	-0.372	3.028	8,177	8,731	Stress
8	40	8	2.075*	8	0.24	0.316	0.282	1,888	2,356	Strength
8	45	8	2.001*	8	0.24	0.086	0.429	2,293	2,356	Strength
8	50	8	2.489*	10	0.37	0.150	0.516	2,747	2,931	Strength
8	55	8	2.961*	12	0.53	0.192	0.619	3,226	3,501	Strength
8	60	8	3.392	14	0.69	0.197	0.753	3,729	4,045	Strength
8	65	8	3.808	16	0.86	0.182	0.901	4,257	4,584	Strength
8	70	8	4.210	18	1.03	0.146	1.065	4,809	5,117	Strength
8	75	8	4.598	20	1.19	0.090	1.243	5,386	5,645	Strength
8	80	8	4.973	22	1.31	0.014	1.436	5,988	6,168	Strength
8	85	8	5.335	24	1.41	-0.081	1.644	6,614	6,686	Strength
8	90	8	6.122	28	1.77	0.038	1.844	7,265	7,667	Strength
8	95	8	6.430	30	1.57	-0.113	2.096	7,941	8,149	Strength
10	40	8	2.075*	8	0.22	0.198	0.314	2,147	2,365	Strength
10	45	8	2.571*	10	0.34	0.262	0.393	2,607	2,945	Strength
10	50	8	3.051	12	0.49	0.292	0.493	3,122	3,521	Strength
10	55	8	3.489	14	0.64	0.283	0.624	3,665	4,072	Strength
10	60	8	3.913	16	0.80	0.251	0.771	4,237	4,619	Strength
10	65	8	4.322	18	0.97	0.196	0.935	4,836	5,162	Strength
10	70	8	4.718	20	1.11	0.120	1.115	5,462	5,700	Strength
10	75	8	5.101	22	1.24	0.023	1.311	6,117	6,234	Strength
10	80	8	5.935	26	1.65	0.156	1.487	6,799	7,270	Strength
10	85	8	6.263	28	1.66	-0.001	1.730	7,510	7,772	Strength
10	90	8	6.578	30	1.46	-0.180	1.989	8,248	8,270	Strength
12	40	9	2.075*	8	0.19	0.180	0.325	2,130	2,410	Strength
12	45	9	2.571*	10	0.30	0.255	0.408	2,538	3,004	Strength
12	50	9	2.489*	10	0.25	-0.018	0.586	2,991	3,004	Strength
12	55	9	2.961*	12	0.35	0.009	0.705	3,463	3,593	Strength
12	60	9	3.392	14	0.44	-0.002	0.857	3,957	4,159	Strength
12	65	9	3.808	16	0.51	-0.035	1.027	4,471	4,721	Strength
12	70	9	4.210	18	0.57	-0.090	1.214	5,008	5,280	Strength
12	75	9	4.598	20	0.58	-0.165	1.419	5,568	5,835	Strength
12	80	9	4.973	22	0.53	-0.262	1.641	6,150	6,386	Stress
12	85	9	5.335	24	0.41	-0.379	1.881	6,755	6,934	Stress
12	90	9	6.122	28	0.52	-0.293	2.119	7,415	7,980	Stress
12	95	9	6.430	30	0.01	-0.491	2.413	8,129	8,497	Stress

PRELIMINARY DESIGN

*A minimum concrete transfer strength of 3.0 ksi is recommended by PCI MNL-116 section 5.3.17.

6.10 Preliminary Design Data

**Final camber is net deflection after all losses and noncomposite and composite dead loads are applied.

Table BT-2 (continued)

Spacing ft	Span ft	Slab Thickness in.	f'_{ci} ksi	No. of Strands	Final Camber in.**	f_b @ L/2 ksi	f_t @ L/2 ksi	M_u @ L/2 ft-kips	M_r @ L/2 ft-kips	Control
AASHTO-PCI Bulb-Tee, 54-in.-Deep Interior Beam										
6	60	8	2.300*	10	0.33	0.081	0.703	2,577	2,908	Strength
6	65	8	2.757*	12	0.48	0.170	0.799	2,918	3,467	Strength
6	70	8	2.643*	12	0.33	-0.069	0.982	3,274	3,467	Strength
6	75	8	3.050	14	0.45	-0.025	1.119	3,645	4,000	Strength
6	80	8	3.444	16	0.55	0.002	1.267	4,032	4,525	Strength
6	85	8	3.306	16	0.22	-0.274	1.485	4,435	4,525	Stress
6	90	8	3.679	18	0.25	-0.275	1.658	4,854	5,044	Stress
6	95	8	4.038	20	0.22	-0.292	1.843	5,288	5,555	Stress
6	100	8	4.384	22	0.13	-0.326	2.041	5,739	6,060	Stress
6	105	8	4.717	24	-0.04	-0.375	2.251	6,206	6,558	Stress
6	110	8	5.013	26	-0.33	-0.456	2.489	6,690	7,030	Stress
6	115	8	5.758	30	-0.50	-0.304	2.702	7,190	7,954	Stress
6	120	8	6.026	32	-1.30	-0.418	2.965	7,706	8,406	Stress
6	125	8	6.661	36	-2.08	-0.357	3.249	8,239	8,957	Stress
8	45	8	2.001*	8	0.24	0.212	0.384	1,970	2,356	Strength
8	55	8	2.399*	10	0.32	0.084	0.620	2,692	2,931	Strength
8	60	8	2.864*	12	0.47	0.154	0.720	3,076	3,501	Strength
8	65	8	2.757*	12	0.34	-0.105	0.908	3,478	3,501	Strength
8	70	8	3.172	14	0.44	-0.082	1.051	3,897	4,045	Strength
8	75	8	3.574	16	0.54	-0.078	1.207	4,334	4,584	Strength
8	80	8	3.961	18	0.61	-0.092	1.378	4,789	5,117	Strength
8	85	8	4.334	20	0.64	-0.123	1.562	5,261	5,645	Strength
8	90	8	4.695	22	0.62	-0.172	1.760	5,752	6,168	Strength
8	95	8	5.042	24	0.54	-0.239	1.972	6,262	6,686	Strength
8	100	8	5.353	26	0.35	-0.337	2.212	6,789	7,179	Stress
8	105	8	5.651	28	-0.01	-0.453	2.466	7,336	7,667	Stress
8	110	8	6.392	32	-0.39	-0.342	2.698	7,901	8,627	Stress
8	115	8	6.640	34	-1.25	-0.508	2.994	8,485	9,080	Stress
10	40	8	2.075*	8	0.22	0.286	0.288	1,917	2,365	Strength
10	45	8	2.001*	8	0.21	0.065	0.433	2,282	2,365	Strength
10	50	8	2.489*	10	0.32	0.141	0.518	2,688	2,945	Strength
10	55	8	2.961*	12	0.46	0.197	0.619	3,111	3,521	Strength
10	60	8	3.392	14	0.59	0.218	0.751	3,553	4,072	Strength
10	65	8	3.286	14	0.46	-0.072	0.955	4,013	4,072	Strength
10	70	8	3.695	16	0.55	-0.087	1.116	4,493	4,619	Strength
10	75	8	4.090	18	0.63	-0.120	1.292	4,992	5,162	Strength
10	80	8	4.471	20	0.65	-0.173	1.484	5,512	5,700	Strength
10	85	8	4.838	22	0.62	-0.245	1.691	6,051	6,234	Strength
10	90	8	5.193	24	0.54	-0.336	1.912	6,611	6,764	Stress
10	95	8	5.510	26	0.35	-0.460	2.164	7,192	7,270	Stress
10	100	8	6.274	30	0.24	-0.356	2.395	7,794	8,270	Stress
10	105	8	6.563	32	-0.40	-0.519	2.677	8,416	8,763	Stress
12	40	9	2.075*	8	0.19	0.174	0.326	2,145	2,410	Strength
12	45	9	2.571*	10	0.30	0.249	0.410	2,555	3,004	Strength
12	50	9	3.051	12	0.42	0.291	0.513	3,010	3,593	Strength
12	55	9	2.961*	12	0.35	0.001	0.707	3,485	3,593	Strength
12	60	9	3.392	14	0.44	-0.011	0.859	3,981	4,159	Strength
12	65	9	3.808	16	0.51	-0.045	1.029	4,498	4,721	Strength
12	70	9	4.210	18	0.57	-0.100	1.217	5,038	5,280	Strength
12	75	9	4.598	20	0.58	-0.177	1.422	5,599	5,835	Strength
12	80	9	4.973	22	0.53	-0.274	1.644	6,184	6,386	Stress
12	85	9	5.335	24	0.41	-0.392	1.884	6,791	6,934	Stress
12	90	9	6.122	28	0.52	-0.296	2.119	7,422	7,980	Stress
12	95	9	6.430	30	0.01	-0.473	2.409	8,077	8,497	Stress

PRELIMINARY DESIGN

6.10 Preliminary Design Data

*A minimum concrete transfer strength of 3.0 ksi is recommended by PCI MNL-116 section 5.3.17.

**Final camber is net deflection after all losses and noncomposite and composite dead loads are applied.

Table BT-3

AASHTO-PCI Bulb-Tee BT-63

Spacing ft	Span ft	Slab Thickness in.	f'_{ci} ksi	No. of Strands	Final Camber in.**	f_b @ L/2 ksi	f_t @ L/2 ksi	M_u @ L/2 ft-kips	M_r @ L/2 ft-kips	Control
AASHTO-PCI Bulb-Tee, 63-in.-Deep Exterior Beam										
6	65	8	2.097*	10	0.28	0.055	0.698	2,990	3,347	Strength
6	70	8	2.525*	12	0.42	0.153	0.779	3,355	3,994	Strength
6	75	8	2.419*	12	0.28	-0.055	0.944	3,735	3,994	Strength
6	80	8	2.821*	14	0.41	0.010	1.051	4,144	4,628	Strength
6	85	8	2.701*	14	0.17	-0.231	1.241	4,595	4,628	Strength
6	90	8	3.069	16	0.25	-0.208	1.382	5,065	5,241	Strength
6	95	8	3.425	18	0.31	-0.200	1.534	5,556	5,847	Strength
6	100	8	3.769	20	0.34	-0.206	1.698	6,066	6,446	Strength
6	105	8	4.102	22	0.31	-0.227	1.872	6,596	7,038	Strength
6	110	8	4.423	24	0.24	-0.262	2.057	7,145	7,623	Strength
6	115	8	4.742	26	0.13	-0.306	2.248	7,715	8,209	Stress
6	120	8	5.021	28	-0.09	-0.381	2.467	8,304	8,761	Stress
6	125	8	5.291	30	-0.43	-0.469	2.697	8,913	9,306	Stress
6	130	8	6.001	34	-0.74	-0.327	2.886	9,541	10,272	Stress
6	135	8	6.262	36	-1.52	-0.435	3.128	10,189	10,616	Stress
8	50	8	2.351*	10	0.34	0.313	0.394	2,769	3,370	Strength
8	55	8	2.274*	10	0.33	0.089	0.545	3,252	3,370	Strength
8	60	8	2.715*	12	0.47	0.147	0.634	3,760	4,028	Strength
8	65	8	3.136	14	0.62	0.182	0.740	4,294	4,673	Strength
8	70	8	3.530	16	0.78	0.192	0.868	4,852	5,300	Strength
8	75	8	3.911	18	0.95	0.184	1.008	5,436	5,921	Strength
8	80	8	4.280	20	1.10	0.160	1.160	6,044	6,537	Strength
8	85	8	4.638	22	1.24	0.119	1.325	6,678	7,147	Strength
8	90	8	4.984	24	1.36	0.061	1.502	7,337	7,752	Strength
8	95	8	5.326	26	1.46	-0.007	1.687	8,020	8,360	Strength
8	100	8	5.630	28	1.50	-0.108	1.900	8,729	8,935	Strength
8	105	8	5.924	30	1.47	-0.224	2.126	9,463	9,505	Strength
8	110	8	6.654	34	1.46	-0.114	2.313	10,222	10,651	Strength
10	50	8	2.351*	10	0.31	0.173	0.436	3,144	3,385	Strength
10	55	8	2.799*	12	0.44	0.219	0.524	3,692	4,048	Strength
10	60	8	3.227	14	0.59	0.241	0.629	4,268	4,701	Strength
10	65	8	3.627	16	0.74	0.236	0.757	4,873	5,336	Strength
10	70	8	4.015	18	0.90	0.213	0.898	5,506	5,966	Strength
10	75	8	4.391	20	1.04	0.171	1.053	6,166	6,592	Strength
10	80	8	4.754	22	1.16	0.111	1.221	6,856	7,214	Strength
10	85	8	5.107	24	1.27	0.033	1.403	7,573	7,831	Strength
10	90	8	5.455	26	1.36	-0.057	1.593	8,319	8,452	Strength
10	95	8	6.200	30	1.73	0.055	1.774	9,093	9,626	Strength
10	100	8	6.495	32	1.56	-0.089	2.008	9,895	10,207	Strength
12	50	9	2.351*	10	0.26	0.160	0.450	3,075	3,443	Strength
12	55	9	2.799*	12	0.37	0.216	0.540	3,560	4,120	Strength
12	60	9	2.715*	12	0.30	-0.037	0.717	4,066	4,120	Strength
12	65	9	3.136	14	0.39	-0.017	0.839	4,594	4,788	Strength
12	70	9	3.530	16	0.47	-0.024	0.984	5,145	5,438	Strength
12	75	9	3.911	18	0.54	-0.049	1.144	5,718	6,084	Strength
12	80	9	4.280	20	0.57	-0.092	1.319	6,315	6,727	Strength
12	85	9	4.638	22	0.56	-0.153	1.508	6,935	7,366	Strength
12	90	9	4.984	24	0.50	-0.230	1.711	7,578	8,002	Strength
12	95	9	5.326	26	0.40	-0.320	1.924	8,246	8,641	Stress
12	100	9	5.630	28	0.19	-0.451	2.170	8,960	9,250	Stress
12	105	9	6.355	32	0.10	-0.376	2.394	9,741	10,456	Stress

PRELIMINARY DESIGN

*A minimum concrete transfer strength of 3.0 ksi is recommended by PCI MNL-116 section 5.3.17.

6.10 Preliminary Design Data

**Final camber is net deflection after all losses and noncomposite and composite dead loads are applied.

Table BT-3 (continued)

Spacing ft	Span ft	Slab Thickness in.	f'_{ci} ksi	No. of Strands	Final Camber in.**	f_b @ L/2 ksi	f_t @ L/2 ksi	M_u @ L/2 ft-kips	M_r @ L/2 ft-kips	Control
AASHTO-PCI Bulb-Tee, 63-in.-Deep Interior Beam										
6	65	8	2.097*	10	0.28	0.050	0.700	3,007	3,347	Strength
6	70	8	2.525*	12	0.42	0.147	0.782	3,374	3,994	Strength
6	75	8	2.419*	12	0.28	-0.062	0.947	3,756	3,994	Strength
6	80	8	2.806*	14	0.40	-0.002	1.062	4,154	4,614	Strength
6	85	8	2.686*	14	0.16	-0.232	1.245	4,569	4,614	Strength
6	90	8	3.054	16	0.23	-0.196	1.380	5,000	5,227	Strength
6	95	8	3.410	18	0.30	-0.174	1.526	5,448	5,833	Strength
6	100	8	3.755	20	0.32	-0.166	1.682	5,912	6,432	Strength
6	105	8	3.609	20	-0.18	-0.436	1.905	6,393	6,432	Stress
6	110	8	3.936	22	-0.30	-0.451	2.081	6,890	7,024	Stress
6	115	8	4.252	24	-0.47	-0.479	2.267	7,405	7,609	Stress
6	120	8	4.537	26	-0.74	-0.533	2.477	7,936	8,168	Stress
6	125	8	5.251	30	-0.51	-0.362	2.655	8,484	9,266	Stress
6	130	8	5.511	32	-1.23	-0.445	2.886	9,050	9,805	Stress
6	135	8	6.132	36	-1.84	-0.349	3.123	9,632	10,484	Stress
6	140	8	6.314	38	-2.98	-0.495	3.409	10,231	10,725	Stress
8	55	8	2.274*	10	0.33	0.241	0.484	2,772	3,370	Strength
8	60	8	2.189*	10	0.28	0.038	0.633	3,168	3,370	Strength
8	65	8	2.623*	12	0.41	0.119	0.719	3,581	4,028	Strength
8	70	8	2.525*	12	0.29	-0.108	0.888	4,012	4,028	Strength
8	75	8	2.918*	14	0.39	-0.066	1.009	4,461	4,660	Strength
8	80	8	3.299	16	0.49	-0.040	1.142	4,928	5,286	Strength
8	85	8	3.668	18	0.58	-0.030	1.286	5,414	5,907	Strength
8	90	8	4.025	20	0.64	-0.034	1.442	5,918	6,523	Strength
8	95	8	3.893	20	0.28	-0.317	1.665	6,441	6,523	Stress
8	100	8	4.232	22	0.22	-0.347	1.843	6,984	7,134	Stress
8	105	8	4.560	24	0.11	-0.392	2.033	7,545	7,739	Stress
8	110	8	4.857	26	-0.08	-0.463	2.246	8,126	8,319	Stress
8	115	8	5.582	30	0.14	-0.311	2.430	8,725	9,464	Stress
8	120	8	5.853	32	-0.45	-0.413	2.667	9,345	10,029	Stress
8	125	8	6.485	36	-0.96	-0.338	2.911	9,983	11,085	Stress
8	130	8	6.679	38	-1.93	-0.505	3.205	10,641	11,576	Stress
10	50	8	2.351*	10	0.31	0.290	0.397	2,767	3,385	Strength
10	55	8	2.274*	10	0.28	0.075	0.546	3,202	3,385	Strength
10	60	8	2.715*	12	0.40	0.143	0.634	3,656	4,048	Strength
10	65	8	3.121	14	0.52	0.181	0.746	4,128	4,687	Strength
10	70	8	3.023	14	0.41	-0.072	0.930	4,621	4,687	Strength
10	75	8	3.411	16	0.50	-0.062	1.067	5,134	5,322	Strength
10	80	8	3.786	18	0.59	-0.069	1.217	5,667	5,953	Strength
10	85	8	4.149	20	0.64	-0.092	1.380	6,221	6,579	Strength
10	90	8	4.501	22	0.65	-0.130	1.555	6,796	7,200	Strength
10	95	8	4.840	24	0.62	-0.185	1.744	7,392	7,818	Strength
10	100	8	5.150	26	0.52	-0.268	1.956	8,009	8,411	Strength
10	105	8	5.448	28	0.35	-0.365	2.181	8,647	9,000	Stress
10	110	8	5.737	30	0.08	-0.478	2.419	9,307	9,586	Stress
10	115	8	6.424	34	-0.27	-0.387	2.641	9,989	10,724	Stress

PRELIMINARY DESIGN

6.10 Preliminary Design Data

*A minimum concrete transfer strength of 3.0 ksi is recommended by PCI MNL-116 section 5.3.17.

**Final camber is net deflection after all losses and noncomposite and composite dead loads are applied.

Table BT-3 (continued)

Spacing ft	Span ft	Slab Thickness in.	f'_{ci} ksi	No. of Strands	Final Camber in.**	f_b @ L/2 ksi	f_t @ L/2 ksi	M_u @ L/2 ft-kips	M_r @ L/2 ft-kips	Control
AASHTO-PCI Bulb-Tee, 63-in.-Deep Interior Beam (continued)										
12	50	9	2.351*	10	0.26	0.154	0.451	3,095	3,443	Strength
12	55	9	2.799*	12	0.37	0.210	0.542	3,583	4,120	Strength
12	60	9	2.715*	12	0.30	-0.045	0.718	4,091	4,120	Strength
12	65	9	3.121	14	0.38	-0.034	0.850	4,622	4,774	Strength
12	70	9	3.515	16	0.46	-0.042	0.995	5,175	5,424	Strength
12	75	9	3.897	18	0.53	-0.067	1.155	5,751	6,071	Strength
12	80	9	4.266	20	0.56	-0.111	1.330	6,350	6,713	Strength
12	85	9	4.624	22	0.55	-0.172	1.519	6,972	7,353	Strength
12	90	9	4.970	24	0.49	-0.251	1.723	7,619	7,988	Strength
12	95	9	5.286	26	0.35	-0.359	1.952	8,289	8,600	Stress
12	100	9	5.591	28	0.14	-0.483	2.197	8,983	9,209	Stress
12	105	9	6.316	32	0.04	-0.390	2.415	9,702	10,416	Stress

PRELIMINARY DESIGN

6.10 Preliminary Design Data

*A minimum concrete transfer strength of 3.0 ksi is recommended by PCI MNL-116 section 5.3.17.

**Final camber is net deflection after all losses and noncomposite and composite dead loads are applied.

Table BT-4

AASHTO-PCI Bulb-Tee BT-72

Spacing ft	Span ft	Slab Thickness in.	f'_{ci} ksi	No. of Strands	Final Camber in.**	f_b @ L/2 ksi	f_t @ L/2 ksi	M_u @ L/2 ft-kips	M_r @ L/2 ft-kips	Control
AASHTO-PCI Bulb-Tee, 72-in.-Deep Exterior Beam										
6	40	8	0.833*	4	0.05	0.031	0.244	1,449	1,537	Strength
6	45	8	1.292*	6	0.13	0.201	0.260	1,731	2,294	Strength
6	50	8	1.231*	6	0.11	0.067	0.362	2,044	2,294	Strength
6	55	8	1.671*	8	0.21	0.212	0.398	2,372	3,044	Strength
6	60	8	1.598*	8	0.18	0.061	0.516	2,715	3,044	Strength
6	65	8	2.021*	10	0.30	0.183	0.569	3,074	3,786	Strength
6	70	8	1.936*	10	0.22	0.015	0.703	3,449	3,786	Strength
6	75	8	2.340*	12	0.36	0.116	0.774	3,840	4,521	Strength
6	80	8	2.244*	12	0.23	-0.071	0.925	4,248	4,521	Strength
6	85	8	2.614*	14	0.34	-0.001	1.024	4,673	5,229	Strength
6	90	8	2.505*	14	0.12	-0.211	1.194	5,137	5,229	Strength
6	95	8	2.859*	16	0.21	-0.173	1.316	5,635	5,930	Strength
6	100	8	3.203	18	0.28	-0.148	1.447	6,154	6,623	Strength
6	105	8	3.536	20	0.34	-0.135	1.588	6,693	7,309	Strength
6	110	8	3.405	20	-0.09	-0.387	1.796	7,252	7,309	Stress
6	115	8	3.723	22	-0.14	-0.395	1.955	7,831	7,989	Stress
6	120	8	4.030	24	-0.23	-0.416	2.123	8,430	8,661	Stress
6	125	8	4.312	26	-0.40	-0.459	2.311	9,050	9,307	Stress
6	130	8	4.584	28	-0.62	-0.514	2.509	9,690	9,946	Stress
6	135	8	5.264	32	-0.29	-0.355	2.672	10,349	11,205	Stress
6	140	8	5.499	34	-0.87	-0.445	2.898	11,029	11,657	Stress
6	145	8	6.100	38	-1.19	-0.350	3.111	11,730	12,365	Stress
6	150	8	6.286	40	-2.10	-0.484	3.375	12,450	12,640	Stress
8	40	8	1.347*	6	0.11	0.185	0.220	1,916	2,303	Strength
8	45	8	1.799*	8	0.20	0.312	0.254	2,329	3,059	Strength
8	50	8	1.738*	8	0.20	0.135	0.375	2,791	3,059	Strength
8	55	8	2.172*	10	0.31	0.229	0.433	3,279	3,810	Strength
8	60	8	2.100*	10	0.29	0.028	0.574	3,792	3,810	Strength
8	65	8	2.516*	12	0.42	0.095	0.653	4,331	4,555	Strength
8	70	8	2.903*	14	0.55	0.135	0.753	4,895	5,275	Strength
8	75	8	3.279	16	0.70	0.161	0.865	5,485	5,989	Strength
8	80	8	3.644	18	0.86	0.172	0.987	6,101	6,698	Strength
8	85	8	3.998	20	1.01	0.168	1.120	6,741	7,401	Strength
8	90	8	4.343	22	1.14	0.151	1.264	7,408	8,099	Strength
8	95	8	4.676	24	1.27	0.119	1.419	8,100	8,792	Strength
8	100	8	4.984	26	1.37	0.064	1.594	8,817	9,460	Strength
8	105	8	5.283	28	1.44	-0.005	1.779	9,560	10,122	Strength
8	110	8	5.572	30	1.47	-0.088	1.975	10,329	10,779	Strength
8	115	8	5.852	32	1.47	-0.183	2.181	11,123	11,431	Strength
8	120	8	6.108	34	1.23	-0.301	2.408	11,942	12,059	Strength
8	125	8	6.727	38	1.17	-0.235	2.623	12,787	13,279	Strength

PRELIMINARY DESIGN

6.10 Preliminary Design Data

*A minimum concrete transfer strength of 3.0 ksi is recommended by PCI MNL-116 section 5.3.17.

**Final camber is net deflection after all losses and noncomposite and composite dead loads are applied.

Table BT-4 (continued)

Spacing ft	Span ft	Slab Thickness in.	f'_{ci} ksi	No. of Strands	Final Camber in.**	f_b @ L/2 ksi	f_t @ L/2 ksi	M_u @ L/2 ft-kips	M_r @ L/2 ft-kips	Control
AASHTO-PCI Bulb-Tee, 72-in.-Deep Exterior Beam (continued)										
10	40	8	1.347*	6	0.11	0.105	0.242	2,175	2,308	Strength
10	45	8	1.799*	8	0.19	0.216	0.283	2,642	3,068	Strength
10	50	8	2.239*	10	0.29	0.301	0.339	3,166	3,824	Strength
10	55	8	2.172*	10	0.28	0.091	0.478	3,719	3,824	Strength
10	60	8	2.594*	12	0.40	0.147	0.556	4,300	4,575	Strength
10	65	8	2.987*	14	0.52	0.176	0.657	4,910	5,302	Strength
10	70	8	3.368	16	0.66	0.188	0.769	5,549	6,025	Strength
10	75	8	3.739	18	0.81	0.185	0.893	6,216	6,743	Strength
10	80	8	4.099	20	0.95	0.166	1.029	6,912	7,457	Strength
10	85	8	4.449	22	1.07	0.132	1.176	7,637	8,166	Strength
10	90	8	4.788	24	1.19	0.082	1.335	8,390	8,871	Strength
10	95	8	5.101	26	1.27	0.008	1.516	9,172	9,552	Strength
10	100	8	5.405	28	1.33	-0.081	1.707	9,983	10,229	Strength
10	105	8	5.699	30	1.35	-0.185	1.91	10,822	10,902	Strength
10	110	8	6.377	34	1.57	-0.091	2.093	11,691	12,215	Strength
10	115	8	6.635	36	1.33	-0.235	2.328	12,587	12,855	Strength
12	40	9	1.347*	6	0.09	0.070	0.252	2,249	2,341	Strength
12	45	9	1.799*	8	0.16	0.185	0.294	2,678	3,114	Strength
12	50	9	2.239*	10	0.25	0.276	0.350	3,154	3,882	Strength
12	55	9	2.172*	10	0.22	0.074	0.491	3,651	3,882	Strength
12	60	9	2.594*	12	0.32	0.138	0.571	4,169	4,647	Strength
12	65	9	2.987*	14	0.42	0.175	0.675	4,710	5,389	Strength
12	70	9	2.903*	14	0.32	-0.064	0.850	5,273	5,389	Strength
12	75	9	3.279	16	0.40	-0.054	0.977	5,860	6,127	Strength
12	80	9	3.644	18	0.47	-0.060	1.117	6,470	6,861	Strength
12	85	9	3.998	20	0.52	-0.081	1.269	7,105	7,592	Strength
12	90	9	4.343	22	0.52	-0.117	1.434	7,763	8,319	Strength
12	95	9	4.676	24	0.50	-0.168	1.611	8,446	9,042	Strength
12	100	9	4.984	26	0.43	-0.244	1.810	9,153	9,742	Strength
12	105	9	5.283	28	0.29	-0.334	2.021	9,885	10,438	Stress
12	110	9	5.572	30	0.09	-0.443	2.246	10,657	11,131	Stress
12	115	9	6.245	34	0.09	-0.364	2.453	11,505	12,486	Stress
12	120	9	6.498	36	-0.44	-0.526	2.716	12,383	13,149	Stress

PRELIMINARY DESIGN

*A minimum concrete transfer strength of 3.0 ksi is recommended by PCI MNL-116 section 5.3.17.

6.10 Preliminary Design Data

**Final camber is net deflection after all losses and noncomposite and composite dead loads are applied.

Table BT-4 (continued)

Spacing ft	Span ft	Slab Thickness in.	f'_{ci} ksi	No. of Strands	Final Camber in.**	f_b @ L/2 ksi	f_t @ L/2 ksi	M_u @ L/2 ft-kips	M_r @ L/2 ft-kips	Control
AASHTO-PCI Bulb-Tee, 72-in.-Deep Interior Beam										
6	40	8	0.833*	4	0.05	0.028	0.246	1,459	1,537	Strength
6	45	8	1.292*	6	0.13	0.198	0.262	1,742	2,294	Strength
6	50	8	1.231*	6	0.11	0.064	0.364	2,057	2,294	Strength
6	55	8	1.671*	8	0.21	0.208	0.400	2,386	3,044	Strength
6	60	8	1.598*	8	0.18	0.056	0.518	2,731	3,044	Strength
6	65	8	2.021*	10	0.30	0.179	0.571	3,092	3,786	Strength
6	70	8	1.936*	10	0.22	0.009	0.706	3,468	3,786	Strength
6	75	8	2.340*	12	0.36	0.110	0.777	3,861	4,521	Strength
6	80	8	2.244*	12	0.23	-0.077	0.928	4,271	4,521	Strength
6	85	8	2.614*	14	0.34	-0.007	1.027	4,697	5,229	Strength
6	90	8	2.505*	14	0.12	-0.212	1.195	5,140	5,229	Strength
6	95	8	2.859*	16	0.21	-0.164	1.311	5,600	5,930	Strength
6	100	8	3.203	18	0.28	-0.127	1.437	6,077	6,623	Strength
6	105	8	3.077	18	-0.10	-0.358	1.629	6,571	6,623	Stress
6	110	8	3.405	20	-0.09	-0.342	1.772	7,083	7,309	Stress
6	115	8	3.723	22	-0.14	-0.338	1.924	7,611	7,989	Stress
6	120	8	4.030	24	-0.23	-0.345	2.085	8,158	8,661	Stress
6	125	8	4.312	26	-0.40	-0.374	2.266	8,721	9,307	Stress
6	130	8	4.584	28	-0.62	-0.414	2.455	9,302	9,946	Stress
6	135	8	4.848	30	-0.90	-0.464	2.653	9,900	10,579	Stress
6	140	8	5.102	32	-1.27	-0.526	2.860	10,516	11,205	Stress
6	145	8	5.726	36	-1.58	-0.399	3.053	11,150	12,039	Stress
6	150	8	5.929	38	-2.46	-0.504	3.297	11,801	12,365	Stress
6	155	8	6.448	42	-3.20	-0.458	3.558	12,469	12,597	Stress
8	40	8	1.347*	6	0.11	0.229	0.201	1,750	2,303	Strength
8	45	8	1.292*	6	0.11	0.091	0.300	2,086	2,303	Strength
8	50	8	1.738*	8	0.20	0.224	0.337	2,458	3,059	Strength
8	55	8	1.671*	8	0.18	0.060	0.456	2,847	3,059	Strength
8	60	8	2.100*	10	0.29	0.170	0.512	3,254	3,810	Strength
8	65	8	2.021*	10	0.23	-0.013	0.650	3,678	3,810	Strength
8	70	8	2.431*	12	0.35	0.074	0.725	4,120	4,555	Strength
8	75	8	2.813*	14	0.47	0.136	0.821	4,581	5,275	Strength
8	80	8	2.716*	14	0.33	-0.076	0.986	5,060	5,275	Strength
8	85	8	3.081	16	0.43	-0.037	1.101	5,558	5,989	Strength
8	90	8	3.435	18	0.53	-0.011	1.227	6,076	6,698	Strength
8	95	8	3.322	18	0.25	-0.252	1.419	6,613	6,698	Strength
8	100	8	3.660	20	0.29	-0.248	1.563	7,169	7,401	Strength
8	105	8	3.989	22	0.27	-0.257	1.718	7,745	8,099	Strength
8	110	8	4.307	24	0.23	-0.278	1.882	8,340	8,792	Strength
8	115	8	4.599	26	0.11	-0.322	2.066	8,956	9,460	Stress
8	120	8	4.881	28	-0.05	-0.378	2.260	9,591	10,122	Stress
8	125	8	5.155	30	-0.28	-0.447	2.464	10,245	10,779	Stress
8	130	8	5.420	32	-0.58	-0.527	2.677	10,920	11,431	Stress
8	135	8	6.052	36	-0.84	-0.418	2.878	11,615	12,681	Stress
8	140	8	6.621	40	-1.30	-0.359	3.119	12,329	13,852	Stress
8	145	8	6.794	42	-2.27	-0.518	3.401	13,064	14,401	Stress

PRELIMINARY DESIGN

6.10 Preliminary Design Data

*A minimum concrete transfer strength of 3.0 ksi is recommended by PCI MNL-116 section 5.3.17.

**Final camber is net deflection after all losses and noncomposite and composite dead loads are applied.

Table BT-4 (continued)

Spacing ft	Span ft	Slab Thickness in.	f'_{ci} ksi	No. of Strands	Final Camber in.**	f_b @ L/2 ksi	f_t @ L/2 ksi	M_u @ L/2 ft-kips	M_r @ L/2 ft-kips	Control
AASHTO-PCI Bulb-Tee, 72-in.-Deep Interior Beam (continued)										
10	40	8	1.347*	6	0.11	0.144	0.228	2,028	2,308	Strength
10	45	8	1.799*	8	0.19	0.275	0.261	2,413	3,068	Strength
10	50	8	1.738*	8	0.18	0.103	0.380	2,841	3,068	Strength
10	55	8	2.172*	10	0.28	0.203	0.437	3,287	3,824	Strength
10	60	8	2.100*	10	0.24	0.009	0.575	3,752	3,824	Strength
10	65	8	2.516*	12	0.35	0.084	0.653	4,237	4,575	Strength
10	70	8	2.903*	14	0.46	0.134	0.752	4,742	5,302	Strength
10	75	8	2.813*	14	0.35	-0.092	0.920	5,268	5,302	Strength
10	80	8	3.183	16	0.44	-0.067	1.040	5,814	6,025	Strength
10	85	8	3.543	18	0.53	-0.056	1.171	6,382	6,743	Strength
10	90	8	3.892	20	0.59	-0.060	1.312	6,970	7,457	Strength
10	95	8	4.231	22	0.63	-0.077	1.465	7,581	8,166	Strength
10	100	8	4.559	24	0.64	-0.107	1.628	8,213	8,871	Strength
10	105	8	4.436	24	0.22	-0.396	1.857	8,867	8,871	Stress
10	110	8	4.733	26	0.09	-0.460	2.051	9,543	9,552	Stress
10	115	8	5.439	30	0.36	-0.308	2.213	10,241	10,902	Strength
10	120	8	5.714	32	0.14	-0.401	2.429	10,961	11,570	Stress
10	125	8	5.964	34	-0.36	-0.517	2.665	11,703	12,215	Stress
10	130	8	6.579	38	-0.69	-0.448	2.890	12,468	13,472	Stress
12	40	9	1.347*	6	0.09	0.066	0.253	2,264	2,341	Strength
12	45	9	1.799*	8	0.16	0.180	0.295	2,696	3,114	Strength
12	50	9	2.239*	10	0.25	0.271	0.352	3,175	3,882	Strength
12	55	9	2.172*	10	0.22	0.068	0.492	3,674	3,882	Strength
12	60	9	2.594*	12	0.32	0.131	0.573	4,195	4,647	Strength
12	65	9	2.987*	14	0.42	0.168	0.677	4,738	5,389	Strength
12	70	9	2.903*	14	0.32	-0.072	0.852	5,304	5,389	Strength
12	75	9	3.279	16	0.40	-0.063	0.979	5,894	6,127	Strength
12	80	9	3.644	18	0.47	-0.069	1.120	6,507	6,861	Strength
12	85	9	3.998	20	0.52	-0.090	1.272	7,144	7,592	Strength
12	90	9	4.343	22	0.52	-0.127	1.437	7,805	8,319	Strength
12	95	9	4.676	24	0.50	-0.179	1.614	8,490	9,042	Strength
12	100	9	4.984	26	0.43	-0.255	1.813	9,200	9,742	Strength
12	105	9	5.283	28	0.29	-0.346	2.025	9,935	10,438	Stress
12	110	9	5.572	30	0.09	-0.451	2.248	10,694	11,131	Stress
12	115	9	6.245	34	0.09	-0.358	2.452	11,479	12,486	Stress
12	120	9	6.498	36	-0.44	-0.504	2.710	12,288	13,149	Stress

PRELIMINARY DESIGN

6.10 Preliminary Design Data

*A minimum concrete transfer strength of 3.0 ksi is recommended by PCI MNL-116 section 5.3.17.

**Final camber is net deflection after all losses and noncomposite and composite dead loads are applied.

Table DBT-1

Deck Bulb-Tees – Maximum Span vs. Section Depth

DBT Depth, in.	35	41	53	65
Span, ft	90	100	140	170

Table DBT-2

Deck Bulb-Tee, 6-ft-Wide Flange Beams

Spacing ft	Span ft	Slab Thickness in.	f'_{ci} ksi	No. of Strands	Final Camber in.**	f_b @ L/2 ksi	f_t @ L/2 ksi	M_u @ L/2 ft-kips	M_r @ L/2 ft-kips	Control
Deck Bulb-Tee, 35-in.-Deep Exterior Beam										
6	50	0	2.717*	10	0.85	-0.121	0.853	1,497	1,558	Strength
6	55	0	3.217	12	1.21	-0.132	1.003	1,760	1,857	Strength
6	60	0	3.640	14	1.57	-0.194	1.181	2,037	2,133	Strength
6	65	0	4.035	16	1.96	-0.285	1.371	2,328	2,405	Stress
6	70	0	4.404	18	2.38	-0.401	1.574	2,633	2,673	Stress
6	75	0	5.351	22	3.23	-0.250	1.748	2,953	3,197	Stress
6	80	0	5.662	24	3.50	-0.424	1.978	3,286	3,454	Stress
6	85	0	6.440	28	4.24	-0.385	2.205	3,633	3,918	Stress
Deck Bulb-Tee, 35-in.-Deep Interior Beam										
6	45	0	2.932*	10	0.88	0.246	0.678	1,309	1,558	Strength
6	50	0	2.743*	10	0.91	-0.074	0.869	1,548	1,558	Strength
6	55	0	3.254	12	1.30	-0.032	1.003	1,799	1,857	Strength
6	60	0	3.686	14	1.72	-0.039	1.163	2,063	2,133	Strength
6	65	0	4.092	16	2.18	-0.067	1.335	2,339	2,405	Strength
6	70	0	4.473	18	2.67	-0.114	1.518	2,628	2,673	Strength
6	75	0	4.829	20	3.20	-0.182	1.712	2,930	2,937	Strength
6	80	0	5.774	24	4.07	0.068	1.868	3,245	3,454	Strength
6	85	0	6.029	26	4.30	-0.068	2.10	3,573	3,688	Strength
6	90	0	6.262	28	4.71	-0.222	2.344	3,915	3,918	Strength
Deck Bulb-Tee, 41-in.-Deep Exterior Beam										
6	50	0	2.677*	10	0.81	0.256	0.627	1,512	1,851	Strength
6	55	0	2.508*	10	0.82	-0.023	0.794	1,778	1,851	Strength
6	60	0	2.995*	12	1.18	0.036	0.910	2,058	2,209	Strength
6	65	0	3.419	14	1.56	0.055	1.048	2,353	2,543	Strength
6	70	0	3.821	16	1.99	0.057	1.196	2,662	2,873	Strength
6	75	0	4.201	18	2.46	0.041	1.354	2,985	3,199	Strength
6	80	0	4.559	20	2.96	0.007	1.522	3,323	3,521	Strength
6	85	0	4.897	22	3.48	-0.043	1.699	3,675	3,840	Strength
6	90	0	5.215	24	3.76	-0.109	1.886	4,042	4,155	Strength
6	95	0	5.477	26	3.94	-0.213	2.094	4,423	4,444	Strength
6	100	0	6.773	32	5.87	0.247	2.245	4,818	4,961	Strength
Deck Bulb-Tee, 41-in.-Deep Interior Beam										
6	50	0	2.677*	10	0.81	0.181	0.677	1,604	1,851	Strength
6	55	0	3.178	12	1.16	0.264	0.779	1,861	2,209	Strength
6	60	0	2.995*	12	1.18	-0.022	0.949	2,130	2,209	Strength
6	65	0	3.419	14	1.56	0.008	1.080	2,412	2,543	Strength
6	70	0	3.821	16	1.99	0.021	1.221	2,707	2,873	Strength
6	75	0	4.201	18	2.46	0.017	1.370	3,015	3,199	Strength
6	80	0	4.559	20	2.96	-0.003	1.529	3,337	3,521	Strength
6	85	0	4.897	22	3.48	-0.039	1.696	3,671	3,840	Strength
6	90	0	5.215	24	3.76	-0.091	1.873	4,019	4,155	Strength
6	95	0	5.477	26	3.94	-0.180	2.071	4,381	4,444	Strength
6	100	0	6.250	30	4.98	0.007	2.245	4,756	4,808	Strength

PRELIMINARY DESIGN

6.10 Preliminary Design Data

*A minimum concrete transfer strength of 3.0 ksi is recommended by PCI MNL-116 section 5.3.17.

**Final camber is net deflection after all losses and noncomposite and composite dead loads are applied.

Table DBT-2 (continued)

Spacing ft	Span ft	Slab Thickness in.	f'_{ci} ksi	No. of Strands	Final Camber in.**	f_b @ L/2 ksi	f_t @ L/2 ksi	M_u @ L/2 ft-kips	M_r @ L/2 ft-kips	Control
Deck Bulb-Tee, 53-in.-Deep Exterior Beam										
6	60	0	2.251*	10	0.69	0.132	0.636	2,100	2,437	Strength
6	65	0	2.105*	10	0.67	-0.086	0.768	2,402	2,437	Strength
6	70	0	2.548*	12	0.98	0.000	0.855	2,719	2,911	Strength
6	75	0	2.946*	14	1.30	0.058	0.957	3,051	3,362	Strength
6	80	0	3.326	16	1.67	0.103	1.067	3,398	3,809	Strength
6	85	0	3.138	16	1.57	-0.159	1.226	3,760	3,809	Strength
6	90	0	3.492	18	1.95	-0.138	1.350	4,137	4,252	Strength
6	95	0	3.830	20	2.37	-0.129	1.480	4,529	4,691	Strength
6	100	0	4.151	22	2.81	-0.132	1.618	4,935	5,126	Strength
6	105	0	4.457	24	3.26	-0.147	1.763	5,357	5,557	Strength
6	110	0	4.724	26	3.50	-0.188	1.922	5,794	5,965	Strength
6	115	0	4.976	28	3.61	-0.240	2.089	6,245	6,369	Strength
6	120	0	5.214	30	3.67	-0.304	2.262	6,712	6,769	Stress
6	125	0	5.897	34	4.57	-0.127	2.418	7,193	7,539	Strength
6	130	0	6.057	36	4.49	-0.243	2.622	7,690	7,889	Strength
6	135	0	6.182	38	4.25	-0.384	2.841	8,201	8,216	Stress
6	140	0	6.627	42	4.45	-0.359	3.083	8,727	8,801	Stress
Deck Bulb-Tee, 53-in.-Deep Interior Beam										
6	55	0	2.386*	10	0.68	0.242	0.577	1,987	2,437	Strength
6	60	0	2.251*	10	0.69	0.039	0.699	2,270	2,437	Strength
6	65	0	2.704*	12	0.99	0.140	0.777	2,566	2,911	Strength
6	70	0	2.548*	12	0.98	-0.083	0.912	2,874	2,911	Strength
6	75	0	2.946*	14	1.30	-0.019	1.011	3,195	3,362	Strength
6	80	0	3.326	16	1.67	0.033	1.116	3,529	3,809	Strength
6	85	0	3.690	18	2.07	0.073	1.227	3,877	4,252	Strength
6	90	0	3.492	18	1.95	-0.192	1.387	4,239	4,252	Strength
6	95	0	3.830	20	2.37	-0.174	1.512	4,615	4,691	Strength
6	100	0	4.151	22	2.81	-0.168	1.643	5,004	5,126	Strength
6	105	0	4.457	24	3.26	-0.173	1.781	5,408	5,557	Strength
6	110	0	4.724	26	3.50	-0.204	1.934	5,825	5,965	Strength
6	115	0	4.976	28	3.61	-0.247	2.093	6,257	6,369	Strength
6	120	0	5.214	30	3.67	-0.300	2.259	6,703	6,769	Stress
6	125	0	5.437	32	3.91	-0.364	2.432	7,163	7,165	Stress
6	130	0	6.057	36	4.49	-0.217	2.603	7,638	7,889	Strength
6	135	0	6.182	38	4.25	-0.346	2.814	8,126	8,216	Stress
6	140	0	6.627	42	4.45	-0.310	3.047	8,629	8,801	Strength

PRELIMINARY DESIGN

*A minimum concrete transfer strength of 3.0 ksi is recommended by PCI MNL-116 section 5.3.17.

6.10 Preliminary Design Data

**Final camber is net deflection after all losses and noncomposite and composite dead loads are applied.

Table DBT-2 (continued)

Spacing ft	Span ft	Slab Thickness in.	f'_{ci} ksi	No. of Strands	Final Camber in.**	f_b @ L/2 ksi	f_t @ L/2 ksi	M_u @ L/2 ft-kips	M_r @ L/2 ft-kips	Control
Deck Bulb-Tee, 65-in.-Deep Exterior Beam										
6	65	0	2.024*	10	0.59	0.179	0.555	2,452	3,022	Strength
6	70	0	1.900*	10	0.58	0.005	0.662	2,777	3,022	Strength
6	75	0	2.312*	12	0.84	0.107	0.728	3,117	3,614	Strength
6	80	0	2.171*	12	0.79	-0.084	0.846	3,473	3,614	Strength
6	85	0	2.541*	14	1.07	-0.011	0.929	3,845	4,182	Strength
6	90	0	2.896*	16	1.39	0.051	1.018	4,232	4,746	Strength
6	95	0	2.730*	16	1.28	-0.166	1.152	4,634	4,746	Strength
6	100	0	3.065	18	1.61	-0.121	1.252	5,053	5,306	Strength
6	105	0	3.385	20	1.98	-0.087	1.358	5,486	5,862	Strength
6	110	0	3.693	22	2.37	-0.062	1.468	5,935	6,413	Strength
6	115	0	3.496	22	2.10	-0.311	1.624	6,400	6,413	Stress
6	120	0	3.783	24	2.47	-0.303	1.746	6,880	6,961	Stress
6	125	0	4.040	26	2.81	-0.315	1.879	7,376	7,486	Stress
6	130	0	4.285	28	3.04	-0.336	2.018	7,888	8,006	Stress
6	135	0	4.519	30	3.07	-0.366	2.162	8,414	8,522	Stress
6	140	0	4.741	32	3.05	-0.405	2.311	8,957	9,035	Stress
6	145	0	4.934	34	2.93	-0.462	2.472	9,515	9,524	Stress
6	150	0	5.493	38	3.25	-0.325	2.631	10,088	10,433	Stress
6	155	0	5.612	40	2.85	-0.432	2.822	10,677	10,853	Stress
6	160	0	6.038	44	2.96	-0.378	3.028	11,282	11,623	Stress
6	165	0	6.085	46	2.29	-0.533	3.248	11,902	11,973	Stress
6	170	0	6.647	52	2.45	-0.424	3.531	12,537	12,888	Stress
Deck Bulb Tee, 65-in.-Deep Interior Beam										
6	65	0	2.024*	10	0.59	0.073	0.629	2,718	3,022	Strength
6	70	0	2.444*	12	0.85	0.185	0.690	3,042	3,614	Strength
6	75	0	2.312*	12	0.84	0.004	0.801	3,378	3,614	Strength
6	80	0	2.690*	14	1.13	0.088	0.877	3,728	4,182	Strength
6	85	0	2.541*	14	1.07	-0.108	0.998	4,091	4,182	Strength
6	90	0	2.896*	16	1.39	-0.041	1.084	4,468	4,746	Strength
6	95	0	3.238	18	1.75	0.017	1.175	4,859	5,306	Strength
6	100	0	3.065	18	1.61	-0.203	1.311	5,264	5,306	Strength
6	105	0	3.385	20	1.98	-0.163	1.412	5,683	5,862	Strength
6	110	0	3.693	22	2.37	-0.131	1.519	6,117	6,413	Strength
6	115	0	3.988	24	2.77	-0.109	1.630	6,565	6,961	Strength
6	120	0	4.252	26	3.16	-0.107	1.754	7,028	7,486	Strength
6	125	0	4.505	28	3.46	-0.113	1.882	7,506	8,006	Strength
6	130	0	4.285	28	3.04	-0.378	2.048	7,998	8,006	Stress
6	135	0	4.519	30	3.07	-0.400	2.187	8,506	8,522	Stress
6	140	0	4.741	32	3.05	-0.431	2.331	9,027	9,035	Stress
6	145	0	5.348	36	3.51	-0.255	2.466	9,564	9,990	Strength
6	150	0	5.493	38	3.25	-0.335	2.639	10,115	10,433	Stress
6	155	0	5.612	40	2.85	-0.434	2.823	10,682	10,853	Stress
6	160	0	6.038	44	2.96	-0.371	3.023	11,263	11,623	Stress
6	165	0	6.085	46	2.29	-0.518	3.236	11,859	11,973	Stress
6	170	0	6.385	50	1.97	-0.536	3.484	12,470	12,606	Stress

PRELIMINARY DESIGN

6.10 Preliminary Design Data

*A minimum concrete transfer strength of 3.0 ksi is recommended by PCI MNL-116 section 5.3.17.

**Final camber is net deflection after all losses and noncomposite and composite dead loads are applied.

Table IB-1

AASHTO I-Beams – Maximum Span (ft) vs. Beam Spacing

Spacing Beam	6 ft	8 ft	10 ft	12 ft
TYPE II	75	65	60	55
TYPE III	100	90	80	70
TYPE IV	125	125	115	100
TYPE V	140	140	130	120
TYPE VI	150	150	140	130

Table IB-2

AASHTO I-Beam Type II

Spacing ft	Span ft	Slab Thickness in.	f'_{ci} ksi	No. of Strands	Final Camber in.**	f_b @ L/2 ksi	f_t @ L/2 ksi	M_u @ L/2 ft-kips	M_r @ L/2 ft-kips	Control
AASHTO I-Beam Type II, Exterior Beam										
6	20	8	1.876*	4	0.12	0.538	-0.070	492	810	Strength
6	25	8	1.810*	4	0.15	0.312	0.110	650	834	Strength
6	30	8	1.730*	4	0.14	0.058	0.323	818	834	Strength
6	35	8	2.602*	6	0.32	0.316	0.358	997	1,240	Strength
6	40	8	2.496*	6	0.27	0.005	0.637	1,189	1,240	Stress
6	45	8	3.320	8	0.45	0.171	0.753	1,418	1,638	Strength
6	50	8	4.033	10	0.61	0.225	0.976	1,687	2,010	Strength
6	55	8	3.888	10	0.33	-0.228	1.374	1,985	2,010	Stress
6	60	8	4.560	12	0.38	-0.258	1.674	2,299	2,375	Stress
6	65	8	5.204	14	0.35	-0.328	2.012	2,630	2,732	Stress
6	70	8	5.822	16	0.25	-0.438	2.388	2,977	3,083	Stress
8	20	8	1.876*	4	0.11	0.434	-0.042	599	812	Strength
8	25	8	1.810*	4	0.13	0.170	0.157	788	838	Strength
8	30	8	2.695*	6	0.29	0.415	0.186	989	1,249	Strength
8	35	8	2.602*	6	0.27	0.088	0.463	1,203	1,249	Strength
8	40	8	3.439	8	0.44	0.254	0.576	1,431	1,653	Strength
8	45	8	4.164	10	0.59	0.301	0.800	1,704	2,033	Strength
8	50	8	4.033	10	0.38	-0.161	1.202	2,006	2,033	Stress
8	55	8	4.717	12	0.42	-0.199	1.510	2,321	2,408	Stress
8	60	8	5.373	14	0.40	-0.279	1.861	2,650	2,777	Stress
8	65	8	6.002	16	0.27	-0.399	2.254	2,992	3,140	Stress
10	20	8.5	1.876*	4	0.10	0.337	-0.012	697	823	Strength
10	25	8.5	2.774*	6	0.23	0.573	0.004	918	1,268	Strength
10	30	8.5	2.695*	6	0.25	0.234	0.275	1,152	1,268	Strength
10	35	8.5	3.544	8	0.40	0.381	0.390	1,401	1,682	Strength
10	40	8.5	3.439	8	0.31	-0.034	0.754	1,666	1,682	Stress
10	45	8.5	4.164	10	0.38	-0.051	1.031	1,984	2,072	Strength
10	50	8.5	4.860	12	0.43	-0.131	1.361	2,337	2,457	Stress
10	55	8.5	5.528	14	0.39	-0.291	1.745	2,750	2,838	Stress
10	60	8.5	6.170	16	0.26	-0.501	2.180	3,185	3,214	Stress
12	20	9.5	1.876*	4	0.09	0.241	0.036	789	843	Strength
12	25	9.5	2.774*	6	0.20	0.394	0.090	1,091	1,301	Strength
12	30	9.5	3.635	8	0.34	0.478	0.209	1,424	1,727	Strength
12	35	9.5	4.386	10	0.47	0.449	0.451	1,784	2,130	Strength
12	40	9.5	5.107	12	0.59	0.357	0.754	2,174	2,529	Strength
12	45	9.5	5.800	14	0.67	0.167	1.120	2,641	2,924	Strength
12	50	9.5	6.465	16	0.69	-0.103	1.548	3,164	3,316	Strength

PRELIMINARY DESIGN

*A minimum concrete transfer strength of 3.0 ksi is recommended by PCI MNL-116 section 5.3.17.

6.10 Preliminary Design Data

**Final camber is net deflection after all losses and noncomposite and composite dead loads are applied.

Table IB-2 (continued)

Spacing ft	Span ft	Slab Thickness in.	f'_{ci} ksi	No. of Strands	Final Camber in.**	f_b @ L/2 ksi	f_t @ L/2 ksi	M_u @ L/2 ft-kips	M_r @ L/2 ft-kips	Control
AASHTO I-Beam Type II, Interior Beam										
6	20	8	1.876*	4	0.12	0.535	-0.068	496	810	Strength
6	25	8	1.810*	4	0.15	0.308	0.111	655	834	Strength
6	30	8	1.730*	4	0.14	0.052	0.324	824	834	Strength
6	35	8	2.602*	6	0.32	0.310	0.360	1,004	1,240	Strength
6	40	8	2.496*	6	0.27	-0.002	0.640	1,197	1,240	Stress
6	45	8	3.320	8	0.45	0.163	0.756	1,427	1,638	Strength
6	50	8	4.033	10	0.61	0.228	0.975	1,683	2,010	Strength
6	55	8	3.888	10	0.33	-0.199	1.365	1,950	2,010	Stress
6	60	8	4.560	12	0.38	-0.198	1.655	2,228	2,375	Stress
6	65	8	5.204	14	0.35	-0.235	1.982	2,519	2,732	Stress
6	70	8	5.822	16	0.25	-0.309	2.347	2,822	3,083	Stress
6	75	8	6.342	18	-0.09	-0.465	2.806	3,138	3,408	Stress
8	20	8	1.876*	4	0.11	0.430	-0.041	604	812	Strength
8	25	8	1.810*	4	0.13	0.165	0.159	795	838	Strength
8	30	8	2.695*	6	0.29	0.409	0.187	997	1,249	Strength
8	35	8	2.602*	6	0.27	0.081	0.465	1,212	1,249	Strength
8	40	8	3.439	8	0.44	0.245	0.578	1,441	1,653	Strength
8	45	8	4.164	10	0.59	0.291	0.802	1,715	2,033	Strength
8	50	8	4.033	10	0.38	-0.172	1.204	2,019	2,033	Stress
8	55	8	4.717	12	0.42	-0.211	1.513	2,336	2,408	Stress
8	60	8	5.373	14	0.40	-0.292	1.864	2,667	2,777	Stress
8	65	8	6.002	16	0.27	-0.414	2.258	3,011	3,140	Stress
10	20	8.5	1.876*	4	0.10	0.333	-0.011	703	823	Strength
10	25	8.5	2.774*	6	0.23	0.568	0.005	925	1,268	Strength
10	30	8.5	2.695*	6	0.25	0.227	0.276	1,160	1,268	Strength
10	35	8.5	3.544	8	0.40	0.373	0.391	1,411	1,682	Strength
10	40	8.5	3.439	8	0.31	-0.044	0.755	1,678	1,682	Stress
10	45	8.5	4.164	10	0.38	-0.061	1.033	1,997	2,072	Strength
10	50	8.5	4.860	12	0.43	-0.142	1.363	2,352	2,457	Stress
10	55	8.5	5.528	14	0.39	-0.268	1.742	2,721	2,838	Stress
10	60	8.5	6.170	16	0.26	-0.44	2.172	3,106	3,214	Stress
12	20	9.5	1.876*	4	0.09	0.236	0.036	796	843	Strength
12	25	9.5	2.774*	6	0.20	0.426	0.089	1,050	1,301	Strength
12	30	9.5	3.635	8	0.34	0.555	0.205	1,321	1,727	Strength
12	35	9.5	3.544	8	0.29	0.116	0.580	1,611	1,727	Strength
12	40	9.5	4.282	10	0.37	0.095	0.876	1,921	2,130	Strength
12	45	9.5	4.990	12	0.39	-0.013	1.234	2,290	2,529	Strength
12	50	9.5	5.671	14	0.34	-0.191	1.653	2,700	2,924	Stress
12	55	9.5	6.324	16	0.19	-0.421	2.131	3,128	3,316	Stress

PRELIMINARY DESIGN

6.10 Preliminary Design Data

*A minimum concrete transfer strength of 3.0 ksi is recommended by PCI MNL-116 section 5.3.17.

**Final camber is net deflection after all losses and noncomposite and composite dead loads are applied.

Table IB-3

AASHTO I-Beam Type III

Spacing ft	Span ft	Slab Thickness in.	f'_{ci} ksi	No. of Strands	Final Camber in.**	f_b @ L/2 ksi	f_t @ L/2 ksi	M_u @ L/2 ft-kips	M_r @ L/2 ft-kips	Control
AASHTO I-Beam Type III, Exterior Beam										
6	50	8	2.110*	8	0.24	-0.004	0.719	1,827	1,990	Strength
6	60	8	2.512*	10	0.19	-0.195	1.100	2,424	2,469	Stress
6	70	8	3.410	14	0.24	-0.189	1.509	3,136	3,366	Strength
6	80	8	4.238	18	0.12	-0.284	2.012	3,928	4,235	Stress
6	90	8	4.961	22	-0.38	-0.496	2.636	4,793	5,058	Stress
6	100	8	6.582	30	-0.52	-0.297	3.261	5,730	6,586	Stress
8	40	8	2.311*	8	0.30	0.313	0.355	1,554	2,005	Strength
8	50	8	2.755*	10	0.39	0.130	0.696	2,180	2,492	Strength
8	60	8	3.107	12	0.29	-0.169	1.165	2,883	2,954	Strength
8	70	8	3.989	16	0.27	-0.230	1.627	3,647	3,862	Stress
8	80	8	4.802	20	0.01	-0.386	2.188	4,476	4,749	Stress
8	90	8	5.980	26	-0.25	-0.414	2.845	5,370	5,981	Stress
10	40	8.5	2.311*	8	0.25	0.151	0.435	1,801	2,033	Strength
10	50	8.5	2.755*	10	0.26	-0.108	0.830	2,527	2,530	Strength
10	60	8.5	3.693	14	0.32	-0.169	1.265	3,340	3,472	Strength
10	70	8.5	4.559	18	0.18	-0.363	1.820	4,280	4,396	Stress
10	80	8.5	5.831	24	0.06	-0.439	2.463	5,356	5,711	Stress
12	40	9.5	2.955*	10	0.33	0.253	0.426	2,226	2,589	Strength
12	50	9.5	3.932	14	0.49	0.116	0.844	3,245	3,559	Strength
12	60	9.5	4.838	18	0.52	-0.173	1.400	4,414	4,514	Strength
12	70	9.5	6.147	24	0.55	-0.347	2.059	5,704	5,881	Stress

AASHTO I-Beam Type III, Interior Beam										
6	50	8	2.110*	8	0.24	-0.010	0.721	1,839	1,990	Strength
6	60	8	2.512*	10	0.19	-0.202	1.104	2,439	2,469	Stress
6	70	8	3.410	14	0.24	-0.167	1.499	3,093	3,366	Strength
6	80	8	4.238	18	0.12	-0.222	1.982	3,804	4,235	Strength
6	90	8	4.961	22	-0.38	-0.387	2.583	4,574	5,058	Stress
6	100	8	6.086	28	-0.94	-0.396	3.240	5,402	6,214	Stress
8	40	8	2.311*	8	0.30	0.307	0.357	1,565	2,005	Strength
8	50	8	2.755*	10	0.39	0.122	0.699	2,195	2,492	Strength
8	60	8	3.107	12	0.29	-0.178	1.168	2,901	2,954	Strength
8	70	8	3.989	16	0.27	-0.240	1.631	3,669	3,862	Stress
8	80	8	4.802	20	0.01	-0.398	2.193	4,501	4,749	Stress
8	90	8	5.980	26	-0.25	-0.428	2.851	5,399	5,981	Stress
10	40	8.5	2.311*	8	0.25	0.145	0.437	1,814	2,033	Strength
10	50	8.5	3.348	12	0.46	0.215	0.729	2,543	3,003	Strength
10	60	8.5	3.693	14	0.32	-0.178	1.268	3,361	3,472	Strength
10	70	8.5	4.559	18	0.18	-0.348	1.816	4,249	4,396	Stress
10	80	8.5	5.831	24	0.06	-0.374	2.445	5,211	5,711	Stress
12	40	9.5	2.311*	8	0.18	-0.036	0.550	2,066	2,079	Strength
12	50	9.5	3.348	12	0.29	-0.057	0.918	2,904	3,076	Strength
12	60	9.5	4.270	16	0.24	-0.238	1.452	3,846	4,038	Stress
12	70	9.5	5.637	22	0.22	-0.261	2.055	4,873	5,435	Stress

PRELIMINARY DESIGN

6.10 Preliminary Design Data

*A minimum concrete transfer strength of 3.0 ksi is recommended by PCI MNL-116 section 5.3.17.

**Final camber is net deflection after all losses and noncomposite and composite dead loads are applied.

Table IB-4
AASHTO I-Beam Type IV

Spacing ft	Span ft	Slab Thickness in.	f'_{ci} ksi	No. of Strands	Final Camber in.**	f_b @ L/2 ksi	f_t @ L/2 ksi	M_u @ L/2 ft-kips	M_r @ L/2 ft-kips	Control
AASHTO I-Beam Type IV, Exterior Beam										
6	65	8	2.108*	12	0.25	-0.001	0.908	2,997	3,467	Strength
6	75	8	2.294*	14	0.06	-0.210	1.282	3,747	4,000	Strength
6	80	8	2.591*	16	0.02	-0.221	1.457	4,175	4,525	Strength
6	85	8	2.875*	18	-0.05	-0.251	1.649	4,630	5,044	Strength
6	90	8	3.148	20	-0.18	-0.296	1.856	5,105	5,555	Strength
6	95	8	3.409	22	-0.36	-0.356	2.079	5,600	6,060	Stress
6	100	8	3.658	24	-0.62	-0.431	2.318	6,115	6,558	Stress
6	105	8	3.871	26	-1.02	-0.537	2.589	6,650	7,030	Stress
6	110	8	4.461	30	-1.01	-0.447	2.821	7,205	7,954	Stress
6	115	8	5.031	34	-1.03	-0.380	3.071	7,780	8,771	Stress
6	120	8	5.206	36	-1.72	-0.533	3.389	8,375	9,067	Stress
6	125	8	5.699	40	-2.36	-0.533	3.706	8,990	9,541	Stress
8	60	8	2.222*	12	0.28	0.014	0.804	3,127	3,501	Strength
8	65	8	2.548*	14	0.35	0.025	0.949	3,536	4,045	Strength
8	70	8	2.426*	14	0.14	-0.224	1.187	3,962	4,045	Strength
8	75	8	2.731*	16	0.11	-0.242	1.364	4,406	4,584	Strength
8	80	8	3.024	18	0.04	-0.277	1.556	4,869	5,117	Strength
8	85	8	3.304	20	-0.07	-0.327	1.765	5,350	5,645	Stress
8	90	8	3.573	22	-0.25	-0.393	1.99	5,849	6,168	Stress
8	95	8	3.830	24	-0.51	-0.474	2.232	6,368	6,686	Stress
8	100	8	4.441	28	-0.46	-0.374	2.452	6,905	7,667	Stress
8	105	8	4.648	30	-0.93	-0.503	2.744	7,461	8,149	Stress
8	110	8	5.225	34	-1.01	-0.443	3.000	8,036	9,100	Stress
8	115	8	5.760	38	-1.27	-0.420	3.290	8,631	10,011	Stress
8	120	8	6.254	42	-2.05	-0.432	3.615	9,244	10,884	Stress
8	125	8	6.731	46	-2.55	-0.464	3.957	9,877	11,550	Stress
10	55	8.5	2.328*	12	0.29	0.063	0.686	3,152	3,550	Strength
10	60	8.5	2.662*	14	0.36	0.059	0.835	3,601	4,106	Strength
10	65	8.5	2.548*	14	0.18	-0.206	1.080	4,070	4,106	Strength
10	70	8.5	2.862*	16	0.15	-0.243	1.265	4,560	4,658	Strength
10	75	8.5	3.163	18	0.08	-0.297	1.468	5,069	5,206	Stress
10	80	8.5	3.452	20	-0.04	-0.369	1.689	5,603	5,749	Stress
10	85	8.5	3.728	22	-0.22	-0.474	1.935	6,209	6,288	Stress
10	90	8.5	4.385	26	-0.14	-0.383	2.145	6,841	7,334	Stress
10	95	8.5	4.997	30	-0.12	-0.332	2.393	7,499	8,343	Stress
10	100	8.5	5.209	32	-0.56	-0.511	2.714	8,183	8,841	Stress
10	105	8.5	5.786	36	-0.68	-0.506	3.003	8,893	9,826	Stress
10	110	8.5	6.645	42	-0.94	-0.374	3.312	9,629	11,213	Stress
12	45	9.5	2.042*	10	0.20	0.069	0.470	2,785	3,028	Strength
12	50	9.5	2.424*	12	0.28	0.059	0.594	3,342	3,622	Strength
12	55	9.5	2.767*	14	0.33	0.011	0.758	3,931	4,193	Strength
12	60	9.5	3.097	16	0.35	-0.060	0.945	4,553	4,760	Strength
12	65	9.5	3.415	18	0.35	-0.154	1.153	5,207	5,324	Strength
12	70	9.5	4.142	22	0.54	-0.035	1.309	5,893	6,440	Strength
12	75	9.5	4.431	24	0.46	-0.175	1.562	6,612	6,993	Strength
12	80	9.5	4.684	26	0.30	-0.351	1.853	7,362	7,522	Stress
12	85	9.5	5.311	30	0.36	-0.338	2.113	8,145	8,571	Stress
12	90	9.5	5.916	34	0.37	-0.354	2.397	8,960	9,605	Stress
12	95	9.5	6.480	38	0.25	-0.411	2.721	9,807	10,606	Stress

PRELIMINARY DESIGN

6.10 Preliminary Design Data

*A minimum concrete transfer strength of 3.0 ksi is recommended by PCI MNL-116 section 5.3.17.

**Final camber is net deflection after all losses and noncomposite and composite dead loads are applied.

Table IB-4 (continued)

Spacing ft	Span ft	Slab Thickness in.	f'_{ci} ksi	No. of Strands	Final Camber in.**	f_b @ L/2 ksi	f_t @ L/2 ksi	M_u @ L/2 ft-kips	M_r @ L/2 ft-kips	Control
AASHTO I-Beam Type IV, Interior Beam										
6	65	8	2.108*	12	0.25	-0.007	0.912	3,014	3,467	Strength
6	75	8	2.294*	14	0.06	-0.217	1.286	3,767	4,000	Strength
6	80	8	2.591*	16	0.02	-0.219	1.456	4,168	4,525	Strength
6	85	8	2.875*	18	-0.05	-0.236	1.640	4,586	5,044	Strength
6	90	8	2.718*	18	-0.57	-0.506	1.915	5,020	5,044	Stress
6	95	8	3.409	22	-0.36	-0.314	2.053	5,471	6,060	Stress
6	100	8	3.658	24	-0.62	-0.374	2.282	5,938	6,558	Stress
6	105	8	3.871	26	-1.02	-0.464	2.543	6,423	7,030	Stress
6	110	8	4.461	30	-1.01	-0.358	2.765	6,925	7,954	Stress
6	115	8	4.650	32	-1.60	-0.477	3.056	7,443	8,406	Stress
6	120	8	5.206	36	-1.72	-0.409	3.310	7,979	9,067	Stress
6	125	8	5.699	40	-2.36	-0.390	3.613	8,532	9,541	Stress
8	60	8	2.222*	12	0.28	0.008	0.807	3,146	3,501	Strength
8	65	8	2.548*	14	0.35	0.018	0.952	3,557	4,045	Strength
8	70	8	2.426*	14	0.14	-0.231	1.191	3,985	4,045	Strength
8	75	8	2.731*	16	0.11	-0.250	1.367	4,431	4,584	Strength
8	80	8	3.024	18	0.04	-0.285	1.560	4,896	5,117	Strength
8	85	8	3.304	20	-0.07	-0.336	1.770	5,379	5,645	Stress
8	90	8	3.573	22	-0.25	-0.403	1.995	5,880	6,168	Stress
8	95	8	3.830	24	-0.51	-0.485	2.237	6,400	6,686	Stress
8	100	8	4.441	28	-0.46	-0.385	2.458	6,940	7,667	Stress
8	105	8	4.648	30	-0.93	-0.514	2.750	7,498	8,149	Stress
8	110	8	5.225	34	-1.01	-0.455	3.006	8,075	9,100	Stress
8	115	8	5.760	38	-1.27	-0.432	3.297	8,672	10,011	Stress
8	120	8	6.254	42	-2.05	-0.444	3.622	9,287	10,884	Stress
8	125	8	6.731	46	-2.55	-0.478	3.965	9,922	11,550	Stress
10	55	8.5	2.328*	12	0.29	0.057	0.688	3,171	3,550	Strength
10	60	8.5	2.662*	14	0.36	0.052	0.838	3,623	4,106	Strength
10	65	8.5	2.548*	14	0.18	-0.214	1.083	4,095	4,106	Strength
10	70	8.5	2.862*	16	0.15	-0.251	1.268	4,586	4,658	Strength
10	75	8.5	3.163	18	0.08	-0.305	1.471	5,098	5,206	Stress
10	80	8.5	3.452	20	-0.04	-0.377	1.693	5,631	5,749	Stress
10	85	8.5	3.728	22	-0.22	-0.467	1.933	6,185	6,288	Stress
10	90	8.5	4.385	26	-0.14	-0.359	2.135	6,760	7,334	Stress
10	95	8.5	4.612	28	-0.51	-0.499	2.430	7,356	7,840	Stress
10	100	8.5	5.209	32	-0.56	-0.450	2.689	7,974	8,841	Stress
10	105	8.5	5.786	36	-0.68	-0.425	2.969	8,614	9,826	Stress
10	110	8.5	6.300	40	-1.21	-0.451	3.302	9,275	10,755	Stress
10	115	8.5	6.796	44	-1.85	-0.500	3.654	9,958	11,668	Stress
12	45	9.5	2.042*	10	0.20	0.112	0.458	2,637	3,028	Strength
12	50	9.5	2.424*	12	0.28	0.126	0.575	3,111	3,622	Strength
12	55	9.5	2.328*	12	0.17	-0.142	0.810	3,605	3,622	Strength
12	60	9.5	2.662*	14	0.18	-0.180	0.986	4,122	4,193	Strength
12	65	9.5	2.984*	16	0.14	-0.239	1.184	4,663	4,760	Strength
12	70	9.5	3.293	18	0.06	-0.317	1.402	5,227	5,324	Stress
12	75	9.5	3.590	20	-0.07	-0.416	1.642	5,815	5,884	Stress
12	80	9.5	3.875	22	-0.29	-0.534	1.903	6,427	6,440	Stress
12	85	9.5	4.539	26	-0.27	-0.457	2.130	7,064	7,522	Stress
12	90	9.5	5.158	30	-0.33	-0.421	2.397	7,726	8,571	Stress
12	95	9.5	5.756	34	-0.45	-0.413	2.688	8,413	9,605	Stress
12	100	9.5	6.312	38	-0.73	-0.444	3.018	9,126	10,606	Stress

PRELIMINARY DESIGN

*A minimum concrete transfer strength of 3.0 ksi is recommended by PCI MNL-116 section 5.3.17.

6.10 Preliminary Design Data

**Final camber is net deflection after all losses and noncomposite and composite dead loads are applied.

Table IB-5
AASHTO I-Beam Type V

Spacing ft	Span ft	Slab Thickness in.	f'_{ci} ksi	No. of Strands	Final Camber in.**	f_b @ L/2 ksi	f_t @ L/2 ksi	M_u @ L/2 ft-kips	M_r @ L/2 ft-kips	Control
AASHTO I-Beam Type V, Exterior Beam										
6	85	8	2.034*	16	0.01	-0.213	1.144	4,967	5,227	Strength
6	90	8	2.271*	18	0.00	-0.218	1.275	5,461	5,833	Strength
6	95	8	2.497*	20	-0.03	-0.240	1.417	5,997	6,432	Strength
6	100	8	2.714*	22	-0.09	-0.273	1.570	6,554	7,024	Strength
6	105	8	2.921*	24	-0.18	-0.318	1.733	7,134	7,609	Strength
6	110	8	3.103	26	-0.38	-0.384	1.914	7,736	8,168	Stress
6	115	8	3.276	28	-0.65	-0.461	2.105	8,361	8,720	Stress
6	120	8	3.774	32	-0.55	-0.366	2.268	9,007	9,805	Stress
6	125	8	3.928	34	-0.94	-0.467	2.479	9,676	10,237	Stress
6	130	8	4.384	38	-0.96	-0.411	2.672	10,366	10,924	Stress
6	135	8	4.811	42	-1.04	-0.379	2.885	11,079	11,481	Stress
8	65	8	2.119*	14	0.33	-0.016	0.730	4,500	4,660	Strength
8	70	8	2.386*	16	0.41	-0.028	0.848	5,091	5,286	Strength
8	75	8	2.642*	18	0.48	-0.054	0.978	5,710	5,907	Strength
8	80	8	2.889*	20	0.55	-0.093	1.119	6,357	6,523	Strength
8	85	8	3.126	22	0.60	-0.146	1.271	7,031	7,134	Strength
8	90	8	3.353	24	0.62	-0.212	1.434	7,732	7,739	Strength
8	95	8	3.892	28	0.86	-0.114	1.578	8,461	8,894	Strength
8	100	8	4.083	30	0.80	-0.217	1.772	9,218	9,464	Strength
8	105	8	4.265	32	0.68	-0.332	1.977	10,002	10,029	Strength
8	110	8	4.765	36	0.87	-0.281	2.156	10,813	11,143	Strength
8	115	8	4.912	38	0.63	-0.431	2.392	11,652	11,673	Stress
8	120	8	5.357	42	0.69	-0.430	2.612	12,519	12,719	Stress
8	125	8	5.787	46	0.44	-0.444	2.843	13,413	13,519	Stress
10	60	8	2.214*	14	0.34	0.050	0.621	4,444	4,687	Strength
10	65	8	2.488*	16	0.42	0.028	0.739	5,079	5,322	Strength
10	70	8	2.751*	18	0.50	-0.008	0.869	5,745	5,953	Strength
10	75	8	3.005	20	0.56	-0.059	1.010	6,441	6,579	Strength
10	80	8	3.249	22	0.62	-0.124	1.163	7,168	7,200	Strength
10	85	8	3.821	26	0.87	-0.016	1.290	7,926	8,411	Strength
10	90	8	4.028	28	0.86	-0.121	1.476	8,714	9,000	Strength
10	95	8	4.225	30	0.81	-0.240	1.674	9,534	9,586	Strength
10	100	8	4.742	34	1.01	-0.191	1.847	10,383	10,743	Strength
10	105	8	4.920	36	0.87	-0.338	2.068	11,264	11,316	Strength
10	110	8	5.381	40	0.98	-0.342	2.283	12,175	12,409	Strength
10	115	8	5.827	44	0.94	-0.363	2.511	13,117	13,487	Strength
10	120	8	6.260	48	0.66	-0.402	2.751	14,090	14,548	Stress
12	60	9	2.214*	14	0.27	0.043	0.622	4,320	4,774	Strength
12	65	9	2.488*	16	0.32	0.030	0.740	4,886	5,424	Strength
12	70	9	2.751*	18	0.36	0.002	0.870	5,477	6,071	Strength
12	75	9	3.005	20	0.38	-0.041	1.013	6,094	6,713	Strength
12	80	9	3.249	22	0.38	-0.097	1.168	6,736	7,353	Strength
12	85	9	3.483	24	0.35	-0.167	1.335	7,404	7,988	Strength
12	90	9	3.692	26	0.23	-0.261	1.523	8,098	8,600	Strength
12	95	9	3.892	28	0.06	-0.369	1.724	8,818	9,209	Stress
12	100	9	4.083	30	-0.18	-0.490	1.938	9,565	9,814	Stress
12	105	9	4.594	34	-0.17	-0.443	2.126	10,339	11,014	Stress
12	110	9	5.074	38	-0.22	-0.425	2.337	11,141	12,179	Stress
12	115	9	5.525	42	-0.33	-0.448	2.575	12,035	13,312	Stress
12	120	9	5.961	46	-0.79	-0.489	2.826	12,959	14,431	Stress

PRELIMINARY DESIGN

6.10 Preliminary Design Data

*A minimum concrete transfer strength of 3.0 ksi is recommended by PCI MNL-116 section 5.3.17.

**Final camber is net deflection after all losses and noncomposite and composite dead loads are applied.

Table IB-5 (continued)

Spacing ft	Span ft	Slab Thickness in.	f'_{ci} ksi	No. of Strands	Final Camber in.**	f_b @ L/2 ksi	f_t @ L/2 ksi	M_u @ L/2 ft-kips	M_r @ L/2 ft-kips	Control
AASHTO I-Beam Type V, Interior Beam										
6	85	8	2.034*	16	0.01	-0.219	1.148	4,992	5,227	Strength
6	90	8	2.271*	18	0.00	-0.220	1.276	5,470	5,833	Strength
6	95	8	2.497*	20	-0.03	-0.232	1.413	5,967	6,432	Strength
6	100	8	2.714*	22	-0.09	-0.256	1.560	6,484	7,024	Strength
6	105	8	2.561*	22	-0.58	-0.491	1.765	7,020	7,024	Stress
6	110	8	2.762*	24	-0.76	-0.534	1.930	7,574	7,609	Stress
6	115	8	3.276	28	-0.65	-0.410	2.074	8,149	8,720	Stress
6	120	8	3.441	30	-0.99	-0.486	2.267	8,742	9,266	Stress
6	125	8	3.928	34	-0.94	-0.391	2.432	9,355	10,237	Stress
6	130	8	4.072	36	-1.43	-0.489	2.644	9,987	10,605	Stress
6	135	8	4.504	40	-1.55	-0.440	2.847	10,639	11,216	Stress
8	70	8	2.016*	14	0.23	-0.053	0.805	4,322	4,660	Strength
8	75	8	2.276*	16	0.27	-0.047	0.919	4,812	5,286	Strength
8	80	8	2.526*	18	0.31	-0.053	1.042	5,323	5,907	Strength
8	85	8	2.402*	18	0.07	-0.275	1.226	5,854	5,907	Strength
8	90	8	2.635*	20	0.04	-0.303	1.370	6,408	6,523	Strength
8	95	8	2.858*	22	-0.03	-0.343	1.524	6,982	7,134	Stress
8	100	8	3.072	24	-0.13	-0.395	1.688	7,578	7,739	Stress
8	105	8	3.261	26	-0.33	-0.468	1.871	8,195	8,319	Stress
8	110	8	3.776	30	-0.23	-0.367	2.026	8,834	9,464	Stress
8	115	8	3.945	32	-0.55	-0.465	2.230	9,495	10,029	Stress
8	120	8	4.433	36	-0.51	-0.395	2.407	10,177	11,143	Stress
8	125	8	4.567	38	-1.02	-0.525	2.641	10,881	11,673	Stress
8	130	8	5.000	42	-1.17	-0.502	2.858	11,608	12,719	Stress
8	135	8	5.419	46	-1.71	-0.495	3.085	12,356	13,519	Stress
8	140	8	5.810	50	-2.46	-0.512	3.332	13,126	14,093	Stress
10	65	8	2.119*	14	0.26	-0.024	0.721	4,412	4,687	Strength
10	70	8	2.386*	16	0.31	-0.029	0.836	4,945	5,322	Strength
10	75	8	2.642*	18	0.36	-0.046	0.963	5,500	5,953	Strength
10	80	8	2.889*	20	0.38	-0.076	1.100	6,078	6,579	Strength
10	85	8	3.126	22	0.39	-0.119	1.248	6,679	7,200	Strength
10	90	8	3.353	24	0.36	-0.174	1.407	7,303	7,818	Strength
10	95	8	3.556	26	0.25	-0.252	1.587	7,951	8,411	Strength
10	100	8	3.749	28	0.09	-0.342	1.777	8,623	9,000	Strength
10	105	8	3.933	30	-0.14	-0.445	1.979	9,319	9,586	Stress
10	110	8	4.438	34	-0.08	-0.379	2.153	10,038	10,743	Stress
10	115	8	4.602	36	-0.44	-0.507	2.377	10,782	11,316	Stress
10	120	8	5.051	40	-0.53	-0.490	2.593	11,550	12,409	Stress
10	125	8	5.486	44	-0.80	-0.490	2.821	12,341	13,487	Stress
10	130	8	5.906	48	-1.37	-0.507	3.061	13,158	14,548	Stress
12	60	9	2.214*	14	0.27	0.038	0.624	4,346	4,774	Strength
12	65	9	2.488*	16	0.32	0.023	0.742	4,915	5,424	Strength
12	70	9	2.751*	18	0.36	-0.005	0.873	5,509	6,071	Strength
12	75	9	3.005	20	0.38	-0.048	1.015	6,128	6,713	Strength
12	80	9	3.249	22	0.38	-0.105	1.170	6,772	7,353	Strength
12	85	9	3.483	24	0.35	-0.176	1.338	7,443	7,988	Strength
12	90	9	3.692	26	0.23	-0.270	1.527	8,140	8,600	Strength
12	95	9	3.892	28	0.06	-0.378	1.728	8,863	9,209	Stress
12	100	9	4.083	30	-0.18	-0.500	1.941	9,613	9,814	Stress
12	105	9	4.594	34	-0.17	-0.454	2.130	10,389	11,014	Stress
12	110	9	5.074	38	-0.22	-0.436	2.341	11,192	12,179	Stress
12	115	9	5.525	42	-0.33	-0.445	2.574	12,022	13,312	Stress
12	120	9	5.961	46	-0.79	-0.472	2.820	12,879	14,431	Stress
12	125	9	6.370	50	-1.42	-0.526	3.088	13,764	15,516	Stress

PRELIMINARY DESIGN

*A minimum concrete transfer strength of 3.0 ksi is recommended by PCI MNL-116 section 5.3.17.

6.10 Preliminary Design Data

**Final camber is net deflection after all losses and noncomposite and composite dead loads are applied.

Table IB-6
AASHTO I-Beam Type VI

Spacing ft	Span ft	Slab Thickness in.	f'_{ci} ksi	No. of Strands	Final Camber in.**	f_b @ L/2 ksi	f_t @ L/2 ksi	M_u @ L/2 ft-kips	M_r @ L/2 ft-kips	Control
AASHTO I-Beam Type VI, Exterior Beam										
6	95	8	2.083*	18	-0.02	-0.184	1.209	6,121	6,623	Strength
6	100	8	2.299*	20	-0.03	-0.186	1.331	6,671	7,309	Strength
6	105	8	2.166*	20	-0.39	-0.393	1.512	7,263	7,309	Stress
6	110	8	2.368*	22	-0.48	-0.417	1.653	7,878	7,989	Stress
6	115	8	2.562*	24	-0.61	-0.451	1.802	8,516	8,661	Stress
6	120	8	2.735*	26	-0.80	-0.502	1.967	9,176	9,307	Stress
6	125	8	3.219	30	-0.68	-0.387	2.102	9,859	10,579	Stress
6	130	8	3.374	32	-0.98	-0.459	2.284	10,564	11,205	Stress
6	135	8	3.834	36	-0.91	-0.369	2.436	11,293	12,151	Stress
6	140	8	3.960	38	-1.37	-0.468	2.643	12,044	12,542	Stress
6	145	8	4.373	42	-1.43	-0.418	2.828	12,818	13,235	Stress
8	75	8	2.182*	16	0.34	-0.041	0.841	5,776	5,989	Strength
8	80	8	2.425*	18	0.41	-0.051	0.955	6,432	6,698	Strength
8	85	8	2.659*	20	0.47	-0.073	1.079	7,115	7,401	Strength
8	90	8	2.885*	22	0.53	-0.106	1.212	7,827	8,099	Strength
8	95	8	3.102	24	0.57	-0.150	1.355	8,567	8,792	Strength
8	100	8	3.298	26	0.55	-0.212	1.514	9,335	9,460	Strength
8	105	8	3.803	30	0.78	-0.111	1.645	10,131	10,779	Strength
8	110	8	3.981	32	0.72	-0.197	1.823	10,955	11,431	Strength
8	115	8	4.151	34	0.60	-0.293	2.011	11,807	12,078	Strength
8	120	8	4.314	36	0.43	-0.400	2.207	12,687	12,720	Stress
8	125	8	4.751	40	0.54	-0.364	2.392	13,596	13,949	Strength
8	130	8	4.885	42	0.24	-0.501	2.614	14,532	14,557	Stress
8	135	8	5.587	48	0.52	-0.337	2.790	15,497	15,874	Strength
10	65	8	2.020*	14	0.29	0.007	0.642	5,129	5,302	Strength
10	70	8	2.277*	16	0.36	0.000	0.747	5,802	6,025	Strength
10	75	8	2.526*	18	0.43	-0.020	0.861	6,507	6,743	Strength
10	80	8	2.766*	20	0.49	-0.052	0.986	7,243	7,457	Strength
10	85	8	2.998*	22	0.55	-0.096	1.121	8,011	8,166	Strength
10	90	8	3.221	24	0.59	-0.152	1.266	8,809	8,871	Strength
10	95	8	3.741	28	0.81	-0.051	1.390	9,639	10,229	Strength
10	100	8	3.933	30	0.78	-0.140	1.563	10,501	10,902	Strength
10	105	8	4.117	32	0.72	-0.240	1.746	11,393	11,570	Strength
10	110	8	4.602	36	0.91	-0.182	1.902	12,317	12,894	Strength
10	115	8	4.757	38	0.75	-0.314	2.112	13,272	13,530	Strength
10	120	8	5.195	42	0.86	-0.299	2.303	14,258	14,791	Strength
10	125	8	5.333	44	0.58	-0.454	2.533	15,276	15,414	Stress
10	130	8	5.750	48	0.45	-0.467	2.745	16,325	16,650	Stress
12	65	9	2.020*	14	0.21	-0.006	0.643	5,017	5,389	Strength
12	70	9	2.277*	16	0.26	-0.007	0.748	5,624	6,127	Strength
12	75	9	2.526*	18	0.30	-0.020	0.863	6,256	6,861	Strength
12	80	9	2.766*	20	0.32	-0.046	0.989	6,914	7,592	Strength
12	85	9	2.998*	22	0.33	-0.083	1.125	7,599	8,319	Strength
12	90	9	2.885*	22	0.07	-0.321	1.319	8,311	8,319	Strength
12	95	9	3.423	26	0.24	-0.201	1.436	9,050	9,742	Strength
12	100	9	3.617	28	0.12	-0.282	1.611	9,815	10,438	Strength
12	105	9	3.803	30	-0.06	-0.374	1.796	10,609	11,131	Stress
12	110	9	3.981	32	-0.30	-0.477	1.991	11,429	11,820	Stress
12	115	9	4.461	36	-0.28	-0.421	2.160	12,277	13,188	Stress
12	120	9	4.904	40	-0.33	-0.396	2.355	13,153	14,502	Stress
12	125	9	5.333	44	-0.42	-0.393	2.564	14,098	15,802	Stress
12	130	9	5.750	48	-0.72	-0.411	2.786	15,101	17,089	Stress

PRELIMINARY DESIGN

6.10 Preliminary Design Data

*A minimum concrete transfer strength of 3.0 ksi is recommended by PCI MNL-116 section 5.3.17.

**Final camber is net deflection after all losses and noncomposite and composite dead loads are applied.

Table IB-6 (continued)

Spacing ft	Span ft	Slab Thickness in.	f'_{ci} ksi	No. of Strands	Final Camber in.**	f_b @ L/2 ksi	f_t @ L/2 ksi	M_u @ L/2 ft-kips	M_r @ L/2 ft-kips	Control
AASHTO I-Beam Type VI, Interior Beam										
6	95	8	2.083*	18	-0.02	-0.190	1.213	6,149	6,623	Strength
6	100	8	2.299*	20	-0.03	-0.188	1.333	6,682	7,309	Strength
6	105	8	2.166*	20	-0.39	-0.387	1.509	7,234	7,309	Stress
6	110	8	2.368*	22	-0.48	-0.403	1.644	7,806	7,989	Stress
6	115	8	2.562*	24	-0.61	-0.427	1.787	8,398	8,661	Stress
6	120	8	2.735*	26	-0.8	-0.469	1.946	9,009	9,307	Stress
6	125	8	2.900*	28	-1.07	-0.520	2.113	9,641	9,946	Stress
6	130	8	3.374	32	-0.98	-0.405	2.249	10,293	11,205	Stress
6	135	8	3.522	34	-1.37	-0.475	2.432	10,965	11,707	Stress
6	140	8	3.960	38	-1.37	-0.392	2.593	11,657	12,542	Stress
6	145	8	4.079	40	-1.92	-0.489	2.799	12,370	12,903	Stress
6	150	8	4.483	44	-2.05	-0.437	2.985	13,102	13,444	Stress
8	80	8	2.080*	16	0.22	-0.057	0.901	5,476	5,989	Strength
8	85	8	2.317*	18	0.25	-0.051	1.009	6,024	6,698	Strength
8	90	8	2.203*	18	0.04	-0.247	1.175	6,592	6,698	Strength
8	95	8	2.425*	20	0.02	-0.259	1.301	7,183	7,401	Strength
8	100	8	2.639*	22	-0.02	-0.281	1.435	7,796	8,099	Strength
8	105	8	2.845*	24	-0.08	-0.314	1.578	8,431	8,792	Strength
8	110	8	3.029	26	-0.22	-0.364	1.737	9,088	9,460	Stress
8	115	8	3.206	28	-0.41	-0.424	1.905	9,768	10,122	Stress
8	120	8	3.374	30	-0.670	-0.494	2.082	10,470	10,779	Stress
8	125	8	3.849	34	-0.60	-0.401	2.229	11,194	12,078	Stress
8	130	8	4.000	36	-0.96	-0.491	2.423	11,941	12,720	Stress
8	135	8	4.427	40	-1.01	-0.439	2.603	12,711	13,949	Stress
8	140	8	4.842	44	-1.11	-0.400	2.794	13,503	15,088	Stress
8	145	8	4.956	46	-1.75	-0.528	3.021	14,318	15,496	Stress
8	150	8	5.337	50	-2.39	-0.52	3.237	15,155	16,207	Stress
10	75	8	2.182*	16	0.25	-0.050	0.831	5,653	6,025	Strength
10	80	8	2.425*	18	0.30	-0.053	0.943	6,247	6,743	Strength
10	85	8	2.659*	20	0.33	-0.067	1.063	6,864	7,457	Strength
10	90	8	2.885*	22	0.34	-0.093	1.193	7,506	8,166	Strength
10	95	8	3.102	24	0.33	-0.129	1.333	8,172	8,871	Strength
10	100	8	2.976*	24	0.00	-0.363	1.528	8,861	8,871	Stress
10	105	8	3.486	28	0.16	-0.249	1.655	9,576	10,229	Strength
10	110	8	3.666	30	-0.01	-0.325	1.830	10,315	10,902	Strength
10	115	8	3.839	32	-0.24	-0.411	2.014	11,078	11,570	Stress
10	120	8	4.003	34	-0.53	-0.508	2.207	11,867	12,234	Stress
10	125	8	4.457	38	-0.53	-0.453	2.380	12,680	13,530	Stress
10	130	8	4.885	42	-0.58	-0.420	2.571	13,518	14,791	Stress
10	135	8	5.301	46	-0.70	-0.401	2.772	14,381	16,034	Stress
10	140	8	5.692	50	-1.21	-0.404	2.990	15,269	17,242	Stress

PRELIMINARY DESIGN

*A minimum concrete transfer strength of 3.0 ksi is recommended by PCI MNL-116 section 5.3.17.

6.10 Preliminary Design Data

**Final camber is net deflection after all losses and noncomposite and composite dead loads are applied.

Table IB-6 (continued)

Spacing ft	Span ft	Slab Thickness in.	f'_{ci} ksi	No. of Strands	Final Camber in.**	f_b @ L/2 ksi	f_t @ L/2 ksi	M_u @ L/2 ft-kips	M_r @ L/2 ft-kips	Control
AASHTO I-Beam Type VI, Interior Beam (continued)										
12	65	9	2.020*	14	0.21	-0.011	0.645	5,047	5,389	Strength
12	70	9	2.277*	16	0.26	-0.013	0.750	5,656	6,127	Strength
12	75	9	2.526*	18	0.30	-0.027	0.865	6,291	6,861	Strength
12	80	9	2.766*	20	0.32	-0.053	0.991	6,952	7,592	Strength
12	85	9	2.998*	22	0.33	-0.091	1.127	7,639	8,319	Strength
12	90	9	3.221	24	0.32	-0.140	1.274	8,354	9,042	Strength
12	95	9	3.423	26	0.24	-0.210	1.439	9,095	9,742	Strength
12	100	9	3.617	28	0.12	-0.290	1.614	9,864	10,438	Strength
12	105	9	3.803	30	-0.06	-0.383	1.799	10,660	11,131	Stress
12	110	9	3.981	32	-0.30	-0.487	1.995	11,483	11,820	Stress
12	115	9	4.461	36	-0.28	-0.431	2.164	12,334	13,188	Stress
12	120	9	4.904	40	-0.33	-0.406	2.359	13,213	14,502	Stress
12	125	9	5.333	44	-0.42	-0.397	2.565	14,119	15,802	Stress
12	130	9	5.750	48	-0.72	-0.403	2.782	15,053	17,089	Stress

PRELIMINARY DESIGN

6.10 Preliminary Design Data

Table NEXT-1

NEXT Beam Type D – Maximum Span vs. Section Depth

NEXT D-8 (in.)	28	32	36	40
Span, ft.	60	70	80	85

NEXT D-10 (in.)	28	32	36	40
Span, ft.	55	65	75	80

PRELIMINARY DESIGN

*A minimum concrete transfer strength of 3.0 ksi is recommended by PCI MNL-116 section 5.3.17.

6.10 Preliminary Design Data

**Final camber is net deflection after all losses and noncomposite and composite dead loads are applied.

Table NEXT-2
NEXT Beam Type D x 96

Spacing ft	Span ft	Slab Thickness in.	f'_{ci} ksi	No. of Strands	Final Camber in.**	f_b @ L/2 ksi	f_t @ L/2 ksi	M_u @ L/2 ft-kips	M_r @ L/2 ft-kips	Control
NEXT Beam 28 D x 8-ft-Wide Exterior Beam										
8	20	0	0.509*	6	-0.01	-0.169	0.386	357	362	Stress
8	30	0	1.601*	10	0.13	-0.046	0.515	672	869	Strength
8	40	0	2.034*	12	0.11	-0.386	0.817	1,061	1,086	Stress
8	50	0	3.473	18	0.50	-0.371	1.102	1,570	1,720	Stress
8	60	0	5.185	26	1.22	-0.327	1.458	2,164	2,467	Stress
8	70	0	6.680	34	1.80	-0.503	1.939	2,831	3,114	Stress
NEXT Beam 28 D x 8-ft-Wide Interior Beam										
8	20	0	1.102*	8	0.05	-0.056	0.436	524	591	Strength
8	30	0	2.120*	12	0.24	-0.060	0.647	922	1,086	Strength
8	40	0	3.056	16	0.52	-0.226	0.951	1,395	1,511	Strength
8	50	0	4.407	22	1.09	-0.372	1.343	2,020	2,109	Stress
8	60	0	6.031	30	2.00	-0.499	1.815	2,742	2,815	Stress
NEXT Beam 32 D x 8-ft-Wide Exterior Beam										
8	20	0	0.414*	6	-0.01	-0.123	0.335	364	398	Stress
8	30	0	0.870*	8	-0.01	-0.237	0.499	689	707	Strength
8	40	0	1.791*	12	0.11	-0.213	0.666	1,090	1,242	Strength
8	50	0	2.647*	16	0.22	-0.358	0.936	1,617	1,745	Stress
8	60	0	3.891	22	0.56	-0.400	1.229	2,231	2,459	Stress
8	70	0	5.407	30	1.20	-0.378	1.565	2,923	3,319	Stress
NEXT Beam 32 D x 8-ft-Wide Interior Beam										
8	20	0	0.942*	8	0.04	0.001	0.366	531	663	Strength
8	30	0	1.392*	10	0.10	-0.186	0.580	938	986	Strength
8	40	0	2.257*	14	0.27	-0.259	0.812	1,425	1,495	Strength
8	50	0	3.556	20	0.73	-0.262	1.094	2,067	2,237	Strength
8	60	0	4.690	26	1.20	-0.458	1.491	2,809	2,895	Stress
8	70	0	6.445	36	2.29	-0.412	1.907	3,638	3,879	Stress
NEXT Beam 36 D x 8-ft-Wide Exterior Beam										
8	20	0	0.345*	6	-0.01	-0.093	0.299	372	434	Stress
8	30	0	0.758*	8	-0.01	-0.166	0.431	706	785	Strength
8	40	0	1.596*	12	0.10	-0.105	0.561	1,120	1,398	Strength
8	50	0	1.961*	14	0.02	-0.404	0.832	1,664	1,690	Stress
8	60	0	3.153	20	0.31	-0.356	1.052	2,298	2,549	Stress
8	70	0	4.212	26	0.53	-0.451	1.357	3,014	3,322	Stress
8	80	0	5.539	34	0.98	-0.472	1.693	3,811	4,277	Stress
NEXT Beam 36 D x 8-ft-Wide Interior Beam										
8	20	0	0.820*	8	0.03	0.031	0.319	542	735	Strength
8	30	0	1.228*	10	0.08	-0.100	0.493	961	1,103	Strength
8	40	0	2.022*	14	0.23	-0.117	0.676	1,461	1,690	Strength
8	50	0	2.800*	18	0.43	-0.274	0.950	2,121	2,265	Strength
8	60	0	3.902	24	0.84	-0.349	1.253	2,881	3,067	Stress
8	70	0	4.942	30	1.24	-0.535	1.625	3,734	3,824	Stress
8	80	0	6.506	40	2.18	-0.512	2.021	4,675	4,935	Stress

PRELIMINARY DESIGN

6.10 Preliminary Design Data

*A minimum concrete transfer strength of 3.0 ksi is recommended by PCI MNL-116 section 5.3.17.

**Final camber is net deflection after all losses and noncomposite and composite dead loads are applied.

Table NEXT-2 (Continued)

Spacing ft	Span ft	Slab Thickness in.	f'_{ci} ksi	No. of Strands	Final Camber in.**	f_b @ L/2 ksi	f_t @ L/2 ksi	M_u @ L/2 ft-kips	M_r @ L/2 ft-kips	Control
NEXT Beam 40 D x 8-ft-Wide Exterior Beam										
8	20	0	0.308*	6	-0.01	-0.072	0.271	378	470	Stress
8	30	0	0.701*	8	0.00	-0.116	0.380	719	863	Strength
8	40	0	1.091*	10	-0.02	-0.237	0.534	1,144	1,220	Strength
8	50	0	1.853*	14	0.06	-0.267	0.711	1,701	1,885	Strength
8	60	0	2.600*	18	0.12	-0.378	0.938	2,352	2,538	Stress
8	70	0	3.665	24	0.38	-0.389	1.176	3,087	3,457	Stress
8	80	0	4.674	30	0.56	-0.490	1.469	3,906	4,330	Stress
8	90	0	6.208	40	1.34	-0.368	1.770	4,810	5,633	Stress
NEXT Beam 40 D x 8-ft-Wide Interior Beam										
8	20	0	0.756*	8	0.02	0.054	0.283	552	807	Strength
8	30	0	1.146*	10	0.07	-0.039	0.427	979	1,220	Strength
8	40	0	1.501*	12	0.10	-0.226	0.627	1,491	1,554	Strength
8	50	0	2.256*	16	0.24	-0.322	0.852	2,165	2,213	Strength
8	60	0	3.358	22	0.61	-0.312	1.088	2,942	3,160	Strength
8	70	0	4.376	28	0.99	-0.414	1.391	3,811	4,042	Stress
8	80	0	5.632	36	1.63	-0.453	1.728	4,775	5,120	Stress

PRELIMINARY DESIGN

*A minimum concrete transfer strength of 3.0 ksi is recommended by PCI MNL-116 section 5.3.17.

6.10 Preliminary Design Data

**Final camber is net deflection after all losses and noncomposite and composite dead loads are applied.

Table NEXT-3

NEXT Beam Type D x 120

Spacing ft	Span ft	Slab Thickness in.	f'_{ci} ksi	No. of Strands	Final Camber in.**	f_b @ L/2 ksi	f_t @ L/2 ksi	M_u @ L/2 ft-kips	M_r @ L/2 ft-kips	Control
NEXT Beam 28 D x 10-ft-Wide Exterior Beam										
12	20	0	1.089*	8	0.05	-0.033	0.354	515	591	Strength
12	30	0	2.082*	12	0.23	-0.08	0.556	950	1,086	Strength
12	40	0	2.995*	16	0.47	-0.305	0.848	1,475	1,511	Stress
12	50	0	4.749	24	1.22	-0.293	1.179	2,165	2,289	Strength
12	60	0	6.285	32	2.04	-0.534	1.641	2,962	2,966	Stress
NEXT Beam 28 D x 10-ft-Wide Interior Beam										
12	20	0	1.665*	10	0.11	0.082	0.392	681	818	Strength
12	25	0	2.129*	12	0.21	0.037	0.506	910	1,086	Strength
12	30	0	2.588*	14	0.35	-0.043	0.637	1,159	1,300	Strength
12	35	0	3.042	16	0.50	-0.158	0.787	1,430	1,511	Strength
12	40	0	3.980	20	0.87	-0.048	0.897	1,723	1,925	Strength
12	45	0	4.366	22	1.06	-0.303	1.123	2,074	2,109	Strength
12	50	0	5.594	28	1.75	-0.158	1.294	2,468	2,643	Strength
12	55	0	6.330	32	2.23	-0.305	1.541	2,884	2,966	Strength
NEXT Beam 32 D x 10-ft-Wide Exterior Beam										
12	20	0	0.937*	8	0.04	0.021	0.298	523	666	Strength
12	25	0	1.412*	10	0.10	0.060	0.359	733	993	Strength
12	30	0	1.373*	10	0.09	-0.195	0.500	967	993	Strength
12	35	0	1.799*	12	0.16	-0.239	0.604	1,224	1,253	Strength
12	40	0	2.220*	14	0.24	-0.313	0.723	1,505	1,510	Stress
12	45	0	3.087	18	0.53	-0.202	0.820	1,838	2,017	Strength
12	50	0	3.495	20	0.64	-0.373	0.994	2,212	2,267	Stress
12	55	0	4.256	24	0.96	-0.381	1.154	2,609	2,721	Stress
12	60	0	5.003	28	1.33	-0.419	1.329	3,030	3,165	Stress
12	65	0	5.699	32	1.68	-0.509	1.531	3,474	3,581	Stress
12	70	0	6.686	38	2.33	-0.464	1.731	3,941	4,160	Stress
NEXT Beam 32 D x 10-ft-Wide Interior Beam										
12	20	0	1.451*	10	0.09	0.137	0.325	700	930	Strength
12	25	0	1.412*	10	0.10	-0.109	0.464	935	993	Strength
12	30	0	1.838*	12	0.18	-0.141	0.564	1,191	1,253	Strength
12	35	0	2.259*	14	0.29	-0.202	0.678	1,468	1,510	Strength
12	40	0	3.126	18	0.56	-0.055	0.755	1,769	2,017	Strength
12	45	0	3.533	20	0.73	-0.205	0.919	2,129	2,267	Strength
12	50	0	4.294	24	1.08	-0.210	1.079	2,534	2,721	Strength
12	55	0	5.040	28	1.49	-0.243	1.254	2,960	3,165	Strength
12	60	0	5.736	32	1.90	-0.328	1.455	3,410	3,581	Strength
12	65	0	6.384	36	2.30	-0.463	1.683	3,882	3,970	Stress

PRELIMINARY DESIGN

6.10 Preliminary Design Data

*A minimum concrete transfer strength of 3.0 ksi is recommended by PCI MNL-116 section 5.3.17.

**Final camber is net deflection after all losses and noncomposite and composite dead loads are applied.

Table NEXT-3 (Continued)

Spacing ft	Span ft	Slab Thickness in.	f'_{ci} ksi	No. of Strands	Final Camber in.**	f_b @ L/2 ksi	f_t @ L/2 ksi	M_u @ L/2 ft-kips	M_r @ L/2 ft-kips	Control
NEXT Beam 36 D x 10-ft-Wide Exterior Beam										
12	20	0	0.819*	8	0.03	0.052	0.258	530	738	Strength
12	25	0	0.786*	8	0.02	-0.131	0.363	745	790	Strength
12	30	0	1.216*	10	0.08	-0.101	0.422	984	1,111	Strength
12	35	0	1.607*	12	0.14	-0.114	0.503	1,247	1,409	Strength
12	40	0	1.995*	14	0.21	-0.153	0.598	1,535	1,705	Strength
12	45	0	2.378*	16	0.29	-0.235	0.719	1,876	1,999	Strength
12	50	0	2.757*	18	0.38	-0.352	0.859	2,259	2,290	Stress
12	55	0	3.505	22	0.66	-0.295	0.973	2,666	2,846	Strength
12	60	0	3.842	24	0.72	-0.477	1.149	3,097	3,110	Stress
12	65	0	4.539	28	1.03	-0.487	1.298	3,553	3,632	Stress
12	70	0	5.518	34	1.63	-0.363	1.441	4,033	4,360	Stress
12	75	0	6.129	38	1.93	-0.457	1.635	4,537	4,821	Stress
NEXT Beam 36 D x 10-ft-Wide Interior Beam										
12	20	0	0.819*	8	0.03	-0.072	0.337	717	738	Strength
12	25	0	1.249*	10	0.08	-0.035	0.395	959	1,111	Strength
12	30	0	1.640*	12	0.15	-0.039	0.473	1,221	1,409	Strength
12	35	0	2.027*	14	0.24	-0.066	0.564	1,505	1,705	Strength
12	40	0	2.411*	16	0.34	-0.118	0.667	1,813	1,999	Strength
12	45	0	2.790*	18	0.46	-0.218	0.799	2,183	2,290	Strength
12	50	0	3.538	22	0.76	-0.158	0.914	2,597	2,846	Strength
12	55	0	3.874	24	0.88	-0.336	1.089	3,034	3,110	Strength
12	60	0	4.571	28	1.23	-0.341	1.238	3,495	3,632	Strength
12	65	0	5.225	32	1.59	-0.388	1.409	3,980	4,126	Stress
12	70	0	5.840	36	1.93	-0.476	1.601	4,489	4,591	Stress
12	75	0	6.734	42	2.58	-0.434	1.789	5,026	5,253	Stress
NEXT Beam 40 D x 10-ft-Wide Exterior Beam										
12	20	0	0.759*	8	0.03	0.076	0.237	533	810	Strength
12	25	0	0.730*	8	0.02	-0.08	0.328	749	868	Strength
12	30	0	1.139*	10	0.07	-0.033	0.375	990	1,228	Strength
12	35	0	1.516*	12	0.13	-0.023	0.442	1,256	1,565	Strength
12	40	0	1.487*	12	0.09	-0.242	0.568	1,546	1,565	Strength
12	45	0	1.860*	14	0.15	-0.29	0.669	1,890	1,900	Strength
12	50	0	2.623*	18	0.38	-0.162	0.740	2,276	2,563	Strength
12	55	0	2.984*	20	0.47	-0.262	0.870	2,687	2,891	Strength
12	60	0	3.316	22	0.53	-0.397	1.019	3,122	3,197	Stress
12	65	0	3.997	26	0.82	-0.363	1.141	3,582	3,801	Stress
12	70	0	4.668	30	1.15	-0.350	1.274	4,067	4,396	Stress
12	75	0	5.276	34	1.44	-0.388	1.435	4,577	4,943	Stress
12	80	0	5.876	38	1.74	-0.447	1.608	5,111	5,482	Stress
12	85	0	6.725	44	2.33	-0.387	1.778	5,670	6,233	Stress

PRELIMINARY DESIGN

*A minimum concrete transfer strength of 3.0 ksi is recommended by PCI MNL-116 section 5.3.17.

6.10 Preliminary Design Data

**Final camber is net deflection after all losses and noncomposite and composite dead loads are applied.

Table NEXT-3 (Continued)

Spacing ft	Span ft	Slab Thickness in.	f'_{ci} ksi	No. of Strands	Final Camber in.**	$f_b @ L/2$ ksi	$f_t @ L/2$ ksi	$M_u @ L/2$ ft-kips	$M_r @ L/2$ ft-kips	Control
NEXT Beam 40 D x 10-ft-Wide Interior Beam										
12	20	0	0.759*	8	0.03	-0.034	0.309	730	810	Strength
12	25	0	1.168*	10	0.07	0.018	0.355	976	1,228	Strength
12	30	0	1.544*	12	0.13	0.036	0.420	1,241	1,565	Strength
12	35	0	1.516*	12	0.13	-0.175	0.542	1,529	1,565	Strength
12	40	0	1.888*	14	0.2	-0.198	0.628	1,841	1,900	Strength
12	45	0	2.257*	16	0.29	-0.262	0.740	2,215	2,233	Strength
12	50	0	3.013	20	0.55	-0.153	0.823	2,633	2,891	Strength
12	55	0	3.344	22	0.66	-0.284	0.972	3,075	3,197	Strength
12	60	0	4.025	26	0.98	-0.246	1.094	3,541	3,801	Strength
12	65	0	4.348	28	1.08	-0.417	1.265	4,031	4,100	Stress
12	70	0	4.987	32	1.42	-0.435	1.417	4,546	4,671	Stress
12	75	0	5.591	36	1.75	-0.489	1.588	5,085	5,214	Stress
12	80	0	6.470	42	2.40	-0.409	1.749	5,649	5,991	Stress

PRELIMINARY DESIGN

6.10 Preliminary Design Data

Table NEXT-4

NEXT Beam Type F – Maximum Span vs. Section Depth

NEXT F-8 (in.)	24	28	32	36
Span, ft.	55	65	75	80

NEXT F-12 (in.)	24	28	32	36
Span, ft.	50	60	65	75

PRELIMINARY DESIGN

*A minimum concrete transfer strength of 3.0 ksi is recommended by PCI MNL-116 section 5.3.17.

6.10 Preliminary Design Data

**Final camber is net deflection after all losses and noncomposite and composite dead loads are applied.

Table NEXT-5
NEXT Beam Type F x 96

Spacing ft	Span ft	Slab Thickness in.	f'_{ci} ksi	No. of Strands	Final Camber in.**	f_b @ L/2 ksi	f_t @ L/2 ksi	M_u @ L/2 ft-kips	M_r @ L/2 ft-kips	Control
NEXT Beam 24 F x 8-ft-Wide Beam										
8	20	8	1.055*	8	0.01	-0.116	0.457	616	753	Strength
8	25	8	1.688*	10	0.07	-0.049	0.502	820	1,034	Strength
8	30	8	2.232*	12	0.13	-0.074	0.602	1,041	1,277	Strength
8	35	8	2.769*	14	0.18	-0.144	0.727	1,279	1,515	Strength
8	40	8	3.299	16	0.22	-0.26	0.877	1,535	1,748	Stress
8	45	8	3.822	18	0.20	-0.449	1.061	1,839	1,977	Stress
8	50	8	4.816	22	0.41	-0.427	1.237	2,177	2,400	Stress
8	55	8	5.716	26	0.53	-0.501	1.467	2,532	2,785	Stress
NEXT Beam 28 F x 8-ft-Wide Beam										
8	20	8	1.133*	8	0.04	0.071	0.332	640	904	Strength
8	25	8	1.098*	8	0.01	-0.182	0.457	853	922	Strength
8	30	8	1.652*	10	0.07	-0.132	0.511	1,083	1,229	Strength
8	35	8	2.139*	12	0.11	-0.154	0.609	1,331	1,511	Strength
8	40	8	2.621*	14	0.16	-0.212	0.727	1,598	1,788	Strength
8	45	8	3.097	16	0.18	-0.328	0.875	1,916	2,060	Stress
8	50	8	3.567	18	0.15	-0.492	1.048	2,268	2,326	Stress
8	55	8	4.470	22	0.35	-0.440	1.199	2,638	2,826	Stress
8	60	8	5.301	26	0.49	-0.464	1.394	3,028	3,287	Stress
8	65	8	6.117	30	0.60	-0.527	1.610	3,436	3,730	Stress
NEXT Beam 32 F x 8-ft-Wide Beam										
8	20	8	0.613*	6	0	-0.123	0.332	663	711	Stress
8	25	8	1.112*	8	0.04	-0.030	0.357	884	1,078	Strength
8	30	8	1.604*	10	0.10	0.032	0.400	1,123	1,424	Strength
8	35	8	1.574*	10	0.04	-0.230	0.544	1,381	1,424	Strength
8	40	8	2.015*	12	0.07	-0.251	0.640	1,659	1,745	Strength
8	45	8	2.451*	14	0.09	-0.322	0.762	1,989	2,060	Stress
8	50	8	2.882*	16	0.09	-0.431	0.905	2,356	2,371	Stress
8	55	8	3.760	20	0.32	-0.310	1.004	2,741	2,977	Stress
8	60	8	4.135	22	0.22	-0.503	1.201	3,146	3,253	Stress
8	65	8	4.903	26	0.35	-0.499	1.371	3,571	3,790	Stress
8	70	8	5.657	30	0.46	-0.528	1.561	4,016	4,309	Stress
8	75	8	6.661	36	0.75	-0.449	1.778	4,482	4,996	Stress
NEXT Beam 36 F x 8-ft-Wide Beam										
8	20	8	0.645*	6	0.01	-0.029	0.265	685	825	Stress
8	25	8	1.095*	8	0.05	0.066	0.284	914	1,234	Strength
8	30	8	1.068*	8	0.03	-0.132	0.396	1,162	1,234	Strength
8	35	8	1.512*	10	0.07	-0.086	0.446	1,430	1,619	Strength
8	40	8	1.915*	12	0.12	-0.086	0.526	1,718	1,979	Strength
8	45	8	2.314*	14	0.16	-0.127	0.629	2,060	2,333	Strength
8	50	8	2.708*	16	0.19	-0.201	0.750	2,440	2,682	Strength
8	55	8	3.099	18	0.20	-0.299	0.888	2,840	3,027	Stress
8	60	8	3.485	20	0.17	-0.421	1.040	3,261	3,366	Stress
8	65	8	4.205	24	0.32	-0.376	1.178	3,702	3,990	Stress
8	70	8	4.912	28	0.47	-0.359	1.332	4,165	4,595	Stress
8	75	8	5.576	32	0.56	-0.391	1.516	4,649	5,161	Stress
8	80	8	6.198	36	0.55	-0.471	1.730	5,155	5,690	Stress

PRELIMINARY DESIGN

6.10 Preliminary Design Data

*A minimum concrete transfer strength of 3.0 ksi is recommended by PCI MNL-116 section 5.3.17.

**Final camber is net deflection after all losses and noncomposite and composite dead loads are applied.

Table NEXT-6
NEXT Beam Type F x 144

Spacing ft	Span ft	Slab Thickness in.	f'_{ci} ksi	No. of Strands	Final Camber in.**	f_b @ L/2 ksi	f_t @ L/2 ksi	M_u @ L/2 ft-kips	M_r @ L/2 ft-kips	Control
NEXT Beam 24 F x 12-ft-Wide Beam										
12	20	8	1.738*	10	0.08	0.090	0.293	830	1,035	Strength
12	25	8	2.266*	12	0.15	0.029	0.372	1,103	1,309	Strength
12	30	8	2.788*	14	0.22	-0.085	0.476	1,397	1,559	Strength
12	35	8	3.303	16	0.28	-0.253	0.604	1,714	1,805	Stress
12	40	8	4.359	20	0.53	-0.162	0.702	2,055	2,286	Strength
12	45	8	4.786	22	0.49	-0.514	0.908	2,460	2,502	Stress
12	50	8	6.132	28	0.90	-0.411	1.077	2,909	3,131	Stress
NEXT Beam 28 D x 12-ft-Wide Beam										
12	20	8	1.140*	8	0.04	-0.070	0.283	860	915	Strength
12	25	8	1.675*	10	0.09	-0.052	0.328	1,143	1,251	Strength
12	30	8	2.148*	12	0.14	-0.107	0.410	1,448	1,543	Strength
12	35	8	2.615*	14	0.20	-0.205	0.513	1,777	1,832	Strength
12	40	8	3.571	18	0.41	-0.063	0.583	2,130	2,398	Strength
12	45	8	4.022	20	0.45	-0.275	0.733	2,550	2,675	Stress
12	50	8	4.845	24	0.63	-0.329	0.888	3,016	3,182	Stress
12	55	8	5.653	28	0.80	-0.428	1.064	3,505	3,675	Stress
12	60	8	6.762	34	1.15	-0.397	1.259	4,018	4,351	Stress
NEXT Beam 32 F x 12-ft-Wide Beam										
12	20	8	1.141*	8	0.04	0.059	0.219	889	1,067	Strength
12	25	8	1.617*	10	0.09	0.096	0.256	1,182	1,447	Strength
12	30	8	2.045*	12	0.16	0.075	0.324	1,497	1,777	Strength
12	35	8	2.468*	14	0.22	0.019	0.408	1,837	2,105	Strength
12	40	8	2.886*	16	0.29	-0.071	0.510	2,202	2,428	Strength
12	45	8	3.300	18	0.33	-0.219	0.636	2,636	2,748	Strength
12	50	8	4.107	22	0.53	-0.185	0.746	3,118	3,359	Strength
12	55	8	4.470	24	0.50	-0.435	0.922	3,624	3,649	Stress
12	60	8	5.216	28	0.64	-0.495	1.080	4,155	4,219	Stress
12	65	8	6.254	34	0.98	-0.423	1.247	4,712	5,011	Stress
NEXT Beam 36 D x 12-ft-Wide Beam										
12	20	8	1.113*	8	0.04	0.139	0.173	916	1,218	Strength
12	25	8	1.085*	8	0.04	-0.073	0.265	1,218	1,249	Strength
12	30	8	1.515*	10	0.09	-0.050	0.310	1,544	1,642	Strength
12	35	8	1.905*	12	0.13	-0.075	0.380	1,894	2,012	Strength
12	40	8	2.292*	14	0.18	-0.130	0.466	2,271	2,378	Strength
12	45	8	2.675*	16	0.22	-0.233	0.574	2,719	2,740	Strength
12	50	8	3.456	20	0.41	-0.144	0.651	3,216	3,455	Strength
12	55	8	3.796	22	0.4	-0.333	0.802	3,739	3,787	Stress
12	60	8	4.495	26	0.56	-0.342	0.931	4,287	4,442	Stress
12	65	8	5.181	30	0.71	-0.382	1.076	4,862	5,083	Stress
12	70	8	5.798	34	0.77	-0.490	1.258	5,464	5,671	Stress
12	75	8	6.720	40	1.07	-0.450	1.432	6,093	6,530	Stress

Table U-1***U-Beams – Maximum Span (ft) vs. Beam Spacing***

Spacing Beam	10 ft	14 ft	18 ft
U40	105	95	80
U54	120	110	95
U66	130	120	105
U78	135	125	110

See **Appendix C** for spliced U-Beams and curved spliced U-Beams from PCI Zone 6.

PRELIMINARY DESIGN

6.10 Preliminary Design Data

*A minimum concrete transfer strength of 3.0 ksi is recommended by PCI MNL-116 section 5.3.17.

**Final camber is net deflection after all losses and noncomposite and composite dead loads are applied.

Table U-2
Texas U-40 Beam

Spacing ft	Span ft	Slab Thickness in.	f'_{ci} ksi	No. of Strands	Final Camber in.**	f_b @ L/2 ksi	f_t @ L/2 ksi	M_u @ L/2 ft-kips	M_r @ L/2 ft-kips	Control
Texas U-40 Exterior Beam										
10	55	8	2.138*	18	0.03	-0.161	1.388	3,619	3,621	Strength
10	60	8	2.668*	22	0.14	-0.087	1.577	4,187	4,421	Strength
10	65	8	2.863*	24	0.04	-0.211	1.849	4,785	4,815	Strength
10	70	8	3.361	28	0.12	-0.181	2.087	5,411	5,590	Strength
10	75	8	3.663	31	0.00	-0.272	2.399	6,065	6,142	Strength
10	80	8	4.082	35	-0.10	-0.314	2.727	6,749	6,850	Strength
10	85	8	4.485	39	-0.26	-0.378	3.079	7,461	7,543	Strength
10	90	8	4.873	43	-0.53	-0.464	3.456	8,201	8,220	Stress
10	95	8	5.517	49	-0.53	-0.429	3.825	8,971	9,209	Stress
14	45	8	2.014*	16	0.09	0.027	0.992	2,887	3,255	Strength
14	50	8	2.244*	18	0.07	-0.073	1.217	3,465	3,672	Strength
14	55	8	2.462*	20	-0.01	-0.194	1.470	4,077	4,086	Strength
14	60	8	2.987*	24	0.05	-0.161	1.691	4,722	4,904	Strength
14	65	8	3.494	28	0.10	-0.155	1.941	5,400	5,710	Strength
14	70	8	3.805	31	-0.05	-0.272	2.268	6,112	6,287	Strength
14	75	8	4.233	35	-0.19	-0.343	2.616	6,857	7,034	Strength
14	80	8	4.645	39	-0.42	-0.439	2.991	7,636	7,768	Stress
14	85	8	5.316	45	-0.45	-0.414	3.361	8,448	8,849	Stress
18	40	10	2.101*	16	0.07	0.007	0.920	3,054	3,434	Strength
18	45	10	2.340*	18	0.02	-0.130	1.169	3,722	3,876	Strength
18	50	10	2.889*	22	0.05	-0.126	1.398	4,469	4,754	Strength
18	55	10	3.418	26	0.06	-0.155	1.662	5,261	5,621	Strength
18	60	10	3.773	29	-0.06	-0.301	1.991	6,098	6,266	Strength
18	65	10	4.223	33	-0.23	-0.420	2.369	6,978	7,077	Stress
18	70	10	4.935	39	-0.28	-0.419	2.749	7,902	8,278	Stress
18	75	10	5.623	45	-0.40	-0.456	3.166	8,871	9,457	Stress
Texas U-40 Interior Beam										
10	60	8	2.022*	18	-0.25	-0.145	1.520	3,229	3,621	Strength
10	65	8	2.221*	20	-0.42	-0.218	1.761	3,667	4,023	Strength
10	70	8	2.408*	22	-0.66	-0.307	2.024	4,126	4,421	Strength
10	75	8	2.584*	24	-1.01	-0.412	2.309	4,607	4,815	Stress
10	80	8	2.749*	26	-1.47	-0.534	2.616	5,108	5,205	Stress
10	85	8	3.349	31	-1.56	-0.429	2.881	5,632	6,142	Stress
10	90	8	3.751	35	-1.97	-0.447	3.218	6,177	6,850	Stress
10	95	8	4.137	39	-2.51	-0.484	3.579	6,744	7,543	Stress
10	100	8	4.784	45	-2.77	-0.397	3.929	7,333	8,554	Stress
10	105	8	5.136	49	-3.6	-0.477	4.336	7,944	9,209	Stress
14	55	8	2.138*	18	-0.17	-0.197	1.451	3,486	3,672	Strength
14	60	8	2.346*	20	-0.34	-0.30	1.712	4,000	4,086	Strength
14	65	8	2.863*	24	-0.35	-0.246	1.941	4,538	4,904	Strength
14	70	8	3.046	26	-0.66	-0.388	2.254	5,102	5,309	Stress
14	75	8	3.374	29	-0.95	-0.464	2.564	5,690	5,910	Stress
14	80	8	3.797	33	-1.28	-0.504	2.915	6,305	6,662	Stress
14	85	8	4.485	39	-1.41	-0.417	3.258	6,945	7,768	Stress
14	90	8	4.873	43	-1.97	-0.506	3.663	7,612	8,492	Stress
14	95	8	5.517	49	-2.32	-0.475	4.062	8,304	9,555	Stress

PRELIMINARY DESIGN

*A minimum concrete transfer strength of 3.0 ksi is recommended by PCI MNL-116 section 5.3.17.

6.10 Preliminary Design Data

**Final camber is net deflection after all losses and noncomposite and composite dead loads are applied.

Table U-2 (continued)

Spacing ft	Span ft	Slab Thickness in.	f'_{ci} ksi	No. of Strands	Final Camber in.**	$f_b @ L/2$ ksi	$f_t @ L/2$ ksi	$M_u @ L/2$ ft-kips	$M_r @ L/2$ ft-kips	Control
Texas U-40 Interior Beam (continued)										
18	45	10	2.014	16	-0.09	-0.161	1.193	3,179	3,434	Strength
18	50	10	2.244	18	-0.22	-0.292	1.469	3,772	3,876	Strength
18	55	10	2.784	22	-0.26	-0.268	1.719	4,397	4,754	Strength
18	60	10	2.987	24	-0.54	-0.450	2.063	5,053	5,189	Stress
18	65	10	3.494	28	-0.72	-0.482	2.383	5,743	6,051	Stress
18	70	10	4.091	33	-0.94	-0.487	2.753	6,467	7,077	Stress
18	75	10	4.795	39	-1.15	-0.456	3.151	7,224	8,278	Stress
18	80	10	5.474	45	-1.46	-0.461	3.586	8,016	9,457	Stress

PRELIMINARY DESIGN

6.10 Preliminary Design Data

*A minimum concrete transfer strength of 3.0 ksi is recommended by PCI MNL-116 section 5.3.17.

**Final camber is net deflection after all losses and noncomposite and composite dead loads are applied.

Table U-3
Texas U-54 Beam

Spacing ft	Span ft	Slab Thickness in.	f'_{ci} ksi	No. of Strands	Final Camber in.**	f_b @ L/2 ksi	f_t @ L/2 ksi	M_u @ L/2 ft-kips	M_r @ L/2 ft-kips	Control
Texas U-54 Exterior Beam										
10	65	8	2.095*	20	0.19	-0.002	1.143	4,927	5,388	Strength
10	70	8	2.274*	22	0.17	-0.061	1.320	5,576	5,922	Strength
10	75	8	2.444*	24	0.12	-0.132	1.513	6,255	6,452	Strength
10	80	8	2.606*	26	0.04	-0.216	1.720	6,964	6,978	Strength
10	85	8	2.896*	29	0.03	-0.237	1.917	7,704	7,758	Strength
10	90	8	3.283	33	0.07	-0.215	2.129	8,474	8,745	Strength
10	95	8	3.657	37	0.09	-0.208	2.357	9,275	9,716	Strength
10	100	8	3.767	39	-0.23	-0.352	2.635	10,106	10,196	Strength
10	105	8	4.120	43	-0.32	-0.373	2.893	10,967	11,142	Strength
10	110	8	4.461	47	-0.46	-0.41	3.166	11,858	12,073	Stress
14	65	8	2.376*	22	0.16	-0.029	1.198	5,542	5,999	Strength
14	70	8	2.553*	24	0.11	-0.117	1.397	6,277	6,543	Strength
14	75	8	2.721*	26	0.02	-0.219	1.612	7,046	7,084	Strength
14	80	8	3.018	29	-0.02	-0.259	1.819	7,851	7,889	Strength
14	85	8	3.412	33	-0.02	-0.257	2.043	8,691	8,914	Strength
14	90	8	3.792	37	-0.06	-0.272	2.284	9,566	9,926	Strength
14	95	8	4.160	41	-0.14	-0.305	2.543	10,476	10,926	Strength
14	100	8	4.268	43	-0.58	-0.488	2.853	11,421	11,422	Stress
14	105	8	4.860	49	-0.49	-0.420	3.112	12,402	12,891	Stress
18	50	10	2.074*	18	0.12	0.037	0.815	4,554	5,106	Strength
18	55	10	2.276*	20	0.10	-0.059	1.001	5,363	5,683	Strength
18	60	10	2.470*	22	0.05	-0.173	1.207	6,219	6,257	Strength
18	65	10	2.931*	26	0.10	-0.151	1.386	7,120	7,397	Strength
18	70	10	3.241	29	0.05	-0.226	1.611	8,068	8,246	Strength
18	75	10	3.648	33	0.02	-0.264	1.856	9,061	9,331	Strength
18	80	10	4.041	37	-0.06	-0.322	2.124	10,100	10,406	Strength
18	85	10	4.422	41	-0.19	-0.401	2.413	11,185	11,471	Strength
18	90	10	4.791	45	-0.40	-0.500	2.723	12,315	12,527	Stress
Texas U-54 Interior Beam										
10	80	8	2.048*	22	-0.40	-0.206	1.606	5,418	5,922	Strength
10	85	8	2.205*	24	-0.59	-0.264	1.802	5,976	6,452	Strength
10	90	8	2.352*	26	-0.84	-0.333	2.012	6,558	6,978	Strength
10	95	8	2.492*	28	-1.17	-0.413	2.235	7,163	7,499	Stress
10	100	8	2.745*	31	-1.45	-0.438	2.460	7,792	8,254	Stress
10	105	8	3.109	35	-1.65	-0.410	2.686	8,445	9,233	Stress
10	110	8	3.208	37	-2.28	-0.533	2.963	9,121	9,716	Stress
10	115	8	3.551	41	-2.65	-0.531	3.218	9,822	10,671	Stress
10	120	8	4.130	47	-2.68	-0.410	3.453	10,547	12,073	Stress
14	75	8	2.165*	22	-0.37	-0.318	1.601	5,991	5,999	Strength
14	80	8	2.606*	26	-0.35	-0.247	1.766	6,640	7,084	Strength
14	85	8	2.759*	28	-0.59	-0.345	1.997	7,317	7,622	Strength
14	90	8	3.026	31	-0.80	-0.389	2.231	8,022	8,403	Strength
14	95	8	3.147	33	-1.24	-0.521	2.505	8,755	8,914	Stress
14	100	8	3.514	37	-1.48	-0.527	2.759	9,516	9,926	Stress
14	105	8	4.120	43	-1.48	-0.413	2.995	10,305	11,422	Stress
14	110	8	4.461	47	-1.86	-0.452	3.283	11,123	12,404	Stress

PRELIMINARY DESIGN

*A minimum concrete transfer strength of 3.0 ksi is recommended by PCI MNL-116 section 5.3.17.

6.10 Preliminary Design Data

**Final camber is net deflection after all losses and noncomposite and composite dead loads are applied.

Table U-3 (continued)

Spacing ft	Span ft	Slab Thickness in.	f'_{ci} ksi	No. of Strands	Final Camber in.**	$f_b @ L/2$ ksi	$f_t @ L/2$ ksi	$M_u @ L/2$ ft-kips	$M_r @ L/2$ ft-kips	Control
Texas U-54 Interior Beam (continued)										
18	60	10	2.189*	20	-0.08	-0.154	1.201	5,276	5,683	Strength
18	65	10	2.376*	22	-0.20	-0.253	1.418	5,998	6,257	Strength
18	70	10	2.553*	24	-0.37	-0.368	1.655	6,755	6,828	Strength
18	75	10	2.997*	28	-0.42	-0.345	1.863	7,547	7,964	Strength
18	80	10	3.277	31	-0.65	-0.427	2.128	8,376	8,790	Stress
18	85	10	3.667	35	-0.85	-0.461	2.401	9,241	9,869	Stress
18	90	10	4.044	39	-1.13	-0.513	2.696	10,142	10,939	Stress
18	95	10	4.657	45	-1.23	-0.451	2.977	11,080	12,527	Stress

PRELIMINARY DESIGN

6.10 Preliminary Design Data

*A minimum concrete transfer strength of 3.0 ksi is recommended by PCI MNL-116 section 5.3.17.

**Final camber is net deflection after all losses and noncomposite and composite dead loads are applied.

Table U-4

Washington U66G5 Beam

Spacing ft	Span ft	Slab Thickness in.	f'_{ci} ksi	No. of Strands	Final Camber in.**	f_b @ L/2 ksi	f_t @ L/2 ksi	M_u @ L/2 ft-kips	M_r @ L/2 ft-kips	Control
Washington U66G5 Exterior Beam										
10	50	8	0.950*	10	0.05	-0.033	0.593	3,226	3,433	Strength
10	55	8	1.134*	12	0.06	-0.033	0.709	3,797	4,106	Strength
10	60	8	1.310*	14	0.07	-0.044	0.841	4,400	4,775	Strength
10	65	8	1.477*	16	0.07	-0.066	0.988	5,034	5,439	Strength
10	70	8	1.636*	18	0.05	-0.099	1.151	5,699	6,099	Strength
10	75	8	1.787*	20	0.00	-0.144	1.330	6,397	6,754	Strength
10	80	8	1.930*	22	-0.09	-0.199	1.524	7,126	7,405	Strength
10	85	8	2.065*	24	-0.22	-0.264	1.734	7,886	8,052	Strength
10	90	8	2.304*	27	-0.32	-0.278	1.936	8,679	8,994	Strength
10	95	8	2.411*	29	-0.57	-0.372	2.188	9,502	9,610	Strength
10	100	8	2.744*	33	-0.67	-0.348	2.400	10,358	10,831	Strength
10	105	8	2.834*	35	-1.07	-0.464	2.683	11,245	11,434	Stress
10	110	8	3.147	39	-1.29	-0.463	2.927	12,164	12,629	Stress
10	115	8	3.450	43	-1.56	-0.475	3.187	13,114	13,808	Stress
10	120	8	3.742	47	-1.91	-0.500	3.464	14,096	14,970	Stress
14	45	8	1.019*	10	0.06	0.034	0.466	3,007	3,450	Strength
14	50	8	1.210*	12	0.08	0.028	0.580	3,613	4,130	Strength
14	55	8	1.392*	14	0.09	0.010	0.712	4,255	4,807	Strength
14	60	8	1.566*	16	0.09	-0.021	0.862	4,934	5,481	Strength
14	65	8	1.732*	18	0.07	-0.064	1.029	5,649	6,151	Strength
14	70	8	1.890*	20	0.01	-0.120	1.214	6,400	6,818	Strength
14	75	8	2.039*	22	-0.08	-0.187	1.416	7,188	7,482	Strength
14	80	8	2.181*	24	-0.22	-0.267	1.635	8,013	8,143	Strength
14	85	8	2.427*	27	-0.33	-0.297	1.849	8,873	9,109	Strength
14	90	8	2.774*	31	-0.42	-0.278	2.059	9,770	10,374	Strength
14	95	8	2.879*	33	-0.74	-0.402	2.343	10,704	11,001	Strength
14	100	8	3.206	37	-0.93	-0.410	2.588	11,674	12,247	Stress
14	105	8	3.523	41	-1.18	-0.433	2.852	12,680	13,480	Stress
14	110	8	3.829	45	-1.50	-0.469	3.135	13,722	14,701	Stress
14	115	8	4.125	49	-1.91	-0.519	3.435	14,801	15,910	Stress
18	40	10	1.081*	10	0.05	0.033	0.406	3,149	3,557	Strength
18	45	10	1.279*	12	0.06	0.010	0.532	3,841	4,260	Strength
18	50	10	1.468*	14	0.06	-0.033	0.682	4,617	4,961	Strength
18	55	10	1.649*	16	0.04	-0.093	0.854	5,440	5,660	Strength
18	60	10	1.821*	18	0.00	-0.168	1.048	6,310	6,356	Strength
18	65	10	2.237*	22	0.02	-0.116	1.193	7,227	7,741	Strength
18	70	10	2.392*	24	-0.10	-0.223	1.431	8,191	8,429	Strength
18	75	10	2.651*	27	-0.21	-0.282	1.667	9,203	9,438	Strength
18	80	10	3.011	31	-0.31	-0.296	1.904	10,261	10,761	Strength
18	85	10	3.129	33	-0.62	-0.456	2.219	11,367	11,419	Stress
18	90	10	3.468	37	-0.84	-0.502	2.500	12,520	12,728	Stress
18	95	10	4.024	43	-0.94	-0.441	2.750	13,719	14,673	Stress
18	100	10	4.339	47	-1.30	-0.523	3.077	14,966	15,957	Stress

PRELIMINARY DESIGN

*A minimum concrete transfer strength of 3.0 ksi is recommended by PCI MNL-116 section 5.3.17.

6.10 Preliminary Design Data

**Final camber is net deflection after all losses and noncomposite and composite dead loads are applied.

Table U-4 (continued)

Spacing ft	Span ft	Slab Thickness in.	f'_{ci} ksi	No. of Strands	Final Camber in.**	f_b @ L/2 ksi	f_t @ L/2 ksi	M_u @ L/2 ft-kips	M_r @ L/2 ft-kips	Control
Washington U66G5 Interior Beam										
10	60	8	1.051*	12	-0.03	-0.06	0.806	3,553	4,106	Strength
10	70	8	1.123*	14	-0.23	-0.213	1.150	4,550	4,775	Strength
10	75	8	1.277*	16	-0.31	-0.231	1.307	5,085	5,439	Strength
10	80	8	1.422*	18	-0.43	-0.258	1.479	5,644	6,099	Strength
10	85	8	1.560*	20	-0.59	-0.296	1.665	6,228	6,754	Strength
10	90	8	1.690*	22	-0.82	-0.343	1.866	6,837	7,405	Strength
10	95	8	1.812*	24	-1.11	-0.400	2.081	7,470	8,052	Stress
10	100	8	1.801*	25	-1.60	-0.537	2.346	8,128	8,373	Stress
10	105	8	2.132*	29	-1.82	-0.488	2.545	8,812	9,610	Stress
10	110	8	2.453*	33	-2.12	-0.452	2.759	9,521	10,831	Stress
10	115	8	2.762*	37	-2.46	-0.428	2.990	10,255	12,034	Stress
10	120	8	3.061	41	-2.89	-0.416	3.236	11,014	13,221	Stress
10	125	8	3.349	45	-3.40	-0.415	3.497	11,799	14,391	Stress
10	130	8	3.627	49	-4.02	-0.427	3.774	12,609	15,546	Stress
14	55	8	1.134*	12	0.00	-0.068	0.741	3,793	4,130	Strength
14	60	8	1.310*	14	-0.02	-0.081	0.879	4,356	4,807	Strength
14	65	8	1.477*	16	-0.06	-0.105	1.033	4,945	5,481	Strength
14	70	8	1.636*	18	-0.12	-0.141	1.205	5,563	6,151	Strength
14	75	8	1.787*	20	-0.22	-0.188	1.393	6,210	6,818	Strength
14	80	8	1.930*	22	-0.38	-0.246	1.597	6,885	7,482	Strength
14	85	8	2.065*	24	-0.59	-0.315	1.819	7,589	8,143	Strength
14	90	8	2.067*	25	-0.97	-0.465	2.092	8,322	8,473	Strength
14	95	8	2.411*	29	-1.15	-0.431	2.301	9,084	9,743	Stress
14	100	8	2.744*	33	-1.38	-0.411	2.527	9,876	11,001	Stress
14	105	8	2.834*	35	-1.93	-0.532	2.828	10,697	11,625	Stress
14	110	8	3.147	39	-2.32	-0.537	3.089	11,548	12,865	Stress
14	115	8	3.676	45	-2.51	-0.431	3.314	12,429	14,701	Stress
14	120	8	3.966	49	-3.06	-0.464	3.612	13,339	15,910	Stress
18	45	10	1.019*	10	0.00	-0.079	0.582	3,417	3,557	Strength
18	50	10	1.210*	12	-0.02	-0.104	0.723	4,056	4,260	Strength
18	55	10	1.392*	14	-0.05	-0.142	0.886	4,729	4,961	Strength
18	60	10	1.566*	16	-0.11	-0.195	1.070	5,438	5,660	Strength
18	65	10	1.732*	18	-0.20	-0.262	1.275	6,182	6,356	Strength
18	70	10	1.890*	20	-0.35	-0.343	1.501	6,963	7,050	Strength
18	75	10	2.290*	24	-0.41	-0.296	1.678	7,781	8,429	Strength
18	80	10	2.306*	25	-0.75	-0.476	1.982	8,637	8,773	Stress
18	85	10	2.662*	29	-0.95	-0.474	2.227	9,530	10,101	Stress
18	90	10	3.007	33	-1.21	-0.489	2.493	10,461	11,419	Stress
18	95	10	3.341	37	-1.56	-0.520	2.782	11,430	12,728	Stress
18	100	10	3.890	43	-1.75	-0.442	3.039	12,437	14,673	Stress
18	105	10	4.200	47	-2.25	-0.507	3.372	13,482	15,957	Stress

PRELIMINARY DESIGN

6.10 Preliminary Design Data

*A minimum concrete transfer strength of 3.0 ksi is recommended by PCI MNL-116 section 5.3.17.

**Final camber is net deflection after all losses and noncomposite and composite dead loads are applied.

Table U-5

Washington U78G5 Beam

Spacing ft	Span ft	Slab Thickness in.	f'_{ci} ksi	No. of Strands	Final Camber in.**	f_b @ L/2 ksi	f_t @ L/2 ksi	M_u @ L/2 ft-kips	M_r @ L/2 ft-kips	Control
Washington U78G5 Exterior Beam										
10	65	8	1.151*	14	0.04	-0.076	0.789	5,149	5,595	Strength
10	70	8	1.302*	16	0.05	-0.092	0.911	5,833	6,376	Strength
10	75	8	1.447*	18	0.03	-0.118	1.046	6,551	7,153	Strength
10	80	8	1.585*	20	0.01	-0.153	1.193	7,301	7,925	Strength
10	85	8	1.715*	22	-0.06	-0.199	1.353	8,084	8,693	Strength
10	90	8	1.838*	24	-0.15	-0.254	1.525	8,900	9,457	Strength
10	95	8	1.841*	25	-0.37	-0.380	1.740	9,749	9,837	Strength
10	100	8	2.159*	29	-0.39	-0.343	1.893	10,631	11,307	Strength
10	105	8	2.253*	31	-0.63	-0.433	2.111	11,546	12,036	Stress
10	110	8	2.340*	33	-0.92	-0.532	2.341	12,495	12,761	Stress
10	115	8	2.633*	37	-1.05	-0.53	2.534	13,476	14,197	Stress
10	120	8	3.124	43	-0.99	-0.434	2.692	14,490	16,321	Stress
10	125	8	3.395	47	-1.21	-0.461	2.914	15,537	17,715	Stress
14	55	8	1.063*	12	0.05	-0.021	0.571	4,338	4,833	Strength
14	60	8	1.228*	14	0.06	-0.034	0.680	5,032	5,627	Strength
14	65	8	1.385*	16	0.06	-0.057	0.804	5,764	6,418	Strength
14	70	8	1.536*	18	0.05	-0.092	0.942	6,534	7,205	Strength
14	75	8	1.679*	20	0.02	-0.138	1.094	7,342	7,990	Strength
14	80	8	1.815*	22	-0.05	-0.195	1.260	8,188	8,771	Strength
14	85	8	1.944*	24	-0.15	-0.262	1.439	9,071	9,549	Strength
14	90	8	2.170*	27	-0.23	-0.285	1.611	9,992	10,690	Strength
14	95	8	2.276*	29	-0.42	-0.380	1.827	10,951	11,441	Strength
14	100	8	2.375*	31	-0.67	-0.485	2.057	11,947	12,189	Stress
14	105	8	2.680*	35	-0.79	-0.490	2.250	12,981	13,674	Stress
14	110	8	2.975*	39	-0.96	-0.509	2.458	14,053	15,147	Stress
14	115	8	3.467	45	-0.95	-0.438	2.635	15,163	17,334	Stress
14	120	8	3.741	49	-1.21	-0.488	2.876	16,310	18,776	Stress
18	50	10	1.128*	12	0.04	-0.051	0.535	4,685	4,963	Strength
18	55	10	1.299*	14	0.03	-0.086	0.660	5,522	5,781	Strength
18	60	10	1.462*	16	0.02	-0.135	0.803	6,408	6,597	Strength
18	65	10	1.618*	18	-0.02	-0.198	0.962	7,342	7,410	Strength
18	70	10	1.997*	22	0.02	-0.149	1.076	8,325	9,029	Strength
18	75	10	2.137*	24	-0.07	-0.240	1.271	9,356	9,835	Strength
18	80	10	2.374*	27	-0.15	-0.290	1.461	10,436	11,019	Strength
18	85	10	2.491*	29	-0.33	-0.413	1.698	11,564	11,799	Strength
18	90	10	2.814*	33	-0.43	-0.438	1.902	12,741	13,352	Stress
18	95	10	3.127	37	-0.57	-0.480	2.124	13,966	14,894	Stress
18	100	10	3.636	43	-0.60	-0.434	2.317	15,240	17,190	Stress
18	105	10	3.927	47	-0.84	-0.512	2.578	16,562	18,708	Stress

PRELIMINARY DESIGN

*A minimum concrete transfer strength of 3.0 ksi is recommended by PCI MNL-116 section 5.3.17.

6.10 Preliminary Design Data

**Final camber is net deflection after all losses and noncomposite and composite dead loads are applied.

Table U-5 (continued)

Spacing ft	Span ft	Slab Thickness in.	f'_{ci} ksi	No. of Strands	Final Camber in.**	f_b @ L/2 ksi	f_t @ L/2 ksi	M_u @ L/2 ft-kips	M_r @ L/2 ft-kips	Control
Washington U78G5 Interior Beam										
10	80	8	1.118*	16	-0.27	-0.231	1.168	5,875	6,376	Strength
10	85	8	1.252*	18	-0.35	-0.252	1.308	6,485	7,153	Strength
10	90	8	1.145*	18	-0.64	-0.409	1.523	7,122	7,153	Stress
10	95	8	1.265*	20	-0.80	-0.446	1.686	7,784	7,925	Stress
10	100	8	1.379*	22	-1.02	-0.493	1.861	8,474	8,693	Stress
10	105	8	1.601*	25	-1.20	-0.486	2.016	9,189	9,837	Stress
10	110	8	1.909*	29	-1.34	-0.440	2.170	9,932	11,307	Stress
10	115	8	1.991*	31	-1.73	-0.520	2.389	10,701	12,036	Stress
10	120	8	2.282*	35	-1.96	-0.496	2.569	11,496	13,481	Stress
10	125	8	2.562*	39	-2.24	-0.484	2.762	12,319	14,909	Stress
10	130	8	2.833*	43	-2.58	-0.485	2.968	13,168	16,321	Stress
10	135	8	3.095	47	-2.99	-0.497	3.188	14,044	17,715	Stress
14	65	8	1.151*	14	-0.03	-0.110	0.816	5,116	5,627	Strength
14	70	8	1.302*	16	-0.06	-0.128	0.942	5,758	6,418	Strength
14	75	8	1.447*	18	-0.11	-0.156	1.082	6,429	7,205	Strength
14	80	8	1.352*	18	-0.31	-0.321	1.299	7,130	7,205	Strength
14	85	8	1.484*	20	-0.43	-0.368	1.465	7,862	7,990	Strength
14	90	8	1.609*	22	-0.60	-0.425	1.644	8,624	8,771	Stress
14	95	8	1.727*	24	-0.82	-0.491	1.836	9,417	9,549	Stress
14	100	8	1.942*	27	-1.01	-0.513	2.020	10,241	10,690	Stress
14	105	8	2.253*	31	-1.17	-0.491	2.196	11,095	12,189	Stress
14	110	8	2.553*	35	-1.36	-0.483	2.387	11,981	13,674	Stress
14	115	8	2.843*	39	-1.61	-0.489	2.593	12,898	15,147	Stress
14	120	8	3.124	43	-1.92	-0.508	2.814	13,846	16,608	Stress
14	125	8	3.600	49	-2.04	-0.438	3.003	14,825	18,776	Stress
18	50	10	1.128*	12	0.04	0.005	0.509	4,172	4,963	Strength
18	55	10	1.063*	12	-0.04	-0.145	0.692	4,865	4,963	Strength
18	60	10	1.228*	14	-0.06	-0.176	0.826	5,596	5,781	Strength
18	65	10	1.385*	16	-0.11	-0.219	0.976	6,364	6,597	Strength
18	70	10	1.536*	18	-0.18	-0.274	1.143	7,169	7,410	Strength
18	75	10	1.679*	20	-0.28	-0.342	1.327	8,013	8,221	Strength
18	80	10	1.815*	22	-0.44	-0.422	1.527	8,896	9,029	Stress
18	85	10	1.944*	24	-0.64	-0.515	1.744	9,818	9,835	Stress
18	90	10	2.386*	29	-0.71	-0.450	1.903	10,779	11,799	Stress
18	95	10	2.704*	33	-0.88	-0.462	2.112	11,780	13,352	Stress
18	100	10	3.012	37	-1.10	-0.490	2.339	12,820	14,894	Stress
18	105	10	3.310	41	-1.38	-0.535	2.583	13,900	16,427	Stress
18	110	10	3.803	47	-1.54	-0.492	2.800	15,020	18,708	Stress

This page intentionally left blank

LOADS AND LOAD DISTRIBUTION

Table of Contents

NOTATION..... 7 - 3

7.1 SCOPE..... 7 - 5

7.2 LOAD TYPES..... 7 - 5

 7.2.1 Permanent Loads..... 7 - 5

 7.2.1.1 Dead Loads 7 - 5

 7.2.1.2 Superimposed Dead Loads..... 7 - 5

 7.2.1.3 Earth Pressures 7 - 5

 7.2.2 Live Loads 7 - 6

 7.2.2.1 Gravity Vehicular Live Load..... 7 - 6

 7.2.2.1.1 Number of Design Lanes 7 - 6

 7.2.2.1.2 Multiple Presence of Live Load 7 - 6

 7.2.2.1.3 Design Vehicular Live Load—LRFD Specifications 7 - 6

 7.2.2.1.4 Dynamic Load Allowance..... 7 - 8

 7.2.2.1.5 Fatigue Load 7 - 8

 7.2.2.2 Other Vehicular Forces 7 - 8

 7.2.2.2.1 Longitudinal (Braking) Forces 7 - 8

 7.2.2.2.2 Centrifugal Forces 7 - 8

 7.2.2.2.3 Vehicular Collision Forces 7 - 8

 7.2.2.3 Pedestrian Loads 7 - 8

 7.2.3 Water and Stream Loads 7 - 8

 7.2.3.1 Stream Forces and Wave Loads 7 - 9

 7.2.3.2 Ice Forces 7 - 9

 7.2.4 Wind Loads..... 7 - 9

 7.2.5 Earthquake Loads and Effects..... 7 - 9

 7.2.5.1 Introduction..... 7 - 9

 7.2.6 Forces Due to Imposed Deformations..... 7 - 9

7.3 LOAD COMBINATIONS AND DESIGN METHODS..... 7 - 10

7.4 SIMPLIFIED DISTRIBUTION METHODS 7 - 14

 7.4.1 Background 7 - 14

 7.4.1.1 Introduction..... 7 - 14

 7.4.2 Approximate Distribution Formulas for Moments (Two Lanes Loaded)..... 7 - 16

 7.4.2.1 I-Beam, Bulb-Tee, or Single or Double Tee Beams with Transverse Post-Tensioning..... 7 - 17

 7.4.2.2 Open or Closed Precast Spread Box Beams with Cast-In-Place Deck..... 7 - 17

 7.4.2.3 Adjacent Box Beams with Cast-In-Place Overlay or Transverse Post-Tensioning..... 7 - 18

 7.4.2.4 Channel Sections, or Box or Tee Sections Connected by “Hinges” at Interface 7 - 18

 7.4.3 Approximate Distribution Formulas for Shear (Two Lanes Loaded) 7 - 18

 7.4.3.1 I-Beam, Bulb-Tee, or Single or Double Tee Beams with Transverse Post-Tensioning..... 7 - 18

 7.4.3.2 Open or Closed Spread Box Beams with Cast-In-Place Deck 7 - 19

 7.4.3.3 Adjacent Box Beams in Multi-Beam Decks..... 7 - 19

LOADS AND LOAD DISTRIBUTION

Table of Contents

7.4.3.4 Channel Sections or Tee Sections Connected by “Hinges” at Interface 7 - 19

7.4.4 Correction Factors for Skews 7 - 19

 7.4.4.1 Multipliers for Moments in Longitudinal Beams..... 7 - 20

 7.4.4.2 Multipliers for Support Shear at Obtuse Corners of Exterior Beams 7 - 20

7.4.5 Lateral Bolting or Post-Tensioning Requirements 7 - 20

 7.4.5.1 Monolithic Behavior 7 - 20

 7.4.5.2 Minimum Post-Tensioning Requirement 7 - 20

 7.4.5.3 Concrete Overlay Alternative..... 7 - 20

7.5 REFINED ANALYSIS METHODS..... 7 - 21

 7.5.1 Introduction and Background 7 - 21

 7.5.2 The Economic Perspective 7 - 21

 7.5.2.1 Moment Reductions 7 - 21

 7.5.2.2 Increasing Span Capability..... 7 - 21

 7.5.3 St. Venant Torsional Constant, J..... 7 - 21

 7.5.4 Related Publications..... 7 - 21

 7.5.5 Modeling Guidelines..... 7 - 22

 7.5.6 Finite Element Study for Moment Distribution Factors..... 7 - 22

7.6 REFERENCES 7 - 22

LOADS AND LOAD DISTRIBUTION

7.1 Scope/7.2.1.4 Superimposed Deformations

NOTATION

A	= area of stringer or beam
A_o	= area enclosed by centerlines of elements (walls)
BR	= vehicular braking force
b	= width of beam
c_1	= constant related to skew factor
C	= stiffness parameter
CE	= vehicular centrifugal force
CR	= force effects due to creep
CT	= vehicular collision force
CV	= vessel collision force
D	= width of distribution per lane
DC	= dead load of structural components and nonstructural attachments
DD	= downdrag
DW	= dead load of wearing surfaces and utilities
d	= depth of beam
d	= precast beam depth
d_e	= horizontal distance from the centerline of the exterior web of the exterior beam at deck level and interior edge of curb or traffic barrier
EH	= horizontal earth pressure load
EL	= miscellaneous locked-in force effects resulting from the construction process, including jacking apart of cantilevers in segmental construction
EQ	= earthquake effects
ES	= earth surcharge load
EV	= vertical pressure from dead load of earth fill
e	= correction factor
e	= eccentricity of a lane from the center of gravity of the pattern of beams
e_g	= distance between the centers of gravity of the beam and deck
FR	= friction force
g	= distribution factor
I	= moment of inertia
I	= moment of inertia of beam
IC	= ice load
IM	= dynamic load allowance
J	= St. Venant torsional constant
K	= a non-dimensional constant
K_g	= longitudinal stiffness parameter

LOADS AND LOAD DISTRIBUTION

7.1 Scope/7.2.1.4 Superimposed Deformations

L	= span of beam
LL	= vehicular live load
LS	= live load surcharge
m	= multiple presence factor
N_b	= number of beams
N_L	= number of loaded lanes under consideration
N_L	= number of traffic lanes
n	= modular ratio between beam and deck material
PL	= pedestrian live load
PS	= secondary forces from post-tensioning
Q	= total factored load
Q_i	= load effect
q_i	= specified loads
R	= reaction on exterior beam in terms of lanes
R_n	= nominal resistance
S	= center-to-center beam spacing
s	= length of a side element
SE	= force effect due to settlement
SH	= force effects due to shrinkage
TG	= force effect due to temperature gradient
TU	= force effect due to uniform temperature
t	= thickness of a side element
t_s	= depth of concrete slab
V	= distance between axles
W	= edge-to-edge width of bridge
W	= wind load on structure
WA	= water load and stream pressure
WL	= wind load on live load
X_{ext}	= horizontal distance from the center of gravity of the pattern of beams to the exterior beam
x	= horizontal distance from the center of gravity of the pattern of beams to each beam
γ_i	= load factors specified in Tables 7.3-1, 7.3-2, and 7.3-3
η	= variable load modifier which depends on ductility, redundancy and operational classification
ϕ	= capacity reduction or resistance factor
μ	= Poisson's ratio, usually assumed equal to 0.20
θ	= skew angle

LOADS AND LOAD DISTRIBUTION

7.1 SCOPE

One main task in bridge design is to collect information on the various permanent and transient loads that may act on a bridge, as well as on how these forces are distributed to the various structural components. This chapter presents the load and load distribution provisions of the AASHTO *LRFD Bridge Design Specifications* (“*LRFD Specifications*”). The in-depth discussions will be limited to live load and its distribution to precast, prestressed concrete superstructure systems. Detailed discussion of other load effects, such as seismic forces and soil pressures, are covered in other chapters of the manual. Although *LRFD Specifications* forms a consistent set of guidelines for bridge design, the engineer should be aware that many state DOTs have additional requirements for loads, load distribution or load combinations. Such requirements are not discussed in this chapter.

This chapter is based on the provisions of the *LRFD Specifications*, 5th Edition, 2010 and the 2011 Interim Revisions.

7.2 LOAD TYPES

In the design of bridge structure components, the engineer should consider all loads which the component must resist. These forces may vary depending on duration (permanent or transient), direction (vertical, transverse, longitudinal, etc.) and deformation (thermal, shrinkage, and creep). Furthermore, the type of effect (bending, shear, axial, etc.) will sometimes influence the magnitude of such forces. A brief description of these forces is detailed below.

7.2.1 Permanent Loads

These loads are sustained by the bridge throughout its life. In general, permanent loads may be subdivided into the following categories.

7.2.1.1 Dead Loads

One of the first tasks in superstructure design is to identify all elements contributing to loads on the beams before composite deck concrete, if any, has cured (some concrete decks are designed to remain noncomposite). These noncomposite dead loads include the weight of the beams, deck slab, haunch, stay-in-place forms and diaphragms.

7.2.1.2 Superimposed Dead Loads

All permanent loads placed on the superstructure after deck curing is completed are usually designated superimposed dead loads. These include the wearing surface, parapets, railings, sidewalk, utilities, and signage. In the *LRFD Specifications*, the load factors for wearing surface and utilities are higher than those for other dead loads to recognize the increased variability of these loads.

7.2.1.3 Earth Pressures

These forces, which primarily affect substructure elements, are usually considered permanent loads. However, they may occasionally affect the superstructure elements at locations where substructure and superstructure interface (abutment backwall, etc.). Detailed equations are listed in the *LRFD Specifications*. Generally, these pressures do not affect superstructure design.

7.2.1.4 Superimposed Deformations

These are permanent loads which vary over a long time period including volume changes from post-tensioning, and force effects due to creep and shrinkage.

LOADS AND LOAD DISTRIBUTION

7.2.2 Live Loads/7.2.2.1.3 Design Vehicular Live Load – LRFD Specifications

7.2.2 Live Loads

7.2.2.1 Gravity Vehicular Live Load

7.2.2.1.1 Number of Design Lanes

Unless otherwise specified, the number of design lanes should be determined by taking the integer part of: roadway width in feet between barriers or curbs divided by 12.0. The loads are assumed to occupy 10.0 ft transversely within a design lane.

7.2.2.1.2 Multiple Presence of Live Load

In view of the improbability of coincident maximum loading in all lanes, *LRFD Specifications* Article 3.6.1.1.2 provides a multiple presence factor, *m*, which applies when using the refined method [LRFD Articles 4.4 and 4.6.3] or the lever rule for distribution of live load. When considering one loaded lane, the multiple presence factor must be used. For three or more loaded lanes, the multiple presence factor is optional. The extreme live load force effect is determined by considering each possible combination of number of loaded lanes multiplied by the corresponding factor given below. The multiple presence factors are not to be used with the approximate load assignment methods of LRFD Articles 4.6.2.2 and 4.6.2.3 because these factors are already incorporated in the distribution factors for both single and multiple lanes loaded.

One loaded lane	$m = 1.20$
Two loaded lanes	$m = 1.00$
Three loaded lanes	$m = 0.85$
Four (or more) loaded lanes	$m = 0.65$

7.2.2.1.3 Design Vehicular Live Load—LRFD Specifications

[LRFD Art. 3.6]

The vehicular live loading on bridges, designated as HL-93, consists of a combination of the:

Design truck OR Design tandem
AND
Design lane load

The design truck is the HS20 vehicle previously used in the AASHTO *Standard Specifications for Highway Bridges* (referred to as the “*Standard Specifications*” in the following), **Figure 7.2.2.1.3-1**. The design tandem consists of a pair of 25.0 kip axles spaced 4.0 ft apart. In either case, the transverse spacing of wheels is taken as 6.0 ft. The design lane load consists of a uniform load of 0.64 klf in the longitudinal direction. It is distributed transversely over a 10.0 ft width.

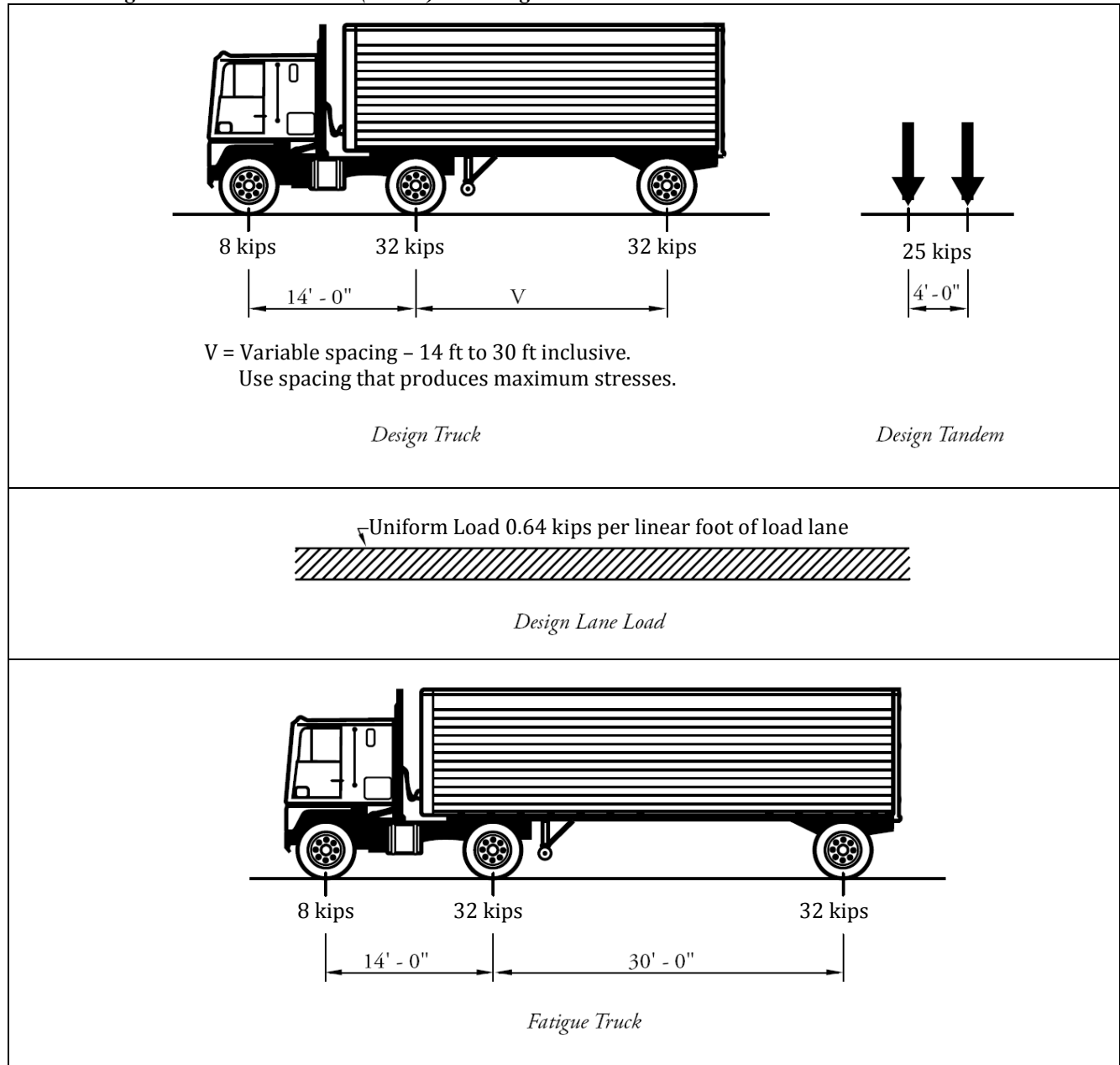
The extreme force effect for the vehicular live load is the larger of the following:

- The effect of the design tandem combined with the design lane load
or
- The effect of one design truck with the variable axle spacing combined with the design lane load
and
- For continuous members, for negative moment between points of dead load contraflexure and reaction at interior piers only: the combination of 90% of the effect of two design trucks (spaced a minimum of 50.0 ft between the lead axle of one and the rear axle of the other truck) with 90% of the effect of the design lane load. The distance between the 32.0 kip axles of each truck is taken as 14.0 ft. The two design trucks must be placed in adjacent spans to produce maximum force effects.

LOADS AND LOAD DISTRIBUTION

7.2.2.1.3 Design Vehicular Live Load – LRFD Specifications

*Figure 7.2.2.1.3-1
LRFD Design Vehicular Live Loads (HL-93) and Fatigue Load*



Axles that do not contribute to the extreme force effect under consideration are neglected. Both the design lanes and the position of the 10.0 ft loaded width in each lane is positioned to produce extreme force effects. The design truck or tandem is positioned transversely so that the center of any wheel load is not closer than 2.0 ft from the edge of the design lane when designing beams.

Unless otherwise specified, the lengths of design lanes, or parts thereof, which contribute to the extreme force effect under consideration are loaded with the design lane load. Only those portions of the span that contribute to maximizing the force effect should be loaded. Influence lines can be used to determine those portions of the span that should be loaded for maximum effect.

LOADS AND LOAD DISTRIBUTION**7.2.2.1.4 Dynamic Load Allowance/7.2.3 Water and Stream Load****7.2.2.1.4 Dynamic Load Allowance**

In *LRFD Specifications* Article 3.6.2, the static effects of the design truck or tandem are multiplied by $(1 + IM)$, where IM is the Dynamic Load Allowance as given for different bridge components below:

[LRFD Table 3.6.2.1-1]

Deck joints: All limit states	75% (0.75)
All other components:	
Fatigue and Fracture Limit State	15% (0.15)
All Other Limit States	33% (0.33)

This dynamic allowance is not applied to the design lane load or to pedestrian loads.

Previously in the *Standard Specifications*, dynamic load allowance was called impact.

7.2.2.1.5 Fatigue Load

In the *LRFD Specifications*, there is a provision for a single fatigue truck, **Figure 7.2.2.1.3-1**, but with a constant spacing of 30.0 ft between the 32.0-kip axles. The applicable dynamic load allowance is 15%. When the bridge is analyzed using approximate methods, the distribution factor for one traffic lane is to be used and the force effect is to be divided by 1.20 (except if the lever rule is used).

7.2.2.2 Other Vehicular Forces**7.2.2.2.1 Longitudinal (Braking) Forces**

[LFRD Art. 3.6.4]

These forces result from vehicles accelerating or braking while traveling over a bridge. Forces are transferred from the wheels to the deck surface.

The braking forces are taken as the greater of:

- 25% of the axle weights of the truck or tandem
- 5% of the truck plus lane load
- 5% of the tandem plus lane load

This braking force is placed in all lanes carrying traffic headed in the same direction. The multiple presence factor, m , is applicable here.

7.2.2.2.2 Centrifugal Forces

[LFRD Art. 3.6.3]

This effect must be considered for bridge structures on horizontal curves. The ratio of this force to the truck (or tandem) axle loads is proportional to the square of the design speed and inversely proportional to the curve radius. This force is applied at 6.0 ft above the roadway surface. Usually, concrete decks resist centrifugal forces within their own plane, and transmit them to the substructure through end diaphragms.

7.2.2.2.3 Vehicular Collision Forces

[LFRD Art. 3.6.5]

These forces need to be considered whenever piers or abutments are not adequately protected to prevent vehicle or railway collisions and for the design of barriers.

7.2.2.3 Pedestrian Loads

[LFRD Art. 3.6.1.6]

In LRFD Article 3.6.1.6, a load of 0.075 ksf is applied to all sidewalks wider than 2.0 ft and must be considered with the vehicular live load. For bridges carrying only pedestrian and/or bicycle traffic, use the *2009 AASHTO Guide LRFD Specifications for the Design of Pedestrian Bridges* and the live load is set at 0.090 ksf.

7.2.3 Water and Stream Loads

These forces primarily affect substructure elements and are due to water course related characteristics. Static water pressure is assumed perpendicular to the surface which is retaining the water, while buoyancy is an uplift force acting on all submerged components.

LOADS AND LOAD DISTRIBUTION**7.2.3.1 Stream Forces and Wave Loads / 7.2.6 Forces Due to Imposed Deformations****7.2.3.1 Stream Forces and Wave Loads**

Stream flow pressure (LRFD Art. 3.7.3) affects the design of piers or supports located in water courses. The average pressure of flowing water on a pier is proportional to the square of water velocity, to the drag coefficient for specific pier geometry and to the projected pier surface exposed to the design flood. Buoyancy shall be considered for all elements below design water level (LRFD Art. 3.7.2). Wave action shall be considered for structures exposed to significant forces. (LRFD Art. 3.7.4)

7.2.3.2 Ice Forces

Floating ice sheets and ice floes on streams cause major dynamic (and static) forces to act on piers in cold weather climates. If clearance is low, the superstructure may also be affected, often with severe damage. Usually, the dynamic force on a pier is a function of ice thickness, ice strength, pier width and inclination of the nose to vertical. The *LRFD Specifications* contains detailed equations and factors for calculation of stream flow and floating ice loads on piers and supports. (LRFD Art. 3.9)

7.2.4 Wind Loads

[LRFD Art. 3.8]

Wind is a dynamic load. However, it is generally approximated as a uniformly distributed static load on the exposed area of a bridge. This area is taken as the combined surfaces of both superstructure and substructure as seen in elevation (orthogonal to the assumed wind direction). AASHTO loads are based on an assumed "base wind velocity" of 100 mph. The specifications also requires varying the wind load direction to determine extreme force effects, and the consideration of a vertical upward force acting on the deck (especially when checking overturning of the bridge).

The *LRFD Specifications* allows some simplifications. For typical girder and slab bridges having an individual span length of not more than 125 ft and a maximum height of 30.0 ft above low ground or water level, the following wind loading may be used for wind on the structure:

- 0.05 ksf, transverse
- 0.012 ksf, longitudinal

Both forces must be applied simultaneously.

For typical girder and slab bridges having an individual span length of not more than 125 ft and a maximum height of 30.0 ft above low ground or water level the following wind loading on live load may be used:

- 0.10 klf, transverse
- 0.04 klf, longitudinal

Both forces must be applied simultaneously.

7.2.5 Earthquake Loads and Effects**7.2.5.1 Introduction**

These temporary natural forces are assumed to act in the horizontal direction and are dependent on the geographic location of the bridge, the structure dead weight (mass), the ground motion (duration and acceleration), the period of the structural system and type of soil. In some cases, a vertical component of acceleration may have to be considered. These factors enter into the seismic analysis which is a simplification of the actual effects of an earthquake. The bridge response assumes the form of an equivalent static load which is applied to the structure to calculate forces and deformations of bridge elements.

For most pretensioned structures, where the superstructure is not integral with the substructure, earthquake forces do not affect beam design, see Chapter 15 for additional information about seismic design of prestressed beam bridges.

7.2.6 Forces Due to Imposed Deformations

These effects include temperature, creep and differential settlement. Some general guidelines are offered in the *LRFD Specifications*. Normally, the difference between the base construction temperature and the temperature

LOADS AND LOAD DISTRIBUTION**7.2.6 Forces Due to Imposed Deformations / 7.3 Load Combinations and Design Methods**

range limits in a region is used to calculate thermal deformation effects for complex concrete box structures. Nearly all engineers neglect the effect of temperature gradient in pretensioned multi-beam bridges. This practice of ignoring thermal gradient for pretensioned multi-beam bridges has been used for over 40 years with good performance. For other types of bridges, judgment and experience should be used in deciding to consider the effects of temperature gradient. Where appropriate, the effects of differential settlements should be considered.

7.3 LOAD COMBINATIONS AND DESIGN METHODS

Vehicle live loads may act on a bridge simultaneously with other live loads. The design engineer is responsible to size and reinforce the structural components to safely resist the possible combinations of loads that may act on a bridge. Therefore, the *LRFD Specifications* contains load combinations, subdivided into various groups, which represent probable simultaneous loadings on the structure. In theory, all structural elements should be designed to resist all groups of loads. In practice, many of the load combinations do not control the design of a typical pretensioned girder.

The method of design in the *LRFD Specifications* employs the LRFD equation specifying that the factored resistance must equal or exceed the factored load for all limit states.

The nominal resistance of a member, R_n , is computed using procedures given in the specifications. This value is then modified by a resistance factor, ϕ , appropriate for the specific conditions of design to obtain the provided strength. The load effects, Q_i , are usually calculated using conventional elastic analysis procedures. These are then modified by the specified load factors, γ_i , to obtain the required strength. In a concise form, the LRFD equation can be expressed as follows:

$$\phi R_n \geq \sum \gamma_i Q_i \quad (\text{Eq. 7.3-1})$$

where Q_i is the load effect.

The total factored load, Q , is given by:

$$Q = \eta \sum \gamma_i q_i \quad (\text{Eq. 7.3-2})$$

where

- η = variable load modifier which depends on ductility, redundancy and operational classification. Its value is often set by state DOTs
- q_i = specified loads
- γ_i = load factors specified in **Tables 7.3-1, 7.3-2 and 7.3-3**

LOADS AND LOAD DISTRIBUTION

7.3 Load Combinations and Design Methods

Table 7.3-1

[LRFD Table 3.4.1-1]

Load Combinations and Load Factors, LRFD Specifications

Load Combination Limit State	DC										Use One of These at a Time															
	DD	EH	EV	ES	EL	PS	CR	SH	LL	IM	CE	BR	PL	LS	WA	WS	WL	FR	TU	TG	SE	EQ	IC	CT	CV	
STRENGTH-I	γ_p	1.75	1.00	—	—	1.00	0.50/1.20	γ_{TG}	γ_{SE}	—	—	—	—	—	—	—	—	—	—	—	—	—	—	—	—	—
STRENGTH-II	γ_p	1.35	1.00	—	—	1.00	0.50/1.20	γ_{TG}	γ_{SE}	—	—	—	—	—	—	—	—	—	—	—	—	—	—	—	—	—
STRENGTH-III	γ_p	—	1.00	1.40	—	1.00	0.50/1.20	γ_{TG}	γ_{SE}	—	—	—	—	—	—	—	—	—	—	—	—	—	—	—	—	—
STRENGTH-IV	γ_p	—	1.00	—	—	1.00	0.50/1.20	—	—	—	—	—	—	—	—	—	—	—	—	—	—	—	—	—	—	—
STRENGTH-V	γ_p	1.35	1.00	0.40	1.0	1.00	0.50/1.20	γ_{TG}	γ_{SE}	—	—	—	—	—	—	—	—	—	—	—	—	—	—	—	—	—
EXTREME EVENT-I	γ_p	γ_{EQ}	1.00	—	—	1.00	—	—	—	1.00	—	—	—	—	—	—	—	—	—	—	—	—	—	—	—	—
EXTREME EVENT-II	γ_p	0.50	1.00	—	—	1.00	—	—	—	—	—	—	—	—	—	—	—	—	—	—	—	1.00	1.00	1.00	—	—
SERVICE-I	1.00	1.00	1.00	0.30	1.0	1.00	1.00/1.20	γ_{TG}	γ_{SE}	—	—	—	—	—	—	—	—	—	—	—	—	—	—	—	—	—
SERVICE-II	1.00	1.30	1.00	—	—	1.00	1.00/1.20	—	—	—	—	—	—	—	—	—	—	—	—	—	—	—	—	—	—	—
SERVICE-III	1.00	0.80	1.00	—	—	1.00	1.00/1.20	γ_{TG}	γ_{SE}	—	—	—	—	—	—	—	—	—	—	—	—	—	—	—	—	—
SERVICE-IV	1.00	—	1.00	0.70	—	1.00	1.00/1.20	—	1.0	—	—	—	—	—	—	—	—	—	—	—	—	—	—	—	—	—
FATIGUE I—LL, IM & CE only	—	1.50	—	—	—	—	—	—	—	—	—	—	—	—	—	—	—	—	—	—	—	—	—	—	—	—
FATIGUE II—LL, IM & CE only	—	0.75	—	—	—	—	—	—	—	—	—	—	—	—	—	—	—	—	—	—	—	—	—	—	—	—

For notes on γ_p , γ_{EQ} , γ_{TG} and γ_{SE} , refer to LRFD Specifications

LOADS AND LOAD DISTRIBUTION

7.3 Load Combinations and Design Methods

Table 7.3-2 [LRFD Table 3.4.1-2]
Load Factors for Permanent Loads, γ_p

Type of Load	Load Factor		
	Maximum	Minimum	
DC: Component and Attachments	1.25	0.90	
DC: Strength IV Only	1.50	0.90	
DD: Downdrag	Piles, α -Tomlinson Method	1.40	0.25
	Piles, λ -Method	1.05	0.30
	Drilled Shafts. O'Neil and Reese Method	1.25	0.35
DW: Wearing Surfaces and Utilities	1.50	0.65	
EH: Horizontal Earth Pressure			
• Active	1.50	0.90	
• At-Rest	1.35	0.90	
EL: Locked-in Construction Stresses	1.00	1.00	
EV: Vertical Earth Pressure			
• Overall Stability	1.00	N/A	
• Retaining Walls and Abutments	1.35	1.00	
• Rigid Buried Structure	1.30	0.90	
• Rigid Frames	1.35	0.90	
ES: Earth Surcharge	1.50	0.75	

The above is excerpted from LRFD Table 3.4.1-2

Table 7.3-3 [LRFD Table 3.4.1-3]
Load Factors for Permanent Loads due to Superimposed Deformations, γ_p

Bridge Component	PS	CR, SH
Superstructures—Segmental Concrete Substructures supporting Segmental Superstructures (see LRFD Articles 3.12.4 and 3.12.5)	1.0	See γ_p for DC, Table 7.3-2
Concrete Superstructures—non-segmental Substructures supporting non-segmental Superstructures	1.0	1.0
• using I_g	0.5	0.5
• using $I_{effective}$	1.0	1.0
Steel substructures	1.0	1.0

Components (and connections) of a bridge structure must satisfy the applicable combinations of factored extreme force effects as specified at each of the limit states. The following load designations are used:

• Permanent Loads

- | | |
|--|--|
| <i>DD</i> = downdrag | <i>EH</i> = horizontal earth pressure load |
| <i>DC</i> = dead load of structural components and nonstructural attachments | <i>ES</i> = earth surcharge load |
| <i>DW</i> = dead load of wearing surfaces and utilities | <i>EV</i> = vertical pressure from dead load of earth fill |
| <i>EL</i> = accumulated locked-in force effects resulting from the construction process, including the secondary forces from post-tensioning | <i>PS</i> = secondary forces from post-tensioning |
| <i>CR</i> = force effects due to creep | <i>SH</i> = force effects due to shrinkage |

LOADS AND LOAD DISTRIBUTION

7.3 Load Combinations and Design Methods

• Transient Loads

<i>BR</i>	= vehicular braking force	<i>LS</i>	= live load surcharge
<i>CE</i>	= vehicular centrifugal force	<i>PL</i>	= pedestrian live load
<i>CT</i>	= vehicular collision force	<i>SE</i>	= settlement
<i>CV</i>	= vessel collision force	<i>TG</i>	= temperature gradient
<i>EQ</i>	= earthquake effects	<i>TU</i>	= uniform temperature
<i>FR</i>	= friction force	<i>WA</i>	= water load and stream pressure
<i>IC</i>	= ice load	<i>WL</i>	= wind on live load
<i>IM</i>	= vehicular dynamic load allowance	<i>WS</i>	= wind load on structure
<i>LL</i>	= vehicular live load		

As has always been the case, the owner or designer may determine that not all of the loads in a given load combination apply to the situation being investigated. The various applicable load factors are in **Tables 7.3-1, 7.3-2, and 7.3-3**. The minimum load factors are especially important in the negative moment regions of continuous beams.

The factors must be selected to produce the total extreme factored force effect. For each load combination, both positive and negative extremes must be investigated. In load combinations where one force effect decreases the effect of another, the minimum value is applied to the load reducing the force effect. For permanent force effects, the load factor (maximum or minimum) which produces the more critical combination is selected **from Table 7.3-2 or 7.3-3**.

The design of pretensioned superstructure beams using the *LRFD Specifications* usually consists of satisfying the requirements of Service I, Service III, and Strength I load combinations. Use of the new larger HL-93 live load for working stress design of prestressed concrete members would result in overly-conservative designs. Also, since no significant cracking has been observed in existing bridges that were designed for the relatively lower loads of the *Standard Specifications*, the Service III load combination was introduced. Service III specifies a load factor of 0.80 to reduce the effect of live load at the service limit state. This combination is only applicable when checking allowable tensile stresses in prestressed concrete superstructure members. Service I is used when checking compressive stresses only. The load combination Strength I is used for design at the strength limit state. Other load combinations for the strength and extreme event limit states are not considered here, but may be required by specific agencies or DOTs—such as Strength II combination for permit vehicles.

The various load combinations applicable to prestressed beams and substructures (Service IV) and shown in **Table 7.3-1** are described below.

- STRENGTH I — Basic load combination relating to the normal vehicular use of the bridge without wind.
- STRENGTH II — Load combination relating to the use of the bridge by permit vehicles without wind. If a permit vehicle is traveling unescorted, or if control is not provided by the escorts, the other lanes may be assumed to be occupied by the vehicular live load herein specified. For bridges longer than the permit vehicle, addition of the lane load, preceding and following the permit load in its lane, should be considered.
- SERVICE I — Load combination relating to the normal operational use of the bridge with 55 mph wind. All loads are taken at their nominal values and extreme load conditions are excluded. Compression in prestressed concrete components and tension in prestressed bent caps is investigated using this load combination.
- SERVICE III — Load combination for longitudinal analysis relating to prestressed concrete superstructures with the primary objective of crack control. Tensile stress in prestressed concrete superstructure members is investigated using this load combination.
- SERVICE IV — Load combination relating only to tension in prestressed concrete columns with the primary objective of crack control. Tensile stress in prestressed concrete substructure members is investigated using this load combination.
- FATIGUE I — Fatigue and fracture load combination related to infinite load-induced fatigue life.
- FATIGUE II — Fatigue and fracture load combination related to finite load-induced fatigue life.

LOADS AND LOAD DISTRIBUTION

7.4.1.1 Introduction

7.4 SIMPLIFIED DISTRIBUTION METHODS

The following sections will focus on precast, prestressed concrete bridges using box, I-, bulb-tee or multi-stem beam cross sections. The majority of the live load distribution formulas in the *LRFD Specifications* are based on an NCHRP project (Zokaie, 1991). However, as with any new technology, revisions and clarifications are inevitable.

7.4.1 Background

Advanced computer technology and refined procedures of analysis—such as the finite element method—constitute the basis for development of the approximate formulas given in the *LRFD Specifications*. First, a large database of more than 800 actual bridges was randomly compiled from various states to achieve national representation. Then, average bridges were obtained for each slab and beam category. Finally, refined analyses were implemented on selected bridges from each group.

Approximate formulas were developed to capture the variation of load distribution factors with each of the dominant geometric and material parameters. It was assumed that the effect of each parameter could be modeled by an exponential function of the form ax^b where 'x' is the value of the given parameter (span, spacing, box depth, etc.) and 'b' is an exponent to be defined. The final distribution factor is given in the following general format which is based on a multiple regression analysis:

$$D.F. = A + B(x)^b(y)^c(z)^d \dots \quad (\text{Eq. 7.4.1-1})$$

The multiple exponential procedure is practical and conservative due to the following assumptions:

- Midspan diaphragms were disregarded thereby increasing moments in interior beams and reducing moments in exterior beams
- The width of the concrete parapet (1 ft 6 in. or 1 ft 9 in.) was often neglected, thereby increasing the load factors for the first two beams

Furthermore, in order to assure conservative results, the constants in the formulas were adjusted so that the ratio of the average value computed using the approximate method to the accurate distribution factor should be in most cases larger than 1.0.

7.4.1.1 Introduction

LRFD Article 4.6.2.2 presents approximate live load distribution factors that may be used when a refined method is not used. Different structure types are identified descriptively and graphically in **LRFD Table 4.6.2.2.1-1** to assist the designer in using the correct distribution factor for the structure being designed. There are 12 structure types included in the table, eight of which utilize precast concrete.

Longitudinal joints connecting adjacent members are shown for five of the types of structures. If adjacent beams are "sufficiently connected to act as a unit," they may be considered to act monolithically. Those types without composite structural concrete topping may require transverse post-tensioning. (See Section 7.4.5.)

The following general conditions must be satisfied for the approximate distribution factor equations to be used:

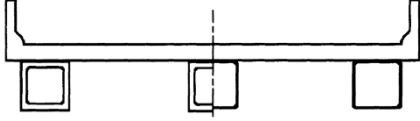
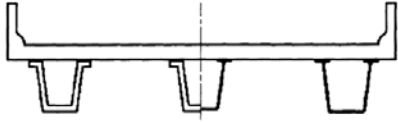
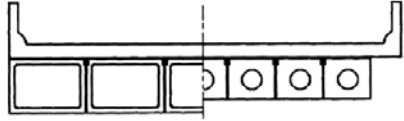
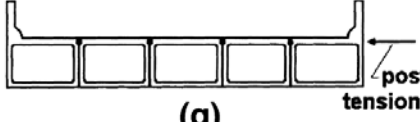
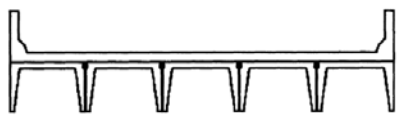
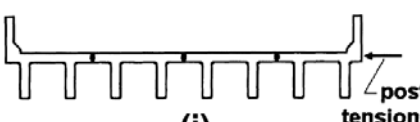
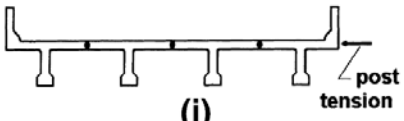
- The width of deck is constant
- The number of beams is not less than three, four or five depending on the case
- Beams are parallel and have approximately the same stiffness
- Unless otherwise specified, the roadway part of the overhang, d_e , does not exceed 3.0 ft
- Limits on girder spacings
- Limits on span lengths
- Curvature in plan is less than the specified limit
- The cross-section is consistent with one of the cross-sections shown in **Figure 7.4.1-1**
- For beams, other than box beams, used in multi-beam decks with shear keys:
 - deep, rigid end diaphragms are required
 - if the stem spacing of stemmed beams is less than 4.0 ft or more than 10.0 ft, a refined analysis must be used

LOADS AND LOAD DISTRIBUTION

7.4.1.1 Introduction

Figure 7.4.1-1
Common Deck Superstructures

[partial LRFD Table 4.6.2.2.1-1]

SUPPORTING COMPONENTS	TYPE OF DECK	TYPICAL CROSS SECTION
Closed Steel or Precast Concrete Boxes	Cast-in-place concrete slab	 <p style="text-align: center;">(b)</p>
Open Steel or Precast Concrete Boxes	Cast-in-place concrete slab, precast concrete deck slab	 <p style="text-align: center;">(c)</p>
Precast Solid, Voided or Cellular Concrete Boxes with Shear Keys	Cast-in-place concrete overlay	 <p style="text-align: center;">(f)</p>
Precast Solid, Voided or Cellular Concrete Boxes with Shear Keys and with or without Transverse Post-Tensioning	Integral Concrete	 <p style="text-align: center;">(g)</p>
Precast Concrete Channel Sections with Shear Keys	Cast-in-place concrete overlay	 <p style="text-align: center;">(h)</p>
Precast Concrete Double Tee Section with Shear Keys and with or without Transverse Post-Tensioning	Integral Concrete	 <p style="text-align: center;">(i)</p>
Precast Concrete Tee Section with Shear Keys and with or without Transverse Post-Tensioning	Integral Concrete	 <p style="text-align: center;">(j)</p>
Precast Concrete I or Bulb-Tee Sections	Cast-in-place concrete, precast concrete	 <p style="text-align: center;">(k)</p>

LOADS AND LOAD DISTRIBUTION**7.4.1.1 Introduction/7.4.2 Approximate Distribution Formulas for Moments (Two Lanes Loaded)**

All formulas in the tables in the *LRFD Specifications* provide the live load distribution per lane. Where roadway width is larger than 20 ft, the formulas for “Two or More Design Lanes Loaded” must be used for the following limit states: Strength I, Service I and Service III. For the Strength II limit state, the same distribution factor may be used. However, results can be overly conservative if the permit load is heavy. To circumvent this situation, where it controls the design, the engineer can use a refined method as discussed in Section 7.5. Finally, when checking for fatigue, the formulas for “One Design Lane Loaded” must be used. In the following sections, two loaded lanes will be assumed.

Specific limitations for each equation are given in the tables. These must also be satisfied before the equations can be used.

Where bridges meet the specified conditions, permanent superimposed loads, such as parapets and wearing surface, may be distributed equally between all beams in the bridge.

The live load distribution factors specified herein may also be used for permit and rating vehicles whose overall width is comparable to the width of the design truck.

7.4.2 Approximate Distribution Formulas for Moments (Two Lanes Loaded)

[LRFD Art. 4.6.2.2]
[LRFD Table 4.6.2.2b-1]
[LRFD Table 4.6.2.2d-1]

The following notation is used in the distribution factor equations:

- A = area of stringer, or beam, in.²
- b = width of beam, in.
- C = stiffness parameter = $K(W/L)$
- d = depth of beam, in.
- d_e = Horizontal distance between the centerline of the exterior web of the exterior beam at the deck level and interior edge of curb or traffic barrier, ft
- D = width of distribution per lane, ft
- e = correction factor
- g = distribution factor
- J = St. Venant torsional constant, in.⁴
- K = a non-dimensional constant
- K_g = longitudinal stiffness parameter, in.⁴
- L = span of beam, ft
- N_b = number of beams
- N_L = number of design lanes
- S = spacing of beams or webs, ft
- t_s = depth of concrete slab, in.
- W = edge-to-edge width of bridge, ft
- θ = skew angle, deg
- μ = Poisson's ratio, usually assumed equal to 0.20

The longitudinal stiffness parameter, K_g , is taken as:

$$K_g = n(I + Ae_g^2) \quad \text{[LRFD Eq. 4.6.2.2.1-1]}$$

where

- n = modular ratio between beam and deck materials, generally ≥ 1
- I = moment of inertia of beam, in.⁴
- e_g = distance between the centers of gravity of the beam and deck, in.

LOADS AND LOAD DISTRIBUTION

7.4.2.1 I-Beam, Bulb-Tee, or Single or Double Tee Beams with Transverse Post-Tensioning/7.4.2.2 Open or Closed Precast Spread Box Beams with Cast-In-Place Deck

7.4.2.1 I-Beam, Bulb-Tee, or Single or Double Tee Beams with Transverse Post-Tensioning

The applicable live load distribution factor equation for interior beams [Figure 7.4.1-1, types (i), (j) and (k)] is:

$$g = 0.075 + \left(\frac{S}{9.5}\right)^{0.6} \left(\frac{S}{L}\right)^{0.2} \left(\frac{K_g}{12.0Lt_s^3}\right)^{0.1} \tag{Eq. 7.4.2.1-1}$$

The only practical conditions affecting applicability of this equation are that N_b must be equal to or larger than 4 and $10,000 \leq K_g \leq 7,000,000$. The latter limit may be exceeded in the case of I-beams that are 96 in. deep or more. With the owner’s concurrence, simplifications to Eq. 7.4.2.1-1 may be used as shown in Table 7.4.2.1-1.

Table 7.4.2.1-1 Simplified Values for LRFD Articles 4.6.2.2.2 and 4.6.2.2.3		[LRFD Table 4.6.2.2.1-2]			
Equation Parameter	Table Reference	Simplified Value			
		<i>a</i>	<i>e</i>	<i>k</i>	<i>f,g,i,j</i>
$\left(\frac{K_g}{12Lt_s^3}\right)^{0.1}$	4.6.2.2.2b-1	1.02	1.05	1.09	—
$\left(\frac{K_g}{12Lt_s^3}\right)^{0.25}$	4.6.2.2.2e-1	1.03	1.07	1.15	—
$\left(\frac{12Lt_s^3}{K_g}\right)^{0.3}$	4.6.2.2.3c-1	0.97	0.93	0.85	—
$\frac{I}{\bar{J}}$	4.6.2.2.2b-1 4.6.2.2.3a-1	—	—	—	$0.54\left(\frac{d}{b}\right) + 0.16$

The equation for exterior beams without midspan diaphragms is:

$$g = eg_{interior} \tag{Eq. 7.4.2.1-2}$$

where $e = 0.77 + (d_e/9.1) \geq 1.0$ (Eq. 7.4.2.1-2a)

If rigid midspan diaphragms are used in the cross section, an additional check is required using an interim, conservative procedure for I- and bulb-tee beam sections and applying the related multiple presence factor, m :

$$g \geq R = \frac{N_L}{N_b} + \frac{X_{ext} \sum^{N_L} e}{\sum^{N_b} x^2} \tag{Eq. 7.4.2.1-3}$$

[LRFD Eq. C4.6.2.2d-1]

where

- R = reaction on exterior beam in terms of lanes
- N_L = number of loaded lanes under consideration
- N_b = number of beams
- e = eccentricity of a lane from the center of gravity of the pattern of beams, ft
- x = horizontal distance from the center of gravity of the pattern of beams to each beam, ft
- X_{ext} = horizontal distance from the center of gravity of the pattern of beams to the exterior beam, ft

7.4.2.2 Open or Closed Precast Spread Box Beams with Cast-In-Place Deck

The live load flexural moment for interior beams [Figure 7.4.1-1, types (b) and (c)] may be determined by applying the following lane fraction:

$$g = \left(\frac{S}{6.3}\right)^{0.6} \left(\frac{Sd}{12.0L^2}\right)^{0.125} \tag{Eq. 7.4.2.2-1}$$

where d = precast beam depth.

This formula is subject to two practical limitations: $N_b \geq 3$ and $6.0 \leq S \leq 18.0$ ft. The other geometric conditions are usually met.

LOADS AND LOAD DISTRIBUTION

7.4.2.2 Open or Closed Precast Spread Box Beams with Cast-In-Place Deck/7.4.3.1 I-Beam, Bulb-Tee, or Single or Double Tee Beams with Transverse Post-Tensioning

The corresponding formula for exterior beams is:

$$g = eg_{interior} \quad (\text{Eq. 7.4.2.2-2})$$

$$\text{where } e = 0.97 + (d_e/28.5) \quad (\text{Eq. 7.4.2.2-2a})$$

Equation (7.4.2.1-3) must also be checked in the case of rigid midspan diaphragms.

7.4.2.3 Adjacent Box Beams with Cast-In-Place Overlay or Transverse Post-Tensioning

The applicable distribution factor equation for interior beams [Figure 7.4.1-1, types (f) and (g)], is given by:

$$g = k \left(\frac{b}{305} \right)^{0.6} \left(\frac{b}{12.0L} \right)^{0.2} \left(\frac{I}{J} \right)^{0.06} \quad (\text{Eq. 7.4.2.3-1})$$

$$\text{where } k = 2.5(N_b)^{-0.2} \geq 1.5 \quad (\text{Eq. 7.4.2.3-1a})$$

In a preliminary design situation one may assume $(I/J)^{0.06} = 1.0$. These equations are limited to box beam widths not exceeding 5.0 ft and to span lengths $L \leq 120$ ft.

The bending moment for exterior beams is determined by applying the following lane fraction:

$$g = eg_{interior} \quad (\text{Eq. 7.4.2.3-2})$$

$$\text{where } e = 1.04 + (d_e/25), d_e \leq 2.0 \quad (\text{Eq. 7.4.2.3-2a})$$

7.4.2.4 Channel Sections, or Box or Tee Sections Connected by "Hinges" at Interface

For interior beams, [Figure 7.4.1-1, types (g), (h), (i) and (j)], the applicable formula for the distribution factor, regardless of the number of loaded lanes, is:

$$g = S/D \quad (\text{Eq. 7.4.2.4-1})$$

where

$$D = 11.5 - N_L + 1.4N_L(1 - 0.2C)^2 \text{ when } C \leq 5 \quad (\text{Eq. 7.4.2.4-1a})$$

$$D = 11.5 - N_L \text{ when } C > 5 \quad (\text{Eq. 7.4.2.4-1b})$$

where

$$C = K(W/L) \leq K \quad (\text{Eq. 7.4.2.4-1c})$$

$$\text{where } K = [(1 + \mu)(I/J)]^{0.5} \quad (\text{Eq. 7.4.2.4-1d})$$

LRFD Table 4.6.2.2.2b-1 suggests values of K for preliminary design.

The specified procedure for exterior beams is simply the lever rule in conjunction with the multiple presence factor, m (see Section 7.2.2.1.2). However, this presents some interpretation problems regarding how many lanes should be loaded (say 2, 3, or 4 lanes if roadway width is 48 ft or more). Until this question is resolved, it is prudent to at least assign the same live load distribution factor for exterior beams as for interior beams, which is the approach used in the *Standard Specifications*. Furthermore, LRFD Article 2.5.2.7 requires that, in general, the load carrying capacity of an exterior beam be not less than the one for an interior beam.

7.4.3 Approximate Distribution Formulas for Shear (Two Lanes Loaded)

The live load shear for interior and exterior beams is determined by applying the lane fractions specified for the categories below. The shear distribution factors are normally higher than the moment factors for the same cross section and span.

7.4.3.1 I-Beam, Bulb-Tee, or Single or Double Tee Beams with Transverse Post-Tensioning

The applicable live load distribution factor equation for interior beams, [Figure 7.4.1-1, types (i), (j) and (k)], is:

$$g = 0.2 + \left(\frac{S}{12} \right) - \left(\frac{S}{35} \right)^{2.0} \quad (\text{Eq. 7.4.3.1-1})$$

The only practical limitation on its applicability is $N_b \geq 4$.

LOADS AND LOAD DISTRIBUTION**7.4.3.1 I-Beam, Bulb-Tee, or Single or Double Tee Beams with Transverse Post-Tensioning/7.4.4 Correction Factors for Skew**

The corresponding equation for exterior beams without midspan diaphragm is:

$$g = eg_{interior} \quad (\text{Eq. 7.4.3.1-2})$$

$$\text{where } e = 0.6 + (d_e/10) \quad (\text{Eq. 7.4.3.1-2a})$$

If rigid midspan diaphragms are present, then the conservative approach in Eq. (7.4.2.1-3) must be used.

7.4.3.2 Open or Closed Spread Box Beams with Cast-In-Place Deck

The live load shear for interior beams [Figure 7.4.1-1, types (b) and (c)], may be determined by applying the following lane fraction:

$$g = \left(\frac{S}{7.4}\right)^{0.8} \left(\frac{d}{12.0L}\right)^{0.1} \quad (\text{Eq. 7.4.3.2-1})$$

The formula is subject to two practical limits: $N_b \geq 3$ and $6.0 \leq S \leq 18.0$ ft. The other conditions are generally satisfied.

The related equation for exterior beams is:

$$g = eg_{interior} \quad (\text{Eq. 7.4.3.2-2})$$

$$\text{where } e = 0.8 + (d_e/10) \quad (\text{Eq. 7.4.3.2-2a})$$

7.4.3.3 Adjacent Box Beams in Multi-Beam Decks

The applicable distribution factor equation for interior beams [Figure 7.4.1-1, types (f) and (g)], is:

$$g = \left(\frac{b}{156}\right)^{0.4} \left(\frac{b}{12.0L}\right)^{0.1} \left(\frac{I}{J}\right)^{0.05} \left(\frac{b}{48}\right) \text{ where } \left(\frac{b}{48}\right) \geq 1.0 \quad (\text{Eq. 7.4.3.3-1})$$

These equations are limited to box widths not exceeding 5.0 ft, to span lengths $L \leq 120$ ft and to I or $J \leq 610,000$ in⁴. The latter value may be exceeded if depth exceeds 66 in.

The shear for exterior beams is determined by applying the following lane fraction:

$$g = e g_{interior} \left(\frac{48}{b}\right) \text{ where } \left(\frac{48}{b}\right) \leq 1.0 \quad (\text{Eq. 7.4.3.3-2})$$

$$\text{where } e = 1 + \left[\frac{d_e + \frac{b}{12} - 2.0}{40}\right]^{0.5} \geq 1.0 \quad (\text{Eq. 7.4.3.3-2a})$$

7.4.3.4 Channel Sections or Tee Sections Connected by "Hinges" at Interface

For interior or exterior beams [Figure 7.4.1-1, types (h), (i) and (j)], the lever rule in conjunction with the multiple presence factor, m , is specified.

7.4.4 Correction Factors for Skews

Skewed beam layout is generally dictated by complex highway intersections and/or by the lack of space in urban areas. When the skew angle of a bridge is small, say, less than 20 degrees, it is often considered safe to ignore the effects of skew and to analyze the bridge as a zero-skew bridge whose span is equal to the skew span. This approach is generally conservative for moments in the beams, and slightly unsafe (<5%) for slab-on-beam decks for longitudinal shears.

LRFD Table 4.6.2.2.2e-1, lists reduction multipliers for moments in longitudinal beams. Also listed in LRFD Table 4.6.2.2.3c-1 are correction factors (> 1.0) applicable to the distribution factors for support shears at the obtuse corner of exterior beams. The commentary reminds the designer to check the possibility of uplift at the acute corners of large skews. Reliable multipliers and correction factors are missing for some bridge cross-sections.

LOADS AND LOAD DISTRIBUTION

7.4.4.1 Multipliers for Moments in Longitudinal Beams/7.4.5.3 Concrete Overlay Alternative

7.4.4.1 Multipliers for Moments in Longitudinal Beams

Bending moments in interior and exterior beams on skewed supports may be reduced using the following multipliers: [LRFD Table 4.6.2.2.2e-1]

- a) I-Beam, Bulb-Tee, Single or Double Tee Beams with Transverse Post-Tensioning [Figure 7.4.1-1, types (i), (j) and (k)]:
Use: $1 - c_1(\tan\theta)^{1.5}$ (Eq. 7.4.4.1-1)

$$\text{where } c_1 = 0.25 \left(\frac{K_g}{12.0L t_s^3} \right)^{0.25} \left(\frac{S}{L} \right)^{0.5} \quad (\text{Eq. 7.4.4.1-1a})$$

Set $c_1 = 0$ when $\theta < 30^\circ$

Set $\theta = 60^\circ$ when $\theta > 60^\circ$

- b) Spread Box Beams, Adjacent Box Beams with Concrete Overlays or Transverse Post-Tensioning, and Double Tees in Multi-Beam Decks [Figure 7.4.1-1, types (b), (c), (f) and (g)]:
Use: $1.05 - 0.25\tan\theta \leq 1.0$ (Eq. 7.4.4.1-2)

Set $\theta = 60^\circ$ if $\theta > 60^\circ$

7.4.4.2 Multipliers for Support Shear at Obtuse Corners of Exterior Beams

Shears in exterior beams on the obtuse corner of the bridge may be reduced using the following multipliers: [LRFD Table 4.6.2.2.3c-1]

- a) I-Beam, Bulb-Tee, Single or Double Tee Beams with Transverse Post-Tensioning [Figure 7.4.1-1, types (i), (j) and (k)]:
Use: $1.0 + 0.20 \left(\frac{12.0L t_s^3}{K_g} \right)^{0.3} \tan\theta$ (Eq. 7.4.4.2-1)

This formula is valid for $\theta < 60^\circ$.

- b) Spread Box Beams [Figure 7.4.1-1, types (b) and (c)]:
Use: $1.0 + \left\{ \left(\frac{Ld}{12.0} \right)^{0.5} \left(\frac{\tan\theta}{6S} \right) \right\}$ (Eq. 7.4.4.2-2)

Two practical limits apply, $\theta < 60^\circ$ and $N_b \geq 3$.

- c) Adjacent Box Beams with Cast-In-Place Overlay or Transverse Post-Tensioning [Figure 7.4.1-1, types (f) and (g)]:
Use: $1.0 + \left\{ \frac{12.0L (\tan\theta)^{0.5}}{90d} \right\}$ (Eq. 7.4.4.2-3)

7.4.5 Lateral Bolting or Post-Tensioning Requirements

The following discussion concerns apparent inconsistencies in provisions of the *LRFD Specifications* related to the transverse connection between adjacent members.

7.4.5.1 Monolithic Behavior

As noted earlier, the *LRFD Specifications* indicates that adjacent beams connected by longitudinal joints may be considered to act monolithically if they are "sufficiently connected to act as a unit." The *LRFD Specifications* also notes that transverse post-tensioning provides the best connection between adjacent beams to achieve monolithic behavior but that a reinforced structural concrete overlay may also be used.

7.4.5.2 Minimum Post-Tensioning Requirement

LRFD Commentary Article C4.6.2.2.1 recommends a minimum transverse post-tensioning stress of 0.250 ksi to make the beams act as a unit. This post-tensioning is required for service considerations to achieve appropriate durability (Arockiasamy, et al., 1991). The 0.250 ksi stress is not needed over the entire contact surface between beams (for example, not needed on full depth of the box beam webs), but should be provided where a direct transverse load path is available such as over the entire cross section of transverse diaphragms and grouted keyways creating the top surface [LRFD Table 4.6.2.1.1-1 Cross Sections (g), (i) and (j)].

7.4.5.3 Concrete Overlay Alternative

LRFD Article 5.14.4.3.3.f gives requirements for a structural concrete topping that can also be used to achieve monolithic action, according to LRFD Commentary Article C4.6.2.2.1.

LOADS AND LOAD DISTRIBUTION

7.5 Refined Analysis Methods/7.5.4 Related Publications

7.5 REFINED ANALYSIS METHODS

7.5.1 Introduction and Background

LRFD Article 4.6.3 allows the use of refined methods of analysis for lateral load distribution in lieu of the tabulated simplified equations. Although the simplified equations are based on a statistical approach, they are often conservative.

7.5.2 The Economic Perspective

The refined methods most often used to study the behavior of bridges are the grillage analysis and the finite element methods. The finite element analysis (FEA) requires the fewest simplifying assumptions to account for the greatest number of variables which govern the structural response of the bridge deck. However, input preparation time, and derivation of overall forces for the composite beam are usually quite tedious. Data preparation for the grillage method is simpler and integration of stresses is not needed.

7.5.2.1 Moment Reductions

Analyses by Aswad and Chen (1994) have shown that using the FEA may result in a reduction of the lateral load distribution factor for moments by at least 18% for interior I-beams when compared to the simplified LRFD approach. The analysis for exterior I-beams and spread box beams showed a smaller but significant reduction.

7.5.2.2 Increasing Span Capability

Detailed prestress designs by Aswad (1994) have shown that the percentage reduction in strands and release strength for interior beams is roughly one-half of the reduction in the distribution factor. For instance, a 22% reduction of midspan moment will result in about 11% less strands and less required release strength, or may allow a 4 to 5% increase in span length without having to use a deeper section. Clearly, there is a significant incentive for both the owner and the industry to use refined methods in many future projects. This is especially significant for beams with higher span-to-depth ratios.

7.5.3 St. Venant Torsional Constant, J

An important step in the FEA method is the computation of the torsional constant, *J*, for the basic precast beam. The torsional constant of a thin-walled, hollow box section, is given by the familiar formula from standard textbooks (Hambly, 1976):

$$J = 4A_o^2 / \Sigma(s/t) \tag{Eq. 7.5.3-1}$$

where

- A_o* = the area enclosed by centerlines of elements (walls)
- s* = the length of a side element
- t* = the thickness of that element

Table 7.5.3-1
Torsional Constant J for AASHTO I-Beams

Shape	J value, in. ⁴
Type I	4,745
Type II	7,793
Type III	17,044
Type IV	32,924
Type V	35,433
Type VI	36,071

For I-beams, the engineer should use rational methods such as those given in the report by Eby (1973). The use of formulas for open, thin sections is not appropriate. A list of St. Venant torsional constants for AASHTO I-beams is shown in **Table 7.5.3-1**.

7.5.4 Related Publications

The following reports by Lehigh University are recommended:

- For I-beams Reports by Wegmuller (1973) and Zellin (1976)
- For spread box beams Reports by Lin (1968), Guilford (1968), VanHorn (1969), Motarjemi (1969) and Chen (1970).

7.5.5 Modeling Guidelines

The following guidelines are suggested for refined analysis methods:

- A minimum of 9 nodes per beam span is preferred
- Aspect ratio of finite elements and grid panels should not exceed 5.0 (Note: this ratio should be reduced to approximately 2.0 for better accuracy)
- Nodal loads should be statically equivalent to the actual point load being applied
- For FEA, relative vertical distances should be maintained between various elements
- For grillage analysis, composite properties should be used
- St. Venant torsional constant, J , is to be determined rationally
- For grillage analysis, only one-half of the effective flange width of the flexural section, before transformation, should be used in computing J . In finite element analysis, an element should have membrane capability with sufficient discretization. Therefore, a shell element is ideal for modeling the cast-in-place slab.

7.5.6 Finite Element Study for Moment Distribution Factors

A parametric study for distribution factors was conducted by Chen and Aswad (1996) using FEA and the ADINA (1991) software. The number of beam elements per span was 16. There were two 4-noded shell elements between adjacent beam lines.

The study covered 10 different I-beam superstructures with spans, L , varying between 90 and 140 ft, and spacings, S , between 8 and 10 ft. The number of beam lines was 5, 6 or 7 while the total slab width (out-to-out) was either 48 or 60 ft. The midspan diaphragm was separated from the cast-in-place deck slab by a 6-in.-deep gap.

The investigation also covered six various superstructures with a spacing, S , of either 8 ft 3 in. or 10 ft 6 in. and spans, L , varying between 60 and 100 ft. There were either 4 or 5 beam lines. The total slab width was either 39 ft 6 in. or 41 ft 0 in. which corresponds to 3 design lanes.

The following paragraphs summarize the findings of the study:

1. Refined methods of analysis may reduce the midspan moment by 18 to 23% in the case of interior I-beams, and by 4 to 12% for exterior I-beams when compared to the LRFD simplified method.
2. The same FEA may reduce the midspan moment by 6 to 12% for spread box beams. However, the reduction may reach 30% for exterior beams when midspan diaphragms are used. This is so because the *AASHTO LRFD Specifications* requires an exterior beam analysis that assumes an infinitely rigid diaphragm which results in conservative midspan moments.
3. The approximate equations for computing distribution factors are generally quite conservative when the span-to-depth ratios approach the upper limits of the span capability.

Based on this study, it is recommended that finite element or grillage analysis be used for the design of bridges with high span-to-depth ratios because they allow a significant reduction in the required release strength or, alternatively, an increase in the span capability.

7.6 REFERENCES

1. AASHTO. 2010. *AASHTO LRFD Bridge Design Specifications*, 5th Edition with 2011 Interim Revisions. American Association of State Highway and Transportation Officials, Washington, DC.
<https://bookstore.transportation.org> (Fee)
2. AASHTO. 2002. *Standard Specifications for Highway Bridges*, 17th Edition. American Association of State Highway and Transportation Officials, Washington, DC.
https://bookstore.transportation.org/collection_detail.aspx?ID=15
3. Arockiasamy, M., A. P. Badve, B. V. Rao, and D. V. Reddy. 1991. "Fatigue Strength of Joints in a Precast Prestressed Concrete Double Tee Bridge." *PCI Journal*, Precast/Prestressed Concrete Institute, Chicago, IL. V. 36, No. 1, (January-February), pp. 84-97
http://www.pci.org/view_file.cfm?file=JL-91-JANUARY-FEBRUARY-7.pdf

4. Aswad, A. and Y. Chen. 1994. "Impact of LRFD Specification on Load Distribution of Prestressed Concrete Bridges." *PCI Journal*, Precast/Prestressed Concrete Institute, Chicago, IL. V.39, No. 5 (September-October), pp. 78-89.
http://www.pci.org/view_file.cfm?file=JL-94-SEPTEMBER-OCTOBER-9.pdf
5. Aswad, G. 1994. Comparison of Refined and Simplified Analysis Methods for P/S Concrete I-Beam Bridge Decks. University of Colorado at Denver, Denver, CO, M.Sc. Thesis.
6. Chen, Y. and A. Aswad. 1996. "Stretching Span Capability of Prestressed Concrete Bridges under AASHTO-LRFD." *ASCE Journal of Bridge Engineering*, American Society of Civil Engineers, Reston, VA. Vol. 1, No. 3, (August), pp. 112-120.
http://ascelibrary.org/beo/resource/1/ibenf2/v1/i3/p112_s1?isAuthorized=no
7. Chen, Y. L. and D. A. VanHorn. 1970. "Structural Behavior of a Prestressed Concrete Box-Beam Bridge—Hazleton Bridge." Report No. 315A.1. Fritz Engineering Laboratory, Lehigh University, Bethlehem, PA.
http://digital.lib.lehigh.edu/fritz/pdf/315A_1.pdf
8. Eby, C. C., J. M. Kulicki, and C. N. Kostem. 1973. "The Evaluation of St. Venant Torsional Constants for Prestressed Concrete I-Beam." Report No. 400.12. Fritz Engineering Laboratory, Lehigh University, Bethlehem, PA.
http://digital.lib.lehigh.edu/fritz/pdf/400_12.pdf
9. Guilford, A. A. and D. A. VanHorn. 1968. "Lateral Distribution of Vehicular Loads in a Prestressed Concrete Box-Beam Bridge —White Haven Bridge." Report No. 315.7. Fritz Engineering Laboratory, Lehigh University, Bethlehem, PA.
http://digital.lib.lehigh.edu/fritz/pdf/315_7.pdf
10. Hambly, E.C. 1976. *Bridge Deck Behavior*, J. Wiley & Sons, New York, NY.
<http://www.amazon.com/Hambly-Bridge-Deck-Behaviour/dp/0470346361> (Fee)
11. Lin, C. S. and D. A. VanHorn. 1968. "The Effect of Midspan Diaphragms on Load Distribution in a Prestressed Concrete Box-Beam Bridge—Philadelphia Bridge." Report No. 315.6. Fritz Engineering Laboratory, Lehigh University, Bethlehem, PA.
http://digital.lib.lehigh.edu/fritz/pdf/315_6.pdf
12. Motarjemi, D. and D. A. VanHorn. 1969. "Theoretical Analysis of Load Distribution in Prestressed Concrete Box-Beam Bridges." Report No. 315.9. Fritz Engineering Laboratory, Lehigh University, Bethlehem, PA.
http://digital.lib.lehigh.edu/fritz/pdf/315_9.pdf
13. VanHorn, D. A. 1969. "Structural Behavior Characteristics of Prestressed Concrete Box-Beam Bridges." Report 315.8. Fritz Engineering Laboratory, Lehigh University, Bethlehem, PA.
http://digital.lib.lehigh.edu/fritz/pdf/315_8.pdf
14. Wegmuller, A. W. and C. N. Kostem. 1973. "Finite Element Analysis of Plates and Eccentrically Stiffened Plates." Report No. 378A.3. Fritz Engineering Laboratory, Lehigh University, Bethlehem, PA.
http://digital.lib.lehigh.edu/fritz/pdf/378A_3.pdf
15. Zellin, M. A., C. N. Kostem, D. A. VanHorn, and J. M. Kulicki. 1976. "Live Load Distribution Factors for Prestressed Concrete I-Beam Bridges." Report No. 387.2B. Fritz Engineering Laboratory, Lehigh University, Bethlehem, PA.
16. Zokaie, T., T. A. Osterkamp, and R. A. Imbsen. 1991. "Distribution of Wheel Loads on Highway Bridges." NCHRP Project Report 12-26. Transportation Research Board, Washington, DC.
<http://apps.trb.org/cmsfeed/trbnetprojectdisplay.asp?projectid=297>

This page intentionally left blank

DESIGN THEORY AND PROCEDURE

Table of Contents

NOTATION.....	8 - 7
8.0 AASHTO SPECIFICATION REFERENCES.....	8 - 17
8.1 PRINCIPLES AND ADVANTAGES OF PRESTRESSING.....	8 - 17
8.1.1 History.....	8 - 17
8.1.2 High-Strength Steel.....	8 - 17
8.1.3 Prestressing Versus Conventional Reinforcing.....	8 - 19
8.1.4 Concrete to Steel Bond.....	8 - 21
8.2 FLEXURE.....	8 - 21
8.2.1 Service Limit States.....	8 - 22
8.2.1.1 Theory.....	8 - 22
8.2.1.1.1 Stage 1 Loading.....	8 - 22
8.2.1.1.2 Stage 2 Loading.....	8 - 22
8.2.1.1.3 Stage 3 Loading.....	8 - 24
8.2.1.1.4 Stage 4 Loading.....	8 - 25
8.2.1.1.5 Stage 5 Loading.....	8 - 25
8.2.1.1.5.1 Tensile Stresses - Normal Strength Concrete.....	8 - 25
8.2.1.1.5.3 Tensile Stresses-Service III limit-state load combination.....	8 - 25
8.2.1.2 Concrete Stress Limits.....	8 - 25
8.2.1.3 Design Procedure.....	8 - 26
8.2.1.4 Composite Section Properties.....	8 - 27
8.2.1.4.1 Theory.....	8 - 27
8.2.1.4.2 Procedure.....	8 - 27
8.2.1.5 Harped Strand Considerations.....	8 - 28
8.2.1.6 Debonded Strand Considerations.....	8 - 28
8.2.1.7 Minimum Strand Cover and Spacing.....	8 - 28
8.2.1.8 Design Example.....	8 - 29
8.2.1.8.1 Design Requirement 1.....	8 - 30
8.2.1.8.2 Design Requirement 2.....	8 - 31
8.2.1.8.3 Design Requirement 3.....	8 - 32
8.2.1.8.3.1 Strand Debonding.....	8 - 34
8.2.1.8.3.2 Harped Strands.....	8 - 34
8.2.1.8.3.3 Other Methods to Control Stresses.....	8 - 35
8.2.1.8.4 Design Requirement 4.....	8 - 35
8.2.1.9 Fatigue.....	8 - 35
8.2.2 Strength Limit State.....	8 - 36
8.2.2.1 Theory.....	8 - 36
8.2.2.2 Nominal Flexural Resistance.....	8 - 36
8.2.2.2.1 Required Parameters.....	8 - 36
8.2.2.2.2 Rectangular Sections.....	8 - 37

DESIGN THEORY AND PROCEDURE

Table of Contents

8.2.2.2.3 Flanged Sections 8 - 37

8.2.2.3 Maximum Reinforcement Limit 8 - 38

8.2.2.4 Minimum Reinforcement Limit 8 - 38

8.2.2.5 Flexural Strength Design Example 8 - 38

 8.2.2.5.1 Design Requirement 1 8 - 38

 8.2.2.5.2 Design Requirement 2 8 - 39

8.2.2.6 Strain Compatibility Approach 8 - 40

8.2.2.7 Design Example – Strain Compatibility 8 - 42

 8.2.2.7.1 Part 1 – Flexural Capacity 8 - 42

 8.2.2.7.2 Part 2 – Comparative Results 8 - 43

8.3 STRAND TRANSFER AND DEVELOPMENT LENGTHS 8 - 44

 8.3.1 Strand Transfer Length 8 - 45

 8.3.1.1 Impact on Design 8 - 45

 8.3.1.2 Specifications 8 - 45

 8.3.1.3 Factors Affecting Transfer Length 8 - 45

 8.3.1.4 Research Results 8 - 45

 8.3.1.5 Recommendations 8 - 46

 8.3.1.6 End Zone Reinforcement 8 - 46

 8.3.2 Strand Development Length 8 - 46

 8.3.2.1 Impact on Design 8 - 46

 8.3.2.2 LRFD Specifications 8 - 46

 8.3.2.3 Factors Affecting Development Length 8 - 47

 8.3.2.4 Bond Studies 8 - 47

 8.3.2.5 Recommendations 8 - 47

8.4 SHEAR 8 - 47

 8.4.1 LRFD Specifications 8 - 48

 8.4.1.1 Shear Design Provisions 8 - 48

 8.4.1.1.1 Nominal Shear Resistance 8 - 48

 8.4.1.1.2 Concrete Contribution, V_c 8 - 48

 8.4.1.1.3 Web Reinforcement Contribution, V_s 8 - 49

 8.4.1.1.4 MCFT Model: Values of β and θ 8 - 49

 8.4.1.1.5 Simplified Procedure: Values of V_{ci} and V_{cw} 8 - 50

 8.4.1.2 Design Procedure 8 - 51

 8.4.1.3 Longitudinal Reinforcement Requirement 8 - 51

8.5 HORIZONTAL INTERFACE SHEAR 8 - 52

 8.5.1 Theory 8 - 52

 8.5.2 LRFD Specifications 8 - 53

8.6 LOSS OF PRESTRESS 8 - 54

 8.6.1 Introduction 8 - 54

DESIGN THEORY AND PROCEDURE

Table of Contents

8.6.2 Definition.....8 - 54

8.6.3 Significance of Losses on Design.....8 - 55

8.6.4 Effects of Estimation of Losses8 - 55

 8.6.4.1 Effects at Transfer8 - 55

 8.6.4.2 Effect on Production Costs8 - 56

 8.6.4.3 Effect on Camber.....8 - 56

 8.6.4.4 Effect of Underestimating Losses8 - 56

8.6.5 Methods for Estimating Losses8 - 56

8.6.6 Elastic Shortening Loss at Transfer.....8 - 56

 8.6.6.1 Computation of Elastic Shortening Loss8 - 56

 8.6.6.2 Elastic Shortening Example8 - 56

8.6.7 Time-Dependent Losses8 - 57

 8.6.7.2 Refined Estimates.....8 - 57

 8.6.7.2.1 Time-Dependent Losses between Transfer and Deck Placement8 - 58

 8.6.7.2.1.1 Shrinkage of Concrete8 - 58

 8.6.7.2.1.2 Creep of Concrete.....8 - 59

 8.6.7.2.1.3 Relaxation of Prestressing Strands8 - 59

 8.6.7.2.2 Time-Dependent Losses between Deck Placement and Final Time8 - 60

 8.6.7.2.2.1 Shrinkage of Concrete8 - 60

 8.6.7.2.2.2 Creep of Concrete.....8 - 60

 8.6.7.2.2.3 Relaxation of Prestressing Strands8 - 61

 8.6.7.2.2.4 Shrinkage of Deck Concrete.....8 - 61

 8.6.7.3 Recommended Treatment of Deck Shrinkage8 - 61

 8.6.7.4 Prestress Loss Example8 - 62

8.7 CAMBER AND DEFLECTION8 - 62

 8.7.1 Multiplier Method.....8 - 64

 8.7.2 Example8 - 64

8.8 DECK SLAB DESIGN8 - 65

 8.8.1 Introduction.....8 - 65

 8.8.2 Design of Bridge Decks Using Precast Panels8 - 65

 8.8.2.1 Determining Prestress Force.....8 - 66

 8.8.2.2 Service Load Stresses and Flexural Strength8 - 66

 8.8.2.3 LRFD Specifications8 - 67

 8.8.2.3.1 LRFD Specifications Refined Analysis8 - 67

 8.8.2.3.2 LRFD Specifications Strip Method8 - 67

 8.8.2.3.2.1 Minimum Thickness.....8 - 67

 8.8.2.3.2.2 Minimum Concrete Cover.....8 - 68

 8.8.2.3.2.3 Live Load.....8 - 68

 8.8.2.3.2.4 Location of Critical Sections8 - 68

DESIGN THEORY AND PROCEDURE

Table of Contents

8.8.2.3.2.5 Design Criteria..... 8 - 68

8.8.2.3.2.6 Reinforcement Requirements 8 - 69

8.8.2.3.2.7 Shear Design..... 8 - 69

8.8.2.3.2.8 Crack Control 8 - 69

8.8.3 Other Precast Bridge Deck Systems 8 - 70

8.8.3.1 Continuous Precast Concrete SIP Panel System, NUDECK..... 8 - 70

8.8.3.1.1 Description of NUDECK..... 8 - 70

8.8.3.2 Full-Depth Precast Concrete Panels..... 8 - 73

8.8.4 Empirical Design Method..... 8 - 74

8.9 TRANSVERSE DESIGN OF ADJACENT BOX BEAM BRIDGES 8 - 75

8.9.1 Background 8 - 75

8.9.1.1 Current Practice 8 - 75

8.9.1.2 Canadian Bridge Design Code Procedure 8 - 75

8.9.2 Empirical Design..... 8 - 76

8.9.2.1 Tie System 8 - 76

8.9.2.2 Production..... 8 - 77

8.9.2.3 Installation 8 - 78

8.9.3 Suggested Design and Construction Procedure..... 8 - 79

8.9.3.1 Transverse Diaphragms 8 - 81

8.9.3.2 Longitudinal Joints Between Beams 8 - 82

8.9.3.3 Tendons 8 - 82

8.9.3.4 Modeling and Loads for Analysis 8 - 82

8.9.3.5 Post-Tensioning Design Chart 8 - 82

8.9.4 Lateral Post-Tensioning Detailing for Skewed Bridges..... 8 - 83

8.10 LATERAL STABILITY OF SLENDER MEMBERS 8 - 83

8.10.1 Introduction 8 - 84

8.10.1.1 Hanging Beams 8 - 84

8.10.1.2 Beams Supported from Beneath 8 - 85

8.10.2 Suggested Factors of Safety..... 8 - 88

8.10.2.1 Conditions Affecting FS_c 8 - 88

8.10.2.2 Effects of Creep and Impact 8 - 88

8.10.2.3 Effects of Overhangs..... 8 - 88

8.10.2.4 Increasing the Factor of Safety 8 - 89

8.10.3 Measuring Roll Stiffness of Vehicles..... 8 - 89

8.10.4 Bearing Pads 8 - 90

8.10.5 Wind Loads..... 8 - 90

8.10.6 Temporary King-Post Bracing 8 - 90

8.10.7 Lateral Stability Examples 8 - 90

8.10.7.1 Hanging Beam Example..... 8 - 91

DESIGN THEORY AND PROCEDURE

Table of Contents

8.10.7.2 Supported Beam Example.....	8 - 93
8.11 BENDING MOMENTS AND SHEAR FORCES DUE TO VEHICULAR LIVE LOADS.....	8 - 94
8.11.1 Design Truck Loading.....	8 - 95
8.11.2 Design Lane Loading, 0.640 kips/ft.....	8 - 95
8.11.3 Fatigue Truck Loading.....	8 - 96
8.12 STRUT-AND-TIE MODELING OF DISTURBED REGIONS.....	8 - 96
8.12.1 Introduction.....	8 - 96
8.12.2 Strut-and-Tie Models.....	8 - 97
8.12.2.1 Truss Geometry Layout.....	8 - 98
8.12.2.2 Nodal Zone and Member Dimensions.....	8 - 101
8.12.2.3 Strength of Members.....	8 - 102
8.12.3 LRFD Specifications Provisions for Strut-and-Tie Models.....	8 - 102
8.12.3.1 Compression Struts.....	8 - 102
8.12.3.1.1 Unreinforced Concrete Struts.....	8 - 102
8.12.3.1.2 Reinforced Concrete Struts.....	8 - 103
8.12.3.2 Tension Ties.....	8 - 103
8.12.3.2.1 Tie Anchorage.....	8 - 104
8.12.3.3 Proportioning Node Regions.....	8 - 104
8.12.3.4 Crack Control Reinforcement.....	8 - 104
8.12.4 Steps for Developing Strut-and-Tie Models.....	8 - 104
8.12.4.1 Design Criteria.....	8 - 105
8.12.4.2 Summary of Steps.....	8 - 105
8.12.5 Pier Cap Example.....	8 - 106
8.12.5.1 Flow of Forces and Truss Geometry.....	8 - 107
8.12.5.2 Forces in Assumed Truss.....	8 - 107
8.12.5.3 Bearing Stresses.....	8 - 108
8.12.5.4 Reinforcement for Tension Tie DE.....	8 - 108
8.12.5.5 Strut Capacities.....	8 - 108
8.12.5.6 Nodal Zone at Pier.....	8 - 110
8.12.5.7 Minimum Reinforcement for Crack Control.....	8 - 110
8.13 DETAILED METHODS OF TIME-DEPENDENT ANALYSIS.....	8 - 111
8.13.1 Introduction.....	8 - 111
8.13.1.1 Properties of Concrete.....	8 - 112
8.13.1.1.1 Stress-Strain-Time Relationship.....	8 - 112
8.13.1.2 Effective Modulus.....	8 - 114
8.13.1.3 Age-Adjusted Effective Modulus.....	8 - 115
8.13.1.4 Properties of Prestressing Steel.....	8 - 116
8.13.1.5 Reduced Relaxation under Variable Strain.....	8 - 116
8.13.2 Analysis of Composite Cross Sections.....	8 - 117

DESIGN THEORY AND PROCEDURE

Table of Contents

8.13.2.1 Initial Strains 8 - 117

8.13.2.2 Method for Time-Dependent Cross-Section Analysis..... 8 - 117

 8.13.2.2.1 Steps for Analysis 8 - 118

 8.13.2.2.2 Example Calculations..... 8 - 119

8.13.3 Analysis of Composite Simple-Span Members 8 - 120

 8.13.3.1 Relaxation of Strands Prior to Transfer..... 8 - 121

 8.13.3.2 Transfer of Prestress Force..... 8 - 121

 8.13.3.2.1 Example Calculation (at Transfer) 8 - 122

 8.13.3.3 Creep, Shrinkage and Relaxation after Transfer..... 8 - 124

 8.13.3.3.1 Example Calculation (after Transfer) 8 - 124

 8.13.3.4 Placement of Cast-in-Place Deck..... 8 - 126

 8.13.3.5 Creep, Shrinkage and Relaxation..... 8 - 126

 8.13.3.6 Application of Superimposed Dead Load..... 8 - 126

 8.13.3.7 Long-Term Behavior 8 - 126

8.13.4 Continuous Bridges..... 8 - 126

 8.13.4.1 Effectiveness of Continuity..... 8 - 127

 8.13.4.2 Applying Time-Dependent Effects 8 - 127

 8.13.4.3 Methods of Analysis..... 8 - 128

 8.13.4.3.1 General Method 8 - 128

 8.13.4.3.2 Approximate Method 8 - 129

 8.13.4.3.2.1 Restraint Moment Due to Creep 8 - 129

 8.13.4.3.2.2 Restraint Moment Due to Differential Shrinkage..... 8 - 129

8.14 REFERENCES 8 - 130

NOTATION

A	= area of cross-section of the precast beam	
a	= distance to pickup points from each end of the beam	
A_c	= area of concrete on the flexural tension side of the member	
A_c	= area of core of spirally reinforced compression member measured to the outside diameter of the spiral	
A_c	= area of beam cross-section	
A_{cv}	= area of concrete section resisting shear transfer	[LRFD]
A_{cs}	= cross-sectional area of a concrete strut	[LRFD]
A_g	= gross area of section	[LRFD]
A_k	= area of cross-section of element k	
A_o	= area enclosed by centerlines of the elements of the beam	[LRFD]
A_{ps}	= area of prestressing steel	[LRFD]
A_s	= area of non-prestressed tension reinforcement	[LRFD]
A_s	= total area of vertical reinforcement located within a distance $(h/5)$ from the end of the beam	[LRFD]
A_{ss}	= area of reinforcement in strut	[LRFD]
A_{st}	= area of longitudinal mild steel reinforcement in tie	[LRFD]
A'_s	= area of compression reinforcement	[LRFD]
A_v	= area of transverse reinforcement within a distance s	[LRFD]
A_{vf}	= area of shear-friction reinforcement	[LRFD]
A_{vh}	= area of web reinforcement required for horizontal shear	
A_{v-min}	= minimum area of web reinforcement	
a	= depth of the equivalent rectangular stress block	[LRFD]
A	= length of overhang	
b	= effective flange width	
b	= width of top flange of beam	
b	= width of the compression face of a member for rectangular sections	[LRFD]
b_b	= width of bottom flange of beam	
b_v	= effective web width	[LRFD]
b_v	= width of interface	[LRFD]
b_w	= web width	[LRFD]
$C(t, t_0)$	= creep coefficient of the concrete member at a certain age	
$C(t, t_j)$	= creep coefficient at time t_j ($j = 0, 1, 2, \dots$)	

DESIGN THEORY AND PROCEDURE

Notation

$C_b(t, t_3)$	= creep at time t for beam concrete loaded at time t_3	
$C_d(t, t_3)$	= creep at time t for deck concrete loaded at time t_3	
C_u	= ultimate creep coefficient for concrete at time of release of prestressing	
C'_u	= ultimate creep coefficient for concrete at time of application of superimposed dead loads	
c	= distance from the extreme compression fiber to the neutral axis	[LRFD]
c	= cohesion factor	[LRFD]
DC	= dead load of structural components and non-structural attachments	[LRFD]
DW	= load of wearing surfaces and utilities	[LRFD]
d_b	= nominal reinforcing bar, wire, and prestressing strand diameter	[LRFD]
d_e	= effective depth from the extreme compression fiber to the centroid of the tensile force in the tension reinforcement	[LRFD]
d_{ext}	= depth of the extreme steel layer from extreme compression fiber	
d_i	= depth of steel layer from extreme compression fiber	
d_p	= distance from extreme compression fiber to the centroid of the prestressing tendons	[LRFD]
d_s	= distance from extreme compression fiber to the centroid of nonprestressed tensile reinforcement	[LRFD]
d_v	= effective shear depth	
d'_s	= distance from extreme compression fiber to the centroid of nonprestressed compression reinforcement	[LRFD]
E	= modulus of elasticity	
E_c	= modulus of elasticity of concrete	[LRFD]
$E_{cb}(t_3)$	= age-adjusted modulus of elasticity for beam concrete at time t_3	
$E_{cd}(t_3)$	= age-adjusted modulus of elasticity for deck concrete at time t_3	
$E_c(t_j)$	= modulus of elasticity at time t_j ($j = 0, 1, 2, \dots$)	
$E_c(t_0)$	= initial modulus of elasticity	
$E_c(t, t_j)$	= modulus of elasticity at a certain time	
E_{ci}	= modulus of elasticity of the beam concrete at transfer	
E_p	= modulus of elasticity of prestressing tendons	[LRFD]
E_s	= modulus of elasticity of reinforcing bars	[LRFD]
E^*_c	= age-adjusted, effective modulus of elasticity of concrete for a gradually applied load at the time of transfer of prestressing	
E^*_{cb}	= age-adjusted, effective modulus of elasticity of the beam	
E^*_{cd}	= age-adjusted, effective modulus of elasticity of the deck	

DESIGN THEORY AND PROCEDURE

Notation

$E_c^*(t, t_0)$	= effective modulus of elasticity at certain time	
E_{ck}^*	= age-adjusted, effective modulus of element k	
e	= eccentricity of prestressing strands	
e_c	= eccentricity of the strand at midspan	
e_d	= eccentricity of deck with respect to the transformed composite section	[LRFD]
e_i	= initial lateral eccentricity of the center of gravity with respect to the roll axis	
e_m	= average eccentricity at midspan	[LRFD]
e_{pc}	= eccentricity of the prestressing strands with respect to the centroid of the composite section	
e_{pg}	= eccentricity of strands with respect to the centroid of the girder	
FS_c	= factor of safety against cracking	
FS_f	= factor of safety against failure	
F_b	= allowable tensile stress in the precompressed tension zone at service loads	
F_{cj}	= force in concrete for the j th component	
F_{pi}	= total force in strands before release	
f	= stress	
f_b	= concrete stress at the bottom fiber of the beam	
f'_c	= specified compressive strength at 28 days	[LRFD]
f'_{ci}	= specified compressive strength of concrete at time of initial loading or pretensioning (transfer)	[LRFD]
f_{cgp}	= concrete stress at the center of gravity of pretensioning tendons, due to pretensioning force at transfer and the self-weight of the member at the section of maximum positive moment	[LRFD]
f_{cu}	= the limiting concrete compressive stress for designing by strut-and-tie model	[LRFD]
f_{pbt}	= stress in prestressing steel immediately prior to transfer	[LRFD]
f_{pc}	= compressive stress in concrete after all prestress losses have occurred either at the centroid of the cross-section resisting live load or at the junction of the web and flange when the centroid lies in the flange. In a composite section, f_{pc} is the resultant compressive stress at the centroid of the composite section, or at the junction of the web and flange when the centroid lies within the flange, due to both prestress and to the bending moments resisted by the precast member acting alone.	[LRFD]
f_{pe}	= effective stress in the prestressing steel after losses	[LRFD]
f_{pi}	= initial stress immediately before transfer	
f_{pj}	= stress in the prestressing steel at jacking	[LRFD]
f_{po}	= stress in the prestressing steel when the stress in the surrounding concrete is zero	[LRFD]
f_{ps}	= average stress in prestressing steel at the time for which the nominal resistance	[LRFD]

DESIGN THEORY AND PROCEDURE

Notation

	of member is required	
f_{pu}	= specified tensile strength of prestressing steel	[LRFD]
f_{py}	= yield strength of prestressing steel	[LRFD]
f_r	= modulus of rupture of concrete	[LRFD]
f_s	= allowable stress in steel under service loads	
f_{se}	= effective final pretension stress	
f_{si}	= effective initial pretension stress	
$f(t_j)$	= stress at time t_j	
$f_r(t, t_0)$	= relaxation stress at a certain time	
$f(t_0)$	= tensile stress at the beginning of the interval	
f_y	= specified minimum yield strength of reinforcing bars	[LRFD]
f'_y	= specified minimum yield strength of compression reinforcement	[LRFD]
f_{yh}	= specified yield strength of transverse reinforcement	[LRFD]
H	= average annual ambient mean relative humidity	[LRFD]
H	= length of a single segment	
h	= overall depth of a member	[LRFD]
h_{cg}	= height of center of gravity of beam above road	
h_d	= deck thickness	
h_f	= compression flange depth	[LRFD]
h_r	= height of roll center above road	
I	= moment of inertia about the centroid of the non-composite precast beam, major axis moment of inertia of beam	[LRFD]
I_k	= moment of inertia of element k	
IM	= dynamic load allowance	[LRFD]
I_{eff}	= effective cracked section lateral (minor axis) moment of inertia	
I_g	= gross lateral (minor axis) moment of inertia	
K	= factor used for calculating time-dependent losses	
K_r	= factor used for calculating relaxation loss in strand that occurs prior to transfer	
K_θ	= sum of rotational spring constants of supports	
K	= factor used in calculation of average stress in pretensioning steel for strength limit state; factor related to type of strand	[LRFD]
k	= factor for type of prestressing steel	[LRFD]
k_c	= product of applicable correction factors for creep = $k_{la} k_h k_s$	
k_{cp}	= correction factor for curing period	
k_{la}	= correction factor for loading age	

DESIGN THEORY AND PROCEDURE

Notation

k_h	= correction factor for relative humidity	
k_s	= correction factor for size of member	
k_{sh}	= product of applicable correction factors for shrinkage = $k_{cp} k_h k_s$	
k_{st}	= correction factor for concrete strength	
L	= overall beam length or design span	
L	= span length	[LRFD]
LL	= vehicular live load	[LRFD]
L_r	= intrinsic relaxation of the strand	
ℓ	= overall length of beam	
ℓ_d	= development length	
ℓ_t	= transfer length	
M_c	= moment in concrete beam section	
M_{cr}	= cracking moment	[LRFD]
$M_{cr}(t)$	= restraint moment due to creep at time t	
M_{el}	= fictitious elastic restraint moment at the supports	
M_g	= unfactored bending moment due to beam self-weight	
M_g	= self-weight bending moment of beam at harp point	
M_{gmsp}	= self-weight bending moment at midspan	
M_k	= element moment	
$M_{lat=}$	= lateral bending moment at cracking	
M_{LL}	= unfactored bending moment due to lane load per beam	
M_n	= nominal flexural resistance	[LRFD]
$M_{n/dc}$	= non-composite dead load moment at the section	
M_r	= factored flexural resistance of a section in bending	[LRFD]
M_{sh}	= shrinkage moment	
$M_{sr}(t)$	= restraint moment due to differential shrinkage at time t	
M_{sw}	= moment at section of interest due to self-weight of the member plus any permanent loads acting on the member at time of release	
M_u	= factored bending moment at section	[LRFD]
M_x	= bending moment at a distance x from the support	
M_o	= theoretical total moment in sections	
M_{ok}	= theoretical moment in section of element k	
m	= stress ratio	
N	= number of segments between nodes (must be even number)	

DESIGN THEORY AND PROCEDURE

Notation

N_k	= element normal force	
N_c	= internal element force in concrete	
N_s	= internal element force in steel	
N_u	= applied factored axial force taken as positive if tensile	[LRFD]
N_{ok}	= theoretical normal force in section of element k, positive when tensile	
N_o	= theoretical total normal force in sections	
n	= modular ratio between slab and beam materials	[LRFD]
n_k	= modular ratio of element k	
n_s	= modular ratio of steel element	
PPR	= partial prestressing ratio	[LRFD]
P_c	= permanent net compression force	[LRFD]
P_n	= nominal axial resistance of strut or tie	[LRFD]
P_r	= factored axial resistance of strut or tie	[LRFD]
P_{se}	= effective pretension force after allowing for all losses	
P_{si}	= effective pretension force after allowing for the initial losses	
Q	= first moment of inertia of the area above the fiber being considered	
R	= radius of curvature	
R_n	= strength design factor	
R_u	= flexural resistance factor	
r	= radius of gyration of the gross cross-section	
r	= radius of stability	
S	= spacing of beams	[LRFD]
S	= slab span	[LRFD]
S	= span between the inside faces of the beam webs	[LRFD]
S_b	= section modulus for the extreme bottom fiber of the non-composite precast beam	
S_{bc}	= composite section modulus for extreme bottom fiber of the precast beam	
S_N	= the value of the integral	
$S(t, t_0)$	= shrinkage coefficient at a certain age	
S_t	= section modulus for the extreme top fiber of the non-composite precast beam	
S_u	= ultimate free shrinkage strain in the concrete adjusted for member size and relative humidity	
s	= length of a side element	[LRFD]
s	= spacing of rows of ties	[LRFD]
t	= time, days; age of concrete at the time of determination of creep effects, days; age of concrete at time of determination of shrinkage effects, days; time after loading,	

DESIGN THEORY AND PROCEDURE

Notation

	days	
t	= thickness of web	
t	= thickness of an element of the beam	
t_f	= thickness of flange	
f_0	= age of concrete when curing ends; age of concrete when load is initially applied, days	
t_s	= cast-in-place concrete slab thickness	
t_s	= depth of concrete slab	[LRFD]
V_c	= nominal shear resistance provided by tensile stresses in the concrete	[LRFD]
V_n	= nominal shear resistance of the section considered	[LRFD]
V_p	= component of the effective prestressing force, in the direction of the applied shear, positive if resisting the applied shear	[LRFD]
V_s	= shear resistance provided by shear reinforcement	[LRFD]
V_u	= factored shear force at the section	[LRFD]
v_u	= average factored shear stress	[LRFD]
W	= total weight of beam	
w	= a uniformly distributed load	[LRFD]
w	= width of clear roadway	[LRFD]
w	= weight per unit length of beam	
w_c	= unit weight of concrete	[LRFD]
x	= distance from the support to the section under question	
y	= height of center of gravity of beam above roll axis (beam supported from below)	
y_b	= distance from centroid to the extreme bottom fiber of the non-composite beam	
y_{bc}	= distance from centroid to the bottom of beam of the composite section	
y_{bs}	= distance from the center of gravity of strands to the bottom fiber of the beam	
y_k	= distance of the centroid of element k from edge	
y_r	= height of roll axis above center of gravity of beam (hanging beam)	
y_s	= height above soffit of centroid of prestressing force	
y_t	= distance from centroid to the extreme top fiber of the non-composite beam	
y_{tc}	= distance from centroid to the top of deck of the composite section	
z	= lateral deflection of center of gravity of beam	
z_{max}	= distance from centerline of vehicle to center of dual tires	
z_o	= theoretical lateral deflection of center of gravity of beam with the full dead weight applied laterally	

DESIGN THEORY AND PROCEDURE

Notation

z'_o	= theoretical lateral deflection of center of gravity of beam with the full dead weight applied laterally, computed using I_{eff} for tilt angle α under consideration	
α	= super-elevation angle or tilt angle of support in radians	
α	= factor used in calculating elastic shortening loss	
α	= coefficient defined by (Eq. 8.6.2.5.1-3) to account for interaction between steel and concrete in prestressing loss calculations	
α_s	= angle between compressive strut and adjoining tension tie	[LRFD]
β	= factor indicating ability of diagonally cracked concrete to transmit tension (a value indicating concrete contribution)	[LRFD]
β_1	= ratio of the depth of the equivalent uniformly stressed compression zone assumed in the strength limit state to the depth of the actual compression zone	[LRFD]
δ_c	= time-dependent multiplier	
Δ	= deflection	
Δ	= camber measured with respect to the beam-ends	
Δf_{cdp}	= change in concrete stress at center of gravity of prestressing steel due to dead loads except the dead load acting at the time the prestressing force is applied	[LRFD]
Δf_{pCR}	= loss in prestressing steel stress due to creep	[LRFD]
Δf_{pES}	= loss in prestressing steel stress due to elastic shortening	[LRFD]
Δf_{pR}	= loss in prestressing steel stress due to relaxation of steel	[LRFD]
Δf_{pR1}	= loss in prestressing steel stress due to relaxation of steel at transfer	[LRFD]
Δf_{pR2}	= loss in prestressing steel stress due to relaxation of steel after transfer	[LRFD]
Δf_{pSR}	= loss in prestressing steel stress due to shrinkage	[LRFD]
Δf_{pT}	= total loss in prestressing steel stress	[LRFD]
Δf_s	= total loss of prestressing	
ϵ	= strain	
ϵ_c	= strain in concrete beam	
ϵ_{cr}	= the time dependent creep strain	
ϵ_f	= the immediate strain due to the applied stress f	
ϵ_{fc}	= elastic strain in concrete	
ϵ_{fk}	= element strain	
ϵ_{fs}	= elastic strain in steel	
ϵ_k	= strain in element k	
ϵ_p	= strain in prestressing steel	
ϵ_s	= strain in mild steel	
ϵ_s	= tensile strain in cracked concrete in direction of tensile tie	[LRFD]
ϵ_{sh}	= free shrinkage strain	

DESIGN THEORY AND PROCEDURE

Notation

$\epsilon_{shb}(t, t_2)$	= shrinkage strain of the beam from time t_2 to time t	
$\epsilon_{shb}(t_3, t_2)$	= shrinkage strain of the beam from time t_2 to time t_3	
$\epsilon_{shd}(t, t_3)$	= shrinkage strain of the deck from time t_3 to time t	
ϵ_{shu}	= ultimate free shrinkage strain in the concrete, adjusted for member size and relative humidity	
ϵ_{si}	= strain in tendons corresponding to initial effective pretension stress	
ϵ_x	= longitudinal strain in the web reinforcement on the flexural tension side of the member	[LRFD]
ϵ_{0c}	= initial strain in concrete	
ϵ_1	= principal tensile strain in cracked concrete due to factored loads	[LRFD]
ϕ	= resistance factor	[LRFD]
Φ	= curvature	
Φ_c	= curvature at midspan	
Φ_{cr}	= curvature due to creep	
Φ_{fk}	= element curvature	
Φ_k	= curvature of element k	
Φ_0	= curvature at support	
λ	= parameter used to determine friction coefficient μ	[LRFD]
μ	= coefficient of friction	[LRFD]
θ	= angle of inclination of diagonal compressive stresses	[LRFD]
θ	= roll angle of major axis of beam with respect to vertical	
θ_L	= left end rotation of beam due to simple span loads	
θ_R	= right end rotation of beam due to simple span loads	
θ_i	= initial roll angle of a rigid beam	
θ_{max}	= tilt angle at which cracking begins, based on tension at the top corner equal to the modulus of rupture	
θ'_{max}	= tilt angle at maximum factor of safety against failure	
ψ	= a factor that reflects the fact that the actual relaxation is less than the intrinsic relaxation	
χ	= aging coefficient	
$\chi(t, t_0)$	= aging coefficient at certain time	

This page intentionally left blank

Design Theory And Procedure

8.0 AASHTO SPECIFICATION REFERENCES

The references to the AASHTO Specifications in this chapter are based on the provisions of the *LRFD Bridge Design Specifications*, Fifth Edition, 2010 and the 2011 Interim Revisions.

8.1 PRINCIPLES AND ADVANTAGES OF PRESTRESSING

8.1.1 History

The principles of prestressing have been used for centuries. For example, wooden barrels have always been made by tightening metal straps around barrel staves. In the making of early wheels, the wooden spokes and rim were first held together by a hot metal tire which, upon cooling, became tensioned. This induced radial compression on the rim and spokes. Other forms of mechanical, chemical, and thermal prestressing have been attempted or used with varying degrees of success.

The use of prestressing for concrete bridge members has been employed with great success for over six decades. Concrete is strong in compression but relatively weak in tension. Therefore, prestressing is used to control tensile stresses and to precompress the concrete. This is analogous to providing the concrete with a “storage” capacity to resist loads which would otherwise produce tension and cracking in the concrete.

The prestressing of precast concrete bridge members is accomplished by stretching high-strength steel strands, then casting concrete around them. As the concrete hardens, it bonds to the strands. When the clamps holding the tensioned strands are released, the force in the strands is applied to (or resisted by) the concrete. This puts the concrete into compression. This technique of prestressing, through the placing of concrete around prestretched strands, is called pretensioning. The high-strength steel strands used for pretensioning typically have an ultimate strength, f_{pu} , of 270 ksi and a yield strength, f_{py} , of 243 ksi.

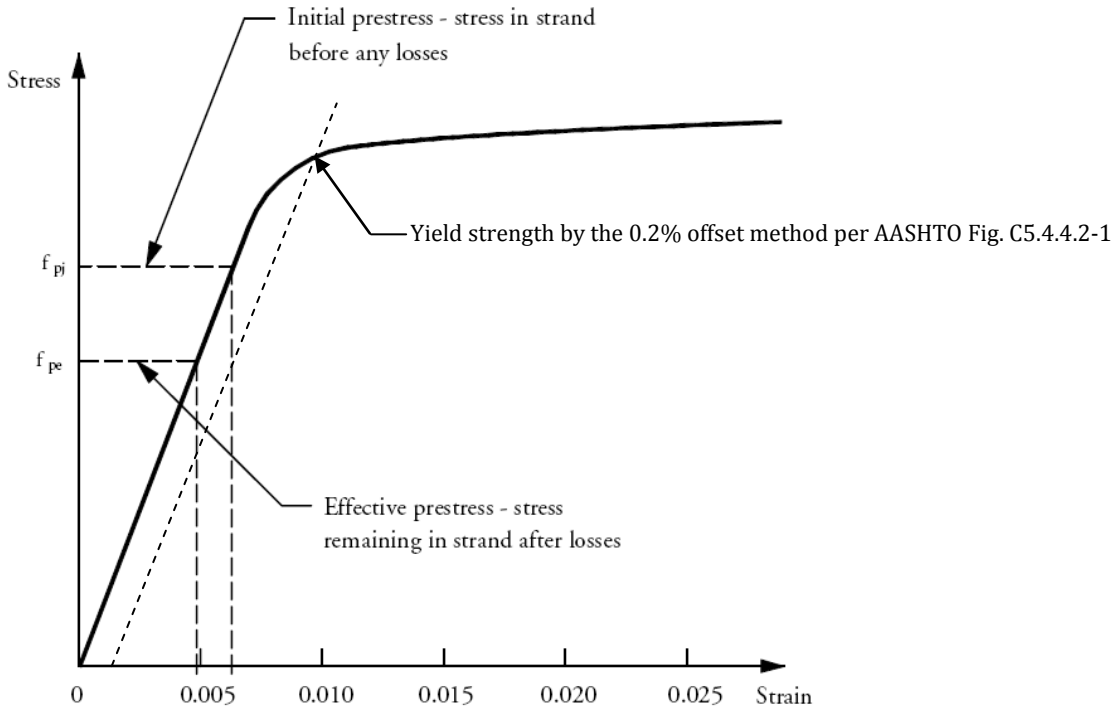
8.1.2 Prestressing Steel

High-strength steel is necessary for achieving prestressed concrete. Strands are typically tensioned initially to $0.75f_{pu} = 202.5$ ksi. Although high, this stress is still safely less than the yield strength ($f_{py} = 243$ ksi). Any loss of stress from this level will be elastic, related to strains by the modulus of elasticity. With time, creep and shrinkage cause shortening of the member, and, since they are bonded to the concrete, shortening of the strands. The shortening of the strands relieves some of the prestrain in the strands, so the prestress is also reduced.

To illustrate why high-strength steel is necessary, consider a concrete member pretensioned with high-strength strand versus mild steel reinforcement (see **Figure 8.1.2-1**). Assume that the shortening of the member produces a corresponding loss of prestress of 40ksi. The stress remaining in the strand after losses, which is called the “effective prestress,” would therefore be $202.5 - 40 = 162.5$ ksi. While the 40 ksi loss is significant, over 80% of the initial prestress remains. Compare this with the same member being prestressed using mild reinforcement ($f_y = 60$ ksi). In this case, the initial stress can only be about 50 ksi in order to remain safely below the yield strength and within the elastic range. Since the member and the prestress force are the same, the losses would also be the same, i.e., 40 ksi. However, in this case, the final conditions are much different, with the effective prestress dropping to 10 ksi, which leaves only 20% of the prestress remaining. So much of the prestress is lost using mild reinforcement for prestressing that it becomes ineffective and unreliable. The high level of prestrain in the strand due to the initial prestress is what makes high-strength strand an effective method of prestressing. The large prestrain reduces the significance of losses.

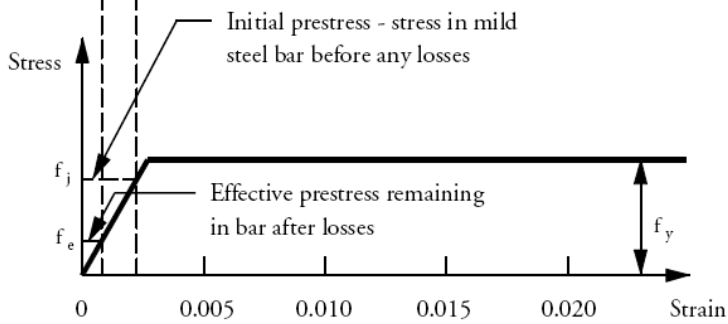
Another outstanding benefit of high-strength (Grade 270) strand is relative cost. While strand may cost nearly twice as much as mild reinforcement per pound, it provides over four times the strength of mild reinforcement. Furthermore, prestressing provides a significant enhancement in the behavior of reinforced concrete members. Thus, the combination of high-quality, plant-cast concrete with prestressing using high-strength steel, results in the most economical bridge for most situations.

Figure 8.1.2-1
Use of High-Strength Versus
Mild Steel for Prestressing Concrete



High Strength Prestressing Steel

← → Loss of pre-strain due to shortening of concrete



Mild Prestressing Steel

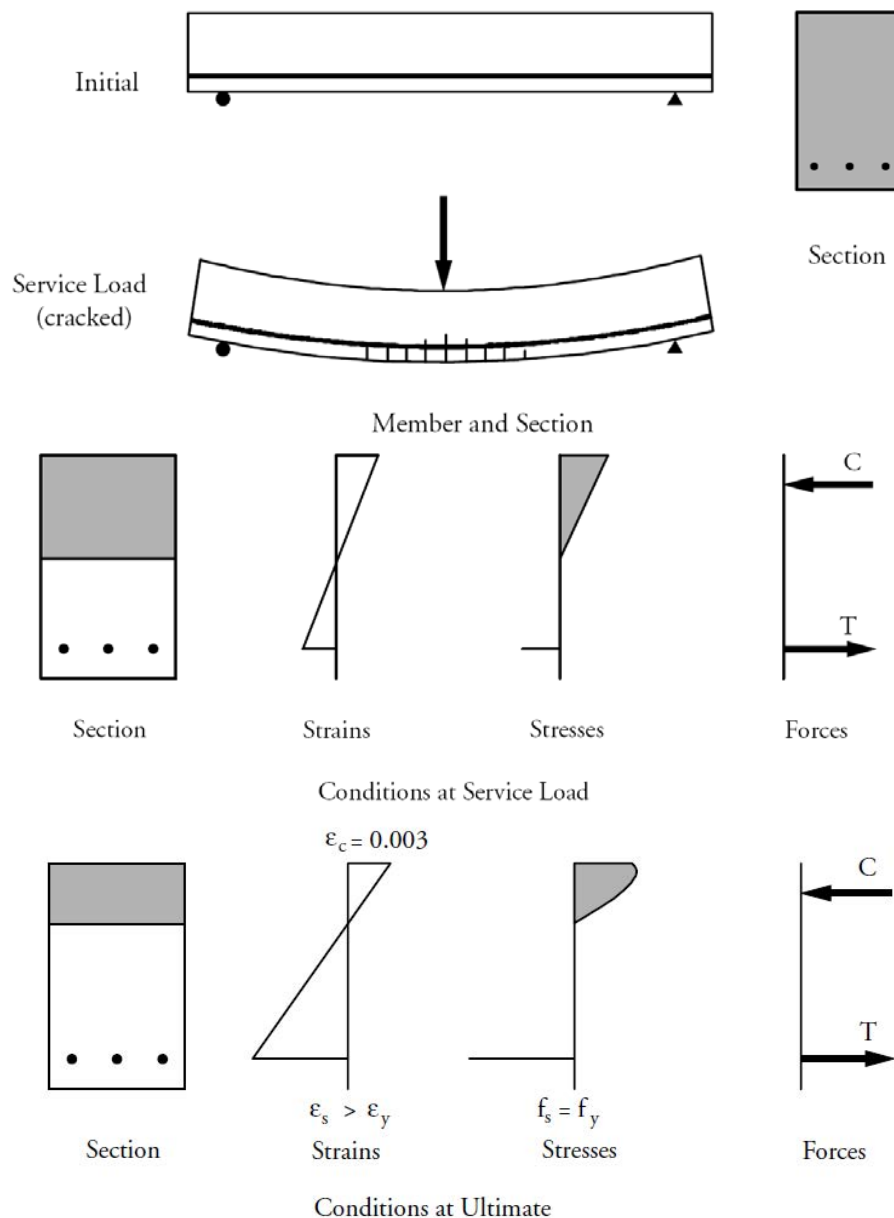
DESIGN THEORY AND PROCEDURE

8.1.3 Prestressing Versus Conventional Reinforcing

8.1.3 Prestressing Versus Conventional Reinforcing

The behavior of flexural members is illustrated using **Figures 8.1.3-1, -2 and -3**. **Figure 8.1.3-1** shows the conditions in a reinforced concrete member that has mild reinforcement and no prestressing. Under service load conditions, concrete on the tension side of the neutral axis is assumed to be cracked. Only concrete on the compression side is effective in resisting loads. In comparison, a prestressed concrete member is normally designed to remain uncracked under service loads (see **Figure 8.1.3-2**). Since the full cross-section is effective, the prestressed member is much stiffer than a conventionally reinforced concrete member resulting in reduced deflection (see **Figure 8.1.3-3**). No unsightly cracks are expected to be seen. Reinforcement is better protected against corrosion. Fatigue of strand due to repeated truck loading is generally not a design issue when the concrete surrounding the strands is not allowed to crack.

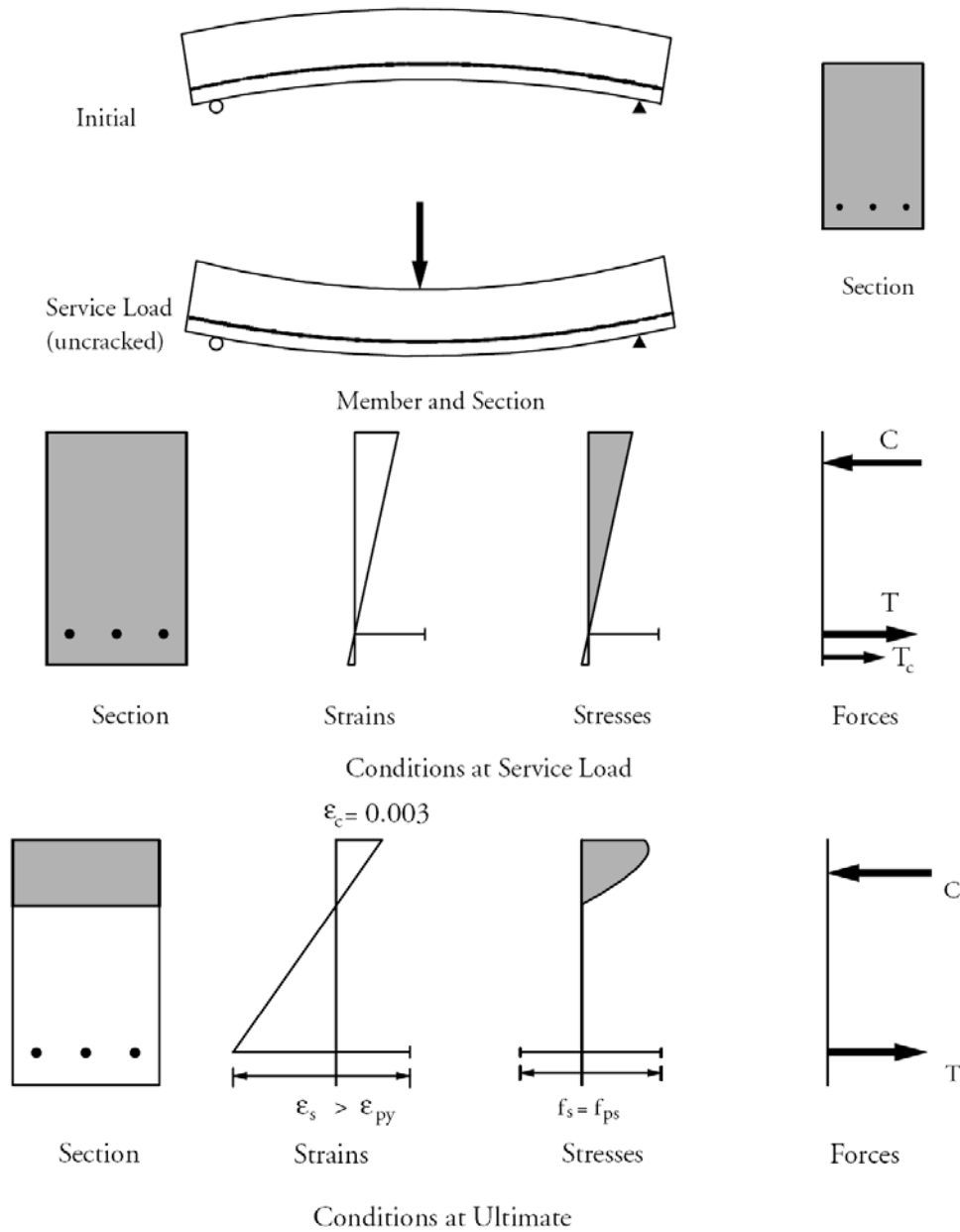
Figure 8.1.3-1
Behavior of Conventionally Reinforced Concrete Members



DESIGN THEORY AND PROCEDURE

8.1.3 Prestressing Versus Conventional Reinforcing

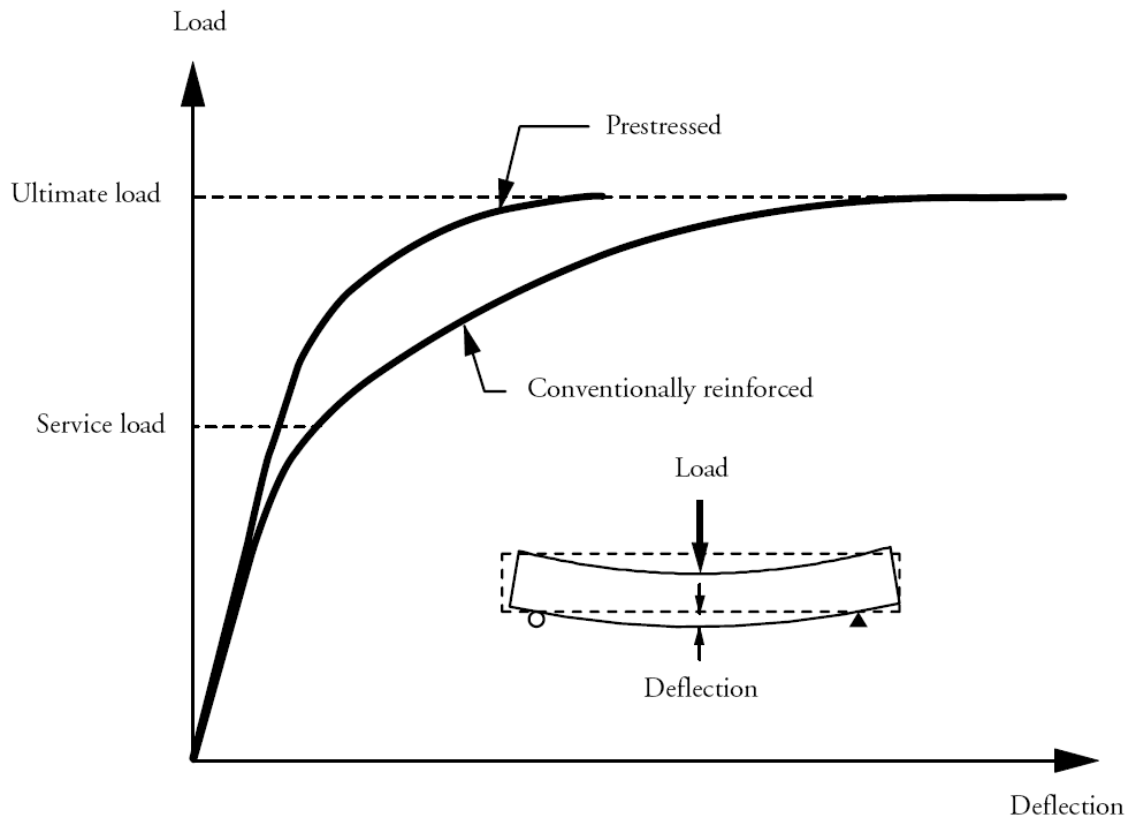
Figure 8.1.3-2
Behavior of Prestressed
Concrete Members



At ultimate load conditions (termed the nominal resistance in the *LRFD Specifications*), conventionally reinforced concrete and prestressed concrete behave similarly. However, due to the lower strength of mild steel bars, a larger steel quantity is needed to achieve the same strength as a prestressed member. This increases the member material costs for a conventionally reinforced member. It should be noted, however, that strand has a lower ultimate elongation at rupture (about 4 to 6%) than that of Grade 60 reinforcement (about 10 to 15%). This lower strain capacity or material ductility may lead one to expect that prestressed concrete members may lack ductility or the capacity to deflect adequately prior to failure. However, prestressed concrete members have been shown both analytically and experimentally to have more than adequate deflection capability prior to failure. It is not unusual in laboratory experiments to observe 10 to 15 in. deflection in a 40 ft-long prestressed concrete member before it fails. This deflection easily exceeds minimum ductility requirements.

DESIGN THEORY AND PROCEDURE**8.1.3 Prestressing Versus Conventional Reinforcing/8.2.Flexure**

Figure 8.1.3-3
Typical Load-Deflection Behavior of Conventional Reinforced and Prestressed Concrete Beams



Another major advantage of prestressing is the improvement in the member's ability to resist shear forces. As a result of the concrete being precompressed, prestressed concrete members have a higher shear capacity, V_c , than conventionally reinforced concrete. This is why thin-webbed I-beam and box-beam bridges have been used very successfully without shear problems. In addition, harped strand, when used, provides a vertical force component that tends to balance part of the gravity load shear force.

8.1.4 Concrete to Steel Bond

Because of the high strength of prestressing strand and the absence of deformations like those found on the surface of reinforcing bars, anchorage of strand in concrete must be carefully assessed. For example, while a Grade 60 #4 bar has a typical development length of 12 to 15 in, the development length of a ½-in.-diameter strand is about 72 to 100 in. Development length can be a limiting design factor in short members such as precast stay-in-place deck panels. It may also be significant for piles that are subjected to moment near the top end. However, the design and performance of most precast bridge beams are not significantly affected by strand development length.

8.2 FLEXURE

The design of prestressed concrete members in flexure normally starts with determination of the required prestressing level to satisfy conditions at the service limit states. All load stages that may be critical during the life of the structure from the time prestressing is first applied are considered. This is followed by a resistance check of the entire member at the strength limit states. The service limit states control the design of most prestressed concrete bridges. Except for rare situations where strand development length is inadequate, and for some adjacent box beam applications, the strength limit states seldom require the addition of reinforcement or other

DESIGN THEORY AND PROCEDURE**8.2.Flexure/8.2.1.1.2 Stage 2 Loading**

design changes. As a result, the flexural resistance of prestressed concrete bridges may be significantly larger than that required. This gives prestressed concrete bridges reserve strength, typically greater than reinforced concrete and most structural steel bridges. Another significant fact is that prestressed concrete members are essentially “proof tested” during fabrication. When prestress forces are transferred in the plant, the prestress level is the highest a member will ever experience while the concrete strength is at its lowest.

8.2.1 Service Limit States

Various service limit state load combinations are considered in design. A load factor of 1.0 is used to reflect the nominal or most likely loading on the structure. There are exceptions to this unity factor as explained in Chapter 7 and later in Section 8.2.1.2. The basic assumptions for flexural design are as follows:

- a. Plane sections remain plane and strains vary linearly over the entire member depth regardless of load level. Therefore, composite members consisting of precast concrete beams and cast-in-place decks must be adequately connected so that this assumption is valid and all elements respond to superimposed loads as one unit.
- b. Before cracking, stress is linearly proportional to strain; i.e. $f = \epsilon E$ where f is stress, E is modulus of elasticity and ϵ is strain.
- c. After cracking, tension in the concrete is neglected.
- d. Spans made continuous for live load through placement of reinforcing bars in the deck slab, or by other means not involving prestressing, are assumed to be treated as prestressed members in the positive moment zone between supports and as conventionally reinforced members in the negative moment zones over the supports. Therefore, no allowable tension limit is imposed on the top fiber stresses in the negative moment zone. However, crack width, fatigue and ultimate strength should be checked.

8.2.1.1 Theory

The various stages of loading for a prestressed concrete beam bridge are shown in **Figure 8.2.1.1-1** and **Figure 8.2.1.1-2**.

8.2.1.1.1 Stage 1 Loading

Stage 1 involves tensioning the strand in the prestressing bed. The tensile stress in the strand is higher at this stage than at any other stage during the service life of the member. Seating losses in the bed, relaxation losses, and any temperature increase reduce the stress in the strand. However, if the temperature drops, or harped strand is deflected after tensioning, the stress in the strand will increase. Producers take these factors into account as part of manufacturing and quality control processes, so the designers do not need to be concerned with controlling strand stresses before transfer.

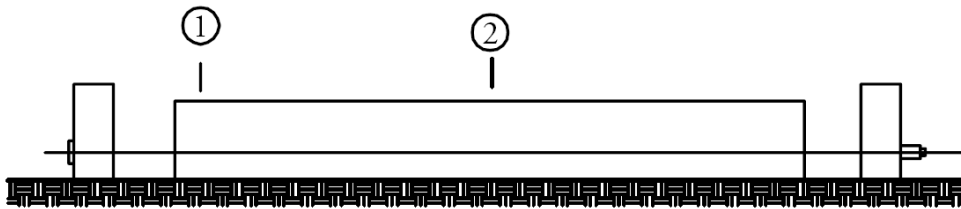
8.2.1.1.2 Stage 2 Loading

Concrete is placed in the forms at Stage 2 and cured until it reaches the initial strength required by design.

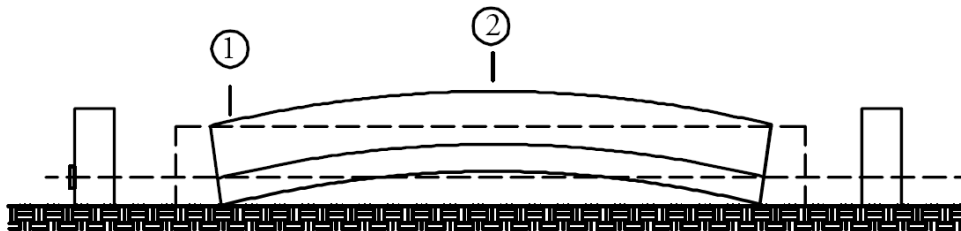
*Figure 8.2.1.1-1
Loading Stages of a
Precast Prestressed Concrete Bridge Beam*



Stage 1: Tensioning of prestressing strands in stressing bed before casting concrete



Stage 2: Placement of concrete in forms and around tensioned strands



Stage 3: Release of strands causing shortening of member

Stage 4: Member placed on piers and/or abutments and deck slab, if any, cast

Stage 5: Full service load after all prestress losses

DESIGN THEORY AND PROCEDURE

8.2.1.1.2 Stage 2 Loading/8.2.1.1.3 Stage 3 Loading

Figure 8.2.1.1-2
Loading Stages, Stress Diagrams and Corresponding
Stress Limits from LRFD Specifications

Stage	1	2	3	4	5
	Tensioning of prestressing strands	Concrete placement	Release of strands	Member installation	Full load
Location 1 (at transfer length)			$< 0.24 \sqrt{f'_{ci}}$ $< 0.6 f'_{ci}$		
Location 2 (at midspan)					$< 0.6 f'_c$ $< 0.19 \sqrt{f'_c}$

8.2.1.1.3 Stage 3 Loading

The force is transferred to the concrete in Stage 3. This is accomplished by flame cutting or by a gradual transfer of the jacking force at the stressing abutment (see Chapter 3, Sect. 3.3.2.8 for details). As the prestress is gradually transferred, the concrete member begins to shorten and camber. When the prestress is fully transferred, the member resists its own weight and the prestress force. The stress distribution is shown in **Figure 8.2.1.1-2**. Regions near the ends of the member do not receive the benefit of bending stresses due to member weight. Therefore, they may be more critical at transfer than the midspan section. It should be noted that the very end of the member has zero stresses. A finite distance from the end, called the transfer length, is required for the prestress to be fully transferred to the concrete through bond between the concrete and steel. Thus, for straight strands that are bonded throughout member length, the critical section for transfer stresses is Location 1 shown in **Figure 8.2.1.1-1**. In most applications, this is not the most effective utilization of available prestress.

There are several methods to relieve excessive stresses at Location 1. They include the following: 1) harping, where some of the strands are deflected upward from one or two points in the member in order to decrease the end eccentricity, 2) debonding, where the strands are kept straight but are wrapped in plastic over a predetermined distance to eliminate concrete bond, or 3) a combination of harping and debonding. The amount of harping or debonding is a design parameter intended to address the maximum allowed concrete compressive or tensile stress near the ends of a member.

Studies, Pang (1997), Huo and Tadros (1997-A), reveal that concrete is capable of resisting more compression than the $0.60f'_{ci}$ allowed by the *LRFD Specifications*. If the results of this research are adopted, designers should expect some relief of the requirements of harping and/or debonding. Concrete tensile stresses in the top fibers at Location 1 in Stage 3 are also a critical design parameter. Often these stresses are controlled by providing straight top strands. It is advisable to use strand whenever possible (as opposed to bars) due to availability and economy. Top strand may be stressed to a nominal 10 to 15 ksi tension, unless higher prestress is needed by design to control bottom concrete compression. The nominal amount of tension in the strands provides taut straight lines which may be useful in providing firm and accurate anchors for attachment of nonprestressed reinforcement.

DESIGN THEORY AND PROCEDURE**8.2.1.1.4 Stage 4 Loading/8.2.1.2 Concrete Stress Limits****8.2.1.1.4 Stage 4 Loading**

Stage 4 represents conditions several weeks to several months after prestress transfer. Camber growth and prestress losses are design factors at this stage. If a cast-in-place composite deck is placed, its top surface must follow the required roadway profile. Field adjustments to the haunch (fillet) thickness above the beam top flanges are usually needed to provide the required grade. Reliable estimates of deflection and camber are needed to prevent fillet thickness from being excessive, to avoid intrusion of the beam flange into the deck, or to avoid adjustments of beam seats or roadway approaches. Stresses at this stage are generally not critical.

8.2.1.1.5 Stage 5 Loading

Stage 5 is assumed to occur after an extended period of time during which all prestress losses have occurred and loads are at their maximum. In contrast to Stage 3, this is the condition described as “service load after losses,” or “maximum service load, minimum prestress.” The tensile stress in the bottom fibers of the midspan section generally controls the design.

8.2.1.1.5.1 Tensile Stresses - Normal Strength Concrete

The tensile stress limit varies from zero to $0.19\sqrt{f'_c}$ (ksi) depending on the severity of exposure and local practices. Generally, it is not advisable to exceed $0.19\sqrt{f'_c}$ (ksi) as cracking might occur under service loads. Some engineers have proposed that prestressed concrete members be allowed to crack, similar to conventional reinforced concrete design. However, until crack control, fatigue, and deflection control issues are well researched and design criteria established, the stress should be maintained below cracking in the positive moment zone at service limit states.

8.2.1.1.5.2 Tensile Stresses-Service III Limit-State Load Combination

The Service III limit state load combination of the *LRFD Specifications* require only 80% of the live load moments to be applied to the bridge when checking the tensile stress at service conditions. This reduced live load was determined by comparing a number of bridges designed by both the *Standard Specifications* and the *LRFD Specifications*. This “calibration” is an acknowledgment of the satisfactory service performance of the very large number of bridges designed by the *Standard Specifications*. Designs using the two Specifications give approximately the same number of strands, except for long spans where the *LRFD Specifications* may still be too conservative in requiring more.

8.2.1.2 Concrete Stress Limits

Stress limits for concrete at transfer:

[LRFD Art. 5.9.4]

1. Compression for pretensioned or post-tensioned members, $0.60\sqrt{f'_{ci}}$
2. Tension:
 - a. In areas without bonded reinforcement, $0.0948\sqrt{f'_{ci}} \leq 0.2$ ksi
 - b. In areas with bonded reinforcement (reinforcing bars or prestressing steel) sufficient to resist the tensile force in the concrete computed assuming an uncracked section, where reinforcement is proportioned using a stress of $0.5f_y$, not to exceed 30 ksi, $0.24\sqrt{f'_{ci}}$, ksi

Stress limits for concrete at service limit state for fully prestressed components are given in LRFD Article 5.9.4.2 (for more information about Load Combinations, see Section 7.3.2).

1. Compression using the service limit state Load Combination I:
 - a. Due to effective prestress and permanent (dead) load, (i.e. beam self-weight, deck slab weight, diaphragm weight, wearing surface and barrier weights), $0.45f'_c$
 - b. Due to effective prestress and permanent and transient loads (i.e., all dead loads and live loads) and during shipping and handling, $0.60\phi_w f'_c$
 - c. Due to live load and one-half the sum of effective prestress and permanent loads, $0.40f'_c$

DESIGN THEORY AND PROCEDURE**8.2.1.2 Concrete Stress Limits/8.2.1.3 Design Procedure**

2. Tension using the service limit state Load Combination III, where only 80% of the live load effects are considered:
 - a. For components with bonded prestressing tendons or reinforcement subjected to not worse than moderate corrosion conditions, $0.19 \sqrt{f'_c}$, ksi
 - b. For components with bonded prestressing tendons or reinforcement subjected to severe corrosive conditions, $0.0948 \sqrt{f'_c}$ ksi
 - c. For components with unbonded prestressing, no tension is allowed

The reduction factor, ϕ_w , should be taken equal to 1.0 when the web and flange slenderness ratio, calculated according to LRFD Article 5.7.4.7.1 for hollow rectangular cross-sections, is not greater than 15. For most beams, $\phi_w = 1$.

8.2.1.3 Design Procedure

Generally, the tensile stresses at midspan due to full dead and live loads plus effective prestress (after losses) control the design. The following steps are used:

1. Compute the tensile stress due to beam self-weight plus any other non-composite loads such as the deck, stay-in-place deck forms, haunches, diaphragms, etc., if any, applied to the beam section only.
2. Compute the tensile stress due to superimposed dead loads plus 0.8 live load (reflecting the Service III limit state load combination of the *LRFD Specifications*) applied to the composite section. Note: the use of transformed section properties (see **Chapter 9**) may have conflict with 0.8 live load factor at Service III limit state. Transformed section properties should be cautiously used until the service limit calibration projects by NCHRP and SHRP2 are completed.
3. The net stress, f_b , due to loads in Steps 1 plus 2, minus the allowable tensile stress is the stress that needs to be offset by prestressing:

$$\frac{P_{se}}{A} + \frac{P_{se}e_c}{S_b}$$

where P_{se} is the effective prestress, e_c is strand eccentricity at midspan, and A and S_b are beam area and bottom fiber modulus.

Solve for P_{se} . The estimated number of strands = $P_{se}/(\text{area of one strand})(f_{pe})$, where f_{pe} is the effective prestress after all losses which may be approximated as 160 ksi for Grade 270 strand.

4. Perform a detailed calculation of prestress losses and repeat Step 3 if necessary.
5. Check stresses at the ends (transfer length) and midspan at transfer and at service. Check stresses at the harp point at transfer. Under typical load conditions, stresses at harp points do not govern at service limit state and are therefore not checked. Determine the amount of harping and/or debonding required to control stresses at the end of the beam. This may be done by computing the required strand eccentricity, e , for the selected effective prestress, P_{se} when harping is used, or by computing the required effective prestress (P_{se}) for the given eccentricity (e) when debonding is used.
6. Check the strength limit state.
7. If necessary, revise number of strands and repeat Steps 4 and 5.

DESIGN THEORY AND PROCEDURE**8.2.1.4 Composite Section Properties/8.2.1.4.2 Procedure****8.2.1.4 Composite Section Properties****8.2.1.4.1 Theory**

Certain bridge superstructures, such as I-beams and spread box beams, require cast-in-place (CIP) concrete deck slabs to provide a continuous riding surface. Sometimes, a CIP topping is provided for adjacent precast concrete members, such as solid slabs, voided slab beams and box beams. When the CIP topping is adequately bonded or connected to the precast concrete member, it provides a “composite section” which is capable of resisting superimposed loads introduced after the deck concrete has cured.

Satisfactory composite action is achieved through verification that the interface shear is adequately resisted through bond between the precast and the CIP concrete, and the addition of shear connectors where needed. Composite (horizontal) shear design is considered in Section 8.5.

Once the composite deck has hardened, the member with deck is considered to act as a unit. The assumption that plane sections remain plane after bending is assumed valid for the entire depth of the composite member, at all loading stages through ultimate capacity.

All loads placed on the bridge after the deck concrete has hardened are applied to the composite member. Since the deck concrete usually has a lower strength than the precast concrete, its modulus of elasticity is also lower. The analysis for service limit state is simplified by transforming the deck concrete into equivalent beam concrete to obtain a section with uniform material properties. This is done by reducing the width of the CIP concrete using the modular ratio, n , of the CIP to precast concrete. It is generally acceptable to use the modular ratio for the 28-day strength. In reality, the two concretes begin to interact with one another upon initial set of the deck concrete.

Designers are advised to specify sufficient field curing procedures for the deck concrete. The concrete surface should be covered with wet blankets as soon as it is able to accept them, and continued for a period of at least 7 days. This is important to avoid premature shrinkage cracks in the CIP deck, especially over the piers in multi-span bridges with continuously cast decks. Time-dependent analysis that accounts for differential creep and shrinkage of the two concretes may alter the stresses obtained from the elastic analysis given below. However, analysis which includes these time dependent effects is complex and requires specialized computer programs, such as CREEP3 described in work by Tadros (1977-B) and Abdel-Karim and Tadros (1993).

8.2.1.4.2 Procedure

1. Compute modular ratio (n) between slab and beam concrete:

$$n = \frac{E_c(\text{slab})}{E_c(\text{beam})}$$

2. Compute effective flange width:

For composite prestressed concrete where slab or flanges are assumed to act integrally with the precast beam, the effective flange width may be calculated as follows:

[LRFD Art. 4.6.2.6.1]

- For interior beams, effective flange width may be taken as one-half the distance to the adjacent beam on each side of the component.
- For exterior beams, effective flange width may be taken as one-half the distance to the adjacent beam plus the full overhang width.
- For closed precast concrete boxes, the distance between the outside of webs at their tops will be used in lieu of the web thickness, and the spacing will be taken as the spacing between the centerline of boxes.

3. Compute transformed section properties:

Transformed flange width = (n) (effective flange width).

If the haunch is considered in the composite section properties, its width should be transformed before it is used in calculations. Note that the haunch thickness should not be included unless the design drawings show a minimum thickness specified after adjustment for camber and deflection.

DESIGN THEORY AND PROCEDURE**8.2.1.5 Harped Strand Considerations/8.2.1.7 Minimum Strand Cover and Spacing****8.2.1.5 Harped Strand Considerations**

When concrete stresses exceed allowable limits, strand harping becomes an attractive option to reduce prestress eccentricity. The designer should be familiar with the practice and limitations of local producers when considering whether or not the calculated force and harp angle can be tolerated. The following are some options to consider if the hold-down force exceeds that which the fabricators can accommodate:

1. Split the strands into two or more groups with separate hold-downs.
2. Change slope of harp by moving harp points closer to centerline of the beam, or by lowering harp elevation at beam ends, or both. Also, refer to Chapter 3 for additional discussion on uplift force and harp angle.
3. Decrease the number of harped strands.
4. Use debonding instead of harping or combine debonding with harping to reduce harping requirements. Refer to Chapter 3, Fabrication, Section 3.3.2.2 for additional details.

8.2.1.6 Debonded Strand Considerations

An alternative to strand harping is to reduce the total prestress force by debonding some strands at the ends of members. After prestress is transferred to the concrete member, the debonded length of the strand has zero stress. Strand debonding may be more economical for some precast producers than harping. However, designers should take into account the effects of the reduction of precompression, (P/A), as well as the loss of the vertical component of prestress, which contributes to shear resistance near the member ends. In addition, the calculated strand development length at the end of a debonded strand is required to be doubled by the *LRFD Specifications*. Debonded strands have been shown by recent studies, Russell and Burns (1993, 1994-A and 1994-B), to perform adequately. LRFD Article 5.11.4.3 provides the following rules if debonded prestressing strands are used:

1. The number of partially debonded strands should not exceed 25% of the total number of strands.
2. The number of debonded strands in any horizontal row shall not exceed 40% of the strands in that row.
3. Debonded strands should be symmetrically distributed about the centerline of the member.
4. Exterior strands in each horizontal row should be fully bonded.

The 25% limitation of Rule 1 has been deemed too conservative with respect to current practice by several states and studies by Russell and Burns (1993, 1994-A, and 1994-B). Consequently, NCHRP Project 12-91 has been created to develop a rational approach for establishing debonding limits for various pretensioned transportation products, and is slated to begin in the first quarter of 2012. The current limitation is based on research by the Florida DOT, and was established to mitigate unacceptable failure modes.

It is good practice to limit the number of debonded strands that are terminated at any section to 40% of the shielded strands, or 4, whichever is greater in order to control the Hoyer effect.

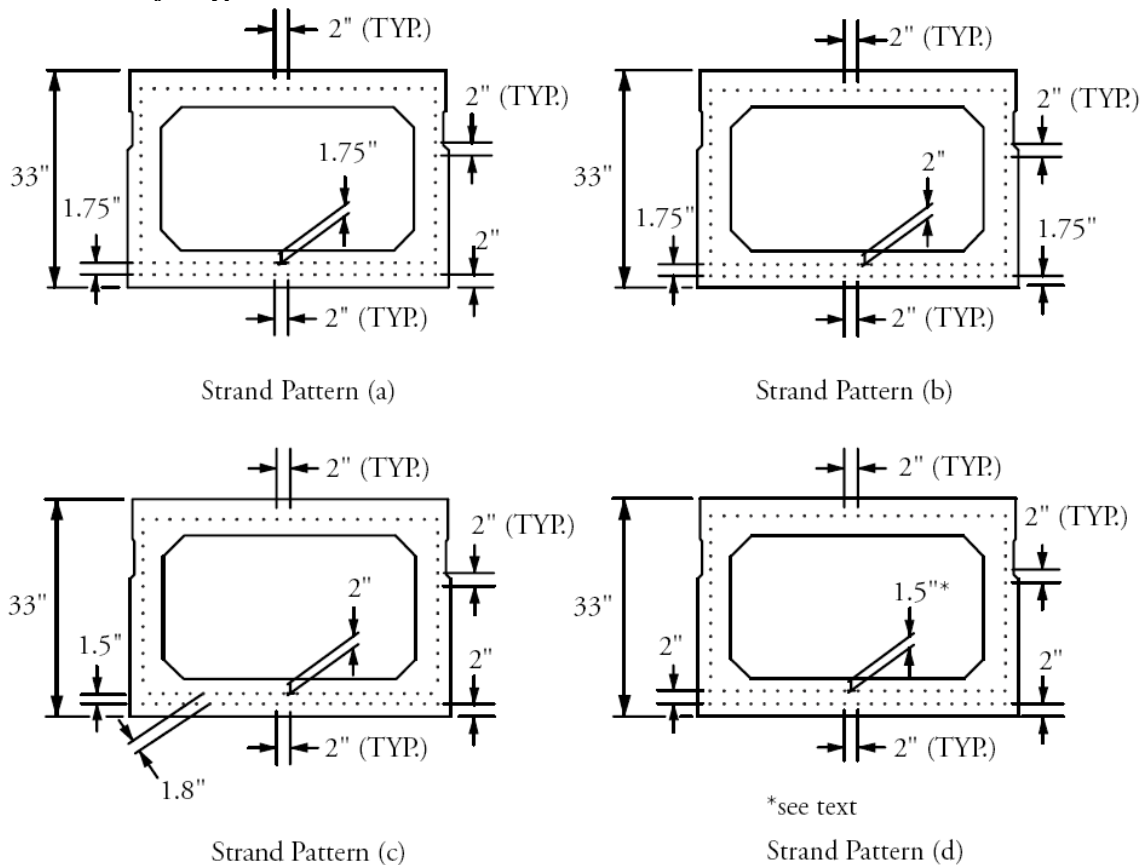
8.2.1.7 Minimum Strand Cover and Spacing

The *LRFD Specifications* are unclear regarding concrete cover over prestressing strand in precast concrete beams. For precast soffit form panels (stay-in-place deck panels), the minimum cover is 0.80 in. and for members subject to exterior exposure, the minimum is 2.0 in. regardless of whether the member is precast or cast-in-place. It is recommended here to use the 1.50 in. minimum cover previously specified in the *Standard Specifications* for bridge beams.

Figure 8.2.1.7-1 shows four possible strand patterns to accomplish various strand spacing and cover requirements. Dimensions are to centerlines of strands. Pattern (d) would require a thicker bottom flange with adjusted void depth if 1.5 in. clear cover is required over the second row to the void.

The Federal Highway Administration has approved use of ½-in.-diameter strand at a spacing of 1.75 in., and 0.6-in.-diameter strand at 2.00 in. on center. As a result, box beams, for example, may have two layers of ½-in.-diameter strands in the bottom flange using one of the alternative patterns shown in **Figure 8.2.1.7-1**. If the vertical strand spacing is desired to be 2 in., the bottom flange thickness may have to be increased to satisfy the minimum cover requirements.

Figure 8.2.1.7-1
Alternative 1/2-in.-Diameter
Strand Patterns for Typical AASHTO Box Beam



8.2.1.8 Design Example

The following information is given for the box beam design example shown in **Figure 8.2.1.8-1**.

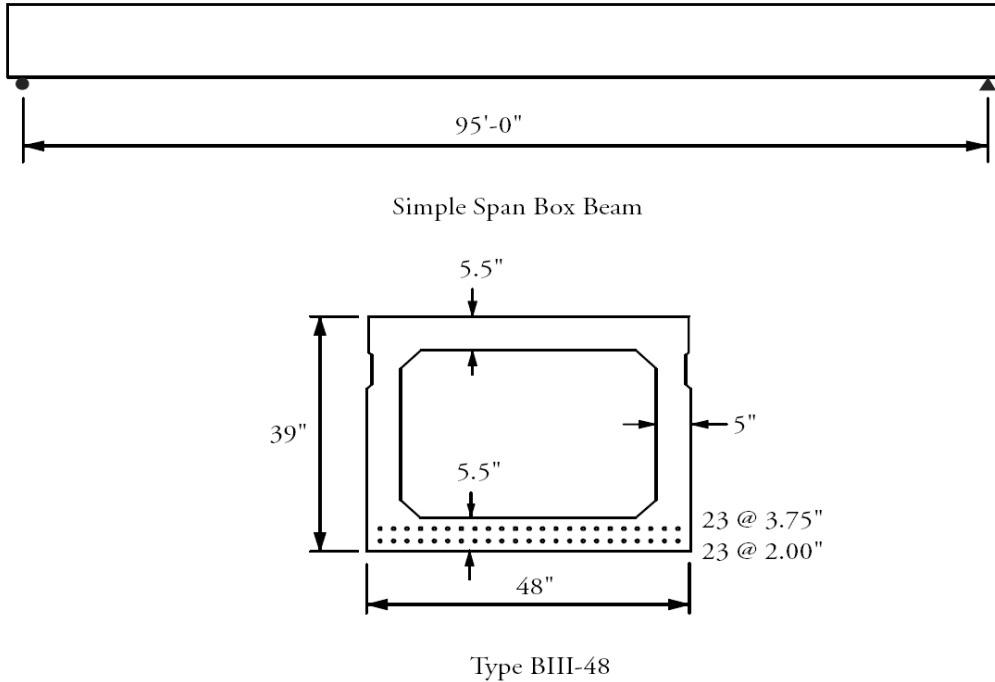
- Design span, $L = 95.0$ ft
- Self-weight of the beam = 0.847 kips/ft
- Superimposed live load = 1.840 kips/ft (This live load does not represent an HL-93 loading. A uniform load is assumed for simplicity.)
- Concrete strength at transfer, $f'_{ci} = 4.000$ ksi (This is an assumed value that must be calculated later in the design process)
- 28-day concrete strength, $f'_c = 5.000$ ksi (This is an assumed value that must be calculated later in the design process)
- Prestressing strands: 1/2-in.-diameter, low-relaxation, 270 ksi steel
- Stress in the strand just after transfer, $f_{si} = 192$ ksi (This is an assumed value that must be calculated later in the design process)
- Strand stress after all losses, $f_{se} = 172$ ksi (This is an assumed value that must be calculated later in the design process)
- Area of box beam cross-section, $A = 813$ in.²
- Section modulus for the extreme bottom fiber of the precast section, $S_b = 8,728$ in.³
- Section modulus for the extreme top fiber of the precast section, $S_t = 8,542$ in.³
- Distance from the centroid of the cross section to extreme bottom fiber, $y_b = 19.29$ in.

DESIGN THEORY AND PROCEDURE

8.2.1.8 Design Example/8.2.1.8.1 Design Requirement 1

Note that the numbers of strand used in this example and in the examples of Sections 8.2.2.4 and 8.2.2.6 is unusually large. They have been selected to illustrate the capacity of standard precast concrete beam shapes and to demonstrate how to resolve challenging design issues.

Figure 8.2.1.8-1
Elevation and Cross-Section of the Box Beam



8.2.1.8.1 Design Requirement 1

Determine the amount of prestressing force required to produce a tensile stress in the bottom fiber at the midspan section under all loads equal to $0.19 \sqrt{f'_c} = 0.424$ ksi.

First calculate the moments due to self-weight and superimposed live load using the following equation at different points along the span, L.

$$M_x = 0.5wx(L - x) \tag{Eq. 8.2.1.8.1-1}$$

where

x = distance between the support and the point on the span under consideration

w = uniformly distributed load

Eq. (8.2.1.8.1-1) above reduces to $\frac{wL^2}{8}$ when $x = L/2$. The general formulation is given here because it is needed

to calculate subsequent requirements

The equation for bottom fiber stress due to applied loads for non-composite sections is:

$$f_b = \frac{P_{se}}{A} + \frac{P_{se}e}{S_b} - \frac{M_g + M_{LL}}{S_b} \tag{Eq. 8.2.1.8.1-2}$$

where

P_{se} = effective prestress force after all losses

DESIGN THEORY AND PROCEDURE

8.2.1.8.1 Design Requirement 1/8.2.1.8.2 Design Requirement 2

e = strand eccentricity at the section being considered (assumed at 16.42 in.)

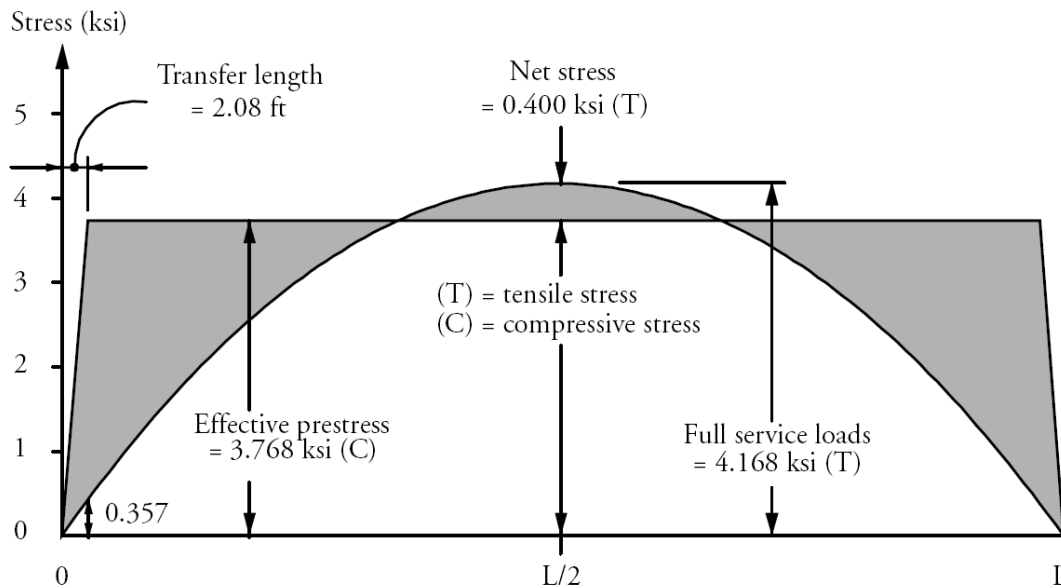
M_g = bending moment due to self-weight

M_{LL} = bending moment due to live load. (As mentioned previously, M_{LL} in this example is based on a simple uniform load for simplicity. If M_{LL} were based on HL-93 loading, a dynamic load allowance IM would be applicable, as would the 0.8 load factor on M_{LL+IM} for Service III tensile stresses.)

The calculations for the required number of strands are computed here at the midspan section. Other design problems may have to be checked at other locations where tensile stresses are higher, e.g. members with harped strands or exterior span members made continuous with interior spans.

Next, the value of P_{se} can be obtained using Eq. (8.2.1.8-2). Set the bottom stress equal to 0.424 ksi (T) and solve for P_{se} . This will yield P_{se} equal to 1,203 kips. Since the prestressing force per strand is equal to 0.153 (172) = 26.32 kips, the required number of strands is 45.7 (use 46 strands) as shown in **Figure 8.2.1.8-1**. **Figure 8.2.1.8.1-1** shows the bottom fiber stress distribution due to full service loads plus the effective prestress force, assuming that the strands are fully-bonded straight strands for the entire length of the member. Note that this figure and the following figures show the stress diagrams due to prestress and due to gravity loads superimposed on each other to get an appreciation for the relative impact of the various components on the net stresses.

Figure (8.2.1.8.1-1)
Bottom Fiber Stress Distribution Due to Full Service Load Plus Effective Prestress



8.2.1.8.2 Design Requirement 2

Find the compressive stress in the top fibers at midspan due to the full service loads and the effective prestress force.

Using the formulas in Section 8.2.1.8.1 with the proper section modulus and stress signs and P_{se}
 $= (46)(0.153)(172) = 1,211$ kips, the top fiber stress distribution is given in **Figure 8.2.1.8.2-1**. The net compressive stress is equal to 3.420 ksi. This exceeds the allowable compressive stress which is equal to $0.60f'_c$
 $= 0.6(5.000) = 3.000$ ksi

This problem may be solved by increasing the 28-day concrete strength to:

$$\frac{3.420}{0.6} = 5.700 \text{ ksi.}$$

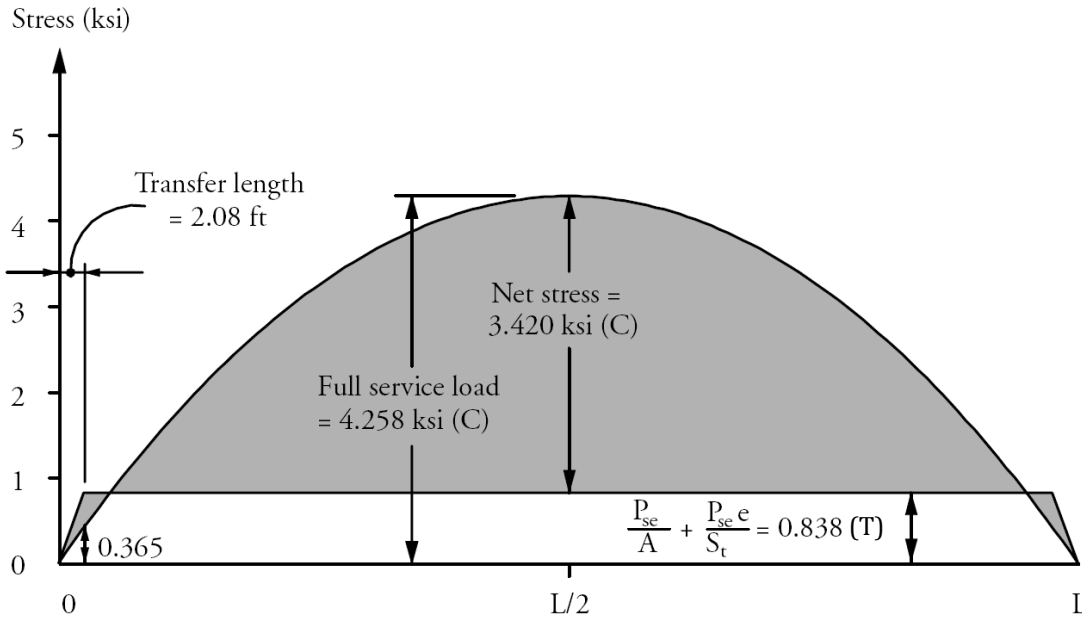
DESIGN THEORY AND PROCEDURE

8.2.1.8.2 Design Requirement 2/8.2.1.8.3 Design Requirement 3

Another option is to add bottom strands if space is available. Note that in this section, all practical available strand locations are utilized for purposes of illustration. Follow-up examples show that other design criteria are not met and indicate how to address deficiencies.

Note that the *LRFD Specifications* require additional compressive stress checks due to other loading combinations.

Figure 8.2.1.8.2-1
Top Fiber Stress Distribution
Due to Full Service Load Plus Effective Prestress

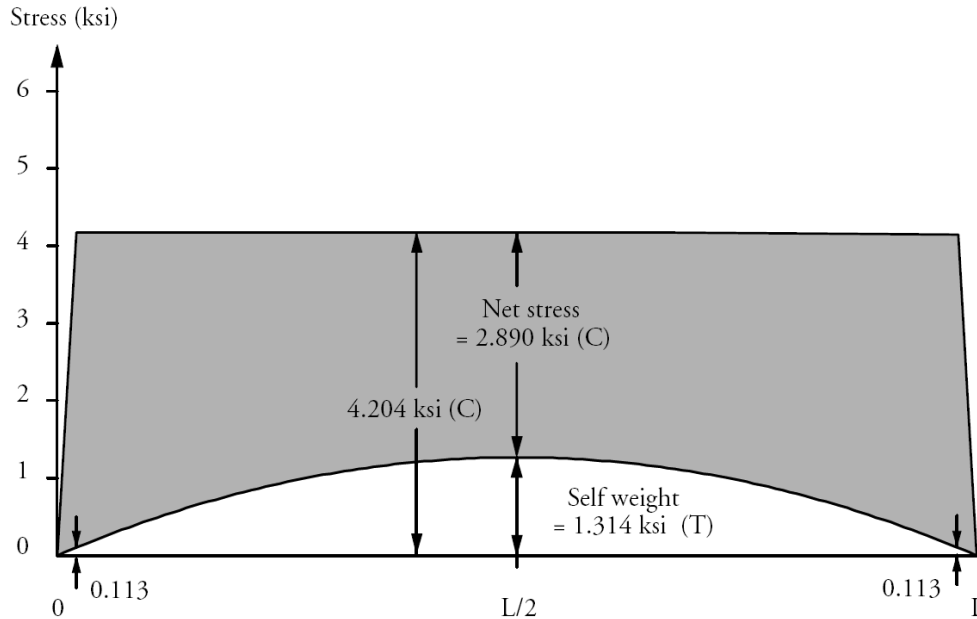


8.2.1.8.3 Design Requirement 3

Determine the compressive stress in the bottom fibers due to the member weight and the initial prestress force and find solutions for excessive stresses.

Using Eq. (8.2.1.8.1-2), with $(M_g + M_{LL})$ replaced by (M_g) only and with P_{se} replaced by $P_{si} = 46(0.153)(192) = 1,351$ kips, the net bottom fiber stress can be calculated to be 2.890 ksi as shown in **Figure 8.2.1.8.3-1**. This exceeds the allowable compressive stress which is equal to $0.60f'_{ci} = 0.6(4.000) = 2.400$ ksi.

Figure 8.2.1.8.3-1
Bottom Fiber Stress Distribution Due to
Self-Weight Plus Initial Prestress, Using Fully
Bonded Straight Strand



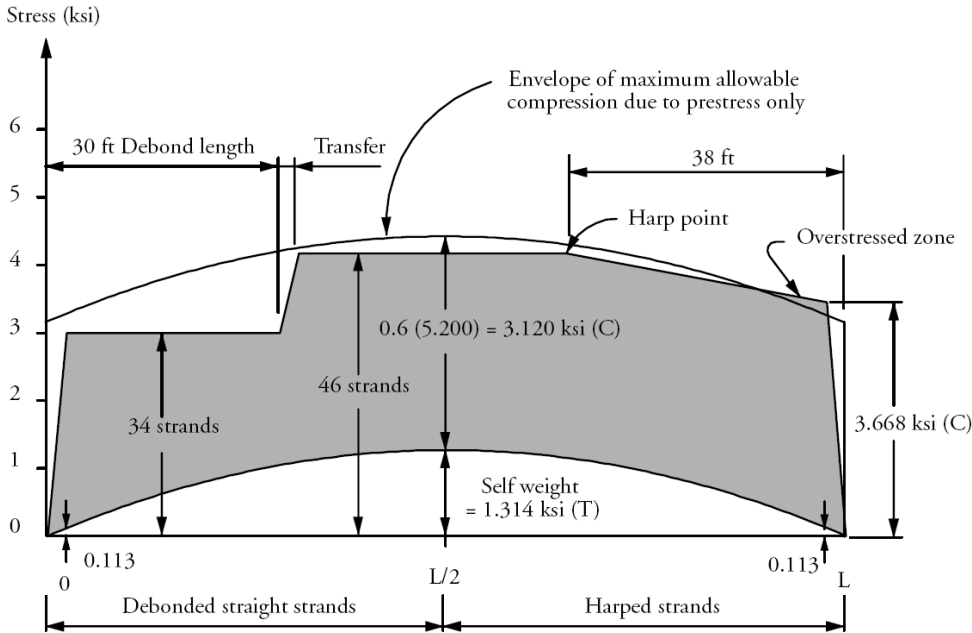
This stress would be acceptable if the initial concrete strength at transfer (f'_{ci}), is increased to:

$$\frac{2.890}{0.6} = 4.817 \text{ ksi.}$$

Note that $f'_{ci} = 4.817$ ksi would satisfy the stress limits only at the midspan section. It must be increased somewhat to allow the 46 strands to be used for a reasonable distance within the middle zone of the member as illustrated in **Figure 8.2.1.8.3-1**.

Assume $f'_{ci} = 5.200$ ksi and proceed with strand debonding and harping accordingly. Of course, this would imply that f'_c at service would have to be specified to be at least equal to 5.200 ksi. Please note that the stress diagram has been modified to reflect gradual transfer of the prestress over a transfer length equal to 25 in. as shown in **Figure 8.2.1.8.3-2**. A strand debonding pattern is attempted for the left half of the beam and a strand harping pattern for the right half. Obviously, only one solution would be used for both halves of a beam in actual design.

Figure 8.2.1.8.3-2
Bottom Fiber Stress Distribution Due to Self-Weight
Plus Initial Prestress, Using Debonded or Harped Strands



8.2.1.8.3.1 Strand Debonding

The diagram in **Figure 8.2.1.8.3-2** should be utilized to determine the number and length of strands to be debonded at the member end. The stress diagram due to initial prestress should always be within the maximum compressive stress envelope shown. The number of debonded strands and the arrangement within a section should be carefully determined to avoid possible stress concentrations. The *LRFD Specifications* give guidelines that should be followed. **Figure 8.2.1.8.3-2** shows that debonding 12 strands for a length equal to 30 ft from the end is sufficient. In actual design, it would be advisable to debond the strands in three groups of 4 strands each over lengths of about 10, 20, and 30 ft.

8.2.1.8.3.2 Harped Strands

A similar analysis can be done for the right half of the beam, with harped strand. Strand harping offers two advantages over strand debonding:

- the average prestress, P/A is higher
- the vertical prestress component due to harping produces a shear force that “balances” part of the shear due to gravity load

However, there are two disadvantages:

- hold down devices and the labor involved in harping may make it a more expensive solution
- only a limited number of strands can be harped

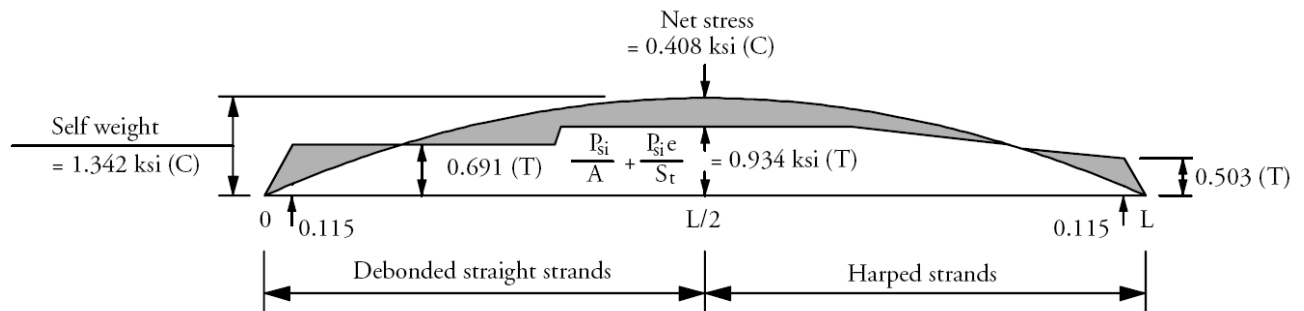
The maximum number of strands to be harped is dictated by their location. Only strands that can be raised into the webs may be harped. Therefore, using the strand pattern shown in **Figure 8.2.1.8-1**, the maximum number of strands that can be harped is four in each web. It is common practice to harp the strands at 0.30 to 0.45L from the member end. Use 0.40L for this example. Also, harp using the maximum possible slope, which corresponds to minimum cover required of the top layer of harped strands, assumed here to be 3 in. Also note that prestressing bed capacity may control the maximum hold-down force of harped strands. Based on this configuration and using $P_{si} = 1,351$ kips, $e = 13.69$ in., and $M_g = 81.85$ kip-ft, the concrete compressive stress at transfer = 3.668 ksi which

exceeds the allowable limit. This solution is therefore unsatisfactory. To allow a harped-strand solution to work, a number of options may be exercised. They include rearranging the pattern of the 46 strands to allow more strands to be harped in the webs.

8.2.1.8.3.3 Other Methods to Control Stresses

It is possible to combine harping strands with a minor amount of debonding, which seems attractive for this example as there is only a small region where the stress limits are exceeded. Finally, it is possible to control the transfer stresses by means of temporary pretensioned straight top strands. This option involves shielding the strands for most of the member length, except perhaps 5 to 10 ft at each end of the member. The shielding will allow this temporary prestress to be eliminated in most of the member length after it is no longer needed. When enough gravity load is introduced, when the concrete strength is increased, or when time dependent losses take effect, the tension in these strands can be transferred by cutting them through a pre-formed pocket. Sometimes, it may be acceptable to avoid cutting top strands if the compression due to effective prestress plus full loads is not critical, however, tension in the bottom fibers may also be a problem if the top strands are not cut. Temporary strands may be utilized to control stresses during transportation. It may also be necessary to remove these temporary strands after girder erection.

Figure 8.2.1.8.4-1
Top Fiber Stress Distribution Due to Self-Weight
Plus Initial Prestress, Using Debonded or Harped Strands



8.2.1.8.4 Design Requirement 4

Calculate the net stress in the top fibers due to the self-weight of the beam and the initial prestress force. Consider both patterns of strand debonding and harping.

Using Eq. (8.2.1.8.1-2), modified with $P_{se} = P_{si} = 1,351$ kips and S_b replaced with $S_t = 8,542$ in.³, the top fiber stress can be obtained, as shown in **Figure 8.2.1.8.4-1**. The two solutions have been shown here for comparison purposes. For complete design examples, see Chapter 9. At midspan, there is a net compressive stress of 0.408 ksi, while a net tension of 0.200 ksi or $0.0948\sqrt{f'_{ci}} = 0.0948\sqrt{5.200} = 0.216$ ksi is allowed. There is tension, however, at other locations as shown in the diagram. If the 0.200 ksi limit is exceeded, the *LRFD Specifications* allow the stress to be as high as $0.24\sqrt{f'_{ci}} = 0.24\sqrt{5.200} = 0.541$ ksi if bonded reinforcement is provided to resist the entire tension force at the section being considered.

8.2.1.9 Fatigue

Article 5.5.3.1 exempts fully prestressed components satisfying the required tensile stress limits of the Service III Limit State from the general fatigue check for reinforcement. Fatigue of concrete in compression is very unlikely to occur in actual practice. However, this issue is addressed in *LRFD Specifications* by setting a maximum concrete compressive stress limit due to full live load combined with 1/2 of permanent loads plus effective prestress.

DESIGN THEORY AND PROCEDURE**8.2.2 Strength Limit State/8.2.2.1 Required Parameters****8.2.2 Strength Limit State****8.2.2.1 Theory**

Approximate formulas for pretensioning steel stress at nominal flexural resistance are given in the *LRFD Specifications* (in this manual Section 8.2.2.3, LRFD Eq. 5.7.3.1.1-1). Use of these formulas simplifies the process of calculating the nominal flexural resistance, M_n , by eliminating consideration of nonlinear material properties of both concrete and prestressing steel at ultimate conditions termed the nominal resistance in LRFD. However, due to their simplified nature, these formulas should be used with caution especially beyond the limits for which they were developed. As will be shown in Section 8.2.2.5, the general strain compatibility approach can be used to avoid difficulties in applying the approximate formulas or inaccuracies associated with their use.

In addition to the standard assumptions used in flexural strength analysis, e.g., equivalent rectangular stress block with ultimate concrete strain of 0.003, the approximate formulas (LRFD Eq. 5.7.3.1.1-1) for calculation of strand stress at ultimate flexure are based on the following simplified assumptions:

- The compression zone is either rectangular or T-shaped.
- The compression zone is within only one type of concrete; for composite members, it is assumed to be within the deck concrete.
- Only fully-tensioned strands near the tension face of the member may be used. No strands near the compression face of the member, or uniformly distributed in the cross-section, can be accurately accounted for.
- Effective pretension is not less than 50% of the ultimate strength of the strands.
- The formulas are only intended as an interpolation function between the yield and ultimate strengths of the steel. Therefore, the area of tension steel must be small enough so that at nominal flexural strength, the calculated stress in the steel is higher than the yield strength.

Examples are given in Section 8.2.2.4 to illustrate how to apply the approximate procedures, and in Section 8.2.2.6 to discuss their accuracy compared to the more general strain compatibility procedure.

8.2.2.2 Nominal Flexural Resistance**8.2.2.2.1 Required Parameters**

The average stress in bonded prestressing steel is:

$$f_{ps} = f_{pu} \left(1 - k \frac{c}{d_p} \right) \quad \text{[LRFD Eq. 5.7.3.1.1-1]}$$

Assuming rectangular section behavior, the neutral axis depth, c , is computed as:

$$c = \frac{A_{ps}f_{pu} + A_s f_y - A'_s f'_y}{0.85 f'_c \beta_1 b + k A_{ps} \frac{f_{pu}}{d_p}} \quad \text{[LRFD Eq. 5.7.3.1.1-4]}$$

where

- c = distance between the neutral axis and the compressive face
- A_{ps} = area of prestressing steel
- f_{pu} = specified tensile strength of prestressing steel
- A_s = area of mild steel tension reinforcement
- f_y = yield strength of tension reinforcement

DESIGN THEORY AND PROCEDURE**8.2.2.2.1 Required Parameters/8.2.2.2.3 Flanged Sections**

A'_s = area of compression reinforcement

f'_y = yield strength of compression reinforcement

β_1 = ratio of depth of equivalent compression zone to depth to the neutral axis [see LRFD Art. 5.7.2.2]

b = width of compression flange

k = factor related to type of strand:

$$= 2 \left(1.04 - \frac{f_{py}}{f_{pu}} \right) \quad [\text{LRFD Eq. 5.7.3.1.1-2}]$$

= 0.28 for low-relaxation strand

f_{py} = yield strength of prestressing steel

d_p = distance from extreme compression fiber to the centroid of the prestressing strand

The depth of the compression block may be computed by, $a = \beta_1 c$. If the depth of the compression flange is less than c , as computed by LRFD Eq. 5.7.3.1.1-4, flanged section behavior must be used with c calculated by:

$$c = \frac{A_{ps}f_{pu} + A_s f_y - A'_s f'_y - 0.85 f'_c (b - b_w) h_f}{0.85 f'_c \beta_1 b_w + k A_{ps} \frac{f_{pu}}{d_p}} \quad [\text{LRFD Eq. 5.7.3.1.1-3}]$$

where

b_w = width of web

8.2.2.2.2 Rectangular Sections

The nominal flexural capacity of a rectangular section is computed using the following equation according to LRFD Article 5.7.3.2.3:

$$M_n = A_{ps} f_{ps} \left(d_p - \frac{a}{2} \right) + A_s f_y \left(d_s - \frac{a}{2} \right) - A'_s f'_y \left(d' - \frac{a}{2} \right) \quad (\text{Eq. 8.2.2.2.2-1})$$

8.2.2.2.3 Flanged Sections

The nominal flexural capacity of a flanged section is computed using the following equation:

$$M_n = A_{ps} f_{ps} \left(d_p - \frac{a}{2} \right) + A_s f_y \left(d_s - \frac{a}{2} \right) - A'_s f'_y \left(d' - \frac{a}{2} \right) + 0.85 f'_c (b - b_w) h_f \left(\frac{a}{2} - \frac{h_f}{2} \right) \quad [\text{LRFD Eq. 5.7.3.2.2-1}]$$

where

f_{ps} = average stress in prestressing steel

a = depth of the equivalent stress block = ($\beta_1 c$)

A_s = area of nonprestressed tension reinforcement

d_s = distance from extreme compression fiber to the centroid of nonprestressed tensile reinforcement

A'_s = area of compression reinforcement

d' = distance from extreme compression fiber to the centroid of nonprestressed compression reinforcement

Factored flexural resistance:

$$M_r = \phi M_n \quad [\text{LRFD Eq. 5.7.3.2.1-1}]$$

where ϕ = resistance factor = 1.0 for tension-controlled prestressed concrete sections (see LRFD Article 5.5.4.2.1 for values of ϕ for sections other than tension-controlled prestressed concrete).

DESIGN THEORY AND PROCEDURE**8.2.2.3 Maximum Reinforcement Limit/8.2.2.5.1 Design Reinforcement 1****8.2.2.3 Maximum Reinforcement Limit**

[LRFD Art. 5.7.3.3.1]

The current provisions of LRFD eliminate any maximum-reinforcement limit and unify the design of prestressed and nonprestressed tension- and compression-controlled members. Below a net tensile strain in the extreme tension steel of 0.005, as the tension reinforcement quantity increases, the factored resistance of prestressed and nonprestressed sections is reduced through a reduced resistance factor. This reduction compensates for decreasing ductility with increasing overstrength. Only the addition of compression reinforcement in conjunction with additional tension reinforcement can result in an increase in the factored flexural resistance of the section.

8.2.2.4 Minimum Reinforcement Limit

[LRFD Art. 5.7.3.3.2]

At any section, the amount of prestressed and nonprestressed reinforcement should be adequate to developed a factored flexural resistance, M_r , at least equal to the lesser of 1.2 times the cracking moment determined on the basis of elastic stress distribution, or 1.33 times the factored moment required by the applicable strength load combinations.

$$M_{cr} = (f_r + f_{cpe})S_c - M_{dnc} \left(\frac{S_c}{S_{bc}} - 1 \right) \geq S_{cpe} f_r$$

where, f_r = modulus of rupture = $0.37\sqrt{f'_c}$

[LRFD Art. 5.4.2.6]

The LRFD Specifications require that this criterion be met at all sections. Editor's note: These minimum reinforcement provisions are current through the AASHTO 2011 Interims. At the time of printing this manual, it appears that these provisions will be revised significantly in the AASHTO 2012 Interims.

8.2.2.5 Flexural Strength Design Example

Consider the information given for the design example in Section 8.2.1.8. Use $f'_c = 5.800$ ksi, and 46 strands as shown in **Figure 8.2.1.8-1**.

8.2.2.5.1 Design Requirement 1

Does the midspan section have adequate flexural strength to resist a factored moment, $M_u = 4,900$ kip-ft?

Using LRFD Eq. 5.7.3.1.1-3, the neutral axis depth, $c = 16.67$ in.

where

$$\begin{aligned} A_{ps} &= 7.038 \text{ in.}^2 \\ f_{pu} &= 270 \text{ ksi} \\ \beta_1 &= 0.76 \\ f'_c &= 5.8 \text{ ksi} \\ (b - b_w) &= 38 \text{ in.} \\ h_f &= 5.50 \text{ in.} \\ b_w &= 10.00 \text{ in.} \\ k &= 2(1.04 - 0.9) = 0.28 \\ d_p &= 36.13 \text{ in.} \end{aligned}$$

The net tensile strain at the centroid of the tension reinforcement is calculated as

$$\left(\frac{0.003}{c} \right) d_t - 0.003 = \left(\frac{0.003}{16.67} \right) (37) - 0.003 = 0.0037$$

where

d_t = distance from the extreme compression fiber to the centroid of the extreme tension steel element

$$d_t = 39 - 2 = 37$$

DESIGN THEORY AND PROCEDURE**8.2.2.5.1 Design Requirement 1/8.2.2.5.2 Design Requirement 2**

Thus the section falls within the transition zone between tension- and compression-controlled and ϕ is calculated using LRFD Eq. 5.5.4.2.1-1.

$$\phi = 0.583 + 0.25 \left(\frac{d_t}{c} - 1 \right) = 0.583 + 0.25 \left(\frac{37}{16.67} - 1 \right) = 0.89$$

Compute the average stress in the prestressing steel at the nominal resistance, f_{ps}

$$f_{ps} = f_{pu} \left(1 - k \left(\frac{c}{d_p} \right) \right) = 270 \left(1 - 0.28 \left(\frac{16.67}{36.13} \right) \right) = 235 \text{ ksi}$$

It should be noted that the stress in the prestressing steel is less than the yield strength and does not satisfy the requirements indicated in Section 8.2.2.1 of this Manual,

Compute the nominal flexural resistance:

$$M_n = A_{ps} f_{ps} \left(d_p - \frac{a}{2} \right) + 0.85 f'_c (b - b_w) h_f \left(\frac{a}{2} - \frac{h_f}{2} \right)$$

$$M_n = 7.038(235) \left(36.13 - \frac{12.67}{2} \right) + 0.85(5.8)(38)(5.5) \left(\frac{12.67}{2} - \frac{5.5}{2} \right)$$

$$M_n = 49,279 + 3,694 = 52,973 \text{ kip-in.} = 4,414 \text{ kip-ft}$$

$$M_r = \phi M_n = 0.89(4,414) = 3,929 \text{ kip-ft}$$

The factored resistance is less than the factored load so the section is not adequate.

If f'_c is increased to 8.5 ksi, using LRFD Eq. 5.7.3.1.1-4 as we now find that the section behaves as a rectangular section, the neutral axis depth = 7.91 in., and the section is calculated to be tension controlled as $\left(\frac{0.003}{c} \right) d_t - 0.003 = \left(\frac{0.003}{7.91} \right) (37) - 0.003 = 0.011 > 0.005$. Thus, a resistance factor is 1.00.

Using Eq. 8.2.2.2-1 with $a = \beta_1 c = 5.14$ in., $f_{ps} = 270[1 - 0.28(7.91)/36.13] = 253$ ksi with $\phi M_n = 4,987$ kip-ft. This value is greater than the capacity needed.

8.2.2.5.2 Design Requirement 2

Does the beam have adequate flexural capacity, ϕM_n , in the end regions?

Assume that the strand development length = 7 ft for bonded strands and 14 ft for debonded strands. Determine the envelope of the flexural capacity along the span length. Assume 12 of the 46 strands are debonded, six in each row, see **Figures 8.2.1.8.3-2** and **8.2.1.8-1**.

Calculate the capacity for the 34 bonded strands when fully developed at 7 ft from the end of the beam. Assume the depth of the compression block, a , falls within the top flange.

Compute the stress in the prestressing steel at the nominal flexural resistance, f_{ps} using LRFD Eq. 5.7.3.1-1, with $f_{pu} = 270$ ksi, $f'_c = 8.500$ ksi, and $k = 0.28$:

$$\text{Therefore, } f_{ps} = 258 \text{ ksi}$$

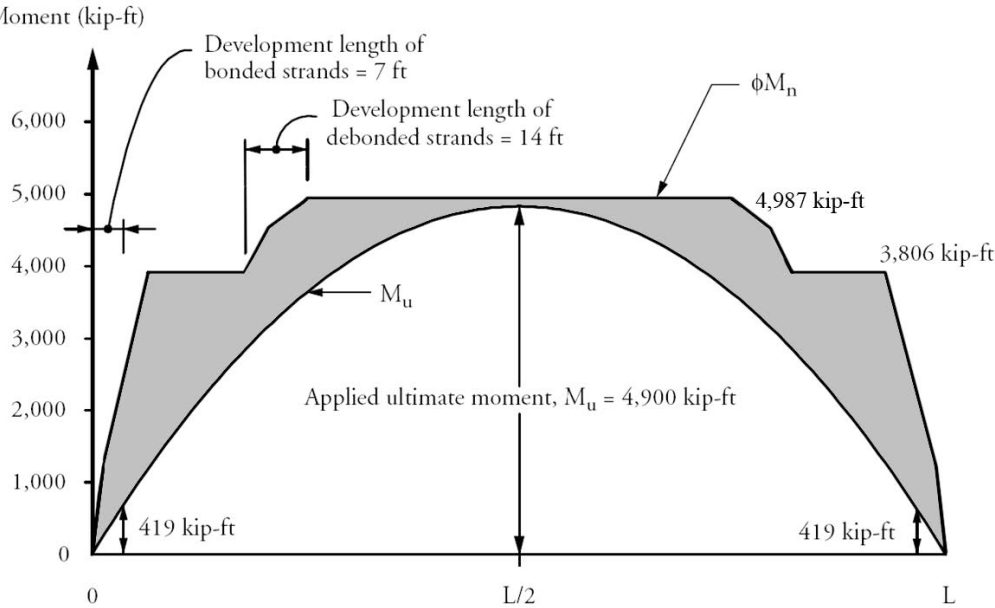
$$\text{The compression block depth, } a = \frac{A_{ps} f_{ps}}{0.85 f'_c b} = \frac{34(0.153)(258)}{0.85(8.5)(48)} = 3.87 \text{ in.}$$

This is less than the flange thickness (5.50 in.). Therefore, the section is considered a rectangular section, and the corresponding ϕM_n (LRFD Art. 5.7.3.2.3) is 3,806 kip-ft. The nominal flexural resistance diagram is shown in **Figure 8.2.2.4.2-1**. Note that even though 14 ft is a very conservative estimate of development length for debonded strands, it has little impact on the flexural strength of this member.

DESIGN THEORY AND PROCEDURE

8.2.2.5.2 Design Requirement 2/8.2.2.6 Strain Compatibility Approach

Figure 8.2.2.5.2-1
Nominal Flexural Resistance for the Beam



8.2.2.6 Strain Compatibility Approach

The strain compatibility approach is based on three well accepted fundamental assumptions:

- Plane sections remain plane after bending
- Compatibility of strains, i.e., full bond between steel and concrete at the section being considered
- Equilibrium of forces within a section

In addition, the standard assumptions of concrete stresses at ultimate flexure being represented by a rectangular stress block is adopted, with the intensity = $0.85f'_c$ and depth $a = \beta_1c$ where c is neutral axis depth and β_1 is a coefficient defined in LRFD Art. 5.7.2.2. (For a “full” strain compatibility analysis utilizing a stress-strain relationship for the concrete as well as the reinforcement, see Seguirant, Brice and Khaleghi (2005).) The steel stress-strain relationship may be defined using any representative formula or graph. For 270 ksi, low-relaxation strands:

$$f_{si} = \epsilon_{si} \left[887 + \frac{27,613}{([1 + (112.4\epsilon_{si})^{7.36}]^{1/7.36})} \right] \leq 270 \text{ ksi} \tag{Eq. 8.2.2.6-1}$$

where f_{si} is the stress in a given layer of reinforcement whose strain is ϵ_{si} and ϵ_{si} is the strain in a given layer of reinforcement.

The above “power formula” is based on a lower bound curve fitting of actual stress-strain relationships and on satisfaction of the minimum ASTM limits (Devalapura and Tadros, 1992). Alternatively, the graph given in Fig. 2.11-1, which is taken from the *PCI Design Handbook* may be used.

For mild reinforcement, an elastic-plastic stress-strain relationship is assumed:

$$f_{si} = E_s \epsilon_{si} \leq f_y \tag{Eq. 8.2.2.6-2}$$

In order to maintain equilibrium, the sum of the tension and compression forces must equal zero. The sum of the moments of these forces about any horizontal axis is equal to the moment acting on the section for the assumed conditions. The process is iterative due to the non-linearity of the stress-strain relationship of the prestressing steel. The following 6 steps, adapted from Skogman, et al (1988), demonstrate the application of this approach:

DESIGN THEORY AND PROCEDURE

8.2.2.6 Strain Compatibility Approach

Step 1: Assume a neutral axis depth c and substitute in Eq (8.2.2.6-3) to obtain the corresponding strain in each steel layer “ i ”. A layer “ i ” is defined here as a group of bars or tendons with the same stress-strain properties (prestressing strand or mild reinforcement), the same effective prestress, and which can be assumed to have a combined area with a single centroid. The strain in each layer of steel can be estimated using the equation:

$$\epsilon_{si} = 0.003 \left(\frac{d_i}{c} - 1 \right) + \left(\frac{f_{se}}{E_s} \right)_i \tag{Eq. 8.2.2.6-3}$$

where

d_i = depth of steel layer from extreme compression fiber

f_{se} = effective prestress. For partially tensioned tendons or for non-tensioned reinforcing bars, f_{se} may be assumed = $f_{pi} - 25$ ksi where f_{pi} is initial tension (assumed zero for non-tensioned reinforcing bars).

Step 2: Use Eq. (8.2.2.6-1) and Eq. (8.2.2.6-2) to estimate the stress in each steel layer.

Step 3: Use equilibrium of forces to check assumed neutral axis depth:

$$\sum A_{si} f_{si} + \sum F_{cj} = 0 \tag{Eq. 8.2.2.6-4}$$

where i refers to steel “layer” and j refers to concrete components within the compression block.

Each concrete component would have a force:

$$F_{cj} = 0.85 f'_c A_{cj} \tag{Eq. 8.2.2.6-5}$$

For example, the cross-section shown in Figure 8.2.2.6-1 has the following three steel “layers:”

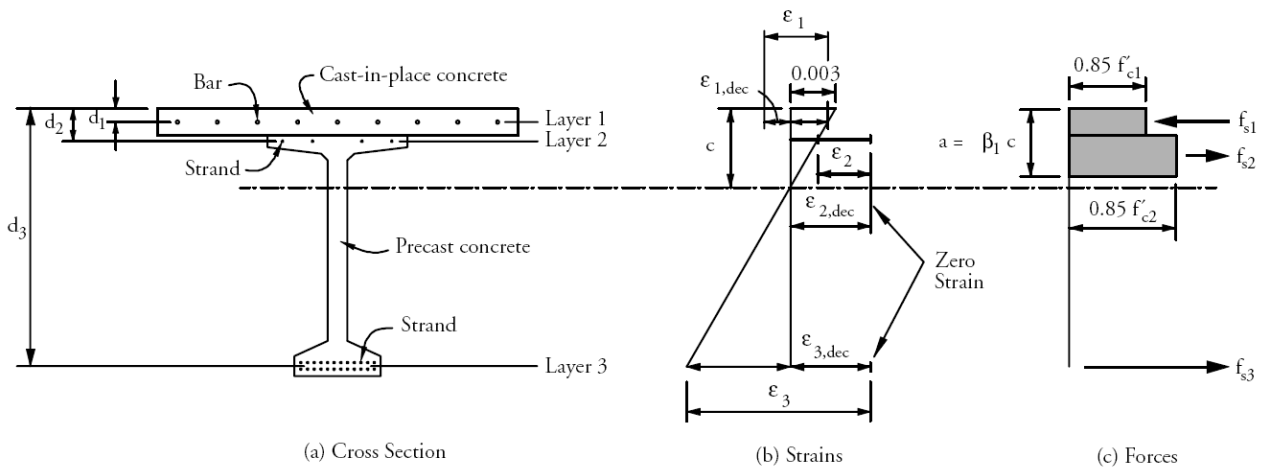
- Bottom flange group of strands
- Top flange group of strands
- Group of deck reinforcing bars

It has three concrete components as follows:

- Cast-in-place deck
- Overhanging portions of the top beam flange
- Portion of the beam web within the compression block depth

The flange overhangs may also be subdivided into rectangular and triangular components, although the additional calculations will not significantly affect the accuracy in this case.

Figure 8.2.2.6-1
Flexural Strength Relationships for Strain Compatibility Analysis



DESIGN THEORY AND PROCEDURE

8.2.2.6 Strain Compatibility Approach/8.2.2.7 Design Example – Strain Compatibility

In composite construction, the stress block factor, β_1 , may be different for different components of the compression block. In this case an average β_1 may be assumed as follows:

$$\beta_{1ave} = \frac{\sum_j (f'_c A_c \beta_1)_j}{\sum_j (f'_c A_c)_j} \tag{Eq. 8.2.2.6-6}$$

The β_{1ave} method may become unconservative at higher reinforcement ratios. See Seguirant, Brice and Khaleghi (2005).

Step 4: Revise “c” and repeat Steps 1-3, until Eq. 8.2.2.6-4 is satisfied.

Step 5: Calculate the nominal flexural capacity by summing moments of all forces about any horizontal axis. If the top fiber is used,

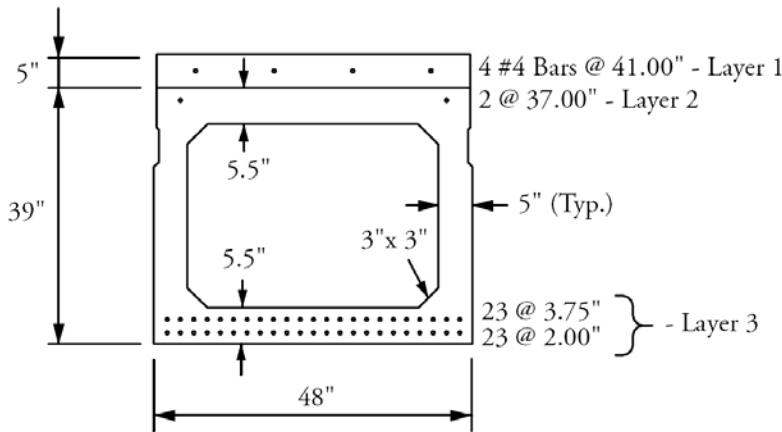
$$M_n = \sum_i A_{si} f_{si} d_i + \sum_j F_{cj} d_j \tag{Eq. 8.2.2.6-7}$$

Step 6: Calculate the design moment capacity ϕM_n , where ϕ is determined in accordance with LRFD Art. 5.5.4.2.1 .

8.2.2.7 Design Example – Strain Compatibility

Consider the precast concrete cross-section shown in **Figure 8.2.1.8-1**. In addition to the 46 strands in the bottom of the section, two strands initially tensioned at 15 ksi are provided near the top as shown in **Figure 8.2.2.7-1**. The section is made composite with a 5.00-in.-thick cast-in-place slab whose f'_c is 3 ksi and reinforced with 4 No. 4 Grade 60 bars. The modulus of elasticity of the pretensioning strands is 28,500 ksi and of the reinforcing bars is 29,000 ksi.

Figure 8.2.2.7-1
Cross-Section of the Box Beam



Type BIII-48

8.2.2.7.1 Part 1 – Flexural Capacity

Determine the flexural capacity and the corresponding steel stresses.

The steps given in Section 8.2.2.6 may be followed iteratively until a solution is achieved. For brevity, only the last iteration will be shown here.

Step 1: Neutral axis depth = c = 12.31 in.

For layer 1: $d_1 = 3$ in., $f_{se1} = -25$ ksi, $E_s = 29,000$ ksi, and ϵ_{s1} from Eq. (8.2.2.6-3), $\epsilon_{s1} = -0.00313$ (positive sign indicates tension). Similarly, $\epsilon_{s2} = -0.00164$ and $\epsilon_{s3} = +0.0131$.

DESIGN THEORY AND PROCEDURE

8.2.2.7 Design Example – Strain Compatibility/8.2.2.7.2 Part 2 – Comparative Results

Step 2: Steel stresses, Eq. (8.2.2.6-2) yields $f_{s1} = -60$ ksi, and Eq. (8.2.2.6-1) yields $f_{s2} = -46.9$ ksi and $f_{s3} = +255.4$ ksi.

Step 3: Check equilibrium of forces using Eq. (8.2.2.6-4).

$$\sum_i A_{si}f_{si} = 4(0.2)(-60) + 2(0.153)(-46.9) + 46(0.153)(255.4) = -48 - 14 + 1,798 = 1,736 \text{ kips}$$

This must be equal and opposite to $\sum_j F_{cj}$

The coefficient β_1 must first be averaged over the two concrete materials since the depth of the compression block is greater than the depth of the cast-in-place topping. β_1 of the 5.8 ksi precast concrete is 0.76 and of the 3.0 ksi cast-in-place concrete is 0.85. Using an initial β_{1ave} of 0.80, $a = \beta_1c = 9.85$ in. Substituting into Eq. (8.2.2.6-6):

$$\beta_{1ave} = [(3)(5)(48)(0.85) + (5.8)(4.85)(48)(0.76)]/[(3)(5)(48) + (5.8)(4.85)(48)] = 0.79$$

Thus, revised $a = 9.72$ in., $c = 9.72/0.79 = 12.30$ in. and

$$\sum_j F_{cj} = -[0.85(3)(5)(48) + 0.85(5.8)(9.72 - 5)(48)] - [612 + 1,117] = -1,729 \text{ kips}$$

$$\sum_i A_{si}f_{si} + \sum_j F_{cj} = 1,736 - 1,729 = 7 \text{ kips} \cong 0.0 \quad \text{O.K.}$$

Step 4: No revision of c or further iteration is needed.

Step 5: Taking moments about the top fiber:

$$M_n = \sum_i A_{si}f_{si}d_i + \sum_j F_{cj}d_j = [-48(3) - 14(7) + 1,798(41.13) - 612(2.5) - 1,117(7.36)]/12 = 5,333 \text{ kip-ft}$$

The approximate formulas of the AASHTO Specifications can be conservatively used if the concrete properties of the CIP topping are used and the two top strands are ignored, which in many cases may be sufficient.

8.2.2.7.2 Part 2 – Comparative Results

Table 8.2.2.7.2-1 compares results of the strain compatibility approach for $f'_c = 5.8$ ksi and 8.5 ksi with the results of flexural design of the example of Section 8.2.2.5.

Table 8.2.2.7.2-1
Flexural Capacity Prediction by Various Methods at Midspan

	$f'_c = 5.8$ ksi		$f'_c = 8.5$ ksi	
	LRFD Spec.	Strain Comp.	LRFD Spec.	Strain Comp.
Neutral Axis Depth, c , in.	16.67	16.39	7.91	8.12
Compression Block Depth, a , in.	12.67	12.46	5.14	5.28
Steel Stress at Ultimate Flexure, ksi	235	240	253	260
ϕM_n , kip-ft	3929	4,222	4,987	5,106
	93%	100%	98%	100%

The table clearly shows the advantage of using the accurate strain compatibility approach.

DESIGN THEORY AND PROCEDURE

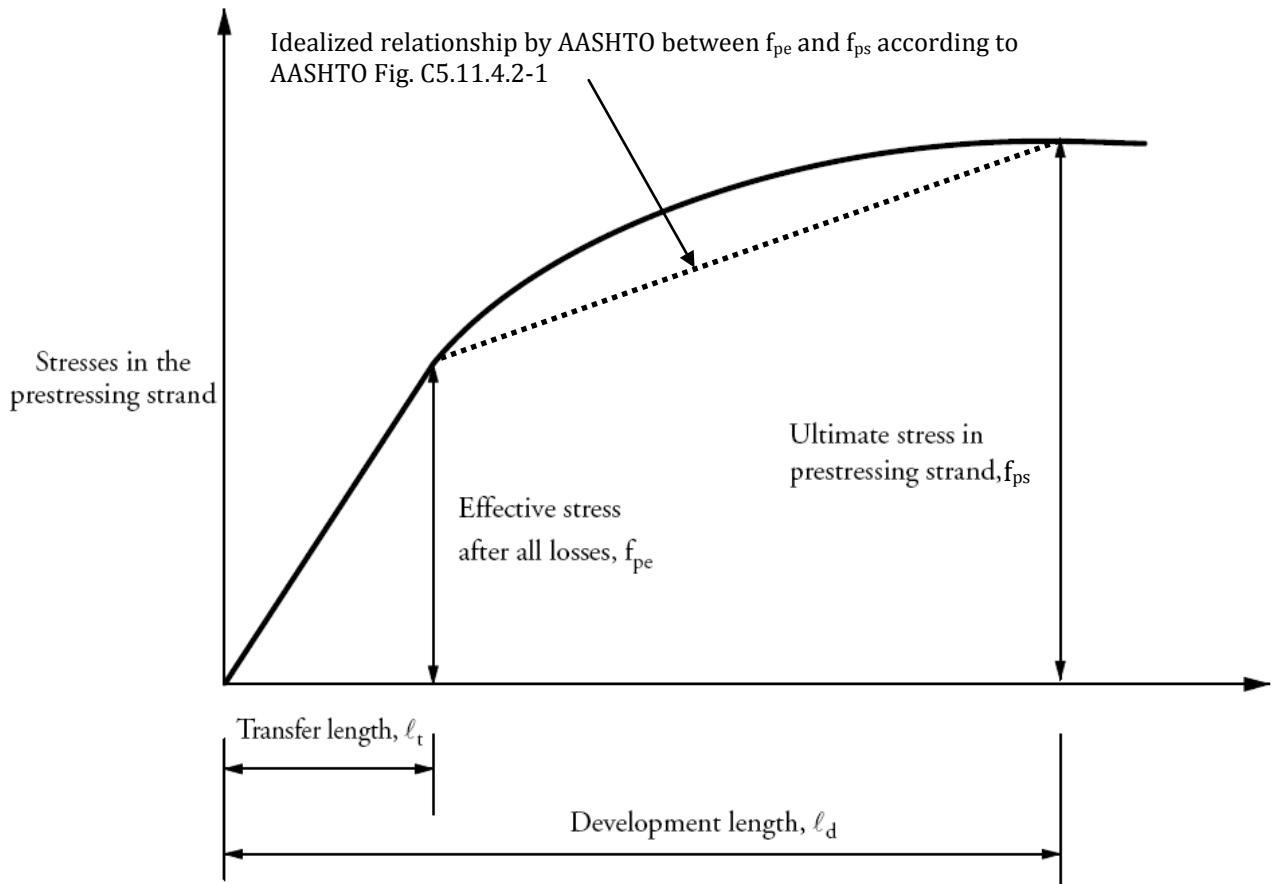
8.2.2.7.2 Part 2 – Comparative Results/8.3 Strand Transfer and Development Lengths

Some designers compound the errors resulting from the approximate procedures by lumping all pretensioning steel in a section into a single location for the purpose of establishing the effective depth. This is incorrect. Only the reinforcement near the tension face of the member should be considered in determining the steel stress using LRFD Eq. 5.7.3.1.1-1.

8.3 STRAND TRANSFER AND DEVELOPMENT LENGTHS

The transfer length, ℓ_t , is the length of strand over which the prestress force in pretensioned members is transferred to the concrete by bond and friction. The development length, ℓ_d , is the length of strand required to develop the stress in the strand corresponding to the nominal flexural resistance of the member. The transfer length is included as part of the development length. These two parameters are used differently in design as discussed below. **Figure 8.3-1** illustrates the relationship between the transfer and development lengths, and the strand stress.

Figure 8.3-1
Strand Transfer and Development Lengths



Much research has been conducted in recent years on methods of predicting ℓ_t and ℓ_d . Prediction formulas have been developed with no clear consensus among researchers. It should be emphasized, however, that the impact of variability of the transfer length on design of bridge beams is very small, and is limited to the 2 to 3 ft at the end of a member. The impact of variability of development length on bridge beams is also small. An over-estimation of ℓ_d will not significantly increase the cost of beams. However, ℓ_d may become a significant design parameter for some prestressed concrete members, such as deck panels, which have very short spans, and piles, which may have their largest bending moment at the pile/cap interface.

DESIGN THEORY AND PROCEDURE**8.3.1 Strand Transfer Length/8.3.1.4 Research Results****8.3.1 Strand Transfer Length****8.3.1.1 Impact on Design**

Transfer length is the bonded length of strand required to transfer the prestress force in the strand to the surrounding concrete in a pretensioned member. At any section which falls within the transfer length, the prestress force should be reduced in proportion to its distance from the end of the member. Specifically, within the transfer length, the stress in the strand is assumed to vary linearly from zero at the end of member, or the point where the strand is bonded if debonding is used, to the full effective prestress force at the end of the transfer length.

Overestimation of transfer length is generally conservative for shear design but may be unconservative when evaluating flexural stress limits in the end regions. Shear strength is reduced within the transfer length due to the reduced precompression in the concrete. On the other hand, the reduced prestress force in the transfer length zone protects the end of the beam from excessive tensile stresses. Such excessive stresses may require that the end of the beam be reinforced with additional bonded steel reinforcement near the top fibers.

8.3.1.2 Specifications

LRFD Article 5.11.4.1 requires a transfer length of 60 times the diameter of the strand for the purposes of estimation of development length.

8.3.1.3 Factors Affecting Transfer Length

The transfer length for prestressing strand is affected by many parameters. Some of the most important are as follows:

- Type of prestressing strand
- Strand diameter
- Strand stress level
- Surface condition of strand (i.e., clean, oiled, rusted, epoxy-coated, etc.)
- Concrete strength
- Type of loading (i.e., static, repeated or impact)
- Method of strand detensioning (i.e., gradual or sudden)
- Confining reinforcement around strand
- Consolidation and consistency of concrete around strand
- Concrete cover around the strand
- Strand spacing
- Time-dependent effects
- Vertical location in concrete (top versus bottom locations)

8.3.1.4 Research Results

The Federal Highway Administration (FHWA), in 1996, approved the use of ½-in. diameter strands at a center-to-center spacing of 1.75 in. and 0.6-in.-diameter strands at a spacing of 2 in. These spacings are less than the four strand diameters previously required in the *Standard Specifications*. This decision was based on studies which demonstrate that the transfer length for the more closely spaced strands remains conservatively estimated using the relationship found in the *Standard Specifications*. With only a 20% increase in diameter from 0.5 to 0.6 in., the prestress force per strand is increased by 40%. Using 0.6-in.-diameter strands at a 2 in. spacing, it is possible now to increase the amount of pretensioning force by up to 40% and still preserve the same prestress eccentricity. This dramatically improves the load carrying capacity of a given cross-section. For more information on this research, see Section 8.3.2.4.

DESIGN THEORY AND PROCEDURE**8.3.1 Strand Transfer Length/8.3.1.4 Research Results****8.3.1.5 Recommendations**

The current recommendations of the *LRFD Specifications* to use 60 strand diameters are adequate for design of typical structures. For unusually short span products or for strands with marginal surface conditions, this transfer length may not be adequate. For high-strength concrete, the provisions may overestimate the transfer length (Ramirez and Russell, 2008).

8.3.1.6 End Zone Reinforcement

LRFD Article 5.10.10.1 requires that an area of nonprestressed reinforcing steel be provided near the ends of pretensioned members to resist 4% of the prestressing force. The stress in the reinforcement resisting this force is limited to 20.0 ksi. This reinforcement is usually provided as stirrups and must be placed within a distance equal to $h/4$ from the beam end, where h is the overall depth of the pretensioned element.

The requirement is a simplification of the equation proposed by Marshall and Mattock (1962). It appears to be reasonable for modest levels of prestressing. However, in recent years, larger prestressing forces are being used with high-strength concrete. This is especially true for sections such as the NU Bulb-Tee beams*, where up to 58 strands can be placed in the bottom flange.

When this large number of strands is used with relatively shallow beams, such as the 43.3 in.-deep NU-1100, the specifications require that as much as 3.6 in.² of reinforcement be placed within a distance of 9.0 in. from the end of the beam. It is very difficult to satisfy this requirement and provide adequate clearance to place and consolidate the concrete. Alternative details have been proposed by Tadros et al. (2010)

Designers should be aware that the most critical time is at prestress transfer. Areas of end zone reinforcement that are less than the required areas and that have been consistently used in actual production without objectionable cracking at member end may be acceptable.

* a family of metric-dimensioned beams developed at the University of Nebraska

8.3.2 Strand Development Length**8.3.2.1 Impact on Design**

Strand development length is the length required for bond to develop the strand tension at the nominal flexural resistance. As shown in Section 8.2.2, this tension is generally lower than the specified ultimate strength of the strand. For bridge beams, the development length is insignificant unless the bridge beams are less than about 24 ft in length, or unless the beams are subjected to large bending moments near their ends. The development length becomes significant in deck panels used as stay-in-place forms.

8.3.2.2 LRFD Specifications

The equation for development length in the *LRFD Specifications* is similar to that used previously in the *Standard Specifications*. However, based on work by Cousins et al. (1986), which indicated that the existing equation was unconservative, the Federal Highway Administration (FHWA) imposed a 1.6 multiplier on the earlier AASHTO equation. As a result, the *LRFD Specifications* include a K factor in the equation as follows:

$$\ell_d \geq K \left(f_{ps} - \frac{2}{3} f_{pe} \right) d_b \quad \text{[LRFD Eq. 5.11.4.2-1]}$$

where

$K = 1.6$ for bonded strands in precast, prestressed beams

When a portion of the strand is debonded or “shielded” and where tension exists in the precompressed tensile zone under service loads, the development length must be determined using LRFD Eq. 5.11.4.2-1 with a value of $K = 2.0$.

DESIGN THEORY AND PROCEDURE**8.3.2.3 Factors Affecting Development Length/8.4 Shear****8.3.2.3 Factors Affecting Development Length**

The development length of the strand depends on a number of factors in addition to the factors already stated for the transfer length. These factors include the following:

- The difference between the stress in the prestressing steel at the ultimate member strength and the effective prestress after all losses.
- Use of bonded or debonded prestressing steel.
- Flexure-shear interaction.

8.3.2.4 Bond Studies

Numerous studies have been conducted on both ½-in. and 0.6-in.-diameter strands, often with conflicting conclusions. A summary of research on ½-in. strand was reported by Buckner (1994 and 1995). He proposed modification of the l_d formula, which takes into account the effect of strand stress at the nominal flexural resistance. He suggests that a strand with a stress at the nominal resistance close to the ultimate strength of the steel should have a development length almost twice as long as a strand with a stress at nominal resistance equal to the yield point of the steel.

Shahawy (2001) suggests that for members with depths greater than 24 in., LRFD Eq. 5.11.4.2-1 (with $K = 1.6$) yields conservative results. For members with depths less than 24 in., the K multiplier in LRFD Eq. 5.11.4.2-1 is not warranted. Shahawy also concludes that flexure-shear interaction has a significant effect on the development length of prestressing strands and should be incorporated into the design equations. For high-strength concrete, the provisions may overestimate the development length (Ramirez and Russell, 2008).

8.3.2.5 Recommendations

It is recommended that the formula given in the *LRFD Specifications* be used unless an improved formula emerges. Even though the factor of 2 applied to debonded strands may be too conservative, it is not expected to have significant impact on bridge beam design.

8.4 SHEAR

The design and analysis of precast, prestressed concrete bridge members for vertical shear are presented in this section. Design and analysis for combined torsion and shear are not included. The applicable sections in the *LRFD Specifications* are covered in detail.

Generally, the design of vertical web reinforcement is one of the last steps performed in the design of a prestressed concrete bridge beam. The precast member cross-section, beam spacing, span geometry and flexural reinforcement have already been established. Unlike flexural design, for which conditions at both service and factored load are evaluated, shear design is only evaluated for factored loads (strength limit state).

Shear design is essentially based on the truss analogy which has been used for concrete design since the early 1900s. In the truss analogy, a concrete member resists loads by a truss composed of concrete “compression struts” and steel “tension ties.” However, while this model is an effective tool for estimating the ultimate shear capacity of concrete members, it may be overly conservative in calculating the cracking shear capacity when compared to test results.

Therefore, the *LRFD Specifications* provide two sectional shear design methods for prestressed concrete members. These methods attempt to provide more realistic estimates of shear capacity of a concrete member by adding a concrete contribution to the basic truss analogy. And thus, the nominal shear strength, V_n , is considered to be a combination of the concrete contribution, V_c , and web reinforcement contribution, V_s . In members with harped strand, the vertical component of the prestressing force, V_p , is also considered to resist the factored shear force. The nominal shear resistance can, therefore, be expressed as:

$$V_n = V_c + V_s + V_p$$

DESIGN THEORY AND PROCEDURE**8.4 Shear/8.4.1.1.2 Concrete Contribution V_c**

The factored shear force at the section under investigation must be less than or equal to the nominal shear resistance reduced by a resistance factor, ϕ :

$$V_u \leq \phi V_n = \phi(V_c + V_s + V_p)$$

While both the methods of the *LRFD Specifications* are based on the truss analogy as discussed above, there is a significant difference in the way in which it is used. The difference is discussed below. To ensure ductile behavior, the designer must properly detail the web reinforcement to provide adequate development and to satisfy maximum and minimum limits on the quantity and spacing of the reinforcement. Each of the shear design procedures is discussed in detail in the following sections.

8.4.1 LRFD Specifications

There are three methods of shear design presented in the *LRFD Specifications* for prestressed members. The most general method is the strut-and-tie model. This model can be applied to any design situation, including members with irregular cross-sections or discontinuities. It is also used to design a member for all load effects, not just shear. This method is discussed in Section 8.12.

The methods used for typical shear design are sectional design models: the modified compression field theory (MCFT) developed by Collins, Mitchell (1980) and others; and the simplified procedure developed by Hawkins et al. (2005). The MCFT method is based on the variable angle truss model in which the inclination of the diagonal compression field is allowed to continuously vary. The simplified procedure fixes the inclination at 45° in regions of flexure-shear cracking but allows it to vary in regions of web-shear cracking. The varying inclination is especially significant for prestressed concrete members where the inclination is typically 20° to 40° degrees due to the effect of the prestressing force.

The MCFT model also differs from the simplified procedure because the concrete contribution, V_c , is attributed to tension being carried across the compression diagonals. This contribution has been determined experimentally and has been related to the strain in the tension side of the member. In general, the higher the strain in the tension side at ultimate, the wider the shear cracks, and in turn the smaller the concrete contribution.

Chapter 5 of the *LRFD Specifications* is applicable to conventionally reinforced concrete, and fully-prestressed concrete, as well as partially-prestressed concrete design. "Flexural Regions" as defined in LRFD Article 5.8.1.1 are discussed below. Design of regions near discontinuities are covered in Section 8.12.

8.4.1.1 Shear Design Provisions

The *LRFD Specifications*, Article 5.8.3, introduces the sectional design models. Subsections 1 and 2 describe the applicable geometry required to use this technique to design web reinforcement.

8.4.1.1.1 Nominal Shear Resistance

The nominal resistance is taken the lesser of:

$$V_n = V_c + V_s + V_p, \text{ or,} \quad [\text{LRFD Eq. 5.8.3.3-1}]$$

$$V_n \leq 0.25f'_c b_v d_v + V_p \quad [\text{LRFD Eq. 5.8.3.3-2}]$$

where

b_v = effective web width

d_v = effective shear depth

LRFD Eq. 5.8.3.3-2 represents an upper limit of V_n to assure that the concrete in the web will not crush prior to yield of the transverse reinforcement.

8.4.1.1.2 Concrete Contribution, V_c

The *LRFD Specifications* defines the concrete contribution as the nominal shear resistance provided by the tensile stresses in the concrete. This resistance is computed using the following equations:

$$V_c = 0.0316\beta\sqrt{f'_c}b_v d_v \text{ for the MCFT model, and} \quad [\text{LRFD Eq. 5.8.3.3-3}]$$

DESIGN THEORY AND PROCEDURE**8.4.1.1.2 Concrete Contribution V_c /8.4.1.1.4 MCFT Model: Values of β and θ**

V_c = the lesser of V_{ci} or V_{cw} for the simplified procedure.

The units used in the *LRFD Specifications* are kips and inches. The factor 0.0316 of the MCFT-model equation is equal to

$$\frac{1}{\sqrt{1,000}}$$

which converts the expression from psi to ksi units for the concrete compressive strength, f'_c .

8.4.1.1.3 Web Reinforcement Contribution, V_s

The contribution of the web reinforcement is given by the general equation:

$$V_s = \frac{A_v f_y d_v (\cot \theta + \cot \alpha) \sin \alpha}{s} \quad [\text{LRFD Eq. 5.8.3.3-4}]$$

where the angles, θ and α , represent the inclination of the diagonal compressive stresses measured from the horizontal beam axis and the angle of the web reinforcement relative to the horizontal beam axis, respectively.

For cases of vertical web reinforcement, the expression for V_s simplifies to:

$$V_s = \frac{A_v f_y d_v \cot \theta}{s} \quad [\text{LRFD Eq. C5.8.3.3-1}]$$

Transverse shear reinforcement shall be provided when:

$$V_u > 0.5 \phi (V_c + V_p) \quad [\text{LRFD Eq. 5.8.2.4-1}]$$

When the reaction introduces compression into the end of the member, LRFD Article 5.8.3.2 specifies that the critical section for shear is the larger of $0.5d_v \cot \theta$, or d_v , measured from the face of the support, where d_v and θ are measured at the critical section for shear.

8.4.1.1.4 MCFT Model: Values of β and θ

To determine the nominal resistance for the MCFT model, the design engineer must determine β and θ from LRFD Article 5.8.3.4.2. For reinforced nonprestressed concrete sections, the values of β and θ may be taken as 2 and 45° respectively [LRFD Art.5.8.3.4.1]. However, for prestressed concrete, the engineer can take advantage of the precompression and use lower angles of θ , which optimizes the web reinforcement.

For sections containing at least the minimum amount of transverse reinforcement specified in LRFD Article 5.8.2.5,

$$\beta = \frac{4.8}{1 + 750\varepsilon_x}$$

otherwise

$$\beta = \frac{4.8}{1 + 750\varepsilon_x} - \frac{51}{39 - s_{xc}}$$

where

$$\varepsilon_x = \frac{\left(\frac{|M_u|}{d_v} + 0.5N_u + |V_u - V_p| - A_{ps}f_{po} \right)}{E_s A_s + E_p A_{ps}}$$

and

$$s_{xc} = s_x \frac{1.38}{a_g + 0.63}$$

DESIGN THEORY AND PROCEDURE**8.4.1.1.4 MCFT Model: Values of β and θ /8.4.1.1.5 Simplified Procedure: Values of V_{ci} and V_{cw}**

where

s_x = the lesser of either d_v or the maximum distance between layers of longitudinal crack control reinforcement

a_g = maximum aggregate size, in.

The specifications indicate that the area of prestressing steel, A_{ps} , must account for lack of development near the ends of prestressed beams. Any nonprestressed reinforcement or strand in the compression zone of the member, which is taken as one-half of the overall depth ($h/2$), should be neglected when computing A_s and A_{ps} for use in this calculation. This is very important when evaluating members with harped strand, since near the end of typical beams, harped strands are near the top of the beam. Because of this, it is recommended that the straight and harped strands be considered separately in the analysis. It is the physical location of each strand that is important and not the centroid of the group.

The variable, f_{po} , represents the modulus of elasticity of prestressing tendons multiplied by the locked-in difference in strain between the prestressing tendons and the surrounding concrete. For usual levels of prestressing, the *LRFD Specifications* suggests a value of $0.7f_{pu}$ is appropriate for both pretensioned and post-tensioned members. However, for pretensioned members, LRFD Article C5.8.3.4.2 indicates that f_{po} can be taken as the stress in the strands when the concrete is cast around them, which is the jacking stress, f_{pi} which equals $0.75f_{pu}$. Therefore, it is recommended that for usual pretensioned beams with low relaxation strands, the value of f_{po} should be taken as $0.75f_{pu}$. Within the transfer length, f_{po} should be increased linearly from zero to its full value along the transfer length.

If the longitudinal strain in the tensile reinforcement (ϵ_x) is negative, ϵ_x should be taken as zero or recomputed using the denominator of the equation replaced by $(E_s A_s + E_p A_{ps} + E_c A_{ct})$, where A_{ct} represents the area of concrete on the flexural tension side of the member as shown in Figure 8.4.1.2-1.

The value of θ , the angle of inclination, in both cases may be taken as

$$\theta = 29 + 3500\epsilon_x$$

Additional requirements of LRFD Article 5.8.3.4.2 should be reviewed

8.4.1.1.5 Simplified Procedure: Values of V_{ci} and V_{cw}

For the simplified procedure, LRFD Article 5.8.3.4.3 specifies the following equations for V_{ci} , nominal shear resistance provided by concrete when inclined cracking results from combined shear and moment, and V_{cw} , nominal shear resistance provided by concrete when inclined cracking results from excessive principal tensions in web :

$$V_{ci} = 0.02\sqrt{f'_c}b_v d_v + V_d + \frac{V_i M_{cre}}{M_{max}} \geq 0.06\sqrt{f'_c}b_v d_v$$

where

V_d = shear force at section due to unfactored dead load and includes both *DC* and *DW*, kips

V_i = factored shear force at section due to externally applied loads occurring simultaneously with M_{max} , kips

M_{cre} = moment causing flexural cracking at section due to externally applied loads, in-kips

M_{max} = maximum factored moment at section due to externally applied loads, in-kips

$$V_{cw} = (0.06\sqrt{f'_c} + 0.30f_{pc})b_v d_v + V_p$$

where

f_{pc} = compressive stress in concrete (after allowance for all prestress losses) at centroid of cross section resisting externally applied loads or at junction of web and flange when the centroid lies within the flange (ksi). In a composite member, f_{pc} is the resultant compressive stress at the centroid of the composite section, or at junction of web and flange, due to both prestress and moments resisted by precast member acting alone.

DESIGN THEORY AND PROCEDURE

8.4.1.2 Design Procedure/8.4.1.3 Longitudinal Reinforcement Requirement

8.4.1.2 Design Procedure

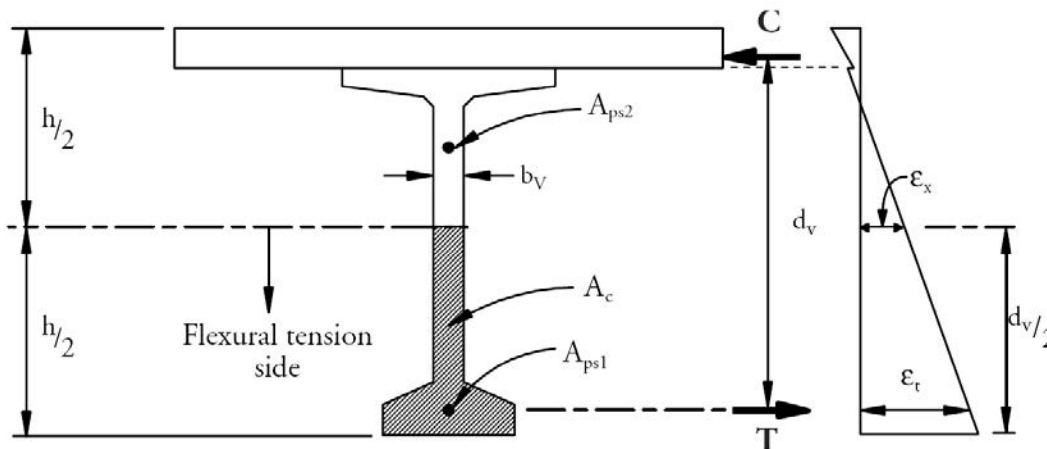
To design the member for shear, the designer first determines the factored shear due to applied loads at the section under investigation. The critical section is located at the larger of d_v or $0.5d_v \cot \theta$ from the face of support. The effective shear depth, d_v , is taken as the distance between the resultants of the tensile and compressive forces due to flexure. It need not be taken less than the greater of $0.9d_e$ or $0.72h$. When strands are straight and compression stays in the top flange, d_v is easily calculated as $d_e - a/2$. When determining d_e , only the steel on the tension side should be considered. However, determination of d_v can get complicated with harped strands as d_v depends on the location of the critical section, which in turn is a function of d_v .

For T-beam analysis, the resultant of the compression force is not at $a/2$. Computer programs may be used to perform these calculations, but some simplifications are warranted for hand calculations. For example, the critical section can initially be assumed to be at $0.72h$, and the value of d_v can be determined at that location. If this value of d_v is larger than $0.72h$ or $0.9 d_e$, then the designer may elect to choose a new location using the value d_v just determined. When calculating d_v , it is convenient to use the depth of the compression block, a , at midspan without introducing significant error.

The shear contribution from harped strand V_p , is then computed.

Next, the concrete contribution, V_c , is estimated based upon Section 8.4.3.1.2 applying either the MCFT model or the simplified procedure.

Figure 8.4.1.2-1
Illustration of Shear Parameters



After V_c has been computed, V_s is calculated using LRFD Eq. 5.8.3.3-4. The quantity of shear reinforcement is then calculated using LRFD Eq. C5.8.3.3.-1 with the value of $\cot \theta$ from either the MCFT model or the simplified procedure.

After determining the amount of shear reinforcement needed, the designer should check the maximum spacing allowed by the specifications as given in LRFD Article 5.8.2.7. Also, the amount of shear reinforcement should be checked to ensure that it is equal to or larger than the minimum value required by the specifications, which is:

$$A_v = 0.0316 \sqrt{f'_c} \frac{b_v s}{f_y} \quad \text{[LRFD Eq. 5.8.2.5-1]}$$

8.4.1.3 Longitudinal Reinforcement Requirement

The longitudinal (flexural) reinforcement must also be able to resist additional force due to shear, i.e., the horizontal component of the diagonal compression field. The tensile capacity of the reinforcement on the flexural

DESIGN THEORY AND PROCEDURE**8.4.1.3 Longitudinal Reinforcement Requirement/8.5.1 Theory**

tension side of the member, taking into account any lack of full development of that reinforcement, must be greater than or equal to the force T , calculated as:

$$T = \left[\frac{M_u}{d_v \phi} + 0.5 \frac{N_u}{\phi} + \left(\frac{V_u}{\phi} - 0.5V_s - V_p \right) \cot \theta \right] \quad [\text{LRFD Eq. 5.8.3.5-1}]$$

The tensile capacity of the reinforcement can be determined by using the appropriate values for $A_s f_y + A_{ps} f_{ps}$. V_s is given by LRFD Eq. 5.8.3.3-4 except that V_s may not be greater than V_u/θ .

Satisfying this equation is very important for prestressed concrete beams, especially near non-continuous supports where a substantial portion of the prestressing strands are harped. Harped strands are not effective in contributing to this longitudinal reinforcement requirement since they are often above midheight of the member.

The *LRFD Specifications* require that this criterion also be checked at the face of the bearing. At this section, which usually lies within the transfer length of the strands, the effective prestressing force in the strands is not fully developed. Thus, the term f_{ps} should be calculated as a portion of the effective prestress force based on linear variation starting from zero at the end of the beam to full effective prestress at the transfer length. The designer should not be confused by the term f_{ps} , which generally refers to the prestress force at Strength Limit State, because the strands at this section do not have enough development length to provide such level of prestress. If the strands are well anchored at the end of the member, by embedment in a diaphragm or by use of a mechanical device, the stress in the strands, f_{ps} , can be considered to equal the stress in the strands at Strength Limit State.

8.5 HORIZONTAL INTERFACE SHEAR**8.5.1 Theory**

Concrete decks designed to act compositely with precast concrete beams must be able to resist the horizontal shearing forces at the interface between the two elements. The basic strength equation for the design of the interface between the deck and beam is:

$$V_{ri} \geq V_{ui} \quad [\text{LRFD Eq. 5.8.4.1-2}]$$

where

V_{ri} = factored interface shear resistance

V_{ui} = factored interface shear force due to total load

Design is carried out at various locations along the span, similar to vertical shear design.

Theoretical calculation of the shearing force acting on the interface at a given section is not simple because the section does not behave as a linear elastic material near ultimate capacity. If it did, the shear stress, horizontal or vertical, at any fiber in a cross-section would be calculated from the familiar equation:

$$v_h = \frac{VQ}{Ib} \quad (\text{Eq. 8.5.1-1})$$

where

V = vertical shear force at the section

I = moment of inertia

b = section width at the fiber being considered

Q = first moment of the area above (or below) the fiber being considered

However, at ultimate conditions, the material is no longer elastic and the concrete may be cracked at the section being considered. Further, the composite cross-section consists of two different types of concrete with different properties. Therefore, application of the above equation to design at ultimate, without modification, would yield questionable results.

DESIGN THEORY AND PROCEDURE

8.5.1 Theory/8.5.2 LRFD Specifications

Loov and Patnaik (1994) determined that the above equation may yield adequate results if both the cracked section moment of inertia and area moment of a transformed composite section are used. The section would be transformed using the slab-to-beam modular ratio used in flexural design by the allowable stress method. However, this approach is still too complicated. It confuses the calculations at two limit states: service and ultimate.

Kamel (1996) used equilibrium of forces to show that:

$$v_h = V/(jd)b_v \quad (\text{Eq. 8.5.1-2})$$

where

V = factored vertical shear at the section in question

d = effective depth of the member

jd = distance between the tension and compression resultant stresses in the section. This is the same distance as d_v used in the *LRFD Specifications* for shear design.

b_v = section width at the interface between the precast and the cast-in-place concrete. It is important to understand that b_v is not the web width.

Another important issue is which loads should be used to calculate V_{ui} at a section. The *LRFD Specifications* mandates that all loads including all noncomposite and composite loads be applied. In the first edition of the LRFD Specifications, a case was made for excluding the self weight of the precast concrete member and the weight of the deck since they are present prior to composite action taking effect. The cohesion and frictions factors were updated to reflect the substantial body of experimental data. [see LRFD Section 5.8.4.3]

To determine the nominal interface shear resistance, the *LRFD Specifications* uses a modification of the well-established shear friction theory.

The requirements of the *LRFD Specifications* are stated in terms of horizontal (interface) shear.

8.5.2 LRFD Specifications

LRFD Article 5.8.4.2 provides guidance for computing interface shear due to factored loads for girder/slab bridges. The factored vertical shear force is V_u . The factored interface shear force per unit length in kips/ft, V_{ui} , is given by the following equation:

$$V_{ui} = \frac{12V_u}{d_v}$$

where

V_{ui} = factored horizontal shear force per unit length of beam

V_u = factored vertical shear force at specified section due to all loads

d_v = the distance between the centroid of the tension steel and the mid-thickness of the slab

Factored load \leq factored resistance, or:

$$V_{ui} \leq \phi V_{ni}$$

where V_{ni} = nominal interface shear resistance

$$= cA_{cv} + \mu[A_{vffy} + P_c]$$

[LRFD Eq. 5.8.4.1-3]

DESIGN THEORY AND PROCEDURE

8.5.2 LRFD Specifications/8.6.2 Definition

where

c = cohesion factor
 = 0.28 ksi for this case [LRFD Art. 5.8.4.3]

A_{cv} = interface area of concrete engaged in shear transfer

μ = friction factor
 = 1.0 for this case [LRFD Art. 5.8.4.3]

A_{vf} = area of shear reinforcement crossing the shear plane where the shear plane under consideration must be consistent with the units used

f_y = yield strength of shear reinforcement

P_c = permanent net compressive force normal to the shear plane (may be conservatively neglected)

The values for c and μ apply when the top surface is intentionally roughened to an amplitude of $\frac{1}{4}$ in. Typically, any compressive force across the interface is neglected (i.e., $P_c = 0$).

Nominal shear resistance must also satisfy:

$V_{ni} \leq K_1 f'_c A_{cv}$, and [LRFD Eq. 5.8.4.1-4]

$V_{ni} \leq K_2 A_{cv}$ [LRFD Eq. 5.8.4.1-5]

where $K_1 = 0.3$ for this case [LRFD Art. 5.8.4.3]

$K_2 = 1.8$ ksi for normal weight concrete [LRFD Art. 5.8.4.3]

The minimum reinforcement required of A_{vf} may be waived where v_{ui} is less than 0.210 ksi. It would seem to be impractical and an unnecessary expense to provide connectors in a number of common applications, such as precast stay-in-place panels if the interface shear stress is lower than 0.210 ksi.

8.6 LOSS OF PRESTRESS

8.6.1 Introduction

Concrete is a material that exhibits time-dependent behavior. Under the effects of sustained stress, “creep” causes concrete to experience ongoing strains. Even when no loads are present, concrete specimens will undergo “shrinkage” strains. Prestressing steel, when strained at levels normal in prestressed concrete bridge members, exhibits a gradual loss of stress under constant strain that is referred to as “relaxation.” **Chapter 2** and Section 8.13 provide equations, representative material constants and more information related to predicting creep, shrinkage, and relaxation.

Under the combined effects of creep and shrinkage of concrete and the relaxation of prestressing steel, prestressed concrete members gradually deform with time. These time-dependent changes manifest themselves in the shortening of the member, in some loss of prestress and, therefore, in a change in camber or deflection.

Several techniques are available to the designer to account for these effects. Approximate methods suitable for conventional designs are given in this section. More detailed methods suitable for unusual or complex designs are presented in Section 8.13.

8.6.2 Definition

Loss of prestress is defined as the difference between the initial stress in the strands (just after seating of strands in the anchorage), and the effective prestress in the member (at a time when concrete stresses are to be calculated). This definition of loss of prestress includes both instantaneous (elastic) losses and losses that are time dependent.

DESIGN THEORY AND PROCEDURE**8.6.2 Definition/8.6.4.1 Effects at Transfer**

Total prestress loss:

$$\Delta f_{pT} = \Delta f_{pES} + \Delta f_{pLT}$$

where

Δf_{pT} = total loss in prestressing steel stress

Δf_{pES} = sum of all losses or gains due to elastic shortening or extension at the time of application of prestress and/or external loads

Δf_{pLT} = long-term losses due to shrinkage and creep of concrete, and relaxation of steel after transfer

It should be emphasized that this definition of loss of prestress differs from previous methods of estimating prestress losses in that elastic changes in the steel stress due to the application of external loads are now considered. Traditionally, calculated prestress losses in pretensioned members included only the elastic shortening loss at release of prestress and inelastic long-term losses. In reality, when a member is loaded externally, the resulting moment and/or axial load changes the strain in both the concrete and bonded reinforcement. For simple-span flexural members, applied loads normally result in tensile stresses in the bottom concrete fibers and additional tensile stresses in the prestressed reinforcement. The effects of dead loads and deck shrinkage are permanent and could be considered to offset some of the prestress losses. The effects of live load are transient but exist whenever the load is present. Proper accounting of these gains in tension in the prestressed reinforcement is necessary to compare the tension in the reinforcement under service conditions with the allowable stresses specified in LRFD. (see **Design Examples 9.1a, 9.1b, & 9.1c**)

In post-tensioning applications, friction between the tendon and the duct as well as anchorage seating losses during the post-tensioning operation must be considered in design. Post-tensioning applications are included in **Chapter 11**.

8.6.3 Significance of Losses on Design

For design, there are two important stages in the life of a prestressed concrete bridge beam when loss of prestress plays a significant role. First, a reasonable estimate of the prestress level is needed immediately following transfer of prestress. This is to avoid overstressing the concrete beam when the prestress force is the highest and concrete strength is lowest. The second stage that requires an estimate of effective prestress is under long-term service conditions. This is required to ensure that calculated stresses in the concrete are below the limits prescribed by the specifications. Other design criteria, including such critical matters as nominal flexural resistance and nominal shear resistance, are relatively insensitive to the designer's estimate of loss of prestress. It is primarily the service limit-state stresses in the bottom flange of a concrete beam that the designer is attempting to control through estimates of loss of prestress.

8.6.4 Effects of Estimation of Losses

It is important to recognize the variables that affect the loss of prestress in a beam. Some of the important variables affecting time-dependent behavior, and therefore loss of prestress, are the concrete's modulus of elasticity, and creep and shrinkage properties. These variables can be somewhat unpredictable for a given concrete mixture and cannot be fully controlled by the designer. Therefore, the estimation of loss of prestress should not be overemphasized at the expense of other more important issues during the design process.

8.6.4.1 Effects at Transfer

An exception to the previous statement should be made with regard to estimation of loss of prestress at the time of transfer. It is important that losses at transfer not be grossly overestimated. If this were to happen, sudden failure of the member at prestress transfer, while not likely, could possibly occur. At least, significant cracking could be expected. Fortunately, estimates of losses at this time are subject to fewer unknown variables, allowing a more accurate estimate to be made in almost all cases.

DESIGN THEORY AND PROCEDURE**8.6.4.2 Effect on Production Costs/8.6.6.2 Elastic Shortening Example****8.6.4.2 Effect on Production Costs**

In the case of overestimation of loss of prestress, the beam is likely to be constructed with more strands than necessary. The increase in strand cost is usually not significant, but if additional strands are provided, the concrete strength at transfer may have to be increased to accommodate the larger prestress force. This could require a longer curing time or a more expensive concrete mix. An increase in beam costs may result, particularly if the increase in strength at transfer requires an additional day to complete the casting cycle.

8.6.4.3 Effect on Camber

Another issue associated with overestimation of loss of prestress, and the addition of strands, is unexpected camber. Excessive camber of a bridge member can cause problems for constructors and can result in the need to adjust bridge grades. Finally, if a designer significantly overestimates loss of prestress for a member near the limits of its span range, it may be necessary to specify a larger beam. Foundation and substructure costs may also increase.

From the above discussion, it should be apparent that it is not beneficial to overestimate loss of prestress. The designer, therefore, is cautioned against overestimation.

8.6.4.4 Effect of Underestimating Losses

Conversely, underestimation of loss of prestress can theoretically result in excessive tensile stresses in the concrete member under service limit-state conditions. No known instances of problems resulting from this condition have been reported. The nominal flexural resistance requirements of bridge design specifications serve to impose a lower limit on the number of strands in a member, thereby indirectly preventing a low estimate for loss of prestress from having a significant adverse impact on a member. Underestimating losses may also result in lower than anticipated camber or even an unsightly sag in the final structure, but again, this is unlikely to occur in practice.

8.6.5 Methods for Estimating Losses

Several methods are available to predict loss of prestress. They fall into three main categories, listed in order of increasing complexity:

1. Lump sum estimate methods
2. Rational approximate methods
3. Detailed time-dependent analyses

The *LRFD Specifications* provides two methods in the second category above. The time-dependent analysis procedure described in Section 8.13 fits into the third category.

8.6.6 Elastic Shortening Loss at Transfer

Elastic shortening is the immediate shortening of the member under the application of prestressing force. Elastic shortening at the transfer of pretensioning occurs instantaneously and is not a time-dependent effect.

8.6.6.1 Computation of Elastic Shortening Loss

Elastic shortening is computed using LRFD Equation 5.9.5.1-1.

$$\Delta f_{pES} = \frac{E_p}{E_{ci}} f_{cgp}$$

where

- E_p = modulus of elasticity of prestressing strands
- E_{ci} = modulus of elasticity of beam concrete at transfer
- f_{cgp} = sum of concrete stresses at the center of gravity of prestressing strands due to prestressing force at transfer and the self weight of the member at sections of maximum moment

8.6.6.2 Elastic Shortening Example

Complete elastic-shortening examples are given in the design examples in Chapter 9 (see 9.1a.6.1).

DESIGN THEORY AND PROCEDURE

8.6.7 Time-Dependent Losses/8.6.7.2 Refined Estimates

8.6.7 Time-Dependent Losses

The *LRFD Specifications* provides two methods for estimating time-dependent losses: an approximate estimate of time-dependent losses (LRFD Article 5.9.5.3) and refined estimates of time-dependent losses (LRFD Article 5.9.5.4). The first method is intended for standard precast, pretensioned members subject to normal loading and environmental conditions. The second method provides more accurate values of creep-, shrinkage-, and relaxation-related losses. Both methods are described in the following sections.

8.6.7.1 Approximate Estimate

The approximate estimate method is applicable for standard precast, pretensioned members, when the following conditions apply:

- Normal loading and environmental conditions
- Members are made from normal weight concrete
- Concrete is either steam- or moist-cured
- Prestressing uses bars or strands with normal- or low-relaxation properties

Using the notation of the *LRFD Specifications*, the total time-dependent loss of prestress, Δf_{pLT} is given by:

$$\Delta f_{pLT} = 10.0 \frac{f_{pi} A_{ps}}{A_g} \gamma_h \gamma_{st} + 12 \gamma_h \gamma_{st} + \Delta f_{pR} \quad [\text{LRFD Eq. 5.9.5.3-1}]$$

where

- f_{pi} = prestressing steel stress immediately prior to transfer
- A_{ps} = total area for prestressing reinforcement
- A_g = area of cross section of the precast concrete beam
- γ_h = correction factor for relative humidity of the ambient air
- γ_{st} = correction factor for specified concrete strength at time of prestress transfer to the concrete member
- Δf_{pR} = an estimate of relaxation loss taken as 2.4 ksi for low-relaxation strand, 10.0 ksi for stress-relieved strand, and in accordance with manufacturers recommendation for other types of strand

The correction factor for relative humidity (normalized to 1.0 for $H = 70\%$):

$$\gamma_h = 1.7 - 0.01H \quad [\text{LRFD Eq. 5.9.5.3-2}]$$

where H = the average annual ambient relative humidity

The correction factor for specified concrete strength (normalized to 1.0 for $f'_{ci} = 4$ ksi):

$$\gamma_{st} = \frac{5}{(1 + f'_{ci})} \quad [\text{LRFD Eq. 5.9.5.3-3}]$$

8.6.7.2 Refined Estimates

Using the notation of the *LRFD Specifications*, total time-dependent loss of prestress, Δf_{pLT} is given by:

$$\Delta f_{pLT} = (\Delta f_{pSR} + \Delta f_{pCR} + \Delta f_{pR1})_{id} + (\Delta f_{pSD} + \Delta f_{pCD} + \Delta f_{pR2} - \Delta f_{pSS})_{df} \quad [\text{LRFD Eq. 5.9.5.4.1-1}]$$

where

- Δf_{pSR} = loss of pretensioning steel stress due to shrinkage of girder concrete between transfer and deck placement
- Δf_{pCR} = loss of pretensioning steel stress due to creep of girder concrete between transfer and deck placement

DESIGN THEORY AND PROCEDURE**8.6.7.2 Refined Estimates/8.6.7.2.1.1 Shrinkage of Concrete**

Δf_{pR1} = loss of pretensioning steel stress due to relaxation of prestressing strands between time of transfer and deck placement

Δf_{pSD} = loss of pretensioning steel stress due to shrinkage of girder concrete between the time of deck placement and final time

Δf_{pCD} = loss of pretensioning steel stress due to creep of girder concrete between deck placement and final time

Δf_{pR2} = loss of pretensioning steel stress due to relaxation of prestressing strands in composite section between time of deck placement and final time.

Δf_{pSS} = prestress gain due to shrinkage of the deck in the composite section.

Although Eq. 5.9.5.4.1-1 accurately represents the provisions in AASHTO LRFD, PCI recommends that the term Δf_{pSS} be deleted from the equation, and that deck shrinkage be treated as an applied load. (See discussion in **8.6.7.3.** and **Design Examples 9.1a, 9.1b, and 9.1c**)

8.6.7.2.1 Time-Dependent Losses between Transfer and Deck Placement

The total time-dependent loss between time of transfer and deck placement is the summation of prestress losses due to shrinkage of concrete, creep of concrete, and relaxation of prestressing strands.

8.6.7.2.1.1 Shrinkage of Concrete

The prestress loss due to shrinkage of concrete between time of transfer and deck placement is calculated by:

$$\Delta f_{pSR} = \epsilon_{bid} E_p K_{id} \quad [\text{LRFD Eq. 5.9.5.4.2a-1}]$$

where

ϵ_{bid} = concrete shrinkage strain of girder for time period between time of transfer and deck placement

E_p = modulus of elasticity of prestressing strands, ksi

K_{id} = transformed section coefficient that accounts for time-dependent interaction between concrete and bonded steel in the section being considered for time period between transfer and deck placement

The concrete shrinkage strain ϵ_{bid} is taken as:

$$\epsilon_{bid} = k_{vs} k_{hs} k_f k_{td} 0.48 \times 10^{-3} \quad [\text{LRFD Eq. 5.4.2.3.3-1}]$$

where

The factor for the effect of the volume-to-surface ratio of the beam:

$$k_{vs} = 1.45 - 0.13(V/S) \quad [\text{LRFD Eq. 5.4.2.3.2-2}]$$

The minimum value of k_{vs} is 1.0

The humidity factor for shrinkage:

$$k_{hs} = 2.00 - 0.014H \quad [\text{LRFD Eq. 5.4.2.3.3-2}]$$

where H = average annual mean relative humidity

The factor for the effect of concrete strength:

$$k_f = \frac{5}{1 + f'_{ci}} \quad [\text{LRFD Eq. 5.4.2.3.2-4}]$$

where f'_{ci} = specified compressive strength of concrete at time of transfer

DESIGN THEORY AND PROCEDURE**8.6.7.2.1.1 Shrinkage of Concrete/8.6.7.2.1.3 Relaxation of Prestressing Strands**

The time development factor at deck placement:

$$k_{td} = \frac{t}{61 - 4f'_{ci} + t} \quad [\text{LRFD Eq. 5.4.2.3.2-5}]$$

where

$$t = \text{maturity of concrete (days)} = t_d - t_i$$

$$t_i = \text{concrete age at transfer usually taken as 1 day}$$

$$t_d = \text{concrete age at deck placement, days}$$

$$K_{id} = \frac{1}{1 + \frac{E_p}{E_{ci}} \frac{A_{ps}}{A_g} \left(1 + \frac{A_g (e_{pg})^2}{I_g} \right) [1 + 0.7\Psi_b(t_f, t_i)]} \quad [\text{LRFD Eq. 5.9.5.4.2a-2}]$$

where

$$e_{pg} = \text{eccentricity of prestressing strand with respect to centroid of girder, in.}$$

$$\Psi_b(t_f, t_i) = \text{girder creep coefficient at final time due to loading introduced at transfer}$$

For the time between transfer and final time:

$$\Psi_b(t_f, t_i) = 1.9k_{vs} k_{hc} k_f k_{td} t_i^{-0.118} \quad [\text{LRFD Eq. 5.4.2.3.2-1}]$$

$$k_{hc} = 1.56 - 0.008H \quad [\text{LRFD Eq. 5.4.2.3.2-3}]$$

8.6.7.2.1.2 Creep of Concrete

The prestress loss due to creep of girder concrete between time of transfer and deck placement is:

$$\Delta f_{pCR} = \frac{E_p}{E_{ci}} f_{cgp} \Psi_b(t_d, t_i) K_{id} \quad [\text{LRFD Eq. 5.9.5.4.2b-1}]$$

where

$$\Psi_b(t_d, t_i) = \text{girder creep coefficient at time of deck placement due to loading introduced at transfer}$$

$$= 1.9k_s k_{hc} k_f k_{td} t_i^{-0.118} \quad [\text{LRFD Eq. 5.4.2.3.2-1}]$$

8.6.7.2.1.3 Relaxation of Prestressing Strands

The prestress loss due to relaxation of prestressing strands between time of transfer and deck placement is determined as:

$$\Delta f_{pR1} = \frac{f_{pt}}{K_L} \left(\frac{f_{pt}}{f_{py}} - 0.55 \right) \quad [\text{LRFD Eq. 5.9.5.4.2c-1}]$$

where

$$f_{pt} = \text{stress in prestressing strands immediately after transfer, taken not less than } 0.55f_y$$

$$K_L = 30 \text{ for low-relaxation strands and } 7 \text{ for other prestressing steel, unless more accurate manufacturer's data are available}$$

According to LRFD Art. 5.9.5.4.2c, the relaxation loss may also be assumed equal to 1.2 ksi for low-relaxation strands.

DESIGN THEORY AND PROCEDURE

8.6.7.2.2 Time-Dependent Losses between Deck Placement and Final Time/8.6.7.2.2.2 Creep of Concrete

8.6.7.2.2 Time-Dependent Losses between Deck Placement and Final Time

The total time-dependent loss between deck placement and final time is the summation of prestress losses due to shrinkage of beam concrete, creep of beam concrete, relaxation of prestressing strands, and shrinkage of deck concrete.

8.6.7.2.2.1 Shrinkage of Concrete

The prestress loss due to shrinkage of concrete between time of deck placement and final time is calculated by:

$$\Delta f_{pSD} = \epsilon_{bdf} E_p K_{df} \quad \text{[LRFD Eq. 5.9.5.4.2a-1]}$$

where

- ϵ_{bdf} = concrete shrinkage strain of girder for time period between deck placement and final time
- E_p = modulus of elasticity of prestressing strands, ksi
- K_{df} = transformed section coefficient that accounts for time-dependent interaction between concrete and bonded steel in the section being considered for time period between deck placement and final time

The total girder concrete shrinkage strain between transfer and final time is taken as:

$$\epsilon_{bdf} = k_{vs} k_{hs} k_f k_{tdf} 0.48 \times 10^{-3} \quad \text{[LRFD Eq. 5.4.2.3.3-1]}$$

The girder concrete shrinkage strain between deck placement and final time is:

$$\epsilon_{bdf} = \epsilon_{bif} - \epsilon_{bid}$$

The beam concrete transformed section coefficient between deck placement and final time is:

$$K_{df} = \frac{1}{1 + \frac{E_p}{E_{ci}} \frac{A_{ps}}{A_c} \left(1 + \frac{A_c (e_{pg})^2}{I_c} \right) [1 + 0.7 \Psi_b(t_f, t_i)]} \quad \text{[LRFD Eq. 5.9.5.4.3a-2]}$$

where

- A_c = area of the composite section
- I_c = moment of inertia of the composite section
- e_{pc} = eccentricity of strands with respect to centroid of composite section

8.6.7.2.2.2 Creep of Concrete

The prestress loss due to creep of beam concrete between time of deck placement and final time is determined as:

$$\Delta f_{pCD} = \frac{E_p}{E_{ci}} f_{cgp} [\Psi_b(t_f, t_i) - \Psi_b(t_d, t_i)] K_{df} + \frac{E_p}{E_c} \Delta f_{cd} \Psi_b(t_f, t_d) K_{df} \quad \text{[LRFD Eq. 5.9.5.4.3b-1]}$$

where

$$\begin{aligned} \Psi_b(t_f, t_d) &= \text{girder creep coefficient at final time due to loading at deck placement} \\ &= 1.9 k_{vs} k_{hc} k_f k_{tdf} t_d^{-0.118} \quad \text{[LRFD Eq. 5.4.2.3.2-1]} \end{aligned}$$

$$k_{tdf} = \frac{t}{(61 - 4f'_{ci} + t)} \quad \text{[LRFD Eq. 5.4.2.3.2-5]}$$

Δf_{cd} = change in concrete stress at centroid of prestressing strands due to long-term losses between transfer and deck placement, combined with deck weight and superimposed loads, ksi

$$\Psi_b(t_f, t_d) = -(\Delta f_{pSR} + \Delta f_{pCR} + \Delta f_{pR1}) \frac{A_{ps}}{A_g} \left(1 + \frac{A_g (e_{pg})^2}{I_g} \right) - \left(\frac{M_s e_{tf}}{I_{tf}} + \frac{(M_b + M_{ws}) e_{tc}}{I_{tc}} \right)$$

DESIGN THEORY AND PROCEDURE

8.6.7.2.2.2 Creep of Concrete/8.6.7.3 Recommended Treatment of Deck Shrinkage

The gross section properties are used in the equation to calculate Δf_{cd} for the long-term losses since the transformed section effect has already been included in the factor K_{id} when calculating the losses between initial time and deck placement.

8.6.7.2.2.3 Relaxation of Prestressing Strands

The prestress loss due to relaxation of prestressing strands in composite section between time of deck placement and final time is taken as:

$$\Delta f_{pR2} = \Delta f_{pR1} \quad [\text{LRFD Eq. 5.9.5.4.3c-1}]$$

8.6.7.2.2.4 Shrinkage of Deck Concrete

The prestress gain due to shrinkage of deck concrete is calculated by:

$$\Delta f_{pSS} = \frac{E_p}{E_c} \Delta f_{cdf} K_{df} [1 + 0.7\Psi_b(t_f, t_d)] \quad [\text{LRFD Eq. 5.9.5.4.3d-1}]$$

where Δf_{cdf} = change in concrete stress at centroid of prestressing strands due to shrinkage of deck concrete, ksi

$$\Delta f_{cdf} = \frac{\varepsilon_{ddf} A_d E_{cd}}{1 + 0.7\Psi_d(t_f, t_d)} \left(\frac{1}{A_c} - \frac{e_{pc} e_d}{I_c} \right) \quad [\text{LRFD Eq. 5.9.5.4.3d-2}]$$

where

ε_{ddf} = shrinkage strain of deck concrete between placement and final time by LRFD Eq. 5.4.2.3.3-1

A_d = area of deck concrete, in.²

$\Psi_d(t_f, t_d)$ = creep coefficient of deck concrete at final time due to loading introduced shortly after deck placement

E_{cd} = modulus of elasticity of deck concrete, ksi

e_d = eccentricity of deck with respect to the gross composite section, in.

$\varepsilon_{ddf} = k_{vs} k_{hs} k_{fj} k_{td} 0.48 \times 10^{-3}$ [LRFD Eq. 5.4.2.3.3-1]

$\Psi_d(t_f, t_d) = 1.9 k_{vs} k_{hc} k_{fj} k_{td} t_i^{-0.118}$ [LRFD Eq. 5.4.2.3.2-1]

Creep of the deck concrete is assumed to start at 1 day.

8.6.7.3 Recommended Treatment of Deck Shrinkage

PCI believes that it is not appropriate to include the prestressing gain caused by the deck shrinkage, Δf_{pSS} , in calculating the prestress losses. Alternatively, the effect of deck shrinkage should be analyzed by considering it as an external force applied to the composite nontransformed section for load combination Service III. This force is applied at the center of the deck with an eccentricity from the center of the deck to the composite center of gravity. The nontransformed section properties are used instead of the transformed section properties to provide a more conservative approach.

It is important to differentiate elastic gains from prestress losses. They are simply part of the elastic response of a beam to applied loads. They are implicit in the calculation of stresses when using transformed sections, but should be tracked separately so that the stress in the prestressing steel at service loads can be checked against the allowable limits in the *LRFD Specifications* (see LRFD Article 5.9.3). The objective is to control tensile stresses (see **Chapter 9**). If gross section properties are used in the analysis, elastic gains must be calculated explicitly and added back into the prestress. Elastic gains are permanent for dead loads and deck shrinkage and transient for live loads.

It is likely, however, that the full calculated force from deck shrinkage will not occur because of the presence of deck cracking and deck reinforcement. PCI recommends that in lieu of a more refined analysis, 50% of the deck shrinkage be applied.

DESIGN THEORY AND PROCEDURE**8.6.7.4 Prestress Loss Example/8.7 Camber and Deflection****8.6.7.4 Prestress Loss Example**

Complete design examples illustrating the application of the prestress-loss and recommended deck-shrinkage methodologies is given in the design examples of Chapter 9 (see Section 9.1a.6).

8.7 CAMBER AND DEFLECTION

Generally, there are three sets of beam deformations of interest to the designer:

- vertical deflections (typically at midspan)
- end rotations
- axial shortening

Of these, midspan deflection, or camber, is usually of greatest interest. Unexpected camber at the time of erection may require adjustment of bridge grades to prevent intrusion of the beam top flange into the deck. Additionally, estimates of the final midspan deflections under the action of permanent dead load and live load may be required to ensure serviceability of the bridge.

End rotations are of importance when continuity is introduced at the time of casting the deck. When these rotations are restrained or partially restrained by adjacent spans, secondary time-dependent stresses are introduced in the structure. These stresses must be considered in the design of connections and detailing of the end regions of beams.

Finally, axial shortening of precast, prestressed bridge members must be considered when designing bearings and expansion devices. This information is also helpful in assessing the impact of superstructure restraint against shortening in jointless bridge systems.

This section discusses the computations of camber and deflection including the changes that occur in these quantities with time. The methods that are available to estimate long-term cambers and other deflections of precast, prestressed members fall into three categories, listed in order of increasing complexity and accuracy:

- multiplier methods
- improved multiplier methods, based on estimates of loss of prestress
- detailed analytical methods

Camber in a prestressed beam occurs immediately upon the transfer of the prestressing force. The magnitude of the initial camber is dependent on the length, weight, and moment of inertia of the member; the modulus of elasticity of the concrete; and the arrangement and amount of prestressing. Values for several prestressing arrangements are given in **Table 8.7-1**. The modulus of elasticity of the concrete usually cannot be predicted with precision at the time of the design of the member. The standard prediction formulas are based on values assumed by the designer for concrete unit weight and strength at the time of prestress transfer. These assumed values do not include actual material properties, nor account for such important factors as type of aggregates and ratio of coarse-to-fine aggregate. For these reasons, initial camber predictions using assumed material properties must be regarded as estimates and the designer is cautioned against placing a high degree of confidence in calculated initial cambers (Tadros et al., 2011).

After transfer, camber generally increases with time. Creep of the concrete is primarily responsible for this camber growth. Simultaneously, the gradual loss of prestress due to creep, shrinkage, and strand relaxation has the effect of reducing the initial rate of growth of camber. The magnitude and rates of both creep and shrinkage, and therefore changes in camber, are affected by environmental conditions such as ambient relative humidity and temperature.

From the preceding discussion, it should be obvious that the task of predicting both initial camber and the growth of camber with time is difficult because the large number of random variables that affect this behavior are beyond the designer's control. Estimates of these effects should be recognized as being approximations only.

DESIGN THEORY AND PROCEDURE

8.7 Camber and Deflection

Table 8.7-1
Camber (deflection) and rotation coefficients for prestress force and loads*

Prestress Pattern	Equivalent Moment or Load	Equivalent Loading	Camber	End Rotation
(1)	$M = Pe$		$\frac{M\ell^2}{16EI} + \frac{M\ell^2}{16EI}$	$\frac{M\ell}{3EI} + \frac{M\ell}{6EI}$
(2)	$M = Pe$		$\frac{M\ell^2}{16EI} + \frac{M\ell^2}{16EI}$	$\frac{M\ell}{3EI} + \frac{M\ell}{6EI}$
(3)	$M = Pe$		$\frac{M\ell^2}{8EI} + \frac{M\ell^2}{8EI}$	$\frac{M\ell}{2EI} + \frac{M\ell}{2EI}$
(4)	$N = \frac{4Pe'}{\ell}$		$\frac{N\ell^3}{48EI} + \frac{N\ell^3}{48EI}$	$\frac{N\ell^2}{16EI} + \frac{N\ell^2}{16EI}$
(5)	$N = \frac{Pe'}{b\ell}$		$\frac{b(3 - 4b^2)N\ell^3}{24EI} + \frac{b(3 - 4b^2)N\ell^3}{24EI}$	$\frac{b(1 - b)N\ell^2}{2EI} + \frac{b(1 - b)N\ell^2}{2EI}$
(6)	$w = \frac{8Pe'}{\ell^2}$		$\frac{5w\ell^4}{384EI} + \frac{5w\ell^4}{384EI}$	$\frac{w\ell^3}{24EI} + \frac{w\ell^3}{24EI}$
(7)	$M = Pe'$		$\frac{M\ell^2}{8EI} (1 - 2b_1^2 - 2b_2^2) + \frac{M\ell^2}{8EI} (1 - 2b_1^2 - 2b_2^2)$	$\frac{M\ell}{2EI} [(1 - 2b_1)^2 - b_2^2] + \frac{M\ell}{2EI} [(1 - 2b_1)^2 - b_2^2]$

* The tabulated values apply to the effects of prestressing. By adjusting the directional rotation, they may also be used for the effects of loads. For patterns 4 to 7, superimpose on 1, 2 or 3 for other C.G. locations

DESIGN THEORY AND PROCEDURE

8.7.1 Multiplier Method/8.7.2 Example

8.7.1 Multiplier Method

Perhaps the most used method for predicting time-dependent camber of precast, prestressed members is the set of multipliers given in **Table 8.7.1-1** (Martin, 1977). This method is fairly straightforward. First, elastic deflections caused by the effects of prestressing, beam self-weight, and other dead loads are calculated using conventional elastic analysis techniques. These are multiplied by the appropriate factors selected from **Table 8.7.1-1** to determine the deflections that occur as a result of time-dependent behavior.

Table 8.7.1-1
Suggested Multipliers to be Used as a Guide in
Estimating Long-Term Cambers and Deflections for Typical Members

	Without Composite Topping	With Composite Topping
At erection:		
(1) Deflection (\downarrow) component – apply to the elastic deflection due to the member weight at transfer of prestress	1.85	1.85
(2) Camber (\uparrow) component – apply to the elastic camber due to prestress at the time of transfer of prestress	1.80	1.80
Final:		
(3) Deflection (\downarrow) component – apply to the elastic deflection due to the member weight at transfer of prestress	2.70	2.40
(4) Camber (\uparrow) component – apply to the elastic camber due to prestress at the time of transfer of prestress	2.45	2.20
(5) Deflection (\downarrow) component – apply to elastic deflection due to superimposed dead load only	3.00	3.00
(6) Deflection (\downarrow) component – apply to elastic deflection caused by the composite topping	---	2.30

This method gives reasonable estimates for cambers at the time of erection. The method does not, however, properly account for the significant effects of a large cast-in-place deck. The presence of a deck, once cured, drastically changes the stiffness of a typical bridge member. This has the effect of restraining the beam creep strains that are the result of prestressing, member self weight, and the dead load of the deck itself. Also, differential creep and shrinkage between the precast beam and the cast-in-place concrete can produce changes in member deformation. The multipliers for long-term deflection suggested by this method, therefore, should not be used for bridge beams with structurally composite cast-in-place decks.

In addition, it is not recommended that prestressing levels be increased in order to reduce or eliminate long-term downward deflection that might be predicted if the multipliers in **Table 8.7.1-1** are used.

8.7.2 Example

Calculate initial and erection cambers, as well as the immediate camber after construction of the deck, for the beam presented in Design Example 9.1a of Chapter 9. Use the multiplier method.

Use the following information from Design Example 9.1a to calculate initial and erection camber:

Initial camber due to prestress:

$$\Delta_p = 3.81 \text{ in. } \uparrow$$

Deflection at transfer due to self-weight:

$$\Delta_g = 1.53 \text{ in. } \downarrow$$

$$\text{So, net camber at transfer} = 3.81 - 1.53 = 2.28 \text{ in. } \uparrow$$

DESIGN THEORY AND PROCEDURE**8.7.2 Example/8.8.2 Design of Bridge Decks Using Precast Panels**

Deflection at erection due to self-weight:

$$\Delta_g = 1.48 \text{ in.} \downarrow$$

Applying the multipliers at erection from **Table 8.7.1-1** to the initial values computed above, erection camber = $(1.80)(3.81) - (1.85)(1.48) = 4.12 \text{ in.} \uparrow$

Deflection due to deck and haunch weights:

$$\Delta_s = 1.61 \text{ in.} \downarrow$$

Net camber immediately after application of deck weights:

$$\text{Camber} = 4.12 - 1.61 = 2.51 \text{ in.}$$

8.8 DECK SLAB DESIGN

8.8.1 Introduction

This section considers concrete slabs that act compositely with precast beams and where the slab span and main reinforcement are transverse to traffic. Cast-in-place (CIP) concrete is sometimes used as a topping on longitudinal, “full-deck” members such as adjacent box beams, double tees, and deck bulb tees. However, this type of deck slab generally does not require flexural design and is not covered in this section. The majority of deck slabs in new bridge construction use CIP concrete with or without precast stay-in-place (SIP) deck panels. The CIP topping provides flexibility to adjust for roadway profile and for differences in beam elevations. The use of precast SIP panels is gaining popularity due to their cost-effectiveness and improvement in jobsite construction time and safety.

This section focuses on the design of CIP decks using precast SIP panels according to both the “Traditional Design” method of the *LRFD Specifications*. In addition, a subsection summarizes the “Empirical Design” method of full-depth CIP slabs. This method is becoming more popular due to the relatively small amount of reinforcement it requires. However, at this time, the *LRFD Specifications* does not permit this method for design of precast SIP deck panel systems. Also in this section, two different precast concrete deck systems are introduced. The first system is an improved SIP panel that allows for better construction speed and structural performance than for the conventional SIP panel system. The second is a full-depth precast, prestressed concrete panel that is best suited for rapid replacement of decks on high-traffic bridges.

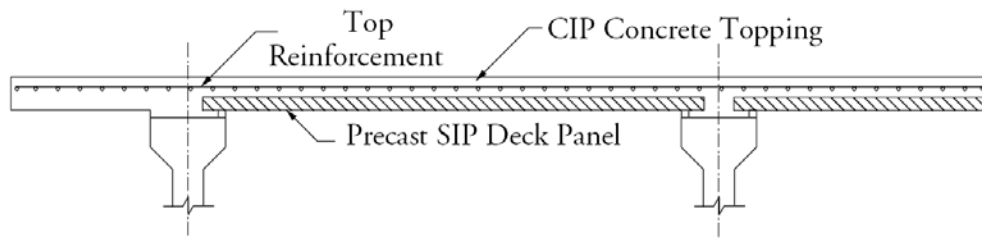
8.8.2 Design of Bridge Decks Using Precast Panels

A precast SIP deck panel system typically consists of thin precast, concentrically prestressed, concrete panels that span between supporting beams, and a CIP concrete topping which acts compositely with the SIP panels to form the fully composite deck. Precast concrete panels as thin as 2.5 in. have successfully been used. Because most panels are thin, strict quality control practices are recommended to avoid panel cracking or camber (PCI Committee Report, 1988). The prestress force should be released as gradually as possible. The strands should be maintained concentric with the concrete cross-section. Research by Kumar (1996) showed that prestressed SIP deck panels with a 0.05 to 0.075-in. amplitude, broom-finished surface do not require horizontal shear connectors to achieve full composite action with the CIP topping providing the nominal horizontal shear stress is less than 0.116 ksi.

Positive moment sections between the supporting beams are designed as prestressed concrete composite sections with the prestressing strands as the main reinforcement. Negative moment sections over beam lines are designed as conventionally reinforced sections with the reinforcing bars in the topping slab as the main reinforcement as shown in **Figure 8.8.2-1**.

DESIGN THEORY AND PROCEDURE**8.8.2 Design of Bridge Decks Using Precast Panels/8.8.2.2 Service Load Stresses and Flexural Strength**

Fig. 8.8.2-1
Cross-Section of CIP Deck with Precast SIP Panel

**8.8.2.1 Determining Prestress Force**

The first step in design is to estimate the required amount of prestress force. This estimate is governed by the allowable tensile stress in the precast SIP panel due to service loads at the maximum positive moment section. The weight of the precast SIP deck panel and the CIP topping act on the non-composite section, i.e. the precast SIP deck panel alone. The superimposed dead loads (wearing surface, barriers, etc.) and live loads act on the precast SIP panel-CIP topping composite section. After the required prestress force is determined, the unfactored load stresses and the ultimate flexural capacity at various construction stages are checked.

8.8.2.2 Service Load Stresses and Flexural Strength

Service load stresses should be checked in the panel and in the completed deck at a number of stages. The first stage is at the time of prestress transfer or release. The strands are normally concentric within the precast SIP deck panel. Therefore, prestress introduces uniformly distributed compressive stresses. However, accidental misplacement of the strands may be conservatively assumed to produce 0.25 in. prestress eccentricity.

The second loading stage occurs at the time of topping placement. Loads at this stage act only on the SIP panel. Service load stresses and ultimate capacity of the precast SIP panel should be checked due to the weight of the precast panel and the CIP topping in addition to a construction load, estimated as 50 psf unless a more accurate figure is available. The construction load represents people, material, and equipment used to place, finish, and cure the topping but it does not include concentrated loads representing finishing machine reactions. Special brackets directly supported on beam seats are used to resist finishing machine loads. Other loads at this stage act only on the SIP panel.

The third loading stage occurs after the CIP topping cures and the superimposed loads are introduced. At this stage, the stresses are calculated using a transformed section analysis similar to that done in composite I-beam analysis. The ultimate strength of the composite section at the maximum positive moment section, is checked against factored dead and live loads. One of the most important issues in determining the flexural strength of the positive moment section is the strand development length. Since the strands are terminated at panel ends over beam lines, the maximum positive moment sections may be closer to the end of the panel than the development length of the strands. Thus, only partial strand development can be expected. In this situation, the average stress in prestressing steel at the time for which the nominal resistance of the member is required, f_{ps} , should be limited to:

$$f_{ps} = \left(\frac{L_x}{d_p \kappa} + \frac{2}{3} f_{pe} \right) \quad [\text{LRFD Art 5.11.4.2}]$$

where

f_{ps} = average stress in prestressing steel at the time for which the nominal resistance of the member is required (ksi)

L_x = distance from end to center of the panel, in.

d_p = nominal diameter of the strand, in.

f_{se} = effective stress in the prestressing steel after losses (ksi)

κ = 1.0 for pretensioned panels, piling, and other pretensioned members with a depth of less than or equal to 24.0 in.

DESIGN THEORY AND PROCEDURE**8.8.2.2 Service Load Stresses and Flexural Strength/8.8.2.3.1 Minimum Thickness**

Non-prestressing reinforcement provided in the CIP topping is determined on the basis of flexural strength. The critical sections over interior beams are designed for superimposed dead and live loads. In addition, the region near the exterior beams should be designed for crash loading combined with dead and live loads. Design Example 9.10 in Chapter 9 gives complete details of the design of overhangs for this type of loading. In negative moment zones, proper distribution of the flexural reinforcement is required to control top fiber cracking.

8.8.2.3 LRFD Specifications

An entire section in the *LRFD Specifications*, Section 9, is devoted to deck systems. Three levels of analysis are permitted in the *LRFD Specifications*:

1. Refined analysis
2. Approximate analysis, generally known as the Strip Method
3. Empirical Method

As noted earlier, the specifications do not permit the empirical method to be used in the design of SIP panel deck systems.

8.8.2.3.1 LRFD Specifications Refined Analysis

LRFD Articles 4.4 and 4.6.3.2 allow the use of refined methods of analysis. These methods should satisfy the requirements of equilibrium and compatibility and utilize stress-strain relationships for the proposed materials. Refined analysis methods include, but are not limited to:

1. grillage analogy method,
2. finite strip method, and
3. finite element method.

However, some conditions should be considered that accurately model the behavior of the deck slabs as observed in actual bridges. These conditions are as follows:

1. Flexural and torsional deformation of the deck in skewed bridges.
2. In-plane shear deformation, which affects the effective width of composite bridge decks.
3. Locations of flexural discontinuity through which shear is transmitted, should be modeled as hinges.
4. Wheel loads should be modeled as patch loads over the tire contact area, given by the specifications, extended by half of the deck depth on all four sides.

A structurally continuous railing, barrier, or median, acting compositely with the supporting components, can be considered to be structurally active only at service and fatigue limit states.

8.8.2.3.2 LRFD Specifications Strip Method

In this method, the deck slab is divided into strips perpendicular to the supporting beams. To calculate the bending moments and shear forces, the strips are treated as a continuous member and the supporting beams are assumed to be infinitely rigid. The width of the strip is determined so that the effects of flexure in the secondary direction and of torsion are accounted for to obtain flexural force effects approximating those that would be provided by refined methods of analysis. However, the strip method model was developed based on non-skewed bridges, thus, more accurate analysis may be warranted for end zones of skewed bridges.

8.8.2.3.2.1 Minimum Thickness

LRFD Article 9.7.1.1 states that the depth of the concrete deck, excluding any provision for grinding, grooving, and sacrificial surface, should not be less than 7.0 in. LRFD Article 2.5.2.4 states that concrete decks without an initial overlay should have an additional thickness of ½ in. to allow for correction of the deck profile by grinding and to compensate for thickness loss due to abrasion. For concrete deck overhangs which support a deck-mounted post system or concrete parapets or barriers, a minimum depth of 8.0 in. is required unless a lesser thickness can be proven satisfactory during the crash testing procedure. (LRFD Art. 13.7.3.1.2). LRFD Article 9.7.4.3.1 states that

DESIGN THEORY AND PROCEDURE**8.8.2.3.2.1 Minimum Thickness/8.8.2.3.2.5 Design Criteria**

the thickness of the precast SIP deck panel should neither exceed 55% of the total slab depth nor be less than 3.5-in. thick. However, as noted earlier, SIP panels 3.0 in. thick or even as thin as 2.5 in. have been used in recent years with satisfactory performance.

8.8.2.3.2.2 Minimum Concrete Cover

LRFD Article 5.12.3 provides minimum concrete cover requirements. The minimum cover values are stated for concrete mixes with water-cement ratios from 0.40 to 0.50. For concrete mixes with different water-cement ratios, a modification factor is provided. When epoxy-coated bars are used, the *LRFD Specifications* allow the minimum cover requirement for uncoated bars in interior exposure to be used. However, special provisions for development length and lap splices for coated reinforcement must be satisfied as given in LRFD Article 5.11.

8.8.2.3.2.3 Live Load

The standard live load used in the *LRFD Specifications* is the HL-93, which consists of the combination of a design truck or tandem, and a design lane load (LRFD Art. 3.6.1.2). However, LRFD Article 3.6.1.3.3 states that for deck slabs where the strips are in the transverse direction of the bridge and their span does not exceed 15 ft, only the wheels of the 32.0-kip axle of the design truck, spaced at 6.0 ft, need be considered. If the transverse strip span exceeds 15 ft, both the 32-kip axle and the design lane load should be used in conjunction with the strip widths for slab-type bridges. One or more design lanes may be assumed to be loaded simultaneously. Within each design lane, the truck axle can be positioned so that the center of a wheel is not closer than 2.0 ft to the edge of the design lane or closer than 1.0 ft to the face of the curb or rail for the deck overhang. The location of the design lanes can be shifted laterally relative to the longitudinal axis of the deck, to produce the maximum force effects. LRFD Article 4.6.2.1.3 gives the width of the strip in inches as:

Width = $26.0 + 6.6S$ (for positive moment calculations)

Width = $48.0 + 3.0S$ (for negative moment calculations)

where S = span of the slab between beam centerlines, ft

For overhangs, the negative moment strip width is:

Width = $45.0 + 10.0X$

where X = distance from the wheel load to point of support, ft

These equations are based on three-dimensional finite element analyses of a large number of one- and two-span bridges covering the practical range of number of beams, beam stiffness, beam spacing, span length, and slab thickness. Because a three-dimensional analysis was used to develop the strip width equations, the effects of flexure in the secondary direction and torsion are already accounted for. The maximum positive and negative bending moments calculated using the strip method are considered to apply to all regions along the bridge length. Dynamic allowance of 33% and a multiple presence factor as specified in LRFD Articles 3.6.2 and 3.6.1.1.2 should be included in design. Table A4-1 in Appendix A4 of the *LRFD Specifications* gives the maximum design bending moment values for different beam arrangements, where the multiple presence factors and the dynamic load allowance are included in the tabulated values. Appendix A4 is applicable only to bridge decks supported on at least three parallel beams and having a width measured between the centerlines of the exterior beams not less than 14 ft.

8.8.2.3.2.4 Location of Critical Sections

For precast I-beam bridges, the location of the design section for negative moments and shear forces may be taken as one-third of the flange width, but not more than 15 in. from the support centerline (LRFD Art. 4.6.2.1.6).

8.8.2.3.2.5 Design Criteria

LRFD Article 9.7.4.1 states that prestressed concrete stay-in-place panels should remain in the elastic range under construction loads. Construction loads include the weight of the SIP panel, weight of the CIP topping, and an additional 0.050 ksf. Flexural stresses due to unfactored construction loads should not exceed 75% of the steel yield strength or 65% of the 28-day compressive strength for concrete in compression, or the modulus of rupture

DESIGN THEORY AND PROCEDURE**8.8.2.3.2.5 Design Criteria/8.8.2.3.2.8 Crack Control**

for concrete in tension. Also, LRFD Article 9.7.4.1 states that elastic deflection caused by the weights of the panel, the plastic concrete, and reinforcement should not exceed:

- span length/180 with an upper limit of 0.50 in. for span lengths of 10 ft or less or
- span length/240 with an upper limit of 0.75 in. for span lengths greater than 10 ft.

At service loads, the stresses in the composite section have to be checked under Service I Limit State for prestressed concrete in compression. For Service III Limit State, which is used to check tensile stresses in the precast SIP panel, the full live load moment should be used, i.e. the 0.8 factor associated with live load should be replaced by 1.0. This is because the 0.8 factor was developed for application only to longitudinal prestressed concrete beams.

Finally, Strength I Limit State is used to check the nominal flexural resistance of the composite section. Check stress in prestressing steel according to the available development length, ℓ_d , as follows:

$$\ell_d = K \left(f_{ps} - \frac{2}{3} f_{pe} \right) d_b \quad \text{[LRFD Eq. 5.11.4.2-1]}$$

where

d_b = nominal strand diameter

f_{pe} = effective stress in prestressing steel after losses

ℓ_d = available development length at midspan of the SIP panel

K = 1.6 for precast, prestressed slabs

8.8.2.3.2.6 Reinforcement Requirements

Minimum reinforcement should be provided so that the factored flexural resistance is not less than 1.2 times the cracking moment (LRFD Art. 5.7.3.3.2). Alternatively, the minimum reinforcement requirement may be satisfied by providing at least one-third more reinforcement than required by analysis.

The *LRFD Specifications* do not give guidance for the required amount of distribution reinforcement for the concrete SIP panel system that provides for the lateral distribution of concentrated live loads. However, LRFD Article 9.7.3.2 specifies the minimum amount of reinforcement in the longitudinal direction for slabs that have four layers of reinforcement, as $220/\sqrt{S} \leq 67\%$ of the primary reinforcement, where S = span between the inside faces of the beam webs, ft.

Applying this provision yields a higher amount of longitudinal reinforcement than that required by the Empirical Design method.

Editor's note: at the time of printing of this manual, which is current through the AASHTO 2011 Interims, it appears the AASHTO 2012 code changes will modify the above LRFD Art. 5.7.3.3.2.

8.8.2.3.2.7 Shear Design

Two-way shear should be checked assuming that the contact area of one or two tires is a single rectangular, 20 in. wide by 10 in. long, as specified in LRFD Article 3.6.1.2.5. The two-way shear capacity is given in LRFD Article 5.13.3.6.3. One-way shear should be checked as specified in LRFD Article 5.13.3.6.2.

8.8.2.3.2.8 Crack Control

For crack control in the negative moment areas, provisions of LRFD Article 5.7.3.4 should be applied. Because positive moment regions for precast SIP deck panel systems are prestressed, they are designed to be uncracked under service load conditions.

In order to control possible cracking due to shrinkage and temperature changes, a minimum amount of reinforcement, in each direction, should be provided:

$$A_s \geq 1.30bh/(2b+h)f_y \quad \text{[LRFD Eq. 5.10.8.2-1]}$$

and

$$0.11 \text{ in}^2 \leq A_s \leq 0.60 \text{ in}^2$$

DESIGN THEORY AND PROCEDURE

8.8.2.3.28 Crack Control/8.8.3.1.1 Description of NUDECK

where

b = least width of component section, in.

h = least thickness of component section, in.

This reinforcement should be equally distributed on both faces and should not be spaced farther apart than three times the slab thickness or 18.0 in. It is reasonable to waive this requirement in precast, prestressed concrete panels in the direction that is prestressed.

8.8.3 Other Precast Bridge Deck Systems

Rapid replacement of bridge decks is becoming increasingly important in high traffic areas due to public intolerance to extended bridge closures. This section covers two bridge deck systems developed at the University of Nebraska for rapid replacement of bridge decks (Tadros, 1998). The first system is a continuous precast concrete stay-in-place panel system, called NUDECK (Badie, 1998). It is intended for applications similar to the conventional SIP panel previously discussed. The second system is a full-depth precast concrete panel system intended for very rapid construction (Takashi, 1998). The following sections briefly introduce these two new systems.

8.8.3.1 Continuous Precast Concrete SIP Panel System, NUDECK

Although conventional SIP precast panels have proven cost-effective and have been widely used in several states, they do have drawbacks. These include the following:

1. The need for forming overhangs with wood forming
2. The possible appearance of reflective cracking over joints between SIP panels
3. The lack of development of the pretensioning strands in the SIP panel caused by strand discontinuity at beam lines and relatively small beam spacing.

The continuous stay-in-place (CSIP) system – NUDECK – has the following advantages:

1. The CSIP panel covers the entire width of the bridge eliminating the necessity of forming the overhang.
2. The CSIP panel is continuous longitudinally and transversely which results in minimized reflective cracks, full development of the pretensioning reinforcement, and better live load distribution.

Cost studies conducted by contractors and consulting engineers (Tadros, 1998), estimated that the NUDECK system would be cost-competitive with CIP systems. The slight increase in panel cost would be offset by the reduction in field costs due to installation of fewer pieces and elimination of overhang forming. However, the novelty of the system, panel forming challenges and panel weight are potential disadvantages of this system.

8.8.3.1.1 Description of NUDECK

Figure 8.8.3.1.1-1 shows a cross-section of a bridge and a plan view of the precast panel. The system consists of a 4.5-in.-thick precast panel and a 3.5- to 4.5-in.-thick CIP reinforced topping. The length of the panel in the direction of traffic can vary from 8 to 12 ft depending on the transportation and lifting equipment available in the field. At each beam position, there is a full-length gap to accommodate shear connectors. The width of the gap, G , depends on the shear connector detail used in the precast beam. As an example, for a beam spacing of 12 ft and overhang of 4 ft subjected to HS25 truck loading, an 8-ft-wide panel would require twelve ½-in.-diameter strands and a 28-day concrete compressive strength of 8.0 ksi. The strands are located in two layers and uniformly spaced at 16 in. A minimum clear concrete cover of 1 in. is used for both the top and bottom layers of strands.

In order to maintain the gap over the beam, and to transmit the pretensioning force from one section to another across the gap, 24 short pieces of No. 7 reinforcing bars are used in two layers. These bars transmit the prestress compression force across the gap. To maintain continuity in the longitudinal direction between the adjacent precast panels, shear keys, and reinforced pockets are provided as shown in **Figures 8.8.3.1.1-2** and **8.8.3.1.1-3**. The panel is reinforced longitudinally with No. 4 bars spaced at 2 ft at the location of the pockets. To provide for

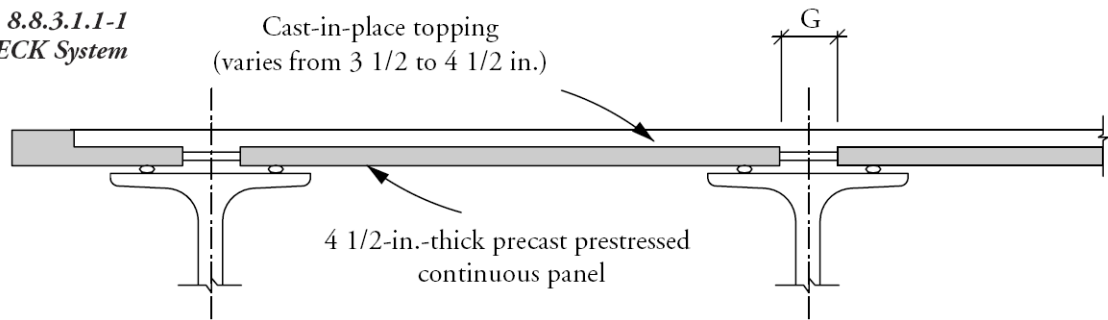
DESIGN THEORY AND PROCEDURE

8.8.3.1.1 Description of NUDECK

full tension development of the No. 4 bars, they are spliced using an innovative confinement technique as shown in **Figure 8.8.3.1.1-4**. A pocket, only 5-in. deep, is needed to fully develop the No. 4 bar. The panels are erected using shims and leveling bolts. The longitudinal gaps are then filled with fine aggregate concrete. When the concrete attains a strength of 4.0 ksi, the finishing machine can then be installed and the CIP topping cast in one continuous operation. Full-scale laboratory testing (Yehia, 1999) has shown this system has almost two-times the load capacity of an equivalent conventional SIP panel system.

Figure 8.8.3.1.1-1
The NUDECK System

Figure 8.8.3.1.1-1
The NUDECK System



(a) Cross Section of the NUDECK System

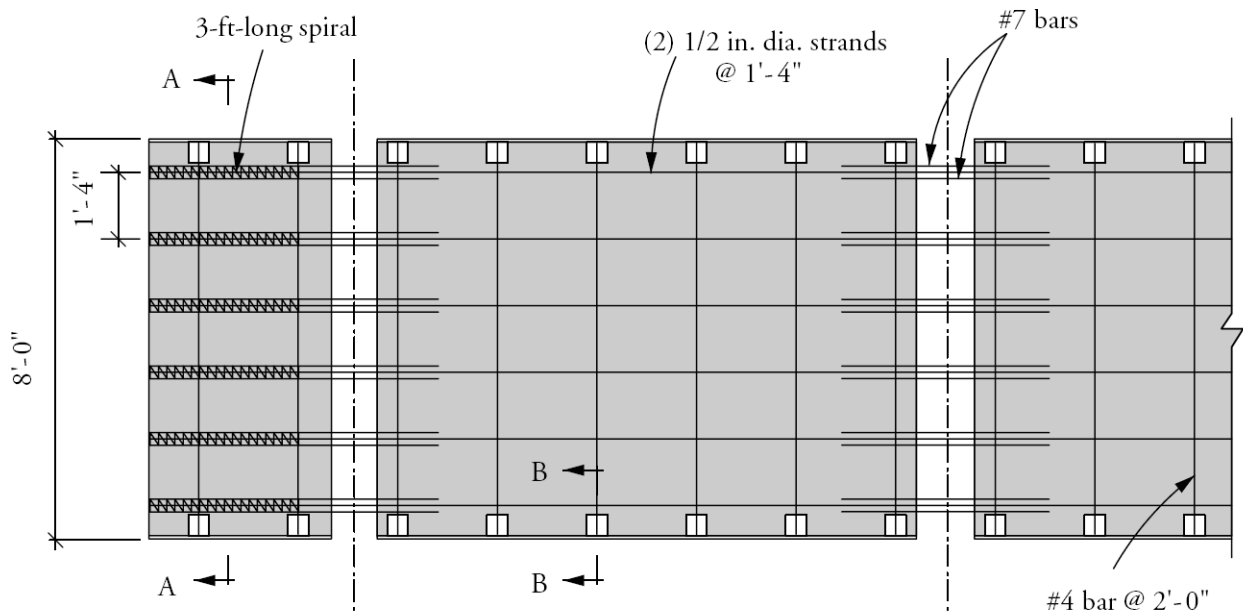


Figure 8.8.3.1.1-2
Cross-Section of the NUDECK Panel

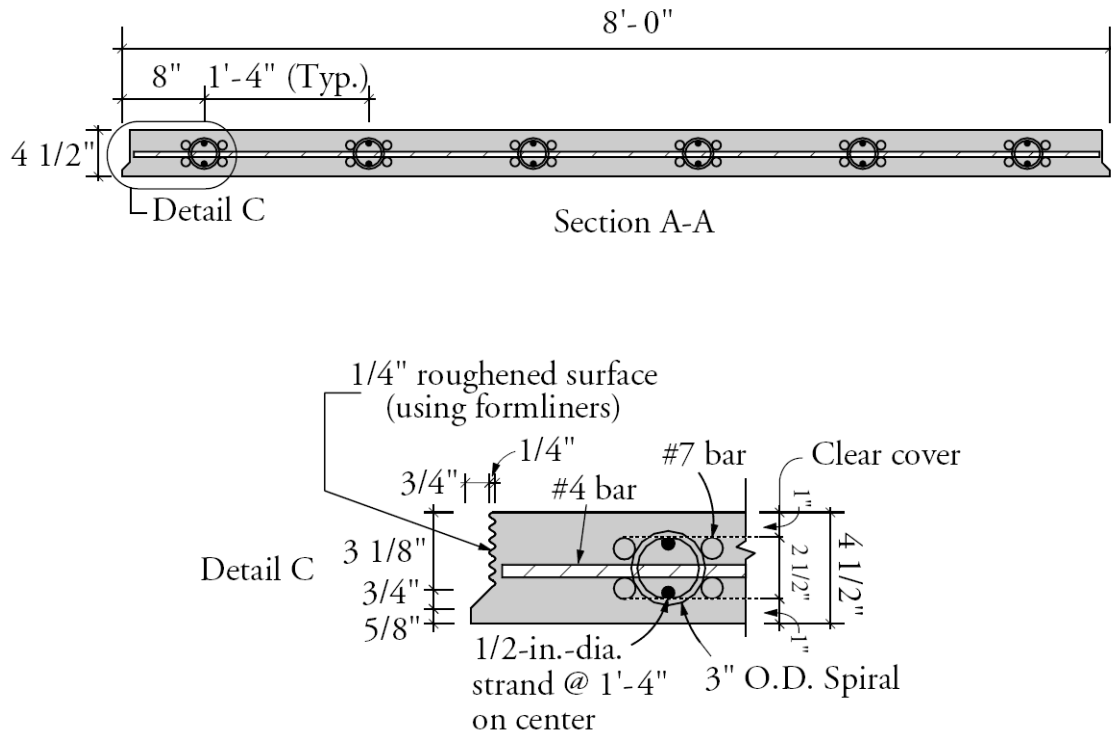
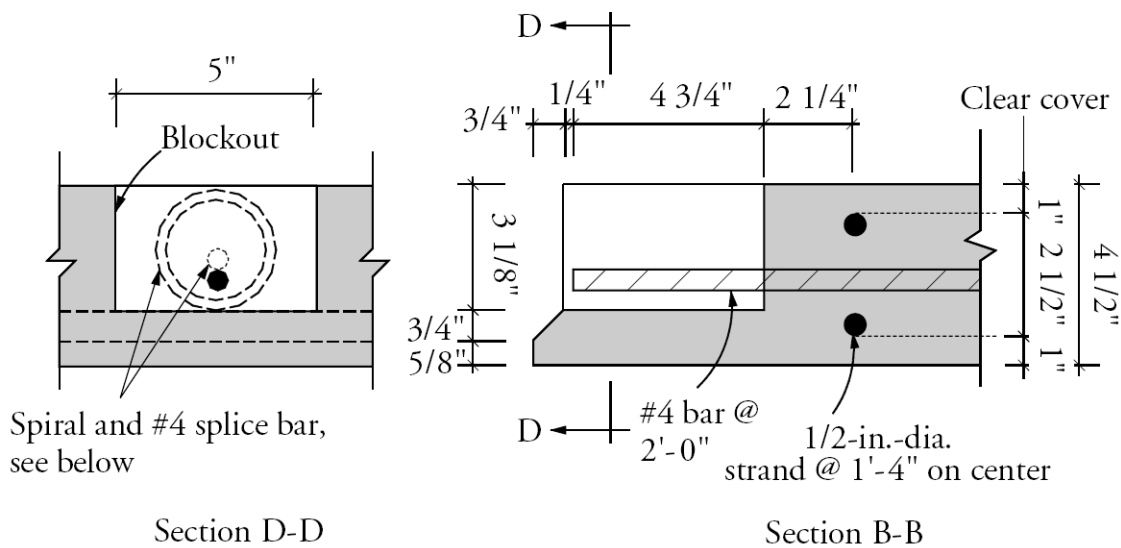


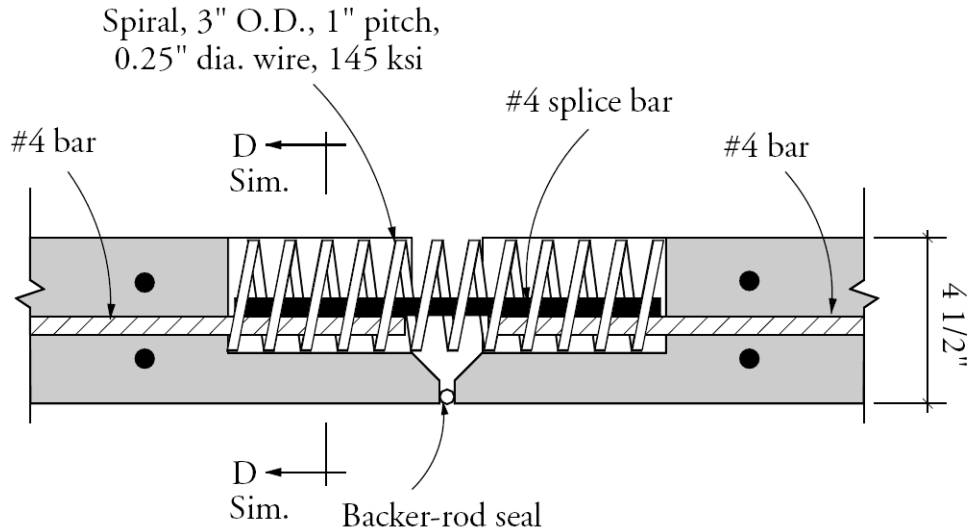
Figure 8.8.3.1.1-3
Details of Reinforced Pockets



DESIGN THEORY AND PROCEDURE

8.8.3.1.1 Description of NUDECK/8.8.3.2 Full-Depth Precast Concrete Panels

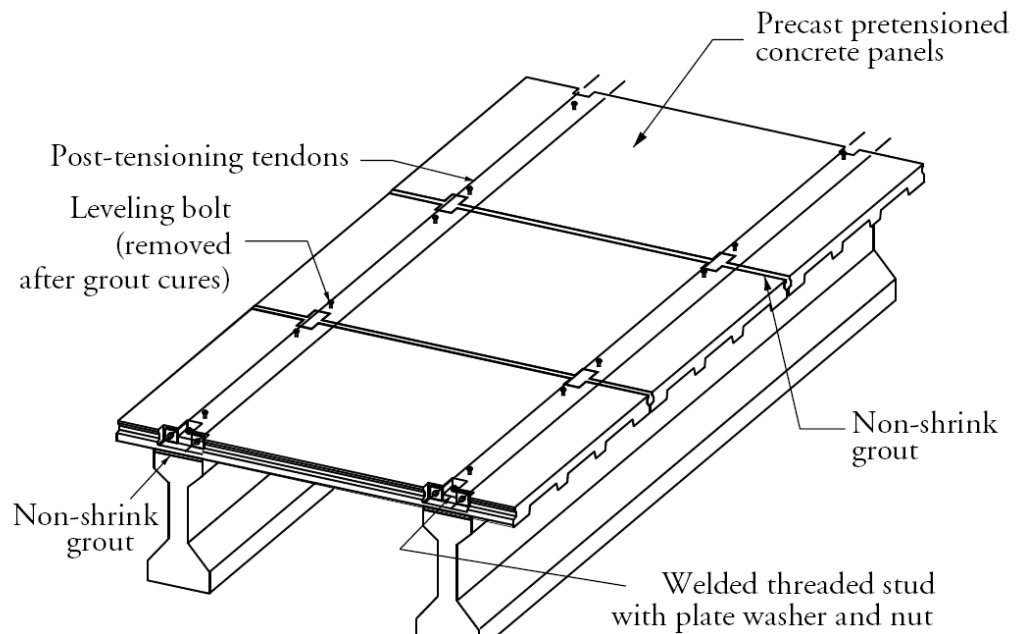
Figure 8.8.3.1.1-4
Panel-to-Panel Connection (At 2'- 0" Centers)



8.8.3.2 Full-Depth Precast Concrete Panels

An overview of this system is shown in **Figure 8.8.3.2-1**. It consists mainly of precast, transversely pretensioned concrete panels, welded threaded studs, grout-filled shear keys, leveling bolts, and longitudinal post-tensioning tendons.

Figure 8.8.3.2-1
Overview of Full-Depth Panel System



The overall geometry is determined by the arrangement of pretensioning strands for positive moments and to provide an adequate compressive zone for negative moments. One layer of welded wire reinforcement is provided in the upper portion of the slab. Pretensioning strands are arranged in two layers and eccentricity is minimized because the panel is subjected to both negative and positive moments. Two important functions of the

DESIGN THEORY AND PROCEDURE**8.8.3.2 Full-Depth Precast Concrete Panels/8.8.4 Empirical Design Method**

transverse joints between panels are to transfer live loads and to prevent water leakage. For these two requirements, a shear key with a rapid-set, non-shrink grout is used. Longitudinal post-tensioning is applied after the transverse shear keys are grouted but before the deck is made composite with the underlying beams.

The full-depth precast pretensioned system has the following benefits:

- It has an equivalent slab thickness of 5.9 in., which makes it significantly lighter than other systems.
- The system is prestressed both directions, resulting in superior performance compared to conventionally reinforced decks.
- The system does not need a CIP topping, which reduces the time of construction.
- The panel includes ½-in. extra cover to be used for grinding the deck to a smooth surface.
- The panels can be rapidly produced and constructed, or removed.
- The grouted, post-tensioned transverse joints between panels prevent cracking and possible leakage throughout the service life of the deck.
- Deflection under service load is small in comparison to non-prestressed systems.

Full-scale fatigue and ultimate strength testing has demonstrated superior performance of this system. No cracks or joint leakage were observed after two million cycles of loading. The strength of the system was governed by punching shear of the slab at about 5 times the maximum wheel load of an HS25 truck.

The disadvantages of this system include the following:

- The deck surface is required to be ground in order to attain a smooth riding surface.
- Longitudinal post-tensioning significantly increases the number of construction steps required.
- Panel weight requires availability of cranes.

8.8.4 Empirical Design Method

The empirical-design procedure of the *LRFD Specifications* [LRFD Art. 9.7.2] is attractive in that it provides less reinforcement than calculated by analytical methods, including finite element and strip analysis. Less steel reinforcement should result in less deck deterioration due to reinforcement corrosion. The method is based on full-scale testing. The empirical design method may be used only if certain specified conditions are met. If the specified amount of reinforcement is provided, the deck is considered to satisfy all design requirements without need for design calculations. The conditions are as follows:

- The supporting components are steel and/or concrete beams.
- The deck is fully cast-in-place and water-cured.
- The deck is of uniform depth, except for haunches at beam flanges and other local thickening.
- The ratio of effective length, between inside faces of beam webs, to the design depth does not exceed 18.0 and is not less than 6.0.
- Core depth of the slab, between the extreme faces of top and bottom reinforcement, is not less than 4.0 in.
- The effective length, between the inside faces of the beam webs, does not exceed 13.5 ft.
- The minimum depth of the slab is not less than 7.0 in. excluding a sacrificial wearing surface where applicable.
- There is an overhang beyond the centerline of the outside beam of at least 5 times the depth of the slab. This condition is satisfied if the overhang is at least 3 times the depth of the slab, and a structurally continuous concrete barrier is made composite with the overhang.
- The specified 28-day strength of the deck concrete is not less than 4.0 ksi.
- The deck is made composite with the supporting structural components.
- The reinforcement required consists of four layers.

DESIGN THEORY AND PROCEDURE**8.8.4 Empirical Design Method/8.9.1.2 Canadian Bridge Design Code Procedure**

- Minimum amount of reinforcement is 0.27 in.²/ft for each bottom layer and 0.18 in.²/ft for each top layer
- Maximum spacing of bars is 18 in.

The provisions of the empirical design method are not applied to overhangs. The overhang should be designed for all of the following cases:

- Wheel loads for decks with discontinuous railings and barriers using the equivalent strip method
- Equivalent line loads for decks with continuous barriers (LRFD Art. 3.6.1.3.4)
- Collision loads using a failure mechanism

Note that negative overhang moments require reinforcement that must be extended into the adjacent span.

8.9 TRANSVERSE DESIGN OF ADJACENT BOX BEAM BRIDGES

8.9.1 Background

Adjacent box beam bridges are constructed by placing precast, prestressed concrete box beams next to each other so that a deck slab is not required to complete the structure. The small longitudinal joint between beams – the “shear key” or “keyway” – is normally filled with grout. Often, a composite concrete topping or a non-structural asphalt concrete overlay is used to provide the riding surface. Typically, longitudinal keyways are dimensioned for standard products shown in Appendix B. Transverse connections are made between beams to mitigate differential deflection and to improve the distribution of live loads.

The design of the transverse connections between adjacent box beams has been identified as an important issue by bridge owners and designers. Without an adequate transverse connection, beams will not deflect equally under live loads. Differential movement between beams may lead to longitudinal cracking of the grouted keyways and reflective cracking in the overlay, if one is present. Surveys of adjacent box beam bridges have revealed that cracks of these types are a recurring problem in some areas (Russell, 2009). In rural locations where deicing chemicals are not used, such cracks may be tolerated. However, in most locations, these cracks should be prevented because water and deicing chemicals penetrate the cracks and cause concrete staining and eventually structural deterioration of the box beams from corrosion of reinforcement and subsequent spalling of the concrete cover.

In addition, a transverse connection between box beams is necessary to provide more effective load transfer between beams. Without adequate transverse connection, live load cannot be distributed across the bridge. Each beam in that case would have to be designed to resist the full effect of a set of wheel loads.

8.9.1.1 Current Practice

When a transverse connection is provided between adjacent box beams, it is typically made using threaded rods, post-tensioning bars or strands, or welded connections. The bars and strands may be either bonded or unbonded. A 5- or 6-in.-thick reinforced concrete composite slab may also be used to provide a transverse connection between adjacent members. When a structural concrete topping is not used, a non-structural overlay, such as a 2.0-in.-thick asphalt concrete wearing surface, is often applied as a final riding surface. However, for some secondary roads, a topping is not used because the surface of the precast beam is more than adequate to use for a riding surface.

The number and location of transverse ties, the erection details, and procedures for installing transverse connections vary from state to state. Several different types of connections have been found to provide good performance, although in other cases, similar details and procedures may perform very differently. The selection of a system for connecting adjacent box beam bridges depends on initial cost, long-term maintenance costs, experience of the owner, capabilities of local contractors, and availability of materials.

8.9.1.2 Canadian Bridge Design Code Procedure

The Canadian Bridge Design Code provides a procedure for the design of adjacent box beam bridges. The Canadian Code assumes that the load is transferred from one beam to another primarily through transverse

DESIGN THEORY AND PROCEDURE

8.9.1.2 Canadian Bridge Design Code Procedure/8.9.2.1 Tie System

shear; transverse flexural rigidity is neglected, (Bakht, 1983). Charts are provided to determine the transverse shear force to be resisted. A reinforced concrete structural slab with a minimum thickness of 5.9 in. is required to be placed on the bridge to provide the shear transfer between beams. Therefore, the grouted keyway is not relied upon to transfer shear between boxes.

8.9.2 Empirical Design

Several users of adjacent beams have developed empirical design guidelines for transverse connection of adjacent slabs and box beams, with varying degree of success. One procedure, developed by the State of Oregon and refined over many years of practice, has demonstrated satisfactory field performance in controlling longitudinal cracking and moisture leakage between beams. This method is described in detail in the following sections.

8.9.2.1 Tie System

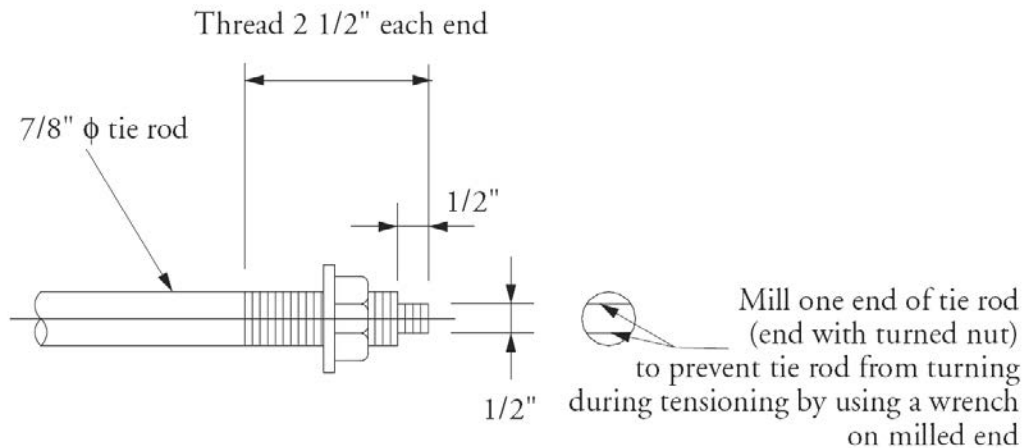
Transverse ties should be capable of providing a total transverse force at least equal to the weight of each beam. The ties are provided in the form of 1 or 2 rods at mid-depth of the member at locations along the span according to **Table 8.9.2.1-1**. This spacing and number of tie rods has been found to produce satisfactory field performance.

*Table 8.9.2.1-1
Number and Spacing of Tie Rods*

Span, ft	Number of rods and spacing
≤ 20	One at midspan
> 20, but ≤ 40	One at third points
> 40, but ≤ 70	Two at third points
> 70, but ≤ 100	Two rods at ≤ 24 ft spacing, with first set at 8 ft from end

A 7/8 -in.-diameter, 8-ft 2-in.-long smooth rod with 2½-in. threaded length is used for each location. The rod material is ASTM A449 high-strength steel. Each rod is tensioned to 39.25 kips, using a torque wrench and a direct tension indicating (DTI) washer, conforming to ASTM F959. A heavy hexagonal nut, conforming to ASTM A194 and a 5x5x1-in. ASTM A36 bearing plate complete the tensioning and anchorage assembly, as shown in **Figure 8.9.2.1-1**. On the non-tensioning end of the rod, the DTI washer is replaced with a hardened steel ASTM F436 flat circular washer. All hardware is hot-dip galvanized after fabrication.

*Figure 8.9.2.1-1
Hardware Used for Tie Rods*



8.9.2.2 Production

Each member is produced with shear keys as shown in **Figure 8.9.2.2-1**. The shear key shown has a well-defined and bulbous shape with an adequate opening at the top to provide access for installation of grout. The face of the key is sandblasted at the precast plant to remove loose materials and to provide a good bonding surface. Other states may use different shape keyways.

Figure 8.9.2.2-1
Shear Key Detail

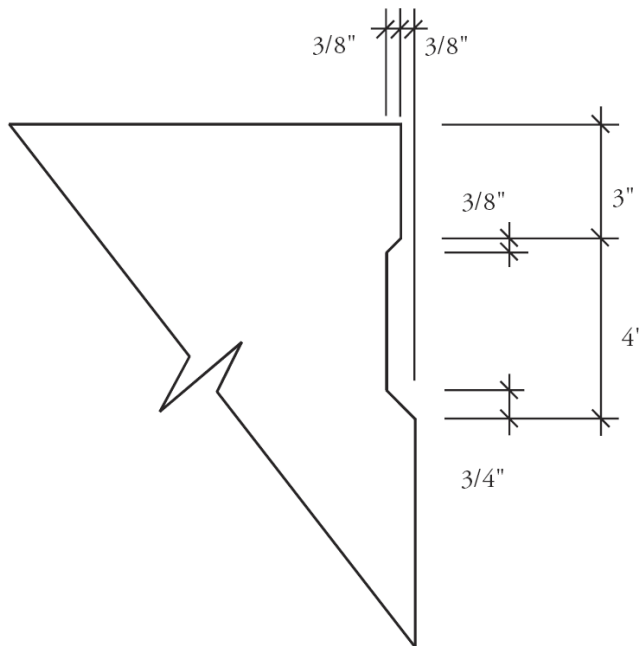
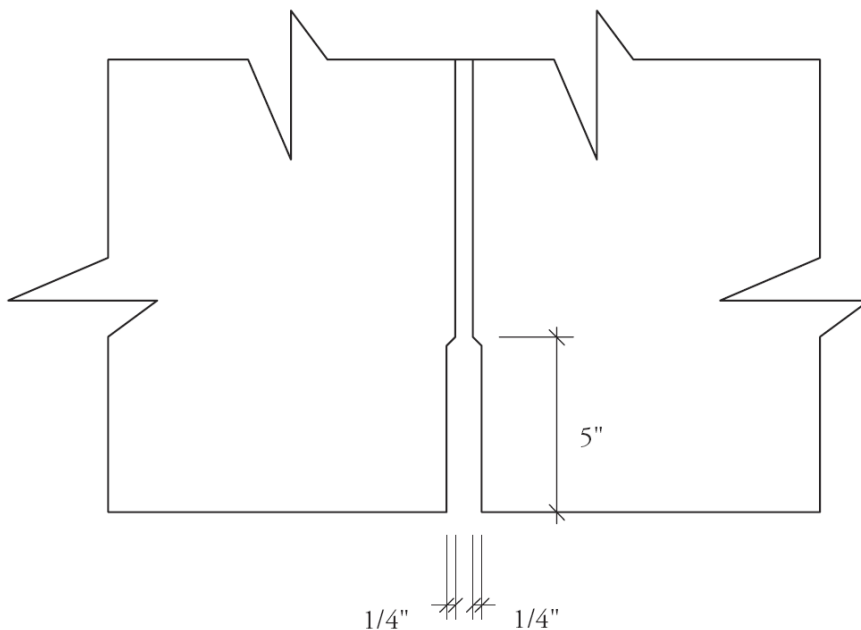


Figure 8.9.2.2-2
Joint Detail



DESIGN THEORY AND PROCEDURE

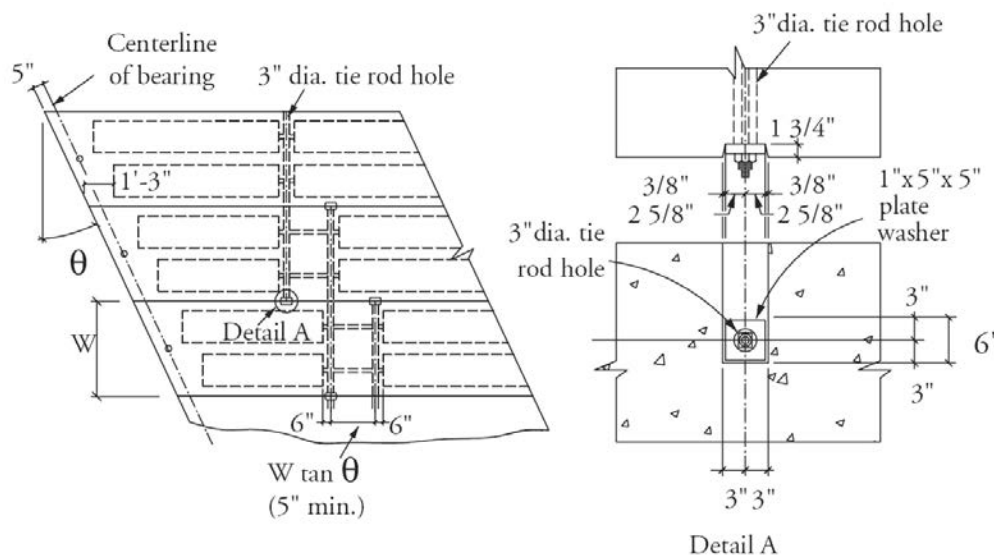
8.9.2.2 Production/8.9.2.3 Installation

It is advisable to provide a recess along the bottom edge of the beam, as shown in **Figure 8.9.2.2-2**, to prevent spalling due to a stress concentration that could result from possible formed surface bulges or protrusions. All beams must have diaphragms at their ends and at tie rod locations. Diaphragm dimensions and locations are determined with consideration of the skew angle. A 3-in. diameter hole is formed at each tie rod location.

8.9.2.3 Installation

Erection of precast units begins at either exterior beam or at the center of the bridge depending upon the width of the bridge and the desired crane placement. After placing the first two adjacent units the tie rods are installed and the nuts are tightened until the ridges on the load indicator washers collapse (see **Figure 8.9.2.3-1**). Prior to installing the nuts on the tie rod, the threads are lubricated with a suitable wax or tension control fluid to allow the required tension on the rods to be developed. The sequence continues by placing a beam and installing the required number of tie rods each time a beam is set. Handholes are provided in the concrete beams at each end of the bolts to provide access to the non-turned nut located on the far side of the previous unit set. After all the units in a span are set, the grout may be installed in the shear keys. The grout should be non-shrink, non-ferrous, non-epoxy grout with a minimum design strength of 5.0 ksi. The surface of the keys should be kept damp for twenty-four hours before and after installing the grout. If the space between beams is wide enough to allow the grout to run through, a strip of foam rod stock is installed at the bottom of the shear key to seal it. In order to provide a positive seal, the grout is tooled-down from the top of the deck to provide a recess for the installation of caulking or a poured joint filler. This area must again be cleaned to remove any loose grout before installing the sealant, as shown in **Figure 8.9.2.3-2**.

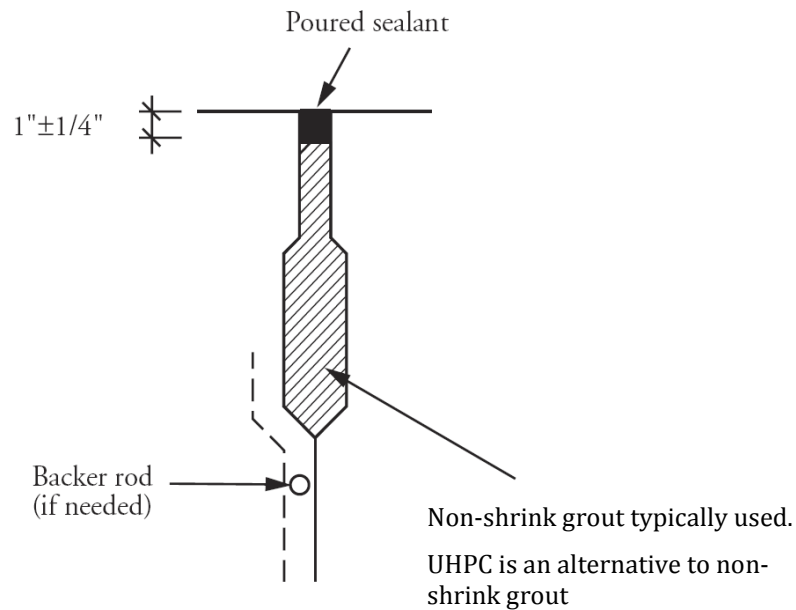
Figure 8.9.2.3-1
Tie Rod Recess Detail



In some jurisdictions, transverse rods are not used because they become problematic particularly for skewed bridges as shown above. This issue is compounded further in camber variations in longer spans. A half-depth CIP slab with one layer of reinforcement eliminates the need for transverse rods, improves longevity, and facilitates continuity at intermediate supports.

DESIGN THEORY AND PROCEDURE**8.9.2.3 Installation/8.9.3 Suggested Design and Construction Procedure**

Figure 8.9.2.3-2
Keyway Grout Detail



Different installation procedures are used by other states (Russell, 2009). As an alternative to connecting one beam at a time, all beams can be erected first and then connected together at one time. The transverse post-tensioning can then be applied to all beams at the same time. Some states prefer to grout the longitudinal joint before post-tensioning. Some states prefer to use full-depth grouting rather than partial-depth grouting. The selected procedures seem to depend on local practices.

8.9.3 Suggested Design and Construction Procedure

A design procedure has been developed (El-Remaily, 1996) which assumes that post-tensioned transverse diaphragms serve as the primary mechanism for the distribution of wheel loads across the bridge. Five diaphragms are provided in each span: one at each end and one at each quarter-point. A typical detail at a diaphragm is shown in **Figure 8.9.3-1**. The amount of post-tensioning required at each diaphragm depends on the bridge geometry and loading. Charts, **Figures 8.9.3-2 through 8.9.3-4**, that have been developed (Hanna, et al., 2007) for the determination of the required amount of transverse post-tensioning, along with a proposed design equation will be described in Section 8.9.3.5.

DESIGN THEORY AND PROCEDURE

8.9.3 Suggested Design and Construction Procedure

Figure 8.9.3-1
Transverse Post-Tensioning Arrangement

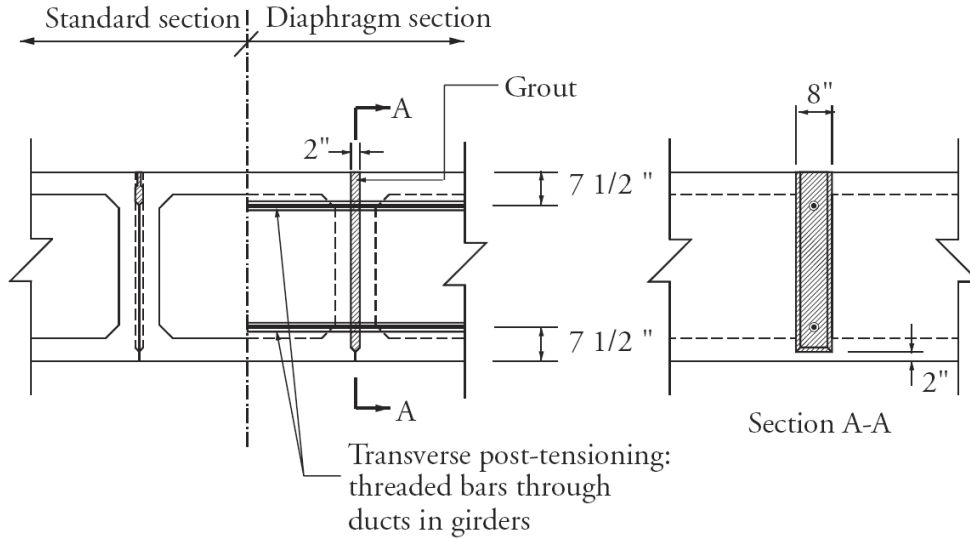
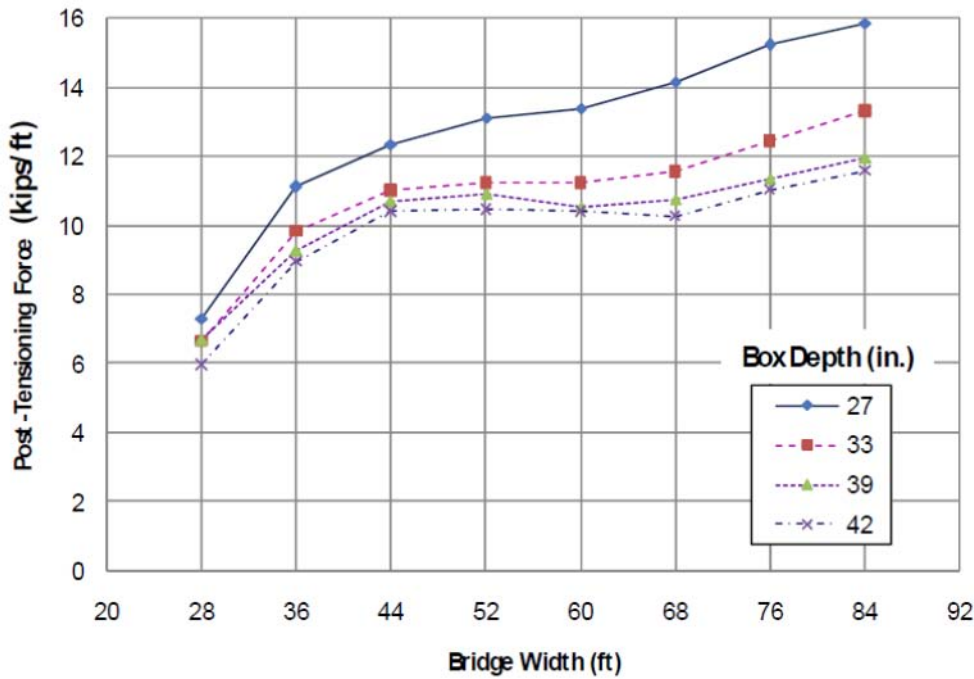


Figure 8.9.3-2
Required Effective Post-Tensioning Force as a Function of Bridge Width



DESIGN THEORY AND PROCEDURE

8.9.3 Suggested Design and Construction Procedure/8.9.3.1 Transverse Diaphragms

Figure 8.9.3-3
 Required Effective Post-Tensioning Force for Different Span-to-Depth Ratios

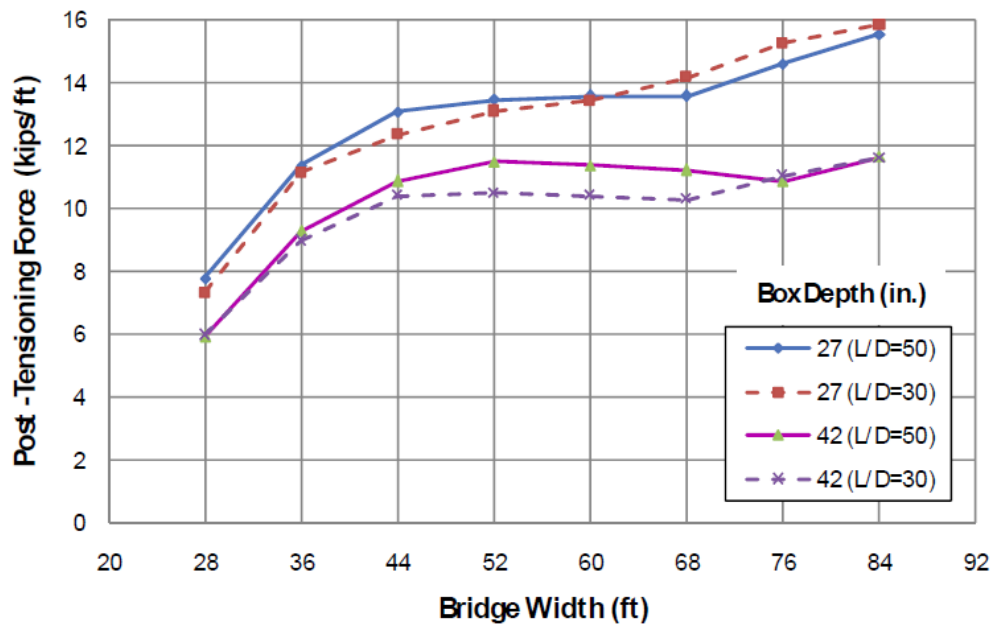
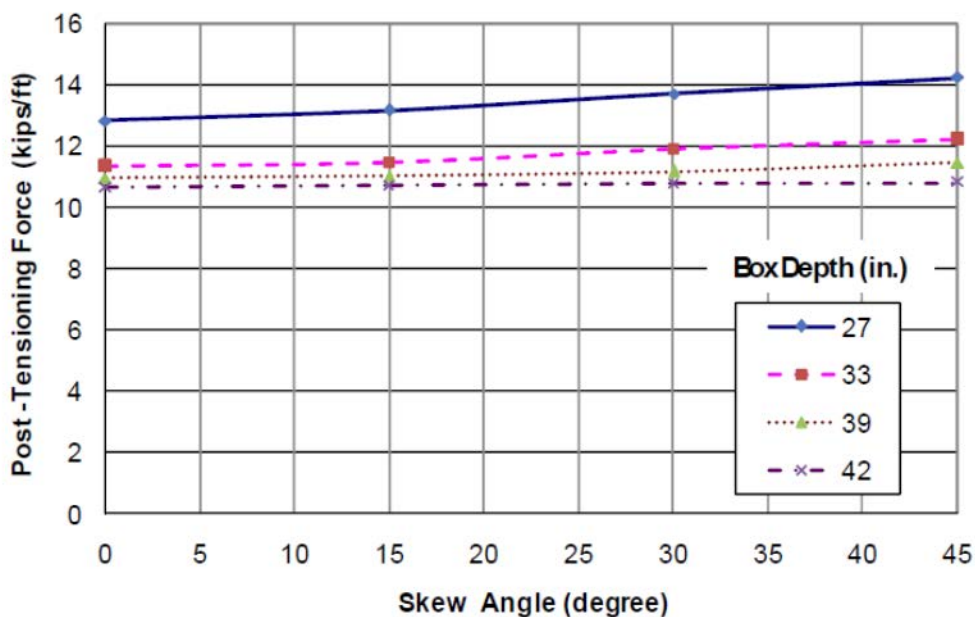


Figure 8.9.3-4
 Required Effective Post-Tensioning Force as a function of Skew Angle



8.9.3.1 Transverse Diaphragms

The transverse diaphragms are made continuous across the entire width of the bridge by providing grout pockets in the faces of the joints at each diaphragm location. These vertical pockets, which are filled with grout prior to post-tensioning, extend nearly the full depth of the beam (see **Figure 8.9.3-1**). The grout must be installed and

DESIGN THEORY AND PROCEDURE**8.9.3.1 Transverse Diaphragms/8.9.3.5 Post-Tensioning Design Chart**

cured prior to post-tensioning so that it will be compressed. This precompression of the grout is necessary to avoid cracking in the diaphragm. The 1-in.-deep by 8-in.-wide grout pocket is formed into the side of each box beam by attaching a breakout to the interior of the steel side form. Installation of the breakout is a simple and inexpensive modification to the box beam form.

It has been found that for spans of up to 100 ft, the use of five post-tensioned diaphragms limit differential deflection between adjacent box beams to 0.02 in., which is an acceptable amount. The use of three diaphragms, one at each end and one at midspan, was found to reduce the required quantity of post-tensioning, but the differential deflection between beams increased to an unacceptable level, i.e. higher than 0.02 in. As a guideline, for spans up to 60 ft, three diaphragms, at ends and at midspan, may be used. For spans over 60 ft, five diaphragms, located at the ends, midspan, and quarter points, may be used.

Diaphragms are post-tensioned because of the difficulty of providing continuous, conventionally reinforced diaphragms across the width of the bridge. Conventionally reinforced diaphragms would also be subject to cracking, which would reduce their effectiveness and possibly allow water penetration. Post-tensioned diaphragms are precompressed and should not crack.

8.9.3.2 Longitudinal Joints Between Beams

The transverse connection between adjacent box beams is made at the diaphragms, so longitudinal shear keys are not required for the structural performance of the bridge. However, the gap between beams should be sealed with grout or an appropriate nonstructural sealant to prevent water leakage between beams. Longitudinal shear keys tend to seal the gap between girders much more effectively when grouted than those without grout.

8.9.3.3 Tendons

In most cases, a pair of post-tensioning tendons is placed in each diaphragm. Each tendon may consist of a single post-tensioning bar or strand. The use of post-tensioning bars may be preferred because they are easier to install, achieve a higher force for a single bar as compared to a single strand, provide greater stiffness across the joint, and generally have a lower anchorage seating loss, which is especially significant for short tendons. Strands may be used if power seating of the anchorage is used to minimize the seating loss. The tendons are placed symmetrically about the mid-height of the section in order to provide equal resistance to the positive and negative moments that are caused by live load and temperature gradients. The vertical distance between tendons should be as large as possible in order to maximize the flexural resistance of the diaphragm.

Tendons may be either bonded, by grouting after post-tensioning, or left unbonded. Bonded tendons provide higher capacity at ultimate conditions and are protected from corrosion by the grout, but grouting is an additional operation that must be performed in the field. Unbonded tendons are easier to install and can be more easily removed if a damaged box beam must be replaced. However, the tendon must be protected in some way from corrosion and the force in the tendon at ultimate is lower than for bonded tendons. In either case, the tendon anchorages must be protected from corrosion by encasing the anchorage in grout or by using galvanized hardware and sealing anchorages with grease caps.

8.9.3.4 Modeling and Loads for Analysis

The bridge is modeled using grid analysis to determine member forces. A series of beam elements is used to represent the beams. These elements are connected by a series of crossing beam elements, representing the diaphragms. The joints between elements allow the transmission of shear, bending moment and torsion.

Barrier rails and live loads are the main sources of transverse bending moments generated in the diaphragms. The live loads are positioned to produce the maximum positive and negative moments in the diaphragms. To obtain the maximum transverse positive moment in the diaphragm at midspan, the live load is placed over the center of the deck. For maximum transverse negative moment at the same location, the load is placed as close to the barrier rail as possible or as required by the specifications.

8.9.3.5 Post-Tensioning Design Chart

Design charts developed by Hanna, et al. (2007) using the above procedure are shown in **Figures 8.9.3-2** through **8.9.3-4**. These charts provide the required transverse post-tensioning force for the standard box beam depths of

DESIGN THEORY AND PROCEDURE**8.9.3.5 Post-Tensioning Design Chart/8.10 Lateral Stability of Slender Members**

27, 33, 39, and 42 in. To prepare the chart, bridges with widths of 28, 36, 44, 52, 60, 76, and 84 ft were considered. For each combination of section depth and bridge width, two different span-to-depth ratios appropriate for the beam size, were considered. These charts may be used for both 3- and 4-ft-wide beams and for bridges with zero skew. Use of the charts should satisfy both service and strength limit states. Similar charts can be generated for other box beam depths and for bridges with skews.

The required transverse post-tensioning force was found to be almost linearly proportional to the span length. The forces shown in the design charts were obtained by dividing the required effective post-tensioning force for the midspan diaphragm by the spacing between diaphragms, and then taking the average of the three span lengths analyzed. The chart was developed assuming that bonded post-tensioning is used. If unbonded post-tensioning is used, the required post-tensioning force would increase about 30%.

The required post-tensioning force for the diaphragms at the quarter points was found to be similar to the midspan diaphragm. It is therefore recommended that the same force be used at all diaphragms within the span. The end diaphragms, however, are subjected to very small bending moments because they are continually supported at the piers or abutments. The same prestressing force may be provided for the end diaphragms or a minimum prestress force of 0.250 ksi on the area of the diaphragm may be provided.

Although the chart was developed for bridges with no skew, it can be used for bridges with skews up to 15 degrees. For bridges with high skews, over 15 degrees, grid analysis or the application of the following design equation should be conducted. Grid analysis is relatively simple to conduct with commercially available computer programs.

The following design equation was developed for calculating the required post-tensioning force (P) for intermediate diaphragms per unit length of the bridge (Hanna, et al., 2007) from the data from the grid analyzes:

$$P = \left(\frac{0.9W}{D} - 1.0 \right) K_L K_S \leq \left(\frac{0.2W}{D} + 8.0 \right) K_L K_S$$

Where,

D = box depth, ft

W = bridge width, ft

L = bridge span, ft

θ = skew angle, degrees

K_L = correction factor for span-to-depth ratio more than 30

$$K_L = 1.0 + 0.003 \left(\frac{L}{D} - 30 \right)$$

K_S = correction factor for skew angle more than 0°

$$K_S = 1.0 + 0.002\theta$$

8.9.4 Lateral Post-Tensioning Detailing for Skewed Bridges

Diaphragms in skewed bridges can either be skewed or perpendicular to the longitudinal axis of the beam. Diaphragms that are skewed are normally limited to skew angles of 20° or less. Use of skewed diaphragms allows for placement of grout between beams all at one time, then post-tensioning in one operation. For multistage or phased construction, it is possible to use staggered post-tensioning with skewed or perpendicular diaphragms. Refer to Sections 3.6.3.4 and 3.6.3.5 in Chapter 3 for illustrations and Section 8.9.2 for details used in Oregon.

8.10 LATERAL STABILITY OF SLENDER MEMBERS

Prestressed concrete members are generally stiff enough to prevent lateral buckling. However, during handling and transportation, support conditions may result in lateral displacements of the beam, thus producing lateral bending about the weak axis.

8.10.1 Introduction

There are two important cases: that of a beam hanging from lifting devices and that of a beam supported on flexible supports. For hanging beams, the tendency to roll is governed primarily by the properties of the beam. For supported beams, the tendency to roll is significantly influenced by the conditions of the supports and the roadway geometry (cross-slope). Detailed explanations of these two cases are given in Mast (1989, 1993).

8.10.1.1 Hanging Beams

The equilibrium conditions for a hanging beam are shown in **Figures 8.10.1.1-1** and **8.10.1.1-2a-2b**. When a beam hangs from lifting points, it may roll about an axis through the lifting points. The safety and stability of long beams subject to roll are dependent upon:

- e_i = the initial lateral eccentricity of the center of gravity with respect to the roll axis
- y_r = the height of the roll axis above the center of gravity of the beam
- \bar{x}_o = the theoretical lateral deflection of the center of gravity of the beam, computed with the full weight applied as a lateral load, measured to the center of gravity of the deflected arc of the beam
- θ_{max} = tilt angle at which cracking begins, based on tension at the top corner equal to the modulus of rupture

Figure 8.10.1.1-1
Perspective of a Beam Free to Roll and Deflect Laterally

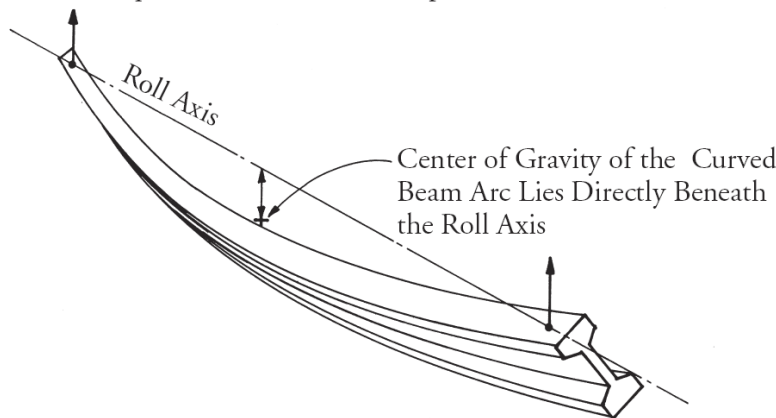
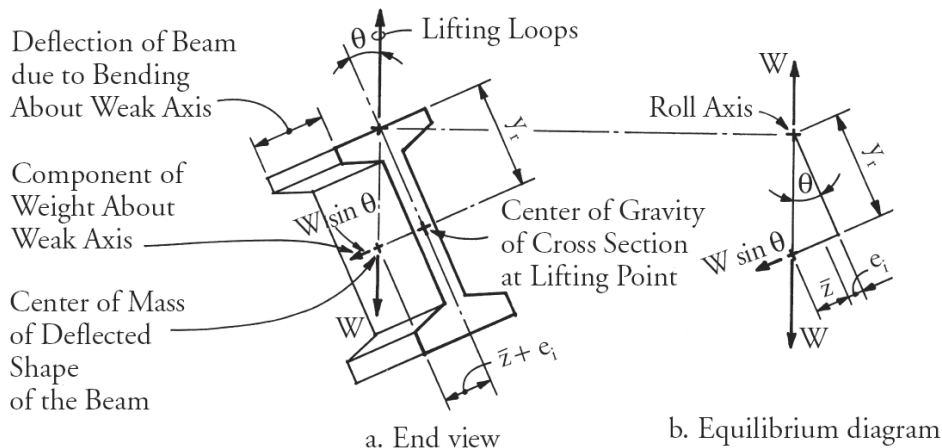


Figure 8.10.1.1-2a-2b
Equilibrium of Beam in Tilted Position



For a beam with overall length, ℓ , and equal overhangs of length, a , at each end:

$$\bar{z}_o = \frac{w}{12EI_g \ell} [0.1(\ell_1)^5 - a^2(\ell_1)^3 + 3a^4(\ell_1) + 1.2(a^5)] \tag{Eq. 8.10.1.1-1}$$

where

$$\ell_1 = \ell - 2a$$

$$I_g = \text{moment of inertia of beam about weak axis}$$

The factor of safety against cracking, FS_c , is given by:

$$FS_c = \frac{1}{\frac{\bar{z}_o}{y_r} + \frac{\theta_i}{\theta_{max}}} \tag{Eq. 8.10.1.1-2}$$

where θ_i = the initial roll angle of a rigid beam = $\frac{e_i}{y_r}$

It is recommended that e_i be based, as a minimum, on $\frac{1}{4}$ in. plus one-half the PCI tolerance for sweep. The PCI sweep tolerance is $\frac{1}{8}$ in. per 10 ft of member length.

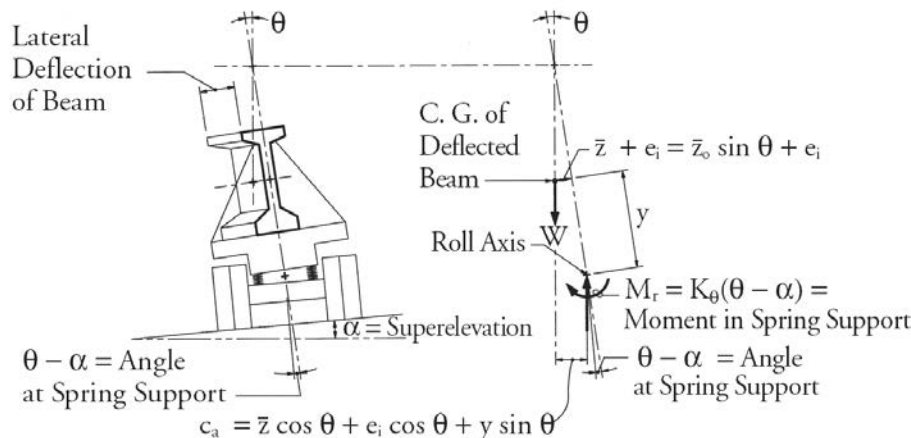
When cracking occurs, the lateral stiffness decreases and \bar{z}_o increases. Thus, failure may occur shortly after cracking as the tilt angle increases rapidly due to the loss of stiffness. In this case, FS_c must be greater than 1.5 for the beam to be considered stable. See Section 8.10.2 for suggested factors of safety.

8.10.1.2 Beams Supported from Beneath

When a beam is supported on flexible supports such as bearing pads or truck and trailer, there is a tendency for the beam to roll about the roll center below the beam (**Figure 8.10.1.2-1**). Because the roll axis is beneath the center of gravity of the beam, the support must be capable of providing resistance to rotation. This resistance is expressed as an elastic rotational spring constant, K_θ .

The rotational spring constant of an elastic support is found by applying a moment and measuring the rotation. The quantity, K_θ is equal to the moment divided by the rotation angle with units of moment per radian.

Figure 8.10.1.2-1
Equilibrium of Beam on Elastic Support



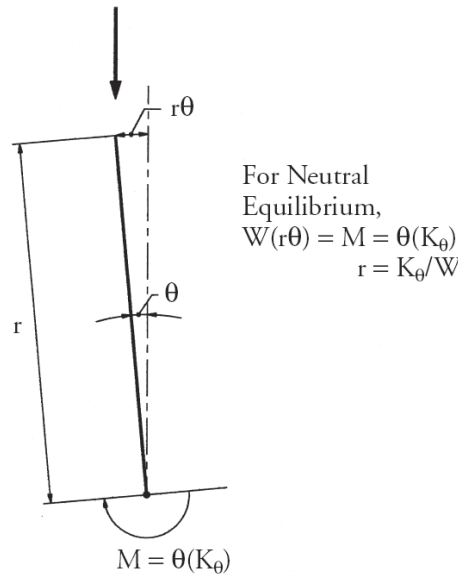
DESIGN THEORY AND PROCEDURE

8.10.1.2 Beams Supported from Beneath

It is convenient to define a quantity, $r = \frac{K_\theta}{W}$, where W is the weight of the beam, as shown in Figure 8.10.1.2- 2.

The quantity, r , has a physical interpretation: it is the height at which the beam weight would be placed in neutral equilibrium with the spring for a given small angle.

Figure 8.10.1.2-2
Definition of radius of stability, r



The equilibrium tilt angle, θ , of the major axis of the beam is given by:

$$\theta = \frac{\alpha r + e_i}{r - y - \bar{z}_o} \tag{Eq. 8.10.1.2-1}$$

where

- α = superelevation angle or tilt angle of supports in radians
- y = height of center of gravity of beam above roll axis (beam supported from beneath)
= $h_{cg} - h_r$

where

- h_{cg} = height of center of gravity of beam above road
- h_r = height of roll center above road

When r is very large (i.e., the support is very stiff), θ approaches α .

The factor of safety against cracking, FS_c , is:

$$FS_c = \frac{r(\theta_{max} - \alpha)}{\bar{z}_o\theta_{max} + e_i + y\theta_{max}} \tag{Eq. 8.10.1.2-2}$$

where θ_{max} = the tilt angle at which cracking begins, based on tension in the top corner equal to the modulus of rupture

DESIGN THEORY AND PROCEDURE

8.10.1.2 Beams Supported from Beneath

For shipping, sweep may be larger (due to creep) and tolerances on location of the support may be larger. Therefore, it is recommended that, e_i , for shipping, be based on 1 in. plus the PCI tolerance for sweep.

Prestressed concrete I-beams possess significant post-cracking strength. After cracking, the beams resist lateral bending by a lateral shift in the centroid of the internal compressive force.

A simplified relationship for the strength and effective stiffness of long prestressed concrete I-beams of ordinary proportions, such as the PCI BT-72, is given by Mast (1993).

- For tilt angles that produce top flange tensile stresses less than the modulus of rupture, $0.24\sqrt{f'_c}$, use the gross moment of inertia, I_g about the weak axis.
- For tilt angles that produce top flange tensile stresses in excess of $0.24\sqrt{f'_c}$ use an effective stiffness:

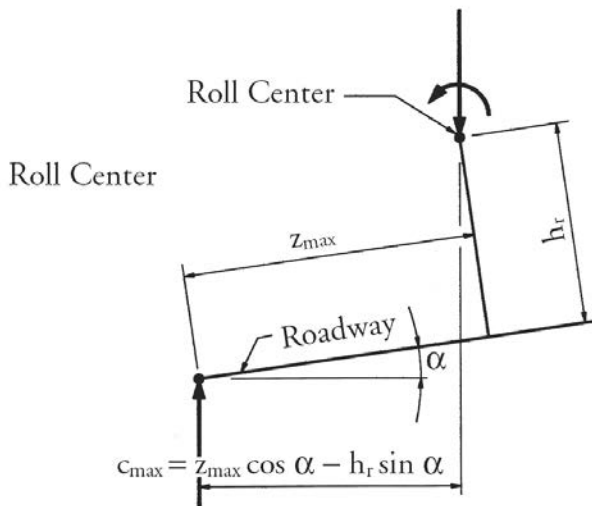
$$I_{eff} = \frac{I_g}{(1 + 2.5\theta)} \tag{Eq. 8.10.1.2-3}$$

- Assume the maximum θ at failure, θ'_{max} , to be 0.4 radians (or 23 degrees).

The maximum tilt angle at failure, θ'_{max} , may be limited by rollover of the transport rig, not by the strength of the beam.

The resisting moment arm is limited by the geometry of the hauling rig. Assuming a height of roll center, h_r normally about 24 in.), and a transverse distance from centerline of the beam to the center of dual tires, z_{max} (normally about 36 in.), the maximum resisting moment arm may be found (see Figure 8.10.1.2-3):

Figure 8.10.1.2-3
Maximum Resisting Moment
Arm for a Beam on Truck and Trailer



Using the usual small angle approximations:

$$\theta'_{max} = \frac{z_{max} - h_r\alpha}{r} \tag{Eq. 8.10.1.2-4}$$

To find the factor of safety, FS_s , against rollover (overturning) failure, Eq. 8.10.1.2-2 may be modified by substituting the cracked section \bar{z}'_o for \bar{z}_o and θ'_{max} for θ_{max}

$$FS_f = \frac{r(\theta'_{max} - \alpha)}{\bar{z}'_o \theta'_{max} + e_i + y \theta'_{max}} \tag{Eq. 8.10.1.2-5}$$

For the angle θ'_{max} , the quantity, \bar{z}'_o , is computed using I_{eff} from Eq. 8.10.1.2-3 for that angle. The calculation is:

$$\bar{z}'_o = \bar{z}_o(1 + 2.5\theta'_{max}) \tag{Eq. 8.10.1.2-6}$$

8.10.2 Suggested Factors of Safety

The necessary factor of safety cannot be determined from scientific laws; it must be determined from experience. It is suggested to use a factor of safety of 1.0 against cracking, FS_c , and 1.5 against failure, FS_f . This applies to both hanging and supported beams.

8.10.2.1 Conditions Affecting FS_c

For supported beams, the major unknowns are the roll stiffness of the supporting vehicles and the transverse slope of the roadway. It should be noted that transverse slopes occur for reasons other than superelevation. On soft ground (on a shoulder or at the construction site) one side of the hauling rig may sink into the ground, creating a large transverse slope.

These unknowns primarily affect the factor of safety against cracking. It is believed that many beams have been successfully shipped with a theoretical factor of safety against cracking of less than unity. But until the factors of safety used in the past can be better documented, a minimum factor of safety against cracking of 1.0 is recommended. The factor of safety against failure is essentially the factor of safety against overturning of the hauling rig. A factor of safety against overturning of 1.5 is believed to be adequate.

8.10.2.2 Effects of Creep and Impact

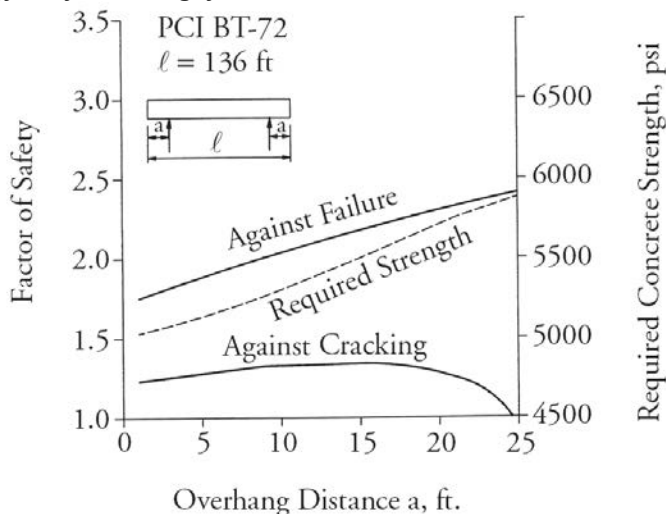
The recommended minimum factors of safety apply to calculations that do not account for creep and impact. Impact is normally of significance during hauling, but stability is primarily a problem when traveling along sections of high superelevation at low speeds. It is recommended that the effects of impact and superelevation be accounted for separately. This was also recommended by Imper and Laszlo (1987).

8.10.2.3 Effects of Overhangs

Figure 8.10.2.3-1 shows the factors of safety for a supported beam on a 6% slope and with supports having a K_θ of 40,500 in.-kips per radian. The factors of safety for supported beams are much less sensitive to overhang distance. For supported beams, the stability of the beam is more a function of the stiffness of the support than the stiffness of the beam. However, the factor of safety against cracking is determined by the top fiber stresses in the beam. Past practice has been to support the beam on the truck at the lifting points. Figure 8.10.2.3-1 would indicate that some deviation in location of support points on the truck and trailer is permissible.

Unequal overhangs are sometimes necessary during shipping. It is sufficiently accurate to use the average overhang in stability calculations, but the stress at the support should be checked using the actual overhang.

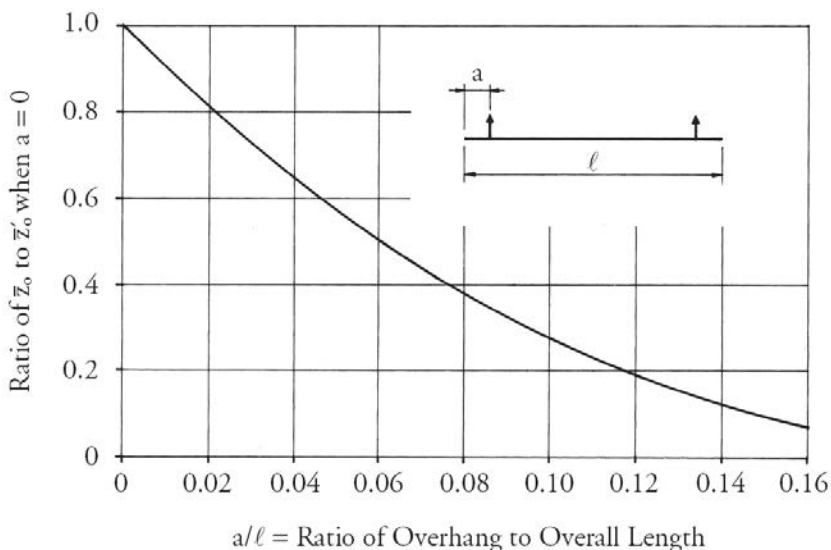
Figure 8.10.2.3-1
Effect of Overhangs for Beam on Truck and Trailer



DESIGN THEORY AND PROCEDURE**8.10.2.4 Increasing the Factor of Safety/8.10.3 Measuring Roll Stiffness of Vehicles****8.10.2.4 Increasing the Factor of Safety**

For safe handling of long members, resistance can be improved by several methods. These are listed below in order of effectiveness and relative ease of accomplishment, with the easiest and most effective first:

1. Move the lifting points inward (**see Figure 8.10.2.4-1**). Decreasing the distance between lifting points by just a small amount can significantly increase the safety factor. Stresses must be checked; temporary post-tensioning can be introduced to control stresses
2. Increase the distance between the center of mass and the lifting point, y_r , by use of a rigid lifting yoke
3. Provide temporary lateral bracing, in the form of a stiffening truss, composed of structural steel shapes
4. Change the shape of the cross-section of the member
5. Increase the stiffness of the member by increasing the concrete modulus of elasticity, E_c , and tensile strength

Figure 8.10.2.4-1**Reduction of \bar{z}_o with Overhangs****8.10.3 Measuring Roll Stiffness of Vehicles**

The roll stiffness (rotational spring stiffness) of transport vehicles is a very important parameter in evaluating the safety of slender beams during transportation. Information on the roll stiffness of transport vehicles is normally not available, however, roll stiffness may be determined by placing a weight on the vehicle at various eccentricities to the vehicle longitudinal centerline. The weight should be of the same order of magnitude as the beam, a convenient weight is the beam itself. One end of the beam may be secured, and the other end placed on the vehicle at eccentricities of, say, 10 and 20 in. either side of the centerline.

Rotations may be determined by measuring the vertical movement at either end of the bolster or cross-member used for chaining the beam. The roll stiffness is the average of the values obtained by dividing the eccentric moment by the rotation in radians. Because the bolster tilts under eccentric loads, it is necessary to use a narrow bearing strip of hard material between the beam and the cross-member, in order to know the eccentricity of the load on the trailer.

A very limited number of measurements indicates that the rotational spring constant, K_θ may be expected to be in the range of 3,000 to 6,000 in.-kips per radian per dual-tire axle. The higher values apply to rigs without leaf

DESIGN THEORY AND PROCEDURE**8.10.3 Measuring Roll Stiffness of Vehicles/8.10.7 Lateral Stability Examples**

springs, in which the spring is primarily in the tires. For instance, a steel trailer with four dual axles plus a single axle might be expected to have a roll stiffness of 4.5 times (3,000 to 6,000) = 13,500 to 27,000 in.-kips per radian. The total, K_θ , is the sum of that for the tractor and the trailer.

The above figures are based on very limited data and must be used with caution until more data are available. Also, these values apply to axles for which the load is balanced mechanically. Axles with air suspension may contribute little, if any, to roll stiffness. For critical shipments, measuring the roll stiffness of the vehicles that will be used is strongly recommended. Rigs with independent axle systems may give inconsistent results.

8.10.4 Bearing Pads

Elastomeric bearing pads also provide a resilient support for prestressed concrete beams. The rotational spring constant, K_θ , is determined by the dimensions and properties of the pad. When the load is outside the kern of the bearing pad, the rotational spring constant becomes highly nonlinear. Test results for this situation are lacking since the objective is generally to keep the load within the kern. In addition, there may be stability problems with thick plain (unreinforced) pads; laminated pads provide more stability.

8.10.5 Wind Loads

Wind forces on beams produce applied moments that must be added to other moments. This causes an additional initial eccentricity due to the deflection caused by the wind load. Additionally, the wind load itself causes an overturning moment about the bottom of the bearing pads which, divided by the beam weight, produces a moment arm. The total moment arm at zero tilt angle, θ , is the sum of assumed initial eccentricity, e_i , plus these two added quantities. This emphasizes the importance of bracing the ends of bridge beams against rollover as soon as they are erected.

8.10.6 Temporary King-Post Bracing

Long prestressed concrete I-beams are often braced during transportation using a king-post truss system. This system uses external prestressing strands which are partially tensioned against bearing plates at each end of the beam. One or two steel king posts are mounted against each side of the beam at opposing points and harp (push) the strands out to a large eccentricity at or near the mid-point of the beam. This provides a truss-like frame around the beam.

Such bracing is of very little benefit, however. The steel area of the prestressing strands is too small to make a significant contribution to the lateral stiffness of the beam. Temporary prestressing of the top flange, as recommended by Imper and Laszlo (1987), is a more effective way to improve the factor of safety against cracking. Horizontal stiffening trusses fabricated with mild steel chords are also effective.

8.10.7 Lateral Stability Examples

These calculations are based on the example given in Imper and Laszlo (1987). Refer to Imper and Laszlo (1987) and Mast (1993) for additional details.

The following information is provided:

AASHTO-PCI BT-72 bridge beam

Depth, $h = 72$ in.

Top flange width, $b = 42$ in.

Bottom flange width, $b_b = 26$ in.

Unit weight of concrete, $w_c = 0.155$ ksf

Beam cross-sectional area, $A_c = 767$ in.²

Strong axis, $I = 545,894$ in.⁴

$y_b = 36.6$ in.

Weak axis, $I_g = 37,634 \text{ in.}^4$

Overall length, $\ell = 136 \text{ ft}$

Pickup (lift) points, $a = 9 \text{ ft}$ from each end

Harp points, 0.4ℓ

Initial prestress force, $P_i = 1,232 \text{ kips}$ (after initial losses)

Location of $P_i, y_{bs} = 5 \text{ in.}$ above soffit at harp points

8.10.7.1 Hanging Beam Example

Find the factors of safety against cracking and against failure when the beam hangs from lifting loops.

1. Check stresses at harp points and required concrete strength:
 $w = 0.826 \text{ klf}$

$$W = wL = 0.826(136) = 112.3 \text{ kips}$$

$$M_g \text{ at harp point at } 0.4\ell = 15,926 \text{ in.-kips}$$

The corresponding concrete stresses:

$$f_t = 0.114 \text{ ksi and } f_b = 3.149 \text{ ksi}$$

$$f'_{ci} \text{ required} = f_b/0.6 = 5.248 \text{ ksi. Use } f'_{ci} = 5.25 \text{ ksi}$$

2. Calculate modulus of elasticity at release of prestress:
 in the absence of local data, assume $K_1 = 1.0$

$$E_c = 33,000K_1w_c^{1.5} \left(\sqrt{f'_{ci}} \right) = 4,613 \text{ ksi}$$

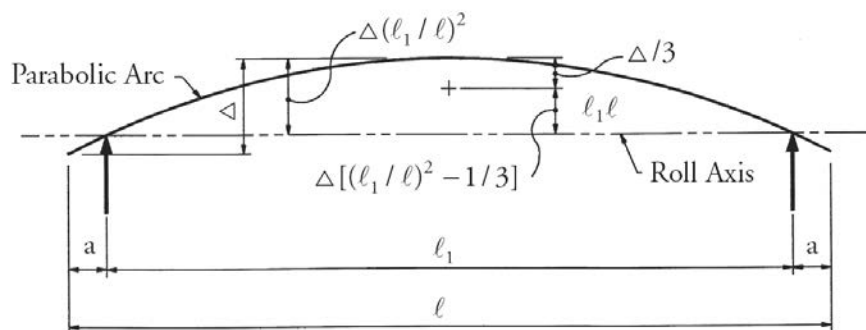
3. Compute initial eccentricity, e_i :

For beams hanging from lifting loops, use a sweep dimension of one-half the PCI sweep tolerance and a lifting loop placement tolerance of $\frac{1}{4}$ in. Or, calculate e_i based on observations of the tilt angles of actual beams. To evaluate e_i due to sweep, the distance between the roll axis and the center of gravity of the arc of the curved beam must be found (see **Figure 8.10.7.1-1**). The curved shape is assumed to be a parabola, and the formulas are derived from the properties of a parabola. $l_1 = l - 2a$

$$\text{offset factor} = \left(\frac{l_1}{l} \right)^2 - \frac{1}{3} = \left(\frac{118}{136} \right)^2 - \frac{1}{3} = 0.419$$

$$e_i = 0.85(0.419) + 0.25 = 0.607$$

Figure 8.10.7.1-1
Offset of Centroid of a Parabolic Arc



DESIGN THEORY AND PROCEDURE

8.10.7.1 Hanging Beam Example

4. Estimate camber and correct the value of y_r for camber.

Camber may be estimated from the midspan radius of curvature, R :

$$R = \frac{EI}{M} \quad (\text{Eq. 8.10.7.1-1})$$

where

$$M = P_1 e - M_{gmsp}$$

where

$$\begin{aligned} M_{gmsp} &= \text{self-weight bending moment at midspan} \\ &= \frac{W}{2} \left[\frac{\ell}{4} - a \right] = \frac{112.28}{2} \left[\frac{136}{4} - 9 \right] (12) = 16,842 \text{ in.} \cdot \text{kips} \end{aligned}$$

$$M = (1,232)(31.6) - 16,842 = 22,089 \text{ in.} \cdot \text{kips}$$

$$R = \frac{4,613(545,894)}{22,089} = 114,000 \text{ in.}$$

The camber, Δ , measured with respect to the beam ends, is computed as follows:

$$\Delta = \frac{\ell^2}{8R} = \frac{[136(12)]^2}{8(114,000)} = 2.92 \text{ in.} \quad (\text{Eq. 8.10.7.1-2})$$

The height of the center of gravity of the cambered arc below the roll axis is computed:

$$y_r = y_t - \Delta(0.419) = (72-36.6) - 2.92(0.419) = 34.18 \text{ in.}$$

Camber has only a small effect on y_r . One may simply subtract an estimate (say between one and two in.) from y_r .

5. Compute \bar{z}_o from Eq. (8.10.1.1-1):

$$\bar{z}_o = \frac{w}{12EI_g \ell} (0.1 \ell_1^5 - a^2 \ell_1^3 + 3a^4 \ell_1 + 1.2a^5) = 10.86 \text{ in.}$$

6. Compute θ_i :

$$\theta_i = \frac{e_i}{y_r} = \frac{0.607}{34.18} = 0.01775$$

7. Compute the tilt angle, θ_{max} , at cracking:

$$f_r = 0.24\sqrt{f'_{ci}} = 0.550 \text{ ksi (tension)}, f_t = 0.114 \text{ ksi (compression) from Step 1.}$$

$$M_{lat} = \frac{(f_r + f_t)(I_g)}{\frac{b}{2}} = 1,190 \text{ kip} \cdot \text{in}$$

$$\theta_{max} = \frac{M_{lat}}{M_g} = \frac{1,190}{15,926} = 0.0747$$

8. Compute factor of safety against cracking, FS_c :

$$FS_c = \frac{1}{\frac{\bar{z}_o}{y_r} + \theta_{max}} = \frac{1}{\frac{10.86}{34.18} + \frac{0.01775}{0.0747}} = 1.80$$

Minimum $FS_c = 1.5$ OK

9. Note that the factor of safety against failure must also be checked in a similar manner.

8.10.7.2 Supported Beam Example

Find the factors of safety against cracking and rollover during transportation for the same beam described in Section 8.10.7.

The following information is provided:

$$f'_c = \text{concrete strength at 28 days} = 5.5 \text{ ksi}$$

Add two strands in top flange, per Imper and Laszlo (1987)

$$P = \text{prestress force} = 1,251.5 \text{ kips}$$

$$y_s = \text{the distance between the center of gravity of the strand to soffit} = 7.91 \text{ in.}$$

$$\alpha = \text{superelevation angle} = 0.06 \text{ radians (different from the 0.08 radians used in Imper and Laszlo, 1987)}$$

Tractor and steer trailer each with four dual axles and one single axle, stiff suspension

$$h_r = \text{height of roll center above road} = 24 \text{ in.}$$

$$h_{cg} = \text{height of center of gravity of beam above road} = 108 \text{ in.}$$

1. Estimate K_θ and find r :

Assume:

$$K_\theta = 4,500 \text{ in.-kips per radian per dual axle}$$

$$K_\theta = 4.5(4,500) = 20,250 \text{ each for tractor and for trailer}$$

Use two times this constant for total, K_θ , for hauling rig. $K_\theta = 40,500 \text{ in.-kips per radian}$

$$r = \frac{K_\theta}{W} = \frac{40,500}{112.28} = 360.7 \text{ in.}$$

2. Find tilt angle, θ , from Eq. (8.10.1.2-1):

$$\theta = \frac{\alpha r + e_i}{r - y - \bar{z}_o}$$

$$y = h_{cg} - h_r = 108 - 24 = 84 \text{ in.}$$

Increase y by 2%, to allow for camber. Then, $y = 85.68 \text{ in.}$, say 86 in.

For shipping, assume PCI sweep tolerances plus 1 in. off-center of truck/trailer. Use offset factor of 0.419 as computed in Step 3 of the previous example. $e_i = 1.70(0.419) + 1 = 1.71 \text{ in.}$

Adjust \bar{z}_o from Step 5 of the previous example, by the square root of ratio of concrete strengths to account for the change in modulus of elasticity.

$$\bar{z}_o = 10.86 \sqrt{\frac{5,248}{5,500}} = 10.61 \text{ in.}$$

$$\theta = 0.0883$$

3. Check stresses at harp points:

$$f_t = \frac{P}{A} - \frac{P_e}{S_t} + \frac{M_g}{S_t} = 0.336 \text{ ksi}$$

$$f_b = 2.971 \text{ ksi}$$

DESIGN THEORY AND PROCEDURE**8.10.7.2 Supported Beam Example/8.11 Bending Moments and Shear Forces due to Vehicular Live Loads**

4. Add lateral bending stress to f_b , and find required concrete strength:

$$M_{lat} = \theta(M_g) = 0.0883 (15,926) = 1,406 \text{ in.-kips}$$

$$f_b = 2.971 + 1,406(13)/37,634 = 3.457 \text{ ksi}$$

$$f'_c = \frac{f_b}{0.6} = 5.759 \text{ ksi and } E_c = 4,833 \text{ ksi}$$

Adjust \bar{z}_o from Step 5 of the previous example by the ratio of E_c 's:

$$\bar{z}_o = 10.86 \left(\frac{4613}{4833} \right) = 10.37 \text{ in.}$$

5. Find the tilt angle, θ_{max} , at cracking:

$$f_r = 0.24\sqrt{5.759} = 0.576 \text{ ksi (tendon)}$$

$$f_t = 0.336 \text{ ksi (compression) from Step 3}$$

$$M_{lat} = \frac{(f_r + f_t)(I_g)}{\frac{b}{2}} = 1,634 \text{ in. - kips}$$

$$\theta_{max} = \frac{M_{lat}}{M_g} = \frac{1,634}{15,962} = 0.1024$$

6. Compute factor of safety against cracking, FS_c , from Eq. (8.10.1.2-2):

$$FS_c = \frac{r(\theta_{max} - \alpha)}{\bar{z}_o\theta_{max} + e_i + y\theta_{max}} = \frac{360.7(0.1024 - 0.06)}{10.37(0.1024) + 1.71 + 86(0.1024)} = 1.32 > 1.0 \quad \text{OK}$$

7. Find tilt angle, θ'_{max} , at maximum resisting moment arm from Eq. (8.10.1.2-4):

$$\theta'_{max} = \frac{z_{max} - h_r\alpha}{r} + \alpha = \frac{36 - 24(0.06)}{360.7} + 0.06 = 0.1558$$

8. Compute \bar{z}'_o at θ'_{max} from Eq. (8.10.1.2-6):

$$\bar{z}'_o = \bar{z}_o(1 + 2.5\theta'_{max}) = 10.37[1 + 2.5(0.1558)] = 14.41 \text{ in.}$$

9. Compute factor of safety against rollover, FS_f , from Eq. (8.10.1.2-5):

$$FS_f = \frac{r(\theta'_{max} - \alpha)}{\bar{z}'_o\theta'_{max} + e_i + y\theta'_{max}} = \frac{360.7(0.1558 - 0.06)}{14.41(0.1558) + 1.71 + 86(0.1558)} = 1.99 > 1.5 \quad \text{OK}$$

8.11 BENDING MOMENTS AND SHEAR FORCES DUE TO VEHICULAR LIVE LOADS

In designing longitudinal members of bridges, the maximum bending moment and shear force at each section along the span, are computed for live loads. The load position must be determined to give the maximum values of shears and moments. The *LRFD Specifications* use the HL-93 loading which is a superposition of the design truck or the design tandem and the design lane loading of 0.640 kips/ft. Design for the fatigue limit state in the *LRFD Specifications*, requires that a special fatigue truck be used. This section gives formulas which may be combined to get the maximum bending moments and shear forces due to the above loading cases.

Readers are referred to the *LRFD Specifications* for details about the effects of the superposition of the design tandem and the design lane loading, which must also be considered in design. It can be shown that this superposition may govern the design of shorter spans.

DESIGN THEORY AND PROCEDURE

8.11.1 Design Truck Loading/8.11.2 Design Lane Loading, 0.640 kips/ft

8.11.1 Design Truck Loading

The following formulas may be used to calculate the maximum bending moment and maximum shear force per lane at any point on a span for the design truck. Certain limitations apply, as noted in the tables. The computed values should be multiplied by a factor of 1/2 to obtain forces per line of wheels. The formulas are valid only for simple spans and dynamic load allowance (impact) is not included (see *AASHTO Manual for Bridge Evaluation*, AASHTO, 2008).

Table 8.11.1-1
Maximum Bending Moment
per Lane for HL-93 Design Truck Load

Load Type	x/L*	Formula for Maximum Bending Moment, kip-ft	Minimum	
			x, ft	L, ft
HL-93 Design Truck	0-0.333	$\frac{72(x)[(L-x)-9.33]}{L}$	0	28
	0.333 - 0.500	$\frac{72(x)[(L-x)-4.67]}{L} - 112$	14	28

* x is the distance from left support to the section being considered and L is the span length, ft

Table 8.11.1-2
Maximum Shear Force per
Lane for HL-93 Design Truck Load

Load Type	x/L*	Formula for Maximum Shear Force, kips	Minimum		Maximum
			x, ft	L, ft	L, ft
HL-93 Design Truck	0-0.500	$\frac{72[(L-x)-4.67]}{L}$	14	28	42
	0 - 0.500	$\frac{72[(L-x)-9.33]}{L}$	0	42	

* x is the distance from left support to the section being considered and L is the span length, ft

8.11.2 Design Lane Loading, 0.640 kips/ft

The following formulas may be used to calculate the maximum bending moment and the maximum shear force per lane at any point on a span for the design lane load of 0.640 kips/ft. The formulas are valid only for simple spans and dynamic load allowance is not included.

$$\text{Maximum bending moment} = \frac{0.64(x)(L-x)}{2}, \text{ ft-kips}$$

$$\text{Maximum shear force} = \frac{0.64}{2L}(L-x)^2, \text{ kips}$$

where

x = distance from left support to the section being considered, ft

L = Span length, ft

DESIGN THEORY AND PROCEDURE

8.11.3 Fatigue Truck Loading/8.12.1 Introduction

8.11.3 Fatigue Truck Loading

When designing using the *LRFD Specifications*, consideration of the fatigue limit state may be required (see LRFD Article 5.5.3.1). A special fatigue truck load is defined in LRFD Article 3.6.1.4.1. This loading consists of a single design truck that has the same axle weights used in all other limit states, but with a constant spacing of 30.0 ft between the 32.0-kip axles. The following equations may be used to calculate the maximum bending moment per lane at any point on the span for the fatigue truck loading. These values should be multiplied by a factor of $\frac{1}{2}$ to obtain values per line of wheels. These formulas are valid only for simple spans and dynamic load allowance is not included.

Table 8.11.3-1
Maximum Bending Moment per Lane
for HL-93 Fatigue Truck Loading

Load Type	x/L^*	Formula for Maximum Bending Moment, kip-ft	Minimum	
			x ,ft	L , ft
Fatigue Truck	0-0.241	$\frac{72(x)[(L-x)-18.22]}{L}$	0	44
	0.241 - 0.500	$\frac{72(x)[(L-x)-11.78]}{L} - 112$	14	28

* x is the distance from left support to the section being considered and L is the span length, ft

8.12 STRUT-AND-TIE MODELING OF DISTURBED REGIONS

Traditionally, models used in the analysis and design of concrete structures have been based on elastic theory and the basic assumption that plane sections remain plane, regardless of the loading. However, it is well known that disturbances do occur in regions near discontinuities, for example, at concentrated loads and abrupt changes in member dimensions. Such regions are referred to as “disturbed regions.”

Methods used to analyze and design disturbed regions must include procedures that reflect the actual flow of stresses in such regions. In considering stress distribution before cracking, it is customary to apply elastic methods of analysis, especially when predicting where significant cracking will occur. Since significant stress redistribution takes place after concrete cracks, elastic methods cannot adequately predict stresses subsequent to cracking.

8.12.1 Introduction

A rational method for dealing with disturbed regions subsequent to cracking is the use of strut-and-tie models. These models can give an excellent representation of the flow of forces in disturbed regions of cracked concrete systems.

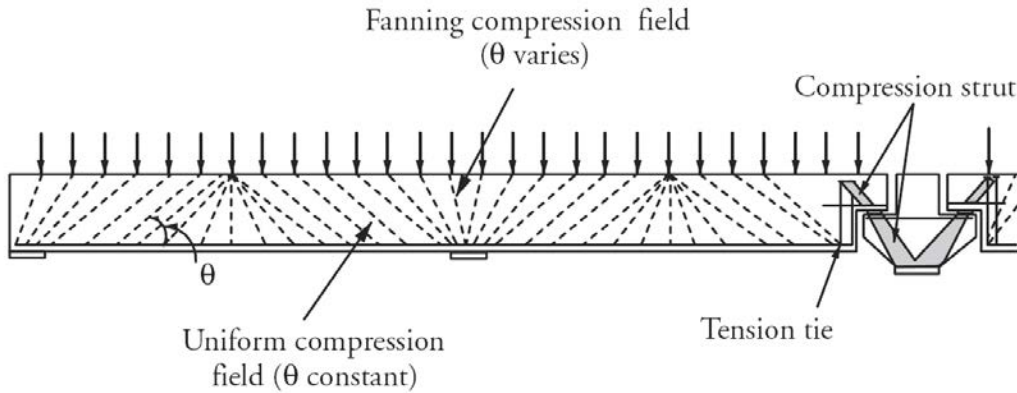
In a typical calculation for shear reinforcement using the various sectional models of the *LRFD Specifications* [Article 5.8.3], the sectional dimensions, prestressing steel, and material strengths have been chosen and the shear design involves selection of adequate shear reinforcement and, if necessary, additional longitudinal reinforcement.

Figure 8.12.1-1 shows that there are three types of regions that need to be considered in general shear design of a beam as follows:

1. Disturbed regions that can be appropriately treated as a system of struts and ties. This approach is discussed in this section.
2. Regions of fanning compressive stresses characterized by radiating compressive stresses near supports and regions where the shear changes sign but remains uniform. In such regions the value of θ varies.
3. Regions of uniform compressive stress fields where the value of θ is constant.

The second and third types of regions are discussed in Section 8.4 using the various sectional models of the *LRFD Specifications*.

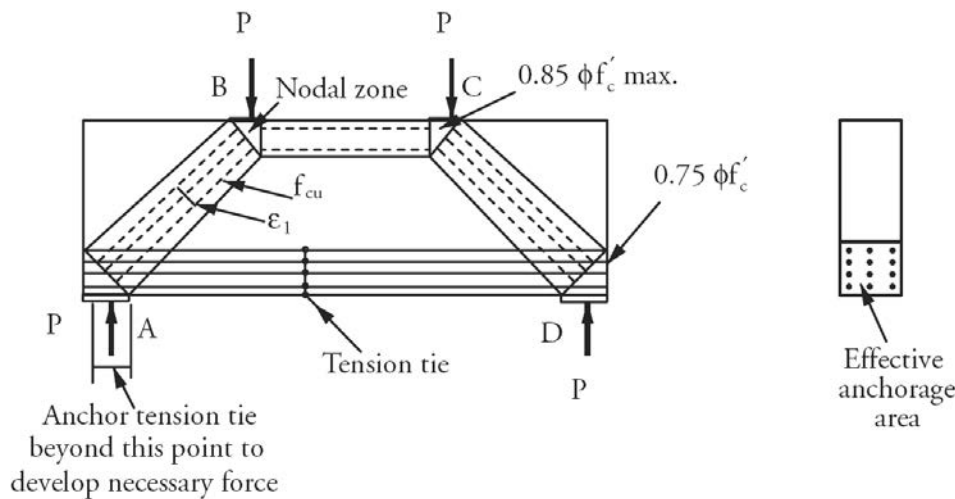
Figure 8.12.1-1
Disturbed Regions and Regions of Uniform Shear Distributions



8.12.2 Strut-and-Tie Models

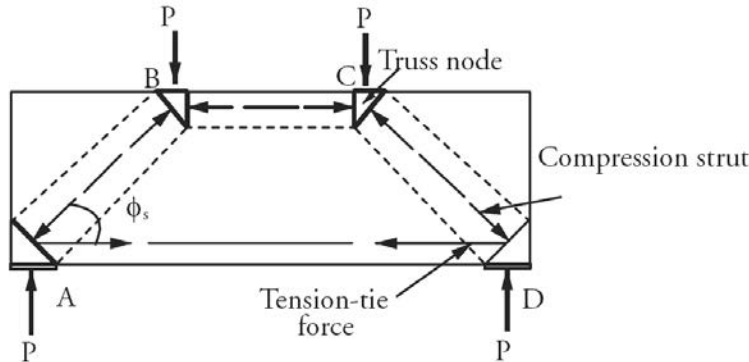
The *LRFD Specifications* encourage the use of strut-and-tie models in design where appropriate. It has been determined through sophisticated analysis and laboratory testing, that cracked reinforced concrete carries load mainly by development of a truss system represented by compressive stresses in the concrete and tensile stresses in the reinforcement. Furthermore, upon the occurrence of significant cracking, the originally curved principal stress trajectories in concrete tend toward straight lines, and it is appropriate to regard the resulting compressive forces as being carried by straight compressive struts. Examples of strut-and-tie modeling of a simply supported and a continuous deep beam are shown in **Figures 8.12.2-1a-1b** and **8.12.2-2**.

Figure 8.12.2-1a
Strut-and-Tie Model for a Simple Deep Beam



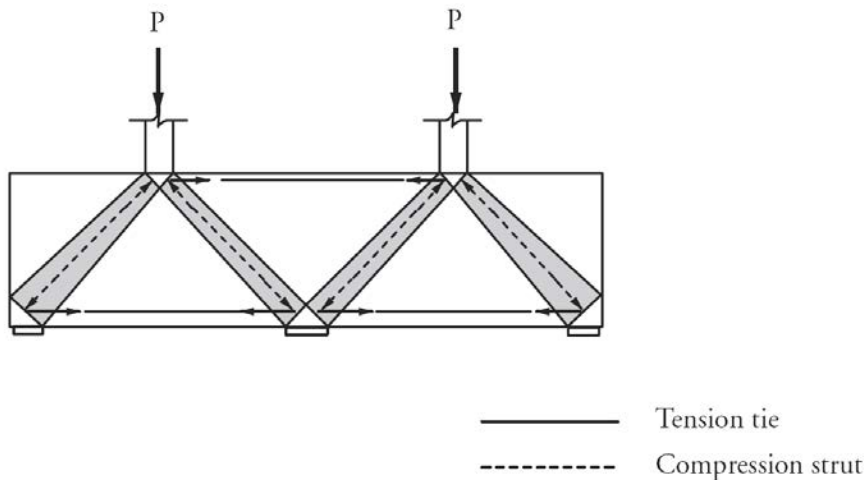
a) Flow of Forces

Figure 8.12.2-1b
Strut-and-Tie Model for a Simple Deep Beam



b) Truss Model

Figure 8.12.2-2
Strut-and-Tie Model for a Continuous Deep Beam



Important considerations in strut-and-tie modeling include the geometry of the truss system, the nodal zone and member dimensions, and the strengths of the compression and tension members.

8.12.2.1 Truss Geometry Layout

The significance of using appropriate geometry in defining a truss should be obvious in the necessity to have an equilibrated system of struts and ties. At first glance, the use of a strut-and-tie truss system to resist loads seems like an easy solution that any engineer should be readily able to accomplish. Since the real structure is a continuum, however, there are an infinite variety of trusses that could be designed inside a concrete member. The best or most efficient truss layout will be one that most closely fits the applied load and reaction conditions while resisting forces through the shortest load paths.

Identification of the existing boundary conditions is the first step in selecting a truss layout for the strut-and-tie system. In the hammerhead pier cap of **Figure 8.12.2.1-1a-1b**, two different sets of boundary conditions are shown depending on the locations of the design lanes and loading on the roadway above. In **Figure 8.12.2.1-1a**, the two 12 ft. design lanes are placed symmetric about the pier centerline and the girder reactions on the pier cap, representing the top boundary condition, are all identical. In **Figure 8.12.2.1-1b**, the two design lanes are shifted to the left side of the roadway and the reactions vary across the top of the pier cap, giving a second top boundary condition.

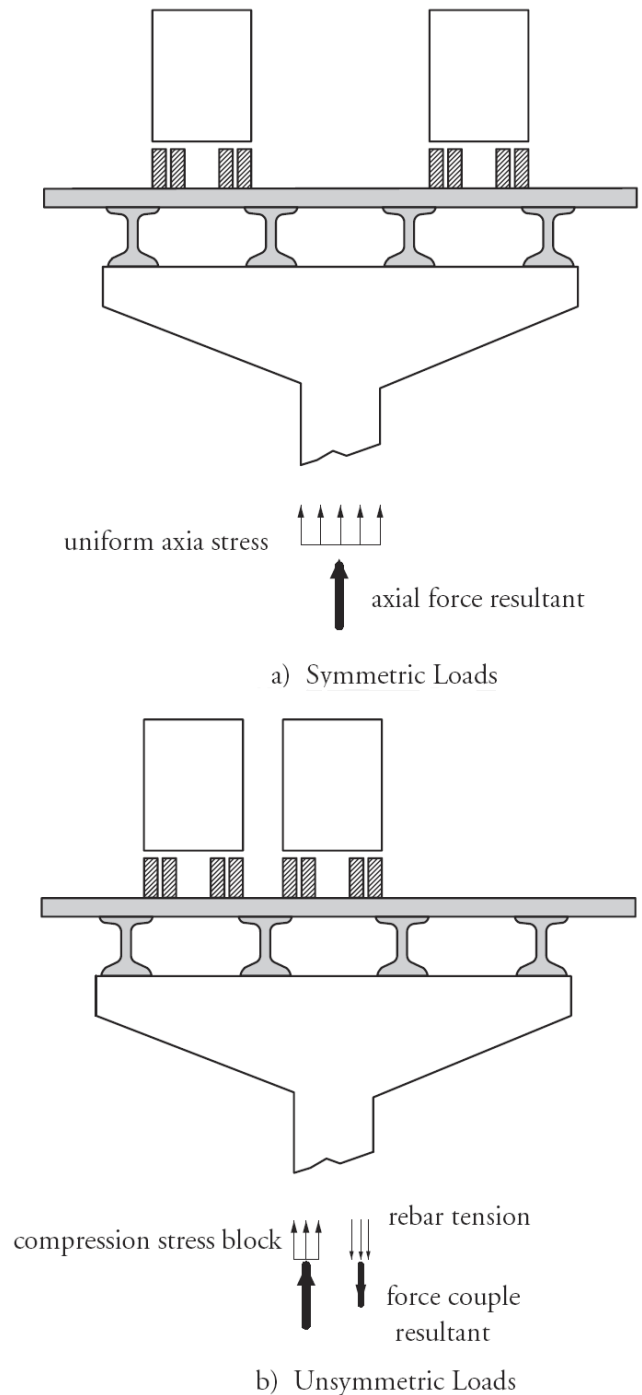
Regardless of the truss layout that might be selected within the pier cap, the forces in the pier column can be directly calculated: with pure axial compression in the first case and compression plus bending in the second case

DESIGN THEORY AND PROCEDURE

8.12.2.1 Truss Geometry Layout

as shown in **Figure 8.12.2.1-1a-1b**. In the first case, the bottom boundary condition is simply an axial force acting at the middle of the pier. The boundary condition in the second case, however, must be calculated and includes a column compression block and tension component as shown in **Figure 8.12.2.1-1b**. The forces shown in the pier of **Figure 8.12.2.1-1b** are assumed to exist at a distance “*d*” from the bottom of the pier cap – away from the disturbed region and in the portion of the column assumed to have sectional model behavior.

Figure 8.12.2.1-1a-1b
Pier Cap under Symmetric and Unsymmetric Lane Loading

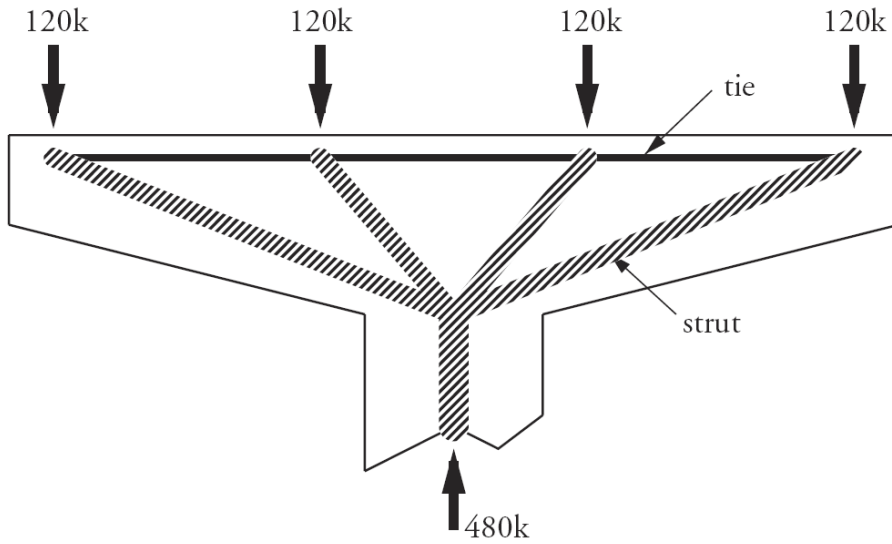


DESIGN THEORY AND PROCEDURE

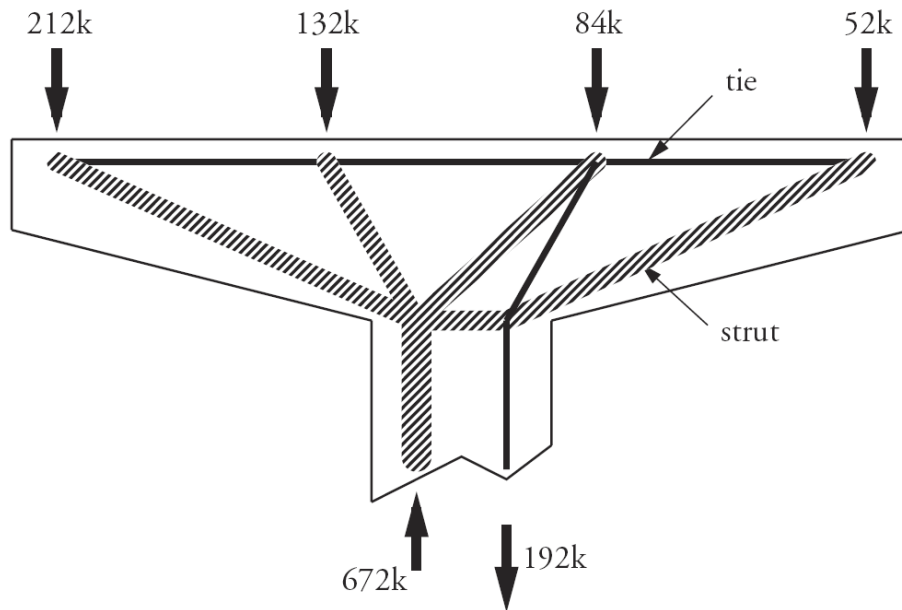
8.12.2.1 Truss Geometry Layout

In the first case of **Figure 8.12.2.1-1a**, the truss layout in the pier cap need only meet the condition of developing a compression thrust at the bottom of the cap. In the second case of **Figure 8.12.2.1-1b**, the truss must develop both the compression and the tension force in the pier column. Clearly two different truss layouts could be designed depending on which set of loads/boundary conditions was being considered as shown in **Figure 8.12.2.1-2a-2b**. The truss in the **Figure 8.12.2.1-2b** would be inverted if the trucks were at the other side of the roadway.

*Figure 8.12.2.1-2a-2b
Truss Layouts for the Different Load Cases*



a) Symmetric Truss



b) Unsymmetric Truss

DESIGN THEORY AND PROCEDURE

8.12.2.1 Truss Geometry Layout/8.12.2.2 Nodal Zone and Member Dimensions

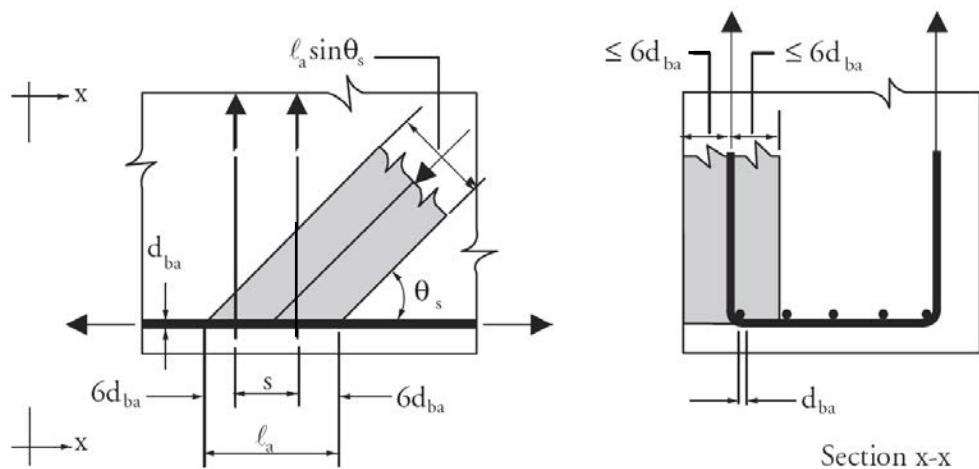
It is essential in the development of a truss layout for strut-and-tie design that:

1. all of the possible load combinations be identified,
2. boundary forces, including internal forces from portions of the structure having sectional type behavior, be calculated for each controlling load condition, and
3. appropriate strut-and-tie models be laid out and designed for each set of boundary conditions.

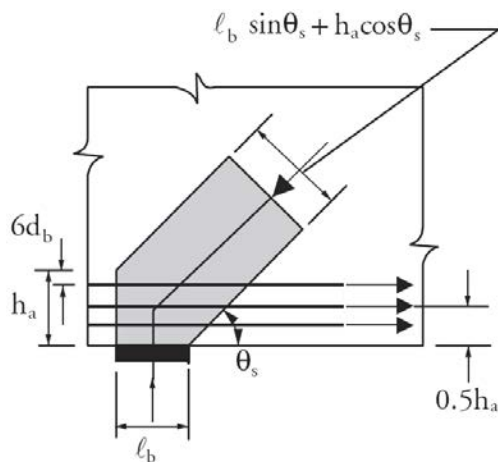
8.12.2.2 Nodal Zone and Member Dimensions

The nodal zones are regions where the struts and ties of the truss join. While the truss diagrams of **Figure 8.12.2.1-2a-2b** idealize the truss members as connecting at points, the actual structure has struts and ties with finite dimensions. The nodal zone sizes are related to both the effective tie member sizes and the mechanism by which exterior loads are transferred into the structure. As shown in **Figure 8.12.2.2-1a-1c** [LRFD Specifications Commentary Figure 5.6.3.3.2-1] the dimensions of the nodal zone and adjoining struts are controlled by the anchorage conditions of reinforcing tie bars or bearing areas of applied loads.

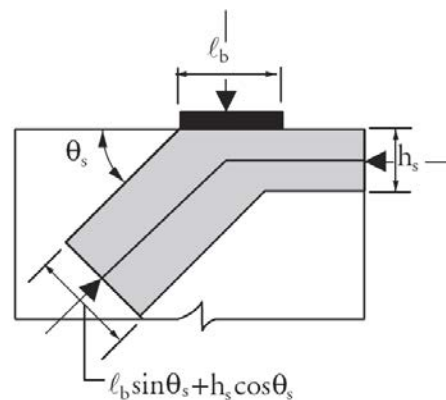
Figure 8.12.2.2-1a-1c
Effects of Anchorage Conditions on Cross-Sectional Area of Strut



a) Strut Anchored by Reinforcement



b) Strut Anchored by Bearing and Reinforcement



c) Strut Anchored by Bearing and Strut

DESIGN THEORY AND PROCEDURE**8.12.2.3 Strength of Members/8.12.3.1.1 Unreinforced Concrete Struts****8.12.2.3 Strength of Members**

The strength of tension ties depends directly on the type and strength of reinforcing used in the ties. Strengths of the individual truss strut members are normally controlled by the limits on stresses within the nodal zones. The nodal zone compressive stresses are defined by the relationship between compressive stress capacity and perpendicular tension strains invoked by compression stress field theory. **Figure 8.12.2-1a** shows the principal tension strain, ε_1 , which may exist perpendicular to the compression strut, BA. The strain, ε_1 , is dependent on the truss geometry and the tensile strain in adjoining truss members. The adverse effect of this tensile strain in the cracked concrete must be considered in calculating the capacity of a strut. In such struts the limiting compressive stress, f_{cu} , is a function of f'_c and ε_1 . The value of ε_1 is, in turn, a function of the tension strain, ε_s , in the cracked concrete in the direction of the tension tie, and the angle between strut and tie.

8.12.3 LRFD Specifications Provisions for Strut-and-Tie Models

LRFD Article 5.6.3.1 states that “strut-and-tie models may be used to determine internal force effects near supports and the points of application of concentrated loads at strength and extreme event limit states.” The statement appearing in the second paragraph of this article is stronger, and more specific, namely, “the strut-and-tie model should be considered for the design of deep footings and pile caps or other situations in which the distance between the centers of applied load and the supporting reactions is less than about twice the member thickness.”

LRFD Article 5.6.3 provides the following specifications for strut-and-tie modeling.

8.12.3.1 Compression Struts

The factored resistance of strut, P_r , may be calculated as:

$$P_r = \phi P_n \quad \text{[LRFD Eq. 5.6.3.2-1]}$$

where

$$\phi = \text{resistance factor} = 0.7 \text{ for bearing in concrete and for strut-and-tie models} \quad \text{[LRFD Art. 5.5.4.2.1]}$$

$$P_n = \text{nominal resistance of a compressive strut}$$

8.12.3.1.1 Unreinforced Concrete Struts

The nominal axial resistance of unreinforced struts is calculated as:

$$P_n = f_{cu} A_{cs} \quad \text{[LRFD Eq. 5.6.3.3.1-1]}$$

where

f_{cu} = limiting compressive stress in strut and is calculated from:

$$f_{cu} = f'_c / (0.8 + 170\varepsilon_1) \leq 0.85f'_c \quad \text{[LRFD Eq. 5.6.3.3.3-1]}$$

where

ε_1 is the principal tensile strain in cracked concrete, and is taken as:

$$\varepsilon_1 = (\varepsilon_s + 0.002) \cot^2 \alpha_s \quad \text{[LRFD Eq. 5.6.3.3.3-2]}$$

where

α_s = smallest angle between the compressive strut and adjoining tension ties, degrees

ε_s = tensile strain in the concrete in the direction of the tension tie, in./in.

$$A_{cs} = \text{effective cross-sectional area of the strut determined from a consideration of the available concrete area and the anchoring or bearing conditions at the ends of the strut} \quad \text{[LRFD Art. 5.6.3.3.2.]}$$

DESIGN THEORY AND PROCEDURE**8.12.3.1.1 Unreinforced Concrete Struts/8.12.3.2 Tension Ties**

For an individual strut, the more basic expression for ϵ_1 includes an additional term, ϵ_s , outside the bracket of LRFD Eq. 5.6.3.3.3-2.

For a value of principal tensile strain, $\epsilon_1 = 0.002$, the concrete in the compression strut can resist a compressive stress of $0.85f'_c$ i.e., the limit for regions of the strut not crossed by or joined to tension ties. It is thus conservatively assumed that the principal compressive strain, ϵ_2 , in the direction of the strut is equal to 0.002.

In the presence of a tension tie at a node, if the reinforcing bars are to yield in tension, there must exist significant tensile strains in the concrete. In LRFD Eq. 5.6.3.3.3-2, as ϵ_s increases, ϵ_1 increases, and f_{cu} in LRFD Eq. 5.6.3.3.3-1 decreases. From LRFD Eq. 5.6.3.3.3-2, it is seen that as α_s decreases, $\cot^2\alpha_s$ and ϵ_1 increase, and therefore f_{cu} decreases. In the limit when $\alpha_s = 0$, the compressive strut direction coincides with that of the tension tie (i.e., incompatibility occurs, and $f_{cu} = 0$ which is an impractical case).

The value of A_{cs} depends on conditions of anchoring of the strut at the node (as shown in **Figure 8.12.2.2-1a-1c**); e.g.

- Strut anchored by reinforcement
- Strut anchored by bearing and reinforcement
- Strut anchored by bearing and strut

The following rules are prescribed for calculating the value of ϵ_s for substitution in LRFD Eq. 5.6.3.3.3-2:

- For a tension tie consisting of reinforcing bars:
 $\epsilon_s =$ tensile strain in reinforcing bars due to factored loads
- For tension tie consisting of prestressing reinforcement:
 $\epsilon_s = 0.0$, up to decompression of concrete (i.e., f_{pe})
 $\epsilon_s = (f_{ps} - f_{pe})/E_p$, beyond decompression

If ϵ_s varies over the width of the strut, ϵ_s is taken as the strain at centerline of the strut.

8.12.3.1.2 Reinforced Concrete Struts

For a strut containing longitudinal reinforcement, which is detailed to develop its yield stress, the nominal resistance is calculated as:

$$P_n = f_{cu}A_{cs} + f_yA_{ss} \quad \text{[LRFD Eq. 5.6.3.3.4-1]}$$

where

$A_{ss} =$ area of reinforcement in strut

$A_{cs} =$ area of concrete strut, calculated as shown earlier

8.12.3.2 Tension Ties

LRFD Article 5.6.3.4.1 states that the nominal strength of a tension tie should be calculated as:

$$P_n = f_yA_{st} + A_{ps}(f_{pe} + f_y) \quad \text{[LRFD Eq. 5.6.3.4.1-1]}$$

where

$f_y =$ yield strength of longitudinal mild steel reinforcement

$f_{pe} =$ stress in prestressing steel due to prestress (after losses)

$A_{st} =$ area of longitudinal mild steel reinforcement in tie

$A_{ps} =$ area of prestressing steel in tie

In the absence of mild steel, a value of $f_y \approx 60$ ksi may be assumed in the equation, in order to reflect the fact that the stress in the prestressing elements will be increased due to the strain which will cause concrete to crack. [LRFD Art. C5.6.3.4.1]

DESIGN THEORY AND PROCEDURE**8.12.3.2.1 Tie Anchorage/8.12.4 Steps for Developing Strut-and-Tie Models****8.12.3.2.1 Tie Anchorage**

The tension tie reinforcement must be anchored in accordance with LRFD Article 5.11 which deals with development of reinforcement. This ensures the satisfactory transfer of the tension force to the node regions.

8.12.3.3 Proportioning Node Regions

In the absence of effective confining reinforcement, it is specified in LRFD Article 5.6.3.5, that the concrete compressive stress in the node regions should not exceed the following:

- $0.85\phi f'_c$ for node regions bounded by compressive struts and bearing areas
- $0.75\phi f'_c$ for node regions anchoring only one tension tie
- $0.65\phi f'_c$ for node regions anchoring tension ties in more than one direction

where ϕ = resistance factor for bearing on concrete = 0.7

[LRFD Art. 5.5.4.2.1]

Stress limits at a nodal zone are controlled by the type of truss members meeting at the node. At nodes B and C (**Figure 8.12.2-1a**) where compression members meet, and at bearing areas at these locations, a higher compressive stress ($0.85\phi f'_c$) is allowed than at A and D where it is necessary to anchor the tension tie, AD. In the latter case, the allowable maximum compressive stress is reduced to $0.75\phi f'_c$. This limit is reduced even further to $0.65\phi f'_c$ when tension ties converge from more than one direction at a node.

The above reductions in the presence of tension ties reflect the detrimental effect of tensile strain in nodes in which tensile reinforcement is anchored. It can be seen that stresses in nodal zones can be reduced by increasing the size of bearing plates, or by increasing the dimensions of struts and tension ties.

LRFD Commentary Article C5.6.3.5 states that if ties consist of post-tensioned tendons, and if the stress in the concrete does not exceed f_{pc} (at centroid of the tie's cross-section), there is no tensile strain in the nodal zone and the limit for concrete compressive stress may be taken as $0.85\phi f'_c$.

8.12.3.4 Crack Control Reinforcement

In order to control crack widths in members designed with the strut-and-tie model (except slabs and footings), and to ensure minimum ductility so that significant redistribution of internal stresses is possible, LRFD Article 5.6.3.6 states that an orthogonal reinforcing grid must be provided near each face. The spacing of bars in such a grid should not exceed 12.0 in., and the ratio of reinforcement area to the width of the member's web times the crack-control reinforcement spacing should be at least 0.003 in each direction.

In general, these crack control requirements lead to a substantial amount of well-distributed reinforcement throughout the member. Accordingly, the *LRFD Specifications* allow for crack control reinforcement located within the region of a tension tie to be included in calculating the resistance of the tie.

8.12.4 Steps for Developing Strut-and-Tie Models

The use of strut-and-tie models typically involves a trial-and-error procedure. The following steps, if followed, should help reduce the effort required:

1. Use strut-and-tie modeling for disturbed regions of the structural member. Solve for internal forces, and their resultants outside the disturbed regions using sectional analysis with all controlling load combinations. These forces from sectional analysis may be considered as boundary forces for the disturbed region model. Apply the resultant forces to the disturbed region along with any external loads that fall on that part of the member.
2. Assume initial models for each of the appropriate controlling load cases and boundary condition force sets. Estimate likely member widths. Elastic stress distribution may be used as a guide. Static equilibrium is then used to determine forces in members due to factored loads. These forces are used in checking member dimensions. It may be necessary to modify the assumed model if the members are determined to be inadequate. A number of appropriate models for different applications are available in the literature [Martin and Sanders (2007), Guyon, (1960); Gergely and Sozen, (1967); Schlaich, et. al., (1987); Collins and Mitchell, (1991); Breen, et. al. (1994)].
3. Draw the strut-and-tie model to a reasonably large scale. This will help avoid errors and give a better appreciation of the proportions of the structure.

DESIGN THEORY AND PROCEDURE**8.12.4 Steps for Developing Strut-and-Tie Models/8.12.4.2 Summary of Steps**

4. There is no single strut-and-tie model for a particular system. Generally, the forces will flow in accordance with the pattern of reinforcement. Well-distributed reinforcement should be provided to ensure the redistribution of internal forces in the cracked concrete.
5. Good detailing of the structure is essential to ensure that the assumed flow of forces can be achieved in the cracked structure. Accordingly, reinforcement in tension ties must be effectively anchored to develop the strength of the member. Nodal zones must be checked to ensure satisfactory load transfer between struts and ties.
6. Complicated stress fields such as fans, arches and bands can usually be replaced by simple line struts. Unnecessary complication of the model is not warranted.

8.12.4.1 Design Criteria

Regardless of the strut-and-tie model adopted, the following design criteria must be met:

1. Limits on bearing stresses and on compressive stresses in struts
2. Satisfactory anchorage and careful detailing of tension tie reinforcement
3. Critical examination of nodal zones to determine their maximum capacities
4. Provision of adequate crack control reinforcement throughout, to ensure the redistribution of internal stresses after cracking of concrete

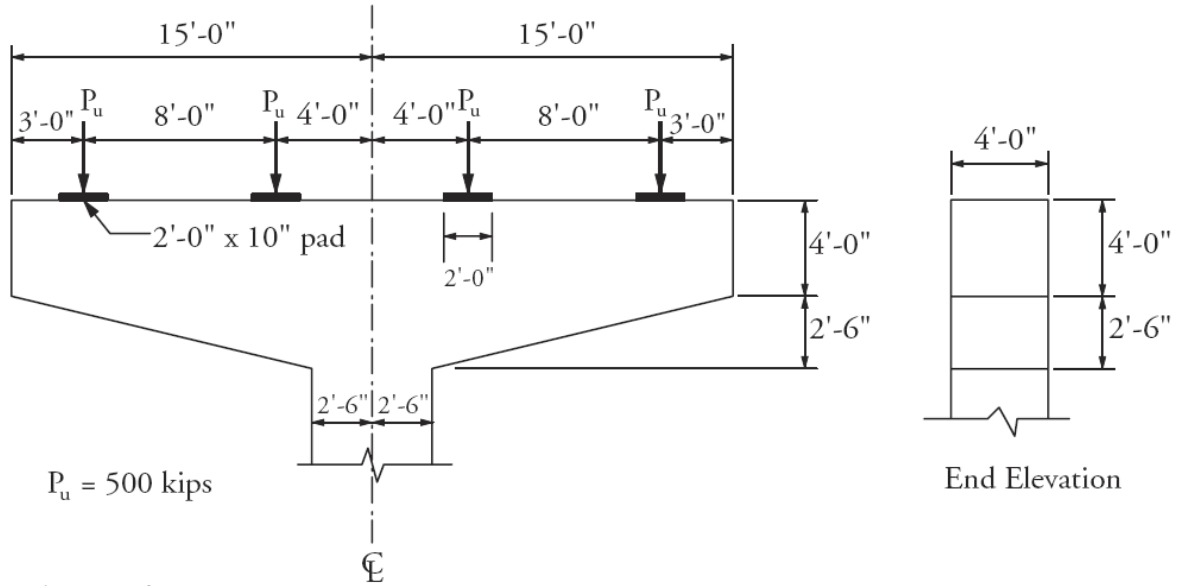
8.12.4.2 Summary of Steps

Step 1	Determine bearing areas	[LRFD Arts. 5.6.3.5 and 5.7.5]
Step 2	Assume appropriate truss geometry (draw a large-scale diagram)	
Step 3	Select tension-tie reinforcement	[LRFD Art. 5.6.3.4]
	Select reinforcement distribution	[LRFD Art. 5.6.3.5]
Step 4	Check development of tension-tie reinforcement	[LRFD Arts. 5.6.3.4.2 and 5.11]
Step 5	Check strength of compression struts	[LRFD Art. 5.6.3.3.1]
Step 6	Select crack control reinforcement	[LRFD Art. 5.6.3.6]
Step 7	Detail structure carefully	

8.12.5 Pier Cap Example

Design the pier cap shown in the figure below.

Figure 8.12.5-1
Pier Cap Dimensions



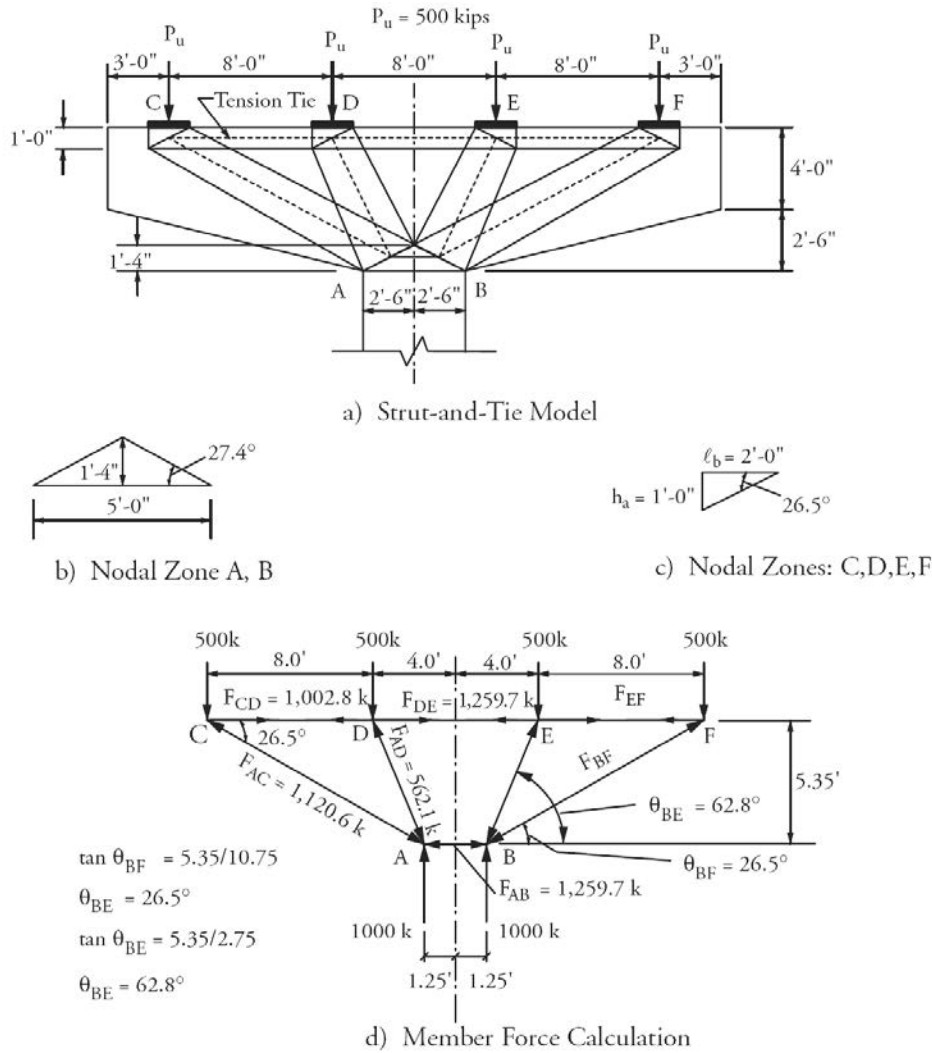
Assumptions
 $f'_c = 5,000$ psi
 $f_y = 60$ ksi

DESIGN THEORY AND PROCEDURE

8.12.5.1 Flow of Forces and Truss Geometry/8.12.5.2 Forces in Assumed Truss

8.12.5.1 Flow of Forces and Truss Geometry

Figure 8.12.5.1-1a-1d
Assumed Truss Geometry



8.12.5.2 Forces in Assumed Truss

Node C:

$$F_{CD} = \frac{500}{\tan(26.5^\circ)} = 1,002.8 \text{ kips}$$

$$F_{AC} = \frac{500}{\sin(26.5^\circ)} = -1,120.6 \text{ kips}$$

Node D:

$$F_{AD} = \frac{500}{\sin(62.8^\circ)} = -562.1 \text{ kips}$$

$$F_{DE} = F_{CD} + F_{AD} \cos(62.8^\circ) = 1,002.8 + 562.1 \cos(62.8^\circ) = 1,259.7 \text{ kips}$$

DESIGN THEORY AND PROCEDURE

8.12.5.2 Forces in Assumed Truss/8.12.5.5 Strut Capacities

Node A:

$$F_{AB} = F_{AD} \cos(62.8^\circ) + F_{Ac} \cos(26.5^\circ) = 562.1 \cos(62.8^\circ) + 1,120.6 \cos(26.5^\circ) = -1,259.7 \text{ kips}$$

$$= -F_{DE} \quad \text{OK}$$

8.12.5.3 Bearing Stresses

Bearing Stresses at C and D:

$$F < P_r = \phi P_n = \phi(0.85 f'_c A_1 m), \text{ assume } m = 1$$

[LRFD Eq.5.7.5-2]

$$\text{Allowable } F/A_1 = 0.7(0.85 \times 5) = 2.98 \text{ ksi}$$

$$\text{Actual } F/A_1 = \frac{500 \text{ k}}{24(10)} = 2.08 \text{ ksi} < \text{maximum allowable of } 2.98 \text{ ksi} \quad \text{OK}$$

Bearing Stresses at A and B:

$$F/A_1 = \frac{2,000 \text{ k}}{60(48)} = 0.69 \text{ ksi} < \text{maximum allowable of } 2.98 \text{ ksi} \quad \text{OK}$$

Therefore, bearing stresses are acceptable.

8.12.5.4 Reinforcement for Tension Tie DE

$$F_{DE} = 1,259.7 \text{ kips}$$

$$\phi f_y A_{st} \geq 1,259.7 \text{ kips}$$

$$A_{st} \geq 1,259.7 / 0.9(60) = 23.3 \text{ in.}^2$$

Because 3 ft -9 in. is available for development at C (at inner edge), choose a bar that can be developed in this distance, i.e., choose No. 10, $\ell_{db} = 43.1 \text{ in.} < 45 \text{ in.}$ available [LRFD Art. 5.11.2.1].

$$\text{No. of bars required} = 23.3 / 1.27 = 18.34 \text{ bars}$$

Use (20) No. 10 bars (25.4 in.²) in 2 layers

$$F_{CD} = 1,002.8 \text{ kips}$$

$$A_{st} > 1,002.8 / 0.9(60) = 18.6 \text{ in.}^2$$

$$\text{If (20) No. 10 bars are used as in DE, } \frac{A_s \text{ required}}{A_s \text{ provided}} = \frac{18.6}{25.4} = 0.73$$

Top bars:

$$\text{Required development length} = 1.3(0.73)(43.1) = 40.9 \text{ in.} < 45 \text{ in. available} \quad \text{O.K.}$$

8.12.5.5 Strut Capacities

Note that each strut is traversed by a tie at one end.

Strut AC:

Strut AC is critical due to the small angle it makes with the tension tie, CD.

$$F_{AC} = 1,120.6 \text{ kips (compression)}$$

End C: (Anchored by bearing and reinforcement)

Tensile strain in tie:

$$F_{CD} / A_s E_s = 1,002.8 / [(20)(1.27)(29,000)] = 1.36 \times 10^{-3} \text{ in./in.}$$

The tension-tie reinforcing bars are developed in the nodal zone. Therefore, the strain in these bars will increase from zero at the ends to 1.36×10^{-3} .

$$\text{Strain at center of strut, } \varepsilon_s = (1/2)(1.36 \times 10^{-3}) = 0.68 \times 10^{-3}$$

$$\varepsilon_1 = (\varepsilon_s + 0.002)\cot^2\alpha_s$$

where

$$\alpha_s = 26.5^\circ \quad [\text{LRFD Art. 5.6.3.3.3}]$$

$$\varepsilon_1 = (0.68 \times 10^{-3} + 2.0 \times 10^{-3})\cot^2(26.5^\circ) = 10.8 \times 10^{-3}$$

$$f_{cu} = f'_c / (0.8 + 170 \varepsilon_1) \leq 0.85 f'_c \quad [\text{LRFD Art. 5.6.3.3.3}]$$

$$= 5.0 / [0.8 + 170(10.8 \times 10^{-3})] = 1.90 \text{ ksi} < (0.85 f'_c = 4.25 \text{ ksi})$$

$$\text{Capacity of strut, AC at C} = \phi f_{cu} A_{cs}$$

where

$$A_{cs} = (\ell_b \sin \theta_s + h_a \cos \theta_s)(48) \quad (\text{Figure 8.12.2.2-1c})$$

$$= (24 \sin(26.5^\circ) + 12 \cos(26.5^\circ)) \times 48 = (21.4 \times 48) \text{ in.}^2$$

$$\text{Capacity of AC at C} = (0.70)(1.90)(48 \times 21.4)$$

$$= 1,366.2 \text{ kips} > F_{AC} = 1,120.6 \text{ kips} \quad \text{OK}$$

End A of AC is obviously not critical (not crossed by tension tie and wider dimensions than at C).

Strut AD:

Strut AD is anchored by bearing and reinforcement at end A, and crossed by tie at end D.

$$F_{AD} = 562.1 \text{ kips}$$

$$\text{End D: Tensile strain in tie, DE} = 1,259.7 / [(20)(1.27)(29,000)] = 1.71 \times 10^{-3}$$

$$\text{Strain at center of strut, } \varepsilon_s = (1/2)(1.71 \times 10^{-3}) = 0.86 \times 10^{-3}$$

$$\varepsilon_1 = (\varepsilon_s + 0.002)\cot^2\alpha_s$$

where

$$\alpha_s = 62.8^\circ$$

$$\varepsilon_1 = (0.86 + 2.0)10^{-3}\cot^2(62.8^\circ) = 0.755 \times 10^{-3}$$

$$f_{cu} = f'_c / (0.8 + 170 \varepsilon_1) \leq 0.85 f'_c$$

$$f_{cu} = 5.0 / [0.8 + 170(0.775 \times 10^{-3})] = 5.39 \text{ ksi} > 0.85 f'_c = 4.25 \text{ ksi}$$

$$\text{Capacity of strut AD at D: } \phi f_{cu} A_{cs}$$

$$A_{cs} = (\ell_b \sin \theta_s + h_a \cos \theta_s)(48) = (24 \sin(62.8^\circ) + 12 \cos(62.8^\circ)) \times 48 = 1,288 \text{ in.}^2$$

$$\text{Capacity of strut} = (0.7)(4.25)(1,288) = 3,831 \text{ kips} > F_{AD} = 562.1 \text{ kips} \quad \text{OK}$$

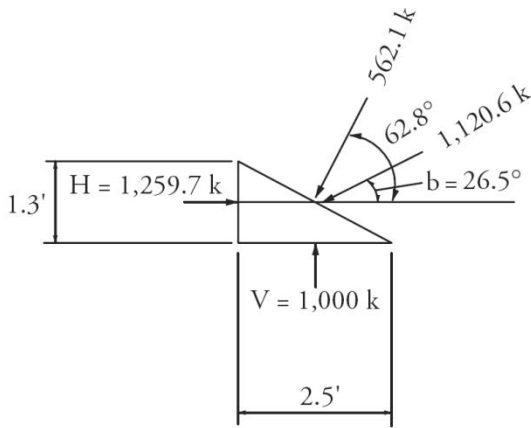
End A is obviously not critical (not crossed by tie).

DESIGN THEORY AND PROCEDURE

8.12.5.6 Nodal Zone at Pier/8.12.5.7 Minimum Reinforcement for Crack Control

8.12.5.6 Nodal Zone at Pier

*Figure 8.12.5.6-1
Nodal Zone at Pier*



Horizontal component, $H = 562.1\cos(62.8^\circ) + 1,120.6\cos(26.5^\circ) = 1,259.7 \text{ kips} = F_{AB}$ OK

This nodal zone is bounded only by compressive struts and bearing areas:

Allowable compressive stress, $f = 0.85f'_c = 2.98 \text{ ksi}$

[LRFD Art. 5.6.3.5]

Due to H: $F/A = 1,259.7/[(1.3)(12)(48)] = 1.68 \text{ ksi} < 2.98$ OK

Due to V: $F/A = 1,000/[(2.5)(12)(48)] = 0.69 \text{ ksi}$ OK.

8.12.5.7 Minimum Reinforcement for Crack Control

Check at throat and provide this reinforcement throughout (assuming 12 in. spacing).

Minimum A_s required = $0.003(12)(48) = 1.73 \text{ in.}^2/\text{ft}$

[LRFD Art. 5.6.3.6]

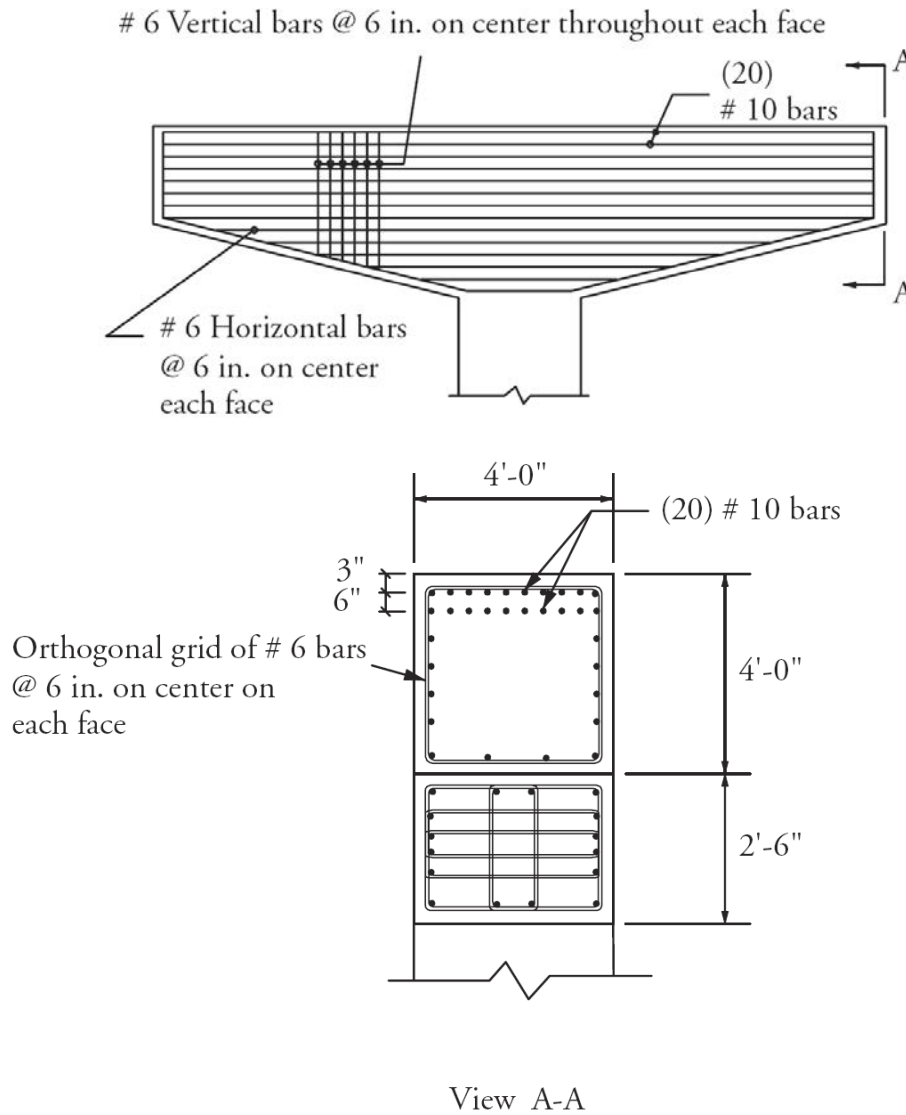
Use , No.9 bars each face at 12 in. on center = $2 \times 1.00 = 2.00 \text{ in.}^2/\text{ft}$, or No. 6 bars each face at 6 in. on center = $4 \times 0.44 = 1.76 \text{ in.}^2/\text{ft}$

Use No. 6 bars @ 6 in. on center vertically and horizontally.

DESIGN THEORY AND PROCEDURE

8.12.5.7 Minimum Reinforcement for Crack Control/8.13.1 Introduction

Figure 8.12.5.7-1
Reinforcement Details



8.13 DETAILED METHODS OF TIME-DEPENDENT ANALYSIS

Section 8.6 of this chapter presents a variety of practical and relatively simple methods to estimate time-dependent effects in prestressed concrete members. Those methods are suitable for a wide range of bridge projects but may not be applicable to certain special situations. More detailed methods are available when the designer feels that a more rigorous estimate of time-dependent effects is warranted.

8.13.1 Introduction

The following sections describe a method that can be used to perform time-dependent analysis of a composite prestressed concrete bridge member of any cross section. This method is based on traditional composite section analysis, using transformed elastic properties of steel elements and any cast-in-place concrete elements. Adjustments are made to the elastic modulus of the concrete elements to reflect creep characteristics. So-called *initial strains* are introduced in the analysis to account for concrete shrinkage, steel relaxation, and residual concrete creep. By analyzing discrete cross-sections, and then performing the numerical integration described in Section 8.7.4, whole members may also be analyzed using the methods that follow.

DESIGN THEORY AND PROCEDURE**8.13.1.1 Properties of Concrete/8.13.1.1.1 Stress-Strain-Time Relationship****8.13.1.1 Properties of Concrete**

The mechanical properties of concrete vary with time. As hydration progresses, compressive strength and modulus of elasticity continually increase, but at a decreasing rate. In addition, it has long been recognized that concrete exhibits creep, defined as the time-dependent increase in strain that occurs while the material is subjected to constant stress. Finally, concrete undergoes shrinkage caused by drying. Chapter 2 and Section 8.6.7 provide more detailed discussion of these time-dependent behaviors.

There exists a wide range of methods used to produce precast concrete bridge components. Concrete mixes, aggregates, admixtures, and curing methods all have significant effects on the time-dependent properties of concrete as a structural material. Because of these variations, the recommendations in Chapter 2 and Section 8.6 should be used only as a starting point. For applications where it is critical to accurately predict time-dependent behavior, the properties of the actual materials used should be determined by testing.

8.13.1.1.1 Stress-Strain-Time Relationship

In order to perform time-dependent analysis, it is necessary to establish the stress-strain-time relationship for the concrete material. This relationship will predict the total strain, ϵ , at a future time, t , that results from a stress increment applied at time, t_0 . The total concrete strain at any time, t , can be separated into three components:

ϵ_f = the immediate strain due to the applied stress, f

ϵ_{cr} = the time-dependent creep strain

ϵ_{sh} = free shrinkage strain

It is important to recognize that both the modulus of elasticity, E , and the creep coefficient, C , are functions of time. In addition, because concrete is an aging material, C depends on the loading age, t_0 , as well.

1. Constant Stress

Total concrete strain is ($\epsilon_f + \epsilon_{cr} + \epsilon_{sh}$) which is usually expressed as follows:

$$\epsilon = \frac{f(t_0)}{E_c(t_0)} [1 + C(t, t_0)] + \epsilon_{sh} \quad (\text{Eq. 8.13.1.1.1-1})$$

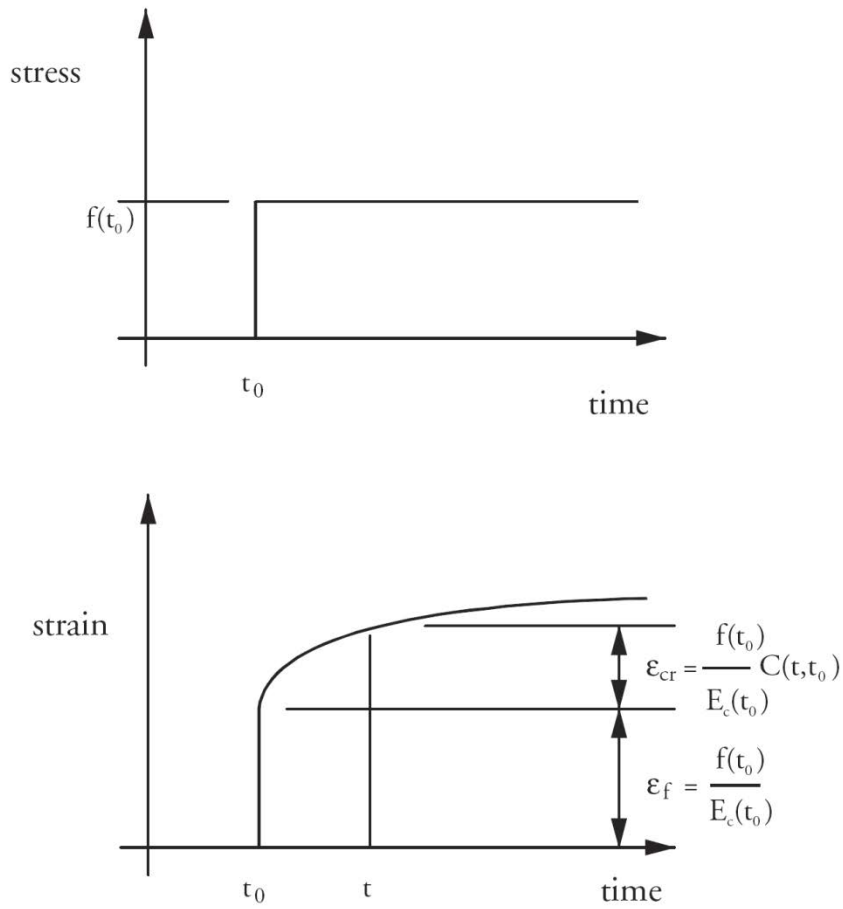
where

$E_c(t_0)$ = modulus of elasticity at time, t_0 , the beginning of the time interval

$C(t, t_0)$ = creep coefficient over a time interval from t_0 to t

Eq. (8.13.1.1.1-1) applies as long as stress, f , is a constant, sustained stress. **Figure 8.13.1.1.1-1** shows the gradual development of creep strains with time under the effects of a constant stress.

Figure 8.13.1.1.1-1
Concrete Strain vs. Time Under Constant Stress



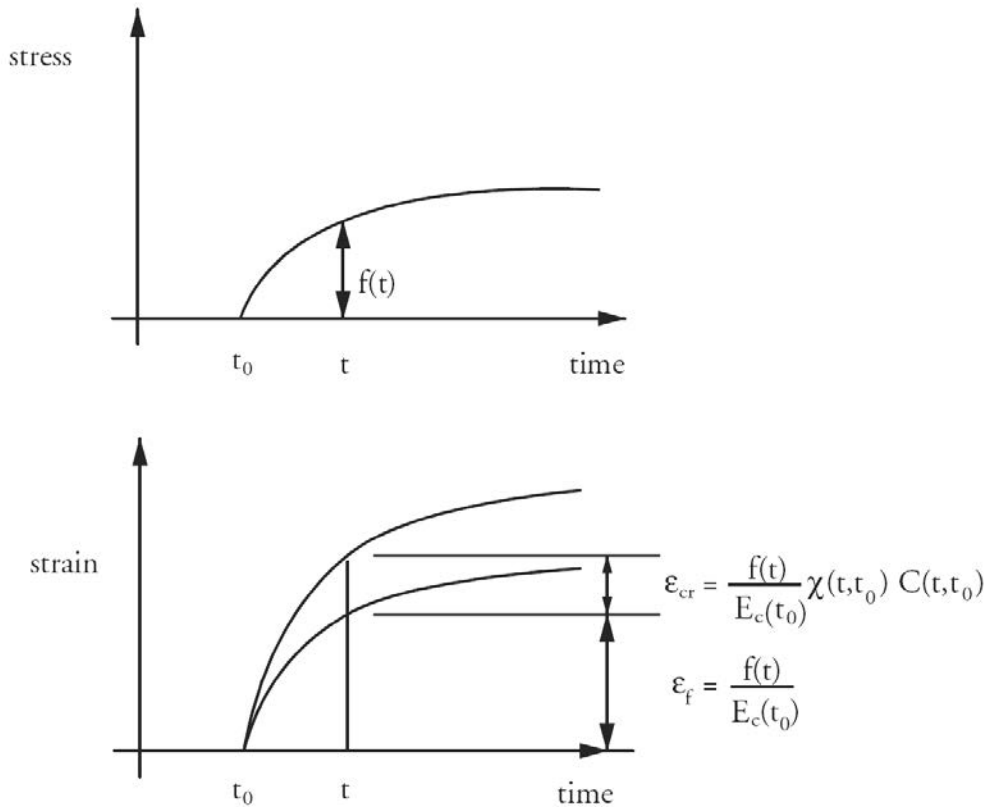
DESIGN THEORY AND PROCEDURE

8.13.1.1.1 Stress-Strain-Time Relationship/8.13.1.2 Effective Modulus

2. Variable Stress

Where the applied stress, f , is variable, Eq. (8.13.1.1.1-1) cannot be used directly. **Figure 8.13.1.1.1-2** depicts the development of creep strains under the effects of an increasing applied stress.

Figure 8.13.1.1.1-2
Concrete Strain vs. Time Under Variable Stress



At most stress levels experienced due to service loads, the principle of superposition applies. Using superposition, the effects of a series of applied stress increments can be determined individually, using the above equation, and then combined to give the total time-dependent concrete strain. For a series of stress increments, f_j , applied at times, t_j , the total concrete strain can be expressed as:

$$\epsilon = \sum \frac{f(t_j)}{E_c(t_j)} [1 + C(t, t_j)] + \epsilon_{sh} \tag{Eq. 8.13.1.1.1-2}$$

Therefore, a method for predicting concrete strain, ϵ , under conditions where stress is not constant, is to break the time interval over which ' f ' is applied into many discrete steps and perform a summation using Eq. (8.13.1.1.1-2). While this approach is general and can be easily implemented on a computer, it is not effective for hand calculations. However, an accurate, but simplified method exists and will be discussed further in Section 8.13.1.3.

8.13.1.2 Effective Modulus

The effective-modulus concept is used frequently to simplify creep analysis. The effective modulus is defined as follows:

$$E_c^*(t, t_0) = \frac{E_c(t_j)}{1 + C(t, t_0)} \tag{Eq 8.13.1.2-1}$$

DESIGN THEORY AND PROCEDURE

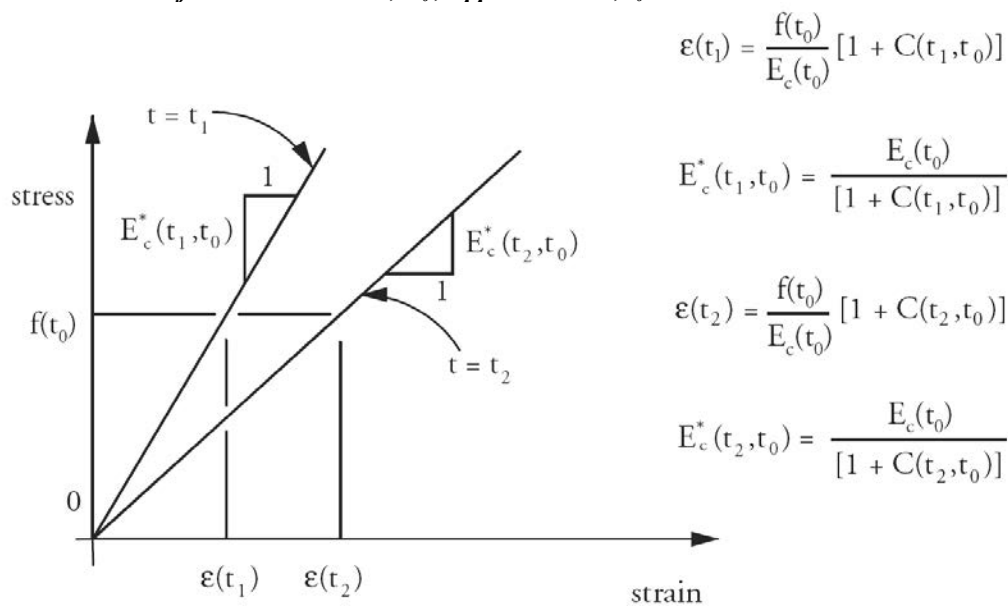
8.13.1.2 Effective Modulus/8.13.1.3 Age-Adjusted Effective Modulus

Comparison with Eq. (8.13.1.1.1-1) shows that E_c^* relates both the immediate strain, ϵ_f , and the time-dependent creep strain, ϵ_{cr} , to the applied stress, f . **Figure 8.13.1.2-1** illustrates the effective-modulus concept. Notice that the effective modulus, or the slope of the stress vs. strain curve, depends on both the time of application of the load, t_0 , and the time at which strains are to be determined, t_1 or t_2 . The use of an effective modulus allows a pseudo-elastic analysis to be performed within a given time interval.

Eq. (8.13.1.1.1-1) can be rewritten to take advantage of the effective-modulus concept:

$$\epsilon = \frac{f(t)}{E_c^*(t, t_0)} + \epsilon_{sh} \tag{Eq. 8.13.1.2-2}$$

Figure 8.13.1.2-1
Stress vs. Strain for Constant Stress, F_0 , Applied at time, t_0



8.13.1.3 Age-Adjusted Effective Modulus

Eqs. (8.13.1.1.1-1) and (8.13.1.2-2) are valid only when the stress, f , is constant. In many situations, however, ' f ' will vary with time. **Figure 8.13.1.1.1-2** graphically depicts this condition.

For instance, consider a hollow precast concrete cylinder that is filled with fresh concrete shortly after the cylinder has been subjected to a constant axial compressive force. When hardened, the cast-in-place concrete fill will be subjected to a load that increases with time as creep strains develop in the surrounding precast cylinder. A similar condition exists in a reinforced concrete member under sustained loads as the reinforcing steel resists creep strains. Solutions of time-dependent problems such as these require the ability to predict creep strains under varying load.

As discussed in Section 8.13.1.1.1, one approach would be to divide the problem into many small time intervals. The stress increment during each interval could be treated as a new load and, since superposition is valid, Eq. (8.13.1.1.1-2) could be used to calculate the total response of the member.

An alternative approach, Bazant (1972), uses the aging coefficient, χ , to adjust the creep coefficient. The aging coefficient accounts for three separate effects:

1. When the applied stress, $f(t)$, is increasing, the concrete experiences the maximum force for only an instant at the end of the time interval (t_0, t) . At all other times, the concrete experiences a load that is less than the maximum.

DESIGN THEORY AND PROCEDURE

8.13.1.3 Age-Adjusted Effective Modulus/8.13.1.5 Reduced Relaxation under Variable Strain

- The concrete is gaining strength, and therefore its modulus is increasing with time. Portions of the time-varying load that occur earlier are acting on concrete which is less stiff. Later in the interval, when the loads are larger, the concrete is also stiffer.
- As shown in Chapter 2, for a given concrete in a given environment, the total creep potential for loads applied to young concrete is larger than for the same loads applied to old concrete.

Eq. (8.13.1.3-1) should be used when the stress varies over the interval (t_0, t) :

$$\varepsilon = \frac{f(t)}{E_c(t_0)} [1 + \chi(t, t_0)C(t, t_0)] + \varepsilon_{sh} \quad (\text{Eq. 8.13.1.3-1})$$

The corresponding age-adjusted effective modulus is given by:

$$E_c^*(t, t_0) = \frac{E_c(t_0)}{1 + \chi(t, t_0)C(t, t_0)} \quad (\text{Eq. 8.13.1.3-2})$$

From here on the effective-modulus will be referred to as defined by Eq. (8.13.1.3-2), with the understanding that Eq. (8.13.1.2-1) represents the special case of an instantaneously applied load for which $\chi = 1$.

There are methods available (Bazant, 1972) by which the aging coefficient can be computed precisely for different ages at loading and for different concrete properties. In most practical problems, however, it is sufficiently accurate to use a value of 0.7 or 0.8 for χ , depending on the age of concrete at the beginning of the time interval. For loads applied at a relatively young concrete age, 0.7 should be used. For all other situations, 0.8 is generally sufficiently accurate given all of the other uncertainties present in this type of analysis.

8.13.1.4 Properties of Prestressing Steel

Most prestressing materials, including steel bars and strand, exhibit relaxation. Relaxation is similar to creep but is defined as the loss of stress in a stressed material held at constant length. The following equation may be used to estimate the relaxation, f_r , occurring in steel prestressing materials during the interval (t, t_0) :

$$f_r(t, t_0) = \frac{f(t_0)}{K_r} \left[\frac{f(t_0)}{f_y} - 0.55 \right] \log_{10} \left(\frac{24t + 1}{24t_0 + 1} \right) \quad (\text{Eq. 8.13.1.4-1})$$

for $\frac{f(t_0)}{f_y} \geq 0.55$

where

$f(t_0)$ = tensile stress at the beginning of the interval

f_y = yield strength of the strand

K_r = constant for the material. Values of K_r and f_y for some prestressing strand are provided in **Table 8.13.1.4-1**.

Table 8.13.1.4-1
Values of Material Constant, K_r , and Yield Strength, f_y

Grade 270 Strand	K_r	f_y , ksi
Low-Relaxation	45*	243.0
Stress-Relieved (Normal-Relaxation)	10	229.5

* Also, see Note accompanying Eq. (8.6.5.3-1)

8.13.1.5 Reduced Relaxation under Variable Strain

The relaxation predicted by Eq. (8.13.1.4-1) is the intrinsic relaxation, i.e., the relaxation that occurs under the theoretical condition of constant strain. In an actual prestressed concrete member, strain in the prestressing

DESIGN THEORY AND PROCEDURE**8.13.1.5 Reduced Relaxation under Variable Strain/8.13.2.2 Method for Time-Dependent Cross Section Analysis**

materials is not constant, and is usually decreasing due to creep and shrinkage of the concrete. Under these circumstances, Eq. (8.13.1.4-1) will somewhat over-predict relaxation. Various researchers, Ghali and Travino (1985), Glodowski and Lorenzetti (1972), Hernandez and Gamble (1975), and others have studied this problem and have proposed various methods of calculating the reduced relaxation that occurs during intervals of decreasing strain.

With modern low-relaxation prestressing materials, however, relaxation effects are very small compared to concrete creep and shrinkage. Therefore, it is sufficiently accurate to adopt a single, standard reduction factor to adjust the intrinsic relaxation during intervals in which the strain is decreasing. In most practical situations, a factor equal to 0.8 may be applied to that portion of the relaxation that occurs under conditions of gradually reducing strain.

8.13.2 Analysis of Composite Cross Sections

The method of analysis illustrated here is essentially no different than a conventional elastic analysis of a prestressed concrete cross-section using transformed section properties. Instead of a conventional modulus of elasticity, however, the age-adjusted, effective modulus is used for all concrete elements in the section. In addition, initial strains must be considered. The following sections will illustrate the procedure.

8.13.2.1 Initial Strains

An initial strain is defined as one that is not directly due to an applied stress. Other than time-dependent analysis, temperature strain may be the most familiar example of an initial strain.

In time-dependent analysis of concrete members, the initial strains normally considered are

- free shrinkage of the concrete occurring during the time interval being considered,
- creep strains of the concrete, occurring during the time interval being considered, that are due to previously applied loads, and
- the apparent steel strain due to relaxation of prestressing steel during the time interval being considered.

To incorporate initial strains into cross-section analysis, it is convenient to calculate a fictitious restraining load which will restrain the initial strains described above. The restraining load is then subtracted from any real loads applied to the section. Using the net load, an analysis is performed in a manner similar to conventional transformed section analysis. Finally, the internal forces are calculated using the two components. The internal forces associated with the net load applied to the entire composite section are calculated. These are then added to the individual element restraint forces to give the total actual forces on an individual element of the cross-section. The following section provides a detailed description of the procedure used.

8.13.2.2 Method for Time-Dependent Cross-Section Analysis

Several researchers have published methods to perform the time-dependent analysis of cross-sections of prestressed concrete members. Two approximate methods, suitable for manual calculations, and rigorous time-step methods suitable only for computerized solutions have been presented. References such as Branson and Kripanarayanan (1971); Tadros, et al. (1975); Tadros, et al. (1977A and B); Dilger (1982-A and B); Tadros, et al. (1985); and Collins and Mitchell (1991) can be consulted for additional information.

All of the methods in the cited references, as well as the method presented here, are based on a pseudo-elastic analysis with the following assumptions and conditions:

- The superposition of creep strains from different stress increments is valid.
- Concrete members remain uncracked.
- Stress levels are low compared to the compressive strength of the concrete.

It is necessary to consider the entire history of a cross-section in determining its time-dependent behavior. This history is usually composed of time intervals of varying lengths. Discrete events (such as the transfer of

DESIGN THEORY AND PROCEDURE

8.13.2.2 Method for Time-Dependent Cross Section Analysis/8.13.2.2.1 Steps for Analysis

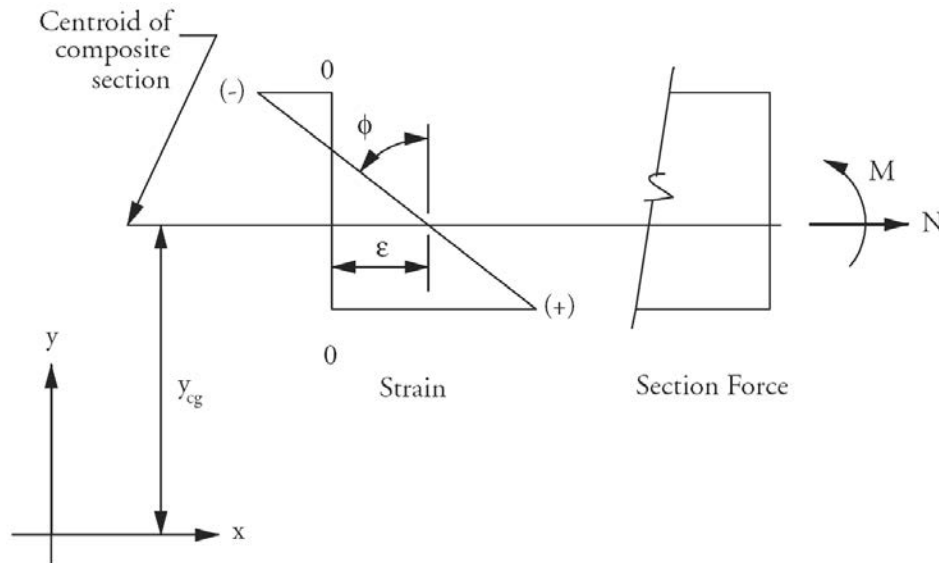
prestressing force or the application of the weight of a cast-in-place topping) mark the beginning and end of each time interval. During the time between these discrete events there is continual creep, shrinkage and relaxation, as well as internal redistribution of stresses. It is convenient to consider each discrete event (such as the transfer of prestressing force) as though it occurred during a time interval whose length is zero.

Within a given time interval an elastic analysis with initial strains is performed for the cross-section being analyzed. Transformed composite section properties are recalculated for the analysis in each time interval since the properties of the concrete are time dependent. A unique set of initial strains, dependent upon all of the stress increments applied during the history of the member, is calculated for each time interval to be analyzed.

The most rigorous methods of time-dependent analysis reduce the time history into many small steps. As the size of the time-step decreases, the accuracy of the analysis increases. One such method is described by Tadros et al. (1977B). A slightly less accurate, but greatly simplified, method is presented by Dilger (1982A and B) and will be used as the basis for the procedure described here. That method uses creep-transformed section properties based on the age-adjusted, effective modulus for a given time interval.

The sign convention for strain, curvature, and section forces in the following procedure are shown in **Figure 8.13.2.2-1**.

Figure 8.13.2.2-1
Sign Conventions for Composite Section Analysis



8.13.2.2.1 Steps for Analysis

The following steps are repeated for each time interval that is to be analyzed over the entire time history of a single cross section:

1. Calculate the age-adjusted, effective modulus, E_{ck}^* , for the interval under consideration for each element, k , comprising the composite section. (Take the effective modulus, E_c^* , of the composite section to be that of the concrete beam).
2. Calculate the modular ratio, n_k , for each element in the section.

$$n_k = \frac{E_{ck}^*}{E_c^*} \tag{Eq. 8.13.2.2.1-1}$$

DESIGN THEORY AND PROCEDURE**8.13.2.2.1 Steps for Analysis/8.13.2.2.2 Example Calculations**

3. Calculate the transformed composite section area, A , center of gravity, y , and moment of inertia, I .

$$A = \Sigma A_k n_k \quad (\text{Eq. 8.13.2.2.1-2})$$

$$y = \frac{1}{A} \Sigma y_k A_k n_k \quad (\text{Eq. 8.13.2.2.1-3})$$

$$I = \Sigma [I_k + (y - y_k)^2 A_k] n_k \quad (\text{Eq. 8.13.2.2.1-4})$$

4. Calculate the total initial strains, ϵ_{0k} , and curvature, ϕ_{0k} , for each element in the composite section. For concrete elements, the total initial strains will be those due to free shrinkage plus those due to creep resulting from previously applied stresses. For prestressed steel elements, the initial strain will be the apparent strain due to relaxation. Typically, non-prestressed steel will have no initial strain. Calculations of initial strains will be presented in the examples that follow.

5. For each element, k , calculate N_{0k} and M_{0k} , the theoretical restraint forces. Sum all the N_{0k} and M_{0k} over the section to give N_0 and M_0 .

$$N_{0k} = -E_c^* \epsilon_{0k} A_k \quad (\text{Eq. 8.13.2.2.1-5})$$

$$N_0 = \Sigma N_{0k} \quad (\text{Eq. 8.13.2.2.1-6})$$

$$M_{0k} = -E_{ck}^* I_k \phi_{0k} \quad (\text{Eq. 8.13.2.2.1-7})$$

$$M_0 = \Sigma [M_{0k} - N_{0k}(y_k - y)] \quad (\text{Eq. 8.13.2.2.1-8})$$

6. Subtract the restraint forces, N_0 and M_0 , from the real applied forces, N and M , and calculate the total strain, ϵ , and curvature, ϕ , in the section.

$$\epsilon = \frac{N - N_0}{E_c^* A} \quad (\text{Eq. 8.13.2.2.1-9})$$

$$\phi = \frac{M - M_0}{E_c^* I} \quad (\text{Eq. 8.13.2.2.1-10})$$

7. Calculate the strains and curvatures for each element in the composite section.

$$\epsilon_k = \epsilon - \phi(y_k - y) \quad (\text{Eq. 8.13.2.2.1-11})$$

$$\phi_k = \phi \quad (\text{Eq. 8.13.2.2.1-12})$$

8. Calculate the element forces, N_k and M_k , and elastic strains, ϵ_{fk} and ϕ_{fk} , based on the element strains and the effective modulus, E_{ck}^* , for each section element.

$$N_k = E_{ck}^* A_k \epsilon_k + N_{0k} \quad (\text{Eq. 8.13.2.2.1-13})$$

$$\epsilon_{fk} = \frac{N_k}{E_{ck}^* A_k} \quad (\text{Eq. 8.13.2.2.1-14})$$

$$M_k = E_{ck}^* I_k \phi_k + M_{0k} \quad (\text{Eq. 8.13.2.2.1-15})$$

$$\phi_{fk} = \frac{M_k}{E_{ck}^* I_k} \quad (\text{Eq. 8.13.2.2.1-16})$$

Steps 1 through 8 are repeated for each time interval to be analyzed over the time history of the cross-section.

8.13.2.2.2 Example Calculations

A 12 x 12 in. concrete prism, reinforced with four No. 9 reinforcing bars, was loaded with a 216-kip axial compressive force immediately after being wet-cured for seven days. Find the concrete and steel stresses 90 days after loading.

DESIGN THEORY AND PROCEDURE

8.13.2.2 Example Calculations/8.13.3 Analysis of Composite Simple-Span Members

The creep coefficient, $C(97,7)$, is 1.65 and the total free shrinkage strain, ϵ_{shu} , occurring during this period is -400×10^{-6} . The initial modulus of elasticity of the concrete, E_{ci} , is 3,500 ksi and the modulus of elasticity of the steel bars is 29,000 ksi. The strain in the section immediately after initial loading was calculated to be -0.0003564 . The concrete and steel compressive stresses were 1.248 ksi and 10.34 ksi, respectively.

Step 1 Calculate the age-adjusted, effective modulus for the concrete:

$$E_c^* = \frac{3,500}{1 + (0.7)(1.65)} = 1,624 \text{ ksi}$$

Step 2 Calculate the modular ratio for the steel elements:

$$n_s = \frac{29,000}{1,624} = 17.86$$

Step 3 Calculate the transformed area of the composite section:

$$A = [(12)(12)-4](1.0) + (4.00)(17.86) = 211.4 \text{ in.}^2$$

Step 4 Calculate the initial strain in the concrete (due to both creep and shrinkage):

$$\epsilon_{0c} = -0.000400 + (1.65)(-0.0003564) = -0.0009881$$

Step 5 Calculate the restraint forces for the concrete element and the composite section:

$$N_0 = N_{0c} = -(1,624)(-0.0009881)(140) = 224.7 \text{ kips}$$

Step 6 Calculate the composite section strain:

$$\epsilon = \frac{0 - 224.7}{(1,624)(211.4)} = -0.0006544$$

Step 7 Calculating the element strains is straightforward for this example. Both the concrete and steel strains are equal to the composite section strain, -0.0006544 .

Step 8 Calculate the internal element forces and elastic strains on the concrete and steel:

$$N_c = (-0.0006544)(1,624)(140) + 224.7 = 75.9 \text{ kips (tension)}$$

$$N_s = (-0.0006544)(29,000)(4.00) = -75.9 \text{ kips (compression)}$$

$$\epsilon_{fc} = \frac{-75.9}{(140.0)(1,624)} = -0.000334$$

$$f_c = \frac{75.9}{140.0} = 0.542 \text{ ksi (tension)}$$

$$\epsilon_{fs} = \frac{-75.9}{(29,000)(4.00)} = -0.000654$$

$$f_s = \frac{-75.9}{4.00} = -19.0 \text{ ksi (compression)}$$

Therefore, the total concrete and steel stresses at 90 days are $(1.248 - 0.542) = 0.706$ ksi and $(10.34 + 19.0) = 29.3$ ksi, respectively. In this example, the initial strains at 90 days were the result of gradual changes that had occurred during the preceding time interval. The aging coefficient in this example was taken to be 0.7 since loading occurred when the concrete was still relatively young.

8.13.3 Analysis of Composite Simple-Span Members

A typical simple-span prestressed concrete bridge beam is shown in **Figure 8.13.3-1**. Detailed information about this bridge is given in Section 8.13.3.2.1. During its history, this beam will experience several different discrete events. Creep, shrinkage, and relaxation will continue between these discrete events, accompanied by an internal redistribution of stresses. **Table 8.13.3-1** summarizes the significant time intervals during the life of this typical beam.

DESIGN THEORY AND PROCEDURE

8.13.3 Analysis of Composite Simple-Span Members/8.13.3.2 Transfer of Prestress Force

Figure 8.13.3-1
Beam Used for Example Calculations

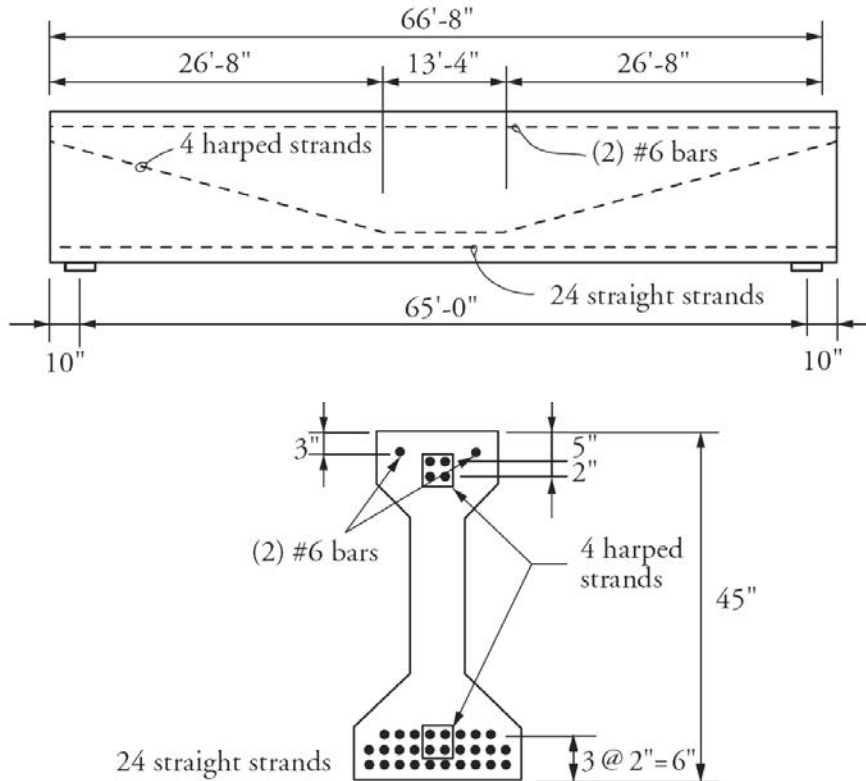


Table 8.13.3-1
Beam Lifetime Intervals

Interval	Event	Typical Duration
1	Strand relaxation before transfer	12 to 24 hours
2	Transfer of prestress	0
3	Creep, shrinkage, and relaxation of beam after transfer	30 days to 1 year
4	Placement of cast-in-place deck	0
5	Creep, shrinkage, and relaxation of composite deck and beam	7 days to 6 months
6	Application of superimposed dead load on the composite deck and beam	0
7	Creep, shrinkage, and relaxation of composite deck and beam	25 years or more

The following sections will describe the analyses performed for each time interval during the life of the beam. This is an incremental analysis and the state of stress or strain in the system at any point in time is equal to the sum of the previous intervals.

8.13.3.1 Relaxation of Strands Prior to Transfer

Eq. (8.13.1.4-1) may be used without adjustment to calculate the intrinsic relaxation of the strands prior to release or transfer. While the strands are anchored at the ends of the casting bed, the strain is constant, so the intrinsic relaxation is the correct quantity in this situation.

8.13.3.2 Transfer of Prestress Force

The method described in Section 8.13.2.2 is used to calculate the effects of transferring the prestressing force. Transformed section properties, including the strands, the concrete, and any additional mild steel, are calculated as described. Because this is considered to be an interval of zero duration, the creep coefficient is zero for the

DESIGN THEORY AND PROCEDURE**8.13.3.2 Transfer of Prestress Force/8.13.3.2.1 Example Calculation (at Transfer)**

concrete. The effective modulus of elasticity of the concrete, therefore, will be equal to the modulus of elasticity at the time of transfer.

The total prestress force in the strands is treated as an external compressive load applied to the transformed section at the centroid of the strands.

8.13.3.2.1 Example Calculation (at Transfer)

Analyze the midspan section of the beam shown in **Figure 8.13.3-1** immediately after the transfer of prestress. To simplify, assume that the strands were tensioned and the concrete cast 18 hours prior to transfer. In practice, it is more likely that strands might be tensioned 18 hours, and concrete cast 12 hours before release. The beam self-weight moment at midspan is 3,694 in.-kips.

Beam data:

Strands: $\frac{1}{2}$ -in.-diameter strand, Grade 270, low-relaxation

Eccentricity at midspan = 16.413 in.

Eccentricity at end of beam = 11.556 in.

Reinforcing bars: No. 6, Grade 60

Beam concrete: $f'_{ci} = 4.95$ ksi at 18 hours, $E_{ci} = 4,054$ ksi

$f'_c = 6.750$ ksi at 28 days, $E_c = 4,734$ ksi

$\epsilon_{shu} = -0.0004$ in./in.

$C_u = 1.4$

Beam section properties: AASHTO-PCI Type II

$A = 560$ in.²

$I = 125,390$ in.⁴

$y_b = 20.27$ in.

Composite section properties: $I_c = 382,372$ in.⁴

$y_{bc} = 36.02$ in.

Deck properties: Width = 104 in.

Thickness = 8 in.

$f'_c = 4.50$ ksi at 28 days

$\epsilon_{shu} = -0.0004$ in./in.

$C_u = 1.4$

Dead loads: Self-weight = 583 plf

Deck weight = 867 plf

Haunch weight = 40 plf

Diaphragm weight = 100 plf

Superimposed dead load = 360 plf

DESIGN THEORY AND PROCEDURE

8.13.3.2.1 Example Calculation (at Transfer)

The total force in the strands, prior to release, is equal to the jacking force less relaxation losses occurring prior to release:

$$f_{pj} = (0.75)(270.0) = 202.5 \text{ ksi}$$

$$f_r = \frac{202.5}{45} \left[\frac{202.5}{243.0} - 0.55 \right] \log_{10} \left(\frac{(24)(0.75) + 1}{(24)(0.0) + 1} \right) = 1.63 \text{ ksi}$$

The force applied to the transformed section at release is:

$$P_i = (202.5 - 1.63)(28)(0.153) = 860.5 \text{ kips} = -N$$

Calculation of transformed composite section properties, i.e. Steps 1 through 3 from Section 8.13.2.2.1, is shown in **Table 8.13.3.2.1-1**. The modulus of elasticity of the beam concrete is based on the concrete strength at release. (The section properties of the bare beam have been adjusted in this example to remove the concrete area occupied by strands and mild steel bars. In practice, this refinement may be omitted with no significant loss of accuracy).

Table 8.13.3.2.1-1

Calculation of Transformed Composite Section Properties at Transfer

Item	Area in. ²	y_{cg} in.	Moment of Inertia in. ⁴	Modulus of Elasticity ksi	Modular Ratio, n	(1) × (5) in. ²	(1) × (5) × (2) in. ³	(3) × (5) in. ⁴	$[y - (2)]^2 \times (1)$ in. ⁴	(8) + (9) in. ⁴
	(1)	(2)	(3)	(4)	(5)	(6)	(7)	(8)	(9)	(10)
Beam	554.836	20.362	123,805	4,054	1.000	554.8	11,298	123,805	207	124,011
Strands	4.284	3.857	10.93	28,500	7.030	30.1	116	77	7,609	7,686
Mild steel	0.880	42.000	0.0	29,000	7.154	6.3	264		3,116	3,116
Composite Section		19.752				591.2	11,678			134,813

Because this is a zero-length time interval, there are no initial strains. Steps 4 and 5 may be omitted for zero-length time intervals.

Use Eqs. (8.13.2.2.1-9) and (8.13.2.2.1-10) to calculate the strain and curvature of the composite section immediately after release:

$$\varepsilon = \frac{-860.5}{(4,054)(591.2)} = -0.000359$$

$$\Phi = \frac{3,694 - (860.5)(19.752 - 3.857)}{(4,054)(134,813)} = -1.83 \times 10^{-5} \text{ in.}^{-1}$$

Next, calculate the individual element strains. The strain due to transfer of prestress at the centroid of the strands is:

$$\varepsilon_p = -0.000359 - (-1.83 \times 10^{-5})(3.857 - 19.752) = -0.000649$$

The strain at the centroid of the mild steel bars is:

$$\varepsilon_s = -0.000359 - (-1.83 \times 10^{-5})(42.00 - 19.752) = 0.0000474$$

The strain at the centroid of the concrete beam section is:

$$\varepsilon_c = -0.000359 - (-1.83 \times 10^{-5})(20.362 - 19.752) = -0.000348$$

Finally, calculate the element forces and elastic strains. For this example, since there are no initial strains, the elastic strains are equal to the total strains that were calculated above. The force on the strands:

$$N_p = (28,500)(4.284)(-0.000649) = -79.3 \text{ kips}$$

DESIGN THEORY AND PROCEDURE

8.13.3.2.1 Example Calculation (at Transfer)/8.13.3.3.1 Example Calculation (after Transfer)

With this information, the remaining stress in the prestressing strands can be calculated:

$$f_p = \frac{860.5 - 79.3}{4.284} = 182.4 \text{ ksi}$$

The force in the mild steel bars:

$$N_s = (29,000)(0.88)(0.0000474) = 1.2 \text{ kip}$$

The axial force and moment on the concrete beam section:

$$N_c = (4,054)(554.8)(-0.000348) = -782.7 \text{ kips}$$

$$M_c = (4,054)(123,805)(-1.83 \times 10^{-5}) = -9,185 \text{ in.-kips}$$

8.13.3.3 Creep, Shrinkage and Relaxation after Transfer

Following the transfer of prestress, but before casting the deck, the beam will undergo gradual changes due to creep and shrinkage of the concrete and relaxation of the prestressing steel. The procedure of Section 8.13.2.2 can be used to analyze these gradual changes. Initial strains due to concrete creep and shrinkage, as well as the apparent strain due to strand relaxation, are included in the analysis. Since the changes occur gradually over this interval, the age-adjusted modulus is used.

8.13.3.3.1 Example Calculation (after Transfer)

Analyze the midspan section of the beam in **Figure 8.13.3-1**, using the results of Example 8.13.3.2.1. Perform the analysis for a time 90 days after casting the beam.

First, calculate the age-adjusted, effective modulus for the concrete beam. The creep coefficient is:

$$C(90,0.75) = \frac{(90 - 0.75)^{0.6}}{10 + (90 - 0.75)^{0.6}} (1.4) = 0.836$$

Using an aging coefficient of 0.7, the age-adjusted, effective modulus for the concrete is:

$$E_c^* = \frac{4,054}{1 + (0.7)(0.836)} = 2,558 \text{ ksi}$$

Calculation of the transformed composite section properties is similar to the procedure in Example 8.13.3.2.1 (see **Table 8.13.3.3.1-1**). The modulus of elasticity of the beam concrete is based on the concrete strength at the beginning of the interval, i.e., 4.95 ksi.

Table 8.13.3.3.1-1

Calculation of Transformed Composite Section Properties After Transfer

Item	Area in. ²	y_{cg} in.	Moment of Inertia in. ⁴	Modulus of Elasticity ksi	Modular Ratio, n	(1) × (5) in. ²	(1) × (5) × (2) in. ³	(3) × (5) in. ⁴	$[y - (2)]^2 \times (1)$ in. ⁴	(8) + (9) in. ⁴
	(1)	(2)	(3)	(4)	(5)	(6)	(7)	(8)	(9)	(10)
Beam	554.836	20.362	123,805	2,558	1.000	554.8	11,298	123,805	484	124,289
Strands	4.284	3.857	10.93	28,500	11.142	47.7	184	122	11,574	11,696
Mild steel	0.880	42.000	0.0	29,000	11.338	10.0	419		5,083	5,083
Composite Section		19.429				612.5	11,901			141,067

Unlike the previous example, there are initial strains to consider in association with the current time interval. First, calculate the initial strain due to shrinkage of the beam concrete:

$$\epsilon_{sh} = S(90,0.75) = \frac{90 - 0.75}{55 + (90 - 0.75)} (-0.000400) = -0.000247$$

DESIGN THEORY AND PROCEDURE

8.13.3.3.1 Example Calculation (after Transfer)

Next, calculate the creep strain in the beam for this interval. The creep coefficient has already been computed. The elastic strain and curvature from the previous example will be used to compute the creep strains occurring during the current interval:

$$\varepsilon_{cr} = (0.836)(-0.000348) = -0.000291$$

$$\Phi_{cr} = (0.836)(-1.83 \times 10^{-5}) = -1.53 \times 10^{-5} \text{ in.}^{-1}$$

The theoretical restraint forces for the concrete are calculated next:

$$N_c = -(2,558)(-0.000247 - 0.000291)(554.8) = 763.7 \text{ kips}$$

$$M_{0c} = -(2,558)(123,805)(-1.53 \times 10^{-5}) = 4,845 \text{ in.-kips}$$

The theoretical restraint force for the strands is due to the apparent strain due to relaxation. Eq. (8.13.1.4-1) is used, along with a reduction factor of 0.8, to compute the reduced relaxation occurring in the strands during the interval:

$$f_r(90,0.75) = (0.8) \frac{182.4}{45} \left[\frac{182.4}{243.0} - 0.55 \right] \log_{10} \left(\frac{(24)(90) + 1}{(24)(0.75) + 1} \right) = 1.34 \text{ ksi}$$

The relaxation of stress in the strand is treated as an apparent positive initial strain in the strand, i.e., an apparent increase in strain without a change in stress. Using Eq. (8.13.2.2.1-5), with a positive value for ε_{0p} gives the following value for N_{0p} :

$$N_{0p} = -(28,500) \left(\frac{1.34}{28,500} \right) (4.284) = -5.7 \text{ kips}$$

Summing the individual restraint forces gives the theoretical restraint forces on the composite transformed section [Eqs. (8.13.2.2.1-6) and (8.13.2.2.1-8)]:

$$N_0 = 763.7 + (-5.7) = 758.0 \text{ kips}$$

$$M_0 = 4,845 - (763.7)(20.362 - 19.429) - (-5.7)(3.857 - 19.429) = 4,044 \text{ in.-kips}$$

Eqs (8.13.2.2.1-9) and (8.13.2.2.1-10) are used to compute section strain and curvature:

$$\varepsilon = \frac{(0) - (758.0)}{(2,558)(612.5)} = -0.000484$$

$$\Phi = \frac{(0.0) - (4,044)}{(2,558)(141,067)} = -1.12 \times 10^{-5} \text{ in.}^{-1}$$

The element strains in the concrete beam, strands, and mild steel (Eqs. 8.13.2.2.1-11 and 8.13.2.2.1-12) are:

$$\varepsilon_c = -0.000484 - (-1.12 \times 10^{-5})(20.362 - 19.429) = -0.000474$$

$$\varepsilon_p = -0.000484 - (-1.12 \times 10^{-5})(3.857 - 19.429) = -0.000658$$

$$\varepsilon_s = -0.000484 - (-1.12 \times 10^{-5})(42.0 - 19.429) = -0.000231$$

The element forces (Eqs 8.13.2.2.1-13 and 8.12.2.2.1-14) are:

$$N_c = (2,558)(554.8)(-0.000474) + 763.7 = 91.0 \text{ kips}$$

$$N_p = (28,500)(4.284)(-0.000658) + (-5.7) = -86.0 \text{ kips}$$

$$N_s = (29,000)(0.88)(-0.000231) + 0.0 = -5.9 \text{ kips}$$

$$M_c = (2,558)(123,805)(-1.12 \times 10^{-5}) + 4,845 = 1,298 \text{ in.-kips}$$

DESIGN THEORY AND PROCEDURE**8.13.3.3.1 Example Calculation (after Transfer)/8.13.4 Continuous Bridges**

Finally, calculate the elastic strains, i.e. the strains due to stress, in the concrete that occurred during this time interval. These strains will be used to compute creep strains during future time intervals:

$$\varepsilon_{fc} = \frac{91.0}{(2,558)(554.8)} = 6.41 \times 10^{-5}$$

$$\Phi_{fc} = \frac{1,298}{(2,558)(123,805)} = 4.10 \times 10^{-6} \text{ in.}^{-1}$$

8.13.3.4 Placement of Cast-in-Place Deck

In a typical prestressed concrete beam bridge, the dead weight of a cast-in-place deck, plus intermediate diaphragms (where required) will be carried by the bare precast beam. The placement of these loads on the beam is assumed to occur during a time interval of zero length. Analysis of this interval is essentially an elastic analysis using transformed composite section properties calculated on the basis of the modulus of elasticity of the concrete at the time of deck placement.

8.13.3.5 Creep, Shrinkage and Relaxation

Following casting and curing, shrinkage of the deck concrete affects the state of stress and strain in the composite system. Since the beam will typically have undergone 40 to 60% of its ultimate shrinkage by the time the slab is cast, the ongoing shrinkage of the slab will usually be larger than the combination of the ongoing shrinkage and creep of the beam. This produces positive curvatures and moments, i.e. tending to cause tension in the bottom of the beam, that gradually diminish with time.

8.13.3.6 Application of Superimposed Dead Load

Application of the superimposed dead load on the composite deck/beam system may occur within 14 days of placement of deck concrete or may be delayed for several months. Concrete barriers and wearing surfaces are the most common instances of superimposed dead loads. Usually, it is assumed that these loads are applied during an interval of zero length, requiring the performance of an elastic analysis for this interval. The appropriate values of concrete modulus of elasticity for both the deck and the beam, based on their respective ages, are used in calculating the transformed composite section properties.

8.13.3.7 Long-Term Behavior

Following the application of superimposed dead loads, the bridge will typically remain in a constant configuration for several years. During this period, shrinkage of both the deck and beam will continue, but at a steadily decreasing rate. Similarly, creep strains in both the deck and beam will continue to develop. Total creep strains during this interval will be the sum of the creep strains caused by each stress increment applied during the preceding intervals.

By the time the superimposed dead load is applied, 60% or more of the creep due to transfer of prestress probably will have occurred. However, only a small percentage of the creep due to the dead weight of the deck will have occurred at the start of this final interval.

Usually the largest stress increments on the beam are associated with transfer of prestress, application of deck dead weight, and application of superimposed dead loads. It is these large, sudden stress increments which produce the majority of the creep strains. In addition to these stresses, however, we must consider the gradually developing stresses that occur between the major events in the life of the member. These gradually developing stresses are due to restrained or differential shrinkage, relaxation of the strands, and restrained or differential creep. For the purpose of calculating future creep strains, it is customary to assume that these gradually developing stresses can be represented by a sudden stress increment applied at the midpoint of the interval during which they occur. As long as these gradually developing stresses are small compared to the stresses associated with discrete events, the error is small.

8.13.4 Continuous Bridges

In simple-span bridges there will be little or no change in the distribution of forces and moments within the structure as a result of time-dependent deformations. However, multiple-span bridges which are made

DESIGN THEORY AND PROCEDURE**8.13.4 Continuous Bridges/8.13.4.2 Applying Time-Dependent Effects**

continuous for live loads and superimposed dead loads, become statically indeterminate after the deck has cured. As a result, any time-dependent deformations that occur after the time that the deck is cured will generally induce forces and moments in the beams (Freyermuth, 1969).

Creep of the beams under the net effects of prestressing, self-weight, deck weight, and superimposed dead loads will tend to produce additional upward camber with time. Shrinkage of the deck concrete will tend to produce downward camber of the composite system with time. In addition, loss of prestress due to creep, shrinkage, and relaxation will result in downward camber. Depending on the properties of the concrete materials and the age at which the beams are erected and subsequently made continuous, either positive or negative moments may occur over continuous supports (Oesterle, et al., 1989).

In the situation where beams are made continuous at a relatively young age it is more likely that positive moments will develop with time at the supports. These positive restraint moments are the result of the tendency of the beams to continue to camber upwards as a result of ongoing creep strains associated with the transfer of prestress. Shrinkage of the deck concrete, loss of prestress, and creep strains due to self-weight, deck weight, and superimposed dead loads all have a tendency to reduce this positive moment.

The alternate situation, i.e. where mature beams are erected and made continuous, could result in negative moments at the supports. In this situation, the time-dependent creep strains associated with the transfer of prestress have diminished to the point where the effects that produce downward deflection are more significant. This will induce negative moments as the end rotations that are associated with this sagging at midspan are restrained over the supports.

For the more typical condition of positive moments developing at the piers it is recommended that reinforcing steel be provided to minimize the detrimental effects of cracking at the bottom of the concrete diaphragm. This reinforcement may be accomplished by extending and bending strands from the bottom rows of the beam into the pier diaphragms. Alternatively, mild steel reinforcing bars protruding from the ends of the beams can be extended and bent into the diaphragms. If mild steel bars are utilized, it is essential that these bars extend far enough into the beam to adequately develop the bars. In addition, different length bars should be used to avoid the situation where all the bars terminate at one location.

8.13.4.1 Effectiveness of Continuity

The effects of positive moments and associated diaphragm cracking on bridge performance continues to be a hotly debated subject. An argument can be made (Oesterle, et al., 1989) that continuity for live loads becomes unreliable after a small crack has opened near the bottom of the diaphragm. It is pointed out that a finite end rotation is required to close this crack, forcing the beam to carry live loads as a simple-span member. Theoretically, this simple-span action results in live load moments that are significantly higher than those predicted by the design calculations that assume full continuity.

Countering this argument, however, is the successful experience of the many agencies that routinely design precast, prestressed concrete bridges under the assumption of full continuity for live loads. Higher stresses in the midspan regions of these bridges, predicted by the preceding discussion, have not been reported. In addition, only service load behavior is significantly affected. Under ultimate loads, end rotations of the beams will be large enough to close any crack that may have opened, restoring full continuity. Ultimate capacity, therefore, is relatively unaffected by this phenomenon.

It is unlikely that this issue will be settled completely in the near future. In the meantime, on the basis of the excellent performance of structures of this type, it is recommended that designers continue to rely on continuous action for the design of routine bridges and use details at the piers that have proven to be successful. Further details are given in Article 5.14.1.4 of the *LRFD Specifications*.

8.13.4.2 Applying Time-Dependent Effects

For unusual or special bridges, a time-dependent analysis to predict restraint moments at the piers may be performed according to the procedure in the following section. Construction sequence restrictions, special pier details, and beam design modifications are alternatives the designer may consider should such an analysis predict excessive positive moments.

DESIGN THEORY AND PROCEDURE**8.13.4.2 Applying Time-Dependent Effects/8.13.4.3.1 General Method**

Specifically, the designer may wish to consider such an analysis when one or more of the following conditions are present:

- Spans 140 ft and longer in humid climates (shorter span lengths should be considered for analysis in arid climates due to increased creep and shrinkage).
- Concrete materials whose creep properties are either unknown, i.e. the mix has not been used previously, or whose creep behavior is known to be poor.
- Situations where thermal movements due to daily heating and cooling of the deck are expected to be unusually high.

For more information, the reader is advised to consult the references by Mattock (1961); Freyermuth (1969); Oesterle, et al., (1989); Dilger (1982-A and B); and Miller, et al. (2004) regarding analysis of the effects of creep movements in continuous bridges.

8.13.4.3 Methods of Analysis

The following sections describe two methods to evaluate restraint moments in continuous bridges. The first is a general method and the second is a simplification of the first.

8.13.4.3.1 General Method

The analysis of restraint moments in continuous bridges is a relatively straightforward extension of the methods described in previous sections. Specifically, the following procedure is used:

1. Calculate the time-dependent beam end rotations that would occur under the effects of prestressing, self-weight, and deck weight acting on the simple-span beam using the methods described in Section 8.13.3. Consider only the portions of time-dependent end rotations that occur after the system is made continuous.
2. Using the age-adjusted, effective-modulus method, calculate the rotational stiffness of the beams by conventional stiffness analysis methods. If the beam is prismatic, use of the gross section properties including the deck, is sufficiently accurate. The stiffness factors are given by Eqs. (8.13.4.3.1-1) and (8.13.4.3.1-2) for interior spans and end spans, respectively.

$$M_L = \frac{4E_c^*I}{L}\theta_L + \frac{2E_c^*I}{L}\theta_R \quad (\text{Eq. 8.13.4.3.1-1})$$

$$M_R = \frac{2E_c^*I}{L}\theta_L + \frac{4E_c^*I}{L}\theta_R \quad (\text{Eq. 8.13.4.3.1-2})$$

where

θ_L = left end rotation of beam due to simple span loads

θ_R = right end rotation of beam due to simple span loads

E_c^* = age-adjusted, effective modulus of elasticity of concrete

I = moment of inertia of the gross concrete section

L = span length measured center-to-center of the supports for the continuous structure

3. Calculate restraint moments equal to the product of the time-dependent end rotations calculated in Step 1 and the rotational stiffness calculated in Step 2. Any sign convention may be used, as long as it is consistent.
4. Perform moment distribution analysis for the continuous structure, using the restraint moments as the fixed end moments and the stiffness properties calculated in Step 2.

The age-adjusted, effective modulus used in Step 2 must be based on gradually varying loads, i.e., use a value of χ that is appropriate for the age and creep coefficient of the concrete. A value of 0.8 may be used with relatively little error.

DESIGN THEORY AND PROCEDURE**8.13.4.3.1 General Method/8.13.4.3.2 Restraint Moment Due to Different Shrinkage**

The effects of permanent loads applied to the structure after continuity is achieved may be computed using a similar analysis. Theoretically, the age-adjusted, effective modulus for this second analysis, however, should be based on a value of χ equal to unity since the application of the load is considered to be instantaneous. As a practical matter, however, this distinction will only affect the distribution of moments in the structure when different creep coefficients are used in different spans. For almost all situations, it would be sufficiently accurate to incorporate the effects of the superimposed dead loads directly into the continuity analysis described above.

8.13.4.3.2 Approximate Method

The above general steps can be further simplified into the following approximate procedures of calculating the restraint moment due to the time-dependent effects.

8.13.4.3.2.1 Restraint Moment Due to Creep

Only loads introduced before continuity can cause time-dependent restraint moments due to creep. Typically, there are pretensioning forces, member self-weight, and possibly deck weight. Each loading case is considered separately. The total effect is obtained by simple superposition.

The following assumptions are made. The load is introduced at time, t_0 , and the modulus of elasticity of concrete at this time is $E(t_0)$. The continuity is made at time, t_1 , and the modulus of elasticity of the concrete at this time is $E(t_1)$. Specifically, the following procedure is used for each load:

1. Calculate time-dependent material properties:

$C(t, t_0)$ is creep at time, t , for concrete loaded at time, t_0

$C(t, t_1)$ is creep at time, t , for concrete loaded at time, t_1

$C(t_1, t_0)$ is creep at time, t_1 , for concrete loaded at time, t_0

Age-adjusted, effective modulus of elasticity of concrete subjected to gradual loading:

$$E_c^*(t, t_1) = \frac{E_c(t_1)}{1 + 0.7C(t, t_1)} \quad (\text{Eq. 8.13.4.3.2.1-1})$$

$$E_c^*(t, t_0) = \frac{E_c(t_0)}{C(t, t_0) - C(t_1, t_0)} \quad (\text{Eq. 8.13.4.3.2.1-2})$$

Perform elastic analysis, assuming that the load was introduced to a continuous member. Determine the fictitious elastic restraint moments at the supports, M_{el}

2. Determine the time-dependent multiplier, δ_c , corresponding to the load:

$$\delta_c = \frac{E_c^*(t, t_1)}{E_c^*(t, t_0)} \quad (\text{Eq. 8.13.4.3.2.1-3})$$

3. Determine the restraining moment, $M_{cr}(t)$:

$$M_{cr}(t) = \delta_c M_{el} \quad (\text{Eq. 8.13.4.3.2.1-4})$$

8.13.4.3.2.2 Restraint Moment Due to Differential Shrinkage

The following assumptions are made: (1) The curing of the beam concludes at time, t_2 . (2) The curing of the deck ends at time, t_3 . Specifically, the following procedure is used for calculating the restraint moment due to differential shrinkage:

1. Calculate time-dependent material properties:

Deck:

$C_d(t, t_3)$ is the creep at time, t , for deck concrete loaded at time, t_3

$\varepsilon_{shd}(t, t_3)$ is the shrinkage strain of the deck from time t_3 to time, t

$E_{cd}(t_3)$ is the modulus of elasticity for deck concrete at time, t_3

Beam:

$C_b(t, t_3)$ is the creep at time, t , for beam concrete loaded at time, t_3

$\varepsilon_{shb}(t, t_2)$ is the shrinkage strain of the beam from time t_2 to time, t

$\varepsilon_{shb}(t_3, t_2)$ is the shrinkage strain of the beam from time t_2 to time, t_3

$E_{cb}(t_3)$ is the modulus of elasticity for beam concrete at time, t_3

The age-adjusted, effective modulus for concrete subjected to gradual loading:

$$E_{cd}^* = \frac{E_{cd}(t_3)}{1 + 0.7C_d(t, t_3)} \quad (\text{Eq. 8.13.4.3.2.2-1})$$

$$E_{cb}^* = \frac{E_{cb}(t_3)}{1 + 0.7C_b(t, t_3)} \quad (\text{Eq. 8.13.4.3.2.2-2})$$

2. Calculate the shrinkage moment, M_{sh} :

$$M_{sh} = Sh_d E_{cd}^* \varepsilon_{shd}(t, t_3) \left(y_{tc} - \frac{h_d}{2} \right) - A E_{cb}^* [\varepsilon_{shb}(t, t_2) - \varepsilon_{shb}(t_3, t_2)] (y_{bc} - y_b) \quad (\text{Eq. 8.13.4.3.2.2-3})$$

where

S = beam spacing

h_d = deck thickness

y_{tc} = distance from centroidal axis of the composite section to the top of the deck

A = gross area of the non-composite beam

y_{bc} = distance from centroidal axis of composite section to the bottom of the beam

y_b = distance from centroidal axis of non-composite section to the bottom of the beam

3. Perform moment distribution analysis for the continuous structure, using the shrinkage moments as the fixed end moments and the stiffness properties calculated from the composite section. The moment at the supports after moment distribution is the restraint moment, $M_{sr}(t)$, due to the differential shrinkage.

Should this analysis predict net positive moments at the piers, the results should probably be treated as an upper bound to the actual moments in the structure. It is likely that the non-prestressed section of the diaphragm between the ends of the beams would experience some cracking at relatively low moments. This would have the effect of introducing a slightly "softer" joint than the fully continuous joint that is assumed by this analysis.

8.14 REFERENCES

1. AASHTO. 2011. *Manual for Bridge Evaluation*, Second Edition. American Association of State Highway and Transportation Officials, Washington, DC.
https://bookstore.transportation.org/item_details.aspx?id=1750 (Fee)
2. AASHTO. 2010. *AASHTO LRFD Bridge Design Specifications*, Fifth Edition. American Association of State Highway and Transportation Officials, Washington, DC, and 2011 Interim Revisions.
https://bookstore.transportation.org/item_details.aspx?id=1750 (Fee)

DESIGN THEORY AND PROCEDURE

8.14 References

3. Abdel-Karim, A. M. and M. K. Tadros. 1993. "Computer Analysis of Spliced Girder Bridges." *ACI Structural Journal*, V. 90, No. 1 (January-February), pp. 21-31.
<http://www.concrete.org/PUBS/JOURNALS/AbstractDetails.asp?SearchID=-1&date=between&aftermonth=1&afterday=1&afteryear=1993&beforemonth=1&beforeday=1&beforeyear=1993&searchmonth=1&searchday=1&searchyear=2011&authors=Abdel%2DKarim&volume=90&issue=1&ID=419> (Fee)
4. ACI Committee 209. 1992. *Prediction of Creep Shrinkage and Temperature Effects in Concrete Structures* (ACI 209R-92). American Concrete Institute, Farmington Hills, MI.
<http://www.concrete.org/BookstoreNet/ProductDetail.aspx?SACode=20992> (Fee)
5. ACI Committee 318. 2008. *Building Code Requirements for Reinforced Concrete*, (ACI 318-08). American Concrete Institute, Farmington Hills, MI.
6. ACI-ASCE Joint Committee 323. 1958. "Tentative Recommendations for Prestressed Concrete." *ACI Journal*, American Concrete Institute, Farmington Hills, MI. V. 54, pp. 545-1299.
<http://www.concrete.org/PUBS/JOURNALS/AbstractDetails.asp?srctype=ALL&keywords=Tentative+Recommendations+for+prestressed+concrete&ID=11455> (Fee)
7. Badie, S. S., M. C. Baishya, and M. K. Tadros. 1998. "NUDECK – An Efficient and Economical Precast Prestressed Bridge Deck System." *PCI Journal*, Precast/Prestressed Concrete Institute, Chicago, IL. V. 43, No. 5 (September-October), pp. 56-74.
http://www.pci.org/view_file.cfm?file=JL-98-SEPTEMBER-OCTOBER-6.pdf
http://www.pci.org/view_file.cfm?file=JL-98-SEPTEMBER-OCTOBER-7.pdf
8. Bakht, B., L. G. Jaeger, and M. S. Cheung. 1983. "Transverse Shear in Multibeam Bridges." *Journal of Structural Engineering*, American Society of Civil Engineers, Reston, VA. V. 109, No. 4 (April), pp. 936-949.
http://ascelibrary.org/sto/resource/1/jsendh/v109/i4/p936_s1?isAuthorized=no (Fee)
9. Bazant, Z. P. 1972. "Prediction of Concrete Creep Effects Using Age-Adjusted Effective Modulus Method." *ACI Journal*, American Concrete Institute, Farmington Hills, MI. V. 69, No. 2, pp. 212-217.
<http://www.civil.northwestern.edu/people/bazant/PDFs/Papers/052.pdf>
10. Birkeland, P. W. and H. W. Birkeland. 1996. "Connections in Precast Concrete Construction." *ACI Journal*, American Concrete Institute, Farmington Hills, MI. V. 63, No. 3 (March), pp. 345-367.
<http://www.concrete.org/PUBS/JOURNALS/AbstractDetails.asp?SearchID=-1&date=anytime&aftermonth=1&afterday=1&afteryear=1972&beforemonth=12&beforeday=31&beforeyear=1972&searchmonth=1&searchday=1&searchyear=2011&authors=Birkeland&volume=63&issue=3&ID=7627> (Fee)
11. Branson, D. E. and K. M. Kripanarayanan. 1971. "Loss of Prestress, Camber and Deflection of Non-Composite and Composite Concrete Structures." *PCI Journal*, Precast/Prestressed Concrete Institute, Chicago, IL. V. 16, No. 5 (September-October), pp. 22-52.
http://www.pci.org/view_file.cfm?file=JL-71-SEPTEMBER-OCTOBER-3.pdf
12. Breen, J. E., O. Burdet, C. Roberts, D. Sanders, and G. Wollmann. 1994. *Anchorage Zone Reinforcement for Post-Tensioned Concrete Girders*. NCHRP Report 356. Transportation Research Board, Washington, DC. 204 pp.
<http://www.worldcat.org/title/anchorage-zone-reinforcement-for-post-tensioned-concrete-girders/oclc/30315575> (Fee)
13. Buckner, C. D. 1994. *An Analysis of Transfer and Development Lengths for Pretensioned Concrete Structures*. Publication No. FHWA-RD-94-049, Federal Highway Administration, Turner-Fairbank Highway Research Center, McLean, VA. 108 pp.

DESIGN THEORY AND PROCEDURE

8.14 References

14. Buckner, C. D. 1995. "A Review of Strand Development Length for Pretensioned Concrete Members." *PCI Journal*, Precast/Prestressed Concrete Institute, Chicago, IL. V. 40, No. 2 (March-April), pp. 84-105.
http://www.pci.org/view_file.cfm?file=JL-95-MARCH-APRIL-11.pdf
http://www.pci.org/view_file.cfm?file=JL-95-MARCH-APRIL-12.pdf
15. Collins, M. P. and D. Mitchell. 1991. *Prestressed Concrete Structures*. Prentice Hall, Englewood Cliffs, NJ. 766 pp.
<http://www.amazon.com/Prestressed-Structures-Prentice-Hall-International-Engineering/dp/013691635X> (Fee)
16. Collins, M. P. and D. Mitchell. 1980. "Shear and Torsion-Design of Prestressed and Non-Prestressed Concrete Beams." *PCI Journal*, Precast/Prestressed Concrete Institute, Chicago, IL. V. 25, No. 5 (September-October), pp. 32-100.
17. Cousins, T., D. W. Johnston, and P. Zia. 1986. *Bond of Epoxy Coated Prestressing Strand*. Publication No. FHWA/NC/87-005. Federal Highway Administration, Washington, DC.
18. Devalapura, R. K. and M. K. Tadros. 1992A. "Critical Assessment of ACI 318 Eq. (18-3) for Prestressing Steel Stress at Ultimate Flexure." *ACI Structural Journal*, American Concrete Institute, Farmington Hills, MI. V. 89, No. 5 (September-October), pp. 538-546.
<http://www.concrete.org/PUBS/JOURNALS/AbstractDetails.asp?SearchID=-1&date=anytime&aftermonth=1&afterday=1&afteryear=2011&beforemonth=1&beforeday=1&beforeyear=2011&searchmonth=1&searchday=1&searchyear=2011&volume=89&issue=5&ID=9641> (Fee)
19. Devalapura, R. K. and M. K. Tadros. 1992B. "Stress-Strain Modeling of 270 ksi Low-Relaxation Prestressing Strands." *PCI Journal*, Precast/Prestressed Concrete Institute, Chicago, IL. V. 37, No. 2 (March-April), pp. 100-106.
http://www.pci.org/view_file.cfm?file=JL-92-MARCH-APRIL-28.pdf
20. Dilger, W. H. 1982. "Creep Analysis of Prestressed Concrete Structures using Creep-Transformed Section Properties." *PCI Journal*, Precast/Prestressed Concrete Institute, Chicago, IL. V. 27, No. 1 (January-February), pp. 98-118.
21. Dilger, W. H. 1982. "Methods of Structural Creep Analysis," *Creep and Shrinkage in Concrete Structures*. Z. P. Bazant and F. H. Wittmann (Editors), John Wiley & Sons Ltd.
<http://www.amazon.com/Shrinkage-Concrete-Structures-Numerical-Engineering/dp/0471104094> (Fee)
22. Einea, A., S. Yehia, and M. K. Tadros. 1999. "Lap Splice in Confined Concrete." *ACI Structural Journal*, American Concrete Institute, Farmington Hills, MI. V. 96, No. 6 (November-December), pp. 947-955.
<http://www.concrete.org/PUBS/JOURNALS/AbstractDetails.asp?SearchID=-1&date=anytime&aftermonth=1&afterday=1&afteryear=2011&beforemonth=1&beforeday=1&beforeyear=2011&searchmonth=1&searchday=1&searchyear=2011&volume=96&issue=6&ID=769> (Fee)
23. El-Remaily, A., M. K. Tadros, T. Yamane, and G. Krause. 1996. "Transverse Design of Adjacent Precast Prestressed Concrete Box Girder Bridge." *PCI Journal*, Precast/Prestressed Concrete Institute, Chicago, IL. V. 41, No. 4 (July-August), pp. 96-113.
http://www.pci.org/view_file.cfm?file=JL-96-JULY-AUGUST-11.pdf
http://www.pci.org/view_file.cfm?file=JL-96-JULY-AUGUST-12.pdf
24. Farrington, E.W. 1996. "Creep and Shrinkage of High Performance Concrete." The University of Texas at Austin, Austin, TX. M.Sc. Thesis.
25. Freyermuth, C. L. 1969. "Design of Continuous Highway Bridges with Precast, Prestressed Concrete Girders." *PCI Journal*, Precast/Prestressed Concrete Institute, Chicago, IL. V. 14, No. 2 (March-April), pp. 14-39.

DESIGN THEORY AND PROCEDURE

8.14 References

26. Gallt, J. G. 1996. *Computer Program TDA: Time Dependent Analysis of Prestressed Beam*. Version 2.02.
27. Gamble, W. L. 1972. *Proposed Amendment to the AASHTO Standard Specifications for Highway Bridges, Article 1.6.7(B), Prestressed Losses*. Department of Civil Engineering, University of Illinois, Urbana, IL.
28. Gergely, P. and M. A. Sozen. 1967. "Design of Anchorage Zone Reinforcement in Prestressed Concrete Beams." *PCI Journal*, Precast/Prestressed Concrete Institute, Chicago, IL. V. 12, No. 2 (March-April), pp. 63-75.
29. Ghali, A. and J. Trevino. 1985. "Relaxation of Steel in Prestressed Concrete." *PCI Journal*, Precast/Prestressed Concrete Institute, Chicago, IL. V. 30, No. 5 (September-October), pp. 82-94.
30. Glodowski, R. J. and J. J. Lorenzetti. 1972. "A Method for Predicting Prestress Losses in a Prestressed Concrete Structure." *PCI Journal*, Precast/Prestressed Concrete Institute, Chicago, IL. V. 17, No. 2 (March-April), pp. 17-31.
http://www.pci.org/view_file.cfm?file=JL-72-MARCH-APRIL-3.pdf
31. Guyon, Y. 1951. *Béton Précontrainte – etude Théorique et expérimentale*, Editions Eyrolles. Paris, France. Also available as *Prestressed Concrete*. John Wiley & Sons Inc., New York, NY, 1960, two volumes, 1300 pp.
32. Hanna, K. E., G. Morcouc, and M. K. Tadros. 2007. "Transverse Design and Detailing of Adjacent Box Beam Bridges." PCI Concrete Bridge Conference, *Proceedings*, Phoenix, AZ, October 22-24.
https://netforum.pci.org/eweb/DynamicPage.aspx?Site=PCI_NF&WebKey=9766331d-1b7d-4c4b-89cb-fc801bc30745&ListSearchFor=proceedings%202007 (Fee)
33. Hawkins, N., D. A. Kuchma, R. L. Mast, M. L. Marsh, and K. Reineck. 2005. *Simplified Shear Design of Structural Concrete Members*. NCHRP Report 549. Transportation Research Board, Washington, DC.
http://onlinepubs.trb.org/onlinepubs/nchrp/nchrp_rpt_549.pdf
34. Hernandez, H. D. and W. L. Gamble. 1975. *Time Dependent Prestress Losses in Pretensioned Concrete Construction*. Report No. 417. University of Illinois, Urbana, IL.
<https://www.ideals.illinois.edu/bitstream/handle/2142/13830/SRS-417.pdf?sequence=2>
35. Hofbeck, J. A., I. O. Ibrahim, and A. H. Mattock. 1969. "Shear Transfer in Reinforced Concrete." *ACI Journal*, American Concrete Institute, Farmington Hills, MI. V. 66, No. 2 (February), pp. 119-128.
<http://www.concrete.org/PUBS/JOURNALS/AbstractDetails.asp?SearchID=-1&date=betweendate&aftermonth=2&afterday=1&afteryear=1969&beforemonth=3&beforeday=31&beforeyear=1969&searchmonth=1&searchday=1&searchyear=2011&ID=7349> (Fee)
36. Huo, X., M. K. Tadros, and N. Al-Omaishi. 2001. "Creep Shrinkage and Modulus of Elasticity of High Performance Concrete." *ACI Materials Journal*, American Concrete Institute, Farmington Hills, MI. V. 89, No. 6 (November-December), pp. 429-439.
<http://www.concrete.org/PUBS/JOURNALS/AbstractDetails.asp?SearchID=-1&date=betweendate&aftermonth=11&afterday=1&afteryear=2001&beforemonth=12&beforeday=31&beforeyear=2001&searchmonth=1&searchday=1&searchyear=2011&ID=10842> (Fee)
37. Huo, X. and M. K. Tadros. 1997A. "Allowable Compressive Strength of Concrete at Prestress Release." Problems & Solutions, *PCI Journal*, Precast/Prestressed Concrete Institute, Chicago, IL. V. 42, No. 1 (January-February), pp. 95-99.
38. Huo, X. and M. K. Tadros. 1997B. "Application of High Performance Concrete in Bridge Design." Problems & Solutions, *PCI Journal*, Precast/Prestressed Concrete Institute, Chicago, IL. V. 42, No. 1 (January-February) p. 94.

DESIGN THEORY AND PROCEDURE

8.14 References

39. Huo, X. 1997. Time Dependent Analysis and Applications of High Performance Concrete Bridges. Department of Civil Engineering, University of Nebraska-Lincoln, Omaha, NE. 211 pp. Ph.D. Dissertation.
<http://digitalcommons.unl.edu/dissertations/AAI9805510/>
40. Imper, R. R. and G. Laszlo. 1987. "Handling and Shipping of Long Span Bridge Beams." *PCI Journal*, Precast/Prestressed Concrete Institute, Chicago, IL. V. 32, No. 6 (November-December), pp. 86-101.
http://www.pci.org/view_file.cfm?file=JL-87-NOVEMBER-DECEMBER-6.pdf
41. Kamel, M. 1996. Innovative Precast Concrete Composite Bridge Systems. Department of Civil Engineering, University of Nebraska-Lincoln, Omaha, NE. Ph.D. Dissertation.
<http://digitalcommons.unl.edu/dissertations/AAI9623625/>
42. Kriz, L. B. and C. H. Raths. 1965. "Connections in Precast Concrete Structures – Strength of Corbels." *PCI Journal*, Precast/Prestressed Concrete Institute, Chicago, IL. V. 10, No. 1 (January-February), pp. 16-61.
43. Kumar, N. V. and J. A. Ramirez. 1996. "Interface Horizontal Shear Strength in Composite Decks with Precast Concrete Panels." *PCI Journal*, Precast/Prestressed Concrete Institute, Chicago, IL. V. 41, No. 2 (March-April), pp. 42-55.
http://www.pci.org/view_file.cfm?file=JL-96-MARCH-APRIL-5.pdf
44. Loov, E. R. and A. K. Patnaik. 1994. "Horizontal Shear Strength of Composite Concrete Beams with a Rough Interface." *PCI Journal*, Precast/Prestressed Concrete Institute, Chicago, IL. V. 39, No. 1 (January-February), pp. 48-69, and also Reader Comments. *PCI Journal*, V. 39, No. 5 (September-October), 1994, pp. 106-109.
http://www.pci.org/view_file.cfm?file=JL-94-JANUARY-FEBRUARY-6.pdf
http://www.pci.org/view_file.cfm?file=JL-94-JANUARY-FEBRUARY-7.pdf
http://www.pci.org/view_file.cfm?file=JL-94-SEPTEMBER-OCTOBER-12.pdf
45. Ma, Z. (John), M. Saleh, and M. K. Tadros. 1997. "Shear Design of Stemmed Bridge Members – How Complex Should It Be?" Problems & Solutions, *PCI Journal*, Precast/Prestressed Concrete Institute, Chicago, IL. V. 42, No. 5 (September-October), pp. 88-93.
http://www.pci.org/view_file.cfm?file=JL-97-SEPTEMBER-OCTOBER-10.pdf
46. Marshall, W.T. and A.H. Mattock. 1962. "Control of Horizontal Cracking in Ends of Pretensioned Prestressed Concrete Girders." *PCI Journal*, Precast/Prestressed Concrete Institute, Chicago, IL. V. 7, No. 5 (September-October), pp. 56-74.
47. Martin, B. T. and D. H. Sanders. 2007. *Verification and Implementation of Strut-and-Tie Model in LRFD Bridge Design Specifications*. Final Report, NCHRP Project 20-07, Task 217, Transportation Research Board, Washington, DC.
[http://onlinepubs.trb.org/onlinepubs/archive/NotesDocs/20-07\(217\)_FR.pdf](http://onlinepubs.trb.org/onlinepubs/archive/NotesDocs/20-07(217)_FR.pdf)
48. Martin, L. D. 1977. "A Rational Method for Estimating Camber and Deflection of Precast Prestressed Members." *PCI Journal*, Precast/Prestressed Concrete Institute, Chicago, IL. V. 22, No. 1 (January-February), pp. 100-108.
http://www.pci.org/view_file.cfm?file=JL-77-JANUARY-FEBRUARY-6.pdf
49. Mast, R. F. 1968. "Auxiliary Reinforcement in Concrete Connections." *ASCE Journal*, American Society of Civil Engineers, Reston, VA. V. 94, No. ST6 (June), pp. 1485-1504.

50. Mast, R. F. 1992. "Unified Design Provisions for Reinforced and Prestressed Concrete Flexural and Compression Members." *ACI Structural Journal*, American Concrete Institute, Farmington Hills, MI. V. 89, No. 2 (March-April), pp. 185-199.
<http://www.concrete.org/PUBS/JOURNALS/AbstractDetails.asp?SearchID=-1&date=betweendate&aftermonth=3&afterday=1&afteryear=1992&beforemonth=4&beforeday=30&beforeyear=1992&searchmonth=1&searchday=1&searchyear=2011&ID=3209> (Fee)
51. Mast, R. F. 1989. "Lateral Stability of Long Prestressed Concrete Beams – Part 1." *PCI Journal*, Precast/Prestressed Concrete Institute, Chicago, IL. V. 34, No. 1 (January-February), pp. 34-53.
http://www.pci.org/view_file.cfm?file=JL-89-JANUARY-FEBRUARY-3.pdf
52. Mast, R. F. 1993. "Lateral Stability of Long Prestressed Concrete Beams – Part 2." *PCI Journal*, Precast/Prestressed Concrete Institute, Chicago, IL. V. 38, No. 1 (January-February), pp. 70-88.
http://www.pci.org/view_file.cfm?file=JL-93-JANUARY-FEBRUARY-30.pdf
http://www.pci.org/view_file.cfm?file=JL-93-JANUARY-FEBRUARY-31.pdf
53. Mattock, A. H. 1961. *Precast-Prestressed Concrete Bridges 5: Creep and Shrinkage Studies*. Bulletin D46, Development Department, Research and Development Laboratories, Portland Cement Association, Skokie, IL, 36 pp.
54. Miller, R. A., R. Castrodale, A. Mirmiran, and M. Hastak. 2004. *Connection of Simple-Span Precast Concrete Girders for Continuity*, NCHRP Report 519, Transportation Research Board, Washington, DC.
http://onlinepubs.trb.org/onlinepubs/nchrp/nchrp_rpt_519.pdf
55. Oesterle, R. G., J. D. Glikin, and S. C. Larson. 1989. *Design of Precast Prestressed Bridge Girders Made Continuous*. NCHRP Report 322, Transportation Research Board, Washington, DC.
<http://books.trbbookstore.org/nr322.aspx>
56. Pang, J. P. 1997. *Allowable Compressive Stresses for Prestressed Concrete*. The University of Oklahoma, Norman, OK. May, 178 pp. M.Sc. Thesis.
57. PCI Bridge Producers Committee. 1988. "Recommended Practice for Precast Prestressed Concrete Composite Bridge Deck Panels." *PCI Journal*, Precast/Prestressed Concrete Institute, Chicago, IL. V. 33, No. 2 (March-April), pp. 67-109.
http://www.pci.org/view_file.cfm?file=JL-88-MARCH-APRIL-6.pdf
http://www.pci.org/view_file.cfm?file=JL-88-MARCH-APRIL-7.pdf
58. PCI Committee on Prestress Losses. 1975. "Recommendations for Estimating Prestress Losses." *PCI Journal*, Precast/Prestressed Concrete Institute, Chicago, IL. V. 20, No. 4 (July-August), pp. 43-75.
http://www.pci.org/view_file.cfm?file=JL-75-JULY-AUGUST-4.pdf
59. PCI. 2010. *PCI Design Handbook*, Seventh Edition. MNL 120-10 Precast/Prestressed Concrete Institute, Chicago, IL.
https://netforum.pci.org/eweb/dynamicpage.aspx?webcode=category&ptc_key=6ccabfe6-c4d9-4379-83b5-d257a2bde354&ptc_code=Design%20Guides%20and%20Standards (Fee)
60. Ralls, M. L. 1996. "Proceedings of the High Performance Concrete Regional Showcase," Omaha, NE, November 18-20.
61. Ramirez, J. A. and B. W. Russell. 2008. *Transfer, Development, and Splice Length for Strand/Reinforcement in High-Strength Concrete*, NCHRP Report 603. Transportation Research Board, Washington, DC.
http://onlinepubs.trb.org/onlinepubs/nchrp/nchrp_rpt_603.pdf

DESIGN THEORY AND PROCEDURE

8.14 References

62. Russell, B. W. and N. H. Burns. 1993. *Design Guidelines for Transfer, Development and Debonding of Large Diameter Seven Wire Strands in Pretensioned Concrete Girders*. Research Report 1210-5F, Project 3-5-89/2-1210, Center for Transportation Research, Bureau of Engineering Research, The University of Texas at Austin, Austin, Texas.
63. Russell, B. W. and N. H. Burns. 1994A. "Fatigue Tests on Prestressed Concrete Beams With Debonded Strands." *PCI Journal*, Precast/Prestressed Concrete Institute, Chicago, IL. V. 39, No. 6 (November-December), pp. 70-88.
http://www.pci.org/view_file.cfm?file=JL-94-NOVEMBER-DECEMBER-7.pdf
64. Russell, B. W. and N. H. Burns. 1994B. "Predicting the Bond Behavior of Prestressed Concrete Beams Containing Debonded Strands." *PCI Journal*, Precast/Prestressed Concrete Institute, Chicago, IL. V. 39, No. 5 (September-October), pp. 60-77.
http://www.pci.org/view_file.cfm?file=JL-94-SEPTEMBER-OCTOBER-7.pdf
http://www.pci.org/view_file.cfm?file=JL-94-SEPTEMBER-OCTOBER-8.pdf
65. Russell, H. G. 2009. *NCHRP Synthesis 393: Adjacent Precast Concrete Box Beam Bridges: Connection Details*. Transportation Research Board, Washington, DC. 75 pp.
http://onlinepubs.trb.org/onlinepubs/nchrp/nchrp_syn_393.pdf
66. Schlaich, J., K. Schafer, and N. Jennewein. 1987. "Towards a Consistent Design of Reinforced Structural Concrete." *PCI Journal*, Precast/Prestressed Concrete Institute, Chicago, IL. V. 32, No. 3 (May-June), pp. 74-150.
http://www.pci.org/view_file.cfm?file=JL-87-MAY-JUNE-5.pdf
http://www.pci.org/view_file.cfm?file=JL-87-MAY-JUNE-6.pdf
http://www.pci.org/view_file.cfm?file=JL-87-MAY-JUNE-7.pdf
http://www.pci.org/view_file.cfm?file=JL-87-MAY-JUNE-8.pdf
67. Seguirant, S. J. 1998. "New Deep WSDOT Standard Sections Extend Spans of Prestressed Concrete Girders," *PCI Journal*, Precast/Prestressed Concrete Institute, Chicago, IL. V. 43, No. 4, July-August, pp. 92-119
http://www.pci.org/view_file.cfm?file=JL-98-JULY-AUGUST-7.pdf
http://www.pci.org/view_file.cfm?file=JL-98-JULY-AUGUST-8.pdf
68. Seguirant, S.J., R. Brice and B. Khaleghi. 2005. "Flexural Strength of Reinforced and Prestressed Concrete T-Beams." *PCI Journal*, Precast/Prestressed Concrete Institute, Chicago, IL. V. 50, No. 1 (January-February), pp. 44-73.
69. Shahawy, M. 2001. "A Critical Evaluation of the AASTHO Provisions for Strand Development Length of Prestressed Concrete Members." *PCI Journal*, Precast/Prestressed Concrete Institute, Chicago, IL. V. 46, No. 4 (July-August), pp. 94-117.
70. Skogman, B. C., M. K. Tadros, and R. Grasmick. 1988. "Flexural Strength of Prestressed Concrete Members." *PCI Journal*, Precast/Prestressed Concrete Institute, Chicago, IL. V. 33, No. 5 (September-October), pp. 96-123.
http://www.pci.org/view_file.cfm?file=JL-88-SEPTEMBER-OCTOBER-5.pdf
http://www.pci.org/view_file.cfm?file=JL-88-SEPTEMBER-OCTOBER-6.pdf
71. Tadros, M. K., A. Ghali, and W. H. Dilger. 1975. "Time-Dependent Prestress Loss and Deflection in Prestressed Concrete Members." *PCI Journal*, Precast/Prestressed Concrete Institute, Chicago, IL. V. 20, No. 3, May-June, pp. 86-98.
72. Tadros, M. K., A. Ghali, and W. H. Dilger. 1977A. "Effects of Non-Prestressed Steel on Prestress Loss and Deflection." *PCI Journal*, Precast/Prestressed Concrete Institute, Chicago, IL. V. 22, No. 2 (March-April), pp. 50-63.

DESIGN THEORY AND PROCEDURE

8.14 References

73. Tadros, M. K., A.Ghali, and W. H. Dilger. 1977B. "Time-Dependent Analysis of Composite Frames." *Journal of the Structural Division*, American Society of Civil Engineers, Reston, VA. V. 103, No. 4 (April), pp. 871-884.
<http://cedb.asce.org/cgi/WWWdisplay.cgi?7333> (Fee)
74. Tadros, M. K., A.Ghali, and A. W. Mey. 1985. "Prestress Loss and Deflection of Precast Concrete Members," *PCI Journal*, Precast/Prestressed Concrete Institute, Chicago, IL. V. 30, No. 1 (January-February), pp. 114-141.
75. Tadros, M. K. 1996. *Proceedings of the High Performance Concrete Regional Showcase*. Omaha, NE. November 18-20.
76. Tadros, M. K. 1998. *Rapid Replacement of Bridge Decks*. NCHRP Report 407, Transportation Research Board, Washington, DC.
http://onlinepubs.trb.org/onlinepubs/nchrp/nchrp_rpt_407.pdf
77. Tadros, M. K., S.S. Badie, and C. Y. Tuan. 2010. *Evaluation and Repair Procedures for Precast/Prestressed Concrete Girders with Longitudinal Cracking in the Web*. NCHRP Report 654, Transportation Research Board, Washington, DC.
http://onlinepubs.trb.org/onlinepubs/nchrp/nchrp_rpt_654.pdf
78. Tadros, M. K., F. Fawzy, and K. E. Hanna. 2011. "Precast, Prestressed Girder Camber Variability." *PCI Journal*, Precast/Prestressed Concrete Institute, Chicago, IL, V. 56, No. 1 (Winter), pp. 135-154.
http://www.pci.org/view_file.cfm?file=IL-11-WINTER-11.pdf
79. Zia, P., H. K. Preston, N. L. Scott, and E. B. Workman, 1979. "Estimating Prestress Losses." *Concrete International*, American Concrete Institute, Farmington Hills, MI. June, pp. 32-38.
<http://www.concrete.org/PUBS/JOURNALS/AbstractDetails.asp?srctype=ALL&keywords=Estimating+prest+ress+losses&ID=15031> (Fee)

This page intentionally left blank

DESIGN EXAMPLES

Table of Contents

NOTATION.....	9.0 - 3
9.0 INTRODUCTION	9.0 - 13
9.0.1 Service Life	9.0 - 13
9.0.2 Sign Convention.....	9.0 - 13
9.0.3 Level of Precision.....	9.0 - 13
9.1a Design Example – Bulb-Tee (BT-72), Single Span with Composite Deck. Designed using Transformed Section Properties, General Shear Procedure, and Refined Estimates of Prestress Losses	
9.1b Design Example – Bulb-Tee (BT-72), Single Span with Composite Deck. Designed using Gross Section Properties, Appendix B5 Shear Procedure, and Refined Estimates of Prestress Losses	
9.1c Design Example – Bulb-Tee (BT-72), Single Span with Composite Deck. Designed using Transformed Section Properties, Simplified Shear, and Approximate Prestress Losses	
9.2 Design Example – Bulb-Tee (BT-72), Three Spans with Composite Deck. Designed using Transformed Section Properties, General Shear Procedure, and Refined Estimates of Prestress Losses	
9.3 Design Example – Deck Bulb-Tee (DBT-53), Single Span with Noncomposite Surface. Designed using Transformed Section Properties, General Shear Procedure, and Refined Estimates of Prestress Losses	
9.4 Design Example – Box Beam (BIII-48), Single Span with Noncomposite Surface. Designed using Transformed Section Properties, General Shear Procedure, and Refined Estimates of Prestress Losses	
9.5 Design Example – Box Beam (BIII-48), Single Span with Composite Deck. Designed using Transformed Section Properties, General Shear Procedure, and Refined Estimates of Prestress Losses	
9.6 Design Example – U-Beam (TX-U54), Single Span with Precast Panels and Composite Deck. Designed using Transformed Section Properties, General Shear Procedure, and Refined Estimates of Prestress Losses	
9.7 Design Example – Double-Tee Beam (NEXT 36 D), Single Span with Noncomposite Surface. Designed using Transformed Section Properties, General Shear Procedure, and Refined Estimates of Prestress Losses	
9.8 Design Example – Double-Tee Beam (NEXT 36 F), Single Span with Composite Deck. Designed using Transformed Section Properties, General Shear Procedure, and Refined Estimates of Prestress Losses	
9.9 Design Example – Precast Composite Slab System. To be included in the next edition.	
9.10 Design Example – Precast Concrete Stay-in-Place Deck Panel System. Designed using Transformed Section Properties and Refined Estimates of Prestress Losses	

Note: Each design example contains a separate detailed table of contents.

This page intentionally left blank

NOTATION

The section number with each notation is the location where the notation is first used. The [LRFD] identifies that similar notation is used in the *LRFD Specifications*.

A_{bs}	= cross-sectional area of beam stems (9.7.4.2.2.1)	
A_c	= total area of the composite section (9.1a.3)	
A_c	= area of concrete on the flexural tension side of the member (9.1b.11.2.1.1)	
A_{cv}	= area of concrete section resisting shear transfer (9.1a.12.3)	[LRFD]
A_d	= area of deck concrete (9.1a.6.3.4)	[LRFD]
A_g	= cross-sectional area of the precast beam or section (9.1a.3)	[LRFD]
A_o	= area enclosed by centerlines of the elements of the beam (9.4.4.2.2-1)	[LRFD]
A_{ps}	= area of prestressing strand (9.1a.5.3)	[LRFD]
A_{PT}	= area of transverse post-tensioning reinforcement (9.4.1.5)	
A'_s	= area of compression reinforcement (9.1a.9)	[LRFD]
A_s	= area of nonprestressed tension reinforcement (9.1a.9)	[LRFD]
A_s	= total area of vertical reinforcement located within a distance $h/4$ from the end of the beam, in. ² (9.1a.14.1)	[LRFD]
A_{tc}	= area of transformed composite section at final time (9.1a.5.5)	
A_{tf}	= area of transformed section at final time (9.1a.5.5-1)	
A_{ti}	= area of transformed section at transfer (9.1a.5.5-1)	
A_v	= area of shear reinforcement within a distance s (9.1a.11.3.2)	[LRFD]
A_{vf}	= area of shear reinforcement crossing the shear plane (9.1a.12.3)	[LRFD]
a	= depth of equivalent stress block (9.1a.9)	[LRFD]
a	= distance from the end of beam to harp point (9.1a.15) or concentrated load (9.6.15.3)	
b	= effective width of compression flange (9.1a.9)	[LRFD]
b	= width of beam (9.4.4.2.2.1)	[LRFD]
b	= width of the compression face of a member (9.4.6)	[LRFD]
b_v	= effective web width (9.1a.11.2.3)	[LRFD]
b_v	= width of interface or actual contact width between the slab and the beam (9.1a.12.3)	[LRFD]
b_w	= web width (9.2.6.1)	[LRFD]
C	= compression force for flexural resistance (9.10.14.2)	
C	= stiffness parameter (9.3.4.2.2.1)	[LRFD]
c	= cohesion factor (9.1a.12.3)	[LRFD]
c	= distance from the extreme compressive fiber to the neutral axis (9.1a.9)	[LRFD]
D	= width of distribution per lane (9.3.4.2.2.1)	[LRFD]
DC	= dead load of structural components and non-structural attachments (9.1a.4.1.1)	[LRFD]
DFD	= distribution factor for deflection (9.1a.15.6)	[LRFD]
DFM	= distribution factor for bending moment (9.1a.4.2.2.1)	[LRFD]

DESIGN EXAMPLES**Notation**

DFV	= distribution factor for shear force (9.1a.4.2.2.2)	[LRFD]
DW	= dead load of wearing surfaces and utilities (9.1a.4.1.1)	[LRFD]
d_b	= nominal strand diameter (9.10.11)	[LRFD]
d_c	= thickness of concrete cover measured from extreme tension fiber to center of the flexural reinforcement located closest thereto (9.10.13.5)	[LRFD]
d_e	= effective depth from the extreme compression fiber to the centroid of the tensile force in the tensile reinforcement (9.1a.11.1)	[LRFD]
d_e	= roadway part of the overhang = distance from the centerline of the exterior web of exterior beam to the interior edge of curb or traffic barrier (9.1a.4.1.1)	[LRFD]
d_p	= distance from extreme compression fiber to the centroid of the prestressing strands (9.1a.9)	[LRFD]
d_v	= distance between the centroid of the tension steel and the mid-thickness of the slab (9.1a.12.1)	[LRFD]
d_v	= effective shear depth (9.1a.11.1)	[LRFD]
E_c	= modulus of elasticity of concrete (9.1a.3)	[LRFD]
E_{cd}	= modulus of elasticity of deck concrete (9.1a.6.3.4)	[LRFD]
E_{ci}	= modulus of elasticity of the beam concrete at transfer (9.1a.6.1)	[LRFD]
E_p	= modulus of elasticity of prestressing tendons or strands (9.1a.2)	[LRFD]
E_s	= modulus of elasticity of reinforcing bars (9.1a.2)	[LRFD]
e	= eccentricity of the strand group at transfer length (9.1a.7.2)	
e'	= difference between eccentricity of prestressing steel at midspan and at end of the beam (9.1a.15.1)	
e_c	= eccentricity of the prestressing strands at midspan (9.1a.5.3)	
e_d	= eccentricity of deck with respect to the gross composite section (9.1a.6.3.4)	[LRFD]
e_e	= eccentricity of prestressing force at end of beam (9.1a.15.1)	
e_g	= distance between the centers of gravity of the precast beam and the slab (9.1a.4.2.2.1)	
e_g	= distance between the centers of gravity of the stems and the flange of the precast beam (9.7.4.2.2.1)	
e_{pc}	= eccentricity of prestressing strands with respect to centroid of composite section (9.1a.6.3.1)	[LRFD]
e_{pg}	= strand eccentricity at midspan with respect to centroid of girder (9.1a.5.4)	[LRFD]
e_{tc}	= eccentricity of strands with respect to transformed composite section at final time (9.1a.5.5)	
e_{tf}	= eccentricity of strands with respect to transformed section at final time (9.1a.5.5)	
e_{ti}	= eccentricity of strands with respect to transformed section at transfer (9.1a.5.5)	
f_b	= concrete stress at the bottom fiber of the beam (9.1a.5)	
f'_c	= specified compressive strength of concrete for use in design (9.1a.2)	[LRFD]
f_{cgp}	= sum of concrete stresses at the center of gravity of prestressing tendons due to prestressing force at transfer and the self-weight of the member at sections of maximum moment (9.1a.6.1)	[LRFD]

DESIGN EXAMPLES**Notation**

f'_{ci}	= specified compressive strength of concrete at time of initial loading or prestressing (9.1a.2)	[LRFD]
f_{cpe}	= compressive stress in concrete due to effective prestress force only (after allowance for all prestress losses) at extreme fiber of section where tensile stress is caused by externally applied loads (9.1a.10.2)	[LRFD]
f_{pb}	= compressive stress at bottom fiber of the beam due to prestress force (9.1a.5.3)	
f_{pbt}	= stress in the prestressing strand before transfer (9.1a.2)	[LRFD]
f_{pc}	= compressive stress in concrete after all prestress losses have occurred either at the centroid of the cross section resisting live load or at the junction of the web and flange when the centroid lies in the flange. In a composite section, f_{pc} is the resultant compressive stress at the centroid of the composite section, or at the junction of the web and flange when the centroid lies within the flange, due to both prestress and to the bending moments resisted by the precast member acting alone (9.1c.11.2)	[LRFD]
f_{pe}	= effective stress in the prestressing strands after all losses (9.1a.6.6)	[LRFD]
f_{pi}	= strand stress before transfer (9.1a.5.3)	[LRFD]
f_{po}	= a parameter taken as modulus of elasticity of prestressing tendons multiplied by the locked-in difference in strain between the prestressing tendons and the surrounding concrete (9.1a.11.2.1)	[LRFD]
f_{ps}	= average stress in prestressing strand at the time for which the nominal resistance of member is required (9.1a.9)	[LRFD]
f_{pt}	= stress in prestressing strand immediately after transfer (9.1a.6.2.3)	[LRFD]
f_{pu}	= specified tensile strength of prestressing strand (9.1a.2)	[LRFD]
f_{py}	= yield strength of prestressing strand (9.1a.2)	[LRFD]
f_r	= modulus of rupture of concrete (9.1a.10.2)	[LRFD]
f_s	= allowable stress in steel (9.1a.14.1)	
f_{ss}	= tensile stress in steel reinforcement at the service limit state (9.10.13.5)	[LRFD]
f_t	= concrete stress at top fiber of the beam for the non-composite section (9.1a.7.2)	
f_{tc}	= concrete stress at top fiber of the slab for the composite section (9.1a.8.2)	
f_{tg}	= concrete stress at top fiber of the beam for the transformed section (9.1a.8.2)	
f_{tg}	= concrete stress at top fiber of the beam for the transformed section under fatigue loading (9.1a.8.4)	
f_y	= specified yield strength of reinforcing bars (9.1a.13)	[LRFD]
f'_y	= specified yield strength of compression reinforcement (9.1a.9)	[LRFD]
f_{yh}	= specified yield strength of shear or transverse reinforcement (9.1a.11.3.2)	[LRFD]
H	= average annual ambient mean relative humidity, percent (9.1a.6.2.1)	[LRFD]
H	= height of wall (9.10.14.2)	[LRFD]
h	= overall depth of a member (9.1a.3.1)	[LRFD]
h_c	= overall depth of the composite section (9.1a.3.2.3)	
h_f	= compression flange depth (9.4.6)	[LRFD]
I	= moment of inertia (9.1a.3.2.3)	[LRFD]

DESIGN EXAMPLES

Notation

IM	= dynamic load allowance (9.1a.4.2.3)	[LRFD]
I_{bs}	= moment of inertia of beam stems (9.7.4.2.2.1)	
I_c	= moment of inertia of the composite section (9.1a.3.2.3)	[LRFD]
I_g	= moment of inertia about the centroid of the non-composite precast beam (9.1a.3.1)	[LRFD]
I_{ti}	= moment of inertia of the transformed section at transfer (9.1a.5.5)	
I_{tf}	= moment of inertia of the transformed section at final time (9.1a.5.5)	
I_{tc}	= moment of inertia of the transformed composite section at final time (9.1a.5.5)	
J_g	= St. Venant torsional inertia (9.3.3)	[LRFD]
j	= a factor relating lever arm to effective depth (9.10.13.5)	
K	= factor used in the calculation of development length (9.10.11)	
K_1	= correction factor for source of aggregate (9.1a.3)	[LRFD]
K_1	= fraction of concrete strength available to resist interface shear (9.1a.12.3)	[LRFD]
K_2	= limiting interface shear resistance (9.1a.12.3)	
K_{df}	= transformed section coefficient that accounts for time-dependent interaction between concrete and bonded steel in the section being considered for time period between deck placement and final time (9.1a.6.3.1)	[LRFD]
K_g	= longitudinal stiffness parameter (9.1a.4.2.2.1)	[LRFD]
K_{id}	= transformed section coefficient that accounts for time-dependent interaction between concrete and bonded steel in the section being considered for time period between transfer and deck placement (9.1a.6.2.1)	
K_L	= factor accounting for type of steel taken as 30 for low relaxation strands and 7 for other prestressing steel, unless more accurate manufacturer's data are available (9.1a.6.2.3)	[LRFD]
k	= a factor used to calculate j (9.10.13.5)	
k	= factor used in calculation of distribution factor for multi-beam bridges (9.5.4.2.2.1)	[LRFD]
k	= factor used in calculation of average stress in prestressing strand for Strength Limit State (9.1a.9)	[LRFD]
k_f	= factor for the effect of concrete strength (9.1a.6.2.1)	[LRFD]
k_{hc}	= humidity factor for creep (9.1a.6.2.1)	[LRFD]
k_{hs}	= humidity factor for shrinkage (9.1a.6.2.1)	[LRFD]
k_{td}	= time development factor (9.1a.6.2.1)	[LRFD]
k_{tdd}	= time development factor at deck placement (9.1a.6.2.1)	
k_{tdf}	= time development factor at final time (9.1a.6.2.1)	
k_{vs}	= factor for the effect of volume-to-surface ratio (9.1a.6.2.1)	[LRFD]
L	= overall beam length or design span length (9.1a.4.1.2)	[LRFD]
LL	= vehicular live load (9.1a.4.3)	[LRFD]
L_c	= critical length of yield line failure pattern (9.10.14.2)	[LRFD]
ℓ_d	= development length (9.10.11)	[LRFD]

M_a	= negative moment at the end of the span being considered (9.2.15.6)	
M_b	= negative moment at the end of the span being considered (9.2.15.6)	
M_b	= unfactored bending moment due to barrier weight (9.1a.4-1)	
M_c	= flexural resistance of barrier at its base (9.10.14.2)	
M_{CIP}	= unfactored bending moment due to cast-in-place slab weight (9.10.6.1)	
M_{const}	= unfactored bending moment due to construction load (9.10.9.2)	
M_{cr}	= cracking moment (9.1a.10.2)	[LRFD]
M_d	= unfactored bending moment due to diaphragm weight per beam (9.4.4-1)	
M_{dnc}	= noncomposite dead load moment at the section (9.1a.10.2)	[LRFD]
M_f	= unfactored bending moment due to fatigue truck per beam (9.1a.4.2.4.1)	
M_g	= unfactored bending moment due to beam self-weight (9.1a.5.1)	[LRFD]
M_j	= unfactored bending moment due to joint concrete weight (9.7.5.1)	
M_{LL}	= unfactored bending moment due to lane load per beam (9.1a.4.2.4.2)	
M_{LL+I}	= unfactored bending moment due to live load plus impact (9.10.6.1)	
M_{LL+LT}	= unfactored bending moment due to truck load plus impact and lane load = $M_{LT} + M_{LL}$ (Table 9.2.4-1)	
M_{LT}	= unfactored bending moment per beam due to truck load with dynamic allowance (9.1a.4.)	
M_{max}	= maximum factored moment at section due to externally applied loads (9.1c.11.2)	
M_n	= nominal flexural resistance (9.1a.9)	[LRFD]
M_r	= factored flexural resistance of a section in bending (9.1a.9)	[LRFD]
M_s	= unfactored bending moment due to slab and haunch weights (9.1a.5.1)	
$M_{service}$	= total bending moment for service load combination (9.10.13.2)	
M_{SIP}	= unfactored bending moment due to stay-in-place panel self weight (9.10.6.1)	
M_u	= factored moment at a section (9.1a.9)	[LRFD]
M_{ws}	= unfactored bending moment due to wearing surface T (9.1a.4-1)	
M_x	= bending moment at a distance (x) from the support (9.1a.4.1.2)	
m	= multiple presence factor (9.1a.4.2.2.1)	[LRFD]
m	= stress ratio = $(f_y/0.85f'_c)$ (9.2.9.2.1)	[LRFD]
N_b	= number of beams (9.1a.4.1.1)	[LRFD]
N_u	= applied factored axial force taken as positive if tensile (9.1a.11.2.1)	[LRFD]
n	= modular ratio between deck slab and beam concrete (9.1a.3.2.2)	
n	= modular ratio between beam and deck slab concrete (9.1a.4.2.2.1)	
n	= modular ratio between prestressing strand and concrete (9.1a.5.5)	[LRFD]
P_c	= permanent net compressive force normal to the shear plane (9.1a.12.3)	[LRFD]
P_d	= diaphragm weight (9.4.15.3)	
P_{pe}	= total prestressing force after all losses (9.1a.5.3)	

P_{pi}	= total prestressing force before transfer (9.1a.6.1)	
P_{pt}	= total prestressing force immediately after transfer (9.1a.6.5)	
P_r	= factored bursting resistance of pretensioned anchorage zone provided by transverse reinforcement (9.1a.14.1)	[LRFD]
Q	= total factored load (9.1a.4.3)	[LRFD]
Q_i	= force effects from specified loads (9.1a.4.3)	[LRFD]
R	= reaction at support (9.3.4.2.2.2)	
R_u	= flexural resistance factor (9.2.9.2.1)	
R_w	= total transverse resistance of the railing or barrier (9.10.14.2)	[LRFD]
S	= spacing of beams (9.1a.4.2.2.1)	[LRFD]
S	= effective span length of the deck slab; clear span plus distance from extreme flange tip to face of web (9.10.15)	[LRFD]
S_b	= section modulus for the extreme bottom fiber of the non-composite precast beam (9.1a.3)	
S_{bc}	= composite section modulus for extreme bottom fiber of the precast beam (9.1a.3.2.3) or panel (9.10.5.2)	
S_{btc}	= section modulus for the extreme bottom fiber of the transformed composite section at final time (9.1a.5.5)	
S_{btf}	= section modulus for the extreme bottom fiber of the transformed section at final time (9.1a.5.5)	
S_{bti}	= section modulus for the extreme bottom fiber of the transformed section at transfer (9.1a.5.5)	
S_c	= section modulus of cast-in-place deck (9.10.14.3)	
S_{dtc}	= composite section modulus for the extreme top fiber of the deck for transformed section at final time (9.1a.5.5)	
S_t	= section modulus for the extreme top fiber of the non-composite precast beam (9.1a.3.2.3)	
S_{tc}	= composite section modulus for top fiber of the structural deck slab (9.1a.3.2.3) or panel (9.10.5.2)	
S_{tg}	= composite section modulus for top fiber of the precast beam (9.1a.3.2.3) or panel (9.10.5.2)	
S_{ttc}	= composite section modulus for the extreme top fiber of the precast beam for transformed section at final time (9.1a.5.5)	
S_{ttf}	= section modulus for the extreme top fiber of the transformed section at final time (9.1a.5.5)	
S_{tti}	= section modulus for the extreme top fiber of the transformed section at transfer (9.1a.5.5)	
s	= spacing of rows of ties or stirrups (9.1a.11.3.2)	[LRFD]
T	= collision force at deck slab level (9.10.14.2)	[LRFD]
t	= thickness of an element (9.4.4.2.2.1)	[LRFD]
t_d	= concrete age at deck placement (9.1a.6.2)	[LRFD]

DESIGN EXAMPLES

Notation

t_f	= concrete age at final stage (9.1a.6.2)	[LRFD]
t_i	= concrete age at transfer (9.1a.6.2)	[LRFD]
t_s	= structural depth of concrete deck (9.1a.2)	
V_b	= unfactored shear force due to barrier weight per beam (9.1a.4-1)	
V_c	= nominal shear resistance provided by tensile stresses in the concrete (9.1a.11)	[LRFD]
V_{ci}	= nominal shear resistance provided by concrete when inclined cracking results from combined shear and moment (9.1c.11.2)	[LRFD]
V_{cw}	= nominal shear resistance provided by concrete when inclined cracking results from excessive principal tensions in web (9.1c.11.2)	[LRFD]
V_d	= unfactored shear force due to barrier weight/lane (9.4.4-1)	
V_d	= shear force at section due to unfactored dead load and includes both DC and DW (9.1c.11.2)	[LRFD]
V_{hi}	= horizontal factored shear force per unit length of the beam (9.1a.12.1)	
V_i	= factored shear force at section due to externally applied loads occurring simultaneously with M_{max} (9.1c.11.2)	
V_{LL}	= unfactored shear force due to lane load per beam (9.1a.4.2.4.1)	
V_{LL+LT}	= unfactored shear force due truck load plus impact and lane load = $V_{LT} + V_{LL}$ (Table 9.2.4-1)	
V_{LT}	= unfactored shear force due to truck load with dynamic allowance per beam (9.1a.4)	
V_n	= nominal shear resistance of the section considered (9.1a.11.3.2)	[LRFD]
V_{ni}	= nominal horizontal shear resistance (9.1a.12.2)	[LRFD]
V_p	= component in the direction of the applied shear of the effective prestressing force, positive if resisting the applied shear (9.1a.11)	[LRFD]
V/S	= volume-to-surface ratio of the beam (9.1a.6.2.1)	
V_s	= shear resistance provided by shear reinforcement (9.1a.11.3.2)	[LRFD]
V_s	= unfactored shear force due to slab and haunch weight/beam (Table 9.1a.4-1)	
V_u	= factored shear force at section (9.1a.11)	[LRFD]
V_{ws}	= unfactored shear force due to wearing surface weight/beam (Table 9.1a.4-1)	
v_u	= factored shear stress on the concrete (9.1a.11.3.3)	[LRFD]
V_x	= shear force at a distance (x) from the support (9.1a.4.1.2)	
W	= edge-to-edge width of bridge (9.3.4.2.2.1)	[LRFD]
w	= a uniformly distributed load (9.1a.4.1.2)	
w	= width of clear roadway (9.1a.4.2.2)	[LRFD]
w_b	= weight of barriers per unit length (9.1a.4.1.1)	
w_c	= unit weight of concrete (9.1a.2)	[LRFD]
w_g	= beam self-weight per unit length (9.1a.4.1.1)	
w_j	= weight of joint concrete per unit length (9.7.15.3)	
w_s	= slab and haunch weights per unit length (9.1a.4.1.1)	

w_{ws}	= weight of future wearing surface per unit length (9.1a.4.1.1)	
X	= distance from load to point of support (9.10.14.2)	
x	= distance from the support to the section under question (9.1a.4)	
y_b	= distance from centroid of the component to the extreme bottom fiber of the non-composite precast beam (9.1a.3.2.3)	
y_{bc}	= distance from the centroid of the composite section to extreme bottom fiber of the precast beam (9.1a.3.2.3)	
y_{bs}	= distance from the center of gravity of strands to the bottom fiber of the beam (9.1a.5.3) or panel (9.10.5.2)	
y_{btc}	= distance from the centroid of the composite transformed section to the extreme bottom fiber of the beam at final time (9.1a.5.5)	
y_{btf}	= distance from the centroid of the noncomposite transformed section to the extreme bottom fiber of the beam at final time (9.1a.5.5)	
y_{bti}	= distance from the centroid of the transformed section to the extreme bottom fiber of the beam at transfer (9.1a.5.5)	
y_t	= distance from centroid to the extreme top fiber of the non-composite precast beam (9.1a.3)	
y_{tc}	= distance from the centroid of the composite section to extreme top fiber of the structural deck (9.1a.3.2.3) or panel (9.10.5.2)	
y_{tg}	= distance from the centroid of the composite section to extreme top fiber of the precast beam (9.1a.3) or panel (9.10.5.2)	
α	= angle of inclination of transverse reinforcement to longitudinal axis (9.1a.11.3.2)	[LRFD]
β	= factor indicating ability of diagonally cracked concrete to transmit tension (a value indicating concrete contribution) (9.1a.11.2)	[LRFD]
β_1	= ratio of the depth of the equivalent uniformly stressed compression zone assumed in the strength limit state to the depth of the actual compression zone (9.1a.9)	[LRFD]
γ	= load factor for Fatigue I load combination (9.4.9.2)	[LRFD]
γ_e	= exposure factor (9.10.13.5)	[LRFD]
γ_h	= correction factor for relative humidity of the ambient air (9.1c.6.2)	[LRFD]
γ_i	= load factors (9.1a.4.3)	[LRFD]
γ_{st}	= correction factor for specified concrete strength at time of prestress transfer (9.1c.6.2)	[LRFD]
$(\Delta F)_{TH}$	= constant-amplitude fatigue threshold (9.4.9.3)	[LRFD]
Δ_{b+ws}	= deflection due to barrier and wearing surface weights (9.1a.15.4)	
Δ_d	= deflection due to diaphragm weight (9.4.14.3)	
Δf	= force effect, live load stress range for fatigue (9.4.9.2)	[LRFD]
Δf_{cd}	= change in concrete stress at centroid of prestressing strands due to long-term losses between transfer and deck placement, combined with deck weight and superimposed loads (9.1a.6.3.2)	[LRFD]
Δf_{cdf}	= change in concrete stress at centroid of prestressing strands due to shrinkage of deck concrete (9.1a.6.3.4)	[LRFD]

DESIGN EXAMPLES

Notation

Δf_{pCD}	= prestress due to creep of girder concrete between time of deck placement and final time (9.1a.6.3.2)	[LRFD]
Δf_{pCR}	= loss in prestressing steel stress due to creep between time of transfer and deck placement (9.1a.6.2.2)	[LRFD]
Δf_{pES}	= sum of all losses or gains due to elastic shortening or extension at the time of application of prestress and/or external loads (9.1a.6)	[LRFD]
Δf_{pi}	= total loss in prestressing strand stress immediately after transfer (9.1a.6.5)	
Δf_{pLT}	= long-term losses due to shrinkage and creep of concrete, and relaxation of steel after transfer (9.1a.6)	
Δf_{pR}	= loss in pretensioning steel stress due to relaxation of steel (9.1c.6.2)	[LRFD]
Δf_{pR1}	= loss in prestressing steel stress due to relaxation of steel between transfer and deck placement (9.1a.6.2.3)	[LRFD]
Δf_{pR2}	= loss in prestressing steel stress due to relaxation of steel between time of deck placement and final time (9.1a.6.3.3)	[LRFD]
Δf_{pSD}	= prestress loss due to shrinkage of concrete between time of deck placement and final time (9.1a.6.3.1)	[LRFD]
Δf_{pSR}	= loss in prestressing steel stress due to shrinkage between time of transfer and deck placement (9.1a.6.2.1)	[LRFD]
Δf_{pSS}	= prestress gain due to shrinkage of deck concrete (9.1a.6.3.4)	[LRFD]
Δf_{pT}	= total loss in prestressing steel stress (9.1a.6)	[LRFD]
Δg	= deflection due to beam self weight (9.1a.15.2)	
Δ_{j+b+ws}	= deflection due to joint concrete, barrier, and wearing surface (9.7.15.3)	
Δ_L	= deflection due to specified live load (9.2.15.6)	
Δ_{LL}	= deflection due to lane load (9.1a.15.6)	
Δ_{LT}	= deflection due to design truck load and impact (9.1a.15.6)	
Δ_p	= camber due prestressing force at transfer (9.1a.15.1)	
Δ_S	= deflection due to slab and haunch weight (9.1a.13.5)	
ϵ_{bdf}	= concrete shrinkage strain of girder for time period between deck placement and final time (9.1a.6.3.1)	[LRFD]
ϵ_{bid}	= concrete shrinkage strain of girder for time period between time of transfer and deck placement (9.1a.6.2.1)	[LRFD]
ϵ_{bif}	= total concrete shrinkage strain of girder between time of transfer and final time (9.1a.6.3.1)	
ϵ_{ddf}	= shrinkage strain of deck concrete between time of placement and final time (9.1a.6.3.4)	[LRFD]
ϵ_s	= longitudinal tensile strain in the section at the centroid of the tension reinforcement (9.1a.11.2.1)	[LRFD]
ϵ_x	= longitudinal strain in the web of the member (9.1b.11.2.1)	[LRFD]
η_i	= load modifier relating to ductility, redundancy, and operational importance (9.1a.4.3)	[LRFD]
θ	= angle of inclination of diagonal compressive stresses (9.1a.11.2.1)	

Notation

μ	= coefficient of friction (9.1a.12.2)	[LRFD]
μ	= Poisson's ratio (9.3.4.2.2.1)	[LRFD]
ρ	= ratio of nonprestressed reinforcement (9.2.9.2.1)	
ρ_a	= actual ratio of non-pretensioned reinforcement (9.10.13.5)	
ϕ	= resistance factor (9.1a.9)	[LRFD]
ϕ_c	= resistance factor for axial load (9.1a.13)	[LRFD]
ϕ_f	= resistance factor for moment (9.1a.13)	[LRFD]
ϕ_v	= resistance factor for shear (9.1a.13)	[LRFD]
ψ	= angle of harped pretensioned reinforcement (9.1a.7.2)	
$\Psi_b(t_d, t_i)$	= girder creep coefficient at time of deck placement due to loading introduced at transfer (9.1a.6.2.2)	[LRFD]
$\Psi_b(t_f, t_d)$	= girder creep coefficient at final time due to loading at deck placement (9.1a.6.3.2)	[LRFD]
$\Psi_b(t_f, t_i)$	= girder creep coefficient at final time due to loading introduced at transfer (9.1a.6.2.1)	[LRFD]
$\Psi_d(t_f, t_d)$	= deck concrete creep coefficient at final time due to loading introduced shortly after deck placement (9.1a.6.3.4)	[LRFD]

Design Examples

9.0 INTRODUCTION

Design examples included in this chapter illustrate the step-by-step procedure used in the design of precast, prestressed concrete bridges. Each design is based on the *AASHTO LRFD Bridge Design Specifications*, Fifth Edition, 2010, and the 2011 Interim Revisions.

Design examples for nine different bridge types and span lengths are included to illustrate the range of possibilities with precast, prestressed components. A tenth design example is for a precast concrete stay-in-place deck panel system. The complete list of design examples is shown in **Table 9.0-1**. Design Example 9.1 has three sets of calculations to illustrate the use of transformed or gross section properties; determination of prestress losses by the approximate method or refined estimates; and design for shear using the general method, Appendix B5 method, or the simplified method. All other design examples use transformed section properties, refined estimates for prestress losses, and the general method for shear design.

All design examples except 9.2 are for simple span bridges. Design example 9.2 is for a bridge that is simply supported for dead load but made continuous for subsequent superimposed dead loads and live loads.

For the nine bridge types, the design examples are for an interior beam. In some situations, the design of the exterior beams may require more strands than the interior beam depending on the assumed distribution of the barrier weight and top flange overhang on the outside of the bridge. Some owners prefer to use the same beam cross sections for interior and exterior beams to facilitate casting and to avoid confusion during erection. The steps in the design procedure are the same for both interior and exterior beams.

The design examples do not always represent the optimum solution for each span length but serve to demonstrate the wide variety of options that exist for a precast, prestressed concrete superstructure. Ideally, the designer would try to match the beam concrete stress level under Service III load combination with the Service III tensile stress limit by incrementally reducing the number of strands and repeating the relevant design steps.

9.0.1 Service Life

Design calculations for prestress losses are based on a final age of 20,000 days or 54.8 years to be consistent with previous editions of the manual. These losses, however, are applicable to longer service lives such as 75 or 100 years because the time development factor only changes by 0.2% after 20,000 days.

9.0.2 Sign Convention

The following sign convention is used where it is necessary to differentiate between compressive and tensile stresses.

- For concrete stresses:
 - Compression is positive (+ ve)
 - Tension is negative (- ve)
- For steel stresses:
 - Compression is negative (- ve)
 - Tension is positive (+ ve)

9.0.3 Level of Precision

The levels of precision shown in **Table 9.0.3-1** are used for most calculations. Some calculations were carried out to a higher number of significant figures than common practice with hand calculations. Depending on available computation resources and designer preference, other levels of precision may be used.

Table 9.0.3-1
Level of Precision

Item	Units	Precision
Concrete Stresses	ksi	1/1000
Steel Stresses	ksi	1/10
Prestress Forces	kips	1/10
Moments	ft-kips	1/10
Shears	kips	1/10
For the Beam:		
Cross-Section Dimensions	in.	1/100
Section Properties	in.	1
Length	ft	1/100
Area of Prestressing Steel	in. ²	1/1000
Area of Nonprestressed Reinforcement	in. ²	1/100

Table 9.0-1
Design Examples

Example Number	Bridge Type	AASHTO Type	Beam Type	Span Lengths ft	Bridge Width ft	Beam Spacing ft	Beam f'_{ci} ksi	Beam f'_c ksi	CIP Deck f'_c ksi	Strand Dia. in.	Cross Section	Prestress Losses	Shear
9.1a	Bulb-tee beams with CIP composite deck	<i>k</i>	BT-72	120	51.0	9.0	5.8	6.5	4.0	0.5	Transformed	Refined 5.9.5.4	General 5.8.3.4.2
9.1b	Bulb-tee beams with CIP composite deck	<i>k</i>	BT-72	120	51.0	9.0	5.8	6.5	4.0	0.5	Gross	Refined 5.9.5.4	Appendix B5
9.1c	Bulb-tee beams with CIP composite deck	<i>k</i>	BT-72	120	51.0	9.0	5.8	6.5	4.0	0.5	Transformed	Approx. 5.9.5.3	Simplified 5.8.3.4.3
9.2	Bulb-tee beams with composite deck continuous for live load	<i>k</i>	BT-72	110, 120, 110	44.5	12.0	5.5	7.0	4.0	0.5	Transformed	Refined 5.9.5.4	General 5.8.3.4.2
9.3	Deck bulb-tee beams w/o CIP deck, with noncomposite wearing surface	<i>j</i>	DBT-53	95	54.0	6.0	5.5	7.0	N/A	0.6	Transformed	Refined 5.9.5.4	General 5.8.3.4.2
9.4	Adjacent box beams without CIP deck, with transverse P/T	<i>g</i>	BIII-48	95	28.0	Adjacent 4.0	4.0	5.0	N/A	0.5	Transformed	Refined 5.9.5.4	General 5.8.3.4.2
9.5	Adjacent box beams with 5.5-in. thick CIP composite deck	<i>f</i>	BIII-48	95	28.0	Adjacent 4.0	4.0	5.0	4.0	0.5	Transformed	Refined 5.9.5.4	General 5.8.3.4.2
9.6	U-beams with 3-½-in.-thick precast panels and 4-in.-thick CIP composite deck	<i>c</i>	TX U54	110	50.0	12.0	6.0	10.0	4.0	0.6	Transformed	Refined 5.9.5.4	General 5.8.3.4.2
9.7	Double-tee beams without CIP deck, with transverse post-tensioning	<i>i</i>	NEXT 36 D	80	44.33	9.0	6.0	8.0	N/A	0.6	Transformed	Refined 5.9.5.4	General 5.8.3.4.2
9.8	Double-tee beams with 6-in.-thick CIP deck and no P/T	<i>k</i>	NEXT 36 F	80	44.33	8.88	6.0	8.0	4.0	0.6	Transformed	Refined 5.9.5.4	General 5.8.3.4.2
9.9	Precast composite slab span system	Details to be determined and included in the next release of material for the Third Edition of the manual.									Transformed	Refined 5.9.5.4	General 5.8.3.4.2
9.10	Precast concrete stay-in-place deck panel system	N/A	3.5 in.-thick SIP	9.5	44.5	Adjacent	6.5	8.0	4.0	0.5	Transformed	Refined 5.9.5.4	General 5.8.3.4.2

This page intentionally left blank

BULB-TEE (BT-72), SINGLE SPAN, COMPOSITE DECK

Transformed Sections, Shear General Procedure, Refined Losses

Table of Contents

9.1a.1 INTRODUCTION	9.1a - 5
9.1a.1.1 Terminology.....	9.1a - 5
9.1a.2 MATERIALS	9.1a - 6
9.1a.3 CROSS-SECTION PROPERTIES FOR A TYPICAL INTERIOR BEAM	9.1a - 7
9.1a.3.1 Noncomposite Nontransformed Beam Section.....	9.1a - 7
9.1a.3.2 Composite Section.....	9.1a - 7
9.1a.3.2.1 Effective Flange Width.....	9.1a - 7
9.1a.3.2.2 Modular Ratio between Slab and Beam Concrete.....	9.1a - 8
9.1a.3.2.3 Section Properties.....	9.1a - 8
9.1a.4 SHEAR FORCES AND BENDING MOMENTS.....	9.1a - 9
9.1a.4.1 Shear Forces and Bending Moments Due to Dead Loads	9.1a - 9
9.1a.4.1.1 Dead Loads	9.1a - 9
9.1a.4.1.2 Unfactored Shear Forces and Bending Moments.....	9.1a - 10
9.1a.4.2 Shear Forces and Bending Moments Due to Live Loads	9.1a - 10
9.1a.4.2.1 Live Loads.....	9.1a - 10
9.1a.4.2.2 Live Load Distribution Factors for a Typical Interior Beam	9.1a - 10
9.1a.4.2.2.1 Distribution Factor for Bending Moment.....	9.1a - 11
9.1a.4.2.2.2 Distribution Factor for Shear Force.....	9.1a - 12
9.1a.4.2.3 Dynamic Allowance.....	9.1a - 12
9.1a.4.2.4 Unfactored Shear Forces and Bending Moments.....	9.1a - 12
9.1a.4.2.4.1 Due To Truck Load; V_{LT} and M_{LT}	9.1a - 12
9.1a.4.2.4.2 Due To Design Lane Load; V_{LL} and M_{LL}	9.1a - 13
9.1a.4.3 Load Combinations.....	9.1a - 13
9.1a.5 ESTIMATE REQUIRED PRESTRESS	9.1a - 15
9.1a.5.1 Service Load Stresses at Midspan	9.1a - 15
9.1a.5.2 Stress Limits for Concrete	9.1a - 15
9.1a.5.3 Required Number of Strands.....	9.1a - 15
9.1a.5.4 Strand Pattern.....	9.1a - 16
9.1a.5.5 Steel Transformed Section Properties.....	9.1a - 17
9.1a.6 PRESTRESS LOSSES.....	9.1a - 19
9.1a.6.1 Elastic Shortening	9.1a - 19
9.1a.6.2 Time-Dependent Losses between Transfer and Deck Placement	9.1a - 19
9.1a.6.2.1 Shrinkage of Concrete	9.1a - 20
9.1a.6.2.2 Creep of Concrete.....	9.1a - 21
9.1a.6.2.3 Relaxation of Prestressing Strands.....	9.1a - 21
9.1a.6.3 Time-Dependent Losses between Deck Placement and Final Time	9.1a - 21
9.1a.6.3.1 Shrinkage of Concrete	9.1a - 21
9.1a.6.3.2 Creep of Concrete.....	9.1a - 22
9.1a.6.3.3 Relaxation of Prestressing Strands.....	9.1a - 23

BULB-TEE (BT-72), SINGLE SPAN, COMPOSITE DECK

Transformed Sections, Shear General Procedure, Refined Losses

Table of Contents

9.1a.6.3.4 Shrinkage of Deck Concrete..... 9.1a - 23

9.1a.6.4 Total Time-Dependent Loss 9.1a - 24

9.1a.6.5 Total Losses at Transfer 9.1a - 24

9.1a.6.6 Total Losses at Service Loads 9.1a - 25

9.1a.7 CONCRETE STRESSES AT TRANSFER..... 9.1a - 25

9.1a.7.1 Stress Limits for Concrete 9.1a - 25

9.1a.7.2 Stresses at Transfer Length Section..... 9.1a - 26

9.1a.7.3 Stresses at Harp Points 9.1a - 28

9.1a.7.4 Stresses at Midspan..... 9.1a - 28

9.1a.7.5 Hold-Down Forces 9.1a - 28

9.1a.7.6 Summary of Stresses at Transfer 9.1a - 29

9.1a.8 CONCRETE STRESSES AT SERVICE LOADS 9.1a - 29

9.1a.8.1 Stress Limits for Concrete 9.1a - 29

9.1a.8.2 Stresses at Midspan..... 9.1a - 29

9.1a.8.3 Fatigue Stress Limit..... 9.1a - 30

9.1a.8.4 Summary of Stresses at Midspan at Service Loads 9.1a - 30

9.1a.8.5 Effect of Deck Shrinkage..... 9.1a - 31

9.1a.8.5.1 Total Time-Dependent Loss 9.1a - 31

9.1a.8.5.2 Effective Prestressing Force..... 9.1a - 31

9.1a.8.5.3 Concrete Stress in Bottom of Beam, Load Combination Service III:..... 9.1a - 31

9.1a.8.5.4 Stresses from Deck Shrinkage 9.1a - 31

9.1a.9 STRENGTH LIMIT STATE..... 9.1a - 32

9.1a.10 LIMITS OF REINFORCEMENT 9.1a - 33

9.1a.10.1 Maximum Reinforcement 9.1a - 33

9.1a.10.2 Minimum Reinforcement 9.1a - 33

9.1a.11 SHEAR DESIGN..... 9.1a - 34

9.1a.11.1 Critical Section 9.1a - 34

9.1a.11.2 Contribution of Concrete to Nominal Shear Resistance 9.1a - 35

9.1a.11.2.1 Strain in Flexural Tension Reinforcement 9.1a - 35

9.1a.11.2.2 Values of β and θ 9.1a - 35

9.1a.11.2.3 Compute Concrete Contribution 9.1a - 36

9.1a.11.3 Contribution of Reinforcement to Nominal Shear Resistance..... 9.1a - 36

9.1a.11.3.1 Requirement for Reinforcement..... 9.1a - 36

9.1a.11.3.2 Required Area of Reinforcement..... 9.1a - 36

9.1a.11.3.3 Determine Spacing of Reinforcement..... 9.1a - 36

9.1a.11.3.4 Minimum Reinforcement Requirement 9.1a - 37

9.1a.11.4 Maximum Nominal Shear Resistance 9.1a - 37

9.1a.12 INTERFACE SHEAR TRANSFER..... 9.1a - 37

9.1a.12.1 Factored Horizontal Shear 9.1a - 37

BULB-TEE (BT-72), SINGLE SPAN, COMPOSITE DECK

Transformed Sections, Shear General Procedure, Refined Losses

Table of Contents

9.1a.12.2 Required Nominal Resistance 9.1a - 37

9.1a.12.3 Required Interface Shear Reinforcement 9.1a - 37

 9.1a.12.3.1 Minimum Interface Shear Reinforcement 9.1a - 38

9.1a.12.4 Maximum Nominal Shear Resistance 9.1a - 38

9.1a.13 MINIMUM LONGITUDINAL REINFORCEMENT REQUIREMENT 9.1a - 38

 9.1a.13.1 Required Reinforcement at Face of Bearing 9.1a - 39

9.1a.14 PRETENSIONED ANCHORAGE ZONE 9.1a - 40

 9.1a.14.1 Anchorage Zone Reinforcement 9.1a - 40

 9.1a.14.2 Confinement Reinforcement 9.1a - 40

9.1a.15 DEFLECTION AND CAMBER 9.1a - 40

 9.1a.15.1 Deflection Due to Prestressing Force at Transfer 9.1a - 40

 9.1a.15.2 Deflection Due to Beam Self Weight 9.1a - 41

 9.1a.15.3 Deflection Due to Slab and Haunch Weights 9.1a - 41

 9.1a.15.4 Deflection Due to Barrier and Future Wearing Surface Weights 9.1a - 41

 9.1a.15.5 Deflection and Camber Summary 9.1a - 42

 9.1a.15.6 Deflection Due to Live Load and Impact 9.1a - 42

This page intentionally left blank

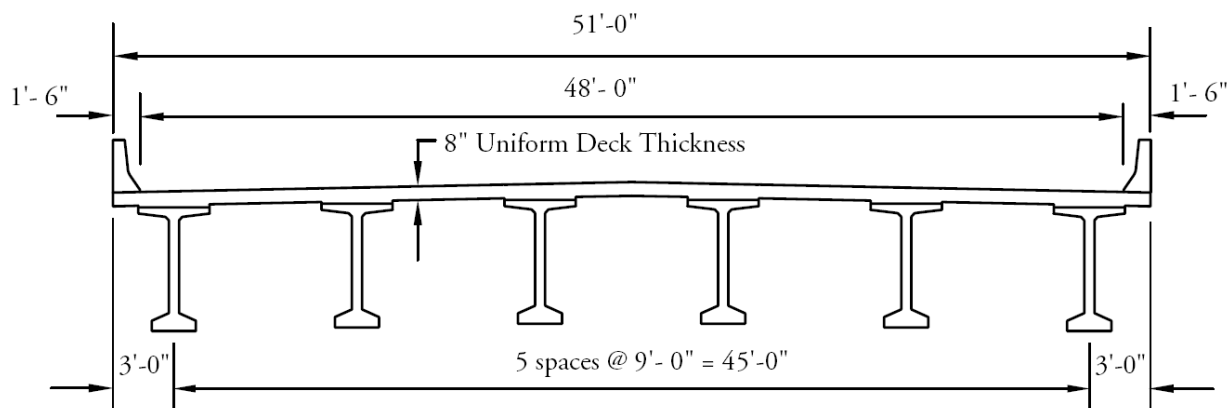
BULB-TEE (BT-72), SINGLE SPAN, COMPOSITE DECK

9.1a.1 Introduction/9.1a.1.1 Terminology

9.1a Transformed Sections, Shear General Procedure, Refined Losses**9.1a.1 INTRODUCTION**

This design example demonstrates the design of a 120-ft, single span, AASHTO-PCI bulb-tee beam bridge with no skew. This example illustrates in detail the design of a typical interior beam at the critical sections in positive flexure, shear, and deflection due to prestress, dead loads, and live load. The superstructure consists of six beams spaced at 9 ft 0 in. centers, as shown in **Figure 9.1a.1-1**. Beams are designed to act compositely with the 8-in.-thick cast-in-place concrete deck to resist all superimposed dead loads, live loads, and impact. A ½-in.-thick wearing surface is considered to be an integral part of the 8-in.-thick deck. Design live load is HL-93. The design is accomplished in accordance with the *AASHTO LRFD Bridge Design Specifications*, Fifth Edition, 2010 and the 2011 Interim Revisions. Elastic stresses from external loads are calculated using transformed sections. Shear strength is calculated using the general procedure. Time-dependent prestress losses are calculated using the refined estimates.

Figure 9.1a.1-1
Bridge Cross Section

**9.1a.1.1 Terminology**

The following terminology is used to describe cross sections in this design example:

noncomposite section—the concrete beam cross section.

noncomposite nontransformed section—the concrete beam cross section without the strands transformed. Also called the gross section.

noncomposite transformed section—the concrete beam cross section with the strands transformed to provide cross-sectional properties equivalent to the girder concrete.

composite section—the concrete beam plus the concrete deck and haunch.

composite nontransformed section—the concrete beam plus the concrete deck and haunch transformed to provide cross-sectional properties equivalent to the girder concrete but without the strands transformed.

composite transformed section—the concrete beam plus the concrete deck and haunch and the strands transformed to provide cross-sectional properties equivalent to the girder concrete.

The term "composite" implicitly includes the transformation of the concrete deck and haunch.

The term "transformed" generally refers to transformation of the strands.

BULB-TEE (BT-72), SINGLE SPAN, COMPOSITE DECK

9.1a.2 Materials

9.1a.2 MATERIALS

Cast-in-place concrete slab: Actual thickness = 8.0 in.

Structural thickness, $t_s = 7.5$ in.

Note that a 1/2-in.-thick wearing surface is considered to be an integral part of the 8-in.-thick deck.

Specified concrete compressive strength for use in design, $f'_c = 4.0$ ksi

Precast concrete beams: AASHTO-PCI bulb-tee beams as shown in **Figure 9.1a.2-1**

Required concrete compressive strength at transfer, $f'_{ci} = 5.8$ ksi

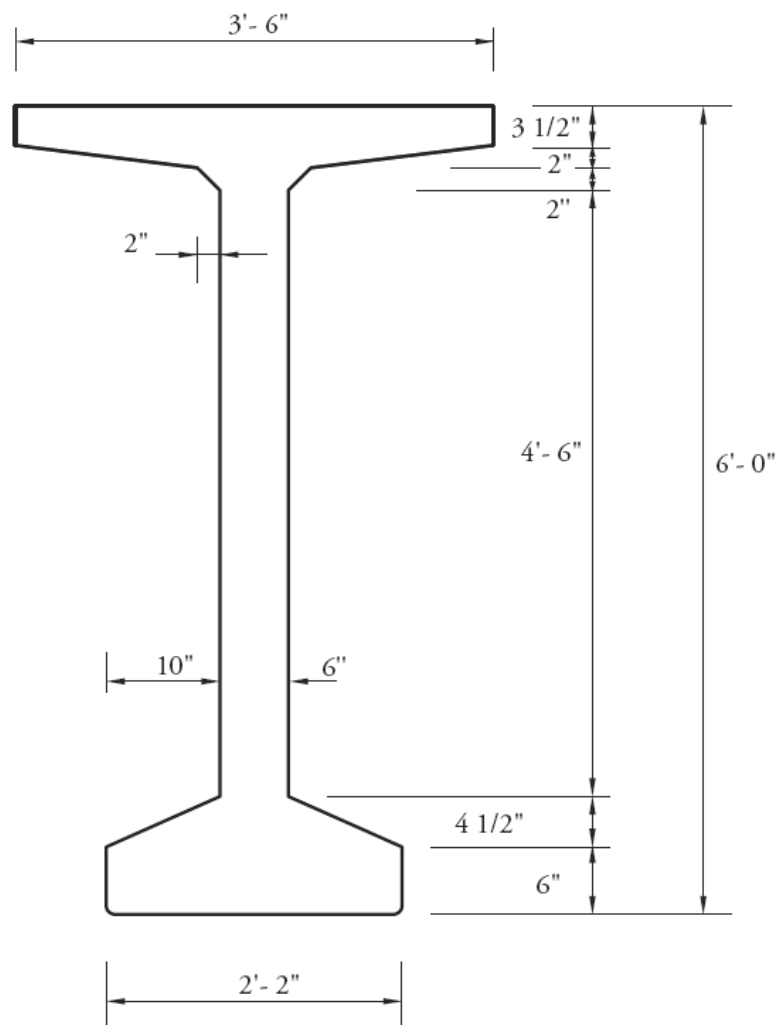
Specified concrete compressive strength for use in design, $f'_c = 6.5$ ksi

Concrete unit weight, $w_c = 0.150$ kcf

Overall beam length = 121.0 ft

Design span = 120.0 ft

Figure 9.1a.2-1
AASHTO-PCI BT-72 Dimensions



BULB-TEE (BT-72), SINGLE SPAN, COMPOSITE DECK

9.1a.2 Materials/9.1a.3.2.1 Effective Flange Width

Prestressing strands: 1/2-in.-dia., seven-wire, low-relaxation

Area of one strand = 0.153 in.²

Specified tensile strength, $f_{pu} = 270.0$ ksi

Yield strength, $f_{py} = 0.9f_{pu} = 243.0$ ksi

[LRFD Table 5.4.4.1-1]

Stress limits for prestressing strands:

[LRFD Table 5.9.3-1]

- before transfer, $f_{pi} \leq 0.75f_{pu} = 202.5$ ksi

- at service limit state (after all losses), $f_{pe} \leq 0.80f_{py} = 194.4$ ksi

Modulus of elasticity, $E_p = 28,500$ ksi

[LRFD Art. 5.4.4.2]

Reinforcing bars:

Yield strength, $f_y = 60.0$ ksi

Modulus of elasticity, $E_s = 29,000$ ksi

[LRFD Art. 5.4.3.2]

Future wearing surface: 2 in. additional concrete, unit weight = 0.150 kcf

New Jersey-type barrier: unit weight = 0.300 kips/ft/side

9.1a.3 CROSS-SECTION PROPERTIES FOR A TYPICAL INTERIOR BEAM**9.1a.3.1 Noncomposite Nontransformed Beam Section**

A_g = area of cross section of beam = 767 in.²

h = overall depth of beam = 72 in.

I_g = moment of inertia about the centroid of the noncomposite precast beam = 545,894 in.⁴

y_b = distance from centroid to extreme bottom fiber of the noncomposite precast beam = 36.60 in.

y_t = distance from centroid to extreme top fiber of the noncomposite precast beam = 35.40 in.

S_b = section modulus for the extreme bottom fiber of the noncomposite precast beam = $I_g/y_b = 14,915$ in.³

S_t = section modulus for the extreme top fiber of the noncomposite precast beam = $I_g/y_t = 15,421$ in.³

w_g = beam weight per unit length = $(767/144)(0.150) = 0.799$ kips/ft

E_c = modulus of elasticity of concrete, ksi = $33,000K_1(w_c)^{1.5}\sqrt{f'_c}$ [LRFD Eq. 5.4.2.4-1]

where

K_1 = correction factor for source of aggregate taken as 1.0

w_c = unit weight of concrete = 0.150 kcf

LRFD Table 3.5.1-1 states that, in the absence of more precise data, the unit weight of concrete may be taken as $0.140 + 0.001f'_c$ for $5.0 < f'_c \leq 15.0$ ksi. For $f'_c = 6.5$ ksi, the unit weight would be 0.1465 kcf. However, precast concrete mixes typically have a relatively low water-cementitious materials ratio and high density. Therefore, a unit weight of 0.150 kcf is used in this example. For high-strength concrete, this value may need to be increased based on test results. For simplicity, a value of 0.150 kcf is also used for the cast-in-place concrete.

f'_c = specified compressive strength of concrete, ksi

Therefore, the modulus of elasticity for:

cast-in-place slab, $E_c = 33,000(1.00)(0.150)^{1.5}\sqrt{4.0} = 3,834$ ksi

precast beam at transfer, $E_{ci} = 33,000(1.00)(0.150)^{1.5}\sqrt{5.80} = 4,617$ ksi

precast beam at service loads, $E_c = 33,000(1.00)(0.150)^{1.5}\sqrt{6.50} = 4,888$ ksi

9.1a.3.2 Composite Section**9.1a.3.2.1 Effective Flange Width**

[LRFD Art. 4.6.2.6.1]

Effective flange width is taken as the tributary width perpendicular to the axis of the beam. For the interior beam, the effective flange width is calculated as one-half the distance to the adjacent beam on each side.

$2 \times (4.5 \times 12) = 108.00$ in.

Therefore, the effective flange width is 108.00 in.

BULB-TEE (BT-72), SINGLE SPAN, COMPOSITE DECK

9.1a.3.2.2 Modular Ratio between Slab and Beam Concrete/9.1a.3.2.3 Section Properties

9.1a.3.2.2 Modular Ratio between Slab and Beam Concrete

Modular ratio between slab and beam concrete, $n = \frac{E_c(\text{slab})}{E_c(\text{beam})} = \frac{3,834}{4,888} = 0.7845$

9.1a.3.2.3 Section Properties

The effective flange width must be transformed by the modular ratio to provide cross-sectional properties equivalent to the girder concrete.

Transformed flange width = $n(\text{effective flange width}) = (0.7845)(108) = 84.73 \text{ in.}$

Transformed flange area = $n(\text{effective flange width})(t_s) = (0.7845)(108.00)(7.50) = 635.45 \text{ in.}^2$

Transformed flange moment of inertia = $(84.73)(7.5)^3/12 = 2,978.79 \text{ in.}^4$

Note: Only the structural thickness of the deck, 7.50 in., is considered.

Due to camber of the precast, prestressed beam, a minimum haunch thickness of 1/2 in. at midspan is considered in the structural properties of the composite section. Also, the width of haunch must be transformed by the modular ratio.

Transformed width of haunch = $(0.7845)(42.00) = 32.95 \text{ in.}$

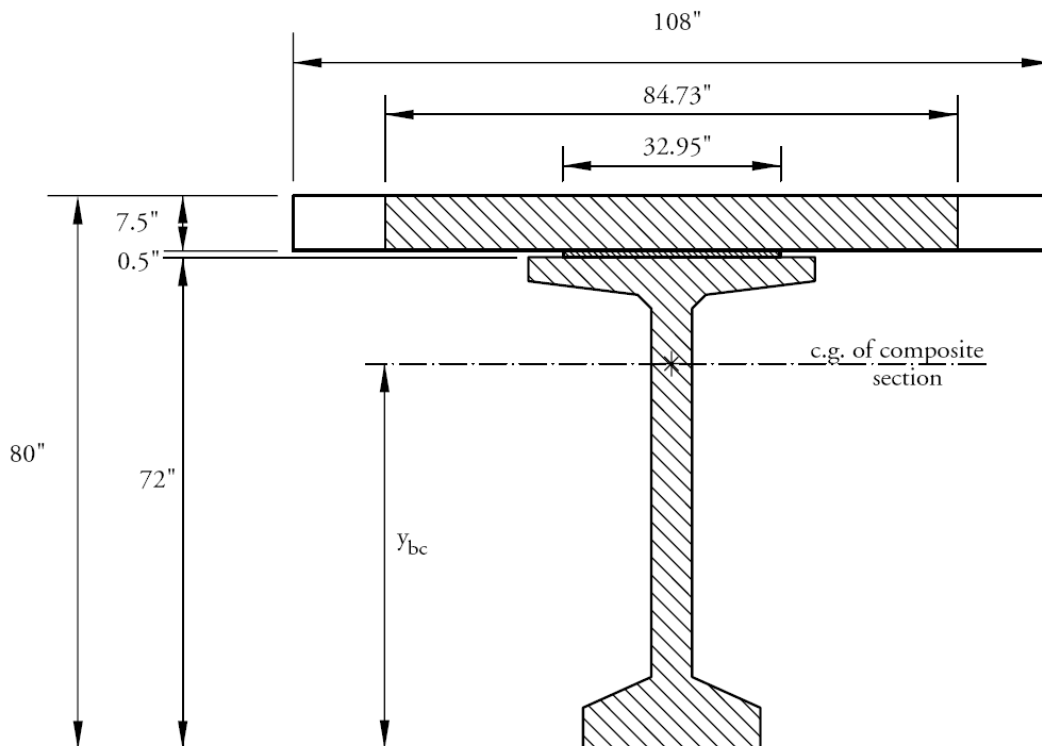
Transformed area of haunch = $(0.7845)(42.00)(0.5) = 16.47 \text{ in.}^2$

Transformed moment of inertia of haunch = $(32.95)(0.5)^3/12 = 0.34 \text{ in.}^4$

Note that the haunch should only be considered to contribute to section properties if it is required to be provided in the completed structure. Therefore, some designers neglect its contribution to the section properties.

Figure 9.1a.3.2.3-1

Dimensions of the Composite Section



BULB-TEE (BT-72), SINGLE SPAN, COMPOSITE DECK

9.1a.3.2.3 Section Properties/9.1a.4.1.1 Dead Loads

Table 9.1a.3.2.3-1
Properties of Composite Section

	Area, in. ²	y_b in.	Ay_b in. ³	$A(y_{bc} - y_b)^2$ in. ⁴	I in. ⁴	$I + A(y_{bc} - y_b)^2$ in. ⁴
Beam	767.00	36.60	28,072	253,224	545,894	799,118
Haunch	16.47	72.25	1,190	5,032	0.34	5,032
Deck	635.45	76.25	48,453	293,191	2,979	296,170
Σ	1,418.9		77,715			1,100,320

A_c = total area of the composite section = 1,418.9 in.²

h_c = overall depth of the composite section = 80.00 in.

I_c = moment of inertia of the composite section = 1,100,320 in.⁴

y_{bc} = distance from the centroid of the composite section to the extreme bottom fiber of the precast beam
 = $77,715/1,418.9 = 54.77$ in.

y_{tg} = distance from the centroid of the composite section to the extreme top fiber of the precast beam = 72.00
 – 54.77 = 17.23 in.

y_{tc} = distance from the centroid of the composite section to the extreme top fiber of the structural deck =
 80.00 – 54.77 = 25.23 in.

S_{bc} = composite section modulus for the extreme bottom fiber of the precast beam
 = $(I_c/y_{bc}) = \frac{1,100,320}{54.77} = 20,090$ in.³

S_{tg} = composite section modulus for the extreme top fiber of the precast beam
 = $(I_c/y_{tg}) = \frac{1,100,320}{17.23} = 63,861$ in.³

S_{tc} = composite section modulus for extreme top fiber of the structural deck slab
 $\left(\frac{1}{n}\right)(I_c/y_{tc}) = \left(\frac{1}{0.7845}\right)\left(\frac{1,100,320}{25.23}\right) = 55,592$ in.³

9.1a.4 SHEAR FORCES AND BENDING MOMENTS

The self weight of the beam and the weight of the deck and haunch act on the noncomposite, simple-span structure, while the weight of barriers, future wearing surface, and live loads with impact act on the composite, simple-span structure. Refer to **Tables 9.1a.4-1** and **9.1a.4-2**, which follow Section 9.1a.4.3 for a summary of unfactored values calculated below.

9.1a.4.1 Shear Forces and Bending Moments Due to Dead Loads**9.1a.4.1.1 Dead Loads**

[LRFD Art. 3.3.2]

DC = Dead load of structural components and nonstructural attachments

Dead loads acting on the noncomposite structure:

Beam self weight, $w_g = 0.799$ kips/ft

8-in.-thick deck weight = $(8/12 \text{ ft})(9 \text{ ft})(0.150 \text{ kcf}) = 0.900$ kips/ft

½-in.-thick haunch weight = $(0.5)(42/144)(0.150) = 0.022$ kips/ft

$w_s = 0.900 + 0.022 = 0.922$ kips/ft

Notes:

1. Actual deck thickness (8 in.) is used for computing dead load.
2. A ½-in. minimum haunch thickness is assumed in the computations of dead load. If a deeper haunch will be used because of final beam camber, the weight of the actual haunch should be used.
3. For this design example, the unit weight of the reinforced concrete is taken as 0.150 kcf. Some designers use a higher unit weight to account for the weight of the reinforcement.
4. The weight of cross-diaphragms is ignored since most agencies are changing from cast-in-place concrete diaphragms to lightweight steel diaphragms.

BULB-TEE (BT-72), SINGLE SPAN, COMPOSITE DECK

9.1a.4.1.1 Dead Loads/9.1a.4.2.2 Live Load Distribution Factors for a Typical Interior Beam

Dead loads placed on the composite structure:

LRFD Article 4.6.2.2.1 states that permanent loads (curbs and wearing surface) may be distributed uniformly among all beams if the following conditions are met:

- Width of the deck is constant OK
- Number of beams, N_b , is not less than four ($N_b = 6$) OK
- Beams are parallel and have the same stiffness OK
- The roadway part of the overhang, $d_e \leq 3.0$ ft
 $d_e = 3.0 - 1.5 - 0.5(6/12) = 1.25$ ft OK
- Curvature in plan is less than specified in the *LRFD Specifications* (curvature = 0.0°) OK
- Cross section of the bridge is consistent with one of the cross sections given in LRFD Table 4.6.2.2.1-1 OK

Since these criteria are satisfied, the barrier and wearing surface loads are distributed equally among the six beams.

$$\text{Barrier weight} = (2 \text{ barriers})(0.300 \text{ kips/ft}) / (6 \text{ beams}) = 0.100 \text{ kips/ft/beam} = w_b$$

DW = Dead load of wearing surface

$$= (2/12)(0.150) = 0.025 \text{ ksf}$$

$$= (0.025 \text{ ksf})(48.0 \text{ ft}) / (6 \text{ beams}) = 0.200 \text{ kips/ft/beam} = w_{ws}$$

9.1a.4.1.2 Unfactored Shear Forces and Bending Moments

For a simply supported beam with span length (L) loaded with a uniformly distributed load (w), the shear force (V_x) and bending moment (M_x) at any distance (x) from the support are given by:

$$V_x = w(0.5L - x) \quad \text{(Eq. 9.1a.4.1.2-1)}$$

$$M_x = 0.5wx(L - x) \quad \text{(Eq. 9.1a.4.1.2-2)}$$

Using the above equations, values of shear forces and bending moments for a typical interior beam, under self weight of beam, weight of slab and haunch, weight of barriers and wearing surface are computed and shown in **Table 9.1a.4-1** that is located at the end of Section 9.1a.4.3. For these calculations, the span length (L) is the design span, 120 ft. However, for calculations of stresses and deformation at the time prestress is transferred, the overall length of the precast member, 121 ft, is used as illustrated later in this example.

9.1a.4.2 Shear Forces and Bending Moments Due to Live Loads**9.1a.4.2.1 Live Loads**

Design live load is HL-93, which consists of a combination of: [LRFD Art. 3.6.1.2.1]

1. Design truck or design tandem with dynamic allowance [LRFD Art. 3.6.1.2.2]
 The design truck consists of 8.0-, 32.0-, and 32.0-kip axles with the first pair spaced at 14.0 ft and the second pair spaced at 14.0 to 30.0 ft. The design tandem consists of a pair of 25.0-kip axles spaced at 4.0 ft apart. [LRFD Art. 3.6.1.2.3]
2. Design lane load of 0.64 kips/ft without dynamic allowance [LRFD Art. 3.6.1.2.4]

9.1a.4.2.2 Live Load Distribution Factors for a Typical Interior Beam

The live load bending moments and shear forces are determined by using the simplified distribution factor formulas, [LRFD Art. 4.6.2.2]. To use the simplified live load distribution factor formulas, the following conditions must be met: [LRFD Art. 4.6.2.2.1]

- Width of deck is constant OK
- Number of beams, N_b not less than four ($N_b = 6$) OK
- Beams are parallel and have approximately the same stiffness OK

BULB-TEE (BT-72), SINGLE SPAN, COMPOSITE DECK**9.1a.4.2.2 Live Load Distribution Factors for a Typical Interior Beam/9.1a.4.2.2.1 Distribution Factor for Bending Moment**

- The roadway part of the overhang, $d_e \leq 3.0$ ft ($d_e = 1.5$ ft) OK
- Curvature is less than specified in the *LRFD Specifications* (curvature = 0.0°) OK

For precast concrete I- or bulb-tee beams with cast-in-place concrete deck, the bridge type is (k).

[LRFD Table 4.6.2.2.1-1]

The number of design lanes is computed as:

Number of design lanes = the integer part of the ratio of $(w/12)$, where (w) is the clear roadway width, in ft, between the curbs

[LRFD Art. 3.6.1.1.1]

From **Figure 9.1a.1-1**, $w = 48$ ft

Number of design lanes = integer part of $(48/12) = 4$ lanes

9.1a.4.2.2.1 Distribution Factor for Bending Moment

- For all limit states except fatigue limit state:

For two or more lanes loaded:

$$DFM = 0.075 + \left(\frac{S}{9.5}\right)^{0.6} \left(\frac{S}{L}\right)^{0.2} \left(\frac{K_g}{12.0Lt_s^3}\right)^{0.1} \quad \text{[LRFD Table 4.6.2.2.2b-1]}$$

Provided that: $3.5 \leq S \leq 16.0$; $S = 9.0$ ft OK
 $4.5 \leq t_s \leq 12.0$; $t_s = 7.5$ in. OK
 $20 \leq L \leq 240$; $L = 120$ ft OK
 $N_b \geq 4$; $N_b = 6$ OK
 $10,000 \leq K_g \leq 7,000,000$ OK (see below)

where

DFM = distribution factor for bending moment for interior beam

S = beam spacing, ft

L = beam span, ft

t_s = structural depth of concrete deck, in.

K_g = longitudinal stiffness parameter, $\text{in.}^4 = n(I_g + A_g e_g^2)$

[LRFD Eq. 4.6.2.2.1-1]

where

n = modular ratio between beam and deck slab concrete

$$= \frac{E_c(\text{beam})}{E_c(\text{slab})} = \frac{4,888}{3,834} = 1.2749$$

A_g = cross-sectional area of the precast beam (noncomposite section), in.^2

I_g = moment of inertia of the precast beam (noncomposite section), in.^4

e_g = distance between the centers of gravity of the precast beam and slab, in.
 $= (7.5/2 + 0.5 + 35.4) = 39.65$ in.

Therefore,

$$K_g = 1.2749[545,894 + 767(39.65)^2] = 2,233,258 \text{ in.}^4$$

$$DFM = 0.075 + \left(\frac{9}{9.5}\right)^{0.6} \left(\frac{9}{120}\right)^{0.2} \left(\frac{2,233,258}{12.0(120)(7.5)^3}\right)^{0.1}$$

$$= 0.075 + (0.968)(0.596)(1.139) = 0.732 \text{ lanes/beam}$$

For one design lane loaded:

$$DFM = 0.06 + \left(\frac{S}{14}\right)^{0.4} \left(\frac{S}{L}\right)^{0.3} \left(\frac{K_g}{12.0Lt_s^3}\right)^{0.1} \quad \text{[LRFD Table 4.6.2.2.2b-1]}$$

$$= 0.06 + \left(\frac{9}{14}\right)^{0.4} \left(\frac{9}{120}\right)^{0.3} \left(\frac{2,233,258}{12.0(120)(7.5)^3}\right)^{0.1}$$

$$= 0.06 + (0.838)(0.460)(1.139) = 0.499 \text{ lanes/beam}$$

Thus, the case of two or more lanes loaded controls and $DFM = 0.732$ lanes/beam.

BULB-TEE (BT-72), SINGLE SPAN, COMPOSITE DECK**9.1a.4.2.1 Distribution Factor for Bending Moment/9.1a.4.2.4.1 Due To Truck Load; V_{LT} and M_{LT}**

- For fatigue limit state:

The *LRFD Specifications*, Art. C3.4.1, states that for Fatigue Limit State, a single design truck should be used. However, live load distribution factors given in LRFD Article 4.6.2.2 take into consideration the multiple presence factor, m . LRFD Article 3.6.1.1.2 states that the multiple presence factor, m , for one design lane loaded is 1.2. Therefore, the distribution factor for one design lane loaded with the multiple presence factor removed, should be used. The distribution factor for fatigue limit state is: $0.499/1.2 = 0.416$ lanes/beam.

9.1a.4.2.2.2 Distribution Factor for Shear Force

For two or more lanes loaded:

$$DFV = 0.2 + \left(\frac{S}{12}\right) - \left(\frac{S}{35}\right)^2 \quad \text{[LRFD Table 4.6.2.2.3a-1]}$$

Provided that: $3.5 \leq S \leq 16.0$; $S = 9.0$ ft OK
 $20 \leq L \leq 240$; $L = 120$ ft OK
 $4.5 \leq t_s \leq 12.0$; $t_s = 7.5$ in. OK
 $N_b \geq 4$; $N_b = 6$ OK

where

DFV = distribution factor for shear force for interior beam
 S = beam spacing, ft

Therefore, the distribution factor for shear force is:

$$DFV = 0.2 + \left(\frac{9}{12}\right) - \left(\frac{9}{35}\right)^2 = 0.884 \text{ lanes/beam}$$

For one design lane loaded:

$$DFV = 0.36 + \left(\frac{S}{25.0}\right) = 0.36 + \left(\frac{9}{25.0}\right) = 0.720 \text{ lanes/beam} \quad \text{[LRFD Table 4.6.2.2.3a-1]}$$

Thus, the case of two or more lanes loaded controls and $DFV = 0.884$ lanes/beam.

9.1a.4.2.3 Dynamic Allowance

$IM = 15\%$ for fatigue limit state

$IM = 33\%$ for all other limit states

[LRFD Table 3.6.2.1-1]

where IM = dynamic load allowance, applied to design truck load only

9.1a.4.2.4 Unfactored Shear Forces and Bending Moments**9.1a.4.2.4.1 Due To Truck Load; V_{LT} and M_{LT}**

- For all limit states except for fatigue limit state:

Shear force and bending moment envelopes on a per-lane-basis are calculated at tenth-points of the span using the equations given in Chapter 8 of this manual. However, this is generally done by means of commercially available computer software that has the ability to deal with moving loads. Therefore, truck load shear forces and bending moments per beam are:

$$\begin{aligned} V_{LT} &= (\text{shear force per lane})(DFV)(1 + IM) \\ &= (\text{shear force per lane})(0.884)(1 + 0.33) \\ &= (\text{shear force per lane})(1.176) \text{ kips} \end{aligned}$$

$$\begin{aligned} M_{LT} &= (\text{bending moment per lane})(DFM)(1 + IM) \\ &= (\text{bending moment per lane})(0.732)(1 + 0.33) \\ &= (\text{bending moment per lane})(0.974) \text{ ft-kips} \end{aligned}$$

Values of V_{LT} and M_{LT} at different points are given in **Table 9.1a.4-2**.

BULB-TEE (BT-72), SINGLE SPAN, COMPOSITE DECK

9.1a.4.2.4.1 Due To Truck Load; V_{LT} and M_{LT} /9.1a.4.3 Load Combinations

- For fatigue limit state:

Art. 3.6.1.4.1 in the *LRFD Specifications* states that the fatigue load is a single design truck which has the same axle weight used in all other limit states but with a constant spacing of 30.0 ft between the 32.0-kip axles. Bending moment envelope on a per-lane-basis is calculated using the equation given in Chapter 8 of this manual.

Therefore, bending moment of fatigue truck load is:

$$\begin{aligned} M_f &= (\text{bending moment per lane})(DFM)(1 + IM) \\ &= (\text{bending moment per lane})(0.416)(1 + 0.15) \\ &= (\text{bending moment per lane})(0.478) \text{ ft-kips} \end{aligned}$$

Values of M_f at different points are given in **Table 9.1a.4-2**.

9.1a.4.2.4.2 Due To Design Lane Load; V_{LL} and M_{LL}

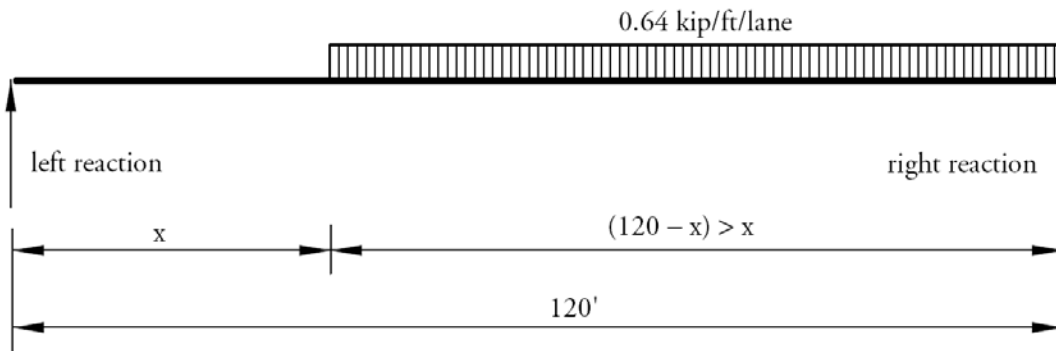
To obtain the maximum shear force at a section located at a distance (x) from the left support under a uniformly distributed load of 0.64 kips/ft, load the member to the right of section under consideration as shown in **Figure 9.1a.4.2.4.2-1**. Therefore, the maximum shear force per lane is:

$$V_x = \frac{0.32(L - x)^2}{L} \text{ for } x \leq 0.5L \tag{Eq. 9.1a.4.2.4.2-1}$$

where V_x is in kips/lane and L and x are in ft

Figure 9.1a.4.2.4.2-1

Maximum Shear Force Due to Design Lane Load



To calculate the maximum bending moment at any section, use Eq. (9.1a.4.1.2-2).

Lane load shear force and bending moment per typical interior beam are as follows:

$$\begin{aligned} V_{LL} &= (\text{lane load shear force})(DFV) \\ &= (\text{lane load shear force})(0.884) \text{ kips} \end{aligned}$$

For all limit states except for fatigue limit state:

$$\begin{aligned} M_{LL} &= (\text{lane load bending moment})(DFM) \\ &= (\text{lane load bending moment})(0.732) \text{ ft-kips} \end{aligned}$$

Note that the dynamic allowance is not applied to the design lane loading.

Values of shear forces and bending moments, V_{LL} and M_{LL} , are given in **Table 9.1a.4-2**.

9.1a.4.3 Load Combinations

[LRFD Art. 3.4]

Total factored load is taken as:

$$Q = \sum \eta_i \gamma_i Q_i \tag{LRFD Eq. 3.4.1-1}$$

BULB-TEE (BT-72), SINGLE SPAN, COMPOSITE DECK

9.1a.4.3 Load Combinations

where

- η_i = a load modifier relating to ductility, redundancy, and operational importance (Here, η_i is considered to be 1.0 for typical bridges) [LRFD Art. 1.3.2]
- γ_i = load factors [LRFD Table 3.4.1-1]
- Q_i = force effects from specified loads

Investigating different limit states given in LRFD Article 3.4.1, the following limit states are applicable:

Service I: check compressive stresses in prestressed concrete components:

$$Q = 1.00(DC + DW) + 1.00(LL + IM) \quad \text{[LRFD Table 3.4.1-1]}$$

This load combination is the general combination for service limit state stress checks and applies to all conditions other than Service III.

Service III: check tensile stresses in prestressed concrete components:

$$Q = 1.00(DC + DW) + 0.80(LL + IM) \quad \text{[LRFD Table 3.4.1-1]}$$

This load combination is a special combination for service limit state stress checks that applies only to tension in prestressed concrete structures to control cracks.

Strength I: check ultimate strength:

[LRFD Tables 3.4.1-1 and -2]

$$\text{Maximum } Q = 1.25(DC) + 1.50(DW) + 1.75(LL + IM)$$

$$\text{Minimum } Q = 0.90(DC) + 0.65(DW) + 1.75(LL + IM)$$

This load combination is the general load combination for strength limit state design.

Note: For simple-span bridges, the maximum load factors produce maximum effects. However, use minimum load factors for dead load (DC), and wearing surface (DW) when dead load and wearing surface stresses are opposite to those of live load.

Fatigue I: check stress range in strands:

[LRFD Table 3.4.1-1]

$$Q = 1.50(LL + IM)$$

This load combination is a special load combination to check the tensile stress range in the strands due to live load and dynamic allowance.

Table 9.1a.4-1

Unfactored Shear Forces and Bending Moments Due to Dead Loads for a Typical Interior Beam

Distance x, ft	Section x/L	Beam Weight		Slab + Haunch Weight		Barrier Weight		Wearing Surface Weight	
		Shear V_g kips	Moment M_g ft-kips	Shear V_s kips	Moment M_s ft-kips	Shear V_b kips	Moment M_b ft-kips	Shear V_{ws} kips	Moment M_{ws} ft-kips
0	0.0	47.9	0.0	55.3	0.0	6.0	0.0	12.0	0.0
*6.10	0.051	43.1	277.6	49.7	320.3	5.4	34.7	10.8	69.5
12	0.1	38.4	517.8	44.3	597.5	4.8	64.8	9.6	129.6
24	0.2	28.8	920.4	33.2	1,062.1	3.6	115.2	7.2	230.4
36	0.3	19.2	1,208.1	22.1	1,394.1	2.4	151.2	4.8	302.4
48	0.4	9.6	1,380.7	11.1	1,593.2	1.2	172.8	2.4	345.6
60	0.5	0.0	1,438.2	0.0	1,659.6	0.0	180.0	0.0	360.0

* Critical section for shear (see Sect. 9.1a.11)

BULB-TEE (BT-72), SINGLE SPAN, COMPOSITE DECK

9.1a.4.3 Load Combinations/9.1a.5.3 Required Number of Strands

Table 9.1a.4-2**Unfactored Shear Forces and Bending Moments Due to Live Loads for a Typical Interior Beam**

Distance <i>x</i> , ft	Section <i>x/L</i>	Truck Load with Impact		Lane Load		Fatigue Truck with Impact
		Shear V_{LT} kips	Moment M_{LT} ft-kips	Shear V_{LL} kips	Moment M_{LL} ft-kips	Moment M_f ft-kips
0	0.0	78.1	0.0	33.9	0.0	0.0
*6.10	0.051	73.8	372.6	30.6	162.7	167.5
12	0.1	69.6	691.6	27.5	303.6	309.2
24	0.2	61.1	1,215.0	21.7	539.7	535.8
36	0.3	52.7	1,570.2	16.6	708.3	692.7
48	0.4	44.2	1,778.8	12.2	809.5	776.1
60	0.5	35.7	1,830.2	8.5	843.3	776.9

* Critical section for shear (see Sect. 9.1a.11)

9.1a.5 ESTIMATE REQUIRED PRESTRESS

The required number of strands is usually governed by concrete tensile stresses at the bottom fiber for load combination Service III at the section of maximum moment or at the harp points. For estimating the number of strands, only the stresses at midspan are considered.

9.1a.5.1 Service Load Stresses at Midspan

Bottom tensile stress due to applied dead and live loads using load combination Service III is:

$$f_b = \frac{M_g + M_s}{S_b} + \frac{M_b + M_{ws} + (0.8)(M_{LT} + M_{LL})}{S_{bc}}$$

where

- f_b = concrete tensile stress at bottom fiber of the beam, ksi
- M_g = unfactored bending moment due to beam self weight, ft-kips
- M_s = unfactored bending moment due to slab and haunch weights, ft-kips
- M_b = unfactored bending moment due to barrier weight, ft-kips
- M_{ws} = unfactored bending moment due to future wearing surface, ft-kips
- M_{LT} = unfactored bending moment due to truck load, ft-kips
- M_{LL} = unfactored bending moment due to lane load, ft-kips

Using values of bending moments from **Tables 9.1a.4-1 and 9.1a.4-2**, bottom tensile stress at midspan is:

$$f_b = \frac{(1,438.2 + 1,659.6)}{14,915}(12) + \frac{(180 + 360) + (0.8)(1,830.2 + 843.3)}{20,090}(12)$$

$$= (2.492 + 1.600) = 4.092 \text{ ksi}$$

9.1a.5.2 Stress Limits for Concrete

Tensile stress limit at service loads = $0.19 \sqrt{f'_c}$

[LRFD Table 5.9.4.2.2-1]

where f'_c = specified concrete compressive strength of beam for design, ksi

Concrete tensile stress limit = $-0.19\sqrt{6.50} = -0.484 \text{ ksi}$

9.1a.5.3 Required Number of Strands

The required precompressive stress at the bottom fiber of the beam is the difference between bottom tensile stress due to the applied loads and the concrete tensile stress limit:

$$f_{pb} = (4.092 - 0.484) = 3.608 \text{ ksi}$$

BULB-TEE (BT-72), SINGLE SPAN, COMPOSITE DECK

9.1a.5.3 Required Number of Strands/9.1a.5.4 Strand Pattern

The location of the strand center of gravity at midspan ranges from 5 to 15% of the beam depth, measured from the bottom of the beam. A value of 5% is appropriate for newer efficient sections like the bulb-tee beams and 15% for less efficient AASHTO standard shapes.

Assume the distance between the center of gravity of bottom strands and the bottom fiber of the beam:

$$y_{bs} = 0.05h = 0.05(72) = 3.60 \text{ in.}, \text{ use } y_{bs} = 4.0 \text{ in.}$$

Therefore, strand eccentricity at midspan, $e_c = (y_b - y_{bs}) = (36.6 - 4.0) = 32.6 \text{ in.}$

If P_{pe} is the total prestressing force after all losses, the stress at the bottom fiber due to prestress is:

$$f_{pb} = \frac{P_{pe}}{A_g} + \frac{P_{pe}e_c}{S_b} \text{ or } 3.608 = \frac{P_{pe}}{767} + \frac{P_{pe}(32.6)}{14,915}$$

Solving for P_{pe} , the required $P_{pe} = 1,034.0 \text{ kips.}$

Final prestress force per strand = (area of strand)(f_{pi})(1 - losses)

where f_{pi} = initial strand stress before transfer, ksi (see Section 9.1a.2) = 202.5 ksi

Assuming final loss of 25% of f_{pi} , the prestress force per strand after all losses

$$= (0.153)(202.5)(1 - 0.25) = 23.2 \text{ kips}$$

Number of strands required = $(1,034.0/23.2) = 44.6 \text{ strands}$

As an initial trial, (46) ½-in.-diameter, 270 ksi strands are selected. The center of gravity of the 46 strands at midspan is 6.35 in. from the bottom of the concrete, which is higher than the assumed value, 4.0 in. Thus, a second iteration using the new value of strand eccentricity indicates that 48 strands are required. The strand pattern at midspan for the 48 strands is shown in **Figure 9.1a.5.3-1**. Each available position is filled beginning with the bottom row.

Total area of prestressing strands, $A_{ps} = 48(0.153) = 7.344 \text{ in.}^2$

Note: This is a conservative estimate of the number of strands because nontransformed section properties are used in lieu of transformed section properties. The number of strands can be refined later in the design process as more accurate section properties and prestress losses are determined.

9.1a.5.4 Strand Pattern

The distance between the center of gravity of bottom strands and the bottom concrete fiber of the beam at midspan is:

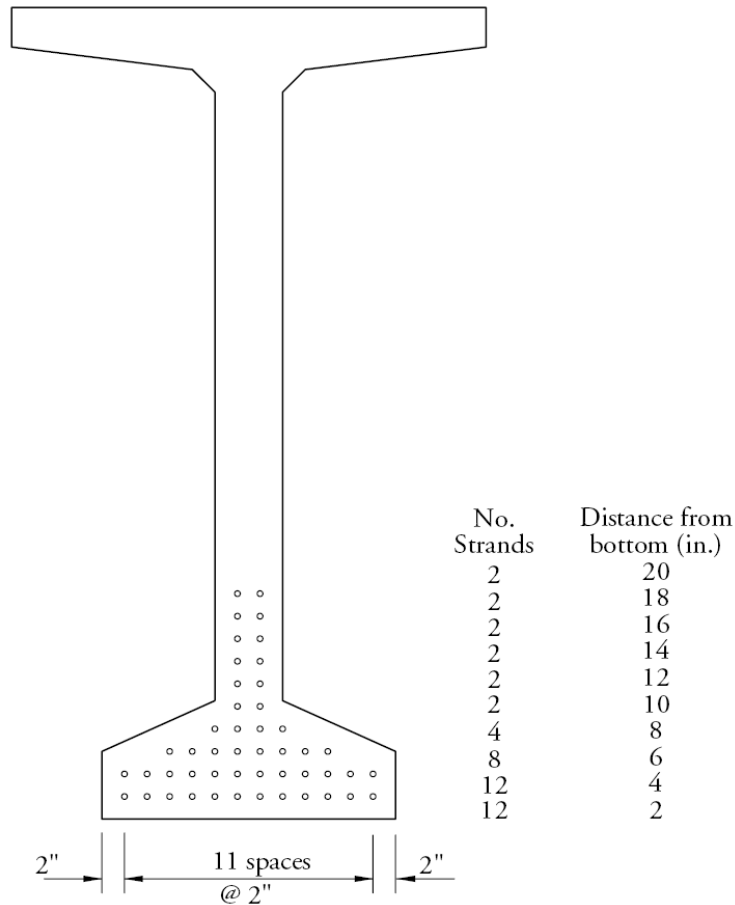
$$y_{bs} = [12(2) + 12(4) + 8(6) + 4(8) + 2(10) + 2(12) + 2(14) + 2(16) + 2(18) + 2(20)]/(48) = 6.92 \text{ in.}$$

Strand eccentricity at midspan, $e_c = y_b - y_{bs} = 36.60 - 6.92 = 29.68 \text{ in.} = e_{pg}$

BULB-TEE (BT-72), SINGLE SPAN, COMPOSITE DECK

9.1a.5.4 Strand Pattern/9.1a.5.5 Steel Transformed Section Properties

Figure 9.1a.5.3-1
Assumed Strand Pattern at Midspan



9.1a.5.5 Steel Transformed Section Properties

From the earliest years of prestressed concrete design, the gross section was conservatively used in analysis since the prestressing forces were smaller and computer programs were not widely used. However, the use of transformed section, which is obtained from the gross section by adding transformed steel area, yields more accurate results than the gross section analysis.

For each row of the prestressing strands shown in **Figure 9.1a.5.3-1**, the steel area is multiplied by $(n - 1)$ to calculate the transformed section properties, where n is the modular ratio between prestressing strand and concrete. Since the modulus of elasticity of concrete is different at transfer and final time, the transformed section properties should be calculated separately for the two stages. Using similar procedures as in Section 9.1a.3.2.3, a sample calculation is shown in **Table 9.1a.5.5-1**.

At transfer:

$$n - 1 = \frac{28,500}{4,617} - 1 = 5.173$$

At final:

$$n - 1 = \frac{28,500}{4,888} - 1 = 4.831$$

BULB-TEE (BT-72), SINGLE SPAN, COMPOSITE DECK

9.1a.5.5 Steel Transformed Section Properties

Table 9.1a.5.5-1
Properties of Composite Transformed Section at Final Time

	Transformed Area, in. ²	y_b in.	Ay_b in. ³	$A(y_{btc} - y_b)^2$ in. ⁴	I in. ⁴	$I + A(y_{btc} - y_b)^2$ in. ⁴
Deck	635.45	76.25	48,453	326,000	2,979	328,979
Haunch	16.47	72.25	1,190	5,729	0.34	5,729
Beam	767.00	36.60	28,072	221,663	545,894	767,557
Row 1	8.87	2.00	17.74	23,617		23,617
Row 2	8.87	4.00	35.48	21,822		21,822
Row 3	5.90	6.00	35.48	13,368		13,368
Row 4	2.96	8.00	23.68	6,155		6,155
Row 5	1.48	10.00	14.80	2,813		2,813
Row 6	1.48	12.00	17.76	2,561		2,561
Row 7	1.48	14.00	20.72	2,321		2,321
Row 8	1.48	16.00	23.68	2,092		2,092
Row 9	1.48	18.00	26.64	1,876		1,876
Row 10	1.48	20.00	29.60	1,671		1,671
Σ	1,454.4		77,961			1,180,561

Note: The moment of inertia of strand about its own centroid is neglected.

The transformed section properties are calculated as:

Noncomposite transformed section at transfer:

A_{ti} = area of transformed section at transfer = 805.0 in.²

I_{ti} = moment of inertia of the transformed section at transfer = 578,827 in.⁴

e_{ti} = eccentricity of strands with respect to transformed section at transfer = 28.28 in.

y_{bti} = distance from the centroid of the transformed section to the extreme bottom fiber of the beam at transfer = 35.20 in.

S_{bti} = section modulus for the extreme bottom fiber of the transformed section at transfer = 16,444 in.³

S_{tti} = section modulus for the extreme top fiber of the transformed section at transfer = 15,729 in.³

Noncomposite transformed section at final time:

A_{tf} = area of transformed section at final time = 802.5 in.²

I_{tf} = moment of inertia of the transformed section at final time = 576,757 in.⁴

e_{tf} = eccentricity of strands with respect to transformed section at final time = 28.37 in.

y_{btf} = distance from the centroid of the noncomposite transformed section to the extreme bottom fiber of the beam at final time = 35.29 in.

S_{btf} = section modulus for the extreme bottom fiber of the transformed section at final time = 16,343 in.³

S_{ttf} = section modulus for the extreme top fiber of the transformed section at final time = 15,711 in.³

Composite transformed section at final time:

A_{tc} = area of transformed composite section at final time = 1,454.4 in.²

I_{tc} = moment of inertia of the transformed composite section at final time = 1,180,561 in.⁴

e_{tc} = eccentricity of strands with respect to transformed composite section at final time = 46.68 in.

y_{btc} = distance from the centroid of the composite transformed section to the extreme bottom fiber of the beam at final time = 53.60 in.

S_{btc} = section modulus for the extreme bottom fiber of the transformed composite section at final time = 22,025 in.³

S_{ttc} = composite section modulus for the extreme top fiber of the precast beam for transformed section at final time = 64,161 in.³

S_{dtc} = composite section modulus for the extreme top fiber of the deck for transformed section at final time = 57,002 in.³

BULB-TEE (BT-72), SINGLE SPAN, COMPOSITE DECK

9.1a.6 Prestress Losses/9.1a.6.2 Time-Dependent Losses Between Transfer and Deck Placement

9.1a.6 PRESTRESS LOSSES

Total prestress loss:

$$\Delta f_{pT} = \Delta f_{pES} + \Delta f_{pLT} \quad [\text{LRFD Eq. 5.9.5.1-1}]$$

where

- Δf_{pT} = total loss in prestressing steel stress
- Δf_{pES} = sum of all losses or gains due to elastic shortening or extension at the time of application of prestress and/or external loads
- Δf_{pLT} = long-term losses due to shrinkage and creep of concrete, and relaxation of steel after transfer. In this design example, the refined estimates of time-dependent losses are used.

9.1a.6.1 Elastic Shortening

$$\Delta f_{pES} = \frac{E_p}{E_{ci}} f_{cgp} \quad [\text{LRFD Eq. 5.9.5.2.3a-1}]$$

where

- E_p = modulus of elasticity of prestressing strands = 28,500 ksi
- E_{ci} = modulus of elasticity of beam concrete at transfer = 4,617 ksi
- f_{cgp} = sum of concrete stresses at the center of gravity of prestressing strands due to prestressing force at transfer and the self weight of the member at sections of maximum moment.

If the gross (or net) cross-section properties are used, it is necessary to perform numerical iterations. The elastic loss Δf_{pES} is usually assumed to be 10% of the initial prestress to calculate f_{cgp} , which is then used in the equation above to calculate a refined Δf_{pES} . The process is repeated until the assumed Δf_{pES} and refined Δf_{pES} converge.

However, when transformed section properties are used to calculate the concrete stress, the effects of losses and gains due to elastic deformations are implicitly accounted for. Therefore, Δf_{pES} should not be included in calculating f_{cgp} .

$$\begin{aligned} \text{Force per strand before transfer} &= (\text{area of strand})(\text{prestress stress before transfer}) \\ &= (0.153)(202.5) = 30.98 \text{ kips} \end{aligned}$$

$$f_{cgp} = \frac{P_{pi}}{A_{ti}} + \frac{P_{pi}e_{ti}^2}{I_{ti}} - \frac{M_g e_{ti}}{I_{ti}}$$

where

- e_{ti} = eccentricity of strands at midspan with respect to the transformed section at transfer = 28.28 in.
- P_{pi} = total prestressing force before transfer = (48 strands)(30.98) = 1,487.0 kips
- M_g should be calculated based on the overall beam length of 121 ft. Since the elastic shortening loss is a part of the total loss, f_{cgp} will be conservatively computed based on M_g using the design span length of 120 ft.

$$f_{cgp} = \frac{1,487.0}{805.0} + \frac{(1,487.0)(28.28)^2}{578,827} - \frac{(1,438.2)(12)(28.28)}{578,827} = 3.059 \text{ ksi}$$

Therefore, loss due to elastic shortening:

$$\Delta f_{pES} = \frac{28,500}{4,617} (3.059) = 18.9 \text{ ksi}$$

AASHTO LRFD C5.9.5.3 indicates that the loss due to elastic shortening at transfer should be added to the time-dependent losses to determine total losses. However, this loss at transfer is directly accounted for if transformed section properties are used in the stress analysis.

9.1a.6.2 Time-Dependent Losses between Transfer and Deck Placement

The following construction schedule is assumed in calculating the time-dependent losses:

- Concrete age at transfer: $t_i = 1$ day
- Concrete age at deck placement: $t_d = 90$ days
- Concrete age at final stage: $t_f = 20,000$ days

BULB-TEE (BT-72), SINGLE SPAN, COMPOSITE DECK

9.1a.6.2 Time-Dependent Losses Between Transfer and Deck Placement/9.1a.6.2.1 Shrinkage of Concrete

The total time-dependent loss between time of transfer and deck placement is the summation of prestress losses due to shrinkage of concrete, creep of concrete, and relaxation of prestressing strands.

9.1a.6.2.1 Shrinkage of Concrete

The prestress loss due to shrinkage of concrete between time of transfer and deck placement is calculated by:

$$\Delta f_{PSR} = \epsilon_{bid} E_p K_{id} \quad \text{[LRFD Eq. 5.9.5.4.2a-1]}$$

where

- ϵ_{bid} = concrete shrinkage strain of girder for time period between transfer and deck placement
- E_p = modulus of elasticity of prestressing strands, ksi
- K_{id} = transformed section coefficient that accounts for time-dependent interaction between concrete and bonded steel in the section being considered for time period between transfer and deck placement

The concrete shrinkage strain ϵ_{bid} is taken as:

$$\epsilon_{bid} = k_{vs} k_{hs} k_f k_{td} 0.48 \times 10^{-3} \quad \text{[LRFD Eq. 5.4.2.3.3-1]}$$

where

The factor for the effect of the volume-to-surface ratio of the beam:

$$k_{vs} = 1.45 - 0.13(V/S) = 1.45 - 0.13 \times 3.01 = 1.059$$

The minimum value of k_{vs} is 1.0 OK

V/S is the volume-to-surface ratio of the beam in **Table 2.5.7.1-1**.

The humidity factor for shrinkage:

$$k_{hs} = 2.00 - 0.014H = 2.00 - 0.014(70) = 1.020$$

where H = average annual mean relative humidity (assume 70%)

The factor for the effect of concrete strength:

$$k_f = \frac{5}{1 + f'_{ci}} = \frac{5}{1 + 5.8} = 0.735$$

The time development factor at deck placement:

$$k_{td} = \frac{t}{61 - 4f'_{ci} + t} = \frac{89}{61 - 4(5.8) + 89} = 0.702 = k_{tda}$$

where t is the maturity of concrete, days = $t_d - t_i = 90 - 1 = 89$ days

$$\epsilon_{bid} = (1.059)(1.020)(0.735)(0.702)(0.48 \times 10^{-3}) = 0.000268$$

$$K_{id} = \frac{1}{1 + \frac{E_p}{E_{ci}} \frac{A_{ps}}{A_g} \left(1 + \frac{A_g (e_{pg})^2}{I_g}\right) [1 + 0.7\Psi_b(t_f, t_i)]} \quad \text{[LRFD Eq. 5.9.5.4.2a-2]}$$

where

- e_{pg} = eccentricity of prestressing strand with respect to centroid of girder, in.
- $\Psi_b(t_f, t_i)$ = girder creep coefficient at final time due to loading introduced at transfer

For the time between transfer and final time:

$$\Psi_b(t_f, t_i) = 1.9k_{vs}k_{hc}k_fk_{td}t_i^{-0.118} \quad \text{[LRFD Eq. 5.4.2.3.2-1]}$$

$$k_{hc} = 1.56 - 0.008H = 1.56 - 0.008(70) = 1.000$$

$$k_{td} = \frac{t}{61 - 4f'_{ci} + t} = \frac{20,000 - 1}{61 - 4(5.8) + (20,000 - 1)} = 0.998 = k_{tdf}$$

$$\begin{aligned} \Psi_b(t_f, t_i) &= 1.9(1.059)(1.000)(0.735)(0.998)(1)^{-0.118} \\ &= 1.476 \end{aligned}$$

BULB-TEE (BT-72), SINGLE SPAN, COMPOSITE DECK

9.1a.6.2.1 Shrinkage of Concrete/9.1a.6.3.1 Shrinkage of Concrete

$$K_{id} = \frac{1}{1 + \frac{28,500}{4,617} \frac{7.344}{767} \left(1 + \frac{767(29.68)^2}{545,894}\right) [1 + 0.7(1.476)]} = 0.788$$

The prestress loss due to shrinkage of concrete between transfer and deck placement is:

$$\Delta f_{pSR} = (0.000268)(28,500)(0.788) = 6.019 \text{ ksi}$$

9.1a.6.2.2 Creep of Concrete

The prestress loss due to creep of girder concrete between time of transfer and deck placement is:

$$\Delta f_{pCR} = \frac{E_p}{E_{ci}} f_{cgp} \Psi_b(t_d, t_i) K_{id} \quad [\text{LRFD Eq. 5.9.5.4.2b-1}]$$

where

$$\begin{aligned} \Psi_b(t_d, t_i) &= \text{girder creep coefficient at time of deck placement due to loading introduced at transfer} \\ &= 1.9k_{vs}k_{hc}k_fk_{td}t_i^{-0.118} \quad [\text{LRFD Eq. 5.4.2.3.2-1}] \\ &= 1.9(1.059)(1.000)(0.735)(0.702)(1)^{-0.118} \\ &= 1.038 \end{aligned}$$

$$\Delta f_{pCR} = \frac{28,500}{4,617} (3.059)(1.038)(0.788) = 15.445 \text{ ksi}$$

9.1a.6.2.3 Relaxation of Prestressing Strands

The prestress loss due to relaxation of prestressing strands between time of transfer and deck placement is determined as:

$$\Delta f_{pR1} = \frac{f_{pt}}{K_L} \left(\frac{f_{pt}}{f_{py}} - 0.55 \right) \quad [\text{LRFD Eq. 5.9.5.4.2c-1}]$$

where

$$\begin{aligned} f_{pt} &= \text{stress in prestressing strands immediately after transfer, taken not less than } 0.55f_y \\ K_L &= 30 \text{ for low-relaxation strands and 7 for other prestressing steel, unless more accurate} \\ &\quad \text{manufacturer's data are available} \end{aligned}$$

$$\Delta f_{pR1} = \frac{(202.5 - 18.9)}{30} \left(\frac{(202.5 - 18.9)}{243} - 0.55 \right) = 1.258 \text{ ksi}$$

According to LRFD Art. 5.9.5.4.2c, the relaxation loss may also be assumed equal to 1.2 ksi for low-relaxation strands.

9.1a.6.3 Time-Dependent Losses between Deck Placement and Final Time

The total time-dependent loss between time of deck placement and final time is the summation of prestress losses due to shrinkage of beam concrete, creep of beam concrete, relaxation of prestressing strands, and shrinkage of deck concrete.

9.1a.6.3.1 Shrinkage of Concrete

The prestress loss due to shrinkage of concrete between time of deck placement and final time is calculated by:

$$\Delta f_{pSD} = \epsilon_{bdf} E_p K_{df} \quad [\text{LRFD Eq. 5.9.5.4.3a-1}]$$

where

$$\begin{aligned} \epsilon_{bdf} &= \text{concrete shrinkage strain of girder for time period between deck placement and final time} \\ E_p &= \text{modulus of elasticity of prestressing strands, ksi} \\ K_{df} &= \text{transformed section coefficient that accounts for time-dependent interaction between concrete and} \\ &\quad \text{bonded steel in the section being considered for time period between deck placement and final time} \end{aligned}$$

BULB-TEE (BT-72), SINGLE SPAN, COMPOSITE DECK

9.1a.6.3.1 Shrinkage of Concrete/9.1a.6.3.2 Creep of Concrete

The total girder concrete shrinkage strain between transfer and final time is taken as:

$$\begin{aligned} \epsilon_{bif} &= k_{vs}k_{hs}k_{f}k_{tdf}0.48 \times 10^{-3} && \text{[LRFD Eq. 5.4.2.3.3-1]} \\ &= (1.059)(1.020)(0.735)(0.998)(0.48 \times 10^{-3}) = 0.000380 \end{aligned}$$

The girder concrete shrinkage strain between deck placement and final time is:

$$\epsilon_{bdf} = \epsilon_{bif} - \epsilon_{bid} = 0.000380 - 0.000268 = 0.000112$$

The beam concrete transformed section coefficient between deck placement and final time is:

$$K_{df} = \frac{1}{1 + \frac{E_p}{E_{ci}} \frac{A_{ps}}{A_c} \left(1 + \frac{A_c(e_{pc})^2}{I_c}\right) [1 + 0.7\Psi_b(t_f, t_i)]} \quad \text{[LRFD Eq. 5.9.5.4.3a-2]}$$

where

- A_c = area of the composite section = 1,418.9 in.²
- I_c = moment of inertia of the composite section = 1,100,320 in.⁴
- e_{pc} = eccentricity of strands with respect to centroid of composite section = 54.77 - 6.92 = 47.85 in.

$$K_{df} = \frac{1}{1 + \frac{28,500}{4,617} \frac{7.344}{1,418.9} \left(1 + \frac{1,418.9(47.85)^2}{1,100,320}\right) [1 + 0.7(1.476)]} = 0.796$$

The prestress loss due to shrinkage of concrete between deck placement and final time is:

$$\Delta f_{psD} = (0.000112)(28,500)(0.796) = 2.541 \text{ ksi}$$

9.1a.6.3.2 Creep of Concrete

The prestress loss due to creep of beam concrete between time of deck placement and final time is determined as:

$$\Delta f_{pCD} = \frac{E_p}{E_{ci}} f_{cgp} [\Psi_b(t_f, t_i) - \Psi_b(t_d, t_i)] K_{df} + \frac{E_p}{E_c} \Delta f_{cd} \Psi_b(t_f, t_d) K_{df} \quad \text{[LRFD Eq. 5.9.5.4.3b-1]}$$

where

$$\begin{aligned} \Psi_b(t_f, t_d) &= \text{girder creep coefficient at final time due to loading at deck placement} \\ &= 1.9k_{vs}k_{hc}k_{f}k_{tdf}t_d^{-0.118} && \text{[LRFD Eq. 5.4.2.3.2-1]} \end{aligned}$$

$$k_{tdf} = \frac{t}{61 - 4f'_{ci} + t} = \frac{(20,000 - 90)}{61 - 4(5.8) + (20,000 - 90)} = 0.998$$

$$\Psi_b(t_f, t_d) = 1.9(1.059)(1.000)(0.735)(0.998)(90)^{-0.118} = 0.868$$

Δf_{cd} = change in concrete stress at centroid of prestressing strands due to long-term losses between transfer and deck placement, combined with deck weight and superimposed loads (ksi)

$$\begin{aligned} &= -(\Delta f_{psR} + \Delta f_{pCR} + \Delta f_{pR1}) \frac{A_{ps}}{A_g} \left(1 + \frac{A_g e_{pg}^2}{I_g}\right) - \left(\frac{M_s e_{tf}}{I_{tf}} + \frac{(M_b + M_{ws}) e_{tc}}{I_{tc}}\right) \\ &= -(6.019 + 15.445 + 1.258) \frac{7.344}{767} \left(1 + \frac{767(29.68)^2}{545,894}\right) \\ &\quad - \left(\frac{1,659.6(12)(28.37)}{576,757} + \frac{(180 + 360)(12)(46.68)}{1,180,561}\right) \\ &= -1.723 \text{ ksi} \end{aligned}$$

The gross section properties are used in the equation to calculate Δf_{cd} for the long-term losses since the transformed section effect has already been included in the factor K_{id} when calculating the losses between initial time and deck placement.

$$\begin{aligned} \Delta f_{pCD} &= \frac{28,500}{4,617} (3.059)(1.476 - 1.038)(0.796) + \frac{28,500}{4,888} (-1.723)(0.868)(0.796) \\ &= -0.358 \text{ ksi} \end{aligned}$$

The negative sign indicates a prestressing gain.

BULB-TEE (BT-72), SINGLE SPAN, COMPOSITE DECK

9.1a.6.3.3 Relaxation of Prestressing Strands/9.1a.6.3.4 Shrinkage of Deck Concrete

9.1a.6.3.3 Relaxation of Prestressing Strands

The prestress loss due to relaxation of prestressing strands in composite section between time of deck placement and final time is taken as:

$$\Delta f_{pR2} = \Delta f_{pR1} = 1.258 \text{ ksi} \quad [\text{LRFD Eq. 5.9.5.4.3c-1}]$$

9.1a.6.3.4 Shrinkage of Deck Concrete

The prestress gain due to shrinkage of deck concrete is calculated by:

$$\Delta f_{pSS} = \frac{E_p}{E_c} \Delta f_{cdf} K_{df} [1 + 0.7 \Psi_b(t_f, t_d)] \quad [\text{LRFD Eq. 5.9.5.4.3d-1}]$$

where Δf_{cdf} = change in concrete stress at centroid of prestressing strands due to shrinkage of deck concrete, ksi

$$\Delta f_{cdf} = \frac{\epsilon_{ddf} A_d E_{cd}}{1 + 0.7 \Psi_d(t_f, t_d)} \left(\frac{1}{A_c} - \frac{e_{pc} e_d}{I_c} \right) \quad [\text{LRFD Eq. 5.9.5.4.3d-2}]$$

where

- ϵ_{ddf} = shrinkage strain of deck concrete between placement and final time by LRFD Eq. 5.4.2.3.3-1
- A_d = area of deck concrete, in.²
- E_{cd} = modulus of elasticity of deck concrete, ksi
- $\Psi_d(t_f, t_d)$ = deck concrete creep coefficient at final time due to loading introduced shortly after deck placement
- e_d = eccentricity of deck with respect to the gross composite section, in.

Assume the initial strength of concrete at deck placement is 0.8(4.0 ksi) = 3.2 ksi, and use a volume-to-surface (V/S) ratio of 3.582 for the deck:

$$k_{vs} = 1.45 - 0.13(V/S) = 1.45 - 0.13(3.582) = 0.984 < 1.0$$

Use $k_{vs} = 1.000$

$$k_f = \frac{5}{1 + f'_{ci}} = \frac{5}{1 + 3.2} = 1.190$$

$$k_{td} = \frac{t}{61 - 4f'_{ci} + t} = \frac{20,000 - 90}{61 - 4(3.2) + (20,000 - 90)} = 0.998$$

$$\begin{aligned} \epsilon_{ddf} &= k_{vs} k_{hs} k_f k_{td} 0.48 \times 10^{-3} \quad [\text{LRFD Eq. 5.4.2.3.3-1}] \\ &= (1.000)(1.020)(1.190)(0.998)(0.48 \times 10^{-3}) \\ &= 0.000581 \end{aligned}$$

$$\begin{aligned} \Psi_d(t_f, t_d) &= 1.9 k_{vs} k_{hc} k_f k_{td} t_i^{-0.118} \quad [\text{LRFD Eq. 5.4.2.3.2-1}] \\ &= 1.9(1.000)(1.000)(1.190)(0.998)(1)^{-0.118} = 2.256 \end{aligned}$$

Creep of the deck concrete is assumed to start at 1 day.

$$\Delta f_{cdf} = \frac{0.000581(108)(7.5)(3,834)}{1 + 0.7(2.256)} \left(\frac{1}{1,418.9} - \frac{47.85(80 - 7.5/2 - 54.77)}{1,100,320} \right)$$

= -0.160 ksi The negative sign indicates a prestressing gain. The prestress gain due to shrinkage of the deck in the composite section:

$$\Delta f_{pSS} = \frac{28,500}{4,888} (-0.160)(0.796)[1 + 0.7(0.868)] = -1.194 \text{ ksi}$$

Note: The effect of deck shrinkage on the calculation of prestress gain is discussed further in Section 9.1a.8.5.

BULB-TEE (BT-72), SINGLE SPAN, COMPOSITE DECK

9.1a.6.4 Total Time-Dependent Loss/9.1a.6.5 Total Losses at Transfer

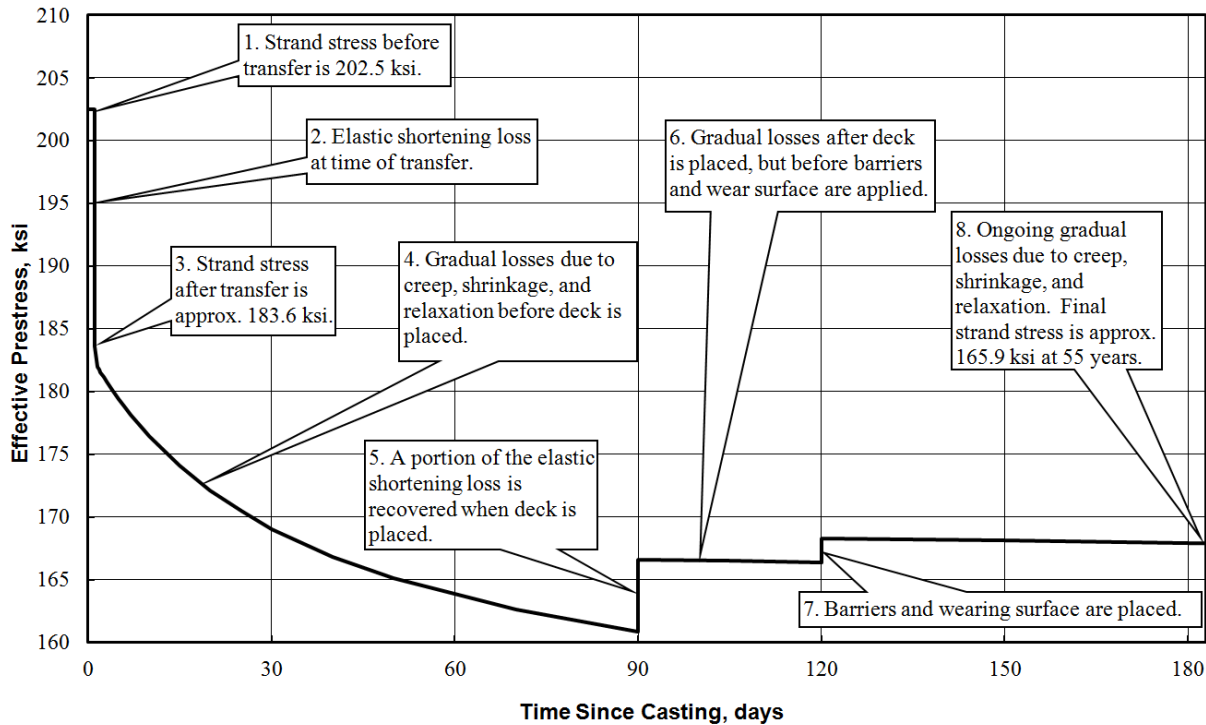
9.1a.6.4 Total Time-Dependent Loss

The total time-dependent loss, Δf_{pLT} , is determined as:

$$\begin{aligned} \Delta f_{pLT} &= (\Delta f_{pSR} + \Delta f_{pCR} + \Delta f_{pR1}) + (\Delta f_{pSD} + \Delta f_{pCD} + \Delta f_{pR2} - \Delta f_{pSS}) && \text{[LRFD Eq. 5.9.5.4.1-1]} \\ &= (6.019 + 15.445 + 1.258) + (2.541 - 0.358 + 1.258 - 1.194) \\ &= 22.722 + 2.247 = 25.0 \text{ ksi} \end{aligned}$$

The history of the development of the effective stress in the prestressing strands is illustrated in **Figure 9.1a.6.4-1**.

Figure 9.1a.6.4-1
Effective Stress in the Prestressing Strands



9.1a.6.5 Total Losses at Transfer

AASHTO LRFD C5.9.5.2.3a and C5.9.5.3 indicate that the losses or gains due to elastic deformation must be taken equal to zero if transformed section properties are used in stress analysis. However, the losses or gains due to elastic deformation must be included in determining the total prestress losses and effective stress in the prestressing strands.

$$\Delta f_{pi} = \Delta f_{pES} = 18.9 \text{ ksi}$$

$$\text{Effective stress in tendons immediately after transfer, } f_{pt} = f_{pi} - \Delta f_{pi} = (202.5 - 18.9) = 183.6 \text{ ksi}$$

$$\text{Force per strand} = (f_{pt})(\text{area of strand}) = 183.6(0.153) = 28.09 \text{ kips}$$

$$\text{Therefore, the total prestressing force after transfer, } P_{pt} = 28.09(48) = 1,348 \text{ kips}$$

$$\text{Initial loss, \%} = (\text{Total losses at transfer})/(f_{pi}) = 18.9/(202.5) = 9.3\%$$

When determining the concrete stresses using transformed section properties, the strand force is that before transfer:

$$\text{Force per strand} = (202.5)(0.153) = 30.98 \text{ kips}$$

$$\text{The total prestressing force before transfer, } P_{pi} = 30.98(48) = 1,487 \text{ kips}$$

BULB-TEE (BT-72), SINGLE SPAN, COMPOSITE DECK

9.1a.6.6 Total Losses at Service Loads/9.1a.7.1 Stress Limits for Concrete

9.1a.6.6 Total Losses at Service Loads

Total loss due to elastic shortening at transfer and long-term losses is:

$$\Delta f_{pT} = \Delta f_{pES} + \Delta f_{pLT} = 18.9 + 25.0 = 43.9 \text{ ksi}$$

The elastic gain due to deck weight, superimposed dead load, and live load (Service III) is:

$$\begin{aligned} & \left(\frac{M_s e_{tf}}{I_{tf}} + \frac{(M_b + M_{ws}) e_{tc}}{I_{tc}} \right) \frac{E_p}{E_c} + 0.8 \left(\frac{(M_{LT} + M_{LL}) e_{tc}}{I_{tc}} \right) \frac{E_p}{E_c} \\ &= \left(\frac{1,659.6(12)(28.37)}{576,757} + \frac{(180 + 360)(12)(46.68)}{1,180,561} \right) \frac{28,500}{4,888} + 0.8 \left(\frac{(1830.2 + 843.3)(12)(46.68)}{1,180,561} \right) \frac{28,500}{4,888} \\ &= 7.2 + 5.9 = 13.1 \text{ ksi} \end{aligned}$$

The effective stress in strands after all losses and gains:

$$f_{pe} = f_{pi} - \Delta f_{pT} + 13.1 = 202.5 - 43.9 + 13.1 = 171.7 \text{ ksi}$$

Check prestressing stress limit at service limit state:

[LRFD Table 5.9.3-1]

$$f_{pe} \leq 0.8 f_{py} = 0.8(243) = 194.4 \text{ ksi} > 171.7 \text{ ksi} \quad \text{OK}$$

The effective stress in strands after all losses and permanent gains:

$$f_{pe} = f_{pi} - \Delta f_{pT} = 202.5 - 43.9 + 7.2 = 165.8 \text{ ksi}$$

Force per strand without live load gains = $(f_{pe})(\text{area of strand}) = 165.8 (0.153) = 25.37 \text{ kips}$.

Therefore, the total prestressing force after all losses = $25.37(48) = 1,218 \text{ kips}$

Final loss percentage = $(\text{total losses and gains})/(f_{pi}) = (202.5 - 165.8)/(202.5) = 18.1\%$

Without consideration of prestressing gains at deck placement, the final loss percentage = $\text{total losses}/(f_{pi}) = (43.9)/(202.5) = 21.7\%$

When determining the concrete stress using transformed section properties, all the elastic losses and gains are implicitly accounted for.

Force per strand with only total time-dependent losses = $(f_{pi} - \Delta f_{pLT})(\text{area of strand}) = (202.5 - 25.0)(0.153) = 27.16 \text{ kips}$.

Total prestressing force, $P_{pe} = 27.16(48) = 1,304 \text{ kips}$

9.1a.7 CONCRETE STRESSES AT TRANSFER

Because the transformed section is used, the total prestressing force before transfer $P_{pi} = 1,487 \text{ kips}$.

9.1a.7.1 Stress Limits for Concrete

[LRFD Art. 5.9.4]

Compression:

- $0.6 f'_{ci} = 0.6(5.8) = +3.480 \text{ ksi}$

where f'_{ci} = concrete strength at transfer = 5.800 ksi

Tension:

- without bonded auxiliary reinforcement

$$-0.0948 \sqrt{f'_{ci}} \leq -0.200 \text{ ksi} = -0.0948 \sqrt{5.800} = -0.228 \text{ ksi}$$

Therefore, -0.200 ksi (Controls)

- with bonded auxiliary reinforcement that is sufficient to resist 120% of the tension force in the cracked concrete

$$-0.24 \sqrt{f'_{ci}} = -0.24 \sqrt{5.800} = -0.578 \text{ ksi}$$

BULB-TEE (BT-72), SINGLE SPAN, COMPOSITE DECK

9.1a.7.2 Stresses at Transfer Length Section

9.1a.7.2 Stresses at Transfer Length Section

Stresses at this location need only be checked at transfer because this stage almost always governs. Also, losses with time will reduce the concrete stresses making them less critical.

Transfer length = 60(strand diameter) = 60(0.5) = 30 in. = 2.5 ft [LRFD Art. 5.11.4]

Due to camber of the beam at transfer, the beam self weight acts on the overall beam length, 121 ft. Therefore, values for bending moment given in **Table 9.1a.4-1** cannot be used because they are based on the design span of 120 ft. Using statics, bending moment at transfer length due to beam self weight is:

$$M_g = 0.5w_gx(L - x) = (0.5)(0.799)(2.5)(121 - 2.5) = 118.4 \text{ ft-kips}$$

Compute stress in the top of beam:

$$f_t = \frac{P_{pi}}{A_{ti}} - \frac{P_{pi}e_{ti}}{S_{tti}} + \frac{M_g}{S_{tti}} = \frac{1,487}{805} - \frac{(1,487)(28.28)}{15,729} + \frac{(118.4)(12)}{15,729}$$

$$= 1.847 - 2.674 + 0.090 = -0.737 \text{ ksi}$$

Tensile stress limit for concrete with bonded reinforcement: -0.578 ksi NG

Compute stress in the bottom of beam:

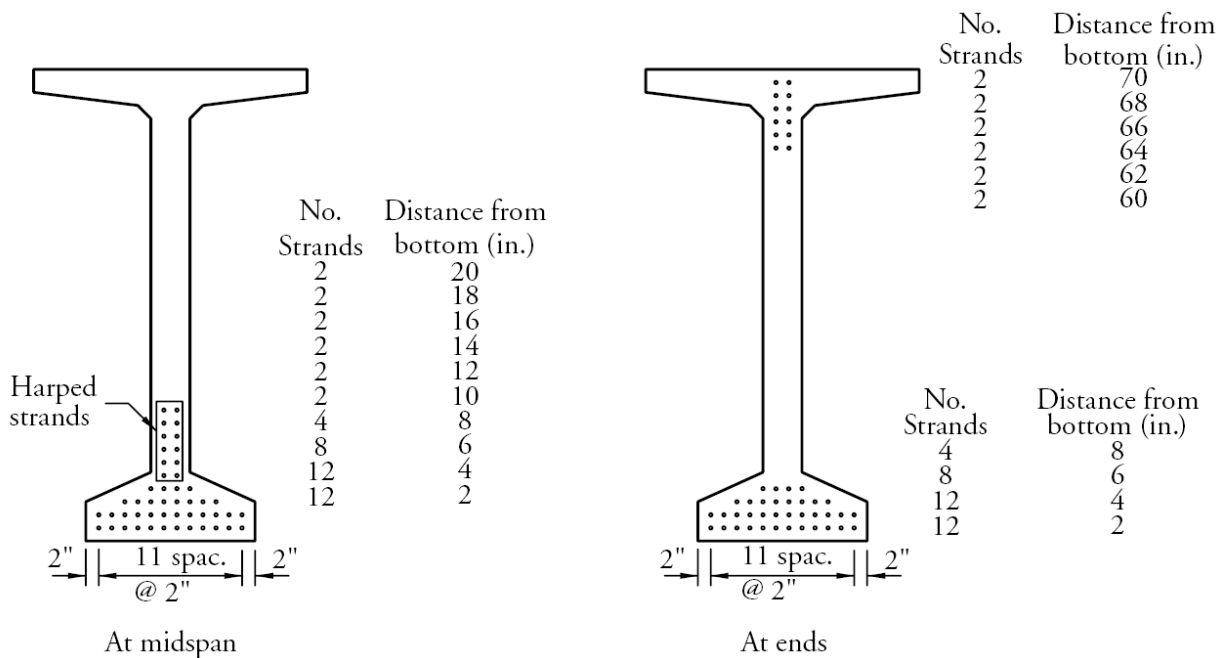
$$f_b = \frac{P_{pi}}{A_{ti}} + \frac{P_{pi}e_{ti}}{S_{bti}} - \frac{M_g}{S_{bti}} = \frac{1,487}{805} + \frac{(1,487)(28.28)}{16,444} - \frac{(118.4)(12)}{16,444}$$

$$= 1.847 + 2.557 - 0.086 = 4.318 \text{ ksi}$$

Compressive stress limit for concrete: +3.480 ksi NG

Since stresses at the top and bottom exceed the stress limits, harp strands to satisfy the specified limits. Harp 12 strands at the 0.4L points, as shown in **Figures 9.1a.7.2-1** and **9.1a.7.2-2**.

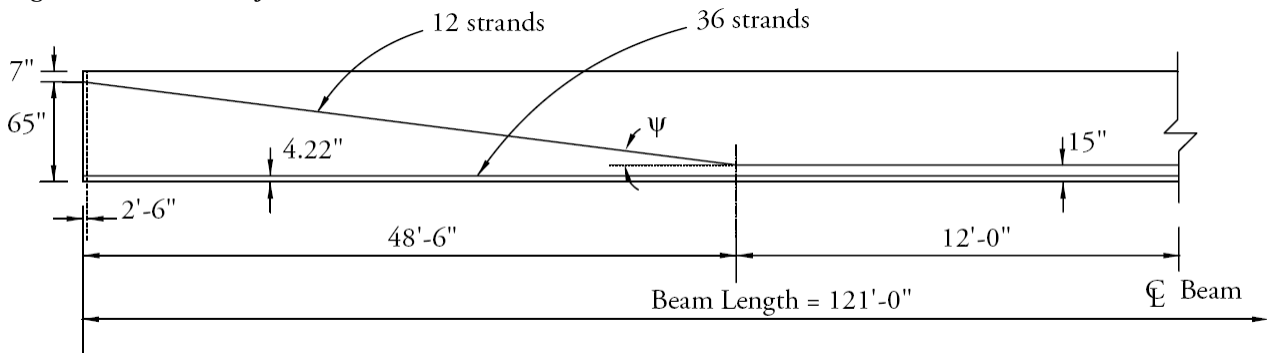
Figure 9.1a.7.2-1
Strand Pattern



BULB-TEE (BT-72), SINGLE SPAN, COMPOSITE DECK

9.1a.7.2 Stresses at Transfer Length Section

Figure 9.1a.7.2-2
Longitudinal Strand Profile



Compute the center of gravity of the prestressing strands at the transfer length section using the harped pattern.

The distance between the center of gravity of the 12 harped strands at the end of the beam and the top fiber of the precast beam is:

$$\frac{2(2) + 2(4) + 2(6) + 2(8) + 2(10) + 2(12)}{12} = 7.0 \text{ in.}$$

The distance between the center of gravity of the 12 harped stands at the harp point and the bottom fiber of the beam is:

$$\frac{2(10) + 2(12) + 2(14) + 2(16) + 2(18) + 2(20)}{12} = 15.0 \text{ in.}$$

The distance between the center of gravity of the 12 harped strands and the top fiber of the beam at the transfer length section:

$$7 \text{ in.} + \frac{(72 - 15 - 7) \text{ in.}}{48.5 \text{ ft}} (2.5 \text{ ft}) = 9.58 \text{ in.}$$

The distance between the center of gravity of the 36 straight bottom strands and the extreme bottom fiber of the beam is:

$$\frac{12(2) + 12(4) + 8(6) + 4(8)}{36} = 4.22 \text{ in.}$$

Therefore, the distance between the center of gravity of the total number of strands measured to the bottom of the precast beam at transfer length is:

$$\frac{36(4.22) + 12(72 - 9.58)}{48} = 18.77 \text{ in.}$$

The center of gravity of all prestressing strand with respect to the extreme bottom fiber at the end of the beam, y_{bs} , is:

$$\frac{36(4.22) + 12(72 - 7)}{48} = 19.42 \text{ in.}$$

Eccentricity of the 48 strand group at transfer length, e , is: $35.76 - 18.77 = 16.99 \text{ in.}$

Recompute top and bottom stresses at the transfer length section with harped strands. Note that the transformed section properties here are different than those at midspan and have been re-calculated.

Concrete stress in top of beam:

$$f_t = \frac{1,487}{805} - \frac{(1,487)(16.99)}{16,103} + \frac{(118.4)(12)}{16,103} = 1.847 - 1.569 + 0.088 = +0.366 \text{ ksi}$$

Compressive stress limit: +3.480 ksi OK

BULB-TEE (BT-72), SINGLE SPAN, COMPOSITE DECK

9.1a.7.2 Stresses at Transfer Length Section/9.1a.7.5 Hold-Down Forces

Concrete stress in bottom of beam:

$$f_b = \frac{1,487}{805} + \frac{(1,487)(16.99)}{16,269} - \frac{(118.4)(12)}{16,269} = 1.847 + 1.553 - 0.087 = +3.313 \text{ ksi}$$

Compressive stress limit: +3.480 ksi OK

9.1a.7.3 Stresses at Harp Points

The strand eccentricity at the harp points is the same as at midspan, $e_{ti} = 28.28$ in.

Bending moment at the harp points ($0.4L$) due to the self weight of the beam is:

$$(0.5)(0.799)(48.5)(121 - 48.5) = 1,405 \text{ ft-kips}$$

Therefore, top and bottom stresses are:

Concrete stress in top of beam:

$$f_t = \frac{1,487}{805} - \frac{(1,487)(28.28)}{15,729} + \frac{(1,405)(12)}{15,729} = 1.847 - 2.674 + 1.072 = +0.245 \text{ ksi}$$

Compressive stress limit: +3.480 ksi OK

Concrete stress in bottom of beam:

$$f_b = \frac{1,487}{805} + \frac{(1,487)(28.28)}{16,444} - \frac{(1,405)(12)}{16,444} = 1.847 + 2.557 - 1.025 = +3.379 \text{ ksi}$$

Compressive stress limit: +3.480 ksi OK

9.1a.7.4 Stresses at Midspan

Bending moment at midspan due to the beam self weight is:

$$M_g = 0.5(0.799)(60.5)(121 - 60.5) = 1,462.3 \text{ ft-kips}$$

$$f_t = \frac{1,487}{805} - \frac{(1,487)(28.28)}{15,729} + \frac{(1,462)(12)}{15,729} = 1.847 - 2.674 + 1.115 = +0.288 \text{ ksi}$$

Compressive stress limit: +3.480 ksi OK

$$f_b = \frac{1,487}{805} + \frac{(1,487)(28.28)}{16,444} - \frac{(1,462)(12)}{16,444} = 1.847 + 2.557 - 1.067 = +3.337 \text{ ksi}$$

Compressive stress limit: +3.480 ksi OK

9.1a.7.5 Hold-Down Forces

Assume that the stress in the strand at the time of prestressing, before seating losses, is:

$$0.80 f_{pu} = 0.80(270) = 216 \text{ ksi}$$

Thus, the prestress force per strand before seating losses is: $0.153(216) = 33.0$ kips

From **Figure 9.1a.7.2-2**, the harp angle,

$$\psi = \tan^{-1} \left(\frac{50}{48.5(12)} \right) = 4.91^\circ$$

Therefore, hold-down force/strand = $1.05(\text{force per strand})(\sin \psi)$

$$= 1.05(33.0)\sin 4.91^\circ = 2.97 \text{ kips/strand}$$

Note the factor 1.05 is applied to account for friction.

Total hold-down force = $12 \text{ strands}(2.97) = 35.6$ kips

The hold-down force and the harp angle should be checked against maximum limits for local practices. Refer to Chapter 3, Fabrication and Construction and Chapter 8, Design Theory and Procedures for additional details.

BULB-TEE (BT-72), SINGLE SPAN, COMPOSITE DECK

9.1a.7.6 Summary of Stresses at Transfer/9.1a.8.2.1 Concrete Stress at Top Fiber of the Beam

9.1a.7.6 Summary of Stresses at Transfer

	Top Fiber Stresses f_t , ksi	Bottom Fiber Stresses f_b , ksi
At transfer length section	+0.366	+3.313
At harp points	+0.245	+3.379
At midspan	+0.288	+3.337

9.1a.8 CONCRETE STRESSES AT SERVICE LOADS

Using transformed section properties and refined losses, $P_{pe} = 1,304$ kips

9.1a.8.1 Stress Limits for Concrete

[LRFD Art. 5.9.4.2]

Compression:

Due to permanent loads, (i.e. beam self weight, weight of slab and haunch, weight of future wearing surface, and weight of barriers), for load combination Service I:

$$\text{for precast beams: } 0.45 f'_c = 0.45(6.500) = +2.925 \text{ ksi}$$

$$\text{for deck: } 0.45 f'_c = 0.45(4.000) = +1.800 \text{ ksi}$$

Due to permanent and transient loads (i.e. all dead loads and live loads), for load combination Service I:

$$\text{for precast beams: } 0.60 f'_c = 0.60(6.500) = +3.900 \text{ ksi}$$

$$\text{for deck: } 0.60 f'_c = 0.60(4.000) = +2.400 \text{ ksi}$$

Tension:

For components with bonded prestressing tendons:

$$\text{for load combination Service III: } -0.19 \sqrt{f'_c}$$

$$\text{for precast beam: } -0.19 \sqrt{6.500} = -0.484 \text{ ksi}$$

9.1a.8.2 Stresses at Midspan**9.1a.8.2.1 Concrete Stress at Top Fiber of the Beam**

To check top compressive stresses, two cases are considered:

1. Under permanent loads, load combination Service I:

Using bending moment values given in **Table 9.1a.4-1**, compute the top fiber stresses:

$$\begin{aligned} f_{tg} &= \frac{P_{pe}}{A_{tf}} - \frac{P_{pe}e_{tf}}{S_{ttf}} + \frac{(M_g + M_s)}{S_{ttf}} + \frac{(M_{ws} + M_b)}{S_{ttc}} \\ &= \frac{1,304}{802.5} - \frac{(1,304)(28.37)}{15,711} + \frac{(1,438.2 + 1,659.6)(12)}{15,711} + \frac{(360 + 180)(12)}{64,161} \\ &= 1.625 - 2.355 + 2.366 + 0.101 = 1.737 \text{ ksi} \end{aligned}$$

Compressive stress limit: +2.925 ksi OK

2. Under permanent and transient loads, load combination Service I:

$$\begin{aligned} f_{tg} &= +1.737 + \frac{(M_{LT} + M_{LL})}{S_{ttc}} \\ &= +1.737 + \frac{(1,830.2 + 843.3)(12)}{64,161} \\ &= +1.737 + 0.500 = +2.237 \text{ ksi} \end{aligned}$$

Compressive stress limit: +3.900 ksi OK

BULB-TEE (BT-72), SINGLE SPAN, COMPOSITE DECK**8.1a.8.2.2 Concrete Stress at the Top Fiber of the Deck/9.1a.8.4 Summary of Stresses at Midspan at Service Loads****9.1a.8.2.2 Concrete Stress at the Top Fiber of the Deck**

Note: Compressive stress in the deck slab at service loads never controls the design for typical applications. The calculations shown below are for illustration purposes and may not be necessary in most practical applications.

1. Under permanent loads, load combination Service I:

$$f_{tc} = \frac{M_{ws} + M_b}{S_{dtc}} = \frac{(360 + 180)(12)}{57,002} = +0.114 \text{ ksi}$$

Compressive stress limit: +1.800 ksi OK

2. Under permanent and transient loads, load combination Service I:

$$f_{tc} = \frac{M_{ws} + M_b}{S_{dtc}} + \frac{M_{LT} + M_{LL}}{S_{dtc}} = 0.114 + \frac{(1,830.3 + 843.3)(12)}{57,002} = +0.677 \text{ ksi}$$

Compressive stress limit: +2.400 ksi OK

9.1a.8.2.3 Concrete Stress in Bottom of Beam, Load Combination Service III:

$$\begin{aligned} f_b &= \frac{P_{pe}}{A_{tf}} + \frac{P_{pe}e_{tf}}{S_{btf}} - \frac{(M_g + M_s)}{S_{btf}} - \frac{(M_{ws} + M_b) + 0.8(M_{LT} + M_{LL})}{S_{btc}} \\ &= \frac{1,304}{802.5} + \frac{(1,304)(28.37)}{16,343} - \frac{(1,438.2 + 1,659.6)(12)}{16,343} - \frac{[(360 + 180) + (0.8)(1,830.2 + 843.3)](12)}{22,025} \\ &= 1.625 + 2.264 - 2.275 - 1.460 = 0.154 \text{ ksi} \end{aligned}$$

Tensile stress limit: -0.484 ksi

The stress is in compression. OK

9.1a.8.3 Fatigue Stress Limit

LRFD Article 5.5.3.1 states that in fully prestressed components other than segmentally constructed bridges, the compressive stress due to Fatigue I load combination and one half the sum of effective prestress and permanent loads shall not exceed $0.40f'_c$, after losses.

From **Table 9.1a.4-2**, the unfactored fatigue bending moment at midspan, M_f , is 776.9 ft-kips. Therefore, stress at the top fiber of the beam due to fatigue load combination I is:

$$f_{tgf} = \frac{1.50(M_f)}{S_{ttc}} = \frac{1.50(776.9)(12)}{64,161} = +0.218 \text{ ksi}$$

At midspan, the top compressive stress due to permanent loads and prestress is:

$$\begin{aligned} f_{tg} &= \frac{P_{pe}}{A_{tf}} - \frac{P_{pe}e_{tf}}{S_{ttf}} + \frac{(M_g + M_s)}{S_{ttf}} + \frac{(M_{ws} + M_b)}{S_{ttc}} \\ &= \frac{1,304}{802.5} - \frac{(1,304)(28.37)}{15,711} + \frac{(1,438.2 + 1,659.6)(12)}{15,711} + \frac{(360 + 180)(12)}{64,161} \\ &= 1.625 - 2.355 + 2.366 + 0.101 = 1.737 \text{ ksi} \end{aligned}$$

Therefore:

$$f_{tgf} + \frac{f_b}{2} = 0.218 + \frac{1.737}{2} = 1.087 < 0.40(f'_c) = 0.40(6.50) = 2.6 \text{ ksi} \quad \text{OK}$$

This condition should be satisfied at all locations along the beam.

9.1a.8.4 Summary of Stresses at Midspan at Service Loads

The stresses calculated using the above methods are summarized in **Table 9.1a.8.5-1**. For comparison, the stresses calculated for the same design example using the previous method of calculating prestress losses are also shown in the table (Example 9.4 in the previous edition of the manual).

BULB-TEE (BT-72), SINGLE SPAN, COMPOSITE DECK

9.1a.8.4 Summary of Stresses at Midspan at Service Loads/9.1a.8.5.4 Stresses from Deck Shrinkage

Table 9.1a.8.4-1
Stresses at Midspan at Service Loads

Design Example	Top of Deck, ksi Service I		Top of Beam, ksi Service I		Bottom of Beam, ksi Service III
	Permanent Loads	Total Loads	Permanent Loads	Total Loads	
9.1a	+0.114	+0.677	+1.737	+2.237	+0.154
9.4	+0.117	+0.694	+1.833	+2.335	-0.487

9.1a.8.5 Effect of Deck Shrinkage

The calculations in Section 9.1a.8.2 comply with the *LRFD Specifications*. However, PCI believes that it is not appropriate to include the prestressing gain caused by the deck shrinkage, Δf_{pSS} , in calculating the prestress losses. Alternatively, the effect of deck shrinkage should be analyzed by considering it as an external force applied to the composite nontransformed section as illustrated in this section for load combination Service III. The nontransformed section properties are used instead of the transformed section properties to provide a more conservative approach.

9.1a.8.5.1 Total Time-Dependent Loss

The total time-dependent loss, Δf_{pLT} , is determined as:

$$\begin{aligned}\Delta f_{pLT} &= (\Delta f_{pSR} + \Delta f_{pCR} + \Delta f_{pR1}) + (\Delta f_{pSD} + \Delta f_{pCD} + \Delta f_{pR2}) && \text{[LRFD Eq. 5.9.5.4.1-1]} \\ &= (6.019 + 15.445 + 1.258) + (2.541 - 0.358 + 1.258) \\ &= 22.722 + 3.441 = 26.2 \text{ ksi}\end{aligned}$$

9.1a.8.5.2 Effective Prestressing Force

Force per strand = $(f_{pi} - \Delta f_{pLT})(\text{area of strand}) = (202.5 - 26.2)(0.153) = 26.97$ kips

Total prestressing force, $P_{pe} = 26.97(48) = 1,295$ kips

9.1a.8.5.3 Concrete Stress in Bottom of Beam, Load Combination Service III:

$$\begin{aligned}f_b &= \frac{P_{pe}}{A_{tf}} + \frac{P_{pe}e_{tf}}{S_{btf}} - \frac{(M_g + M_s)}{S_{btf}} - \frac{(M_{ws} + M_b) + 0.8(M_{LT} + M_{LL})}{S_{btc}} \\ &= \frac{1,295}{802.5} + \frac{(1,295)(28.37)}{16,343} - \frac{(1,438.2 + 1,659.6)(12)}{16,343} - \frac{[(360 + 180) + (0.8)(1,830.2 + 843.3)](12)}{22,025} \\ &= 1.614 + 2.248 - 2.275 - 1.460 = 0.127 \text{ ksi}\end{aligned}$$

9.1a.8.5.4 Stresses from Deck Shrinkage

Restraining force due to deck shrinkage, ΔP_{ds} , is calculated as shown in Section 9.1a.6.3.4:

$$\Delta P_{ds} = \frac{\epsilon_{ddf} A_d E_{cd}}{1 + 0.7\Psi_d(t_f, t_d)} = \frac{0.000581(108)(7.5)(3,834)}{1 + 0.7(2.256)} = 700 \text{ kips}$$

This force is applied at the center of the deck with an eccentricity from the center the deck to the composite center, $e_d = 21.48$ in.

The corresponding bottom fiber stress, f_{bds} , using the composite nontransformed section properties and assuming the force is 100% effective is:

$$f_{bds} = \frac{\Delta P_{ds}}{A_c} - \frac{\Delta P_{ds}e_d}{S_{bc}} = \frac{700}{1,418.9} - \frac{(700)(21.48)}{20,090} = 0.493 - 0.748 = -0.255 \text{ ksi}$$

Under service load, Load Combination Service III:

$$f_b = 0.127 - 0.255 = -0.128 \text{ ksi} > -0.484 \text{ ksi} \quad \text{OK}$$

BULB-TEE (BT-72), SINGLE SPAN, COMPOSITE DECK

9.1a.8.5.4 Stresses from Deck Shrinkage/9.1a.9 Strength Limit State

It is likely, however, that the full calculated force from deck shrinkage will not occur because of the presence of deck cracking and deck reinforcement. **Table 9.1a.8.5.2-1** summarizes the effect of applying 0, 50, or 100% of the calculated deck force on the stresses at load combination Service III.

Table 9.1a.8.5.4-1

Stresses at Midspan for Load Combination Service III Including the Effect of Deck Shrinkage.

Deck Shrinkage Force, %	Bottom of Beam, ksi Service III
0	+0.127
+50	-0.001
100	-0.128

9.1a.9 STRENGTH LIMIT STATE

Total ultimate bending moment for Strength I is:

$$M_u = 1.25(DC) + 1.5(DW) + 1.75(LL + IM)$$

Using the values of unfactored bending moment given in **Tables 9.1a.4-1** and **9.1a.4-2**, the ultimate bending moment at midspan is:

$$M_u = 1.25(1,438.2 + 1,659.6 + 180) + 1.5(360) + 1.75(1,830.3 + 843.3) = 9,316 \text{ ft-kips}$$

Average stress in prestressing strands when $f_{pe} \geq 0.5 f_{pu}$:

$$f_{ps} = f_{pu} \left(1 - k \frac{c}{d_p} \right) \quad \text{[LRFD Eq. 5.7.3.1.1-1]}$$

where

f_{ps} = average stress in prestressing strand, ksi

f_{pu} = specified tensile strength of prestressing strand = 270.0 ksi

$$k = 2 \left(1.04 - \frac{f_{py}}{f_{pu}} \right) \quad \text{[LRFD Eq. 5.7.3.1.1-2]}$$

= 0.28 for low-relaxation strands [LRFD Table C5.7.3.1.1-1]

d_p = distance from extreme compression fiber to the centroid of the prestressing strands = $h - y_{bs}$ = 80.00 - 6.92 = 73.08 in.

c = distance from the extreme compression fiber to the neutral axis, in.
To compute c , assume rectangular section behavior and check if the depth of the equivalent compression stress block, a , is less than or equal to t_s : [LRFD C5.7.3.2.2]

where $a = \beta_1 c$

$$c = \frac{A_{ps} f_{pu} + A_s f_y - A'_s f'_y}{0.85 f'_c \beta_1 b + k A_{ps} \frac{f_{pu}}{d_p}} \quad \text{[LRFD Eq. 5.7.3.1.1-4]}$$

where

a = depth of the equivalent stress block

A_{ps} = area of prestressing strand = 48(0.153) = 7.344 in.²

A_s = area of nonprestressed tension reinforcement = 0 in.²

A'_s = area of compression reinforcement = 0 in.²

f'_c = specified compressive strength of deck concrete = 4.0 ksi

f_y = specified yield strength of tension reinforcement, ksi

f'_y = specified yield strength of compression reinforcement = 60.0 ksi

β_1 = stress factor of compression block [LRFD Art. 5.7.2.2]

= 0.85 for $f'_c \leq 4.0$ ksi

= $0.85 - 0.05 (f'_c - 4.0) \geq 0.65$ for $f'_c > 4.0$ ksi

= 0.85

b = effective width of compression flange = 108 in.

BULB-TEE (BT-72), SINGLE SPAN, COMPOSITE DECK

9.1a.9 Strength Limit State/9.1a.10.2 Minimum Reinforcement

$$c = \frac{7.344(270.0) + 0 - 0}{0.85(4.0)(0.85)(108) + 0.28(7.344)\left(\frac{270.0}{73.80}\right)} = 6.20 \text{ in.} < t_s = 7.5 \text{ in.} \quad \text{OK}$$

$$a = \beta_1 c = 0.85(6.20) = 5.27 \text{ in.}$$

Therefore, the rectangular section behavior assumption is valid.

The average stress in prestressing strand is:

$$f_{ps} = 270.0 \left(1 - 0.28 \frac{6.20}{73.08}\right) = 263.6 \text{ ksi}$$

Nominal flexural resistance:

[LRFD Art. 5.7.3.2.3]

$$M_n = A_{ps} f_{ps} \left(d_p - \frac{a}{2}\right)$$

[LRFD Eq. 5.7.3.2.2-1]

The above equation is a simplified form of LRFD Equation 5.7.3.2.2-1 because no compression reinforcement or nonprestressed reinforcement is considered and the section behaves as a rectangular section.

$$M_n = (7.344)(263.6) \left(73.08 - \frac{5.27}{2}\right) / 12 = 11,364 \text{ ft-kips}$$

Factored flexural resistance:

$$M_r = \phi M_n$$

[LRFD Eq. 5.7.3.2.1-1]

where

$$\phi = \text{resistance factor}$$

[LRFD Art. 5.5.4.2.1]

$$= 1.00, \text{ for tension controlled prestressed concrete sections}$$

$$M_r = 11,364 \text{ ft-kips} > M_u = 9,316 \text{ ft-kips} \quad \text{OK}$$

9.1a.10 LIMITS OF REINFORCEMENT

[LRFD Art. 5.7.3.3.1]

9.1a.10.1 Maximum Reinforcement

The check of maximum reinforcement limits in LRFD Article 5.7.3.3.1 was removed from the *LRFD Specifications* in 2005.

Adequate ductility of the beam is ensured by evaluating whether the member can be classified as tension-controlled. If the member does not satisfy the requirements to be tension-controlled, the resistance factor for the strength limit state 1 check will be reduced in accordance with LRFD Article 5.5.4.2.1.

9.1a.10.2 Minimum Reinforcement

[LRFD Art. 5.7.3.3.2]

At any section, the amount of prestressed and nonprestressed tensile reinforcement must be adequate to develop a factored flexural resistance, M_r , equal to the lesser of:

- 1.2 times the cracking strength determined on the basis of elastic stress distribution and the modulus of rupture, and
- 1.33 times the factored moment required by the applicable strength load combination.

Check at midspan:

$$M_{cr} = S_{btc}(f_r + f_{cpe}) - M_{dnc} \left(\frac{S_{btc}}{S_{btf}} - 1\right) \geq S_{btc} f_r \quad \text{[LRFD Eq. 5.7.3.3.2-1]}$$

where

$$f_r = \text{modulus of rupture of concrete} \quad \text{[LRFD Art. 5.4.2.6]}$$

$$= 0.37\sqrt{f'_c} = 0.37\sqrt{6.500} = 0.943 \text{ ksi}$$

$$f_{cpe} = \text{compressive stress in concrete due to effective prestress force only (after allowance for all prestress losses) at extreme fiber of section where tensile stress is caused by externally applied loads}$$

$$= \frac{P_{pe}}{A_{tf}} + \frac{P_{pe} e_{tf}}{S_{btf}} = \frac{1,304}{802.5} + \frac{1,304(28.37)}{16,343} = 3.889 \text{ ksi}$$

$$M_{dnc} = \text{noncomposite dead load moment at the section}$$

$$= M_g + M_s = 1,438.2 + 1,659.6 = 3,098 \text{ ft-kips}$$

BULB-TEE (BT-72), SINGLE SPAN, COMPOSITE DECK

9.1a.10.2 Minimum Reinforcement/9.1a.11.1 Critical Section

S_{btc} = section modulus for the extreme bottom fiber of the transformed composite section where the tensile stress is caused by externally applied loads = 22,025 in.³

S_{btf} = section modulus for the extreme bottom fiber of the transformed noncomposite section where the tensile stress is caused by externally applied loads = 16,343 in.³

$$M_{cr} = (0.943 + 3.889) \frac{22,025}{12} - (3,098) \left(\frac{22,025}{16,343} - 1 \right) = 7,792 \text{ ft-kips}$$

$$1.2 M_{cr} = 1.2(7,792) = 9,350 \text{ ft-kips}$$

At midspan, the factored moment required by the Strength I load combination is:

$$M_u = 9,316 \text{ ft-kips (as calculated in Section 9.1a.9)}$$

$$\text{Thus, } 1.33M_u = 1.33(9,316) = 12,390 \text{ ft-kips}$$

Since $1.2M_{cr} < 1.33M_u$, the $1.2M_{cr}$ requirement controls.

$$M_r = 11,364 \text{ ft-kips} > 1.2M_{cr} = 9,350 \text{ ft-kips} \quad \text{OK}$$

Note: The *LRFD Specifications* requires that this criterion be met at every section.

Illustrated based on 2011 *LRFD Specifications*.

Editor's Note: 2012 *LRFD Specifications* changes will revise minimum reinforcement.

9.1a.11 SHEAR DESIGN

The area and spacing of shear reinforcement must be determined at regular intervals along the entire length of the beam. In this design example, transverse shear design procedures are demonstrated below by determining these values at the critical section near the supports.

Transverse shear reinforcement is required when:

$$V_u > 0.5\phi(V_c + V_p) \quad \text{[LRFD Eq. 5.8.2.4-1]}$$

where

V_u = total factored shear force, kips

V_c = nominal shear resistance provided by tensile stresses in the concrete, kips

V_p = component in the direction of the applied shear of the effective prestressing force, kips

ϕ = resistance factor = 0.9 for normal weight concrete [LRFD Art. 5.5.4.2.1]

9.1a.11.1 Critical Section

[LRFD Art. 5.8.3.2]

The critical section near the supports is taken as the effective shear depth d_v from the internal face of the support.

$$d_v = \text{distance between resultants of tensile and compressive forces, } (d_e - a/2), \text{ but not less than } (0.9d_e) \text{ or } (0.72h_c) \quad \text{[LRFD Art. 5.8.2.9]}$$

where

d_e = the corresponding effective depth from the extreme compression fiber to the centroid of the tensile force in the tensile reinforcement [LRFD Art. 5.8.2.9]

a = depth of compression block = 5.27 in. at midspan (assumed adequate)

h_c = overall depth of the composite section = 80.0 in.

Since some of the strands are harped, the effective depth, d_e , varies from point-to-point. However, d_e must be calculated at the critical section in shear which is not yet determined; therefore, for the first iteration, d_e is calculated based on the center of gravity of the straight strand group at the end of the beam, y_{bs} .

$$d_e = h_c - y_{bs} = 80.0 - 4.22 = 75.78 \text{ in.}$$

$$d_v = 75.78 - (5.27/2) = 73.14 \text{ in.}$$

$$\geq 0.9 d_e = 0.9(75.78) = 68.20 \text{ in.}$$

$$\geq 0.72h_c = 0.72(80) = 57.60 \text{ in.}$$

OK

Therefore, $d_v = 73.14$ in.

Because the width of the bearing is not yet determined, it is conservatively assumed to be zero. Therefore, the critical section in shear is located at a distance of:

$$73.14 \text{ in.} = 6.10 \text{ ft from centerline of support}$$

BULB-TEE (BT-72), SINGLE SPAN, COMPOSITE DECK9.1a.11.1 Critical Section/9.1a.11.2.2 Values of β and θ

$$(x/L) = 6.10/120 = 0.051L$$

The effective depth, d_e , and the position of the critical section in shear may be refined based on the position of the critical section calculated above. However, the difference is small. Therefore, no more refinement is performed.

9.1a.11.2 Contribution of Concrete to Nominal Shear Resistance

The contribution of the concrete to the nominal shear resistance is:

$$V_c = 0.0316\beta\sqrt{f'_c}b_vd_v \quad [\text{LRFD Eq. 5.8.3.3-3}]$$

where β = a factor indicating the ability of diagonally cracked concrete to transmit tension (a value indicating concrete contribution).

Several quantities must be determined before this expression can be evaluated.

9.1a.11.2.1 Strain in Flexural Tension Reinforcement

Calculate the strain at the centroid of the tension reinforcement, ϵ_s :

$$\epsilon_s = \frac{\frac{|M_u|}{d_v} + 0.5N_u + |(V_u - V_p)| - A_{ps}f_{po}}{(E_sA_s + E_pA_{ps})} \quad [\text{LRFD Eq. 5.8.3.4.2-4}]$$

where

$$\begin{aligned} M_u &= \text{applied factored bending moment at the specified section, } 0.051L \\ &= 1.25(277.6 + 320.3 + 34.7) + 1.50(69.5) + 1.75(372.6 + 162.7) \quad (\text{Tables 9.1a.4-1 and 9.1a.4-2}) \\ &= 1,832 \text{ ft-kips} \end{aligned}$$

$$N_u = \text{applied factored axial force at the specified section, } 0.051L = 0 \text{ kips}$$

$$\begin{aligned} V_u &= \text{applied factored shear force at the specified section, } 0.051L \\ &= 1.25(43.1 + 49.7 + 5.4) + 1.50(10.8) + 1.75(73.8 + 30.6) = 321.7 \text{ kips} \\ &\quad (\text{Tables 9.1a.4-1 and 9.1a.4-2}) \end{aligned}$$

$$\begin{aligned} V_p &= (\text{Force per strand without live load gains})(\text{Number of harped strands})(\sin \psi) \\ &= (25.37)(12)\sin 4.91^\circ = 26.1 \text{ kips is a conservative resistance} \end{aligned}$$

$$A_{ps} = \text{area of prestressing strands on the flexural tension side of the member} = 36(0.153) = 5.508 \text{ in.}^2$$

$$\begin{aligned} f_{po} &= \text{a parameter taken as modulus of elasticity of prestressing tendons multiplied by the locked-in difference in strain between the prestressing tendons and the surrounding concrete (ksi). For pretensioned members, LRFD Article 5.8.3.4.2 indicates that } f_{po} \text{ can be taken as } 0.7f_{pu}. \text{ (Note: use this for both pretensioned and post-tensioned systems made with stress relieved and low relaxation strands).} \\ &= 0.7(270.0) = 189.0 \text{ ksi} \end{aligned}$$

$$\epsilon_s = \frac{\frac{1,832(12)}{73.14} + 0 + |(321.7 - 26.1)| - 5.508(189.0)}{[0 + 28,500(5.508)]}$$

$$= -2.834 \times 10^{-3}$$

ϵ_s is less than zero. Use $\epsilon_s = 0$.

9.1a.11.2.2 Values of β and θ

Assume the section contains at least the minimum amount of transverse reinforcement:

$$\beta = \frac{4.8}{(1 + 750\epsilon_s)} = \frac{4.8}{(1 + 0)} = 4.8 \quad [\text{LRFD Eq. 5.8.3.4.2-1}]$$

Angle of diagonal compressive stresses is:

$$\theta = 29 + 3,500\epsilon_s = 29 + 3,500(0) = 29^\circ \quad [\text{LRFD Eq. 5.8.3.4.2-3}]$$

BULB-TEE (BT-72), SINGLE SPAN, COMPOSITE DECK

9.1a.11.2.3 Compute Concrete Contribution/9.1a.11.3.3 Determine Spacing of Reinforcement

9.1a.11.2.3 Compute Concrete Contribution

The nominal shear resisted by the concrete is:

$$V_c = 0.0316\beta\sqrt{f'_c}b_vd_v \quad [\text{LRFD Eq. 5.8.3.3-3}]$$

where b_v = effective web width = 6 in.

$$V_c = 0.0316(4.8)\sqrt{6.5}(6)(73.14) = 169.7 \text{ kips}$$

9.1a.11.3 Contribution of Reinforcement to Nominal Shear Resistance**9.1a.11.3.1 Requirement for Reinforcement**

Check if $V_u > 0.5\phi(V_c + V_p)$ [LRFD Eq. 5.8.2.4-1]

$$0.5\phi(V_c + V_p) = 0.5(0.9)(169.7 + 26.1) = 88.1 \text{ kips} < 321.7 \text{ kips}$$

Therefore, transverse shear reinforcement must be provided.

9.1a.11.3.2 Required Area of Reinforcement

$$V_u/\phi \leq V_n = V_c + V_s + V_p \quad [\text{LRFD Eq. 5.8.3.3-1}]$$

where

$$\begin{aligned} V_s &= \text{shear resistance provided by shear reinforcement} \\ &= (V_u/\phi) - V_c - V_p = (321.7/0.9) - 169.7 - 26.1 = 161.6 \text{ kips} \end{aligned}$$

$$V_s = \frac{A_v f_{yh} d_v (\cot \theta + \cot \alpha) (\sin \alpha)}{s} \quad [\text{LRFD Eq. 5.8.3.3-4}]$$

where

$$\begin{aligned} A_v &= \text{area of shear reinforcement within a distance } s, \text{ in.}^2 \\ s &= \text{spacing of stirrups, in.} \\ f_{yh} &= \text{specified yield strength of shear reinforcement, ksi} \\ \alpha &= \text{angle of inclination of transverse reinforcement to longitudinal axis} \\ &= 90^\circ \text{ for vertical stirrups} \end{aligned}$$

Therefore, area of shear reinforcement within a distance s , is:

$$\begin{aligned} A_v &= (sV_s)/(f_{yh}d_v \cot \theta) \\ &= [(s)(161.6)]/[60(73.14)\cot 29^\circ] = 0.020(s) \text{ in.}^2 \end{aligned}$$

If $s = 12$ in., required $A_v = 0.24 \text{ in.}^2/\text{ft}$

9.1a.11.3.3 Determine Spacing of Reinforcement

Check maximum spacing of transverse reinforcement. [LRFD Art 5.8.2.7]

Check if $v_u < 0.125f'_c$

$$v_u = \frac{|V_u - \phi V_p|}{\phi b_v d_v} = \frac{|321.7 - (0.9)(26.2)|}{(0.9)(6)(73.14)} = 0.755 \text{ ksi} \quad [\text{LRFD Eq. 5.8.2.9-1}]$$

$$0.125f'_c = (0.125)(6.5) = 0.813 \text{ ksi}$$

Since $v_u < 0.125f'_c$ [LRFD Eq. 5.8.2.7-1]

then, $s \leq 24$ in.

$$s \leq 0.8d_v = 0.8(73.14) = 58.5 \text{ in.}$$

Therefore, maximum $s = 24$ in. $> s$ provided OK

Use No. 4 bar double legs at 12 in., $A_v = 0.40 \text{ in.}^2/\text{ft} > 0.24 \text{ in.}^2/\text{ft}$

BULB-TEE (BT-72), SINGLE SPAN, COMPOSITE DECK

9.1a.11.3.3 Determine Spacing of Reinforcement/9.1a.12.3 Required Interface Shear Reinforcement

$$V_s = \frac{0.4(60)73.14 \cot 29^\circ}{12} = 263.9 \text{ kips}$$

A smaller amount of shear reinforcement could have been selected. However, calculations for minimum interface shear reinforcement require more. (See Sect. 9.1a.12.3.1)

9.1a.11.3.4 Minimum Reinforcement Requirement

The area of transverse reinforcement should not be less than:

[LRFD Eq. 5.8.2.5-1]

$$0.0316 \sqrt{f'_c} \frac{b_v s}{f_{yh}} = 0.0316 \sqrt{6.5} \frac{(6)(12)}{60.0} = 0.10 \text{ in.}^2/\text{ft} < A_v \text{ provided} \quad \text{OK}$$

9.1a.11.4 Maximum Nominal Shear Resistance

In order to ensure that the concrete in the web of the beam will not crush prior to yielding of the transverse reinforcement, the *LRFD Specifications* gives an upper limit of V_n as follows:

$$V_n = 0.25 f'_c b_v d_v + V_p \quad \text{[LRFD Eq. 5.8.3.3-2]}$$

Comparing this equation with LRFD Eq. 5.8.3.3-1, it can be concluded that

$$V_c + V_s \text{ must not be greater than } 0.25 f'_c b_v d_v$$

$$169.7 + 263.9 = 433.6 \text{ kips} \leq 0.25(6.5)(6)(73.14) = 713.1 \text{ kips} \quad \text{OK}$$

Using the above procedures, the transverse reinforcement can be determined at increments along the entire length of the beam.

9.1a.12 INTERFACE SHEAR TRANSFER**9.1a.12.1 Factored Horizontal Shear**

[LRFD Art. 5.8.4]

At the strength limit state, the horizontal shear at a section on a per unit basis can be taken as:

$$V_{hi} = \frac{V_u}{d_v} \quad \text{[LRFD Eq. C5.8.4.2-7]}$$

where

V_{hi} = horizontal factored shear force per unit length of the beam, kips/in.

V_u = factored shear force at specified section due to superimposed loads after the deck is cast, kips

d_v = the distance between the centroid of the tension steel and the mid-thickness of the slab = $(d_e - t_s/2)$
= $75.78 - 7.5/2 = 72.03$ in.

The *LRFD Specifications* does not identify the location of the critical section. For convenience, it will be assumed here to be the same location as the critical section for vertical shear, at point 0.051L.

Using load combination Strength I:

$$V_u = 1.25(43.1+49.7+5.4) + 1.5(10.8) + 1.75(73.8 + 30.6) = 321.7 \text{ kips} \quad \text{(Tables 9.1a.4-1 and 9.1a.4-2)}$$

Therefore, the applied factored horizontal shear is:

$$V_{hi} = \frac{321.7}{72.03} = 4.47 \text{ kips/in.}$$

9.1a.12.2 Required Nominal Resistance

Required $V_{ni} = V_{hi}/\phi = 4.47/0.9 = 4.97$ kips/in.

[LRFD Eq. 5.8.4.1-1]

9.1a.12.3 Required Interface Shear Reinforcement

The nominal shear resistance of the interface surface is:

$$V_{ni} = cA_{cv} + \mu[A_v f_{yh} + P_c] \quad \text{[LRFD Eq. 5.8.4.1-3]}$$

BULB-TEE (BT-72), SINGLE SPAN, COMPOSITE DECK

9.1a.12.3 Required Interface Shear Reinforcement/9.1a.13 Minimum Longitudinal Reinforcement Requirement

where

c = cohesion factor, ksi

μ = coefficient of friction

A_{cv} = area of concrete section resisting shear transfer, in.²

A_{vf} = area of shear reinforcement crossing the shear plane, in.²

P_c = permanent net compressive force normal to the shear plane, kips

f_{yh} = specified yield strength of shear reinforcement, ksi

For cast-in-place concrete slabs placed on clean concrete girder surface intentionally [LRFD Art. 5.8.4.3] roughened.

c = 0.28 ksi

μ = 1.0

The actual contact width, b_v , between the slab and the beam is 42 in.

A_{cv} = (42.0 in.)(1.0 in.) = 42.0 in.²

LRFD Eq. 5.8.4.1-3 can be solved for A_{vf} as follows:

$$4.97 = 0.28(42.0) + 1.0[A_{vf}(60) + 0]$$

Solving for A_{vf} :

$$A_{vf}(\text{req'd}) < 0$$

Since the resistance provided by cohesion is greater than the applied force, provide the minimum required interface reinforcement.

9.1a.12.3.1 Minimum Interface Shear Reinforcement

$$A_{vf} \geq (0.05A_{cv})/f_{yh} \quad \text{[LRFD Eq. 5.8.4.4-1]}$$

From the design of vertical shear reinforcement, a No. 4 double-leg bar at 12-in. spacing is provided from the beam extending into the deck. Therefore, $A_{vf} = 0.40 \text{ in.}^2/\text{ft}$

$$A_{vf} = (0.40 \text{ in.}^2/\text{ft}) < (0.05A_{cv})/f_{yh} = 0.05(42)/60 = 0.035 \text{ in.}^2/\text{in.} = 0.42 \text{ in.}^2/\text{ft} \quad \text{NG}$$

However, LRFD Article 5.8.4.4 states that the minimum reinforcement need not exceed the amount needed to resist $1.33V_{hi}/\phi$ as determined using Eq. 5.8.4.1-3.

$$1.33(4.47/0.9) = 0.28(42.0) + 1.0[A_{vf}(60) + 0]$$

solving for A_{vf} :

$$A_{vf}(\text{req'd}) < 0 \quad \text{OK}$$

9.1a.12.4 Maximum Nominal Shear Resistance

$$V_{ni} \leq K_1 f'_c A_{cv} \text{ or } K_2 A_{cv}$$

$$V_{ni} \text{ provided} = (0.28)(42) + 1.0 \left(\frac{0.40}{12} (60.0) + 0 \right) = 13.76 \text{ kips/in.}$$

$$K_1 f'_c A_{cv} = (0.3)(4.0)(42) = 50.4 \text{ kips/in.} \quad \text{[LRFD Eq. 5.8.4.1-4]}$$

$$K_2 A_{cv} = 1.8(42) = 75.6 \text{ kips/in.} \quad \text{[LRFD Eq. 5.8.4.1-5]}$$

Since provided $V_{ni} = 13.76 \text{ kips/in.} < 50.4 \text{ kips/in.}$ OK

9.1a.13 MINIMUM LONGITUDINAL REINFORCEMENT REQUIREMENT

[LRFD Art. 5.8.3.5]

Longitudinal reinforcement should be proportioned so that at each section the following equation is satisfied:

$$A_{ps} f_{ps} + A_s f_y \geq \frac{M_u}{d_v \phi_f} + 0.5 \frac{N_u}{\phi_c} + \left(\left| \frac{V_u}{\phi_v} - V_p \right| - 0.5 V_s \right) \cot \theta \quad \text{[LRFD Eq. 5.8.3.5-1]}$$

where

A_s = area of nonprestressed tension reinforcement, in.²

f_y = specified yield strength of reinforcing bars, ksi

BULB-TEE (BT-72), SINGLE SPAN, COMPOSITE DECK**9.1a.13 Minimum Longitudinal Reinforcement Requirement/9.1a.13.1 Required Reinforcement at Face of Bearing**

- A_{ps} = area of prestressing strand at the tension side of the section, in.²
 f_{ps} = average stress in prestressing strand at the time for which the nominal resistance is required, ksi
 M_u = factored moment at the section corresponding to the factored shear force, ft-kips
 N_u = applied factored axial force, kips
 V_u = factored shear force at section, kips
 V_s = shear resistance provided by shear reinforcement, kips
 V_p = component in the direction of the applied shear of the effective prestressing force, kips
 d_v = effective shear depth, in.
 ϕ = resistance factor as appropriate for moment, shear, and axial resistance. [LRFD Art. 5.5.4.2]
 Therefore, different ϕ factors will be used for the terms in LRFD Equation 5.8.3.5-1, depending on the type of action being considered.
 θ = angle of inclination of diagonal compressive stresses

9.1a.13.1 Required Reinforcement at Face of Bearing

For simple end supports, the longitudinal reinforcement on the flexural tension side of the member at inside face of bearing should satisfy:

$$A_{ps}f_{ps} + A_s f_y \geq \left(\frac{V_u}{\phi} - 0.5V_s - V_p \right) \cot \theta \quad [\text{LRFD Eq. 5.8.3.5-2}]$$

$$M_u = 0 \text{ ft-kips}$$

$$N_u = 0 \text{ kips}$$

Because the width of the bearing is not yet determined, it is assumed to be zero. This assumption is conservative for these calculations. Therefore, the failure crack assumed for this analysis radiates from the centerline of the bearing, 6 in. from the end of the beam.

From **Tables 9.1a.4-1** and **9.1a.4-2** using load combination Strength I, the factored shear force at this section is:

$$V_u = 1.25(47.9 + 55.3 + 6.0) + 1.5(12.0) + 1.75(78.1 + 33.9) = 350.5 \text{ kips}$$

$$\left(\frac{V_u}{\phi} - 0.5V_s - V_p \right) \cot \theta = \left(\frac{350.5}{0.9} - 0.5(263.9) - 26.1 \right) \cot 29^\circ = 417.4 \text{ kips}$$

As shown in **Figure 9.1a.13.1-1**, the assumed crack plane crosses the centroid of the 36 straight strands at a distance of $(6 + 4.22 \cot 29^\circ = 13.61 \text{ in.})$ from the end of the beam. Since the transfer length is 30 in. from the end of the beam (60 times the strand diameter), the available prestress from the 36 straight strands is a fraction of the effective prestress, f_{pe} , in these strands. The 12 harped strands do not contribute to the tensile capacity since they are not on the flexural tension side of the member.

Therefore, the available prestress force is:

$$\begin{aligned}
 A_{ps}f_{ps} + A_s f_y &= (36)(0.153) \left((202.5 - 43.9) \frac{13.61}{30} \right) + 0 \\
 &= 396.3 + 0 = 396.3 \text{ kips} < 417.4 \text{ kips} \quad \text{NG}
 \end{aligned}$$

Assume a bearing width of 6 in. The failure crack then extends from the edge of the bearing. The assumed crack plane then crosses the centroid of the 36-straight strands at a distance of $(6 + 6/2 + 4.22 \cot 29^\circ = 16.61 \text{ in.})$ from the end of the beam.

Therefore, the available prestressing force is

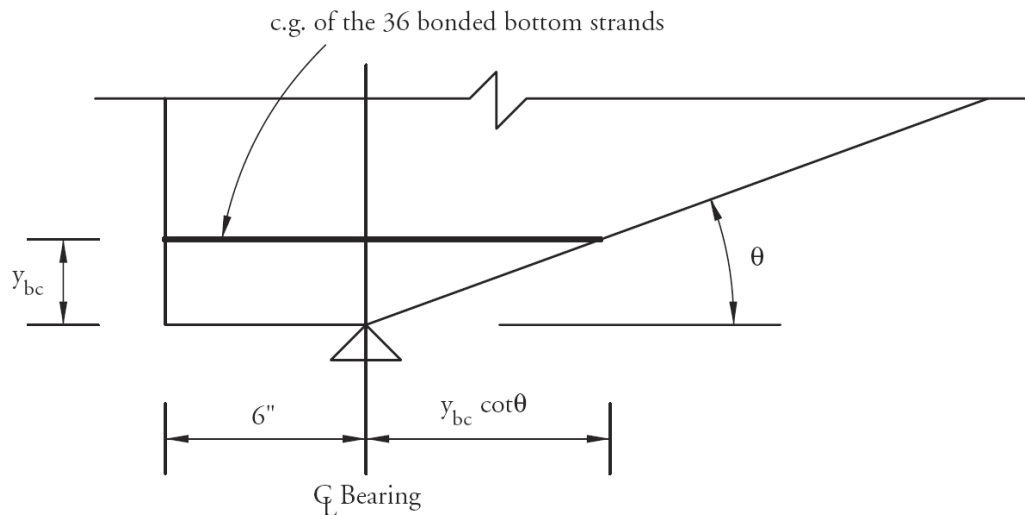
$$\begin{aligned}
 A_{ps}f_{ps} + A_s f_y &= (36)(0.153) \left((202.5 - 43.9) \frac{16.61}{30} \right) + 0 \\
 &= 483.7 + 0 = 483.7 \text{ kips} > 417.4 \text{ kips} \quad \text{OK}
 \end{aligned}$$

Note: An alternative approach for the calculation of available prestressing force excluding the gains from deck shrinkage is illustrated in Section 9.6.13.1

BULB-TEE (BT-72), SINGLE SPAN, COMPOSITE DECK

9.1a.13.1 Required Reinforcement at Face of Bearing/9.1a.15.1 Deflection due to Prestressing Force at Transfer

Figure 9.1a.13.1-1
Assumed Failure Crack



9.1a.14 PRETENSIONED ANCHORAGE ZONE

[LRFD Art. 5.10.10]

9.1a.14.1 Anchorage Zone Reinforcement

[LRFD Art. 5.10.10.1]

Design of the anchorage zone reinforcement is computed using the force in the strands just prior to transfer:

Force in the strands before transfer = $P_{pi} = 48(0.153)(202.5) = 1,487$ kips

The bursting resistance, P_r , should not be less than 4.0% of P_{pi} .

$P_r = f_s A_s \geq 0.04 P_{pi} = 0.04(1,487) = 59.5$ kips

where

- A_s = total area of vertical reinforcement located within a distance $h/4$ from the end of the beam, in.²
- f_s = allowable stress in steel, but taken not greater than 20 ksi

Solving for the required area of steel, $A_s = 59.5/20 = 2.98$ in.²

At least 2.98 in.² of vertical transverse reinforcement should be provided within a distance of ($h/4 = 72/4 = 18.0$ in.) from the end of the beam.

Use five No. 5 double leg bars at 4 in. spacing starting at 2 in. from the end of the beam

The provided $A_s = 5(2)(0.31) = 3.10$ in.² > 2.98 in.² OK

9.1a.14.2 Confinement Reinforcement

[LRFD Art. 5.10.10.2]

For a distance of $1.5h = 1.5(72) = 108$ in., from the end of the beam, reinforcement is placed to confine the prestressing steel in the bottom flange. The reinforcement may not be less than No. 3 deformed bars with spacing not exceeding 6 in. The reinforcement should be of a shape that will confine (enclose) the strands.

9.1a.15 DEFLECTION AND CAMBER

[LRFD Art. 5.7.3.6.2]

Deflections are calculated using the modulus of elasticity of concrete calculated in Section 9.1a.3.1, and the gross section properties of the noncomposite precast beam.

9.1a.15.1 Deflection Due to Prestressing Force at Transfer

Force per strand after transfer = 28.09 kips

BULB-TEE (BT-72), SINGLE SPAN, COMPOSITE DECK**9.1a.15.1 Deflection due to Prestressing Force at Transfer/9.1a.15.4 Deflection due to Barrier and Future Wearing Surface Weights**

$$\Delta_p = \frac{P_{pt}}{E_{ci}I_g} \left(\frac{e_c L^2}{8} - \frac{e' a^2}{6} \right)$$

where

- Δ_p = camber due to prestressing force at transfer, in.
- P_{pt} = total prestressing force after transfer = $48 \times 28.09 = 1,348$ kips
- e_c = eccentricity of prestressing strand at midspan = 29.68 in.
- e' = difference between eccentricity of prestressing strand at midspan and at end of the beam
= $e_c - e_e = 29.68 - (y_b - y_{bs}) = 29.68 - (36.6 - 19.42) = 12.50$ in.
- a = distance from end of the beam to the harp point = 48.5 ft
- L = overall beam length = 121.0 ft
- E_{ci} = modulus of elasticity at transfer = 4,617 ksi
- I_g = moment of inertia of the noncomposite precast beam = 545,894 in.⁴

$$\Delta_p = \frac{1,348}{(4,617)(545,894)} \left(\frac{29.68(121 \times 12)^2}{8} - \frac{12.50(48.5 \times 12)^2}{6} \right) = 3.81 \text{ in. } \uparrow$$

9.1a.15.2 Deflection Due to Beam Self Weight

$$\Delta_g = \frac{5w_g L^4}{384E_{ci}I_g}$$

where

- Δ_g = deflection due to beam self weight, in.
- w_g = beam self weight = 0.799 kips/ft (Sect. 9.1a.3.1)
- E_{ci} = modulus of elasticity of precast beam at transfer = 4,617 ksi
- I_g = gross moment of inertia of the precast beam = 545,894 in.⁴
- L = beam length = 121.0 ft at transfer = 120.0 ft at erection

Deflection due to beam self weight after transfer:

$$\Delta_g = \frac{5 \left(\frac{0.799}{12} \right) (121 \times 12)^4}{(384)(4,617)(545,894)} = 1.53 \text{ in. } \downarrow$$

Deflection due to beam self weight used to compute deflection at erection:

$$\Delta_g = \frac{5 \left(\frac{0.799}{12} \right) (120 \times 12)^4}{(384)(4,617)(545,894)} = 1.48 \text{ in. } \downarrow$$

9.1a.15.3 Deflection Due to Slab and Haunch Weights

$$\Delta_s = \frac{5w_s L^4}{384E_c I_g}$$

where

- Δ_s = deflection due to slab and haunch weights, in.
- w_s = slab and haunch weight = $0.900 + 0.022$ kips/ft = 0.922 kips/ft (Sect. 9.1a.4.1.1)
- L = design span = 120.0 ft
- E_c = modulus of elasticity of precast beam at service loads = 4,888 ksi
- I_g = gross moment of inertia of the precast beam = 545,894 in.⁴

$$\Delta_s = \frac{5 \left(\frac{0.922}{12} \right) (120 \times 12)^4}{(384)(4,888)(545,894)} = 1.61 \text{ in. } \downarrow$$

9.1a.15.4 Deflection Due to Barrier and Future Wearing Surface Weights

$$\Delta_{b+ws} = \frac{5(w_b + w_{ws})L^4}{384E_c I_c}$$

BULB-TEE (BT-72), SINGLE SPAN, COMPOSITE DECK**9.1a.15.4 Deflection due to Barrier and Future Wearing Surface Weights/9.1a.15.6 Deflection Due to Live Load and Impact**

where

Δ_{b+ws} = deflection due to barrier and wearing surface weights, in.

w_b = barrier weight = 0.100 kips/ft (Sect. 9.1a.4.1.1)

w_{ws} = wearing surface weight = 0.200 kips/ft

L = design span = 120.0 ft

E_c = modulus of elasticity of precast beam at service loads = 4,888 ksi

I_c = gross moment of inertia of the composite section = 1,100,320 in.⁴ (Table 9.1a.3.2.3-1)

$$\Delta_{b+ws} = \frac{(5) \left(\frac{0.300}{12} \right) (120 \times 12)^4}{(384)(4,888)(1,100,320)} = 0.26 \text{ in. } \downarrow$$

9.1a.15.5 Deflection and Camber Summary

After transfer, $(\Delta_p + \Delta_g) = 3.81 - 1.53 = 2.28 \text{ in. } \uparrow$

Total deflection at erection, using PCI multipliers (see *PCI Design Handbook*)

$$= 1.8(3.81) - 1.85(1.48) = 4.12 \text{ in. } \uparrow$$

Long-Term Deflection:

LRFD Article 5.7.3.6.2 states that the long-time deflection may be taken as the instantaneous deflection multiplied by a factor 4.0, if the instantaneous deflection is based on the gross moment of inertia. However, a factor of 4.0 is not appropriate for this type of precast construction. Therefore, it is recommended that the designer follow the guidelines of the owner agency for which the bridge is being designed, or undertake a more rigorous, time-dependent analysis.

9.1a.15.6 Deflection Due to Live Load and Impact

Live load deflection limit (optional) = Span/800 [LRFD Art. 2.5.2.6.2]

$$= \left(120 \times \frac{12}{800} \right) = 1.80 \text{ in.}$$

If the owner invokes the optional live load deflection criteria specified in LRFD Art. 2.5.2.6.2, the deflection is the greater of:

- that resulting from the design truck plus impact Δ_{LT} , or [LRFD Art. 3.6.1.3.2]
- that resulting from 25% of the design truck plus impact Δ_{LT} , taken together with the design lane load, Δ_{LL} .

Note: LRFD Article 2.5.2.6.2 states that the dynamic load allowance be included in the calculation of live load deflection.

The *LRFD Specifications* states that all the beams should be assumed to deflect equally under the applied live load and impact. [LRFD Art. 2.5.2.6.2]

Therefore, the distribution factor for deflection, DFD , is calculated as follows:

$$\begin{aligned} DFD &= (\text{number of lanes/number of beams}) && \text{[LRFD Art. C2.5.2.6.2]} \\ &= 4/7 = 0.571 \text{ lanes/beam} \end{aligned}$$

However, it is more conservative to use the distribution factor for moment, DFM .

Deflection due to lane load

Design lane load, $w = 0.64DFM = 0.64(0.732) = 0.468 \text{ kips/ft/beam}$

$$\Delta_{LL} = \frac{5wL^4}{384E_cI_c} = \frac{5 \left(\frac{0.468}{12} \right) (120 \times 12)^4}{(384)(4,888)(1,100,320)} = 0.41 \text{ in } \downarrow$$

Deflection due to Design Truck Load and Impact

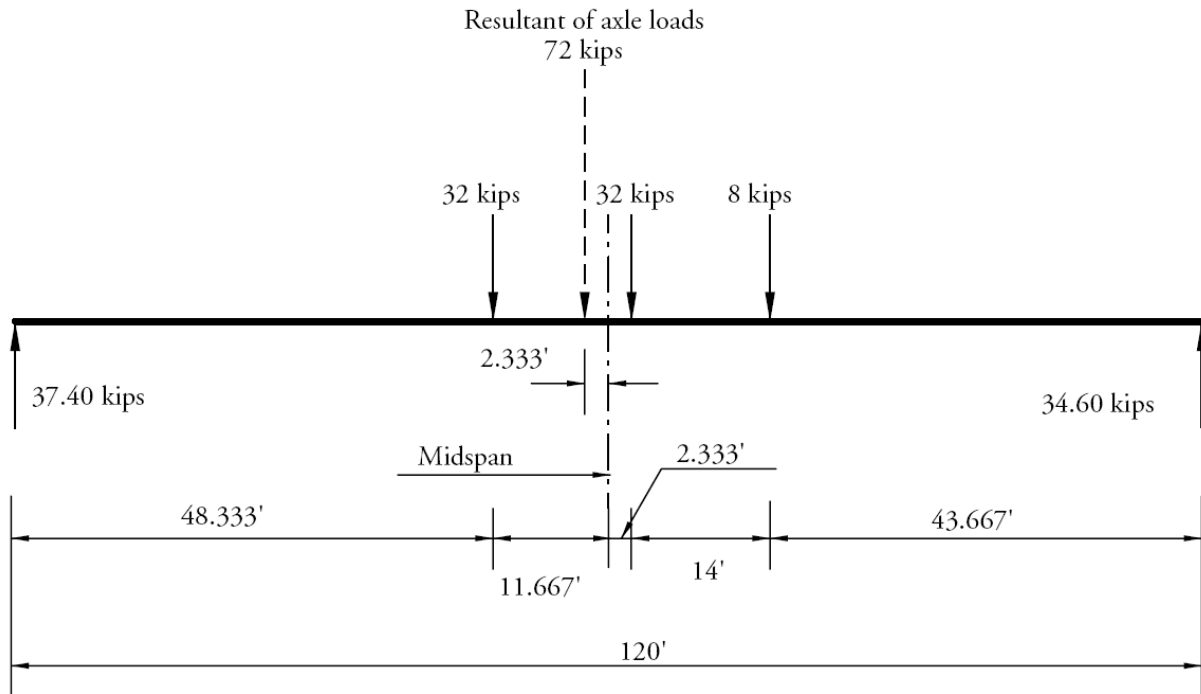
BULB-TEE (BT-72), SINGLE SPAN, COMPOSITE DECK

9.1a.15.6 Deflection Due to Live Load and Impact

To obtain maximum moment and deflection at midspan due to the truck load, let the centerline of the beam coincide with the middle point of the distance between the inner 32-kip axle and the resultant of the truck load, as shown in **Figure 9.1a.15.6-1**.

Figure 9.1a.15.6-1

Design Truck Axle Load Position for Maximum Bending Moment



Using the elastic moment area or influence lines, deflection at midspan is:

$$\Delta_{LT} = (0.803)(IM)(DFM) = (0.803)(1.33)(0.732) = 0.78 \text{ in. } \downarrow$$

Therefore, live load deflection is the greater of:

$$\Delta_{LT} = 0.78 \text{ in. (Controls)}$$

$$0.25\Delta_{LT} + \Delta_{LL} = 0.25(0.78) + 0.41 = 0.61 \text{ in.}$$

Therefore, live load deflection = 0.78 in. < allowable deflection = 1.8 in.

This page intentionally left blank

BULB-TEE (BT-72), SINGLE SPAN, COMPOSITE DECK

Gross Sections, Shear Appendix B5, Refined Losses

Table of Contents

9.1b.1 INTRODUCTION 9.1b - 3

9.1b.2 MATERIALS 9.1b - 3

9.1b.3 CROSS-SECTION PROPERTIES FOR A TYPICAL INTERIOR BEAM 9.1b - 3

9.1b.4 SHEAR FORCES AND BENDING MOMENTS 9.1b - 3

9.1b.5 ESTIMATE REQUIRED PRESTRESS 9.1b - 3

9.1b.6 PRESTRESS LOSSES 9.1b - 4

 9.1b.6.1 Elastic Shortening 9.1b - 4

 9.1b.6.2 Time-Dependent Losses between Transfer and Deck Placement 9.1b - 5

 9.1b.6.2.1 Shrinkage of Concrete 9.1b - 5

 9.1b.6.2.2 Creep of Concrete 9.1b - 7

 9.1b.6.2.3 Relaxation of Prestressing Strands 9.1b - 7

 9.1b.6.3 Time-Dependent Losses between Deck Placement and Final Time 9.1b - 7

 9.1b.6.3.1 Shrinkage of Concrete 9.1b - 7

 9.1b.6.3.2 Creep of Concrete 9.1b - 8

 9.1b.6.3.3 Relaxation of Prestressing Strands 9.1b - 8

 9.1b.6.3.4 Shrinkage of Deck Concrete 9.1b - 9

 9.1b.6.4 Total Time-Dependent Loss 9.1b - 9

 9.1b.6.5 Total Losses at Transfer 9.1b - 10

 9.1b.6.6 Total Losses at Service Loads 9.1b - 10

9.1b.7 CONCRETE STRESSES AT TRANSFER 9.1b - 10

 9.1b.7.1 Stress Limits for Concrete 9.1b - 10

 9.1b.7.2 Stresses at Transfer Length Section 9.1b - 11

 9.1b.7.3 Stresses at Harp Points 9.1b - 13

 9.1b.7.4 Stresses at Midspan 9.1b - 13

 9.1b.7.5 Hold-Down Forces 9.1b - 14

 9.1b.7.6 Summary of Stresses at Transfer 9.1b - 14

9.1b.8 CONCRETE STRESSES AT SERVICE LOADS 9.1b - 14

 9.1b.8.1 Stress Limits for Concrete 9.1b - 14

 9.1b.8.2 Stresses at Midspan 9.1b - 15

 9.1b.8.2.1 Concrete Stress at Top Fiber of the Beam 9.1b - 15

 9.1b.8.2.2 Concrete Stress at the Top Fiber of the Deck 9.1b - 15

 9.1b.8.2.3 Concrete Stress in Bottom of Beam, Load Combination Service III 9.1b - 15

 9.1b.8.3 Fatigue Stress Limit 9.1b - 15

 9.1b.8.4 Summary of Stresses at Midspan at Service Loads 9.1b - 16

 9.1b.8.5 Effect of Deck Shrinkage 9.1b - 16

9.1b.9 STRENGTH LIMIT STATE 9.1b - 16

9.1b.10 LIMITS OF REINFORCEMENT 9.1b - 16

 9.1b.10.1 Maximum Reinforcement 9.1b - 16

 9.1b.10.2 Minimum Reinforcement 9.1b - 16

BULB-TEE (BT-72), SINGLE SPAN, COMPOSITE DECK

Gross Sections, Shear Appendix B5, Refined Losses

Table of Contents

9.1b.11 SHEAR DESIGN9.1b - 17

 9.1b.11.1 Critical Section9.1b - 18

 9.1b.11.2 Contribution of Concrete to Nominal Shear Resistance9.1b - 18

 9.1b.11.2.1 Strain in Flexural Tension Reinforcement.....9.1b - 18

 9.1b.11.2.1.1 Calculation for Negative Strain.....**9.1b - 19**

 9.1b.11.2.1.2 Compute Shear Stress.....**9.1b - 20**

 9.1b.11.2.2 Values of β and θ 9.1b - 20

 9.1b.11.2.3 Compute Concrete Contribution9.1b - 20

 9.1b.11.3 Contribution of Reinforcement to Nominal Shear Resistance9.1b - 20

 9.1b.11.3.1 Requirement for Reinforcement.....9.1b - 20

 9.1b.11.3.2 Required Area of Reinforcement9.1b - 20

 9.1b.11.3.3 Determine Spacing of Reinforcement.....9.1b - 21

 9.1b.11.3.4 Minimum Reinforcement Requirement.....9.1b - 21

 9.1b.11.4 Maximum Nominal Shear Resistance.....9.1b - 21

9.1b.12 INTERFACE SHEAR TRANSFER9.1b - 22

9.1b.13 MINIMUM LONGITUDINAL REINFORCEMENT REQUIREMENT9.1b - 22

 9.1b.13.1 Required Reinforcement at Face of Bearing9.1b - 22

9.1b.14 PRETENSIONED ANCHORAGE ZONE9.1b - 23

9.1b.15 DEFLECTION AND CAMBER9.1b - 23

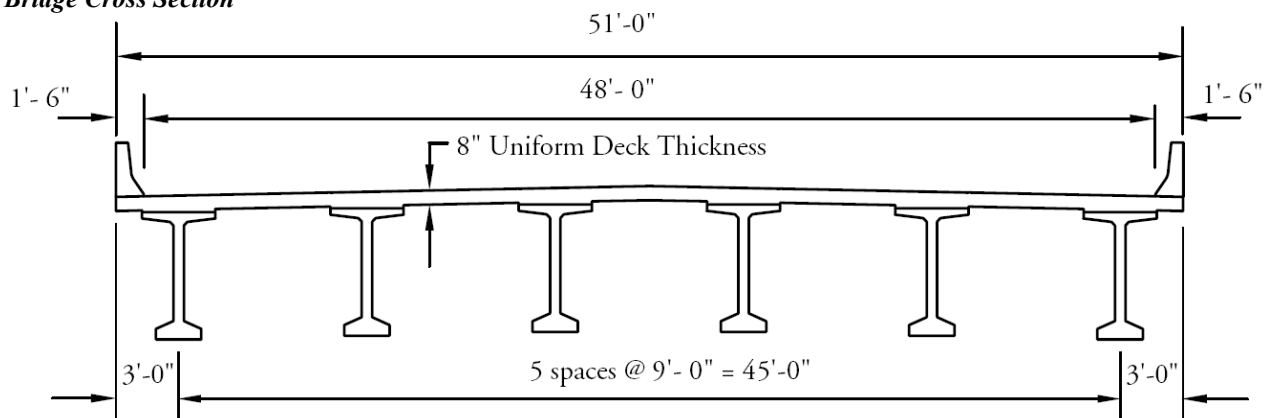
BULB-TEE (BT-72), SINGLE SPAN, COMPOSITE DECK

9.1b.1 Introduction/9.1b.5 Estimate Required Prestress

9.1b Gross Sections, Shear Appendix B5, Refined Losses**9.1b.1 INTRODUCTION**

This design example demonstrates the design of a 120-ft, single span, AASHTO-PCI bulb-tee beam bridge with no skew. This example illustrates in detail the design of a typical interior beam at the critical sections in positive flexure, shear, and deflection due to prestress, dead loads, and live load. The superstructure consists of six beams spaced at 9 ft 0 in. centers, as shown in **Figure 9.1b.1-1**. Beams are designed to act compositely with the 8-in.-thick cast-in-place concrete deck to resist all superimposed dead loads, live loads, and impact. A ½-in.-thick wearing surface is considered to be an integral part of the 8-in.-thick deck. Design live load is HL-93. The design is accomplished in accordance with the *AASHTO LRFD Bridge Design Specifications*, Fifth Edition, 2010, and the 2011 Interim Revisions. Elastic stresses from external loads are calculated using gross sections. Shear strength is calculated using the general procedure of Appendix B5 of the *LRFD Specifications*. Time-dependent prestress losses are calculated using the refined estimates.

Figure 9.1b.1-1
Bridge Cross Section

**9.1b.2 MATERIALS**

See Section 9.1a.2.

9.1b.3 CROSS-SECTION PROPERTIES FOR A TYPICAL INTERIOR BEAM

See Section 9.1a.3.

9.1b.4 SHEAR FORCES AND BENDING MOMENTS

See Section 9.1a.4.

9.1b.5 ESTIMATE REQUIRED PRESTRESS

See Section 9.1a.5.

BULB-TEE (BT-72), SINGLE SPAN, COMPOSITE DECK

9.1b.5 Estimate Required Prestress/9.1b.6.1 Elastic Shortening

For convenience, the section properties are shown in **Table 9.1b.5-1**.

Table 9.1b.5-1.
Summary of Section Properties at Transfer and at Final Time

Property	Noncomposite Gross		Composite Gross at Final	
Area, in ²	A_g	767	A_c	1,418.9
Total Depth, in.	h	72.00	h_c	80.00
Moment of Inertia, in. ⁴	I_g	545,894	I_c	1,100,320
Centroid of Section to Centroid of Prestress, in.	e_{pg}	29.68	e_{pc}	47.85
Centroid to Bottom Fiber of Beam, in.	y_b	36.60	y_{bc}	54.77
Centroid of Section to Top Fiber of Beam, in.	y_t	35.40	y_{tg}	17.23
Centroid of Section to Top Fiber of Deck, in.			y_{tc}	25.23
Centroid of Section to Centroid of Deck, in.			e_d	21.48
Section Modulus for Beam Bottom Fiber, in. ³	S_b	14,915	S_{bc}	20,090
Section Modulus for Beam Top Fiber, in. ³	S_t	15,421	S_{tg}	63,861
Section Modulus for Deck Top Fiber, in. ³			S_{tc}	55,592

9.1b.6 PRESTRESS LOSSES

Total prestress loss:

$$\Delta f_{pT} = \Delta f_{pES} + \Delta f_{pLT} \quad \text{[LRFD Eq. 5.9.5.1-1]}$$

where

- Δf_{pT} = total loss in prestressing steel stress
- Δf_{pES} = sum of all losses or gains due to elastic shortening or extension at the time of application of prestress and/or external loads
- Δf_{pLT} = long-term losses due to shrinkage and creep of concrete, and relaxation of steel after transfer. In this design example, the refined estimates of time-dependent losses are used.

9.1b.6.1 Elastic Shortening

$$\Delta f_{pES} = \frac{E_p}{E_{ci}} f_{cgp} \quad \text{[LRFD Eq. 5.9.5.2.3a-1]}$$

where

- E_p = modulus of elasticity of prestressing reinforcement = 28,500 ksi
- E_{ci} = modulus of elasticity of beam concrete at transfer = 4,617 ksi
- f_{cgp} = sum of concrete stresses at the center of gravity of prestressing tendons due to prestressing force at transfer and the self weight of the member at sections of maximum moment.

Common practice is to assume the initial losses are a percentage of the prestressing stress before transfer, f_{pi} . Calculated losses are compared with the assumed initial losses and if different from the assumed value, a second iteration should be carried out. In this example, 9% f_{pi} initial loss is assumed.

BULB-TEE (BT-72), SINGLE SPAN, COMPOSITE DECK

9.1b.6.1 Elastic Shortening/9.1b.6.2.1 Shrinkage of Concrete

Force per strand after transfer = (area of strand)(prestress stress after transfer)

$$= (0.153)(202.5)(1 - 0.09) = 28.19 \text{ kips}$$

$$f_{cgp} = \frac{P_{pt}}{A_g} + \frac{P_{pt}e_c^2}{I_g} - \frac{M_g e_c}{I_g}$$

where

e_c = eccentricity of prestressing strands at midspan

P_{pt} = total prestressing force after transfer = (48 strands)(28.19) = 1,353.1 kips

M_g should be calculated based on the overall beam length of 121 ft. Since the elastic shortening loss is a part of the total loss, f_{cgp} will be conservatively computed based on M_g using the design span length of 120 ft.

$$f_{cgp} = \frac{1,353.1}{767} + \frac{(1,353.1)(29.68)^2}{545,894} - \frac{[(1,438.2)(12)](29.68)}{545,894}$$

$$= 1.764 + 2.183 - 0.938 = 3.009 \text{ ksi}$$

Therefore, loss due to elastic shortening:

$$\Delta f_{pES} = \frac{28,500}{4,617} (3.009) = 18.6 \text{ ksi}$$

$$\text{Percent actual loss due to elastic shortening } \square = \frac{18.6}{202.5} (100) = 9.2\%$$

Since the calculated loss of 9.2% is approximately equal to the initial loss assumption of 9%, a second iteration is not necessary.

9.1b.6.2 Time-Dependent Losses between Transfer and Deck Placement

The following construction schedule is assumed in calculating the time-dependent losses:

Concrete age at transfer: $t_i = 1$ day

Concrete age at deck placement: $t_d = 90$ days

Concrete age at final stage: $t_f = 20,000$ days

The total time-dependent loss between time of transfer and deck placement is the summation of prestress losses due to shrinkage of concrete, creep of concrete, and relaxation of prestressing strands.

9.1b.6.2.1 Shrinkage of Concrete

The prestress loss due to shrinkage of concrete between time of transfer and deck placement is calculated by:

$$\Delta f_{pSR} = \varepsilon_{bid} E_p K_{id} \quad [\text{LRFD Eq. 5.9.5.4.2a-1}]$$

where

ε_{bid} = concrete shrinkage strain of girder for time period between transfer and deck placement

E_p = modulus of elasticity of prestressing strands, ksi

K_{id} = transformed section coefficient that accounts for time-dependent interaction between concrete and bonded steel in the section being considered for time period between transfer and deck placement

The concrete shrinkage strain ε_{bid} is taken as:

$$\varepsilon_{bid} = k_{vs} k_{ns} k_f k_{td} 0.48 \times 10^{-3} \quad [\text{LRFD Eq. 5.4.2.3.3-1}]$$

BULB-TEE (BT-72), SINGLE SPAN, COMPOSITE DECK

9.1b.6.2.1 Shrinkage of Concrete

where

The factor for the effect of the volume-to-surface ratio of the beam:

$$k_{vs} = 1.45 - 0.13(V/S) = 1.45 - 0.13 \times 3.01 = 1.059$$

The minimum value of k_{vs} is 1.0 OK

V/S is the volume-to-surface ratio of the beam in **Table 2.5.7.1-1**.

The humidity factor for shrinkage:

$$k_{hs} = 2.00 - 0.014H = 2.00 - 0.014(70) = 1.020$$

where H = average annual mean relative humidity (assume 70%)

The factor for the effect of concrete strength:

$$k_f = \frac{5}{1 + f'_{ci}} = \frac{5}{1 + 5.8} = 0.735$$

The time development factor at deck placement:

$$k_{td} = \frac{t}{61 - 4f'_{ci} + t} = \frac{89}{61 - 4(5.8) + 89} = 0.702 = k_{tda}$$

where t is the maturity of concrete (days) = $t_d - t_i = 90 - 1 = 89$ days

$$\epsilon_{bid} = (1.059)(1.020)(0.735)(0.702)(0.48 \times 10^{-3}) = 0.000268$$

$$K_{id} = \frac{1}{1 + \frac{E_p}{E_{ci}} \frac{A_{ps}}{A_g} \left(1 + \frac{A_g(e_{pg})^2}{I_g}\right) [1 + 0.7\Psi_b(t_f, t_i)]} \quad \text{[LRFD Eq. 5.9.5.4.2a-2]}$$

where

e_{pg} = eccentricity of prestressing strand with respect to centroid of girder, in.

$\Psi_b(t_f, t_i)$ = girder creep coefficient at final time due to loading introduced at transfer

For the time between transfer and final time:

$$\Psi_b(t_f, t_i) = 1.9k_{vs}k_{hc}k_fk_{td}t_i^{-0.118} \quad \text{[LRFD Eq. 5.4.2.3.2-1]}$$

$$k_{hc} = 1.56 - 0.008H = 1.56 - 0.008(70) = 1.000$$

$$k_{td} = \frac{t}{61 - 4f'_{ci} + t} = \frac{20,000 - 1}{61 - 4(5.8) + (20,000 - 1)} = 0.998 = k_{tdf}$$

$$\begin{aligned} \Psi_b(t_f, t_i) &= 1.9(1.059)(1.000)(0.735)(0.998)(1)^{-0.118} \\ &= 1.476 \end{aligned}$$

$$K_{id} = \frac{1}{1 + \frac{28,500}{4,617} \frac{7,344}{767} \left(1 + \frac{767(29.68)^2}{545,894}\right) [1 + 0.7(1.476)]} = 0.788$$

The prestress loss due to shrinkage of concrete between transfer and deck placement is:

$$\Delta f_{psR} = (0.000268)(28,500)(0.788) = 6.019 \text{ ksi}$$

BULB-TEE (BT-72), SINGLE SPAN, COMPOSITE DECK

9.1b.6.2.2 Creep of Concrete/9.1b.6.3.1 Shrinkage of Concrete

9.1b.6.2.2 Creep of Concrete

The prestress loss due to creep of girder concrete between time of transfer and deck placement is determined as:

$$\Delta f_{pCR} = \frac{E_p}{E_{ci}} f_{cgp} \Psi_b(t_d, t_i) K_{id} \quad [\text{LRFD Eq. 5.9.5.4.2b-1}]$$

where

$$\begin{aligned} \Psi_b(t_d, t_i) &= \text{girder creep coefficient at time of deck placement due to loading introduced at transfer} \\ &= 1.9k_{vs}k_{hc}k_f k_{td} t_i^{-0.118} \quad [\text{LRFD Eq. 5.4.2.3.2-1}] \\ &= 1.9(1.059)(1.000)(0.735)(0.702)(1)^{-0.118} = 1.038 \end{aligned}$$

$$\Delta f_{pCR} = \frac{28,500}{4,617} (3.009)(1.038)(0.788) = 15.193 \text{ ksi}$$

9.1b.6.2.3 Relaxation of Prestressing Strands

The prestress loss due to relaxation of prestressing strands between time of transfer and deck placement is determined as:

$$\Delta f_{pR1} = \frac{f_{pt}}{K_L} \left(\frac{f_{pt}}{f_{py}} - 0.55 \right) \quad [\text{LRFD Eq. 5.9.5.4.2c-1}]$$

where

$$\begin{aligned} f_{pt} &= \text{stress in prestressing strands immediately after transfer, taken not less than } 0.55f_y \\ K_L &= 30 \text{ for low relaxation strands and } 7 \text{ for other prestressing steel, unless more accurate} \\ &\quad \text{manufacturer's data are available} \end{aligned}$$

$$\Delta f_{pR1} = \frac{(202.5 - 18.6)}{30} \left(\frac{(202.5 - 18.6)}{243} - 0.55 \right) = 1.268 \text{ ksi}$$

According to LRFD Art. 5.9.5.4.2c, the relaxation loss may also be assumed equal to 1.2 ksi for low-relaxation strands.

9.1b.6.3 Time-Dependent Losses between Deck Placement and Final Time

The total time-dependent loss between time of deck placement and final time is the summation of prestress losses due to shrinkage of beam concrete, creep of beam concrete, relaxation of prestressing strands, and shrinkage of deck concrete.

9.1b.6.3.1 Shrinkage of Concrete

The prestress loss due to shrinkage of concrete between time of deck placement and final time is calculated by:

$$\Delta f_{pSD} = \varepsilon_{bdf} E_p K_{df} \quad [\text{LRFD Eq. 5.9.5.4.2a-1}]$$

where

$$\begin{aligned} \varepsilon_{bdf} &= \text{concrete shrinkage strain of girder for time period between deck placement and final time} \\ E_p &= \text{modulus of elasticity of prestressing strands, ksi} \\ K_{df} &= \text{transformed section coefficient that accounts for time-dependent interaction between concrete and} \\ &\quad \text{bonded steel in the section being considered for time period between deck placement and final time} \end{aligned}$$

The total girder concrete shrinkage strain between transfer and final time is taken as:

$$\begin{aligned} \varepsilon_{bif} &= k_{vs} k_{hs} k_f k_{td} 0.48 \times 10^{-3} \quad [\text{LRFD Eq. 5.4.2.3.3-1}] \\ &= (1.059)(1.020)(0.735)(0.998)(0.48 \times 10^{-3}) = 0.000380 \end{aligned}$$

The girder concrete shrinkage strain between deck placement and final time is:

$$\varepsilon_{bdf} = \varepsilon_{bif} - \varepsilon_{bid} = 0.000380 - 0.000268 = 0.000112$$

BULB-TEE (BT-72), SINGLE SPAN, COMPOSITE DECK

9.1b.6.3.1 Shrinkage of Concrete / 9.1b.6.3.3 Relaxation of Prestressing Strands

The beam concrete transformed section coefficient between deck placement and final time is:

$$K_{df} = \frac{1}{1 + \frac{E_p A_{ps}}{E_{ci} A_c} (1 + [1 + 0.7\Psi_b(t_f, t_i)])} \quad [\text{LRFD Eq. 5.9.5.4.3a-2}]$$

where

$$\begin{aligned} A_c &= \text{area of the composite section} = 1,418.9 \text{ in.}^2 \\ I_c &= \text{moment of inertia of the composite section} = 1,100,320 \text{ in.}^4 \\ e_{pc} &= \text{eccentricity of strands with respect to centroid of composite section} \\ &= 54.77 - 6.92 = 47.85 \text{ in.} \end{aligned}$$

$$K_{df} = \frac{1}{1 + \frac{28,500}{4,617} \frac{7.344}{1,418.9} \left(1 + \frac{1,418.9(47.85)^2}{1,100,320}\right) [1 + 0.7(1.476)]} = 0.796$$

The prestress loss due to shrinkage of concrete between deck placement and final time is:

$$\Delta f_{pSD} = (0.000112)(28,500)(0.796) = 2.541 \text{ ksi}$$

9.1b.6.3.2 Creep of Concrete

The prestress loss due to creep of beam concrete between time of deck placement and final time is determined as:

$$\Delta f_{pCD} = \frac{E_p}{E_{ci}} f_{cgp} [\Psi_b(t_f, t_i) - \Psi_b(t_d, t_i)] K_{df} + \frac{E_p}{E_c} \Delta f_{cd} \Psi_b(t_f, t_d) K_{df} \quad [\text{LRFD Eq. 5.9.5.4.3b-1}]$$

where

$$\begin{aligned} \Psi_b(t_f, t_d) &= \text{girder creep coefficient at final time due to loading at deck placement} \\ &= 1.9k_{vs}k_{hc}k_fk_{td}t_d^{-0.118} \quad [\text{LRFD Eq. 5.4.2.3.2-1}] \end{aligned}$$

$$k_{tdf} = \frac{t}{61 - 4f'_{ci} + t} = \frac{(20,000 - 90)}{61 - 4(5.8) + (20,000 - 90)} = 0.998$$

$$\Psi_b(t_f, t_d) = 1.9(1.059)(1.000)(0.735)(0.998)(90)^{-0.118} = 0.868$$

Δf_{cd} = change in concrete stress at centroid of prestressing strands due to long-term losses between transfer and deck placement, combined with deck weight and superimposed loads, ksi

$$\begin{aligned} &= -(\Delta f_{pSR} + \Delta f_{pCR} + \Delta f_{pR1}) \frac{A_{ps}}{A_g} \left(1 + \frac{A_g e_{pg}^2}{I_g}\right) - \left(\frac{M_s e_{pg}}{I_g} + \frac{(M_b + M_{ws}) e_{pc}}{I_c}\right) \\ &= -(6.019 + 15.193 + 1.268) \frac{7.344}{767} \left(1 + \frac{767(29.68)^2}{545,894}\right) \\ &\quad - \left(\frac{1,659.6(12)(29.68)}{545,894} + \frac{(180 + 360)(12)(47.85)}{1,100,320}\right) \\ &= -1.846 \text{ ksi} \end{aligned}$$

$$\Delta f_{pCD} = \frac{28,500}{4,617} (3.009)(1.476 - 1.038)(0.796) + \frac{28,500}{4,888} (-1.846)(0.868)(0.796)$$

= -0.961 ksi The negative sign indicates a prestressing gain.

9.1b.6.3.3 Relaxation of Prestressing Strands

The prestress loss due to relaxation of prestressing strands in composite section between time of deck placement and final time is taken as:

$$\Delta f_{pR2} = \Delta f_{pR1} = 1.268 \text{ ksi} \quad [\text{LRFD Eq. 5.9.5.4.3c-1}]$$

BULB-TEE (BT-72), SINGLE SPAN, COMPOSITE DECK

9.1b.6.3.4 Shrinkage of Deck Concrete/9.1b.6.4 Total Time-Dependent Loss

9.1b.6.3.4 Shrinkage of Deck Concrete

The prestress gain due to shrinkage of deck concrete is calculated by:

$$\Delta f_{pSS} = \frac{E_p}{E_c} \Delta f_{cdf} K_{df} [1 + 0.7 \Psi_b(t_f, t_d)] \quad [\text{LRFD Eq. 5.9.5.4.3d-1}]$$

Where Δf_{cdf} = change in concrete stress at centroid of prestressing strands due to shrinkage of deck concrete (ksi)

$$\Delta f_{cdf} = \frac{\epsilon_{ddf} A_d E_{cd}}{1 + 0.7 \Psi_d(t_f, t_d)} \left(\frac{1}{A_c} - \frac{e_{pc} e_d}{I_c} \right) \quad [\text{LRFD Eq. 5.9.5.4.3d-2}]$$

where

ϵ_{ddf} = shrinkage strain of deck concrete between placement and final time by LRFD Eq. 5.4.2.3.3-1

A_d = area of deck concrete, in.²

E_{cd} = modulus of elasticity of deck concrete, ksi

$\Psi_d(t_f, t_d)$ = deck concrete creep coefficient at final time due to loading introduced shortly after deck placement

e_d = eccentricity of deck with respect to the gross composite section, in.

Assume the initial strength of concrete at deck placement is 0.8(4.0 ksi) = 3.2 ksi, and use a volume-to-surface (V/S) ratio of 3.582 for the deck:

$$k_{vs} = 1.45 - 0.13(V/S) = 1.45 - 0.13(3.582) = 0.984 < 1.0$$

$$\text{Use } k_{vs} = 1.000$$

$$k_f = \frac{5}{1 + f'_{ci}} = \frac{5}{1 + 3.2} = 1.190$$

$$k_{td} = \frac{t}{61 - 4f'_{ci} + t} = \frac{20,000 - 90}{61 - 4(3.2) + (20,000 - 90)} = 0.998$$

$$\epsilon_{ddf} = k_{vs} k_{hs} k_f k_{td} 0.48 \times 10^{-3} \quad [\text{LRFD Eq. 5.4.2.3.3-1}]$$

$$= (1.000)(1.020)(1.190)(0.998)(0.48 \times 10^{-3}) = 0.000581$$

$$\Psi_d(t_f, t_d) = 1.9 k_{vs} k_{hc} k_f k_{td} t_i^{-0.118} \quad [\text{LRFD Eq. 5.4.2.3.2-1}]$$

$$= 1.9(1.000)(1.000)(1.190)(0.998)(1)^{-0.118} = 2.256$$

Creep of the deck concrete is assumed to start at 1 day.

$$\Delta f_{cdf} = \frac{0.000581(108)(7.5)(3,834)}{1 + 0.7(2.256)} \left(\frac{1}{1418.9} - \frac{47.85(80 - 7.5/2 - 54.77)}{1,100,320} \right)$$

$$= -0.160 \text{ ksi} \quad \text{The negative sign indicates a prestressing gain.}$$

The prestress gain due to shrinkage of the deck in the composite section:

$$\Delta f_{pSS} = \frac{28,500}{4,888} (0.160)(0.796)[1 + 0.7(0.868)] = 1.194 \text{ ksi}$$

Note: The effect of deck shrinkage on the calculation of prestress gain is discussed further in Section 9.1a.8.5.

9.1b.6.4 Total Time-Dependent Loss

The total time-dependent loss, Δf_{pLT} , is determined as:

$$\begin{aligned} \Delta f_{pLT} &= (\Delta f_{pSR} + \Delta f_{pCR} + \Delta f_{pR1}) + (\Delta f_{pSD} + \Delta f_{pCD} + \Delta f_{pR2} - \Delta f_{pSS}) \quad [\text{LRFD Eq. 5.9.5.4.1-1}] \\ &= (6.019 + 15.193 + 1.268) + (2.541 - 0.961 + 1.268 - 1.194) \\ &= 22.480 + 1.654 = 24.1 \text{ ksi} \end{aligned}$$

BULB-TEE (BT-72), SINGLE SPAN, COMPOSITE DECK

9.1b.6.5 Total Losses at Transfer/9.1b.7.1 Stress Limits for Concrete

9.1b.6.5 Total Losses at Transfer

$$\Delta f_{pi} = \Delta f_{pES} = 18.6 \text{ ksi}$$

Effective stress in tendons immediately after transfer, $f_{pt} = f_{pi} - \Delta f_{pi} = (202.5 - 18.6) = 183.9 \text{ ksi}$

$$\text{Force per strand} = (f_{pt})(\text{area of strand}) = 183.9(0.153) = 28.14 \text{ kips}$$

Therefore, the total prestressing force after transfer, $P_{pt} = 28.14(48) = 1,351 \text{ kips}$

$$\text{Initial loss, \%} = (\text{Total losses at transfer})/(f_{pi}) = 18.6/(202.5) = 9.2\%$$

The first estimation of loss at transfer, 9%, is very close to the actual computed initial loss of 9.2%. Thus, there is no need to perform a second iteration to refine the initial losses.

9.1b.6.6 Total Losses at Service Loads

Total loss due to elastic shortening at transfer and long-term losses is:

$$\Delta f_{pT} = \Delta f_{pES} + \Delta f_{pLT} = 18.6 + 24.1 = 42.7 \text{ ksi}$$

The elastic gain due to deck weight, superimposed dead load, and live load (Service III) is:

$$\begin{aligned} & \left(\frac{M_s e_{pg}}{I_g} + \frac{(M_b + M_{ws}) e_{pc}}{I_c} \right) \frac{E_p}{E_c} + 0.8 \left(\frac{(M_{LT} + M_{LL}) e_{tc}}{I_{tc}} \right) \frac{E_p}{E_c} \\ &= \left(\frac{1,659.6(12)(29.68)}{545,894} + \frac{(180 + 360)(12)(47.85)}{1,100,320} \right) \frac{28,500}{4,888} + 0.8 \left(\frac{(1830.2 + 843.3)(12)(46.68)}{1,100,320} \right) \frac{28,500}{4,888} \\ &= 8.0 + 6.3 = 14.3 \text{ ksi} \end{aligned}$$

The effective stress in strands after all losses and gains:

$$f_{pe} = f_{pi} - \Delta f_{pT} + 8.0 = 202.5 - 42.7 + 14.3 = 174.1 \text{ ksi}$$

Check prestressing stress limit at service limit state:

[LRFD Table 5.9.3-1]

$$f_{pe} \leq 0.8f_{py} = 0.8(243) = 194.4 \text{ ksi} > 174.1 \text{ ksi} \quad \text{OK}$$

The effective stress in strands after all losses and permanent gains:

$$f_{pe} = f_{pi} - \Delta f_{pT} + 8.0 = 202.5 - 42.7 + 8.0 = 167.8 \text{ ksi}$$

Force per strand without live load gains = $(f_{pe})(\text{area of strand}) = 167.8 (0.153) = 25.67 \text{ kips}$

Therefore, the total prestressing force after all losses = $25.67(48) = 1,232 \text{ kips}$

$$\text{Final loss percentage} = (\text{total losses and gains})/(f_{pi}) = (202.5 - 167.8)/(202.5) = 17.1\%$$

Without consideration of prestressing gains at deck placement, the final loss percentage = $\text{total losses}/(f_{pi}) = (42.7)/(202.5) = 21.1\%$

9.1b.7 CONCRETE STRESSES AT TRANSFER

Because the gross section is used, the total prestressing force after transfer, $P_{pt} = 1,351 \text{ kips}$

9.1b.7.1 Stress Limits for Concrete

[LRFD Art. 5.9.4]

Compression:

$$\bullet 0.6f'_{ci} = 0.6(5.8) = +3.480 \text{ ksi}$$

where f'_{ci} = concrete strength at transfer = 5.800 ksi

Tension:

• without bonded auxiliary reinforcement

$$-0.0948\sqrt{f'_{ci}} \leq 0.200 \text{ ksi}; \quad -0.0948\sqrt{5.800} = -0.228 \text{ ksi}$$

Therefore, -0.200 ksi (Controls)

BULB-TEE (BT-72), SINGLE SPAN, COMPOSITE DECK**9.1b.7.1 Stress Limits for Concrete/9.1b.7.2 Stresses at Transfer Length Section**

- with bonded auxiliary reinforcement that is sufficient to resist 120% of the tension force in the cracked concrete

$$-0.24\sqrt{f'_{ci}} = -0.24\sqrt{5.800} = -0.578 \text{ ksi}$$

9.1b.7.2 Stresses at Transfer Length Section

Stresses at this location need only be checked at transfer since this stage almost always governs. Also, losses with time will reduce the concrete stresses making them less critical.

$$\text{Transfer length} = 60(\text{strand diameter}) = 60(0.5) = 30 \text{ in.} = 2.5 \text{ ft} \quad [\text{LRFD Art. 5.11.4}]$$

Due to camber of the beam at release, the beam self weight acts on the overall beam length, 121 ft. Therefore, values for bending moment given in **Table 9.1a.4-1** cannot be used because they are based on the design span of 120 ft. Using statics, bending moment at transfer length due to beam self weight is:

$$M_g = 0.5w_gx(L - x) = (0.5)(0.799)(2.5)(121 - 2.5) = 118.4 \text{ ft-kips}$$

Compute stress in the top of beam:

$$f_t = \frac{P_{pt}}{A_g} - \frac{P_{pt}e_{pg}}{S_t} + \frac{M_g}{S_t} = \frac{1,351}{767} - \frac{(1,351)(29.68)}{15,421} + \frac{(118.4)(12)}{15,421}$$

$$= 1.761 - 2.600 + 0.092 = -0.747 \text{ ksi}$$

Tensile stress limit for concrete with bonded reinforcement: -0.578 ksi NG

Compute stress in the bottom of beam:

$$f_b = \frac{P_{pt}}{A_g} + \frac{P_{pt}e_{pg}}{S_b} - \frac{M_g}{S_b} = \frac{1,351}{767} + \frac{(1,351)(29.68)}{14,915} - \frac{(118.4)(12)}{14,915}$$

$$= 1.761 + 2.688 - 0.095 = 4.354 \text{ ksi}$$

Compressive stress limit for concrete: $+3.480 \text{ ksi}$ NG

Since stresses at the top and bottom exceed the stress limits, harp strands to satisfy the specified limits. Harp 12 strands at the $0.4L$ points, as shown in **Figures 9.1b.7.2-1** and **9.1b.7.2-2**.

BULB-TEE (BT-72), SINGLE SPAN, COMPOSITE DECK

9.1b.7.2 Stresses at Transfer Length Section

Figure 9.1b.7.2-1
Strand Pattern

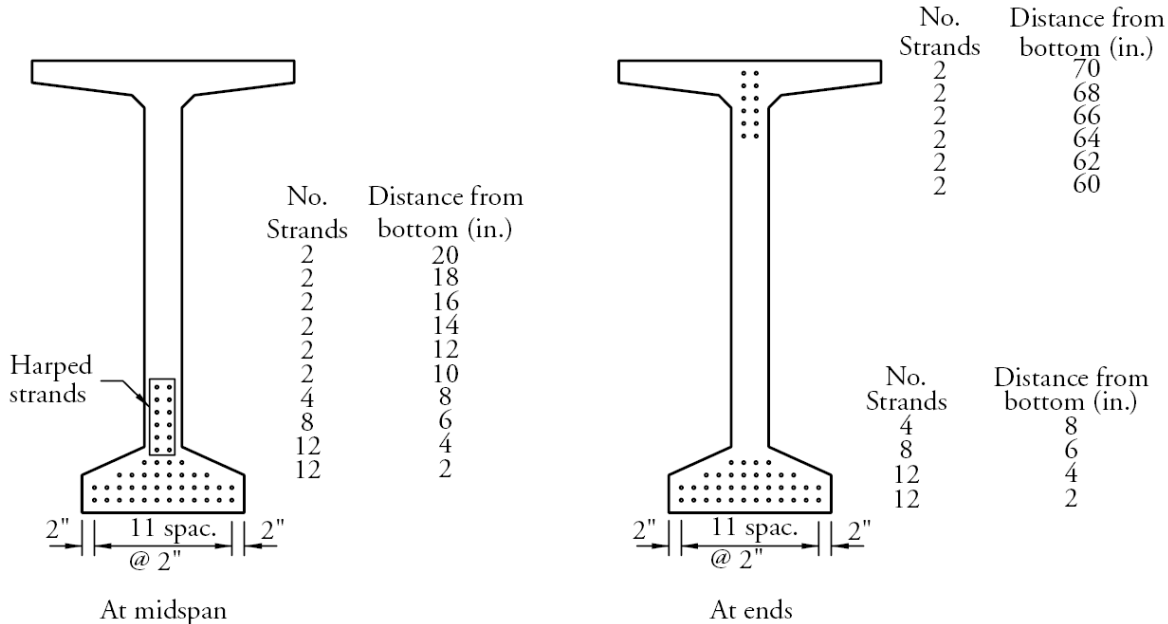
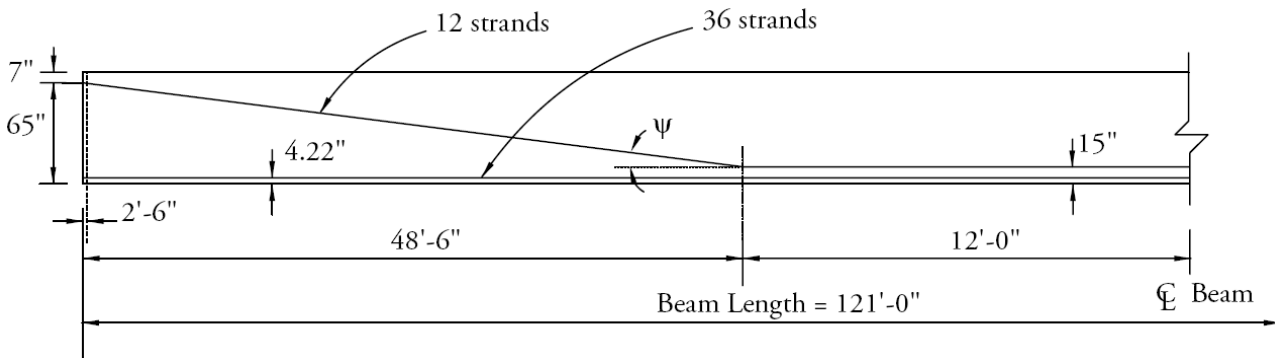


Figure 9.1b.7.2-2
Longitudinal Strand Profile



Compute the center of gravity of the prestressing strands at the transfer length section using the harped pattern.

The distance between the center of gravity of the 12 harped strands at the end of the beam and the top fiber of the precast beam is:

$$\frac{2(2) + 2(4) + 2(6) + 2(8) + 2(10) + 2(12)}{12} = 7.0 \text{ in.}$$

The distance between the center of gravity of the 12 harped stands at the harp point and the bottom fiber of the beam is:

$$\frac{2(10) + 2(12) + 2(14) + 2(16) + 2(18) + 2(20)}{12} = 15.0 \text{ in.}$$

The distance between the center of gravity of the 12 harped strands and the top fiber of the beam at the transfer length section:

$$7 \text{ in.} + \frac{(72 - 15 - 7) \text{ in.}}{48.5 \text{ ft}} (2.5 \text{ ft}) = 9.58 \text{ in.}$$

BULB-TEE (BT-72), SINGLE SPAN, COMPOSITE DECK

9.1b.7.2 Stresses at Transfer Length Section/9.1b.7.4 Stresses at Midspan

The distance between the center of gravity of the 36 straight bottom strands and the extreme bottom fiber of the beam is:

$$\frac{12(2) + 12(4) + 8(6) + 4(8)}{36} = 4.22 \text{ in.}$$

Therefore, the distance between the center of gravity of the total number of 36 strands and the extreme bottom fiber of the precast beam at transfer length is:

$$\frac{36(4.22) + 12(72 - 9.58)}{48} = 18.77 \text{ in.}$$

The center of gravity of all prestressing strand with respect to the extreme bottom fiber at the end of the beam, y_{bs} , is:

$$\frac{36(4.22) + 12(72 - 7)}{48} = 19.42 \text{ in.}$$

Eccentricity of the 48 strand group at transfer length, e , is: $36.60 - 18.77 = 17.83 \text{ in.}$

Recompute the top and bottom stresses at the transfer length section with harped strands:

Concrete stress in top of beam:

$$f_t = \frac{1,351}{767} - \frac{(1351)(17.83)}{15,421} + \frac{(118.4)(12)}{15,421} = 1.761 - 1.562 + 0.092 = 0.291 \text{ ksi}$$

Compressive stress limit: + 3.480 ksi OK

Concrete stress in bottom of beam:

$$f_b = \frac{1,351}{767} + \frac{(1351)(17.83)}{14,915} - \frac{(118.4)(12)}{14,915} = 1.761 + 1.615 - 0.095 = 3.281 \text{ ksi}$$

Compressive stress limit: + 3.480 ksi OK

9.1b.7.3 Stresses at Harp Points

The strand eccentricity at the harp points is the same as at midspan, $e_{pg} = 29.68 \text{ in.}$

Bending moment at the harp points ($0.4L$) due to the self weight of the beam is:

$$(0.5)(0.799)(48.5)(121 - 48.5) = 1,405 \text{ ft-kips}$$

Therefore, top and bottom stresses are:

Concrete stress in top of beam:

$$f_t = \frac{1,351}{767} - \frac{(1351)(29.68)}{15,421} + \frac{(1,405)(12)}{15,421} = 1.761 - 2.600 + 1.093 = +0.254 \text{ ksi}$$

Compressive stress limit: +3.480 ksi OK

Concrete stress in bottom of beam:

$$f_b = \frac{1,351}{767} + \frac{(1351)(29.68)}{14,915} - \frac{(1,405)(12)}{14,915} = 1.761 + 2.688 - 1.130 = +3.319 \text{ ksi}$$

Compressive stress limit: +3.480 ksi OK

9.1b.7.4 Stresses at Midspan

Bending moment at midspan due to the beam self weight is:

$$M_g = 0.5(0.799)(60.5)(121 - 60.5) = 1,462.3 \text{ ft-kips}$$

$$f_t = \frac{1,351}{767} - \frac{(1351)(29.68)}{15,421} + \frac{(1,462)(12)}{15,421} = 1.761 - 2.600 + 1.138 = +0.299 \text{ ksi}$$

BULB-TEE (BT-72), SINGLE SPAN, COMPOSITE DECK

9.1b.7.4 Stresses at Midspan/9.1b.8.1 Stress Limits for Concrete

Compressive stress limit: +3.480 ksi OK

$$f_b = \frac{1,351}{767} + \frac{(1351)(29.68)}{14,915} - \frac{(1,462)(12)}{14,915} = 1.761 + 2.688 - 1.176 = +3.273 \text{ ksi}$$

Compressive stress limit: + 3.480 ksi OK

9.1b.7.5 Hold-Down Forces

Assume that the stress in the strand at the time of prestressing, before seating losses, is:

$$0.80f_{pu} = 0.80(270) = 216 \text{ ksi}$$

Thus, the prestress force per strand before seating losses is: $0.153(216) = 33.0$ kipsFrom **Figure 9.1b.7.2-2**, the harp angle,

$$\psi = \tan^{-1}\left(\frac{50}{48.5(12)}\right) = 4.91^\circ$$

Therefore, hold-down force/strand = $1.05(\text{force per strand})(\sin \psi)$

$$= 1.05(33.0)\sin 4.91^\circ = 2.97 \text{ kips/strand}$$

Note the factor 1.05 is applied to account for friction.

Total hold-down force = 12 strands(2.97) = 35.6 kips

The hold-down force and the harp angle should be checked against maximum limits for local practices. Refer to Chapter 3, Fabrication and Construction and Chapter 8, Design Theory and Procedures for additional details.

9.1b.7.6 Summary of Stresses at Transfer

	Top Fiber Stresses f_t , ksi	Bottom Fiber Stresses f_b , ksi
At transfer length section	+0.291	+3.281
At harp points	+0.254	+3.319
At midspan	+0.299	+3.273

9.1b.8 CONCRETE STRESSES AT SERVICE LOADSUsing gross sections and refined losses, $P_{pe} = 1,232$ kips**9.1b.8.1 Stress Limits for Concrete**

[LRFD Art. 5.9.4.2]

Compression

Due to permanent loads, (i.e. beam self weight, weight of slab and haunch, weight of future wearing surface, and weight of barriers), for load combination Service I:

$$\text{for precast beams: } 0.45 f'_c = 0.45(6.500) = +2.925 \text{ ksi}$$

$$\text{for deck: } 0.45 f'_c = 0.45(4.000) = +1.800 \text{ ksi}$$

Due to permanent and transient loads (i.e. all dead loads and live loads), for load combination Service I:

$$\text{for precast beam: } 0.60 f'_c = 0.60(6.500) = +3.900 \text{ ksi}$$

$$\text{for deck: } 0.60 f'_c = 0.60(4.000) = +2.400 \text{ ksi}$$

Tension:

For components with bonded prestressing tendons:

$$\text{for load combination Service III: } -0.19\sqrt{f'_c}$$

$$\text{for precast beam: } -0.19\sqrt{6.500} = -0.484 \text{ ksi}$$

BULB-TEE (BT-72), SINGLE SPAN, COMPOSITE DECK

9.1b.8.2 Stresses at Midspan/9.1b.8.3 Fatigue Stress Limit

9.1b.8.2 Stresses at Midspan**9.1b.8.2.1 Concrete Stress at Top Fiber of the Beam**

To check top compressive stresses, two cases are considered:

1. Under permanent loads, load combination Service I:

Using bending moment values given in **Table 9.1a.4-1**, compute the top fiber stresses:

$$f_{tg} = \frac{P_{pe}}{A_g} - \frac{P_{pe}e_{pg}}{S_t} + \frac{(M_g + M_s)}{S_t} + \frac{(M_{ws} + M_b)}{S_{tg}}$$

$$= \frac{1,232}{767} - \frac{(1,232)(29.68)}{15,421} + \frac{(1,438.2 + 1,659.6)(12)}{15,421} + \frac{(360 + 180)(12)}{63,861}$$

$$= 1.606 - 2.371 + 2.411 + 0.101 = +1.747 \text{ ksi}$$

Compressive stress limit: +2.925 ksi OK

2. Under permanent and transient loads, load combination Service I:

$$f_{tg} = +1.747 + \frac{(M_{LT} + M_{LL})}{S_{tc}} = +1.747 + \frac{(1,830.3 + 843.3)(12)}{63,861}$$

$$= 1.747 + 0.502 = +2.249 \text{ ksi}$$

Compressive stress limit: +3.900 ksi OK

9.1b.8.2.2 Concrete Stress at the Top Fiber of the Deck

Note: Compressive stress in the deck slab at service loads never controls the design for typical applications. The calculations shown below are for illustration purposes and may not be necessary in most practical applications.

1. Under permanent loads, load combination Service I:

$$f_{tc} = \frac{M_{ws} + M_b}{S_{tc}} = \frac{(360 + 180)(12)}{55,592} = +0.117 \text{ ksi}$$

Compressive stress limit: +1.800 ksi OK

2. Under permanent and transient loads, load combination Service I:

$$f_{tc} = \frac{M_{ws} + M_b}{S_{tc}} + \frac{M_{LT} + M_{LL}}{S_{tc}} = 0.117 + \frac{(1,830.3 + 843.3)(12)}{55,592} = +0.694 \text{ ksi}$$

Compressive stress limit: +2.400 ksi OK

9.1b.8.2.3 Concrete Stress in Bottom of Beam, Load Combination Service III

$$f_b = \frac{P_{pe}}{A_g} + \frac{P_{pe}e_{pg}}{S_b} - \frac{(M_g + M_s)}{S_b} - \frac{(M_{ws} + M_b) + 0.8(M_{LT} + M_{LL})}{S_{bc}}$$

$$= \frac{1,232}{767} + \frac{(1,232)(29.68)}{14,915} - \frac{(1,438.2 + 1,659.6)(12)}{14,915} - \frac{[(360 + 180) + (0.8)(1,830.3 + 843.3)](12)}{20,090}$$

$$= 1.606 + 2.452 - 2.492 - 1.600 = -0.034 \text{ ksi}$$

Tensile stress limit: -0.484 ksi OK

9.1b.8.3 Fatigue Stress Limit

LRFD Article 5.5.3.1 states that in fully prestressed components other than segmentally constructed bridges, the compressive stress due to Fatigue I load combination and one half the sum of effective prestress and permanent loads shall not exceed $0.40f'_c$, after losses.

From **Table 9.1a.4-2**, the unfactored fatigue bending moment at midspan, M_f , is 776.9 ft-kips. Therefore, stress at the top fiber of the beam due to fatigue load combination I is:

$$f_{tgf} = \frac{1.50(M_f)}{S_{tg}} = \frac{1.50(776.9)(12)}{63,861} = +0.219 \text{ ksi}$$

BULB-TEE (BT-72), SINGLE SPAN, COMPOSITE DECK

9.1b.8.3 Fatigue Stress Limit/9.1b.10.2 Minimum Reinforcement

From **Table 9.1a.4-2**, the unfactored fatigue bending moment at midspan, M_f , is 776.9 ft-kips. Therefore, stress at the top fiber of the beam due to fatigue load combination I is:

$$f_{t_{gf}} = \frac{1.50(M_f)}{S_{t_g}} = \frac{1.50(776.9)(12)}{63,861} = +0.219 \text{ ksi}$$

At midspan, the top compressive stress due to permanent loads and prestress is:

$$f_{t_g} = \frac{P_{pe}}{A_g} - \frac{P_{pe}e_{pg}}{S_t} + \frac{(M_g + M_s)}{S_t} + \frac{(M_{ws} + M_b)}{S_{t_g}}$$

$$= \frac{1,353.1}{767} - \frac{(1,353.1)(29.68)}{15,421} + \frac{(1,438.2 + 1,659.6)(12)}{15,421} + \frac{(360 + 180)(12)}{63,861}$$

$$= 1.764 - 2.604 + 2.411 + 0.101 = 1.672 \text{ ksi}$$

Therefore:

$$f_{t_{gf}} + \frac{f_{t_g}}{2} = 0.219 + \frac{1.672}{2} = 1.055 < 0.40(f'_c) = 0.40(6.50) = 2.6 \text{ ksi OK}$$

This condition should be satisfied at all locations along the beam.

9.1b.8.4 Summary of Stresses at Midspan at Service Loads

The stresses calculated using the above methods are summarized in **Table 9.1b.8.4-1**. For comparison, the stresses calculated for the same design example using the previous method of calculating prestress losses are also shown in the table (Example 9.4 in the previous edition of the manual).

Table 9.1b.8.4-1

Stresses at Midspan at Service Loads

Design Example	Top of Deck, ksi Service I		Top of Beam, ksi Service I		Bottom of Beam, ksi Service III
	Permanent Loads	Total Loads	Permanent Loads	Total Loads	
9.1b	+0.117	+0.694	+1.747	+2.249	-0.034
9.4	+0.117	+0.694	+1.833	+2.335	-0.487

9.1b.8.5 Effect of Deck Shrinkage

The calculations in Section 9.1b.8.2 comply with the *LRFD Specifications*. However, PCI believes that it is not appropriate to include the prestressing gain caused by the deck shrinkage, Δf_{pss} , in calculating the prestress losses. Alternatively, the effect of deck shrinkage should be analyzed by considering it as an external force applied to the composite section as illustrated in 9.1a.8.5.

9.1b.9 STRENGTH LIMIT STATE

See Section 9.1a.9.

9.1b.10 LIMITS OF REINFORCEMENT

[LRFD Art. 5.7.3.3.1]

9.1b.10.1 Maximum Reinforcement

The check of maximum reinforcement limits in LRFD Article 5.7.3.3.1 was removed from the *LRFD Specifications* in 2005.

Adequate ductility of the beam is ensured by evaluating whether the member can be classified as tension-controlled. If the member does not satisfy the requirements to be tension-controlled, the resistance factor for the strength limit state 1 check will be reduced in accordance with LRFD Article 5.5.4.2.1.

9.1b.10.2 Minimum Reinforcement

[LRFD Art. 5.7.3.3.2]

At any section, the amount of prestressed and nonprestressed tensile reinforcement must be adequate to develop a factored flexural resistance, M_r , equal to the lesser of:

- 1.2 times the cracking strength determined on the basis of elastic stress distribution and the modulus of rupture, and
- 1.33 times the factored moment required by the applicable strength load combination.

BULB-TEE (BT-72), SINGLE SPAN, COMPOSITE DECK

9.1b.10.2 Minimum Reinforcement/9.1b.11 Shear Design

Check at midspan:

$$M_{cr} = S_{bc}(f_r + f_{cpe}) - M_{dnc} \left(\frac{S_{bc}}{S_b} - 1 \right) \geq S_{bc} f_r \quad [\text{LRFD Eq. 5.7.3.3.2-1}]$$

where

$$f_r = \text{modulus of rupture of concrete} \quad [\text{LRFD Art. 5.4.2.6}]$$

$$= 0.37\sqrt{f'_c} = 0.37\sqrt{6.500} = 0.943 \text{ ksi}$$

$$f_{cpe} = \text{compressive stress in concrete due to effective prestress force only (after allowance for all prestress losses) at extreme fiber of section where tensile stress is caused by externally applied loads}$$

$$= \frac{P_{pe}}{A_g} + \frac{P_{pe}e_{pg}}{S_b} = \frac{1,232}{767} + \frac{1,232(29.68)}{14,915} = 4.058 \text{ ksi}$$

$$M_{dnc} = \text{noncomposite dead load moment at the section}$$

$$= M_g + M_s = 1,438.2 + 1,659.6 = 3,098 \text{ ft-kips}$$

$$S_{bc} = \text{composite section modulus for the extreme fiber of section where the tensile stress is caused by externally applied loads} = 20,090 \text{ in.}^3$$

$$S_b = \text{noncomposite section modulus for the extreme fiber of section where the tensile stress is caused by externally applied loads} = 14,915 \text{ in.}^3$$

$$M_{cr} = (0.943 + 4.058) \frac{20,090}{12} - (3,098) \left(\frac{20,090}{14,915} - 1 \right) = 7,298 \text{ ft-kips}$$

$$1.2 M_{cr} = 1.2(7,298) = 8,758 \text{ ft-kips}$$

At midspan, the factored moment required by the Strength I load combination is:

$$M_u = 9,316 \text{ ft-kips (as calculated in Section 9.1a.9)}$$

$$\text{Thus, } 1.33M_u = 1.33(9,316) = 12,390 \text{ ft-kips}$$

Since $1.2M_{cr} < 1.33M_u$, the $1.2 M_{cr}$ requirement controls.

$$M_r = 11,364 \text{ ft-kips} > 1.2 M_{cr} = 8,758 \text{ ft-kips} \quad \text{OK}$$

Note: The *LRFD Specifications* requires that this criterion be met at every section.Illustrated based on 2011
LRFD Specifications.Editor's Note: 2012 *LRFD Specifications* changes will revise minimum reinforcement.**9.1b.11 SHEAR DESIGN**

The area and spacing of shear reinforcement must be determined at regular intervals along the entire length of the beam. In this design example, transverse shear design procedures are demonstrated below by determining these values at the critical section near the supports.

Transverse shear reinforcement is required when:

$$V_u > 0.5\phi(V_c + V_p) \quad [\text{LRFD Eq. 5.8.2.4-1}]$$

where

$$V_u = \text{total factored shear force, kips}$$

$$V_c = \text{nominal shear resistance provided by tensile stresses in the concrete, kips}$$

$$V_p = \text{component in the direction of the applied shear of the effective prestressing force, kips}$$

$$\phi = \text{resistance factor} = 0.9 \text{ for normal weight concrete} \quad [\text{LRFD Art. 5.5.4.2.1}]$$

BULB-TEE (BT-72), SINGLE SPAN, COMPOSITE DECK

9.1b.11.1 Critical Section/9.1b.11.2.1 Strain in Flexural Tension Reinforcement

9.1b.11.1 Critical Section

[LRFD Art. 5.8.3.2]

The critical section near the supports is taken as the effective shear depth d_v from the internal face of the support.

$$d_v = \text{distance between resultants of tensile and compressive forces, } (d_e - a/2), \text{ but not less than } (0.9d_e) \text{ or } (0.72h_c) \quad \text{[LRFD Art. 5.8.2.7]}$$

where

$$d_e = \text{the corresponding effective depth from the extreme compression fiber to the centroid of the tensile force in the tensile reinforcement} \quad \text{[LRFD Art. 5.8.2.9]}$$

$$a = \text{depth of compression block} = 5.27 \text{ in. at midspan (assumed adequate)}$$

$$h_c = \text{total depth of the composite section} = 80.0 \text{ in.}$$

Since some of the strands are harped, the effective depth, d_e , varies from point-to-point. However, d_e must be calculated at the critical section in shear which is not yet determined; therefore, for the first iteration, d_e is calculated based on the center of gravity of the straight strand group at the end of the beam, y_{bs} .

$$d_e = h_c - y_{bs} = 80.0 - 4.22 = 75.78 \text{ in.}$$

$$d_v = 75.78 - (5.27/2) = 73.14 \text{ in.}$$

$$\geq 0.9 d_e = 0.9(75.78) = 68.20 \text{ in.}$$

$$\geq 0.72 h_c = 0.72(80) = 57.60 \text{ in.} \quad \text{OK}$$

Therefore, $d_v = 73.14$ in.

Because the width of the bearing is not yet determined, it is conservatively assumed to be zero. Therefore, the critical section in shear is located at a distance of:

$$73.14 \text{ in.} = 6.10 \text{ ft from centerline of support}$$

$$(x/L) = 6.10/120 = 0.051L$$

The effective depth, d_e , and the position of the critical section in shear may be refined based on the position of the critical section calculated above. However, the difference is small. Therefore, no more refinement is performed.

9.1b.11.2 Contribution of Concrete to Nominal Shear Resistance

The contribution of the concrete to the nominal shear resistance is:

$$V_c = 0.0316\beta\sqrt{f'_c}b_vd_v \quad \text{[LRFD Eq. 5.8.3.3-3]}$$

where β = a factor indicating the ability of diagonally cracked concrete to transmit tension (a value indicating concrete contribution)

Several quantities must be determined before this expression can be evaluated.

9.1b.11.2.1 Strain in Flexural Tension Reinforcement

Calculate the strain at the centroid of the tension reinforcement, ϵ_x :

$$\epsilon_x = \frac{\frac{|M_u|}{d_v} + 0.5N_u + 0.5|V_u - V_p| \cot \theta - A_{ps}f_{po}}{2(E_sA_s + E_pA_{ps})} \quad \text{[LRFD Eq. B5.2-1]}$$

where

$$M_u = \text{applied factored bending moment at the specified section, } 0.051L.$$

$$= 1.25(277.6 + 320.3 + 34.7) + 1.50(69.5) + 1.75(372.6 + 162.7) \quad \text{[Tables 9.1a.4-1 and 9.1a.4-2]}$$

$$= 1,832 \text{ ft-kips}$$

$$N_u = \text{applied factored normal force at the specified section, } 0.051L = 0 \text{ kips}$$

$$V_u = \text{applied factored shear force at the specified section, } 0.051L$$

BULB-TEE (BT-72), SINGLE SPAN, COMPOSITE DECK

9.1b.11.2.1 Strain in Flexural Tension Reinforcement/9.1b.11.2.1.1 Calculation for Negative Strain

$$= 1.25(43.1 + 49.7 + 5.4) + 1.50(10.8) + 1.75(73.8 + 30.6) = 321.7 \text{ kips} \quad [\text{Tables 9.1a.4-1 and 9.1a.4-2}]$$

$$V_p = (\text{Force per strand without live load gains})(\text{Number of harped strands})(\sin \psi)$$

$$= (25.37)(12)\sin 4.91^\circ = 26.1 \text{ kips is a conservative resistance}$$

$$A_{ps} = \text{area of prestressing strands on the flexural tension side of the member} = 36(0.153) = 5.508 \text{ in.}^2$$

f_{po} = a parameter taken as modulus of elasticity of prestressing tendons multiplied by the locked-in difference in strain between the prestressing tendons and the surrounding concrete (ksi). For pretensioned members, LRFD Article B5.2 indicates that f_{po} can be taken as $0.7f_{pu}$. (Note: use this for both pretensioned and post-tensioned systems made with stress relieved and low relaxation strands).

$$= 0.7(270.0) = 189.0 \text{ ksi}$$

θ = angle of inclination of diagonal compressive stresses, assume θ is 23° (slope of compression field)

The shear design at any section depends on the angle of diagonal compressive stresses at the section. Shear design is an iterative process that begins with assuming a value for θ . For this example, only the final cycle of calculations is shown. As a guide, for areas which have high shear forces and low bending moments, the angle θ ranges from 20° to 30° . For areas of low shear forces and high bending moments, the angle θ ranges to 45° . Using the previously stated guidelines, two iterations are enough in most cases.

M_u need not to be taken less than $(V_u - V_p)d_v$:

$$= (V_u - V_p)d_v = (321.7 - 26.1)(73.14)/12 = 1,801 \text{ ft-kips}$$

Since $(V_u - V_p)d_v \leq M_u$; M_u Controls.

$$\epsilon_x = \frac{\frac{1,832(12)}{73.14} + 0 + 0.5(321.7 - 26.1)(\cot 23^\circ) - 5.508(189.0)}{2[0 + 28,500(5.508)]} = \frac{-392.2}{313,956}$$

$$= -1.249 \times 10^{-3}$$

9.1b.11.2.1.1 Calculation for Negative Strain

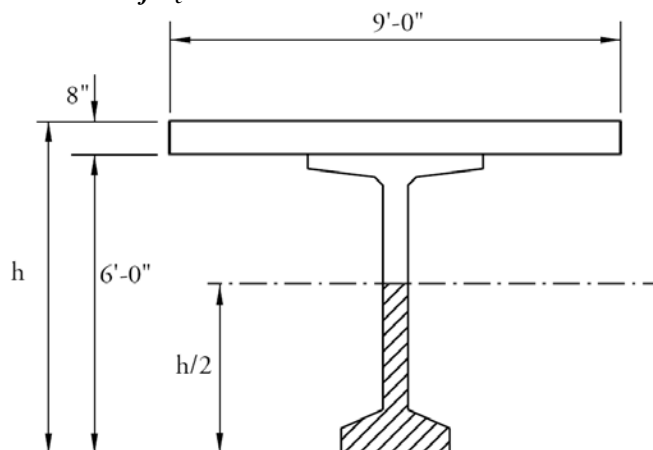
Since the value of ϵ_x is negative, a different equation for ϵ_x must be used.

$$\epsilon_x = \frac{\frac{|M_u|}{d_v} + 0.5N_u + 0.5|V_u - V_p| \cot \theta - A_{ps}f_{po}}{2(E_cA_c + E_sA_s + E_pA_{ps})} \quad [\text{LRFD Eq. B5.2-3}]$$

where A_c = area of concrete (in.²) on the flexural tension side of the member, as shown in **Figure 9.1b.11.2.1-1** (area of concrete below $h/2 = 80/2 = 40$ in.)

Figure 9.1b.11.2.1-1

Illustration of A_c



BULB-TEE (BT-72), SINGLE SPAN, COMPOSITE DECK

9.9.1b.11.2.1.1 Calculation for Negative Strain/9.1b.11.3.2 Required Area of Reinforcement

$$A_c = [26(6) + (2)(0.5)(10)(4.5) + 6(34)] = 405 \text{ in.}^2$$

$$\text{Therefore, } \epsilon_x = \frac{-392.2}{2[(4,888)(405) + 0 + (28,500)(5.508)]} = -0.092 \times 10^{-3}$$

Note that the negative sign of ϵ_x should be maintained.

9.1b.11.2.1.2 Compute Shear Stress

$$v_u = \frac{V_u - \phi V_p}{\phi b_v d_v} \quad [\text{LRFD Eq. 5.8.2.9-1}]$$

where

v_u = shear stress on the concrete, ksi

ϕ = resistance factor = 0.9 [LRFD Art. 5.5.4.2.1]

V_p = component in the direction of the applied shear of the effective prestressing force (calculated in Sect. 9.1b.11.2.1) = 26.1 kips

$$v_u = \frac{321.7 - (0.9)(26.1)}{(0.9)(6)(73.14)} = 0.755 \text{ ksi}$$

$$(v_u/f'_c) = (0.755/6.5) = 0.116$$

9.1b.11.2.2 Values of β and θ

Having computed ϵ_x and v_u/f'_c , find a better estimate of θ from LRFD Table B5.2-1. Since the computed value of v_u/f'_c is likely to fall between two rows in the table, a linear interpolation may be performed. However, for hand calculations, interpolation is not recommended (LRFD Art. CB5.2). The values of θ in the lower row that bounds the computed value may be used. Similarly, the values of θ in the first column to the right of the computed value may be used. For this example, the applicable row and column are the ones labeled " ≤ 0.125 " and " ≤ -0.05 ", respectively. The values of θ and β contained in the cell at the intersection of that row and column are:

$$\theta = 22.8^\circ \cong \text{assumed value of } 23^\circ \quad \text{OK}$$

Therefore, no further iteration is needed

$$\beta = 2.94$$

9.1b.11.2.3 Compute Concrete Contribution

The nominal shear resisted by the concrete is:

$$V_c = 0.0316\beta\sqrt{f'_c}b_v d_v \quad [\text{LRFD Eq. 5.8.3.3-3}]$$

where b_v = effective web width = 6 in.

$$V_c = 0.0316(2.94)\sqrt{6.5}(6)(73.14) = 103.9 \text{ kips}$$

9.1b.11.3 Contribution of Reinforcement to Nominal Shear Resistance**9.1b.11.3.1 Requirement for Reinforcement**

Check if $V_u > 0.5\phi(V_c + V_p)$ [LRFD Eq. 5.8.2.4-1]

$$0.5\phi(V_c + V_p) = 0.5(0.9)(103.9 + 26.1) = 58.5 \text{ kips} < 321.7 \text{ kips}$$

Therefore, transverse shear reinforcement must be provided.

9.1b.11.3.2 Required Area of Reinforcement

$$V_u/\phi \leq V_n = V_c + V_s + V_p \quad [\text{LRFD Eq. 5.8.2.4-1}]$$

BULB-TEE (BT-72), SINGLE SPAN, COMPOSITE DECK

9.1b.11.3.2 Required Area of Reinforcement/9.1b.11.4 Maximum Nominal Shear Resistance

where

$$\begin{aligned}
 V_s &= \text{shear resistance provided by shear reinforcement} \\
 &= (V_u/\phi) - V_c - V_p = (321.7/0.9) - 103.9 - 26.1 = 227.4 \text{ kips} \\
 V_s &= \frac{A_v f_{yh} d_v (\cot \theta + \cot \alpha) (\sin \alpha)}{s} \quad \text{[LRFD Eq. 5.8.3.3-4]}
 \end{aligned}$$

Where

$$\begin{aligned}
 A_v &= \text{area of shear reinforcement within a distance } s, \text{ in.}^2 \\
 s &= \text{spacing of stirrups, in.} \\
 f_{yh} &= \text{specified yield strength of shear reinforcement, ksi} \\
 \alpha &= \text{angle of inclination of transverse reinforcement to longitudinal axis} \\
 &= 90^\circ \text{ for vertical stirrups}
 \end{aligned}$$

Therefore, area of shear reinforcement within a distance s , is:

$$\begin{aligned}
 A_v &= (sV_s)/(f_{yh}d_v \cot \theta) \\
 &= [(s)(227.4)]/[60(73.14)\cot 23^\circ] = 0.022(s)
 \end{aligned}$$

If $s = 12$ in., required $A_v = 0.26$ in.²/ft**9.1b.11.3.3 Determine Spacing of Reinforcement**

Check maximum spacing of transverse reinforcement.

[LRFD Art 5.8.2.7]

Check if $v_u < 0.125f'_c$

$$v_u = 0.755 \text{ ksi (calculated in Sect. 9.1b.11.2.1.2)}$$

$$0.125f'_c = (0.125)(6.5) = 0.813 \text{ ksi}$$

Since $v_u < 0.125f'_c$

[LRFD Eq. 5.8.2.7-1]

then, $s \leq 24$ in.

$$s \leq 0.8d_v = 0.8(73.14) = 58.5 \text{ in.}$$

Therefore, maximum $s = 24$ in. $> s$ provided OK**Use No. 4 bar double legs at 12 in., $A_v = 0.40$ in.²/ft > 0.26 in.²/ft**

$$V_s = \frac{0.4(60)73.14 \cot 23^\circ}{12} = 344.6 \text{ kips}$$

9.1b.11.3.4 Minimum Reinforcement Requirement

The area of transverse reinforcement should not be less than:

[LRFD Eq. 5.8.2.5-1]

$$0.0316\sqrt{f'_c} \frac{b_v s}{f_{yh}} = 0.0316\sqrt{6.5} \frac{(6)(12)}{60.0} = 0.10 \text{ in.}^2/\text{ft} < A_v \text{ provided OK}$$

9.1b.11.4 Maximum Nominal Shear ResistanceIn order to ensure that the concrete in the web of the beam will not crush prior to yielding of the transverse reinforcement, the *LRFD Specifications* gives an upper limit of V_n as follows:

$$V_n = 0.25f'_c b_v d_v + V_p \quad \text{[LRFD Eq. 5.8.3.3-2]}$$

Comparing this equation with LRFD Eq. 5.8.3.3-1, it can be concluded that

$$V_c + V_s \text{ must not be greater than } 0.25f'_c b_v d_v$$

$$103.9 + 344.6 = 448.5 \text{ kips} \leq 0.25(6.5)(6)(73.14) = 713.1 \text{ kips OK}$$

Using the above procedures, the transverse reinforcement can be determined at increments along the entire length of the beam.

BULB-TEE (BT-72), SINGLE SPAN, COMPOSITE DECK

9.1b.12 Interface Shear Transfer/9.1b.13.1 Required Reinforcement at Face of Bearing

9.1b.12 INTERFACE SHEAR TRANSFER

See Section 9.1a.12.

9.1b.13 MINIMUM LONGITUDINAL REINFORCEMENT REQUIREMENT

[LRFD Art. 5.8.3.5]

Longitudinal reinforcement should be proportioned so that at each section the following equation is satisfied:

$$A_{ps}f_{ps} + A_s f_y \geq \frac{M_u}{d_v \phi_f} + 0.5 \frac{N_u}{\phi_c} + \left(\left| \frac{V_u}{\phi_v} - V_p \right| - 0.5V_s \right) \cot \theta \quad [\text{LRFD Eq. 5.8.3.5-1}]$$

where

 A_s = area of nonprestressed tension reinforcement, in.² f_y = specified yield strength of reinforcing bars, ksi A_{ps} = area of prestressing strand at the tension side of the section, in.² f_{ps} = average stress in prestressing strand at the time for which the nominal resistance is required, ksi M_u = factored moment at the section corresponding to the factored shear force, ft-kips N_u = applied factored axial force, kips V_u = factored shear force at section, kips V_s = shear resistance provided by shear reinforcement, kips V_p = component in the direction of the applied shear of the effective prestressing force, kips d_v = effective shear depth, in.

ϕ = resistance factor as appropriate for moment, shear and axial resistance. [LRFD Art. 5.5.4.2]
Therefore, different ϕ factors will be used for the terms in LRFD Equation (5.8.3.5-1), depending on the type of action being considered

 θ = angle of inclination of diagonal compressive stresses**9.1b.13.1 Required Reinforcement at Face of Bearing**

For simple end supports, the longitudinal reinforcement on the flexural tension side of the member at inside face of bearing should satisfy:

$$A_{ps}f_{ps} + A_s f_y \geq \left(\frac{V_u}{\phi} - 0.5V_s - V_p \right) \cot \theta \quad [\text{LRFD Eq. 5.8.3.5-2}]$$

 $M_u = 0$ ft-kips $N_u = 0$ kips

Because the width of the bearing is not yet determined, it is assumed to be zero. This assumption is conservative for these calculations. Therefore, the failure crack assumed for this analysis radiates from the centerline of the bearing, 6 in. from the end of the beam.

From **Tables 9.1a.4-1** and **9.1a.4-2**, using load combination Strength I, the factored shear force at this section is:

$$V_u = 1.25(47.9 + 55.3 + 6.0) + 1.5(12.0) + 1.75(78.1 + 33.9) = 350.5 \text{ kips}$$

$$\left(\frac{V_u}{\phi} - 0.5V_s - V_p \right) \cot \theta = \left(\frac{350.5}{0.9} - 0.5(344.6) - 26.1 \right) \cot 23^\circ = 450.1 \text{ kips}$$

As shown in **Figure 9.1b.13.1-1**, the assumed crack plane crosses the centroid of the 36 straight strands at a distance of $(6 + 4.22 \cot 23^\circ = 15.94 \text{ in.})$ from the end of the beam. Since the transfer length is 30 in. from the end

BULB-TEE (BT-72), SINGLE SPAN, COMPOSITE DECK

9.1b.13.1 Required Reinforcement at Face of Bearing/9.1b.15 Deflection and Camber

of the beam (60 times the strand diameter), the available prestress from the 36 straight strands is a fraction of the effective prestress, f_{pe} , in these strands. The 12 harped strands do not contribute to the tensile capacity since they are not on the flexural tension side of the member.

Therefore, the available prestress force is:

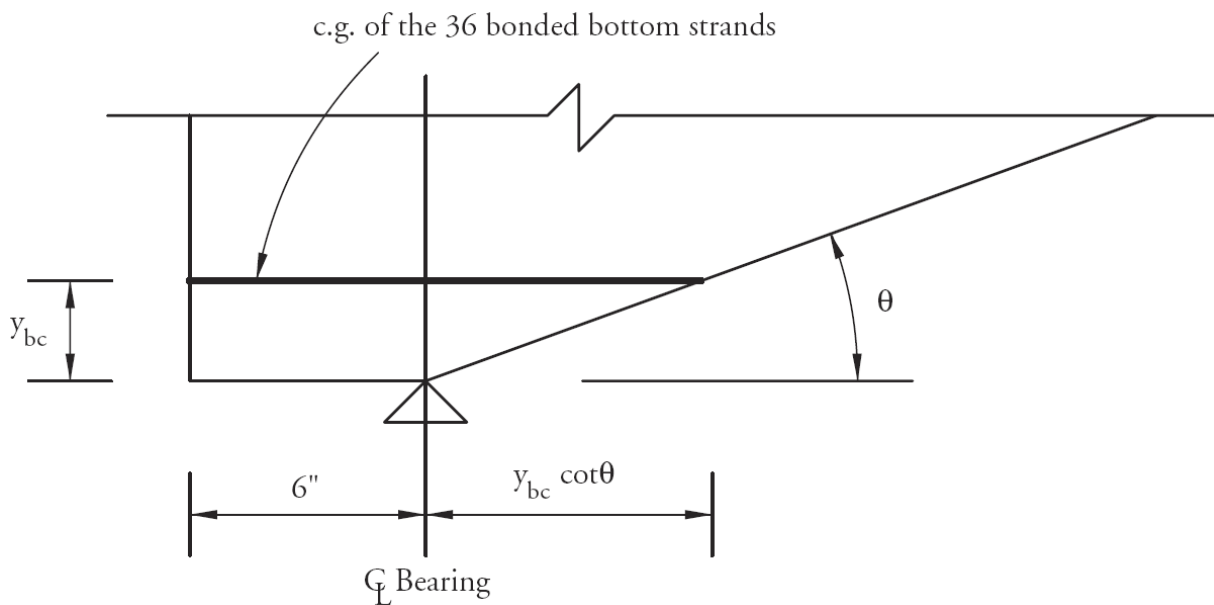
$$A_{ps}f_{ps} + A_s f_y = (36)(0.153) \left((202.5 - 42.7) \frac{15.94}{30} \right) + 0$$

$$= 467.7 + 0 = 467.7 \text{ kips} > 450.1 \text{ kips} \quad \text{OK}$$

No additional reinforcement is required.

Note: An alternative approach for the calculation of available prestressing force excluding the gains from deck shrinkage is illustrated in Section 9.6.13.1.

Figure 9.1b.13.1-1
Assumed Failure Crack



9.1b.14 PRETENSIONED ANCHORAGE ZONE

See Section 9.1a.14.

9.1b.15 DEFLECTION AND CAMBER

See Section 9.1a.15.

This page intentionally left blank

BULB-TEE (BT-72), SINGLE SPAN, COMPOSITE DECK

Transformed Sections, Simplified Shear, Approximate Losses

Table of Contents

9.1c.1 INTRODUCTION.....	9.1c - 3
9.1c.2 MATERIALS	9.1c - 4
9.1c.3 CROSS-SECTION PROPERTIES FOR A TYPICAL INTERIOR BEAM.....	9.1c - 4
9.1c.4 SHEAR FORCES AND BENDING MOMENTS	9.1c - 4
9.1c.5 ESTIMATE REQUIRED PRESTRESS	9.1c - 4
9.1c.6 PRESTRESS LOSSES	9.1c - 4
9.1c.6.1 Elastic Shortening	9.1c - 5
9.1c.6.2 Time-Dependent Losses between Transfer and Deck Placement	9.1c - 5
9.1c.6.3 Time-Dependent Losses between Deck Placement and Final Time	9.1c - 5
9.1c.6.4 Approximate Estimate of Time-Dependent Losses.....	9.1c - 5
9.1c.6.5 Total Losses at Transfer	9.1c - 5
9.1c.6.6 Total Losses at Service Loads	9.1c - 6
9.1c.7 CONCRETE STRESSES AT TRANSFER	9.1c - 6
9.1c.8 CONCRETE STRESSES AT SERVICE LOADS.....	9.1c - 6
9.1c.8.1 Stress Limits for Concrete	9.1c - 6
9.1c.8.2 Stresses at Midspan.....	9.1c - 7
9.1c.8.3 Fatigue Stress Limit.....	9.1c - 8
9.1c.8.4 Summary of Stresses at Midspan at Service Loads	9.1c - 8
9.1c.8.5 Effect of Deck Shrinkage	9.1c - 8
9.1c.9 STRENGTH LIMIT STATE	9.1c - 9
9.1c.10 LIMITS OF REINFORCEMENT.....	9.1c - 9
9.1c.10.1 Maximum Reinforcement.....	9.1c - 9
9.1c.10.2 Minimum Reinforcement	9.1c - 9
9.1c.11 SHEAR DESIGN.....	9.1c - 10
9.1c.11.1 Critical Section	9.1c - 10
9.1c.11.2 Contribution of Concrete to Nominal Shear Resistance	9.1c - 10
9.1c.11.2.1 Calculate V_{ci}	9.1c - 11
9.1c.11.2.2 Calculate V_{cw}	9.1c - 12
9.1c.11.2.3 Calculate V_c	9.1c - 12
9.1c.11.3 Contribution of Reinforcement to Nominal Shear Resistance.....	9.1c - 12
9.1c.11.3.1 Requirement for Reinforcement.....	9.1c - 12
9.1c.11.3.2 Required Area of Reinforcement.....	9.1c - 13
9.1c.11.3.3 Determine Spacing of Reinforcement.....	9.1c - 13
9.1c.11.3.4 Minimum Reinforcement Requirement	9.1c - 14
9.1c.11.4 Maximum Nominal Shear Resistance	9.1c - 14
9.1c.12 INTERFACE SHEAR TRANSFER.....	9.1c - 14
9.1c.12.1 Factored Horizontal Shear.....	9.1c - 14
9.1c.12.2 Required Nominal Resistance.....	9.1c - 14
9.1c.12.3 Required Interface Shear Reinforcement	9.1c - 14

BULB-TEE (BT-72), SINGLE SPAN, COMPOSITE DECK

Transformed Sections, Simplified Shear, Approximate Losses
Table of Contents

9.1c.12.3.1 Minimum Interface Shear Reinforcement..... 9.1c - 15

9.1c.12.4 Maximum Nominal Shear Resistance 9.1c - 15

9.1c.13 MINIMUM LONGITUDINAL REINFORCEMENT REQUIREMENT 9.1c - 15

9.1c.14 PRETENSIONED ANCHORAGE ZONE 9.1c - 16

9.1c.15 DEFLECTION AND CAMBER..... 9.1c - 16

BULB-TEE (BT-72), SINGLE SPAN, COMPOSITE DECK

9.1c.2 Materials/9.1c.6 Prestress Losses

9.1c.2 MATERIALS

See Section 9.1a.2.

9.1c.3 CROSS-SECTION PROPERTIES FOR A TYPICAL INTERIOR BEAM

See Section 9.1a.3.

9.1c.4 SHEAR FORCES AND BENDING MOMENTS

See Section 9.1a.4.

9.1c.5 ESTIMATE REQUIRED PRESTRESS

See Section 9.1a.5.

For convenience, the section properties are shown in **Table 9.1c.5-1**.

Table 9.1c.5-1.
Summary of Section Properties at Transfer and at Final Time

Property	Noncomposite Gross		Noncomposite Transformed at Transfer		Noncomposite Transformed at Final		Composite Gross at Final		Composite Transformed at Final	
	A_g		A_{ti}		A_{tf}		A_c		A_{tc}	
Area, in ²	767		805.0		802.5		1,418.9		1,454.4	
Total Depth, in.	h	72.00	h	72.00	h	72.00	h_c	80.00	h_c	80.00
Moment of Inertia, in. ⁴	I_g	545,894	I_{ti}	578,827	I_{tf}	576,757	I_c	1,100,320	I_{tc}	1,180,561
Centroid of Section to Centroid of Prestress, in.	e_{pg}	29.68	e_{ti}	28.28	e_{tf}	28.37	e_{pc}	47.85	e_{tc}	46.68
Centroid to Bottom Fiber of Beam, in.	y_b	36.60	y_{bti}	35.20	y_{btf}	35.29	y_{bc}	54.77	y_{btc}	53.60
Centroid of Section to Top Fiber of Beam, in.	y_t	35.40	y_{tti}	36.80	y_{ttf}	36.71	y_{tg}	17.23		18.40
Centroid of Section to Top Fiber of Deck, in.							y_{tc}	25.23		26.40
Centroid of Section to Centroid of Deck, in.							e_d	21.48		
Section Modulus for Beam Bottom Fiber, in. ³	S_b	14,915	S_{bti}	16,444	S_{btf}	16,343	S_{bc}	20,090	S_{btc}	22,025
Section Modulus for Beam Top Fiber, in. ³	S_t	15,421	S_{tti}	15,729	S_{ttf}	15,711	S_{tg}	63,861	S_{ttc}	64,161
Section Modulus for Deck Top Fiber, in. ³							S_{tc}	55,592	S_{dtc}	57,002

9.1c.6 PRESTRESS LOSSES

Total prestress loss:

$$\Delta f_{pT} = \Delta f_{pES} + \Delta f_{pLT} \quad \text{[LRFD Eq. 5.9.5.1-1]}$$

where

Δf_{pT} = total loss in prestressing steel stress

Δf_{pES} = sum of all losses or gains due to elastic shortening or extension at the time of application of prestress and/or external loads

Δf_{pLT} = long-term losses due to shrinkage and creep of concrete, and relaxation of steel after transfer. In this design example, the approximate estimate of time-dependent losses is used.

BULB-TEE (BT-72), SINGLE SPAN, COMPOSITE DECK

9.1c.6.1 Elastic Shortening/9.1c.6.5 Total Losses at Transfer

9.1c.6.1 Elastic Shortening

See Section 9.1a.6.1.

9.1c.6.2 Time-Dependent Losses between Transfer and Deck Placement

Not applicable.

9.1c.6.3 Time-Dependent Losses between Deck Placement and Final Time

Not applicable.

9.1c.6.4 Approximate Estimate of Time-Dependent Losses

The approximate estimate of time-dependent losses is valid if

- Members are made from normal weight concrete, OK
- The concrete is either steam- or moist-cured, OK
- Prestressing is by bars or strands with normal and low-relaxation properties, and OK
- Average exposure conditions and temperatures characterize the site. OK

The long-term prestress loss, Δf_{pLT} , due to creep of concrete, shrinkage of concrete, and relaxation of steel is determined using the following equation:

$$\Delta f_{pLT} = 10.0 \frac{f_{pi} A_{ps}}{A_g} \gamma_h \gamma_{st} + 12 \gamma_h \gamma_{st} + \Delta f_{pR} \quad [\text{LRFD Eq. 5.9.5.3-1}]$$

where

f_{pi} = prestressing steel stress immediately prior to transfer = 202.5 ksi

A_{ps} = area for prestressing strand = 7.344 in.²

A_g = area of cross section of the precast concrete beam = 767 in.²

γ_h = correction factor for relative humidity of the ambient air

γ_{st} = correction factor for specified concrete strength at time of prestress transfer to the concrete member

Δf_{pR} = an estimate of relaxation loss taken as 2.4 ksi for low-relaxation strand, 10.0 ksi for stress-relieved strand, and in accordance with manufacturers recommendation for other types of strand, ksi

The correction factor for relative humidity:

$$\gamma_h = 1.7 - 0.01H \quad [\text{LRFD Eq. 5.9.5.3-2}]$$

where

H = the average annual ambient relative humidity (assume 70%)

$$\gamma_h = 1.7 - 0.01(70) = 1.000$$

The correction factor for specified concrete strength:

$$\begin{aligned} \gamma_{st} &= \frac{5}{(1 + f'_{ci})} \quad [\text{LRFD Eq. 5.9.5.3-3}] \\ &= \frac{5}{1 + 5.8} = 0.735 \end{aligned}$$

Long-term prestress loss:

$$\begin{aligned} \Delta f_{pLT} &= \frac{10.0(202.5)(7.344)}{767} (1.000)(0.735) + 12.0(1.000)(0.735) + 2.4 \\ &= 14.251 + 8.820 + 2.4 = 25.5 \text{ ksi} \end{aligned}$$

9.1c.6.5 Total Losses at Transfer

See Section 9.1a.6.5.

BULB-TEE (BT-72), SINGLE SPAN, COMPOSITE DECK

9.1c.6.6 Total Losses at Service Loads/9.1c.8.1 Stress Limits for Concrete

9.1c.6.6 Total Losses at Service Loads

Total loss due to elastic shortening at transfer and long-term losses is:

$$\Delta f_{pT} = \Delta f_{pES} + \Delta f_{pLT} = 18.9 + 25.5 = 44.4 \text{ ksi}$$

The elastic gain due to deck weight, superimposed dead load, and live load (Service III) is:

$$\begin{aligned} & \left(\frac{M_s e_{tf}}{I_{tf}} + \frac{(M_b + M_{ws}) e_{tc}}{I_{tc}} \right) \frac{E_p}{E_c} + 0.8 \left(\frac{(M_{LT} + M_{LL}) e_{tc}}{I_{tc}} \right) \frac{E_p}{E_c} \\ &= \left(\frac{1,659.6(12)(28.37)}{576,757} + \frac{(180 + 360)(12)(46.68)}{1,180,561} \right) \frac{28,500}{4,888} + 0.8 \left(\frac{(1830.2 + 843.3)(12)(46.68)}{1,180,561} \right) \frac{28,500}{4,888} \\ &= 7.2 + 5.9 = 13.1 \text{ ksi} \end{aligned}$$

The effective stress in strands after all losses and gains:

$$f_{pe} = f_{pi} - \Delta f_{pT} + 13.1 = 202.5 - 44.4 + 13.1 = 171.2 \text{ ksi}$$

Check prestressing stress limit at service limit state:

[LRFD Table 5.9.3-1]

$$f_{pe} \leq 0.8f_{py} = 0.8(243) = 194.4 \text{ ksi} > 171.2 \text{ ksi} \quad \text{OK}$$

The effective stress in strands after all losses and permanent gains:

$$f_{pe} = f_{pi} - \Delta f_{pT} + 7.2 = 202.5 - 44.4 + 7.2 = 165.3 \text{ ksi}$$

Force per strand without live load gains = $(f_{pe})(\text{area of strand}) = 165.3 (0.153) = 25.29 \text{ kips}$

Therefore, the total prestressing force after all losses = $25.29 (48) = 1,214 \text{ kips}$

Final loss percentage = $(\text{total losses and gains}) / (f_{pi}) = (202.5 - 165.3) / (202.5) = 18.4\%$

Without consideration of prestressing gains at deck placement, the final loss percentage = $\text{total losses} / (f_{pi}) = (44.4) / (202.5) = 21.9\%$

When determining the concrete stress using transformed section properties, all the elastic losses and gains are implicitly accounted for.

Force per strand with only total time-dependent losses = $(f_{pi} - \Delta f_{pLT})(\text{area of strand}) = (202.5 - 25.5)(0.153) = 27.08 \text{ kips}$

Total prestressing force $P_{pe} = 27.08(48) = 1,300 \text{ kips}$

9.1c.7 CONCRETE STRESSES AT TRANSFER

See Section 9.1a.7.

9.1c.8 CONCRETE STRESSES AT SERVICE LOADS

Using transformed section properties and approximate time-dependent losses, $P_{pe} = 1,300 \text{ kips}$

9.1c.8.1 Stress Limits for Concrete

LRFD Art. 5.9.4.2]

Compression:

Due to permanent loads, (i.e. beam self weight, weight of slab and haunch, weight of future wearing surface, and weight of barriers), for load combination Service I:

$$\text{for precast beams: } 0.45 f'_c = 0.45(6.500) = +2.925 \text{ ksi}$$

$$\text{for deck: } 0.45 f'_c = 0.45(4.000) = +1.800 \text{ ksi}$$

Due to permanent and transient loads (i.e. all dead loads and live loads), for load combination Service I:

$$\text{for precast beams: } 0.60 f'_c = 0.60(6.500) = +3.900 \text{ ksi}$$

$$\text{for deck: } 0.60 f'_c = 0.60(4.000) = +2.400 \text{ ksi}$$

BULB-TEE (BT-72), SINGLE SPAN, COMPOSITE DECK

9.1c.8.1 Stress Limits for Concrete/9.1c.8.2.2 Concrete Stress at the Top Fiber of the Deck

Tension:

For components with bonded prestressing tendons:

$$\text{for load combination Service III: } -0.19 \sqrt{f'_c}$$

$$\text{for precast beam: } -0.19\sqrt{6.500} = -0.484 \text{ ksi}$$

9.1c.8.2 Stresses at Midspan**9.1c.8.2.1 Concrete Stress at Top Fiber of the Beam**

To check top compressive stresses, two cases are considered:

1. Under permanent loads, load combination Service I:

Using bending moment values given in **Table 9.1a.4-1**, compute the top fiber stresses:

$$\begin{aligned} f_{tg} &= \frac{P_{pe}}{A_{tf}} - \frac{P_{pe}e_{tf}}{S_{ttf}} + \frac{(M_g + M_s)}{S_{ttf}} + \frac{(M_{ws} + M_b)}{S_{ttc}} \\ &= \frac{1,300}{802.5} - \frac{(1,300)(28.37)}{15,711} + \frac{(1,438.2 + 1,659.6)(12)}{15,711} + \frac{(360 + 180)(12)}{64,161} \\ &= 1.620 - 2.347 + 2.366 + 0.101 = 1.740 \text{ ksi} \end{aligned}$$

Compressive stress limit: +2.925 ksi OK

2. Under permanent and transient loads, load combination Service I:

$$\begin{aligned} f_{tg} &= +1.740 + \frac{(M_{LT} + M_{LL})}{S_{ttc}} \\ &= +1.740 + \frac{(1,830.2 + 843.3)(12)}{64,161} \\ &= +1.740 + 0.500 = +2.240 \text{ ksi} \end{aligned}$$

Compressive stress limit: +3.900 ksi OK

9.1c.8.2.2 Concrete Stress at the Top Fiber of the Deck

Note: Compressive stress in the deck slab at service loads never controls the design for typical applications. The calculations shown below are for illustration purposes and may not be necessary in most practical applications.

1. Under permanent loads, Service I:

$$f_{tc} = \frac{M_{ws} + M_b}{S_{dtc}} = \frac{(360 + 180)(12)}{57,002} = +0.114 \text{ ksi}$$

Compressive stress limit: +1.800 ksi OK

2. Under permanent and transient loads, load combination Service I:

$$f_{tc} = \frac{M_{ws} + M_b}{S_{dtc}} + \frac{M_{LT} + M_{LL}}{S_{dtc}} = 0.114 + \frac{(1,830.3 + 843.3)(12)}{57,002} = +0.677 \text{ ksi}$$

Compressive stress limit: +2.400 ksi OK

BULB-TEE (BT-72), SINGLE SPAN, COMPOSITE DECK

9.1c.8.2 Concrete Stress in Bottom of Beam, Load Combination Service III/9.1c.8.5 Effect of Deck Shrinkage

9.1c.8.2.3 Concrete Stress in Bottom of Beam, Load Combination Service III

$$f_b = \frac{P_{pe}}{A_{tf}} + \frac{P_{pe}e_{tf}}{S_{btf}} - \frac{(M_g + M_s)}{S_{btf}} - \frac{(M_{ws} + M_b) + 0.8(M_{LT} + M_{LL})}{S_{btc}}$$

$$= \frac{1,300}{802.5} + \frac{(1,300)(28.37)}{16,343} - \frac{(1,438.2 + 1,659.6)(12)}{16,343} - \frac{[(360 + 180) + (0.8)(1,830.2 + 843.3)](12)}{22,025}$$

$$= 1.620 + 2.257 - 2.275 - 1.460 = 0.142 \text{ ksi}$$

Tensile stress limit: -0.484 ksi

The stress is in compression. OK

9.1c.8.3 Fatigue Stress Limit

From **Table 9.1a.4-2**, the unfactored fatigue bending moment at midspan, M_f , is 776.9 ft-kips. Therefore, stress at the top fiber of the beam due to fatigue load combination I is:

$$f_{tgf} = \frac{1.50(M_f)}{S_{ttc}} = \frac{1.50(776.9)(12)}{64,161} = +0.218 \text{ ksi}$$

At midspan, the top compressive stress due to permanent loads and prestress is:

$$f_{tg} = \frac{P_{pe}}{A_{tf}} - \frac{P_{pe}e_{tf}}{S_{ttf}} + \frac{(M_g + M_s)}{S_{ttf}} + \frac{(M_{ws} + M_b)}{S_{ttc}}$$

$$= \frac{1,300}{802.5} - \frac{(1,300)(28.37)}{15,711} + \frac{(1,438.2 + 1,659.6)(12)}{15,711} + \frac{(360 + 180)(12)}{64,161}$$

$$= 1.620 - 2.347 + 2.366 + 0.101 = 1.740 \text{ ksi}$$

Therefore:

$$f_{tgf} + \frac{f_{tg}}{2} = 0.218 + \frac{1.737}{2} = 1.087 < 0.40(f'_c) = 0.40(6.50) = 2.6 \text{ ksi OK}$$

This condition should be satisfied at all locations along the beam.

9.1c.8.4 Summary of Stresses at Midspan at Service Loads

The stresses calculated using the above methods are summarized in **Table 9.1c.8.4-1**. For comparison, the stresses calculated for the same design example using the previous method of calculating prestress losses are also shown in the table (Example 9.4 in the previous edition of the manual).

Table 9.1a.8.4-1

Stresses at Midspan at Service Loads

Design Example	Top of Deck, ksi Service I		Top of Beam, ksi Service I		Bottom of Beam, ksi Service III
	Permanent Loads	Total Loads	Permanent Loads	Total Loads	
9.1c	+0.114	+0.677	+1.740	+2.240	+0.142
9.4	+0.117	+0.694	+1.833	+2.335	-0.487

9.1c.8.5 Effect of Deck Shrinkage

The calculations in Section 9.1c.8.2 comply with the *LRFD Specifications*. However, PCI believes that it is not appropriate to include the prestressing gain caused by the deck shrinkage, Δf_{pss} , in calculating the prestress losses. Alternatively, the effect of deck shrinkage should be analyzed by considering it as an external force applied to the composite nontransformed section as illustrated in Section 9.1a.8.5.

BULB-TEE (BT-72), SINGLE SPAN, COMPOSITE DECK

9.1c.9 Strength Limit State/9.1c.10.2 Minimum Reinforcement

9.1c.9 STRENGTH LIMIT STATE

See Section 9.1a.9.

9.1c.10 LIMITS OF REINFORCEMENT

[LRFD Art. 5.7.3.3.1]

9.1c.10.1 Maximum Reinforcement

The check of maximum reinforcement in LRFD Article 5.7.3.3.1 was removed from the *LRFD Specifications* in 2005.

9.1c.10.2 Minimum Reinforcement

[LRFD Art. 5.7.3.3.2]

At any section, the amount of prestressed and nonprestressed tensile reinforcement must be adequate to develop a factored flexural resistance, M_r , equal to the lesser of:

- 1.2 times the cracking strength determined on the basis of elastic stress distribution and the modulus of rupture, and
- 1.33 times the factored moment required by the applicable strength load combination.

Check at midspan:

$$M_{cr} = S_{btc}(f_r + f_{cpe}) - M_{dnc} \left(\frac{S_{btc}}{S_{btf}} - 1 \right) \geq S_{btc}f_r \quad \text{[LRFD Eq. 5.7.3.3.2-1]}$$

where

$$f_r = \text{modulus of rupture of concrete} \quad \text{[LRFD Art. 5.4.2.6]}$$

$$= 0.37\sqrt{f'_c} = 0.37\sqrt{6.500} = 0.943 \text{ ksi}$$

$$f_{cpe} = \text{compressive stress in concrete due to effective prestress force only (after allowance for all prestress losses) at extreme fiber of section where tensile stress is caused by externally applied loads}$$

$$= \frac{P_{pe}}{A_{tf}} + \frac{P_{pe}e_{tf}}{S_{btf}} = \frac{1,300}{802.5} + \frac{1,300(28.37)}{16,343} = 3.877 \text{ ksi}$$

$$M_{dnc} = \text{noncomposite dead load moment at the section}$$

$$= M_g + M_s = 1,438.2 + 1,659.6 = 3,098 \text{ ft-kips}$$

$$S_{btc} = \text{section modulus for the extreme bottom fiber of the transformed composite section where the tensile stress is caused by externally applied loads} = 22,025 \text{ in.}^3$$

$$S_{btf} = \text{section modulus for the extreme bottom fiber of transformed noncomposite section where the tensile stress is caused by externally applied loads} = 16,343 \text{ in.}^3$$

$$M_{cr} = (0.943 + 3.877) \frac{22,025}{12} - (3,098) \left(\frac{22,025}{16,343} - 1 \right) = 7,770 \text{ ft-kips}$$

$$1.2 M_{cr} = 1.2(7,770) = 9,324 \text{ ft-kips}$$

At midspan, the factored moment required by the Strength I load combination is:

$$M_u = 9,316 \text{ ft-kips (as calculated in Section 9.1a.9)}$$

$$\text{Thus, } 1.33M_u = 1.33(9,316) = 12,390 \text{ ft-kips}$$

Since $1.2M_{cr} < 1.33M_u$, the $1.2M_{cr}$ requirement controls.

$$M_r = 11,364 \text{ ft-kips} > 1.2M_{cr} = 9,350 \text{ ft-kips} \quad \text{OK}$$

Note: The *LRFD Specifications* requires that this criterion be met at every section.

Illustrated based on 2011
LRFD Specifications.

Editor's Note: 2012 *LRFD Specifications* changes will revise minimum reinforcement.

BULB-TEE (BT-72), SINGLE SPAN, COMPOSITE DECK

9.1c.11 Shear Design/9.1c.11.2 Contribution of Concrete to Nominal Shear Resistance

9.1c.11 SHEAR DESIGN

The area and spacing of shear reinforcement must be determined at regular intervals along the entire length of the beam. In this design example, transverse shear design procedures are demonstrated below by determining these values at the critical section near the supports and using the simplified procedure of LRFD Article 5.8.3.4.3.

Transverse shear reinforcement is required when:

$$V_u > 0.5\phi(V_c + V_p) \quad [\text{LRFD Eq. 5.8.2.4-1}]$$

where

- V_u = total factored shear force, kips
- V_c = nominal shear resistance provided by tensile stresses in the concrete, kips
- V_p = component in the direction of the applied shear of the effective prestressing force, kips
- ϕ = resistance factor = 0.9 for normal weight concrete [LRFD Art. 5.5.4.2.1]

9.1c.11.1 Critical Section

[LRFD Art. 5.8.3.2]

The critical section near the supports is taken as the effective shear depth d_v from the internal face of the support.

$$d_v = \text{distance between resultants of tensile and compressive forces, } (d_e - a/2), \text{ but } \geq 0.9d_e \text{ or } 0.72h_c \quad [\text{LRFD Art. 5.8.2.7}]$$

where

- d_e = the corresponding effective depth from the extreme compression fiber to the centroid of the tensile force in the tensile reinforcement [LRFD Art. 5.8.2.9]
- a = depth of compression block = 5.27 in. at midspan (assumed adequate)
- h_c = overall depth of the composite section = 80.0 in.

Since some of the strands are harped, the effective depth, d_e , varies from point-to-point. However, d_e must be calculated at the critical section in shear which is not yet determined; therefore, for the first iteration, d_e is calculated based on the center of gravity of the straight strand group at the end of the beam, y_{bs} .

$$d_e = h_c - y_{bs} = 80.0 - 4.22 = 75.78 \text{ in.}$$

$$d_v = 75.78 - (5.27/2) = 73.14 \text{ in.}$$

$$\geq 0.9 d_e = 0.9(75.78) = 68.20 \text{ in.}$$

$$\geq 0.72 h_c = 0.72(80) = 57.60 \text{ in.} \quad \text{OK}$$

Therefore, $d_v = 73.14$ in.

Because the width of the bearing is not yet determined, it was conservatively assumed to be zero. Therefore the critical section in shear is located at a distance of:

$$73.14 \text{ in.} = 6.10 \text{ ft from centerline of support}$$

$$(x/L) = 6.10/120 = 0.051L$$

The effective depth, d_e , and the position of the critical section in shear may be refined based on the position of the critical section calculated above. However, the difference is small and on the conservative side. Therefore, no more refinement is performed.

9.1c.11.2 Contribution of Concrete to Nominal Shear Resistance

The contribution of the concrete, V_o to the nominal shear resistance is taken as the lesser of V_{ci} and V_{cw} :

$$V_{ci} = 0.02\sqrt{f'_c}b_vd_v + V_d + \frac{V_iM_{cr}}{M_{max}} \geq 0.06\sqrt{f'_c}b_vd_v \quad [\text{LRFD Eq. 5.8.3.4.3-1}]$$

$$V_{cw} = (0.06\sqrt{f'_c} + 0.30f_{pc})b_vd_v + V_p \quad [\text{LRFD Eq. 5.8.3.4.3-3}]$$

BULB-TEE (BT-72), SINGLE SPAN, COMPOSITE DECK9.1c.11.2 Contribution of Concrete to Nominal Shear Resistance/9.1c.11.2.1 Calculate V_{ci}

where

- V_{ci} = nominal shear resistance provided by concrete when inclined cracking results from combined shear and moment, kips
- V_{cw} = nominal shear resistance provided by concrete when inclined cracking results from excessive principal tensions in web, kips
- b_v = effective web = 6 in.
- d_v = effective shear depth = 73.14 in.
- V_d = shear force at section due to unfactored dead load and includes both DC and DW , kips
- V_i = factored shear force at section due to externally applied loads occurring simultaneously with M_{max} , kips
- M_{cr} = moment causing flexural cracking at section due to externally applied loads, ft-kips
- M_{max} = maximum factored moment at section due to externally applied loads, ft-kips
- f_{pc} = compressive stress in concrete (after allowance for all prestress losses) at centroid of cross section resisting externally applied loads or at junction of web and flange when the centroid lies within the flange (ksi). In a composite member, f_{pc} is the resultant compressive stress at the centroid of the composite section, or at junction of web and flange, due to both prestress and moments resisted by precast member acting alone, ksi

9.1c.11.2.1 Calculate V_{ci}

$$V_d = 43.1 + 49.7 + 5.4 + 10.8 = 109.0 \text{ kips}$$

(Table 9.1a.4-1)

$$M_{cr} = S_{btc} \left(f_r + f_{cpe} - \frac{M_{dnc}}{S_{btf}} \right)$$

[LRFD Art. 5.8.3.4.3-2]

where

- f_r = modulus of rupture of concrete = $0.20\sqrt{6.5} = 0.510$ ksi
- f_{cpe} = compressive stress in concrete due to effective prestress forces only (after allowance for all prestress losses) at extreme fiber of section where tensile stress is caused by externally applied loads, ksi
- M_{dnc} = total unfactored dead load moment acting on the monolithic or noncomposite section, ft-kips
- S_{btc} = section modulus for the extreme bottom fiber of the transformed composite section where the tensile stress is caused by externally applied loads = 22,025 in.³
- S_{btf} = section modulus for the extreme bottom fiber of the monolithic of transformed noncomposite section where tensile stress is caused by externally applied loads = 16,343 in.³

$$f_{cpe} = \frac{P_{pe}}{A_{tf}} + \frac{P_{pe} e_{tf}}{S_{btf}}$$

Note that the transformed properties, e_{tf} , A_{tf} , and S_{btf} are at the critical section and could be re-calculated. For simplicity the values of A_{tf} and S_{btf} are assumed to be the same as those at midspan and the value of e_{tf} is calculated to be 18.08 in.

$$f_{cpe} = \frac{1,300}{802.5} + \frac{(1,300)(18.08)}{16,343}$$

$$= 1.620 + 1.438 = 3.058 \text{ ksi}$$

$$M_{dnc} = M_g + M_s = 277.6 + 320.3$$

(Table 9.1a.4-1)

$$= 598 \text{ ft-kips}$$

$$M_{cr} = \frac{22,025}{12} \left(0.510 + 3.058 - \frac{598}{16,343} (12) \right)$$

$$= 5,743 \text{ ft-kips}$$

BULB-TEE (BT-72), SINGLE SPAN, COMPOSITE DECK9.1c.11.2.1 Calculate V_{ci} /9.1c.11.3.1 Requirement for Reinforcement

$$M_{max} = M_u - M_{dnc} \quad [\text{LRFD C5.8.3.4.3}]$$

$$\begin{aligned} M_u &= 1.25 (M_g + M_s + M_b) + 1.5 (M_{ws}) + 1.75 (M_{LL+I} + M_{LT}) \\ &= 1.25 (277.6 + 320.3 + 34.7) + 1.5 (69.5) + 1.75 (372.6 + 162.7) \\ &= 1,832 \text{ ft-kips} \end{aligned}$$

(Tables 9.1a.4-1 and 9.1a.4-2)

$$M_{max} = 1,832 - 598 = 1,234 \text{ ft-kips}$$

$$V_i = V_u - V_d$$

$$\begin{aligned} V_u &= 1.25 (V_g + V_s + V_b) + 1.50 (V_{ws}) + 1.75 (V_{LL+I} + V_{LT}) \\ &= 1.25 (43.1 + 49.7 + 5.4) + 1.50 (10.8) + 1.75 (73.8 + 30.6) \\ &= 321.7 \text{ kips} \end{aligned}$$

(Tables 9.1a.4-1 and 9.1a.4-2)

$$V_d = (43.1 + 49.7 + 5.4) + 10.8 = 109.0 \text{ kips}$$

$$V_i = 321.7 - 109.0 = 212.7 \text{ kips}$$

$$V_{ci} = 0.02\sqrt{6.5}(6.0)(73.14) + 109.0 + \frac{(212.7)(5,743)}{1,234}$$

$$= 1,121.3 \text{ kips} \geq 0.06\sqrt{6.5}(6.0)(73.14) = 67.1 \text{ kips}$$

9.1c.11.2.2 Calculate V_{cw}

$$f_{pc} = \frac{P_{pe}}{A_{tf}} - \frac{P_{pe}e_{tf}}{I_{tf}} (y_{btc} - y_{btf}) + \frac{M_{dnc}(y_{btc} - y_{btf})}{I_{tf}}$$

where

e_{tf} = eccentricity of strands with respect to transformed section at final time = 18.08 in.

y_{btc} = distance from the centroid of the composite transformed section to the extreme bottom fiber of the beam at final time = 53.60 in.

y_{btf} = distance from the centroid of the noncomposite transformed section to the extreme bottom fiber of the beam at final time = 35.29 in.

$$\begin{aligned} f_{pc} &= \frac{1,300}{802.5} - \frac{(1,300)(18.08)}{576,757} (53.60 - 35.29) + \frac{(598)(53.60 - 35.29)(12)}{576,757} \\ &= 1.102 \text{ ksi} \end{aligned}$$

$$V_p \text{ (without live load gains)} = (25.29)(12) \sin 4.91^\circ = 26.0 \text{ kips}$$

$$\begin{aligned} V_{cw} &= \left(0.06\sqrt{6.5} + (0.30)(1.102)\right) (6.0)(73.14) + 26.0 \\ &= 238.2 \text{ kips} \end{aligned}$$

9.1c.11.2.3 Calculate V_c

$$V_c = \text{lesser of } V_{ci} \text{ and } V_{cw} = 238.2 \text{ kips}$$

9.1c.11.3 Contribution of Reinforcement to Nominal Shear Resistance**9.1c.11.3.1 Requirement for Reinforcement**

$$\text{Check if } V_u > 0.5\phi(V_c + V_p)$$

[LRFD Eq. 5.8.2.4-1]

$$0.5\phi(V_c + V_p) = 0.5(0.9)(238.2 + 26.0) = 118.9 \text{ kips} < 321.7 \text{ kips}$$

Therefore, transverse shear reinforcement must be provided.

BULB-TEE (BT-72), SINGLE SPAN, COMPOSITE DECK

9.1c.11.3.2 Required Area of Reinforcement/9.1c.11.3.3 Determine Spacing of Reinforcement

9.1c.11.3.2 Required Area of Reinforcement

$$V_u / \phi \leq V_n = V_c + V_s + V_p \quad [\text{LRFD Eq. 5.8.3.3-1}]$$

where

$$\begin{aligned} V_s &= \text{shear resistance provided by shear reinforcement} \\ &= (V_u / \phi) - V_c - V_p = (321.7 / 0.9) - 238.2 - 0 = 119.2 \text{ kips} \\ V_p &\text{ is taken as zero in accordance with LRFD Article 5.8.3.4.3} \end{aligned}$$

$$V_s = \frac{A_v f_{yh} d_v (\cot \theta + \cot \alpha) (\sin \alpha)}{s} \quad [\text{LRFD Eq. 5.8.3.3-4}]$$

where

$$\begin{aligned} A_v &= \text{area of shear reinforcement within a distance } s, \text{ in.}^2 \\ s &= \text{spacing of stirrups, in.} \\ f_{yh} &= \text{specified yield strength of shear reinforcement, ksi} \\ \alpha &= \text{angle of inclination of transverse reinforcement to longitudinal axis} \\ &= 90^\circ \text{ for vertical stirrups} \\ \theta &= \text{angle of inclination of diagonal compressive stress} \end{aligned}$$

Because $V_{ci} > V_{cw}$

$$\begin{aligned} \cot \theta &= 1.0 + 3 \left(\frac{f_{pc}}{\sqrt{f'_c}} \right) \leq 1.8 \quad [\text{LRFD Eq. 5.8.3.4.3-4}] \\ &= 1.0 + 3 \left(\frac{1.102}{\sqrt{6.5}} \right) = 2.297 \end{aligned}$$

Use $\cot \theta = 1.8$

Therefore, area of shear reinforcement within a distance s , is:

$$\begin{aligned} A_v &= (sV_s) / (f_{yh} d_v \cot \theta) \\ &= (s)(119.2) / [60(73.14)(1.8)] = 0.015(s) \text{ in.}^2 \end{aligned}$$

If $s = 12$ in., required $A_v = 0.18 \text{ in.}^2/\text{ft}$

9.1c.11.3.3 Determine Spacing of Reinforcement

Check maximum spacing of transverse reinforcement.

[LRFD Art. 5.8.2.7]

Check if $v_u < 0.125f'_c$

$$v_u = \frac{|V_u - \phi V_p|}{\phi b_v d_v} = \frac{|321.7 - (0.9)(26.0)|}{(0.9)(6)(73.14)} = 0.755 \text{ ksi} \quad [\text{LRFD Eq. 5.8.2.9-1}]$$

$$0.125f'_c = (0.125)(6.5) = 0.813 \text{ ksi}$$

Since $v_u < 0.125f'_c$

[LRFD Eq. 5.8.2.7-1]

then, $s \leq 24$ in.

$$s \leq 0.8d_v = 0.8(73.14) = 58.5 \text{ in.}$$

Therefore, maximum $s = 24$ in. $> s$ provided OK

Use No. 4 bar double legs at 12 in., $A_v = 0.40 \text{ in.}^2/\text{ft} > 0.18 \text{ in.}^2/\text{ft}$

BULB-TEE (BT-72), SINGLE SPAN, COMPOSITE DECK**9.1c.11.3.3 Determine Spacing of Reinforcement/9.1c.12.3 Required Interface Shear Reinforcement**

$$V_s = \frac{0.4(60)(73.14)(1.8)}{12} = 263.3 \text{ kips}$$

A smaller amount of shear reinforcement could have been selected. However, calculations for minimum interface shear reinforcement require more. (See Sect. 9.1c.12.3.1)

9.1c.11.3.4 Minimum Reinforcement Requirement

The area of transverse reinforcement should not be less than:

$$0.0316\sqrt{f'_c} \frac{b_v s}{f_{yh}} = 0.0316\sqrt{6.5} \frac{(6)(12)}{60} = 0.10 \text{ in.}^2/\text{ft} < A_v \text{ provided} \quad \text{OK} \quad [\text{LRFD Eq. 5.8.2.5-1}]$$

9.1c.11.4 Maximum Nominal Shear Resistance

In order to ensure that the concrete in the web of the beam will not crush prior to yielding of the transverse reinforcement, the *LRFD Specifications* gives an upper limit of V_n as follows:

$$V_n = 0.25f'_c b_v d_v + V_p \quad [\text{LRFD Eq. 5.8.3.3-2}]$$

Comparing this equation with LRFD Eq. 5.8.3.3-1, it can be concluded that

$$V_c + V_s \text{ must not be greater than } 0.25f'_c b_v d_v$$

$$238.2 + 263.3 = 501.5 \text{ kips} \leq 0.25(6.5)(6)(73.14) = 713.1 \text{ kips} \quad \text{OK}$$

Using the above procedures, the transverse reinforcement can be determined at increments along the entire length of the beam.

9.1c.12 INTERFACE SHEAR TRANSFER**9.1c.12.1 Factored Horizontal Shear**

[LRFD Art. 5.8.4]

At the strength limit state, the horizontal shear at a section on a per unit basis can be taken as:

$$V_{hi} = \frac{V_u}{d_v} \quad [\text{LRFD Eq. C5.8.4.2-7}]$$

where

V_{hi} = horizontal factored shear force per unit length of the beam, kips/in.

V_u = factored shear force at specified section due to superimposed loads after the deck is cast, kips

d_v = the distance between the centroid of the tension steel and the mid-thickness of the slab = $(d_e - t_s/2)$
 $= 75.78 - 7.5/2 = 72.03 \text{ in.}$

The *LRFD Specifications* does not identify the location of the critical section. For convenience, it will be assumed here to be the same location as the critical section for vertical shear, at point 0.051L.

Using load combination Strength I:

$$V_u = 1.25(43.1+49+5.4) + 1.5(10.8) + 1.75(73.8 + 30.6) = 321.7 \text{ kips} \quad (\text{Tables 9.1a.4-1 and 9.1a.4-2})$$

Therefore, the applied factored horizontal shear is:

$$V_{hi} = \frac{321.7}{73.14} = 4.40 \text{ kips/in.}$$

9.1c.12.2 Required Nominal Resistance

Required $V_{ni} = V_{hi}/\phi = 4.40/0.9 = 4.89 \text{ kips/in.}$

[LRFD Eq. 5.8.4.1-1]

9.1c.12.3 Required Interface Shear Reinforcement

The nominal shear resistance of the interface surface is:

BULB-TEE (BT-72), SINGLE SPAN, COMPOSITE DECK**9.1c.12.3 Required Interface Shear Reinforcement/9.1c.13 Minimum Longitudinal Reinforcement Requirement**

$$V_{ni} = cA_{cv} + \mu(A_{vf}f_{yh} + P_c) \quad [\text{LRFD Eq. 5.8.4.1-3}]$$

where

c = cohesion factor, ksi

μ = coefficient of friction

A_{cv} = area of concrete section resisting shear transfer, in.²

A_{vf} = area of shear reinforcement crossing the shear plane, in.²

P_c = permanent net compressive force normal to the shear plane, kips

f_{yh} = specified yield strength of shear reinforcement, ksi

For cast-in-place concrete slabs placed on clean, concrete girder surface intentionally roughened:

[LRFD Art. 5.8.4.3]

c = 0.28 ksi

μ = 1.0

The actual contact width, b_v , between the slab and the beam is 42 in.

$A_{cv} = (42.0 \text{ in.})(1.0 \text{ in.}) = 42.0 \text{ in.}^2$

LRFD Eq. 5.8.4.1-3 can be solved for A_{vf} as follows:

$$4.89 = 0.28(42.0) + 1.0(A_{vf}(60) + 0)$$

Solving for A_{vf} ,

$$A_{vf}(\text{req'd}) < 0$$

Since the resistance provided by cohesion is greater than the applied force, provide the minimum required interface reinforcement.

9.1c.12.3.1 Minimum Interface Shear Reinforcement

$$A_{vf} \geq (0.05A_{cv})/f_{yh} \quad [\text{LRFD Eq. 5.8.4.4-1}]$$

From the design of vertical shear reinforcement, a No. 4 double-leg bar at 12-in. spacing is provided from the beam extending into the deck. Therefore, $A_{vf} = 0.40 \text{ in.}^2/\text{ft}$

$$A_{vf} = 0.40 \text{ in.}^2/\text{ft} < (0.05A_{cv})/f_{yh} = 0.05(42)/60 = 0.035 \text{ in.}^2/\text{in.} = 0.42 \text{ in.}^2/\text{ft} \quad \text{NG}$$

However, LRFD Article 5.8.4.4 states that the minimum reinforcement need not exceed the amount needed to resist $1.33V_{hi}/\phi$ as determined using Eq. 5.8.4.1-3.

$$1.33(4.40/0.9) = 0.28(42.0) + 1.0(A_{vf}(60) + 0)$$

solving for A_{vf} ,

$$A_{vf}(\text{req'd}) < 0 \quad \text{OK}$$

9.1c.12.4 Maximum Nominal Shear Resistance

$$V_{ni} \leq K_1f'_cA_{cv} \text{ or } K_2A_{cv}$$

$$V_n \text{ provided} = (0.28)(42) + 1.0\left(\frac{0.40}{12}(60) + 0\right) = 13.76 \text{ kips/in.}$$

$$K_1f'_cA_{cv} = (0.3)(4.0)(42) = 50.4 \text{ kips/in.}$$

[LRFD Eq. 5.8.4.1-4]

$$K_2A_{cv} = 1.8(42) = 75.6 \text{ kips/in.}$$

[LRFD Eq. 5.8.4.1-5]

Since provided $V_n = 13.76 \text{ kips/in.} < 50.4 \text{ kips/in.} \quad \text{OK}$

9.1c.13 MINIMUM LONGITUDINAL REINFORCEMENT REQUIREMENT

See Section 9.1a.13. Although the values of V_s and $\cot \theta$ are slightly different in Example 9.1c.13, the calculations and end result are essentially the same.

BULB-TEE (BT-72), SINGLE SPAN, COMPOSITE DECK

9.1c.14 Pretensioned Anchorage Zone/9.1c.15 Deflection and Camber

9.1c.14 PRETENSIONED ANCHORAGE ZONE

See Section 9.1a.14.

9.1c.15 DEFLECTION AND CAMBER

See Section 9.1a.15.

BULB-TEE (BT-72), THREE SPANS, COMPOSITE DECK

Transformed Sections, Shear General Procedure, Refined Losses

Table of Contents

9.2.1 INTRODUCTION	9.2 - 5
9.2.1.1 Terminology.....	9.2 - 6
9.2.2 MATERIALS	9.2 - 6
9.2.3 CROSS-SECTION PROPERTIES FOR A TYPICAL INTERIOR BEAM	9.2 - 8
9.2.3.1 Noncomposite Nontransformed Beam Section	9.2 - 8
9.2.3.2 Composite Section.....	9.2 - 8
9.2.3.2.1 Effective Flange Width	9.2 - 8
9.2.3.2.2 Modular Ratio between Slab and Beam Concrete.....	9.2 - 8
9.2.3.2.3 Transformed Section Properties	9.2 - 8
9.2.4 SHEAR FORCES AND BENDING MOMENTS.....	9.2 - 10
9.2.4.1 Shear Forces and Bending Moments Due to Dead Loads	9.2 - 10
9.2.4.1.1 Dead Loads	9.2 - 10
9.2.4.1.2 Unfactored Shear Forces and Bending Moments.....	9.2 - 11
9.2.4.2 Shear Forces and Bending Moments Due to Live Loads	9.2 - 11
9.2.4.2.1 Live Loads.....	9.2 - 11
9.2.4.2.2 Distribution Factor for a Typical Interior Beam.....	9.2 - 12
9.2.4.2.2.1 Distribution Factor for Bending Moment.....	9.2 - 12
9.2.4.2.2.2 Distribution Factor for Shear Force	9.2 - 13
9.2.4.2.3 Dynamic Allowance	9.2 - 14
9.2.4.2.4 Unfactored Shear Forces and Bending Moments.....	9.2 - 14
9.2.4.2.4.2 Due To Design Lane Load; V_{LL} and M_{LL}	9.2 - 14
9.2.4.3 Load Combinations.....	9.2 - 14
9.2.5 ESTIMATE REQUIRED PRESTRESS	9.2 - 17
9.2.5.1 Service Load Stresses at Midspan	9.2 - 17
9.2.5.3 Required Number of Strands.....	9.2 - 17
9.2.5.4 Strand Pattern.....	9.2 - 18
9.2.6 PRESTRESS LOSSES.....	9.2 - 20
9.2.6.1 Elastic Shortening.....	9.2 - 20
9.2.6.2 Time-Dependent Losses between Transfer and Deck Placement.....	9.2 - 21
9.2.6.2.1 Shrinkage of Concrete	9.2 - 21
9.2.6.2.2 Creep of Concrete	9.2 - 22
9.2.6.2.3 Relaxation of Prestressing Strands.....	9.2 - 23
9.2.6.3 Time-Dependent Losses between Deck Placement and Final Time	9.2 - 23
9.2.6.3.1 Shrinkage of Concrete	9.2 - 23
9.2.6.3.2 Creep of Concrete	9.2 - 24
9.2.6.3.3 Relaxation of Prestressing Strands.....	9.2 - 24
9.2.6.3.4 Shrinkage of Deck Concrete.....	9.2 - 24
9.2.6.4 Total Time-Dependent Loss.....	9.2 - 25
9.2.6.5 Total Losses at Transfer	9.2 - 26

BULB-TEE (BT-72), THREE SPANS, COMPOSITE DECK

Transformed Sections, Shear General Procedure, Refined Losses

Table of Contents

9.2.6.6 Total Losses at Service Loads 9.2 - 26

9.2.7 CONCRETE STRESSES AT TRANSFER 9.2 - 27

 9.2.7.1 Stress Limits For Concrete 9.2 - 27

 9.2.7.2 Stresses at Transfer Length Section 9.2 - 27

 9.2.7.3 Stresses at the Harp Points 9.2 - 29

 9.2.7.4 Stresses at Midspan 9.2 - 29

 9.2.7.5 Hold-Down Forces 9.2 - 30

 9.2.7.6 Summary of Stresses at Transfer 9.2 - 30

9.2.8 CONCRETE STRESSES AT SERVICE LOADS 9.2 - 30

 9.2.8.1 Stress Limits For Concrete 9.2 - 30

 9.2.8.2 Stresses at Midspan 9.2 - 31

 9.2.8.3 Fatigue Stress Limit 9.2 - 32

 9.2.8.3.1 Positive Moment Section 9.2 - 32

 9.2.8.3.2 Negative Moment Section 9.2 - 32

 9.2.8.4 Summary of Stresses at Service Loads 9.2 - 32

 9.2.8.5 Effect of Deck Shrinkage 9.2 - 32

9.2.9 STRENGTH LIMIT STATE 9.2 - 32

 9.2.9.1 Positive Moment Section 9.2 - 32

 9.2.9.2 Negative Moment Section 9.2 - 34

 9.2.9.2.1 Design of the Section 9.2 - 34

 9.2.9.2.2 Fatigue Stress Limit and Crack Control 9.2 - 35

 9.2.10.1 Positive Moment Section 9.2 - 35

 9.2.10.1.1 Maximum Reinforcement 9.2 - 35

 9.2.10.1.2 Minimum Reinforcement 9.2 - 35

 9.2.10.2 Negative Moment Section 9.2 - 36

 9.2.10.2.1 Maximum Reinforcement 9.2 - 36

 9.2.10.2.2 Minimum Reinforcement 9.2 - 36

9.2.11 SHEAR DESIGN 9.2 - 36

 9.2.11.1 Critical Section 9.2 - 37

 9.2.11.1.1 Effective Shear Depth 9.2 - 37

 9.2.11.1.2 Calculation of Critical Section 9.2 - 37

 9.2.11.1.3 Forces at the Critical Section 9.2 - 38

 9.2.11.2 Contribution of Concrete to Nominal Shear Resistance 9.2 - 38

 9.2.11.2.1 Strain in Flexural Tension Reinforcement 9.2 - 39

 9.2.11.2.2 Values of β and θ 9.2 - 39

 9.2.11.2.3 Compute Concrete Contribution 9.2 - 39

 9.2.11.3 Contribution of Reinforcement to Nominal Shear Resistance 9.2 - 39

 9.2.11.3.1 Requirement for Reinforcement 9.2 - 39

 9.2.11.3.2 Required Area of Reinforcement 9.2 - 40

BULB-TEE (BT-72), THREE SPANS, COMPOSITE DECK

Transformed Sections, Shear General Procedure, Refined Losses

Table of Contents

9.2.11.3.3 Determine Spacing of Reinforcement..... 9.2 - 40

9.2.11.3.4 Minimum Reinforcement Requirement..... 9.2 - 40

9.2.11.4 Maximum Nominal Shear Resistance 9.2 - 40

9.2.12 INTERFACE SHEAR TRANSFER..... 9.2 - 41

9.2.12.1 Factored Horizontal Shear 9.2 - 41

9.2.12.2 Required Nominal Resistance 9.2 - 41

9.2.12.3 Required Interface Shear Reinforcement 9.2 - 41

9.2.12.3.1 Minimum Interface Shear Reinforcement 9.2 - 42

9.2.12.4 Maximum Nominal Shear Resistance 9.2 - 42

9.2.14 PRETENSIONED ANCHORAGE ZONE..... 9.2 - 43

9.2.14.1 Anchorage Zone Reinforcement..... 9.2 - 43

9.2.14.2 Confinement Reinforcement..... 9.2 - 43

9.2.15 DEFLECTION AND CAMBER 9.2 - 43

9.2.15.1 Deflection Due to Prestressing Force at Transfer 9.2 - 43

9.2.15.2 Deflection Due to Beam Self Weight..... 9.2 - 44

9.2.15.3 Deflection Due to Slab and Haunch and Deck Weights 9.2 - 44

9.2.15.4 Deflection Due to Barrier and Future Wearing Surface Weights 9.2 - 45

9.2.15.5 Deflection and Camber Summary..... 9.2 - 45

9.2.15.6 Deflection Due to Live Load and Impact..... 9.2 - 45

This page intentionally left blank

BULB-TEE (BT-72), THREE SPANS, COMPOSITE DECK

9.2.1 Introduction

9.2 Transformed Sections, Shear General Procedure, Refined Losses

9.2.1 INTRODUCTION

This design example demonstrates the design of a three-span, AASHTO-PCI bulb-tee beam bridge with span lengths of 110, 120, and 110 ft and no skew, as shown in **Figure 9.2.1-1**. This example illustrates in detail the design of a typical interior beam in the center span at the critical sections in positive flexure, negative flexure, shear, and deflection due to prestress, dead loads, and live load. The superstructure consists of four beams spaced at 12 ft 0 in. centers as shown in **Figure 9.2.1-2**. Beams are designed to act compositely with the 8-in.-thick cast-in-place concrete deck slab to resist all superimposed dead loads, live loads, and impact. A ½-in.-thick wearing surface is considered to be an integral part of the 8-in.-thick deck. Design live load is AASHTO LRFD HL-93. The design is accomplished in accordance with the *AASHTO LRFD Bridge Design Specifications*, Fifth Edition, 2010 and the 2011 Interim Revisions. Elastic stresses from external loads are calculated using transformed sections. Shear strength is calculated using the general procedure. Time-dependent prestress losses are calculated using the refined estimates.

Figure 9.2.1-1
Longitudinal Section

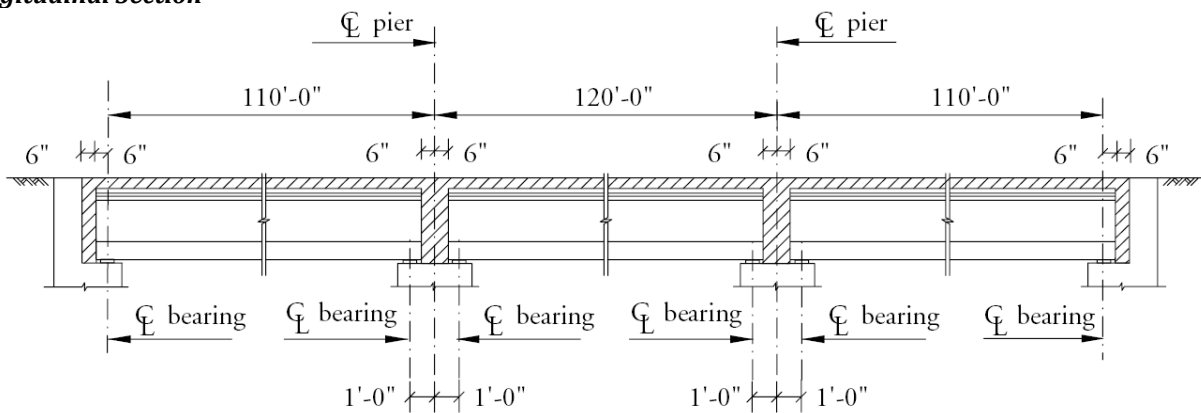
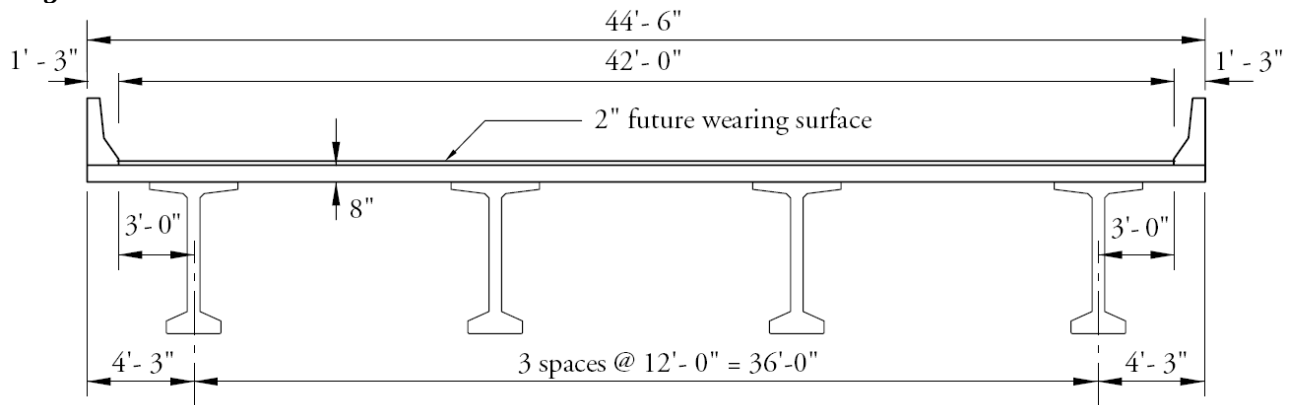


Figure 9.2.1-2
Bridge Cross Section



BULB-TEE (BT-72), THREE SPANS, COMPOSITE DECK

9.2.1.1 Terminology/9.2.2 Materials

9.2.1.1 Terminology

The following terminology is used to describe cross sections in this design example:

noncomposite section—the concrete beam cross section.

noncomposite nontransformed section—the concrete beam cross section without the strands transformed. Also called the gross section.

noncomposite transformed section—the concrete beam cross section with the strands transformed to provide cross-sectional properties equivalent to the beam concrete.

composite section—the concrete beam plus the concrete deck and haunch.

composite nontransformed section—the concrete beam plus the concrete deck and haunch transformed to provide cross-sectional properties equivalent to the beam concrete but without the strands transformed.

composite transformed section—the concrete beam plus the concrete deck and haunch and the strands transformed to provide cross-sectional properties equivalent to the beam concrete.

The term "composite" implicitly includes the transformation of the concrete deck and haunch.

The term "transformed" generally refers to transformation of the strands.

9.2.2 MATERIALS

Cast-in-place concrete slab: Actual thickness, = 8.0 in.

Structural thickness $t_s = 7.5$ in.

Note that a ½-in.-thick wearing surface is considered to be an integral part of the 8-in.-thick deck.

Specified concrete compressive strength for use in design, $f'_c = 4.0$ ksi

Concrete unit weight, $w_c = 0.150$ kcf

Precast concrete beams: AASHTO-PCI BT-72 bulb-tee beams as shown in **Figure 9.2.2-1**.

Required concrete compressive strength at transfer, $f'_{ci} = 5.5$ ksi

Specified concrete compressive strength for use in design, $f'_c = 7.0$ ksi

Concrete unit weight, $w_c = 0.150$ kcf

Overall beam length (**Figure 9.2.1-1**) = 110.0 ft (end spans) and 119.0 ft (center span)

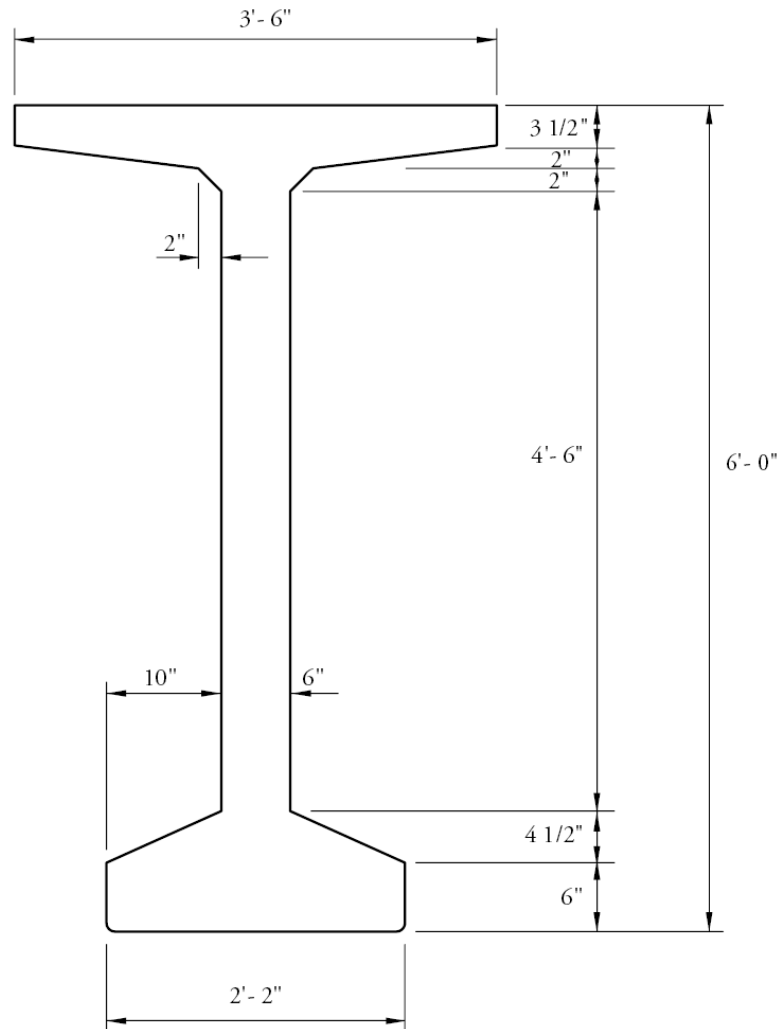
Design spans (**Figure 9.2.1-1**):

For noncomposite beam: 109.0 ft (end spans) and 118.0 ft (center span)

For composite beam: 110.0 ft (end spans) and 120.0 ft (center span)

BULB-TEE (BT-72), THREE SPANS, COMPOSITE DECK

Figure 9.2.2-1
AASHTO-PCI BT-72 Dimensions



Prestressing strands: 1/2-in.-dia., seven wire, low-relaxation

Area of one strand = 0.153 in.²

Specified tensile strength, $f_{pu} = 270.0$ ksi

Yield strength, $f_{py} = 0.9f_{pu} = 243.0$ ksi

[LRFD Table 5.4.4.1-1]

Stress limits for prestressing strands:

[LRFD Table 5.9.3-1]

- before transfer, $f_{pi} \leq 0.75f_{pu} = 202.5$ ksi
- at service limit state (after all losses), $f_{pe} \leq 0.80f_{py} = 194.4$ ksi

Modulus of elasticity, $E_p = 28,500$ ksi

[LRFD Art. 5.4.4.2]

Reinforcing bars:

Yield strength, $f_y = 60.0$ ksi

Modulus of elasticity, $E_s = 29,000$ ksi

[LRFD Art. 5.4.3.2]

Future wearing surface: 2 in. additional concrete, unit weight = 0.150 kcf

New Jersey-type barrier: Unit weight = 0.300 kips/ft/side

BULB-TEE (BT-72), THREE SPANS, COMPOSITE DECK

9.2.3 Cross-Section Properties for a Typical Interior Beam/9.2.3.2.3 Transformed Section Properties

9.2.3 CROSS-SECTION PROPERTIES FOR A TYPICAL INTERIOR BEAM**9.2.3.1 Noncomposite Nontransformed Beam Section**

A_g = area of cross section of beam = 767 in.²

h = overall depth of beam = 72 in.

I_g = moment of inertia about the centroid of the noncomposite precast beam = 545,894 in.⁴

y_b = distance from centroid to extreme bottom fiber of the noncomposite precast beam = 36.60 in.

y_t = distance from centroid to extreme top fiber of the noncomposite precast beam = 35.40 in.

S_b = section modulus for the extreme bottom fiber of the noncomposite precast beam = I_g/y_b = 14,915 in.³

S_t = section modulus for the extreme top fiber of the noncomposite precast beam = I_g/y_t = 15,421 in.³

w_g = beam weight per unit length = $(767/144)(0.150)$ = 0.799 kips/ft

E_c = modulus of elasticity of concrete, ksi = $33,000K_1(w_c)^{1.5}\sqrt{f'_c}$ [LRFD Eq. 5.4.2.4-1]

where

K_1 = correction factor for source of aggregate taken as 1.0

w_c = unit weight of concrete = 0.150 kcf

LRFD Table 3.5.1-1 states that, in the absence of more precise data, the unit weight of concrete may be taken as $0.140 + 0.001f'_c$ for $5.0 < f'_c \leq 15.0$ ksi. For $f'_c = 6.5$ ksi, the unit weight would be 0.1465 kcf. However, precast concrete mixes typically have a relatively low water-cementitious materials ratio and high density. Therefore, a unit weight of 0.150 kcf is used in this example. For high-strength concrete, this value may need to be increased based on test results. For simplicity, a value of 0.150 kcf is also used for the cast-in-place concrete.

f'_c = specified compressive strength of concrete, ksi

Therefore, the modulus of elasticity for:

cast-in-place slab, $E_c = 33,000(1.00)(0.150)^{1.5}\sqrt{4.0} = 3,834$ ksi

precast beam at transfer, $E_{ci} = 33,000(1.00)(0.150)^{1.5}\sqrt{5.5} = 4,496$ ksi

precast beam at service loads, $E_c = 33,000(1.00)(0.150)^{1.5}\sqrt{7.0} = 5,072$ ksi

9.2.3.2 Composite Section**9.2.3.2.1 Effective Flange Width**

[LRFD Art. 4.6.2.6.1]

Effective flange width is taken as the tributary width perpendicular to the axis of the beam. For the interior beam, the effective flange width is calculated as one-half the distance to the adjacent beam on each side.

Therefore, the effective flange width is $(2)(6)(12) = 144$ in.

9.2.3.2.2 Modular Ratio between Slab and Beam Concrete

Modular ratio between slab and beam concrete, $n = \frac{E_c(\text{slab})}{E_c(\text{beam})} = \frac{3,834}{5,072} = 0.7559$

9.2.3.2.3 Transformed Section Properties

The effective flange width must be transformed by the modular ratio to provide cross-sectional properties equivalent to the beam concrete.

Transformed flange width = n (effective flange width) = $(0.7559)(144) = 108.85$ in.

Transformed flange area = n (effective flange width)(t_s)
 = $(0.7559)(144)(7.5) = 816.37$ in.²

BULB-TEE (BT-72), THREE SPANS, COMPOSITE DECK

9.2.3.2.3 Transformed Section Properties

Transformed flange area moment of inertia = $(108.85)(7.5)^3/12 = 3826.76 \text{ in.}^4$

Note: only the structural thickness of the deck, 7.5 in., is considered.

Due to camber of the precast, prestressed beam, a minimum haunch thickness of 1/2 in., at midspan, is considered in the structural properties of the composite section. Also, the width of haunch must be transformed by the modular ratio.

Transformed haunch width = $(0.7559)(42) = 31.75 \text{ in.}$

Transformed area of haunch = $(0.7559)(42)(0.5) = 15.87 \text{ in.}^2$

Transformed moment of inertia of haunch = $(31.75)(0.5)^3/12 = 0.33 \text{ in.}^4$

Note that the haunch should only be considered to contribute to section properties if it is required to be provided in the completed structure. Some designers neglect its contribution to the section properties.

Figure 9.2.3.2.3-1 shows the dimensions of the composite section.

Figure 9.2.3.2.3-1
Dimensions of the Composite Section

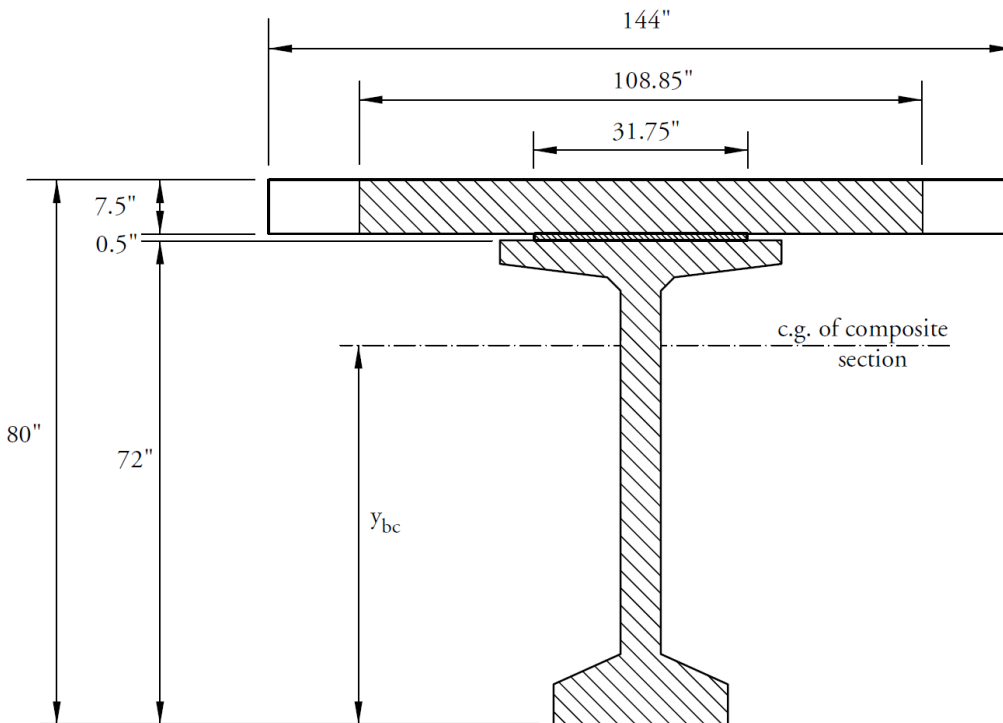


Table 9.2.3.2.3-1
Properties of Composite Section DAC Line weights revised

	Area, in. ²	y_b in.	Ay_b in. ³	$A(y_{bc} - y_b)^2$ in. ⁴	I in. ⁴	$I + A(y_{bc} - y_b)^2$ in. ⁴
Beam	767.00	36.60	28,072	325,484	545,894	871,378
Haunch	15.87	72.25	1,147	3,595	0.3	3,595
Deck	816.37	76.25	62,248	296,263	3,827	300,090
Σ	1,599.24		91,467			1,175,063

BULB-TEE (BT-72), THREE SPANS, COMPOSITE DECK

9.2.3.2.3 Transformed Section Properties/9.2.4.1.1 Dead Loads

$$A_c = \text{total area of composite section} = 1,599 \text{ in.}^2$$

$$h_c = \text{overall depth of the composite section} = 80.00 \text{ in.}$$

$$I_c = \text{moment of inertia of the composite section} = 1,175,063 \text{ in.}^4$$

$$y_{bc} = \text{distance from the centroid of the composite section to the extreme bottom fiber of the precast beam}$$

$$= \frac{91,467}{1,599} = 57.20 \text{ in.}$$

$$y_{tg} = \text{distance from the centroid of the composite section to the extreme top fiber of the precast beam}$$

$$= 72.00 - 57.20 = 14.80 \text{ in.}$$

$$y_{tc} = \text{distance from the centroid of the composite section to the extreme top fiber of the structural deck}$$

$$= 80.00 - 57.20 = 22.80 \text{ in.}$$

$$S_{bc} = \text{composite section modulus for the extreme bottom fiber of the precast beam}$$

$$= (I_c/y_{bc}) = \left(\frac{1,175,063}{57.20}\right) = 20,543 \text{ in.}^3$$

$$S_{tg} = \text{composite section modulus for the extreme top fiber of the precast beam}$$

$$= (I_c/y_{tg}) = \left(\frac{1,175,063}{14.80}\right) = 79,396 \text{ in.}^3$$

$$S_{tc} = \text{composite section modulus for extreme top fiber of the structural deck slab}$$

$$= \left(\frac{1}{n}\right)(I_c/y_{tc}) = \left(\frac{1}{0.7559}\right)\left(\frac{1,175,063}{22.80}\right) = 68,181 \text{ in.}^3$$

9.2.4 SHEAR FORCES AND BENDING MOMENTS

The self weight of the beam and the weight of the slab and haunch act on the noncomposite, simple-span structure, while the weight of barriers, future wearing surface, and live loads with impact act on the composite, continuous structure. Refer to **Table 9.2.4-1**, which follows Section 9.2.4.3 for a summary of unfactored values calculated below.

9.2.4.1 Shear Forces and Bending Moments Due to Dead Loads

[LRFD Art. 3.3.2]

9.2.4.1.1 Dead Loads

DC = Dead load of structural components and nonstructural attachments

Dead loads acting on the simple-span structure, noncomposite section:

$$\text{Beam self weight, } w_g = 0.799 \text{ kips/ft}$$

$$\text{8-in.-thick deck weight} = (8/12 \text{ ft})(12 \text{ ft})(0.150 \text{ kcf}) = 1.200 \text{ kips/ft}$$

$$\text{1/2-in.-thick haunch weight} = (0.5)(42/144)(0.150) = 0.022 \text{ kips/ft}$$

$$w_s = 1.200 + 0.022 = 1.222 \text{ kips/ft}$$

Notes:

1. Actual slab thickness (8 in.) is used for computing dead load.
2. A 1/2-in.-minimum haunch thickness is assumed in the computations of dead load. If a deeper haunch will be used because of final beam camber, the weight of the actual haunch should be used.
3. For this design example, the unit weight of the reinforced concrete is taken as 0.150 kcf. Some designers use a higher unit weight to account for the weight of the reinforcement.
4. The weight of cross-diaphragms is ignored since most agencies are changing from cast-in-place concrete diaphragms to lightweight steel diaphragms.

BULB-TEE (BT-72), THREE SPANS, COMPOSITE DECK

9.2.4.1.1 Dead Loads/9.2.4.2.1 Live Loads

Dead loads placed on the continuous structure, composite section:

LRFD Article 4.6.2.2.1 states that permanent loads (curbs and future wearing surface) may be distributed uniformly among all beams if the following conditions are met:

- Width of the deck is constant OK
- Number of beams, N_b , is not less than four ($N_b = 4$) OK
- Beams are parallel and have the same stiffness OK
- Roadway part of the overhang, $d_e \leq 3.0$ ft

$$d_e = 3.0 - 0.5 \left(\frac{6}{12} \right) = 2.75 \text{ ft OK}$$

- Curvature in plan is less than specified in the *LRFD Specifications* (curvature = 0.0°) OK
- Cross section of the bridge is consistent with one of the cross sections given in LRFD Table 4.6.2.2.1-1 OK

Since these criteria are satisfied, the barrier and wearing surface loads are distributed equally among the four beams.

$$\text{Barrier weight} = (2 \text{ barriers})(0.300 \text{ kips/ft}) / (4 \text{ beams}) = 0.150 \text{ kips/ft/beam} = w_b$$

DW = Dead load of future wearing surface

$$= (2/12)(0.150) = 0.0250 \text{ ksf}$$

$$= (0.025 \text{ ksf})(42.0 \text{ ft}) / (4 \text{ beams}) = 0.263 \text{ kips/ft/beam} = w_{ws}$$

9.2.4.1.2 Unfactored Shear Forces and Bending Moments

For a simply supported beam with a span length (L) loaded with a uniformly distributed load (w), the shear force (V_x) and bending moment (M_x) at any distance (x) from the support are given by:

$$V_x = w(0.5L - x) \quad \text{[Eq. 9.2.4.1.2-1]}$$

$$M_x = 0.5wx(L - x) \quad \text{[Eq. 9.2.4.1.2-2]}$$

Using the above equations, values of shear forces and bending moments for a typical interior beam, under self weight of beam and weight of slab and haunch are computed and shown in **Table 9.2.4-1** that is located at the end of Section 9.2.4.3. The span length for each span to be considered depends on the construction stage:

- overall length immediately after prestress transfer = 110.0 and 119.0 ft
- centerline-to-centerline distance between beam bearings at the time of deck placement = 109.0 and 118.0 ft
- centerline-to-centerline distance between supports after beams are made continuous = 110.0 and 120.0 ft

Shear forces and bending moments due to barrier weight and future wearing surface are calculated based on the continuous span lengths, 110, 120, and 110 ft. The three-span structure was analyzed using a continuous beam program. The shear forces and bending moments are given in **Table 9.2.4-1** that is located at the end of Section 9.2.4.3.

9.2.4.2 Shear Forces and Bending Moments Due to Live Loads**9.2.4.2.1 Live Loads**

Design live load is HL-93, which consists of a combination of: [LRFD Art. 3.6.1.2.1]

1. Design truck or design tandem with dynamic allowance. [LRFD Art. 3.6.1.2.2]

The design truck consists of 8.0-, 32.0-, and 32.0-kip axles with the first pair spaced at 14.0 ft and the second pair spaced at 14.0 to 30.0 ft. The design tandem consists of a pair of 25.0-kip axles spaced 4.0 ft apart.

[LRFD Art. 3.6.1.2.3]

Spans in the range used in this example are much larger than those controlled by the tandem loading. For this reason, tandem loading effects are not included.

BULB-TEE (BT-72), THREE SPANS, COMPOSITE DECK

9.2.4.2.1 Live Loads/9.2.4.2.1 Distribution Factor for Bending Moment

2. Design lane load of 0.64 kips/ft without dynamic allowance [LRFD Art. 3.6.1.2.4]

Art. 3.6.1.3.1 in the *LRFD Specifications* requires that for negative moment between points of dead load contraflexure and for reactions at interior piers only, 90% of the effect of two design trucks spaced at a minimum of 50.0 ft between the lead axle of one truck and the rear axle of the other truck, combined with 90% of the effect of the design lane load be considered. The distance between the 32-kip axles of each truck should be taken as 14 ft.

This three-span structure was analyzed using a continuous beam program that has the ability to generate live load shear force and bending moment envelopes in accordance with the *LRFD Specifications* on a per-lane basis. The span lengths used are the continuous span lengths, 110, 120, and 110 ft.

9.2.4.2.2 Distribution Factor for a Typical Interior Beam

The live load bending moments and shear forces are determined by using the simplified distribution factor formulas. To use the simplified live load distribution factor formulas, the following conditions must be met. [LRFD Art. 4.6.2.2] [LRFD Art. 4.6.2.2.1]

- Width of deck is constant OK
- Number of beams, N_b not less than four ($N_b = 4$) OK
- Beams are parallel and have approximately the same stiffness OK
- Roadway part of overhang, $d_e \leq 3.0$ ft $d_e = 3.0 - 0.5(6/12) = 2.75$ ft OK
- Curvature is less than specified in the *LRFD Specifications* (Curvature = 0.0°) OK

For precast concrete I- or bulb-tee beams with cast-in-place concrete deck slab, the bridge type is (k). [LRFD Table 4.6.2.2.1-1]

The number of design lanes is computed as:
 Number of design lanes = the integer part of the ratio of ($w/12$), where (w) is the clear roadway width, in ft, between the curbs. [LRFD Art. 3.6.1.1.1]

From **Figure 9.2.1-2**, $w = 42$ ft

Number of design lanes = integer part of ($42/12$) = 3 lanes

9.2.4.2.2.1 Distribution Factor for Bending Moment

- For all limit states except for fatigue limit state:

For two or more lanes loaded:

$$DFM = 0.075 + \left(\frac{S}{9.5}\right)^{0.6} \left(\frac{S}{L}\right)^{0.2} \left(\frac{K_g}{12.0Lt_s^3}\right)^{0.1}$$

[LRFD Table 4.6.2.2.2b-1]

Provided that: $3.5 \leq S \leq 16.0$; $S = 12.0$ ft OK
 $4.5 \leq t_s \leq 12.0$; $t_s = 7.5$ in. OK
 $20 \leq L \leq 240$; $L = 120$ ft OK
 $N_b \geq 4$; $N_b = 4$ OK
 $10,000 \leq K_g \leq 7,000,000$ OK (see below)

where

- DFM = distribution factor for bending moment for interior beam
- S = beams spacing, ft
- L = beam span, ft
- t_s = structural depth of concrete deck, in.
- K_g = longitudinal stiffness parameter, $\text{in.}^4 = n(I_g + A_g e_g^2)$ [LRFD Eq. 4.6.2.2.1-1]

BULB-TEE (BT-72), THREE SPANS, COMPOSITE DECK

9.2.4.2.2.1 Distribution Factor for Bending Moment/9.2.4.2.2.2 Distribution Factor for Shear Force

where

n = modular ratio between beam and deck slab concrete

$$= \frac{E_c(\text{beam})}{E_c(\text{slab})} = \frac{5,072}{3,834} = 1.323$$

A_g = cross-section area of the precast beam (noncomposite section), in.²

I_g = moment of inertia of the precast beam (noncomposite section), in.⁴

e_g = distance between the centers of gravity of the beam and deck, in.

$$= (7.5/2 + 0.5 + 35.4) = 39.65 \text{ in.}$$

Therefore,

$$K_g = (1.323)[545,894 + 767(39.65)^2] = 2,317,515 \text{ in.}^4$$

At center span:

$$\begin{aligned} DFM &= 0.075 + \left(\frac{12}{9.5}\right)^{0.6} \left(\frac{12}{120}\right)^{0.2} \left(\frac{2,317,515}{(12.0)(120)(7.5)^3}\right)^{0.1} \\ &= 0.075 + \boxed{(1.150)(0.631)(1.143)} = 0.904 \text{ lanes/beam} \end{aligned}$$

For one design lane loaded:

$$\begin{aligned} DFM &= 0.06 + \left(\frac{S}{14}\right)^{0.4} \left(\frac{S}{L}\right)^{0.3} \left(\frac{K_g}{12.0Lt_s^3}\right)^{0.1} && \text{[LRFD Table 4.6.2.2b-1]} \\ &= 0.06 + \left(\frac{12}{14}\right)^{0.4} \left(\frac{12}{120}\right)^{0.3} \left(\frac{2,317,515}{(12.0)(120)(7.5)^3}\right)^{0.1} \\ &= 0.06 + (0.940)(0.501)(1.143) = 0.598 \text{ lanes/beam} \end{aligned}$$

Thus, the case of the two design lanes loaded controls, $DFM = 0.904$ lanes/beam.

- For fatigue limit state:

Fatigue limit state is not checked in this example. The live load moment that would be used to compute the fatigue stress range is the moment due to a truck load with a constant spacing of 30 ft between the 32.0-kip axles plus a dynamic load allowance.

9.2.4.2.2.2 Distribution Factor for Shear Force

For two or more lanes loaded:

$$DFV = 0.2 + \left(\frac{S}{12}\right) - \left(\frac{S}{35}\right)^2 \quad \text{[LRFD Table 4.6.2.2.3a-1]}$$

Provided that: $3.5 \leq S \leq 16.0$; $S = 12.0$ ft OK

$20 \leq L \leq 240$; $L = 120$ ft OK

$4.5 \leq t_s \leq 12.0$; $t_s = 7.5$ in. OK

$N_b \geq 4$; $N_b = 4$ OK

where

DFV = distribution factor for shear force for interior beam

S = beam spacing, ft

Therefore, the distribution factor for shear force for both end spans and center span is:

$$DFV = 0.2 + \left(\frac{12}{12}\right) - \left(\frac{12}{35}\right)^2 = 1.082 \text{ lanes/beam}$$

BULB-TEE (BT-72), THREE SPANS, COMPOSITE DECK

9.2.4.2.2 Distribution Factor for Shear Force/9.2.4.3 Load Combinations

For one design lane loaded:

$$DFV = 0.36 + \left(\frac{S}{25.0}\right) = 0.36 + \left(\frac{12}{25.0}\right) = 0.840 \text{ lanes/beam}$$

Thus, the case of two or more lanes loaded controls, $DFV = 1.082$ lanes/beam.

9.2.4.2.3 Dynamic Allowance

$IM = 15\%$ for fatigue limit state

$IM = 33\%$ for all other limit states

[LRFD Table 3.6.2.1-1]

where IM = dynamic load allowance, applied to design truck load only

9.2.4.2.4 Unfactored Shear Forces and Bending Moments**9.2.4.2.4.1 Due To Truck Load; V_{LT} and M_{LT}**

- For all limit states except for fatigue limit state:

Shear force and bending moment envelopes on a per-lane-basis are calculated at tenth-points of the span using the equations given in Chapter 8 of this manual. However, this is generally done by means of commercially available computer software that has the ability to deal with moving loads. Therefore, truck load shear force and bending moments per beam are:

$$\begin{aligned} V_{LT} &= (\text{shear force per lane})(DFV)(1 + IM) = (\text{shear force per lane})(1.082)(1 + 0.33) \\ &= (\text{shear force per lane})(1.439) \text{ kips} \end{aligned}$$

$$\begin{aligned} M_{LT} &= (\text{bending moment per lane})(DFM)(1 + IM) \\ &= (\text{bending moment per lane})(0.904)(1 + 0.33) \\ &= (\text{bending moment per lane})(1.202) \text{ ft-kips} \end{aligned}$$

9.2.4.2.4.2 Due To Design Lane Load; V_{LL} and M_{LL}

$$\begin{aligned} V_{LL} &= (\text{lane load shear force})(DFV) \\ &= (\text{lane load shear force})(1.082) \text{ kips} \end{aligned}$$

$$\begin{aligned} M_{LL} &= (\text{lane load bending moment})(DFM) \\ &= (\text{lane load bending moment})(0.904) \text{ ft-kips} \end{aligned}$$

Note that the dynamic allowance is not applied to the design lane loading.

Values of $V_{LL+LT} = V_{LL} + V_{LT}$ and $M_{LL+LT} = M_{LL} + V_{LT}$ at different points are given in **Table 9.2.4-1**.

9.2.4.3 Load Combinations

[LRFD Art. 3.4]

Total factored load is taken as:

$$Q = \sum \eta_i \gamma_i Q_i \quad \text{[LRFD Eq. 3.4.1-1]}$$

where

η_i = a load multiplier relating to ductility, redundancy, and operational importance. (Here, η_i is considered to be 1.0 for typical bridges) [LRFD Art. 1.3.2]

γ_i = load factors

Q_i = force effects from specified loads [LRFD Table 3.4.1-1]

Investigating different limit states given in LRFD Article 3.4.1, the following limit states are applicable:

Service I: check compressive stresses in prestressed concrete components:

$$Q = 1.00(DC + DW) + 1.00(LL + IM) \quad \text{[LRFD Table 3.4.1-1]}$$

This load combination is the general combination for service limit state stress checks and applies to all conditions other than Service III.

BULB-TEE (BT-72), THREE SPANS, COMPOSITE DECK

9.2.4.3 Load Combinations

Service III: check tensile stresses in prestressed concrete components:

$$Q = 1.00(DC + DW) + 0.80(LL + IM) \quad \text{[LRFD Table 3.4.1-1]}$$

This load combination is a special combination for the service limit state stress check that applies only to tension in prestressed concrete structures to control cracks.

Strength I: check ultimate strength: [LRFD Table 3.4.1-1 and 2]

$$\text{Maximum } Q = 1.25(DC) + 1.50(DW) + 1.75(LL + IM)$$

$$\text{Minimum } Q = 0.90(DC) + 0.65(DW) + 1.75(LL + IM)$$

This load combination is the general load combination for strength limit state design. The minimum load factors for dead load (DC) and future wearing surface (DW) are used when dead load and future wearing surface stresses are of an opposite sign to that of the live load.

Fatigue I: check stress range in strands: [LRFD Table 3.4.1-1]

$$Q = 1.50(LL + IM)$$

This load combination is a special load to check the tensile stress range in the strands due to live load and dynamic allowance.

Note: The live load used in the above equation results from a single design truck only with a 30-ft constant spacing between the 32.0-kip axles with the special dynamic allowance, (IM) for fatigue.

BULB-TEE (BT-72), THREE SPANS, COMPOSITE DECK

9.2.4.3 Load Combinations

**Table 9.2.4-1
Unfactored Shear Forces and Bending Moments for a Typical Interior Beam**

Location		Beam Weight (Simple Span)		Deck + Haunch Weight (Simple Span)		Barrier Weight (Continuous Span)		Future Wearing Surface (Continuous Span)		HL-93 Live Load Envelope (Continuous Span)	
Distance <i>x</i> , ft	Section <i>x/L</i> [4]	Shear <i>V_g</i> kips	Moment <i>M_g</i> ft-kips	Shear <i>V_s</i> kips	Moment <i>M_s</i> ft-kips	Shear <i>V_b</i> kips	Moment <i>M_b</i> ft-kips	Shear <i>V_{ws}</i> kips	Moment <i>M_{ws}</i> ft-kips	Shear <i>V_{LL+LT}</i> kips	Moment <i>M_{LL+LT}</i> ft-kips
0.0[1]	0.000	43.5	0.0	66.6	0.0	6.0	0.0	11.0	0.0	128.4	0.0
11.0	0.100	34.8	430.7	53.2	658.7	5.0	62.0	8.0	109.0	111.6	1,026.3
22.0	0.200	26.0	764.6	39.7	1169.5	3.0	106.0	6.0	186.0	91.9	1,749.4
33.0	0.300	17.2	1,001.9	26.3	1532.4	2.0	132.0	3.0	231.0	72.0	2,186.5
44.0	0.400	8.4	1142.6	12.8	1747.5	0.0	139.0	0.0	244.0	57.1	2,382.9
55.0	0.500	0.4	1186.5	0.6	1814.7	2.0	128.0	3.0	225.0	68.9	2,348.5
66.0	0.600	9.2	1133.8	14.1	1734.0	3.0	100.0	6.0	175.0	85.2	2,108.7
77.0	0.700	18.0	984.4	27.5	1505.5	5.0	53.0	9.0	93.0	101.4	1,654.3
88.0	0.800	26.8	738.3	40.9	1129.1	7.0	-12.0	12.0	-21.0	114.7	1,021.7
99.0	0.900	35.6	395.5	54.4	604.9	8.0	-95.0	15.0	-167.0	120.3	-1,316.8
109.0[1]	0.991	43.5	0.0	66.6	0.0	9.8*	-187.7*	17.7*	-328.8*	144.6*	-2,235.8*
110.0	1.000	0.0	0.0	0.0	0.0	10.0	-197.0	18.0	-345.0	147.0	-2,327.7
0.0[2]	0.000	0.0	0.0	0.0	0.0	9.0	-197.0	16.0	-345.0	144.6	-2,327.7
1.0[1]	0.008	47.1	0.0	72.0	0.0	8.8*	-188.9*	15.8*	-336.6*	143.6*	-2,276.9*
7.1[3]	0.059	42.3	272.7	64.6	417.1	7.8*	-139.6*	14.2	-244.4*	137.3*	-1,717.8*
12.0	0.100	38.4	470.2	58.7	719.1	7.0	-100.0	13.0	-175.0	132.3	-1,296.9
24.0	0.200	28.8	872.9	44.0	1335.0	5.0	-24.0	10.0	-42.0	113.8	1,044.4
36.0	0.300	19.2	1160.5	29.3	1775.0	4.0	30.0	6.0	53.0	92.6	1,641.7
48.0	0.400	9.6	1333.1	14.7	2038.9	2.0	62.0	3.0	109.0	76.7	2,006.4
60.0	0.500	0.0	1390.7	0.0	2126.9	0.0	73.0	0.0	128.0	58.2	2,115.0

[1] Centerline of bearing

[2] Centerline of pier

[3] Critical section in shear

[4] *L* is taken as 110 or 120 ft

* Determined using linear interpolation

Note: Shear values shown are absolute values.

BULB-TEE (BT-72), THREE SPANS, COMPOSITE DECK

9.2.5 Estimate Required Prestress/9.2.5.3 Required Number of Strands

9.2.5 ESTIMATE REQUIRED PRESTRESS

The required number of strands is usually governed by concrete tensile stresses at the bottom fiber for the load combination Service III at the section of maximum moment or at the harp points. For estimating the number of strands, only the stresses at midspan are considered.

9.2.5.1 Service Load Stresses at Midspan

Bottom tensile stress due to applied dead and live loads using load combination Service III, is:

$$f_b = \frac{M_g + M_s}{S_b} + \frac{M_b + M_{ws} + (0.8)(M_{LL+LT})}{S_{bc}}$$

where

- f_b = concrete tensile stress at bottom fiber of the beam, ksi
- M_g = unfactored bending moment due to beam self weight, ft-kips
- M_s = unfactored bending moment due to slab and haunch weights, ft-kips
- M_b = unfactored bending moment due to barrier weight, ft-kips
- M_{ws} = unfactored bending moment due to weight of future wearing surface, ft-kips
- M_{LL+LT} = unfactored bending moment due to truck load plus impact and lane load, ft-kips

Using values of bending moments from **Tables 9.2.4-1** and **9.2.4-2**, the bottom tensile stress at midspan of the center span (point 0.5, centerspan), is:

$$f_b = \frac{(1,390.7 + 2,126.9)(12)}{14,915} + \frac{(73.0 + 128.0 + 0.8 \times 2,115.0)(12)}{20,543}$$

$$= 2.830 + 1.106 = 3.936 \text{ ksi}$$

9.2.5.2 Stress Limits for Concrete

[LRFD Table 5.9.4.2.2-1]

The tensile stress limit at service loads = $0.19\sqrt{f'_c}$

where f'_c = specified concrete compressive strength for design, ksi

Concrete tensile stress limit = $-0.19\sqrt{7.0} = -0.503$ ksi

9.2.5.3 Required Number of Strands

The required precompressive stress at the bottom fiber of the beam is the difference between bottom tensile stress due to the applied loads and the concrete tensile stress limit:

$$f_{pb} = (3.936 - 0.503) = 3.433 \text{ ksi.}$$

The location of the strand center of gravity at midspan ranges from 5 to 15% of the beam depth, measured from the bottom of the beam. A value of 5% is appropriate for newer efficient sections like the bulb-tee beams and 15% for less efficient AASHTO standard shapes.

Assume the distance from the center of gravity of strands to the bottom fiber of the beam, y_{bs} , is equal to 7% of the beam depth.

$$y_{bs} = 0.07h = 0.07(72) = 5.04 \text{ in.}$$

Then, the strand eccentricity at midspan, e_c , is $(y_b - y_{bs}) = (36.60 - 5.04) = 31.56$ in.

If P_{pe} is the total prestressing force after all losses, the stress at the bottom fiber due to prestress is:

$$f_{pb} = \frac{P_{pe}}{A_g} + \frac{P_{pe}e_c}{S_b} \quad \text{or} \quad 3.433 = \frac{P_{pe}}{767.0} + \frac{P_{pe}(31.56)}{14,915}$$

Solving for P_{pe} , the required $P_{pe} = 1,003.9$ kips

BULB-TEE (BT-72), THREE SPANS, COMPOSITE DECK

9.2.5.3 Required Number of Strands/9.2.5.5 Steel Transformed Section Properties

Final prestress force per strand = (area of strand)(f_{pi})(1 – losses)

where f_{pi} = initial strand stress before transfer (see Section 9.2.2) = 202.5 ksi

Assuming final loss of 25% of f_{pi} , the prestress force per strand after all losses

$$= (0.153)(202.5)(1 - 0.25) = 23.2 \text{ kips}$$

Number of strands required = $(1,003.9/23.2) = 43.3$ strands

Try forty four 1/2-in.-diameter, 270 ksi, low-relaxation strands

Total area of prestressing stands, $A_{ps} = 44(0.153) = 6.732 \text{ in.}^2$

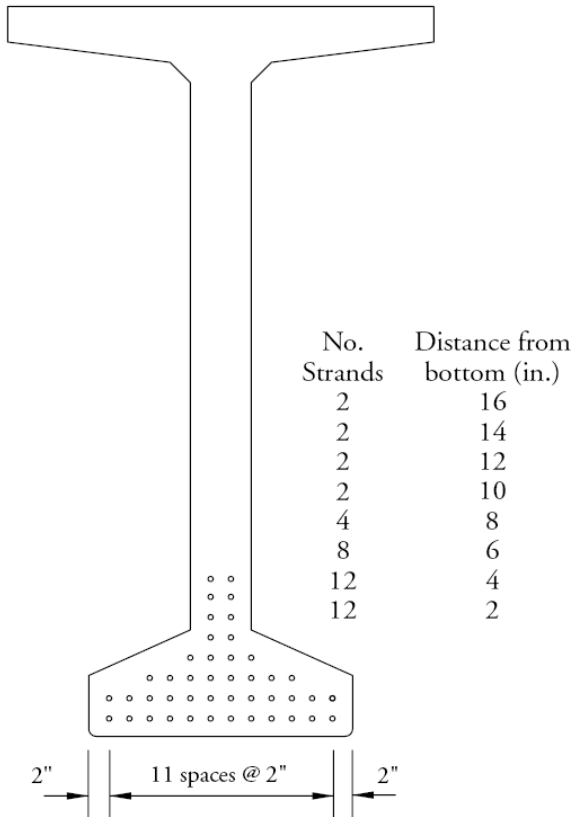
Note: This is a conservative estimate of the number of strands because nontransformed section properties are used in lieu of transformed section properties. The number of strands can be refined later in the design process as more accurate section properties and prestress losses are determined.

9.2.5.4 Strand Pattern

The assumed strand pattern for the 44 strands at midspan is shown in **Figure 9.2.5.4-1**. Each available position is filled beginning with the bottom row.

Figure 9.2.5.4-1

Assumed Strand Pattern at Midspan



The distance between the center of gravity of strands and the bottom concrete fiber of the beam at midspan is:

$$y_{bs} = [(12(2) + 12(4) + 8(6) + 4(8) + 2(10) + 2(12) + 2(14) + 2(16)]/44 = 5.82 \text{ in.}$$

$$\text{Strand eccentricity at midspan, } e_c = y_b - y_{bs} = 36.60 - 5.82 = 30.78 \text{ in.} = e_{pg}$$

9.2.5.5 Steel Transformed Section Properties

From the earliest years of prestressed concrete design, the gross section was conservatively used in analysis since the prestressing forces were smaller and computer programs were not widely used. However, the use of transformed section, which is obtained from the gross section by adding transformed steel area, yields more accurate results than the gross section analysis.

BULB-TEE (BT-72), THREE SPANS, COMPOSITE DECK

9.2.5.5 Steel Transformed Section Properties

For each row of the prestressing strands shown in **Figure 9.2.5.4-1**, the steel area is multiplied by $(n - 1)$ to calculate the transformed section properties, where n is the modular ratio between prestressing strand and concrete. Since the modulus of elasticity of concrete is different at transfer and final time, the transformed section properties should be calculated separately for the two stages. Using the similar procedures as in Section 9.2.3.2.3, the transformed composite section properties at final time are calculated in **Table 9.2.5.5-1**.

At transfer:

$$n - 1 = \frac{28,500}{4,496} - 1 = 5.339$$

At final:

$$n - 1 = \frac{28,500}{5,072} - 1 = 4.619$$

Table 9.2.5.5-1
Properties of Composite Transformed Section at Final Time

	Transformed Area, in. ²	y_b in.	Ay_b in. ³	$A(y_{btc} - y_b)^2$ in. ⁴	I in. ⁴	$I + A(y_{btc} - y_b)^2$ in. ⁴
Deck	816.37	76.25	62,248	327,528	3,826.75	331,355
Haunch	15.87	72.25	1147	4078	0.34	4078
Beam	767.00	36.60	28,072	295,252	545,894	841,146
Row 1	8.48	2.00	16.96	24,930		24,930
Row 2	8.48	4.00	33.92	23,124		23,124
Row 3	5.65	6.00	33.90	14,244		14,224
Row 4	2.83	8.00	22.64	6,580		6,580
Row 5	1.41	10.00	14.10	3,012		3,012
Row 6	1.41	12.00	16.92	2,757		2,757
Row 7	1.41	14.00	19.74	2,513		2,513
Row 8	1.41	16.00	22.56	2,281		2,281
Σ	1,630.3		91,648			1,256,000

Note: The moment of inertia of strand about its own centroid is neglected.

The transformed section properties are calculated as follows:

Noncomposite transformed section at transfer:

$$A_{ti} = \text{area of transformed section at transfer} = 802.9 \text{ in.}^2$$

$$I_{ti} = \text{moment of inertia of the transformed section at transfer} = 578,964 \text{ in.}^4$$

$$e_{ti} = \text{eccentricity of strands with respect to transformed section at transfer} = 29.40 \text{ in.}$$

$$y_{bti} = \text{distance from the centroid of the transformed section to the extreme bottom of the beam at transfer} \\ = 35.22 \text{ in.}$$

$$S_{bti} = \text{section modulus for the extreme bottom fiber of the transformed section at transfer} = 16,439 \text{ in.}^3$$

$$S_{tti} = \text{section modulus for the extreme top fiber of the transformed section at transfer} = 15,741 \text{ in.}^3$$

Noncomposite transformed section at final time:

$$A_{tf} = \text{area of transformed section at final time} = 798.1 \text{ in.}^2$$

$$I_{tf} = \text{moment of inertia of the transformed section at final time} = 574,703 \text{ in.}^4$$

$$e_{tf} = \text{eccentricity of strands with respect to transformed section at final time} = 29.58 \text{ in.}$$

BULB-TEE (BT-72), THREE SPANS, COMPOSITE DECK

9.2.5.5 Steel Transformed section Properties/9.2.6.1 Elastic Shortening

y_{btf} = distance from the centroid of the noncomposite transformed section to the extreme bottom fiber of the beam at final time = 35.4 in.

S_{btf} = section modulus for the extreme bottom fiber of the transformed section at final time = 16,235 in.³

S_{ttf} = section modulus for the extreme top fiber of the transformed section at final time = 15,702 in.³

Composite transformed section at final time:

A_{tc} = area of transformed composite section at final time = 1,630.3 in.²

I_{tc} = moment of inertia of the transformed composite section at final time = 1,256,000 in.⁴

e_{tc} = eccentricity of strands with respect to transformed composite section at final time = 50.40 in.

y_{btc} = distance from the centroid of the composite transformed section to the extreme bottom fiber of the beam at final time = 56.22 in.

S_{btc} = section modulus for the extreme bottom fiber of the transformed composite section at final time = 22,341 in.³

S_{ttc} = composite section modulus for the extreme top fiber of the precast beam for transformed section at final time = 79,594 in.³

S_{dtc} = composite section modulus for the extreme top fiber of the deck for transformed section at final time = 69,874 in.³

9.2.6 PRESTRESS LOSSES

Total prestress loss:

$$\Delta f_{pT} = \Delta f_{pES} + \Delta f_{pLT} \quad [\text{LRFD Eq. 5.9.5.1-1}]$$

where

Δf_{pT} = total loss in prestressing steel stress

Δf_{pES} = sum of all losses or gains due to elastic shortening or extension at the time of application of prestress and/or external loads

Δf_{pLT} = long-term losses due to shrinkage and creep of concrete, and relaxation of steel after transfer. In this design example, the refined estimates of time-dependent losses are used.

9.2.6.1 Elastic Shortening

$$\Delta f_{pES} = \frac{E_p}{E_{ci}} f_{cgp} \quad [\text{LRFD Eq. 5.9.5.2.3a-1}]$$

where

E_p = modulus of elasticity of prestressing strands = 28,500 ksi

E_{ci} = modulus of elasticity of beam concrete at transfer = 4,496 ksi

f_{cgp} = sum of concrete stresses at the center of gravity of prestressing tendons due to prestressing force at transfer and the self weight of the member at sections of maximum moment.

If the gross (or net) cross-section properties are used, it is necessary to perform numerical iterations. The elastic loss Δf_{pES} is usually assumed to be 10% of the initial prestress to calculate f_{cgp} , which is then used in the equation above to calculate a refined Δf_{pES} . The process is repeated until the assumed Δf_{pES} and refined Δf_{pES} converge. However, when transformed section properties are used to calculate the concrete stress, the effects of losses and gains due to elastic deformations are implicitly accounted for. Therefore, Δf_{pES} should not be included in calculating f_{cgp} .

BULB-TEE (BT-72), THREE SPANS, COMPOSITE DECK

9.2.6.1 Elastic Shortening/9.2.6.2.1 Shrinkage of Concrete

$$\begin{aligned} \text{Force per strand before transfer} &= (\text{area of strand})(\text{prestress stress before transfer}) \\ &= (0.153)(202.5) = 30.98 \text{ kips} \end{aligned}$$

$$f_{cgp} = \frac{P_{pi}}{A_{ti}} + \frac{P_{pi}e_{ti}^2}{I_{ti}} - \frac{M_g e_{ti}}{I_{ti}}$$

where

$$P_{pi} = \text{total prestressing force before transfer} = (44 \text{ strands})(30.98) = 1,363.1 \text{ kips}$$

$$e_{ti} = \text{eccentricity of strands at midspan with respect to the transformed section at transfer} = 29.40 \text{ in.}$$

M_g is calculated based on the overall beam length of 119 ft.

$$f_{cgp} = \frac{1,363.1}{802.9} + \frac{(1,363.1)(29.40)^2}{578,964} - \frac{(1,414.3)(12)(29.40)}{578,964} = 2.871 \text{ ksi}$$

Therefore, loss due to elastic shortening:

$$\Delta f_{pes} = \frac{28,500}{4,496} (2.871) = 18.2 \text{ ksi}$$

AASHTO LRFD C5.9.5.3 indicates that the loss due to elastic shortening at transfer should be added to the time-dependent losses to determine total losses. However, this loss at transfer is directly accounted for if transformed section properties are used in stress analysis.

9.2.6.2 Time-Dependent Losses between Transfer and Deck Placement

The following construction schedule is assumed in calculating the time-dependent losses:

$$\text{Concrete age at transfer: } t_i = 1 \text{ day}$$

$$\text{Concrete age at deck placement: } t_d = 90 \text{ days}$$

$$\text{Concrete age at final stage: } t_f = 20,000 \text{ days}$$

The total time-dependent loss between time of transfer and deck placement is the summation of prestress losses due to shrinkage of concrete, creep of concrete, and relaxation of prestressing strands.

9.2.6.2.1 Shrinkage of Concrete

The prestress loss due to shrinkage of concrete between transfer and deck placement is calculated by:

$$\Delta f_{pSR} = \epsilon_{bid} E_p K_{id} \quad [\text{LRFD Eq. 5.9.5.4.2a-1}]$$

where

$$\epsilon_{bid} = \text{concrete shrinkage strain of girder for time period between transfer and deck placement}$$

$$E_p = \text{modulus of elasticity of prestressing strands, ksi}$$

$$K_{id} = \text{transformed section coefficient that accounts for time-dependent interaction between concrete and bonded steel in the section being considered for time period between transfer and deck placement}$$

The concrete shrinkage strain ϵ_{bid} is taken as:

$$\epsilon_{bid} = k_{vs} k_{hs} k_f k_{td} 0.48 \times 10^{-3} \quad [\text{LRFD Eq. 5.4.2.3.3-1}]$$

where

The factor for the effect of the volume-to-surface ratio of the beam:

$$k_{vs} = 1.45 - 0.13(V/S) = 1.45 - 0.13 \times 3.01 = 1.059$$

The minimum value of k_s is 1.0 OK

V/S is the volume-to-surface ratio of the beam from **Table 2.5.7.1-1**.

BULB-TEE (BT-72), THREE SPANS, COMPOSITE DECK

9.2.6.2.1 Shrinkage of Concrete/9.2.6.2.2 Creep of Concrete

The humidity factor for shrinkage:

$$k_{hs} = 2.00 - 0.014H = 2.00 - 0.014(70) = 1.020$$

where H = average annual mean relative humidity (assume 70%)

The factor for the effect of concrete strength:

$$k_f = \frac{5}{1 + f'_{ci}} = \frac{5}{1 + 5.5} = 0.769$$

The time development factor at deck placement:

$$k_{td} = \frac{t}{61 - 4f'_{ci} + t} = \frac{89}{61 - 4(5.5) + 89} = 0.695 = k_{tda}$$

where t is the maturity of concrete (days) = $t_d - t_i = 90 - 1 = 89$ days

$$\varepsilon_{bid} = (1.059)(1.020)(0.769)(0.695)(0.48 \times 10^{-3}) = 0.000277$$

$$K_{id} = \frac{1}{1 + \frac{E_p}{E_{ci}} \frac{A_{ps}}{A_g} \left(1 + \frac{A_g (e_{pg})^2}{I_g}\right) [1 + 0.7\Psi_b(t_f, t_i)]} \quad \text{[LRFD Eq. 5.9.5.4.2a-2]}$$

where

e_{pg} = eccentricity of prestressing strand with respect to centroid of girder in. = 30.78 in.

$\Psi_b(t_f, t_i)$ = girder creep coefficient at final time due to loading introduced at transfer

For the time between transfer and final time:

$$\Psi_b(t_f, t_i) = 1.9k_{vs}k_{hc}k_fk_{td}t_i^{-0.118} \quad \text{[LRFD Eq. 5.4.2.3.2-1]}$$

$$k_{hc} = 1.56 - 0.008H = 1.56 - 0.008(70) = 1.000$$

$$k_{td} = \frac{t}{61 - 4f'_{ci} + t} = \frac{20,000 - 1}{61 - 4(5.5) + (20,000 - 1)} = 0.998 = k_{tdf}$$

$$\Psi_b(t_f, t_i) = 1.9(1.059)(1.000)(0.769)(0.998)(1)^{-0.118} = 1.544$$

$$K_{id} = \frac{1}{1 + \frac{28,500}{4,496} \frac{6,732}{767} \left(1 + \frac{767(30.78)^2}{545,894}\right) [1 + 0.7(1.544)]} = 0.787$$

The prestress loss due to shrinkage of concrete between transfer and deck placement is:

$$\Delta f_{pSR} = (0.000277)(28,500)(0.787) = 6.213 \text{ ksi}$$

9.2.6.2.2 Creep of Concrete

The prestress loss due to creep of beam concrete between time of transfer and deck placement is determined as:

$$\Delta f_{pCR} = \frac{E_p}{E_{ci}} f_{cgp} \Psi_b(t_d, t_i) K_{id} \quad \text{[LRFD Eq. 5.9.5.4.2b-1]}$$

where

$\Psi_b(t_d, t_i)$ = girder creep coefficient at time of deck placement due to loading introduced at transfer

$$= 1.9k_{vs}k_{hc}k_fk_{td}t_i^{-0.118} \quad \text{[LRFD Eq. 5.4.2.3.2-1]}$$

$$= 1.9(1.059)(1.000)(0.769)(0.695)(1)^{-0.118} = 1.075$$

$$\Delta f_{pCR} = \frac{28,500}{4,496} (2.871)(1.075)(0.787) = 15.397 \text{ ksi}$$

BULB-TEE (BT-72), THREE SPANS, COMPOSITE DECK

9.2.6.2.3 Relaxation of Prestressing Strands/9.2.6.3.1 Shrinkage of Concrete

9.2.6.2.3 Relaxation of Prestressing Strands

The prestress loss due to relaxation of prestressing strands between time of transfer and deck placement is determined as:

$$\Delta f_{pR1} = \frac{f_{pt}}{K_L} \left(\frac{f_{pt}}{f_{py}} - 0.55 \right) \quad [\text{LRFD Eq. 5.9.5.4.2c-1}]$$

where

- f_{pt} = stress in prestressing strands immediately after transfer, taken not less than $0.55f_y$
 K_L = 30 for low relaxation strands and 7 for other prestressing steel, unless more accurate manufacturer's data are available

$$\Delta f_{pR1} = \frac{(202.5 - 18.2)}{30} \left(\frac{(202.5 - 18.2)}{243} - 0.55 \right) = 1.281 \text{ ksi} \quad [\text{LRFD Eq. 5.9.5.4.2c-1}]$$

According to LRFD Art. 5.9.5.4.2c, the relaxation loss may also be assumed equal to 1.2 ksi for low-relaxation strands.

9.2.6.3 Time-Dependent Losses between Deck Placement and Final Time

The total time-dependent loss between time of deck placement and final time is the summation of prestress losses due to shrinkage of beam concrete, creep of beam concrete, relaxation of prestressing strands, and shrinkage of deck concrete.

9.2.6.3.1 Shrinkage of Concrete

The prestress loss due to shrinkage of concrete between deck placement and final time is calculated by:

$$\Delta f_{pSD} = \epsilon_{bdf} E_p K_{df} \quad [\text{LRFD Eq. 5.9.5.4.3a-1}]$$

where

- ϵ_{bdf} = concrete shrinkage strain of girder for the time period between deck placement and final time
 E_p = modulus of elasticity of prestressing strands, ksi
 K_{df} = transformed section coefficient that accounts for time-dependent interaction between concrete and bonded steel in the section being considered for time period between deck placement and final time

The total girder concrete shrinkage strain between transfer and final time is taken as:

$$\begin{aligned} \epsilon_{bif} &= k_{vs} k_{hs} k_{jt} k_{tdf} 0.48 \times 10^{-3} \quad [\text{LRFD Eq. 5.4.2.3.3-1}] \\ &= (1.059)(1.020)(0.769)(0.998)(0.48 \times 10^{-3}) = 0.000398 \end{aligned}$$

The girder concrete shrinkage strain between deck placement and final time is:

$$\epsilon_{bdf} = \epsilon_{bif} - \epsilon_{bid} = 0.000398 - 0.000277 = 0.000121$$

The girder concrete transformed section coefficient between deck placement and final time is:

$$K_{df} = \frac{1}{1 + \frac{E_p}{E_{ci}} \frac{A_{ps}}{A_c} \left(1 + \frac{A_c (e_{pc})^2}{I_c} \right) [1 + 0.7\Psi_b(t_f, t_i)]} \quad [\text{LRFD Eq. 5.9.5.4.3a-2}]$$

where

- A_c = area of the composite section = 1,599 in.²
 e_{pc} = eccentricity of strands with respect to centroid of composite section
 = 57.20 – 5.82 = 51.38 in.
 I_c = moment of inertia of the composite section = 1,175,063 in.⁴

BULB-TEE (BT-72), THREE SPANS, COMPOSITE DECK

9.2.6.3.1 Shrinkage of Concrete/9.2.6.3.4 Shrinkage of Deck Concrete

$$K_{df} = \frac{1}{1 + \frac{28,500}{4,496} \frac{6.732}{1,599} \left(1 + \frac{1,599(51.38)^2}{1,175,063}\right) [1 + 0.7(1.544)]} = 0.797$$

The prestress loss due to shrinkage of concrete between deck placement and final time is:

$$\Delta f_{pSD} = (0.000121)(28,500)(0.797) = 2.748 \text{ ksi}$$

9.2.6.3.2 Creep of Concrete

The prestress loss due to creep of beam concrete between time of deck placement and final time is determined as:

$$\Delta f_{pCD} = \frac{E_p}{E_c} f_{cgp} [\Psi_b(t_f, t_i) - \Psi_b(t_d, t_i)] K_{df} + \frac{E_p}{E_c} \Delta f_{cd} \Psi_b(t_f, t_d) K_{df} \quad [\text{LRFD Eq. 5.9.5.4.3b-1}]$$

where

$$\begin{aligned} \Psi_b(t_f, t_d) &= \text{girder creep coefficient at final time due to loading at deck placement} \\ &= 1.9 k_{vs} k_{hc} k_{fj} k_{td} t_d^{-0.118} \quad [\text{LRFD Eq. 5.4.2.3.2-1}] \end{aligned}$$

$$k_{tdf} = \frac{t}{61 - 4f'_{ci} + t} = \frac{(20,000 - 90)}{61 - 4(5.5) + (20,000 - 90)} = 0.998$$

$$\Psi_b(t_f, t_d) = 1.9(1.059)(1.000)(0.769)(0.998)(90)^{-0.118} = 0.908$$

Δf_{cd} = change in concrete stress at centroid of prestressing strands due to long-term losses between transfer and deck placement, combined with deck weight and superimposed loads, ksi

$$\begin{aligned} &= -(\Delta f_{pSR} + \Delta f_{pCR} + \Delta f_{pR1}) \frac{A_{ps}}{A_g} \left(1 + \frac{A_g e_{pg}^2}{I_g}\right) - \left(\frac{M_s e_{tf}}{I_{tf}} + \frac{(M_b + M_{ws}) e_{tc}}{I_{tc}}\right) \\ &= -(6.213 + 15.397 + 1.281) \frac{6.732}{767} \left(1 + \frac{767(30.78)^2}{545,894}\right) \\ &\quad - \left(\frac{2,126.9(12)(29.58)}{574,703} + \frac{(73 + 128)(12)(50.40)}{1,256,000}\right) \\ &= -1.879 \text{ ksi} \end{aligned}$$

The gross section properties are used in the equation to calculate Δf_{cd} for the long-term losses since the transformed section effect has already been included in the factor K_{id} when calculating the losses between initial time and deck placement.

$$\begin{aligned} \Delta f_{pCD} &= \frac{28,500}{4,496} (2.871)(1.544 - 1.075)(0.797) + \frac{28,500}{5,072} (-1.879)(0.908)(0.797) \\ &= -0.838 \text{ ksi} \quad \text{The negative sign indicates a prestressing gain.} \end{aligned}$$

9.2.6.3.3 Relaxation of Prestressing Strands

The prestress loss due to relaxation of prestressing strands in composite section between time of deck placement and final time is taken as:

$$\Delta f_{pR2} = \Delta f_{pR1} = 1.281 \text{ ksi} \quad [\text{LRFD Eq. 5.9.5.4.3c-1}]$$

9.2.6.3.4 Shrinkage of Deck Concrete

The prestress gain due to shrinkage of deck concrete is calculated by:

$$\Delta f_{pSS} = \frac{E_p}{E_c} \Delta f_{cdf} K_{df} [1 + 0.7 \Psi_b(t_f, t_d)] \quad [\text{LRFD Eq. 5.9.5.4.3d-1}]$$

where Δf_{cdf} = change in concrete stress at centroid of prestressing strands due to shrinkage of deck concrete, ksi

BULB-TEE (BT-72), THREE SPANS, COMPOSITE DECK**9.2.6.3.4 Shrinkage of Deck Concrete/9.6.2.4 Total Time-Dependent Loss**

$$\Delta f_{cdf} = \frac{\epsilon_{ddf} A_d E_{cd}}{1 + 0.7 \Psi_d(t_f, t_d)} \left(\frac{1}{A_c} - \frac{e_{pc} e_d}{I_c} \right) \quad [\text{LRFD Eq. 5.9.5.4.3d-2}]$$

where

- ϵ_{ddf} = shrinkage strain of deck concrete between placement and final time
- A_d = area of deck concrete, in.²
- E_{cd} = modulus of elasticity of deck concrete, ksi
- $\Psi_d(t_f, t_d)$ = deck concrete creep coefficient at final time due to loading introduced shortly after deck placement
- e_d = eccentricity of deck with respect to the gross composite section, in.

Assume the initial strength of concrete at deck placement is $0.8(4.0 \text{ ksi}) = 3.2 \text{ ksi}$, and use a volume-to-surface (V/S) ratio of 3.622 for the deck:

$$k_{vs} = 1.45 - 0.13(V/S) = 1.45 - 0.13(3.622) = 0.979 < 1.0$$

Use $k_{vs} = 1.000$

$$k_f = \frac{5}{1 + f'_{ci}} = \frac{5}{1 + 3.2} = 1.190$$

$$k_{td} = \frac{t}{61 - 4f'_{ci} + t} = \frac{20,000 - 90}{61 - 4(3.2) + (20,000 - 90)} = 0.998$$

$$\begin{aligned} \epsilon_{ddf} &= k_{vs} k_{hs} k_f k_{td} 0.48 \times 10^{-3} & [\text{LRFD Eq. 5.4.2.3.3-1}] \\ &= (1.000)(1.020)(1.190)(0.998)(0.48 \times 10^{-3}) \\ &= 0.000581 \end{aligned}$$

$$\begin{aligned} \Psi_d(t_f, t_d) &= 1.9 k_{vs} k_{hc} k_f k_{td} t_i^{-0.118} & [\text{LRFD Eq. 5.4.2.3.2-1}] \\ &= 1.9(1.000)(1.000)(1.190)(0.998)(1)^{-0.118} \\ &= 2.256 \end{aligned}$$

Creep of the deck concrete is assumed to start at 1 day

$$\begin{aligned} \Delta f_{cdf} &= \frac{0.000581(144)(7.5)(3,834)}{1 + 0.7(2.256)} \left(\frac{1}{1,599} - \frac{51.38(80 - 7.5/2 - 57.20)}{1,175,063} \right) \\ &= -0.194 \text{ ksi} \quad \text{The negative sign indicates a prestressing gain.} \end{aligned}$$

The prestress gain due to shrinkage of the deck in the composite section:

$$\Delta f_{pSS} = \frac{28,500}{5,072} (-0.194)(0.797)[1 + 0.7(0.908)] = -1.421 \text{ ksi}$$

Note: The effect of deck shrinkage on the calculation of prestress gain is discussed further in Section 9.1a.8.5

9.2.6.4 Total Time-Dependent Loss

The total time-dependent loss, Δf_{pLT} , is determined as:

$$\begin{aligned} \Delta f_{pLT} &= (\Delta f_{pSR} + \Delta f_{pCR} + \Delta f_{pR1}) + (\Delta f_{pSD} + \Delta f_{pCD} + \Delta f_{pR2} + \Delta f_{pSS}) & [\text{LRFD Eq. 5.9.5.4.1-1}] \\ &= (6.213 + 15.397 + 1.281) + (2.748 - 0.838 + 1.281 - 1.421) \\ &= 22.891 + 1.770 = 24.7 \text{ ksi} \end{aligned}$$

BULB-TEE (BT-72), THREE SPANS, COMPOSITE DECK**9.2.6.5 Total Losses at Transfer/9.2.6.6 Total Losses at Service Loads****9.2.6.5 Total Losses at Transfer**

AASHTO LRFD C5.9.5.2.3a and C5.9.5.3 indicate that the losses or gains due to elastic deformation must be taken equal to zero if transformed section properties are used in stress analysis. However, the losses or gains due to elastic deformation must be included in determining the total prestress losses and effective stress in the prestressing strands.

$$\Delta f_{pi} = \Delta f_{pES} = 18.2 \text{ ksi}$$

Effective stress in tendons immediately after transfer, $f_{pt} = f_{pi} - \Delta f_{pi} = (202.5 - 18.2) = 184.3 \text{ ksi}$

Force per strand = $(f_{pt})(\text{area of strand}) = 184.3(0.153) = 28.20 \text{ kips}$

Therefore, the total prestressing force after transfer, $P_{pt} = 28.20(44) = 1,240.8 \text{ kips}$

Initial loss, % = $(\text{Total losses at transfer})/(f_{pi}) = 18.2/(202.5) = 9.0 \%$

When determining the concrete stress using transformed section properties, the strand force is that before transfer:

Force per strand = $(202.5)(0.153) = 30.98 \text{ kips}$

The total prestressing force before transfer, $P_{pi} = 30.98(44) = 1,363.1 \text{ kips}$

9.2.6.6 Total Losses at Service Loads

Total loss due to elastic shortening at transfer and long-term losses is:

$$\Delta f_{pT} = \Delta f_{pES} + \Delta f_{pLT} = 18.2 + 24.7 = 42.9 \text{ ksi}$$

The elastic gain due to deck weight, superimposed dead load, and live load (Service III) is:

$$\begin{aligned} & \left(\frac{M_s e_{tf}}{I_{tf}} + \frac{(M_b + M_{ws}) e_{tc}}{I_{tc}} \right) \frac{E_p}{E_c} + 0.8 \left(\frac{(M_{LL+LT}) e_{tc}}{I_{tc}} \right) \frac{E_p}{E_c} \\ &= \left(\frac{(2,126.9)(12)(29.58)}{574,703} + \frac{(73 + 128)(12)(50.40)}{1,256,000} \right) \frac{28,500}{5,072} + 0.8 \left(\frac{(2,115.0)(12)(50.4)}{1,256,000} \right) \frac{28,500}{5,072} \\ &= 7.9 + 4.6 = 12.5 \text{ ksi} \end{aligned}$$

The effective stress in strands after all losses and gains:

$$f_{pe} = f_{pi} - \Delta f_{pT} + 7.9 = 202.5 - 42.9 + 12.5 = 172.1 \text{ ksi}$$

Check prestressing stress limit at service limit state:

[LRFD Table 5.9.3-1]

$$f_{pe} = \leq 0.8f_{py} = 0.8(243) = 194.4 \text{ ksi} > 172.1 \text{ ksi} \quad \text{OK}$$

The effective stress in strands after all losses and permanent gains:

$$f_{pe} = f_{pi} - \Delta f_{pT} + 7.9 = 202.5 - 42.9 + 7.9 = 167.5 \text{ ksi}$$

Force per strand without live load gains = $(f_{pe})(\text{area of strand}) = 167.5 (0.153) = 25.63 \text{ kips}$

Therefore, the total prestressing force after all losses = $25.63(44) = 1,127.7 \text{ kips}$

Final loss percentage = $(\text{total losses and gains})/(f_{pi}) = (42.9 - 7.9)/(202.5) = 17.3\%$

Without consideration of prestressing gains at deck placement, the final loss percentage = $\text{total losses}/(f_{pi}) = (42.9)/202.5 = 21.2\%$

When determining the concrete stress using transformed section properties, all the elastic gains and losses are implicitly accounted for:

Force per strand with only total time-dependent losses = $(f_{pi} - \Delta f_{pLT})(\text{area of strand}) = (202.5 - 24.7)(0.153) = 27.20 \text{ kips}$

Total prestressing force, $P_{pe} = 27.20(44) = 1,196.8 \text{ kips}$

BULB-TEE (BT-72), THREE SPANS, COMPOSITE DECK

9.2.7 Concrete Stresses at Transfer/9.2.7.2 Stresses at Transfer Length Section

9.2.7 CONCRETE STRESSES AT TRANSFER

Because the transformed section is used, the total prestressing force before and after transfer $P_{pi} = 1,363.1$ kips

9.2.7.1 Stress Limits For Concrete

[LRFD Art. 5.9.4]

Compression:

- $0.6f'_{ci} = 0.6(5.5) = +3.300$ ksi

where f'_{ci} = concrete strength at transfer

Tension:

- without bonded auxiliary reinforcement:

$$-0.0948\sqrt{f'_{ci}} \leq -0.200 \text{ ksi}; -0.0948\sqrt{5.500} = -0.222 \text{ ksi} < \boxed{-0.200} \text{ ksi}$$

Therefore, -0.200 ksi (Controls)

- with bonded auxiliary reinforcement that is sufficient to resist 120% of the tension force in the cracked concrete:

$$-0.24\sqrt{f'_{ci}} = -0.24\sqrt{5.500} = -0.563 \text{ ksi}$$

9.2.7.2 Stresses at Transfer Length Section

Stresses at this location need only be checked at transfer because this stage almost always governs. Also, losses with time will reduce the concrete stresses making them less critical.

$$\text{Transfer length} = 60(\text{strand diameter}) = 60(0.5) = 30 \text{ in.} = 2.5 \text{ ft}$$

[LRFD Art. 5.11.4]

Due to the camber of the beam at transfer, the beam self weight acts on the overall beam length (119 ft).

Therefore, values of bending moment given in **Table 9.2.4-1** cannot be used since they are based on the span between centerlines of bearings (118 ft). Using Equation Eq. 9.2.4.1.2-2 given previously, the bending moment at a distance 2.5 ft from the end of the beam is calculated due to beam self weight:

$$M_g = (0.5)(0.799)(2.5)(119 - 2.5) = 116.4 \text{ ft-kips}$$

Compute stress in the top of beam:

$$f_t = \frac{P_{pi}}{A_{ti}} - \frac{P_{pi}e_{ti}}{S_{tti}} + \frac{M_g}{S_{tti}} = \frac{1,363.1}{802.9} - \frac{(1,363.1)(29.40)}{15,741} + \frac{(116.4)(12)}{15,741}$$

$$= 1.698 - 2.546 + 0.089 = -0.759 \text{ ksi}$$

Tensile stress limit for concrete with bonded reinforcement: -0.563 ksi NG

Compute stress in the bottom fiber of the beam:

$$f_b = \frac{P_{pi}}{A_{ti}} + \frac{P_{pi}e_{ti}}{S_{bti}} - \frac{M_g}{S_{bti}} = \frac{1,363.1}{802.9} + \frac{(1,363.1)(29.40)}{16,439} - \frac{(116.4)(12)}{16,439}$$

$$= 1.698 + 2.438 - 0.085 = +4.051 \text{ ksi}$$

Compressive stress limit for concrete: $+3.300$ ksi NG

Since the stresses at the top and bottom exceed the stress limits, harp strands to make stresses fall within the specified limits. Harp 12 strands at the $0.3L$ points, as shown in **Figures 9.2.7.2-1** and **9.2.7.2-2**. This harp location is more appropriate for the end spans of multi-span continuous bridges because the maximum positive moment is closer to the abutment than in the interior spans. For simple spans, it is more common to use a harp point at least $0.4L$ from the ends.

BULB-TEE (BT-72), THREE SPANS, COMPOSITE DECK

9.2.7.2 Stresses at Transfer Length Section

**Figure 9.2.7.2-1
Strand Pattern**

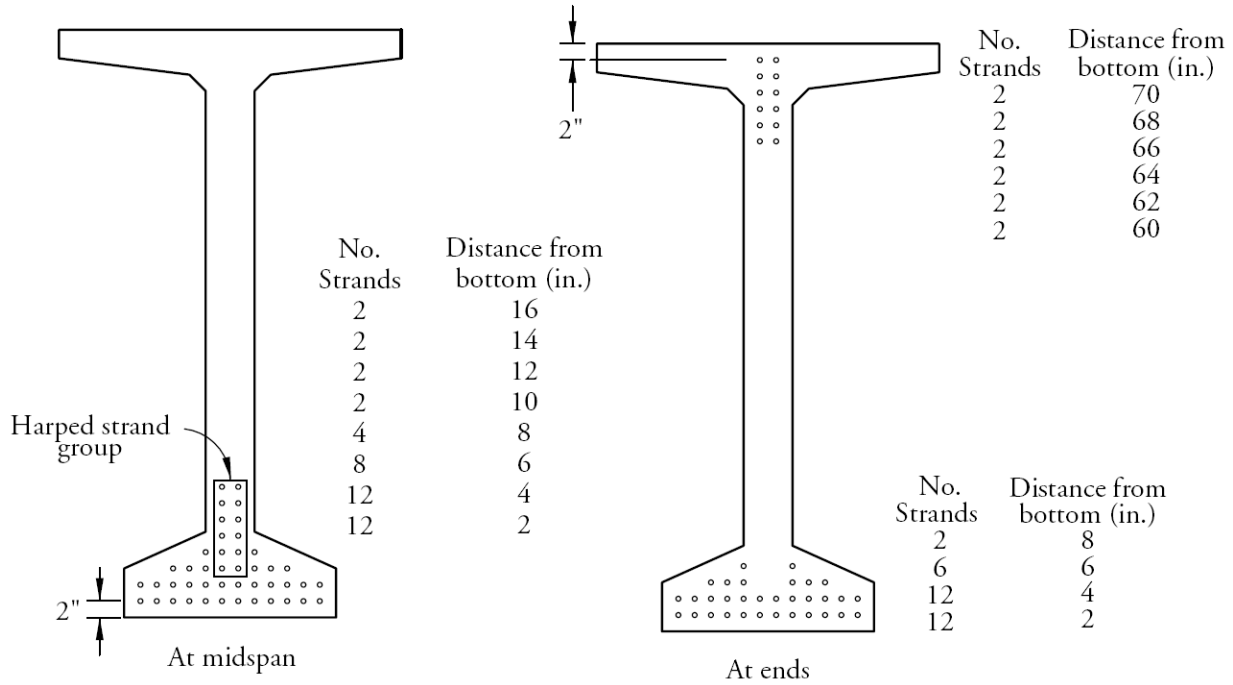
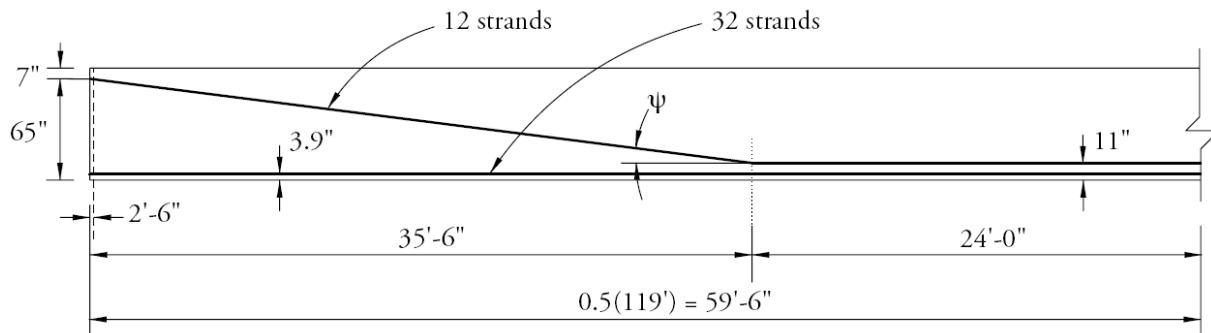


**Figure 9.2.7.2-2
Longitudinal Strand Profile**



Compute the center of gravity of the prestressing strands at the transfer length using the harped pattern.

The distance between the center of gravity of the 12 harped strands at the end of the beam and the top fiber of the precast beam is:

$$\frac{2(2) + 2(4) + 2(6) + 2(8) + 2(10) + 2(12)}{12} = 7.00 \text{ in.}$$

The distance between the center of gravity of the 12 harped stands at the harp point and the bottom fiber of the beam is:

$$\frac{2(6) + 2(8) + 2(10) + 2(12) + 2(14) + 2(16)}{12} = 11.0 \text{ in.}$$

The distance between the center of gravity of the 12 harped strands and the top fiber of the beam at the transfer length section is:

$$7 \text{ in.} + \frac{(72 - 11 - 7) \text{ in.}}{35.5 \text{ ft}} (2.5) \text{ ft} = 10.80 \text{ in.}$$

BULB-TEE (BT-72), THREE SPANS, COMPOSITE DECK

9.2.7.2 Stresses at Transfer Length Section/9.2.7.2 Stresses at Midspan

The distance between the center of gravity of the 32 straight bottom strands and the extreme bottom fiber of the beam is:

$$\frac{12(2) + 12(4) + 6(6) + 2(8)}{32} = 3.88 \text{ in.}$$

Therefore, the distance between the center of gravity of the total number of the strands and the bottom fiber of the precast beam at transfer length is:

$$\frac{12(72 - 10.80) + 32(3.88)}{44} = 19.51 \text{ in.}$$

Eccentricity of the 44 strand group at transfer length, e , is: $35.84 - 19.51 = 16.33 \text{ in.}$

The distance between the center of gravity of the total number of the strands and the bottom fiber of the precast beam at the end of the beam is:

$$\frac{12(72 - 7) + 32(3.88)}{44} = 20.55 \text{ in.} = y_{bs}$$

Recompute top and bottom stresses at the transfer length section using the harped strands. Note that the transformed section properties are now different than those at midspan and have been re-calculated.

Concrete stress at top of the beam:

$$f_t = \frac{1,363.1}{802.9} - \frac{(1,363.1)(16.33)}{16,027} + \frac{(116.4)(12)}{16,027} = 1.698 - 1.389 + 0.087 = +0.396 \text{ ksi}$$

Compressive stress limit for concrete: +3.300 ksi OK

Concrete stress at bottom of the beam,

$$f_b = \frac{1,363.1}{802.9} + \frac{(1,363.1)(16.33)}{16,170} - \frac{(116.4)(12)}{16,170} = 1.698 + 1.377 - 0.086 = +2.989 \text{ ksi}$$

Compressive stress limit for concrete: +3.300 ksi OK

9.2.7.3 Stresses at the Harp Points

The strand eccentricity at the harp points is the same as at midspan, $e_{ti} = 29.40 \text{ in.}$

Bending moment due to beam self weight at a distance 35.5 ft (0.3L) from the end of the beam is:

$$M_g = (0.5)(0.799)(35.5)(119 - 35.5) = 1,184.2 \text{ ft-kips}$$

Concrete stress at top of the beam,

$$f_t = \frac{1,363.1}{802.9} - \frac{(1,363.1)(29.40)}{15,741} + \frac{(1,184.2)(12)}{15,741} = 1.698 - 2.546 + 0.903 = +0.055 \text{ ksi}$$

Compressive stress limit for concrete: +3.300 ksi OK

Concrete stress at bottom of the beam:

$$f_b = \frac{1,363.1}{802.9} + \frac{(1,363.1)(29.40)}{16,439} - \frac{(1,184.2)(12)}{16,439} = 1.698 + 2.438 - 0.864 = +3.272 \text{ ksi}$$

Compressive stress limit for concrete: +3.300 ksi OK

9.2.7.4 Stresses at Midspan

The bending moment due to beam self weight at a distance 59.5 feet from the end of the beam is:

$$M_g = (0.5)(0.799)(59.5)(119 - 59.5) = 1,414.3 \text{ ft-kips}$$

Concrete stress at top of the beam:

$$f_t = \frac{1,363.1}{802.9} - \frac{(1,363.1)(29.40)}{15,741} + \frac{(1,414.3)(12)}{15,741} = 1.698 - 2.546 + 1.078 = +0.230 \text{ ksi}$$

BULB-TEE (BT-72), THREE SPANS, COMPOSITE DECK

9.2.7.4 Stresses at Midspan/9.2.8.1 Stress Limits for Concrete

Compressive stress limit for concrete: +3.300 ksi OK

Concrete stress at bottom of the beam,

$$f_b = \frac{1,363.1}{802.9} + \frac{(1,363.1)(29.40)}{16,439} - \frac{(1,414.3)(12)}{16,439} = 1.698 + 2.438 - 1.032 = +3.104 \text{ ksi}$$

Compressive stress limit for concrete: +3.300 ksi OK

9.2.7.5 Hold-Down Forces

Assume that the stress in the strand at the time of prestressing, before any losses, is:

$$0.80f_{pu} = 0.80(270) = 216 \text{ ksi}$$

Then, the prestress force per strand before any losses is: $0.153(216) = 33.0$ kipsFrom **Figure 9.2.7.2-2**, the harp angle,

$$\psi = \tan^{-1} \left(\frac{72 - 7 - 11}{35.5(12)} \right) = 7.2^\circ$$

Therefore, hold-down force/strand = 1.05 (force per strand)(sin ψ)

$$= 1.05(33.0) \sin 7.2^\circ = 4.34 \text{ kips/strand}$$

Note that the factor 1.05 is applied to account for friction.

$$\text{Total hold-down force} = 12 \text{ strands } (4.34) = 52.08 \text{ kips}$$

The hold-down force and the harp angle should be checked against maximum limits for local practices. Refer to Chapter 3, Fabrication and Construction, and Chapter 8, Design Theory and Procedures, for additional details.

9.2.7.6 Summary of Stresses at Transfer

	Top Fiber Stresses f_t , ksi	Bottom Fiber Stresses f_b , ksi
At transfer length section	+0.396	+2.989
At harp points	+0.055	+3.272
At midspan	+0.230	+3.104

Note that the bottom stresses at the harp points are now more critical than the ones at midspan.

9.2.8 CONCRETE STRESSES AT SERVICE LOADSUsing transformed section properties and refined losses, $P_{pe} = 1,196.8$ kips**9.2.8.1 Stress Limits For Concrete**

[LRFD Art. 5.9.4.2]

Compression:

Due to permanent loads, (i.e., beam self weight, weight of slab and haunch, weight of future wearing surface, and weight of barriers), for load combination Service I:

$$\text{for precast beams: } 0.45f'_c = 0.45(7.000) = +3.150 \text{ ksi}$$

$$\text{for deck: } 0.45f'_c = 0.45(4.000) = +1.800 \text{ ksi}$$

Due to permanent and transient loads (i.e., all dead loads and live loads), for load combination Service I:

$$\text{for precast beams: } 0.60f'_c = 0.60(7.000) = +4.200 \text{ ksi}$$

$$\text{for deck: } 0.60f'_c = 0.60(4.000) = +2.400 \text{ ksi}$$

BULB-TEE (BT-72), THREE SPANS, COMPOSITE DECK**9.2.8.1 Stress Limits for Concrete/9.2.8.2.3 Concrete Stress at the Bottom Fiber of Beam, Load Combination Service III**

Tension:

For components with bonded prestressing tendons:

$$\text{for load combination Service III: } -0.19\sqrt{f'_c}$$

$$\text{for precast beam: } -0.19\sqrt{7.000} = -0.503 \text{ ksi}$$

9.2.8.2 Stresses at Midspan**9.2.8.2.1 Concrete Stresses at the Top Fiber of the Beam**

To check top compressive stress, two cases are considered:

1. Under permanent loads, load combination Service I:

Using bending moment values given in **Table 9.2.4-1**, concrete stress at top fiber of the beam is:

$$\begin{aligned} f_{tg} &= \frac{P_{pe}}{A_{tf}} - \frac{P_{pc}e_{tf}}{S_{ttf}} + \frac{(M_g + M_s)}{S_{ttf}} + \frac{(M_{ws} + M_b)}{S_{ttc}} \\ &= \frac{1,196.8}{798.1} - \frac{(1,196.8)(29.58)}{15,702} + \frac{(1,390.7 + 2,126.9)(12)}{15,702} + \frac{(128.0 + 73.0)(12)}{79,594} \\ &= 1.500 - 2.255 + 2.688 + 0.030 = +1.963 \text{ ksi} \end{aligned}$$

Compressive stress limit for concrete: +3.150 ksi OK

2. Under permanent and transient loads, load combination Service I:

$$\begin{aligned} f_{tg} &= +1.963 + \frac{(M_{LL+LT})}{S_{ttc}} \\ &= +1.963 + \frac{(2,115.0)(12)}{79,594} \\ &= 1.963 + 0.319 = +2.282 \text{ ksi} \end{aligned}$$

Compressive stress limit for concrete: +4.200 ksi OK

9.2.8.2.2 Concrete Stress at the Top Fiber of the Deck, Load Combination Service I

Note: Compression stress in the deck slab at service loads never controls the design for typical applications. The calculations shown below are for illustration and may not be necessary in most practical applications.

1. Under permanent loads, load combination Service 1:

$$f_{tc} = \frac{(M_{ws} + M_b)}{S_{dtc}} = \frac{(128.0 + 73.0)(12)}{69,874} = +0.035 \text{ ksi}$$

Compressive stress limit for concrete: +1.800 ksi OK

2. Under permanent and transient loads, load combination Service I:

$$f_{tc} = \frac{(M_{ws} + M_b + M_{LL+LT})}{S_{dtc}} = \frac{(128.0 + 73.0 + 2,115.0)(12)}{69,874} = +0.398 \text{ ksi}$$

Compressive stress limit for concrete: +2.400 ksi OK

9.2.8.2.3 Concrete Stress at the Bottom Fiber of Beam, Load Combination Service III

$$\begin{aligned} f_b &= \frac{P_{pe}}{A_{tf}} + \frac{P_{pe}e_{tf}}{S_{btf}} - \frac{(M_g + M_s)}{S_{btf}} - \frac{(M_{ws} + M_b) + 0.8(M_{LL+LT})}{S_{btc}} \\ &= \frac{1,196.8}{798.1} + \frac{(1,196.8)(29.58)}{16,235} - \frac{(1,390.7 + 2,126.9)(12)}{16,235} - \frac{(128.0 + 73.0)(12) + 0.8(2,115.0)(12)}{22,341} \\ &= 1.500 + 2.181 - 2.600 - 1.017 = -+0.064 \text{ ksi} \end{aligned}$$

Compressive stress limit for concrete: +3.300 ksi OK

BULB-TEE (BT-72), THREE SPANS, COMPOSITE DECK

9.2.8.3 Fatigue Stress Limit/9.2.9.1 Positive Moment Section

9.2.8.3 Fatigue Stress Limit

9.2.8.3.1 Positive Moment Section

Fatigue limit state is not checked in this example. For an example of this calculation, refer to Example 9.1a, Section 9.1a.8.3.

9.2.8.3.2 Negative Moment Section

In order to perform the fatigue check, the reinforcement of the section should be determined. Therefore, the fatigue check for the negative moment section is addressed in Section 9.2.9.2.2.

9.2.8.4 Summary of Stresses at Service Loads

The stresses calculated using the above methods are summarized in **Table 9.2.8.4-1**. For comparison, the stresses calculated for the same design example using the previous method of calculating prestress losses are also shown in the table (Example 9.6 in the previous edition of the manual).

Table 9.2.8.4-1
Stresses at Midspan at Service Loads

Design Example	Top of Deck, ksi Service I		Top of Beam, ksi Service I		Bottom of Beam, ksi Service III
	Permanent Loads	Total Loads	Permanent Loads	Total Loads	
9.1b	+0.035	+0.398	+1.963	+2.282	+ 0.064
9.6	+0.042	+0.485	+2.062	+2.463	-0.495

9.2.8.5 Effect of Deck Shrinkage

The calculations in Section 9.2.8.2 comply with the *LRFD Specifications*. However, PCI believes that it is not appropriate to include the prestressing gain caused by the deck shrinkage, Δf_{pss} , in calculating the prestress losses. Alternatively, the effect of deck shrinkage should be analyzed by considering it as an external force applied to the composite nontransformed section as illustrated in Section 9.1a.8.5.

9.2.9 STRENGTH LIMIT STATE

9.2.9.1 Positive Moment Section

Total ultimate bending moment for Strength I is:

$$M_u = 1.25(DC) + 1.5(DW) + 1.75(LL + IM) \quad \text{[LRFD Tables 3.4.1-1\&2]}$$

Using the values of unfactored bending moment given in **Table 9.2.4-1**, the ultimate bending moment at midspan of the center span is:

$$M_u = 1.25(1,390.7 + 2,126.9 + 73.0) + 1.5(128.0) + 1.75(2,115.0) \\ = 4,488.3 + 192.0 + 3,701.3 = 8,381.6 \text{ ft-kips}$$

Average stress in prestressing strands when $f_{pe} \geq 0.5 f_{pu}$:

$$f_{ps} = f_{pu} \left(1 - k \frac{c}{d_p} \right) \quad \text{[LRFD Eq. 5.7.3.1.1-1]}$$

where

$$f_{ps} = \text{average stress in prestressing strand, ksi}$$

$$f_{pu} = \text{specified tensile strength of prestressing strand} = 270.0 \text{ ksi}$$

$$k = 2 \left(1.04 - \frac{f_{py}}{f_{pu}} \right) \quad \text{[LRFD Eq. 5.7.3.1.1-2]}$$

$$= 0.28 \text{ for low-relaxation strands} \quad \text{[LRFD Table C5.7.3.1.1-1]}$$

BULB-TEE (BT-72), THREE SPANS, COMPOSITE DECK

9.2.9.1 Positive Moment Section

$$c = \text{distance from the extreme compression fiber to the neutral axis, in.} \quad [\text{LRFD 5.7.3.2.2}]$$

$$d_p = \text{distance from extreme compression fiber to the centroid of the prestressing strands} \\ = h_c - y_{bs} = 80.00 - 5.82 = 74.18 \text{ in.}$$

To compute c , assume rectangular section behavior, and check if the depth of the equivalent compression block, a , is equal to or less than t_s :

$$c = \frac{A_{ps}f_{pu} + A_s f_y - A'_s f'_y}{0.85f'_c \beta_1 b + k A_{ps} \frac{f_{pu}}{d_p}} \quad [\text{LRFD Eq. 5.7.3.1.1-4}]$$

where

$$A_{ps} = \text{area of prestressing strand} = 44(0.153) = 6.732 \text{ in.}^2$$

$$A_s = \text{area of nonprestressed tension reinforcement} = 0.0 \text{ in.}^2$$

$$f_y = \text{specified yield strength of tension reinforcement} = 60.0 \text{ ksi}$$

$$A'_s = \text{area of compression reinforcement} = 0.0 \text{ in.}^2$$

$$f'_y = \text{specified yield strength of compression reinforcement} = 60.0 \text{ ksi}$$

$$f'_c = \text{compressive strength of deck concrete} = 4.0 \text{ ksi}$$

$$\beta_1 = \text{stress factor of compression block} \quad [\text{LRFD Art. 5.7.2.2}]$$

$$= 0.85 \text{ for } f'_c \leq 4.0 \text{ ksi}$$

$$= 0.85 - 0.05(f'_c - 4.0) \geq 0.65 \text{ for } f'_c > 4.0 \text{ ksi}$$

$$= 0.85$$

$$b = \text{effective width of compression flange} = 144 \text{ in.}$$

$$c = \frac{(6.732)(270.0) + 0.0 - 0.0}{(0.85)(4.0)(0.85)(144) + 0.28(6.732) \frac{270.0}{74.18}} = 4.30 \text{ in.} < t_s = 7.5 \text{ in.} \quad \text{OK}$$

$$a = \text{depth of the equivalent stress block} = \beta_1 c \quad [\text{LRFD Eq. 9.6.9.1-1}]$$

$$= 0.85(4.30) = 3.66 \text{ in.}$$

Therefore, the assumption of rectangular section behavior is valid.

The average stress in prestressing strand is:

$$f_{ps} = 270.0 \left(1 - 0.28 \frac{4.30}{74.18} \right) = 265.6 \text{ ksi}$$

$$\text{Nominal flexural resistance:} \quad [\text{LRFD Art. 5.7.3.2.3}]$$

$$M_n = A_{ps} f_{ps} \left(d_p - \frac{a}{2} \right) \quad [\text{LRFD Eq. 5.7.3.2.2-1}]$$

The above equation is a simplified form of LRFD Equation 5.7.3.2.2-1 because no compression reinforcement or nonprestressed reinforcement is considered and the section behaves as a rectangular section.

$$M_n = (6.732)(265.6) \left(74.18 - \frac{3.66}{2} \right) / 12 = 10,780 \text{ ft-kips}$$

Factored flexural resistance:

$$M_r = \phi M_n \quad [\text{LRFD Eq. 5.7.3.2.1-1}]$$

where ϕ = resistance factor

$$[\text{LRFD Art. 5.5.4.2.1}]$$

$$= 1.00, \text{ for tension controlled prestressed concrete sections}$$

$$M_r = 0,780 \text{ ft-kips} > M_u = 8,381.6 \text{ ft-kips} \quad \text{OK}$$

BULB-TEE (BT-72), THREE SPANS, COMPOSITE DECK

9.2.9.2 Negative Moment Section/9.2.9.2.1 Design of the Section

9.2.9.2 Negative Moment Section**9.2.9.2.1 Design of the Section**

Total ultimate bending moment for Strength I is:

$$M_u = 1.25(DC) + 1.5(DW) + 1.75(LL + IM) \quad [\text{LRFD Tables 3.4.1-1\&2}]$$

At the pier section:

$$M_u = 1.25(-197) + 1.5(-345) + 1.75(-2,327.7) = -4,837.2 \text{ ft-kips}$$

Notes:

1. At the negative moment section, the compression face is the bottom flange of the beam and is 26 in. wide.

Therefore, the design strength of the concrete is 7.0 ksi.

2. This section is a nonprestressed reinforced concrete section, thus $\phi = 0.9$ for flexure.

Assume the deck reinforcement is at mid-height of the deck. The effective depth:

$$d_e = 72 + 0.5 + 0.5(7.5) = 76.25 \text{ in.}$$

$$R_u = \frac{M_u}{\phi b d_e^2} = \frac{4,837.2 (12)}{(0.9)(26)(76.25)^2} = 0.427 \text{ ksi}$$

$$m = \frac{f_y}{0.85 f'_c} = \frac{60.0}{(0.85)(7.0)} = 10.084$$

$$\rho = \frac{1}{m} \left[1 - \sqrt{1 - \frac{2R_u m}{f_y}} \right] = \frac{1}{10.084} \left[1 - \sqrt{1 - \frac{2(0.427)(10.084)}{60.0}} \right] = 0.00739$$

$$A_s = (\rho b d_e) = (0.00739)(26)(76.25) = 14.65 \text{ in.}^2$$

This is the amount of nonprestressed reinforcement required in the slab to resist the negative moment. Assume that the typical deck reinforcement consists of a bottom mat of No. 5 bars @ 12 in. and a top mat of No. 4 bars @ 12 in. for a total $A_s = 0.20 + 0.31 = 0.51 \text{ in.}^2/\text{ft}$.

Since the *LRFD Specifications* does not provide guidance on the width over which this reinforcement is to be distributed, it is assumed here to be the same as the effective compression flange width which was determined earlier to be 144 in.

The typical reinforcement provided over this width is equal to $(144 \times 0.51/12) = 6.12 \text{ in.}^2$. Therefore, the required additional reinforcement at the negative moment section = $14.65 - 6.12 = 8.53 \text{ in.}^2$.

Provide twelve No. 8 bars additional reinforcement at 12-in. spacing (one No. 8 bar in each space between the No. 4 bars).

$$A_s = 12(0.79) = 9.48 \text{ in.}^2$$

Therefore, the total A_s provided = $9.48 + 6.12 = 15.60 \text{ in.}^2 > 14.65 \text{ in.}^2$ OK

Compute the capacity of the section in flexure at the pier:

Compute the depth of the compression block:

$$a = \frac{A_s f_y}{0.85 b f'_c} = \frac{15.60(60.0)}{(0.85)(26)(7.0)} = 6.05 \text{ in.}$$

Note that this value is slightly larger than the flange thickness of 6.0 in. However, the adjustment in the moment capacity, ϕM_n , when using a more accurate nonrectangular section analysis, is extremely small.

$$\phi M_n = \phi A_s f_y \left(d - \frac{a}{2} \right)$$

BULB-TEE (BT-72), THREE SPANS, COMPOSITE DECK

9.2.9.2.1 Design of the Section/9.2.10.1.2 Minimum Reinforcement

$$\phi M_n = 0.9(15.60)(60.0) \left(76.25 - \frac{6.05}{2} \right) / 12 = 5,140.4 \text{ ft-kips} > 4,837.2 \text{ ft-kips} \quad \text{OK}$$

With time, creep of concrete members heavily pretensioned may cause camber growth. Because this bridge is designed to have rigid connections between beams at the piers, camber growth is restrained. As a result, time-dependent positive moments at the piers will develop. Therefore, it is recommended that a nominal amount of positive moment continuity reinforcement be used over the piers to control potential cracking in this region. A common way to provide this reinforcement is to extend approximately 25% of the strands from the bottom flange and bend them up into the diaphragm. Another common detail is the addition of a quantity of nonprestressed reinforcement required to resist a moment equal to $1.2M_{cr}$. This reinforcement is also extended from the ends of the beam and bent up into the diaphragm. This topic is addressed in Article 5.14.1.4 of the *LRFD Specifications*, which requires that connections between girders at the continuity diaphragm be designed for all effects that cause moment at the connection.

9.2.9.2.2 Fatigue Stress Limit and Crack Control

The fatigue limit state and crack control for the negative moment zone over the piers are important design criteria that must be checked. This zone is expected to be cracked due to service loads and the steel stress range is expected to be high.

For moment calculations, the fatigue truck loading must be introduced to the three-span continuous structure. The resulting moments are then used to determine whether or not the stress range in the longitudinal reinforcement is within the acceptable limits.

In order to control flexural cracking, the spacing of the nonprestressed steel reinforcement at service limit state, should not exceed the value given by LRFD Eq. 5.7.3.4-1 for the exposure condition required by the owner.

9.2.10 LIMITS OF REINFORCEMENT**9.2.10.1 Positive Moment Section**

This section is a prestressed concrete section.

9.2.10.1.1 Maximum Reinforcement

[LRFD Art. 5.7.3.3.1]

The check of maximum reinforcement limits was removed from the *LRFD Specifications* in 2005.

9.2.10.1.2 Minimum Reinforcement

[LRFD Art. 5.7.3.3.2]

At any section, the amount of prestressed and nonprestressed tensile reinforcement must be adequate to develop a factored flexural resistance, M_r , equal to the lesser of:

- 1.2 times the cracking strength determined on the basis of elastic stress distribution and the modulus of rupture, and
- 1.33 times the factored moment required by the applicable strength load combination.

Check at midspan:

$$M_{cr} = S_{btc}(f_r + f_{cpe}) - M_{anc} \left(\frac{S_{btc}}{S_{btf}} - 1 \right) \geq S_{btc}f_r \quad \text{[LRFD Eq. 5.7.3.3.2-1]}$$

where

- f_r = modulus of rupture of concrete [LRFD Art. 5.4.2.6]
- = $0.37\sqrt{f'_c} = 0.37\sqrt{7.000} = 0.979 \text{ ksi}$
- f_{cpe} = compressive stress in concrete due to effective prestress force only (after allowance for all prestress losses) at extreme fiber of section where tensile stress is caused by externally applied loads

BULB-TEE (BT-72), THREE SPANS, COMPOSITE DECK

9.2.10.1.2 Minimum Reinforcement/9.2.11 Shear Design

$$= \frac{P_{pe}}{A_{tf}} + \frac{P_{pe}e_{tf}}{S_{btf}} = \frac{1,196.8}{798.1} + \frac{(1,196.8)(29.58)}{16,235} = 1.500 + 2.181 = 3.681 \text{ ksi}$$

M_{dnc} = noncomposite dead load moment at the section

$$= M_g + M_s = 1,390.7 + 2,126.9 = 3,517.6 \text{ ft-kips}$$

S_{btc} = section modulus for the extreme bottom fiber of the transformed composite section where the tensile stress is caused by externally applied loads = 22,341 in.³

S_{btf} = section modulus for the extreme bottom fiber of the transformed noncomposite section where the tensile stress is caused by externally applied loads = 16,235 in.³

$$M_{cr} = (0.979 + 3.681) \left(\frac{22,341}{12} \right) - 3,517.6 \left(\frac{22,341}{16,235} - 1 \right) = 7,352.8 \text{ ft-kips}$$

$$1.2M_{cr} = 1.2(7,352.8) = 8,823.4 \text{ ft-kips}$$

At midspan, the factored moment required by the Strength I load combination is:

$$M_u = 8,381.6 \text{ ft-kips (as calculated in Section 9.2.9.1)}$$

$$\text{Therefore, } 1.33M_u = 1.33(8,381.6) = 11,147.5 \text{ ft-kips}$$

Since $1.2M_{cr} < 1.33M_u$, $1.2M_{cr}$ requirement controls

$$M_r = 10,780 \text{ ft-kips} > 1.2M_{cr} = 8,823.4 \text{ ft-kips} \quad \text{OK}$$

The *LRFD Specifications* requires that this criterion be met at every section.

Illustrated based on 2011
LRFD Specifications.

Editor's Note: 2012 *LRFD Specifications* changes will revise minimum reinforcement.

9.2.10.2 Negative Moment Section**9.2.10.2.1 Maximum Reinforcement**

[LRFD Art. 5.7.3.3.1]

The check of maximum reinforcement was removed from the *LRFD Specifications* in 2005.

9.2.10.2.2 Minimum Reinforcement

[LRFD Art. 5.7.3.3.2]

For negative moment sections, the LRFD Eq. 5.7.3.3.2-1 can be reduced to:

$$M_{cr} = S_{tc} f_r$$

where

$$S_{tc} = 68,181 \text{ in.}^3$$

$$f_r = 0.37\sqrt{f'_c} = 0.37\sqrt{4.0} = 0.740 \text{ ksi}$$

Note: Gross section properties are used here for the negative moment section.

$$M_{cr} = 0.740(68,181)/12 = 4,204.5 \text{ ft-kips}$$

$$1.2M_{cr} = 1.2(4,204.5) = 5,045.4 \text{ ft-kips}$$

$$M_u = -4,837.2 \text{ ft-kips as calculated in Section 9.2.9.2.1}$$

$$\text{Thus, } 1.33M_u = 1.33(4,837.2) = 6,433.5 \text{ ft-kips}$$

Since $1.2M_{cr} < 1.33M_u$, the $1.2M_{cr}$ requirement controls

$$M_r = 5,140.4 \text{ ft-kips} > 1.2M_{cr} = 5,045.4 \text{ ft-kips} \quad \text{OK}$$

9.2.11 SHEAR DESIGN

The area and spacing of shear reinforcement must be determined at regular intervals along the entire length of the beam. In this design example, transverse shear design procedures are demonstrated below by determining these values for the center span at the critical section near the supports.

BULB-TEE (BT-72), THREE SPANS, COMPOSITE DECK

9.2.11 Shear Design/9.2.11.1.2 Calculation of Critical Section

Transverse shear reinforcement is required when:

$$V_u > 0.5\phi(V_c + V_p) \quad [\text{LRFD Eq. 5.8.2.4-1}]$$

where

V_u = total factored shear force, kips

V_c = nominal shear resistance provided by tensile stresses in the concrete, kips

V_p = component in the direction of the applied shear of the effective prestressing force, kips

ϕ = resistance factor = 0.9 for normal weight concrete [LRFD Art. 5.5.4.2.1]

9.2.11.1 Critical Section

The critical section near the supports is taken as the effective shear depth, d_v , from the internal face of the support. [LRFD Art. 5.8.3.2]

d_v = distance between resultants of tensile and compressive forces, $(d_e - a/2)$ but not less than $0.9d_e$ or $0.72h_c$ [LRFD Art. 5.8.2.7]

where

d_e = the corresponding effective depth from the extreme compression fiber to the centroid of the tensile force in the tensile reinforcement = 76.25 in. (Sect. 9.2.9.2.1)

(Note: d_e is calculated considering the nonprestressed reinforcement in the slab as the main reinforcement and neglecting the prestressing strand. This is because this section lies in the negative moment zone.)

a = equivalent depth of the compression block = 6.05 in. (Sect. 9.2.9.2.1)

h_c = overall depth of the composite section = 80.0 in.

9.2.11.1.1 Effective Shear Depth

$$d_v = 76.25 - 0.5(6.05) = 73.23 \text{ in.}$$

$$\geq 0.9d_e = 0.9(76.25) = 68.63 \text{ in.}$$

$$\geq 0.72h_c = 0.72(80.0) = 57.60 \text{ in.}$$

Therefore, $d_v = 73.23$ in.

9.2.11.1.2 Calculation of Critical Section

The critical section is taken as d_v from the face of the support:

$$d_v = 73.23 \text{ in.}$$

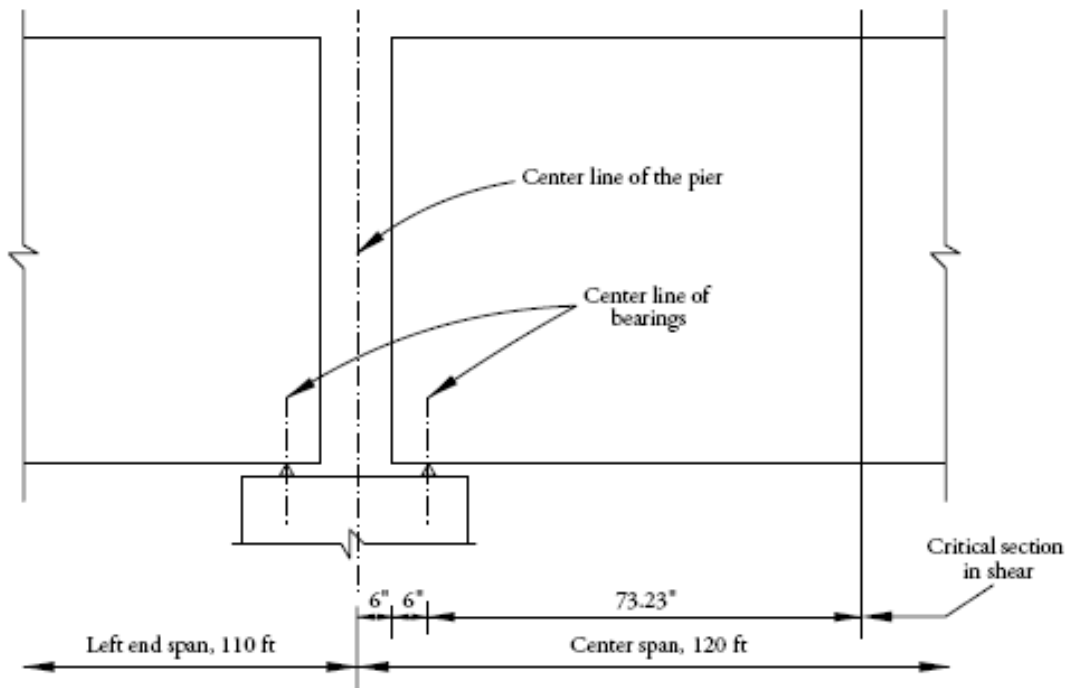
Because the width of the bearing is not yet determined, the width of bearing was conservatively assumed to be equal to zero for the computation of the critical section of shear, as shown in **Figure 9.2.11.1.2-1**. Therefore the critical section in shear is at a distance of $0.5 + 0.5 + 73.23/12 = 7.10$ ft from the centerline of the first interior support (pier).

$$x/L = 7.10/120 = 0.059L \text{ from the centerline of the first interior support (pier)}$$

BULB-TEE (BT-72), THREE SPANS, COMPOSITE DECK

9.2.11.1.2 Calculation of Critical Section/9.2.11.2 Contribution of Concrete to Nominal Shear Resistance

Figure 9.2.11.1.2-1
Critical Section in Shear of the Center Span



9.2.11.1.3 Forces at the Critical Section

Using values from **Table 9.2.4-1**, compute the factored shear force and bending moment at the critical section for shear (center span point $0.059L$), according to Strength I load combination.

$$V_u = 1.25(42.3 + 64.6 + 7.8) + 1.50(14.2) + 1.75(137.3) = 405.0 \text{ kips}$$

$$M_u = 1.25(272.7 + 417.1 - 139.6) + 1.50(-44.4) + 1.75(-717.8) = -2,685.0 \text{ ft-kips}$$

or

$$V_u = 0.9(42.3 + 64.6 + 7.8) + 1.50(14.2) + 1.75(137.3) = 364.8 \text{ kips}$$

$$M_u = 0.9(272.7 + 417.1 - 139.6) + 1.50(-44.4) + 1.75(-1,717.8) = -2,877.6 \text{ ft-kips}$$

When determining M_u at a particular section, it is conservative to take M_u as the highest factored moment that will occur at that section, rather than the moment corresponding to maximum V_u . [LRFD Art. C5.8.3.4.2]

Therefore,

$$V_u = 405.0 \text{ kips}$$

$$M_u = -2,877.6 \text{ ft-kips}$$

9.2.11.2 Contribution of Concrete to Nominal Shear Resistance

The contribution of the concrete to the nominal shear resistance is:

$$V_c = 0.0316\beta\sqrt{f'_c}b_vd_v \quad \text{[LRFD Eq. 5.8.3.3-3]}$$

where β = a factor indicating the ability of diagonally cracked concrete to transmit tension (a value indicating concrete contribution)

Several quantities must be determined before this expression can be evaluated.

BULB-TEE (BT-72), THREE SPANS, COMPOSITE DECK

9.2.11.2.1 Strain in Flexural Tension Reinforcement/9.2.11.3.1 Requirement for Reinforcement

9.2.11.2.1 Strain in Flexural Tension Reinforcement

Calculate strain at the centroid of the tension reinforcement, ϵ_s :

$$\epsilon_s = \frac{\frac{|M_u|}{d_v} + 0.5N_u + |V_u - V_p| - A_{ps}f_{po}}{(E_s A_s + E_p A_{ps})} \quad [\text{LRFD Eq. 5.8.3.4.2-4}]$$

where

N_u = applied factored normal force at the specified section, $0.59L = 0$ kips

V_p = (Force per strand without live loads gains)(Number of harped strands)($\sin \psi$)

= $(25.63)(12)\sin 7.2^\circ = 38.5$ kips is a conservative resistance

f_{po} = a parameter taken as modulus of elasticity of prestressing tendons multiplied by the locked-in difference in strain between the prestressing tendons and the surrounding concrete (ksi). For pretensioned members, LRFD Article 5.8.3.4.2 indicates that f_{po} can be taken as $0.7f_{pu}$. (Note: use this for both pretensioned and post-tensioned systems made with stress relieved and low relaxation strands).

= $0.70(270.0) = 189.0$ ksi

A_s = area of nonprestressed tension reinforcement on the flexural side of the member = 15.60 in.^2

A_{ps} = area of prestressing strands on the flexural tension side of the member. The flexural tension side of the member should be taken as the half-depth containing the flexural tension zone as illustrated in LRFD Figure 5.8.3.4.2-1.

= $12(0.153) = 1.836 \text{ in.}^2$

$$\epsilon_s = \frac{\frac{2,877.6(12)}{73.23} + 0 + (405.0 - 38.5) - 1.836(189.0)}{29,000(15.60) + 28,500(1.836)} = +0.973 \times 10^{-3}$$

9.2.11.2.2 Values of β and θ

Assume the section contains at least the minimum amount of transverse reinforcement:

$$\beta = \frac{4.8}{(1 + 750\epsilon_s)} = \frac{4.8}{(1 + 750(0.973 \times 10^{-3}))} = 2.775 \quad [\text{LRFD Eq. 5.8.3.4.2-1}]$$

Angle of diagonal compressive stresses is:

$$\theta = 29 + 3,500\epsilon_s = 29 + 3,500(0.973 \times 10^{-3}) = 32.4^\circ \quad [\text{LRFD Eq. 5.8.3.4.2-3}]$$

9.2.11.2.3 Compute Concrete Contribution

The nominal shear resisted by the concrete is:

$$V_c = 0.0316\beta\sqrt{f'_c}b_v d_v \quad [\text{LRFD Eq. 5.8.3.3-3}]$$

where b_v = effective web width = 6 in.

$$V_c = 0.0316(2.775)\sqrt{7.0}(6)(73.23) = 101.9 \text{ kips}$$

9.2.11.3 Contribution of Reinforcement to Nominal Shear Resistance**9.2.11.3.1 Requirement for Reinforcement**

Check if $V_u > 0.5\phi(V_c + V_p)$

[LRFD Eq. 5.8.2.4-1]

$$0.5\phi(V_c + V_p) = 0.5(0.9)(101.9 + 38.5) = 63.2 \text{ kips} < 405.0 \text{ kips}$$

Therefore, transverse reinforcement must be provided.

BULB-TEE (BT-72), THREE SPANS, COMPOSITE DECK

9.2.11.3.2 Required Area of Reinforcement/9.2.11.4 Maximum Nominal Shear Resistance

9.2.11.3.2 Required Area of Reinforcement

$$V_u/\phi \leq V_n = V_c + V_s + V_p \quad [\text{LRFD Eq. 5.8.3.3-1}]$$

where

$$\begin{aligned} V_s &= \text{shear resistance provided by shear reinforcement} \\ &= (V_u/\phi) - V_c - V_p = 405.0/0.9 - 101.9 - 38.5 = 309.6 \text{ kips} \end{aligned}$$

$$V_s = \frac{A_v f_{yh} d_v (\cot \theta + \cot \alpha) (\sin \alpha)}{s} \quad [\text{LRFD Eq. 5.8.3.3-4}]$$

where

$$\begin{aligned} A_v &= \text{area of shear reinforcement within a distance } s, \text{ in.}^2 \\ s &= \text{spacing of stirrups, in.} \\ f_{yh} &= \text{specified yield strength of shear reinforcement, ksi} \\ \alpha &= \text{angle of inclination of transverse reinforcement to longitudinal axis} \\ &= 90^\circ \text{ for vertical stirrups} \end{aligned}$$

Therefore, area of shear reinforcement within a spacing, s , is:

$$\begin{aligned} A_v &= (sV_s)/(f_{yh}d_v \cot \theta) \\ &= s(309.6)/(60)(73.23 \cot 32.4^\circ) = 0.045(s) \text{ in.}^2 \end{aligned}$$

if $s = 12$ in., required $A_v = 0.54 \text{ in.}^2$ **9.2.11.3.3 Determine Spacing of Reinforcement**

Check maximum spacing of transverse reinforcement:

[LRFD Art. 5.8.2.7]

Check if $v_u < 0.125f'_c$

[LRFD Eq. 5.8.2.7-1]

$$v_u = \frac{V_u - \phi V_p}{\phi b_v d_v} = \frac{405.0 - 0.9(38.5)}{(0.9)(6)(73.23)} = 0.937 \text{ ksi}$$

$$0.125f'_c = (0.125)(7.0) = 0.875 \text{ ksi}$$

Since $v_u > 0.125f'_c$

$$\text{Then } s \leq 12 \text{ in.} \leq 0.4d_v = 0.4(73.23) = 29.3 \text{ in.}$$

Therefore, $s \leq 12$ in.**Use No. 5 double leg bars at 12 in., $A_v = 0.62 \text{ in.}^2/\text{ft} > 0.54 \text{ in.}^2/\text{ft}$**

$$V_s = \frac{(0.62)(60)(73.23) \cot 32.4^\circ}{12} = 357.7 \text{ kips}$$

9.2.11.3.4 Minimum Reinforcement Requirement

The area of transverse reinforcement should not be less than:

$$0.0316 \sqrt{f'_c} \frac{b_v s}{f_{yh}} = 0.0316 \sqrt{7.0} \left(\frac{6(12)}{60.0} \right) = 0.10 \text{ in.}^2 < A_v \text{ provided} \quad \text{OK} \quad [\text{LRFD Eq. 5.8.2.5-1}]$$

9.2.11.4 Maximum Nominal Shear ResistanceIn order to ensure that the concrete in the web of the beam will not crush prior to yielding of the transverse reinforcement, the *LRFD Specifications* specifies an upper limit of V_n as follows:

$$V_n = 0.25f'_c b_v d_v + V_p \quad [\text{LRFD Eq. 5.8.3.3-2}]$$

Comparing this equation with LRFD Eq. 5.8.3.3-1, it can be concluded that,

BULB-TEE (BT-72), THREE SPANS, COMPOSITE DECK**9.2.11.4 Maximum Nominal Shear Resistance/9.2.12.3 Required Interface Shear Reinforcement**

$V_c + V_s$ must not be greater than $0.25f'_c b_v d_v$

$$101.9 + 357.7 = 459.6 \text{ kips} \leq 0.25(7.0)(6)(73.23) = 768.9 \text{ kips} \quad \text{OK}$$

Using the above procedures, the transverse reinforcement can be determined at increments along the entire length of the beam.

9.2.12 INTERFACE SHEAR TRANSFER

[LRFD Art. 5.8.4]

9.2.12.1 Factored Horizontal Shear

At the strength limit state, the horizontal shear at a section on a per unit basis can be taken as:

$$V_{hi} = \frac{V_u}{d_v} \quad \text{[LRFD Eq. C5.8.4.2-7]}$$

where

V_{hi} = horizontal factored shear force per unit length of the beam, kips/in.

V_u = factored shear force at specified section due to superimposed loads after the deck is cast, kips

d_v = distance between the centroid of the tension steel and the mid-thickness of the slab = $(d_e - t_s/2)$
 $= 76.25 - 7.5/2 = 72.50$ in.

The *LRFD Specifications* does not identify the location of the critical section. For convenience, it will be assumed here to be the same location as the critical section for vertical shear, at point $0.059L$ of the center span.

Using load combination Strength I:

$$V_u = 1.25(42.3+64.6+7.8) + 1.50(14.2) + 1.75(137.3) = 405.0 \text{ kips} \quad \text{(Table 9.2.4-1)}$$

Therefore, the applied factored horizontal shear is:

$$V_{hi} = \frac{405.0}{72.50} = 5.59 \text{ kips/in.}$$

9.2.12.2 Required Nominal Resistance

$$\text{Required } V_{ni} = V_{hi}/0.9 = 5.59/0.9 = 6.21 \text{ kips/in.} \quad \text{[LRFD Eq. 5.8.4.1-1]}$$

9.2.12.3 Required Interface Shear Reinforcement

The nominal shear resistance of the interface plane is:

$$V_{ni} = c A_{cv} + \mu[A_{vf}f_{yh} + P_c] \quad \text{[LRFD Eq. 5.8.4.1-3]}$$

where

c = cohesion factor, ksi [LRFD Art. 5.8.4.2]

A_{cv} = area of concrete section resisting shear transfer, in.²

μ = coefficient of friction [LRFD Art. 5.8.4.2]

A_{vf} = area of shear reinforcement crossing the shear plane, in.²

f_{yh} = specified yield strength of shear reinforcement, ksi

P_c = permanent net compressive force normal to the shear plane, kips

For a cast-in-place concrete slabs placed on clean concrete girder surface intentionally roughened: [LRFD Art. 5.8.4.3]

$$c = 0.28 \text{ ksi}$$

$$\mu = 1.0$$

BULB-TEE (BT-72), THREE SPANS, COMPOSITE DECK**9.2.12.3 Required Interface Shear Reinforcement/9.2.13 Minimum Longitudinal Reinforcement Requirement**

The actual contact width, b_v , between the deck and the beam is 42 in. Therefore,

$$A_{cv} = (42 \text{ in.})(1 \text{ in.}) = 42 \text{ in.}^2/\text{in.}$$

LRFD Eq. 5.8.4.1-3 can be solved for A_{vf} as follows:

$$6.21 = 0.28(42) + 1.0[A_{vf}(60.0) + 0]$$

$$A_{vf}(\text{req'd}) < 0$$

Since the resistance provided by cohesion is greater than the applied force, provide the minimum required interface reinforcement.

9.2.12.3.1 Minimum Interface Shear Reinforcement

Minimum shear reinforcement, $A_{vf} \geq (0.05A_{cv})/f_{yh}$

[LRFD Eq. 5.8.4.4-1]

From the design of vertical shear reinforcement, a No. 5 double-leg bar at 12-in. spacing is provided from the beam extending into the deck. Therefore, $A_{vf} = 0.62 \text{ in.}^2/\text{ft}$

$$A_{vf} = (0.62 \text{ in.}^2/\text{ft}) > (0.05 A_{cv})/f_{yh} = 0.05(42)/60 = 0.035 \text{ in.}^2/\text{in.} = 0.42 \text{ in.}^2/\text{ft} \quad \text{OK}$$

Consider further that LRFD Article 5.8.4.4 states that the minimum reinforcement requirement may be waived if $V_{hi}/A_{cv} < 0.210 \text{ ksi}$ with surface roughened to an amplitude of 0.25 in.

$$4.16 \text{ kips/in.}/42.0 \text{ in.} = 0.099 \text{ ksi} < 0.210 \text{ ksi}$$

Therefore, the minimum reinforcement requirement could be waived had it governed.

9.2.12.4 Maximum Nominal Shear Resistance

$$V_{ni} \leq K_1 f'_c A_{cv} \text{ or } K_2 A_{cv}$$

$$V_{ni} \text{ provided} = (0.28)(42) + 1.0 \left(\frac{0.62}{12} (60.0) + 0 \right) = 14.9 \text{ kips/in.}$$

$$K_1 f'_c A_{cv} = (0.3)(4.0)(42) = 50.4 \text{ kips/in.}$$

[LRFD Eq. 5.8.4.1-4]

$$K_2 A_{cv} = 1.8(42) = 75.6 \text{ kips/in.}$$

[LRFD Eq. 5.8.4.1-5]

$$V_{ni} \text{ provided} \leq 0.3 f'_c A_{cv} \quad \text{OK}$$

$$\leq 1.8 A_{cv} \quad \text{OK}$$

9.2.13 MINIMUM LONGITUDINAL REINFORCEMENT REQUIREMENT

[LRFD Art. 5.8.3.5]

The *LRFD Specifications* states that if the reaction force or the load at the maximum moment location introduces direct compression into the flexural compression face of the member, the area of longitudinal reinforcement on the flexural tension side of the member need not exceed the area required to resist the maximum moment acting alone.

This reason that the longitudinal reinforcement requirement is relaxed for this condition, is based on the following explanation. At maximum moment locations, the shear force changes sign and, hence, the inclination of the diagonal compressive stresses also changes. At direct supports and point loads, this change of inclination is associated with a fan-shaped pattern of compressive stresses radiating from the point load or the direct support. This fanning of the diagonal stresses reduces the tension in the longitudinal reinforcement caused by the shear, i.e., angle θ becomes steeper.

The conditions mentioned above exist at the interior supports. Directly over the support, the angle θ becomes 90° and the contribution of shear to the longitudinal reinforcement requirement is zero. Therefore, at this location, the longitudinal reinforcement is sized only for the moment applied to the section and there is no need to check the minimum longitudinal reinforcement requirement.

However, for sections within a distance of $(d_v \cot \theta)/2$ from the interior supports, the shear will again affect the required longitudinal reinforcement and the requirement must be checked. It should be noted that at locations

BULB-TEE (BT-72), THREE SPANS, COMPOSITE DECK**9.2.13 Minimum Longitudinal Reinforcement Requirement/9.2.15.1 Deflection Due to Prestressing Force at Transfer**

near the interior supports of continuous members, the minimum longitudinal reinforcement requirement is used to check the quantity of reinforcement in the deck. The longitudinal reinforcement requirement must also be checked for the prestressing strands at the simply-supported ends of continuous span units. Refer to Design Example 9.1a, Section 9.1a.13.

9.2.14 PRETENSIONED ANCHORAGE ZONE

[LRFD Art. 5.10.10]

9.2.14.1 Anchorage Zone Reinforcement

[LRFD Art. 5.10.10.1]

Design of the anchorage zone reinforcement is computed using the force in the strands just before transfer.

Force in the strands before transfer = $P_{pi} = 1,363.1$ kips

The bursting resistance, P_r , should not be less than 4.0% of P_{pi} .

$$P_r = f_s A_s \geq 0.04 P_{pi} = 0.04(1,363.1) = 54.5 \text{ kips}$$

where

f_s = allowable stress in steel, but taken not greater than 20 ksi

A_s = total area of vertical reinforcement located within a distance $h/4$ from the end of the beam, in.²

Solving for the required area of steel, $A_s = 54.5/(20) = 2.73$ in.²

At least 2.73 in.² of vertical transverse reinforcement should be provided at the end of the beam for a distance equal to one-fourth of the depth of the beam, $h/4 = 72/4 = 18.0$ in.

The shear reinforcement was determined in Section 9.2.11 to be No. 5 (double legs) @ 12 in. However, the minimum vertical reinforcement criteria controls.

Use five No. 5 double leg bars at 4 in. spacing starting at 2 in. from the end of the beam

Provided $A_s = 5(2)(0.31) = 3.1$ in.² > 2.73 in.² OK

9.2.14.2 Confinement Reinforcement

[LRFD Art. 5.10.10.2]

For a distance of $1.5h = 1.5(72) = 108$ in., from the end of the beam, reinforcement is placed to confine the prestressing steel in the bottom flange. The reinforcement should not be less than No. 3 deformed bars, with spacing not exceeding 6.0 in., and shaped to enclose the strands.

9.2.15 DEFLECTION AND CAMBER

[LRFD Art. 5.7.3.6.2]

Deflections are calculated using the modulus of elasticity of concrete calculated in Section 9.2.2 and the gross moment of inertia of the noncomposite precast beam.

9.2.15.1 Deflection Due to Prestressing Force at Transfer

Force per strand at transfer = 28.20 kips

$$\Delta_p = \frac{P_{pt}}{E_{ci} I_g} \left(\frac{e_c L^2}{8} - \frac{e' a^2}{6} \right)$$

where

Δ_p = camber due to prestressing force at transfer, in.

P_{pt} = total prestressing force at transfer = $44(28.20) = 1,240.8$ kips

E_{ci} = modulus of elasticity at transfer = 4,496 ksi

I_g = moment of inertia of the noncomposite precast beam = 545,894 in.⁴

e_c = eccentricity of prestressing strand at midspan = 30.78 in.

BULB-TEE (BT-72), THREE SPANS, COMPOSITE DECK

9.2.15.1 Deflection Due to Prestressing Force at Transfer/9.2.15.3 Deflection Due to Slab and Haunch and Deck Weights

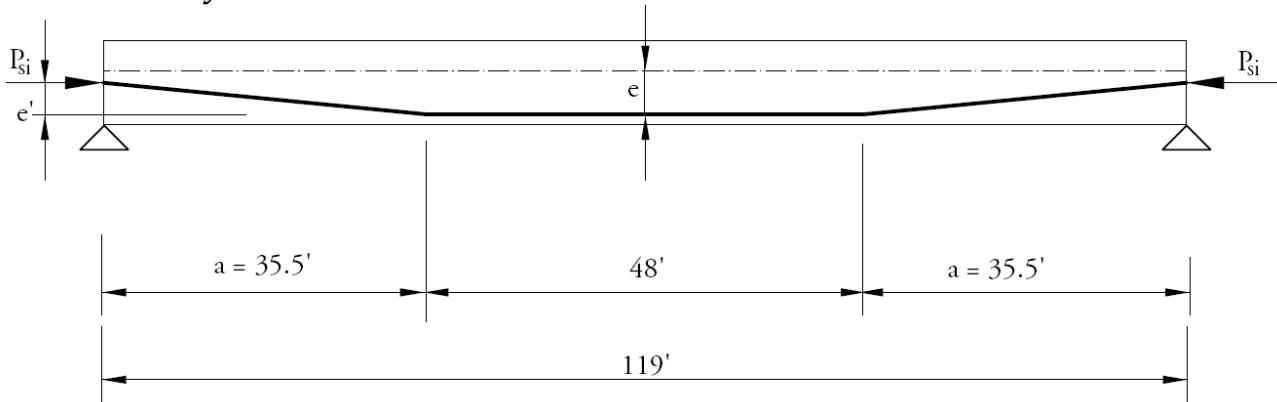
$L =$ overall beam length = 119.0 ft

$e' =$ difference between eccentricity of prestressing strand at midspan and at end of the beam, as shown in **Figure 9.2.15.1-1**

$$= e_c - e_e = 30.78 - (y_b - y_{bs}) = 30.78 - (36.60 - 20.55) = 14.73 \text{ in.}$$

$a =$ distance from end of beam to the harp point = 35.5 ft

Figure 9.2.15.1-1
Strand Eccentricity



$$\Delta_p = \frac{1,240.8}{4,496(545,894)} \left(\frac{30.78(119 \times 12)^2}{8} - \frac{14.73(35.5 \times 12)^2}{6} \right) = 3.74 \text{ in. } \uparrow$$

9.2.15.2 Deflection Due to Beam Self Weight

$$\Delta_g = \frac{5w_g L^4}{384E_{ci}I_g}$$

where

$\Delta_g =$ deflection due to beam self weight, in.

$w_g =$ beam self weight, = 0.799 kips/ft

Deflection due to beam self weight after transfer:

$L =$ overall beam length = 119 ft

$$\Delta_g = \frac{5 \left(\frac{0.799}{12} \right) (119 \times 12)^4}{(384)(4,496)(545,894)} = 1.47 \text{ in. } \downarrow$$

Deflection due to beam self weight at erection:

$L =$ span length between centerlines of bearings = 118 ft

$$\Delta_g = \frac{5 \left(\frac{0.799}{12} \right) (118 \times 12)^4}{(384)(4,496)(545,894)} = 1.42 \text{ in. } \downarrow$$

9.2.15.3 Deflection Due to Slab and Haunch and Deck Weights

$$\Delta_s = \frac{5w_s L^4}{384E_c I_g}$$

where

$\Delta_s =$ deflection due to slab and haunch weights, in.

$w_s =$ slab and haunch weight = 1.200 + 0.022 = 1.222, kips/ft

BULB-TEE (BT-72), THREE SPANS, COMPOSITE DECK

9.2.15.3 Deflection Due to Slab and Haunch and Deck Weights/9.2.15.6 Deflection Due to Live Load and Impact

$L =$ design span = 118.0 ft

$E_c =$ modulus of elasticity of precast beam at service loads = 5,072 ksi

$$\Delta_s = \frac{5 \left(\frac{1.222}{12} \right) (118 \times 12)^4}{(384)(5,072)(545,894)} = 1.93 \text{ in. } \downarrow$$

9.2.15.4 Deflection Due to Barrier and Future Wearing Surface Weights

$\Delta_{b+ws} = 0.048 \text{ in. } \downarrow$

(This value was calculated using a continuous beam program.)

9.2.15.5 Deflection and Camber Summary

For midspan:

At transfer, $(\Delta_p + \Delta_g) = 3.74 - 1.47 = 2.27 \text{ in. } \uparrow$

Total deflection at erection, using PCI multipliers (see the *PCI Design Handbook*)

$= 1.8(3.74) - 1.85(1.42) = 4.19 \text{ in. } \uparrow$

Long-Term Deflection

LRFD Article 5.7.3.6.2 states that the long-term deflection may be taken as the instantaneous deflection multiplied by a factor of 4.0, if the instantaneous deflection is based on the gross moment of inertia. However, a factor of 4.0 is not appropriate for this type of precast construction. Therefore, it is recommended that the designer follow the guidelines of the owner agency for whom the bridge is being designed, or undertake a more rigorous time-dependent analysis.

9.2.15.6 Deflection Due to Live Load and Impact

Live load deflection is not a required check, according to the provisions of the *LRFD Specifications*. Further, live load deflections are usually not a problem for prestressed concrete I- and bulb-tee shapes especially when they are constructed to act as a continuous structure under superimposed loads. If the designer chooses to check deflection, the following recommendations are from the *LRFD Specifications*.

Live load deflection limit: $\text{Span}/800 = 120(12)/800 = 1.80 \text{ in.}$ [LRFD Art. 2.5.2.6.2]

If the owner invokes the optional live load deflection criteria specified in LRFD Article 2.5.2.6.2, the deflection is the greater of: [LRFD Art. 3.6.1.3.2]

- that resulting from the design truck plus impact, Δ_{LT} , or
- that resulting from 25% of the design truck plus impact, Δ_{LT} , taken together with the design lane load, Δ_{LL} .

Note: LRFD Article 2.5.2.6.2 states that the dynamic load allowance be included in the calculation of live load deflection.

The *LRFD Specifications* states that all beams may be assumed to be deflecting equally under the applied live load and impact. [LRFD Art. 2.5.2.6.2]

Therefore, the distribution factor for deflection, DFD , is calculated as follows:

$$DFD = (\text{number of lanes}/\text{number of beams}) = 3/4 = 0.75 \text{ lanes/beams}$$
 [LRFD Art. C2.5.2.6.2]

However, it is more conservative to use the distribution factor for moment, DFM .

The live load deflection may be conservatively estimated using the following formula:

$$\Delta_{LL} = \frac{5L^2}{48E_c I_c} [M_s - 0.1(M_a + M_b)]$$
 (Eq. 9.2.15.6-1)

BULB-TEE (BT-72), THREE SPANS, COMPOSITE DECK

9.2.15.6 Deflection Due to Live Load and Impact

where

M_s = the maximum positive moment

M_a and M_b = the corresponding negative moments at the ends of the span being considered.

The live load combination specified in LRFD Article 3.6.1.3.2 calls for the greater of design truck with impact alone or 0.25 design truck with impact plus lane load.

In this example, a conservative approximation may be made by using the positive moment for Service III load combination, 0.8 truck plus lane load, and by ignoring the effect of M_a and M_b .

$$\Delta_{LL} = \frac{5(120 \times 12)^2}{48(5,072)(1,175,063)} [0.8 \times 2,115.0 \times 12] = 0.74 \text{ in.} \downarrow < 1.80 \text{ in.} \quad \text{OK}$$

DECK BULB-TEE (DBT-53), SINGLE SPAN, NONCOMPOSITE SURFACE

Transformed Sections, Shear General Procedure, Refined Losses

Table of Contents

9.3.1 INTRODUCTION.....	9.3 - 3
9.3.1.1 Terminology.....	9.3 - 3
9.3.2 MATERIALS	9.3 - 3
9.3.3 CROSS-SECTION PROPERTIES FOR A TYPICAL INTERIOR BEAM.....	9.3 - 4
9.3.4 SHEAR FORCES AND BENDING MOMENTS	9.3 - 5
9.3.4.1 Shear Forces and Bending Moments Due to Dead Loads	9.3 - 5
9.3.4.1.1 Dead Loads	9.3 - 5
9.3.4.1.2 Unfactored Shear Forces and Bending Moments.....	9.3 - 6
9.3.4.2 Shear Forces and Bending Moments due to Live Loads.....	9.3 - 6
9.3.4.2.1 Live Loads.....	9.3 - 6
9.3.4.2.2 Live Load Distribution Factors for a Typical Interior Beam	9.3 - 6
9.3.4.2.2.1 Distribution Factor for Bending Moments.....	9.3 - 6
9.3.4.2.2.2 Distribution Factor for Shear Force	9.3 - 7
9.3.4.2.3 Dynamic Allowance	9.3 - 8
9.3.4.2.4 Unfactored Shear Forces and Bending Moments.....	9.3 - 9
9.3.4.2.4.1 Due to Truck Load; V_{LT} and M_{LT}	9.3 - 9
9.3.4.2.4.2 Due To Design Lane Load; V_{LL} and M_{LL}	9.3 - 9
9.3.4.3 Load Combinations.....	9.3 - 10
9.3.5 ESTIMATE REQUIRED PRESTRESS.....	9.3 - 11
9.3.5.1 Service Load Stresses at Midspan	9.3 - 11
9.3.5.2 Stress Limits for Concrete.....	9.3 - 12
9.3.5.3 Required Number of Strands.....	9.3 - 12
9.3.5.4 Strand Pattern.....	9.3 - 12
9.3.5.5 Steel Transformed Section Properties	9.3 - 13
9.3.6 PRESTRESS LOSSES	9.3 - 14
9.3.6.1 Elastic Shortening.....	9.3 - 14
9.3.6.2 Time-Dependent Losses between Transfer and Deck Placement.....	9.3 - 15
9.3.6.2.1 Shrinkage of Concrete	9.3 - 15
9.3.6.2.2 Creep of Concrete.....	9.3 - 16
9.3.6.2.3 Relaxation of Prestressing Strands.....	9.3 - 16
9.3.6.3 Time-Dependent Losses between Deck Placement and Final Time	9.3 - 17
9.3.6.3.1 Shrinkage of Concrete	9.3 - 17
9.3.6.3.2 Creep of Concrete.....	9.3 - 17
9.3.6.3.3 Relaxation of Prestressing Strands.....	9.3 - 18
9.3.6.3.4 Shrinkage of Deck Concrete.....	9.3 - 18
9.3.6.4 Total Time-Dependent Loss.....	9.3 - 18
9.3.6.5 Total Losses at Transfer	9.3 - 18
9.3.6.6 Total Losses at Service Loads.....	9.3 - 19
9.3.7 CONCRETE STRESSES AT TRANSFER.....	9.3 - 19

DECK BULB-TEE (DBT-53), SINGLE SPAN, NONCOMPOSITE SURFACE

Transformed Sections, Shear General Procedure, Refined Losses

Table of Contents

9.3.7.1 Stress Limits for Concrete 9.3 - 19

9.3.7.2 Stresses at Transfer Length Section..... 9.3 - 20

9.3.7.3 Stresses at Harp Points 9.3 - 22

9.3.7.4 Stresses at Midspan..... 9.3 - 22

9.3.7.5 Hold-Down Forces 9.3 - 23

9.3.7.6 Summary of Stresses at Transfer 9.3 - 23

9.3.8 CONCRETE STRESSES AT SERVICE LOADS..... 9.3 - 23

 9.3.8.1 Stress Limits for Concrete 9.3 - 23

 9.3.8.2 Stresses at Midspan..... 9.3 - 23

 9.3.8.3 Fatigue Stress Limit..... 9.3 - 24

 9.3.8.4 Summary of Stresses at Midspan at Service Loads 9.3 - 25

9.3.9 STRENGTH LIMIT STATE 9.3 - 25

9.3.10 LIMITS OF REINFORCEMENT..... 9.3 - 26

 9.3.10.1 Maximum Reinforcement 9.3 - 26

 9.3.10.2 Minimum Reinforcement..... 9.3 - 26

9.3.11 SHEAR DESIGN 9.3 - 27

 9.3.11.1 Critical Section 9.3 - 27

 9.3.11.2 Contribution of Concrete to Nominal Shear Resistance 9.3 - 28

 9.3.11.2.1 Strain in Flexural Tension Reinforcement 9.3 - 28

 9.3.11.2.2 Values of β and θ 9.3 - 29

 9.3.11.2.3 Compute Concrete Contribution..... 9.3 - 29

 9.3.11.3 Contribution of Reinforcement to Nominal Shear Resistance..... 9.3 - 29

 9.3.11.3.1 Requirement for Reinforcement..... 9.3 - 29

 9.3.11.3.2 Required Area of Reinforcement..... 9.3 - 29

 9.3.11.3.3 Determine Spacing of Reinforcement..... 9.3 - 29

 9.3.11.3.4 Minimum Reinforcement Requirement..... 9.3 - 30

 9.3.11.4 Maximum Nominal Shear Resistance 9.3 - 30

9.3.12 INTERFACE SHEAR TRANSFER..... 9.3 - 30

9.3.13 MINIMUM LONGITUDINAL REINFORCEMENT REQUIREMENT 9.3 - 30

 9.3.13.1 Required Reinforcement at Face of Bearing..... 9.3 - 31

9.3.14 PRETENSIONED ANCHORAGE ZONE..... 9.3 - 32

 9.3.14.1 Anchorage Zone Reinforcement..... 9.3 - 32

 9.3.14.2 Confinement Reinforcement..... 9.3 - 32

9.3.15 DEFLECTION AND CAMBER..... 9.3 - 32

 9.3.15.1 Deflection Due to Prestressing Force at Transfer 9.3 - 33

 9.3.15.2 Deflection Due to Beam Self Weight..... 9.3 - 33

 9.3.15.3 Deflection Due to Barrier and Future Wearing Surface Weights 9.3 - 33

 9.3.15.4 Deflection and Camber Summary..... 9.3 - 34

 9.3.15.5 Deflection Due to Live Load and Impact..... 9.3 - 34

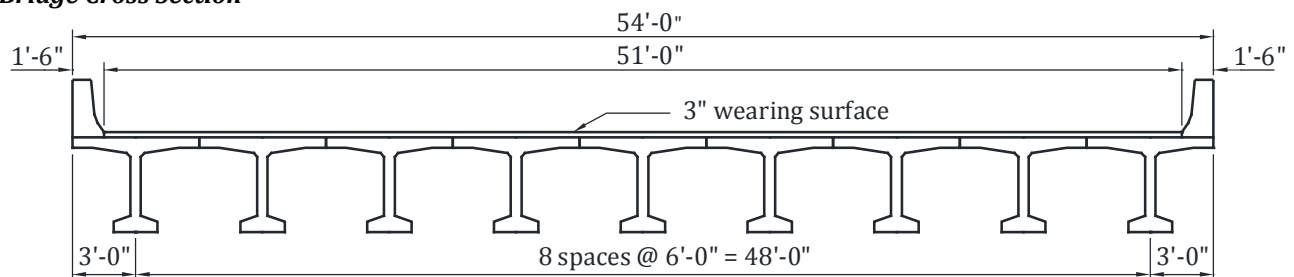
DECK BULB-TEE (DBT-53), SINGLE SPAN, NONCOMPOSITE SURFACE

9.3.1 Introduction/9.3.2 Materials

9.3 Transformed Sections, Shear General Procedure, Refined Losses**9.3.1 INTRODUCTION**

This design example demonstrates the design of a 95-ft, single span, AASHTO Type DBT-53 bulb-tee beam bridge with no skew. This example illustrates in detail the design of a typical interior beam at the critical sections in positive flexure, shear, and deflection due to prestress, dead loads, and live load. The superstructure consists of nine beams spaced at 6 ft 0 in. centers, as shown in **Figure 9.3.1-1**. Beams are designed with a noncomposite wearing surface and are transversely connected by shear keys. Design live load is HL-93. The design is accomplished in accordance with the *AASHTO LRFD Bridge Design Specifications*, Fifth Edition, 2010, and the 2011 Interim Revisions. Elastic stresses from external loads are calculated using transformed sections. Shear strength is calculated using the general procedure. Time-dependent prestress losses are calculated using the refined estimates.

Figure 9.3.1-1
Bridge Cross Section

**9.3.1.1 Terminology**

The following terminology is used to describe cross sections in this design example:

noncomposite section—the concrete beam cross section.

noncomposite nontransformed section—the concrete beam cross section without the strands transformed. Also called the gross section.

noncomposite transformed section—the concrete beam cross section with the strands transformed to provide cross-sectional properties equivalent to the beam concrete.

The term "transformed" refers to transformation of the strands.

9.3.2 MATERIALS

Precast concrete beams: AASHTO deck bulb-tee beam, Type DBT-53 as shown in **Figure 9.3.2-1**.

Required concrete compressive strength at transfer, $f'_{ci} = 5.5$ ksi

Specified concrete compressive strength for use in design, $f'_c = 7.0$ ksi

Concrete unit weight, $w_c = 0.150$ kcf

Overall beam length = 96.0 ft

Design span = 95.0 ft

Prestressing strands: 0.6-in.-dia., seven-wire, low-relaxation

Area of one strand = 0.217 in.²

Specified tensile strength, $f_{pu} = 270.0$ ksi

Yield strength, $f_{py} = 0.9 f_{pu} = 243.0$ ksi

[LRFD Table 5.4.4.1-1]

DECK BULB-TEE (DBT-53), SINGLE SPAN, NONCOMPOSITE SURFACE

9.3.2 Materials/9.3.3 Cross-Section Properties for a Typical Interior Beam

Stress limits for prestressing strands: [LRFD Table 5.9.3-1]

- before transfer, $f_{pi} \leq 0.75f_{pu} = 202.5$ ksi
- at service limit state (after all losses), $f_{pe} \leq 0.80f_{py} = 194.4$ ksi

Modulus of elasticity, $E_p = 28,500$ ksi [LRFD Table 5.4.4.2]

Reinforcing bars:

Yield strength, $f_y = 60.0$ ksi [LRFD Art. 5.4.3.2]

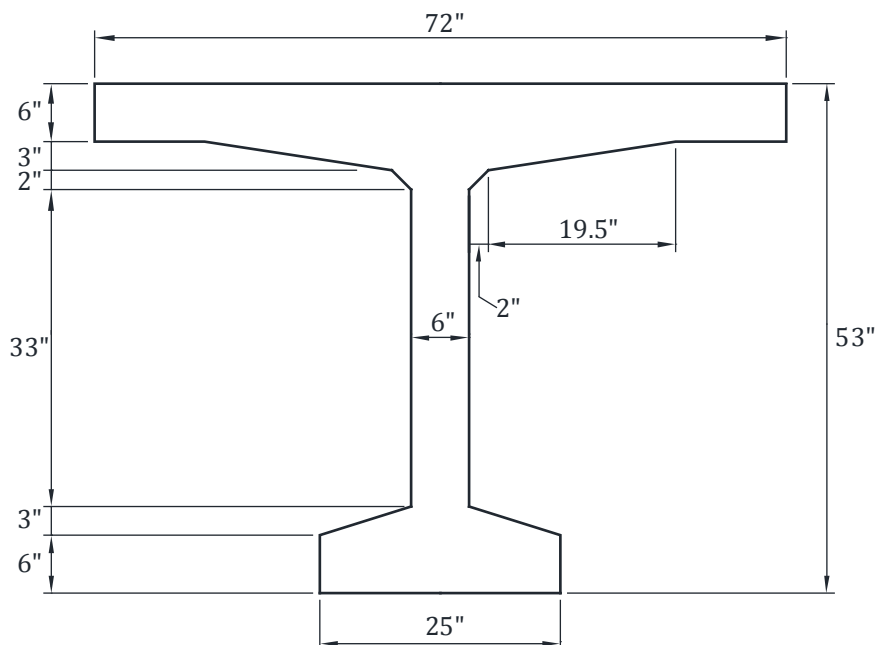
Modulus of elasticity, $E_s = 29,000$ ksi

Bituminous surfacing 3-in. thick: unit weight = 0.140 kcf [LRFD Table 3.5.1-1]

New Jersey-type barrier: unit weight = 0.300 kips/ft/side

Figure 9.3.2-1

AASHTO Deck Bulb-Tee Beam Type DBT-53 Dimensions



9.3.3 CROSS-SECTION PROPERTIES FOR A TYPICAL INTERIOR BEAM

A_g = area of cross section of beam = 931 in.²

h = overall depth of beam = 53 in.

I_g = moment of inertia about the centroid of the noncomposite precast beam = 335,679 in.⁴

J_g = St. Venant's torsional inertia = 34,697 in.⁴

y_b = distance from centroid to the extreme bottom fiber of the noncomposite precast beam = 34.56 in.

y_t = distance from centroid to the extreme top fiber of the noncomposite precast beam = 18.44 in.

S_b = section modulus for extreme bottom fiber of the noncomposite precast beam = $I_g/y_b = 9,713$ in.³

S_t = section modulus for extreme top fiber of the noncomposite precast beam = $I_g/y_t = 18,204$ in.³

w_g = beam weight per unit length = $(931/144)(0.150) = 0.970$ kips/ft

E_c = modulus of elasticity, ksi = $33,000K_1(w_c)^{1.5}\sqrt{f'_c}$ [LRFD Eq. 5.4.2.4-1]

DECK BULB-TEE (DBT-53), SINGLE SPAN, NONCOMPOSITE SURFACE**9.3.3 Cross-Section Properties for a Typical Interior Beam/9.3.4.1.1 Dead Loads**

where

K_1 = correction factor for source of aggregate taken as 1.00

w_c = unit weight of concrete, = 0.150 kcf

LRFD Table 3.5.1-1 states that, in the absence of more precise data, the unit weight of concrete may be taken as $0.140 + 0.001f'_c$ for $5.0 < f'_c \leq 15.0$ ksi. For $f'_c = 6.5$ ksi, the unit weight would be 0.1465 kcf. However, precast concrete mixes typically have a relatively low water-cementitious materials ratio and high density. Therefore, a unit weight of 0.150 kcf is used in this example. For high-strength concrete, this value may need to be increased based on test results. For simplicity, a value of 0.150 kcf is also used for the cast-in-place concrete.

f'_c = specified compressive strength of concrete, ksi

Therefore, the modulus of elasticity for:

precast beam at transfer, $E_{ci} = 33,000(1.00)(0.150)^{1.5}\sqrt{5.50} = 4,496$ ksi

precast beam at service loads, $E_c = 33,000(1.00)(0.150)^{1.5}\sqrt{7.00} = 5,072$ ksi

9.3.4 SHEAR FORCES AND BENDING MOMENTS

Refer to **Tables 9.3.4-1** and **9.3.4-2**, which follow Section 9.3.4.3 for a summary of unfactored values calculated below.

9.3.4.1 Shear Forces and Bending Moments Due to Dead Loads**9.3.4.1.1 Dead Loads**

[LRFD Art. 3.3.2]

DC = Dead load of structural components and nonstructural attachments

Beam self weight, $w_g = 0.970$ kips/ft

LRFD Article 4.6.2.2.1 states that permanent loads (barrier and wearing surface loads) may be distributed uniformly among the beams if the following conditions are met:

- Width of the deck is constant. OK
- Number of beams, N_b , is not less than four ($N_b = 9$) OK
- Beams are parallel and have the same stiffness OK
- The roadway part of the overhang, $d_e \leq 3.0$ ft
 $d_e = (54 - 51)/2 = 1.5$ ft OK
- Curvature in plan is less than specified in the *LRFD Specifications* (curvature = 0.0°) OK
- Cross section of the bridge is consistent with one of the cross sections given in LRFD Table 4.6.2.2.1-10K

Since these criteria are satisfied, the barrier and wearing surface loads are distributed equally among the nine beams.

Barrier weight = (2 barriers)(0.300 kips/ft)/9 beams = 0.067 kips/ft = w_b

DW = Dead load of wearing surface (weight of 3 in. bituminous wearing surface at 0.140 kcf)

= (3/12)(0.140) = 0.035 ksf

= (0.035)(51.0 ft)/9 beams = 0.198 kips/ft/beam = w_{ws}

DW load should be kept separately from DC because of a higher load factor is applied to it.

DECK BULB-TEE (DBT-53), SINGLE SPAN, NONCOMPOSITE SURFACE**9.3.4.1.2 Unfactored Shear Forces and Bending Moments/9.3.4.2.2.1 Distribution Factor for Bending Moments****9.3.4.1.2 Unfactored Shear Forces and Bending Moments**

For a simply supported beam with a span length (L) loaded with a uniformly distributed load (w), the shear force (V_x) and bending moment (M_x) at any distance (x) from the support are given by:

$$V_x = w(0.5L - x) \quad (\text{Eq. 9.3.4.1.2-1})$$

$$M_x = 0.5wx(L - x) \quad (\text{Eq. 9.3.4.1.2-2})$$

Using the above equations, values of shear forces and bending moments for a typical interior beam under the self weight of beam, barriers, and wearing surface are computed and given in **Table 9.3.4-1** that is located at the end of Section 9.3.4.3. For these calculations, the span length (L) is the design span, 95 ft. However, for calculations of stresses and deformations at the time the prestress is transferred, the overall length of the precast member, 96 ft, is used as illustrated later in this example.

9.3.4.2 Shear Forces and Bending Moments due to Live Loads**9.3.4.2.1 Live Loads**

Design live load is HL-93, which consists of a combination of: [LRFD Art. 3.6.1.2.1]

1. Design truck or design tandem with dynamic allowance [LRFD Art. 3.6.1.2.2]

The design truck consists of 8.0-, 32.0-, and 32.0-kip axles with the first pair spaced at 14.0 ft and the second pair spaced at 14.0 to 30.0 ft. The design tandem consists of a pair of 25.0-kip axles spaced at 4.0 ft apart.

[LRFD Art. 3.6.1.2.3]

2. Design lane load of 0.64 kips/ft without dynamic allowance [LRFD Art. 3.6.1.2.4]

9.3.4.2.2 Live Load Distribution Factors for a Typical Interior Beam

The live load bending moments and shear forces are determined by using the simplified distribution factor formulas. To use the simplified live load distribution factor formulas, the following conditions must be met: [LRFD Art. 4.6.2.2]
[LRFD Art. 4.6.2.2.1]

- Width of deck is constant OK
- Number of beams, N_b not less than four ($N_b = 9$) OK
- Beams are parallel and have approximately the same stiffness OK
- The roadway part of the overhang, $d_e \leq 3.0$ ft ($d_e = 1.5$ ft) OK
- Curvature is less than specified in the *LRFD Specifications*, (curvature = 0.0°) OK

For a precast deck bulb-tee beam, the bridge type is (j). [LRFD Table 4.6.2.2.1-1]

The number of design lanes is computed as:

Number of design lanes = the integer part of the ratio $w/12$, where (w) is the clear roadway width, in ft, between the curbs. [LRFD Art. 3.6.1.1.1]

From **Figure 9.3.1-1**, $w = 51$ ft

Number of design lanes = integer part of $(51/12) = 4$ lanes

9.3.4.2.2.1 Distribution Factor for Bending Moments

- For all limit states except fatigue limit state:

Assume the beams are connected only enough to prevent relative vertical displacement at the interface.

Regardless of number of loaded lanes:

$$DFM = \frac{S}{D} \quad [\text{LRFD Table 4.6.2.2.2b-1}]$$

DECK BULB-TEE (DBT-53), SINGLE SPAN, NONCOMPOSITE SURFACE

9.3.4.2.2.1 Distribution Factor for Bending Moments/9.3.4.2.2.2 Distribution Factor for Shear Force

where

DFM = distribution factor for bending moment for interior beam

S = beam spacing = 6 ft

D = width of distribution per lane, ft

The stiffness parameter, C , needs to be determined first in order to calculate D .

$$C = K \left(\frac{W}{L} \right) \leq K \quad \text{[LRFD Table 4.6.2.2.2b-1]}$$

Provided that: skew $\leq 45^\circ$; no skew OK

$$N_L \leq 6; \quad N_L = 4 \quad \text{OK}$$

where

W = edge-to-edge width of the bridge = 54 ft

L = span length of the bridge = 95 ft

N_L = number of design lanes = 4 lanes

$$K = \sqrt{\frac{(1 + \mu)I_g}{J_g}} \quad \text{[LRFD Table 4.6.2.2.2b-1]}$$

where

μ = Poisson's ratio = 0.2 for normal weight concrete [LRFD Art. 5.4.2.5]

I_g = moment of inertia about the centroid of the noncomposite precast beam, in.⁴

J_g = St. Venant's torsional inertia = 34,697 in.⁴

$$K = \sqrt{\frac{(1 + 0.2)(335,679)}{(34,697)}} = 3.41$$

Using the equations above,

$$C = 3.41 \left(\frac{54}{95} \right) = 1.94 \leq 3.41 \quad \text{OK}$$

Since $C \leq 5$, use the following equation to calculate D :

$$\begin{aligned} D &= 11.5 - N_L + 1.4N_L(1 - 0.2C)^2 && \text{[LRFD Table 4.6.2.2.2b-1]} \\ &= 11.5 - 4 + 1.4(4)[1 - 0.2(1.94)]^2 = 9.60 \end{aligned}$$

$$DFM = (6/9.60) = 0.625 \text{ lanes/beam}$$

• For fatigue limit state:

The *LRFD Specifications*, Art. C3.4.1, states that for Fatigue Limit State, a single design truck should be used. However, live load distribution factors given in LRFD Article 4.6.2.2 take into consideration the multiple presence factor, m . LRFD Article 3.6.1.1.2 states that the multiple presence factor, m , for one design lane loaded is 1.2. Therefore, the distribution factor for one design lane loaded with the multiple presence factor removed, should be used. The distribution factor for fatigue limit state is: $0.625/1.2 = 0.521$ lanes/beam.

9.3.4.2.2.2 Distribution Factor for Shear Force

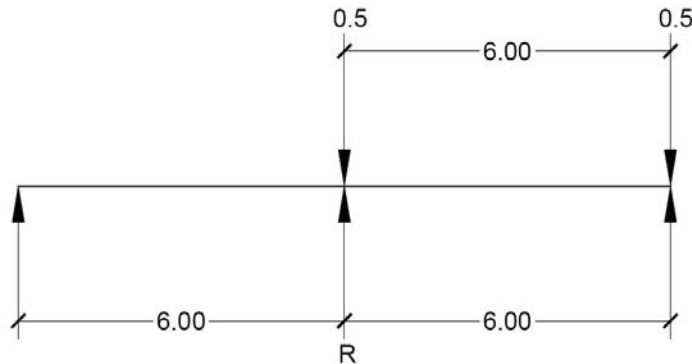
For Type (j) bridge connected only enough to prevent relative vertical displacement at the interface, DFV (Shear distribution factor) for interior beam is determined using the Lever Rule. Refer to **Figures 9.3.4.2.2.2-1** and **9.3.4.2.2.2-2**.

DECK BULB-TEE (DBT-53), SINGLE SPAN, NONCOMPOSITE SURFACE

9.3.4.2.2.2 Distribution Factor for Shear Force/9.3.4.2.3 Dynamic Allowance

Figure 9.3.4.2.2.2-1

Lever Rule for one lane loaded



For one lane loaded:

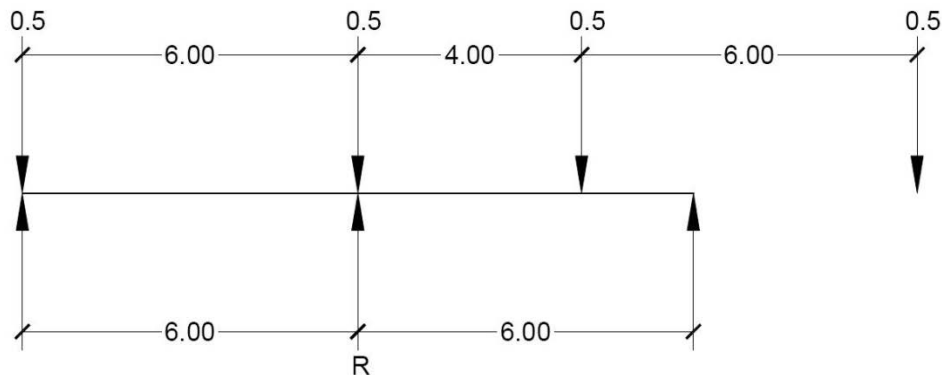
$R = \text{reaction at support} = 0.5$

$DFV = (\text{multiple presence factor})(R) = (1.2)(0.5) = 0.6$

Figure 9.3.4.2.2.2-2

Lever rule for two lanes loaded

For two lanes loaded:



$$\sum M \text{ at support} = R(6) - 0.5(6) - 0.5(2) = 0$$

Therefore, $R = 0.667$

$$DFV = (\text{multiple presence factor})(R) = (1.0)(0.667) = 0.667$$

Thus the case of two lanes loaded controls,

$$DFV = 0.667 \text{ lanes/beam}$$

9.3.4.2.3 Dynamic Allowance

$IM = 15\%$ for fatigue limit state

$IM = 33\%$ for all other limit states

where $IM = \text{dynamic load allowance, applied to design truck load only}$

[LRFD Table 3.6.2.1-1]

DECK BULB-TEE (DBT-53), SINGLE SPAN, NONCOMPOSITE SURFACE

9.3.4.2.4 Unfactored Shear Forces and Bending Moments/9.3.4.2.4.2 Due to Design Lane Load; V_{LL} and M_{LL}

9.3.4.2.4 Unfactored Shear Forces and Bending Moments

9.3.4.2.4.1 Due to Truck Load; V_{LT} and M_{LT}

- For all limit states except for fatigue limit state:

Shear force and bending moment envelopes on a per-lane-basis are calculated at tenth-points of the span using the equations given in Chapter 8 of this manual. However, this is generally done by means of commercially available computer software that has the ability to deal with moving loads. Therefore, truck load shear force and bending moments per beam are:

$$\begin{aligned}
 V_{LT} &= (\text{shear force per lane}) (DFV) (1 + IM) \\
 &= (\text{shear force per lane}) (0.667) (1 + 0.33) \\
 &= (\text{shear force per lane}) (0.887) \text{ kips} \\
 M_{LT} &= (\text{bending moment per lane}) (DFM) (1 + IM) \\
 &= (\text{bending moment per lane}) (0.625) (1 + 0.33) \\
 &= (\text{bending moment per lane}) (0.831) \text{ ft-kips}
 \end{aligned}$$

Values for V_{LT} and M_{LT} at different points are given in **Table 9.3.4-2**.

- For fatigue limit state:

Article 3.6.1.4.1 in the *LRFD Specifications* states that fatigue load is a single design truck which has the same axle weight used in all other limit states but with a constant spacing of 30.0 ft between the 32.0-kip axles. Bending moment envelope on a per-lane-basis is calculated using the equation given in Chapter 8 of this manual.

Therefore, bending moment of the fatigue truck load is:

$$\begin{aligned}
 M_f &= (\text{bending moment per lane}) (DFM)(1 + IM) \\
 &= (\text{bending moment per lane}) (0.521) (1 + 0.15) \\
 &= (\text{bending moment per lane}) (0.599) \text{ ft-kips}
 \end{aligned}$$

Values of M_f at different points are given in **Table 9.3.4-2**.

9.3.4.2.4.2 Due To Design Lane Load; V_{LL} and M_{LL}

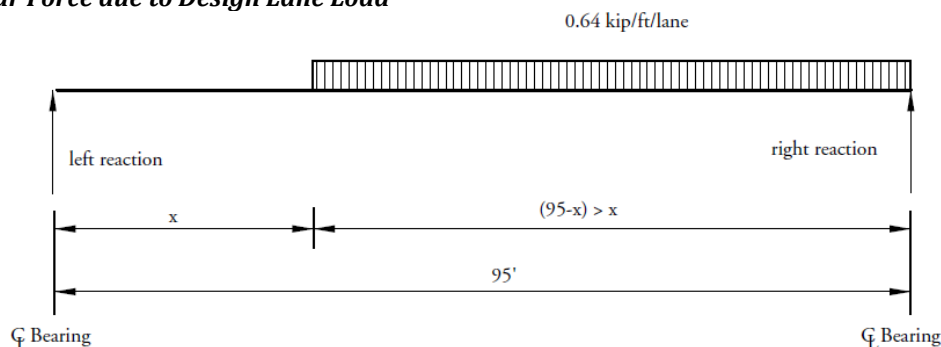
To obtain the maximum shear force at a section located at a distance (x) from the left support under a uniformly distributed load of 0.64 kips/ft, load the member to the right of the section under consideration as shown in **Figure 9.3.4.2.4.2-1**. Therefore, the maximum shear force per lane is:

$$V_x = \frac{0.32(L - x)^2}{L} \text{ for } x \leq 0.5L \tag{Eq. 9.3.4.2.4.2-1}$$

where V_x is in kips/lane and L and x are in ft

Figure 9.3.4.2.4.2-1

Maximum Shear Force due to Design Lane Load



DECK BULB-TEE (DBT-53), SINGLE SPAN, NONCOMPOSITE SURFACE

9.3.4.2.4.2 Due to Design Land Load; V_{LL} and M_{LL} /9.3.4.3 Load Combinations

To calculate the maximum bending moment at any sections, use Eq. (9.3.4.1.2-2).

Lane Load shear force and bending moment per typical interior beam are as follows:

$$\begin{aligned} V_{LL} &= (\text{lane load shear force})(DFV) \\ &= (\text{lane load shear force})(0.667) \text{ kips} \end{aligned}$$

For all limit states except for fatigue limit state:

$$\begin{aligned} M_{LL} &= (\text{lane load bending moment})(DFM) \\ &= (\text{lane load bending moment})(0.625) \text{ ft-kips} \end{aligned}$$

Note that dynamic allowance is not applied to the design lane loading.

Values of shear forces and bending moments, V_{LL} and M_{LL} , are given in **Table 9.3.4-2**.

9.3.4.3 Load Combinations

Total factored load is taken as:

$$Q = \sum \eta_i \gamma_i Q_i \quad \text{[LRFD Eq. 3.4.1-1]}$$

where

$$\eta_i = \text{a load modifier relating to ductility, redundancy, and operational importance} \quad \text{[LRFD Art. 1.3.2]}$$

(Here, η_i is considered to be 1.0 for typical bridges.)

$$\gamma_i = \text{loads factors} \quad \text{[LRFD Table 3.4.1-1]}$$

$$Q_i = \text{force effects from specified loads}$$

Investigating different limit states given in LRFD Article 3.4.1, the following limit states are applicable:

Service I: check compressive stresses in prestressed concrete components:

$$Q = 1.00(DC + DW) + 1.00(LL + IM) \quad \text{[LRFD Table 3.4.1-1]}$$

This load combination is a special combination for service limit state stress checks and applies to all conditions other than Service III.

Service III: check tensile stresses in prestressed concrete components:

$$Q = 1.00(DC + DW) + 0.80(LL + IM) \quad \text{[LRFD Table 3.4.1-1]}$$

This load combination is a special combination for service limit state stress checks that applies only to tension in prestressed concrete structures to control cracks.

Strength I: check ultimate strength:

[LRFD Tables 3.4.1-1 and 2]

$$\text{Maximum } Q = 1.25(DC) + 1.50(DW) + 1.75(LL + IM)$$

$$\text{Minimum } Q = 0.90(DC) + 0.65(DW) + 1.75(LL + IM)$$

This load combination is the general load combination for strength limit state design.

Note: For simple-span bridges, the maximum load factors produce maximum effects. However, use minimum load factors for dead load (DC), and wearing surface (DW) when the dead load and wearing surface stresses are opposite to those of the live load.

Fatigue I: check stress range in strands:

[LRFD Table 3.4.1-1]

$$Q = 1.50(LL + IM)$$

This load combination is a special load combination to check the tensile stress range in the strands due to live load and dynamic allowance.

Note: The LL used in the above equation results only from a single design truck with a 30-ft constant spacing between 32.0-kip axles with the special dynamic allowance, (IM) for fatigue.

DECK BULB-TEE (DBT-53), SINGLE SPAN, NONCOMPOSITE SURFACE

9.3.4.3 Load Combinations/9.3.5.1 Service Load Stresses at Midspan

Table 9.3.4-1**Unfactored Shear Forces and Bending Moments Due to Dead Loads for a Typical Interior Beam**

Distance <i>x</i> , ft	Section <i>x/L</i>	Beam Weight		Barrier Weight		Wearing Surface Weight	
		Shear <i>V_g</i> kips	Moment <i>M_g</i> ft-kips	Shear <i>V_b</i> kips	Moment <i>M_b</i> ft-kips	Shear <i>V_{ws}</i> kips	Moment <i>M_{ws}</i> ft-kips
0	0.0	46.1	0.0	3.2	0.0	9.4	0.0
*4.04	0.043	42.2	178.2	2.9	12.3	8.6	36.4
9.5	0.1	36.9	393.9	2.5	27.2	7.5	80.4
19.0	0.2	27.6	700.3	1.9	48.4	5.7	143.0
28.5	0.3	18.4	919.2	1.3	63.5	3.8	187.6
38.0	0.4	9.2	1,050.5	0.6	72.6	1.9	214.4
47.5	0.5	0.0	1,094.3	0.0	75.6	0.0	223.4

*Critical section for shear (see Sect. 9.3.11)

Table 9.3.4-2**Unfactored Shear Forces and Bending Moments Due to Live Loads for a Typical Interior Beam**

Distance <i>x</i> , ft	Section <i>x/L</i>	Truck Load with Impact		Lane load		Fatigue Truck with Impact
		Shear <i>V_{LT}</i> kips	Moment <i>M_{LT}</i> ft-kips	Shear <i>V_{LL}</i> kips	Moment <i>M_{LL}</i> ft-kips	Moment <i>M_f</i> ft-kips
0	0.0	57.6	0.0	20.3	0.0	0.0
*4.04	0.043	54.9	207.8	18.6	73.5	133.4
9.50	0.1	51.2	455.9	16.4	162.5	290.2
19.0	0.2	44.8	798.0	13.0	288.8	498.5
28.50	0.3	38.4	1,026.5	9.9	379.1	641.1
38.00	0.4	32.1	1,159.7	7.3	433.2	713.2
47.50	0.5	25.7	1,188.6	5.1	451.3	703.4

*Critical section for shear (see Sect. 9.3.11)

9.3.5 ESTIMATE REQUIRED PRESTRESS

The required number of strands is usually governed by concrete tensile stresses at the bottom fiber for load combination Service III at the section of maximum moment and in some cases at Strength Limit State (Strength I). For estimating the number of strands, only the stresses at midspan are considered.

9.3.5.1 Service Load Stresses at Midspan

Bottom tensile stresses due to applied dead and live loads using load combination Service III is:

$$f_b = \frac{M_g + M_b + M_{ws} + (0.8)(M_{LT} + M_{LL})}{S_b}$$

where

- f_b = concrete tensile stresses at bottom fiber of the beam, ksi
- M_g = unfactored bending moment due to beam self weight, ft-kips
- M_b = unfactored bending moment due to barrier weight, ft-kips
- M_{ws} = unfactored bending moment due to wearing surface, ft-kips
- M_{LT} = unfactored bending moment due to truck load, ft-kips
- M_{LL} = unfactored bending moment due to lane load, ft-kips

DECK BULB-TEE (DBT-53), SINGLE SPAN, NONCOMPOSITE SURFACE**9.3.5.1 Service Load Stresses at Midspan/9.3.5.4 Strand Pattern**

Using values of bending moments from **Tables 9.3.4-1** and **9.3.4-2**, bottom tensile stress at midspan is:

$$f_b = \frac{1,094.3 + 75.6 + 223.4 + (0.8)(1,188.6 + 451.3)}{9,713} (12) = 3.342 \text{ ksi}$$

9.3.5.2 Stress Limits for Concrete

$$\text{Tensile stress limit at service loads} = 0.19\sqrt{f'_c} \quad [\text{LRFD Table 5.9.4.2.2-1}]$$

where f'_c = specified concrete compressive strength for design, ksi

$$\text{Concrete tensile stress limit} = -0.19\sqrt{7,000} = -0.503 \text{ ksi}$$

9.3.5.3 Required Number of Strands

The required precompressive stress at the bottom fiber of the beam is the difference between the bottom tensile stress due to the applied loads and the concrete tensile stress limit:

$$f_{pb} = (3.342 - 0.503) = 2.839 \text{ ksi}$$

The location of the strand center of gravity at midspan ranges from 5 to 15% of the beam depth, measured from the bottom of the beam. A value of 5% is appropriate for newer efficient sections like the bulb-tee beams and 15% for less efficient AASHTO standard shapes.

Assume the distance between the center of gravity of strands and the bottom fiber of the beam:

$$y_{bs} = 0.05h = 0.05(53) = 2.65 \text{ in.}, \text{ use } y_{bs} = 3.00 \text{ in.}$$

Therefore, strand eccentricity at midspan, $e_c = (y_b - y_{bs}) = (34.56 - 3.00) = 31.56 \text{ in.}$

If P_{pe} is the total prestress force after all losses, the stress at the bottom fiber due to prestress is:

$$f_{pb} = \frac{P_{pe}}{A_g} + \frac{P_{pe}e_c}{S_b} \text{ or } 2.839 = \frac{P_{pe}}{931} + \frac{P_{pe}(31.56)}{9,713}$$

Solving for P_{pe} , the required $P_{pe} = 656.7 \text{ kips}$

Final prestress force per strand = (area of strand)(f_{pi})(1 - final losses)

where f_{pi} = initial stress before transfer, ksi (see Section 9.3.2) = 202.5 ksi

Assuming final loss of 25% of f_{pi} , prestress force per strand after all losses

$$= (0.217)(202.5)(1 - 0.25) = 33.0 \text{ kips}$$

Number of strands required = $(656.7/33.0) = 19.9$ strands

Try twenty two 0.6-in.-diameter, 270 ksi low-relaxation strands

Total area of prestressing strands, $A_{ps} = 22(0.217) = 4.774 \text{ in.}^2$

Note: This is a conservative estimate of the number of strands because nontransformed section properties are used in lieu of transformed section properties. The number of strands can be refined later in the design process as more accurate section properties and prestress losses are determined.

9.3.5.4 Strand Pattern

The assumed strand pattern for the 22 strands at midspan is shown in **Figure 9.3.5.4-1**. Each available position is filled beginning with the bottom row.

The distance between the center of gravity of strands and the bottom concrete fiber of the beam at midspan is:

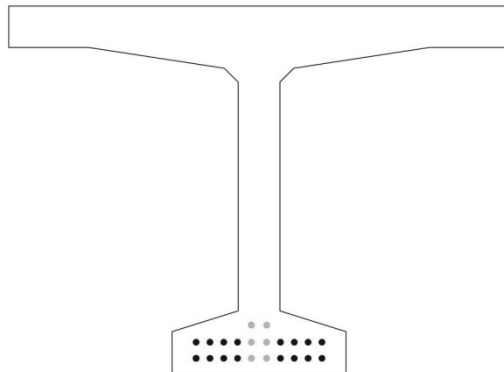
$$y_{bs} = [10(2) + 10(4) + 2(6)]/(22) = 3.27 \text{ in.}$$

Strand eccentricity at midspan, $e_c = y_b - y_{bs} = 34.56 - 3.27 = 31.29 \text{ in.} = e_{pg}$

DECK BULB-TEE (DBT-53), SINGLE SPAN, NONCOMPOSITE SURFACE

9.3.5.4 Strand Pattern/9.3.5.5 Steel Transformed Section Properties

Figure 9.3.5.4-1
Assumed Strand Pattern at Midspan



No. of Strands	Distance from bottom (in.)
2	6
10	4
10	2

9.3.5.5 Steel Transformed Section Properties

From the earliest years of prestressed concrete design, the gross section was conservatively used in analysis since the prestressing forces were smaller and computer programs were not widely used. However, the use of transformed section, which is obtained from the gross section by adding transformed steel area, yields more accurate results than the gross section analysis.

For each row of prestressing strands shown in **Figure 9.3.5.4-1**, the steel area is multiplied by $(n - 1)$ to calculate the transformed section properties, where n is the modular ratio between prestressing strand and concrete. Since the modulus of elasticity of concrete is different at transfer and final time, the transformed section properties should be calculated separately for the two stages. A sample calculation is shown in **Table 9.3.5.5-1** below.

At transfer:

$$n - 1 = \frac{28,500}{4,496} - 1 = 5.339$$

At final:

$$n - 1 = \frac{28,500}{5,072} - 1 = 4.619$$

Table 9.3.5.5-1
Properties of Transformed Section at Final Time

	Transformed Area, in. ²	y_b in.	Ay_b in. ³	$A(y_{btf} - y_b)^2$ in. ⁴	I , in. ⁴	$I + A(y_{btf} - y_b)^2$ in. ⁴
Beam	931	34.56	32,175	483	335,679	336,162
Row 1	10.02	2.00	20.04	10,158		10,158
Row 2	10.02	4.00	40.08	8,922		8,922
Row 3	2.00	6.00	12.00	1,550		1,550
Σ	953.0		32,247			356,792

Note: The moment of inertia of strand about its own centroid is neglected.

Noncomposite transformed section at transfer:

A_{ti} = area of transformed section at transfer = 956.5 in.²

I_{ti} = moment of inertia of the transformed section at transfer = 360,017 in.⁴

e_{ti} = eccentricity of strands with respect to transformed section at transfer = 30.46 in.

y_{bti} = distance from the centroid of the transformed section to the extreme bottom fiber of the beam at transfer = 33.73 in.

S_{bti} = section modulus for the extreme bottom fiber of the transformed section at transfer = 10,673 in.³

S_{tti} = section modulus for the extreme top fiber of the transformed section at transfer = 18,683 in.³

DECK BULB-TEE (DBT-53), SINGLE SPAN, NONCOMPOSITE SURFACE**9.3.5.5 Steel Transformed Section Properties/9.3.6.1 Elastic Shortening**

Noncomposite transformed section at final time:

$$A_{tf} = \text{area of transformed section at final time} = 953.0 \text{ in.}^2$$

$$I_{tf} = \text{moment of inertia of the transformed section at final time} = 356,792 \text{ in.}^4$$

$$e_{tf} = \text{eccentricity of strands with respect to transformed section at final time} = 30.57 \text{ in.}$$

$$y_{btf} = \text{distance from the centroid of the noncomposite transformed section to the extreme bottom fiber of the beam at final time} = 33.84 \text{ in.}$$

$$S_{btf} = \text{section modulus for the extreme bottom fiber of the transformed section at final time} = 10,543 \text{ in.}^3$$

$$S_{ttf} = \text{section modulus for the extreme top fiber of the transformed section at final time} = 18,622 \text{ in.}^3$$

9.3.6 PRESTRESS LOSSES

Total prestress loss:

$$\Delta f_{pT} = \Delta f_{pES} + \Delta f_{pLT} \quad [\text{LRFD Eq. 5.9.5.1-1}]$$

where

$$\Delta f_{pT} = \text{total loss in prestressing steel stress}$$

$$\Delta f_{pES} = \text{sum of all losses or gains due to elastic shortening or extension at the time of application of prestress and/or external loads}$$

$$\Delta f_{pLT} = \text{long-term losses due to shrinkage and creep of concrete, and relaxation of steel after transfer. In this design example, the refined estimates of time-dependent losses are used.}$$

9.3.6.1 Elastic Shortening

$$\Delta f_{pES} = \frac{E_p}{E_{ci}} f_{cgp} \quad [\text{LRFD Eq. 5.9.5.2.3a-1}]$$

where

$$E_p = \text{modulus of elasticity of prestressing strands} = 28,500 \text{ ksi}$$

$$E_{ci} = \text{modulus of elasticity of beam concrete at transfer} = 4,496 \text{ ksi}$$

$$f_{cgp} = \text{sum of concrete stresses at the center of gravity of prestressing tendons due to prestressing force at transfer and the self weight of the member at sections of maximum moment.}$$

If the gross (or net) cross-section properties are used, it is necessary to perform numerical iterations. The elastic loss Δf_{pES} is usually assumed to be 10% of the initial prestress to calculate f_{cgp} , which is then used in the equation above to calculate a refined Δf_{pES} . The process is repeated until the assumed Δf_{pES} and refined Δf_{pES} converge. However, when transformed section properties are used to calculate concrete stress, the effects of losses and gains due to elastic deformations are implicitly accounted for. Therefore, Δf_{pES} should not be included in calculating f_{cgp} .

$$\begin{aligned} \text{Force per strand at transfer} &= (\text{area of strand})(\text{prestress stress at transfer}) \\ &= (0.217)(202.5) = 43.94 \text{ ksi} \end{aligned}$$

$$f_{cgp} = \frac{P_{pi}}{A_{ti}} + \frac{P_{pi}e_{ti}^2}{I_{ti}} - \frac{M_g e_{ti}}{I_{ti}}$$

where

$$P_{pi} = \text{total prestressing force before transfer} = (22 \text{ strands})(43.94) = 966.7 \text{ kips}$$

$$e_{ti} = \text{eccentricity of strands at midspan with respect to the transformed section at transfer} = 30.46 \text{ in.}$$

M_g should be calculated based on the overall beam length of 96 ft. Since the elastic shortening loss is a part of the total loss, f_{cgp} will be conservatively computed based on M_g using the design span length of 95 ft.

$$f_{cgp} = \frac{966.7}{956.5} + \frac{(966.7)(30.46)^2}{360,017} - \frac{(1,094.3)(12)(30.46)}{360,017} = 2.391 \text{ ksi}$$

DECK BULB-TEE (DBT-53), SINGLE SPAN, NONCOMPOSITE SURFACE

9.3.6.1 Elastic Shortening/9.3.6.2.1 Shrinkage of Concrete

Therefore, loss due to elastic shortening:

$$\Delta f_{pES} = \left(\frac{28,500}{4,496} \right) (2.391) = 15.2 \text{ ksi}$$

AASHTO LRFD C5.9.5.3 indicates that the loss due to elastic shortening at transfer should be added to the time-dependent losses to determine total losses. However, this loss at transfer is directly accounted for if transformed section properties are used in stress analysis.

9.3.6.2 Time-Dependent Losses between Transfer and Deck Placement

AASHTO LRFD Art. 5.9.5.4.4 indicates that the time of "deck placement" may be taken as (LRFD Art. 5.9.5.4.4) time of noncomposite deck placement. In this example the term "deck placement" is interchangeable with topping placement.

The following construction schedule is assumed in calculating the time-dependent losses:

Concrete age at transfer:	$t_i = 1$ day
Concrete age at deck placement:	$t_d = 90$ days
Concrete age at final stage:	$t_f = 20,000$ days

The total time-dependent loss between time of transfer and deck placement is the summation of prestress losses due to shrinkage of concrete, creep of concrete, and relaxation of prestressing strands.

9.3.6.2.1 Shrinkage of Concrete

The prestress loss due to shrinkage of concrete between time of transfer and deck placement is calculated by:

$$\Delta f_{pSR} = \epsilon_{bid} E_p K_{id} \quad \text{[LRFD Eq. 5.9.5.4.2a-1]}$$

where

- ϵ_{bid} = concrete shrinkage strain of girder for time period between transfer and deck placement
- E_p = modulus of elasticity of prestressing strands, ksi
- K_{id} = transformed section coefficient that accounts for time-dependent interaction between concrete and bonded steel in the section being considered for time period between transfer and deck placement

The concrete shrinkage strain ϵ_{bid} is taken as:

$$\epsilon_{bid} = k_{vs} k_{hs} k_f k_{td} 0.48 \times 10^{-3} \quad \text{[LRFD Eq. 5.4.2.3.3.-1]}$$

where

The factor for the effect of the volume-to-surface ratio of the beam:

$$k_{vs} = 1.45 - 0.13(V/S) = 1.45 - 0.13 \times 3.51 = 0.994$$

The minimum value of k_{vs} is 1.0, therefore use $k_{vs} = 1.0$

V/S is the volume-to-surface ratio of the beam.

The humidity factor for shrinkage:

$$k_{hs} = 2.00 - 0.14H = 2.00 - 0.14(70) = 1.020$$

where H = average annual mean relative humidity (assume 70%)

The factor for the effect of the concrete strength:

$$k_f = \frac{5}{1 + f'_{ci}} = \frac{5}{1 + 5.5} = 0.769$$

The time development factor at deck placement:

$$k_{td} = \frac{t}{61 - 4f'_{ci} + t} = \frac{89}{61 - (4)(5.5) + 89} = 0.695 = k_{td}$$

where t is the maturity of concrete(days) = $t_d - t_i = 90 - 1 = 89$ days

DECK BULB-TEE (DBT-53), SINGLE SPAN, NONCOMPOSITE SURFACE

9.3.6.2.1 Shrinkage of Concrete/9.3.6.2.3 Relaxation of Prestressing Strands

$$\epsilon_{bid} = (1.000)(1.020)(0.769)(0.695)(0.48 \times 10^{-3}) = 0.000262$$

$$K_{id} = \frac{1}{1 + \frac{E_p}{E_{ci}} \frac{A_{ps}}{A_g} \left(1 + \frac{A_g(e_{pg})^2}{I_g}\right) [1 + 0.7\Psi_b(t_f, t_i)]} \quad \text{[LRFD Eq. 5.9.5.4.2a-2]}$$

where

- e_{pg} = eccentricity of prestressing force with respect to centroid of girder, in.
- $\Psi_b(t_f, t_i)$ = girder creep coefficient at final time due to loading introduced at transfer

For the time between transfer and final time:

$$\Psi_b(t_f, t_i) = 1.9k_{vs}k_{hc}k_{fj}k_{td}t_i^{-0.118} \quad \text{[LRFD Eq. 5.4.2.3.2-1]}$$

$$k_{hc} = 1.56 - 0.008H = 1.56 - 0.008(70) = 1.000$$

$$k_{td} = \frac{t_f - t_i}{61 - 4f'_{ci} + (t_f - t_i)} = \frac{20,000 - 1}{61 - 4(5.5) + (20,000 - 1)} = 0.998 = k_{tdf}$$

$$\begin{aligned} \Psi_b(t_f, t_i) &= 1.9(1.000)(1.000)(0.769)(0.998)(1.000)^{-0.118} \\ &= 1.458 \end{aligned}$$

$$K_{id} = \frac{1}{1 + \frac{28,500}{4,496} \frac{4,774}{931} \left(1 + \frac{931(31.29)^2}{335,679}\right) [1 + 0.7(1.458)]} = 0.804$$

The prestress loss due to shrinkage of concrete between transfer and deck placement is:

$$\Delta f_{psR} = (0.000262)(28,500)(0.804) = 6.003 \text{ ksi}$$

9.3.6.2.2 Creep of Concrete

The prestress loss due to creep of girder concrete between time of transfer and deck placement is determined as:

$$\Delta f_{pCR} = \frac{E_p}{E_{ci}} f_{cgp} \Psi_b(t_d, t_i) K_{id} \quad \text{[LRFD Eq. 5.9.5.4.2b-1]}$$

where

- $\Psi_b(t_d, t_i)$ = girder creep coefficient at time of deck placement due to loading introduced at transfer
- = $1.9k_{vs}k_{hc}k_{fj}k_{td}t_i^{-0.118}$ [LRFD Eq. 5.4.2.3.2-1]
- = $1.9(1.000)(1.000)(0.769)(0.695)(1)^{-0.118}$
- = 1.015

$$\Delta f_{pCR} = \frac{28,500}{4,496} (2.391)(1.015)(0.804) = 12.369 \text{ ksi}$$

9.3.6.2.3 Relaxation of Prestressing Strands

The prestress loss due to relaxation of prestressing strands between time of transfer and deck placement is determined as:

$$\Delta f_{pR1} = \frac{f_{pt}}{K_L} \left(\frac{f_{pt}}{f_{py}} - 0.55 \right) \quad \text{[LRFD Eq. 5.9.5.4.2c-1]}$$

where

- f_{pt} = stress in prestressing strands immediately after transfer, taken not less than $0.55f_y$
- K_L = 30 for low-relaxation strands and 7 for other prestressing steel, unless more accurate manufacturer's data are available

DECK BULB-TEE (DBT-53), SINGLE SPAN, NONCOMPOSITE SURFACE**9.3.6.2.3 Relaxation of Prestressing Strands/9.3.6.3.2 Creep of Concrete**

$$\Delta f_{pR1} = \frac{(202.5 - 15.2)}{30} \left(\frac{(202.5 - 15.2)}{243} - 0.55 \right) = 1.378 \text{ ksi}$$

According to LRFD Art. 5.9.5.4.2c, the relaxation loss may also be assumed equal to 1.2 ksi for low-relaxation strands.

9.3.6.3 Time-Dependent Losses between Deck Placement and Final Time

The total time-dependent loss between time of deck placement and final time is the summation of prestress loss due to shrinkage of beam concrete, creep of beam concrete, and relaxation of prestressing strands.

9.3.6.3.1 Shrinkage of Concrete

The prestress loss due to shrinkage of concrete between time of deck placement and final time is calculated by:

$$\Delta f_{pSD} = \epsilon_{bdf} E_p K_{df} \quad [\text{LRFD Eq. 5.9.5.4.2a-1}]$$

where

ϵ_{bdf} = concrete shrinkage strain of girder for time period between the deck placement and final time

E_p = modulus of elasticity of prestressing strands, ksi

K_{df} = transformed section coefficient that accounts for time-dependent interaction between concrete and bonded steel in the section being considered for time period between deck placement and final time

The total girder concrete shrinkage strain between transfer and final time is taken as:

$$\begin{aligned} \epsilon_{bif} &= k_{vs} k_{hs} k_f k_{tdf} (0.48 \times 10^{-3}) \quad [\text{LRFD Eq. 5.4.2.3.3-1}] \\ &= (1.000)(1.020)(0.769)(0.998)(0.48 \times 10^{-3}) \\ &= 0.000376 \end{aligned}$$

The girder concrete shrinkage strain between deck placement and final time is:

$$\epsilon_{bdf} = \epsilon_{bif} - \epsilon_{bid} = 0.000376 - 0.000262 = 0.000114$$

The beam concrete transformed section coefficient between deck placement and final time is:

$$K_{df} = \frac{1}{1 + \frac{E_p}{E_{ci}} \frac{A_{ps}}{A_c} \left(1 + \frac{A_c (e_{pc})^2}{I_c} \right) [1 + 0.7 \Psi_b(t_f, t_i)]} \quad [\text{LRFD Eq. 5.9.5.4.3a-2}]$$

As there is no composite deck in this example, the composite section properties are taken as:

$A_c = A_g =$ area of the precast beam section = 931 in.²

$e_{pc} = e_{pg} =$ eccentricity of strands with respect to centroid of beam = 31.29 in.

$I_c = I_g =$ moment of inertia of the beam = 335,679 in.⁴

$$K_{df} = \frac{1}{1 + \frac{28,500}{4,496} \frac{4.774}{931} \left(1 + \frac{(931)(31.29)^2}{335,679} \right) [1 + 0.7(1.458)]} = 0.804$$

The prestress loss due to shrinkage of concrete between deck placement and final time is:

$$\Delta f_{pSD} = (0.000114)(28,500)(0.804) = 2.612 \text{ ksi}$$

9.3.6.3.2 Creep of Concrete

The prestress loss due to creep of girder concrete between time of deck placement and final time is determined as:

$$\Delta f_{pCD} = \frac{E_p}{E_{ci}} f_{cpg} [\Psi_b(t_f, t_i) - \Psi_b(t_d, t_i)] K_{df} + \frac{E_p}{E_c} \Delta f_{cd} \Psi_b(t_f, t_d) K_{df} \quad [\text{LRFD Eq. 5.9.5.4.3b-1}]$$

DECK BULB-TEE (DBT-53), SINGLE SPAN, NONCOMPOSITE SURFACE

9.3.6.3.2 Creep of Concrete/9.3.6.5 Total Losses at Transfer

where

$$\begin{aligned}\Psi_b(t_f, t_d) &= \text{girder creep coefficient at final time due to loading at deck placement} \\ &= 1.9k_{vs}k_{hc}k_{jt}k_{td}t_d^{-0.118} \quad \text{[LRFD Eq. 5.4.2.3.2-1]}\end{aligned}$$

$$k_{tdf} = \frac{t}{61 - 4f'_{ci} + t} = \frac{(20,000 - 90)}{61 - 4(5.5) + (20,000 - 90)} = 0.998$$

$$\Psi_b(t_f, t_d) = 1.9(1.000)(1.000)(0.769)(0.998)(90)^{-0.118} = 0.857$$

Δf_{cd} = change in concrete stress at centroid of prestressing strands due to long term losses between transfer and deck placement, combined with deck weight and superimposed loads, ksi

$$\begin{aligned}&= -(\Delta f_{pSR} + \Delta f_{pCR} + \Delta f_{pR1}) \frac{A_{ps}}{A_g} \left(1 + \frac{A_g e_{pg}^2}{I_g} \right) - \left(\frac{(M_b + M_{ws})e_{tf}}{I_{tf}} \right) \\ &= -(6.003 + 12.369 + 1.378) \frac{4.774}{931} \left(1 + \frac{(931)(31.29)^2}{335,679} \right) - \left(\frac{(75.6 + 223.4)(12)(30.57)}{356,792} \right) \\ &= -0.684 \text{ ksi}\end{aligned}$$

The gross section properties are used in the equation to calculate Δf_{pcd} for the long-term losses since the transformed section effect has already been included in the factor K_{id} when calculating the losses between initial time and deck placement.

$$\Delta f_{pcd} = \frac{28,500}{4,496} 2.391[1.458 - 1.015](0.804) + \frac{28,500}{5,072} (-0.684)(0.857)(0.804) = 2.750 \text{ ksi}$$

9.3.6.3.3 Relaxation of Prestressing Strands

The prestress loss due to relaxation of prestressing strands between time of deck placement and final time is taken as:

$$\Delta f_{pR2} = \Delta f_{pR1} = 1.378 \text{ ksi} \quad \text{[LRFD Eq. 5.9.5.4.3c-1]}$$

9.3.6.3.4 Shrinkage of Deck Concrete

The prestress gain due to shrinkage of deck concrete is taken as zero for this bridge because there is no composite deck.

$$\Delta f_{pSS} = 0.0 \text{ ksi}$$

9.3.6.4 Total Time-Dependent Loss

The total time-dependent loss, Δf_{pLT} , is determined as:

$$\begin{aligned}\Delta f_{pLT} &= (\Delta f_{pSR} + \Delta f_{pCR} + \Delta f_{pR1}) + (\Delta f_{pSD} + \Delta f_{pcd} + \Delta f_{pR2} + \Delta f_{pSS}) \quad \text{[LRFD Eq. 5.9.5.4.1-1]} \\ &= (6.003 + 12.369 + 1.378) + (2.612 + 2.750 + 1.378 + 0.0) \\ &= 26.5 \text{ ksi}\end{aligned}$$

9.3.6.5 Total Losses at Transfer

AASHTO LRFD C5.9.5.2.3a and C5.9.5.3 indicate that the losses or gains due to elastic deformation must be taken equal to zero if transformed section properties are used in stress analysis. However, the losses or gains due to elastic deformation must be included in determining the total prestress losses and the effective stress in the prestressing strands.

$$\Delta f_{pi} = \Delta f_{pES} = 15.2 \text{ ksi}$$

Effective stress in tendons immediately after transfer, $f_{pt} = f_{pi} - \Delta f_{pi} = (202.5 - 15.2) = 187.3 \text{ ksi}$

DECK BULB-TEE (DBT-53), SINGLE SPAN, NONCOMPOSITE SURFACE**9.3.6.5 Total Losses at Transfer/9.3.7.1 Stress Limits for Concrete**

Force per strand = $(f_{pt})(\text{area of strand}) = (187.3)(0.217) = 40.64$ kips

Therefore, the total prestressing force after transfer, $P_{pt} = 40.64(22) = 894.1$ kips

Initial loss, % = $(\text{Total losses at transfer})/(f_{pi}) = 15.2/202.5 = 7.5\%$

When determining the concrete stresses using transformed section properties, the strand force is that before transfer:

Force per strand = $(202.5)(0.217) = 43.94$ kips

The total prestressing force before transfer, $P_{pi} = 43.94(22) = 967$ kips

9.3.6.6 Total Losses at Service Loads

Total loss due to elastic shortening at transfer and long-term losses is:

$$\Delta f_{pT} = \Delta f_{pES} + \Delta f_{pLT} = 15.2 + 26.5 = 41.7 \text{ ksi}$$

The elastic gain due to deck weight, superimposed dead load, and live load (Service III) is:

$$\begin{aligned} & \left(\frac{(M_b + M_{ws})e_{tf}}{I_{tf}} \right) \frac{E_p}{E_c} + 0.8 \left(\frac{(M_{LT} + M_{LL})e_{tf}}{I_{tf}} \right) \frac{E_p}{E_c} \\ &= \left(\frac{(75.6 + 223.4)(12)(30.57)}{356,792} \right) \frac{28,500}{5,072} + 0.8 \left(\frac{(1,188.6 + 451.3)(12)(30.57)}{356,792} \right) \frac{28,500}{5,072} \\ &= 1.7 + 7.6 = 9.3 \text{ ksi} \end{aligned}$$

The effective stress in tendons after all losses and gains:

$$f_{pe} = f_{pi} - \Delta f_{pT} + 9.3 = 202.5 - 41.7 + 9.3 = 170.1 \text{ ksi}$$

Check prestressing stress limit at service limit state:

[LRFD Table 5.9.3-1]

$$f_{pe} \leq 0.8 f_{py} = 0.8(243) = 194.4 \text{ ksi} > 170.1 \text{ ksi} \quad \text{OK}$$

The effective stress in strands after all losses and permanent gains:

$$f_{pe} = f_{pi} - \Delta f_{pT} + 1.7 = 202.5 - 41.7 + 1.7 = 162.5 \text{ ksi}$$

Force per strand without live load gains = $(f_{pe})(\text{area of strand}) = (162.5)(0.217) = 35.26$ kips

Therefore, the total prestressing force after all losses = $35.26(22) = 775.7$ kips

Final loss percentage = $(\text{total losses and gains})/(f_{pi}) = (41.7 - 1.7)/(202.5) = 19.8\%$

When determining the concrete stress using transformed section properties, all the elastic losses and gains are implicitly accounted for:

Force per strand with only total time-dependent losses = $(f_{pi} - \Delta f_{pLT})(\text{area of strand}) = (202.5 - 26.5)(0.217) = 38.19$ kips

Total prestressing force, $P_{pe} = (38.19)(22) = 840.2$ kips

9.3.7 CONCRETE STRESSES AT TRANSFER

Because the transformed section is used, the total prestressing force before and after transfer, $P_{pi} = 967$ kips

9.3.7.1 Stress Limits for Concrete

[LRFD Art.5.9.4]

Compression:

- $0.6 f'_{ci} = 0.6(5.5) = +3.300$ ksi

where f'_{ci} = concrete strength at transfer = 5.500 ksi

Tension:

- without bonded auxiliary reinforcement

$$-0.0948 \sqrt{f'_{ci}} \leq 0.200 \text{ ksi} = -0.0948 \sqrt{5.500} = -0.222 \text{ ksi}$$

Therefore, -0.200 ksi (Controls)

DECK BULB-TEE (DBT-53), SINGLE SPAN, NONCOMPOSITE SURFACE

9.3.7.1 Stress Limits for Concrete/9.3.7.2 Stresses at Transfer Length Section

- with bonded auxiliary reinforcement that is sufficient to resist 120% of the tension force in the cracked concrete:

$$-0.24 \sqrt{f'_{ci}} = -0.24 \sqrt{5.500} = -0.563 \text{ ksi}$$

9.3.7.2 Stresses at Transfer Length Section

Stresses at this location need only be checked at transfer since this stage almost always governs. Also, losses with time will reduce the concrete stresses making them less critical.

Transfer length = 60(strand diameter) = 60(0.6) = 36 in. = 3.0 ft [LRFD Art. 5.11.4]

Due to camber of the beam at transfer, the beam self weight acts on the overall beam length, 96 ft. Therefore, the values for bending moment given in **Table 9.3.4-1** cannot be used because they are based on the design span length of 95 ft. Using statics, bending moment at transfer length due to beam self weight is:

$$0.5w_gx(L - x) = (0.5)(0.970)(3.0)(96.0 - 3.0) = 135.3 \text{ ft-kips}$$

Compute stress in the top of the beam:

$$f_t = \frac{P_{pi}}{A_{ti}} - \frac{P_{pi}e_{ti}}{S_{tti}} + \frac{M_g}{S_{tti}} = \frac{967}{956.5} - \frac{(967)(30.46)}{18,683} + \frac{(135.3)(12)}{18,683} = -0.479 \text{ ksi}$$

Tensile stress limit for concrete with bonded reinforcement: -0.563 ksi OK

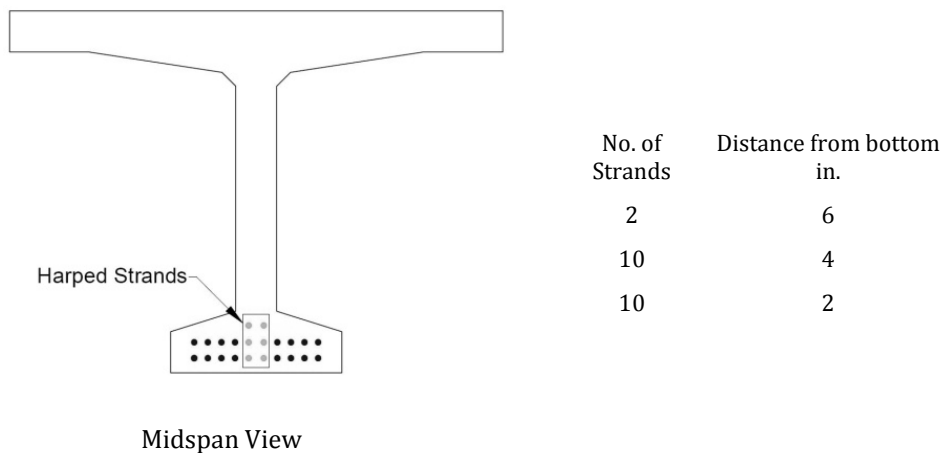
Compute stress in the bottom of the beam:

$$f_b = \frac{P_{pi}}{A_{ti}} + \frac{P_{pi}e_{ti}}{S_{bti}} - \frac{M_g}{S_{bti}} = \frac{967}{956.5} + \frac{(967)(30.46)}{10,673} - \frac{(135.3)(12)}{10,673} = +3.619 \text{ ksi}$$

Compressive stress limit for concrete: +3.300 ksi NG

Since the stress at the bottom exceeds the stress limit, harp strands to satisfy the specified limits. Harp six strands at the 0.4L points, as shown in **Figures 9.3.7.2-1** and **9.3.7.2-2**.

Figure 9.3.7.2-1
Strand Pattern



DECK BULB-TEE (DBT-53), SINGLE SPAN, NONCOMPOSITE SURFACE

9.3.7.2 Stresses at Transfer Length Section

**Figure 9.3.7.2-1 (cont.)
Strand Pattern**

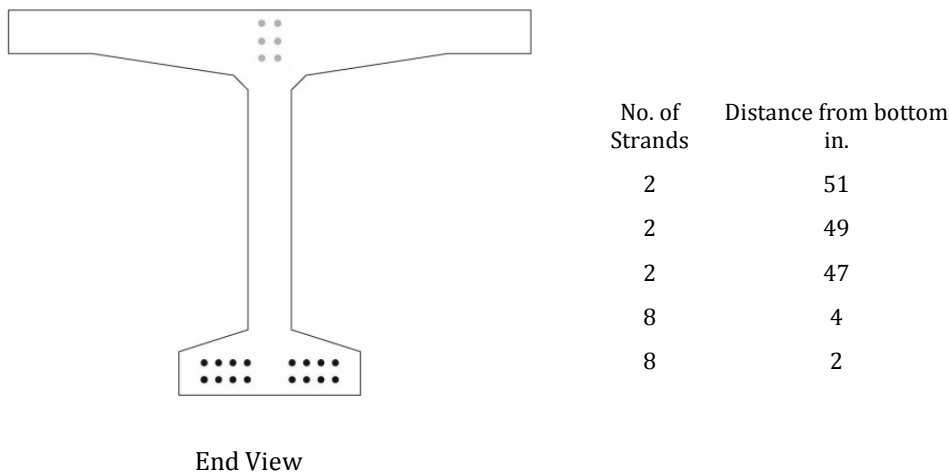
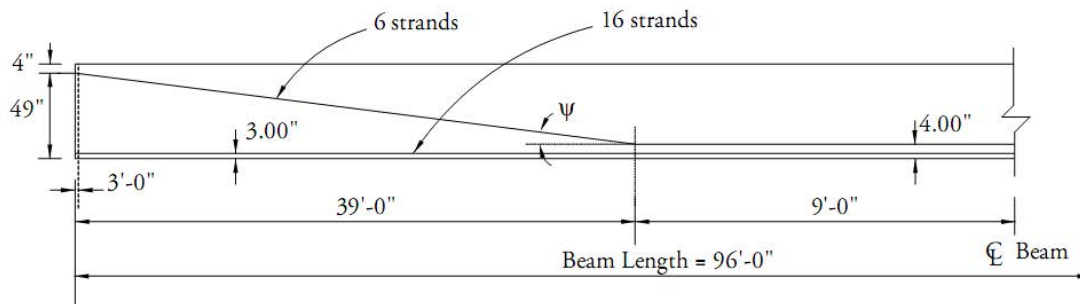


**Figure 9.3.7.2-2
Longitudinal Strand Profile**



Compute the center of gravity of the prestressing strands at the transfer length section using the harped pattern.

The distance between the center of gravity of the six harped strands at the end of the beam and the top fiber of the precast beam is:

$$\frac{2(2) + 2(4) + 2(6)}{6} = 4.0 \text{ in.}$$

The distance between the center of gravity of the six harped strands at the harp point and the bottom fiber of the beam is:

$$\frac{2(2) + 2(4) + 2(6)}{6} = 4.0 \text{ in.}$$

The distance between the center of gravity of the six harped strands and the top fiber of the beam at the transfer length section:

$$4 \text{ in.} + \frac{(53 - 4 - 4) \text{ in.}}{39 \text{ ft}} (3 \text{ ft}) = 7.46 \text{ in.}$$

The distance between the center of gravity of the bottom straight 16 strands and the extreme bottom fiber of the beam is:

$$\frac{8(2) + 8(4)}{16} = 3.0 \text{ in.}$$

DECK BULB-TEE (DBT-53), SINGLE SPAN, NONCOMPOSITE SURFACE

9.3.7.2 Stresses at Transfer Length Section/9.3.7.4 Stresses at Midspan

Therefore, the distance between the center of gravity of the total number of strands measured to the bottom of the precast beam at transfer length:

$$\frac{16(3) + 6(53 - 7.46)}{22} = 14.60 \text{ in.}$$

Eccentricity of the strand group at transfer length, e , is: $34.05 - 14.60 = 19.45 \text{ in.}$

The center of gravity of all prestressing strands with respect to the extreme bottom fiber at the end of the beam, y_{bs} , is:

$$\frac{16(3) + 6(53 - 4)}{22} = 15.55 \text{ in.}$$

Recompute top and bottom stresses at the transfer length section with harped strands. Note that the transformed section properties here are different than those at midspan and have been re-calculated.

Concrete stress in top of the beam:

$$f_t = \frac{967}{956.5} - \frac{(967)(19.45)}{18,754} + \frac{(135.3)(12)}{18,754} = +0.095 \text{ ksi}$$

Compressive stress limit: +3.300 ksi OK

Concrete stress in bottom of beam:

$$f_b = \frac{967}{956.5} + \frac{(967)(19.45)}{10,437} - \frac{(135.3)(12)}{10,437} = +2.657 \text{ ksi}$$

Compressive stress limit: +3.300 ksi OK

9.3.7.3 Stresses at Harp Points

The strand eccentricity at the harp points is the same as at midspan, $e_{ti} = 30.46 \text{ in.}$

Bending moment at the harp points ($0.4L$) due to the self weight of the beam is:

$$(0.5)(0.970)(39)(96-39) = 1078.2 \text{ ft-kips}$$

Therefore, the top and bottom stresses are:

Concrete stress in top of beam:

$$f_t = \frac{967}{956.5} - \frac{(967)(30.46)}{18,683} + \frac{(1,078.2)(12)}{18,683} = +0.127 \text{ ksi}$$

Compressive stress limit is: +3.300 ksi OK

Concrete stress in bottom of beam:

$$f_b = \frac{967}{956.5} + \frac{(967)(30.46)}{10,673} - \frac{(1,078.2)(12)}{10,673} = +2.558 \text{ ksi}$$

Compressive stress limit: +3.300 ksi OK

9.3.7.4 Stresses at Midspan

Bending moment at midspan due to the beam self weight is:

$$M_g = 0.5(0.970)(48)(96-48) = 1,117.4 \text{ ft-kips}$$

$$f_t = \frac{967}{956.5} - \frac{(967)(30.46)}{18,683} + \frac{(1,117.4)(12)}{18,683} = +0.152 \text{ ksi}$$

Compressive stress limit: +3.300 ksi OK

$$f_b = \frac{967}{956.5} + \frac{(967)(30.46)}{10,673} - \frac{(1,117.4)(12)}{10,673} = +2.514 \text{ ksi}$$

Compressive stress limit: +3.300 ksi OK

DECK BULB-TEE (DBT-53), SINGLE SPAN, NONCOMPOSITE SURFACE

9.3.7.5 Hold-Down Forces/9.3.8.2.1 Concrete Stress at Top Fiber of the Beam

9.3.7.5 Hold-Down Forces

Assume that the stress in the strand at the time of prestressing, before seating losses, is:

$$0.8 f_{pu} = 0.8(270) = 216 \text{ ksi}$$

Thus, the prestress force per strand before seating losses is: $0.217 (216) = 46.9$ kips

From **Figure 9.3.7.2-2**, the harp angle,

$$\psi = \tan^{-1} \left(\frac{45}{39(12)} \right) = 5.49^\circ$$

Therefore, hold-down force/strand = $1.05(\text{force per strand})(\sin \psi)$

$$= 1.05(46.9)\sin 5.49^\circ = 4.71 \text{ kips/strand}$$

Note the factor 1.05 is applied to account for friction.

Total hold-down force = $6 \text{ strands}(4.71) = 28.3$ kips

The hold-down force and the harp angle should be checked against maximum limits for local practices. Refer to Chapter 3, Fabrication and Construction and Chapter 8, Design Theory and Procedures for additional details.

9.3.7.6 Summary of Stresses at Transfer

	Top Fiber Stresses f_t , ksi	Bottom Fiber Stresses f_b , ksi
At transfer length section	+0.095	+2.657
At harp points	+0.127	+2.558
At midspan	+0.152	+2.514

9.3.8 CONCRETE STRESSES AT SERVICE LOADS

Using transformed section properties and refined losses, $P_{pe} = 840.2$ kips

9.3.8.1 Stress Limits for Concrete

[LRFD Art. 5.9.4.2]

Compression:

Due to permanent loads, (i.e. beam self weight, weight of wearing surface, and weight of barriers), for load combination Service I:

$$\text{for precast beams: } 0.45 f'_c = (0.45)(7.000) = +3.150 \text{ ksi}$$

Due to permanent and transient loads (i.e. all dead loads and live loads), for load combination Service I:

$$\text{for precast beam: } 0.6 f'_c = 0.6(7.000) = +4.200 \text{ ksi}$$

Tension:

For components with bonded prestressing tendons:

$$\text{for load combination Service III: } -0.19 \sqrt{f'_c}$$

$$\text{for precast beam: } -0.19 \sqrt{7.000} = -0.503 \text{ ksi}$$

9.3.8.2 Stresses at Midspan

9.3.8.2.1 Concrete Stress at Top Fiber of the Beam

To check top compressive stresses, two cases are considered:

DECK BULB-TEE (DBT-53), SINGLE SPAN, NONCOMPOSITE SURFACE**9.3.8.2.1 Concrete Stress at Top Fiber of the Beam/9.3.8.3 Fatigue Stress Limit**

1. Under permanent loads, load combination Service I:

Using bending moment values given in **Table 9.3.4-1**, compute the top fiber stresses:

$$\begin{aligned} f_{tg} &= \frac{P_{pe}}{A_{tf}} - \frac{P_{pe}e_{tf}}{S_{ttf}} + \frac{(M_g + M_{ws} + M_b)}{S_{ttf}} \\ &= \frac{840.2}{953.0} - \frac{(840.2)(30.57)}{18,622} + \frac{(1,094.3 + 223.4 + 75.6)(12)}{18,622} \\ &= 0.882 - 1.379 + 0.898 = +0.401 \text{ ksi} \end{aligned}$$

Compressive stress limit: +3.150 ksi OK

2. Under permanent and transient loads, load combination Service I:

$$\begin{aligned} f_{tg} &= +0.401 + \frac{(M_{LT} + M_{LL})}{S_{ttf}} \\ &= +0.401 + \frac{(1,188.6 + 451.3)(12)}{18,622} = +1.458 \text{ ksi} \end{aligned}$$

Compressive stress limit: +4.200 ksi OK

9.3.8.2.2 Concrete Stress in Bottom of Beam, Load Combination Service III

$$\begin{aligned} f_b &= \frac{P_{pe}}{A_{tf}} + \frac{P_{pe}e_{tf}}{S_{btf}} - \frac{(M_g + M_{ws} + M_b) + 0.8(M_{LT} + M_{LL})}{S_{btf}} \\ &= \frac{840.2}{953.0} + \frac{(840.2)(30.57)}{10,543} - \frac{[(1,094.3 + 223.4 + 75.6) + 0.8(1,188.6 + 451.3)](12)}{10,543} \\ &= 0.882 + 2.436 - 3.079 = +0.239 \text{ ksi} \end{aligned}$$

Tensile stress limit: -0.503 ksi

The stress is in compression. OK

9.3.8.3 Fatigue Stress Limit

LRFD Article 5.5.3.1 states that in fully prestressed components other than segmentally constructed bridges, the compressive stress due to Fatigue I load combination and one half the sum of effective prestress and permanent loads shall not exceed $0.40f'_c$, after losses.

From **Table 9.3.4-2**, the unfactored fatigue bending moment at midspan, M_f , is 703.4 ft-kips. Therefore, stress at the top fiber of the beam due to fatigue load combination I is:

$$f_{tgf} = \frac{1.50(M_f)}{S_{ttf}} = \frac{1.50(703.4)(12)}{18,622} = +0.680 \text{ ksi}$$

At midspan, the top compressive stress due to permanent loads and prestress is:

$$\begin{aligned} f_{tg} &= \frac{P_{pe}}{A_{tf}} - \frac{P_{pe}e_{tf}}{S_{ttf}} + \frac{(M_g)}{S_{ttf}} + \frac{(M_{ws} + M_b)}{S_{ttf}} \\ &= \frac{840.2}{953} - \frac{(840.2)(30.57)}{18,622} + \frac{(1,094.3)(12)}{18,622} + \frac{(223.4 + 75.6)(12)}{18,622} \\ &= 0.882 - 1.379 + 0.705 + 0.193 = 0.401 \text{ ksi} \end{aligned}$$

Therefore:

$$f_{tgf} + \frac{f_{tg}}{2} = 0.680 + \frac{0.401}{2} = 0.881 < 0.40(f'_c) = 0.40(7.00) = 2.8 \text{ ksi OK}$$

This condition should be satisfied at all locations along the beam.

DECK BULB-TEE (DBT-53), SINGLE SPAN, NONCOMPOSITE SURFACE**9.3.8.4 Summary of Stresses at Midspan at Service Loads/9.3.9 Strength Limit State****9.3.8.4 Summary of Stresses at Midspan at Service Loads**

	Top of Beam, ksi Service I		Bottom of Beam, ksi Service III
	Permanent Loads	Total Loads	
At midspan	+0.401	+1.458	+0.239

9.3.9 STRENGTH LIMIT STATE

Total ultimate bending moment for Strength I is:

$$M_u = 1.25(DC) + 1.5(DW) + 1.75(LL + IM)$$

Using values of unfactored bending moment given in **Tables 9.3.4-1** and **9.3.4-2**, the ultimate bending moment at midspan is:

$$M_u = 1.25(1,094.3 + 75.6) + 1.5(223.4) + 1.75(1,188.6 + 451.3) = 4,667.3 \text{ ft-kips}$$

Average stress in prestressing steel when $f_{pe} \geq 0.5f_{pu}$:

$$f_{ps} = f_{pu} \left(1 - k \frac{c}{d_p} \right) \quad [\text{LRFD Eq. 5.7.3.1.1-1}]$$

where

f_{ps} = average stress in prestressing strand, ksi

f_{pu} = specified tensile strength of prestressing strand = 270.0 ksi

$$k = 2 \left(1.04 - \frac{f_{py}}{f_{pu}} \right) \quad [\text{LRFD Eq. 5.7.3.1.1-2}]$$

= 0.28 for low-relaxation strands [LRFD Table C5.7.3.1.1-1]

c = distance from the extreme compression fiber to the neutral axis, in.

d_p = distance from extreme compression fiber to the centroid of the prestressing tendons

$$= h - y_{bs} = 53.00 - 3.27 = 49.73 \text{ in.}$$

To compute c , assume rectangular section behavior and check if the depth of the equivalent compression stress block, a , is less than or equal to t_s : [LRFD C5.7.3.2.2]

$$c = \frac{A_{ps}f_{pu} + A_s f_y - A'_s f'_y}{0.85 f'_c \beta_1 b + k A_{ps} \frac{f_{pu}}{d_p}} \quad [\text{LRFD Eq. 5.7.3.1.1-4}]$$

where

A_{ps} = area of prestressing strand = $(22)(0.217) = 4.774 \text{ in.}^2$

A_s = area of nonprestressed tension reinforcement = 0 in.^2

f_y = specified yield strength of tension reinforcement = 60.0 ksi

A'_s = area of compression reinforcement = 0 in.^2

f'_y = specified yield strength of compression reinforcement, ksi

f'_c = compressive strength of concrete = 7.0 ksi

β_1 = stress factor of compression block [LRFD Art. 5.7.2.2]

$$= 0.85 \text{ for } f'_c \leq 4.0 \text{ ksi}$$

$$= 0.85 - 0.05(f'_c - 4.0) \text{ for } f'_c > 4.0 \text{ ksi}$$

$$= 0.85 - 0.05(7.0 - 4.0) = 0.70$$

b = effective width of compression flange = 72 in.

DECK BULB-TEE (DBT-53), SINGLE SPAN, NONCOMPOSITE SURFACE**9.3.9 Strength Limit State/9.3.10.2 Minimum Reinforcement**

$$c = \frac{4.774(270.0) + 0 - 0}{0.85(7.0)(0.7)(72) + 0.28(4.774)\frac{270.0}{49.73}} = 4.197 \text{ in.}$$

$a =$ depth of the equivalent stress block $= \beta_1 c = (0.7)(4.197) = 2.94 \text{ in.} < t_s = 6.0 \text{ in.}$ OK

Therefore, the rectangular section behavior is valid.

The average stress in prestressing strand is:

$$f_{ps} = 270.0 \left(1 - 0.28 \frac{4.197}{49.73} \right) = 263.6 \text{ ksi} \quad [\text{LRFD Art. 5.7.3.2.3}]$$

Nominal flexural resistance:

$$M_n = A_{ps} f_{ps} \left(d_p - \frac{a}{2} \right) \quad [\text{LRFD Eq. 5.7.3.2.2-1}]$$

The above equation is a simplified form of LRFD Equation 5.7.3.2.2-1 because no compression reinforcement or nonprestressed reinforcement is considered and the section behaves as a rectangular section.

$$M_n = (4.774)(263.6) \left(49.73 - \frac{2.94}{2} \right) / 12 = 5,061.0 \text{ ft-kips}$$

Factored flexural resistance:

$$M_r = \phi M_n \quad [\text{LRFD Eq. 5.7.3.2.1-1}]$$

where

$$\phi = \text{resistance factor} \quad [\text{LRFD Art. 5.5.4.2.1}]$$

$$= 1.00, \text{ for tension controlled prestressed concrete sections}$$

$$M_r = 5,061.0 \text{ ft-kips} > M_u = 4,667.3 \text{ ft-kips} \quad \text{OK}$$

9.3.10 LIMITS OF REINFORCEMENT**9.3.10.1 Maximum Reinforcement**

[LRFD Art. 5.7.3.3.1]

The check of maximum reinforcement limits in LRFD Article 5.7.3.3.1 was removed from the *LRFD Specifications* in 2005.

9.3.10.2 Minimum Reinforcement

[LRFD Art. 5.7.3.3.2]

At any section, the amount of prestressed and nonprestressed tensile reinforcement must be adequate to develop a factored flexural resistance, M_r , equal to the lesser of:

- 1.2 times the cracking strength determined on the basis of elastic stress distribution and the modulus of rupture, and
- 1.33 times the factored moment required by the applicable strength load combination.

Check at midspan:

$$M_{cr} = S_{btf} (f_r + f_{cpe}) \quad [\text{LRFD Eq. 5.7.3.3.2-1}]$$

The above equation is a simplified form of LRFD Eq. 5.7.3.3.2-1 because a composite section does not exist. Therefore, the composite section modulus and noncomposite section modulus are the same.

where

$$f_r = \text{modulus of rupture of concrete} \quad [\text{LRFD Art. 5.4.2.6}]$$

$$= 0.37 \sqrt{f'_c} = 0.37 \sqrt{7.000} = 0.979 \text{ ksi}$$

$$f_{cpe} = \text{compressive stress in concrete due to effective prestress force only (after allowance for all prestress losses) at extreme fiber of section where tensile stress is caused by externally applied loads}$$

DECK BULB-TEE (DBT-53), SINGLE SPAN, NONCOMPOSITE SURFACE

9.3.10.2 Minimum Reinforcement/9.3.11.1 Critical Section

$$= \frac{P_{pe}}{A_{tf}} + \frac{P_{pe}e_{tf}}{S_{btf}} = \frac{840.2}{953.0} + \frac{(840.2)(30.57)}{10,543} = 3.318 \text{ ksi}$$

$$M_{cr} = (0.979 + 3.318) \frac{10,543}{12} = 3,775 \text{ ft-kips}$$

$$1.2 M_{cr} = 1.2(3,775) = 4,530 \text{ ft-kips}$$

At midspan, the factored moment required by the Strength I load combination is:

$$M_u = 4,667.3 \text{ ft-kips (as calculated in Section 9.3.9)}$$

$$\text{Thus, } 1.33M_u = 1.33(4,667.3) = 6,208 \text{ ft-kips}$$

Since $1.2M_{cr} < 1.33M_u$, the $1.2M_{cr}$ requirement controls.

$$M_r = 5,061.0 \text{ ft-kips} > 1.2M_{cr} = 4,530 \text{ ft-kips} \quad \text{OK}$$

Note: The *LRFD Specifications* requires that this criterion be met at every section.

Illustrated based on 2011
LRFD Specifications.

Editor's Note: 2012 *LRFD Specifications* changes will revise minimum reinforcement.

9.3.11 SHEAR DESIGN

The area and spacing of shear reinforcement must be determined at regular intervals along the entire length of the beam. In this design example, transverse shear design procedures are demonstrated below by determining these values at the critical section near the supports.

Transverse shear reinforcement is required when:

$$V_u > 0.5 \phi(V_c + V_p) \quad \text{[LRFD Eq. 5.8.2.4-1]}$$

where

V_u = total factored shear force, kips

V_c = nominal shear resistance provided by tensile stresses in the concrete, kips

V_p = component in the direction of the applied shear of the effective prestressing force, kips

ϕ = resistance factor = 0.9 for normal weight concrete [LRFD Art. 5.5.4.2.1]

9.3.11.1 Critical Section

[LRFD Art.5.8.3.2]

The critical section near the supports is taken as the effective shear depth, d_v , from the internal face of the support.

d_v = distance between resultants of tensile and compressive forces, $(d_e - a/2)$, but not less than $(0.9d_e)$ or $(0.72h)$ [LRFD Art.5.8.2.7]

where

d_e = the corresponding effective depth from the extreme compression fiber to the centroid of the tensile force in the tensile reinforcement [LRFD Art.5.8.2.9]

a = depth of compression block = 2.94 in. at midspan (assumed adequate)

h = overall depth of the section = 53.00 in.

Since some of the strands are harped, the effective depth, d_e , varies from point-to-point. However, d_e must be calculated at the critical section in shear which is not yet determined; therefore, for the first iteration, d_e is calculated based on the center of gravity of the straight strand group at the end of the beam, y_{bs} .

$$d_e = h - y_{bs} = 53.00 - 3.00 = 50.00 \text{ in.}$$

$$d_v = 50.00 - (2.94/2) = 48.53 \text{ in.}$$

$$\geq 0.9d_e = 0.9(50.00) = 45.00 \text{ in.}$$

$$\geq 0.72h = 0.72(53) = 38.16 \text{ in.} \quad \text{OK}$$

Therefore, $d_v = 48.53 \text{ in.}$

DECK BULB-TEE (DBT-53), SINGLE SPAN, NONCOMPOSITE SURFACE

9.3.11.1 Critical Section/9.3.11.2.1 Strain in Flexural Tension Reinforcement

Because the width of the bearing is not yet determined, it was conservatively assumed to be zero. Therefore, the critical section in shear is located at a distance of:

$$48.53 \text{ in.} = 4.04 \text{ ft from centerline of support}$$

$$(x/L) = 4.04/95 = 0.043L$$

The effective depth, d_e , and the position of the critical section in shear may be refined based on the position of the critical section calculated above. However, the difference is small and on the conservative side. Therefore, no more refinement is performed.

9.3.11.2 Contribution of Concrete to Nominal Shear Resistance

The contribution of the concrete to the nominal shear resistance is:

$$V_c = 0.0316\beta\sqrt{f'_c} b_v d_v \quad [\text{LRFD Eq.5.8.3.3-3}]$$

where β = a factor indicating the ability of diagonally cracked concrete to transmit tension (a value indicating concrete contribution).

Several quantities must be determined before this expression can be evaluated.

9.3.11.2.1 Strain in Flexural Tension Reinforcement

Calculate the strain at the centroid of the tension reinforcement, ϵ_s :

$$\epsilon_s = \frac{\frac{|M_u|}{d_v} + 0.5N_u + |(V_u - V_p) - A_{ps}f_{po}}{(E_s A_s + E_p A_{ps})}}{\quad} \quad [\text{LRFD Eq. 5.8.3.4.2-4}]$$

where

$$N_u = \text{applied factored normal force at the specified section, } 0.043L = 0 \text{ kips}$$

$$V_u = \text{applied factored shear force at the specified section, } 0.043L \\ = 1.25(42.2 + 2.9) + 1.5(8.6) + 1.75(54.9 + 18.6) = 197.9 \text{ kips}$$

$$V_p = \text{component of the effective prestressing force in the direction of the applied shear} \\ = (\text{Force per strand without live load gains})(\text{Number of harped strands})(\sin \Psi) \\ = (35.26)(6)\sin 5.49^\circ = 20.2 \text{ kips is a conservative resistance.}$$

$$M_u = \text{applied factored bending moment at the specified section, } 0.043L \\ = 1.25(178.2 + 12.3) + 1.5(36.4) + 1.75(207.8 + 73.5) \\ = 785.0 \text{ ft-kips}$$

$$M_u \text{ should not be taken less than } (V_u - V_p) d_v.$$

$$(V_u - V_p)d_v = (197.9 - 20.2)(48.53)/12 = 718.6 \text{ ft-kips}$$

Since 785.0 ft-kips > 718.6 ft-kips, use $M_u = 785.0$ ft-kips.

$$A_{ps} = \text{area of prestressing strands on the flexural tension side of the member} = (0.217)(16) = 3.472 \text{ in.}^2$$

$$f_{po} = \text{a parameter taken as modulus of elasticity of prestressing tendons multiplied by the locked-in} \\ \text{difference in strain between the prestressing tendons and the surrounding concrete (ksi). For pre-} \\ \text{tensioned members, LRFD Article 5.8.3.4.2 indicates that } f_{po} \text{ can be taken as } 0.7f_{pu}. \text{ (Note: use this} \\ \text{for both pretensioned and post-tensioned systems made with stress relieved and low relaxation} \\ \text{strands).}$$

$$= 0.7(270) = 189.0 \text{ ksi}$$

$$\epsilon_s = \frac{\frac{|785.0(12)|}{48.53} + 0 + |(197.9 - 20.2) - (3.472)(189.0)}{(0 + (28,500)(3.472))}} = -2.87 \times 10^{-3}$$

ϵ_s is less than zero. Use $\epsilon_s = 0$.

DECK BULB-TEE (DBT-53), SINGLE SPAN, NONCOMPOSITE SURFACE

9.3.11.2.2 Values of β and θ / 9.3.11.3.3 Determine Spacing of Reinforcement

9.3.11.2.2 Values of β and θ

Assume the section contains at least the minimum amount of transverse reinforcement:

$$\beta = \frac{4.8}{(1 + 750\varepsilon_s)} = \frac{4.8}{(1 + 0)} = 4.8 \quad \text{[LRFD Eq. 5.8.3.4.2-1]}$$

Angle of diagonal compressive stresses is:

$$\theta = 29 + 3,500(\varepsilon_s) = 29 + 3,500(0) = 29^\circ \quad \text{[LRFD Eq. 5.8.3.4.2-3]}$$

9.3.11.2.3 Compute Concrete Contribution

The nominal shear resisted by the concrete is:

$$V_c = 0.0316 \beta \sqrt{f'_c} b_v d_v \quad \text{[LRFD Eq. 5.8.3.3-3]}$$

where b_v = effective web width = 6 in.

$$V_c = 0.0316 (4.8) \sqrt{7,000} (6) (48.53) = 116.9 \text{ kips}$$

9.3.11.3 Contribution of Reinforcement to Nominal Shear Resistance

9.3.11.3.1 Requirement for Reinforcement

Check if $V_u > 0.5\phi(V_c + V_p)$ [LRFD Eq. 5.8.2.4-1]

$$0.5\phi(V_c + V_p) = 0.5(0.9)(116.9 + 20.2) = 61.7 \text{ kips} < 197.9 \text{ kips}$$

Therefore, transverse shear reinforcement must be provided.

9.3.11.3.2 Required Area of Reinforcement

$$V_u/\phi \leq V_n = V_c + V_s + V_p \quad \text{[LRFD Eq. 5.8.3.3-1]}$$

where

$$\begin{aligned} V_s &= \text{shear resistance provided by shear reinforcement} \\ &= (V_u/\phi) - V_c - V_p = (197.9/0.9) - 116.9 - 20.2 = 82.8 \text{ kips} \end{aligned}$$

$$V_s = \frac{A_v f_{yh} d_v (\cot \theta + \cot \alpha) (\sin \alpha)}{s} \quad \text{[LRFD Eq. 5.8.3.3-4]}$$

where

$$\begin{aligned} A_v &= \text{area of shear reinforcement within a distance, } s, \text{ in.}^2 \\ f_{yh} &= \text{specified yield strength of shear reinforcement, ksi} \\ \alpha &= \text{angle of inclination of transverse reinforcement to longitudinal axis} \\ &= 90^\circ \text{ for vertical stirrups} \\ s &= \text{spacing of stirrups, in.} \end{aligned}$$

Therefore, area of shear reinforcement within a distance, s , is:

$$\begin{aligned} A_v &= (sV_s)/(f_{yh}d_v \cot \theta) \\ &= [(s)(82.8)]/[(60)(48.53)\cot 29^\circ] = 0.016(s) \text{ in.}^2 \end{aligned}$$

If $s = 12$ in., required $A_v = 0.19$ in.²/ft

9.3.11.3.3 Determine Spacing of Reinforcement

Check maximum spacing of transverse reinforcement. [LRFD Art 5.8.2.7]

Check if $v_u < 0.125f'_c$

DECK BULB-TEE (DBT-53), SINGLE SPAN, NONCOMPOSITE SURFACE**9.3.11.3.3 Determine Spacing of Reinforcement/9.3.13 Minimum Longitudinal Reinforcement Requirement**

$$v_u = \frac{|V_u - \phi V_p|}{\phi b_v d_v} = \frac{|(197.9) - (0.9)(20.2)|}{(0.9)(6)(48.53)} = 0.686 \text{ ksi} \quad [\text{LRFD Eq. 5.8.2.9-1}]$$

$$0.125 f'_c = (0.125)(7) = 0.875 \text{ ksi} \quad [\text{LRFD Eq. 5.8.2.7-1}]$$

Since $v_u < 0.125 f'_c$

then, $s \leq 24 \text{ in.}$ (Controls)

$$s \leq 0.8d_v = 0.8(48.53) = 38.8 \text{ in.}$$

Therefore, maximum $s = 24 \text{ in.} > s$ provided OK

Use double legs of W20 or D20 welded wire reinforcement at 12 in., centers

A_v provided = 0.40 in.²/ft. > 0.19 in.²/ft

$$V_s = \frac{0.4(60)48.53 (\cot 29^\circ)}{12} = 175.1 \text{ kips}$$

9.3.11.3.4 Minimum Reinforcement Requirement

[LRFD Eq. 5.8.2.5-1]

The area of transverse reinforcement should not be less than:

$$0.0316 \sqrt{f'_c} \frac{b_v s}{f_y h} = 0.0316 \sqrt{7.000} \frac{(6)(12)}{60.0} = 0.10 \text{ in.}^2/\text{ft} < A_v \text{ provided OK}$$

9.3.11.4 Maximum Nominal Shear Resistance

In order to ensure that the concrete in the web of the beam will not crush prior to yielding of the transverse reinforcement, the *LRFD Specifications* gives an upper limit of V_n as follows:

$$V_n = 0.25 f'_c b_v d_v + V_p \quad [\text{LRFD Eq. 5.8.3.3-2}]$$

Comparing this equation with Eq. 5.8.3.3-1, it can be concluded that

$$V_c + V_s \text{ must not be greater than } 0.25 f'_c b_v d_v$$

$$116.9 + 175.1 = 292.0 \text{ kips} \leq 0.25(7)(6)(48.53) = 509.6 \text{ kips OK}$$

Using the above procedures, the transverse reinforcement can be determined at increments along the entire length of the beam.

9.3.12 INTERFACE SHEAR TRANSFER

Because there is no cast-in-place composite deck, calculations for interface shear transfer are not required.

9.3.13 MINIMUM LONGITUDINAL REINFORCEMENT REQUIREMENT

Longitudinal reinforcement should be proportioned so that at each section the following equation is satisfied:

$$A_{ps} f_{ps} + A_s f_y \geq \frac{M_u}{d_v \phi_f} + 0.5 \frac{N_u}{\phi_c} + \left(\left| \frac{V_u}{\phi_v} - V_p \right| - 0.5 V_s \right) \cot \theta \quad [\text{LRFD Eq. 5.8.3.5-1}]$$

where

A_{ps} = area of prestressing strand at the tension side of the section, in.²

f_{ps} = average stress in prestressing strand at the time for which the nominal resistance is required, ksi

A_s = area of nonprestressed tension reinforcement, in.²

f_y = specified yield strength of reinforcing bars, ksi

M_u = factored moment at the section corresponding to the factored shear force, ft-kips

d_v = effective shear depth, in.

DECK BULB-TEE (DBT-53), SINGLE SPAN, NONCOMPOSITE SURFACE**9.3.13 Minimum Longitudinal Reinforcement Requirement/9.3.13.1 Required Reinforcement at Face of Bearing**

ϕ = resistance factor as appropriate for moment, shear, and axial resistance.

Therefore, different ϕ factors will be used for the terms in LRFD Equation (5.8.3.5-1), depending on the type of action being considered. [LRFD Art.5.5.4.2]

N_u = applied factored axial force, kips

V_u = factored shear force at section, kips

V_p = component in the direction of the applied shear of the effective prestressing force, kips

V_s = shear resistance provided by shear reinforcement, kips

θ = angle of inclination of diagonal compressive stresses

9.3.13.1 Required Reinforcement at Face of Bearing

[LRFD Art.5.8.3.5]

For simple end supports, the longitudinal reinforcement on the flexural tension side of the member at inside face of bearing should satisfy:

$$A_{ps}f_{ps} + A_s f_y \geq \left(\frac{V_u}{\phi} - 0.5V_s - V_p \right) \cot \theta \quad \text{[LRFD Eq.5.8.3.5-2]}$$

$$M_u = 0 \text{ ft-kips}$$

$$N_u = 0 \text{ kips}$$

Because the width of the bearing is not yet determined, it is assumed to be zero. This assumption is conservative for these calculations. Therefore, the failure crack assumed for this analysis radiates from the centerline of the bearing, 6 in. from the end of the beam.

From **Tables 9.3.4-1** and **9.3.4-2**, using load combination Strength I, the factored shear force at this section is:

$$V_u = 1.25(46.1 + 3.2) + 1.5(9.4) + 1.75(57.6 + 20.3) = 212.1 \text{ kips}$$

$$\left(\frac{V_u}{\phi} - 0.5V_s - V_p \right) \cot \theta = \left(\frac{212.1}{0.9} - 0.5(175.1) - 20.2 \right) \cot 29^\circ = 230.8 \text{ kips}$$

As shown in **Figure 9.3.13.1-1**, the assumed crack plane crosses the centroid of the 16 straight strands at a distance of $(6 + 3.0 \cot 29^\circ = 11.41 \text{ in.})$ from the end of the beam. Since the transfer length is 36 in. from the end of the beam (60 times the strand diameter), the available prestress from the 16 straight strands is a fraction of the effective prestress, f_{pe} , in these strands. The six harped strands do not contribute to the tensile capacity since they are not on the flexural tension side of the member.

Therefore, the available prestress force is:

$$\begin{aligned} A_{ps}f_{ps} + A_s f_y &= (16)(0.217) \left((202.5 - 41.7) \frac{11.41}{36} \right) + 0 = 176.9 + 0 \\ &= 176.9 \text{ kips} < 230.8 \text{ kips} \quad \text{NG} \end{aligned}$$

The strands are not adequate to resist the longitudinal force. Therefore, provide additional nonprestressed reinforcement to carry the difference.

$$\text{Force to be resisted by additional reinforcement} = 230.8 - 176.9 = 53.9 \text{ kips}$$

$$\text{Additional reinforcement required} = (53.9 \text{ kips}) / (60 \text{ ksi}) = 0.90 \text{ in.}^2$$

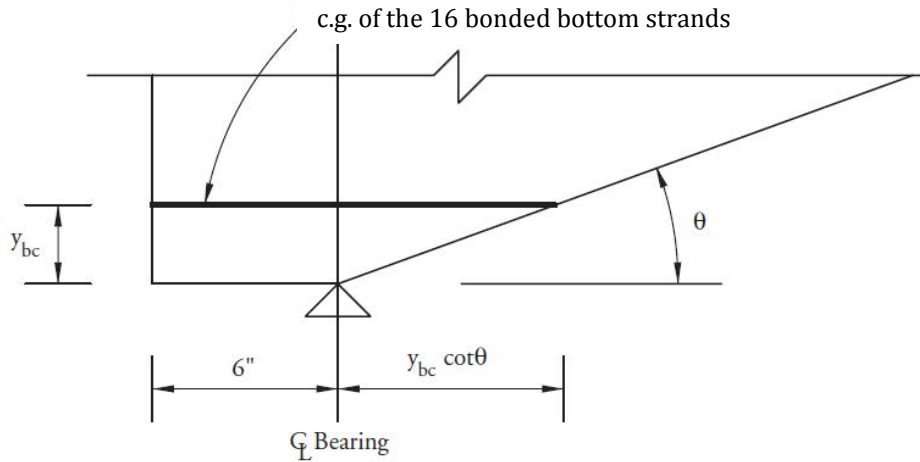
Use three No. 5 bars. The area of steel provided = $(3)(0.31) = 0.93 \text{ in.}^2$

Note: An alternative approach for the calculation of available prestressing force excluding the gains from deck shrinkage is illustrated in Section 9.6.13.1.

DECK BULB-TEE (DBT-53), SINGLE SPAN, NONCOMPOSITE SURFACE

9.3.13.1 Required Reinforcement at Face of Bearing/9.3.15 Deflection and Camber

Figure 9.3.13.1-1
Assumed Failure Crack



9.3.14 PRETENSIONED ANCHORAGE ZONE

[LRFD Art. 5.10.10]

9.3.14.1 Anchorage Zone Reinforcement

Design of the anchorage zone reinforcement is computed using the force in the strands just prior to transfer:

Force in the strands before transfer = $P_{pi} = 22(0.217)(202.5) = 966.7$ kips

The bursting resistance, P_r , should not be less than 4.0% of P_{pi} .

[LRFD Arts 5.10.10.1]

$P_r = f_s A_s \geq 0.04 P_{pi} = 0.04(966.7) = 38.7$ kips

where

f_s = allowable stress in steel, but taken not greater than 20 ksi

A_s = total area of vertical reinforcement located within a distance $h/4$ from the end of the beam, in.²

Solving for the required area of steel, $A_s = 38.7/20 = 1.94$ in.²

At least 1.94 in.² of vertical transverse reinforcement should be provided within a distance of ($h/4 = 53/4 = 13.3$ in.) from the end of the beam.

Use double leg bars of W18 or D18 welded wire reinforcement at 2 in. spacing, starting at 2 in. from the end of the beam.

The provided $A_s = 6(2)(0.18) = 2.16$ in.² > 1.94 in.² OK

9.3.14.2 Confinement Reinforcement

[LRFD Art. 5.10.10.2]

For a distance of $1.5h = 1.5(53) = 79.5$ in., from the end of the beam, reinforcement is placed to confine the prestressing steel in the bottom flange. The reinforcement may not be less than No. 3 deformed bars with spacing not exceeding 6 in. The reinforcement should be of a shape that will confine (enclose) the strands.

9.3.15 DEFLECTION AND CAMBER

[LRFD Art. 5.7.3.6.2]

Deflections are calculated using the modulus of elasticity of concrete calculated in Section 9.4.3.1, and the gross section properties of the noncomposite precast beam.

DECK BULB-TEE (DBT-53), SINGLE SPAN, NONCOMPOSITE SURFACE

9.3.15.1 Deflection Due to Prestressing Force at Transfer/9.3.15.3 Deflection Due to Barrier and Future Wearing Surface Weights

9.3.15.1 Deflection Due to Prestressing Force at Transfer

Force per strand at transfer = 40.6 kips

$$\Delta_p = \frac{P_{pt}}{E_{ci}I_g} \left(\frac{e_c L^2}{8} - \frac{e' a^2}{6} \right)$$

where

Δ_p = camber due to prestressing force at transfer, in.

P_{pt} = total prestressing force after transfer = 22(40.6) = 893.2 kips

E_{ci} = modulus of elasticity at transfer = 4,496 ksi

I_g = gross moment of inertia of the precast beam = 335,679 in.⁴

e_c = eccentricity of prestressing strand at midspan = 31.29 in.

L = overall beam length = 96.0 ft

e' = difference between eccentricity of prestressing strand at midspan and at end of the beam
 = $e_c - e_e = 31.29 - (y_b - y_{bs}) = 31.29 - (34.56 - 15.55) = 12.28$ in.

a = distance from end of the beam to the harp point = 39 ft

$$\Delta_p = \frac{893.2}{(4,496)(335,679)} \left(\frac{(31.29)(96 \times 12)^2}{8} - \frac{(12.28)(39 \times 12)^2}{6} \right) = 2.81 \text{ in. } \uparrow$$

9.3.15.2 Deflection Due to Beam Self Weight

$$\Delta_g = \frac{5w_g L^4}{384E_{ci}I_g}$$

where

Δ_g = deflection due to beam self weight, in.

w_g = beam self weight = 0.970 kips/ft

L = beam length = 96.0 ft at transfer = 95.0 ft at erection

E_{ci} = modulus of elasticity of precast beam at transfer = 4,496 ksi

I_g = gross moment of inertia of the precast beam = 335,679 in.⁴

Deflection due to beam self weight after transfer:

$$\Delta_g = \frac{5 \left(\frac{0.970}{12} \right) (96 \times 12)^4}{384(4,496)(335,679)} = 1.23 \text{ in. } \downarrow$$

Deflection due to beam self weight at erection:

$$\Delta_g = \frac{5 \left(\frac{0.970}{12} \right) (95 \times 12)^4}{384(4,496)(335,679)} = 1.18 \text{ in. } \downarrow$$

9.3.15.3 Deflection Due to Barrier and Future Wearing Surface Weights

$$\Delta_{b+ws} = \frac{5(w_b + w_{ws})L^4}{384E_{ci}I_g}$$

where

Δ_{b+ws} = deflection due to barrier and wearing surface, in.

w_b = barrier weight = 0.067 kips/ft

w_{ws} = wearing surface weight = 0.198 kips/ft

DECK BULB-TEE (DBT-53), SINGLE SPAN, NONCOMPOSITE SURFACE**9.3.15.3 Deflection Due to Barrier and Future Wearing Surface Weights/9.3.15.5 Deflection Due to Live Load and Impact**

L = design span = 95.0 ft

E_c = modulus of elasticity of precast beam at service loads = 5,072 ksi

I_g = gross moment of inertia = 335,679 in.⁴

$$\Delta_{b+ws} = \frac{5 \left(\frac{0.067 + 0.198}{12} \right) (95 \times 12)^4}{384(5,072)(335,679)} = 0.29 \text{ in. } \downarrow$$

9.3.15.4 Deflection and Camber Summary

After transfer, $(\Delta_p + \Delta_g) = 2.81 - 1.23 = 1.58 \text{ in. } \uparrow$

Total deflection at erection, using PCI multipliers (see *PCI Design Handbook*)

$$= 1.8(2.81) - 1.85(1.18) = 2.88 \text{ in. } \uparrow$$

Long-Term Deflection:

LRFD Article 5.7.3.6.2 states that the long-time deflection may be taken as the instantaneous deflection multiplied by a factor of 4.0, if the instantaneous deflection is based on the gross moment of inertia. However, a factor of 4.0 is not appropriate for this type of precast construction. Therefore, it is recommended that the designer follow the guidelines of the owner agency for whom the bridge is being designed, or undertake a more rigorous, time-dependent analysis.

9.3.15.5 Deflection Due to Live Load and Impact

Live load deflection limit (optional) = Span/800

[LRFD Art.2.5.2.6.2]

$$= \left(95 \times \frac{12}{800} \right) = 1.43 \text{ in.}$$

If the owner invokes the optional live load deflection criteria specified in LRFD Art. 2.5.2.6.2, the deflection is the greater of:

- that resulting from the design truck plus impact, Δ_{LT} , or
- that resulting from 25% of the design truck plus impact, Δ_{LT} , taken together with the design lane load, Δ_{LL} .

Note: LRFD Article 2.5.2.6.2 states that the dynamic load allowance be included in the calculation of live load deflection.

The *LRFD Specifications* states that all beams should be assumed to deflect equally under the applied live load and impact.

[LRFD Art. 2.5.2.6.2]

Therefore, the distribution factor for deflection, DFD , is calculated as follows:

$$DFD = (\text{number of lanes/number of beams})$$

[LRFD Art. C2.5.2.6.2]

$$= 4/9 = 0.444 \text{ lanes/beam}$$

However, it is more conservative to use the distribution factor for moment, DFM .

Deflection due to lane load

Design lane load, $w = 0.64 (DFM) = 0.64(0.625) = 0.400 \text{ kips/ft/beam}$

$$\Delta_{LL} = \frac{5wL^4}{384E_{ci}I_g} = \frac{5 \left(\frac{0.400}{12} \right) (95 \times 12)^4}{384(5,072)(335,679)} = 0.43 \text{ in.}$$

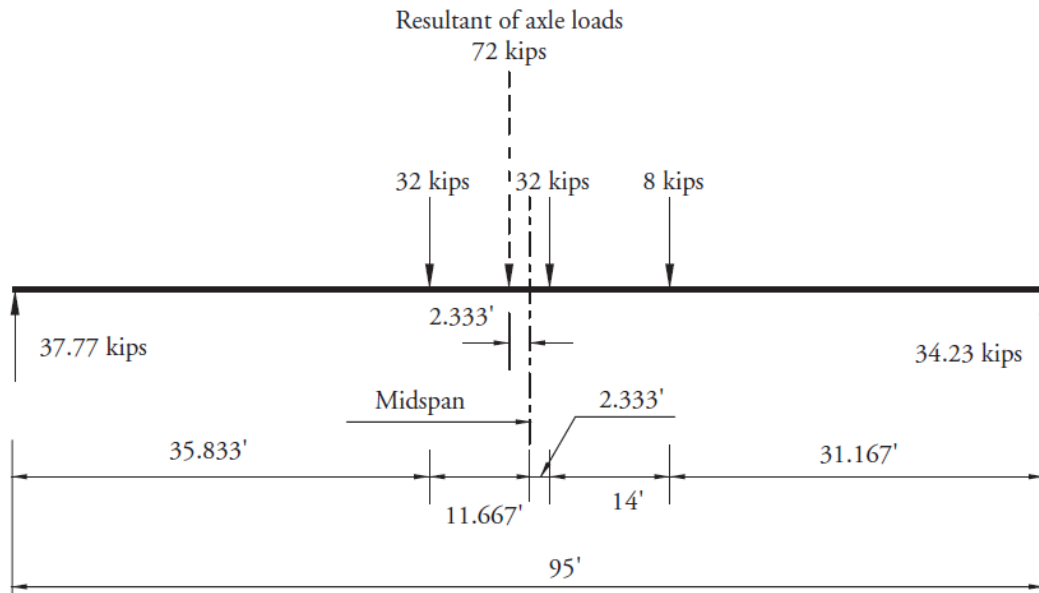
Deflection due to Design Truck Load and Impact:

To obtain the maximum moment and deflection at midspan due to truck load, let the centerline of the beam coincide with the middle point of the distance between the inner 32-kip axle and the resultant of the truck load, as shown in **Figure 9.3.15.5-1**.

DECK BULB-TEE (DBT-53), SINGLE SPAN, NONCOMPOSITE SURFACE

9.3.15.5 Deflection Due to Live Load and Impact

Figure 9.3.15.5-1
Design Truck Axle Load Position for Maximum Bending Moment



Using the elastic moment area or influence lines, deflection at midspan is:

$$\Delta_{LT} = (1.25)(IM)(DFM) = (1.25)(1.33)(0.625) = 1.04 \text{ in. } \downarrow$$

Therefore, live load deflection is the greater of:

$$\Delta_{LT} = 1.04 \text{ in. (Controls)}$$

$$0.25\Delta_{LT} + \Delta_{LL} = 0.25(1.04) + 0.43 = 0.69 \text{ in.}$$

Therefore, live load deflection = 1.04 in. < allowable deflection = 1.43 in. OK

This page intentionally left blank

BOX BEAM (BIII-48), SINGLE SPAN, NONCOMPOSITE SURFACE

Transformed Sections, Shear General Procedure, Refined Losses

Table of Contents

9.4.1 INTRODUCTION.....	9.4 - 3
9.4.1.1 Terminology.....	9.4 - 3
9.4.2 MATERIALS	9.4 - 3
9.4.3 CROSS-SECTION PROPERTIES FOR A TYPICAL INTERIOR BEAM.....	9.4 - 4
9.4.4 SHEAR FORCES AND BENDING MOMENTS	9.4 - 5
9.4.4.1. Shear Forces and Bending Moments Due to Dead Loads	9.4 - 5
9.4.4.1.1 Dead Loads	9.4 - 5
9.4.4.1.2 Unfactored Shear Forces and Bending Moments.....	9.4 - 6
9.4.4.2 Shear Forces and Bending Moments Due to Live Loads	9.4 - 6
9.4.4.2.1 Live Loads.....	9.4 - 6
9.4.4.2.2 Live Load Distribution Factors for a Typical Interior Beam	9.4 - 7
9.4.4.2.2.1 Distribution Factor for Bending Moments.....	9.4 - 7
9.4.4.2.2.2 Distribution Factor for Shear Forces.....	9.4 - 8
9.4.4.2.3 Dynamic Allowance	9.4 - 8
9.4.4.2.4 Unfactored Shear Forces and Bending Moments.....	9.4 - 8
9.4.4.2.4.1 Due to Design Truck Load; V_{LT} and M_{LT}	9.4 - 8
9.4.4.2.4.2 Due to Design Lane Load; V_{LL} and M_{LL}	9.4 - 9
9.4.4.3 Load Combinations.....	9.4 - 10
9.4.5 ESTIMATE REQUIRED PRESTRESS.....	9.4 - 11
9.4.5.1 Service Load Stresses at Midspan	9.4 - 11
9.4.5.2 Stress Limits for Concrete.....	9.4 - 12
9.4.5.3 Required Number of Strands.....	9.4 - 12
9.4.5.4 Strand Pattern.....	9.4 - 12
9.4.5.5 Steel Transformed Section Properties	9.4 - 13
9.4.6 STRENGTH LIMIT STATE	9.4 - 14
9.4.7 PRESTRESS LOSSES	9.4 - 16
9.4.7.1 Elastic Shortening.....	9.4 - 16
9.4.7.2 Time-Dependent Losses between Transfer and Deck Placement.....	9.4 - 17
9.4.7.2.1 Shrinkage of Concrete	9.4 - 17
9.4.7.2.2 Creep of Concrete	9.4 - 18
9.4.7.2.3 Relaxation of Prestressing Strands.....	9.4 - 18
9.4.7.3 Time-Dependent Losses between Deck Placement and Final Time	9.4 - 19
9.4.7.3.1 Shrinkage of Concrete	9.4 - 19
9.4.7.3.2 Creep of Concrete	9.4 - 19
9.4.7.3.3 Relaxation of Prestressing Strands.....	9.4 - 20
9.4.7.3.4 Shrinkage of Deck Concrete.....	9.4 - 20
9.4.7.4 Total Time-Dependent Loss.....	9.4 - 20
9.4.7.5 Total Losses at Transfer	9.4 - 20
9.4.7.6 Total Losses at Service Loads.....	9.4 - 21

BOX BEAM (BIII-48), SINGLE SPAN, NONCOMPOSITE SURFACE

Transformed Sections, Shear General Procedure, Refined Losses

Table of Contents

9.4.8 CONCRETE STRESSES AT TRANSFER 9.4 - 21

 9.4.8.1 Stress Limits for Concrete 9.4 - 22

 9.4.8.2 Stresses at Transfer Length Section of Bonded Strands 9.4 - 22

 9.4.8.3 Stresses at Transfer Length Section of Debonded Strands 9.4 - 23

 9.4.8.4 Stresses at Midspan 9.4 - 24

 9.4.8.5 Summary of Stresses at Transfer 9.4 - 24

9.4.9 CONCRETE STRESSES AT SERVICE LOADS 9.4 - 24

 9.4.9.1 Stress Limits for Concrete 9.4 - 24

 9.4.9.2 Stresses at Midspan 9.4 - 25

 9.4.9.3 Fatigue Stress Limit 9.4 - 25

 9.4.9.4 Summary of Stresses at Midspan at Service Loads 9.4 - 26

9.4.10 LIMITS OF REINFORCEMENT 9.4 - 26

 9.4.10.1 Maximum Reinforcement 9.4 - 26

 9.4.10.2 Minimum Reinforcement 9.4 - 26

9.4.11 SHEAR DESIGN 9.4 - 27

 9.4.11.1 Critical Section 9.4 - 27

 9.4.11.2 Contribution of Concrete to Nominal Shear Resistance 9.4 - 28

 9.4.11.2.1 Strain in Flexural Tension Reinforcement 9.4 - 28

 9.4.11.2.3 Compute Concrete Contribution 9.4 - 29

 9.4.11.3 Contribution of Reinforcement to Nominal Shear Resistance 9.4 - 29

 9.4.11.3.1 Requirement for Reinforcement 9.4 - 29

 9.4.11.3.2 Required Area of Reinforcement 9.4 - 29

 9.4.11.3.3 Determine Spacing of Reinforcement 9.4 - 30

 9.4.11.3.4 Minimum Reinforcement Requirement 9.4 - 30

 9.4.11.4 Maximum Nominal Shear Resistance 9.4 - 30

9.4.12 interface shear transfer 9.4 - 32

9.4.13 MINIMUM LONGITUDINAL REINFORCEMENT REQUIREMENT 9.4 - 32

 9.4.13.1 Required Reinforcement at Face of Bearing 9.4 - 32

9.4.14 PRETENSIONED ANCHORAGE ZONE 9.4 - 33

 9.4.14.1 Anchorage Zone Reinforcement 9.4 - 33

 9.4.14.2 Confinement Reinforcement 9.4 - 34

9.4.15 DEFLECTION AND CAMBER 9.4 - 34

 9.4.15.1 Deflection Due to Prestressing Force at Transfer 9.4 - 34

 9.4.15.2 Deflection Due to Beam Self Weight 9.4 - 34

 9.4.15.3 Deflection Due to Diaphragm Weight 9.4 - 35

 9.4.15.4 Deflection Due to Barrier and Wearing Surface Weights 9.4 - 35

 9.4.15.5 Deflection and Camber Summary 9.4 - 35

 9.4.15.6 Deflection Due to Live Load and Impact 9.4 - 35

9.4.16 TRANSVERSE POST-TENSIONING 9.4 - 37

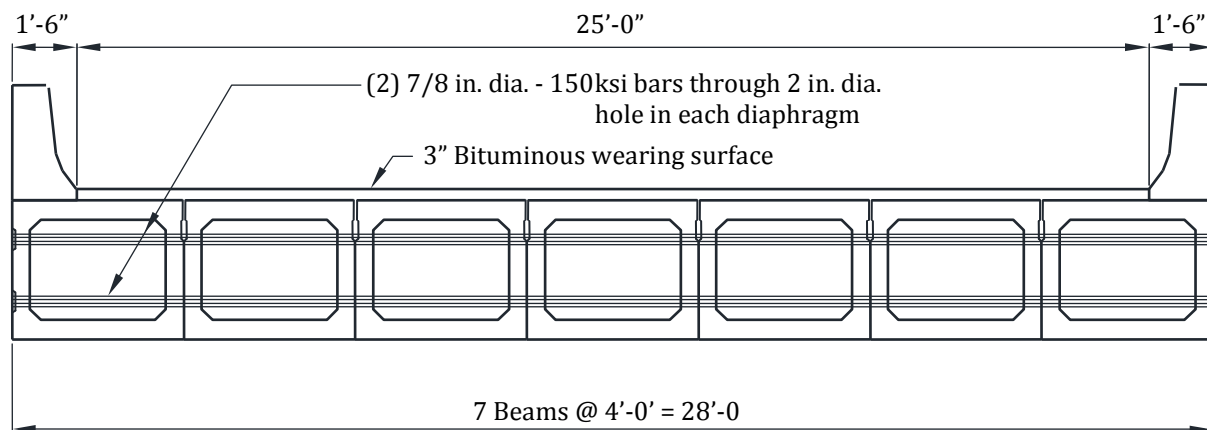
BOX BEAM (BIII-48), SINGLE SPAN, NONCOMPOSITE SURFACE

9.4.1 Introduction/9.4.2 Materials

9.4 Transformed Sections, Shear General Procedure, Refined Losses**9.4.1 INTRODUCTION**

This design example demonstrates the design of a 95-ft, single-span, AASHTO Type BIII-48 box beam bridge with no skew. This example illustrates in detail the design of a typical interior beam at the critical sections in positive flexure, shear, and deflection due to prestress, dead loads, and live loads. The superstructure consists of seven beams abutted as shown in **Figure 9.4.1-1**. A 3-in.-thick bituminous surfacing will be placed on the beams as a wearing surface. Beams are transversely post-tensioned through 8-in.-thick full-depth diaphragms located at the quarter-points. Design live load is HL-93. The design is accomplished in accordance with the *AASHTO LRFD Bridge Design Specifications*, Fifth Edition, 2010, and the 2011 Interim Revisions. Elastic stresses from external loads are calculated using transformed sections. Shear strength is calculated using the general procedure. Time-dependent prestress losses are calculated using the refined estimates.

Figure 9.4.1-1
Bridge Cross Section

**9.4.1.1 Terminology**

The following terminology is used to describe cross sections in this design example:

noncomposite section—the concrete beam cross section.

noncomposite nontransformed section—the concrete beam cross section without the strands transformed. Also called the gross section.

noncomposite transformed section—the concrete beam cross section with the strands transformed to provide cross-sectional properties equivalent to the beam concrete.

The term "transformed" refers to transformation of the strands.

9.4.2 MATERIALS

Precast concrete beams: AASHTO Box Beams, Type BIII-48, as shown in **Figure 9.4.2-1**

Required concrete compressive strength at transfer, $f'_{ci} = 4.0$ ksi

Specified concrete compressive strength for use in design, $f'_c = 5.0$ ksi

Concrete unit weight, $w_c = 0.150$ kcf

Overall beam length = 96.0 ft

Design span = 95.0 ft

BOX BEAM (BIII-48), SINGLE SPAN, NONCOMPOSITE SURFACE

9.4.2 Materials/9.4.3.1 Nontransformed Beam Section

Prestressing strands: 1/2-in.-dia., seven-wire, low-relaxation

Area of one strand = 0.153 in.²

Specified tensile strength, $f_{pu} = 270.0$ ksi

Yield strength, $f_{py} = 0.9f_{pu} = 243.0$ ksi

[LRFD Table 5.4.4.1-1]

Stress limits for prestressing strands:

[LRFD Table 5.9.3-1]

- before transfer, $f_{pi} \leq 0.75f_{pu} = 202.5$ ksi
- at service limit state (after all losses), $f_{pe} \leq 0.8f_{py} = 194.4$ ksi

Modulus of elasticity, $E_p = 28,500$ ksi

[LRFD Art. 5.4.4.2]

Reinforcing bars:

Yield strength, $f_y = 60.0$ ksi

Modulus of elasticity, $E_s = 29,000$ ksi

[LRFD Art. 5.4.3.2]

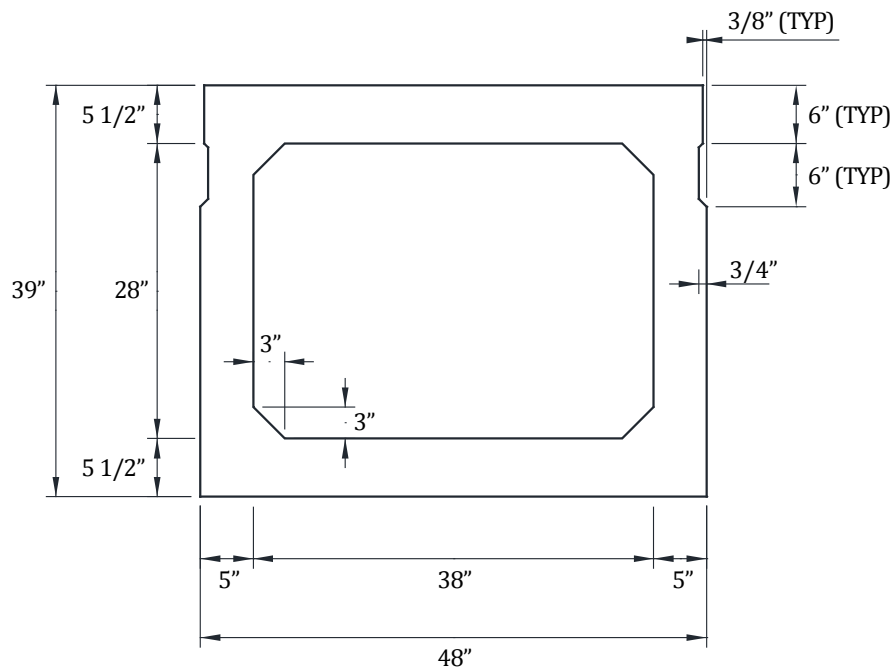
Bituminous surfacing, 3 in. thick: unit weight = 0.140 kcf

[LRFD Table 3.5.1-1]

New Jersey-type barrier: unit weight = 0.300 kips/ft/side

Figure 9.4.2-1

AASHTO Box Beam Type BIII-48



9.4.3 CROSS-SECTION PROPERTIES FOR A TYPICAL INTERIOR BEAM

9.4.3.1 Nontransformed Beam Section

A_g = area of cross section of precast beam = 813 in.²

h = overall depth of precast beam = 39 in.

I_g = moment of inertia about the centroid of the noncomposite precast beam = 168,367 in.⁴

y_b = distance from centroid to the extreme bottom fiber of the noncomposite precast beam = 19.29 in.

y_t = distance from centroid to the extreme top fiber of the noncomposite precast beam = 19.71 in.

BOX BEAM (BIII-48), SINGLE SPAN, NONCOMPOSITE SURFACE

9.4.3.1 Nontransformed Beam Section/9.4.4.1.1 Dead Loads

S_b = section modulus for extreme bottom fiber of the noncomposite precast beam = $I_g/y_b = 8,728 \text{ in.}^3$

S_t = section modulus for extreme top fiber of the noncomposite precast beam = $I_g/y_t = 8,542 \text{ in.}^3$

w_g = beam weight per unit length = $(813/144)0.150 = 0.847 \text{ kips/ft}$

E_c = modulus of elasticity of concrete, ksi, = $33,000K_1(w_c)^{1.5}\sqrt{f'_c}$ [LRFD Eq. 5.4.2.4-1]

where

K_1 = correction factor for source of aggregate taken as 1.0

w_c = unit weight of concrete = 0.150 kcf

LRFD Table 3.5.1-1 states that, in the absence of more precise data, the unit weight of concrete may be taken as $0.140 + 0.001f'_c$ for $5.0 < f'_c \leq 15.0$ ksi. For $f'_c = 5.0$ ksi, the unit weight would be 0.1450 kcf. However, precast concrete mixes typically have a relatively low water-cementitious materials ratio and high density. Therefore, a unit weight of 0.150 kcf is used in this example. For high-strength concrete, this value may need to be increased based on test results. For simplicity, a value of 0.150 kcf is also used for the cast-in-place concrete.

f'_c = specified compressive strength of concrete, ksi

Therefore, the modulus of elasticity for:

precast beam at transfer, $E_{ci} = 33,000(1.00)(0.150)^{1.5}\sqrt{4.0} = 3,834 \text{ ksi}$

precast beam at service loads, $E_c = 33,000(1.00)(0.150)^{1.5}\sqrt{5.0} = 4,287 \text{ ksi}$

9.4.4 SHEAR FORCES AND BENDING MOMENTS**9.4.4.1. Shear Forces and Bending Moments Due to Dead Loads**

[LRFD Art. 3.3.2]

9.4.4.1.1 Dead Loads

Refer to **Tables 9.4.4-1** and **9.4.4-2**, which follow Section 9.4.4.3 for a summary of unfactored values calculated below.

DC = Dead load of structural components and nonstructural attachments

Dead loads acting on the noncomposite structure:

Beam self weight, $w_g = 0.847 \text{ kip/ft}$

Diaphragm weight = $\left(\frac{8}{12}\right) \left[\frac{(48-10)}{12} \times \frac{(39-11)}{12} - 4 \left(\frac{1}{2}\right) \left(\frac{3}{12}\right) \left(\frac{3}{12}\right) \right] (0.150) = 0.73 \text{ kips/diaphragm}$

Generally, the unit weight of reinforced concrete should be slightly greater than the unit weight of concrete alone because of the added weight of reinforcement. However, in this example, the difference is considered negligible. The weights of the diaphragms are considered concentrated loads acting at quarter points as shown in **Figure 9.4.4.1.1-1**.

LRFD Article 4.6.2.2.1 states that permanent loads (barrier and wearing surface) may be distributed uniformly among the beams if the following conditions are met:

- Width of the deck is constant OK
- Number of beams, N_b , is not less than four ($N_b = 7$) OK
- Beams are parallel and have the same stiffness OK
- The roadway part of the overhang, $d_e \leq 3.0 \text{ ft}$ ($d_e = 0.0$) OK
- Curvature in plan is less than specified in the *LRFD Specifications* (curvature = 0.0°) OK
- Cross section of the bridge is consistent with one of the cross sections given in LRFD Table 4.6.2.2.1-1 OK

BOX BEAM (BIII-48), SINGLE SPAN, NONCOMPOSITE SURFACE

9.4.4.1.1 Dead Loads/9.4.4.2.1 Live Loads

Since these criteria are satisfied, the barrier and wearing surface loads are distributed equally among the seven beams.

$$\text{Barrier weight} = (2 \text{ barriers})(0.300 \text{ kips/ft}) / (7 \text{ beams}) = 0.086 \text{ kips/ft/beam} = w_b$$

$$DW = \text{Dead load of wearing surface (weight of 3 in. bituminous wearing surface)} \quad [\text{LRFD Table 3.5.1-1}]$$

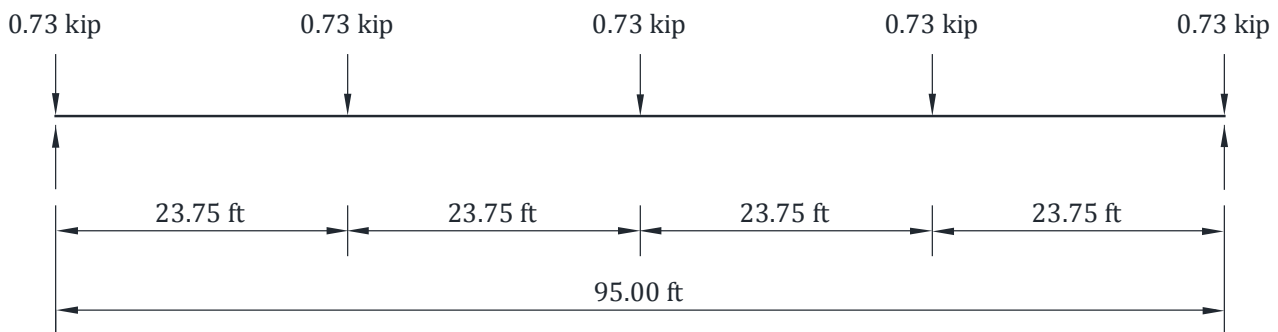
$$= 0.140 \text{ kcf}$$

$$= (3/12)(0.140) = 0.035 \text{ ksf}$$

$$= (0.035 \text{ ksf})(25.0 \text{ ft}) / 7 \text{ beams} = 0.125 \text{ kips/ft/beam} = w_{ws}$$

The *DW* load should be kept separately from *DC* loads because a higher load factor is applied to it.

Figure 9.4.4.1.1-1
Diaphragm Loads per Beam



9.4.4.1.2 Unfactored Shear Forces and Bending Moments

For a simply supported beam with a span length (*L*) loaded with a uniformly distributed load (*w*), the shear force (*V_x*) and the bending moment (*M_x*) at a distance (*x*) from the support are given by:

$$V_x = w(0.5L - x) \quad (\text{Eq. 9.4.4.1.2-1})$$

$$M_x = 0.5wx(L - x) \quad (\text{Eq. 9.4.4.1.2-2})$$

Using the above equations, values of shear forces and bending moments for a typical interior beam under the self weight of beam, diaphragms, barriers, and wearing surface are computed and given in **Table 9.4.4-1** that is located at the end of Section 9.4.4.3. Using statics, values of shear forces and bending moments due to diaphragm weight are calculated and given in **Table 9.4.4-1**. For these calculations, the span length (*L*) is the design span, 95 ft. However, for calculation of stresses and deformations at the time prestress is transferred, the overall length of the precast member, 96 ft, is used as illustrated later in this example.

9.4.4.2 Shear Forces and Bending Moments Due to Live Loads

9.4.4.2.1 Live Loads

Design live load is HL-93, which consists of a combination of [LRFD Art. 3.6.1.2.1]

1. Design truck or design tandem with dynamic allowance. [LRFD Art. 3.6.1.2.2]

The design truck consists of 8.0-, 32.0-, and 32.0-kip axles with the first pair spaced at 14.0 ft and the second pair spaced at 14.0 to 30.0 ft. The design tandem consists of a pair of 25.0-kip axles spaced at 4.0 ft apart. [LRFD Art. 3.6.1.2.3]

2. Design lane load of 0.64 kips/ft without dynamic allowance [LRFD Art. 3.6.1.2.4]

BOX BEAM (BIII-48), SINGLE SPAN, NONCOMPOSITE SURFACE

9.4.4.2.2 Live Load Distribution Factors for a Typical Interior Beam/9.4.4.2.1 Distribution Factor for Bending Moments

9.4.4.2.2 Live Load Distribution Factors for a Typical Interior Beam

The live load bending moments and shear forces are determined by using the simplified distribution factor formulas [LRFD Art. 4.6.2.2]. To use the simplified live load distribution factor formulas, the following conditions must be met: [LRFD Art. 4.6.2.2.1]

- Width of deck is constant OK
- Number of beams, N_b not less than four ($N_b = 7$) OK
- Beams are parallel and have approximately the same stiffness OK
- The roadway part of the overhang, $d_e \leq 3.0$ ft. ($d_e = 0.0$) OK
- Curvature is less than specified in the *LRFD Specifications* (Curvature = 0.0°) OK

For a precast cellular concrete box with shear keys and with or without transverse post-tensioning, the bridge type is (g) and is sufficiently connected to act as a unit. [LRFD Table 4.6.2.2.1-1]

The number of lanes design lanes is computed as:

Number of design lanes = the integer part of the ratio of ($w/12$), where (w) is the clear roadway width, in ft, between the curbs [LRFD Art. 3.6.1.1.1]

From **Figure 9.4.1-1**, $w = 25$ ft

Number of design lanes = Integer part of ($25/12$) = 2 lanes

9.4.4.2.2.1 Distribution Factor for Bending Moments

- For all limit states except fatigue limit state

For two or more lanes loaded

$$DFM = k \left(\frac{b}{305} \right)^{0.6} \left(\frac{b}{12.0L} \right)^{0.2} \left(\frac{I_g}{J_g} \right)^{0.06} \quad \text{[LRFD Table 4.6.2.2.2b-1]}$$

Provided that: $35 \leq b \leq 60$; $b = 48$ in OK
 $20 \leq L \leq 120$; $L = 95$ ft OK
 $5 \leq N_b \leq 20$; $N_b = 7$ OK

where

DFM = distribution factor for moment for interior beam

$$k = 2.5(N_b)^{-0.2} \geq 1.5 = 2.5(7)^{-0.2} = 1.694 > 1.5 \quad \text{OK}$$

N_b = number of beams

b = beam width, in.

L = beam span, ft

I_g = moment of inertia of the beam, in⁴

J_g = St. Venant torsional inertia, in⁴

$$J_g \sim \frac{4A_o^2}{\sum \frac{s}{t}} \quad \text{[LRFD Eq. C4.6.2.2.1-3]}$$

where

$$A_o = \text{area enclosed by centerlines of the elements of the beam} \\ = (48 - 5)(39 - 5.5) = 1,440.5 \text{ in.}^2$$

s = length of a side element

t = thickness of an element

$$J_g = \frac{4(1,440.5)^2}{2 \left(\frac{48 - 5}{5.5} \right) + 2 \left(\frac{39 - 5.5}{5} \right)} = 285,854 \text{ in.}^2$$

BOX BEAM (BIII-48), SINGLE SPAN, NONCOMPOSITE SURFACE

9.4.4.2.1 Distribution Factor for Bending Moments/9.4.4.2.1 Due to Design Truck Load, V_{LT} and M_{LT}

Therefore:

$$DFM = 1.694 \left(\frac{48}{305}\right)^{0.6} \left(\frac{48}{12.0 \times 95}\right)^{0.2} \left(\frac{168,367}{285,854}\right)^{0.06} = 0.287 \text{ lanes/beam}$$

For one design lane loaded, if sufficiently connected to act as a unit:

$$DFM = k \left(\frac{b}{33.3L}\right)^{0.5} \left(\frac{I_g}{J_g}\right)^{0.25} = 1.694 \left(\frac{48}{33.3 \times 95}\right)^{0.5} \left(\frac{168,367}{285,854}\right)^{0.25} \quad [\text{LRFD Table 4.6.2.2.2b-1}]$$

$$= 0.183 \text{ lanes/beam}$$

Thus, the case of two or more lanes loaded controls and $DFM = 0.287$ lanes/beam.

- For fatigue limit state:

The *LRFD Specifications*, Art. C3.4.1, states that for Fatigue Limit State, a single design truck should be used. However, live load distribution factors given in LRFD Article 4.6.2.2 take into consideration the multiple presence factor, m . LRFD Article 3.6.1.1.2 states that the multiple presence factor, m , for one design lane loaded is 1.2. Therefore, the distribution factor for one design lane loaded with the multiple presence factor removed, should be used. The distribution factor for fatigue limit state is: $0.183/1.2 = 0.153$ lanes/beam

9.4.4.2.2 Distribution Factor for Shear Forces

For two or more lanes loaded:

$$DFV = \left(\frac{b}{156}\right)^{0.4} \left(\frac{b}{12.0L}\right)^{0.1} \left(\frac{I_g}{J_g}\right)^{0.05} \left(\frac{b}{48}\right) \quad [\text{LRFD Table 4.6.2.2.3a-1}]$$

Provided that: $35 \leq b \leq 60$; $b = 48$ in OK
 $20 \leq L \leq 120$; $L = 95$ ft OK
 $5 \leq N_b \leq 20$; $N_b = 7$ OK
 $25,000 \leq J_g \leq 610,000$; $J_g = 285,854 \text{ in.}^4$ OK
 $40,000 \leq I_g \leq 610,000$; $I_g = 168,367 \text{ in.}^4$ OK

where DFV = distribution factor for shear for interior beam

$$DFV = \left(\frac{48}{156}\right)^{0.4} \left(\frac{48}{12.0 \times 95}\right)^{0.1} \left(\frac{168,367}{285,854}\right)^{0.05} \left(\frac{48}{48}\right) = 0.443 \text{ lanes/beam}$$

For one design lane loaded:

$$DFV = \left(\frac{b}{130L}\right)^{0.15} \left(\frac{I_g}{J_g}\right)^{0.05} = \left(\frac{48}{130 \times 95}\right)^{0.15} \left(\frac{168,367}{285,854}\right)^{0.05} = 0.424 \text{ lanes/beam} \quad [\text{LRFD Table 4.6.2.2.3a-1}]$$

Thus, the case of two lanes loaded controls and $DFV = 0.443$ lanes/beam.

9.4.4.2.3 Dynamic Allowance

[LRFD Art. 3.6.2]

$IM = 15\%$ for fatigue limit state

$IM = 33\%$ for all other limit states

[LRFD Table 3.6.2.1-1]

where IM = dynamic load allowance, applied to design truck load only

9.4.4.2.4 Unfactored Shear Forces and Bending Moments

9.4.4.2.4.1 Due to Design Truck Load; V_{LT} and M_{LT}

- For all limit states except fatigue limit state:

Shear force and bending moment envelopes on a per-lane-basis are calculated at tenth-points of the span using the equations given in Chapter 8 of this manual. However, this is generally done by means of commercially

BOX BEAM (BIII-48), SINGLE SPAN, NONCOMPOSITE SURFACE

9.4.4.2.4.1 Due to Design Truck Load; V_{LT} and M_{LT} /9.4.4.2.4.2 Due to Design Load; V_{LL} and M_{LL}

available computer software that has the ability to deal with moving loads. Therefore, truck load shear forces and bending moments per beam are:

$$\begin{aligned}
 V_{LT} &= (\text{shear force per lane})(DFV)(1 + IM) \\
 &= (\text{shear force per lane})(0.443)(1 + 0.33) \\
 &= (\text{shear force per lane})(0.589) \text{ kips} \\
 M_{LT} &= (\text{bending moment per lane})(DFM)(1 + IM) \\
 &= (\text{bending moment per lane})(0.287)(1 + 0.33) \\
 &= (\text{bending moment per lane})(0.382) \text{ ft-kips}
 \end{aligned}$$

Values of V_{LT} and M_{LT} at different points are given in **Table 9.4.4-2**.

- For fatigue limit state:

Article 3.6.1.4.1 in the *LRFD Specifications* states that the fatigue load is a single design truck which has the same axle weight used in all other limit states but with a constant spacing of 30.0 ft between the 32.0-kip axles. Bending moment envelope on a per-lane-basis is calculated using the equation given in Chapter 8 of this manual.

Therefore, bending moment of fatigue truck load is:

$$\begin{aligned}
 M_f &= (\text{bending moment per lane})(DFM)(1 + IM) \\
 &= (\text{bending moment per lane})(0.153)(1 + 0.15) \\
 &= (\text{bending moment per lane})(0.176) \text{ ft-kips}
 \end{aligned}$$

Values of M_f at different points are given in **Table 9.4.4-2**.

9.4.4.2.4.2 Due to Design Lane Load; V_{LL} and M_{LL}

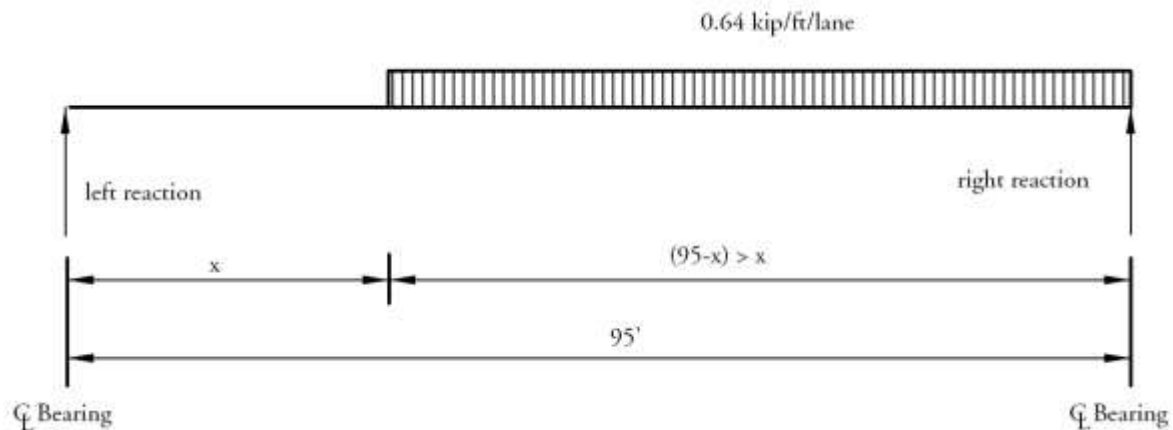
To obtain the maximum shear force at a section located at a distance (x) from the left support under a uniformly distributed load of 0.64 kips/ft, load the member to the right of the section under consideration as shown in **Figure 9.4.4.2.4.2-1**. Therefore, the maximum shear force per lane is:

$$V_x = \frac{0.32(L - x)^2}{L} \text{ for } x \leq 0.5L \tag{Eq. 9.4.4.2.4.2-1}$$

where V_x is in kips/lane and L and x are in ft

Figure 9.4.4.2.4.2-1

Maximum Shear Force due to Design Lane Load



To calculate the maximum bending moment at any section, use Eq. (9.4.4.1.2-2).

Lane load shear force and bending moment per typical interior beam are as follows:

$$\begin{aligned}
 V_{LL} &= (\text{lane load shear force})(DFV) \\
 &= (\text{lane load shear force})(0.443) \text{ kips}
 \end{aligned}$$

BOX BEAM (BIII-48), SINGLE SPAN, NONCOMPOSITE SURFACE9.4.4.2.4.2 Due to Design Load; V_{LL} and M_{LL} /9.4.4.3 Load Combinations

For all limit states except for fatigue limit state:

$$M_{LL} = (\text{lane load bending moment})(DFM)$$

$$= (\text{lane load bending moment})(0.287) \text{ ft-kips}$$

Note that the dynamic allowance is not applied to the design lane loading. [LRFD Art. 3.4]

Values of shear forces and bending moments, V_{LL} and M_{LL} , are given in **Table 9.4.4-1**.

9.4.4.3 Load Combinations

Total factored load, Q , is taken as:

$$Q = \sum \eta_i \gamma_i Q_i \quad \text{[LRFD Eq. 3.4.1-1]}$$

where

η_i = a load modifier relating to ductility, redundancy, and operational importance [LRFD Art. 1.3.2.1]
(Here, η_i is considered to be 1.0 for typical bridges.)

γ_i = load factors [LRFD Table 3.4.1-1]

Q_i = force effects from specified loads

Investigating different limit states given in LRFD Article 3.4.1, the following limit states are applicable:

Service I: check compressive stress in prestressed concrete components:

$$Q = 1.00(DC + DW) + 1.00(LL + IM) \quad \text{[LRFD Table 3.4.1-1]}$$

This load combination is the general combination for service limit state stress checks and applies to all conditions other than Service III.

Service III: check tensile stress in prestressed concrete components:

$$Q = 1.00(DC + DW) + 0.80(LL + IM) \quad \text{[LRFD Table 3.4.1-1]}$$

This load combination is a special combination for service limit state stress checks that applies only to tension in prestressed concrete structures to control cracks.

Strength I: check ultimate strength: [LRFD Tables 3.4.1-1 and -2]

$$\text{Maximum } Q = 1.25(DC) + 1.50(DW) + 1.75(LL + IM)$$

$$\text{Minimum } Q = 0.90(DC) + 0.65(DW) + 1.75(LL + IM)$$

This load combination is the general load combination for strength limit state design.

Note: For simple-span bridges, the maximum load factors produce maximum effects. However, use minimum load factors for dead load (DC), and wearing surface (DW) when dead load and wearing surface stresses are opposite to those of the live load.

Fatigue I: check stress range in strands: [LRFD Table 3.4.1-1]

$$Q = 1.5(LL + IM)$$

This load combination is a special load combination to check the tensile stress range in the strands due to live load and dynamic allowance.

BOX BEAM (BIII-48), SINGLE SPAN, NONCOMPOSITE SURFACE

9.4.4.3 Load Combinations/9.4.5.1 Service Load Stresses at Midspan

Table 9.4.4-1

Unfactored Shear Forces and Bending Moments Due to Dead Loads for a Typical Interior Beam

Distance x, ft	Section x/L	Beam Weight		Diaphragm Weight		Barrier Weight		Wearing Surface Weight	
		Shear V_g kips	Moment M_g ft-kips	Shear V_d kips	Moment M_d ft-kips	Shear V_b kips	Moment M_b ft-kips	Shear V_{ws} kips	Moment M_{ws} ft-kips
0	0.0	40.2	0.0	1.1	0.0	4.1	0.0	5.9	0.0
*2.80	0.029	37.9	109.3	1.1	3.1	3.8	11.1	5.6	16.1
9.5	0.1	32.2	344.0	1.1	10.4	3.3	34.9	4.8	50.8
19.0	0.2	24.1	611.5	1.1	20.8	2.5	62.1	3.6	90.3
28.5	0.3	16.1	802.6	0.4	27.7	1.6	81.5	2.4	118.5
38.0	0.4	8.0	917.3	0.4	31.2	0.8	93.1	1.2	135.4
47.5	0.5	0.0	955.5	0.4	34.7	0.0	97.0	0.0	141.0

* Critical section for shear (see Sect. 9.4.11)

Table 9.4.4-2

Unfactored Shear Forces and Bending Moments Due to Live Load for a Typical Interior Beam

Distance x, ft	Section x/L	Design Truck with Impact		Lane Load		Fatigue Truck with Impact
		Shear V_{LT} kips	Moment M_{LT} ft-kips	Shear V_{LL} kips	Moment M_{LL} ft-kips	Moment M_f ft-kips
0	0.0	38.3	0.0	13.5	0.0	0.0
*2.80	0.029	37.0	67.1	12.7	23.7	27.6
9.5	0.1	34.0	209.3	10.9	74.6	85.2
19.0	0.2	29.8	366.5	8.6	132.6	146.4
28.5	0.3	25.5	471.4	6.6	174.1	188.3
38.0	0.4	21.3	532.5	4.8	198.9	209.4
47.5	0.5	17.0	545.8	3.4	207.2	206.6

*Critical section for shear (see Sect. 9.4.11)

9.4.5 ESTIMATE REQUIRED PRESTRESS

The required number of strands is usually governed by concrete tensile stresses at the bottom fiber for load combination Service III at the section of maximum moment. For estimating the number of strands, only the stresses at midspan are considered.

9.4.5.1 Service Load Stresses at Midspan

Bottom tensile stress due to applied loads using load combination Service III is:

$$f_b = \frac{M_g + M_d + M_b + M_{ws} + (0.8)(M_{LT} + M_{LL})}{S_b}$$

where

- f_b = concrete tensile stress at bottom fiber of the beam, ksi
- M_g = unfactored bending moment due to beam self weight, ft-kips
- M_d = unfactored bending moment due to diaphragm weight, ft-kips
- M_b = unfactored bending moment due to barrier weight, ft-kips
- M_{ws} = unfactored bending moment due to wearing surface, ft-kips
- M_{LT} = unfactored bending moment due to truck load, ft-kips
- M_{LL} = unfactored bending moment due to lane load, ft-kips

BOX BEAM (BIII-48), SINGLE SPAN, NONCOMPOSITE SURFACE

9.4.5.1 Service Load Stresses at Midspan/9.4.5.4 Strand Pattern

Using values of bending moments from **Tables 9.4.4-1** and **9.4.4-2**, bottom tensile stress at midspan is:

$$f_b = \frac{(955.5 + 34.7) + (97.0 + 141.0) + (0.8)(545.8 + 207.2)}{8,728}(12) = 2.517 \text{ ksi}$$

9.4.5.2 Stress Limits for Concrete

$$\text{Tensile stress limit at service loads} = 0.19\sqrt{f'_c} \quad [\text{LRFD Table. 5.9.4.2.2-1}]$$

where f'_c = specified concrete compressive strength for design, ksi

$$\text{Concrete tensile stress limit} = -0.19\sqrt{5.00} = -0.425 \text{ ksi}$$

9.4.5.3 Required Number of Strands

The required precompressive stress at the bottom fiber of the beam is the difference between bottom tensile stress due to the applied loads and the concrete tensile stress limit:

$$f_{pb} = (2.517 - 0.425) = 2.092 \text{ ksi}$$

Assume the distance between the center of gravity of bottom strands and the bottom fiber of the beam, y_{bs} , = 4.5 in. at midspan.

Therefore, strand eccentricity at midspan, $e_c = y_b - y_{bs} = 19.29 - 4.5 = 14.79$ in.

If P_{pe} is the total prestressing force after all losses, the stress at the bottom fiber due to prestress is:

$$f_{pb} = \frac{P_{pe}}{A_g} + \frac{P_{pe}e_c}{S_b} \text{ or } 2.092 = \frac{P_{pe}}{813} + \frac{P_{pe}(14.79)}{8,728}$$

Solving for P_{pe} , the required $P_{pe} = 715.3$ kips.

Final prestress force per strand = (area of strand)(f_{pi})(1 – losses)

where f_{pi} = initial stress before transfer = 202.5 ksi (Sect. 9.2.2)

Assuming final loss of 20% of f_{pi} , the final prestress force per strand after all losses

$$= (0.153)(202.5)(1 - 0.20) = 24.8 \text{ kips}$$

Number of strands required = $715.3/24.8 = 28.84$ strands

Try (31) ½-in.-diameter, 270 ksi strands

Total area of prestressing strands, $A_{ps} = 31(0.153) = 4.743 \text{ in.}^2$

Note: This is a conservative estimate of the number of strands because nontransformed section properties are used in lieu of transformed section properties. The number of strands can be refined later in the design process as more accurate section properties and prestress losses are determined.

9.4.5.4 Strand Pattern

Figure 9.4.5.4-1 shows the assumed strand pattern for the 31 strands at midspan of the beam. All strands are straight.

The distance between the center of gravity of the strands and the bottom concrete fiber of the beam at midspan is:

$$y_{bs} = \frac{23(2) + 6(4) + 2(36)}{31} = 4.58 \text{ in.}$$

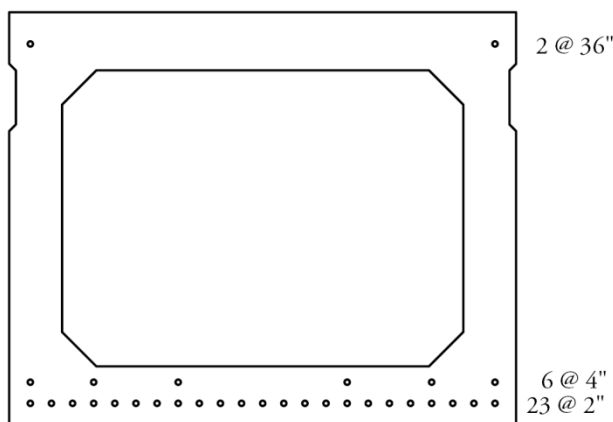
Strand eccentricity at midspan:

$$e_c = y_b - y_{bs} = 19.29 - 4.58 = 14.71 \text{ in.} = e_{pg}$$

BOX BEAM (BIII-48), SINGLE SPAN, NONCOMPOSITE SURFACE

9.4.5.4 Strand Pattern/9.4.5.5 Steel Transformed Section Properties

Figure 9.4.5.4-1
Strand Pattern at Midspan



9.4.5.5 Steel Transformed Section Properties

From the earliest years of prestressed concrete design, the gross section was conservatively used in analysis since the prestressing forces were smaller and computer programs were not widely used. However, the use of transformed section, which is obtained from the gross section by adding transformed steel area, yields more accurate results than the gross section analysis.

For each row of the prestressing strands shown in **Figure 9.4.5.4-1**, the steel area is multiplied by $(n - 1)$ to calculate the transformed section properties, where n is the modular ratio between prestressing strand and concrete. Since the modulus of elasticity of concrete is different at transfer and final time, the transformed section properties should be calculated separately for the two stages. The transformed section properties are calculated as shown in **Table 9.4.5.5-1**.

At transfer:

$$n - 1 = \frac{28,500}{3,834} - 1 = 6.433$$

At final:

$$n - 1 = \frac{28,500}{4,287} - 1 = 5.648$$

Table 9.4.5.5-1
Properties of Transformed Section at Final Time

	Transformed Area, in. ²	y_b in.	Ay_b in. ³	$A(y_{btf} - y_b)^2$ in. ³	I in. ⁴	$I + A(y_{btf} - y_b)^2$ in. ⁴
Beam	813.00	19.29	15,683	180	168,367	168,547
Row 1	19.88	2.00	39.76	5,624		5,624
Row 2	5.18	4.00	20.72	1,138		1,138
Row 3	1.73	36.00	62.28	511		511
Σ	839.8		15,806			175,820

Note: The moment of inertia of strand about its own centroid is neglected.

The transformed section properties are calculated as:

Transformed section at transfer:

$$A_{ti} = \text{area of transformed section at transfer} = 843.5 \text{ in.}^2$$

$$I_{ti} = \text{moment of inertia of the transformed section at transfer} = 176,829 \text{ in.}^4$$

$$e_{ti} = \text{eccentricity of strands with respect to transformed section at transfer} = 14.18 \text{ in.}$$

BOX BEAM (BIII-48), SINGLE SPAN, NONCOMPOSITE SURFACE

9.4.5.5 Steel Transformed Section Properties/9.4.6 Strength Limit State

y_{bti} = distance from the centroid of the transformed section to the extreme bottom fiber of the beam at transfer = 18.76 in.

S_{bti} = section modulus for the extreme bottom fiber of the transformed section at transfer = 9,426 in.³

S_{tti} = section modulus for the extreme top fiber of the transformed section at transfer = 8,737 in.³

Transformed section at final time:

A_{tf} = area of transformed section at final time = 839.8 in.²

I_{tf} = moment of inertia of the transformed section at final time = 175,820 in.⁴

e_{tf} = eccentricity of strands with respect to transformed section at final time = 14.24 in.

y_{btf} = distance from the centroid of the transformed section to the extreme bottom fiber of the beam at final time = 18.82 in.

S_{btf} = section modulus for the extreme bottom fiber of the transformed section at final time = 9,342 in.³

S_{ttf} = section modulus for the extreme top fiber of the transformed section at final time = 8,713 in.³

9.4.6 STRENGTH LIMIT STATE

For box sections, it is common that the flexural strength controls design. It is therefore recommended that the strength calculations be conducted prior to the stress check. As the state-of-the-art continues to develop into the use of high-strength concrete and emphasis continues to be placed on the importance of member strength, it is possible that future designs using other cross sections will be controlled by the strength limit state.

Total ultimate bending moment for Strength I is:

$$M_u = 1.25(DC) + 1.5(DW) + 1.75(LL + IM)$$

Using the values of unfactored bending moment given in **Tables 9.4.4-1** and **9.4.4-2**, the ultimate bending moment at midspan is:

$$M_u = 1.25(955.5 + 34.7 + 97.0) + 1.5(141.0) + 1.75(545.8 + 207.2) = 2,888.3 \text{ ft-kips}$$

Average stress in prestressing strands when $f_{pe} \geq 0.5 f_{pu}$:

$$f_{ps} = f_{pu} \left(1 - k \frac{c}{d_p} \right) \quad \text{[LRFD Eq. 5.7.3.1.1-1]}$$

where

f_{ps} = average stress in prestressing strand, ksi

f_{pu} = specified tensile strength of prestressing strand = 270.0 ksi

$$k = 2 \left(1.04 - \frac{f_{py}}{f_{pu}} \right) = 2 \left(1.04 - \frac{243}{270} \right) \quad \text{[LRFD Eq. 5.7.3.1.1-2]}$$

$$= 0.28 \text{ for low-relaxation strands} \quad \text{[LRFD Table C5.7.3.1.1-1]}$$

d_p = distance from extreme compression fiber to the centroid of the prestressing strands, in.

c = distance from extreme compression fiber to the neutral axis, in.

To compute c , assume rectangular section behavior and check if the depth of the equivalent compression stress block, a , is less than or equal to compression flange depth, t_s . [LRFD Art. C5.7.3.2.2]

where $a = \beta_1 c$

$$c = \frac{A_{ps} f_{pu} + A_s f_y - A'_s f'_y}{0.85 f'_c \beta_1 b + k A_{ps} \frac{f_{pu}}{d_p}} \quad \text{[LRFD Eq. 5.7.3.1.1-4]}$$

BOX BEAM (BIII-48), SINGLE SPAN, NONCOMPOSITE SURFACE

9.4.6 Strength Limit State

where

- a = depth of the equivalent stress block
 A_{ps} = area of prestressing strand = $29(0.153) = 4.437 \text{ in.}^2$
 A_s = area of nonprestressed tension reinforcement = 0 in.^2
 f_y = specified yield strength of tension reinforcement = 60.0 ksi
 A'_s = area of compression reinforcement = 0 in.^2
 f'_y = specified yield strength of compression reinforcement
 β_1 = stress factor of compression block [LRFD Art. 5.7.2.2]
 = 0.85 for $f'_c \leq 4.0 \text{ ksi}$
 = $0.85 - 0.05(f'_c - 4.0) \geq 0.65$ for $f'_c > 4.0 \text{ ksi}$
 = $0.85 - 0.05(5.0 - 4.0) = 0.80$
 b = width of compression flange = 48 in.

Note: In computing the flexural strength of members with strands placed near the compression face of the member, it is not correct to use the combined centroid of the entire strand group for establishing the effective depth, d_p , and the area of prestressing steel, A_{ps} . This is because the top strands will have different strain from that of the bottom strands. An accurate solution can be achieved using the detailed strain compatibility approach, which accounts for the steel strain at various distances from the neutral axis. However, a reasonable approximation is to ignore all strands placed on the compression side.

For the 29 bottom strands, the distance between the center of gravity of the strands and the bottom fiber of the beam, y_{bs} , is:

$$\frac{23(2) + 6(4)}{29} = 2.41 \text{ in.}$$

Thus, $d_p = 39 - 2.41 = 36.59 \text{ in.}$

$$c = \frac{4.437(270.0) + 0 - 0}{(0.85)(5.0)(0.80)(48) + 0.28(4.437)\left(\frac{270.0}{36.59}\right)} = 6.95 \text{ in.}$$

$$a = \beta_1 c = 0.80(6.95) = 5.56 \text{ in.} > t_s = 5.5 \text{ in.} \quad \text{NG}$$

Therefore, compute c using T-section behavior.

$$c = \frac{A_{ps}f_{pu} + A_s f_y - A'_s f'_y - 0.85 f'_c (b - b_w) h_f}{0.85 f'_c \beta_1 b_w + k A_{ps} \frac{f_{pu}}{d_p}} \quad \text{[LRFD Eq. 5.7.3.1.1-3]}$$

where

$$h_f = \text{compression flange depth} = t_s = 5.5 \text{ in.}$$

$$b_w = \text{width of web} = 2(5) = 10 \text{ in.}$$

$$c = \frac{4.437(270) + 0 - 0 - 0.85(5.0)(48 - 10)(5.5)}{(0.85)(5.0)(0.80)(10) + 0.28(4.437)\left(\frac{270}{36.59}\right)} = 7.18 \text{ in.}$$

$$a = \beta_1 c = 0.80(7.18) = 5.74 \text{ in.} > t_s = 5.5 \text{ in.} \quad \text{OK}$$

Therefore, the average stress in the prestressing strand:

$$f_{ps} = 270.0 \left(1 - 0.28 \frac{7.18}{36.59} \right) = 255.2 \text{ ksi}$$

BOX BEAM (BIII-48), SINGLE SPAN, NONCOMPOSITE SURFACE**9.4.6 Strength Limit State/9.4.7.1 Elastic Shortening**

Nominal flexural resistance:

[LRFD Art. 5.7.3.2.2]

$$M_n = A_{ps}f_{ps} \left(d_p - \frac{a}{2} \right) + 0.85f'_c (b - b_w)h_f \left(\frac{a}{2} - \frac{h_f}{2} \right) \quad \text{[LRFD Eq. 5.7.3.2.2-1]}$$

$$M_n = (4.437)(255.2) \left(36.59 - \frac{5.74}{2} \right) / 12 + 0.85(5.0)(48 - 10)(5.5) \left(\frac{5.74}{2} - \frac{5.5}{2} \right) / 12 = 3,190.7 \text{ ft-kips}$$

Factored flexural resistance, M_r :

$$M_r = \phi M_n \quad \text{[LRFD Eq. 5.7.3.2.1-1]}$$

where ϕ = resistance factor

[LRFD Art. 5.5.4.2.1]

= 1.00 for tension controlled prestressed concrete sections

$$M_r = 3,190.7 \text{ ft-kips} > M_u = 2,888.3 \text{ ft-kips} \quad \text{OK}$$

9.4.7 PRESTRESS LOSSES

Total prestress loss:

$$\Delta f_{pT} = \Delta f_{pES} + \Delta f_{pLT} \quad \text{[LRFD Eq. 5.9.5.1-1]}$$

where

 Δf_{pT} = total loss in prestressing steel stress Δf_{pES} = sum of all losses or gains due to elastic shortening or extension at the time of application of prestress and/or external loads Δf_{pLT} = long-term losses due to shrinkage and creep of concrete, and relaxation of steel after transfer. In this design example, the refined estimates of time-dependent losses are used.**9.4.7.1 Elastic Shortening**

$$\Delta f_{pES} = \frac{E_p}{E_{ci}} f_{cgp} \quad \text{[LRFD Eq. 5.9.5.2.3a-1]}$$

where

 E_p = modulus of elasticity of prestressing strands = 28,500 ksi E_{ci} = modulus of elasticity of beam concrete at transfer = 3,834 ksi f_{cgp} = sum of concrete stresses at the center of gravity of prestressing tendons due to prestressing force at transfer and the self weight of the member at sections of maximum moment.

If the gross (or net) cross-section properties are used, it is necessary to perform numerical iterations. The elastic loss Δf_{pES} is usually assumed to be 10% of the initial prestress to calculate f_{cgp} , which is then used in the equation above to calculate a refined Δf_{pES} . The process is repeated until the assumed Δf_{pES} and refined Δf_{pES} converge.

However, when transformed section properties are used to calculate the concrete stress, the effects of losses and gains due to elastic deformations are implicitly account for. Therefore, Δf_{pES} should not be included in calculating f_{cgp} .

Force per strand before transfer = (area of strand)(prestress stress before transfer)

$$= (0.153)(202.5) = 30.98 \text{ kips}$$

$$f_{cgp} = \frac{P_{pi}}{A_{ti}} + \frac{P_{pi}e_{ti}^2}{I_{ti}} - \frac{(M_g + M_d)e_{ti}}{I_{ti}}$$

where

 P_p = total prestressing force before transfer = (31 strands)(30.98) = 960.4 kips e_{ti} = eccentricity of strands at midspan with respect to the transformed section at transfer = 14.18 in.

BOX BEAM (BIII-48), SINGLE SPAN, NONCOMPOSITE SURFACE

9.4.7.1 Elastic Shortening/9.4.7.2.1 Shrinkage of Concrete

M_g and M_d should be calculated based on the overall beam length of 96 ft. However, since the elastic shortening loss is a part of the total loss, f_{cgp} will be conservatively computed based on M_g using the design span length of 95 ft

$$f_{cgp} = \frac{960.4}{843.5} + \frac{(960.4)(14.18)^2}{176,829} - \frac{(955.5 + 34.7)(12)(14.18)}{176,829} = 1.278 \text{ ksi}$$

herefore, loss due to elastic shortening:

$$\Delta f_{pES} = \frac{28,500}{3,834}(1.278) = 9.5 \text{ ksi}$$

AASHTO LRFD C5.9.5.3 indicates that the loss due to elastic shortening at transfer should be added to the time-dependent losses to determine total losses. However, this loss is directly accounted for if transformed section properties are used in the stress analysis.

9.4.7.2 Time-Dependent Losses between Transfer and Deck Placement

AASHTO LRFD Art. 5.9.5.4.4 indicates that the time of "deck placement" may be taken as [LRFD Art. 5.9.5.4.4] time of noncomposite topping placement. In this example, the term "deck placement" is interchangeable with topping placement.

The following construction schedule is assumed in calculating the time-dependent losses:

Concrete age at transfer:	$t_i = 1$ day
Concrete age at deck placement:	$t_d = 90$ days
Concrete age at final stage:	$t_f = 20,000$ days

The total time-dependent loss between time of transfer and deck placement is the summation of prestress losses due to shrinkage of concrete, creep of concrete, and relaxation of prestressing strands.

9.4.7.2.1 Shrinkage of Concrete

The prestress loss due to shrinkage of concrete between transfer and deck placement is calculated by:

$$\Delta f_{pSR} = \epsilon_{bid} E_p K_{id} \quad \text{[LRFD Eq. 5.9.5.4.2a-1]}$$

where

- ϵ_{bid} = concrete shrinkage strain of girder for time period between transfer and deck placement
- E_p = modulus of elasticity of prestressing strand, ksi
- K_{id} = transformed section coefficient that accounts for time-dependent interaction between concrete and bonded steel in the section being considered for time period between transfer and deck placement

The concrete shrinkage strain ϵ_{bid} is taken as:

$$\epsilon_{bid} = k_{vs} k_{hs} k_f k_{td} 0.48 \times 10^{-3} \quad \text{[LRFD Eq. 5.4.2.3.3-1]}$$

where

The factor for the effect of the volume-to-surface ratio of the beam:

$$k_{vs} = 1.45 - 0.13(V/S) = 1.45 - 0.13 \times 2.72 = 1.096$$

The minimum value of k_{vs} is 1.0. OK

V/S is the volume-to-surface ratio of the beam.

The humidity factor for shrinkage:

$$k_{hs} = 2.00 - 0.014H = 2.00 - 0.014(70) = 1.020$$

where H = average annual relative humidity (assume 70%)

The factor for the effect of concrete strength:

$$k_f = \frac{5}{1 + f'_{ci}} = \frac{5}{1 + 4.0} = 1.000$$

BOX BEAM (BIII-48), SINGLE SPAN, NONCOMPOSITE SURFACE

9.4.7.2.1 Shrinkage of Concrete/9.4.7.2.3 Relaxation of Prestressing Strands

The time development factor:

$$k_{td} = \frac{t}{61 - 4f'_{ci} + t} = \frac{89}{61 - 4(4.0) + 89} = 0.664 = k_{td}$$

where t is the maturity of concrete (days) = $t_d - t_i = 90 - 1 = 89$ days

$$\epsilon_{bid} = (1.096)(1.020)(1.000)(0.664)(0.48 \times 10^{-3}) = 0.000356$$

$$K_{id} = \frac{1}{1 + \frac{E_p}{E_{ci}} \frac{A_{ps}}{A_g} \left(1 + \frac{A_g (e_{pg})^2}{I_g}\right) [1 + 0.7\Psi_b(t_f, t_i)]} \quad [\text{LRFD Eq. 5.9.5.4.2a-2}]$$

where

e_{pg} = eccentricity of prestressing strand with respect to centroid of girder, in.

$\Psi_b(t_f, t_i)$ = girder creep coefficient at final time due to loading introduced at transfer

For the time between transfer and final time:

$$\Psi_b(t_f, t_i) = 1.9k_{vs}k_{hc}k_{kj}k_{td}t_i^{-0.118} \quad [\text{LRFD Eq. 5.4.2.3.2-1}]$$

$$k_{hc} = 1.56 - 0.008H = 1.56 - 0.008(70) = 1.000$$

$$k_{td} = \frac{t}{61 - 4f'_{ci} + t} = \frac{20000 - 1}{61 - 4(4.0) + (20000 - 1)} = 0.998 = k_{td}$$

$$\Psi_b(t_f, t_i) = 1.9(1.096)(1.000)(1.000)(0.998)(1)^{-0.118} = 2.078$$

$$K_{id} = \frac{1}{1 + \frac{28,500}{3,834} \frac{4.743}{813} \left(1 + \frac{813(14.71)^2}{168,367}\right) [1 + 0.7(2.078)]} = 0.821$$

The prestress loss due to shrinkage of concrete between transfer and deck placement is:

$$\Delta_{pSR} = (0.000356)(28,500)(0.821) = 8.330 \text{ ksi}$$

9.4.7.2.2 Creep of Concrete

The prestress loss due to creep of girder concrete between time of transfer and deck placement is:

$$\Delta f_{pCR} = \frac{E_p}{E_{ci}} f_{cgp} \Psi_b(t_d, t_i) K_{id} \quad [\text{LRFD Eq. 5.9.5.4.2b-1}]$$

where

$\Psi_b(t_d, t_i)$ = girder creep coefficient at time of deck placement due to loading introduced at transfer

$$= 1.9k_{vs}k_{hc}k_{kj}k_{td}t_i^{-0.118} \quad [\text{LRFD Eq. 5.4.2.3.2-1}]$$

$$= 1.9(1.096)(1.000)(1.000)(0.664)(1)^{-0.118} = 1.383$$

$$\Delta f_{pCR} = \frac{28,500}{3,834} (1.278)(1.383)(0.821) = 10.787 \text{ ksi}$$

9.4.7.2.3 Relaxation of Prestressing Strands

The prestress loss due to relaxation of prestressing strands between time of transfer and deck placement is determined as:

$$\Delta f_{pR1} = \frac{f_{pt}}{K_L} \left(\frac{f_{pt}}{f_{py}} - 0.55 \right) \quad [\text{LRFD Eq. 5.9.5.4.2c-1}]$$

where

f_{pt} = stress in prestressing strands immediately after transfer, taken not less than $0.55f_y$

K_L = 30 for low-relaxation strands and 7 for other prestressing steel, unless more accurate manufacturer's data are available

BOX BEAM (BIII-48), SINGLE SPAN, NONCOMPOSITE SURFACE

9.4.7.2.3 Relaxation of Prestressing Strands/9.4.7.3.2 Creep of Concrete

$$\Delta f_{pR1} = \frac{(202.5 - 9.5)}{30} \left(\frac{(202.5 - 9.5)}{243} - 0.55 \right) = 1.571 \text{ ksi}$$

According to LRFD Art. 5.9.5.4.2c, the relaxation loss may also be assumed equal to 1.2 ksi for low-relaxation strands.

9.4.7.3 Time-Dependent Losses between Deck Placement and Final Time

The total time-dependent loss between time of deck placement and final time is the summation of prestress loss due to shrinkage of beam concrete, creep of beam concrete, relaxation of prestressing strands.

9.4.7.3.1 Shrinkage of Concrete

The prestress loss due to shrinkage of concrete between deck placement and final time is calculated by:

$$\Delta f_{pSD} = \epsilon_{bdf} E_p K_{df} \quad [\text{LRFD Eq. 5.9.5.4.2a-1}]$$

where

ϵ_{bdf} = concrete shrinkage strain of girder for time period between deck placement and final time

E_p = modulus of elasticity of prestressing strands, ksi

K_{df} = transformed section coefficient that accounts for time-dependent interaction between concrete and bonded steel in the section being considered for time period between deck placement and final time

The total girder concrete shrinkage strain between transfer and final time is taken as:

$$\begin{aligned} \epsilon_{bif} &= k_{vs} k_{hs} k_{f} k_{tdf} 0.48 \times 10^{-3} \quad [\text{LRFD Eq. 5.4.2.3.3-1}] \\ &= (1.096)(1.020)(1.000)(0.998)(0.48 \times 10^{-3}) = 0.000536 \end{aligned}$$

The girder concrete shrinkage strain between deck placement and final time is:

$$\epsilon_{bdf} = \epsilon_{bif} - \epsilon_{bid} = 0.000536 - 0.000356 = 0.000180$$

The beam concrete transformed section coefficient between deck placement and final time is:

$$K_{df} = \frac{1}{1 + \frac{E_p}{E_{ci}} \frac{A_{ps}}{A_c} \left(1 + \frac{A_c (e_{pc})^2}{I_c} \right) [1 + 0.7 \Psi_b(t_f, t_i)]} \quad [\text{LRFD Eq. 5.9.5.4.3a-2}]$$

where

A_c = A_g = area of the precast beam = 813 in.²

I_c = I_g = moment of inertia of the precast beam = 168,367 in.⁴

e_{pc} = e_{pg} = eccentricity of prestressing strands with respect to centroid of precast beam = 14.71 in.

Because there is no composite deck, the noncomposite beam section properties are used in the calculation.

$$K_{df} = \frac{1}{1 + \frac{28,500}{3,834} \frac{4.743}{813} \left(1 + \frac{813(14.71)^2}{168,367} \right) [1 + 0.7(2.078)]} = 0.821$$

The prestress loss due to shrinkage of concrete between deck placement and final time is:

$$\Delta f_{pSD} = (0.000180)(28,500)(0.821) = 4.212 \text{ ksi}$$

9.4.7.3.2 Creep of Concrete

The prestress loss due to creep of beam concrete between time of deck placement and final time is determined as:

$$\Delta f_{pCD} = \frac{E_p}{E_{ci}} f_{cgp} [\Psi_b(t_f, t_i) - \Psi_b(t_d, t_i)] K_{df} + \frac{E_p}{E_c} \Delta f_{cd} \Psi_b(t_f, t_d) K_{df} \quad [\text{LRFD Eq. 5.9.5.4.3b-1}]$$

BOX BEAM (BIII-48), SINGLE SPAN, NONCOMPOSITE SURFACE

9.4.7.3.2 Creep of Concrete/9.4.7.5 Total Losses at Transfer

where

$$\begin{aligned}\Psi_b(t_f, t_d) &= \text{beam creep coefficient at final time due to loading at deck placement} \\ &= 1.9k_{vs}k_{hc}k_{\beta}k_{tdf}t_d^{-0.118} \quad \text{[LRFD Eq. 5.4.2.3.2-1]}\end{aligned}$$

$$k_{tdf} = \frac{t}{61 - 4f'_{ci} + t} = \frac{(20,000 - 90)}{61 - 4(4.0) + (20,000 - 90)} = 0.998$$

$$\Psi_b(t_f, t_d) = 1.9(1.096)(1.000)(1.000)(0.998)(90)^{-0.118} = 1.222$$

Δf_{cd} = change in concrete stress at centroid of prestressing strands due to long-term losses between transfer and deck placement, combined with deck weight and superimposed loads, ksi

$$\begin{aligned}&= -(\Delta f_{pSR} + \Delta f_{pCR} + \Delta f_{pR1}) \frac{A_{ps}}{A_g} \left(1 + \frac{A_g e_{pg}^2}{I_g} \right) - \left(\frac{(M_b + M_{ws}) e_{tf}}{I_{tf}} \right) \\ &= -(8.330 + 10.787 + 1.571) \frac{4.743}{813} \left(1 + \frac{813(14.71)^2}{168,367} \right) - \left(\frac{(97.0 + 141.0)(12)(14.24)}{175,820} \right) \\ &= -0.478 \text{ ksi}\end{aligned}$$

The gross section properties are used in the equation to calculate Δf_{cd} for the long-term losses since the transformed section effect has already been included in the factor K_{td} when calculating the losses between initial time and deck placement.

$$\Delta f_{pCD} = \frac{28,500}{3,834} (1.278)(2.078 - 1.383)(0.821) + \frac{28,500}{4,287} (-0.478)(1.222)(0.821) = 2.233 \text{ ksi}$$

9.4.7.3.3 Relaxation of Prestressing Strands

The prestress loss due to relaxation of prestressing strands between time of deck placement and final time is taken as:

$$\Delta f_{pR2} = \Delta f_{pR1} = 1.571 \text{ ksi} \quad \text{[LRFD Eq. 5.9.5.4.3c-1]}$$

9.4.7.3.4 Shrinkage of Deck Concrete

The prestress gain due to shrinkage of deck concrete is taken as zero for this bridge because there is no composite deck.

$$\Delta f_{pSS} = 0.0 \text{ ksi}$$

9.4.7.4 Total Time-Dependent Loss

The total time-dependent loss, Δf_{pLT} , is determined as:

$$\begin{aligned}\Delta f_{pLT} &= (\Delta f_{pSR} + \Delta f_{pCR} + \Delta f_{pR1}) + (\Delta f_{pSD} + \Delta f_{pCD} + \Delta f_{pR2} + \Delta f_{pSS}) \quad \text{[LRFD Eq. 5.9.5.4.1-1]} \\ &= (8.330 + 10.787 + 1.571) + (4.212 + 2.233 + 1.571 + 0.0) \\ &= 28.7 \text{ ksi}\end{aligned}$$

9.4.7.5 Total Losses at Transfer

AASHTO LRFD C5.9.5.2.3a and C5.9.5.3 indicate that the losses or gains due to elastic deformation must be taken equal to zero if transformed section properties are used in stress analysis. However, the losses or gains due to elastic deformation must be included in determining the total prestress losses and effective stress in the prestressing strands.

BOX BEAM (BIII-48), SINGLE SPAN, NONCOMPOSITE SURFACE

9.4.7.5 Total Losses at Transfer/9.4.8 Concrete Stresses at Transfer

$$\Delta f_{pi} = \Delta f_{pES} = 9.5 \text{ ksi}$$

Effective stress in tendons immediately after transfer, $f_{pt} = f_{pi} - \Delta f_{pi} = (202.5 - 9.5) = 193.0 \text{ ksi}$

Force per strand = $(f_{pt})(\text{area of strand}) = 193.0(0.153) = 29.5 \text{ kips}$

Therefore, the total prestressing force after transfer, $P_{pt} = 29.5(31) = 914.5 \text{ kips}$

Initial loss percentage = $(\text{Total losses at transfer})/(f_{pi}) = 9.5/(202.5) = 4.7\%$

When determining the concrete stress using transformed section properties, the strand force is that before transfer:

Force per strand = $(202.5)(0.153) = 30.98 \text{ kips}$

The total prestressing force before transfer, $P_{pi} = (30.98)(31) = 960.4 \text{ kips}$

9.4.7.6 Total Losses at Service Loads

Total loss due to elastic shortening at transfer and long-term losses is:

$$\Delta f_{pT} = \Delta f_{pES} + \Delta f_{pLT} = 9.5 + 28.7 = 38.2 \text{ ksi}$$

The elastic gain due to deck weight, superimposed dead load and live load (Service III) is:

$$\begin{aligned} & \left(\frac{(M_b + M_{ws})e_{tf}}{I_{tf}} \right) \frac{E_p}{E_c} + 0.8 \left(\frac{(M_{LT} + M_{LL})e_{tf}}{I_{tf}} \right) \frac{E_p}{E_c} \\ &= \left(\frac{(97.0 + 141.0)(12)(14.24)}{175,820} \right) \frac{28,500}{4,287} + 0.8 \left(\frac{(545.8 + 207.2)(12)(14.24)}{175,820} \right) \frac{28,500}{4,287} \\ &= 1.5 + 3.9 = 5.4 \text{ ksi} \end{aligned}$$

The effective stress in strands after all losses and gains:

$$f_{pe} = f_{pi} - \Delta f_{pT} + 5.4 = 202.5 - 38.2 + 5.4 = 169.7 \text{ ksi}$$

Check prestressing stress limit at service limit state:

[LRFD Table 5.9.3-1]

$$f_{pe} \leq 0.8f_{py} = 0.8(243) = 194.4 \text{ ksi} > 169.7 \text{ ksi} \quad \text{OK}$$

The effective stress in strands after all losses and permanent gains:

$$f_{pe} = f_{pi} - \Delta f_{pT} + 1.5 = 202.5 - 38.2 + 1.5 = 165.8 \text{ ksi}$$

Force per strand without live load gains = $(f_{pe})(\text{area of strand}) = 165.8(0.153) = 25.4 \text{ kips}$

Therefore, the total prestressing force after all losses = $25.4(31) = 787.4 \text{ kips}$

Final loss percentage = $(\text{total losses and gains})/(f_{pi}) = (38.2-1.5)/(202.5) = 18.1\%$

The initial estimate of final losses of 20%, which was used to determine the number of strands, is conservative. Because the assumed initial loss and final loss are close, there is no need to perform a second iteration with the computed total losses.

When determining the concrete stress using transformed section properties, all the elastic gains and losses are implicitly accounted for:

Force per strand with only total time-dependent losses = $(f_{pi} - \Delta f_{pLT})(\text{area of strand}) = (202.5 - 28.7)(0.153) = 26.59 \text{ kips}$

Total prestressing force, $P_{pe} = 26.59(31) = 824.3 \text{ kips}$

9.4.8 CONCRETE STRESSES AT TRANSFER

Because the transformed section is used, total prestressing force before and after transfer, $P_{pi} = 960.4 \text{ kips}$

BOX BEAM (BIII-48), SINGLE SPAN, NONCOMPOSITE SURFACE

9.4.8.1 Stress Limits for Concrete/9.4.8.2 Stresses at Transfer Length Section of Bonded Strands

9.4.8.1 Stress Limits for Concrete

[LRFD Art. 5.9.4]

Compression:

- $0.6f'_{ci} = 0.6(4.0) = +2.400$ ksi

where f'_{ci} = concrete strength at transfer = 4.000 ksi

Tension:

- without bonded auxiliary reinforcement

$$-0.0948 \sqrt{f'_{ci}} \leq -0.200 \text{ ksi} = -0.0948 \sqrt{4.000} = -0.190 \text{ ksi} \leq -0.200 \text{ ksi} \quad \text{OK}$$

- with bonded auxiliary reinforcement that is sufficient to resist 120% of the tension force in the cracked concrete

$$-0.24 \sqrt{f'_{ci}} = -0.24 \sqrt{4.000} = -0.480 \text{ ksi}$$

9.4.8.2 Stresses at Transfer Length Section of Bonded Strands

Stresses at this location need only be checked at transfer, because this stage almost always governs. Also, losses with time will reduce the concrete stresses making them less critical.

Transfer length = 60(strand diameter) = 60(0.5) = 30 in. = 2.5 ft

[LRFD Art. 5.11.4]

The transfer length extends to approximately 2.5 ft from the end of the beam or 2.0 ft from centerline of the bearing. Due to the camber of the beam at transfer, the self weight of the beam and diaphragms act on the overall beam length, 96 ft. Therefore, the values of bending moment given in **Table 9.4.4-1** cannot be used at transfer length because they are based on the design span, 95 ft. Using statics, bending moments at the end of the transfer length due to beam and diaphragm weights, are

$$M_g = 0.5w_g x(L - x) = 0.5(0.847)(2.5)(96 - 2.5) = 99.0 \text{ ft-kips, and}$$

$$M_d = (0.73 + 0.73/2)(2.5) = 2.7 \text{ ft-kips}$$

Compute stress in top of beam:

$$f_t = \frac{P_{pi}}{A_{ti}} - \frac{P_{pi}e_{ti}}{S_{tti}} + \frac{(M_g + M_d)}{S_{tti}} = \frac{960.4}{843.5} - \frac{(960.4)(14.18)}{8,737} + \frac{(99.0 + 2.7)(12)}{8,737}$$

$$= 1.139 - 1.559 + 0.140 = -0.280 \text{ ksi}$$

Tensile stress limit for concrete with no bonded reinforcement: -0.190 ksi NGTensile stress limit for concrete with bonded reinforcement: -0.480 ksi OK

Compute stress in bottom of beam:

$$f_b = \frac{P_{pi}}{A_{ti}} + \frac{P_{pi}e_{ti}}{S_{bti}} - \frac{(M_g + M_d)}{S_{bti}} = \frac{960.4}{843.5} + \frac{(960.4)(14.18)}{9,426} - \frac{(99.0 + 2.7)(12)}{9,426}$$

$$= 1.139 + 1.445 - 0.129 = 2.455 \text{ ksi}$$

Compression stress limit for concrete: 2.400 ksi NG

Therefore, try debonding seven strands from the strand group at 2 in. from bottom for a distance of 5 ft 0 in. from the end of the beam or 4 ft 6 in. from centerline of bearing.

To minimize the shock impact of detensioning and cracks at corners and bottom, assume the strand pattern shown in **Figure 9.4.8.2-1**. LRFD Article 5.11.4.3 requires that the following conditions be satisfied if debonding is used:

- Percentage debonded of total = $7/31 = 22.6\% < 25\%$ OK
- Percentage debonded of row = $7/23 = 30.4\% < 40\%$ OK
- All limit states should be satisfied OK
- Debonded strands should be symmetrically distributed OK
- Exterior strands in each horizontal line are fully bonded OK

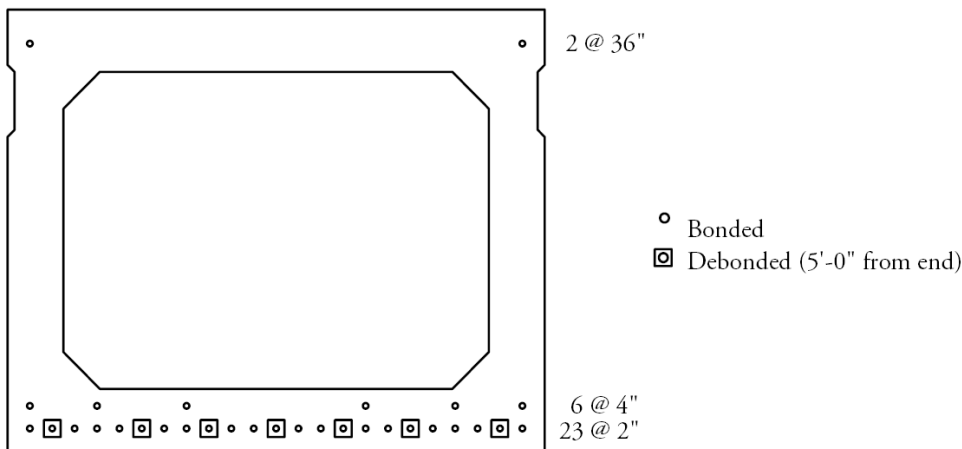
BOX BEAM (BIII-48), SINGLE SPAN, NONCOMPOSITE SURFACE

9.4.8.2 Stresses at Transfer Length Section of Bonded Strands /9.4.8.3 Stresses at Transfer length Section of Debonded Strands

Recompute the stresses at the transfer length section. Note that the transformed section properties here are different than those at midspan after debonding. Using the same method as described in Sect. 9.4.5.5, the transformed section properties at end of beam are computed as:

$$A_{ti} = 836.6 \text{ in.}^2 \qquad y_{bti} = 18.90 \text{ in.} \qquad S_{bti} = 9,253 \text{ in.}^3 \qquad S_{tti} = 8,700 \text{ in.}^3$$

Figure 9.4.8.2-1
Strand Pattern at End of Beam



The distance from the center of gravity of strands to the bottom fiber of the beam is:

$$y_{bs} = [16(2) + 6(4) + 2(36)] / (24) = 5.33 \text{ in.}$$

and the strand eccentricity for the transformed section at end of beam is:

$$e_{eti} = 18.90 - 5.33 = 13.57 \text{ in.}$$

Total prestressing force before transfer at end section = 24(30.98) = 743.5 kips

Concrete stress in top of beam:

$$f_t = \frac{743.5}{836.6} - \frac{743.5(13.57)}{8,700} + \frac{(99.0 + 2.7)(12)}{8,700} = 0.889 - 1.160 + 0.140 = -0.131 \text{ ksi}$$

Tension stress limit for concrete with no bonded reinforcement: -0.190 ksi OK

Thus, there is no need for additional bonded reinforcement.

Concrete stress in bottom of beam:

$$f_b = \frac{743.5}{836.6} + \frac{743.5(13.57)}{9,253} - \frac{(99.0 + 2.7)(12)}{9,253} = 0.889 + 1.090 - 0.132 = +1.847 \text{ ksi}$$

Compressive stress limit for concrete: +2.400 ksi OK

9.4.8.3 Stresses at Transfer Length Section of Debonded Strands

All strands are effective at this location, therefore, use the full value of P_{pi} . Bending moments due to the self weight of the beam and diaphragm, at (5 ft + 2.5 ft = 7.5 ft) from the end of the beam, based on overall length, are:

$$M_g = 0.5w_g x(L - x) = 0.5 (0.847)(7.5)(96 - 7.5) = 281.1 \text{ ft-kips}$$

$$M_d = (0.73 + 0.73/2)7.5 = 8.2 \text{ ft-kips}$$

Concrete stress in top of beam:

$$f_t = \frac{P_{pi}}{A_{ti}} - \frac{P_{pi}e_{ti}}{S_{tti}} + \frac{(M_g + M_d)}{S_{tti}} = \frac{960.4}{843.5} - \frac{(960.4)(14.18)}{8,737} + \frac{(281.1 + 8.2)(12)}{8,737}$$

$$= 1.139 - 1.559 + 0.397 = -0.023 \text{ ksi}$$

Tension stress limit for concrete with no bonded reinforcement: -0.190 ksi OK

BOX BEAM (BIII-48), SINGLE SPAN, NONCOMPOSITE SURFACE

9.4.8.3 Stresses at Transfer length Section of Debonded Strands/9.4.9.1 Stress Limits for Concrete

Concrete stress in bottom of beam:

$$f_b = \frac{P_{pi}}{A_{ti}} + \frac{P_{pi}e_{ti}}{S_{bti}} - \frac{(M_g + M_d)}{S_{bti}} = \frac{960.4}{843.5} + \frac{(960.4)(14.18)}{9,426} - \frac{(281.1 + 8.2)(12)}{9,426}$$

$$= 1.139 + 1.445 - 0.368 = 2.216 \text{ ksi}$$

Compressive stress limit for concrete: +2.400 ksi OK

9.4.8.4 Stresses at Midspan

Bending moments due to beam self weight and diaphragm weight at midspan are

$$M_g = 0.5w_g x(L - x) = 0.5 (0.847)(48)(96 - 48) = 975.7 \text{ ft-kips}$$

$$M_d = \left(0.73 + \frac{0.73}{2}\right)(48) - 0.73(23.75) = 35.2 \text{ ft-kips}$$

$$f_t = \frac{P_{pi}}{A_{ti}} - \frac{P_{pi}e_{ti}}{S_{tti}} + \frac{(M_g + M_d)}{S_{tti}} = \frac{960.4}{843.5} - \frac{(960.4)(14.18)}{8,737} + \frac{(975.7 + 35.2)(12)}{8,737}$$

$$= 1.139 - 1.559 + 1.388 = +0.968 \text{ ksi}$$

Tension stress limit for concrete with no bonded reinforcement: -0.190 ksi OK

and,

$$f_b = \frac{P_{pi}}{A_{ti}} + \frac{P_{pi}e_{ti}}{S_{bti}} - \frac{(M_g + M_d)}{S_{bti}} = \frac{960.4}{843.5} + \frac{(960.4)(14.18)}{9,426} - \frac{(975.7 + 35.2)(12)}{9,426}$$

$$= 1.139 + 1.445 - 1.287 = +1.297 \text{ ksi}$$

Compressive stress limit for concrete: +2.400 ksi OK

9.4.8.5 Summary of Stresses at Transfer

	Top Fiber Stresses f_t , ksi	Bottom Fiber Stresses f_b , ksi
At transfer length section of bonded strands	-0.131	+1.847
At transfer length section of debonded strands	-0.023	+2.216
At midspan	+0.968	+1.297

9.4.9 CONCRETE STRESSES AT SERVICE LOADS

[LRFD Art. 5.9.4.2]

Using transformed section properties and refined losses, $P_{pe} = 824.3$ kips

9.4.9.1 Stress Limits for Concrete

Compression:

Due to permanent loads, i.e., beam self weight, diaphragm weight, wearing surface, and barrier load, for load combination Service I:

$$\text{for precast beams: } 0.45f'_c = 0.45(5.000) = 2.250 \text{ ksi}$$

Due to permanent and transient loads, i.e., all dead loads and live loads, for load combination Service I:

$$\text{for precast beams: } 0.60f'_c = 0.60(5.000) = 3.000 \text{ ksi}$$

Tension:

For components with bonded prestressing tendons:

for load combination Service III:

$$\text{for precast beams: } -0.19\sqrt{f'_c} = -0.19\sqrt{5.000} = -0.425 \text{ ksi}$$

BOX BEAM (BIII-48), SINGLE SPAN, NONCOMPOSITE SURFACE

9.4.9.2 Stresses at Midspan/9.4.9.3 Fatigue Stress Limit

9.4.9.2 Stresses at Midspan**9.4.9.2.1 Concrete Stress at Top Fiber of the Beam**

To check compressive stresses at the top of the beam, two cases are considered.

1: Under permanent load, load combination Service I:

Using values in **Tables 9.4.4-1** and **9.4.4-2**, compute the top fiber stresses:

$$f_{tg} = \frac{P_{pe}}{A_{tf}} - \frac{P_{pe}e_{tf}}{S_{ttf}} + \frac{(M_g + M_d + M_b + M_{ws})}{S_{ttf}}$$

$$= \frac{824.3}{839.8} - \frac{824.3(14.24)}{8,713} + \frac{(955.5 + 34.7 + 97.0 + 141.0)(12)}{8,713}$$

$$= 0.982 - 1.347 + 1.692 = +1.327 \text{ ksi}$$

Compression stress limit for concrete: +2.250 ksi OK

2. Under permanent and transient loads, load combination Service I:

$$f_t = +1.327 + \frac{(M_{LT} + M_{LL})(12)}{S_{ttf}}$$

$$= +1.327 + \frac{(545.8 + 207.2)(12)}{8,713}$$

$$= +1.327 + 1.037 = +2.364 \text{ ksi}$$

Compressive stress limit for concrete: +3.000 ksi OK

9.4.9.2.2 Concrete Stress in Bottom of Beam, Load Combination Service III

$$f_b = \frac{P_{pe}}{A_{tf}} + \frac{P_{pe}e_{tf}}{S_{btf}} - \frac{(M_g + M_d + M_b + M_{ws}) + 0.8(M_{LT} + M_{LL})}{S_{btf}}$$

$$= \frac{824.3}{839.8} + \frac{824.3(14.24)}{9,342} - \frac{[(955.5 + 34.7 + 97.0 + 141.0) + 0.8(545.8 + 207.2)](12)}{9,342}$$

$$= +0.982 + 1.256 - 2.351 = -0.113 \text{ ksi}$$

Tension stress limit for concrete: -0.425 ksi OK

9.4.9.3 Fatigue Stress Limit

LRFD Article 5.5.3.1 also states that in fully prestressed components other than segmentally constructed bridges, the compressive stress due to the Fatigue I load combination and one-half the sum of effective prestress and permanent loads shall not exceed $0.40f'_c$ after losses.

From **Table 9.4.4-2**, the unfactored fatigue bending moment at midspan, M_f , is 206.6 ft-kips. Therefore, stress at the top fiber of the beam due to fatigue load combination I is:

$$f_{tgf} = \frac{1.50(M_f)}{S_{ttf}} = \frac{1.50(206.6)(12)}{8,713} = +0.427 \text{ ksi}$$

At midspan, the top compressive stress due to permanent loads and prestress is:

$$f_{tg} = \frac{P_{pe}}{A_{tf}} - \frac{P_{pe}e_{tf}}{S_{ttf}} + \frac{(M_g + M_d)}{S_{ttf}} + \frac{(M_{ws} + M_b)}{S_{ttf}}$$

$$= \frac{824.3}{839.8} - \frac{(824.3)(14.24)}{8,713} + \frac{(955.5 + 34.7)(12)}{8,713} + \frac{(141 + 97)(12)}{8,713}$$

$$= 0.982 - 1.347 + 1.364 + 0.328 = 1.327 \text{ ksi}$$

BOX BEAM (BIII-48), SINGLE SPAN, NONCOMPOSITE SURFACE

9.4.9.3 Fatigue Stress Limit/9.4.10.2 Minimum Reinforcement

Therefore:

$$f_{tgf} + \frac{f_{tg}}{2} = 0.427 + \frac{1.327}{2} = 1.091 < 0.40(f'_c) = 0.40(5.000) = 2.0 \text{ ksi} \quad \text{OK}$$

This condition should be satisfied at all locations along the beam.

9.4.9.4 Summary of Stresses at Midspan at Service Loads

The stresses calculated using the above methods are summarized in **Table 9.4.9.4 -1**. For comparison, the stresses calculated for the same design example using the previous method of calculating prestress losses are also shown in the table (Example 9.2 in the previous edition of the manual).

Table 9.4.9.4-1
Stresses at Midspan at Service Loads

Design Example	Top of Beam, ksi Service I		Bottom of Beam, ksi Service III
	Permanent Loads	Total Loads	
9.4	+1.327	+2.364	-0.113
9.2	+1.328	+2.386	-0.168

9.4.10 LIMITS OF REINFORCEMENT

9.4.10.1 Maximum Reinforcement

The check of maximum reinforcement in LRFD Article 5.7.3.3.1 was removed from the *LRFD Specifications* in 2005.

9.4.10.2 Minimum Reinforcement

[LRFD Art. 5.7.3.3.2]

At any section, the amount of prestressed and nonprestressed tensile reinforcement must be adequate to develop a factored flexural resistance, M_r , equal to the lesser of:

- 1.2 times the cracking strength determined on the basis of elastic stress distribution and the modulus of rupture, and
- 1.33 times the factored moment required by the applicable strength load combination.

Check at midspan:

$$M_{cr} = S_{btf}(f_r + f_{cpe}) \quad \text{[LRFD Eq. 5.7.3.3.2-1]}$$

The above equation is a simplified form of LRFD Eq. 5.7.3.3.2-1 because a composite section does not exist. Therefore, the composite section modulus and noncomposite section modulus are the same.

where

$$f_r = \text{modulus of rupture of concrete} \quad \text{[LRFD Art. 5.4.2.6]}$$

$$= 0.37\sqrt{f'_c} = 0.37\sqrt{5.000} = 0.827 \text{ ksi}$$

f_{cpe} = compressive stress in concrete due to effective prestress force only (after allowance for all prestress losses) at extreme fiber of section where tensile stress is caused by externally applied loads

$$= \frac{P_{pe}}{A_{tf}} + \frac{P_{pe}e_{tf}}{S_{btf}} = \frac{824.3}{839.8} + \frac{824.3(14.24)}{9,342} = 2.238 \text{ ksi}$$

$$M_{cr} = (0.827 + 2.238)9,342/12 = 2,386 \text{ ft-kips}$$

$$1.2M_{cr} = 1.2(2,386) = 2,863 \text{ ft-kips}$$

BOX BEAM (BIII-48), SINGLE SPAN, NONCOMPOSITE SURFACE

9.4.10.2 Minimum Reinforcement/9.4.11.1 Critical Section

At midspan, the factored moment required by Strength I load combination is:

$$M_u = 2,888.3 \text{ ft-kips (as calculated in Sect. 9.4.6)}$$

$$\text{Thus, } 1.33M_u = 1.33(2,888.3) = 3,841.4 \text{ ft-kips}$$

Since $1.2M_{cr} < 1.33M_u$, the $1.2M_{cr}$ requirement controls.

$$M_r = 3,190.7 \text{ ft-kips} > 1.2M_{cr} \quad \text{OK}$$

Note: The *LRFD Specifications* requires that this criterion be met at every section.

Illustrated based on 2011
LRFD Specifications.

Editor's Note: 2012 *LRFD Specifications* changes will revise minimum reinforcement.

9.4.11 SHEAR DESIGN

The area and spacing of shear reinforcement must be determined at regular intervals along the entire length of the beam. In this design example, transverse shear design procedures are demonstrated below by determining these values at the critical section near the supports.

Transverse shear reinforcement is required when:

$$V_u > 0.5\phi(V_c + V_p) \quad \text{[LRFD Eq. 5.8.2.4-1]}$$

where

V_u = total factored shear force, kips

V_c = nominal shear resistance provided by tensile stresses in the concrete, kips

V_p = component in the direction of the applied shear of the effective prestressing force, kips

ϕ = resistance factor = 0.9 for normal weight concrete [LRFD Art. 5.5.4.2.1]

9.4.11.1 Critical Section

[LRFD Art. 5.8.3.2]

The critical section near the supports is taken as the effective shear depth d_v from the internal face of the support.

d_v = distance between resultants of tensile and compressive forces, $(d_e - a/2)$, but not less than $(0.9d_e)$ or $(0.72h)$ [LRFD Art. 5.8.2.7]

where

d_e = the corresponding effective depth from the extreme compression fiber to the centroid of the tensile force in the tensile reinforcement

a = depth of compression block = 5.74 in. (assumed adequate)

h = overall depth = 39.00 in.

Note: Only 22 strands (16 at 2 in. and 6 at 4 in.) are effective at the critical section for shear, because seven strands are debonded for a distance equal to 5 ft from the end of the beam and the top level of strands is ignored.

Because the beam is a flanged section, the effective shear depth, d_v , should be determined using LRFD Eq. C5.8.2.9-1. However, d_v can be conservatively approximated as $d_e - a/2$ using a as determined in the midspan flexural analysis in Sect. 9.4.6.

$$y_{bs} = [16(2) + 6(4)]/(22) = 2.55 \text{ in.}$$

$$d_e = h - y_{bs} = 39.00 - 2.55 = 36.45 \text{ in.}$$

$$d_v = d_e - a/2 = [36.45 - (5.74/2)] = 33.58 \text{ in.}$$

$$0.9d_e = 0.9(36.45) = 32.81 \text{ in.}$$

$$0.72h = 0.72(39) = 28.08 \text{ in.}$$

Therefore, $d_v = 33.58 \text{ in.}$

BOX BEAM (BIII-48), SINGLE SPAN, NONCOMPOSITE SURFACE

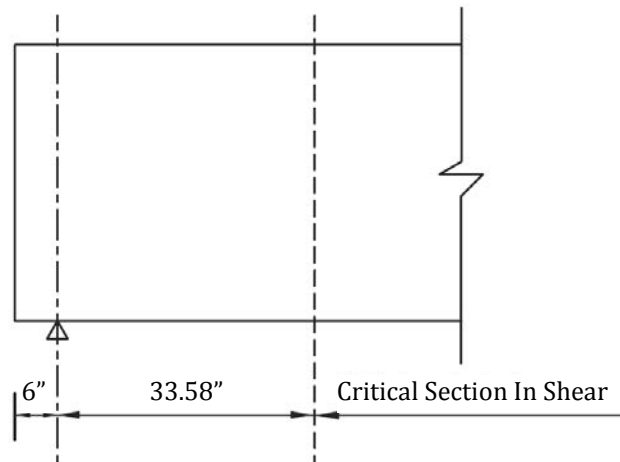
9.4.11.1 Critical Section/9.4.11.2.1 Strain in Flexural Tension Reinforcement

Because the width of the bearing is not yet determined, it is conservatively assumed to be zero for determining the critical section for shear, as shown in **Figure 9.4.11.1-1**. Therefore, the critical section for shear is at a distance of:

33.58 in. = 2.80 ft from centerline of support

$$x/L = 2.80/95 = 0.029L$$

Figure 9.4.11.1-1
Critical Section in Shear



9.4.11.2 Contribution of Concrete to Nominal Shear Resistance

The contribution of the concrete to the nominal shear resistance is:

$$V_c = 0.031\beta\sqrt{f'_c}b_vd_v \quad \text{[LRFD Eq. 5.8.3.3-3]}$$

where β = factor indicating the ability of diagonally cracked concrete to transmit tension (a value indicating concrete contribution).

Several quantities must be determined before this expression can be evaluated.

9.4.11.2.1 Strain in Flexural Tension Reinforcement

Calculate the strain at the centroid of the tension reinforcement, ϵ_s :

$$\epsilon_s = \frac{\frac{|M_u|}{d_v} + 0.5N_u + |(V_u - V_p)| - A_{ps}f_{po}}{(E_sA_s + E_pA_{ps})} \quad \text{[LRFD Eq. 5.8.3.4.2-4]}$$

where

N_u = applied factored axial force at the specified section, $0.029L = 0$ kips

V_u = applied factored shear force at the specified section, $0.029L$

$$= 1.25(37.9 + 1.1 + 3.8) + 1.50(5.6) + 1.75(37.0 + 12.7) \quad \text{(Tables 9.4.4-1 and 9.4.4-2)}$$

$$= 148.9 \text{ kips}$$

V_p = component of the effective prestressing force in the direction of the applied shear

= 0 kips since strand pattern is straight

M_u = applied factored bending moment at the specified section, $0.029L$, or, conservatively taken as the maximum M_u .

$$= 1.25(109.3 + 3.1 + 11.1) + 1.50(16.1) + 1.75(67.1 + 23.7) \quad \text{(Tables 9.4.4-1 and 9.4.4-2)}$$

$$= 337.4\text{ft-kips}$$

BOX BEAM (BIII-48), SINGLE SPAN, NONCOMPOSITE SURFACE

9.4.11.2.1 Strain in Flexural Tension Reinforcement/9.4.11.3.2 Required Area of Reinforcement

M_u need not to be taken less than $(V_u - V_p)d_v = (148.9 - 0)(33.58)/12 = 416.7$ ft-kips. Controls.

A_{ps} = area of prestressing strands on the flexural tension side of the member = $22(0.153) = 3.366$ in.²

f_{po} = a parameter taken as modulus of elasticity of prestressing tendons multiplied by the locked in difference in strain between the prestressing tendons and the surrounding concrete (ksi). For pretensioned members, LRFD Article C5.8.3.4.2 indicates that f_{po} can be taken as $0.70f_{pu}$. (Note: use this for both pretensioned and post-tensioned systems made with stress relieved and low relaxation strands).

$$= 0.70(270.0) = 189.0 \text{ ksi}$$

$$\epsilon_s = \frac{\frac{|416.7(12)|}{33.58} + 0 + |(149.0 - 0)| - 3.366(189.0)}{(0 + 28,500(3.366))} = -3.526 \times 10^{-3}$$

ϵ_s is less than zero. Use $\epsilon_s = 0$.

9.4.11.2.2 Values of β and θ

Assume the section contains at least the minimum amount of transverse reinforcement:

$$\beta = \frac{4.8}{(1 + 750\epsilon_s)} = \frac{4.8}{(1 + 0)} = 4.8 \quad [\text{LRFD Eq. 5.8.3.4.2-1}]$$

Angle of diagonal compressive stresses is:

$$\theta = 29 + 3,500\epsilon_s = 29 + 3,500(0) = 29^\circ \quad [\text{LRFD Eq. 5.8.3.4.2-3}]$$

9.4.11.2.3 Compute Concrete Contribution

The nominal shear resisted by the concrete is:

$$\begin{aligned} V_c &= 0.0316\beta\sqrt{f'_c} b_v d_v & [\text{LRFD Eq. 5.8.3.3-3}] \\ &= 0.0316(4.8)\sqrt{5.0} (10)(33.58) = 113.9 \text{ kips} \end{aligned}$$

9.4.11.3 Contribution of Reinforcement to Nominal Shear Resistance**9.4.11.3.1 Requirement for Reinforcement**

Check if $V_u > 0.5\phi(V_c + V_p)$ [LRFD Eq. 5.8.2.4-1]

$$V_u = 148.9 \text{ kips} > 0.5\phi(V_c + V_p) = [0.5(0.9)](113.9 + 0) = 51.3 \text{ kips}$$

Therefore, transverse shear reinforcement must be provided.

9.4.11.3.2 Required Area of Reinforcement

$$V_u/\phi \leq V_n = V_c + V_s + V_p \quad [\text{LRFD Eq. 5.8.3.3-1}]$$

where

$$\begin{aligned} V_s &= \text{shear resistance provided by shear reinforcement} \\ &= (V_u/\phi) - V_c - V_p = (148.9/0.9) - 113.9 - 0 = 51.5 \text{ kips} \end{aligned}$$

$$V_s = \frac{A_v f_{yh} d_v (\cot \theta + \cot \alpha) (\sin \alpha)}{s} \quad [\text{LRFD Eq. 5.8.3.3-4}]$$

where

$$\begin{aligned} A_v &= \text{area of shear reinforcement within a distance } s, \text{ in.}^2 \\ f_{yh} &= \text{specified yield strength of shear reinforcement, ksi} \\ \alpha &= \text{angle of inclination of transverse reinforcement to longitudinal axis} \\ &= 90^\circ \text{ for vertical stirrups} \\ s &= \text{spacing of stirrups, in.} \end{aligned}$$

BOX BEAM (BIII-48), SINGLE SPAN, NONCOMPOSITE SURFACE

9.4.11.3.2 Required Area of Reinforcement/9.4.11.4 Maximum Nominal Shear Resistance

Therefore, area of shear reinforcement within a spacing, s , is:

$$A_v = (sV_s)/(f_{yh}d_v \cot \theta)$$

$$= s(51.5)/[(60)(33.58)\cot 29^\circ] = 0.0142(s) \text{ in.}^2$$

If $s = 12$ in., then $A_v = 0.17 \text{ in.}^2/\text{ft}$

9.4.11.3.3 Determine Spacing of Reinforcement

Check maximum spacing of transverse reinforcement:

[LRFD Art. 5.8.2.7]

Check if $v_u < 0.125f'_c$

$$v_u = \frac{|V_u - \phi V_p|}{\phi b_v d_v} = \frac{|148.9 - 0|}{(0.9)(10)(33.58)} = 0.493 \text{ ksi} \quad \text{[LRFD Eq. 5.8.2.9-1]}$$

$$0.125f'_c = 0.125(5.0) = 0.625 \text{ ksi}$$

Since $v_u < 0.125f'_c$

[LRFD Eq. 5.8.2.7-1]

$s \leq 24$ in. (Controls)

$$s \leq 0.8d_v = (0.8)(33.58) = 26.86 \text{ in.}$$

s provided = 12 in. < 24 in. OK

Use No. 3 single leg in each web at 12 in. spacing

A_v provided = 0.22 in.²/ft > A_v required = 0.17 in.² OK

$$V_s = \frac{0.22(60)(33.58)(\cot 29^\circ)}{12} = 66.6 \text{ kips}$$

9.4.11.3.4 Minimum Reinforcement Requirement

[LRFD Art. 5.8.2.5]

The area of transverse reinforcement should not be less than:

$$0.0316\sqrt{f'_c} \frac{b_v s}{f_{yh}} = 0.0316\sqrt{5} \frac{(10)(12)}{60.0} = 0.14 \text{ in.}^2/\text{ft} < 0.22 \text{ in.}^2/\text{ft} \quad \text{OK} \quad \text{[LRFD Eq. 5.8.2.5-1]}$$

9.4.11.4 Maximum Nominal Shear Resistance

In order to assure that the concrete in the web of the beam will not crush prior to yield of the transverse reinforcement, the *LRFD Specifications* gives an upper limit for V_n as follows:

$$V_n = 0.25f'_c b_v d_v + V_p \quad \text{[LRFD Eq. 5.8.3.3-2]}$$

Comparing this equation with [LRFD Eq. 5.8.3.3-1], it can be concluded that

$$V_c + V_s \text{ must not be greater than } 0.25f'_c b_v d_v$$

$$113.9 + 66.6 = 180.5 \text{ kips} \leq 0.25(5.0)(10)(33.58) = 419.8 \text{ kips} \quad \text{OK}$$

Using the above procedures, shear design was carried out at tenth points along the span. The results are shown below in **Table 9.4.11.4-1**.

BOX BEAM (BIII-48), SINGLE SPAN, NONCOMPOSITE SURFACE

9.4.11.4 Maximum Nominal Shear Resistance

*Table 9.4.11.4-1 [Changes highlighted]
Design for Vertical Shear*

Distance x , ft	Section x/L	Shear V_u kips	Moment M_u ft-kips	d_v in.	A_{ps} in. ²	Strain ϵ_s in./in. $\times 10^{-3}$	Actual θ deg	β	V_c kips	V_s kips	Maximum Spacing in.	A_v in. ² /ft	Minimum A_v in. ² /ft
2.80 ^[1]	0.029	148.9	416.7	33.58	3,366	-3.526	29.0	4.8	113.9	51.5	24	0.17	0.14
9.5	0.1	131.0	1,060	33.59	4,437	-2.601	29.0	4.8	113.9	31.7	24	0.07	0.14
19.0	0.2	106.7	1,877	33.41	4,437	-0.457	29.0	4.8	113.3	5.3	24	0.01	0.14
28.5	0.3	82.0	2,448	33.41	4,437	0.970	32.4	2.8	66.1	25.0	24	0.06	0.14
38.0	0.4	58.7	2,771	33.41	4,437	1.703	35.0	2.1	49.6	15.6	24	0.04	0.14
47.5	0.5	35.9	2,889	33.41	4,437	1.858	35.5	2.0	47.2	—	24	—	0.14

[1] Critical section for shear (see Sect. 9.4.11.1)

BOX BEAM (BIII-48), SINGLE SPAN, NONCOMPOSITE SURFACE

9.4.12 Interface Shear Transfer/9.4.13.1 Required Reinforcement at Face of Bearing

9.4.12 INTERFACE SHEAR TRANSFER

Because there is no cast-in-place composite deck, calculations for interface shear transfer are not required.

9.4.13 MINIMUM LONGITUDINAL REINFORCEMENT REQUIREMENT [LRFD ART. 5.8.3.5]

Longitudinal reinforcement should be proportioned so that at each section the following equation is satisfied:

$$A_{ps}f_{ps} + A_s f_y \geq \frac{M_u}{d_v \phi_f} + 0.5 \frac{N_u}{\phi_c} + \left(\left| \frac{V_u}{\phi_v} - V_p \right| - 0.5V_s \right) \cot \theta \quad [\text{LRFD Eq. 5.8.3.5-1}]$$

where

A_{ps} = area of prestressing strand at the tension side of the section, in.²

f_{ps} = average stress in prestressing strand at the time for which nominal resistance is required, ksi

A_s = area of nonprestressed tension reinforcement, in.²

f_y = specified yield strength of reinforcing bars, ksi

M_u = factored moment at the section corresponding to the factored shear force, ft-kips

d_v = effective shear depth, in.

ϕ = resistance factor as appropriate for moment, shear, and axial resistance. Therefore, different ϕ factors will be used for the terms in LRFD Eq. 5.8.3.5-1, depending on the type of action considered.

N_u = applied factored axial force = 0 kips

V_u = factored shear force at section, kips

V_p = component in the direction of the applied shear of the effective prestressing force, kips

V_s = shear resistance provided by shear reinforcement, kips

θ = angle of inclination of diagonal compressive stresses

9.4.13.1 Required Reinforcement at Face of Bearing

For simple end supports, the longitudinal reinforcement on the flexural tension side of the member at inside face of bearing should satisfy:

$$A_{ps}f_{ps} + A_s f_y \geq \left(\left| \frac{V_u}{\phi_v} - 0.5V_s - V_p \right| \right) \cot \theta \quad [\text{LRFD Eq. 5.8.3.5-2}]$$

$M_u = 0$ ft-kips

$N_u = 0$ kips

Because the width of the bearing is not yet determined, it is assumed to be zero. This assumption is conservative for these calculations. Therefore, the failure crack assumed for this analysis radiates from the centerline of the bearing, 6 in. from the end of the beam.

From **Tables 9.4.4-1** and **9.4.4-2**, using load combination Strength I, the factored shear force at this section is:

$$V_u = 1.25(40.2 + 1.1 + 4.1) + 1.5(5.9) + 1.75(38.3 + 13.5) = 156.3 \text{ kips}$$

$$\left(\frac{V_u}{\phi} - 0.5V_s - V_p \right) \cot \theta = \left(\frac{156.3}{0.9} - 0.5(66.6) - 0 \right) \cot 29^\circ = 253.2 \text{ kips}$$

As shown in **Figure 9.4.13.1-1**, the assumed crack plane crosses the centroid of the 22 bonded bottom strands at a distance of $(6 + y_{bc} \cot \theta)$ from the end of the beam. Since the transfer length is 30 in. from the end of the beam (60 times the strand diameter), the available prestress from the 22 straight strands is a fraction of the effective prestress, f_{pe} , in these strands.

BOX BEAM (BIII-48), SINGLE SPAN, NONCOMPOSITE SURFACE**9.4.13.1 Required Reinforcement at Face of Bearing/9.4.14.1 Anchorage Zone Reinforcement**

Note: This crack is quite unlikely because it would form in the end block, which is a large solid section of concrete. However, the analysis does not account for the area of concrete involved. It simply assumes a crack.

For the 22 bonded bottom strands, $y_{bc} = \frac{2(16) + 6(4)}{22} = 2.55$ in.

Therefore, $6 + y_{bc} \cot \theta = 6 + 2.55(\cot 29^\circ) = 10.60$ in. < 30 in.

Since the location is within the transfer length, the available prestressing force is less than the effective prestressing force. The prestressing force at the center line of bearing is:

$$A_{ps}f_{ps} + A_s f_y = (22)(0.153) \left((202.5 - 38.2) \frac{10.60}{30} \right) + 0 = 195.4 \text{ kips} < 253.2 \text{ kips} \quad \text{NG}$$

The strands are not adequate to resist the required longitudinal force. Therefore, provide additional nonprestressed reinforcement to carry the difference.

Force to be resisted by additional reinforcement = $253.2 - 195.4 = 57.8$ kips

Additional nonprestressed reinforcement required = $(57.8 \text{ kips}) / (60 \text{ ksi}) = 0.96 \text{ in.}^2$

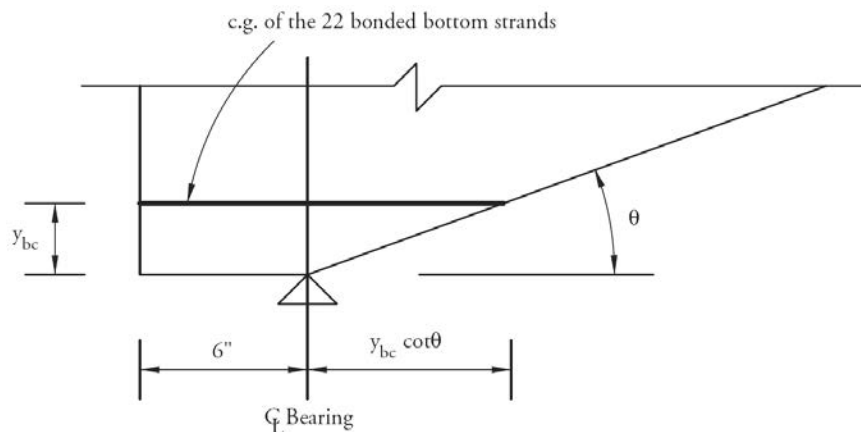
Use five No. 4 bars

The area of steel provided = $5 \times 0.20 = 1.00 \text{ in.}^2$

This reinforcement could be eliminated by using a 7-in. wide bearing:

$$A_{ps} f_s = 22(0.153) \left[(202.5 - 38.2) \left(\frac{10.60 + 3.5}{30} \right) \right] = 259.9 \text{ kips} > 253.2 \text{ kips} \quad \text{OK}$$

Note: An alternative approach for the calculation of available prestressing force excluding the gains from deck shrinkage is illustrated in Section 9.6.13.1.

Figure 9.4.13.1-1**Assumed Failure Crack****9.4.14 PRETENSIONED ANCHORAGE ZONE**

[LRFD Art. 5.10.10]

9.4.14.1 Anchorage Zone Reinforcement

Design of the anchorage zone reinforcement is computed using the force in the strands just before transfer. Since seven strands are debonded at the ends of the beam, the force in the remaining strands before transfer is:

$$P_{pi} = 24(0.153)(202.5) = 743.6 \text{ kips}$$

The bursting resistance, P_r , should not be less than 4.0% of P_{pi}

$$P_r = f_s A_s \geq 0.04 P_{pi} = 0.04(743.6) = 29.7 \text{ kips}$$

where

A_s = total area of vertical reinforcement located within the distance $h/4$ from the end of the beam, in.²

f_s = allowable stress in steel, but taken not greater than 20 ksi

BOX BEAM (BIII-48), SINGLE SPAN, NONCOMPOSITE SURFACE

9.4.14.1 Anchorage Zone Reinforcement/9.4.15.2 Deflection Due to Beam Self Weight

Solving for the required area of steel, $A_s = 29.7/(20) = 1.49 \text{ in.}^2$

At least 1.49 in.^2 of vertical transverse reinforcement should be provided within a distance of $h/4 = 39/4 = 9.75 \text{ in.}$ from the end of the beam.

Use orthogonal welded wire reinforcement (WWR) of W20 or D20 wires at 12 in. centers vertically and horizontally.

Space two layers of WWR at 3 in. starting at 2 in. from, and parallel to the end of the beam in the diaphragm. The layers of WWR each provide four vertical and three horizontal wires. Area of steel provided is $2(4 + 3)(0.2) = 2.80 \text{ in.}^2$ Alternatively, a reinforcing bar cage could be used. Provide adequate embedment for bars.

9.4.14.2 Confinement Reinforcement

LRFD Article 5.10.10.2 requires that transverse reinforcement be provided in the bottom flange and anchored by extending the leg of the stirrup into the web of the girder. The article does not state how much transverse reinforcement should be provided in box beams.

9.4.15 DEFLECTION AND CAMBER

[LRFD Art. 5.7.3.6.2]

Deflections are calculated using the modulus of elasticity of concrete calculated in Section 9.4.3, and the gross section properties of the noncomposite precast beam.

9.4.15.1 Deflection Due to Prestressing Force at Transfer

$$\Delta_p = \frac{P_{pt} e_c L^2}{8E_{ci} I_g}$$

where

Δ_p = camber due to prestressing force after transfer, in.

P_{pt} = total prestressing force after transfer = $31(29.5) = 914.5 \text{ kips}$

e_c = eccentricity of prestressing strand at midspan = 14.71 in.

L = overall beam length = 96.0 ft

E_{ci} = modulus of elasticity at transfer = $3,834 \text{ ksi}$

I_g = moment of inertia of the noncomposite precast beam = $168,367 \text{ in.}^4$

$$\Delta_p = \frac{(914.5)(14.71)(96 \times 12)^2}{(8)(3,834)(168,367)} = 3.46 \text{ in. } \uparrow$$

9.4.15.2 Deflection Due to Beam Self Weight

$$\Delta_g = \frac{5w_g L^4}{384E_{ci} I_g}$$

where

Δ_g = deflection due to beam self weight, in.

w_g = beam self weight = 0.847 kips/ft

Deflection due to beam self weight at transfer:

L = overall beam length = 96.0 ft

$$\Delta_g = \frac{5 \left(\frac{0.847}{12} \right) (96 \times 12)^4}{(384)(3,834)(168,367)} = 2.51 \text{ in. } \downarrow$$

Deflection due to beam self weight at erection:

L = design span = 95.0 ft

$$\Delta_g = \frac{5 \left(\frac{0.847}{12} \right) (95 \times 12)^4}{(384)(3,834)(168,367)} = 2.40 \text{ in. } \downarrow$$

BOX BEAM (BIII-48), SINGLE SPAN, NONCOMPOSITE SURFACE

9.4.15.3 Deflection Due to Diaphragm Weight/9.4.15.6 Deflection Due to Live Load and Impact

9.4.15.3 Deflection Due to Diaphragm Weight

$$\Delta_d = \frac{19P_d L^3}{384E_{ci}I_g}$$

where

 Δ_d = deflection due to diaphragm weight, in. P_d = diaphragm weight concentrated at quarter points = 0.73 kips

Deflection due to diaphragm weight at transfer:

 L = overall beam length = 96.0 ft

$$\Delta_d = \frac{19(0.73)(96 \times 12)^3}{(384)(3,834)(168,367)} = 0.09 \text{ in. } \downarrow$$

Deflection due to diaphragm weight at erection:

 L = design span = 95.0 ft

$$\Delta_d = \frac{19(0.73)(95 \times 12)^3}{(384)(3,834)(168,367)} = 0.08 \text{ in. } \downarrow$$

9.4.15.4 Deflection Due to Barrier and Wearing Surface Weights

$$\Delta_{b+ws} = \frac{5(w_b + w_{ws})L^4}{384E_c I_g}$$

where

 Δ_{b+ws} = deflection due to barrier and wearing surface weights, in. w_b = barrier weight = 0.086 kips/ft w_{ws} = wearing surface weight = 0.125 kips/ft L = design span = 95.0 ft because these loads are applied to the structure in its final location

$$\Delta_{b+ws} = \frac{5 \left(\frac{0.211}{12} \right) (95 \times 12)^4}{(384)(4,287)(168,367)} = 0.54 \text{ in. } \downarrow$$

9.4.15.5 Deflection and Camber SummaryAt transfer: $(\Delta_p + \Delta_g + \Delta_d) = 3.46 - 2.51 - 0.09 = 0.86 \text{ in. } \uparrow$

Total deflection at erection using PCI multipliers (see PCI Design Handbook):

$$1.8(3.46) - 1.85(2.51 + 0.09) = 1.42 \text{ in. } \uparrow$$

Long-Term Deflection:

LRFD Article 5.7.3.6.2, states that the long-time deflection may be taken as the instantaneous deflection multiplied by a factor, 4.0, if the instantaneous deflection is based on gross moment of inertia. However, a factor of 4.0 is not appropriate for this type of precast construction. Therefore, it is recommended that the designer follow the guidelines of the owner agency for which the bridge is being designed, or undertake a more rigorous time-dependent analysis.

9.4.15.6 Deflection Due to Live Load and Impact

Live load deflection limit (optional) = Span/800

[LRFD Art. 2.5.2.6.2]

$$= \left(95 \times \frac{12}{800} \right) = 1.43 \text{ in.}$$

BOX BEAM (BIII-48), SINGLE SPAN, NONCOMPOSITE SURFACE

9.4.15.6 Deflection Due to Live Load and Impact

If the owner invokes the optional live load deflection criteria specified in Art. 2.5.2.6.2, the deflection is the greater of

- that resulting from the design truck plus impact, Δ_{LT} , or
- that resulting from 25% of the design truck plus impact, Δ_{LT} , taken together with the design lane load, Δ_{LL} .

Note: LRFD Article 2.5.2.6.2 states that the dynamic load allowance be included in the calculation of live load deflection.

The *LRFD Specifications* state that all the beams should be assumed to deflect equally [LRFD Art. 2.5.2.6.2]
under the applied live load and impact.

Therefore, the distribution factor for deflection, *DFD*, is calculated as follows:

$$DFD = (\text{number of lanes/number of beams}) \qquad \qquad \qquad \text{[LRFD Art. C2.5.2.6.2]}$$

$$= (2/7) = 0.286 \text{ lanes/beam}$$

However, it is more conservative to use the distribution factor for moment, *DFM*.

Deflection due to lane load

Design lane load, $w = 0.64DFM = 0.64(0.287) = 0.184 \text{ kips/ft/beam}$

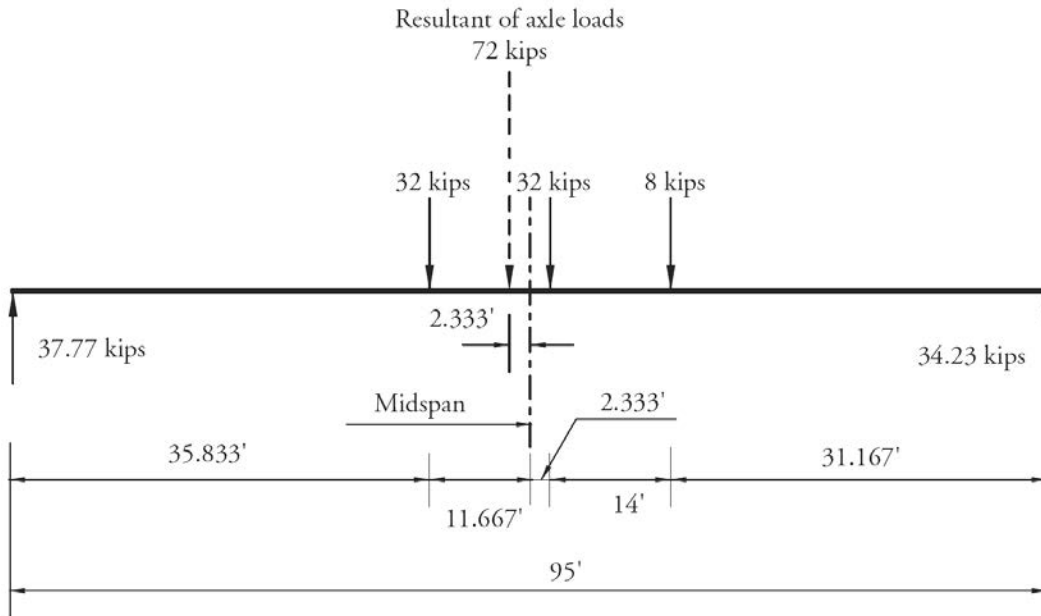
$$\Delta_{LL} = \frac{5wL^4}{384E_cI_g} = \frac{5\left(\frac{0.184}{12}\right)(95 \times 12)^4}{(384)(4,287)(168,367)} = 0.47 \text{ in.} \downarrow$$

Deflection due to Design Truck Load with Impact:

To obtain maximum moment and deflection at midspan due to the truck load, let the centerline of the beam coincide with the middle point of the distance between the inner 32-kip axle and the resultant of the truck load, as shown in **Figure 9.4.15.6-1**.

Figure 9.4.15.6-1

Design Truck Axle Load Position on the Span for Maximum Moment [use larger arrowheads on dimension lines]



Using the elastic moment area, deflection at midspan is:

$$\Delta_{LT} = 2.90(IM)(DFM) = 2.90(1.33)(0.287) = 1.11 \text{ in.} \downarrow$$

BOX BEAM (BIII-48), SINGLE SPAN, NONCOMPOSITE SURFACE

9.4.15.6 Deflection Due to Live Load and Impact/9.4.16 Transverse Post-Tensioning

Therefore, live load deflection is the greater of:

$$\Delta_{LT} = 1.11 \text{ in. } \downarrow \text{ (Controls)}$$

$$0.25 \Delta_{LT} + \Delta_{LL} = 0.25(1.11) + 0.47 = 0.75 \text{ in. } \downarrow$$

Allowable live load deflection: 1.43 in. > 1.11 in. OK

9.4.16 TRANSVERSE POST-TENSIONING

Article C4.6.2.2.1 in the *LRFD Specifications* states that for bridge type (*g*), the structure acts as a monolithic unit if sufficiently interconnected. To satisfy this requirement, the *LRFD Specifications* recommends that a minimum average transverse prestress of 0.250 ksi be used. However, definition of the contact area for that post-tensioning is unclear as to whether it is the shear key, the diaphragm, or the entire box side surface. Instead of an empirical minimum, El-Remaly (1996) recommends that the entire deck surface be modeled as a rigid assembly of gridwork with adequate post-tensioning to provide for a continuous transverse member at the diaphragm locations. A design chart based on this theory is given in Chapter 8 for the required transverse post-tensioning per unit length of span.

According to the chart, for a 28 ft-wide bridge with 39 in. deep beams, an effective post-tensioning force of 4.0 kips/ft is required. Since diaphragms are provided at quarter-points of the span, the post-tensioning force required is:

$$4.0(23.75) = 95 \text{ kips/diaphragm}$$

It is recommended that transverse post-tensioning consist of one tendon near the top and another near the bottom in order to provide sufficient flexural strength.

Use 160-ksi prestressing bars. Assume the effective prestress to be 55 percent of the ultimate strength of the bar.

$$P_{eff} = 0.55(160)A_{PT} = 88.0A_{PT} \text{ kips}$$

$$\text{Thus, total required } A_{PT} = \frac{95.0}{88.0} = 1.08 \text{ in.}^2/\text{diaphragm}$$

Try (2) $\frac{7}{8}$ in. diameter, 160 ksi, bars.

$$\text{The total area provided is } A_{PT} = 2(0.601) = 1.202 \text{ in.}^2$$

$$\text{Total provided post-tensioning force} = (1.202)(0.55)(160) = 105.8 \text{ kips/diaphragm} > 95.0 \text{ kips/diaphragm} \quad \text{OK}$$

If the post-tensioning bars are positioned so that they are concentric with the diaphragm cross section, concrete stress due to the effective prestressing force is:

$$105.8/(8)(39) = 0.339 \text{ ksi}$$

This page intentionally left blank

BOX BEAM (BIII-48), SINGLE SPAN, COMPOSITE DECK

Transformed Sections, Shear General Procedure, Refined Losses

Table of Contents

9.5.1 INTRODUCTION.....	9.5 - 5
9.5.1.1 Terminology.....	9.5 - 5
9.5.2 MATERIALS.....	9.5 - 6
9.5.3 CROSS-SECTION PROPERTIES FOR A TYPICAL INTERIOR BEAM.....	9.5 - 7
9.5.3.1 Noncomposite, Nontransformed Beam Section.....	9.5 - 7
9.5.3.2 Composite Section.....	9.5 - 8
9.5.3.2.1 Effective Flange Width.....	9.5 - 8
9.5.3.2.2 Modular Ratio between Slab and Beam Concrete.....	9.5 - 8
9.5.3.2.3 Transformed Section Properties.....	9.5 - 8
9.5.4 SHEAR FORCES AND BENDING MOMENTS.....	9.5 - 10
9.5.4.1 Shear Forces and Bending Moments Due to Dead Loads.....	9.5 - 10
9.5.4.1.1 Dead Loads.....	9.5 - 10
9.5.4.1.2 Unfactored Shear Forces and Bending Moments.....	9.5 - 11
9.5.4.2 Shear Forces and Bending Moments Due to Live Loads.....	9.5 - 11
9.5.4.2.1 Live Load Distribution Factors for a Typical Interior Beam.....	9.5 - 11
9.5.4.2.2.1 Distribution Factor for Bending Moments.....	9.5 - 12
9.5.4.2.2.2 Distribution Factor for Shear Force.....	9.5 - 13
9.5.4.2.3 Dynamic Allowance.....	9.5 - 13
9.5.4.2.4 Unfactored Shear Forces and Bending Moments.....	9.5 - 13
9.5.4.2.4.1 Due to Truck Load; V_{LT} and M_{LT}	9.5 - 13
9.5.4.2.4.2 Due to Design Lane Load; V_{LL} and M_{LL}	9.5 - 14
9.5.4.3 Load Combinations.....	9.5 - 15
9.5.5 ESTIMATE REQUIRED PRESTRESS.....	9.5 - 16
9.5.5.1 Service Load Stresses at Midspan.....	9.5 - 16
9.5.5.2 Stress Limits for Concrete.....	9.5 - 17
9.5.5.3 Required Number of Strands.....	9.5 - 17
9.5.5.4 Strand Pattern.....	9.5 - 17
9.5.5.5 Steel Transformed Section Properties.....	9.5 - 18
9.5.6 STRENGTH LIMIT STATE.....	9.5 - 19
9.5.7 PRESTRESS LOSSES.....	9.5 - 21
9.5.7.1 Elastic Shortening.....	9.5 - 21
9.5.7.2 Time-Dependent Losses between Transfer and Deck Placement.....	9.5 - 22
9.5.7.2.1 Shrinkage of Concrete.....	9.5 - 22
9.5.7.2.2 Creep of Concrete.....	9.5 - 24
9.5.7.2.3 Relaxation of Prestressing strands.....	9.5 - 24
9.5.7.3 Time-Dependent Losses between Deck Placement and Final Time.....	9.5 - 24
9.5.7.3.1 Shrinkage of Concrete.....	9.5 - 24
9.5.7.3.2 Creep of Concrete.....	9.5 - 25
9.5.7.3.3 Relaxation of Prestressing Strands.....	9.5 - 26

BOX BEAM (BIII-48), SINGLE SPAN, COMPOSITE DECK

Transformed Sections, Shear General Procedure, Refined Losses

Table of Contents

9.5.7.3.4 Shrinkage of Deck Concrete 9.5 - 26

9.5.7.3.5 Total Time-Dependent Loss..... 9.5 - 27

9.5.7.3.6 Total Losses at Transfer 9.5 - 27

9.5.7.3.7 Total Losses at Service Loads..... 9.5 - 27

9.5.8 CONCRETE STRESSES AT TRANSFER 9.5 - 28

9.5.8.1 Stress Limits for Concrete..... 9.5 - 28

9.5.8.2 Stresses at Transfer Length Section 9.5 - 28

9.5.8.3 Stresses at Transfer Length Section of Debonded Strands 9.5 - 30

9.5.8.4 Stresses at Midspan 9.5 - 30

9.5.8.5 Summary of Stresses at Transfer..... 9.5 - 30

9.5.9 CONCRETE STRESSES AT SERVICE LOADS..... 9.5 - 31

9.5.9.1 Stress Limits for Concrete..... 9.5 - 31

9.5.9.2 Stresses at Midspan 9.5 - 31

9.5.9.3 Fatigue Stress Limit 9.5 - 32

9.5.9.4 Summary of Stresses at Service Loads..... 9.5 - 32

9.5.9.5 Effect of Deck Shrinkage 9.5 - 32

9.5.10 LIMITS OF REINFORCEMENT..... 9.5 - 33

9.5.10.1 Maximum Reinforcement..... 9.5 - 33

9.5.10.2 Minimum Reinforcement 9.5 - 33

9.5.11 SHEAR DESIGN..... 9.5 - 33

9.5.11.1 Critical Section..... 9.5 - 34

9.5.11.2 Contribution of Concrete to Nominal Shear Resistance 9.5 - 35

9.5.11.2.1 Strain in Flexural Tension Reinforcement..... 9.5 - 35

9.5.11.2.2 Values of β and θ 9.5 - 36

9.5.11.3 Compute Concrete Contribution 9.5 - 36

9.5.11.3 Contribution of Reinforcement to Nominal Shear Resistance 9.5 - 36

9.5.11.3.1 Requirement for Reinforcement 9.5 - 36

9.5.11.3.2 Required Area of Reinforcement 9.5 - 36

9.5.11.3.3 Determine Spacing of Reinforcement 9.5 - 37

9.5.11.3.4 Minimum Reinforcement Requirement..... 9.5 - 37

9.5.11.4 Maximum Nominal Shear Resistance..... 9.5 - 37

9.5.12 INTERFACE SHEAR TRANSFER..... 9.5 - 37

9.5.12.1 Factored Horizontal Shear 9.5 - 37

9.5.12.2 Required Nominal Resistance 9.5 - 38

9.5.12.3 Required Interface Shear Reinforcement..... 9.5 - 38

9.5.12.3.1 Minimum Interface Shear Reinforcement 9.5 - 38

9.5.12.4 Maximum Nominal Shear Resistance..... 9.5 - 39

9.5.13 MINIMUM LONGITUDINAL REINFORCEMENT REQUIREMENT 9.5 - 39

9.5.13.1 Required Reinforcement at Face of Bearing..... 9.5 - 39

BOX BEAM (BIII-48), SINGLE SPAN, COMPOSITE DECK

Transformed Sections, Shear General Procedure, Refined Losses

Table of Contents

9.5.14 PRETENSIONED ANCHORAGE ZONE 9.5 - 41

 9.5.14.2 Confinement Reinforcement 9.5 - 41

9.5.15 DEFLECTION AND CAMBER 9.5 - 41

 9.5.15.1 Deflection Due to Prestressing Force at Transfer 9.5 - 41

 9.5.15.2 Deflection Due to Beam Self Weight 9.5 - 42

 9.5.15.3 Deflection Due to Slab and Haunch Weights 9.5 - 42

 9.5.15.4 Deflection Due to Diaphragm Weight 9.5 - 42

 9.5.15.5 Deflection Due to Barrier and Wearing Surface Weights 9.5 - 43

 9.5.15.6 Deflection and Camber Summary 9.5 - 43

 9.5.15.7 Deflection Due to Live Load and Impact 9.5 - 43

BOX BEAM (BIII-48), SINGLE SPAN, COMPOSITE DECK

This page intentionally left blank

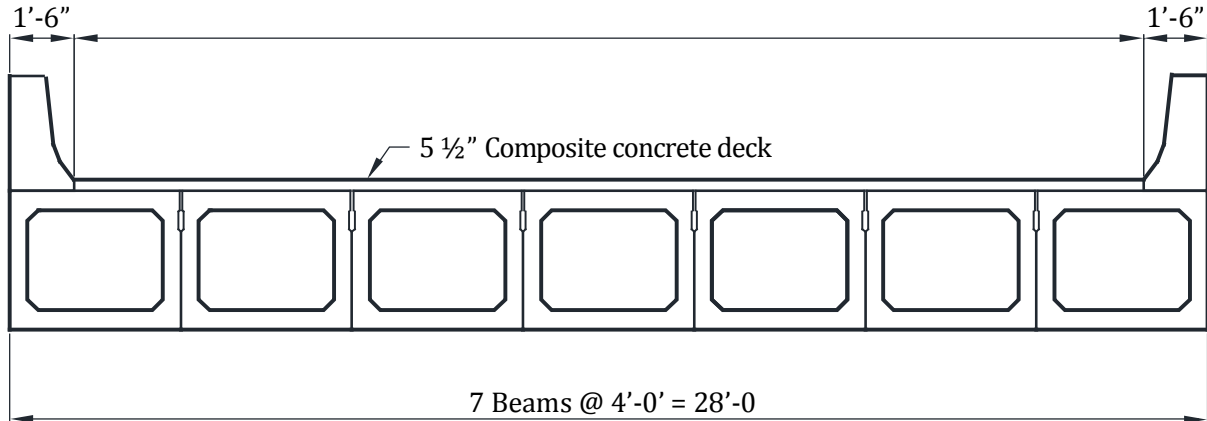
BOX BEAM (BIII-48), SINGLE SPAN, COMPOSITE DECK

9.5.1 Introduction/9.5.1.1 Terminology

9.5 Transformed Sections, Shear General Procedure, Refined Losses**9.5.1 INTRODUCTION**

This design example demonstrates the design of a 95-ft-long, single span, AASHTO Type BIII-48 box beam bridge with no skew. This example illustrates, in detail, the design of a typical interior beam at the critical sections in positive flexure, shear, and deflection due to prestress, dead loads, and live loads. The superstructure consists of seven adjacent beams, as shown in **Figure 9.5.1-1**. Beams are designed to act compositely with a 5.5-in.-thick cast-in-place concrete deck to resist all superimposed dead loads, live loads, and impact. A ½-in.-thick wearing surface is considered to be an integral part of the 5.5-in.-thick deck. Design live load is HL-93. The design is accomplished in accordance with the *AASHTO LRFD Bridge Design Specifications*, Fifth Edition, 2010, and the 2011 Interim Revisions. Elastic stresses from external loads are calculated using transformed sections. Shear strength is calculated using the general procedure. Time-dependent prestress losses are calculated using the refined estimates.

Figure 9.5.1-1
Bridge Cross Section

**9.5.1.1 Terminology**

The following terminology is used to describe cross sections in this design example:

noncomposite section—the concrete beam cross section.

noncomposite nontransformed section—the concrete beam cross section without the strands transformed. Also called the gross section.

noncomposite transformed section—the concrete beam cross section with the strands transformed to provide cross-sectional properties equivalent to the beam concrete.

composite section—the concrete beam plus the concrete deck and haunch.

composite nontransformed section—the concrete beam plus the concrete deck and haunch transformed to provide cross-sectional properties equivalent to the beam concrete but without the strands transformed.

composite transformed section—the concrete beam plus the concrete deck and haunch and the strands transformed to provide cross-sectional properties equivalent to the beam concrete.

The term "composite" implicitly includes the transformation of the concrete deck and haunch.

The term "transformed" generally refers to transformation of the strands.

BOX BEAM (BIII-48), SINGLE SPAN, COMPOSITE DECK**9.5.2 Materials****9.5.2 MATERIALS**

Cast-in-place concrete slab: Actual thickness = 5.5 in.

Structural thickness, $t_s = 5.0$ in.

Note that a ½-in.-thick wearing surface is considered to be an integral part of the deck.

Specified concrete compressive strength for use in design, $f'_c = 4.0$ ksi

Precast concrete beams: AASHTO BIII-48 box beams as shown in **Figure 9.5.2-1**

Required concrete compressive strength at transfer, $f'_{ci} = 4.0$ ksi

Specified concrete compressive strength for use in design, $f'_c = 5.0$ ksi

Concrete unit weight, $w_c = 0.150$ kcf

Overall beam length = 96.0 ft

Design span = 95.0 ft

Prestressing strands: ½-in. diameter, low-relaxation

Area of one strand = 0.153 in.²

Specified tensile strength, $f_{pu} = 270.0$ ksi

Yield strength, $f_{py} = 0.9 f_{pu} = 243.0$ ksi

[LRFD Table 5.4.4.1-1]

Stress limits for prestressing strands:

[LRFD Table 5.9.3-1]

- Before transfer, $f_{pi} \leq 0.75 f_{pu} = 202.5$ ksi
- At service limit state (after all losses), $f_{pe} \leq 0.80 f_{py} = 194.4$ ksi

Modulus of elasticity, $E_p = 28,500$ ksi

[LRFD Art.5.4.4.2]

Reinforcing bars:

Yield strength, $f_y = 60.0$ ksi

Modulus of elasticity, $E_s = 29,000$ ksi

[LRFD Art.5.4.3.2]

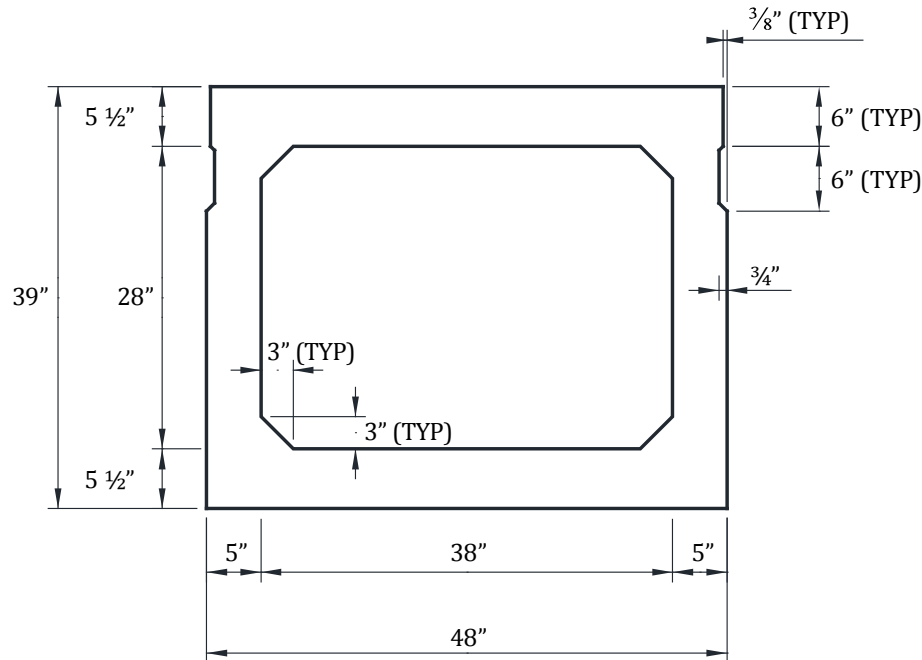
Future wearing surface: 2 in. additional concrete, unit weight = 0.150 kcf

New Jersey-type barrier: unit weight = 0.300 kips/ft/side

BOX BEAM (BIII-48), SINGLE SPAN, COMPOSITE DECK

9.5.2 Materials/9.5.3.1 Noncomposite, Nontransformed Beam Section

Figure 9.5.2-1
AASHTO BIII-48 Box Beam Dimensions



9.5.3 CROSS-SECTION PROPERTIES FOR A TYPICAL INTERIOR BEAM

9.5.3.1 Noncomposite, Nontransformed Beam Section

A_g = area of cross section of precast beam = 813 in.²

h = overall depth of precast beam = 39 in.

I_g = moment of inertia about the centroid of the noncomposite precast beam = 168,367 in.⁴

y_b = distance from centroid to extreme bottom fiber of the noncomposite precast beam = 19.29 in.

y_t = distance from centroid to extreme top fiber of the noncomposite precast beam = 19.71 in.

S_b = section modulus for the extreme bottom fiber of the noncomposite precast beam = I_g/y_b = 8,728 in.³

S_t = section modulus for the extreme top fiber of the noncomposite precast beam = I_g/y_t = 8,542 in.³

w_g = beam weight per unit length = $(813/144)0.150$ = 0.847 kips/ft

E_c = modulus of elasticity of concrete, ksi = $33,000K_1(w_c)^{1.5}\sqrt{f'_c}$ [LRFD Eq. 5.4.2.4-1]

where

K_1 = correction factor for source of aggregate taken as 1.0

w_c = unit weight of concrete = 0.150 kcf

LRFD Table 3.5.1-1 states that, in the absence of more precise data, the unit weight of concrete may be taken as $0.140 + 0.001f'_c$ for $5.0 < f'_c \leq 15.0$ ksi. For $f'_c = 5.0$ ksi, the unit weight would be 0.1450 kcf. However, precast concrete mixes typically have a relatively low water-cementitious materials ratio and high density. Therefore, a unit weight of 0.150 kcf is used in this example. For high-strength concrete, this value may need to be increased based on test results. For simplicity, a value of 0.150 kcf is also used for the cast-in-place concrete.

f'_c = specified compressive strength of concrete, ksi

BOX BEAM (BIII-48), SINGLE SPAN, COMPOSITE DECK

9.5.3.1 Noncomposite, Nontransformed Beam Section/9.5.3.2.3 Transformed Section Properties

Therefore, the modulus of elasticity for:

$$\text{cast-in-place slab, } E_c = 33,000(1.0)(0.150)^{1.5}\sqrt{4.0} = 3,834 \text{ ksi}$$

$$\text{precast beam at transfer, } E_{ci} = 33,000(1.0)(0.150)^{1.5}\sqrt{4.0} = 3,834 \text{ ksi}$$

$$\text{precast beam at service loads, } E_c = 33,000(1.0)(0.150)^{1.5}\sqrt{5.0} = 4,287 \text{ ksi}$$

9.5.3.2 Composite Section**9.5.3.2.1 Effective Flange Width**

[LRFD Art.4.6.2.6.1]

Effective flange width is taken as the tributary width perpendicular to the axis of the beam. For the interior beam, the effective flange width is calculated as one-half the distance to the adjacent beam on each side.

$$2 \times (24) = 48.00 \text{ in.}$$

Therefore, the effective flange width is = 48.00 in.

9.5.3.2.2 Modular Ratio between Slab and Beam Concrete

$$\text{Modular ratio between slab and beam concrete, } n = \frac{E_c(\text{slab})}{E_c(\text{beam})} = \frac{3,834}{4,287} = 0.8943$$

9.5.3.2.3 Transformed Section Properties

The effective flange width must be transformed by the modular ratio to provide cross-sectional properties equivalent to the beam concrete.

$$\text{Transformed flange width} = n(\text{effective flange width}) = (0.8943)(48) = 42.93 \text{ in.}$$

$$\begin{aligned} \text{Transformed flange area} &= n(\text{effective flange width})(t_s) \\ &= (0.8943)(48)(5) = 214.63 \text{ in.}^2 \end{aligned}$$

$$\text{Transformed flange moment of inertia} = 42.93(5.0)^3/12 = 447.19 \text{ in.}^4$$

Note: Only the structural thickness of the deck, 5.0 in., is considered.

Due to the camber of the precast, prestressed beam, a minimum haunch thickness of $\frac{1}{2}$ in., at midspan is considered in the structural properties of the composite section. Also, the width of haunch must be transformed by the modular ratio.

$$\text{Transformed width of haunch} = (0.8943)(48) = 42.93 \text{ in.}$$

$$\text{Transformed area of haunch} = (0.8943)(48)(0.5) = 21.46 \text{ in.}^2$$

$$\text{Transformed moment of inertia of haunch} = 42.93(0.5)^3/12 = 0.447 \text{ in.}^4$$

Note that the haunch should only be considered to contribute to section properties if it is required to be provided in the completed structure. Therefore, some designers neglect its contribution to the section properties.

BOX BEAM (BIII-48), SINGLE SPAN, COMPOSITE DECK

9.5.3.2.3 Transformed Section Properties

Figure 9.5.3.2.3-1
Dimensions of the Composite Section

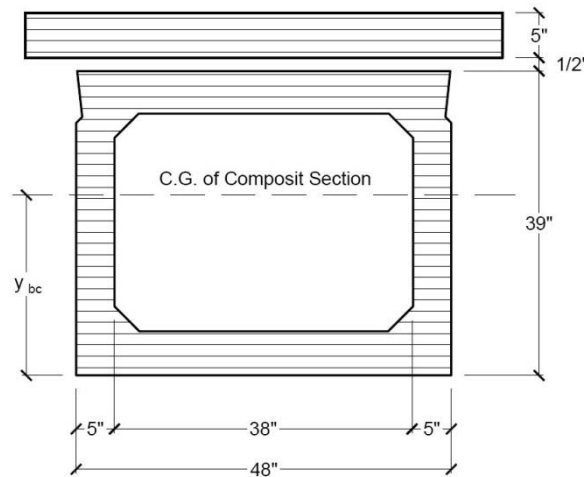


Table 9.5.3.2.3-1
Properties of Composite Section

	Area in. ²	y_b in.	Ay_b in. ³	$A(y_{bc} - y_b)^2$ in. ⁴	I in. ⁴	$I + A(y_{bc} - y_b)^2$ in. ⁴
Beam	813.00	19.29	15,683	20,734	168,367	189,101
Haunch	21.46	39.25	842	4,771	0.45	4,771
Deck	214.63	42.00	9,014	66,938	447	67,385
Σ	1,049.1		25,539			261,257

A_c = total area of the composite section = 1,049.1 in.²

h_c = overall depth of the composite section = 44.50 in.

I_c = moment of inertia of the composite section = 261,257 in.⁴

y_{bc} = distance from the centroid of the composite section to the extreme bottom fiber of the precast beam
 = 25,539/1,049.1 = 24.34 in.

y_{tg} = distance from the centroid of the composite section to the extreme top fiber of the precast beam
 = 39.00 - 24.34 = 14.66 in.

y_{tc} = distance from the centroid of the composite section to the extreme top fiber of the deck
 = 44.50 - 24.34 = 20.16 in.

S_{bc} = composite section modulus for the extreme bottom fiber of the precast beam

$$= (I_c / y_{bc}) = \frac{261,257}{24.34} = 10,734 \text{ in.}^3$$

S_{tg} = composite section modulus for the top fiber of the precast beam

$$= (I_c / y_{tg}) = \frac{261,257}{14.66} = 17,821 \text{ in.}^3$$

S_{tc} = composite section modulus for extreme top fiber of the structural deck slab

$$= \frac{1}{n} \left(\frac{I_c}{y_{tc}} \right) = \frac{1}{0.8943} \left(\frac{261,257}{20.16} \right) = 14,491 \text{ in.}^3$$

BOX BEAM (BIII-48), SINGLE SPAN, COMPOSITE DECK**9.5.4 Shear Forces and Bending Moments/9.5.4.1.1 Dead Loads****9.5.4 SHEAR FORCES AND BENDING MOMENTS**

The self weight of the beam and the weight of the deck and haunch act on the noncomposite, simple-span structure, while the weight of barriers, future wearing surface, and live loads with impact act on the composite, simple-span structure. Refer to **Tables 9.5.4-1** and **9.5.4-2**, which follow Section 9.5.4.3 for a summary of unfactored values calculated below.

9.5.4.1 Shear Forces and Bending Moments Due to Dead Loads**9.5.4.1.1 Dead Loads**

[LRFD Art. 3.3.2]

DC = Dead load of structural components and nonstructural attachments

Dead loads acting on the noncomposite structure:

Beam self weight, $w_g = 0.847$ kips/ft

$$\text{Diaphragm weight} = \left(\frac{8}{12}\right) \left[\frac{(48-10)}{12} \times \frac{(39-11)}{12} - 4 \left(\frac{1}{2}\right) \left(\frac{3}{12}\right) \left(\frac{3}{12}\right) \right] (0.150) = 0.73 \text{ kips/diaphragm}$$

$$5.5\text{-in.-thick deck weight} = (5.5/12)(4 \text{ ft})(0.150 \text{ kcf}) = 0.275 \text{ kips/ft}$$

$$\frac{1}{2}\text{-in.-thick haunch weight} = (0.5)(48/144)(0.150) = 0.025 \text{ kips/ft}$$

$$w_s = 0.275 + 0.025 = 0.300 \text{ kips/ft}$$

Notes:

1. Actual deck thickness (5.5 in.) is used for computing dead load.
2. A $\frac{1}{2}$ -in. minimum haunch thickness is assumed in the computations of dead load. If a deeper haunch will be used because of final beam camber, the weight of the actual haunch should be used.
3. For this design example, the unit weight of the reinforced concrete is taken as 0.150 kcf. Some designers use a higher unit weight to account for the weight of the reinforcement.
4. The weights of the diaphragms are considered concentrated loads acting at the ends, center, and quarter points as shown in **Figure 9.5.4.1.1-1**.

Dead loads placed on the composite structure:

LRFD Article 4.6.2.2.1 states that permanent loads (curbs and future wearing surface) may be distributed uniformly among all beams if the following conditions are met:

- Width of the deck is constant OK
- Number of beams, N_b , is not less than four ($N_b = 7$) OK
- Beams are parallel and have the same stiffness OK
- The roadway part of the overhang, $d_e \leq 3.0$ ft ($d_e = 0.0$ ft) OK
- Curvature in plan is less than specified in the *LRFD Specifications* (curvature = 0.0°) OK
- Cross section of the bridge is consistent with one of the cross sections given in LRFD Table 4.6.2.2.1-1 OK

Since these criteria are satisfied, the barrier and wearing surface loads are equally distributed among the seven beams.

$$\text{Barrier weight} = (2 \text{ barriers})(0.300 \text{ kips/ft}) / (7 \text{ beams}) = 0.086 \text{ kips/ft/beam} = w_b$$

DW = dead load of future wearing surface

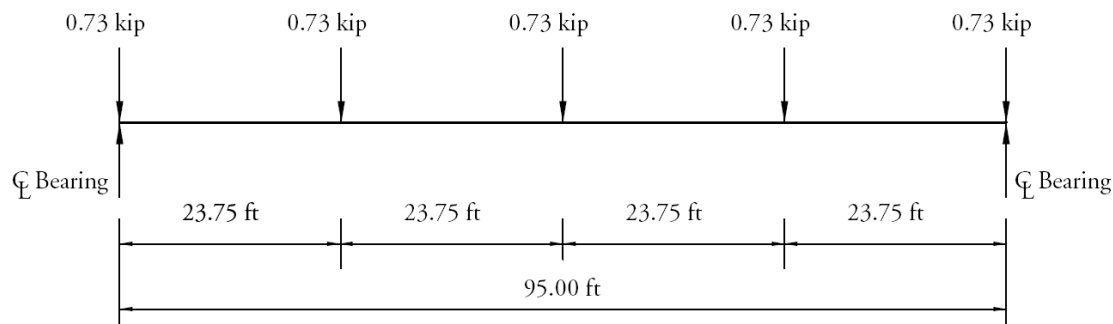
$$= (2/12)(0.150) = 0.025 \text{ ksf}$$

$$= (0.025 \text{ ksf})(25.0 \text{ ft}) / (7 \text{ beams}) = 0.089 \text{ kips/ft} = w_w$$

BOX BEAM (BIII-48), SINGLE SPAN, COMPOSITE DECK

9.5.4.1.1 Dead Loads/9.5.4.2.2 Live Load Distribution Factors for a Typical Interior Beam

Figure 9.5.4.1.1-1
Diaphragm Loads per Beam

**9.5.4.1.2 Unfactored Shear Forces and Bending Moments**

For a simply supported beam with span length (L) loaded with a uniformly distributed load (w), the shear force (V_x) and bending moment (M_x) at any distance (x) from the support given by:

$$V_x = w(0.5L - x) \quad \text{(Eq.9.5.4.1.2-1)}$$

$$M_x = 0.5wx(L - x) \quad \text{(Eq.9.5.4.1.2-2)}$$

Using the above equations, values of shear forces and bending moments for a typical interior beam, under self weight of beam, weight of slab and haunch, weight of barriers, and future wearing surface are computed and shown in **Table 9.5.4-1** that is located at the end of Section 9.5.4.3. For these calculations, the span length (L) is the design span, 95 ft. However, for calculations of stresses and deformation at the time prestress is transferred, the overall length of the precast member, 96 ft, is used, as illustrated later in this example.

9.5.4.2 Shear Forces and Bending Moments Due to Live Loads**9.5.4.2.1 Live Loads**

Design live load is HL-93 which consists of a combination of: [LRFD Art. 3.6.1.2.1]

1. Design truck or design tandem with dynamic allowance [LRFD Art.3.6.1.2.2]

The design truck consists of 8.0-, 32.0-, and 32.0-kip axles with the first pair spaced at 14.0 ft and the second pair spaced at 14.0 to 30.0 ft. The design tandem consists of a pair of 25.0-kip axles spaced at 4.0 ft apart.

[LRFD Art.3.6.1.2.3]

2. Design lane load of 0.64 kips/ft without dynamic allowance [LRFD Art. 3.6.1.2.4]

9.5.4.2.2 Live Load Distribution Factors for a Typical Interior Beam

The live load bending moments and shear forces are determined by using the simplified distribution factor formulas, [LRFD Art. 4.6.2.2]. To use the simplified live load distribution factor formulas, the following conditions must be met: [LRFD Art. 4.6.2.2.1]

- Width of deck is constant OK
- Number of beams, N_b not less than four ($N_b = 7$) OK
- Beams are parallel and have approximately the same stiffness OK
- The roadway part of the overhang, $d_e \leq 3.0$ ft ($d_e = 0.0$ ft) OK
- Curvature is less than specified in the *LRFD Specifications* (curvature = 0.0°) OK

BOX BEAM (BIII-48), SINGLE SPAN, COMPOSITE DECK**9.5.4.2.2 Live Load Distribution Factors for a Typical Interior Beam/9.5.4.2.2.1 Distribution Factor for Bending Moments**

For a precast cellular concrete box with shear keys and a cast-in-place concrete overlay, the bridge type is (f). [LRFD Table 4.6.2.2.1-1]

The number of design lanes is computed as:

The number of design lanes = the integer part of the ratio $w/12$, where (w) is the clear roadway width, in ft, between the curbs [LRFD Art.3.6.1.1.1]

From **Figure 9.5.1-1**, $w = 25$ ft

Number of design lanes = Integer part of $(25/12) = 2$ lanes

9.5.4.2.2.1 Distribution Factor for Bending Moments

- For all limit states except fatigue limit state:

For two or more lanes loaded when members are sufficiently connected by the cast-in-place deck to act as a unit:

$$DFM = k \left(\frac{b}{305} \right)^{0.6} \left(\frac{b}{12.0L} \right)^{0.2} \left(\frac{I_c}{J_g} \right)^{0.06} \quad [\text{LRFD Table 4.6.2.2.2b-1}]$$

Provided that: $35 \leq b \leq 60$; $b = 48$ in. OK

$20 \leq L \leq 120$; $L = 95$ ft OK

$5 \leq N_b \leq 20$; $N_b = 7$ OK

where

DFM = distribution factor for moment of interior beam

$k = 2.5(N_b)^{-0.2} \geq 1.5 = 2.5(7)^{-0.2} = 1.694 > 1.5$ OK

N_b = number of beams

b = beam width, in.

L = beam span, ft

I_c = moment of inertia of the composite beam, in.⁴

J_g = St. Venant torsional inertia (derived using composite section properties), in.⁴

For closed, thin-walled shapes:

$$J_g \sim \frac{4A_o^2}{\sum \frac{s}{t}} \quad [\text{LRFD Eq. C4.6.2.2.1-3}]$$

where

A_o = area enclosed by centerlines of the elements of the beam

$$= (48 - 5) \left(44.5 - \left(\frac{5.0 + 0.5 + 5.5}{2} + \frac{5.5}{2} \right) \right) = 1,559 \text{ in.}^2$$

s = length of a side element

t = thickness of an element

$$J_g = \frac{4(1,559)^2}{2 \left(\frac{44.5 - \left(\frac{11}{2} + \frac{5.5}{2} \right)}{5} \right) + \left(\frac{48 - 5}{5.5} \right) + \left(\frac{48 - 5}{11} \right)} = 370,680 \text{ in.}^4$$

Therefore,

$$DFM = 1.694 \left(\frac{48}{305} \right)^{0.6} \left(\frac{48}{12.0 \times 95.0} \right)^{0.2} \left(\frac{261,257}{370,680} \right)^{0.06} = 0.290 \text{ lanes/beam}$$

BOX BEAM (BIII-48), SINGLE SPAN, COMPOSITE DECK**9.5.4.2.2.1 Distribution Factor for Bending Moments/9.5.4.2.4.1 Due to Truck Load; V_{LT} and M_{LT}**

For one lane loaded, when sufficiently connected to act as a unit:

$$DFM = k \left(\frac{b}{33.3L} \right)^{0.5} \left(\frac{I_c}{J_g} \right)^{0.25} \quad [\text{LRFD Table 4.6.2.2.2b-1}]$$

$$= 1.694 \left(\frac{48}{33.3 \times 95} \right)^{0.5} \left(\frac{261,257}{370,680} \right)^{0.25} = 0.191 \text{ lanes/beam}$$

Thus, the case of two or more lanes loaded controls and $DFM = 0.290$ lanes/beam.

- For fatigue limit state:

The *LRFD Specifications* Art. C3.4.1 states that for Fatigue Limit State, a single design truck should be used. However, live load distribution factors given in Article 4.6.2.2 take into consideration the multiple presence factor, m . LRFD Article 3.6.1.1.2 states that the multiple presence factor, m , for one design lane loaded is 1.2. Therefore, the distribution factor for one design lane loaded should be used. Distribution factor for fatigue limit state is: $0.191/1.2 = 0.159$ lanes/beam

9.5.4.2.2.2 Distribution Factor for Shear Force

For two or more lanes loaded:

$$DFV = \left(\frac{b}{156} \right)^{0.4} \left(\frac{b}{12.0L} \right)^{0.1} \left(\frac{I_c}{J_g} \right)^{0.05} \left(\frac{b}{48} \right) \quad [\text{LRFD Table 4.6.2.2.3a-1}]$$

Provided that: $35 \leq b \leq 60$; $b = 48$ in. OK

$20 \leq L \leq 120$; $L = 95$ ft OK

$5 \leq N_b \leq 20$; $N_b = 7$ OK

$25,000 \leq J_g \leq 610,000$; $J_g = 370,680$ in.⁴ OK

$40,000 \leq I_c \leq 610,000$; $I_c = 261,257$ in.⁴ OK

where DFV = distribution factor for shear force for interior beam

$$DFV = \left(\frac{48}{156} \right)^{0.4} \left(\frac{48}{12.0 \times 95} \right)^{0.1} \left(\frac{261,257}{370,680} \right)^{0.05} \left(\frac{48}{48} \right) = 0.447 \text{ lanes/beam}$$

For one design lane loaded:

$$DFV = \left(\frac{b}{130L} \right)^{0.15} \left(\frac{I_c}{J_g} \right)^{0.05} = \left(\frac{48}{130 \times 95} \right)^{0.15} \left(\frac{261,257}{370,680} \right)^{0.05} = 0.427 \text{ lanes/beam} \quad [\text{LRFD Table 4.6.2.2.3a-1}]$$

Thus, the case of two lanes loaded controls and $DFV = 0.447$ lanes/beam.

9.5.4.2.3 Dynamic Allowance

[LRFD Art. 3.6.2]

$IM = 15\%$ for fatigue limit state

$IM = 33\%$ for all other limit states

Where IM = dynamic load allowance, applied to design truck load only

9.5.4.2.4 Unfactored Shear Forces and Bending Moments**9.5.4.2.4.1 Due to Truck Load; V_{LT} and M_{LT}**

- For all limit states except for fatigue limit state:

Shear force and bending moment envelopes on a per-lane-basis are calculated at tenth-points of the span, using the equations given in Chapter 8 of this manual. However, this is generally done by means of commercially available computer software that has the ability to deal with moving loads. Therefore, truck load shear forces and bending moments per beam are:

BOX BEAM (BIII-48), SINGLE SPAN, COMPOSITE DECK

9.5.4.2.4.1 Due to Truck Load; V_{LT} and M_{LT} /9.5.4.2.4.2 Due to Design Lane Load; V_{LL} and M_{LL}

$$\begin{aligned}
 V_{LT} &= (\text{shear force per lane})(DFV)(1 + IM) \\
 &= (\text{shear force per lane})(0.447)(1 + 0.33) \\
 &= (\text{shear force per lane})(0.595) \text{ kips} \\
 M_{LT} &= (\text{bending moment per lane})(DFM)(1 + IM) \\
 &= (\text{bending moment per lane})(0.290)(1 + 0.33) \\
 &= (\text{bending moment per lane})(0.386) \text{ ft-kips}
 \end{aligned}$$

Values of V_{LT} and M_{LT} at different points are given in **Table 9.5.4-2**.

- For fatigue limit state:

Article 3.6.1.4.1 in the *LRFD Specifications* states that the fatigue load is a single design truck which has the same axle weight used in all other limit states, but with a constant spacing of 30.0 ft between the 32.0-kip axles. Bending moment envelope on a per-lane-basis is calculated using the equation given in Chapter 8 of this manual.

Therefore, bending moment of fatigue truck load is:

$$\begin{aligned}
 M_f &= (\text{bending moment per lane})(DFM)(1 + IM) \\
 &= (\text{bending moment per lane})(0.159)(1 + 0.15) \\
 &= (\text{bending moment per lane})(0.183) \text{ ft-kips}
 \end{aligned}$$

Values of M_f at different points are given in **Table 9.5.4-2**.

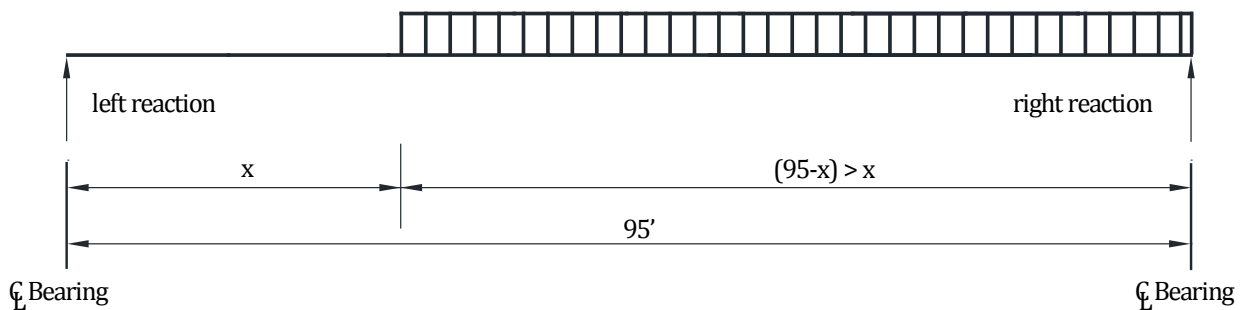
9.5.4.2.4.2 Due to Design Lane Load; V_{LL} and M_{LL}

To obtain the maximum shear force at a section located at a distance (x) from the left support under a uniformly distributed load of 0.64 kips/ft, load the member to the right of the section under consideration, as shown in **Figure 9.5.4.2.4.2-1**. Therefore, the maximum shear force per lane is:

$$V_x = \frac{0.32(L - x)^2}{L} \text{ for } x \leq 0.5L \tag{Eq. 9.5.4.2.4.2-1}$$

where V_x is in kips/lane and L and x are in ft

Figure 9.5.4.2.4.2-1
Maximum Shear Force due to Design Lane Load



To calculate the maximum bending moment at any section, use Eq. (9.5.4.1.2-2).

Lane load shear forces and bending moments per beam are as follows:

$$\begin{aligned}
 V_{LL} &= (\text{lane load shear force})(DFV) \\
 &= (\text{lane load shear force})(0.447) \text{ kips}
 \end{aligned}$$

BOX BEAM (BIII-48), SINGLE SPAN, COMPOSITE DECK9.5.4.2.4.2 Due to Design Lane Load; V_{LL} and M_{LL} /9.5.4.3 Load Combinations

For all limit states except fatigue limit state:

$$M_{LL} = (\text{lane load bending moment})(DFM)$$

$$= (\text{lane load bending moment})(0.290) \text{ ft-kips}$$

Note that the dynamic allowance is not applied to the design lane loading.

Values of shear forces and bending moments, V_{LL} and M_{LL} , are given in **Table 9.5.4-2**.

9.5.4.3 Load Combinations

[LRFD Art. 3.4]

Total factored load shall be taken as:

$$Q = \sum \eta_i \gamma_i Q_i \quad \text{[LRFD Eq. 3.4.1-1]}$$

where

η_i = a load modifier relating to ductility, redundancy, and operational importance [LRFD Art.1.3.2.1]
(Here, η_i is considered to be 1.0 for typical bridges.)

γ_i = load factors [LRFD Table 3.4.1-1]

Q_i = force effects from specified loads

Investigating the various limit states given in LRFD Article 3.4.1, the following limit states are applicable:

Service I: check compressive stresses in prestressed concrete components:

$$Q = 1.00(DC + DW) + 1.00(LL + IM) \quad \text{[LRFD Table 3.4.1-1]}$$

This load combination is the general combination for service limit state stress and applies to all conditions other than Service III.

Service III: check tensile stresses in prestressed concrete components:

$$Q = 1.00(DC + DW) + 0.80(LL + IM) \quad \text{[LRFD Table 3.4.1-1]}$$

This load combination is a special combination for service limit state stress that applies only to tension in prestressed concrete structures to control cracks.

Strength I: check ultimate strength:

[LRFD Tables 3.4.1-1 and 2]

$$\text{Maximum } Q = 1.25(DC) + 1.50(DW) + 1.75(LL + IM)$$

$$\text{Minimum } Q = 0.90(DC) + 0.65(DW) + 1.75(LL + IM)$$

This load combination is the general load combination for strength limit state design.

Note: For simple-span bridges, the maximum load factors produce maximum effects. However, use minimum load factors for dead load (DC) and wearing surface (DW) when dead load and wearing surface stresses are opposite to those of live load.

Fatigue I: check stress range in strands:

[LRFD Table 3.4.1-1]

$$Q = 1.50(LL + IM)$$

This load combination is a special load combination to check the tensile stress range in the strands due to live load and dynamic allowance.

BOX BEAM (BIII-48), SINGLE SPAN, COMPOSITE DECK

9.5.4.3 Load Combinations/9.5.5.1 Service Load Stresses at Midspan

Table 9.5.4-1

Unfactored Shear Forces and Bending Moments Due to Dead Loads for a Typical Interior Beam

Distance x, ft	Section x/L	Beam Weight		Slab and Haunch Weight		Barrier Weight		Wearing Surface Weight		Diaphragm Weight	
		Shear V_g kips	Moment M_g ft-kips	Shear V_s kips	Moment M_s ft-kips	Shear V_b kips	Moment M_b ft-kips	Shear V_{ws} kips	Moment M_{ws} ft-kips	Shear V_d kips	Moment M_d ft-kips
0	0	40.2	0	14.3	0	4.1	0	4.2	0	1.1	0
*3.21	0.034	37.5	124.8	13.3	44.2	3.8	12.7	3.9	13.1	1.1	3.5
9.5	0.1	32.2	344.0	11.4	121.8	3.3	34.9	3.4	36.1	1.1	10.4
19.0	0.2	24.1	611.5	8.6	216.6	2.5	61.1	2.5	64.3	1.1	20.8
28.5	0.3	16.1	802.6	5.7	284.3	1.6	81.5	1.7	84.3	0.4	27.7
38.0	0.4	8.0	917.3	2.9	324.9	0.8	93.1	0.8	96.4	0.4	31.2
47.5	0.5	0.0	955.5	0.0	338.4	0.0	97.0	0.0	100.4	0.4	34.7

* Critical section for shear (see Sect. 9.5.11)

Table 9.5.4-2

Unfactored Shear Forces and Bending Moments Due to Live Loads for a Typical Interior Beam

Distance x, ft	Section x/L	Truck Load with Impact		Lane Load		Fatigue Truck with Impact
		Shear V_{LT} kips	Moment M_{LT} ft-kips	Shear V_{LL} kips	Moment M_{LL} ft-kips	Moment M_f ft-kips
0	0	38.6	0	13.6	0	0
*3.21	0.034	37.2	77.1	12.7	27.3	32.6
9.5	0.1	34.3	211.5	11.0	75.4	88.6
19	0.2	30.0	370.8	8.7	134.0	152.1
28.5	0.3	25.8	476.3	6.7	175.8	195.6
38	0.4	21.5	538.1	4.9	201.0	217.7
47.5	0.5	17.2	551.5	3.4	209.4	214.7

* Critical section for shear (see Sect. 9.5.11)

9.5.5 ESTIMATE REQUIRED PRESTRESS

The required number of strands is usually governed by concrete tensile stresses at the bottom fiber for load combination Service III and in some cases at load combination Strength I. For estimating the number of strands, only the stresses at midspan are considered.

9.5.5.1 Service Load Stresses at Midspan

Bottom tensile stress due to applied dead and live loads using load combination Service III is:

$$f_b = \frac{M_g + M_s + M_d}{S_b} + \frac{M_b + M_{ws} + (0.8)(M_{LT} + M_{LL})}{S_{bc}}$$

where

- f_b = concrete tensile stress at bottom fiber of the beam, ksi
- M_g = unfactored bending moment due to beam self weight, ft-kips
- M_s = unfactored bending moment due to slab and haunch weights, ft-kips
- M_d = unfactored bending moment due to diaphragm weight, ft-kips
- M_b = unfactored bending moment due to barrier weight, ft-kips
- M_{ws} = unfactored bending moment due to future wearing surface, ft-kips

BOX BEAM (BIII-48), SINGLE SPAN, COMPOSITE DECK

9.5.5.1 Service Load Stresses at Midspan/9.5.5.4 Strand Pattern

M_{LT} = unfactored bending moment due to truck load, ft-kips

M_{LL} = unfactored bending moment due to lane load, ft-kips

Using values of bending moments from **Tables 9.5.4-1** and **9.5.4-2**, bottom tensile stress at midspan is:

$$f_b = \frac{(955.5 + 338.4 + 34.7)(12)}{8,728} + \frac{(97.0 + 100.4 + (0.8)(551.5 + 209.4))(12)}{10,734} = 2.728 \text{ ksi}$$

9.5.5.2 Stress Limits for Concrete

Tensile stress limit at service limit state = $0.19\sqrt{f'_c}$

[LRFD Art. 5.9.4.2]

where f'_c = specified concrete compressive strength of beam for design, ksi

Concrete tensile stress limit = $-0.19\sqrt{5.0} = -0.425$ ksi

9.5.5.3 Required Number of Strands

The required precompressive stress at the bottom fiber of the beam after all losses is the difference between the bottom tensile stress due to the applied loads and the concrete tensile stress limit:

$$f_{pb} = 2.728 - 0.425 = 2.303 \text{ ksi}$$

Assume the distance between the center of gravity of strands and the bottom fiber of the beam $y_{bs} = 4.0$ in. at midspan.

Therefore, strand eccentricity at midspan, $e_c = y_b - y_{bs} = 19.29 - 4.0 = 15.29$ in.

If P_{pe} is the total prestressing force after all losses, the stress at the bottom fiber due to prestress is:

$$f_{pb} = \frac{P_{pe}}{A_g} + \frac{P_{pe}e_c}{S_b} \quad \text{or} \quad 2.303 = \frac{P_{pe}}{813} + \frac{(P_{pe})(15.29)}{8,728}$$

Solving for P_{pe} , the required $P_{pe} = 772.3$ kips

Final prestress force per strand = (area of strand)(f_{pi})(1 - final losses)

where f_{pi} = initial stress before transfer = 202.5 ksi

(Section 9.5.2)

Assuming a final loss of 20% of f_{pi} , the prestress force per strand after all losses:

$$= (0.153)(202.5)(1-0.20) = 24.8 \text{ kips}$$

Number of strands required = $772.3/24.8 = 31.1$ strands

Try (31) ½-in.-diameter, 270 ksi strands

Total area of prestressing strands, $A_{ps} = 31(0.153) = 4.473$ in.²

Note: This is a conservative estimate of the number of strands because nontransformed section properties are used in lieu of transformed section properties. The number of strands can be refined later in the design process as more accurate section properties and prestress losses are determined.

9.5.5.4 Strand Pattern

Figure 9.5.5.4-1 shows the assumed strand pattern for the 31 strands at midspan of the beam. All strands are straight.

The distance between the center of gravity of the strands and the bottom concrete fiber of the beam at midspan:

$$y_{bs} = \frac{23(2) + 6(4) + 2(36)}{31} = 4.58 \text{ in.}$$

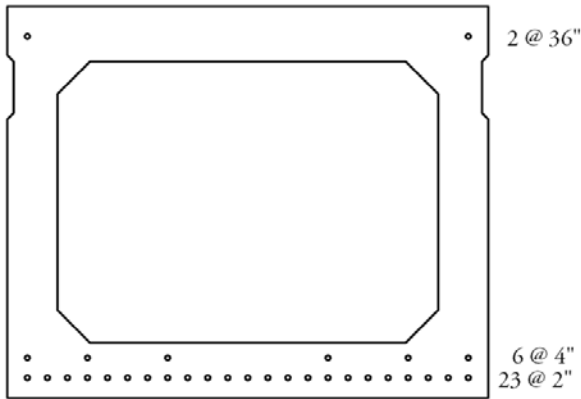
Strand eccentricity at midspan:

$$e_c = y_b - y_{bs} = 19.29 - 4.58 = 14.71 \text{ in.} = e_{pg}$$

BOX BEAM (BIII-48), SINGLE SPAN, COMPOSITE DECK

9.5.5.4 Strand Pattern/9.5.5.5 Steel Transformed Section Properties

Figure 9.5.5.4-1
Strand Pattern at Midspan



9.5.5.5 Steel Transformed Section Properties

From the earliest years of prestressed concrete design, the gross section was conservatively used in analysis since the prestressing forces were smaller and computer programs were not widely used. However, the use of transformed section, which is obtained from the gross section by adding transformed steel area, yields more accurate results than the gross section analysis.

For each row of prestressing strands shown in **Figure 9.5.5.4-1**, the steel area is multiplied by $(n - 1)$ to calculate the transformed section properties, where n is the modular ratio between prestressing strand and concrete. Since the modulus of elasticity of concrete is different at transfer and final time, the transformed section properties should be calculated separately in the two stages. Using similar procedures as in Section 9.5.3.2.3, a sample calculation is shown in **Table 9.5.5.5-1** below.

At transfer:

$$n - 1 = \frac{28,500}{3,834} - 1 = 6.433$$

At final:

$$n - 1 = \frac{28,500}{4,287} - 1 = 5.648$$

Table 9.5.5.5-1
Properties of Transformed Section at Final Time

	Transformed Area, in. ²	y_b in.	Ay_b in. ³	$A(y_{btc} - y_b)^2$ in. ⁴	I in. ⁴	$I + A(y_{btc} - y_b)^2$ in. ⁴
Deck	214.63	42.00	9,014	70,704	447	71,151
Haunch	21.46	39.25	842	5,089	0.45	5,089
Beam	813.00	19.29	15,683	16,905	168,367	185,272
Row1	19.88	2.00	39.76	9,491		9,491
Row2	5.18	4.00	20.72	2,041		2,041
Row3	1.73	36.00	62.28	255		255
Σ	1,075.9		25,662			273,299

Note: The moment of inertia of strand about its own centroid is neglected.

BOX BEAM (BIII-48), SINGLE SPAN, COMPOSITE DECK

9.5.5.5 Steel Transformed Section Properties/9.5.6 Strength Limit State

The transformed section properties are calculated as:

Noncomposite transformed section at transfer:

$$A_{ti} = \text{area of transformed section at transfer} = 843.5 \text{ in.}^2$$

$$I_{ti} = \text{moment of inertia of the transformed section at transfer} = 176,829 \text{ in.}^4$$

$$e_{ti} = \text{eccentricity of strands with respect to transformed section at transfer} = 14.18 \text{ in.}$$

$$y_{bti} = \text{distance from the centroid of the transformed section to the extreme bottom fiber of the beam at transfer} = 18.76 \text{ in.}$$

$$S_{bti} = \text{section modulus for the extreme bottom fiber of the transformed section at transfer} = 9,426 \text{ in.}^3$$

$$S_{tti} = \text{section modulus for the extreme top fiber of the transformed section at transfer} = 8,737 \text{ in.}^3$$

Noncomposite transformed section at final time:

$$A_{tf} = \text{area of transformed section at final time} = 839.8 \text{ in.}^2$$

$$I_{tf} = \text{moment of inertia of the transformed section at final time} = 175,822 \text{ in.}^4$$

$$e_{tf} = \text{eccentricity of strands with respect to transformed section at final time} = 14.24 \text{ in.}$$

$$y_{btf} = \text{distance from the centroid of the noncomposite transformed section to the extreme bottom fiber of the beam at final time} = 18.82 \text{ in.}$$

$$S_{btf} = \text{section modulus for the extreme bottom fiber of the transformed section at final time} = 9,342 \text{ in.}^3$$

$$S_{ttf} = \text{section modulus for the extreme top fiber of the transformed section at final time} = 8,713 \text{ in.}^3$$

Composite transformed section at final time:

$$A_{tc} = \text{area of transformed composite section at final time} = 1,075.9 \text{ in.}^2$$

$$I_{tc} = \text{moment of inertia of the transformed composite section at final time} = 273,299 \text{ in.}^4$$

$$e_{tc} = \text{eccentricity of strands with respect to transformed composite section at final time} = 19.27 \text{ in.}$$

$$y_{btc} = \text{distance from the centroid of the composite transformed section to the extreme bottom fiber of the beam at final time} = 23.85 \text{ in.}$$

$$S_{btc} = \text{section modulus for the extreme bottom fiber of the transformed composite section at final time} = 11,459 \text{ in.}^3$$

$$S_{ttc} = \text{composite section modulus for the extreme top fiber of the precast beam for transformed section at final time} = 18,040 \text{ in.}^3$$

$$S_{dte} = \text{composite section modulus for the extreme top fiber of the deck for transformed section at final time} = 14,799 \text{ in.}^3$$

9.5.6 STRENGTH LIMIT STATE

For box sections, it is common that the flexural strength controls the design. It is therefore recommended that the strength calculations be conducted prior to the stress check. As the state-of-the-art continues to develop into the use of high-strength concrete and emphasis continues to be placed on the importance of member strength, it is possible that the future designs using other cross sections will be controlled by the strength limit state.

Total ultimate bending moment for Strength I is:

$$M_u = 1.25(DC) + 1.5(DW) + 1.75(LL + IM)$$

BOX BEAM (BIII-48), SINGLE SPAN, COMPOSITE DECK

9.5.6 Strength Limit State

Using the values of unfactored bending moment given in **Tables 9.5.4-1** and **9.5.4-2**, the ultimate bending moment at midspan is:

$$M_u = 1.25(955.5 + 338.4 + 97.0 + 34.7) + 1.5(100.4) + 1.75(209.4 + 551.5) = 3,264.2 \text{ ft-kips}$$

Average stress in prestressing strands when $f_{pe} \geq 0.5f_{pu}$:

$$f_{ps} = f_{pu} \left(1 - k \frac{c}{d_p} \right) \quad [\text{LRFD Eq.5.7.3.1.1-1}]$$

where

f_{ps} = average stress in prestressing strand, ksi

f_{pu} = specified tensile strength of prestressing strand = 270.0 ksi

$$k = 2 \left(1.04 - \frac{f_{py}}{f_{pu}} \right) \quad [\text{LRFD Eq.5.7.3.1.1-2}]$$

= 0.28 for low-relaxation strands

d_p = distance from extreme compression fiber to the centroid of the prestressing strands, in.

c = distance from extreme compression fiber to the neutral axis, in.

To compute c , assume rectangular section behavior and check if the depth of the equivalent stress block, a , is less than or equal to t_s + haunch thickness + precast beam top flange thickness: [LRFD Art.C5.7.3.2.2]

where $a = \beta_1 c$,

$$c = \frac{A_{ps}f_{pu} + A_s f_y - A'_s f'_y}{0.85 f'_c \beta_1 b + k A_{ps} \frac{f_{pu}}{d_p}} \quad [\text{LRFD Eq.5.7.3.1.1-4}]$$

where

A_{ps} = area of prestressing strand = $29(0.153) = 4.437 \text{ in.}^2$

A_s = area of nonprestressed tension reinforcement = 0 in.^2

f_y = specified yield strength of tension reinforcement = 60.0 ksi

A'_s = area of compression reinforcement = 0 in.^2

f'_y = specified yield strength of compression reinforcement = 60.0 ksi

f'_c = specified compressive strength of deck concrete = 4.0 ksi

LRFD C5.7.2.2 states that if the compressive block includes two types of concrete, the lower of the concrete strengths can be conservatively used.

β_1 = stress factor of compression block

= 0.85 for $f'_c \leq 4.0 \text{ ksi}$

= $0.85 - 0.05(f'_c - 4.0) \geq 0.65$ for $f'_c > 4.0 \text{ ksi}$

= 0.85

b = effective width of compression flange = 48 in.

Note: In computing the flexural strength of members with strands placed near the compression face of the member, it is not correct to use the combined centroid of the entire strand group for establishing the effective depth, d_p , and the area of prestressing steel, A_{ps} . This is because the top strands will have different strain from that of the bottom strands. An accurate solution can be achieved using the detailed strain compatibility approach, which accounts for the steel strain at various distances from the neutral axis. However, a reasonable approximation is to ignore all strands placed on the compression side.

BOX BEAM (BIII-48), SINGLE SPAN, COMPOSITE DECK

9.5.6 Strength Limit States/9.5.7.1 Elastic Shortening

For the 29 bottom strands, the distance between the center of gravity of the strands and the bottom fiber of the beam, y_{bs} , is:

$$\frac{23(2) + 6(4)}{29} = 2.41 \text{ in.}$$

Therefore, $d_p = 44.5 - 2.41 = 42.09$ in.

$$c = \frac{(4.437)(270.0) + 0 - 0}{0.85(4.0)(0.85)(48) + (0.28)(4.437)\left[\frac{270.0}{42.09}\right]} = 8.17 \text{ in.}$$

$$a = \beta_1 c = (0.85)(8.17) = 6.94 \text{ in.} \leq 5.0 + 0.5 + 5.5 = 11.0 \text{ in.} \quad \text{OK}$$

Therefore, the average stress in the prestressing strand is:

$$f_{ps} = 270.0 \left(1 - 0.28 \frac{8.17}{42.09}\right) = 255.3 \text{ ksi}$$

Nominal flexural resistance:

[LRFD Art.5.7.3.2.2]

$$M_n = A_{ps} f_{ps} \left(d_p - \frac{a}{2}\right)$$

[LRFD Eq.5.7.3.2.2-1]

$$M_n = \frac{(4.437)(255.3)\left(42.09 - \frac{6.94}{2}\right)}{12} = 3,645.6 \text{ ft-kips}$$

Factored flexural resistance, M_r :

$$M_r = \phi M_n$$

[LRFD Eq.5.7.3.2.1-1]

where

$$\phi = \text{resistance factor} = 1.00 \text{ for flexure and tension controlled prestressed concrete sections}$$

[LRFD Art.5.5.4.2.1]

$$M_r = 3,645.6 \text{ ft-kips} > M_u = 3,264.2 \text{ ft-kips} \quad \text{OK}$$

9.5.7 PRESTRESS LOSSES

[LRFD Art.5.9.5]

Total prestress loss:

$$\Delta f_{pT} = \Delta f_{pES} + \Delta f_{pLT}$$

[LRFD Eq. 5.9.5.1-1]

where

$$\Delta f_{pT} = \text{total loss in prestressing steel strands}$$

$$\Delta f_{pES} = \text{sum of all losses or gains due to elastic shortening or extension at the time of application of prestress and/or external loads}$$

$$\Delta f_{pLT} = \text{long-term losses due to shrinkage and creep of concrete, and relaxation of steel after transfer. In this design example, the refined estimates of time-dependent losses are used.}$$

9.5.7.1 Elastic Shortening

$$\Delta f_{pES} = \frac{E_p}{E_{ci}} f_{cgp}$$

[LRFD Eq.5.9.5.2.3a-1]

where

$$E_p = \text{modulus of elasticity of prestressing strands} = 28,500 \text{ ksi}$$

$$E_{ci} = \text{modulus of elasticity of beam concrete at transfer} = 3,834 \text{ ksi}$$

$$f_{cgp} = \text{sum of concrete stresses at the center of gravity of prestressing strands due to prestressing force at transfer and the self weight of the member at sections of maximum moment.}$$

BOX BEAM (BIII-48), SINGLE SPAN, COMPOSITE DECK**9.5.7.1 Elastic Shortening/9.5.7.2.1 Shrinkage of Concrete**

If the gross (or net) cross-section properties are used, it is necessary to perform numerical iterations. The elastic loss Δf_{pES} is usually assumed to be 10% of the initial prestress to calculate f_{cgp} , which is then used in the equation above to calculate a refined Δf_{pES} . The process is repeated until the assumed Δf_{pES} and refined Δf_{pES} converge.

However, when transformed section properties are used to calculate concrete stress, the effects of losses and gains due to elastic deformations are implicitly accounted for. Therefore, Δf_{pES} should not be included in calculating f_{cgp} .

$$\begin{aligned} \text{Force per strand before transfer} &= (\text{area of strand})(\text{prestress stress before transfer}) \\ &= (0.153)(202.5) = 30.98 \text{ ksi} \end{aligned}$$

$$f_{cgp} = \frac{P_{pi}}{A_{ti}} + \frac{P_{pi}e_{ti}^2}{I_{ti}} - \frac{(M_g + M_d)e_{ti}}{I_{ti}}$$

where

$$P_{pi} = \text{total prestressing force before transfer} = (31 \text{ strands})(30.98) = 960.4 \text{ kips}$$

$$e_{ti} = \text{eccentricity of strands with respect to the transformed section at transfer} = 14.18 \text{ in.}$$

M_g and M_d should be calculated based on the overall beam length of 96 ft. Since the elastic shortening loss is a part of the total loss, f_{cgp} will be conservatively computed based on M_g using the design span length of 95 ft.

$$f_{cgp} = \frac{960.4}{843.5} + \frac{(960.4)(14.18)^2}{176,829} - \frac{(955.5 + 34.7)(12)(14.18)}{176,829} = 1.278$$

Therefore, loss due to elastic shortening:

$$\Delta f_{pES} = \left(\frac{28,500}{3,834} \right) (1.278) = 9.5 \text{ ksi}$$

AASHTO LRFD C5.9.5.3 indicates that the loss due to elastic shortening at transfer should be added to the time-dependent losses to determine total losses. However, this loss at transfer is directly accounted for if transformed section properties are used in stress analysis.

9.5.7.2 Time-Dependent Losses between Transfer and Deck Placement

The following construction schedule is assumed in calculating the time-dependent losses:

$$\text{Concrete age at transfer:} \quad t_i = 1 \text{ day}$$

$$\text{Concrete age at deck placement:} \quad t_d = 90 \text{ days}$$

$$\text{Concrete age at final stage:} \quad t_f = 20,000 \text{ days}$$

The total time-dependent loss between time of transfer and deck placement is the summation of prestress loss due to shrinkage of concrete, creep of concrete, and relaxation of prestressing strands.

9.5.7.2.1 Shrinkage of Concrete

The prestress loss due to shrinkage of concrete between transfer and deck placement:

$$\Delta f_{pSR} = \varepsilon_{bid} E_p K_{id} \quad [\text{LRFD Eq. 5.9.5.4.2a-1}]$$

where

$$\varepsilon_{bid} = \text{concrete shrinkage strain of girder for time period between transfer and deck placement}$$

$$E_p = \text{modulus of elasticity of prestressing strands, ksi}$$

$$K_{id} = \text{transformed section coefficient that accounts for time-dependent interaction between concrete and bonded steel in the section being considered for time period between transfer and deck placement.}$$

BOX BEAM (BIII-48), SINGLE SPAN, COMPOSITE DECK

9.5.7.2.1 Shrinkage of Concrete

The concrete shrinkage strain, ϵ_{bi} , is taken as:

$$\epsilon_{bid} = k_{vs}k_{hs}k_fk_{td}0.48 \times 10^{-3} \quad [\text{LRFD Eq. 5.4.2.3.3.-1}]$$

where

The factor for the effect of the volume-to-surface ratio of the beam

$$k_{vs} = 1.45 - 0.13(V/S) = 1.45 - 0.13(2.72) = 1.096$$

The minimum value of k_{vs} is 1.0 OK

V/S is the volume-to-surface ratio of the beam.

The humidity factor for shrinkage:

$$k_{hs} = 2.00 - 0.014H = 2.00 - 0.014(70) = 1.020$$

where H = average annual mean relative humidity (assume 70%)

The factor for the effect of the concrete strength:

$$k_f = \frac{5}{1 + f'_{ci}} = \frac{5}{1 + 4.0} = 1.000$$

The time development factor at deck placement:

$$k_{td} = \frac{t}{61 - (4f'_{ci}) + t} = \frac{89}{61 - 4(4.0) + 89} = 0.664 = k_{tda}$$

where t is the maturity of concrete(days) = $t_d - t_i = 90 - 1 = 89$ days

$$\epsilon_{bid} = (1.096)(1.020)(1.000)(0.664)(0.48 \times 10^{-3}) = 0.000356$$

$$K_{id} = \frac{1}{1 + \frac{E_p A_{ps}}{E_{ci} A_g} \left(1 + \frac{A_g (e_{pg})^2}{I_g} \right) [1 + 0.7\Psi_b(t_f, t_i)]} \quad [\text{LRFD Eq. 5.9.5.4.2a-2}]$$

where

e_{pg} = eccentricity of prestressing strand with respect to centroid of girder, in.

$\Psi_b(t_f, t_i)$ = girder creep coefficient at final time due to loading introduced at transfer

For the time between transfer and final time:

$$\Psi_b(t_f, t_i) = 1.9 k_{vs}k_{hc}k_fk_{td}t_i^{-0.118} \quad [\text{LRFD Eq. 5.4.2.3.2-1}]$$

$$k_{hc} = 1.56 - 0.008H = 1.56 - 0.008(70) = 1.000$$

$$k_{td} = \frac{t}{61 - 4f'_{ci} + t} = \frac{20,000 - 1}{61 - 4(4.0) + (20,000 - 1)} = 0.998 = k_{tdf}$$

$$\begin{aligned} \Psi_b(t_f, t_i) &= 1.9(1.096)(1.000)(1.000)(0.998)(1)^{-0.118} \\ &= 2.078 \end{aligned}$$

$$K_{id} = \frac{1}{1 + \frac{28,500}{3,834} \frac{4.743}{813} \left(1 + \frac{813(14.71)^2}{168,367} \right) [1 + 0.7(2.078)]} = 0.821 \text{ ksi}$$

The prestress loss due to shrinkage of concrete between transfer and deck placement is:

$$\Delta f_{psr} = (0.000356)(28,500)(0.821) = 8.330 \text{ ksi}$$

BOX BEAM (BIII-48), SINGLE SPAN, COMPOSITE DECK

9.5.7.2.2 Creep of Concrete/9.5.7.3.1 Shrinkage of Concrete

9.5.7.2.2 Creep of Concrete

The prestress loss due to creep of girder concrete between time of transfer and deck placement is:

$$\Delta f_{pCR} = \frac{E_p}{E_{ci}} f_{cgp} \Psi_b(t_d, t_i) K_{id} \quad [\text{LRFD Eq. 5.9.5.4.2b-1}]$$

where

$$\begin{aligned} \Psi_b(t_d, t_i) &= \text{girder creep coefficient at time of deck placement due to loading introduced at transfer} \\ &= 1.9k_{vs}k_{hc}k_fk_{td}t_i^{-0.118} \quad [\text{LRFD Eq. 5.4.2.3.2-1}] \\ &= 1.9(1.096)(1.000)(1.000)(0.664)(1)^{-0.118} \\ &= 1.383 \end{aligned}$$

$$\Delta f_{pCR} = \frac{28,500}{3,834} (1.278)(1.383)(0.821) = 10.787 \text{ ksi}$$

9.5.7.2.3 Relaxation of Prestressing strands

The prestress loss due to relaxation of prestressing strands between time of transfer and deck placement is determined as:

$$\Delta f_{pR1} = \frac{f_{pt}}{K_L} \left(\frac{f_{pt}}{f_{py}} - 0.55 \right) \quad [\text{LRFD Eq. 5.9.5.4.2c-1}]$$

where

$$\begin{aligned} f_{pt} &= \text{stress in prestressing strands immediately after transfer, taken not less than } 0.55f_y \\ K_L &= 30 \text{ for low-relaxation strands and } 7 \text{ for other prestressing steel, unless more accurate} \\ &\quad \text{manufacturer's data are available} \end{aligned}$$

$$\Delta f_{pR1} = \frac{(202.5 - 9.5)}{30} \left(\frac{(202.5 - 9.5)}{243} - 0.55 \right) = 1.571 \text{ ksi}$$

According to LRFD Art. 5.9.5.4.2c, the relaxation loss may also be assumed equal to 1.2 ksi for low-relaxation strands.

9.5.7.3 Time-Dependent Losses between Deck Placement and Final Time

The total time-dependent loss between time of deck placement and final time is the summation of prestress loss due to shrinkage of beam concrete, creep of beam concrete, relaxation of prestressing strands, and shrinkage of deck concrete.

9.5.7.3.1 Shrinkage of Concrete

The prestress loss due to shrinkage of concrete between deck placement and final time is calculated by:

$$\Delta f_{pSD} = \varepsilon_{bdf} E_p K_{df} \quad [\text{LRFD Eq. 5.9.5.4.3a-1}]$$

where

$$\begin{aligned} \varepsilon_{bdf} &= \text{concrete shrinkage strain of girder for the time period between deck placement and final time} \\ E_p &= \text{modulus of elasticity of prestressing strands, ksi} \\ K_{df} &= \text{transformed section coefficient that accounts for time-dependent interaction between concrete and} \\ &\quad \text{bonded steel in the section being considered for time period between deck placement and final time} \end{aligned}$$

The total girder concrete shrinkage strain between transfer and final time is taken as:

$$\begin{aligned} \varepsilon_{bif} &= k_{vs}k_{hs}k_fk_{td}(0.48 \times 10^{-3}) \quad [\text{LRFD Eq. 5.4.2.3.3-1}] \\ &= (1.096)(1.020)(1.000)(0.998)(0.48 \times 10^{-3}) = 0.000536 \end{aligned}$$

The girder concrete shrinkage strain between deck placement and final time is:

$$\varepsilon_{bdf} = \varepsilon_{bif} - \varepsilon_{bid} = 0.000536 - 0.000356 = 0.000180$$

BOX BEAM (BIII-48), SINGLE SPAN, COMPOSITE DECK

9.5.7.3.1 Shrinkage of Concrete/9.5.7.3.2 Creep of Concrete

The beam concrete transformed section coefficient between deck placement and final time is:

$$K_{df} = \frac{1}{1 + \frac{E_p}{E_{ci}} \frac{A_{ps}}{A_c} \left(1 + \frac{A_c (e_{pc})^2}{I_c} \right) [1 + 0.7 \Psi_b(t_f, t_i)]} \quad [\text{LRFD Eq. 5.9.5.4.3a-2}]$$

where

$$A_c = \text{area of the composite section} = 1,049.1 \text{ in.}^2$$

$$I_c = \text{moment of inertia of the composite section,} = 261,257 \text{ in.}^4$$

$$e_{pc} = \text{eccentricity of strands with respect to centroid of composite section} \\ = 24.34 - 4.58 = 19.76 \text{ in.}$$

$$K_{df} = \frac{1}{1 + \left(\frac{28,500}{3,834} \right) \left(\frac{4.743}{1,049.1} \right) \left(1 + \frac{(1,049.1)(19.76)^2}{261,257} \right) [1 + 0.7(2.078)]} = 0.825$$

The prestress loss due to shrinkage of concrete between deck placement and final time is:

$$\Delta f_{pSD} = (0.000180)(28,500)(0.825) = 4.232 \text{ ksi}$$

9.5.7.3.2 Creep of Concrete

The prestress loss due to creep of beam concrete between deck placement and final time is determined as:

$$\Delta f_{pCD} = \frac{E_p}{E_{ci}} f_{cp} g [\Psi_b(t_f, t_i) - \Psi_b(t_d, t_i)] K_{df} + \frac{E_p}{E_c} \Delta f_{cd} \Psi_b(t_f, t_d) K_{df} \quad [\text{LRFD Eq. 5.9.5.4.3b-1}]$$

where

Δf_{cd} = change in concrete stress at centroid of prestressing strands due to long term losses between transfer and deck placement, combined with deck weight and superimposed loads, ksi

$$\begin{aligned} &= -(\Delta f_{pSR} + \Delta f_{pCR} + \Delta f_{pR1}) \frac{A_{ps}}{A_g} \left(1 + \frac{A_g (e_{pg})^2}{I_g} \right) - \left(\frac{M_s e_{tf}}{I_{tf}} + \frac{(M_b + M_{ws}) e_{tc}}{I_{tc}} \right) \\ &= -(8.330 + 10.787 + 1.571) \frac{4.743}{813} \left(1 + \frac{(813)(14.71)^2}{168,367} \right) \\ &\quad - \left(\frac{(338.4)(12)(14.24)}{175,822} + \frac{(97.0 + 100.4)(12)(19.27)}{273,299} \right) = -0.743 \text{ ksi} \end{aligned}$$

$\Psi_b(t_f, t_d)$ = beam creep coefficient at final time due to loading at deck placement

$$= 1.9 k_{vs} k_{hc} k_f k_{tdf} t_d^{-0.118} \quad [\text{LRFD Eq. 5.4.2.3.2-1}]$$

$$k_{tdf} = \frac{t}{61 - 4f'_{ci} + t} = \frac{20,000 - 90}{61 - 4(4.0) + (20,000 - 90)} = 0.998$$

$$\Psi_b(t_f, t_d) = 1.9(1.096)(1.000)(1.000)(0.998)(90)^{-0.118} = 1.222$$

The gross section properties are used in the equation to calculate Δf_{cd} for the long-term losses since the transformed section effect has already been included in the factor K_{df} when calculating the losses between initial time and deck placement.

$$\begin{aligned} \Delta f_{pCD} &= \frac{28,500}{3,834} (1.278)(2.078 - 1.383)(0.825) + \frac{28,500}{4,287} (-0.743)(1.222)(0.825) \\ &= 0.467 \text{ ksi} \end{aligned}$$

BOX BEAM (BIII-48), SINGLE SPAN, COMPOSITE DECK

9.5.7.3.3 Relaxation of Prestressing Strands/9.5.7.3.4 Shrinkage of Deck Concrete

9.5.7.3.3 Relaxation of Prestressing Strands

The prestress loss due to relaxation of prestressing strands in the composite section between time of deck placement and final time is taken as:

$$\Delta f_{pR2} = \Delta f_{pR1} = 1.571 \text{ ksi} \quad [\text{LRFD Eq. 5.9.5.4.3c-1}]$$

9.5.7.3.4 Shrinkage of Deck Concrete

The prestress gain due to shrinkage of deck concrete is calculated by:

$$\Delta f_{pSS} = \frac{E_p}{E_c} \Delta f_{cdf} K_{df} [1 + 0.7\Psi_b(t_f, t_d)] \quad [\text{LRFD Eq.5.9.5.4.3d-1}]$$

where

Δf_{cdf} = change in concrete stress at centroid of prestressing strands due to shrinkage of deck concrete, ksi

$$= \frac{\epsilon_{ddf} A_d E_{cd}}{1 + 0.7\Psi_d(t_f, t_d)} \left(\frac{1}{A_c} - \frac{e_{pc} e_d}{I_c} \right) \quad [\text{LRFD Eq.5.9.5.4.3d-2}]$$

where

ϵ_{ddf} = shrinkage strain of deck concrete between placement and final time

A_d = area of deck concrete, in.²

E_{cd} = modulus of elasticity of deck concrete, ksi

$\Psi_d(t_f, t_d)$ = deck concrete creep coefficient at final time due to loading introduced shortly after deck placement

e_d = eccentricity of deck with respect to the gross composite section, in.

Assume the initial strength of concrete at deck placement is $0.8(4.0 \text{ ksi}) = 3.2 \text{ ksi}$, and use a volume-to-surface ratio (V/S) of 2.466 for the deck:

$$k_{vs} = 1.45 - 0.13(V/S) = 1.45 - 0.13(2.466) = 1.129 > 1.0$$

Use $k_{vs} = 1.129$

$$k_f = \frac{5}{1 + f'_{ci}} = \frac{5}{1 + 3.2} = 1.190$$

$$k_{td} = \frac{t}{61 - 4f'_{ci} + t} = \frac{20,000 - 90}{61 - 4(3.2) + (20,000 - 90)} = 0.998$$

$$\epsilon_{ddf} = k_{vs} k_{hs} k_f k_{td} 0.48 \times 10^{-3} \quad [\text{LRFD Eq. 5.4.2.3.3-1}]$$

$$= (1.129)(1.020)(1.190)(0.998)(0.48 \times 10^{-3})$$

$$= 0.000656$$

$$\Psi_d(t_f, t_d) = 1.9 k_{vs} k_{nc} k_f k_{td} t_i^{-0.118} \quad [\text{LRFD Eq. 5.4.2.3.2-1}]$$

$$= 1.9(1.129)(1.000)(1.190)(0.998)(1)^{-0.118} = 2.548$$

Creep of deck concrete is assumed to start at 1 day.

$$\Delta f_{cdf} = \frac{0.000656(48 \times 5)(3,834)}{1 + 0.7(2.548)} \left(\frac{1}{1,049.1} - \frac{(19.77)(44.5 - (5/2) - 24.34)}{261,257} \right)$$

$$= -0.083 \text{ ksi} \quad \text{The negative sign indicates a prestressing gain.}$$

The prestress gain due to shrinkage of the deck in the composite section:

$$\Delta f_{pSS} = \frac{28,500}{4,287} (-0.083)(0.825)[1 + 0.7(1.222)] = -0.845 \text{ ksi}$$

Note: The effect of deck shrinkage on the calculation of prestress gain is discussed further in Section 9.1a.8.5

BOX BEAM (BIII-48), SINGLE SPAN, COMPOSITE DECK

9.5.7.3.5 Total Time-Dependent Loss/9.5.7.3.7 Total Losses at Service Loads

9.5.7.3.5 Total Time-Dependent Loss

The total time-dependent loss, Δf_{pLT} , is determined as:

$$\begin{aligned}\Delta f_{pLT} &= (\Delta f_{pSR} + \Delta f_{pCR} + \Delta f_{pR1}) + (\Delta f_{pSD} + \Delta f_{pCD} + \Delta f_{pR2} + \Delta f_{pSS}) && \text{[LRFD Eq. 5.9.5.4.1-1]} \\ &= (8.330 + 10.787 + 1.571) + (4.232 + 0.467 + 1.571 - 0.845) \\ &= 26.1 \text{ ksi}\end{aligned}$$

9.5.7.3.6 Total Losses at Transfer

AASHTO LRFD C5.9.5.2.3a and C5.9.5.3 indicate that the losses or gains due to elastic deformation must be taken equal to zero if transformed section properties are used in stress analysis. However, the losses or gains due to elastic deformation must be included in determining the total prestress losses and the effective stress in prestressing strands.

$$\Delta f_{pi} = \Delta f_{pES} = 9.5 \text{ ksi}$$

$$\text{Effective stress in tendons immediately after transfer, } f_{pt} = f_{pi} - \Delta f_{pi} = (202.5 - 9.5) = 193.0 \text{ ksi}$$

$$\text{Force per strand} = (f_{pt})(\text{area of strand}) = (193.0)(0.153) = 29.5 \text{ kips}$$

$$\text{Therefore, the total prestressing force after transfer, } P_{pt} = 29.5(31) = 914.5 \text{ kips}$$

$$\text{Initial loss, \%} = (\text{Total losses at transfer})/(f_{pi}) = 9.5/202.5 = 4.7\%$$

When determining the concrete stress using transformed section properties, the strand force is that before transfer:

$$\text{Force per strand} = (202.5)(0.153) = 30.98 \text{ kips}$$

$$\text{The total prestressing force after transfer, } P_{pi} = 30.98(31) = 960.4 \text{ kips}$$

9.5.7.3.7 Total Losses at Service Loads

Total loss due to elastic shortening at transfer and long-term losses is:

$$\Delta f_{pT} = \Delta f_{pES} + \Delta f_{pLT} = 9.5 + 26.1 = 35.6 \text{ ksi}$$

The elastic gain due to deck weight, superimposed dead load and live load (Service III) is:

$$\begin{aligned}&\left(\frac{M_s e_{tf}}{I_{tf}} + \frac{(M_b + M_{ws})e_{tc}}{I_{tc}}\right)\frac{E_p}{E_c} + 0.8\left(\frac{(M_{LT} + M_{LL})e_{tc}}{I_{tc}}\right)\frac{E_p}{E_c} \\ &= \left(\frac{(338.4)(12)(14.24)}{175,822} + \frac{(97.0 + 100.4)(12)(19.27)}{273,299}\right)\frac{28,500}{4,287} \\ &\quad + 0.8\left(\frac{(551.5 + 209.4)(12)(14.24)}{273,299}\right)\frac{28,500}{4,287} \\ &= 3.3 + 2.5 = 5.8 \text{ ksi}\end{aligned}$$

The effective stress in strands after all losses and gains:

$$f_{pe} = f_{pi} - \Delta f_{pT} + 5.8 = 202.5 - 35.6 + 5.8 = 172.7 \text{ ksi}$$

Check prestressing stress limit at service limit state:

[LRFD Table 5.9.3-1]

$$f_{pe} \leq 0.8 f_{py} = 0.8(243) = 194.4 \text{ ksi} > 172.7 \text{ ksi} \quad \text{OK}$$

The effective stress in strands after all losses and permanent gains:

$$f_{pe} = f_{pi} - \Delta f_{pT} + 3.3 = 202.5 - 35.6 + 3.3 = 170.2 \text{ ksi}$$

$$\text{Force per strand without live load gains} = (f_{pe})(\text{area of strand}) = (170.2)(0.153) = 26.04 \text{ kips}$$

$$\text{Therefore, the total prestressing force after all losses} = 26.04(31) = 807.2 \text{ kips}$$

$$\text{Final losspercentage} = (\text{total losses and gains})/(f_{pi}) = (35.6 - 3.30)/(202.5) = 16.0 \%$$

The initial estimate of final losses of 20.0%, which was used to determine the number of strands, is conservative and a second iteration is not necessary. For greater accuracy, a second iteration could be performed.

BOX BEAM (BIII-48), SINGLE SPAN, COMPOSITE DECK

9.5.7.3.7 Total Losses at Service Loads/9.5.8.2 Stresses at Transfer Length Section

When determining the concrete stress using transformed section properties, all the elastic gains and losses are implicitly accounted for:

Force per strand with only total time-dependent losses = $(f_{pi} - \Delta f_{pLT})(\text{area of strand}) = (202.5 - 26.1)(0.153) = 26.99$ kips

Total prestressing force, $P_{pe} = (26.99)(31) = 836.7$ kips

9.5.8 CONCRETE STRESSES AT TRANSFER

Because the transformed section is used, the total prestressing force before transfer, $P_{pi} = 914.5$ kips.

9.5.8.1 Stress Limits for Concrete

Compression:

[LRFD Art. 5.9.4]

- $0.6f'_{ci} = 0.6(4.0) = +2.400$ ksi

where f'_{ci} = concrete strength at transfer = 4.000 ksi

Tension:

- without bonded auxiliary reinforcement

$$-0.0948 \sqrt{f'_{ci}} \leq -0.200 \text{ ksi} = -0.0948 \sqrt{4.000} = -0.190 \text{ ksi} \leq -0.200 \text{ ksi} \quad \text{OK}$$

- with bonded auxiliary reinforcement that is sufficient to resist 120% of the tension force in the cracked concrete

$$-0.24 \sqrt{f'_{ci}} = -0.24 \sqrt{4.000} = -0.480 \text{ ksi}$$

9.5.8.2 Stresses at Transfer Length Section

Stresses at this location need only be checked at transfer, because this stage almost always governs. Also, losses with time will reduce the concrete stresses making them less critical.

Transfer length = 60(strand diameter) = 60(0.5) = 30 in. = 2.5 ft

[LRFD Art. 5.11.4]

The transfer length extends to approximately 2.5 ft from the end of the beam or 2.0 ft from centerline of the bearing. Due to the camber of the beam at release, the self weight of the beam and diaphragm act on the overall beam length, 96 ft. Therefore, the values of bending moment given in **Table 9.5.4-1** cannot be used at transfer because they are based on the design span, 95 ft. Using Eq. 9.5.4.1.2-2 given previously, the bending moments at the end of the transfer zone due to beam and diaphragm weights, are:

$$M_g = 0.5wx(L - x) = 0.5(0.847)(2.5)(96 - 2.5) = 99.0 \text{ ft-kips, and}$$

$$M_d = (0.73 + 0.73/2)2.5 = 2.7 \text{ ft-kips}$$

Compute stress in top of beam:

$$f_t = \frac{P_{pi}}{A_{ti}} - \frac{P_{pi}e_{ti}}{S_{tti}} + \frac{(M_g + M_d)}{S_{tti}} = \frac{960.4}{843.5} - \frac{(960.4)(14.18)}{8,737} + \frac{(99.0 + 2.7)(12)}{8,736}$$

$$= 1.139 - 1.559 + 0.140 = -0.280 \text{ ksi}$$

The tension stress limit for concrete with no bonded reinforcement: -0.190 ksi NG

Tension stress limit for concrete with bonded reinforcement: -0.480 ksi OK

Compute stress in bottom of beam:

$$f_b = \frac{P_{pi}}{A_{ti}} + \frac{P_{pi}e_{ti}}{S_{bti}} - \frac{(M_g + M_d)}{S_{bti}} = \frac{960.4}{843.5} + \frac{(960.4)(14.18)}{9,426} - \frac{(99.0 + 2.7)(12)}{9,426}$$

$$= 1.139 + 1.445 - 0.129 = +2.455 \text{ ksi}$$

Compression stress limit for concrete: $+2.400$ ksi NG

Therefore, try debonding seven strands from the strand group at 2 in. from bottom for a distance of 5 ft 0 in. from the end of the beam or 4 ft 6 in. from centerline of bearing.

BOX BEAM (BIII-48), SINGLE SPAN, COMPOSITE DECK

9.5.8.2 Stresses at Transfer Length Section

To minimize the shock impact of detensioning and cracks at corners and bottom, assume the strand pattern shown in **Figure 9.5.8.2-1**. LRFD Article 5.11.4.3 requires that the following conditions be satisfied if debonding is used:

- Percentage of debonded of total = $7/31 = 22.6\% < 25\%$ OK
- Percentage of debonded of row = $7/23 = 30.4\% < 40\%$ OK
- All limit states should be satisfied OK
- Debonded strands should be symmetrically distributed OK
- Exterior strands in each horizontal line are fully bonded OK

Recompute the stresses at the transfer length section. Note that the transformed section properties here are different than those at midspan after debonding. Using the same method as described in Sect. 9.5.5.5, the transformed section properties at the end of the beam are computed as:

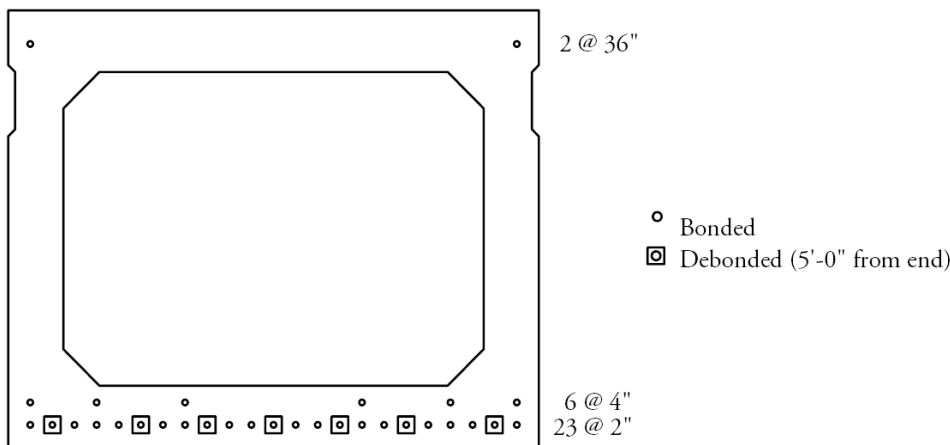
$$A_{ti} = 836.6 \text{ in.}^2$$

$$y_{bti} = 18.90 \text{ in.}$$

$$S_{tti} = 8,700 \text{ in.}^3$$

$$S_{bti} = 9,253 \text{ in.}^3$$

Figure 9.5.8.2-1
Strand Pattern at End of Beam



Distance from the center of gravity of strands to the bottom fiber of the beam is:

$$y_{bs} = [16(2) + 6(4) + 2(36)]/24 = 5.33 \text{ in.}$$

and the strand eccentricity for the transformed section at end of the beam is:

$$e_{eti} = 18.90 - 5.33 = 13.57 \text{ in.}$$

Total prestressing force before transfer at end section = $24(30.98) = 743.5$ kips

Concrete stress in top of beam:

$$f_t = \frac{743.5}{836.6} - \frac{(743.5)(13.57)}{8,700} + \frac{(99.0 + 2.7)(12)}{8,700} = 0.889 - 1.160 + 0.140 = -0.131 \text{ ksi}$$

Tension stress limit for concrete with no bonded reinforcement: -0.190 ksi OK

BOX BEAM (BIII-48), SINGLE SPAN, COMPOSITE DECK

9.5.8.2 Stresses at Transfer Length Section/9.5.8.5 Summary of Stresses at Transfer

Thus, there is no need for additional bonded reinforcement; and

$$f_b = \frac{743.5}{836.6} + \frac{(743.5)(13.57)}{9,253} - \frac{(99.0 + 2.7)(12)}{9,253} = 0.889 + 1.090 - 0.132 = +1.847 \text{ ksi}$$

Compression stress limit for concrete: +2.400 ksi OK

9.5.8.3 Stresses at Transfer Length Section of Debonded Strands

All strands are effective at this location, therefore use the full value of P_{pi} . Bending moments due to the self weight of the beam and diaphragm, at (5 ft + 2.5 ft = 7.5 ft) from the end of the beam, based on overall length, are:

$$M_g = 0.5w_g x(L - x) = 0.5 (0.847)(7.5)(96 - 7.5) = 281.1 \text{ ft-kips}$$

$$M_d = (0.73 + 0.73/2)7.5 = 8.2 \text{ ft-kips}$$

Concrete stress in top of beam:

$$f_t = \frac{P_{pi}}{A_{ti}} - \frac{P_{pi}e_{ti}}{S_{tti}} + \frac{(M_g + M_d)}{S_{tti}} = \frac{960.4}{843.5} - \frac{(960.4)(14.18)}{8,737} + \frac{(281.1 + 8.2)(12)}{8,737}$$

$$= 1.139 - 1.559 + 0.397 = -0.023 \text{ ksi}$$

Tension stress limit for concrete with no bonded reinforcement: -0.190 ksi OK

Concrete stress in bottom of beam:

$$f_b = \frac{P_{pi}}{A_{ti}} + \frac{P_{pi}e_{ti}}{S_{bti}} - \frac{(M_g + M_d)}{S_{bti}} = \frac{960.4}{843.5} + \frac{(960.4)(14.18)}{9,426} - \frac{(281.1 + 8.2)(12)}{9,426}$$

$$= 1.139 + 1.445 - 0.368 = +2.216 \text{ ksi}$$

Compression stress limit for concrete: +2.400 ksi OK

9.5.8.4 Stresses at Midspan

Bending moments due to beam self weight and diaphragm weight at midspan are:

$$M_g = 0.5w_g x(L - x) = 0.5 (0.847)(48)(96 - 48) = 975.7 \text{ ft-kips}$$

$$M_d = (0.73 + 0.73/2)(48) - 0.73(23.75) = 35.2 \text{ ft-kips}$$

All strands are effective at this location; therefore use the full value of P_{pi} .

$$f_t = \frac{P_{pi}}{A_{ti}} - \frac{P_{pi}e_{ti}}{S_{tti}} + \frac{(M_g + M_d)}{S_{tti}} = \frac{960.4}{843.5} - \frac{(960.4)(14.18)}{8,737} + \frac{(975.7 + 35.2)(12)}{8,737}$$

$$= 1.139 - 1.559 + 1.388 = +0.968 \text{ ksi}$$

Tension stress limit for concrete with no bonded reinforcement: -0.190 ksi OK

$$f_b = \frac{P_{pi}}{A_{ti}} + \frac{P_{pi}e_{ti}}{S_{bti}} - \frac{(M_g + M_d)}{S_{bti}} = \frac{960.4}{843.5} + \frac{(960.4)(14.18)}{9,426} - \frac{(975.7 + 35.2)(12)}{9,426}$$

$$= 1.139 + 1.445 - 1.287 = +1.297 \text{ ksi}$$

Compression stress limit for concrete: +2.400 ksi OK

9.5.8.5 Summary of Stresses at Transfer

	Top Fiber Stresses	Bottom Fiber Stresses
	f_t , ksi	f_b , ksi
At transfer length section of bonded strands	-0.131	+1.847
At transfer length section of debonded strands	-0.023	+2.216
At midspan	+0.968	+1.297

BOX BEAM (BIII-48), SINGLE SPAN, COMPOSITE DECK**9.5.9 Concrete Stresses at Service Loads/9.5.9.2.2 Concrete Stress at the Top Fiber of the Deck****9.5.9 CONCRETE STRESSES AT SERVICE LOADS**

Using transformed section properties and refined losses, $P_{pe} = 836.7$ kips

9.5.9.1 Stress Limits for Concrete

Compression:

[LRFD Art.5.9.4.2]

Due to permanent loads, (i.e., beam self weight, diaphragm weight, weight of slab and haunch, wearing surface weight, and barrier loads), for load combination Service I:

$$\text{for precast beams: } 0.45f'_c = 0.45(5.000) = +2.250 \text{ ksi}$$

$$\text{for deck: } 0.45f'_c = 0.45(4.000) = +1.800 \text{ ksi}$$

Due to permanent and transient loads, i.e., all dead loads and live loads, for load combination Service I:

$$\text{for precast beams: } 0.60f'_c = 0.60(5.000) = +3.000 \text{ ksi}$$

$$\text{for deck: } 0.60f'_c = 0.60(4.000) = +2.400 \text{ ksi}$$

Tension:

For components with bonded prestressing tendons:

$$\text{for load combination Service III: } -0.19\sqrt{f'_c}$$

$$\text{for precast beam: } -0.19\sqrt{5.000} = -0.425 \text{ ksi}$$

9.5.9.2 Stresses at Midspan**9.5.9.2.1 Concrete Stress at Top Fiber of the Beam**

To check top compressive stresses, two cases are considered:

1. Under permanent loads, load combination Service I:

Using bending moment values given in **Table 9.5.4-1**, compute the top fiber stresses:

$$\begin{aligned} f_{tg} &= \frac{P_{pe}}{A_{tf}} - \frac{P_{pe}e_{tf}}{S_{ttf}} + \frac{(M_g + M_d + M_s)}{S_{ttf}} + \frac{(M_{ws} + M_b)}{S_{ttc}} \\ &= \frac{836.7}{839.8} - \frac{(836.7)(14.24)}{8,713} + \frac{(955.5 + 34.7 + 338.4)(12)}{8,713} + \frac{(100.4 + 97.0)(12)}{18,040} \\ &= 0.996 - 1.367 + 1.830 + 0.131 = +1.590 \text{ ksi} \end{aligned}$$

Compressive stress limit: +2.250 ksi OK

2. Under permanent and transient loads, load combination Service I:

$$\begin{aligned} f_{tg} &= +1.590 + \frac{(M_{LT} + M_{LL})(12)}{S_{ttc}} \\ &= +1.590 + \frac{(551.5 + 209.4)(12)}{18,040} \\ &= +1.590 + 0.506 = +2.096 \text{ ksi} \end{aligned}$$

Compressive stress limit for concrete = +3.000 ksi OK

9.5.9.2.2 Concrete Stress at the Top Fiber of the Deck

Note: Compressive stress in the deck slab at service loads never controls the design for typical applications. The calculations shown below are for illustration purposes and may not be necessary in most practical applications.

1. Under permanent loads, load combination Service I:

$$f_{tc} = \frac{M_{ws} + M_b}{S_{dte}} = \frac{(100.4 + 97.0)(12)}{14,799} = +0.160 \text{ ksi}$$

Compressive stress limit: +1.800 ksi OK

BOX BEAM (BIII-48), SINGLE SPAN, COMPOSITE DECK

9.5.9.2.2 Concrete Stress at the Top Fiber of the Deck/9.5.9.5 Effect of Deck Shrinkage

2. Under permanent and transient loads, load combination Service I:

$$f_{tc} = \frac{M_{ws} + M_b}{S_{dte}} + \frac{M_{LT} + M_{LL}}{S_{dte}} = +0.160 + \frac{(551.5 + 209.4)(12)}{14,799}$$

$$= +0.160 + 0.617 = +0.777 \text{ ksi}$$

Compressive stress limit: +2.400 ksi OK

• **9.5.9.2.3 Concrete Stress in Bottom of Beam, Load Combination Service III**

$$f_b = \frac{P_{pe}}{A_{tf}} + \frac{P_{pe}e_{tf}}{S_{btf}} - \frac{(M_g + M_d + M_s)}{S_{btf}} - \frac{(M_{ws} + M_b) + 0.8(M_{LT} + M_{LL})}{S_{bte}}$$

$$= \frac{836.7}{839.8} + \frac{(836.7)(14.24)}{9,342} - \frac{(955.5 + 34.7 + 338.4)(12)}{9,342} - \frac{[(100.4 + 97.0) + 0.8(551.5 + 209.4)](12)}{11,459}$$

$$= 0.996 + 1.275 - 1.707 - 0.844 = -0.280 \text{ ksi}$$

Tensile stress limit: -0.425 ksi OK

9.5.9.3 Fatigue Stress Limit

From **Table 9.1a.4-2**, the unfactored fatigue bending moment at midspan, M_f , is 214.7 ft-kips. Therefore, stress at the top fiber of the beam due to fatigue load combination I is:

$$f_{tgf} = \frac{1.50(M_f)}{S_{ttc}} = \frac{1.50(214.7)(12)}{18,040} = +0.214 \text{ ksi}$$

At midspan, the top compressive stress due to permanent loads and prestress is:

$$f_{tg} = \frac{P_{pe}}{A_{tf}} - \frac{P_{pe}e_{tf}}{S_{ttf}} + \frac{(M_g + M_d + M_s)}{S_{ttf}} + \frac{(M_{ws} + M_b)}{S_{ttc}}$$

$$= \frac{836.7}{839.8} - \frac{(836.7)(14.24)}{8,713} + \frac{(955.5 + 34.7 + 338.4)(12)}{8,713} + \frac{(100.4 + 97.0)(12)}{18,040}$$

$$= 0.996 - 1.367 + 1.830 + 0.131 = 1.590 \text{ ksi}$$

Therefore:

$$f_{tgf} + \frac{f_b}{2} = 0.214 + \frac{1.590}{2} = 1.009 < 0.40(f'_c) = 0.40(5.0) = 2.0 \text{ ksi OK}$$

This condition should be satisfied at all locations along the beam.

9.5.9.4 Summary of Stresses at Service Loads

	Top of Deck Service I ksi		Top of Beam Service I ksi		Bottom of Beam ksi
	Permanent Loads	Total Loads	Permanent Loads	Total Loads	Service III
At midspan	+0.160	+0.777	+1.590	+2.096	-0.280

9.5.9.5 Effect of Deck Shrinkage

The calculations in Section 9.5.9.2 comply with the *LRFD Specifications*. However, PCI believes that it is not appropriate to include the prestressing gain caused by the deck shrinkage, Δf_{pss} , in calculating the prestress losses. Alternatively, the effect of deck shrinkage should be analyzed by considering it as an external force applied to the composite nontransformed section as illustrated in Section 9.1a.8.5.

BOX BEAM (BIII-48), SINGLE SPAN, COMPOSITE DECK

9.5.10 Limits of Reinforcement/9.5.11 Shear Design

9.5.10 LIMITS OF REINFORCEMENT

[LRFD Art.5.7.3.3.1]

9.5.10.1 Maximum Reinforcement

The check of maximum reinforcement limits in LRFD Article 5.7.3.3.1 was removed from the *LRFD Specifications* in 2005.

9.5.10.2 Minimum Reinforcement

[LRFD Art.5.7.3.3.2]

At any section, the amount of prestressed and nonprestressed tensile reinforcement must be adequate to develop a factored flexural resistance, M_r , equal to the lesser of:

- 1.2 times the cracking strength determined on the basis of elastic stress distribution and the modulus of rupture, and
- 1.33 times the factored moment required by the applicable strength load combination.

Check at midspan:

$$M_{cr} = S_{btc}(f_r + f_{cpe}) - M_{dnc} \left(\frac{S_{btc}}{S_{btf}} - 1 \right) \geq S_{btc}f_r \quad \text{[LRFD Eq.5.7.3.3.2-1]}$$

where

$$f_r = \text{modulus of rupture of concrete} \quad \text{[LRFD Art.5.4.2.6]}$$

$$= 0.37\sqrt{f'_c} = 0.37\sqrt{5.000} = 0.827 \text{ ksi}$$

f_{cpe} = compressive stress in concrete due to effective prestress force only (after allowance for all prestress losses) at extreme fiber of section where tensile stress is caused by externally applied loads

$$= \frac{P_{pe}}{A_{tf}} + \frac{P_{pe}e_{tf}}{S_{btf}} = \frac{836.7}{839.8} + \frac{(836.7)(14.24)}{9,342} = 2.272 \text{ ksi}$$

M_{dnc} = noncomposite dead load moment at the section

$$= M_g + M_s + M_d = 955.5 + 338.4 + 34.7 = 1,328.6 \text{ ft-kips}$$

S_{btc} = section modulus for the extreme bottom fiber of transformed composite section where the tensile stress is caused by externally applied loads = 11,459 in.³

S_{btf} = section modulus for the extreme bottom fiber of transformed section where the tensile stress is caused by externally applied loads = 9,342 in.³

$$M_{cr} = \frac{11,459}{12}(0.827 + 2.272) - (1,328.6) \left(\frac{11,459}{9,342} - 1 \right) = 2,657 \text{ ft-kips}$$

$$1.2M_{cr} = 1.2(2,657) = 3,188 \text{ ft-kips}$$

At midspan, the factored moment required by the Strength I load combination is:

$$M_u = 3,264.2 \text{ ft-kips (as calculated in Section 9.5.6)}$$

$$\text{Thus, } 1.33M_u = 1.33(3,264.2) = 4,341 \text{ ft-kips}$$

Since $1.2M_{cr} < 1.33M_u$, the $1.2M_{cr}$ requirement controls.

$$M_r = 3,645.6 \text{ ft-kips} > 1.2M_{cr} = 3,188.6 \text{ ft-kips} \quad \text{OK}$$

Note: The *LRFD Specifications* requires that this criterion be met at every section.

Illustrated based on
2011 *LRFD*
Specifications.

Editor's Note: 2012
LRFD Specifications
changes will revise
minimum
reinforcement.

9.5.11 SHEAR DESIGN

The area and spacing of shear reinforcement must be determined at regular intervals along the entire length of the beam. In this design example, transverse shear design procedures are demonstrated below by determining these values at the critical section near the supports.

BOX BEAM (BIII-48), SINGLE SPAN, COMPOSITE DECK

9.5.11 Shear Design/9.5.11.1 Critical Section

Transverse shear reinforcement is provided when:

$$V_u > 0.5\phi(V_c + V_p) \quad [\text{LRFD Eq.5.8.2.4-1}]$$

where

V_u = total factored shear force, kips

V_c = nominal shear strength provided by tensile stresses in the concrete, kips

V_p = component in the direction of the applied shear of the effective prestressing force, kips

ϕ = resistance factor = 0.9 for normal weight concrete [LRFD Art.5.5.4.2.1]

9.5.11.1 Critical Section

[LRFD Art.5.8.3.2]

The critical section near the supports is taken as the effective shear depth, d_v , from the internal face of the support.

d_v = distance between resultants of tensile and compressive forces, $(d_e - a/2)$, but not less than $(0.9d_e)$ or $(0.72h_c)$ [LRFD Art.5.8.2.7]

where

d_e = the corresponding effective depth from the extreme compression fiber to the centroid of the tensile force in the tensile reinforcement [LRFD Art. 5.8.2.9]

a = depth of compression block = 6.94 in. (at midspan, conservative estimate)

h_c = overall depth of the composite section = 44.5 in.

Note: Only 22 strands (16 at 2 in. and 6 at 4 in.) are effective at the critical section for shear, because seven strands are debonded for a distance equal to 5 ft from the end of the beam and the top level of strands is ignored.

Because the beam is a flanged section, the effective shear depth, d_v , should be determined using LRFD Eq. C5.8.2.9-1. However, d_v can be conservatively approximated as $d_e - a/2$ using the a as determined in the midspan flexural analysis in Sect. 9.5.6.

$$y_{bs} = [16(2) + 6(4)/22] = 2.55 \text{ in.}$$

$$d_e = h_c - y_{bs} = 44.5 - 2.55 = 41.95$$

$$d_v = d_e - a/2 = [41.95 - 0.5(6.94)] = 38.48 \text{ in.}$$

$$0.9d_e = 0.9(41.95) = 37.76 \text{ in.}$$

$$0.72h_c = 0.72(44.5) = 32.04 \text{ in.}$$

Therefore, $d_v = 38.48$ in.

Because the width of the bearing is not yet determined, it is conservatively assumed to be equal to zero for determining the critical section for shear, as shown in **Figure 9.5.11.1-1**. Therefore, the critical section for shear is at a distance of:

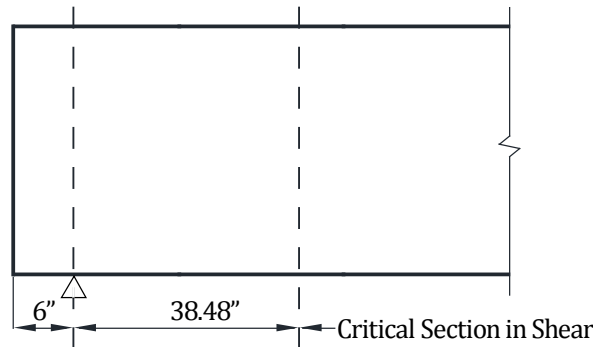
38.48 in. = 3.21 ft from centerline of support

$$x/L = 3.21/95 = 0.034L$$

BOX BEAM (BIII-48), SINGLE SPAN, COMPOSITE DECK

9.5.11.1 Critical Section/9.5.11.2.1 Strain in Flexural Tension Reinforcement

Figure 9.5.11.1-1
Critical Section in Shear



9.5.11.2 Contribution of Concrete to Nominal Shear Resistance

The contribution of the concrete to the nominal shear resistance is:

$$V_c = 0.0316\beta\sqrt{f'_c}b_vd_v \quad \text{[LRFD Eq.5.8.3.3-3]}$$

where β = a factor indicating the ability of diagonally cracked concrete to transmit tension (a value indicating concrete contribution).

Several quantities must be determined before this expression can be evaluated.

9.5.11.2.1 Strain in Flexural Tension Reinforcement

Calculate the strain at the centroid of the tension reinforcement, ϵ_s :

$$\epsilon_s = \frac{\frac{|M_u|}{d_v} + 0.5N_u + |(V_u - V_p)| - A_{ps}f_{po}}{(E_sA_s + E_pA_{ps})} \quad \text{[LRFD Eq. 5.8.3.4.2-4]}$$

where

N_u = applied factored axial force at the specified section, $0.034L = 0$ kips

V_u = applied factored shear force at the specified section, $0.034L$
 $= 1.25(37.5 + 13.3 + 1.1 + 3.8) + 1.5(3.9) + 1.75(37.2 + 12.7)$ (Tables 9.5.4-1 and 9.5.4-2)
 $= 162.8$ kips

V_p = component of the effective prestressing force in the direction of the applied shear
 $= 0$ kips since the strand pattern is straight

M_u = applied factored bending moment at the specified section, $0.034L$, which occurs simultaneously with V_u , or conservatively taken as the maximum M_u .
 $= 1.25(124.8 + 44.2 + 3.5 + 12.7) + 1.5(13.1) + 1.75(77.1 + 27.3)$ [Tables 9.5.4-1 and 9.5.4-2]
 $= 433.9$ ft-kips

M_u need not to be taken less than $(V_u - V_p)d_v$
 $= (163.0 - 0.0)(38.48)/12$
 $= 522.7$ ft-kips. (Controls)

f_{po} = a parameter taken as modulus of elasticity of prestressing tendons multiplied by the locked-in difference in strain between the prestressing tendons and the surrounding concrete, ksi. For pretensioned members, LRFD Article C5.8.3.4.2 indicates that f_{po} can be taken as $0.7f_{pu}$. (Note: use this for both pretensioned and post-tensioned systems made with stress relieved and low relaxation strands).
 $= 0.7(270.0) = 189.0$ ksi

BOX BEAM (BIII-48), SINGLE SPAN, COMPOSITE DECK**9.5.11.2.1 Strain in Flexural Tension Reinforcement/9.5.11.3.2 Required Area of Reinforcement**

$$A_{ps} = \text{area of prestressing strands on the flexural tension side of the member}$$

$$= 22(0.153) = 3.366 \text{ in.}^2 \text{ (Only 22 strands of the 29 strands are effective in the flexural tension side because 7 strands are debonded.)}$$

$$A_s = \text{area of nonprestressing steel on the flexural tension side of the member}$$

$$= 0.0 \text{ in.}^2$$

$$\epsilon_s = \frac{\frac{|(522.7)(12)|}{38.48} + 0 + |(162.8 - 0)| - 3.366(189.0)}{(0 + 28,500(3.366))} = -3.235 \times 10^{-3}$$

ϵ_s is less than zero. Use $\epsilon_s = 0$.

9.5.11.2.2 Values of β and θ

Assume the section contains at least the minimum amount of transverse reinforcement:

$$\beta = \frac{4.8}{(1 + 750\epsilon_s)} = \frac{4.8}{(1 + 0)} = 4.8 \quad \text{[LRFD Eq.5.8.3.4.2-1]}$$

Angle of diagonal compressive stresses is:

$$\theta = 29 + 3,500\epsilon_s = 29 + 3,500(0) = 29^\circ \quad \text{[LRFD Eq.5.8.3.4.2-3]}$$

9.5.11.3 Compute Concrete Contribution

The nominal shear resisted by the concrete is:

$$V_c = 0.0316\beta\sqrt{f'_c}b_vd_v \quad \text{[LRFD Eq.5.8.3.3-3]}$$

where b_v = effective web width = 10 in.

$$V_c = 0.0316(4.8)\sqrt{5.0}(10)(38.48) = 130.5 \text{ kips}$$

9.5.11.3 Contribution of Reinforcement to Nominal Shear Resistance**9.5.11.3.1 Requirement for Reinforcement**

$$\text{Check if } V_u > 0.5\phi(V_c + V_p) \quad \text{[LRFD Eq.5.8.2.4-1]}$$

$$V_u = 163.0 \text{ kips} > 0.5\phi(V_c + V_p) = [0.5(0.9)](130.5 + 0) = 58.7 \text{ kips}$$

Therefore, transverse shear reinforcement must be provided.

9.5.11.3.2 Required Area of Reinforcement

$$V_u/\phi \leq V_n = V_c + V_s + V_p \quad \text{[LRFD Eq.5.8.3.3-1]}$$

where

$$V_s = \text{shear resistance provided by shear reinforcement}$$

$$= (V_u/\phi) - V_c - V_p = (163.0/0.9) - 130.5 - 0 = 50.6 \text{ kips}$$

$$V_s = \frac{A_v f_{yh} d_v (\cot \theta + \cot \alpha) (\sin \alpha)}{s} \quad \text{[LRFD Eq. 5.8.3.3-4]}$$

where

$$A_v = \text{area of shear reinforcement within a distance } s, \text{ in.}^2$$

$$s = \text{spacing of stirrups, in.}$$

$$f_{yh} = \text{specified yield strength of shear reinforcement, ksi}$$

$$\alpha = \text{angle of inclination of transverse reinforcement to longitudinal axis}$$

$$= 90^\circ \text{ for vertical stirrups}$$

BOX BEAM (BIII-48), SINGLE SPAN, COMPOSITE DECK

9.5.11.3.2 Required Area of Reinforcement/9.5.12.1 Factored Horizontal Shear

Therefore, area of shear reinforcement within a spacing s is:

$$A_v = (sV_s)/(f_{yh}d_v \cot \theta)$$

$$= [s(50.6)]/[(60.0)(38.48) \cot 29^\circ] = 0.0121(s)$$

If $s = 12$ in., then $A_v = 0.15$ in.²/ft

9.5.11.3.3 Determine Spacing of Reinforcement

Check maximum spacing of transverse reinforcement.

[LRFD Art.5.8.2.7]

$$v_u = \frac{|V_u - \phi V_p|}{\phi b_v d_v} = \frac{|163.0 - 0|}{(0.9)(10)(38.48)} = 0.471 \text{ ksi}$$

[LRFD Eq.5.8.2.9-1]

$$0.125f'_c = 0.125(5.0) = 0.625 \text{ ksi}$$

Since $v_u = 0.471 \text{ ksi} < 0.125f'_c$

$$s \leq 24 \text{ in. (Controls)}$$

[LRFD Eq.5.8.2.7-1]

$$s \leq 0.8d_v = (0.8)(38.48) = 30.78 \text{ in.}$$

s provided = 12 in. < 24 in. OK

Use No. 3 single leg in each web at 12 in. spacing

A_v provided = 0.22 in.²/ft > A_v required = 0.15 in.² OK

$$V_s = \frac{(0.22)(60)(38.48)(\cot 29^\circ)}{12} = 76.4 \text{ kips}$$

9.5.11.3.4 Minimum Reinforcement Requirement

[LRFD Art.5.8.2.5]

The area of transverse reinforcement should not be less than:

$$0.0316\sqrt{f'_c} \frac{b_v s}{f_{yh}} = 0.0316\sqrt{5.0} \frac{(10)(12)}{60.0} = 0.14 \text{ in.}^2/\text{ft} < 0.22 \text{ in.}^2/\text{ft} \quad \text{OK}$$

[LRFD Eq.5.8.2.5-1]

9.5.11.4 Maximum Nominal Shear Resistance

In order to assure that the concrete in the web of the beam will not crush prior to yield of the transverse reinforcement, the *LRFD Specifications* gives an upper limit for V_n as follows:

$$V_n = 0.25f'_c b_v d_v + V_p \quad \text{[LRFD Eq.5.8.3.3-2]}$$

Comparing this equation with [LRFD Eq.5.8.3.3-1], it can be concluded that

$$V_c + V_s \text{ must not be greater than } 0.25f'_c b_v d_v$$

$$130.5 + 76.4 = 206.9 \text{ kips} \leq 0.25(5.0)(10)(38.48) = 481.0 \text{ kips} \quad \text{OK}$$

Using the above procedures, the transverse reinforcement can be determined at increments along the entire length of the beam.

9.5.12 INTERFACE SHEAR TRANSFER**9.5.12.1 Factored Horizontal Shear**

[LRFD Art.5.8.4]

At the strength limit state, the horizontal shear at a section on a per unit basis can be taken as:

$$V_{hi} = \frac{V_u}{d_v} \quad \text{[LRFD Eq.C5.8.4.2-7]}$$

where

$$V_{hi} = \text{horizontal factored shear force per unit length of the beam, kips/in.}$$

BOX BEAM (BIII-48), SINGLE SPAN, COMPOSITE DECK**9.5.12.1 Factored Horizontal Shear/9.5.12.3.1 Minimum Interface Shear Reinforcement**

V_u = factored shear force at specified section due to superimposed loads after the deck is cast, kips

d_v = the distance between the centroid of the tension steel and the mid-thickness of the slab = $(d_e - t_s/2)$
 $= 41.95 - (5.0/2) = 39.45$ in.

The *LRFD Specifications* does not identify the location of the critical section. For convenience, it will be assumed here to be the same location as the critical section for vertical shear, at point 0.034L.

Using load combination Strength I:

$$V_u = 1.25(37.5+13.3+3.8) + 1.5(3.9) + 1.75(37.2 + 12.7) = 161.4 \text{ kips} \quad (\text{Tables 9.5.4-1 and 9.5.4-2})$$

Therefore, the applied factored horizontal shear is:

$$V_{hi} = \frac{161.4}{39.45} = 4.09 \text{ kips/in.}$$

9.5.12.2 Required Nominal Resistance

$$\text{Required } V_{ni} = V_{hi}/\phi = 4.09/0.9 = 4.54 \text{ kips/in.} \quad [\text{LRFD Eq. 5.8.4.1-1}]$$

9.5.12.3 Required Interface Shear Reinforcement

The nominal shear resistance of the interface surface is:

$$V_{ni} = cA_{cv} + \mu[A_{vf}f_{yh} + P_c] \quad [\text{LRFD Eq.5.8.4.1-3}]$$

where

c = cohesion factor, ksi [LRFD Art. 5.8.4.3]

A_{cv} = area of concrete section resisting shear transfer, in.²

μ = coefficient of friction [LRFD Art. 5.8.4.3]

A_{vf} = area of shear reinforcement crossing the shear plane, in.²

f_{yh} = specified yield strength of shear reinforcement, ksi

P_c = permanent net compressive force normal to the shear plane, kips

For cast-in-place concrete slabs placed on clean concrete girder surface intentionally roughened: [LRFD Art.5.8.4.3]

c = 0.28 ksi

μ = 1.0

The actual contact width, b_v , between the slab and the beam is 48 in.

$$A_{cv} = (48.0 \text{ in})(1.0 \text{ in.}) = 48.0 \text{ in.}^2$$

LRFD Eq.5.8.4.1-3 can be solved for A_{vf} as follows:

$$4.54 = (0.28)(48.0) + 1.0[A_{vf}(60.0) + 0]$$

Solving for A_{vf} ,

$$A_{vf}(\text{req'd}) < 0$$

Since the resistance provided by cohesion is greater than the applied force, provide the minimum required interface reinforcement.

9.5.12.3.1 Minimum Interface Shear Reinforcement

$$A_{vf} \geq (0.05A_{cv})/f_{yh} \quad [\text{LRFD Eq.5.8.4.4-1}]$$

From the design of vertical shear reinforcement, a No. 3 single-leg bar in each web at 12-in. spacing is provided from the beam extending into the deck. Therefore, $A_{vf} = 0.22 \text{ in.}^2/\text{ft}$.

$$A_{vf} = (0.22 \text{ in.}^2/\text{ft}) < (0.05A_{cv})/f_{yh} = 0.05(48)/60 = 0.04 \text{ in.}^2/\text{in.} = 0.48 \text{ in.}^2/\text{ft} \quad \text{NG}$$

BOX BEAM (BIII-48), SINGLE SPAN, COMPOSITE DECK**9.5.12.3.1 Minimum Interface Shear Reinforcement/9.5.13.1 Required Reinforcement at Face of Bearing**

However, LRFD Article 5.8.4.4 states that the minimum reinforcement need not exceed the amount needed to resist $1.33 V_{hi}/\phi$ as determined using LRFD Eq. 5.8.4.1-3.

$$(1.33 \times 4.09/0.9) = (0.28 \times 48.0) + 1.0[A_{vf}(60) + 0]$$

Solving for A_{vf} ,

$$A_{vf}(\text{req'd}) < 0 \quad \text{OK}$$

9.5.12.4 Maximum Nominal Shear Resistance

$$V_{ni} \leq K_1 f'_c A_{cv} \text{ or } K_2 A_{cv}$$

$$V_{ni} \text{ provided} = (0.28)(48) + 1.0 \left(\frac{0.22}{12} (60.0) + 0 \right) = 14.54 \text{ kips/in.}$$

$$K_1 f'_c A_{cv} = (0.3)(4.0)(48) = 57.6 \text{ kips/in.}$$

$$K_2 A_{cv} = (1.8)(48) = 86.4 \text{ kips/in.}$$

$$\text{Since provided } V_{ni} \leq 0.3 f'_c A_{cv} \quad \text{OK}$$

[LRFD Eq.5.8.4.1-4]

$$\leq 1.8 A_{cv} \quad \text{OK}$$

[LRFD Eq.5.8.4.1-5]

9.5.13 MINIMUM LONGITUDINAL REINFORCEMENT REQUIREMENT [LRFD Art.5.8.3.5]

Longitudinal reinforcement should be proportioned so that at each section the following equation is satisfied:

$$A_{ps} f_{ps} + A_s f_y \geq \frac{M_u}{d_v \phi_f} + 0.5 \frac{N_u}{\phi_c} + \left(\left| \frac{V_u}{\phi_v} - V_p \right| - 0.5 V_s \right) \cot \theta \quad \text{[LRFD Eq.5.8.3.5-1]}$$

where

A_{ps} = area of prestressing strand at the tension side of the section, in.²

f_{ps} = average stress in prestressing strand at the time for which nominal resistance is required, ksi

A_s = area of nonprestressed tension reinforcement, in.²

f_y = specified yield strength of reinforcing bars, ksi

M_u = factored moment at the section corresponding to the factored shear force, ft-kips

d_v = effective shear depth, in.

ϕ = resistance factor as appropriate moment, shear, and axial resistance. Therefore, [LRFD Art. 5.5.4.2] different ϕ factors will be used for the terms in LRFD Eq. 5.8.3.5-1, depending on the type of action considered.

N_u = applied factored axial force = 0.0 kips

V_u = factored shear force at section, kips

V_p = component in the direction of the applied shear of the effective prestressing force, kips

V_s = shear resistance provided by shear reinforcement, kips

θ = angle of inclination of diagonal compressive stresses

9.5.13.1 Required Reinforcement at Face of Bearing

[LRFD Art.5.8.3.5]

For simple end supports, the longitudinal reinforcement on the flexural tension side of the member at inside face of bearing should satisfy:

$$A_{ps} f_{ps} + A_s f_y \geq \left(\frac{V_u}{\phi_v} - 0.5 V_s - V_p \right) \cot \theta \quad \text{[LRFD Eq.5.8.3.5-2]}$$

BOX BEAM (BIII-48), SINGLE SPAN, COMPOSITE DECK

9.5.13.1 Required Reinforcement at Face of Bearing

$$M_u = 0 \text{ ft-kips}$$

$$N_u = 0 \text{ kips}$$

Because the width of the bearing is not yet determined, it is assumed to be zero. This assumption is conservative for these calculations. Therefore, the failure crack assumed for this analysis radiates from the centerline of the bearing, 6 in. from the end of the beam.

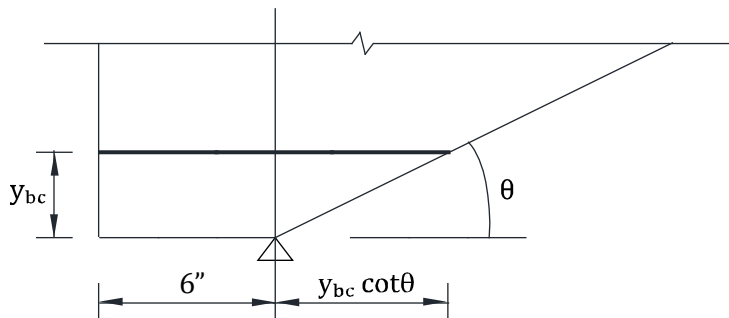
From **Tables 9.5.4-1** and **9.5.4-2**, using load combination Strength I, the factored shear force at this section is :

$$V_u = 1.25(40.2 + 14.3 + 4.1 + 1.1) + 1.5(4.2) + 1.75(38.6 + 13.6) = 172.3 \text{ kips}$$

$$\left(\frac{V_u}{\phi_v} - 0.5V_s - V_p\right) \cot \theta = \left(\frac{172.3}{0.9} - 0.5(76.4) - 0\right) \cot 29^\circ = 276.5 \text{ kips}$$

As shown in **Figure 9.5.13.1-1**, the assumed crack plane crosses the centroid of the 22 bonded bottom strands at a distance of $(6 + y_{bc} \cot \theta)$ from the end of the beam. Since the transfer length is 30 in. from the end of the beam (60 times the strand diameter), the available prestress from the 22 straight strands is a fraction of the effective prestress, f_{pe} , in these strands.

Figure 9.5.13.1-1
Assumed Failure Crack



Note: This crack is unlikely because it would form in the end block, which is a large solid section of concrete. However, the analysis does not account for the area of concrete involved. It simply assumes a crack.

$$\text{For the 22 bonded bottom strands, } y_{bc} = \frac{2(16) + 6(4)}{22} = 2.55 \text{ in.}$$

$$\text{Therefore, } 6 + y_{bc} \cot \theta = 6 + (2.55)(\cot 29^\circ) = 10.60 \text{ in.} < 30 \text{ in.}$$

Since the location is within the transfer length, the available prestress is less than the effective prestress. The prestressing force at the center line of bearing is:

$$A_{ps}f_{ps} + A_s f_y = \left[(22)(0.153) \left((202.5 - 35.6) \frac{10.60}{30} \right) \right] + 0 = 198.5 \text{ kips} < 276.5 \text{ kips}$$

The strands are not adequate to resist the required longitudinal force. Therefore, provide additional nonprestressed reinforcement to carry the difference.

$$\text{Force to be resisted by additional reinforcement} = 276.5 - 198.5 = 78.0 \text{ kips}$$

$$\text{Additional mild steel reinforcement required} = (78.0 \text{ kips}) / (60 \text{ ksi}) = 1.30 \text{ in.}^2$$

Use five No. 5 bars.

$$\text{The area of steel provided} = 5 \times 0.31 = 1.55 \text{ in.}^2$$

Note: An alternative approach for the calculation of available prestressing force excluding the gains from deck shrinkage is illustrated in Section 9.6.13.1.

BOX BEAM (BIII-48), SINGLE SPAN, COMPOSITE DECK

9.5.14 Pretensioned Anchorage Zone/9.5.15.1 Deflection Due to Prestressing Force at Transfer

9.5.14 PRETENSIONED ANCHORAGE ZONE

[LRFD Art.5.10.10]

9.5.14.1 Anchorage Zone Reinforcement

Design of the anchorage zone reinforcement is computed using the force in the strands just before transfer. Since seven strands are debonded at the ends of the beam, the force in the remaining strands before transfer is:

$$P_{pi} = 24(0.153)(202.5) = 743.6 \text{ kips}$$

The bursting resistance, P_r , should not be less than 4.0% of the prestress force at transfer.

$$P_r = f_s A_s \geq 0.04 P_{pi} = 0.04(743.6) = 29.7 \text{ kips}$$

where

A_s = total area of vertical reinforcement located within the distance $h/4$ from the end of the beam, in.²

f_s = allowable stress in steel, but taken not greater than 20 ksi

Solving for the required area of steel, $A_s = 29.7/(20) = 1.49 \text{ in.}^2$

At least 1.49 in.² of vertical transverse reinforcement should be provided within a distance of $h/4 = 39/4$ from the end of the beam.

Use orthogonal welded wire reinforcement of W20 or D20 wires at 12 in. centers vertically and horizontally.

Space two layers of WWR at 3 in. spacing starting at 2 in. from, and parallel to the end of the beam in the diaphragm. The layers of WWR each provide four vertical and three horizontal wires. Area of steel provided is $2(4 + 3)(0.2) = 2.80 \text{ in.}^2$. A reinforcing bar cage could be used. Provide adequate embedment for bars.

9.5.14.2 Confinement Reinforcement

LRFD Article 5.10.10.2 requires that transverse reinforcement be provided in the bottom flange and anchored by extending the leg of the stirrup into the web of the girder. The article does not state how much transverse reinforcement should be provided in box beams.

9.5.15 DEFLECTION AND CAMBER

[LRFD Art.5.7.3.6.2]

Deflections are calculated using the modulus of elasticity of concrete calculated in Section 9.5.3, and the gross section properties.

9.5.15.1 Deflection Due to Prestressing Force at Transfer

$$\Delta_p = \frac{P_{pt} e_c L^2}{8 E_{ci} I_g}$$

where

Δ_p = camber due to prestressing force at transfer, in.

P_{pt} = total prestressing force after transfer = 914.5 kips

e_c = eccentricity of prestressing strand at midspan = 14.71 in.

L = overall beam length = 96.0 ft

E_{ci} = modulus of elasticity at transfer = 3,834 ksi

I_g = moment of inertia of noncomposite precast beam = 168,367 in.⁴

$$\Delta_p = \frac{(914.5)(14.71)(96 \times 12)^2}{(8)(3,834)(168,367)} = 3.46 \text{ in. } \uparrow$$

BOX BEAM (BIII-48), SINGLE SPAN, COMPOSITE DECK

9.5.15.2 Deflection Due To Beam Self Weight/9.5.15.4 Deflection Due To Diaphragm Weight

9.5.15.2 Deflection Due to Beam Self Weight

$$\Delta_g = \frac{5w_g L^4}{384E_{ci}I_g}$$

where

Δ_g = deflection due to beam self weight, in.

w_g = beam self weight = 0.847 kips/ft

Deflection due to beam self weight at transfer:

L = overall beam length = 96.0 ft

$$\Delta_g = \frac{5\left(\frac{0.847}{12}\right)(96 \times 12)^4}{384(3,834)(168,367)} = 2.51 \text{ in. } \downarrow$$

Deflection due to beam self weight used to compute deflection at erection:

L = design span = 95.0 ft

$$\Delta_g = \frac{5\left(\frac{0.847}{12}\right)(95 \times 12)^4}{384(3,834)(168,367)} = 2.40 \text{ in. } \downarrow$$

9.5.15.3 Deflection Due to Slab and Haunch Weights

$$\Delta_s = \frac{5w_s L^4}{384E_c I_g}$$

where

Δ_s = deflection due to slab and haunch weights, in.

w_s = slab and haunch weight = 0.275 + 0.025 = 0.300 kips/ft

L = design span = 95.0 ft

E_c = modulus of elasticity of precast beam at service loads = 4,287 ksi

$$\Delta_s = \frac{5\left(\frac{0.300}{12}\right)(95 \times 12)^4}{384(4,287)(168,367)} = 0.76 \text{ in. } \downarrow$$

9.5.15.4 Deflection Due to Diaphragm Weight

$$\Delta_d = \frac{19P_d L^3}{384E_{ci}I_g}$$

where

Δ_d = deflection due to diaphragm weight, in.

P_d = diaphragm weight concentrated at quarter points = 0.73 kips

Deflection due to diaphragm self weight at transfer:

L = overall beam length = 96.0 ft

$$\Delta_d = \frac{19(0.73)(96 \times 12)^3}{384(3,834)(168,367)} = 0.09 \text{ in. } \downarrow$$

BOX BEAM (BIII-48), SINGLE SPAN, COMPOSITE DECK

9.5.15.4 Deflection Due To Diaphragm Weight/9.5.15.7 Deflection Due To Live Load and Impact

Deflection due to diaphragm self weight at erection:

$$L = \text{design span} = 95.0 \text{ ft}$$

$$\Delta_d = \frac{19(0.73)(95 \times 12)^3}{384(3,834)(168,367)} = 0.08 \text{ in. } \downarrow$$

9.5.15.5 Deflection Due to Barrier and Wearing Surface Weights

$$\Delta_{b+ws} = \frac{5(w_b + w_{ws})L^4}{384E_cI_c}$$

where

$$\Delta_{b+ws} = \text{deflection due to barrier and wearing surface weights, in.}$$

$$w_b = \text{barrier} = 0.086 \text{ kips/ft}$$

$$w_{ws} = \text{wearing surface weight} = 0.089 \text{ kips/ft}$$

$$I_c = \text{gross moment of inertia of composite section} = 261,268 \text{ in.}^4$$

$$L = \text{design span} = 95.0 \text{ ft}$$

$$\Delta_{b+ws} = \frac{5\left(\frac{0.175}{12}\right)(95 \times 12)^4}{384(4,287)(261,257)} = 0.29 \text{ in. } \downarrow$$

9.5.15.6 Deflection and Camber Summary

$$\text{At transfer, } (\Delta_p + \Delta_g + \Delta_d) = 3.46 - 2.51 - 0.09 = 0.86 \text{ in. } \uparrow$$

Total deflection at erection, using PCI multipliers (see PCI Design Handbook):

$$1.8(3.46) - 1.85(2.51 + 0.09) = 1.42 \text{ in. } \uparrow$$

Long-Term Deflection:

LRFD Article 5.7.3.6.2 states that the long-time deflection may be taken as the instantaneous deflection multiplied by a factor 4.0, if the instantaneous deflection is based on the gross moment of inertia. However, a factor of 4.0 is not appropriate for this type of precast construction. Therefore, it is recommended that the designer follow the guidelines of the owner agency for whom the bridge is being designed, or undertake a more rigorous, time-dependent analysis.

9.5.15.7 Deflection Due to Live Load and Impact

$$\text{Live load deflection limit (optional)} = \text{Span}/800$$

[LRFD Art.2.5.2.6.2]

$$= \left(95 \times \frac{12}{800}\right) = 1.43 \text{ in.}$$

If the owner invokes the optional live load deflection criteria specified in Art.2.5.2.6.2, the deflection is the greater of:

[LRFD Art.3.6.1.3.2]

- that resulting from the design truck plus impact, Δ_{LT} , or
- that resulting from 25% of the design truck plus impact, Δ_{LT} taken together with the design lane load, Δ_{LL} .

Note: LRFD Article 2.5.2.6.2 states that the dynamic load allowance be included in the calculation of live load deflection.

The *LRFD Specifications* states that all the beams should be assumed to deflect equally under the applied live load and impact. [LRFD Art. 2.5.2.6.2]

Therefore, the distribution factor for deflection, *DFD*, is calculated as follows:

$$DFD = (\text{number of lanes}/\text{number of beams})$$

[LRFD Art.C2.5.2.6.2]

$$= 2/7 = 0.286 \text{ lanes/beam}$$

BOX BEAM (BIII-48), SINGLE SPAN, COMPOSITE DECK

9.5.15.7 Deflection Due to Live Load and Impact

However, it is more conservative to use the distribution factor for moment, *DFM*.

Deflection due to lane load;

Design lane load, $w = 0.64DFM = 0.64(0.290) = 0.186$ kips/ft/beam

$$\Delta_{LL} = \frac{5wL^4}{384E_cI_c} = \frac{5\left(\frac{0.186}{12}\right)(95 \times 12)^4}{384(4,287)(261,257)} = 0.30 \text{ in.} \downarrow$$

Deflection due to Design Truck Load and Impact;

To obtain maximum moment and deflection at midspan due to the truck load, let the centerline of the beam coincide with the middle point of the distance between the inner 32-kip axle and the resultant of the truck load, as shown in **Figure 9.5.15.7-1**.

Using the elastic moment area or influence lines, deflection at midspan is:

$$\Delta_{LT} = (1.87)(IM)(DFM) = (1.87)(1.33)(0.290) = 0.72 \text{ in.} \downarrow$$

Therefore, live load deflection is the greater of:

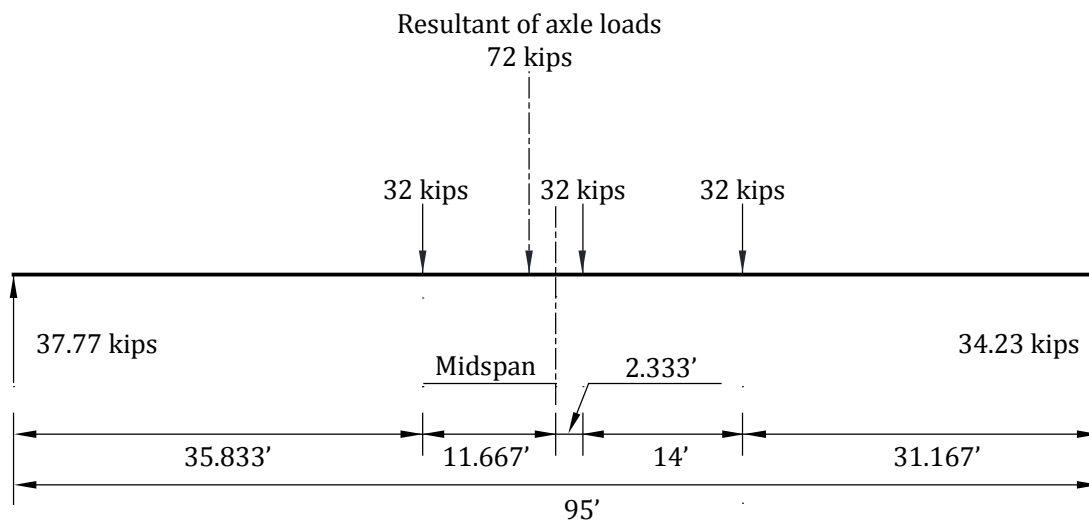
$$\Delta_{LT} = 0.72 \text{ in.} \downarrow \text{ (Controls)}$$

$$0.25 \Delta_{LT} + \Delta_{LL} = 0.25(0.72) + 0.30 = 0.48 \text{ in.}$$

Allowable live load deflection: 1.43 in. > 0.72 in. OK

Figure 9.5.15.7-1

Design Truck Axle Load Position on the Span for Maximum Moment



U-BEAM (TX-U54), SINGLE SPAN, PRECAST DECK PANELS, COMPOSITE DECK

Transformed Sections, Shear General Procedure, Refined Losses

Table of Contents

9.6.1 INTRODUCTION.....	9.6 - 5
9.6.1.1 Terminology.....	9.6 - 5
9.6.2 MATERIALS	9.6 - 6
9.6.3 CROSS-SECTION PROPERTIES FOR A TYPICAL INTERIOR BEAM.....	9.6 - 7
9.6.3.2 Composite Section.....	9.6 - 7
9.6.3.2.1 Effective Flange Width	9.6 - 7
9.6.3.2.2 Modular Ratio between Slab and Beam Concrete.....	9.6 - 8
9.6.3.2.3 Transformed Section Properties	9.6 - 8
9.6.4 SHEAR FORCES AND BENDING MOMENTS	9.6 - 9
9.6.4.1 Shear Forces and Bending Moments Due to Dead Loads	9.6 - 9
9.6.4.1.1 Dead Loads	9.6 - 9
9.6.4.1.2 Unfactored Shear Forces and Bending Moments.....	9.6 - 11
9.6.4.2 Shear Forces and Bending Moments Due to Live Loads	9.6 - 11
9.6.4.2.1 Live Loads.....	9.6 - 11
9.6.4.2.2 Live Load Distribution Factors for a Typical Interior Beam	9.6 - 11
9.6.4.2.2.1 Distribution Factor for Bending Moment.....	9.6 - 11
9.6.4.2.2.2 Distribution Factor for Shear Force	9.6 - 12
9.6.4.2.3 Dynamic Allowance	9.6 - 13
9.6.4.2.4 Unfactored Shear Forces and Bending Moments.....	9.6 - 13
9.6.4.2.4.1 Due to Truck Load; V_{LT} and M_{LT}	9.6 - 13
9.6.4.2.4.2 Due To Design Lane Load; V_{LL} and M_{LL}	9.6 - 13
9.6.4.3 Load Combinations.....	9.6 - 14
9.6.5 ESTIMATE REQUIRED PRESTRESS.....	9.6 - 15
9.6.5.1 Service Load Stresses at Midspan	9.6 - 15
9.6.5.2 Stress Limits for Concrete.....	9.6 - 16
9.6.5.3 Required Number of Strands.....	9.6 - 16
9.6.5.4 Strand Pattern.....	9.6 - 17
9.6.5.5 Steel Transformed Section Properties	9.6 - 17
9.6.6 PRESTRESS LOSSES	9.6 - 19
9.6.6.1 Elastic Shortening.....	9.6 - 19
9.6.6.2 Time-Dependent Losses between Transfer and Deck Placement.....	9.6 - 20
9.6.6.2.1 Shrinkage of Concrete	9.6 - 20
9.6.6.2.2 Creep of Concrete	9.6 - 21
9.6.6.2.3 Relaxation of Prestressing Strands.....	9.6 - 21
9.6.6.3 Time-Dependent Losses between Deck Placement and Final Time	9.6 - 22
9.6.6.3.1 Shrinkage of Concrete	9.6 - 22
9.6.6.3.2 Creep of Concrete.....	9.6 - 22
9.6.6.3.3 Relaxation of Prestressing Strands.....	9.6 - 23
9.6.6.3.4 Shrinkage of Deck Concrete.....	9.6 - 23

U-BEAM (TX-U54), SINGLE SPAN, PRECAST DECK PANELS, COMPOSITE DECK

Transformed Sections, Shear General Procedure, Refined Losses

Table of Contents

9.6.6.4 Total Time-Dependent Loss 9.6 - 24

9.6.6.5 Total Losses at Transfer 9.6 - 24

9.6.6.6 Total Losses at Service Loads 9.6 - 25

9.6.7 CONCRETE STRESSES AT TRANSFER 9.6 - 25

9.6.7.1 Stress Limits for Concrete 9.6 - 25

9.6.7.2 Stresses at Transfer Length Section..... 9.6 - 26

9.6.7.3 Stresses at Transfer Length Section of Debonded Strands..... 9.6 - 27

9.6.7.4 Stresses at Midspan..... 9.6 - 28

9.6.7.5 Summary of Stresses at Transfer 9.6 - 28

9.6.8 CONCRETE STRESSES AT SERVICE LOADS..... 9.6 - 28

9.6.8.1 Stress Limits for Concrete 9.6 - 28

9.6.8.2 Stresses at Midspan..... 9.6 - 29

9.6.8.2.3 Concrete Stress in Bottom of Beam, Load Combination Service III 9.6 - 30

9.6.8.3 Fatigue Stress Limit..... 9.6 - 30

9.6.8.4 Summary of Stresses at Midspan at Service Loads 9.6 - 30

9.6.8.5 Effect of Deck Shrinkage 9.6 - 30

9.6.9 STRENGTH LIMIT STATE 9.6 - 31

9.6.10 LIMITS OF REINFORCEMENT..... 9.6 - 32

9.6.10.1 Maximum Reinforcement 9.6 - 32

9.6.10.2 Minimum Reinforcement 9.6 - 32

9.6.11 SHEAR DESIGN 9.6 - 33

9.6.11.1 Critical Section 9.6 - 33

9.6.11.2 Contribution of Concrete to Nominal Shear Resistance 9.6 - 34

9.6.11.2.1 Strain in Flexural Tension Reinforcement 9.6 - 34

9.6.11.2.2 Values of β and θ 9.6 - 35

9.6.11.2.3 Compute Concrete Contribution..... 9.6 - 35

9.6.11.3 Contribution of Reinforcement to Nominal Shear Resistance..... 9.6 - 35

9.6.11.3.1 Requirement for Reinforcement..... 9.6 - 35

9.6.11.3.2 Required Area of Reinforcement..... 9.6 - 35

9.6.11.3.3 Determine Spacing of Reinforcement..... 9.6 - 36

9.6.11.3.4 Minimum Reinforcement Requirement..... 9.6 - 36

9.6.11.4 Maximum Nominal Shear Resistance 9.6 - 36

9.6.12 INTERFACE SHEAR TRANSFER..... 9.6 - 37

9.6.12.1 Factored Horizontal Shear 9.6 - 37

9.6.12.2 Required Nominal Resistance..... 9.6 - 37

9.6.12.3 Required Interface Shear Reinforcement 9.6 - 37

9.6.12.3.1 Minimum Interface Shear Reinforcement 9.6 - 38

9.6.12.4 Maximum Nominal Shear Reinforcement..... 9.6 - 38

9.6.13 MINIMUM LONGITUDINAL REINFORCEMENT REQUIREMENT 9.6 - 38

U-BEAM (TX-U54), SINGLE SPAN, PRECAST DECK PANELS, COMPOSITE DECK

Transformed Sections, Shear General Procedure, Refined Losses

Table of Contents

9.6.13.1 Required Reinforcement at Face of Bearing 9.6 - 39

9.6.14 PRETENSIONED ANCHORAGE ZONE 9.6 - 40

 9.6.14.1 Anchorage Zone Reinforcement 9.6 - 40

 9.6.14.2 Confinement Reinforcement 9.6 - 40

9.6.15 DEFLECTION AND CAMBER 9.6 - 40

 9.6.15.1 Deflection Due to Prestressing Force at Transfer 9.6 - 40

 9.6.15.2 Deflection Due to Beam Self Weight 9.6 - 41

 9.6.15.3 Deflection Due to Diaphragm Weight 9.6 - 41

 9.6.15.4 Deflection Due to Slab and Haunch Weights 9.6 - 42

 9.6.15.5 Deflection Due to Barrier and Future Wearing Surface Weights 9.6 - 42

 9.6.15.6 Deflection and Camber Summary 9.6 - 42

 9.6.15.7 Deflection Due to Live Load and Impact 9.6 - 43

This page intentionally left blank

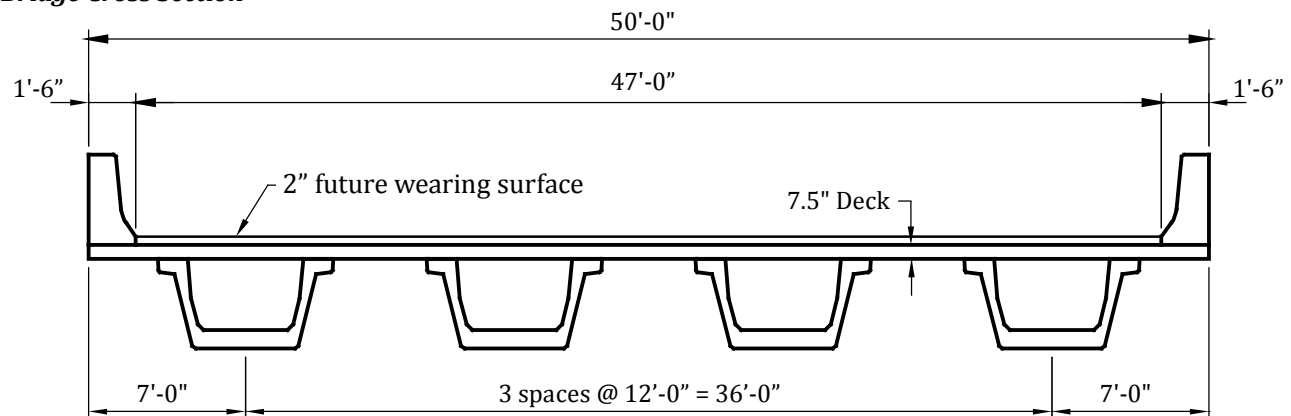
U-BEAM (TX-U54), SINGLE SPAN, PRECAST DECK PANELS, COMPOSITE DECK

9.6.1 Introduction/9.6.1.1 Terminology

9.6 Transformed Sections, Shear General Procedure, Refined Losses**9.6.1 INTRODUCTION**

This design example demonstrates the design of a 110-ft, single span, Texas U-Beam (TX-U54) bridge with no skew. This example illustrates in detail the design of a typical interior beam at the critical sections in positive flexure, shear, and deflection due to prestress, dead loads, and live loads. The superstructure consists of four beams spaced at 12 ft 0 in. centers, as shown in **Figure 9.6.1-1**. Beams are designed to act compositely with the deck, which consists of 4-in.-thick cast-in-place concrete on 3.5-in.-thick precast concrete deck panels, to resist all superimposed dead loads, live loads, and impact. A ½-in.-thick wearing surface is considered to be an integral part of the 7.5-in.-thick deck. Design live load is HL-93. The design is accomplished in accordance with *AASHTO LRFD Bridge Design Specifications*, Fifth Edition, 2010 and the 2011 Interim Revisions. Elastic stresses from external loads are calculated using transformed sections. Shear strength is calculated using the general procedure. Time-dependent prestress losses are calculated using the refined estimates.

Figure 9.6.1-1
Bridge Cross Section

**9.6.1.1 Terminology**

The following terminology is used to describe cross sections in this design example:

noncomposite section—the concrete beam cross section.

noncomposite nontransformed section—the concrete beam cross section without the strands transformed. Also called the gross section.

noncomposite transformed section—the concrete beam cross section with the strands transformed to provide cross-sectional properties equivalent to the beam concrete.

composite section—the concrete beam plus the concrete deck and haunch.

composite nontransformed section—the concrete beam plus the concrete deck and haunch transformed to provide cross-sectional properties equivalent to the beam concrete but without the strands transformed.

composite transformed section—the concrete beam plus the concrete deck and haunch and the strands transformed to provide cross-sectional properties equivalent to the beam concrete.

The term "composite" implicitly includes the transformation of the concrete deck and haunch.

The term "transformed" generally refers to transformation of the strands.

U-BEAM (TX-U54), SINGLE SPAN, PRECAST DECK PANELS, COMPOSITE DECK

9.6.2 Materials/9.6.3.2.1 Effective Flange Width

Reinforcing bars:

Yield strength, $f_y = 60.0$ ksiModulus of elasticity, $E_s = 29,000$ ksi

[LRFD Art. 5.4.3.2]

Future wearing surface: 2 in. additional concrete, unit weight = 0.150 kcf

New Jersey type barrier: unit weight = 0.300 kips/ft/side

9.6.3 CROSS-SECTION PROPERTIES FOR A TYPICAL INTERIOR BEAM**9.6.3.1 Noncomposite, Nontransformed Beam Section** A_g = area of cross section of precast beam = 1,120 in.² h = overall depth of precast beam = 54 in. I_g = moment of inertia about the centroid of the noncomposite precast beam = 403,020 in.⁴ y_b = distance from centroid to the extreme bottom fiber of the noncomposite precast beam = 22.36 in. y_t = distance from centroid to the extreme top fiber of the noncomposite precast beam = 31.58 in. S_b = section modulus for extreme bottom fiber of the noncomposite precast beam = $I_g/y_b = 18,024$ in.³ S_t = section modulus for extreme top fiber of the noncomposite precast beam = $I_g/y_t = 12,762$ in.³ w_g = beam weight per unit length = $(1,120/144)(0.150) = 1.167$ kips/ft E_c = modulus of elasticity, ksi = $33,000K_1(w_c)^{1.5}\sqrt{f'_c}$ [LRFD Eq. 5.4.2.4-1]

Where

 K_1 = correction factor for source of aggregate taken as 1.0 w_c = unit weight of concrete = 0.150 kcf

LRFD Table 3.5.1-1 states that, in the absence of more precise data, the unit weight of concrete may be taken as $0.140 + 0.001f'_c$ for $5.0 < f'_c \leq 15.0$ ksi. For $f'_c = 10.0$ ksi, the unit weight is 0.150 kcf. However, precast concrete mixes typically have a relatively low water-cementitious materials ratio and high density. Therefore, this value may need to be increased based on test results. For simplicity, a value of 0.150 kcf is also used for the cast-in-place concrete.

 f'_c = specified compressive strength of concrete, ksi

Therefore, the modulus of elasticity for:

cast-in-place slab and precast panels, $E_c = 33,000(1.0)(0.150)^{1.5}\sqrt{4.0} = 3,834$ ksiprecast beam at transfer, $E_{ci} = 33,000(1.0)(0.150)^{1.5}\sqrt{6.00} = 4,696$ ksiprecast beam at service loads, $E_c = 33,000(1.0)(0.150)^{1.5}\sqrt{10.00} = 6,062$ ksi**9.6.3.2 Composite Section****9.6.3.2.1 Effective Flange Width**

[LRFD Eq. 4.6.2.6.1]

Effective flange width is taken as the tributary width perpendicular to the axis of the beam. For the interior beam, the effective flange width is calculated as one-half the distance to the adjacent beam on each side.

 $2 \times (6.0 \times 12) = 144.00$ in.

Therefore, the effective flange width is 144.00 in.

U-BEAM (TX-U54), SINGLE SPAN, PRECAST DECK PANELS, COMPOSITE DECK

9.6.3.2.2 Modular Ratio between Slab and Beam Concrete/9.6.3.2.3 Transformed Section Properties

9.6.3.2.2 Modular Ratio between Slab and Beam Concrete

Modular ratio between slab and beam concrete, $n = \frac{E_c(\text{slab})}{E_c(\text{beam})} = \frac{3,834}{6,062} = 0.6325$

9.6.3.2.3 Transformed Section Properties

The effective flange width must be transformed by the modular ratio to provide cross-sectional properties equivalent to the beam concrete.

Transformed flange width = $n(\text{Effective flange width}) = (0.6325)(144) = 91.08 \text{ in.}$

Transformed flange area = $n(\text{Effective flange width})(t_s)$
 $= (0.6325)(144)(7.0) = 637.56 \text{ in.}^2$

Transformed flange moment of inertia = $(91.08)(7.0)^3/12 = 2,603.37 \text{ in.}^4$

Note: Because the precast panels and cast-in-place deck have the same modulus of elasticity, they are considered as a combined unit for purposes of transformed flange section properties. In addition, only the structural thickness of the cast-in-place deck, 3.5 in., is considered.

Due to camber of the precast, prestressed beam, a minimum haunch thickness of 1/2 in. at midspan is considered in the structural properties of the composite section. Also, the width of haunch must be transformed by the modular ratio.

Transformed width of haunch = $(0.6325)(15.75)(2) = 19.92 \text{ in.}$

Transformed area of haunch = $(0.6325)(15.75)(2)(0.5) = 9.96 \text{ in.}^2$

Transformed moment of inertia of haunch = $(19.92)(0.5)^3/12 = 0.21 \text{ in.}^4$

Note that the haunch should only be considered to contribute to the section properties if it is required to be provided in the completed structure. Therefore, some designers neglect its contribution to the section properties.

Figure 9.6.3.2.3-1

Dimensions of the Composite Section [DAC Convert to black and white]

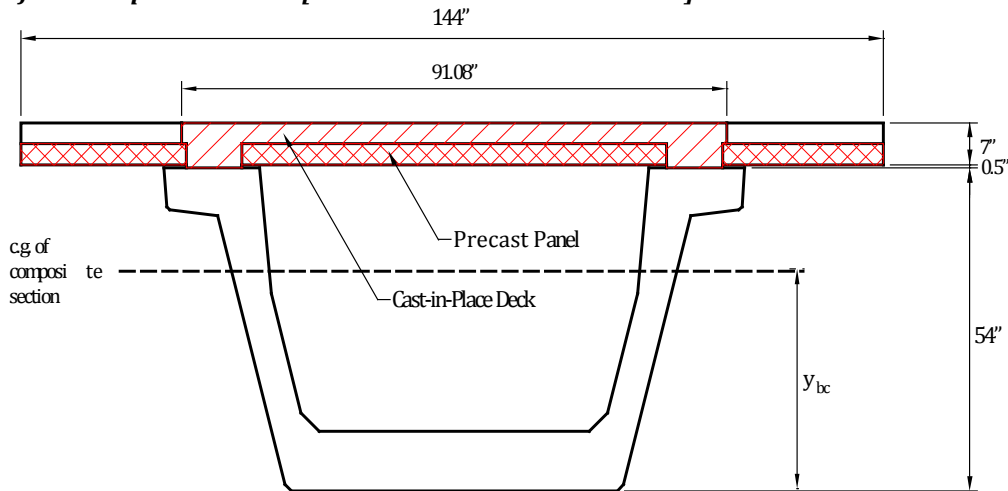


Table 9.6.3.2.3-1

Properties of the Composite Section

	Area, in. ²	y _b , in.	Ay _b , in. ³	A(y _{bc} - y _b) ² , in. ⁴	I, in. ⁴	I + A(y _{bc} - y _b) ² , in. ⁴
Beam	1,120.00	22.36	25,043	190,447	403,020	593,467
Haunch	9.96	54.25	540	3,539	0.21	3,539
Deck	637.56	58.00	36,978	325,640	2,603	328,243
Σ	1,767.5		62,561			925,249

U-BEAM (TX-U54), SINGLE SPAN, PRECAST DECK PANELS, COMPOSITE DECK

9.6.3.2.3 Transformed Section Properties/9.6.4.1.1 Dead Loads

$$\begin{aligned}
 A_c &= \text{total area of the composite section} = 1,768 \text{ in.}^2 \\
 h_c &= \text{overall depth of the composites section} = 61.50 \text{ in.} \\
 I_c &= \text{moment of inertia of the composite section} = 925,249 \text{ in.}^4 \\
 y_{bc} &= \text{distance from the centroid of the composite section to the extreme bottom fiber of the precast beam} \\
 &= 62,561/1,767.5 = 35.40 \text{ in.} \\
 y_{tg} &= \text{distance from the centroid of the composite section to the extreme top fiber of the precast beam} \\
 &= 54.00 - 35.40 = 18.60 \text{ in.} \\
 y_{tc} &= \text{distance from the centroid of the composite section to the extreme top fiber of the deck slab} \\
 &= 61.50 - 35.40 = 26.10 \text{ in.} \\
 S_{bc} &= \text{composite section modulus for the extreme bottom fiber of the precast beam} \\
 &= (I_c/y_{bc}) = \frac{925,249}{35.40} = 26,137 \text{ in.}^3 \\
 S_{tg} &= \text{composite section modulus for the extreme top fiber of the precast beam} \\
 &= (I_c/y_{tg}) = \frac{925,249}{18.60} = 49,745 \text{ in.}^3 \\
 S_{tc} &= \text{composite section modulus for extreme top fiber of the structural deck slab} \\
 &= \left(\frac{1}{n}\right)(I_c/y_{tc}) = \left(\frac{1}{0.6325}\right)\left(\frac{925,249}{26.10}\right) = 56,048 \text{ in.}^3
 \end{aligned}$$

9.6.4 SHEAR FORCES AND BENDING MOMENTS

The self weight of the beam and the weight of the deck, haunch, and diaphragms act on the noncomposite, simple-span structure, while the weight of barriers, future wearing surface, and live loads with impact act on the composite, simple-span structure. Refer to **Tables 9.6.4-1** and **9.6.4-2**, which follow Section 9.6.4.3 for a summary of unfactored values calculated below.

9.6.4.1 Shear Forces and Bending Moments Due to Dead Loads**9.6.4.1.1 Dead Loads**

DC = Dead load of structural components and nonstructural attachments

[LRFD Art. 3.3.2]

Dead loads acting on the noncomposite structure:

Beam self weight, $w_g = 1.167$ kips/ft

7.5-in.-thick deck and precast panel weight = $(7.5/12 \text{ ft})(12 \text{ ft})(0.150 \text{ kcf}) = 1.125$ kips/ft

½-in.-thick haunch weight = $(0.5)(31.5/144)(0.150 \text{ kcf}) = 0.016$ kips/ft

$w_s = 1.125 + 0.016 = 1.141$ kips/ft

Assume an 18-in.-thick diaphragm at each end and two 8-in.-thick intermediate diaphragms located at a distance of 42 ft from each bearing. The diaphragm area is based on three trapezoids that make up the inside of the U-beam. The diaphragm placement layout is based on the Texas Department of Transportation standard drawings. See **Figure 9.6.4.1.1-1**.

Cross-sectional area of diaphragm

$$= \left(\frac{(21.625)(64.5 + 61.0)}{2 \cdot 144} + \frac{(21.125)(61.0 + 50.5)}{2 \cdot 144} + \frac{(3.0)(50.5 + 43.0)}{2 \cdot 144} \right) = 18.576 \text{ ft}^2$$

U-BEAM (TX-U54), SINGLE SPAN, PRECAST DECK PANELS, COMPOSITE DECK

9.6.4.1.1 Dead Loads

End diaphragm self weight = $(18/12 \text{ ft})(18.576 \text{ ft}^2)(0.150 \text{ kcf})$
 = 4.180 kips/diaphragm

Interior diaphragm self weight = $(8/12 \text{ ft})(18.576 \text{ ft}^2)(0.150 \text{ kcf})$
 = 1.858 kips/diaphragm

Notes:

1. Actual deck thickness (7.5 in.) is used for computing dead load.
2. A ½-in. minimum haunch thickness is assumed in the computations of dead load. If a deeper haunch will be used because of final beam camber, the weight of the actual haunch should be used.
3. For this design example, the unit weight of the reinforced concrete is taken as 0.150 kcf. Some designers use a higher unit weight to account for the weight of the reinforcement.

Dead loads placed on the composite structure:

LRFD Article 4.6.2.2.1 states that permanent loads (barrier and future wearing surface loads) may be distributed uniformly among all beams if the following conditions are met:

- Width of the deck is constant OK
- Number of beams, N_b is not less than four ($N_b = 4$) OK
- Beams are parallel and have the same stiffness OK
- The roadway part of the overhang, $d_e \leq 3.0 \text{ ft}$ OK

$d_e = (36 - 18) + 15\frac{3}{4} = 33\frac{3}{4} \text{ in.} = 2.81 \text{ ft}$ OK

For simplicity, d_e is taken from the inside face of the barrier to the inside face of the web at the deck level.

- Curvature in plan is less than specified in the *LRFD Specifications* (curvature = 0.0°) OK
- Cross section of the bridge is consistent with one of the cross sections given in LRFD Table 4.6.2.2.1-1 OK

Since these criteria are satisfied, the barrier and wearing surface loads are distributed equally among the four beams.

Barrier weight = $(2 \text{ barriers})(0.300 \text{ kips}) / (4 \text{ beams}) = 0.150 \text{ kips/ft/beam} = w_b$

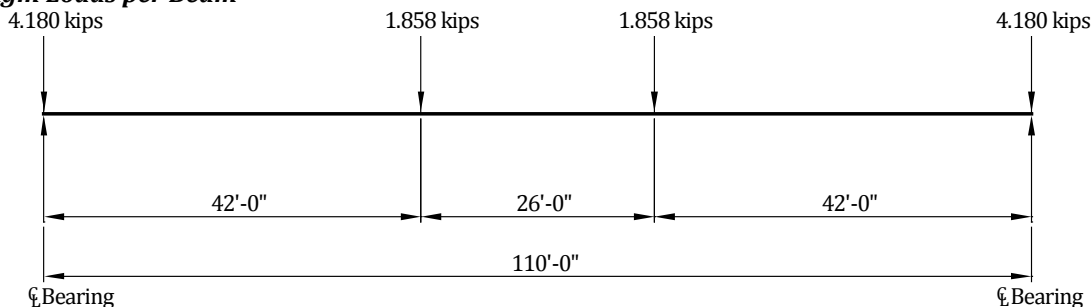
DW = Dead load of 2-in.-thick future wearing surface

= $(2/12)(0.150) = 0.025 \text{ ksf}$

= $(0.025 \text{ ksf})(47.0 \text{ ft}) / (4 \text{ beams}) = 0.294 \text{ kips/ft/beam} = w_{ws}$

DW load should be kept separately from DC because of the higher load factor applied to it.

Figure 9.6.4.1.1-1
Diaphragm Loads per Beam



U-BEAM (TX-U54), SINGLE SPAN, PRECAST DECK PANELS, COMPOSITE DECK**9.6.4.1.2 Unfactored Shear Forces and Bending Moments/9.6.4.2.2.1 Distribution Factor for Bending Moment****9.6.4.1.2 Unfactored Shear Forces and Bending Moments**

For a simply supported beam with span length (L) loaded with a uniformly distributed load (w), the shear force (V_x) and bending moment (M_x) at any distance (x) from the support are given by:

$$V_x = w(0.5L - x) \quad \text{[Eq. 9.6.4.1.2-1]}$$

$$M_x = 0.5wx(L - x) \quad \text{[Eq. 9.6.4.1.2-2]}$$

Using the above equations, values of shear forces and bending moments for a typical interior beam under the self weight of beam, weight of slab and haunch, and weight of barriers and future wearing surface are computed and given in **Table 9.6.4-1** that is located at the end of Section 9.6.4.3. For these calculations, the span length (L) is the design span, 110 ft. However, for calculations of stresses and deformation at the time prestress is transferred, the overall length of the precast member, 111 ft, is used as illustrated later in this example.

9.6.4.2 Shear Forces and Bending Moments Due to Live Loads**9.6.4.2.1 Live Loads**

[LRFD Art. 3.6.1.2]

Design live load is HL-93, which consists of a combination of:

[LRFD Art. 3.6.1.2.1]

1. Design truck or design tandem with dynamic allowance

[LRFD Art. 3.6.1.2.2]

The design truck consists of 8.0-, 32.0-, and 32.0-kip axles with the first pair spaced at 14.0 ft and the second pair spaced at 14.0 to 30.0 ft. The design tandem consists of a pair of 25.0-kip axles spaced at 4.0 ft apart.

[LRFD Art. 3.6.1.2.3]

2. Design lane load of 0.64 kips/ft without dynamic allowance

[LRFD Art. 3.6.1.2.4]

9.6.4.2.2 Live Load Distribution Factors for a Typical Interior Beam

The live load bending moments and shear forces are determined by using the simplified distribution factor formulas, [LRFD Art. 4.6.2.2]. To use the simplified live load distribution factor formulas, the following conditions must be met:

[LRFD Art. 4.6.2.2.1]

- Width of deck is constant OK
- Number of beams, N_b not less than four ($N_b = 4$) OK
- Beams are parallel and approximately of the same stiffness OK
- The roadway part of the overhang, $d_e \leq 3.0$ ft ($d_e = 2.81$ ft) OK
- Curvature is less than in the *LRFD Specifications*, (curvature = 0.0°) OK

For a precast concrete U-section with cast-in-place concrete deck, the bridge type is (c). [LRFD Table 4.6.2.2.1-1]

The number of design lanes is computed as:

Number of design lanes = the integer part of the ratio $w/12$, where (w) is the clear roadway width, in ft, between the curbs. [LRFD Art. 3.6.1.1.1]

From **Figure 9.6.1-1**, $w = 47$ ft

Number of design lanes = integer part of $(47/12) = 3$ lanes

9.6.4.2.2.1 Distribution Factor for Bending Moment

- For all limit states except fatigue limit state:

For two or more lanes loaded:

$$DFM = \left(\frac{S}{6.3}\right)^{0.6} \left(\frac{Sh}{12.0L^2}\right)^{0.125} \quad \text{[LRFD Table 4.6.2.2.2b-1]}$$

Provided that: $6.0 \leq S \leq 18.0$; $S = 12.0$ ft OK

$20 \leq L \leq 140$; $L = 110$ ft OK

$18 \leq h \leq 65$; $h = 54$ in. OK

$N_b \geq 3$; $N_b = 4$ OK

U-BEAM (TX-U54), SINGLE SPAN, PRECAST DECK PANELS, COMPOSITE DECK

9.6.4.2.2.1 Distribution Factor for Bending Moment/9.6.4.2.2.2 Distribution Factor for Shear Force

where

DFM = distribution factor for bending moment for interior beam

S = beam spacing, ft

L = beam span, ft

$$DFM = \left(\frac{12.0}{6.3}\right)^{0.6} \left(\frac{(12.0)(54)}{(12.0)(110)^2}\right)^{0.125}$$

$$= (1.472)(0.508) = 0.748 \text{ lanes/beam}$$

For one design lane loaded:

$$DFM = \left(\frac{S}{3.0}\right)^{0.35} \left(\frac{Sh}{12.0L^2}\right)^{0.25} \quad [\text{LRFD Table 4.6.2.2.2b-1}]$$

$$= \left(\frac{12.0}{3.0}\right)^{0.35} \left(\frac{(12.0)(54)}{(12.0)(110)^2}\right)^{0.25}$$

$$= (1.625)(0.258) = 0.419 \text{ lanes/beam}$$

Thus, the case of two or more lanes loaded controls and $DFM = 0.748$ lanes/beam.

- For fatigue limit state:

The *LRFD Specifications*, Art. C3.4.1, states that for Fatigue Limit State, a single design truck should be used. However, live load distribution factors given in LRFD Article 4.6.2.2 take into consideration the multiple presence factor, m . LRFD Article 3.6.1.1.2 states that the multiple presence factor, m , for one design lane loaded is 1.2. Therefore, the distribution factor for one design lane loaded with the multiple presence factor removed, should be used. The distribution factor for fatigue limit state is $0.419/1.2 = 0.349$ lanes/beam.

9.6.4.2.2.2 Distribution Factor for Shear Force

For two or more lanes loaded:

$$DFV = \left(\frac{S}{7.4}\right)^{0.8} \left(\frac{h}{12.0L}\right)^{0.1} \quad [\text{LRFD Table 4.6.2.2.3a-1}]$$

Provided that: $6.0 \leq S \leq 18.0$; $S = 12.0$ ft OK

$20 \leq L \leq 140$; $L = 110$ ft OK

$18 \leq h \leq 65$; $h = 54$ in. OK

$N_b \geq 3$; $N_b = 4$ OK

where

DFV = distribution factor for shear for interior beam

S = beam spacing, ft

Therefore, the distribution factor for shear force is:

$$DFV = \left(\frac{12.0}{7.4}\right)^{0.8} \left(\frac{54}{(12.0)(110)}\right)^{0.1} = 1.069 \text{ lanes/beam}$$

For one design lane loaded:

$$DFV = \left(\frac{S}{10}\right)^{0.6} \left(\frac{d}{12.0L}\right)^{0.1} = \left(\frac{12.0}{10}\right)^{0.6} \left(\frac{54}{(12.0)(110)}\right)^{0.1} = 0.810 \text{ lanes/beam}$$

Thus, the case of two or more lanes loaded controls and $DFV = 1.069$ lanes/beam.

U-BEAM (TX-U54), SINGLE SPAN, PRECAST DECK PANELS, COMPOSITE DECK9.6.4.2.3 Dynamic Allowance/9.6.4.2.4.2 Due to Design Lane Load; V_{LL} and M_{LL} **9.6.4.2.3 Dynamic Allowance** $IM = 15\%$ for fatigue limit state

[LRFD Table 3.6.2.1-1]

 $IM = 33\%$ for all other limit stateswhere IM = dynamic load allowance applied to design truck load only**9.6.4.2.4 Unfactored Shear Forces and Bending Moments****9.6.4.2.4.1 Due to Truck Load; V_{LT} and M_{LT}**

- For all limit states except for fatigue limit state:

Shear force and bending moment envelopes on a per-lane basis are calculated at tenth-points of the span using the equations given in Chapter 8 of this manual. However, this is generally done by means of commercially available computer software that has the ability to deal with moving loads. Therefore, truck load shear forces and bending moments per beam are:

$$\begin{aligned} V_{LT} &= (\text{shear force per lane})(DFV)(1 + IM) \\ &= (\text{shear force per lane})(1.069)(1 + 0.33) \\ &= (\text{shear force per lane})(1.422) \text{ kips} \end{aligned}$$

$$\begin{aligned} M_{LT} &= (\text{bending moment per lane})(DFM)(1 + IM) \\ &= (\text{bending moment per lane})(0.748)(1 + 0.33) \\ &= (\text{bending moment per lane})(0.995) \text{ ft-kips} \end{aligned}$$

Values for V_{LT} and M_{LT} at different points are given in **Table 9.6.4-2**.

- For fatigue limit state:

Art. 3.6.1.4.1 in the *LRFD Specifications* states that the fatigue load is a single design truck which has the same axle weight used in all other limit states but with a constant spacing of 30.0 ft between the 32.0-kip axles. Bending moment envelope on a per-lane basis is calculated using the equation given in Chapter 8 of this manual.

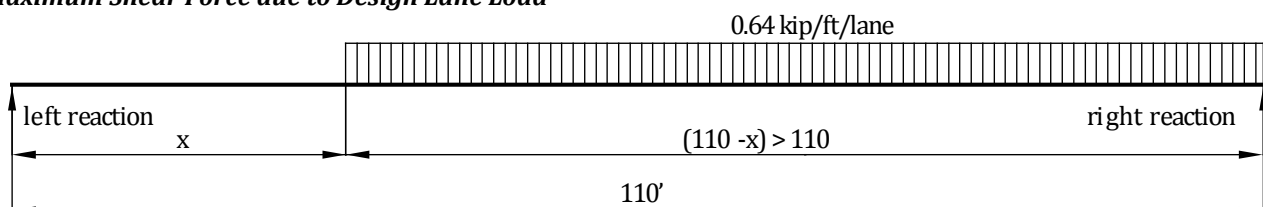
Therefore, the bending moment of the fatigue truck load is:

$$\begin{aligned} M_f &= (\text{bending moment per lane})(DFM)(1+IM) \\ &= (\text{bending moment per lane})(0.349)(1+ 0.15) \\ &= (\text{bending moment per lane})(0.401) \text{ ft-kips} \end{aligned}$$

Values of M_f at different points are given in **Table 9.6.4-2**.**9.6.4.2.4.2 Due to Design Lane Load; V_{LL} and M_{LL}**

To obtain the maximum shear force at a section located at a distance (x) from the left support under a uniformly distributed load of 0.64 kips/ft, load the member to the right of the section under consideration as shown in **Figure 9.6.4.2.4.2-1**. Therefore, the maximum shear force per lane is:

$$V_x = \frac{0.32(L - x)^2}{L} \text{ for } x \leq 0.5L \quad (\text{Eq. 9.6.4.2.4.2-1})$$

where V_x is in kips/lane and L and x are in ft**Figure 9.6.4.2.4.2-1****Maximum Shear Force due to Design Lane Load**

U-BEAM (TX-U54), SINGLE SPAN, PRECAST DECK PANELS, COMPOSITE DECK9.6.4.2.4.2 Due to Design Lane Load; V_{LL} and M_{LL} /9.6.4.3 Load Combinations

To calculate the maximum bending moment at any sections, use Eq. (9.6.4.1.2-2).

Lane load shear forces and bending moments per typical interior beam are as follows:

$$\begin{aligned} V_{LL} &= (\text{lane load shear force})(DFV) \\ &= (\text{lane load shear force})(1.069) \text{ kips} \end{aligned}$$

For all limit states except for fatigue limit state:

$$\begin{aligned} M_{LL} &= (\text{lane load bending moment})(DFM) \\ &= (\text{lane load bending moment})(0.748) \text{ ft-kips} \end{aligned}$$

Note that dynamic allowance is not applied to the design lane loading.

Values of shear forces and bending moments, V_{LL} and M_{LL} , are given in **Table 9.6.4-2**.

9.6.4.3 Load Combinations

[LRFD Art. 3.4]

Total factored load is taken as:

$$Q = \sum \eta_i \gamma_i Q_i \quad \text{[LRFD Eq. 3.4.1-1]}$$

where

$$\eta_i = \text{a load modifier relating to ductility, redundancy, and operational importance (Here, } \eta_i \text{ is considered to be 1.0 for typical bridges.)} \quad \text{[LRFD Art. 1.3.2]}$$

$$\gamma_i = \text{load factors} \quad \text{[LRFD Table 3.4.1-1]}$$

$$Q_i = \text{force effect from specified loads}$$

Investigating different limit states given in LRFD Article 3.4.1, the following limit states are applicable:

Service I: check compressive stresses in prestressed concrete components:

$$Q = 1.00(DC + DW) + 1.00(LL + IM) \quad \text{[LRFD Table 3.4.1-1]}$$

This load combination is a special combination for a service limit state stress checks and applies to all conditions other than Service III.

Service III: check tensile stresses in prestressed concrete components:

$$Q = 1.00(DC + DW) + 0.80(LL + IM) \quad \text{[LRFD Table 3.4.1-1]}$$

This load combination is a special combination for service limit state stress checks that applies only to tension in prestressed concrete structures to control cracks.

Strength I: check ultimate strength:

[LRFD Tables 3.4.1-1 and -2]

$$\text{Maximum } Q = 1.25(DC) + 1.50(DW) + 1.75(LL + IM)$$

$$\text{Minimum } Q = 0.90(DC) + 0.65(DW) + 1.75(LL + IM)$$

This load combination is the general load combination for strength limit state design.

Note: For simple-span bridges, the maximum load factors produce maximum effects. However, use minimum load factors for dead load (DC), and wearing surface (DW) when dead load and wearing surface stresses are opposite to those of live load.

Fatigue I: check stress range in strands:

[LRFD Table 3.4.1-1]

$$Q = 1.50(LL + IM)$$

This load combination is a special load combination to check the tensile stress range in the strands due to live load and dynamic allowance.

U-BEAM (TX-U54), SINGLE SPAN, PRECAST DECK PANELS, COMPOSITE DECK

9.6.4.3 Load Combinations/9.6.5.1 Service Load Stresses at Midspan

Table 9.6.4-1

Unfactored Shear Forces and Bending Moments Due to Dead Loads for a Typical Interior Beam

Distance x, ft	Section x/L	Beam Weight		Internal Diaphragm Weight		Slab + Haunch Weight		Barrier Weight		Wearing Surface Weight	
		Shear V_g kips	Moment M_g ft-kips	Shear V_d kips	Moment M_d ft-kips	Shear V_s kips	Moment M_s ft-kips	Shear V_b kips	Moment M_b ft-kips	Shear V_{ws} kips	Moment M_{ws} ft-kips
0	0	64.2	0.0	1.9	0.0	62.8	0.0	8.3	0.0	16.2	0.0
*4.70	0.043	58.7	288.8	1.9	8.7	57.4	282.3	7.5	37.1	14.8	72.8
11	0.1	51.3	635.4	1.9	20.4	50.2	621.3	6.6	81.7	12.9	160.1
22	0.2	38.5	1,129.7	1.9	40.9	37.7	1,104.5	5.0	145.2	9.7	284.6
33	0.3	25.7	1,482.7	1.9	61.3	25.1	1,449.6	3.3	190.6	6.5	373.5
44	0.4	12.8	1,694.5	0.0	78.0	12.6	1,656.7	1.7	217.8	3.2	426.9
55	0.5	0.0	1,765.1	0.0	78.0	0.0	1,725.8	0.0	226.9	0.0	444.7

*Critical section for shear (see Sect. 9.6.11)

Table 9.6.4-2

Unfactored Shear Forces and Bending Moments Due to Live Loads for a Typical Interior Beam

Distance x, ft	Section x/L	Truck Load with Impact		Lane Load		Fatigue Truck with Impact
		Shear V_{LT} kips	Moment M_{LT} ft-kips	Shear V_{LL} kips	Moment M_{LL} ft-kips	Moment M_f ft-kips
0	0	93.7	0.0	37.6	0.0	0.0
*4.70	0.043	89.3	293.7	34.5	118.5	107.4
11	0.1	83.4	642.3	30.5	260.7	233.2
22	0.2	73.2	1,127.0	24.1	463.4	402.9
33	0.3	63.0	1,454.1	18.4	608.2	520.0
44	0.4	52.7	1,645.8	13.5	695.1	581.3
55	0.5	42.5	1,691.1	9.4	724.1	579.0

* Critical section for shear (see Sect. 9.6.11)

9.6.5 ESTIMATE REQUIRED PRESTRESS

The required number of strands is usually governed by concrete tensile stresses at the bottom fiber for load combination Service III at the section of maximum moment or at the harp points and in some cases Strength I. For estimating the number of strands, only the stresses at midspan are considered.

9.6.5.1 Service Load Stresses at Midspan

Bottom tensile stress due to applied dead and live loads using load combination Service III is:

$$f_b = \frac{M_g + M_s + M_d}{S_b} + \frac{M_b + M_{ws} + (0.8)(M_{LT} + M_{LL})}{S_{bc}}$$

where

- f_b = concrete tensile stress at bottom fiber of the beam, ksi
- M_g = unfactored bending moment due to beam self weight, ft-kips
- M_s = unfactored bending moment due to slab and haunch weights, ft-kips
- M_d = unfactored bending moment due to diaphragm weights, ft-kips
- M_b = unfactored bending moment due to barrier weight, ft-kips

U-BEAM (TX-U54), SINGLE SPAN, PRECAST DECK PANELS, COMPOSITE DECK**9.6.5.1 Service Load Stresses at Midspan/9.6.5.3 Required Number of Strands**

M_{ws} = unfactored bending moment due to future wearing surface, ft-kips

M_{LT} = unfactored bending moment due to truck load and impact, ft-kips

M_{LL} = unfactored bending moment due to lane load, ft-kips

Using values of bending moments from **Tables 9.6.4-1** and **9.6.4-2**, bottom tensile stress at midspan is:

$$f_b = \frac{1,765.1 + 1,725.8 + 78.0}{18,024}(12) + \frac{(226.9 + 444.7) + (0.8)(1,691.1 + 724.1)}{26,137}(12)$$

$$= (2.376 + 1.195) = 3.571 \text{ ksi}$$

9.6.5.2 Stress Limits for Concrete

Tensile stress limit at service loads = $0.19\sqrt{f'_c}$ [LRFD Table 5.9.4.2.2-1]

where f'_c = specified concrete compressive strength of beam for design, ksi

Concrete tensile stress limit = $-0.19\sqrt{10.00} = -0.601$ ksi

9.6.5.3 Required Number of Strands

The required precompressive stress at the bottom fiber of the beam is the difference between the bottom tensile stress due to the applied loads and the concrete tensile stress limit:

$$f_{pb} = (3.571 - 0.601) = 2.970 \text{ ksi}$$

Assume the distance between the center of gravity of strands and the bottom fiber of the beam:

Try $y_{bs} = 3.00$ in.

Therefore, strand eccentricity at midspan, $e_c = (y_b - y_{bs}) = (22.36 - 3.0) = 19.36$ in.

If P_{pe} is the total prestress force after all losses, stress at the bottom fiber due to prestress is:

$$f_{pb} = \frac{P_{pe}}{A_g} + \frac{P_{pe}e_c}{S_b} \text{ or } 2.970 = \frac{P_{pe}}{1,120} + \frac{P_{pe}(19.36)}{18,024}$$

Solving for P_{pe} , the required $P_{pe} = 1,509.9$ kips.

Final prestress force per strand = (area of strand)(f_{pi})(1 - losses)

where f_{pi} = initial stress before transfer, ksi (see Section 9.6.2) = 202.5 ksi

Assuming final loss of 15% of f_{pi} , the prestress force per strand after all losses

$$= (0.217)(202.5)(1 - 0.15) = 37.4 \text{ kips}$$

Number of strands required = $(1,509.9/37.4) = 40.4$ strands

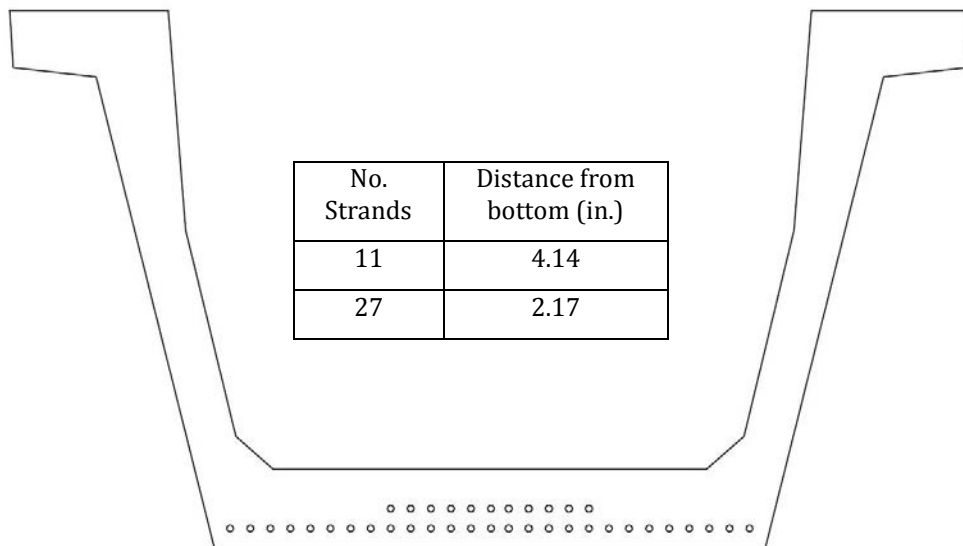
Considering that the steel transformed section properties are used, as an initial trial, try (38) 0.6-in.-diameter, 270 ksi strands. The strand pattern at midspan for the 38 strands is shown in **Figure 9.6.5.3-1**. Each available position is filled beginning with the bottom row.

Total area of prestressing strands, $A_{ps} = 38(0.217) = 8.246$ in.²

U-BEAM (TX-U54), SINGLE SPAN, PRECAST DECK PANELS, COMPOSITE DECK

9.6.5.3 Required Number of Strands/9.6.5.5 Steel Transformed Section Properties

Figure 9.6.5.3-1
Assumed Strand Pattern at Midspan



Note: This is a non-standard strand pattern. Typically rows are spaced vertically at 2" apart.

9.6.5.4 Strand Pattern

The distance between the center of gravity of bottom strands and the bottom concrete fiber of the beam at midspan is:

$$y_{bs} = [27(2.17) + 11(4.14)] / (38) = 2.74 \text{ in. This is close to the assumed value of 3.0 in. OK}$$

$$\text{Strand eccentricity at midspan, } e_c = y_b - y_{bs} = 22.36 - 2.74 = 19.62 \text{ in.} = e_{pg}$$

9.6.5.5 Steel Transformed Section Properties

From the earliest years of prestressed concrete design, the gross section was conservatively used in analysis since the prestressing forces were smaller and computer programs were not widely used. However, the use of transformed section, which is obtained from the gross section by adding transformed steel area, yields more accurate results than the gross section analysis.

For each row of prestressing strands shown in **Figure 9.6.5.4-1**, the steel area is multiplied by $(n - 1)$ to calculate the transformed section properties, where n is the modular ratio between prestressing strand and concrete. Since the modulus of elasticity of concrete is different at transfer and final time, the transformed section properties should be calculated separately for the two stages. Using similar procedures as in Section 9.6.3.2.3, a sample calculation is shown in **Table 9.6.5.5-1**.

At transfer:

$$n - 1 = \frac{28,500}{4,696} - 1 = 5.069$$

At final:

$$n - 1 = \frac{28,500}{6,062} - 1 = 3.701$$

U-BEAM (TX-U54), SINGLE SPAN, PRECAST DECK PANELS, COMPOSITE DECK

9.6.5.5 Steel Transformed Section Properties

Table 9.6.5.5-1

Properties of Composite Transformed Section at Final Time

	Transformed Area, in. ²	y_b in.	Ay_b in. ³	$A(y_{btc} - y_b)^2$ in. ⁴	I in. ⁴	$I + A(y_{btc} - y_b)^2$ in. ⁴
Deck	637.56	58.00	36,978	341,978	2,603	344,581
Haunch	9.96	54.25	540	3,752	0.21	3,752
Beam	1,120.00	22.36	25,043	174,440	403,020	577,460
Row 1	21.68	2.17	47.05	23,140		23,140
Row 2	8.83	4.14	36.56	8,322		8,322
Σ	1,798.03		62,645			957,255

Note: The moment of inertia of strand about its own centroid is neglected.

The transformed section properties are calculated as:

Noncomposite transformed section at transfer:

A_{ti} = area of transformed section at transfer = 1,161.8 in.²

I_{ti} = moment of inertia of the transformed section at transfer = 418,565 in.⁴

e_{ti} = eccentricity of strands with respect to transformed section at transfer = 18.91 in.

y_{bti} = distance from the centroid of the transformed section to the extreme bottom fiber of the beam at transfer = 21.65 in.

S_{bti} = section modulus for the extreme bottom fiber of the transformed section at transfer = 19,333 in.³

S_{tti} = section modulus for the extreme top fiber of the transformed section at transfer = 12,939 in.³

Noncomposite transformed section at final time:

A_{tf} = area of transformed section at final time = 1,151 in.²

I_{tf} = moment of inertia of the transformed section at final time = 414,519 in.⁴

e_{tf} = eccentricity of strands with respect to transformed section at final time = 19.10 in.

y_{btf} = distance from the centroid of the noncomposite transformed section to the extreme bottom fiber of the beam at final time = 21.84 in.

S_{btf} = section modulus for the extreme bottom fiber of the transformed section at final time = 18,980 in.³

S_{ttf} = section modulus for the extreme top fiber of the transformed section at final time = 12,889 in.³

Composite transformed section at final time:

A_{tc} = area of transformed composite section at final time = 1,798 in.²

I_{tc} = moment of inertia of the transformed composite section at final time = 957,255 in.⁴

e_{tc} = eccentricity of strands with respect to transformed composite section at final time = 32.10 in.

y_{btc} = distance from the centroid of the composite transformed section to the extreme bottom fiber of the beam at final time = 34.84 in.

S_{btc} = section modulus for the extreme bottom fiber of the transformed composite section at final time = 27,476 in.³

S_{ttc} = composite section modulus for the extreme top fiber of the precast beam for transformed section at final time = 49,961 in.³

S_{dtc} = composite section modulus for the extreme top fiber of the deck for the transformed composite section at final time = 56,768 in.³

U-BEAM (TX-U54), SINGLE SPAN, PRECAST DECK PANELS, COMPOSITE DECK**9.6.6 PRESTRESS LOSSES**

Total prestress loss:

$$\Delta f_{pT} = \Delta f_{pES} + \Delta f_{pLT}$$

where

Δf_{pLT} = total loss in prestressing steel stress

Δf_{pES} = sum of all losses or gains due to elastic shortening or extension at the time of application of prestress and/or external loads

Δf_{pLT} = long-term losses due to shrinkage and creep of concrete, and relaxation of steel after transfer. In this example, the refined estimates of time-dependent losses are used.

9.6.6.1 Elastic Shortening

$$\Delta f_{pES} = \frac{E_p}{E_{ci}} f_{cgp}$$

where

E_p = modulus of elasticity of prestressing strands = 28,500 ksi

E_{ci} = modulus of elasticity of beam concrete at transfer = 4,696 ksi

f_{cgp} = sum of concrete stresses at the center of gravity of prestressing strands due to prestressing force at transfer and the self weight of the member at sections of maximum moment.

If the gross (or net) cross-section properties are used, it is necessary to perform numerical iterations. The elastic loss Δf_{pES} is usually assumed to be 10% of the initial prestress to calculate f_{cgp} , which is then used in the equation above to calculate a refined Δf_{pES} . The process is repeated until the assumed Δf_{pES} and refined Δf_{pES} converge.

However, when transformed section properties are used to calculate concrete stress, the effects of losses and gains due to elastic deformations are implicitly accounted for. Therefore, Δf_{pES} should not be included in calculating f_{cgp} .

$$\begin{aligned} \text{Force per strand before transfer} &= (\text{area of strand})(\text{prestress stress before transfer}) \\ &= (0.217)(202.5) = 43.94 \text{ kips} \end{aligned}$$

$$f_{cgp} = \frac{P_{pi}}{A_{ti}} + \frac{P_{pi}e_{ti}^2}{I_{ti}} - \frac{(M_g + M_d)e_{ti}}{I_{ti}}$$

where

e_{ti} = eccentricity of strands at midspan with respect to the transformed section at transfer = 18.91 in.

P_{pi} = total prestressing force before transfer = (38 strands)(43.94) = 1,669.7 kips

M_g and M_d should be calculated based on the overall beam length of 111 ft. Since the elastic shortening loss is a part of the total loss, f_{cgp} will be conservatively computed based on M_g and M_d using the design span length of 110 ft.

$$f_{cgp} = \frac{1,669.7}{1,161.8} + \frac{(1,669.7)(18.91)^2}{418,565} - \frac{(1,765.1 + 78.0)(12)(18.91)}{418,565} = 1.864 \text{ ksi}$$

Therefore, loss due to elastic shortening:

$$\Delta f_{pES} = \frac{28,500}{4,696} 1.864 = 11.3 \text{ ksi}$$

AASHTO LRFD C5.9.5.3 indicates that the loss due to elastic shortening at transfer should be added to the time-dependent losses to determine total losses. However, this loss at transfer is directly accounted for if transformed section properties are used in the stress analysis.

U-BEAM (TX-U54), SINGLE SPAN, PRECAST DECK PANELS, COMPOSITE DECK**9.6.6.2 Time-Dependent Losses between Transfer and Deck Placement/9.6.6.2.1 Shrinkage of Concrete****9.6.6.2 Time-Dependent Losses between Transfer and Deck Placement**

The following construction schedule is assumed in calculating the time-dependent losses.

Concrete age at transfer: $t_i = 1$ day

Concrete age at deck placement: $t_d = 90$ days

Concrete age at final stage: $t_f = 20,000$ days

The total time-dependent loss between time of transfer and deck placement is the summation of prestress losses due to shrinkage of concrete, creep of concrete, and relaxation of prestressing strands.

9.6.6.2.1 Shrinkage of Concrete

The prestress loss due to shrinkage of concrete between time of transfer and deck placement is calculated by:

$$\Delta f_{pSR} = \epsilon_{bid} E_p K_{id} \quad [\text{LRFD 5.9.5.4.2a-1}]$$

where

ϵ_{bid} = concrete shrinkage strain of girder for time period between transfer and deck placement

E_p = modulus of elasticity of prestressing strands, ksi

K_{id} = transformed section coefficient that accounts for time-dependent interaction between concrete and bonded steel in the section being considered for time period between transfer and deck placement

The concrete shrinkage strain, ϵ_{bid} , is taken as:

$$\epsilon_{bid} = k_{vs} k_{hs} k_f k_{td} 0.48 \times 10^{-3} \quad [\text{LRFD Eq. 5.4.2.3.3.-1}]$$

where

The factor for the effect of the volume-to-surface ratio of the beam:

$$k_{vs} = 1.45 - 0.13(V/S) = 1.45 - 0.13 \times 3.19 = 1.035$$

The minimum value of k_{vs} is 1.0 OK

V/S is the volume-to-surface ratio of the beam.

The humidity factor for shrinkage:

$$k_{hs} = 2.00 - 0.14H = 2.00 - 0.014(70) = 1.020$$

where H = average annual mean relative humidity (assume 70%)

The factor for the effect of the concrete strength:

$$k_f = \frac{5}{1 + f'_{ci}} = \frac{5}{1 + 6.0} = 0.714$$

The time development factor at deck placement:

$$k_{td} = \frac{t}{61 - 4f'_{ci} + t} = \frac{89}{61 - 4(6.0) + 89} = 0.706 = k_{tdd}$$

where t is the maturity of concrete(days) = $t_d - t_i = 90 - 1 = 89$ days

$$\epsilon_{bid} = (1.035)(1.020)(0.714)(0.706)(0.48 \times 10^{-3}) = 0.000255$$

$$K_{id} = \frac{1}{1 + \frac{E_p}{E_{ci}} \frac{A_{ps}}{A_g} \left(1 + \frac{A_g (e_{pg})^2}{I_g}\right) [1 + 0.7\Psi_b(t_f, t_i)]} \quad [\text{LRFD Eq. 5.9.5.4.2a-2}]$$

U-BEAM (TX-U54), SINGLE SPAN, PRECAST DECK PANELS, COMPOSITE DECK

9.6.6.2.1 Shrinkage of Concrete/9.6.6.2.3 Relaxation of Prestressing Strands

where

e_{pg} = eccentricity of prestressing strand with respect to the centroid of the girder, in.

$\Psi_b(t_f, t_i)$ = girder creep coefficient at final time due to loading introduced at transfer

For the time between transfer and final time:

$$\Psi_b(t_f, t_i) = 1.9k_{vs}k_{hc}k_fk_{td}t_i^{-0.118} \quad [\text{LRFD Eq. 5.4.2.3.2-1}]$$

$$k_{hc} = 1.56 - 0.008H = 1.56 - 0.008(70) = 1.000$$

$$k_{td} = \frac{t}{61 - 4f'_{ci} + t} = \frac{20,000 - 1}{61 - 4(6.0) + (20,000 - 1)} = 0.998 = k_{tdf}$$

$$\Psi_b(t_f, t_i) = 1.9(1.035)(1.000)(0.714)(0.998)(1)^{-0.118} = 1.401$$

$$K_{id} = \frac{1}{1 + \frac{28,500}{4,696} \frac{8.246}{1,120} \left(1 + \frac{1,120(19.62)^2}{403,020}\right) [1 + 0.7(1.401)]} = 0.845$$

The prestress loss due to shrinkage of concrete between transfer and deck placement is:

$$\Delta f_{pSR} = (0.000255)(28,500)(0.845) = 6.141 \text{ ksi}$$

9.6.6.2.2 Creep of Concrete

The prestress loss due to creep of girder concrete between time of transfer and deck placement is:

$$\Delta f_{pCR} = \frac{E_p}{E_{ci}} f_{cgp} \Psi_b(t_d, t_i) K_{id} \quad [\text{LRFD Eq. 5.9.5.4.2b-1}]$$

where

$\Psi_b(t_d, t_i)$ = girder creep coefficient at time of deck placement due to loading introduced at transfer

$$= 1.9k_{vs}k_{hc}k_fk_{td}t_i^{-0.118} \quad [\text{LRFD Eq. 5.4.2.3.2-1}]$$

$$= 1.9(1.035)(1.000)(0.714)(0.706)(1)^{-0.118} = 0.991$$

$$\Delta f_{pCR} = \frac{28,500}{4,696} (1.864)(0.991)(0.845) = 9.473 \text{ ksi}$$

9.6.6.2.3 Relaxation of Prestressing Strands

The prestress loss due to relaxation of prestressing strands between time of transfer and deck placement is determined as:

$$\Delta f_{pR1} = \frac{f_{pt}}{K_L} \left(\frac{f_{pt}}{f_{py}} - 0.55 \right) \quad [\text{LRFD Eq. 5.9.5.4.2c-1}]$$

where

f_{pt} = stress in prestressing strands immediately after transfer, taken not less than $0.55f_y$

K_L = 30 for low-relaxation strands and 7 for other prestressing steel, unless more accurate manufacturer's data are available

$$\Delta f_{pR1} = \frac{(202.5 - 11.3)}{30} \left(\frac{(202.5 - 11.3)}{243} - 0.55 \right) = 1.509 \text{ ksi}$$

According to LRFD Art. 5.9.5.4.2c, the relaxation loss may also be assumed equal to 1.2 ksi for low-relaxation strands.

U-BEAM (TX-U54), SINGLE SPAN, PRECAST DECK PANELS, COMPOSITE DECK**9.6.6.3 Time-Dependent Losses between Deck Placement and Final Time/9.6.6.3.2 Creep of Concrete****9.6.6.3 Time-Dependent Losses between Deck Placement and Final Time**

The total time-dependent loss between time of deck placement and final time is the summation of prestress losses due to shrinkage of beam concrete, creep of beam concrete, relaxation of prestressing strands, and shrinkage of deck concrete.

9.6.6.3.1 Shrinkage of Concrete

The prestress loss due to shrinkage of concrete between time of deck placement and final time is calculated by:

$$\Delta f_{pSD} = \epsilon_{bdf} E_p K_{df} \quad [\text{LRFD Eq. 5.9.5.4.3a-1}]$$

where

ϵ_{bdf} = concrete shrinkage strain of girder for time period between deck placement and final time

E_p = modulus of elasticity of prestressing strands, ksi

K_{df} = transformed section coefficient that accounts for time-dependent interaction between concrete and bonded steel in the section being considered for time period between deck placement and final time

The total concrete shrinkage strain between transfer and final time is taken as:

$$\begin{aligned} \epsilon_{bid} &= \epsilon_{bid} = k_{vs} k_{hs} k_f k_{tdf} 0.48 \times 10^{-3} & [\text{LRFD Eq. 5.4.2.3.3-1}] \\ &= (1.035)(1.020)(0.714)(0.998)(0.48 \times 10^{-3}) = 0.000361 \end{aligned}$$

The concrete shrinkage strain between deck placement and final time is:

$$\epsilon_{bdf} = \epsilon_{bif} - \epsilon_{bid} = 0.000361 - 0.000255 = 0.000106$$

The beam concrete transformed section coefficient between deck placement and final time is:

$$K_{df} = \frac{1}{1 + \frac{E_p}{E_{ci}} \frac{A_{ps}}{A_c} \left(1 + \frac{A_c (e_{pc})^2}{I_c}\right) [1 + 0.7 \Psi_b(t_f, t_i)]} \quad [\text{LRFD Eq. 5.9.5.4.3a-2}]$$

where

A_c = area of the composite section = 1,768 in.²

I_c = moment of inertia of the composite section = 925,249 in.⁴

e_{pc} = eccentricity of strands with respect to centroid of composite section = 35.40 – 2.74 = 32.66 in.

$$K_{df} = \frac{1}{1 + \frac{28,500}{4,696} \frac{8.246}{1,768} \left(1 + \frac{1,768(32.66)^2}{925,249}\right) [1 + 0.7(1.401)]} = 0.854$$

The prestress loss due to shrinkage of concrete between deck placement and final time is:

$$\Delta f_{pSD} = (0.000106)(28,500)(0.854) = 2.580 \text{ ksi}$$

9.6.6.3.2 Creep of Concrete

The prestress loss due to creep of beam concrete between time of deck placement and final time is:

$$\Delta f_{pCD} = \frac{E_p}{E_{ci}} f_{cgp} [\Psi_b(t_f, t_i) - \Psi_b(t_d, t_i)] K_{df} + \frac{E_p}{E_c} \Delta f_{cd} \Psi_b(t_f, t_d) K_{df} \quad [\text{LRFD Eq. 5.9.5.4.3b-1}]$$

where

$\Psi_b(t_f, t_d)$ = girder creep coefficient at final time due to loading at deck placement

$$= 1.9 k_{vs} k_{hc} k_f k_{tdf} t_d^{-0.118} \quad [\text{LRFD Eq. 5.4.2.3.2-1}]$$

U-BEAM (TX-U54), SINGLE SPAN, PRECAST DECK PANELS, COMPOSITE DECK

9.6.6.3.2 Creep of Concrete/9.6.6.3.4 Shrinkage of Deck Concrete

$$k_{tdf} = \frac{t}{61 - 4f'_{ci} + t} = \frac{20,000 - 90}{61 - 4(6.0) + (20,000 - 90)} = 0.998$$

$$\Psi_b(t_f, t_d) = 1.9(1.035)(1.000)(0.714)(0.998)(90)^{-0.118} = 0.824$$

Δf_{cd} = change in concrete stress at centroid of prestressing strands due to long-term losses between transfer and deck placement, combined with deck weight and superimposed loads, ksi

$$\begin{aligned} &= -(\Delta f_{pSR} + \Delta f_{pCR} + \Delta f_{pR1}) \frac{A_{ps}}{A_g} \left(1 + \frac{A_g (e_{pg})^2}{I_g} \right) - \left(\frac{M_s e_{tf}}{I_{tf}} + \frac{(M_b + M_{ws}) e_{tc}}{I_{tc}} \right) \\ &= -(6.141 + 9.473 + 1.509) \frac{8.246}{1,120} \left(1 + \frac{1,120(19.62)^2}{403,020} \right) \\ &\quad - \left(\frac{1,725.8(19.10)(12)}{414,519} + \frac{(226.9 + 444.7)(32.10)(12)}{957,255} \right) \\ &= -1.485 \text{ ksi} \end{aligned}$$

The gross section properties are used in the equation to calculate Δf_{cd} for the long-term losses since the transformed section effect has already been included in the factor K_{id} when calculating the losses between initial time and deck placement.

$$\begin{aligned} \Delta f_{pCD} &= \frac{28,500}{4,696} (1.864)(1.401 - 0.991)(0.854) + \frac{28,500}{6,062} (-1.485)(0.824)(0.854) \\ &= -0.952 \text{ ksi} \end{aligned}$$

The negative sign indicates a prestressing gain.

9.6.6.3.3 Relaxation of Prestressing Strands

The prestress loss due to relaxation of prestressing strands in the composite section between time of deck placement and final time is taken as:

$$\Delta f_{pR2} = \Delta f_{pR1} = 1.509 \text{ ksi}$$

9.6.6.3.4 Shrinkage of Deck Concrete

For simplicity, the shrinkage of the CIP deck concrete and the precast panel concrete are both assumed to start 1 day after the deck is cast. In reality, shrinkage of the deck panels after the CIP deck is placed will be less than that of the CIP deck. The effect on the total calculated prestress losses is minimal.

The prestress gain due to shrinkage of deck concrete is calculated by:

$$\Delta f_{pSS} = \frac{E_p}{E_c} \Delta f_{cdf} K_{df} [1 + 0.7\Psi_b(t_f, t_d)] \quad \text{[LRFD Eq. 5.9.5.4.3d-1]}$$

where Δf_{cdf} = change in concrete stress at centroid of prestressing strands due to shrinkage of deck concrete, ksi

$$\Delta f_{cdf} = \frac{\varepsilon_{ddf} A_d E_{cd}}{1 + 0.7\Psi_d(t_f, t_d)} \left[\frac{1}{A_c} - \frac{e_{pc} e_d}{I_c} \right] \quad \text{[LRFD Eq. 5.9.5.4.3d-2]}$$

where

ε_{ddf} = shrinkage strain of deck concrete between placement and final time by LRFD Eq. 5.4.2.3.3-1

A_d = area of deck concrete, in.²

E_{cd} = modulus of elasticity of deck concrete, ksi

$\Psi_d(t_f, t_d)$ = deck concrete creep coefficient at final time due to loading introduced shortly after deck placement

e_d = eccentricity of deck with respect to the gross composite section, in.

U-BEAM (TX-U54), SINGLE SPAN, PRECAST DECK PANELS, COMPOSITE DECK**9.6.6.3.4 Shrinkage of Deck Concrete/9.6.6.5 Total Losses at Transfer**

Assume the initial strength of concrete at deck placement is $0.8(4.0 \text{ ksi}) = 3.2 \text{ ksi}$, and use a volume-to-surface ratio 3.379 for the deck:

$$k_{vs} = 1.45 - 0.13(V/S) = 1.45 - 0.13(3.379) = 1.011 > 1.0 \quad \text{OK}$$

$$k_f = \frac{5}{1 + f'_{ci}} = \frac{5}{1 + 3.2} = 1.190$$

$$k_{td} = \frac{t}{61 - 4f'_{ci} + t} = \frac{20,000 - 90}{61 - 4(3.2) + (20,000 - 90)} = 0.998$$

$$\varepsilon_{ddf} = k_{vs}k_{hs}k_fk_{td}0.48 \times 10^{-3} \quad \text{[LRFD Eq. 5.4.2.3.3-1]}$$

$$= (1.011)(1.020)(1.190)(0.998)(0.48 \times 10^{-3}) = 0.000588$$

$$\Psi_d(t_f, t_d) = 1.9k_{vs}k_{hc}k_fk_{td}t_i^{-0.118} \quad \text{[LRFD Eq. 5.4.2.3.2-1]}$$

$$= 1.9(1.011)(1.000)(1.190)(0.998)(1)^{-0.118} = 2.281$$

Creep of the deck concrete is assumed to start at 1 day.

$$\Delta f_{cdf} = \frac{0.000588(144)(7.0)(3,834)}{1 + 0.7(2.281)} \left(\frac{1}{1,768} - \frac{32.66(61.5 - 7.0/2 - 35.40)}{925,249} \right)$$

$$= -0.203 \text{ ksi} \quad \text{The negative sign indicates a prestressing gain.}$$

The prestress gain due to shrinkage of the deck in the composite section:

$$\Delta f_{pSS} = \frac{28,500}{6,062} (-0.203)(0.854)[1 + 0.7(0.824)] = -1.285 \text{ ksi}$$

Note: The effect of deck shrinkage on the calculation of prestress gain is discussed further in Section 9.1a.8.5.

9.6.6.4 Total Time-Dependent Loss

The total time-dependent loss, Δf_{pLT} , is determined as:

[LRFD Eq. 5.9.5.4.1-1]

$$\Delta f_{pLT} = (\Delta f_{pSR} + \Delta f_{pCR} + \Delta f_{pR1}) + (\Delta f_{pSD} + \Delta f_{pCD} + \Delta f_{pR2} + \Delta f_{pSS})$$

$$= (6.141 + 9.473 + 1.509) + (2.580 - 0.952 + 1.509 - 1.285)$$

$$= 19.0 \text{ ksi}$$

9.6.6.5 Total Losses at Transfer

AASHTO LRFD C5.9.5.2.3a and C5.9.5.3 indicates that the losses or gains due to elastic deformation must be taken equal to zero if transformed section properties are used in stress analysis. However, the losses or gains due to elastic deformation must be included in determining the total prestress losses and the effective stress in prestressing strands.

$$\Delta f_{pi} = \Delta f_{pES} = 11.3 \text{ ksi}$$

Effective stress in tendons immediately after transfer, $f_{pt} = f_{pi} - \Delta f_{pi} = (202.5 - 11.3) = 191.2 \text{ ksi}$

Force per strand = $(f_{pt})(\text{area of strand}) = (191.2)(0.217) = 41.49 \text{ kips}$

Therefore, the total prestressing force after transfer, $P_{pt} = 41.49(38) = 1,577 \text{ kips}$

Initial loss, % = $(\text{Total losses at transfer})/(f_{pi}) = 11.3/(202.5) = 5.6\%$

When determining the concrete stress using transformed section properties, the strand force is that before transfer:

Force per strand = $(202.5)(0.217) = 43.94 \text{ kips}$

The total prestressing force before transfer, $P_{pi} = 43.94(38) = 1,670 \text{ kips}$

U-BEAM (TX-U54), SINGLE SPAN, PRECAST DECK PANELS, COMPOSITE DECK**9.6.6.6 Total Losses at Service Loads/9.6.7.1 Stress Limits for Concrete****9.6.6.6 Total Losses at Service Loads**

Total loss due to elastic shortening at transfer and long-term losses is:

$$\Delta f_{pT} = \Delta f_{pES} + \Delta f_{pLT} = 11.3 + 19.0 = 30.3 \text{ ksi}$$

The elastic gain due to deck weight, superimposed dead load, and live load (Service III) is:

$$\begin{aligned} &= \left(\frac{M_s e_{tf}}{I_{tf}} + \frac{(M_b + M_{ws}) e_{tc}}{I_{tc}} \right) \frac{E_p}{E_c} + 0.8 \left(\frac{(M_{LT} + M_{LL}) e_{tc}}{I_{tc}} \right) \frac{E_p}{E_c} \\ &= \left(\frac{(1,725.8)(12)(19.10)}{414,519} + \frac{(226.9 + 444.7)(12)(32.10)}{957,255} \right) \frac{28,500}{6,062} + 0.8 \left(\frac{(1,691.1 + 724.1)(12)(32.1)}{957,255} \right) \frac{28,500}{6,062} \\ &= 5.8 + 3.7 = 9.5 \text{ ksi} \end{aligned}$$

The effective stress in strands after all losses and gains:

$$f_{pe} = f_{pi} - \Delta f_{pT} + 5.8 = 202.5 - 30.3 + 9.5 = 181.7 \text{ ksi}$$

Check prestressing stress limit at service limit state:

[LRFD Table 5.9.3-1]

$$f_{pe} \leq 0.8 f_{py} = 0.8(243) = 194.4 \text{ ksi} > 181.7 \text{ ksi} \quad \text{OK}$$

The effective stress in strands after all losses and permanent gains:

$$f_{pe} = f_{pi} - \Delta f_{pT} + 8.0 = 202.5 - 30.3 + 5.8 = 178.0 \text{ ksi}$$

Force per strand without live load gains = $(f_{pe})(\text{area of strand}) = (178.0)(0.217) = 38.63 \text{ kips}$

Therefore, the total prestressing force after all losses = $38.63(38) = 1,468 \text{ kips}$

Final loss percentage = $(\text{total losses and gains})/(f_{pi}) = (30.3 - 5.8)/(202.5) = 12.1\%$

Without consideration of prestressing gains at deck placement, the final loss percentage = $\text{total losses}/(f_{pi}) = (30.3)/202.5 = 15.0\%$

When determining the concrete stress using transformed section properties, all the elastic gains and losses are implicitly accounted for.

Force per strand with only total time-dependent losses = $(f_{pi} - \Delta f_{pLT})(\text{area of strand}) = (202.5 - 19.0)(0.217) = 39.82 \text{ kips}$

Total prestressing force, $P_{pe} = (39.82)(38) = 1,513 \text{ kips}$

9.6.7 CONCRETE STRESSES AT TRANSFER

Because the transformed section is used, the total prestressing force before transfer $P_{pi} = 1,670 \text{ kips}$.

9.6.7.1 Stress Limits for Concrete

[LRFD Art. 5.9.4]

Compression:

- $0.6 f'_{ci} = 0.6(6.0) = +3.600 \text{ ksi}$

where f'_{ci} = concrete strength at release = 6.000 ksi

Tension:

- without bonded auxiliary reinforcement

$$-0.0948 \sqrt{f'_{ci}} \leq -0.200 \text{ ksi}; \quad -0.0948 \sqrt{6.000} = -0.232 \text{ ksi}$$

Therefore, -0.200 ksi (Controls)

- with bonded auxiliary reinforcement that is sufficient to resist 120% of the tension force in the cracked concrete

$$-0.24 \sqrt{f'_{ci}} = -0.24 \sqrt{6.000} = -0.588 \text{ ksi}$$

U-BEAM (TX-U54), SINGLE SPAN, PRECAST DECK PANELS, COMPOSITE DECK**9.6.7.2 Stresses at Transfer Length Section****9.6.7.2 Stresses at Transfer Length Section**

Stresses at this location need only be checked at transfer because this stage almost always governs. Also, losses with time will reduce the concrete stresses making them less critical.

$$\text{Transfer length} = 60(\text{strand diameter}) = 60(0.6) = 36 \text{ in.} = 3 \text{ ft} \quad [\text{LRFD Art. 5.11.4}]$$

Due to camber of the beam at transfer, the beam self weight and diaphragm weight act on the overall beam length, 111 ft. Therefore, values for bending moment given in **Table 9.6.4-1** cannot be used because they are based on the design span length of 110 ft. Using Equation 9.6.4.1.2-2, the bending moment at transfer length due to beam and diaphragm weights, are:

$$M_g = 0.5w_gx(L - x) = (0.5)(1.167)(3)(111 - 3) = 189.1 \text{ ft-kips}$$

$$M_d = 1.858(3) = 5.6 \text{ ft-kips}$$

Compute concrete stress in the top of beam:

$$f_t = \frac{P_{pi}}{A_{ti}} - \frac{P_{pi}e_{ti}}{S_{tti}} + \frac{(M_g + M_d)}{S_{tti}} = \frac{1,670}{1,161.8} - \frac{1,670(18.91)}{12,939} + \frac{(189.1 + 5.6)(12)}{12,939}$$

$$= 1.437 - 2.441 + 0.181 = -0.823 \text{ ksi}$$

Tensile stress limit for concrete with bonded reinforcement: -0.588 ksi NG

Compute concrete stress in the bottom of beam:

$$f_b = \frac{P_{pi}}{A_{ti}} + \frac{P_{pi}e_{ti}}{S_{bti}} - \frac{(M_g + M_d)}{S_{bti}} = \frac{1,670}{1,161.8} + \frac{1,670(18.91)}{19,333} - \frac{(189.1 + 5.6)(12)}{19,333}$$

$$= 1.437 + 1.633 - 0.121 = +2.949 \text{ ksi}$$

Compressive stress limit for concrete: +3.600 ksi OK

Since stress at the top exceeds the stress limit, debond strands to satisfy the specified limits. Debond nine strands for a distance of 10 ft from the end of the beam.

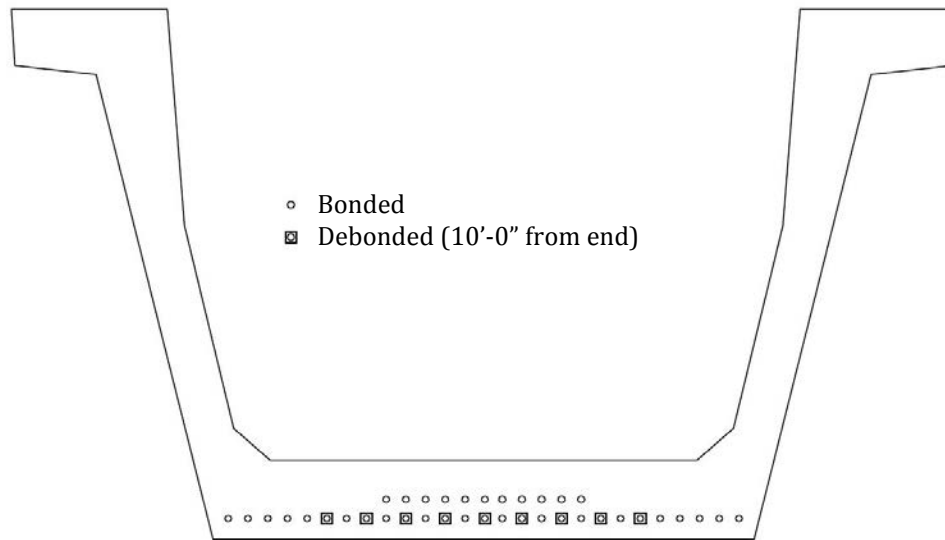
To minimize the shock impact of detensioning and cracks at corners and bottom, assume the strand pattern shown in **Fig. 9.6.7.2-1**. LRFD Article 5.11.4.3 requires that the following conditions be satisfied if debonding is used:

- percentage debonding of total = $9/38 = 24\% \leq 25\%$ OK
- percentage debonding of row = $9/27 = 33\% \leq 40\%$ OK
- All limit states should be satisfied OK
- Debonded strands should be symmetrically distributed OK
- Exterior strands in each horizontal line are fully bonded OK

U-BEAM (TX-U54), SINGLE SPAN, PRECAST DECK PANELS, COMPOSITE DECK

9.6.7.2 Stresses at Transfer Length Section/9.6.7.3 Stresses at Transfer Length Section of Debonded Strands

Figure 9.6.7.2-1
Strand Pattern at End of Beam



Compute the center of gravity of the bonded prestressing strands at the end of the beam.

The distance from the center of gravity of bonded strands to the bottom fiber of the beam is:

$$y_{bs} = [18(2.17) + 11(4.14)] / (29) = 2.92 \text{ in.}$$

and the strand eccentricity for the transformed section at end of the beam is:

$$e_{ti} = 21.82 - 2.92 = 18.90 \text{ in.}$$

Recompute the stresses at the transfer length section. Note that the transformed section properties here are different than those at midspan after debonding. Using the same method as described in Section 9.6.5.5, the transformed section properties at end of beam are computed as:

$$A_{ti} = 1,152 \text{ in.}^2 \quad y_{bi} = 21.82 \text{ in.} \quad S_{bti} = 19,183 \text{ in.}^3 \quad S_{tti} = 13,007 \text{ in.}^3$$

Total prestressing force at release at end section = 29(43.94) = 1,274 kips

Concrete stress in top of beam:

$$f_t = \frac{1,274}{1,152} - \frac{1,274(18.90)}{13,007} + \frac{(189.1 + 5.6)(12)}{13,007}$$

$$= 1.106 - 1.851 + 0.180 = -0.565 \text{ ksi}$$

Tensile stress limit for concrete is: -0.588 ksi OK

Concrete stress in bottom of beam:

$$f_b = \frac{1,274}{1,152} + \frac{1,274(18.90)}{19,183} - \frac{(189.1 + 5.6)(12)}{19,183}$$

$$= 1.106 + 1.255 - 0.122 = +2.239 \text{ ksi}$$

Compressive stress limit for concrete is: +3.600 ksi OK

9.6.7.3 Stresses at Transfer Length Section of Debonded Strands

All strands are effective at this location; therefore use the full value of P_{pi} . Bending moments due to the self weight of the beam and diaphragms at (10 ft + 3 ft = 13 ft) from the end of the beam are:

$$M_g = 0.5w_gx(L - x) = (0.5)(1.167)(13)(111 - 13) = 743.4 \text{ ft-kips}$$

$$M_d = 1.858(13) = 24.2 \text{ ft-kips}$$

U-BEAM (TX-U54), SINGLE SPAN, PRECAST DECK PANELS, COMPOSITE DECK

9.6.7.3 Stresses at Transfer Length Section of Debonded Strands/9.6.8.1 Stress Limits for Concrete

Concrete stress in top of beam:

$$f_t = \frac{P_{pi}}{A_{ti}} - \frac{P_{pi}e_{ti}}{S_{tti}} + \frac{(M_g + M_d)}{S_{tti}} = \frac{1,670}{1,161.8} - \frac{1,670(18.91)}{12,939} + \frac{(743.4 + 24.2)(12)}{12,939}$$

$$= 1.437 - 2.441 + 0.712 = -0.292 \text{ ksi}$$

Tensile stress limit for concrete: -0.588 ksi OK

Concrete stress in bottom of beam:

$$f_b = \frac{P_{pi}}{A_{ti}} + \frac{P_{pi}e_{ti}}{S_{bti}} - \frac{M_g}{S_{bti}} = \frac{1,670}{1,161.8} + \frac{1,670(18.91)}{19,333} - \frac{(743.4 + 24.2)(12)}{19,333}$$

$$= 1.437 + 1.633 - 0.476 = 2.594 \text{ ksi}$$

Compressive stress limit for concrete: +3.600 ksi OK

9.6.7.4 Stresses at Midspan

Bending moment at midspan due to the beam and diaphragm weights are:

$$M_g = 0.5(1.167)(55.5)(111 - 55.5) = 1,797.3 \text{ ft-kips}$$

$$M_d = 1.858(42.5) = 79.0 \text{ ft-kips}$$

Concrete stress in top bottom of beam:

$$f_t = \frac{1,670}{1,161.8} - \frac{1,670(18.91)}{12,939} + \frac{(1,797.3 + 79.0)(12)}{12,939} = 1.437 - 2.441 + 1.740 = +0.736 \text{ ksi}$$

Tensile stress limit for concrete: -0.588 ksi OK

Concrete stress in bottom of beam:

$$f_b = \frac{1,670}{1,161.8} + \frac{1,670(18.91)}{19,333} - \frac{(1,797.3 + 79.0)(12)}{19,333} = 1.437 + 1.633 - 1.165 = +1.905 \text{ ksi}$$

Compressive stress limit for concrete: +3.600 ksi OK

9.6.7.5 Summary of Stresses at Transfer

	Top Fiber Stresses f_t , ksi	Bottom Fiber Stresses f_b , ksi
At transfer length section	-0.565	+2.239
At end of debonded strands + transfer length	-0.292	+2.594
At midspan	+0.736	+1.905

9.6.8 CONCRETE STRESSES AT SERVICE LOADS

Using transformed section properties and refined losses, $P_{pe} = 1,513$ kips

9.6.8.1 Stress Limits for Concrete

Compression:

[LRFD Art. 5.9.4.2.]

Due to permanent loads, (i.e. beam self weight, weight of slab and haunch, diaphragm weight, weight of future wearing surface, and weight of barriers,), for load combination Service I:

for precast beams: $0.45 f'_c = (0.45)(10.000) = +4.500$ ksi

for deck: $0.45 f'_c = (0.45)(4.000) = +1.800$ ksi

U-BEAM (TX-U54), SINGLE SPAN, PRECAST DECK PANELS, COMPOSITE DECK**9.6.8.1 Stress Limits for Concrete/9.6.8.2 Concrete Stress at the Top Fiber of the Deck**

Due to permanent and transient loads (i.e. all dead loads and live loads), for load combination Service I:

$$\text{for precast beams: } 0.60 f'_c = 0.6(10.000) = +6.000 \text{ ksi}$$

$$\text{for deck: } 0.60 f'_c = 0.60(4.000) = +2.400 \text{ ksi}$$

Tension:

For components with bonded prestressing tendons:

$$\text{for load combination Service III: } 0.19\sqrt{f'_c}$$

$$\text{for precast beam: } -0.19\sqrt{10.000} = -0.601 \text{ ksi}$$

9.6.8.2 Stresses at Midspan**9.6.8.2.1 Concrete Stress at Top Fiber of the Beam**

To check top compressive stresses, two cases are considered:

1. Under permanent loads, load combination Service I:

Using bending moment values given in **Table 9.6.4-1**, compute the top fiber stresses:

$$\begin{aligned} f_{tg} &= \frac{P_{pe}}{A_{tf}} - \frac{P_{pe}e_{tf}}{S_{ttf}} + \frac{M_g + M_d + M_s}{S_{ttf}} + \frac{(M_{ws} + M_b)}{S_{ttc}} \\ &= \frac{1,513}{1,151} - \frac{(1,513)(19.10)}{12,889} + \frac{(1,765.1 + 78.0 + 1,725.8)(12)}{12,889} + \frac{(444.7 + 226.9)(12)}{49,961} \\ &= 1.315 - 2.242 + 3.323 + 0.161 = +2.557 \text{ ksi} \end{aligned}$$

Compressive stress limit for concrete: +4.500 ksi OK

2. Under permanent and transient loads, load combination Service I:

$$\begin{aligned} f_{tg} &= +2.557 + \frac{(M_{LT} + M_{LL})}{S_{ttc}} \\ &= +2.557 + \frac{(1,691.1 + 724.1)(12)}{49,961} \\ &= 2.557 + 0.580 = +3.137 \text{ ksi} \end{aligned}$$

Compressive stress limit for concrete: +6.000 ksi OK

9.6.8.2.2 Concrete Stress at the Top Fiber of the Deck

Note: Compressive stress in the deck slab at service loads never controls the design for typical applications. The calculations shown below are for illustration purposes and may not be necessary in most practical applications.

1. Under permanent loads, load combination Service I:

$$f_{tc} = \frac{(M_{ws} + M_b)}{S_{dtc}} = \frac{(444.7 + 226.9)(12)}{56,768} = +0.142 \text{ ksi}$$

Compressive stress limit for concrete: +1.800 ksi OK

2. Under permanent and transient loads, load combination Service I:

$$\begin{aligned} f_{tc} &= \frac{(M_{ws} + M_b)}{S_{dtc}} + \frac{(M_{LT} + M_{LL})}{S_{dtc}} = +0.142 + \frac{(1,691.1 + 724.1)(12)}{56,768} \\ &= 0.142 + 0.511 = +0.653 \end{aligned}$$

Compressive stress limit for concrete: +2.400 ksi OK

U-BEAM (TX-U54), SINGLE SPAN, PRECAST DECK PANELS, COMPOSITE DECK

9.6.8.2.3 Concrete Stress in Bottom of Beam, Load Combination Service III/9.6.8.5 Effect of Deck Shrinkage

9.6.8.2.3 Concrete Stress in Bottom of Beam, Load Combination Service III

$$f_b = \frac{P_{pe}}{A_{tf}} + \frac{P_{pe}e_{tf}}{S_{btf}} - \frac{(M_g + M_d + M_s)}{S_{btf}} - \frac{(M_{ws} + M_b) + 0.8(M_{LT} + M_{LL})}{S_{btcc}}$$

$$= \frac{1,513}{1,151} + \frac{(1,513)(19.10)}{18,980} - \frac{(1,765.1 + 78.0 + 1,725.8)(12)}{18,980}$$

$$- \frac{(444.7 + 226.9)(12) + 0.8(1,691.1 + 724.1)(12)}{27,476}$$

= 1.315 + 1.523 – 2.256 – 1.137 = –0.555 ksi

Tensile stress limit for concrete: –0.601 ksi OK

9.6.8.3 Fatigue Stress Limit

LRFD Article 5.5.3.1 states that in fully prestressed components other than segmentally constructed bridges, the compressive stress due to Fatigue I load combination and one half the sum of effective prestress and permanent loads shall not exceed $0.40f'_c$, after losses.

From **Table 9.6.4-2**, the unfactored fatigue bending moment at midspan, M_f , is 579.0 ft-kips. Therefore, stress at the top fiber of the beam due to fatigue load combination I is:

$$f_{tgf} = \frac{1.50(M_f)}{S_{ttc}} = \frac{1.50(579.0)(12)}{49,961} = +0.209 \text{ ksi}$$

At midspan, the top compressive stress due to permanent loads and prestress is:

$$f_{tg} = \frac{P_{pe}}{A_{tf}} - \frac{P_{pe}e_{tf}}{S_{ttf}} + \frac{(M_g + M_d + M_s)}{S_{ttf}} + \frac{(M_{ws} + M_b)}{S_{ttc}}$$

$$= \frac{1,513}{1,151} - \frac{(1,513)(19.10)}{12,889} + \frac{(1,765.1 + 78.0 + 1,725.8)(12)}{12,889} + \frac{(444.7 + 226.9)(12)}{49,961}$$

$$= 1.315 - 2.242 + 3.323 + 0.161 = 2.557 \text{ ksi}$$

Therefore:

$$f_{tgf} + \frac{f_b}{2} = 0.209 + \frac{2.257}{2} = 1.488 < 0.40(f'_c) = 0.40(10.0) = 4.0 \text{ ksi OK}$$

This condition should be satisfied at all locations along the beam.

9.6.8.4 Summary of Stresses at Midspan at Service Loads

	Top of Beam, ksi Service I		Top of Deck, ksi Service I		Bottom of Beam, ksi Service III
	Permanent Loads	Total Loads	Permanent Loads	Total Loads	
At midspan	+2.557	+3.137	+0.142	+0.653	–0.555

9.6.8.5 Effect of Deck Shrinkage

The calculations in Section 9.6.8.2 comply with the *LRFD Specifications*. However, PCI believes that it is not appropriate to include the prestressing gain caused by the deck shrinkage, Δf_{pss} , in calculating the prestress losses. Alternatively, the effect of deck shrinkage should be analyzed by considering it as an external force applied to the composite nontransformed section as illustrated in Section 9.1a.8.5.

U-BEAM (TX-U54), SINGLE SPAN, PRECAST DECK PANELS, COMPOSITE DECK

9.6.9 Strength Limit State

9.6.9 STRENGTH LIMIT STATE

Total ultimate bending moment for Strength I is:

$$M_u = 1.25(DC) + 1.5(DW) + 1.75(LL + IM)$$

Using the values of unfactored bending moment given in **Tables 9.6.4-1** and **9.6.4-2**, the ultimate bending moment at midspan is:

$$M_u = 1.25(1,765.1 + 78.0 + 1,725.8 + 226.9) + 1.5(444.7) + 1.75(1,691.1 + 724.1) = 9,638.4 \text{ ft-kips}$$

Average stress in prestressing steel when $f_{pe} \geq 0.5f_{pu}$:

$$f_{ps} = f_{pu} \left(1 - k \frac{c}{d_p} \right) \quad \text{[LRFD Eq. 5.7.3.1.1-1]}$$

where

f_{ps} = average stress in prestressing strand, ksi

f_{pu} = specified tensile strength of prestressing strand = 270.0 ksi

$$k = 2 \left(1.04 - \frac{f_{py}}{f_{pu}} \right) = 2 \left(1.04 - \frac{243}{270} \right) \quad \text{[LRFD Eq. 5.7.3.1.1-2]}$$

$$= 0.28 \text{ for low-relaxation strands}$$

c = distance from the extreme compression fiber to the neutral axis, in.

d_p = distance from extreme compression fiber to the centroid of the prestressing strands = $h_c - y_{bs} = 61.50 - 2.74 = 58.76$ in.

To compute c , assume rectangular section behavior and check if the depth of the equivalent compression stress block, a , is less than or equal to t_s : [LRFD C5.7.3.2.2]

where $a = \beta_1 c$

$$c = \frac{A_{ps} f_{pu} + A_s f_y - A'_s f'_y}{0.85 f'_c \beta_1 b + k A_{ps} \frac{f_{pu}}{d_p}} \quad \text{[LRFD Eq. 5.7.3.1.1-4]}$$

where

a = depth of the equivalent stress block

A_{ps} = area of prestressing strand = $38(0.217) = 8.246 \text{ in.}^2$

A_s = area of nonprestressed tension reinforcement = 0.0 in.^2

f_y = specified yield strength of tension reinforcement, = 60.0 ksi

A'_s = area of compression reinforcement = 0.0 in.^2

f'_y = specified yield strength of compression reinforcement = 60.0 ksi

f'_c = specified compressive strength of deck concrete = 4.0 ksi

β_1 = stress factor of compression block [LRFD Art. 5.7.2.2]

= 0.85 for $f'_c \leq 4.0$ ksi

= $0.85 - 0.05(f'_c - 4.0) \geq 0.65$ for $f'_c > 4.0$ ksi

= 0.85

b = effective width of compression flange = 144.0 in.

U-BEAM (TX-U54), SINGLE SPAN, PRECAST DECK PANELS, COMPOSITE DECK

9.6.9 Strength Limit State/9.6.10.2 Minimum Reinforcement

$$c = \frac{8.246(270.0) + 0 - 0}{0.85(4.0)(0.85)(144.0) + (0.28)(8.246)\left(\frac{270.0}{58.76}\right)} = 5.22 \text{ in.}$$

$$a = \beta_1 c = (0.85)(5.22) = 4.44 \text{ in.} < t_s = 7.0 \text{ in.} \quad \text{OK}$$

Therefore, the rectangular section behavior assumption is valid.

Therefore, the average stress in the prestressing strand is:

$$f_{ps} = 270.0 \left(1 - 0.28 \frac{5.22}{58.76} \right) = 263.3 \text{ ksi}$$

Nominal flexural resistance:

$$M_n = A_{ps} f_{ps} \left(d_p - \frac{a}{2} \right) \quad \text{[LRFD Art. 5.7.3.2.2-1]}$$

The above equation is a simplified form of LRFD Equation 5.7.3.2.2-1 because no compression reinforcement or mild tension reinforcement is present.

$$M_n = (8.246)(263.3) \left(58.76 - \frac{4.44}{2} \right) / 12 = 10,229.8 \text{ ft-kips}$$

Factored flexural resistance:

$$M_r = \phi M_n \quad \text{[LRFD Eq. 5.7.3.2.1-1]}$$

$$\text{where } \phi = \text{resistance factor} \quad \text{[LRFD Art. 5.5.4.2.1]}$$

$$= 1.00, \text{ for tension controlled prestressed concrete sections}$$

$$M_r = 10,229.8 \text{ ft-kips} > M_u = 9,638.4 \text{ ft-kips} \quad \text{OK}$$

9.6.10 LIMITS OF REINFORCEMENT**9.6.10.1 Maximum Reinforcement**

[LRFD Art. 5.7.3.3.1]

The check of maximum reinforcement limits in LRFD Article 5.7.3.3.1 was removed from the *LRFD Specifications* in 2005.

9.6.10.2 Minimum Reinforcement

[LRFD Art. 5.7.3.3.2]

At any section, the amount of prestressed and nonprestressed tensile reinforcement must be adequate to develop a factored flexural resistance, M_r , equal to the lesser of:

- 1.2 times the cracking strength determined on the basis of elastic stress distribution and the modulus of rupture, and
- 1.33 times the factored moment required by the applicable strength load combination.

Check at midspan:

$$M_{cr} = S_{btc}(f_r + f_{cpe}) - M_{dnc} \left(\frac{S_{btc}}{S_{btf}} - 1 \right) \geq S_{btc} f_r \quad \text{[LRFD Art. 5.7.3.3.2-1]}$$

where

$$f_r = \text{modulus of rupture of concrete} \quad \text{[LRFD Art. 5.4.2.6]}$$

$$= 0.37\sqrt{f'_c} = 0.37\sqrt{10,000} = 1.170 \text{ ksi}$$

$$f_{cpe} = \text{compressive stress in concrete due to effective prestress force only (after allowance for all prestress losses) at extreme fiber of section where tensile stress is caused by externally applied loads}$$

U-BEAM (TX-U54), SINGLE SPAN, PRECAST DECK PANELS, COMPOSITE DECK

9.6.10.2 Minimum Reinforcement/9.6.11.1 Critical Section

$$= \frac{P_{pe}}{A_{tf}} + \frac{P_{pe}e_{tf}}{S_{btf}} = \frac{1,513}{1,151} + \frac{(1,513)(19.10)}{18,980} = 2.837 \text{ ksi}$$

M_{dnc} = noncomposite dead load moment at the section

$$= M_g + M_d + M_s = 1,765.1 + 78.0 + 1,725.8 = 3,568.9 \text{ ft-kips}$$

S_{btc} = section modulus for the extreme bottom fiber of transformed composite section where the tensile stress is caused by externally applied loads = 27,476 in.³

S_{btf} = section modulus for the extreme bottom fiber of transformed noncomposite section where the tensile stress is caused by externally applied loads = 18,980 in.³

$$M_{cr} = (1.170 + 2.837) \frac{27,476}{12} - (3,568.9) \left(\frac{27,476}{18,980} - 1 \right) = 7,577.2 \text{ ft-kips}$$

$$1.2M_{cr} = 1.2(7,577.2) = 9,092.6 \text{ ft-kips}$$

At midspan, the factored moment required by the Strength I load combination is:

$$M_u = 9,638.4 \text{ ft-kips (as calculated in Section 9.6.9)}$$

$$1.33 M_u = 1.33(9,638.4) = 12,819.1 \text{ ft-kips}$$

Since $1.2M_{cr} < 1.33M_u$, the $1.2M_{cr}$ requirement controls.

$$M_r = 10,229.8 \text{ ft-kips} > 1.2M_{cr} = 9,092.6 \quad \text{OK}$$

Note: The *LRFD Specifications* requires that this criterion be met at every section.

Illustrated based on 2011 *LRFD Specifications*.

Editor's Note: 2012 *LRFD Specifications* changes will revise minimum reinforcement.

9.6.11 SHEAR DESIGN

The area and spacing of shear reinforcement must be determined at regular intervals along the entire length of the beam. In this design example, transverse shear design procedures are demonstrated below by determining these values at the critical section near the supports.

Transverse shear reinforcement is required when:

$$V_u > 0.5\phi(V_c + V_p) \quad \text{[LRFD Eq. 5.8.2.4-1]}$$

where

V_u = total factored shear force, kips

V_c = nominal shear resistance provided by tensile stresses in the concrete, kips

V_p = component in the direction of the applied shear of the effective prestressing force, kips

ϕ = resistance factor = 0.9 for normal weight concrete [LRFD Art. 5.5.4.2.1]

9.6.11.1 Critical Section

[LRFD Art. 5.8.3.2]

The critical section near the supports is taken as the effective shear depth, d_v , from the internal face of the support.

d_v = distance between resultants of tensile and compressive forces, $(d_e - a/2)$, but not less than $(0.9d_e)$ or $(0.72h_c)$ [LRFD Art. 5.8.2.7]

where

d_e = the corresponding effective depth from the extreme compression fiber to the centroid of the tensile force in the tensile reinforcement [LRFD Art. 5.8.2.9]

a = depth of compression block = 4.44 in. (at midspan, assumed adequate)

h_c = overall depth of the composite section = 61.5 in.

U-BEAM (TX-U54), SINGLE SPAN, PRECAST DECK PANELS, COMPOSITE DECK

9.6.11.1 Critical Section/9.6.11.2.1 Strain in Flexural Tension Reinforcement

Note: Only 29 strands are effective at the critical section for shear, because nine strands are debonded for a distance of 10 ft from the end of the beam.

$$y_{bs} = 2.92 \text{ in., calculated in Section 9.6.7.2}$$

$$d_e = h_c - y_{bs} = 61.50 - 2.92 = 58.58 \text{ in.}$$

$$d_v = 58.58 - (0.5)(4.44) = 56.36 \text{ in. (Controls)}$$

$$\geq 0.9d_e = 0.9(58.58) = 52.72 \text{ in. OK}$$

$$\geq 0.72h_c = 0.72(61.50) = 44.28 \text{ in. OK}$$

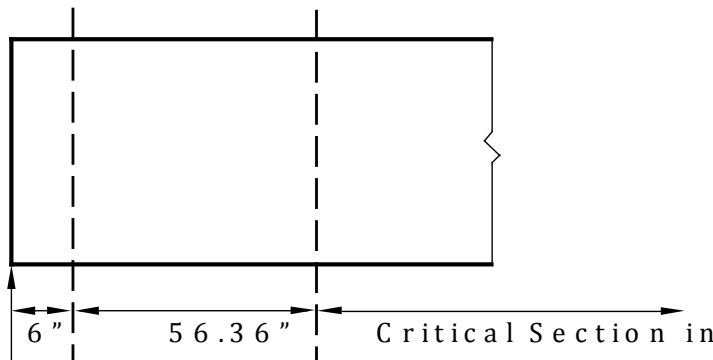
Therefore, $d_v = 56.36 \text{ in.}$

Because the width of the bearing is not yet determined, it was conservatively assumed to be zero for determining the critical section for shear, as shown in **Figure 9.6.11.1-1**. Therefore, the critical section in shear is located at a distance of:

$$56.36 \text{ in.} = 4.70 \text{ ft from centerline of support}$$

$$(x/L) = 4.70/110 = 0.043L$$

Figure 9.6.11.1-1
Critical Section in Shear



9.6.11.2 Contribution of Concrete to Nominal Shear Resistance

The contribution of the concrete to the nominal shear resistance is:

$$V_c = 0.0316\beta\sqrt{f'_c} b_v d_v \quad \text{[LRFD Eq.5.8.3.3-3]}$$

where β = a factor indicating the ability of diagonally cracked concrete to transmit tension (a value indicating concrete contribution)

Several quantities must be determined before this expression can be evaluated.

9.6.11.2.1 Strain in Flexural Tension Reinforcement

Calculate the strain at the centroid of the tension reinforcement, ϵ_s :

$$\epsilon_s = \frac{\frac{|M_u|}{d_v} + 0.5N_u + |(V_u - V_p)| - A_{ps}f_{po}}{(E_s A_s + E_p A_{ps})} \quad \text{[LRFD Eq. 5.8.3.4.2-4]}$$

where

$$N_u = \text{applied factored axial force at the specified section, } 0.043L = 0 \text{ kips}$$

$$V_u = \text{applied factored shear force at the specified section, } 0.043L$$

$$= 1.25(58.7 + 57.4 + 7.5 + 1.9) + 1.50(14.8) + 1.75(89.3 + 34.5) \quad \text{(Tables 9.6.4-1 and 9.6.4-2)}$$

$$= 395.7 \text{ kips}$$

U-BEAM (TX-U54), SINGLE SPAN, PRECAST DECK PANELS, COMPOSITE DECK

9.6.11.2.1 Strain in Flexural Tension Reinforcement/9.6.11.3.2 Required Area of Reinforcement

V_p = component of the effective prestressing force in the direction of the applied shear
= 0 kips since strand pattern is straight

M_u = applied factored bending moment at the specified section, $0.043L$
= $1.25(288.8 + 282.3 + 37.1 + 8.7) + 1.50(72.8) + 1.75(293.7 + 118.5)$
= 1,601.7 ft-kips

M_u need not to be taken less than $(V_u - V_p)d_v$:
 $(V_u - V_p)d_v = [(395.7 - 0)(56.36/12)] = 1,858.5$ ft-kips
Since $(V_u - V_p)d_v \geq M_u$, $M_u = 1,858.5$ ft-kips Controls

A_{ps} = area of prestressing strands on the flexural tension side of the member = $29(0.217) = 6.293$ in.²
(Only 29 of the 38 strands in the flexural tension side are effective because nine strands are debonded).

f_{po} = a parameter taken as modulus of elasticity of prestressing tendons multiplied by the locked-in difference in strain between the prestressing tendons and the surrounding concrete (ksi). For pretensioned members, LRFD Article C5.8.3.4.2 indicates that f_{po} can be taken as $0.7f_{pu}$. (Note: use this for both pretensioned and post-tensioned systems made with stress relieved and low relaxation strands).
= $0.7(270.0) = 189.0$ ksi

$$\varepsilon_s = \frac{\frac{1,858.5 \times (12)}{56.36} + 0.5(0) + |(395.7 - 0)| - 6.293(189)}{[0 + 28,500(6.293)]} = -2.219 \times 10^{-3}$$

ε_s is less than zero. Use $\varepsilon_s = 0$.

9.6.11.2.2 Values of β and θ

Assume the section contains at least the minimum amount of traverse reinforcement:

$$\beta = \frac{4.8}{(1 + 750\varepsilon_s)} = \frac{4.8}{(1 + 0)} = 4.8 \quad \text{[LRFD Eq. 5.8.3.4.2-1]}$$

Angle of diagonal compressive stress is:

$$\theta = 29 + 3,500\varepsilon_s = 29 + 3,500(0) = 29^\circ \quad \text{[LRFD Eq. 5.8.3.4.2-3]}$$

9.6.11.2.3 Compute Concrete Contribution

The nominal shear resisted by the concrete is:

$$V_c = 0.0316\beta\sqrt{f'_c} b_v d_v \quad \text{[LRFD Eq. 5.8.3.3-3]}$$

where b_v = effective web width = 10.0 in.

$$V_c = 0.0316(4.8) \sqrt{10.0} (10.0)(56.36) = 270.3 \text{ kips}$$

9.6.11.3 Contribution of Reinforcement to Nominal Shear Resistance**9.6.11.3.1 Requirement for Reinforcement**

Check if $V_u > 0.5\phi(V_c + V_p)$ [LRFD Eq. 5.8.2.4-1]

$$V_u = 395.7 \text{ kips} > 0.5\phi(V_c + V_p) = 0.5(0.9)(270.3 + 0) = 121.6 \text{ kips}$$

Therefore, transverse shear reinforcement must be provided.

9.6.11.3.2 Required Area of Reinforcement

$$V_u / \phi \leq V_n = V_c + V_s + V_p \quad \text{[LRFD Eq. 5.8.3.3-1]}$$

U-BEAM (TX-U54), SINGLE SPAN, PRECAST DECK PANELS, COMPOSITE DECK

9.6.11.3.2 Required Area of Reinforcement/9.6.11.4 Maximum Nominal Shear Resistance

where

$$\begin{aligned} V_s &= \text{shear resistance provided by shear reinforcement} \\ &= (V_u / \phi) - V_c - V_p = (395.7 / 0.9) - 270.3 - 0.0 = 169.4 \text{ kips} \end{aligned}$$

$$V_s = \frac{A_v f_{yh} d_v (\cot \theta + \cot \alpha) (\sin \alpha)}{s} \quad [\text{LRFD Eq. 5.8.3.3-4}]$$

where

$$\begin{aligned} A_v &= \text{area of shear reinforcement within a distance, } s, \text{ in.}^2 \\ s &= \text{spacing of stirrups, in.} \\ f_{yh} &= \text{specified yield strength of shear reinforcement} = 60.0 \text{ ksi} \\ \alpha &= \text{angle of inclination of transverse reinforcement to longitudinal axis} \\ &= 90^\circ \text{ for vertical stirrups} \end{aligned}$$

Therefore, area of shear reinforcement within a distance s , is:

$$\begin{aligned} A_v &= (sV_s) / (f_{yh} d_v \cot \theta) \\ &= [(s)(169.4)] / [60(56.36) \cot 29^\circ] = 0.028s \text{ in.}^2 \end{aligned}$$

If $s = 10$ in., required $A_v = 0.28 \text{ in.}^2/\text{ft}$ **9.6.11.3.3 Determine Spacing of Reinforcement**

Check maximum spacing of transverse reinforcement:

[LRFD Art 5.8.2.7]

Check if $v_u < 0.125f'_c$

$$v_u = \frac{|V_u - \phi V_p|}{\phi b_v d_v} = \frac{|395.7 - 0|}{(0.9)(10.0)(56.36)} = 0.780 \text{ ksi} \quad [\text{LRFD Eq. 5.8.2.9-1}]$$

$$0.125f'_c = (0.125)(10.0) = 1.250 \text{ ksi} \quad [\text{LRFD Eq. 5.8.2.7-1}]$$

Since $v_u < 0.125f'_c$ then, $s \leq 24$ in. (Controls)

$$s \leq 0.8d_v = 0.8(56.36) = 45.1 \text{ in.}$$

Therefore, maximum $s = 24$ in. $> s$ provided = 10 in. OK**Use No. 4 bar two-leg stirrups at 10 in., $A_v = 0.48 \text{ in.}^2/\text{ft} > 0.28 \text{ in.}^2/\text{ft}$**

$$V_s = \frac{0.40(60.0)(56.36) \cot 29^\circ}{10} = 244.0 \text{ kips}$$

9.6.11.3.4 Minimum Reinforcement Requirement

The area of traverse reinforcement should not be less than:

$$0.0316 \sqrt{f'_c} \frac{b_v s}{f_{yh}} = 0.0316 \sqrt{10.0} \frac{10.0(10.0)}{60.0} = 0.167 \text{ in.}^2/\text{ft} < A_v \text{ provided OK} \quad [\text{LRFD Eq. 5.8.2.5-1}]$$

9.6.11.4 Maximum Nominal Shear ResistanceIn order to ensure that the concrete in the web of the beam will not crush prior to yielding of the transverse reinforcement, the *LRFD Specifications* gives an upper limit of V_n as follows:

$$V_n = 0.25f'_c b_v d_v + V_p \quad [\text{LRFD Eq. 5.8.3.3-2}]$$

Comparing this equation with LRFD Eq. 5.8.3.3-1, it can be concluded that

$$V_c + V_s \text{ must not be greater than } 0.25f'_c b_v d_v$$

U-BEAM (TX-U54), SINGLE SPAN, PRECAST DECK PANELS, COMPOSITE DECK**9.6.11.4 Maximum Nominal Shear Resistance/9.6.12.3 Required Interface Shear Reinforcement**

$$270.3 + 244.0 = 514.3 \text{ kips} \leq 0.25(10)(10.0)(56.36) = 1,409.0 \text{ kips} \quad \text{OK}$$

Using the above procedures, the transverse reinforcement can be determined at increments along the entire length of the beam.

9.6.12 INTERFACE SHEAR TRANSFER**9.6.12.1 Factored Horizontal Shear**

[LRFD Art. 5.8.4]

At the strength limit state, the horizontal shear at a section on a per unit basis can be taken as:

$$V_{hi} = \frac{V_u}{d_v} \quad \text{[LRFD Eq. C5.8.4.2-7]}$$

where

V_{hi} = horizontal factored shear force per unit length of the beam, kips/in.

V_u = factored shear force at specified section due to superimposed loads after the deck is cast, kips

d_v = the distance between the centroid of the tension steel and the mid-thickness of the slab
 $= (d_e - t_s/2) = 58.58 - (7.00/2) = 55.08 \text{ in.}$

The *LRFD Specifications* does not identify the location of the critical section. For convenience, it will be assumed here to be the same location as the critical section for vertical shear at point 0.043L.

Using load combination Strength I:

$$V_u = 1.25(58.7+1.9+57.4+7.5) + 1.50(14.8) + 1.75(89.3 + 34.5) = 395.7 \text{ kips} \quad \text{(Tables 9.6.4-1 and 9.6.4-2)}$$

Therefore, the applied factored horizontal shear is:

$$V_{hi} = \frac{395.7}{55.08} = 7.18 \text{ kips/in.}$$

9.6.12.2 Required Nominal Resistance

Required $V_{ni} = V_{hi}/\phi = 7.18/0.9 = 7.98 \text{ kips/in.}$

[LRFD Eq. 5.8.4.1-1]

9.6.12.3 Required Interface Shear Reinforcement

The nominal shear resistance of the interface surface is:

$$V_{ni} = cA_{cv} + \mu[A_{vf}f_{yh} + P_c] \quad \text{[LRFD Eq. 5.8.4.1-3]}$$

where

c = cohesion factor, ksi [LRFD Art. 5.8.4.3]

μ = coefficient of friction [LRFD Art. 5.8.4.3]

A_{cv} = area of concrete section resisting shear transfer, in.²

A_{vf} = area of shear reinforcement crossing the shear plane, in.²

P_c = permanent net compressive force normal to the shear plane, kips

f_{yh} = specified yield strength of shear reinforcement, ksi

For cast-in-place concrete slabs placed on clean concrete girder surface intentionally roughened: [LRFD Art. 5.8.4.3]

c = 0.28 ksi

μ = 1.0

The actual contact width, b_v , between the slab and the beam is $2(15.75) = 31.5 \text{ in.}$

$$A_{cv} = (31.5 \text{ in.})(1.0 \text{ in.}) = 31.5 \text{ in.}^2$$

U-BEAM (TX-U54), SINGLE SPAN, PRECAST DECK PANELS, COMPOSITE DECK**9.6.12.3 Required Interface Shear Reinforcement/9.6.13 Minimum Longitudinal Reinforcement Requirement**

LRFD Eq. 5.6.4.1-3 can be solved for A_{vf} as follows:

$$7.98 = 0.28(31.5) + 1.0[A_{vf}(60) + 0]$$

Solving for A_{vf}

$$A_{vf}(\text{req'd}) < 0.0 \text{ in.}^2/\text{ft}$$

Since the resistance provided by cohesion is greater than the applied force, provide the minimum required interface reinforcement.

9.6.12.3.1 Minimum Interface Shear Reinforcement

Minimum shear reinforcement, $A_{vf} \geq (0.05A_{cv})/f_{yh}$

[LRFD Eq. 5.8.4.4-1]

From the design of vertical shear reinforcement, a No. 4 two leg bar at 10 in. spacing is provided from the beam extending into the deck. Therefore, $A_{vf} = 0.48 \text{ in.}^2/\text{ft}$.

$$A_{vf} = (0.48 \text{ in.}^2/\text{ft}) > (0.05 A_{cv})/f_{yh} = 0.05(31.5)/60 = 0.026 \text{ in.}^2/\text{in.} = 0.31 \text{ in.}^2/\text{ft} \quad \text{OK}$$

Consider further that LRFD Article 5.8.4.4 states that the minimum reinforcement requirement may be waived if $v_{hi}/A_{cv} < 0.210 \text{ ksi}$ with surface roughened to an amplitude of 0.25 in.

$$7.18 \text{ kips/in.}/31.5 \text{ in.} = 0.228 \text{ ksi} > 0.210 \text{ ksi}$$

Therefore, the minimum reinforcement requirement cannot be waived.

9.6.12.4 Maximum Nominal Shear Reinforcement

$$V_{ni} \leq K_1 f'_c A_{cv} \text{ or } K_2 A_{cv}$$

$$V_n \text{ provided} = 0.28(31.5) + 1.0 \left(\frac{0.96}{12} (60) + 0 \right) = 13.62 \text{ kips/in.}$$

$$K_1 f'_c A_{cv} = (0.3)(4.0)(31.5) = 37.8 \text{ kips/in.}$$

$$K_2 A_{cv} = 1.8(31.5) = 56.7 \text{ kips/in.}$$

$$\text{Since provided } V_n \leq 0.3 f'_c A_{cv} \quad \text{OK}$$

[LRFD Eq. 5.8.4.1-4]

$$\leq 1.8 A_{cv} \quad \text{OK}$$

[LRFD Eq. 5.8.4.1-5]

9.6.13 MINIMUM LONGITUDINAL REINFORCEMENT REQUIREMENT [LRFD Art. 5.8.3.5]

Longitudinal reinforcement should be proportioned so that at each section, the following equation is satisfied:

$$A_{ps} f_{ps} + A_s f_y \geq \frac{M_u}{d_v \phi_f} + 0.5 \frac{N_u}{\phi_c} \left(\left| \frac{V_u}{\phi_v} - V_p \right| - 0.5 V_s \right) \cot \theta \quad \text{[LRFD Eq. 5.8.3.5-1]}$$

where

A_{ps} = area of prestressing strand at the tension side of the section, in.²

f_{ps} = average stress in prestressing strand at the time for which the nominal resistance is required, ksi

A_s = area of nonprestressed tension reinforcement, in.²

f_y = specified yield strength of reinforcing bars, ksi

M_u = factored moment at the section corresponding to the factored shear force, ft-kips

d_v = effective shear depth, in.

ϕ = resistance factor as appropriate for moment, shear and axial resistance. [LRFD Art. 5.5.4.2]
Therefore, different ϕ factors will be used for the terms in LRFD Equation 5.8.3.5-1, depending on the type of action being considered

N_u = applied factored axial force, kips

U-BEAM (TX-U54), SINGLE SPAN, PRECAST DECK PANELS, COMPOSITE DECK**9.6.13 Minimum Longitudinal Reinforcement Requirement/9.6.13.1 Required Reinforcement at Face of Bearing**

V_u = factored shear force at section, kips

V_s = shear resistance provided by shear reinforcement, kips

V_p = component in the direction of the applied shear of the effective prestressing force, kips

θ = angle of inclination of diagonal compressive stresses

9.6.13.1 Required Reinforcement at Face of Bearing

[LRFD Art.5.8.3.5]

For simple end supports, the longitudinal reinforcement on the flexural tension side of the member at inside face of bearing should satisfy:

$$A_{ps}f_{ps} + A_s f_y \geq \left(\frac{V_u}{\phi} - 0.5V_s - V_p \right) \cot \theta \quad \text{[LRFD Eq.5.8.3.5-2]}$$

$$M_u = 0 \text{ ft-kips}$$

$$N_u = 0 \text{ kips}$$

Because the width of the bearing is not yet determined, it is assumed to be zero. This assumption is conservative for these calculations. Therefore, the failure crack assumed for this analysis radiates from the centerline of the bearing, 6 in. from the end of the beam.

From **Tables 9.6.4-1** and **9.6.4-2** using load combination Strength I, the factored shear force at this section is:

$$V_u = 1.25(64.2 + 62.8 + 8.3 + 1.9) + 1.50(16.2) + 1.75(93.7 + 37.6) = 425.6 \text{ kips}$$

$$\left(\frac{V_u}{\phi} - 0.5V_s - V_p \right) \cot \theta = \left(\frac{425.6}{0.9} - 0.5(244.0) - 0.0 \right) \cot 29^\circ = 633.0 \text{ kips}$$

As shown in **Figure 9.6.13.1-1**, the assumed crack plane crosses the centroid of the 29 bonded strands at a distance of $(6 + 2.92 \cot 29^\circ = 11.27 \text{ in.})$ from the end of the beam. Since the transfer length is 36 in. from the end of the beam (60 times the strand diameter), the available prestress from the 29 bonded strands is a fraction of the effective prestress, f_{pe} , in these strands. Note: 29 effective strands because nine are debonded and use f_{ps} without gains at beam end to be conservative.

Therefore, the available prestress force is:

$$\begin{aligned} A_{ps}f_{ps} + A_s f_y &= (29)(0.217) \left((202.5 - 30.3) \frac{11.27}{36} \right) \\ &= 339.2 \text{ kips} < 633.0 \text{ kips} \quad \text{NG} \end{aligned}$$

Additional reinforcement required:

$$(633.0 - 343.7)/60.0 = 4.897 \text{ in.}^2$$

Provide (12) No. 6 bars = (5.28 in.²)

An alternative approach is to exclude all permanent gains from the available prestressing force. The prestress force at the girder ends is slightly different because of varying influence of losses/gains as compared to midspan. The available prestressing force then becomes:

$$\begin{aligned} A_{ps}f_{ps} + A_s f_y &= (29)(0.217) \left(\left(202.5 - (\Delta f_{pT} - \Delta f_{pCD} - \Delta f_{pSS}) \right) \frac{11.27}{36} \right) + 0 \\ &= (29)(0.217) \left((202.5 - (30.3 - 0.952 - 1.285)) \frac{11.27}{36} \right) + 0 \\ &= 343.7 \text{ kips} < 633.0 \text{ kips} \quad \text{NG} \end{aligned}$$

Additional reinforcement required:

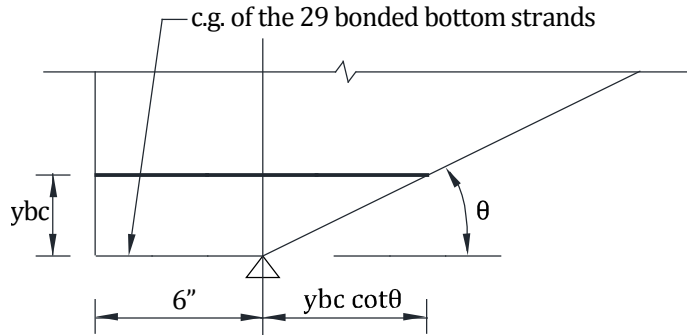
$$(633.0 - 343.7)/60.0 = 4.822 \text{ in.}^2 \text{ (Note: difference is not significant)}$$

Provide (12) No. 6 bars = (5.28 in.²)

U-BEAM (TX-U54), SINGLE SPAN, PRECAST DECK PANELS, COMPOSITE DECK

9.6.13.1 Required Reinforcement at Face of Bearing/9.6.15.Deflection and Camber

Figure 9.6.13.1-1
Assumed Failure Crack



9.6.14 PRETENSIONED ANCHORAGE ZONE

[LRFD Art. 5.10.10]

9.6.14.1 Anchorage Zone Reinforcement

[LRFD Art. 5.10.10.1]

Design of the anchorage zone reinforcement is computed using the force in the strands just prior to transfer. Since nine strands are debonded at the ends of the beam, the force in the remaining strands before transfer is:

$$P_{pi} = 29(0.217)(202.5) = 1,274.3 \text{ kips}$$

The bursting resistance, P_r , should not be less than 4.0% of P_{pi} .

$$P_r = f_s A_s \geq 0.04 P_{pi} = 0.04(1,274.3) = 51.0 \text{ kips}$$

where

- A_s = total area of horizontal reinforcement located within a distance $h/4$ from the end of the beam, in.²
- f_s = allowable stress in steel, but taken not greater than 20 ksi

Solving for the required area of steel, $A_s = 51.0/20 = 2.55 \text{ in.}^2$

At least 2.55 in.² of horizontal transverse reinforcement should be provided within a distance of ($h/4 = 54/4 = 13.5 \text{ in.}$) from the end of the beam.

Use two transverse horizontal layers of reinforcement in the bottom flange to resist splitting forces in the horizontal direction as shown in *LRFD Specifications* Fig. C5.10.10.1-1. Each layer of reinforcement to consist of three No. 6 bars at 5.5-in. centers starting at 2 in. from end of the beam. Area of reinforcement provided = $6(0.44) = 2.64 \text{ in.}^2 > 2.5 \text{ in.}^2$ OK

9.6.14.2 Confinement Reinforcement

[LRFD Art. 5.10.10.2]

For a distance of $1.5h = 1.5(54) = 81 \text{ in.}$, from the end of the beam, reinforcement is placed to confine the prestressing steel in the bottom flange. The reinforcement may not be less than No. 3 deformed bars with spacing not exceeding 6 in. The reinforcement should be of a shape that will confine (enclose) the strands.

9.6.15 DEFLECTION AND CAMBER

[LRFD Art. 5.7.3.6.2]

Deflections are calculated using the modulus of elasticity of concrete calculated in Section 9.6.3.1, and the gross section properties of the precast beam.

9.6.15.1 Deflection Due to Prestressing Force at Transfer

$$\Delta_p = \frac{P_{pt} e_c L^2}{8 E_{ci} I_g}$$

U-BEAM (TX-U54), SINGLE SPAN, PRECAST DECK PANELS, COMPOSITE DECK

9.6.15 Deflection and Camber/9.6.15.3 Deflection due to Diaphragm Weight

where

Δ_p = camber due to prestressing force at transfer, in.

P_{pt} = total prestressing force after transfer = $38(41.49) = 1,577$ kips

e_c = eccentricity of prestressing force at midspan = 19.62 in.

L = overall beam length = 111.0 ft

E_{ci} = modulus of elasticity at transfer = 4,696 ksi

I_g = moment of inertia of the noncomposite precast beam = 403,020 in.⁴

$$\Delta_p = \frac{1,577.0(19.62)(111 \times 12)^2}{(8)(4,696)(403,020)} = 3.63 \text{ in. } \uparrow$$

9.6.15.2 Deflection Due to Beam Self Weight

$$\Delta_g = \frac{5w_g L^4}{384E_{ci}I_g}$$

where

Δ_g = deflection due to beam self weight, in.

w_g = beam self weight = 1.167 kips/ft

E_{ci} = modulus of elasticity of precast beam at transfer = 4,696 ksi

I_g = moment of inertia of the noncomposite precast beam = 403,020 in.⁴

L = beam length = 111.0 ft at transfer = 110.0 ft at erection

Deflection due to beam self weight at transfer:

$$\Delta_g = \frac{5\left(\frac{1.167}{12}\right)(111 \times 12)^4}{(384)(4,696)(403,020)} = 2.11 \text{ in. } \downarrow$$

Deflection due to beam self weight used to compute deflection at erection:

$$\Delta_g = \frac{5\left(\frac{1.167}{12}\right)(110 \times 12)^4}{(384)(4,696)(403,020)} = 2.03 \text{ in. } \downarrow$$

9.6.15.3 Deflection Due to Diaphragm Weight

For two equal concentrated loads symmetrically placed, the deflection at midspan is calculated as:

$$\Delta_d = \frac{P_d a}{24E_{ci}I_g}(3L^2 - 4a^2)$$

where

P_d = diaphragm weight concentrated at 42 ft from each support = 1.858 kips

a = distance from the concentrated load to beam end = 42.5 ft at transfer

= 42.0 ft at erection

E_{ci} = modulus of elasticity of precast beam at transfer = 4,696 ksi

I_g = moment of inertia of the noncomposite precast beam = 403,020 in.⁴

L = beam length = 111.0 ft at transfer = 110.0 ft at erection

U-BEAM (TX-U54), SINGLE SPAN, PRECAST DECK PANELS, COMPOSITE DECK

9.6.15.3 Deflection due to Diaphragm Weight/9.6.15.6 Deflection and Camber Summary

Deflection due to diaphragm weight at transfer:

$$\Delta_d = \frac{(1.858)(42.5 \times 12)}{(24)(4,696)(403,020)} [3(111 \times 12)^2 - 4(42.5 \times 12)^2] = 0.09 \text{ in. } \downarrow$$

Deflection due to diaphragm weight used to compute deflection at erection:

$$\Delta_d = \frac{(1.858)(42.0 \times 12)}{(24)(4,696)(403,020)} [3(110 \times 12)^2 - 4(42.0 \times 12)^2] = 0.09 \text{ in. } \downarrow$$

9.6.15.4 Deflection Due to Slab and Haunch Weights

$$\Delta_s = \frac{5w_s L^4}{384E_c I_g}$$

where

Δ_s = deflection due to slab and haunch weights, in.

w_s = slab and haunch weight = 1.125 + 0.016 = 1.141 kips/ft (Sect. 9.6.4.1.1)

L = design span = 110.0 ft

E_c = modulus of elasticity of precast beam at service loads = 6,062 ksi

I_g = gross moment of inertia of the precast beam = 403,020 in.⁴

$$\Delta_s = \frac{5 \left(\frac{1.141}{12} \right) (110 \times 12)^4}{(384)(6,062)(403,020)} = 1.54 \text{ in. } \downarrow$$

9.6.15.5 Deflection Due to Barrier and Future Wearing Surface Weights

$$\Delta_{b+ws} = \frac{5(w_b + w_{ws})L^4}{384E_c I_c}$$

where

Δ_{b+ws} = deflection due to barrier and wearing surface weights, in.

w_b = barrier weight = 0.150 kips/ft

w_{ws} = wearing surface weight = 0.294 kips/ft

L = design span = 110.0 ft

E_c = modulus of elasticity of precast beam at service loads = 6,062 ksi

I_c = gross moment of inertia of the composite section = 925,249 in.⁴ (Table 9.6.3.2.3-1)

$$\Delta_{b+ws} = \frac{5 \left(\frac{0.444}{12} \right) (110 \times 12)^4}{(384)(6,062)(925,249)} = 0.26 \text{ in. } \downarrow$$

9.6.15.6 Deflection and Camber Summary

At transfer, $(\Delta_p + \Delta_g + \Delta_d) = 3.63 - 2.11 - 0.09 = 1.43 \text{ in. } \uparrow$

Total deflection at erection, using PCI multipliers (see *PCI Design Handbook*)

$= 1.8(3.63) - 1.85(2.03 + 0.09) = 2.61 \text{ in. } \uparrow$

Long-Term Deflection:

LRFD Article 5.7.3.6.2 states that the long-time deflection may be taken as the instantaneous deflection multiplied by a factor of 4.0, if the instantaneous deflection is based on the gross moment of inertia. However, a factor of 4.0 is not appropriate for this type of precast construction. Therefore, it is recommended that the designer follow the guidelines of the owner agency for which the bridge is being designed, or undertake a more rigorous, time-dependent analysis.

U-BEAM (TX-U54), SINGLE SPAN, PRECAST DECK PANELS, COMPOSITE DECK

9.6.15.7 Deflection Due to Live Load and Impact

9.6.15.7 Deflection Due to Live Load and Impact

Live load deflection limit (optional) = Span/800

[LRFD Art.2.5.2.6.2]

$$= \left(110 \times \frac{12}{800} \right) = 1.65 \text{ in.}$$

If the owner invokes the optional live load deflection criteria specified in Art. 2.5.2.6.2, the deflection is the greater of:

[LRFD Art. 3.6.1.3.2]

- that resulting from the design truck plus impact, Δ_{LT} , or
- that resulting from 25% of the design truck plus impact, Δ_{LT} , taken together with the design lane load, Δ_{LL}

Note: LRFD Article 2.5.2.6.2 states that the dynamic load allowance be included in the calculation of live load deflection.

The *LRFD Specifications* states that all beams should be assumed to deflect equally under the applied live load and impact.

[LRFD Art. 2.5.2.6.2]

Therefore, the distribution factor for deflection, *DFD*, is calculated as follows:

$$DFD = (\text{number of lanes/number of beams}) = 3/4 = 0.75 \text{ lanes/beam}$$

[LRFD Art. C2.5.2.6.2]

However, it is more conservative to use the distribution factor for moment, *DFM*

Deflection due to lane load:

$$\text{Design lane load, } w = 0.64DFM = 0.64(0.748) = 0.479 \text{ kips/ft/beam}$$

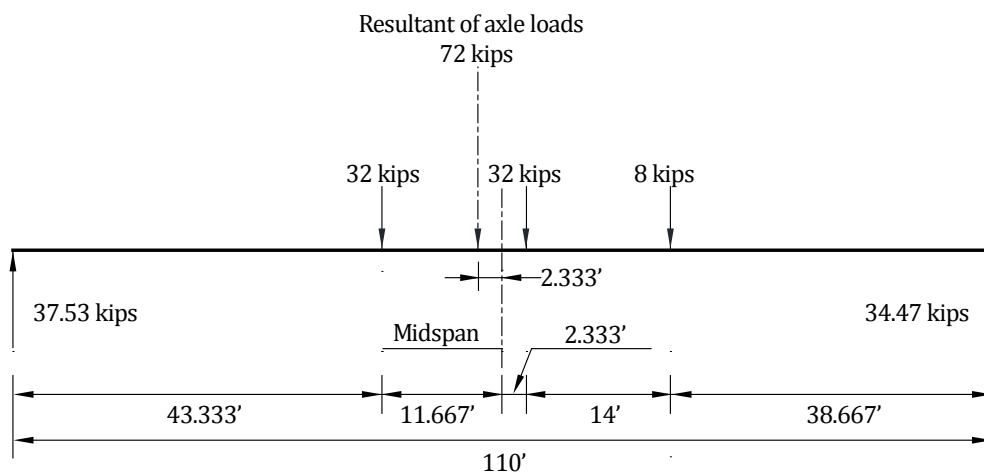
$$\Delta_{LL} = \frac{5wL^4}{384E_cI_c} = \frac{5 \left(\frac{0.479}{12} \right) (110 \times 12)^4}{(384)(6,062)(925,249)} = 0.28 \text{ in.} \downarrow$$

Deflection due to Design Truck Load and Impact:

To obtain the maximum moment and deflection at midspan due to truck load, let the centerline of the beam coincide with the middle point of the distance between the inner 32-kip axle and the resultant of the truck load, as shown in **Figure 9.6.15.7-1**.

Figure 9.6.15.7-1

Design Truck Axle Load Position for Maximum Bending Moment



Using the elastic moment area or influence lines, deflection at midspan is:

$$\Delta_{LT} = (0.589)(IM)(DFD) = (0.589)(1.33)(0.75) = 0.59 \text{ in.} \downarrow$$

U-BEAM (TX-U54), SINGLE SPAN, PRECAST DECK PANELS, COMPOSITE DECK

9.6.15.7 Deflection Due to Live Load and Impact

Therefore, live load deflection is the greater of:

$$\Delta_{LT} = 0.59 \text{ in.} \downarrow \text{ (Controls)}$$

$$0.25\Delta_{LT} + \Delta_{LL} = 0.25(0.59) + 0.28 = 0.43 \text{ in.} \downarrow$$

Therefore, live load deflection = 0.59 in. < allowable deflection = 1.65 in. OK

DOUBLE-TEE BEAM (NEXT 36 D), SINGLE SPAN, NONCOMPOSITE SURFACE

Transformed Sections, Shear General Procedure, Refined Losses

Table of Contents

9.7.1 INTRODUCTION	9.7 - 3
9.7.1.1 Terminology.....	9.7 - 3
9.7.2 MATERIALS	9.7 - 3
9.7.3 CROSS-SECTION PROPERTIES FOR A TYPICAL INTERIOR BEAM	9.7 - 4
9.7.4 SHEAR FORCES AND BENDING MOMENTS	9.7 - 5
9.7.4.1 Shear Forces and Bending Moments Due to Dead Loads	9.7 - 5
9.7.4.1.1 Dead Loads	9.7 - 5
9.7.4.1.2 Unfactored Shear Forces and Bending Moments	9.7 - 6
9.7.4.2 Shear Forces and Bending Moments Due to Live Loads	9.7 - 6
9.7.4.2.1 Live Loads	9.7 - 6
9.7.4.2.2 Live Load Distribution Factors for a Typical Interior Beam	9.7 - 6
9.7.4.2.2.1 Distribution Factor for Bending Moments	9.7 - 6
9.7.4.2.2.2 Distribution Factor for Shear Force	9.7 - 7
9.7.4.2.3 Dynamic Allowance	9.7 - 8
9.7.4.2.4 Unfactored Shear Forces and Bending Moments	9.7 - 8
9.7.4.2.4.1 Due to Truck Load; V_{LT} and M_{LT}	9.7 - 8
9.7.4.2.4.2 Due To Design Lane Load; V_{LL} and M_{LL}	9.7 - 9
9.7.4.3 Load Combinations	9.7 - 9
9.7.5 ESTIMATE REQUIRED PRESTRESS	9.7 - 11
9.7.5.1 Service Load Stresses at Midspan	9.7 - 11
9.7.5.2 Stress Limits for Concrete	9.7 - 11
9.7.5.3 Required Number of Strands	9.7 - 11
9.7.5.4 Strand Pattern	9.7 - 12
9.7.5.5 Steel Transformed Section Properties	9.7 - 12
9.7.6 PRESTRESS LOSSES	9.7 - 13
9.7.6.1 Elastic Shortening	9.7 - 14
9.7.6.2 Time-Dependent Losses between Transfer and Deck Placement	9.7 - 14
9.7.6.2.1 Shrinkage of Concrete	9.7 - 15
9.7.6.2.2 Creep of Concrete	9.7 - 16
9.7.6.2.3 Relaxation of Prestressing Strands	9.7 - 16
9.7.6.3 Time-Dependent Losses between Deck Placement and Final Time	9.7 - 16
9.7.6.3.1 Shrinkage of Concrete	9.7 - 16
9.7.6.3.2 Creep of Concrete	9.7 - 17
9.7.6.3.3 Relaxation of Prestressing Strands	9.7 - 18
9.7.6.3.4 Shrinkage of Deck Concrete	9.7 - 18
9.7.6.4 Total Time-Dependent Loss	9.7 - 18
9.7.6.5 Total Losses at Transfer	9.7 - 18
9.7.6.6 Total Losses at Service Loads	9.7 - 18
9.7.7 CONCRETE STRESSES AT TRANSFER	9.7 - 19

DOUBLE-TEE BEAM (NEXT 36 D), SINGLE SPAN, NONCOMPOSITE SURFACE

Transformed Sections, Shear General Procedure, Refined Losses

Table of Contents

9.7.7.1 Stress Limits for Concrete 9.7 - 19

9.7.7.2 Stresses at Transfer Length Section of Bonded Strands 9.7 - 19

9.7.7.3 Stresses at Transfer Length Section of Debonded Strands 9.7 - 21

9.7.7.4 Stresses at Midspan 9.7 - 21

9.7.7.5 Summary of Stresses at Transfer 9.7 - 21

9.7.8 CONCRETE STRESSES AT SERVICE LOADS 9.7 - 21

9.7.8.1 Stress Limits for Concrete 9.7 - 22

9.7.8.2 Stresses at Midspan 9.7 - 22

9.7.8.3 Fatigue Stress Limit 9.7 - 22

9.7.8.4 Summary of Stresses at Midspan at Service Loads 9.7 - 23

9.7.9 STRENGTH LIMIT STATE 9.7 - 23

9.7.10 LIMITS OF REINFORCEMENT 9.7 - 25

9.7.10.1 Maximum Reinforcement 9.7 - 25

9.7.10.2 Minimum Reinforcement 9.7 - 25

9.7.11 SHEAR DESIGN 9.7 - 26

9.7.11.1 Critical Section 9.7 - 26

9.7.11.2 Contribution of Concrete to Nominal Shear Resistance 9.7 - 27

9.7.11.2.1 Strain in Flexural Tension Reinforcement 9.7 - 27

9.7.11.2.2 Values of β and θ 9.7 - 28

9.7.11.2.3 Compute Concrete Contribution 9.7 - 28

9.7.11.3 Contribution of Reinforcement to Nominal Shear Resistance 9.7 - 28

9.7.11.3.1 Requirement for Reinforcement 9.7 - 28

9.7.11.3.2 Required Area of Reinforcement 9.7 - 28

9.7.11.3.3 Determine Spacing of Reinforcement 9.7 - 29

9.7.11.4 Maximum Nominal Shear Resistance 9.7 - 29

9.7.12 INTERFACE SHEAR TRANSFER 9.7 - 29

9.7.13 MINIMUM LONGITUDINAL REINFORCEMENT REQUIREMENT 9.7 - 29

9.7.13.1 Required Reinforcement at Face of Bearing 9.7 - 30

9.7.14 PRETENSIONED ANCHORAGE ZONE 9.7 - 31

9.7.14.2 Confinement Reinforcement 9.7 - 31

9.7.15 DEFLECTION AND CAMBER 9.7 - 31

9.7.15.1 Deflection Due to Prestressing Force at Transfer 9.7 - 31

9.7.15.2 Deflection Due to Beam Self Weight 9.7 - 32

9.7.15.3 Deflection Due to Joint Concrete, Barrier, and Wearing Surface Weights 9.7 - 32

9.7.15.4 Deflection and Camber Summary 9.7 - 33

9.7.15.5 Deflection Due to Live Load and Impact 9.7 - 33

9.7.16 TRANSVERSE POST-TENSIONING 9.7 - 34

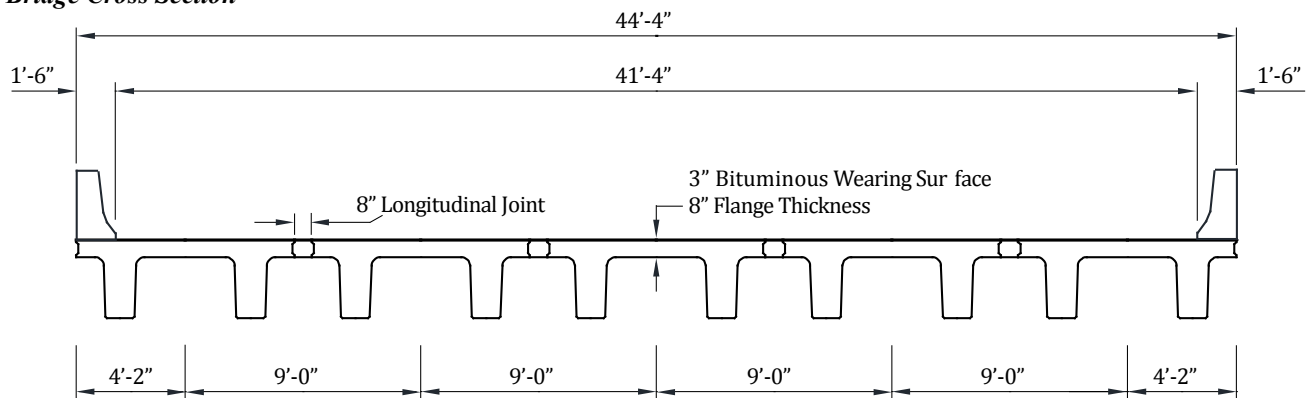
DOUBLE-TEE BEAM (NEXT 36 D), SINGLE SPAN, NONCOMPOSITE SURFACE

9.7.1 Introduction/9.7.2 Materials

9.7 Transformed Sections, Shear General Procedure, Refined Losses**9.7.1 INTRODUCTION**

This design example demonstrates the design of an 80-ft, single span, PCI Northeast Extreme double-tee deck bridge with no skew. This example illustrates in detail the design of a typical interior beam at the critical sections in positive flexure, shear, and deflection due to prestress, dead loads, and live loads. The superstructure consists of five beams spaced at 9 ft 0 in. centers, as shown in **Figure 9.7.1-1**. A 3-in.-thick bituminous surfacing will be placed on the beams as a wearing surface. Beams are transversely post-tensioned through the flange of the beams. Design live load is HL-93. The design is accomplished in accordance with *AASHTO LRFD Bridge Design Specifications*, Fifth Edition, 2010, and the 2011 Interim Revisions. Elastic stresses from external loads are calculated using transformed sections. Shear strength is calculated using the general procedure. Time-dependent prestress losses are calculated using the refined estimates.

Figure 9.7.1-1
Bridge Cross Section

**9.7.1.1 Terminology**

The following terminology is used to describe cross sections in this design example:

noncomposite section—the concrete beam cross section.

noncomposite nontransformed section—the concrete beam cross section without the strands transformed. Also called the gross section.

noncomposite transformed section—the concrete beam cross section with the strands transformed to provide cross-sectional properties equivalent to the beam concrete.

The term "transformed" generally refers to transformation of the strands.

9.7.2 MATERIALS

Precast concrete beams: PCI double-tee beams, Type NEXT 36 D as shown in **Figure 9.7.2-1**

Required concrete compressive strength at transfer, $f'_{ci} = 6.0$ ksi

Specified concrete compressive strength for use in design, $f'_c = 8.0$ ksi

Concrete unit weight, $w_c = 0.150$ kcf

Overall beam length = 81.0 ft

Design span = 80.0 ft

DOUBLE-TEE BEAM (NEXT 36 D), SINGLE SPAN, NONCOMPOSITE SURFACE

9.7.2 Materials/9.7.3 Cross-Section Properties for a Typical Interior Beam

Prestressing strands: 0.6-in.-dia., seven-wire, low-relaxation

Area of one strand = 0.217 in.²

Specified tensile strength, $f_{pu} = 270.0$ ksi

Yield strength, $f_{py} = 0.9f_{pu} = 243.0$ ksi

[LRFD Table 5.4.4.1-1]

Stress limits for prestressing strands:

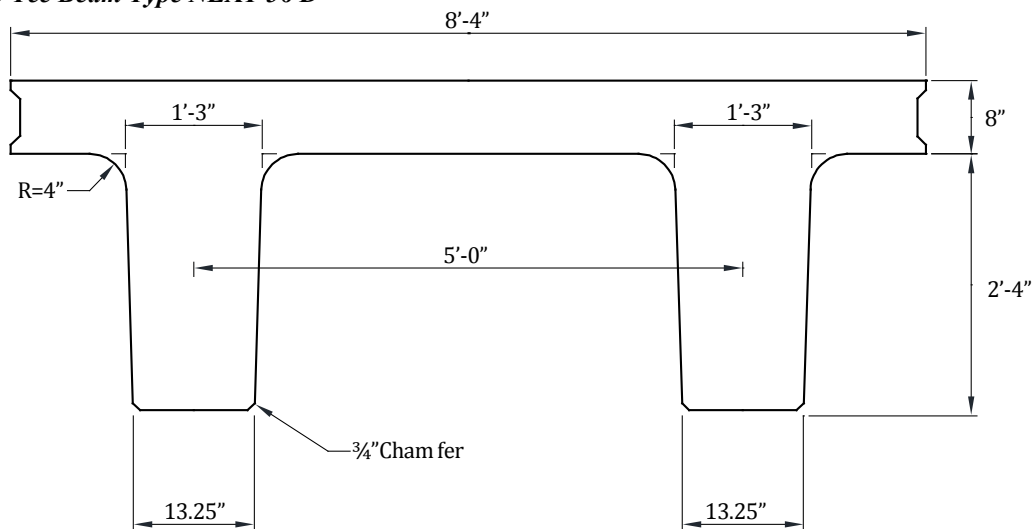
[LRFD Table 5.9.3-1]

- before transfer, $f_{pi} \leq 0.75f_{pu} = 202.5$ ksi
- at service limit state (after all losses), $f_{pe} \leq 0.80f_{py} = 194.4$ ksi

Modulus of elasticity, $E_p = 28,500$ ksi

[LRFD Art. 5.4.4.2]

Figure 9.7.2-1
PCI Double-Tee Beam Type NEXT 36 D



Reinforcing bars:

Yield strength, $f_y = 60.0$ ksi

Modulus of elasticity, $E_s = 29,000$ ksi

[LRFD Art. 5.4.3.2]

3-in.-thick bituminous wearing surface: unit weight = 0.140 kcf

[LRFD Table 3.5.1-1]

New Jersey-type barrier: unit weight = 0.300 kips/ft/side

9.7.3 CROSS-SECTION PROPERTIES FOR A TYPICAL INTERIOR BEAM

A_g = area of cross section of precast beam = 1,595.0 in.²

h = overall depth of precast beam = 36 in.

I_g = moment of inertia about the centroid of the noncomposite precast beam = 179,629 in.⁴

y_b = distance from centroid to the extreme bottom fiber of the noncomposite precast beam = 23.20 in.

y_t = distance from centroid to the extreme top fiber of the noncomposite precast beam = 12.80 in.

S_b = section modulus for extreme bottom fiber of the noncomposite precast beam = $I_g/y_b = 7,743$ in.³

S_t = section modulus for extreme top fiber of the noncomposite precast beam = $I_g/y_t = 14,034$ in.³

w_g = beam weight per unit length = $(1,595/144)(0.150) = 1.661$ kips/ft

E_c = modulus of elasticity, ksi = $33,000K_1(w_c)^{1.5}\sqrt{f'_c}$

[LRFD Eq. 5.4.2.4-1]

DOUBLE-TEE BEAM (NEXT 36 D), SINGLE SPAN, NONCOMPOSITE SURFACE

9.7.3 Cross-Section Properties for a Typical Interior Beam/9.7.4.1.1 Dead Loads

where

K_1 = correction factor for source of aggregate taken as 1.0

w_c = unit weight of concrete = 0.150 kcf

LRFD Table 3.5.1-1 states that, in the absence of more precise data, the unit weight of concrete may be taken as $0.140 + 0.001f'_c$ for $5.0 < f'_c \leq 15.0$ ksi. For $f'_c = 8.0$ ksi, the unit weight would be 0.1480 kcf. However, precast concrete mixes typically have a relatively low water-cementitious materials ratio and high density. Therefore, a unit weight of 0.150 kcf is used in this example. For high-strength concrete, this value may need to be increased based on test results. For simplicity, a value of 0.150 kcf is also used for the cast-in-place concrete.

f'_c = specified compressive strength of concrete, ksi

Therefore, the modulus of elasticity for:

precast beam at transfer: $E_{ci} = 33,000(1.00)(0.150)^{1.5}\sqrt{6.0} = 4,696$ ksi

precast beam at service loads: $E_c = 33,000(1.00)(0.150)^{1.5}\sqrt{8.0} = 5,422$ ksi

9.7.4 SHEAR FORCES AND BENDING MOMENTS**9.7.4.1 Shear Forces and Bending Moments Due to Dead Loads****9.7.4.1.1 Dead Loads**

DC = Dead load of structural components and nonstructural attachments

[LRFD Art. 3.3.2]

Beam self weight, $w_g = 1.661$ kips/ft

Joint concrete = 8×8 in. cast-in-place, longitudinal joint

= $((8)(8)/144 \text{ ft}^2)(0.150 \text{ kcf}) = 0.067$ kips/ft/beam

Generally, the unit weight of reinforced concrete should be slightly greater than the unit weight of concrete alone because of the added weight of reinforcement. However, in this example, the difference is considered negligible.

LRFD Article 4.6.2.2.1 states that permanent loads (barrier and wearing surface loads) may be distributed uniformly among all the beams if the following conditions are met:

- Width of deck is constant OK
- Number of beams, N_b , is not less than four ($N_b = 5$) OK
- Beams are parallel and have approximately the same stiffness OK
- The roadway part of the overhang, $d_e \leq 3.0$ ft

$d_e = 4.17 - 2.50 - 1.50 = 0.17$ ft OK

- Curvature in plan is less than specified in the *LRFD Specifications* (curvature = 0.0°) OK
- Cross section of the bridge is consistent with one of the cross sections given in LRFD Table 4.6.2.2.1-1. The bridge is "sufficiently connected to act as unit" and the bridge type is (i). OK

Since these criteria are satisfied, the barrier and wearing surface loads are distributed equally among the five beams.

Barrier weight = $(2 \text{ barriers})(0.300 \text{ kips})/(5 \text{ beams}) = 0.120$ kips/ft/beam = w_b

DW = Dead load of wearing surface

= $(3/12)(0.140) = 0.035$ ksf

= $(0.035 \text{ ksf})(41.33 \text{ ft})/(5 \text{ beams}) = 0.289$ kips/ft/beam = w_{ws}

The DW loads should be kept separately from DC loads because a higher load factor is applied to them.

DOUBLE-TEE BEAM (NEXT 36 D), SINGLE SPAN, NONCOMPOSITE SURFACE

9.7.4.1.2 Unfactored Shear Forces and Bending Moments/9.7.4.2.1 Distribution Factor for Bending Moments

9.7.4.1.2 Unfactored Shear Forces and Bending Moments

For a simply supported beam with a span length (L) loaded with a uniformly distributed load (w), the shear force (V_x) and bending moment (M_x) at any distance (x) from the support are given by:

$$V_x = w(0.5L - x) \quad \text{[Eq. 9.7.4.1.2-1]}$$

$$M_x = 0.5wx(L - x) \quad \text{[Eq. 9.7.4.1.2-2]}$$

Using the above equations, values of shear forces and bending moments for a typical interior beam under the self weight of beam and weights of longitudinal joint concrete, barriers, and wearing surface are computed and given in **Table 9.7.4-1** that is located at the end of Section 9.7.4.3. For these calculations, the span length (L) is the design span, 80 ft. However, for calculations of stresses and deformations at the time prestress is transferred, the overall length of the precast member, 81 ft, is used as illustrated later in this example.

9.7.4.2 Shear Forces and Bending Moments Due to Live Loads**9.7.4.2.1 Live Loads**

Design live load is HL-93, which consists of a combination of: [LRFD 3.6.1.2.1]

1. Design truck or design tandem with dynamic allowance [LRFD 3.6.1.2.2]

The design truck consists of 8.0-, 32.0-, and 32.0-kip axles with the first pair spaced at 14.0 ft and the second pair spaced at 14.0 to 30.0 ft. The design tandem consists of a pair of 25.0-kip axles spaced at 4.0 ft apart. [LRFD Art. 3.6.1.2.3]

2. Design lane load of 0.64 kips/ft without dynamic allowance [LRFD Art. 3.6.1.2.4]

9.7.4.2.2 Live Load Distribution Factors for a Typical Interior Beam

The live load bending moments and shear forces are determined by using the simplified distribution factor formulas [LRFD Art. 4.6.2.2]. To use the simplified live load distribution factor formulas, the following conditions must be met: [LRFD Art. 4.6.2.2.1]

- Width of deck is constant OK
- Number of beams, N_b not less than four ($N_b = 5$) OK
- Beams are parallel and approximately of the same stiffness OK
- The roadway part of the overhang, $d_e \leq 3.0$ ft ($d_e = 0.17$ ft) OK
- Curvature is less than specified in the *LRFD Specifications*, (curvature = 0.0°) OK

For a precast concrete double-tee section with shear keys and with transverse post-tensioning, the bridge type is (i). [LRFD Table 4.6.2.2.1-1]

The number of design lanes is computed as:

Number of design lanes = the integer part of the ratio ($w/12$), where w is the clear roadway width, in ft, between the curbs [LRFD Art. 3.6.1.1.1]

From **Figure 9.7.1-1**, $w = 41.33$ ft

Number of design lanes = integer part of $(41.33/12) = 3$ lanes

9.7.4.2.2.1 Distribution Factor for Bending Moments

- For all limit states except fatigue limit state:

For two or more lanes loaded:

$$DFM = 0.075 + \left(\frac{S}{9.5}\right)^{0.6} \left(\frac{S}{L}\right)^{0.2} \left(\frac{K_g}{12.0Lt^3}\right)^{0.1} \quad \text{[LRFD Table 4.6.2.2.2b-1]}$$

DOUBLE-TEE BEAM (NEXT 36 D), SINGLE SPAN, NONCOMPOSITE SURFACE

9.7.4.2.2.1 Distribution Factor for Bending Moments/9.7.4.2.2.2 Distribution Factor for Shear Force

Provided that: $3.5 \leq S \leq 16.0$; $S = 9.0$ ft OK
 $4.5 \leq t_s \leq 12.0$; $t_s = 8.0$ in. OK
 $20 \leq L \leq 240$; $L = 80$ ft OK
 $N_b \geq 4$; $N_b = 5$ OK
 $10,000 \leq K_g \leq 7,000,000$ OK (see below)

where

DFM = distribution factor for moment in interior beam

S = beam spacing, ft

L = beam span, ft

t_s = structural depth of concrete deck, in.

K_g = longitudinal stiffness parameter, $\text{in.}^4 = n(I_{bs} + A_{bs}e_g^2)$ [LRFD Eq. 4.6.2.2.1-1]

where

n = modular ratio between beam and deck slab concrete

$$= \frac{E_c(\text{beam})}{E_c(\text{slab})} = \frac{5,422}{5,422} = 1.0000$$

I_{bs} = moment of inertia of the stems, $\text{in.}^4 = 53,462 \text{ in.}^4$

A_{bs} = cross-sectional area of the beam stems, $\text{in.}^2 = 803 \text{ in.}^2$

e_g = distance between the centers of gravity of the stems and the flange, $\text{in.} = 17.49 \text{ in.}$

LRFD Article 4.6.2.2 is unclear on how to calculate K_g for bridges without a composite deck. For this example, because the beams are connected to act as a unit, the stem is considered as the “beam” and the flange is considered as the “deck” in calculating K_g .

Therefore,

$$K_g = 1.0000[53,462 + 803(17.49^2)] = 299,100 \text{ in.}^4$$

$$DFM = 0.075 + \left(\frac{9}{9.5}\right)^{0.6} \left(\frac{9}{80}\right)^{0.2} \left(\frac{299,100}{12.0(80)(8)^3}\right)^{0.1}$$

$$= 0.075 + (0.968)(0.646)(0.952) = 0.670 \text{ lanes/beam}$$

For one design lane loaded:

$$DFM = 0.06 + \left(\frac{S}{14}\right)^{0.4} \left(\frac{S}{L}\right)^{0.3} \left(\frac{K_g}{12.0Lt_s^3}\right)^{0.1}$$

[LRFD Table 4.6.2.2.2b-1]

$$= 0.06 + \left(\frac{9}{14}\right)^{0.4} \left(\frac{9}{80}\right)^{0.3} \left(\frac{299,100}{12.0(80)(8)^3}\right)^{0.1}$$

$$= 0.06 + (0.838)(0.519)(0.952) = 0.474 \text{ lanes/beam}$$

Thus, the case of two or more lanes loaded controls and $DFM = 0.670$ lanes/beam.

- For fatigue limit state:

The *LRFD Specifications*, Art. C3.4.1, states that for Fatigue Limit State, a single design truck should be used. However, live load distribution factors given in LRFD Article 4.6.2.2 take into consideration the multiple presence factor, m . LRFD Article 3.6.1.1.2 states that the multiple presence factor, m , for one design lane loaded is 1.2. Therefore, the distribution factor for one design lane loaded with the multiple presence factor removed, should be used. The distribution factor for fatigue limit state is: $0.474/1.2 = 0.395$ lanes/beam.

9.7.4.2.2.2 Distribution Factor for Shear Force

For two or more lanes loaded:

$$DFV = 0.2 + \left(\frac{S}{12}\right) - \left(\frac{S}{35}\right)^{2.0}$$

[LRFD Table 4.6.2.2.3a-1]

DOUBLE-TEE BEAM (NEXT 36 D), SINGLE SPAN, NONCOMPOSITE SURFACE9.7.4.2.2.2 Distribution Factor for Shear Force/9.7.4.2.4.1 Due to Truck Load; V_{LT} and M_{LT}

Provided that: $3.5 \leq S \leq 16.0$; $S = 9.0$ ft OK
 $20 \leq L \leq 240$; $L = 80$ ft OK
 $4.5 \leq t_s \leq 12.0$; $t_s = 8.0$ in. OK
 $N_b \geq 4$; $N_b = 5$ OK

where

DFV = distribution factor for shear for interior beam
 S = beam spacing, ft

Therefore, the distribution factor for shear force is:

$$DFV = 0.2 + \left(\frac{9}{12}\right) - \left(\frac{9}{35}\right)^{2.0} = 0.884 \text{ lanes/beams}$$

For one design lane loaded:

$$DFV = 0.36 + \left(\frac{S}{25}\right) = 0.36 + \left(\frac{9}{25}\right) = 0.720 \text{ lanes/beams} \quad [\text{LRFD Table 4.6.2.2.3a-1}]$$

Thus, the case of two or more lanes loaded controls and $DFV = 0.884$ lanes/beam.

9.7.4.2.3 Dynamic Allowance

$IM = 15\%$ for fatigue limit state

[LRFD Table 3.6.2.1-1]

$IM = 33\%$ for all other limit states

where IM = dynamic load allowance, applied to design truck load only

9.7.4.2.4 Unfactored Shear Forces and Bending Moments**9.7.4.2.4.1 Due to Truck Load; V_{LT} and M_{LT}**

- For all limit states except for fatigue limit state:

Shear force and bending moment envelopes on a per-lane basis are calculated at tenth-points of the span using the equations given in Chapter 8 of this manual. However, this is generally done by means of commercially available computer software that has the ability to deal with moving loads. Therefore, truck load shear forces and bending moments per beam are:

$$\begin{aligned} V_{LT} &= (\text{shear force per lane})(DFV)(1 + IM) \\ &= (\text{shear force per lane})(0.884)(1 + 0.33) \\ &= (\text{shear force per lane})(1.176) \text{ kips} \end{aligned}$$

$$\begin{aligned} M_{LT} &= (\text{bending moment per lane})(DFM)(1 + IM) \\ &= (\text{bending moment per lane})(0.670)(1 + 0.33) \\ &= (\text{bending moment per lane})(0.891) \text{ ft-kips} \end{aligned}$$

Values for V_{LT} and M_{LT} at different points are given in **Table 9.7.4-2**.

- For fatigue limit state:

Article 3.6.1.4.1 in the *LRFD Specifications* states that fatigue load is a single design truck which has the same axle weight used in all other limit states but with a constant spacing of 30.0 ft between the 32.0-kip axles. Bending moment envelope on a per-lane basis is calculated using the equation given in Chapter 8 of this manual.

Therefore, bending moment of fatigue truck load is:

$$\begin{aligned} M_f &= (\text{bending moment per lane})(DFM)(1 + IM) \\ &= (\text{bending moment per lane})(0.395)(1 + 0.15) \\ &= (\text{bending moment per lane})(0.454) \text{ ft-kips} \end{aligned}$$

Values of M_f at different points are given in **Table 9.7.4-2**.

DOUBLE-TEE BEAM (NEXT 36 D), SINGLE SPAN, NONCOMPOSITE SURFACE

9.7.4.2.4.2 Due to Design Lane Load; V_{LL} and M_{LL} /9.7.4.3 Load Combinations

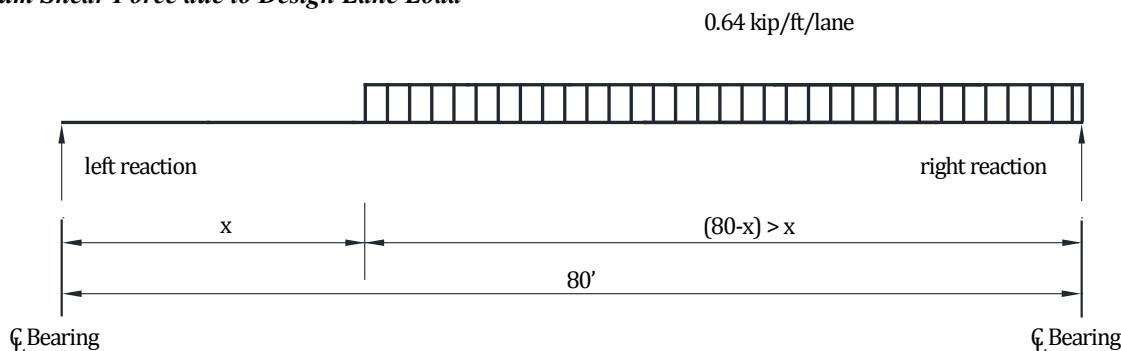
9.7.4.2.4.2 Due To Design Lane Load; V_{LL} and M_{LL}

To obtain the maximum shear force at a section located at a distance (x) from the left support under a uniformly distributed load of 0.64 kips/ft, load the member to the right of the section under consideration as shown in **Figure 9.7.4.2.4.2-1**. Therefore, the maximum shear force per lane is:

$$V_x = \frac{0.32(L - x)^2}{L} \text{ for } x \leq 0.5L \tag{Eq. 9.7.4.2.4.2-1}$$

where V_x is in kips/lane and L and x are in ft

Figure 9.7.4.2.4.2-1
Maximum Shear Force due to Design Lane Load



To calculate the maximum bending moment at any section, use Eq. (9.7.4.1.2-2).

Lane load shear force and bending moment per typical interior beam are as follows:

$$\begin{aligned} V_{LL} &= (\text{lane load shear force})(DFV) \\ &= (\text{lane load shear force})(0.884) \text{ kips} \end{aligned}$$

For all limit states except for fatigue limit state:

$$\begin{aligned} M_{LL} &= (\text{lane load bending moment})(DFM) \\ &= (\text{lane load bending moment})(0.670) \text{ ft-kips} \end{aligned}$$

Note that dynamic allowance is not applied to the design lane loading.

Values of shear forces and bending moments, V_{LL} and M_{LL} , are given in **Table 9.7.4-2**.

9.7.4.3 Load Combinations

[LRFD Art. 3.4]

Total factored load is taken as:

$$Q = \sum \eta_i \gamma_i Q_i \tag{LRFD Eq. 3.4.1-1}$$

where

η_i = a load modifier relating to ductility, redundancy, and operational importance. [LRFD Art. 1.3.2.1]
(Here, η_i is considered to be 1.0 for typical bridges.)

γ_i = load factors [LRFD Table 3.4.1-1]

Q_i = force effects from specified loads

Investigating different limit states given in LRFD Article 3.4.1, the following limit states are applicable:

Service I: check compressive stresses in prestressed concrete components:

$$Q = 1.00(DC + DW) + 1.00(LL + IM)$$

This load combination is a special combination for a service limit state stress and applies to all conditions other than Service III.

DOUBLE-TEE BEAM (NEXT 36 D), SINGLE SPAN, NONCOMPOSITE SURFACE

9.7.4.3 Load Combinations

Service III: check tensile stresses in prestressed concrete components:

$$Q = 1.00(DC + DW) + 0.80(LL + IM) \quad \text{[LRFD Table 3.4.1-1]}$$

This load combination is a special combination for service limit state stress checks that applies only to tension in prestressed concrete structures to control cracks.

Strength I: check ultimate strength: [LRFD Tables 3.4.1-1 and 3.4.1-2]

$$\text{Maximum } Q = 1.25(DC) + 1.50(DW) + 1.75(LL + IM)$$

$$\text{Minimum } Q = 0.90(DC) + 0.65(DW) + 1.75(LL + IM)$$

This load combination is the general load combination for strength limit state design.

Note: For simple-span bridges, the maximum load factors produce maximum effects. However, use minimum load factors for dead load (DC), and wearing surface (DW) when the dead load and wearing surface stresses are opposite to those of live load.

Fatigue I: check stress range in strands:

$$Q = 1.50(LL + IM) \quad \text{[LRFD Table 3.4.1-1]}$$

This load combination is a special load combination to check the tensile stress range in the strands due to live load and dynamic allowance.

Table 9.7.4-1

Unfactored Shear Forces and Bending Moments Due to Dead Loads for a Typical Interior Beam

Distance x, ft	Section x/L	Beam Weight		Joint Concrete Weight		Barrier Weight		Wearing Surface Weight	
		Shear V_g kips	Moment M_g ft-kips	Shear V_j kips	Moment M_j ft-kips	Shear V_b kips	Moment M_b ft-kips	Shear V_{ws} kips	Moment M_{ws} ft-kips
0	0	66.4	0.0	2.7	0.0	4.8	0.0	11.6	0.0
*2.38	0.03	62.5	153.4	2.5	6.2	4.5	11.1	10.9	26.7
8	0.1	53.2	478.4	2.1	19.3	3.8	34.6	9.2	83.3
16	0.2	39.9	850.4	1.6	34.3	2.9	61.4	6.9	148.0
24	0.3	26.6	1,116.2	1.1	45.0	1.9	80.6	4.6	194.2
32	0.4	13.3	1,275.6	0.5	51.5	1.0	92.2	2.3	222.0
40	0.5	0	1,328.8	0.0	53.6	0.0	96.0	0	231.2

*Critical section for shear (see Sect. 9.7.11)

Table 9.7.4-2

Unfactored Shear Forces and Bending Moments Due to Live Loads for a Typical Interior Beam

Distance x, ft	Section x/L	Truck Load with Impact		Lane Load		Fatigue Truck with Impact
		Shear V_{LT} kips	Moment M_{LT} ft-kips	Shear V_{LL} kips	Moment M_{LL} ft-kips	Moment M_f ft-kips
0	0	74.8	0.0	22.6	0.0	0.0
*2.38	0.03	72.3	130.3	21.3	39.6	64.2
8	0.1	66.3	402.1	18.3	123.5	204.7
16	0.2	57.8	701.5	14.5	219.5	357.2
24	0.3	49.4	898.3	11.1	288.2	457.3
32	0.4	40.9	1,012.2	8.1	329.3	516.0
40	0.5	32.5	1,033.6	5.7	343.0	526.9

*Critical section for shear (see Sect. 9.7.11)

DOUBLE-TEE BEAM (NEXT 36 D), SINGLE SPAN, NONCOMPOSITE SURFACE

9.7.5 Estimate Required Prestress/9.7.5.3 Required Number of Strands

9.7.5 ESTIMATE REQUIRED PRESTRESS

The required number of strands is usually governed by concrete tensile stresses at the bottom fiber for load combination Service III at the section of maximum moment or at the harp points and in some cases Strength I. For estimating the number of strands, only the stresses at midspan are considered.

9.7.5.1 Service Load Stresses at Midspan

Bottom tensile stresses, due to applied dead and live loads using load combination Service III is:

$$f_b = \frac{M_g + M_j + M_b + M_{ws} + (0.8)(M_{LT} + M_{LL})}{S_b}$$

where

- f_b = concrete tensile stress at bottom fiber of the beam, ksi
- M_g = unfactored bending moment due to beam self weight, ft-kips
- M_j = unfactored bending moment due to joint concrete weight, ft-kips
- M_b = unfactored bending moment due to barrier weight, ft-kips
- M_{ws} = unfactored bending moment due to wearing surface, ft-kips
- M_{LT} = unfactored bending moment due to truck load, ft-kips
- M_{LL} = unfactored bending moment due to lane load, ft-kips

Using values of bending moments from **Tables 9.7.4-1 and 9.7.4-2**, bottom tensile stress at midspan is:

$$f_b = \frac{1,328.8 + 53.6 + 96.0 + 231.2 + (0.8)(1,033.6 + 343.0)}{7,743}(12) = 4.356 \text{ ksi}$$

9.7.5.2 Stress Limits for Concrete

Tensile stress limit at service loads = $0.19\sqrt{f'_c}$

[LRFD Table 5.9.4.2.2-1]

where f'_c = specified concrete compressive strength of beam for design, ksi

Concrete tensile stress limit = $-0.19\sqrt{8.0} = -0.537$ ksi

9.7.5.3 Required Number of Strands

The required precompressive stress at the bottom fiber of the beam is the difference between the bottom tensile stress due to the applied loads and the concrete tensile stress limit:

$$f_{pb} = (4.356 - 0.537) = 3.819 \text{ ksi}$$

Assume the distance between the center of gravity of bottom strands and the bottom fiber of the beam:

$$y_{bs} = 6.0 \text{ in.}$$

Therefore, strand eccentricity at midspan, $e_c = (y_b - y_{bs}) = (23.20 - 6.0) = 17.2$ in.

If P_{pe} is the total prestressing force after all losses, the bottom fiber stress due to prestress is:

$$f_{pb} = \frac{P_{pe}}{A_g} + \frac{P_{pe}e_c}{S_b} \text{ or } 3.819 = \frac{P_{pe}}{1,595} + \frac{P_{pe}(17.2)}{7,743}$$

Solving for P_{pe} , the required $P_{pe} = 1,340.8$ kips

Final prestress force per strand = (area of strand)(f_{pi})(1 - final losses)

where f_{pi} = initial strand stress before transfer, ksi (see Section 9.7.2) = 202.5 ksi

Assuming a final loss of 20% of f_{pi} , the prestress force per strand after all losses

$$= (0.217)(202.5)(1 - 0.20) = 35.2 \text{ kips}$$

Number of strands required = $(1,340.8/35.2) = 38.09$ strands

DOUBLE-TEE BEAM (NEXT 36 D), SINGLE SPAN, NONCOMPOSITE SURFACE

9.7.5.3 Required Number of Strands/9.7.5.5 Steel Transformed Section Properties

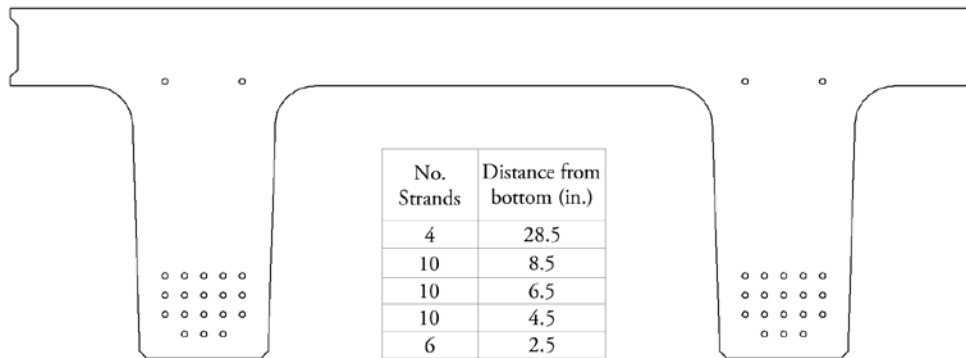
As an initial trial, (38) 0.6-in.-diameter, 270 ksi strands are selected. The center of gravity of the 38 strands at midspan is 8.08 in. from the bottom of the concrete, which is higher than the assumed value, 6.0 in. Thus, a second iteration using the new value of strand eccentricity indicates that 40 strands are required. The strand pattern at midspan for the 40 strands is shown in **Figure 9.7.5.3-1**. Each available position is filled beginning with the bottom row.

Try (40) 0.6-in.-diameter, 270 ksi strands

Total area of prestressing strands, $A_{ps} = 40 (0.217) = 8.680 \text{ in.}^2$

Note: This is a conservative estimate of the number of strands because nontransformed section properties are used in lieu of transformed section properties. The number of strands can be refined later in the design process as more accurate section properties and prestress losses are determined.

Figure 9.7.5.3-1
Assumed Strand Pattern at Midspan



9.7.5.4 Strand Pattern

The distance between the center of gravity of strands and the bottom concrete fiber of the beam at midspan is:

$$y_{bs} = [6(2.5) + 10(4.5) + 10(6.5) + 10(8.5) + 4(28.5)] / (40) = 8.10 \text{ in.}$$

$$\text{Strand eccentricity at midspan, } e_c = y_b - y_{bs} = 23.20 - 8.10 = 15.10 \text{ in.} = e_{pg}$$

9.7.5.5 Steel Transformed Section Properties

From the earliest years of prestressed concrete design, the gross section was conservatively used in analysis because the prestressing forces were smaller and computer programs were not widely used. However, the use of transformed section, which is obtained from the gross section by adding transformed steel area, yields more accurate results than the gross section analysis.

For each row of prestressing strands shown in **Figure 9.7.5.3-1**, the steel area is multiplied by $(n - 1)$ to calculate the transformed section properties, where n is the modular ratio between prestressing strand and concrete. Since the modulus of elasticity of concrete is different at transfer and final time, the transformed section properties should be calculated separately for the two stages. A sample calculation of the transformed section properties is shown in **Table 9.7.5.5-1**.

At transfer:

$$n - 1 = \frac{28,500}{4,696} - 1 = 5.069$$

At final:

$$n - 1 = \frac{28,500}{5,422} - 1 = 4.256$$

DOUBLE-TEE BEAM (NEXT 36 D), SINGLE SPAN, NONCOMPOSITE SURFACE

9.7.5.5 Steel Transformed Section Properties/9.7.6 Prestress Losses

Table 9.7.5.5-1
Properties of Transformed Section at Final Time

	Transformed Area, in. ²	y_b in.	Ay_b in. ³	$A(y_{btf} - y_b)^2$ in. ⁴	I in. ⁴	$I + A(y_{btf} - y_b)^2$ in. ⁴
Beam	1,595.00	23.20	37,004	184	179,629	179,813
Row 1	5.54	2.50	13.85	2,296		2,296
Row 2	9.24	4.50	41.58	3,115		3,115
Row 3	9.24	6.50	60.06	2,473		2,473
Row 4	9.24	8.50	78.54	1,905		1,905
Row 5	3.69	28.50	105.17	117		117
Σ	1,632.0		37,303			189,719

Note: The moment of inertia of strand about its own centroid is neglected.

The transformed section properties are calculated as:

Noncomposite transformed section at transfer:

$$A_{ti} = \text{area of transformed section at transfer} = 1,639.0 \text{ in.}^2$$

$$I_{ti} = \text{moment of inertia of the transformed section at transfer} = 191,602 \text{ in.}^4$$

$$e_{ti} = \text{eccentricity of strands with respect to transformed section at transfer} = 14.69 \text{ in.}$$

$$y_{bti} = \text{distance from the centroid of the transformed section to the extreme bottom fiber of the beam at transfer} = 22.79 \text{ in.}$$

$$S_{bti} = \text{section modulus for the extreme bottom fiber of the transformed section at transfer} = 8,407 \text{ in.}^3$$

$$S_{tti} = \text{section modulus for the extreme top fiber of the transformed section at transfer} = 14,504 \text{ in.}^3$$

Noncomposite transformed section at final time:

$$A_{tf} = \text{area of transformed section at final time} = 1,632.0 \text{ in.}^2$$

$$I_{tf} = \text{moment of inertia of the transformed section at final time} = 189,719 \text{ in.}^4$$

$$e_{tf} = \text{eccentricity of strands with respect to transformed section at final time} = 14.76 \text{ in.}$$

$$y_{btf} = \text{distance from the centroid of the transformed section to the extreme bottom fiber of the beam at final time} = 22.86 \text{ in.}$$

$$S_{btf} = \text{section modulus for the extreme bottom fiber of the transformed section at final time} = 8,299 \text{ in.}^3$$

$$S_{ctf} = \text{section modulus for the extreme top fiber of the transformed section at final time} = 14,438 \text{ in.}^3$$

Note: The 8-in.-wide cast-in-place concrete joint between the girders would change the section properties at service. However, the difference is small so it is conservatively ignored in this example.

9.7.6 PRESTRESS LOSSES

Total prestress loss:

$$\Delta f_{pT} = \Delta f_{pES} + \Delta f_{pLT} \quad [\text{LRFD Eq. 5.9.5.1-1}]$$

where

$$\Delta f_{pT} = \text{total loss in prestressing steel stress}$$

$$\Delta f_{pES} = \text{sum of all losses or gains due to elastic shortening or extension at the time of application of prestress and/or external loads}$$

$$\Delta f_{pLT} = \text{long-term losses due to shrinkage and creep of concrete, and relaxation of steel after transfer. In this design example, the refined estimates of time-dependent losses are used.}$$

DOUBLE-TEE BEAM (NEXT 36 D), SINGLE SPAN, NONCOMPOSITE SURFACE

9.7.6.1 Elastic Shortening/9.7.6.2 Time-Dependent Losses between Transfer and Deck Placement

9.7.6.1 Elastic Shortening

$$\Delta f_{pES} = \frac{E_p}{E_{ci}} f_{cgp} \quad [\text{LRFD Eq. 5.9.5.2.3a-1}]$$

where

E_p = modulus of elasticity of prestressing strands = 28,500 ksi

E_{ci} = modulus of elasticity of beam concrete at transfer = 4,696 ksi

f_{cgp} = sum of concrete stresses at the center of gravity of prestressing strands due to prestressing force at transfer and the self weight of the member at sections of maximum moment.

If the gross (or net) cross-section properties are used, it is necessary to perform numerical iterations. The elastic loss Δf_{pES} is usually assumed to be 10% of the initial prestress to calculate f_{cgp} , which is then used in the equation above to calculate a refined Δf_{pES} . The process is repeated until the assumed Δf_{pES} and refined Δf_{pES} converge.

However, when transformed section properties are used to calculate concrete stress, the effects of losses and gains due to elastic deformations are implicitly accounted for. Therefore, Δf_{pES} should not be included in calculating f_{cgp} .

Force per strand before transfer = (area of strand)(prestressing stress before transfer) = (0.217)(202.5) = 43.94 ksi

$$f_{cgp} = \frac{P_{pi}}{A_{ti}} + \frac{P_{pi}e_{ti}^2}{I_{ti}} - \frac{M_g e_{ti}}{I_{ti}}$$

where

e_{ti} = eccentricity of strands at midspan with respect to the transformed section at transfer = 14.69 in.

P_{pi} = total prestressing force before transfer = (40 strands)(43.94) = 1757.6 kips

M_g should be calculated based on the overall beam length of 81 ft. Since the elastic shortening loss is a part of the total loss, f_{cgp} will be conservatively computed based on M_g using the design span length of 80 ft.

$$f_{cgp} = \frac{1,757.6}{1,639.0} + \frac{(1,757.6)(14.69)^2}{191,602} - \frac{(1,328.8)(12)(14.69)}{191,602} = 1.829 \text{ ksi}$$

Therefore, loss due to elastic shortening:

$$\Delta f_{pES} = \left(\frac{28,500}{4,696} \right) (1.829) = 11.1 \text{ ksi}$$

AASHTO LRFD C5.9.5.3 indicates that the loss due to elastic shortening at transfer should be added to the time-dependent losses to determine total losses. However, this loss at transfer is directly accounted for if transformed section properties are used in stress analysis.

9.7.6.2 Time-Dependent Losses between Transfer and Deck Placement

AASHTO LRFD 5.9.5.4.4 states that the values for time of "deck placement" can be taken as time of noncomposite topping placement. For convenience, this example will use the term "deck placement" to be interchangeable with topping placement. The following construction schedule is assumed in calculating the time-dependent losses.

Concrete age at transfer: $t_i = 1$ day

Concrete age at deck placement: $t_d = 90$ days

Concrete age at final stage: $t_f = 20,000$ days

The total time-dependent loss between time of transfer and deck placement is the summation of prestress losses due to shrinkage of concrete, creep of concrete, and relaxation of prestressing strands.

DOUBLE-TEE BEAM (NEXT 36 D), SINGLE SPAN, NONCOMPOSITE SURFACE

9.7.6.2.1 Shrinkage of Concrete

9.7.6.2.1 Shrinkage of Concrete

The prestress loss due to shrinkage of concrete between time of transfer and deck placement is calculated by:

$$\Delta f_{pSR} = \epsilon_{bid} E_p K_{id} \quad [\text{LRFD 5.9.5.4.2a-1}]$$

where

ϵ_{bid} = concrete shrinkage strain of girder for time period between transfer and deck placement

E_p = modulus of elasticity of prestressing strands, ksi

K_{id} = transformed section coefficient that accounts for time-dependent interaction between concrete and bonded steel in the section being considered for time period between transfer and deck placement

The concrete shrinkage strain, ϵ_{bid} , is taken as:

$$\epsilon_{bid} = k_{vs} k_{hs} k_f k_{td} 0.48 \times 10^{-3} \quad [\text{LRFD Eq. 5.4.2.3.3.-1}]$$

where

The factor for the effect of the volume-to-surface ratio of the beam:

$$k_{vs} = 1.45 - 0.13(V/S) = 1.45 - 0.13(5.138) = 0.782$$

The minimum value of k_{vs} is 1.0. Therefore, use $k_{vs} = 1.000$

V/S is the volume-to-surface ratio of the beam.

The humidity factor for shrinkage:

$$k_{hs} = 2.00 - 0.014H = 2.00 - 0.014(70) = 1.020$$

where H = average annual mean relative humidity (assume 70%)

The factor for the effect of the concrete strength:

$$k_f = \frac{5}{1 + f'_{ci}} = \frac{5}{1 + 6.0} = 0.714$$

The time development factor at deck placement:

$$k_{td} = \frac{t}{61 - 4f'_{ci} + t} = \frac{89}{61 - 4(6.0) + 89} = 0.706 = k_{tda}$$

where t is the maturity of concrete(days) = $t_d - t_i = 90 - 1 = 89$ days

$$\epsilon_{bid} = (1.000)(1.020)(0.714)(0.706)(0.48 \times 10^{-3}) = 0.000247$$

$$K_{id} = \frac{1}{1 + \frac{E_p A_{ps}}{E_{ci} A_g} \left(1 + \frac{A_g (e_{pg})^2}{I_g} \right) [1 + 0.7\Psi_b(t_f, t_i)]} \quad [\text{LRFD Eq. 5.9.5.4.2a-2}]$$

where

e_{pg} = eccentricity of prestressing strand with respect to the centroid of the girder = 15.10 in.

$\Psi_b(t_f, t_i)$ = girder creep coefficient at final time due to loading introduced at transfer

For the time between transfer and final time:

$$\Psi_b(t_f, t_i) = 1.9k_{vs}k_{hc}k_fk_{td}t_i^{-0.118} \quad [\text{LRFD Eq. 5.4.2.3.2-1}]$$

$$k_{hc} = 1.56 - 0.008H = 1.56 - 0.008(70) = 1.000$$

$$k_{td} = \frac{t_f - t_i}{61 - 4f'_{ci} + (t_f - t_i)} = \frac{20,000 - 1}{61 - 4(6.0) + (20,000 - 1)} = 0.998 = k_{tdf}$$

$$\Psi_b(t_f, t_i) = 1.9(1.000)(1.000)(0.714)(0.998)(1)^{-0.118} = 1.354$$

DOUBLE-TEE BEAM (NEXT 36 D), SINGLE SPAN, NONCOMPOSITE SURFACE

9.7.6.2.1 Shrinkage of Concrete/9.7.6.3.1 Shrinkage of Concrete

$$K_{id} = \frac{1}{1 + \frac{28,500}{4,696} \frac{8.680}{1,595} \left(1 + \frac{1,595(15.10)^2}{179,629}\right) [1 + 0.7(1.354)]} = 0.837$$

The prestress loss due to shrinkage of concrete between transfer and deck placement is:

$$\Delta f_{pSR} = (0.000247)(28,500)(0.837) = 5.892 \text{ ksi}$$

9.7.6.2.2 Creep of Concrete

The prestress loss due to creep of girder concrete between time of transfer and deck placement is determined as:

$$\Delta f_{pCR} = \frac{E_p}{E_{ci}} f_{cgp} \Psi_b(t_d, t_i) K_{id} \quad \text{[LRFD Eq. 5.9.5.4.2b-1]}$$

where

$$\begin{aligned} \Psi_b(t_d, t_i) &= \text{girder creep coefficient at time of deck placement due to loading introduced at transfer} \\ &= 1.9k_{vs}k_{nc}k_fk_{td}t_i^{-1.18} \quad \text{[LRFD Eq. 5.4.2.3.2-1]} \\ &= 1.9(1.000)(1.000)(0.714)(0.706)(1)^{-0.118} = 0.958 \end{aligned}$$

$$\Delta f_{pCR} = \frac{28,500}{4,696} (1.829)(0.958)(0.837) = 8.901 \text{ ksi}$$

9.7.6.2.3 Relaxation of Prestressing Strands

The prestress loss due to relaxation of prestressing strands between time of transfer and deck placement is determined as:

$$\Delta f_{pR1} = \frac{f_{pt}}{K_L} \left(\frac{f_{pt}}{f_{py}} - 0.55 \right) \quad \text{[LRFD Eq. 5.9.5.4.2c-1]}$$

where

$$\begin{aligned} f_{pt} &= \text{stress in prestressing strands immediately after transfer, taken not less than } 0.55f_y \\ K_L &= 30 \text{ for low-relaxation strands and } 7 \text{ for other prestressing steel, unless more accurate} \\ &\quad \text{manufacturer's data are available} \end{aligned}$$

$$\Delta f_{pR1} = \frac{(202.5 - 11.1)}{30} \left(\frac{(202.5 - 11.1)}{243} - 0.55 \right) = 1.516 \text{ ksi}$$

According to LRFD Art. 5.9.5.4.2c, the relaxation loss may also be assumed equal to 1.2 ksi for low-relaxation strands.

9.7.6.3 Time-Dependent Losses between Deck Placement and Final Time

The total time-dependent loss between time of deck placement and final time is the summation of prestress losses due to shrinkage of beam concrete, creep of beam concrete, relaxation of prestressing strands, and shrinkage of deck concrete.

9.7.6.3.1 Shrinkage of Concrete

The prestress loss due to shrinkage of concrete between deck placement and final time is calculated by:

$$\Delta f_{pSD} = \epsilon_{bdf} E_p K_{df} \quad \text{[LRFD Eq. 5.9.5.4.3a-1]}$$

where

$$\begin{aligned} \epsilon_{bdf} &= \text{concrete shrinkage strain of girder for time period between deck placement and final time} \\ E_p &= \text{modulus of elasticity of prestressing strands, ksi} \\ K_{df} &= \text{transformed section coefficient that accounts for time-dependent interaction between concrete} \\ &\quad \text{and bonded steel in the section being considered for time period between deck placement and final} \\ &\quad \text{time} \end{aligned}$$

DOUBLE-TEE BEAM (NEXT 36 D), SINGLE SPAN, NONCOMPOSITE SURFACE

9.7.6.3.1 Shrinkage of Concrete/9.7.6.3.2 Creep of Concrete

The total concrete shrinkage strain between transfer and final time is taken as:

$$\begin{aligned}\varepsilon_{bif} &= k_{vs}k_{hs}k_fk_{tdf}0.48 \times 10^{-3} && \text{[LRFD Eq. 5.4.2.3.3-1]} \\ &= (1.000)(1.020)(0.714)(0.998)(0.48 \times 10^{-3}) = 0.000349\end{aligned}$$

The girder concrete shrinkage strain between deck placement and final time is:

$$\varepsilon_{bdf} = \varepsilon_{bif} - \varepsilon_{bid} = 0.000349 - 0.000247 = 0.000102$$

The beam concrete transformed section coefficient between deck placement and final time is:

$$K_{df} = \frac{1}{1 + \frac{E_p}{E_{ci}} \frac{A_{ps}}{A_c} \left(1 + \frac{A_c (e_{pc})^2}{I_c} \right) [1 + 0.7\Psi_b(t_f, t_i)]} \quad \text{[LRFD Eq. 5.9.5.4.3a-2]}$$

where

Since there is no composite deck for this example, the beam section properties will be used in place of the composite section properties:

$$\begin{aligned}A_c &= A_g &= \text{area of the precast beam} &= 1,595 \text{ in.}^2 \\ I_c &= I_g &= \text{moment of inertia of the precast beam} &= 179,629 \text{ in.}^4 \\ e_{pc} &= e_{pg} &= \text{eccentricity of strands with respect to centroid of the precast beam} \\ &= 15.10 \text{ in.}\end{aligned}$$

$$K_{df} = \frac{1}{1 + \frac{28,500}{4,696} \frac{8,680}{1,595} \left(1 + \frac{(1,595)(15.10)^2}{179,629} \right) [1 + 0.7(1.354)]} = 0.837$$

The prestress loss due to shrinkage of concrete between deck placement and final time is:

$$\Delta f_{pSD} = (0.000102)(28,500)(0.837) = 2.433 \text{ ksi}$$

9.7.6.3.2 Creep of Concrete

The prestress loss due to creep of beam concrete between time of deck placement and final time is:

$$\Delta f_{pCD} = \frac{E_p}{E_{ci}} f_{cgp} [\Psi_b(t_f, t_i) - \Psi_b(t_d, t_i)] K_{df} + \frac{E_p}{E_c} \Delta f_{cd} \Psi_b(t_f, t_d) K_{df} \quad \text{[LRFD Eq. 5.9.5.4.3b-1]}$$

where

$$\begin{aligned}\Psi_b(t_f, t_d) &= \text{girder creep coefficient at final time due to loading at deck placement} \\ &= 1.9k_{vs}k_{hc}k_fk_{tdf}t_d^{-0.118} && \text{[LRFD Eq. 5.4.2.3.2-1]}\end{aligned}$$

$$k_{tdf} = \frac{t_f - t_d}{61 - 4f'_{ci} + (t_f - t_d)} = \frac{20,000 - 90}{61 - 4(6.0) + (20,000 - 90)} = 0.998$$

$$\Psi_b(t_f, t_d) = 1.9(1.000)(1.000)(0.714)(0.998)(90)^{-0.118} = 0.796$$

Δf_{cd} = change in concrete stress at centroid of prestressing strands due to long-term losses between transfer and deck placement, combined with deck weight and superimposed loads, ksi

$$\begin{aligned}&= -(\Delta f_{pSR} + \Delta f_{pCR} + \Delta f_{pR1}) \frac{A_{ps}}{A_g} \left(1 + \frac{A_g e_{pg}^2}{I_g} \right) - \left(\frac{(M_j + M_b + M_{ws})e_{tf}}{I_{tf}} \right) \\ &= -(5.892 + 8.901 + 1.516) \frac{8,680}{1,595} \left(1 + \frac{(1,595)(15.10)^2}{179,629} \right) - \left(\frac{(53.6 + 96.0 + 231.5)(12)(14.76)}{189,719} \right) \\ &= -0.624 \text{ ksi}\end{aligned}$$

DOUBLE-TEE BEAM (NEXT 36 D), SINGLE SPAN, NONCOMPOSITE SURFACE

9.7.6.3.2 Creep of Concrete/9.7.6.6 Total Losses at Service Loads

The gross section properties are used in the equation to calculate Δf_{cd} for the long-term losses since the transformed section effect has already been included in the factor K_{id} when calculating the losses between initial time and deck placement.

$$\begin{aligned}\Delta f_{pCD} &= \frac{28,500}{4,696} 1.829[1.354 - 0.958](0.837) + \frac{28,500}{5,422} (-0.624)(0.796)(0.837) \\ &= 1.494 \text{ ksi}\end{aligned}$$

9.7.6.3.3 Relaxation of Prestressing Strands

The prestress loss due to relaxation of prestressing strands between time of deck placement and final time is taken as:

$$\Delta f_{pR2} = \Delta f_{pR1} = 1.516 \text{ ksi} \quad [\text{LRFD Eq. 5.9.5.4.3c-1}]$$

9.7.6.3.4 Shrinkage of Deck Concrete

The prestress gain due to shrinkage of deck concrete is taken a zero for this bridge because there is no composite deck.

$$\Delta f_{pSS} = 0.0 \text{ ksi}$$

9.7.6.4 Total Time-Dependent Loss

The total time-dependent loss, Δf_{pLT} , is determined as:

[LRFD Eq. 5.9.5.4.1-1]

$$\begin{aligned}\Delta f_{pLT} &= (\Delta f_{pSR} + \Delta f_{pCR} + \Delta f_{pR1}) + (\Delta f_{pSD} + \Delta f_{pCD} + \Delta f_{pR2} + \Delta f_{pSS}) \\ &= (5.892 + 8.901 + 1.516) + (2.433 + 1.494 + 1.516 + 0.0) = 21.8 \text{ ksi}\end{aligned}$$

9.7.6.5 Total Losses at Transfer

AASHTO LRFD C5.9.5.2.3a and C5.9.5.3 indicate that the losses or gains due to elastic deformation must be taken equal to zero if transformed section properties are used in stress analysis. However, the losses or gains due to elastic deformation must be included in determining the total prestress losses and the effective stress in prestressing strands.

$$\Delta f_{pi} = \Delta f_{pES} = 11.1 \text{ ksi}$$

Effective stress in tendons immediately after transfer, $f_{pt} = f_{pi} - \Delta f_{pi} = (202.5 - 11.1) = 191.4 \text{ ksi}$

Force per strand = $(f_{pt})(\text{area of strand}) = (191.4)(0.217) = 41.5 \text{ kips}$

Therefore, the total prestressing force after transfer, $P_{pt} = 41.5(40) = 1660.0 \text{ kips}$

Initial loss, % = $(\text{Total losses at transfer})/(f_{pi}) = 11.1/202.5 = 5.5\%$

When determining the concrete stress using transformed section properties, the strand force is that before transfer:

Force per strand = $(202.5)(0.217) = 43.9 \text{ kips}$

The total prestressing force before transfer, $P_{pi} = 43.9(40) = 1,756 \text{ kips}$

9.7.6.6 Total Losses at Service Loads

Total loss due to elastic shortening at transfer and long-term losses (Service III) is:

$$\Delta f_{pT} = \Delta f_{pES} + \Delta f_{pLT} = 11.1 + 21.8 = 32.9 \text{ ksi}$$

The elastic gain due to superimposed dead load, and live load is:

$$\begin{aligned}&= \left(\frac{(M_j + M_b + M_{ws})e_{tf}}{I_{tf}} \right) \frac{E_p}{E_c} + 0.8 \left(\frac{(M_{LT} + M_{LL})e_{tf}}{I_{tf}} \right) \frac{E_p}{E_c} \\ &= \left(\frac{(53.6 + 96.0 + 231.5)(12)(14.76)}{189,719} \right) \frac{28,500}{5,422} + 0.8 \left(\frac{(1,033.6 + 343.0)(12)(14.76)}{189,719} \right) \frac{28,500}{5,422} \\ &= 1.9 + 5.4 = 7.3 \text{ ksi}\end{aligned}$$

DOUBLE-TEE BEAM (NEXT 36 D), SINGLE SPAN, NONCOMPOSITE SURFACE

9.7.6.6 Total Losses at Service Loads/9.7.7.2 Stresses at Transfer Length Section of Bonded Strands

The effective stress in strands after all losses and gains:

$$f_{pe} = f_{pi} - \Delta f_{pT} + 7.3 = 202.5 - 32.9 + 7.3 = 176.9 \text{ ksi}$$

Check prestressing stress limit at service limit state:

[LRFD Table 5.9.3-1]

$$f_{pe} \leq 0.8 f_{py} = 0.8(243) = 194.4 \text{ ksi} > 176.9 \text{ ksi} \quad \text{OK}$$

The effective stress in strands after all losses and permanent gains:

$$f_{pe} = f_{pi} - \Delta f_{pT} + 1.9 = 202.5 - 32.9 + 1.9 = 171.5 \text{ ksi}$$

Force per strand without live load gains = $(f_{pe})(\text{area of strand}) = (171.5)(0.217) = 37.22 \text{ kips}$

Therefore, the total prestressing force after all losses = $37.22(40) = 1,488.8 \text{ kips}$

Final loss percentage = $(\text{total losses and gains})/(f_{pi}) = (32.9 - 1.9)/(202.5) = 15.3\%$

When determining the concrete stress using transformed section properties, all the elastic gains and losses are implicitly accounted for:

Force per strand with only total time-dependent losses = $(202.5 - 21.8)(0.217) = 39.21 \text{ kips}$

Total prestressing force, $P_{pe} = (39.21)(40) = 1,568 \text{ kips}$

9.7.7 CONCRETE STRESSES AT TRANSFER

Because the transformed section is used, the total prestressing force before transfer, $P_{pi} = 1,756 \text{ kips}$.

9.7.7.1 Stress Limits for Concrete

[LRFD Art. 5.9.4]

Compression:

- $0.6 f'_{ci} = 0.6(6.0) = +3.600 \text{ ksi}$

where f'_{ci} = concrete strength at transfer = 6.000 ksi

Tension:

- without bonded auxiliary reinforcement

$$-0.0948 \sqrt{f'_{ci}} \leq 0.200 \text{ ksi} = -0.0948 \sqrt{6.000} = -0.232 \text{ ksi}$$

Therefore, -0.200 ksi (Controls)

- with bonded auxiliary reinforcement that is sufficient to resist 120% of the tension force in the cracked concrete

$$-0.24 \sqrt{f'_{ci}} = -0.24 \sqrt{6.000} = -0.588 \text{ ksi}$$

9.7.7.2 Stresses at Transfer Length Section of Bonded Strands

Stresses at this location need only be checked at transfer since this stage almost always governs. Also, losses with time will reduce the concrete stresses, making them less critical.

Transfer length = $60(\text{strand diameter}) = 60(0.6) = 36 \text{ in.} = 3 \text{ ft}$

[LRFD Art. 5.11.4]

Due to camber of the beam at transfer, the beam self weight acts on the overall beam length, 81 ft. Therefore, values for bending moment given in **Table 9.7.4-1** cannot be used because they are based on the design span length of 80 ft. Using Equation 9.7.4.1.2-2, the bending moment at transfer length due to beam self weight is:

$$M_g = 0.5 w_g x(L - x) = (0.5)(1.661)(3)(81 - 3) = 194.3 \text{ ft-kips}$$

Compute concrete stress in the top of beam:

$$f_t = \frac{P_{pi}}{A_{ti}} - \frac{P_{pi} e_{ti}}{S_{tti}} + \frac{M_g}{S_{tti}} = \frac{1,756}{1,639} - \frac{(1,756)(14.69)}{14,504} + \frac{194.3(12)}{14,504} = 1.071 - 1.779 + 0.161 = -0.547 \text{ ksi}$$

DOUBLE-TEE BEAM (NEXT 36 D), SINGLE SPAN, NONCOMPOSITE SURFACE

9.7.7.2 Stresses at Transfer Length Section of Bonded Strands

Tensile stress limit for concrete with bonded reinforcement: -0.588 ksi OK

Compute concrete stress in bottom of beam:

$$f_b = \frac{P_{pi}}{A_{ti}} + \frac{P_{pi}e_{ti}}{S_{bti}} - \frac{M_g}{S_{bti}} = \frac{1,756}{1,639} + \frac{(1,756)(14.69)}{8,407} - \frac{194.3(12)}{8,407} = 1.071 + 3.068 - 0.277 = +3.862 \text{ ksi}$$

Compressive stress limit for concrete: +3.600 ksi NG

Therefore, try debonding four strands from the strand group at 4.5 in. from the bottom for a distance of 5 ft 0 in. from the end of the beam or 4 ft 6 in. from centerline of bearing.

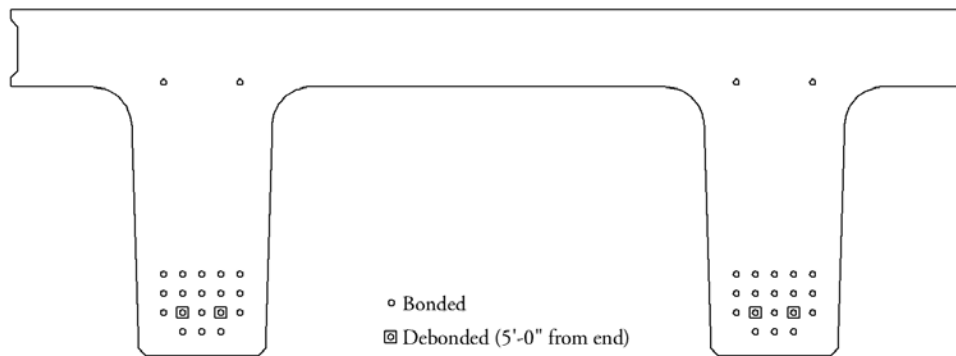
To minimize the shock impact of detensioning and cracks at corners and bottom, assume the strand pattern shown in **Figure 9.7.7.2-1**. LRFD Article 5.11.4.3 requires that the following conditions be satisfied if debonding is used:

- percentage debonding of total = 4/40 = 10% ≤ 25% OK
- percentage debonding of row = 4/10 = 40% ≤ 40% OK
- All limit states should be satisfied OK
- Debonded strands should be symmetrically distributed OK
- Exterior strands in each horizontal line are fully bonded OK

Recompute top and bottom the stresses at the transfer length section. Note that the transformed section properties here are different than those at midspan after debonding. Using the same method as described in Section 9.7.5.5, the transformed section properties at end of beam are computed as:

$$A_{ti} = 1,635 \text{ in.}^2 \quad y_{bti} = 22.84 \text{ in.} \quad S_{bti} = 8,324 \text{ in.}^3 \quad S_{tti} = 14,447 \text{ in.}^3$$

Figure 9.7.7.2-1
Strand Pattern at End of Beam



Distance from the center of gravity of bonded strands to the bottom fiber of the beam is:

$$y_{bs} = [6(2.5) + 6(4.5) + 10(6.5) + 10(8.5) + 4(28.5)] / (36) = 8.50 \text{ in.}$$

and the strand eccentricity for the transformed section at end of beam is:

$$e_{ti} = 22.84 - 8.50 = 14.34 \text{ in.}$$

Total prestressing force before transfer at end section = 36(43.9) = 1580 kips

Concrete stress in top of beam:

$$f_t = \frac{1,580}{1,635} - \frac{(1,580)(14.34)}{14,447} + \frac{(194.3)(12)}{14,447} = 0.966 - 1.568 + 0.161 = -0.441 \text{ ksi}$$

Tensile stress limit is: -0.558 ksi OK

DOUBLE-TEE BEAM (NEXT 36 D), SINGLE SPAN, NONCOMPOSITE SURFACE**9.7.7.2 Stresses at Transfer Length Section of Bonded Strands/9.7.8 Concrete Stresses at Service Loads**

Bonded auxiliary reinforcement must be provided in the top of the beam.

Concrete stress in bottom of beam:

$$f_b = \frac{1,580}{1,635} + \frac{(1,580)(14.34)}{8,324} - \frac{(194.3)(12)}{8,324} = 0.966 + 2.722 - 0.280 = +3.408 \text{ ksi}$$

Compressive stress limit is: +3.600 ksi OK

9.7.7.3 Stresses at Transfer Length Section of Debonded Strands

All strands are effective at this location; therefore use the full value of P_{pi} . Bending moment due to the self weight of the beam at (5 ft + 3 ft = 8 ft) from the end of the beam:

$$M_g = 0.5w_gx(L - x) = (0.5)(1.661)(8)(81 - 8) = 485.0 \text{ ft-kips}$$

Concrete stress in top of beam:

$$f_t = \frac{P_{pi}}{A_{ti}} - \frac{P_{pi}e_{ti}}{S_{tti}} + \frac{M_g}{S_{tti}} = \frac{1,756}{1,639} - \frac{(1,756)(14.69)}{14,504} + \frac{485.0(12)}{14,504} = 1.071 - 1.779 + 0.401 = -0.307 \text{ ksi}$$

Tensile stress limit: -0.588 ksi OK

Concrete stress in bottom of beam:

$$f_b = \frac{P_{pi}}{A_{ti}} + \frac{P_{pi}e_{ti}}{S_{bti}} - \frac{M_g}{S_{bti}} = \frac{1,756}{1,639} + \frac{(1,756)(14.69)}{8,407} - \frac{485.0(12)}{8,407} = 1.071 + 3.068 - 0.692 = +3.447 \text{ ksi}$$

Compressive stress limit: +3.600 ksi OK

9.7.7.4 Stresses at Midspan

Bending moment at midspan due to the beam self weight is:

$$M_g = 0.5(1.661)(40.5)(81-40.5) = 1,362.2 \text{ ft-kips}$$

$$f_t = \frac{1,756}{1,639} - \frac{(1,756)(14.69)}{14,504} + \frac{(1,362)(12)}{14,504} = 1.071 - 1.779 + 1.127 = +0.419 \text{ ksi}$$

Compressive stress limit: +3.600 ksi OK

$$f_b = \frac{1,756}{1,639} + \frac{(1,756)(14.69)}{8,407} - \frac{(1,362)(12)}{8,407} = 1.071 + 3.068 - 1.944 = +2.195 \text{ ksi}$$

Compressive stress limit: +3.600 ksi OK

9.7.7.5 Summary of Stresses at Transfer

	Top Fiber Stresses f_t , ksi	Bottom Fiber Stresses f_b , ksi
At transfer length section of bonded strands	-0.441	+3.408
At transfer length section of debonded strands	-0.307	+3.447
At midspan	+0.419	+2.195

9.7.8 CONCRETE STRESSES AT SERVICE LOADS

[LRFD Art. 5.9.4.2]

Using transformed section properties and refined losses, $P_{pe} = 1568$ kips

DOUBLE-TEE BEAM (NEXT 36 D), SINGLE SPAN, NONCOMPOSITE SURFACE**9.7.8 Concrete Stresses at Service Loads//9.7.8.3 Fatigue Stress Limit****9.7.8.1 Stress Limits for Concrete**

Compression:

[LRFD Table 5.9.4.2.1-1]

Due to permanent loads (i.e. beam self weight, weight of future wearing surface, weight of barriers, and weight of joint concrete), for load combination Service I:

$$\text{for precast beams: } 0.45f'_c = (0.45)(8.000) = +3.600 \text{ ksi}$$

Due to permanent and transient loads (i.e. all dead loads and live loads), for load combination Service I:

$$\text{for precast beams: } 0.60f'_c = 0.6(8.000) = +4.800 \text{ ksi}$$

Tension:

[LRFD Table 5.9.4.2.2-1]

For components with bonded prestressing tendons:

for load combination Service III:

$$\text{for precast beams } -0.19\sqrt{f'_c} = -0.19\sqrt{8.000} = -0.537 \text{ ksi}$$

9.7.8.2 Stresses at Midspan**9.7.8.2.1 Concrete Stress at Top Fiber of the Beam**

To check top compressive stresses, two cases are considered:

- Under permanent loads, load combination Service I:

Using bending moment values given in **Table 9.7.4-1** and **9.7.4-2**, compute the top fiber stresses:

$$\begin{aligned} f_{tg} &= \frac{P_{pe}}{A_{tf}} - \frac{P_{pe}e_{tf}}{S_{ttf}} + \frac{(M_g + M_j + M_{ws} + M_b)}{S_{ttf}} \\ &= \frac{1,568}{1,632} - \frac{(1,568)(14.76)}{14,438} + \frac{(1,328.8 + 53.6 + 231.2 + 96.0)(12)}{14,438} = 0.961 - 1.603 + 1.421 = +0.779 \text{ ksi} \end{aligned}$$

Compressive stress limit: +3.600 ksi OK

- Under permanent and transient loads, load combination Service I:

$$f_{tg} = +0.779 + \frac{(M_{LT} + M_{LL})}{S_{ttf}} = +0.779 + \frac{(1,033.6 + 343.0)(12)}{14,438} = +0.779 + 1.144 = +1.923 \text{ ksi}$$

Compressive stress limit: +4.800 ksi OK

9.7.8.2.2 Concrete Stress in Bottom of Beam, Load Combination Service III

$$\begin{aligned} f_b &= \frac{P_{pe}}{A_{tf}} + \frac{P_{pe}e_{tf}}{S_{btf}} - \frac{(M_g + M_j + M_{ws} + M_b) + 0.8(M_{LT} + M_{LL})}{S_{btf}} \\ &= \frac{1,568}{1,632} + \frac{(1,568)(14.76)}{8,299} - \frac{(1,328.8 + 53.6 + 231.2 + 96.0)(12) + 0.8(1,033.6 + 343.0)(12)}{8,299} \\ &= 0.961 + 2.789 - 4.064 = -0.314 \text{ ksi} \end{aligned}$$

Tensile stress limit: -0.537 ksi OK

9.7.8.3 Fatigue Stress Limit

LRFD Article 5.5.3.1 states that in fully prestressed components other than segmentally constructed bridges, the compressive stress due to Fatigue I load combination and one half the sum of effective prestress and permanent loads shall not exceed $0.40f'_c$, after losses.

From **Table 9.7.4-2**, the unfactored fatigue bending moment at midspan, M_f , is 526.9 ft-kips. Therefore, stress at the top fiber of the beam due to fatigue load combination I is:

$$f_{tgf} = \frac{1.50(M_f)}{S_{ttf}} = \frac{1.50(526.9)(12)}{14,438} = +0.657 \text{ ksi}$$

DOUBLE-TEE BEAM (NEXT 36 D), SINGLE SPAN, NONCOMPOSITE SURFACE

9.7.8.3 Fatigue Stress Limit/9.7.9 Strength Limit State

At midspan, the top compressive stress due to permanent loads and prestress is:

$$f_{tg} = \frac{P_{pe}}{A_{tf}} - \frac{P_{pe}e_{tf}}{S_{ttf}} + \frac{(M_g + M_j + M_{ws} + M_b)}{S_{ttf}}$$

$$= \frac{1,568}{1,632} - \frac{(1,568)(14.76)}{14,438} + \frac{(1,328.8 + 53.6 + 231.2 + 96.0)(12)}{14,438}$$

$$= 0.961 - 1.603 + 1.421 = 0.779 \text{ ksi}$$

Therefore:

$$f_{tgf} + \frac{f_b}{2} = 0.657 + \frac{0.779}{2} = 1.047 < 0.40(f'_c) = 0.40(8.00) = 3.2 \text{ ksi OK}$$

This condition should be satisfied at all locations along the beam.

9.7.8.4 Summary of Stresses at Midspan at Service Loads

	Top of Beam, ksi Service I		Bottom of Beam, ksi Service III
	Permanent Loads	Total Loads	
At midspan	+0.779	+1.923	-0.314

9.7.9 STRENGTH LIMIT STATE

Total ultimate bending moment for Strength I is:

$$M_u = 1.25(DC) + 1.5(DW) + 1.75(LL + IM)$$

Using the values of unfactored bending moment given in **Tables 9.7.4-1 and 9.7.4-2**, the ultimate bending moment at midspan is:

$$M_u = 1.25(1,328.8 + 53.6 + 96.0) + 1.5(231.2) + 1.75(1,033.6 + 343.0) = 4,603.9 \text{ ft-kips}$$

Average stress in prestressing strands when $f_{pe} \geq 0.5f_{pu}$:

$$f_{ps} = f_{pu} \left(1 - k \frac{c}{d_p} \right) \quad \text{[LRFD Eq. 5.7.3.1.1-1]}$$

where

f_{ps} = average stress in prestressing strand, ksi

f_{pu} = specified tensile strength of prestressing strand = 270.0 ksi

$$k = 2 \left(1.04 - \frac{f_{py}}{f_{pu}} \right) = 2 \left(1.04 - \frac{243}{270} \right) \quad \text{[LRFD Eq. 5.7.3.1.1-2]}$$

= 0.28 for low-relaxation strands [LRFD Table C5.7.3.1.1-1]

d_p = distance from extreme compression fiber to the centroid of the prestressing strands

c = distance from extreme compression fiber to the neutral axis, in.

To compute c , assume rectangular section behavior and check if the depth of the equivalent compression stress block, a , is less than or equal to t_s :

where $a = \beta_1 c$

$$c = \frac{A_{ps}f_{pu} + A_s f_y - A'_s f'_y}{0.85 f'_c \beta_1 b + k A_{ps} \frac{f_{pu}}{d_p}} \quad \text{[LRFD Eq. 5.7.3.1.1-4]}$$

DOUBLE-TEE BEAM (NEXT 36 D), SINGLE SPAN, NONCOMPOSITE SURFACE

9.7.9 Strength Limit State

where

 a = depth of the equivalent stress block, in. A_{ps} = area of prestressing strand = $36(0.217) = 7.812 \text{ in.}^2$ A_s = area of nonprestressed tension reinforcement = 0 in.^2 A'_s = area of compression reinforcement = 0 in.^2 f'_c = specified compressive strength of concrete = 8.0 ksi f_y = specified yield strength of tension reinforcement = 60.0 ksi f'_y = specified yield strength of compression reinforcement, ksi β_1 = stress factor of compression block [LRFD Art. 5.7.2.2]= 0.85 for $f'_c \leq 4.0$ ksi= $0.85 - 0.05(f'_c - 4.0) \geq 0.65$ for $f'_c > 4.0$ ksi= $0.85 - 0.05(8.0 - 4.0) = 0.65$ b = width of compression flange = 100 in.

Note: In computing the flexural strength of members with strands placed near the compression face of the member, it is not correct to use the combined centroid of the entire strand group for establishing the effective depth, d_p , and the area of prestressing steel, A_{ps} . This is because the top strands will have different strain from that of the bottom strands. An accurate solution can be achieved using the detailed strain compatibility approach, which accounts for the steel strain at various distances from the neutral axis. However, a reasonable approximation is to ignore all strands placed on the compression side.

For the 36 bottom strands, the distance between the center of gravity of the strands and the bottom fiber of the beam, y_{bs} , is:

$$y_{bs} = [6(2.5) + 10(4.5) + 10(6.5) + 10(8.5)] / (36) = 5.83 \text{ in.}$$

$$d_p = h - y_{bs} = 36.00 - 5.83 = 30.17 \text{ in.}$$

$$c = \frac{7.812(270) + 0 - 0}{0.85(8.0)(0.65)(100) + (0.28)(7.812)\left(\frac{270}{30.17}\right)} = 4.57 \text{ in.}$$

$$a = \beta_1 c = (0.65)(4.57) = 2.97 \text{ in.} < t_s = 8.0 \text{ in.} \quad \text{OK}$$

Therefore, the rectangular section behavior is valid.

The average stress in prestressing strand is:

$$f_{ps} = 270.0 \left(1 - 0.28 \frac{4.57}{30.17} \right) = 258.5 \text{ ksi}$$

Nominal flexural resistance:

$$M_n = A_{ps} f_{ps} \left(d_p - \frac{a}{2} \right)$$

The above equation is a simplified form of LRFD Equation 5.7.3.2.2-1 because no compression reinforcement or nonprestressed tension reinforcement is considered and the section behaves as a rectangular section.

$$M_n = \frac{(7.812)(258.5) \left(30.17 - \frac{2.97}{2} \right)}{12} = 4,827 \text{ ft-kips}$$

Factored flexural resistance:

$$M_r = \phi M_n \quad \text{[LRFD Eq. 5.7.3.2.1-1]}$$

DOUBLE-TEE BEAM (NEXT 36 D), SINGLE SPAN, NONCOMPOSITE SURFACE

9.7.9 Strength Limit State/9.7.10.2 Minimum Reinforcement

where

$$\phi = \text{resistance factor} \quad [\text{LRFD Art. 5.5.4.2.1}]$$

$$= 1.00, \text{ tension controlled prestressed concrete sections}$$

$$M_r = 4,827 \text{ ft-kips} > M_u = 4,603.9 \text{ ft-kips} \quad \text{OK}$$

9.7.10 LIMITS OF REINFORCEMENT**9.7.10.1 Maximum Reinforcement**

[LRFD Art. 5.7.3.3.1]

The check of maximum reinforcement limits was removed from the *LRFD Specifications* in 2005.

9.7.10.2 Minimum Reinforcement

[LRFD Art. 5.7.3.3.2]

At any section, the amount of prestressed and nonprestressed tensile reinforcement must be adequate to develop a factored flexural resistance, M_r , equal to the lesser of:

- 1.2 times the cracking strength determined on the basis of elastic stress distribution and the modulus of rupture, and
- 1.33 times the factored moment required by the applicable strength load combination.

Check at midspan:

$$M_{cr} = S_{btf}(f_r + f_{cpe}) \quad [\text{LRFD Eq. 5.7.3.3.2-1}]$$

The above equation is a simplified form of LRFD Equation 5.7.3.3.2-1 because no composite section exists, therefore the composite and noncomposite section modulus are the same.

where

$$f_r = \text{modulus of rupture of concrete} \quad [\text{LRFD Art. 5.4.2.6}]$$

$$= 0.37\sqrt{f'_c} = 0.37\sqrt{8,000} = 1.047 \text{ ksi}$$

$$f_{cpe} = \text{compressive stress in concrete due to effective prestress force only (after allowance for all prestress losses) at extreme fiber of section where tensile stress is caused by externally applied loads}$$

$$= \frac{P_{pe}}{A_{tf}} + \frac{P_{pe}e_{tf}}{S_{btf}} = \frac{1,568}{1,632} + \frac{(1,568)(14.76)}{8,299} = 3.750 \text{ ksi}$$

$$S_{btf} = \text{section modulus for the extreme bottom fiber of transformed section where the tensile stress is caused by externally applied loads. For this example, use noncomposite transformed section modulus} = 8,299 \text{ in.}^3$$

$$M_{cr} = \frac{8,299}{12}(1.047 + 3.750) = 3,318 \text{ ft-kips}$$

At midspan, the factored moment required by the Strength I load combination is:

$$1.2M_{cr} = 1.2(3,318) = 3,982 \text{ ft-kips}$$

$$M_u = 4,603.9 \text{ ft-kips} \quad (\text{Sect. 9.7.9})$$

$$\text{Thus, } 1.33M_u = 1.33(4,603.9) = 6,123 \text{ ft-kips}$$

Since $1.2M_{cr} < 1.33M_u$, the $1.2M_{cr}$ requirement controls.

$$M_r = 4,827 \text{ ft-kips} > 1.2M_{cr} = 3,982 \text{ ft-kips} \quad \text{OK}$$

Note: The *LRFD Specifications* requires that this criterion be met at every section.

Illustrated based on
2011 *LRFD*
Specifications.

Editor's Note: 2012
LRFD Specifications
changes will revise
minimum
reinforcement.

DOUBLE-TEE BEAM (NEXT 36 D), SINGLE SPAN, NONCOMPOSITE SURFACE

9.7.11 Shear Design/9.7.11.1 Critical Section

9.7.11 SHEAR DESIGN

The area and spacing of shear reinforcement must be determined at regular intervals along the entire length of the beam. In this design example, transverse shear design procedures are demonstrated below by determining these values at the critical section near the supports.

Transverse shear reinforcement is required when:

$$V_u > 0.5\phi(V_c + V_p) \quad \text{[LRFD Eq. 5.8.2.4-1]}$$

where

- V_u = total factored shear force, kips
- V_c = nominal shear resistance provided by tensile stresses in the concrete, kips
- V_p = component in the direction of the applied shear of the effective prestressing force, kips
- ϕ = resistance factor = 0.9 for normal weight concrete [LRFD Art. 5.5.4.2.1]

9.7.11.1 Critical Section

[LRFD Art. 5.8.3.2]

The critical section near the supports is taken as the effective shear depth, d_v , from the internal face of the support.

$$d_v = \text{distance between resultants of tensile and compressive forces, } (d_e - a/2), \text{ but not less than } (0.9d_e) \text{ or } (0.72h) \quad \text{[LRFD Art. 5.8.2.7]}$$

where

- d_e = the corresponding effective depth from the extreme compression fiber to the centroid of the tensile force in the tensile reinforcement
- a = depth of compression block = 2.97 in. at midspan (assumed adequate) (Sect. 9.7.9)
- h = overall depth of the section = 36 in.

Note: Only 32 strands are effective at the critical section for shear, because four strands are debonded for a distance equal to 5 ft from the end of the beam and the top level of strands is ignored.

$$y_{bs} = [6(2.5) + 6(4.5) + 10(6.5) + 10(8.5)] / (32) = 6.00 \text{ in.}$$

$$d_e = h - y_{bs} = 36.00 - 6.00 = 30.00 \text{ in.}$$

$$d_v = 30.00 - (0.5)(2.97) = 28.52 \text{ in.}$$

$$\geq 0.9 d_e = 0.9(30.00) = 27.00 \text{ in.}$$

$$\geq 0.72 h = 0.72(36) = 25.92 \text{ in.} \quad \text{OK}$$

Therefore, $d_v = 28.52$ in.

Because the width of the bearing is not yet determined, it is conservatively assumed to be zero for determining the critical section for shear, as shown in **Figure 9.7.11.1-1**. Therefore, the critical section in shear is located at a distance of:

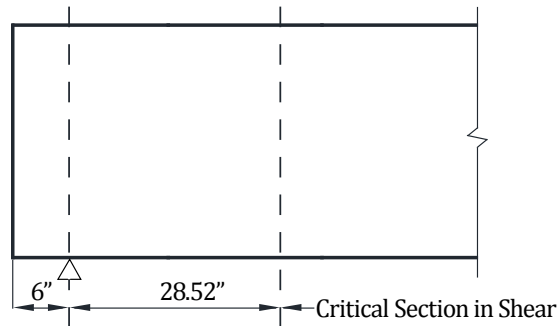
$$28.52 \text{ in.} = 2.38 \text{ ft from centerline of support}$$

$$(x/L) = 2.38/80 = 0.030L$$

DOUBLE-TEE BEAM (NEXT 36 D), SINGLE SPAN, NONCOMPOSITE SURFACE

9.7.11.1 Critical Section/9.7.11.2.1 Strain in Flexural Tension Reinforcement

Figure 9.7.11.1-1
Critical Section in Shear



9.7.11.2 Contribution of Concrete to Nominal Shear Resistance

The contribution of the concrete to the nominal shear resistance is:

$$V_c = 0.0316\beta\sqrt{f'_c} b_v d_v \quad \text{[LRFD Eq.5.8.3.3-3]}$$

where β = a factor indicating the ability of diagonally cracked concrete to transmit tension (a value indicating concrete contribution).

Several quantities must be determined before this expression can be evaluated.

9.7.11.2.1 Strain in Flexural Tension Reinforcement

Calculate the strain at the centroid of the tension reinforcement, ϵ_s :

$$\epsilon_s = \frac{\frac{|M_u|}{d_v} + 0.5N_u + |(V_u - V_p)| - A_{ps}f_{po}}{(E_s A_s + E_p A_{ps})} \quad \text{[LRFD Eq. 5.8.3.4.2-4]}$$

where

N_u = applied factored normal axial force at the specified section, $0.030L = 0$

V_u = applied factored shear force at the specified section, $0.030L$
 = $1.25(62.5 + 2.5 + 4.5) + 1.50(10.9) + 1.75(72.3 + 21.3)$ (Tables 9.7.4-1 and 9.7.4-2)
 = 267.0 kips

V_p = component of the effective prestressing force in the direction of the applied shear
 = 0 since strand pattern is straight

M_u = applied factored bending moment at the specified section, $0.030L$
 = $1.25(153.4 + 6.2 + 11.1) + 1.50(26.7) + 1.75(130.3 + 39.6)$ (Tables 9.7.4-1 and 9.7.4-2)
 = 550.8 ft-kips

M_u need not to be taken less than $(V_u - V_p)d_v$:

$$(V_u - V_p)d_v = [(267.0 - 0)28.52]/12 = 634.6 \text{ ft-kips}$$

Since $(V_u - V_p)d_v \geq M_u$, $M_u = 634.6$ ft-kips Controls

A_{ps} = area of prestressing strands on the flexural tension side of the member = $32(0.217) = 6.944 \text{ in.}^2$
 (Only 32 strands of the 36 strands are effective in the flexural tension side because four strands are debonded). Transfer length $60(0.60) = 36$ inches. Use critical section = $6 + 28.52$ inches. Use $34.52/36(6.944 \text{ in.}^2) = 6.659 \text{ in.}^2$

DOUBLE-TEE BEAM (NEXT 36 D), SINGLE SPAN, NONCOMPOSITE SURFACE

9.7.11.2.1 Strain in Flexural Tension Reinforcement/9.7.11.3.2 Required Area of Reinforcement

f_{po} = a parameter taken as modulus of elasticity of prestressing tendons multiplied by the locked-in difference in strain between the prestressing tendons and the surrounding concrete (ksi). For pretensioned members, LRFD Article C5.8.3.4.2 indicates that f_{po} can be taken as $0.7f_{pu}$. (Note: use this for both pretensioned and post-tensioned systems made with stress-relieved and low relaxation strands).

$$= 0.7(270.0) = 189.0 \text{ ksi}$$

$$\epsilon_s = \frac{\frac{|634.6(12)|}{28.52} + 0.5(0) + |267.0 - 0| - 6.659(189)}{(0 + 28,500(6.659))} = -3.8 \times 10^{-3}$$

ϵ_s is less than zero. Use $\epsilon_s = 0$.

9.7.11.2.2 Values of β and θ

Assume the section contains at least the minimum amount of traverse reinforcement:

$$\beta = \frac{4.8}{(1 + 750\epsilon_s)} = \frac{4.8}{(1 + 0)} = 4.8 \quad \text{[LRFD Eq. 5.8.3.4.2-1]}$$

Angle of diagonal compressive stress is:

$$\theta = 29 + 3,500\epsilon_s = 29 + 3,500(0) = 29^\circ \quad \text{[LRFD Eq. 5.8.3.4.2-3]}$$

9.7.11.2.3 Compute Concrete Contribution

The nominal shear resisted by the concrete is:

$$V_c = 0.0316\beta\sqrt{f'_c} b_v d_v \quad \text{[LRFD Eq. 5.8.3.3-3]}$$

where b_v = effective web width = $2(13.25) = 26.5$ in.

LRFD Article 5.8.2.9 states that b_v is the minimum web width between the tensile and compressive forces due to flexure. In this example the beam web is slightly sloped. The minimum width at the bottom of the beam is conservatively used in the calculation.

$$V_c = 0.0316(4.8) \sqrt{8.0} (26.5)(28.52) = 324.2 \text{ kips}$$

9.7.11.3 Contribution of Reinforcement to Nominal Shear Resistance**9.7.11.3.1 Requirement for Reinforcement**

Check if $V_u > 0.5\phi(V_c + V_p)$ [LRFD Eq. 5.8.2.4-1]

$$V_u = 267.0 \text{ kips} > 0.5\phi(V_c + V_p) = 0.5(0.9)(324.2 + 0) = 145.9 \text{ kips}$$

Therefore, transverse shear reinforcement must be provided.

9.7.11.3.2 Required Area of Reinforcement

$V_u/\phi \leq V_n = V_c + V_s + V_p$ [LRFD Eq. 5.8.3.3-1]

where

$$\begin{aligned} V_s &= \text{shear resistance provided by shear reinforcement} \\ &= (V_u/\phi - V_c - V_p) = (267.0/0.9) - 324.2 - 0.0 = -27.5 \text{ kips} \end{aligned}$$

$$V_s = \frac{A_v f_{yh} d_v (\cot \theta + \cot \alpha) (\sin \alpha)}{s} \quad \text{[LRFD Eq. 5.8.3.3-4]}$$

where

- A_v = area of shear reinforcement within a distance, s , in.²
- s = spacing of stirrups, in.
- f_{yh} = specified yield strength of shear reinforcement, ksi
- α = angle of inclination of transverse reinforcement to longitudinal axis
- = 90° for vertical stirrups

DOUBLE-TEE BEAM (NEXT 36 D), SINGLE SPAN, NONCOMPOSITE SURFACE**9.7.11.3.2 Required Area of Reinforcement/9.7.13 Minimum Longitudinal Reinforcement Requirement**

Since the required V_s is negative the minimum transverse reinforcement requirement is used to determine the area of the shear reinforcement. The area of transverse reinforcement should not be less than:

$$A_v \geq 0.0316 \sqrt{f'_c} \frac{b_v s}{f_{yh}} = 0.0316 \sqrt{8.0} \frac{(26.5)(s)}{60} = 0.039(s) \quad [\text{LRFD Eq. 5.8.2.5-1}]$$

If $s = 15$ in., required $A_v = 0.59$ in²/ft

9.7.11.3.3 Determine Spacing of Reinforcement

Check maximum spacing of transverse reinforcement:

[LRFD Art 5.8.2.7]

Check if $v_u < 0.125f'_c$

$$v_u = \frac{|V_u - \phi V_p|}{\phi b_v d_v} = \frac{|(267.0) - (0)|}{(0.9)(26.5)(28.52)} = 0.393 \text{ ksi}$$

$$0.125f'_c = (0.125)(8.0) = 1.000 \text{ ksi}$$

[LRFD Eq. 5.8.2.7-1]

Since $v_u < 0.125f'_c$

then, $s \leq 24$ in.

$$s \leq 0.8 d_v = 0.8(28.52) = 22.8 \text{ in. Controls}$$

Therefore, maximum $s = 22.8$ in. $> s$ provided = 15 in. OK

Use No. 4 bar four-leg stirrups at 15 in., $A_v = 0.64$ in.²/ft > 0.59 in.²/ft

$$V_s = \frac{0.80(60)(28.52) (\cot 29^\circ)}{15} = 164.6 \text{ kips}$$

9.7.11.4 Maximum Nominal Shear Resistance

In order to ensure that the concrete in the web of the beam will not crush prior to yielding of the transverse reinforcement, the *LRFD Specifications* gives an upper limit of V_n as follows:

$$V_n = 0.25f'_c b_v d_v + V_p \quad [\text{LRFD Eq. 5.8.3.3-2}]$$

Comparing this equation with LRFD Eq. 5.8.3.3-1, it can be concluded that

$$V_c + V_s \text{ must not be greater than } 0.25f'_c b_v d_v$$

$$324.2 + 164.6 = 488.8 \text{ kips} \leq 0.25(8)(26.5)(28.52) = 1,511.6 \text{ kips OK}$$

Using the above procedures, the transverse reinforcement can be determined at increments along the entire length of the beam.

9.7.12 INTERFACE SHEAR TRANSFER

Because there is no cast-in-place composite deck, calculations for interface shear transfer are not required.

9.7.13 MINIMUM LONGITUDINAL REINFORCEMENT REQUIREMENT

Longitudinal reinforcement should be proportioned so that at each section the following equation is satisfied:

$$A_{ps} f_{ps} + A_s f_y \geq \frac{M_u}{d_v \phi_f} + 0.5 \frac{N_u}{\phi_c} + \left(\left| \frac{V_u}{\phi_v} - V_p \right| - 0.5V_s \right) \cot \theta \quad [\text{LRFD Eq. 5.8.3.5-1}]$$

Where

A_{ps} = area of prestressing strand at the tension side of the section, in.²

f_{ps} = average stress in prestressing strand at the time for which the nominal resistance is required, ksi

A_s = area of nonprestressed tension reinforcement, in.²

f_y = specified yield strength of reinforcing bars, ksi

DOUBLE-TEE BEAM (NEXT 36 D), SINGLE SPAN, NONCOMPOSITE SURFACE**9.7.13 Minimum Longitudinal Reinforcement Requirement/9.7.13.1 Required Reinforcement at Face of Bearings**

- M_u = factored moment at the section corresponding to the factored shear force, ft-kips
 d_v = effective shear depth, in.
 ϕ = resistance factor as appropriate for moment, shear, and axial resistance. Therefore, different ϕ factors will be used for the terms in LRFD Equation (5.8.3.5-1), depending on the type of action being considered
 N_u = applied factored axial force, kips
 V_u = factored shear force at section, kips
 V_p = component in the direction of the applied shear of the effective prestressing force, kips
 V_s = shear resistance provided by shear reinforcement, kips
 θ = angle of inclination of diagonal compressive stresses

9.7.13.1 Required Reinforcement at Face of Bearing

[LRFD Art.5.8.3.5]

For simple end supports, the longitudinal reinforcement on the flexural tension side of the member at inside face of bearing should satisfy:

$$A_{ps}f_{ps} + A_s f_y \geq \left(\frac{V_u}{\phi_v} - 0.5V_s - V_p \right) \cot \theta \quad \text{[LRFD Eq.5.8.3.5-2]}$$

$$M_u = 0 \text{ ft-kips}$$

$$N_u = 0 \text{ kips}$$

Because the width of the bearing is not yet determined, it is assumed to be zero. This assumption is conservative for these calculations. Thus, the failure crack assumed for this analysis radiates from the centerline of the bearing, 6 in. from the end of the beam.

From **Tables 9.7.4-1 and 9.7.4-2** using load combination, Strength I, the factored shear force at this section is:

$$V_u = 1.25(66.4 + 2.7 + 4.8) + 1.50(11.6) + 1.75(74.8 + 22.6) = 280.2 \text{ kips} \quad \text{(Tables 9.7.4-1 and 9.7.4-2)}$$

$$\left(\frac{V_u}{\phi_v} - 0.5V_s - V_p \right) \cot \theta = \left(\frac{280.2}{0.9} - 0.5(164.6) - 0.0 \right) \cot 29^\circ = 413.2 \text{ kips}$$

As shown in **Figure 9.7.13.1-1**, the assumed crack plane crosses the centroid of the 32 bonded strands at a distance of $(6 + 6.00 \cot 29^\circ = 16.82 \text{ in.})$ from the end of the beam. Since the transfer length is 36 in. from the end of the beam (60 times the strand diameter), the available prestress from the 32 bonded strands is a fraction of the effective prestress, f_{pe} , in these strands. Note: 32 effective strands, and $y_{bc} = y_{bs} = 6.00 \text{ in.}$ comes from Section 9.7.11.1.

Therefore, the available prestress force is:

$$A_{ps}f_{ps} + A_s f_y = \left[(32)(0.217) \left((171.5) \frac{16.82}{36} \right) \right] + 0 = 556.4 \text{ kips} > 413.2 \text{ kips} \quad \text{OK}$$

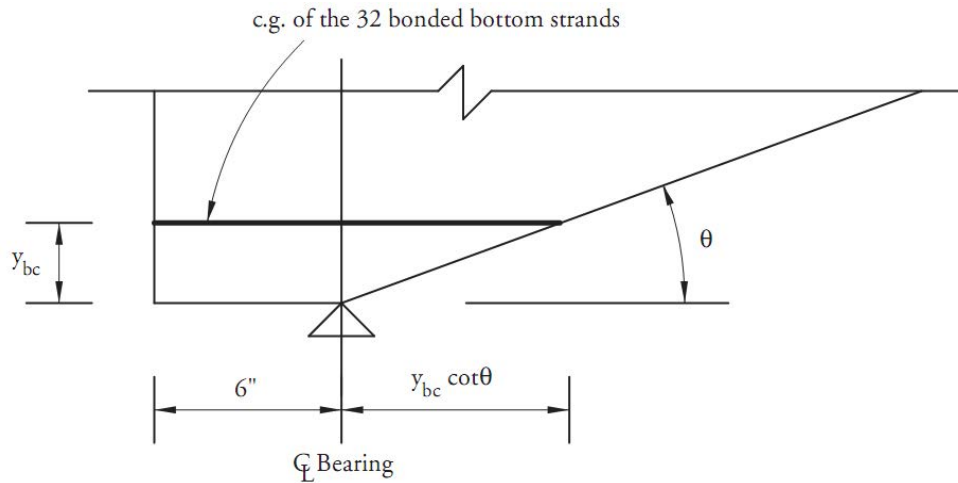
No additional reinforcement is required.

Note: An alternative approach for the calculation of available prestressing force excluding the gains from deck shrinkage is illustrated in Section 9.6.13.1.

DOUBLE-TEE BEAM (NEXT 36 D), SINGLE SPAN, NONCOMPOSITE SURFACE

9.7.13.1 Required Reinforcement at Face of Bearings/9.7.15.1 Deflection Due to Prestressing Force at Transfer

Figure 9.7.13.1-1
Assumed Failure Crack



9.7.14 PRETENSIONED ANCHORAGE ZONE

[LRFD Art. 5.10.10]

9.7.17.1 Anchorage Zone Reinforcement

Design of the anchorage zone reinforcement is computed using the force in the strands just prior to transfer. Since four strands are debonded at the ends of the beam, the force in the remaining strands before transfer is:

$$P_{pi} = 36(0.217)(202.5) = 1,582 \text{ kips}$$

The bursting resistance, P_r , should not be less than 4.0% of P_{pi} .

$$P_r = f_s A_s \geq 0.04 P_{pi} = 0.04(1,582) = 63.3 \text{ kips}$$

where

A_s = total area of vertical reinforcement located within a distance $h/4$ from the end of the beam, in.²

f_s = stress in steel, but not taken greater than 20 ksi

Solving for the required area of steel, $A_s = 63.3/20 = 3.17 \text{ in.}^2$

At least 3.17 in.² of vertical transverse reinforcement should be provided within a distance of ($h/4 = 36/4 = 9.0$ in.) from the end of the beam.

Use four No. 4 four-leg bars at 2 in. spacing starting at 2 in. from the end of the beam

The provided $A_s = 4(4)(0.20) = 3.20 \text{ in.}^2 > 3.17 \text{ in.}^2$ OK

9.7.14.2 Confinement Reinforcement

[LRFD Art. 5.10.10.2]

For a distance of $1.5h = 1.5(36) = 54$ in., from the end of the beam, reinforcement is placed to confine the prestressing steel in the bottom flange. The reinforcement may not be less than No. 3 deformed bars with spacing not exceeding 6 in. The reinforcement should be of a shape that will confine (enclose) the strands.

9.7.15 DEFLECTION AND CAMBER

[LRFD Art. 5.7.3.6.2]

Deflections are calculated using the modulus of elasticity of concrete calculated in Section 9.7.3.1 and gross section properties of the precast beam.

9.7.15.1 Deflection Due to Prestressing Force at Transfer

Force per strand after transfer = 41.5 kips

$$\Delta_p = \frac{P_{pt} e_c L^2}{8 E_{ci} I_g}$$

DOUBLE-TEE BEAM (NEXT 36 D), SINGLE SPAN, NONCOMPOSITE SURFACE**9.7.15.1 Deflection Due to Prestressing Force at Transfer/9.7.15.3 Deflection Due to Joint Concrete, Barrier, and Wearing Surface Weights**

where

Δ_p = camber due to prestressing force at transfer, in.

P_{pt} = total prestressing force after transfer = $40(41.5) = 1,660.0$ kips

e_c = eccentricity of prestressing force at midspan = 15.10 in.

L = overall beam length = 81.0 ft

E_{ci} = modulus of elasticity at transfer = 4,696 ksi

I_g = moment of inertia of the noncomposite precast beam = 179,629 in.⁴

$$\Delta_p = \frac{1,660.0(15.10)(81 \times 12)^2}{(8)(4,696)(179,629)} = 3.51 \text{ in. } \uparrow$$

9.7.15.2 Deflection Due to Beam Self Weight

$$\Delta_g = \frac{5w_g L^4}{384E_{ci}I_g}$$

where

Δ_g = deflection due to beam self weight, in.

w_g = beam self weight = 1.661 kips/ft

E_{ci} = modulus of elasticity of precast beam at transfer = 4,696 ksi

I_g = moment of inertia of the noncomposite precast beam = 179,629 in.⁴

L = beam length = 81.0 ft at transfer = 80.0 ft at erection

Deflection due to beam self weight after transfer:

$$\Delta_g = \frac{5 \left(\frac{1.661}{12} \right) (81 \times 12)^4}{(384)(4,696)(179,629)} = 1.91 \text{ in. } \downarrow$$

Deflection due to beam self weight used to compute deflection at erection:

$$\Delta_g = \frac{5 \left(\frac{1.661}{12} \right) (80 \times 12)^4}{(384)(4,696)(179,629)} = 1.81 \text{ in. } \downarrow$$

9.7.15.3 Deflection Due to Joint Concrete, Barrier, and Wearing Surface Weights

$$\Delta_{j+b+ws} = \frac{5(w_j + w_b + w_{ws})L^4}{384E_c I_g}$$

where

Δ_{j+b+ws} = deflection due to joint concrete, barrier, and wearing surface weights, in.

w_j = joint concrete weight = 0.067 kips/ft

w_b = barrier weight = 0.120 kips/ft

w_{ws} = wearing surface weight = 0.289 kips/ft

L = design span = 80.0 ft

E_c = modulus of elasticity of precast beam at service loads = 5,422 ksi

I_g = moment of inertia of the noncomposite precast beam = 179,629 in.⁴

$$\Delta_{j+b+ws} = \frac{5 \left(\frac{0.067 + 0.120 + 0.289}{12} \right) (80 \times 12)^4}{(384)(5,422)(179,629)} = 0.45 \text{ in. } \downarrow$$

DOUBLE-TEE BEAM (NEXT 36 D), SINGLE SPAN, NONCOMPOSITE SURFACE

9.7.15.4 Deflection and Camber Summary/9.7.15.5 Deflection Due to Live Load and Impact

9.7.15.4 Deflection and Camber SummaryAt transfer, $(\Delta_p + \Delta_g) = 3.51 - 1.91 = 1.60$ in. \uparrow Total deflection at erection, using PCI multipliers (see *PCI Design Handbook*)

$$= 1.8(3.51) - 1.85(1.81) = 2.97 \text{ in. } \uparrow$$

Long-Term Deflection:

LRFD Article 5.7.3.6.2 states that the long-time deflection may be taken as the instantaneous deflection multiplied by a factor of 4.0, if the instantaneous deflection is based on the gross moment of inertia. However, a factor of 4.0 is not appropriate for this type of precast construction. Therefore, it is recommended that the designer follow the guidelines of the owner agency for which the bridge is being designed, or undertake a more rigorous, time-dependent analysis.

9.7.15.5 Deflection Due to Live Load and Impact

Live load deflection limit (optional) = Span/800

[LRFD Art.2.5.2.6.2]

$$= \left(80 \times \frac{12}{800}\right) = 1.20 \text{ in.}$$

If the owner invokes the optional live load deflection criteria specified in Art. 2.5.2.6.2, the deflection is the greater of:

- that resulting from the design truck plus impact, Δ_{LT} , or
- that resulting from 25% of the design truck plus impact, Δ_{LT} , taken together with the design lane load, Δ_{LL} .

Note: LRFD Article 2.5.2.6.2 states that the dynamic load allowance be included in the calculations for live load deflection.

The *LRFD Specifications* state that all beams should be assumed to deflect equally under the applied live load and impact.

[LRFD Art. 2.5.2.6.2]

Therefore, the distribution factor for deflection, DFD , is calculated as follows:

$$DFD = (\text{number of lanes/number of beams})$$

[LRFD Art. C2.5.2.6.2]

$$= 3/5 = 0.60 \text{ lanes/beam}$$

However, it is more conservative to use the distribution factor for moment, DFM .

Deflection due to lane load:

$$\text{Design lane load, } w = 0.64 \text{ } DFM = 0.64(0.670) = 0.429 \text{ kips/ft/beam}$$

$$\Delta_{LL} = \frac{5wL^4}{384E_cI_g} = \frac{5\left(\frac{0.429}{12}\right)(80 \times 12)^4}{(384)(5,422)(179,629)} = 0.41 \text{ in. } \downarrow$$

Deflection due to Design Truck Load and Impact:

To obtain the maximum moment and deflection at midspan due to truck load, let the centerline of the beam coincide with the middle point of the distance between the inner 32-kip axle and the resultant of the truck load, as shown in **Figure 9.7.15.5-1**.

Using the elastic moment area or influence lines, deflection at midspan is:

$$\Delta_{LT} = (1.258)(IM)(DFM) = (1.258)(1.33)(0.670) = 1.12 \text{ in. } \downarrow$$

Therefore, live load deflection is the greater of:

$$\Delta_{LT} = 1.12 \text{ in. (Controls)}$$

$$0.25\Delta_{LT} + \Delta_{LL} = 0.25(1.12) + 0.41 = 0.69 \text{ in. } \downarrow$$

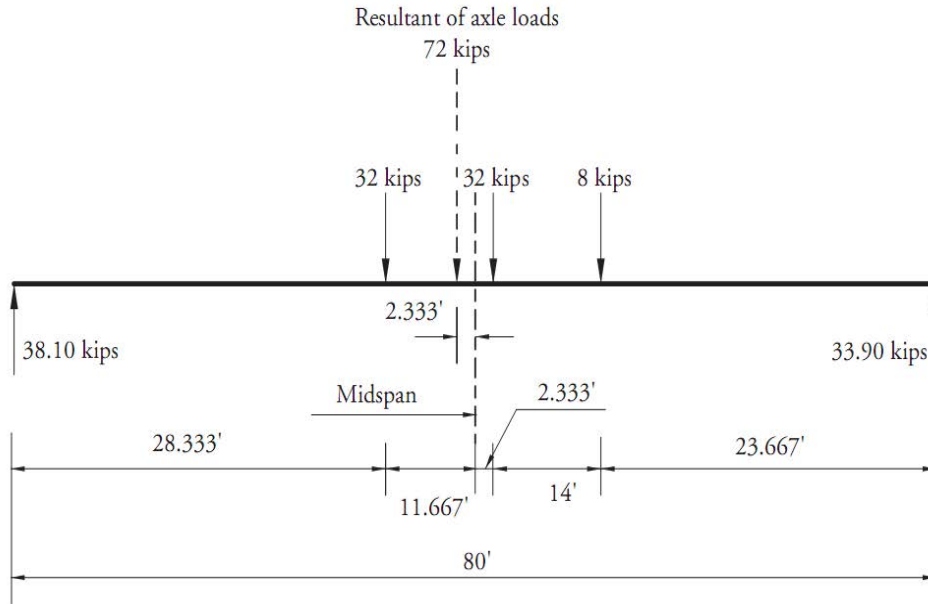
Therefore, live load deflection = 1.12 in. < allowable deflection = 1.20 in. OK

DOUBLE-TEE BEAM (NEXT 36 D), SINGLE SPAN, NONCOMPOSITE SURFACE

9.7.15.5 Deflection Due to Live Load and Impact/9.7.16 Transverse Post-Tensioning

Figure 9.7.15.5-1

Design Truck Axle Load Position for Maximum Bending Moment



9.7.16 TRANSVERSE POST-TENSIONING

Article C4.6.2.2.1 in the *LRFD Specifications* states that for bridge Type (i), the structure acts as a monolithic unit if sufficiently interconnected. To satisfy this requirement, the *LRFD Specifications* recommends that a minimum average traverse prestress of 0.250 ksi be used. However, definition of the contact area for the post-tensioning is unclear. LRFD Article 5.14.4.3.3c states that the compressed depth of the joint shall not be less than 7.0 in. for shear-flexure joints that are required to provide full continuity and monolithic behavior of the deck. In this example, the contact area is the 8-in.-thick flange. The post-tensioning force required is:

$$0.250(8)(12) = 24 \text{ kips/ft}$$

According to common practice, post-tensioning ducts incorporating four seven-wire strands are used for applications such as these. Therefore, **use four 270 ksi, 0.6-in.-diameter seven wire strands per duct**. Assume the effective prestress to be 55% of the ultimate strength of the strand.

$$P_{eff} = 4(0.217)(0.55)(270) = 128.9 \text{ kips/duct}$$

$$\text{Spacing between ducts} = 128.9/(24) = 5.37 \text{ ft between ducts} \quad \text{OK}$$

Use 5.00 ft between ducts

Total provided post-tensioning force

$$= 128.9 \text{ kips/duct} > \text{required post-tensioning force} = 5.00(24) = 120 \text{ kips/duct} \quad \text{OK}$$

The concrete stress due to the effective post-tensioning force is:

$$128.9/(8)(5.0 \times 12) = 0.269 \text{ ksi} > 0.250 \text{ ksi} \quad \text{OK}$$

DOUBLE-TEE BEAM (NEXT 36 F), SINGLE SPAN, COMPOSITE DECK

Transformed Sections, Shear General Procedure, Refined Losses

Table of Contents

9.8.1 INTRODUCTION9.8 - 5

 9.8.1.1 Terminology.....9.8 - 5

9.8.2 MATERIALS9.8 - 5

9.8.3 CROSS-SECTION PROPERTIES FOR A TYPICAL INTERIOR BEAM9.8 - 6

 9.8.3.1 Noncomposite, Nontransformed, Beam Section9.8 - 6

 9.8.3.2 Composite Section.....9.8 - 7

 9.8.3.2.1 Effective Flange Width9.8 - 7

 9.8.3.2.2 Modular Ratio between Slab and Beam Concrete.....9.8 - 7

 9.8.3.2.3 Transformed Section Properties9.8 - 7

9.8.4 SHEAR FORCES AND BENDING MOMENTS9.8 - 9

 9.8.4.1 Shear Forces and Bending Moments Due to Dead Loads9.8 - 9

 9.8.4.1.2 Unfactored Shear Forces and Bending Moments.....9.8 - 10

 9.8.4.2 Shear Forces and Bending Moments Due to Live Loads9.8 - 10

 9.8.4.2.1 Live Loads.....9.8 - 10

 9.8.4.2.2 Live Load Distribution Factors for a Typical Interior Beam9.8 - 10

 9.8.4.2.2.1 Distribution Factor for Bending Moments **9.8 - 10**

 9.8.4.2.2.2 Distribution Factor for Shear Force **9.8 - 11**

 9.8.4.2.3 Dynamic Allowance9.8 - 12

 9.8.4.2.4 Unfactored Shear Forces and Bending Moments.....9.8 - 12

 9.8.4.2.4.1 Due to Truck Load; V_{LT} and M_{LT} **9.8 - 12**

 9.8.4.2.4.2 Due To Design Lane Load; V_{LL} and M_{LL} **9.8 - 13**

 9.8.4.3 Load Combinations.....9.8 - 13

9.8.5 ESTIMATE REQUIRED PRESTRESS9.8 - 15

 9.8.5.1 Service Load Stresses at Midspan9.8 - 15

 9.8.5.2 Stress Limits for Concrete.....9.8 - 15

 9.8.5.3 Required Number of Strands.....9.8 - 15

 9.8.5.4 Strand Pattern.....9.8 - 16

 9.8.5.5 Steel Transformed Section Properties9.8 - 16

9.8.6 PRESTRESS LOSSES.....9.8 - 18

 9.8.6.1 Elastic Shortening.....9.8 - 18

 9.8.6.2 Time-Dependent Losses between Transfer and Deck Placement.....9.8 - 19

 9.8.6.2.1 Shrinkage of Concrete9.8 - 19

 9.8.6.2.2 Creep of Concrete9.8 - 20

 9.8.6.2.3 Relaxation of Prestressing Strands.....9.8 - 20

 9.8.6.3 Time-Dependent Losses between Deck Placement and Final Time9.8 - 20

 9.8.6.3.1 Shrinkage of Concrete9.8 - 20

 9.8.6.3.2 Creep of Concrete9.8 - 21

 9.8.6.3.3 Relaxation of Prestressing Strands.....9.8 - 22

 9.8.6.3.4 Shrinkage of Deck Concrete9.8 - 22

DOUBLE-TEE BEAM (NEXT 36 F), SINGLE SPAN, COMPOSITE DECK

Transformed Sections, Shear General Procedure, Refined Losses

Table of Contents

9.8.6.4 Total Time-Dependent Loss 9.8 - 23

9.8.6.5 Total Losses at Transfer 9.8 - 23

9.8.6.6 Total Losses at Service Loads 9.8 - 23

9.8.7 CONCRETE STRESSES AT TRANSFER 9.8 - 24

9.8.7.1 Stress Limits for Concrete [LRFD Art. 5.9.4] 9.8 - 24

9.8.7.2 Stresses at Transfer Length Section 9.8 - 24

9.8.7.3 Stresses at Transfer Length Section of Debonded Strands 9.8 - 26

9.8.7.4 Stresses at Midspan 9.8 - 26

9.8.7.5 Summary of Stresses at Transfer 9.8 - 26

9.8.8 CONCRETE STRESSES AT SERVICE LOADS 9.8 - 27

9.8.8.1 Stress Limits for Concrete 9.8 - 27

9.8.8.2 Stresses at Midspan 9.8 - 27

9.8.8.3 Fatigue Stress Limit 9.8 - 28

9.8.8.4 Summary of Stresses at Midspan at Service Loads 9.8 - 28

9.8.8.5 Effect of Deck Shrinkage 9.8 - 28

9.8.9 STRENGTH LIMIT STATE 9.8 - 28

9.8.10 LIMITS OF REINFORCEMENT 9.8 - 30

9.8.10.1 Maximum Reinforcement 9.8 - 30

9.8.10.2 Minimum Reinforcement 9.8 - 31

9.8.11 SHEAR DESIGN 9.8 - 31

9.8.11.1 Critical Section 9.8 - 32

9.8.11.2 Contribution of Concrete to Nominal Shear Resistance 9.8 - 33

9.8.11.2.1 Strain in Flexural Tension Reinforcement 9.8 - 33

9.8.11.2.2 Values of β and θ 9.8 - 33

9.8.11.2.3 Compute Concrete Contribution 9.8 - 34

9.8.11.3 Contribution of Reinforcement to Nominal Shear Resistance 9.8 - 34

9.8.11.3.1 Requirement for Reinforcement 9.8 - 34

9.8.11.3.2 Required Area of Reinforcement 9.8 - 34

9.8.11.3.3 Determine Spacing of Reinforcement 9.8 - 34

9.8.11.4 Maximum Nominal Shear Resistance 9.8 - 35

9.8.12 INTERFACE SHEAR TRANSFER 9.8 - 35

9.8.12.1 Factored Horizontal Shear 9.8 - 35

9.8.12.2 Required Nominal Resistance 9.8 - 35

9.8.12.3 Required Interface Shear Reinforcement 9.8 - 35

9.8.12.3.1 Required Interface Shear Reinforcement 9.8 - 36

9.8.12.4 Maximum Nominal Shear Resistance 9.8 - 36

9.8.13 MINIMUM LONGITUDINAL REINFORCEMENT REQUIREMENT 9.8 - 37

9.8.13.1 Required Reinforcement at Face of Bearing 9.8 - 37

9.8.14 PRETENSIONED ANCHORAGE ZONE 9.8 - 38

DOUBLE-TEE BEAM (NEXT 36 F), SINGLE SPAN, COMPOSITE DECK

Transformed Sections, Shear General Procedure, Refined Losses

Table of Contents

9.8.14.1 Anchorage Zone Reinforcement..... 9.8 - 38

9.8.14.2 Confinement Reinforcement..... 9.8 - 39

9.8.15 DEFLECTION AND CAMBER 9.8 - 39

9.8.15.1 Deflection Due to Prestressing Force at Transfer 9.8 - 39

9.8.15.2 Deflection Due to Beam Self Weight..... 9.8 - 39

9.8.15.3 Deflection Due to Slab and Haunch Weights 9.8 - 40

9.8.15.4 Deflection Due to Barrier and Future Wearing Surface Weights 9.8 - 40

9.8.15.5 Deflection and Camber Summary..... 9.8 - 40

9.8.15.6 Deflection Due to Live Load and Impact..... 9.8 - 40

This page intentionally left blank

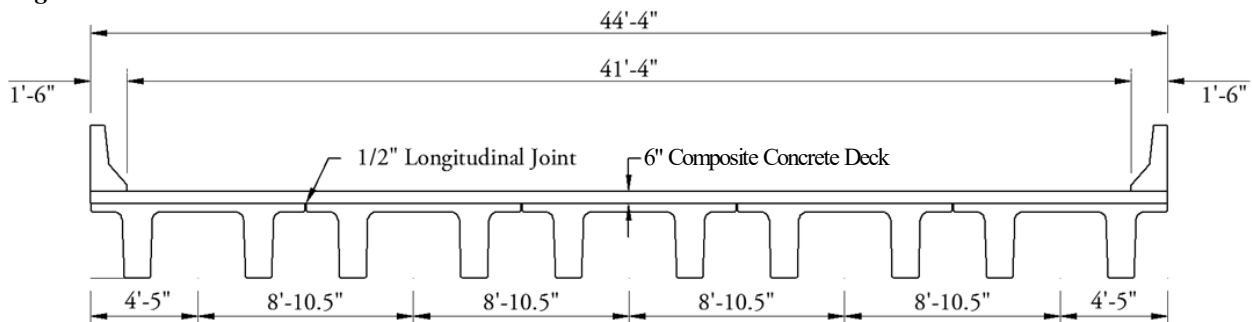
DOUBLE-TEE BEAM (NEXT 36 F), SINGLE SPAN, COMPOSITE DECK

9.8 Transformed Sections, Shear General Procedure, Refined Losses/9.8.2 Materials

9.8 Transformed Sections, Shear General Procedure, Refined Losses**9.8.1 INTRODUCTION**

This design example demonstrates the design of an 80-ft, single span, PCI Northeast Extreme Double-Tee bridge with no skew. This example illustrates in detail the design of a typical interior beam at the critical sections in positive flexure, shear, and deflection due to prestress, dead loads, and live load. The superstructure consists of five beams spaced at 8-ft 10½-in. centers, as shown in **Figure 9.8.1-1**. Beams are designed to act compositely with the 6-in.-thick cast-in-place concrete deck to resist all superimposed dead loads, live loads, and impact. A ½-in.-thick wearing surface is considered to be an integral part of the 6-in.-thick deck. Design live load is HL-93. The design is accomplished in accordance with *AASHTO LRFD Bridge Design Specifications*, Fifth Edition, 2010, and the 2011 Interim Revisions. Elastic stresses from external loads are calculated using transformed sections. Shear strength is calculated using the general procedure. Time-dependent prestress losses are calculated using the refined estimates.

Figure 9.8.1-1
Bridge Cross Section

**9.8.1.1 Terminology**

The following terminology is used to describe cross sections in this design example:

noncomposite section—the concrete beam cross section.

noncomposite nontransformed section—the concrete beam cross section without the strands transformed. Also called the gross section.

noncomposite transformed section—the concrete beam cross section with the strands transformed to provide cross-sectional properties equivalent to the beam concrete.

composite section—the concrete beam plus the concrete deck and haunch.

composite nontransformed section—the concrete beam plus the concrete deck and haunch transformed to provide cross-sectional properties equivalent to the beam concrete but without the strands transformed.

composite transformed section—the concrete beam plus the concrete deck and haunch and the strands transformed to provide cross-sectional properties equivalent to the beam concrete.

The term "composite" implicitly includes the transformation of the concrete deck and haunch.

The term "transformed" generally refers to transformation of the strands.

9.8.2 MATERIALS

Cast-in-place concrete slab: Actual thickness = 6.0 in.

Structural thickness, $t_s = 5.5$ in.

Note that a ½-in.-thick wearing surface is considered to be an integral part of the 6-in.-thick deck.

Specified concrete compressive strength for use in design, $f'_c = 4.0$ ksi

DOUBLE-TEE BEAM (NEXT 36 F), SINGLE SPAN, COMPOSITE DECK

9.8.2 Materials/9.8.3 Cross-Section Properties for a Typical Interior Beam

Precast concrete beams: PCI Northeast Double-Tee Beams, Type NEXT 36 F as shown in **Figure 9.8.2-1**

- Required concrete compressive strength at transfer, $f'_{ci} = 6.0$ ksi
- Specified concrete compressive strength for use in design, $f'_c = 8.0$ ksi
- Concrete unit weight, $w_c = 0.150$ kcf
- Overall beam length = 81.0 ft
- Design span = 80.0 ft

Prestressing strands: 0.6-in.-dia., seven-wire, low-relaxation

- Area of one strand = 0.217 in.²
- Specified tensile strength, $f_{pu} = 270.0$ ksi
- Yield strength, $f_{py} = 0.9f_{pu} = 243.0$ ksi [LRFD Table 5.4.4.1-1]
- Stress limits for prestressing strands: [LRFD Table 5.9.3-1]
 - before transfer, $f_{pi} \leq 0.75f_{pu} = 202.5$ ksi
 - at service limit state (after all losses), $f_{pe} \leq 0.8f_{py} = 194.4$ ksi
- Modulus of elasticity, $E_p = 28,500$ ksi [LRFD Table 5.4.4.2]

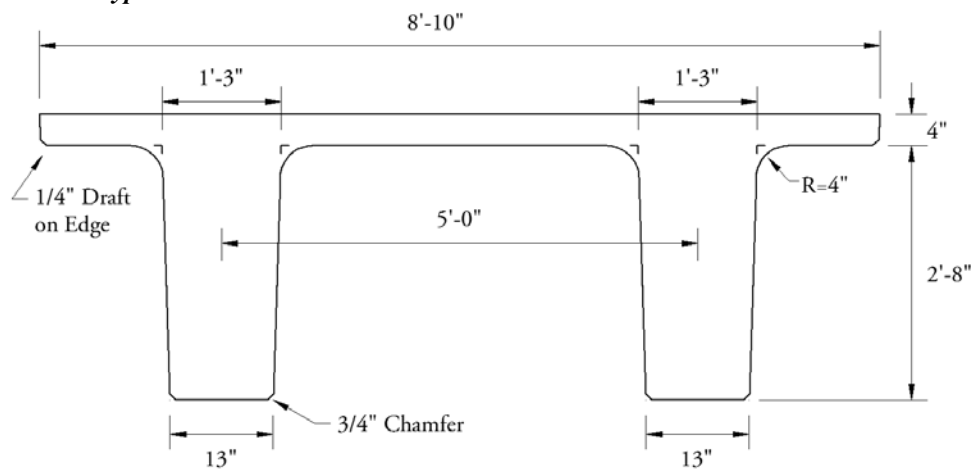
Reinforcing bars:

- Yield strength, $f_y = 60.0$ ksi
- Modulus of elasticity, $E_s = 29,000$ ksi [LRFD Art. 5.4.3.2]

Future wearing surface: 2 in. additional concrete, unit weight = 0.150 kcf

New Jersey-type barrier: unit weight = 0.300 kips/ft/side

Figure 9.8.2-1
PCI Double-Tee Beam Type NEXT 36 F



9.8.3 CROSS-SECTION PROPERTIES FOR A TYPICAL INTERIOR BEAM

9.8.3.1 Noncomposite, Nontransformed, Beam Section

- A_g = area of cross section of precast beam = 1,330 in.²
- h = overall depth of precast beam = 36 in.
- I_g = moment of inertia about the centroid of the noncomposite precast beam = 166,569 in.⁴
- y_b = distance from centroid to the extreme bottom fiber of the noncomposite precast beam = 22.13 in.
- y_t = distance from centroid to the extreme top fiber of the noncomposite precast beam = 13.87 in.

DOUBLE-TEE BEAM (NEXT 36 F), SINGLE SPAN, COMPOSITE DECK**9.8.3.1 Noncomposite, Nontransformed, Beam Section/9.8.3.2.3 Transformed Section Properties**

S_b = section modulus for extreme bottom fiber of the noncomposite precast beam = $I_g/y_b = 7,527 \text{ in.}^3$

S_t = section modulus for extreme top fiber of the noncomposite precast beam = $I_g/y_t = 12,009 \text{ in.}^3$

w_g = beam weight per unit length $(1,330/144)(0.150) = 1.385 \text{ kips/ft}$

E_c = modulus of elasticity, ksi = $33,000K_1(w_c)^{1.5}\sqrt{f'_c}$ [LRFD Eq. 5.4.2.4-1]

where

K_1 = correction factor for source of aggregate taken as 1.0

w_c = unit weight of concrete = 0.150 kcf

LRFD Table 3.5.1-1 states that, in the absence of more precise data, the unit weight of concrete may be taken as $0.140 + 0.001f'_c$ for $5.0 < f'_c \leq 15.0$ ksi. For $f'_c = 8.0$ ksi, the unit weight would be 0.1480 kcf. However, precast concrete mixes typically have a relatively low water-cementitious materials ratio and high density. Therefore, a unit weight of 0.150 kcf is used in this example. For high-strength concrete, this value may need to be increased based on test results. For simplicity, a value of 0.150 kcf is also used for the cast-in-place concrete.

f'_c = specified compressive strength of concrete, ksi

Therefore, the modulus of elasticity for:

cast-in-place slab, $E_c = 33,000(1.00)(0.150)^{1.5}\sqrt{4.0} = 3,834 \text{ ksi}$

precast beam at transfer, $E_{ci} = 33,000(1.00)(0.150)^{1.5}\sqrt{6.0} = 4,696 \text{ ksi}$

precast beam at service loads, $E_c = 33,000(1.00)(0.150)^{1.5}\sqrt{8.0} = 5,422 \text{ ksi}$

9.8.3.2 Composite Section**9.8.3.2.1 Effective Flange Width**

[LRFD Eq. 4.6.2.6.1]

Effective flange width is taken as the tributary width perpendicular to the axis of the beam. For the interior beam, the effective flange width is calculated as one-half the distance to the adjacent beam on each side.

$$106.0 + 0.25 + 0.25 = 106.5 \text{ in.}$$

Therefore, the effective flange width is 106.5 in.

9.8.3.2.2 Modular Ratio between Slab and Beam Concrete

$$\text{Modular ratio between slab and beam concrete, } n = \frac{E_c(\text{slab})}{E_c(\text{beam})} = \frac{3,834}{5,422} = 0.7071$$

9.8.3.2.3 Transformed Section Properties

The effective flange width must be transformed by the modular ratio to provide cross-sectional properties equivalent to the beam concrete.

$$\text{Transformed flange width} = n(\text{Effective flange width}) = (0.7071)(106.5) = 75.31 \text{ in.}$$

$$\begin{aligned} \text{Transformed flange area} &= n(\text{Effective flange width})(t_s) \\ &= (0.7071)(106.5)(5.5) = 414.18 \text{ in.}^2 \end{aligned}$$

$$\text{Transformed flange moment of inertia} = (75.31)(5.5)^3/12 = 1,044.14 \text{ in.}^4$$

Note: Only the structural thickness of the deck, 5.5 in., is considered.

Due to camber of the precast, prestressed beam, a minimum haunch thickness of ½ in. at midspan is considered in the structural properties of the composite section. Also, the width of haunch must be transformed by the modular ratio.

$$\text{Transformed width of haunch} = (0.7071)(106) = 74.95 \text{ in.}$$

$$\text{Transformed area of haunch} = (0.7071)(106)(0.5) = 37.48 \text{ in.}^2$$

$$\text{Transformed moment of inertia of haunch} = (74.95)(0.5)^3/12 = 0.78 \text{ in.}^4$$

DOUBLE-TEE BEAM (NEXT 36 F), SINGLE SPAN, COMPOSITE DECK

9.8.3.2.3 Transformed Section Properties

Note that the haunch should only be considered to contribute to section properties if it is required to be provided in the completed structure. Therefore, some designers neglect its contribution to the section properties.

Figure 9.8.3.2.3-1

Dimensions of the Composite Section

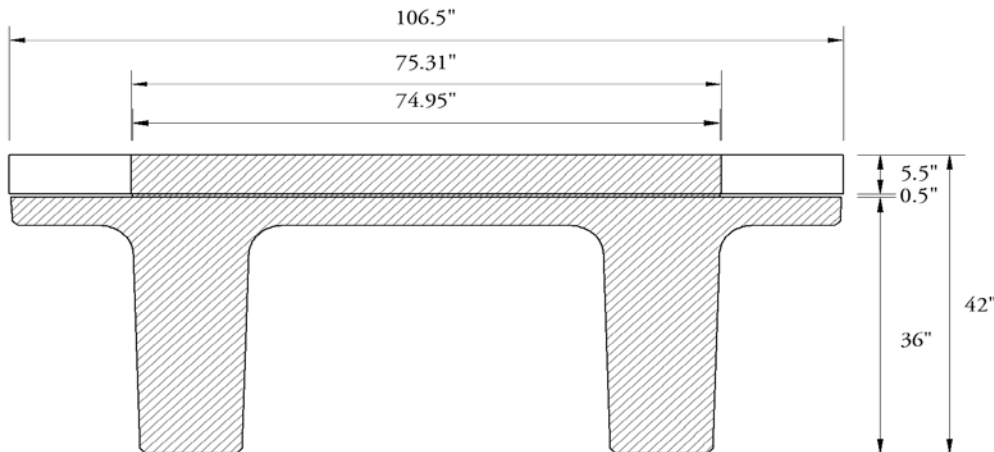


Table 9.8.3.2.3-1

Dimensions of the Composite Section

	Area, in. ²	y_b in.	$A y_b$ in. ³	$A(y_{bc} - y_b)^2$ in. ⁴	I in. ⁴	$I + A(y_{bc} - y_b)^2$ in. ⁴
Beam	1,330.00	22.13	29,433	24,363	166,569	190,932
Haunch	37.48	36.25	1,359	3,629	0.78	3,630
Deck	414.18	39.25	16,257	68,284	1,044	69,328
Σ	1,781.7		47,049			263,890

A_c = total area of the composite section = 1,782 in.

h_c = overall depth of the composite section = 42.00 in.

I_c = moment of inertia of the composite section = 263,890 in.⁴

y_{bc} = distance from the centroid of the composite section to the extreme bottom fiber of the precast beam = 47,049/1,781.7 = 26.41 in.

y_{tg} = distance from the centroid of the composite section to the extreme top fiber of the precast beam = 36.00 – 26.41 = 9.59 in.

y_{tc} = distance from the centroid of the composite section to the extreme top fiber of the structural deck = 42.00 – 26.41 = 15.59 in.

S_{bc} = composite section modulus for the extreme bottom fiber of the precast beam

$$= (I_c/y_{bc}) = \frac{263,890}{26.41} = 9,992 \text{ in.}^3$$

S_{tg} = composite section modulus for the extreme top fiber of the precast beam

$$= (I_c/y_{tg}) = \frac{263,890}{9.59} = 27,517 \text{ in.}^3$$

S_{tc} = composite section modulus for extreme top fiber of the structural deck slab

$$= \left(\frac{1}{n}\right)(I_c/y_{tc}) = \left(\frac{1}{0.7071}\right)\left(\frac{263,890}{15.59}\right) = 23,938 \text{ in.}^3$$

DOUBLE-TEE BEAM (NEXT 36F), SINGLE SPAN, COMPOSITE DECK**9.8.4 Shear Forces and Bending Moments/9.8.4.1.1 Dead Loads****9.8.4 SHEAR FORCES AND BENDING MOMENTS**

The self weight of the beam and the weight of the deck and haunch act on the noncomposite, simple-span structure, while the weight of barriers, future wearing surface, and live loads with impact act on the composite, simple-span structure. Refer to **Tables 9.8.4-1** and **9.8.4-2**, which follow Section 9.8.4.3 for a summary of unfactored values calculated below.

9.8.4.1 Shear Forces and Bending Moments Due to Dead Loads**9.8.4.1.1 Dead Loads**

DC = Dead load of structural components and nonstructural attachments

[LRFD Art. 3.3.2]

Dead loads acting on the noncomposite structure:

Beam self weight, $w_g = 1.385$ kips/ft

6-in.-thick deck weight = $(6/12 \text{ ft})(106.5/12 \text{ ft})(0.150 \text{ kcf}) = 0.666$ kips/ft

½-in.-thick haunch weight = $(0.5/12 \text{ ft})(106.5/12 \text{ ft})(0.150 \text{ kcf}) = 0.055$ kips/ft

$w_s = 0.666 + 0.055 = 0.721$ kips/ft

Notes:

1. Actual deck thickness (6 in.) is used for computing dead load.
2. A ½-in. minimum haunch thickness is assumed in the computations of dead load. If a deeper haunch will be used because of final beam camber, the weight of the actual haunch should be used.
3. For this design example, the unit weight of the reinforced concrete is taken as 0.150 kcf. Some designers use a higher unit weight to account for the weight of the reinforcement.
4. The weight of cross-diaphragms is ignored since most agencies are changing from cast-in-place concrete diaphragms to lightweight steel diaphragms.

Dead loads placed on the composite structure:

LRFD Article 4.6.2.2.1 states that permanent loads (barrier and future wearing surface) may be distributed uniformly among the beams if the following conditions are met:

- Width of the deck is constant OK
- Number of beams, N_b , is not less than four ($N_b = 5$) OK
- Beams are parallel and have approximately the same stiffness OK
- The roadway part of the overhang, $d_e \leq 3.0$ ft
- $d_e = (8.83 - 5.00)/2 - 1.5 = 0.42$ ft OK
- Curvature in plan is less than specified in the *LRFD Specifications* (curvature = 0.0°) OK
- Cross section of the bridge is consistent with one of the cross sections given in LRFD Table 4.6.2.2.1-1 (similar to bridge type "k") OK

Since these criteria are satisfied, the barrier and wearing surface loads are equally distributed among the five beams.

Barrier weight = $(2 \text{ barriers})(0.300 \text{ kips/ft})/(5 \text{ beams}) = 0.120$ kips/ft/beam = w_b

DW = Dead load of 2-in. future wearing surface

= $(2/12)(0.150) = 0.025$ ksf

= $(0.025 \text{ ksf})(41.33 \text{ ft})/(5 \text{ beams}) = 0.207$ kips/ft/beam = w_{ws}

DW load should be kept separately from DC because of higher load factor is applied to it

DOUBLE-TEE BEAM (NEXT 36F), SINGLE SPAN, COMPOSITE DECK**9.8.4.1.2 Unfactored Shear Forces and Bending Moments/9.8.4.2.1 Distribution Factor for Bending Moments****9.8.4.1.2 Unfactored Shear Forces and Bending Moments**

For a simply supported beam with a span length (L) loaded with a uniformly distributed load (w), the shear force (V_x) and bending moment (M_x) at any distance (x) from the support are given by:

$$V_x = w(0.5L - x) \quad \text{(Eq. 9.8.4.1.2-1)}$$

$$M_x = 0.5wx(L - x) \quad \text{(Eq. 9.8.4.1.2-2)}$$

Using the above equations, values of shear forces and bending moments for a typical interior beam under self weight of beam, weight of slab and haunch, and weight of barriers and future wearing surface are computed and shown in **Table 9.8.4-1** that is located at the end of Section 9.8.4.3. For these calculations, the span length (L) is the design span, 80 ft. However, for calculations of stresses and deformation at the time prestress is transferred, the overall length of the precast member, 81 ft, is used as illustrated later in this example.

9.8.4.2 Shear Forces and Bending Moments Due to Live Loads**9.8.4.2.1 Live Loads**

Design live load is HL-93, which consists of a combination of: [LRFD 3.6.1.2.1]

1. Design truck or design tandem with dynamic allowance. [LRFD 3.6.1.2.2]

The design truck consists of 8.0-, 32.0-, and 32.0-kip axles with the first pair spaced at 14.0 ft and the second pair spaced at 14.0 to 30.0 ft. The design tandem consists of a pair of 25.0-kip axles spaced at 4.0 ft apart.

[LRFD Art. 3.6.1.2.3]

2. Design lane load of 0.64 kips/ft without dynamic allowance [LRFD Art. 3.6.1.2.4]

9.8.4.2.2 Live Load Distribution Factors for a Typical Interior Beam

The live load bending moments and shear forces are determined by using the simplified distribution factor formulas [LRFD Art. 4.6.2.2]. To use the simplified live load distribution factor formulas, the following conditions must be met: [LRFD Art. 4.6.2.2.1]

- Width of deck is constant OK
- Number of beams, $N_b \geq$ four ($N_b = 5$) OK
- Beams are parallel and have approximately the same stiffness OK
- The roadway part of the overhang, $d_e \leq 3.0$ ft ($d_e = 0.42$ ft) OK
- Curvature is less than specified in the *LRFD Specifications* (Curvature = 0.0°) OK

Note: The precast double-tee section with deck is not included in LRFD Table 4.6.2.2.1-1, therefore, it is analyzed as Type (k) due to similar structural behavior. [LRFD Table 4.6.2.2.1-1]

The number of design lanes is computed as:

Number of design lanes = the integer part of the ratio $w/12$, where w is the clear roadway width, in feet, between the curbs. [LRFD Art. 3.6.1.1.1]

From **Figure 9.8.1-1**, $w = 41.33$ ft

Number of design lanes = integer part of $(41.33/12) = 3$ lanes

9.8.4.2.2.1 Distribution Factor for Bending Moments

- For all limit states except fatigue limit state:

For two or more lanes loaded:

$$DFM = 0.075 + \left(\frac{S}{9.5}\right)^{0.6} \left(\frac{S}{L}\right)^{0.2} \left(\frac{K_g}{12Lt_s^3}\right)^{0.1} \quad \text{[LRFD Table 4.6.2.2.2b-1]}$$

Provided that: $3.5 \leq S \leq 16$; $S = 8.9$ ft OK

$4.5 \leq t_s \leq 12$; $t_s = 5.5$ in. OK

$20 \leq L \leq 240$; $L = 80$ ft OK

$N_b \geq 4$; $N_b = 5$ OK

$10,000 \leq K_g \leq 7,000,000$ OK (see below)

DOUBLE-TEE BEAM (NEXT 36F), SINGLE SPAN, COMPOSITE DECK

9.8.4.2.2.1 Distribution Factor for Bending Moments/9.8.4.2.2.2. Distribution Factor for Shear Force

where

 DFM = distribution factor for bending moment for interior beam S = beam spacing, ft L = beam span, ft t_s = structural depth of concrete deck, in. K_g = longitudinal stiffness parameter, in.⁴ = $n(I_g + A_g e_g^2)$ [LRFD Eq. 4.6.2.2.1-1]

where

 n = modular ratio between beam and deck slab concrete

$$= \frac{E_c(\text{beam})}{E_c(\text{slab})} = \frac{5,422}{3,834} = 1.414$$

 A_g = cross-sectional area of the precast beam (noncomposite section) = 1,330 in.² I_g = moment of inertia of the precast beam (noncomposite section) = 166,569 in.⁴ e_g = distance between the centers of gravity of the precast beam and the deck

$$= [42.00 - (5.5/2) - 22.13] = 17.12 \text{ in.}$$

Therefore,

$$K_g = 1.414[166,569 + 1330(17.12)^2] = 786,728 \text{ in.}^4$$

$$DFM = 0.075 + \left(\frac{8.9}{9.5}\right)^{0.6} \left(\frac{8.9}{80}\right)^{0.2} \left(\frac{786,728}{12.0(80)(5.5)^3}\right)^{0.1}$$

$$= 0.075 + (0.962)(0.645)(1.173) = 0.803 \text{ lanes/beam}$$

For one design lane loaded:

$$DFM = 0.06 + \left(\frac{S}{14}\right)^{0.4} \left(\frac{S}{L}\right)^{0.3} \left(\frac{K_g}{12Lt_s^3}\right)^{0.1} \quad \text{[LRFD Table 4.6.2.2.2b-1]}$$

$$= 0.06 + \left(\frac{8.9}{14}\right)^{0.4} \left(\frac{8.9}{80}\right)^{0.3} \left(\frac{786,728}{12.0(80)(5.5)^3}\right)^{0.1}$$

$$= 0.06 + (0.834)(0.517)(1.173) = 0.566 \text{ lanes/beam}$$

Thus, the case of two or more lanes loaded controls and $DFM = 0.803$ lanes/beam.

For fatigue limit state:

The *LRFD Specifications*, Art. C3.4.1, states that for Fatigue Limit State, a single design truck should be used.However, live load distribution factors given in LRFD Article 4.6.2.2 take into consideration the multiple presence factor, m . LRFD Article 3.6.1.1.2 states that the multiple presence factor, m , for one design lane loaded is 1.2.Therefore, the distribution factor for one design lane loaded with the multiple presence factor removed, should be used. The distribution factor for fatigue limit state is: $0.566/1.2 = 0.472$ lanes/beam.**9.8.4.2.2.2 Distribution Factor for Shear Force**

For two or more lanes loaded:

$$DFV = 0.2 + \left(\frac{S}{12}\right) - \left(\frac{S}{35}\right)^{2.0} \quad \text{[LRFD Table 4.6.2.2.3a-1]}$$

Provided that: $3.5 \leq S \leq 16$; $S = 8.9$ ft OK
 $4.5 \leq t_s \leq 12$; $t_s = 5.5$ in. OK
 $20 \leq L \leq 240$; $L = 80$ ft OK
 $N_b \geq 4$; $N_b = 5$ OK

DOUBLE-TEE BEAM (NEXT 36F), SINGLE SPAN, COMPOSITE DECK9.8.4.2.2 Distribution Factor for Shear Force/9.8.4.2.4.1 Due to Design Lane Load; V_{LL} and M_{LL}

where

DFV = distribution factor for shear for interior beam

S = beam spacing, ft

Therefore, the distribution factor for shear force is:

$$DFV = 0.2 + \left(\frac{8.9}{12}\right) - \left(\frac{8.9}{35}\right)^{2.0} = 0.877 \text{ lanes/beam}$$

For one design lane loaded:

$$DFV = 0.36 + \left(\frac{S}{25}\right) = 0.36 + \left(\frac{8.9}{25}\right) = 0.716 \text{ lanes/beam}$$

Thus, the case of two or more lanes loaded controls and $DFV = 0.877$ lanes/beam.

9.8.4.2.3 Dynamic Allowance

IM = 15% for fatigue limit state

[LRFD Table 3.6.2.1-1]

IM = 33% for all other limit states

where IM = dynamic allowance, applied to design truck load only

9.8.4.2.4 Unfactored Shear Forces and Bending Moments**9.8.4.2.4.1 Due to Truck Load; V_{LT} and M_{LT}**

- For all limit states except for fatigue limit state:

Shear force and bending moment envelopes on a per-lane basis are calculated at tenth-points of the span using the equations given in Chapter 8 of this manual. However, this is generally done by means of commercially available computer software that has the ability to deal with moving loads. Therefore, truck load shear forces and bending moments per beam are:

$$\begin{aligned} V_{LT} &= (\text{shear force per lane})(DFV)(1 + IM) \\ &= (\text{shear force per lane})(0.877)(1 + 0.33) \\ &= (\text{shear force per lane})(1.166) \text{ kips} \end{aligned}$$

$$\begin{aligned} M_{LT} &= (\text{bending moment per lane})(DFM)(1 + IM) \\ &= (\text{bending moment per lane})(0.803)(1 + 0.33) \\ &= (\text{bending moment per lane})(1.068) \text{ ft-kips} \end{aligned}$$

Values for V_{LT} and M_{LT} at different points are given in **Table 9.8.4-2**.

- For fatigue limit state:

Article 3.6.1.4.1 in the *LRFD Specifications* states that fatigue load is a single design truck which has the same axle weight used in all other limit states but with a constant spacing of 30.0 ft between the 32.0-kip axles. Bending moment envelope on a per-lane basis is calculated using the equation given in Chapter 8 of this manual.

Therefore, the bending moment of the fatigue truck load is:

$$\begin{aligned} M_f &= (\text{bending moment per lane})(DFM)(1 + IM) \\ &= (\text{bending moment per lane})(0.472) (1 + 0.15) \\ &= (\text{bending moment per lane})(0.543) \text{ ft-kips} \end{aligned}$$

Values of M_f at different points are given in **Table 9.8.4-2**.

DOUBLE-TEE BEAM (NEXT 36F), SINGLE SPAN, COMPOSITE DECK

9.8.4.2.4.2 Due to Design Lane Load; V_{LL} and M_{LL} /9.8.4.3 Load Combinations

9.8.4.2.4.2 Due To Design Lane Load; V_{LL} and M_{LL}

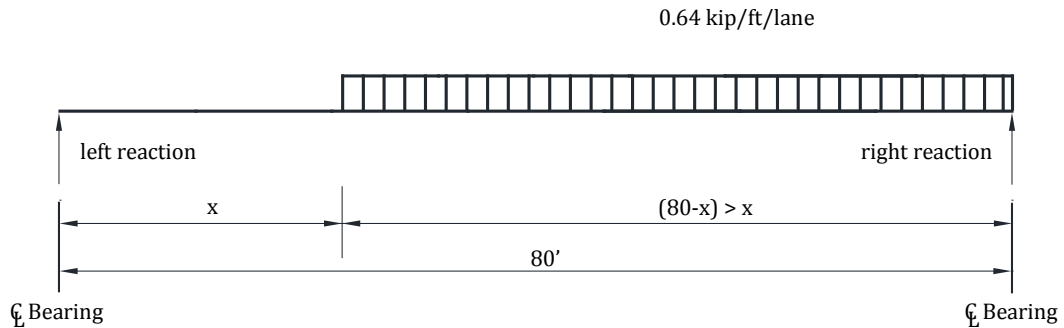
To obtain the maximum shear force at a section located at a distance (x) from the left support under a uniformly distributed load of 0.64 kips/ft, load the member to the right of the section under consideration as shown in **Figure 9.8.4.2.4.2-1**. Therefore, the maximum shear force per lane is:

$$V_x = \frac{0.32(L - x)^2}{L} \text{ for } x \leq 0.5L \tag{Eq. 9.8.4.2.4.2-1}$$

where V_x is in kips/lane and L and x are in ft

Figure 9.8.4.2.4.2-1

Maximum Shear Force due to Design Lane Load



To calculate the maximum bending moment at any sections, use Eq. (9.8.4.1.2-2).

Lane load shear force and bending moment per typical interior beam are as follows:

$$\begin{aligned} V_{LL} &= (\text{lane load shear force})(DFV) \\ &= (\text{lane load shear force})(0.877) \text{ kips} \end{aligned}$$

For all limit states except for fatigue limit state:

$$\begin{aligned} M_{LL} &= (\text{lane load bending moment})(DFM) \\ &= (\text{lane load bending moment})(0.803) \text{ ft-kips} \end{aligned}$$

Note that dynamic allowance is not applied to the design lane loading.

Values of shear forces and bending moments, V_{LL} and M_{LL} , are given in **Table 9.8.4-2**.

9.8.4.3 Load Combinations

Total factored load shall be taken as:

$$Q = \sum \eta_i \gamma_i Q_i \tag{LRFD Eq. 3.4.1-1}$$

where

η_i = a load modifier relating to ductility, redundancy, and operational importance. [LRFD Art. 1.3.2.1]
(Here, η_i is considered to be 1.0 for typical bridges.)

γ_i = load factors [LRFD Table 3.4.1-1]

Q_i = force effects from specified loads

Investigating different limit states given in LRFD Article 3.4.1, the following limit states are applicable:

Service I: check compressive stresses in prestressed concrete components:

$$Q = 1.00(DC + DW) + 1.00(LL + IM) \tag{LRFD Table 3.4.1-1}$$

This load combination is a special combination for service limit state stress and applies to all conditions other than Service III.

DOUBLE-TEE BEAM (NEXT 36F), SINGLE SPAN, COMPOSITE DECK

9.8.4.3 Load Combinations

Service III: check tensile stresses in prestressed concrete components:

$$Q = 1.00(DC + DW) + 0.80(LL + IM) \quad \text{[LRFD Table 3.4.1-1]}$$

This load combination is a special combination for service limit state stress that applies only to tension in prestressed concrete structures to control cracks.

Strength I: check ultimate strength: [LRFD Tables 3.4.1-1 and -2]

$$Q \text{ maximum} = 1.25(DC) + 1.50(DW) + 1.75(LL + IM)$$

$$Q \text{ minimum} = 0.90(DC) + 0.65(DW) + 1.75(LL + IM)$$

This load combination is the general load combination for strength limit state design.

Note: For simple-span bridges, the maximum load factors produce maximum effects. However, use minimum load factors for dead load (DC), and wearing surface (DW) when the dead load and wearing surface stresses are opposite to those of live load.

Fatigue I: check stress range in strands [LRFD Table 3.4.1-1]

$$Q = 1.50(LL + IM)$$

This load combination is a special load combination to check the tensile stress range in the strands due to live load and dynamic allowance.

Table 9.8.4-1
Unfactored Shear Forces and Bending Moments Due to Dead Loads for a Typical Interior Beam

Distance x, ft	Section x/L	Beam Weight		Slab + Haunch Weight		Barrier Weight		Wearing Surface Weight	
		Shear V_g kips	Moment M_g ft-kips	Shear V_s kips	Moment M_s ft-kips	Shear V_b kips	Moment M_b ft-kips	Shear V_{ws} kips	Moment M_{ws} ft-kips
0	0	55.4	0.0	28.8	0.0	4.8	0.0	8.3	0.0
*2.69	0.034	51.7	144.0	26.9	75.0	4.5	12.5	7.7	21.5
8	0.1	44.3	398.9	23.1	207.6	3.8	34.6	6.6	59.6
16	0.2	33.2	709.1	17.3	369.2	2.9	61.4	5.0	106.0
24	0.3	22.2	930.7	11.5	484.5	1.9	80.6	3.3	139.1
32	0.4	11.1	1,063.7	5.8	553.7	1.0	92.2	1.7	159.0
40	0.5	0.0	1,108.0	0.0	576.8	0.0	96.0	0.0	165.6

*Critical section for shear (see Section 9.8.11)

Table 9.8.4-2
Unfactored Shear Forces and Bending Moments Due to Live Loads for a Typical Interior Beam

Distance x, ft	Section x/L	Truck Load with Impact		Lane Load		Fatigue Truck with Impact
		Shear V_{LT} kips	Moment M_{LT} ft-kips	Shear V_{LL} kips	Moment M_{LL} ft-kips	Moment M_f ft-kips
0	0	74.1	0.0	22.5	0.0	0.0
*2.69	0.034	71.4	175.8	21.0	53.4	77.7
8	0.1	65.8	481.9	18.2	148.0	210.2
16	0.2	57.4	840.8	14.4	263.1	357.8
24	0.3	49.0	1,076.6	11.0	345.4	457.7
32	0.4	40.6	1,213.1	8.1	394.7	505.4
40	0.5	32.2	1,238.7	5.6	411.1	490.6

*Critical section for shear (see Section 9.8.11)

DOUBLE-TEE BEAM (NEXT 36F), SINGLE SPAN, COMPOSITE DECK

9.8.5 Estimate Required Prestress/9.8.5.3 Required Number of Strands

9.8.5 ESTIMATE REQUIRED PRESTRESS

The required number of strands is usually governed by concrete tensile stresses at the bottom fiber for load combination Service III at the section of maximum moment and in some cases at Strength I. For estimating the number of strands, only the stresses at midspan are considered.

9.8.5.1 Service Load Stresses at Midspan

Bottom tensile stress due to applied dead and live loads, using load combination III, is:

$$f_b = \frac{M_g + M_s}{S_b} + \frac{M_b + M_{ws} + (0.8)(M_{LT} + M_{LL})}{S_{bc}}$$

where

- f_b = concrete tensile stress at bottom fiber of the beam, ksi
- M_g = unfactored bending moment due to beam self weight, ft-kips
- M_s = unfactored bending moment due to slab and haunch weights, ft-kips
- M_b = unfactored bending moment due to barrier weight, ft-kips
- M_{ws} = unfactored bending moment due to wearing surface, ft-kips
- M_{LT} = unfactored bending moment due to truck load, ft-kips
- M_{LL} = unfactored bending moment due to lane load, ft-kips

Using values of bending moments from **Tables 9.8.4-1** and **9.8.4-2**, bottom tensile stress at midspan is:

$$f_b = \frac{1,108.0 + 576.8}{7,527} (12) + \frac{96.0 + 165.6 + (0.8)(1,238.7 + 411.1)}{9,992} (12) = 4.585 \text{ ksi}$$

9.8.5.2 Stress Limits for Concrete

Tensile stress limit at service limit state = $-0.19\sqrt{f'_c}$ [LRFD Art. 5.9.4.2]

where f'_c = specified concrete compressive strength of beam for design, ksi

Concrete tensile stress limit = $-0.19\sqrt{8.0} = -0.537$ ksi

9.8.5.3 Required Number of Strands

The required precompressive stress at the bottom fiber of the beam is the difference between the bottom tensile stress due to the applied loads and the concrete tensile stress limit:

$$f_{pb} = 4.585 - 0.537 = 4.048 \text{ ksi}$$

Assume the distance between the center of gravity of strands and the bottom fiber of the beam:

Try $y_{bs} = 6.0$ in.

Therefore, strand eccentricity at midspan, $e_c = (y_b - y_{bs}) = (22.13 - 6.0) = 16.1$ in.

If P_{pe} is the total prestress force after all losses, the stress at the bottom fiber due to prestress is:

$$f_{pb} = \frac{P_{pe}}{A_g} + \frac{P_{pe}e_c}{S_b}, \text{ or } 4.048 = \frac{P_{pe}}{1,330} + \frac{P_{pe}(16.1)}{7,527}$$

Solving for P_{pe} , the required $P_{pe} = 1,400.3$ kips.

Final prestress force per strand = (area of strand)(f_{pi})(1 - final losses)

where f_{pi} = initial strand stress before transfer, ksi (see Section 9.8.2) = 202.5 ksi

Assuming final loss of 20% of f_{pi} , prestress force per strand after all losses

$$= (0.217)(202.5)(1-0.20) = 35.2 \text{ kips}$$

Number of strands required = $(1,400.3/35.2) = 39.8$ strands

DOUBLE-TEE BEAM (NEXT 36F), SINGLE SPAN, COMPOSITE DECK

9.8.5.3 Required Number of Strands/9.8.5.5 Steel Transformed Section Properties

As an initial trial, (40) 0.6-in.-diameter, 270 ksi strands were selected. The center of gravity of the 40 strands at midspan is 8.50 in. from the bottom of the concrete, which is higher than the assumed value, 6.0 in. Thus, a second iteration using the new value of strand eccentricity indicates that 46 strands are required. The strand pattern at midspan for the 46 strands is shown in **Figure 9.8.5.4.1**. Each available position is filled beginning with the bottom row.

Try (46) 0.6-in.-diameter, 270 ksi strands

Total area of prestressing stands, $A_{ps} = 46(0.217) = 9.982 \text{ in.}^2$

Note: This is a conservative estimate of the number of strands because nontransformed section properties are used in lieu of transformed section properties. The number of strands can be refined later in the design process as more accurate section properties and prestress losses are determined.

9.8.5.4 Strand Pattern

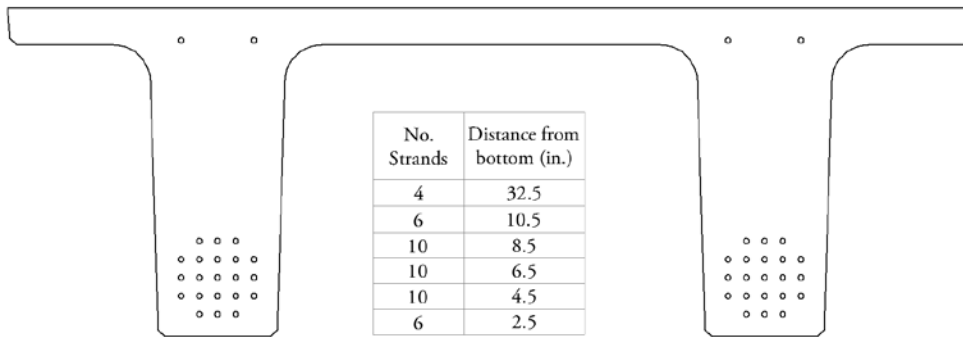
The distance between the center of gravity of strands and the bottom concrete fiber of the beam at midspan is:

$$y_{bs} = [6(2.5) + 10(4.5) + 10(6.5) + 10(8.5) + 6(10.5) + 4(32.5)] / (46) = 8.76 \text{ in.}$$

$$\text{Strand eccentricity at midspan, } e_c = y_b - y_{bs} = 22.13 - 8.76 = 13.37 \text{ in.} = e_{pg}$$

Figure 9.8.5.4-1

Assumed Strand Pattern at Midspan



9.8.5.5 Steel Transformed Section Properties

From the earliest years of prestressed concrete design, the gross section was conservatively used in analysis since the prestressing forces were smaller and computer programs were not widely used. However, the use of transformed section, which is obtained from the gross section by adding transformed steel area, yields more accurate results than the gross section analysis.

For each row of prestressing strands shown in **Figure 9.8.5.4-1**, the steel area is multiplied by $(n - 1)$ to calculate the transformed section properties, where n is the modular ratio between prestressing strand and concrete. Since the modulus of elasticity of concrete is different at transfer and final time, the transformed section properties should be calculated separately for the two stages. Using similar procedures as in Section 9.8.3.2.3, a sample calculation is shown in **Table 9.8.5.5-1**.

At transfer:

$$n - 1 = \frac{28,500}{4,696} - 1 = 5.069$$

At final:

$$n - 1 = \frac{28,500}{5,422} - 1 = 4.25$$

DOUBLE-TEE BEAM (NEXT 36F), SINGLE SPAN, COMPOSITE DECK

9.8.5.5 Steel Transformed Section Properties

Table 9.8.5.5-1
Properties of Composite Transformed Section at Final Time

	Transformed Area, in. ²	y_b in.	Ay_b in. ³	$A(y_{btc} - b_y)^2$ in. ⁴	I in. ⁴	$I + A(y_{btc} - b_y)^2$ in. ⁴
Deck	414.18	39.25	16,257	72,714	1044	73,758
Haunch	37.48	36.25	1,359	3,938	0.78	3,939
Beam	1,330.00	22.13	29,433	19,919	166,569	186,488
Row 1	5.54	2.50	13.85	3,059		3,059
Row 2	9.24	4.50	41.58	4,271		4,271
Row 3	9.24	6.50	60.06	3,514		3,514
Row 4	9.24	8.50	78.54	2,830		2,830
Row 5	5.54	10.50	58.17	1,331		1,331
Row 6	3.69	32.50	119.93	156		156
Σ	1,824.2		47,421			279,346

Note: The moment of inertia of strand about its own centroid is neglected.
The transformed section properties are calculated as:

Noncomposite transformed section at transfer:

$$A_{ti} = \text{area of transformed section at transfer} = 1,381 \text{ in.}^2$$

$$I_{ti} = \text{moment of inertia of the transformed section at transfer} = 178,296 \text{ in.}^4$$

$$e_{ti} = \text{eccentricity of strands with respect to transformed section at transfer} = 12.88 \text{ in.}$$

$$y_{bti} = \text{distance from the centroid of the transformed section to the extreme bottom fiber of the beam at transfer} = 21.64 \text{ in.}$$

$$S_{bti} = \text{section modulus for the extreme bottom fiber of the transformed section at transfer} = 8,239 \text{ in.}^3$$

$$S_{tti} = \text{section modulus for the extreme top fiber of the transformed section at transfer} = 12,416 \text{ in.}^3$$

Noncomposite transformed section at final time:

$$A_{tf} = \text{area of transformed section at final time} = 1,373 \text{ in.}^2$$

$$I_{tf} = \text{moment of inertia of the transformed section at final time} = 176,469 \text{ in.}^4$$

$$e_{tf} = \text{eccentricity of strands with respect to transformed section at final time} = 12.96 \text{ in.}$$

$$y_{btf} = \text{distance from the centroid of the noncomposite transformed section to the extreme bottom fiber of the beam at final time} = 21.72 \text{ in.}$$

$$S_{btf} = \text{section modulus for the extreme bottom fiber of the transformed section at final time} = 8,125 \text{ in.}^3$$

$$S_{ttf} = \text{section modulus for the extreme top fiber of the transformed section at final time} = 12,358 \text{ in.}^3$$

Composite transformed section at final time:

$$A_{tc} = \text{area of transformed composite section at final time} = 1,824 \text{ in.}^2$$

$$I_{tc} = \text{moment of inertia of the transformed composite section at final time} = 279,346 \text{ in.}^4$$

$$e_{tc} = \text{eccentricity of strands with respect to transformed composite section at final time} = 17.24 \text{ in.}$$

$$y_{btc} = \text{distance from the centroid of the composite transformed section to the extreme bottom fiber of the beam at final time} = 26.00 \text{ in.}$$

$$S_{btc} = \text{section modulus for the extreme bottom fiber of the transformed composite section at final time} = 10,744 \text{ in.}^3$$

$$S_{ttc} = \text{composite section modulus for the extreme top fiber of the precast beam for transformed section at final time} = 27,935 \text{ in.}^3$$

$$S_{dtc} = \text{composite section modulus for the extreme top fiber of the deck for transformed section at final time} = 24,691 \text{ in.}^3$$

DOUBLE-TEE BEAM (NEXT 36F), SINGLE SPAN, COMPOSITE DECK**9.8.6 Prestress Losses/9.8.6.1 Elastic Shortening****9.8.6 PRESTRESS LOSSES**

Total prestress loss:

$$\Delta f_{pT} = \Delta f_{pES} + \Delta f_{pLT} \quad [\text{LRFD Eq. 5.9.5.1-1}]$$

where

Δf_{pT} = total loss in prestressing steel stress

Δf_{pES} = sum of all losses or gains due to elastic shortening or extension at the time of application of prestress and/or external loads

Δf_{pLT} = long-term losses due to shrinkage and creep of concrete, and relaxation of steel after transfer. In this design example, the refined estimates of time-dependent losses are used.

9.8.6.1 Elastic Shortening

$$\Delta f_{pES} = \frac{E_p}{E_{ci}} f_{cgp} \quad [\text{LRFD Eq. 5.9.5.2.3a-1}]$$

where

E_p = modulus of elasticity of prestressing strands = 28,500 ksi

E_{ci} = modulus of elasticity of beam concrete at transfer = 4,696 ksi

f_{cgp} = sum of concrete stresses at the center of gravity of prestressing strands due to prestressing force at transfer and the self weight of the member at sections of maximum moment.

If the gross (or net) cross-section properties are used, it is necessary to perform numerical iterations. The elastic loss Δf_{pES} is usually assumed to be 10% of the initial prestress to calculate f_{cgp} , which is then used in the equation above to calculate a refined Δf_{pES} . The process is repeated until the assumed Δf_{pES} and refined Δf_{pES} converge.

However, when transformed section properties are used to calculate concrete stress, the effects of losses and gains due to elastic deformations are implicitly accounted for. Therefore, Δf_{pES} should not be included in calculating f_{cgp} .

$$\begin{aligned} \text{Force per strand before transfer} &= (\text{area of strand})(\text{prestress stress before transfer}) \\ &= (0.217)(202.5) = 43.94 \text{ ksi} \end{aligned}$$

$$f_{cgp} = \frac{P_{pi}}{A_{ti}} + \frac{P_{pi}e_{ti}^2}{I_{ti}} - \frac{M_g e_{ti}}{I_{ti}}$$

where

e_{ti} = eccentricity of strands at midspan with respect to the transformed section at transfer = 12.88 in.

P_i = total prestressing force before transfer = (46 strands)(43.94) = 2,021.2 kips

M_g should be calculated based on the overall beam length of 81 ft. Since the elastic shortening loss is a part of the total loss, f_{cgp} will be conservatively computed based on M_g using the design span length of 80 ft.

$$f_{cgp} = \frac{2,021.2}{1,381} + \frac{(2,021.2)(12.88)^2}{178,296} - \frac{(1,108.0)(12)(12.88)}{178,296} = 1.464 + 1.881 - 0.960 = 2.385 \text{ ksi}$$

Therefore, loss due to elastic shortening:

$$\Delta f_{pES} = \frac{28,500}{4,696} (2.385) = 14.5 \text{ ksi}$$

AASHTO LRFD C5.9.5.3 indicates that the loss due to elastic shortening at transfer should be added to the time-dependent losses to determine total losses. However, this loss at transfer is directly accounted for if transformed section properties are used in the stress analysis.

DOUBLE-TEE BEAM (NEXT 36F), SINGLE SPAN, COMPOSITE DECK**9.8.6.2 Time-Dependent Losses between Transfer and Deck Placement/9.8.6.2.1 Shrinkage of Concrete****9.8.6.2 Time-Dependent Losses between Transfer and Deck Placement**

The following construction schedule is assumed in calculating the time-dependent losses:

Concrete age at transfer: $t_i = 1$ day

Concrete age at deck placement: $t_d = 90$ days

Concrete age at final stage: $t_f = 20,000$ days

The total time-dependent loss between time of transfer and deck placement is the summation of prestress losses due to shrinkage of concrete, creep of concrete, and relaxation of prestressing strands.

9.8.6.2.1 Shrinkage of Concrete

The prestress loss due to shrinkage of concrete between time of transfer and deck placement is calculated by:

$$\Delta f_{pSR} = \epsilon_{bid} E_p K_{id} \quad [\text{LRFD 5.9.5.4.2a-1}]$$

where

ϵ_{bid} = concrete shrinkage strain of girder for time period between transfer and deck placement

E_p = modulus of elasticity of prestressing strands, ksi

K_{id} = transformed section coefficient that accounts for time-dependent interaction between concrete and bonded steel in the section being considered for time period between transfer and deck placement

The concrete shrinkage strain, ϵ_{bid} is taken as:

$$\epsilon_{bid} = k_{vs} k_{hs} k_f k_{td} 0.48 \times 10^{-3} \quad [\text{LRFD Eq. 5.4.2.3.3.-1}]$$

where

The factor for the effect of the volume-to-surface ratio of the beam:

$$k_{vs} = 1.45 - 0.13(V/S) = 1.45 - 0.13(3.816) = 0.954$$

The minimum value of k_{vs} is 1.0. Therefore use $k_{vs} = 1.000$

V/S is the volume-to-surface ratio of the beam.

The humidity factor for shrinkage:

$$k_{hs} = 2.00 - 0.14H = 2.00 - 0.014(70) = 1.020$$

where H = average annual mean relative humidity (assume 70%)

The factor for the effect of concrete strength:

$$k_f = \frac{5}{1 + f'_{ci}} = \frac{5}{1 + 6.0} = 0.714$$

The time development factor at deck placement:

$$k_{td} = \frac{t}{61 - 4f'_{ci} + t} = \frac{89}{61 - 4(6.0) + 89} = 0.706 = k_{td}$$

where t is the maturity of concrete (days) = $t_d - t_i = 90 - 1 = 89$ days

$$\epsilon_{bid} = (1.000)(1.020)(0.714)(0.706)(0.48 \times 10^{-3}) = 0.000247$$

$$K_{id} = \frac{1}{1 + \frac{E_p A_{ps}}{E_{ci} A_g} \left(1 + \frac{A_g (e_{pg})^2}{I_g} \right) [1 + 0.7 \Psi_b(t_f, t_i)]} \quad [\text{LRFD Eq. 5.9.5.4.2a-2}]$$

where

e_{pg} = eccentricity of prestressing strand with respect to the centroid of the girder, in.

$\Psi_b(t_f, t_i)$ = girder creep coefficient at final time due to loading introduced at transfer

DOUBLE-TEE BEAM (NEXT 36F), SINGLE SPAN, COMPOSITE DECK

9.8.6.2.1 Shrinkage of Concrete/9.8.6.3.1 Shrinkage of Concrete

For the time between transfer and final time:

$$\Psi_b(t_f, t_i) = 1.9k_{vs}k_{hc}k_{fj}k_{td}t_i^{-0.118} \quad [\text{LRFD Eq.5.4.2.3.2-1}]$$

$$k_{hc} = 1.56 - 0.008H = 1.56 - 0.008(70) = 1.000$$

$$k_{td} = \frac{t_f - t_i}{61 - 4f'_{ci} + (t_f - t_i)} = \frac{20000 - 1}{61 - 4(6.0) + (20000 - 1)} = 0.998 = k_{tdf}$$

$$\Psi_b(t_f, t_i) = 1.9(1.000)(1.000)(0.714)(0.998)(1)^{-0.118} = 1.354$$

$$K_{id} = \frac{1}{1 + \frac{28,500}{4,696} \frac{9.982}{1,330} \left(1 + \frac{1,330(13.37)^2}{166,569}\right) [1 + 0.7(1.354)]} = 0.823$$

The prestress loss due to shrinkage of concrete between transfer and deck placement is:

$$\Delta f_{pSR} = (0.000247)(28,500)(0.823) = 5.794 \text{ ksi}$$

9.8.6.2.2 Creep of Concrete

The prestress loss due to creep of girder concrete between time of transfer and deck placement is:

$$\Delta f_{pCR} = \frac{E_p}{E_{ci}} f_{cgp} \Psi_b(t_d, t_i) K_{id} \quad [\text{LRFD Eq.5.9.5.4.2b-1}]$$

where

$$\begin{aligned} \Psi_b(t_d, t_i) &= \text{girder creep coefficient at time of deck placement due to loading introduced at transfer} \\ &= 1.9k_{vs}k_{hc}k_{fj}k_{td}t_i^{-0.118} \quad [\text{LRFD Eq. 5.4.2.3.2-1}] \\ &= 1.9(1.000)(1.000)(0.714)(0.706)(1)^{-0.118} = 0.958 \end{aligned}$$

$$\Delta f_{pCR} = \frac{28,500}{4,696} (2.385)(0.958)(0.823) = 11.412 \text{ ksi}$$

9.8.6.2.3 Relaxation of Prestressing Strands

The prestress loss due to relaxation of prestressing strands between time of transfer and deck placement is determined as:

$$\Delta f_{pR1} = \frac{f_{pt}}{K_L} \left(\frac{f_{pt}}{f_{py}} - 0.55 \right) \quad [\text{LRFD Eq. 5.9.5.4.2c-1}]$$

where

$$\begin{aligned} f_{pt} &= \text{stress in prestressing strands immediately after transfer, taken not less than } 0.55f_y \\ K_L &= 30 \text{ for low-relaxation strands and } 7 \text{ for other prestressing steel, unless more accurate} \\ &\quad \text{manufacturer's data are available} \end{aligned}$$

$$\Delta f_{pR1} = \frac{(202.5 - 14.5)}{30} \left(\frac{(202.5 - 14.5)}{243} - 0.55 \right) = 1.402 \text{ ksi}$$

According to LRFD Art. 5.9.5.4.2c, the relaxation loss may also be assumed equal to 1.2 ksi for low-relaxation strands.

9.8.6.3 Time-Dependent Losses between Deck Placement and Final Time

The total time-dependent loss between time of deck placement and final time is the summation of prestress losses due to shrinkage of beam concrete, creep of beam concrete, relaxation of prestressing strands, and shrinkage of deck concrete.

9.8.6.3.1 Shrinkage of Concrete

The prestress loss due to shrinkage of concrete between deck placement and final time is calculated by:

$$\Delta f_{pSD} = \epsilon_{bd} E_p K_{df} \quad [\text{LRFD Eq. 5.9.5.4.3a-1}]$$

DOUBLE-TEE BEAM (NEXT 36F), SINGLE SPAN, COMPOSITE DECK

9.8.6.3.1 Shrinkage of Concrete/9.8.6.3.2 Creep of Concrete

where

ϵ_{bdf} = concrete shrinkage strain of girder for time period between deck placement and final time

E_p = modulus of elasticity of prestressing strands, ksi

K_{df} = transformed section coefficient that accounts for time-dependent interaction between concrete and bonded steel in the section being considered for time period between deck placement and final time

The total concrete shrinkage strain between transfer and final time is taken as:

$$\begin{aligned}\epsilon_{bif} &= k_{vs}k_{ns}k_{fj}k_{tdf}0.48 \times 10^{-3} && \text{[LRFD Eq. 5.4.2.3.3-1]} \\ &= (1.000)(1.020)(0.714)(0.998)(0.48 \times 10^{-3}) = 0.000349\end{aligned}$$

The girder concrete shrinkage strain between deck placement and final time is:

$$\epsilon_{bdf} = \epsilon_{bif} - \epsilon_{bid} = 0.000349 - 0.000247 = 0.000102$$

The beam concrete transformed section coefficient between deck placement and final time is:

$$K_{df} = \frac{1}{1 + \frac{E_p A_{ps}}{E_{ci} A_c} \left(1 + \frac{A_c (e_{pc})^2}{I_c}\right) [1 + 0.7\Psi_b(t_f, t_i)]} \quad \text{[LRFD Eq. 5.9.5.4.3a-2]}$$

where

A_c = area of the composite section = 1,782 in.²

I_c = moment of inertia of the composite section = 236,890 in.⁴

e_{pc} = eccentricity of strands with respect to centroid of composite section
= 26.41 – 8.76 = 17.65 in.

$$K_{df} = \frac{1}{1 + \frac{28,500}{4,696} \frac{9.982}{1,782} \left(1 + \frac{1,782(17.65)^2}{263,890}\right) [1 + 0.7(1.354)]} = 0.830$$

The prestress loss due to shrinkage of concrete between deck placement and final time is:

$$\Delta f_{pSD} = (0.000102)(28,500)(0.830) = 2.413 \text{ ksi}$$

9.8.6.3.2 Creep of Concrete

The prestress loss due to creep of beam concrete between deck placement and final time is:

$$\Delta f_{pCD} = \frac{E_p}{E_{ci}} f_{cgp} [\Psi_b(t_f, t_i) - \Psi_b(t_d, t_i)] K_{df} + \frac{E_p}{E_c} \Delta f_{cd} [\Psi_b(t_f, t_d)] K_{df} \quad \text{[LRFD Eq. 5.9.5.4.3b-1]}$$

where

$\Psi_b(t_f, t_d)$ = girder creep coefficient at final time due to loading at deck placement

$$= 1.9k_{vs}k_{nc}k_{fj}k_{tdf}t_d^{-0.118} \quad \text{[LRFD Eq. 5.4.2.3.2-1]}$$

$$k_{tdf} = \frac{t}{61 - 4f_{ci}' + t} = \frac{(20,000 - 90)}{61 - 4(6.0) + (20,000 - 90)} = 0.998$$

$$\Psi_b(t_f, t_d) = 1.9(1.000)(1.000)(0.714)(0.998)(90)^{-0.118} = 0.796$$

Δf_{cd} = change in concrete stress at centroid of prestressing strands due to long-term losses between transfer and deck placement, combined with deck weight and superimposed loads, ksi

$$= -(\Delta f_{pSR} + \Delta f_{pCR} + \Delta f_{pR1}) \frac{A_{ps}}{A_g} \left(1 + \frac{A_g e_{pg}^2}{I_g}\right) - \left(\frac{M_s e_{tf}}{I_{tf}} + \frac{(M_b + M_{ws}) e_{tc}}{I_{tc}}\right)$$

DOUBLE-TEE BEAM (NEXT 36F), SINGLE SPAN, COMPOSITE DECK

9.8.6.3.2 Creep of Concrete/9.8.6.3.4 Shrinkage of Deck Concrete

$$= -(5.794 + 11.412 + 1.402) \frac{9.982}{1,330} \left(1 + \frac{1,330(13.37)^2}{166,569} \right) - \left(\frac{576.8(12)(12.96)}{176,469} + \frac{(96.0 + 165.6)(12)(17.24)}{279,346} \right) = -1.041 \text{ ksi}$$

The gross section properties are used in the equation to calculate Δf_{cd} for the long-term losses since the transformed section effect has already been included in the factor K_{id} when calculating the losses between initial time and deck placement.

$$\Delta f_{pCD} = \frac{28,500}{4,696} (2.385)(1.354 - 0.958)(0.830) + \frac{28,500}{5,422} (-1.041)(0.796)(0.830) = 1.142 \text{ ksi}$$

9.8.6.3.3 Relaxation of Prestressing Strands

The prestress loss due to relaxation of prestressing strands between time of deck placement and final time is taken as:

$$\Delta f_{pR2} = \Delta f_{pR1} = 1.402 \text{ ksi} \quad \text{[LRFD Eq. 5.9.5.4.3c-1]}$$

9.8.6.3.4 Shrinkage of Deck Concrete

The prestress gain due to shrinkage of deck concrete is calculated by:

$$\Delta f_{pSS} = \frac{E_p}{E_c} \Delta f_{cdf} K_{df} [1 + 0.7\Psi_b(t_f, t_d)] \quad \text{[LRFD Eq. 5.9.5.4.3d-1]}$$

where Δf_{cdf} = change in concrete stress at centroid of prestressing strands due to shrinkage of deck concrete, ksi

$$\Delta f_{cdf} = \frac{\epsilon_{ddf} A_d E_{cd}}{1 + 0.7\Psi_d(t_f, t_d)} \left[\frac{1}{A_c} - \frac{e_{pc} e_d}{I_c} \right] \quad \text{[LRFD Eq. 5.9.5.4.3d-2]}$$

where

- ϵ_{ddf} = shrinkage strain of deck concrete between placement and final time
- A_d = area of deck concrete, in.²
- E_{cd} = modulus of elasticity of deck concrete, ksi
- $\Psi_d(t_f, t_d)$ = deck concrete creep coefficient at final time due to loading introduced shortly after deck placement
- e_d = eccentricity of deck with respect to the gross composite section, in.

Assume the initial strength of concrete at deck placement is $0.8(4.0 \text{ ksi}) = 3.2 \text{ ksi}$, and use a volume-to-surface ratio 2.839 for the deck:

$$k_{vs} = 1.45 - 0.13(V/S) = 1.45 - 0.13(2.839) = 1.081 > 1.0 \quad \text{OK}$$

$$k_f = \frac{5}{1 + f'_{ci}} = \frac{5}{1 + 3.2} = 1.190$$

$$k_{td} = \frac{t}{61 - 4f'_{ci} + t} = \frac{20,000 - 90}{61 - 4(3.2) + (20,000 - 90)} = 0.998$$

$$\begin{aligned} \epsilon_{ddf} &= k_{vs} k_{hs} k_f k_{td} 0.48 \times 10^{-3} && \text{[LRFD Eq. 5.4.2.3.3-1]} \\ &= (1.081)(1.020)(1.190)(0.998)(0.48 \times 10^{-3}) = 0.000629 \end{aligned}$$

$$\begin{aligned} \Psi_d(t_f, t_d) &= 1.9 k_{vs} k_{hc} k_f k_{td} t_i^{-0.118} && \text{[LRFD Eq. 5.4.2.3.2-1]} \\ &= 1.9(1.081)(1.000)(1.190)(0.998)(1)^{-0.118} = 2.439 \end{aligned}$$

DOUBLE-TEE BEAM (NEXT 36F), SINGLE SPAN, COMPOSITE DECK**9.8.6.3.4 Shrinkage of Deck Concrete/9.8.6.6. Total Losses at Service Loads**

Creep of deck concrete is assumed to start at 1 day.

$$\Delta f_{cdf} = \frac{0.000629(106.5)(5.5)(3,834)}{1 + 0.7(2.439)} \left(\frac{1}{1,782} - \frac{17.65(42 - \frac{5.5}{2} - 26.41)}{263,890} \right)$$

$$= -0.155 \text{ ksi} \quad \text{The negative sign indicates a prestressing gain.}$$

The prestress gain due to shrinkage of the deck in the composite section:

$$\Delta f_{pSS} = \frac{28,500}{5,422} (-0.155)(0.830)[1 + 0.7(0.796)] = -1.053 \text{ ksi}$$

Note: The effect of deck shrinkage on the calculation of prestress gain is discussed further in Section 9.1a.8.5.

9.8.6.4 Total Time-Dependent Loss

The total time-dependent loss, Δf_{pLT} , is determined as:

$$\Delta f_{pLT} = (\Delta f_{pSR} + \Delta f_{pCR} + \Delta f_{pR1}) + (\Delta f_{pSD} + \Delta f_{pCD} + \Delta f_{pR2} + \Delta f_{pSS}) \quad [\text{LRFD Eq. 5.9.5.4.1-1}]$$

$$= (5.794 + 11.412 + 1.402) + (2.413 + 1.142 + 1.402 - 1.053)$$

$$= 18.608 + 3.904 = 22.5 \text{ ksi}$$

9.8.6.5 Total Losses at Transfer

AASHTO LRFD C5.9.5.2.3a and C5.9.5.3 indicate that the losses or gains due to elastic deformation must be taken equal to zero if transformed section properties are used in stress analysis. However, the losses or gains due to elastic deformation must be included in determining the total prestress losses and the effective stress in the prestressing strands.

$$\Delta f_{pi} = \Delta f_{pES} = 14.5 \text{ ksi}$$

Effective stress in tendons immediately after transfer, $f_{pt} = f_{pi} - \Delta f_{pi} = (202.5 - 14.5) = 188.0 \text{ ksi}$

Force per strand = $(f_{pt})(\text{area of strand}) = (188.0)(0.217) = 40.80 \text{ kips}$

Therefore, the total prestressing force after transfer, $P_{pt} = 40.80(46) = 1,877 \text{ kips}$

Initial loss, % = $(\text{Total losses at transfer})/(f_{pi}) = 14.5/202.5 = 7.2\%$

When determining the concrete stress using transformed section properties, the strand force is that before transfer:

Force per strand = $(202.5)(0.217) = 43.94 \text{ kips}$

The total prestressing force before transfer $P_{pi} = 43.94(46) = 2,021 \text{ kips}$

9.8.6.6 Total Losses at Service Loads

Total loss due to elastic shortening at transfer and long-term losses is:

$$\Delta f_{pT} = \Delta f_{pES} + \Delta f_{pLT} = 14.5 + 22.5 = 37.0 \text{ ksi}$$

The elastic gain due to deck weight, superimposed dead load, and live load (Service III) is:

$$= \left(\frac{M_s e_{tf}}{I_{tf}} + \frac{(M_b + M_{ws}) e_{tc}}{I_{tc}} \right) \frac{E_p}{E_c} + 0.8 \left(\frac{(M_{LT} + M_{LL}) e_{tc}}{I_{tc}} \right) \frac{E_p}{E_c}$$

$$= \left(\frac{576.8(12)(12.96)}{176,469} + \frac{(96.0 + 165.6)(12)(17.24)}{279,346} \right) \frac{28,500}{5,422} + 0.8 \left(\frac{(1,238.7 + 411.1)(12)(17.24)}{279,346} \right) \frac{28,500}{5,422}$$

$$= 3.7 + 5.1 = 8.8 \text{ ksi}$$

The effective stress in strands after all losses and gains:

$$f_{pe} = f_{pi} - \Delta f_{pT} + 3.7 = 202.5 - 37.0 + 8.8 = 174.3 \text{ ksi}$$

DOUBLE-TEE BEAM (NEXT 36F), SINGLE SPAN, COMPOSITE DECK**9.8.6.6. Total Losses at Service Loads/9.8.7.2 Stresses at Transfer Length Section**

Check prestressing stress limit at service limit state:

[LRFD Table 5.9.3-1]

$$f_{pe} \leq 0.8 f_{py} = 0.8(243) = 194.4 \text{ ksi} > 174.3 \text{ ksi} \quad \text{OK}$$

The effective stress in strands after all losses and permanent gains:

$$f_{pe} = f_{pi} - \Delta f_{pT} + 7.2 = 202.5 - 37.0 + 3.7 = 169.2 \text{ ksi}$$

$$\text{Force per strand without live load gains} = (f_{pe})(\text{area of strand}) = (169.2)(0.217) = 36.72 \text{ kips}$$

$$\text{Therefore, the total prestressing force after all losses} = 36.72(46) = 1,689.1 \text{ kips}$$

$$\text{Final loss percentage} = (\text{total losses and gains}) / (f_{pi}) = (37.0 - 3.7) / (202.5) = 16.4\%$$

$$\text{Without consideration of prestressing gains at deck placement, the final loss percentage} = \text{total losses} / (f_{pi}) = (37.0) / (202.5) = 18.3\%$$

When determining the concrete stress using transformed section properties, all the elastic losses and gains are implicitly accounted for.

$$\text{Force per strand with only total time-dependent losses} = (f_{pi} - \Delta f_{pLT})(\text{area of strand}) = (202.5 - 22.5)(0.217) = 39.06 \text{ kips}$$

$$\text{Total prestressing force, } P_{pe} = (39.06)(46) = 1,797 \text{ kips}$$

9.8.7 CONCRETE STRESSES AT TRANSFER

Because transformed section is used, the total prestressing force before and after transfer, $P_{pi} = 2,021$ kips.

9.8.7.1 Stress Limits for Concrete

[LRFD Art. 5.9.4]

Compression:

- $0.6f'_c = 0.6(6.0) = +3.600 \text{ ksi}$

where f'_c = concrete strength at transfer = 6.000 ksi

Tension:

- without bonded auxiliary reinforcement

$$0.0948\sqrt{f'_{ci}} \leq 0.200 \text{ ksi}; \quad -0.0948\sqrt{6.000} = -0.232 \text{ ksi}$$

Therefore, -0.200 ksi (Controls)

- with bonded auxiliary reinforcement that is sufficient to resist 120% of the tension force in the cracked concrete

$$0.24\sqrt{f'_{ci}} = -0.24\sqrt{6.000} = -0.588 \text{ ksi}$$

9.8.7.2 Stresses at Transfer Length Section

This section is located at a distance equal to the transfer length from the end of the beam. Stresses at this location need only be checked at transfer because this stage almost always governs. Also, losses with time will reduce the concrete stresses, making them less critical.

$$\text{Transfer length} = 60(\text{strand diameter}) = 60(0.6) = 36 \text{ in.} = 3 \text{ ft}$$

[LRFD Art. 5.11.4]

Due to camber of the beam at transfer, the beam self weight acts on the overall beam length, 81 ft. Therefore, values for bending moment given in **Table 9.8.4-1** cannot be used because they are based on the design span length of 80 ft. Using Eq. 9.8.4.1.2-2, the bending moment at transfer length due to beam weight is:

$$M_g = 0.5w_g x(L - x) = (0.5)(1.385)(3)(81 - 3) = 162.0 \text{ ft-kips}$$

Compute stress in the top of beam:

$$f_t = \frac{P_{pi}}{A_{ti}} - \frac{P_{pi}e_{ti}}{S_{tti}} + \frac{M_g}{S_{tti}} = \frac{2,021}{1,381} - \frac{2,021(12.88)}{12,416} + \frac{(162.0)(12)}{12,416}$$

$$= 1.463 - 2.097 + 0.157 = -0.477 \text{ ksi}$$

DOUBLE-TEE BEAM (NEXT 36F), SINGLE SPAN, COMPOSITE DECK

9.8.7.2 Stresses at Transfer Length Section

Tensile stress limit for concrete with bonded reinforcement: -0.588 ksi OK

Compute stress in the bottom of beam:

$$f_b = \frac{P_{pi}}{A_{ti}} + \frac{P_{pi}e_{ti}}{S_{bti}} - \frac{M_g}{S_{bti}} = \frac{2,021}{1,381} + \frac{2,021(12.88)}{8,239} - \frac{(162.0)(12)}{8,239}$$

$$= 1.463 + 3.159 - 0.236 = +4.386 \text{ ksi}$$

Compressive stress limit for concrete: +3.600 ksi NG

Therefore, try debonding eight strands from the strand groups at 4.5 in. and 8.5 in. from the bottom for a distance of 13 ft 0 in. from the end of the beam or 12 ft 6 in. from centerline of bearing.

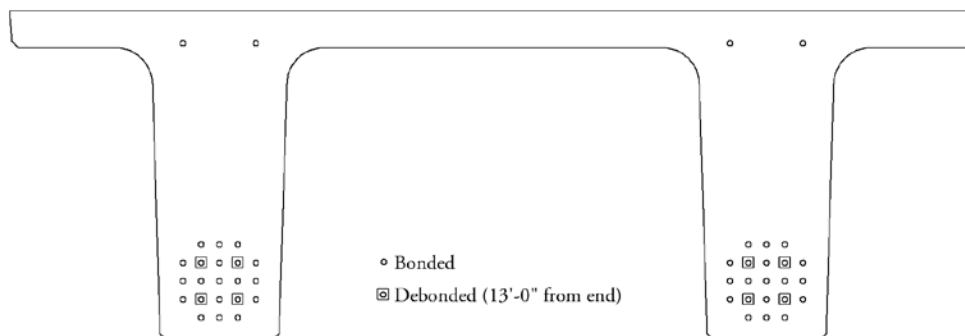
To minimize the shock impact of detensioning and cracks at corners and bottom, assume the strand pattern shown in **Figure 9.8.7.2-1**. LRFD Article 5.11.4.3 requires that the following conditions be satisfied if debonding is used:

- Percentage debonded of total = $8/46 = 17\% \leq 25\%$ OK
- Percentage debonded of row = $4/10 = 40\% \leq 40\%$ OK
- All limit states should be satisfied OK
- Debonded strands should be symmetrically distributed OK
- Exterior strands in each horizontal line are fully bonded OK

Recompute the stresses at the transfer length section. Note that the transformed section properties here are different from those at midspan after debonding. Using the same method as described in Section 9.8.5.5, the transformed section properties at end of beam are computed as:

$$A_{ti} = 1,372 \text{ in.}^2 \qquad y_{bti} = 21.74 \text{ in.} \qquad S_{bti} = 8,201 \text{ in.}^3 \qquad S_{tti} = 12,503 \text{ in.}^3$$

Figure 9.8.7.2-1
Strand Pattern at End of Beam



Distance from the center of gravity of bonded strands to the bottom fiber of the beam is:

$$y_{bs} = [6(2.5) + 6(4.5) + 10(6.5) + 6(8.5) + 6(10.5) + 4(32.5)] / (38) = 9.24 \text{ in.}$$

and the strand eccentricity for the transformed section at end of beam is;

$$e_{ti} = 21.74 - 9.24 = 12.50 \text{ in.}$$

Total prestressing force at release at end section = $38(43.94) = 1,669.7$ kips

Concrete stress in top of beam:

$$f_t = \frac{1,669.7}{1,372} - \frac{1,669.7(12.50)}{12,503} + \frac{(162.0)(12)}{12,503} = 1.217 - 1.669 + 0.155 = -0.297 \text{ ksi}$$

DOUBLE-TEE BEAM (NEXT 36F), SINGLE SPAN, COMPOSITE DECK

9.8.7.2 Stresses at Transfer Length Section/9.8.7.5 Summary of Stresses at Transfer

Tensile stress limit for concrete: -0.588 ksi OK

Concrete stress in bottom of beam:

$$f_b = \frac{1,669.7}{1,372} + \frac{1,669.7(12.50)}{8,201} - \frac{(162.0)(12)}{8,201} = 1.217 + 2.545 - 0.237 = 3.525 \text{ ksi}$$

Compressive stress limit for concrete: +3.600 ksi OK

9.8.7.3 Stresses at Transfer Length Section of Debonded Strands

All strands are effective at this location. Therefore, $P_{pi} = 2,021$ kips

Bending moment due to the self-weight of the beam at (13 + 3 = 16 ft) from the end of the beam is:

$$(0.5)(1.385)(16)(81 - 16) = 720.2 \text{ ft-kips.}$$

Therefore, top and bottom stresses are:

Concrete stress in top of beam:

$$f_t = \frac{2,021}{1,381} - \frac{(2,021)(12.88)}{12,416} + \frac{(720.2)(12)}{12,416} = 1.463 - 2.097 + 0.696 = +0.062 \text{ ksi}$$

Compressive stress limit: +3.600 ksi OK

Concrete stress in bottom of beam:

$$f_b = \frac{2,021}{1,381} + \frac{(2,021)(12.88)}{8,239} - \frac{(720.2)(12)}{8,239} = 1.463 + 3.159 - 1.049 = +3.573 \text{ ksi}$$

Compressive stress limit: +3.600 ksi OK

9.8.7.4 Stresses at Midspan

Bending moment at midspan due to the beam self weight is:

$$M_g = 0.5(1.385)(40.5)(81 - 40.5) = 1,135.9 \text{ ft-kips}$$

$$f_t = \frac{2,021}{1,381} - \frac{(2,021)(12.88)}{12,416} + \frac{(1,135.9)(12)}{12,416} = 1.463 - 2.097 + 1.098 = +0.464 \text{ ksi}$$

Compressive stress limit: +3.600 ksi OK

$$f_b = \frac{2,021}{1,380.61,381} + \frac{2,021(12.88)}{8,239} - \frac{(1,135.9)(12)}{8,239} = 1.463 + 3.159 - 1.654 = +2.968 \text{ ksi}$$

Compressive stress limit: +3.600 ksi OK

9.8.7.5 Summary of Stresses at Transfer

	Top Fiber Stresses f_t , ksi	Bottom Fiber Stresses f_b , ksi
At transfer length section	-0.297	+3.525
At end of debonded strands + transfer length	+0.062	+3.573
At midspan	+0.464	+2.968

DOUBLE-TEE BEAM (NEXT 36F), SINGLE SPAN, COMPOSITE DECK**9.8.8 Concrete Stresses at Service Loads/9.8.8.2.2 Concrete Stresses at the Top Fiber of the Deck****9.8.8 CONCRETE STRESSES AT SERVICE LOADS**

Using transformed section properties and refined losses, $P_{pe} = 1,797$ kips

9.8.8.1 Stress Limits for Concrete

[LRFD Art. 5.9.4.2]

Compression:

Due to permanent loads, (i.e. beam self weight, weight of joint concrete, weight of slab and haunch, weight of future wearing surface, and weight of barrier), for load combination Service I:

$$\text{for precast beams: } 0.45 f'_c = (0.45)(8.000) = +3.600 \text{ ksi}$$

$$\text{for deck: } 0.45 f'_c = (0.45)(4.000) = +1.800 \text{ ksi}$$

Due to permanent and transient loads (i.e. all dead loads and live loads), for load combination Service I:

$$\text{for precast beams: } 0.60 f'_c = 0.6(8.000) = +4.800 \text{ ksi}$$

$$\text{for deck: } 0.60 f'_c = 0.60(4.000) = +2.400 \text{ ksi}$$

Tension:

For components with bonded prestressing tendons:

$$\text{for load combination Service III: } -0.19 \sqrt{f'_c}$$

$$\text{for precast beam: } -0.19 \sqrt{8.000} = -0.537 \text{ ksi}$$

9.8.8.2 Stresses at Midspan**9.8.8.2.1 Concrete Stress at Top Fiber of the Beam**

To check top compressive stresses, two cases are considered:

1. Under permanent loads, load combination Service I:

Using bending moment values given in **Table 9.8.4-1**, compute the top fiber stresses:

$$\begin{aligned} f_{tg} &= \frac{P_{pe}}{A_{tf}} - \frac{P_{pe} e_{tf}}{S_{ttf}} + \frac{M_g + M_s}{S_{ttf}} + \frac{(M_{ws} + M_b)}{S_{ttc}} \\ &= \frac{1,797}{1,373} - \frac{(1,797)(12.96)}{12,358} + \frac{(1,108.0 + 576.8)(12)}{12,358} + \frac{(96 + 165.6)(12)}{27,935} \\ &= 1.309 - 1.885 + 1.636 + 0.112 = +1.172 \text{ ksi} \end{aligned}$$

Compressive stress limit: +3.600 ksi OK

2. Under permanent and transient loads, load combination Service I:

$$f_{tg} = +1.172 + \frac{(M_{LT} + M_{LL})}{S_{ttc}} = +1.172 + \frac{(1,238.7 + 411.1)(12)}{27,935} = 1.172 + 0.709 = +1.881 \text{ ksi}$$

Compressive stress limit: +4.800 ksi OK

9.8.8.2.2 Concrete Stress at the Top Fiber of the Deck

Note: Compressive stress in the deck slab at service loads never controls the design for typical applications. The calculations shown below are for illustration purposes and may not be necessary in most practical applications.

1. Under permanent loads, load combination Service I:

$$f_{tc} = \frac{(M_{ws} + M_b)}{S_{dtc}} = \frac{(165.6 + 96.0)(12)}{24,691} = +0.127 \text{ ksi}$$

Compressive stress limit: +1.800 ksi OK

2. Under permanent and transient loads, load combination Service I:

$$f_{tc} = \frac{(M_{ws} + M_b)}{S_{dtc}} + \frac{(M_{LT} + M_{LL})}{S_{dtc}} = +0.127 + \frac{(1,238.7 + 411.1)(12)}{24,691} = +0.929 \text{ ksi}$$

Compressive stress limit: +2.400 ksi OK

DOUBLE-TEE BEAM (NEXT 36F), SINGLE SPAN, COMPOSITE DECK

9.8.8.2.3 Concrete Stress in Bottom of Beam, Load Combination Service III/9.8.9 Strength Limit State

9.8.8.2.3 Concrete Stress in Bottom of Beam, Load Combination Service III

$$f_b = \frac{P_{pe}}{A_{tf}} + \frac{P_{pe}e_{tf}}{S_{btf}} - \frac{(M_g + M_s)}{S_{btf}} - \frac{(M_{ws} + M_b) + 0.8(M_{LT} + M_{LL})}{S_{btc}}$$

$$= \frac{1,797}{1,373} + \frac{(1,797)(12.96)}{8,125} - \frac{(1,108.0 + 576.8)(12)}{8,125} - \frac{(165.6 + 96.0)(12) + 0.8(1,238.7 + 411.1)(12)}{10,744}$$

$$= 1.309 + 2.866 - 2.488 - 1.766 = -0.079 \text{ ksi}$$

Tensile stress limit: -0.537 ksi OK

9.8.8.3 Fatigue Stress Limit

LRFD Article 5.5.3.1 states that in fully prestressed components other than segmentally constructed bridges, the compressive stress due to Fatigue I load combination and one half the sum of effective prestress and permanent loads shall not exceed $0.40f'_c$, after losses.

From **Table 9.8.4-2**, the unfactored fatigue bending moment at midspan, M_f is 490.6 ft-kips. Therefore, stress at the top fiber of the beam due to fatigue load combination I is:

$$f_{tgf} = \frac{1.50(M_f)}{S_{ttc}} = \frac{1.50(490.6)(12)}{27,935} = +0.316 \text{ ksi}$$

At midspan, the top compressive stress due to permanent loads and prestress is:

$$f_{tg} = \frac{P_{pe}}{A_{tf}} - \frac{P_{pe}e_{tf}}{S_{ttf}} + \frac{(M_g + M_s)}{S_{ttf}} + \frac{(M_{ws} + M_b)}{S_{ttc}}$$

$$= \frac{1,797}{1,373} - \frac{(1,797)(12.96)}{12,358} + \frac{(1,108.0 + 576.8)(12)}{12,358} + \frac{(165.6 + 96.0)(12)}{27,935}$$

$$= 1.309 - 1.885 + 1.636 + 0.112 = 1.172 \text{ ksi}$$

Therefore:

$$f_{tgf} + \frac{f_b}{2} = 0.316 + \frac{1.172}{2} = 0.902 < 0.40(f'_c) = 0.40(6.50) = 2.6 \text{ ksi OK}$$

This condition should be satisfied at all locations along the beam.

9.8.8.4 Summary of Stresses at Midspan at Service Loads

	Top of Deck, ksi Service I		Top of Beam, ksi Service I		Bottom of Beam, ksi Service III
	Permanent Loads	Total Loads	Permanent Loads	Total Loads	
At midspan	+0.127	+0.929	+1.172	+1.881	-0.079

9.8.8.5 Effect of Deck Shrinkage

The calculations in Section 9.8.8.2 comply with the *LRFD Specifications*. However, PCI believes that it is not appropriate to include the prestressing gain caused by the deck shrinkage, Δf_{pss} , in calculating the prestress losses. Alternatively, the effect of deck shrinkage should be analyzed by considering it as an external force applied to the composite nontransformed section as illustrated Section 9.1a.8.5.

9.8.9 STRENGTH LIMIT STATE

Total ultimate bending moment for Strength I is:

$$M_u = 1.25(DC) + 1.5(DW) + 1.75(LL + IM)$$

Using values of unfactored bending moment given in **Tables 9.8.4-1** and **9.8.4-2**, the ultimate bending moment at midspan is:

$$M_u = 1.25(1,108.0 + 576.8 + 96.0) + 1.5(165.6) + 1.75(1,238.7 + 411.1) = 5,361.6 \text{ ft-kips}$$

DOUBLE-TEE BEAM (NEXT 36F), SINGLE SPAN, COMPOSITE DECK

9.8.9 Strength Limit State

Average stress in prestressing steel when $f_{pe} \geq 0.5f_{pu}$:

$$f_{ps} = f_{pu} \left(1 - k \frac{c}{d_p} \right) \quad [\text{LRFD Eq. 5.7.3.1.1-1}]$$

where

 f_{ps} = average stress in prestressing strand, ksi f_{pu} = specified tensile strength of prestressing strand = 270.0 ksi

$$k = 2 \left(1.04 - \frac{f_{py}}{f_{pu}} \right) = 2 \left(1.04 - \frac{243}{270} \right) \quad [\text{LRFD Eq. 5.7.3.1.1-2}]$$

= 0.28 for low-relaxation strands

 d_p = distance from extreme compression fiber to the centroid of the prestressing strands, in.For the 42 bottom strands, the distance between the center of gravity of the strands and the bottom fiber of the beam, y_{bs} , is:

$$y_{bs} = [6(2.5) + 10(4.5) + 10(6.5) + 10(8.5) + 6(10.5)] / (42) = 6.50 \text{ in.}$$

$$d_p = h_c - y_{bs} = 42.00 - 6.50 = 35.50 \text{ in.}$$

 c = distance from the extreme compression fiber to the neutral axis, in.To compute c , assume rectangular section behavior and check if the depth of the equivalent compression stress block, a , is less than or equal to t_s : [LRFD C5.7.3.2.2]where $a = \beta_1 c$

$$c = \frac{A_{ps} f_{pu} + A_s f_y - A'_s f'_y}{0.85 f'_c \beta_1 b + k A_{ps} \frac{f_{pu}}{d_p}} \quad [\text{LRFD Eq. 5.7.3.1.1-4}]$$

where

 a = depth of the equivalent stress block A_{ps} = area of prestressing strand = $42(0.217) = 9.114 \text{ in.}^2$ A_s = area of nonprestressed tension reinforcement = 0 in.^2 A'_s = area of compression reinforcement = 0 in.^2 f'_c = specified compressive strength of deck concrete = 4.0 ksi f_y = specified yield strength of tension reinforcement = 60.0 ksi f'_y = specified yield strength of compression reinforcement, ksi β_1 = stress factor of compression block [LRFD Art. 5.7.2.2]= 0.85 for $f'_c \leq 4.0 \text{ ksi}$ = $0.85 - 0.05(f'_c - 4.0) \geq 0.65$ for $f'_c > 4.0 \text{ ksi}$

= 0.85

 b = effective width of compression flange = 106.5 in.

Note: In computing the flexural strength of members with strands placed near the compression face of the member, it is not correct to use the combined centroid of the entire strand group for establishing the effective depth, d_p , and the area of prestressing steel, A_{ps} . This is because the top strands will have different strain from that of the bottom strands. An accurate solution can be achieved using the detailed strain compatibility approach which accounts for the steel strain at various distances from the neutral axis. However, a reasonable approximation is to ignore all strands placed on the compression side.

DOUBLE-TEE BEAM (NEXT 36F), SINGLE SPAN, COMPOSITE DECK

9.8.9 Strength Limit State/9.8.10.1 Maximum Reinforcement

$$c = \frac{9.114(270.0) + 0 - 0}{0.85(4.0)(0.85)(106.5) + (0.28)(9.114)\left(\frac{270.0}{35.50}\right)} = 7.52 \text{ in.}$$

$$a = \beta_1 c = (0.85)(7.52) = 6.39 \text{ in.} > t_s = 5.5 \text{ in.} \quad \text{NG}$$

Therefore, compute c using T-section behavior.

$$c = \frac{A_{ps}f_{pu} + A_s f_y - A'_s f'_y - 0.85 f'_c (b - b_w) h_f}{0.85 f'_c \beta_1 b_w + k A_{ps} \frac{f_{pu}}{d_p}} \quad \text{[LRFD Eq. 5.7.3.1.1-3]}$$

where

$$h_f = \text{depth of compression flange} = t_s = 5.5 \text{ in.}$$

$$b_w = \text{width of web} = 106.0 \text{ in.}$$

$$c = \frac{9.114(270) + 0 - 0 - 0.85(4.0)(106.5 - 106.0)5.5}{0.85(4.0)(0.85)(106.0) + (0.28)(9.114)\left(\frac{270}{35.50}\right)} = 7.53 \text{ in.}$$

$$a = \beta_1 c = (0.85)(7.53) = 6.40 \text{ in.} > t_s = 5.5 \text{ in.} \quad \text{OK}$$

LRFD C5.7.2.2 states that if the compressive block includes two types of concrete, the lower of the concrete strengths can be conservatively used.

Therefore, the average stress in the prestressing strand is:

$$f_{ps} = 270.0 \left(1 - 0.28 \frac{7.53}{35.50}\right) = 254.0 \text{ ksi}$$

Nominal flexural resistance:

$$M_n = A_{ps} f_{ps} \left(d_p - \frac{a}{2}\right) + 0.85 f'_c (b - b_w) t_s \left(\frac{a}{2} - \frac{h_f}{2}\right)$$

The above equation is a simplified form of LRFD Equation 5.7.3.2.2-1 because no compression reinforcement or nonprestressed tension reinforcement is considered.

$$M_n = \frac{(9.114)(254.0)\left(35.50 - \frac{6.40}{2}\right)}{12} + \frac{0.85(4.000)(106.5 - 106.0)(5.5)\left(\frac{6.40}{2} - \frac{5.5}{2}\right)}{12}$$

$$= 6,231.4 \text{ ft-kips}$$

Factored flexural resistance:

$$M_r = \phi M_n \quad \text{[LRFD Eq. 5.7.3.2.1-1]}$$

where

$$\phi = \text{resistance factor} \quad \text{[LRFD Art. 5.5.4.2.1]}$$

$$= 1.00, \text{ for tension controlled prestressed concrete sections}$$

$$M_r = 6,231.4 \text{ ft-kips} > M_u = 5,361.6 \text{ ft-kips} \quad \text{OK}$$

9.8.10 LIMITS OF REINFORCEMENT**9.8.10.1 Maximum Reinforcement**

The check of maximum reinforcement limits in LRFD Article 5.7.3.3.1 was removed from the *LRFD Specifications* in 2005.

DOUBLE-TEE BEAM (NEXT 36F), SINGLE SPAN, COMPOSITE DECK

9.8.10.2 Minimum Reinforcement/9.8.11 Shear Design

9.8.10.2 Minimum Reinforcement

[LRFD Art. 5.7.3.3.2]

At any section, the amount of prestressed and nonprestressed tensile reinforcement must be adequate to develop a factored flexural resistance, M_r , equal to the lesser of:

- 1.2 times the cracking strength determined on the basis of elastic stress distribution and the modulus of rupture, and
- 1.33 times the factored moment required by the applicable strength load combination.

Check at midspan:

$$M_{cr} = S_{btc}(f_r + f_{cpe}) - M_{dnc} \left(\frac{S_{btc}}{S_{btf}} - 1 \right) \geq S_{btc}f_r \quad \text{[LRFD Art. 5.7.3.3.2-1]}$$

where

$$f_r = \text{modulus of rupture of concrete} \quad \text{[LRFD Art. 5.4.2.6]}$$

$$= 0.37\sqrt{f'_c} = 0.37\sqrt{8.000} = 1.047 \text{ ksi}$$

$$f_{cpe} = \text{compressive stress in concrete due to effective prestress force only (after allowance for all prestress losses) at extreme fiber of section where tensile stress is caused by externally applied loads}$$

$$= \frac{P_{pe}}{A_{tf}} + \frac{P_{pe}e_{tf}}{S_{btf}} = \frac{1,797}{1,373} + \frac{(1,797)(12.96)}{8,125} = 4.175 \text{ ksi}$$

$$M_{dnc} = \text{noncomposite dead load moment at the section}$$

$$= M_g + M_s = 1,108.0 + 576.8 = 1,684.8 \text{ ft-kips}$$

$$S_{btc} = \text{section modulus for the extreme bottom fiber of the transformed composite section where the tensile stress is caused by externally applied loads} = 10,744 \text{ in.}^3$$

$$S_{btf} = \text{section modulus for the extreme bottom fiber of the transformed noncomposite section where the tensile stress is caused by externally applied loads} = 8,125 \text{ in.}^3$$

$$M_{cr} = (1.047 + 4.175) \frac{10,744}{12} - (1,684.8) \left(\frac{10,744}{8,124} - 1 \right) = 4,132.1 \text{ ft-kips}$$

$$1.2M_{cr} = 1.2(4,132.1) = 4,958.5 \text{ ft-kips}$$

At midspan, the factored moment required by the Strength I load combination is:

$$M_u = 5,361.6 \text{ ft-kips (as calculated in Section 9.8.9)}$$

$$\text{Thus, } 1.33 M_u = 1.33(5,361.6) = 7,130.9 \text{ ft-kips}$$

Since $1.2M_{cr} < 1.33M_u$, the $1.2M_{cr}$ requirement controls.

$$M_r = 6,231.4 \text{ ft-kips} > 1.2 M_{cr} = 4,958.5 \quad \text{OK}$$

Note: The *LRFD Specifications* requires that this criterion be met at every section.

Illustrated based on
2011 *LRFD*
Specifications.

Editor's Note: 2012
LRFD Specifications
changes will revise
minimum
reinforcement.

9.8.11 SHEAR DESIGN

The area and spacing of shear reinforcement must be determined at regular intervals along the entire length of the beam. In this design example, transverse shear design procedures are demonstrated below by determining these values at the critical section near the supports.

Transverse shear reinforcement is required when:

$$V_u > 0.5\phi(V_c + V_p) \quad \text{[LRFD Eq. 5.8.2.4-1]}$$

DOUBLE-TEE BEAM (NEXT 36F), SINGLE SPAN, COMPOSITE DECK

9.8.11 Shear Design/9.8.11.1 Critical Section

where

- V_u = total factored shear force, kips
- V_c = nominal shear strength provided by tensile stresses in the concrete, kips
- V_p = component in the direction of the applied shear of the effective prestressing force, kips
- ϕ = resistance factor = 0.9 for normal weight concrete [LRFD Art. 5.5.4.2.1]

9.8.11.1 Critical Section [LRFD Art. 5.8.3.2]

The critical section near the supports is taken as the effective shear depth, d_v , from the internal face of support.

d_v = distance between resultants of tensile and compressive forces, $(d_e - a/2)$, but [LRFD Art. 5.8.2.9]
not less than $(0.9d_e)$ or $(0.72h_c)$

where

- d_e = the corresponding effective depth from the extreme compression fiber to the centroid of the tensile force in the tensile reinforcement [LRFD Art. 5.8.2.7]
- a = depth of compression block = 6.40 in. at midspan (assumed adequate)
- h_c = overall depth of the composite section = 42.0 in.

Note: Only 34 strands are effective at the critical section for shear, because eight strands are debonded for a distance equal to 13 ft from the end of the beam and the top level of strands is ignored.

$d_e = h_c - y_{bs} = 42.00 - 6.50 = 35.50$ in.

$d_v = 35.50 - (6.40)/2 = 32.30$ in.

$\geq 0.9 d_e = 0.9(35.50) = 31.95$ in.

$\leq 0.72 h_c = 0.72(42.00) = 30.24$ in. OK

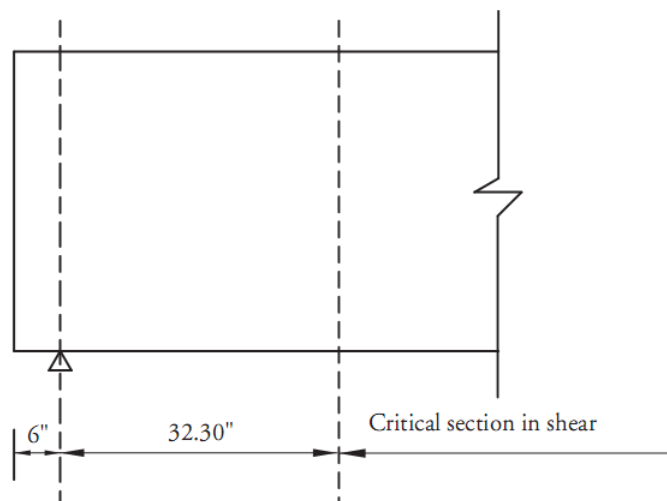
Therefore, $d_v = 32.30$ in.

Because the width of the bearing is not yet determined, it is conservatively assumed to be zero. Therefore, the critical section in shear is located at a distance of:

32.30 in. = 2.69 ft from centerline of support as shown in **Figure 9.8.11-1**.

$(x/L) = 2.69/80 = 0.034L$

Figure 9.8.11-1
Critical Section in Shear



DOUBLE-TEE BEAM (NEXT 36F), SINGLE SPAN, COMPOSITE DECK9.8.11.2 Contribution of Concrete to Nominal Shear Resistance/9.8.11.2.2 Values of β and θ **9.8.11.2 Contribution of Concrete to Nominal Shear Resistance**

The contribution of the concrete to the nominal shear resistance is:

$$V_c = 0.0316\beta\sqrt{f'_c} b_v d_v \quad [\text{LRFD Eq. 5.8.3.3-3}]$$

where β = a factor indicating the ability of diagonally cracked concrete to transmit tension (a value indicating concrete contribution).

Several quantities must be determined before this expression can be evaluated.

9.8.11.2.1 Strain in Flexural Tension ReinforcementCalculate the strain at the centroid of the reinforcement, ϵ_s :

$$\epsilon_s = \frac{\frac{|M_u|}{d_v} + 0.5N_u + |(V_u - V_p)| - A_{ps}f_{po}}{(E_s A_s + E_p A_{ps})} \quad [\text{LRFD Eq. 5.8.3.4.2-4}]$$

where

$$\begin{aligned} M_u &= \text{applied factored bending moment at the specified section, } 0.034L \\ &= 1.25(144.0 + 75.0 + 12.5) + 1.50(21.5) + 1.75(175.8 + 53.4) \quad (\text{Tables 9.8.4-1 and 9.8.4-2}) \\ &= 722.7 \text{ ft-kips} \end{aligned}$$

M_u need not to be taken less than $(V_u - V_p)d_v$:

$$(V_u - V_p)d_v = [(277.1 - 0)(32.30/12)] = 745.9 \text{ ft-kips}$$

Since $(V_u - V_p)d_v \geq M_u$, $M_u = 745.9$ ft-kips Controls

$$N_u = \text{applied factored normal axial force at the specified section, } 0.034L = 0$$

$$\begin{aligned} V_u &= \text{applied factored shear force at the specified section, } 0.034L \\ &= 1.25(51.7 + 26.9 + 4.5) + 1.50(7.7) + 1.75(71.7 + 21.0) \quad (\text{Tables 9.8.4-1 and 9.8.4-2}) \\ &= 277.1 \text{ kips} \end{aligned}$$

$$\begin{aligned} V_p &= \text{component in the direction of the applied shear of the effective prestressing force} \\ &= 0 \text{ kips since strand pattern is straight} \end{aligned}$$

$$\begin{aligned} A_{ps} &= \text{area of prestressing strands on the flexural tension side of the member} = 34(0.217) = 7.378 \text{ in.}^2 \\ &(\text{Only 34 of the 42 strands are effective in the flexural tension side because eight strands are debonded}). \end{aligned}$$

$$\begin{aligned} f_{po} &= \text{a parameter taken as modulus of elasticity of prestressing tendons multiplied by the locked-in difference in strain between the prestressing tendons and the surrounding concrete (ksi). For pretensioned members, LRFD Article C5.8.3.4.2 indicates that } f_{po} \text{ can be taken as } 0.7f_{pu}. \text{ (Note: use this for both pretensioned and post-tensioned systems made with stress-relieved and low relaxation strands).} \\ &= 0.7(270) = 189.0 \text{ ksi} \end{aligned}$$

$$\epsilon_s = \frac{\frac{|722.7(12)|}{32.30} + 0.5(0) + |(277.1 - 0)| - 7.378(189)}{(0 + 28,500(7.378))} = -3.996 \times 10^{-3}$$

ϵ_s is less than zero. Use $\epsilon_s = 0$.

9.8.11.2.2 Values of β and θ

Assume the section contains at least the minimum amount of traverse reinforcement:

$$\beta = \frac{4.8}{(1 + 750\epsilon_s)} = \frac{4.8}{(1 + 0)} = 4.8 \quad [\text{LRFD Eq. 5.8.3.4.2-1}]$$

DOUBLE-TEE BEAM (NEXT 36F), SINGLE SPAN, COMPOSITE DECK9.8.11.2.2 Values of β and θ /9.8.11.3.3 Determine Spacing of Reinforcement

Angle of diagonal compressive stress is:

$$\theta = 29 + 3,500\varepsilon_s = 29 + 3,500(0) = 29^\circ \quad [\text{LRFD Eq. 5.8.3.4.2-3}]$$

9.8.11.2.3 Compute Concrete Contribution

The nominal shear resisted by the concrete is:

$$V_c = 0.0316\beta\sqrt{f'_c}b_vd_v \quad [\text{LRFD Eq. 5.8.3.3-3}]$$

where b_v = effective web width = $2(13.00) = 26.00$ in.

LRFD Article 5.8.2.9 states that b_v is the minimum web width between the tensile and compressive forces due to flexure. In this example, the beam web is slightly sloped. The minimum width at the bottom of the beam is conservatively used in the calculation.

$$V_c = 0.0316(4.8)\sqrt{8.0}(26.00)(32.30) = 360.3 \text{ kips}$$

9.8.11.3 Contribution of Reinforcement to Nominal Shear Resistance**9.8.11.3.1 Requirement for Reinforcement**

Check if $V_u > 0.5\phi(V_c + V_p)$ [LRFD Eq. 5.8.2.4-1]

$$V_u = 277.1 \text{ kips} > 0.5\phi(V_c + V_p) = 0.5(0.9)(360.3 + 0) = 162.1 \text{ kips}$$

Therefore, transverse shear reinforcement must be provided.

9.8.11.3.2 Required Area of Reinforcement

$$V_u/\phi \leq V_n = V_c + V_s + V_p \quad [\text{LRFD Eq. 5.8.3.3-1}]$$

where

$$\begin{aligned} V_s &= \text{shear resistance provided by shear reinforcement} \\ &= (V_u/\phi) - V_c - V_p = (277.1/0.9) - 360.3 - 0.0 = -52.4 \text{ kips} \end{aligned}$$

$$V_s = \frac{A_v f_{yh} d_v (\cot \theta + \cot \alpha) (\sin \alpha)}{s} \quad [\text{LRFD Eq. 5.8.3.3-4}]$$

where

- A_v = area of shear reinforcement within a distance, s , in.²
- s = spacing of stirrups, in.
- f_{yh} = specified yield strength of shear reinforcement, ksi
- α = angle of inclination of transverse reinforcement to longitudinal axis
= 90° for vertical stirrups

Since the required V_s is negative, the minimum transverse reinforcement requirement is used to determine the area of the shear reinforcement. The area of transverse reinforcement should not be less than:

$$A_v \leq 0.0316\sqrt{f'_c} \frac{b_v s}{f_{yh}} = 0.0316\sqrt{8.0} \frac{26.0(s)}{60.0} = 0.039(s) \quad [\text{LRFD Eq. 5.8.2.5-1}]$$

If $s = 15$ in., required $A_v = 0.59$ in.²/ft

9.8.11.3.3 Determine Spacing of Reinforcement

Check maximum spacing of transverse reinforcement: [LRFD Art 5.8.2.7]

Check if $v_u < 0.125f'_c$

$$v_u = \frac{|V_u - \phi V_p|}{\phi b_v d_v} = \frac{|277.1 - 0|}{(0.9)(26.0)(32.30)} = 0.367 \text{ ksi} \quad [\text{LRFD Eq. 5.8.2.9-1}]$$

DOUBLE-TEE BEAM (NEXT 36F), SINGLE SPAN, COMPOSITE DECK

9.8.11.3.3 Determine Spacing of Reinforcement/9.8.12.3 Required Interface Shear Reinforcement

$$0.125f'_c = (0.125)(8) = 1.000 \text{ ksi}$$

$$\text{Since } v_u < 0.125f'_c$$

[LRFD Eq. 5.8.2.7-1]

then, $s \leq 24 \text{ in.}$ Controls

$$s \leq 0.8 d_v = 0.8(32.30) = 25.84 \text{ in.}$$

Therefore, maximum $s = 24.0 \text{ in.}$ $> s$ provided = 15 in. OK

Use No. 4 bar four-leg stirrups at 15 in., $A_v = 0.64 \text{ in.}^2/\text{ft} > 0.59 \text{ in.}^2/\text{ft}$

$$V_s = \frac{0.80(60)(32.30) \cot 29^\circ}{15} = 186.5 \text{ kips}$$

9.8.11.4 Maximum Nominal Shear Resistance

In order to ensure that the concrete in the web of the beam will not crush prior to yielding of the transverse reinforcement, the LRFD *Specifications* gives an upper limit of V_n as follows:

$$V_n = 0.25f'_c b_v d_v + V_p$$

[LRFD Eq. 5.8.3.3-2]

Comparing this equation with LRFD Eq. 5.8.3.3-1, it can be concluded that

$$V_c + V_s \text{ must not be greater than } 0.25 f'_c b_v d_v$$

$$360.3 + 186.5 = 546.8 \text{ kips} \leq 0.25(8)(26.0)(32.30) = 1,679.6 \text{ kips} \quad \text{OK}$$

9.8.12 INTERFACE SHEAR TRANSFER**9.8.12.1 Factored Horizontal Shear**

[LRFD Art. 5.8.4]

At the strength limit state, the horizontal shear at a section on a per unit basis can be taken as:

$$V_{hi} = \frac{V_u}{d_v}$$

[LRFD Eq. C5.8.4.2-7]

where

V_{hi} = horizontal factored shear force per unit length of the beam, kips/in.

V_u = factored shear force at specified section due to superimposed loads after the deck is cast, kips

d_v = the distance between the centroid of the tension steel and the mid-thickness of the slab = $(d_e - t_s/2) = 35.50 - (5.5/2) = 32.75 \text{ in.}$

The LRFD *Specifications* does not identify the location of the critical section. For convenience, it will be assumed here to be the same location as the critical section for vertical shear at point 0.034L.

Using load combination Strength I:

$$V_u = 1.25(51.7+26.9+4.5) + 1.50(7.7) + 1.75(71.4 + 21.0) = 277.1 \text{ kips} \quad [\text{Tables 9.8.4-1 and 9.8.2-2}]$$

Therefore, the applied factored horizontal shear is:

$$V_{hi} = \frac{277.1}{32.75} = 8.46 \text{ kips/in.}$$

9.8.12.2 Required Nominal Resistance

$$\text{Required } V_{ni} = V_{hi}/\phi = 8.46/0.9 = 9.40 \text{ kips/in.}$$

[LRFD Eq. 5.8.4.1-1]

9.8.12.3 Required Interface Shear Reinforcement

The nominal shear resistance of the interface surface is:

$$V_{ni} = cA_{cv} + \mu[A_v f_{yh} + P_c]$$

[LRFD Eq. 5.8.4.1-3]

DOUBLE-TEE BEAM (NEXT 36F), SINGLE SPAN, COMPOSITE DECK**9.8.12.3 Required Interface Shear Reinforcement/9.8.12.4 Maximum Nominal Shear Resistance**

where

c = cohesion factor, ksi [LRFD Art. 5.8.4.3]

μ = coefficient of friction [LRFD Art. 5.8.4.3]

A_{cv} = area of concrete section resisting shear transfer, in.²

A_{vf} = area of shear reinforcement crossing the shear plane, in.²

P_c = permanent net compressive force normal to the shear plane, kips

f_{yh} = specified yield strength of shear reinforcement, ksi

For cast-in-place concrete slabs placed on clean concrete girder surface intentionally roughened : [LRFD Art. 5.8.4.3]

c = 0.28 ksi

μ = 1.0

The actual contact width, b_v , between the slab and the beam is 106.0 in.

$A_{cv} = (106.0 \text{ in.})(1.0 \text{ in.}) = 106.0 \text{ in.}^2$

LRFD Eq. 5.8.4.1-3 can be solved for A_{vf} as follows:

$$9.40 = (0.28 \times 106) + 0.6[A_{vf}(60.0) + 0]$$

Solving for A_{vf}

$$A_{vf}(\text{req'd}) < 0$$

Since the resistance provided by cohesion is greater than the applied force, provide the minimum required interface reinforcement.

9.8.12.3.1 Required Interface Shear Reinforcement

Minimum $A_{vf} \geq (0.05A_{cv})/f_{yh}$ [LRFD Eq. 5.8.4.4-1]

From the design of vertical shear reinforcement, a No. 4 four-leg bar at 15-in. spacing is provided from the beam extending into the deck. Therefore, $A_{vf} = 0.64 \text{ in.}^2/\text{ft}$.

$$A_{vf} = (0.64 \text{ in.}^2/\text{ft}) < (0.05A_{cv})/f_{yh} = 0.05(106)/60.0 = 0.088 \text{ in.}^2/\text{in.} = 1.06 \text{ in.}^2/\text{ft} \quad \text{NG}$$

However, LRFD Article 5.8.4.4 states that the minimum reinforcement need not exceed the amount needed to resist $1.33V_{hi}/\phi$ as determined using LRFD Eq. 5.8.4.1-3.

$$(1.33 \times 8.46/0.9) = (0.28 \times 106.0) + 1.0[A_{vf}(60.0) + 0]$$

Solving for A_{vf}

$$A_{vf}(\text{req'd}) < 0 \quad \text{OK}$$

9.8.12.4 Maximum Nominal Shear Resistance

$$V_{ni} \leq K_1 f'_c A_{cv} \text{ or } K_2 A_{cv}$$

$$V_{ni} \text{ provided} = 0.28(106) + 1.0 \left(\frac{0.64}{12} (60.0) + 0 \right) = 32.88 \text{ kips/in.}$$

$$K_1 f'_c A_{cv} = (0.3)(4.0)(106.0) = 127.20 \text{ kips/in.}$$

$$K_2 A_{cv} = 1.8(106.0) = 190.8 \text{ kips/in.}$$

Since provided $V_{ni} \leq 0.3 f'_c A_{cv}$ OK

[LRFD Eq. 5.8.4.1-4]

$$\leq 1.8 A_{cv} \quad \text{OK}$$

[LRFD Eq. 5.8.4.1-5]

DOUBLE-TEE BEAM (NEXT 36F), SINGLE SPAN, COMPOSITE DECK**9.8.13 Minimum Longitudinal Reinforcement Requirement/9.8.13.1 Required Reinforcement at Face of Bearing****9.8.13 MINIMUM LONGITUDINAL REINFORCEMENT REQUIREMENT**

Longitudinal reinforcement should be proportioned so that at each section the following equation is satisfied:

$$A_{ps}f_{ps} + A_s f_y \geq \frac{M_u}{d_v \phi_f} + 0.5 \frac{N_u}{\phi_c} + \left(\left| \frac{V_u}{\phi_v} - V_p \right| - 0.5V_s \right) \cot \theta \quad [\text{LRFD Eq.5.8.3.5-1}]$$

where

- A_{ps} = area of prestressing strand at the tension side of the section, in.²
- f_{ps} = average stress in prestressing strand at the time for which the nominal resistance is required, ksi
- A_s = area of nonprestressed tension reinforcement, in.²
- f_y = specified yield strength of reinforcing bars, ksi
- M_u = factored moment at the section corresponding to the factored shear force, ft-kips
- d_v = effective shear depth, in.
- ϕ = resistance factor as appropriate for moment, shear, and axial resistance.
Therefore, different ϕ factors will be used for the terms in LRFD Equation 5.8.3.5-1, depending on the type of action being considered.
- N_u = applied factored axial force, kips
- V_u = factored shear force at section, kips
- V_s = shear resistance provided by shear reinforcement, kips
- V_p = component in the direction of the applied shear of the effective prestressing force, kips
- θ = angle of inclination of diagonal compressive stresses

9.8.13.1 Required Reinforcement at Face of Bearing

For simple end supports, the longitudinal reinforcement on the flexural tension side of the member at inside face of bearing should satisfy:

$$A_{ps}f_{ps} + A_s f_y \geq \left(\frac{V_u}{\phi} - 0.5V_s - V_p \right) \cot \theta \quad [\text{LRFD Eq.5.8.3.5-2}]$$

$$M_u = 0 \text{ ft-kips}$$

$$N_u = 0 \text{ kips}$$

Because the width of the bearing is not yet determined, it is assumed to be zero. This assumption is conservative for these calculations. Therefore, the failure crack assumed for this analysis radiates from the centerline of the bearing, 6 in. from the end of the beam.

From **Tables 9.8.4-1** and **9.8.4-2** using load combination Strength I, the factored shear force at this section is:

$$V_u = 1.25(55.4 + 28.8 + 4.8) + 1.50(8.3) + 1.75(74.1 + 22.5) = 292.8 \text{ kips}$$

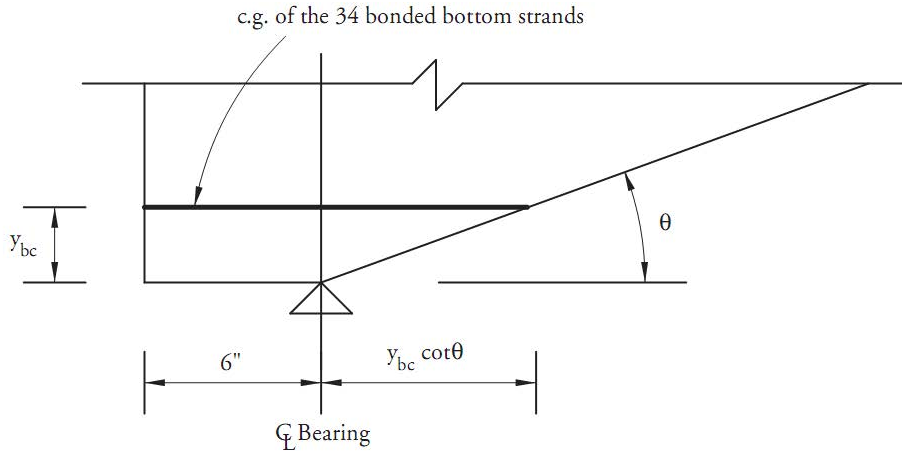
$$\left(\frac{V_u}{\phi} - 0.5V_s - V_p \right) \cot \theta = \left(\frac{292.8}{0.9} - 0.5(186.5) - 0.0 \right) \cot 29^\circ = 418.7 \text{ kips}$$

As shown in **Figure 9.8.13.1-1**, the assumed crack plane crosses the centroid of the 34 bonded strands at a distance of $(6 + 6.50 \cot 29^\circ = 17.73 \text{ in.})$ from the end of the beam. Since the transfer length is 36 in. from the end of the beam (60 times the strand diameter), the available prestress from the 34 bonded strands is a fraction of the effective prestress, f_{pe} , in these strands. Note: 34 effective strands and $y_{bc} = y_{bs} = 6.50 \text{ in.}$ comes from **Section 9.8.11.1**.

DOUBLE-TEE BEAM (NEXT 36F), SINGLE SPAN, COMPOSITE DECK

9.8.13.1 Required Reinforcement at Face of Bearing/9.8.14.1 Anchorage Zone Reinforcement

Figure 9.8.13.1-1
Assumed Failure Crack



Therefore, the available prestressing force is:

$$A_{ps}f_{ps} + A_s f_y = \left[(34)(0.217) \left((202.5 - 37.0) \frac{17.73}{36} \right) \right] + 0 = 601.4 \text{ kips} > 418.7 \text{ kips} \quad \text{OK}$$

Note: An alternative approach for the calculation of available prestressing force excluding the gains from deck shrinkage is illustrated in Section 9.6.13.1.

9.8.14 PRETENSIONED ANCHORAGE ZONE

[LRFD Art. 5.10.10]

9.8.14.1 Anchorage Zone Reinforcement

[LRFD Art. 5.10.10.1]

Design of the anchorage zone reinforcement is computed using the force in the strands just prior to transfer. Since eight strands are debonded at the ends of the beam, the force in the remaining strands before transfer is:

$$P_{pi} = 38(0.217)(202.5) = 1,669.8 \text{ kips}$$

The bursting resistance, P_r , should not be less than 4.0% of P_{pi} .

[LRFD Art. 5.10.10.1]

$$P_r = f_s A_s \geq 0.04 P_{pi} = 0.04(1,669.8) = 66.8 \text{ kips}$$

where

A_s = total area of vertical reinforcement located within a distance $h/4$ from the end of the beam, in.²

f_s = allowable stress in steel, but taken not greater than 20 ksi

Solving for the required area of steel, $A_s = 66.8/20 = 3.34 \text{ in.}^2$

At least 3.34 in.² of vertical transverse reinforcement should be provided within a distance of ($h/4 = 36/4 = 9.0$ in.) from the end of the beam.

Use five No. 4, four-leg bars at 2 in. spacing starting 2 in. from the end of the beam.

The provided $A_s = 5(4)(0.20) = 4.00 \text{ in.}^2 > 3.34 \text{ in.}^2 \quad \text{OK}$

Note:

1. The distance at which the provided five bars extends from the end of the beam, including 2 in. distance from end of the beam and 2 in. spacing in between bars, is 10 in., which is larger than the required $h/4 = 9$ in. However, 10 in. is close enough to 9 in. that it is okay to use this fifth bar in the provided area of steel. Alternatively, a 1¾-in. spacing could be used but this results in an even more congested pattern of reinforcement.
2. A general detail of the NEXT 36 F beam stipulates that No. 4 bars should be used to maximize the cover on the side of the stem. If larger bars are acceptable by the engineer's judgment, 9 in. would be enough to encompass the required amount of steel.

DOUBLE-TEE BEAM (NEXT 36F), SINGLE SPAN, COMPOSITE DECK

9.8.14.2 Confinement Reinforcement/9.8.15.2 Deflection Due to Beam Self Weight

9.8.14.2 Confinement Reinforcement

[LRFD Art. 5.10.10.2]

For a distance of $1.5h = 1.5(36) = 54$ in., from the end of the beam, reinforcement is placed to confine the prestressing steel in the bottom flange. The reinforcement may not be less than No. 3 deformed bars with spacing not exceeding 6 in. The reinforcement should be of a shape that will confine (enclose) the strands.

9.8.15 DEFLECTION AND CAMBER

[LRFD Art. 5.7.3.6.2]

Deflections are calculated using the modulus of elasticity of concrete calculated in Section 9.8.3.1, and the gross section properties.

9.8.15.1 Deflection Due to Prestressing Force at Transfer

Force per strand after transfer = 40.80 kips

$$\Delta_p = \frac{P_{pt}e_cL^2}{8E_{ci}I_g}$$

where

Δ_p = camber due to prestressing force at transfer, in.

P_{pt} = total prestressing force after transfer = $46(40.80) = 1,877$ kips

e_c = eccentricity of prestressing strand at midspan = 13.37 in.

L = overall beam length = 81.0 ft

E_{ci} = modulus of elasticity at transfer = 4,696 ksi

I_g = gross moment of inertia of the noncomposite precast beam = 166,569 in.⁴

$$\Delta_p = \frac{1,877(13.37)(81 \times 12)^2}{(8)(4,696)(166,569)} = 3.79 \text{ in. } \uparrow$$

9.8.15.2 Deflection Due to Beam Self Weight

$$\Delta_g = \frac{5w_gL^4}{384E_{ci}I_g}$$

where

Δ_g = deflection due to beam self weight, in.

w_g = beam self weight = 1.385 kips/ft

E_{ci} = modulus of elasticity of precast beam at transfer = 4,696 ksi

I_g = gross moment of inertia of the noncomposite precast beam = 166,569 in.⁴

L = beam length = 81.0 ft at transfer = 80.0 ft at erection

Deflection due to beam self weight after transfer:

$$\Delta_g = \frac{5\left(\frac{1.385}{12}\right)(81 \times 12)^4}{(384)(4,696)(166,569)} = 1.71 \text{ in. } \downarrow$$

Deflection due to beam self weight used to compute deflection at erection:

$$\Delta_g = \frac{5\left(\frac{1.385}{12}\right)(80 \times 12)^4}{(384)(4,696)(166,569)} = 1.63 \text{ in. } \downarrow$$

DOUBLE-TEE BEAM (NEXT 36F), SINGLE SPAN, COMPOSITE DECK

9.8.15.3 Deflection Due to Slab and Haunch Weights/9.8.15.6 Deflection Due to Live Load and Impact

9.8.15.3 Deflection Due to Slab and Haunch Weights

$$\Delta_s = \frac{5w_s L^4}{384E_c I_g}$$

where

- Δ_s = deflection due to slab and haunch weights, in.
 w_s = slab and haunch weight = 0.666 + 0.055 kips/ft = 0.721 kips/ft
 L = design span = 80.0 ft
 E_c = modulus of elasticity of precast beam at service loads = 5,422 ksi
 I_g = gross moment of inertia of the precast beam = 166,569 in.⁴

$$\Delta_s = \frac{5 \left(\frac{0.721}{12} \right) (80 \times 12)^4}{(384)(5,422)(166,569)} = 0.74 \text{ in. } \downarrow$$

9.8.15.4 Deflection Due to Barrier and Future Wearing Surface Weights

$$\Delta_{b+ws} = \frac{5(w_b + w_{ws})L^4}{384E_c I_c}$$

where

- Δ_{b+ws} = deflection due to barrier and wearing surface weights, in.
 w_b = barrier weight = 0.120 kips/ft
 w_{ws} = wearing surface weight = 0.207 kips/ft
 L = design span = 80.0 ft
 E_c = modulus of elasticity of precast beam at service loads = 5,422 ksi
 I_c = gross moment of inertia of the composite section = 263,890 in.⁴ (Table 9.8.3.2.3-1)

$$\Delta_{b+ws} = \frac{5 \left(\frac{0.120 + 0.207}{12} \right) (80 \times 12)^4}{(384)(5,422)(263,890)} = 0.21 \text{ in. } \downarrow$$

9.8.15.5 Deflection and Camber SummaryAt transfer, $(\Delta_p + \Delta_g) = 3.79 - 1.71 = 2.08 \text{ in. } \uparrow$ Total deflection at erection, using PCI multipliers (see *PCI Design Handbook*)

$$= 1.8(3.79) - 1.85(1.71) = 3.66 \text{ in. } \uparrow$$

Long-Term Deflection:

LRFD Article 5.7.3.6.2 states that the long-time deflection may be taken as the instantaneous deflection multiplied by a factor of 4.0, if the instantaneous deflection is based on the gross moment of inertia. However, a factor of 4.0 is not appropriate for this type of precast construction. Therefore, it is recommended that the designer follow the guidelines of the owner agency for which the bridge is being designed, or undertake a more rigorous, time-dependent analysis.

9.8.15.6 Deflection Due to Live Load and Impact

Live load deflection limit (optional) = Span/800 [LRFD Art.2.5.2.6.2]

$$= \left(80 \times \frac{12}{800} \right) = 1.20 \text{ in.}$$

DOUBLE-TEE BEAM (NEXT 36F), SINGLE SPAN, COMPOSITE DECK

9.8.15.6 Deflection Due To Live Load and Impact

If the owner invokes the optional live load deflection criteria specified in LRFD Art. 2.5.2.6.2, the deflection is the greater of: [LRFD Art 3.6.1.3.2]

- that resulting from the design truck plus impact, Δ_{LT} , or
- that resulting from 25% of the design truck plus impact, Δ_{LT} , taken together with the design lane load, Δ_{LL} .

Note: LRFD Article 2.5.2.6.2 states that the dynamic load allowance be included in the calculation of live load deflection.

The *LRFD Specifications* state that all beams should be assumed to deflect equally under the applied live load and impact. [LRFD Art. 2.5.2.6.2]

Therefore, the distribution factor for deflection, *DFD*, is calculated as follows:

$$DFD = (\text{number of lanes/number of beams}) = 3/5 = 0.60 \text{ lanes/beam} \quad [\text{LRFD Art. C2.5.2.6.2}]$$

However, it is more conservative to use the distribution factor for moment, *DFM*.

Deflection due to lane load:

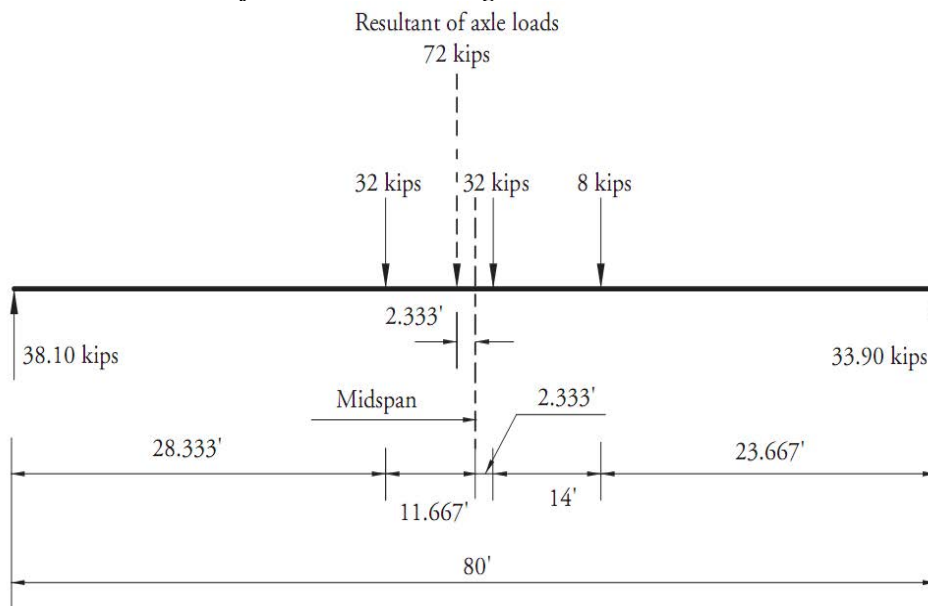
$$\text{Design lane load, } w = 0.64DFM = 0.64(0.803) = 0.514 \text{ kips/ft/beam}$$

$$\Delta_{LL} = \frac{5wL^4}{384E_cI_c} = \frac{5\left(\frac{0.514}{12}\right)(80 \times 12)^4}{(384)(5,422)(263,890)} = 0.33 \text{ in. } \downarrow$$

Deflection due to Design Truck Load and Impact:

To obtain the maximum moment and deflection at midspan due to truck load, let the centerline of the beam coincide with the middle point of the distance between the inner 32-kip axle and the resultant of the truck load, as shown in **Figure 9.8.15.5-1**.

Figure 9.8.15.5-1
Design Truck Axle Load Position for Maximum Bending Moment



Using the elastic moment area or influence lines, deflection at midspan is:

$$\Delta_{LT} = (0.856)(IM)(DFM) = (0.856)(1.33)(0.803) = 0.914 \text{ in. } \downarrow$$

Therefore, live load deflection is the greater of:

$$\Delta_{LT} = 0.914 \text{ in. (Controls)}$$

$$0.25\Delta_{LT} + \Delta_{LL} = 0.25(0.914) + 0.33 = 0.56 \text{ in. } \downarrow$$

Therefore, live load deflection = 0.914 in. < allowable deflection = 1.20 in. OK

This page intentionally left blank

SLAB SYSTEM, SINGLE SPAN, COMPOSITE DECK

Transformed Sections, Shear General Procedure, Refined Losses

9.9 Transformed Sections, Shear General Procedure, Refined Losses**9.9.1 INTRODUCTION**

This design example will demonstrate the design of a single span slab system with a composite cast-in-place concrete deck. This design example will be included in the next release of material for the Third Edition of the manual.

This page intentionally left blank

PRECAST CONCRETE STAY-IN-PLACE DECK PANEL SYSTEM

Transformed Sections, Refined Losses
Table of Contents

9.10.1 INTRODUCTION..... 9.10 - 3

 9.10.1.1 Terminology..... 9.10 - 3

9.10.2 MATERIALS 9.10 - 4

9.10.3 MINIMUM SLAB THICKNESS 9.10 - 5

9.10.4 LOADS 9.10 - 5

 9.10.4.1 Dead Loads..... 9.10 - 5

 9.10.4.2 Wearing Surface and Construction Loads..... 9.10 - 5

 9.10.4.3 Live Loads 9.10 - 5

 9.10.4.4 Load Combination 9.10 - 6

9.10.5 CROSS-SECTION PROPERTIES FOR A TYPICAL PANEL 9.10 - 7

 9.10.5.1 Noncomposite, Nontransformed Panel Section 9.10 - 7

 9.10.5.2 Composite Section 9.10 - 7

9.10.6 ESTIMATE REQUIRED PRESTRESS..... 9.10 - 9

 9.10.6.1 Service Load Stresses at Midspan..... 9.10 - 9

 9.10.6.4 Strand Pattern 9.10 - 10

 9.10.6.5 Steel Transformed Section Properties 9.10 - 10

9.10.7 PRESTRESS LOSSES 9.10 - 12

 9.10.7.1 Elastic Shortening..... 9.10 - 12

 9.10.7.2 Time-Dependent Losses between Transfer and Deck Placement..... 9.10 - 13

 9.10.7.2.1 Shrinkage of Precast Concrete 9.10 - 13

 9.10.7.2.2 Creep of Precast Concrete 9.10 - 14

 9.10.7.2.3 Relaxation of Prestressing Strands 9.10 - 14

 9.10.7.3 Time-Dependent Losses between Deck Placement and Final time..... 9.10 - 15

 9.10.7.3.1 Shrinkage of Precast Concrete 9.10 - 15

 9.10.7.3.2 Creep of Precast Concrete 9.10 - 15

 9.10.7.3.3 Relaxation of Prestressing Strands 9.10 - 16

 9.10.7.3.4 Shrinkage of CIP Concrete 9.10 - 16

 9.10.7.3.5 Total Time-Dependent Loss..... 9.10 - 17

 9.10.7.3.6 Total Losses at Transfer 9.10 - 17

 9.10.7.3.7 Total Losses at Service Loads..... 9.10 - 18

9.10.8 CONCRETE STRESSES IN THE SIP PANEL AT TRANSFER..... 9.10 - 18

 9.10.8.1 Stress Limits for Concrete..... 9.10 - 18

 9.10.8.2 Stresses at Midspan 9.10 - 19

9.10.9 CONCRETE STRESSES IN SIP PANEL AT TIME OF CASTING TOPPING SLAB..... 9.10 - 19

 9.10.9.1 Stress Limits for Concrete..... 9.10 - 19

 9.10.9.2 Stresses at Midspan after all Noncomposite Loads 9.10 - 19

 9.10.9.3 Elastic Deformation 9.10 - 20

9.10.10 CONCRETE STRESSES IN SIP PANEL AT SERVICE LOADS 9.10 - 20

 9.10.10.1 Stress Limits for Concrete 9.10 - 20

PRECAST CONCRETE STAY-IN-PLACE DECK PANEL SYSTEM

Transformed Sections, Refined Losses
Table of Contents

9.10.10.2 Service Load Stresses at Midspan.....9.10 - 20

 9.10.10.2.1 Concrete Stress at Top Surface of the CIP Slab.....9.10 - 20

 9.10.10.2.2 Concrete Stress at Top Fiber of the SIP Panel9.10 - 21

 9.10.10.2.3 Concrete Stress at Bottom Fiber of the SIP Panel.....9.10 - 21

9.10.11 FLEXURAL STRENGTH OF POSITIVE MOMENT SECTION.....9.10 - 21

9.10.12 LIMITS OF REINFORCEMENT FOR POSITIVE MOMENT SECTION.....9.10 - 23

 9.10.12.1 Maximum Reinforcement.....9.10 - 23

 9.10.12.2 Minimum Reinforcement9.10 - 23

9.10.13 NEGATIVE MOMENT SECTION OVER INTERIOR BEAMS.....9.10 - 24

 9.10.13.1 Critical Section9.10 - 24

 9.10.13.2 Bending Moment.....9.10 - 24

 9.10.13.3 Design of Section.....9.10 - 25

 9.10.13.4 Minimum Reinforcement9.10 - 25

 9.10.13.5 Crack Control9.10 - 25

9.10.14 NEGATIVE MOMENT SECTION OVER EXTERIOR BEAMS9.10 - 26

 9.10.14.1 Critical Section9.10 - 26

 9.10.14.2 Design of Section.....9.10 - 26

 9.10.14.3 Minimum Reinforcement9.10 - 29

 9.10.14.4 Crack Control9.10 - 30

9.10.15 DISTRIBUTION REINFORCEMENT.....9.10 - 31

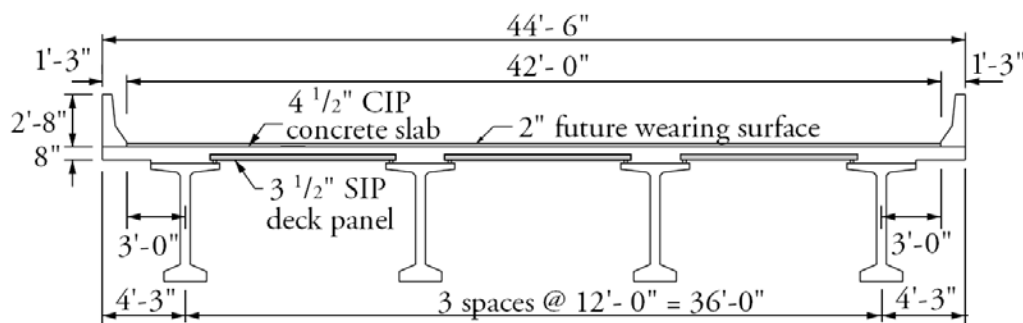
PRECAST CONCRETE STAY-IN-PLACE DECK PANEL SYSTEM

9.10.1 Introduction/9.10.1.1 Terminology

9.10 Transformed Sections, Refined Losses**9.10.1 INTRODUCTION**

This example demonstrates the design of a 3½-in.-thick, precast, pretensioned, stay-in-place (SIP) deck panel with a 4½-in.-thick cast-in-place (CIP) concrete topping. A ½-in.-thick wearing surface is considered to be an integral part of the 4½-in. topping slab. The example bridge has 3-lanes with a total bridge width of 44 ft 6 in. The deck slab is supported over four AASHTO-PCI bulb-tee beams spaced at 12 ft on center and includes overhangs of 4 ft 3 in., as shown in **Figure 9.10.1-1**. The CIP concrete requires a design strength of 4.0 ksi. The SIP panel requires a strength of 6.5 ksi at the time of transfer of the prestress force to the panel and a design strength of 8.0 ksi at the time of casting the CIP slab. A New Jersey-type barrier is included. The design is conducted in accordance with the *LRFD Specifications*, Fifth Edition, 2010, and the 2010 Interim Revisions. Elastic stresses from external loads are calculated using transformed sections. Time-dependent prestress losses are calculated using refined estimates. The strip design method is used.

Figure 9.10.1-1
Bridge Cross Section

**9.10.1.1 Terminology**

The following terminology is used to describe cross sections in this design example:

noncomposite section—the precast concrete SIP panel cross section.

noncomposite nontransformed section—the precast concrete SIP panel cross section without the strands transformed. Also called the gross section.

noncomposite transformed section—precast concrete SIP deck panel cross section with the strands transformed to provide cross-sectional properties equivalent to the panel concrete.

composite section—the precast concrete SIP panel cross section plus the CIP concrete slab and haunch.

composite nontransformed section—the precast concrete SIP panel cross section plus the CIP concrete slab and haunch transformed to provide cross-sectional properties equivalent to the panel concrete but without the strands transformed.

composite transformed section—the precast concrete SIP panel cross section beam plus the CIP concrete slab and haunch and the strands transformed to provide cross-sectional properties equivalent to the panel concrete.

The term "composite" implicitly includes the transformation of the CIP concrete slab and haunch.

The term "transformed" generally refers to transformation of the strands.

PRECAST CONCRETE STAY-IN-PLACE DECK PANEL SYSTEM**9.10.2 Materials****9.10.2 MATERIALS**

Cast-in-place concrete composite slab: Actual thickness = 4½ in.

Structural thickness, $t_s = 4.0$ in.

Note that a ½-in.-thick wearing surface is considered to be an integral part of the deck.

Specified concrete compressive strength for use in design, $f'_c = 4.0$ ksi

Concrete unit weight, $w_c = 0.150$ kcf

Superstructure beams: AASHTO-PCI bulb-tee beams shown in **Figure 9.10.1-1**

Beam spacing = 12.0 ft

Top flange width = 42 in.

Deck overhang = 4.25 ft from the centerline of the exterior beam

Precast, pretensioned concrete SIP deck panels:

Required concrete compressive strength at transfer, $f'_{ci} = 6.5$ ksi

Specified concrete compressive strength for use in design, $f'_c = 8.0$ ksi

Concrete unit weight, $w_c = 0.150$ kcf

Panel dimensions: 8 ft wide × 9 ft 6 in. long × 3½ in. deep as shown in **Fig. 9.10.2-1**.

Prestressing strands: ½-in.-dia., low-relaxation

Area of one strand = 0.153 in.²

Specified tensile strength, $f_{pu} = 270.0$ ksi

Yield strength, $f_{py} = 0.9f_{pu} = 243.0$ ksi

[LRFD Table 5.4.4.1-1]

Stress limits for prestressing strands:

[LRFD Table 5.9.3-1]

- before transfer, $f_{pi} \leq 0.75f_{pu} = 202.5$ ksi
- at service limit state (after all losses) $f_{pe} \leq 0.80f_{py} = 194.4$ ksi

Modulus of elasticity, $E_p = 28,500$ ksi

[LRFD Art. 5.4.4.2]

Reinforcing bars:

Yield strength, $f_y = 60.0$ ksi

Modulus of elasticity, $E_s = 29,000$ ksi

[LRFD Art. 5.4.3.2]

Top reinforcement clear cover = 2.5 in.

[LRFD Table 5.12.3-1]

Bottom reinforcement clear cover = 1.0 in. > 0.8 in. OK

[LRFD Table 5.12.3-1]

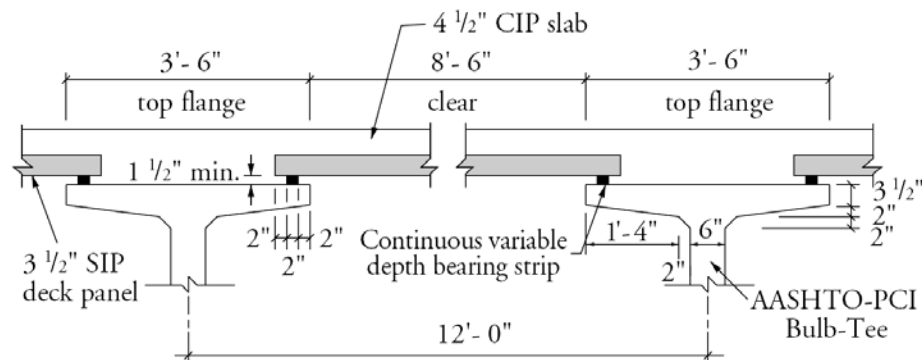
Future wearing surface: 2 in. additional concrete, unit weight = 0.150 kcf

New Jersey-type barrier: unit weight = 0.300 kips/ft/side

PRECAST CONCRETE STAY-IN-PLACE DECK PANEL SYSTEM

9.10.2 Materials/9.10.4.3 Live Loads

Figure 9.10.2-1
Details of the SIP Deck Panel on Supports



9.10.3 MINIMUM SLAB THICKNESS

For interior spans: 8 in. – 0.5 in. sacrificial layer = 7.5 in. = $t_s > 7.0$ in. OK [LRFD Art. 9.7.1.1]

For overhangs: 8 in. [LRFD Art. 13.7.3.1.2]

Depth of the SIP panel: [LRFD Art. 9.7.4.3.1]

SIP thickness should be $\leq 55\%$ (total depth) = $0.55(8.0) = 4.4$ in. > 3.5 in. OK

Select the 3.5-in.-thick precast SIP panel with 4.5-in.-thick CIP slab. A 1/2-in.-thick wearing surface is an integral part of the 4.5-in.-thick topping slab.

9.10.4 LOADS

The precast SIP panels support their own weight, any construction loads, and the weight of the CIP slab. For superimposed dead and live loads, the precast panels are analyzed assuming that they act compositely with the CIP concrete.

9.10.4.1 Dead Loads

Weight of 3.5-in.-thick SIP panel = $(3.5/12)(0.150) = 0.044$ ksf

Weight of 4.5-in.-thick CIP slab = $(4.5/12)(0.150) = 0.056$ ksf

Weight of New Jersey barrier = 0.300 kips/ft/side

9.10.4.2 Wearing Surface and Construction Loads

Weight of 2-in. wearing surface = $(2/12)(0.150) = 0.025$ ksf

Construction load (applied to the SIP precast panel only) = 0.050 ksf [LRFD Art. 9.7.4.1]

Note that LRFD Article 3.4.2.1 requires a load factor of at least 1.5 be used with construction loads.

9.10.4.3 Live Loads

LRFD Article 3.6.1.3.3 states that for decks where the primary strips are transverse and their span does not exceed 15 ft, the transverse strips are designed for the wheels of the 32.0-kip axle of the design truck.

Multiple Presence Factor: [LRFD Art. 3.6.1.1.2]

Single truck = 1.2

Two trucks = 1.0

Dynamic Load Allowance = 33% [LRFD Art. 3.6.2.1]

LRFD Table A4-1 gives the values of maximum positive and negative bending moments for different spans. This table is valid for decks supported on at least three girders and having a width measured between the centerlines of the exterior girders of not less than 14 ft. Multiple presence factors and the dynamic load allowance are

PRECAST CONCRETE STAY-IN-PLACE DECK PANEL SYSTEM

9.10.4.3 Live Loads/9.10.4.4 Load Combinations

included in the tabulated values. Values of negative bending moments provided by this table do not apply to the deck overhang.

For the deck under consideration, where $S = 12.0$ ft, the maximum positive bending moment, with dynamic allowance, $M_{LL+I} = 8.01$ ft-kips/ft.

For the overhang, a minimum distance of 12 in. from center of wheel of the design truck to the inside face of parapet should be considered [LRFD Art. 3.6.1.3]. However, LRFD Article 3.6.1.3.4 states that for overhangs less than 6.0 ft with continuous barrier, the outside row of wheels may be replaced with a uniformly distributed, 1.0-kip/ft line load, located 1.0 ft from railing face. In this example, the case of concentrated wheel loads is considered.

9.10.4.4 Load Combination

[LRFD Art. 3.4]

Total factored load is taken as:

$$Q = \sum \eta_i \gamma_i Q_i \quad \text{[LRFD Eq. 3.4.1-1]}$$

where

η_i = a load modifier relating to ductility, redundancy, and operational importance. (Here, η_i is considered to be 1.0 for typical bridges.) [LRFD Art. 1.3.2]

γ_i = load factors [LRFD Table 3.4.1-1]

Q_i = force effects from specified loads

Investigating different limit states given in LRFD Article 3.4.1, the following limit states are applicable:

Service I: check compressive stresses in prestressed concrete components:

$$Q = 1.00(DC + DW) + 1.00(LL + IM) \quad \text{[LRFD Table 3.4.1-1]}$$

This load combination is the general combination for service limit state stress checks and applies to all conditions other than Service III.

Service III: check tensile stresses in prestressed concrete components:

$$Q = 1.00(DC + DW) + 0.80(LL + IM) \quad \text{[LRFD Table 3.4.1-1]}$$

This load combination is a special combination for service limit state stress checks that applies only to tension in prestressed concrete structures to control cracks. Note that the 0.8 factor provided for the live load with dynamic allowance is intended for application to longitudinal prestressed concrete beams only. Therefore, it is replaced with a factor of 1.0 for use in this example.

Strength I: check ultimate strength: [LRFD Tables 3.4.1-1 and 2]

$$\text{Maximum } Q = 1.25(DC) + 1.50(DW) + 1.75(LL + IM)$$

$$\text{Minimum } Q = 0.90(DC) + 0.65(DW) + 1.75(LL + IM)$$

This load combination is the general load combination for strength limit state design.

Note: For simple-span bridges, the maximum load factors produce maximum effects. Use minimum load factors for dead load (DC) and wearing surface (DW) when dead load and wearing surface stresses are opposite to those of the live load.

Fatigue: [LRFD Art. 9.5.3 and 5.5.3.1]

Fatigue need not be investigated for concrete slabs in multi-beam bridges.

PRECAST CONCRETE STAY-IN-PLACE DECK PANEL SYSTEM

9.10.5 Cross-Section Properties for a Typical Panel/9.10.5.2.2 Transformed Composite Section Properties

9.10.5 CROSS-SECTION PROPERTIES FOR A TYPICAL PANEL**9.10.5.1 Noncomposite, Nontransformed Panel Section**

$$A_g = \text{area of cross section of the precast panel} = (3.5)(12) = 42 \text{ in.}^2/\text{ft}$$

$$I_g = \text{moment of inertia about the centroid of the noncomposite precast panel} = \frac{(3.5)^3 12}{12} = 42.88 \text{ in.}^4/\text{ft}$$

$$S_b = \text{section modulus for the extreme bottom fiber of the noncomposite precast panel} = (12)(3.5)^2/6 = 24.5 \text{ in.}^3/\text{ft}$$

$$S_t = \text{section modulus for the extreme top fiber of the noncomposite precast panel} = (12)(3.5)^2/6 = 24.5 \text{ in.}^3/\text{ft}$$

$$E_c = \text{modulus of elasticity, ksi} = 33,000K_1(w_c)^{1.5}\sqrt{f'_c} \quad [\text{LRFD Eq. 5.4.2.4-1}]$$

where

$$K_1 = \text{correction factor for source of aggregate taken as 1.0}$$

$$w_c = \text{unit weight of concrete} = 0.150 \text{ kcf}$$

LRFD Table 3.5.1-1 states that, in the absence of more precise data, the unit weight of concrete may be taken as $0.140 + 0.001f'_c$ for $5.0 < f'_c \leq 15.0$ ksi. For $f'_c = 8.0$ ksi, the unit weight would be 0.1480 kcf. However, precast concrete mixes typically have a relatively low water-cementitious materials ratio and high density. Therefore, a unit weight of 0.150 kcf is used in this example. For high-strength concrete, this value may need to be increased based on test results. For simplicity, a value of 0.150 kcf is also used for the cast-in-place concrete.

$$f'_c = \text{specified compressive strength of concrete, ksi}$$

Therefore, the modulus of elasticity is:

$$\text{At transfer, } E_{ci} = 33,000(1.00)(0.150)^{1.5}\sqrt{6.5} = 4,888 \text{ ksi}$$

$$\text{At service loads, } E_c = 33,000(1.00)(0.150)^{1.5}\sqrt{8.0} = 5,422 \text{ ksi}$$

9.10.5.2 Composite Section

The pretensioning reinforcement is ignored in the initial calculations of the composite section properties.

$$E_c \text{ (for the SIP panel)} = 5,422 \text{ ksi}$$

$$E_c \text{ (for the CIP slab)} = 33,000(0.150)^{1.5}\sqrt{4.0} = 3,834 \text{ ksi}$$

9.10.5.2.1 Modular Ratio between CIP and SIP Concrete

$$\text{Modular ratio between CIP slab and SIP panel concrete } n = \frac{E_c(\text{slab})}{E_c(\text{panel})} = 3,834/5,422 = 0.707$$

9.10.5.2.2 Transformed Composite Section Properties

$$\text{Transformed width of CIP slab} = (0.707)(12) = 8.48 \text{ in./ft}$$

$$\text{Transformed area of CIP slab} = (0.707)(12)(4.0) = 33.94 \text{ in.}^2$$

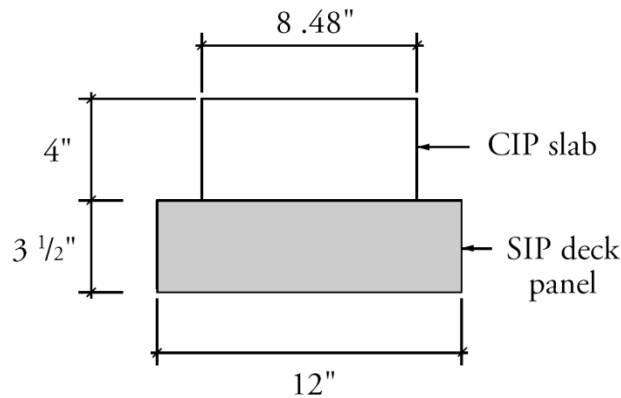
$$\text{Transformed moment of inertia of CIP slab} = 0.707(12)(4.0)^3/12 = 45.25 \text{ in.}^2$$

Figure 9.10.5.2.2-1 shows the dimensions of the composite section. Since a ½-in.-thick wearing surface is considered to be an integral part of the 4½-in.-thick CIP slab, only the structural depth of the CIP slab, 4 in., is considered.

PRECAST CONCRETE STAY-IN-PLACE DECK PANEL SYSTEM

9.10.5.2.2 Transformed Composite Section Properties

Figure 9.10.5.2.2-1
Transformed Composite Section



$$A_c = \text{total area of the composite section} = 12(3.5) + 8.48(4) = 42 + 33.92 = 75.92 \text{ in.}^2/\text{ft}$$

$$y_{bc} = \text{distance from the centroid of the composite section to the extreme bottom fiber of the precast panel} \\ = [42(3.5/2) + 33.92(3.5 + 2)] / (75.92) = 3.43 \text{ in.}$$

$$y_{tg} = \text{distance from the centroid of the composite section to the extreme top fiber of the precast panel} \\ = 3.50 - 3.43 = 0.07 \text{ in.}$$

$$y_{tc} = \text{distance from the centroid of the composite section to the extreme top fiber of the CIP slab} \\ = 3.5 + 4.0 - 3.43 = 4.07 \text{ in.}$$

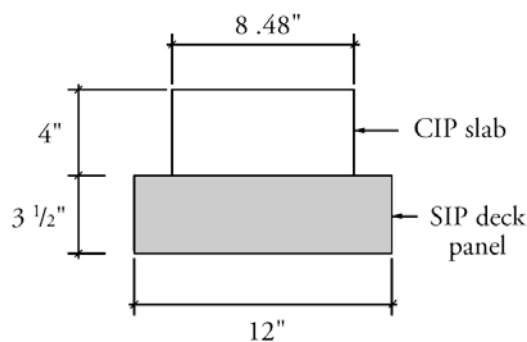
$$I_c = \text{moment of inertia of the composite section} \\ = (42)(3.5)^2/12 + 42(3.43 - 3.5/2)^2 + (33.92)(4)^2/12 + (33.92)(3.5 + 2 - 3.43)^2 = 352 \text{ in.}^4/\text{ft}$$

$$S_{bc} = \text{composite section modulus for the extreme bottom fiber of the precast panel} \\ = (I_c/y_{bc}) = \frac{352}{3.43} = 102.6 \text{ in.}^3/\text{ft}$$

$$S_{tg} = \text{composite section modulus for the top fiber of the precast panel} \\ = (I_c/y_{tg}) = \frac{352}{0.07} = 5,028.6 \text{ in.}^3/\text{ft}$$

$$S_{tc} = \text{composite section modulus for extreme top fiber of the CIP slab} \\ = \left(\frac{1}{n}\right)(I_c/y_{tc}) = \left(\frac{1}{0.707}\right)\left(\frac{352}{4.07}\right) = 122.3 \text{ in.}^3/\text{ft}$$

Figure 9.10.5.2.2-1
Transformed Composite Section



PRECAST CONCRETE STAY-IN-PLACE DECK PANEL SYSTEM

9.10.6 Estimate Required Prestress/9.10.6.1 Service Load Stresses at Midspan

9.10.6 ESTIMATE REQUIRED PRESTRESS

The required number of strands is usually governed by concrete tensile stress at the bottom fiber for load combination Service III.

9.10.6.1 Service Load Stresses at Midspan

Bottom tensile stress due to applied dead and live loads, using the modified Service III load combination (see Section 9.10.4.4), is:

$$f_b = \frac{M_{SIP} + M_{CIP}}{S_b} + \frac{M_{ws} + M_b + M_{LL+I}}{S_{bc}}$$

where

- f_b = concrete tensile stress at bottom fiber of panel, ksi
- M_{SIP} = unfactored bending moment due to SIP panel self weight, ft-kips/ft
- M_{CIP} = unfactored bending moment due to CIP slab weight, ft-kips/ft
- M_{ws} = unfactored bending moment due to future wearing surface, ft-kips/ft
- M_b = unfactored bending moment due to barrier weight, ft-kips/ft
- M_{LL+I} = unfactored bending moment due to live load plus impact, ft-kips/ft
= 8.01 ft-kips/ft (Section 9.10.4.3)

For bending moments due to the weight of the SIP panel and CIP slab, which are acting on the noncomposite section, the span length is taken conservatively as the panel length, 9 ft 6 in.

$$M_{SIP} = (0.044)(9.5)^2/8 = 0.496 \text{ ft-kips/ft}$$

$$M_{CIP} = (0.056)(9.5)^2/8 = 0.632 \text{ ft-kips/ft}$$

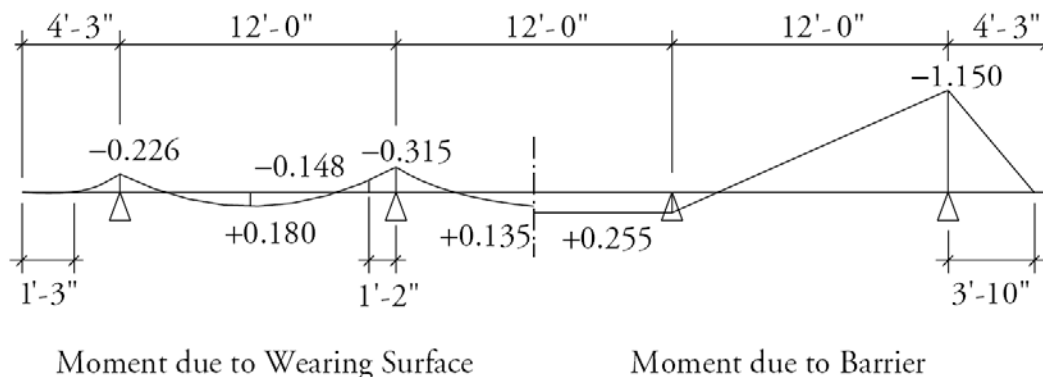
For the superimposed dead and live loads, LRFD Article 4.6.2.1.6 states that force effects should be calculated based on analyzing the strip as a continuous beam supported by infinitely rigid supports. The maximum value of positive moment applies to all positive moment sections [LRFD Art. 4.6.2.1.1]. Also, LRFD Article 4.6.2.1.6 states that the effective span is the center-to-center distance between the supporting beams, which is 12.0 ft. Using software for continuous beam analysis, bending moments due to wearing surface and barrier weight are as shown in **Figure 9.10.6.1-1**.

To arrive at maximum effects, consider the interior span, where

$$M_{ws} = 0.135 \text{ ft-kips/ft}$$

$$M_b = 0.255 \text{ ft-kips/ft}$$

Figure 9.10.6.1-1
Bending Moments in ft-kips/ft



PRECAST CONCRETE STAY-IN-PLACE DECK PANEL SYSTEM**9.10.6.1 Service Load Stresses at Midspan/9.10.6.5 Steel Transformed Section Properties**

$$f_b = \frac{(0.496 + 0.632)12}{24.5} + \frac{(0.135 + 0.255 + 8.01)12}{102.6} = 0.552 + 0.982 = 1.534 \text{ ksi}$$

9.10.6.2 Stress Limits for Concrete

$$\text{Concrete tensile stress limit at service loads} = 0.19\sqrt{f'_c} \quad [\text{LRFD Table 5.9.4.2.2-1}]$$

$$= -0.19\sqrt{8.0} = -0.537 \text{ ksi}$$

9.10.6.3 Required Number of Strands

The required precompressive stress at bottom fiber of the panel is the difference between bottom tensile stress due to the applied loads and the concrete tensile stress limit:

$$f_{pb} = 1.534 - 0.537 = 0.997 \text{ ksi}$$

If P_{pe} is the total effective prestress force after all losses, and the center of gravity of strands is concentric with the center of gravity of the SIP panel:

$$0.997 = \frac{P_{pe}}{A_g} = \frac{P_{pe}}{42}$$

Solving for P_{pe} , the required $P_{pe} = 41.9 \text{ kips/ft} = (41.9)(8.0) = 335.2 \text{ kips/panel}$

Using 1/2-in.-diameter, 270 ksi, low-relaxation strand and assuming 15% final losses, the final prestress force per strand = $f_{pi}(\text{area of strand})(1 - \text{final losses})$

$$= (202.5)(0.153)(1 - 0.15) = 26.3 \text{ kips}$$

The required number of strands = $335.2/26.3 = 12.8 \text{ strands/panel}$

Try (13) 1/2-in.-diameter, 270 ksi, low-relaxation strands per panel.

9.10.6.4 Strand Pattern

The distance between the center of gravity of bottom strands and the bottom concrete fiber of the panel is:

$$y_{bs} = 3.5/2 = 1.75 \text{ in.}$$

The distance from the centroid of the panel to the extreme bottom fiber of the noncomposite panel:

$$y_b = 3.5/2 = 1.75 \text{ in.}$$

Strand eccentricity at midspan, $e_c = y_b - y_{bs} = 1.75 - 1.75 = 0 \text{ in.}$

9.10.6.5 Steel Transformed Section Properties

From the earliest years of prestressed concrete design, the gross section was conservatively used in analysis since the prestressing forces were smaller and computer programs were not widely used. However, the use of transformed section, which is obtained from the gross section by adding transformed steel area, yields more accurate results than the gross section analysis.

For each row of prestressing strands, the steel area is multiplied by $(n - 1)$ to calculate the transformed section properties, where n is the modular ratio between prestressing strand and concrete. Since the modulus of elasticity of concrete is different at transfer and final time, the transformed section properties should be calculated separately in the two stages. Using the similar procedures as in Section 9.10.5.2, the transformed section properties area calculated as shown in **Table 9.10.6.5-1**.

At transfer:

$$n - 1 = \frac{28,500}{4,888} - 1 = 4.831$$

At final:

$$n - 1 = \frac{28,500}{5,422} - 1 = 4.256$$

PRECAST CONCRETE STAY-IN-PLACE DECK PANEL SYSTEM

9.10.6.5 Steel Transformed Section Properties

Table 9.10.6.5-1
Properties of Composite Transformed Section at Final Time

	Transformed Area, in. ²	y_b in	Ay_b in. ³	$A(y_{btc} - y_b)^2$ in. ⁴	I in. ⁴	$I + A(y_{btc} - y_b)^2$ in. ⁴
Panel	42.00	1.75	73.5	114.3	42.88	157.2
Slab	33.94	5.50	186.7	149.7	45.25	195.0
Row 1	1.06	1.75	1.86	2.9		2.9
Σ	77.0		262.1			355.1

Note: The moment of inertia of strand about its own centroid is neglected.

The transformed section properties are calculated as:

Noncomposite transformed section at transfer:

$$A_{ti} = \text{area of transformed section at transfer} = 43.2 \text{ in.}^2/\text{ft}$$

$$I_{ti} = \text{moment of inertia of the transformed section at transfer} = 42.9 \text{ in.}^4/\text{ft}$$

$$e_{ti} = \text{eccentricity of strands with respect to transformed section at transfer} = 0.0 \text{ in.}$$

$$y_{bti} = \text{distance from the centroid of the transformed section to the extreme bottom fiber of the beam at transfer} = 1.75 \text{ in.}$$

$$S_{bti} = \text{section modulus for the extreme bottom fiber of the transformed section at transfer} = 24.5 \text{ in.}^3/\text{ft}$$

$$S_{tti} = \text{section modulus for the extreme top fiber of the transformed section at transfer} = 24.5 \text{ in.}^3/\text{ft}$$

Noncomposite transformed section at final time:

$$A_{tf} = \text{area of transformed section at final time} = 43.1 \text{ in.}^2/\text{ft}$$

$$I_{tf} = \text{moment of inertia of the transformed section at final time} = 42.9 \text{ in.}^4/\text{ft}$$

$$e_{tf} = \text{eccentricity of strands with respect to transformed section at final time} = 0.0 \text{ in.}$$

$$y_{btf} = \text{distance from the centroid of the noncomposite transformed section to the extreme bottom fiber of the beam at final time} = 1.75 \text{ in.}$$

$$S_{btf} = \text{section modulus for the extreme bottom fiber of the transformed section at final time} = 24.5 \text{ in.}^3/\text{ft}$$

$$S_{ttf} = \text{section modulus for the extreme top fiber of the transformed section at final time} = 24.5 \text{ in.}^3/\text{ft}$$

Composite transformed section at final time:

$$A_{tc} = \text{area of transformed composite section at final time} = 77.0 \text{ in.}^2/\text{ft}$$

$$I_{tc} = \text{moment of inertia of the transformed composite section at final time} = 355.1 \text{ in.}^4/\text{ft}$$

$$e_{tc} = \text{eccentricity of strands with respect to transformed composite section at final time} = 1.65 \text{ in.}$$

$$y_{btc} = \text{distance from the centroid of the transformed composite section to the extreme bottom fiber of the beam at final time} = 3.40 \text{ in.}$$

$$S_{btc} = \text{section modulus for the extreme bottom fiber of the transformed composite section at final time} = 104.4 \text{ in.}^3/\text{ft}$$

$$S_{ttc} = \text{section modulus for the extreme top fiber of the transformed composite precast panel at final time} = 3,551.0 \text{ in.}^3/\text{ft}$$

$$S_{dtc} = \text{section modulus for the extreme top fiber of the deck of the transformed composite section at final time} = 122.5 \text{ in.}^3/\text{ft}$$

PRECAST CONCRETE STAY-IN-PLACE DECK PANEL SYSTEM

9.10.7 Prestress Losses/9.10.7.1 Elastic Shortening

9.10.7 PRESTRESS LOSSES

Total prestress loss:

$$\Delta f_{pT} = \Delta f_{pES} + \Delta f_{pLT} \quad [\text{LRFD Eq. 5.9.5.1-1}]$$

where

Δf_{pT} = total loss in prestressing steel stress

Δf_{pES} = sum of all losses or gains due to elastic shortening or extension at the time of application of prestress and/or external loads

Δf_{pLT} = long-term losses due to shrinkage and creep of concrete, and relaxation of steel after transfer. In this design example, the refined estimates of time-dependent losses are used.

Note that the SIP deck panel will be considered as the “girder” and the CIP composite slab will be considered as the “deck” in the analysis.

9.10.7.1 Elastic Shortening

$$\Delta f_{pES} = \frac{E_p}{E_{ci}} f_{cgp} \quad [\text{LRFD Eq. 5.9.5.2.3a-1}]$$

where

E_p = modulus of elasticity of prestressing strands = 28,500 ksi

E_{ci} = modulus of elasticity of beam concrete at transfer = 4,888 ksi

f_{cgp} = sum of concrete stresses at the center of gravity of prestressing tendons due to prestressing force at transfer and the self weight of the member at sections of maximum moment.

If the gross (or net) cross-section properties are used, it is necessary to perform numerical iterations. The elastic loss Δf_{pES} is usually assumed to be 10% of the initial prestress to calculate f_{cgp} , which is then used in the equation above to calculate a refined Δf_{pES} . The process is repeated until the assumed Δf_{pES} and refined Δf_{pES} are close enough.

However, when transformed section properties are used to calculate concrete stress, the effects of loss and gains due to elastic deformations are implicitly accounted for. Therefore, Δf_{pES} should not be included in calculating f_{cgp} .

Force per strand before transfer = (area of strand)(prestress stress before transfer)

$$= (0.153)(202.5) = 30.98 \text{ kips}$$

$$f_{cgp} = \frac{P_{pi}}{A_{ti}} + \frac{P_{pi}e_{ti}^2}{I_{ti}} - \frac{M_{SIP}e_{ti}}{I_{ti}}$$

where

e_{ti} = eccentricity of strands at midspan with respect to the transformed section at transfer = 0.0 in.

P_{pi} = total prestressing force before transfer = 30.98(13)/8 = 50.3 kips/ft

$$f_{cgp} = \frac{50.3}{43.2} + 0 - 0 = 1.164 \text{ ksi}$$

Therefore, loss due to elastic shortening:

$$\Delta f_{pes} = \left(\frac{28,500}{4,888} \right) (1.164) = 6.8 \text{ ksi}$$

AASHTO LRFD C5.9.5.3 indicates that the loss due to elastic shortening at transfer should be added to the time-dependent losses to determine total losses. However, this loss must be taken equal to zero if transformed section properties are used in stress analysis.

PRECAST CONCRETE STAY-IN-PLACE DECK PANEL SYSTEM**9.10.7.2 Time-Dependent Losses between Transfer and Deck Placement/9.10.7.2.1 Shrinkage of Precast Concrete****9.10.7.2 Time-Dependent Losses between Transfer and Deck Placement**

The following construction schedule is assumed in calculating the time-dependent losses:

Concrete age at transfer:	$t_i = 1$ day
Concrete age at deck placement:	$t_d = 90$ days
Concrete age at final stage:	$t_f = 20,000$ days

The total time-dependent loss between time of transfer and deck placement is the summation of prestress loss due to shrinkage of concrete, creep of concrete, and relaxation of prestressing strands.

9.10.7.2.1 Shrinkage of Precast Concrete

The prestress loss due to shrinkage of concrete between time of transfer and deck placement is calculated by:

$$\Delta f_{pSR} = \epsilon_{bid} E_p K_{id} \quad [\text{LRFD Eq. 5.9.5.4.2a-1}]$$

where

- ϵ_{bid} = concrete shrinkage strain of panel for time period between transfer and deck placement
- E_p = modulus of elasticity of prestressing strands, ksi
- K_{id} = transformed section coefficient that accounts for time-dependent interaction between concrete and bonded steel in the section being considered for time period between transfer and deck placement

The concrete shrinkage, ϵ_{bid} , strain is taken as:

$$\epsilon_{bid} = k_{vs} k_{hs} k_f k_{td} 0.48 \times 10^{-3} \quad [\text{LRFD Eq. 5.4.2.3.3.-1}]$$

where

The factor for the effect of the volume-to-surface ratio of the beam:

$$k_{vs} = 1.45 - 0.13(V/S) = 1.45 - 0.13 \times 1.64 = 1.237$$

The minimum value of k_{vs} is 1.0 OK

V/S is the volume-to-surface ratio of the SIP panel.

The humidity factor for shrinkage:

$$k_{hs} = 2.00 - 0.014H = 2.00 - 0.014(70) = 1.020$$

where H = relative humidity (assume 70%)

The factor for the effect of the concrete strength:

$$k_f = \frac{5}{1 + f'_{ci}} = \frac{5}{1 + 6.5} = 0.667$$

The time development factor:

$$k_{td} = \frac{t}{61 - 4f'_{ci} + t} = \frac{89}{61 - 4(6.5) + 89} = 0.718 = k_{tda}$$

where t is the maturity of concrete = $t_d - t_i = 90 - 1 = 89$ days

$$\epsilon_{bid} = (1.237)(1.020)(0.667)(0.718)(0.48 \times 10^{-3}) = 0.000290$$

$$K_{id} = \frac{1}{1 + \frac{E_p}{E_{ci}} \frac{A_{ps}}{A_g} \left(1 + \frac{A_g (e_{pg})^2}{I_g} \right) [1 + 0.7\Psi_b(t_f, t_i)]} \quad [\text{LRFD Eq. 5.9.5.4.2a-2}]$$

PRECAST CONCRETE STAY-IN-PLACE DECK PANEL SYSTEM

9.10.7.2.1 Shrinkage of Precast Concrete/9.10.7.2.3 Relaxation of Prestressing Strands

where

$$A_{ps} = \text{area of prestressing strands per ft} = [(0.153)(13 \text{ strands})]/8 \text{ ft} = 0.249 \text{ in.}^2/\text{ft}$$

$$e_{pg} = \text{eccentricity of prestressing strand with respect to centroid of panel, in.}$$

$$\Psi_b(t_f, t_i) = \text{panel creep coefficient at final time due to loading introduced at transfer}$$

For the time between transfer and final time:

$$\Psi_b(t_f, t_i) = 1.9k_{vs}k_{hc}k_{fd}k_{td}t_i^{-0.118} \quad [\text{LRFD Eq. 5.4.2.3.2-1}]$$

$$k_{hc} = 1.56 - 0.008H = 1.56 - 0.008(70) = 1.000$$

$$k_{td} = \frac{t_f - t_i}{61 - 4f_{ci} + (t_f - t_i)} = \frac{20,000 - 1}{61 - 4(6.5) + (20,000 - 1)} = 0.998 = k_{tdf}$$

$$\Psi_b(t_f, t_i) = 1.9(1.237)(1.000)(0.667)(0.998)(1)^{-0.118} = 1.565$$

$$K_{id} = \frac{1}{1 + \left(\frac{28,500}{4,888}\right) \left(\frac{0.249}{42.0}\right) \left(1 + \frac{42.0(0)^2}{42.88}\right) [1 + 0.7(1.565)]} = 0.932$$

The prestress loss due to shrinkage of concrete between transfer and deck placement is:

$$\Delta f_{pSR} = (0.000290)(28,500)(0.932) = 7.703 \text{ ksi}$$

9.10.7.2.2 Creep of Precast Concrete

The prestress loss due to creep of panel concrete between time of transfer and deck placement is determined as:

$$\Delta f_{pCR} = \frac{E_p}{E_{ci}} f_{cgp} \Psi_b(t_d, t_i) K_{id} \quad [\text{LRFD Eq. 5.9.5.4.2b-1}]$$

where

$$\Psi_b(t_d, t_i) = \text{girder creep coefficient at time of deck placement due to loading introduced at transfer}$$

$$= 1.9k_{vs}k_{hc}k_{fd}k_{td}t_i^{-0.118} \quad [\text{LRFD Eq. 5.4.2.3.2-1}]$$

$$= 1.9(1.237)(1.000)(0.667)(0.718)(1)^{-0.118} = 1.126$$

$$\Delta f_{pCR} = \frac{28,500}{4,888} (1.164)(1.126)(0.932) = 7.122 \text{ ksi}$$

9.10.7.2.3 Relaxation of Prestressing Strands

The prestress loss due to relaxation of prestressing strands between time of transfer and deck placement is determined as:

$$\Delta f_{pR1} = \frac{f_{pt}}{K_L} \left(\frac{f_{pt}}{f_{py}} - 0.55 \right) \quad [\text{LRFD Eq. 5.9.5.4.2c-1}]$$

where

$$f_{pt} = \text{stress in prestressing strands immediately after transfer, taken not less than } 0.55f_y$$

$$K_L = 30 \text{ for low-relaxation strands and } 7 \text{ for other prestressing steel, unless more accurate manufacturer's data are available}$$

$$\Delta f_{pR1} = \frac{(202.5 - 6.8)}{30} \left(\frac{(202.5 - 6.8)}{243} - 0.55 \right) = 1.666 \text{ ksi}$$

According to LRFD Art. 5.9.5.4.2c, the relaxation loss may also be assumed equal to 1.2 ksi for low-relaxation strands.

PRECAST CONCRETE STAY-IN-PLACE DECK PANEL SYSTEM**9.10.7.3 Time-Dependent Losses between Deck Placement and Final Time/9.10.7.3.2 Creep of Precast Concrete****9.10.7.3 Time-Dependent Losses between Deck Placement and Final Time**

The total time-dependent loss between time of deck placement and final time is the summation of prestress losses due to shrinkage of panel concrete, creep of panel concrete, relaxation of prestressing strands, and shrinkage of CIP deck concrete.

9.10.7.3.1 Shrinkage of Precast Concrete

The prestress loss due to shrinkage of concrete between deck placement and final time is calculated by:

$$\Delta f_{pSD} = \epsilon_{bdf} E_p K_{df} \quad [\text{LRFD Eq. 5.9.5.4.3a-1}]$$

where

ϵ_{bdf} = concrete shrinkage strain of panel between deck placement and final time

E_p = modulus of elasticity of prestressing strands, ksi

K_{df} = transformed section coefficient that accounts for time-dependent interaction between concrete and bonded steel in the section being considered for time period between deck placement and final time

The total concrete shrinkage strain between transfer and final time is taken as:

$$\begin{aligned} \epsilon_{bif} &= k_{vs} k_{hs} k_{jt} k_{td} 0.48 \times 10^{-3} \quad [\text{LRFD Eq. 5.4.2.3.3-1}] \\ &= (1.237)(1.020)(0.667)(0.998)(0.48 \times 10^{-3}) = 0.000403 \end{aligned}$$

The concrete shrinkage strain between deck placement and final time is:

$$\epsilon_{bdf} = \epsilon_{bif} - \epsilon_{bid} = 0.000403 - 0.000290 = 0.000113$$

The beam concrete transformed section coefficient between deck placement and final time is:

$$K_{df} = \frac{1}{1 + \frac{E_p}{E_{ci}} \frac{A_{ps}}{A_c} \left(1 + \frac{A_c (e_{pc})^2}{I_c} \right) [1 + 0.7 \Psi_b(t_f, t_i)]} \quad [\text{LRFD Eq. 5.9.5.4.3a-2}]$$

where

A_c = area of the composite section = 75.92 in.²/ft

I_c = moment of inertia of the composite section = 352 in.⁴/ft

e_{pc} = eccentricity of strands with respect to centroid of composite section, in.
= 3.43 – 1.75 = 1.68 in.

$$K_{df} = \frac{1}{1 + \left(\frac{28,500}{4,888} \right) \left(\frac{0.249}{75.92} \right) \left(1 + \frac{(75.92)(1.68)^2}{352} \right) [1 + 0.7(1.565)]} = 0.939$$

The prestress loss due to shrinkage of concrete between deck placement and final time is:

$$\Delta f_{pSD} = (0.000113)(28,500)(0.939) = 3.024 \text{ ksi}$$

9.10.7.3.2 Creep of Precast Concrete

The prestress loss due to creep of girder concrete between deck placement and final time is determined as:

$$\Delta f_{pCD} = \frac{E_p}{E_{ci}} f_{cgp} [\Psi_b(t_f, t_i) - \Psi_b(t_d, t_i)] K_{df} + \frac{E_p}{E_c} \Delta f_{cd} \Psi_b(t_f, t_d) K_{df} \quad [\text{LRFD Eq. 5.9.5.4.3b-1}]$$

where

$\Psi_b(t_f, t_d)$ = panel creep coefficient at final time due to loading at deck placement

$$= 1.9 k_{vs} k_{hc} k_{jt} k_{td} t_d^{-0.118} \quad [\text{LRFD Eq. 5.4.2.3.2-1}]$$

PRECAST CONCRETE STAY-IN-PLACE DECK PANEL SYSTEM

9.10.7.3.2 Creep of Precast Concrete/9.10.7.3.4 Shrinkage of CIP Concrete

$$\begin{aligned}
 k_{tdf} &= \frac{t}{61 - 4f'_{ci} + t} = \frac{(20,000 - 90)}{61 - 4(6.5) + (20,000 - 90)} = 0.998 \\
 \Psi_b(t_f, t_d) &= 1.9(1.237)(1.000)(0.667)(0.998)(90)^{-0.118} = 0.920 \\
 \Delta f_{cd} &= \text{change in concrete stress at centroid of prestressing strands due to long-term losses between transfer and deck placement, combined with deck weight and superimposed loads, ksi} \\
 &= -(\Delta f_{pSR} + \Delta f_{pCR} + \Delta f_{pR1}) \frac{A_{ps}}{A_g} \left(1 + \frac{A_g e_{pg}^2}{I_g} \right) - \left(\frac{M_{CIP} e_{tf}}{I_{tf}} + \frac{(M_b + M_{ws}) e_{tc}}{I_{tc}} \right) \\
 &= -(7.703 + 7.122 + 1.666) \frac{0.249}{42.00} \left(1 + \frac{42.0(0)^2}{42.88} \right) - \left(\frac{(0.632)(0)}{42.9} + \frac{(0.255 + 0.135)(12)(1.65)}{355.1} \right) \\
 &= -0.120 \text{ ksi}
 \end{aligned}$$

The gross section properties are used in the equation to calculate Δf_{cd} for the long-term losses since the transformed section effect has already been included in the factor K_{id} when calculating the losses between initial time and deck placement.

$$\Delta f_{pCD} = \frac{28,500}{4,888} 1.164[1.565 - 1.126](0.939) + \frac{28,500}{5,423} (-0.120)(0.920)(0.939) = 2.253 \text{ ksi}$$

9.10.7.3.3 Relaxation of Prestressing Strands

The prestress loss due to relaxation of prestressing strands in composite section between time of deck placement and final time is taken as:

$$\Delta f_{pR2} = \Delta f_{pR1} = 1.666 \text{ ksi} \quad \text{[LRFD Eq. 5.9.5.4.3c-1]}$$

9.10.7.3.4 Shrinkage of CIP Concrete

The prestress gain due to shrinkage of CIP deck concrete is calculated by:

$$\Delta f_{pSS} = \frac{E_p}{E_c} \Delta f_{cdf} K_{df} [1 + 0.7\Psi_b(t_f, t_d)] \quad \text{[LRFD Eq.5.9.5.4.3d-1]}$$

where Δf_{cdf} = change in concrete stress at centroid of prestressing strands due to shrinkage of deck concrete, ksi

$$= \frac{\epsilon_{ddf} A_d E_{cd}}{1 + 0.7\Psi_d(t_f, t_d)} \left(\frac{1}{A_c} - \frac{e_{pc} e_d}{I_c} \right) \quad \text{[LRFD Eq.5.9.5.4.3d-2]}$$

Where

- ϵ_{ddf} = shrinkage strain of CIP deck concrete between placement and final time
- A_d = area of CIP deck concrete, in.²/ft
- E_{cd} = modulus of elasticity of CIP deck concrete, ksi
- $\Psi_d(t_f, t_d)$ = CIP deck creep coefficient at final time due to loading introduced shortly after CIP deck placement
- e_d = eccentricity of CIP deck with respect to the gross composite section, in.

Assume the initial strength of concrete at deck placement is $0.8(4.0 \text{ ksi}) = 3.2 \text{ ksi}$, and use a volume-to-surface ratio 4.0 (drying from top surface only) for the CIP deck:

$$k_{vs} = 1.45 - 0.13(V/S) = 1.45 - 0.13(4.000) = 0.930 < 1.0$$

Therefore, use $k_{vs} = 1.000$

PRECAST CONCRETE STAY-IN-PLACE DECK PANEL SYSTEM

9.10.7.3.4 Shrinkage of CIP Concrete/9.10.7.3.6 Total Losses at Transfer

$$k_f = \frac{5}{1 + f'_{ci}} = \frac{5}{1 + 3.2} = 1.190$$

$$k_{td} = \frac{t}{61 - 4f'_{ci} + t} = \frac{20,000 - 90}{61 - 4(3.2) + (20,000 - 90)} = 0.998$$

$$\begin{aligned} \varepsilon_{adf} &= k_{vs}k_{hs}k_fk_{td}0.48 \times 10^{-3} \\ &= (1.000)(1.020)(1.190)(0.998)(0.48 \times 10^{-3}) = 0.000581 \end{aligned}$$

$$\begin{aligned} \Psi_d(t_f, t_d) &= 1.9k_{vs}k_{hc}k_fk_{td}t_i^{-0.118} && \text{[LRFD Eq. 5.4.2.3.2-1]} \\ &= 1.9(1.000)(1.000)(1.190)(0.998)(1)^{-0.118} = 2.256 \end{aligned}$$

Creep of the CIP deck concrete is assumed to start at 1 day

$$\Delta f_{cdf} = \frac{0.000581(12 \times 4)(3,834)}{1 + 0.7(2.256)} \left(\frac{1}{75.92} - \frac{(1.68) \left(7.5 - \frac{4}{2} - 3.43 \right)}{352} \right) = 0.136 \text{ ksi}$$

The prestress loss due to shrinkage of the deck in the composite section:

$$\Delta f_{pSS} = \frac{28,500}{5,422} (0.136)(0.939)[1 + 0.7(0.920)] = 1.104 \text{ ksi}$$

Note: The effect of CIP concrete shrinkage on the calculation of prestress gain is discussed further in Section 9.1a.8.5.

9.10.7.3.5 Total Time-Dependent Loss

The total time-dependent loss, Δf_{pLT} , is determined as:

$$\begin{aligned} \Delta f_{pLT} &= (\Delta f_{pSR} + \Delta f_{pCR} + \Delta f_{pR1}) + (\Delta f_{pSD} + \Delta f_{pCD} + \Delta f_{pR2} + \Delta f_{pSS}) && \text{[LRFD Eq. 5.9.5.4.1-1]} \\ &= (7.703 + 7.122 + 1.666) + (3.024 + 2.253 + 1.666 + 1.104) = 24.5 \text{ ksi} \end{aligned}$$

9.10.7.3.6 Total Losses at Transfer

AASHTO LRFD C5.9.5.2.3a and C5.9.5.3 indicate that the losses or gains due to elastic deformation must be taken equal to zero if transformed section properties are used in stress analysis. However, the losses or gains due to elastic deformation must be included in determining the total prestress losses and the effective stress in prestressing strands.

$$\Delta f_{pi} = \Delta f_{pES} = 6.8 \text{ ksi}$$

$$\text{Effective stress in tendons immediately after transfer, } f_{pt} = f_{pi} - \Delta f_{pi} = (202.5 - 6.8) = 195.7 \text{ ksi}$$

$$\text{Force per strand} = (f_{pt})(\text{area of strand}) = (195.7)(0.153) = 29.94 \text{ kips}$$

$$\begin{aligned} \text{Therefore, the total prestressing force after transfer } P_{pt} &= 29.94(13) = 389.2 \text{ kips/panel} = 389.2/8 \text{ kips/ft} \\ &= 48.65 \text{ kips/ft} \end{aligned}$$

$$\text{Initial loss, \%} = (\text{Total losses at transfer})/(f_{pi}) = 6.8/202.5 = 3.4\%$$

When determining the concrete stresses using transformed section properties the strand force is that before transfer:

$$\text{Force per strand} = (202.5)(0.153) = 30.98 \text{ kips}$$

$$\text{The total prestressing force before transfer, } P_{pi} = 30.98(13) = 402.7 \text{ kips/panel} = 50.34 \text{ kips/ft}$$

PRECAST CONCRETE STAY-IN-PLACE DECK PANEL SYSTEM**9.10.7.3.7 Total Losses at Service Loads/9.10.8.1 Stress Limits for Concrete****9.10.7.3.7 Total Losses at Service Loads**

Total loss due to elastic shortening at transfer and long-term losses (Service III) is:

$$\Delta f_{pT} = \Delta f_{pES} + \Delta f_{pLT} = 6.8 + 24.5 = 31.3 \text{ ksi}$$

The elastic gain due to deck weight, superimposed dead load, and live load is:

$$\begin{aligned} & \left(\frac{M_{CIP} e_{tf}}{I_{tf}} + \frac{(M_b + M_{ws}) e_{tc}}{I_{tc}} \right) \frac{E_p}{E_c} + 0.8 \left(\frac{(M_{LL+I}) e_{tc}}{I_{tc}} \right) \frac{E_p}{E_c} \\ & = \left(\frac{(0.632)(12)(0)}{42.9} + \frac{(0.255 + 0.135)(12)(1.65)}{355.1} \right) \frac{28,500}{5,422} + 0.8 \left(\frac{(8.010)(12)(1.65)}{355.1} \right) \frac{28,500}{5,422} = 0.11 + 1.88 \\ & = 1.99 \text{ ksi} \end{aligned}$$

The effective stress in tendons after all losses and gains:

$$f_{pe} = f_{pi} - \Delta f_{pT} + 0.11 = 202.5 - 31.3 + 2.0 = 173.2 \text{ ksi}$$

Check prestressing stress limit at service limit state:

[LRFD Table 5.9.3-1]

$$f_{pe} \leq 0.8f_{py} = 0.8(243) = 194.4 \text{ ksi} > 173.2 \text{ ksi} \quad \text{OK}$$

The effective stress in strands after all losses and permanent gains:

$$f_{pe} = f_{pi} - \Delta f_{pT} + 0.11 = 202.5 - 31.3 + 0.11 = 171.3 \text{ ksi}$$

Force per strand without live load losses = $(f_{pe})(\text{area of strand}) = (171.3)(0.153) = 26.21 \text{ kips}$

Therefore, the total prestressing force after all losses = $26.21(13) = 340.73 \text{ kips/panel} = 340.73/8$

$$= 42.59 \text{ kips/ft}$$

Final loss percentage = $(\text{total losses and gains})/(f_{pi}) = (31.3 - 0.11)/(202.5) = 15.4 \%$

When determining the concrete stress using transformed section properties, all the elastic gains and losses are implicitly accounted for:

Force per strand with only total time-dependent losses $(f_{pi} - \Delta f_{pLT})(\text{area of strand}) = (202.5 - 24.5)(0.153) = 27.23 \text{ kips}$

Total prestressing force, $P_{pe} = (27.23)(13) = 353.99 \text{ kips/panel} = 353.99/8 = 44.25 \text{ kips/ft}$

9.10.8 CONCRETE STRESSES IN THE SIP PANEL AT TRANSFER**9.10.8.1 Stress Limits for Concrete**

[LRFD Art. 5.9.4]

Compression:

- $0.6f'_{ci} = 0.6(6.5) = +3.900 \text{ ksi}$

where f'_{ci} = concrete strength at transfer

Tension:

- without bonded auxiliary reinforcement:

$$0.0948\sqrt{f'_{ci}} \leq 0.200 = -0.0948\sqrt{6.5} = -0.242 \text{ ksi}$$

Therefore, -0.200 ksi (Controls)

- with bonded reinforcement that is sufficient to resist 120% of the tension force in the cracked concrete:

$$0.24\sqrt{f'_{ci}} = -0.24\sqrt{6.5} = -0.612 \text{ ksi}$$

Because the strand group is concentric with the precast concrete panel, the midspan section is the critical section that should be checked.

PRECAST CONCRETE STAY-IN-PLACE DECK PANEL SYSTEM**9.10.8.2 Stresses at Midspan/9.10.9.2 Stresses at Midspan after all Noncomposite Loads****9.10.8.2 Stresses at Midspan**

Effective prestress after transfer, $P_{pi} = 50.34$ kips/ft

Bending moment due to self weight of the panel, $M_{SIP} = 0.496$ ft-kips/ft

Compute stress in the top of SIP panel:

$$f_t = \frac{P_{pi}}{A_{ti}} + \frac{M_{SIP}}{S_{tti}} = \frac{50.34}{43.2} + \frac{0.496(12)}{24.5} = +1.408 \text{ ksi}$$

Compressive stress limit: $+3.900 \text{ ksi} > +1.408 \text{ ksi}$ OK

Bottom concrete stress of the SIP panel:

$$f_b = \frac{P_i}{A_{ti}} - \frac{M_{SIP}}{S_{bti}} = \frac{50.34}{43.2} - \frac{0.496(12)}{24.5} = +0.922 \text{ ksi}$$

Compressive stress limit: $+3.900 \text{ ksi} > +0.922 \text{ ksi}$ OK

9.10.9 CONCRETE STRESSES IN SIP PANEL AT TIME OF CASTING TOPPING SLAB

Using transformed section properties and refined losses, $P_{pe} = 44.25$ kips/ft

9.10.9.1 Stress Limits for Concrete

LRFD Article 9.7.4.1 states that flexural stresses in the SIP formwork due to unfactored construction loads should not exceed 65% of the 28-day compressive strength for concrete in compression, or the modulus of rupture in tension.

Note that the definition of construction loads according to the *LRFD Specifications* includes the weight of the SIP panel, CIP topping, and an additional 0.050 ksf.

Therefore, the stress limit for concrete in compression, for load combination Service I:

$$0.65 f'_c = +0.65(8.0) = +5.200 \text{ ksi}$$

Stress limit for concrete in tension, for load combination Service I:

$$\text{Modulus of rupture, } f_r = 0.24\sqrt{f'_c} = -0.24\sqrt{8.0} = -0.679 \text{ ksi} \quad [\text{LRFD Art. 5.4.2.6}]$$

9.10.9.2 Stresses at Midspan after all Noncomposite Loads

Bending moment due to the self weight of the SIP panel, all losses (creates highest concrete fiber stress and thus a conservative calculation), the CIP topping and construction load:

$$M_{SIP} = 0.496 \text{ ft-kips/ft}$$

$$M_{CIP} = 0.632 \text{ ft-kips/ft}$$

$$M_{const} = (0.050)(9.5)^2/8 = 0.564 \text{ ft-kips/ft}$$

Concrete stress at top fiber of the SIP panel:

$$f_t = \frac{P_{pe}}{A_{tf}} + \frac{M_{SIP} + M_{CIP} + M_{const}}{S_{ttf}} = \frac{44.25}{43.1} + \frac{(0.496 + 0.632 + 0.564)(12)}{24.5} = +1.855 \text{ ksi}$$

Compressive stress limit: $+5.200 \text{ ksi} > +1.855 \text{ ksi}$ OK

Concrete stress at bottom fiber of the SIP panel:

$$f_b = \frac{P_{pe}}{A_{tf}} - \frac{M_{SIP} + M_{CIP} + M_{const}}{S_{btf}} = \frac{44.25}{43.1} - \frac{(0.496 + 0.632 + 0.564)(12)}{24.5} = +0.198 \text{ ksi}$$

Compressive stress limit: $+5.200 \text{ ksi} > +0.196 \text{ ksi}$ OK

PRECAST CONCRETE STAY-IN-PLACE DECK PANEL SYSTEM**9.10.9.3 Elastic Deformation/9.10.10.2.1 Concrete Stress at Top Surface of the CIP Slab****9.10.9.3 Elastic Deformation**

(Art. 9.7.4.1)

LRFD Article 9.7.4.1, states that, for SIP panels spanning less than 10 ft, the elastic deformation due to dead load of the panel plus the CIP topping should not exceed either the panel span divided by 180 or 0.50 in.

$$\begin{aligned} \text{Elastic deformation} &= \frac{5}{48} \frac{(M_{SIP} + M_{CIP})L^2}{E_c I_g} \\ &= \frac{5}{48} \frac{(0.496 + 0.632)(12)[(9.5)(12)]^2}{(5,422)(42.88)} \\ &= 0.08 \text{ in.} < 0.50 \text{ in.} < 9.5 \frac{12}{180} = 0.63 \text{ in.} \quad \text{OK} \end{aligned}$$

9.10.10 CONCRETE STRESSES IN SIP PANEL AT SERVICE LOADS

Using transformed section properties and refined losses, $P_{pe} = 44.25$ kips/ft

9.10.10.1 Stress Limits for Concrete

[LRFD Art. 5.9.4.2]

Compression for load combination Service I:

- Due to permanent loads, (i.e. self weight of SIP panel, CIP slab, wearing surface, and barriers) = $0.45f'_c$
for the SIP panel: $0.45(8.000) = +3.600$ ksi
for the CIP slab: $0.45(4.000) = +1.800$ ksi
- Due to permanent and transient loads, (i.e. all dead and live loads) = $0.60f'_c$
for the SIP panel: $0.60(8.0) = +4.800$ ksi
for the CIP slab: $0.60(4.000) = +2.400$ ksi
- Tension for load combination Service III: $0.19\sqrt{f'_c}$

$$\text{for the SIP panel} = -0.19\sqrt{8.000} = -0.537 \text{ ksi}$$

9.10.10.2 Service Load Stresses at Midspan

Effective prestress after all losses, $P_{pe} = 44.25$ kips

The weights of the SIP panel and the CIP concrete act on the noncomposite section:

$$M_{SIP} = 0.496 \text{ ft-kips/ft}$$

$$M_{CIP} = 0.632 \text{ ft-kips/ft}$$

At the time of opening the bridge to traffic, the wearing surface, barriers, and live loads act on the composite section.

$$M_{ws} = 0.135 \text{ ft-kips/ft}$$

$$M_b = 0.255 \text{ ft-kips/ft}$$

$$M_{LL+I} = 8.01 \text{ ft-kips/ft}$$

9.10.10.2.1 Concrete Stress at Top Surface of the CIP Slab

Due to permanent loads, Service I:

$$f_{tc} = \frac{M_{ws} + M_b}{S_{dtc}} = + \frac{(0.135 + 0.255)(12)}{122.5} = +0.038 \text{ ksi}$$

$$\text{Compressive stress limit: } +1.800 \text{ ksi} > +0.038 \text{ ksi} \quad \text{OK}$$

PRECAST CONCRETE STAY-IN-PLACE DECK PANEL SYSTEM**9.10.10.2.1 Concrete Stress at Top Surface of the CIP Slab/9.10.11 Flexural Strength of Positive Moment Section**

Due to permanent and transient loads, Service I

$$f_{tc} = \frac{M_{ws} + M_b + M_{LL+I}}{S_{dtc}} = + \frac{(0.135 + 0.255 + 8.01)(12)}{122.5} = +0.823 \text{ ksi}$$

Compressive stress limit: +2.400 ksi > +0.823 ksi OK

9.10.10.2.2 Concrete Stress at Top Fiber of the SIP Panel

Due to permanent loads, Service I:

$$\begin{aligned} f_{tg} &= \frac{P_{pe}}{A_{tf}} + \frac{M_{SIP} + M_{CIP}}{S_{ttf}} + \frac{M_{ws} + M_b}{S_{ttc}} \\ &= + \frac{(44.25)}{43.1} + \frac{(0.496 + 0.632)(12)}{24.5} + \frac{(0.135 + 0.255)(12)}{3,551.0} = 1.580 \text{ ksi} \end{aligned}$$

Compressive stress limit: +3.600 ksi > +1.580 ksi OK

Due to permanent and transient loads, Service I:

$$\begin{aligned} f_{tg} &= \frac{P_{pe}}{A_{tf}} + \frac{M_{SIP} + M_{CIP}}{S_{ttf}} + \frac{M_{ws} + M_b + M_{LL+I}}{S_{ttc}} \\ &= + \frac{(44.25)}{43.1} + \frac{(0.496 + 0.632)(12)}{24.5} + \frac{(0.135 + 0.255 + 8.01)(12)}{3,551.0} = 1.608 \text{ ksi} \end{aligned}$$

Compressive stress limit: +4.800 ksi > +1.608 ksi OK

9.10.10.2.3 Concrete Stress at Bottom Fiber of the SIP Panel

$$\begin{aligned} f_b &= \frac{P_{pe}}{A_{tf}} - \frac{M_{SIP} + M_{CIP}}{S_{btf}} - \frac{M_{ws} + M_b + M_{LL+I}}{S_{btc}} \\ &= + \frac{(44.25)}{43.1} - \frac{(0.496 + 0.632)(12)}{24.5} - \frac{(0.135 + 0.255 + 8.01)(12)}{104.4} = -0.491 \text{ ksi} \end{aligned}$$

Tensile stress limit: -0.537 ksi > -0.491 ksi OK

9.10.11 FLEXURAL STRENGTH OF POSITIVE MOMENT SECTION

Total ultimate bending moment for Strength I is:

$$M_u = 1.25(DC) + 1.5(DW) + 1.75(LL + IM) = 1.25(M_{SIP} + M_{CIP} + M_b) + 1.5(M_{ws}) + 1.75M_{LL+I}$$

$$M_{SIP} = 0.496 \text{ ft-kips/ft}$$

$$M_{CIP} = 0.632 \text{ ft-kips/ft}$$

$$M_{ws} = 0.135 \text{ ft-kips/ft}$$

$$M_b = 0.255 \text{ ft-kips/ft}$$

$$M_{LL+I} = 8.01 \text{ ft-kips/ft}$$

$$M_u = 1.25(0.496 + 0.632 + 0.255) + 1.5(0.135) + 1.75(8.01) = 15.9 \text{ ft-kips/ft}$$

Average stress in prestressing strand when $f_{pe} \geq 0.5f_{pu}$:

$$f_{ps} = f_{pu} \left(1 - k \frac{c}{d_p} \right) \quad \text{[LRFD Eq. 5.7.3.1.1-1]}$$

PRECAST CONCRETE STAY-IN-PLACE DECK PANEL SYSTEM

9.10.11 Flexural Strength of Positive Moment Section

where

$$k = 2 \left(1.04 - \frac{f_{py}}{f_{pu}} \right) \quad \text{[LRFD Eq. 5.7.3.1.1-2]}$$

$$= 0.28 \text{ for low-relaxation strands} \quad \text{[LRFD Table C5.7.3.1.1-1]}$$

$$d_p = \text{distance from extreme compression fiber of the composite section to the centroid of the prestressing tendons} = 7.5 - 0.5(3.5) = 5.75 \text{ in.}$$

$$c = \text{distance from the extreme compression fiber to the neutral axis, in.}$$

To compute c , assume rectangular section behavior and check if the depth of the equivalent compression stress block, a , is less than or equal to t_s : [LRFD Art. C5.7.3.2.2]

$$c = \frac{A_{ps}f_{pu} + A_s f_y - A'_s f'_y}{0.85 f'_c \beta_1 b + k A_{ps} \frac{f_{pu}}{d_p}} \quad \text{[LRFD Eq. 5.7.3.1.1-4]}$$

$$a = \text{depth of equivalent rectangular stress block} = \beta_1 c$$

$$A_{ps} = \text{area of prestressing steel} = 13(0.153) = 1.989 \text{ in.}^2$$

$$f_{pu} = \text{specified tensile strength of prestressing steel} = 270.0 \text{ ksi}$$

$$A_s = \text{area of mild steel tension reinforcement} = 0$$

$$f_y = \text{yield strength of nonprestressed tension reinforcement, ksi}$$

$$A'_s = \text{area of compression reinforcement} = 0$$

$$f'_y = \text{yield strength of nonprestressed compression reinforcement, ksi}$$

$$f'_c = \text{compressive strength of slab concrete} = 4.0 \text{ ksi}$$

$$\beta_1 = \text{stress factor of compression block} \quad \text{[LRFD Art. 5.7.2.2]}$$

$$= 0.85 \text{ for } f'_c \leq 4.0 \text{ ksi}$$

$$= 0.85 - 0.05(f'_c - 4.0) \geq 0.65 \text{ for } f'_c > 4.0 \text{ ksi}$$

$$= 0.85$$

$$b = \text{effective width of compression flange} = 8.0(12) = 96.0 \text{ in.}$$

$$c = \frac{1.989(270) + 0 - 0}{0.85(4.0)(0.85)(96) + 0.28(1.989) \left(\frac{270}{5.75} \right)} = 1.77 \text{ in}$$

$$a = \beta_1 c = 0.85(1.77) = 1.50 \text{ in.}$$

Therefore, the rectangular section behavior assumption is valid.

$$f_{ps} = (270.0) \left(1 - 0.28 \frac{1.77}{5.75} \right) = 246.7 \text{ ksi}$$

Check stress in prestressing strand according to available development length, ℓ_d :

$$\ell_d = K \left(f_{ps} - \frac{2}{3} f_{pe} \right) d_b \text{ or} \quad \text{[LRFD Eq. 5.11.4.2-1]}$$

$$f_{ps} = \frac{\ell_d}{K d_b} + \frac{2}{3} f_{pe} \quad \text{(Eq. 9.10.11-1)}$$

PRECAST CONCRETE STAY-IN-PLACE DECK PANEL SYSTEM**9.10.11 Flexural Strength of Positive Moment Section/9.10.12.2 Minimum Reinforcement**

where

$K = 1.0$ for pretensioned panels

$d_b =$ nominal strand diameter

$f_{pe} =$ effective stress in prestressing strands after losses = 171.3 ksi

Available development length at midspan of the SIP panel = $0.5(9.5) = 4.75$ ft

$$f_{ps} = \frac{4.75(12)}{0.5} + \frac{2}{3}(171.3) = 228.2 \text{ ksi} \quad (\text{Controls})$$

Factored flexural resistance:

$$M_r = \phi M_n \quad [\text{LRFD Eq. 5.7.3.2.1-1}]$$

where

$\phi =$ resistance factor [LRFD Art. 5.5.4.2.1]

$= 1.00$ for tension controlled prestressed concrete sections

$M_n =$ nominal flexural resistance [LRFD Art. 5.7.3.2.3]

$$M_n = A_{ps} f_{ps} \left(d_p - \frac{a}{2} \right) \quad [\text{LRFD Eq. 5.7.3.2.2-1}]$$

Therefore, the design flexural strength is:

$$\phi M_n = \frac{1.0(1.989)(228.2) \left(5.75 - \frac{1.50}{2} \right)}{12}$$

$$= 189.1 \text{ ft-kips/panel} = 189.1/8 = 23.6 \text{ ft-kips/ft} > M_u = 15.9 \text{ ft-kips/ft} \quad \text{OK}$$

The calculations were conducted for flexure in the midspan section. It is possible that intermediate sections between midspan and the supports will have critical stresses due to only partial development of the strands.

9.10.12 LIMITS OF REINFORCEMENT FOR POSITIVE MOMENT SECTION**9.10.12.1 Maximum Reinforcement**

[LRFD Art. 5.7.3.3.1]

The check of maximum reinforcement limits in LRFD Article 5.7.3.3.1 was removed from the *LRFD Specifications* in 2005.

9.10.12.2 Minimum Reinforcement

[LRFD Art. 5.7.3.3.2]

At any section, the amount of prestressed and nonprestressed tensile reinforcement must be adequate to develop a factored flexural resistance, M_r , at least equal to the lesser of:

- 1.2 times the cracking strength determined on the basis of elastic stress distribution and the modulus of rupture, and
- 1.33 times the factored moment required by the applicable strength load combination.

Check at midspan

$$M_{cr} = (f_r + f_{cpe})S_{btc} - (M_{dnc})(S_{btc}/S_{btf} - 1) \geq S_{btf}f_r \quad [\text{LRFD Eq. 5.7.3.3.2-1}]$$

where

$f_r =$ modulus of rupture [LRFD Art. 5.4.2.6]

$$= 0.37\sqrt{f'_c} = 0.37\sqrt{8.000} = 1.047 \text{ ksi}$$

$f_{cpe} =$ compressive stress in concrete due to effective prestress force only, (after allowance for all prestress losses) at extreme fiber of section where tensile stress is caused by externally applied loads

PRECAST CONCRETE STAY-IN-PLACE DECK PANEL SYSTEM

9.10.12.2 Minimum Reinforcement/9.10.3.2 Bending Moment

$$= \frac{P_{pe}}{A_{tf}} = \frac{44.25}{43.1} = 1.027 \text{ ksi}$$

M_{dnc} = noncomposite dead load moment at the section

$$= M_{CIP} + M_{SIP} = 0.632 + 0.496 = 1.128 \text{ ft-kips/ft}$$

S_{btc} = section modulus for the extreme fiber of the transformed composite section where the tensile stress is caused by externally applied loads = 104.4 in.³/ft

S_{btf} = section modulus for the extreme fiber of transformed noncomposite section where the tensile stress is caused by externally applied loads = 24.5 in.³/ft

$$M_{cr} = (1.047 + 1.027) \left(\frac{104.4}{12} \right) - (1.128) \left(\frac{104.4}{24.5} - 1 \right) = 14.4 \text{ ft-kips/ft}$$

$$1.2M_{cr} = 1.2(14.4) = 17.3 \text{ ft-kips/ft}$$

At midspan, the factored moment required by Strength I load combination is:

$$M_u = 15.9 \text{ ft-kips/ft (as calculated in Section 9.10.11)}$$

$$\text{Therefore, } 1.33M_u = 1.33(15.9) = 21.1 \text{ ft-kips/ft}$$

Since $1.2M_{cr} < 1.33M_u$, $1.2M_{cr}$ controls.

$$M_r = \phi M_n = 23.6 \text{ ft-kips/ft} > 1.2M_{cr} = 17.3 \text{ ft-kips/ft} \quad \text{OK}$$

Note: The *LRFD Specifications* requires that this criterion be met at every section.

Illustrated based on 2011
LRFD Specifications.

Editor's Note: 2012 *LRFD Specifications* changes will revise minimum reinforcement.

9.10.13 NEGATIVE MOMENT SECTION OVER INTERIOR BEAMS**9.10.13.1 Critical Section**

The design section for negative moments and shear forces, for precast I-shaped concrete beams, is at a distance of $\frac{1}{3}$ of the flange width from the centerline of the support but not exceeding 15 in. [LRFD Art. 4.6.2.1.6]

Since $\frac{1}{3}$ the beam flange width = $\frac{1}{3}(42) = 14 \text{ in.} < 15 \text{ in.}$, the design section for negative moment is at a distance of 14 in. (1.17 ft) from the centerline of the beam.

9.10.13.2 Bending Moment

[LRFD Art. 4.6.2.1.6]

LRFD Article 4.6.2.1.6 states that force effects be calculated based on analyzing the strip as a continuous beam supported by infinitely rigid supports. The maximum value of moment applies at all sections (LRFD Article 4.6.2.1.1). Using appropriate software for beam analysis, the bending moment is:

DC: Because the weight of the barrier produces positive moment at the interior girders, as shown in **Figure 9.10.6.1-1**, bending moment due to this load is conservatively ignored.

DW: Due to wearing surface, $M_{ws} = 0.148 \text{ ft-kips/ft}$

LL + IM From LRFD Table A4.1-1, for $S = 12.0 \text{ ft}$, maximum negative bending moment at 14 in. from beam center line by linear interpolation, with impact and multiple presence factor, $M_{LL+I} = 6.347 \text{ ft-kips/ft}$

Therefore, the negative service bending moment, $M_{service}$, is:

$$M_{service} = 0.148 + 6.347 = 6.495 \text{ ft-kips/ft}$$

Negative factored bending moment:

$$M_u = 1.5(0.148) + 1.75(6.347) = 11.329 \text{ ft-kips/ft}$$

PRECAST CONCRETE STAY-IN-PLACE DECK PANEL SYSTEM

9.10.13.3 Design of Section/9.10.13.5 Crack Control

9.10.13.3 Design of Section

Assume No. 5 reinforcing bars and 2.5-in. clear cover.

$$d_e = 7.5 - 0.5(0.625) - 2.5 = 4.688 \text{ in.}$$

$$R_n = (M_u / \phi b d_e^2) = (11.329)(12) / [(0.9)(12)(4.688)^2] = 0.573 \text{ ksi}$$

$$m = (f_y / 0.85 f'_c) = (60.0) / [(0.85)(4.0)] = 17.65$$

$$\rho = \frac{1}{m} \left(1 - \sqrt{1 - \frac{2mR_n}{f_y}} \right) = \frac{1}{17.65} \left(1 - \sqrt{1 - \frac{2(17.65)(0.573)}{60.0}} \right) = 0.01053$$

$$A_s = \rho(bd_e) = (0.01053)(12)(4.688) = 0.59 \text{ in.}^2/\text{ft}$$

Use No. 5 bars at 6-in. centers, $A_s = 0.31(12/6) = 0.62 \text{ in.}^2/\text{ft}$

Check:

$$a = (A_s f_y) / (0.85 b f'_c) = (0.62)(60) / [(0.85)(12)(4.0)] = 0.91 \text{ in.}$$

$$\begin{aligned} \phi M_n &= 0.9(A_s f_y)(d - a/2) = 0.9(0.62)(60)[4.688 - 0.5(0.91)]/12 \\ &= 11.810 \text{ ft-kips/ft} > M_u = 11.329 \text{ ft-kips/ft} \quad \text{OK} \end{aligned}$$

Note: The critical section for negative moment is $42/3 = 14$ in. from the beam centerline and the panel starts at 15 in. away. Therefore, the strength of the cast-in-place concrete is used in the above calculations.

9.10.13.4 Minimum Reinforcement

[LRFD Art. 5.7.3.3.2]

For the negative moment section, the LRFD Eq. 5.7.3.3.2-1 can be reduced to:

$$M_{cr} = S_{tc} f_r$$

where

$$f_r = 0.37 \sqrt{f'_c} = 0.37 \sqrt{4.0} = 0.740 \text{ ksi}$$

$$S_{tc} = 122.3 \text{ in.}^3$$

Note: Gross section properties should be used here for negative moment section.

$$M_{cr} = 0.740(122.4)/12 = 7.548 \text{ ft-kips}$$

$$1.2M_{cr} = 12(7.548) = 9.058 \text{ ft-kips}$$

$$M_u = 11.329 \text{ ft-kips, as calculated in Section 9.10.13.2.}$$

$$\text{Thus, } 1.33M_u = 1.33(11.329) = 15.1 \text{ ft-kips}$$

Since $1.2M_{cr} < 1.33 M_u$, the $1.2M_{cr}$ requirement controls.

$$M_r = 11.810 \text{ ft-kips} > 1.2M_{cr} = 9.058 \text{ ft-kips} \quad \text{OK}$$

Illustrated based on 2011 *LRFD Specifications*.Editor's Note: 2012 *LRFD Specifications* changes will revise minimum reinforcement.**9.10.13.5 Crack Control**

[LRFD Art 5.7.3.4]

According to the *LRFD Specifications*, the spacing, s , of nonprestressed reinforcement must satisfy the following limitation:

$$s \leq \frac{700\gamma_e}{\beta_s f_{ss}} - 2d_c$$

[LRFD Eq.5.7.3.4-1]

in which

$$\beta_s = 1 + \frac{d_c}{0.7(h - d_c)}$$

PRECAST CONCRETE STAY-IN-PLACE DECK PANEL SYSTEM

9.10.13.5 Crack Control/9.10.14.2 Design of Section

where

γ_e = exposure factor = 1.00 for Class 1 exposure condition

d_c = thickness of concrete cover measured from extreme tension fiber to center of the flexural reinforcement located closest thereto, in.

$$= 2.5 + 0.5 (0.625) = 2.813 \text{ in.}$$

f_{ss} = tensile stress in steel reinforcement at the service limit state, ksi

$$= M_{service}/(jd_e A_s)$$

where

j = a factor relating lever arm to effective depth = $1 - k/3$

$$k = \sqrt{(\rho_a n)^2 + (2\rho_a n)} - \rho_a n$$

$$\rho_a = \text{actual reinforcement ratio} = \frac{A_s}{12(d_e)} = \frac{0.62}{12(4.688)} = 0.011$$

$$n = E_s/E_c = 29,000/3,834 = 7.56$$

Therefore:

$$k = \sqrt{[(0.011)(7.56)]^2 + 2(0.011)(7.56)} - (0.011)(7.56) = 0.33$$

$$j = 1 - 0.33/3 = 0.89$$

$$f_{ss} = M_{service}/(jd_e A_s) = (6.495)(12)/[(0.89)(4.688)(0.62)] = 30.1 \text{ ksi}$$

h = overall thickness or depth of the component, in. = 7.5 in.

$$\text{Therefore, } \beta_s = 1 + \frac{2.813}{0.7(7.5 - 2.813)} = 1.857$$

The spacing limitation for the nonprestressed reinforcement can now be checked:

$$s = \frac{700(1.00)}{(1.857)(30.1)} - 2(2.813) = 6.90 \text{ in.} > 6 \text{ in.} \quad \text{OK}$$

9.10.14 NEGATIVE MOMENT SECTION OVER EXTERIOR BEAMS**9.10.14.1 Critical Section**

The critical section for negative moment over the beams is at a distance of 14 in., 1.17 ft, from the centerline of the beam (Section 9.10.13.1).

Therefore, cantilever span is $4.25 - 1.17 = 3.08$ ft

9.10.14.2 Design of Section

LRFD Article A13.4.1 states that three design cases need to be checked when designing the overhang regions. These cases are:

- **Case 1:** check overhang for horizontal vehicular collision load Extreme Load Combination II:

The deck overhang is designed to provide a flexural resistance in combination with an axial force, T , that exceeds the flexural resistance at the base of the barrier, M_c .

From design of the barrier (not shown in this example):

[LRFD Art. A13.3]

Flexural resistance of the barrier at its base, $M_c = 17.200$ ft-kips/ft

Total transverse resistance of the barrier, i.e. collision horizontal force at top of barrier, $R_w = 166.0$ kips

PRECAST CONCRETE STAY-IN-PLACE DECK PANEL SYSTEM

9.10.14.2 Design of Section

The force, R_w , is distributed over a width of L_c at the top fiber of the barrier = 13.36 ft

Height of the barrier, $H = 32$ in.

Assume that this force is distributed at an angle of 45° from the top fiber of the barrier to its base, thus:

Collision force at deck slab level:

$$T = \frac{R_w}{L_c + 2H} \quad \text{[LRFD Eq. A13.4.2-1]}$$

where L_c = critical length of yield line failure pattern = 160.32 in.

$$T = \frac{166.0}{160.32 + 2(32)} = 0.74 \text{ kips/in.} = 8.88 \text{ kips/ft}$$

Note that the slab thickness is ignored.

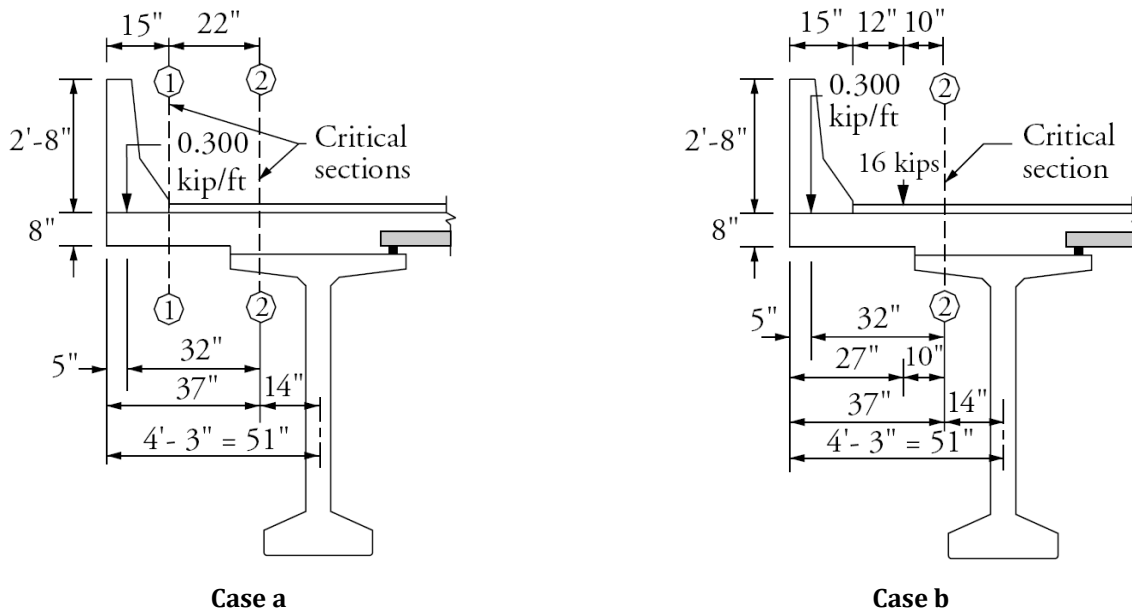
Design the section at the inner face of barrier; i.e. Section 1-1 in Case a in **Figure 9.10.14.2-1**:

Factored bending moment, M_u , at face of barrier due to collision force and dead loads:

$$M_u = M_c + 1.25(M_{CIP} + M_b)$$

$$= 17.200 + 1.25[(0.5)[8(0.150)/12](15/12)^2 + 0.300(15 - 5)/12] = 17.610 \text{ ft-kips/ft}$$

Figure 9.10.14.2-1
Loading Cases for the Overhang



Try No. 6 bars at 5 in. centers, $A_s = 0.44(12)/5 = 1.056 \text{ in.}^2/\text{ft}$

For No. 6 bars and 2.5 in. clear cover, the effective depth,

$d_e = 7.5 - 0.5(0.75) - 2.5 = 4.625$ in. The depth of slab is conservatively taken as 7.5 in.

$b = 12$ in.

Check development length of steel reinforcement:

$$\ell_d = \frac{1.25A_b f_y}{\sqrt{f'_c}} = \frac{1.25(0.44)(60)}{\sqrt{4.0}} = 16.5 \text{ in.} \quad \text{[LRFD Art. 5.11.2.1]}$$

PRECAST CONCRETE STAY-IN-PLACE DECK PANEL SYSTEM

9.10.14.2 Design of Section

Since the width of the barrier, 15 in., is less than the length required to fully develop the No. 6 bars, available stress of the No. 6 bar should be reduced as follows:

$$f_{ss} = 60(15/16.5) = 54.55 \text{ ksi}$$

Alternatively, a 90° hook could be provided at the end of the bar.

$$A_s f_{ss} = 1.056(54.55) = 57.60 \text{ kips/ft}$$

$$T = 8.88 \text{ kips/ft}$$

$$C = A_s f_s - T = 57.60 - 8.88 = 48.72 \text{ kips/ft}$$

where C = compression force for flexural resistance

$$a = C / (0.85 b f'_c) = 48.72 / [0.85(12)(4.0)] = 1.19 \text{ in.}$$

$$\phi = 1.0 \text{ (for extreme event, LRFD Art. 1.3.2.1)}$$

$$\begin{aligned} \phi M_n &= \phi [A_s f_s (d_e - a/2) - T(d_e/2 - a/2)] \\ &= 1.0 [57.60(4.625 - 1.19/2) - 8.88(4.625/2 - 1.19/2)] / 12 \\ &= 18.073 \text{ ft-kips/ft} > M_u = 17.610 \text{ ft-kips/ft} \quad \text{OK} \end{aligned}$$

For the critical section over the exterior beam, Section 2-2 in Case 1 in **Figure 9.10.14.2-1**:

At the inner face of the barrier, the flexural resistance of the barrier at its base, 17.200 ft-kips/ft, is distributed over a length L_c , while the collision axial force T is distributed over a length of $(L_c + 2H)$ where H is the height of the barrier. Assume that the moment at the face of the barrier and the axial force are distributed at an angle of 30° in the slab from the inner face of the barrier to the design section. The collision bending moment at the critical section is:

$$\frac{M_c L_c}{L_c + 2(22) \tan 30^\circ} = \frac{17.200(160.32)}{160.32 + 2(22) \tan 30^\circ} = 14.847 \text{ ft-kips/ft}$$

The factored bending moment at Section 2-2 due to collision force and dead loads is:

$$M_u = 14.847 + 1.25(M_{CP} + M_b) + 1.5 M_{ws} = 14.847 + 1.25[(0.5)(8 \times 0.150/12)(22 + 15)^2 / (12)^2 + 0.300(22 + 10)/12] + 1.5[(0.5)(2 \times 0.150/12)(22/12)^2] = 16.504 \text{ ft-kips/ft}$$

Collision axial force at Section 2-2 is:

$$\begin{aligned} T &= \frac{R_w}{L_c + 2H + 2(22) \tan 30^\circ} \\ &= \frac{166.0}{160.32 + 2(32) + 2(22) \tan 30^\circ} = 0.665 \text{ kips/in.} = 7.98 \text{ kips/ft} \end{aligned}$$

Check No. 6 bars at 5-in. centers:

$$A_s = 0.44(12)/5 = 1.056 \text{ in.}^2$$

$$d_e = 7.5 - 0.5(0.75) - 2.5 = 4.625 \text{ in.}$$

$$T = 7.98 \text{ kips/ft}$$

$$C = A_s f_y - T = 1.056(60) - 7.98 = 55.38 \text{ kips/ft}$$

$$a = C / (0.85 b f'_c) = 55.38 / [0.85(12)(4.0)] = 1.36 \text{ in.}$$

$$\phi = 1.0 \text{ (for extreme event, LRFD Art. 1.3.2.1)}$$

$$\begin{aligned} \phi M_n &= \phi [A_s f_y (d_e - a/2) - T(d_e/2 - a/2)] \\ &= 1.0 [63.36(4.625 - 1.36/2) - 7.98(4.625/2 - 1.36/2)] / 12 \\ &= 19.744 \text{ ft-kips/ft} > M_u = 16.504 \text{ ft-kips/ft} \quad \text{OK} \end{aligned}$$

• **Case 2:** check overhang for vertical collision force

[LRFD Art. A13.4.1]

PRECAST CONCRETE STAY-IN-PLACE DECK PANEL SYSTEM

9.10.14.2 Design of Section/9.10.14.3 Minimum Reinforcement

For concrete parapets, the case of vertical collision never controls.

- **Case 3:** check overhang for dead and live loads:

[LRFD Art. A13.4.1]

DC:

Due to weight of slab, $M_{CIP} = (8 \times 0.150/12)(37/12)^2/2 = 0.475$ ft-kips/ft

Due to barrier load, $M_b = 0.300(32/12) = 0.800$ ft-kips/ft

DW:

Due to wearing surface, $M_{ws} = (2 \times 0.150/12)(22/12)^2/2 = 0.042$ ft-kips/ft

LL + IM:

For maximum negative moment, the truck wheel should be at 12 in. from the face of the barrier, as shown in Case b in **Figure 9.10.14.2-1**.

[LRFD Art. 3.6.1.3.1]

The wheel load is distributed over a length of $(45.0 + 10.0 X)$, inches.

[LRFD Art. 4.6.2.1.3]

where X = distance from load to point of support, ft = $10/12 = 0.833$ ft

Therefore, the width is $45 + 10(0.833) = 53.33$ in. = 4.44 ft

Dynamic allowance = 33%

[LRFD Art. 3.6.2.1]

Multiple presence factor for single truck = 1.2

[LRFD Art. 3.6.1.1.2]

Maximum negative bending moment at Section 2-2, with impact and multiple presence factor is:

$$M_{LL+I} = (16/4.44)(0.833)(1 + 0.33)(1.2) = 4.791 \text{ ft-kips/ft}$$

Therefore, the negative service bending moment at Section 2-2:

$$M_{service} = 0.475 + 0.800 + 0.042 + 4.791 = 6.108 \text{ ft-kips/ft}$$

Negative factored bending moment at Section 2-2:

$$M_u = 1.25(0.475 + 0.800) + 1.5(0.042) + 1.75(4.791) = 10.041 \text{ ft-kips/ft}$$

Check No. 6 bars at 5 in. centers:

$$A_s = 1.056 \text{ in.}^2$$

$$d_e = 7.5 - 0.5(0.75) - 2.5 = 4.625 \text{ in.}$$

$$a = (A_s f_y) / (0.85 b f'_c) = (1.056)(60) / [(0.85)(12)(4.0)] = 1.55 \text{ in.}$$

$$\phi M_n = 0.9(A_s f_y)(d_e - a/2)$$

$$= (0.9)(1.056)(60)(4.625 - 1.55/2) / 12 = 18.295 \text{ ft-kips/ft} > M_u = 10,041 \text{ ft-kips/ft} \quad \text{OK}$$

9.10.14.3 Minimum Reinforcement

[LRFD Art. 5.7.3.3.2]

For the negative moment section, the LRFD Eq. 5.7.3.3.2-1 can be reduced to:

$$M_{cr} = S_c f_r$$

where

$$f_r = 0.37 \sqrt{f'_c} = 0.37 \sqrt{4.0} = 0.740 \text{ ksi}$$

$$S_c = (12)(7.5)^2 / 6 = 112.5 \text{ in.}^3$$

Note: Gross section properties of the CIP slab are used here for negative moment section.

$$M_{cr} = 0.740(112.5) / 12 = 6.938 \text{ ft-kips}$$

PRECAST CONCRETE STAY-IN-PLACE DECK PANEL SYSTEM

9.10.14.3 Minimum Reinforcement/9.10.14.4 Crack Control

$$1.2M_{cr} = 1.2(6.938) = 8.326 \text{ ft-kips}$$

$$M_u = 10.041 \text{ ft-kips (as calculated in Section 9.10.14.2)}$$

$$\text{Thus, } 1.3M_u = 1.33(10.041) = 13.4 \text{ ft-kips}$$

Since $1.2M_{cr} < 1.33M_u$, the $1.2M_{cr}$ requirement controls.

$$M_r = 18.295 \text{ ft-kips} > 1.2M_{cr} = 8.326 \text{ ft-kips} \quad \text{OK}$$

9.10.14.4 Crack Control

[LRFD Art 5.7.3.4]

According to the *LRFD Specifications*, the spacing, s , of nonprestressed reinforcement must satisfy the following limitation:

$$s \leq \frac{700\gamma_e}{\beta_s f_{ss}} - 2d_c \quad \text{[LRFD Eq.5.7.3.4-1]}$$

in which

$$\beta_s = 1 + \frac{d_c}{0.7(h - d_c)}$$

where

γ_e = exposure factor = 1.00 for Class 1 exposure condition

d_c = thickness of concrete cover measured from extreme tension fiber to center of the flexural reinforcement located closest thereto, in.

$$= 2.5 + 0.5(0.75) = 2.875 \text{ in.}$$

f_{ss} = tensile stress in steel reinforcement at the service limit state, ksi

$$= M_{service}/(jd_e A_s)$$

where

j = a factor relating lever arm to effective depth = $1 - k/3$

$$k = \sqrt{(\rho_a n)^2 + (2\rho_a n)} - \rho_a n$$

$$\rho_a = \text{actual reinforcement ratio} = \frac{A_s}{12(d_e)} = \frac{1.056}{12(4.625)} = 0.019$$

$$n = E_s/E_c = 29,000/3,834 = 7.56$$

Therefore:

$$k = \sqrt{[(0.019)(7.56)]^2 + 2(0.019)(7.56)} - (0.019)(7.56) = 0.41$$

$$j = 1 - 0.41/3 = 0.86$$

$$f_{ss} = M_{service}/(jd_e A_s) = (6.108)(12)/[(0.86)(4.625)(1.056)] = 17.5 \text{ ksi}$$

h = overall thickness or depth of the component, in. = 7.5 in.

$$\text{Therefore, } \beta_s = 1 + \frac{2.875}{0.7(7.5 - 2.875)} = 1.888$$

The spacing limitation for the nonprestressed reinforcement can now be checked:

$$s = \frac{700(1.00)}{(1.888)(17.5)} - 2(2.875) = 15.44 \text{ in.} > 6.0 \text{ in.} \quad \text{OK}$$

PRECAST CONCRETE STAY-IN-PLACE DECK PANEL SYSTEM**9.10.15 Distribution Reinforcement****9.10.15 DISTRIBUTION REINFORCEMENT**

The *LRFD Specifications* does not provide guidelines for the distribution reinforcement required for a SIP panel system. However, LRFD Article 9.7.3.2 gives guidance for deck slabs, which have four layers of reinforcement, as follows:

$$(\text{Distribution reinforcement/primary reinforcement}), \% = \frac{220}{\sqrt{S}} \leq 67\%$$

where S = clear span + distance from extreme flange tip to the face of the web

$$= (12.0 - 42/12) + 2(18/12) = 11.5 \text{ ft} \quad [\text{LRFD Art.9.7.2.3}]$$

Therefore, the percentage of distribution reinforcement = $220/\sqrt{11.50} = 64.9 < 67\%$

Based on the area of the strands, which are the main positive reinforcement in the SIP panel, the distribution reinforcement = $(0.649)(13)(0.153)/8.0 = 0.16 \text{ in.}^2/\text{ft}$.

If the strand area is converted to equivalent nonprestressed reinforcement area, the required distribution reinforcement = $0.16(243/60) = 0.65 \text{ in.}^2/\text{ft}$. Note that the yield strength of each material is used as the basis for equivalence.

This amount of reinforcement is 45% higher than that required by the Empirical Design Method, LRFD Article 9.7.2.5, where a total amount of $(0.27 + 0.18) = 0.45 \text{ in.}^2/\text{ft}$ is provided in two layers.

Therefore, the designer may opt to use No. 5 bars at 5.5-in. centers to satisfy LRFD Article 9.7.3.2 or No. 5 bars at 8.0-in. centers to satisfy LRFD Article 9.7.2.5.

This page intentionally left blank

NOTATION.....	10 - 5
10.1 INTRODUCTION.....	10 - 9
10.2 HISTORY OF ELASTOMERIC BEARINGS.....	10 - 9
10.3 SPECIFICATIONS.....	10 - 10
10.4 LOADS AND MOVEMENTS FOR DESIGN.....	10 - 10
10.4.1 Rotational Movements.....	10 - 10
10.4.1.1. Rotation Axes.....	10 - 10
10.4.1.2 Sources of Rotation.....	10 - 12
10.4.1.3 Accounting for Rotation in Bearing Design.....	10 - 12
10.4.2 Translational Movements.....	10 - 13
10.4.3 Vertical Loads.....	10 - 14
10.4.4 Horizontal Loads.....	10 - 14
10.5 PLANNING THE BEARING LAYOUT.....	10 - 14
10.5.1 General.....	10 - 14
10.5.2 Bearing Configurations.....	10 - 15
10.5.2.1 Fixed Bearings.....	10 - 15
10.5.2.2 Movable Bearings.....	10 - 15
10.5.2.2.1 Flexible Bearings.....	10 - 16
10.5.2.2.2 Sliding Bearings.....	10 - 16
10.5.2.3 Guided bearings.....	10 - 17
10.5.2.4 Force Control Bearings.....	10 - 17
10.5.2.5 Special Considerations for Box Beams.....	10 - 17
10.5.2.6 Special Considerations for Fixed and Guided Bearings.....	10 - 18
10.6 TYPES OF ELASTOMERIC BEARINGS.....	10 - 18
10.6.1 Plain Elastomeric Pads.....	10 - 18
10.6.2 Fiberglass-reinforced Pads.....	10 - 18
10.6.3 Cotton Duck-reinforced Pads.....	10 - 18
10.6.4 Steel-reinforced Elastomeric Bearings.....	10 - 18
10.7 BEHAVIOR OF ELASTOMERIC BEARINGS.....	10 - 19
10.7.1 Elastomeric Materials.....	10 - 19
10.7.1.1 General.....	10 - 19
10.7.1.2 Shear Modulus.....	10 - 19
10.7.1.3 Low Temperature Grades.....	10 - 20
10.7.2. Mechanics of Elastomeric Bearings.....	10 - 21
10.7.2.1 Behavior of an Elastomeric Layer.....	10 - 21
10.7.2.2 Elastic Stress-Strain Behavior in Compression.....	10 - 24
10.7.2.3 Creep Strains.....	10 - 25
10.7.3 Stability.....	10 - 25
10.7.4 Tapered Bearings.....	10 - 26

BEARINGS

Table of Contents

10.8 DESIGN OF ELASTOMERIC BEARINGS..... 10 - 27

 10.8.1 Applicable Specifications..... 10 - 27

 10.8.2 Testing Requirements..... 10 - 28

 10.8.3 Steel-Reinforced Elastomeric Bearings– Design using Method B..... 10 - 30

 10.8.3.1 Loads and Movements..... 10 - 30

 10.8.3.2 Design for Shear Displacements..... 10 - 32

 10.8.3.3 Design for Combined Loading..... 10 - 32

 10.8.3.4 Design for Hydrostatic Tension..... 10 - 33

 10.8.3.5 Stability 10 - 34

 10.8.3.6 Steel Reinforcement 10 - 35

 10.8.3.7 Anchorage 10 - 35

 10.8.3.8 Bearing Design Example–Method B 10 - 36

 10.8.3.8.1 Introduction 10 - 36

 10.8.3.8.2 Loads and Movements..... 10 - 36

 10.8.3.8.3 Elastomer Thickness for Shear Displacements 10 - 40

 10.8.3.8.4 Trial Bearing Size..... 10 - 40

 10.8.3.8.5 Design for Combined Loading..... 10 - 41

 10.8.3.8.6 Design for Hydrostatic Tension..... 10 - 42

 10.8.3.8.7 Stability 10 - 42

 10.8.3.8.8 Steel Reinforcement 10 - 43

 10.8.3.8.9 Anchorage 10 - 44

 10.8.3.8.10 Low Temperature Requirements 10 - 44

 10.8.3.8.11 Testing Requirements..... 10 - 44

 10.8.3.8.12 Summary..... 10 - 44

 10.8.4 Design using Method A..... 10 - 44

 10.8.4.1 General..... 10 - 44

 10.8.4.2 Material Properties..... 10 - 45

 10.8.4.3 Testing requirements..... 10 - 45

 10.8.4.4 Loads and Movements..... 10 - 45

 10.8.4.5 Design of Plain Elastomeric Pads, Fiberglass-reinforced Pads, and Steel Reinforced Elastomeric Bearings..... 10 - 45

 10.8.4.6 Design of Cotton Duck Reinforced Pads 10 - 46

 10.8.4.7 Bearing Design Example–Method A 10 - 47

 10.8.4.7.1 Introduction 10 - 47

 10.8.4.7.2 Elastomer Thickness for Shear Displacements 10 - 48

 10.8.4.7.3 Design for Compressive Stress 10 - 48

 10.8.4.7.4 Steel Reinforcement 10 - 50

 10.8.4.7.5 Stability 10 - 50

 10.8.4.7.6 Low Temperature Requirements 10 - 50

BEARINGS

Table of Contents

10.8.4.7.7 Design Shear Force and Anchorage..... 10 - 50

10.8.4.7.8 Summary 10 - 51

10.8.5 Tapered Bearings..... 10 - 51

10.9 BEARING SELECTION GUIDE..... 10 - 52

10.10 REFERENCES..... 10 - 54

This page intentionally left blank

NOTATION

A	= plan area of elastomeric bearing
	= factor for evaluating stability of bearings
A_{slab}	= area of cross section of slab
B	= factor for evaluating stability of bearings
C_{α}	= constant used in evaluation hydrostatic tension stress
C_{rot}	= constant relating beam deflection to end rotation
D	= diameter of a circular bearing
D_a	= constant relating axial stress on bearing to shear strain
D_r	= constant relating rotation on bearing to shear strain
E_c	= effective modulus of elastomeric bearings in compression, assuming incompressible behavior
$E_{c,tot}$	= effective modulus of elastomeric bearings in compression, accounting for bulk compression
E_{gird}	= modulus of elasticity of beam concrete
E_p	= modulus of elasticity of prestressing strand material
E_{slab}	= modulus of elasticity of slab concrete
$(EI)_{tr}$	= transformed moment of inertia of composite beam
F_y	= yield strength of steel reinforcement
$f_{b,tr}$	= bending stress in beam due to transfer of prestress
G	= shear modulus of the elastomer
H_s	= horizontal service load on the bearing
h_{ri}	= thickness of i^{th} elastomeric layer in elastomeric bearing
$h_{r,max}$	= thickness of thickest elastomeric layer in elastomeric bearing
h_{rt}	= total elastomer thickness in an elastomeric bearing
h_s	= thickness of steel laminate in steel-laminated elastomeric bearing
K	= bulk modulus of the elastomer
k_{shear}	= shear stiffness of bearing
L	= length of a rectangular elastomeric bearing (parallel to longitudinal bridge axis)
n	= number of elastomer layers
P	= axial load
P_{cy}	= Cyclic axial load
P_D	= dead load for service limit state at each bearing
P_m	= maximum compressive load considering all appropriate load combinations
P_{st}	= static axial load
P_L	= live load for service limit state at each bearing

P_v	= vertical load on bearing
r	= radius of gyration
S	= shape factor of thickest layer of an elastomeric bearing
t_p	= thickness of cotton duck pad
W	= width of the bearing in the transverse direction
y_b	= distance from centroid to bottom face of beam section
α	= coefficient of thermal expansion
	= parameter in calculation of hydrostatic tension
	= skew angle of bridge
	= dimensionless parameter in design of cotton duck pads
γ_a	= shear strain in the elastomer due to axial load
γ_r	= shear strain in the elastomer due to rotation
γ_s	= shear strain in the elastomer due to shear displacement
γ_{tot}	= total shear strain in the elastomer
Δ_{CR+SH}	= creep and shrinkage movement
$\Delta_{diff,sh}$	= vertical deflection due to differential shrinkage between beam and slab
ΔF_{TH}	= constant amplitude fatigue threshold for Category A as specified in LRFD Article 6.6
Δf_p	= change in stress in the prestressing strands
Δ_H	= horizontal displacement on the bearing
Δ_o	= maximum service horizontal displacement of the bridge deck
ΔL	= change in length
Δ_{LL}	= vertical deflection of the beam due to live load
Δ_{slab}	= vertical deflection of the beam due to slab weight
Δ_s	= maximum shear deformation of the elastomer
	= shear deformation due to compressive load on tapered bearing
ΔT	= change in temperature
Δ_T	= horizontal displacement due to temperature
Δ_v	= vertical deflection of beam at midspan
ϵ_c	= instantaneous compressive strain of a cotton duck pad
$\epsilon_{sh,free}$	= free shrinkage strain of concrete
ϵ_t	= maximum compressive strain due to combined compression and rotation of CDP at the service limit state
θ	= taper of tapered bearing pad
θ_B	= allowance for uncertainties in bearing rotation

θ_i	= rotation of the i^{th} layer of the bearing = θ_s/n if all layers have the same thickness.
θ_t	= torsional rotation of beam
θ_f	= flexural rotation of beam
θ_x	= rotation of beam about the x-axis of the bridge
θ_y	= rotation of beam about the y-axis of the bridge
θ_{end}	= end rotation of beam about the transverse axis
θ_{cy}	= cyclic rotation
θ_{st}	= static rotation
θ_s	= maximum service rotation due to total load
λ	= compressibility index
μ	= coefficient of friction
σ_a	= average axial stress in the load combination being evaluated
σ_D	= average compressive stress due to dead load
σ_{hyd}	= hydrostatic stress
σ_L	= average compressive stress due to live load
σ_s	= service average compressive stress due to total load
σ_{TL}	= average compressive stress due to total dead plus live loads

This page intentionally left blank

Bearings

10.1 INTRODUCTION

Bearings are devices used to connect a bridge superstructure to its substructure. The primary function of a bearing is to transfer concentrated vertical forces from the superstructure into the substructure, but in many cases it must also permit rotation and translation to occur freely between the sub- and superstructure. In practice, the bearing's resistance to such movements is small, but not exactly zero. Consequently, the *LRFD Specifications* requires consideration of the moments and horizontal forces that are introduced into the substructure as a result of bearing movements. Because the forces applied by the bearings are usually much smaller than the members' capacities, they are of little consequence.

In many applications, bearings must allow translational movements of the superstructure relative to the substructure without inducing significant horizontal forces into the substructure. Accommodation of thermal expansion provides an example. In other situations, such as when wind or vehicle braking forces act on the superstructure, the bearings must be designed to restrain the translational movements and resist the horizontal loads. Under seismic load, the flexibility of the bearings may lengthen the period of the structure and so change the induced forces, but the bearing may still be required to resist those reduced forces.

This chapter describes design and selection procedures for bearings. For the vast majority of bridges constructed using precast, prestressed concrete beams, plain elastomeric pads or elastomeric bearings reinforced with steel plates will be the bearings of choice. Most of the discussion in this chapter is dedicated to these types of bearings.

For longer-span precast concrete bridges or for bridges with special loading requirements, it may be necessary for the designer to consider the use of pot, disk or spherical bearings. These bearings are often referred to collectively as high load multi-rotational (HLMR) bearings. They offer the benefits of supporting higher stresses and accommodating larger rotations than typical elastomeric bearings. However, recent changes in the provisions for elastomeric bearings have significantly reduced the extent of those advantages. Because of initial costs and maintenance requirements, the use of HLMR bearings should generally be limited to only those situations where plain or reinforced elastomeric bearings are not suitable.

This chapter does not address diaphragm details that connect superstructure and substructure elements or pentels and sole plates which restrain translation. These details are considered systems or sub-systems that change the static scheme of the structure and should be analyzed separately.

10.2 HISTORY OF ELASTOMERIC BEARINGS

Elastomeric bearings have been widely used in the United States since the 1950s. The first recorded use was in 1957, when neoprene pads were used to support prestressed concrete beams in Victoria, Texas (Muscarella, 1995). The earliest use of elastomeric pads worldwide is reported to have been in Australia where plain rubber pads were used to support a viaduct that was constructed in 1889 (Lindley, 1981). Those pads were reported to still be in service, with very little deterioration, in 1981.

The design of elastomeric bearing pads was first addressed by AASHTO in the eighth edition of the *Standard Specifications*, which was published in 1961. It permitted only neoprene pads and contained only a single page of design information for elastomeric bearings. In contrast, the current *LRFD* and *Standard Specifications* both contain detailed design procedures for elastomeric bearings. The new requirements are based largely on research conducted at the University of Washington (Roeder, et al., 1987; Roeder, et al., 1990; Stanton et al., 2008). The changes in the AASHTO Specifications since 1987 have encouraged the use of steel reinforced elastomeric bearings over plain elastomeric bearings in all but the most lightly loaded conditions, because of the reinforced bearings' much greater capacity and reliability.

Until 1992, tapered elastomeric pads were allowed by the *Standard Specifications* and were routinely used to accommodate the nonparallel bearing surfaces that result from the longitudinal grade of a bridge. Currently, however, the use of tapered pads is restricted by both the *LRFD* and *Standard Specifications*.

10.3 SPECIFICATIONS

AASHTO offers two design specifications, the *Standard Specifications* and the *LRFD Specifications*, and both contain provisions for designing bearings. Both specifications have existed in parallel since 1994, when the *LRFD Specifications* were first published, but the *Standard Specifications* have not been maintained with the same regularity. Their most recent full edition (the 17th) was published in 2002, and the last interims were published in 2005. The goal is to have all designers use the *LRFD Specifications*, and it has for the most part been achieved. In 2009 the provisions for bearings were changed significantly in the *LRFD Specifications*, but not the *Standard Specifications*, so the two are now quite different from each other. For that reason, and to avoid confusion, this document is based solely on the provisions of the Fifth Edition of the *LRFD Specifications*, 2010, and the 2011 Interim Revisions.

10.4 LOADS AND MOVEMENTS FOR DESIGN

The *LRFD Specifications* requires that rotational and translational movements of the bridge be considered in the design of bearings.

10.4.1 Rotational Movements

10.4.1.1. Rotation Axes

Rotations can occur about all three axes, but those associated with beam bending are generally the largest.

Transverse axis rotation of the bearing is associated with bending of the beam about its major axis.

Longitudinal axis rotation of the bearing (i.e. about the beam longitudinal axis) occurs in all bridges, but its magnitude is usually significant only in skew or curved bridges. The value should be taken from the overall structural analysis but, as a first approximation, it may be taken as:

$$\theta_t = \theta_f \tan \alpha \quad (\text{Eq. 10.4-1})$$

where

θ_t = torsional rotation of the beam

θ_f = flexural rotation of the beam

α = skew angle (= 0.0 when the line of support is perpendicular to the longitudinal axis of the bridge).

The torsional rotation may be larger than the bending rotation in a bridge with skew more than 45 degrees.

Equation 10.4-1 can be derived with reference to **Figure 10.4.1.1-1**. The total rotation of the deck can be described by rotations θ_x and θ_y , about axes parallel and perpendicular to the support, or by θ_t and θ_f . Because the supports are rigid vertically, θ_y is zero. Then the flexural and torsional components are given by:

$$\theta_f = \theta_x \cos \alpha - \theta_y \sin \alpha = \theta_x \cos \alpha \quad (\text{Eq. 10.4-2a})$$

$$\theta_t = \theta_y \cos \alpha + \theta_x \sin \alpha = \theta_x \sin \alpha \quad (\text{Eq. 10.4-2b})$$

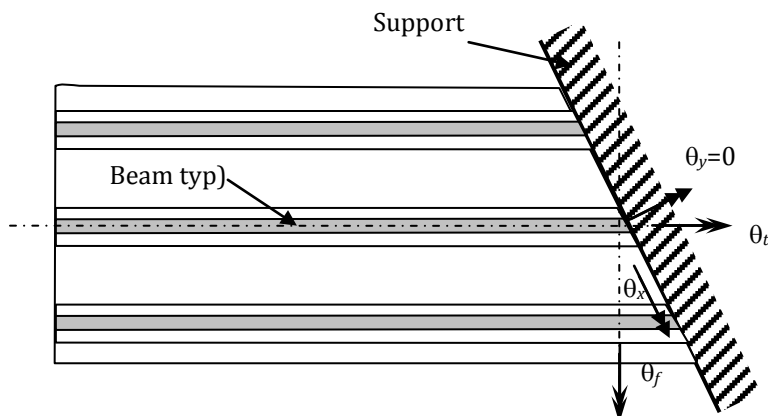


Fig. 10.4.1.1-1. Bearings at a Skewed Support.

This relationship also suggests that the designer has choices for the bearing orientation. Three are illustrated in **Figure 10.4.1.1-2**. Rectangular bearings placed with the long edge parallel to the supports (**Figure 10.4.1.1-2b**) will cause the entire rotation to occur about the weak axis. This is desirable, because it minimizes the stress in the elastomer. However, this orientation means that the bearing is not perpendicular to the beam, in which case it must either be parallelogram-shaped (**Figure 10.4.1.1-2a**) or rectangular and quite small (**Figure 10.4.1.1-2b**) to avoid projecting beyond the beam flange. Parallelogram-shaped bearings are undesirable because they are inefficient at carrying load, and are non-standard and expensive to manufacture. Making the bearings as wide as possible also provides the beams with torsional stability during erection, and that is best achieved by aligning them with the beam rather than the support (**Figure 10.4.1.1-2c**). That orientation is commonly used, even though some stress is induced by torsional rotation of the beam acting about the strong axis of the bearing.

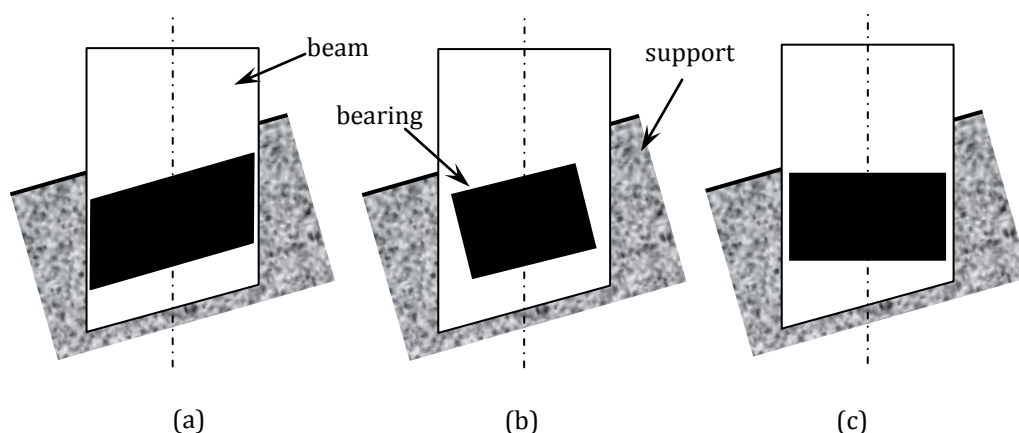


Figure 10.4.1.1-2. Possible Bearing Alignments at a Skew Support.

Twisting of the bearing about a vertical axis occurs in skew bridges, when the whole deck twists due to thermal or other loadings. However the strains induced by this rotation are small compared with those from other sources and are typically ignored.

10.4.1.2 Sources of Rotation

For precast, prestressed concrete beams, the primary sources of bearing rotations are:

1. *Non-parallelism of the bearing surfaces.* The surface that supports the bearing and the bottom flange of the beam may not be parallel, either by design or unintentionally. Typical causes of this non-parallelism include the camber of the beams at the time of erection, the longitudinal grade of the bridge, and the unintended sloping of the supporting surface as a result of construction tolerances. The *LRFD Specifications* requires an allowance for unintended non-parallelism of at least 0.005 radians unless an approved quality control plan justifies a smaller value. [LRFD Art. 14.4.2.1]. For large, stiff bearings, this rotation induces significant stresses, and some agencies have chosen to reduce the value even without a quality control plan, presumably on the basis that their bearings are typically installed to higher accuracy. That practice is ill-advised. 0.005 radians represents a slope of about $1/8$ " in 2 ft., or only one tenth of a bubble length on a typical spirit level, and it is likely that some bearings are not even installed to that accuracy.
2. *Dead load deflections.* When dead loads such as the deck weight are applied to the beams, the resulting deflection causes end rotations. The deflection and associated rotation are typically in the direction that reduces the effects of initial camber. They may have both short-term and long-term components.
3. *Live load deflections (without impact).* The *LRFD Specifications* states, in Section 14.4.1, "that a dynamic load allowance need not be included for bearings."
4. *Thermal camber changes.* Daily fluctuations in camber are caused by solar heat gain on the top of the deck, while the shaded underside of the deck experiences a smaller temperature increase.
5. *Differential shortening of the slab relative to the beam.* A cast-in-place slab on a precast beam will shrink relative to the beam, and will cause downward deflection with corresponding end rotations. Post-tensioning the slab (e.g. a full-depth precast slab) will have a similar effect, and adds to the consequences of differential shrinkage.

The bearing is generally much more flexible in rotation than the beam that it supports. Thus its stiffness has little effect on the global displacements of the structure and the beam end rotation is generally taken as that which would occur if the support were truly pinned. The bearing's low rotational stiffness also causes the moment induced in the member and the substructure to be small compared with the capacities of those elements. Moments on those elements are frequently ignored in design, but should be considered in those rare cases in which they adversely affect the substructure or superstructure.

10.4.1.3 Accounting for Rotation in Bearing Design

The strains in the elastomer caused by the rotation must be accounted for in the bearing design. Their potential for damage to the bearing depends on their magnitude and the number of cycles applied. The *LRFD Specifications* treats static and cyclic loads differently. In all beams, rotations due to live load deflections are cyclic, whereas those due to dead load deflections are static, so the former are more damaging for a given magnitude of rotation. While daily thermal cycles are strictly cyclic, they are treated by the *LRFD Specifications* as static because the number of cycles is so small compared with the number of truck loading cycles.

The live load rotations are typically quite small. In a simply supported beam under truck loading, the end rotation can be shown to be directly related to the mid-span deflection (Stanton et al., 2008, Appendix F), which the *LRFD Specifications* restricts to a value of $L/800$. The end rotation due to live load is then implicitly limited to approximately 0.004 radian. In precast concrete beam bridges, the beam stiffness is usually more than the minimum, so the live load rotation is usually less than 0.004 radians. At the interior supports of continuous beams, the rotations are typically much smaller than those in simply supported beams and are therefore unlikely to contribute significantly to the total strain in the elastomer.

Static rotations are caused by unintended non-parallelism, dead loads, thermal loading, and creep and shrinkage. Some beams remain simply supported throughout their lifetimes, while others are erected as simply supported

but are subsequently made continuous for live load, in which case the rotations that occur before continuity is achieved must be accounted for properly, since they will likely constitute the majority of the total rotation.

If the end rotation due to dead load is large enough to lead to an undesirably thick bearing, a beveled plate or a beveled recess in the bottom flange of the beam may reduce the design rotation imposed on the bearing and provide relief. However, the most recent changes in the *LRFD Specifications* may render such a device unnecessary in many cases, because the *LRFD Specifications* no longer prohibits lift-off of the beam from one side of the bearing. (The previous prohibition was a consequence of the design equations, rather than being stated explicitly in words, and was therefore not obvious to the casual reader). The changes also permit relatively large rotations if the accompanying compressive load is small, and these are precisely the conditions that prevail immediately after setting the beams and that often cause the need for a beveled plate.

Rotation results in an increased compressive strain at one edge of the bearing and a reduced compressive strain (or even net tensile strain) at the opposite edge. As will be discussed below, the design of the bearing must consider the total anticipated rotation to avoid over-compression at the edge of the bearing. In cases where the bearing is attached to both the beam and support in a way that prevents lift-off, hydrostatic tension stresses in the bearing must also be checked.

In circular bearings, the rotations about the two perpendicular axes are additive, and their vector sum should be used for design of the bearing. In rectangular bearings, the peak strains due to compression and rotation occur at the mid-points of the sides, and drop to zero at the corners. Thus the peak strains due to the two rotation components are not additive, and rotation about each axis, in combination with axial load, may be considered independently. In this regard, design of an elastomeric bearing differs from design of a column for axial load and biaxial bending.

10.4.2 Translational Movements

Translational movements of the bearing may occur in two directions:

1. *Longitudinal translations.* These occur directly due to change in length of the superstructure and indirectly due to movement of the bottom flange caused by end rotation of the beam.
2. *Transverse translations.* These occur primarily in curved and skew bridges.

The movements are typically caused by a combination of the following effects:

1. *Temperature changes.* As the ambient temperature changes, the superstructure will expand and contract. For daily thermal changes, concrete bridges experience smaller movements than do steel structures, primarily because concrete bridges have a higher thermal mass and consequently respond more slowly to ambient temperature changes. For seasonal changes, the time scale is slow enough that the thermal mass makes little difference and the two bridge types experience similar movements. The magnitude of the thermal movement is computed based on extreme temperatures defined in the specifications compared to the ambient temperature at the time of construction. The temperature extremes to be used in design are determined using LRFD Article 3.12.2. Care should be exercised with skew bridges, in which thermal changes can cause deformations in unexpected directions (Moorty and Roeder, 1992).
2. *Shrinkage and creep of concrete.* Shrinkage and creep of the precast beams causes an overall shortening of the superstructure. If the beams are precast and the deck slab is cast-in-place, differential shrinkage of the slab will cause some additional overall shortening. It also causes downwards deflection which in turn leads to end rotation and longitudinal movement of the bottom flange. Since this component of movement is outwards, it opposes the inwards movement due to overall shortening of the beam and the net movement at the bearing may be small. Shrinkage and creep deformations theoretically continue forever, but field measurements show that, in a prestressed concrete I-beam bridge, the great majority of the deformation is complete within a year. Creep and shrinkage movements may be estimated using the methods given in Chapter 8 of this manual.

For the global translational movements caused by volume changes, e.g. temperature, shrinkage and creep, the movements at individual bearings are computed based on the distance of that bearing from the apparent point of

fixity of the superstructure. The apparent point of fixity is the point of zero longitudinal movement. It may be determined analytically using the relative stiffnesses of the superstructure and the substructure, the frictional and shearing resistance of the bearings, and other relevant effects. However, most designers simply choose one of the following locations as the point of apparent fixity:

1. The mid-length of the superstructure between expansion joints
2. The central pier for a bridge with an even number of spans between expansion joints
3. The midpoint of the central span for a bridge with an odd number of spans between expansion joints

A small error in the selection of the point of apparent fixity for volume changes will have little effect on the overall performance of the bridge and its bearings.

10.4.3 Vertical Loads

In the *LRFD Specifications*, vertical design loads for bearing design are based on load combinations and load factors for the service limit state, rather than the strength limit state. Furthermore, the *LRFD Specifications* states that no dynamic load allowance needs to be included. Dead loads and live loads should be tabulated separately. Combinations of loads and displacements that occur simultaneously should be identified so that critical combinations, such as low axial force and high rotation (or vice versa), can be considered in design.

10.4.4 Horizontal Loads

In addition to the applied vertical load, horizontal forces must be considered in the design of bearings. Horizontal forces on bearings result from two sources:

1. *Horizontal design loads.* Loads such as wind on the superstructure and traffic, and centrifugal and braking forces must be transmitted to the substructure by the bearings.
2. *Forces induced by bearing deformations.* If the superstructure shortens, the movable bearing deforms in shear and a force is induced. That force induces an equal and opposite force in the bearing at the other end of the beam.

The *LRFD Specifications* no longer contains explicit design procedures for resisting horizontal loads on elastomeric bearings, but rather require that "...bearings shall be provided with adequate... anchorage..." (Article 14.7.5.3.7). Article 14.7.5.4 also contains a requirement that bearings without bonded external plates should be provided with a restraint system if the rotation per layer of elastomer, θ_s/n , exceeds $3\epsilon_a/S_i$. This rotation is about three times the rotation at the start of lift-off, and it would be prudent to lower the threshold for providing restraint against horizontal load.

Anchorage is discussed in Section 10.8.3.7 of this Manual.

10.5 PLANNING THE BEARING LAYOUT

10.5.1 General

The best bearing is no bearing. Bearings of any sort provide the opportunity for errors during design, manufacturing, and installation, so connecting the beams directly to the bent caps or abutments, without bearings, is the best choice if it can be done. For single span bridges of less than about 30 ft span, this may be possible because the thermal deformations are small enough. In a longer single-span bridge, the abutments are likely to be too stiff longitudinally to accommodate the deck expansion without inducing excessive forces, so bearings will be necessary. However, in a multi-span bridge the central piers may be quite tall and may be flexible enough to provide all the longitudinal movement needed regardless of the span.

The designer generally determines the bearing types at each support based on the configuration of the structure, the anticipated movement, the expected superstructure behavior, and any substructure limitations. Then, the movements are evaluated at each support. The designer provides a bearing that is either movable or fixed with respect to translational movements in a given direction. Bearings that are fixed with respect to one horizontal direction may be movable with respect to another perpendicular direction and are referred to as being "guided."

When fixed (or guided) bearings are selected, the designer must provide lateral strength adequate to resist all applied loads and restrain unwanted translation.

When movable bearings are selected, the designer must choose between accommodating this movement through elastic shear deformations of the bearing or by providing low-friction, sliding surfaces. In most situations, shearing of the bearing will be the preferred solution. When large movements are present, a sliding bearing is preferred in order to avoid the use of a thick bearing.

In a multi-span bridge, the engineer should decide where the point of apparent fixity should be, estimate the movements from that point, and select suitable joints and bearings. The bearings located further from the point of fixity will experience larger movements, and bearings with greater movement capacity will be needed there. Because the beam is likely to be discontinuous at the abutment, that bearing will have to accommodate rotation as well as the largest horizontal displacement in the bridge. If elastomeric bearings are used without sliders, the end bearing is typically the thickest.

The installation temperature is usually not known at design time, so the engineer knows only the total design displacement between the two extreme temperatures, but not the individual elongation and shortening relative to the installation temperature. Several options are available. The bearing can be provided with a displacement capacity larger than the minimum necessary, so that the bearings and beams may be installed within a reasonable range of temperature (to be stated on the plans) and still have enough movement capacity in each direction. An alternative is to erect the span at any arbitrary temperature and make provision for subsequently lifting the superstructure when the temperature is at the middle of the expected range, thereby relieving the movement offset. Another alternative is to install the bearings with an imposed offset that is related to the real installation temperature. The latter is feasible with sliding bearings, but it is quite difficult to achieve reliably with elastomeric bearings because it means holding the bearings in a deformed state while they are installed.

In general, the bearings should be designed to have a short length (the direction parallel to the longitudinal axis of the bridge) because this minimizes the moments and stresses due to flexural rotation under service conditions. They should also be as wide as possible to promote torsional stability of the beam during erection. A common approach is to make the bearing about 3 in. narrower than the bottom flange of the beam, and then to select the length based on the area required to achieve an acceptable compressive stress. If the load is light, this approach may lead to a length that is impractically short, in that the ratio of bearing height/length may be excessive and lead to instability by rolling over in the longitudinal direction. The solution is then to select the length needed to provide stability against rollover, in which case the compressive stress will be lower, and the rotation stresses will be higher, than the minimum values that would be possible if each was considered separately.

The expected life of an elastomeric bearing is not known with certainty. Some have been removed after approximately 50 years and found to be in good working order with only a slight increase in stiffness measurable as a result of aging. The bearing discussed by Lindley (Lindley, 1981) was made from a natural rubber compound that was chemically quite primitive, but it was still in good working order even after almost 100 years, albeit with surface blemishes. Thus a well-designed and fabricated bearing may reasonably be expected to last the life of the bridge. However, it is still prudent to provide space on the pier cap for jacking the superstructure should bearing replacement ever be necessary.

10.5.2 Bearing Configurations

10.5.2.1 Fixed Bearings

At a fixed bearing, the superstructure is prevented from moving horizontally relative to the substructure. The fixity is usually achieved by external means, such as steel angles that bear against the beam flange or concrete shear blocks between the beams.

10.5.2.2 Movable Bearings

Movable bearings are intended to accommodate translational movements of the superstructure while imparting relatively small horizontal forces to the substructure and superstructure. Movable bearings are classified as either flexible or sliding, as described below.

10.5.2.2.1 Flexible Bearings

Flexible bearings accommodate translational movements through elastic shear deformation of a deformable material. Elastomers are the only such materials presently permitted by the *LRFD Specifications*. The *LRFD Specifications* permits a shear strain up to 0.50, so the elastomer thickness must be at least 2.0 times the horizontal displacement. The shear stiffness of the bearing is given by

$$k_{shear} = \frac{GA}{h_{rt}} \quad (\text{Eq. 10.5.2.2.1-1})$$

where

G = shear modulus of the elastomer, ksi

A = plan area of the elastomeric bearing, in.²

h_{rt} = total thickness of the elastomer, in.

Low horizontal resistance is therefore achieved with a bearing that has a large thickness and a small plan area. However, the ratio of thickness to plan dimensions is limited by stability considerations, which are discussed in **Section 10.7.3**. Bearings up to about 4 in. thick, with a displacement capacity of ± 2 in., are common. Thicker bearings can be made (the thickest known bearing is about 24 in.) but the difficulty and cost of fabrication, and the bearing weight, increase rapidly with thickness.

10.5.2.2.2 Sliding Bearings

In most bridges constructed with precast, prestressed concrete beams, flexible bearings are capable of handling the required movements. However, when the translational movements exceed the practical capacity of flexible bearings, a sliding surface may be used on top of the bearing. The slider will accommodate most of the translational movement, leaving the elastomeric part of the bearing to accommodate the rotation and the small translation that occurs prior to the start of slip at the sliding surface. The slider usually consists of a polytetrafluoroethylene (PTFE)-stainless steel interface. In bearings with a metal structure, such as pot, disk or spherical bearings, the PTFE is typically recessed into a carbon steel plate that is vulcanized to the top of the bearing and the stainless steel sliding on top of it. In an elastomeric bearing or a cotton duck pad, the PTFE may be applied directly to the elastomeric component. The stainless steel must be longer than the PTFE to ensure full contact during sliding, and the interface should, if possible, be installed with the stainless steel on top facing downwards, so that it does not gather dust and other contaminants.

The *LRFD Specifications* provides friction coefficients only for highly polished (#8 mirror finish) stainless steel. A recent study (Stanton and Taylor, 2010) found that a 2B finish, which is unpolished and therefore less expensive and more readily available, gave results that were in many ways just as good.

It should be recognized that a slider has some friction, in which case small longitudinal movements (such as those caused by truck passage over the span) will be accommodated by shear deformation of the elastomer before sliding starts, while larger movements (such as thermal elongations) will be accommodated by sliding. This unavoidable allocation of movements is fortunate, because there is some evidence that a large number of small sliding movements cause more wear of the PTFE surface than the same total slide path applied in fewer, larger movements. It can be shown that the shear displacement at which sliding starts is:

$$\Delta_s = \frac{\mu\sigma_a}{G} h_{rt} \quad (\text{Eq. 10.5.2.2.2-1})$$

where

μ = coefficient of friction between PTFE and stainless steel

σ_a = average compressive stress on the elastomer, ksi

G = shear modulus of the elastomer, ksi

h_{rt} = total thickness of the elastomer, in.

10.5.2.3 Guided bearings

A guided bearing is free to move in one direction but is restrained against movement in the other. These requirements may exist, for example, if the superstructure must be allowed free longitudinal movement for creep and shrinkage but must resist transverse wind forces with little movement. The guidance may be achieved in several ways, such as concrete shear blocks between beams or steel angles that bear against the sides of the bottom flange. In both cases, provision should be made for free sliding against the guide. A pair of inclined flexible bearings, as shown in **Figure 10.5.2.3-1**, has also been used for the purpose.

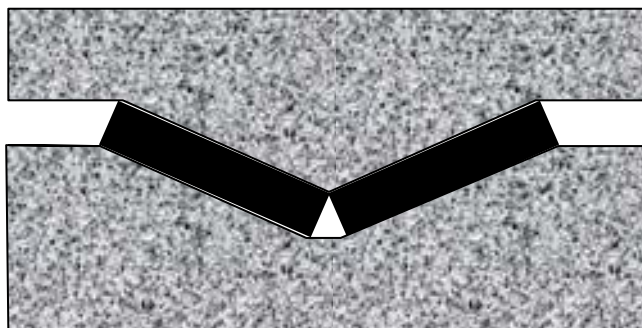


Figure 10.5.2.3-1. Horizontally Opposed Inclined Bearings.

10.5.2.4 Force Control Bearings

While most bridge bearings are designed for vertical forces and slowly applied horizontal movements caused by temperature, creep and shrinkage, they can also be designed to limit horizontal seismic forces using the principles of seismic isolation. Either flexible or sliding bearings may be used for the purpose. If a flexible bearing is used, its shear stiffness is selected to give the structure a long natural period that lies beyond the period of the primary ground motion. The structure then experiences little earthquake excitation so the forces induced in it are low. To control the displacements in the bearing, damping is introduced. This may be done by including a yielding lead plug in the bearing, using high-damping rubber, or adding an external damping device.

Lead-cored elastomeric bearings can also be used to alleviate high thermal loads on substructures while maintaining the desired fixity for short-term service loads. This is due to the ability of lead to creep for slowly applied loading such as expansion or contraction of bridge superstructures. These slowly applied thermal displacements will, therefore, result in much lower forces transmitted to the substructure than if the displacement were applied rapidly.

A sliding bearing system, called the Friction Pendulum System described at the website <http://www.earthquakeprotection.com/product2.html>, has also been widely used for seismic isolation. The superstructure rests on a sliding element in a shallow stainless steel dish. The surface of the dish is a partial sphere, so the sliding element tends to return to the center of the dish. The system possesses a natural period that is defined by the radius of curvature of the stainless steel dish, and the friction between the PTFE and stainless steel provides the necessary damping.

More information on the design of force control bearings, particularly for limiting seismic loads, can be found in *Guide Specifications*, 2010; Buckle and Mays, 1996; HITEC, 1996; Stanton and Roeder, 1991; and Nagarajaiah et al., 1998.

10.5.2.5 Special Considerations for Box Beams

Historically, bearings for adjacent box beam bridges have consisted of either continuous strips of unreinforced or reinforced elastomeric material placed across the full width of the support, or four individual bearings, two at each end of each box beam. Both arrangements present challenges, caused partly by the fact that box beams are very stiff in torsion so the slightest difference in slope between the two ends causes uneven bearing forces. The problem is accentuated in skew bridges. A solution has been used in New England region (Culmo, 2002) in which each beam is set on only three bearings, with two at one end and one at the other. This arrangement is statically determinate and eliminates the problem of uneven loading.

10.5.2.5 Special Considerations for Box Beams/10.6.4 Steel-reinforced Elastomeric Bearings

Unreinforced elastomeric strips present an additional potential problem, because they tend to shift over time, possibly causing the concrete beam to bear directly on the concrete support.

If the box beams are to be bolted or post-tensioned transversely, alignment of the ducts is necessary. The bearing system should be designed so that its deformations do not jeopardize the alignment of the ducts. This is particularly important if the supports are sloped, for example to provide roadway cross-slopes, or if the bridge is skewed. In both of those cases the beam displacements and rotations due to bearing deformations are more difficult to predict and control.

10.5.2.6 Special Considerations for Fixed and Guided Bearings.

If fixed or longitudinally guided bearings are used, allowance should be made for transverse expansion and contraction, especially in wide bridges. If every bearing at a pier were guided to permit only longitudinal movement, large transverse forces might be set up in the guide system. This can be avoided if only a small number of bearings near the mid-width of the bridge are guided, and the bearings under the outer beams are free to move in both directions.

Curved and skew bridges present particular planning challenges. Centrifugal (and wind) forces must be resisted to avoid excessive transverse movement, but the fixed, guided and free bearings must be planned so that they allow free movement in the desired directions needed and do not “fight” each other.

10.6 TYPES OF ELASTOMERIC BEARINGS

Elastomeric bearings may be either made from elastomer alone, or may be reinforced with steel plates, layers of cotton duck, or layers of fiberglass.

10.6.1 Plain Elastomeric Pads

Plain elastomeric pads (PEP) are the most economical, but are suitable only for supporting relatively light vertical loads. In addition, they cannot accommodate large rotations or translations. As the selection guide in **Section 10.9** indicates, plain pads are only applicable over a relatively narrow range of situations.

10.6.2 Fiberglass-reinforced Pads

Fiberglass-reinforced bearing pads (FGP) are reinforced with discrete layers of fiberglass, and their behavior is conceptually similar to that of steel-reinforced bearings. Because fiberglass is not susceptible to corrosion, edge cover is not needed, so the pads can be made in large sheets and cut to size as needed. This offers advantages in terms of cost and delivery time. However, the bond between the fiberglass and elastomer is less good than the bond between steel and elastomer, so the compressive load capacity of FGPs is only slightly higher than that of plain pads. Furthermore, at the time of writing, FGPs are not commercially available.

10.6.3 Cotton Duck-reinforced Pads

Cotton duck pads (CDP) are constructed of closely spaced layers of cotton duck impregnated with elastomer. The layers of cotton duck are specified to be spaced at no more than 1/60 in. and lead to theoretically very high shape factors, if the layer is considered to consist of the elastomer between the layers of cotton. In practice, the cotton is not very stiff in resisting outwards bulging, so the friction on the top and bottom surface of the pad also contributes to restraining the bulging. Thus the shape factor effect is not clearly defined in a CDP. However, it has a high compressive stress capacity but little ability to deform in shear or rotation. Provision of a PTFE slider provides translational capacity, but does nothing to improve the rotation capacity. CDPs are not widely used in prestressed concrete beam bridges.

10.6.4 Steel-reinforced Elastomeric Bearings

Steel-reinforced elastomeric bearings (SREB) are the most versatile type of elastomeric bearings and can be designed to have high compressive stress capacities and to accommodate large horizontal movements. They can also be designed to accommodate quite large rotations, but these detract from the compressive load carrying capacity. They are the bearing type most commonly used for precast, prestressed beam bridges.

One bound on the dimensions of the bearing is provided by permissible stresses. However, the size may also be controlled by stability. The width is usually made as large as possible to provide torsional stability to the beam during erection, and the length may be governed by the need to avoid bearing instability in the longitudinal direction. Its area may then be such that the applied stress is lower than the permissible stress.

The first cost of SREBs is typically higher than for other types, because they have to be molded individually, but their record of long-term performance is excellent.

10.7 BEHAVIOR OF ELASTOMERIC BEARINGS

10.7.1 Elastomeric Materials

10.7.1.1 General

An elastomer is an elastic polymer. Its behavior is classified as elastic because the material returns to its original configuration when the load is removed. The name polymer implies a chemical structure that consists of long, repeating, chain molecules. Natural rubber and neoprene are the elastomers most commonly used in bridge bearings. For most bearings, the differences in behavior between neoprene and natural rubber are not significant and, in the absence of specific requirements from the designer, the elastomer is usually chosen by the bearing manufacturer in order to best meet the overall performance requirements.

The elastomeric compounds used in bearings include many additives, and these, as well as the raw elastomer, affect the properties of the compound. A vulcanization agent such as sulfur is added to cross-link the elastomer molecules and prevent creep, oils are added to soften the rubber during processing, carbon black acts as a filler and increases stiffness, and chemicals are added to increase resistance to ozone and oxidation. The compound is then vulcanized, or cured, by subjecting the mixed materials to heat and pressure, at temperatures of about 280 F (Lee, 1994). Large bearings are more difficult to cure because of their thermal mass and the low thermal conductivity of the elastomer. There is a danger of over-curing the outside before the inside is fully cured, and careful temperature control is needed.

In general, neoprene has a higher resistance to ozone deterioration and is more resistant to attack from many chemicals, but it becomes stiff and brittle at low temperatures more readily than does natural rubber. Thus natural rubber may be preferred in very cold climates. Natural rubber is also the elastomer of choice for almost all seismic isolation bearings because of its greater strain capacity.

During the 1990s, some bearings were found to “walk”, or slip out of place. This behavior was attributed to the addition to the compound of anti-ozonant waxes (Muscarella, 1995), which were used in both neoprene and natural rubber bearings, although in greater quantities in the latter because of their perceived greater sensitivity to ozone. As the waxes migrate to the surfaces of the bearings, they tend to reduce the friction that holds the bearings in position. The real need for ozone protection is open to question, because the bearing identified by Lindley (1981) contained no such protection and had suffered ozone stiffening to a depth below the surface of only about $\frac{1}{8}$ in. after almost 100 years in service. Although anti-ozonants are not formally required in neoprene, paraffin and other waxes have nonetheless been found in neoprene bearings. McDonald et al. (2000) recommend that elastomeric bearings should only be ordered from manufacturers that do not add paraffin to their product. In addition, at least one state agency in the U.S. has a “no-wax” specification (Dunker, 2000). The real dangers of slipping appear to outweigh the possibility of chemical deterioration due to ozone attack, so it would seem preferable to avoid the use of waxes.

10.7.1.2 Shear Modulus

The stiffness of the elastomer is the most important material parameter in bearing design, and may be specified either by the shear modulus (in psi) or by the hardness (on the empirical Shore A scale). Shear modulus is measured in a special rig, defined in ASTM D4014. Hardness is measured using a simple indenter (ASTM D2240), which measures the penetration under a given load. The shear modulus is the quantity on which the design is based and is therefore the one that is needed, but the hardness test is simpler and faster to conduct. While the two are linked (Gent, 1958), the correlation is not exact, if nothing else because the hardness values obtained from a durometer are somewhat user-dependent. Thus, the *LRFD Specifications* encourages the use of the more precise

shear modulus by giving a range of shear moduli that might be expected for any given hardness, but they require that the least advantageous G value from that range be used in the various steps of the design. (The wording for this is unfortunately unclear, and it is hoped that it will be corrected in the AASHTO 2012 Interim). The ranges of hardness and shear modulus are shown in **Table 10.7.1.2-1** [LRFD Table 14.7.6.2-1]. This process is therefore slightly conservative and imposes a small penalty on bearings designed by hardness.

It is very important to specify either hardness or shear modulus, but not both. Specifying both could lead to a combination of values that cannot be achieved by a single elastomer. Specification by shear modulus is the preferred method, because it is more accurate and it imposes no penalty in practice, since every manufacturer of bearings suitable for use under beams has the equipment to run the material test for shear modulus.

Current specifications permit elastomers with a nominal hardness between 50 and 60 durometer to be used for steel-reinforced elastomeric bearings. Elastomers used in plain pads, cotton duck pads, and fiberglass-reinforced pads may have a nominal hardness between 50 and 70 durometer.

Table 10.7.1.2-1
Elastomer Properties at Different Hardnesses

Hardness (Shore A)	50	60	70
Shear modulus, G , at 73 °F (psi)	95-130	130-200	200-300
(Creep deflection at 25 years) ÷ (Instantaneous deflection)	25%	35%	45%

[LRFD Table 14.7.6.2-1]

10.7.1.3 Low Temperature Grades

The material properties of most elastomers vary with temperature. In particular, both neoprene and natural rubber stiffen and become brittle at low temperatures. It is important to use an elastomer that is suitable for the temperatures expected at a specific bridge site. The *LRFD Specifications* requires that bearings be fabricated from AASHTO low temperature grades of elastomer conforming to the requirements of the *AASHTO Bridge Construction Specifications* and the *Material Specification, M 251*.

Table 10.7.1.3-1
Low Temperature Zones and Elastomer Grades

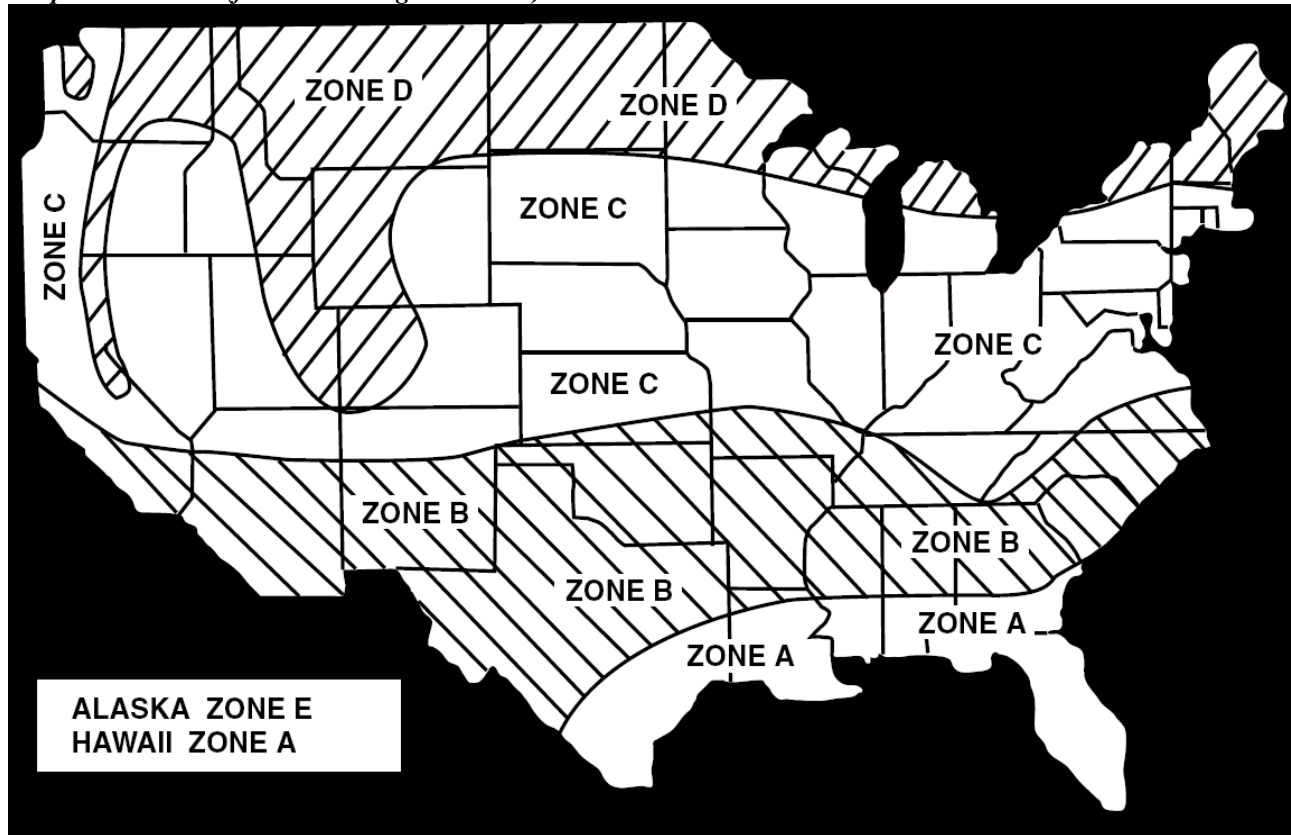
Low Temperature Zone	A	B	C	D	E
50 year low temperature (°F)	0	-20	-30	-45	All other
Max. no. of days below 32 °F	3	7	14	N/A	N/A
Low temperature elastomer grade without special force provisions	0	2	3	4	5*
Low temperature elastomer grade with special force provisions	0	0	2	3	5*

* Grade 5 elastomer may be difficult to obtain

[LRFD Table 14.7.5.2-1]

In the absence of specific requirements from either the owner or the design agency, **Table 10.7.1.3-1**, together with **Figure 10.7.1.3-1**, may be used to establish the minimum low temperature grade required [LRFD Table 14.7.5.2-1 and Fig. 14.7.5.2-1]. The *LRFD Specifications* permits the use of a lesser grade material if a device such as a sliding surface is used to reduce the forces or if the substructure is designed for the additional forces that may result.

Figure 10.7.1.3-1
Temperature Zones (from LRFD Fig. 14.7.5.2-1)



10.7.2. Mechanics of Elastomeric Bearings

10.7.2.1 Behavior of an Elastomeric Layer

Elastomers used in bearings are virtually incompressible, that is, they have a very low G/K ratio, where K is the bulk modulus. This means that a piece of the material changes shape very readily, but has high resistance to changing volume under pressure, so it behaves somewhat like a fluid. Poisson’s ratio, ν , is essentially 0.5.

A single layer of elastomer resting on a lubricated surface and subjected to vertical load will respond by a reduction on thickness and a corresponding increase in lateral dimensions, caused by the Poisson effect. This is shown in **Figure 10.7.2.1-1a**. The relationship between vertical stress and strain would be:

$$\sigma = E\epsilon \tag{Eq. 10.7.2.1-1}$$

where $E = 2(1 + \nu)G \approx 3G$ (Eq. 10.7.2.1-2)

Such a bearing would be too flexible in compression for practical use.

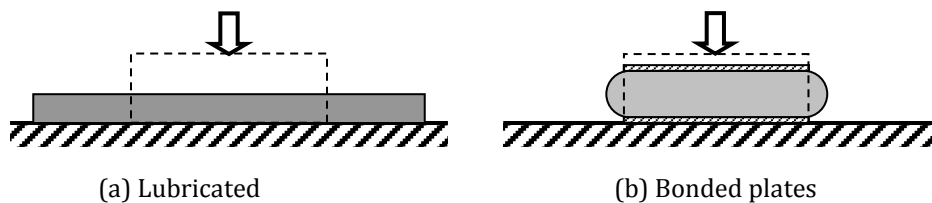


Figure 10.7.2.1-1. Compression of an elastomer layer.

If the elastomer layer is bonded to steel plates on the top and bottom, as in **Figure 10.7.2.1-1b**, the lateral expansion is prevented at the top and bottom surfaces. The vertical displacement can then be accommodated only by lateral bulging between the plates. The plates thus stiffen the system significantly in compression. However, they do not change its shear stiffness, and this allows the designer to create a layered system with the desirable properties of high axial stiffness and low shear stiffness.

The bulging deformations induce shear strains in the elastomer, which are largest at the corners of the layer. They are the critical strains in the material and, in the extreme, they cause shear tearing in the elastomer along the interface between the plate and elastomer, as illustrated in **Figure 10.7.2.1-2**. In thick layers of elastomer, significant bulging (and a correspondingly high level of shear strain) occurs under axial compression. Under the same load, thinner layers of elastomer will bulge less and will therefore experience smaller shear strains. Layers that are thin compared with their plan dimensions are therefore stiffer and stronger in resisting vertical loads.

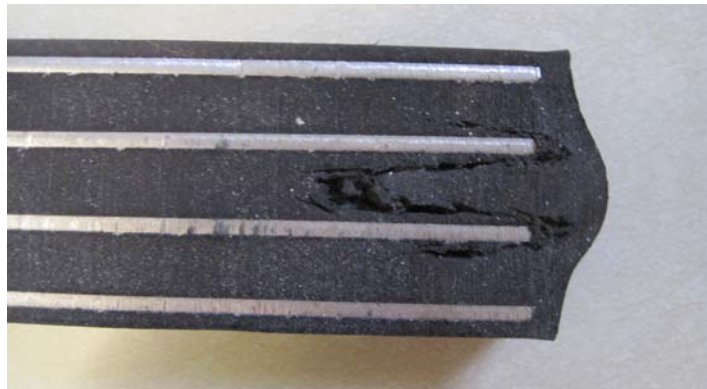


Figure 10.7.2.1-2. Shear Failure in the Elastomer

The shape factor, S , for a layer of elastomer is the parameter that characterizes the restraint of bulging and its effect on the mechanical properties. It is defined as the area of the horizontal loaded surface divided by the area of the vertical perimeter surface that is free to bulge. For a rectangular bearing without holes, the shape factor is computed as:

$$S = \frac{LW}{2h_{ri}(L + W)} \quad [\text{LRFD Eq. 14.7.5.1-1}]$$

where

L = length of a rectangular elastomeric bearing (parallel to the longitudinal bridge axis), in.

W = width of a rectangular elastomeric bearing (perpendicular to the longitudinal bridge axis), in.

h_{ri} = thickness of i^{th} elastomeric layer in elastomeric bearing, in.

For a circular bearing it is:

$$S = \frac{D}{4h_{ri}} \quad [\text{LRFD Eq. 14.7.5.1-2}]$$

Plain pads derive their resistance to lateral expansion by friction at the top and bottom bearing surfaces. In the absence of friction, the lateral expansion would occur freely, and no bulging would occur. In practice, the frictional restraint in a plain pad is insufficient to prevent all lateral expansion, so both slip and bulging occur, and the pad's behavior lies between that of a steel reinforced bearing and a lubricated plain elastomer layer. It is illustrated in Fig 10.7.2.1-3. The slip occurs in the outer region of the pad, and the outer edge moves outwards from its original, unloaded location.

Because the frictional resistance is partial and uncertain, the allowable stress on a plain pad is lower than that on a steel-reinforced bearing with the same shape factor.

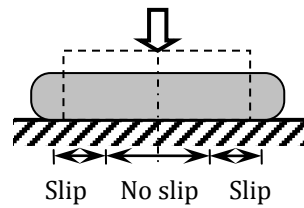


Figure 10.7.2.1-3. Partial Slip at the Surface of a Plain Pad.

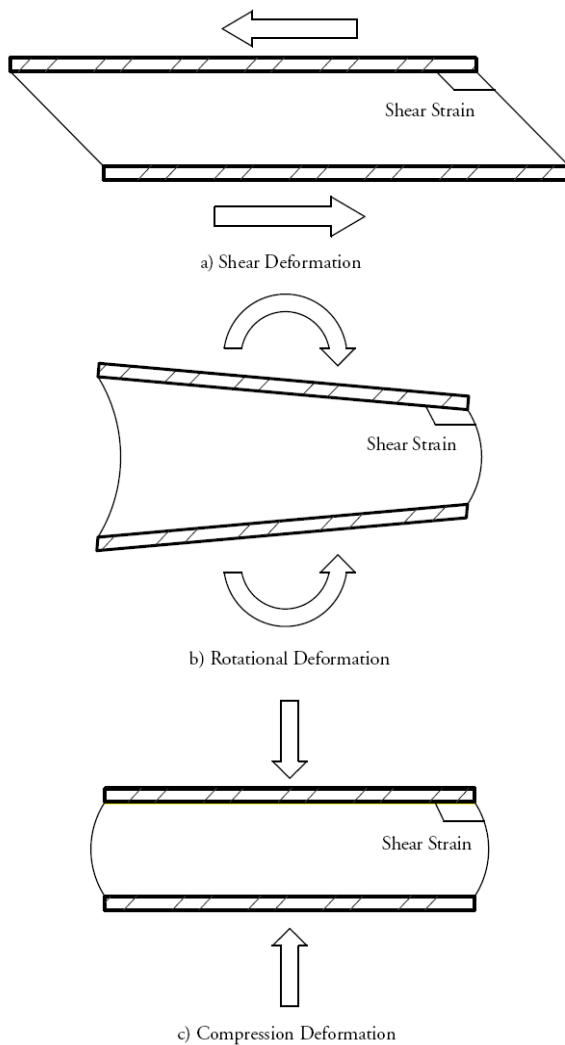
Cotton duck pads gain some of their resistance to vertical load from the lateral restraint provided by the cotton layers, and some from the friction on the top and bottom of the pad.

Rotation causes bulging deformations that are similar in concept to compressive deformations. Under pure rotation (no compression) the elastomer bulges out on one side and in on the other, as shown in **Figure 10.7.2.1-4b**. These bulges cause shear strains, again at the corners of the layer, which add to those due to compression. A high shape factor causes the bearing layer to be very stiff and strong in resisting rotation, and induces high shear strains for even a small rotation. Thus a high shape factor is beneficial for resisting compression loads, but disadvantageous in allowing rotation, so design of an elastomeric bearing is likely to be a compromise between axial and rotational demands. Layer shape factors in the range 6 to 12 are likely to provide the optimum design in most precast prestressed concrete beams.

Shear displacements (**Figure 10.7.2.1-4a**) cause shear strains that are nearly constant throughout the bearing.

Holes in bearings are strongly discouraged because they provide stress concentrations in the steel plates. However, if holes are required and the elastomer around their edges is free to bulge, the shape factor equation should be modified by deducting the area of the holes from the numerator and adding the area associated with the perimeter of the holes to the denominator (see LRFD Eq. C14.7.5.1-1 and 2). If the hole is needed only for fabrication purposes and is subsequently filled completely with elastomer, no modification to the shape factor is needed.

Figure 10.7.2.1-4
Shear Strains in an Elastomeric Bearing



10.7.2.2 Elastic Stress-Strain Behavior in Compression

Early AASHTO Specifications limited the compressive strain in the bearing to 7%, on the basis that larger strains caused damage. That limit is no longer used, partly because the strain in a well-designed bearing will be significantly lower than 7%, and partly because the shear strains, and not the compressive strains, in the elastomer are the best indicators of potential damage.

An elastomeric bearing has a load-deflection curve in compression that is nonlinear stiffening. Part of the nonlinearity is due to geometric effects caused by the fact that the deformed geometry may differ significantly from the undeformed geometry. Furthermore, in a test, the elastomer exhibits “bedding in” effects, which make establishing a true zero for displacement very difficult. (This is one reason why requiring a compressive load-displacement test for establishing the stiffness of a bearing is of dubious value). Gent (1958) developed a linearized effective modulus, based on the initial geometry of the layer, and given by

$$E_c \approx 6GS^2$$

[LRFD Eq. C14.6.3.2-1]

where

E_c = effective modulus in compression, ksi

G = shear modulus of the elastomer, ksi

S = shape factor

The effective modulus, E_c , depends on the bulging of the elastomer and accounts only for that behavior, assuming complete incompressibility. For bearings with a shape factor less than about 5, the error introduced by that assumption is smaller than that due to other uncertainties, so the approximation is acceptable. However, as the shape factor increases, change in volume by bulk compression of the elastomer starts to account for a significant proportion of the total vertical deformation, and $E_{c,tot}$, given by the approximate Equation 10.7.2.2-2 (Gent and Lindley, 1959), which includes the effects of bulk compression, should be used.

$$E_{c,tot} = \frac{K \times E_c}{K + E_c} \quad (\text{Eq. 10.7.2.2-2})$$

Of course, in a bearing with a high shape factor, the compressive deformation will be very small anyway, and its exact magnitude may not be important.

The most important deflection is the one due to live load. Because it occurs after the application of dead load, and because the load-deflection curve is nonlinear stiffening, an estimate of the live load deflection that is based on the initial stiffness will over-predict the true value and thus be conservative.

In a well-designed bearing the vertical stiffness is high, so the vertical deflection, including both elastic and creep components, is low. Vertical deflection is important primarily for maintaining good ride characteristics, but no mandatory limit is given in the *LRFD Specifications*. The Commentary suggests that live load deflection should be limited to $\frac{1}{8}$ in. Since many bridge decks contain surface irregularities that are significantly larger than this (for example expansion joints), it is evident that compressive deflection in bearings is usually not a critical design constraint.

10.7.2.3 Creep Strains

In addition to instantaneous elastic strains, the elastomeric materials used in bearings will exhibit creep behavior. The approximate ratio of ultimate creep strains to initial strains for various elastomers is provided in LRFD Table 14.7.6.2-1. Creep is seldom a controlling parameter. It affects the shear deformations more than the change in volume, so it is likely to be more prevalent in bearings with low shape factors.

10.7.3 Stability

A bearing is an elastomeric column, and may buckle if the slenderness or compressive stress is too high. The mechanics of buckling are more complicated for bearings than for conventional columns because the shear flexibility of a bearing plays a major role. Haryngx (1948) was the first to develop a model for buckling of continuous, linear, shear flexible systems, and Gent (1964) adapted it for discrete layers such as those found in elastomeric bearings. Stanton et al. (1990) then adapted Gent's formulation to include nonlinear corrections to account for the fact that, under the high stresses normally required to cause buckling, the geometry changes significantly. The resulting equations are given in the *LRFD Specifications* and are quite complicated. In some cases those equations lead to a predicted buckling stress that is negative. The implication is that buckling will never occur at any stress and may be ignored. This curious behavior is associated with shear-flexible systems, and is described in Article 2.19 of Timoshenko and Gere (1961). It may be thought of as arising because the column shortens under load. The shorter column has a higher buckling strength, and for certain column geometries the strength increases faster than the load, rendering buckling impossible.

The *LRFD Specifications* includes two methods for checking stability. For bearings designed using Method A, the total bearing height needs only to be less than one third of the smallest plan dimension. For bearings designed using Method B, explicit equations are included. However, if the bearing satisfies the Method A criteria, it will almost certainly satisfy the more complex explicit checks.

10.7.4 Tapered Bearings

Until 1992, tapered bearings were permitted by the *Standard Specifications*. Currently, however, both of the AASHTO Specifications do not allow the use of tapered layers in elastomeric bearings [LRFD Art. 14.7.5.1]. The reasons are related to performance. First, the greater layer thickness on one side creates lower compressive stiffness there, so the load is unevenly distributed across the bearing and exacerbates the internal stresses. Under cyclic loading, it may also promote “walking” of the bearing. Second, some bearings with tapered layers tested by Roeder et al. (1987) were found to debond prematurely from the internal steel plates. This was attributed to the presence of the tapered layers.

If the applied static rotation is too large to be accommodated by deformation of the bearing, a steel tapered plate or a sloping recess in the bottom flange of the beam may be used to correct for it, and the deformation capacity of the bearing can then be used to accommodate live load rotations. If a tapered plate or recess is used, care should be taken to orient it correctly (see **Figure 10.7.4-1**). A reversed tapered plate or recess creates stresses in the bearing that are more severe than those in a system with no tapered plate.



Figure 10.7.4-1. Reversed recess in beam.

The bearing should always be set on a horizontal support and have its surfaces and internal steel plates horizontal. Any tapered plate should be placed on top of it. If the internal plates were to be inclined, a portion of the vertical load would have to be carried by the bearing in shear and, because the shear stiffness is low, the deformations would be significant.

Muscarella (1995) studied the behavior of tapered elastomeric bearings and has provided recommendations for their continued use, which are given in Section 10.8.5. It should be noted that use of tapered bearing layers violates the *LRFD Specifications*, so cannot be recommended, particularly because the cost of replacing a damaged bearing is typically many times the first cost of the bearing itself.

10.8 DESIGN OF ELASTOMERIC BEARINGS

10.8.1 Applicable Specifications

Bearing design is controlled by the *LRFD Specifications*, materials requirements and testing are defined in the *AASHTO M 251 Materials Specifications*, and the *AASHTO Construction Specifications* dictates the ASTM and other tests that the bearings must satisfy. These three documents are maintained by different committees, and consequently they are less well correlated than is desirable.

The *LRFD Specifications* has for many years included two methods by which bearings may be designed. Method A is intended to be relatively simple, at the expense of some conservatism, and can be applied to steel-reinforced bearings, fiberglass-reinforced bearings, cotton duck pads and plain pads. Method B applies only to steel reinforced elastomeric bearings. It is more computationally intensive, generally results in higher capacities, and the bearings designed by it must at present be subjected to more rigorous testing.

Both design methods underwent major revisions in the 2009 *LRFD Interim Revisions* as a result of research conducted under NCHRP Project 12-68 (Stanton et al., 2008). The primary objective of that study was to re-evaluate design for rotation, and in particular to rationalize the provisions for load combinations consisting of light loads and large rotations. These load combinations are common during construction, and may lead to lift-off on one side of the bearing. In previous editions of the *LRFD Specifications*, lift-off was prohibited, albeit indirectly, which meant that in many cases no elastomeric bearing could be designed to satisfy the requirements at both the initial conditions and the final service conditions. The testing conducted for NCHRP Project 12-68 showed that lift-off is not inherently harmful and that the important criterion is not lift-off on the tension side of the bearing, but rather excessive bulging on the compression side, caused by combined axial load and rotation.

The form of the Method B design equations was changed to make the process more transparent, and the previous absolute limit of 1.75 ksi on average compressive stress was removed. In the 2009 approach, the shear strains in the elastomer due to compression, rotation, and shear are each calculated explicitly and are then added. The resulting total shear strain must satisfy a specified limiting value. In addition, the shear strain due to permanent compression alone is subject to a second, independent limit. The outcome is that a bearing can be designed to carry a high compressive stress if it has a high shape factor and experiences only a small rotation. The new design provisions encourage the use of shape factors higher than those typically used in the past (about 4 to 6). The change is supported by both theory and the excellent performance of high shape factor bearings in the tests.

In the past, the main barrier to the use of Method B was the additional testing, which was seen as expensive and time-consuming. A change was proposed that would impose the additional testing requirements on large bearings, (which are more difficult to cure properly, and are therefore at greater risk of failure in the elastomer), rather than on those designed using Method B. This would open the way to more widespread use of Method B for many bearings. The wording with regard to testing in the 2010 *LRFD Specifications* is unclear on the matter. It is expected to be clarified in the 2012 *LRFD Interim Revisions*.

Method A was also changed. The goal was to discard the previous provisions for rotation and to use only a compressive stress criterion, thereby making the method simpler to use. But this can only be done if some guard is introduced to prevent use of the method under circumstances when combined rotation and compression would over-stress the elastomer. To provide this guard, a simple limit was imposed on the use of Method A so that, for common bearing types (e.g., bearings under prestressed concrete beams in highway overpasses) subjected to common amplitudes of rotation, the capacity under Method A would not be greater than that computed using Method B. Under the previous provisions, this was sometimes possible and was clearly not rational. Unfortunately, due to an oversight, the rotation requirements from the previous Method A were retained, when they should have been removed. Furthermore, proposed changes to the allowable stresses on plain pads were not made. That situation is expected to be corrected in the 2012 *Interim Revisions*, and the resulting Method A design procedure will then be simpler than in any previous edition because there will be no explicit checks on rotation.

The following discussion is based on the method that is expected to be in the 2012 *Interim Revisions*, after the foregoing changes have been made.

10.8.2 Testing Requirements

Testing is required both for materials and for some finished bearings. Both types of test are defined in the *M 251 Materials Specification*. The *Construction Specifications* requires that testing be conducted in accordance with M 251. This is unfortunate because the *M 251 Specification* is poorly correlated with the design and construction specifications, and is updated less frequently. At present, the *M 251 Specification* requires that SREBs designed using Method B satisfy additional long-term testing. One of the recommendations of the NCHRP Report 596 was that such additional testing only be required for large bearings, thereby permitting designers to use the more rational Method B for moderate-sized bearings without the cost penalty of additional tests. It is hoped that this change will be adopted in the 2012 *Interim Revisions*.

The rationale underlying the requirements for additional testing is to address uncertainty. Uncertainty exists in design, for example over the accuracy of the design models, the precision with which the material properties are known, etc. It is also present in fabrication and construction, where it depends on the completeness of the curing of the elastomer, the dimensional control of the bearing components, etc. Previously, it was believed that bearings designed by Method B were stressed more highly, in which case some of their reserve capacity was already used up. To compensate, measures to reduce the remaining uncertainty were deemed necessary, and the easiest way of achieving that goal was by rigorous testing to confirm the quality of fabrication. For that reason, additional testing was required for bearings design using Method B.

The recent modifications to the *LRFD Specifications* changed both design methods, with the result that, for common bearing types and sizes, approximately the same stress level can be achieved using either design method. Thus the choice of design method is no longer a good criterion for deciding the testing regime. However curing a large bearing is more difficult than curing a small one because of the need for careful control and monitoring of the temperature throughout the bearing. Therefore NCHRP report 596 recommended that the criterion for additional testing be changed, and to be based on bearing size. It is expected that that change will be incorporated into the 2012 *Interim Revisions*.

Testing requirements, assuming the foregoing changes are adopted, are summarized in **Table 10.8.2-1**.

Short-duration load tests on every steel-reinforced elastomeric bearing, regardless of design method, are advisable. They can usually be conducted in the press that was used for fabrication, and can be conducted quickly and easily. They are a useful indicator of obvious fabrication flaws, such as misplaced internal steel plates, so the cost is low and the benefit is high. By contrast, long-term load tests occupy fabrication equipment for a significant amount of time, or require a special test machine, and so are more costly. It is therefore appropriate that they should be required only when there is some reasonable cause for questioning the integrity of the bearing. This is the case with large bearings, which are defined as any bearing with a plan area greater than 1,000 in.² or a height greater than 8 in. This distinction is included in the *LRFD Specifications* [LRFD Art. C14.7.5.1] but the way that it is intended to be applied is not very clear.

BEARINGS

10.8.2 Testing Requirements

Table 10.8.2-1
Testing Requirements for Elastomeric Bearings

Test	Low Temperature Grades 0, 2, and 3		Low Temperature Grades 4 and 5	
	Large SREBs ⁽³⁾	PEPs, FGPs, small SREBs	Large SREBs ⁽³⁾	PEPs, FGPs, small SREBs
Elastomer material tests at ambient temperature (manufacturer may submit certificate in lieu of shear modulus testing)	R	R	R	R
Instantaneous thermal stiffening	R	R	R	R
Low temperature brittleness	R ⁽¹⁾	R ⁽¹⁾	R	R
Low temperature crystallization	R ⁽²⁾	R ⁽²⁾	R	R
Short-term load test (each bearing)	R	O	R	O
Long-term load test (randomly selected bearings)	R		R	R
Shear modulus (<i>G</i>)	O	O	O	O

R = required

O = optional; required only when specified by the engineer

(1) = not required for Grades 0 and 2

(2) = not required for Grade 0

(3) = >1,000 in.²

10.8.3 Steel-Reinforced Elastomeric Bearings– Design using Method B

Figure 10.8.3-1 shows the configuration of a typical steel-reinforced elastomeric bearing. The following describes the procedure for designing bearings using Method B [LRFD Art. 14.7.5].

Method B may be used for any steel-reinforced elastomeric bearing, but it is especially intended for use with bearings that are large, have unusual geometry, or experience high stress or deformation, because it accounts more precisely than Method A for the strains in the elastomer.

The method consists of checking the stresses in the elastomer, the stresses in the steel plates, overall stability and anchorage against sliding. The elastomer is checked by computing the peak shear strains in it and ensuring that they do not exceed three independent limits: for strains due to shear displacement alone, for strains due to static compressive stress alone, and for strains due to combined loading (compression, rotation, and shear). A fourth limit associated with internal fracture caused by hydrostatic tension applies only to bearings with bonded external plates. It seldom controls, both because external plates are seldom used in concrete bridges, and because the conditions that promote hydrostatic tension include light compressive load (or net tension) combined with large rotations. While these conditions may occur during erection of a steel bridge, they seldom occur in concrete bridges.

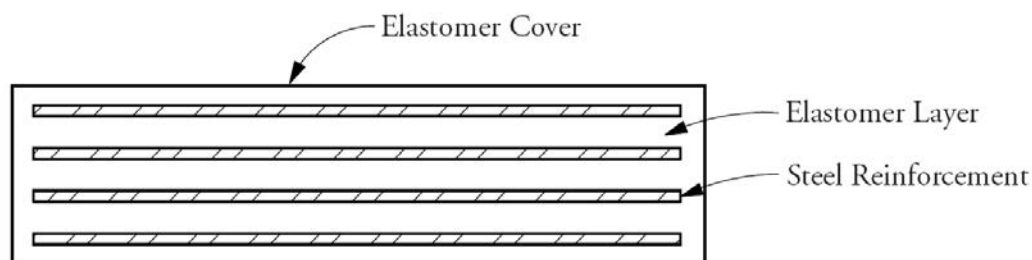


Figure 10.8.3-1 Typical Steel-Reinforced Elastomeric Bearing

Method B bearings are required to use elastomers that have a shear modulus of between 80 and 175 psi and a nominal hardness of between 50 and 60 durometer on the Shore A scale.

10.8.3.1 Loads and Movements

The loads and movements for which the bearing is designed should be tabulated in a rational form. **Figure 10.8.3.1-1** [LRFD Fig. C14.4.1-1] is provided as an example. Vertical dead loads and live loads (without impact) should be identified separately, because, in the design procedure, the live loads are amplified by an additional factor to account for the damage done by repetitive loading. Horizontal loads, if required to be resisted by the bearing, should also be identified. **Figure 10.8.3.1-1** will be useful for the majority of design situations for elastomeric bearings. For more sophisticated bearing designs, various combinations of vertical and lateral loads must be considered. For example, the vertical load and rotation during beam erection should be considered, in addition to the service load combinations.

Translations and rotations due to live loads, dead loads, and time-dependent effects should be computed and tabulated.

BEARINGS

10.8.3.1 Loads and Movements

Figure 10.8.3.1-1 Sample Form—Schedule of Loads and Movements

Bridge Name or Reference							
Bearing Identification Mark							
Number of Bearings Required							
Seating Material		Upper Surface					
		Lower Surface					
Allowable Average Contact Pressure (psi)		Upper Face	Serviceability Strength				
			Lower Face	Serviceability Strength			
Design Load Effects (kips)	Service Limit State			Vertical	Max.		
			Vertical	Perm.			
			Vertical	Min.			
	Strength Limit State		Transverse				
			Longitudinal				
			Vertical				
Translation	Service Limit State		Irreversible		Transverse		
			Irreversible		Longitudinal		
	Reversible		Reversible		Transverse		
			Reversible		Longitudinal		
	Strength Limit State		Irreversible		Transverse		
			Irreversible		Longitudinal		
Rotation (radians)		Service Limit State		Irreversible		Transverse	
				Irreversible		Longitudinal	
Maximum Bearing Dimensions (in.)		Upper Surface		Irreversible		Transverse	
				Irreversible		Longitudinal	
Overall Height		Lower Surface		Reversible		Transverse	
				Reversible		Longitudinal	
Tolerable Movement Of Bearing Under Transient Loads (in.)		Vertical		Vertical			
				Transverse			
				Longitudinal			
Allowable Resistance to Translation Under Service Limit State (kips)		Transverse		Transverse			
				Longitudinal			
Allowable Resistance to Rotation Under Service Limit State (kips/ft)		Transverse		Transverse			
				Longitudinal			
Type of Attachment to Structure and Substructure		Transverse		Transverse			
				Longitudinal			

10.8.3.2 Design for Shear Displacements

The minimum acceptable elastomer thickness is often controlled by design for shear displacements. The total thickness of the elastomer layers in the bearing must satisfy the following:

$$h_{rt} \geq 2\Delta_s \quad [\text{LRFD Eq. 14.7.5.3.2-1}]$$

where

h_{rt} = total elastomeric thickness, in.

Δ_s = maximum shear deformation of elastomer at the service limit state, in.

The shear displacement demand on the bearing is taken as the maximum possible displacement caused by creep, shrinkage, prestressing, and thermal effects [LRFD Section 14.7.5.3.2]. In most precast, prestressed beams, the greatest displacement will be in the shortening direction because shrinkage and creep cause shortening. Calculation of the displacement should take into account the effects of any pier flexibility or construction procedures, including the temperature at which the beams are set, because that may reduce the shear deformation demand on the bearing.

10.8.3.3 Design for Combined Loading

The peak shear strains in the elastomer due to axial load, rotation, and shear displacements are computed, and their sum must satisfy the specified limit. The shear strain due to axial load (usually compression), γ_a , is given by:

$$\gamma_a = D_a \left(\frac{\sigma_s}{GS_i} \right) \quad [\text{LRFD Eq. 14.7.5.3.3-3}]$$

The shear strain due to rotation, γ_r , is given by:

$$\gamma_r = D_r \left(\frac{L}{h_{ri}} \right)^2 \theta_i \quad [\text{LRFD Eq. 14.7.5.3.3-6}]$$

for a rectangular bearing and:

$$\gamma_r = D_r \left(\frac{D}{h_{ri}} \right)^2 \theta_i \quad [\text{LRFD Eq. 14.7.5.3.3-8}]$$

for a circular bearing. The shear strain due to shear displacement, γ_s , is given by:

$$\gamma_s = \frac{\Delta_s}{h_{rt}} \quad [\text{LRFD Eq. 14.7.5.3.3-10}]$$

where

D = diameter of a circular bearing, in.

D_a, D_r = numerical constants

G = shear modulus of the elastomer, ksi

h_{rt} = total thickness of the internal elastomer layers, in.

S = shape factor of thickest layer of an elastomeric bearing

γ = shear strain (subscripts a, r , and s designate axial load, rotation and shear), in./in.

Δ_s = service shear displacement of the bearing, in.

θ_i = rotation in layer i of the bearing, radians, $= \frac{\theta_s}{n}$

θ_s = rotation of the bearing under service load

σ_a = axial stress on the bearing, ksi

The *LRFD Specifications* offers two sets of values for the numerical constants D_a and D_r in the foregoing equations. In the simpler set, which is suitable for hand calculations, the values for a rectangular bearing are $D_a = 1.4$ and $D_r = 0.5$. For a circular bearing, $D_a = 1.0$ and $D_r = 0.375$. In the more complex set, the D_a and D_r values are functions of the compressibility Index, λ , and the bearing aspect ratio, L/W . Their use leads to less conservative designs, but they require more computational effort if they are used in a hand calculation. They are suitable for use in a spreadsheet or other computer application. The compressibility index, λ , reflects the degree to which the elastomer is not completely incompressible. It is given by:

$$\lambda = S \sqrt{\frac{3G}{K}} \quad [\text{LRFD Eq. C14.7.5.3.3-6}]$$

The compressibility index becomes more important as the shape factor increases, so the additional benefit offered by the use of the more complex set of constants is greater for a bearing with a high shape factor. $\lambda = 0.0$ for a completely incompressible material.

These shear strains are computed separately for cyclic and static loads. Only loads due to traffic are considered cyclic so, for example, daily thermal displacements are treated as static. A distinction could be made between the AASHTO truck loading and lane loading on the basis that lane loading creates cycles of deformations with lower amplitudes. The *LRFD Specifications* is silent on the matter, in which case both loads should be treated as cyclic. The strains must satisfy

$$(\gamma_{a,st} + \gamma_{r,st} + \gamma_{s,st}) + 1.75(\gamma_{a,cy} + \gamma_{r,cy} + \gamma_{s,cy}) \leq 5.0 \quad [\text{LRFD Eq. 14.7.5.3.3-1}]$$

$$\gamma_{a,st} \leq 3.0 \quad [\text{LRFD Eq. 14.7.5.3.3-2}]$$

where the subscripts *st* and *cy* refer to the static and cyclic components of the load. The factor 1.75 applied to the cyclic component of the shear strains reflects the fact that cyclic loading causes damage to the elastomer more readily than does static loading. LRFD Equation 14.7.5.3.3-1 addresses debonding or tearing of the elastomer due to combined loading, while LRFD Equation 14.7.5.3.3-2 is intended to prevent damage in a bearing with high dead load. The latter is likely to control only in long-span bridges where the dead load is a significant proportion of the total load. The checks should be made for rotation about both primary axes of the bearing. The combination with rotation about the longitudinal axis of the beam (torsional deformation) is likely to control only in bridges with large skew angles.

A question arises over the way to interpret the rotations, especially when the allowance for nonparallelism is included. If the beams camber upwards under full dead load, the end rotation is also upwards. However, the end rotation due to truck loading will cause downwards rotation, so the total rotation may be less than the dead load rotation. There is thus a need for a rational way of accounting for the rotation components. The rotation tests on which the 2009 *LRFD Specifications* was based were conducted using a fixed static rotation, θ_{st} , plus a cyclic rotation, $\pm \theta_{cy}$. The real loading should thus be broken down into comparable components.

First, the largest total rotation, including the nonparallelism allowance acting in its most disadvantageous sense and the live load rotation should be established. Both directions should be investigated and the larger of the two absolute values should be selected. θ_{st} should be taken as that total rotation minus the (unamplified) cyclic rotation. The nominal live load rotation, due to both truck and lane loading, should be multiplied by 1.75 and added to the static rotation to give the total design rotation. The procedure is illustrated in the design example in Section 10.8.3.8.

10.8.3.4 Design for Hydrostatic Tension

If the bearing is positively attached to the beam, for example through a bonded external steel plate, it must be checked for potential internal fracture caused by hydrostatic tension in the elastomer. If the beam or sole plate can lift off from the bearing, the check is not necessary. Because prestressed concrete beams are generally set on their bearings with no such attachment, the check will seldom be necessary.

The hydrostatic stress must satisfy

$$\sigma_{hyd} \leq 2.25G \quad [\text{LRFD Eq. 14.7.5.3.3-11}]$$

The hydrostatic stress is computed as

$$\sigma_{hyd} \leq 3GS^3\theta_i C_\alpha \quad [\text{LRFD Eq. 14.7.5.3.3-12}]$$

$$\text{where } C_\alpha = \frac{4}{3} \left\{ \left(\alpha^2 + \frac{1}{3} \right)^{1.5} - \alpha(1 - \alpha^2) \right\} \quad [\text{LRFD Eq. 14.7.5.3.3-13}]$$

$$\alpha = \frac{\varepsilon_a}{S\theta_i} \quad [\text{LRFD Eq. 14.7.5.3.3-14}]$$

where ε_a , the average axial strain (taken as positive in compression), is computed using:

$$\varepsilon_a = \frac{\sigma_s}{3B_a G S^2} \quad [\text{LRFD Eq. 14.7.5.3.3-15}]$$

Constant B_a may be taken as 1.6 for all bearings. An alternative, more precise value, which is a function of the aspect ratio and compressibility index, is given in the Commentary to the *LRFD Specifications*.

Hydrostatic tension is caused by axial tension loading on the bearing, large rotation, or a combination of the two. It may occur on the "uplift" side of the bearing even if the axial load is compressive, if the rotation is large enough. Load combinations that lead to excessive hydrostatic tension are expected to be rare, especially with prestressed concrete beams.

The *LRFD Specifications* allows the service average compressive stresses to be computed on the basis of the gross, external dimensions of the bearing. This is an acceptable approximation when the elastomeric side cover lies in the common range of $\frac{1}{8}$ in. to $\frac{1}{4}$ in. If thicker side cover is used, it is recommended that the dimensions of the steel plates be used to define both the shape factor and the compressive stress.

10.8.3.5 Stability

In order to prevent buckling of the bearing, the *LRFD Specifications* limits the average compressive stress to half the predicted buckling stress. Bearings that satisfy LRFD Equation 14.7.5.3.4-1 are considered to be stable at any stress, and require no additional investigation of stability:

$$2A \leq B \quad [\text{LRFD Eq. 14.7.5.3.4-1}]$$

where

$$A = \frac{1.92 \left(\frac{h_{rt}}{L} \right)}{\sqrt{1 + \frac{2.0L}{W}}} \quad [\text{LRFD Eq. 14.7.5.3.4-2}]$$

$$B = \frac{2.67}{(S + 2.0) \left(1 + \frac{L}{4W} \right)} \quad [\text{LRFD Eq. 14.7.5.3.4-3}]$$

where

h_{rt} = total elastomer thickness in bearing, in.

L = length of a rectangular elastomeric bearing (parallel to longitudinal bridge axis), in.

S = shape factor of one layer of an elastomeric bearing

W = width of bearing in the transverse direction (perpendicular to longitudinal bridge axis), in.

If LRFD Equation 14.7.5.3.4-1 is not satisfied, one of the following equations must be satisfied depending on the conditions of restraint for horizontal translation.

If the superstructure is free to translate horizontally, i.e., if the bearing being investigated can buckle in a sidesway mode, the following equation must be satisfied:

$$\sigma_s \leq \frac{GS}{2A - B} \quad [\text{LRFD Eq. 14.7.5.3.4-4}]$$

If the superstructure is fixed against horizontal translation because, for example, it is fixed at one end, the following equation must be satisfied:

$$\sigma_s \leq \frac{GS}{A - B} \quad [\text{LRFD Eq. 14.7.5.3.4-5}]$$

A negative or infinite result on the right hand side of the equation indicates that the bearing is stable under any stress. Note that, if a bridge has fixed bearings at one end and unrestrained bearings at the other, the unrestrained bearings will be free to sway transversely but will be prevented from longitudinal displacement by the bearings at the other end. The foregoing equations address instability in the longitudinal direction. Potential instability in the transverse direction can be investigated by interchanging L and W .

10.8.3.6 Steel Reinforcement

The internal steel plates experience horizontal tension when the bearing is loaded in vertical compression, because they restrain the lateral movement of the elastomer. Therefore they must be strong enough for that purpose. They must also be thick enough to not warp during fabrication of the bearing. To guard against that, it is recommended that they be at least 14-gauge (0.0747 in.), but many fabricators use 11-gauge (0.1196 in.) as a standard, because it is thick enough for almost all bearings and it allows them to buy the steel in quantity. A plate size that is practical for fabrication will often be adequate for strength.

The following equation is intended to assure adequate plate strength at the service limit state:

$$h_s \geq \frac{3.0h_{r,max}\sigma_s}{F_y} \quad [\text{LRFD Eq. 14.7.5.3.5-1}]$$

where

h_s = thickness of steel reinforcement, in.

F_y = yield strength of steel reinforcement, ksi

$h_{r,max}$ = thickness of thickest elastomeric layer in elastomeric bearing, in.

To prevent fatigue failure of the steel reinforcement, LRFD Equation 14.7.5.3.5-2 must also be satisfied:

$$h_s \geq \frac{2.0h_{r,max}\sigma_L}{\Delta F_{TH}} \quad [\text{LRFD Eq. 14.7.5.3.5-2}]$$

where

ΔF_{TH} = constant amplitude fatigue threshold for Category A as specified in LRFD Article 6.6, ksi

σ_L = average compressive stress due to live load, ksi

If holes are necessary, the computed minimum thickness of the reinforcement must be increased by a factor equal to twice the gross width of the plate divided by the net width.

10.8.3.7 Anchorage

Bearings that are required to transmit horizontal forces must be checked for slipping, and restraint must be provided if needed.

For bearings with external bonded plates, restraint is most easily provided by securing the plates to the girder and the support using bolting, welding or other procedures.

For bearings without external plates, restraint may be provided by friction or by a supplementary system, such as anchor bolts. The 2010 *LRFD Specifications* does not give a value for the available coefficient of friction, but the 2005 *Interim Revisions* contained provisions that implied that a friction coefficient of 0.20 could be relied upon. However, friction of polymers is a complex subject and does not obey the common Coulomb friction laws. For example, the friction coefficient of a polymer is not a constant, but rather varies with the contact pressure. It also varies with the material and roughness of the contact surface. Further complications are introduced if anti-ozonant wax is used in the elastomer formulation, because it has been found to diffuse to the surface of the bearing, where it acts as a lubricant and promotes slip.

In the light of those difficulties, it would be prudent to secure actively any bearing that must resist significant horizontal forces.

10.8.3.8 Bearing Design Example–Method B

10.8.3.8.1 Introduction

This example demonstrates the design of an elastomeric bearing in accordance with Method B in the *LRFD Specifications*. The need for long-term testing will depend on the size of the bearing.

The bridge is the same as the one in **Design Example 9.1a** in **Chapter 9** and is, for this example, located in Rosemount, Minn. It consists of six 120-ft simple span BT-72 beams on 9 ft centers, with an 8-in.-thick, cast-in-place concrete deck. It has no skew and all movement is accounted for at one end. The beams have a 26-in.-wide bottom flange. Choose a suitable movable elastomeric bearing.

Criteria in addition to those given in **Example 9.1a** are:

- The design temperature range is to be taken from the LRFD Article 3.12.2.
- Of the shrinkage and creep that occur between transfer and casting the slab, assume that two-thirds occurs before the beams are erected.
- Assume free differential shrinkage of 400×10^{-6} in./in. of the deck slab relative to the beams. This is the difference in free shrinkage between the slab and the girder after slab casting. The free shrinkage of a concrete component is the shrinkage that would occur if the component was not restrained, for example by being connected to another element.

Bearing Type:

Use a rectangular, steel-reinforced elastomeric bearing with a shear modulus of 0.100 ksi.

10.8.3.8.2 Loads and Movements

In the following analysis, the loads and movements are developed in some detail, using data from **Chapter 9, Example 9.1a**. If less precise estimates are used in the interests of simplicity, they should be conservative.

The primary design requirements are the vertical load, horizontal displacement, and rotation about the transverse axis of the beam. Because the bridge has no skew, torsional beam rotations are ignored, but the allowance for nonparallelism must still be included about that axis. The combinations of load, displacement, and rotation change over time, but two times are likely to be critical: directly before the slab is cast, at which time some of the prestressing has been lost, and after all prestress losses have occurred and live load is applied. The bearing will be checked for those two times.

Table 10.8.3.8.2-1
Design Loads and Movements

Event	Time		P _v	P _v	Δ _v	Δ _v	Rotation	Rotation	Δ _H	Δ _H	Δ _H	Δ _H	
			Incr. kips	Cum. kips	Incr. in.	Cum. in.	Incr. Rad (10 ⁻³)	Cum. Rad (10 ⁻³)	CG Incr. in.	Rotation Incr. in.	Cum. in.	After Erection in.	
	Start	End											
Prestress	Start transfer	End transfer		0	-3.810	-3.810	-9.260	-9.260	-1.041				
Girder Self Wt	Start transfer	End transfer		0	1.480	-2.330	3.597	-5.663				-1.041	
Cr + Sh	End transfer	Erection	47.9	47.9	-1.193	-3.523	-2.900	-8.564		-0.835		-1.894	0.000
Cr + Sh	Erection	Before Slab	0	47.9	-0.597	-4.120	-1.450	-10.014		-0.418		-2.312	-0.418
Slab + DL	Before Slab	After slab	73.3	121.2	1.870	-2.250	4.545	-5.469	0.000	0.333	-1.979	-0.085	
Diff Sh	After Slab	Infinite	0	121.2	0.975	-1.275	2.370	-3.099	-0.331	0.260	-2.051	-0.157	
Thermal	Infinite	Infinite	0	121.2	0.000	0.000	0.000	-3.099	-0.786	0.000	-2.837	-0.943	
LL Lane	Infinite	After LL Lane	33.9	155.1	0.410	-0.865	0.997	-2.102	0.000	0.109	-2.728	-0.834	
LL Truck	After LL Lane	After LL Truck	78.1	233.2	0.780	-0.085	1.896	-0.207	0.000	0.208	-2.520	-0.626	

Table 10.8.3.8.2-1 summarizes the response quantities (loads, movements, and rotations) at different times. For each quantity, an increment is computed and added to the cumulative total. The values were obtained as follows.

The beam self-weight reaction, and the additional dead load reactions from the weights of the slab, haunch, barriers, and wearing course, and the truck and lane load reactions, were all taken directly from **Example 9.1a**. No live load impact fraction was used [LRFD Art. 14.4.1].

The beam end rotations, which define the bearing rotations, are not computed in **Example 9.1a**. However, it can be shown (Stanton et al., 2008, Appendix F) that:

$$\theta_{end} = c_{rot} \frac{\Delta_v}{L} \tag{Eq. 10.8.3.8.2-1}$$

where

Δ_v = the mid-span deflection, in.

L = the span length, in.

The value of *c_{rot}* varies slightly with the type of loading. For prestressing with constant eccentricity, *c_{rot}* = 4.0. For prestressing harped at midspan, *c_{rot}* = 3.0. For a uniform load, *c_{rot}* = 3.2. In the interests of simplicity, the end rotations are computed here using *c_{rot}* = 3.5 in all cases. One of the consequences of this relationship is that, if the midspan live load deflection is limited to L/800, the end rotation due to live load will be no greater than 3.5/800 = 0.0044 radian. The live load deflection of a prestressed concrete beam is usually less than L/800, and for live load *c_{rot}* ≈ 3.2, so the live rotation applied to the bearing will be less than 0.0040 radians, and that value may be used as a conservative estimate if a better value is not available. However, in this example the individual components of rotation were obtained from the corresponding vertical deflections. The rotation values in the table are given in 10⁻³ radian.

The vertical deflection components from which the end rotations were computed were taken from **Example 9.1a**. Downwards deflections are treated as positive here, so upwards camber is negative. The elastic camber at transfer is -3.810 in., and the corresponding self-weight deflection is $+1.480$ in. Using the PCI multipliers to approximate the effects of creep and shrinkage, the example gives additional deflections of 0.80 times the prestressing camber and 0.85 times the self-weight deflection between transfer and slab casting. It is assumed here (see the problem statement) that two-thirds of that additional deflection occurs between transfer and beam erection, and the remaining one-third between beam erection and slab casting. Thus the increment before beam erection is:

$$\Delta_{v,inc} = \frac{2}{3}(0.80(-3.810) + 0.85(1.480)) = -1.193 \text{ in.} \quad (\text{Eq. 10.8.3.8.2-2})$$

and the deflection increment between beam erection and slab casting is the remaining one third of the total, or half the value given in Eq. 10.8.3.8.2-2, giving -0.597 in. Those values are shown in **Table 10.8.3.8.2-1**. The value of 1.870 in., shown for elastic vertical deflection due to slab self-weight, also includes the deflections due to the weight of the slab, haunch, barriers, and wearing surface, each computed using the appropriate moment of inertia.

After the slab is cast, it shrinks relative to the beam. Because the slab is bonded to the beam, the relative shrinkage causes positive curvature and downwards deflection of the composite section. A simple analysis that ignores the haunch and any steel in the beam and slab shows that the beam undergoes constant curvature along its length and a corresponding midspan deflection given by:

$$\begin{aligned} \Delta_v &= \frac{L^2}{8} \frac{E_{slab} A_{slab} \bar{y} \varepsilon_{sh,free}}{(EI)_{tr}} = \frac{(1,440)^2}{8} \frac{(3,834)(810)(21.48)(0.0004)}{(4,888)(1,100,320)} \\ &= 1.286 \text{ in.} \end{aligned} \quad (\text{Eq. 10.8.3.8.2-3})$$

where

A_{slab} = Cross-sectional area of the slab, in.²

E_{slab} = Modulus of elasticity of the slab concrete, ksi

$(EI)_{tr}$ = the flexural stiffness of the composite, transformed section, k-in.²

\bar{y} = the distance between the centroid of the transformed section and the centroid of the slab, in.

$\varepsilon_{sh,free}$ = the free shrinkage of the slab relative to the beam, in./in.

Here, all the values were taken from **Example 9.1a**, except for the differential shrinkage between slab and beam which was taken to be 0.0004 in./in., as stated in the assumptions to this example. A more precise calculation, using the same principles but using a numerical solution, included the haunch and the steel in the beam and slab. It gave a downwards deflection of 0.975 in., which is the value used here. In it, the slab was assumed to shrink by a total of 0.0005 in./in., and the beam by 0.0001 in./in., after the slab was cast. The steel in the elements restrains some of the shrinkage and therefore reduces the deflection.

The instantaneous deflections due to lane loading (0.410 in.) and truck loading (0.780 in.) were taken directly from **Example 9.1a**.

Horizontal displacement of the bearing arises from two sources: change in length of the beam at its centroid, and end rotation of the beam about its centroid. In the table, increments in the former are given in the column marked " Δ_H CG Incr.," while increments in the latter are given in the column marked " Δ_H Rotation Incr." In both cases, negative values correspond to shortening of the beam bottom flange. Where possible, the values were taken from **Example 9.1a**. In some cases the two components (caused by axial shortening at the centroid and by end rotation multiplied by the bottom flange distance) were computed together in **Example 9.1a**, so they are reported together in the table.

The shortening of the bottom flange at transfer was obtained from the stress change in the concrete there, given in **Section 9.1a.7.2** as 3.337 ksi at midspan. The stress really varies slightly along the span, but the midspan value was taken as representative for these purposes. The total change in length is given by:

$$\Delta L = \frac{f_{b,tr}L}{E_{gird}} = -\frac{(3.337)(1,440)}{4,617} = -1.041 \text{ in.} \quad (\text{Eq. 10.8.3.8.2-4})$$

where

E_{gird} = modulus of elasticity of the beam concrete at the time of transfer, ksi

$f_{b,tr}$ = bending stress in the concrete due to transfer, ksi

ΔL = change in length, in.

This value includes both the shortening due to prestressing and the elongation due to self-weight.

Creep and shrinkage between transfer and slab casting together cause a stress loss in the tendon of $6.019 + 15.445 = 21.464$ ksi (**Section 9.1a.6.2.2**). The change in length at the tendon centroid is therefore:

$$\Delta L = \frac{\Delta f_p L}{E_p} = -\frac{(21.464)(1,440)}{28,500} = -1.084 \text{ in.} \quad (\text{Eq. 10.8.3.8.2-5})$$

where

Δf_p = change in stress in the prestressing strands, ksi

E_p = Modulus of Elasticity of the prestressing strands, ksi

The negative value indicates shortening. The corresponding value at the bottom flange is:

$$\Delta L = \frac{\left(1 + \frac{e_p y_b}{r^2}\right)}{\left(1 + \frac{e_p^2}{r^2}\right)} (-1.084) = \frac{\left(1 + \frac{(28.28)(36.60)}{(26.68)^2}\right)}{\left(1 + \frac{(28.28)^2}{(26.68)^2}\right)} (-1.084) = -1.253 \text{ in.} \quad (\text{Eq. 10.8.3.8.2-6})$$

where

e_p = eccentricity of the prestressing strands relative to the center of gravity of the transformed beam section at transfer, in.

r = radius of gyration of the beam cross section, in.

y_b = distance from center of gravity to extreme bottom fiber of the noncomposite, nontransformed precast beam, in.

For consistency with the vertical deflections and rotations, two-thirds of this change (-0.835 in.) is assumed to occur between transfer and beam erection, and the remaining one-third (-0.418 in.) between erection and slab casting. This change in length must all be accommodated at the movable bearing.

The movement due to slab casting consists of the end rotation multiplied by the bottom flange distance, given by:

$$\Delta L = \theta_{end} y_b = (0.00454)(36.60) = 0.166 \text{ in.} \quad (\text{Eq. 10.8.3.8.2-7})$$

This change represents an outwards movement, or elongation, so is taken as positive. This movement happens at each end of the girder, so the total movement of one end relative to the other is 0.333 in. Because one end is fixed, the value at the movable end is 0.333 in.

The differential shrinkage causes a strain change of -230×10^{-6} at the centroid of the transformed section, or a change in length there of -0.331 in. The associated vertical deflection is 0.975 in. which leads to an end rotation of 0.00237 radian. The additional component of longitudinal movement due to that rotation is:

$$\Delta L = \theta y_b = (0.00237)(54.77) = 0.130 \text{ in.} \quad (\text{Eq. 10.8.3.8.2-8})$$

Note that y_b , the bottom flange distance, used here is the value for the composite section. Again, because one end of the bridge is fixed but rotation occurs at both ends, the displacement at the movable bearing is twice this value, or 0.260 in. It represents an outward movement, so is positive. Thus the total movement due to differential shrinkage is $(-0.333 + 0.260) = -0.073$ in.

Thermal contraction in cold weather causes the beam to shorten. Changes in camber due to thermal gradients are ignored here, because the solar gain on the deck is small in the winter, and only the movement due to overall change in length is considered. LRFD Article 14.7.5.3.2 stipulates that, unless the bearing is reset at the average temperature, it shall be designed for 65% of the total thermal movement range computed in accordance with LRFD Art. 3.12.2.

The maps in that article show a minimum and maximum temperature for Rosemount of -30 and $+110$ °F respectively. Thus the change in length is:

$$\Delta L = L\alpha\Delta T = (1,440)(0.000006)(0.65)((110) - (-30)) = 0.786 \text{ in.} \quad (\text{Eq. 10.8.3.8.2-9})$$

Strictly, this change in length should be considered in both directions (lengthening and shortening) but, since it is to be combined with creep and shrinkage, shortening will control.

The total movement due to temperature, creep and shrinkage, and differential shrinkage (LRFD Art. 14.7.5.3.2) is therefore

$$\Delta_0 = \Delta_T + \Delta_{CR+SHR} + \Delta_{diff,shr} = (-0.786) + (-0.418) + (-0.073) = -1.277 \text{ in.} \quad (\text{Eq. 10.8.3.8.2-10})$$

Note that this value excludes the elongation due to the weight of the slab and live loads, because LRFD Art. 14.7.5.3.2 does not specify them. Excluding them is conservative because those loadings cause elongation of the bottom flange. However, when the combined loading specified in LRFD Article 14.7.5.3.3 is used, the elongations caused by live load must be accounted for. They must also be multiplied by 1.75 to account for the damaging nature of cyclic loading. Under those circumstances the elongation controls, and the critical length change is given by:

$$\begin{aligned} \Delta L &= \Delta_T + \Delta_{CR+SHR} + \Delta_{slab} + \Delta_{diff,shr} + 1.75\Delta_{LL} \\ &= (+0.786) + (-0.418) + 0.333 + (-0.073) + 1.75(0.109 + 0.208) = +1.183 \text{ in.} \quad (\text{Eq. 10.8.3.8.2-11}) \end{aligned}$$

It should be recognized that the longitudinal displacements that cause shear deformation in the bearing are only those that occur after the beam has been set on the bearings. Thus the last column of **Table 10.8.3.8.2-1** shows the net longitudinal displacements after subtracting the value at erection. However, this principle does not apply to rotations or vertical loads.

The load combinations chosen for use in the design are therefore:

- Initial conditions just before deck casting. ($P = 47.9$ kips, $\theta = -0.01001$ radian, $\Delta = -0.418$ in.)
- Final service condition with truck and lane loads. ($P = 233.2$ kips, $\theta = -0.000207$ radian, $\Delta = +1.183$ in.)

10.8.3.8.3 Elastomer Thickness for Shear Displacements

The supports are considered to be rigid with respect to horizontal movements, so the total thickness of the elastomer must accommodate all of the movement. For the limit on shear displacements, LRFD Article 14.7.5.3.2 only requires consideration of the changes in length due to temperature, creep, shrinkage, and post-tensioning. The total length change, Δ_0 , calculated above, is 1.275 in. Because the supports are rigid:

$$\Delta_s = \Delta_0 = 1.275 \text{ in.} \quad (\text{Eq. 10.8.3.8.3-1})$$

The elastomer thickness must satisfy:

$$h_{rt} > 2\Delta_s = 2(1.275) = 2.55 \text{ in.} \quad [\text{LRFD Eq. 14.7.5.3.2.-1}]$$

10.8.3.8.4 Trial Bearing Size

The bearing should be as wide as possible to promote torsional stability of the beam during erection. The beam bottom flange is 26 in. wide. Try a 23-in.-wide bearing, so as to leave 1.5 in. on each side to accommodate any

chamfer. Using a trial h_{ri} of 2.6 in., 0.25 in. thick top and bottom cover and an estimated seven, 11-gage steel plates, the total bearing height will be approximately $2(0.25) + 2.6 + 7(0.12) = 3.94$ in. The simple stability check of Method A, according to which the total bearing height must not exceed one third of the length, thus suggests a length of at least 11.8 in. Assuming that the Method B stability criteria will lead to a slightly smaller bearing, try 23 by 10 in., with $h_{ri} = 2.6$ in. Assume six internal layers, each 0.433 in. thick. (In practice, a more standard thickness, such as 0.50", would likely be chosen. Here the bearing size is kept to a minimum to demonstrate the possibilities using the new design methods. Minimizing the bearing size inevitably leads to some non-standard values.) The shape factor for each layer is then:

$$S = \frac{LW}{2h_{ri}(L+W)} = \frac{23(10)}{2(0.433)(23+10)} = 8.048 \quad \text{[LRFD Eq. 14.7.5.1-1]}$$

10.8.3.8.5 Design for Combined Loading

The service load combination is evaluated first because it contains the highest axial load. The static axial load is caused by beam self-weight, haunch, deck, barriers, wearing course, and lane load, and is given by:

$$P_{st} = 47.9 + 73.3 = 121.2 \text{ kips} \quad \text{(Eq. 10.8.3.8.5-1)}$$

The live load is caused by the lane and truck loading, and is:

$$P_{cy} = 33.9 + 78.1 = 112 \text{ kips} \quad \text{(Eq. 10.8.3.8.5-2)}$$

The axial stress, including the amplification of the live load for cyclic effects is:

$$\sigma_a = \frac{P_{st} + 1.75(P_{cy})}{A} = \frac{121.2 + 1.75(112)}{23(10)} = \frac{317.2}{230} = 1.379 \text{ ksi} \quad \text{(Eq. 10.8.3.8.5-3)}$$

The corresponding shear strain is:

$$\gamma_a = D_a \frac{\sigma_a}{GS} = 1.40 \left(\frac{1.379}{0.100(8.048)} \right) = 2.399 \quad \text{[LRFD Eq. 14.7.5.3.3-3]}$$

$$\text{Thus, } \gamma_a < 3.0 \quad \text{[LRFD Eq. 14.7.5.3.3-2]}$$

Computing the rotation raises some subtle questions. The primary one is that some of the components of the total rotation counteract each other, and that a way must be found for computing values for the design static and cyclic rotations that reflects the intent of the *LRFD Specifications*, especially in view of the fact that the static allowance for nonparallelism should be taken in the sense that is least advantageous. A simple approach would be to add the absolute values of all rotation components, but it would likely be very conservative. Here the signs of the rotation components are taken into account when the values are added, and the nonparallelism allowance is tried in both senses (+ and -). From **Table 10.8.3.8.2-1** the computed static rotation, without the nonparallelism allowance is -3.099×10^{-3} radian. The negative sign indicates that it is associated with upwards camber. The amplified live load rotation is:

$$\theta_{cy} = 1.75(0.997 + 1.896) \times 10^{-3} = 0.005063 \text{ radian} \quad \text{(Eq. 10.8.3.8.5-4)}$$

If the nonparallelism allowance of 0.005 radian is taken as negative, the static rotation becomes -0.008099 radian, to which must be added the cyclic $+0.005063$ radian. Thus, during the passage of a truck plus lane load, the rotation varies from -0.008099 to -0.003036 radian. If the allowance is taken as positive, the values are $+0.001901$ to $+0.006964$. Of these values, the largest, namely 0.008099, is accepted as the design rotation. Then the shear strain due to rotation is:

$$\gamma_r = D_r \left(\frac{L}{h_{ri}} \right)^2 \theta_i = 0.5 \left(\frac{10}{0.433} \right)^2 \frac{(0.008099)}{6} = 0.360 \quad \text{[LRFD Eq. 14.7.5.3.3-6]}$$

The trial bearing has six interior elastomer layers, so n is taken here as 6. LRFD Article 14.7.5.3.3 permits n to be increased by 1 if the top and bottom cover layers are at least half the thickness of the interior layers, on the basis that they will accommodate some of the total rotation. In this case the 0.25 in. thick cover layers satisfy the

criterion, but the value of n was left unchanged. This choice is conservative, because the true shear strain caused by rotation will be slightly smaller than the calculated value.

The shear strain due to shear displacement used here must include all components, including those caused by applied dead and live loads. In **Section 10.8.3.8.2**, the total horizontal displacement was found to be 1.184 in. (**Eq. 10.8.3.8.2-11**)

Therefore the shear strain due to shear displacement, γ_s , is given by:

$$\gamma_s = \frac{\Delta_s}{h_{rt}} = \frac{1.184}{2.6} = 0.455 \quad [\text{LRFD Eq. 14.7.5.3.3-10}]$$

The combined shear strain is:

$$\gamma_{tot} = \gamma_a + \gamma_r + \gamma_s = 2.399 + 0.360 + 0.455 = 3.214 < 5.000 \quad (\text{Eq. 10.8.3.8.5-5})$$

It can be seen that the axial load provides the largest contribution (2.399) to the total shear strain. It could be reduced, at the expense of increasing the shear strain due to rotation, by using thinner layers and a higher shape factor. By trial and error the lowest total shear strain of 2.314 was found to occur with 16 layers at 0.1625 in. each. Such a bearing would be extremely robust, but would be heavier and more expensive due to the extra steel layers.

Further trial and error, in which the bearing length was varied, shows that a bearing 23 by 8 in., with six layers 0.4333 in. each, also works. It leads to a shape factor of $S = 6.849$ and a total shear strain of 4.209. The components due to axial, rotation, and shear were respectively 3.524, 0.230 and 0.455. That bearing is accepted for use here.

The strains were also checked in the transverse direction. The value of γ_a was the same (3.524), γ_s was 0.0, but γ_r was found to be 1.174. This relatively large value occurs because the bearing is stiff in rotation about its strong axis, but the nonparallelism allowance of 0.005 radians must still be accommodated. The total shear strain in the transverse direction is thus 4.698, and it is this value that controls the design.

The conditions just before deck casting ($P = 47.9$ kips, $\theta = -0.01001$ radians, $\Delta = -0.418$ in.) lead to $\gamma_a = 0.532$, $\gamma_r = 0.426$, $\gamma_s = 0.161$ and $\gamma_{tot} = 1.119$ for rotation about the transverse axis (beam bending), and $\gamma_a = 0.532$, $\gamma_r = 1.174$, $\gamma_s = 0.000$ and $\gamma_{tot} = 1.706$ for rotation about the longitudinal axis (beam torsion). Even though lift-off occurs under these initial conditions, the shear strains are easily acceptable. Thus the service condition controls the design.

10.8.3.8.6 Design for Hydrostatic Tension

The bearing has no bonded external plates. Therefore hydrostatic tension does not need to be considered.

10.8.3.8.7 Stability

The *LRFD Specifications* depend on parameters A and B . For sway in the longitudinal direction they are given by:

$$A = \frac{1.92 \left(\frac{h_{rt}}{L} \right)}{\sqrt{1 + \frac{2.0L}{W}}} = \frac{1.92 \left(\frac{2.6}{8} \right)}{\sqrt{1 + \frac{2.0(8)}{23}}} = 0.523 \quad [\text{LRFD Eq. 14.7.5.3.4-2}]$$

$$B = \frac{2.67}{(S + 2.0) \left(1 + \frac{L}{4W} \right)} = \frac{2.67}{(6.849 + 2.0) \left(1 + \frac{8}{4(23)} \right)} = 0.278 \quad [\text{LRFD Eq. 14.7.5.3.4-3}]$$

where

h_{rt} = total elastomer thickness in bearing, in.

L = length of a rectangular elastomeric bearing (parallel to longitudinal bridge axis), in.

S = shape factor of one layer of an elastomeric bearing

W = width of bearing in the transverse direction (perpendicular to longitudinal bridge axis), in.

If the bridge deck is fixed against horizontal translation, as it is in the longitudinal direction, the simplest and most conservative stability check in the *LRFD Specifications* is:

$$2A \leq B \quad [\text{LRFD Eq. 14.7.5.3.4-1}]$$

or $2(0.523) \leq 0.278$ N.G.

Passing this test would have indicated that the bearing could never buckle at any stress and is therefore unconditionally stable. If LRFD Eq. 14.7.5.3.4-1 is not satisfied, the bearing may still be stable if the applied compressive stress is less than the allowable compressive stress, which depends on the horizontal restraint conditions. If the bridge is not free to translate horizontally, for example because the bridge is fixed at one end, the requirement is:

$$\sigma_s \leq \frac{GS}{A - B} = \frac{0.100(6.849)}{0.479 - 0.278} = 3.407 \text{ ksi} \quad [\text{LRFD Eq. 14.7.5.3.4-5}]$$

Since the applied stress is:

$$\sigma_s = \frac{233.2}{23(8)} = 1.267 \text{ ksi} \quad (\text{Eq. 10.8.3.8.7-1})$$

LRFD Equation 14.7.5.3.4-5 is easily satisfied and the bearing is stable. In the transverse direction, in which the deck is assumed not to be restrained against horizontal translation:

$$A = \frac{1.92 \left(\frac{h_{rt}}{W} \right)}{\sqrt{1 + \frac{2.0W}{L}}} = \frac{1.92 \left(\frac{2.6}{23} \right)}{\sqrt{1 + \frac{2.0(23)}{8}}} = 0.08354 \quad [\text{LRFD Eq. 14.7.5.3.4-2}]$$

$$B = \frac{2.67}{(S + 2.0) \left(1 + \frac{W}{4L} \right)} = \frac{2.67}{(6.849 + 2.0) \left(1 + \frac{23}{4(8)} \right)} = 0.1756 \quad [\text{LRFD Eq. 14.7.5.3.4-3}]$$

$$0.1671 = 2A \leq B = 0.1756, \quad [\text{LRFD Eq. 14.7.5.3.4-1}]$$

so in that direction the bearing is unconditionally stable.

10.8.3.8.8 Steel Reinforcement

The thickness of the steel plates for static strength is determined by

$$h_s \geq \frac{3.0h_{r,max}\sigma_s}{F_y} = \frac{3.0(0.433)(1.267)}{36} = 0.0457 \text{ in.} \quad [\text{LRFD Eq. 14.7.5.3.5-1}]$$

where

h_s = thickness of steel reinforcement, in.

F_y = yield strength of steel reinforcement, ksi

$h_{r,max}$ = thickness of thickest elastomeric layer in elastomeric bearing, in.

To prevent fatigue failure, the thickness must also satisfy:

$$h_s \geq \frac{2.0h_{r,max}\sigma_L}{\Delta F_{TH}} = \frac{2.0(0.433)(0.609)}{24} = 0.0220 \text{ in.} \quad [\text{LRFD Eq. 14.7.5.3.5-2}]$$

where

ΔF_{TH} = constant amplitude fatigue threshold for Category A as specified in LRFD Article 6.6, ksi

σ_L = average compressive stress due to live load = $\frac{112 \text{ kip}}{23(8)} = 0.609 \text{ ksi}$

14 gage plates ($h_s = 0.0747$ in.) are sufficient.

10.8.3.8.9 Anchorage

The maximum shear displacement occurs in the absence of live load but with the extreme low temperature, and it –0.943 in. The maximum horizontal force is then:

$$H_s = \frac{GA\Delta_s}{h_{rt}} = \frac{(0.100)(184)(0.943)}{2.6} = 6.674 \text{ kips} \quad (\text{Eq. 10.8.3.8.9-1})$$

This load occurs under dead load alone, in which case the friction coefficient needed to prevent slipping is:

$$\mu \geq \frac{H_s}{P_D} = \frac{6.674}{121.2} = 0.055 \quad (\text{Eq. 10.8.3.8.9-2})$$

This is significantly lower than the available friction coefficient of 0.20 implied in previous editions of the *LRFD Specifications*, so resistance to slip is taken to be adequate without additional restraint. Checks under other load combinations confirm that it will not slip under any conditions.

10.8.3.8.10 Low Temperature Requirements

From **Figure 10.7.1.3-1**, Rosemount, Minn., lies within Zone D. If no special force provisions are made, a grade 4 elastomer will be required as indicated in **Table 10.7.1.3-1**. Alternatively, if special force provisions are made, then a grade 3 elastomer may be used.

10.8.3.8.11 Testing Requirements

The thickness of the bearing is less than 8 in. and its plan area is less than 1,000 in.², so it does not count as large. Therefore no special test requirements exist.

10.8.3.8.12 Summary

Plan dimensions:	8 in. by 23 in. overall
Steel reinforcement:	Seven 14 ga steel plates: 7.5 in. by 22.5 in. by 0.0747 in.
Elastomer:	Six internal elastomer layers by 0.433 in. thick 2 cover elastomer layers by 0.25 in. thick Low temperature grade 4, $G = 0.100$ ksi
Total thickness	3.62 in.
Total weight	49 lbs

10.8.4 Design using Method A

The AASHTO LRFD design provisions that constitute Method A are expected to change from their existing form. The design methods presented below are those that are expected to be in the 2012 *Interim Revisions*.

10.8.4.1 General

The following procedures refer to pads and bearings designed in accordance with LRFD Article 14.7.6. The design procedure may be used for:

- Plain elastomeric pads (PEP) (see **Section 10.6.1**)
- Pads reinforced with discrete layers of fiberglass (FGP); (see **Section 10.6.2**).
- Cotton duck pads (CDP) with closely spaced layers of cotton duck (see Section 10.6.3) and manufactured and tested under compression in accordance with Military Specification MIL-C-882.
- Steel reinforced elastomeric bearings (SREB) (see **Section 10.6.4**).without bonded external plates, in which $S^2/n < 22$, and for which the primary rotation is about the weak axis. Here S = the shape factor of the thinnest internal layer and n = the number of internal layers of elastomer.

10.8.4.1 General/10.8.4.5 Design of Plain Elastomeric Pads, Fiberglass-reinforced Pads, and Steel Reinforced Elastomeric Bearings

The restriction on S^2/n for steel reinforced bearings is intended to prevent use of Method A for bearings in which rotations of typical magnitudes would cause excessive shear strain. The basis for it is explained in Stanton et al., 2008. This restriction is necessary because the method does not include an explicit calculation of shear strain due to rotation. If a steel-reinforced elastomeric bearing is subjected to unusually large rotations or complex load combinations, or if it has externally bonded steel plates that are attached to the beam, Method B should be used.

10.8.4.2 Material Properties.

Elastomers for plain pads must have a shear modulus of 80 to 250 psi and a nominal hardness of 50 to 70 on the Shore A scale. Steel-reinforced elastomeric bearings designed by Method A must use elastomers with a shear modulus of 80 to 175 psi and have a nominal hardness of between 50 and 60 on the Shore A scale.

10.8.4.3 Testing requirements

Plain pads designed using Method A are not required to undergo either short-term or long-term load testing, unless low temperature grade 4 or 5 elastomers are used (refer to **Table 10.8.2-1**).

10.8.4.4 Loads and Movements

The sources of design loads and movements are identical to those described in Section 10.4. Note that, in Method A, the strains due to cyclic load effects are not multiplied by the amplification factor of 1.75 used in Method B.

10.8.4.5 Design of Plain Elastomeric Pads, Fiberglass-reinforced Pads, and Steel Reinforced Elastomeric Bearings

The procedures for designing PEP, FGP and SREB are similar to each other, although the limiting strain values differ. Thus the design methods for all three types are addressed together here. The AASHTO Technical Committee T-2 on Joints and Bearings recently voted on changes to Article 14.7.6.3 of the LRFD *Specifications*, which addresses design Method A. The following paragraphs reflect the revised requirements and use the revised equation and article numbering. It is expected to be included in the 2011 *Interim Revisions*.

For shear displacements, PEP, FGP and SREB must satisfy:

$$h_{rt} \geq 2\Delta_s \quad \text{[LRFD Eq. 14.7.6.3.4-1]}$$

For stability, the total thickness of the pad or bearing shall not exceed the least of $L/3$, $W/3$, or $D/4$.

PEP must satisfy:

$$\sigma_s \leq 1.0 \text{ GS} \quad \text{[LRFD Eq. 14.7.6.3.2-1]}$$

$$\sigma_s \leq 0.800 \text{ ksi} \quad \text{[LRFD Eq. 14.7.6.3.2-2]}$$

where σ_s = average compressive stress due to total dead plus live loads at service limit state

FGP must satisfy:

$$\sigma_s \leq 1.25 \text{ GS} \quad \text{[LRFD Eq. 14.7.6.3.2-3]}$$

and $\sigma_s \leq 1.00 \text{ ksi}$ [LRFD Eq. 14.7.6.3.2-4]

SREB must satisfy:

$$\sigma_s \leq 1.25 \text{ GS} \quad \text{[LRFD Eq. 14.7.6.3.2-7]}$$

and $\sigma_s \leq 1.25 \text{ ksi}$ [LRFD Eq. 14.7.6.3.2-8]

where

G = shear modulus of the elastomer, ksi

h_{rt} = total elastomer thickness in an elastomeric bearing, in.

S = shape factor of the thickest layer of the bearing

Δ_s = maximum shear displacement of the bearing at the service limit state, in.

σ_s = service average compressive stress due to total load, ksi

BEARINGS**10.8.4.5 Design of Plain Elastomeric Pads, Fiberglass-reinforced Pads, and Steel Reinforced Elastomeric Bearings/10.8.4.6 Design of Cotton Duck Reinforced Pads**

When bearings are not subject to shear deformations, the allowable stresses in the above equations may be increased by 10%.

Steel reinforcement must conform to the requirements specified for Method B (see **Section 10.8.3.6**).

There are no design requirements for rotation.

10.8.4.6 Design of Cotton Duck Reinforced Pads

For shear displacements, CDP must satisfy:

$$h_{rt} \geq 10\Delta_s \quad [\text{LRFD Eq. 14.7.6.3.4-2}]$$

CDP have a much lower tolerance for shear deformation than do PEP, FGP or SREB. Thus, in many cases they are equipped with sliding interfaces to accommodate any horizontal movement.

For stability, the total thickness of the pad must not exceed the least of $L/3$, $W/3$, or $D/4$.

Compressive stress must satisfy

$$\sigma_s \leq 3.0 \text{ ksi} \quad [\text{LRFD Eq. 14.7.6.3.2-5}]$$

$$\text{and } \sigma_L \leq 2.0 \text{ ksi} \quad [\text{LRFD Eq. 14.7.6.3.2-6}]$$

where

σ_s = average compressive stress due to total load from applicable service load combinations

σ_L = average compressive stress at the service limit state due to live load

The total compressive strain at the service limit state due to combined compression and rotation must satisfy:

$$\epsilon_c + \frac{\theta_s L}{2t_p} \leq 0.20 \quad [\text{LRFD Eq. 14.7.6.3.5c-1}]$$

where

$$\epsilon_c = \frac{\sigma_s}{E_c} \quad [\text{LRFD Eq. 14.7.6.3.5c-2}]$$

σ_s = service average compressive stress due to total load associated with the maximum rotation, ksi

E_c = effective modulus in compression of elastomeric bearing, ksi. (E_c may be taken as 30 ksi in lieu of pad-specific test data).

h_{rt} = total elastomer thickness in an elastomeric bearing, in.

L = length of CDP pad in the plane of rotation, in.

t_p = total thickness of CDP pad, in.

Δ_s = maximum shear deformation of elastomer at the service limit state, in.

ϵ_c = maximum uniaxial strain due to compression under total load from applicable service load combinations in LRFD Table 3.4.1-1, in./in.

θ_s = Maximum service rotation due to total load, radians

Note that, unlike the requirements for PEP and FGP, design Method A does impose rotation requirements on CDP. Research on cotton duck pads (Lehman et al., 2005) found that cotton duck pads were adversely affected by lift-off on one side due to large rotations. To avoid it, the rotation must be limited to:

$$\theta_s \leq 0.80 \frac{2t_p \epsilon_c}{L} \quad [\text{LRFD Eq. 14.7.6.3.5c-3}]$$

$$\text{and } \theta_L \leq 0.20 \frac{2t_p \epsilon_c}{L} \quad [\text{LRFD Eq. 14.7.6.3.5c-4}]$$

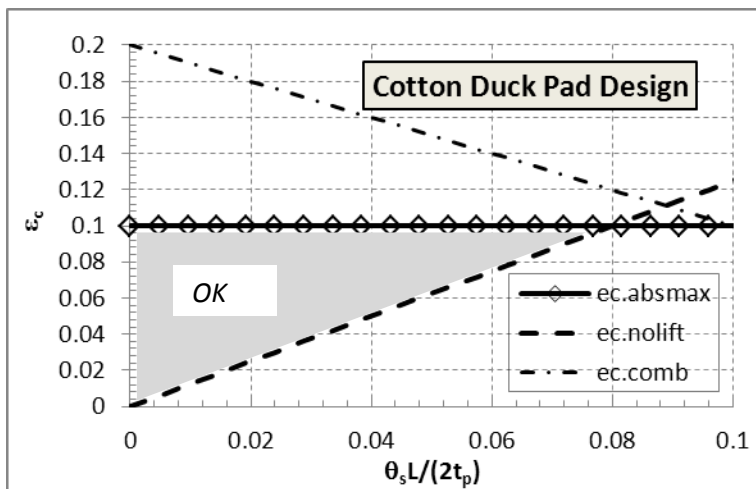


Figure 10.8.4.6-1. Design Limits for Cotton Duck Pads

These two sets of equations relate the average compressive strain and the rotation. The relationship is illustrated in **Figure 10.8.4.6-1**, using values for combined loading. The $(\epsilon_c, \theta_s L / 2t_p)$ pair must lie above the “ec.nolift” line and below the “ec.absmax” line. Similar relationships exist for live load, but the numerical values are different. If Young’s modulus is taken at its default value of 30 ksi the maximum compressive strain, ϵ_c , must be ≤ 0.10 . This is also shown in the figure as the “ec.abs.max” line. It is evident that the combined loading equation [LRFD Eq. 14.7.6.3.5c-1] is never an active constraint and that design is always controlled by a combination of the no lift-off condition of [LRFD Eq. 14.7.6.3.5c-3] and the absolute maximum stress of 3.0 ksi.

The largest possible total rotation capacity is available when the pad is loaded to the largest possible compressive stress of 3 ksi, in which case:

$$\theta_s = 0.08 \frac{2t_p}{L} \tag{Eq. 10.8.4.6-1}$$

10.8.4.7 Bearing Design Example—Method A

10.8.4.7.1 Introduction

This example demonstrates the design of an elastomeric bearing using Method A. It uses the same bridge as was used in **Section 10.8.3.8**, which in turn uses the bridge from **Design Example 9.1a** in **Chapter 9**.

The bridge consists of six simply supported BT-72 beams at 9-ft centers with an 8-in.-thick cast-in-place concrete deck. The span is 120 ft, it has no skew and all movement is accounted for at one end. The beams have a 26-in.-wide bottom flange. Choose a suitable movable elastomeric bearing.

Criteria in addition to those given in **Example 9.1a** are:

- The design temperature range is to be taken from LRFD Article 3.12.2
- Of the shrinkage and creep that occur between transfer and casting the slab, assume that two-thirds occurs before the beams are erected
- Assume free differential shrinkage of 400×10^{-6} in./in. of the deck slab relative to the beams.

Bearing Type:

Use a rectangular, steel-reinforced elastomeric bearing with a Shore A hardness of 50 durometer.

Method A does not account for rotations explicitly. Much of the design work in the Method B Design Example involved determining the loads, displacements and rotations at different stages of construction and subsequent service. The *LRFD Specifications* is not explicit in its guidance about the level of detail with which to determine these parameters when Method A is used, but the intended simplicity of the design method implies the need for a less computationally intensive procedure. This is especially true if the beam and bearings are to be designed by different agencies, in which case the detailed information may not be readily available to the bearing designer. It is thus proposed to consider:

- vertical loads
- change in length due to creep and shrinkage, determined from the corresponding prestress losses
- change in length due to thermal effects.

Longitudinal displacements of the bearing due to beam end rotations caused by thermal gradient, differential shrinkage, and vertical load will be ignored. The first two are not commonly computed and tend to cause low displacements anyway, because the average change in length of the whole composite beam acts in the opposite direction to the movement of the bottom flange due to end rotation, and the two effects largely cancel out. (This was seen in the calculation of horizontal movement due to differential shrinkage in **Section 10.8.3.8.2**). The horizontal movements due to vertical dead and live load on the beam depend on end rotation, which is ignored by Method A. They are also typically less than the horizontal displacements due to creep and shrinkage or thermal effects.

The loads and movements are thus:

$$P_D = 121.2 \text{ kips (includes beam, haunch, slab, barriers and wearing surface)}$$

$$P_L = 112.0 \text{ kips (includes lane and truck loads)}$$

$$\Delta_{CR+SHR} = -0.418 \text{ in. (One third of the creep and shrinkage movement between transfer and slab casting)}$$

$$\Delta_T = -0.786 \text{ in. (due to temperature drop of } 91 \text{ }^\circ\text{F from beam setting temperature)}$$

10.8.4.7.2 Elastomer Thickness for Shear Displacements

The total movement is:

$$\Delta_o = \Delta_{CR+SHR} + \Delta_T = -0.418 - 0.786 = -1.204 \text{ in.} \quad (\text{Eq. 10.8.4.7.2-1})$$

Assume that the substructure is rigid compared to the bearing, so the shear deformation, Δ_s , in the bearing will be equal to the total movement, Δ_o .

$$\Delta_s = \Delta_o = -1.204 \text{ in.} \quad (\text{Eq. 10.8.4.7.2-2})$$

Total thickness of elastomer:

$$h_{rt} \geq 2\Delta_s = (2)(1.204) = 2.408 \text{ in.} \quad [\text{LRFD Eq. 14.7.6.3.4-1}]$$

$$\text{Try } h_{rt} = 2.5 \text{ in.}$$

10.8.4.7.3 Design for Compressive Stress

The following limits apply:

$$\sigma_s \leq 1.25GS_i \quad [\text{LRFD Eq. 14.7.6.3.2-7}]$$

$$\sigma_s \leq 1.25 \text{ ksi} \quad [\text{LRFD Eq. 14.7.6.3.2-8}]$$

Since shear deformation is not prevented, the stress limits may not be increased.

For torsional stability of the beam at erection, use the widest bearing possible. Allow 1.5 in. between the edge of the beam and the edge of the bearing, giving a bearing width, $W = 26 - 2(1.5) = 23 \text{ in.}$

For preliminary purposes, the stress, σ_s , in the bearing can be computed as:

$$\sigma_s = \frac{P_D + P_L}{LW} \quad (\text{Eq. 10.8.4.7.3-1})$$

where

P_D = dead load reaction, kips

P_L = live load reaction, kips

L = length of bearing, in.

W = width of bearing, in.

Eq. 10.8.4.7.3-1 can be solved for L , assuming the maximum value of σ_s :

$$L \geq \frac{P_D + P_L}{\sigma_s W} = \frac{121.2 + 112.0}{(1.25)(23.0)} = 8.11 \text{ in.} \quad (\text{Eq. 10.8.4.7.3-2})$$

The length of the bearing may also be limited by the stability requirements. The trial value for total thickness of the internal layers is 2.5 in. Allow 0.25 in. cover top and bottom and 0.5 in. for internal steel plates, so the total thickness will be about 3.5 in. Since the total thickness must be less than $L/3$ for stability,

$$L \geq 3h_{rt} = 3(3.5) = 10.5 \text{ in.} \quad (\text{Eq. 10.8.4.7.3-3})$$

Try $L = 11$ in. and compute the actual stress, σ_s :

$$\sigma_s = \frac{P_D + P_L}{LW} = \frac{233.2}{(11.0)(23.0)} = 0.922 \text{ ksi} < 1.25 \text{ ksi} \quad \text{OK} \quad (\text{Eq. 10.8.4.7.3-4})$$

Determine the lower limit on shape factor, S , by solving the second expression in LRFD Equation 14.7.6.3.2-7:

$$S \geq \frac{\sigma_s}{1.25G} = \frac{0.922}{(1.25)(0.095)} = 7.764 \quad [\text{Eq. 10.8.4.7.3-5}]$$

Note that $G = 95$ psi, the lowest value in the range, must be used here to obtain the maximum shape factor, because the elastomer properties were defined by hardness. If they had been defined by the shear modulus, the exact value of G value could have been used. It is therefore advantageous to define the properties by the shear modulus.

Determine the maximum acceptable layer thickness, $h_{r,max}$, by solving LRFD Equation 14.7.5.1-1:

$$h_{r,max} \leq \frac{LW}{2S(L+W)} = \frac{(11.0)(23.0)}{(2)(7.764)(11.0+23.0)} = 0.480 \text{ in.} \quad (\text{Eq. 10.8.4.7.3-6})$$

The minimum number of layers = 2.5 in./0.480 in. = 5.2. Use 6 layers of 0.4375 in. (7/16 in.) each, to give a total elastomer thickness of 2.625 in.

Compute final shape factor:

$$S = \frac{LW}{2h_{ri}(L+W)} = \frac{(11.0)(23.0)}{(2)(0.4375)(11.0+23.0)} = 8.504 \quad [\text{LRFD Eq. 14.7.5.1-1}]$$

Check limitation on use of Method A:

$$\frac{S^2}{n} = \frac{(8.504)^2}{6} = 12.1 < 22 \quad \text{OK} \quad (\text{Eq. 10.8.4.7.3-7})$$

10.8.4.7.4 Steel Reinforcement

Use mild steel with 36 ksi yield stress (F_y) and a 24 ksi fatigue limit (ΔF_{TH} , from LRFD Table 6.6.1.2.5-3).

LRFD Article 14.7.6.3.7 indicates that steel reinforcement of bearings designed using Method A must conform to the requirements of Method B [LRFD Art. 14.7.5.3.5]. Note that the stresses are based on loads that are not amplified for cyclic load effects.

Check the strength of the plates at the service limit state:

$$h_s \geq \frac{3.0h_{r,max}\sigma_s}{F_y} = \frac{(3.0)(0.500)(0.922)}{36.0} = 0.0384 \text{ in.} \quad [\text{LRFD Eq. 14.7.5.3.5-1}]$$

Check that fatigue requirements for the plate are satisfied, which requires computation of the live load stress, σ_L :

$$\sigma_L \geq \frac{P_L}{LW} = \frac{112.0}{(11.0)(23)} = 0.443 \text{ ksi} \quad (\text{Eq. 10.8.4.7.4-1})$$

$$h_s \geq \frac{2.0h_{r,max}\sigma_L}{\Delta F_{TH}} = \frac{(2.0)(0.500)(0.443)}{24.0} = 0.0185 \text{ in.} \quad [\text{LRFD Eq. 14.7.5.3.5-2}]$$

The first equation governs, so the plate thickness must be at least 0.0384 in.

The minimum thickness permitted by the M 251 *Material Specification* is 1.52 mm, which corresponds to 16-gage. Keeping such plates flat during molding and curing is difficult. Select 14-gauge steel plate:

$$h_s = 0.0747 \text{ in.} \quad \text{OK}$$

10.8.4.7.5 Stability

LRFD Article 14.7.6.3.6 requires that the total thickness of a rectangular bearing not exceed the least of $L/3$ or $W/3$. For this bearing, $L/3$ will be the governing value.

Total elastomer thickness = $2(0.25) + 2.5 = 3.00$ in.

Total reinforcement thickness = 6 plates(0.0747) = 0.448 in.

Total thickness of bearing = $3.0 + 0.448 = 3.448$ in.

Maximum bearing thickness = $L/3 = 11/3 = 3.667$ in. > 3.448 in. OK

10.8.4.7.6 Low Temperature Requirements

From **Figure 10.7.1.3-1**, Rosemount, Minn. lies within Zone D. If no special force provisions are made, a grade 4 elastomer will be required as indicated in **Table 10.7.1.3-1**. If special force provisions are made, then a grade 3 elastomer may be used.

10.8.4.7.7 Design Shear Force and Anchorage

The requirements for anchorage depend on the low temperature grade of elastomer used. The service design shear force, using the value of G at 73 deg. F, is:

$$H_s = GA \frac{\Delta_s}{h_{rt}} = (0.130)[(11.0)(23.0)] \left(\frac{1.204}{3.125} \right) = 12.67 \text{ kips} \quad (\text{Eq. 10.8.4.7.7-1})$$

Note that $G = 130$ psi. The high value in the range must be used to compute the design shear force because the elastomer properties were defined by hardness, rather than shear modulus. The total elastomer thickness, h_{rt} , consists of both the internal layers (6 layers at 0.4375 in. each) and the top and bottom cover (0.25" each).

Rosemount, MN, lies in low temperature zone C (LRFD *Specifications* Article 14.7.5.2). If no force-control device, such as a sliding interface, is to be provided, the elastomer must satisfy the low-temperature requirements for grade 3. Then the friction coefficient needed to prevent slip would be

$$\mu \geq \frac{H_s}{P_D} = \frac{12.67}{121.2} = 0.105 \quad (\text{Eq. 10.8.4.7.7-1})$$

This is less than the implied available value of 0.20 in the previous editions of the LRFD *Specifications*, so the bearing will be prevented from slipping by friction alone and no special anchorage is required. Because grade 3 requirements can be satisfied without difficulty by most bearing manufacturers, this represents a good design choice. If a suitable grade 3 elastomer is not available, the bearing may be made from a grade 2 elastomer (LRFD Article 14.7.5.2), but the design horizontal force must be increased by a factor of four from the value given in Eq. 10.8.4.7.7-1. This is likely to trigger the need for special restraining devices, such as anchor bolts through the bearing, to prevent slipping. It will also induce larger forces in the components of the bridge superstructure.

A second alternative would be to use the grade 2 elastomer, but to provide a force-control device, such as a sliding interface, to accommodate most of the horizontal movement and to limit the horizontal force on the bearing.

10.8.4.7.8 Summary

Dimensions:	11.0 in. by 23 in. by 3.648 in. overall
Steel reinforcement:	Seven steel plates: 10.75 in. by 22.75 in. by 0.0747 in. (14 ga)
Elastomer:	Six internal layers at 0.4375 in. each 2 cover layers at 0.25 in. 50 durometer (Shore 'A' scale) Low-temperature grade 3

10.8.5 Tapered Bearings

Tapered elastomeric layers in bearing are not permitted by the LRFD *Specifications*. Nonetheless, Muscarella et al., 1995, conducted tests on tapered bearings and concluded that they behave in essentially the same way as flat bearings in almost all regards. That conclusion is not shared by all researchers in the discipline, and tapered layers in elastomeric bearings are used at the risk of the designer. The following recommendations are based on the work of Muscarella et al., 1995.

Tapered pads exhibit a non-negligible horizontal shearing deflection associated with vertically applied loads. This additional shearing deflection must be accounted for in the design of the bearing. The magnitude of this shearing deflection was found to be closely approximated by the following equation:

$$\Delta_s = \frac{0.400P_m h_{rt}}{GA} \quad (\text{Eq. 10.8.5-1})$$

where

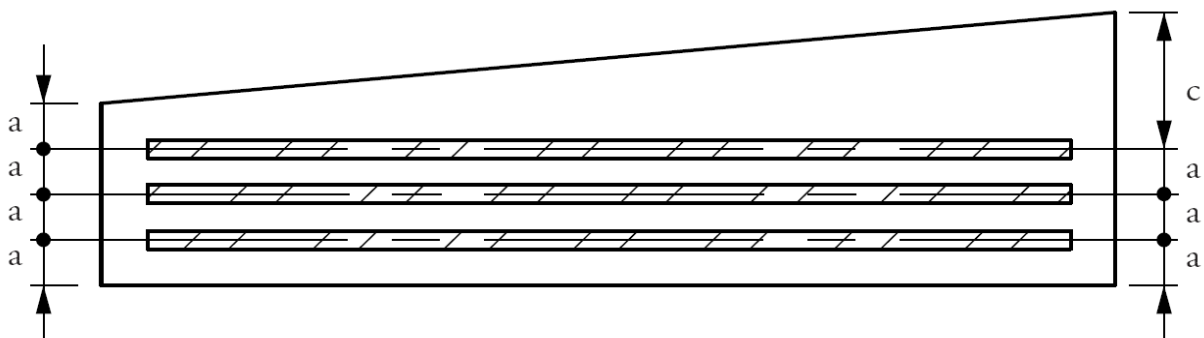
- Δ_s = shear deformation due to compressive load on tapered bearing, in.
- θ = taper of tapered bearing pad, radians
- P_m = maximum compressive load considering all appropriate load combinations, kips
- h_{rt} = total thickness of elastomer, in.
- G = shear modulus of elastomer, ksi
- A = plan area of elastomeric bearing, in.²

The following recommendations are made for the use of tapered bearings:

1. A tapered top cover layer of elastomer should be permitted provided that the designer takes into account the additional horizontal deflection that occurs under vertical load. As described above, it will usually be necessary to increase the total thickness of the elastomer, h_{rt} , by twice the computed horizontal deflection calculated by Eq. (10.8.5-1).

2. The average compressive stress on the bearing due to permanent loads should be between 500 psi and 1,000 psi.
3. A slope mismatch of up to 0.01 radians, including the 0.005 radians allowance for non-parallelism, may be permitted between a tapered bearing and the beam. This degree of mismatch will not result in significant separation between the bearing and the beam if compressive stresses on the bearing are maintained above 500 psi.
4. Compressive deformations for tapered pads can be computed as though the bearings are flat and then increased by 10% for each 0.01 radians of taper.
5. The shape factor, S , for the bearing should be between approximately 9.5 and 10.5.
6. The elastomer should have a Shore A hardness between 50 and 55 durometer.
7. Tapered pads should be constructed with horizontal, parallel steel reinforcement plates. The taper should be built into the bearing by tapering only the top cover layer of elastomer. See **Figure 10.8.5-1**.
8. The average thickness of the tapered cover layer of elastomer shall not exceed 0.333 in.

Figure 10.8.5-1
Tapered Bearing with Parallel Steel Reinforcement



10.9 BEARING SELECTION GUIDE

Table 10.9-1, based on (Roeder and Stanton, 1996) summarizes the most common types of bearings found in bridges constructed with precast, prestressed concrete beams. Ranges of loads, permissible translational and rotational movements, and cost information are provided for each of these common bearing types.

Figure 10.9-1 provides a graphical selection guide. The load range on the vertical scale shows the upper limit of load for each bearing type, and is the same for all displacements. The horizontal scale shows the displacement capacity, which, for each bearing type, is divided into a shaded and a clear area. The shaded areas indicate the translation range without a sliding interface, while in the clear areas a sliding interface, in combination with the bearing type in question, is required to achieve the displacement.

Once the designer has determined the total vertical load that the bearing must support and has estimated the required translational movement, this figure can be used as a guide to the type of bearing that should be considered for an application. The figure is appropriate for use where rotational requirements are moderate, i.e., less than approximately 0.015 radians. The limits depicted on **Figure 10.9-1** are indicative rather than absolute. In situations near the edges of a zone, consideration of more than one type of bearing may be appropriate.

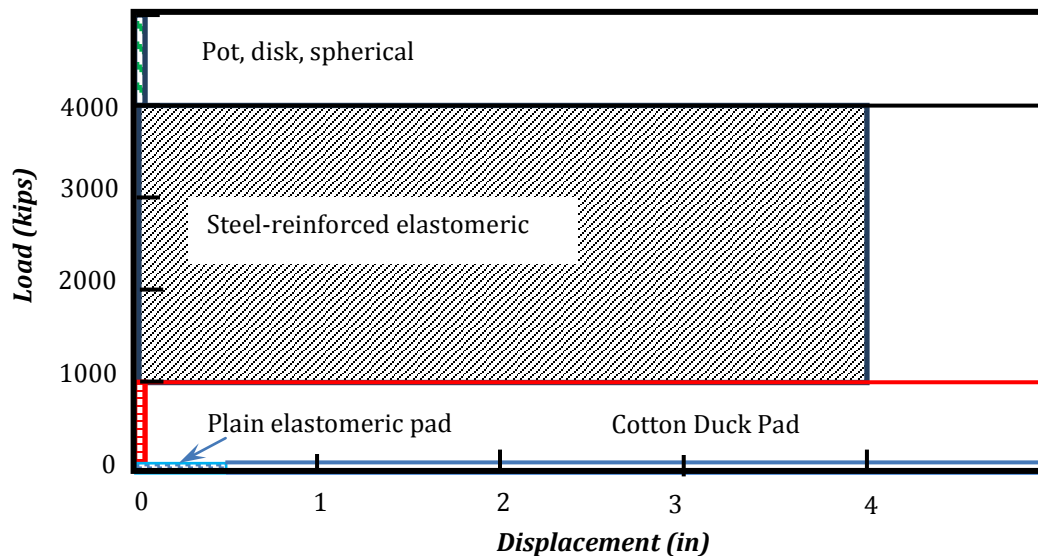
Table 10.9-1
Approximate Demand Limits for Different Bearing Types

Bearing Type	Load		Translation		Rotation	Costs	
	Min. kips	Max. kips	Min. in.	Max. in.	Limit radian	Initial	Maintenance
Elastomeric Pads Plain (PEP)	0	100	0.0	0.50	0.010	Low	Low
Cotton Duck (CDP)	0	750	0.0	0.25	0.003	Low	Low
Fiberglass (FGP)	0	150	0.0	1.00	0.015	Low	Low
Steel Reinforced Elastomeric Bearing (SREB)	0	4,000	0.0	4.00	0.020	Low	Low
Pot Bearing	250	≥ 4,000	0.0	0.00	0.020	Moderate	Moderate
Flat PTFE Slider	0	≥ 4,000	1.0	≥ 4.00	0.000	Low	Moderate

Adapted from NSBA Steel Bridge Bearing Selection and Design Guide.

Note: if a PTFE sliding surface is combined with another bearing type, the composite bearing has the translation capacity of the PTFE sliding surface.

Figure 10.9-1
Bearing Type Selection Guide



Note

10.10 REFERENCES

1. AASHTO. 2010. *AASHTO LRFD Bridge Construction Specifications*, 3rd Edition. American Association of State Highway and Transportation Officials, Washington, DC.
https://bookstore.transportation.org/Item_details.aspx?id=1583 (Fee)
2. AASHTO. 2010. *AASHTO LRFD Bridge Design Specifications*, 5th Edition with 2011 Interim Revisions. American Association of State Highway and Transportation Officials, Washington, DC.
<https://bookstore.transportation.org/search.aspx?Text=LRFD&gclid=CLbkhbKHwawCFQFX7AodIjPHsg> (Fee)
3. AASHTO. 2010. *Guide Specifications for Seismic Isolation Design*, 3rd Edition. American Association of State Highway and Transportation Officials, Washington, DC.
https://bookstore.transportation.org/Item_details.aspx?id=1604 (Fee)
4. AASHTO. 2002. *Standard Specifications for Highway Bridges*, 17th Edition. American Association of State Highway and Transportation Officials, Washington, DC.
https://bookstore.transportation.org/Item_details.aspx?id=51 (Fee)
5. AASHTO. 2006. *AASHTO M251. Standard Specification for Plain and Laminated Elastomeric Bridge Bearings*. American Association of State Highway and Transportation Officials, Washington, DC. 18 pp.
https://bookstore.transportation.org/item_details.aspx?ID=523 (Fee)
6. Buckle, I.G. and R.L. Mayes. 1996. "Seismic Isolation: History, Application, and Performance—A World View." *Earthquake Spectra*, Earthquake Engineering Research Institute (EERI), Oakland, CA. Vol. 6, No. 2, pp. 161-201.
http://eqs.eeri.org/resource/1/easpef/v6/i2/p161_s1?isAuthorized=no
7. Culmo, Michael P. 2002. Three Bearing Concept for Prestressed Concrete Adjacent Box Beam Bridges. Paper 104, Proceedings, Concrete Bridge Conference, Nashville, TN, National Concrete Bridge Council, Skokie, IL, 10 pp.
8. Dunker, K. F. 2000. Personal communication. Iowa Department of Transportation. (May)
9. Gent, A.N. 1958. "On the Relation Between Indentation Hardness and Young's Modulus." *Transactions of the Institution of the Rubber Industry*, now the *Institute of Materials, Minerals and Mining*, London, England. Vol. 34, No. 2, pp. 46-57.
http://www.rubberchemtechnol.org/resource/1/rctea4/v31/i4/p896_s1?isAuthorized=no (Fee)
10. Gent, A.N. 1964. "Elastic Stability of Rubber Compression Springs." *Journal of Mechanical Engineering Science, Institution of Mechanical Engineers*, Westminster, London, England. Vol. 6, No. 4, pp. 318-326.
<http://jms.sagepub.com/content/6/4/318.abstract>
11. Gent, A.N. and P.B. Lindley. 1959. "The Compression of Bonded Rubber Blocks." *Proceedings of the Institution of Mechanical Engineers*, Westminster, London, England. Vol. 173, pp. 111-122.
<http://sdj.sagepub.com/content/6/2/121.abstract>
12. Haryngx, J.A. 1948-1949. "On Highly Compressible Helical Springs and Vibration-free Mountings." Parts 1, II, III. *Philips Research Reports*, maintained by Leibniz Institute for Solid State and Materials Research Dresden, Dresden, Germany.
13. HITEC. 1996. *Guidelines for the Testing of Seismic Isolation and Energy Dissipating Devices*. Report No. 40162. Highway Innovative Technology Evaluation Center, Civil Engineering Research Foundation, American Society of Civil Engineers, Reston, VA.
<http://www.earthquakeprotection.com/product2.html>
14. Lee, David J. 1994. *Bridge Bearings and Expansion Joints*, Second Edition. E & FN Spon, London, UK, 212 pp.
<http://www.abebooks.com/9780419145707/Bridge-Bearings-Expansion-Joints-Lee-0419145702/plp> (Fee)

15. Lehman, D.E, C.W. Roeder, and R. Larson. 2005. "Design of Cotton Duck Bridge Bearing Pads." *ASCE Journal of Bridge Engineering*, American Society of Civil Engineers, Reston, VA. Vol. 10, No. 5, pp. 555-563.
http://www.ce.washington.edu/people/faculty/cv/Lehman_Dawn.pdf
16. Lindley, P. B. 1981. "Natural Rubber Structural Bearings." ACI Special Publication SP-70, Vol. 1, American Concrete Institute, Farmington Hills, MI., pp. 353-378.
17. McDonald, J., E. Heymsfield, and R. R. Avent. 2000. "Slippage of Neoprene Bearing Pads." *ASCE Journal of Bridge Engineering*, American Society of Civil Engineers, Reston, VA. Vol. 5, No. 3, (August), pp. 216-223.
<http://cedb.asce.org/cgi/WWWdisplay.cgi?122820> (Fee)
18. Moorthy, S. and C.W. Roeder. 1992. "Temperature Dependent Bridge Movements." *Journal of Structural Division*, American Society of Civil Engineers, Reston, VA. Vol. 118, No. 4, pp. 1090-1105.
<http://cedb.asce.org/cgi/WWWdisplay.cgi?75546> (Fee)
19. Muscarella, Joseph V. 1995. An Experimental Study of Elastomeric Bridge Bearings with Design Recommendations. University of Texas at Austin, Austin, TX. Ph.D. Dissertation.
http://www.utexas.edu/research/ctr/pdf_reports/1304_3.pdf
20. Nagarajaiah, S., M. C. Constantinou, and A. M Reinhorn. 1989. *Nonlinear Dynamic Analysis of Three-Dimensional Base Isolated Structures*. Report No. NCEER-89-0019. National Center for Earthquake Engineering Research, State University of New York at Buffalo, Buffalo, NY.
<http://mceer.buffalo.edu/publications/resacom/94-sp02/3-dbasis.pdf>
21. Roeder, C. W. and J. F. Stanton. 1996. *Steel Bridge Bearing Selection and Design Guide*. National Steel Bridge Alliance, Chicago, IL.
http://www.inti.gob.ar/cirsoc/pdf/puentes_acero/steel_bridge.pdf
22. Roeder, C. W., J. F. Stanton, and T. Feller. 1990. *Low Temperature Behavior and Acceptance Criteria for Elastomeric Bridge Bearings*. NCHRP Report 325. Transportation Research Board, Washington, DC.
<http://nisee.berkeley.edu/elibrary/Text/201107201>
23. Roeder, C. W., J. F. Stanton, and A. Taylor. 1987. *Elastomeric Bearings—Design Construction and Materials*. NCHRP Report 298. Transportation Research Board, Washington, DC.
<http://nisee.berkeley.edu/elibrary/Text/S20728>
24. Stanton, J. F., G. Scroggins, A. W. Taylor, and C. W. Roeder. 1990. "Stability of Laminated Elastomeric Bearings." *ASCE Journal of Engineering Mechanics*, American Society of Civil Engineers, Reston, VA. Vol. 116, No. 6 (June), pp. 1351-1371.
<http://cedb.asce.org/cgi/WWWdisplay.cgi?9002293> (Fee)
25. Stanton, J.F. and C.W. Roeder. 1991. "Advantages and Limitations of Seismic Isolation." *Earthquake Spectra*, Earthquake Engineering Research Institute (EERI), Oakland, CA. Vol. 7, No. 2 (May), pp. 301-309.
http://eqs.eeri.org/resource/1/easpef/v7/i2/p301_s1?isAuthorized=no (Fee)
26. Stanton, J. F., P. MacKenzie, C.W. Roeder, C. Kuester, C. White, and B. Craig. 2008. *Rotation Limits for Elastomeric Bearings*. NCHRP Report No. 596. National Cooperative Highway Research Program, Washington, DC.
http://onlinepubs.trb.org/onlinepubs/nchrp/nchrp_rpt_596.pdf
27. Stanton, J.F. and J.C. Taylor, 2010. "Friction Coefficients for Stainless Steel (PTFE) Teflon Bearings". Report No. WHRP 10-01, Wisconsin Highway Research Program, Madison, WI, 111 pp.
http://www.whrp.org/research-areas/structures/structures_0092-08-13.html
28. Timoshenko, S.P. and J.M. Gere. 1961. *Theory of Elastic Stability*, 2nd Edition. McGraw-Hill, New York, NY, 603 pp.
http://www.4shared.com/document/YuzrYKHI/Theory_of_Elastic_Stability_Ti.html

This page intentionally left blank

EXTENDING SPANS

Table of Contents

NOTATION..... 11 - 5

11.1 INTRODUCTION..... 11 - 9

11.2 HIGH-PERFORMANCE CONCRETE..... 11 - 10

 11.2.1 High-Strength Concrete 11 - 10

 11.2.1.1 Benefits..... 11 - 10

 11.2.1.2 Costs..... 11 - 10

 11.2.1.3 Effects of Section Geometry and Strand Size..... 11 - 11

 11.2.1.4 Compressive Strength at Transfer 11 - 13

 11.2.1.5 Reduction of Pretensioning Force by Post-Tensioning 11 - 13

 11.2.1.6 Tensile Stress Limit at Service Limit State 11 - 13

 11.2.1.7 Prestress Losses 11 - 14

 11.2.2 Lightweight Aggregate Concrete..... 11 - 14

11.3 CONTINUITY 11 - 15

 11.3.1 Introduction 11 - 15

 11.3.2 Method 1 – Conventional Deck Reinforcement..... 11 - 15

 11.3.3 Method 2 – Post-Tensioning 11 - 15

 11.3.4 Method 3 – Coupled High-Strength Rods 11 - 17

 11.3.5 Method 4 – Coupled Prestressing Strands..... 11 - 19

11.4 SPLICED-BEAM STRUCTURAL SYSTEMS 11 - 19

 11.4.1 Introduction and Discussion..... 11 - 19

 11.4.1.1 Combined Pretensioning and Post-Tensioning..... 11 - 19

 11.4.2 Types of Beams 11 - 20

 11.4.3 Span Arrangements and Splice Location..... 11 - 21

 11.4.4 Details at Beam Splices..... 11 - 21

 11.4.4.1 Cast-In-Place Post-Tensioned Splice 11 - 22

 11.4.4.1.1 “Stitched” Splice 11 - 24

 11.4.4.1.2 Structural Steel Strong Back at Splice..... 11 - 25

 11.4.4.1.3 Structural Steel Hanger at Splice 11 - 26

 11.4.4.2 Match-Cast Splice 11 - 27

 11.4.5 System Optimization 11 - 29

 11.4.5.1 Minimum Web Width to Accommodate Post-Tensioning 11 - 29

 11.4.5.2 Pier Segments (Constant Depth and Haunched) 11 - 31

 11.4.6 Design and Fabrication Details 11 - 31

 11.4.7 Construction Methods and Techniques 11 - 31

 11.4.7.1 Splicing and Shoring Considerations 11 - 31

 11.4.7.2 Construction Sequencing and Impact on Design 11 - 33

 11.4.7.2.1 Single Spans..... 11 - 33

 11.4.7.2.2 Multiple Spans..... 11 - 33

 11.4.8 Grouting of Post-Tensioning Ducts 11 - 34

11.4.9 Deck Removal Considerations	11 - 35
11.4.10 Post-Tensioning Anchorages	11 - 36
11.5 EXAMPLES OF SPLICED-BEAM BRIDGES.....	11 - 36
11.5.1 Eddyville-Cline Hill Section, Little Elk Creek Bridges 1 through 10, Corvallis-Newport Highway (U.S. 20), Oregon. (2000).....	11 - 36
11.5.2 Rock Cut Bridge, Stevens and Ferry Counties, Washington (1997).....	11 - 37
11.5.3 US 27-Moore Haven Bridge, Florida (1999)	11 - 38
11.5.4 Bow River Bridge, Calgary, Alberta (2002).....	11 - 39
11.6 POST-TENSIONING ANALYSIS.....	11 - 40
11.6.1 Introduction	11 - 40
11.6.2 Losses at Post-Tensioning	11 - 40
11.6.2.1 Friction Loss.....	11 - 40
11.6.2.2 Anchorage Set Loss	11 - 41
11.6.2.3 Design Example	11 - 41
11.6.2.3.1 Friction Loss	11 - 42
11.6.2.3.2 Anchor Set Loss	11 - 42
11.6.2.3.2.1 Length Affected by Seating is within L_{ab}	11 - 43
11.6.2.3.2.2 Length Affected by Seating is Within L_{ac}	11 - 43
11.6.2.4 Elastic Shortening Loss	11 - 44
11.6.3 Time-Dependent Analysis.....	11 - 44
11.6.4 Equivalent Loads for Effects of Post-Tensioning.....	11 - 44
11.6.4.1 Conventional Analysis Using Equivalent Uniformly Distributed Loads.....	11 - 45
11.6.4.2 Refined Modeling Using a Series of Nodal Forces	11 - 47
11.6.4.2.1 Example	11 - 48
11.6.4.3 Design Consideration.....	11 - 50
11.6.5 Shear Limits in Presence of Post-Tensioning Ducts	11 - 50
11.7 POST-TENSIONING ANCHORAGES IN I-BEAMS.....	11 - 51
11.8 DESIGN EXAMPLE: TWO-SPAN BEAM SPLICED OVER PIER.....	11 - 53
11.8.1 Introduction	11 - 53
11.8.2 Materials and Beam Cross-Section.....	11 - 54
11.8.3 Cross-Section Properties	11 - 55
11.8.3.1 Non-Composite Section.....	11 - 55
11.8.3.2 Composite Section	11 - 56
11.8.4 Shear Forces and Bending Moments.....	11 - 56
11.8.5 Required Pretensioning.....	11 - 57
11.8.6 Modeling of Post-Tensioning.....	11 - 58
11.8.6.1 Post-Tensioning Profile	11 - 58
11.8.6.2 Equivalent Loads.....	11 - 61
11.8.7 Required Post-Tensioning	11 - 62

EXTENDING SPANS

Table of Contents

11.8.7.1 Stress Limits for Concrete.....	11 - 63
11.8.7.2 Positive Moment Section	11 - 63
11.8.7.3 Negative Moment Section	11 - 64
11.8.8 Prestress Losses	11 - 65
11.8.8.1 Prediction Method.....	11 - 65
11.8.8.2 Time-Dependent Material Properties.....	11 - 65
11.8.8.3 Time Step Analysis	11 - 65
11.8.9 Service Limit State at Section 0.4L.....	11 - 66
11.8.9.1 Stress Limits for Concrete.....	11 - 66
11.8.9.2 Stage 1 Post-Tensioning.....	11 - 67
11.8.9.3 Stage 2 Post-Tensioning.....	11 - 67
11.8.9.4 Compression Due to Service I Loads	11 - 68
11.8.9.5 Tension Due to Service III Loads.....	11 - 68
11.8.10 Stresses at Transfer of Pretensioning Force	11 - 69
11.8.10.1 Stress Limits for Concrete	11 - 69
11.8.10.2 Stresses at Transfer Length Section.....	11 - 69
11.8.10.3 Stresses at Midspan.....	11 - 69
11.8.11 Strength Limit State	11 - 70
11.8.11.1 Positive Moment Section	11 - 70
11.8.11.2 Negative Moment Section.....	11 - 71
11.8.12 Limits of Reinforcement.....	11 - 72
11.8.12.1 Positive Moment Section	11 - 72
11.8.13 Shear Design.....	11 - 73
11.8.14 Comments and Remaining Steps.....	11 - 73
11.9 DESIGN EXAMPLE: SINGLE SPAN, THREE SEGMENT BEAM	11 - 74
11.9.1 Input Data and Design Criteria	11 - 74
11.9.2 Construction Stages	11 - 75
11.9.3 Flexure at Service Limit State.....	11 - 76
11.9.4 Flexure at Strength Limit State	11 - 77
11.9.5 Discussion	11 - 78
11.10 REFERENCES.....	11 - 79

This page intentionally left blank

NOTATION

A	= area of the beam cross section	
A_c	= total area of the composite section	
A_{ps}	= area of prestressing steel	[LRFD]
A_v	= area of a transverse reinforcement within distance, s	[LRFD]
a	= depth of equivalent rectangular stress block	[LRFD]
b_v	= width of the web adjusted for the presence of ducts	[LRFD]
b_w	= width of the member's web	[LRFD]
c	= distance from extreme compression fiber to centroid of the post-tensioning force at location denoted by subscript	
c	= distance from extreme compression fiber to the neutral axis	[LRFD]
DC	= dead load of structural components and nonstructural attachments	[LRFD]
DW	= dead load of wearing surfaces and utilities	[LRFD]
d_v	= effective shear depth	[LRFD]
E_c	= modulus of elasticity of concrete	[LRFD]
E_{ci}	= modulus of elasticity of concrete at transfer	[LRFD]
E_p	= modulus of elasticity of prestressing tendons	[LRFD]
E_s	= modulus of elasticity of reinforcing bars	[LRFD]
e	= base of neperian logarithm	
e	= eccentricity of strands at transfer length or location denoted by subscript	
e_c	= eccentricity of strands at the midspan	
F	= vertical load	
f_b	= concrete stress at the bottom fiber of the beam	
f'_c	= specified compressive strength of concrete for use in design	[LRFD]
f'_{ci}	= specified compressive strength of concrete at the time of initial loading or prestressing	[LRFD]
f_{pb}	= compressive stress at bottom fiber of the beam due to prestress force	
f_{cpe}	= compressive stress in concrete due to effective prestress forces only (after allowance for all prestress losses) at extreme fiber of section where tensile stress is caused by externally applied loads	[LRFD]
f_p	= stress in post-tensioning strands at location denoted by additional subscript	
f'_p	= stress in post-tensioning strands after anchor set loss at location denoted by subscript	
f_{pj}	= stress in the prestressing steel at jacking	[LRFD]
f_{ps}	= average stress in prestressing steel at the time for which the nominal resistance of member is required	[LRFD]
f_{pt}	= stress in prestressing steel immediately after transfer	[LRFD]
f_{pu}	= ultimate strength of prestressing steel	[LRFD]
f_{py}	= yield strength of prestressing steel	[LRFD]

f_r	= modulus of rupture of concrete	[LRFD]
f_{rel}	= assumed allowable tensile stress in concrete at transfer	
f_s	= stress limit for post-tensioning strands prior to seating	
f_s'	= stress in the mild steel compression reinforcement at nominal flexural reinforcement	[LRFD]
f_t	= concrete stress at top fiber of the beam for the non-composite section	
f_{ser}	= assumed allowable tensile stress at service load	
f_{tg}	= concrete stress at top fiber of the beam for the composite section	
f_y	= specified minimum yield strength of reinforcing bars	[LRFD]
h	= overall thickness or depth of a member	[LRFD]
h	= distance from top fiber to centroid of post-tensioning force at location denoted by subscript	
h_c	= total height of composite section	
I	= moment of inertia about the centroid of the non-composite precast beam	[LRFD]
IM	= vehicular dynamic load allowance	[LRFD]
I_c	= moment of inertia for the composite section	
K	= wobble friction coefficient	[LRFD]
L	= span length	[LRFD]
LL	= vehicular live load	[LRFD]
M	= moment at location denoted by subscript	
M_b	= unfactored bending moment due to barrier weight	
M_{cr}	= cracking moment	[LRFD]
M_d	= bending moment at section due to unfactored dead load	
M_{dnc}	= total unfactored dead load moment acting on the monolithic or non-composite section.	[LRFD]
M_g	= unfactored bending moment due to beam self-weight	
M_{LL+I}	= unfactored bending moment due to live load plus impact	
M_n	= nominal flexural resistance	[LRFD]
M_r	= factored flexural resistance of a section in bending	[LRFD]
M_S	= unfactored bending moment due to deck slab and haunch weights	
$M_{secondary}$	= secondary bending moment due to post-tensioning	
M_u	= factored moment at the section	[LRFD]
M_{ws}	= unfactored bending moment due to wearing surface	
n	= modular ratio = E_s/E_c or E_p/E_c ; modular ratio between the deck concrete and reinforcement	[LRFD]
P	= prestressing force	
P_i	= total pretensioning force immediately after transfer	
P_{pe}	= total pretensioning force after all losses	
P_{PT}	= total post-tensioning force after all losses	
S_b	= non-composite section modulus for the extreme bottom fiber of the precast beam	

S_{bc}	= composite section modulus for the extreme bottom fiber of the precast beam	
S_t	= section modulus for extreme top fiber of the non-composite precast beam	
S_c	= section modulus for the extreme fiber of the composite section where tensile stress is caused by the external applied loads.	[LRFD]
S_{nc}	= section modulus for the extreme fiber of the monolithic or non-composite section where tensile stress is caused by the external applied loads.	[LRFD]
S_{tc}	= composite section modulus for top fiber of the slab	
S_{tg}	= composite section modulus for the top fiber of the precast beam	
s	= spacing of reinforcing bars	[LRFD]
t_s	= structural thickness of concrete slab	
V	= shear force	
V_b	= unfactored shear force due to barrier weight per beam	
V_c	= nominal shear resistance provided by tensile stresses in the concrete	[LRFD]
V_g	= unfactored shear force due to girder weight	
V_{LL+I}	= unfactored shear force due to live load plus impact	
V_n	= nominal shear resistance of the section considered	[LRFD]
V_p	= component in the direction of the applied shear of the effective prestressing force, positive if resisting the applied shear	[LRFD]
V_s	= shear resistance provided by shear reinforcement	[LRFD]
V_s	= unfactored shear force due to slab and haunch weight per beam	
$V_{secondary}$	= secondary shear force due to post-tensioning	
V_u	= factored shear force at section	[LRFD]
V_{ws}	= unfactored shear force due wearing surface weight per beam	
w_{eq}	= equivalent load for post-tensioning	
w_c	= unit weight of concrete	[LRFD]
x	= distance from the support to the section under question	
x	= length influenced by anchor set	
x	= length of a prestressing tendon from the jacking end to any point under consideration, ft.	[LRFD]
y_b	= distance from the centroid to the extreme bottom fiber of the non-composite precast beam	
y_{bc}	= distance from the centroid of the composite section to the extreme bottom fiber of the precast beam	
y_{bs}	= distance from the center of gravity of strands to the bottom fiber of the beam	
y_t	= distance from centroid to the extreme top fiber of the non-composite precast beam	
y_{tg}	= distance from the centroid of the composite section to the top fiber of the precast beam	
α	= angle of inclination of transverse reinforcement to longitudinal axis (degrees); total angular change of prestressing steel path from jacking end to a point under investigation (rad.); the angle of inclination of a tendon reinforcement with respect to the centerline of the member (degrees)	[LRFD]

EXTENDING SPANS

Notation

β	= factor relating effect of longitudinal strain on the shear capacity of concrete, as indicated by the ability of diagonally cracked concrete to transmit tension	[LRFD]
β_1	= ratio of the depth of the equivalent uniformly stress compression zone assumed in the strength limit state to the depth of the actual compression zone	[LRFD]
Δf_{pA}	= loss in prestressing steel stress due to anchorage set	[LRFD]
Δf_{pa}	= prestress loss at point, a	
Δf_{pES}	= loss in prestressing steel stress due to elastic shortening	[LRFD]
Δf_{pF}	= loss in prestressing steel stress due to friction	[LRFD]
ΔL	= anchor set	
θ	= angle of inclination of diagonal compressive stresses	[LRFD]
μ	= coefficient of friction	[LRFD]
ϕ	= resistance factor	[LRFD]

EXTENDING SPANS

11.1 INTRODUCTION

Precast, prestressed concrete beams have been used widely for highway bridges throughout the United States and the world. The simplest and most economical application for precast concrete beam bridges is where full-span beams are used in the bridge. The full-span beams have most often been used as simple spans, although continuity has also been established between spans using a continuity diaphragm at interior piers and various methods to counter negative moments.

For simple span, precast, prestressed concrete bridges using conventional materials, the maximum spans for each standard section type are shown in Chapter 6. However, the excellent durability and structural performance, low maintenance, and low cost of bridges using precast, prestressed concrete beams have encouraged designers to find ways to use them for even longer spans.

A number of methods have been identified for extending the typical span ranges of prestressed concrete beams. These include the use of the following:

- High-strength concrete
- Larger strand size or strength
- Modified section dimensions
 - Widening the web
 - Thickening or widening the top flange
 - Thickening the bottom flange
 - Increasing the section depth (haunch) at interior piers
 - Casting the deck with the girder (deck bulb tee)
- Lightweight concrete
- Post-tensioning
- Continuity
- Use of pier tables

Of these methods, the use of high-strength concrete, lightweight aggregate concrete (both of which are considered to be high-performance concrete) and continuity are discussed in this chapter.

As designers attempt to use longer full-span beams, limitations on handling and transportation are encountered. Some of the limitations are imposed by the states regarding the size and weight of vehicles allowed on highways. Some states limit the maximum transportable length of a beam to 120 ft and the weight to 70 tons. Other states, including Pennsylvania, Washington, Nebraska and Florida, for example, have allowed precast beams with lengths up to 210 ft and weights in excess of 150 tons to be shipped by truck. Unique haul rigs capable of expanding their footprint have a capacity of 340 kips (see **Figure 3.5.1-1**). In other cases, the size of the erection equipment may be limited, either by availability to the contractor or by access to the site. There are sites where access will not allow long beams to reach the bridge.

When any of these limitations preclude the use of full-span beams, shorter beam segments can be produced and shipped. These beam segments are then spliced together at or near the jobsite or in their final location. The splices are located in the spans, away from the piers. The beam segments are typically post-tensioned for the full length of the bridge unit, which can be either a simple span or a multiple span continuous unit.

While the introduction of splices and post-tensioning increases the complexity of the construction and adds cost, precast bridges of this type have been found to be very cost competitive with other systems and materials. The longest span in a modern spliced beam bridge in the United States is currently the 325-ft-long river span in a four-span bridge over the Kentucky River near Gratz, Kentucky. This bridge was originally designed using a steel plate girder, but was redesigned at the recommendation of the precaster to reduce project costs, which clearly demonstrates the comparative economy of the spliced concrete beam system.

Since splicing is an important tool for extending span ranges, and since it also incorporates some additional design issues not discussed elsewhere in this Manual, a significant portion of this chapter is devoted to providing

designers with information on this type of bridge. Design theory, post-tensioning analysis and details, segment-to-segment joint details, and examples of recently constructed spliced-beam bridges are given. The chapter includes examples intended to help designers understand the various design criteria and to develop preliminary superstructure designs. A significant additional resource for the design of precast prestressed concrete beams for extended spans is the research project performed as part of the National Cooperative Highway Research Program (NCHRP) titled "Extending Span Ranges of Precast Prestressed Concrete Girders" by Castrodale and White (2004). The final report contains considerable information on methods for extending span ranges, as well as an extended discussion of issues related to the design of spliced beam bridges, including three design examples. The report also identifies nearly 250 spliced beam bridges constructed in the United States and Canada.

11.2 HIGH-PERFORMANCE CONCRETE

High-performance concrete (HPC) has been defined in a number of different ways, but, in general, it includes modifications to concrete that improve the efficiency, durability or structural capability of members over that achieved using conventional concrete. A number of HPC tools can be used to extend the spans of precast, prestressed concrete beams. In this chapter, the discussion will be limited to the use of high-strength and lightweight concrete.

11.2.1 High-Strength Concrete

High-strength concrete (HSC) has several advantages over conventional-strength concrete.

11.2.1.1 Benefits

These benefits include increased:

- compressive strength,
- modulus of elasticity, and
- tensile strength.

In addition, high-strength concrete is nearly always enhanced by these other benefits:

- Smaller creep coefficient
- Less shrinkage strain
- Lower permeability
- Improved durability

Specifically, beams made with high-strength concrete exhibit the following structural benefits:

- Permit the use of high levels of prestress and therefore a greater capacity to carry gravity loads. This, in turn, allows the use of:
 - fewer beam lines for the same width of bridge,
 - longer spans for the same beam depth and spacing, and
 - shallower beams for a given span.
- For the same level of initial prestress, axial shortening and short-term and long-term deflections are reduced.
- For the same level of initial prestress, reduced creep and shrinkage result in lower prestress losses, which can be beneficial for reducing the required number of strands.
- Higher tensile strength results in a slight reduction in the required prestressing force if the tensile stress limit controls the design.
- Strand transfer and development lengths are reduced.

11.2.1.2 Costs

The benefits of high-strength concrete are not attained without cost implications. For example, when high concrete compressive strength is used to increase member capacity, a higher prestress force is required. This in turn offsets the effect of a lower creep coefficient and results in larger losses and deflections. Furthermore, very long and shallow members require an investigation of live load deflections, as well as constructability and stability during design.

EXTENDING SPANS

11.2.1.2 Costs/11.2.1.3 Effects of Section Geometry and Strand Size

High-strength concrete is more expensive per cubic yard than conventional concrete. In some areas, increasing concrete strength from 7.0 ksi to 14.0 ksi could double the cost from \$70 to \$140/yd³. However, a modest increase to 10.0 ksi might add only \$10 to \$20/yd³. Concrete mixes with strengths higher than 10.0 ksi may be difficult to attain with consistency and require large quantities of admixtures. It is difficult to generalize about costs and capabilities. The materials, experience, and equipment may be more a regional issue for the industry. Generally, the technology to produce high-strength precast concrete is advancing very rapidly.

Other consequential costs that should be taken into consideration include the following:

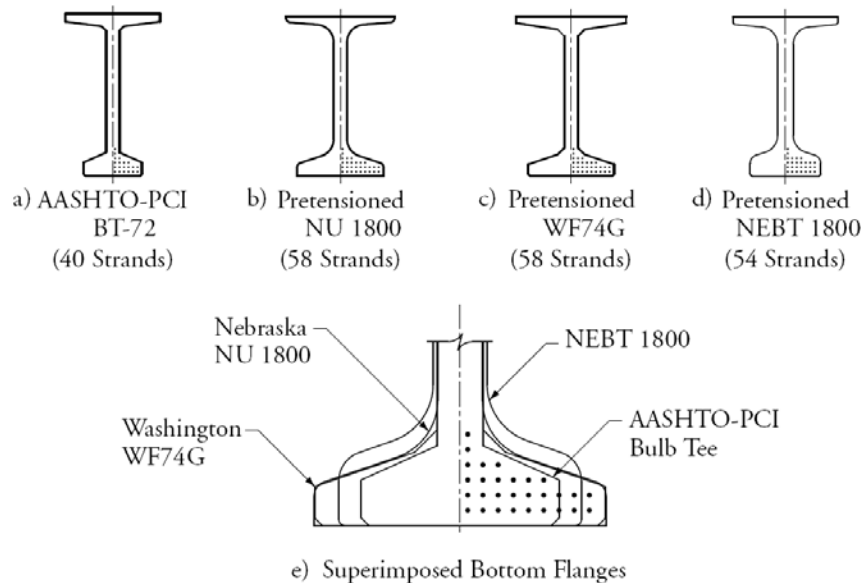
- Achieving high transfer strengths could extended the production cycle to more than one day.
- High prestress forces may exceed available bed capacity for some plants.
- Larger capacity equipment to handle, transport, and erect longer and heavier beams may be required than is normally available.

Costs associated with the production of high-strength concrete should be weighed against the reduction in volume and the net result may well be both initial savings as well as long-term durability enhancements. Producers near the project (and their state and regional associations) should be consulted about these issues.

11.2.1.3 Effects of Section Geometry and Strand Size

High-strength concrete increases the effectiveness of precast, prestressed concrete beams. High concrete strength at prestress transfer permits the application of a larger pretension force, which in turn increases the member’s capacity to resist design loads. The number of strands that can be used is limited by the size of the bottom flange. The primary reason that the NU I-Girders, the Washington Super Girders and the New England Bulb-Tee beams have higher span capacities than the AASHTO-PCI Bulb Tee is that they all have significantly larger bottom flanges as shown in **Figure 11.2.1.3-1**.

Figure 11.2.1.3-1
Bulb Tee and I-Beam Shapes with Large Bottom Flanges to Accommodate More Strand



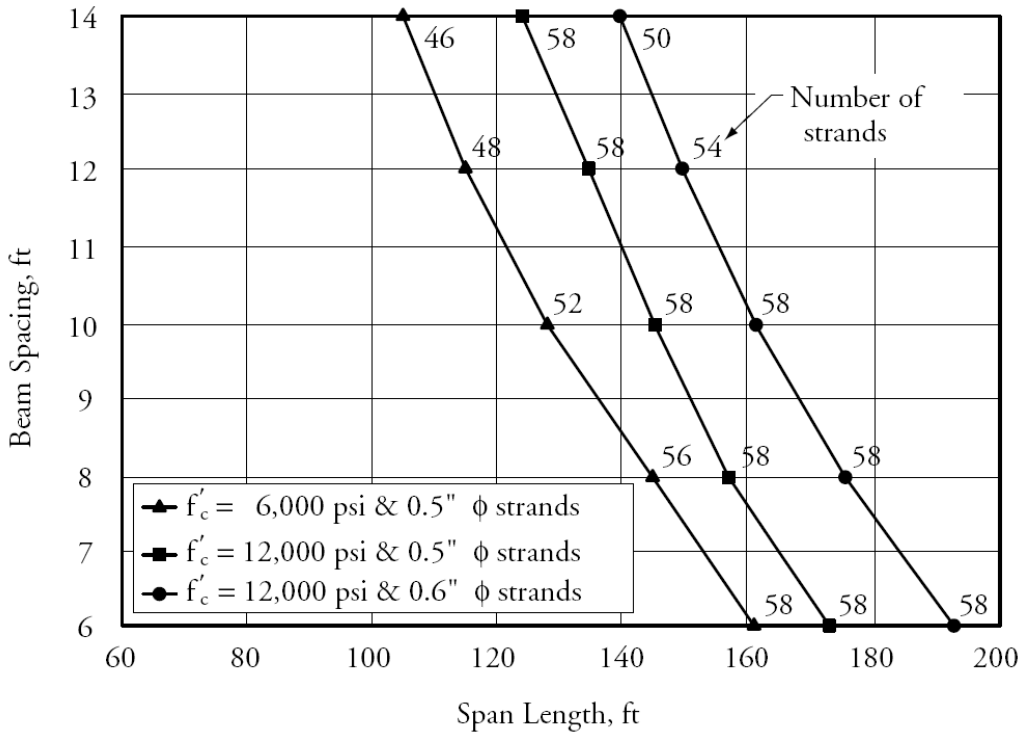
Designers have rapidly implemented the use of 0.6-in.-diameter strands. This will improve the efficiency of all beam shapes because each 0.6-in.-diameter strand provides 40% more pretensioning force for only a 20% increase in diameter. The *LRFD Specifications* allow the same center-to-center spacing for 0.6-in.-diameter strand as for ½-in.-diameter strand.

EXTENDING SPANS

11.2.1.3 Effects of Section Geometry and Strand Size

Figure 11.2.1.3-2 shows the maximum span of a NU2000 (78.7-in.-deep) beam.

Figure 11.2.1.3-2
Maximum Span of NU2000 Beam



The maximum span varies with the beam spacing and number of strands. The number of strands must increase to allow for a greater span length. Likewise, as the beam spacing increases, the number of strands must also increase. An investigation conducted by the Washington State Department of Transportation and the Pacific Northwest PCI shows that the maximum span of the W21MG beam (now referred to as the W83G beam), with 7.5-ksi transfer strength, using 0.6-in.-diameter strands, is 180 ft (Seguirant, 1998).

At a small beam spacing of about 6 to 8 ft, however, the potential for increased span length with high-strength concrete may be limited by the number of strands that can be placed in the bottom flange. For the NU beam with 6.0 ksi concrete and beam spacing of 6 ft, 58 strands are required to achieve the maximum span length of 161 ft. This is the maximum number of strands that can be placed in the bottom flange of the NU beam. If the concrete strength is increased to 12.0 ksi, the maximum span will increase only 12 ft, about 7.5% greater than the original maximum span. However, when the beam spacing is increased to 14 ft, the number of strands can be increased from 46 for concrete with a design strength of 6.0 ksi to 58 for 12.0 ksi concrete with an increase in span from 105 ft to 124 ft.

If concrete strength and strand size are both increased, the span length can be extended further. The 12.0 ksi concrete is still adequate to fully utilize the bottom flange by filling it with 58 strands. This confirms the work by Russell, et al. (1997), who found that concrete with a compressive strength lower than 12.0 ksi would be adequate when 1/2-in.-diameter strands are used.

EXTENDING SPANS**11.2.1.3 Effects of Section Geometry and Strand Size/11.2.1.6 Tensile Stress Limit at Service Limit State**

Based on these results, two conclusions can be made regarding effective utilization of beams with high-strength concrete:

- The effectiveness of HSC is largely dependent on the number of strands that the bottom flange can hold. The more strands contained in the bottom flange, the farther the beam can span and the greater the capacity to resist positive moment. It is recognized that designers do not always have a large number of choices of available beam sections. Nonetheless, a beam that provides for the greatest number of strands in the bottom flange is preferred when using HSC.
- Allowable stresses are increased when using HSC. If these limiting stresses cannot be fully utilized with ½-in.-diameter strands, then 0.6-in.-diameter strands should be used. The tensile strength of 0.6-in.-diameter strands is nearly 40% greater than the capacity of ½-in.-diameter strands. The *LRFD Specifications* permit the use of 0.6-in.-diameter strands at the common 2-in. spacing. The use of 0.6-in.-diameter strands is expected to increase in the future even with the use of conventional strength concrete due to economy in production.

11.2.1.4 Compressive Strength at Transfer

Higher concrete compressive strength at transfer allows a beam to contain more strands and increases the capability of the beam to resist design loads. To achieve the largest span for a given beam size, designers should use concrete with the compressive strength needed to resist the effect of the maximum number of strands that can be accommodated in the bottom flange. However, the availability of high compressive strength concrete at transfer varies throughout the country. Strength at transfer should not be higher than required for the span being designed because strengths in excess of 5.5 to 6.5 ksi may increase the required duration of the production cycle at the manufacturing plant. This would in turn increase the cost of the beams. Early compressive strength is influenced by local materials and sometimes by production facilities and regional practices. Producers should be consulted about available concrete strengths before beginning design.

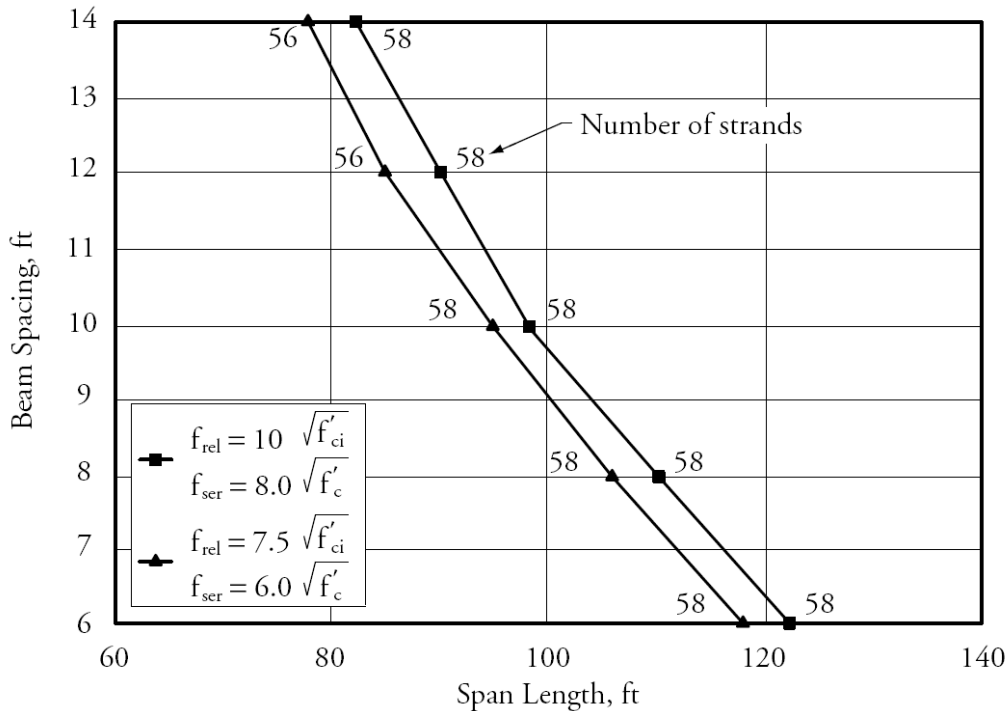
11.2.1.5 Reduction of Pretensioning Force by Post-Tensioning

When it is necessary to reduce compressive strength at transfer or when there are limitations on the capacity of the pretensioning bed, the total amount of prestress can be provided in two stages. The first is pretensioning during production followed by post-tensioning after production. Compared to using only pretensioning during production, combining pre- and post-tensioning generally increases the cost of the beam but has been used very effectively to solve strength and plant constraints.

11.2.1.6 Tensile Stress Limit at Service Limit State

Numerous test results on HSC have shown a modulus of rupture as high as $12\sqrt{f'_c}$ compared to $7.5\sqrt{f'_c}$ indicated for conventional concrete (ACI Committee 363, 2010). Since the limiting tensile stress is directly proportional to the modulus of rupture, some designers and researchers have suggested an increase in the tensile stress limit. As shown in **Figure 11.2.1.6-1**, the use of higher tensile stress limits has relatively small effect on the maximum achievable spans of prestressed concrete I-beams.

Figure 11.2.1.6-1
Variation of Maximum Span of NU1100
Beams with Spacing and Allowable Tensile Stress



11.2.1.7 Prestress Losses

Depending on specific aggregates, the general characteristics of HSC are reduced creep, reduced shrinkage strain, and increased modulus of elasticity. Consequently, prestress losses are lower for HSC compared to conventional concrete at a constant level of prestress. However, higher levels of prestress are generally used in HSC members. Therefore, the absolute value of loss may be comparable, or even higher compared to conventional strength concrete (Seguirant, 1998).

A study for the National Cooperative Highway Research Program (NCHRP) by Tadros, et al. (2002), resulted in recommendations for the determination of certain concrete properties in HSC (modulus of elasticity, creep, and shrinkage), as well as a proposal for prestress loss estimation, which have been adopted by AASHTO. The *LRFD Specifications* provides two methods for estimating time-dependent losses: the approximate method and the refined method. Both methods are described in Chapter 8 with design examples in Chapter 9.

11.2.2 Lightweight Aggregate Concrete

Structural lightweight aggregate concrete has been used extensively to reduce the weight of precast members. The weight of a concrete beam accounts for about one third of its total load, and increases in proportion as the span increases. Reducing member weight allows the beam to carry higher superimposed loads and to span farther. Structural lightweight aggregate (LWA) concrete bridges have been reported in the literature from the earliest days of the prestressed concrete industry and those applications continue. Useful publications on LWA concrete applications are provided by the Expanded Shale, Clay and Slate Institute (ESCSI) (website www.escsi.org). LWA concrete with a specified strength of 10.0 ksi has reportedly been used in Norway and Canada (Meyer and Kahn, 2001). Research performed at Georgia Institute of Technology (Meyer and Kahn, 2002) includes a study of the advantages of lightweight, high-strength concrete to 12.0 ksi. The production and testing of full-size beams has verified the important design and long-term properties of the material. When lighter weight is combined with higher strength and improved durability, the benefits are compounded.

11.3 CONTINUITY

11.3.1 Introduction

Precast, prestressed concrete beams are most often placed on their supports as simple-span beams. In this configuration, the beams support self-weight and the weight of deck formwork. Generally, the weight of the deck slab is also supported by the simple span. If the details used allow for rotation of beam-ends, further loads applied to the bridge may also be applied to the simple span.

Simple span systems have sometimes not performed well. When the deck slab is placed continuously over abutting girder ends at a pier, but the girder ends are allowed to rotate, significant deck cracking can occur. This cracking, as well as alternative joints placed at this location, can lead to leakage through the deck and deterioration of the girder ends, bearings, and the substructure. This is especially critical in cold weather regions where deicing chemicals are used.

However, when beams are made continuous, structural efficiency and long-term performance are significantly improved.

Two methods have been used to create continuity in precast, prestressed concrete beam bridges:

- Deck reinforcement
- Post-tensioning

Two additional methods have been introduced recently for establishing continuity. They are accomplished prior to placing the deck and have shown promising results:

- Coupling beams with high-strength rods
- Coupling beams with prestressing strands

The use of post-tensioning and the latter two methods provide the structural benefit of making the beam continuous to resist the deck weight – a considerable portion of the total load. This significantly improves the structural performance of the bridge.

Discussion of the features of each of the four methods follows.

11.3.2 Method 1 – Conventional Deck Reinforcement

Continuity can be established by casting abutting beam-ends on the pier into cast-in-place concrete diaphragms. Reinforcement is placed in the cast-in-place deck to resist the negative design moments that develop. Section 3.2.3.2.2 provides more details of this method. Design considerations and calculations are shown in Design Example 9.2.

The method has been used very successfully in a number of states beginning as early as the 1950s. It is the simplest of the existing methods because it does not require additional equipment or specialized labor to make the connections between beams to establish continuity. The beam acts as a simple span under its own weight and the weight of the deck slab but as a continuous beam for other dead loads and the live load. Since the deck is mildly reinforced and not pretensioned, decks are design to meet the strength limit state. Designers should meet the owner service limit state design criteria, if required.

11.3.3 Method 2 – Post-Tensioning

This method is somewhat more expensive than the previous method per unit volume of beam concrete. It generally requires full-length post-tensioning of the bridge beams. The beam web must be wider than 6 in. that is common in many pretensioned beams. It also requires enlargement of the webs at the ends of some beams (end blocks) to accommodate post-tensioning anchorage hardware, or special anchorage details in the back wall of the abutment. A specialized contractor may be required to perform the post-tensioning and grouting operations.

However, significant advantages of this method are the ability to:

- splice segments into longer spans,
- create efficient, multiple-span continuous bridges,
- pre-compress the deck in the negative moment regions to virtually eliminate transverse surface cracking in the deck at piers under service loads,
- improve structural efficiency by having a continuous beam for the deck weight and all subsequent loads
- have post-tensioning resist part of the self-weight of the beam, and
- use plant pretensioning only to counteract the weight of the beam and for handling stresses. This relatively small prestress results in small cambers and minimizes the need for high-strength concrete at transfer.

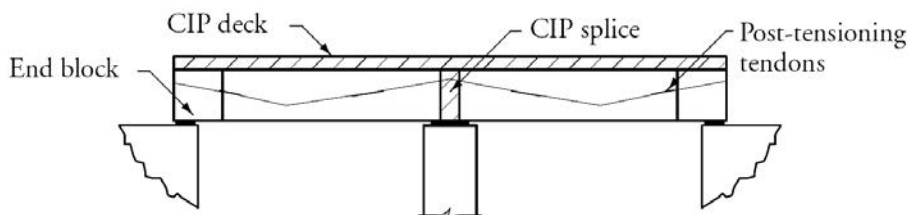
For these reasons, much of the remainder of this chapter is devoted to the use, the analysis, and design of post-tensioning for extending the spans of precast concrete beams.

In general, the construction of a post-tensioned beam bridge proceeds in the following way. The beams or beam segments are erected first, the post-tensioning ducts are spliced and then the beam splices or diaphragms are formed, cast and cured. Some or all of the post-tensioning tendons may then be installed and tensioned. The cast-in-place composite deck is cast. The remainder of the post-tensioning tendons are installed and tensioned. A schematic diagram of a typical splice-girder bridge is shown in **Figure 11.3.3-1**.

The timing of the application of post-tensioning defines three general schemes for spliced girder bridge design and construction:

- Advantages of applying all of the post-tensioning prior to the deck pour include: 1) the beam system will be continuous for the weight of the deck, which makes the beams more efficient, 2) minimal pretensioning is required in the segments themselves for self-weight and handling, which reduces the required concrete release strength, 3) one stage of post-tensioning minimizes the specialized labor required for such operations, and 4) future deck replacement is less complicated since the beams have been designed to handle the prestressing without the composite action of the deck. Disadvantages of this scheme include 1) higher concrete strengths in the girders and cast-in-place splices will normally be required at post-tensioning since the weight of the deck is not present to offset the effects of prestress, and 2) the deck will not be prestressed, which will increase the potential for cracking in the negative moment regions over the piers. This region of the deck can be designed with mild reinforcement in accordance with Article 5.9 of the LRFD Specifications, much like Method 1 in section 11.3.2.
- Advantages of applying all of the post-tensioning after the deck has cured include: 1) the deck can be prestressed to minimize cracking in the negative moment region over the piers (issues associated with applying post-tensioning after the deck has cured are discussed in Section 11.4.9), 2) one stage of post-tensioning minimizes the specialized labor required for such operations, and 3) concrete strengths in the girders and cast-in-place splices can be minimized since the weight of the deck is present to offset the effects of prestress. Disadvantages of this scheme include 1) the beams will not be continuous for the weight of the deck, 2) the segments must be designed to carry the weight of the deck in simple span, which increases the required pretensioning, and 3) future deck replacement is complicated by the fact that the bare beams were not designed to handle the prestressing without the composite action of the deck.
- Two stages of post-tensioning, one before the deck pour and one after the deck has cured, can maximize the advantages of both of the previous schemes while minimizing the disadvantages. Of course, the prime disadvantage here is the added cost of mobilizing a second round of specialized labor for the post-tensioning operation.

Figure 11.3.3-1
Full-Length Post-Tensioned Beam Bridge



EXTENDING SPANS

11.3.3 Method 2 – Post Tensioning/11.3.4 Method 3 – Coupled High-Strength Rods

First-stage post-tensioning must be large enough to control concrete stresses throughout the continuous member for the loads applied before the next post-tensioning stage. If a second post-tensioning stage is used, it is usually applied after the deck has cured and before superimposed dead loads are applied. Issues associated with applying post-tensioning after the deck has been placed are discussed in Section 11.4.9.

In cases where all post-tensioning is applied prior to placement of the deck, tensile stresses in the deck are not usually checked. The provisions of AASHTO Section 5.9 may be used to reinforce an area in tension using mild steel reinforcement.

In cases where the deck is subject to tensile stresses by the application of post-tensioning, tensile stresses in the deck may be checked unless required by the owner. If tensile stresses in the deck in negative moment regions exceed design requirements, one of the following could be considered:

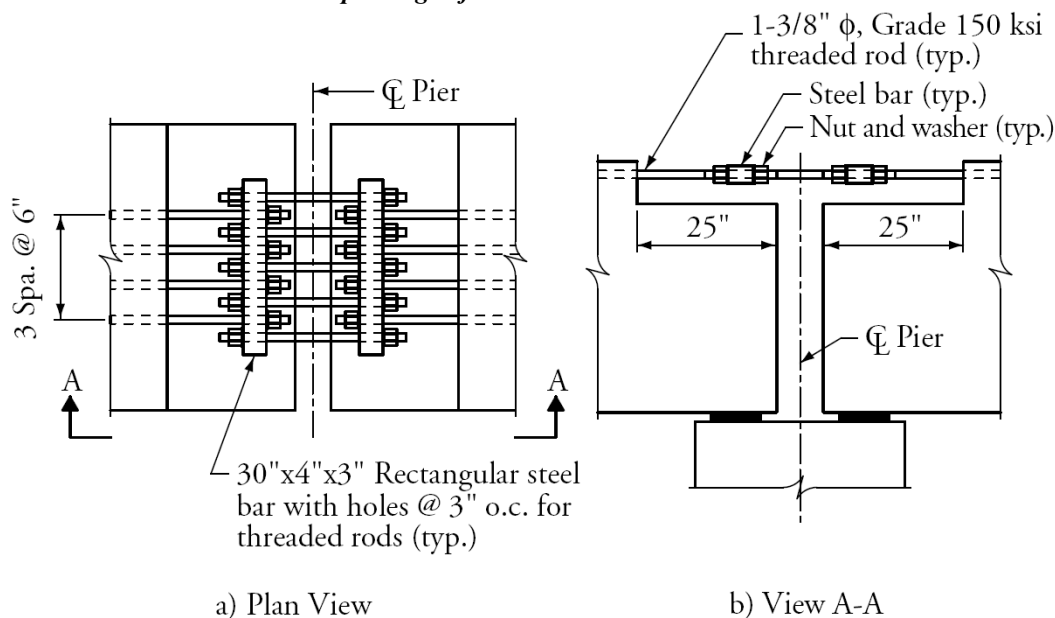
- Consider the deck partially prestressed at this section. This condition would be superior to other continuous beam systems where the deck has no prestressing and is expected to crack under service load.
- Increase post-tensioning to bring deck concrete stresses within limits and recheck positive moment regions for code compliance.
- Increase the specified concrete strength of the deck

11.3.4 Method 3 – Coupled High-Strength Rods

In this method, nonprestressed, high-strength threaded rods are extended from the top of the beam and coupled over the piers to provide resistance to negative moments from the weight of the deck slab. Conventional longitudinal reinforcement as described in Section 11.3.2, Method 1, is placed in the deck in the negative moment to resist the additional negative moments due to superimposed dead and live loads. Therefore, this method provides continuity conditions for deck weight, superimposed dead load and live load.

An earlier version of the connection shown in **Figure 11.3.4-1** has undergone full-scale testing (Ma, et al., 1998). It was shown to be structurally effective and simple to construct. The detail has been adopted by the Nebraska Department of Roads. A similar detail has been used on a four-span, Florida Department of Transportation double tee bridge on U.S. 41 over the Imperial River at Bonita Springs, Florida.

Figure 11.3.4-1
Threaded-Rod Connection in Top Flange of I-Beam



EXTENDING SPANS

11.3.4 Method 3 – Coupled High-Strength Rods

Another application of the method was a successful value-engineering change to a project in Nebraska in 2002. The contractor redesigned the Clarks Bridge from a haunched plate girder system that varied from 4- to 6-ft deep, to a modified, 50-in.-deep bulb tee. The project is shown nearing completion in **Figure 11.3.4-2**.

*Figure 11.3.4-2
Clarks Bridge, over U.S. Highway 30 and the
Union Pacific Railroad, Omaha, Nebraska*



The bridge has four spans of 100, 148, 151, and 128 ft. It has a composite deck thickness of 8 in. and a beam spacing of 10.75 ft to match the original steel beam design. For a precast I-beam system at this relatively wide spacing, the bridge has an impressive span-to-depth ratio of $151 \times 12 / (50 + 8) = 31$. It also uses unique individual cast-in-place pier tables to support the beams. These tables become composite with cast-in-place extensions of the beams and later, with the bridge deck. **Figure 11.3.4-3a** shows a typical beam with high-strength rods extended from the top flange. **Figure 11.3.4-3b** shows the beams on their pier tables with extended rods spliced between ends of the beams (Hennessey and Bexten, 2002).

*Figure 11.3.4-3
Clarks Bridge, Omaha, Nebraska*



a) Beam Showing High-Strength Rods b) Spliced Negative Moment Reinforcement

The coupled-rod splice combines the simplicity of adding reinforcement in the deck (Method 1) with some of the structural efficiency of post-tensioning (Method 2) where the beam may be made continuous for certain dead loads. A cost comparison of this method with Method 1 (Saleh, et al., 1995) indicates that savings in positive moment strands offsets the added cost of the threaded rods and hardware. Moreover, any need for positive moment reinforcement at the piers due to creep restraint is totally eliminated because the compression introduced into the bottom of the splice from the negative dead load moment is expected to counteract any possible positive moment generated from time-dependent effects. This method also increases the span capacity of a given beam size by about 10%.

11.3.5 Method 4 – Coupled Prestressing Strands

This method uses pretensioning strands, which are left extended at beam ends. Strands are positioned so that, after production, they project from the ends of the beam near the top surface. After the pier diaphragm concrete is placed and hardened, but before the cast-in-place deck slab is placed, the strands are spliced and tensioned. This method has been utilized in the construction of a pedestrian/bicycle overpass in Lincoln, Nebraska, and is described in detail in Ficenec, et al. (1993). The prestressing strand continuity method provides all the advantages of full-length post-tensioning but may cost less because it does not require large jacks, end blocks or the grouting associated with post-tensioning. This method is very efficient because it utilizes the existing pretensioning strands. However, the hardware and procedures for strand splicing and the procedures for the transfer of prestress in the plant are somewhat complex.

11.4 SPLICED-BEAM STRUCTURAL SYSTEMS

11.4.1 Introduction and Discussion

In many parts of the country, spans greater than about 165 ft cannot usually be achieved economically with one piece, precast, pretensioned concrete beams because of transportation and lifting restrictions. If erection is over water, longer beams may be transported and erected from barges. Owners tend to specify structural steel for these relatively large spans.

However, many are becoming familiar with the efficiency and economy of spliced concrete beams. This system, which is described in detail in the remainder of this chapter, has been demonstrated in the past several decades to be cost-competitive with structural steel and has advantages with regard to durability and aesthetics (Abdel-Karim, 1991; Abdel-Karim and Tadros, 1992).

To provide simple spans, precast, pretensioned beam segments are sometimes post-tensioned together at or near the project site and lifted as one piece onto final supports. In most cases, however, the precast segments are erected on temporary towers to span the full distance between supports. When the segments are post-tensioned together, they lift off the temporary falsework and span between their permanent pier and abutment supports.

As discussed in Section 11.3.3, these spliced, continuous, post-tensioned beam bridges offer the advantage, over steel and pretensioned, precast concrete bridges, of having pre-compressed concrete in the deck at the negative moment regions. While competitive with steel, they require more design and construction steps, and are generally, but not always, more expensive than pretensioned-only concrete systems.

In situations that require these longer spans, precast concrete beams that are only pretensioned are usually not viable. Today, it is becoming more common for designers to think of spliced post-tensioned I-beam solutions. Owner agencies should be encouraged to develop designs using this system as an alternative to steel plate beams for as many projects as possible. The experience in a number of states of offering a spliced concrete beam and a steel plate beam alternative has resulted in healthy competition and significant savings. Even when the steel alternate is the successful one, its bid price has been shown to be dramatically lower than before competing against a concrete alternative. This has proven to more than justify the cost of preparing alternatives for contractor bidding. In instances when structural steel suppliers sacrifice profits or provide plate beams at a loss, continuing alternative designs have resulted in the concrete solution eventually being selected for construction and further rewarding the owner through lower long-term maintenance costs.

11.4.1.1 Combined Pretensioning and Post-Tensioning

The combination of plant pretensioning and subsequent post-tensioning offers an opportunity for structural optimization of simple spans made continuous, where the prestressing is introduced in stages corresponding to the introduction of design loads. The conventional system is to design a precast, pretensioned beam as simple span for self-weight and deck weight, and to make spans continuous through longitudinal deck reinforcement for superimposed dead loads and live loads. Alternatively, the same beam can be pretensioned to resist self weight as a simple span and then spliced and post-tensioned to resist all other loads as a continuous beam. This optimization can result in the reduction of one or two beam lines or a reduction in structural depth while maintaining the same beam spacing. Several bridges have been built in Nebraska using the combination of two types of prestressing. In nearly all cases, combined prestressing was successfully bid against a structural steel alternate.

EXTENDING SPANS

11.4.1.1 Combined Pretensioning and Post-Tensioning/11.4.2 Types of Beams

This type of system offers a practical introduction for agencies that have little or no experience with spliced-beam bridges or post-tensioning. Once the agency becomes familiar with the design and construction process, and the techniques are introduced in practice, applications can advance to longer span systems that require splices away from the permanent pier supports.

When pretensioning and post-tensioning are combined, additional losses will occur due to the interaction of different prestressing forces.

11.4.2 Types of Beams

Shapes typically used in spliced-beam bridge applications are shown in **Figure 11.4.2-1**. Prestressed I-beams are the most popular, mainly due to their moderate self-weight, ease of fabrication, and ready availability. For these reasons, much of the discussion that follows will focus on I-beams.

As the trend continues toward continuous superstructures, the need becomes evident for optimum I-beam sections. The I-beam geometry should perform well in both the positive and negative moment regions. This is clearly a different goal from shapes that were developed specifically for simple spans. Simple-span beams generally have inadequate sections for negative moment resistance and have webs too thin for post-tensioning ducts. A minimum web width to accommodate the post-tensioning tendon ducts and shear reinforcement is required, as discussed in Section 11.4.5.1.

Open-topped trapezoidal beams, or U-beams, are increasingly popular because of their aesthetic appeal. They are also being used for curved beams as discussed in Chapter 12.

*Figure 11.4.2-1
Shapes Used for Spliced-Beam Bridges*

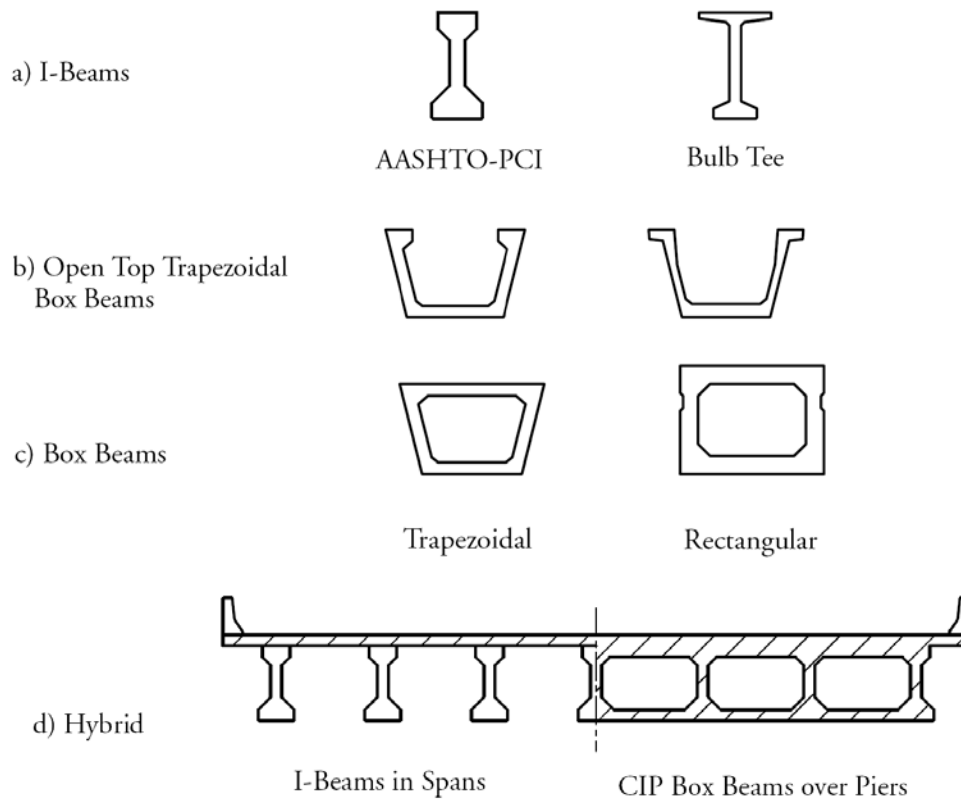


Figure 11.4.2-1d depicts a unique solution, which uses a hybrid combination of precast and cast-in-place concrete. Precast I-beams achieve a slender, light-looking mid-span element and are combined with cast-in-place concrete box beams at the piers where compressive forces caused by negative moments require a large bottom flange. While this solution has the benefit of improved section properties to resist negative moments at the

interior piers, construction is more complex and lengthy than for more conventional precast construction. However, where structure depth is severely restricted, a section like this has proven to be an economical solution for several bridges.

11.4.3 Span Arrangements and Splice Location

By considering spliced beams, the designer has more flexibility to select the most advantageous span lengths, beam depths, number and locations of piers, segment lengths for handling, hauling and construction, and splice locations. As discussed in Section 11.3.3, a commonly used splicing technique is to post-tension a series of beams that are simply supported on piers or abutments. This achieves continuity for deck weight and superimposed loads. In addition to the enhanced structural efficiency of this system, post-tensioning can be used to assure that the deck is stressed below its cracking limit, which improves durability considerably.

Another feature of spliced beams is the ability to adapt to horizontally curved alignments. By casting the beam segments in appropriately short lengths and providing the necessary transverse diaphragms, spliced beams may be chorded along a curved alignment. This is shown clearly in **Figure 11.4.3-1** that shows the Rosebank-Patiki Interchange in New Zealand with a 492-ft radius.

The chorded solution results in an efficient framing system while enhancing aesthetics. More details for chorded curved bridges are given in Chapter 12.

*Figure 11.4.3-1
The Rosebank-Patiki Interchange, New Zealand*



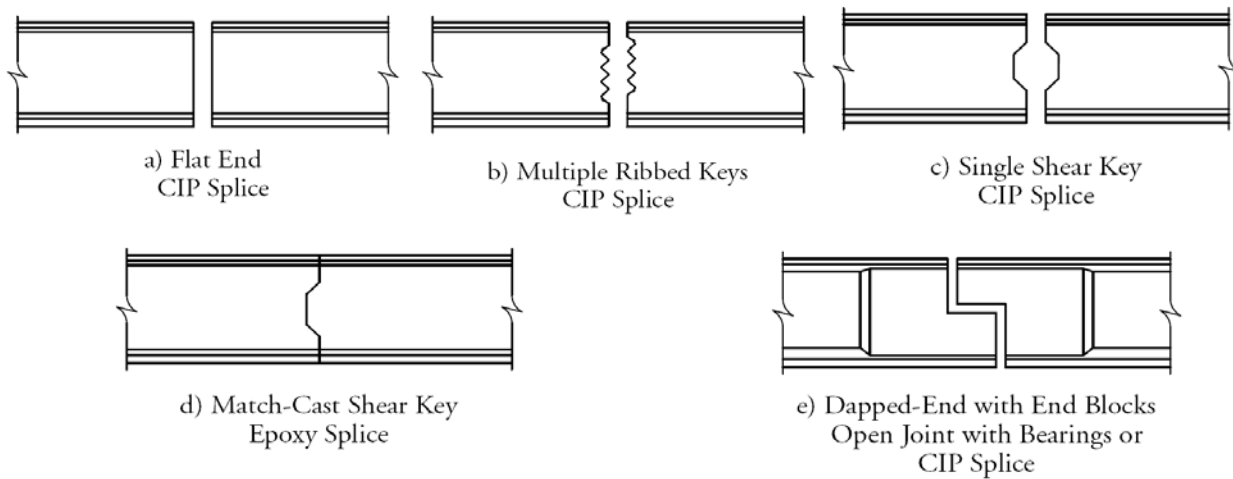
11.4.4 Details at Beam Splices

A wide variety of joint details have been used for splicing between beams. **Figure 11.4.4-1** shows some of the beam splice configurations used for I-beams.

EXTENDING SPANS

11.4.4 Details at Beam Splices/11.4.4.1 Cast-In-Place Post-Tensioned Splice

Figure 11.4.4-1
I-Beam Splice Configurations



Most precast concrete beam splices are cast-in-place as shown in **Figure 11.4.4-1a**, **-1b**, and **-1c**. Cast-in-place splices allow the designer more construction tolerances. These details use a gap width of from 6 to 18 in. or even 24 in. The space is filled with high-early-strength concrete. Detail **a** is not recommended, even when the end of the beam is roughened by sandblasting or other means, because the high vertical interface shear generally requires a more positive shear key system. Detail **d** is an epoxy-coated, match-cast joint. This detail is discouraged because of the difficulty in adequately matching two pretensioned beam-ends, especially when the beams are of different lengths and with different pretensioning levels. Detail **e** is used with continuous post-tensioning but is sometimes used when the designer desires to have an expansion joint in the bridge. For an expansion joint, the post-tensioning tendons are terminated at the joint. While this detail has been used very successfully for a number of bridges, it has not been used for most recent structures.

With proper mix designs and proportions, the required strength and quality of jobsite concrete can be achieved. Three-day concrete strengths in the range of 5.0 ksi can be achieved. It should be noted that more jobsite labor is needed for cast-in-place splices than for other splicing techniques, such as match-cast splicing.

11.4.4.1 Cast-In-Place Post-Tensioned Splice

Cast-in-place, post-tensioned splices are most commonly used because of their simplicity and their ability to accommodate fabrication and construction tolerances. The segments are erected on falsework, the ducts are coupled and post-tensioning tendons installed. Concrete for the deck slab may be placed at the same time as the concrete for the splice, or the deck concrete may be placed after the splice and following the first stage of post-tensioning. **Figure 11.4.4.1-1** shows details of a cast-in-place, post-tensioned splice.

EXTENDING SPANS

11.4.4.1 Cast-In-Place Post-Tensioned Splice

Figure 11.4.4.1-1
Cast-In-Place Post-Tensioned Splice

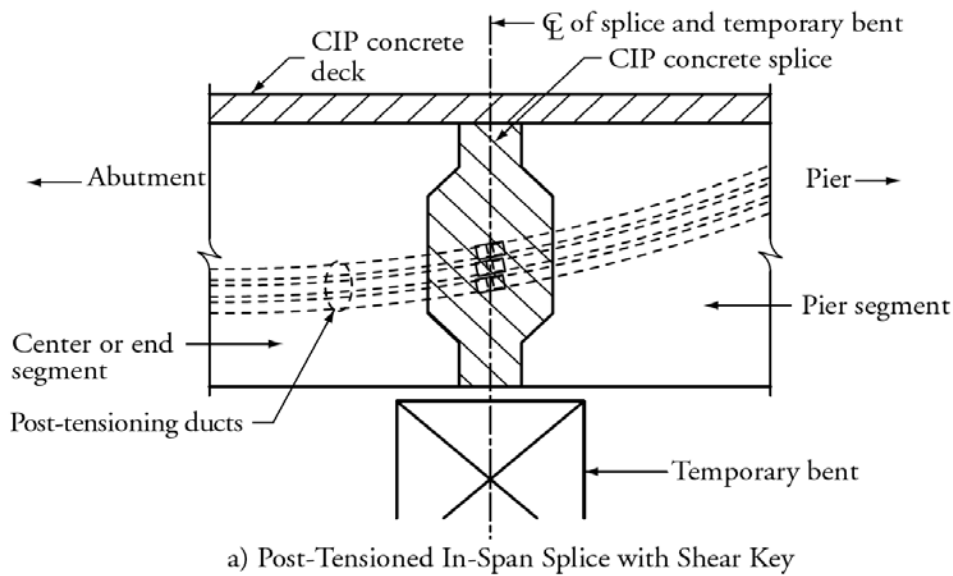


Figure 11.4.4.1-2 shows a typical splice during construction.

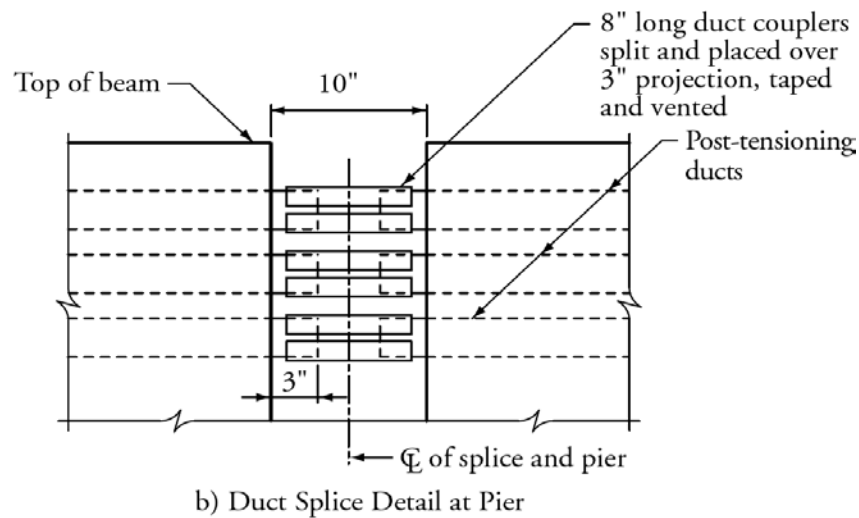
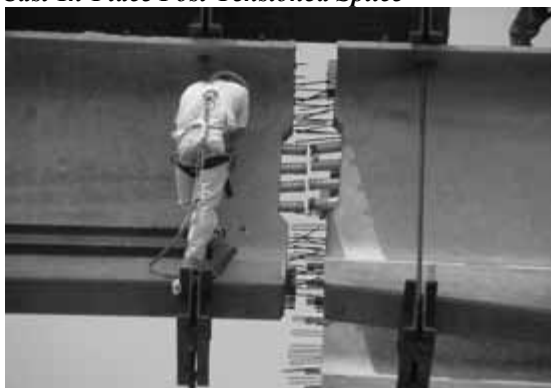


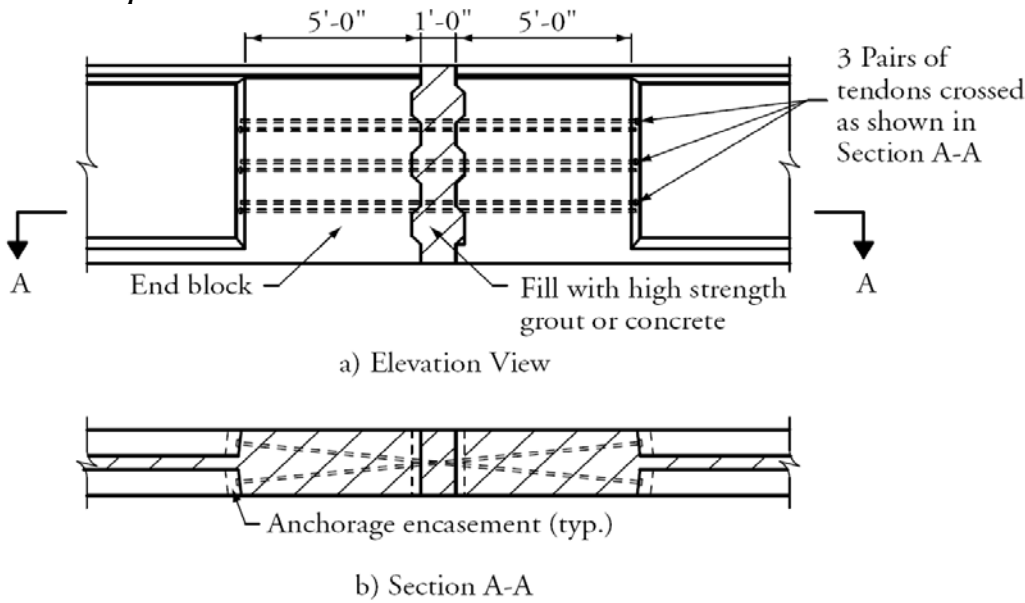
Figure 11.4.4.1-3
Cast-In-Place Post-Tensioned Splice



11.4.4.1.1 "Stitched" Splice

A schematic view of a "stitched" splice is shown in **Figure 11.4.4.1.1-1**.

*Figure 11.4.4.1.1-1
"Stitched" Splice*



A similar splice is shown during construction in **Figure 11.4.4.1.1-2**. The photo is of the Shelby Creek Bridge in Kentucky. The workman is tensioning a stitch tendon at the end of the widened end section. Grout ports are located near each tendon. This project used precast diaphragms that can be seen in the left foreground (See Caroland, et al., 1992).

*Figure 11.4.4.1.1-2
Stitched Splice in the Shelby Creek Bridge, Kentucky*



In this type of cast-in-place splice, the precast, pretensioned segments are post-tensioned across the splice using short tendons or threaded bars. It should be noted that precise alignment of the post-tensioning ducts is essential for the effectiveness of the post-tensioning. If proper alignment is not achieved, considerable frictional losses can

result. Oversized ducts are often used to provide additional tolerance. In addition, because of the short length of the tendons, anchor seating losses could be unacceptably large. To reduce anchor seating losses, the use of a power wrench to tension threaded bars is recommended.

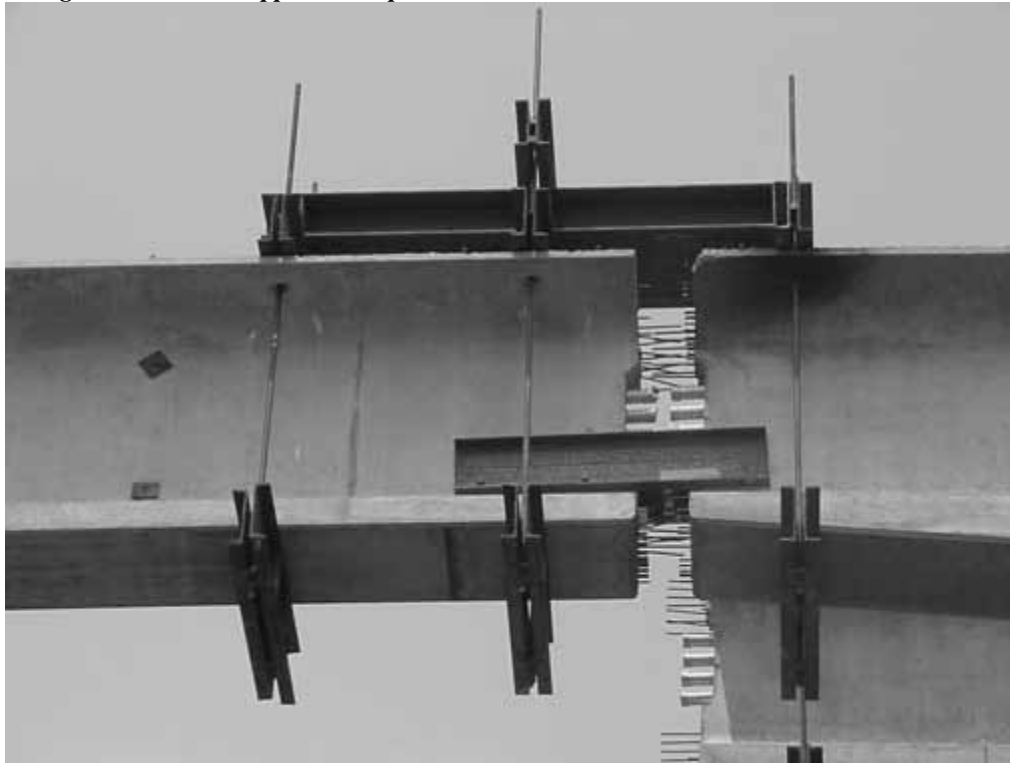
End blocks are required at the ends of the beams at each splice location in order to house the post-tensioning hardware and provide the "end zone" reinforcement to resist concentrated stresses due to the anchorages.

This type of splice may be suitable for long bridges where continuous tendon post-tensioning over the full length produces excessive friction losses.

11.4.4.1.2 Structural Steel Strong Back at Splice

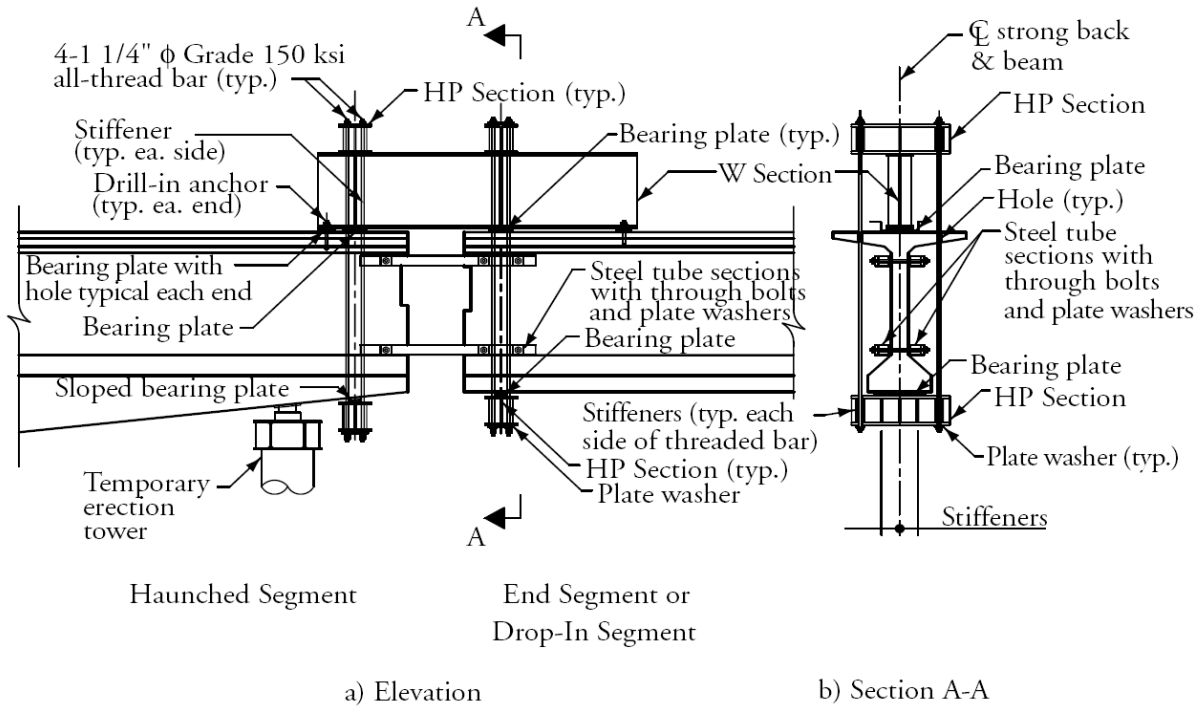
Some projects have used a removable structural steel "strong back" assembly in place of dapped ends or temporary support towers or falsework. **Figure 11.4.4.1.2-1** shows a strong back in use.

Figure 11.4.4.1.2-1
Strong Back Used to Support a Drop-in Beam



Structural steel strong backs are rigidly connected to the top of the "drop-in" or end segments. They are used to hang these segments from the cantilevered pier segments until the splice joint is cast and the beams are post-tensioned. The strong back is attached to the drop-in beam with threaded-rod yokes. It bears on the top of the end of the cantilevered pier segment. Additional supports are used across the joint at the webs to maintain alignment and to prevent the tendency of the cantilevered beam to roll under the weight of the drop-in segment. As for all joint details, alignment of the ducts is important. The strong back is removed after the joint is cast and the segments are post-tensioned together. This device is especially recommended for situations where falsework is not economical. It requires detailed structural design and careful erection due to the large forces involved. A typical detail is shown in **Figure 11.4.4.1.2-2**.

Figure 11.4.4.1.2-2
Strong Back at Splice



11.4.4.1.3 Structural Steel Hanger at Splice

Another device used to avoid falsework towers is a unique adaptation of the “Cazaly Hanger” used for many years in the precast industry. It employs steel shapes that are embedded in both ends of the beams at a joint. The embedments in the pier segment support the hangers that have also been embedded in the drop-in segment. This solution requires even more control of fabrication and erection tolerances, alignment of ducts, and care in construction. The details include “keepers” to assist with alignment and prevent dislodging the hangers from the seats. Additional alignment brackets are required on the webs to provide for stability as in the strong back details previously described. The use of this device is described by Caroland, et al. (1992). **Figure 11.4.4.1.3-1a** shows the large rectangular steel bars extending from pier beams in storage. At the project site, a steel “shoe” will be fitted over and pinned to these bars as shown in **Figure 11.4.4.1.3-1b**. The drop-in beams will sit on the shoe and will in turn be pinned to it.

Figure 11.4.4.1.3-1
Hanger Supports, Shelby Creek Bridge, Kentucky



a) Beam Segment with Hanger Bar



b) Beam Segments with Hanger Support Bars and Guide Shoes in Place

11.4.4.2 Match-Cast Splice

Match-cast segments were used in early applications of spliced beam bridges to eliminate the time and expense of cast-in-place joints. If segments are pretensioned, the segments will camber after release of prestress. When the segments camber, all match-casting is lost, no matter how the match-casting is done. This is the reason they are seldom used today. Match-casting of I- or other beam sections has significant challenges. Beams that are pretensioned and cast on a long-line system, as most are, have continuous pretensioning strands that must be cut before these products are removed from the form. That operation is usually facilitated by the use of “headers” that form the ends of beams. The space between headers is used to cut the strands.

Emulated match-casting has been used where a machined steel header provides precisely formed concrete surfaces. The header is precision-made in a machine shop to exacting tolerances. Installed in the casting bed, it has stubs to accurately position the ends of the post-tensioning ducts and access ports to allow cutting the strands that have been threaded through it.

Figure 11.4.4.2-1 shows the header in the form. **Figure 11.4.4.2-2** shows the resulting match-cast joint on a temporary support tower being compressed through the use of external threaded rods. The mating surfaces of the beams have been coated with epoxy.

Figure. 11.4.4.2-1
Fabrication of a Match-Cast Joint



a) Machined "Match-Cast" Header in Form



b) Close-Up of Header

Figure. 11.4.4.2-2
Match-Cast Joint Being Compressed During Installation



Other necessary details to consider include the following:

- Coupling of post-tensioning ducts. This requires the forming of small recesses around the duct where it meets the header.
- Sealing of the coupling zone against leakage of post-tensioning grout.
- Camber in the pretensioned beams that causes the ends to rotate. The rotation must be accounted for during fit-up of the beams at the joints as shown in **Figure 11.4.4.2-2**.

11.4.5 System Optimization

The main reason for segmenting and post-tensioning precast beams is to overcome the size and weight limitations for handling, shipping, and erection. For example, in a bridge with two spans of 180 ft, the beams can be produced and shipped in three 120-ft-long segments. These pieces are one segment on the pier located between two end segments.

For very long spans, the critical location is generally at the pier due to large negative moments or large shear forces. The beams at the pier may need to be deepened to accommodate these forces. This will result in a considerably heavier pier segment and, therefore, special planning and attention for production and transportation. Haunched pier beams are shown in storage in the manufacturing plant in **Figure 11.4.5-1**.

Figure 11.4.5-1
Haunched Pier Beams



Deepening the pier beam is but one choice available to the designer. This option should be carefully evaluated and compared to other options before a final decision is made on its use. Other options include the following:

- Placement of a cast-in-place bottom slab
- Gradual widening of a member toward the support
- Using higher concrete strength
- Adding compression reinforcement in the bottom flange
- The use of a hybrid system like that discussed in Section 11.4.2
- The use of a composite steel plate in the bottom of the bottom flange as discussed in the design example, Section 11.8.11.2.

11.4.5.1 Minimum Web Width to Accommodate Post-Tensioning

Web width should be as small as possible to optimize cross-section shape and minimize weight. Yet it should be large enough to accommodate a post-tensioning duct, auxiliary reinforcement, and minimum cover for corrosion protection.

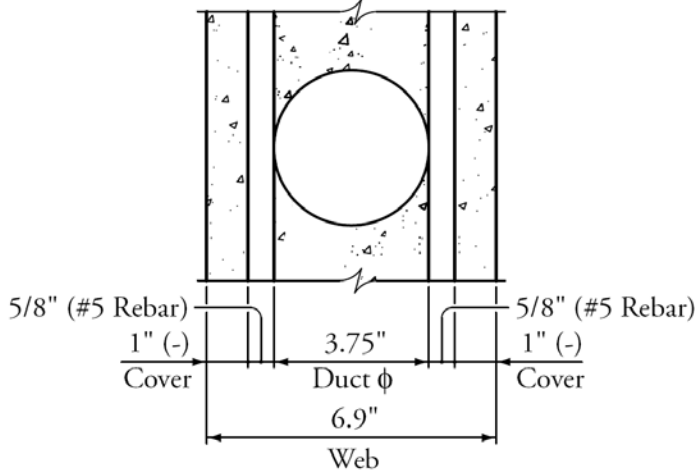
The requirements of the AASHTO specifications changed with the introduction of the *LRFD Specifications*. LRFD Article 5.4.6.2 states that the duct cannot be larger than 40% of the web width. Additionally, the designer is reminded to check the shear capacity. Traditionally, a reduction of 50% of the cross-sectional area of the duct is deducted for bonded tendons. This requirement has been traditionally used to size webs for internal ducts in segmental bridge construction. Historically, this requirement has not existed and has not been used for spliced I-beams. Editor's note: at the time of printing of this manual, which is current through the AASHTO 2011 Interims, it appears the AASHTO T-10 technical sub-committee for concrete design is considering a specification change that will modify this current practice for precast pretensioned straight spliced girders. If ratified, these provisions will be available in the 2013 code changes.

EXTENDING SPANS

11.4.5.1 Minimum Web Width to Accommodate Post-Tensioning

When the NU I-Beam was developed in the early 1990s, a 6.9-in. (175-mm)-thick web was selected to provide approximately 1-in. (25-mm) cover on each side plus two No. 5 (16-mm-diameter) vertical bars plus a 3.75-in. (95-mm)-diameter post-tensioning duct. The dimensions are shown in **Figure 11.4.5.1-1**.

*Figure 11.4.5.1-1
Web Configuration for NU I-Beam*



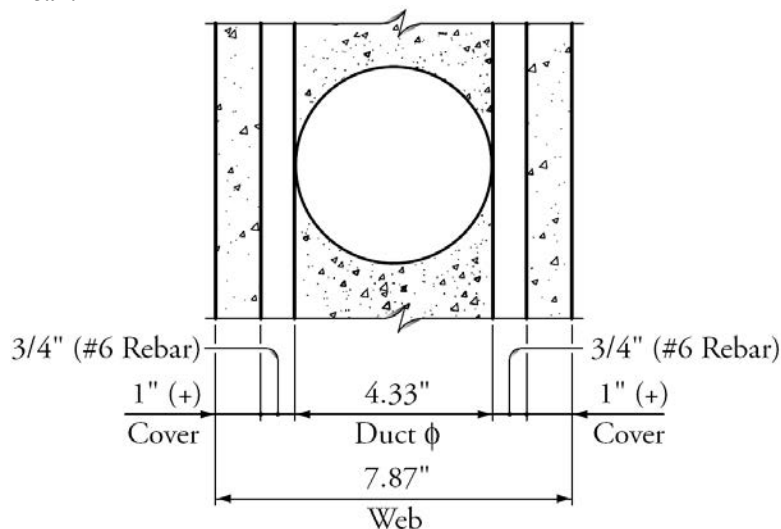
Another requirement of LRFD Article 5.4.6.2, and a requirement of the Post-Tensioning Institute (PTI) *Specifications for Grouting* (2003), is that the inside duct area be at least 2.5 times the tendon cross-sectional area for the “pull through” method of tendon installation and 2.0 times the tendon cross-sectional area for the “push through” method of tendon installation. The NU I-Beam duct diameter satisfied the minimum requirement of 2.5 times the tendon cross-sectional area for the standard fifteen 0.6-in.-diameter tendons used in Nebraska. The corresponding minimum inside duct area is calculated as $2.5(15)(0.217) = 8.14 \text{ in.}^2$. This corresponds to a required inside diameter of 3.22 in. These values have been the standard practice in Nebraska, backed up by significant experimental research and actual bridge applications.

The Washington State Department of Transportation (WSDOT) chose a web width of 200 mm (7.87 in.) for their new series of beams (Seguirant, 1998). This was derived as shown in **Figure 11.4.5.1-2**. The 4.33-in. duct can accommodate commercially available post-tensioning systems of up to nineteen 0.6-in.-diameter strands per tendon, or twenty nine 1/2-in.-diameter strands per tendon. The corresponding distance between the duct and the concrete surface of 1.77 in. is more than twice the maximum aggregate size of 3/4-in. used in Washington. A number of other states and Canadian provinces have adopted similar practices with no reported problems.

EXTENDING SPANS

11.4.5.1 Minimum Web Width to Accommodate Post-Tensioning/11.4.7.1 Splicing and Shoring Considerations

Figure 11.4.5.1-2
Web Configuration, Washington State
I-Beam



Eleven bridges were described in the PCI report on spliced girder bridges (PCI Committee on Bridges, 1992). Of those bridges, two had web widths of 6 in., five had web widths of 7 in., two had web widths of 7.5 in., and two had web widths of 8 in. None of the bridges had a web width that was more than 8 in. Many of the spliced straight I-beam bridges built over the past four decades have not met the limit of duct diameter and web width. Note that the two numerical examples in this chapter do not meet this LRFD requirement on the minimum web width either. However, this is not intended to encourage designers to violate the AASHTO LRFD and PTI Specification requirement. Also, there have been arguments on whether it affects bridge durability. If this requirement is not satisfied, it is important that the designers are aware of this requirement during the early phase of the design.

11.4.5.2 Pier Segments (Constant Depth and Haunched)

In situations where it is not possible to avoid a splice joint in the span, and prismatic constant depth pier segments are not adequate, haunched pier segments can be used effectively. For these haunched segments to be most efficient, Girgis, et. al. (2002) has shown that the haunch depth should be about 1.75 times the standard depth and the haunch length 20% of the span. Shallower depths or shorter lengths may have to be used, with less efficiency, to satisfy clearance criteria. Advantages to constant depth pier segments include conventional form casting and no requirement for massive bulkheads for pretensioning top strands. It can be economical for spans outside the range of prestressed girders, but shorter than required for haunch girders.

11.4.6 Design and Fabrication Details

Wet-cast splice joints are the standard practice. The ends of the beams at splices should have formed shear keys, if required, similar to those shown in **Figure 11.4.4.1-1**. Ducts for post-tensioning should be made of semi-rigid galvanized metal, high-density polyethylene (HDPE) or polypropylene (PP). They must be adequately supported within the beam during casting to maintain alignment and minimize friction losses.

11.4.7 Construction Methods and Techniques

11.4.7.1 Splicing and Shoring Considerations

In a conventionally reinforced or post-tensioned splice away from the piers, it is usually necessary to support the ends of both beam segments on temporary supports. For bridges over inaccessible terrain or for water crossings, structural steel strong backs like those described in Section 11.4.4.1.2 are commonly used to support one beam segment from another instead of using towers. A common solution for a three-span channel crossing is to use towers for the side spans, where land is accessible during construction and strong backs in the center span over the water.

EXTENDING SPANS**11.4.7.1 Splicing and Shoring Considerations**

Important factors to consider when deciding whether to use falsework to support the segments in place or to splice the segments on the ground include the following:

- Space at the site is needed to position the segments, cast the joints, and post-tension the beam.
- The assembled beam will be heavy and require larger cranes.
- Access for trucks and cranes.
- Falsework towers may need to be excessively tall.

The principal advantage of splicing on the ground versus in-place is the saving of the cost of falsework. On the ground, the splice is readily accessible by the workers and is close to material and equipment. The resulting improved labor productivity is an additional advantage. Splicing on the ground requires a large level area and temporary supports such as concrete pads. Segments need to be accurately aligned during splicing. **Figure 11.4.7.1-1** shows segments aligned, ducts spliced and reinforcement installed for splicing on the ground.

Figure 11.4.7.1-1
Segments Aligned for Splicing on the Ground



In-place splicing requires stiff falsework constructed with the capability to make adjustments for final elevations. **Figure 11.4.7.1-2** shows falsework supporting the ends of a pier beam and drop-in beam.

Figure 11.4.7.1-2
Segment Ends Supported on Falsework for Splicing



EXTENDING SPANS**11.4.7.1 Splicing and Shoring Considerations/11.4.7.2.2 Multiple Spans**

Precise vertical alignment of the beam segments is usually accomplished by the use of shims or screw jacks between the falsework and the segments. The major advantages of in-place splicing over splicing on the ground is that the beam segments are handled only once and require smaller lifting equipment. Additional assembly space at the site is not required.

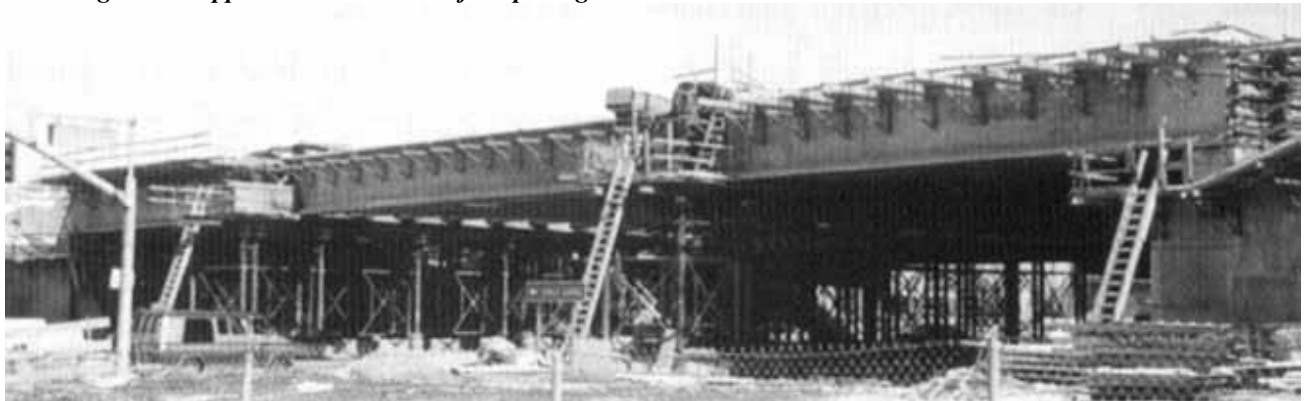
Some or all of the falsework requirements can be eliminated through the use of strong backs or hangers that are described in Sections 11.4.4.1.2 and 11.4.4.1.3.

11.4.7.2 Construction Sequencing and Impact on Design**11.4.7.2.1 Single Spans**

Single-span beams can be made-up of two or more segments. Using three segments as an example, as shown in **Figure 11.4.7.2.1-1**, the segments are installed on temporary towers and braced. Next, the splice joints are cast, tendons inserted in ducts, and post-tensioning applied, completing the assembly of the beam. Before the splice joints are cast, the end elevations of the segments need to be carefully positioned to allow for calculated long-term deflection. This also impacts the aesthetic appearance of the profile due to camber in the beam. These elevations also determine the amount of concrete needed for the haunches – the space between the top of the top flange and the bottom of the deck.

Figure 11.4.7.2.1-1

Three Segments Supported on Falsework for Splicing

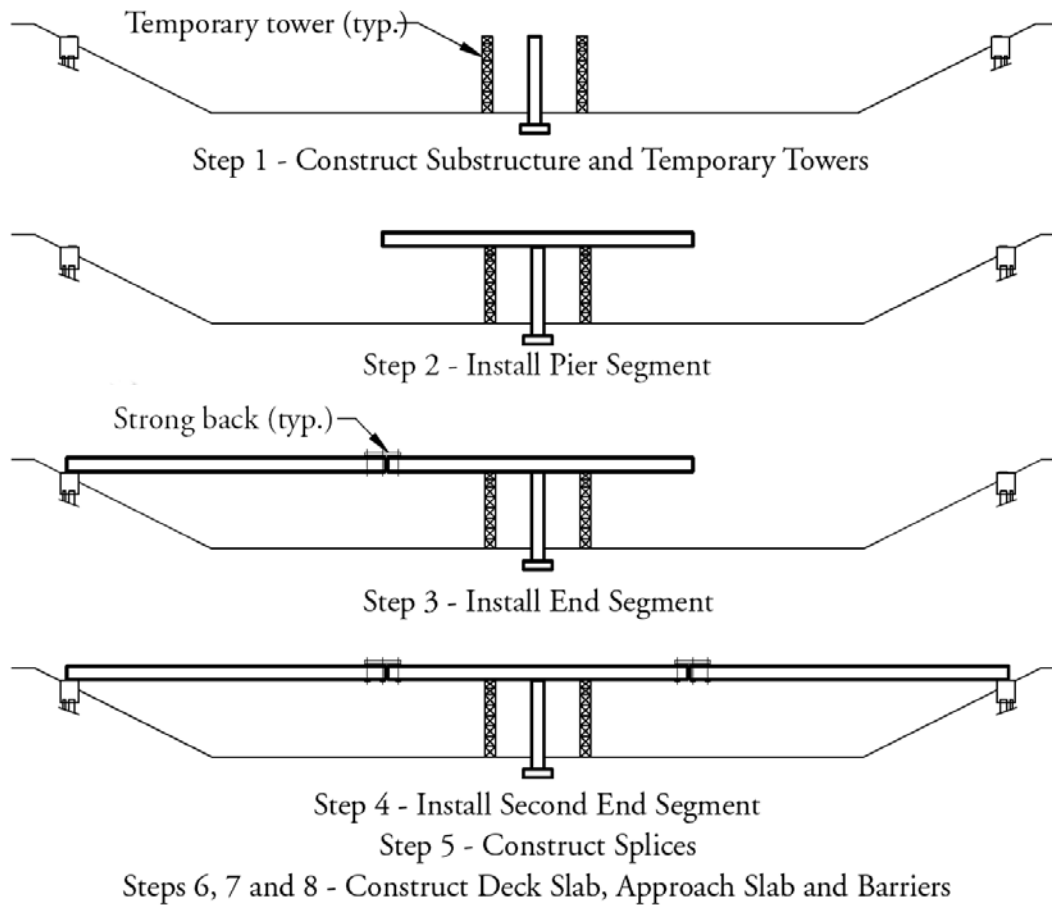


When the post-tensioning is applied, the full-span spliced beam cambers upwards and lifts up away from the temporary towers. The beam reactions that were being carried by the temporary towers are now carried by the spliced girder, so they must be considered in the analysis.

11.4.7.2.2 Multiple Spans

The same issues apply to multi-span spliced beams erected on temporary towers. **Figure 11.4.7.2.2-1** shows the erection sequencing of a two-span overpass where traffic does not allow for temporary towers at the splice joint.

Figure 11.4.7.2.2-1
Two-Span Bridge Construction Sequence



The pier segment is installed on the pier and adjacent towers and a connection is made to the pier. Ideally, for three or more span unit, the pier connection should be one that allows for horizontal displacement of the beam at the time of post-tensioning. However, a fully integral joint can be utilized as long as the supports at the abutment allow for horizontal movement during tensioning of the post-tensioning tendons.

Placement of the first end segment, as shown in Step 3 of **Figure 11.4.7.2.2-1**, creates moments in the pier segment and overturning effects on the tower and pier that must be evaluated. When an end segment is erected on the second span, the temporary overturning effect is reduced or eliminated. After the concrete in the splice has achieved the specified compressive strength and the post-tensioning tendons are stressed, the tower reactions must be considered as applied loads to the continuous two-span system. The balance of construction sequencing is as described earlier.

11.4.8 Grouting of Post-Tensioning Ducts

Grouting of the ducts after tensioning is a critical step in the construction process. Good workmanship in grouting ensures proper performance of the structure and longevity. Inadequate attention to grouting can lead to problems that can compromise the integrity of the bridge.

Grouting of ducts should be performed as soon as possible after completion of the post-tensioning. Leaving the tendons ungrouted for an extended period of time could cause accumulation of moisture and chlorides in coastal areas, and the onset of corrosion. Moisture accumulation in the ducts may result in water lenses and ultimately in air pockets that could compromise the durability of the system.

Specific grouts and grouting techniques must be strictly observed in order to achieve high-quality construction. For example, the grout must be flowable and must be pumped at a pressure high enough to displace the air in the ducts yet low enough to avoid cracking or blow-outs of the concrete cover over the ducts. Air vent tubes must be placed at strategic locations to prevent air encapsulation.

The grout mix generally contains a shrinkage compensating or an expansive admixture. Current recommendations are that the grout be the commercially-packaged type manufactured for this purpose. The current edition of the *PTI Specification for Grouting* (2003) should be followed.

Since proper grouting is such an important step in the construction process, it should be performed by experienced and well-qualified personnel. The American Segmental Bridge Institute (ASBI) has developed grouting training courses and a personnel certification program, which should be required. These will serve as important resources for good grouting practices.

11.4.9 Deck Removal Considerations

The removal of a bridge deck that has been in service has been a subject of concern among bridge owners who are interested in using spliced-beam and segmental box beam bridges. In the snow belt areas of the United States, due to the large number of freeze-thaw cycles and the liberal use of deicing chemicals, it has been common to expect that a bridge deck will deteriorate to the point of needing replacement in 20 to 30 years.

When the deck is in place when the beams are post-tensioned, it becomes an integral part of the resistance system. Removal of the deck for replacement may temporarily overstress the bare beam. This would require an elaborate analysis and possibly a complicated temporary support scheme until the new deck is in place. However, if properly analyzed and the economics are verified, there is no reason this approach should not be considered. Computing power and available software make this a viable alternative.

Some states have avoided this issue by requiring designers to apply the post-tensioning in its entirety before the deck is placed (Nebraska, 2001). An additional benefit of this single-stage post-tensioning is simplified scheduling and coordination of construction. It eliminates multiple mobilizations for specialized subcontractors.

However, there are significant benefits to multistage post-tensioning in terms of structural efficiency, compared with single-stage post-tensioning. A convenient option is to divide the post-tensioning into thirds: two-thirds applied to the bare beam and one-third applied to the composite section. This is demonstrated in the example in Section 11.8. There are a number of benefits to this division. The deck is subject to compression that controls transverse cracking and extends its "first" life before it might need replacement. The ratio of initial post-tensioning on the composite system to total post-tensioning, 0.33, is partially offset by the gain in concrete strength of beam and time-dependent prestress loss which is approximately 20%. Therefore, the beams would not be appreciably more overstressed than when initially post-tensioned.

It may be desirable to apply all of the post-tensioning after the deck becomes part of the composite section. This case would be similar to the conditions of a segmental box beam system where the top flange is an integral part of the cross-section when the post-tensioning tendons are stressed. This solution in the United States and abroad has proven to provide a deck surface of excellent durability, perhaps not requiring any provisions for deck removal and replacement. The position of the ASBI is to provide a small additional thickness of sacrificial concrete in the original deck that can be removed and replaced with a wearing overlay if chloride diffusion measurements warrant such action. However, if the designer wishes to do so, the analysis of deck removal and replacement as part of the original design of the bridge is entirely possible.

Analysis for deck removal and replacement generally requires use of a continuous beam computer program (Tadros, et al., 1977). First, concrete stresses in the deck at time of anticipated deck removal are calculated with due consideration of time-dependent effects. Then, analysis is performed on the continuous precast member due to two sets of loads: the deck weight reversed, and the deck stress resultants reversed. The resulting stress increments in the beam are then added to the stresses just before deck removal and the net values checked against maximum stress limits.

Deck removal and replacement is a temporary loading case requiring temporary measures. If the concrete tensile stress exceeds the stress limit, then one should check if there is enough reinforcement to control cracking. If concrete compressive stress exceeds the $0.6 f_c$ specification limit, then a temporary support may be required. A more practical approach would be that the designer consider waiving that limit temporarily if the resistance strength moment is greater than the factored load, i.e., required strength moment.

11.4.10 Post-Tensioning Anchorages/11.5.1 Eddyville-Cline Hill Section, Little Creek Bridges 1 thru 10, Corvallis-NewPort Highway, Ore.

11.4.10 Post-Tensioning Anchorages

Post-tensioning anchorages require the use of end blocks, which are thickened webs for a short length at the anchorages. End blocks can increase production costs of beams considerably due to the need for special forms and forming changes during production. I-beams with end blocks are also heavier to handle and transport, especially if the dimensions are selected according to LRFD Article 5.10.9.1. It states that the end block length should be at least equal to the beam depth and its width adequate to resist bursting stresses (generally these are taken to be at least equal to the smaller of the widths of the two flanges for Bulb Tee sections). End blocks are shown in **Figure 11.4.10-1** for an I-Beam section. The beam in the center shows the typical cross-section.

It is possible to use the cast-in-place diaphragm at the abutment to house the anchorage located there. This practice is used in the Pacific Northwest because of the availability of contractors experienced with cast-in-place, post-tensioned concrete. For regions where post-tensioning is not prevalent, it is preferred to have the anchorage hardware placed by the precast concrete producer in order to control quality, reduce contractor risk and reduce construction time. Post-tensioning anchorage zones are discussed further in Section 11.7.

*Figure 11.4.10-1
Beam End Block*



11.5 EXAMPLES OF SPLICED-BEAM BRIDGES

The PCI report on spliced-girder bridges (1992) contains information on some of the bridges that had been constructed during the preceding three decades. The following is a brief description of some additional notable bridges not contained in that report.

11.5.1 Eddyville-Cline Hill Section, Little Elk Creek Bridges 1 through 10, Corvallis-Newport Highway (U.S. 20), Oregon. (2000)

In 2000, the Oregon Department of Transportation (ODOT) completed 6.4 miles of U.S. 20 highway realignment between Corvallis and Newport. This two-lane section of highway is located 25 miles from the Pacific Ocean in the Coastal Mountain Range. The new alignment crosses the Little Elk Creek at 10 locations. The creek is environmentally sensitive and has a history of channel shifting during flood conditions; therefore, simple spans ranging from 99 to 184 ft were required to minimize stream impact and eliminate piers in the water.

ODOT selected a three-piece precast, post-tensioned, composite spliced-beam structure for four of the bridges that exceeded a span of 164 ft. **Figure 11.5.1-1** shows Bridge No. 7 upon completion. The roadway width is 46 ft and six lines of beams spaced at 7 ft-10 in. support an 8-in.-thick deck. The precast beam is the ODOT Bulb-I 2440

EXTENDING SPANS**11.5.1 Eddyville-Cline Hill Section, Little Creek Bridges 1 thru 10, Corvallis-NewPort Highway, Ore./11.5.2 Rock Cut Bridge, Stevens and Ferry Counties, Washington**

(BI96). The top and bottom flanges are 24 in. wide and the web is 7.5 in. thick. End blocks were incorporated at the abutment ends to receive the multiple post-tensioning anchorages. Up to five tendons with nineteen, ½-in.-diameter strands each were placed in the beam segments. The beams were supported at the abutments and on two temporary towers located at the third points. The post-tensioning tendons were spliced at the interior, 24-in.-wide closure pours. End diaphragms were cast followed by the deck placement. Post-tensioning was applied to complete the superstructure. Pretensioning was provided to control shipping stresses and to carry the non-composite loads. This method of construction allowed work to continue during critical in-water limitation periods and the project was completed one year ahead of schedule.

Figure 11.5.1-1
Bridge No. 7 over Little Elk Creek

**11.5.2 Rock Cut Bridge, Stevens and Ferry Counties, Washington (1997)**

The Rock Cut Bridge is a single span of 190 ft 6 in. spliced using three segments. It is shown after completion in **Figure 11.5.2-1**.

Figure 11.5.2-1
Rock Cut Bridge



EXTENDING SPANS**11.5.2 Rock Cut Bridge, Stevens & Ferry Counties, Wash./11.5.3 US 27-Moore Haven Bridge, Fla.**

The bridge consists of four, 7.5-ft-deep special beams and is 24.5 ft wide. Transportation difficulties, elimination of a center pier, and environmental restraints presented major design-construction challenges in a mountainous region of northeast Washington State. The restrictions imposed on constructing the new bridge were unusually severe. First, because it is located in an environmentally sensitive area, the surroundings were to be left as undisturbed as possible. Second, for environmental and structural reasons, no center pier (permanent or temporary) was allowed. Third, the route leading to the project site was along a highway with steep slopes and sharp bends. Therefore, even though a one-piece, 200-ft-long prestressed concrete beam was feasible, it was ruled out because such a long beam could not be transported along the winding highway.

The key to solving the problem was to divide the long beam into three, 63-ft-long beam segments with each segment weighing only 40 tons. The segments were fabricated and transported 150 miles to a staging area near the bridge site. There, the segments for each beam were precisely aligned, closures were cast, and post-tensioning tendons threaded and jacked. The fully-assembled beams were then carefully transported to the bridge site. At the site, the leading end of the beam was secured on a rolling trolley on a launching truss. Next, the transport vehicle backed the beam across the truss. When the leading end of the beam reached the opposite side of the river, the beam was picked up and set in place by cranes at both ends. All four beams were erected into final position using this method.

Using precast, prestressed concrete spliced beams for this bridge resulted in several benefits including a shortened construction time (3½ months), protection of the river environment, and cost savings due to constructing the bridge in one restricted construction season. This construction method resulted in a highly successful project. There was no pier in the water, no environmental issues were challenged by agencies, no construction delays occurred due to high water or weather, no stoppage occurred due to fishery constraints, and no special equipment or non-standard concrete strengths were needed. The total cost of the bridge was \$660,471 (\$141.50/ft²). The cost of the precast concrete portion of the project, which included production, transportation, installation, and post-tensioning prior to launching, amounted to \$229,482 (\$49.17/ft²). For more details, see Nicholls and Prussack (1997).

11.5.3 US 27-Moore Haven Bridge, Florida (1999)

The Moore Haven Bridge crosses the Caloosahatchee River. The bridge had record span lengths for a precast, prestressed concrete bridge at the time of its construction. The bridge consists of 11 total spans with a three-span continuous girder over the water. The original design of the three-span unit was steel with a total length of 740 ft and a total width of 105 ft. The main span is 320 ft. The redesign concrete structure is shown in **Figure 11.5.3-1**.

Figure 11.5.3-1
Moore Haven Bridge



EXTENDING SPANS

11.5.3 US 27-Moore Haven Bridge, Fla./11.5.4 Bow River Bridge, Calgary, AB

Each three-span continuous unit consists of five segments: two haunched beams, one center drop-in beam, and two end beams. The haunched beams are 138 ft long and vary in depth from 6.75 to 15 ft. The drop-in beam is 182 ft long and 8 ft deep. The end beams are 141 ft long and 6.75 ft deep. The beams were constructed in straight segments and made continuous using post-tensioning. Notable the splice girder portion of the bridge is located within the horizontal curve.

11.5.4 Bow River Bridge, Calgary, Alberta (2002)

The Bow River Bridge is 774 ft long. It is shown during construction in **Figure 11.5.4-1**.

Figure 11.5.4-1
Bow River Bridge during Construction



The twin structures consist of four spans: two at 174 ft long and two at 213 ft. The project is described by Bexten, et al. (2002). The precast concrete alternative provided a cost savings of about 10% over the steel plate beam option. This bridge marked the first time a single piece, 211-ft-long beam weighing 268,000 lb spanned the entire distance between permanent pier supports without use of spliced I-beams, intermediate splice joints, or temporary falsework towers. Another source of economy was the relatively wide beam spacing of 11.65 ft. This spacing resulted in fewer beam lines despite the relatively long spans and the uncommonly heavy live loading mandated in Alberta due to the heavy hauling demands of its oil refinery industry. The maximum live load moment in Alberta bridge design practice is significantly larger than the moment resulting from the AASHTO specifications.

An NU 2800 beam with a depth of 9.2 ft and a web width of 6.9 in. was used for the 213-ft-long span. The thin web is one of the important reasons for the minimized beam weight and increased span efficiency. The beam is shown in transit in **Figure 11.5.4-2**.

Figure 11.5.4-2
Transportation of the 211-ft-Long Bow River Beam



The largest NU 2800 bridge beam used prior to this project was part of the spliced beam Oldman River Bridge, also in Alberta, which was completed a year earlier. It had a length of 188.6 ft and weighed 240,000 lbs. The Oldman River Bridge, however, utilized pier segments and jobsite-cast joints to span the 230 ft interior spans of the five-span bridge (180, 230, 230, 230, and 180 ft).

EXTENDING SPANS**11.5.4 Bow River Bridge, Calgary, AB/11.6.2.1 Friction Loss**

The Bow River Bridge beams were pretensioned for lifting, shipping, and erection. They were checked for top flange buckling during each of these stages. The stability analysis methods given in Section 8.10 were utilized. A steel stiffening truss was used in the center 100 ft section of the beams and a special lifting device that allowed shifting of the lifting point several feet above the top flange were some of the measures taken to assure safety during beam handling. At the site, the first beam erected in each span was braced to the top of the pier. After erection of the second beam, structural steel diagonal bracing diaphragms were placed between the first and second beams, which provided the necessary stability for both.

After erection, the beams were post-tensioned using four tendons, each with twelve 0.6-in.-diameter strands, placed in 3-in.-diameter ducts. One tendon was stressed prior to placing the deck making the beams continuous for deck weight. The remaining tendons were post-tensioned following placement of the deck.

11.6 POST-TENSIONING ANALYSIS

11.6.1 Introduction

Several issues related to the analysis and design of post-tensioned beams differ significantly from those for pretensioned beams. These include the following:

- Losses in post-tensioning tendons. Additional sources of prestress losses must be considered such as friction and anchorage losses.
- Interaction of losses between pretensioned strands and post-tensioned tendons.
- Time-dependent analysis. The method of analysis should take into account the effects of creep and shrinkage of concrete and relaxation of steel. This analysis is only applicable to statically indeterminate structures.
- Effect of post-tensioning on continuous beams. The method of analysis should properly account for post-tensioning, including secondary moments.
- Effect of post-tensioning ducts on shear capacity.

These issues are discussed in this section. Chapter 8 provides a detailed discussion of prestress losses and deflections. In this chapter, only friction and anchorage set losses are discussed, which are unique to post-tensioning.

Other issues that are significant in the design and analysis of post-tensioned beams include the following:

- Methods used to show post-tensioning on plans. Some jurisdictions indicate the centroid of the group while others illustrate each tendon.
- Analysis and design of anchorage zones. The design must include consideration of potential conflicts between the anchorage hardware with its accompanying reinforcement and other reinforcement in the anchorage zone.
- Estimation of deflection, camber, and end rotation of beams with multiple construction stages.
- Web thickness to accommodate ducts.
- Difference between the center of gravity of the duct and the tendon.
- Flexural strength for post-tensioned tendons.

Information on some of these subjects can be found elsewhere in this chapter, including the design examples. Additional information can be found in texts that discuss design of post-tensioned structures. An additional resource regarding the use of post-tensioning in precast, prestressed concrete beams is NCHRP Report 517 (Castrodale and White, 2004). This document includes an extensive discussion of issues and three design examples related to spliced beam construction.

11.6.2 Losses at Post-Tensioning

11.6.2.1 Friction Loss

In the design of post-tensioned structures, the designer ordinarily provides in the contract plans the geometry of a tendon path and the required design forces at one or more locations along the path. This allows the contractor to select the post-tensioning system and procedures that lead to the best economy for the project without neglecting safety.

EXTENDING SPANS**11.6.2.1 Friction Loss/11.6.2.3 Design Example**

The first step in analyzing a tendon is to plot a diagram of the stress or force along the tendon path. When a tendon is jacked from one or both ends, the stress along the tendon decreases away from the jack due to the effects of friction. The loss of stress may be expressed by the following equation:

$$\Delta f_{pF} = f_{pj} (1 - e^{-(Kx + \mu\alpha)}) \quad [\text{LRFD Eq. 5.9.5.2.2b-1}]$$

where

f_{pj} = stress in the prestressing tendon at jacking

e = base of naperian logarithm

x = length of a prestressing tendon from the jacking end to any point under consideration, ft

K = wobble friction coefficient, typically about 0.0002/ft for rigid and semirigid galvanized metal ducts [LRFD Table 5.9.5.2.2b-1]

μ = coefficient of friction due to local deviations from tendon path, typically about 0.2/radian for rigid and semi-rigid galvanized metal sheathing and polyethylene ducts [LRFD Table 5.9.5.2.2b-1]

α = sum of the absolute values of angular change of post-tensioning tendon from jacking end, or from the nearest jacking end if tensioning is done equally at both ends, to the point under investigation, radians

11.6.2.2 Anchorage Set Loss

Anchorage set loss of prestress occurs in the vicinity of the jacking end of post-tensioned members as the post-tensioning force is transferred from the jack to the anchorage block. During this process, the wedges move inward as they seat and grip the strand. This results in a loss of elongation and therefore force in the tendon.

The value of the strand shortening, generally referred to as anchorage set, ΔL , varies from about 0.125 to 0.375 in. It depends on the anchorage hardware and jacking equipment. An average value of 0.25 in. may be assumed in design with the stipulation on the plans that the post-tensioning contractor is to verify the accuracy of this assumed value and appropriate adjustment be made to the expected force and elongation.

The anchor set loss is highest at the anchorage. It diminishes gradually due to friction effects as the distance from the anchorage increases. Anchorage set loss is more significant in shorter tendons. On very short tendons, the anchorage set loss can be nearly as high as the initial tendon elongation. Therefore, the initial prestress could be ineffective.

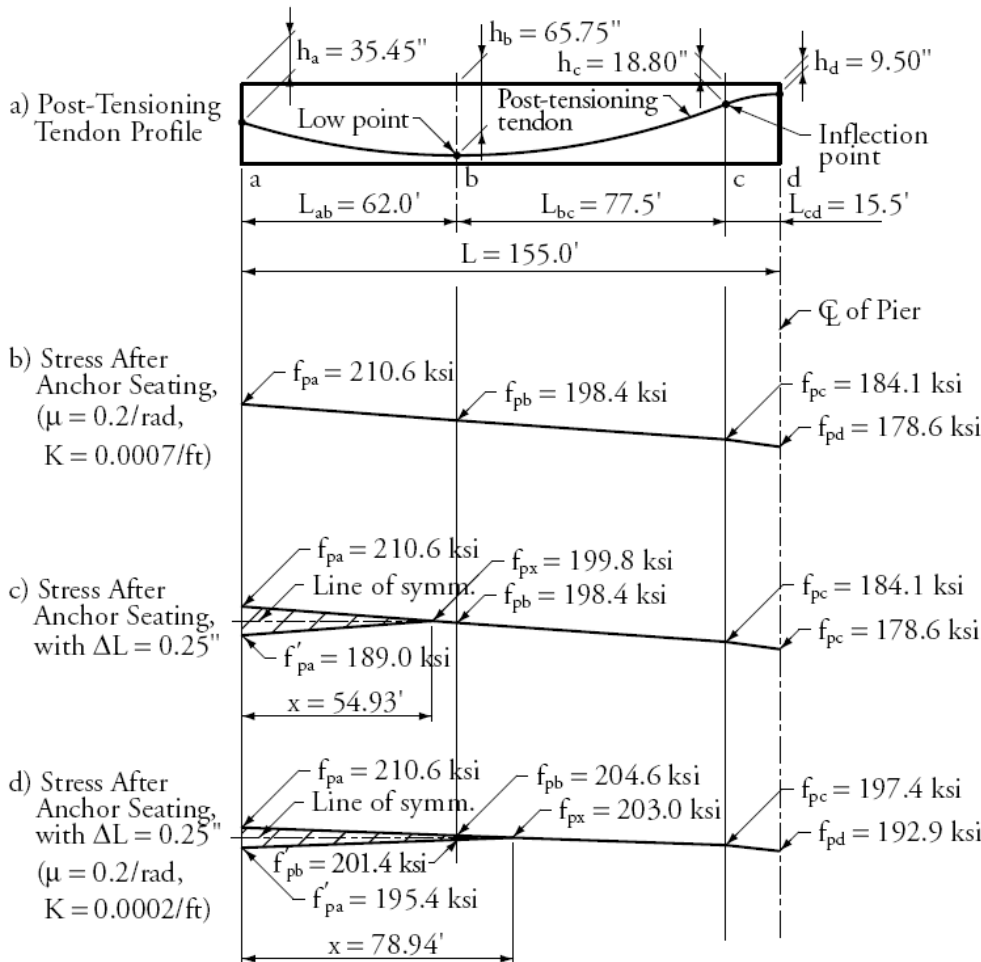
11.6.2.3 Design Example

Calculation of friction and anchorage set losses is best demonstrated by an example.

Figure 11.6.2.3-1a shows the elevation of the end span of a multispan beam. Its length is 155 ft. The tendon profile consists of three segments, L_{ab} , L_{bc} , and L_{cd} with three different curvatures.

A jacking stress, $f_{pa} = 0.78f_{pu} = 210.6$ ksi is often used for design. A curvature coefficient $\mu = 0.20$ /radian, and a wobble coefficient, $K = 0.0007$ /ft are assumed. The value of K in this part of the example is significantly overestimated for simpler presentation of the anchor set loss. The typical value is 0.0002/ft as stated in Section 11.6.2.1.

Figure 11.6.2.3-1
Anchor Set Loss



11.6.2.3.1 Friction Loss

The stress values before seating can be calculated by applying LRFD Eq. 5.9.5.2.2b- 1 for each of the three segments. The results are as follows:

- Strand stress at location b, $f_{pb} = 198.4$ ksi
- Strand stress at location c, $f_{pc} = 184.1$ ksi
- Strand stress at location d, $f_{pd} = 178.6$ ksi

For this reason, the stress diagram before accounting for anchor set loss, shown in **Figure 11.6.2.3-1b**, consists of three linear segments. The slope of each segment is partly a function of the tendon curvature as discussed in Section 11.6.2.1.

11.6.2.3.2 Anchor Set Loss

The hatched area in **Figure 11.6.2.3-1c** and **11.6.2.3-1d** represent the drop in tendon stress over the affected beam length, x , after the post-tensioning tendon is anchored. This total length may be shorter than L_{ab} or as large as the beam length between anchorages. After seating, the highest stress will be at the right end of the hatched area. The stresses before seating and after seating are symmetrical about a horizontal line passing through f_{px} , the tendon stress at distance, x . This symmetry results from the fact that friction effects are equal in both directions, i.e., as the tendon is being pulled out of the beam during stressing, or pulled back into the beam during seating of

EXTENDING SPANS

11.6.2.3.2 Anchor Set Loss/11.6.2.3.2.2 Length Affected by Seating is Within L_{ac}

the anchorage. Since the distance, x , is not yet known, it is best calculated by numerical iteration until the following condition is satisfied:

$$\Delta L = \text{hatched area}/E_p \quad (\text{Eq. 11.6.2.3.2-1})$$

11.6.2.3.2.1 Length Affected by Seating is within L_{ab}

First, assume that x , measured from point a , is equal to $L_{ab} = 62$ ft. Dividing the hatched area in **Figure 11.6.2.3-1c** by the steel modulus of elasticity, $(210.6 - 198.4)(62)(12)/28,500 = 0.318$ in. which is greater than the assumed $\Delta L = 0.25$ in. Thus, the length affected by seating is within L_{ab} , and therefore the hatched area is bounded by straight lines.

In this case, a closed form solution is possible using the below equation or Eq. 11.6.2.3.2-1:

$$x = \sqrt{\frac{\Delta L(E_p)(L_{ab})}{(f_{pa} - f_{pb})}} \quad (\text{Eq. 11.6.2.3.2.1-1})$$

Substituting for ΔL , f_{pa} , f_{pb} , E_p , and L_{ab} , the values 0.25 in., 210.6 ksi, 198.4 ksi, 28,500 ksi, and 62 ft respectively, x is found to be = 54.93 ft, which is less than 62 ft as expected. The corresponding anchor set loss, Δf_{pA} , is:

$$\Delta f_{pA} = \frac{2(f_{pa} - f_{pb})(x)}{L_{ab}} \quad (\text{Eq. 11.6.2.3.2.1-2})$$

Substituting the value of $x = 54.93$ ft, $\Delta f_{pA} = 21.6$ ksi, see **Figure 11.6.2.3-1c**.

Therefore

$$f_{px} = f_{pa} - 0.5 \Delta f_{pA} = 210.6 - 0.5(21.6) = 199.8 \text{ ksi} \leq 0.74 f_{pu} = 199.8 \text{ ksi} \quad (\text{LRFD Table 5.9.3-1})$$

and

$$f'_{pa} = f_{pa} - \Delta f_{pA} = 210.6 - (21.6) = 189.0 \text{ ksi} \leq 0.70 f_{pu} = 189.0 \text{ ksi} \quad (\text{LRFD Table 5.9.3-1})$$

11.6.2.3.2.2 Length Affected by Seating is Within L_{ac}

To illustrate the case where the length affected by seating is greater than the distance to the low point in the tendon profile L_{ab} (hatched area longer than 62 ft), the example will be reworked with $\mu = 0.20/\text{radian}$ and $K = 0.0002/\text{ft}$, which are the typical values according to LRFD Table 5.9.5.2.2-1. With these values, f_{pb} , f_{pc} , and f_{pd} can be found to be equal to 204.6, 197.4, and 192.9 ksi, respectively.

In this case, two quantities are unknown: x and Δf_{pA} . An iterative procedure will be used to reach a solution.

The first condition is that the stress diagrams before and after seating are symmetrical about a horizontal line passing through f_{px} , therefore:

$$\Delta f_{pb} = \frac{2(f_{pb} - f_{pc})(x - L_{ab})}{L_{bc}} \quad (\text{Eq. 11.6.2.3.2.2-1})$$

$$\Delta f_{pA} = 2(f_{pa} - f_{pb}) + \Delta f_{pb} \quad (\text{Eq. 11.6.2.3.2.2-2})$$

The second condition is that the hatched area divided by the steel modulus of elasticity is equal to the anchor seating, ΔL :

$$\Delta L = \frac{1}{E_p} \left[\frac{1}{2} (\Delta f_{pA} + \Delta f_{pb})(L_{ab}) + \frac{1}{2} (\Delta f_{pb})(x - L_{ab}) \right] \quad (\text{Eq. 11.6.2.3.2.2-3})$$

With x assumed equal to L_{ab} , the first estimate of Δf_{pA} , using Eq. (11.6.2.3.2.2-2), is 12 ksi. Substituting this value in Eq. (11.6.2.3.2.2-3) gives a tendon shortening of 0.16 in., which is less than the assumed value of 0.25 in.

The next iteration would be to try $x = L_{ab} + L_{bc}$. The corresponding tendon shortening using this value is 0.76 in., which is greater than 0.25 in. Since the two computed values bracket the assumed value, values of x between the above two limits are tried until a solution is found. The use of spreadsheet software simplifies this iteration. The

EXTENDING SPANS**11.6.2.3.2 Length Affected by Seating is Within L_{ac} /11.6.4 Equivalent Loads for Effects of Post-Tensioning**

results of the iteration are $x = 947.25$ in. (78.94 ft) and $\Delta f_{pa} = 15.2$ ksi. This corresponds to stress at point a of $(210.6 - 15.2) = 195.4$ ksi, stress at point b of $[204.6 - (15.2 - 12.0)] = [204.6 - 3.2] = 201.4$ ksi, and stress at distance x of $(204.6 - 3.2/2) = 203.0$ ksi. **Figure 11.6.2.3-1d** shows the tendon stress diagram for this case.

As noted in the previous section, the *LRFD Specifications* limit tendon stresses f'_{pa} and f'_{px} after seating. The stress f'_{pa} at point a exceeds the limit by 6.4 ksi, while the stress, f'_{px} at point x exceeds the limit by 3.2 ksi. Therefore, tendon stress at point a governs and the initial jacking stress must be reduced by approximately 6.4 ksi. The required maximum jacking stress is therefore $(210.6 - 6.4) = 204.2$ ksi. The tendon stress should be recomputed using this new jacking stress, resulting in the entire tendon stress diagram being lowered by approximately 6.4 ksi.

11.6.2.4 Elastic Shortening Loss

Post-tensioned beams are typically post-tensioned sequentially using one multi-strand tendon jack. It is not generally economical to tension more than one tendon at a time. When the first tendon is tensioned, it is anchored at the end of the beam. Tensioning of subsequent tendons in the same beam, and to some extent moving across the bridge width (if the deck has been cast before the tendons are stressed), causes the concrete along with previously tensioned tendons to shorten. This sequential elastic shortening loss is highest in the first tendon tensioned. There are formulas in the *LRFD Specifications* to estimate the average elastic shortening loss in this situation. A second round of tendon tensioning to restore the original tensile stress in the tendons may substantially eliminate the losses due to sequential shortening, but it is generally not required.

11.6.3 Time-Dependent Analysis

There are differing approaches to complex concrete bridge design. Some believe it is unwarranted to spend a considerable amount of time and resources to model spliced I-beam bridges with sophisticated finite-element, time-dependent programs. There is limited advantage in calculating in detail the effects of differential creep and shrinkage and the effects of temperature gradients, compared to the practice used with conventional, non-post-tensioned I-beam systems when selecting appropriately conservative creep and shrinkage values.

Some commercial computer programs that include time-dependent analysis are based on European creep and shrinkage prediction formulas. These spliced-beam programs tend to follow programs developed for segmental box beam bridges. Time-dependent analysis will pickup problems with differential shrinkage between deck and girder that other approaches miss. Most time-dependent analysis programs also include time-stepped construction with supported added then removed. This accounting process is much more reliable if the program accounts for the changes internally. Friction and anchor set losses are included in these programs.

11.6.4 Equivalent Loads for Effects of Post-Tensioning

In a pretensioned beam, when the prestress force is transferred from the strands to the concrete, it causes the member to camber and become supported at its ends. The beam acts as a simply-supported member. At any section, the effect of the prestress is an axial force equal to the effective prestress force and a bending moment equal to the product of the effective prestress force and its eccentricity. Because the member is statically determinate, the support reactions due to prestressing are zero. The end reactions are caused only by member weight. The same is true for a simple span, post-tensioned beam.

For continuous members, post-tensioning is usually introduced at the construction site. Because the continuous member is statically indeterminate at the time of post-tensioning, its support reactions are affected by the deformations of the beam. The member cannot camber freely as the post-tensioning tendons are stressed.

Support reactions caused by the restrained deformations due to post-tensioning result in additional moments called "secondary" moments. There are secondary shears as well, but usually not additional axial forces, unless the member is restrained by the supports against axial deformation. The term "secondary" is somewhat misleading. The effects are called "secondary" only because they are caused as the result of another effect – the post-tensioning of the beam. The effect of the secondary moments may not be minor as could be implied by the term, because it is conceivable that the secondary moment at the intermediate support of a two-span bridge could totally offset the primary moment caused by post-tensioning. This would result in a uniform stress at that location equal to P/A , where A is the cross-sectional area of the member.

EXTENDING SPANS

11.6.4.1 Conventional Analysis Using Equivalent Uniformly Distributed Loads

11.6.4.1 Conventional Analysis Using Equivalent Uniformly Distributed Loads

A common approach to evaluate secondary moments due to post-tensioning, is to model the effect of the post-tensioning tendon as a series of equivalent uniformly distributed loads. **Figure 11.6.4.1-1** shows the required equations for calculation of the equivalent loads for a typical end span of a post-tensioned beam.

Figure 11.6.4.1-2 shows one span of a two-span continuous bridge beam.

Figure 11.6.4.1-1
Post-Tensioning Equivalent Loads for Two-Span Continuous Bridge

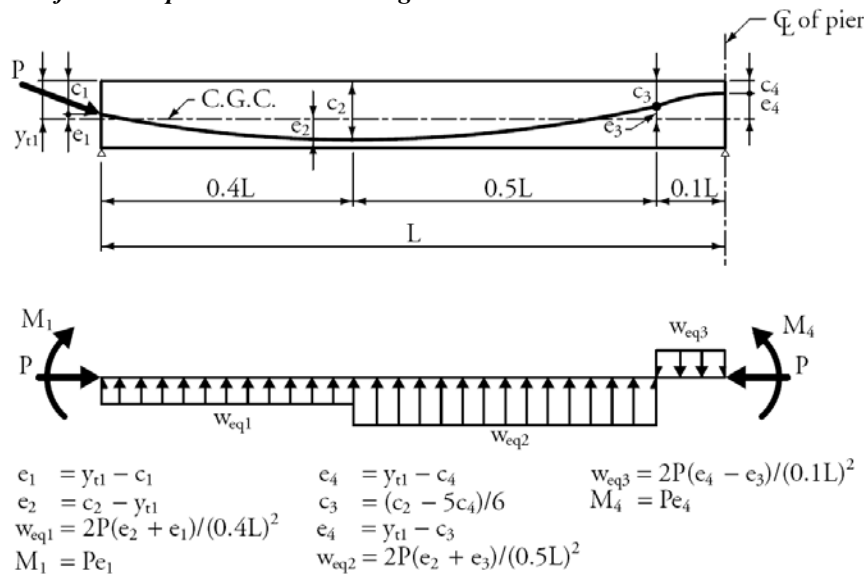
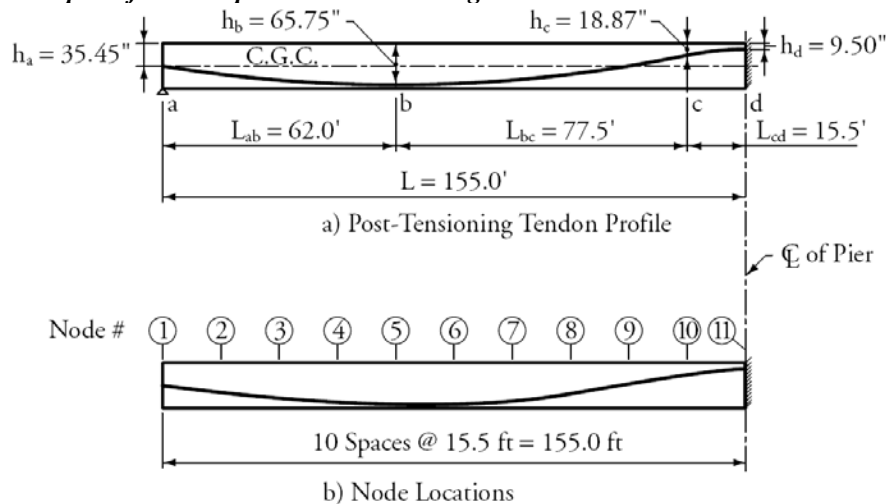


Figure 11.6.4.1-2
One Span of a Two-Span Continuous Bridge



The two spans are equal, 155 ft. The beam depth is 72 in. and the centroidal distance from the top fiber, 35.45 in. The span is divided into 10 segments with 11 nodes. The eccentricities at Nodes 5, 10, and 11, at $0.4L$, $0.9L$, and $1.0L$, are given, based on available concrete cover at the lowest and highest points, and on a common tangent of the curves connected at Node 10. Note that although the $0.9L$ node is commonly used as the inflection point for the tendon as it approaches the pier location ($1.0L$), it may not be the optimal location in terms of overall effects of post-tensioning. The designer may wish to investigate other locations. The geometric properties of the curves between Nodes 1 and 5, 5 and 10, and 10 and 11, are used to determine the tendon eccentricities at the remainder

EXTENDING SPANS

11.6.4.1 Conventional Analysis Using Equivalent Uniformly Distributed Loads

of the nodes. If the curve is a parabola, as is usually assumed, the relationship, $y = ax^2$, can be used. The distance, y , is the height above the lowest point or below the highest point, and x is the horizontal distance from that point. The eccentricities at all 11 nodes for the example have been calculated and are shown in **Table 11.6.4.1-1**.

Table 11.6.4.1-1 shows the post-tensioning stresses at each node after accounting for friction and anchor set losses. The average post-tensioning tendon stress along the length of the span is 184.7 ksi. Assuming the area of post-tensioning tendons is 4.34 in.², which corresponds to a twenty 0.6 in.-diameter strand tendon, the average post-tensioning force is equal to 801.5 kips. Using this average force, equivalent loads are calculated according to **Figure 11.6.4.1-1**. The loads are then input into a continuous beam analysis computer program to obtain the total moments due to post-tensioning. For the analysis of this particular example, only one span needs to be modeled due to symmetry. The support at point 'a' is assumed to be restrained against vertical movement only, while the support at point 'd' is fully restrained due to symmetry. The secondary moments are the difference between the primary and the total moments. The total, primary, and secondary moments using this method are shown in **Table 11.6.4.1-1**.

This approach is appropriate only if the effective prestress force is relatively constant along the entire beam length. However, friction and anchor set losses in large multi-strand tendons, which are generally used in bridge applications, may cause the variation in post-tensioning force over the member length to be as high as 30%. Thus, assuming constant P and uniform equivalent loads may be only appropriate in preliminary design.

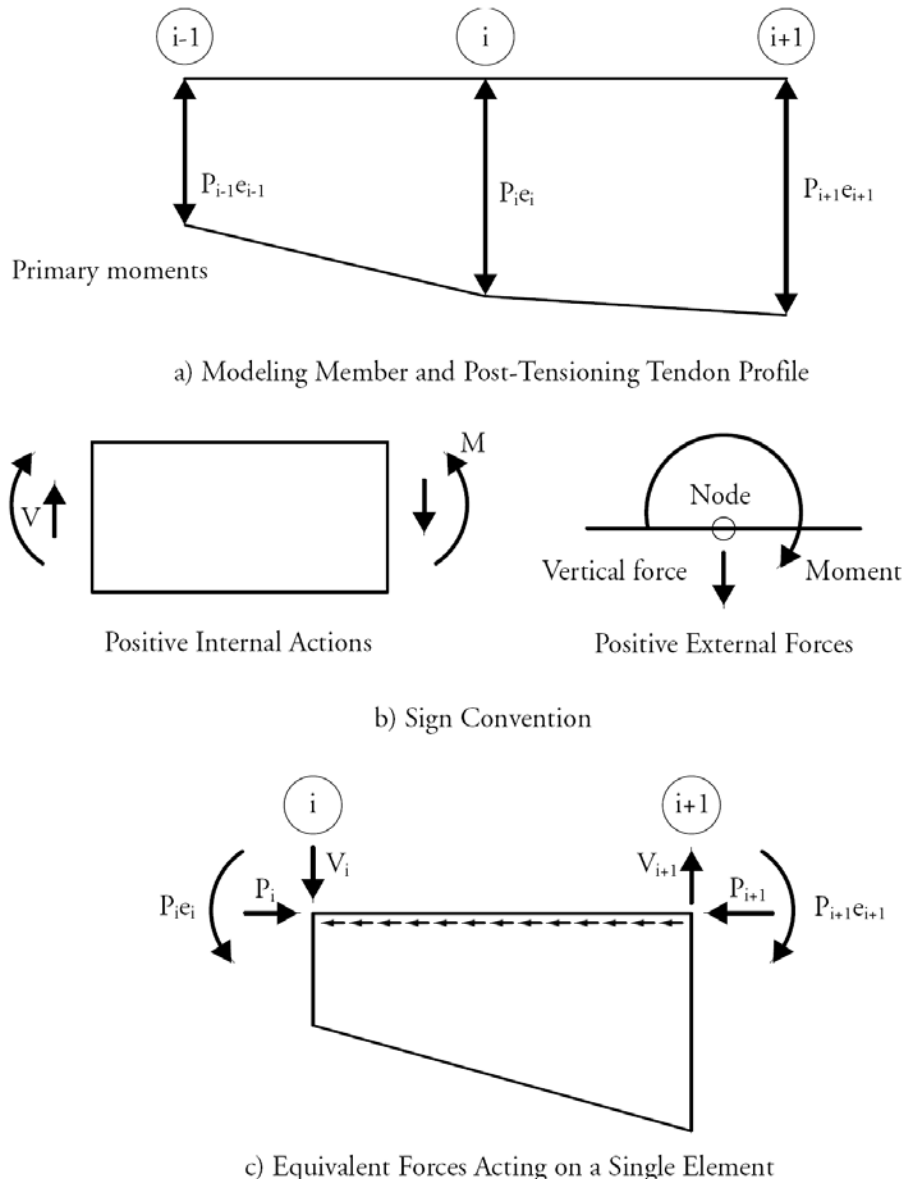
Table 11.6.4.1-1
Post-Tensioning Effect—Approximate Method

Node No.	1	2	3	4	5	6	7	8	9	10	11
Distance from Left End, in.	0	186	372	558	744	930	1,116	1,302	1,488	1,674	1,860
Tendon Eccentricity in.	0.00	-13.26	-22.73	-28.41	-30.30	-28.43	-22.80	-13.43	-0.30	16.58	25.95
Post-tensioning Stress, ksi	181.4	182.9	184.4	185.9	187.4	188.3	187.7	186.3	184.8	183.4	178.9
Equivalent Loads:											
Vertical Force kips/ft	1.05	1.05	1.05	1.05	1.05	0.31	0.31	0.31	0.31	-5.21	-5.21
Moment in.-kips	0	0	0	0	0	0	0	0	0	0	-20,798
Total Moment in.-kips	0	-9,456	-15,969	-19,538	-20,163	-17,859	-12,638	-4,501	6,552	20,520	28,660
Primary Moment in.-kips	0	-10,625	-18,214	-22,767	-24,285	-22,782	-18,274	-10,760	-240	13,285	20,798
Secondary Moment in.-kips	0	786	1,572	2,358	3,145	3,931	4,717	5,503	6,289	7,075	7,862

11.6.4.2 Refined Modeling Using a Series of Nodal Forces

A convenient way to determine the effects of post-tensioning is to use a spreadsheet program. The post-tensioning effects at each of the nodes of an element are converted to equivalent nodal forces: a vertical force, a horizontal force, and a couple at each node. In addition, a distributed horizontal force is applied to the element between each pair of adjacent nodes to account for the change between horizontal nodal forces due to friction and anchor set losses. The beam and post-tensioning modeling are shown in **Figure 11.6.4.2-1**.

*Figure 11.6.4.2-1
Numerical Assumptions and
Sign Convention in Proposed Method*



The only approximation used in this method is to assume the post-tensioning profile is a series of straight lines between the nodes. A structural analysis program for continuous beams is then used to determine the total bending moment diagram. For clarity of presentation, an axial load diagram is not included. It can easily be obtained from the axial nodal and element forces.

EXTENDING SPANS

11.6.4.2 Refined Modeling Using a Series of Nodal Forces/11.6.4.2.1 Example

The primary bending moment diagram can be obtained directly as P_e . It can also be obtained through the same structural analysis program with the same loads, but with enough supports removed to render the beam statically determinate. The example used in Section 11.6.4.1 will be used below to illustrate the calculation steps.

Figure 11.6.4.2-1 shows three nodes in sequence and the sign convention used. The equivalent load at each node is calculated using the post-tensioning force and its eccentricity at that point. The global (structure) sign convention for this analysis is that downward loads are positive, a couple acting clockwise is positive, tendon eccentricity below the concrete centerline is positive, and prestress force is always positive. The standard sign convention for internal forces, including axial force, shearing force, and bending moment is used.

Consistent units of measurement must be maintained throughout the analysis. All supports except one are assumed to be free to move horizontally.

The vertical point load at a node, i , is computed as:

$$F_{yi} = \frac{P_{i-1}e_{i-1} - P_i e_i}{L_{i-1}} - \frac{P_i e_i - P_{i+1} e_{i+1}}{L_i} \quad (\text{Eq. 11.6.4.2-1})$$

where

e_i = tendon eccentricity from concrete section centroid to tendon centroid at node i

L_i = distance between nodes i and $i + 1$, or length of segment i

P_i = post-tensioning force at node i .

The couples shown at element ends, see **Figure 11.6.4.2-1c**, cancel each other when the elements are combined into the full member. Two exceptions to this are the first node, Node 1, and the last node, Node 11, in this example. Thus, the external couples at Nodes 2, 3, 4, 5, 6, 7, 8, 9, and 10 = 0.0. The couples at Nodes 1 and 11 are computed using:

$$M_i = P_i e_i \quad (\text{Eq. 11.6.4.2-2})$$

$$M_1 = -P_1 e_1 \text{ and } M_{11} = P_{11} e_{11}$$

Using the sign convention for moments, M_1 will be negative and M_{11} will be positive.

11.6.4.2.1 Example

As an example, calculate the equivalent loads at Nodes 1 and 2 and on Segment 1. The post-tensioning forces are 787.28 and 793.79 kips. The eccentricities are 0.00 and 13.26 in. The loads at Nodes 1 and 2 are:

$$F_{y1} = 0 - \frac{787.3(0) - 793.8(13.26)}{186} = 56.59 \text{ kips}$$

$$M_1 = (787.3)(0) = 0.00$$

$$F_{y2} = \frac{787.3(0) - 793.8(13.26)}{186} - \frac{793.8(13.26) - 800.3(22.73)}{186} = -15.38 \text{ kips}$$

$$M_2 = 793.8 (13.26) - 793.8 (13.26) = 0.00$$

The post-tensioning force at each node is calculated as the product of the post-tensioning stress, after accounting for friction and anchor set losses, and the area of post-tensioning tendons. The forces at each node are given in **Table 11.6.4.2.1-1** and **Figure 11.6.4.2.1-1a**.

The equivalent vertical loads for this example are shown in **Figure 11.6.4.2.1-1b**. A relatively large number of nodes in a span would result in greater accuracy. For most applications, nodes at tenth or twentieth points provide sufficient accuracy.

After the equivalent loads due to post-tensioning are calculated, the member should be checked for equilibrium; the sum of vertical forces and the sum of the moments about a point should be equal to zero. When the supports are placed and a continuous beam analysis is performed, the total reactions, shears, and moments due to post-tensioning are obtained. The reactions obtained in this step are due to secondary effects that are intended to maintain the restraint conditions at the supports. **Table 11.6.4.2.1-1** shows the total moment using the proposed method.

Figure 11.6.4.2.1-1
Post-Tensioning Profile and Equivalent Loads

The total moments are shown in **Figure 11.6.4.2.1-2b**. Subtracting the primary moments from the total moments results in the secondary moments.

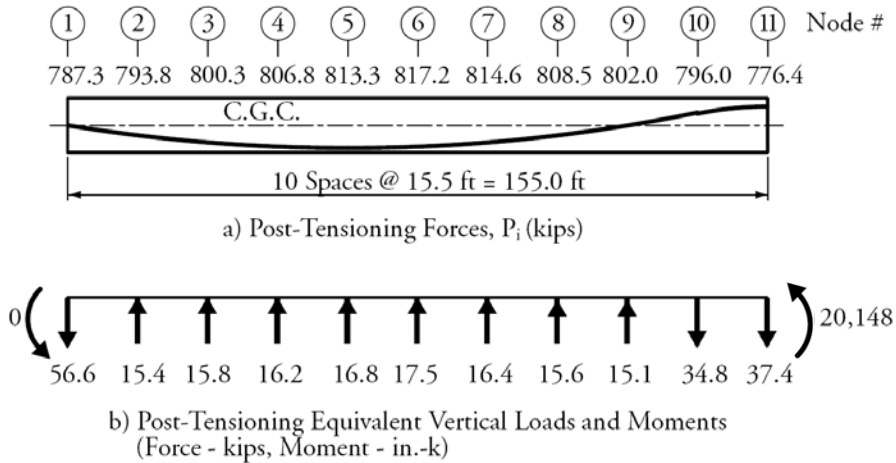
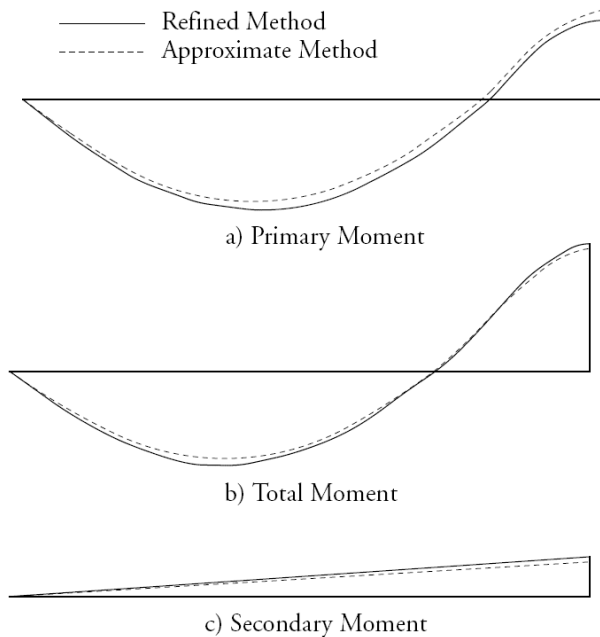


Table 11.6.4.2.1-1
Post-Tensioning Effect—Refined Method

Node No.	1	2	3	4	5	6	7	8	9	10	11
Distance from Left End, in.	0	186	372	558	744	930	1,116	1,302	1,488	1,674	1,860
Tendon Eccentricity in.	0.00	-13.26	-22.73	-28.41	-30.30	-28.43	-22.80	-13.43	-0.30	16.58	25.95
Post-tensioning Stress, ksi	181.4	182.9	184.4	185.9	187.4	188.3	187.7	186.3	184.8	183.4	178.9
Post-tensioning Force, kips	787.3	793.8	800.3	806.8	813.3	817.2	814.6	808.5	802.0	796.0	776.4
Equivalent Loads:											
Vertical Force kips/ft	56.59	-15.38	-15.78	-16.17	-16.84	-17.48	-16.42	-15.61	-15.12	34.79	37.41
Moment in.-kips	0	0	0	0	0	0	0	0	0	0	-20,148
Total Moment in.-kips	0	-9,621	-16,377	-20,194	-20,998	-18,678	-13,102	-4,476	7,051	21,388	29,251
Primary Moment in.-kips	0	-10,526	-18,191	-22,921	-24,644	-23,234	-18,573	-10,859	-241	13,189	20,148
Secondary Moment in.-kips	0	905	1,814	2,727	3,645	4,556	5,471	6,383	7,292	8,199	9,103

Figure 11.6.4.2.1-2
Bending Moment Diagrams



11.6.4.3 Design Consideration

The secondary reactions are the only external forces acting on the member due to post-tensioning. They act at the supports. These reactions must be in equilibrium. For the two-span example, the reaction due to post-tensioning at the center pier is 9.79 kips downward (or pier uplift), and the reaction at each abutment is 9.79/2 = 4.89 kips upward (or downward load on abutment). Accordingly, secondary shears must be constant between supports and secondary moments must be linear between supports. If these characteristics are not observed, the calculations must be reviewed for errors. These characteristics must hold true regardless of the tendon profile and whether or not the member’s cross-section properties vary along its length.

The total (primary plus secondary) effects must be used when checking service limit states, e.g., tension at bottom fibers at final loading conditions, etc. However, the primary and secondary effects must be separated before performing calculations for the strength limit state. Because post-tensioning continuous members creates a set of external loads, i.e. support reactions, these external loads must be considered in the factored load combinations in strength design. The accepted practice is to combine the factored secondary moment using a load factor of 1.0 with the moments due to factored dead and live loads, and to compare the “total factored load” moment at a section against the design flexural strength at that section.

The accuracy of using elastic analysis to calculate the secondary moments and of using a load factor of 1.0 at the strength limit state has occasionally been the subject of debate. However, no better approach has been adopted for standard practice.

11.6.5 Shear Limits in Presence of Post-Tensioning Ducts

In order to ensure that the concrete in the web of the beam will not crush prior to yielding of the transverse reinforcement, the *LRFD Specifications* give an upper limit of V_n :

$$V_n = 0.25f'_c b_v d_v + V_p \tag{LRFD Eq. 5.8.3.3-2}$$

where b_v is taken as the minimum web width within the depth d_v , modified for the presence of ducts where applicable. The LRFD code defines b_w as the width of the members web, therefore $b_v = b_w - \text{duct diameter}$. In determining b_v at a particular level, one-half of the diameters of the ungrouted ducts or one quarter of the diameters of the grouted ducts at that level must be subtracted from the web width. Additional definitions for these terms appear in LRFD Art. 5.8.2.9.

11.7 POST-TENSIONING ANCHORAGES IN I-BEAMS

Anchorage zones are designed to accommodate anchorage hardware with its associated special reinforcement and to provide adequate space for the reinforcement needed to distribute the highly concentrated post-tensioning force. Detailed guidance for the design of anchorage zones is given in the PTI publication, *Anchorage Zone Design* (PTI, 2000). A design example in NCHRP Report 517 (Castrodale and White, 2004) also discusses the design of anchorage zone reinforcement. **Figure 11.7-1** shows reinforcement and anchorages in the end of a beam that has been designed with a top recess. The dapped area provides access for post-tensioning after both abutting beams are erected in place. Multiple levels of tendon protection are required in corrosive environments. (see PTI Specifications (2003), FHWA (2004), and LRFD Construction Specifications Chapter 10).

Figure 11.7-1
*Reinforcement and Anchorages
in an I-Beam End Block*

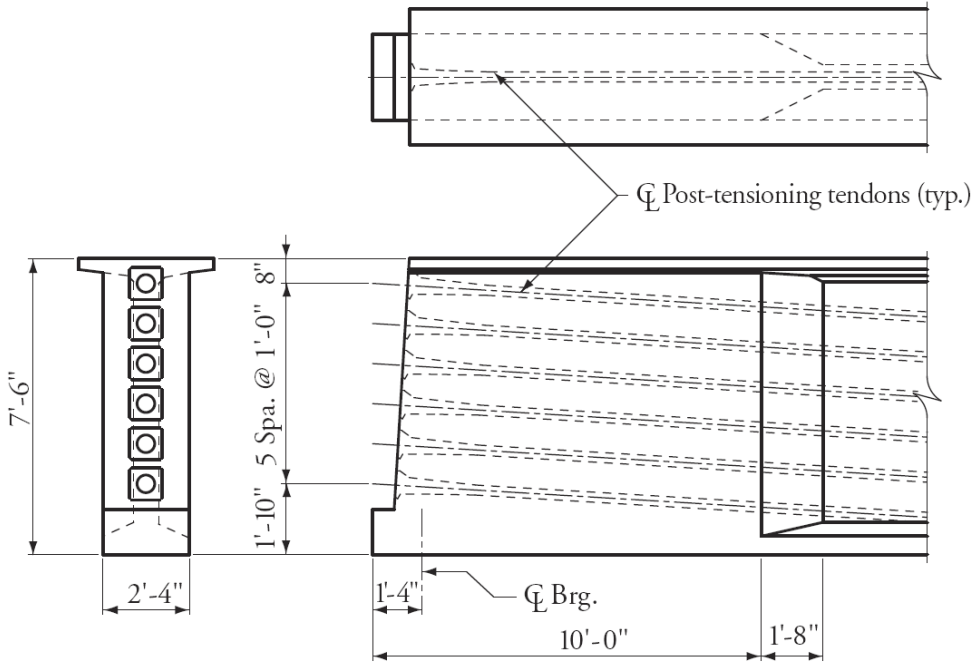


The anchorage zone is typically detailed using an end block that is the same width as the bottom flange in Bulb Tee section and extends for a distance from the end of the beam of at least one beam height before a tapered section returns the cross-section to the width of the web. Typical dimensions are illustrated in **Figure 11.7-2**. The extent of the anchorage zone is based on the principle of St. Venant which proposes that the disturbed stress field introduced at the end of the beam by the concentrated forces at post-tensioning tendon anchorages extends approximately a beam height into the beam (see the discussion in Section 11.4.10 and LRFD Fig. C5.10.9.1-1).

Based on this principle, the cross-section in the anchorage zone (end block) has generally been held constant until the stress distribution from the anchorage forces becomes more uniform. If the cross-section were also decreased within the disturbed region, it is believed that this could compound the stress disturbance and lead to increased cracking.

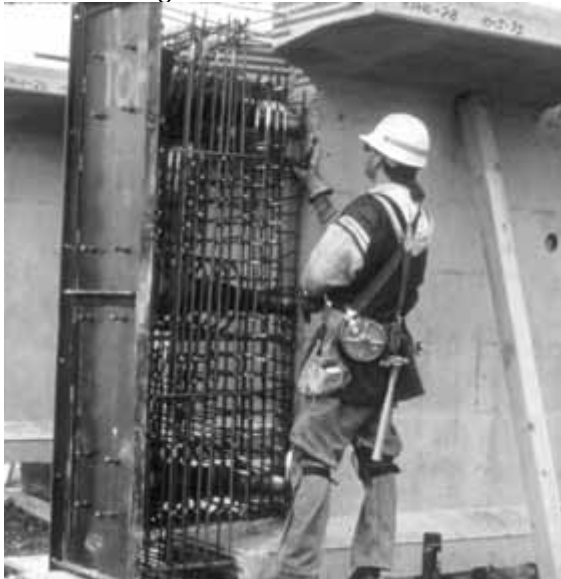
Some research has indicated that a much smaller anchorage zone may be adequate. It has been proposed that the concrete should be the minimum size necessary to house the anchorage hardware and to provide for cover over reinforcement. It is suggested that large concrete dimensions in the anchorage zone are unnecessary and possibly counterproductive, as they may require large amounts of reinforcement to control cracks. A research project by Tadros and Khalifa (1998) for the Federal Highway Administration and the Nebraska Department of Roads tested full-size beams with two concepts for anchorage zones with significantly reduced cross-sections. The new details have been adopted and used on several projects in Nebraska and other areas such as the project shown in **Figure 11.7-3**. A paper by Ma, et al. (1999), discusses the design of this post-tensioned anchorage zone in accordance with the *LRFD Specifications* using strut-and-tie modeling. The paper includes a design example. Experimental testing of post-tensioning anchor zones has been reported by Breen, et al. (1994) and Ma, et al. (1999).

Figure 11.7-2
Typical I-Beam End Block Dimensions



In Washington State, alternative details were used on the Rock Cut Bridge for Stevens and Ferry Counties (Nicholls and Prussack, 1997). This project included casting the end blocks in a secondary cast after the prismatic beams were stripped from the form. This can result in cost savings by not having to use special beam forms to accommodate the widened end block section. **Figure 11.7-3a** shows a workman tying bars and forming the short end block. **Figure 11.7-3b** shows the finished secondary cast. Additional details of the project are discussed in Section 11.5.2.

Figure 11.7-3
Rock Cut Bridge End Block



a) Forming and Tying Steel for End Block



b) Completed End Blocks

11.8 DESIGN EXAMPLE: TWO-SPAN BEAM SPLICED OVER PIER

11.8.1 Introduction

This example is similar to Design Example 9.2. It will provide a comparison in design calculations when post-tensioning is employed for a very common superstructure system. It will also illustrate the increased span length when post-tensioning is used to establish continuity over a pier.

Many of the fundamental calculations in this example are not shown or are not explained in detail. Frequently, the applicable *LRFD Specifications* references are not given. These details are provided in Chapter 8 and in the design examples in Chapter 9.

This example selects the same 72-in.-deep bulb tee (BT-72) used in Example 9.2. However, for this example, two, 155-ft-long spans will be used instead of the 110-ft long end spans and the 120-ft-long center span of the three-span bridge designed in that example. The full-span beam segments are spliced over the pier with post-tensioning and are made composite with the deck. Some of the details already discussed in Example 9.2 are not repeated here. Analysis for post-tensioning effects is emphasized.

Figures 11.8.1-1 and 11.8.1-2 show the longitudinal section and cross-section of the bridge. The cross-section has four beams spaced at 12 ft-0 in. AASHTO-PCI Bulb Tees are modified by widening the section 1-in. to accommodate the post-tensioning ducts. The beams are designed to act compositely with the cast-in-place concrete deck slab. The 8-in.-thick slab includes a ½-in. integral wearing course. Therefore, the full 8-in. thickness is used in load calculations but 7.5-in. is used for the deck to compute composite section properties. A haunch over the top flange averaging ½-in. thick is considered in the load and stress analysis. Design live loading is HL-93.

Figure 11.8.1-1
Longitudinal Section

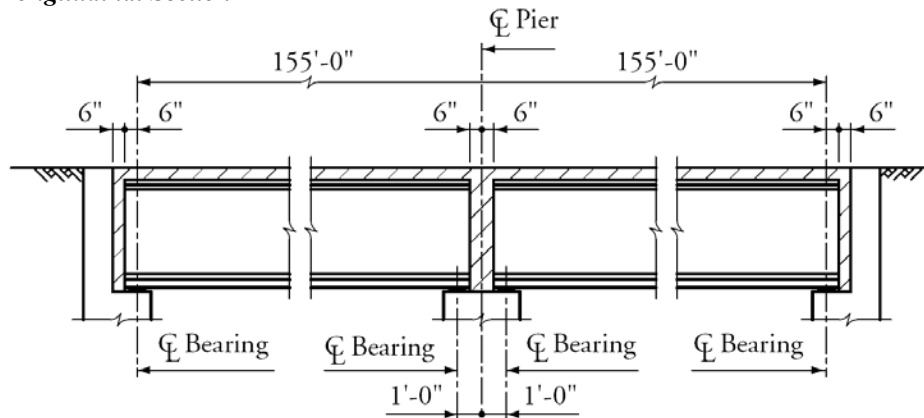
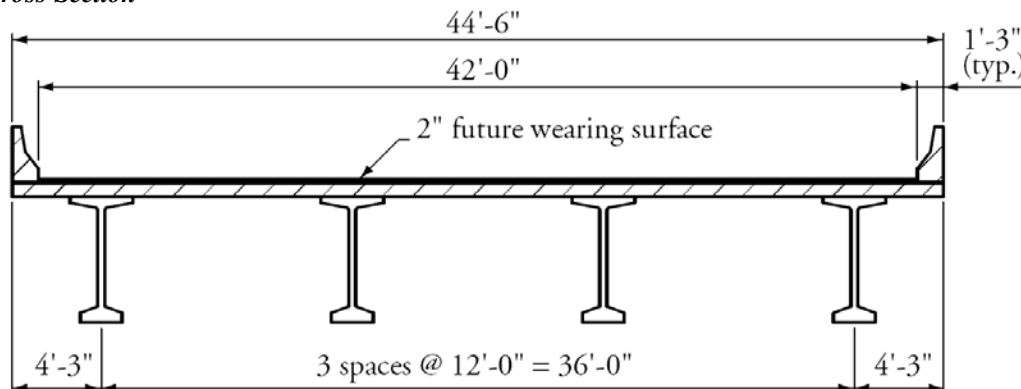


Figure 11.8.1-2
Cross-Section

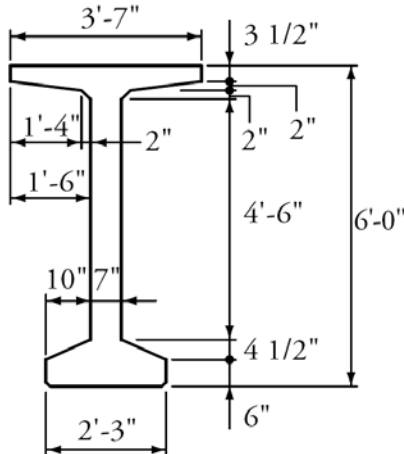


11.8.2 Materials and Beam Cross-Section

The cross-section of the modified AASHTO-PCI Bulb Tee (BT-72) is shown in **Figure 11.8.2-1**. The width of the beam was increased 1 in. to provide a 7-in.-thick web to accommodate post-tensioning ducts.

Figure 11.8.2-1

Modified 72-in. AASHTO-PCI Bulb Tee



Cast-in-place slab:

Total thickness = 8.0 in.

Structural thickness, $t_s = 7.5$ in.

Concrete strength at 28 days, $f'_c = 4.0$ ksi

Concrete unit weight, $w_c = 0.150$ kcf

$$E_c = 33,000(1.0)(0.15)^{1.5}\sqrt{4.0} = 3,834 \text{ ksi}$$

Precast beams:

Concrete strength at transfer, $f'_{ci} = 5.5$ ksi

Concrete strength at 28 days, $f'_c = 7.0$ ksi

Concrete unit weight, $w_c = 0.150$ kcf

$$E_c = 33,000(1.0)(0.15)^{1.5}\sqrt{7.0} = 5,072 \text{ ksi}$$

From **Figure 11.8.1-1**, the design span is assumed to be 154.0 ft when the beam is supported on its bearing pads before it is made continuous, and 155.0 ft after the pier diaphragm concrete is cured and the beam becomes continuous.

Pretensioning strands:

½-in.-diameter, low-relaxation

Area of one strand = 0.153 in.²

Ultimate strength, $f_{pu} = 270.0$ ksi

Yield strength, $f_{py} = 0.9f_{pu} = 243.0$ ksi

[LRFD Table 5.4.4.1-1]

Modulus of elasticity, $E_p = 28,500$ ksi

[LRFD Art. 5.4.4.2]

Stress limits for pretensioning strands:

[LRFD Table 5.9.3-1]

before transfer, $f_{pi} \leq 0.75f_{pu} = 202.5$ ksi

Post-tensioning strands:

0.6-in.-diameter, low-relaxation

Area of one strand = 0.217 in.²

Ultimate strength, $f_{pu} = 270.0$ ksi

Yield strength, $f_{py} = 0.9f_{pu} = 243.0$ ksi

[LRFD Table 5.4.4.1-1]

Modulus of elasticity, $E_p = 28,500$ ksi

[LRFD Art. 5.4.4.2]

Stress limits for post-tensioning strands:

[LRFD Table 5.9.3-1]

prior to seating, $f_s \leq 0.9f_{py} = 218.7$ ksi

immediately after anchor set,

$(f_{pt} + \Delta f_{pES} + \Delta f_{pA}) \leq 0.7f_{pu} = 189.0$ ksi

at end of the seating loss zone immediately after anchor set,

$(f_{pt} + \Delta f_{pES} + \Delta f_{pA}) \leq 0.74f_{pu} = 199.8$ ksi

A maximum of three tendons, each with up to 15 strands, for a total of 45 strands, will be assumed.

Post-Tensioning Tendon Duct:

Rigid galvanized steel duct with outside diameter 3.75-in. Editor's note: When using plastic duct wall profiles are different and generally have larger outside diameters.

Reinforcing bars:

Yield strength, $f_y = 60.0$ ksi

Modulus of elasticity, $E_s = 29,000$ ksi

[LRFD Art. 5.4.3.2]

Future wearing surface:

An additional weight of 0.025 ksf for a future 2-in.-thick concrete wearing surface is included. Unit weight, $w_c = 0.150$ kcf

New Jersey-type barriers:

Two weighing 0.300 kips/ft per barrier are assumed to be distributed equally to all beams.

11.8.3 Cross-Section Properties

11.8.3.1 Non-Composite Section

Standard section properties for PCI BT-72 are modified to reflect the 1-in. increase in width.

A = cross-sectional area of beam = $767 + 72 = 839$ in.²

h = overall depth of beam = 72 in.

I = moment of inertia about the centroid of the non-composite precast beam = 577,022 in.⁴

y_b = distance from centroid to extreme bottom fiber of the non-composite precast beam = 36.55 in.

y_t = distance from centroid to extreme top fiber of the non-composite precast beam = 35.45 in.

S_b = section modulus for the extreme bottom fiber of the non-composite precast beam = 15,789 in.³

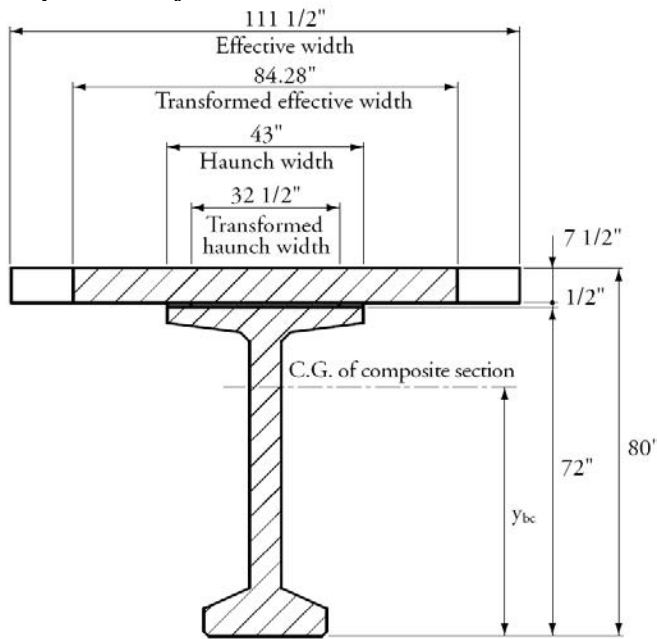
S_t = section modulus for the extreme top fiber of the non-composite precast beam = 16,276 in.³

Beam weight = 0.874 kips/ft

11.8.3.2 Composite Section

The composite section properties are calculated according to the *LRFD Specifications*. **Figure 11.8.3.2-1** shows the cross-section of the composite section.

Figure 11.8.3.2-1
Composite Transformed Section



$n =$ modular ratio of deck and girder concretes $= 3,834/5,072 = 0.7559$

$A_c =$ total area of composite section $= 1,487 \text{ in.}^2$

$h_c =$ overall depth of the composite section $= 72 + 7.5 + 0.5 = 80 \text{ in.}$

$I_c =$ moment of inertia of the composite section $= 1,153,760 \text{ in.}^4$

$y_{bc} =$ distance from the centroid of the composite section to the extreme bottom fiber of the precast beam
 $= (\sum Ay_b / A_c = 80,038 / 1,487 = 53.81 \text{ in.}$

$y_{tg} =$ distance from the centroid of the composite section to the extreme top fiber of the precast beam
 $= 72 - 53.81 = 18.19 \text{ in.}$

$S_{bc} =$ composite section modulus for the extreme bottom fiber of the precast beam
 $= 1,153,760/53.81 = 21,441 \text{ in.}^3$

$S_{tg} =$ composite section modulus for the top fiber of the precast beam
 $= 1,153,760/18.19 = 63,428 \text{ in.}^3$

$S_{tc} =$ composite section modulus of extreme top fiber of the slab
 $= \left(\frac{1}{n}\right)\left(\frac{I_c}{y_{tc}}\right) = \left(\frac{1}{0.7559}\right)\left(\frac{1,153,760}{26.19}\right) = 58,279 \text{ in.}^3$

11.8.4 Shear Forces and Bending Moments

The weight of the beam acts on the non-composite, simple-span beam. The staging of post-tensioning (see Sect. 11.8.6.1) allows the weight of the slab and haunch to act on the non-composite, continuous span beam. The weight of the barriers and the future wearing surface, and the live load act on the composite, continuous-span beam.

EXTENDING SPANS

11.8.4 Shear Forces and Bending Moments/11.8.5 Required Pretensioning

The values of shear forces and bending moments for a typical interior beam, under self-weight of beam, weight of slab and haunch are computed, similar to Example 9.2. These are listed in **Table 11.8.4-1**. The two-span structure was analyzed using a continuous beam program that has the capability to generate live load shear force and bending moment envelopes for a “lane” of HL-93 live loading according to the *LRFD Specifications*. The span lengths used are for the continuous bridge with span lengths of 155 ft.

Table 11.8.4-1

Unfactored Shear Forces and Bending Moments for a Typical Interior Beam

Distance x, ft	Section x/L	Girder Weight (Simple Span)		Slab + Haunch Weight (Continuous Span)		Barrier Weight (Continuous Span)		Wearing Surface (Continuous Span)		HL-93 Live Load Envelope (Continuous Span)	
		Shear V_g kips	Moment M_g ft-kips	Shear V_s kips	Moment M_s ft-kips	Shear V_b kips	Moment M_b ft-kips	Shear V_{ws} kips	Moment M_{ws} ft-kips	Shear V_{LL+I} kips	Moment M_{LL+I} ft-kips
0.0	0.000	67.7	0.0	72.0	0.0	8.7	0.0	15.3	0.0	146.2	1,981.7
15.5	0.100	54.2	944.9	53.0	969.6	6.4	117.1	11.2	205.3	122.1	3,398.6
31.0	0.200	40.6	1,679.8	33.9	1,641.1	4.1	198.2	6.7	347.5	99.7	4,274.2
46.5	0.300	27.1	2,204.8	14.1	2,014.5	1.7	243.3	3.1	426.5	79.4	4,663.8
62.0	0.400	13.5	2,519.7	5.0	2,089.0	0.6	252.3	1.1	442.3	61.1	4,585.9
77.5	0.500	0.0	2,624.7	24.0	1,864.7	2.9	225.2	5.1	394.9	78.8	4,079.0
93.0	0.600	13.5	2,519.7	43.1	1,343.0	5.2	162.2	9.2	284.3	97.6	3,146.6
108.5	0.700	27.1	2,204.8	62.9	522.5	7.6	63.1	13.3	110.6	116.8	-2,541.8
124.0	0.800	40.6	1,679.8	82.0	-597.0	9.9	-72.1	17.3	-126.3	136.3	-3,209.6
139.5	0.900	54.2	944.9	101.0	-2,014.5	12.2	-243.3	21.4	-426.5	155.8	-3,209.6
147.9 ^[1]	0.954	61.5	458.0	111.8	-3,558.7	13.5	-429.8	23.6	-753.6	166.1	-4,279.9
155.0	1.000	67.7	0.0	120.1	-3,730.1	14.5	-450.5	25.4	-789.9	174.8	-4,455.4

Note: Shear is given in absolute values

^[1] Section designed in shear

For all limit states except the Fatigue Limit State, for two or more lanes loaded, the distribution factor for moment (DFM) = 0.849 lanes/beam. For one design lane loaded, DFM = 0.550 lanes/beam. Therefore, the case of the two design lanes loaded controls.

For two or more lanes loaded, distribution factor for shear (DFV) = 1.082 lanes/beam [LRFD Table 4.6.2.2.3a-1]. For one design lane loaded, DFV = 0.840 lanes/beam. Therefore, the case of two design lanes loaded controls.

Values of V_{LL+I} and M_{LL+I} at various points along the span are given in **Table 11.8.4-1**.

11.8.5 Required Pretensioning

The number of pretensioning strands is selected to resist at least 120% of the beam weight. This would allow for a slight camber at prestress transfer and for additional safety during handling and shipping.

Using the value of bending moment from **Table 11.8.4-1**, the bottom tensile stress at midspan (0.5L), due to 1.2 times beam weight is:

$$f_b = -\frac{1.2(2,624.7)(12)}{15,789} = -2.394 \text{ ksi}$$

Tensile stress limit at service loads = $-0.19 \sqrt{f'_c} = -0.503 \text{ ksi}$ [LRFD Table 5.9.4.2.2-1]

The required precompressive stress at bottom fiber of the beam is the difference between bottom tensile stress due to the applied loads and the concrete tensile stress limit:

$$f_{pb} = 2.394 - 0.503 = 1.891 \text{ ksi.}$$

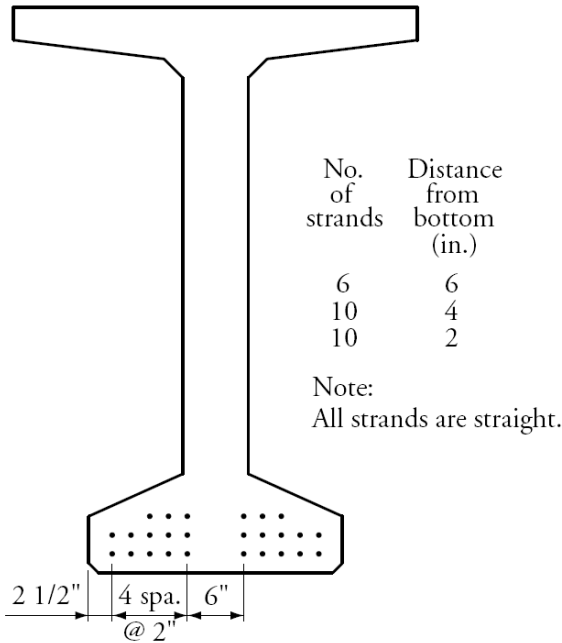
Similar to Example 9.2, assume the distance from the center of gravity of strands to the bottom fiber of the beam, y_{bs} , is equal to 7% of the beam depth, or, $y_{bs} = 0.07h = 0.07(72) = 5.04 \text{ in.}$ Then, strand eccentricity at midspan, e_c , equals $y_b - y_{bs} = 36.55 - 5.04 = 31.51 \text{ in.}$

The minimum required effective prestress force, P_{pe} :

$$1.891 = \frac{P_{pe}}{839} + \frac{P_{pe}(31.51)}{15,789}$$

Therefore, $P_{pe} = 593.2$ kips. Assuming a total prestress loss of 25%, the prestress force per strand after all losses $= 0.153)(202.5)(1 - 0.25) = 23.2$ kips. The number of strands required is $(593.2/23.2) = 25.6$ strands. Use twenty six 1/2-in.-diameter, 270 ksi, low-relaxation strands. The assumed strand pattern for the 26 strands at midspan is shown in **Figure 11.8.5-1**. Each available location, with allowance for post-tensioning ducts, was filled beginning with the bottom row.

Figure 11.8.5-1
Pretensioning Strand Pattern at Midspan



The distance between the center of gravity of strands and the bottom fiber of the beam,

$$y_{bs} = [10(2) + 10(4) + 6(6)]/(26) = 3.69 \text{ in. Strand eccentricity at midspan, } e_c = y_b - y_{bs} = 36.55 - 3.69 = 32.86 \text{ in.}$$

Before continuing with post-tensioning calculations, the designer should investigate if analysis is warranted for slender member stability (see Section 8.10) or for stresses at prestress transfer. In most cases, these two design considerations do not control.

11.8.6 Modeling of Post-Tensioning

In continuous structures, the moments due to post-tensioning may not be proportional to the tendon eccentricity. The difference occurs because the deformations imposed by the post-tensioning are resisted by the continuity of the members at the piers. The moments resulting from the restraint to the post-tensioning deformations are called secondary moments. Also, see Section 11.6.4.

11.8.6.1 Post-Tensioning Profile

The post-tensioning is applied in two stages. In the first stage, two of three equal tendons are post-tensioned before the beams are made composite with the deck. The second stage post-tensioning is applied through one tendon to the composite section. This two-thirds, one-third division of post-tensioning allows for the deck to be precompressed for crack control, yet not compressed enough to require extensive analysis for effects of future deck removal and replacement.

Stage 1:

Place two tendons with two-thirds of the total number of post-tensioning strands in the precast continuous member. Assume an initial post-tensioning force equal to 1,000 kips.

Stage 2:

Place one tendon with one-third of the total number of the post-tensioning strands in the composite member. Assume an initial post-tensioning force equal to 500 kips.

Once the total required post-tensioning force is determined based on various design criteria, the effects of the 1,500 kips (1,000 + 500) are linearly factored to correspond to the calculated force and analysis continues.

Figure 11.8.6.1-1 shows the positions of the tendons in a cross-section of the beam. Note that the clear spacing between ducts is taken as 1 in. This is a good practice as long as maximum aggregate size is not larger than $\frac{3}{4}$ in. The *LRFD* Article 5.10.3.3.2 states that up to three ducts may be bundled as long as they are splayed out in the anchorage area for 3 ft at a spacing of 1.5 in. or 1.33 times the maximum aggregate size.

Figure 11.8.6.1-1
Duct Locations

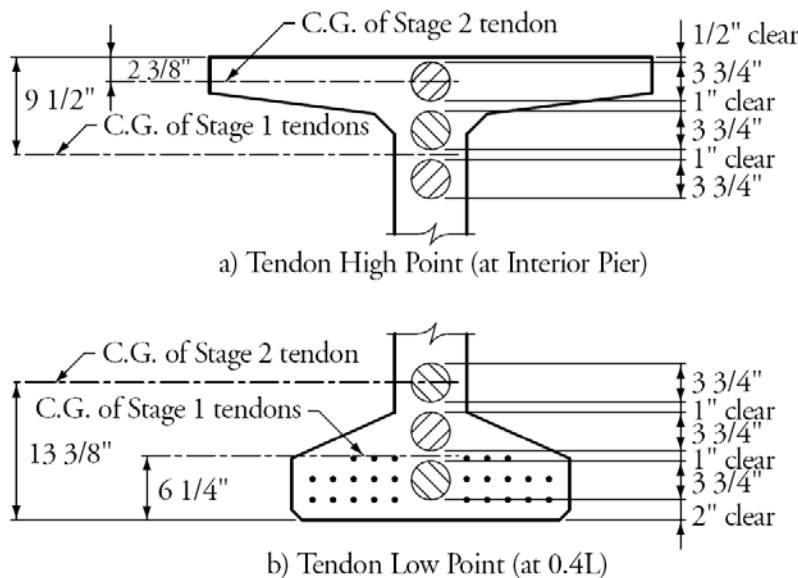


Figure 11.8.6.1-2 shows the post-tensioning tendon profile for both stages. **Tables 11.8.6.2-1** and **11.8.6.2-2**, found in the next section, show tendon eccentricities at various locations. In a detailed analysis, the difference between the centroid of the tendon and the center of the ducts may be accounted for in accordance with *LRFD* Article C5.9.1.6. The difference between the two centers is due to the fact that the strands cluster near the top of the duct in the low segments of the duct profile and cluster near the bottom in the high, negative moment areas of the duct profile. This minor effect is ignored in the calculations of this example.

Figure 11.8.6.1-3 illustrates the equation used to calculate the eccentricity of the post-tension profile at any point of the span. For a tendon geometry to be fully defined, two conditions are required for a straight-line tendon and three conditions for a second-degree curve.

Figure 11.8.6.1-2
Post-Tensioning Tendon Profiles

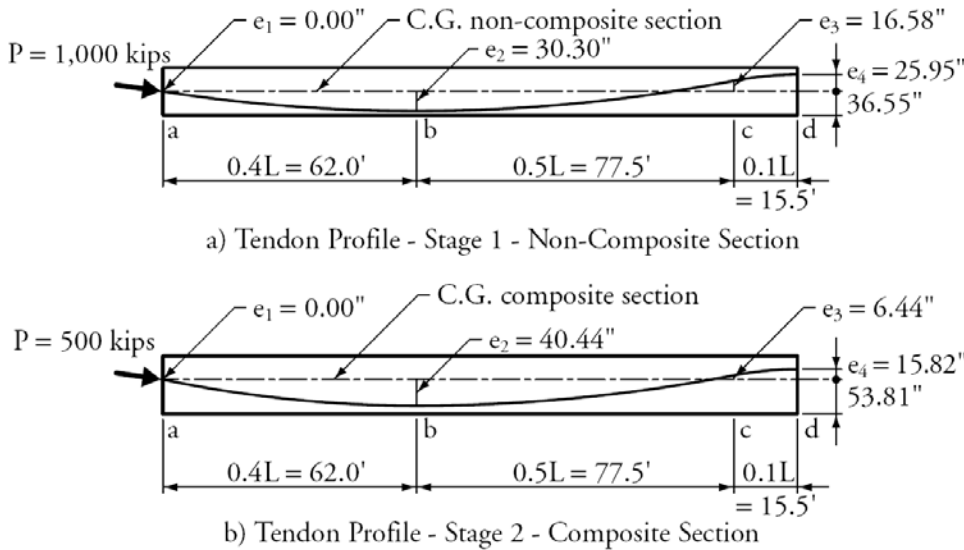
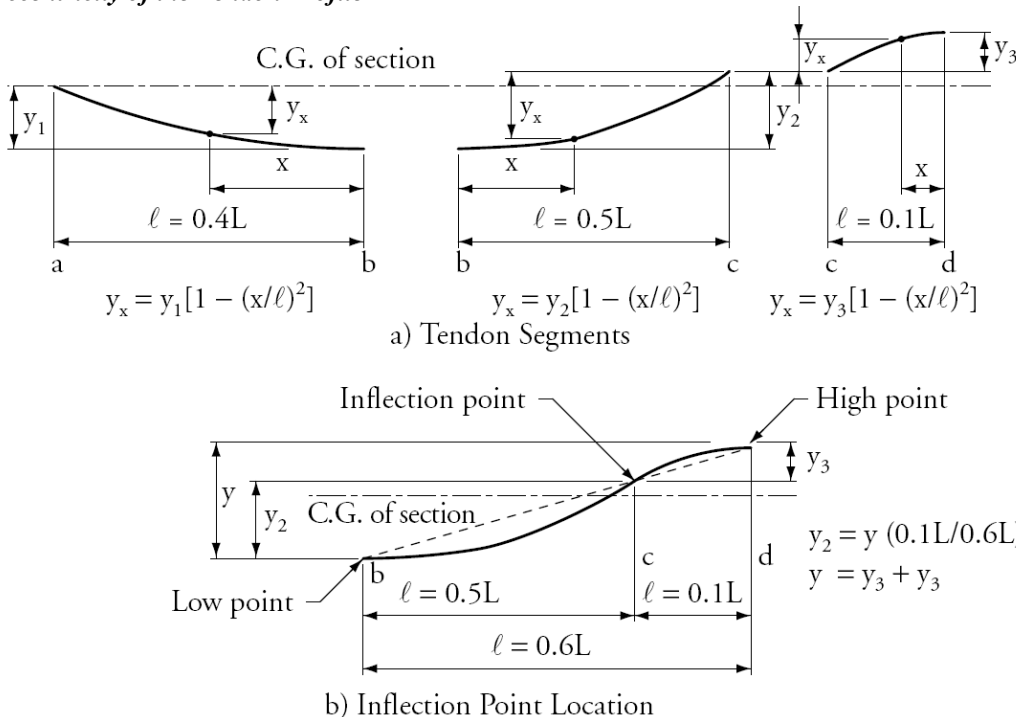


Figure 11.8.6.1-3
Eccentricity of the Tendon Profile



It is common practice to assume a parabolic profile defined by three parabolas in the end span of a continuous beam. The first has zero eccentricity at beam-end and has the maximum allowed bottom position at $0.4L$ with zero slope (or horizontal tangent) at that point. The second parabola has the same eccentricity and tangential slope at $0.4L$ and a common tangent and eccentricity as it joins the third parabola. The third parabola is a small curve dictated by the specification limits of tendon curvature. Generally, it has common eccentricity and is tangent with the second parabola. It has zero slope (horizontal tangent) over the pier centerline and the maximum possible eccentricity. The point of common tangent between the second and third parabolas has

EXTENDING SPANS

11.8.6.1 Post-Tensioning Profile/11.8.6.2 Equivalent Loads

traditionally been taken as $0.1L$ from centerline of support. However, other locations should be examined in an optimization of the tendon profile. The assumptions made for the three parabolas allow the tendon geometry to be fully defined when the eccentricities at the abutment (i.e., $0.0L$), $0.4L$, $0.9L$, and pier (i.e., $1.0L$) are given.

For bridges with interior spans, similar assumptions may be made, namely, horizontal tangents at the ends and at $0.5L$, and common tangents at $0.1L$ and $0.9L$.

11.8.6.2 Equivalent Loads

When equivalent loads are placed on the continuous beam, and structural analysis is performed, the resulting moments, shears and reactions are the total effects. The secondary moments are the total moments minus the primary moments, which are defined as the products of the prestress force and the eccentricity at any given section. **Figure 11.8.6.2-1** shows the equivalent loads for the tendon profiles shown in **Figure 11.8.6.1-2**.

Figure 11.8.6.2-1
Post-Tensioning Equivalent Vertical Loads and Moments (Refined Method)

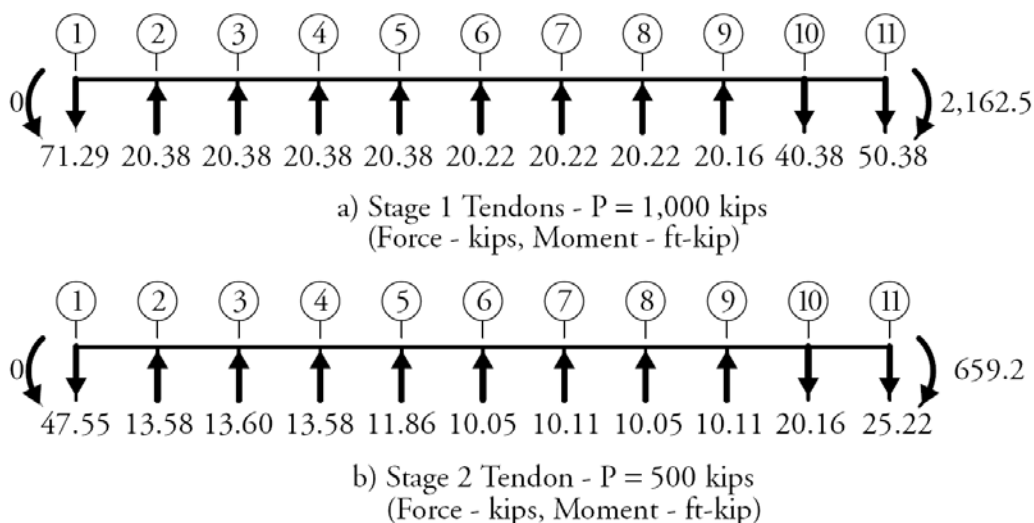


Table 11.8.6.2-1 shows the total moments, primary moments, and secondary moments at tenth-span points due to Stage 1 post-tensioning. **Table 11.8.6.2-2** shows the same quantities for Stage 2 post-tensioning.

Table 11.8.6.2-1
Loads Applied by Post-Tensioning in Stage 1 (P = 1,000 kips)

Point along Span	0.0	0.1	0.2	0.3	0.4	0.5	0.6	0.7	0.8	0.9	1.0
Distance from Top of Girder, in.	35.45	48.71	58.18	63.86	65.75	63.88	58.25	48.88	35.75	18.88	9.50
Tendon Eccentricity, in.	0.00	-13.26	-22.73	-28.41	-30.30	-28.43	-22.80	-13.43	-0.30	16.58	25.95
Equivalent Loads:											
Vertical Force kips/ft	71.29	-20.38	-20.38	-20.38	-20.22	-20.22	-20.22	-20.22	-20.16	40.38	50.38
Moment in.-kips	0	0	0	0	0	0	0	0	0	0	2,163
Total Moment in.-kips	0	-1,014	-1,711	-2,093	-2,159	-1,912	-1,351	-479	706	2,205	3,077
Primary Moment ft-kips	0	-1,105	-1,894	-2,368	-2,525	-2,369	-1,900	-1,119	-25.0	1,382	2,163
Secondary Moment in.-kips	0	91	183	274	366	457	549	640	731	823	914

EXTENDING SPANS

11.8.6.2 Equivalent Loads/11.8.7 Required Post-Tensioning

**Table 11.8.6.2-2
Loads Applied by Post-Tensioning in Stage 2 (P = 500 kips)**

Point along Span	0.0	0.1	0.2	0.3	0.4	0.5	0.6	0.7	0.8	0.9	1.0
Distance from Top of Girder, in.	18.19	35.88	48.52	56.10	58.63	56.75	51.13	41.75	28.63	11.75	2.38
Tendon Eccentricity in.	0.00	-17.69	-30.33	-37.91	-40.44	-38.56	-32.94	-23.56	-10.44	6.44	15.82
Equivalent Loads:											
Vertical Force kips/ft	47.55	-13.58	-13.60	-13.58	-11.86	-10.05	-10.11	-10.05	-10.11	20.16	25.22
Moment in.-kips	0	0	0	0	0	0	0	0	0	0	659
Total Moment in.-kips	0	-630	-1,049	-1,258	-1,256	-1,071	-729	-231	423	1,234	1,732
Primary Moment ft-kips	0	-737	-1,264	-1,580	-1,685	-1,607	-1,373	-982	-435	268	659
Secondary Moment in.-kips	0	107	215	322	429	536	644	751	858	965	1,073

11.8.7 Required Post-Tensioning

At this stage of analysis, the post-tensioning forces are not yet known and prestress losses must be initially assumed. **Table 11.8.7-1** shows the assumed prestressing levels at each of the construction stages.

**Table 11.8.7-1
Assumed Effective Prestress at Various Construction Stages**

Construction Stage	Stress in Pretensioning Strand, ksi	Stress in Post-Tensioning Strand, Stage 1, ksi	Stress in Post-Tensioning Strand, Stage 2, ksi
Pretensioning	$0.92(0.75)f_{pu} = 186.3$	—	—
Post-Tensioning Stage 1	$0.87(0.75)f_{pu} = 176.2$	$0.92(0.78)f_{pu} = 193.8$	—
Post-Tensioning Stage 2	$0.87(0.75)f_{pu} = 176.2$	$0.87(0.78)f_{pu} = 183.2$	$0.92(0.78)f_{pu} = 193.8$
Service Loads	$0.82(0.75)f_{pu} = 166.1$	$0.82(0.78)f_{pu} = 172.7$	$0.82(0.78)f_{pu} = 172.7$

Elastic pretension loss, the total loss at time of post-tensioning and the total loss at final service time are assumed to be 8, 13, and 18%, respectively, of initial prestress which is assumed to be 75% of the specified ultimate strength. Once the prestress forces are determined, primarily based on concrete tension limits at service load conditions, then a detailed analysis of prestress loss should be conducted and the prestress force revised if needed. The process of calculating prestress losses is covered in detail in Chapters 8 and 9.

The pretensioning forces are:

Immediately following transfer:

$$26(0.153)(186.3) = 741.1 \text{ kips}$$

At Stage 1 (assumed to be the same as at Stage 2 post-tensioning):

$$26(0.153)(176.2) = 700.8 \text{ kips}$$

At service:

$$26(0.153)(166.1) = 660.5 \text{ kips}$$

Several factors affect post-tensioning losses. In addition to friction and anchor set described in Section 11.6.2, post-tensioning at any stage affects the prestressing tendons stressed in preceding stages. At this stage of analysis, post-tensioning losses are estimated, as given in **Table 11.8.7-1**, to be verified later with a detailed analysis after the post-tensioning forces are finalized.

Using 0.6-in.-diameter strand (area per strand = 0.217 in.²), the post-tensioning force per strand is: For Stage 1 strands, following jacking, $193.8(0.217) = 42.04$ kips, and at the time of Stage 2 post-tensioning, 39.76 kips, and at service = 37.47 kips. For Stage 2 strands, immediately following jacking, 42.04 kips, and at service, 37.47 kips.

11.8.7.1 Stress Limits for Concrete

[LRFD Art. 5.9.4.2]

The concrete compressive stress limit for the Service I load combination due to weight of beam, slab, future wearing surface, and barriers, is $0.45\sqrt{f'_c}$. For the precast beam alone, the limit is $0.45(7.0) = +3.15$ ksi, and for the slab, $0.45(4.0) = +1.80$ ksi. Due to dead loads plus live loads, for Service I load combination, the limit is $0.60\sqrt{f'_c}$, or $+4.200$ ksi for the precast beam and $+2.400$ ksi for the slab. For the Service III load combination, the tension limit is $-0.19\sqrt{f'_c} = -0.19\sqrt{7.0} = -0.503$ ksi.

The post-tensioning is calculated to satisfy tensile stresses at final service conditions due to full loads. The maximum negative section at the pier and the maximum positive moment section at $0.4L$ from the abutment are the two sections used for this analysis. Once the amount of post-tensioning is estimated, a detailed prestress loss calculation is made and all other design criteria are verified, the post-tensioning is adjusted as needed.

11.8.7.2 Positive Moment Section

The values of the bending moments due to various cases of loading are given in **Table 11.8.4-1**. The critical positive moment section is assumed to be at $0.4L$. The moments shown are:

$$M_g, \text{ due to beam weight} = 2,519.7 \text{ ft-kips}$$

$$M_s, \text{ due to deck weight} = 2,089.0 \text{ ft-kips}$$

$$M_b, \text{ due to barrier weight} = 252.3 \text{ ft-kips}$$

$$M_{ws}, \text{ due to wearing surface weight} = 442.3 \text{ ft-kips}$$

$$M_{LL+I}, \text{ due to live load and impact} = 4,585.9 \text{ ft-kips}$$

The pretensioning force at $0.4L$, $P_{pe} = 660.5$ kips, and its eccentricity is 32.86 in. The total moments due to post-tensioning are shown in **Tables 11.8.6.2-1** and **11.8.6.2-2**, for assumed values of Stage 1 and Stage 2 post-tensioning. Allowing for prestress losses:

$$\begin{aligned} \text{Stage 1 total moment} &= \left(\frac{2(n)37.47}{1,000} \right) (-2,159.3) \\ &= (0.075)(n) (-2,159.3) = -161.95(n) \text{ ft-kips} \end{aligned}$$

$$\begin{aligned} \text{Stage 2 total moment} &= \frac{(n)37.47}{500} (-1,256.0) \\ &= -94.20(n) \text{ ft-kips} \end{aligned}$$

Where (n) is the number of 0.6-in.-diameter strands per tendon. Stage 1 has two post-tensioned tendons, i.e., $2(n)$ strands, and Stage 2 has one tendon, i.e., (n) strands.

The bottom fiber stress due to each of the effects is given as:

$$\begin{aligned} f_b &= -\frac{(M_g + M_s)}{S_b} - \frac{(M_{ws} + M_b) + 0.8M_{LL+I}}{S_{bc}} \\ f_b &= -\frac{(2,519.7 + 2,089.0)(12)}{15,789} = \frac{(442.3 + 252.3)(12) + 0.8(4,585.9)(12)}{21,441} = -5.945 \text{ ksi} \\ f_b &= \frac{(P_{pe})}{A} + \frac{(P_{pe})e}{S_b} = \frac{660.5}{839} + \frac{660.5(32.86)}{15,789} = +0.787 + 1.375 = +2.162 \text{ ksi} \\ f_b &= \frac{(P_{PT})_{\text{Stage 1}}}{A} + \frac{(M_{\text{Total}})_{\text{Stage 1}}}{S_b} = \frac{(n)(37.47)}{839} + \frac{161.95(n)(12)}{15,789} = +0.212(n) \text{ ksi} \\ f_b &= \frac{(P_{PT})_{\text{Stage 2}}}{A_c} + \frac{(M_{\text{Total}})_{\text{Stage 2}}}{S_{bc}} = \frac{(n)(37.47)}{1,487} + \frac{(n)(94.20)(12)}{21,441} = +0.078(n) \text{ ksi} \end{aligned}$$

EXTENDING SPANS

11.8.7.2 Positive Moment Section/11.8.7.3 Negative Moment Section

Therefore, the total stress is $= -5.945 + 2.162 + 0.212(n) + 0.078(n)$ ksi

By setting this value equal to the stress limit, -0.503 ksi, a value of $n = 12$ strands per tendon, or a total of 36 strands total, is found to be required.

11.8.7.3 Negative Moment Section

The section at the centerline of the pier will be used for analysis of negative moment stresses. For the refined analysis, the critical section should be selected at the face of the diaphragm. It is interesting to note here that the requirement for checking tensile stresses in the negative moment zone is not enforced by designers of bridges made continuous without post-tensioning (using conventional reinforcement in the deck slab). This added check has good value in that it controls top cracking in the pier area and therefore increases the performance of the bridge. The claim can be made that the owner is receiving higher value by using a post-tensioning system compared to a conventionally reinforced one.

From **Table 11.8.4-1**, the values of the bending moments are:

$$M_g = 0.0 \text{ ft-kips}; M_s = -3,730.1 \text{ ft-kips}; M_b = -450.5 \text{ ft-kips}; M_{ws} = -789.9 \text{ ft-kips}; M_{LL+I} = -4,455.4 \text{ ft-kips}$$

The post-tensioning force at this section is:

Stage 1, $P_{PT} = 74.94(n)$ kips. The total moment per 1,000 kips of post-tensioning force = 3,076.8 ft-kips. This corresponds to $(0.075)(n)(3,076.8) = 230.76(n)$ ft-kips, where (n) is the number of strands per tendon in the two-tendon Stage 1 post-tensioning.

Stage 2, $P_{PT} = 37.47(n)$ kips. The total moment per 500 kips of Stage 2 post-tensioning = 1,731.8 ft-kips. This corresponds to $(0.075)(n)(1,731.8) = 129.89(n)$ ft-kips.

Solving for the total stress at the top fibers of the beam:

$$f_t = -\frac{(M_g + M_s)}{S_t} - \frac{(M_{ws} + M_b) + 0.8M_{LL+I}}{S_{tc}} + \frac{(P_{PT})_{Stage 1}}{A} + \frac{(M_{Total})_{Stage 1}}{S_b} + \frac{(P_{PT})_{Stage 2}}{A_c} + \frac{(M_{Total})_{Stage 2}}{S_{bc}}$$

$$f_t = -2.750 - 0.909 + \frac{74.94(n)}{839} + \frac{230.76(n)(12)}{16,276} + \frac{37.47(n)}{1,487} + \frac{129.89(n)(12)}{63,428}$$

$$f_t = -3.659 + (0.089 + 0.170 + 0.025 + 0.025)(n) = -0.503 \text{ ksi}$$

Solving for (n) , the minimum number of 0.6-in.-diameter strands per post-tensioning tendon is 10.21, or, rounding, a total of 33 strands for the three tendons.

The positive moment section requires three more post-tensioning strands than the negative moment section. In order to optimize, the post-tensioning required for the negative moment region will be used for the entire beam. An attempt will be made to increase the positive moment capacity by adding pretensioning. However, due to the limitations of the AASHTO-PCI Bulb Tee, the maximum number of strands that can be placed in the bottom flange, outside of the web area (which is reserved for post-tensioning) is 28. So, the design will be attempted using 28, ½-in.-diameter pretensioning strands and three post-tensioning tendons of eleven, 0.6-in.-diameter strands.

The pretensioning force at this section, $P_{pe} = 711.2$ kips.

Strand eccentricity at midspan,

$$e_c = y_b - y_{bs} = 36.55 - [(10(2) + 10(4) + 6(6) + 2(8)) / (28)] = 32.55 \text{ in.}$$

$$\text{Positive moment stress} = -5.945 + \frac{711.2}{839} + \frac{711.2(32.55)}{15,789} + 0.212(11) + 0.078(11)$$

$$= -5.945 + 0.848 + 1.466 + 3.190 = -0.441 \text{ ksi}$$

$$\text{Negative moment stress} = -3.659 + (0.089 + 0.170 + 0.025 + 0.025)(11) = -0.260 \text{ ksi}$$

Both values are within -0.503 ksi allowable tension for load combination, Service III.

11.8.8 Prestress Losses

11.8.8.1 Prediction Method

The *LRFD Specifications* account for level of prestress, concrete strength, and environmental conditions. They also allow for the long-term losses to be broken into increments representing the significant construction stages present in this type of superstructure. All calculations are made for the maximum positive moment section and the resulting elastic shortening and long-term losses are assumed to be constant along the entire length of the member.

11.8.8.2 Time-Dependent Material Properties

For the calculation of prestress losses, the bridge is assumed to be located where the average ambient relative humidity is 70%. The following construction schedule has been assumed:

1. Pretensioning is transferred one day after beam concrete placement
2. Stage 1 post-tensioning occurs at 30 days
3. Deck slab concrete is placed at 60 days
4. Stage 2 post-tensioning and superimposed dead loads are applied shortly after the deck is placed

To simplify the time-dependent calculations, it is reasonable to calculate the creep and shrinkage coefficients for three time periods: 1 to 30 days, 30 to 60 days and 60 to 20,000 days. The selection of 20,000 days is arbitrary and represents a bridge life of 55 years. Creep and shrinkage essentially cease after several years so this assumption is inconsequential. It is further assumed that no time-dependent effects take place between deck placement, Stage 2 post-tensioning, and application of superimposed dead load.

Using the procedures in the *LRFD Specifications*, the beam creep coefficient for a loading age of one day and a loading duration of 29 days is 0.691. Assuming a loading age of 30 applied to all concrete stress components introduced between 1 and 30 days, and a loading duration of 30 days ($60 - 30$), the creep coefficient is 0.507. For concrete loaded at 60 days and for a loading duration of 20,000 days ($\approx 20,000 - 60$), the creep coefficient is 1.00. The corresponding shrinkage strains of the beam are 143×10^{-6} , 65×10^{-6} , and 167×10^{-6} in./in. The strand relaxation is a minor contributor to the prestress losses and it is assumed equal to 1.2 ksi between 1 and 30 days, 1.2 ksi between 30 and 60 days, and zero thereafter. The modulus of elasticity was calculated earlier. These are E_c (deck) = 3,834 ksi; E_c (beam) at one day = 4,496 ksi and at 30 days (assumed the same as at 28 days) = 5,072 ksi.

11.8.8.3 Time Step Analysis

At day one, elastic shortening loss is calculated for pretensioning and beam self-weight. The initial prestress, just before transfer is assumed equal to $0.75f_{pu} = 202.5$ ksi. When the corresponding force and the self-weight moment are introduced to a transformed precast concrete section, with the steel area transformed by the factor, $n_i = E_p/E_{ci}$, the resulting concrete stress is the true stress in the section. The concrete stress at the centroid of the steel, multiplied by the modular ratio results in an elastic shortening loss = 5.458 ksi.

The concrete stress at the centroid of the pretensioning steel is used to calculate the creep loss between 1 and 30 days. With the relaxation loss added, the total long-term loss between 1 and 30 days is 7.987 ksi.

The concrete stress at the centroid of the pretensioning steel due to Stage 1 post-tensioning allows determination of elastic loss due to that stage of post-tensioning. The post-tensioning force is the applied load. The stress in the post-tensioning steel is calculated with due consideration of friction losses as given in Section 11.6.2 to be 187.18 ksi. The corresponding force is introduced to a transformed precast section with the pretensioning steel area transformed by the factor $n = E_p/E_c$. The resulting elastic shortening loss is 13.744 ksi. The net concrete stress at the pretensioning steel level immediately after application of Stage 1 post-tensioning is then used to calculate creep loss between 30 and 60 days. The corresponding long-term loss in the pretensioning steel is 8.922 ksi.

The elastic gain due to deck weight is calculated using the same section properties as for the Stage 1 post-tensioning. It is found to be = 7.102 ksi.

Transformed composite section properties are used for all effects that follow deck placement. The deck slab is transformed to beam concrete using E_c (deck)/ E_c (beam). The pretensioning steel and the post-tensioning steel are transformed using E_p/E_c (beam). The elastic loss due to Stage 2 post-tensioning, and the elastic gain due to superimposed dead load are calculated and the net concrete stress at centroid of pretensioning steel is determined. Combined with the creep and shrinkage properties between 60 days and 20,000 days, the long-term loss is calculated. It is found to be 17.682 ksi.

EXTENDING SPANS

18.8.8.3 Time Step Analysis/11.8.9.1 Stress Limits for Concrete

Similar calculations are carried out for post-tensioning Stage 1, except that concrete stresses are calculated at the centroid of the post-tensioning steel at that stage. Also, note that the transformed section should not include the area of the post-tensioning steel until after that steel is anchored to the concrete and grouted. For purposes of loss calculations, grouting is assumed to be completed immediately after a tendon is post-tensioned.

Stresses in the prestressed reinforcement are summarized in **Table 11.8.8.3-1** and are plotted in **Figure 11.8.8.3-1**.

Figure 11.8.8.3-1
Stresses in the Prestressed Reinforcement

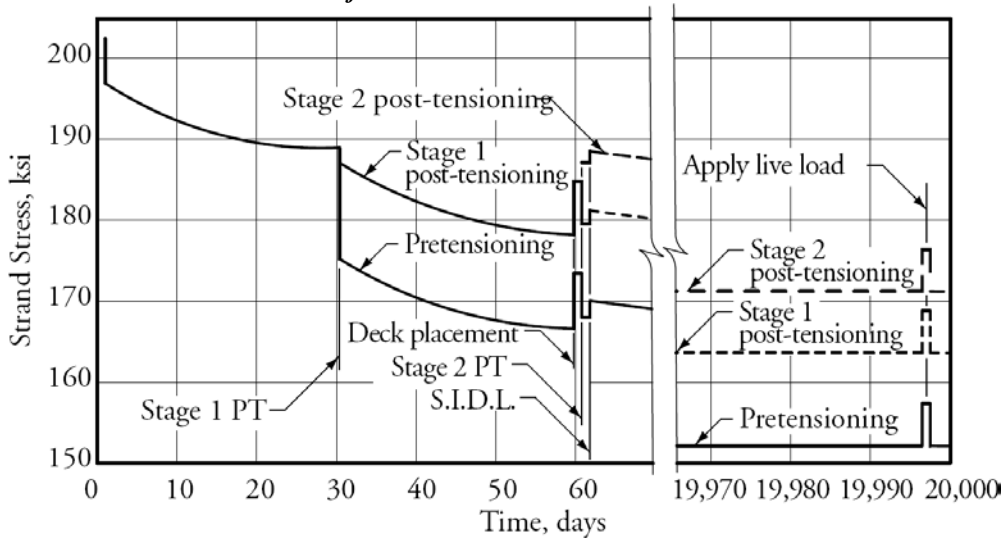


Table 11.8.8.3-1
Prestress Levels at Loading

Loading	Construction Schedule days	Stress, ksi		
		Pretensioning	Stage 1 Post-Tensioning	Stage 2 Post-Tensioning
Pretensioning plus Girder Weight	1	197.0	—	—
Long-Term	1 to 30	189.1	—	—
Stage 1 Post-Tensioning	30	175.3	187.2	—
Long-Term	30 to 60	166.4	178.3	—
Deck Weight	60	173.5	184.9	—
Stage 2 Post-Tensioning	60	168.0	179.6	187.2
Superimposed Dead Load	60	169.8	181.3	188.6
Long-Term	60 to 20,000	152.1	163.7	171.2
Live Load	20,000	163.9	174.9	180.7
80% Live Load (Service III)	20,000	161.6	172.6	178.8

11.8.9 Service Limit State at Section 0.4L

11.8.9.1 Stress Limits for Concrete

[LRFD Art. 5.9.4.2]

Compression:

Due to Service I, permanent load combination:

for the precast beam: $0.45f'_c = 0.45(7.0) = +3.150$ ksi

for the deck slab: $0.45f'_c = 0.45(4.0) = +1.800$ ksi

Due to Service I, full load combination:

for the precast beam: $0.60f'_c = 0.60(7.0) = +4.200$ ksi

for the deck slab: $0.60f'_c = 0.60(4.0) = +2.400$ ksi

Tension:

For Service III, full load combination:

for the precast beam: $-0.19\sqrt{f'_c} = -0.19\sqrt{7.0} = -0.503$ ksi

The conditions at the time of Stage 1 and Stage 2 post-tensioning are considered temporary and tension and compression limits should be the same as for the conditions of Service III.

11.8.9.2 Stage 1 Post-Tensioning

The maximum positive moment section, located at 0.4L, is checked.

- The pretensioning force, $P_{pe} = 28(0.153)(175.311) = 751.0$ kips
- Post-tensioning, Stage 1, $P_{PT} = 22(0.217)(187.18) = 893.6$ kips

$$\begin{aligned}
 f_{tg} &= \frac{(M_g + M_s)}{S_t} + \frac{P_{pe}}{A} - \frac{P_{pe}(e)}{S_t} + \frac{(P_{PT})_{Stage\ 1}}{A} - \frac{(M_{Total})_{Stage\ 1}}{S_t} \\
 &= +\frac{(2,519.7 + 2,089.0)12}{16,276} + \frac{751.0}{839} - \frac{751.0(32.55)}{16,276} + \frac{893.597}{839} - \frac{893.6(2,159.3)}{1,000} \frac{(12)}{16,276} \\
 &= +3.398 + 0.895 - 1.502 + 1.065 - 1.423 = +2.433 \text{ ksi} < +3.150 \text{ ksi} \quad \text{OK}
 \end{aligned}$$

$$\begin{aligned}
 f_b &= \frac{(M_g + M_s)}{S_b} + \frac{P_{pe}}{A} - \frac{P_{pe}(e)}{S_b} + \frac{(P_{PT})_{Stage\ 1}}{A} - \frac{(M_{Total})_{Stage\ 1}}{S_b} \\
 &= +\frac{(2,519.7 + 2,089.0)12}{15,789} + \frac{751.0}{839} - \frac{751.0(32.55)}{15,789} + \frac{893.6}{839} - \frac{893.6(2,159.3)}{1,000} \frac{(12)}{15,789} \\
 &= -3.503 + 0.895 + 1.548 + 1.065 + 1.467 = +1.472 \text{ ksi} < +3.150 \text{ ksi} \quad \text{OK}
 \end{aligned}$$

11.8.9.3 Stage 2 Post-Tensioning

The maximum positive moment section, located at 0.4L, is checked.

Immediately after Stage 2 post-tensioning, the following prestressing forces act on the cross-section:

Pretensioning force, $P_{pe} = 28(0.153)(168.04) = 719.9$ kips

Post-tensioning, Stage 1, $P_{PT} = 22(0.217)(179.59) = 857.4$ kips

Post-tensioning, Stage 2, $P_{PT} = 11(0.217)(187.18) = 446.8$ kips

$$\begin{aligned}
 f_{tg} &= \frac{(M_g + M_s)}{S_t} + \frac{P_{pe}}{A} - \frac{P_{pe}(e)}{S_t} + \frac{(P_{PT})_{Stage\ 1}}{A} + \frac{(M_{Total})_{Stage\ 1}}{S_t} + \frac{(P_{PT})_{Stage\ 2}}{A_c} + \frac{(M_{Total})_{Stage\ 2}}{S_{tg}} \\
 &= \frac{(2,519.7 + 2,089.0)(12)}{16,276} + \frac{719.9}{839} - \frac{719.9(32.55)}{16,276} \\
 &\quad + \frac{857.4}{839} - \frac{857.4(2,159.3)}{1,000} \frac{(12)}{16,276} + \frac{446.8}{1,487} + \frac{446.8(1,256.0)}{500} \frac{(12)}{63,428} \\
 &= +3.398 + 0.858 - 1.440 + 1.022 - 1.365 + 0.300 - 0.212
 \end{aligned}$$

$f_b = +2.561$ ksi < +3.150 ksi OK

$$-\frac{(M_g + M_s)}{S_b} + \frac{P_{pe}}{A} - \frac{P_{pe}(e)}{S_b} + \frac{(P_{PT})_{Stage\ 1}}{A} + \frac{(M_{Total})_{Stage\ 1}}{S_b} + \frac{(P_{PT})_{Stage\ 2}}{A_c} + \frac{(M_{Total})_{Stage\ 2}}{S_{bc}}$$

EXTENDING SPANS

11.8.9.3 Stage 2 Post-Tensioning/11.8.9.5 Tension Due to Service III Loads

$$\begin{aligned}
&= \frac{(2,519.7 + 2,089.0)(12)}{15,789} + \frac{719.9}{839} + \frac{719.9(32.55)}{15,789} \\
&\quad + \frac{857.4}{839} + \frac{857.4(2,159.3)}{1,000} \frac{(12)}{15,789} + \frac{446.8}{1,487} + \frac{446.8(1,256.0)}{500} \frac{(12)}{63,428} \\
&= -3.503 + 0.858 + 1.484 + 1.022 + 1.407 + 0.300 + 0.628 \\
&= +2.196 \text{ ksi} < +3.150 \text{ ksi} \quad \text{OK}
\end{aligned}$$

11.8.9.4 Compression Due to Service I Loads

To check compressive stress at the top fiber of the beam, two cases are checked as follows:

1. Under Permanent Load Combination, Service I:

At long term without the live load effect, the following prestressing forces act on the cross-section:

- Pretensioning force, $P_{pe} = 28(0.153)(152.14) = 651.8$ kips
- Post-tensioning, Stage 1, $P_{PT} = 22(0.217)(163.646) = 781.2$ kips
- Post-tensioning, Stage 2, $P_{PT} = 11(0.217)(171.245) = 408.8$ kips

Using bending moment values given in **Table 11.8.4-1**, concrete stress at the top fiber of the beam is:

$$\begin{aligned}
f_{tg} &= + \frac{(M_g + M_s)}{S_t} + \frac{(M_{ws} + M_b)}{S_{tg}} + \frac{P_{pe}}{A} - \frac{P_{pe}(e)}{S_t} + \frac{(P_{PT})_{Stage 1}}{A} - \frac{(M_{Total})_{Stage 1}}{S_t} + \frac{(P_{PT})_{Stage 2}}{A} - \frac{(M_{Total})_{Stage 2}}{S_{tg}} \\
&= \frac{(2,519.7 + 2,089.0)(12)}{16,276} + \frac{(442.3 + 252.3)(12)}{63,428} + \frac{651.8}{839} - \frac{651.8(32.55)}{16,276} \\
&\quad + \frac{781.2}{839} - \frac{781.2(2,159.3)}{1,000} \frac{(12)}{16,276} + \frac{408.8}{1,487} - \frac{408.8(1,256.0)}{500} \frac{(12)}{63,428} \\
&= 3.398 + 0.131 + 0.777 - 1.304 + 0.931 - 1.244 + 0.275 - 0.194 \\
&= +2.770 \text{ ksi} < +3.150 \text{ ksi} \quad \text{OK}
\end{aligned}$$

2. Under Full Load Combination, Service I:

$$\begin{aligned}
f_{tg} &= 2.770 + \frac{M_{LL+I}}{S_{tg}} = 2.770 + \frac{4,585.9(12)}{63,428} \\
&= 2.770 + 0.868 = +3.638 \text{ ksi} < +4.200 \text{ ksi} \quad \text{OK}
\end{aligned}$$

11.8.9.5 Tension Due to Service III Loads

At long term with 80 percent live load effect, the following prestressing forces act on the cross-section:

Pretensioning force, $P_{pe} = 28(0.153)(161.557) = 692.1$ kips

Post-tensioning, Stage 1, $P_{PT} = 22(0.217)(172.623) = 824.1$ kips

Post-tensioning, Stage 2, $P_{PT} = 11(0.217)(178.828) = 426.9$ kips

$$\begin{aligned}
f_b &= - \frac{(M_g + M_s)}{S_b} - \frac{(M_{ws} + M_b + 0.8M_{LL+I})}{S_{bc}} + \frac{P_{pe}}{A} - \frac{P_{pe}(e)}{S_b} + \frac{(P_{PT})_{Stage 1}}{A} + \frac{(M_{Total})_{Stage 1}}{S_b} + \frac{(P_{PT})_{Stage 2}}{A} \\
&\quad + \frac{(M_{Total})_{Stage 2}}{S_{bc}} \\
&= - \frac{(2,519.7 + 2,089.0)(12)}{15,789} - \frac{(442.3 + 252.3 + 0.8(4,585.9))(12)}{21,441} + \frac{692.1}{839} + \frac{692.1(32.55)}{15,789} \\
&\quad + \frac{824.1}{839} + \frac{824.1(2,159.3)}{1,000} \frac{(12)}{15,789} + \frac{426.9}{1,487} + \frac{426.9(1,256.0)}{500} \frac{(12)}{21,441}
\end{aligned}$$

$$= -3.503 - 2.442 + 0.825 + 1.427 + 0.982 + 1.352 + 0.287 + 0.600$$

$$= -0.472 \text{ ksi} > -0.503 \text{ ksi} \quad \text{OK}$$

The above process should be repeated for several sections along the span, usually 1/10th span points.

11.8.10 Stresses at Transfer of Pretensioning Force

11.8.10.1 Stress Limits for Concrete

[LRFD Art. 5.9.4.1]

Compression: $0.6f'_{ci} = 0.6(5.5) = 3.300 \text{ ksi}$

Tension without bonded auxiliary reinforcement:

$$-0.0948 \sqrt{f'_{ci}} = -0.0948 \sqrt{5.5} = -0.222 \text{ ksi} \leq -0.200 \text{ ksi}$$

Therefore, -0.200 ksi controls.

Tension with bonded auxiliary reinforcement which is sufficient to resist the tension force in the concrete:

$$-0.24 \sqrt{f'_{ci}} = -0.24 \sqrt{5.5} = -0.563 \text{ ksi}$$

11.8.10.2 Stresses at Transfer Length Section

Stresses at the end of the transfer length must be checked at time of transfer. This stage usually governs design. However, the magnitude of losses will lessen with time, rendering the concrete stresses less critical.

$$P_i = (28)(0.153)(189.055) = 809.9 \text{ kips}$$

$$\text{Transfer length} = 60(\text{Strand diameters}) = 60(0.5) = 30 \text{ in.} = 2.5 \text{ ft}$$

[LRFD Art. 5.8.2.3]

Bending moment at a distance 2.5 ft from the end of the beam due to beam self-weight:

$$M_g = (0.5)(0.874)(2.5)(155 - 2.5) = 166.6 \text{ ft-kips.}$$

Stress at the top fiber of the beam:

$$f_t = \frac{P_i}{A} - \frac{P_i e_c}{S_t} + \frac{M_g}{S_t} = \frac{809.911}{839} - \frac{(809.9)(32.55)}{16,276} + \frac{(166.6)(12)}{16,276}$$

$$= 0.965 - 1.620 + 0.123 = -0.532 \text{ ksi} > -0.563 \text{ ksi} \quad \text{OK}$$

Stress at the bottom fiber of the beam:

$$f_b = \frac{P_i}{A} + \frac{P_i e_c}{S_b} - \frac{M_g}{S_b} = \frac{809.9}{839} + \frac{(809.9)(32.55)}{15,789} - \frac{(166.6)(12)}{15,789}$$

$$= 0.965 + 1.670 - 0.127 = +2.508 \text{ ksi} < +3.300 \text{ ksi} \quad \text{OK}$$

Tensile stress satisfies the limit for concrete with bonded reinforcement (-0.563 ksi). Crack control conventional reinforcement at the top of the precast beam is required to satisfy the *LRFD Specifications*. Refer to Chapters 8 and 9 of this manual for additional details. Compressive stress is within the limit of $+3.300 \text{ ksi}$.

11.8.10.3 Stresses at Midspan

Bending moment due to the weight of the beam at midspan:

$$M_g = (0.5)(0.874)(77.5)(155 - 77.5) = 2,624.7 \text{ ft-kips}$$

Concrete stress at the top fiber of the beam:

$$f_t = \frac{809.9}{839} - \frac{809.9(32.55)}{16,276} + \frac{(2,624.7)(12)}{16,276}$$

$$= 0.965 - 1.620 + 1.935 = +1.280 \text{ ksi} \quad \text{OK}$$

Concrete stress at the bottom fiber of the beam:

$$f_b = \frac{809.9}{839} + \frac{809.9(32.55)}{15,789} - \frac{(2,624.7)(12)}{15,789}$$

$$= 0.965 + 1.670 - 1.995 = +0.640 \text{ ksi OK}$$

11.8.11 Strength Limit State

11.8.11.1 Positive Moment Section

Using the values of bending moments from **Tables 11.8.4-1, 11.8.6.2-1 and 11.8.6.2-2**, total ultimate bending moment for Strength I is:

For Stage 1 post-tensioning, $M_{secondary} = \left(\frac{822.08}{1,000}\right)(365.7) = 300.6 \text{ ft-kips}$

For Stage 2 post-tensioning, $M_{secondary} = \left(\frac{411.05}{500}\right)(429.0) = 352.7 \text{ ft-kips}$

$$M_u = 1.25(DC) + 1.5(DW) + 1.75(LL + IM) + 1.0(M_{secondary}) \quad \text{[LRFD Tables 3.4.1-1\&2]}$$

$$M_u = 1.25(2,519.7 + 2,089.0 + 252.3) + 1.5(442.3) + 1.75(4,585.9) + 1.0(300.6 + 352.7) = 15,418.3 \text{ ft-kips}$$

At this section, there are three layers of prestressing steel, as shown in **Table 11.8.11.1-1**.

Table 11.8.11.1-1
Prestressing Steel at 0.4L

Layer	A_{ps} , in. ²	Distance from Bottom of Section, in.
Pretensioned Strands	4.284	4.0
Post-Tensioning Stage 1	4.774	6.25
Post-Tensioning Stage 2	2.387	13.375
Total	11.445	—

This example used the strain compatibility approach to calculate the capacity of the section. For detailed information on the method, please refer to Chapter 8. The *LRFD Specifications* approximate formulas are not recommended in this type of application.

Using the strain compatibility method, the following results are obtained:

The distance from top of the composite section to the neutral axis, $c = 9.97 \text{ in.}$

The depth of the rectangular stress block, $a = 8.36 \text{ in.}$

The nominal moment capacity, $M_n = 17,504.9 \text{ ft-kips}$

Average stress in the pretensioning steel, $f_{ps} = 268.0 \text{ ksi}$

Average stress in the post-tensioning steel, Stage 1, $f_{ps} = 267.9 \text{ ksi}$

Average stress in the post-tensioning steel, Stage 2, $f_{ps} = 266.0 \text{ ksi}$

$$\text{Factored flexural resistance, } M_r = \phi M_n \quad \text{[LRFD Eq. 5.7.3.2.1-1]}$$

where

$$\phi = \text{resistance factor} = 1.00, \text{ for flexure and tension of prestressed concrete} \quad \text{[LRFD Art. 5.5.4.2.1]}$$

$$M_r = 17,504.9 \text{ ft-kips} > M_u = 15,418.3 \text{ ft-kips} \quad \text{OK}$$

11.8.11.2 Negative Moment Section

Ignoring the width of the pier diaphragm and using the values of bending moments from **Table 11.8.4-1**, **Table 11.8.6.2-1** and **Table 11.8.6.2-2**, the total factored bending moment for Strength I is:

$$\text{For Stage 1 post-tensioning, } M_{\text{secondary}} = \left(\frac{822.08}{1,000}\right)(914.3) = 751.6 \text{ ft-kips}$$

$$\text{For Stage 2 post-tensioning, } M_{\text{secondary}} = \left(\frac{411.05}{500}\right)(1,072.6) = 881.8 \text{ ft-kips}$$

The ultimate moment is computed using load factors found in LRFD Tables 3.4.1-1 & 2. The load factor for secondary moments is determined by the factor for "EL" defined in LRFD Article 3.3.2.

$$M_u = 1.25(DC) + 1.5(DW) + 1.75(LL + IM) + 1.0(M_{\text{secondary}}) \quad [\text{LRFD Tables 3.4.1-1 \& 2}]$$

$$M_u = 1.25(-3,730.1 - 450.5) + 1.5(-789.9) + 1.75(-4,455.4) + 1.0(751.6 + 881.8) = -12,574.2 \text{ ft-kips}$$

The compression face is the bottom flange of the beam, which is 27-in. wide. The deck reinforcement in the longitudinal direction is assumed to be No. 6 @ 6-in. top and bottom. At this section there are three layers of reinforcement as shown in **Table 11.8.11.2-1**.

Table 11.8.11.2-1
Reinforcing Steel at the Pier

Layer	Area of Steel in. ²	Distance from Top of the Composite Section, in.
Reinforcement in the Deck	16.72	3.8
Post-Tensioning Stage 1	4.77	17.5
Post-Tensioning Stage 2	2.39	10.4
Total	23.88	—

Using the strain compatibility method, the depth of the compression block is large and the stress in the prestressing steel is low, causing the steel to be used inefficiently. This is due to the relatively small bottom flange of the AASHTO-PCI Bulb Tee, which was not originally developed for continuous post-tensioned applications. If this section is the only one available locally, the compression capacity of the bottom flange can be enhanced in several ways:

- Increase the strength of the concrete in the precast beam.
- Add compression reinforcement in the bottom flange of the precast beam if it does not interfere with the pretensioning strands already there.
- Add a structural steel plate embedded in the bottom of the precast section. Make the plate composite through the use of studs, similar to the connection of plate girders to deck slabs.

In this example, if a 1-in.-thick steel plate is used, strain compatibility analysis produces the following results:

Neutral axis depth, $c = 11.90$ in.

Rectangular stress block depth, $a = 8.33$ in.

Stress in mild reinforcement, $f_{ps} = 60.0$ ksi

Average stress in Stage 1 post-tensioning steel, $f_{ps} = 262.6$ ksi

Stress in Stage 2 post-tensioning, $f_{ps} = 264.2$ ksi

Nominal capacity, $M_n = 16,393.7$ ft-kips

Factored flexural resistance, $M_r = \phi M_n$

[LRFD Eq. 5.7.3.2.1-1]

EXTENDING SPANS

11.8.11.2 Negative Moment Section/11.8.12.1 Positive Moment Section

where

$$\phi = \text{resistance factor} = 1.00, \text{ for flexure and tension of prestressed concrete} \quad [\text{LRFD Art. 5.5.4.2.1}]$$

$$M_r = 16,393.7 \text{ ft-kips} > M_u = 12,574.2 \text{ ft-kips} \quad \text{OK}$$

Further design refinement may prove that a thinner plate is adequate. It will also determine the location where the plate may be terminated.

11.8.12 Limits of Reinforcement

11.8.12.1 Positive Moment Section

This section is a prestressed reinforced concrete section.

According to LRFD Article 5.7.3.3.2, the minimum amount of prestressed and nonprestressed tensile reinforcement should be adequate to develop a factored flexural resistance, M_r , equal to the lesser of 1.2 times the cracking strength determined on the basis of elastic stress distribution and the modulus of rupture, and 1.33 times the factored moment required by the applicable strength load combination.

At midspan:

The cracking moment:

$$M_{cr} = (f_r + f_{cpe})S_c - M_{dnc}(S_c/S_{nc} - 1) \geq S_c f_r \quad [\text{LRFD Eq. 5.7.3.3.2-1}]$$

where

$$f_r = \text{modulus of rupture} = 0.24 \sqrt{f'_c} = 0.24 \sqrt{7.0} = 0.635 \text{ ksi} \quad [\text{LRFD Art. 5.4.2.6}]$$

$$f_{cpe} = \text{compressive stress in concrete due to effective prestress force only (after allowance for all prestress losses) at extreme fiber of the section where tensile stress is caused by externally applied loads}$$

$$\begin{aligned} &= \left(\frac{P_{pe}}{A} + \frac{P_{pe}e_c}{S_b} \right)_{\text{Pretensioning}} + \left(\frac{P_{pe}}{A} + \frac{M_{Total}}{S_b} \right)_{P/T \text{ Stage } 1} + \left(\frac{P_{pe}}{A} + \frac{M_{Total}}{S_{bc}} \right)_{P/T \text{ Stage } 2} \\ &= \left(\frac{651.768}{839} + \frac{651.768(32.55)}{15,789} \right) + \left(\frac{781.246}{839} + \frac{1,686.94(12)}{15,789} \right) + \left(\frac{408.762}{1,487} + \frac{1,026.81(12)}{21,441} \right) \\ &= 2.211 + 2.213 + 0.850 = 5.274 \text{ ksi} \end{aligned}$$

$$M_{dnc} = \text{moment due to non-composite dead loads}$$

$$= M_g + M_s = 2,519.7 + 2,089.0 = 4,608.7 \text{ ft-kips}$$

$$S_c = \text{composite section modulus for the extreme fiber of the section where the tensile stress is caused by externally applied loads} = 21,441 \text{ in.}^3$$

$$S_{nc} = \text{non-composite section modulus for the extreme fiber of the section where the tensile stress is caused by externally applied loads} = 15,789 \text{ in.}^3$$

$$M_{cr} = (0.635 + 5.274) \left(\frac{15,789}{12} \right) - (4,608.7) \left(\frac{21,441}{15,789} - 1 \right) = 6,125.0 \text{ ft-kips}$$

$$1.2M_{cr} = 1.2(6,125.0) = 7,350.0 \text{ ft-kips}$$

At midspan, the factored moment required by the Strength I load combination,

$$M_u = 15,418.3 \text{ ft-kips}$$

$$1.33M_u = 1.33(15,433.4) = 20,506.3 \text{ ft-kips}$$

Since $1.2M_{cr} < 1.33M_u$, $1.2M_{cr}$ controls, and, $M_r = 17,504.87 \text{ ft-kips} > 1.2M_{cr}$ OK

11.8.13 Shear Design

For an example of detailed calculations of shear design, refer to Example 9.1 of Chapter 9. The following calculation is intended to demonstrate the feasibility of this beam size in shear and the order of magnitude of the shear reinforcement required.

A section at 7.1 ft away from the pier centerline is considered. The factored shear, $V_u = 482.7$ kips, and the factored moment, $M_u = 12,056.2$ ft-kips.

Based on the *LRFD Specifications*, the effective web width for shear after the duct is grouted, is the gross web width minus 25% of the duct diameter:

$$b_v = 7.00 - 3.75/4 = 6.06 \text{ in.} \quad [\text{LRFD Art. 5.8.2.7}]$$

The effective depth for shear, $d_v = 61.32$ in. By conservatively assuming that $\beta = 2$ and $\theta = 45^\circ$, the calculated V_c and V_p are 62.1 kips and 56.90 kips respectively, and the required $V_s = 417.3$ kips. Therefore, the required A_v/s is calculated to be 1.36 in.²/ft.

Use WWR D20 with 3 in. spacing. The sum of V_c and V_s is 479.72 kips, which is less than maximum limit of $0.25f'_c b_v d_v = 650.3$ kips.

11.8.14 Comments and Remaining Steps

The calculations presented in Section 11.8 cover the preliminary design steps needed to

- check adequacy of the precast member for the selected span and spacing,
- determine concrete strength,
- determine the amount of pretensioning required, and
- determine the amount of post-tensioning required.

After a solution is established, a thorough and detailed design should be performed. As a minimum, a commercially available continuous beam analysis program is needed for the detailed analysis for post-tensioning and live load effects. Specialized programs for computing moments and shears from LRFD live loads may also be used.

The following items should be considered in completing the design:

1. Calculate the prestress losses at various stages of loading and construction, specifically at pretension transfer, Stage 1 post-tensioning, Stage 2 post-tensioning, and final time.
2. Determine the bending moments and shear forces due to pretensioning, dead loads, and live loads. A spreadsheet table could be used to organize the calculations at equal span increments, say tenth points of each span.
3. Conduct service load analysis and check concrete stresses at various sections and various loading and construction stages. Modify prestressing if necessary and recycle the analysis.
4. Conduct strength analysis. Avoid the unnecessary penalties imposed by the *LRFD Specifications* described earlier in this example, by using the strain compatibility approach in Section 8.2.2.5 of this manual. If there is strength deficiency in a positive moment area, attempt to correct it by providing additional pretensioning. If there is a deficiency in a negative moment area, attempt to correct it by providing additional deck reinforcement.
5. Calculate cambers and deflections. Use this information to determine requirements for setting the build-up over the beam top flange, and for setting the beam seat elevations to match the roadway profile. Also, check to see that live load deflection is within the optimal limits.
6. Conduct a thorough shear design. Systems of this type have a reduced equivalent web width due to the presence of post-tensioning ducts. The *LRFD Specifications* limit of $0.25f'_c b_v d_v$ on the maximum shear force controls the design in many cases.
7. Design and detail the post-tensioning anchorage zone, as suggested in Section 11.7

In addition to the above items, further design considerations could include: treatment of transverse displacement, the accumulation of creep, shrinkage, thermal movement, integral super and substructure, double end stressing, shoring tower and strong back design.

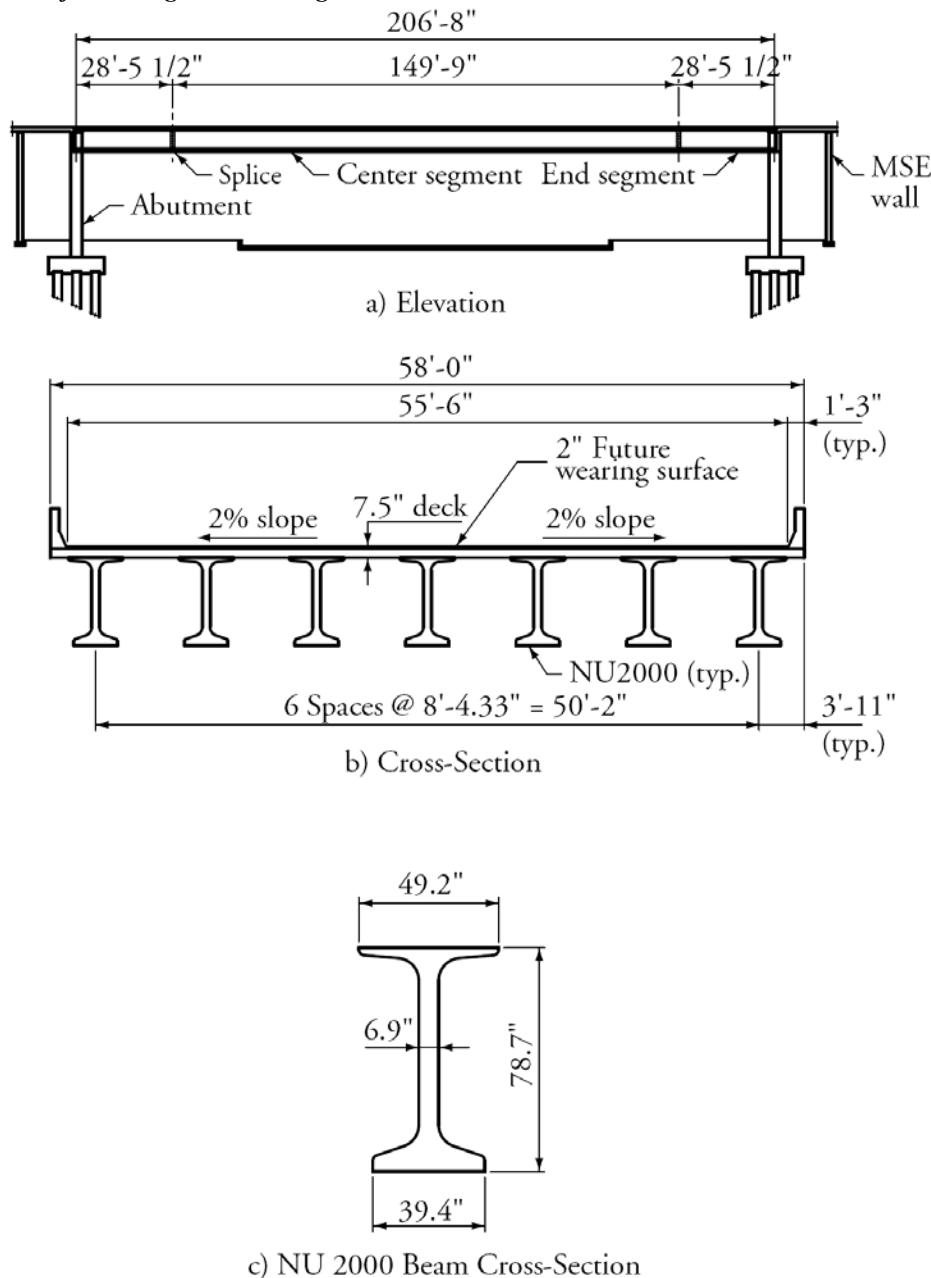
11.9 DESIGN EXAMPLE: SINGLE SPAN, THREE SEGMENT BEAM

This example provides a summary of the calculations for a bridge constructed in 2003 and 2004 in Omaha, Nebraska, at Dodge Street (U.S. Highway 6) and 204th Street (Nebraska Highway 31). Some of the significant considerations are presented in summary.

11.9.1 Input Data and Design Criteria

The length of this single-span bridge is 206.7 ft. The project used the NU2000PT (Nebraska) I-beam. The beam depth is 78.74 in. (2,000 mm) and web width is 6.9 in. The bridge section consists of seven beams spaced at 8 ft-4.3 in. The bridge is 58 ft wide. Details of the bridge are shown in **Figure 11.9.1-1**.

*Figure 11.9.1-1
Details of the Dodge Street Bridge*



EXTENDING SPANS**11.9.1 Input Data and Design Criteria/11.9.2 Construction Stages**

A composite, 8-in.-thick concrete slab (7.5-in. structural depth) is cast-in-place. Each beam line uses three beam segments. The end segments are approximately 28 ft long each and the center segment is nearly 149 ft long. These lengths are in addition to two, 12-in.-wide spaces for the splices. The specified compressive strengths of the precast beam concrete and CIP slab are 10 ksi and 4.3 ksi, respectively. The bridge is designed in accordance with *LRFD Specifications*, 2nd Edition and the 1999 and 2000 Interim Revisions. Design live load is HL-93.

11.9.2 Construction Stages

The construction stages are as follows:

Stage 1a: Fabricate precast beam segments

Stage 1b: Erect precast beam segments on temporary towers and abutments

Stage 2: Splice post-tensioning ducts and cast splice

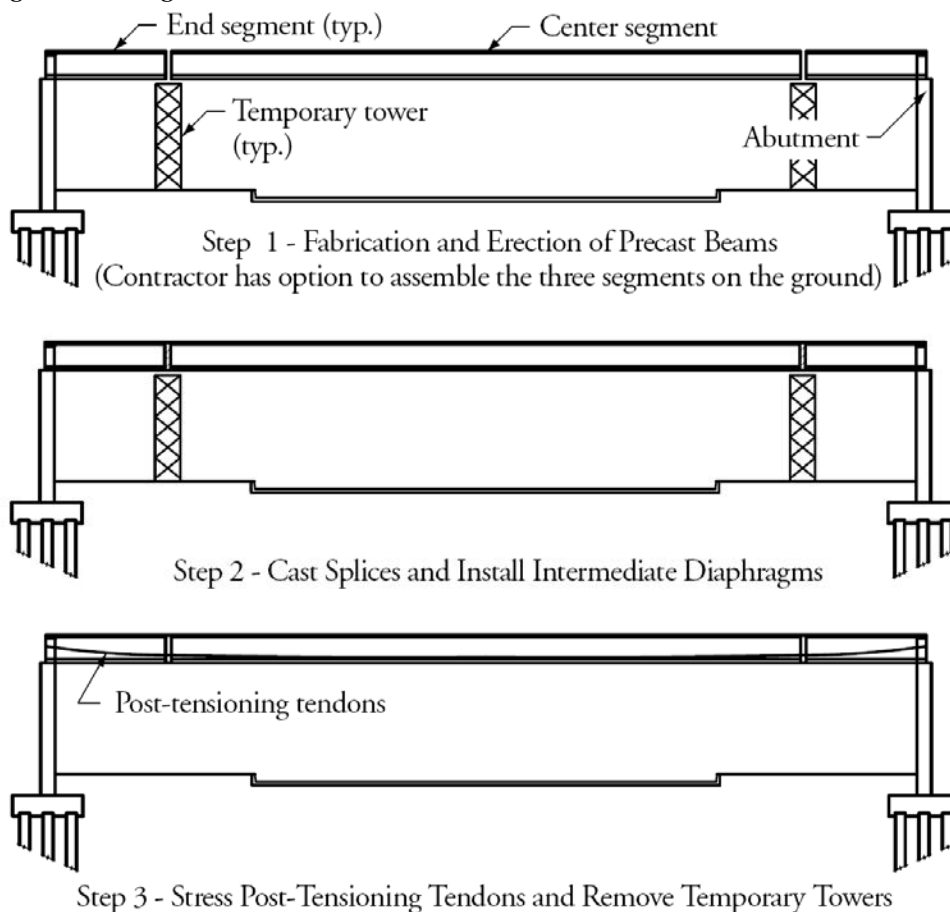
Stage 3: Stress post-tension tendons and remove temporary towers

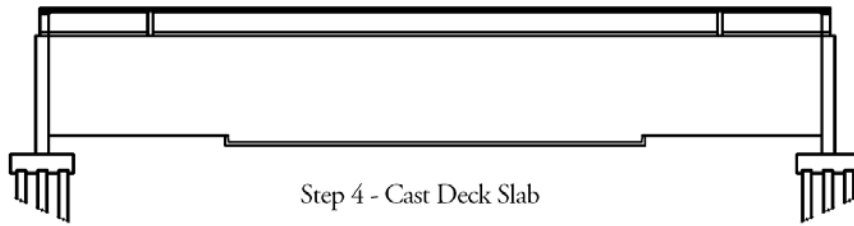
Stage 4: Place deck slab

Stage 5: Construct barriers

The construction stages are summarized in **Figure 11.9.2-1**. This construction schedule does not provide compression in the deck, since all post-tensioning is applied before the deck is cast. This solution is also less efficient, since only the beam is post-tensioned. However, this does permit removal of the deck for replacement.

Figure 11.9.2-1
Construction Sequence of the Dodge Street Bridge





11.9.3 Flexure at Service Limit State

The critical section in flexure, after all losses, due to full loads plus effective prestress, is at midspan. For pretensioning and post-tensioning details, see **Figures 11.9.3-1** and **11.9.3-2** respectively.

Figure 11.9.3-1
Pretensioning Details

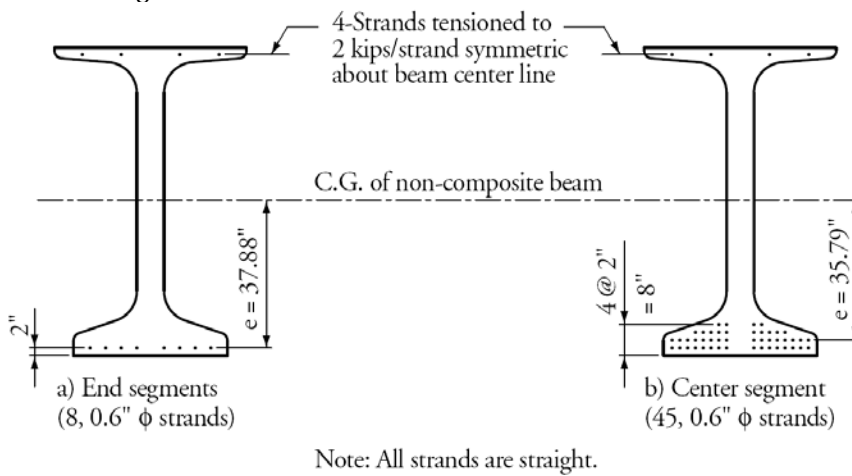
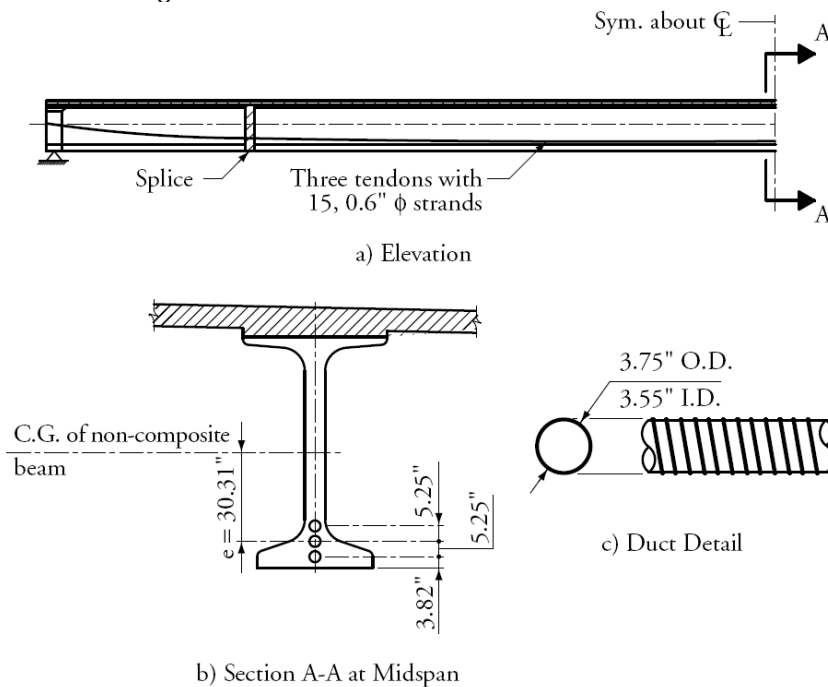


Figure 11.9.3-2
Post-Tensioning Details



EXTENDING SPANS**11.9.3 Flexure at Service Limit State/11.9.4 Flexural at Strength Limit State**

Table 11.9.3-1 provides the bending moments for an interior beam line. **Table 11.9.3-2** gives a summary of the concrete stresses at midspan. The table shows that the most critical stress is concrete compression at the top fibers of the beam due to effective prestress plus permanent loads. The stress limit in the *LRFD Specifications* is $0.45 f'_c$, which required the beam concrete strength to be specified at 10 ksi.

Table 11.9.3-1
Bending Moments at Midspan

Loading	Bending Moment at Midspan Section ft-kips
Girder Weight	2,774.5
Support Removal	2,499.2
Deck Slab	4,464.8
Wearing Surface	1,116.2
Barriers	560.8
Live Loads	5,031.5

Table 11.9.3-2
Service Load Stresses at Midspan

Location	Top of Slab, ksi Service I		Top of Beam, ksi Service I		Bottom of Beam, ksi Service III
	Permanent Loads	Total Loads	Permanent Loads	Total Loads	
At Midspan	0.279	1.117	4.492	5.491	1.054
Allowable Stress	1.935	2.580	4.500	6.000	-0.600

11.9.4 Flexure at Strength Limit State

The required factored bending moment is:

$$M_u = 1.25(DC) + 1.5(DW) + 1.75(LL + IM) + 1.0(M_{secondary}) \quad [\text{LRFD Tables 3.4.1-1 \& 2}]$$

Since this is a statically determinate beam, there are no secondary effects from post-tensioning.

$$M_u = 1.25(2,774.5 + 2,499.2 + 4,464.8 + 560.8) + 1.5(1,116.2) + 1.75(5,031.5) = 23,353.6 \text{ ft-kips}$$

At this section, there are seven layers of prestressing steel as shown in **Table 11.9.4-1**.

Using the strain compatibility method, the following results are found:

Neutral axis depth, $c = 32.3$ in.

Stress block depth, $a = 24.5$ in.

Stress in the pretensioning steel varies from 244.0ksi to 247.9 ksi

Stress in the post-tensioning steel varied from 241.9 ksi to 246.5 ksi

$$M_r = 27,317.7 \text{ ft-kips} > M_u = 23,353.6 \text{ ft-kips} \quad \text{OK}$$

Table 11.9.4-1
Prestressing Steel at Midspan

Layer	A_{ps} in. ²	Distance from Bottom of Section, in.
Layer 1 Pretensioning Strands	3.472	2.00
Layer 2 Pretensioning Strands	3.472	4.00
Layer 3 Pretensioning Strands	2.170	6.00
Layer 4 Pretensioning Strands	0.868	8.00
First Post-Tensioning Tendon	3.255	3.88
Second Post-Tensioning Tendon	3.255	8.63
Second Post-Tensioning Tendon	3.255	13.38

11.9.5 Discussion

This is a simple, yet important application of spliced beams. Single-point urban interchanges such as the Dodge Street Bridge are becoming increasingly important. They require a single long, wide span.

Production and handling of 200-ft-long beams would be challenging in most areas, although it has been achieved, for example, on the Bow River (Sect. 11.5.4). Temporary towers were used to support the segments during construction of the Dodge Street Bridge. However, post-tensioning segments together on the ground, then lifting the full-length beam into place is also challenging and requires careful slenderness calculations and the use of larger erection equipment. Before a decision is made, all of these options should be investigated for each project. Contractors can be an excellent resource to designers in this situation and are usually willing to contribute. Many precasters have had experience furnishing these products and are also good resources. It is practically impossible to achieve the span demonstrated by this example without carefully combining pretensioning with post-tensioning.

The 10 ksi specified concrete strength for the Dodge Street Bridge beams helped keep the compressive stress due to effective prestress plus permanent loads below the *LRFD Specifications* limit of $0.45f'_c$. This strength is now achievable in most parts of the country. In addition, the strength of the deck could be increased to improve behavior at both service and strength limit states.

On bridges of this type, it is important to carefully calculate instantaneous and long-term deflections at various stages of loading and at final conditions. Net long-term deflection may be downward. To compensate for a possible sag in the span, which may be psychologically unacceptable, the elevations of the temporary tower supports can be raised to create a cambered beam.

More useful design and construction details can be found in an article by Van Lund, et al. (2002) on the Twisp River Bridge in Washington State, which is similar to the bridge in this example.

11.10 REFERENCES

1. AASHTO. 2011. *AASHTO LRFD Bridge Design Specifications*, Fifth Edition with 2011 Interims, American Association of State Highway and Transportation Officials, Washington, DC.
https://bookstore.transportation.org/item_details.aspx?id=1560 (Fee)
2. AASHTO. 2011. *AASHTO LRFD Bridge Construction Specifications*, Third Edition with 2011 Interims, American Association of State Highway and Transportation Officials, Washington, DC.
https://bookstore.transportation.org/item_details.aspx?id=1560 (Fee)
3. Abdel-Karim, A. M. 1991. *Analysis and Design of Precast/Prestressed Spliced-Girder Bridges*. University of Nebraska-Lincoln, Omaha, NE, 178 pp. Ph.D. dissertation.
<http://proquest.umi.com/pqdlink?Ver=1&Exp=11-18-2016&FMT=7&DID=747159141&RQT=309&attempt=1&cfc=1> (Fee)
4. Abdel-Karim, A. M. and M. K. Tadros. 1992. "Design and Construction of Spliced I-Girder Bridges," *PCI Journal*, Precast/Prestressed Concrete Institute, Chicago, IL. V. 37, No. 4 (July-August), pp. 114-122.
http://www.pci.org/view_file.cfm?file=JL-92-JULY-AUGUST-33.pdf
5. ACI Committee 363. 2010. *High-Strength Concrete* (ACI 363R-10). American Concrete Institute, Farmington Hills, MI, 65 pp.
<http://www.concrete.org/PUBS/newpubs/36310.htm> (Fee)
6. Bexten, K. A., S. Hennessey, and B. LeBlanc. 2002. "The Bow River Bridge—A Precast Record," *HPC Bridge Views*, Issue No. 22 (July/August), Federal Highway Administration /National Concrete Bridge Council, c/o Portland Cement Association, Skokie, IL.
http://www.cement.org/pdf_files/hpc-22julaug02.pdf
7. Breen, J. E., O. Burdet, C. Roberts, D. Sanders, G. Wollmann. 1994. *Anchorage Zone Reinforcement for Post-Tensioned Concrete Girders*. NCHRP Report 356. Transportation Research Board, Washington, DC,
<http://pubsindex.trb.org/view/1994/m/388973>
8. Caroland, W. B., D. Depp, H. H. Janssen, L. Spaans. 1992. "Spliced Segmental Prestressed Concrete I-Beams for Shelby Creek Bridge," *PCI Journal*, Precast/Prestressed Concrete Institute, Chicago, IL. V. 37, No. 5 (September-October), pp. 22-33.
http://www.pci.org/view_file.cfm?file=JL-92-SEPTEMBER-OCTOBER-4.pdf
http://www.pci.org/view_file.cfm?file=JL-92-SEPTEMBER-OCTOBER-5.pdf
http://www.pci.org/view_file.cfm?file=JL-92-SEPTEMBER-OCTOBER-6.pdf
http://www.pci.org/view_file.cfm?file=JL-92-SEPTEMBER-OCTOBER-7.pdf
http://www.pci.org/view_file.cfm?file=JL-92-SEPTEMBER-OCTOBER-8.pdf
http://www.pci.org/view_file.cfm?file=JL-92-SEPTEMBER-OCTOBER-9.pdf
http://www.pci.org/view_file.cfm?file=JL-92-SEPTEMBER-OCTOBER-10.pdf
9. Castrodale, R. W. and C. D. White. 2004. *Extending Span Ranges of Precast Prestressed Concrete Girders*. NCHRP Report 517. Transportation Research Board, Washington, DC. 552 pp.
http://www.trb.org/Main/Blurbs/Extending_Span_Ranges_of_Precast_Prestressed_Concr_154330.aspx (Fee)
10. Ficenc, J. A., S. D. Kneip, M. K. Tadros, L. G. Fischer. 1993. "Prestressed Spliced IGirders: Tenth Street Viaduct Project, Lincoln, Nebraska," *PCI Journal*, Precast/Prestressed Concrete Institute, Chicago, IL. V. 38, No. 5 (September-October), pp. 38-48.
http://www.pci.org/view_file.cfm?file=JL-93-SEPTEMBER-OCTOBER-11.pdf
http://www.pci.org/view_file.cfm?file=JL-93-SEPTEMBER-OCTOBER-12.pdf
http://www.pci.org/view_file.cfm?file=JL-93-SEPTEMBER-OCTOBER-13.pdf
http://www.pci.org/view_file.cfm?file=JL-93-SEPTEMBER-OCTOBER-14.pdf
http://www.pci.org/view_file.cfm?file=JL-93-SEPTEMBER-OCTOBER-15.pdf
11. FHWA, 2004. "Post-Tensioning Tendon Installation and Grouting Manual"
<http://www.fhwa.dot.gov/bridge/pt/pt.pdf>
12. Girgis, A., C. Sun, and M. K. Tadros. 2002 "Flexural Strength of Continuous Bridge Girders – Avoiding the Penalty in the AASHTO-LRFD Specifications," *PCI Journal*, Precast/Prestressed Concrete Institute, Chicago, IL.

- V. 47, No. 4 (July-August), pp. 138-141.
http://www.pci.org/view_file.cfm?file=JL-02-JULY-AUGUST-8.pdf
13. Girgis, A. M. 2002. Optimization of Spliced Precast Concrete I-Girder Superstructures. University of Nebraska-Lincoln, Omaha, NE. 150 pp. Ph.D. diss.
<http://digitalcommons.unl.edu/dissertations/AAI3092544>
 14. Hennessey, S. A. and K. A. Bexten. 2002. *Value Engineering Results in Successful Precast Bridge Solution*. Proceedings, Concrete Bridge Conference, October, Nashville, TN, National Concrete Bridge Council and Federal Highway Administration . Precast/Prestressed Concrete Institute, Chicago, IL. CD-ROM. 6 pp.
http://www.pci.org/view_file.cfm?file=JL-02-JULY-AUGUST-4.pdf
 15. Ma, Z., X. Huo, M. K. Tadros, M. Baishya. 1998. "Restraint Moments in Precast/Prestressed Concrete Continuous Bridges," *PCI Journal*, Precast/Prestressed Concrete Institute, Chicago, IL. V. 43, No. 6 (November-December), pp. 40-57.
http://www.pci.org/view_file.cfm?file=JL-98-NOVEMBER-DECEMBER-6.pdf
http://www.pci.org/view_file.cfm?file=JL-98-NOVEMBER-DECEMBER-7.pdf
 16. Ma, Z., M. A. Saleh, and M. K. Tadros. 1999. "Optimized Post-Tensioning Anchorage in Prestressed Concrete I-Beams," *PCI Journal*, Precast/Prestressed Concrete Institute, Chicago, IL. V. 44, No. 2 (March-April), pp. 56-73.
http://www.pci.org/view_file.cfm?file=JL-99-MARCH-APRIL-6.pdf
http://www.pci.org/view_file.cfm?file=JL-99-MARCH-APRIL-7.pdf
 17. Meyer, Karl F. and Lawrence F. Kahn. 2001. *Annotated Bibliography for High Strength Lightweight Prestressed Concrete*. Report to the Office of Materials and Research, Georgia Department of Transportation, Atlanta, GA, 12 pp.
 18. Meyer, Karl F. and Lawrence F. Kahn. 2002 "Lightweight Concrete Reduces Weight and Increases Span Length of Pretensioned Concrete Bridge Girders," *PCI Journal*, Precast/Prestressed Concrete Institute, Chicago, IL. V. 47, No. 1 (January-February), pp. 68-75.
http://www.pci.org/view_file.cfm?file=JL-02-JANUARY-FEBRUARY-18.pdf
 19. Nebraska. 2001. *Nebraska Bridge Office Policies and Procedures Manual*. Nebraska Department of Roads, Lincoln, NE.
 20. Nicholls, J. J. and C. Prussack. 1997. "Innovative Design and Erection Methods Solve Construction of Rock Cut Bridge," *PCI Journal*, Precast/Prestressed Concrete Institute, Chicago, IL. V. 42, No. 4 (July-August), pp. 42-55.
http://www.pci.org/view_file.cfm?file=JL-97-JULY-AUGUST-5.pdf
 21. PCI Committee on Bridges. 1992. *State-of-the-Art of Precast/Prestressed Concrete Spliced Girder Bridges*, (SG-92). Precast/Prestressed Concrete Institute, Chicago, IL. 134 pp.
http://www.pci.org/view_file.cfm?file=SG_92.PDF
 22. PTI. 2000. *Post-Tensioning Manual*, 6th Edition, Chapter VIII, *Anchorage Zone Design*, Post-Tensioning Institute, Farmington Hills, MI. 46 pp. (also published by PTI as a stand-alone publication)
<http://www.scribd.com/doc/57832154/2011-Post-Tensioning-Institute-Publications-Catalog> (Fee)
 23. PTI. 2003. *Specification for Grouting of Post-Tensioned Structures*, Second Edition, Post-Tensioning Institute, Farmington Hills, MI. 60 pp.
<http://www.scribd.com/doc/57832154/2011-Post-Tensioning-Institute-Publications-Catalog> (Fee)
 24. Russell, H. G., J. S. Volz, and R. N. Bruce. 1997. *Optimized Sections for High-Strength Concrete Bridge Girders*. Report No. FHWA-RD-95-180. Federal Highway Administration, U. S. Department of Transportation, Washington, DC. 156 pp.
 25. Saleh, M. A., A. Einea, and M. K. Tadros. 1995. "Creating Continuity in Precast Girder Bridges," *Concrete International*, American Concrete Institute, Farmington Hills, MI. Vol. 17, No. 8, pp. 431-595
http://www.concreteinternational.com/pages/featured_article.asp?ID=1038
 26. Seguirant, Stephen J. 1998. "New Deep WSDOT Standard Sections Extend Spans of Prestressed Concrete Girders," *PCI Journal*, Precast/Prestressed Concrete Institute, Chicago, IL. V. 43, No. 4 (July-August) pp. 92-119.
http://www.pci.org/view_file.cfm?file=JL-98-JULY-AUGUST-7.pdf
http://www.pci.org/view_file.cfm?file=JL-98-JULY-AUGUST-8.pdf

27. Tadros, M. K., A. Ghali, and W. H. Dilger, 1977. "Time-Dependent Analysis of Composite Frames," *ASCE Journal of Structural Engineering*, American Society of Civil Engineers, Reston, VA. V. 103, No. 4 (April), pp. 871-884.
28. Tadros, M. K. and M. A. Khalifa. 1998. *Post-Tensioning Anchorages in Concrete I-Girder Bridges*. Report No. FHWA-NE-98-P486, Research Project SPR-PL- 1(31) P486, Nebraska Department of Roads, Federal Highway Administration and University of Nebraska Center for Infrastructure Research, Lincoln, NE. 198 pp.
29. Tadros, M. K., N. Al-Omaishi, S. J. Seguirant, J.G. Gallt. 2002. *Prestress Losses in Pretensioned High-Strength Concrete Bridge Girders*. NCHRP Report 496, Transportation Research Board, Washington, DC. 120 pp.
http://onlinepubs.trb.org/onlinepubs/nchrp/nchrp_rpt_496.pdf
30. Van Lund, J. A., P. D. Kinderman, and S. J. Seguirant. 2002. "New Deep WSDOT Girders used for the Twisp River Bridge," *PCI Journal*, Precast/Prestressed Concrete Institute, Chicago, IL. V. 47, No. 2 (March-April), pp. 20-31.
http://www.pci.org/view_file.cfm?file=JL-02-MARCH-APRIL-2.pdf

This page intentionally left blank

SKEWED AND CURVED BRIDGES

Table of Contents

NOTATION..... 12 - 5

12.1 SCOPE..... 12 - 9

12.2 SKEW AND GRADE EFFECTS..... 12 - 9

 12.2.1 General..... 12 - 9

 12.2.2 Superstructure Behavior 12 - 9

 12.2.3 Substructure Behavior..... 12 - 10

 12.2.4 Temperature and Volume Change Effects 12 - 12

 12.2.5 Response to Lateral Loads 12 - 13

 12.2.6 Detailing..... 12 - 13

 12.2.6.1 Effects of Grade..... 12 - 13

 12.2.6.2 Skewed Beam Ends 12 - 14

 12.2.6.3 Intermediate Diaphragms..... 12 - 14

 12.2.6.4 Deck Reinforcement 12 - 14

 12.2.6.5 Plans 12 - 14

12.3 CURVED BRIDGE CONFIGURATIONS..... 12 - 15

 12.3.1 General..... 12 - 15

 12.3.1.1 Straight Beams Chorded from Pier to Pier 12 - 15

 12.3.1.2 Straight Segments with Spliced Joints in the Span..... 12 - 16

 12.3.1.3 Curved Beams..... 12 - 16

 12.3.2 Beam Cross-Section Considerations..... 12 - 17

 12.3.2.1 Box Beams Versus I-Beams Versus U-Beams 12 - 17

 12.3.2.2 Box Section Configuration 12 - 17

 12.3.2.3 I-Beam Configuration..... 12 - 18

 12.3.2.4 U-Beam Configuration 12 - 18

 12.3.2.5 Continuity..... 12 - 18

 12.3.2.6 Crossbeams..... 12 - 18

 12.3.2.7 Superelevation 12 - 18

12.4 USEFUL GEOMETRIC APPROXIMATIONS..... 12 - 18

 12.4.1 Arc Offset from Chord 12 - 18

 12.4.2 Excess of Slant Length over Plan Length..... 12 - 19

 12.4.3 Excess of Arc Length over Chord Length..... 12 - 19

 12.4.4 Twist Resulting from Grade 12 - 19

 12.4.5 Center of Gravity of an Arc..... 12 - 21

 12.4.6 Curved Surfaces 12 - 21

12.5 STRUCTURAL BEHAVIOR OF CURVED BRIDGES..... 12 - 22

 12.5.1 Longitudinal Flexure 12 - 22

 12.5.1.1 Analysis as a Straight Beam..... 12 - 22

 12.5.1.2 Loads on Outside Beam..... 12 - 22

 12.5.2 Torsion..... 12 - 22

SKEWED AND CURVED BRIDGES

Table of Contents

12.5.2.1 Torsion in Simple-Span Beams..... 12 - 23

12.5.2.2 Torsion in Continuous Beams..... 12 - 24

12.5.2.3 Behavior of Beam Gridworks in Segmental Spans..... 12 - 25

12.5.3 Crossbeams 12 - 26

12.6 DESIGN CONSIDERATIONS 12 - 26

12.6.1 Validity of Approximations 12 - 26

12.6.2 Loading Stages for Simple Span Box Beams 12 - 27

 12.6.2.1 Bare Beam..... 12 - 27

 12.6.2.2 Non-Composite Gridwork..... 12 - 27

 12.6.2.3 Composite Gridwork..... 12 - 27

12.6.3 Loading Stages for Simple Span I-Beams 12 - 27

 12.6.3.1 Individual Segments..... 12 - 27

 12.6.3.2 Shoring Loads..... 12 - 27

 12.6.3.4 Composite Gridwork..... 12 - 27

12.6.4 Other Design Checks..... 12 - 27

12.7 FABRICATION..... 12 - 28

12.7.1 Box Beams..... 12 - 28

 12.7.1.1 Chord Lengths 12 - 28

 12.7.1.2 Bridge Layout 12 - 28

 12.7.1.3 Forms 12 - 29

 12.7.1.4 Casting..... 12 - 30

 12.7.1.5 Post-Tensioning 12 - 30

12.7.2 I-Beams and Bulb-Tee Beams 12 - 30

 12.7.2.1 Chord Lengths 12 - 30

 12.7.2.2 Bridge Layout 12 - 30

 12.7.2.3 Forms 12 - 30

 12.7.2.4 Casting..... 12 - 30

 12.7.2.5 Pretensioning 12 - 31

12.7.3 U-Beams 12 - 31

 12.7.3.1 Beam Lengths 12 - 31

 12.7.3.2 Forms 12 - 31

 12.7.3.3 Fabrication..... 12 - 31

 12.7.3.4 Post-Tensioning 12 - 31

12.8 HANDLING, TRANSPORTATION, AND ERECTION 12 - 32

12.8.1 Box Beams..... 12 - 32

 12.8.1.1 Handling..... 12 - 32

 12.8.1.2 Transportation..... 12 - 32

 12.8.1.3 Erection..... 12 - 32

12.8.2 I-Beams and Bulb-Tee Beams 12 - 33

SKEWED AND CURVED BRIDGES

Table of Contents

12.8.2.1 Handling and Transportation.....	12 - 33
12.8.2.2 Erection and Post-Tensioning.....	12 - 33
12.8.3 U-Beams	12 - 33
12.9 DESIGN EXAMPLE.....	12 - 34
12.9.1 Introduction	12 - 34
12.9.1.1 Plan Geometry.....	12 - 34
12.9.1.2 Construction.....	12 - 34
12.9.2 Materials	12 - 36
12.9.3 Cross-Section Properties for a Typical Interior Beam.....	12 - 37
12.9.3.1 Non-Composite Non-Transformed Beam Section.....	12 - 37
12.9.3.2 Composite Sections.....	12 - 38
12.9.3.2.1 Effective Flange Width	12 - 38
12.9.3.2.2 Modular Ratio.....	12 - 38
12.9.3.2.3 Transformed Section Properties.....	12 - 39
12.9.4 Loads	12 - 39
12.9.4.1 Dead Loads.....	12 - 40
12.9.4.1.1 Dead Loads Acting on the Non-Composite Structure	12 - 40
12.9.4.1.2 Dead Loads Acting on the Composite Structure	12 - 40
12.9.4.1.3 Total Dead Load.....	12 - 40
12.9.4.2 Live Loads	12 - 40
12.9.4.2.1 Lane Loading.....	12 - 41
12.9.4.2.2 Truck Loading	12 - 41
12.9.4.2.3 Total Live Load	12 - 41
12.9.4.2.4 Centrifugal Force.....	12 - 41
12.9.5 Correction Factors.....	12 - 42
12.9.5.1 Additional Span Length Factor	12 - 42
12.9.5.2 Shift in Center of Gravity	12 - 42
12.9.6 Bending Moments – Outside Exterior Beam.....	12 - 44
12.9.7 Stresses – Outside Exterior Beam.....	12 - 44
12.9.8 Beam Gridwork Computer Models.....	12 - 45
12.9.8.1 Model 1 – Beam Segments on Shores	12 - 45
12.9.8.2 Model 2 – Shore Loads.....	12 - 45
12.9.8.3 Model 3 – Weight of Deck and Haunches	12 - 46
12.9.8.4 Model 4 – Weight of Barriers and Future Wearing Surface.....	12 - 46
12.9.8.5 Model 5 – Lane Loading	12 - 47
12.9.8.6 Model 6 – Truck Loading with Centrifugal Force	12 - 48
12.9.8.7 Summary of Bending Moments	12 - 49
12.9.9 Selection of Prestressing Force.....	12 - 50
12.9.9.1 Pretensioning	12 - 50

SKEWED AND CURVED BRIDGES

Table of Contents

12.9.9.2 Post-Tensioning 12 - 50

12.9.9.3 Model 7 - Post-Tensioning 12 - 51

12.9.10 Results 12 - 52

 12.9.10.1 Stresses in Outside Exterior Beam 12 - 52

 12.9.10.2 Strength Limit State 12 - 53

 12.9.10.3 Crossbeams 12 - 53

 12.9.10.4 Behavior Check 12 - 54

 12.9.10.5 Shear and Torsion 12 - 54

12.9.11 Comparison to Straight Bridge 12 - 55

12.10 DETAILED FINAL DESIGN 12 - 56

 12.10.1 Loss of Prestress 12 - 56

 12.10.2 Computer Models 12 - 56

 12.10.3 Crossbeam Details 12 - 56

 12.10.4 Post-Tensioning Anchorages 12 - 56

12.11 REFERENCES 12 - 56

NOTATION

A	= area (Fig. 12.9.5.2-2)
A_c	= total area of the composite section (12.9.3.2.3)
A_{cb}	= area of cross beam (12.9.3.1)
A_{ccb}	= area of cross section in composite cross beam (12.9.3.2.3)
A_{cp}	= area enclosed by outside perimeter of concrete cross-section (12.9.10.5)
A_g	= cross-sectional area of the precast beam (12.9.3.1)
a	= length (Fig. 12.4.1-1)
B	= width (12.4.6)
b_v	= effective web width (12.9.10.5)
C	= coefficient to compute centrifugal force(12.9.4.2.4)
DC	= dead load structural components and nonstructural attachments (12.9.8.7)
DW	= dead load of wearing surfaces and utilities (12.9.8.7)
E_c	= modulus of elasticity of concrete (12.9.3.1)
E_{ci}	= modulus of elasticity of the beam concrete at transfer or at post-tensioning (12.9.3.1)
E_{cd}	= modulus of elasticity of deck concrete (12.9.3.1)
E_p	= modulus of elasticity of post-tensioning strands(12.9.2)
E_s	= modulus of elasticity of reinforcing bars (12.9.2)
e	= eccentricity of strand group (12.9.9.1)
f_b	= concrete stress at the bottom fiber of the beam (12.9.9.2)
f'_c	= specified compressive strength of concrete for use in design (12.9.2)
f'_{ci}	= specified compressive strength of concrete at time of initial loading or at post-tensioning (12.9.2)
f_{pc}	= compressive stress in concrete after prestress losses have occurred either at the centroid of the cross-section resisting live loads or at the junction of the web and flange where the centroid lies in the flange (12.9.10.5)
f_{pe}	= effective stress in the post-tensioning strands after losses (12.9.2)
f_{pu}	= specified tensile strength of post-tensioning strands (12.9.2)
f_{py}	= yield strength of post-tensioning strands (12.9.2)
f_y	= specified minimum yield strength of reinforcing bars (12.9.2)
g	= gravitational acceleration (12.9.4.2.4)
H	= elevation difference between ends of a beam (12.4.2)
h	= overall depth of beam (12.9.3.1)
h_c	= overall depth of composite section (12.9.3.2.3)
I	= moment of inertia (Fig. 12.9.5.2-2)
IM	= dynamic load allowance (impact factor) (12.9.4.2)

I_c	= moment of inertia of composite section (12.9.3.2.3)
I_{cb}	= moment of inertia of cross beam (12.9.3.1)
I_{ccb}	= moment of inertia of composite cross beam (12.9.3.2.3)
$I_{cb\text{lat}}$	= lateral moment of inertia of cross beam (12.9.3.1)
I_{clat}	= lateral moment of inertia of composite section (12.9.3.2.3)
I_{clatcb}	= lateral moment of inertia of composite (12.9.3.2.3)
I_g	= moment of inertia about the centroid of the non-composite precast beam (12.9.3.1)
I_{lat}	= lateral moment of inertia of the non-composite precast beam (12.9.3.1)
I_p	= polar moment of inertia (12.9.3.1)
I_{pc}	= polar moment of inertia of composite section (12.9.3.2.3)
J	= torsional constant (12.9.3.1)
J_c	= torsional constant for composite section (12.9.3.2.3)
J_{ccb}	= torsion constant for composite cross beam (12.9.3.1)
J_{cb}	= torsional constant of cross beam (12.9.3.1)
K_1	= correction factor for source of aggregate (12.9.3.1)
L	= overall beam length or design span (12.4.2.)
LL	= live load (12.9.8.7)
L_a	= arc length (12.3.1.1)
L_c	= chord length (12.3.1.1)
M	= bending moment (Fig. 12.5.2.1-1)
M_c	= moment applied to cross beam (Table 12.9.10.4-1)
M_o	= moment in outside beam (Fig. 12.5.2.3-1)
M_t	= torsional moment (Fig. 12.5.2.1-1)
M_u	= factored bending moment at the section (Table 12.9.10.3-1)
m	= multiple presence factor (12.9.4.2)
n	= modular ratio between deck slab and beam materials (12.9.3.2.2)
P_{pe}	= effective prestressing force (Table 12.9.9.1-1)
p_c	= the length of the outside perimeter of the concrete section (12.9.10.5)
R	= radius of curvature (Fig. 12.4.1-1)
R_i	= reaction of inside beam (Fig. 12.5.2.3-1)
R_o	= reaction of outside beam (Fig. 12.5.2.3-1)
S	= section modulus (12.9.5.2)
S_b	= section modulus for the extreme bottom fiber of the non-composite precast beam (12.9.3.1)
S_{bc}	= composite section modulus for extreme bottom fiber of the precast beam (12.9.3.2.3)
S_t	= section modulus for the extreme top fiber of the non-composite precast beam (12.9.3.1)

S_{tc}	= composite section modulus for top fiber of the structural deck slab (12.9.3.2.3)
S_{tg}	= composite section modulus for top fiber of the precast beam (12.9.3.2.3)
s	= sagitta, arc-to-chord offset (Fig. 12.4.1-1)
T	= unfactored torsional moment (Table 12.9.10.5-1)
T_{cr}	= torsional cracking moment (12.9.10.5)
T_u	= factored torsional moment (12.9.10.5)
t_s	= structural depth of concrete deck (12.9.2)
V	= shear force (Fig. 12.5.2.3-1)
v	= highway design speed (12.9.4.2.4)
W	= weight (Fig. 12.5.2.1-1)
w	= clear width of roadway (12.9.4.2)
w_c	= unit weight of concrete (12.9.2)
w_g	= beam self weight per unit length (12.9.3.1)
w_{gcb}	= cross beam self weight per unit length (12.9.3.1)
x	= An arc length (Fig. 12.5.2.1-1)
y	= distance (Fig. 12.9.5.2-2)
y_b	= distance from centroid to the extreme bottom fiber of the non-composite precast beam (12.9.3.1)
y_{bc}	= distance from the centroid of the composite section to extreme bottom fiber of the precast beam (12.9.3.2.3)
y_{max}	= maximum distance, used in computing section modulus (Fig. 12.9.5.2-2)
y_t	= distance from centroid to the extreme top fiber of the non-composite precast beam (12.9.3.1)
y_{tc}	= distance from the centroid of the composite section to extreme top fiber of the deck slab (12.9.3.2.3)
y_{tg}	= distance from the centroid of the composite section to extreme top fiber of the precast beam (12.9.3.2.3)
γ	= grade angle = H/L expressed as a decimal (12.4.2)
ϕ	= resistance factor (12.9.10.5)
θ	= skew angle (Fig. 12.2.2-1)
ψ	= an angle (Fig. 12.4.4-1)

This page intentionally left blank

Skewed and Curved Bridges

12.1 SCOPE

This chapter deals with the geometric and structural challenges for bridges with curvature in plan, or with skewed supports, and on a grade. The effects of skew and grade are primarily geometric, with some effect on shears and moments. Larger skew angles also have some effect on live load distribution. The effects of curvature are both structural and geometric. This chapter primarily describes the design of curved bridges. Structures with very sharp curvature (say 300-ft radius), such as freeway on or off ramps, may require the use of specially made box beams that are also described in ABAM (1988). Straight beams are normally used on curved bridges with shorter spans, or on longer spans with larger radii, because the offset between arc and chord is small.

12.2 SKEW AND GRADE EFFECTS

12.2.1 General

A skewed bridge is one in which the major axis of the substructure is not perpendicular to the longitudinal axis of the superstructure. For most agencies, the skew angle (usually given in degrees) is the angle between the major axis of the substructure and a perpendicular to the longitudinal axis of the superstructure. This definition is used in this chapter. Some agencies use the angle between the major axis of the substructure and the longitudinal axis of the superstructure. Usually, different substructure units in the same bridge have approximately the same skew angle.

The presence of skew affects the geometry of many bridge details. Skew angles greater than 20 degrees also have an effect on bending moment and on shear in the exterior beams. The structural response of a skewed bridge to seismic loads can be significantly altered by the skew angle of the substructure.

The effects of grade are geometric.

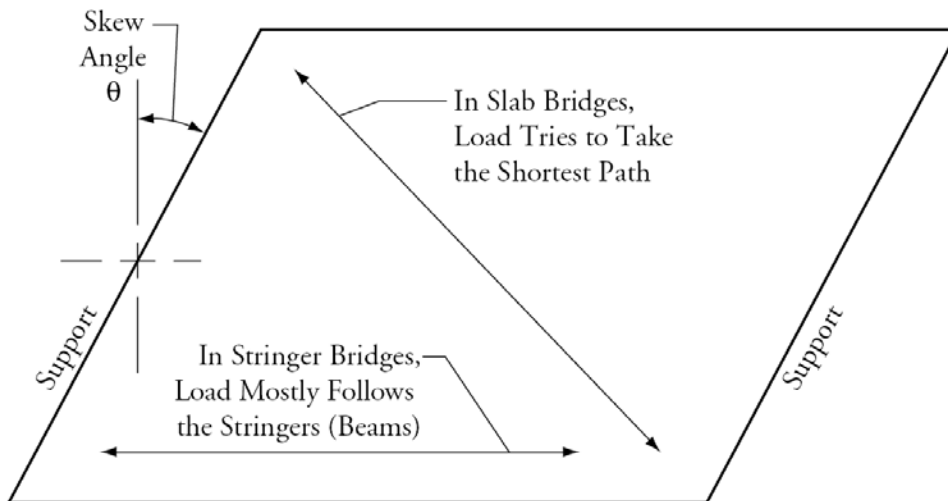
12.2.2 Superstructure Behavior

In bridges supported by longitudinal I- or bulb-tee beams, the load tends to flow along the length of the supporting beams, and the effect of skew on the bending moments is minimized. In solid slab bridges and other bridges with high torsional rigidity, the load tends to take a “short cut” between the obtuse corners of the span, as shown in **Figure 12.2.2-1**. This reduces the longitudinal bending moments, but it increases the shear in the obtuse corners. The same effect occurs in stringer bridges, but is less pronounced. The modification factors due to skew for shear and moment are given in Section 7.5.4.

SKewed AND CURVED BRIDGES

12.2.2 Superstructure Behavior/12.2.3 Substructure Behavior

Figure 12.2.2-1
Load Distribution in Skewed Spans



12.2.3 Substructure Behavior

The relative stiffness of the substructure about its major and minor axis is important. A substructure consisting of round columns and a cap beam is about four times as stiff when acting as a frame resisting loads along its major axis, compared to its stiffness acting as a cantilever for loads along its minor axis. For rectangular cantilever piers, the ratio of major-to-minor-axis stiffness is proportional to the dimension ratio squared. For wall piers, the major axis stiffness is almost infinite compared to the minor axis stiffness.

When a substructure unit deflects due to horizontal loads or superstructure deformations, the deflection is primarily along the minor axis, and the rotation vector at the top is along the major axis. When the superstructure deflects due to vertical loads, the rotation vector at the support is perpendicular to the axis of the beams, as shown in **Figure 12.2.3-1**.

This raises a question of how to orient the “pin” between superstructure and substructure. Concrete bridges are seldom supported by real pins. Bearings consisting of elastomeric pads can provide rotation capacity about all axes, which solves the problem of how to orient the pin. Continuous bridges are sometimes constructed using a concrete hinge between superstructure and substructure, as shown in **Figure 12.2.3-2** (also, see Sect. 3.2.3.2.2). This forces the rotation vector to lie along the major axis of the substructure, which is inconsistent with the end rotation of the superstructure beam. However, live load rotations at an interior support of a continuous bridge are small, and structures so constructed seem to perform satisfactorily.

SKEWED AND CURVED BRIDGES

12.2.3 Substructure Behavior

Figure 12.2.3-1
Rotation Vector for Vertical Loads

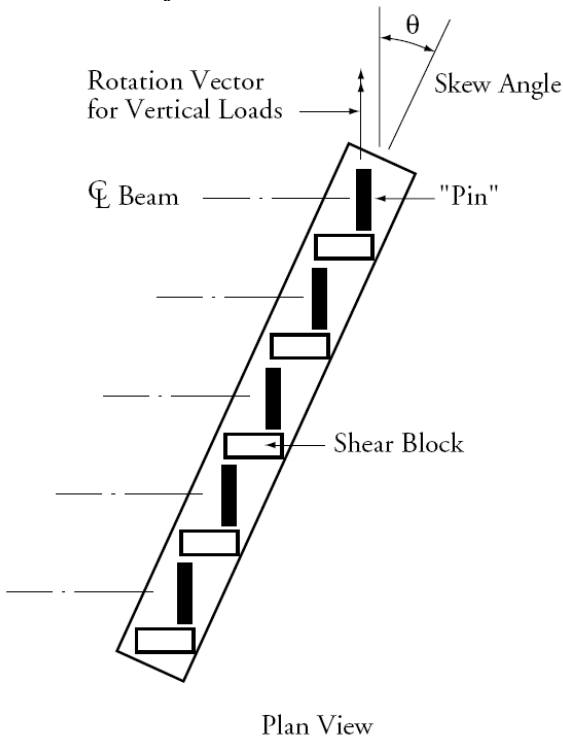
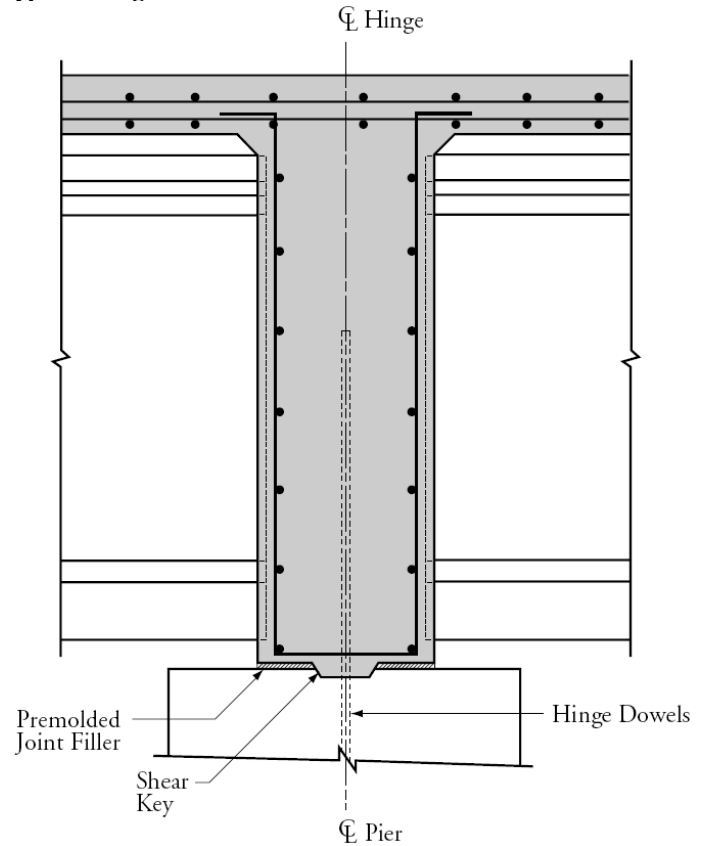


Figure 12.2.3-2
Typical Hinge Section



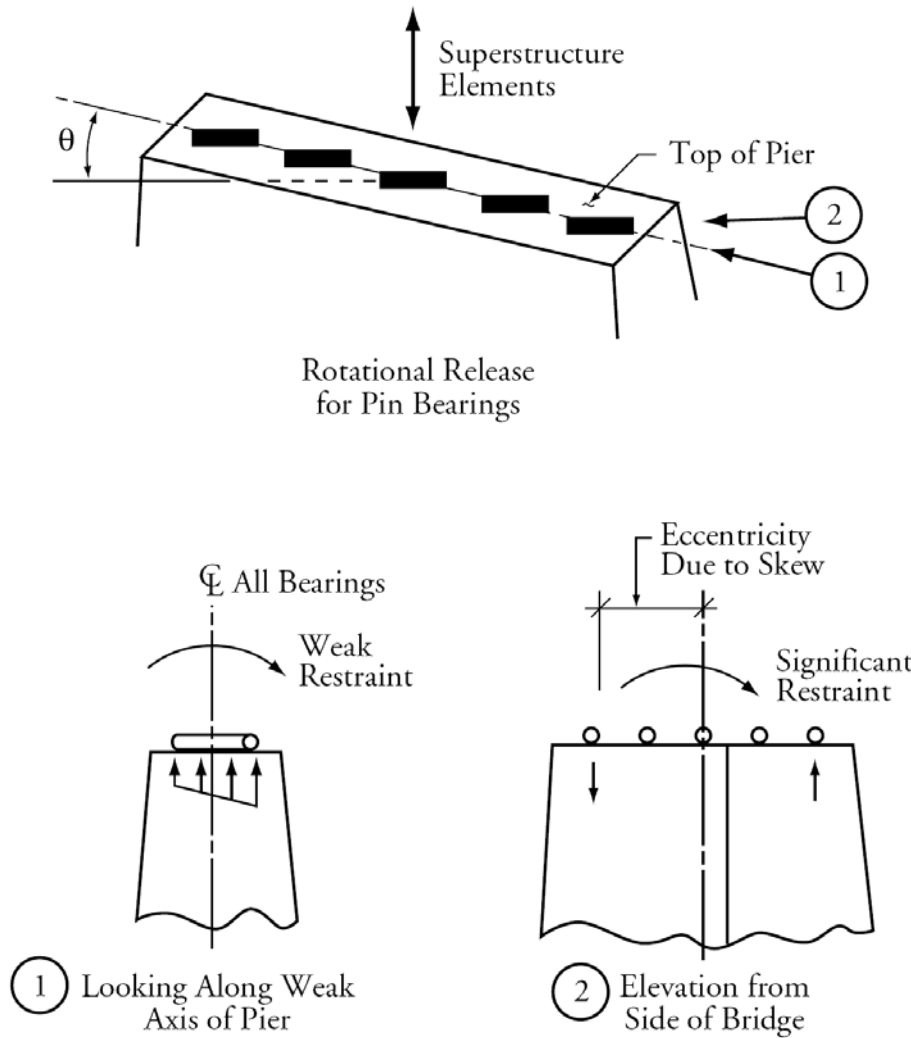
NOTE: Reinforcement from beams extending into diaphragm and other details not shown for clarity.

A sideline to this discussion concerns computer modeling. Orienting the rotational release vector with respect to the superstructure axes may force a component of rotation about the major axis of the substructure. This will create a fictitious moment at the top of the substructure in the computer model, as shown in **Figure 12.2.3-3**. In general, a rotational release between superstructure and substructure should be oriented with respect to the substructure axes.

SKewed AND CURVED BRIDGES

12.2.3 Substructure Behavior/12.2.4 Temperature and Volume Change Effects

Figure 12.2.3-3
Orientation of Pins in Computer Model



Use Rotational Release About Weak Axis of Pier,
Not Perpendicular to Superstructure Beams

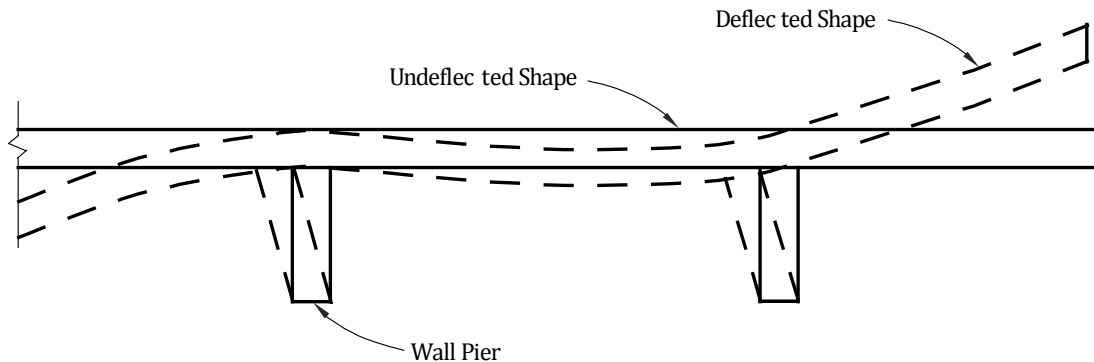
12.2.4 Temperature and Volume Change Effects

The shortening of a skewed span due to creep, shrinkage, and temperature will cause the supporting substructure units to deflect, if they are connected longitudinally to the superstructure. The substructure units will tend to deflect about their minor axes, causing a rotation of the superstructure, as shown in **Figure 12.2.4-1**. If transverse shear blocks are provided at the abutments, transverse forces at the abutments can develop, as well as forces along the major axis of the piers.

SKEWED AND CURVED BRIDGES

12.2.4 Temperature and Volume Change Effects/12.2.6.1 Effects of Grade

Figure 12.2.4-1
Bridge Rotation Caused by Superstructure Shortening



12.2.5 Response to Lateral Loads

Wind and seismic loads transverse to the major axis of the bridge cause both transverse and longitudinal deflection of the superstructure, as the substructure elements deflect about their weak axes. Similarly, longitudinal loads also cause both longitudinal and transverse deflections of the superstructure. This can lead to a coupling of transverse and longitudinal modes in a dynamic seismic analysis. This subject is more fully discussed in FHWA (1996A and 1996B).

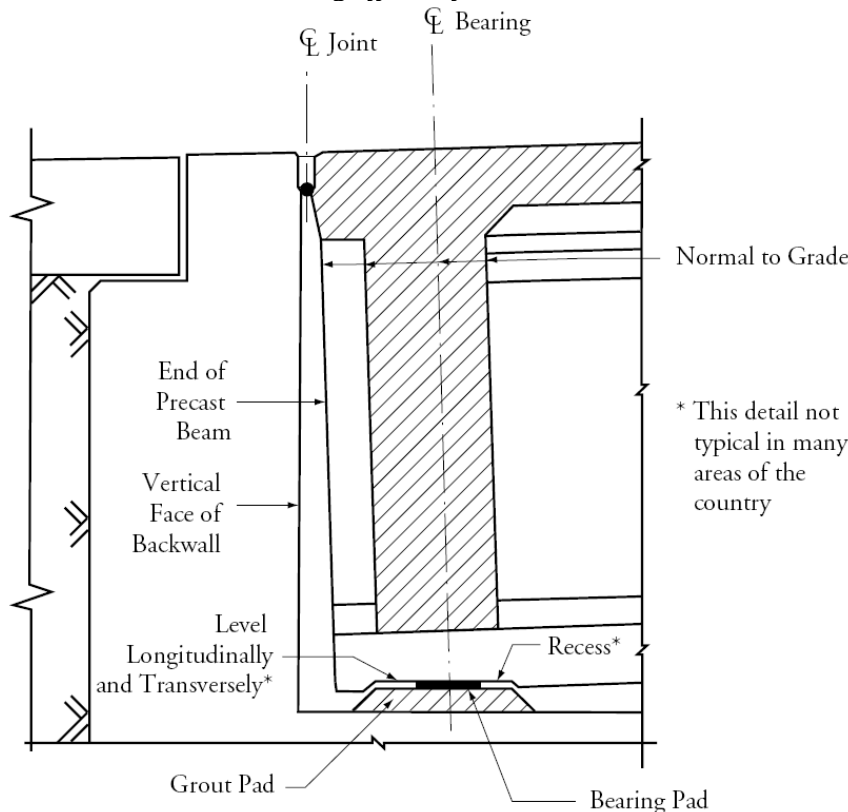
12.2.6 Detailing

12.2.6.1 Effects of Grade

Grade affects the geometry of the precast beams. The slant length is increased over the plan length by an amount $\gamma^2 L/2$, where γ is the grade, expressed as a decimal and L = plan length for beam or span. The precast beam is normally made in the shape of a rectangle, as seen in elevation. That is to say, the ends of the beam are usually square with the longitudinal axis of the beam, rather than being vertical in the final position of the beam. Similarly, the diaphragms are normally square with the axis of the beam.

Cast-in-place substructures are normally cast with vertical surfaces. This needs to be considered in the abutment detail (see **Fig. 12.2.6.1-1**) in which the beam end is not vertical. The bearing pad is set on a level, horizontal surface. Recesses, shims, sloped risers, or grout pads are used to compensate for the difference in planes between the beam soffit and the top of the cap beam. Sometimes, on moderate grades, the bearing pads and bearing surfaces on the abutment and on the underside of the beam are set parallel to the grade.

Figure 12.2.6.1-1
Section at Abutment Showing Effects of Grade



12.2.6.2 Skewed Beam Ends

Skewed beam ends (in plan) are sometimes provided at expansion joints. Skew angles should be grouped into standard increments because each skew angle will require a special end bulkhead to form it. At interior ends in continuous beams, the beam-ends are normally made square in plan. Some end diaphragm details may require that the ends of continuous beams be skewed. In the latter case, when using precast, prestressed box beams, a maximum skew angle of 30 degrees is used by many states to avoid warping or racking of the beams (Russell 2009).

12.2.6.3 Intermediate Diaphragms

Intermediate diaphragms, if used, may be perpendicular to the beam axes, or parallel to the skew. Making them parallel to the skew can have the advantage of making interior beams identical. Making them perpendicular to the beams simplifies their construction in the field.

12.2.6.4 Deck Reinforcement

For skew angles of 25 degrees or less, transverse deck reinforcement may be placed parallel to the skew according to the *LRFD Specifications (AASHTO 2010)*. This simplifies detailing and the placement of reinforcement. For skew angles exceeding 25 degrees, transverse deck reinforcement must be placed normal to the longitudinal axis of the beams, and shorter bars should be used in the acute corners of the deck. The limit of 25 degrees is somewhat arbitrary and some agencies may use a different angle.

12.2.6.5 Plans

The detailing recommendations made in Section 12.2.6 are not universal. The plans must show the geometric effects of skew and grade. It is important to indicate which surfaces are parallel or normal to the skew, and which surfaces are parallel or normal to the beam axis. Similarly, the plans should indicate which surfaces are truly vertical and horizontal, and which surfaces are parallel or normal to the inclined beam axis for beams on a grade.

SKEWED AND CURVED BRIDGES

12.3 Curved Bridge Configurations/12.3.1.1 Straight Beams Chorded from Pier to Pier

12.3 CURVED BRIDGE CONFIGURATIONS**12.3.1 General**

Curved concrete bridges may be created using one or more of the following beam configurations.

- Straight beams chorded from pier to pier
- Straight segments with spliced joints within the span
- Curved beams

12.3.1.1 Straight Beams Chorded from Pier to Pier

The combination of straight beams supporting a concrete deck with curved edges is suitable for short spans and long spans with a large radius of curvature (See **Fig. 12.3.1.1-1**). The limitation for its use is the deck overhang. Normally, the maximum deck overhang at midspan on the outside of the curve is made approximately equal to the overhang on the inside of the curve at the piers. When the overhang is large, the bridge appearance may be objectionable and the structural design for the deck overhang and the exterior beam may be uneconomical.

Figure 12.3.1.1-1

Curved Bridge with Straight Beams from Pier to Pier Photo: BergerABAM.



The maximum offset between an arc and its chord is approximately equal to $L_c^2/8R$ where L_c is the chord length and R is the radius of curvature. Because it is an approximation, the length may be either the arc length, L_a , or the chord length, L_c , whichever is known.

It is desirable that the arc-to-chord offset be limited to 1.5 ft, and that the edge of the top flange of the beam be no closer than 0.5 ft to the slab edge. **Table 12.3.1.1-1** shows the minimum curve radii that satisfy the different maximum offset criterion. The limit of 1.5 ft is often exceeded, but each case should be examined for acceptability.

SKEWED AND CURVED BRIDGES

12.3.1.1 Straight Beams Chorded from Pier to Pier/12.3.1.3 Curved Beams

Table 12.3.1.1-1
Radii that Provide Offsets
Shown for Various Straight Beam Lengths

Beam Length ft	Radius, ft			
	Offsets, ft			
	0.5	1.0	1.5	2.0
70	1,225	613	408	306
80	1,600	800	533	400
90	2,025	1,013	675	506
100	2,500	1,250	833	625
110	3,025	1,513	1,008	756
120	3,600	1,800	1,200	900
130	4,225	2,113	1,408	1,056
140	4,900	2,450	1,633	1,225
150	5,625	2,813	1,875	1,406
160	6,400	3,200	2,133	1,600

Straight beams are by far the simplest and most cost-effective way to use precast, prestressed beams in a curved bridge; they should be used whenever appropriate. This solution is not discussed in detail in this chapter because the analysis is almost identical to that for a straight bridge. The only difference is in the computation of loads on the exterior beams. The “lever rule” [LRFD Art. C4.6.2.2.1] may be used in the same manner as for a straight bridge, as long as the variable overhang is accounted for.

The designer has two possible options for laying out the substructure for a curved bridge with straight-chorded beams. The first option is to arrange the pier caps on radial lines relative to the center of the curve. The primary disadvantage of this arrangement is that each beam within a span is a different length and may have different prestressing requirements. The second option is to layout pier caps parallel to one another. The advantage to this arrangement is that all beams in the same span have the same length. Interior beams within each span will have very similar, if not identical designs, while the exterior beams will be different because of the variable overhang length. The skew for each span will be different, which makes this layout not appropriate for a large angular change of the roadway.

For situations in which the offset exceeds 1.5 ft, the number of chords may need to be increased. One method is to splice I- and bulb-tee-beam segments together in the field using methods described later in this chapter and in Chapter 11. With two chords, the offset will decrease by a factor of 4; and with three chords, the offset will decrease by a factor of 9.

12.3.1.2 Straight Segments with Spliced Joints in the Span

Angular changes between straight chords are seldom noticed. The individual segments may be pretensioned for shipping, handling, and erection and the complete beam post-tensioned. Diaphragms are required at the splice locations to counteract the lateral forces from the post-tensioning. Thicker webs may be needed to accommodate the post-tensioning ducts.

12.3.1.3 Curved Beams

The availability of precast concrete beams with a U-shaped cross section has enabled the development of a full range of straight to curved beams using the same cross section (see Fig. 12.3.1.3-1). Precast concrete U-beams provide bridge owners and the engineering community with an economical alternative to cast-in-place concrete and structural steel for the construction of horizontally curved bridges.

SKewed AND Curved BRIDGES

12.3.1.3 Curved Beams/12.3.2.2 Box Section Configurations

Figure 12.3.1.3-1**Curved Bridge with Curved U-Beams Photos: Summit Engineering Group.**

Continuously-curved precast concrete beams allow a unified appearance throughout the project at an economical cost. They provide aesthetically pleasing superstructures that uniformly follow the curvature of the roadway. The beams may be simply supported or made continuous for superimposed loads. Span lengths can be extended by splicing beams at the site or providing deeper sections at the piers. Span lengths up to 260 ft have been achieved with curved precast U-beams.

12.3.2 Beam Cross-Section Considerations

12.3.2.1 Box Beams Versus I-Beams Versus U-Beams

Full-span-length, curved beams may be cast in the plant and then post-tensioned. Torsional stresses and handling considerations have traditionally caused a closed box section to be preferred for full-length curved beams. However, precast concrete box beams can be fabricated without top flanges or with small top flanges above each web to create a U-beam. Although there are no national standards for U-beams at the present time, several state DOTs have developed standard cross sections and the PCI-certified producers in Zone 6 (Southeast) have developed standards for spliced curved U-beams. Details of these are provided in Appendix C of this manual.

Spliced-beam construction may be used with conventional I-beams. Two or three straight segments may be supported on temporary shores, and post-tensioned in the field after constructing diaphragms at the segment joints. Details are given in Chapter 11.

The feasibility of pretensioned, precast concrete I-beam bridges with straight chord segments has been investigated by Amorn, Tuan, and Tadros (2008). They reported that this type of bridge has been a common practice in the Netherlands for more than a decade but is currently nonexistent in the United States.

12.3.2.2 Box Section Configuration

Box sections will often require new formwork, as standard box sections of the size needed do not exist in many localities. The sides of box beams may be vertical or sloped. Vertical sides are somewhat easier to form. Sloping sides are generally thought to have a better appearance.

The maximum span of box beams is often limited by shipping weight. Field-splicing of shorter segments may be used to minimize weight of individual segments. In order to minimize the thickness of webs and flanges, consideration should be given to the use of “external” post-tensioned tendons inside the box section.

Design charts for continuous, curved box beams are given in ABAM (1988). These charts are useful for preliminary sizing of curved box beams.

SKEWED AND CURVED BRIDGES**12.3.2.3 I-Beam Configuration/12.4.1 Arc Offset from Chord****12.3.2.3 I-Beam Configuration**

The use of post-tensioning requires webs thicker than the 6-in. webs of AASHTO-PCI bulb-tees and other standard I-beams. To accommodate post-tensioning ducts and reinforcement, the minimum web thickness should be 7 to 8 in. Thicker webs can often be obtained by spreading the side forms of standard shapes by 1 or 2 in.

12.3.2.4 U-Beam Configuration

Precast concrete box beams can be fabricated without top flanges or with narrow flanges at the top of each web to produce an open section U-beam. After the deck is cast, the section becomes closed and provides the necessary torsional resistance. For handling, shipping, and erection, intermediate diaphragms in the U-beams may be necessary. Curved precast concrete U-beam projects have generally used beams varying in depth from 48 to 84 in. for span lengths varying from 150 to 240 ft. Variable depth sections have been used to extend span lengths beyond 240 ft.

The use of splices in precast concrete, horizontally curved U-beam bridges requires that web thicknesses be proportioned to accommodate post-tensioning ducts. The *LRFD Specifications* requires that post-tensioning ducts occupy at most 40% of the web thickness. Using this criterion, web thicknesses that vary from 7.5 to 10 in. can be used to accommodate 3- and 4-in.-diameter post-tensioning ducts in webs. The choice of web thickness must also consider the required shear, torsion, and principal tensile stresses.

Bottom slab width and thickness are proportioned to accommodate the post-tensioning ducts and to supply adequate compression in negative moment regions. Top flanges of the U- beam section are optimized to increase capacity for non-composite loading, to enhance beam stability during erection, and to accommodate post-tensioning ducts in negative moment regions.

12.3.2.5 Continuity

Continuity is very desirable in curved bridges. In addition to the benefits that continuity provides for straight bridges, there are two additional benefits for curved bridges. Continuity greatly reduces torsion resulting from applied loads and reduces the excess load on the exterior beam on the outside of the curve.

12.3.2.6 Crossbeams

Transverse members spanning between beams within a span (intermediate diaphragms) are often omitted on straight bridges (see Sect. 3.7). However, in curved bridges, the transverse members, which will be referred to as crossbeams in this chapter due to their unique role, are required to counteract both the effects of torsion and the lateral forces resulting from curvature. The crossbeams should also be deep enough to brace the bottom flange.

12.3.2.7 Superelevation

Standard practice is to keep the beam cross-section vertical, and provide a “haunch” or “pad” of cast-in-place deck concrete to fill the space between the sloping deck and the horizontal top flange.

12.4 USEFUL GEOMETRIC APPROXIMATIONS

Despite the immense computing power now available, simple approximations remain very useful for preliminary design. They are quick to use, and they give the designer a “feel” for how a change in one parameter affects other parameters.

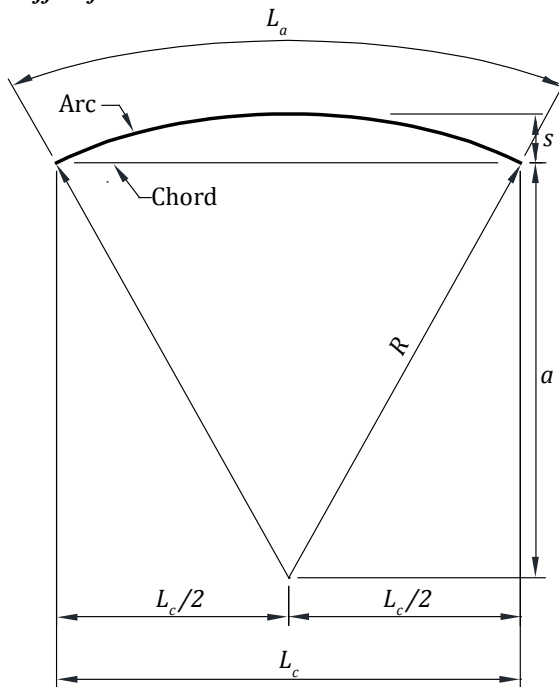
12.4.1 Arc Offset from Chord

The maximum offset between arc and chord is called the middle ordinate or the “sagitta” (sagitta is Latin for “arrow”) and represented by the symbol, s . The sagitta is approximately equal to $L_c^2/8R$. The derivation is simple and is shown in **Figure 12.4.1-1**. Once again, since these are approximations, either the arc length or chord length may be used.

SKewed AND CURVED BRIDGES

12.4.1 Arc Offset from Chord/12.4.4 Twist Resulting from Grade

Figure 12.4.1-1
Arc Offset from Chord



By Pythagorean Theorem:

$$a^2 + (L_c/2)^2 = R^2$$

Also:

$$a = R - s$$

$$R^2 - 2Rs + s^2 + L_c^2/4 = R^2$$

But s is small compared to R and L_c . Therefore, ignore the term s^2 and solve for s .

$$s = \frac{L_c^2}{8R}$$

The formula slightly underestimates the distance, s . The approximation is slightly better if the length is taken as the arc length, L_a .

12.4.2 Excess of Slant Length over Plan Length

The slant length of a beam on a grade is longer than the plan length by an amount $H^2/2L$, where H is the difference in elevation of the two ends of the beam. This is a well-known formula, and is identical to the $\gamma^2 L/2$ formula given in Section 12.2.6.1 (γ is equal to H/L). The derivation is similar to that for the arc-chord offset. The Pythagorean theorem is used, neglecting a small second-order quantity.

12.4.3 Excess of Arc Length over Chord Length

The length of an arc is longer than its chord by an amount $8s^2/3L_c$, where s is the arc-chord offset and L_c the chord length. The excess length may also be expressed as $L_c^3/24R^2$. This formula is derived by approximating the arc length as a series of short chords, then taking the limit as the chord length approaches zero.

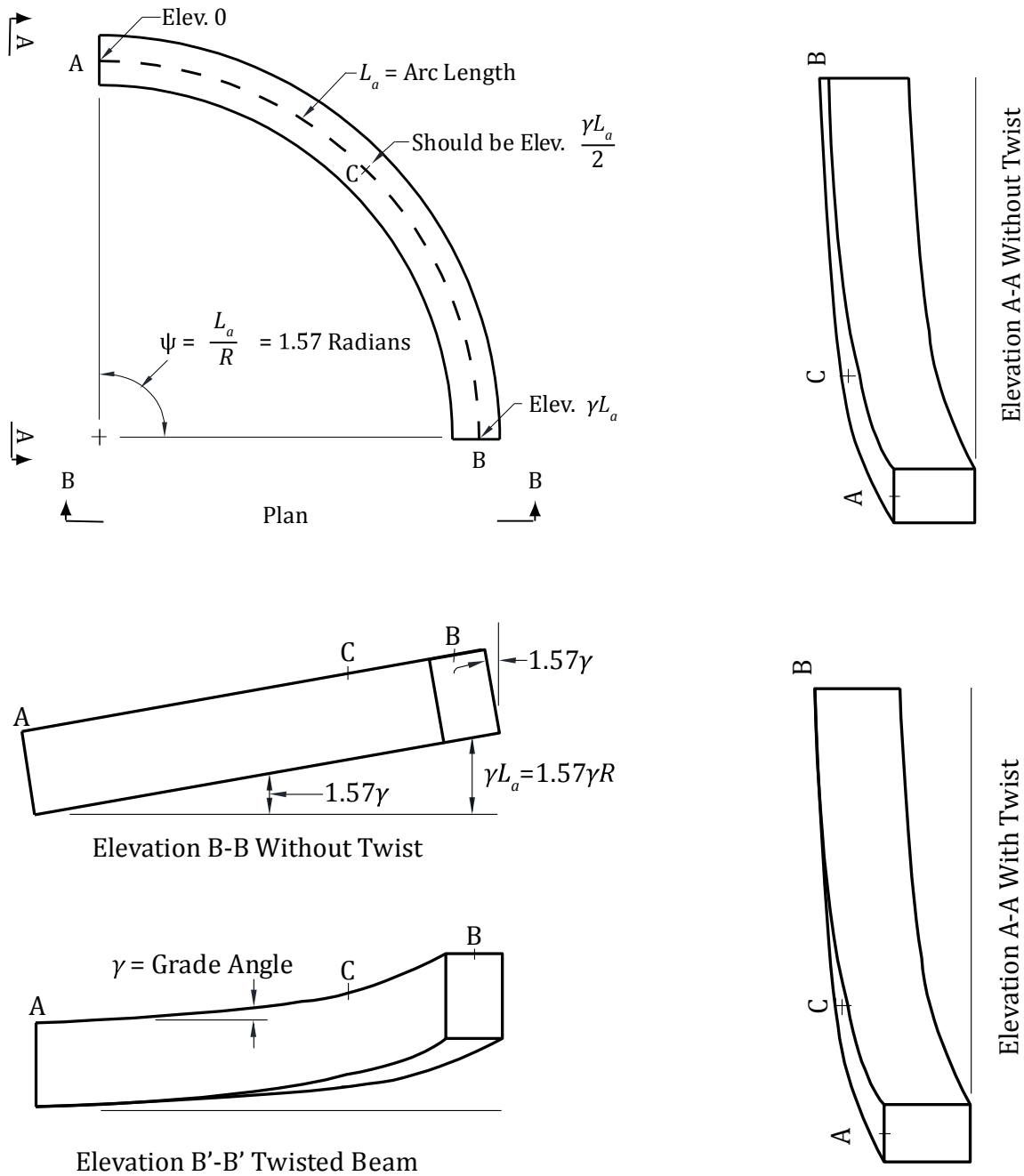
12.4.4 Twist Resulting from Grade

The shape of a curved beam on a grade is a helix. It has the same shape as the railing on a “spiral” (more correctly, helical) stair. Such a railing is twisted. If a section were cut out of the railing and laid flat, the twist would be apparent.

SKewed AND CURVED BRIDGES

12.4.4 Twist Resulting from Grade

Figure 12.4.4-1
Twist Resulting from Grade Change



To understand more fully the twist in a curved beam caused by grade, consider a beam curved 90 degrees (1.57 radians) in plan, made without twist, with square ends as illustrated in the Plan View of **Figure 12.4.4-1**. The bearing at Point B is elevated higher than at Point A by an amount $1.57\gamma R$ as shown in Elevation B-B. Therefore, the beam will be tipped by an angle of 1.57γ . At Point B, the sides of the beam will not be plumb; they will be tipped by an angle 1.57γ . Also, note that at Point C, the midpoint of the beam, the elevation of the beam will not be half of $1.57\gamma R$, as it should be.

SKEWED AND CURVED BRIDGES

12.4.4 Twist Resulting from Grade/12.4.6 Curved Surfaces

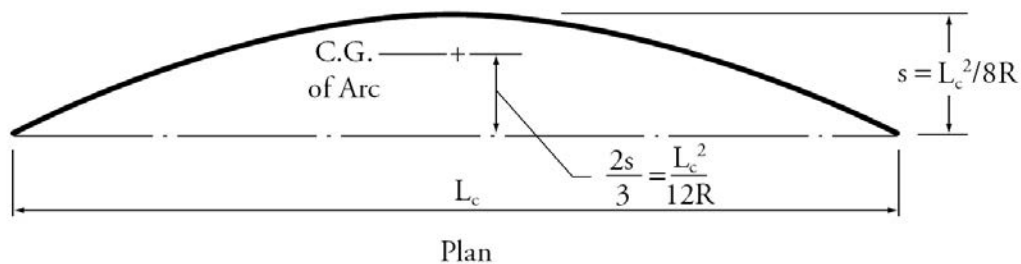
Elevation B'-B', **Figure 12.4.4-1**, shows the elevation of the beam fabricated to a true helix. The ends and sides of the beam will be plumb at Points A and B, and the elevation at C will be correct. The beam must be twisted by an amount 1.57γ . Generalizing for angles other than 1.57 radians, the amount of twist is $\psi\gamma$, or $(L_a/R)\gamma$ where L_a is the arc length.

The approximation is this: The twist angle is normally small enough to be ignored in beam fabrication, except for monorail beams. If the twist is ignored in beam fabrication, it should be realized that when the beam is set in the field, it will not be possible for both ends to be perfectly plumb. If the apparent twist is large enough to be measurable, the beam should be set by "splitting the difference" of the out-of-plumbness at the two ends. This will also result in the midpoint of the beam being at the proper elevation (not including the effects of camber).

12.4.5 Center of Gravity of an Arc

The center of gravity of an arc (and of a uniform load applied along the arc) is offset from the chord by $2s/3$, or $L_c^2/12R$. See **Figure 12.4.5-1**.

*Figure 12.4.5-1
Center of Gravity of Arc*

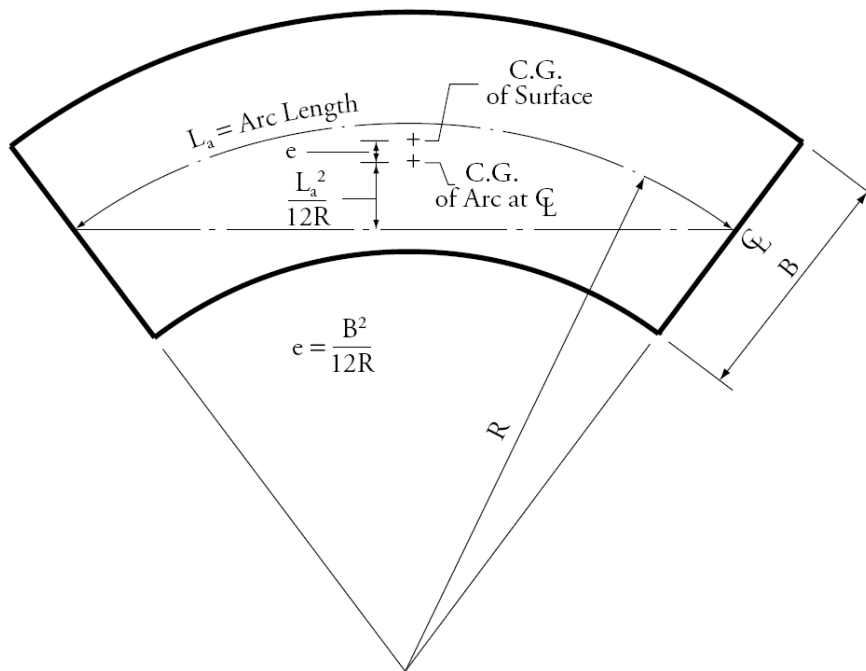


12.4.6 Curved Surfaces

The area of a curved surface with radial ends, such as a bridge deck, is equal to BL_a , where B is the width and L_a is the arc length along the centerline. See **Figure 12.4.6-1**.

The center of gravity of a curved surface lies outside of the center of gravity of the centerline arc, because there is more area outside the centerline than inside. This additional eccentricity, e , is equal to $B^2/12R$. The total offset from the chord to the center of gravity of the surface is therefore $(L_c^2 + B^2)/12R$. Where the ends of the bridge are not radial, a more detailed calculation is required for the area and centroid of the surface.

Figure 12.4.6-1
Properties of a Curved Planar Surface



12.5 STRUCTURAL BEHAVIOR OF CURVED BRIDGES

12.5.1 Longitudinal Flexure

12.5.1.1 Analysis as a Straight Beam

The bending moments from longitudinal flexure are virtually the same as those for a straight beam of span equal to the arc length between supports. This approximation is sufficiently accurate for preliminary design.

12.5.1.2 Loads on Outside Beam

The shears and moments in the exterior beam on the outside of the curve are substantially larger than for other beams in the bridge. This is caused by the following factors:

- The arc length on the outside of the curve is longer than the nominal length at the centerline of the bridge. This increases bending moments in the outer beam by approximately the square of the ratio of the arc lengths.
- The overhang at mid-arc may be increased by an amount equal to the arc-to-chord offset.
- Other beams will shed some of their torsional moment by shifting load toward the next beam to the outside. The outermost beam must resist this shifted load.

12.5.2 Torsion

Although flexural moments may be estimated by analyzing a straight beam of length equal to the arc length of the curved beam, the same cannot be said for torsional moments. Torsional moments are necessary for equilibrium of a curved beam. It is useful to look in more detail at how torsional moments develop in a curved beam. It will be shown that torsional moments are related to the flexural moment, M divided by the radius of curvature, R .

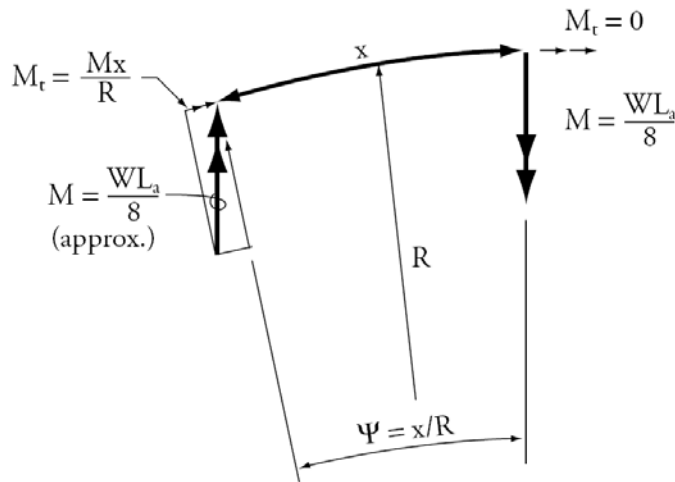
SKEWED AND CURVED BRIDGES

12.5.2.1 Torsion in Simple Span Beams

12.5.2.1 Torsion in Simple-Span Beams

The development of torsional moments in a curved beam may be thought of in the following way. Consider a short segment of length x near midspan of the simple-span curved beam as shown in **Figure 12.5.2.1-1**.

*Figure 12.5.2.1-1
Torsion and Curvature*

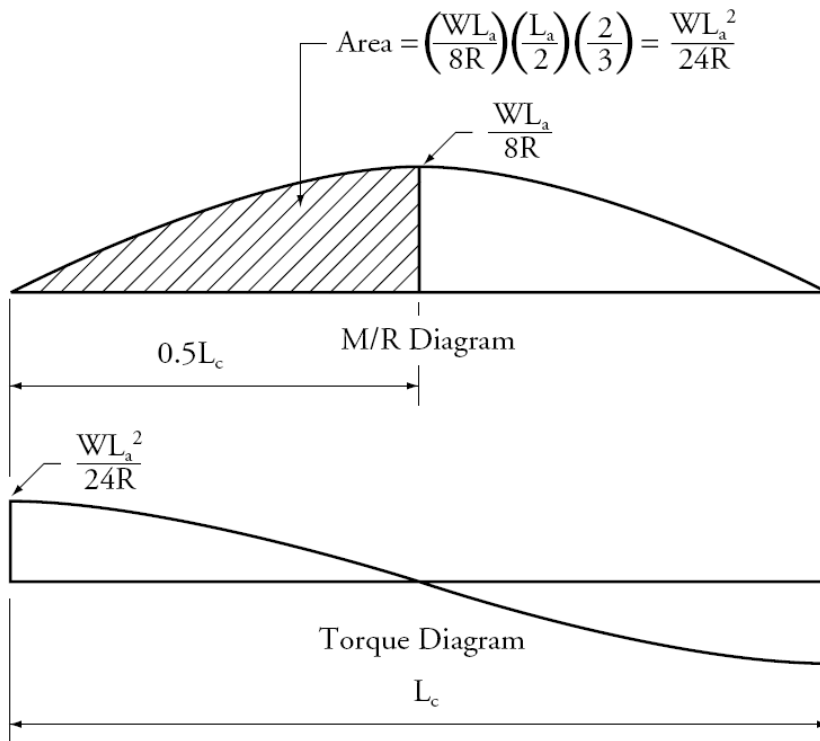


At midspan, the bending moment is $WL_a/8$, and the torsional moment is zero (by symmetry). At a small angle, ψ , away from midspan, the bending moment must “turn” through the angle, ψ , and a torsional moment approximately equal to $xWL_a/8R$ is necessary for equilibrium. Following around the curve to the support, the torsional moment increases by increments of xM/R . However, M changes between midspan and the support. Integrating the M/R diagram from midspan to support, as shown in **Figure 12.5.2.1-2**, a torsional moment of $WL_a^2/24R$ is obtained.

SKEWED AND CURVED BRIDGES

12.5.2.1 Torsion in Simple Span Beams/12.5.2.2 Torsion in Continuous Beams

Figure 12.5.2.1-2
Torsion in a Simple-Span Curved Beam



12.5.2.2 Torsion in Continuous Beams

Torsion in continuous beams may be understood by first examining torsion in a fixed-ended beam. **Figure 12.5.2.2-1** shows the M/R diagram for a fixed-ended beam.

Because the area under the M/EI diagram for a fixed-ended beam must integrate to zero, the area under the M/R diagram will also integrate to zero, given constant EI and R . Thus, the torsion at the support will be zero. The maximum torque occurs at the inflection point, and is 19% of the maximum torque in a simple-span beam.

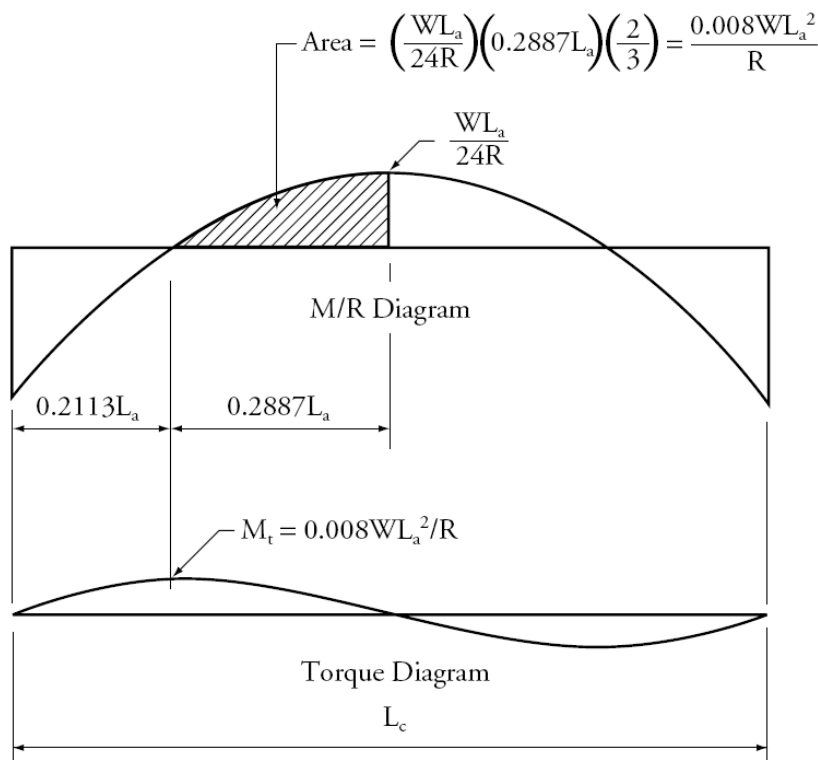
Continuous beams are intermediate between simple-span and fixed-ended beams. Interior spans resemble the fixed case more closely, and the free end of exterior spans may be closer to the simple-span case.

Continuity can significantly reduce torsional moments.

SKEWED AND CURVED BRIDGES

12.5.2.2 Torsion in Continuous Beams/12.5.2.3 Behavior of Beam Gridworks in Segmental Spans

Figure 12.5.2.2-1
Torsion in a Fixed-Ended Curved Beam



12.5.2.3 Behavior of Beam Gridworks in Segmental Spans

Beam gridworks composed of straight beam segments can resist eccentric loads without torsion. **Figure 12.5.2.3-1** shows a simple two-beam, three-segment gridwork.

The beam moment at a joint must “turn the corner.” In this case, equilibrium is supplied by a bending moment in the crossbeam. This bending moment in the crossbeam is equal to the angle (in radians) between the two beam segments multiplied by the bending moment in the main beam.

An equilibrium sketch of the crossbeam is shown in **Figure 12.5.2.3-1**. The moments at the two ends of the beam are equilibrated by shear forces, which transfer load from the inner to outer beam.

Note that for a two-beam gridwork, the reactions may be determined by statics, because the resultant of the reactions at each end must lie on a line through the resultant location of the loads. For multiple beam gridworks, reactions may be estimated by assuming a straight-line distribution of reactions that produces the correct location of the resultant. A procedure similar to that described in the *LRFD Specifications* Commentary Article C4.6.2.2d may be used. This is illustrated in the Design Example in Section 12.9.5.2.

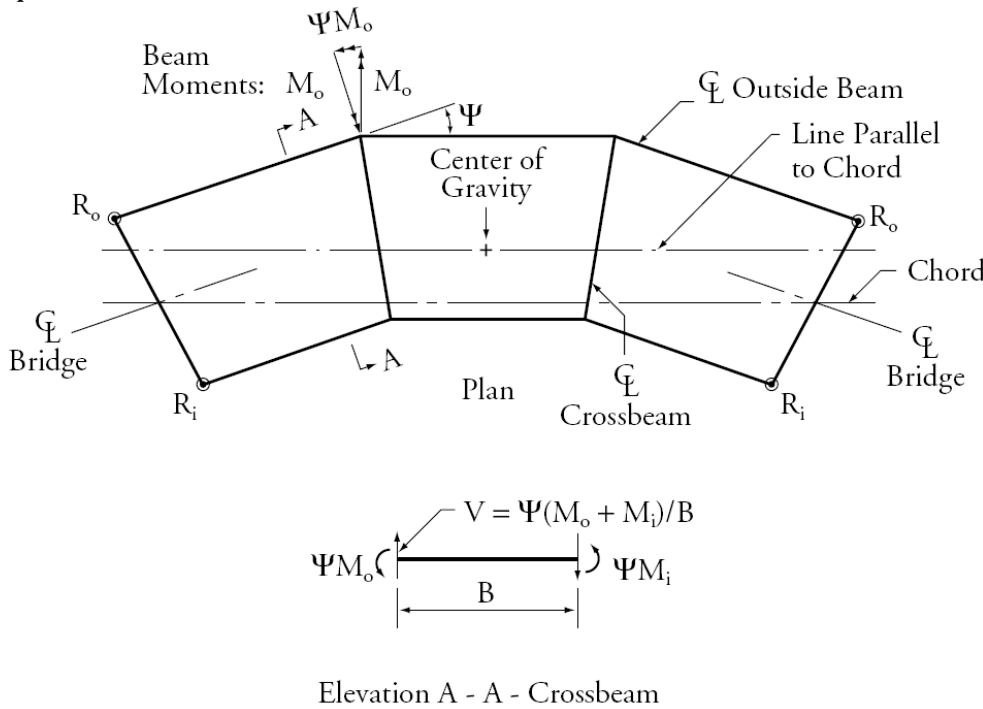
After estimating the end reaction of the outside beam, one may estimate the bending moment in the outside beam. This is done by comparison to the bending moment in a straight beam of length equal to the arc (or chord) length of the centerline of the bridge. Two correction factors are then applied to this bending moment. The first correction is the ratio of the estimated end reaction in the beam grid work of the curved bridge to that in a straight bridge. A simplifying assumption is made that the bending moment is proportional to the end reaction multiplied by the length, giving the second correction factor, the ratio of the length of the outside beam to the centerline length. The bending moment of a straight beam of length equal to the centerline length of the bridge is then multiplied by these two factors to obtain the estimate of bending moment in the outer beam as illustrated in Section 12.9.5 of the design example.

SKewed AND CURVED BRIDGES

12.5.2.3 Behavior of Beam Gridworks in Segmental Spans/12.6.1 Validity of Approximations

Loads applied after the gridwork is completed can theoretically be supported without torsion. Although equilibrium could be obtained without torsion, an analysis will show a small amount of compatibility torsion. If the factored compatibility torsion is below that given in the *LRFD Specifications* [Equation 5.8.2.1-3], the torsion may be safely ignored.

Figure 12.5.2.3-1
Simple Gridwork



12.5.3 Crossbeams

Diaphragms in straight bridges, if used at all, are usually designed empirically, i.e., the design is not based on calculated shears and moments. In curved bridges, crossbeams must be designed for the shears and moments resulting from the change in direction of the primary bending moment in the stringer at the location of the crossbeams. The longitudinal forces in the bottom flange have a transverse component at the location of the crossbeam. The crossbeam must be deep enough to brace the bottom flange to resist this component.

12.6 DESIGN CONSIDERATIONS

This section addresses the various loading stages for a simple span curved bridge made with box beams or I-beams using straight segments spliced in the span.

12.6.1 Validity of Approximations

Detailed design is done using a beam gridwork computer model. For mathematical consistency, it is better to use "exact" plan geometry instead of the approximations used in preliminary design. The computer model may be created in a horizontal plane, ignoring grade and superelevation. However, the extra weight in the "haunch" (or "pad") caused by superelevation should be taken into account.

SKEWED AND CURVED BRIDGES

12.6.2 Loading Stages for Simple Span Box Beams/12.6.4 Other Design Checks

12.6.2 Loading Stages for Simple Span Box Beams**12.6.2.1 Bare Beam**

An initial stage of plant post-tensioning is applied to the bare simple span beam to assemble the beam segments. This effectively applies the post-tensioning and the self weight bending moment at the same time. After erection, crossbeams are cast, and their weight is applied to the bare beam.

12.6.2.2 Non-Composite Gridwork

The weight of the deck is applied to a non-composite gridwork, assuming unshored construction.

12.6.2.3 Composite Gridwork

The weights of future wearing surface, barriers, live load plus impact, and centrifugal force are applied to the composite gridwork. The simplified assumptions for distribution of these loads in straight bridges cannot be used for curved bridges.

Additional field post-tensioning could be applied after casting the deck to partially compensate for the weight of the deck. This should not be done if future replacement of the deck is anticipated.

12.6.3 Loading Stages for Simple Span I-Beams

A three-segment, simple-span I-beam is considered. For continuous spans, more complex loading stages may be required.

12.6.3.1 Individual Segments

The segments are pretensioned in the plant to compensate for self weight bending of the individual segment.

12.6.3.2 Shoring Loads

The individual segments are erected in the field, supported by final bearings and by shores at intermediate locations. Post-tensioning ducts are spliced and crossbeams are cast.

During this loading stage, stresses in the segments do not change as the weight of the concrete in the crossbeams is carried directly by the shoring. Loads from the cast-in-place concrete of the crossbeams are carried directly by the shoring. The completed beam only picks up the weight of the crossbeams when the shoring is removed.

12.6.3.3 Non-Composite Gridwork

Post-tensioning is applied to the non-composite gridwork after the crossbeams have cured sufficiently. This lifts the beams from the shores. The load that was present in the shores becomes a load applied to the non-composite beam gridwork.

The post-tensioning is best modeled as a set of external loads. That is, all the forces applied to the concrete by the tendons and their anchors are applied as external loads to the model. It is important that the transverse forces at the crossbeams are not overlooked. These forces are caused by the tendons that change direction (in plan) at the crossbeams.

The weight of the deck and haunch is also applied to the non-composite gridwork.

12.6.3.4 Composite Gridwork

The weights of the future wearing surface, barriers, live load plus impact, and centrifugal force are applied to the composite gridwork. See Section 12.6.2.3 for additional considerations.

12.6.4 Other Design Checks

Checking allowable stresses, deflection and camber, prestress losses, and ultimate strength is generally similar to that for a straight bridge, keeping in mind the differences between post-tensioning and pretensioning.

Torsion is an additional consideration. For segmental I-beam curved bridges, the torsion will often be below the limit for which the *LRFD Specifications* [Eq. 5.8.2.1-3] permits torsion to be neglected. Full-span box beams have

SKEWED AND CURVED BRIDGES

12.6.4 Other Design Checks/12.7.1.2 Bridge Layout

higher torsion from self weight, and a torsion analysis will be needed. For box sections, the reinforcement to resist torsional shear may be added directly to the reinforcement to resist the vertical shear [LRFD Specifications, 5.8.3.6], and the analysis is similar to that done for vertical shear only.

12.7 FABRICATION

It is generally more economical to ship a full-span beam to the site instead of assembling segments on site. However, curved I-beams seldom have a sufficient torsional strength to permit this; thus, segments are used.

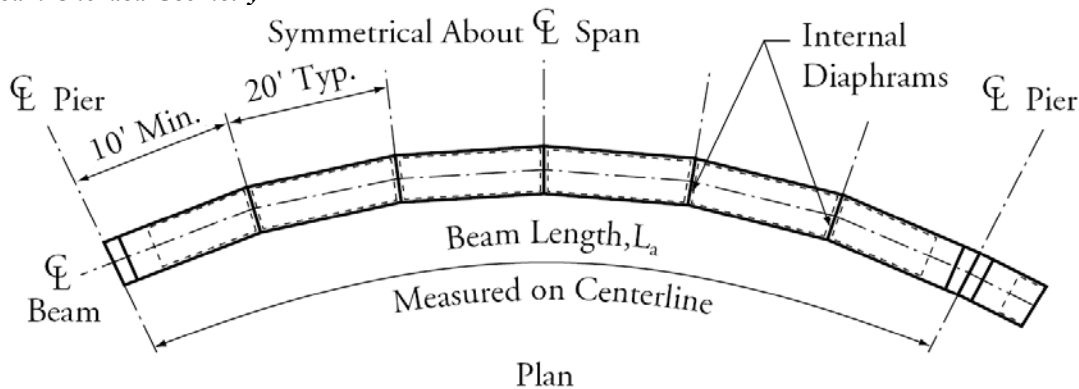
12.7.1 Box Beams

Box beams usually have enough strength to permit shipping a full-span beam. Segments would only be used if the full-span box beam is too large to be shipped.

12.7.1.1 Chord Lengths

Chord lengths of 20 ft are suggested for curved box beams as shown in **Figure 12.7.1.1-1**. This produces a maximum arc-to-chord offset of 1 in. on a 600-ft radius and 2 in. on a 300-ft radius.

*Figure 12.7.1.1-1
Precast Beam Chorded Geometry*



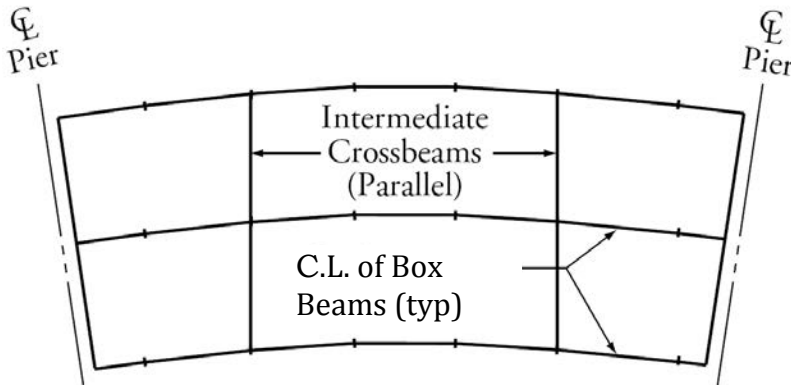
12.7.1.2 Bridge Layout

Using 20-ft chords, lay out the bridge so that the chords at each end are between 10- and 20-ft long. Lay out the crossbeams parallel to each other, so that they intersect the main beams at a form joint. These considerations will simplify beam forming and fabrication. See **Figure 12.7.1.2-1**.

SKEWED AND CURVED BRIDGES

12.7.1.2 Bridge Layout/12.7.1.3 Forms

Figure 12.7.1.2-1
Box-Beam-Bridge Layout

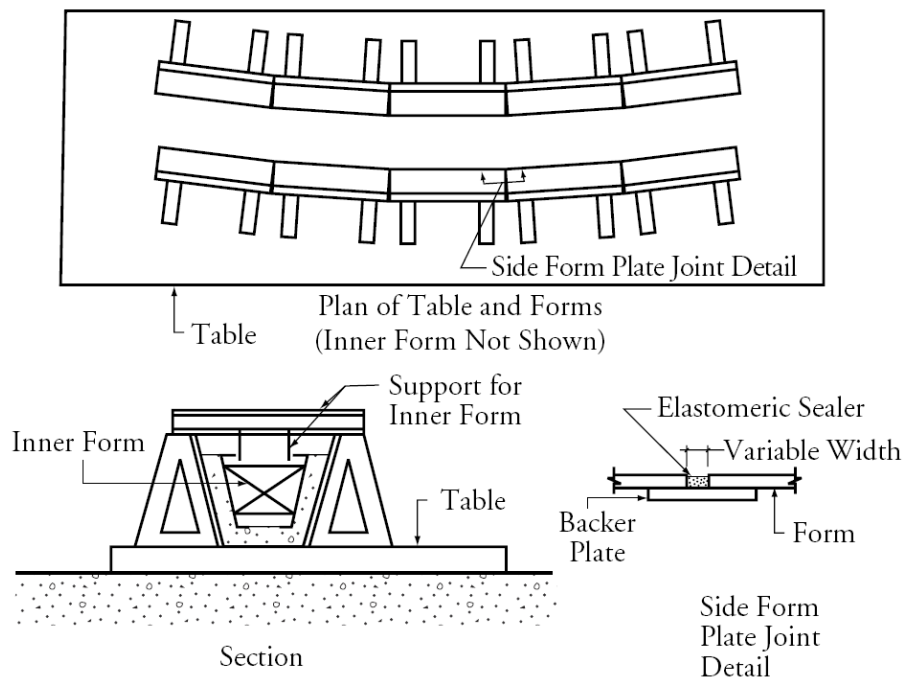


12.7.1.3 Forms

Side forms can be erected on a steel table, as shown in **Figure 12.7.1.3-1**. The table must be wide enough to accommodate the curvature. The 20-ft chorded side forms are secured to the table to the desired geometry.

Another forming method is the use of form sections that form both the sides and the soffit. This is described in ABAM (1988). See **Figure 12.7.1.3-2**.

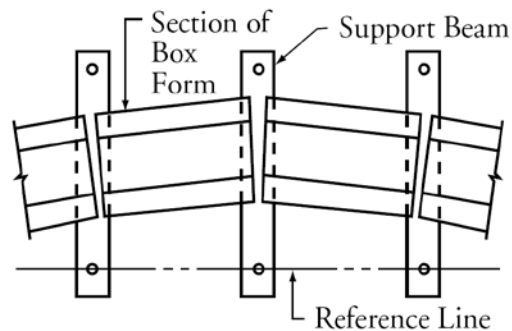
Figure 12.7.1.3-1
Chorded Forms on Flat Table



SKewed AND CURVED BRIDGES

12.7.1.3 Forms/12.7.2.4 Casting

Figure 12.7.1.3-2
Plan View of Forming

**12.7.1.4 Casting**

Using an inner form, the beam is cast up to the underside of the top flange (top of the web). After the concrete hardens, the inner form is removed, and a stay-in-place form is used to form the top flange, which is cast in a second-stage operation. Alternatively, stay-in-place void forms can be used if voids are properly anchored to prevent movement during placement of concrete and if thorough consolidation is attained under the form. The use of self-consolidating concrete facilitates the use of this method.

12.7.1.5 Post-Tensioning

If the complete curved box beam is prefabricated, the beam is post-tensioned and the ducts and anchorages are grouted at the plant. This may be done as a two-stage operation, with the first stage of post-tensioning done at an early age, and the final stage done after the concrete design strength is achieved. Where segments of curved beams are spliced in the field due to haul limitations, additional post-tensioning will be required. If curved beams are made continuous over piers, additional post-tensioning near the piers or of the entire structure may be required in the field.

12.7.2 I-Beams and Bulb-Tee Beams**12.7.2.1 Chord Lengths**

Chord segment lengths should be made as long as possible (see Sect. 12.3.1.1), in order to minimize the field joints in the segmented beam. Generally two, three, or four segments should be used.

12.7.2.2 Bridge Layout

In contrast to the box beam bridge layout, it is recommended that crossbeams be on radial lines. This will result in a more consistent geometry, and the variation in length of beam segments will not cause forming problems.

12.7.2.3 Forms

Standard beam forms may be used. It is usually necessary to thicken the webs to accommodate post-tensioning ducts. This can often be done by spreading the side forms. A new pallet or pan, as well as new end bulkheads, may be required.

If post-tensioning tendons are anchored at the ends of the beams, as is frequently done, end blocks will be required. End blocks are often cast with the segment but may be added later as a secondary casting. End blocks will be needed only at one end of each end segment, so odd lengths can be accommodated by adjusting the bulkhead location at the opposite end. In some cases, end blocks may be eliminated by placing post-tensioning anchorages in the end walls or end diaphragms.

12.7.2.4 Casting

The beam segments are cast in the usual manner with the addition of post-tensioning ducts and anchorages. Splices between segments are generally wet cast, so match-casting is not required.

SKEWED AND CURVED BRIDGES

12.7.2.5 Pretensioning/12.7.3.4 Post-Tensioning

12.7.2.5 Pretensioning

The beam segments may have a small amount of pretensioning to compensate for self weight bending of the individual segments.

12.7.3 U-Beams**12.7.3.1 Beam Lengths**

Precast curved U-beams have been cast to lengths of 120 ft and weights of 260 kips for radii as small as 765 ft. Shorter beams have been field-spliced and erected in lengths up to 150 ft and maximum weights of 350 kips. However, there are no particular limitations to the span lengths that may be obtained using this type of construction. Currently the longest known span using curved precast U-beams is approximately 260 ft. Beam segment lengths are restricted by physical and legal limits on handling and transportation.

12.7.3.2 Forms

Forms for curved precast beams must be versatile to accommodate varying curvatures for different bridges or sometimes for the same bridge. Forms may also need to accommodate variable girder depth, web thickness, and bottom flange thickness. In addition, consideration should be given to the ability of the forming to accommodate "special features" such as integral diaphragms, variable flange/web thicknesses, and stub-outs for post-tensioning anchorages, etc.

Curved U-beams are fabricated using an outer form that conforms to the horizontal alignment. The outer form can consist of a series of short straight sections or a continuous curved section. Both methods have produced consistent results.

Typically the inner core forms consist of a number of short, straight sections that are chorded along the curve. The chorded core forms must maintain the design thickness of the web and flanges along the curve but are not curved themselves for simplicity.

Forming for closed sections is similar to open U-beam casting except that it requires the placement of a top flange between the webs in the final cross section. This can be done as a second stage casting using a removable core form for the first stage and placing a stay-in-place form for the bottom of the top flange. The addition of a lid slab produces heavier beams, which can be undesirable.

12.7.3.3 Fabrication

Straight beams are typically fabricated in pretensioning beds, whereas curved beams are cast in separate beds that can be adjusted for variations in curvature. Fabrication issues such as concrete placement are not significantly different from straight girders of similar shape. Currently, there are no PCI fabrication tolerances that specifically address curved precast girder sections. Past projects have conformed to the owner's specifications and current PCI fabrication tolerances for similar precast girder sections.

In general, reinforcement for curved precast concrete beams does not significantly vary from that of straight precast beams except that supplemental reinforcement around post-tensioning ducts may be necessary to resist radial bursting forces. This reinforcement is particularly important at ends of beams where kinks may form at splice locations. Anchorage areas to accommodate post-tensioning hardware that are used in lieu of pretensioning have been designed and detailed for various projects. While this introduces another variable, these same details could occur in straight beams as well and are not peculiar to curved beam construction.

12.7.3.4 Post-Tensioning

Due to horizontal curvature, precast concrete girders requiring prestressing have all been post-tensioned. Post-tensioning that is anchored within each girder is stressed and grouted in the fabrication yard prior to shipping to the erection site. Currently there are no known commercial facilities that have casting beds capable of pre-tensioning curved girders.

After erection and splicing the segments together, additional post-tensioning is applied in the field.

12.8 HANDLING, TRANSPORTATION, AND ERECTION

12.8.1 Box Beams

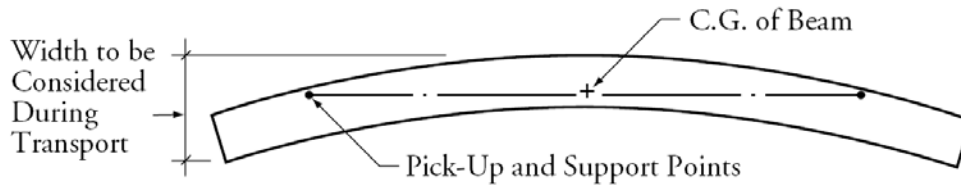
This section addresses handling, transportation, and erection considerations for curved box beams. Handling for individual straight box beam segments to be assembled in the field is similar to the handling of I-beam segments addressed in the following sections.

12.8.1.1 Handling

Pickup and support points must be located on a line through the center of gravity (in plan) of the curved beam. Pickup and temporary support points may be located inward from the beam ends, if the curvature is too great for the beam to be stable when supported at the ends. Of course, the beam stresses must be checked for the pickup and support point location. See **Figure 12.8.1.1-1**.

Figure 12.8.1.1-1

Pick-Up and Support Points for Curved Beam

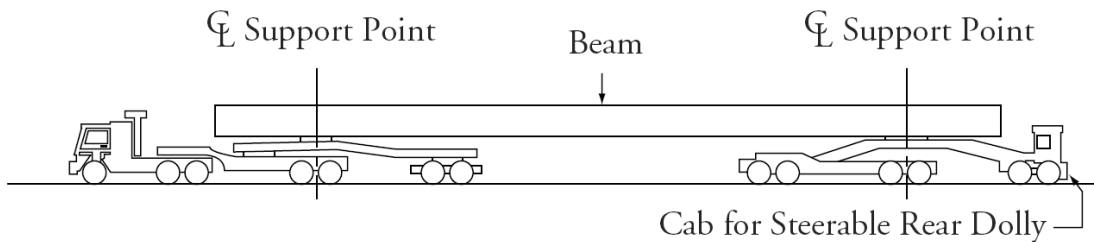


12.8.1.2 Transportation

Long-span box beams are very heavy. The maximum span may be governed by the maximum practical transportable weight or transportable width instead of final design considerations. Curved box beams may also be spliced in the field if weight or width limitations restrict transportable length. Special transporters will usually be required, as illustrated schematically in **Figure 12.8.1.2-1**, to accommodate weight and long overhangs from support points.

Figure 12.8.1.2-1

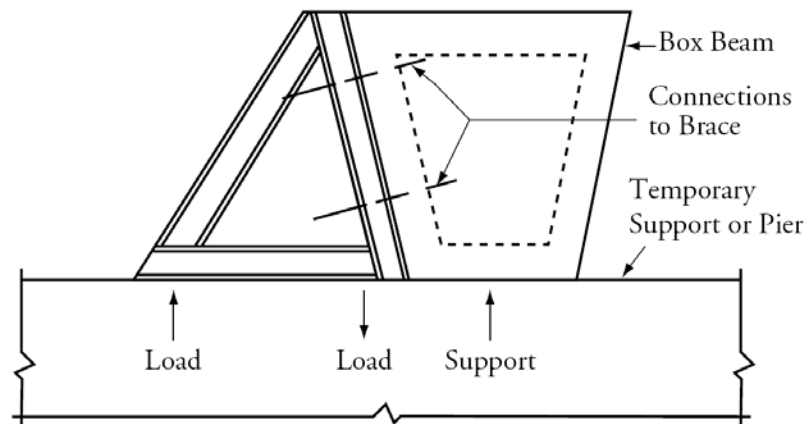
Beam Transporter



12.8.1.3 Erection

A temporary brace will probably be needed to stabilize the beam after erection, as shown in **Figure 12.8.1.3-1**. The brace needs to be located on the appropriate side of the beam to prevent rotation. For example: a simply supported beam needs to be braced on the outside of the curve. For a continuous beam, it could be on the inside or outside of the curve depending on the support locations. This brace needs to remain in place until the end and intermediate diaphragms are cast.

Figure 12.8.1.3-1
Schematic of Temporary Brace to Stabilize Beam



12.8.2 I-Beams and Bulb-Tee Beams

12.8.2.1 Handling and Transportation

Stability of I-shaped precast beams during handling and shipping is an important consideration. Lateral stability of long I- and bulb-tee cross-sections should be checked to ensure safe handling and transportation of the pieces. A procedure for the lateral stability check is detailed in two PCI Journal articles by Mast, R. F. (1989 and 1993). Additionally, transportation routes must be carefully planned to avoid steep inclines and declines, low overhead clearance, tight-radius turns and curves, and other situations that may cause problems for the hauler. Experienced trucking companies and precasters can provide guidance in these areas.

12.8.2.2 Erection and Post-Tensioning

A detailed erection plan is essential for the safe, proper, and efficient erection of the bridge structure. The erection plan should include crane locations and mobilizations, temporary shoring and bracing requirements, precast girder segment orientation, erection sequence, and safety plans. The mark number and mark orientation of the erection plan should match the piece marks shown on the precast girder shop drawings. Any required shoring and bracing must be properly designed to ensure the safety of the worksite through the entire erection process. If shoring towers are to be erected near existing traffic, the shoring must be designed to withstand a vehicle crash impact load.

12.8.3 U-Beams

Curved U-beams require special design consideration for loadings during lifting, handling, and erection. Beam flexural and torsional stresses, crack control, and stability during plant storage, transport, and erection must all be considered during design and construction. Lifting and support locations should be specified to control rolling of the beams during handling, storage, and erection. Handling and construction stresses must be limited to control cracking prior to incorporating the beams into the final structure.

At some point during the construction process, typically prior to casting the deck slab, the open-top precast concrete curved U-beams will require bracing between the top flanges or a secondary concrete placement to close the section, but this is not typically done during fabrication.

Size and weight of horizontally curved precast concrete segments are often limited by the lifting and shipping constraints. Size and weight limitations on transporting beams are important issues that designers need to research during preliminary design. Variables that influence the size and weight of beams include lifting capability of cranes at fabrication yards, capability of trucking companies, lane width restrictions during transport, and limitations on overload haul permits by various agencies. Special hauling rigs are commonly used to transport heavy permit loads in excess of 100 tons in most states.

Curved U-beams must be supported to prevent rolling in the casting yard, during shipping, and at the construction site. Methods to stabilize the beams must be implemented at all stages of construction. Locations of support points during hauling must be considered to ensure the stability of the haul truck while transporting the beams. Because the beams cannot be braced while sitting on the trucking rig, they must be supported as close to the equilibrium points as possible during hauling. Temporary stresses during transportation should be checked if the support points differ significantly from those during storage or erection.

When the beams are erected on falsework or the permanent foundations, they must also be braced to prevent rolling. Welded steel angle bracing, special erection assemblies cast into the precast components, and concrete outriggers have been used on curved beam projects to stabilize the beams during construction.

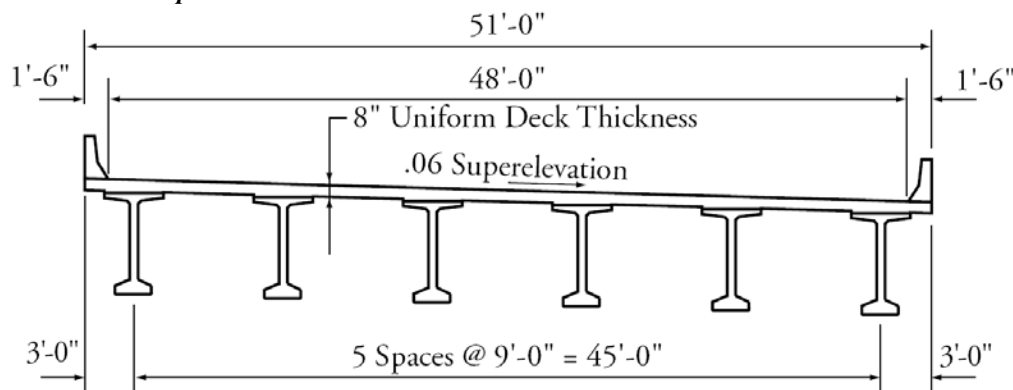
12.9 DESIGN EXAMPLE

12.9.1 Introduction

This design example demonstrates the preliminary design of a 120-ft, simple-span, bulb-tee-beam bridge on a 600-ft radius curve. Except for changes brought about by the curvature, the bridge is the same as that designed in Section 9.1. The 120-ft span is measured along the arc at the centerline of the bridge. The bridge is superelevated 6%, and the design speed is 40 mph. The splices, intermediate diaphragms, and piers are all radial to the curve.

The superstructure consists of six beams spaced at 9 ft 0 in. centers, as shown in **Figure 12.9.1-1**. Beams are designed to act compositely with the 8-in.-thick cast-in-place deck to resist all superimposed dead loads, live loads, and impact. A ½-in.-thick wearing surface is considered an integral part of the 8-in.-thick deck. The design is accomplished in accordance with the *LRFD Specifications*, Fifth Edition, 2010 and the 2011 Interim Revisions. Design live load is HL-93.

Figure 12.9.1-1
Bridge Cross-Section at Midspan



12.9.1.1 Plan Geometry

Check to see if straight beams might be used. The arc-to-chord offset is $L_c^2/8R = (120)^2/(8 \times 600) = 3$ ft. This exceeds the maximum recommended offset of 1.5 ft. If the beam is subdivided into three chords, the maximum offset will be reduced by a factor of $(3)^2$, producing an offset of 4 in. at the center of each chord. This will be barely detectable visually and will be acceptable. In order to minimize the overhang on the outside of the curve, the 3-ft overhang will be set at the middle of each chorded segment. At the ends of the chorded segments, the overhang from beam centerline on the outside will be 2 ft 8 in. and 3 ft 4 in. on the inside. **Figure 12.9.1.1-1** shows the plan geometry.

12.9.1.2 Construction

With a nominal chord offset of 3 ft for the span, the torsion will be too large for a plant cast post-tensioned, full-length beam. Therefore, spliced girder construction will be used. Each 40-ft (nominal length) straight segment will

SKEWED AND CURVED BRIDGES

12.9.12 Construction

be precast with enough pretension to compensate for its self weight on the 40-ft span. Shoring will be erected at the $\frac{1}{3}$ points of the 120-ft span. The 40-ft-long segments will then be set on the shores and on the end bearings at the abutments. Crossbeams, 12-in. thick by 66-in. deep, will be cast at the ends and at the $\frac{1}{3}$ points (splice locations). The beams will then be post-tensioned and the shores removed.

The deck is generally cast after post-tensioning. This procedure makes it feasible to replace the deck in the future, should that become necessary.

Because the beams are post-tensioned, a thicker web will be used to provide necessary cover over the ducts. This may be accomplished by spreading the side forms for an AASHTO-PCI BT-72 by 2 in., creating an 8-in.-thick web. See **Figure 12.9.1.2-1** for modified section dimensions.

Figure 12.9.1.1-1
Beam Framing Plan Geometry

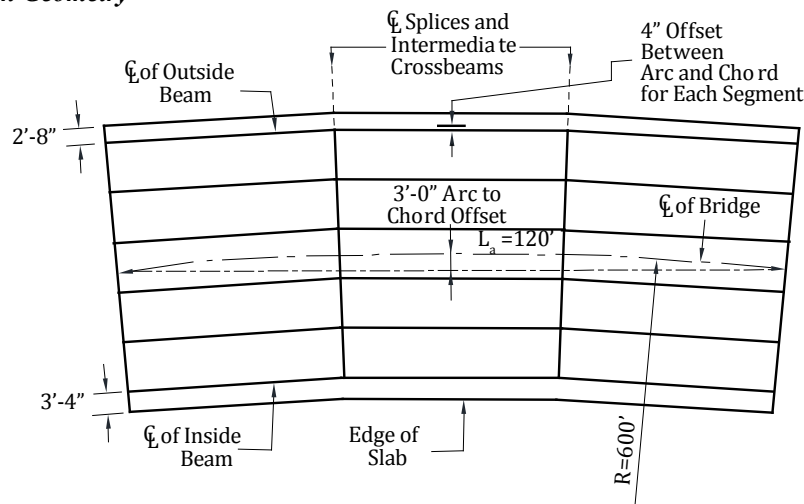
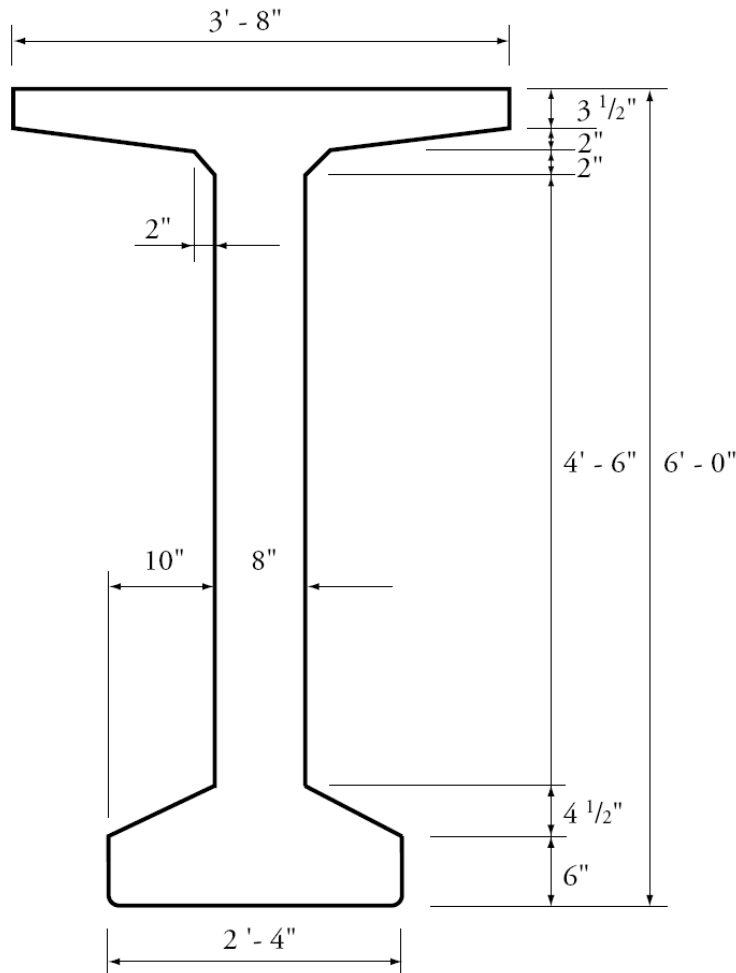


Figure 12.9.1.2-1
AASHTO-PCI BT-72 Dimensions with 2 in. Added to Width



12.9.2 Materials

These are almost identical to those used in the Section 9.1 examples.

Cast-in-place slab:

Actual thickness = 8.0 in.

Structural thickness, $t_s = 7.5$ in.

Note that a 1/2-in.-thick wearing surface is considered an integral part of the 8-in.-thick deck.

Specified concrete strength for design, $f'_c = 4.0$ ksi

Precast beams:

AASHTO-PCI Bulb-tee with 2-in.-added width as shown in **Figure 12.9.1.2-1**

Specified concrete compressive strength of beam at post-tensioning, $f'_{ci} = 6.5$ ksi

Specified concrete compressive strength for design, $f'_c = 6.5$ ksi

Unit weight of concrete, $w_c = 0.150$ kcf

SKEWED AND CURVED BRIDGES**12.9.2 Materials 12.9.3.1 Non-Composite Non-Transformed Beam Section**

Pretensioning strands	½-in. dia., seven-wire, low-relaxation	
	Area of one strand = 0.153 in. ²	
	Specified tensile strength, $f_{pu} = 270.0$ ksi	
	Yield strength, $f_{py} = 0.9f_{pu} = 243.0$ ksi	[LRFD Table 5.4.4.1-1]
	Stress limits for pretensioning strands at service limit state (after all losses):	[LRFD Table 5.9.3-1]
	$f_{pe} < 0.80f_{py} = 194.4$ ksi	
	Modulus of elasticity, $E_p = 28,500$ ksi	[LRFD Art. 5.4.4.2]
Post-tensioning strands:	0.6-in. dia., seven-wire, low-relaxation	
	Area of one strand = 0.217 in. ²	
	Specified tensile strength, $f_{pu} = 270.0$ ksi	
	Yield strength, $f_{py} = 0.9f_{pu} = 243.0$ ksi	[LRFD Table 5.4.4.1-1]
	Stress limits for post-tensioning strands at service limit state (after all losses):	[LRFD Table 5.9.3-1]
	$f_{pe} < 0.80f_{py} = 194.4$ ksi	
	Modulus of elasticity, $E_p = 28,500$ ksi	[LRFD Art. 5.4.4.2]
Reinforcing bars:	Yield strength, $f_y = 60$ ksi	
	Modulus of elasticity, $E_s = 29,000$ ksi	[LRFD Art. 5.4.3.2]
Future wearing surface:	2 in. additional concrete, unit weight = 0.150 kcf	
New Jersey-type barrier:	Unit weight = 0.300 kips/ft/side	

12.9.3 Cross-Section Properties for a Typical Interior Beam**12.9.3.1 Non-Composite Non-Transformed Beam Section**

A_g	= cross-sectional area of the precast beam = 911 in. ²	
h	= overall depth of beam = 72 in.	
I_g	= moment of inertia about the centroid of the non-composite precast beam = 608,109 in. ⁴	
y_b	= distance from centroid to extreme bottom fiber of the non-composite precast beam = 36.51 in.	
y_t	= distance from centroid to extreme top fiber of the non-composite precast beam = 35.49 in.	
S_b	= section modulus for the extreme bottom fiber of the non-composite precast beam = 16,657 in. ³	
S_t	= section modulus for the extreme top fiber of the non-composite precast beam = 17,134 in. ³	
I_{lat}	= lateral moment of inertia of non-composite precast beam = 46,014 in. ⁴	
w_g	= beam self weight per unit length = $(911/144)(0.150) = 0.949$ kips/ft	
E_c	= modulus of elasticity = $33,000K_1(w_c)^{1.5}\sqrt{f'_c}$ ksi	[LRFD Eq. 5.4.2.4-1]

where

K_1 = correction factor for source of aggregate taken as 1.0

w_c = unit weight of concrete = 0.150 kcf

SKewed AND CURVED BRIDGES**12.9.3.1 Non-Composite Non-Transformed Beam Section/12.9.3.2.2 Modular Ratio**

LRFD Table 3.5.1-1 states that, in the absence of more precise data, the unit weight of concrete may be taken as $0.140 + 0.001f'_c$ for $5.0 < f'_c \leq 15.0$ ksi. For $f'_c = 6.5$ ksi, the unit weight would be 0.1465 kcf. However, precast concrete mixes typically have a relatively low water-cementitious materials ratio and high density. Therefore, a unit weight of 0.150 kcf is used in this example. For high-strength concrete, this value may need to be increased based on test results. For simplicity, a value of 0.150 kcf is also used for the cast-in-place concrete.

where f'_c = specified compressive strength of concrete, ksi

Therefore, the modulus of elasticity for:

$$\text{cast-in-placedeck, } E_{cd} = 33,000(1.0)(0.150)^{1.5}\sqrt{4.0} = 3,834 \text{ ksi}$$

precast beam at post-tensioning (at 28 days minimum)

$$E_{ci} = 33,000(1.0)(0.150)^{1.5}\sqrt{6.50} = 4,888 \text{ ksi}$$

$$\text{precast beam at service loads, } E_c = 33,000(0.150)^{1.5}\sqrt{6.50} = 4,888 \text{ ksi}$$

The torsional constant, J , is estimated in accordance with *LRFD Specifications* Article C4.6.2.1.

$$J \approx \frac{A_g^4}{40.0I_p}$$

The polar moment of inertia I_p is equal to the sum of I_g and I_{lat} . $I_p = 654,123 \text{ in.}^4$

$$J \approx \frac{911^4}{40(654,123)} = 26,324 \text{ in.}^4$$

Properties of the 12 by 66-in. crossbeam:

$$A_{cb} = 792 \text{ in.}^2$$

$$I_{cb} = 287,496 \text{ in.}^4$$

$$I_{cb\text{lat}} = 9,504 \text{ in.}^4 \text{ (for lateral bending)}$$

$$J_{cb} = 33,120 \text{ in.}^4$$

$$w_{gcb} = 0.825 \text{ kips/ft}$$

12.9.3.2 Composite Sections**12.9.3.2.1 Effective Flange Width**

Because this is a preliminary design, it is reasonable to assume the same properties for interior and exterior beams. Therefore, the properties for a typical interior beam are used. Final designs will require more thorough calculations.

Effective flange width for interior beams is taken as the average spacing between beams [LRFD Art. 4.6.2.6.1]

$$(9 \times 12) = 108 \text{ in.}$$

Therefore, the effective flange width is 108 in. for the beam.

For the interior crossbeams, the effective flange width is taken as $(12 \times 7.5) + 12 = 102 \text{ in.}$

Note that the crossbeam in a curved bridge is not an ordinary beam spanning between main beams (9 ft in this case). Rather, it transfers load all the way across the bridge from inside to outside beams.

12.9.3.2.2 Modular Ratio

$$\text{Modular ratio between slab and beam concrete, } n = \frac{E_{cd}}{E_c} = \frac{3,834}{4,888} = 0.7845$$

SKewed AND CURVED BRIDGES**12.9.3.2.3 Transformed Section Properties/12.9.4 Loads****12.9.3.2.3 Transformed Section Properties**

Transformed flange width for interior beams = $n(\text{effective flange width})$
 $= (0.7845)(108.00) = 84.73 \text{ in.}$

Transformed flange area for interior beams = $n(\text{effective flange width})(\text{structural thickness})$
 $= (0.7845)(108.00)(7.5) = 635.45 \text{ in.}^2$

Note: Only the structural thickness of the deck, 7.5 in., is considered.

A minimum haunch thickness of $\frac{1}{2}$ in. at midspan is considered in the structural properties of the composite section. The superelevation will cause the average thickness of the haunch to be greater than $\frac{1}{2}$ in. The extra weight will be accounted for, but the extra thickness caused by superelevation will conservatively be neglected in computing composite section properties. In addition, the width of haunch must be transformed.

Transformed width of haunch = $(0.7845)(44.00) = 35.52 \text{ in.}$

Transformed area of haunch = $(0.7845)(44.00)(0.5) = 17.26 \text{ in.}^2$

Note that the haunch should only be considered to contribute to section properties if it is required to be provided in the completed structure. Therefore, some designers neglect its contribution to the section properties.

A_c = total area of the composite section = $1,564 \text{ in.}^2$

h_c = overall depth of the composite section = 80 in.

I_c = moment of inertia of the composite section = $1,208,734 \text{ in.}^4$

y_{bc} = distance from the centroid of the composite section to the extreme bottom fiber of the precast beam = 53.05 in.

y_{tg} = distance from the centroid of the composite section to the extreme top fiber of the precast beam = 18.95 in.

y_{tc} = distance from the centroid of the composite section to the extreme top fiber of the deck = 26.95 in.

S_{bc} = composite section modulus for the extreme bottom fiber of the precast beam = $22,784 \text{ in.}^3$

S_{tg} = composite section modulus for the top fiber of the precast beam = $63,792 \text{ in.}^3$

S_{tc} = composite section modulus for the top fiber of the structural deck slab = $57,176 \text{ in.}^3$

I_{clat} = moment of inertia of composite section for lateral bending = $666,423 \text{ in.}^4$

For computing J_c , the torsional constant for the composite beam, half the composite flange width is used to compute the area A_c and the polar moment of inertia I_{pc} for substitution in Eq. C4.6.2.2.1-2 in the *LRFD Specifications*. The transformed area A_c is $1,246 \text{ in.}^2$ and I_{pc} is $1,118,680 \text{ in.}^4$. This results in a value of J_c of $53,865 \text{ in.}^4$.

Composite properties of interior crossbeams:

A_{ccb} = $1,397 \text{ in.}^2$

I_{ccb} = $765,432 \text{ in.}^4$

I_{clatcb} = $529,860 \text{ in.}^4$ for lateral bending

J_{ccb} = $54,204 \text{ in.}^4$

12.9.4 Loads

For a first approximation, all loads except the truck load will be assumed to be distributed over the area of the deck. Later, after a beam gridwork model is created, the computer program will generate member self weights.

SKewed AND CURVED BRIDGES

12.9.4.1 Dead Loads/12.9.4.2 Live Loads

12.9.4.1 Dead Loads**12.9.4.1.1 Dead Loads Acting on the Non-Composite Structure**

Beam and crossbeam weight:

$$\text{Beams} = (6)(120 \text{ ft})(0.949 \text{ kips/ft}) = 683 \text{ kips}$$

$$\text{Crossbeams} = (4)(45 \text{ ft})(0.825 \text{ kips/ft}) = 149 \text{ kips}$$

$$\text{Total weight of beams and crossbeams} = 683 + 149 = 832 \text{ kips}$$

Deck weight:

$$\text{Gross area of deck} = (120 \text{ ft})(51 \text{ ft}) = 6,120 \text{ ft}^2$$

Actual thickness = 8 in.

$$\text{Deck weight} = [8 \text{ in.}/(12 \text{ in./ft})](0.150 \text{ kcf})(6,120 \text{ ft}^2) = 612 \text{ kips}$$

For a minimum haunch thickness of 0.5 in., the superelevation of 0.06 will cause the average haunch thickness to be 0.5 in. + 0.06(22 in.) = 1.82 in., say 2 in. The haunch weight is 0.150 kcf (2 in.)(44 in.)/(144 in.²/ft²) = 0.092 kips/ft/beam

$$\text{Haunch weight} = (6)(120 \text{ ft})(0.092 \text{ kips/ft}) = 66 \text{ kips}$$

$$\text{Weight of deck, including haunch} = 612 + 66 = 678 \text{ kips}$$

12.9.4.1.2 Dead Loads Acting on the Composite Structure

Barrier weight is given as 0.300 kips/ft/side

$$\text{Barrier weight} = (2)(120 \text{ ft})(0.3 \text{ kips/ft}) = 72 \text{ kips}$$

Future wearing surface is 0.025 ksf

$$(0.025 \text{ ksf})(120 \text{ ft})(48 \text{ ft}) = 144 \text{ kips}$$

$$\text{Dead load on composite structure} = 72 + 144 = 216 \text{ kips}$$

12.9.4.1.3 Total Dead Load

$$\text{Total dead load} = 832 + 678 + 216 = 1,726 \text{ kips}$$

12.9.4.2 Live Loads

Design live load is HL-93, which consists of a combination of:

[LRFD Art. 3.6.1.2.1]

1. Design truck or design tandem with dynamic allowance

[LRFD Art. 3.6.1.2.2]

The design truck consists of 8.0-, 32.0-, and 32.0-kip axles with the first pair spaced at 14.0 ft and the second pair spaced at 14.0 to 30.0 ft. The design tandem consists of a pair of 25.0-kip axles spaced at 4.0 ft apart.

[LRFD Art. 3.6.1.2.3]

2. Design lane load of 0.64 kips/ft not subject to dynamic allowance

[LRFD Art. 3.6.1.2.4]

$$IM = 33\%$$

[LRFD Table 3.6.2.1-1]

where IM = dynamic load allowance, applied to design truck or design tandem only

The number of design lanes is computed as:

Number of design lanes = the integer part of the ratio of $w/12$, where w is the clear roadway width, ft, between the curbs:

[LRFD Art. 3.6.1.1.1]

$$w = 48 \text{ ft}$$

$$\text{Number of design lanes} = \text{integer part of } (48/12) = 4 \text{ lanes}$$

SKEWED AND CURVED BRIDGES

12.9.4.2 Live Loads/12.9.4.2.4 Centrifugal Force

Multiple presence factor, m :

[LRFD Table 3.6.1.1.2-1]

For 4 lanes, $m = 0.65$.

Stresses from truck and lane loads obtained from refined analysis will be multiplied by 0.65.

12.9.4.2.1 Lane Loading

The lane load is positioned over a 10-ft width within the 12-ft design lane.

[LRFD Art. 3.6.1.3.1]

To maximize the effect of the live load, the 10-ft loaded width is shifted to the left within each design lane. This causes the lane load to have an eccentricity of 1 ft relative to the lane centerline, and the four lane loads have an eccentricity of 1 ft relative to the bridge centerline. The average arc length increases by the ratio of 601-ft radius/600-ft radius, to 120.2 ft.

The total lane loading for the four design lanes is $(4)(120.2 \text{ ft})(0.64 \text{ kips/ft})(0.65) = 200.0 \text{ kips}$.

The 0.65 factor above is the factor, m .

12.9.4.2.2 Truck Loading

The total weight of the design truck is $8 + 32 + 32 = 72 \text{ kips}$.

Including 33% impact, $1.33 \times 72 = 95.76 \text{ kips}$.

For 4 trucks, including the multiple presence factor, m :

$$4(95.76)(0.65) = 249.0 \text{ kips}$$

Note that because this is a preliminary design of the main members of a 120-ft span, the tandem load need not be considered at this time.

12.9.4.2.3 Total Live Load

Total live load = $200.0 + 249.0 = 449.0 \text{ kips}$

12.9.4.2.4 Centrifugal Force

[LRFD Art. 3.6.3]

The design speed is 40 mph. The centrifugal force coefficient is given by:

$$C = \left(\frac{4}{3}\right) \frac{v^2}{gR}$$

[LRFD Eq. 3.6.3-1]

where

C = coefficient to compute centrifugal force

v = highway design speed, ft/sec

g = gravitational acceleration, 32.2 ft/sec²

R = radius of curvature of traffic lane, ft

The design speed in ft/sec = $40 \text{ mph}/0.682 = 58.65 \text{ ft/sec}$

$$C = \left(\frac{4}{3}\right) \frac{(58.65)^2}{(32.2)(600)} = 0.2374$$

This is applied to the truck axle loads only, without the dynamic load allowance, and with the factor, m . The centrifugal force for four trucks is $4(72 \text{ kips})(0.2374)(0.65) = 44.4 \text{ kips}$.

SKEWED AND CURVED BRIDGES

12.9.5 Correction Factor/12.9.5.2 Shift in Center of Gravity

12.9.5 Correction Factors

The bending moments in the exterior beam on the outside of the curve will be greater than in a straight bridge for three reasons:

1. The additional span length on the outside of the curve.
2. The center of gravity of the curved centerline lies outside of a line through the centerline of the supports.
3. The center of gravity of an area load is further shifted outward, because there is more area outside the centerline than inward of the centerline.

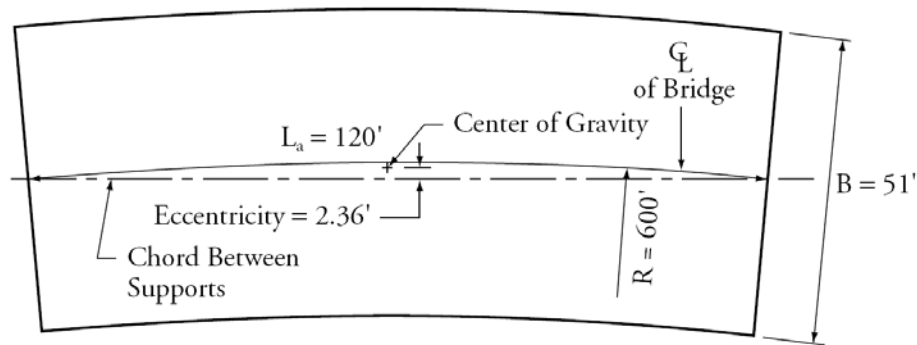
12.9.5.1 Additional Span Length Factor

The outside beam is on a radius of 622.5 ft. This increases the span length by a factor of $622.5/600 = 1.0375$.

12.9.5.2 Shift in Center of Gravity

The center of gravity (in plan) of the centerline arc is offset from a line through the center of the bearings by an amount equal to $\frac{2}{3}$ of the arc-to-chord offset $(\frac{2}{3})(3 \text{ ft}) = 2 \text{ ft}$. The additional eccentricity caused by the extra area outside the centerline is equal to $B^2/12R = (51 \text{ ft})^2/(12)(600) = 0.36 \text{ ft}$, as shown in **Figure 12.9.5.2-1**. For the initial simplification that all dead load is an area load, the eccentricity of the dead load is 2.36 ft.

*Figure 12.9.5.2-1
Center of Gravity of Curved Area*

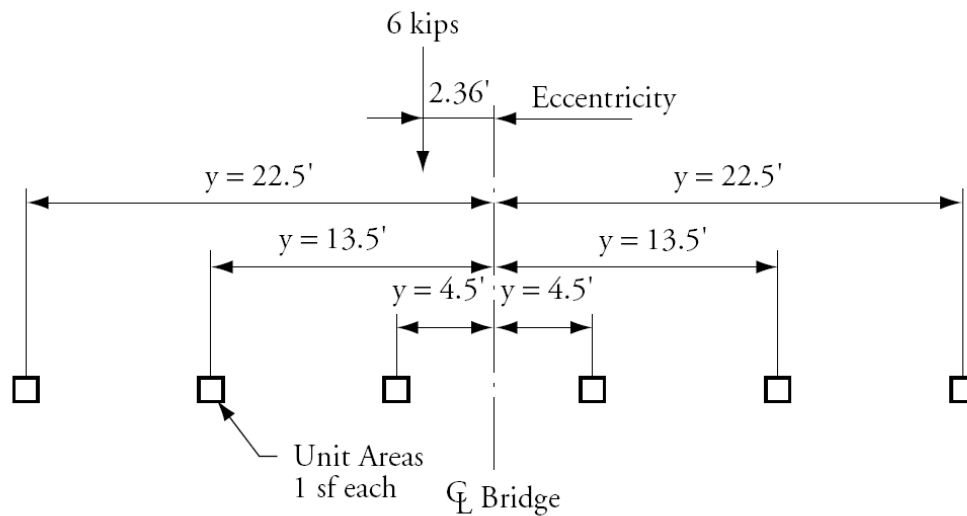


The next step is to find how much the load on the outside beam is increased because of this eccentricity. The procedure is analogous to one described in the LRFD Commentary [Article C4.6.2.2.2d] (see **Fig. 12.9.5.2-2**). For six unit areas at 9-ft spacing, the moment of inertia is 1,417.5 ft⁴ and the section modulus is 63 ft³. For an arbitrary load of 1 kip per bearing, or 6 kips, at 2.36 ft eccentricity, $P/A + Pe/S = 1 + 6(2.36)/63 = 1.2248$. This is the increase in load on the outside exterior beam caused by the eccentricity of the load. The total correction factor for bending moment due to dead load is $(1.0375)(1.2248) = 1.271$.

SKEWED AND CURVED BRIDGES

12.9.5.2 Shift in Center of Gravity

Figure 12.9.5.2-2
Properties of Group of Beam Supports



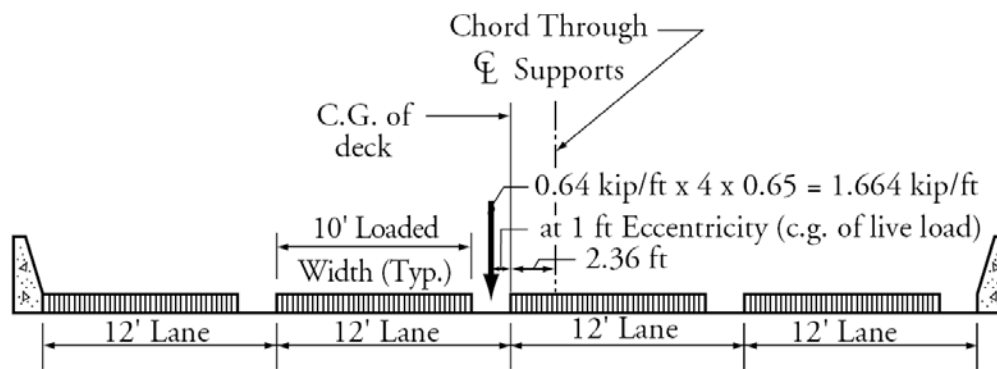
$$A = 6 \text{ ft}^2$$

$$I = \Sigma[(\text{Unit Area})(y^2)] = 1,417.5 \text{ ft}^4$$

$$S = I/y_{\text{max}} = 63 \text{ ft}^3$$

For the lane loading, the LRFD requirement to place the load off-center of the lane adds 1 ft to the eccentricity. See **Figure 12.9.5.2-3**. For a 6-kip load at 3.36-ft eccentricity, the load on the outside beam is $1 + 6(3.36)/63 = 1.32$. The total correction factor for lane loading is $(1.0375)(1.32) = 1.370$.

Figure 12.9.5.2-3
Lane Load Eccentricity



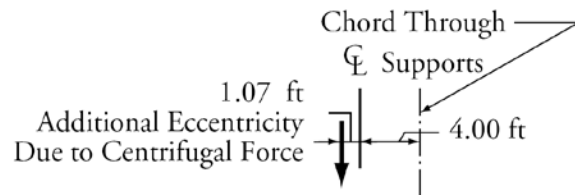
Lane Loading [LRFD Article 3.6.1.2.4]

For the truck loading, LRFD Article 3.6.1.3.1 specifies that the center of the wheel load be placed 2 ft from the curb. This causes the center of the vehicle to be 5 ft from the curb (also the lane edge), so the eccentricity from the centerline of the lane is 1 ft. The trucks are in the center of the bridge, which has a 3-ft eccentricity with respect to the supports. Thus, the vertical truck loading has an eccentricity of 4 ft as shown in **Figure 12.9.5.2-4**.

SKewed AND CURVED BRIDGES

12.9.5.2 Shift in Center of Gravity/12.9.7 Stress – Outside Exterior Beam

Figure 12.9.5.2-4
Truck Load Eccentricity



Truck Loading [LFRD Articles 3.6.1.3.1 and 3.6.3]

The effects of centrifugal force must also be taken into account. The total centrifugal force of 44.4 kips acts at a height of 6 ft [LFRD Art. 3.6.3]. The vertical truck loading is 249 kips. The horizontal force acting at 6 ft increases the eccentricity of the vertical load by $(44.4/249)(6 \text{ ft}) = 1.07 \text{ ft}$. The total eccentricity of the vertical truck load is 5.07 ft, and the correction is $1 + 6(5.07)/63 = 1.483$, as shown in **Figure 12.9.5.2-4**. The total correction factor due to centrifugal force and truck loading is $(1.0375)(1.483) = 1.538$.

12.9.6 Bending Moments – Outside Exterior Beam

The bending moments in the outside exterior beam may now be estimated. For all loads, the bending moment may be estimated as that for a 120-ft straight beam multiplied by the correction factor. For all loads except the truck loadings, the 120-ft straight beam bending moment is $WL/8$ divided by six beams in the bridge. For the truck loading, the bending moment is scaled from that for a standard truck on a 120-ft straight span. **Table 12.9.6-1** is a summary of the estimated midspan bending moments for the outside exterior beam.

Comparing these estimates to the values in the right column taken from **Tables 9.1a.4-1** and **9.1a.4-2**, it may be seen that the dead load moments are substantially increased, compared to the interior beam of a straight bridge. However, the live loads are decreased somewhat, because of the factor, m [LFRD Art. 3.6.1.1.2], which is not used in the approximate distribution method. It should also be noted that the curved beam is almost 20% heavier than the straight beam.

Table 12.9.6-1
Estimated Bending Moments in Outside Beam

	Total Weight W , kips	Moment for 120-ft Straight Beam ft-kips	Correction Factor	Moment for Curved Beam ft-kips	Interior Beam, Straight Bridge, ft-kips*
Beam & Crossbeam	832	2,080	1.271	2,644	1,438
Deck & Haunch	678	1,695	1.271	2,154	1,660
Barrier	72	180	1.271	229	180
Wearing Surface	144	360	1.271	458	360
Truck Loading w/impact	249	1,080	1.538	1,662	1,830
Lane Loading	200	500	1.370	685	843
Total	-	5,895	-	7,832	6,311

* Bending moments in the right column are taken from **Tables 9.1a.4-1** and **9.1a.4-2**.

12.9.7 Stresses – Outside Exterior Beam

The next step is to verify that the chosen beam section is adequate. It is assumed that the bottom fiber stress due to the weight of the beams and crossbeams can be compensated for by the tensioning.

SKewed AND CURVED BRIDGES**12.9.7 Stress – Outside Exterior Beam/12.9.8.2 Model 2 – Shore Loads**

Table 12.9.7-1
Estimate of Bottom Fiber Stress

LOAD	Bending Moment, ft-kips	S_b or S_{bc} , in. ³	Bottom Fiber Stress, ksi
1. Self Weight of Beams and Crossbeams (Compensated by pretensioning)	2,644	16,657	1.905
2. Deck and Haunch	2,154	16,657	1.552
3. Superimposed Dead Load	687	22,784	0.362
4. Live Load (0.8)(2,347) =	1,878	22,784	0.989
5. Sum of 2 + 3 + 4			2.903
Allowable stress at transfer of post-tensioning = $(0.60)f'_{ci} = (0.6)(6.5)$ 5.9.4.1.1] [LRFD Art.			3.900

Table 12.9.7-1 shows the bottom fiber stress caused by deck weight, superimposed dead load, and live load. For service load tensile stress checks, the live load may be taken as 80 percent of the computed live load [LRFD Art. 3.4.1, limit state Service III]. The bottom fiber stress for these loads applied to the beams and crossbeams in **Table 12.9.7-1** is 2.903 ksi. The allowable temporary stress after post-tensioning (before time-dependent losses) is 3.90 ksi. Therefore, because there is sufficient margin between the actual stress after losses and the allowable stress before losses, the beam section should be adequate and the computer model may be constructed using this beam.

12.9.8 Beam Gridwork Computer Models

12.9.8.1 Model 1 – Beam Segments on Shores

This model (not shown) is a variation of Model 2 (see Section 12.9.8.2). The ends of the members are released in bending to model the situation of simple span beam segments supported on shores. The simple span length is conservatively taken as the center-to-center distance of the crossbeams (40 ft). The reactions at each shoring location are computed. These loads are then applied to the Model 2 beam gridwork to represent removal of the shores. These loads are shown on **Figure 12.9.8.2-1**.

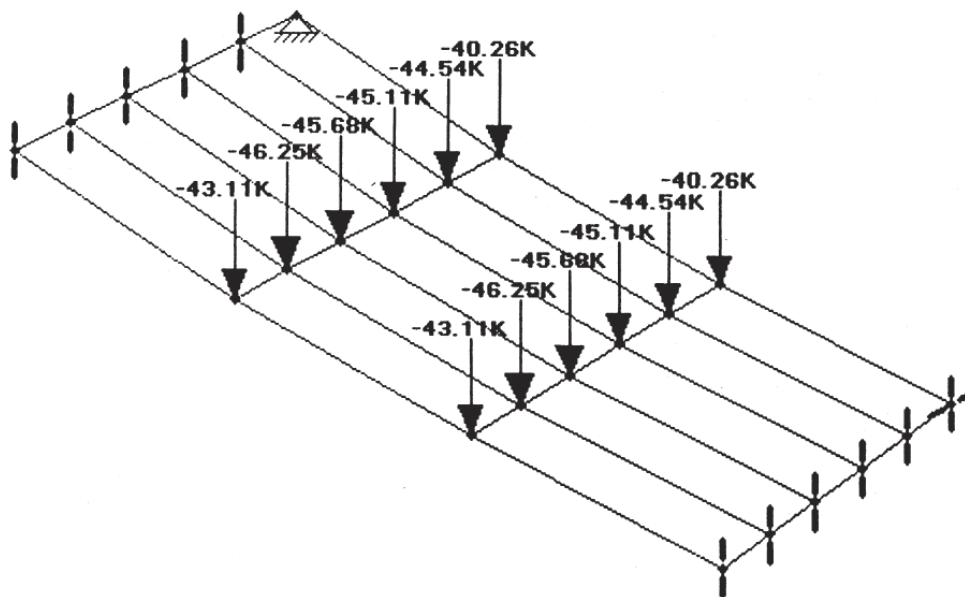
12.9.8.2 Model 2 – Shore Loads

Model 2 is the non-composite beam gridwork on the nominal 120-ft span. The loads applied to Model 2 are the loads that previously existed in the shores, as determined in Model 1. When the shores are removed, the loads previously existing in the shores are loads that are applied to Model 2. These loads are shown in **Figure 12.9.8.2-1**. The analysis done using Model 1 could be skipped, and the self weight loads applied directly to Model 2. The difference in total self weight bending moment in the outside exterior beam is less than 0.1 percent. However, it must be remembered that the moment consists of two parts, that applied to the 40-ft nominal span, and that applied to the 120-ft nominal span.

SKewed AND CURVED BRIDGES

12.9.8.2 Model 2 – Shore Loads/12.9.8.4 Model 4 – Weight of Barriers and Future Wearing Surface

Figure 12.9.8.2-1
Non-Composite Model 2 – Shore Loads



12.9.8.3 Model 3 – Weight of Deck and Haunches

The total weight of the deck and the haunches between the deck and the top flanges of the beam was calculated to be 678 kips in Section 12.9.4.1.1. This load is assumed to be applied as a uniform load of 110.8 psf over the 6,120 ft² gross area of the deck.

The model for deck weight is shown in **Figure 12.9.8.3-1**. The finite elements are only used as a means of applying a uniform load. The structural properties of the deck are zeroed out, because this is a non-composite model. The beam gridwork is the same as in Model 2.

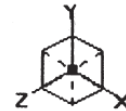
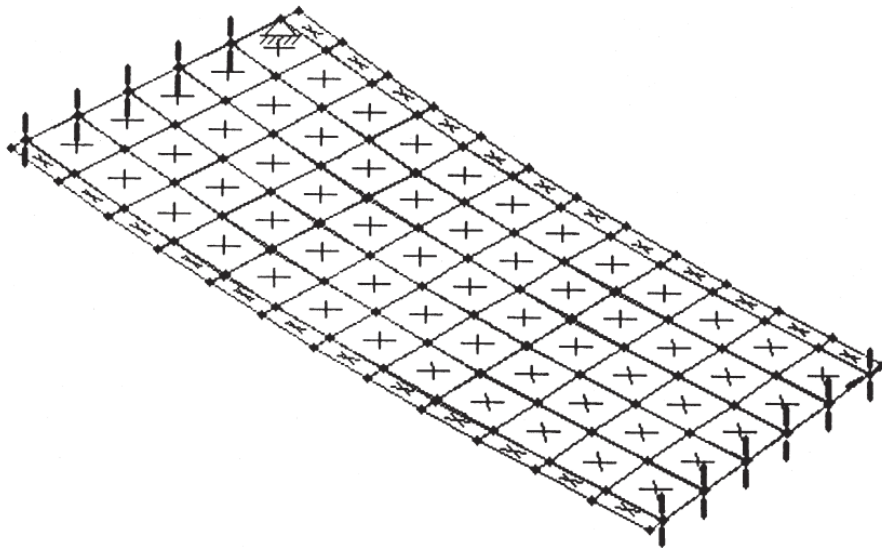
12.9.8.4 Model 4 – Weight of Barriers and Future Wearing Surface

Model 4 represents the composite structure. Composite section properties are used in the beam gridwork. The general appearance of the model is the same as Model 3 (see **Figure 12.9.8.3-1**). The 0.025 ksf uniform load is applied over the entire 51-ft width of the deck for the future wearing surface (FWS). A net barrier load of 0.263 kips/ft (0.3 kips/ft less the 0.025 ksf acting over the 1.5-ft width occupied by the barrier) is applied as a line load along the longitudinal edges of the model.

SKEWED AND CURVED BRIDGES

12.9.8.4 Model 4 – Weight of Barriers and Future Wearing Surface/12.9.8.5 Model 5 – Lane Loading

*Figure 12.9.8.3-1
Non-Composite Model 3 – Deck Weight*



12.9.8.5 Model 5 – Lane Loading

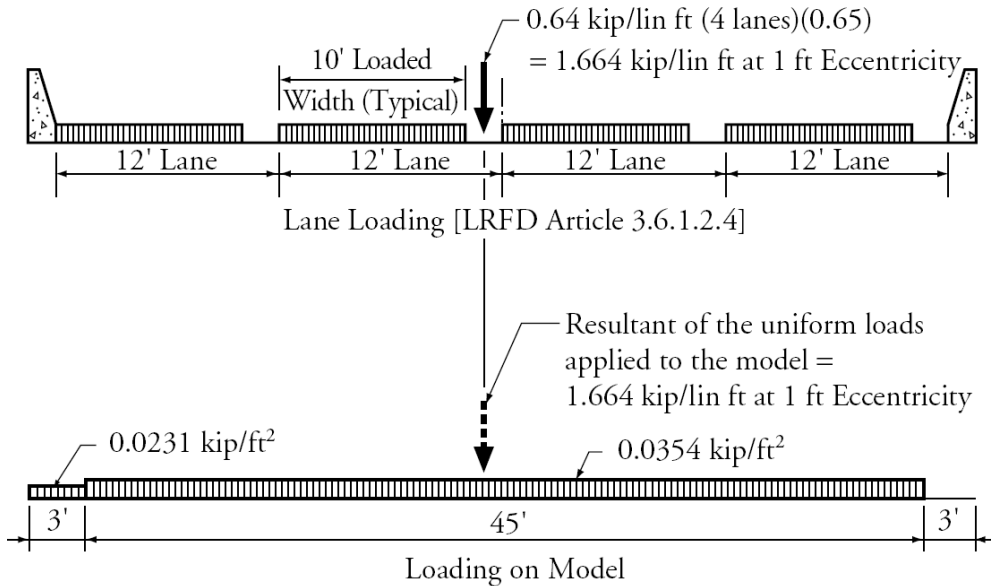
As noted in Section 12.9.4.2.1, LRFD Article 3.6.1.3 specifies that the design lane load be applied over a 10-ft width within the design lane width (of 12 ft in this case). This causes the resultant of the lane loads to be shifted 1 ft towards the outside of the curve.

The upper part of **Figure 12.9.8.5-1** shows the specified location of the lane loads in a cross-section through the bridge. The lower part of **Figure 12.9.8.5-1** shows the actual loads applied to the model. The loads were chosen so that deck elements would be loaded uniformly and the total load would have the correct location of the resultant load.

SKewed AND CURVED BRIDGES

12.9.8.5 Model 5 – Lane Loading/12.9.8.6 Model 6 – Truck Loading with Centrifugal Force

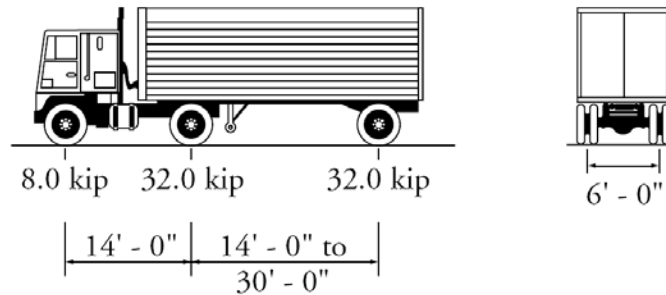
Figure 12.9.8.5-1
Lane Loading



12.9.8.6 Model 6 – Truck Loading with Centrifugal Force

The design truck is shown in **Figure 12.9.8.6-1**, which is Fig. 3.6.1.2.2-1 from the *LRFD Specifications*. For maximum positive moment, the minimum rear axle spacing of 14 ft controls. The maximum bending moment occurs with the middle axle load placed 2.33 ft from midspan.

Figure 12.9.8.6-1
Characteristics of the Design Truck



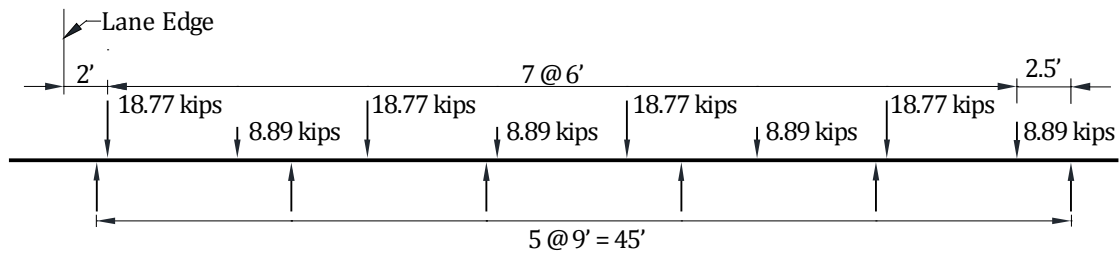
The main axle wheel loads are 16 kips each, plus a 33 percent dynamic allowance, or 21.28 kips. For the design speed of 40 mph, the centrifugal force is 0.2374 of the truck weight (without dynamic allowance). This force acts 6 ft above the roadway. The overturning moment per main axle is 0.2374 times 32 kips times 6 ft, or 45.58 ft-kips. Dividing by the 6-ft wheel spacing, the wheel loads due to centrifugal force are ± 7.6 kips. The total main axle wheel loads, including the 0.65 factor, m , are $0.65 (21.28 \pm 7.6) = 18.77$ kips and 8.89 kips. The front axle wheel loads are one quarter of this, or 4.69 kips and 2.22 kips.

The wheel loads are placed on fictitious, pin-ended members in order to transfer the loads to the main beams, as shown in **Figure 12.9.8.6-2** for the heavier axles.

SKEWED AND CURVED BRIDGES

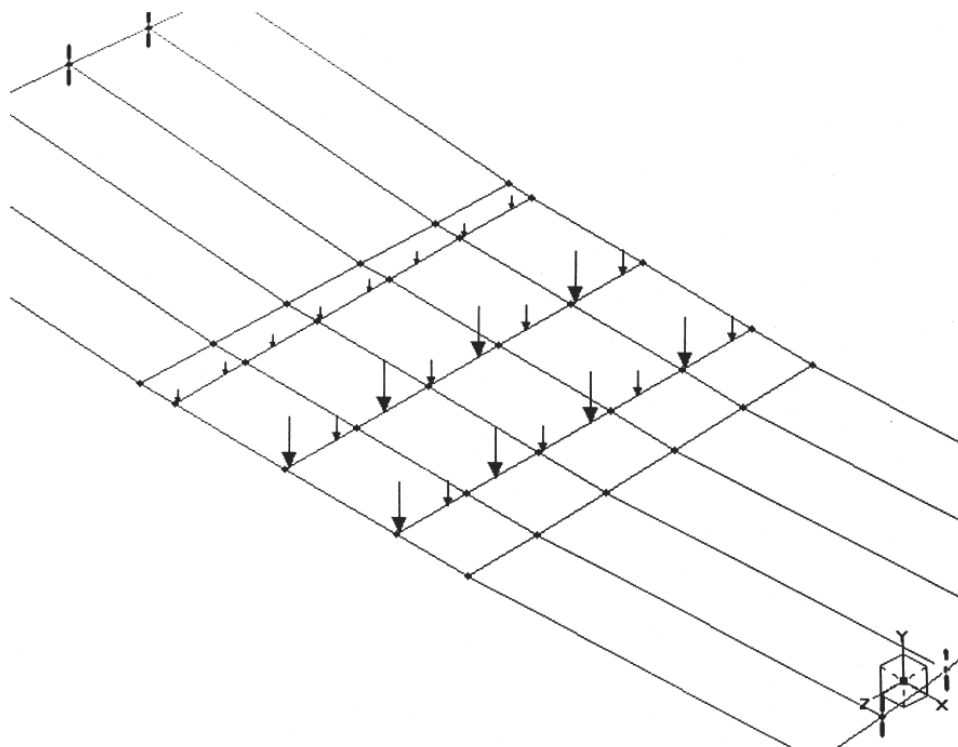
12.9.8.6 Model 6 – Truck Loading with Centrifugal Force/12.9.8.7 Summary of Bending Moments

Figure 12.9.8.6-2
Wheel Load Placement across Model for Heavy Axles



The added pin-ended members and loads that represent the truck loading for the condition producing maximum moment are shown in **Figure 12.9.8.6-3**.

Figure 12.9.8.6-3
Truck Loading on Model 6



12.9.8.7 Summary of Bending Moments

The bending moments for each of the six beams from the six loading models are summarized in **Table 12.9.8.7-1**. Pretensioning counteracts the moments from Model 1 while post-tensioning is used to counteract the moments from Models 2 through 6. The *LRFD Specifications* [Article 3.4.1 and Table 3.4.1.1], states that for checking tension in prestressed concrete members at service load, the Service III load combination may be used. This combination is $1.00 (DC + DW) + 0.8(LL + IM)$.

SKEWED AND CURVED BRIDGES

12.9.8.7 Summary of Bending Moments/12.9.9.2 Post-Tensioning

Table 12.9.8.7-1
Bending Moments in Each Beam

Load	Maximum Bending Moments, ft-kips					
	Beam Number					
	Outside					Inside
	1	2	3	4	5	6
Model 1 – Segments on Shores	204	199	193	187	181	176
Model 2 – Shore Loads	2,249	2,067	1,883	1,694	1,491	1,270
Model 3 – Deck & Haunch	2,119	1,973	1,823	1,662	1,479	1,286
Model 4 – Barrier & FWS	720	610	565	513	444	446
Model 5 – Lane Loading	649	605	551	491	420	341
Model 6 – Truck Loading	1,468	1,324	1,204	1,045	917	603
(0.8)Live Load = (0.8)(Models 5 + 6)	1,694	1,543	1,404	1,229	1,070	755
Models 2 + 3 + 4 + (0.8)(5 + 6)	6,782	6,193	5,675	5,098	4,484	3,757

12.9.9 Selection of Prestressing Force

12.9.9.1 Pretensioning

The maximum self weight bending moment for a beam segment is 204 ft-kips. The bottom fiber stress is M/S_b , or $(204)(12)/(16,657) = 0.147$ ksi. For $y_b = 36.51$ in., the eccentricity, e , is 34.51 in. for strands centered at 2 in. from bottom of the beam. Try (4) ½ in.-dia. strands with a force of 25 kips each.

Table 12.9.9.1-1
Stress Due to Pretensioning

Stress	Fiber Stress, ksi	
	Top	Bottom
$P_{pe}/A = (4)(25) / 911$	0.110	0.110
$P_{pe}/S = (4)(25)(34.51)/S$	-0.201	0.207
$M/S = (204)(12)/S$	0.143	-0.147
Pretension & Self Weight	0.052	0.170

Because this is a temporary condition, a check for minimum reinforcement is not necessary.

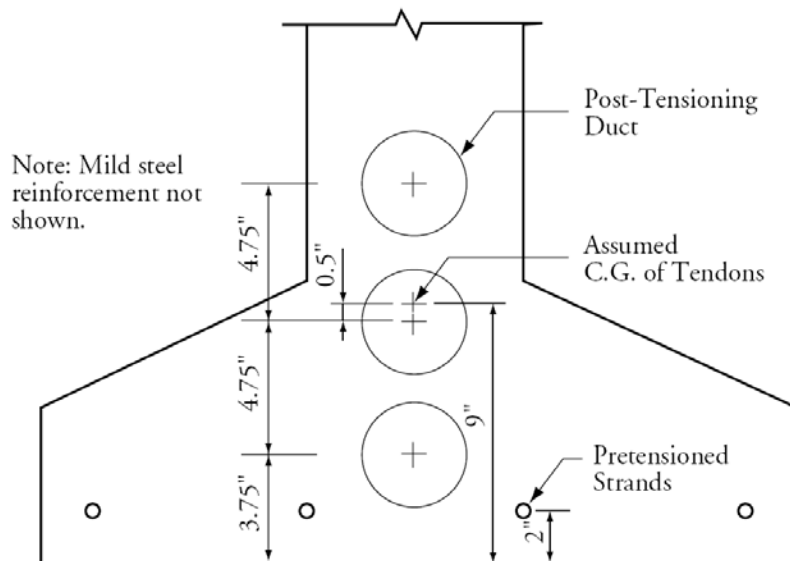
12.9.9.2 Post-Tensioning

Table 12.9.9.2-1 shows the stresses to be resisted by post-tensioning. Assuming three tendons, the maximum eccentricity is estimated to be $y_b - 9$ in. (at the location of maximum moment) as seen in **Figure 12.9.9.2-1**.

Table 12.9.9.2-1
Bottom Fiber Stresses in Outside Beam at Location of Maximum Moment

Load	M/S	Bottom Stress, ksi
Shore Loads	$(2,249)(12)/16,657 =$	1.620
Deck & Haunch	$(2,119)(12)/16,657 =$	1.527
Barrier & FWS	$(720)(12)/22,784 =$	0.379
(0.8) Live Load	$(1,694)(12)/22,784 =$	0.892
Total Stress to be Compensated by Post-Tensioning, $f_b =$		4.418

Figure 12.9.9.2-1
Bottom Flange Detail at Maximum Moment Location



For preliminary design, assume zero tension in the bottom fiber. The required final force, P_{pe} , is computed below, using non-composite section properties because the tensioning is assumed to be completed before casting the deck.

$$P_{pe} = f_b / (1/A + e/S_b)$$

$$P_{pe} = 4.418 / (1/911 + (36.51 - 9.00) / 16,657)$$

$$P_{pe} = 1,607 \text{ kips}$$

Try (48) 0.6-in.-dia. strands at 162 ksi ($0.6f_{pu}$)

$$P_{pe} = (48)(0.217)(162) = 1,687 \text{ kips}$$

A review of the total bending moments in **Table 12.9.8.7-1** indicates that the post-tensioning should be reduced in the other beams. Try 44 strands in Beam 2, 40 in Beam 3, 36 in Beam 4, 32 in Beam 5, and 28 in Beam 6.

12.9.9.3 Model 7 – Post-Tensioning

For the preliminary design, the post-tensioning trajectory is simplified to be three straight segments, with horizontal and vertical angle changes at the interior diaphragms. The tendons are modeled as bar elements, with a thermal coefficient equal to $1/E_p$. The tensioning of the model is done by applying a negative temperature change equal to the effective prestress.

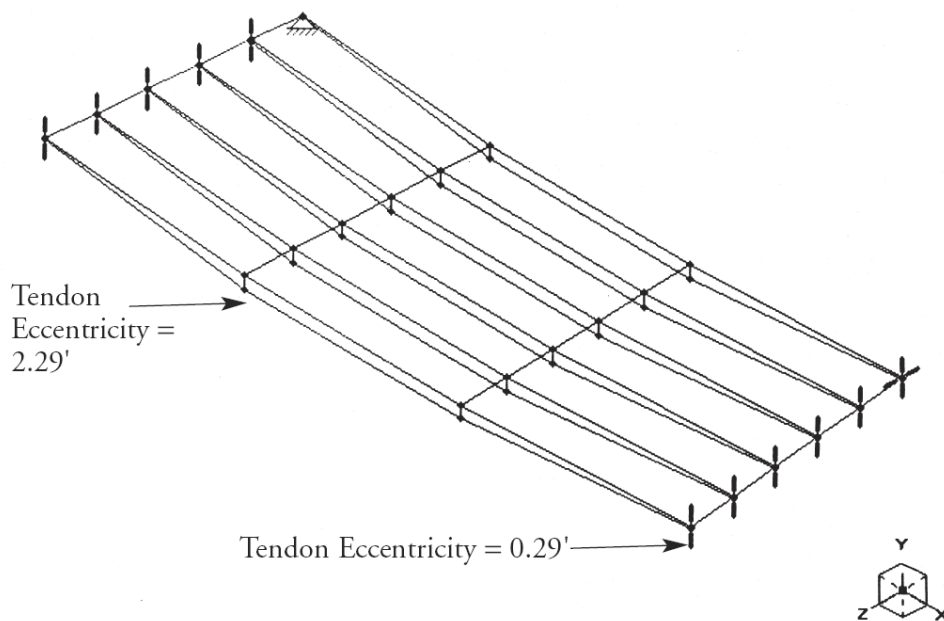
Figure 12.9.9.3-1 shows the post-tensioning model. Short, rigid stubs are used to connect the tendons to the beam gridwork. The length of these stubs is equal to the tendon eccentricity, 0.29 ft at the ends and 2.29 ft at the interior crossbeams. These stubs will also resist the transverse forces caused by the angle change of the tendons at the crossbeams.

For the middle third of the outer beam, the axial force is found to be 1,663 kips, and the bending moment due to post-tensioning is 3,650 ft-kips which agrees well with the assumptions made. The tendon profiles will be held constant but the post-tensioning force changes for the remaining beams.

SKewed and Curved Bridges

12.9.9.3 Model 7 – Post-Tensioning/12.9.12.1 Stresses in Outside Exterior Beam

Figure 12.9.9.3-1
Model - 7 Post-Tensioning



12.9.10 Results

12.9.10.1 Stresses in Outside Exterior Beam

Table 12.9.10.1-1 summarizes the stress history of the outside beam for the stages of service loads. The stresses are within the limits. As stated in LRFD Article 3.4.1, the Service I load combination is used to check compressive stresses, and the Service III load combination is used to check tensile stresses. Service I uses a load factor of 1.0 for live loads, whereas Service III uses a load factor of 0.8 for live loads.

Table 12.9.10.1-1
Stress Summary for Outside Beam

Load	Stresses, ksi		
	Top of Slab	Top of Beam	Bottom of Beam
1. Pretensioning + Beam Segment Self Weight		0.152	0.170
2. Post-Tensioning: $P/A = 1,663/911$		1.825	1.825
3. Post-Tensioning: $M/S = (3,650)(12)/S$		-2.556	2.630
4. Shore Loads: $M/S = (2,249)(12)/S$		1.575	-1.620
5. Stress after Losses*		0.996	3.005
6. Deck & Haunch: $M/S = (2,119)(12)/S$		1.484	-1.527
7. Barrier & FWS: $M/S = (720)(12)/S$	0.151	0.135	-0.379
8. Dead Load**	0.151	2.615	1.099
9a. 0.8 Live Load: $M/S = (1,694)(12)/S$			-0.892
9b. 1.0 Live Load: $M/S = (2,117)(12)/S$	0.445	0.399	
	0.596	3.014	0.207
Stress Limits: $0.60 f'_c$ Compression & 0 Tension	2.400	3.900	0 Tension

SKEWED AND CURVED BRIDGES

12.9.12.1 Stresses in Outside Exterior Beam/12.9.10.3 Crossbeams

*	The stress before losses should also be checked. The allowable temporary compressive stress for this condition is $(0.60) f'_{ci} = (0.60)(6.5) = 3.90$ ksi. It appears, by inspection, that this stress should be OK.	[LRFD Art. 5.9.4.2.1]
**	The allowable compressive stress in the beam under full dead load is $(0.45) f'_{ci} = 2.925$ OK	[LRFD Art. 5.9.4.2.1]

12.9.10.2 Strength Limit State

The check for the strength limit state is done in the same manner as that presented in Section 9.1a.9 for a straight beam. For the straight beam, the provided strength was 22% in excess of that required, and a similar amount of excess strength would be found for the beams in the curved bridge.

12.9.10.3 Crossbeams

The diaphragms function as crossbeams in the beam gridwork. They transfer load from the inside to the outside of the curve. This load transfer maintains equilibrium without the necessity of large torsional moments.

Figure 12.9.10.3-1

Model 2 - Crossbeam Shears and Moments

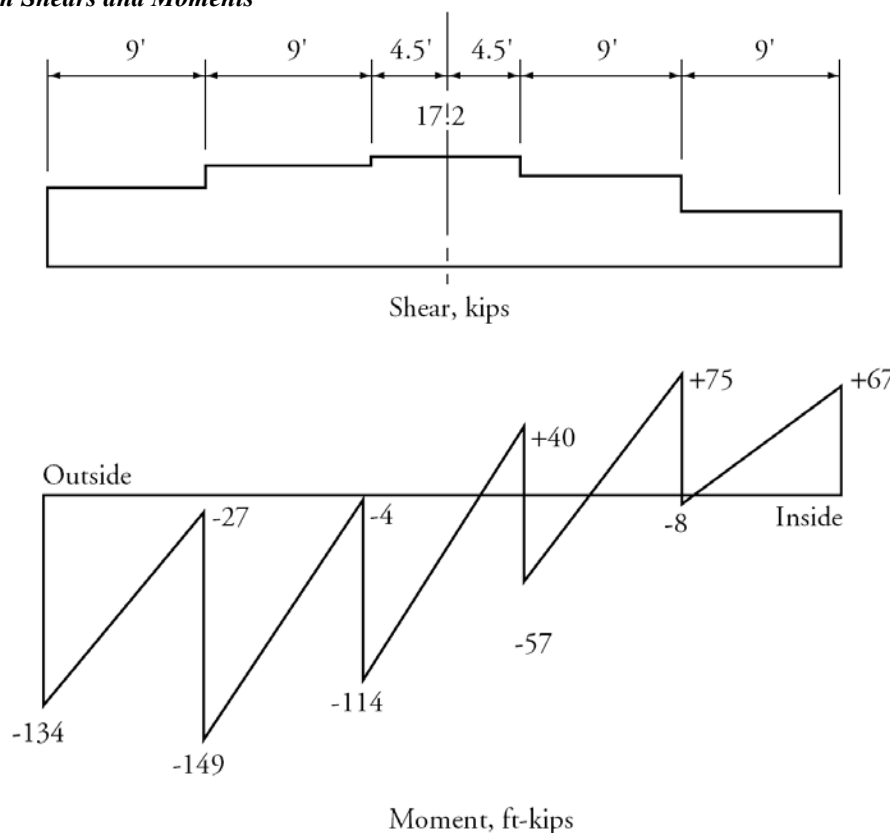


Figure 12.9.10.3-1 shows the shear and moment curves for an interior crossbeam for Model 2. The shear is relatively constant, transferring load to the outside. The crossbeam is also loaded by bending moments at each interior beam. These moments balance the primary bending moments in the stringers as they turn through an angle at the joint with the crossbeam.

The maximum bending moment occurs at the first interior beam. **Table 12.9.10.3-1** shows the factored bending moments at this location. The *LRFD Specifications* do not give a load factor for prestressing. Because the bending from prestressing is additive to that from loads, a load factor of 1.25 (the same as for dead load) is conservatively used. The bending moments are well within the capacity of a nonprestressed beam. Although the crossbeam could be post-tensioned, the simple solution is to use a conventionally reinforced (nonprestressed) member.

SKEWED AND CURVED BRIDGES

12.9.10.3 Crossbeams/12.9.10.5 Shear and Torsion

Table 12.9.10.3-1
Factored Bending Moments in Crossbeam
and at First Interior Beam

Load	M ft-kips	Load Factor	M _u ft-kips
Model 2 – Beams	-149	1.25	-186
Model 3 – Deck	-130	1.25	-163
Model 4 – Barrier & Surface	-138	1.50	-207
Model 5 + 6 – Live Loading	-110	1.75	-193
Model 7 – Prestress	-34	1.25	-42
Total			-791

12.9.10.4 Behavior Check

The behavior of the beam gridwork may be checked manually by observation of the bending moments applied to the crossbeam. The beams are bent through an angle ψ of 0.0667 radians at the crossbeam. The crossbeams must resist a moment of 0.0667 times the flexural bending moment in the beam.

Table 12.9.10.4-1
Beam Gridwork Behavior Check

Beam Number	Beam Bending Moment ft-kips	M x ψ , ft-kips	Moment on Crossbeam M _c ft-kips	Torsion M _t in Beam ft-kips	M _c + M _t ft-kips
1 (outside)	2249	150	134	16	150
2	2,067	138	122	16	138
3	1,883	126	110	16	126
4	1,694	113	97	16	113
5	1,491	99	83	16	99
6 (inside)	1270	85	67	18	85

Table 12.9.10.4-1 shows the flexural bending moment in each of the beams for Model 2, Shore Loads. The third column shows the bending moments multiplied by the angle ψ . The fourth column shows the moments in the crossbeams, from the gridwork analysis. The difference is resisted by torsion in the beams. This is compatibility torsion, caused by the fact that the bridge tilts slightly toward the outside of the curve.

12.9.10.5 Shear and Torsion

The beam gridwork is stable without torsional moments in its members. However, some torsion occurs due to the deformations of the gridwork. LRFD Article 5.8.2.1 requires torsion to be investigated when:

$$T_u > 0.25\phi T_{cr} \quad \text{[LRFD Eq. 5.8.2.1-3]}$$

where

T_u = factored torsional moment, in.-kips

ϕ = resistance factor [LRFD Article 5.5.4.2]

T_{cr} = torsional cracking moment, in.-kips, and where:

$$T_{cr} = 0.125\sqrt{f'_c} \left(\frac{A_{cp}^2}{p_c} \right) \sqrt{1 + \frac{f_{pc}}{0.125\sqrt{f'_c}}} \quad \text{[LRFD Eq. 5.8.2.1-4]}$$

SKEWED AND CURVED BRIDGES

12.9.10.5 Shear and Torsion/12.9.11 Comparison to Straight Bridge

where

A_{cp} = area enclosed by outside perimeter of concrete cross-section, in.²

p_c = the length of the outside perimeter of the concrete section, in.

f_{pc} = compressive stress in concrete after prestress losses have occurred either at the centroid of the cross-section resisting live loads or at the junction of the web and flange where the centroid lies in the flange, ksi

For consistency, the transformed section is used to compute A_{cp} , p_c , and the average f_{pc} on the transformed section.

A_{cp} = A_c = 1,564 in.²

p_c = 400 in.

f_{pc} = P_{pe}/A_c = 1,663/1,564 = 1.063 ksi

$$T_{cr} = 0.125\sqrt{6.5} \left(\frac{(1,564)^2}{400} \right) \sqrt{1 + \frac{1.063}{0.125\sqrt{6.5}}} = 4,058 \text{ in.-kips} = 338 \text{ ft-kips}$$

Check if $T_u < 0.25\phi T_{cr} = 0.25(0.9)(338) = 76.1 \text{ ft-kips}$

Torsion may be neglected if the ultimate torque is less than 76.1 ft-kips. Examine torsion in the outside exterior beam.

Table 12.9.10.5-1
Torsional Moments in Outside Beam

Load	T ft-kips	Load Factor	T_u ft-kips
Model 2 – Beams	-16.1	1.25	-20.1
Model 3 – Deck	-15.9	1.25	-19.9
Model 4 – Barrier & Surface	-9.5	1.50	-14.3
Model 5 + 6 – Live Loads	-15.8	1.75	-27.6
Model 7 – Prestress	+21.7	0.9*	+19.5
Total			62.4

*Because the prestress acts to oppose the other torsional moments, a load factor of 0.9 was conservatively assumed.

Table 12.9.10.5-1 shows that T_u is less than 76.1 ft-kips. Therefore, torsion may be neglected.

The shear design is performed in a manner similar to that shown in Section 9.1a.4.11 for a straight beam. Note that for post-tensioned beams, LRFD Article 5.8.2.9 requires that the effective web width, b_v , be computed deducting one quarter of the diameter of grouted ducts. The actual web width is 8 in., but the effective width, b_v , will be approximately 7 in.

12.9.11 Comparison to Straight Bridge

Compared to the straight bridge of Section 9.1a, the additional cost items for this curved bridge are as follows:

1. Additional design cost.
2. The cost and inconvenience of shoring. This may be at least partially offset by the reduced shipping and erection costs for the beam segments, as compared to full length beams.
3. The additional cost of concrete for 2 in. increase in width of beams (1 cf/lf of added concrete) due to addition of post-tensioning.

SKEWED AND CURVED BRIDGES

12.9.11 Comparison to Straight Bridge/12.11 References

4. The cost of intermediate crossbeams (not required for straight bridge).
5. Additional cost of post-tensioning compared to pretensioning.
6. The cost of additional strand. Less strand is used in the other five beams, but the total strand area (including pretensioned strands) for the six beams is about 20 percent greater than for the straight bridge.
7. A wider cap beam may be necessary to allow clearance for the post-tensioning jacks between the ends of the beams.

12.10 DETAILED FINAL DESIGN

The detailed final design of the curved beam bridge will generally follow the design for a similar straight bridge, as described in Section 9.1a. Some special points relating to the post-tensioned curved bridge are given below.

12.10.1 Loss of Prestress

The calculation of prestress losses for post-tensioned beams is somewhat different from that for pretensioned beams. Refer to *LRFD Specifications*, Article 5.9.5.

12.10.2 Computer Models

The computer models used in the preliminary design to analyze the effect of vertical loads are adequate for use in the detailed final design. The model for the post-tensioning (Model 7) should be refined, using more realistic tendon trajectories and accurate estimates of the initial and final prestressing forces. In addition, the optimum prestressing levels for all six beams needs to be investigated more thoroughly. This is a trial-and-error process.

12.10.3 Crossbeam Details

The detailing of crossbeams between the beam segments is similar to that described in Chapter 11 for spliced beams. Refer to Chapter 11.

Initial stresses in the beams at the crossbeam location need to be calculated in order to determine the required initial concrete strength, f_{ci} , for the crossbeam concrete at the time the beams are post-tensioned.

The post-tensioning tendons undergo an angle change at the crossbeams. This creates an inward radial force equal to the tension in the tendon multiplied by the angle change in radians. At the exterior beam on the inside of the curve, reinforcement must be provided to tie this force back into the crossbeam. See Podolny (1985) for a further discussion of this problem.

12.10.4 Post-Tensioning Anchorages

Post-tensioned beams will generally be detailed with end blocks to contain the tendon anchors. The design of post-tensioned anchorage zones is given in *LRFD Specifications*, Article 5.10.9. An alternate method is to place anchorages in the end walls to eliminate the need for end blocks on the beams.

12.11 REFERENCES

1. AASHTO. 2010. *AASHTO LRFD Bridge Design Specifications*, Fifth Edition, American Association of State Highway and Transportation Officials, Washington, DC, 2010 and 2011 Interim Revisions. <https://bookstore.transportation.org> (Fee)
2. ABAM Engineers Inc. 1988. "Precast Prestressed Concrete Horizontally Curved Bridge Beams," *PCI Journal*, Precast/Prestressed Concrete Institute, Chicago, IL. V. 33, No. 5 (September-October), pp. 50-95. http://www.pci.org/view_file.cfm?file=JL-88-SEPTEMBER-OCTOBER-3.pdf
http://www.pci.org/view_file.cfm?file=JL-88-SEPTEMBER-OCTOBER-4.pdf

SKewed AND CURVED BRIDGES**12.9.11 Comparison to Straight Bridge/12.11 References**

3. Amorn, W., C. Y. Tuan, and M. K. Tadros. 2008. "Curved Precast, Pretensioned Concrete I-Girder Bridges," *PCI Journal*, Precast/Prestressed Concrete Institute, Chicago, IL. V. 53, No. 6 (November-December), pp. 48-66.
http://www.pci.org/view_file.cfm?file=JL-08-NOVEMBER-DECEMBER-7.pdf
4. FHWA. 1996-A. *Seismic Bridge Design Applications*, Part Two, FHWA Publication No. FHWA-SA-97-018, National Highway Institute (NHI) Course No. 13063, National Technical Information Service, Springfield, VA.
<http://isddc.dot.gov/OLPFiles/FHWA/012348.pdf>
5. FHWA. 1996-B. *Seismic Design of Bridges*, Design Example No. 2, FHWA Publication No. FHWA-SA-97-007, National Technical Information Service, Springfield, VA.
<http://www.ntis.gov/search/product.aspx?ABBR=PB97143309> (Fee)
6. Mast, R. F. 1989. "Lateral Stability of Long Prestressed Concrete Beams – Part 1," *PCI Journal*, Precast/Prestressed Concrete Institute, Chicago, IL. V. 34, No. 1 (January –February), pp. 34-53.
http://www.pci.org/view_file.cfm?file=JL-89-JANUARY-FEBRUARY-3.pdf
7. Mast, R. F. 1993. "Lateral Stability of Long Prestressed Concrete Beams – Part 2," *PCI Journal*, Precast/Prestressed Concrete Institute, Chicago, IL. V. 38, No. 1 (January-February), pp. 70-88.
http://www.pci.org/view_file.cfm?file=JL-93-JANUARY-FEBRUARY-30.pdf
http://www.pci.org/view_file.cfm?file=JL-93-JANUARY-FEBRUARY-31.pdf
8. Podolny, Walter, Jr. 1985. "The Cause of Cracking in Post-Tensioned Concrete Box Girder Bridges and Retrofit Procedures," *PCI Journal*, Precast/Prestressed Concrete Institute, Chicago, IL. V. 30, No. 2 (March-April), pp. 82-139 and discussion by Bruggeling, A. S. G., T. Y. Lin, and Walter Podolny, Jr., V. 31, No. 4 (July-August), 1986, pp. 130-133.
http://www.pci.org/view_file.cfm?file=JL-86-JULY-AUGUST-10.pdf
9. Russell, H. G. 2009. "NCHRP Synthesis 393: Adjacent Precast Concrete Box Beam Bridges: Connection Details," National Research Council, Transportation Research Board, Washington, DC, 75 pp.
<http://www.trb.org/main/blurbs/160850.aspx> (Fee)
- 10.

This page intentionally left blank

INTEGRAL BRIDGES

Table of Contents

13.1 INTRODUCTION	13 - 3
13.1.1 Overview	13 - 3
13.2 INTEGRAL (JOINTLESS) BRIDGES	13 - 3
13.2.1 Basic Characteristics	13 - 3
13.2.2 Limitations	13 - 4
13.3 SUPERSTRUCTURE DESIGN	13 - 4
13.3.1 Superstructure Details at Integral Abutments	13 - 4
13.3.2 Continuity at Piers	13 - 5
13.3.3 Movements and Restraint Forces	13 - 8
13.3.4 Approach Slabs	13 - 8
13.4 ABUTMENT DESIGN	13 - 9
13.4.1 Abutment Configurations	13 - 9
13.4.2 Accommodating Superstructure Movement at Abutments	13 - 10
13.4.3 Passive Pressure Reduction	13 - 12
13.4.4 Details at Abutments	13 - 13
13.4.5 Problems and Solutions	13 - 15
13.4.5.1 Problems	13 - 15
13.4.5.2 Solutions	13 - 16
13.5 PIER DESIGN	13 - 16
13.5.1 Introduction	13 - 16
13.5.2 Accommodating Superstructure Movements at Piers	13 - 17
13.5.2.1 Flexible Bents	13 - 17
13.5.2.2 Isolated Rigid Piers	13 - 18
13.5.2.3 Semi-Rigid Piers	13 - 19
13.5.2.4 Hinged-Base Piers	13 - 20
13.5.3 Analysis and Design of Semi-Rigid Piers	13 - 21
13.5.3.1 Longitudinal and Transverse Load Distribution	13 - 21
13.5.3.2 Equivalent Forces Due to Superstructure Movements	13 - 22
13.5.3.3 Estimation of Pier Stiffness Parameters	13 - 22
13.5.3.4 Load Combinations	13 - 23
13.5.3.5 Slenderness Effects	13 - 23
13.6 ANALYSIS CONSIDERATIONS	13 - 23
13.6.1 Introduction	13 - 23
13.6.2 Equivalent Cantilever Method	13 - 27
13.6.3 Forces in Substructure Units	13 - 29
13.6.4 Conclusions from Example	13 - 31
13.7 SURVEY OF CURRENT PRACTICE	13 - 31
13.7.1 Introduction	13 - 31
13.7.2 Data Collection/Survey Response	13 - 32

INTEGRAL BRIDGES

Table of Contents

13.7.3 Lessons Learned..... 13 - 39

13.7.4 Future Research Needs 13 - 39

 13.7.4.1 Design and Analysis..... 13 - 39

 13.7.4.2 Performance..... 13 - 39

13.8 CASE STUDIES 13 - 40

 13.8.1 Section Description..... 13 - 40

 13.8.2 The Nebraska City Viaduct, Nebraska 13 - 40

 13.8.3 I-469 Bridge Over I-69, Indiana 13 - 47

 13.8.4 Menauhant Road Bridge, Massachusetts..... 13 - 53

 13.8.5 Deer Creek Industrial Park Access Bridge, West Virginia 13 - 57

 13.8.6 Tennessee State Route 50 over Happy Hollow Creek, Tennessee 13 - 61

13.9. CONCLUSIONS 13 - 71

13.10. CITED REFERENCES 13 - 71

13.11 BIBLIOGRAPHY 13 - 72

INTEGRAL BRIDGES

13.1 INTRODUCTION

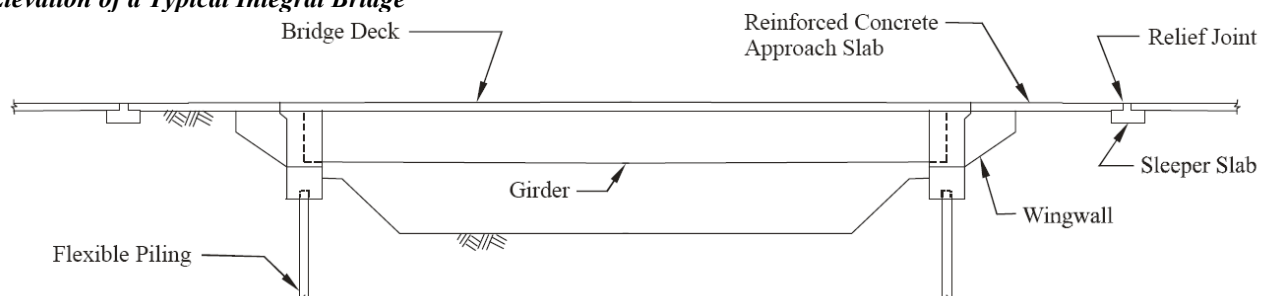
13.1.1 Overview

Traditional bridge design makes use of expansion joints in conjunction with expansion bearings to accommodate superstructure movements. However, leaking expansion joints and frozen bearings are major bridge maintenance issues. To address these issues, many state departments of transportation have adopted a policy of designing and constructing integral bridges, which have no expansion joints, whenever possible. Integral bridge superstructures are constructed to work integrally with the abutments, as shown in **Figure 13.1.1-1**. Movements due to creep, shrinkage and temperature changes are accommodated by using flexible piling and through incorporating relief joints at the ends of the approach slabs.

In addition to reduced maintenance costs, other advantages of this type of bridge include improved structural integrity, reliability and redundancy, improved long term serviceability, improved riding surface, reduced initial cost, and improved aesthetics, since abutment and pier staining and other damage caused by water intrusion are avoided.

The material presented in this chapter is based on the PCI State of the Art Report, SOA IB-01-02 titled, "Precast/Prestressed Integral Bridges", 2001. This report presents discussion, analysis and reviews of the design techniques and considerations used in the United States and Canada. Also included is a comprehensive reference list for related information and selected case studies.

Figure 13.1.1-1
Elevation of a Typical Integral Bridge



Although in recent times, integral bridges have been built in seismically sensitive areas, the committee concluded that seismic issues were beyond the scope of this report at this time. The designer is referred to the extensive publications in the bibliography for additional information.

13.2 INTEGRAL (JOINTLESS) BRIDGES

13.2.1 Basic Characteristics

Integral bridges consist of superstructures, abutments (also called end bents), intermediate piers, and foundations. The design of integral bridges is generally similar to that of conventional bridge design. Special analysis and design considerations required for integral bridges are primarily associated with the need to accommodate volumetric changes in the structure, such as thermal movements.

Integral bridges accommodate superstructure movements without conventional expansion joints. The superstructure is rigidly or semi-rigidly connected to the abutments. The abutment pilings are flexible, allowing the superstructure to expand and contract. Approach slabs, connected to the abutment and/or deck slab with reinforcement, move with the superstructure. Generally, at its junction with the approach pavement, the

INTEGRAL BRIDGES**13.2.1 Basic Characteristics/13.3.1 Superstructure Details at Integral Abutments**

approach slab is supported by a sleeper slab or grade beam. The superstructure movement here is accommodated using flexible pavement joints.

Integral construction is well-suited to both single- and multiple-span bridges. For single-span bridges, stability is provided by passive pressure behind the backwall. For multiple-span bridges, intermediate piers contribute to the bridge's stability. The various pier configurations typically used in integral bridges are discussed in Section 13.5.

13.2.2 Limitations

There are limitations on the use of integral bridges. These involve the following factors:

1. Length of structure. Limitations on length are concerned with passive pressure effects, stresses in the piles, and the movement capacity of the joint between the approach slab and the approach pavement. Many state departments of transportation limit lengths to 300 ft for steel superstructures and 600 ft for prestressed concrete superstructures. A few states, like Tennessee, have successfully used longer lengths.
2. Structure geometry. Only six states have reported application of integral construction to curved bridges. Skew angles have generally been below 40 deg. However, Tennessee has used this method of construction extensively and effectively for curved bridges as well as bridges with skew angles up to 70 deg.
3. Foundations. Integral bridges require that abutment piles be flexible. Therefore, they should not be used with pile foundations where rock is closer than 10 ft from the bottom of the abutment beam, unless pre-augered holes for piles are employed. The New York Department of Transportation specifies a minimum pile penetration of 20 ft into acceptable soils to ensure adequate flexibility and to provide for scour protection. The minimum depth is also meant to provide sufficient lateral support for the pile, particularly when conditions dictate that the top portion of the pile is pre-augered and back-filled with granular material.

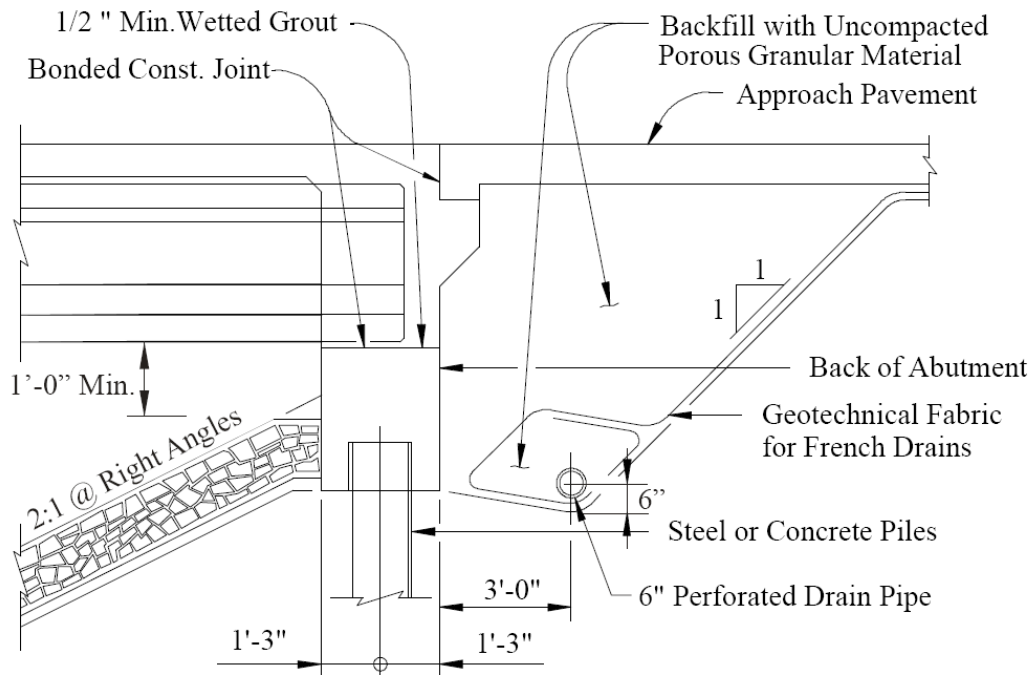
Usually, integral bridges are founded on piles. However, there are instances where they have been supported by spread footings that are founded on rock. They can also be supported on spread footings on soil if the soil is well compacted and the possibility of settlement of the foundation is considered in the design.

13.3 SUPERSTRUCTURE DESIGN**13.3.1 Superstructure Details at Integral Abutments**

The critical detail that makes a bridge an integral bridge is the connection of the superstructure to the integral abutments. As shown in **Figure 13.3.1-1**, the girders are framed into the abutment through encasement in concrete and/or embedded reinforcement. The deck slab is continuous over the abutment. The approach slab is connected to the abutment with reinforcement. Some bridge engineers are of the opinion that it is better to hinge the approach slab to the backwall by means of dowel bars to better accommodate rotation of the abutment or the approach slab.

INTEGRAL BRIDGES**13.3.1 Superstructure Details at Integral Abutments/13.3.2 Continuity at Piers**

Figure 13.3.1-1
Connection of the Superstructure
to the Integral Abutments



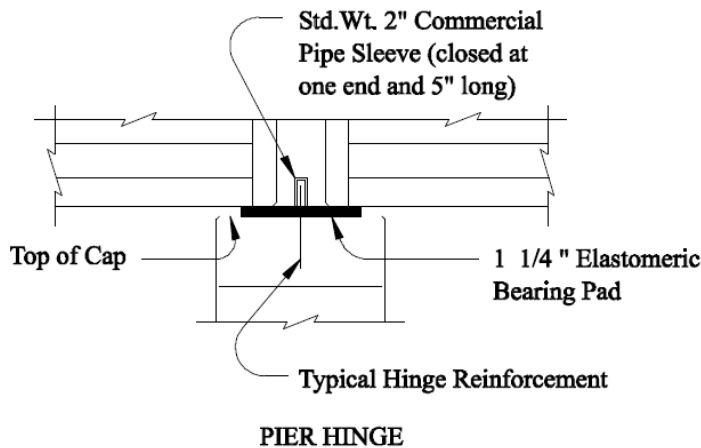
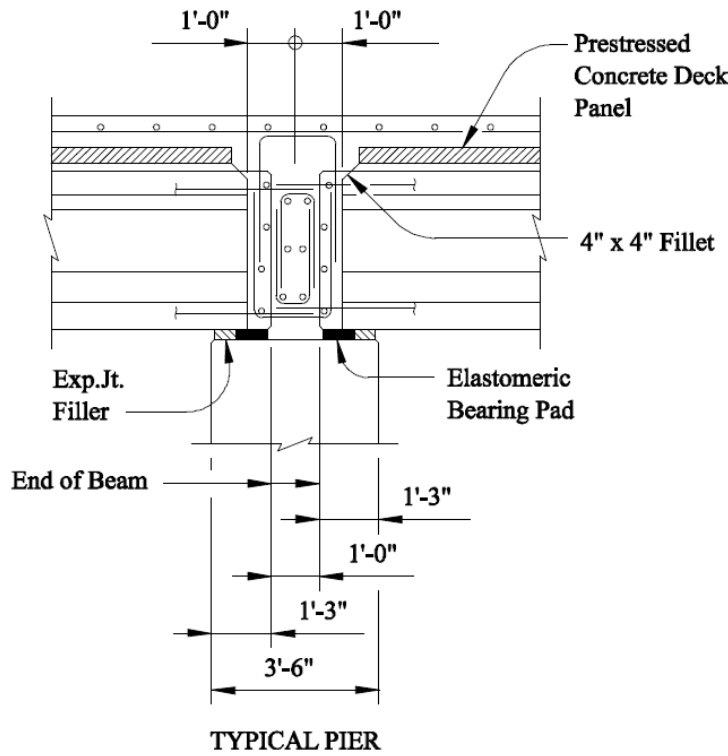
Because the superstructure is moment-connected to the integral abutments, girder rotation will theoretically induce moments in the abutment piles. These moments are usually ignored in the design of superstructure, since the superstructure is generally considerably stiffer than the piles. Girder rotation can be minimized by casting the end span deck slab prior to the backwall. However, in certain situations, particularly in longer span integral bridges, moments due to superstructure rotation are considered in the design of the abutment piles.

13.3.2 Continuity at Piers

Distinction must be made between slab continuity and girder continuity at the piers. For a bridge to be classified as an integral bridge, it is obvious that the slab must be physically continuous. Joints, if used, should be limited to saw-cut control joints or construction joints. Girder continuity at the piers, however, is not a necessity unless the superstructure is designed for continuity. Lack of girder continuity decreases the redundancy of the structure and increases its vulnerability to catastrophic events such as the loss of a pier. Deck continuity at piers not only eliminates the potential leakage of water through expansion joints but also is absolutely necessary for integral bridges.

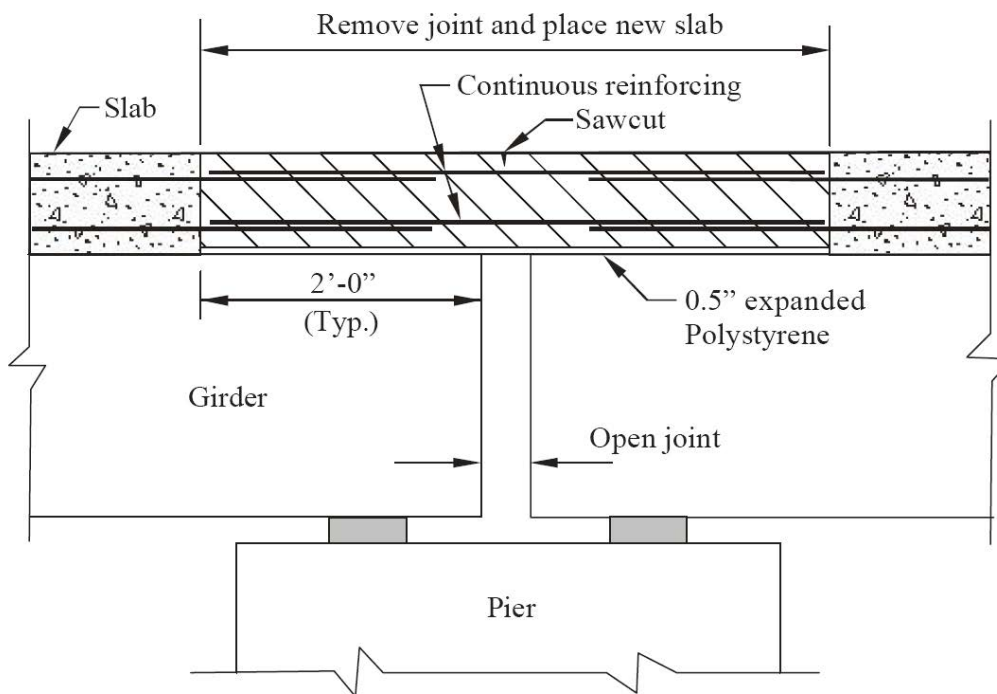
If girder continuity is provided, the superstructure is most commonly assumed to be continuous for live loads (LL) and superimposed dead loads (SDL) only. In a typical structure, girders are erected as simple spans and made continuous by the addition of mild steel in the slab, and by placing concrete diaphragms over the piers, between the ends of the precast girders, as shown in **Figure 13.3.2-1**. Systems that use post-tensioning or other methods of providing girder continuity have also been used successfully.

Figure 13.3.2-1
Typical Pier Details



When slab-only continuity is provided over the piers, girders are designed as simply supported for all loads and only the slab and its reinforcement are continuous over the pier. To control cracking a saw-cut control joint is usually provided. **Figure 13.3.2-2** shows how slab only continuity can be achieved in existing structures by eliminating the expansion joint. The detail shown in **Figure 13.3.2-2** should only be applied to short and medium spans (up to 100 ft). Flexure cracks in the deck are expected at the pier. However, the problems associated with these cracks are much less than the problems resulting from leaking joints.

Figure 13.3.2-2
Retrofitting at Piers for Continuity



At least two agencies reported that they provide girder continuity in the form of extra slab steel and concrete diaphragms, but then do not decrease mid-span positive SDL and LL moments used for prestressed girder design. Although somewhat conservative, the penalty for this approach is small except in span ranges that are approaching the limits of the girder section. Most commonly, however, continuity is considered when calculating SDL and LL moments.

Advantages and disadvantages of girder continuity are well documented, as are design methodologies. In addition, the relative benefits of the positive moment connection between the ends of the individual precast members have received significant attention (Oesterle 1989). These issues are not discussed in this report.

In the special environment of longer span integral bridges, i.e., those with spans over 100 ft, particular attention must be given to the construction sequence if girder continuity is provided. Various agencies have found that casting the concrete diaphragms over the piers should be done concurrently with placement of the slab. Failure to follow this procedure has resulted in the splitting of the diaphragms as the weight of the deck concrete causes the girder ends to rotate, and their restraint to creep and shrinkage effects induces tension in the diaphragms. At least one agency, however, has had success in allowing the placement of diaphragms early, provided that the girders do not have both ends restrained prior to deck concrete placement.

The detailing of the superstructure at the integral abutment is such that girder rotation will theoretically induce moments in the abutment piles. While these moments may be considered in the design of the piles in special situations, they are usually ignored in the design of the superstructure. A typical precast, prestressed concrete superstructure will be significantly stiffer than the abutment piles and will experience negligible moments.

Under-reinforcing positive moment regions in the girders at the piers should be avoided because of crack potential at the diaphragm/girder interface. Hairline cracks, which have been observed in some instances, are found to be harmless. Also, termination of positive moment reinforcement inside the girder should be evaluated carefully to avoid any cracking in the girder. The Canadian Code requires the mild steel reinforcement be developed beyond the strand transfer length. As an alternative, research presented in NCHRP Report 519, demonstrates that development of a sufficient number of prestressing strands projected into the cast-in-place diaphragms provides adequate development lengths into the cast-in-place diaphragms can be found in "Pullout Capacity of Non-Prestressed Bent Strands for Prestressed Concrete Girders", Noppakunwijai, et. al. (2002) published in the July-August 2002 PCI Journal.

INTEGRAL BRIDGES**13.3.2 Continuity at Piers/13.3.4 Approach Slabs**

Prior to specifying the sequence of construction, the designer should evaluate the behavior of the girder-diaphragm system under the combined effects of slab dead load, creep due to prestressing, and differential shrinkage between the deck slab and girder.

13.3.3 Movements and Restraint Forces

Precast, prestressed superstructures have an important advantage over both steel and cast-in-place concrete superstructures for integral bridges. The advantage is that precast, prestressed superstructures experience considerably less thermal movement than steel superstructures, and less long-term movements than cast-in-place concrete superstructures.

Concrete superstructures are less sensitive to temperature changes due to the lag between the air temperature and the interior temperature of a concrete member with its relatively large mass. This phenomenon is reflected in AASHTO specifications, which provides lower design temperature variations for concrete superstructures than for steel. In a moderate climate, a concrete superstructure will expand and contract a total of approximately 0.5 in. per 100 ft of bridge length with seasonal temperature variation. However, a steel superstructure will typically expand and contract approximately 1.0 in. per 100 ft of length.

Thermal movements of a cast-in-place concrete superstructure are similar to those of a precast, prestressed concrete superstructure. However, creep and shrinkage movements are considerably greater for cast-in-place than for precast superstructures. This is because the manufacturing process for precast members is such that much of the long term shrinkage will have occurred prior to erection and establishment of continuity in the superstructure. Moreover, the amount of creep that will occur over time decreases with increasing age of concrete at time of erection. For these reasons, shrinkage and creep movements of precast, prestressed concrete superstructures are frequently ignored for structures of moderate length. However for longer spans the differential shrinkage between the cast-in-place slab and the precast girder in addition to creep and thermal effects should be considered.

Even though thermal movements in precast, prestressed members are minimal, restraint forces in the superstructure will be present. Flexible integral abutments and semi-rigid or flexible piers are used to minimize the restraint forces in integral bridges.

Various reports have shown that piers and abutments do, in fact, restrain thermal movements and induce tensile (or compressive) forces in the superstructure. This is evidenced by discrepancies between predicted thermal movements and those that are actually measured. With properly proportioned piers and abutments, however, these restraint forces are routinely and safely ignored in the design of the superstructure.

In addition, it can be shown that the resultant of the passive soil pressure behind the backwall will generally be eccentric with respect to the superstructure. The magnitude of the stresses produced by this eccentric axial force in the superstructure, however, is negligible and is typically ignored.

13.3.4 Approach Slabs

Although usually not considered as part of the superstructure, approach slabs have been found to be one of the most critical components of an integral bridge. The approach slabs serve two primary purposes:

1. Approach slabs reduce the compaction of the backfill material behind the backwall due to traffic. Control of excessive passive soil resistance to thermal expansion is also achieved.
2. The thermal movements of the system are transferred from the end of the bridge to the point where the approach slab joins the roadway pavement. A flexible pavement joint is provided at this point. Details of the flexible pavement joint vary from agency to agency. In addition, some agencies use plastic sheets or expanded polystyrene boards below the approach slab to provide a positive separation from the subgrade to enhance movement.

An important lesson learned is that the approach slab must be tied to the abutment backwall with mild steel reinforcing. Failure to provide this reinforcing in some early integral bridges resulted in a gradually increasing opening of the joint between the backwall and approach slab. The cause of this problem is the inability of the approach slab to move with the abutment on the contraction portion of the thermal cycle. Accumulation of debris in the joint leads to a successively wider opening of the joint with each expansion portion of the cycle. Many bridge engineers prefer to have hinge style reinforcing bar details across this joint instead of straight horizontal bars in order to accommodate rotation of the abutment or the approach slab.

INTEGRAL BRIDGES

13.3.4 Approach Slabs/13.4.1 Abutment Configurations

Approach slabs are generally about 20-25 ft long and are standardized in most states. The flexible pavement joint should match that of the particular joint material used to accommodate the movement rating desired. Theoretically, the reinforcement needed for connection to the abutment should exceed the weight of the slab multiplied by the coefficient of friction between poured concrete and sub-base material used. No. 6 bars at 12 in. centers have reportedly worked well in some states.

Another method, which has been used in Ontario, is to design the approach slab bottom reinforcement based on a span equal to 50% of the slab length, usually 20-30 ft. Assuming that the approach slab is dragged on the approach fill, the reinforcement to tie the slab to the abutment backwall is nominal. The width of the joint at the free end of the approach slab should be kept small. A 3/4 in. wide sealed saw cut in the pavement at the end of the approach slab has reportedly worked well for bridge lengths up to 300 ft.

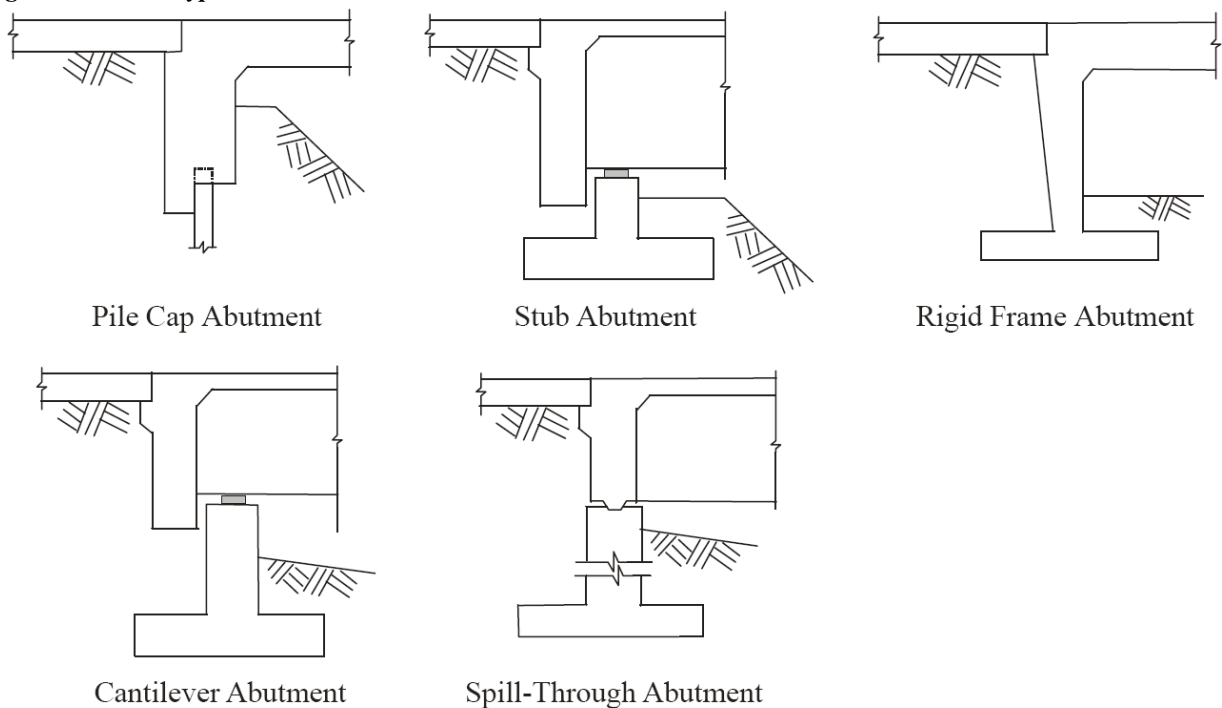
13.4 ABUTMENT DESIGN

13.4.1 Abutment Configurations

The beginning or ending substructure element of a bridge is commonly referred to as an abutment or end bent. There are numerous variations that are used in further describing these units, such as bench-type, spill-through, stub, deep, semideep, etc. **Figure 13.4.1-1** shows different types of integral abutments. For consistency within this report, these units will be collectively referred to as abutments, with only minimal added description of their variation in type.

Figure 13.4.1-2 shows a typical integral abutment. Normally H-piles with bending about their weak axis are used. However piles with bending about their strong axis have also been used. Precast, prestressed concrete piles with their tops encased in a compressible material (Kamal 1996) and steel pipe piles have also been used.

*Figure 13.4.1-1
Integral Abutment Types*

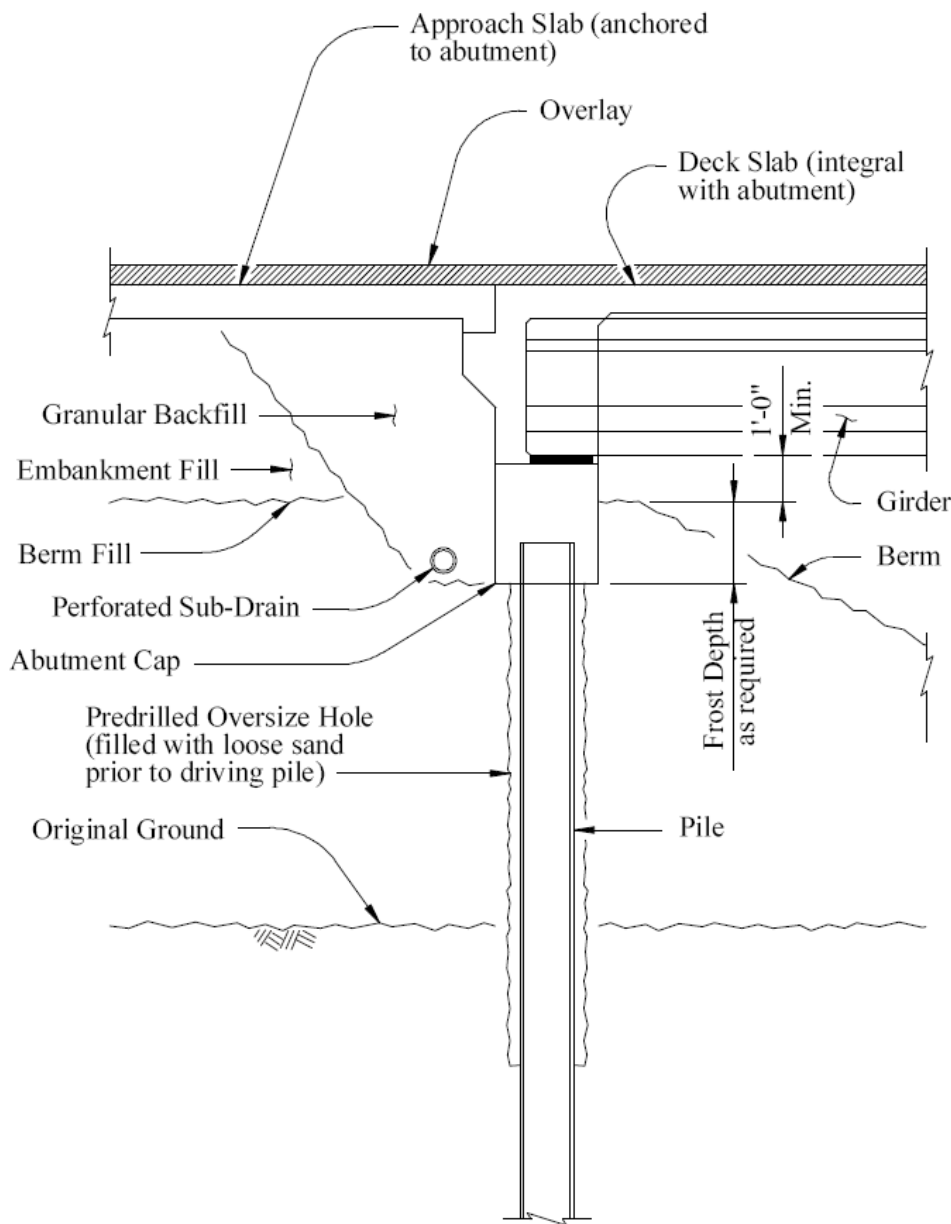


In integral bridges, the ends of the girders are fixed to the abutments. Expansion joints are thus eliminated at these supports. With the expansion joints eliminated, forces are induced in the substructure due to resistance to thermal movement and to creep and shrinkage. These have to be considered in the design of integral abutments.

INTEGRAL BRIDGES

13.4.1 Abutment Configurations/13.4.2 Accommodating Superstructure Movement at Abutments

Figure 13.4.1-2
Typical Integral Abutment



13.4.2 Accommodating Superstructure Movement at Abutments

Generally, integral abutments are supported by a single row of piles. The integral abutment bridge concept is based on the theory that due to the flexibility of these piles, thermal stresses are transferred to the substructure by way of a rigid connection. The concrete abutment contains sufficient bulk to be considered a rigid mass. The moment connection between the girder ends and the abutment transfers temperature variation and live load displacements to the abutment piling.

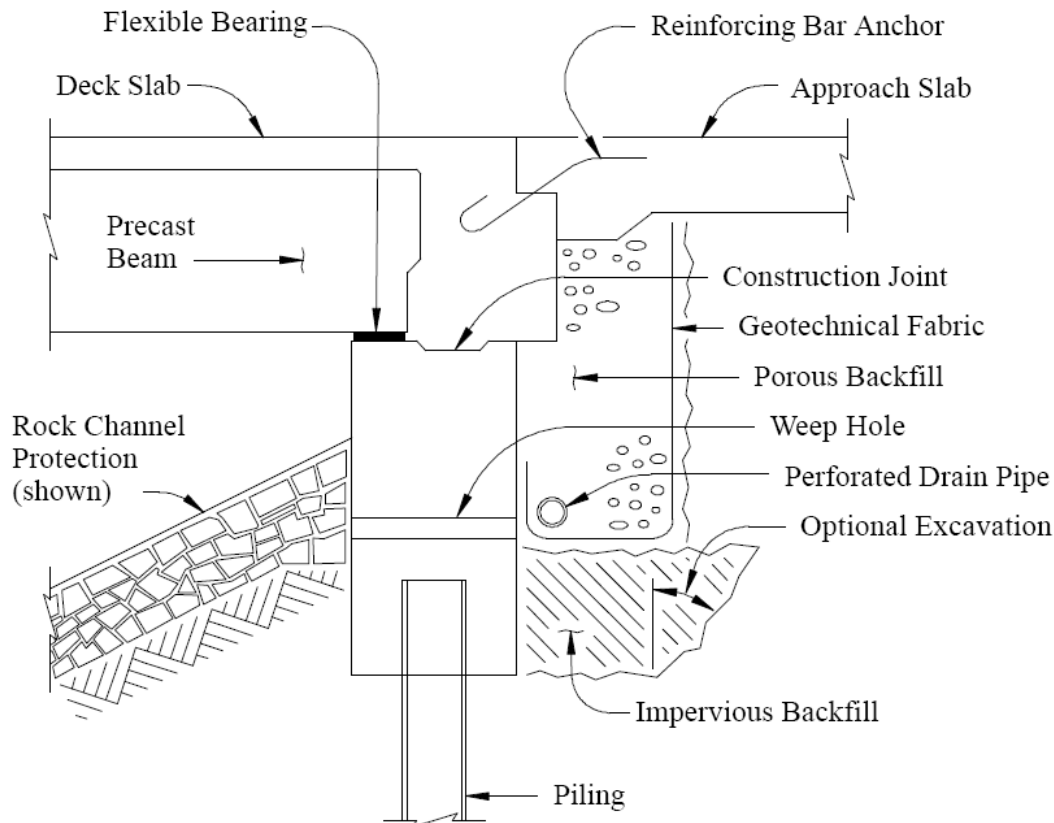
Semi-rigid, or semi-integral abutments may also be used to eliminate expansion joints at these points of support. In the semi-integral concept, the transfer of rotational displacement to the piles is minimized. Rotation is generally accomplished by using a flexible bearing surface at a selected horizontal interface in the abutment backwall. Allowing rotation at the pile top generally reduces pile loads. **Figure 13.4.2-1** shows a typical semi-integral abutment.

INTEGRAL BRIDGES

13.4.2 Accommodating Superstructure Movement at Abutments

To support the integral or semi-integral abutment with its single row of piles, the piles are driven vertically and none are battered longitudinal to the bridge. This arrangement of piles permits the abutment to move in a longitudinal direction under temperature, creep, and shrinkage effects. Steel H piles, steel pipes filled with concrete, precast concrete round, square and octagonal, and mandrel piles have been used.

Figure 13.4.2-1
Typical Semi-Integral Abutment



NOTE: Construction Joint can either be keyed as shown or can be a roughened surface.

Some designers are concerned about pile length when standard precast piles are used. Their concern is that the higher stiffness of a concrete pile will tend to resist thermal movement of the abutment and cause excessive shear stresses in the top of the pile just below the abutment. Conversely, when the piles are long (about 40 ft or longer for a 14 in. square concrete pile) there is sufficient flexibility in the pile to allow movement and to avoid high shear. However, the type of soil surrounding the pile also substantially affects the ability of the top of the pile to move laterally for both steel piles and concrete piles. To improve flexibility, piles are often driven through pre-bored holes. The annular space is filled with granular material after installation of the piles.

Research has demonstrated that rotation and translation fixity of the embedded portion of the pile into the abutment create significant relief of the stresses at the top of the pile. Such relief can be achieved by enclosing a portion of the pile embedment at the top in expanded polystyrene (EPS) board or a similar compressible material.

Opinions differ on the proper orientation for steel H piles in an integral abutment. Some designers prefer to align the strong axis of the pile parallel to the abutment wall. Others prefer to place the piles with the weak axis aligned parallel to the longitudinal dimension of the abutment wall (parallel to the centerline of roadway for a 0 deg skew). Overall, the consensus seems to be toward designs to permit weak axis bending. The amount of movement will be approximately the same for either orientation; however, strong axis bending will create more resisting force than weak axis bending. Due to a greater moment of inertia, stresses in an H-pile oriented for strong axis

INTEGRAL BRIDGES

13.4.2 Accommodating Superstructure Movement at Abutments/13.4.3 Passive Pressure Reduction

bending will be less than for weak axis bending. Stresses due to the $P-\Delta$ effect are inversely proportional to moment of inertia (I), and will therefore be larger for bending about the weak axis.

If precast, prestressed concrete piles are used, the stresses along either of the major axes will be the same. Recent studies by Construction Technology Laboratories have shown that steel pipe piles have performed equal to or better than other types of piling.

13.4.3 Passive Pressure Reduction

Various means of reducing the resistance of integral abutments to passive pressures that are caused by thermal movement have also been successfully put into practice. Generally, these methods consist of placing granular, non-compacted materials as backfill at the abutments, as shown in **Figure 13.4.3-1**. When this is done, it is also necessary to provide an approach slab supported at one end on the abutment bridge seat to prevent future compaction of voids in the granular materials. Both **Figures 13.4.3-1** and **13.4.3-2** show typical details of the approach slab at the transition with the roadway slab.

Figure 13.4.3-1
Typical Approach Slab

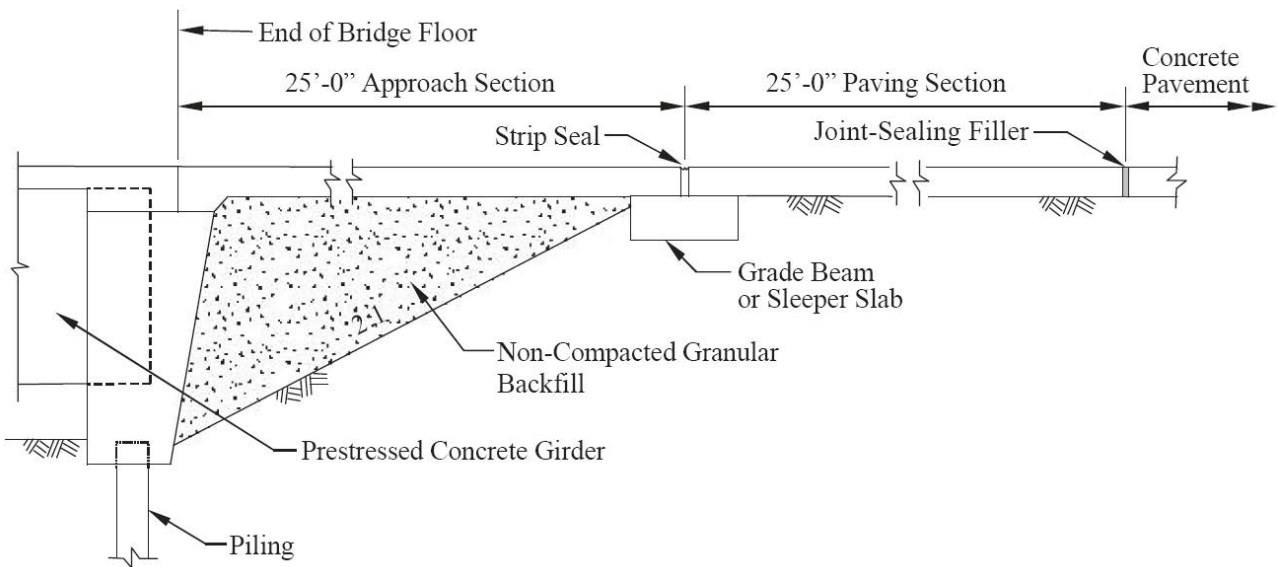
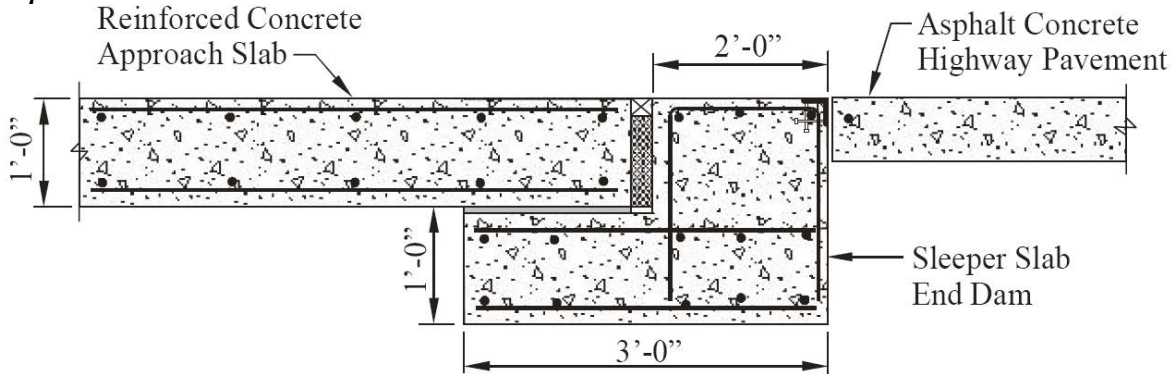


Figure 13.4.3-2
Sleeper Slab Detail



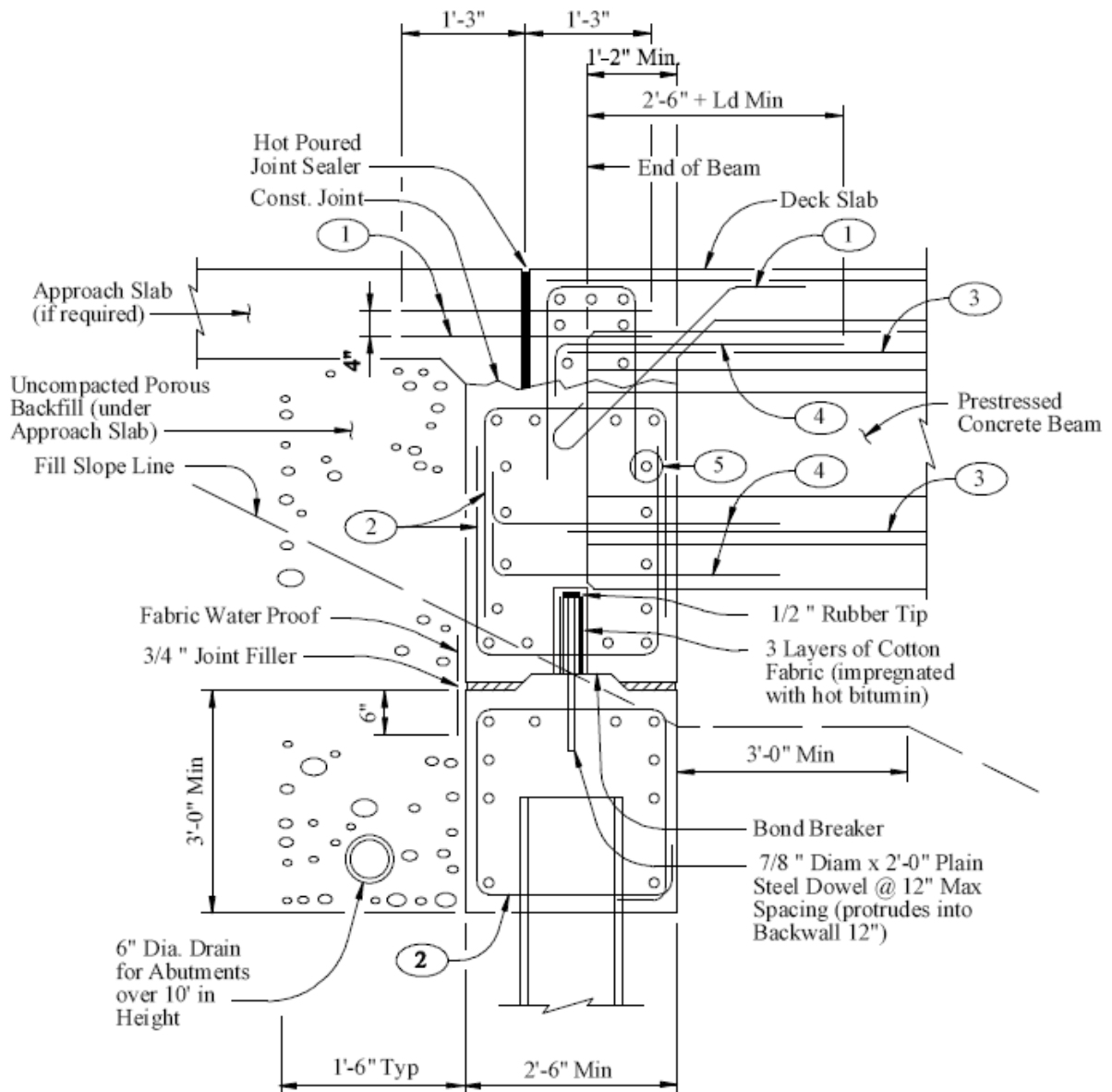
INTEGRAL BRIDGES

13.4.3 Passive Pressure Reduction/13.4.4 Details at Abutment

13.4.4 Details at Abutments

The Virginia Department of Transportation reports well over ten years of satisfactory performance of integral bridges. They have developed a guide for use in the design of integral bridges with particular emphasis on the design and details for the abutments and approach slabs. Some of this information is depicted in **Figures 13.4.4-1 to 13.4.4-1**.

*Figure 13.4.4-1
Integral Bridge Abutment Detail 1*

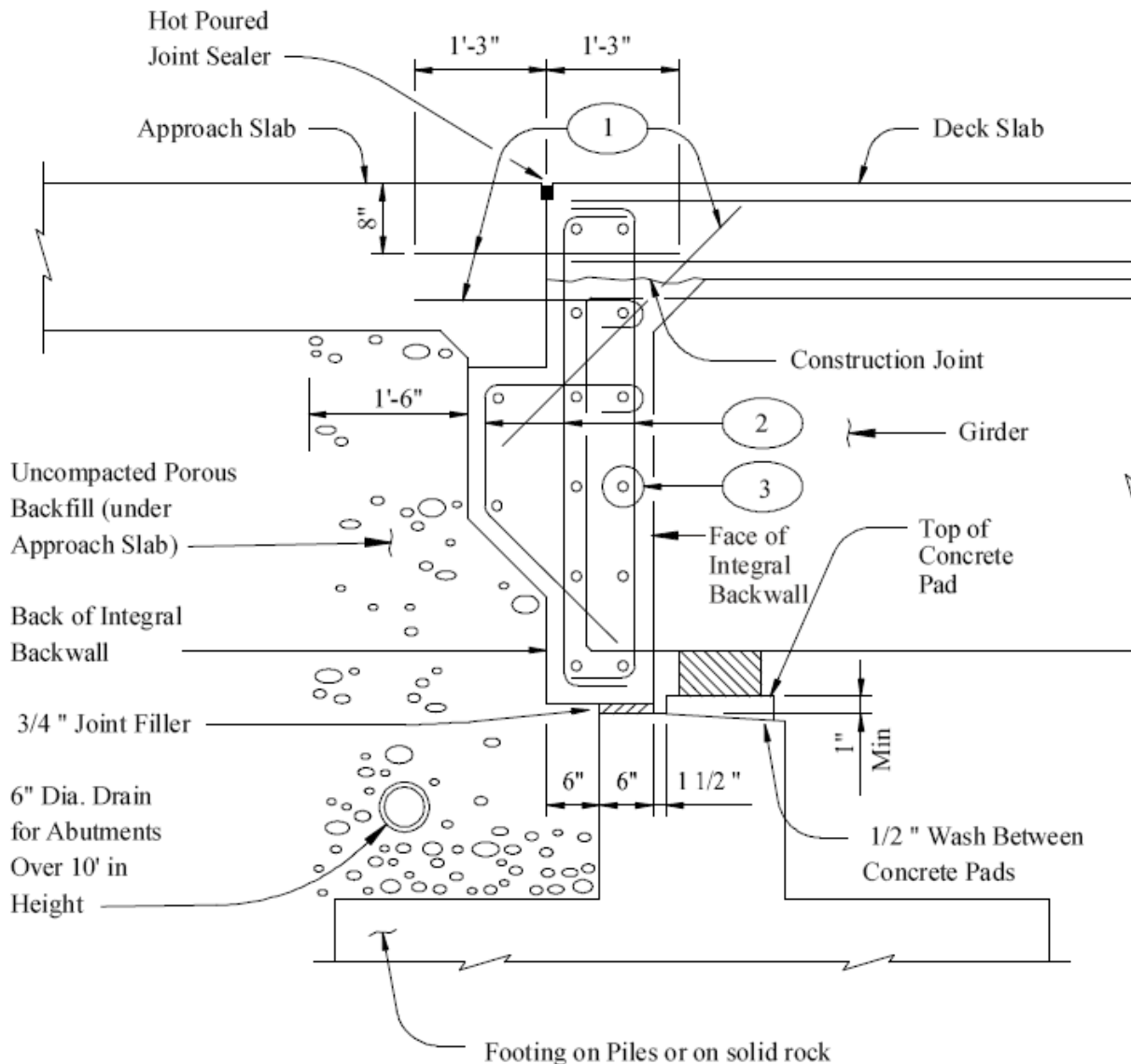


NOTES:

1. Integral backwall concrete to be placed and cured prior to placement of deck concrete. Beams/girders shall be held in place and rest on temporary supports (acceptable to the engineer) until backwall concrete gains a minimum strength of 3000 psi.
2. Backfill, behind both bridge abutments, shall be placed simultaneously.

- | | |
|--|---|
| <ul style="list-style-type: none"> ① #5 @ 12" Max ② #4 @ 12" Max ③ 2 ~ #5 | <ul style="list-style-type: none"> ④ 2 ~ #6 Min at each location - shall protrude beyond beam and into abutment by <i>Ld</i> ⑤ #6 Typ - through holes in beam web as needed |
|--|---|

Figure 13.4.4-2
Integral Bridge Abutment
Detail 2



NOTES:

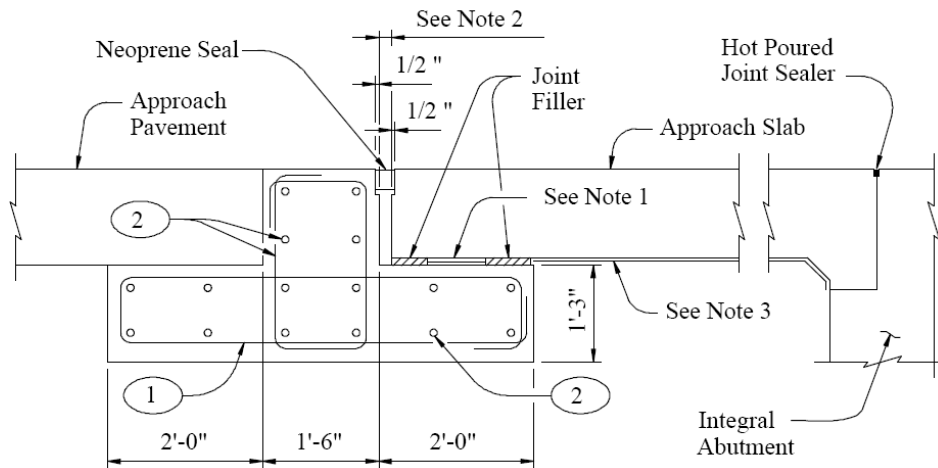
1. Integral backwall concrete to be placed and cured prior to placement of deck concrete.
2. Backfill, behind backwalls of both bridge abutments, to be placed simultaneously when needed.

- (1) #5 @ 12" Max
- (2) #4 @ 12" Max
- (3) #6 Typ - through holes in Beam web as needed

INTEGRAL BRIDGES

13.4.4 Details at Abutment/13.4.5.1 Problems

Figure 13.4.4-3
Integral Bridge Abutment Detail 3

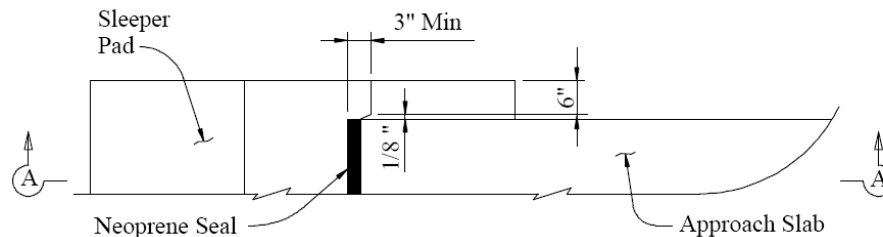


SECTION A-A THRU SLEEPER PAD

NOTES:

1. 2 ~ 1/8 " Preformed bedding material pads full length of bridge seat. Between the pads, use either a powdered graphite lubricant or Molykote 321 by Dow-Corning or Mantek Dri-guard.
2. Minimum at 60°F = 1/2 total thermal movement due to expansion and contraction plus 1/4 "
3. 10 mil plastic moisture barrier

- | | |
|---|--------------|
| 1 | #5 @ 12" Max |
| 2 | #4 @ 12" Max |



PARTIAL PLAN OF SLEEPER PAD

13.4.5 Problems and Solutions

During preparation of their design policies, the Pennsylvania Department of Transportation conducted a study of problems encountered by various state highway agencies using integral abutments. Some of the problems they reported with their corresponding solutions are as follows:

13.4.5.1 Problems

- Backfill settling into the void between the abutment and fill when the bridge superstructure contracts.
- Settling of roadway fill under the approach slabs due to traffic compaction.
- Undermining of the abutments due to drainage at the bridge ends.
- Movement at the abutment caused by shortening of prestressed concrete superstructures due to creep and shrinkage.
- Cracking of wing walls due to rotation and contraction of the super structure.
- Development of a bump in the asphalt pavement at abutments due to movement of the bridge.
- Cracking observed in abutment stem due to rotational forces in skewed integral bridges.
- Wrong size joints.

INTEGRAL BRIDGES**13.4.5.1 Problems/13.5.1 Introduction**

- Opening of the joints between the bridge and the approach pavement over several years of cycling through the extremes of summer and winter temperatures.
- Continuous maintenance of the approach embankments due to settlement at the paving notch and along the wing walls.
- Damage to the approach embankment and pavement by water intrusion between the abutment and approach roadway.

13.4.5.2 Solutions

Many of the states that are currently building integral abutment bridges have found solutions to the above noted problems. For example:

- Provisions for a reinforced concrete approach slab tied to the abutment stem and bridge deck solved many of these problems. With a properly-sized roadway expansion joint placed over a sleeper slab or grade beam located 20 to 50 ft away from the end of the bridge deck, the settlement due to traffic compaction and backfill settling into the void when the bridge contracts can be avoided.
- Adverse effects from longitudinal shortening due to creep in prestressed concrete bridge superstructures have been solved in some states by pouring the wing walls after a specified period of time has passed, allowing most of the creep to have already occurred. Also, pre-drilling oversize holes for the top 8 to 20 ft of piles and filling the holes with a loose granular material is another effective method for eliminating the same problem. From Canada, it has been reported that expanded polystyrene pellets have also been used successfully to fill pre-drilled holes.
- Undermining and other erosion problems have been eliminated through the use of granular backfill to allow free drainage. Providing granular backfill, along with a proper drainage system, also eliminates hydrostatic pressure buildup behind the abutment.
- Abutment cracking due to rotation and contraction has been reduced or eliminated by limiting the skew and orienting the piles for weak-axis bending and by using pre-drilled oversized holes to reduce stresses, or both. Various depths of the pre-drilled oversize hole are required by the states using them with integral abutment bridges. Iowa, for example, requires a minimum depth of 8 ft for integral abutment bridges longer than 130 ft. Other states require depths of up to 20 ft or more.
- Pre-drilled oversize holes create a hinge effect in the substructure, which increases the flexibility of the piles and the abutment wall. These pre-drilled oversize holes also aid in minimizing pile down-drag forces when used in compressible soils.
- At least two states have used a corrugated metal pressure-relief system behind the backwall to reduce passive earth pressures on the abutment and to help reduce the formation of void spaces caused by contraction of the superstructure.
- One state has used expanded polystyrene board behind the abutment backwall.

An item needing further study and evaluation is the interface between the slope protection and the abutment stem. Because of the flexibility of the abutment, gaps have formed at this interface in some of the bridges. Until this condition can be permanently prevented, periodic inspection and corrective measures should be considered.

13.5 PIER DESIGN**13.5.1 Introduction**

Piers for integral bridges have similar design requirements and share common design procedures with those of piers of more traditional bridge types. The primary distinguishing features of the piers of an integral bridge involve accommodation of potentially large superstructure movements and the sharing of transverse (perpendicular to the longitudinal centerline of the bridge) and longitudinal (parallel to the centerline of the bridge) forces among substructure units.

INTEGRAL BRIDGES**13.5.2. Accommodating Superstructure Movements at Pier/13.5.2.1 Flexible Bents****13.5.2 Accommodating Superstructure Movements at Piers**

Like integral abutments, the piers of an integral bridge must be designed to accommodate the superstructure movements. Thermal movements are usually the major concern, although superstructure movements due to concrete creep and shrinkage will also be present to some degree. Creep and shrinkage movements of precast, prestressed girders are frequently ignored; however for longer integral bridges, these effects must also be considered in the design of the piers.

It is normally assumed that any reduction of free superstructure movements due to pier stiffness are negligible. Although reductions on the order of 17 percent of calculated thermal movements have been attributed to substructure restraint, (University of Tennessee 1982), most pier designs do not take advantage of any reduction.

To successfully design the piers to accommodate potentially large superstructure movements, the designer has several options:

1. Flexible bents - rigidly connected to the superstructure;
2. Isolated rigid piers - connected to the superstructure by means of flexible bearings;
3. Semi-rigid piers - connected to the superstructure with dowels and neoprene bearing pads; or
4. Hinged-base piers - connected to the superstructure with dowels and neoprene bearing pads.

13.5.2.1 Flexible Bents

A single row of piles, with a concrete cap that may be rigidly attached to the superstructure, provides a typical example of a flexible bent (**Figure 13.5.2-1**). This type of bent is assumed to provide vertical support only. The small moments induced in the piles due to superstructure rotation or translation are usually ignored (Burke 1991 and Burke 1993).

A bridge constructed with flexible bents relies entirely on the integral abutments for stability in the bridge's longitudinal direction and for resisting longitudinal forces. Passive pressures behind the backwalls, friction, and passive pressures on abutment piles are mobilized to resist transverse and longitudinal forces.

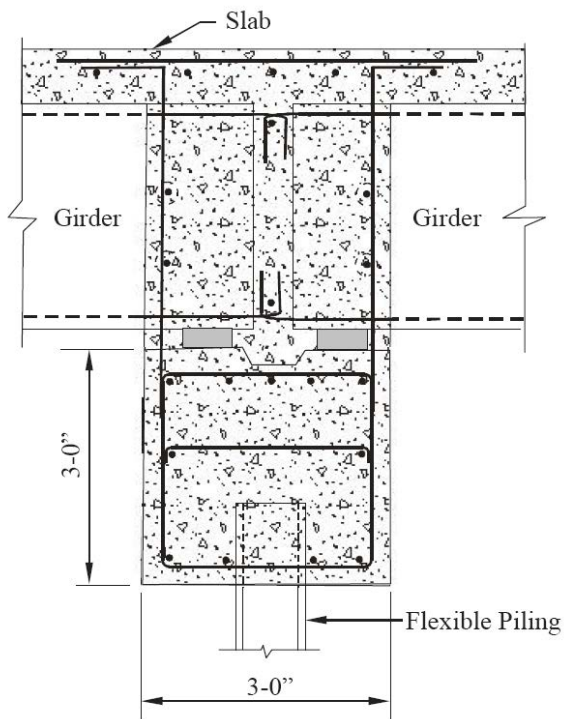
The advantage of this system is that by virtue of the flexibility and ductility of the bents, no special considerations need be made to accommodate the thermal movements associated with long integral bridges. Bents are, therefore, economical and easy to construct. A very simple system results.

Two potential disadvantages are introduced with this type of bent. First, the possible need for temporary bracing to provide stability during construction must be considered. Second, a reasonable amount of backfill compaction is required to mobilize passive pressure due to modest displacement of the backwall.

INTEGRAL BRIDGES

13.5.2.1 Flexible Bents/13.5.2.2 Isolated Rigid Piers

Figure 13.5.2-1
Typical Flexible Bent



13.5.2.2 Isolated Rigid Piers

Rigid piers are defined as piers whose base is considered fixed against rotation and translation, either by large footings bearing on soil or rock, or by pile groups designed to resist moment. The connection to the superstructure is usually detailed in a way that allows free longitudinal movement of the superstructure, but restrains transverse movements. This type of detailing permits the superstructure to undergo thermal movements freely, yet allows the pier to participate in carrying transverse forces.

In modern precast concrete bridges with this type of pier, the superstructure is supported on relatively tall laminated neoprene bearing pads. A shear block, isolated from the pier diaphragm with a compressible material such as cork, is cast on the top of the pier cap to guide the movement longitudinally, while restraining transverse movements (**Figure 13.5.2.2-1**).

If the designer does not wish to rely solely on the integral abutments to provide resistance to transverse and/or longitudinal forces, one or more rigid piers near the center of the structure may be provided to restrain transverse and/or longitudinal movements and thus reduce the amount of thermal movement at the abutments.

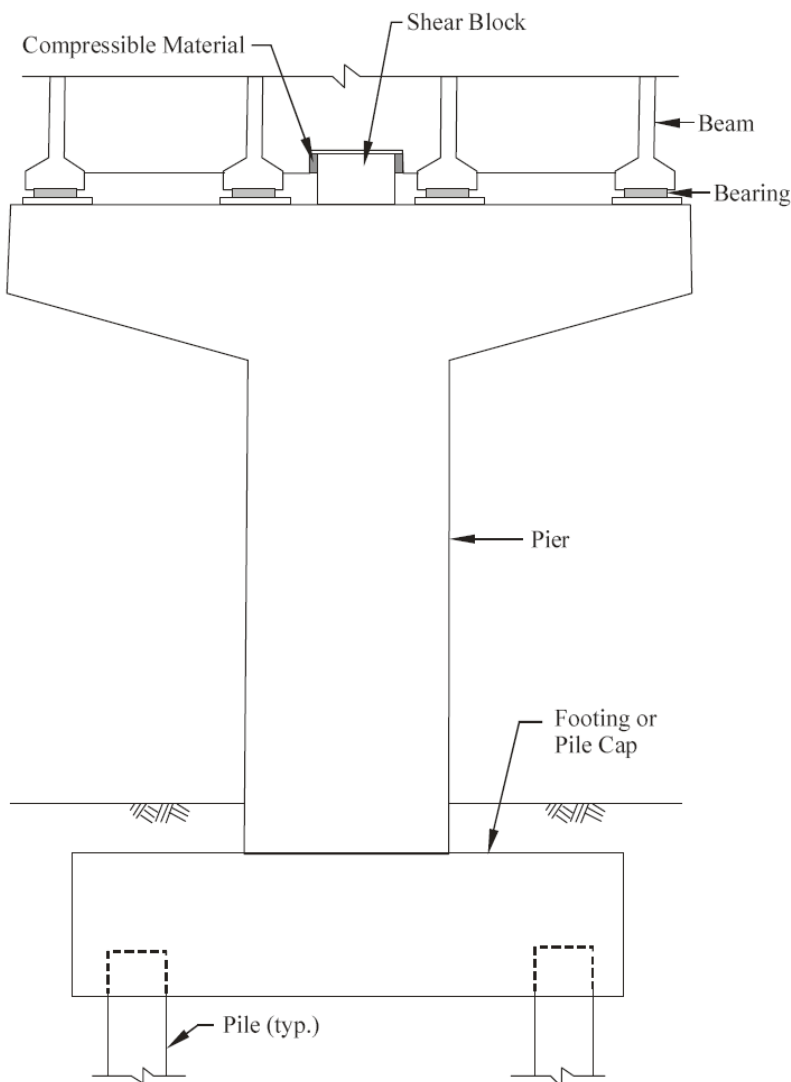
This approach represents the traditional solution taken with steel girder bridges at so-called expansion piers. It offers the advantage of eliminating the stresses associated with superstructure thermal movements. It also provides piers that require no temporary shoring for stability during construction.

The primary disadvantage of this system lies in the additional expense associated with the taller bearing pads and the detailing associated with the shear key. In addition, because the pier and the superstructure are isolated longitudinally, the designer must ensure that the bearing seats are wide enough to accommodate seismic movements.

INTEGRAL BRIDGES

13.5.2.2 Isolated Rigid Piers/13.5.2.3 Semi-Rigid Piers

Figure 13.5.2.2-1
Typical Isolated Rigid Pier



13.5.2.3 Semi-Rigid Piers

Semi-rigid piers are the preferred type of pier among many agencies and designers of integral bridges. These piers are similar to rigid piers, described above, with bases considered fixed by either large spread footings or pile groups. However, the connection of the piers to the superstructure differs significantly.

A typical semi-rigid pier superstructure connection is shown in **Figure 13.5.2.3-1**. Here, the precast girders bear on elastomeric pads, 0.5 to 1.5 in. thick. A diaphragm is placed between the ends of the girders, and dowels, perhaps combined with a shear key between girders, connect the diaphragm to the pier cap. Compressible materials are frequently introduced along the edges of the diaphragm and, along with the elastomeric bearing pads, allow the girders to rotate freely under live load.

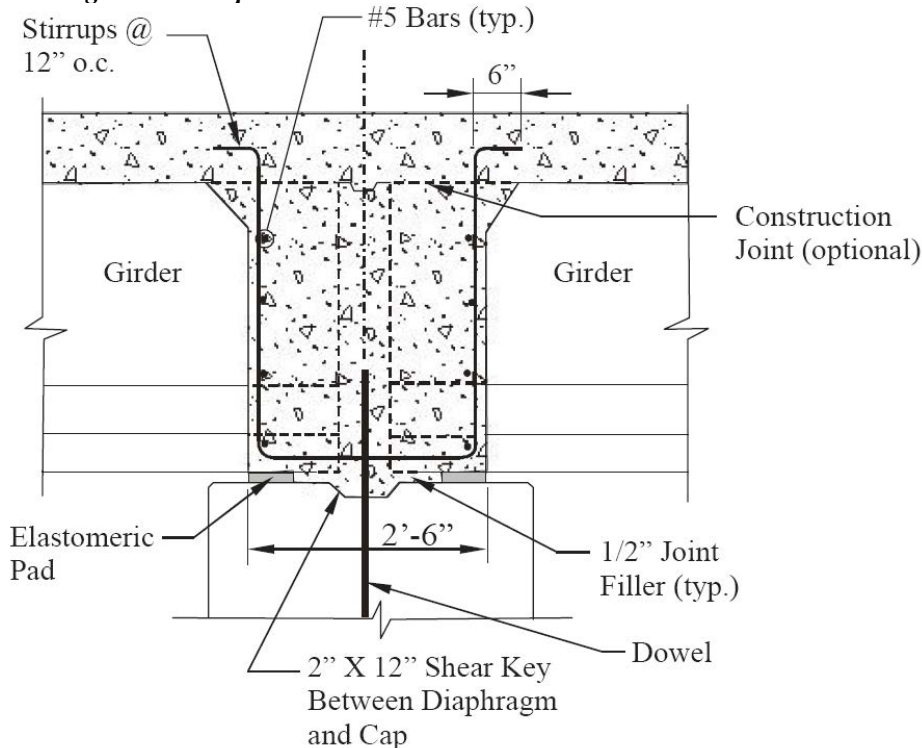
The dowels force the pier to move with the superstructure as it undergoes thermal expansion and contraction, and, to a lesser extent, creep and shrinkage. Accommodation of these movements requires careful analysis during the design of the piers. Normally, the stiffness of the piers is reduced due to cracking and creep of the pier concrete, which should be factored into the analysis.

INTEGRAL BRIDGES

13.5.2.3 Semi-Rigid Piers/13.5.2.4 Hinged-Based Piers

The advantages of this type of simplified pier detailing are: thin elastomeric pads are relatively inexpensive, temporary shoring is not required during construction, all piers participate in resisting seismic forces, and the girders are positively attached to the piers. In addition, with multiple piers active in resisting longitudinal and transverse forces, the designer need not rely solely on passive soil pressures at the integral abutments to resist lateral forces.

Figure 13.5.2.3-1
Semi-Rigid Pier to Superstructure Connection



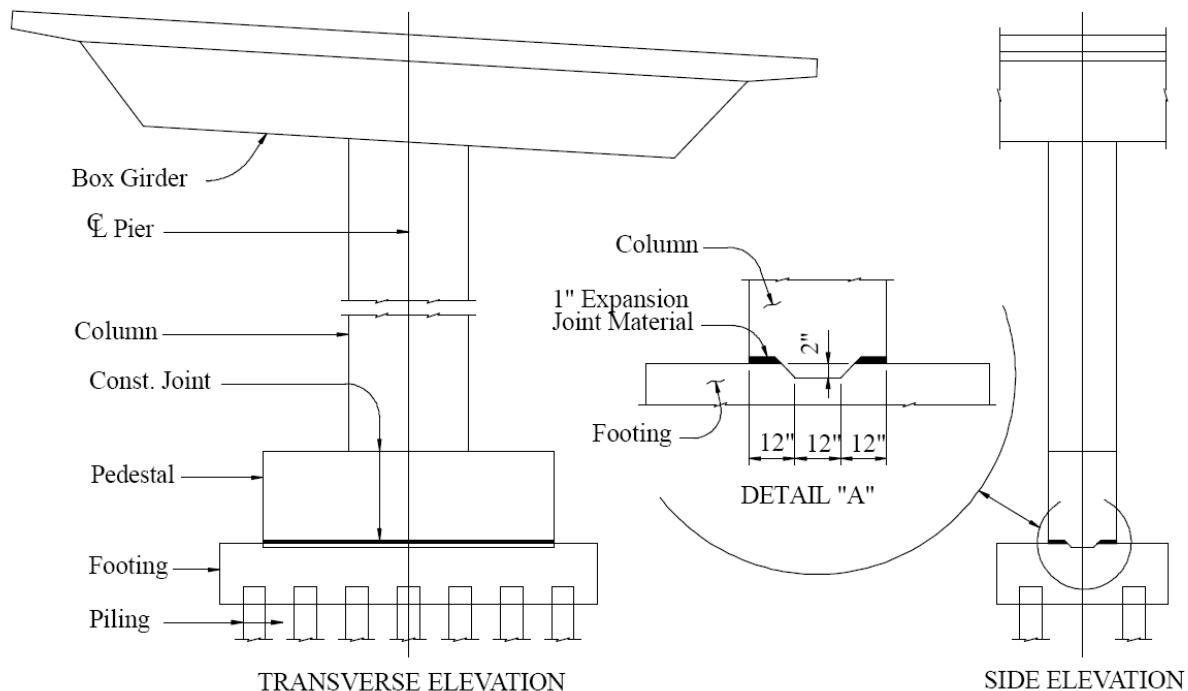
The main disadvantage of semi-rigid piers is that they are slightly more complicated than other types because careful assessment of foundation conditions, pier stiffness, and estimated movements are required. Indeed, in some situations, semi-rigid piers are inappropriate. For example, short piers bearing on solid rock may not have adequate flexibility to accommodate large movements without distress to the piers.

13.5.2.4 Hinged-Base Piers

The Tennessee Department of Transportation has utilized a hinged-base pier similar to the one shown in **Figure 13.5.2.4-1**. This type of detail may be used to avoid the need for an expansion pier in a situation where semi-rigid piers have inadequate flexibility. Temporary construction shoring is required, and additional detailing requirements at the top of the footing may increase cost. However, the designer should keep this alternative in mind for use under special circumstances where the other pier types are not feasible. (Wasserman 1987)

INTEGRAL BRIDGES**13.5.2.4 Hinged-Based Piers/13.5.3.1 Longitudinal and Transverse Load Distribution**

Figure 13.5.2.4-1
Typical Hinged-Base Pier



13.5.3 Analysis and Design of Semi-Rigid Piers

Piers supporting long, multiple-span integral superstructures frequently require specialized analytical models to predict transverse load distributions, forces induced as a result of superstructure movements, pier stiffness, and slenderness effects. Although traditional bridges require similar analytical models, the relatively large substructure movements associated with integral bridges place special emphasis on the topics covered below. Whereas this discussion is based on the semi-rigid pier type, it is generally applicable to other types of piers with minor modifications.

13.5.3.1 Longitudinal and Transverse Load Distribution

As part of the overall structural system, semi-rigid piers will typically be required to carry a portion of the externally applied longitudinal and transverse loads on the bridge. In addition, thermal movements of the superstructure will induce forces as the piers attempt to restrain those movements.

In order to distribute external loads to the substructure units, one of two possible assumptions is commonly made:

1. **Flexible Superstructure / Rigid Substructure:** A carryover from the traditional simple span, jointed bridge deck, this method assigns a "tributary length" of superstructure to each substructure unit. This tributary length is usually based on a simple span assumption between supports. This method satisfies equilibrium, but is usually inconsistent with geometric compatibility of displacements;
2. **Rigid Superstructure / Flexible Substructure:** This method, preferred for integral bridges, distributes loads to the substructure elements in relation to their stiffness and satisfies geometric compatibility of displacements. This analysis becomes a three-dimensional frame problem when skewed supports are present.

The first method offers simplicity and is straightforward. Results may be somewhat unreliable, however, in situations where substructure stiffness and span lengths vary significantly.

The second method, although requiring additional effort on the part of the designer, is preferred for integral bridges that utilize semi-rigid piers.

INTEGRAL BRIDGES**13.5.3.1 Longitudinal and Transverse Load Distribution/13.5.3.3 Estimation of Pier Stiffness Parameters**

Both methods require that the designer exercise judgment regarding the extent to which integral abutments will participate in carrying longitudinal and transverse loads. Reasonable assumptions regarding abutment stiffness can be made using documented methods. (Reese 1989) Current practice varies from assuming that all forces are carried by the abutments (Burke 1993), to a conservative assumption that no forces are resisted by the abutments. (Penn DOT Q&A) Using very low or zero stiffness to model the abutments results in a conservative pier design.

13.5.3.2 Equivalent Forces Due to Superstructure Movements

As the superstructure expands and contracts with seasonal temperature changes and, to a lesser extent, due to creep and shrinkage, the tops of the piers will be forced to undergo displacements relative to their bases. These displacements will produce curvatures in the pier columns that can be closely estimated based on the magnitude of the movements, the fixity conditions at the top and bottom of the columns, and the height of the columns.

It is significant to mention that if footing rotations and pier cap deformations are ignored, the curvatures are essentially independent of the column stiffness (EI), and depend only on the pier geometry and the magnitude of the displacements.

For a skewed multi-column type pier, displacements and curvatures in the direction transverse to the pier cap and along the pier cap must be considered separately.

Once curvatures are estimated, an effective EI must be chosen in order to compute internal moments and shears. A set of equivalent external forces, in equilibrium with the computed internal moments and shears, can be computed by statics. This set of equivalent forces is used in subsequent analysis to represent the effects of superstructure movements on the piers.

13.5.3.3 Estimation of Pier Stiffness Parameters

To compute the forces induced by superstructure movements and for calculating the distribution of externally applied loads to the substructure units, it is necessary to estimate the effective EI of the piers. Several approaches are common in selecting the effective EI , varying in terms of both complexity and accuracy. At one extreme is the use of the full uncracked, elastic section properties of the gross column section to calculate EI . This approach is simple and well suited for figuring the distribution of external loads to the substructure units. However, this method is overly conservative for calculating forces due to superstructure movement and could result in impractical foundation and column designs.

At the other extreme is the use of a non-linear moment-curvature relationship that accounts for the effects of cracking, non-linear stress-strain curves, time dependent behavior (creep and shrinkage), and axial load. These methods can be complicated and time-consuming and are seldom justified. In critical design situations or in analyzing an existing pier, however, this type of analysis may be required. Computerized methods that are capable of providing an accurate estimation of the restraint forces caused by displacements of the superstructure using nonlinear moment-curvature relationships are available to the designer. Linear approximations to theoretical non-linear moment-curvature relationships (Manzelli 1993) are also available for some standard bridge pier sections, which may represent a compromise between rigorous solutions and simplified methods.

Most commonly, simplified methods are used. These methods calculate an effective EI , reduced from the linear elastic value, to account for concrete cracking and creep. Several factors may reduce the effective EI :

1. Cracking, if present under the load combination considered, will result in a significant reduction in moment of inertia;
2. Relaxation and/or creep of the concrete will occur as a result of the gradually varied curvatures associated with seasonal temperature variations; and
3. Column base rotation will occur to some extent, depending upon foundation conditions. Charts that can be used to estimate the stiffness of a footing bearing on various foundation materials are available. (PCI 1992) Further discussion of foundation stiffness is presented in Section 13.6.

The Tennessee Department of Transportation uses an effective E of 1,000 ksi to account for concrete relaxation/creep and cracking. The effective stiffness is further reduced by an additional 50 percent if footing rotation is expected. (Tennessee DOT 1989)

INTEGRAL BRIDGES**13.5.3.3 Estimation of Pier Stiffness Parameters/13.6.1 Introduction**

The SR 137 bridge over the Holston River in Tennessee demonstrates how effective EI values can accurately predict the equivalent forces due to superstructure movement. (University of Tennessee 1982) This bridge is 2,700 ft long and consists of 29 spans of precast, prestressed concrete box girders with a cast-in-place concrete deck. Each semi-rigid pier is connected to the superstructure with dowels.

During construction, strain gauges were placed at various points in the structure, including selected reinforcing bars at the base of the first pier. At this location, approximately 1,250 ft of superstructure would be expected to contribute to the movement at the top of the pier.

Under a 40 °F temperature rise, curvature at the base of the pier was calculated based on measured bar strains. This curvature was found to be consistent with a cracked section and a corresponding steel stress of approximately 18 ksi. Assuming a linear variation of the computed curvature, a prediction of the displacement at the top of the pier was made.

The prediction based on computed curvature agreed exactly with the measured movement at that point. Although cracking was reportedly observed in the pier, no distress was noted. The use of elastic uncracked properties would have significantly overestimated the forces for this bridge. This example also demonstrates that cracking of the piers, as a means of relief of restraint forces, can be tolerated in a long bridge.

13.5.3.4 Load Combinations

Similar to the design of a traditional pier, piers of integral bridges are designed for the load combinations specified in the relevant design code. Often, load combinations involving temperature, creep, and shrinkage control the design of integral bridges as opposed to combinations containing external loads only. Under the AASHTO Standard Specifications, load Groups IV and VI will frequently control the design of a pier. The pier must be capable of undergoing the imposed superstructure movements while simultaneously resisting external forces.

13.5.3.5 Slenderness Effects

The piers supporting an integral bridge are commonly designed as individual elements using the moment magnification factor method specified in the ACI and AASHTO codes. However, some designers advocate using effective length factors of less than one for the columns in an integral bridge, thus resisting side sway both longitudinally and transversely by the integral abutments (Burke 1991). Under this condition, slenderness effects and moment magnification would be significantly reduced.

If it is conservatively assumed that longitudinal sidesway of piers is not resisted by abutments, advantage can still be taken of the fact that all the semi-rigid piers in the bridge must fail before a sidesway instability is reached. Reducing the effective length factor, resulting in an increased P_c , is often justified, thereby reducing moment magnification factors. If the controlling load group includes externally applied loads plus rib shortening (R), shrinkage (S) and temperature (T), the designer should be aware that the effects of $R+S+T$ will reduce the effect of the external loads in approximately 50 percent of the semi-rigid piers supporting an integral bridge. These mostly unloaded piers provide a stabilizing effect, reducing the moment magnification on the loaded piers due to sidesway. While these effects are seldom considered directly in design, they should assist the designer in avoiding excessively conservative pier designs.

13.6 ANALYSIS CONSIDERATIONS**13.6.1 Introduction**

For typical integral bridges, a two-dimensional structural analysis is usually sufficient for the determination of vertical, longitudinal and time-dependent loading effects. However, more complex structures, such as those with large skews or horizontal curvature may require a three-dimensional finite element analysis. The complexity of the model and degree of analysis that is utilized should reflect site specific conditions and the desired results.

Most significant in the analysis of integral bridges are the calculations and assumptions that are to be made concerning foundation stiffness. The required level of detail in the calculations varies according to the complexity of the structure.

For typical integral grade separation structures of moderate overall length with minimal skew and flexible piling, zero stiffness against rotation and lateral movement is commonly assumed at the abutment foundations. Accordingly, fixity between the superstructure and the abutment piles is neglected in the design of the superstructure. The piles are designed for vertical loads only, neglecting the effects of bending due to temperature change, creep, shrinkage and $P-\Delta$ effects. Pier stiffness may be calculated using the methods given in Section 13.5.

In longer multiple-span bridges where semi-rigid piers are used, refinements in the analyses may be necessary to properly distribute external forces and forces due to superstructure movement to the substructure units. This analysis may also be desirable when designing moderate length structures that have abutments with stiffer pile-type foundations.

As stated in Section 13.5, a semi-rigid pier is generally pinned to the superstructure. If the pier is assumed fixed at the footing, then the translational stiffness (K) of an intermediate pier on a spread footing can be calculated as:

$$K = \frac{3E_c I_c}{H_1^3}$$

Where E_c and I_c are modulus of elasticity and moment of inertia of the concrete column, respectively, and H_1 is the distance from bottom of the superstructure to the top of footing. For actual applications, E_c and I_c are usually reduced to account for creep and shrinkage and might also be reduced to account for cracking.

For footings on piles, the rotational flexibility of the pile group should be accounted for as a reduction in stiffness. The modified stiffness term can be expressed as:

$$K = \frac{1}{\left(\frac{H_1^3}{3E_c I_c} + \frac{H_2^2 L_p}{I_g A_p E_p} \right)}$$

Where:

H_2 = Distance from top of pier cap to bottom of footing (ft)

L_p = Effective Pile length (ft)

I_g = Moment of inertia of the pile group about the axis under consideration (ft²)

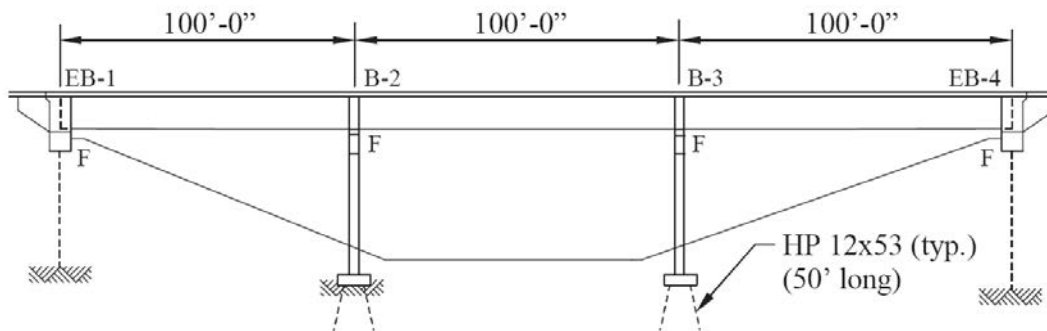
A_p = Cross-sectional area of a typical pile (in²)

E_p = Modulus of elasticity of typical pile (ksi)

The second term in the denominator represents the stiffness of a group of axially loaded "truss" members (the piles) subjected to compression or tension due to footing rotation.

Figures 13.6.1-1 and 13.6.1-2 show the details of a three-span continuous structure. The stiffness of the pier footing, using the above equations, can be computed as follows:

Figure 13.6.1-1
Elevation of Structure



First, considering the pier to be fixed at the footing for the spread footings:

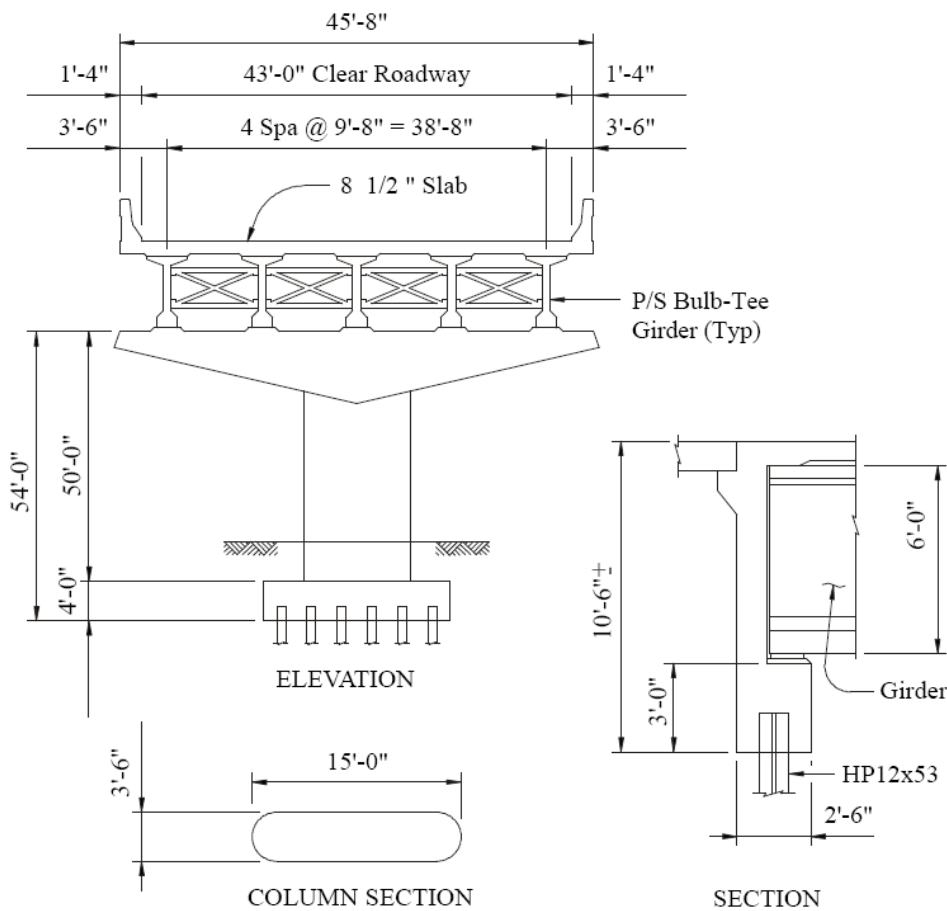
$$E_c = 57\sqrt{3,000} = 3,122 \text{ ksi (449,570 ksf)}$$

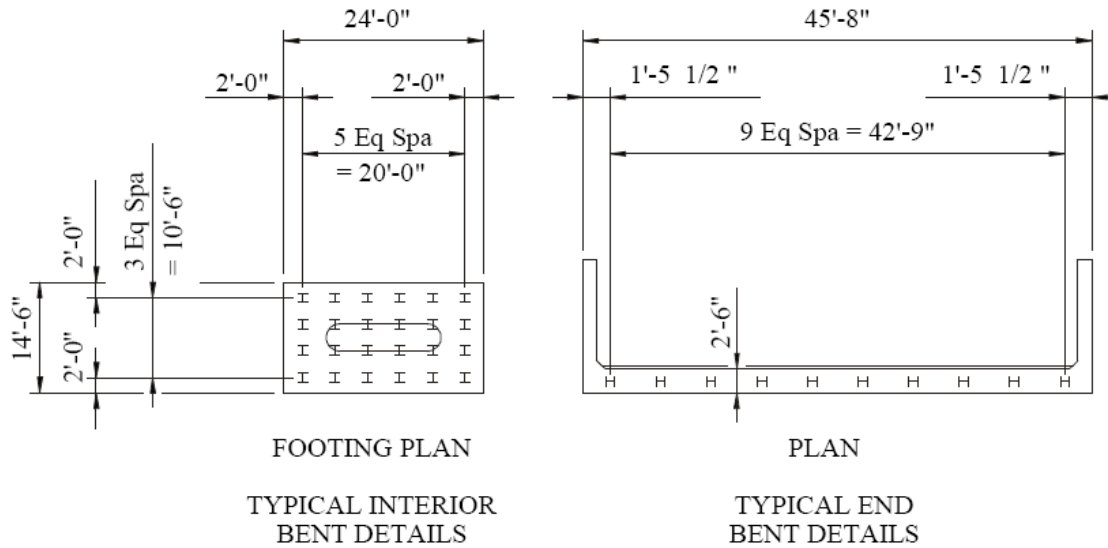
$$I_c = \frac{11.5(3.5)^3}{12} + \frac{\pi(3.5)^4}{64} = 48.45 \text{ ft}^4$$

$$H_1 = 50 \text{ ft}$$

$$K = \frac{3(449,570)(48.45)}{50^3} = 522. \text{ kip/ft}$$

Figure 13.6.1-2
Substructure Details





Second, including the effects of footing rotation for a pile foundation with an assumed end bearing pile length of 50 ft:

$$I_g = 12(1.75^2 + 5.25^2) = 367.5 \text{ ft}^2$$

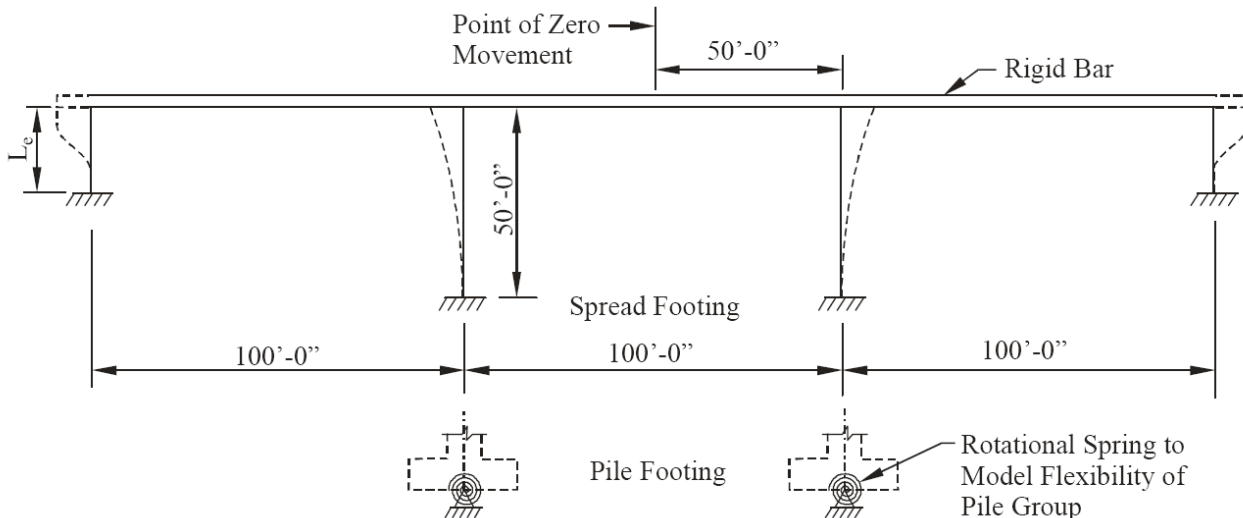
$$E_p = 29,000 \text{ k/in}^2$$

$$A_p = 15.5 \text{ in}^2$$

$$K = \frac{1}{522.76} + \frac{(54^2)(50)}{(367.5)(15.5)(29,000)} = 357.7 \text{ kip/ft}$$

This example shows that the reduction in stiffness is considerable when footing rotation is included in the analysis. Reduced stiffness due to cracking is not considered in the above example. The effect of lowered stiffness will be to reduce the forces in the structure. Advantage should be taken of this effect. **Figure 13.6.1-3** shows the stiffness assumptions graphically.

Figure 13.6.1-3
Stiffness Assumptions



INTEGRAL BRIDGES**13.6.1 Introduction/13.6.2 Equivalent Cantilever Method**

Due to the integral concrete diaphragms at the end bents, the tops of the piles are usually considered rigidly attached to the superstructure. Also, the flexural stiffness of the superstructure is several times larger than the stiffness of the intermediate bents and the end bent piles, allowing the superstructure to be modeled as a rigid bar. Intermediate bents are considered hinged to the superstructure.

For very long integral bridges, soil structure interaction analysis can be used to obtain a sufficiently accurate distribution of forces. The analysis proceeds as follows:

1. Initial stiffness assumptions are made for the foundations of each substructure unit.
2. The structure is analyzed for each required load combination.
3. Foundation forces are extracted and the pile groups are analyzed for the applied forces and actual subsurface profiles.
4. New foundation stiffness factors are calculated.
5. Steps 2 through 4 are repeated until convergence.

The Equivalent Cantilever Method described in Section 6.1 may be used to obtain the initial foundation stiffness.

13.6.2 Equivalent Cantilever Method

This example illustrates a procedure for calculating the equivalent cantilever for piles in an integral end bent. The procedure is similar for groups of piles, as long as none of the piles are battered.

A simplified model for pile deformation is shown in **Figure 13.6.2-1**. Equivalent length " L_e " can be determined by considering soil-pile interaction. To accomplish this, the soil will be modeled with a series of translational springs resisting the horizontal movement of the piles. For simplicity of this example, the lateral stiffness of the soil mass will be taken as constant with depth. (Constant modulus of subgrade reaction in kip/ft³). For most soil types, the lateral stiffness of the soil mass would increase with depth. The model shown in **Figure 13.6.2-2** was developed using a two-dimensional frame program.

Figure 13.6.2-1
Simplified Pile Deformation Model

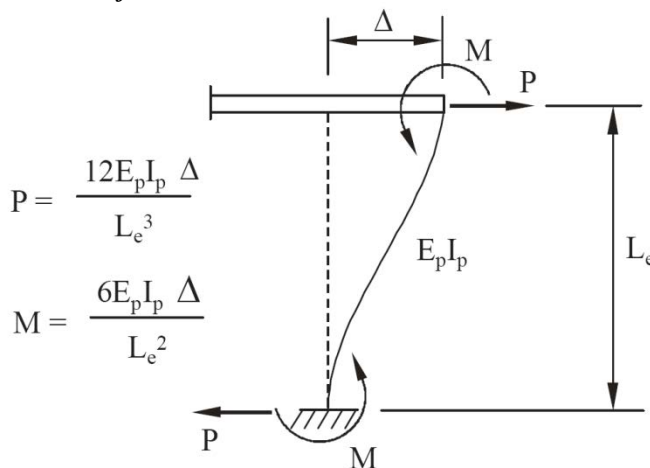
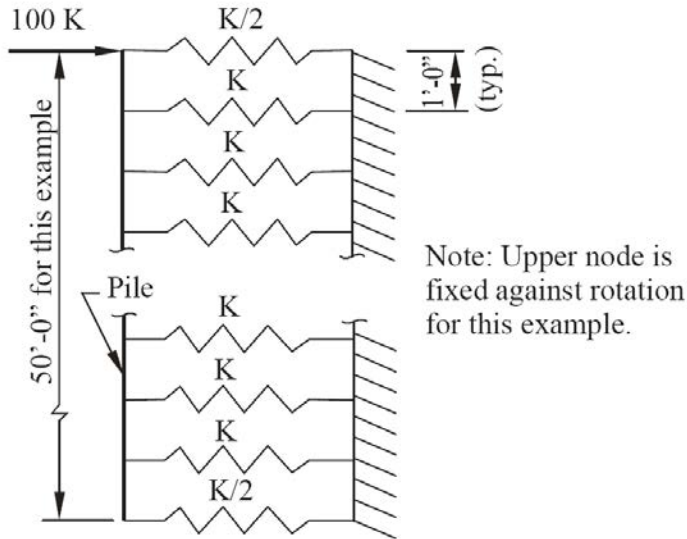


Figure 13.6.2-2
Soil-Pile Interaction Model



The value of the soil spring stiffness, k , is dependent on the modulus of subgrade reaction (K in kip/ft³). For this example, both a loose soil and a dense soil will be considered.

Table 13.6.2-1
Soil Spring Stiffnesses for Loose and Dense Soils

Soil Type	K_h (kip/ft ³)
Loose	100
Dense	400

Spring stiffness, $k = K_h ds$

where:

$d =$ pile width or diameter (ft)

$s =$ spacing of springs in the model (ft)

The pile modeled for each soil density case was a HP 12 x 53 pile about its minor axis ($I_p = 127$ in⁴). Displacement and Moment at top of pile bent due to 100 kip horizontal load are as follows:

Table 13.6.2-2
Displacement and Moment Versus Soil Type

Soil Type	K_h (kip/ft ³)	Displacement (in.)	Moment (kip-in.)
Loose	100	2.13	3,376
Dense	400	0.750	2,374

INTEGRAL BRIDGES

13.6.2 Equivalent Cantilever Method/13.6.3 Forces in Substructure Units

Table 13.6.2-3
Effective Length of Pile

Soil Type	Effective Length, L_e (in.), Based on:		Stiffness, K (kip-in.)
	Moment	100kip Load	
Formula	$\sqrt{\frac{6E_p I_p \Delta}{M}}$	$\sqrt[3]{\frac{12E_p I_p \Delta}{P}}$	$\frac{12E_p I_p}{L_e^3}$
Loose	117.8 (9.8 ft)	97.9 (8.2 ft)	35.1 (421 kip-ft)
Dense	83.6 (7.0 ft)	69.2 (5.8 ft)	118.4 (1421 kip-ft)

Where:

$$E_p = 29,000 \text{ ksi/in}^2$$

$$I_p = 2127 \text{ in}^4$$

$$M = (\text{See Table 13.6.2-2})$$

$$\Delta = (\text{See Table 13.6.2-2})$$

$$P = 100 \text{ kips}$$

$$n = \text{number of piles}$$

The value of K in **Table 13.6.2-2** is based on $L_e = 9.0$ ft for loose soil and 6.0 ft for dense soil. The value is computed for the end bent, which has 10-HP 12x53 piles.

Since calculated L_e values based on P and M are not equal for each soil density case, it can be concluded that the simplified pile model is only an approximate representation of soil-pile interaction. However, for normal design applications, the simplified model should be adequate when a single soil type is encountered along the length of the pile. In practice mostly multiple soil types are encountered along the length of the pile. In such situations, L-pile, group or similar programs which consider multiple soil profiles may be used to determine effective length of pile (L_e). These programs have moment and deflection plot capabilities. From these plots, L_e can be determined.

13.6.3 Forces in Substructure Units

Because the translational stiffness of the substructure units are symmetrical, the point of zero movement of the superstructure will be at the mid-point of the center span in this example. For a temperature fall of 40 °F and temperature rise of 30 °F:

Forces at Intermediate Bents:

$$\Delta_{fall} = \alpha \Delta T L = (6.0 \times 10^{-6})(40)(50) = 0.012 \text{ ft}$$

$$\Delta_{rise} = \alpha \Delta T L = (6.0 \times 10^{-6})(30)(50) = 0.009 \text{ ft}$$

Pile Footings:

$$F_{fall} = (0.012)(357.7) = 4.3 \text{ kips}$$

$$F_{rise} = (0.009)(357.7) = 3.2 \text{ kips}$$

Spread Footings:

$$F_{fall} = (0.012)(522.8) = 6.3 \text{ kips}$$

$$F_{rise} = (0.009)(522.8) = 4.7 \text{ kips}$$

Forces at End Bents:

$$\Delta_{fall} = (6.0 \times 10^{-6})(40)(150) = 0.036 \text{ ft}$$

$$\Delta_{rise} = (6.0 \times 10^{-6})(30)(150) = 0.027 \text{ ft}$$

Loose Soil:

$$F_{fall} = (0.036)(421) = 15.2 \text{ kips}$$

$$F_{rise} = (0.027)(421) = 11.4 \text{ kips}$$

Dense Soil:

$$F_{fall} = (0.036)(1,421) = 51.2 \text{ kips}$$

$$F_{rise} = (0.027)(1,421) = 38.4 \text{ kips}$$

For the case of temperature rise, a theoretical passive pressure force is mobilized behind the end bents, which may be considered in addition to the resistance due to soil-pile interaction. Effects of soil placed in front of the abutment are ignored. To determine the passive pressure force for this example, an internal angle of friction, ϕ , for the backfill material will be taken as 28° . Using 120 pcf for the density of the soil:

$$F_{passive} = 120 \tan^2 \left(45 + \frac{\phi}{2} \right) \left(\frac{H^2}{2} \right) (L)$$

where H = total depth of the end bent (ft)

L = length of end bent (ft)

$$F_{passive} = 120 \tan^2 \left(45 + \frac{28}{2} \right) \left(\frac{10.5^2}{2} \right) \left(\frac{45.67}{1,000} \right) = 836.8 \text{ kips}$$

Total force for the loose soil case:

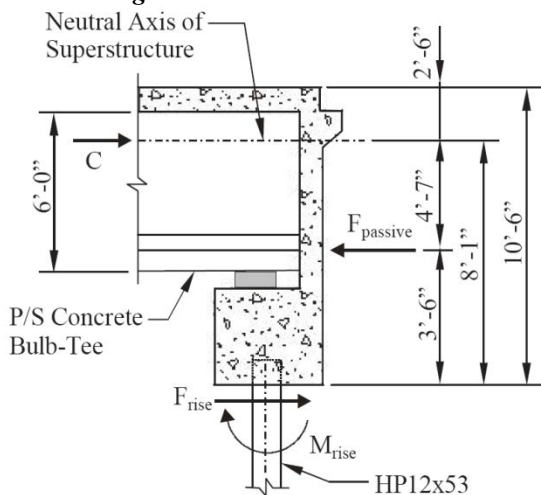
$$F_{total} = F_{rise} + F_{passive} = 11.4 + 836.8 = 848.2 \text{ kips (169.6 kip/girder)}$$

Total force for the dense soil case:

$$F_{total} = F_{rise} + F_{passive} = 38.4 + 836.8 = 875.2 \text{ kips (175.0 kip/girder)}$$

The passive pressure force developed behind the backwall is resisted by backwall bending (see **Figure 13.6.3-1**). This backwall bending is usually not significant and can readily be accommodated by nominal reinforcing in the backwall.

Figure 13.6.3-1
Forces Acting on End Bent



Consider pile moments caused by soil-pile interaction:

$$f_b = \frac{M}{S} = \frac{6E_p I_p \Delta / L_e^2}{S}$$

Where:

$$E_p = 29,000 \text{ kip/in}^2$$

$$I_p = 127 \text{ in}^4$$

$$L_e = 9 \text{ ft for loose soil (6 ft for dense soil)}$$

$$\Delta = 0.036 \text{ ft}$$

$$S_{pile} = 21.1 \text{ in}^3$$

Loose Soil:

$$M_{pile} = \frac{6(29,000)(127)(0.036)(12)}{(12 \times 9)^2} = 818.4 \text{ in- kip}$$

$$f_b = 818.4/21.1 = 38.8 \text{ ksi} > 36 \text{ ksi}$$

Dense Soil:

$$M_{pile} = \frac{6(29,000)(127)(0.036)(12)}{(12 \times 6)^2} = 1,841 \text{ in- kip}$$

$$f_b = 1,841.5/21.1 = 87.3 \text{ ksi} > 36 \text{ ksi}$$

For the conditions assumed in this illustration, a pile bending stress beyond yield occurs for both the loose and dense soil conditions. In particular, the dense soil example indicates the pile to be highly overstressed and could therefore be highly strained. As this is a repetitive movement, pile damage could occur even though a plastic hinge forms at this point. Where piles are driven in dense soils, predrilled oversized holes filled with loose sand may be provided to reduce resistance to lateral movement and to reduce the pile stresses. In any event, the piles must also be checked for adequacy as columns and interaction diagrams should be drawn. Then the Loading Cases of AASHTO Table 3.22.1A are plotted on the interaction diagrams to complete an analysis based on actual conditions.

13.6.4 Conclusions from Example

The following conclusions can be drawn from this example:

1. Intermediate bents are relatively flexible compared to integral end bents. As a result, they experience very small longitudinal temperature forces. For this example, the temperature force generated at the end bents is independent of the forces generated at the intermediate bents. This will be true if there is symmetry in the longitudinal stiffness of the substructure.
2. Temperature rise can generate large passive pressure forces at the end bent backwall. However, these large passive forces usually have little effect on the end bent and can readily be accommodated by backwall reinforcement.
3. Due to the larger magnitude and less effect from passive resistance, temperature fall has the greatest effect on the end bent foundation.
4. Thermal expansion and contraction occurs in all structures. Expansion joints in the approach slabs of the bridge should accommodate thermal movements when integral end bents are used.

13.7 SURVEY OF CURRENT PRACTICE

13.7.1 Introduction

To obtain the current information on integral bridges, the Subcommittee on Integral Bridges distributed a questionnaire to the departments of transportation in all 50 states and ministries of transportation in nine Canadian provinces. In addition, the questionnaire was sent to 17 design consultants.

INTEGRAL BRIDGES

13.7.1 Introduction/13.7.2 Data Collection/Survey Response

The questionnaire solicited the following information:

1. Organization's experience with integral bridges
2. Geometric restrictions
3. Design criteria
4. Design methodology
5. Method of handling creep, shrinkage, and temperature
6. Any applications to curved bridges
7. Any known research
8. Future research requirements
9. Lessons learned

The questionnaire also requested sample drawings of integral bridges.

The response was excellent, with 49 of the 50 states, seven of the nine Canadian Provinces, six of the 17 consultants, plus St. Louis County, Missouri responding to the questionnaire.

13.7.2 Data Collection/Survey Response

The effort for this report began by developing a questionnaire. The first question asked was whether or not the responding entity had an integral bridge in service, in the design stage, or currently under construction in its jurisdiction. If the answer was negative, further response was not required. If the answer was affirmative, information in the above-mentioned areas was collected.

Table 13.7.2-1 summarizes the responses to the questionnaires, and **Table 13.7.2-2** details the responses from each individual state department of transportation and Canadian provincial ministry of transportation. **Table 13.7.2-3** summarizes the responses to the question, "Why do Integral Bridges Work?". Only those states having integral bridges at the time of the survey are listed. The responses to this question were diverse, but mainly centered on the idea that actual movements in superstructures due to creep, shrinkage and temperature are less than theoretical predictions, that backfill can allow small movements, and that foundations can be flexible.

*Table 13.7.2-1
Summary of Responses*

Question	Response
Designed and/or built integral bridges?	54 (Yes)
Overall experience?	Good to Excellent
Geometric restrictions?	31 (Yes)
Applied to curved bridges?	12 (Yes)
Any design methodology?	28 (Yes)
Any abutment design parameters?	23 (Exists)
Any temperature, creep and Shrinkage criteria?	20 (Yes)
Need for future research?	10 (Yes)
Lessons learned?	9 (Yes)

INTEGRAL BRIDGES

13.7.2 Data Collection/Survey Response

Table 13.7.2-4 reflects the geometric constraints imposed by the responding entities on precast concrete integral bridges. Most of the states limit such bridges to a maximum of 300-400 ft in total length. Some states have gone well beyond this limit. The skew angles of integral bridges are also mostly limited to about 30°. Only 12 states have had experience in curved integral bridges.

Based on the information available, and on the detailed design criteria supplied by some respondents, the matrix shown in **Table 13.7.2-5** was prepared to illustrate the various design criteria used. The states and provinces who supplied very detailed design criteria were Illinois, Indiana, New York, Pennsylvania, Tennessee and Ontario.

Table 13.7.2-2
Responses from each Agency

	Response received?	Have jointless bridges?	Overall experience	Temp., creep & shrink. criteria?	Any design methodology?	Any abutment design parameters?	Any geometric restrictions?	Opinion on why they work?	Applied to curved bridges?	Aware of any research?	Need for future research?	Lessons learned?	Provided list of jointless bridges?	Samples provided?
Alaska	Y	Y	S	Y	N	N	Y	Y	N	Y	N	Y	Y	N
Arizona	Y	Y	D	-	-	-	-	-	-	-	-	-	-	-
California	Y	Y	S	Y	Y	Y	Y	Y	Y	N	N	Y	N	Y
Colorado	Y	Y	E	Y	Y	Y	Y	N	Y	N	Y	Y	N	Y
Georgia	Y	Y	S	N	Y	N	N	Y	Y	N	N	N	Y	Y
Hawaii	Y	Y	S	N	N	Y	NC	Y	N	N	Y	N	N	N
Idaho	Y	Y	G	Y	Y	Y	Y	Y	Y	N	Y	N	Y	N
Illinois	Y	Y	G	N	Y	Y	Y	Y	N	N	Y	N	Y	Y
Indiana	Y	Y	G	N	Y	Y	Y	Y	N	Y	Y	N	N	Y
Iowa	Y	Y	E	Y	Y	Y	Y	NC	N	Y	N	Y	N	Y
Kansas	Y	Y	VG	N	Y	Y	Y	Y	N	Y	N	Y	N	Y
Kentucky	Y	Y	S	Y	Y	Y	Y	Y	Y	N	N	N	Y	Y
Louisiana	Y	Y	VG	N	N	N	Y	NC	N	N	N	NC	N	Y
Maine	Y	Y	VG	N	Y	Y	Y	Y	N	Y	Y	Y	Y	N
Maryland	Y	Y	-	-	-	-	-	-	-	-	-	-	-	-
Massachusetts	Y	Y	G	Y	Y	Y	Y	Y	N	Y	N	N	Y	Y
Michigan	Y	Y	S	Y	Y	Y	Y	N	N	N	Y	N	N	N
Minnesota	Y	Y	P	Y	Y	Y	Y	Y	N	N	N	Y	N	Y
Missouri	Y	Y	E	Y	Y	Y	Y	Y	Y	N	N	N	N	Y
Nebraska	Y	Y	G	Y	N	Y	Y	-	N	-	-	-	N	Y
Nevada	Y	Y	G	N	Y	N	Y	N	Y	N	N	N	N	Y
New York	Y	Y	VG	Y	Y	Y	Y	Y	Y	Y	Y	Y	Y	Y
North Dakota	Y	Y	G	N	N	Y	Y	Y	N	N	N	N	N	Y

INTEGRAL BRIDGES

13.7.2 Data Collection/Survey Response

Ohio	Y	Y	G	N	N	N	Y	N	N	N	N	N	N	Y
Oklahoma	Y	Y	G	N	Y	N	N	Y	Y	Y	Y	Y	Y	Y
Oregon	Y	Y	G	Y	Y	Y	N	Y	N	N	N	Y	Y	Y
Pennsylvania	Y	Y	G	Y	Y	Y	Y	Y	N	Y	Y	N	N	Y
South Carolina	Y	Y	S	Y	Y	Y	Y	N	N	Y	Y	N	Y	N
South Dakota	Y	Y	VG	Y	Y	N	Y	Y	N	Y	N	N	N	Y
Tennessee	Y	Y	VG	Y	Y	Y	Y	Y	Y	Y	N	Y	Y	Y
Utah	Y	Y	VG	N	Y	Y	Y	Y	N	N	N	N	N	N
Virginia	Y	Y	VG	Y	Y	Y	Y	Y	N	Y	Y	Y	Y	Y
Washington	Y	Y	G	Y	Y	Y	Y	Y	Y	Y	Y	Y	Y	Y
Wisconsin	Y	Y	G	N	Y	N	Y	Y	N	N	N	Y	Y	Y
Wyoming	Y	Y	G	N	Y	N	Y	Y	Y	N	Y	Y	N	Y
Alberta	Y	Y	NC	N	Y	N	N	Y	N	N	Y	N	N	Y
Nova Scotia	Y	Y	S	N	-	N	N	Y	N	N	N	N	Y	Y
Ontario	Y	Y	G	Y	Y	Y	Y	Y	N	N	Y	Y	N	Y

Experience Key: E - Excellent, VG - Very Good, G - Good, S - Satisfactory, F - Fair, P - Poor, U - Unacceptable

Other abbreviations: Y - Yes, N - No or None, NC - No Comment, D - Discontinued

Table 13.7.2-3

Why Integral Bridges Work

Backfill may be resilient to allow small movements.
Flexibility of supports, including piles, piers & abutments.
Limit on length, lateral & rotational movements.
Actual movements are less than theoretical.
Bridges work as frames.
Bridges experience less thermal movement than anticipated.
Issues are shifted from bridge to approach roadway.
Plastic hinge is created at piles.
End Bents are flexible. They can move up to 2" without damage, if properly detailed

Table 13.7.2-4

Geometrical Constraints

Location	Maximum Length (ft)	Maximum Skew Angle (deg.)	Radius of Curvature (ft)
Arkansas	260	33	No
California	(Note 1)	30 - 45	700
Georgia	410 259	0 30 - 40	250
Hawaii	250		
Illinois	300	30	
Indiana	300	30	
Idaho	400	30	Yes
Iowa	300 (flexible)	30	
Kansas	450	None	

INTEGRAL BRIDGES

13.7.2 Data Collection/Survey Response

Kentucky	400	30	Yes
Louisiana	1,000	0	
Maine	150	30	
Michigan	None	30	
Missouri	500		
Massachusetts	300	30	1,146
North Dakota	400	30	
Nevada	200	45	
New York	300	30	
Ohio	375	30	
Oklahoma	210	0	
Pennsylvania	600	20	
Ontario	330	15	
Oregon	203	25	
South Dakota	700	35	
South Carolina	500	30	
Tennessee	(Note 2)	No limit	No limit
Utah	300	20	
Wyoming	360		
Washington	450	30	Yes
Wisconsin	300	40	
Virginia	500	30	

Note 1 - Δ = ½" - 1"

Note 2 - Δ = 2"

Table 13.7.2-5
Agency Design Criteria

Illinois

Length Criteria/Type of Superstructure	Steel Structures: 200' max. Concrete Structures: 300' max. Analysis of thermal forces not required if structure is within these limitations. Longer structures may be permitted provided that thermal analysis is performed.
Alignment/Geometry Criteria	Maximum skew is 30 deg. Tangent alignment only - no curved girders. Abutments and piers must be parallel
Movement Criteria	NA
Approach Slab	NA
Backfill	Abutment backfill must be well drained and non compacted porous granular embankment. Geotextile and 6" perforated drain pipe required.
Foundation	Steel H piles required for structures up to 200' long and required for structures between 200' and 300' long. Concrete piles permitted for structures up to 200' long.
End Bent/Abutment	All abutments must be provided with "dog-ear" type wingwalls.

INTEGRAL BRIDGES

13.7.2 Data Collection/Survey Response

Bearing at End Bent	Steel beams are set on lead plates and bolted to the abutments cap. PPC I-beams are set on a 1/2" grout bed.
Joint Details/Expansion Provisions	NA
Remarks	

Indiana

Length Criteria/Type of Superstructure	Steel Structures: 250' max. (125' from fixed pt. to end bent). Concrete Structures: 300' max. (150' from fixed pt. to end bent). Longer structures may be permitted if analysis indicates feasibility. Concrete slab bridges: 200' max.
Alignment/Geometry Criteria	Maximum skew is 30 deg. Concrete slab bridges shall have integral end bents regardless of skew.
Movement Criteria	NA
Approach Slab	Reinforced concrete approach slab required. 2 layers of 6 mil (minimum) PE sheeting required between approach slab and subgrade.
Backfill	Indiana "Type B" backfill drained with 6" perforated pipe required behind end bents.
Foundation	Only steel H piles or steel encased concrete piles permitted at end bents. H piles preferred. If N>35 blows/ft. within 10' below cap, 8' deep predrilled hole, filled with pea gravel required.
End Bent/Abutment	2'-6" minimum width. Piling extends 2' min. into cap for beams placed directly on piles and 1'-3" min. into C.I.P. caps. Beams extend 1'-9" into bent.
Bearing at End Bent	NA
Joint Details/Expansion Provisions	2'-wide terminal joint or pavement relief joint required between approach slab and roadway if roadway pavement is concrete. Not required if pavement is bituminous.
Remarks	

New York

Length Criteria/Type of Superstructure	For steel or prestressed concrete bridges: 300' max. Lengths between 300' and 400' approved on an individual basis. Lengths over 400' not recommended.
Alignment/Geometry Criteria	Max. skew: 30 deg. for single spans over 90' and all multiple span steel bridges; 45 deg. for single spans 90' or less. Straight beams only. Beams must be parallel to each other. Abutments must be parallel to each other. 5% max. grade.
Movement Criteria	NA
Approach Slab	Always required for integral abutments. Sawcut or construction joint required between approach slab and backwall to provide controlled crack location.
Backfill	Geotextile and 6" perforated drain pipe required.

INTEGRAL BRIDGES

13.7.2 Data Collection/Survey Response

Foundation	C.I.P piles are allowed for bridges with spans of 150' and less, otherwise steel H-piles req'd. Single line only. H piles webs oriented perpendicular to centerline of beams. Top 8' of pile is augered and backfilled with sand.
End Bent/Abutment	In-line wingwalls preferred. Flared walls considered on a case by case basis. U-walls normally not allowed. Wingwall length over 10' to be avoided. 3' min. pile cap width.
Bearing at End Bent	Individual plain rubber pads or 8" dia. concrete pad for prestressed beams. Load plate, load cap or bearing pad required for steel beams.
Joint Details/Expansion Provisions	For lengths up to 150', no expansion joint req'd at end of appr. slab unless highway pavement is rigid. Exp. Joint req'd for lengths over 150'. Short sleeper slab provided beneath exp. joint.
Remarks	Scour criteria should be reviewed and evaluated prior to use of this type of structure where scour potential exists.

Pennsylvania

Length Criteria/Type of Superstructure	Steel Structures: 400' max. Concrete Structures: 600' max. Lengths over these limits approved on an individual basis. Lengths over 600' not recommended.
Alignment/Geometry Criteria	Max. skew: 30 deg. for single spans over 90' and all multiple span steel bridges; 45 deg. for single spans 90' or less. Straight beams only. Beams must be parallel to each other. Abuts. must be parallel to each other. 5% max. grade.
Movement Criteria	Temperature ranges: Metal Structures = 120 deg. F., Concrete Structures = 90 deg. F.
Approach Slab	25' long approach slab required. 2 layers of 6 mil (minimum) PE sheeting required between approach slab and subgrade. Contraction joint required between approach slab and backwall to provide controlled crack location.
Backfill	Area behind abutment backfilled with granular material. Geotextile and 6" perforated drain pipe required.
Foundation	Steel H or steel encased concrete piles for total structure length 150' and less, otherwise steel H-piles req'd. Single line only. H piles webs oriented perpendicular to centerline of beams. Top 10' to 20' of pile is augered and backfilled with sand.
End Bent/Abutment	In-line wingwalls preferred. Flared or U walls considered on a case by case basis. Wingwall length over 10' to be avoided. 3' min. pile cap width.
Bearing at End Bent	NA
Joint Details/Expansion Provisions	For lengths up to 150', no expansion joint req'd at end of appr. slab unless highway pavement is rigid. Exp. Joint req'd for lengths over 150'. Short sleeper slab provided beneath exp. joint.
Remarks	Scour criteria should be reviewed and evaluated prior to use of this type of structure where scour potential exists.

INTEGRAL BRIDGES

13.7.2 Data Collection/Survey Response

Tennessee

Length Criteria/Type of Superstructure	Steel structures: 536' max; Concrete structures: 1175' max. Lengths up to 427' in steel and 800' in concrete require no special approvals.
Alignment/Geometry Criteria	No limit on maximum skew. Substructures may have varying skews.
Movement Criteria	Temperature range: Steel = 0 to 120 deg. F. Concrete = 25 to 95 deg. F. Unrestrained abutments to be integral for total movement at abut <2" - no exp. joint required. Abut. to be integral for movement <1/4" regardless of support conditions.
Approach Slab	Construction joint required between approach slab and backwall. Provision shall be made for movement between approach pavement and roadway interface.
Backfill	Area behind abutment backfilled with granular material. Geotextile and 6" perforated drain pipe required.
Foundation	For movement at each abutment <1/4", spread footing on rock may be used. For movement >1/4" one row of piling is required.
End Bent/Abutment	Piling extends 1' into abutment beam. Wingwalls are parallel to bridge axis.
Bearing at End Bent	1/2" thick 60 durometer elastomeric pad.
Joint Details/Expansion Provisions	Expansion joint provided at approach slab to roadway interface.
Remarks	Designers encouraged to use integral abutments on all sharply skewed and curved bridges

Ontario

Length Criteria/Type of Superstructure	Overall length 100m (328') max. Superstructure types: Steel girders with concrete deck, CPCI girders with concrete deck, and prestressed concrete box girders with concrete deck.
Alignment/Geometry Criteria	20 deg. maximum skew.
Movement Criteria	NA
Approach Slab	Provide weak joint between approach slab and roadway pavement.
Backfill	Granular material and 150 mm perforated drain pipe.
Foundation	Single row of vertical steel H-piles with weak axis normal to the direction of movement. In stiff soil, predrill holes at least 3 meters below abutment and fill with loose sand.
End Bent/Abutment	Maximum recommended abut. height is 5 m. Use parallel type wingwalls, size minimized. Max wingwall length = 6 m. Embed piles 600 mm into abut.
Bearing at End Bent	Thin rubber pad
Joint Details/Expansion Provisions	NA
Remarks	

13.7.3 Lessons Learned

A number of important lessons learned were reported by the respondents. The main ones (not in order of priority) were:

1. Place concrete in pier and abutment diaphragms with deck to avoid diaphragm cracking due to downward rotation of the beams.
2. Use semi-integral type abutments to avoid spalling and slab cracking inside abutment.
3. Provide proper details to allow movement, otherwise girder failure and support spalling can occur.
4. Avoid drainage structures in the area of the end diaphragms.
5. Limit span lengths, depending on location, to accommodate thermal, creep, and shrinkage movements.
6. Abutment support should be flexible, with single row of piles.
7. Consider using hinges at abutment and piers.
8. Provide a positive connection between the approach slab and the abutment.
9. Provide a sleeper slab at end of the approach slab to eliminate settlement due to traffic and backfill.
10. Consider placing piles in pre-drilled oversize holes filled with loose granular material such as pea gravel or dry sand (upper 8 to 20 ft).
11. Limit skew angles.
12. Orient the abutment piles for weak axis bending.
13. Provide granular backfill behind abutment backwall and a proper draining system.

13.7.4 Future Research Needs

For convenience, the future research needs that were reported are divided into design and analysis issues and actual performance issues. In no particular order, they are:

13.7.4.1 Design and Analysis

1. Establish design criteria and design guidelines for both superstructure and substructure for the effects of temperature, shrinkage, and creep.
2. Identify rational limitations for this type of structure taking into account the combined effects of actual rotations, translations, skews, and horizontal curvature.
3. Determine how these structures should be designed to resist earthquakes and determine how they will actually perform during earthquakes. (Seismic considerations may require increased abutment stiffness whereas the thermal movements require the abutments to be flexible.)
4. Determine how to design and detail the approach pavement.
5. Determine the best type of wingwall to use and describe how it should be designed.

13.7.4.2 Performance

1. Investigate earth pressure effects behind abutments due to thermal expansion, particularly for severely skewed bridges.
2. Investigate stresses in steel and concrete piles caused by large longitudinal movements.
3. Monitor temperature effects on existing bridges with integral or semi-integral abutments.
4. Investigate the effect of frost on the flexibility of abutments.

INTEGRAL BRIDGES

13.7.4.2 Performance/13.8.2 The Nebraska City Viaduct, Nebraska

5. Identify the cost effectiveness of various alternatives including approach slabs with and without joints, pre-drilling of holes for piles and providing compressible material behind backwalls.
6. Summarize past experience, particularly from bridge maintenance staff.
7. Determine the susceptibility of these bridges to deck cracking as compared to conventional bridges.

13.8 CASE STUDIES

13.8.1 Section Description

Five case studies are presented in the Appendix. They were drawn from the following areas of the country:

- The Nebraska City Viaduct, Nebraska
- I-469 Bridge over I-69, Indiana
- Menauhant Road Bridge, Massachusetts
- Deer Creek Industrial Park Access Bridge, West Virginia
- Tennessee State Route 50 over Happy Hollow Creek, Tennessee

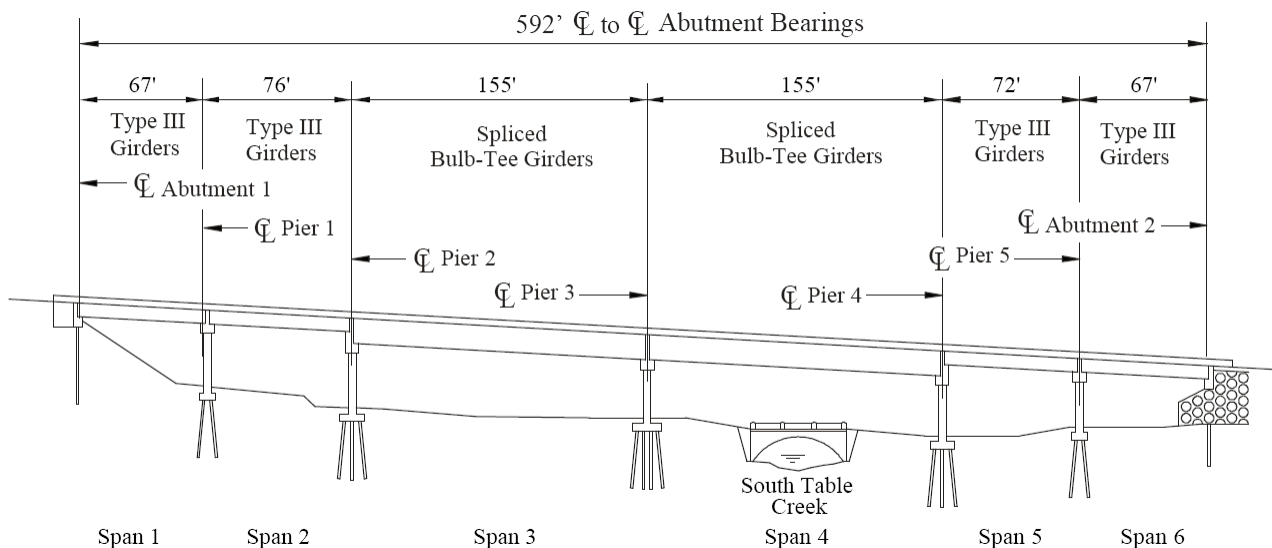
13.8.2 The Nebraska City Viaduct, Nebraska

The U. S. Highway 75 Viaduct in Nebraska City, Neb., built in 1992, is a six-span highway structure that provides a crossing of two railroad tracks, a small creek and a city access type road. The viaduct replaced a fifty-year old steel girder bridge that was obsolete and in poor structural condition. AASHTO Type III girders are used for four spans and spliced bulb-tee girders are used for two spans. It is designed for live load and superimposed dead load continuity. The piers are hinged at the superstructure.

The roadway of the new structure provides for two lanes of highway traffic. A sidewalk is included on one side of the roadway deck.

The alignment for the new structure could not be offset nor altered from the existing street alignment. This required the new bridge piers to be located to clear the existing pier foundations, thus avoiding substantial removal costs. These restrictions resulted in an overall structure length of 592 ft with span arrangement as shown in **Figure 13.8.2-1**. Continuity for live load and for dead load applied to the composite section was assumed in design, and the structure was constructed as an integral (jointless) bridge.

Figure 13.8.2-1
Elevation



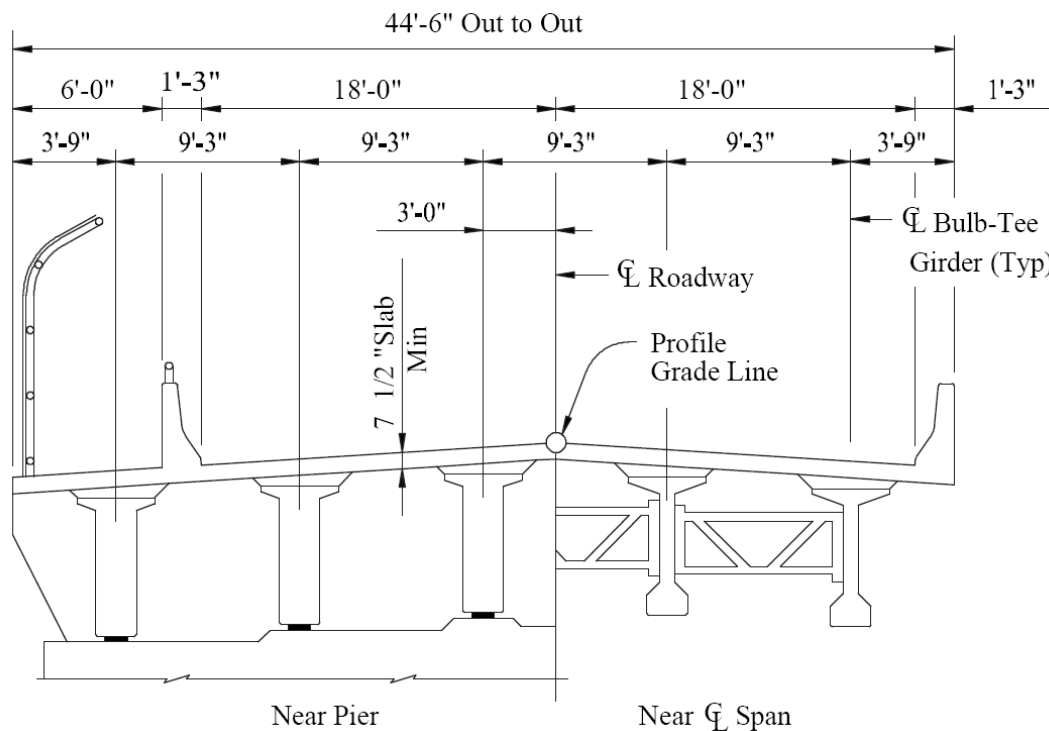
INTEGRAL BRIDGES

13.8.2 The Nebraska City Viaduct, Nebraska

Prestressed concrete girders are used throughout the superstructure to support the cast-in-place reinforced concrete deck. Bulb-tee girders were used for the two 155 ft spans. Each of these spans is comprised of three bulb-tee segments which were match cast in the prestressing plant and shipped to the site. The segments were then spliced and post-tensioned together prior to placement on the piers. The shorter spans are AASHTO Type III girders. All bulb-tee and Type III sections were designed in accordance with standards of the Nebraska Department of Roads. A typical section of the bridge superstructure at the bulb-tee spans is shown in **Figure 13.8.2-2**.

All piers are of reinforced concrete design and conform to NDOR standards. Both abutments were designed and constructed integrally with the superstructure, requiring special design considerations and detail in regard to thermal effects, creep, and shrinkage. All substructure units are supported on steel bearing piles driven to bedrock.

Figure 13.8.2-2
Cross Section

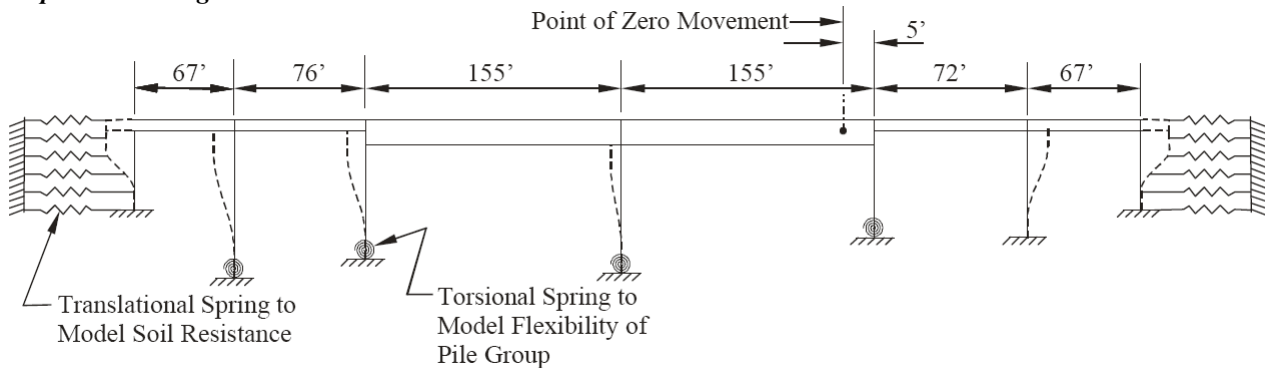


Longitudinal forces were distributed to the substructure units in proportion to their relative stiffness. The five piers vary substantially in height and therefore vary in stiffness. The point of fixity, i.e. point of zero longitudinal temperature movement, was located between Pier Numbers 3 and 4, somewhat closer to the shorter and stiffer piers. The stiffness of each pier as assumed in design included consideration of both the concrete frame and its pile supported foundation. A point of fixity of the pile group was assumed to be at some point below the base of footings. The abutment stiffness was modeled using spring restraints that approximated the passive earth resistance to movement of the diaphragm. For analysis, the structure was modeled as indicated in **Figure 13.8.2-3**.

INTEGRAL BRIDGES

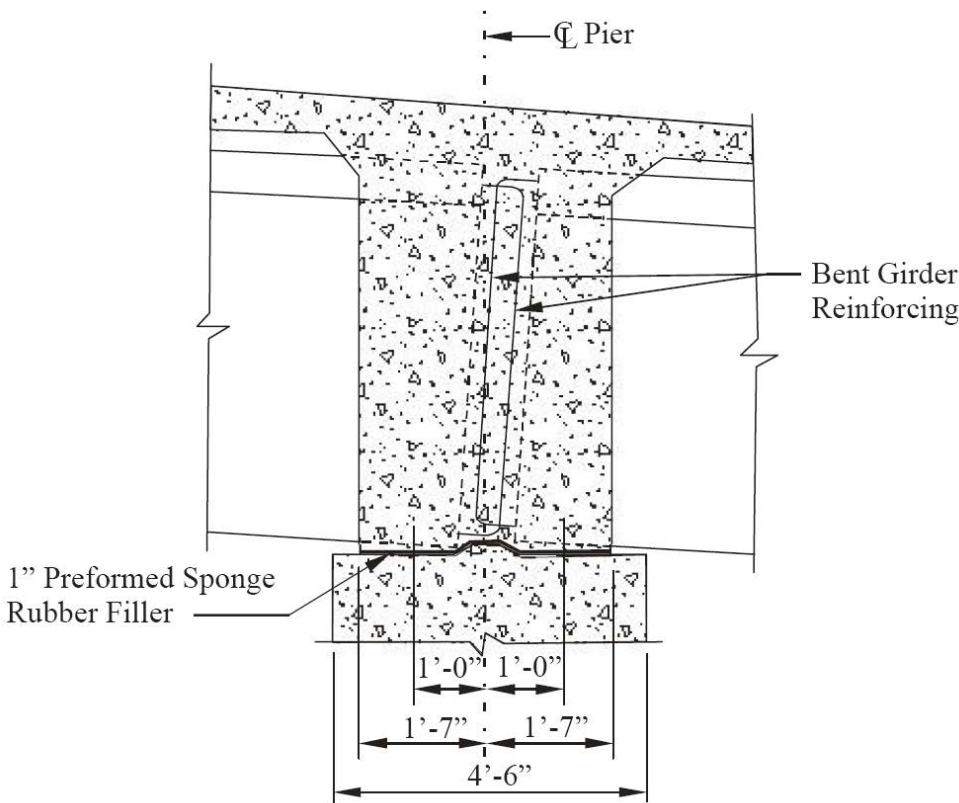
13.8.2 The Nebraska City Viaduct, Nebraska

Figure 13.8.2-3
Computer Modeling



Due to the integral concrete diaphragms at the abutments, the tops of the piles were considered to be rigidly attached to the superstructure. Also, the flexural stiffness of the superstructure is several times larger than the stiffness of the piers and the abutment piles, allowing the superstructure to be modeled as a rigid bar. The piers were considered to be hinged to the superstructure. This hinge was developed as shown in **Figure 13.8.2-4**.

Figure 13.8.2-4
Pier Hinge Detail



Special consideration was given to the abutments for the effects of thermal expansion and contraction. Temperature rise can generate a high passive pressure on the abutment diaphragm. While this pressure has little effect on the abutment itself, the effects of axial loads and moments due to eccentricity transferred to the superstructure were considered in the design. Temperature fall has the greater effect on the abutment design. The piles were driven with their weak axis perpendicular to the line of movement. In addition, at Abutment

INTEGRAL BRIDGES

13.8.2 The Nebraska City Viaduct, Nebraska

Number 2, where a mechanically stabilized earthwall was required, corrugated metal pipes were placed over the pile protrusions and were filled with sand. This was done to allow the piles to displace independently of the completed retaining walls. Joints to permit thermal movements were provided only at the ends of the approach slab pavement sections about 25 ft from the ends of the bridge deck. The general scheme at the abutments is shown in **Figure 13.8.2-5**.

Figure 13.8.2-5
Longitudinal Section at Approach Slab

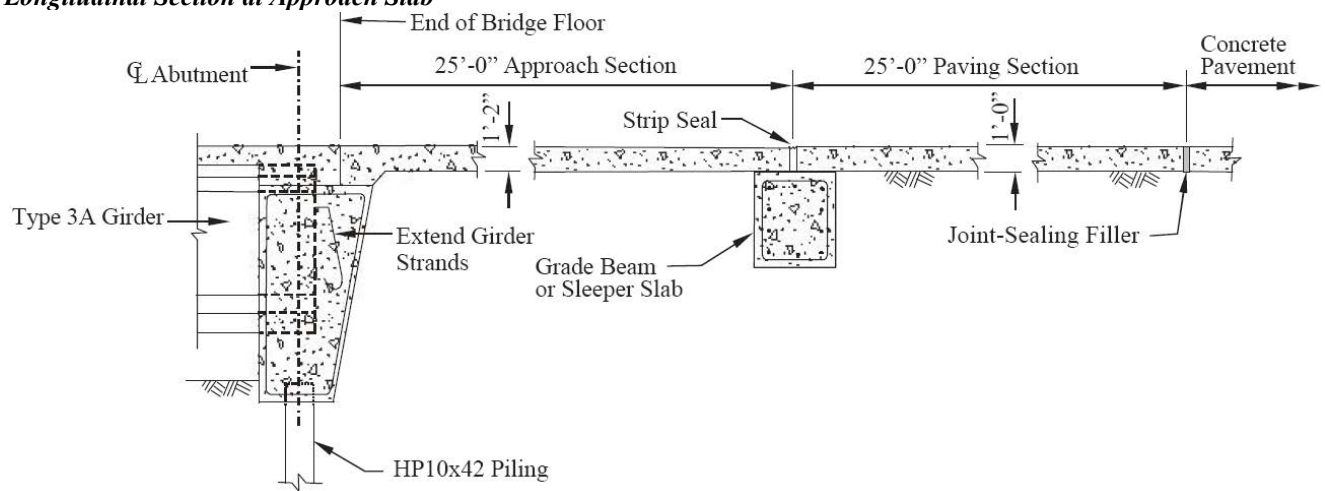


Figure 13.8.2-6
Abutment 2 Piles Encased in Corrugated Metal Pipes



INTEGRAL BRIDGES

13.8.2 The Nebraska City Viaduct, Nebraska

Figure 13.8.2-7
Abutment 2 Girder in Place
Before Abutment Pour



The bridge was completed for the Nebraska Department of Roads in November 1992 at a cost of approximately \$975,000, exclusive of approach street work and removal of the previous structure. All design was in accordance with NDOR policy and procedure of their Bridge Division. Current policy of the department is to limit the design of integral bridges to an overall length of about 600 ft. **Figures 13.8.2-6** through **13.8.2-11** are photographs of the bridge under construction and at completion.

INTEGRAL BRIDGES

13.8.2 The Nebraska City Viaduct, Nebraska

*Figure 13.8.2-8
Abutment 1 Abutment Forms in Place*



*Figure 13.8.2-9
Pipe Sleeves Through Abutment
to Accommodate Conduits*



INTEGRAL BRIDGES

13.8.2 The Nebraska City Viaduct, Nebraska

*Figure 13.8.2-10
The Completed Nebraska City Viaduct*



*Figure 13.8.2-11
Aerial View of the Completed Nebraska City Viaduct*

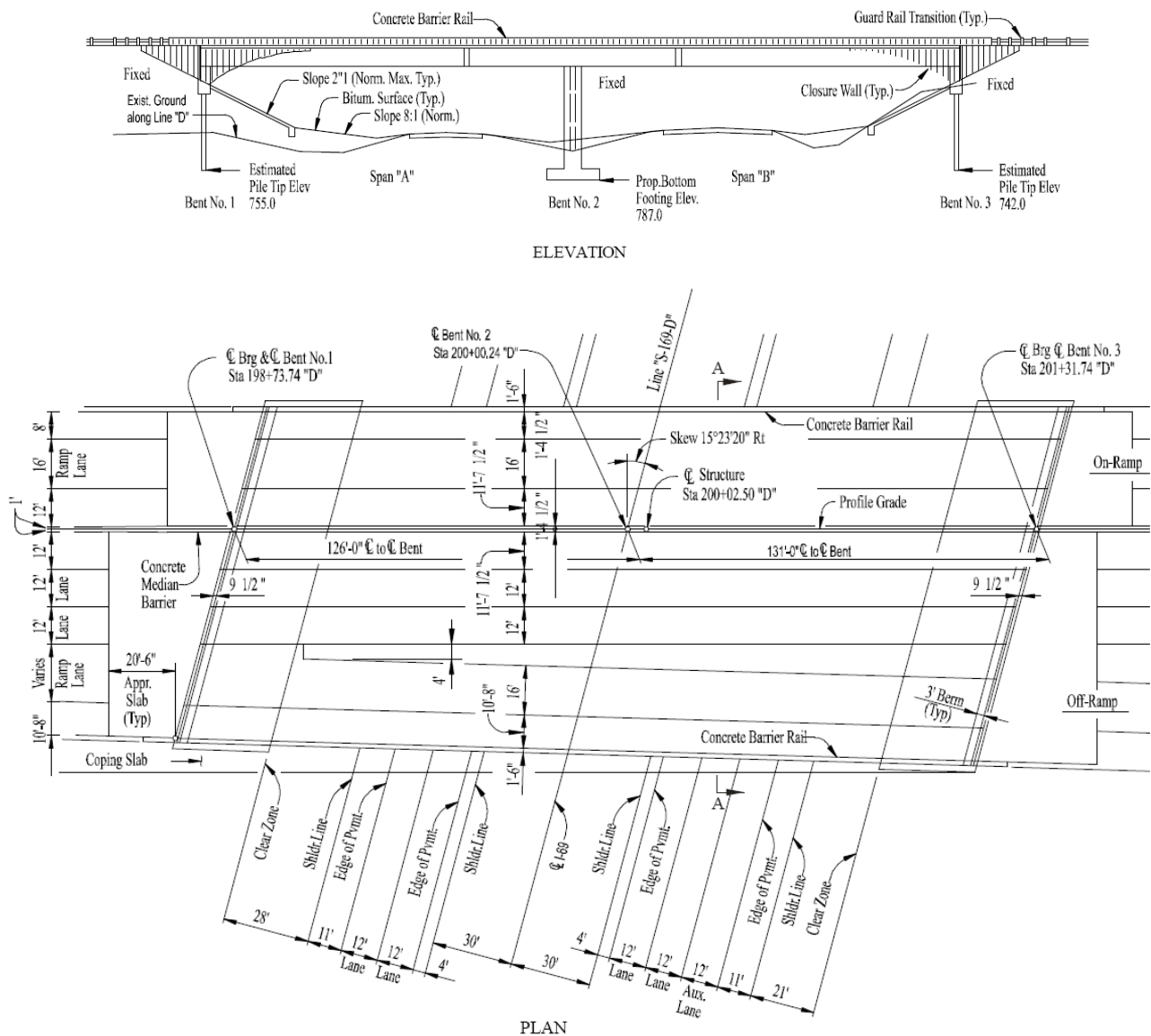


13.8.3 I-469 Bridge Over I-69, Indiana

The I-469 overpass bridge, a two-span highway structure over I-69 on the north side of Fort Wayne, Ind., is part of the final portion of the Fort Wayne Bypass completed in 1995. This is a two-span skewed structure, 258 ft long with a variable width due to an offramp taper. This section of highway includes 3.5 miles of new interstate roadway and seven new bridges. All of the bridges incorporate precast, prestressed, bulb-tee I-girders with no joints in the bridge decks. It is the first bridge to use a spliced girder technique with posttensioning anchors anchored to the abutment backwalls.

The bridge over I-69 is an unsymmetrical twin structure with one 16-ft off-ramp lane, one 16-ft on-ramp lane, and two 12-ft westbound through lanes. The bridge has two spans of 126.5 and 131.5 ft and varies in width from 106 to 116.25 ft due to the off-ramp taper across the structure. The plan and elevation of the overpass are shown in **Figure 13.8.3-1**.

Figure 13.8.3-1
Plan and Elevation

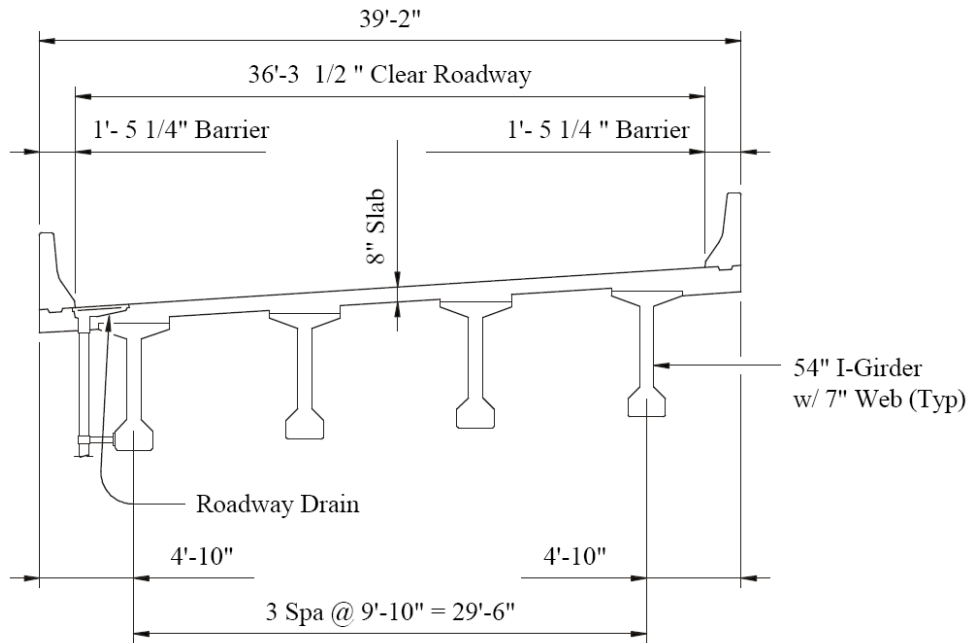


Precast, prestressed, post-tensioned concrete bulb-tee I-girders are used throughout the superstructure to support the cast-in-place reinforced concrete deck. The I-girders are 54 in. deep and incorporate a 4-ft top flange. The bridge cross sections are shown in **Figure 13.8.3-2**.

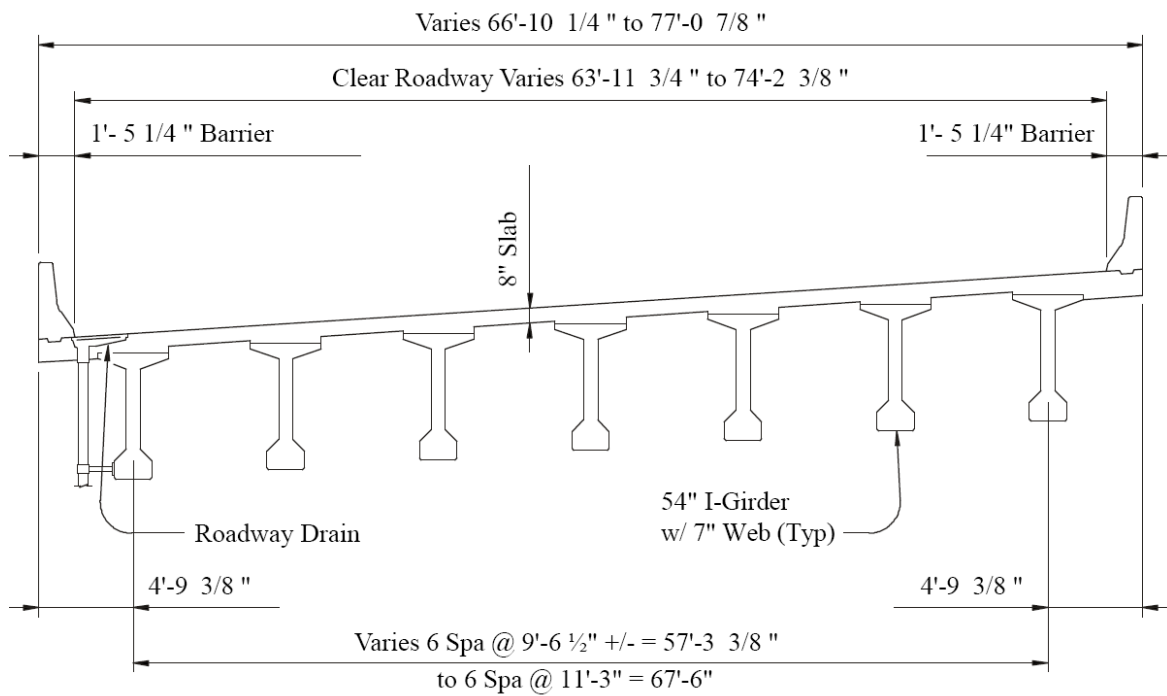
INTEGRAL BRIDGES

13.8.3 I-469 Bridge Over I-69, Indiana

Figure 13.8.3-2
Cross Sections



PARTIAL SECTION A-A



PARTIAL SECTION A-A

INTEGRAL BRIDGES

13.8.3 I-469 Bridge Over I-69, Indiana

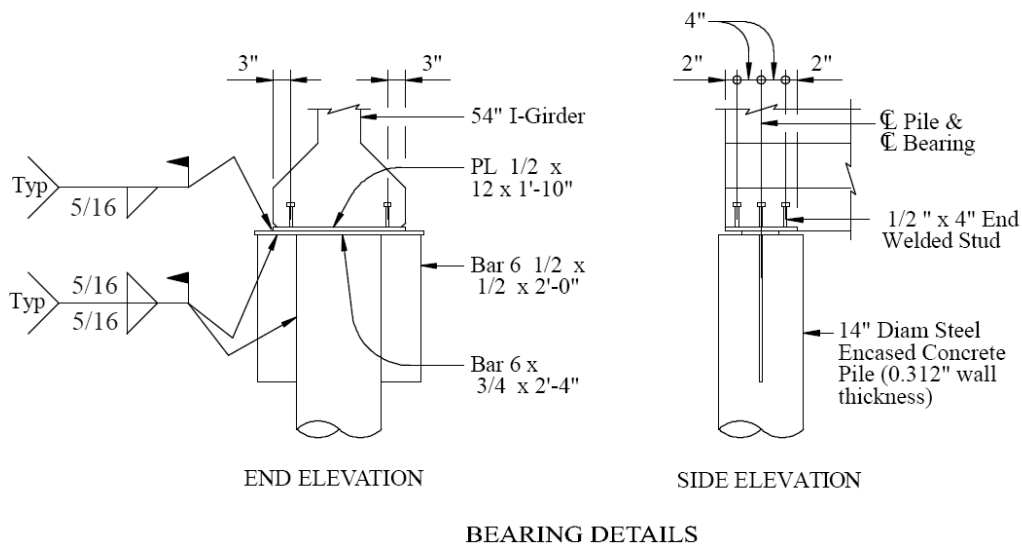
This structure incorporates many firsts for the state of Indiana. They are as follows:

1. First overpass bridge to use fully integral construction for both the piers end bents.
2. First integral end bents to use expanded polystyrene to pin the top of the piles to reduce the moments in the pile.
3. First overpass structure to use post-tensioned segmental, bulb-tee I-girder construction with all of the post-tensioned anchors located behind the integral end bents, outside the limits of the I-girder.
4. First overpass bridge to use a new concrete mix using high-range water reducer, lower water-cement ratio of 0.40, and an extended curing time for the deck utilizing soaker hoses.
5. First bridge to incorporate a concrete barrier rail base isolation system to reduce or eliminate cracking in the railing.
6. First concrete I-beam bridge to incorporate a slab between the bottom flanges of the beams in order to eliminate the need for increasing the depths of the beams over the interior supports.

The decision to pin the tops of the piles at the end bents was due to the shortening that would result from the longitudinal post-tensioning of the structure and the fact that the end bent concrete had to be cast to the top of the beam prior to pouring of concrete in the deck. It was calculated that the moments in the pile could be reduced by approximately 50 percent due to the pinned connection. One and one half in. of spray-on expanded polystyrene was placed around the pile within the limits of the concrete. **Figure 13.8.3-3** shows the end bent section and beam bearing details. Photographs of the bridge are shown in **Figures 13.8.3-4** through **13.8.3-8**.

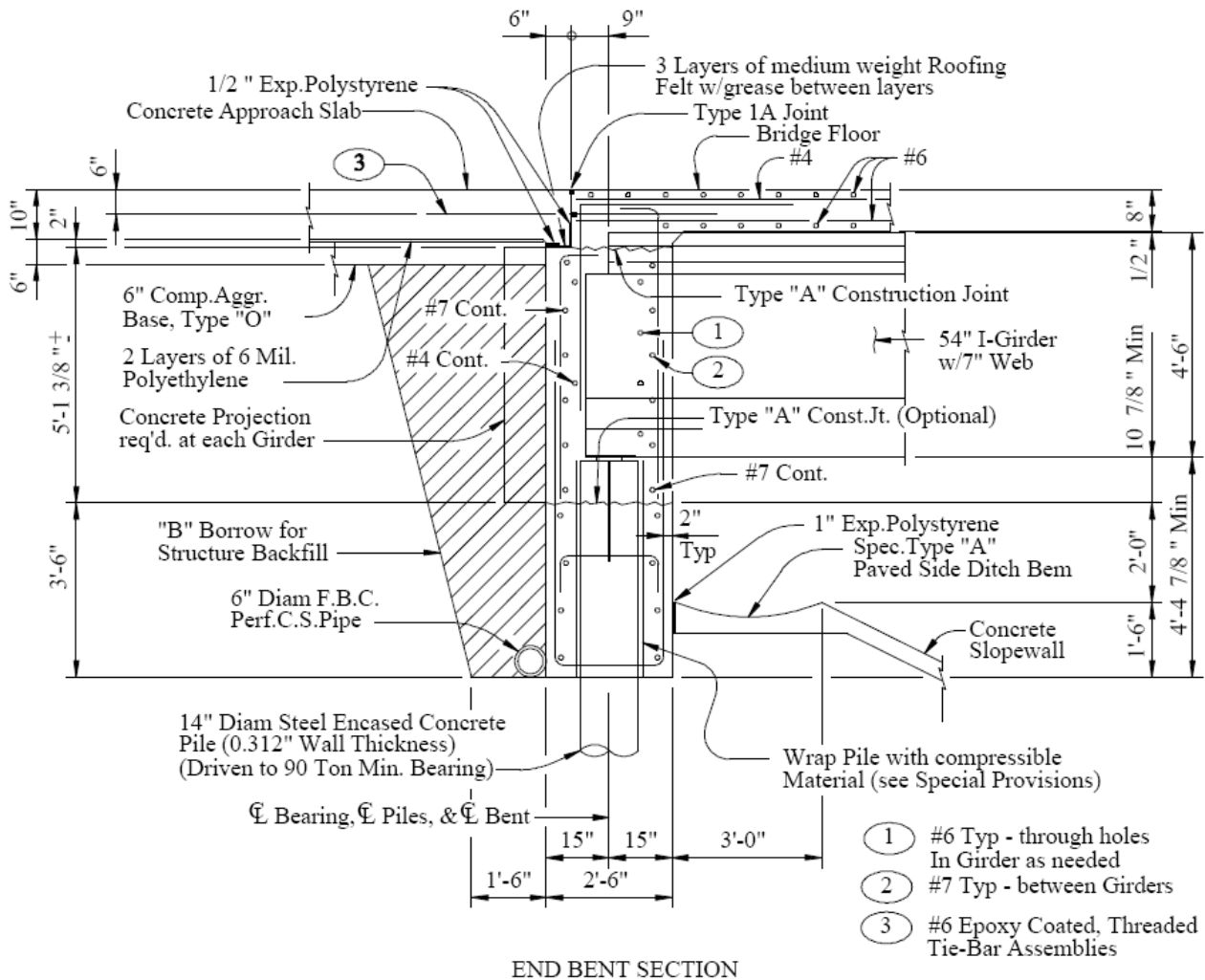
The cost of the bridge was approximately \$1,900,000 or \$65/ft² of deck surface.

Figure 13.8.3-3
Bearing and Abutment Details



INTEGRAL BRIDGES

13.8.3 I-469 Bridge Over I-69, Indiana



END BENT SECTION

INTEGRAL BRIDGES

13.8.3 I-469 Bridge Over I-69, Indiana

*Figure 13.8.3-4
The Completed Structure*



*Figure 13.8.3-5
View of the Underside of the Bridge*



Figure 13.3.8-6
Abutment



Figure 13.8.3-7
Pier Details



Figure 13.3.8-8
Girder Ends



INTEGRAL BRIDGES

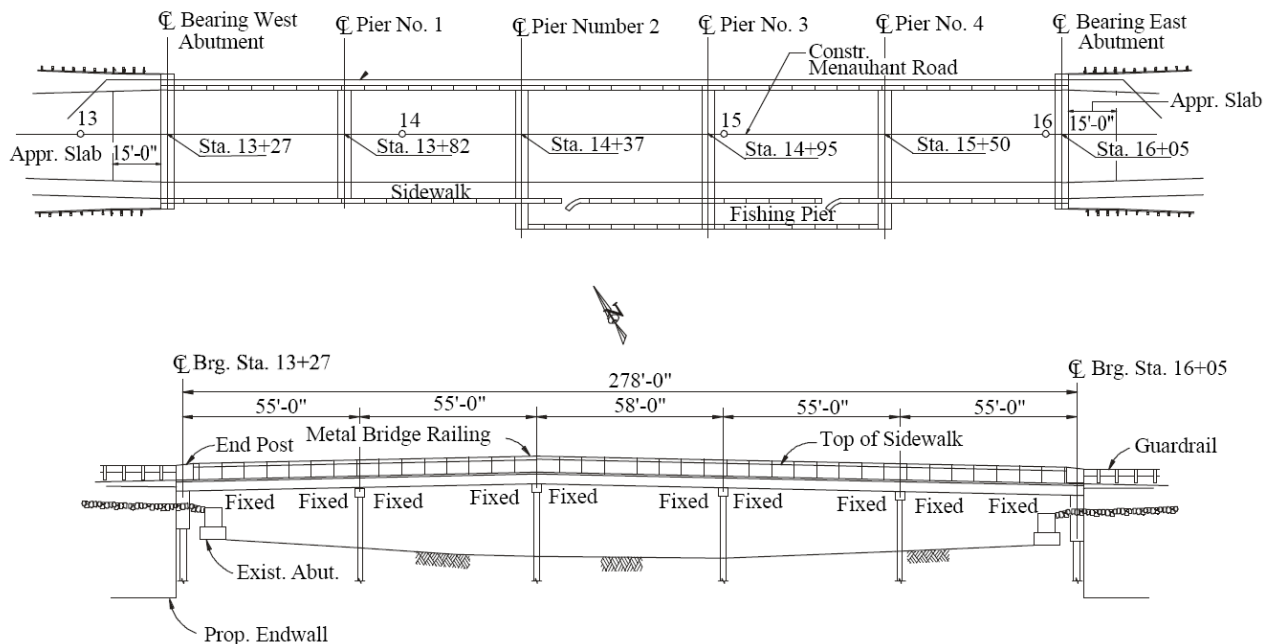
13.8.4 Menauhant Road Bridge Massachusetts

13.8.4 Menauhant Road Bridge, Massachusetts

The Menauhant Road Bridge, a five-span highway structure, provides a crossing over Green Pond. Green Pond is a tidal inlet located on the south side of Cape Cod in the Town of Falmouth and is highly used by the local boating community. The bridge replaced a 10-span, 250-ft long concrete structure constructed in 1926 that was structurally deficient. The bridge was widened to accommodate two 11-ft travel lanes, two 4-ft shoulders and a 5-ft sidewalk on one side. An 8-ft wide fishing pier is located off the sidewalk on two center spans of the new bridge. The new bridge, completed in 1995, is 278 ft long, includes precast deck beams and was designed for seismic forces.

The horizontal alignment of the new bridge, the same as the existing bridge, is located on a tangent. Since the vertical clearance of the existing bridge did not allow passageway of many boats under the structure during high tide, the vertical alignment of the new bridge was raised approximately 2 ft. The new bridge piers and abutments were located to clear the existing pier and abutment foundations, thus avoiding substantial removal costs. The resulting layout of the structure consists of four 55-ft spans and one 58-ft center span. The plan and profile of the Menauhant Road Bridge are shown in **Figure 13.8.4-1**.

Figure 13.8.4-1
Plan and Profile of
Menauhant Road Bridge



Prestressed concrete deck beams are used throughout the superstructure to support the cast-in-place reinforced concrete deck. The composite beam and deck design was assumed continuous for the entire length of the structure to support live loads and superimposed dead loads. A combination of 3-ft and 4-ft wide deck beams are utilized throughout the superstructure and are 1 ft - 9 in. deep. All deck beams were designed in accordance with the standards of the Massachusetts Highway Department. The bridge cross sections are shown in **Figures 13.8.4-2** and **13.8.4-3**.

Environmental requirements limited the option for intermediate piers to the use of concrete pile bents. Both abutments were designed and constructed integrally with the superstructure, which provided an economical means of resisting the resulting seismic loads and proved to be one of the only practical methods. The Massachusetts Highway Department established a base rock acceleration of 0.10 g, and the depth to rock-like material was determined to be over 150 ft. Soft alluvial soils with organics limited the lateral capacity of the piles to values much lower than seismic demand. The abutments became the only economical means to resist the sizable longitudinal forces. (See **Figure 13.8.4-4** for a typical abutment section.)

INTEGRAL BRIDGES

13.8.4 Menauhant Road Bridge Massachusetts

Figure 13.8.4-2
Bridge Section with Fishing Pier

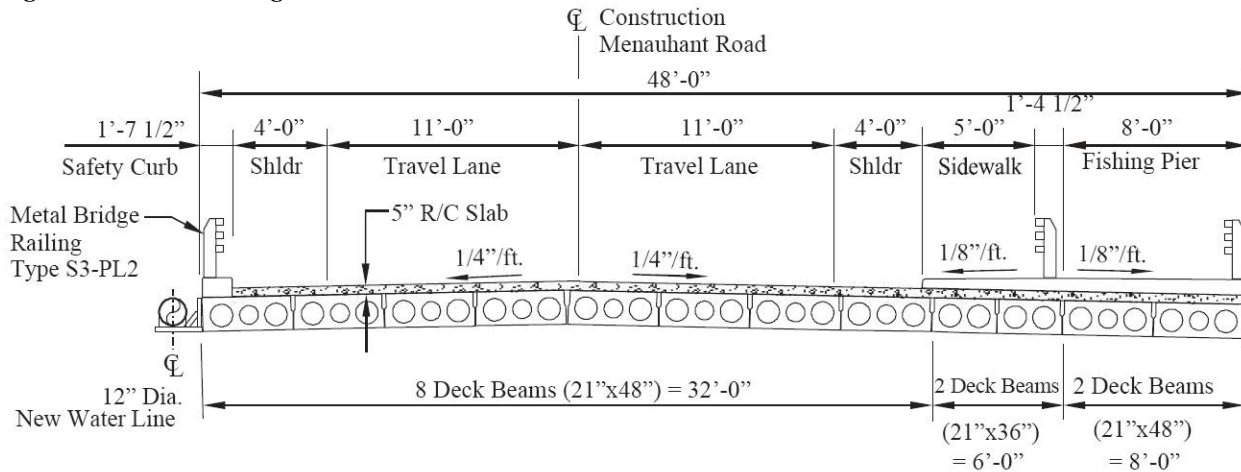
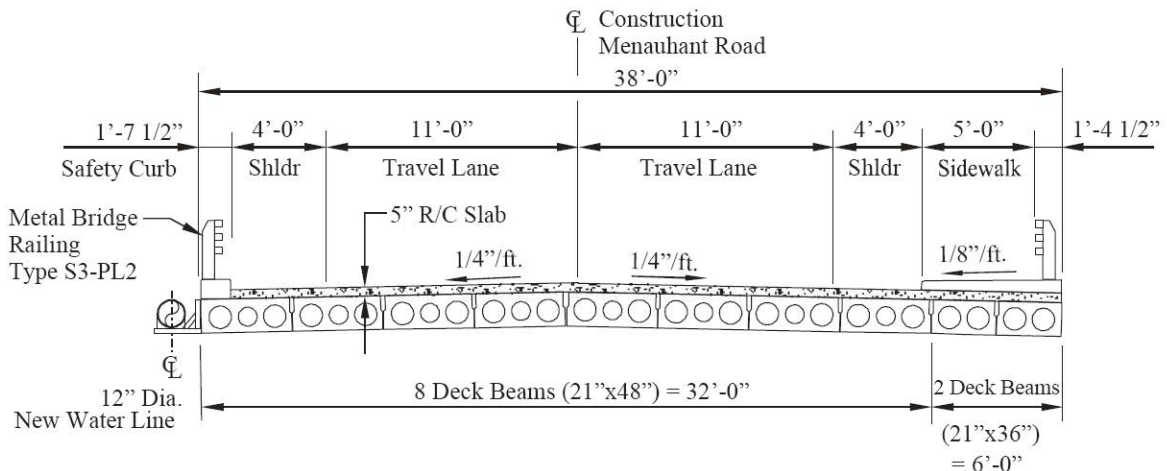


Figure 13.8.4-3
Bridge Section without Fishing Pier



Engaging the passive resistance of the abutment backfill provided the required additional seismic resistance. However, computing the concurrent contribution of the abutment and the interior bent piles and confirming that no piles were overloaded required an involved process. Passive soil pressure requires measurable movements in order to be mobilized. Furthermore, the load-deflection relationship is nonlinear due to the elasto-plastic response of the soil mass. Complicating the fact was that the soil structure interaction of the laterally loaded piles follows a similar nonlinear, but uncoupled model.

Using an integrative procedure, an assumed translational deflection of 1 in. was used to estimate the spring constants for modeling the abutment backfill and lateral soil support of the piles. The lateral pile program LPILE was used to compute the load deflection response of both the abutment and interior bents. The LPILE analysis is based on modeling the soil layers with a set of P-Y curves which are a function of soil type and strength. To obtain the initial values, a deflection of 1 in. was induced at the pile heads.

The load-deflection results for the piles, as well as the simulated backfill response, were entered as spring constants in the bridge seismic analysis program SEISAB. After performing the dynamic analysis, the computed deflections were compared to the assumed values. The elastic dynamic analysis predicted longitudinal deflections of 1.16 in. New spring constants were computed for the soil backfill using an assumed deflection of 1.2 in. and input into the SEISAB model. The deflections computed during this iteration matched the assumed values within 3%, so further iterations were not necessary.

INTEGRAL BRIDGES

13.8.4 Menauhant Road Bridge Massachusetts

*Figure 13.8.4-5
Aerial View of Structure*



*Figure 13.8.4-6
Box Beams Being Set into Place*



INTEGRAL BRIDGES

13.8.5 Deer Creek Industrial Park Access Bridge, West Virginia

13.8.5 Deer Creek Industrial Park Access Bridge, West Virginia

Since the late 1930s, the West Virginia Department of Transportation has designed structures that are continuous over the piers. In 1992, they adopted a policy to eliminate joints at the abutments. The new policy was developed to eliminate deck expansion joints wherever practical. Since then, 90 integral and semi-integral bridges have been designed in West Virginia. Approximately half of these designs included prestressed concrete superstructures.

The Deer Creek Access Bridge, located in Barboursville, W. Va. was built in 1996. It provides highway access to an area of land that was once landlocked between the river and the railroad. The land is currently being developed into an industrial park.

The bridge is a three-span continuous structure, totaling 301 ft-9 in. length that spans the Guyandotte River (**Figure 13.8.5-1**). The substructure consists of two integral abutments and two reinforced concrete hammerhead piers. Each abutment is founded on a single row of steel H-piles. One of the piers is hinged to the superstructure and is founded on spread footing whereas the second pier has expansion bearings on top and rests on piles. The end bents are supported on single line of piles. The two-lane superstructure is made up of five AASHTO Type IV prestressed concrete beams, a reinforced concrete deck, and parapets (**Figure 13.8.5-2**). The bridge length/opening was dictated by the required waterway opening to prevent additional backwater. The bridge was designed for an HS25 live load, using load factor design and in accordance with the current AASHTO specifications.

Figure 13.8.5-1
Bridge Elevation

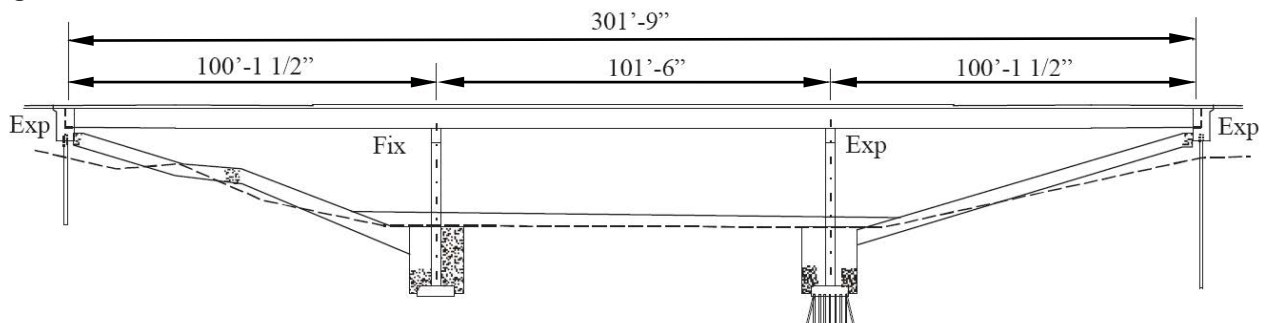
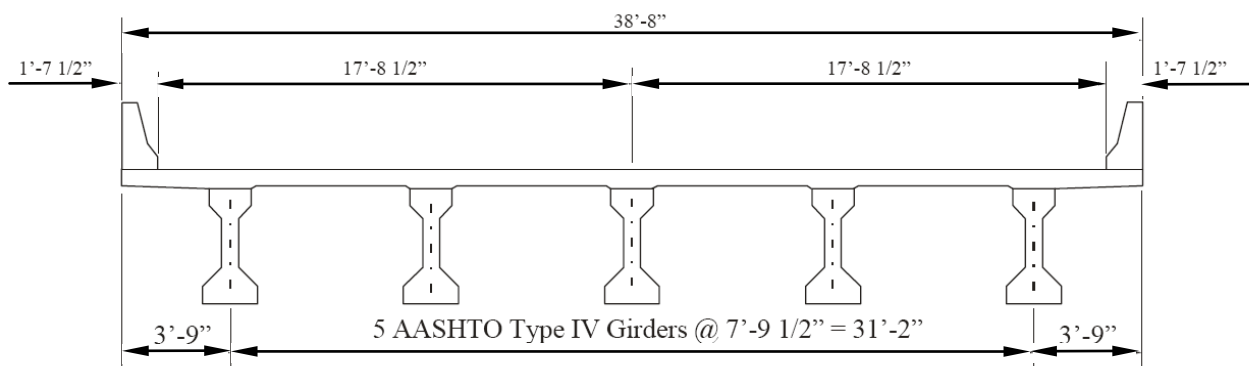


Figure 13.8.5-2
Cross Section



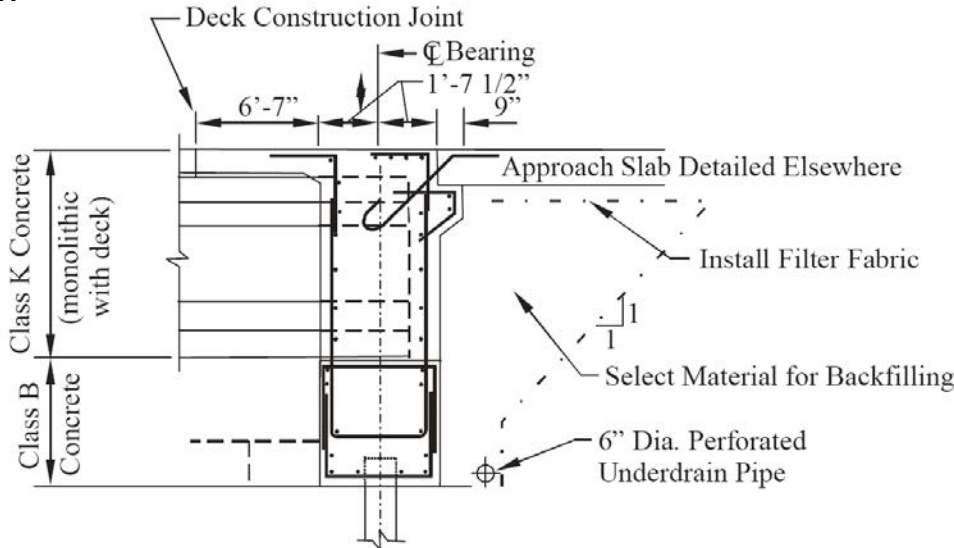
The Deer Creek Access bridge was designed assuming roller connections at the abutments and a pinned connection at one of the piers. Basically, it was designed no differently from a bridge with joints at the abutments and continuous over the piers. The abutments were designed by simply dividing the vertical dead and live loads by the allowable bearing pile capacity. The piles are oriented to allow weak axis bending (**Figure 13.8.5-3**). By paying proper attention to detailing, the majority of concerns regarding pile bending and the effects of passive earth pressure were eliminated.

INTEGRAL BRIDGES

13.8.5 Deer Creek Industrial Park Access Bridge, West Virginia

The jointless bridge policy gives a maximum movement range (2") allowed at the abutments, rather than a maximum bridge length. Since concrete superstructures can be designed for a smaller temperature range than steel (approximately 50 percent that of steel-due) to the way that concrete absorbs heat in comparison to steel, it is possible to use concrete beams with integral abutments for bridges that are twice as long as those allowed for jointless steel bridges. This structure was on the borderline for using a steel integral abutment design.

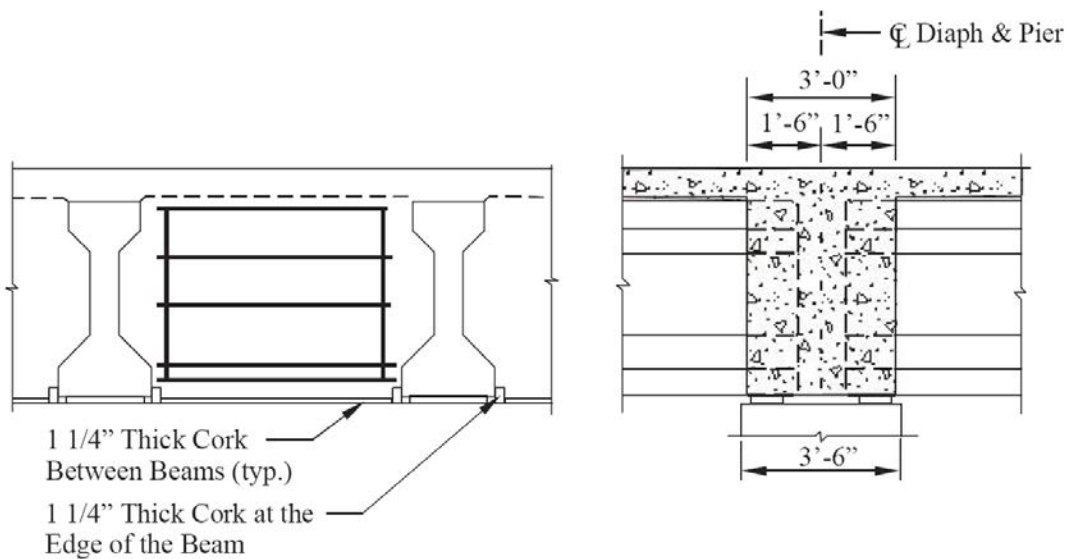
Figure 13.8.5-3
Typical Abutment Section



The total cost of this project was \$1,250,000, of which \$786,000 was for the bridge beams. This resulted in a cost of approximately \$67/ft², which is a very good price for bridges constructed in West Virginia. Both steel and concrete superstructures were considered. Steel was ruled out due to cost savings. It was estimated that using concrete beams resulted in a cost savings of approximately 10 percent.

Photographs of the bridge are shown in **Figures 13.8.5-5 through 13.8.5-9**.

Figure 13.8.5-4
Pier Diaphragm Details



INTEGRAL BRIDGES

13.8.5 Deer Creek Industrial Park Access Bridge, West Virginia

*Figure 13.8.5-5
Elevation View: Three-Span Continuous for Live Load and Integral Abutments*



*Figure 13.8.5-6
Plan View: Deer Creek Industrial Park Access Bridge.*



INTEGRAL BRIDGES

13.8.5 Deer Creek Industrial Park Access Bridge, West Virginia

*Figure 13.8.5-7
Continuous for Live Load at Piers*



*Figure 13.8.5-8
Erection of AASHTO Type IV Girders*



*Figure 13.8.5-9
Erection of Girders*



INTEGRAL BRIDGES

13.8.6 Tennessee State Route 50 over Happy Hollow Creek, Tennessee

13.8.6 Tennessee State Route 50 over Happy Hollow Creek, Tennessee

The bridge carrying State Route 50 over Happy Hollow Creek is composed of 9 spans of precast, prestressed concrete bulb-tee beams designed as simple spans for non-composite dead loads and as continuous spans for live loads and subsequent composite dead loads (**Figure 13.8.6-1**). The 46-ft, wide, 8 ¼-in thick composite concrete slab conforms to a 4 degree, 45-minute curve for approximately 976 ft of its length while the remaining 199 ft conforms to a spiral curve. Span lengths along the centerline of the roadway vary from 129 ft to 140 ft. The bridge was built in 1997, the layout is shown in **Figure 13.8.6-2**.

Figure 13.8.6-1

Aerial View of S.R. 50 Over Happy Hollow Creek



Supporting the six-beam cross section, shown in **Figure 13.8.6-3(a)**, are two-column bents varying in height from approximately 51 ft to 91 ft (**Figure 13.8.6-4**). These bents vary in skew such that they are arranged to allow all beams in all spans, but one, be equal length. Since the beams are chorded, the slab overhang on each side of the bridge varies from 3-ft 6-in to 5-ft 6-in along the span length.

To accomplish continuity, a common diaphragm, shown in **Figures 13.8.6-3(b)** and **13.8.6-3(c)** join both the ends of girders in adjacent spans and the cast-in-place slab. Since the dead load and slab deflections of the 72-in bulb-tees are relatively large and their depths significant, Tennessee DOT requires one of several options be used by the contractor. He may choose to pour the entire deck in one operation, concurrently pouring the diaphragms. If the deck cannot be poured in one operation, then no construction joint may be located closer than 10 ft nor further than 15 ft from an interior support and no diaphragm at an interior support may be poured unless the slab in the positive movement area of the adjacent spans have been poured. This prevents cracking of the common diaphragms at the supports. To steady the beams in the interim, permanent intermediate diaphragms, composed of galvanized steel angles in an x-brace configuration are placed at 1/3 points in the span and temporarily near supports. After pouring the deck, the x-braces near supports may be removed. Pouring sequences require either the end 3 to 4 ft of the slab, or all the positive movement area of the end span, to be poured concurrently with the abutment backwall and wingwalls, thus achieving a jointless deck with integral abutments.

Details of the integral abutment are shown in **Figures 13.8.6-5** and **13.8.6-6**. Due to the magnitude of thermal movements, the abutments are supported on a single row of HP10x42 steel piles for flexibility.

Tennessee DOT prefers the piles to be oriented with the strong axis in bending. Tennessee's choice of orientation is evolutionary, being a logical extension of pile orientation used in jointed abutments. However, calculations

INTEGRAL BRIDGES

13.8.6 Tennessee State Route 50 over Happy Hollow Creek, Tennessee

using the COM624P Laterally Loaded Pile Analysis Program, developed for the FHWA at the University of Texas, indicates slightly higher vertical load capacity in the deflected piles than can be achieved with piles oriented to bend about the weak axis.

The "analysis" procedures used for a jointless bridge depends on the size and complexity of the bridge being considered. In Tennessee, with 30 years of experience in integral construction, little analysis is performed on routine bridges. For concrete superstructure construction, bridges up to 800 ft in length require no analysis provided that conditions are such that the total movement at an abutment does not exceed 2 in, that the abutments are stub-type and founded on one row of piles for flexibility. If the supporting bents are not integrally connected to the superstructure, then columns are analyzed as cantilever beams to identify the force required to deflect the free end the required distance to accommodate thermal effects. A free end condition at the top is assumed in the longitudinal direction. In calculating this moment, experience has shown that substituting the long term modulus of elasticity of 1,000,000 psi gives satisfactory results and adequately models the actual cracked column behavior without the need of rigorous computations. Where the resulting thermal moments, combined with other appropriate longitudinal moments, become too large to conveniently provide for reinforcement, expansion devices under the superstructure can be added to reduce the applied moments. However, in the latter case, the designer must verify that the force required to cause the expansion bearings to move does not exceed the force required to cause the bent to deflect. Should the force to move the bent be less, then the expansion bearing cannot function and alternate arrangements to accommodate thermal movements in the bridge must be made.

Since the State Route 50 bridge over Happy Hollow Creek exceeded Tennessee's standards of practice, special considerations had to be made. First, it was desirable to eliminate expansion joints and expansion bearings, not only because of their high initial and maintenance costs, but because of the skew of the substructures and curvature in alignment. It is not an easy matter to predict the path of movement in curved structures: Is it along the radial axis of the deck; the chord line of the end span girders; or along a chord struck from abutment to abutment? What affect do column stiffnesses and skew play in influencing the path of expansion? The wrong choice in orientation of the expansion joint and bearings can lead to their destruction or structural damage to the beams and abutments.

In order to arrive at the decision not to use joints at the abutments in the bridge, the designer considered two options that appear to be the boundaries for the bridge's behavior due to thermal effects. First, the bridge could be considered to act as a curved bar, fixed at one end, at an abutment. **Figure 13.8.6-7** represents this model.

If the radius of curvature of the bar is large, compared to its cross-sectional dimensions, ordinary beam deflection formulas may be used to calculate the lateral deflection of the curved bar under the influence of a concentrated force, P , acting at the free end. If the free end is considered to be at a distance equal to the bridge length and the lateral deflection is identified as equal to the total thermal expansive movement at the free end, then the concentrated force, P , resisting the deflection can be quantified. This force can then be visualized as the reaction force needed to be exerted by the abutment to cause the bridge to bow outward should the abutment remain stationary.

Since the designer has no control over the temperature at which the completed structure will be made fully integral at the abutments, it was presumed that the required lateral deflection must be equal to the maximum movement expected at the abutment, in this case 2.97 in. From the geometry of the structure, the deflection relationship is derived as follows:

$$\Delta = \int_0^L \frac{-R(1 - \cos \theta)[-PR(1 - \cos \theta)]Rd\theta}{EI}$$

where

$L =$ Angle of the arc subtended in radians (or bridge length)

$L = \frac{\text{Bridge Length}}{\text{Radius}} = \frac{1,175.19}{1,206.23} = 0.9742 \text{ Rads}$

$E =$ Modulus of elasticity of the concrete deck = 3,834 ksi

INTEGRAL BRIDGES

13.8.6 Tennessee State Route 50 over Happy Hollow Creek, Tennessee

$I =$ Transverse Inertia of the Superstructure = 115,600,000 in⁴

$$\Delta = 0.03918 \frac{PR^3}{EI}$$

Solving for P yields the following:

$$P = \frac{EI\Delta}{0.03918R^3}$$

If Δ is 2.967 in., the force required to cause or restrain this displacement is:

$$P = \frac{2.967(3,864,000)(115,600,000)}{0.03918(1,206.23)^3(12)^3} = 11 \text{ kips}$$

This force is much less than the force required to overcome the passive pressure behind the abutment, 2,606 kips. Therefore, the bridge will bow laterally under thermal expansion and contraction rather than mobilize the abutments. This simplified solution ignores the stiffness of the bents and is far from an exact analysis. However, the forces required to deflect the tall columns of this structure are small and the large difference between the force to deflect the structure vs. the force to move the abutment makes further refinement unnecessary.

The other boundary condition is to consider the bridge as being straight. In this case, each abutment would be required to move a total amount of 2.97 in. Tests conducted recently by the University of Tennessee for the department indicate that HP10x42 piles with an embedment of 12 in. into the abutment beam, as shown in **Figure 13.8.6-5**, can sustain this amount of movement repeatedly without detriment to the serviceability of either the piles or abutment beam.

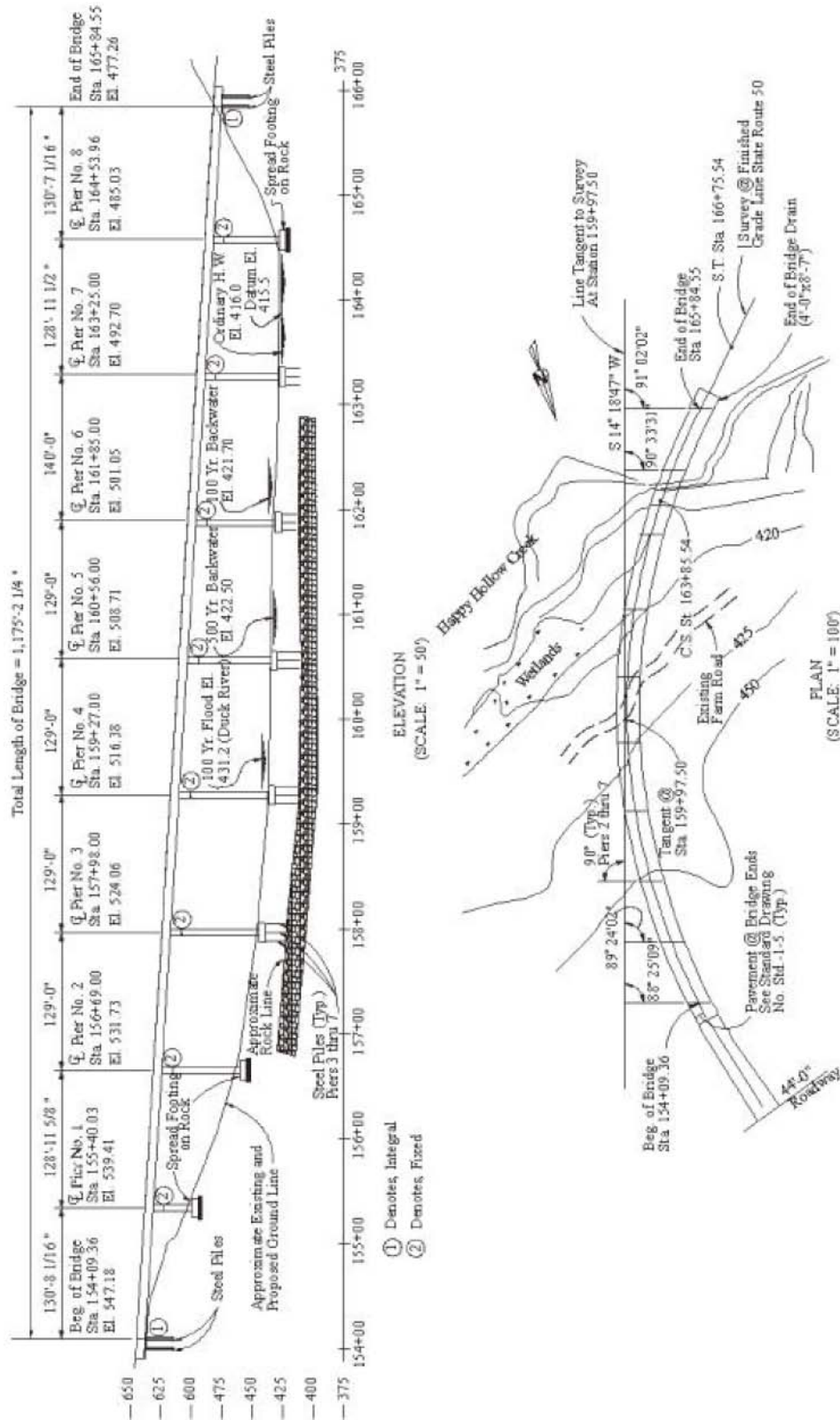
With these boundary conditions identified, the department decided to construct the State Route 50 bridge as jointless with integral abutments.

To account for the possibility of movements at the abutments, approach pavements equipped with silicone expansion joints adjacent to the asphalt paving of the roadway were installed. The details of the approach pavements, standard of Tennessee's jointless bridges, are shown in **Figures 13.8.6-8** and **13.8.6-9**.

INTEGRAL BRIDGES

13.8.6 Tennessee State Route 50 over Happy Hollow Creek, Tennessee

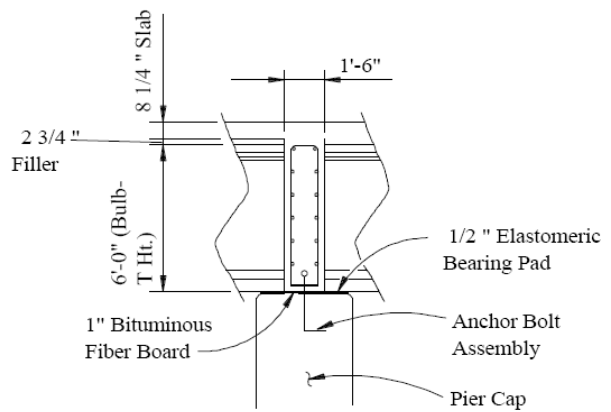
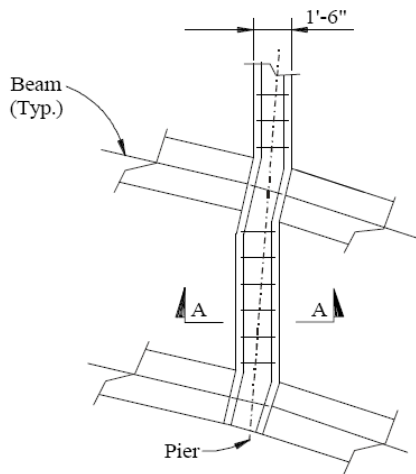
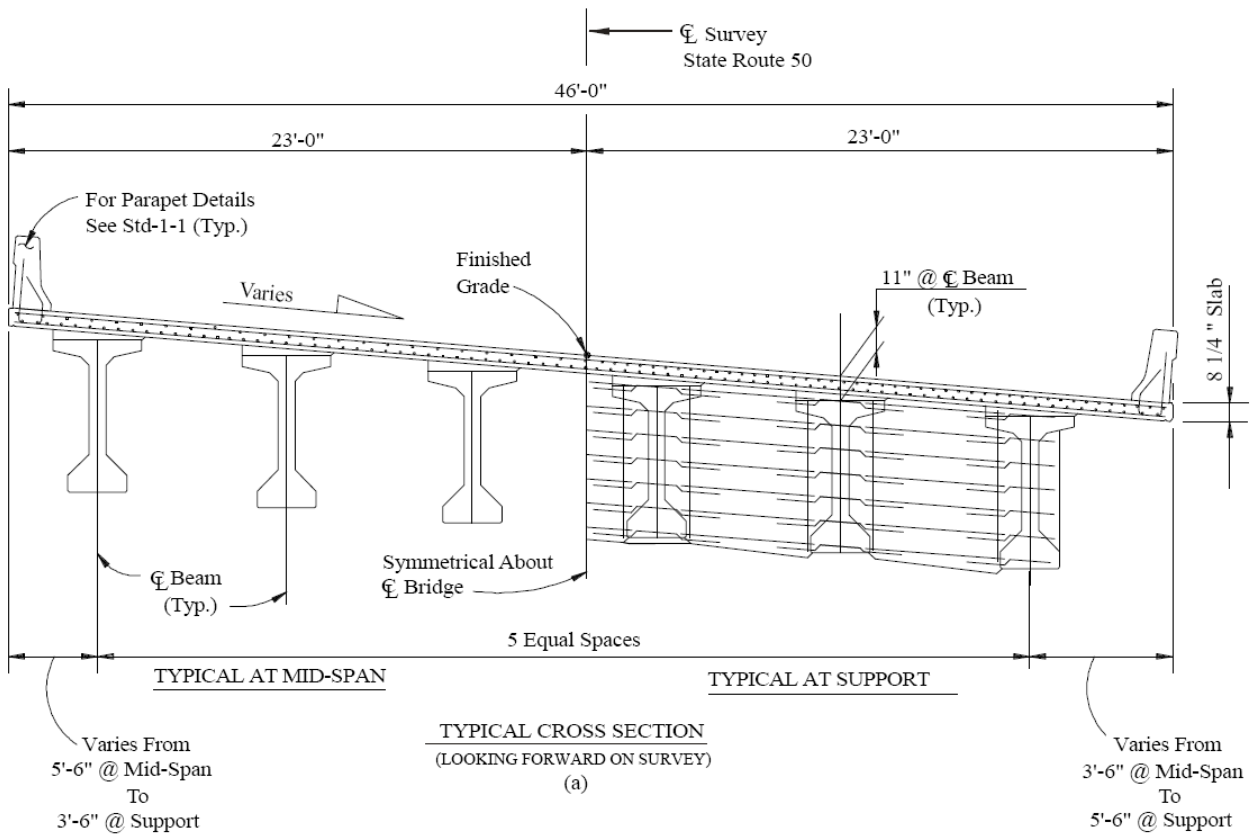
Figure 13.8.6-2
Plan and Elevation



INTEGRAL BRIDGES

13.8.6 Tennessee State Route 50 over Happy Hollow Creek, Tennessee

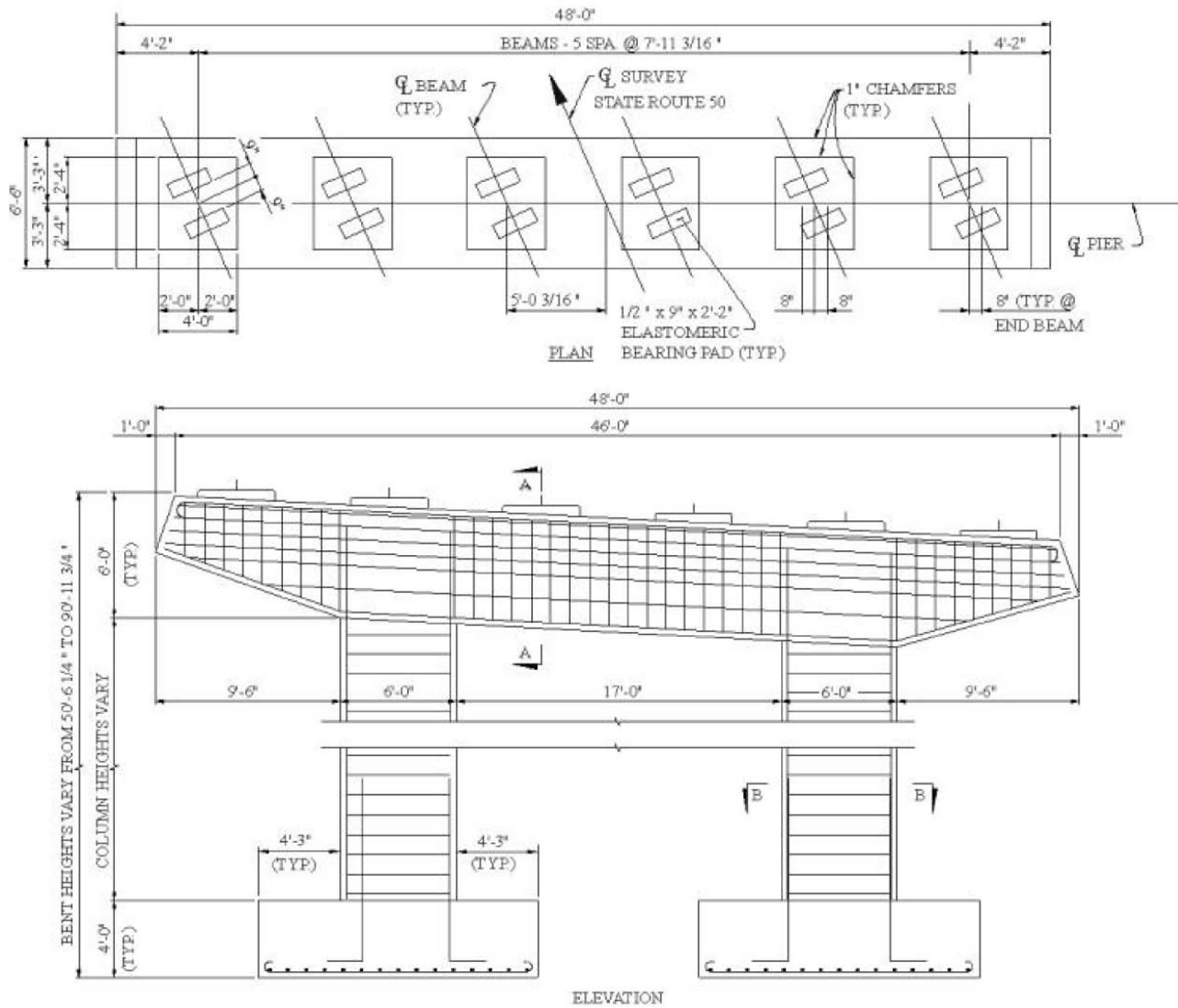
Figure 13.8.6-3
Cross-Section and Details



INTEGRAL BRIDGES

13.8.6 Tennessee State Route 50 over Happy Hollow Creek, Tennessee

Figure 13.8.6-4
Pier Plan and Elevation



INTEGRAL BRIDGES

13.8.6 Tennessee State Route 50 over Happy Hollow Creek, Tennessee

Figure 13.8.6-6
Abutment Details

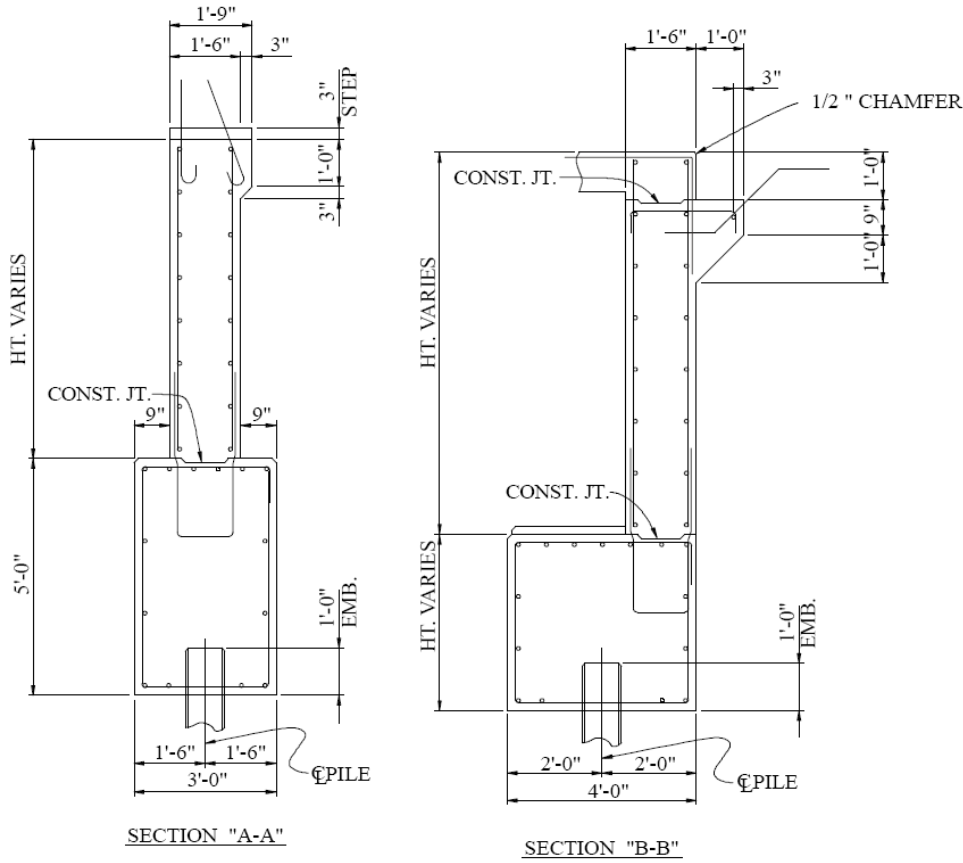
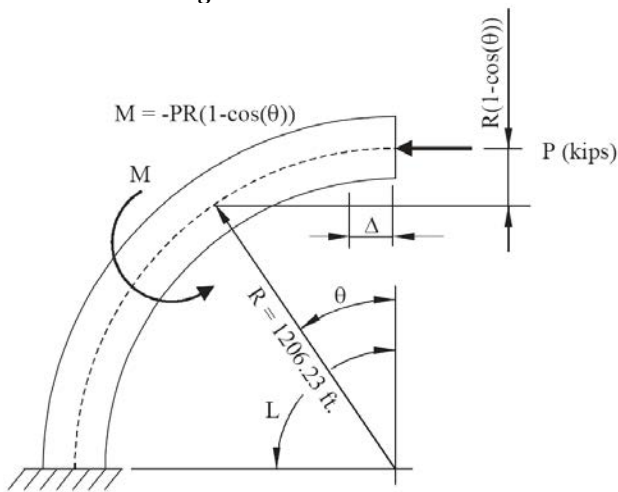


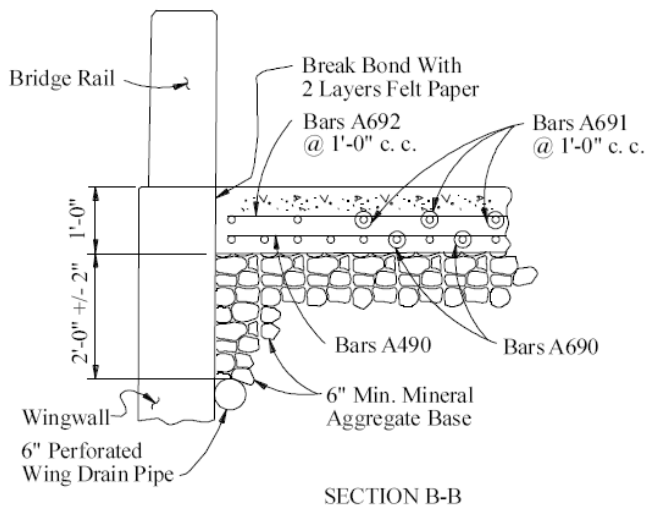
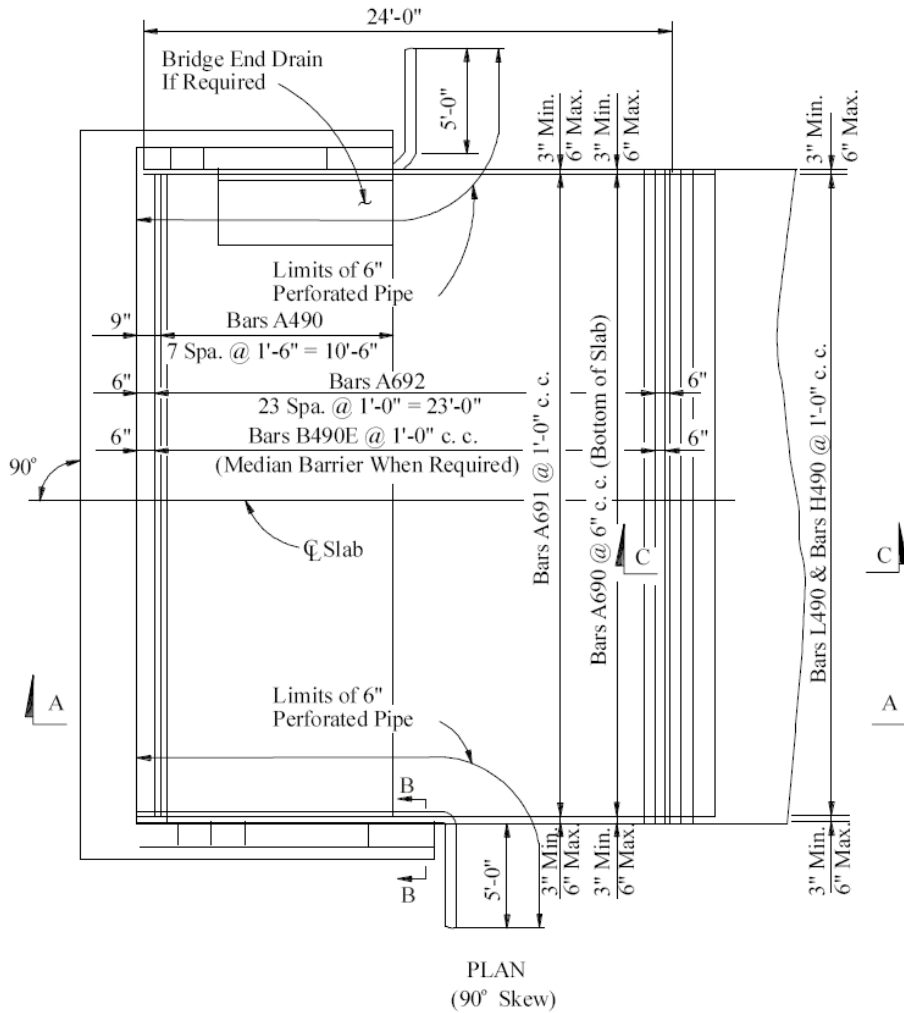
Figure 13.8.6-7
Structural Modeling



INTEGRAL BRIDGES

13.8.6 Tennessee State Route 50 over Happy Hollow Creek, Tennessee

Figure 13.8.6-8
Slab Details

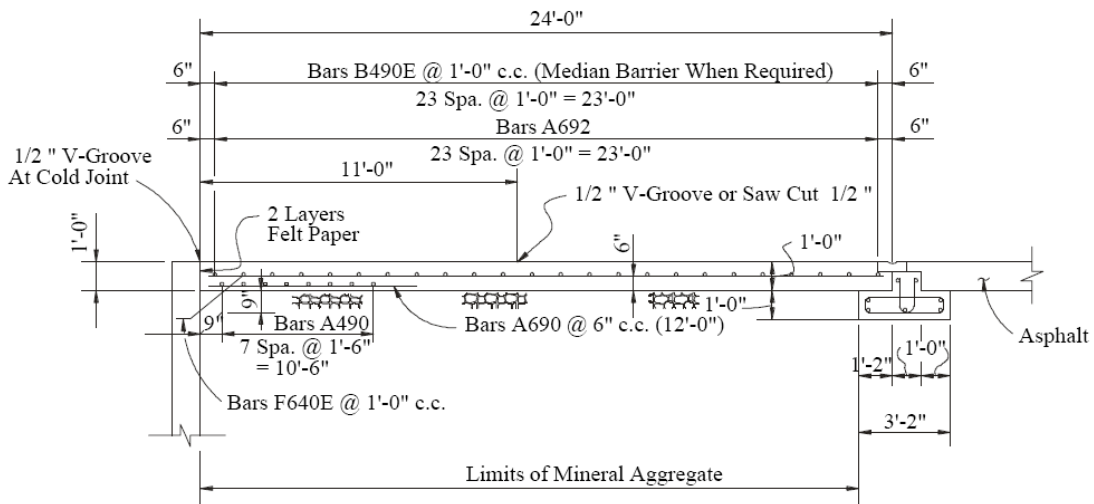


NOTE: Slab to be Poured Directly on Mineral Aggregate Base Stone.

INTEGRAL BRIDGES

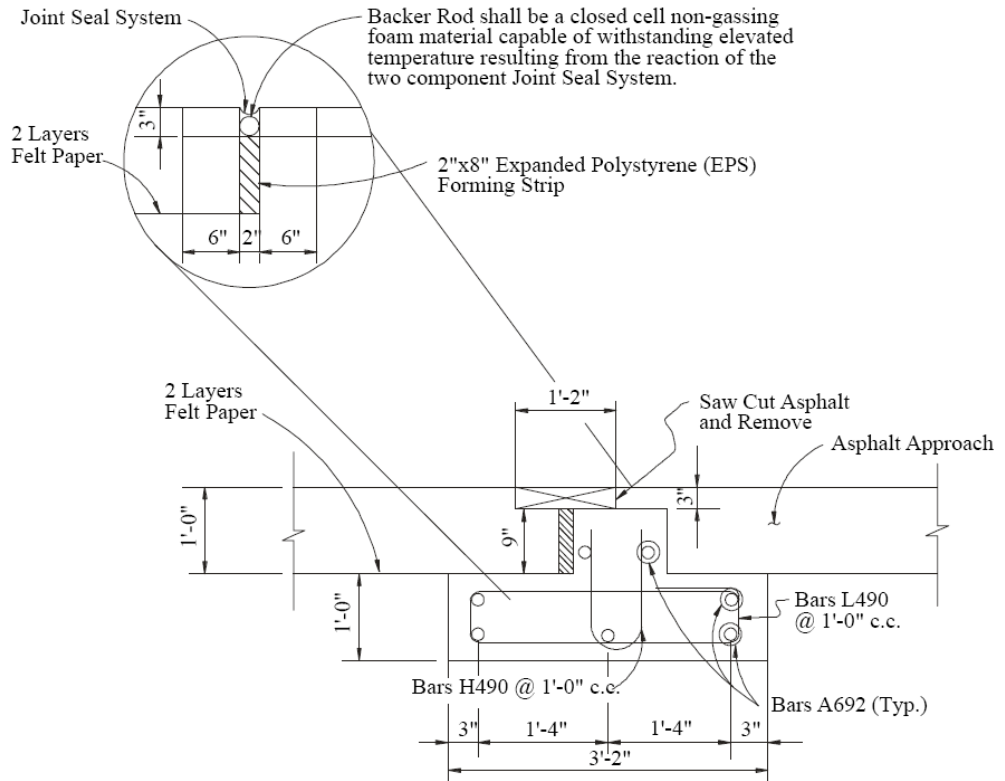
13.8.6 Tennessee State Route 50 over Happy Hollow Creek, Tennessee

Figure 13.8.6-9
Approach Slab Details



NOTE: Top of slab to conform to roadway slope and drain.

* NOTE: When Bridge End Drains are required, any Reinforcing Steel interfering with Bridge End Drain shall be cut in field.



SECTION C - C

13.9. CONCLUSIONS

This report has presented the state-of-the-art on precast, prestressed concrete integral bridges. Historically, conventional bridges with bearings and expansion joints have developed severe maintenance problems due to corrosive environments and excessive use of deicing salts in the northern parts of the United States and in Canada. Although many bearing types used have performed well during their 10-20 year service life, eventually replacement is required at considerable cost. The presence of bearings and expansion joints in a superstructure results in increased cost for inspection, maintenance and replacement. In order to avoid or to decrease these costs, integral bridges are a welcome addition to the bridge market. By eliminating the expansion joints and bearings in shorter bridges, two of the main problem elements on bridges have been removed.

A significant number of precast, prestressed concrete integral bridges have been designed, built and are performing well. However, as the responses to the survey have indicated, further research into the behavior of integral bridges is still needed. This report has highlighted some of the research needs.

Lessons learned have been many, but in most instances the issues have been resolved and better details have been developed.

This report has addressed many of the complex issues both in design and analysis of the overall bridge, as well as its components, and has brought to focus the different practices followed by the responding entities to the survey. But the report, intentionally, has not recommended any particular design procedure. Instead, each of the different chapters has offered only general suggestions in order to guide the designer during the design of precast/prestressed concrete integral bridges.

13.10. CITED REFERENCES

- Section 13.3** 1. Oesterle, R. G., et al, "Design of Precast Prestressed Bridge Girders Made Continuous," National Cooperative Highway Research Program Report 322, Transportation Research Board, Washington, DC, Nov. 1989
<http://pubsindex.trb.org/view/1989/m/302086> (Fee)
- Section 13.4** 1. Kamal, M.R., Benak, J.V., Tadros, M.K., and Jamshidi, M., "Prestressed Concrete Piles In Jointless Bridges," PCI Journal, March-April 1996, pp. 56-65.
http://www.pci.org/view_file.cfm?file=JL-96-MARCH-APRIL-6.pdf
- Section 13.5** 1. University of Tennessee, Civil Engineering Department, "Final Report: Thermal Movements of Continuous Concrete and Steel Structures," Tennessee Department of Transportation Research Project No. 77-272, January 1982.
<http://trid.trb.org/view.aspx?id=849668>
2. Burke, M.P. and Weintraut, S.F., "Integral Bridge Seminar for Massachusetts Department of Public Works (Lecture Notes)", June 10-11, 1991.
3. Burke, Martin P. Jr., "The Design of Integral Concrete Bridges," Concrete International, June 1993, pp. 37-42
http://concreteinternational.com/pages/featured_article.asp?FromSearch=True&srctype=ALL&date=specificdate&searchmonth=6&searchday=1&searchyear=1993&authors=Burke&ID=4218
4. Wasserman, E.P., "Jointless Bridge Decks," Engineering Journal, American Institute of Steel Construction, Inc., Vol. 24, No. 3, Third Quarter 1987, pp. 93-100.
<http://www.aisc.org/store/p-716-jointless-bridge-decks.aspx> (Fee)
5. Reese, L.C., and Wang, S.T., Documentation of the Computer Program LPILE, Version 3.0, Ensoft, Inc., Austin, TX, 1989.

6. Pennsylvania Department of Transportation, Integral and Semi-Integral Abutment Bridges, unpublished material received in response to questionnaire.
7. Manzelli, A.A., and Harik, I.E., "Prismatic and Nonprismatic Slender Columns and Bridge Piers," Journal of Structural Engineering, American Society of Civil Engineers, Vol. 119, No. 4, April 1993, pp. 1133-1149.
http://ascelibrary.org/sto/resource/1/jsendh/v119/i4/p1133_s1?isAuthorized=no
8. Precast/Prestressed Concrete Institute, PCI Design Handbook, Fourth Edition, Chicago, IL, 1992.
9. Tennessee Department of Transportation, Structural Memorandum SM045-04/06, July 1989.
10. Miller, R. A., R. Castrodale, A. Mirmiran, M. Hastak, "Connection of Simple-Span Precast Concrete Girders for Continuity", NCHRP Report 519, 2004
http://onlinepubs.trb.org/onlinepubs/nchrp/nchrp_rpt_519.pdf
11. Noppakunwijai, P., N. Jungpitakseel, Z. J. Ma, S. A. Yehia, M. K. Tadros, "Pullout Capacity of Non-Prestressed Bent Strands for Prestressed Concrete Girders", PCI Journal, Precast/Prestressed Concrete Institute, July-August 2002, pp. 90-104-
http://www.pci.org/view_file.cfm?file=JL-02-July-August-13.pdf

13.11 BIBLIOGRAPHY

1. Abdul-Ahad, R. B., "Effects of Restrained Thermal Movement in a Continuous Prestressed Concrete Bridge without Interior Expansion Joints," Ph.D. Dissertation, The University of Tennessee, Knoxville, Department of Civil Engineering, June 1981, 147 pp.
2. Abendroth, R. E., Greimann, L. F., and Ebner, P. B., "Abutment Pile Design for Jointless Bridges," Journal of Structural Engineering, American Society of Civil Engineers, Vol. 115, No. 11, Nov. 1989, pp. 2914-2929.
http://ascelibrary.org/sto/resource/1/jsendh/v115/i11/p2914_s1?isAuthorized=no (Fee)
3. ACI Committee 209, "Prediction of Creep, Shrinkage and Temperature Effects in Concrete Structures," ACI 209R-92, American Concrete Institute, Detroit, MI, 1992.
<http://www.concrete.org/BookstoreNet/ProductDetail.aspx?ItemID=20992> (Fee)
4. Anon, "Bridge Approach Design and Construction Practices," National Cooperative Highway Research Program (NCHRP) Synthesis of Highway Practice 2, 1969.
<http://pubsindex.trb.org/view/1969/m/118491>
5. Anon, "Bridge Bearings," National Cooperative Highway Research Program, Synthesis Highway Practice 41, Washington, DC, 1977, 62 pp.
<http://pubsindex.trb.org/view/1977/m/58810> (Fee)
6. Anon, "Thermal Movements of Continuous Concrete and Steel Structures -Final Report," Tennessee Department of Transportation Research Project No. 77-27-2, The University of Tennessee, Civil Engineering Department, January 1982.
7. Anon, "Thermal Expansion and Contraction," Tennessee Structures Memorandum -045, July 1989, 6 pp.
8. Anon, "Tennessee's Holton River Bridge Jointless Over 2650 ft," Bridge Report SR248.01E, Portland Cement Association, Skokie, IL, 4 pp.
9. Bishop, G. F., "Design of Bridge Approach Slabs," Proceedings, 1965 Kentucky Highway Conference, Vol. 21, No. 1, Jan. 1966, pp. 72-80.
10. Broms, B. B. and Ingleson, I., "Earth Pressure against the Abutments of a Rigid Frame Bridge," Geotechnique, Vol. 21, No. 1, 1971, pp. 15-28.
<http://www.icevirtuallibrary.com/content/article/10.1680/geot.1971.21.1.15> (Fee)
11. Burke, M. P., "Bridge Approach Pavements, Integral Bridges, and Cycle Control Joints," Burgess and Niple, Limited, Columbus, OH, Presented at Transportation Research Board's 66th Annual Meeting, Jan. 1987.

INTEGRAL BRIDGES

13.11 Bibliography

12. Burke, Martin P. Jr., "The Design of Integral Concrete Bridges," *Concrete International*, June 1993, pp. 37-42.
http://concreteinternational.com/pages/featured_article.asp?FromSearch=True&srctype=ALL&date=anytime&searchmonth=6&searchday=1&searchyear=1993&authors=Burke&ID=4218 (Fee)
13. Churchward, A. and Sokal, Y. J., "Prediction of Temperatures in Concrete Bridges," *Journal of the Structural Division, American Society of Civil Engineers*, Vol. 107, No. S+11, No. 1981, pp. 2163-2176.
<http://cedb.asce.org/cgi/WWWdisplay.cgi?10575> (Fee)
14. Coyle, H.M., et al, "Field Measurements of Lateral Earth Pressures on a Cantilever Retaining Wall," *Performance of Earth Retaining Structures and Pile Foundations, Transportation Research Record 517, Transportation Research Board, Washington, DC, 1974, pp. 16-29.*
<http://pubsindex.trb.org/view/1974/C/26659> (Fee)
15. Dagher, H. J., et al, "Analytical Investigation of Slab Bridges with Integral Wall Abutments," *Bridge and Hydrology Research, Transportation Research Record No. 1319, Transportation Research Board, Washington, DC, 1991.*
<http://pubsindex.trb.org/view/1991/C/365413> (Fee)
16. Dagher, H., et al, "Skew Slab Bridges with Integral Slab Abutments – Final Report, Vol. I: Design Guide, Vol. II: Design Curves, Vol. III: Computer Program Skewslab, Vol. IV: Analysis of Smith Bridge," *University of Maine, Department of Civil Engineering, Oct. 1991.*
17. Dilger, W. H., et al, "Temperature Stresses in Composite Box Girder Bridges," *Journal of Structural Engineering, American Society of Civil Engineers*, Vol. 109, No. 6, Jan. 1983, pp. 1460-1479.
http://ascelibrary.org/sto/resource/1/jsendh/v109/i6/p1460_s1?isAuthorized=no (Fee)
18. Elgaaly, M., et al, "Monitoring the Forks Bridge," *Research Report ST 91-1, GT 91-2, Maine Department of Transportation, December 1990, 75 pp.*
19. Fattal, S. G., et al, "Analysis of Thermal Stresses in Internally Sealed Concrete Bridge Decks, National Engineering Lab., FHWA/RD-80/085, National Bureau of Standards, Washington, DC, Apr. 1981.
20. Freyermuth, C. L., "Design of Continuous Highway Bridges with Precast, Prestressed Concrete Girders," *Journal of the Prestressed Concrete Institute*, Vol. 14, No. 1, 19, 1969, pp. 14-39.
21. GangaRao, H., Thippeswamy, H., Dickson, B., and Franco, J., "Survey and Design Of Integral Abutment Bridges," *Workshop on Integral Abutment Bridges, November 13-15, 1996, Pittsburgh, PA.*
22. Gastal, F. P., "Instantaneous and Time-Dependent Response and Strength of Jointless Bridge Beams," *North Carolina State University at Raleigh, 1987, 289 pp.*
23. Girton, D. D., et al, "Validation of Design Recommendations for Integral-Abutment Piles," *Journal of Structural Engineering, American Society of Civil Engineers*, Vol. 117, No. 7, July 1991, pp. 2117-2134.
http://ascelibrary.org/sto/resource/1/jsendh/v117/i7/p2117_s1?isAuthorized=no (Fee)
24. Glikin, J. D. and Oesterle, R. G., "Creep and Shrinkage Analysis of Simple-Span Precast, Prestressed Bridge Girders Made Continuous," *Fourth RILEM International Symposium on Creep and Shrinkage of Concrete: Mathematical Modeling, Northwestern University, IL, Aug. 1986, pp. 765-775.*
25. Greimann, L. F., et al, "Finite Element Model for Soil-Pile Interaction in Integral Abutment Bridges," *Computers and Geotechnics, 1987, pp. 127-149.*
26. Greimann, L. and Wolde-Tinsae, A. M., "Design Model for Piles in Jointless Bridges," *Journal of Structural Engineering, American Society of Civil Engineers*, Vol. 114, No. 6, June 1988, pp. 1354-1371.
http://ascelibrary.org/sto/resource/1/jsendh/v114/i6/p1354_s1?isAuthorized=no (Fee)
27. Greimann, L. F., et al, "Nonlinear Analysis of Integral Abutment Bridges," *Journal of Structural Engineering, American Society of Civil Engineers*, Vol. 112, No. 10, Oct. 1986, pp. 2263-2280.
http://ascelibrary.org/sto/resource/1/jsendh/v112/i10/p2263_s1?isAuthorized=no (Fee)

28. Greimann, L. F., et al, "Final Report, Design of Piles for Integral Abutment Bridges," Department of Civil Engineering, Engineering Research Institute, Iowa State University, Ames, IA, Aug. 1984.
http://books.google.com/books?id=ZjVbGwAACAAJ&dq=Engineering+research+institute,+Iowa+state+university,+1984,+Greimann,+Final+Report,+Design+of+Piles+for+Integral+Abutment+Bridges&hl=en&ei=aYzeTo7zC83lggeGwriRBg&sa=X&oi=book_result&ct=result&resnum=2&ved=0
29. Greimann, L. F., et al, "Skewed Bridges with Integral Abutments," Bridges and Culverts, Transportation Research Record 903, Transportation Research Board, Washington, DC, 1983, pp. 64-72.
<http://trid.trb.org/view.aspx?id=195803> (Fee)
30. Holmes, J.R., et al, "Investigation of the Contraction of Prestressed Concrete Bridges," Nebraska Research Study 66-6, Report No. FHWA-NE-DOR-R-77-1, Nebraska Department of Roads, Lincoln, NE, March 1977, 389 pp.
<http://trid.trb.org/view.aspx?id=50578> (Fee)
31. Hulsey, J. L. and Emanuel, J. H., "Environmental Stresses in Flexibly Supported Bridges," Bridge Engineering - Vol. 1, Transportation Research Record 664, Transportation Research Board, Washington, DC, 1978.
<http://trid.trb.org/view.aspx?id=80040> (Fee)
32. Hulsey, J. L., "Environmental Effects on Composite - Girder Bridge Structures," Ph.D. Dissertation, University of Missouri-Rolla, Department of Civil Engineering, 1976, 339 pp.
http://books.google.com/books/about/Environmental_effects_on_composite_girde.html?id=3zZuNwAACAAI (Fee)
33. Imbsen, R. A., et al, "Thermal Effects in Concrete Bridge Superstructures," National Cooperative Highway Research Program Report 276, Transportation Research Board, Washington, DC, Sept. 1985, 99 pp.
<http://pubsindex.trb.org/view/1985/M/271760> (Fee)
34. Joo, Y., "Time-Dependent Analysis of Partially Prestressed Composite Members," Ph.D. Dissertation, University of Nebraska, Department of Civil Engineering, Lincoln, NE, 1989, 233 pp.
<http://digitalcommons.unl.edu/dissertations/AAI9013640/>
35. Jorgenson, J. L., "Behavior of Abutment Piles in an Integral Abutment Bridge," Engineering Experiment Station, FHWA-ND-I-75-B, North Dakota State University, Fargo, ND, Nov. 1981.
36. Kramer, S. L., and Sajar, P., "Bridge Approach Slab Effectiveness – Final Report," Washington State Transportation Center, University of Washington, Seattle, WA, Dec. 1991.
<http://www.wsdot.wa.gov/Research/Reports/200/227.1.htm>
37. Loveall, C. L., "Jointless Bridge Decks," Civil Engineering, American Society of Civil Engineers, ISSN: 0360-0556, Nov. 1985, pp. 64-67.
38. Maher, R. H. and Aust, M. I. E., "The Effects of Differential Temperature on Continuous Prestressed Concrete Bridges," The Institution of Engineers, Australia, Civil Engineering Transactions, Apr. 1970, pp. 29-32.
39. Maragakis, E. A. and Siddharthan, R., "Estimation of Inelastic Longitudinal Abutment Stiffness of Bridges," Journal of Structural Engineering, American Society of Civil Engineers, Vol. 115, No. 9, September 1989, pp. 2382-2399.
http://ascelibrary.org/sto/resource/1/jsendh/v115/i9/p2382_s1?isAuthorized=no (Fee)
40. Oesterle, R. G., et al, "Design of Precast Prestressed Bridge Girders Made Continuous," National Cooperative Highway Research Program Report 322, Transportation Research Board, Washington, DC, Nov. 1989.
<http://pubsindex.trb.org/view/1989/M/302086> (Fee)
41. Paduana, J.A. and Yee, W.S., "Lateral Load Tests on Piles in Bridge Embankments," Performance of Earth Retaining Structures and Pile Foundations, Transportation Research Record 517, Transportation Research Board, Washington, DC, 1974, pp. 77-92.
<http://pubsindex.trb.org/view/1974/C/26664> (Fee)

42. Pierce, P., "Jointless Redecking," Civil Engineering, Sept. 1991, pp. 60-61. Potgieter, I. C. and Gamble, W. L., "Nonlinear Temperature Distributions in Bridges at Different Locations in the United States," PCI Journal, Precast/Prestressed Concrete Institute, July-Aug. 1989, pp. 80-103.
<http://cedb.asce.org/cgi/WWWdisplay.cgi?73365> (Fee)
http://www.pci.org/view_file.cfm?file=JL-89-JULY-AUGUST-5.pdf
http://www.pci.org/view_file.cfm?file=JL-89-JULY-AUGUST-6.pdf
43. Potgieter, I. C. and Gamble, W. L., "Response of Highway Bridges to Nonlinear Temperature Distributions," Civil Engineering Studies, Structural Research Series No. 505, UILU-ENG-85-2007, ISSN-0069-4274, University of Illinois at Urbana-Champaign, Urbana, IL, April 1983, 291 pp.
<https://www.ideals.illinois.edu/handle/2142/14113>
44. Priestley, M. J. N. and Buckle, I. G., "Ambient Thermal Response of Concrete Bridges," Bridge Seminar 1978 - Volume 2, Road Research Unit Bulletin 42, National Roads Board, Wellington, New Zealand, 1979, 83 pp.
45. Priestley, M. J. N., "Design of Concrete Bridges for Temperature Gradients," ACI Journal, American Concrete Institute, No. 5, May 1978, pp. 209-217.
<http://www.concrete.org/PUBS/JOURNALS/AbstractDetails.asp?SearchID=-1&date=betweendate&aftermonth=5&afterday=1&afteryear=1978&beforemonth=5&beforeday=31&beforeyear=1978&searchmonth=1&searchday=1&searchyear=2011&authors= Priestley&ID=10934> (Fee)
46. Priestley, M. J. N., "Thermal Gradients in Bridges - Some Design Considerations," New Zealand Engineering, Vol. 27(7), July 1972, pp. 228-233.
<http://www.ipenz.org.nz/ipenz/publications> (Fee)
47. Radolli, M., et al, "Thermal Stress Analysis of Concrete Bridge Superstructures," Bridge Design, Testing, and Evaluation, Transportation Research Board 607, Transportation Research Board, Washington, DC 1977, pp. 7-13.
<http://pubsindex.trb.org/view/1976/C/53650> (Fee)
48. Russell, H. G., et al, "Evaluation and Verification of Time-Dependent Deformations in Post-Tensioned Box-Girder Bridges," Segmental and System Bridge Construction: Concrete Box Girder and Steel Design, Transportation Research Board, Washington, DC, 1983.
<http://pubsindex.trb.org/view/1982/C/188134> (Fee)
49. Sandford, T. C. and Elgaaly, M., "Skew Effects on Backfill Pressures at Frame Bridge Abutments," Civil Engineering Department, University of Maine, Orono, ME, Transportation Research Board 72nd Annual Meeting, Paper No. 930930, January 1993.
<http://pubsindex.trb.org/view/1993/C/389610> (Fee)
50. Soltani, A. A. and Kukreti, A. R., "Performance Evaluation of Integral Abutment Bridges, Paper No. 920179, Preprint Copy Submitted to The Transportation Research Board 71st Annual Meeting, Washington, DC, Jan. 1992, 29 pp.
<http://pubsindex.trb.org/view/1992/C/371579> (Fee)
51. Stewart, C. F., "Long Highway Structures Without Expansion Joints," Report by California Department of Transportation, FHWA/CA/SD-82-8, California Department of Transportation, Sacramento, CA, May 1983.
52. Tart, R. G., "A Study of the End Movement of a Reinforced Concrete Bridge under Variable Thermal Conditions," Virginia Highway Research Council, Charlottesville, VA, March 1965, 13 pp.
53. Tyler, R. G., "Creep, Shrinkage and Elastic Strain in Concrete Bridges in the United Kingdom, 1963 -71, " Magazine of Concrete Research, Vol. 28, No. 95, Cement and Concrete Association, June 1976, pp. 55-84.
54. Wah, T. and Kirksey, R. E., "Thermal Characteristics of Highway Bridges," Unpublished report to the National Cooperative Highway Research Program (NCHRP), Summary of Progress, Highway Research Board, Washington, DC, 1970, pp. 79-85.
55. Wasserman, E. P., "Jointless Bridge Decks," Engineering Journal, American Institute of Steel Construction, Inc., Vol. 24, No. 3, Third Quarter 1987, pp. 93-100.
<http://www.aisc.org> (Fee)

56. Wolde-Tinsae, A. M., et al, "End-Bearing Piles in Jointless Bridges," Journal of Structural Engineering, American Society of Civil Engineers, Vol. 114, No. 8, Aug. 1988, pp. 1870-1884.
http://ascelibrary.org/sto/resource/1/jsendh/v114/i8/p1870_s1?isAuthorized=no (Fee)
57. Wolde-Tinsae, A. M. and Aggour, M. S., "Structural and Soil Provisions for Approaches to Bridges - Final Report," Maryland University, Maryland Department of Transportation, State Highway Administration, June 1990.
58. Wolde-Tinsae, A. M and Greimann, L. F., "General Design Details for Integral Abutment Bridges," Civil Engineering Practice, Journal of the Boston Society of Civil Engineers Section/ASCE, Vol. 3, No. 2, ISSN:0886-9685, Fall 1988, pp. 7-20.
59. Wolde-Tinsae, A. M., et al, "Performance of Jointless Bridges," Journal of Performance and Constructed Facilities, American Society of Civil Engineers, Vol. 2, No. 2, May 1988, pp. 110-125.
http://ascelibrary.org/cfo/resource/1/jpcfev/v2/i2/p111_s1?isAuthorized=no (Fee)
60. Wolde-Tinsae, A. M., et al, "Performance and Design of Jointless Bridges," Final Report, Contract No. DTFH61-85-C-00092, Department of Civil Engineering, University of Maryland, Prepared in Cooperation with the U.S. Department of Transportation, Federal Highway Administration, June, 1987, 281 pp.
61. Wolde-Tinsae, A. M., et al, "Bridge Deck Joint Rehabilitation or Retrofitting," State Highway Administration Research Report, Maryland Department of Transportation, Grant No. AW089-327-046, Dec. 1988, 270 pp.
62. Zederbaum, J., "Factors Influencing the Longitudinal Movement of Concrete Bridge System with Special Reference to Deck Contraction," Concrete Bridge Design, ACI Publication SP-23, American Concrete Institute, Detroit, MI, 1969, pp. 75-95.
<http://www.concrete.org/PUBS/JOURNALS/AbstractDetails.asp?SearchID=-1&publication=Special+Publication&volume=23&ID=17229> (Fee)
63. Zuk, W., "Jointless Bridges," Report by Virginia Highway Research Council, Report No. VHTRC-81-R48, for the Federal Highway Administration, Richmond, VA, June 1981, 47 pp.
64. Zuk, W., "End-Movement Studies of Various Types of Highway Bridges," Highway Research Record No. 295, Highway Research Board, Washington, DC, 1969, pp. 1-4.
<http://pubsindex.trb.org/view/1969/C/105618> (Fee)
65. Zuk W., "Summary Review of Studies Relating to Thermal Stresses in Highway Bridges," Virginia Highway Research Council, Charlottesville, VA, June 1965, 7 pp.

PRECAST SEGMENTAL BRIDGES

Table of Contents

14.1 INTRODUCTION	14 - 3
14.1.1 Balanced Cantilever Method	14 - 3
14.1.2 Span-by-Span Method	14 - 5
14.2 PRECAST SEGMENTS	14 - 7
14.3 TRANSVERSE ANALYSIS	14 - 7
14.3.1 Modeling for Transverse Analysis	14 - 8
14.3.2 Analysis for Uniformly Repeating Loads	14 - 10
14.3.3 Analysis for Concentrated Wheel Live Loads	14 - 11
14.3.3.1 Live Load Moments in Cantilever Wings	14 - 12
14.3.3.2 Negative Live Load Moments in the Top Flange	14 - 14
14.3.3.3 Positive Live Load Moments at Centerline of the Top Flange	14 - 17
14.3.4 Transverse Post-Tensioning	14 - 19
14.3.4.1 Transverse Post-Tensioning Tendon Layouts	14 - 19
14.3.4.2 Required Prestressing Force	14 - 19
14.3.4.3 Transverse Post-Tensioning Tendon Placement and Tensioning	14 - 21
14.4 BALANCED CANTILEVER CONSTRUCTION	14 - 22
14.5 SPAN-BY-SPAN CONSTRUCTION	14 - 22
14.6 DIAPHRAGMS, ANCHOR BLOCKS AND DEVIATION DETAILS	14 - 22
14.6.1 Transfer of Vertical Shear Forces to Bearings	14 - 22
14.6.2 Transfer of Longitudinal Moment to Bearings	14 - 24
14.6.3 Transfer of Torsion to Bearings	14 - 26
14.6.4 Shear-Friction Resistance	14 - 27
14.6.5 Diaphragm Face Tension	14 - 28
14.7 GEOMETRY CONTROL	14 - 29
14.8 PRESTRESSING WITH POST-TENSIONING	14 - 29
14.8.1 Introduction	14 - 29
14.8.2 Cross Section and Sign Convention	14 - 29
14.8.3 Selection of Prestressing Force for a Given Eccentricity	14 - 29
14.8.4 Permissible Eccentricities for a Given Prestressing Force	14 - 31
14.9 CITED REFERENCES	14 - 32
14.10 PCI JOURNAL SEGMENTAL BRIDGE BIBLIOGRAPHY	14 - 32

PRECAST SEGMENTAL BRIDGES

This page intentionally left blank

Precast Segmental Bridges

14.1 INTRODUCTION

Since first introduced in the 1970s, precast concrete segmental bridges have significantly impacted major bridge construction in the United States. Precast concrete segmental bridges are comprised of short, full-width concrete sections called segments. The precast segments are fabricated either in an established precast concrete fabrication plant or a casting yard built near the project. The segments are then transported to the bridge site and erected to form the bridge. Specialized precasting and construction methods have produced cost effective bridges that are widely adaptable to a variety of span lengths, highway geometry, and other site constraints. Typical applications include:

- Long-span bridges
- Long bridges over water
- Complex urban interchanges and viaducts
- Bridges over sensitive environments
- Rail and transit aerial bridges
- Cable-stayed bridges

The clean lines and smooth surfaces of segmental box girders, along with the ability to minimize the size of substructure elements, have produced award-winning bridge aesthetics. Many segmental bridges have become signatures and icons of the regions in which they are located.

Additional information regarding the design and construction of precast post-tensioned segmental bridges can be found on the websites of the American Segmental Bridge Institute (ASBI), FHWA, and the Post-Tensioning Institute (PTI). PCI recommends using the ASBI “Construction Practices Handbook for Concrete Segmental and Cable-Supported Bridges” (2008) and the FHWA “Post-Tensioning Tendon Installation and Grouting Manual” (2004).

Precast segmental bridges are typically classified by the method by which the precast segments are incorporated into the structure. The two most common types of precast segment bridge erection are the balanced cantilever and span-by-span methods.

14.1.1 Balanced Cantilever Method

Precast segmental balanced cantilever construction involves the symmetrical placement of segments about a supporting pier. Each segment is lifted into position and abutting faces are coated with epoxy. Temporary post-tensioning bars are then tensioned connecting the segment to the cantilever. When two balancing segments are in place, post-tensioning tendons are tensioned across both cantilevers. In this way, as segments are added to the cantilevers, more top tendons are added. The number of cantilever tendons is a maximum at the segment over the pier and decreases along the length of the cantilevers. Once all of the segments of adjacent cantilevers are erected and tendons tensioned, superstructure continuity is achieved by casting a midspan closure joint and tensioning continuity post-tensioning tendons. These operations repeat until all spans of the bridge are assembled. **Figure 14.1.1-1** shows schematics of two common methods of placing precast segments in cantilever: placement by ground-based crane and overhead erection gantry.

PRECAST SEGMENTAL BRIDGES

14.1.2 Balanced Cantilever Method

Figure 14.1.1-1
Balanced Cantilever Erection by Ground Based Crane and Overhead Gantry

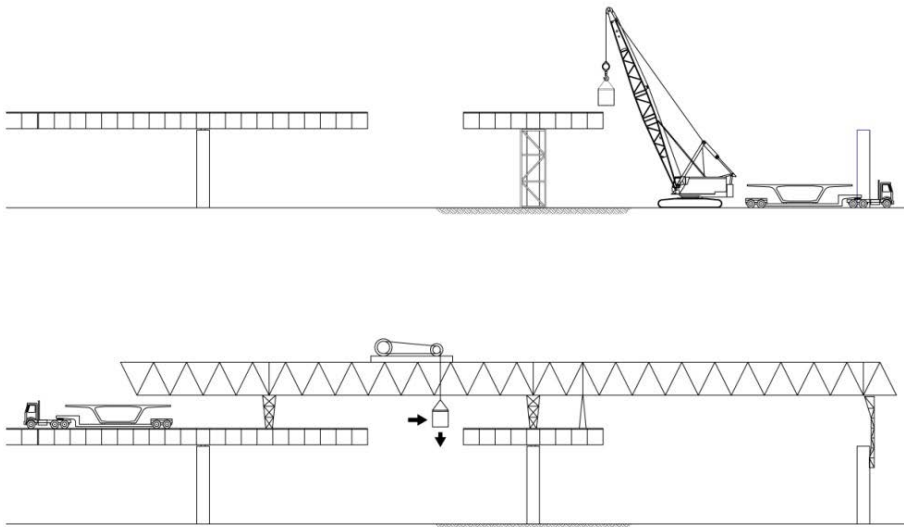


Figure 14.1.1-2 shows a ground-based crane used to erect precast segments in the balanced cantilevers of the SE Ramp of the I-95/I-295 North Interchange in Jacksonville, Fla. Precast segments for this 2,250-ft-long bridge were cast in a project casting yard established by the contractor. As the erection sequence required, the precast segments were trucked to the site on a low-boy trailer. A lifting frame was attached to the top of the segments to avoid overstressing the top slab during lifting. Cantilever overturning due to out-of-balance moments before the balancing segment is placed on the other end of the cantilever is provided by a temporary stability tower at the pier. The stability tower also provides transverse overturning stability for moments caused by the curvature of the cantilever.

Figure 14.1.1-2
Balanced Cantilever Construction for the I-95/I-295 North Interchange Ramp SE in Jacksonville, Fla., using a ground-based crane. (Photo Courtesy of Corven Engineering)



This 2,250-ft-long bridge demonstrates the cost effectiveness of precast segmental balanced cantilever construction over heavily traveled urban highways. Construction of the 274-ft-long spans crossing I-295 used lane shifts and nighttime construction to keep traffic moving throughout the project. **Figure 14.1.2-3** shows segment placement during night shift work.

PRECAST SEGMENTAL BRIDGES

14.1.2 Balanced Cantilever Method/14.1.2 Span-by-Span Method

Figure 14.1.1-3

Nighttime Segment Placement at the I-95/I-295 North Interchange Ramp SE in Jacksonville, FL. (Photo Courtesy of Corven Engineering)



Figure 14.1.1-4 shows cantilever erection of the Seabreeze Bridge in Daytona Beach, Fla., using an overhead gantry. The precast segments were delivered to the end of the gantry over the completed portion of bridge. The gantry winch lifts the segment and transports it to the free end of the cantilever. In this system of erection, cantilever stability can be provided by struts between the cantilever and the erection gantry.

Figure 14.1.1-4

Balanced Cantilever Erection using Overhead Gantr. (Photo Courtesy of Scott McNary)



14.1.2 Span-by-Span Method

Span-by-span construction calls for the temporary support of all segments of a span on erection trusses, while full-span tendons are installed and tensioned. The erection trusses may be either overhead or under-slung to the concrete segments. The precast segments are delivered to the site and are placed on the erection trusses by crane, segment hauler, or gantry winch systems. **Figure 14.1.2-5** illustrates a typical cycle of construction for span-by-span erection using under-slung trusses and a ground based crane.

PRECAST SEGMENTAL BRIDGES

14.1.2 Span-by-Span Method

Figure 14.1.2-5
Span-by-Span Erection Schematic. 1) Segments are placed on the erection truss; 2) Closure joints are cast and full-span tendons are tensioned; 3) the erection truss is launched forward to begin erection of the next span.

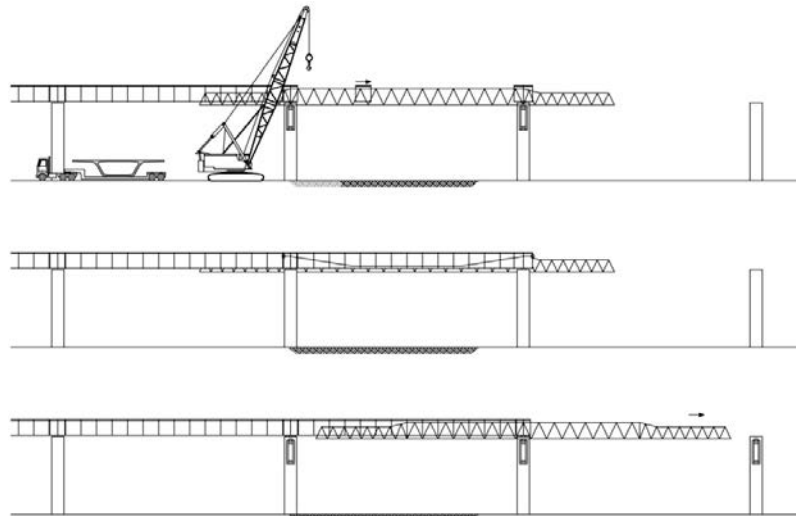


Figure 14.1.2-6 shows the construction of the Lyons Bridge in Stuart, Fla. Twin, under-slung trusses support the segments below the root of the cantilever wings. Segments were delivered by truck to the span to be erected over the completed portion of bridge. A deck mounted segment hauler lifted the segments from the transporting trailer and placed them on the temporary trusses. Each segment is supported on the temporary trusses by sliding jacks that could be adjusted to position each segments to the required roadway geometry.

Figure 14.1.2-6
Span-by-span Construction using Under-slung Erection Girders. (Photo Courtesy of PCL Civil Constructors)



Span-by-span construction of the Dulles Corridor Metrorail Project through Tysons Corner, Va., using an overhead truss is shown in **Figure 14.1.2-7**. The segments for these twin, single track bridges are delivered either at street level or over the completed structure. Individual segments of a span are lifted, and if necessary, translated to their final location in the span. Once one girder in a span is completed, the overhead truss is launched laterally to build the adjacent girder. The combination of erection truss supports and rigging enable the erection truss to be self-launching in the longitudinal direction

PRECAST SEGMENTAL BRIDGES

14.1.2 Span-by-Span Method/14.3 Transverse Analysis

Figure 14.1.2-7**Span-by-Span Erection using an Overhead Truss (Photo: Corven Engineering, Inc.)**

Post-tensioning tendons in span-by-span construction are anchored in pier segment diaphragms at both ends of the span and external to concrete for the length of the span. The external tendons are placed within polyethylene ducts that are then filled with grout. The draped profile of tendons within the span is achieved by deviating the tendons vertically through deviation saddles and diaphragms. The benefit of using external tendons is that the webs in which they would normally be placed can be made thinner, reducing the weight of the bridge and improving the efficiency of the cross section. These two benefits lead to a reduction of the required amount of prestressing.

Spans built using this method of segment assembly can be either simple spans or made continuous to reduce superstructure expansion joints. Link slabs can also be used to connect simple span superstructures to reduce the number of expansion joints. Spans are made continuous by overlapping post-tensioning tendons in pier segment diaphragms centered over the piers. Closure joints located on one or both sides of the pier segments are used to accommodate variations in actual segment lengths, and sometimes to uncouple the casting of typical segments from the pier segments.

Simple spans are commonly used for transit rail aerial structures where rail interaction forces transmitted to the substructure can be more evenly distributed. Post-tensioning tendons for these spans are anchored at the ends of the simple spans, with the net eccentricity of the tendons at the ends near the center of gravity of the cross section. **Figure 14.1.2-8** shows an end view of twin single track girders for the Dulles Corridor Metrorail Project. The anchorages for these twin segmental simple spans can be seen anchored in the pier segment diaphragms.

14.2 PRECAST SEGMENTS

To be released in 2012

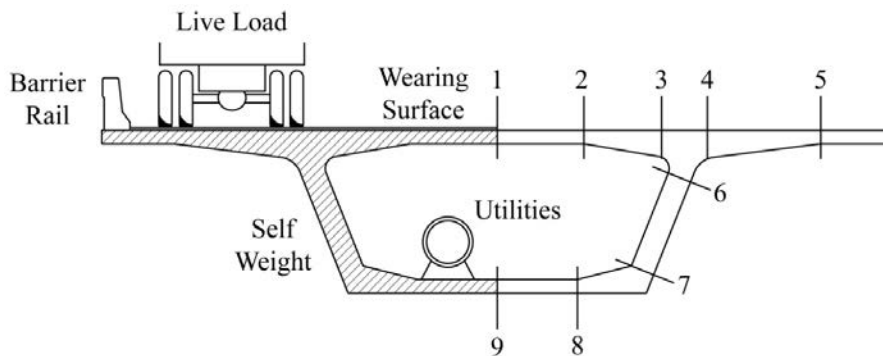
14.3 TRANSVERSE ANALYSIS

The cross section of a precast segmental box girder bridge is designed to resist bending moments acting transverse to the longitudinal direction of the bridge span. Transverse analyses are performed to evaluate transverse bending moments resulting from both permanent and live loads. Permanent loads include self weight, barrier rails, sidewalks, wearing surfaces, and utilities that may be attached inside or outside of the box-girder superstructure. Live loads are comprised of the *LRFD Specifications* HL-93 Design Truck (LRFD Art. 3.6.1.2.2) and Design Tandem (LRFD Art. 3.6.1.2.3), arranged in travel lanes to produce maximum bending moments at critical sections. Figure 14.3-1 shows a typical box-girder superstructure, applied loads and likely critical sections. The results of the transverse analysis are used to design the reinforcement in the cantilever wings, top flange, webs, and bottom flange and post-tensioning in the top flange.

PRECAST SEGMENTAL BRIDGES

14.3 Transverse Analysis/14.3.1 Modeling for Transverse Analysis

Figure 14.3-1
Loads and Design Sections for Transverse Analysis of a Precast Segmental Box Girder

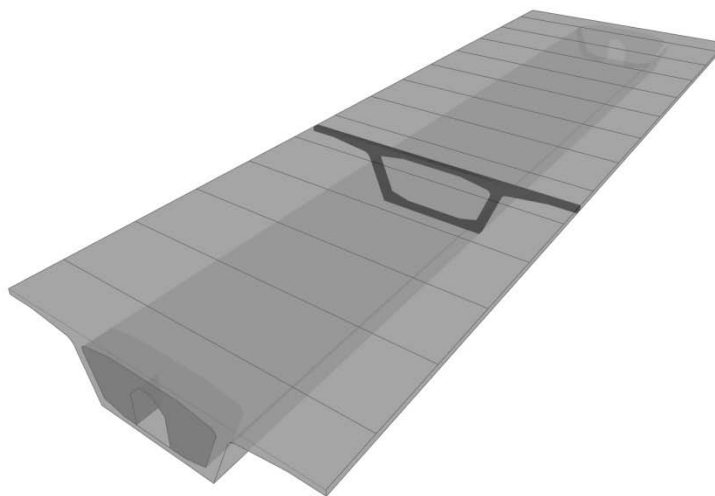


The magnitude and distribution of transverse bending moments due to permanent and live loads vary along the length of a span as a function of the deflection behavior of the box girder. Near supports, where deflections are restrained, localized bending moments remain concentrated. Within the span, general longitudinal deflections reduce maximum transverse moments as they are distributed along a greater portion of the span. Rigorous transverse analyses could be made using three-dimensional finite element methods with sufficient load cases to generate an envelope of transverse design moments. The practicality of fabricating segments with uniform reinforcing and post-tensioning details typically overrides refinements gained by a rigorous solution.

14.3.1 Modeling for Transverse Analysis

An accepted approach for the transverse analysis of a concrete box girder superstructure is a simplified, two-dimensional method, with sufficient consideration for longitudinal load distribution. Figure 14.3-2 shows a perspective of a span of precast segmental superstructure. A typical cross section with a unit length is identified in the span for a two-dimensional analysis in the plane of the cross section. The extracted typical section for analysis is shown in Figure 14.3-3. The cross section shown in Figure 14.3-3 is that of the AASHTO-PCI-ASBI 2700-2 Segment. Results of example calculations presented in this section are for this standard segment.

Figure 14.3-2
Typical Precast Segmental Span with Cross Section Defined at Midspan



PRECAST SEGMENTAL BRIDGES

14.3.1 Modeling for Transverse Analysis

*Figure 14.3-3**One Foot Section of Typical Cross Section of the AASHTO-PCI-ASBI 2700-2 Segment*

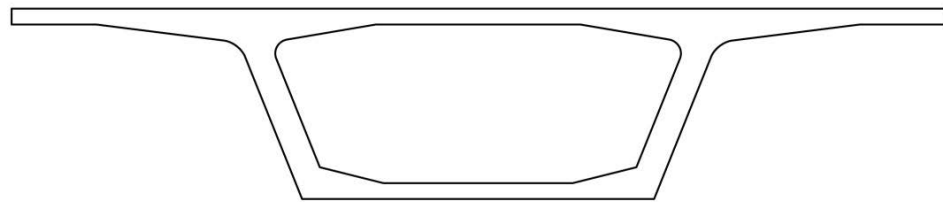
The typical cross section is modeled using beam elements in a general two-dimensional structural analysis program. Figure 14.3-4 shows the transition from typical cross section, to idealized beam members, to node and element layout for a typical analysis model. Special transverse modeling considerations include:

- The model shown in Figure 14.3-4b shows beam elements extending to nodes at the top of web/cantilever/top slab intersection and the bottom of web/bottom slab intersection. Often, designers will model a portion of these intersecting members as rigid elements, as the size of the connection can be significant with regard to member length.
- Many precast segmental cross sections include linear or circular fillets at the cantilever/top of web and top slab/top of web connections. The choice of the critical sections for design of flexure at these sections is left to the discretion of the engineer who must consider the particular geometry of the cross section.
- Vertical supports are placed under the webs as shown in Figure 14.3-4c. One horizontal support is required for model stability. A second horizontal support has been added to restrain side-sway of the two-dimensional model. This support helps account for the torsional rigidity of the box girder in the actual three-dimensional structure. This second horizontal support can be problematic for some load cases such as transverse post-tensioning. Use and placement of the second support is left to the discretion of the engineer.

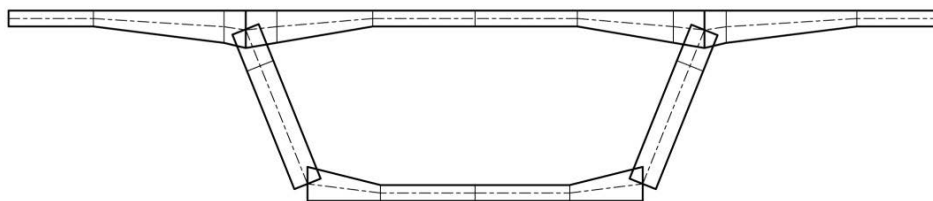
PRECAST SEGMENTAL BRIDGES

14.3.1 Modeling for Transverse Analysis/14.3.2 Analysis for Uniformly Repeating Loads

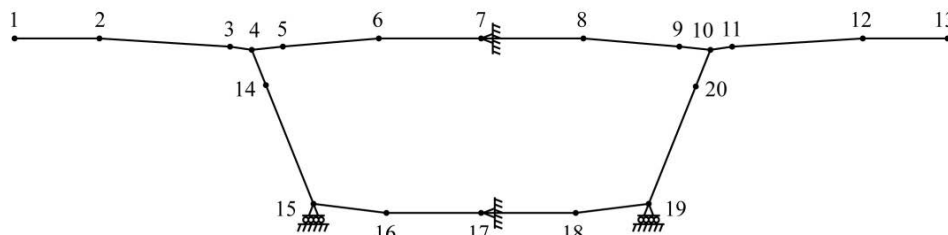
Figure 14.3-4
Developing the Two-Dimensional Transverse Model



a) Typical Cross Section



b) Idealized Members



c) Computer Model

14.3.2 Analysis for Uniformly Repeating Loads

Transverse bending moments for loads that repeat uniformly along the span can be determined directly from the two-dimensional analysis mode. Self weight bending moments can typically be generated internally by the analysis software once the unit weight of the concrete has been defined. The per-unit length values of superimposed dead loads are applied directly to the two-dimensional analysis model as either concentrated or distributed loads.

To serve as an example, the AASHTO-PCI-ASBI 2700-2 Segment shown in Figure 14.3-4 was analyzed for the following loads:

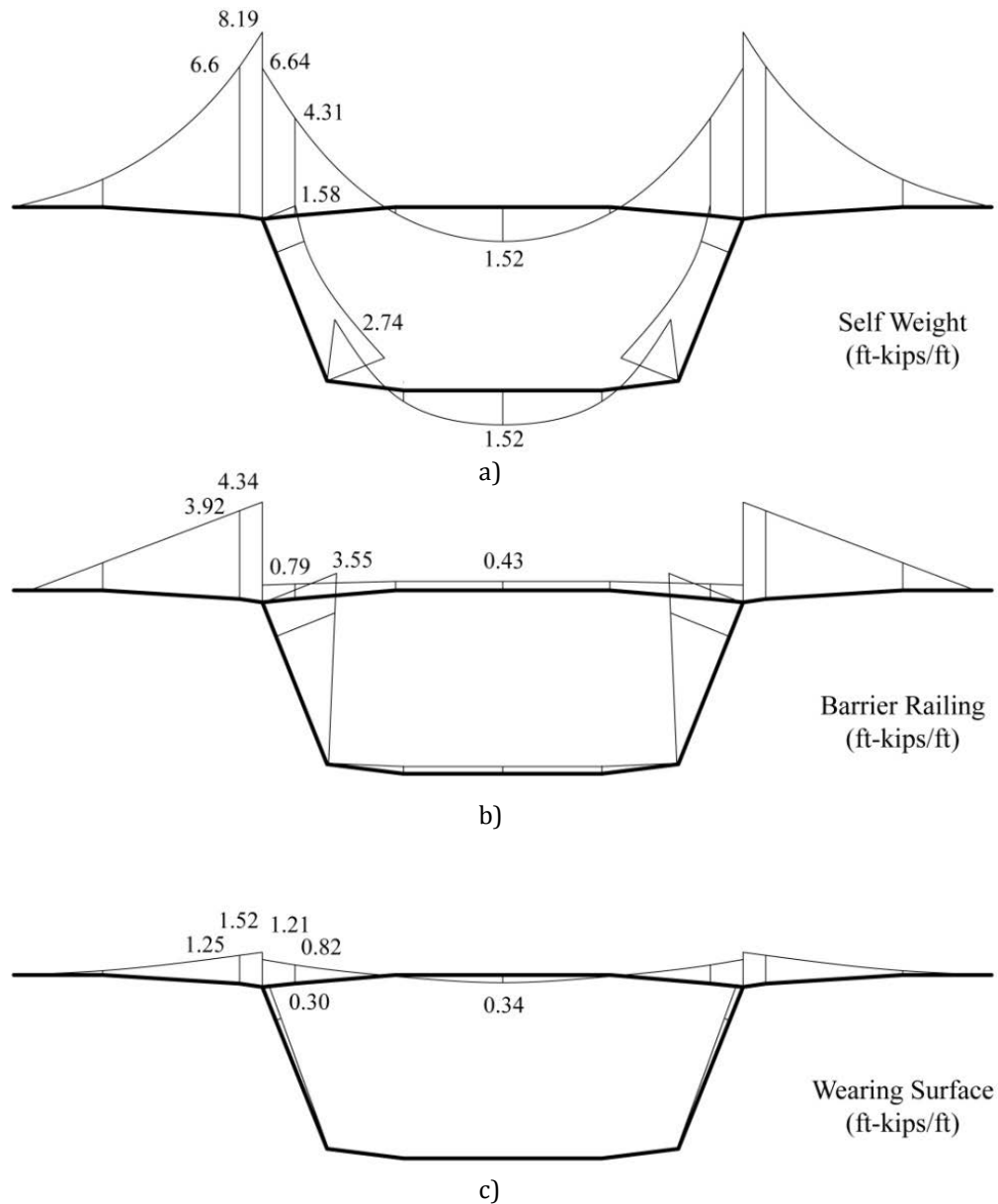
- Self Weight: Concrete unit weight = 0.150 kip/ft³
- Barrier Railing: p = 0.420 kips/ft (8 in. from edge of the cantilevers)
- Future Wearing Surface: 2 in. concrete, p = 0.025 kips/ft/ft

The transverse bending moments resulting from these three load cases are shown in Figure 14.3-5.

PRECAST SEGMENTAL BRIDGES

14.3.2 Analysis for Uniformly Repeating Loads/14.3.3 Analysis for Concentrated Wheel Live Loads

Figure 14.3-5
Transverse Bending Moments for Uniformly Repeating Loads in the 2700-2 Segment



14.3.3 Analysis for Concentrated Wheel Live Loads

Figure 14.3-6 shows the perspective of a precast segmental box girder superstructure loaded with the Design Truck portion of the HL-93 notional load. Travel lanes, and the trucks/tandems within the lanes, are positioned in number and location in accordance with *LRFD Specifications* requirements to produce maximum transverse bending moments at critical sections. The appropriate multi-presence factor of LRFD Article 3.6.1.1.2 should be considered in choosing the number of design lanes to apply for a given critical section. Truck and tandem locations within the lanes should be in accordance with LRFD Article 3.6.1.3.1.

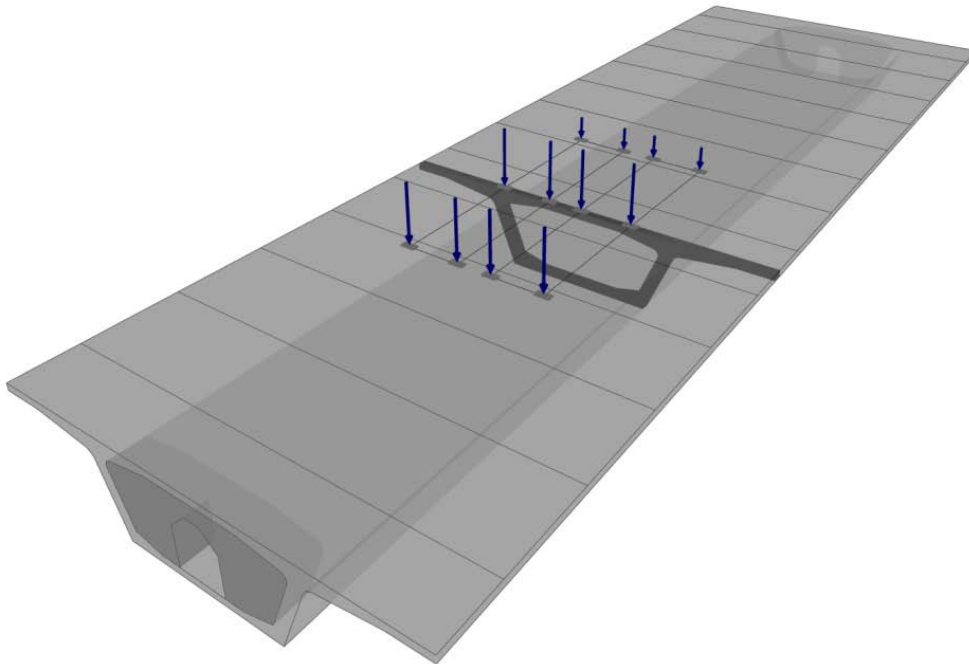
PRECAST SEGMENTAL BRIDGES**14.3.3 Analysis for Concentrated Wheel Live Loads/14.3.3.1 Live Load Moments in Cantilever Wings**

Transverse bending moments resulting from the application of concentrated loads in the span are determined in a three step process:

1. Determine maximum transverse bending moments at critical sections of the cantilever wing and top flange considering these members as separate three-dimensional, fixed-end slab structures.
2. Use the two-dimensional model to distribute “fixed-end” slab moments around the cross-sectional model.
3. Sum the fixed-end moments and redistributed moments to determine live load moments for design.

The fixed-end slab structures are typically analyzed using finite element methods or other tools such as influence surfaces. When modeled using finite elements, the slab structures are supported by full restraints at their intersection with the top of the webs. The longitudinal length of the flange structure should be sufficient to not impact transverse bending behavior. Flanges with shorter spans may warrant the application of wheel loads as surface loads. The areas over which the loads are distributed are the LRFD Tire Contact Area (LRFD Art. 3.6.1.2.5) projected to the center of gravity of the top flange using a 45-degree distribution in both longitudinal and transverse directions. Bending moments computed in the examples included in this section use influence surfaces and consider only the HL-93 Design Truck.

Figure 14.3-6
Truck Loads on a Segmental Box-Girder Span

**14.3.3.1 Live Load Moments in Cantilever Wings.**

The maximum fixed-end moment in the cantilever wing is determined by positioning the HL-93 Truck 1 ft away from the face of the barrier railing in accordance with LRFD Art. 3.6.1.3.1. Figure 14.3-7 shows this loading for the 2700-2 Segment. Figure 14.3-8 shows an influence surface for negative moment at the root of the cantilever, along the centerline of the influence surface. This Figure also shows the location of wheel loads to produce the maximum fixed-end moment in the cantilever flange. The negative maximum bending moment found using this cantilever influence surface is 15.2 ft-kips.

PRECAST SEGMENTAL BRIDGES

14.3.3.1 Live Load Moments in Cantilever Wings

Figure 14.3-7
Truck Location for Maximum Transverse Bending Moment at Root of Cantilever

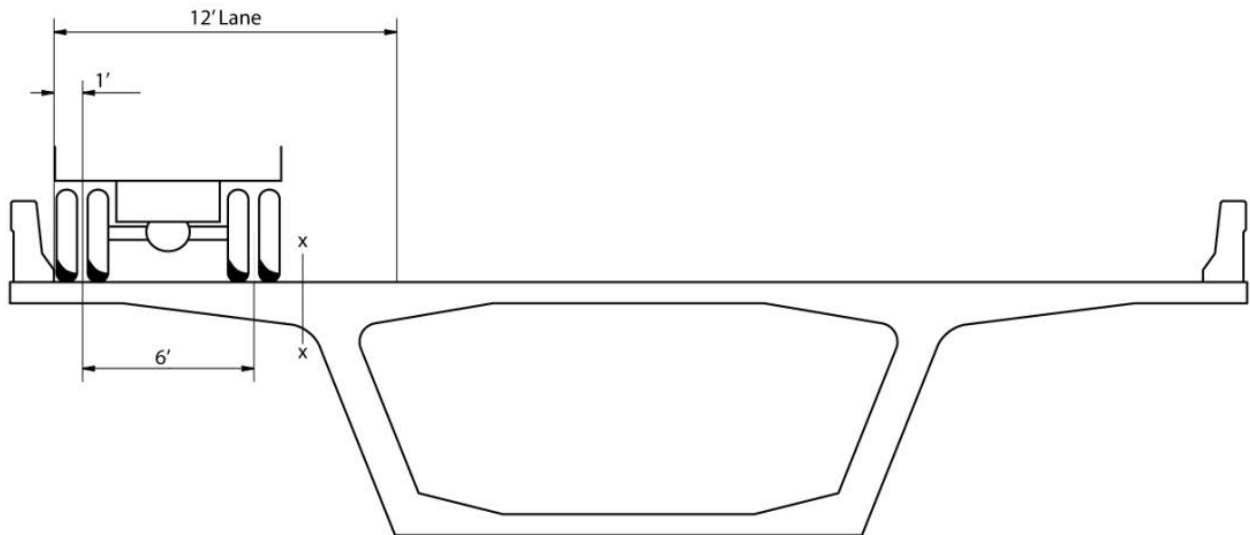
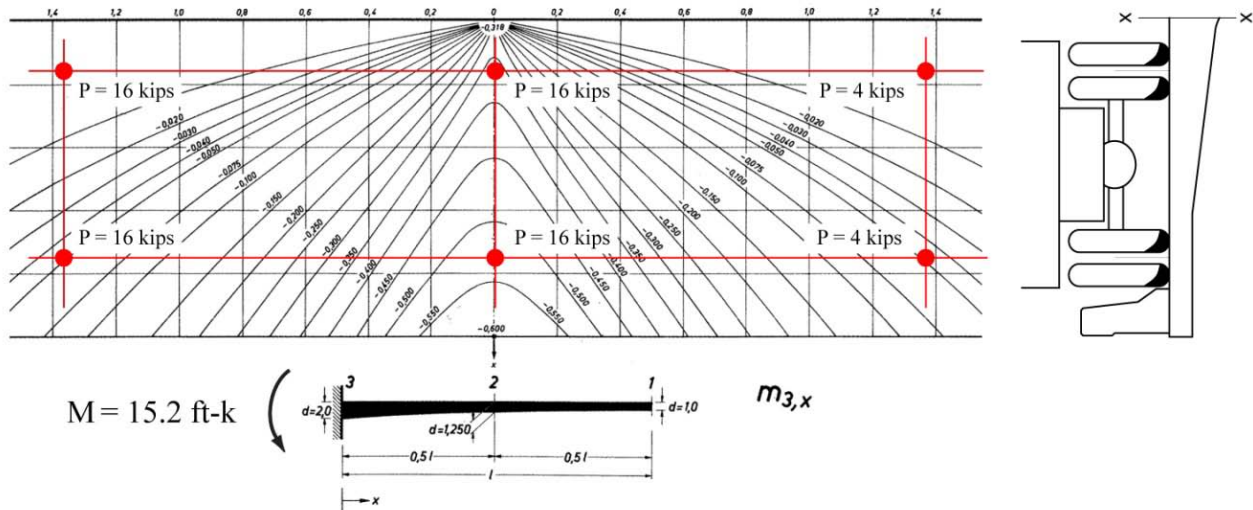


Figure 14.3-8
Loaded Influence Surface for the Cantilever Flange



Transverse bending moments in the other members of the cross section resulting from live load on the cantilever are determined by applying the cantilever moment to the cantilever-top flange -web intersection in the two-dimensional model. Figure 14.3-9 shows the distribution of 15.2 ft-kip cantilever moment around the cross section. Superimposing the cantilever moments with the distributed moments produces the final transverse bending moment diagram shown in Figure 14.3-10.

PRECAST SEGMENTAL BRIDGES

14.3.3.1 Live Load Moments in Cantilever Wings/14.3.3.2 Negative Live Load Moments in the Top Flange

Figure 14.3-9
Distribution of Cantilever Live Load Moments in the Cross Section

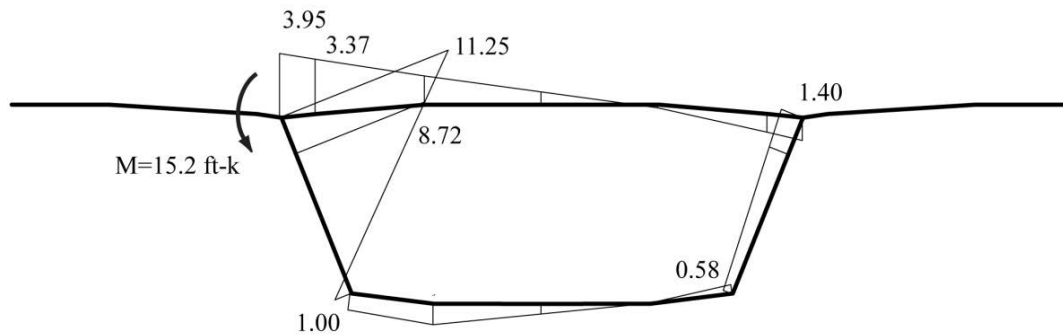
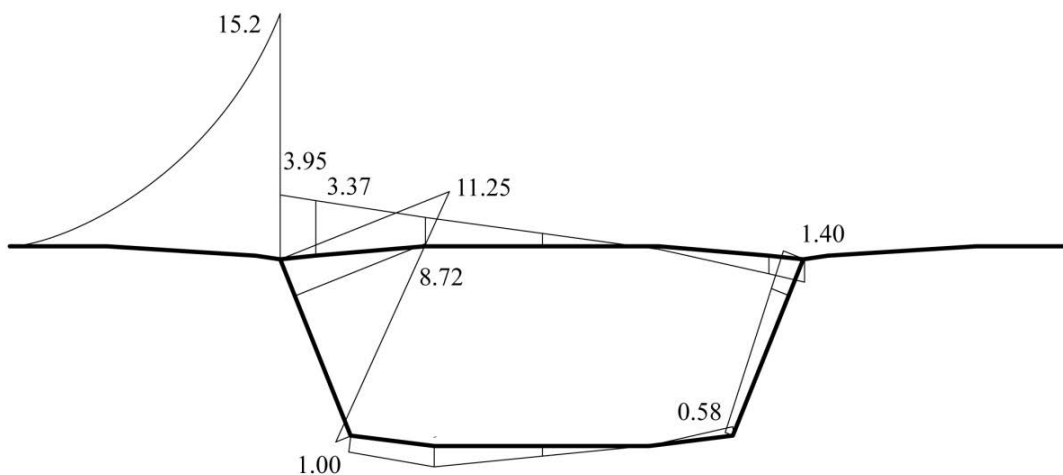


Figure 14.3-10
Final Bending Moments for Live Load on Cantilever



The shape of the bending moment diagram in the loaded cantilever flange is approximate, as the influence surface used, only provides the bending moment at the root of the cantilever. Plate solutions using finite element methods could be used to produce moments along the loaded cantilever.

14.3.3.2 Negative Live Load Moments in the Top Flange.

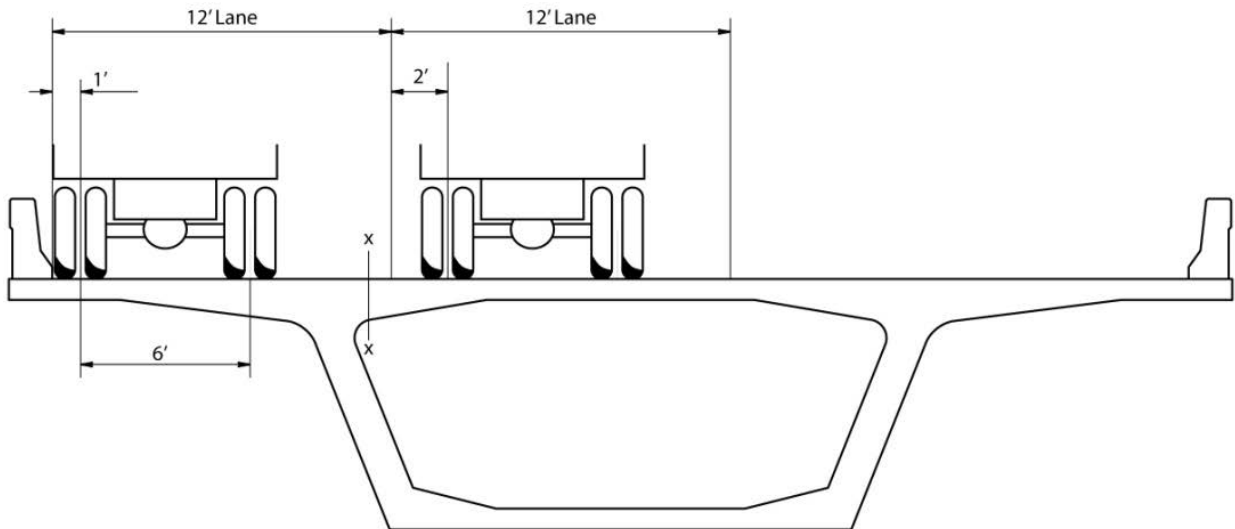
Negative live load moments in the top slab require positioning the Design Truck and Tandem for maximum negative effect at the end of the isolated top flange structure. In the example of the 2700-2 Segment, the maximum negative moment at the left end of the top flange is produced by locating one truck in the top flange and adding the effect of one truck in the cantilever wing. Figure 14.3-11 shows the locations of these two travel lanes. This loading arrangement can be evaluated as a superposition of the moments due to a truck on the cantilever shown in Figure 14.3-10 and moments resulting from the single truck located between the webs as shown in Figure 14.3-12.

PRECAST SEGMENTAL BRIDGES

14.3.3.2 Negative Live Load Moments in the Top Flange

Figure 14.3-11

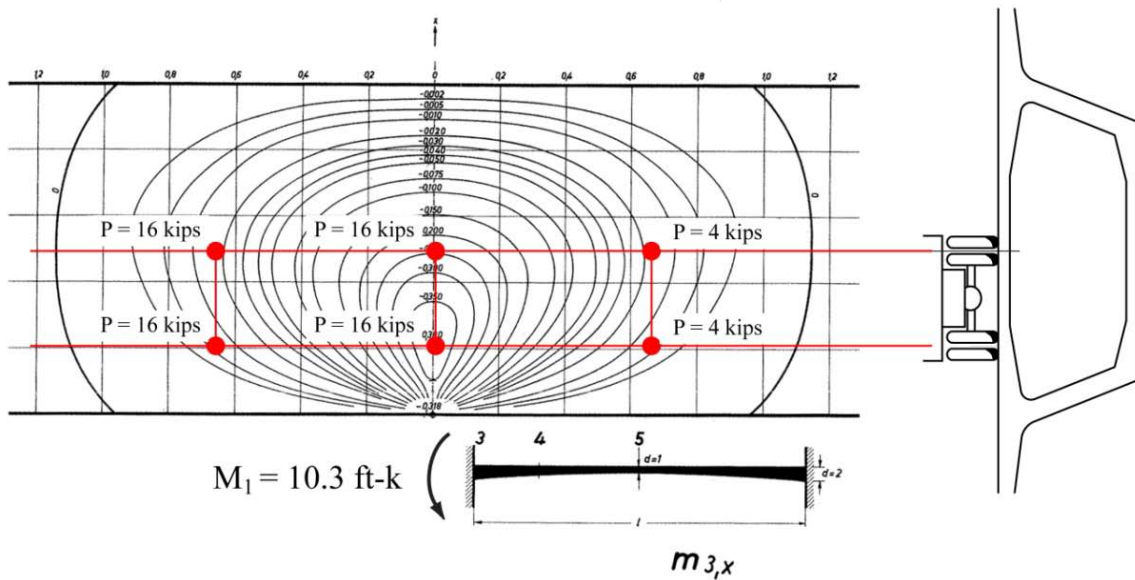
Truck Location for Maximum Transverse Bending Moment at Middle of Top Flange



The fixed-end moments for the top flange plate structure are determined using influence surfaces for a doubly fixed plate. Figure 14.3-12 shows the influence surface for the maximum negative moment at the left end of the flange (10.3 ft-kips). Figure 14.3-13 shows the inverted influence surface used to compute the corresponding moment at the right end of the slab (5.1 ft-kips).

Figure 14.3-12

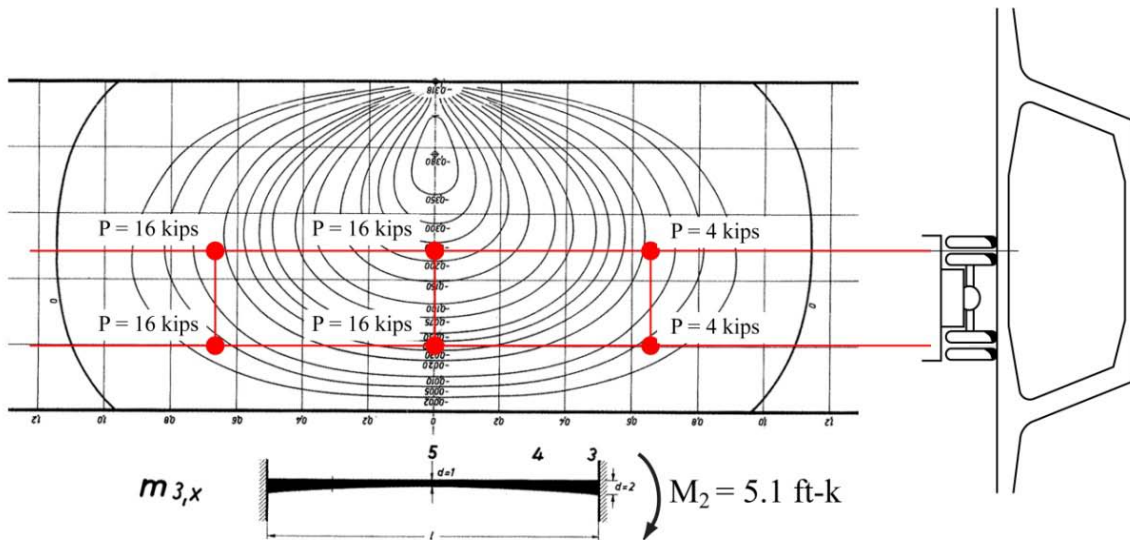
Influence Surface for Maximum Negative Bending at the Left End of the Top Flange



PRECAST SEGMENTAL BRIDGES

14.3.3.2 Negative Live Load Moments in the Top Flange

Figure 14.3-13
Influence Surface for Maximum Negative Bending at the Right End of the Top Flange



The two fixed-end moments can be “released” on the cross section by applying them as concentrated moments at the cantilever-top flange -web intersection. Figure 14.3-14 shows the results of the application of the concentrated couples on the two-dimensional analysis model. The concentrated couples, though applied as external loads, are actually internal fixed-end moments. When applied as external loads with signs opposite to the internally fixed-end moments, the moments in the unloaded members (webs and bottom flange) are the final moments due to the loading. The moments in the top slab represent the differential moments in the loaded member in moving from fixed-end conditions to the actual flexibility of the box girder. The final bending moment diagram, shown in Figure 14.3-15, is determined by reducing the fixed-end moments by these differential moments.

The total negative moment at the left end of the top flange for Design Trucks arranged in two lanes as shown in Figure 14.3-11 are found by summing the maximum moment from the distributed cantilever moment (Figure 14.3-10) and the moment resulting from the truck in the top slab (Figure 14.3-15). The moment at the left end of the top slab is:

$$M_{neg} = 3.95 + 8.09 = 12.04 \text{ ft - k}$$

The results of this analysis are valid only at the location of known fixed moments and their redistributed differential moments. The shape of the top flange bending moment between the two known extremity moments is not an exact representation, but general in nature. Efforts have been made in past practice to develop approaches using equivalent forces in equilibrium with the extremity moments to determine bending moments within the top flange for a given loading. The results of these methods do not prove accurate or necessary for the design of the top flange.

PRECAST SEGMENTAL BRIDGES

14.3.3.2 Negative Live Load Moments in the Top Flange/14.3.3.3 Positive Live Load Moments at Centerline of the Top Flange

Figure 14.3-14

Distribution of Fixed-End Live Load Moments for Maximum Negative Moment Case

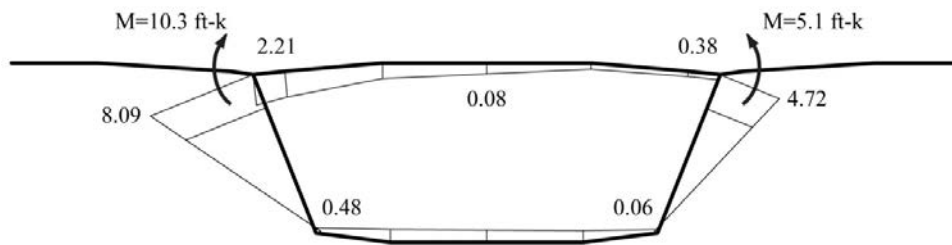
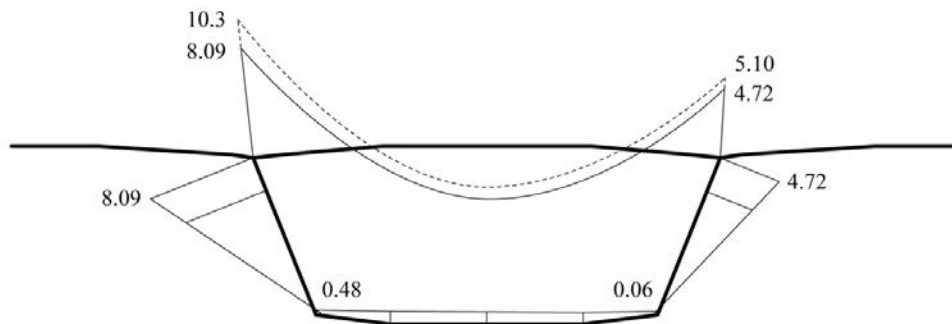


Figure 14.3-15

Summed Live Load Moments for the Maximum Negative Moment Case



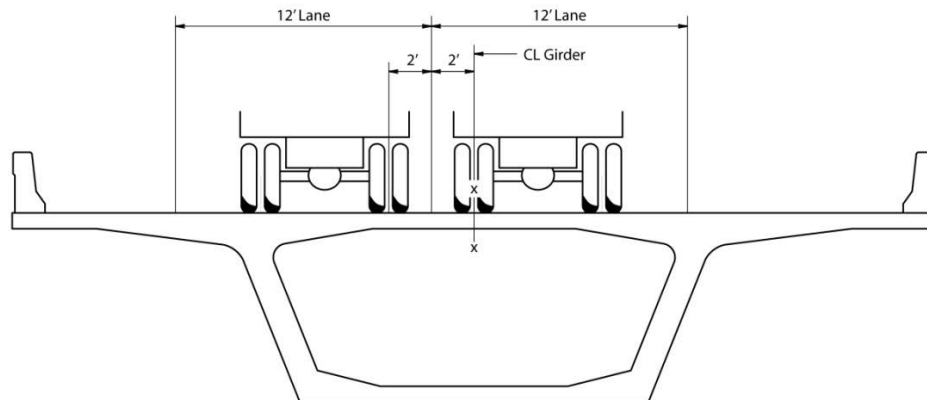
14.3.3.3 Positive Live Load Moments at Centerline of the Top Flange

Positive live load moments at the centerline of the top flange are computed in a fashion similar to the negative moments at the ends of the slab, with one additional initial step. An influence surfaces for moment at the center of the isolated top flange structure, or a finite element model, is first used to determine the arrangement of loads to produce maximum positive moment. Fixed-end negative moments are then determined for this load arrangement and distributed around the cross section. The final positive moment at the centerline of the slab is the positive moment in the fixed-end top flange structure, increased by the release of the end moments.

Figure 14.3-16 shows the load arrangement for maximum positive bending moment at the center of the top flange. Figure 14.3-17 shows an influence surface for the maximum positive transverse bending moment at the center of the top flange for this loading arrangement. The value of this bending moment with fixed-end supports is 3.88 ft-kips. The fixed-end bending moments at the ends of the top flange structure for the same loading arrangement are 12.0 ft-kips at the left end and 11.1 ft-kips at the right end.

Figure 14.3-16

Summed Live Load Moments for the Maximum Negative Moment Case



PRECAST SEGMENTAL BRIDGES

14.3.3.3 Positive Live Load Moments at Centerline of the Top Flange

These fixed-end moments are released on the cross section as previously presented in Section 14.3.3.2. Figure 14.3-18 shows the differential moments, and Figure 14.3-19 shows the summed values. The release of the fixed-end moments shifts the bending moment diagram in the top slab, increasing the bending moment at the centerline of the top flange. The fixed-end centerline moment increases from 3.88 ft-kips/ft to 5.08 ft-kips/ft. Again, the shape of the top slab bending moment diagram between known locations is only an approximation.

Figure 14.3-17
Maximum Positive Moment in the Top Flange for Fixed-End Conditions

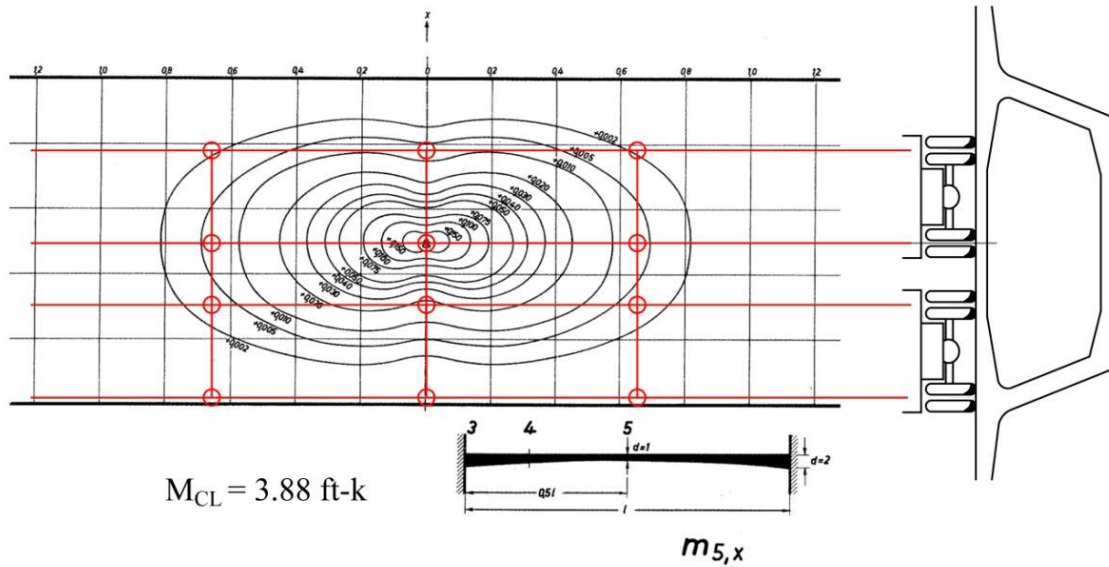
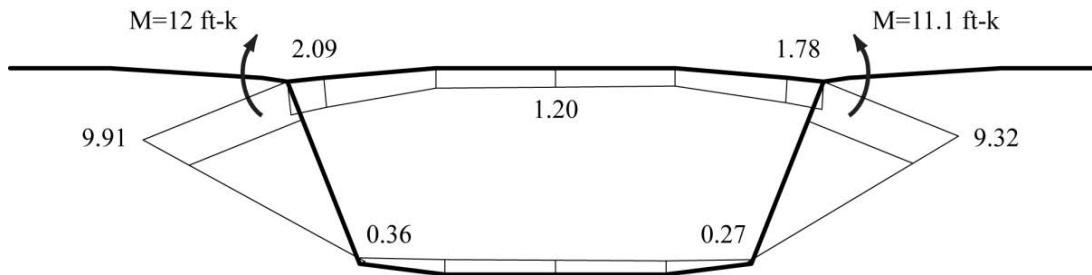


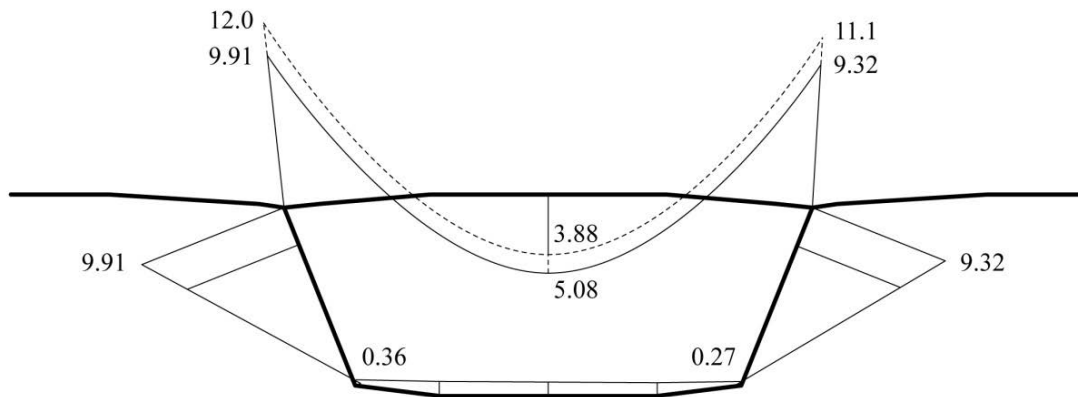
Figure 14.3-18
Distribution of Fixed-End Live Load Moments for Maximum Negative Moment Case



PRECAST SEGMENTAL BRIDGES

14.3.3.3 Positive Live Load Moments at Centerline of the Top Flange/14.3.4.2 Required Prestressing Force

*Figure 14.3-19
Summed Live Load Moments for the Maximum Positive Moment Case*



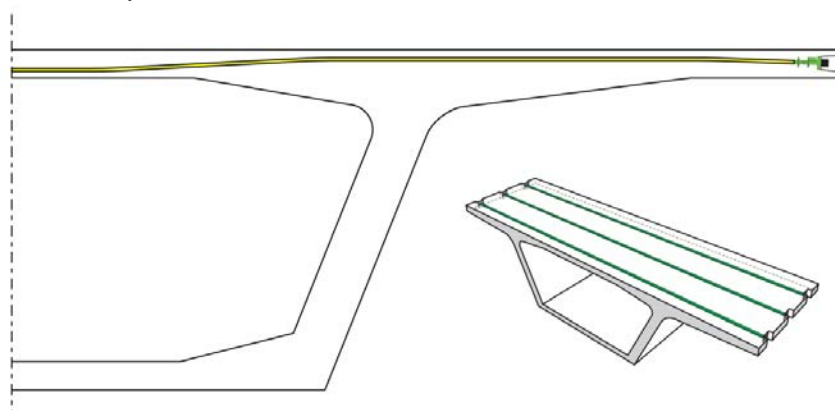
14.3.4 Transverse Post-Tensioning

14.3.4.1 Transverse Post-Tensioning Tendon Layouts

The cantilever wings and top flange of precast segmental box girder superstructures are typically prestressed transversely by post-tensioning to offset tensile stresses resulting from permanent and live loads. Narrow precast box girders with widths of 16 ft or less, often used for single track transit systems, may not greatly benefit from transverse post-tensioning. Rails that carry the normal operating train loads can be positioned adjacent to webs, causing small top flange bending moments.

Figure 14.3-20 shows a typical transverse post-tensioning tendon layout for the 2700-2 Standard Segment. The transverse tendons are typically comprised of three or four strands, of either 0.5-in. or 0.6 in. diameter each, placed in flat (oval shaped) ducts. The profile of the tendons varies to provide needed eccentricity over the webs and at the centerline of the top flange. The perspective view in Figure 14.3-20 shows three transverse tendons in a single segment, typical for 10-ft-long segments of bridges from 30 to 50 ft wide.

*Figure 14.3-20
Typical Transverse Tendon Layout*



14.3.4.2 Required Prestressing Force

The determination of the required prestressing force on a unit length basis is made by summing the moments at critical sections, evaluating each section’s prestressing requirement, and choosing the greatest required force. *LRFD Specifications* Service I is the appropriate limit state for transverse prestressing design based on permissible concrete tension (LRFD Art. 3.4.1). The load factors for permanent and live loads at this limit state are equal to 1.0.

PRECAST SEGMENTAL BRIDGES

14.3.4.2 Required Prestressing Force

Considering the example presented in this section for the 2700-2 standard segment, the summary of moments at the three sections studied are:

Section	Root of Cantilever	Edge of Top Flange	Centerline of Top Slab
Self Weight	-8.19	-6.64	1.52
Barrier Railing	-4.34	-0.79	-0.43
Wearing Surface	-1.52	-1.21	0.34
Live Load	-15.2	-12.04	5.08
Multi-Presence	1.20	1.00	1.00
Dynamic Allowance (IM)	1.33	1.33	1.33
Total Service I Moment	-38.4	-24.7	8.19

From Appendix G, the equations governing post-tensioning selection are:

$$F \geq \frac{-M + M_a}{\rho c_2 - e} \quad (\text{Negative Moment}) \qquad F \geq \frac{M - M_a}{\rho c_1 + e} \quad (\text{Positive Moment})$$

where:

- M = total applied service load moment
- M_a = moment causing allowable tensile stress
- c_1 = distance from neutral axis to extreme top fiber
- c_2 = distance from neutral axis to extreme bottom fiber
- ρ = cross-section efficiency = $\frac{1}{3}$ for a rectangular section
- e = tendon eccentricity considering location of strands within the duct

The moment causing allowable tensile stress (M_a) is equal to the allowable tensile stress (f_a) multiplied by the section modulus ($S = bh^2/6$ for a rectangular section), or:

$$M_a = f_a \left(\frac{h^2}{6} \right)$$

The allowable transverse flexural stress in the top flange of a precast segment is equal to $0.0948\sqrt{f'_c}$. Using 6 ksi concrete, the allowable stress would be 0.232 ksi (33.4 ksf). Solving for the prestress force requirements:

Section	Root of Cantilever	Edge of Top Flange	Centerline of Top Flange
Moment	-38.4	-24.7	8.19
$h/2 = c_1 = c_2$	0.87	0.87	0.369
Efficiency (ρ)	$\frac{1}{3}$	$\frac{1}{3}$	$\frac{1}{3}$
Eccentricity (e)	-0.60	-0.60	0.19
Moment Causing f_a	-16.9	-16.9	4.12
Required PT Force/ft	24.2	8.8	13.0

PRECAST SEGMENTAL BRIDGES**14.3.4.2 Required Prestressing Force /14.3.4.3 Transverse Post-Tensioning Tendon Placement and Tensioning**

Considering the limited example presented in this section, the governing cross section for required prestress force is the root of the cantilever. The prestress force required at this section is 24.2 kips/ft.

The final selection of the number and size of the post-tensioning tendons requires a study to determine the final force in the tendons. This work must include initial losses caused by friction, wobble and anchor set, and long-term losses resulting from concrete creep and shrinkage, as well as prestressing steel relaxation. Several commercially available software packages include modeling of the actual geometry of post-tensioning tendons, automatic generation of internal forces due to tendon tensioning, losses during tensioning, and long-term, time-dependent loss calculations.

Depending on the tendon profile in the top slab, the flexural restraint provided by the webs can result in secondary prestressing moments. These moments should be included in the summation of service limit state moments when determining the required prestressing force. The final value of the secondary moments is a function of the resulting prestress demand, thwarting a direct solution and slightly complicating the final prestress force. For the example in this section, a concordant tendon profile was used that produced no secondary moments.

The selection of the required prestress force satisfies just a part of the design requirements for the cross section. Other tasks that need to be performed include:

- Tensile and compressive stresses at all sections of the cantilever wings and top flange need to be verified at appropriate service limit states.
- Reinforcing requirements in the top flange need to be verified at appropriate strength limit states.
- Transverse bending moments in the webs need to be combined with shear reinforcing requirements to select final web reinforcement.

14.3.4.3 Transverse Post-Tensioning Tendon Placement and Tensioning

Figures 14.3-21 and 14.3-22 show photographs of the installation and tensioning of the transverse top flange tendons in a casting yard. Figure 14.3-21 shows the placement of the transverse oval duct within the reinforcing cage after positioning into the casting machine. The transverse ducts pass over the longitudinal tendons of this cantilever bridge and are connected to the anchorages, which are fixed to the cantilever wing bulkhead during the concrete pour. The ducts shown are plastic (typically polypropylene), which provide an important layer of corrosion protection to the transverse post-tensioning strands. Vertical grout inspection ports are located at the top of the anchorages to permit post-grouting inspections within the tendon.

Figure 14.3-21

Transverse Duct Placement in Casting Machine

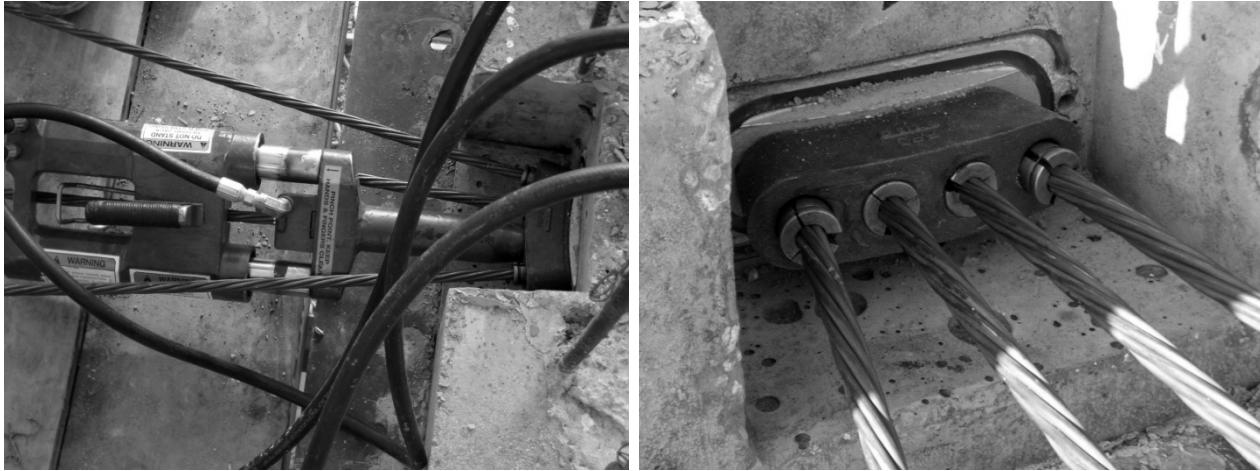


PRECAST SEGMENTAL BRIDGES**14.3.4.3 Transverse Post-Tensioning Tendon Placement and Tensioning/14.6.1 Transfer of Vertical Shear Forces to Bearings**

The photograph on the left of Figure 14.3-22 shows the tensioning of a four-strand transverse tendon using a mono-strand tensioning ram. The photograph on the right is a close view of the transverse tendon anchorage and wedge block after tensioning the two center strands. Following tensioning, strand “tails” are cut off, permanent grout caps are placed over the anchorages, the tendons are grouted, anchorage block-outs are filled with concrete, and protective coatings are applied.

Figure 14.3-22

Mono-Strand Tensioning of a Four-Strand Tendon (left). Anchorage after Tensioning Second Strand (right).

**14.4 BALANCED CANTILEVER CONSTRUCTION**

To be released in 2012

14.5 SPAN-BY-SPAN CONSTRUCTION

To be released in 2012

14.6 DIAPHRAGMS, ANCHOR BLOCKS AND DEVIATION DETAILS

Special precast segments at piers, expansion joints, and abutments contain diaphragms to stiffen and strengthen the typical segment to transfer loads from the superstructure to the supporting substructure. Diaphragms work to transfer shear forces in the webs to the bridge bearings, stiffen the box girder with regard to torsion, and provide a location for anchoring and deviating post-tensioning tendons. This section develops basic load-carrying considerations for diaphragm design.

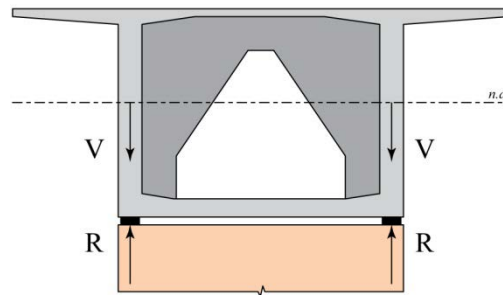
14.6.1 Transfer of Vertical Shear Forces to Bearings

Figure 14.6-1 shows a fundamental arrangement of a vertical web box girder supported by bearings on a pier. In this arrangement, the pier is sufficiently wide to allow the bearings to be placed directly below the axes of the vertical webs. The diaphragm in this arrangement sees no real force under the action of vertical loads.

PRECAST SEGMENTAL BRIDGES

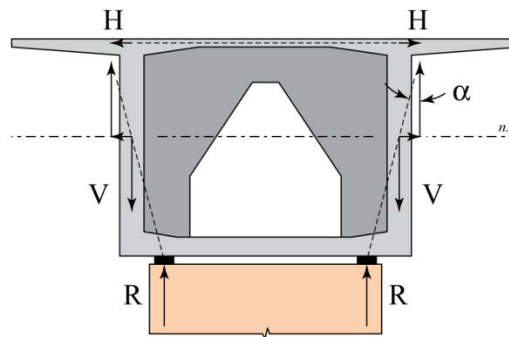
14.6.1 Transfer of Vertical Shear Forces to Bearings

Figure 14.6-1
Concentric Web/Bearing Orientation



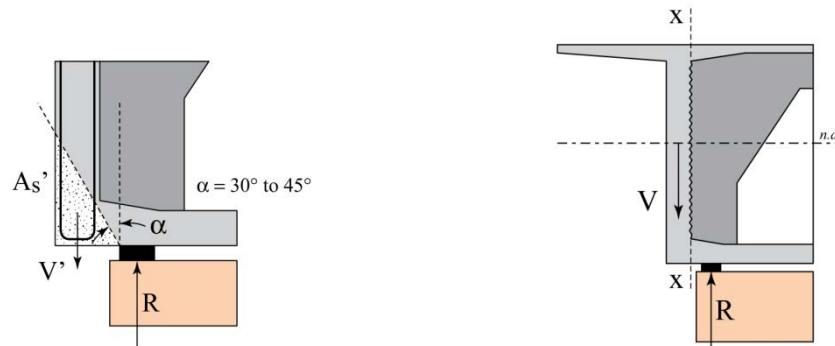
Using the diaphragm to transfer vertical forces, the spacing of bearings may be reduced and the width of the pier cap greatly reduced. This narrowing of the pier cap provides significant cost reduction while greatly enhancing aesthetics. **Figure 14.6-2** shows this bearing configuration for the case of the vertical web box girder. Using strut and tie modeling the horizontal forces developed by the eccentricity of the web to the bearing can be computed. Though occurring over the depth of the box girder, the transverse reinforcing or post-tensioning used to resist the horizontal forces is typically placed near the top of the diaphragm, detailed to fully develop the width of the webs.

Figure 14.6-2
Eccentric Web Bearing Orientation



In addition to horizontal transverse tension, **Figure 14.6-3** shows two other force transfer mechanisms that need to be investigated when the line of action of the web is eccentric to the bearings. Shear friction at the interface of the web and diaphragm, as shown in the sketch on the left in **Figure 14.6-3**, should be evaluated and reinforced in accordance with *LRFD Specifications* requirements. Locally, web reinforcement at the bottom of the web is subjected to a direct tension that should be included in the web reinforcing selection for the pier or abutment segment.

Figure 14.6-3
General Shear-Friction and Localized Direct Tension

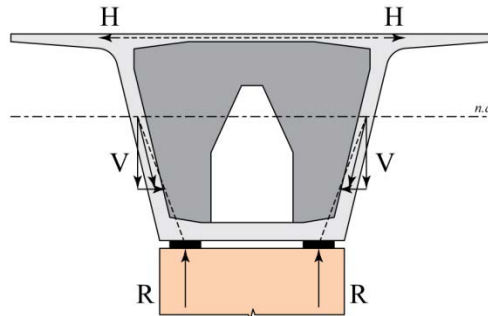


PRECAST SEGMENTAL BRIDGES

14.6.1 Transfer of Vertical Shear Forces to Bearings/14.6.2 Transfer of Longitudinal Moment to Bearings

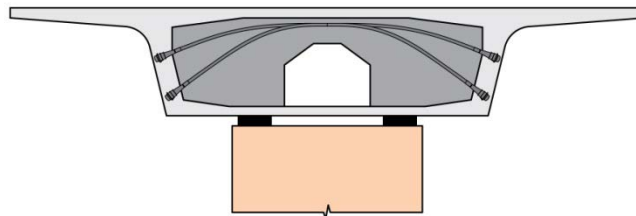
Further cost savings and improved aesthetics are achieved in precast segmental construction through the use of inclined webs. **Figure 14.6-4** shows the impact on transverse horizontal forces when inclined webs are used. The combination of web slope and bearing offset work to increase transverse horizontal force in the diaphragm.

Figure 14.6-4
Vertical Force Transfer with Inclined Webs



As in the case of the vertical web box girders, the bearing spacing can be further reduced in bridges with inclined webs to again reduce substructure costs and improve aesthetics. **Figure 14.6-5** depicts a box girder with significant eccentricity between the web line of action and bearings. In this instance, transverse post-tensioning is used to “lift” the web forces to the top of the diaphragm where they may then be transferred to the bearings.

Figure 14.6-5
Transverse Post-Tensioning in Diaphragms



14.6.2 Transfer of Longitudinal Moment to Bearings

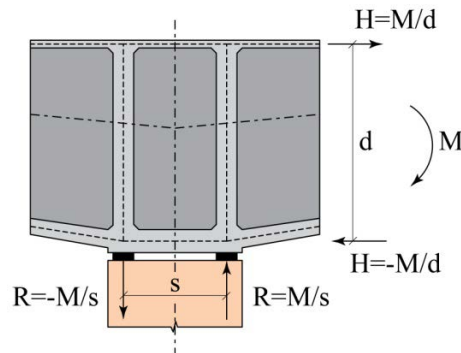
Overall structural behavior may lead a designer to use a moment-resisting connection between the superstructure and substructure. This is typically achieved in precast segmental construction with the use of two rows of bearings. The longitudinal bending moments in the superstructure are transferred through differential reactions on the bearings as shown in **Figure 14.6-6**. In this figure, two vertical diaphragms are used to transfer forces to the bearings. The differential forces resulting from the moment transferred to the bearings is coupled with vertical forces from the webs to design the particular diaphragm.

PRECAST SEGMENTAL BRIDGES

14.6.2 Transfer of Longitudinal Moment to Bearings

Figure 14.6-6

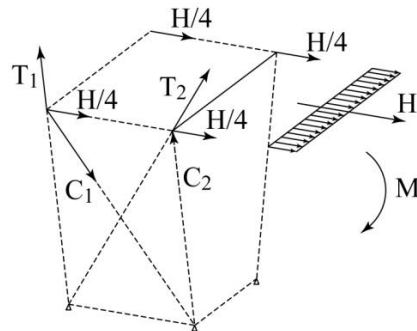
“Fixed” Connection Between Precast Superstructure and Substructure—Vertical Diaphragms



Within the pier segment, the flow of forces needs to be resolved between the diaphragms and portion of web between the diaphragms. **Figure 14.6-7** presents one strut-and-tie layout for this consideration. The horizontal force in the top flange produced by the moment being transferred is distributed to four nodal points at the top of the diaphragm-web intersections. Compression and tensile forces in the strut-and-tie model are developed considering the specific geometry of the members. The resulting forces in the webs are superimposed with other loads to select appropriate reinforcing in the webs between the diaphragms.

Figure 14.6-7

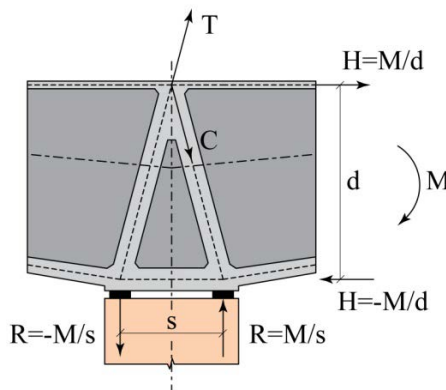
“Fixed” Connection Between Precast Superstructure and Substructure—Vertical Diaphragms



One option available to the designer to minimize the web forces between the bearings is by using inclined diaphragms shown in **Figure 14.6-8**. The differential bearing forces are resolved directly into the inclined diaphragms. The downside to this solution is the forming difficulties for the precast pier segment.

Figure 14.6-8

“Fixed” Connection Between Precast Superstructure and Substructure—Inclined Diaphragms



14.6.3 Transfer of Torsion to Bearings

Forces acting on the superstructure eccentric to the center of torsion will produce torsional moments in the precast segmental box girder. The torsional moments are resisted in shear flow around the closed box section. The shear flow and resulting shear stress due to torsion are given by:

$$\phi = \frac{M_t}{2A_o}$$

$$\tau_i = \frac{\phi}{t_i}$$

Where: M_t = applied torsional moment (length-force)

A_o = sectoral area (length²)

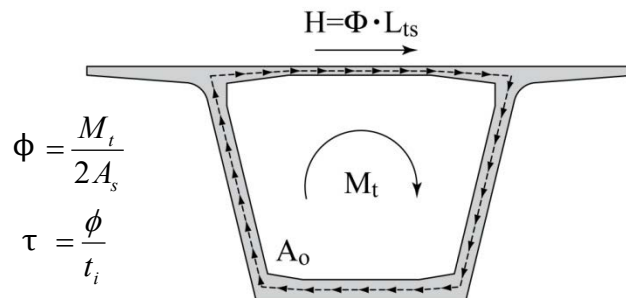
t_i = thickness of the i^{th} member of the cross section (length)

ϕ = shear flow (force/length)

τ_i = shear stress in the i^{th} member of the cross section (force/length²)

The sectoral area is that area bounded by the centerlines of the members of the closed box cross section. **Figure 14.6-9** shows the concept of shear flow and the limits of the sectoral area. The equations presented here, along with those typically used for the torsional stiffness of a precast segmental superstructure, are simplified from more complete expressions that include the effect of the cantilever wings. Generally speaking, for most precast segmental bridges, this behavior is small and may be neglected.

Figure 14.6-9
Shear Flow Resulting from Torsional Forces



Torsional moments along a span are transferred to the substructure at the bearings. The shear flow in the top flange caused by the torsional moment reaction produces a horizontal force in the top flange as shown in **Figure 14.6-9**. Diaphragms located in the pier segments are designed to resist the horizontal force in the top flange, and maintain the integrity of the transverse cross section of the superstructure. **Figure 14.6-10** and **Figure 14.6-11** show two common configurations of torsion-resisting diaphragms. The diaphragm in **Figure 14.6-10** resists torsion in an “A-shaped” configuration, while the diaphragm in **Figure 14.6-11** resists torsion in a “V-shaped” fashion. The tension and compression components are evaluated by strut-and-tie models. Tension forces are resisted by either mild reinforcing or inclined post-tensioning. Compressive stresses produced by the compressive forces are verified to establish the minimum concrete dimensions.

PRECAST SEGMENTAL BRIDGES

14.6.3 Transfer of Torsion to Bearings/14.6.4 Shear-Friction Resistance

Figure 14.6-10
"A"-Shaped Torsion Diaphragm

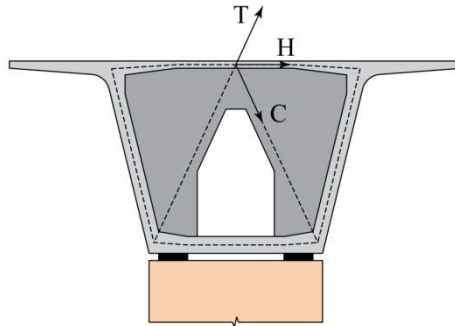
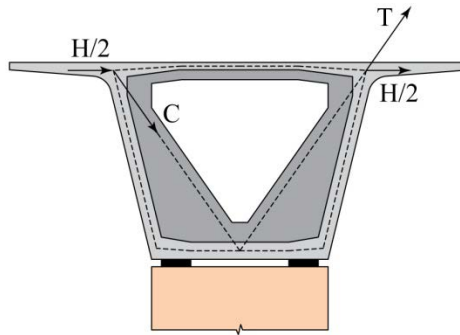
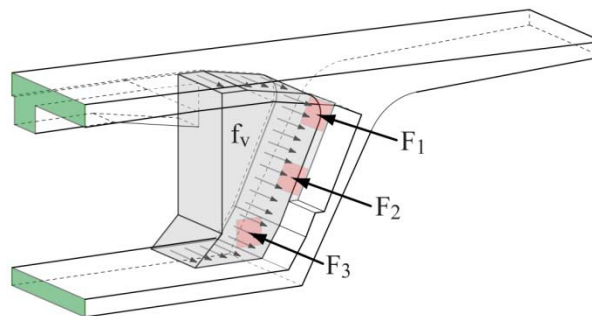


Figure 14.6-11
"V"-Shaped Torsion Diaphragm



14.6.4 Shear-Friction Resistance

Figure 14.6-12
Shear-Friction Forces from Post-Tensioning



14.6.5 Diaphragm Face Tension

Figure 14.6-13
Typical Anchorage Configuration in Span-By-Span Construction

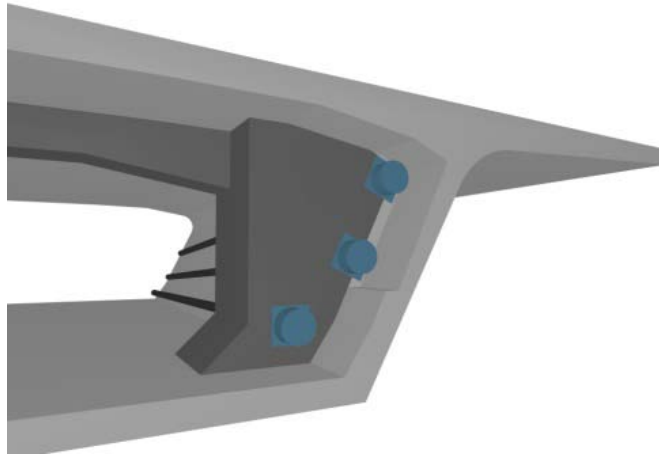


Figure 14.6-14
Strut-and-Tie Modeling for Back-face Tension

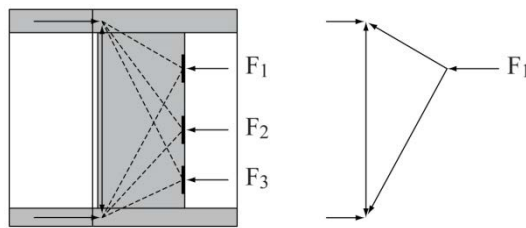
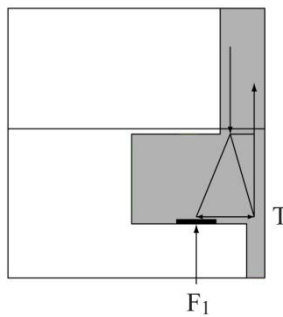


Figure 14.6-15
Strut-and-Tie Modeling for Front-Face Tension



PRECAST SEGMENTAL BRIDGES

14.7 Geometry Control/14.8.3 Selection of Prestressing Force for a Given Eccentricity

14.7 GEOMETRY CONTROL

To be released in 2012

14.8 PRESTRESSING WITH POST-TENSIONING

14.8.1 Introduction

Service limit state flexural verification of prestressed concrete members typically involves summing stresses due to applied forces with comparison to permissible stresses. It is often more convenient, however, to work with moments and forces when designing prestressed members. This section provides expressions for prestressing based on force and eccentricity.

14.8.2 Cross Section and Sign Convention

Consider a beam shown in **Figure 14.8.2-1**, with the following cross-section properties:

A = area (length²)

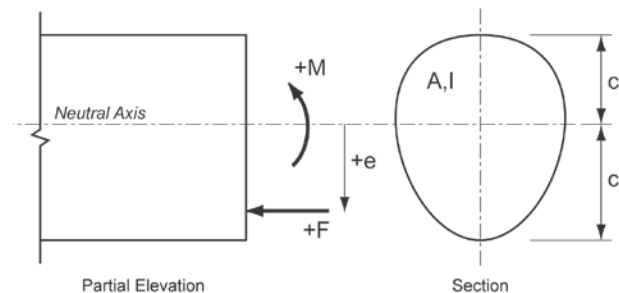
I = moment of inertia (length⁴)

c_1 = distance from neutral axis to the extreme top fiber

c_2 = distance from neutral axis to extreme bottom fiber

Figure 14.8.2-1

Cross Section Nomenclature and Sign Convention



The cross section is assumed to be symmetrical about its vertical axis and the prestressing is symmetrically applied so that there is no biaxial bending. **Figure 14.8.2-1** also shows positive sign conventions for prestressing force (F), eccentricity of prestressing (e), and externally applied bending moments (M). For the conventions of this section, compressive stresses in the concrete are positive (+) and tensile stresses in the concrete are negative (-).

14.8.3 Selection of Prestressing Force for a Given Eccentricity

Stresses are determined at the extreme top and bottom fibers by the familiar equations:

$$f_T = \frac{F}{A} - \frac{Fec_1}{I} + \frac{Mc_1}{I} \quad (\text{Eq. 14.8.3-1})$$

$$f_B = \frac{F}{A} + \frac{Fec_2}{I} - \frac{Mc_2}{I} \quad (\text{Eq. 14.8.3-2})$$

These equations can be rearranged to express the required prestressing force as a function of the other equation variables.

PRECAST SEGMENTAL BRIDGES**14.8.3 Selection of Prestressing Force for a Given Eccentricity**

Consider first the prestressing requirements for midspan of a simple-span beam. The minimum required prestressing force would be that which satisfies Equation 14.8.3-2 when the bottom stress f_B is set to a permissible concrete stress f_A . Making this substitution and multiplying Equation 14.8.3-2 by the moment of inertia and dividing by the distance from the neutral axis to the extreme bottom fiber the equation becomes:

$$\frac{f_A I}{c_2} \leq \frac{F I}{A c_2} + F e - M \quad (\text{Eq. 14.8.3-3})$$

This equation can be reduced further by noting that the left hand side of the equation is a bending moment that produces the permissible stress in the concrete:

$$M_A = \frac{f_A I}{c_2} \quad (\text{Eq. 14.8.3-4})$$

Equation 14.8.3-3 now becomes:

$$M_A \leq \frac{F I}{A c_2} + F e - M \quad (\text{Eq. 14.8.3-5})$$

Further simplification is made by defining the dimensionless parameter:

$$\rho = \frac{I}{A c_1 c_2} \quad (\text{Eq. 14.8.3-6})$$

The parameter ρ is termed the “efficiency” of the cross section with regard to prestressing. Recognizing that:

$$\rho c_2 = \frac{I}{A c_1} \quad (\text{Eq. 14.8.3-7})$$

Equation 14.8.3-5 is now simplified to:

$$M_A \leq F \rho c_2 + F e - M \quad (\text{Eq. 14.8.3-8})$$

Solving for the prestressing force:

$$F \geq \frac{M + M_A}{\rho c_2 + e} \quad (\text{Eq. 14.8.3-9})$$

The numerator of this equation is the bending moment at the cross section under study, adjusted by the moment causing allowable stress. The sign of M_A is established by the sign of the allowable stress at the section. A permissible tension would cause M_A to be negative, reducing the required prestressing force. A requirement for a residual compressive stress would cause M_A to be positive, increasing the required prestressing force.

The denominator of Equation 14.8.3-9 is the lever arm of the prestressing force required to offset the net bending moment about the upper kern of the cross section. For precast segmental construction, where no tension is allowed at the joints between segments ($M_A = 0$), Equation 14.8.3-9 becomes:

$$F \geq \frac{M}{\rho c_2 + e} \quad (\text{Eq. 14.8.3-10})$$

This exercise can be repeated for minimum stress control at the top of a cross section. Typical cases are cross sections at the face of piers during balanced cantilever construction of precast segmental construction. In this case, Equation 14.8.3-1 can be adjusted to find:

$$F \geq \frac{M - M_A}{e - \rho c_2} \quad (\text{Eq. 14.8.3-11})$$

PRECAST SEGMENTAL BRIDGES**14.8.3 Selection of Prestressing Force for a Given Eccentricity/14.8.4 Permissible Eccentricities for a Given Prestressing Force**

For precast segmental construction, where no tension is allowed at the joints between segments ($M_A = 0$), Equation 14.8.3-11 becomes:

$$F \geq \frac{M}{e - \rho c_2} \quad (\text{Eq. 14.8.3-12})$$

14.8.4 Permissible Eccentricities for a Given Prestressing Force

Equations for determining prestressing force as a function of a given eccentricity were developed. These equations can be used to solve for the prestressing force at a critical section. With the required prestressing force established, it is necessary to locate the tendon profile such that the stress limitations are met along the entire length of the member. Permissible ranges of eccentricity can be determined in a fashion similar to those expressions for force in the previous section.

First, consider the question: How low can the eccentricity be while not exceeding a specified minimum stress at the top of the member. Beginning again with Equation 14.8.3-1:

$$f_T \leq \frac{F}{A} - \frac{Fec_1}{I} + \frac{Mc_1}{I} \quad (\text{Eq. 14.8.3-1})$$

Again, multiply Equation 14.8.3-1 by the moment of inertia (I) and divide through by the distance to the extreme top fiber (c_1):

$$\frac{f_T I}{c_1} \leq \frac{FI}{Ac_1} - Fe + M \quad (\text{Eq. 14.8.4-13})$$

Substituting M_A and ρc_2 :

$$M_A \leq F\rho c_2 - Fe + M \quad (\text{Eq. 14.8.4-14})$$

Solving for the eccentricity:

$$e \leq \rho c_2 + \left(\frac{M - M_A}{F} \right) \quad (\text{Eq. 14.8.4-15})$$

If a tensile stress is allowed, M_A will be negative, negating the negative sign in the numerator. The result is that the tendon eccentricity can be lowered (made more positive). In the opposite sense, a residual compression reduces the permissible eccentricity. For precast segmental construction, M_A is equal to zero and Equation 14.8.4-15 may be simplified to:

$$e \leq \rho c_2 + \frac{M}{F} \quad (\text{Eq. 14.8.4-16})$$

When no moment is acting on the cross section, this equation reduces further to:

$$e \leq \rho c_2 \quad (\text{Eq. 14.8.4-17})$$

The equality portion of this equation defines the lower limit of the kern of the cross section. The lower kern limit is the lowest eccentricity of a force on a cross section that does not produce a tensile stress on the opposite extreme fiber.

This exercise can be repeated for determining the highest eccentricity (most negative) at which a force can be applied while not producing tension on the extreme bottom fiber. The resulting equation is:

$$e \leq -\rho c_1 + \left(\frac{M + M_A}{F} \right) \quad (\text{Eq. 14.8.4-18})$$

PRECAST SEGMENTAL BRIDGES**14.8.4 Permissible Eccentricities for a Given Prestressing Force /14.10 PCI Journal Segmental Bridge Bibliography**

If a tensile stress is allowed, M_A will be negative, reducing the numerator. The result is that the tendon eccentricity can be raised (made more negative). In the opposite sense, a residual compression increases the permissible eccentricity. For precast segmental construction, M_A is equal to zero and Equation 14.8.4-18 may be simplified to:

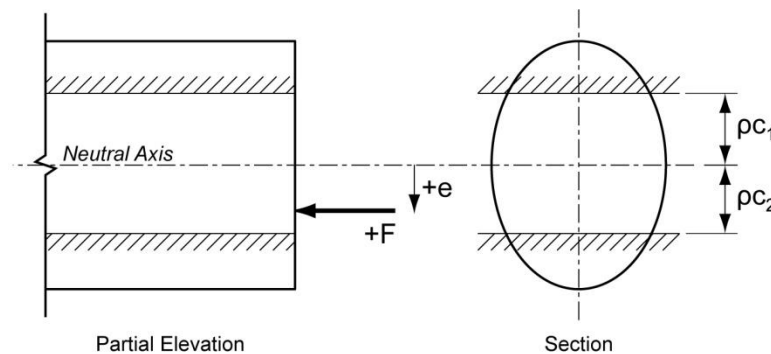
$$e \leq -\rho c_1 + \frac{M}{F} \quad (\text{Eq. 14.8.4-19})$$

When no moment is acting on the cross section, this equation reduces further to:

$$e \leq -\rho c_1 \quad (\text{Eq. 14.8.4-20})$$

The equality portion of this equation defines the upper limit of the kern of the cross section. The upper kern limit is the lowest eccentricity of a force on a cross section that does not produce a tensile stress on the opposite extreme fiber.

Figure 14.8.4-1
Limits of Eccentricity for a Prestressing Force, F

**14.9 CITED REFERENCES**

1. American Segmental Bridge Institute
<http://asbi-assoc.org>
2. ASBI 2008 "Construction Practices Handbook for Concrete Segmental and Cable-Supported Bridges", Second Edition
<http://www.asbi-assoc.org/cfcs/cmsIT/baseComponents/fileManagerProxy.cfc?method=GetFile&fileID=0F83A220-F1F6-B13E-8924C226E711CC5E> (Fee)
3. FHWA, 2004. "Post-Tensioning Tendon Installation and Grouting Manual"
<http://www.fhwa.dot.gov/bridge/pt/pt.pdf>
4. Post-Tensioning Institute
<http://www.post-tensioning.org>

14.10 PCI JOURNAL SEGMENTAL BRIDGE BIBLIOGRAPHY

1. Abdel-Halim, M. R. M. McClure, and H. H. West. 1987. "Overload Behavior of an Experimental Precast Prestressed Concrete Segmental Bridge." *PCI Journal*, Precast/Prestressed Concrete Institute, Chicago, IL. Vol. 32, No. 6, (November-December), pp. 102-123.
http://www.pci.org/view_file.cfm?file=JL-87-NOVEMBER-DECEMBER-7.pdf
http://www.pci.org/view_file.cfm?file=JL-87-NOVEMBER-DECEMBER-8.pdf

PRECAST SEGMENTAL BRIDGES**14.8.4 Permissible Eccentricities for a Given Prestressing Force /14.10 PCI Journal Segmental Bridge Bibliography**

2. Abrahams, M. J. and G. Wilson. 1998. "Precast Prestressed Segmental Floating Drawspan for Admiral Clarey Bridge." *PCI Journal*, Precast/Prestressed Concrete Institute, Chicago, IL. Vol. 43, No. 4. (July-August), pp. 60-79.
http://www.pci.org/view_file.cfm?file=JL-98-JULY-AUGUST-4.pdf
http://www.pci.org/view_file.cfm?file=JL-98-JULY-AUGUST-5.pdf
3. Alberdi Jr., T. 1980. "Value Engineering vs. Alternate Designs in Bridge Bidding." *PCI Journal*, Precast/Prestressed Concrete Institute, Chicago, IL, Vol. 25, No. 4, (July-August), pp. 41-47.
http://www.pci.org/view_file.cfm?file=JL-80-JULY-AUGUST-6.pdf
http://www.pci.org/view_file.cfm?file=JL-80-JULY-AUGUST-7.pdf
4. Barbaux, S. H. and C. C. Zollman. 1986. "Rehabilitation of the Boivre Viaduct—A Multispan Prestressed Box Girder Bridge." *PCI Journal*, Precast/Prestressed Concrete Institute, Chicago, IL. Vol. 31, No. 3, (May-June), pp. 22-47.
http://www.pci.org/view_file.cfm?file=JL-86-MAY-JUNE-2.pdf
http://www.pci.org/view_file.cfm?file=JL-86-MAY-JUNE-3.pdf
5. Barker, J. M. 1980. "Construction Techniques for Segmental Concrete Bridges." *PCI Journal*, Precast/Prestressed Concrete Institute, Chicago, IL. Vol. 25, No. 4, (July-August), pp. 66-86.
http://www.pci.org/view_file.cfm?file=JL-80-JULY-AUGUST-9.pdf
6. Bassi, K. G., W. L. Lin, G. Al-Bazi, and O. E. Ramkko. 1984. "The Twelve Mile Creek Precast Prestressed Segmental Bridges." *PCI Journal*, Precast/Prestressed Concrete Institute, Chicago, IL. Vol. 29, No. 6, (November-December), pp. 30-47.
7. Bazant, Z. P. and L. Panula. 1980. "Creep and Shrinkage Characterization for Analyzing Prestressed Concrete Structures." *PCI Journal*, Precast/Prestressed Concrete Institute, Chicago, IL. Vol. 25, No. 3, (May-June), pp. 86-122.
http://www.pci.org/view_file.cfm?file=JL-80-MAY-JUNE-5.pdf
8. Bender, B. F. 1977. "Provisions for Possible Reconstruction of Decks on Segmental Box Girder Bridges." *PCI Journal*, Precast/Prestressed Concrete Institute, Chicago, IL. Vol. 22, No. 4, (July-August), pp. 80-84
http://www.pci.org/view_file.cfm?file=JL-77-JULY-AUGUST-7.pdf
9. Bender, B. F. and H. H. Janssen. 1982. "Geometry Control of Precast Segmental Concrete Bridges." *PCI Journal*, Precast/Prestressed Concrete Institute, Chicago, IL. Vol. 27, No. 4, (July-August), pp. 72-86.
10. Billington, S. L., R. W. Barnes, and J. E. Breen. 1999. "A Precast Segmental Substructure System for Standard Bridges." *PCI Journal*, Precast/Prestressed Concrete Institute, Chicago, IL. Vol. 44. No. 4, (July-August), pp. 56-73.
http://www.pci.org/view_file.cfm?file=JL-99-JULY-AUGUST-4.pdf
http://www.pci.org/view_file.cfm?file=JL-99-JULY-AUGUST-5.pdf
11. Breen, J. E. 1985. "Controlling Twist in Precast Segmental Concrete Bridges." *PCI Journal*, Precast/Prestressed Concrete Institute, Chicago, IL. Vol. 30, No. 4, (July-August), pp. 86-111.
12. Breen, J. E. 1990. "Prestressed Concrete: The State of the Art in North America." *PCI Journal*, Precast/Prestressed Concrete Institute, Chicago, IL. Vol. 35, No. 6, (November-December), pp. 62-67.
http://www.pci.org/view_file.cfm?file=JL-90-NOVEMBER-DECEMBER-5.pdf
13. Bridges, C. P. and C. S. Coulter. 1979. "Geometry Control for Intercity Bridge." *PCI Journal*, Precast/Prestressed Concrete Institute, Chicago, IL. Vol. 24, No. 3, (May-June), pp. 112-125.

PRECAST SEGMENTAL BRIDGES**14.8.4 Permissible Eccentricities for a Given Prestressing Force /14.10 PCI Journal Segmental Bridge Bibliography**

14. Brockmann, C. and H. Rogenhofer. 2000. "Bang Na Expressway, Bangkok, Thailand—World's Longest Bridge and Largest Precasting Operation." *PCI Journal*, Precast/Prestressed Concrete Institute, Chicago, IL. Vol. 45, No. 1, (January-February), pp. 26-38.
http://www.pci.org/view_file.cfm?file=JL-00-JANUARY-FEBRUARY-5.pdf
15. Chandra, V. and A. L. Ricci. 2000. "Central Artery/Tunnel Project: A Precast Bonanza—Part 1." *PCI Journal*, Precast/Prestressed Concrete Institute, Chicago, IL. Vol. 45, No. 3, (May-June), pp. 14-20.
http://www.pci.org/view_file.cfm?file=JL-00-MAY-JUNE-1.pdf
16. Chandra, V. and A. L. Ricci. 2001. "Central Artery/Tunnel Project: Boston's Engineering Marvel—Where We Are Now." *PCI Journal*, Precast/Prestressed Concrete Institute, Chicago, IL. Vol. 45, No. 2, (March-April).
http://www.pci.org/view_file.cfm?file=JL-01-MARCH-APRIL-3.pdf
17. Donington, K., P. Towell, and V. Chandra. 2000. "Central Artery/Tunnel Project: Precast/Prestressed Structures Span the Big Dig." *PCI Journal*, Precast/Prestressed Concrete Institute, Chicago, IL. Vol. 45, No. 5, (September-October), pp. 30-33.
http://www.pci.org/view_file.cfm?file=JL-00-SEPTEMBER-OCTOBER-5.pdf
18. Dudra, J. 1966. "Design and Construction of Hudson Hope Bridge." *PCI Journal*, Precast/Prestressed Concrete Institute, Chicago, IL. Vol. 11, No. 2, (April), pp. 52-72.
19. Elbadry, M. M. and A. Ghali. 1989. "Serviceability Design of Continuous Prestressed Concrete Structures." *PCI Journal*, Precast/Prestressed Concrete Institute, Chicago, IL. Vol. 34, No. 1, (January-February), pp. 54-91.
http://www.pci.org/view_file.cfm?file=JL-89-JANUARY-FEBRUARY-4.pdf
http://www.pci.org/view_file.cfm?file=JL-89-JANUARY-FEBRUARY-5.pdf
20. Eriksson, R. L. and S. Zendegui. 1985. "Segmental Design of the Harbour Island People Mover." *PCI Journal*, Precast/Prestressed Concrete Institute, Chicago, IL. Vol. 30, No. 4, (July-August), pp. 38-51.
21. Figg Jr., E. C. 1997. "Proposed AASHTO Standards for Segmental Bridges Represent a Growing Market for the Precast Concrete Industry." *PCI Journal*, Precast/Prestressed Concrete Institute, Chicago, IL. Vol. 42, No. 5, (September-October), pp. 30-31.
http://www.pci.org/view_file.cfm?file=JL-97-SEPTEMBER-OCTOBER-4.pdf
22. Figg, L. and D. Pate. 2004. "Precast Concrete Segmental Bridges—America's Beautiful and Affordable Icons," *PCI Journal*, Precast/Prestressed Concrete Institute, Chicago, IL. Vol. 49, No. 5, (September-October), pp. 26-39.
http://www.pci.org/view_file.cfm?file=JL-04-SEPTEMBER-OCTOBER-9.pdf
23. Freyermuth, C. L. 1982. "Post-Tensioning Details for Long-Span Concrete Bridges." *PCI Journal*, Precast/Prestressed Concrete Institute, Chicago, IL. Vol. 27, No. 6, (November-December), pp. 48-65.
24. Freyermuth, C. L. 1997. "AASHTO-PCI-ASBI Segmental Box Girder Standards: A New Product for Grade Separations and Interchange Bridges." *PCI Journal*, Precast/Prestressed Concrete Institute, Chicago, IL. Vol. 42, No. 5, (September-October), pp. 32-42.
http://www.pci.org/view_file.cfm?file=JL-97-SEPTEMBER-OCTOBER-5.pdf
25. Freyermuth, C. L. 1999. "Ten Years of Segmental Achievements and Projections for the Next Century." *PCI Journal*, Precast/Prestressed Concrete Institute, Chicago, IL. Vol. 44, No. 3, (May-June), pp. 36-52.
http://www.pci.org/view_file.cfm?file=JL-99-MAY-JUNE-4.pdf
http://www.pci.org/view_file.cfm?file=JL-99-MAY-JUNE-5.pdf

PRECAST SEGMENTAL BRIDGES**14.8.4 Permissible Eccentricities for a Given Prestressing Force /14.10 PCI Journal Segmental Bridge Bibliography**

26. Gallaway, T. M. 1980. "Design Features and Prestressing Aspects of Long Key Bridge." *PCI Journal*, Precast/Prestressed Concrete Institute, Chicago, IL. Vol. 25, No. 6, (November-December), pp. 84-96.
27. Gentilini, B. and L. Gentilini. 1975. "Precast Prestressed Segmental Elevated Urban Motorway in Italy." *PCI Journal*, Precast/Prestressed Concrete Institute, Chicago, IL. Vol. 20, No. 5, (September-October), pp. 26-43.
28. Gerwick Jr., B. C. 1966. "Bridge over the Eastern Scheldt." *PCI Journal*, Precast/Prestressed Concrete Institute, Chicago, IL. Vol. 11, No. 1, (February), pp. 53-59.
29. Gerwick Jr., B. C. 1982. "Causes and Prevention of Problems in Large-Scale Prestressed Concrete Construction." *PCI Journal*, Precast/Prestressed Concrete Institute, Chicago, IL. Vol. 27, No. 3, (May-June), pp. 58-75.
30. Goñi Baamonde, J. J. and A. M. García y Benitez. 2009. "Metrorrey's Linea 2 Extension Viaduct: A Revolution for Light-Rail Precast Concrete Segmental Bridges," *PCI Journal*, Precast/Prestressed Concrete Institute, Chicago, IL. Vol. 54, No. 4, (Fall), pp. 175-188.
http://www.pci.org/view_file.cfm?file=JL-09-FALL-15.pdf
31. Goodyear, D. and M. J. Smith. 1988. "A Practical Look at Creep and Shrinkage in Bridge Design." *PCI Journal*, Precast/Prestressed Concrete Institute, Chicago, IL. Vol. 33, No. 3, (May-June), pp. 108-121.
http://www.pci.org/view_file.cfm?file=JL-88-MAY-JUNE-8.pdf
32. Grant, A. 1979. "The Pasco-Kennewick Intercity Bridge." *PCI Journal*, Precast/Prestressed Concrete Institute, Chicago, IL. Vol. 24, No. 3, (May-June), pp. 90-111.
33. Grant, A. 1987. "Design and Construction of the East Huntington Bridge." *PCI Journal*, Precast/Prestressed Concrete Institute, Chicago, IL. Vol. 32, No. 1, (January-February), pp. 20-29.
http://www.pci.org/view_file.cfm?file=JL-87-JANUARY-FEBRUARY-2.pdf
34. Harwood, A. C. 1982. "I-205 Columbia River Bridge—Design and Construction Highlights." *PCI Journal*, Precast/Prestressed Concrete Institute, Chicago, IL. Vol. 27, No. 2, (March-April), pp. 56-77.
35. Herbert, T. J. 1990. "Computer Analysis of Deflections and Stresses in Stage Constructed Concrete Bridges." *PCI Journal*, Precast/Prestressed Concrete Institute, Chicago, IL. Vol. 35, No. 3, (May-June), pp. 52-63.
http://www.pci.org/view_file.cfm?file=JL-90-MAY-JUNE-5.pdf
36. Hoffman, P. C., R. M. McClure, and H. H. West, 1983. "Temperature Study of an Experimental Segmental Concrete Bridge." *PCI Journal*, Precast/Prestressed Concrete Institute, Chicago, IL. Vol. 28, No. 2, (March-April), pp. 78-97.
37. Hugenschmidt, F. 1974. "Epoxy Adhesives in Precast Prestressed Concrete Construction." *PCI Journal*, Precast/Prestressed Concrete Institute, Chicago, IL. Vol. 19, No. 2, (March-April), pp. 112-124.
http://www.pci.org/view_file.cfm?file=JL-74-MARCH-APRIL-8.pdf
38. Iverson, J. K., C. Banchik, R. Brantley, and J. Sage. 1999. "Precast Segmental Seismic Retrofit for the San Mateo-Hayward Bridge." *PCI Journal*, Precast/Prestressed Concrete Institute, Chicago, IL. Vol. 44, No. 6, (November-December), pp. 28-40.
http://www.pci.org/view_file.cfm?file=JL-99-NOVEMBER-DECEMBER-3.pdf
39. Joint PCI-PTI Committee on Segmental Construction 1982. "Recommended Practice for Precast Post-Tensioned Segmental Construction." *PCI Journal*, Precast/Prestressed Concrete Institute, Chicago, IL. Vol. 27, No. 1, (January-February), pp. 14-61.

PRECAST SEGMENTAL BRIDGES**14.8.4 Permissible Eccentricities for a Given Prestressing Force /14.10 PCI Journal Segmental Bridge Bibliography**

40. Kulka, F. and S. J. Thoman. 1983. "Feasibility Study of Standard Sections for Segmental Prestressed Concrete Box Girder Bridges." *PCI Journal*, Precast/Prestressed Concrete Institute, Chicago, IL. Vol. 28, No. 5, (September-October), pp. 54-77.
http://www.pci.org/view_file.cfm?file=JL-83-SEPTEMBER-OCTOBER-4.pdf
41. Lacey, G. C., J. E. Breen, and N. H. Burns. 1971. "State of the Art for Long Span Prestressed Concrete Bridges of Segmental Construction." *PCI Journal*, Precast/Prestressed Concrete Institute, Chicago, IL. Vol. 16, No. 5, (September-October), pp. 53-77.
http://www.pci.org/view_file.cfm?file=JL-71-SEPTEMBER-OCTOBER-4.pdf
42. Leonhardt, F. 1968. "Aesthetics of Bridge Design." *PCI Journal*, Precast/Prestressed Concrete Institute, Chicago, IL. Vol. 13, No. 1, (February), pp. 14-31.
43. Leonhardt, F. 1987. "Cable Stayed Bridges with Prestressed Concrete." *PCI Journal*, Precast/Prestressed Concrete Institute, Chicago, IL. Vol. 32, No. 5, (September-October), pp. 52-80.
http://www.pci.org/view_file.cfm?file=JL-87-SEPTEMBER-OCTOBER-4.pdf
44. Leonhardt, F. 1988. "Cracks and Crack Control in Concrete Structures." *PCI Journal*, Precast/Prestressed Concrete Institute, Chicago, IL. Vol. 33, No. 4, (July-August), pp. 124-145.
http://www.pci.org/view_file.cfm?file=JL-88-JULY-AUGUST-10.pdf
45. Lester, B. and G. Tadros. 1995. "Northumberland Strait Crossing: Design Development of Precast Prestressed Bridge Structure." *PCI Journal*, Precast/Prestressed Concrete Institute, Chicago, IL. Vol. 40, No. 5, (September-October), pp. 32-44.
http://www.pci.org/view_file.cfm?file=JL-95-SEPTEMBER-OCTOBER-4.pdf
46. Lin, T. Y. and C. Redfield. 1982. "Some Design Issues Facing American Bridge Constructors." *PCI Journal*, Precast/Prestressed Concrete Institute, Chicago, IL. Vol. 27, No. 4, (July-August), pp. 58-71.
47. Lovell, J. A. B. 1980. "The Islington Avenue Bridge." *PCI Journal*, Precast/Prestressed Concrete Institute, Chicago, IL. Vol. 25, No. 3, (May-June), pp. 32-66.
http://www.pci.org/view_file.cfm?file=JL-80-MAY-JUNE-3.pdf
48. Massicotte, B., A. Picard, Y. Gaumond, and C. Ouellet. 1994. "Strengthening of a long Span Prestressed Segmental Box Girder Bridge." *PCI Journal*, Precast/Prestressed Concrete Institute, Chicago, IL. Vol. 39, No. 3, (May-June), pp. 52-65.
http://www.pci.org/view_file.cfm?file=JL-94-MAY-JUNE-6.pdf
http://www.pci.org/view_file.cfm?file=JL-94-MAY-JUNE-7.pdf
49. Massicotte, B. and A. Picard. 1994. "Monitoring of a Prestressed Segmental Box Girder Bridge During Strengthening." *PCI Journal*, Precast/Prestressed Concrete Institute, Chicago, IL. Vol. 39, No.3, (May-June), pp. 66-80.
http://www.pci.org/view_file.cfm?file=JL-94-MAY-JUNE-8.pdf
http://www.pci.org/view_file.cfm?file=JL-94-MAY-JUNE-9.pdf
50. Matt, P. 1983. "Status of Segmental Bridge Construction in Europe." *PCI Journal*, Precast/Prestressed Concrete Institute, Chicago, IL. Vol. 28, No. 3, (May-June), pp. 104-125.
51. Megally, S., F. Seible, M. Garg, and R. K. Dowell. 2002. "Seismic Performance of Precast Segmental Bridge Superstructures with Internally Bonded Prestressing Tendons." *PCI Journal*, Precast/Prestressed Concrete Institute, Chicago, IL. Vol. 47, No. 2, (March-April), pp. 40-56.
http://www.pci.org/view_file.cfm?file=JL-02-MARCH-APRIL-4.pdf

PRECAST SEGMENTAL BRIDGES**14.8.4 Permissible Eccentricities for a Given Prestressing Force /14.10 PCI Journal Segmental Bridge Bibliography**

52. Megally, S., F. Seible, and R. K. Dowell. 2003. "Seismic Performance of Precast Segmental Bridges: Segment-to-Segment Joints Subjected to High Flexural Moments and Low Shears." *PCI Journal*, Precast/Prestressed Concrete Institute, Chicago, IL. Vol. 48, No. 2, (March-April), pp. 80-96.
http://www.pci.org/view_file.cfm?file=JL-03-MARCH-APRIL-6.pdf
53. Megally, S., M. J. Veletzos, K. Burnell, J. I. Restrepo, and F. Seible. 2009. "Seismic Performance of Precast Concrete Segmental Bridges: Summary of Experimental Research on Segment-to-Segment Joints." *PCI Journal*, Precast/Prestressed Concrete Institute, Chicago, IL. Vol. 54, No. 2, (Spring), pp. 116-142.
http://www.pci.org/view_file.cfm?file=JL-09-SPRING-12.pdf
http://www.pci.org/view_file.cfm?file=JL-09-SPRING-13.pdf
54. Miller, M. 1995. "Durability Survey of Segmental Concrete Bridges." *PCI Journal*, Precast/Prestressed Concrete Institute, Chicago, IL. Vol. 40, No. 3, (May-June), pp. 110-123.
http://www.pci.org/view_file.cfm?file=JL-95-MAY-JUNE-11.pdf
http://www.pci.org/view_file.cfm?file=JL-95-MAY-JUNE-12.pdf
55. Mondorf, P. E. 1993. "Design-Construction of Precast Segmental Elevated Metro Line for Monterrey, Nuevo León, Mexico." *PCI Journal*, Precast/Prestressed Concrete Institute, Chicago, IL. Vol. 38, No. 2, (March-April), pp. 42-56.
http://www.pci.org/view_file.cfm?file=JL-93-MARCH-APRIL-17.pdf
http://www.pci.org/view_file.cfm?file=JL-93-MARCH-APRIL-18.pdf
http://www.pci.org/view_file.cfm?file=JL-93-MARCH-APRIL-19.pdf
http://www.pci.org/view_file.cfm?file=JL-93-MARCH-APRIL-20.pdf
http://www.pci.org/view_file.cfm?file=JL-93-MARCH-APRIL-21.pdf
http://www.pci.org/view_file.cfm?file=JL-93-MARCH-APRIL-22.pdf
http://www.pci.org/view_file.cfm?file=JL-93-MARCH-APRIL-23.pdf
http://www.pci.org/view_file.cfm?file=JL-93-MARCH-APRIL-24.pdf
http://www.pci.org/view_file.cfm?file=JL-93-MARCH-APRIL-25.pdf
http://www.pci.org/view_file.cfm?file=JL-93-MARCH-APRIL-26.pdf
http://www.pci.org/view_file.cfm?file=JL-93-MARCH-APRIL-27.pdf
56. Moreton, A. J. 1989. "Segmental Bridge Construction in Florida—A Review and Perspective." *PCI Journal*, Precast/Prestressed Concrete Institute, Chicago, IL. Vol. 34, No. 3, (May-June), pp. 36-77.
http://www.pci.org/view_file.cfm?file=JL-89-MAY-JUNE-3.pdf
http://www.pci.org/view_file.cfm?file=JL-89-MAY-JUNE-4.pdf
57. Moustafa, S. E. 1974. "Ultimate Load Test of a Segmentally Constructed Prestressed Concrete I-Beam." *PCI Journal*, Precast/Prestressed Concrete Institute, Chicago, IL. Vol. 19, No. 4, (July-August), pp. 54-75.
http://www.pci.org/view_file.cfm?file=JL-74-JULY-AUGUST-5.pdf
58. Muller, J. 1975. "Ten Years of Experience in Precast Segmental Construction—A Special Report." *PCI Journal*, Precast/Prestressed Concrete Institute, Chicago, IL. Vol. 20, No. 1, (January-February), pp. 28-61.
http://www.pci.org/view_file.cfm?file=JL-75-JANUARY-FEBRUARY-3.pdf
http://www.pci.org/view_file.cfm?file=JL-75-JANUARY-FEBRUARY-4.pdf
59. Muller, J. 1980. "Construction of Long Key Bridge." *PCI Journal*, Precast/Prestressed Concrete Institute, Chicago, IL. Vol. 25, No. 6, (November-December), pp. 97-111.
60. Muller, J. and J. M. Barker. 1982. "Joint Heating Allows Winter Construction on Linn Cove Viaduct." *PCI Journal*, Precast/Prestressed Concrete Institute, Chicago, IL. Vol. 27, No. 5, (September-October), pp. 120-130.
61. Muller, J. M. and J. M. Barker. 1985. "Design and Construction of Linn Cove Viaduct." *PCI Journal*, Precast/Prestressed Concrete Institute, Chicago, IL. Vol. 30, No. 5, (September-October), 38-53.

PRECAST SEGMENTAL BRIDGES**14.8.4 Permissible Eccentricities for a Given Prestressing Force /14.10 PCI Journal Segmental Bridge Bibliography**

62. Nair, R. S. and J. K. Iverson. 1982. "Design and Construction of the Kishwaukee River Bridges." *PCI Journal*, Precast/Prestressed Concrete Institute, Chicago, IL. Vol. 27, No. 6, (November-December), pp. 22-47.
63. Palmer, A. M. 2006. "Fundamentals of Launching a Precast Concrete Segmental Operation for Bridge Construction Projects." *PCI Journal*, Precast/Prestressed Concrete Institute, Chicago, IL. Vol. 51, No. 3, (May-June), pp. 32-44.
http://www.pci.org/view_file.cfm?file=JL-06-MAY-JUNE-6.pdf
64. Pate, D. 1995. "The Chesapeake and Delaware Canal Bridge—Design-Construction Highlights." *PCI Journal*, Precast/Prestressed Concrete Institute, Chicago, IL. Vol. 40, No. 5, (September-October), pp. 20-30.
http://www.pci.org/view_file.cfm?file=JL-95-SEPTEMBER-OCTOBER-3.pdf
65. PCI Committee on Segmental Construction. 1975. "Recommended Practice for Segmental Construction in Prestressed Concrete." *PCI Journal*, Precast/Prestressed Concrete Institute, Chicago, IL. Vol. 20, No. 2, (March-April), pp. 22-41.
66. PCI Bridge Committee. 1975. "Tentative Design and Construction Specifications for Precast Segmental Box Girder Bridges." *PCI Journal*, Precast/Prestressed Concrete Institute, Chicago, IL. Vol. 20, No. 4, (July-August), pp. 34-42.
http://www.pci.org/view_file.cfm?file=JL-75-JULY-AUGUST-3.pdf
67. PCI Committee on Segmental Construction. 1975. "Recommended Practice for Segmental Construction in Prestressed Concrete." *PCI Journal*, Precast/Prestressed Concrete Institute, Chicago, IL. Vol. 20, No. 2, (March-April), pp. 22-41.
68. Pfeifer, D. 1982. "Development of the Concrete Technology for a Precast Prestressed Concrete Segmental Bridge." *PCI Journal*, Precast/Prestressed Concrete Institute, Chicago, IL. Vol. 27, No. 5, (September-October), pp. 78-99.
69. Phipps, A. R. and Q.D. Spruill Jr. 1990. "Biloxi Interstate-110 Viaduct." *PCI Journal*, Precast/Prestressed Concrete Institute, Chicago, IL. Vol. 35, No. 1, (January-February), pp. 120-132.
http://www.pci.org/view_file.cfm?file=JL-90-JANUARY-FEBRUARY-14.pdf
70. Polgieter, I. C. and W. L. Gamble. 1989. "Nonlinear Temperature Distributions in Bridges at Different Locations in the United States." *PCI Journal*, Precast/Prestressed Concrete Institute, Chicago, IL. Vol. 34, No. 4, (July-August), pp. 80-103.
http://www.pci.org/view_file.cfm?file=JL-89-JULY-AUGUST-5.pdf
http://www.pci.org/view_file.cfm?file=JL-89-JULY-AUGUST-6.pdf
71. Podolny Jr., W. 1979. "An Overview of Precast Prestressed Segmental Bridges." *PCI Journal*, Precast/Prestressed Concrete Institute, Chicago, IL. Vol. 24, No. 1, (January-February), pp. 56-87.
http://www.pci.org/view_file.cfm?file=JL-79-JANUARY-FEBRUARY-4.pdf
http://www.pci.org/view_file.cfm?file=JL-79-JANUARY-FEBRUARY-5.pdf
72. Podolny Jr., W. and A. A. Mireles. 1983. "Kuwait's Bubiyan Bridge—A 3-D Precast Segmental Space Frame." *PCI Journal*, Precast/Prestressed Concrete Institute, Chicago, IL. Vol. 28, No. 1, (January-February), pp. 68-107.
73. Podolny Jr., W. 1985. "The Cause of Cracking in Post-Tensioned Concrete Box Girder Bridges and Retrofit Procedures." *PCI Journal*, Precast/Prestressed Concrete Institute, Chicago, IL. Vol. 30, No. 2, (March-April), pp. 82-139.

PRECAST SEGMENTAL BRIDGES**14.8.4 Permissible Eccentricities for a Given Prestressing Force /14.10 PCI Journal Segmental Bridge Bibliography**

74. Podolny, Jr., W. 1986. "Evaluation of Transverse Flange Forces Induced by Laterally Inclined Longitudinal Post-Tensioning in Box Girder Bridges." *PCI Journal*, Precast/Prestressed Concrete Institute, Chicago, IL. Vol. 31, No. 1, (January-February), pp. 44-61.
75. Poston, R. W., J. E. Breen, and R. L. Carrasquillo. 1989. "Design of Transversely Prestressed Concrete Bridge Decks." *PCI Journal*, Precast/Prestressed Concrete Institute, Chicago, IL. Vol. 34, No. 5, (September-October), pp. 68-109.
http://www.pci.org/view_file.cfm?file=JL-89-SEPTEMBER-OCTOBER-5.pdf
http://www.pci.org/view_file.cfm?file=JL-89-SEPTEMBER-OCTOBER-6.pdf
76. Project Story. 1967. "Report of the FIP Commission on Prefabrication." *PCI Journal*, Precast/Prestressed Concrete Institute, Chicago, IL. Vol. 12, No. 5, (October), pp. 41-53.
77. Project Story. 1979. "Quebec's Grand'Mere Bridge—935-ft Long Post-Tensioned Segmental Structure." *PCI Journal*, Precast/Prestressed Concrete Institute, Chicago, IL. Vol. 24, No. 1, (January-February), pp. 94-99.
http://www.pci.org/view_file.cfm?file=JL-79-JANUARY-FEBRUARY-7.pdf
78. Project Story. 1984. "Dauphin Island Bridge." *PCI Journal*, Precast/Prestressed Concrete Institute, Chicago, IL. Vol. 29, No. 1, (January-February).
79. Project Story. 1985. "MARTA Rapid Transit Bridges." *PCI Journal*, Precast/Prestressed Concrete Institute, Chicago, IL. Vol. 30, No. 2, (March-April), pp. 188-194.
80. Project Story. 1986. "Microcomputer Technology Assists Florida DOT." *PCI Journal*, Precast/Prestressed Concrete Institute, Chicago, IL. Vol. 31, No. 3, (May-June), pp. 139-143.
http://www.pci.org/view_file.cfm?file=JL-86-MAY-JUNE-11.pdf
81. Project Story. 1986. "Ramp 'I' Over I-75 and the Florida Turnpike Extension." *PCI Journal*, Precast/Prestressed Concrete Institute, Chicago, IL. Vol. 31, No.4, (July-August), pp. 116-119.
82. Project Story. 1989. "Ramp B Bridge Over U.S. Highway 23." *PCI Journal*, Precast/Prestressed Concrete Institute, Chicago, IL. Vol. 34, No. 1, (January-February), pp. 144-147.
http://www.pci.org/view_file.cfm?file=JL-89-JANUARY-FEBRUARY-10.pdf
83. Quinn, S. B. and M. J. Kopetz. 1982. "Design and Construction of the Houston Ship Channel Bridge." *PCI Journal*, Precast/Prestressed Concrete Institute, Chicago, IL. Vol. 27, No. 3, (May-June), pp. 30-57.
84. Rabbat, B. G. 1987. "Testing of Segmental Concrete Girders with External Tendons." *PCI Journal*, Precast/Prestressed Concrete Institute, Chicago, IL. Vol. 32, No. 2, (March-April), pp. 86-107.
http://www.pci.org/view_file.cfm?file=JL-87-MARCH-APRIL-7.pdf
85. Roberts-Wollmann, C. L., J. E. Breen, and M. E. Kreger. 1995. "Temperature Induced Deformations in Match-Cast Segments." *PCI Journal*, Precast/Prestressed Concrete Institute, Chicago, IL. Vol. 40, No. 4, (July-August), pp. 62-71.
http://www.pci.org/view_file.cfm?file=JL-95-JULY-AUGUST-9.pdf
86. Rodriguez, J., M. Hedayati, A. Taddeo, and J. Parks. 2004. "Precast Concrete Light Rail System Provides Mass Transit Solution for JFK International Airport." *PCI Journal*, Precast/Prestressed Concrete Institute, Chicago, IL. Vol. 49, No. 1, (January-February), pp. 32-44.
http://www.pci.org/view_file.cfm?file=JL-04-JANUARY-FEBRUARY-3.pdf

PRECAST SEGMENTAL BRIDGES**14.8.4 Permissible Eccentricities for a Given Prestressing Force /14.10 PCI Journal Segmental Bridge Bibliography**

87. Rosignoli, M. 2010. "Self-launching Erection Machines for Precast Concrete Bridges," *PCI Journal*, Precast/Prestressed Concrete Institute, Chicago, IL. Vol. 55, No. 1, (Winter 2010), pp. 36-57.
http://www.pci.org/view_file.cfm?file=JL-10-WINTER-9.pdf
88. Salas, R., A. Schokker, J. West, J. Breen, and M. Kreger. 2008. "Corrosion Risk of Bonded, Post-tensioned Concrete Elements." *PCI Journal*, Precast/Prestressed Concrete Institute, Chicago, IL. Vol. 53, No. 1, (January-February), pp. 89-107.
http://www.pci.org/view_file.cfm?file=JL-08-JANUARY-FEBRUARY-13.pdf
89. Sason, A. S. 1992. "Evaluation of Degree of Rusting on Prestressed Concrete Strand." *PCI Journal*, Precast/Prestressed Concrete Institute, Chicago, IL. Vol. 37, No. 3, (May-June), pp. 25-30.
http://www.pci.org/view_file.cfm?file=JL-92-MAY-JUNE-4.pdf
http://www.pci.org/view_file.cfm?file=JL-92-MAY-JUNE-5.pdf
90. Schupack, M. 1971. "Grouting Tests on Large Post-Tensioning Tendons for Secondary Nuclear Containment Structures." *PCI Journal*, Precast/Prestressed Concrete Institute, Chicago, IL. Vol. 16, No. 2, (March-April), pp. 85-97.
http://www.pci.org/view_file.cfm?file=JL-71-MARCH-APRIL-8.pdf
91. Schlaich, J., K. Schafer, and M. Jennewein. 1987. "Toward a Consistent Design of Structural Concrete." *PCI Journal*, Precast/Prestressed Concrete Institute, Chicago, IL. Vol. 32, No. 3, (May-June), pp. 74-150.
http://www.pci.org/view_file.cfm?file=JL-87-MAY-JUNE-5.pdf
http://www.pci.org/view_file.cfm?file=JL-87-MAY-JUNE-6.pdf
http://www.pci.org/view_file.cfm?file=JL-87-MAY-JUNE-7.pdf
http://www.pci.org/view_file.cfm?file=JL-87-MAY-JUNE-8.pdf
92. Shiu, K. N. and H. G. Russell. 1983. "Knowledge Gained from Instrumentation of the Kishwaukee River Bridge." *PCI Journal*, Precast/Prestressed Concrete Institute, Chicago, IL. Vol. 28, No. 5, (September-October), pp. 32-53.
http://www.pci.org/view_file.cfm?file=JL-83-SEPTEMBER-OCTOBER-3.pdf
93. Shushkewich, K. W. 1998. "Design of Segmental Bridges for Thermal Gradient." *PCI Journal*, Precast/Prestressed Concrete Institute, Chicago, IL. Vol. 43, No. 4, (July-August), pp. 120-137.
http://www.pci.org/view_file.cfm?file=JL-98-JULY-AUGUST-12.pdf
http://www.pci.org/view_file.cfm?file=JL-98-JULY-AUGUST-13.pdf
94. Shushkewich, K. W. 2003. "The Strutted Box Widening Method for Prestressed Concrete Segmental Bridges." *PCI Journal*, Precast/Prestressed Concrete Institute, Chicago, IL. (November-December), pp. 64-81.
http://www.pci.org/view_file.cfm?file=JL-03-NOVEMBER-DECEMBER-1.pdf
95. Sofia, M. J. and E. H. Homsy. 1994. "Fabrication and Erection of Precast Concrete Segmental Boxes for Baldwin Bridge." *PCI Journal*, Precast/Prestressed Concrete Institute, Chicago, IL. Vol. 39, No. 6, (November-December), pp. 36-52.
http://www.pci.org/view_file.cfm?file=JL-94-NOVEMBER-DECEMBER-5.pdf
96. Sowlat, K. and B. G. Rabbat. 1987. "Testing of Segmental Concrete Girders With External Tendons." *PCI Journal*, Precast/Prestressed Concrete Institute, Chicago, IL. Vol. 32, No. 2, (March-April), pp. 86-107.
http://www.pci.org/view_file.cfm?file=JL-87-MARCH-APRIL-7.pdf
97. Strasky, J. and M. Korenek. 1986. "Short Span Segmental Bridged in Czechoslovakia." *PCI Journal*, Precast/Prestressed Concrete Institute, Chicago, IL. Vol. 31, No. 1, (January-February), pp. 106-132.
http://www.pci.org/view_file.cfm?file=JL-86-JANUARY-FEBRUARY-4.pdf

PRECAST SEGMENTAL BRIDGES**14.8.4 Permissible Eccentricities for a Given Prestressing Force /14.10 PCI Journal Segmental Bridge Bibliography**

98. Tadros, M. K., A. Ghali, and W. H. Dilger. 1979. "Long-Term Stresses and Deformation of Segmental Bridges." *PCI Journal*, Precast/Prestressed Concrete Institute, Chicago, IL. Vol. 24, No. 4, (July-August), pp. 66-87.
http://www.pci.org/view_file.cfm?file=JL-79-JULY-AUGUST-6.pdf
99. Tang, M. 1987. "Construction of East Huntington Bridge." *PCI Journal*, Precast/Prestressed Concrete Institute, Chicago, IL. Vol. 32, No. 6, (November-December), pp. 32-48.
http://www.pci.org/view_file.cfm?file=JL-87-NOVEMBER-DECEMBER-3.pdf
100. Tassin, D. 2006. "Jean M. Muller: Bridge Engineer with Flair for the Art Form." *PCI Journal*, Precast/Prestressed Concrete Institute, Chicago, IL. (March-April), pp. 2-15.
http://www.pci.org/view_file.cfm?file=JL-06-MARCH-APRIL-7.pdf
101. Towell, P. J., P. A. Mainville, V. Chandra, and E. Homsy. 2000. "Central Artery/Tunnel Project: Innovative Use of Precast Segmental Technology." *PCI Journal*, Precast/Prestressed Concrete Institute, Chicago, IL. Vol. 45, No. 4, (July-August), pp. 44-50.
http://www.pci.org/view_file.cfm?file=JL-00-JULY-AUGUST-4.pdf
102. Veletzos, M. J. and J. I. Restrepo. 2009. "Influence of Vertical Earthquake Motion and Pre-earthquake Stress on Joint Response of Precast Concrete Segmental Bridges." *PCI Journal*, Precast/Prestressed Concrete Institute, Chicago, IL. Vol. 54, No. 3, (Summer), pp. 99-128.
http://www.pci.org/view_file.cfm?file=JL-09-SUMMER-10.pdf
103. Walker, H. M., H. H. Janssen, and J. B. Kelly. 1981. "The Kentucky River Bridge—Variable Depth Precast Prestressed Segmental Concrete Structure." *PCI Journal*, Precast/Prestressed Concrete Institute, Chicago, IL. Vol. 26, No. 4, (July-August), pp. 60-85.
104. Ward, D. J. 1983. "An Overview of Prestressed Segmental Concrete Bridges." *PCI Journal*, Precast/Prestressed Concrete Institute, Chicago, IL. Vol. 28, No. 2, (March-April), pp. 120-131.
105. West, J. S., J. E. Breen, and R. P. Vignos. 2002. "Evaluation of Corrosion Protection for Internal Prestressing Tendons in Precast Segmental Bridges." *PCI Journal*, Precast/Prestressed Concrete Institute, Chicago, IL. Vol. 47, No. 5, (September-October), pp. 76-91.
http://www.pci.org/view_file.cfm?file=JL-02-SEPTEMBER-OCTOBER-3.pdf
106. Wilkes, W. J. 1980. "Segmental Bridge Construction—The Wave of the Future." *PCI Journal*, Precast/Prestressed Concrete Institute, Chicago, IL. Vol. 25, No. 5, (September-October), pp. 24-30.
107. Yazdani, N. and M. Issa. 2003. "Reduction of Joint Seepage and Cross-Grouting in Bridge Segments." *PCI Journal*, Precast/Prestressed Concrete Institute, Chicago, IL. Vol. 48, No. 1, (January-February), pp. 82-90.
http://www.pci.org/view_file.cfm?file=JL-03-JANUARY-FEBRUARY-1.pdf
108. Yu, C. K. 1984. "Segmental Box Girders for the High Level West Seattle Bridge." *PCI Journal*, Precast/Prestressed Concrete Institute, Chicago, IL. Vol. 29, No. 4, (July-August) 1984, pp. 52-67.

This page intentionally left blank

SEISMIC DESIGN

TABLE OF CONTENTS

NOTATION 15 - 5

15.1 INTRODUCTION 15 - 11

 15.1.1 General 15 - 11

 15.1.2 Objective 15 - 11

 15.1.3 Potential Causes of Earthquake Damage to Bridges with Precast Components 15 - 12

 15.1.4 Seismic Hazard Maps 15 - 12

 15.1.5 Performance Criteria 15 - 13

 15.1.6 Precast Systems and Components 15 - 13

 15.1.6.1 Superstructure Types 15 - 13

 15.1.6.2 Substructure Components 15 - 13

 15.1.6.3 Precast Systems and Components Not Addressed 15 - 14

 15.1.7 Scope 15 - 14

15.2 STRUCTURAL SYSTEM CONSIDERATIONS 15 - 14

 15.2.1 Foundations 15 - 14

 15.2.2 Response Characteristics of Precast Concrete Bridge Systems 15 - 15

 15.2.2.1 Concept A—Simple-span Precast Beams Supported on a Drop Cap 15 - 15

 15.2.2.2 Concept B—Continuous Precast Beams Supported on a Drop Cap—Hinge Support 15 - 15

 15.2.2.3 Concept C—Continuous Precast Beams Bearing on a Partially Precast Bent Cap 15 - 16

 15.2.2.4 Concept D—Precast Beams Constructed Integrally with Bent Cap 15 - 17

 15.2.3 Bent Cap Types 15 - 17

 15.2.3.1 Simple-span Precast Beams on a Drop Bent Cap—Continuous for Live Load 15 - 17

 15.2.3.2 Partially Dropped Bent Cap 15 - 18

 15.2.3.3 Precast Concrete Bent Cap 15 - 19

 15.2.3.4 Precast Spliced Beam 15 - 19

 15.2.4 Advantages and Disadvantages of Various Systems 15 - 19

 15.2.5 Preliminary Design Considerations 15 - 20

15.3 SEISMIC DESIGN CRITERIA 15 - 20

 15.3.1 Early Seismic Design Criteria 15 - 20

 15.3.2 Seismic Design Criteria of the AASHTO Specifications 15 - 21

 15.3.2.1 AASHTO Standard Specifications for Highway Bridges 15 - 21

 15.3.2.2 AASHTO LRFD Bridge Design Specifications 15 - 21

 15.3.2.3 LRFD Seismic Guide Specifications 15 - 22

 15.3.3 California Seismic Design Criteria 15 - 23

 15.3.4 Other Seismic Design Criteria 15 - 23

 15.3.4.1 Japan Criteria 15 - 23

 15.3.4.2 New Zealand Criteria 15 - 23

15.4 SEISMIC ANALYSIS 15 - 23

 15.4.1 General 15 - 23

 15.4.2 Force Based Analysis 15 - 23

15.4.2.1 Elastic Dynamic Analysis (EDA).....	15 - 24
15.4.2.2 Column Analysis Criteria.....	15 - 24
15.4.2.3 Secondary Effect of Axial Loads	15 - 24
15.4.2.4 Flexural Resistance.....	15 - 25
15.4.2.5 Column-to-Superstructure Connection Design	15 - 25
15.4.3 Displacement-Based Analysis.....	15 - 25
15.4.4 Computer Modeling.....	15 - 26
15.5 CONNECTION DETAILS.....	15 - 26
15.5.1 Details of Current Practice.....	15 - 27
15.5.1.1 Beam Continuity through the Deck	15 - 27
15.5.1.2 Hinged Diaphragm Connection	15 - 27
15.5.1.3 Fixed Diaphragm Connection.....	15 - 27
15.5.1.4 Positive Moment Connection at Pier Diaphragms	15 - 28
15.5.2 Abutment Connection for Precast, Prestressed Beam Bridges	15 - 31
15.5.2.1 Introduction.....	15 - 31
15.5.2.2 Semi-integral End Diaphragm.....	15 - 31
15.5.2.3 Traditional L-shaped Abutment.....	15 - 32
15.5.2.4 Support Length Requirement.....	15 - 33
15.5.2.4.1 Support Length for Bridges Assigned to Seismic Design Category D.....	15 - 33
15.5.2.4.2 Beam Stop Details.....	15 - 33
15.5.3 Pile-to-Pile Cap Connection.....	15 - 34
15.5.4 Haunched Beam-to-Cast-in-Place Inverted-Tee Bent.....	15 - 35
15.5.5 Precast Pile-to-Partial Precast Cap.....	15 - 36
15.5.6 Precast Segmental Columns in Seismic Applications	15 - 39
15.5.6.1 Grouted Duct Connection.....	15 - 41
15.5.7 Precast Abutments	15 - 43
15.5.8 Precast Spliced Beam Superstructure with Integral Cap	15 - 44
15.6 DESIGN EXAMPLES.....	15 - 47
15.6.1 Configure Spans, Balance Stiffness, and Design Practice in California	15 - 47
15.6.1.1 Adjust Dynamic Characteristics	15 - 47
15.6.1.1.1 Outline of Procedure.....	15 - 48
15.6.1.1.1.1 Determine Preliminary Member Sizes and Span Configuration.....	15 - 48
15.6.1.1.1.2 Check for Balanced Stiffness.....	15 - 49
15.6.1.2 Assess Preliminary Ductility—“Lollipop Model”	15 - 49
15.6.1.3 Transverse Pushover Analysis.....	15 - 50
15.6.1.3.1 Design Column Shear	15 - 50
15.6.1.3.2 Design of Bent Cap	15 - 51
15.6.1.4 Longitudinal Pushover Analysis	15 - 51
15.6.1.5 Final Displacement Demand Assessment.....	15 - 51

SEISMIC DESIGN

TABLE OF CONTENTS

- 15.6.2 Precast Substructure and Superstructure Bridge with CIP Connections..... 15 - 51
 - 15.6.2.1 Introduction 15 - 51
 - 15.6.2.2 Design Procedure for Positive Earthquake Loading Reinforcement at Interior Pier of a Precast Beam Bridge..... 15 - 52
 - 15.6.2.2.1 Given..... 15 - 53
 - 15.6.2.2.2 Design Steps:..... 15 - 54
- 15.6.3 Pushover Analysis: Two-Column Bent in the Transverse Direction..... 15 - 55
 - 15.6.3.1. Introduction 15 - 55
 - 15.6.3.2. General Model Information 15 - 56
 - 15.6.3.2.1 Model Description 15 - 56
 - 15.6.3.2.2 Spread Footings..... 15 - 56
 - 15.6.3.2.3 Concrete Material Modeling..... 15 - 56
 - 15.6.3.2.4 Columns 15 - 56
 - 15.6.3.2.5 Superstructure..... 15 - 59
 - 15.6.3.2.6 Loads 15 - 60
 - 15.6.3.3. Modal Analysis 15 - 60
 - 15.6.3.3.1 Mass Source..... 15 - 60
 - 15.6.3.3.2 Column Cracking..... 15 - 61
 - 15.6.3.3.3 Analysis Case Setup 15 - 62
 - 15.6.3.4. Response Spectrum Analysis..... 15 - 62
 - 15.6.3.4.1 Seismic Hazard..... 15 - 62
 - 15.6.3.4.2 Response Spectrum 15 - 63
 - 15.6.3.4.3 Analysis Case Setup 15 - 64
 - 15.6.3.4.4 Column Displacements..... 15 - 64
 - 15.6.3.4.5 Column Inflection Points 15 - 65
 - 15.6.3.5. Displacement Demand..... 15 - 65
 - 15.6.3.5.1 Response Spectrum Displacements..... 15 - 65
 - 15.6.3.5.2 Displacement Magnification 15 - 66
 - 15.6.3.6. P-Delta Effect Check..... 15 - 66
 - 15.6.3.7. Hinge Definitions/Assignments 15 - 66
 - 15.6.3.7.1 Hinge Lengths..... 15 - 66
 - 15.6.3.7.2 Assign Hinges 15 - 67
 - 15.6.3.8. Pushover Analysis 15 - 68
 - 15.6.3.8.1 Load Distribution..... 15 - 68
 - 15.6.3.8.2 Analysis Case Setup 15 - 68
 - 15.6.3.9. Check Displacement Capacity..... 15 - 74
 - 15.6.3.10 Check Hinge Ductility 15 - 75
 - 15.6.3.11. Check Column Shear Capacity 15 - 77
- 15.6.4 Precast Concrete Bridges in Washington 15 - 77

15.6.4.1 Introduction	15 - 77
15.6.4.2 Geometry	15 - 77
15.6.4.3 Material Properties	15 - 78
15.6.4.4 Section Properties	15 - 79
15.6.4.5 Stage 1 Bent Cap Design	15 - 81
15.6.4.5.1 Check Flexural Capacity.....	15 - 81
15.6.4.5.2 Check Shear Capacity.....	15 - 82
15.6.4.5.3 Torsional Capacity	15 - 84
15.6.4.5.4 Shear Interface Calculation	15 - 84
15.6.4.6 Entire Bent Cap Design	15 - 84
15.6.4.6.1 Superimposed Dead and Live Loads	15 - 84
15.6.4.6.2 Extreme Event Load Demands	15 - 85
15.6.4.6.3 Load Summary.....	15 - 86
15.6.4.7 Additional Bent Cap Design Checks.....	15 - 86
15.6.5 Two-Span Spliced U-Beam.....	15 - 86
15.6.5.1 Introduction	15 - 86
15.6.5.2 Description of Bridge	15 - 87
15.6.5.3 Load Combinations	15 - 89
15.6.5.4 Seismic Considerations	15 - 89
15.6.5.5 Seismic Forces.....	15 - 89
15.6.5.6 Joint Shear Design	15 - 91
15.6.5.7 Bent Cap Torsion	15 - 94
15.6.5.8 Superstructure Demands	15 - 95
15.7 CITED REFERENCES	15 - 96

NOTATION

A	= area of section considered (for section properties) = acceleration coefficient
A_b	= area of individual reinforcing bar of column transverse reinforcement
A_e	= effective concrete area resisting shear strength
A_g	= gross cross-sectional area of column
A_S^{J-bar}	= total area of J-bars in the bent cap
A_S^H	= total area of horizontal shear reinforcement anchored in the joint
A_S^V	= total area of vertical shear reinforcement anchored in the joint
A_ℓ	= longitudinal column steel
A_{ps}	= area of prestressing strand
A_s	= effective peak ground acceleration = area of all reinforcement passing through the shear plane = area of longitudinal column reinforcement
A_{sc}	= total area of column reinforcement anchored in the joint
$A_{s\ max}$	= maximum area of longitudinal column steel
$A_{s\ min}$	= minimum area of longitudinal column steel
A_{st}	= area of hoops
A_v	= area of shear reinforcement
a	= acceleration = depth of the equivalent concrete stress block
b	= effective flange width
B_{cap}	= width of cap
B_{eff}	= effective width of superstructure for resisting longitudinal seismic moments
b_v	= width of the section resisting shear
C	= component capacity
c	= depth of neutral axis
c_s	= distance from center of gravity of extended strands to bottom of beam
D	= component force demand
D_c	= diameter of column
D_s	= depth of superstructure including cap beam
d	= distance from top of slab to center of gravity of extended strands = depth of the section, less the clear cover to the bottom of the stirrup
d'	= diameter of column concrete core
d_b	= nominal strand diameter

d_{be}	= nominal diameter of longitudinal column reinforcing steel bars
d_p	= distance from extreme compression fiber to centroid of prestressing strands
d_s	= total depth of the section
d_v	= critical shear depth
E_c	= modulus of elasticity of concrete
E_s	= modulus of elasticity of steel
F_1	= factor, a function of ductility demand
F_2	= factor, a function of compressive axial stress
F_a	= short-period site coefficient at 0.2 second period spectral acceleration
F_v	= long-period site coefficient at 1.0 second period spectral acceleration
F_{PGA}	= site coefficient for PGA coefficient
f'_c	= specified concrete compressive strength
f'_{ce}	= expected concrete compressive strength
f_{pu}	= specified tensile strength of prestressing strands
f_{py}	= yield strength of prestressing steel
f_r	= modulus of rupture
f_{ue}	= expected tensile stress of longitudinal column reinforcing steel bars for seismic design
f_{ye}	= expected yield stress of longitudinal column reinforcing steel bars for seismic design
f_{yh}	= nominal yield stress of transverse column reinforcement
H	= average height of abutment wall supporting the superstructure = beam depth
H_s	= height of superstructure
h	= distance from top of column to center of gravity of superstructure
h_c	= inside depth of u-beam
I	= moment of inertia of section
IC	= importance classification
$I_{cracked}$	= moment of inertia of the cracked section
I_e	= effective moment of inertia
I_{eff}	= effective flexural stiffness
I_g	= moment of inertia of the gross concrete section about the centroidal axis, neglecting the reinforcement
k_e	= effective stiffness of column
k_i^e	= effective stiffness of bent or column i
k_j^e	= effective stiffness of bent or column j
L	= bridge length to the adjacent expansion joint, or to the end of the bridge = column height

	= length of column from point of maximum moment to the point of moment contraflexure
L_1	= length of column from point of maximum moment at base to inflection point
	= span length
L_2	= length of column from point of maximum moment at top to inflection point
	= span length
L_c	= column clear distance between top of footing and bottom face of bent cap
L_p	= length of plastic hinge
ℓ_{ac}	= length of column bar extension into core of bent cap
M	= design moment obtained from elastic frame analysis
	= ductility demand
M_{sei}^{Avg}	= average moment per beam
M_{po}^{Base}	= plastic overstrength moment at base of column
M_{po}^{CG}	= design moment at the center of gravity of the superstructure
M_{cr}	= cracking moment
M_{des}	= design moment per beam
M_{DL}	= moment due to dead load
M_{EQ}	= elastic moment demand
M_{sei}^{Ext}	= moment per beam for nonadjacent beams
M_F	= column moment from elastic frame analysis
M_{sei}^{Int}	= moment per beam for adjacent beams
M_n	= nominal flexural resistance
M_o	= overstrength moment
M_o^{Base}	= column overstrength moments at the base of column
M_o^{CG}	= column overstrength moments at the center of gravity of the superstructure
M_o^{Top}	= column overstrength moments at the top of column
M_{OT}	= overturning moment
M_p	= plastic moment
M_{PR}	= moment corresponding to Δ_{PR}
M_r	= factored flexural resistance of a section in bending
M_{SIDL}	= moment per beam due to superimposed dead load
M_{sei}	= seismic moment
M_{po}^{top}	= plastic overstrength moment at top of column
M_u	= factored moment
M_x	= transverse elastic moments
M_y	= longitudinal elastic moment
m	= gravitational constant

m_i	= tributary mass of column or bent i
m_j	= tributary mass of column or bent j
N	= minimum support length
N_g^{ext}	= number of beams outside the effective width
N_g^{int}	= number of beams encompassed by the effective width
N_{ps}	= number of extended straight strands
n	= modular ratio
P	= axial load
PGA	= peak seismic ground acceleration coefficient on rock
P_f	= prestress force after all losses
p_c	= principal compression stress
p_t	= principal tension stress
R	= response modification factor = permissible force reduction factor
$R_{d,Trans}$	= displacement magnification factor
S	= skew angle of the support measured normal to span = section modulus = spacing of transverse reinforcement = site effects
S_1	= mapped spectral acceleration coefficient, 5% damped, for a 1-second period on Class B rock
S_{D1}	= 5% damped design spectral response acceleration coefficient at 1-second period
SDC	= Seismic Design Category
S_{DS}	= 5% damped design spectral response acceleration coefficients at short periods
S_b	= section modulus for extreme bottom fiber
S_G	= spacing of beams
SPC	= Seismic Performance Category
S_s	= mapped spectral acceleration coefficient, 5% damped, for short periods on Class B rock
S_t	= section modulus for extreme top fiber
s	= spacing of column transverse reinforcement
T_c	= portion of column force clamped by D1
T'_c	= remaining column tension force clamped by D2 and D3 assumed to be 25% of the total column longitudinal reinforcement.
T_s	= S_{D1}/S_{DS} period
T^*	= characteristic ground motion period
T_{Trans}	= natural period of vibration for transverse direction of bridge

T_w	= web thickness of u-beam
t_s	= effective slab thickness
V_c	= shear resistance of the concrete
v_c	= shear stress in the concrete
V_n	= nominal shear resistance of the section
V_o	= overstrength shear
V_{PR}	= shear force corresponding to displacement Δ_{PR}
V_s	= shear resistance of the reinforcement
W_S	= equivalent effective width of superstructure
w_c	= unit weight of concrete
	= inside depth of u-beam
Y_{CG}	= distance from top of column (bottom face of bent cap) to center of gravity of the superstructure
y_b	= distance from center of gravity to bottom fiber
y_t	= distance from center of gravity to top fiber
y_{t-slab}	= c.g. of superstructure to top of slab
β	= factor relating effect of longitudinal strain on the shear capacity of concrete, as indicated by the ability of diagonally cracked concrete to transmit tension
β_1	= ratio of the depth of the equivalent uniformly stressed compression zone assumed in the strength limit state to the depth of the actual compression zone
δ_b	= dead load coefficient
δ_s	= seismic moment coefficient
Δ	= displacement
Δ_c	= displacement capacity taken along the local principal axis corresponding to Δ_d
Δ_{cr+sh}	= displacement due to creep and shrinkage
Δ_d	= global seismic displacement demand
$\Delta_{L_D_Trans}$	= displacement demand from response-spectrum analysis
Δ_p	= plastic displacement
Δ_y	= yield displacement taken along the local principal axis corresponding to Δ_d = displacement at which the hinge yields during the pushover analysis when foundation effects are included
Δ_{yi}	= idealized yield displacement
Δ_{PR}	= primary elastic deflection
Δ_{EQ}	= elastic deflection computed from the complete quadratic combination (CQC) method
Δ_{eq}	= seismic displacement demand of the long period frame on one side of the expansion joint = displacement due to earthquake loads
$\Delta_{p/s}$	= displacement due to prestressing

Δ_{temp}	= displacement due to temperature effects
γ_p	= load factor for permanent loading
μ_c	= local displacement ductility capacity
μ_Δ	= structural ductility
ϕ	= resistance factor
ϕ_p	= curvature corresponding to plastic moment = soil spring
ϕ_v	= resistance factor for shear
ϕ_y	= yield curvature
ϕ_{yi}	= idealized first yield curvature
ρ_s	= reinforcement ratio
θ	= angle of shear failure plane
θ_p	= plastic rotation

Seismic Design

15.1 INTRODUCTION

In 2013, the Precast/Prestressed Concrete Institute (PCI) published the *Seismic Design of Precast Concrete Bridges State-of-the-Art Report* (PCI, 2013). It is referred to here as the *Seismic Design Report*. The report was written by a subcommittee of experts from the Committee on Bridges and underwent a sequence of reviews by several groups and selected specialists as required by PCI. This chapter is taken from that report. The report contains more information including three appendices that summarize the relevant research that pertains to the use of precast concrete in seismically active regions; the results of an international survey about the use of precast concrete in seismic-resistant bridges; and a summary of seismic design criteria in Japan and New Zealand. There are references to those appendices in this chapter. An internet link is given to the report in the references at the end of the chapter.

15.1.1 General

Precast concrete bridge components and systems provide effective and economical design solutions for new bridge construction and for the rehabilitation of existing bridges. The use of precast components can shorten road closure times, minimize interference with traffic flow, and accomplish the objective often cited by officials to “get in, get out, and stay out.”

Seismic design of precast concrete bridges begins with a global analysis of the response of the structure to earthquake loadings and a detailed evaluation of connections between precast beams and of connections between the superstructure and the supporting substructure. Ductile behavior is desirable under earthquake loadings for both the longitudinal and transverse directions of the bridge. Further, the substructure must be made to either protect the superstructure from force effects due to ground motions through fusing or plastic hinging, or to transmit the inertial forces that act on the bridge to the ground through a continuous load path.

The information in this chapter is intended to augment, and not replace the *AASHTO Guide Specifications for LRFD Seismic Bridge Design* (AASHTO, 2009) (referred to herein as the *LRFD Seismic Guide Specifications*) or any agency requirements for seismic analysis or design. The designer should verify the latest applicable standards with the owner and discuss any necessary exceptions before beginning design. For the current state-of-the-practice, the seismic design of precast concrete bridges employs an AASHTO-LRFD Type 1 design strategy and uses connections between precast concrete elements and between cast-in-place (CIP) concrete and precast concrete elements that are intended to emulate the behavior of CIP concrete connections.

Seismic design is complex. Bridges of similar characteristics in different locations may behave very differently during an earthquake. The engineer should not copy details that have been used on previous projects without a complete understanding of the reasons behind the original design.

15.1.2 Objective

This chapter presents state-of-the-practice information on the seismic design of ordinary highway bridges containing precast components. Ordinary bridges are defined as:

- Well-proportioned structures with span lengths less than 300 ft
- Structures where stiffness and frame geometry are balanced and without unusual geometry such as splayed beams or abrupt changes in superstructure stiffness
- Structures without outrigger caps, changes in beam type, variable numbers of beams between spans or variable beam spacing
- Structures constructed with either normal or lightweight concrete
- Structures either simply supported or continuous at piers or bents with beams either supported on dropped bent caps or made integral with bent caps Structures supported on elastomeric bearings, cotton duck pads, disc bearings, or other bearings and without the intentional use of seismic isolation or other energy dissipating technology in the supports
- Structures supported on spread footings, driven piles, drilled shafts, or a combination of these foundation types

15.1.3 Potential Causes of Earthquake Damage to Bridges with Precast Components

Precast concrete bridge failures during an earthquake have been attributed to:

- Unseating of the superstructure at abutments, hinges, intermediate supports, or expansion joints due to insufficient support length
- Column failure due to longitudinal bar buckling caused by inadequately confined reinforcement, unraveling of spiral reinforcement, poor quality butt welds, or necking of mechanical splices
- Column failure due to lateral forces causing shear failures due to inadequate transverse reinforcement
- Column failure due to architectural flares reducing effective column height, increasing column stiffness, and attracting more load to one column than others
- Column failure due to inadequate or nonstaggered lap splices, poor quality butt welds or necking at mechanical splices in plastic hinging regions of column
- Column failure due to barrier rail being attached to the column and thereby shortening, stiffening, and attracting more load to the column
- Joint shear failure at critical superstructure-to-substructure connections
- Columns punching through the superstructure due to inadequate shear resistance of the deck following loss of the column bearing during liquefaction
- Moment failure at the base of a column due to lack of a top layer of reinforcement in the footing
- Inadequate transverse support or transverse stop mechanism at beam supports
- Pile-to-pile cap connection failure
- Concrete bearing failure due to the yield of elastomeric bearings, or tipping of steel rocker bearings
- Inadequate detailing of reinforcement in support

15.1.4 Seismic Hazard Maps

Seismic hazard is not limited to the western United States. Although most states nationwide have not had significant levels of earthquake activity during recent history, the occurrence of past notable earthquakes demonstrates that significant earthquake hazards exist in the Missouri–Illinois–Tennessee tri-state region, in South Carolina, and along the St. Lawrence Seaway, as well as in the western United States, Alaska, Hawaii, Puerto Rico and the U. S. Virgin Islands. Mapping of fault zones and discovery of hidden or inactive faults have brought increased concerns. Most states include some form of seismic criteria in their bridge design policies.

Seismic maps typically depict peak ground acceleration, determined as the lesser of probabilistic and deterministic ground motion parameters. Maps for bridges and buildings are available from the United States Geological Service (USGS) website: <http://earthquake.usgs.gov/hazards/designmaps/usdesign.php>. The maps for bridges and buildings are not the same because of differences in the targeted earthquake return period, the targeted risk rather than uniform-hazard ground motion, and the use of the maximum direction rather than the geometric mean for the spectral response acceleration. Probabilistic maps are based on the strain rate for each documented event.

One of the most significant recent revisions by the *LFRD Seismic Guide Specifications* has been the adoption of seismic maps that use a 1,000 year return period (7% probability of exceedance in 75 years). The maps for bridge design on the USGS website are available in downloadable form and were created by the USGS under agreement with the American Association of State Highway and Transportation Officials (AASHTO). The USGS software provides a ground motion tool that develops peak seismic ground accelerations (PGA), spectral accelerations, and response spectra for a given postal zip code or grid location.

Prior to September 2009, the California Department of Transportation (Caltrans) used deterministic maps based on seismic records, the maximum credible event for each known fault, and a specific seismic attenuation relationship. After September 2009, the hazard maps were revised to reflect values based on hybrid deterministic-probabilistic relationships.

Earthquake motions can result in ground and hydrological response modifications that can subject bridges to forces different from, and additional to, the forces associated with earthquake motions alone. Ground response can result in lateral spreading and liquefaction that markedly affect the substructure and consequently the response of the superstructure of the bridge. Where such effects are likely, a thorough soils investigation should

be completed and its results taken into account before any detailed seismic design is undertaken. In coastal areas of the western United States, subduction zone motions can give rise to tsunamis and marked ground elevation changes. The National Tsunami Hazard Mitigation Program is led by the National Oceanic and Atmospheric Administration (NOAA) and the USGS. Tsunami inundation maps are available on a state-by-state basis and the extent of those areas should be considered for design of coastal bridges.

15.1.5 Performance Criteria

Acceptable seismic performance criteria for precast concrete bridge structures must satisfy both safety and economic criteria. A bridge is part of a highway system and most agencies have earthquake response and recovery plans that identify primary, secondary, and tertiary response routes within that system. Ideally, the acceptable seismic performance for bridges on a given route will vary with the priority of the route and may need to be higher than that for collapse prevention as specified in the *LRFD Seismic Guide Specifications*. Requiring all bridges to be serviceable immediately after an earthquake is not economically feasible for most agencies. Still, preventing bridge collapse and possible loss of life should be achievable if, as required by the *LRFD Seismic Guide Specifications*, bridges are designed for a life safety performance objective considering the seismic hazard corresponding to a 7% probability of exceedance in 75 years. This chapter is concerned with seismic design for the collapse-prevention performance level. Higher levels of performance, with operational objectives, may be deemed necessary for a given bridge, and the research results reported in Appendix A of the *Seismic Design Report* (PCI, 2013), can help provide information for desirable response guidelines for higher levels of performance.

Designing for life safety means that significant damage can result. Significant damage includes permanent offsets, damage between approach structures and the bridge superstructure, between spans at expansion joints, permanent changes in bridge span lengths, and permanent displacements at the top of bridge columns. Damage also consists of severe concrete cracking, yielding and buckling of reinforcement, major spalling of concrete, and severe cracking of the bridge deck slab. These conditions may require closure of the bridge to repair the damages. Partial or complete replacement of columns may be required in some cases. For sites with lateral flow due to liquefaction, piles may suffer significant inelastic deformation and partial or complete replacement of the columns and piles may be necessary. If replacement of columns or other components is to be avoided, a design strategy that produces minimal or moderate damage—such as seismic isolation or a control and reparability design concept—should be used. Designing for life safety means that significant disruption to service level performance is likely, resulting in the need for limited access (reduced lanes, light emergency traffic) on the bridge and possible requirements for shoring.

15.1.6 Precast Systems and Components

The precast structural systems covered in this chapter are as follows:

15.1.6.1 Superstructure Types

- Precast, pretensioned concrete beams with CIP concrete deck
- Precast, post-tensioned concrete spliced beams with CIP concrete deck

15.1.6.2 Substructure Components

- Precast concrete column segments post-tensioned together in the field
- Precast concrete bent caps (“dropped caps” where the beams sit on the top surface; also known as hammerhead caps)
- Partially precast bent caps (beams sit on a precast “yoke” that fits over columns and has stirrup extensions; top-half of cap is CIP with deck concrete)
- Integral bent caps (CIP concrete that encapsulates beam ends; bottom of cap is flush with bottom of beams)
- Precast columns on CIP footings
- Precast drop caps on precast columns
- Precast piles
- Precast pile caps
- Precast abutments
- Precast walls

15.1.6.3 Precast Systems and Components Not Addressed

Precast segmental members and systems for bridges constructed using the balanced cantilever method are not covered in this chapter. Seismic design considerations for extraordinary bridges and major bridges are not covered in this chapter.

15.1.7 Scope

Considerations for the selection of structural systems for precast concrete bridges are addressed in depth in Section 15.2. Structural response varies from hinged, in the case of simply-supported beams, to emulative of fixity, where monolithic cast-in-place concrete, beam-to-cap and column details are used. Because modeling techniques have not yet been implemented for jointed details, the focus of this chapter is on procedures for the evaluation of system response and the detailing of connections for emulative behavior. Since the desired structural response is noncollapse of the superstructure, the preferred approach is to force damage into the columns that are more easily repaired or replaced than the deck. The bent cap details are essential to forcing this desired behavior and therefore bent cap details are the primary focus of Section 15.2.

Relevant seismic design criteria are discussed in Section 15.3. The criteria of early years are summarized along with the current criteria of the *LRFD Seismic Guide Specifications, Standard Specifications* (AASHTO, 2002), the *LRFD Specifications* (AASHTO, 2007), and the Seismic Design Criteria (Caltrans, 2006), *Specifications for Highway Bridges* (Japan, 2002) and Chapter 5 of the New Zealand Bridge Manual (New Zealand, 2003) requirements.

Seismic analysis procedures are discussed in Section 15.4. While the primary emphasis is on force-based analysis procedures, displacement-based analysis and computer modeling are also discussed.

Relevant information on connection details used in current practice, additional to the information on bent cap details of Section 15.2, are discussed in Section 15.5. Issues covered include details of beam-to-diaphragm connections, abutment connections, pile-to-pile cap connections, and use of precast elements for segmental columns. Design for low and moderate, as well as high seismic risk applications, is discussed.

Cited references and references for additional information are provided in Section 15.7.

Design examples, in addition to the bent cap example details covered in Section 15.2, are provided in Section 15.6. Examples include details of calculations for a bridge with cast-in-place concrete sub- and superstructure connections, a pushover design example for design of a two-column bent loaded in the transverse direction, some typical details used for Washington State Department of Transportation (WSDOT) bridges, and design considerations for a two-span spliced U-beam bridge.

In the *Seismic Design Report* (PCI, 2013), Appendix A contains summary details of relevant precast concrete bridge research by several agencies. Caltrans has done much testing, numerical modeling, and research on framed structures. Similar efforts on emulative structures have recently been completed by WSDOT and are continuing as part of the agency's Highways for Life (HfL) project, funded in part by the Federal Highway Administration (FHWA) through its HfL program. Included is information related to superstructure-substructure connections, substructure connections, and precast piers. The appendices contain the results of a survey of DOTs on their usage of precast elements.

15.2 STRUCTURAL SYSTEM CONSIDERATIONS

15.2.1 Foundations

As more is learned about the effect of soil-structure interaction (SSI), new guidelines and procedures continue to be developed to enhance the accuracy of predictions of bridge response to seismic loading. However, practical limitations prevent detailed incorporation of SSI effects into every project.

Where a situation warrants the development of a site-specific spectra, extra effort in site investigation, laboratory testing and modeling may be required. On very long bridges, the subsurface conditions may vary to the extent that a single-response spectrum is not an accurate representation of the soil conditions. In these cases, multiple-support excitations may be required. SSI modeling may not be required if site-specific spectra are used.

15.2.1 Foundations/15.2.2 Concept B—Continuous Precast Beams Supported on a Drop Cap—Hinge Support

In addition to SSI analyses, site stability should be considered. Issues include soil liquefaction, basin effects, soft-clay sites, and slope hazards. Investigation into soil liquefaction includes analysis for lateral spread, loss of support, and dynamic settlement, as well as mitigation of such effects through site improvements. Large site amplification effects are possible for soft-clay sites. Slope failure has been recognized as one of the major causes of bridge collapse due to earthquakes.

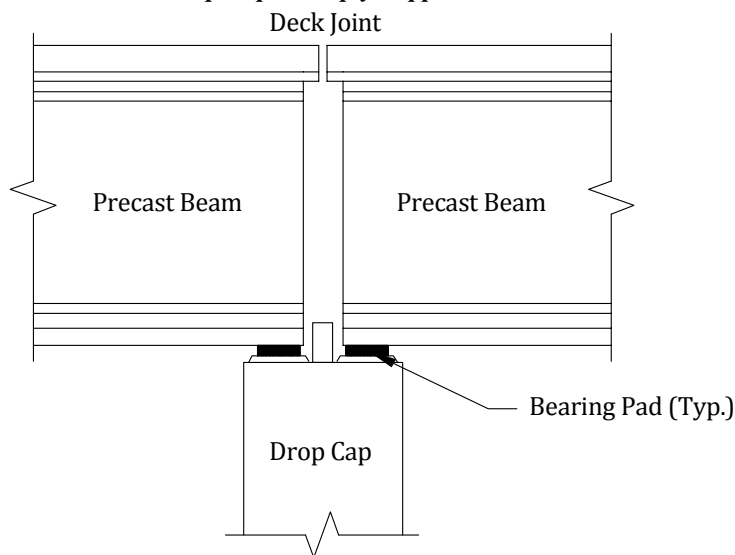
15.2.2 Response Characteristics of Precast Concrete Bridge Systems

The structural response of a precast bridge varies from hinged in the case of simply-supported beams to emulative of fixity for bridges with monolithic cast-in-place beam–cap–column details. The desired seismic structural response is collapse prevention of the superstructure. This response can be accomplished by forcing damage into the columns, which are then more easily repaired or replaced than the superstructure. For precast concrete construction, bent cap detail is a key to the implementation of that strategy. Four bent cap–beam connection concepts, Concepts A through D, are discussed in the following four sections. Each provides progressively less jointed behavior and progressively more ability to drive plastic hinging into the columns.

15.2.2.1 Concept A—Simple-span Precast Beams Supported on a Drop Cap

This connection type is shown in **Figure 15.2.2.1-1**. The bearings for the precast beams sit directly on the top of the drop caps. The beams can be either simply supported or the deck slab made continuous for live load and superimposed dead loads. The joint between the beams is left open. Such structures exhibit jointed behavior and are practical for regions of low and moderate seismic hazard. Such structures are widely used in the Midwest and East regions and are easy to build, but can require maintenance of bearings and joints (Martin and Sanders, 2007).

Figure 15.2.2.1-1
Precast Beams on a Drop Cap—Simply Supported



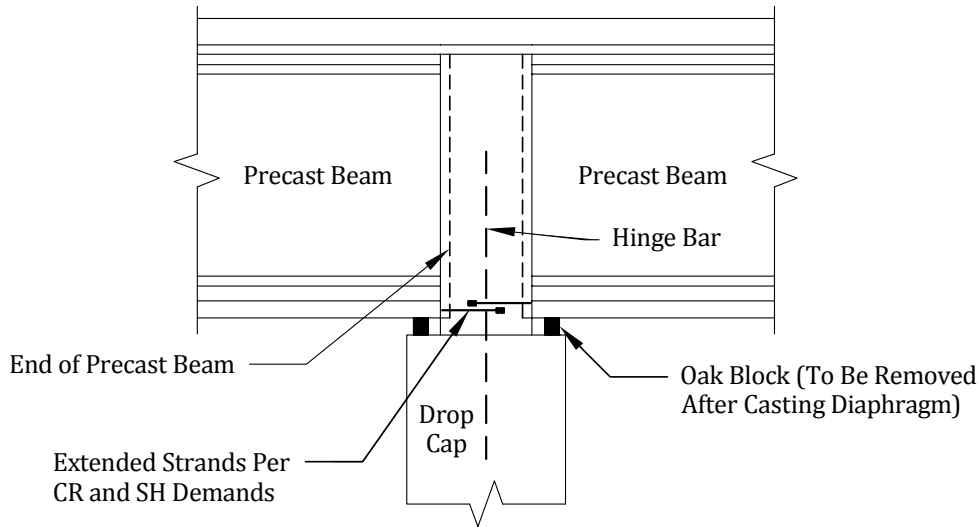
15.2.2.2 Concept B—Continuous Precast Beams Supported on a Drop Cap—Hinge Support

This concept is illustrated in **Figure 15.2.2.2-1**. The precast beams sit directly on the top of the drop caps. The beams are made continuous at intermediate piers by providing full-height diaphragms that fill the gap between the beams of adjacent spans. The deck slab is made continuous for live load and superimposed dead loads. Reinforcement extending from the bottom of the beams and spliced within the diaphragm is proportioned to resist creep and shrinkage demands. A central hinge bar extends from the drop cap up into the diaphragm. Such structures behave as if they possess a continuous superstructure with a pinned connection to the substructure (Martin and Sanders, 2007). They are suitable for use in regions of moderate and high seismic hazard.

SEISMIC DESIGN

**15.2.2.2 Concept B—Continuous Precast Beams Supported on a Drop Cap—Hinge Support/
15.2.2.3 Concept C—Continuous Precast Beams Bearing on a Partially Bent Cap**

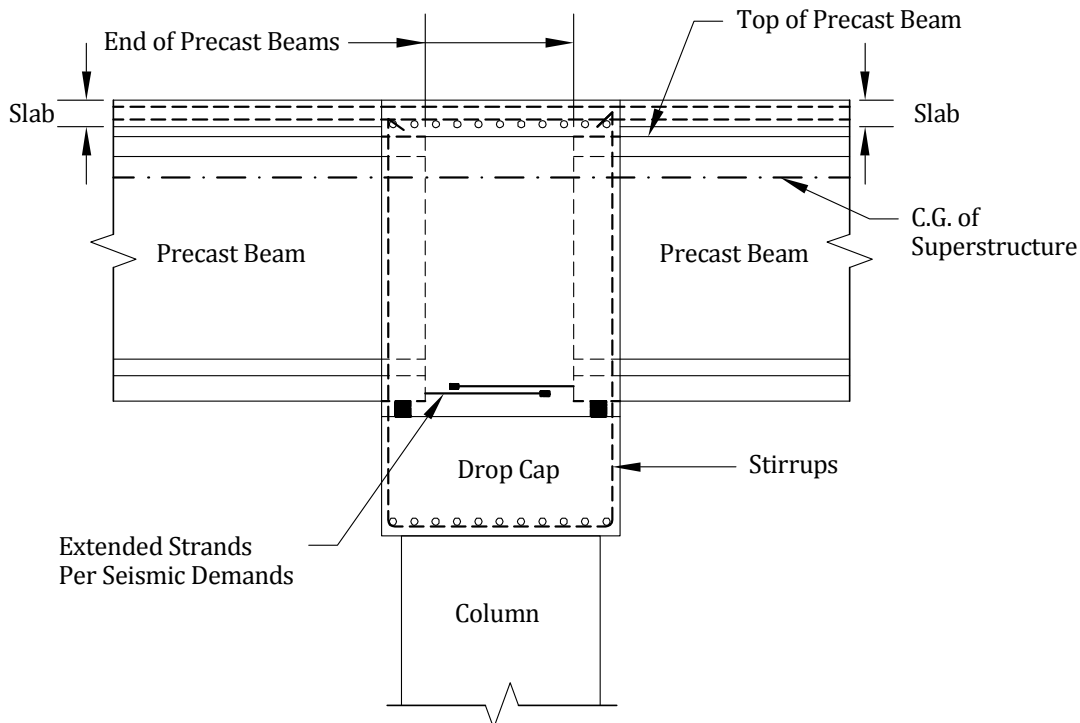
*Figure 15.2.2.2-1
Precast Beams on Drop Cap—WSDOT*



15.2.2.3 Concept C—Continuous Precast Beams Bearing on a Partially Precast Bent Cap

This concept is illustrated in **Figure 15.2.2.3-1**. Beams and deck slab are continuous at the intermediate pier with beams framed into the pier diaphragm. Such structures are thought to exhibit behavior as a continuous superstructure with a fixed moment resistant connection to the substructure. This connection concept is commonly used by WSDOT for bridges in moderate and high seismic zones, but has not yet been proof tested (Martin and Sanders, 2007).

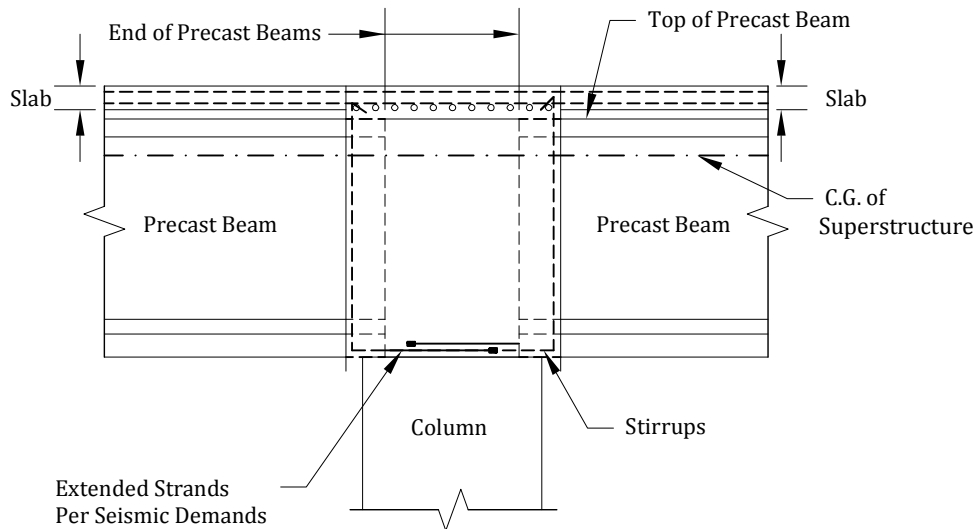
*Figure 15.2.2.3-1
Precast Beams on Partial Drop Cap (WSDOT)*



SEISMIC DESIGN

15.2.2.4 Concept D—Precast Beams Constructed Integrally with Bent Cap/
15.2.3.1 Simple-span Precast Beams on a Drop Bent Cap—Continuous for Live Load**15.2.2.4 Concept D—Precast Beams Constructed Integrally with Bent Cap**

This type of connection is illustrated in **Figure 15.2.2.4-1**. Beams are framed into the bent cap, so that generally, the bottoms of the beams are flush with the bottom of the cap. The column(s) or pier top(s) are effectively fixed, and the bent cap is made integral with the superstructure. The behavior emulates that of a framed structure (Martin and Sanders, 2007) and the connection is appropriate for regions of high seismic hazard. This connection concept has not yet been proof tested.

*Figure 15.2.2.4-1**Precast Beams and Integral Bent Cap—Fixed Connection***15.2.3 Bent Cap Types**

This section describes in more detail the characteristics of some of the different types of bent caps. Test results for some typical bent cap details are also reported in Restrepo et al., 2011.

15.2.3.1 Simple-span Precast Beams on a Drop Bent Cap—Continuous for Live Load

Where traditional simple-span precast beams and precast beams made continuous in the deck for live loads and superimposed dead loads (Concepts A and B) are supported on dropped bent caps, there is an absence of monolithic action between the superstructure and the bent cap. The beam seats on the bent cap act as rollers or pinned connections. Consequently, for multi-column bents with a continuous end diaphragm, good frame stability exists in the cap in the transverse direction. However, stability in the longitudinal direction requires the column bases to be fixed to the foundation supports. This requirement can result in substantial force demands on the foundations, particularly in areas of moderate to high seismicity.

Providing a moment connection between the superstructure and substructure makes it possible to introduce a pinned connection at the column bases. The resultant hinging at the base of the column permits foundation design for the lesser of the unreduced elastic or plastic moment of the column.

The longitudinal moment demand in a typical beam system near the pier consists of the sum of the permanent loads and a portion of the column seismic (plastic) moment on one side of the pier, and the difference between permanent loads and the remaining portion of the column seismic (plastic) moment on the other side. During a seismic event the moment rapidly changes with the cyclic behavior. On one side the moments are additive while a relatively smaller and constant positive moment occurs on the opposite side. This distribution is reversible depending on the direction of the earthquake force and is intensified by vertical ground motion in larger events. Therefore, the beams must be designed to carry both a high negative moment near the pier and a smaller positive moment for an extended length on each side of the pier.

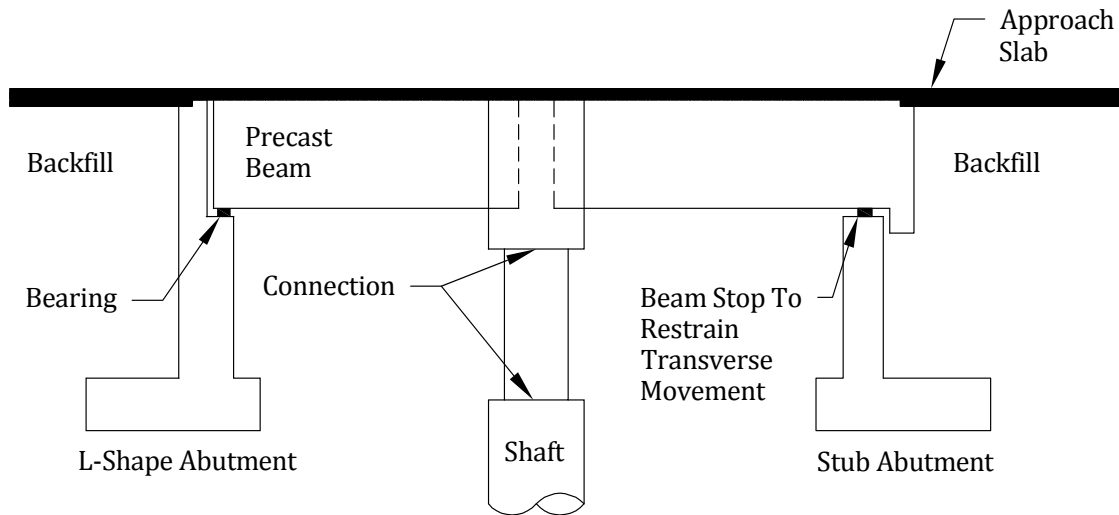
SEISMIC DESIGN

15.2.3.1 Simple-span Precast Beams on a Drop Bent Cap—Continuous for Live Load/15.2.3.2 Partially Dropped Bent Cap

Structures that are skewed in plan are subjected to in-plane rotation toward the obtuse corners due to lateral seismic forces. Fuses, in the form of concrete shear keys, may be required in moderate to high seismic regions.

Where precast beams frame into the bent cap, similar to **Figure 15.2.3.1-1**, if the bottom of the beam is flush with the bottom of the cap, and the column(s) or pier top(s) are fixed, then the bent cap is integral with the superstructure.

*Figure 15.2.3.1-1
Continuous Bridge with Semi-raised Bent Cap (WSDOT)*



15.2.3.2 Partially Dropped Bent Cap

In a partially dropped bent cap (Concept C), to emulate frame behavior between the superstructure and substructure at intermediate supports, the beams are encapsulated into the cap and the entire cap is post-tensioned in the transverse direction. Beams are also spliced monolithically at the supports and at approximately the third points along each span. Typical details for this form of construction for the Sacramento Bridge are shown in **Figure 15.2.3.2-1**.

*Figure 15.2.3.2-1
Continuous Bridge with Semi-raised Bent Cap at Intermediate Pier*

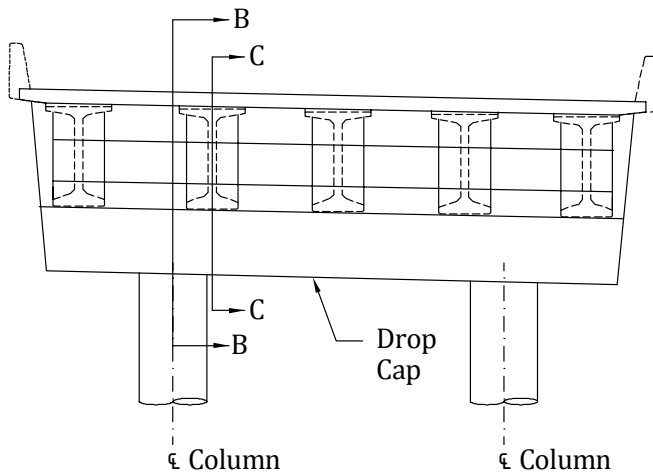
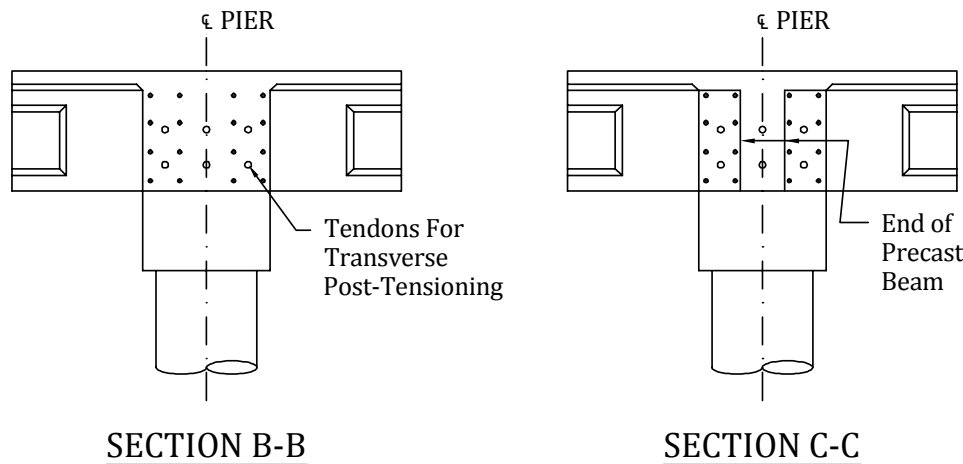


Figure 15.2.3.2-1**Continuous Bridge with Semi-raised Bent Cap at Intermediate Pier (continued)****15.2.3.3 Precast Concrete Bent Cap**

Successful use of precast concrete bent caps requires attention to constructability in addition to consideration of the seismic performance of the connections. Early uses of precast bent caps were limited to nonseismic applications where minimal moment and shear transfer were required at connections. In seismic regions, the bottom half of the cap must be able to develop the strength of the columns for the transverse and longitudinal directions and also provide a connection with adequate joint shear reinforcement. Constructability requires attention to both the strength and flow of concrete. Connections must often be made using grouted bars. Relevant research on grouted sleeves by the University of Washington is summarized in Appendix A of the *Seismic Design Report* (PCI, 2013), Section A.2.1.3. (Pang et al., 2010). Precast bent caps can also be post-tensioned to the piers.

15.2.3.4 Precast Spliced Beam

Caltrans has tested an integral precast spliced system that utilizes a continuous bulb tee or U-beam section erected over the support. Splices are only necessary at third points in the spans.

Temporary supports are then erected at approximately third points so that the mid-span beams can be erected and post-tensioned for continuity. This system is described later in this chapter.

15.2.4 Advantages and Disadvantages of Various Systems

- Precast beams: very economical for multi-span bridges where repetition can be utilized.
- Precast bent caps: suitable for accelerated construction, but tolerances may be restrictive when fixity is required at the tops of columns or piers. Recent research and bridge construction projects (WSDOT) have proven the suitability of this method for accelerated bridge construction.
- Precast columns and bents: suitable for accelerated construction in seismic regions but may be more expensive without the need for significant time savings.
- Precast spliced continuous beams: good performance, but falsework or hangers are required to support drop-in segments. See Sections 5.8 and 6.5.
- Precast decks: These accelerate construction, but performance of deck connection details during seismic events is not well understood. Deck durability and longevity may be reduced due to opening and closing of joints during seismic events.

The use of precast, prestressed concrete spliced beams permits rapid construction and longer spans that reduce the number of piers. Through the use of post-tensioned continuous members, the bridge superstructure depth can be minimized to obtain necessary vertical clearance for rail or vehicular traffic. The resultant minimization of falsework improves traffic flow and improves safety for traffic and construction workers. The beam spacing can also be increased so that the number of beam lines and the total project cost are reduced.

15.2.5 Preliminary Design Considerations

The following suggestions should be considered during bridge type selection. Use of these guidelines can enhance seismic performance and help avoid problems during final design.

- Use columns preferably of equal height in multi-column bents. Short columns are stiffer than tall columns of equal diameter, and will attract more loads.
- Avoid highly irregular or suddenly changing member stiffness so as to prevent concentration of load demands on a particular bent or frame. This constraint will also minimize any tendency of the bridge to undergo in-plane rotation.
- Use continuous frames and plastic hinging design concepts, i.e. plastic hinges at the top or bottom of selected columns, piers, and bents. Jointed behavior may be permissible in the future only after more research and testing.
- Do not allow plastic hinges to form in the superstructure.
- Ask the owner if “drive-by” inspection after a major earthquake is required. If so, all plastic-hinging of vertical members must be above grade.
- Consider a depth of flexibility for piers and shafts below the actual ground level. Isolation materials have been used around the upper portions of some foundations in California.
- Consider using larger shaft diameters for columns below ground than above ground in order to force hinging above ground.
- Avoid skews for abutments, intermediate supports, and hinges that are greater than 30 degrees from the centerline of the bridge.
- Make the superstructure depth at integral bent caps, or wherever the top of the column is fixed to the cap, equal to or greater than the maximum column diameter. This improves performance of the joint in a seismic event.
- Make the bent cap width greater than the column diameter or pier width. Caltrans requires bent caps to extend at least 1 ft beyond the face of the column on each side.
- Use isolation details for architectural flares at the top of columns, or if the flares are to be relied upon structurally, use proper confinement and analyze for the reduced column height.
- Consider using integral and semi-integral abutments for shorter bridges in low seismic areas and where rapid post-earthquake inspection is not required.
- Do not use integral abutments in high seismic areas. Inspection requires earth-moving equipment and repair can be complicated and costly.

15.3 SEISMIC DESIGN CRITERIA

15.3.1 Early Seismic Design Criteria

The American Association of State Highway Officials (AASHO), predecessor to AASHTO, published the first bridge design standards for the United States in 1931. Neither the first edition nor subsequent editions of the standards published prior to 1941 addressed seismic design. The editions published in the 1940s mentioned seismic loading only to the extent that bridge structures must be proportioned for earthquake stresses.

Seismic design commenced with Caltrans' requirement that bridges resist lateral forces that were a percentage of their self-weight. In 1940, a lateral load of 6% of the dead load was required. In 1965, the period of the structure was added as a main design variable and the maximum lateral seismic design force was increased to 13% of the self-weight for select bridges. Provisions were in part based on the lateral force requirements for buildings developed by the Structural Engineers Association of California (SEAOC).

The collapse of several California bridge structures during the 1971 San Fernando earthquake was a major turning point in the development of seismic design criteria for bridges in the United States. In 1973, Caltrans developed a specification based on research that considered the relationship of the site to known active faults, the seismic response of the soils at the site and dynamic response characteristics of the bridge. In 1975, AASHTO adopted interim specifications that were a slightly modified version of the 1973 Caltrans provisions.

SEISMIC DESIGN**15.3.1 Early Seismic Design Criteria/15.3.2.2 AASHTO LRFD Bridge Design Specifications**

The 1971 San Fernando earthquake was a catalyst for research activity by the FHWA. In 1978, FHWA funded a major research project headed by the Applied Technology Council (ATC) that focused on development of improved seismic design guidelines for highway bridges in all regions of the United States. *Seismic Retrofitting Guidelines for Highway Bridges* (ATC-06, 1983) provided guidelines to incorporate elastic Response Spectrum Analysis (RSA), and factors to account for redundancy in the structure, ductility of the structural components, and risk. Proper detailing for ductile behavior and prevention of collapse even after significant structural damage occurs was emphasized.

15.3.2 Seismic Design Criteria of the AASHTO Specifications**15.3.2.1 AASHTO Standard Specifications for Highway Bridges**

AASHTO adopted the ATC-06 recommendations as a guide specification in 1983, and incorporated them into the *Standard Specifications* in 1992. After the earthquakes in Loma Prieta, Calif. (1989), Costa Rica (1991), and the Philippines (1991), AASHTO requested that the Transportation Research Board (TRB) review the provisions and prepare revised specifications as appropriate. Funded by the National Cooperative Highway Research Program (NCHRP), the National Center for Earthquake Engineering Research (NCEEER, now MCEER) developed seismic design provisions that were adopted in Division I-A of the *Standard Specifications*.

The principles used in the development of the AASHTO provisions were:

- The design ground motion must have a low probability of being exceeded during the normal lifetime of the bridge (10% probability of being exceeded in 50 years or a 475-year return period).
- The bridge must have a low probability of collapse due to the design ground motion.
- Structural damage is acceptable as long as it does not result in collapse or loss of life; and, where possible, damage that does occur should be readily detectable and accessible for inspection and repair. Small and moderate earthquakes should be resisted within the elastic range of the structural components without significant damage.
- Functionality of essential bridges must be maintained.
- The provisions must be applicable to all regions of the United States.

15.3.2.2 AASHTO LRFD Bridge Design Specifications

The “force-based” seismic provisions of the 1992 *Standard Specifications* were rewritten in load-and-resistance-factor-design (LRFD) format, and included in the *LRFD Specifications* beginning with the 1st Edition. Research findings available at that time, which had not been included in the *Standard Specifications* were also added.

Additional items included:

1. Separate soil profile site coefficients and seismic response coefficients (response spectra) for soft soil conditions.
2. Three levels of importance—“critical,” “essential,” and “other”—as opposed to the two levels defined in previous AASHTO provisions. The *R* factors were adjusted accordingly.

The 2008, Interim Revisions to the 4th Edition of the *LRFD Specifications* revised the design event to have a 1,000-year return period, that is, a 7% chance of exceedance in 75 years. An extensive set of maps was provided for the United States showing peak ground acceleration and spectral response acceleration for structures with natural periods of 0.2 and 1.0 second. Alaska, Hawaii, and Puerto Rico were included, and enlarged diagrams with improved resolution were provided for California, the New Madrid, Salt Lake City, and Charleston areas with more frequent seismic activity. Significant changes were also made to site (soil) classification. The analysis, design, and detailing procedures remained for the most part unchanged from those for the 1st Edition except for the following:

1. Some structures were placed in a higher hazard zone due to changes in mapping and soil classification.
2. Eccentric axial load *P*-Delta (*P*- Δ) effects on columns had to be kept to less than 25% of the factored resistance.
3. The amount of longitudinal column steel A_l had to be between 1% and 6% of the gross cross-sectional area A_g in Zone 2, and between 1% and 4% in Zones 3 and 4.
4. The resistance factor for column flexural design was revised to have a constant value of 0.9.
5. Support length requirements for beams were increased

SEISMIC DESIGN**15.3.2.2 AASHTO LRFD Bridge Design Specifications/15.3.2.3 LRFD Seismic Guide Specifications**

Bridges are assigned to one of four seismic zones. Single-span bridges need only satisfy seat length and minimum horizontal force requirements, regardless of zone. Multi-span bridges in Zone 1 require no seismic analysis. Multi-span bridges in Zones 2 through 4 require either single- or multi-mode equivalent static analysis, or multi-mode elastic spectral or time–history dynamic analysis, depending on the bridge location, importance, and the regularity of the structure geometry. Guidance is given for developing both standard and site-specific seismic response spectra. Coefficients are plotted as a function of period, and the appropriate coefficient is then multiplied by the equivalent static weight. The resulting elastic forces are divided by a response modification factor R that varies according to member function. Columns and piers have R -values greater than one to compensate for inelastic behavior and energy dissipation. Design is performed for these reduced force effects with some additional reductions permitted on foundation components in Zone 2. Detailing requirements for each zone are successively more stringent. Displacements are evaluated to check for adequate support lengths only.

15.3.2.3 LRFD Seismic Guide Specifications

The *LRFD Seismic Guide Specifications*, 1st Edition, is “displacement-based,” meaning that bridges designed to this guide should have adequate displacement capacity to accommodate earthquake demands. The commentary to Article 3.10.1 recommends that the displacement capacity of bridges be checked using a displacement-based procedure, especially for those bridges located in regions of high seismic risk. The “force-based” methodology of the *LRFD Specifications* (2007) has been found to both “miss” potential seismic weaknesses in some cases, and lead to over-design in others.

The overall objective of the performance criteria is life safety during a 1,000-year seismic event. The *LRFD Seismic Guide Specifications* says, “the bridge has a low probability of collapse but may suffer significant damage and significant disruption to service. Partial or complete replacement may be required.” In a major event, offsets, cracking, reinforcement yielding, and major spalling of concrete are expected. While the 1,000-year return period is judged as applicable to most bridges, higher levels of performance may be required by the bridge owner, as in the case of “critical” or “essential” bridges that provide life safety transportation, bridges that are essential to the economy, or bridges required for local emergency plans. Site- or project-specific design criteria are generally developed for such projects.

Three global seismic design strategies are identified. The seismic designs of most structures with precast concrete components in service prior to 2011 have used the Type 1 design strategy: a ductile substructure with an essentially elastic superstructure. Type 1 behavior emulates that of a concrete frame structure. Rather than describe the methodology here, the reader is urged to study the seismic design flow charts that are part of the *LRFD Seismic Guide Specifications*. The Type 2 strategy uses an essentially elastic substructure with a ductile superstructure and applies only to steel structures. The Type 3 strategy uses an elastic sub- and superstructure with a fusing mechanism between them, involves use of isolation devices, and is beyond the scope of this chapter.

The soil classification, P - Δ effect checks of eccentrically loaded columns, and the hazard maps described for the 2008 Interim Revisions to the *Standard Specifications* (2002) are also used in the *LRFD Seismic Guide Specifications* (2009). Other seismic technology that is new to *LRFD Seismic Guide Specifications* (2009) includes:

- Displacement-based design methodology; plastic-hinge definition, plastic hinge length calculations, and transverse reinforcement requirements
- Permissible earthquake-resisting-systems (ERS) and permissible earthquake-resisting-elements (ERE), including ERE requiring owner-approval and unacceptable ERE
- Use of expected rather than specified material properties
- Balanced bent stiffness and frame geometry requirements for improved seismic behavior
- Curvature-based methodology for evaluating shear resistance
- Joint-shear requirements for integral bent caps that must be 1 ft wider than the face of the column or pier width and principal stress check
- Load factor taken as 1.0 for permanent loads; all resistance factors taken as 1.0

The *LRFD Seismic Guide Specifications* does not explicitly address precast, pretensioned or post-tensioned elements. The precast beams made continuous for live loads must have beam-to-beam or beam-to-cap connections that can be expected to remain undamaged during the 1,000-year seismic event. Opening and closing of the bottom flange-to-flange or flange-to-cap joint connection is not permitted. Precast segmental superstructures must also be designed so that the joints do not open during a seismic event, and essentially follow

a Type 1 design strategy. Segmentally-precaster, post-tensioned columns or piers do not clearly fit into either the Type 1 or Type 3 design strategies.

15.3.3 California Seismic Design Criteria

Under a Caltrans-funded project, the Applied Technology Council (ATC) reviewed and recommended seismic design standards, performance criteria, specifications, and practices. The project synthesized the results of recent research in the field of bridge seismic design, observations on the performance of Caltrans-designed bridges in the 1989 Loma Prieta earthquake, and studies of other structures in other recent earthquakes. The work was published as Report No. ATC-32, *Improved Seismic Design Criteria for California Bridges: Provisional Recommendations* (ATC, 1996) and used as one of the fundamental references in the preparation of Caltrans' original *Seismic Design Criteria* (Caltrans, 2006).

Caltrans' ongoing support of seismic research and further knowledge gained after the Northridge, Kobe, and other earthquakes have resulted in ongoing improvements to *Seismic Design Criteria*. An interim revision 1.5 (2009), the latest version 1.6, and the original v1.4 are available on-line at <http://www.dot.ca.gov/hq/esc/techpubs/manual/othermanual/other-engin-manual/seismic-design-criteria/sdc.html>. V1.6 was introduced to provide hybrid deterministic-probabilistic fault maps. The prior version, v1.4, which was issued in 2006, was the version used in 2011 and is the basis for some of the examples included in this chapter.

15.3.4 Other Seismic Design Criteria

15.3.4.1 Japan Criteria

Specifications for Highway Bridges (JRA, 2002) is available from the Japan Road Association. "Seismic Design" is Part V. Following the Hyogo-ken Nanbu Kobe Earthquake in 1995, these requirements were revised in 1996 and then again in 2002. Many seismic retrofit projects have since taken place.

15.3.4.2 New Zealand Criteria

Specifications for earthquake-resistant design of bridges are published in Chapter 5 of the *Bridge Manual* (New Zealand, 2004). The manual requires that the primary objective of the seismic design is to ensure that the bridge can safely perform its function of maintaining communications after a seismic event. The extent to which this is possible will depend on the severity of the event, and thus by implication, on its return period. For design purposes, bridges are categorized according to their importance, and assigned a Risk Factor related to the seismic return period. This approach results in an equivalent design earthquake hazard and consequent loading.

Brief descriptions of seismic design specifications of Japan and New Zealand are provided in Appendix C of the *Seismic Design Report* (PCI, 2013).

15.4 SEISMIC ANALYSIS

15.4.1 General

Two general approaches are available for evaluation of the seismic response of a bridge. The first approach is conventional force-based analysis, while the second involves the use of a displacement ductility criterion. The *LRFD Specifications* (2007) prescribes the force-based approach while the new *LRFD Seismic Guide Specifications* (2009) uses the displacement ductility method. In recent years, more emphasis has been placed on the latter because of its better accuracy in predicting displacements.

15.4.2 Force Based Analysis

In the force-based analysis method, a linear elastic multi-modal response spectrum analysis is performed and the force effects in various bridge or structure components are determined. Equivalent static analysis of lateral loads based on a percentage of the dead load is also permitted by some agencies. The capacities of the components are evaluated and the component demand/capacity (D/C) ratios are then calculated. A particular component is said to have adequate capacity if its D/C ratio is less than the permissible force reduction factor, R , for that component.

When the R factor is greater than 1.0, limited inelastic behavior is being permitted. The R factor depends on the type of component.

15.4.2.1 Elastic Dynamic Analysis (EDA)

A linear elastic multi-modal spectral analysis uses the appropriate response spectrum selected by the designer. The number of degrees of freedom and the number of modes considered in the analysis needs to capture at least 90% mass participation in the longitudinal and transverse directions. A minimum of three elements per column and four elements per span should be used in the linear elastic mode. The EDA model results should be combined using the complete quadratic combination (CQC) method. The CQC method (*LFRD Seismic Guide Specifications*) is a statistical rule for combining modal responses from an earthquake load applied in a single direction to obtain the maximum response due to this earthquake load.

EDA, based on design spectral accelerations, can produce stresses in some elements that exceed their elastic limit. The presence of such stresses indicates nonlinear behavior. The forces generated by linear elastic analysis could vary considerably from the actual force demands on the structure. Sources of nonlinear response that are not captured by EDA include the effect of the surrounding soil, yielding of structural components, opening and closing of expansion joints, and nonlinear restrainer and abutment behavior.

15.4.2.2 Column Analysis Criteria

An effective flexural stiffness, I_{eff} , should be used when modeling the response of reinforced concrete columns for seismic analysis purposes. I_{eff} can be assumed to be either $0.5I_g$, or derived from empirical curves that depend on the axial load, P , and reinforcement ratio, P/A_g , for the column. Such curves are provided in Figure 5.6.2-1 of the *LFRD Seismic Guide Specifications* for rectangular and circular columns. More accurate I_{eff} values can also be determined by column moment-curvature analysis.

15.4.2.3 Secondary Effect of Axial Loads

Consideration of the secondary force effect due to geometric nonlinearity, ($P-\Delta$ due to axial loads), is required by the *LFRD Seismic Guide Specifications* Article 4.11.5. A modified approach that can be used to perform a second-order analysis to magnify the extreme event moments is as follows:

$$M_u = \delta_b M_{DL} + \delta_s (M_{EQ}/R)$$

where

M_{EQ} = elastic moment demand obtained from the seismic analysis, ft-kips

R = response modification factor defined in the *LFRD Seismic Guide Specifications* Table 3.10.7.1-1

δ_b, δ_s = dead load and seismic moment coefficients, respectively

The design procedure may be summarized as follows:

Columns are designed to form plastic hinges at a specified percentage of the computed fully elastic seismic moment demand. This hinging will occur at a deflection and shear force corresponding to M_{EQ}/R . Beyond this point, inelastic deflections will continue to some unknown maximum, but bending moments and shear forces in the columns will theoretically not increase. Therefore, the problem is to compute the additional design moment, M , due to the slenderness effect such that:

$$M_{EQ}/R + M = \delta_s M_{EQ}/R$$

A recommended second-order analysis is as follows:

Estimate the maximum primary elastic deflection, Δ_{PR} , of the frame:

$$\Delta_{PR} = \Delta_{EQ}/R$$

where Δ_{EQ} = the CQC elastic deflection computed from the seismic analysis

Apply Δ_{PR} to the frame model. This will yield a set of primary deflections and forces, M_{PR} and V_{PR} , corresponding to Δ_{PR} . (Note that these forces may not agree exactly with the results of the seismic analysis. An approximation of $\pm 5\%$ is commonly acceptable). The design moments for the columns are then given by:

$$M_u = M_{DL} + M_{EQ}/R + M$$

where

$M = M_F - M_{PR}$ obtained from the elastic frame analysis

where $M_F =$ the column moment from elastic frame analysis, ft-kips

The response modification factor, R , used for footing or pile design is generally less than the value used for columns. Therefore a separate analysis may be required to obtain the footing design moment.

15.4.2.4 Flexural Resistance

Once the magnified moment has been established, the resisting capacity of the column section must be made adequate to carry the magnified moment. In addition, the superstructure and the foundation must also be designed to resist this magnified moment.

The biaxial strength of columns cannot be less than that required for flexure, as specified in Article 5.7.4 of the *LRFD Specifications* and in Article 3.10.8 for the extreme event limit state. The resistance factor for columns with either spiral or tie reinforcement is taken as equal to 0.9, as specified in Article 5.7.4.

15.4.2.5 Column-to-Superstructure Connection Design

The *LRFD Specifications* requires that connections to the superstructure be designed for the elastic demand moment at the top of the column using either the unreduced elastic moment or the plastic moment capacity of the top of the column, whichever is less. These column moments are to be carried into the diaphragm of the superstructure and accounted for in the design of the beam connections.

15.4.3 Displacement-Based Analysis

Displacement-based or inelastic quasi-static analysis is commonly referred to as pushover analysis. Displacement capacities of a structure or frame as it reaches its limit of structural stability are determined. Expected material properties of modeled members are used.

Pushover analysis addresses typical sources of material nonlinearity as well as geometric nonlinearity. Material nonlinearity includes soil, concrete, soil-structure interaction, and yielding of the reinforcement. Geometric nonlinearity refers to the $P-\Delta$ effect. The bridge frame is pushed laterally along both its longitudinal and transverse directions until the target displacement is obtained. Some software offers two types of the lateral loading patterns, namely acceleration and modal load patterns. The collapse mechanism and plastic hinge sequence of formation for the typical bridge structure due to the two loading patterns are similar. The analysis indicates where the first and subsequent plastic hinges are formed at the top or bottom of the column.

The analysis is incrementally linearly elastic and captures the overall nonlinear behavior of the elements, including soil effects, by pushing the frame laterally to initiate plastic action. Each increment pushes the frame until a plastic hinge forms, and redefines the structural system after each hinge forms until the potential collapse mechanism is achieved. Because the analytical model accounts for the redistribution of internal actions as components respond inelastically, a more realistic measure of behavior can be obtained from pushover procedures than from elastic analysis procedures.

The following steps outline the displacement-based design procedure currently used by Caltrans. This procedure is intended to achieve a "No Collapse" condition for standard ordinary bridges using one level of seismic safety evaluation. The basic assumption is that the displacement demand obtained from linear-elastic response spectrum analysis is an upper bound to the displacement demand even if there is considerable nonlinear plastic hinging.

Pushover steps:

1. Choose a well-balanced span configuration—design for service and strength loads.
2. Perform linear elastic response spectrum analysis of the bridge using design acceleration spectra specified by national or local specifications.
3. Note the transverse and longitudinal displacement demands.

SEISMIC DESIGN**15.4.3 Displacement-Based Analysis/15.5 Connection Details**

4. Develop moment-curvature diagrams for each column, and from those diagrams determine the elastic, plastic, and ultimate curvatures for each column.
5. Using the above information and pier geometry (single or multi-column configuration), compute the plastic displacement of each column, and the ultimate displacement capacity. The displacement ductility should be based on: $\mu_c = \Delta_c/\Delta_y > 3$, $\Delta_d < \Delta_c$.
where
 - Δ_d = global seismic displacement demand
 - Δ_c = displacement capacity taken along the local principal axis corresponding to Δ_d
 - Δ_y = yield displacement taken along the local principal axis corresponding to Δ_d
6. Perform pushover analysis of each bent for its transverse direction. For this purpose, the plastic hinging moment for each column must be computed, and it may be necessary to incorporate foundation flexibility by use of soil springs.
7. Compare the total displacement capacity of the bent to the displacement demand from the elastic analysis. If the capacity is insufficient, then higher ductility is required.
8. Perform similar pushover analysis for the longitudinal direction of the entire bridge and for each frame in the case of a multi-frame bridge, and check the displacement capacity versus displacement demand.
9. Design the superstructure (cap) and foundation (e.g., footing) for 20% higher capacity than the plastic capacity of the columns to ensure that plastic hinges occur within the column.

15.4.4 Computer Modeling

In most cases, the solutions to the equations of motion to determine the force and displacement demands are based on a linear elastic multi-mode Response Spectrum Analysis (RSA). This type of analysis is considered acceptable for continuous precast beam bridges with integral caps or other details such that hinging is only at the top or bottom of columns. RSA offers the following advantages:

1. It is usually simple to use.
2. It eliminates the need for extensive testing (modeling nonlinearity often requires additional data to describe the behavior of the material).
3. It provides acceptable limit state solutions. Limit states are often used in conjunction with an iterative process to envelop the behavior of the structure. Each limit state is a worst-case scenario corresponding to a set of boundary conditions or material properties. Examples of commonly used limit states are the tension and compression models of a bridge with expansion hinges and abutment supports. The tension model corresponds to the opening of all expansion hinges and lack of abutment soil springs (stiffness), while the compression model corresponds to the closing of all gaps and the engaging of the soil at one or both abutments.
4. It uses pre-defined acceleration response curves, except when the size of the project and/or the geology requires site-specific information. The curves take into account such factors as proximity to fault zone and site geology (primarily depth-to-rock).

15.5 CONNECTION DETAILS

Seismic design practices and requirements vary from region to region, depending on the level of anticipated seismic activity and philosophy of the governing jurisdictions. Similarly, connection details vary. Nevertheless, good seismic performance depends on well thought out details that accommodate the load path and overall seismic strategy.

Plastic moment demands at tops of the columns must be transferred into the superstructure without yielding either the beam seat or the ends of the precast beams. In other words, the beams should not lift or rotate relative to the cap. To achieve this condition, the connection of the beam ends to the cap must be designed to resist the forces transferred from the column. Ideally, longitudinal moment from the top of the column is distributed to multiple beams in the vicinity of the column.

15.5.1 Details of Current Practice

15.5.1.1 Beam Continuity through the Deck

The most basic precast bridge consists of precast, prestressed concrete beams made continuous for live load by forming and placing a continuous deck. Precast beams are erected onto the cap and temporarily supported on elastomeric bearings or wood blocks until the cast-in-place concrete diaphragm is complete. The strands from the beam ends are sometimes extended for additional continuity. As previously shown in **Figure 15.2.2.2-1**, the wood block location should be away from the edge of bent cap to prevent edge failure, or spalling, due to dead loads from beam, slab, and construction loads.

15.5.1.2 Hinged Diaphragm Connection

A hinge connection used by WSDOT is shown in **Figure 15.2.2.2-1** for continuous spans at intermediate pier diaphragms. The requirements for using this detail are:

- All beams of adjoining spans should be of equal depth, spacing, and type
- Reinforcement for negative moments due to live loads and superimposed dead loads from traffic barriers, pedestrian walkways, utilities, etc. is provided in the deck at intermediate piers

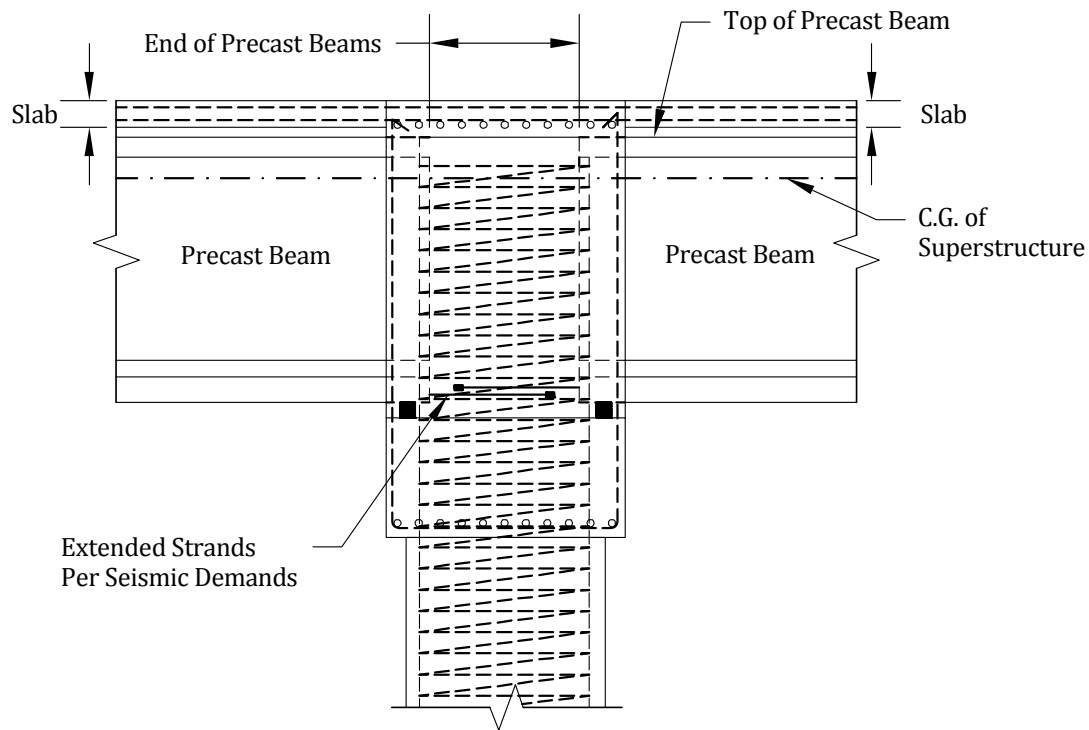
The hinge bar size and spacing is designed for anticipated lateral loads due to seismic and other load combinations.

15.5.1.3 Fixed Diaphragm Connection

The connection shown in **Figure 15.5.1.3-1** is used by WSDOT for continuous spans and assumed to provide a moment resistant connection between the superstructure and the substructure at intermediate piers. Pier caps are wider for fixed connections than hinged connections. Precast beams are supported on blocks or pads on the bent caps. The diaphragm is cast in place in two stages. The first stage, a portion of the depth, is to ensure precast beam stability after erection, and the second stage, the balance of the depth, is cast after slab casting and initial creep has occurred. Adequate extended strands and reinforcing bars are provided to ensure elastic performance of the connection during a major seismic event. The design recommendations for this detail are:

- All beams of adjoining spans are of equal depth, spacing, and preferably the same type
- Negative moment reinforcement for live loads, impact, and superimposed dead loads from traffic barriers, pedestrian walkways, utilities, etc. is provided in the deck at intermediate piers
- Resultant plastic hinging forces at the centroid of the superstructure are evaluated
- The number of extended strands resists seismic positive moment and restraint moment due to time-dependent forces
- The diaphragm reinforcement is designed to resist the resultant seismic forces acting at the centroid of the diaphragm
- Beam ends are designed for interface shear transfer between the precast beams and the cast-in-place concrete diaphragms

Figure 15.5.1.3-1
Fixed Diaphragm at Intermediate Piers (WSDOT)

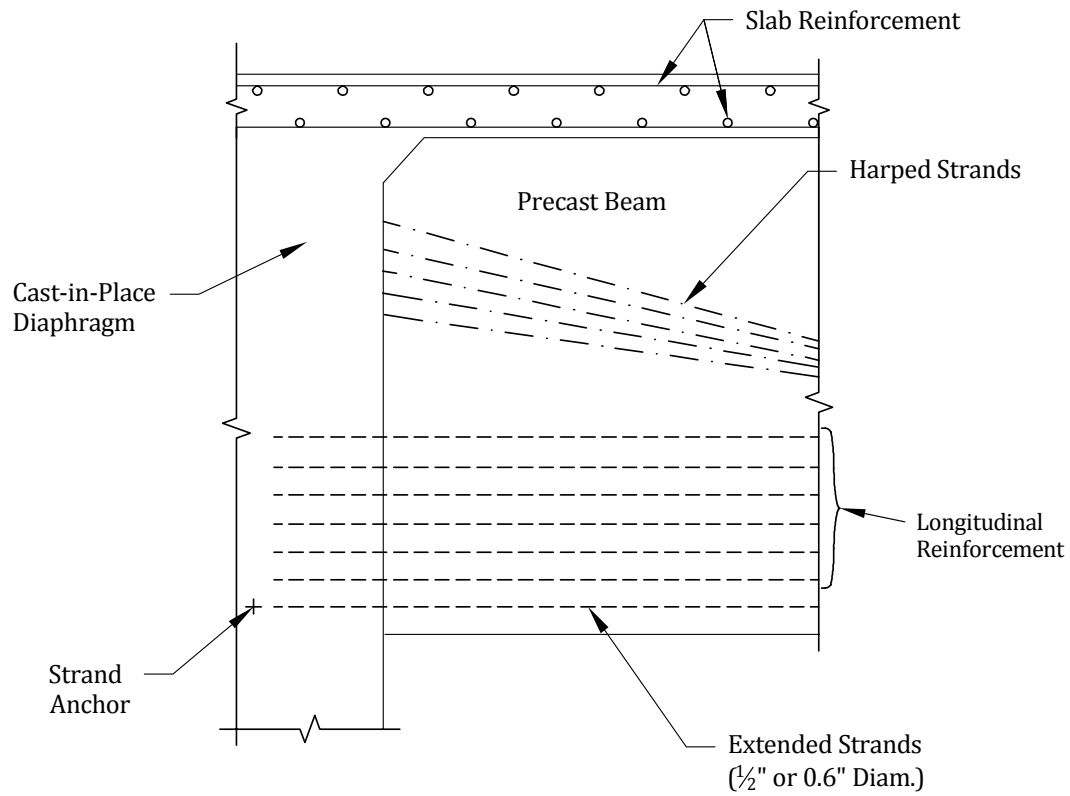


15.5.1.4 Positive Moment Connection at Pier Diaphragms

Strand extension details with strand extensions and strand anchor chucks used for continuous spans at fixed diaphragms for WSDOT bridges are shown in **Figure 15.5.1.4-1**, and are suitable for use with most common prestressed concrete beam bridges. Note that it is necessary to seat the wedges in the chucks. The effect of time-dependent positive moments from creep and shrinkage should be considered in determination of the positive moment capacity available. A minimum of four extended strands is desirable regardless of design requirements.

The procedure used to calculate the required number of extended strands is described in this section. Calculations assume development of the tensile strength of the strands at ultimate loads. Strands used for this purpose must be developed within the short distance between the two beam ends. A minimum distance of 2 ft between beam ends is desirable. Strand anchors are then installed at 1 ft 9 in. from the beam ends. The number of extended strands cannot exceed the number of straight strands available in the beam.

Figure 15.5.1.4-1
Strand Extension Details



a) Schematic Drawing of Strands and Reinforcement Extended into Diaphragm



b) Extended Strands with Anchor Chucks and Plates



c) Extended Strands and Reinforcement without Additional Anchorage

SEISMIC DESIGN

15.5.1.4 Positive Moment Connection at Pier Diaphragms

The design moment at the center of gravity of the superstructure, M_{po}^{CG} is calculated using the following equation:

$$M_{po}^{CG} = M_{po}^{top} + \frac{(M_{po}^{top} + M_{po}^{Base})}{L_c} h$$

where

M_{po}^{top} = plastic overstrength moment at top of column, ft-kips

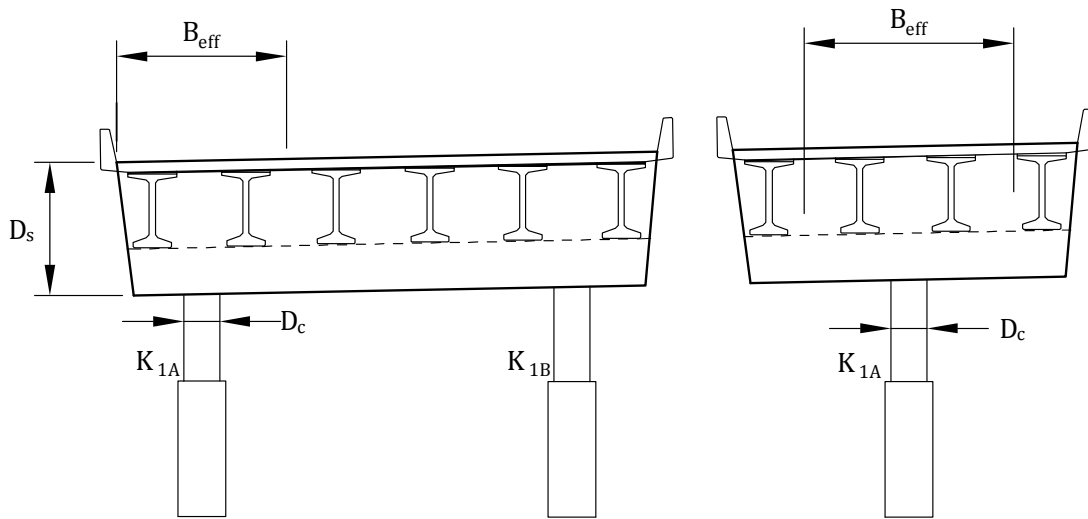
M_{po}^{Base} = plastic overstrength moment at base of column, ft-kips

h = distance from top of column to c.g. of superstructure, ft

L_c = column clear height used to determine overstrength shear associated with the overstrength moments, ft

This moment is resisted by the bent cap through torsion. The torsion in the bent cap is distributed into the superstructure based on the relative flexibility of the superstructure and the bent cap. Hence, the superstructure does not resist column overstrength moments uniformly across its width. To account for this, an effective width approximation is used, where the maximum resistance per unit of superstructure width is distributed over an equivalent effective width to provide an equivalent resistance. The equivalent width concept is illustrated in **Figure 15.5.1.4-2**.

*Figure 15.5.1.4-2
Effective Superstructure Width for Extended Strand Design*



For concrete bridges, with the exception of box beams and solid superstructure, this effective width can be calculated as follows:

$$B_{eff} = D_c + D_s$$

where

D_c = diameter of column, ft

D_s = depth of superstructure including cap beam, ft

Structural testing at the University of California at San Diego in the late 1990s (Holombo, 2000) recommended that roughly two-thirds of the column plastic moment should be resisted by the two beams adjacent to the column (encompassed by the effective width) and the other one-third should be resisted by the nonadjacent beams.

Based on this effective width, B_{eff} , the moment per beam line is calculated as follows:

- For adjacent beams (encompassed by the effective width):

$$M_{sei}^{Int} = \frac{2M_{po}^{CG}}{3N_g^{int}}$$

- For nonadjacent beams:

$$M_{sei}^{Ext} = \frac{M_{po}^{CG}}{3N_g^{ext}}$$

The seismic moment is then calculated:

If $M_{sei}^{Int} \geq M_{sei}^{Ext}$ then $M_{sei} = M_{sei}^{Int}$

If $M_{sei}^{Int} < M_{sei}^{Ext}$ then $M_{sei} = \frac{M_{po}^{CG}}{N_g^{int} + N_g^{ext}}$

where

N_g^{int} = number of beams encompassed by the effective width

N_g^{ext} = number of beams outside the effective width

Total number of extended straight strands, N_{ps} , needed to develop the required moment capacity at the end of beam is based on the yield strength of the strands:

$$N_{ps} = 12[M_{sei}(K - M_{SIDL})] \frac{1}{0.9\phi A_{ps} f_{py} d}$$

where

A_{ps} = area of each extended strand, in.²

f_{py} = yield strength of prestressing steel specified in *LRFD Specifications* Table 15.5.4.4.1-1, ksi

d = distance from top of slab to c.g. of extended strands, in.

M_{SIDL} = moment due to superimposed dead loads (traffic barrier, sidewalk, etc.) per beam, ft-kips

K = span moment distribution factor. Use maximum of $K1$ and $K2$

ϕ = strength reduction factor for flexure

15.5.2 Abutment Connection for Precast, Prestressed Beam Bridges

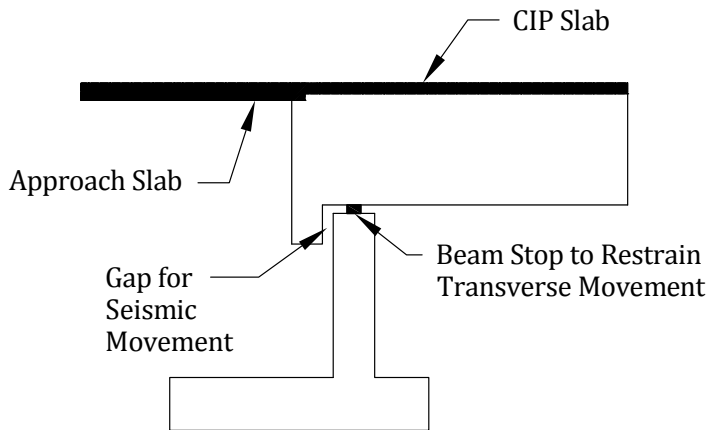
15.5.2.1 Introduction

The typical abutment in regions of moderate and high seismic hazard is a cast-in-place concrete pier wall supported on spread footings, piles, or shaft foundations. Precast beams are often supported on elastomeric bearing pads at end piers. Semi-integral end diaphragms may be used for shorter bridges. An L-shaped abutment (**Figs. 15.2.3.1-1** and **15.5.2.3-1**) is often used for longer precast bridges. In this type of connection, the bridge ends are free for longitudinal movement but restrained for transverse seismic movement by beam stops. The bearing system is designed for the service load condition but may not be adequate to resist seismic loading. The bearings are designed to be accessible so that the superstructure can be lifted and the bearings replaced after a major seismic event. Approach slabs rest on a notch provided at the superstructure end, thereby providing a ramp up to and on to the bridge, should soil behind the abutment settle during a seismic event.

15.5.2.2 Semi-integral End Diaphragm

Figure 15.5.2.2-1 shows a semi-integral end pier detail used by WSDOT. This type of end diaphragm eliminates the need for expansion joints at end piers. The gap between the end pier wall and the end diaphragm is designed to be greater than the longitudinal seismic movement requirement for the extreme event limit state, and thermal expansions at the service limit state for bridge lengths less than 450 ft.

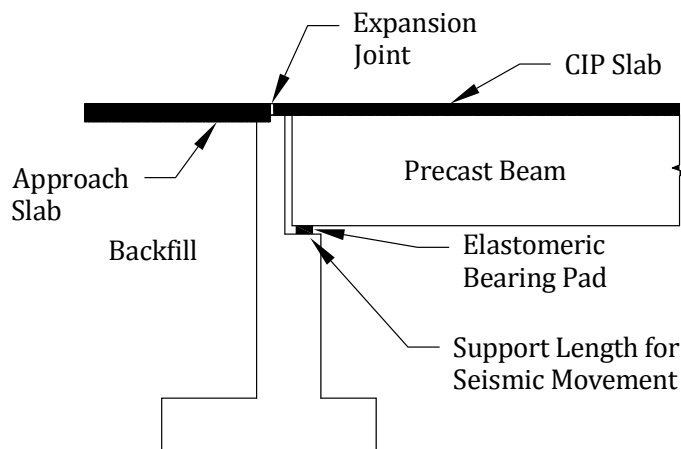
Figure 15.5.2.2-1
Semi-integral End Pier Connection (WSDOT)



15.5.2.3 Traditional L-shaped Abutment

A typical abutment detail for medium to long spans is shown in **Figure 15.5.2.3-1**. The diaphragm is cast in place between the beams and is not shown. The seat width must be greater than the anticipated longitudinal seismic movement in the extreme event limit state. The gap between the superstructure and the back wall must be designed to accommodate the longitudinal seismic movement for the extreme event limit state, and the thermal expansion for the service limit state. For bridges with large longitudinal movement, the back wall could be designed to shear during a seismic event.

Figure 15.5.2.3-1
Traditional Abutment on Spread Footing



15.5.2.4 Support Length Requirement

The minimum displacement requirements at the expansion bearing should accommodate the greater of the maximum displacement calculated from a displacement analysis or a percentage of the empirical seat width, N , specified in Equation 4.12.2-1 of Restrepo et al., 2011.

$$N = (8 + 0.02L + 0.08H)(1 + 0.000125S^2) \quad (\text{Restrepo et al., 2011, Eq. 4.12.2-1})$$

where

N = minimum support length, in.

L = bridge length to the adjacent expansion joint, or to the end of the bridge, ft

H = average height of abutment wall supporting the superstructure in ft as described in *LRFD Specifications* Article 4.7.4.4

S = skew angle of the support measured normal to span, degrees

The empirical seat width is modified as shown in **Table 15.5.2.4-1** for different seismic zones.

Table 15.5.2.4-1
Percentage N by SDC and Effective Peak Ground Acceleration, A_s

Seismic Zone	Effective Peak Ground Acceleration, A_s	Percentage N
A	< 0.05	≥ 75
A	≥ 0.05	100
B	All Applicable	150
C	All Applicable	150

15.5.2.4.1 Support Length for Bridges Assigned to Seismic Design Category D

For SDC D, the beam bearing support length, N , must accommodate the relative longitudinal earthquake displacement demand at the supports or at a hinge within a span between two frames. That length is determined as:

$$N = (4 + 1.65\Delta_{eq})(1 + 0.00025S^2) \geq 24 \quad (\text{LRFD Seismic Guide Specifications Eq. 4.12.3-1})$$

where Δ_{eq} = relative earthquake loading longitudinal displacement demand

Caltrans' *Seismic Design Criteria* (2006) permits the hinge seat length in "well-balanced frames" (adjacent frames for which the ratio of the natural periods is equal to or greater than 0.7) to be evaluated as follows:

$$N = \Delta_{p/s} + \Delta_{cr+sh} + \Delta_{temp} + \Delta_{eq} + 4 \text{ in.} \quad (\text{Caltrans Seismic Design Criteria Eq. 7.5})$$

where

$\Delta_{p/s}$ = displacement due to prestressing

Δ_{cr+sh} = displacement due to creep and shrinkage

Δ_{temp} = displacement due to temperature effects

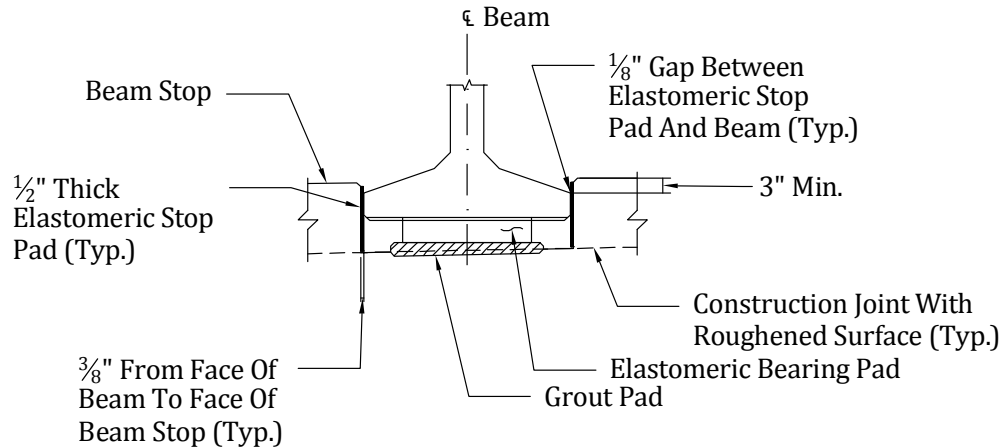
Δ_{eq} = relative earthquake loading longitudinal displacement demand

15.5.2.4.2 Beam Stop Details

A typical beam stop detail used at end piers is shown in **Figure 15.5.2.4.2-1**. Elastomeric pads are provided at the sides of the beam stops to prevent concrete-to-concrete impact during a seismic event while also allowing bridge longitudinal movement under service motions. The beam stops need to be adequately dimensioned and reinforced to resist the transverse seismic force. The abutment foundation must also be able to transmit the lateral load, or resist the design load if the beam stops are designed to shear in a seismic event.

Finally, the lateral resistance of any pile- or shaft-supported abutment should exceed the transverse seismic force to avoid below-grade damage that cannot be easily detected.

Figure 15.5.2.4.2-1
Beam Stop at End Piers

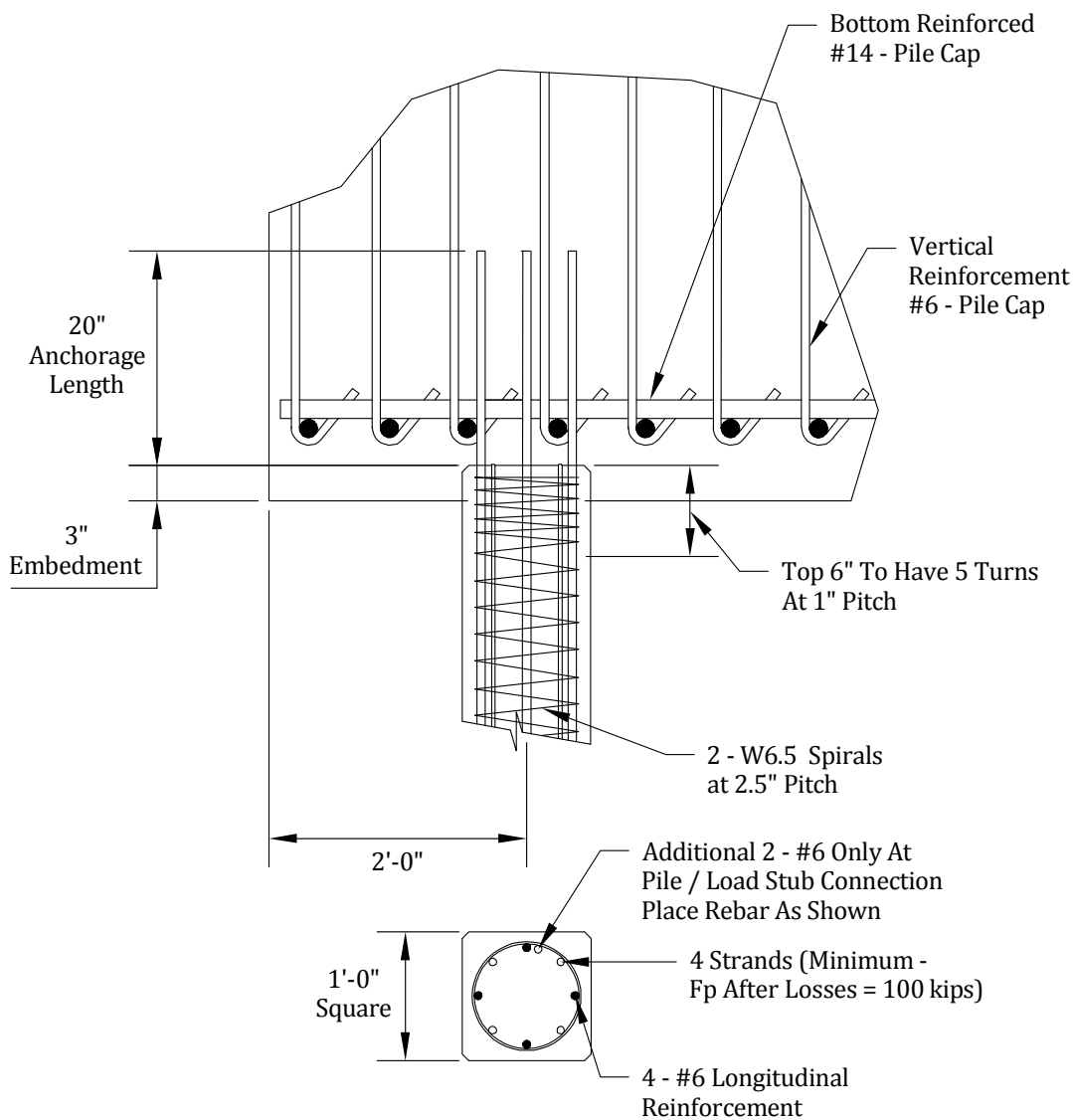


15.5.3 Pile-to-Pile Cap Connection

Precast concrete 12- and 16-in.-square piles are frequently used under cast-in-place abutment, bent, and retaining wall footings. Caltrans requires that “the size and number of piles and the pile group layout be designed to resist service level moments, shears, and axial loads and the moment demand induced by the column plastic hinging mechanism” in competent soils. Marginal soils may call for a more ductile pile that can withstand larger deflections.

Different philosophies exist concerning the optimum pile embedment into the cap, especially when the piles are to be fixed against rotation. A larger embedment may improve fixity, but it also reduces the effective flexural depth in the footing at locations over the piles. Resistance to punching shear is also diminished. Simulated seismic loads on a test specimen with 3-in. embedment conducted at the University of California at San Diego resulted in a brittle failure after spalling of the concrete cover around the pile. The unit, however, did reach its theoretical flexural capacity under compressive and tensile axial loading, and exhibited sufficient displacement ductility. Test specimen details are shown in **Figure 15.5.3-1**. Anchorage bars are left straight for driving, but may be hooked in the field around the top mat of footing reinforcement. In this event, the bars should be rechecked for appropriate development length.

Figure 15.5.3-1
Precast Pile-to-Cast-in-Place Concrete Cap Connection

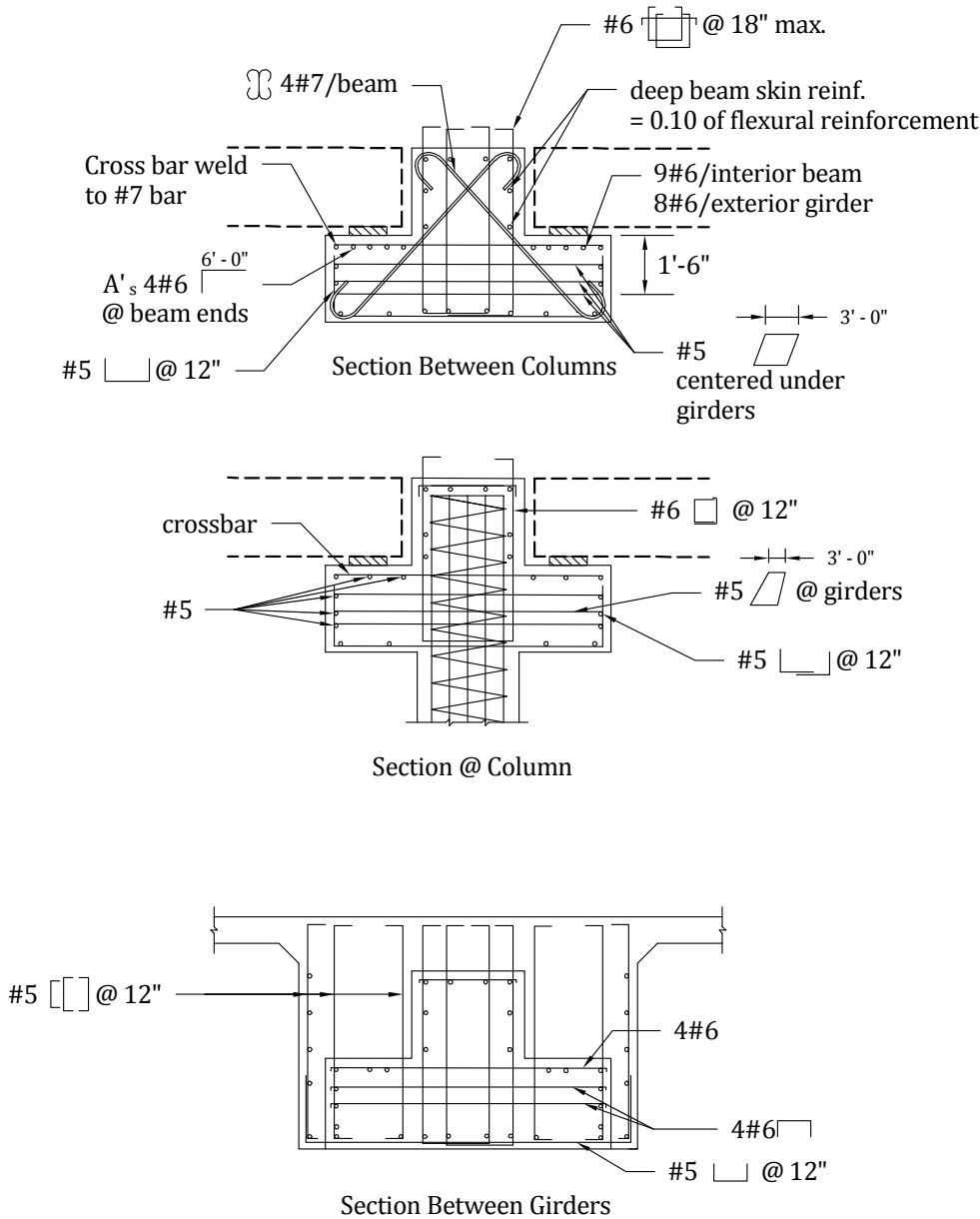


Longitudinal reinforcement must be properly confined in the top 15 ft of the pile when in place, and be developed into the cap. If a pile meets refusal at an elevation higher than that for which it was designed, obvious issues arise with confinement and cutting of prestressing steel.

15.5.4 Haunched Beam-to-Cast-in-Place Inverted-Tee Bent

When haunched precast beams are placed on a cast-in-place inverted-T bent cap, as shown in **Figure 15.5.4-1**, there is no positive moment connection. Testing may eventually show that the confinement provided on each side of the beam is adequate to compensate for the lack of beam connection. But until that testing is completed and corresponding analytical tools are developed, this detail should be used only in regions of low-to-moderate seismic risk. A strut-and-tie model is needed to design the inverted-T bent cap. A design example can be found in Martin and Sanders, 2007.

Figure 15.5.4-1
Haunched Precast Beams on Cast-In-Place Inverted-T Bent Cap



15.5.5 Precast Pile-to-Partial Precast Cap

The current approach to seismic design of precast bent caps is to emulate the behavior of cast-in-place concrete caps. For the San Mateo-Hayward Bridge, a precast "yoke" was lifted into place over the columns/piles and temporarily supported. This precast unit ultimately became the lower half of the bent cap, and it supports the precast I-beams or bulb-tee beams during their erection. After the beams are placed, the top half of the bent cap is formed, reinforced, and cast. Details are shown in **Figures 15.5.5-1 and 15.5.5-2**. Precast deck panels were used. Seismic analysis of the cap was the same as that for a similar cast-in-place cap.

Figure 15.5.5-1
Precast Pile-to-Partial Precast Cap—1

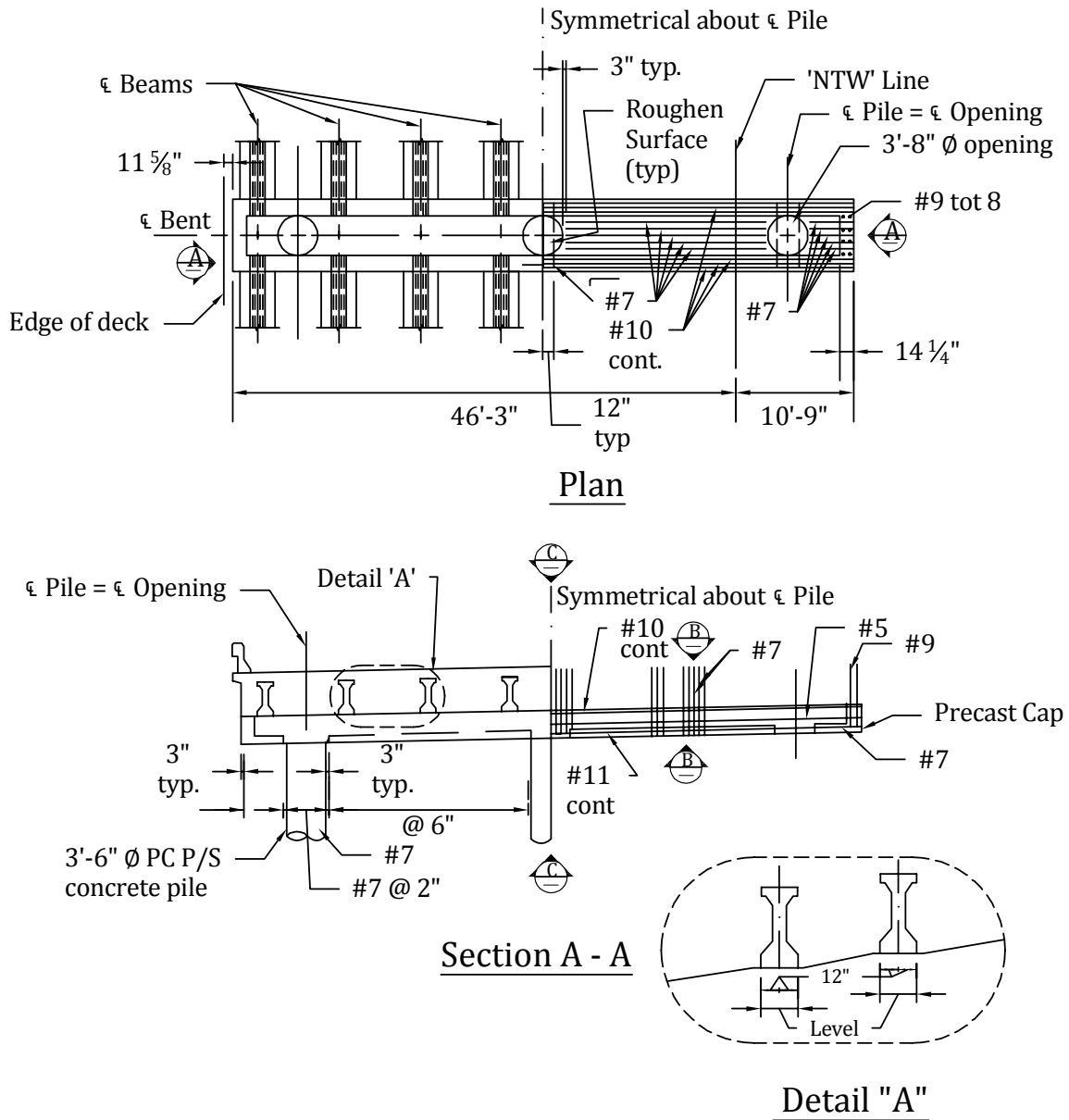
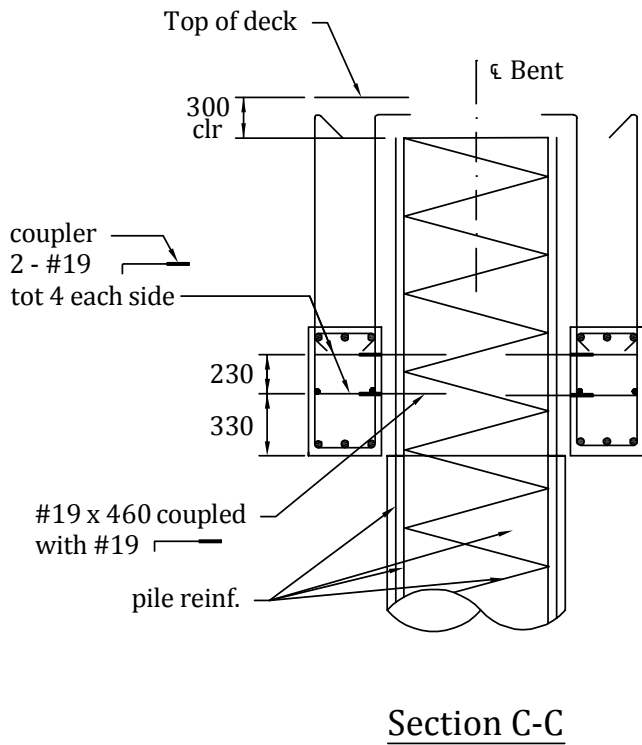
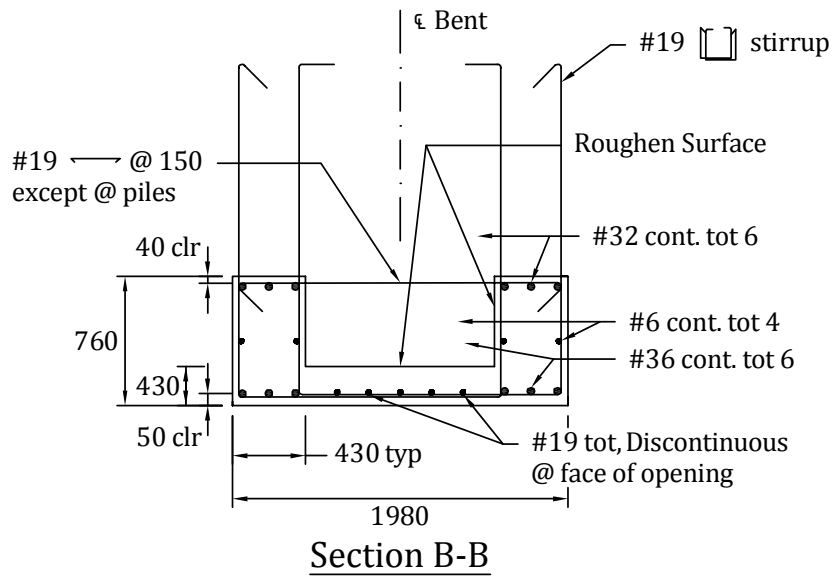


Figure 15.5.5-2
Precast Pile-to-Partial Precast Cap—2



15.5.6 Precast Segmental Columns in Seismic Applications

Precast segmental substructures can be a very efficient solution especially when there is repetition of shapes. Precasting can also be the best solution for unique sections that require high quality concrete or geometry control, and when there is a long lead time for deep foundations that allows the contractor to fabricate pier sections concurrently with foundation work. The major advantage of precasting piers is the speed of construction.

The WSDOT Highways for Life (HfL) project involved the development of a totally prefabricated bridge bent system, including prefabricated segmental columns, prefabricated bent cap, and prefabricated superstructure as shown in **Figures 15.5.6-1** through **15.5.6-3**. To accelerate construction without sacrificing seismic resistance, the beam-to-column connections were made with a small number of large-diameter reinforcing bars that were grouted into much larger diameter ducts. The HfL project demonstrated that the product could be deployed in a wide range of applications. The HfL project was accomplished in four phases:

1. Proof testing of project-specific and alternative-design variations of the system
2. Development of project-specific and general design provisions and specifications
3. Development of design examples
4. Deployment of the basic system in the field

In order for precast column design to be economical, segments should be dimensioned for practical fabrication, transport, and erection. The resulting sections are typically sized for a maximum weight on the order of 50 tons or less, enabling erection by standard cranes. Column segments can be assembled with mild reinforcement, post-tensioning tendons, or high strength bars.

Figure 15.5.6-1
Precast Segmental Column

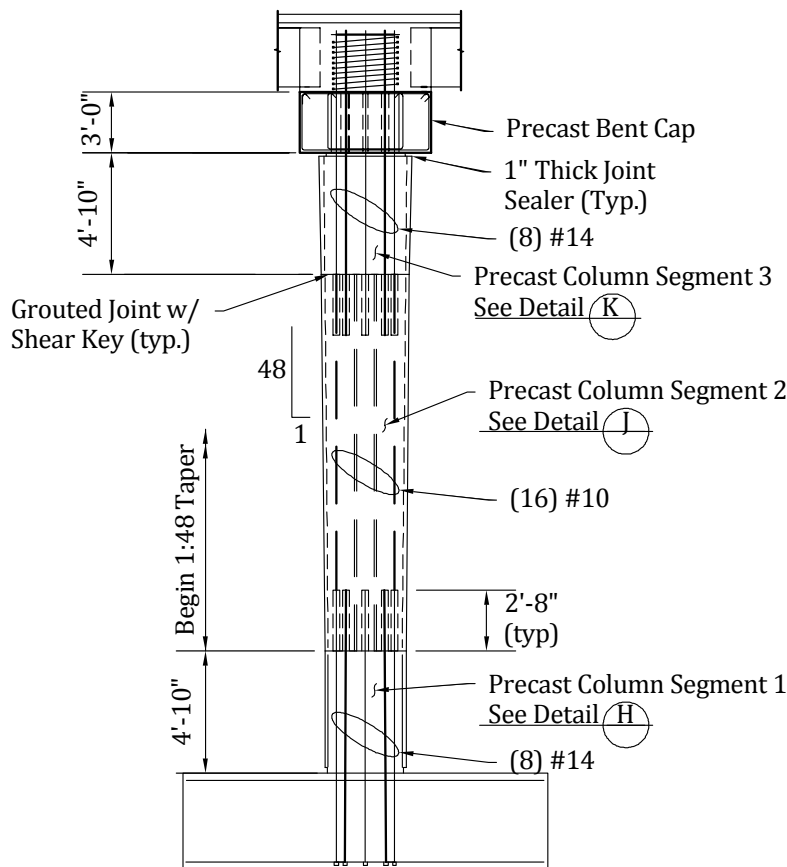
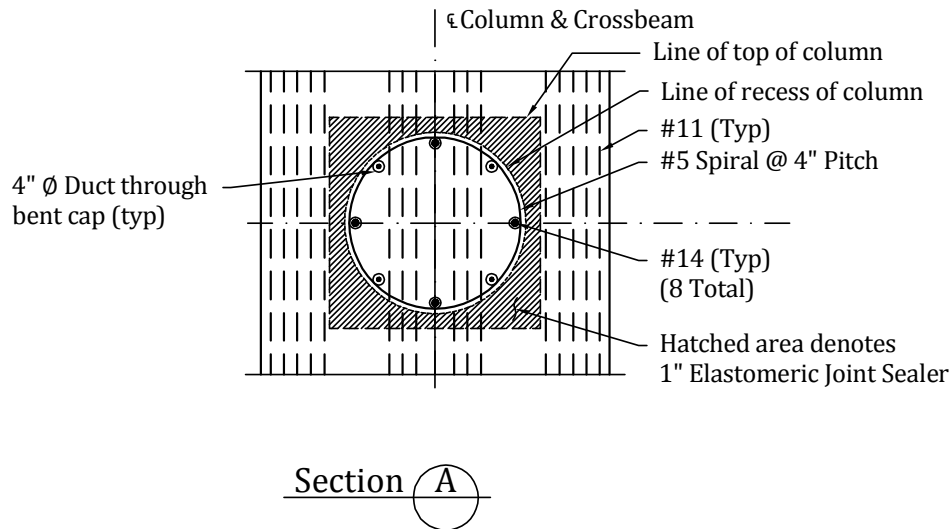


Figure 15.5.6-3
Precast Segmental Column (continued)



15.5.6.1 Grouted Duct Connection

Where grouted connections are used, transverse reinforcement in the form of tied column reinforcement, spirals, hoops, or intersecting spirals or hoops must be provided. The minimum transverse reinforcement in the joint for grouted duct connections should be based on Equation 8.15.3.1-1 of Article 8.15.3.1 of Restrepo et al. (2011). Spacing of transverse reinforcement should not exceed $0.3D_s$ or 12 in. Articles 8.15.5 and C8.15.5 in the same reference summarize related design provisions and background information on nonintegral bent cap systems completed using grouted duct or cap pocket connections.

Minimum transverse joint reinforcement is required in the joint to ensure that the connection does not become a weak point in a precast bent system. However, the additional joint shear reinforcement required for SDC B, C, and D is not required.

Grouted duct connections should be reinforced in accordance with the requirements of Article 8.13.4.2.2a. Details of the connection include ducts, vertical stirrups inside the joint, and bedding layer reinforcement. The embedment lengths shown in **Table 15.5.6.1-1** were validated by University of Washington pullout tests of large diameter bars embedded in grouted ducts, as summarized in Appendix A, Section A.2.1.3 of the *Seismic Design Report* (PCI, 2013). These embedment lengths were adopted in the *WSDOT Bridge Design Manual*.

Table 15.5.6.1-1
Embedment Requirements for Grouted Duct Connections

Bar Size No.	Nominal Duct Size, in.	Embedment Length, in.	Embedment/Bar Diameter
3	2	12	29
4	2.5	15	27
5	3	15	21
6	3	15	18
7	3	20	21
8	3.5	20	18
9	3.5	20	16
10	3.5	25	18
11	4	25	16
14	4	30	16
18	4.5	40	16

The grout specification for the grouted duct connection is shown in **Table 15.5.6.1-2**.

Table 15.5.6.1-2 Grout Specification for Grouted Duct Connection
(Restrepo et al., 2011)

Property	Value	
Mechanical Compressive strength (ASTM C109, 2 in. cubes)	Age	Compressive strength (psi)
	1 day	2,500
	3 days	4,000
	7 days	5,000
	28 days	Maximum [6,000 1.25($f'_{ccap} + 500$)]
Compatibility Expansion requirements (ASTM C827 & ASTM C1090) Modulus of elasticity (ASTM C469) Coefficient of thermal expansion (ASTM C531)	Grade B or C—expansion per ASTM C1107	
	2.8–5.0×10 ⁶ psi	
	3.0–10.0×10 ⁻⁶ /deg F	
Constructability Flowability (ASTM C939; CRD-C611 Flow Cone) Set Time (ASTM C191) Initial Final	Fluid consistency efflux time: 20–30 seconds	
	2.5–5.0 hrs	
	4.0–8.0 hrs	
Durability Freeze Thaw (ASTM C666) Sulfate Resistance (ASTM C1012)	300 cycles, RDF 90%	
	Expansion at 26 weeks < 0.1%	

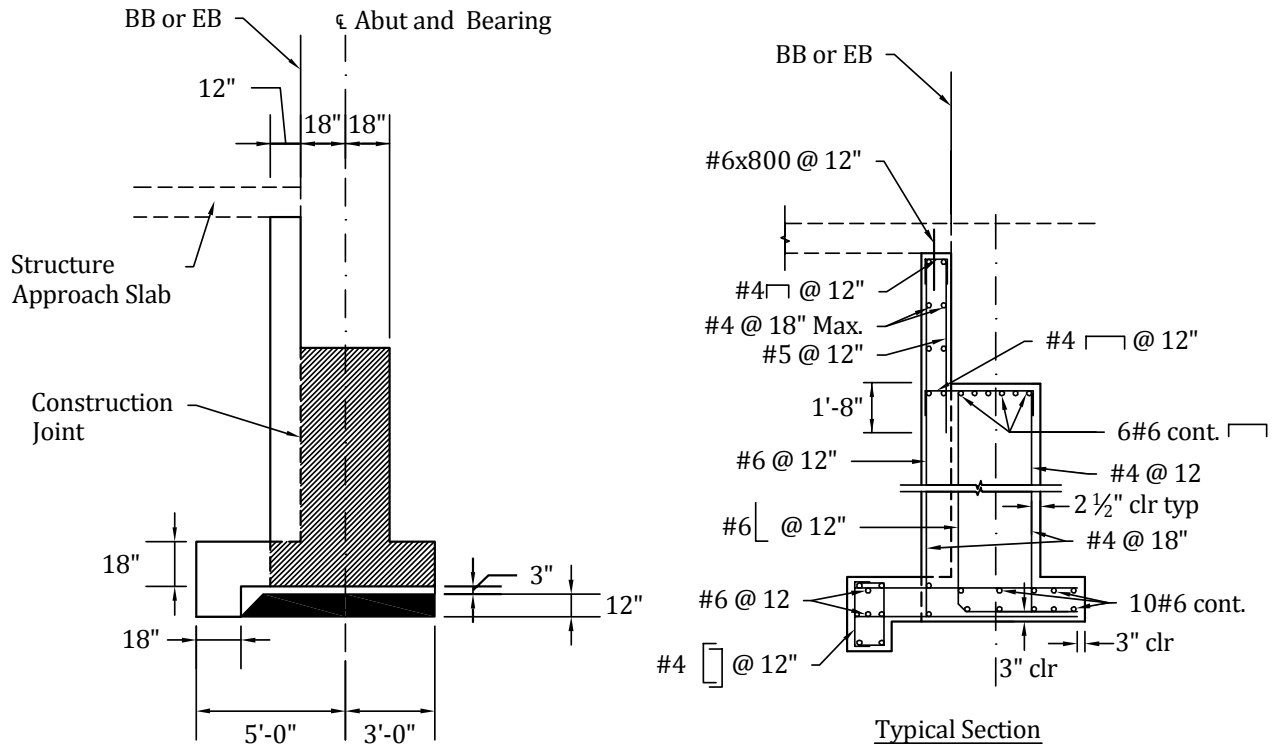
15.5.7 Precast Abutments

Precast abutments can be a very efficient solution for standard pier shapes or when accelerated bridge construction is necessary. Precasting can also be the best solution for unique sections that require high-quality concrete or geometry control, when there is a long lead time that allows the contractor to fabricate abutment sections concurrently with precast superstructure members, and when a precasting yard is located in the region. **Figures 15.5.7-1** and **15.5.7-2** show the use of a precast abutment for accelerated bridge construction. The cast-in-place backwall and the shear key are designed to resist the lateral seismic forces from the retained soil.

Figure 15.5.7-1
Use of Precast Abutment for Bridge Construction



Figure 15.5.7-2
Abutment Details



15.5.8 Precast Spliced Beam Superstructure with Integral Cap

With the increasing desire for bridges with longer spans, the need for increased vertical clearances, and the demand for faster construction, precast, prestressed, spliced concrete beams have been successfully used. A spliced beam is a precast, prestressed concrete member that is fabricated in several relatively long pieces (beam segments). These beams are assembled into a single beam or a continuous beam onsite. Post-tensioning is generally used to reinforce the connection longitudinally between beam segments. The bridge cross section is typically a conventional shape in which multiple precast beams support a cast-in-place concrete composite deck. The spliced beam, with longitudinal post-tensioning, can provide not only superstructure continuity, but also an integral cap-to-column connection if designed properly.

Figures 15.5.8-1 through 15.5.8-3 show details for a precast spliced beam superstructure with an integral bent cap that provides optimal clearance.

SEISMIC DESIGN

15.5.8 Precast Spliced Beam Superstructure with Integral Cap

Figure 15.5.8-1
Precast Box Beam Elevation

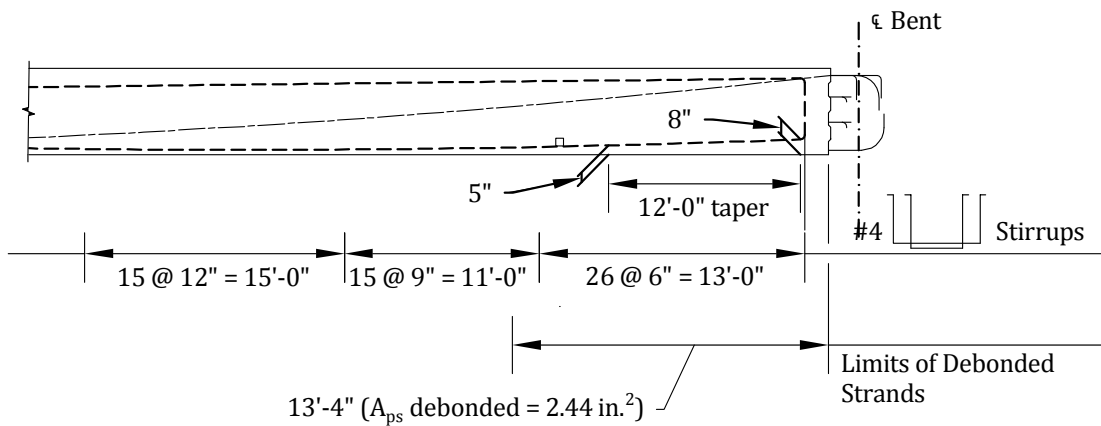
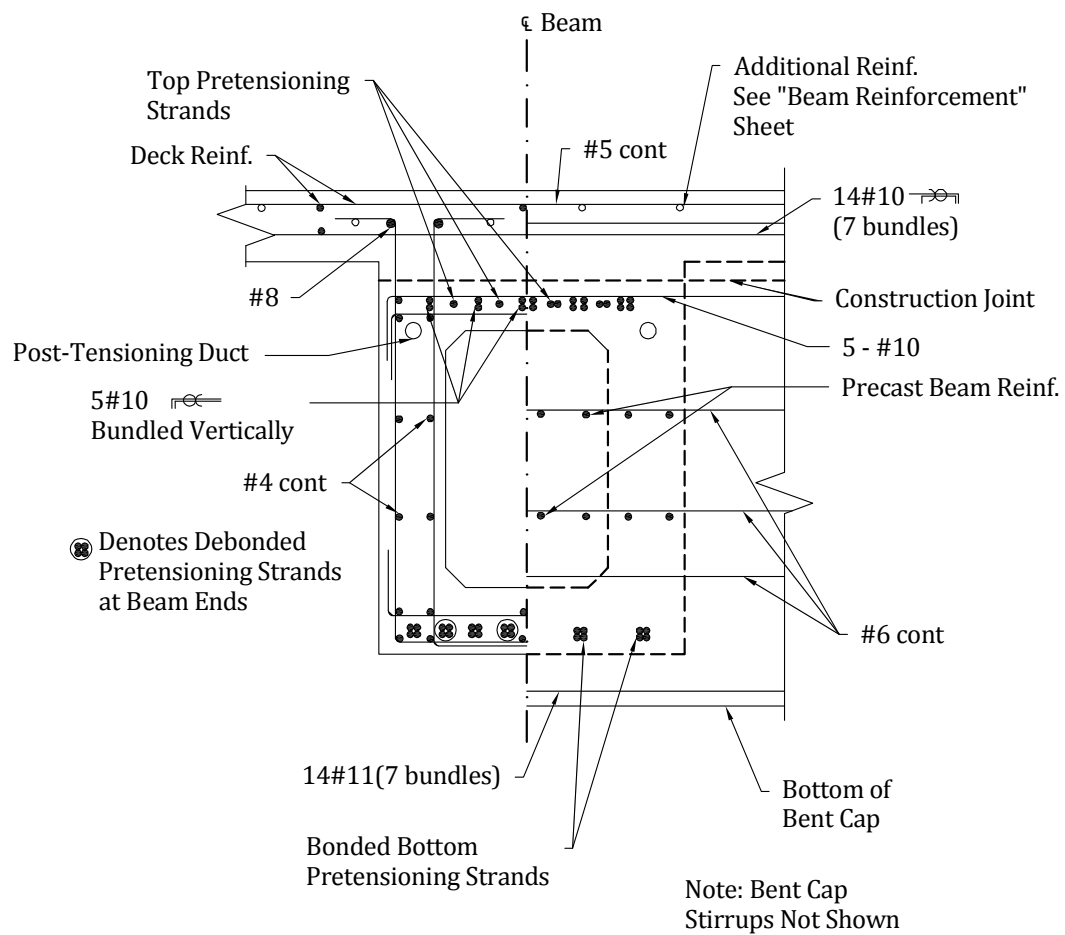


Figure 15.5.8-2
Integral Bent Cap Details



SEISMIC DESIGN

15.5.8 Precast Spliced Beam Superstructure with Integral Cap

Figure 15.5.8-2
Integral Bent Cap Details (continued)

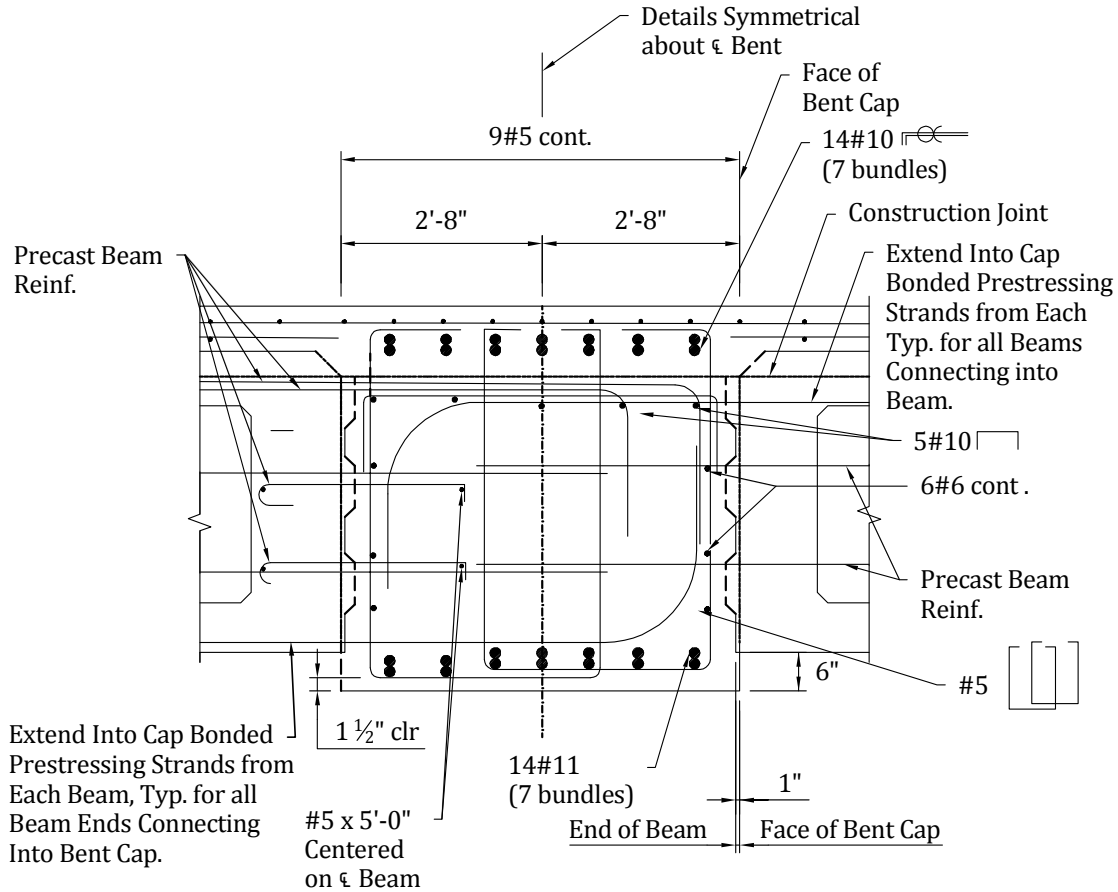
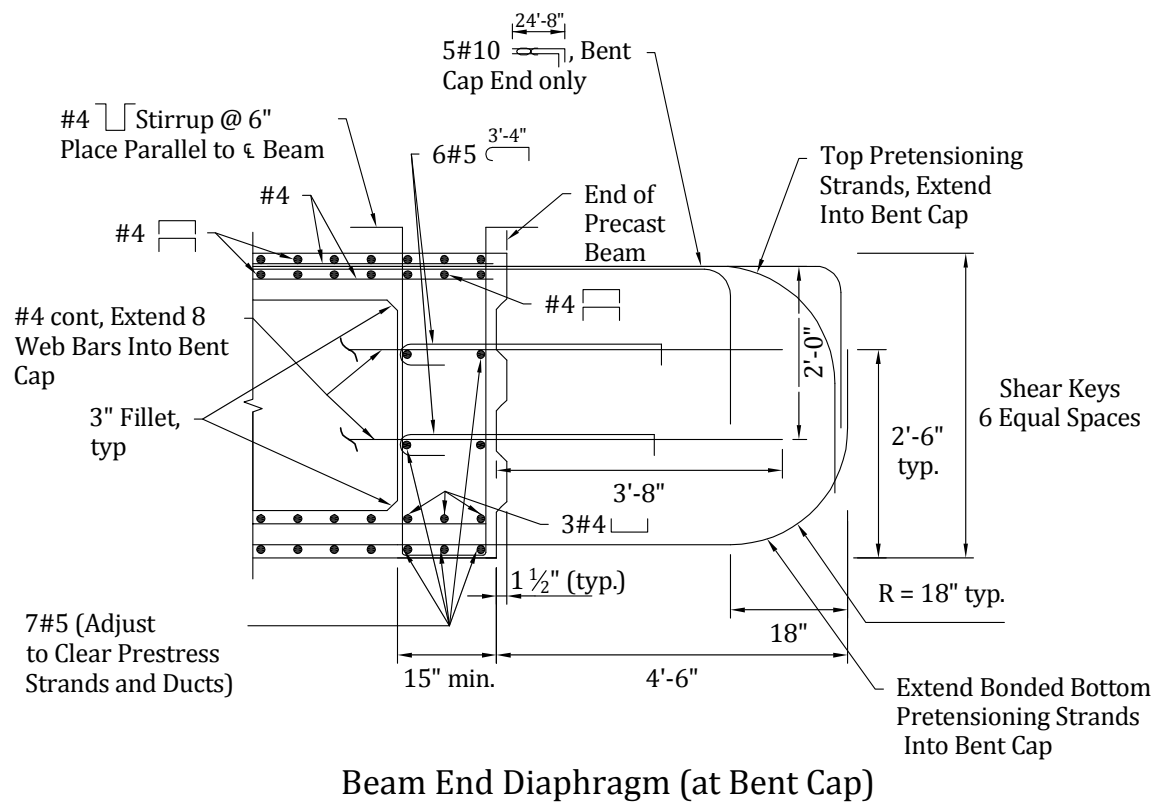


Figure 15.5.8-3
End Diaphragm at Bent Cap



15.6 DESIGN EXAMPLES

15.6.1 Configure Spans, Balance Stiffness, and Design Practice in California

15.6.1.1 Adjust Dynamic Characteristics

During preliminary design, the following should be considered to achieve acceptable seismic performance (**Figs. 15.6.1.1-1 and 15.6.1.1-2**).

Column:

- Adjust effective column lengths (lower footing, pile cap, or shaft)
- Vary cross section
- Vary longitudinal reinforcement details
- Add, subtract, or relocate columns

Frame:

- Use or modify end flexibility
- Reduce or redistribute superstructure mass
- Modify the hinge or expansion joint layout

15.6.1.1 Adjust Dynamic Characteristics/15.6.1.1.1 Determine Preliminary Member Sizes and Span Configuration

Figure 15.6.1.1-1
Balance Stiffness

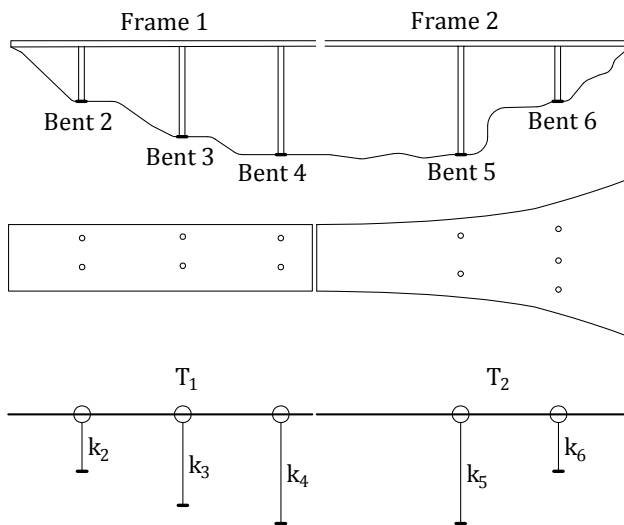
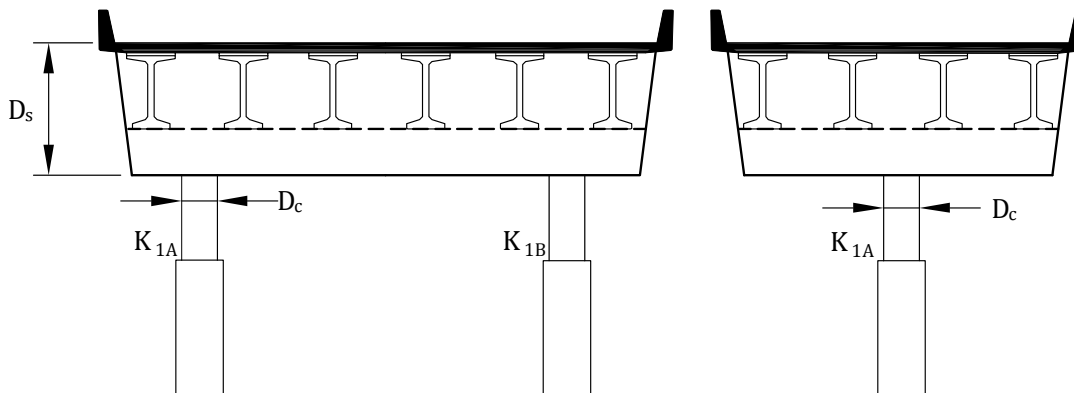


Figure 15.6.1.1-2
Bridge Typical Sections



15.6.1.1.1 Outline of Procedure

15.6.1.1.1.1 Determine Preliminary Member Sizes and Span Configuration

$$0.70 < \frac{D_c}{D_s} < 1.00$$

(Caltrans Seismic Design Criteria Eq. 7.24)

where

D_c = column diameter, ft

D_s = superstructure depth, ft

For the column, A_{s max} < 0.04A_g and A_{s min} > 0.01A_g

(Caltrans SDC Eqs. 3.28, 3.29)

SEISMIC DESIGN**15.6.1.1.1 Determine Preliminary Member Sizes and Span Configuration/15.6.1.2 Assess Preliminary Ductility—“Lollipop Model”**

where

A_s = area of longitudinal column steel, in.²

A_g = gross cross-sectional area of column, in.²

$$\rho_s = \frac{4A_b}{d's} \quad (\text{Caltrans SDC Eq. 3.31})$$

where

ρ_s = volumetric ratio of column lateral reinforcement

A_b = area of column transverse reinforcement, in.²

d' = diameter of column concrete core, in.

s = spacing of column transverse reinforcement, in.

For the cap, $B_{cap} = D_c + 2$ (Caltrans SDC Eq. 7.10)

where B_{cap} = width of cap, ft

15.6.1.1.1.2 Check for Balanced Stiffness

$$\frac{k_i^e m_j}{k_j^e m_i} \geq 0.5 \quad (\text{Caltrans SDC Eq. 7.1a})$$

where

k_i^e, k_j^e = effective stiffness of any two bents within a frame or between any two columns within a bent

m_i, m_j = tributary mass of column or bent i and j

$$\frac{k_i^e m_j}{k_j^e m_i} \geq 0.75 \quad (\text{Caltrans SDC Eq. 7.2a})$$

where

k_i^e, k_j^e = effective stiffness between adjacent bents or between adjacent columns within a bent

m_i, m_j = tributary mass of column or bent i and j

15.6.1.2 Assess Preliminary Ductility—“Lollipop Model”

Material properties:

$$f'_{ce} = \text{greater of } 1.3\sqrt{f'_c} \text{ or } 5.0, \text{ ksi} \quad (\text{Caltrans SDC Eq. 3.13})$$

where f'_{ce} = expected concrete compressive strength, ksi

$$E_c = 33,000(w_c)^{1.5}\sqrt{f'_c}, \text{ ksi} \quad (\text{Caltrans SDC Eq. 3.11})$$

Use idealized bilinear moment-curvature (M - ϕ) relationship to estimate plastic rotation

$$\theta_p = L_p \phi_p$$

where

θ_p = plastic rotation capacity

L_p = plastic hinge length, in.

ϕ_p = idealized plastic curvature (assumed constant over length L_p)

$$L_p = 0.08L + 0.15f_{ye}d_{be} \geq 0.3f_{ye}d_{be} \quad (\text{Caltrans SDC Eq. 7.25})$$

where

f_{ye} = expected yield, ksi

d_{be} = diameter of longitudinal bars, in.

L = column height, in.

SEISMIC DESIGN**15.6.1.2 Assess Preliminary Ductility—“Lollipop Model”/15.6.1.3.1 Design Column Shear**

Evaluate plastic displacement: $\Delta_p = \theta_p(L - 0.5L_p)$

Evaluate displacement capacity: $\Delta_c = \Delta_y + \Delta_p$

where Δ_y = yield displacement taken along the local principal axis corresponding to Δ_d

Evaluate displacement demand:

$$\Delta_d = \frac{(m)(a)}{k_e}$$

where

a is taken from the appropriate Caltrans Acceleration Response Spectrum (ARS) curve based on the period of the fundamental mode of vibration, and multiplied by the gravitational constant

k_e = effective stiffness of column

$$\mu_c = \frac{\Delta_c}{\Delta_y} > 3 \quad (\text{Caltrans SDC Eq. 3.6})$$

where μ_c is the local displacement ductility capacity, calculated for each bent

Finally, check preliminary $\Delta_d < \Delta_c$ (Caltrans SDC Eq. 4.1)

15.6.1.3 Transverse Pushover Analysis

Software input includes section properties, M_p , I_e , and soil springs ϕ_y , ϕ_p

where

M_p = plastic moment capacity, ft-kips

I_e = effective stiffness, in.⁴

ϕ_y = yield curvature

ϕ_p = plastic curvature

Except for single-column bents, the designer must iterate for change in column axial force (until less than 5%) due to earthquake loading and revise M_p . The lateral force at the first yield displacement, Δ_y , is then multiplied by the bent height to determine the overturning moment M_{OT} .

Repeat steps in 15.6.1.2 for maximum tension and maximum compression in columns.

Check that P - Δ effects are less than 20% of the seismic demand.

15.6.1.3.1 Design Column Shear

$\phi V_n > V_o$ (Caltrans SDC Eq. 3.14)

where

V_o = overstrength shear = M_o/L , kips

$V_n = V_c + V_s$

where

M_o = column overstrength moment = $1.2M_p$, ft-kips

L = member length from point of maximum moment to point of contra-flexure, ft

$V_c = v_c A_e$

where

A_e = effective area resisting shear = $0.8A_g$, in.² (Caltrans SDC Eqs. 3.16, 3.17)

$v_c = F_1 F_2 \sqrt{f'_c} < 4\sqrt{f'_c}$, ksi (inside plastic hinge zone) (Caltrans SDC Eq. 3.18)

where F_1 is a function of ductility demand and F_2 is a function of compressive axial stress

15.6.1.3.2 Design of Bent Cap

Design bent cap for flexure and shear. Note that exterior column-to-cap connection may behave as a knee joint. For typical T-joints, calculate principal tension and compression stresses.

$$\text{Principal compression } p_c \leq 0.25\sqrt{f'_c}, \text{ psi} \quad (\text{Caltrans SDC Eq. 7.8})$$

$$\text{Principal tension } p_t \leq 12\sqrt{f'_c}, \text{ psi} \quad (\text{Caltrans SDC Eq. 7.9})$$

Minimum volumetric ratio of transverse column reinforcement when $p_t \leq 3.5\sqrt{f'_c}$, psi:

$$\rho_s \leq \frac{3.5\sqrt{f'_c}}{f_{yh}}, \text{ psi} \quad (\text{Caltrans SDC Eq. 7.18})$$

where

f_{yh} = yield strength of hoops otherwise, minimum ratio

$$\rho_s \leq 0.4 \frac{A_{st}}{l_{ac}^2} \quad (\text{Caltrans SDC Eq. 7.23})$$

where

l_{ac} = length of column bar extension into core, in.

A_{st} = area of hoops, in.²

Vertical stirrups are taken as 20% of column reinforcement anchored in joint region (Caltrans SDC Eq. 7.19)

15.6.1.4 Longitudinal Pushover Analysis

Steps for longitudinal pushover analysis:

- Determine abutment soil springs.
- Lump columns together; ignore overturning.
- Determine ductility capacity and demand, including P - Δ . Perform analysis similar to that for transverse pushover analysis. Check shear in longitudinal direction.
- Determine seismic strength of concrete superstructure (not addressed explicitly for precast members in Caltrans' *Seismic Design Criteria*, but must remain elastic), including effects of continuity forces.
- Check seat widths including effects due to creep, shrinkage, temperature, and earthquake.

15.6.1.5 Final Displacement Demand Assessment

If any modifications were made to the original design, the displacement demand in the transverse and longitudinal directions must be re-evaluated using pushover analysis.

15.6.2 Precast Substructure and Superstructure Bridge with CIP Connections**15.6.2.1 Introduction**

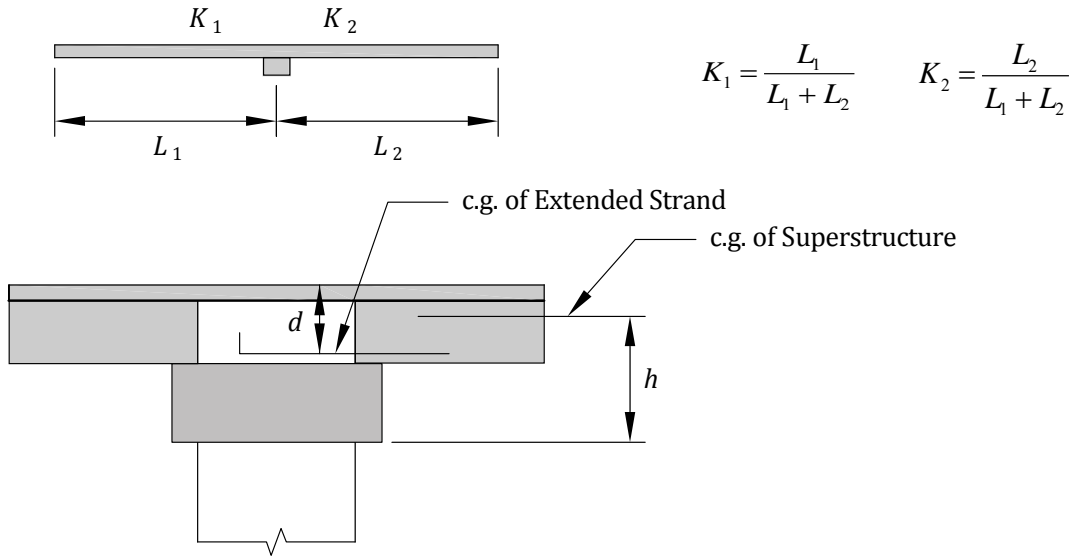
The recommended design procedure for the following precast pier system is as follows:

- Configure spans and balance stiffness for optimum seismic performance
- Perform seismic analysis (force-based or displacement-based analysis)

The top diameter of the column should be at least 12 in. smaller than the bottom of the column for ease of construction. The column stiffness for seismic analysis should be kept constant based on the section properties of the bottom of the column (or balance stiffness as suggested in Caltrans' *Seismic Design Criteria*). Effective sectional properties based on actual column axial load and reinforcement ratio, as shown in **Figure 15.6.2.1-1** (*Seismic Design Criteria*, 2006), should be used for seismic analysis.

15.6.2.1 Introduction/15.6.2.2 Design Procedure for Positive Earthquake Loading Reinforcement at Interior Pier of a Precast Beam Bridge

Figure 15.6.2.1-1
Extended Strands at Pier of Continuous Bridges



Where force-based design is used, determine the applicable response modification factors, design the column reinforcement and calculate the plastic moment capacity at the top and bottom of the column. Discrete hoops should be used for transverse reinforcement, and must be used in the plastic hinge region. Spiral reinforcement should be avoided in large-diameter columns to avoid unraveling in the event of failure in one location and to facilitate material inspection.

Mechanical splices should not be used in the plastic hinge region as bars may neck outside of the device under ultimate strain.

- Increase area of reinforcement in the top of the column to obtain approximately equal plastic moment capacity at the top and bottom of the column.
- Perform complete redistribution of forces for multiple-column bents. This step is not necessary if a frame-pushover analysis is performed. Calculate plastic shear. Perform joint shear analysis.
- Design precast bent cap for flexure and shear capacity to resist strength load combinations.
- Design for interface shear between cast-in-place concrete and precast bent cap. Check interface shear capacity based on capacity provided by shear keys. Reinforcing bars with mechanical couplers may be used in addition to shear keys to satisfy interface shear demand.
- Design foundation and bent cap connections for the lesser of full elastic or plastic hinging moment and associated shear. The above type of precast construction is also applicable where precast trapezoidal U-beams are used rather than I-beams. The construction sequences and the design procedures are identical to those for I-beam superstructures.

Strand extension details as used to produce continuous spans at fixed diaphragms for WSDOT bridges are shown in Figure 15.5.1.4-1. The effects of time-dependent positive moments from creep and shrinkage are considered in determination of the positive moment capacity.

The design procedure to calculate the required number of extended strands was described in Section 15.5.1.4. The calculations in this example follow that procedure. The strands must be developed within the distance between the two beam ends which is 2 ft. Strand anchors are installed at 1 ft 9 in. from the end of each beam.

15.6.2.2 Design Procedure for Positive Earthquake Loading Reinforcement at Interior Pier of a Precast Beam Bridge

Consider a two-span precast concrete bridge for which the interior support is a fixed connection.

The design moment at the center of gravity of superstructure is calculated as follows:

SEISMIC DESIGN

15.6.2.2 Design Procedure for Positive Earthquake Loading Reinforcement at Interior Pier of a Precast Beam Bridge/15.6.2.2.1 Given

$$N_{ps} = 12[M_{sei}K - M_{SIDL}] \frac{1}{0.9\phi A_{ps} f_{py} d}$$

$$M_{po}^{CG} = M_{po}^{top} + \frac{(M_{po}^{top} + M_{po}^{Base})}{L_c} h$$

$$M_{sei}^{Int} = \frac{2M_{po}^{CG}}{3N_g^{int}}$$

$$M_{sei}^{Ext} = \frac{M_{po}^{CG}}{3N_g^{ext}}$$

$$\text{If } M_{sei}^{Int} \geq M_{sei}^{Ext} \text{ then } M_{sei} = M_{sei}^{Int}$$

$$\text{If } M_{sei}^{Int} < M_{sei}^{Ext} \text{ then } M_{sei} = \frac{M_{po}^{CG}}{N_g^{int} + N_g^{ext}}$$

The effective width is calculated from:

$$B_{eff} = D_c + D_s$$

Based on that effective width, the seismic moment per beam line is calculated along with the required number of strands, N_{ps} . The notation used is that of Section 15.5.1.4.

EI is assumed to be constant and beams are assumed to have fixed-fixed supports for both spans.

15.6.2.2.1 Given

D_c = 5.00 ft = diameter of column

D_s = 12.93 ft = depth of superstructure including cap beam

B_{eff} = 5.00 + 12.93 = 17.93 ft

f'_c = 4.00 ksi, = specified compressive strength of deck concrete, Class 4000D.

d_b = 0.6 in. = nominal strand diameter ($A_{ps} = 0.217 \text{ in.}^2$)

f_{pu} = 270 ksi = specified tensile strength of prestressing strands

f_{py} = 243 ksi = yield strength for low relaxation strand

ϕ = 1.00 = resistance factor (LRFD Art. C1.3.2.1, for extreme event limit state)

N_g^{int} = 3 = number of beams encompassed by the effective width

N_g^{ext} = 2 = number of prestressed beams in the pier

Typical beam is the W83G.

H = depth of beam = 82.625 in.

A = 9.50 in. (Includes ½ in. wearing surface integral with slab. Measured from top of beam to top slab at support)

t_s = 7.50 in. = effective slab thickness (not including ½ in. integral with slab.)

y_{t-slab} = 36.86 in. = c.g. of superstructure to top of slab (see PG Super output)

b = 41.00 in. = effective flange width (PG Super Output & LRFD Art. 4.6.2.6.1)

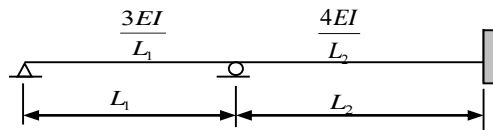
h = 116.64 in. = distance from top of column to c.g. of superstructure

L_1 = 176.63 ft = Span length of Span 1 Factor = 1.33

L_2 = 180.00 ft = Span length of Span 2 Factor = 1.00

SEISMIC DESIGN

15.6.2.2.1 Given/15.6.2.2.2 Design Steps



Far End Condition	
Pin	1.33
Fixed	1.00

- L_c = 25.00 ft = column clear height used to determine overstrength shear associated with the overstrength moments
- M^{top}_{po} = 16,000.0 ft-kips = plastic overstrength moment at top of column
- M^{Base}_{po} = 16,500.0 ft-kips = plastic overstrength moment at base of column
- M_{SIDL} = 517.0 ft-kips = moment due to superimposed dead load (traffic barrier, sidewalk, etc.) per beam, (see QconBridge Output)
- γ_p = 0.90

15.6.2.2.2 Design Steps:

Step 1: Calculate the design moment at the center of gravity of superstructure:

$$M_{po}^{CG} = 16,000 + ((16,000 + 16,500)/25)(116.64)/12 = 28,636 \text{ ft-kips}$$

Step 2: Calculate the design moment per beam:

$$M_{sei}^{Int} = (2/3)28,636/3 = 6,363.6 \text{ ft-kips}$$

$$M_{sei}^{Ext} = (1/3)28,636/2 = 4,772.7 \text{ ft-kips}$$

$$M_{sei}^{Avg} = 28,636/(3 + 2) = 5,727.2 \text{ ft-kips} < 6,363.6 \text{ ft-kips}$$

$$L_1 = 234.9 \text{ ft (Modified)} \quad K_1 = 180/(234.9 + 180) = 0.434$$

$$L_2 = 180.0 \text{ ft (Modified)} \quad K_2 = 234.9/(234.9 + 180) = 0.566$$

$$K = 0.566$$

Design Moment per beam

$$M_{des} = (0.566)(6,363.6) - (0.9)(517) = 3,137.6 \text{ ft-kips per beam}$$

Step 3: Calculate the number of extended strands required:

$c_s = 3.00 \text{ in.}$ = distance from center of gravity of extended strands to bottom of beam

$$d = 9.5 - 0.5 + 82.625 - 3 = 88.625 \text{ in.}$$

assume $f_{py} = 243 \text{ ksi}$

Number of extended strands required =

$$12(3,137.6)/((0.9)(1)(0.217)(243)(88.625)) = 9 \text{ strands}$$

Use $N_{ps} = 10$ extended strands—even number of strands desired

Step 4: Check moment capacity of extended strands:

$c_s = 3.00 \text{ in.}$ = distance from c.g. of extended strands to bottom of beam

From LRFD 5.7.3.2, the factored flexural resistance: $M_r = \phi M_n$

where

$$M_n = A_{ps}f_{py} \left(d_p - \frac{a}{2} \right)$$

$$A_{ps} = \text{area of prestressing steel} = (10)0.217 = 2.17 \text{ in.}^2$$

$$d_p = \text{distance from extreme compression fiber to centroid of prestressing tendons} \\ = 9.5 - 0.5 + 82.625 - 3 = 88.625 \text{ in.}$$

Assume linear behavior and find N.A. depth, c :

$$c = \frac{A_{ps}f_{py}}{0.85f'_{ce}\beta_1b}$$

where

$$\beta_1 = 0.85 \text{ for } f'_{ce} \leq 4 \text{ ksi}$$

$$\beta_1 = 0.85 - 0.05(f'_{ce} - 4) \geq 0.65 \text{ for } f'_{ce} > 4 \text{ ksi}$$

$$f'_c = 4.00 \text{ ksi} \quad f'_{ce} = (1.3)4 = 5.2 \text{ ksi} \quad \beta_1 = 0.79$$

$$c = (2.17)243 / ((0.85)(5.2)(0.79)(81)) = 1.864 \text{ in.}$$

$$a = (0.79)1.864 = 1.473 \text{ in. depth of the equivalent stress block}$$

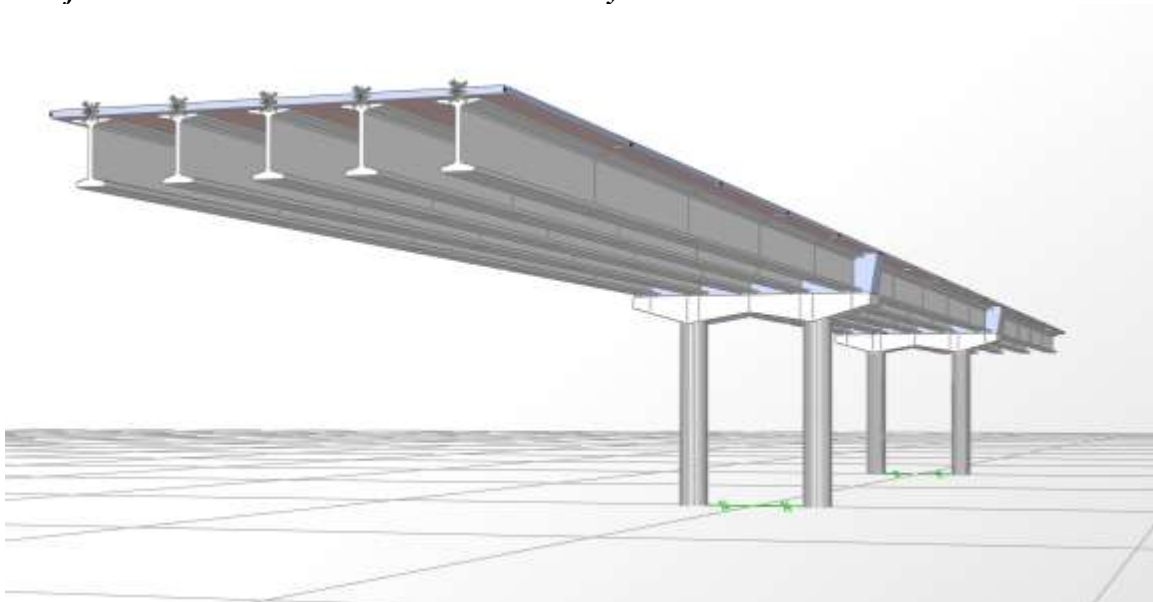
$$M_n = (2.17)(243)(88.625 - 1.473/2) / 12 = 3,862.0 \text{ ft-kips}$$

$$M_r = (1)3,862.0 = 3,862.0 \text{ ft-kips} \geq 3,137.6 \text{ ft-kips} \quad \text{OK}$$

15.6.3 Pushover Analysis: Two-Column Bent in the Transverse Direction

Figure 15.6.3-1

Structure for Two-Column Bent Transverse Pushover Analysis



15.6.3.1. Introduction

This example serves to illustrate the procedure used to perform a nonlinear static “pushover” analysis on a two-column bent in the transverse direction in accordance with the *LRFD Seismic Guide Specifications* using SAP2000. A full model of the bridge is used to compute the displacement demand from a response-spectrum analysis. To perform the pushover analysis in the transverse direction, the bent is isolated using the SAP2000 “staged construction” feature. The example bridge is symmetrical about all axes and has three spans. This example does not provide explicit step-by-step instructions for creating and defining a model in SAP2000. It is assumed the reader has previous knowledge about the use of SAP2000.

15.6.3.2. General Model Information

15.6.3.2.1 Model Description

The superstructure is modeled using beam-column elements for each of the beams and shell elements for the deck. Shell elements are also used to model the diaphragms at the piers. Nonprismatic sections are used to model the crossbeams since they have variable depth. The longitudinal direction is along the X-axis and the Z-axis is vertical. The following summarizes the characteristics of the bridge being modeled:

- Spread footings, 60 ft long by 24 ft wide by 5 ft deep at each bent
- Abutment is free in longitudinal direction and fixed in transverse direction
- Two 5-ft-diameter columns at bents
- Five lines of prestressed concrete beams (WF74G) at 9 ft 6 in. center-to-center spacing
- 8 in. deck with 46 ft 11 in. outside-to-outside width

15.6.3.2.2 Spread Footings

Each bent is supported by a spread footing. The footings are modeled using springs. Rigid links connect the bases of the columns to a center joint to which the spring properties are assigned. The soil springs are generated using the method for spread footings outlined in Chapter 7 of the *Bridge Design Manual* (WSDOT, 2008). The assumed parameters are $G = 2,150$ ksf and $\nu = 0.35$. The spring values used in the model are the following:

$$kX = 334,821 \text{ kips/ft}$$

$$kY = 309,181 \text{ kips/ft}$$

$$kZ = 335,349 \text{ kips/ft}$$

$$kRX = 232,222,833 \text{ kip-ft/rad}$$

$$kRY = 58,748,246 \text{ kip-ft/rad}$$

$$kRZ = 267,521,076 \text{ kip-ft/rad}$$

The beams are fixed torsionally at the abutments, but are free to rotate about the strong and weak axes.

15.6.3.2.3 Concrete Material Modeling

SAP2000 default concrete material properties have moduli of elasticity based on concrete densities of 144 psf. The *PCI Bridge Design Manual* (PCI, 2011) suggests that moduli of elasticity be based on concrete densities of 160 psf. Therefore, the default material properties are updated to reflect the difference. **Table 15.6.3.2.3-1** provides a summary of the concrete properties used in the model.

**Table 15.6.3.2.3-1
Concrete Properties**

Element	f'_c , ksi	E_c , ksi
Columns	5.2	4,816
Crossbeams	4.0	4,224
Beams	6.0	5,173
Deck	4.0	4,224

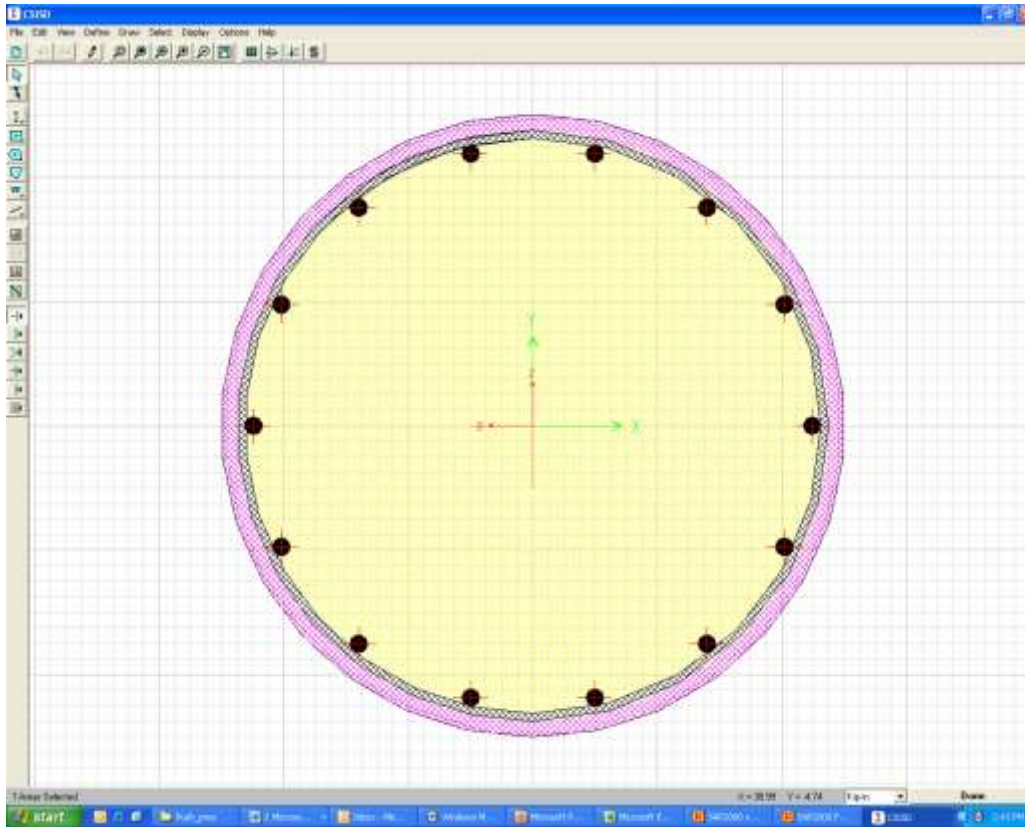
Nonlinear concrete modeling is implemented using Mander’s model in accordance with the *LRFD Seismic Guide Specifications* and is discussed in more detail in the following section. The nonlinear steel model also conforms to the same specifications.

15.6.3.2.4 Columns

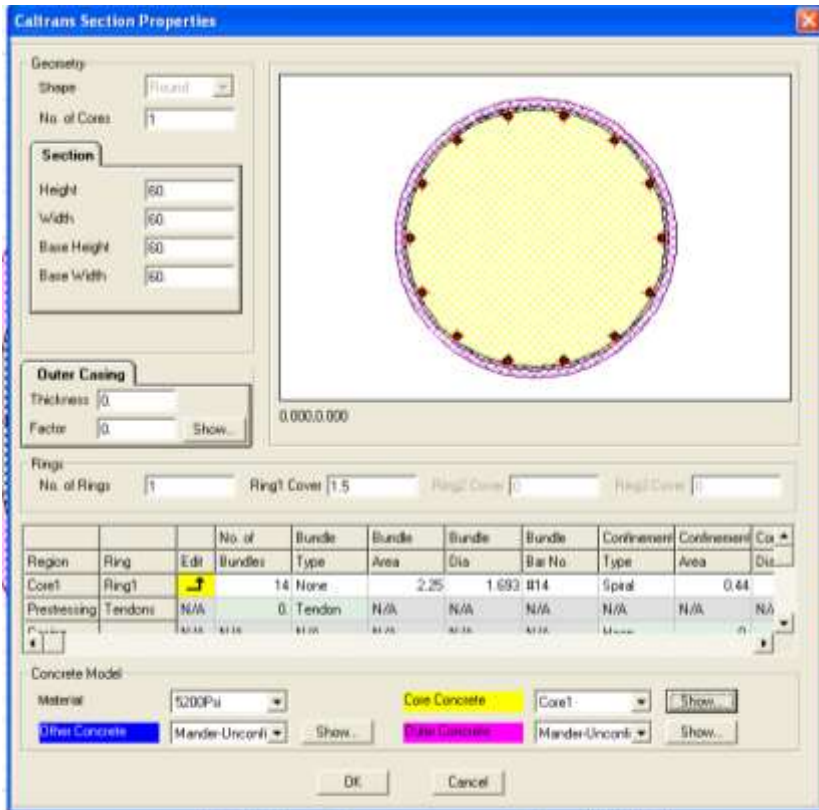
There are two columns at each bent. They are 5 ft in diameter and have fourteen No. 14 bars as longitudinal steel, corresponding to a steel-to-concrete area ratio of about 1%. In the hinge zones, the columns have confinement steel consisting of No. 6 spiral bars at a 2.25-in. pitch.

The column elements have rigid end offsets assigned to them at the footings and crossbeams. The net clear height of the columns is 29 ft 2 in. The columns are split into three elements as required by Article 5.4.3 of the *LRFD Seismic Guide Specifications*.

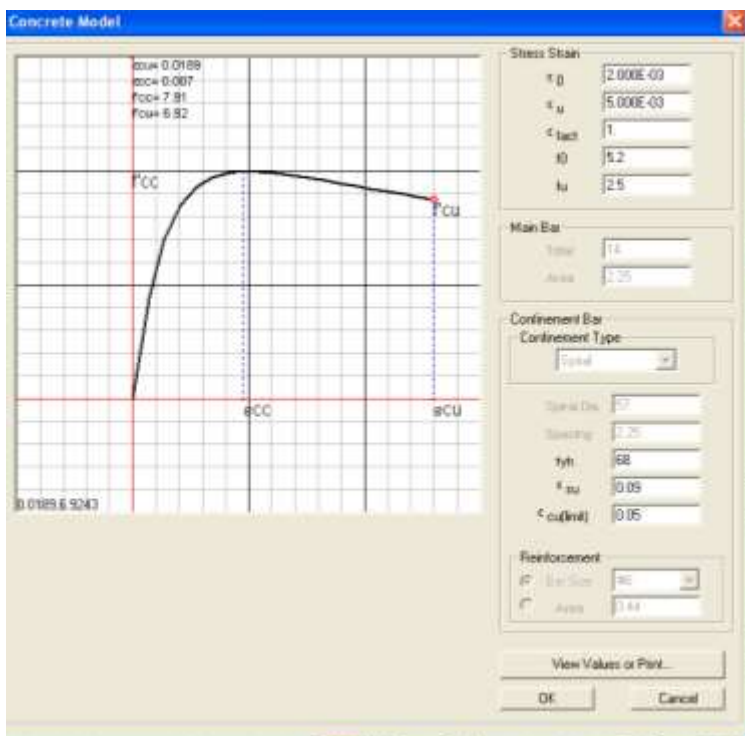
The columns' frame sections are defined using a round Caltrans shape in Section Designer. A view of the section as shown in Section Designer is shown below.



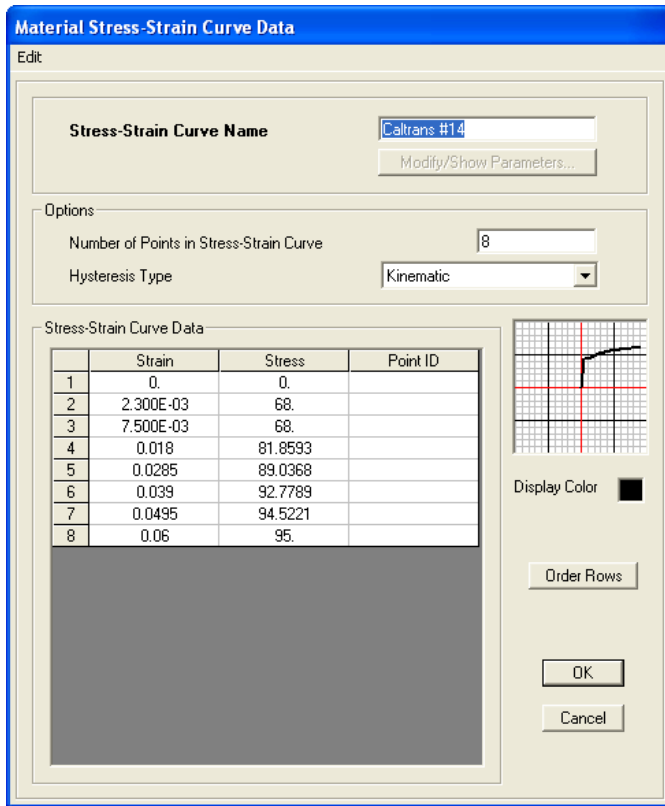
The parameter input window for the Caltrans shape is shown below.



The nonlinear concrete model parameter input window for the core concrete is shown below.

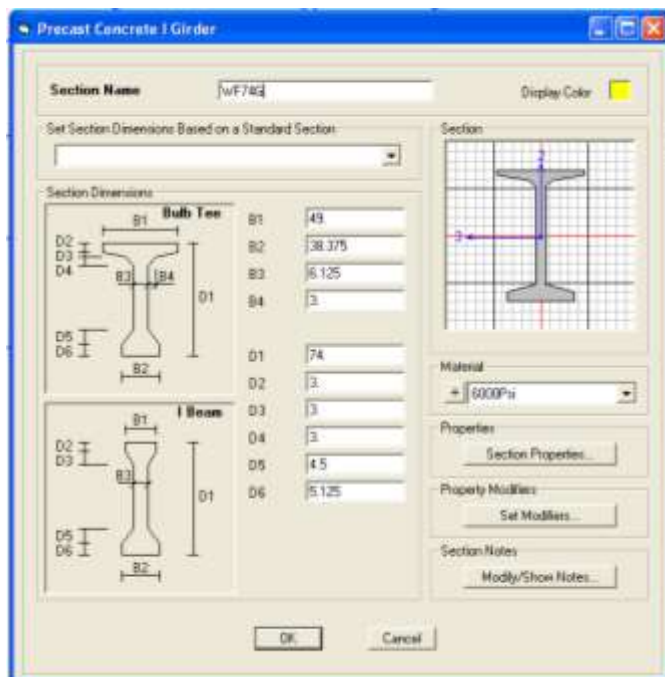


The nonlinear steel model for the No. 14 bars is shown below.

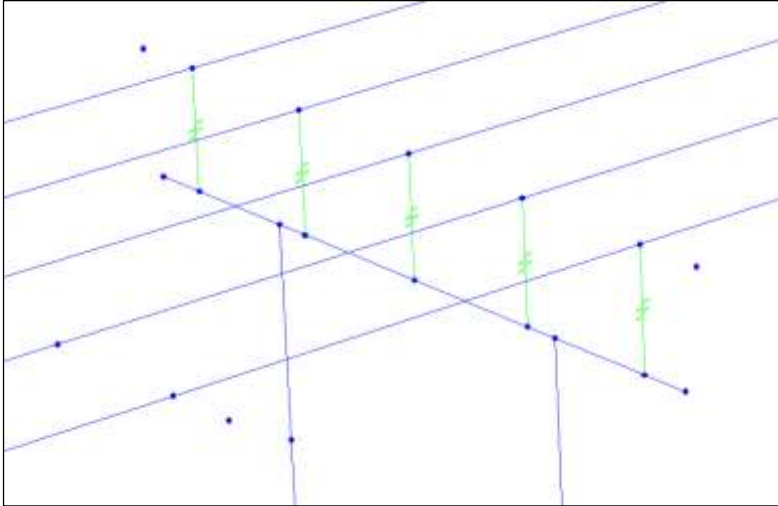


15.6.3.2.5 Superstructure

The beams are Washington State Department of Transportation WF76G. The frame section definition is shown below.



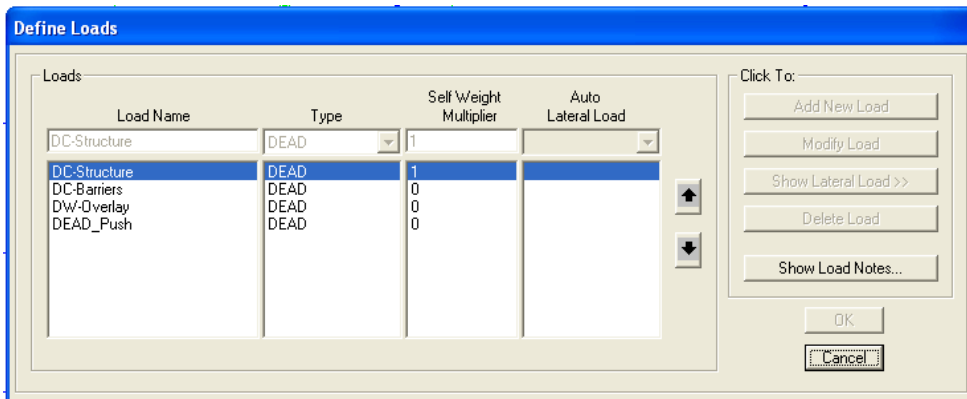
The beams are assigned insertion points such that they frame to the same joints as the deck elements but are below the deck. There is also a 3-in. gap between the top of the beam and the soffit of the deck to model the “A” dimension measured from top of beam to top of deck slab at support. Links connect the beams to the crossbeams to transfer moment, shear, and axial loads. The corresponding screen shot is shown below.



There are five elements per span of the superstructure. Article 5.4.3 of the *LRFD Seismic Guide Specifications* requires that a minimum of four elements per span be used.

15.6.3.2.6 Loads

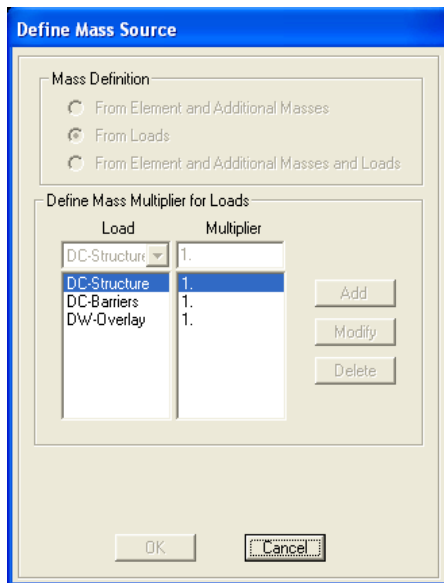
There are four dead load cases in the model: DC-Structure, DC-Barriers, DW-Overlay, and DEAD-Push. The DC-Structure case includes the self-weight of the structural components. The DC-Barriers case includes the dead load of the barriers, which is applied to the outermost deck shells. The DW-Overlay case includes the future overlay loads applied to the deck shells. The DEAD-Push case is used to apply the column axial loads to the isolated bent during pushover analysis in the transverse direction since the remainder of the structure will not be in place, and therefore, cannot apply the dead load. The load case definitions are shown below.



15.6.3.3. Modal Analysis

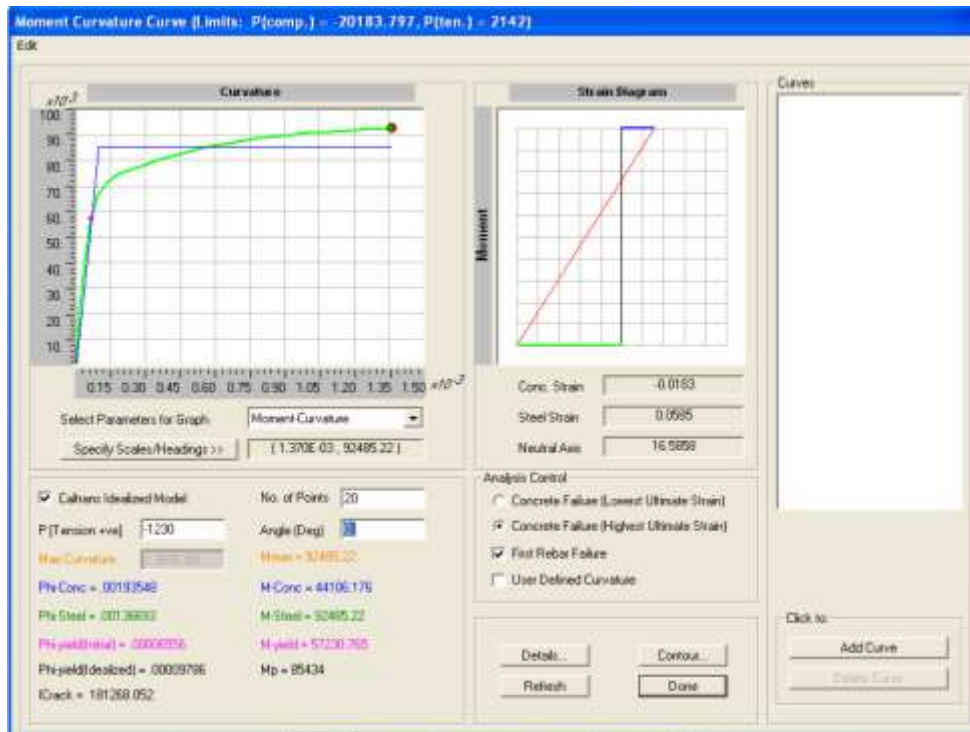
15.6.3.3.1 Mass Source

All of the dead loads are considered as contributing mass (except the DEAD-Push) for the modal analysis case. A display of the mass source definition window from SAP2000 is shown below.

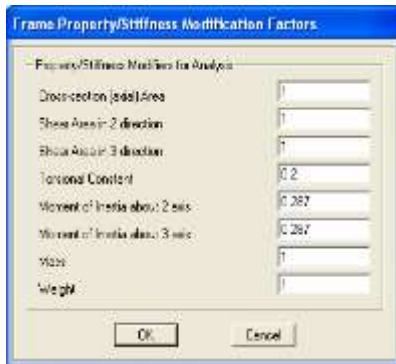


15.6.3.3.2 Column Cracking

Article 5.6 of the *LRFD Seismic Guide Specifications* provides diagrams that can be used to determine the cracked section properties of the columns. However, these diagrams are based on sections having a concrete modulus of elasticity computed using a concrete density of 0.144 ksf. The columns in this model have a modulus of elasticity computed using a material density of 0.160 ksf. Therefore SAP2000's Section Designer is used to compute the effective section properties. The column axial dead load is 1,230 kips. By having Section Designer perform a moment curvature analysis on the column section with an axial load of 1,230 kips, it is found that $I_{cracked} = 181,268 \text{ in.}^4$. The gross moment of inertia is 630,500 in.^4 . Therefore, the ratio is $181,268/630,500 = 0.29$. The result of the moment curvature analysis is shown below:



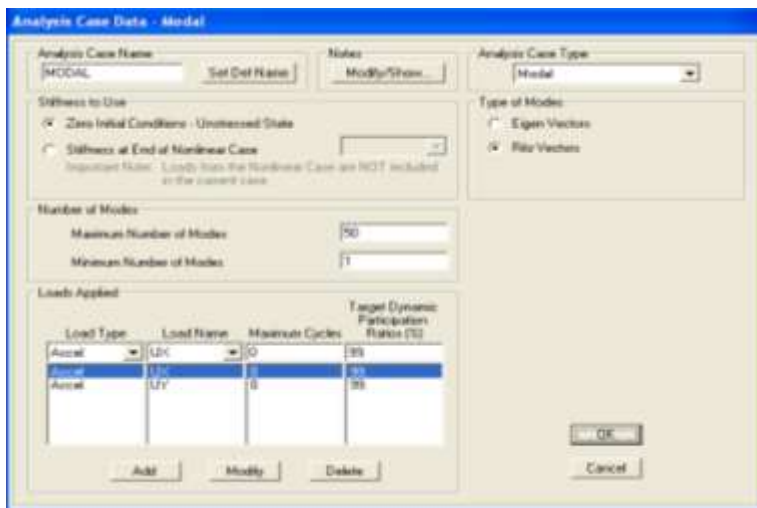
The property modifiers are then applied, as shown below.



The torsional constant is 0.2 for columns as required by Article 5.6.5 of the *LRFD Seismic Guide Specifications*.

15.6.3.3.3 Analysis Case Setup

The modal analysis case uses Ritz vectors and is defined in SAP2000 as shown below.



Note that Article 5.4.3 of the *LRFD Seismic Guide Specifications* requires a minimum of 90% mass participation in both directions.

15.6.3.4. Response Spectrum Analysis

15.6.3.4.1 Seismic Hazard

The bridge is located in Redmond, Wash., (Postal Zip Code 98052). The mapped spectral acceleration coefficients are:

$$PGA = 0.396 g$$

$$S_s = 0.883 g$$

$$S_1 = 0.294 g$$

The soil site class is *D* and the site coefficients are:

$$F_{PGA} = 1.10$$

$$F_a = 1.15$$

$$F_v = 1.81$$

Therefore, the response spectrum is generated using the following parameters:

$$A_s = (F_{PGA})PGA = 0.436 g$$

$$S_{DS} = (F_a)S_s = 1.016 g$$

$$S_{D1} = (F_v)S_1 = 0.533 g$$

Since S_{D1} exceeds 0.50, the Seismic Design Category is D per Table 3.5-1 of the *LRFD Seismic Guide Specifications*.

Note: All these terms are standard in descriptions of earthquake ground motions.

F_v = long-period site coefficient at 1.0-sec period

F_a = short-period site coefficient at 0.2-sec period

F_{PGA} = factor for peak ground acceleration

PGA = mapped MCE_g (Maximum Considered Earthquake) peak ground motion

S_1 = mapped MCE_g , 5% damped, spectral response acceleration parameter at a period of 1 sec

S_s = mapped MCE_g , 5% damped, spectral response acceleration parameter at short periods

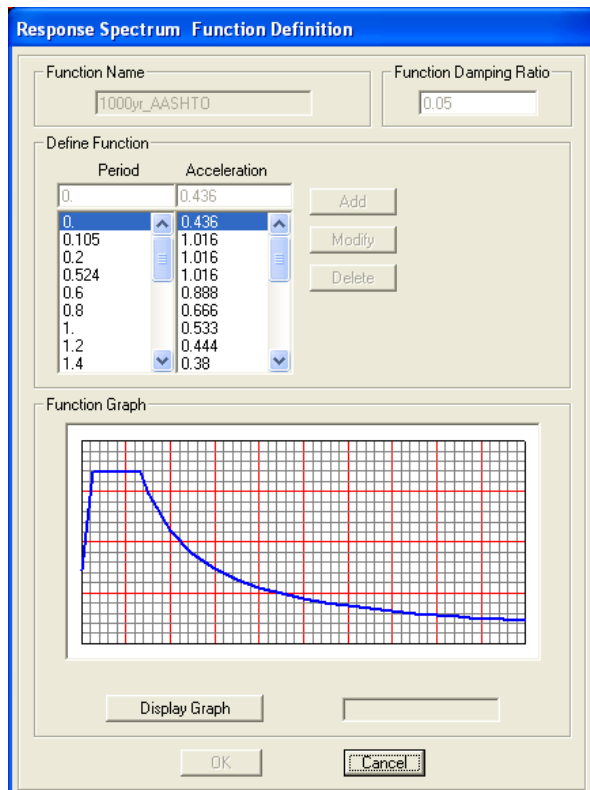
$A_s = F_{PGA}PGA$

S_{DS} = design, 5% damped, spectral response acceleration parameter at short periods

S_{D1} = design, 5% damped, spectral response acceleration parameter at a period of 1 sec

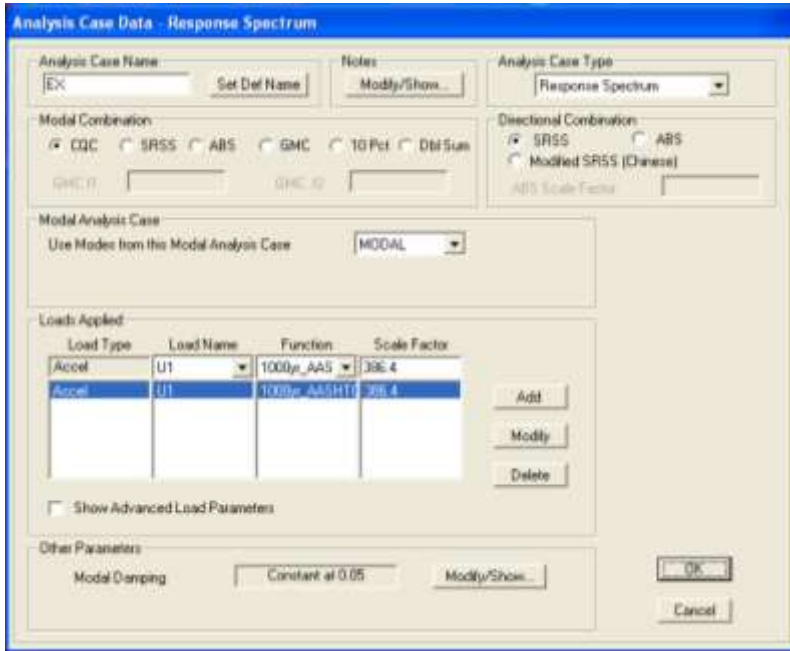
15.6.3.4.2 Response Spectrum

A screen shot of the response spectrum as input in SAP2000 is shown below.



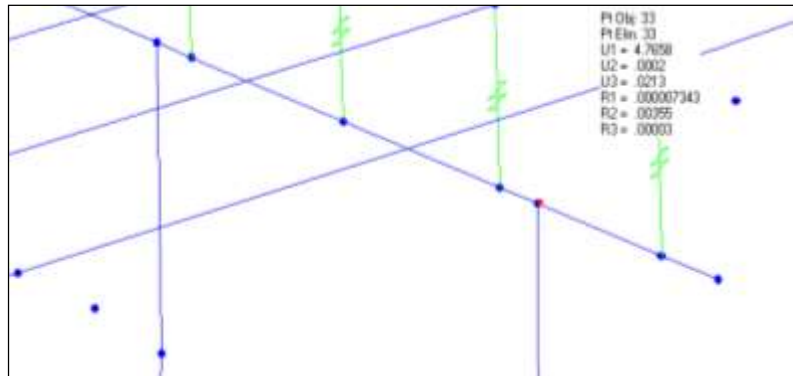
15.6.3.4.3 Analysis Case Setup

Two analysis cases are setup in SAP2000, one for each orthogonal direction. The analysis case definition for the X-direction (longitudinal direction) is shown below.

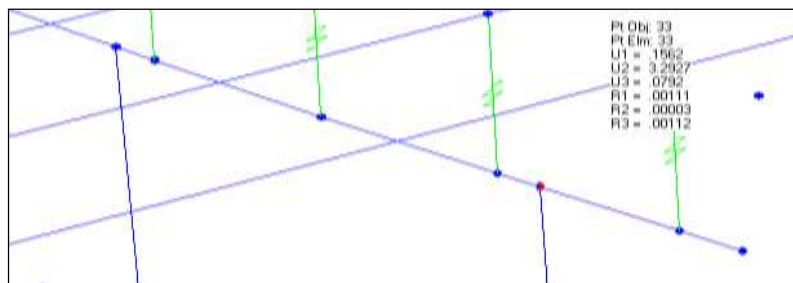


15.6.3.4.4 Column Displacements

The horizontal displacements at the top of the column from the EX analysis case are $U1 = 4.766$ in. and $U2 = 0.000$ in. This is shown below as displayed in SAP2000.

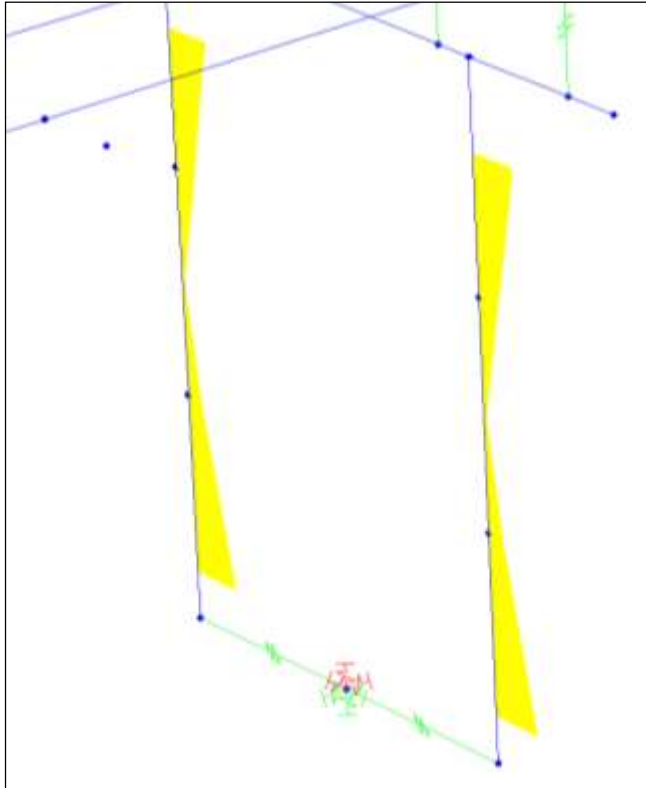


The horizontal displacements at the top of the column from the EY analysis case are $U1 = 0.156$ in. and $U2 = 3.293$ in. This is shown below as displayed in SAP2000.



15.6.3.4.5 Column Inflection Points

The results from the response spectrum analysis can also be used to find the column inflection points, which will be used to define the hinge lengths. Shown below is the column moment diagram for the EY analysis case as displayed in SAP2000. Note that there is no moment shown in the rigid offset zones.



From this information it is found that the inflection point is halfway between the column joints, and the following are computed:

$$L_1 = \text{length from point of maximum moment at base of column to inflection point} \\ = \text{total column height}/2 - \text{lower offset} = (438/2) - 30 = 189 \text{ in.}$$

$$L_2 = \text{length from point of maximum moment at top of column to inflection point} \\ = \text{total column height}/2 - \text{upper offset} = (438/2) - 58 = 161 \text{ in.}$$

15.6.3.5. Displacement Demand**15.6.3.5.1 Response Spectrum Displacements**

Article 4.4 of the *LRFD Seismic Guide Specifications* requires that 100% plus 30% of the displacements from each orthogonal seismic analysis case be combined to determine the displacement demands. This example considers the transverse direction only, so that the applicable combination is the 100EY + 30EX. The UY displacement is computed:

$$UY \text{ (due to } EY) = 3.293 \text{ in.}$$

$$UY \text{ (due to } EX) = 0.000 \text{ in.}$$

Therefore,

$$\Delta_y = (1.0)3.293 + (0.3)0.000 = 3.293 \text{ in.}$$

15.6.3.5.2 Displacement Magnification

Displacement magnification must be performed in accordance with Article 4.3.3 of the *LRFD Seismic Guide Specifications*.

$$T_s = S_{D1}/S_{DS} = 0.533/1.016 = 0.525 \text{ sec}$$

$$T^* = 1.25T_s = (1.25)0.525 = 0.656 \text{ sec}$$

where T^* = characteristic ground motion period

$$T_{Trans} = 0.595 \text{ sec}$$

where T_{Trans} = natural period of vibration for transverse direction of example bridge

$$T^*/T_{Trans} = 0.656/0.595 = 1.103 > 1.0 \quad \text{Magnification is required}$$

$$R_{d,Trans} = (1 - 1/\mu_D)(T^*/T) + 1/\mu_D = (1 - 1/6)(1.103) + 1/6 = 1.085$$

where $R_{d,Trans}$ = magnification factor to account for short period structure for transverse direction of example bridge

$$\Delta^L_{D,Trans} = (R_{d,Trans})\Delta_y = (1.085)3.293 = 3.574 \text{ in. This is the Displacement Demand.}$$

15.6.3.6. P-Delta Effect Check

The requirements of Article 4.11.5 of the *LRFD Seismic Guide Specifications* must be met, or a nonlinear time history analysis must be performed.

15.6.3.7. Hinge Definitions/Assignments**15.6.3.7.1 Hinge Lengths**

The hinge lengths must be computed at both the tops and bottoms of the columns using the equation in Article 4.11.6 of the *LRFD Seismic Guide Specifications*.

The hinge length is computed as follows:

$$L_p = 0.08L + 0.15 f_{ye} d_{be} \geq 0.3 f_{ye} d_{be}$$

where

L = length of column from point of maximum moment to the point of moment contra-flexure, in.

L_1 = distance from point of inflection to the base of the columns = 189 in.

L_2 = distance from point of inflection to the top of the columns = 161 in.

f_{ye} = expected yield strength of longitudinal column reinforcing steel bars, ksi
= 68 ksi (ASTM A706 bars)

d_{be} = nominal diameter of longitudinal column reinforcing steel bars
= 1.693 in. (No. 14 bars)

For the bottom of the columns:

$$L_{p1} = (0.08)189 + (0.15)(68)1.693 \geq (0.3)(68)1.693 = 32.4 \text{ in.} \geq 34.5 \text{ in.} \quad \text{Use 34.5 in.}$$

For the top of the columns:

$$L_{p2} = (0.08)161 + (0.15)(68)1.693 \geq (0.3)(68)1.693 = 30.1 \text{ in.} \geq 34.5 \text{ in.} \quad \text{Use 34.5 in.}$$

15.6.3.7.2 Assign Hinges

In order to assign the hinges to the column elements the relative locations of the hinges must be computed.

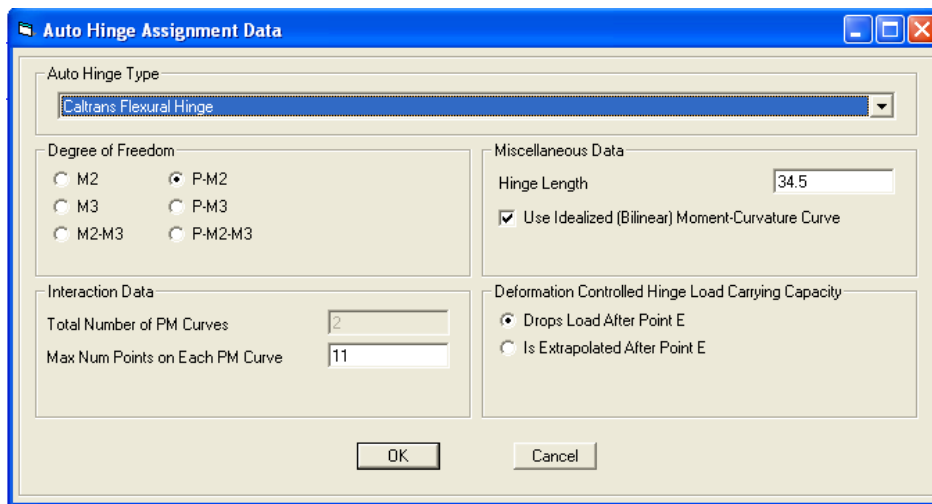
For the bottom of the columns:

$$\begin{aligned} \text{Relative Length} &= (\text{Footing Offset} + (\text{Hinge Length}/2))/\text{Element Length} \\ &= (30 + (34.5/2))/146 = 0.324 \end{aligned}$$

For the top of the columns:

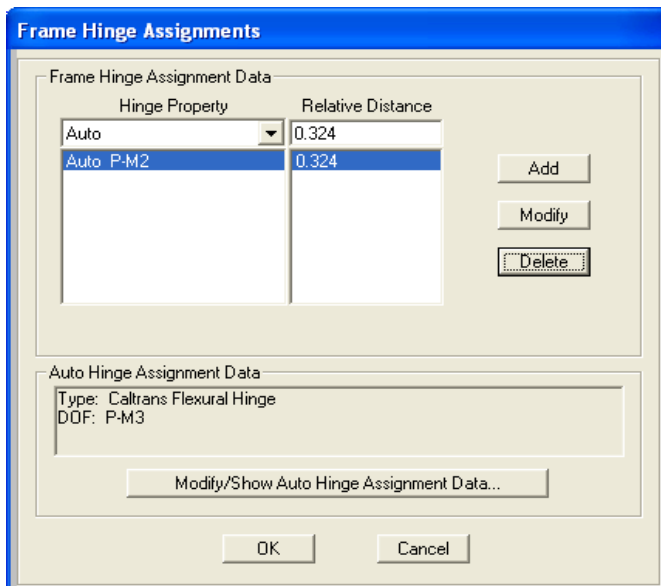
$$\begin{aligned} \text{Relative Length} &= (\text{Element Length} - \text{Xbeam Offset} - (\text{Hinge Length}/2))/\text{Element Length} \\ &= (146 - 58 - (34.5/2))/146 = 0.484 \end{aligned}$$

The hinge input parameters in SAP2000 are as shown below.

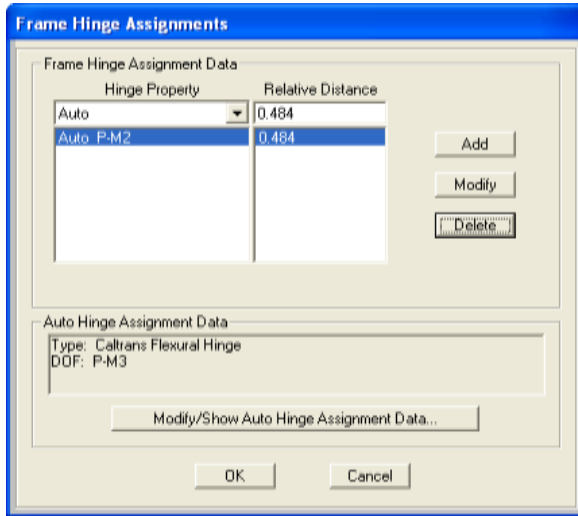


Note that the hinge is a Caltrans Flexural Hinge, has *P-M2* degrees of freedom, has a length of 34.5 in., uses the idealized moment-curvature curve, and drops load after point E. These parameters are the same for all of the hinges since they are all of the same length and are all acting in the same direction.

The hinges at the bottoms of the columns are assigned as shown below.



The hinges at the tops of the columns are assigned as shown below.



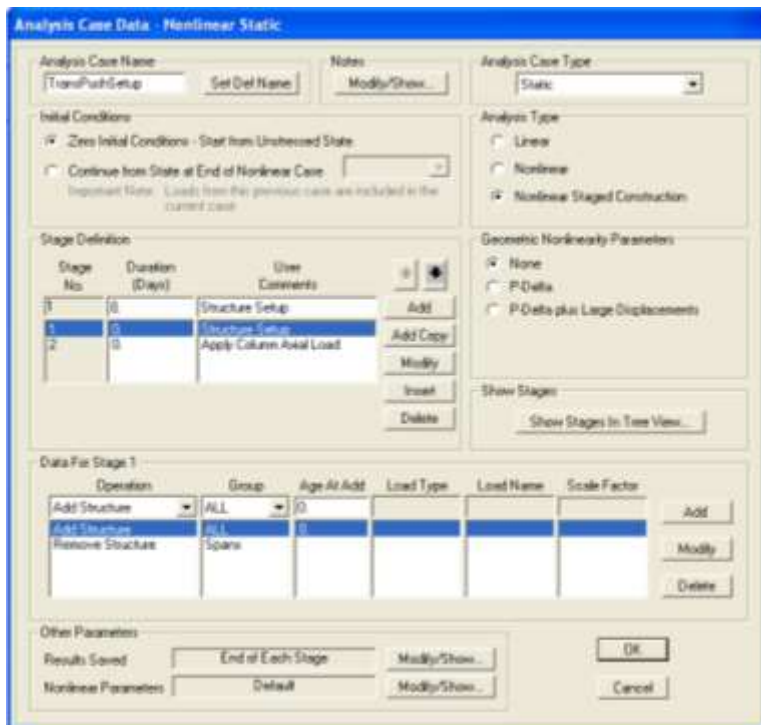
15.6.3.8. Pushover Analysis

15.6.3.8.1 Load Distribution

The lateral load distribution used in this example for the pushover analysis is a direct acceleration on the mass of the structure. However, since the bent is isolated, the acceleration does not include the mass of the superstructure. A lateral load distribution consisting of only a horizontal point load applied at the centroid of the superstructure is also a reasonable method of applying the lateral load.

15.6.3.8.2 Analysis Case Setup

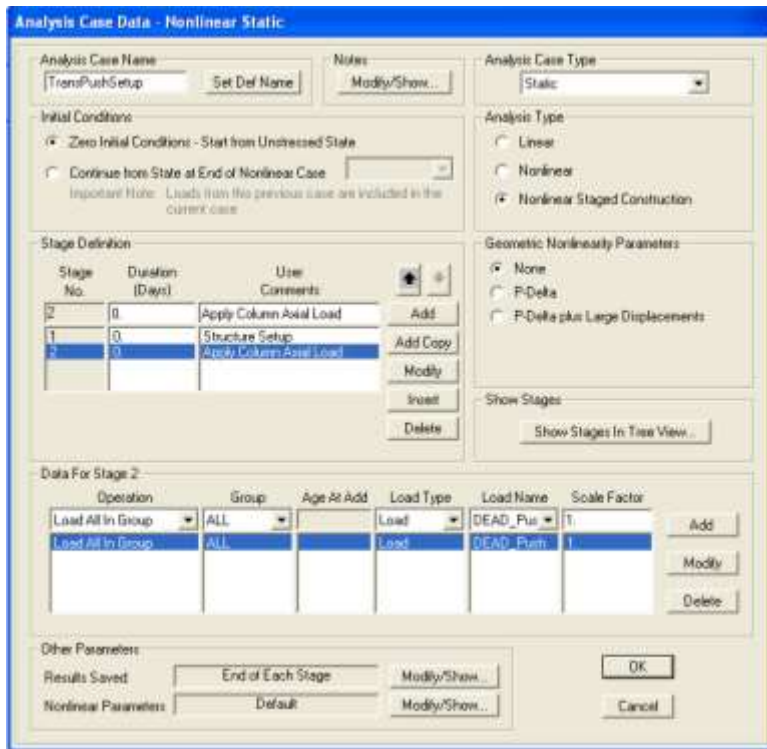
The transverse pushover analysis case is preceded by a staged construction analysis case called “TransPushSetup,” which is used to isolate the bent and apply the static loads to the columns equivalent to the axial dead loads from the entire structure. The “TransPushSetup” analysis case definition is shown below.



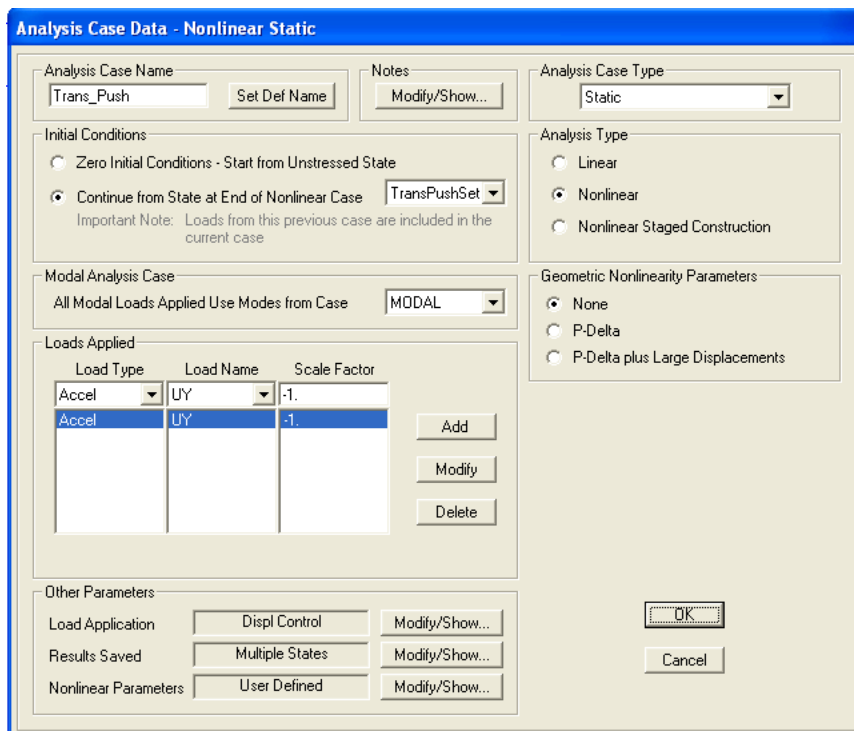
SEISMIC DESIGN

15.6.3.8.2 Analysis Case Setup

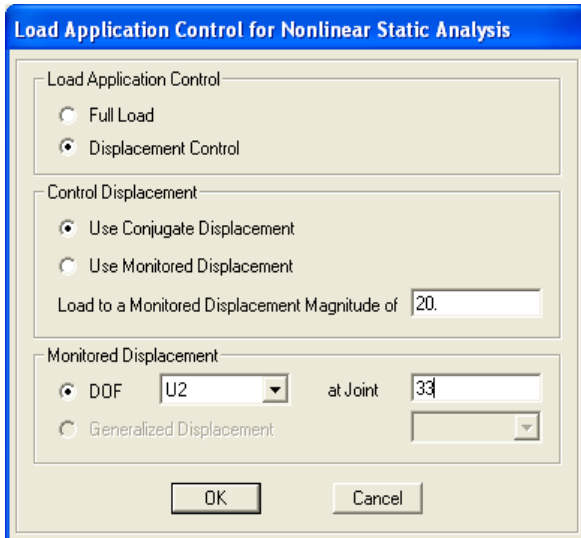
The “TransPushSetup” analysis case has two stages, one to isolate the bent, and one to apply the column axial loads. Note these two stages could be combined into one stage without altering the results. The “TransPushSetup” analysis case definition is shown below with the data for Stage 2 in view.



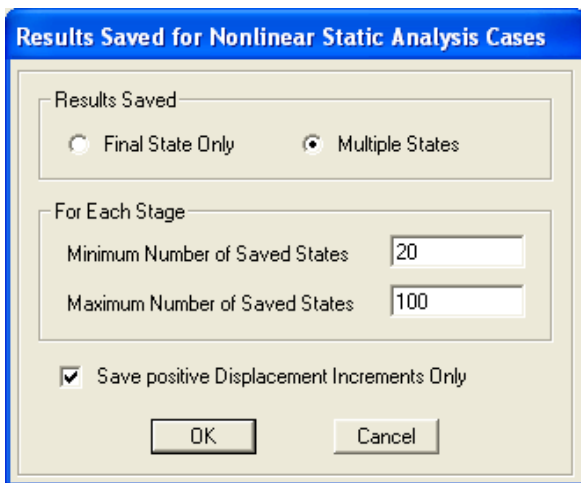
The pushover analysis case is called “Trans_Push” and is continued from the “TransPushSetup” analysis case. The “Trans_Push” analysis case definition is shown below.



Note that the load applied is acceleration in the UY direction, a nonlinear static analysis is used, and no geometric nonlinearities are included. The load application is displacement control as shown in the load application parameter input window.

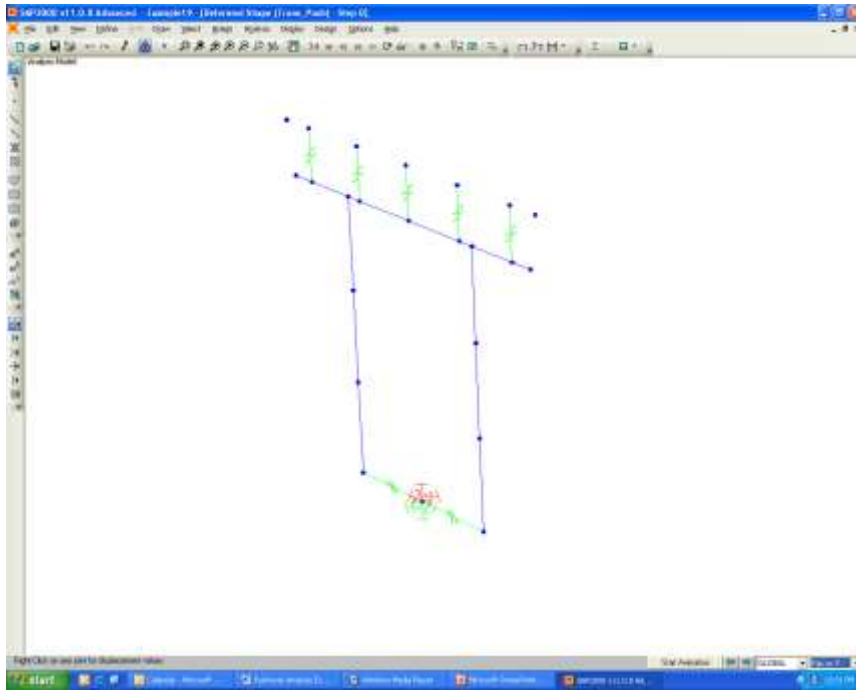


The results are also saved as shown in the window below.

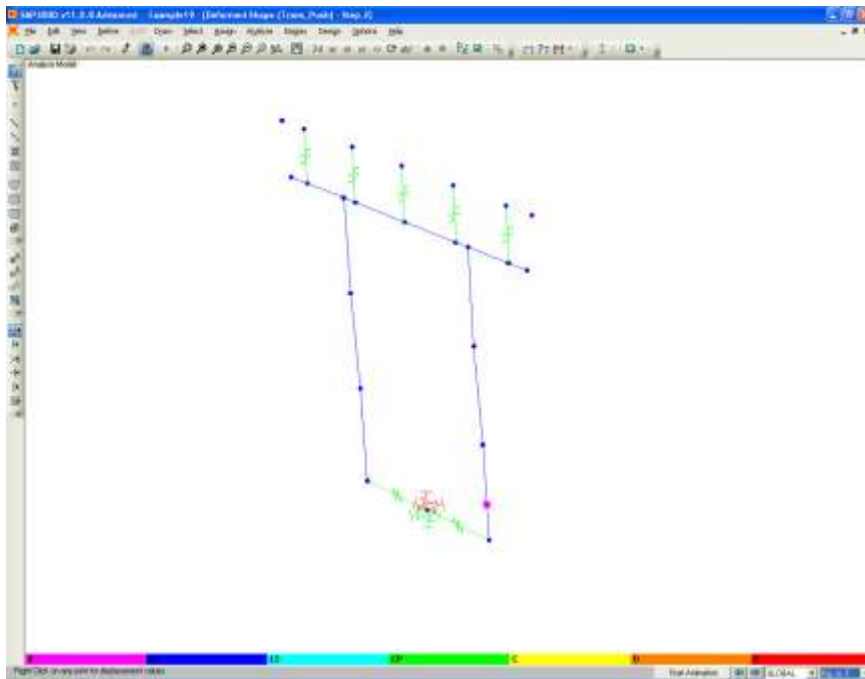


The following screen shots show the deformed shape of the bent at various displacements.

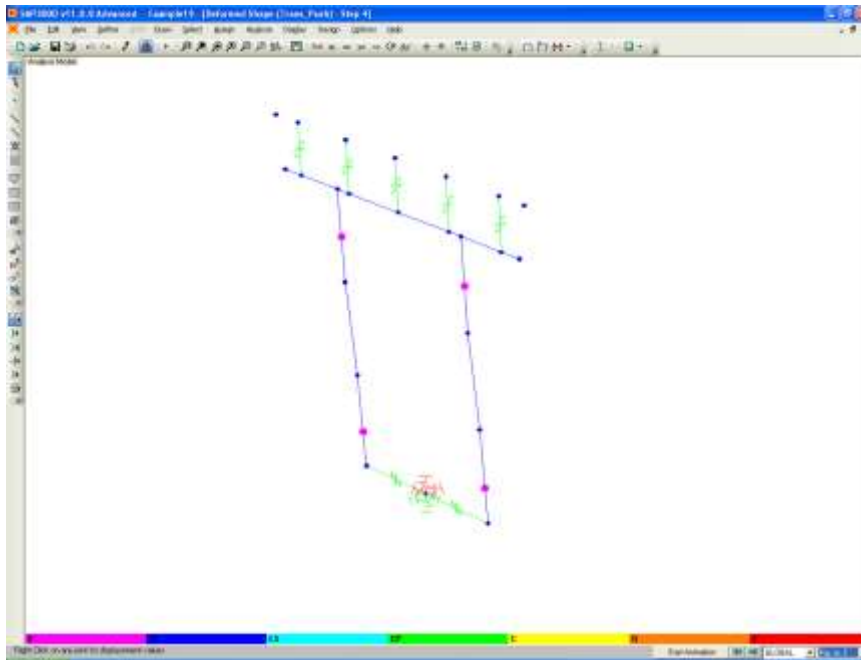
At $DY = 0.00$ in.



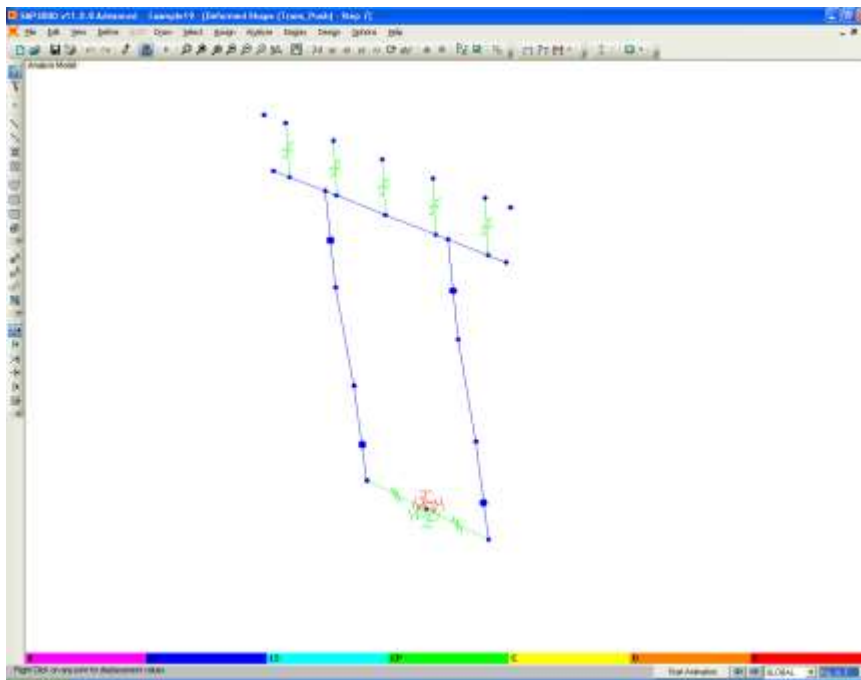
At $DY = 1.98$ in.



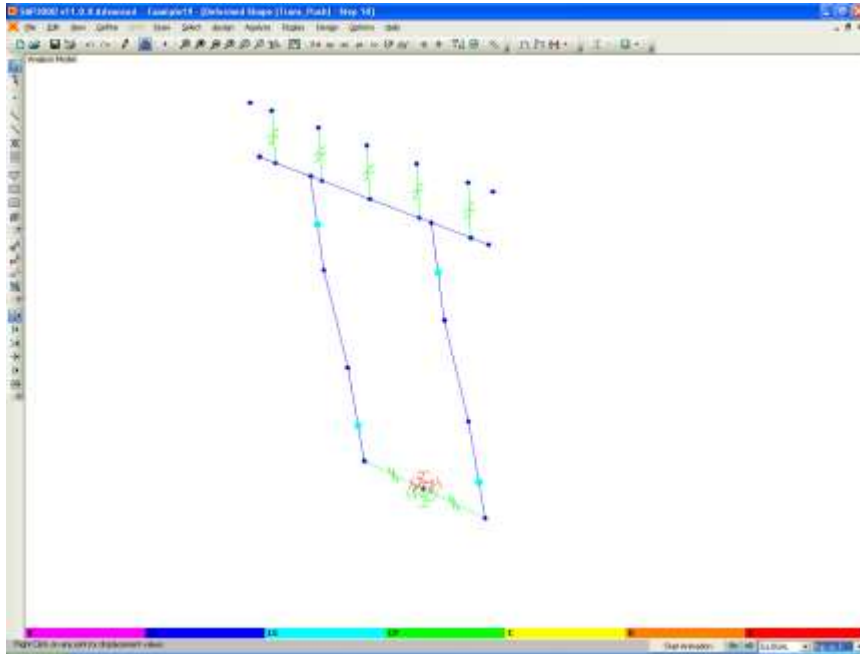
At DY = 3.29 in.



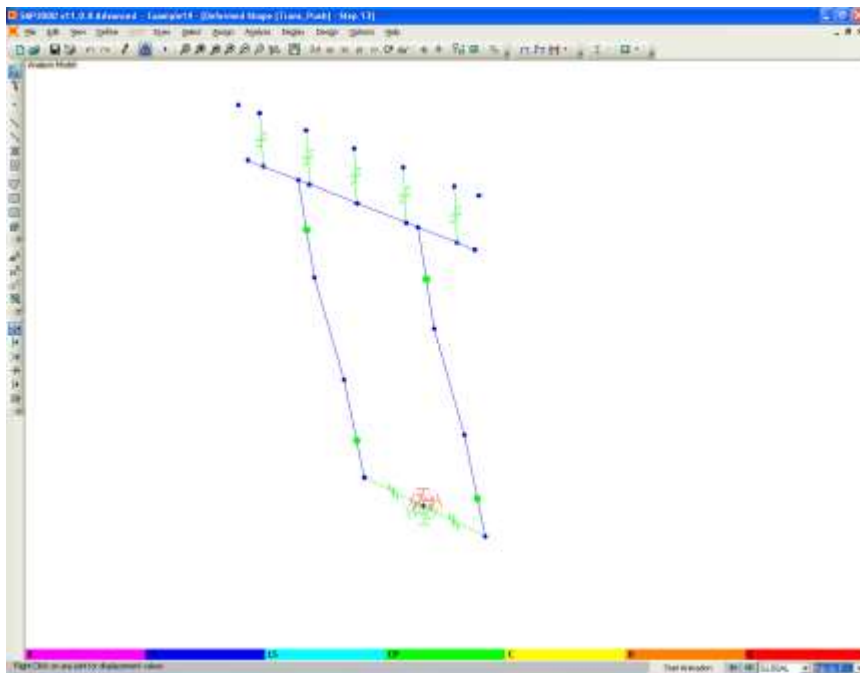
At DY = 6.29 in.



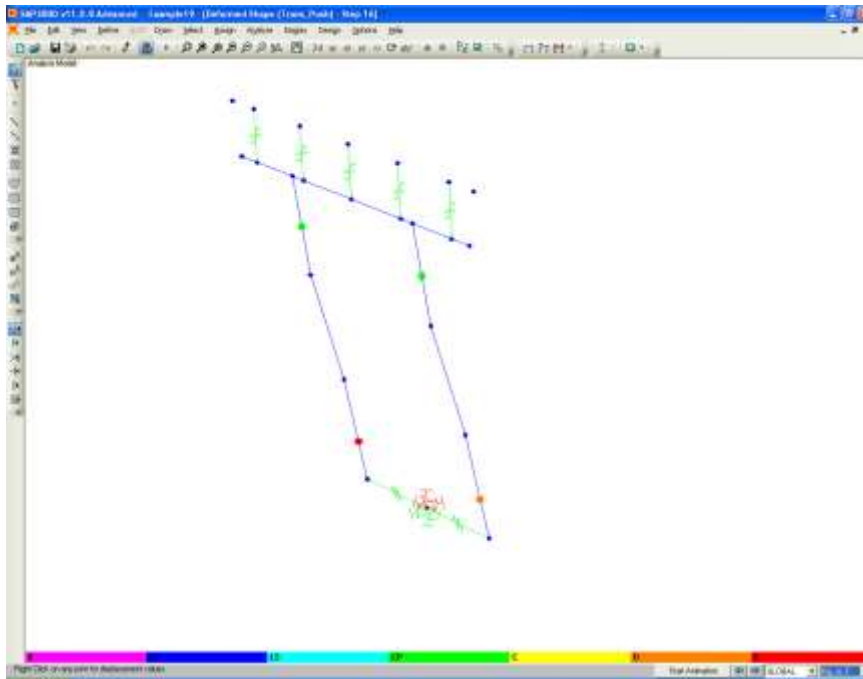
At DY = 9.29 in.



At DY = 12.29 in.



At DY = 14.29 in.

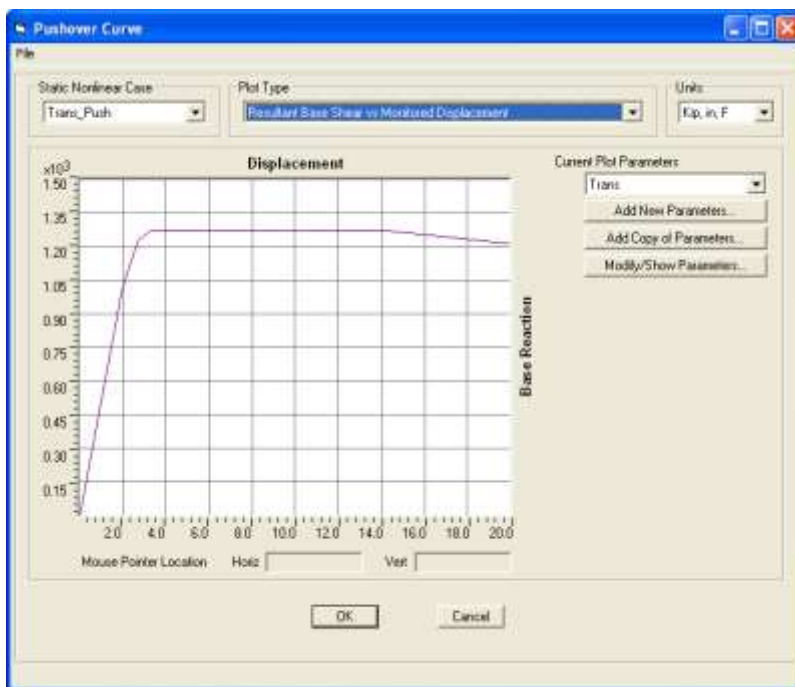


15.6.3.9. Check Displacement Capacity

The overall displacement capacity of the bent is 14.29 in. which is much greater than the displacement demand of 3.29 in.

$$\Delta^L_{C_Trans} = 14.29 \text{ in.} \geq 3.29 \text{ in.} \quad \text{OK}$$

The pushover curve is shown below.



15.6.3.10 Check Hinge Ductility

The requirements for hinge ductility demands in Article 4.9 of the *LRFD Seismic Guide Specifications* must be met for all hinges in the structure. In this example the hinge at the base of the right column controls. To determine the hinge ductility demand the following values must be determined:

$$M = \text{ductility demand} = 1 + \Delta_{pd}/\Delta_{yi} = 1 + (\Delta_{D_Trans} - \Delta_y)/\Delta_{yi}$$

where

$$\begin{aligned} \Delta_{yi} &= \text{idealized yield displacement (does not include spring effects)} \\ &= (L_1^2 + L_2^2)\phi_{yi}/3 \end{aligned}$$

where L_1, L_2 = lengths from point of maximum moments to the inflection point

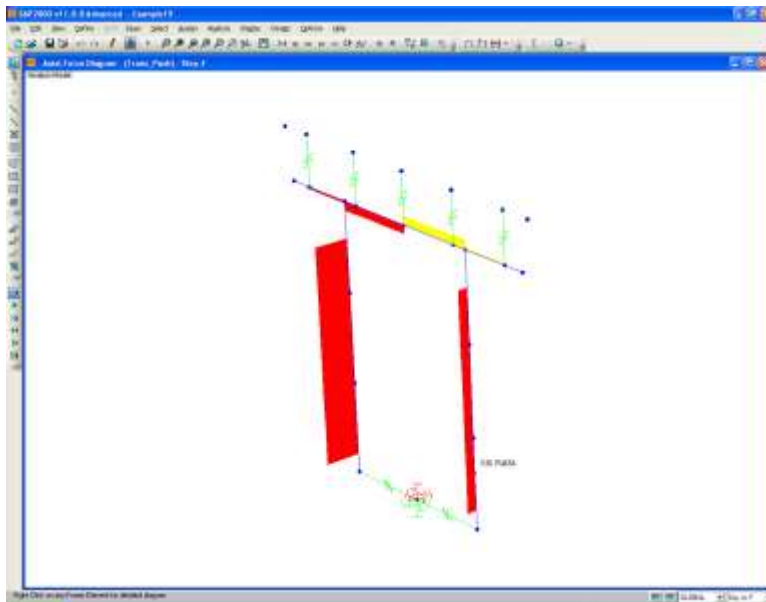
Δ_y = displacement at which the hinge yields during the pushover analysis when foundation effects are included

Δ_{D_Trans} = displacement demand from response-spectrum analysis = 3.29 in.

Determine Δ_{yi} :

First, use the pushover analysis to find the axial load on the column at yield. From scrolling through the deformed shape described previously, it is known that the hinge first forms in Step 2. Therefore, determine the axial load on the column at Step 2.

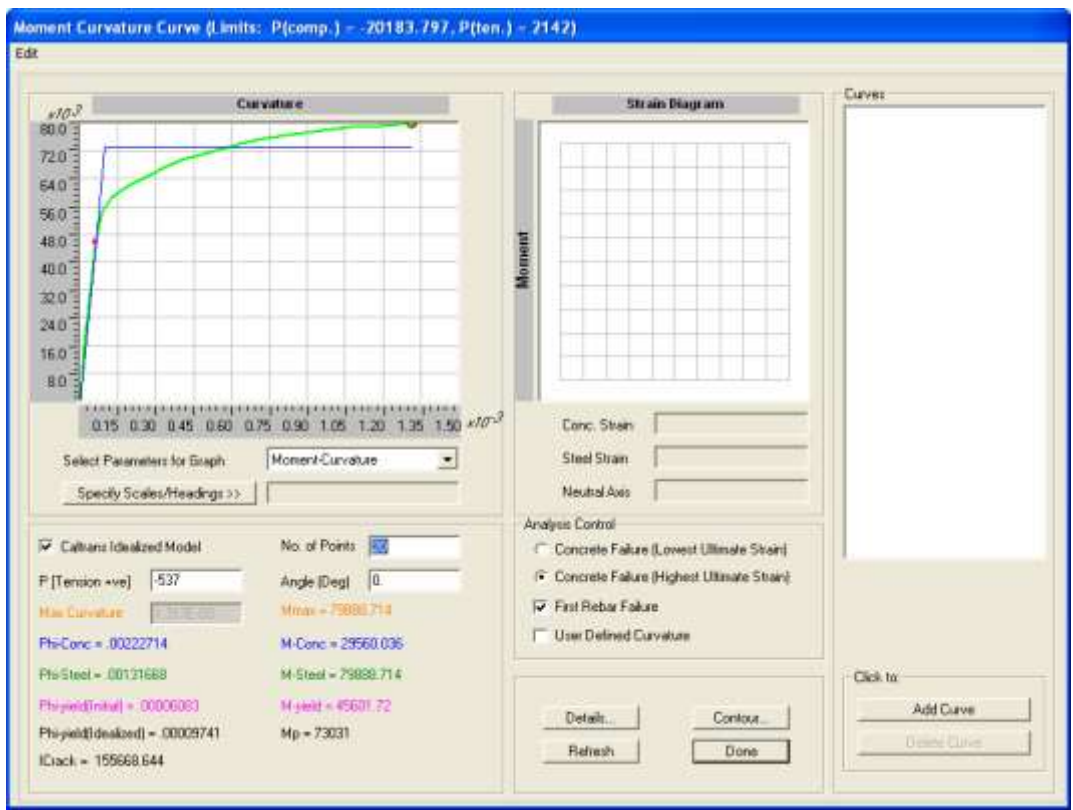
Zooming in on the bent on the right and placing the mouse cursor over the column will make the screen appear as shown below.



From the screen, the axial force is 537 kips. The column length between maximum moment and the inflection point must now be determined. The hinge length definitions are based on the column moment distribution from the response-spectrum analysis. However, the length used in this calculation will be based on the column moment distribution at the analysis step when the hinge in question first yields. For this hinge, the analysis step when first yield occurred was Step 2.

By right-clicking on the members and considering the offsets for the footing and the cross beam, it is determined that the distance from the top of the footing (maximum moment) to the inflection point is 174 in. (L_1) and the distance from the bottom of the cross beam (maximum moment) to the inflection point is 176 in. (L_2).

Use Section Designer to determine the idealized curvature at $P = 537$ kips:
The screen should appear as shown below.



The model shows that ϕ_y (idealized) = 0.00009741

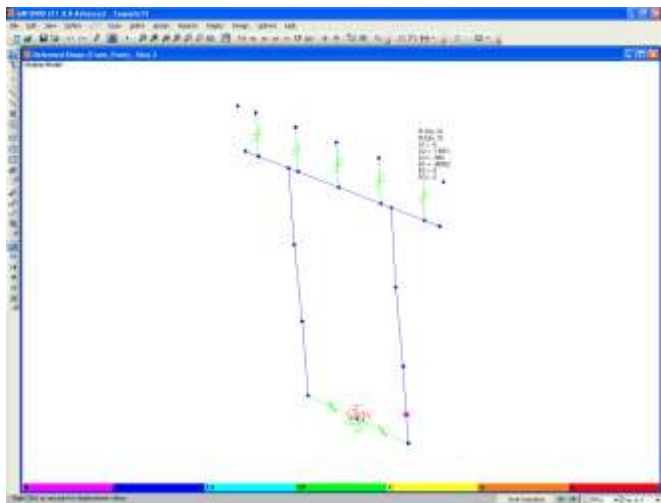
Δ_{yi} can now be computed as:

$$\Delta_{yi} = (L_1^2 + L_2^2)\phi_{yi}/3 = ((174)^2 + (176)^2)0.00009741/3 = 1.98 \text{ in.}$$

where ϕ_{yi} = idealized first yield curvature

Determine Δ_y :

The yield displacement (displacement at Step 2) must now be determined.



The screen shows $\Delta_y = 1.98$ in. This implies there is very little rotation from the footing since

$$\Delta_{yi} = \Delta_y = 1.98 \text{ in.}$$

Compute μ :

$$\begin{aligned} \mu = \text{ductility demand} &= 1 + \Delta_{pd}/\Delta_{yi} = 1 + (\Delta^{L_{D_Trans}} - \Delta_y)/\Delta_{yi} \\ &= 1 + (3.29 - 1.98)/1.98 = 1.7 \quad \text{OK since less than 5} \end{aligned}$$

This likely means the columns are well over sized and could be a smaller diameter.

15.6.3.11. Check Column Shear Capacity

The column shear requirements in Article 8.6 of the *LRFD Seismic Guide Specifications* must also be checked.

15.6.4 Precast Concrete Bridges in Washington

15.6.4.1 Introduction

There are two objectives for the following design example. One is to demonstrate the standard design practices followed by WSDOT in the seismic design of cast-in-place concrete bent caps supporting precast concrete superstructures. The second is to show a parallel design process that can be implemented for the design of a precast, nonprestressed, Stage 1 bent cap, in-lieu of cast-in-place construction. Utilizing a Stage 1 precast bent cap can reduce the amount of formwork that is needed to construct the bent cap, which can reduce construction time and costs. In Stage 2, the precast cap is filled with cast-in-place concrete. The cast-in-place diaphragm is considered as part of the bent cap.

This example replicates the calculations made for the Susie Creek Bridge Replacement Project. The bridge was designed in 1995, and constructed in 1996. It is located in Clallam County in the State of Washington, west of Port Angeles, on SR 112. It utilized cast-in-place concrete bent caps. Alongside the replicated bridge calculations, an alternate calculation will be made to show how the same bridge could have been designed with precast concrete bent caps.

For this example, the design calculations are carried out as if the bridge were designed in accordance with the *LRFD Specifications*, 4th Edition, using the force-based approach for seismic analysis and design.

15.6.4.2 Geometry

The bridge is a three-span continuous precast beam bridge with a composite cast-in-place deck. The bridge is aligned with a horizontal tangent, and does not have any vertical curvature. The total bridge length is 364.0 ft with three equal spans of 124 ft 8 in., as shown in **Figure 15.6.4.2-1**. The roadway width, measured from curb line to curb line, is 31 ft 6 in., and the deck thickness is 8 in. with an "A"-dimension (top of beam to top of deck slab at the support) of 13 in. The deck is supported within each span by five W74MG precast beams spaced at 6.73 ft on center. The barriers are WSDOT Standard Type F barriers with standard BP railing. A typical section of the bridge superstructure at a pier is shown in **Figure 15.6.4.2-2**.

Figure 15.6.4.2-1
Bridge Profile

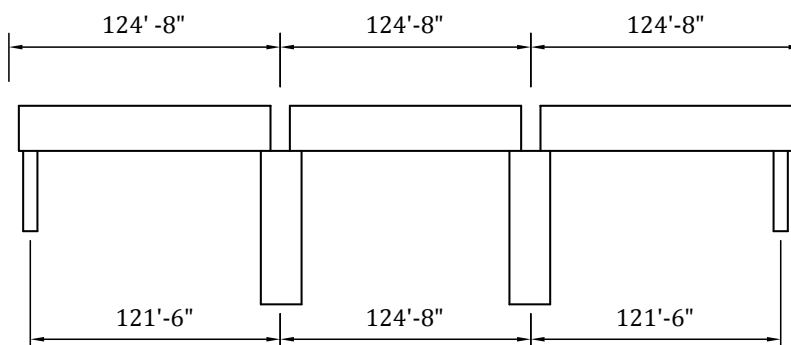
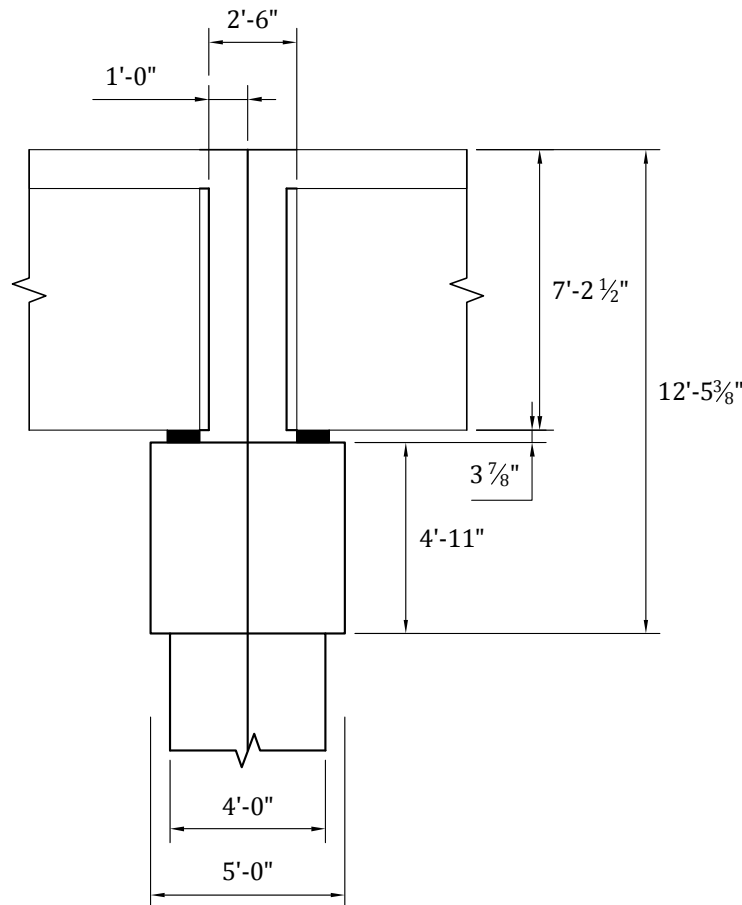


Figure 15.6.4.2-2
Bridge Section at Pier



The bridge abutments and piers are all oriented perpendicular to the alignment. At piers, the beams are made continuous for superimposed dead loads and live loads including impact. The piers consist of two-stage caps which are supported by two 48 in. diameter cast-in-place columns, which in turn, are each supported by a 72-in.-diameter drilled shaft. The Stage 1 portion of the bent cap is 4 ft 11 in. wide by 4 ft 11 in. deep. The 7 ft 6 in. height of the Stage 2 portion of the bent cap accounts for the height of the beams and the thickness of the oak shims, pads, and deck. The 30 in. width of the Stage 2 portion of the bent cap was set so that reinforcement placement could be made between beam ends. The 3 in. extension of the beam ends into the Stage 2 portion of the bent cap is a WSDOT standard for intermediate piers being made continuous for superimposed dead loads and live loads including impact.

15.6.4.3 Material Properties

The following material properties were used in the design of the precast concrete, cast-in-place concrete, and reinforcement in the bent cap:

Precast

Unit Weight, $w_c = 0.16 \text{ k/ft}^3$ (includes weight of reinforcement)

Concrete Strength, $f'_{c,pc} = 9 \text{ ksi}$

Modulus of Elasticity of Concrete, $E_c = 33,000K_1w_c^{1.5}\sqrt{f'_c} = 6,336 \text{ ksi}$ (LRFD Eq. 5.4.2.4-1)

Cast-In-Place

Unit Weight, $w_c = 0.16$ kips/ft³

Concrete Strength, $f'_{c_cip} = 4$ ksi

Modulus of Elasticity of Concrete, $E_c = 33,000K_1w_c^{1.5}\sqrt{f'_c} = 4,224$ ksi (LRFD Eq. 5.4.2.4-1)

Reinforcement

Yield Strength, $f_y = 60$ ksi

Modulus of Elasticity of Steel, $E_s = 29,000$ ksi

15.6.4.4 Section Properties

As previously noted, the Stage 1 cast-in-place section was 59 in. wide by 59 in. deep. The associated uncracked section properties are as follows (the uncracked section properties are used for simplicity and based on the assumption the members adjacent to plastic hinging regions remain elastic at the design earthquake):

CIP. (Stage 1)

$f'_c = 4$ ksi

Area, $A = 3,481$ in.²

Moment of Inertia, $I = 1,009,780$ in.⁴

Center of Gravity to Top Fiber, $y_t = -29.50$ in.

Center of Gravity to Bottom Fiber, $y_b = 29.50$ in.

Section Modulus for Extreme Top Fiber, $S_t = 34,230$ in.³

Section Modulus for Extreme Bottom Fiber, $S_b = 34,230$ in.³

The total cast-in-place concrete gross bent cap properties for the combined Stages 1 and 2 placements is as follows:

CIP. (Total)

$f'_c = 4$ ksi

Area, $A = 6,132$ in.²

Inertia, $I = 10,909,627$ in.⁴

Center of Gravity to Top Fiber, $y_t = -86.02$ in.

Center of Gravity to Bottom Fiber, $y_b = 61.36$ in.

Section Modulus for Extreme Top Fiber, $S_t = 126,822$ in.³

Section Modulus for Extreme Bottom Fiber, $S_b = 177,788$ in.³

If the cast-in-place option is replaced by a precast option, multiple stages need to be checked. The first stage is when the precast cap beam is erected and the precast beams are set in place. The cap beam being used in the design example is shown in **Figure 15.6.4.4-1**, with section properties as follows:

Precast (U-beam)

$f'_c = 9$ ksi

Area, $A = 1,131$ in.²

Inertia, $I = 373,372$ in.⁴

Center of Gravity to Top Fiber, $y_t = -38.85$ in.

Center of Gravity to Bottom Fiber, $y_b = 20.15$ in.

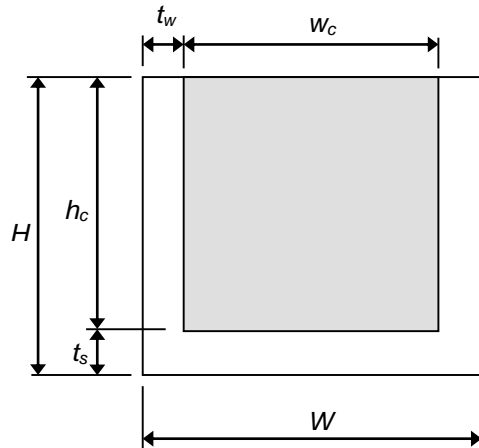
Section Modulus for Extreme Top Fiber, $S_t = 9,620$ in.³

Section Modulus for Extreme Bottom Fiber, $S_b = 18,548$ in.³

Parameters

$W = 4 \text{ ft } 11 \text{ in.}$, $w_c = 3 \text{ ft } 11 \text{ in.}$, $H = 4 \text{ ft } 11 \text{ in.}$, $h_c = 4 \text{ ft } 2 \text{ in.}$, $t_s = 9 \text{ in.}$, $t_w = 6 \text{ in.}$

Figure 15.6.4.4-1
Precast Cap Beam Section



Center-to-center of stems = 53 in. vs. for reactions = 42.52 in.

After all the Stage 1 bent cap reinforcement has been placed, and the beams are set, the Stage 1 cast-in-place portion of the bent cap will be placed. Once this has reached sufficient strength, the bridge deck and Stage 2 reinforcement will be placed. The section properties for this case are presented below.

Composite (Stage 1)

$f'_c = 9 \text{ ksi}$

Area, $A = 2,697 \text{ in.}^2$

Inertia, $I = 826,077 \text{ in.}^4$

Center of Gravity about Top of Section, $y_t = -30.81 \text{ in.}$

Center of Gravity about Bottom of Section, $y_b = 28.19 \text{ in.}$

Section Modulus about Top of Section, $S_t = 26,815 \text{ in.}^3$

Section Modulus about Bottom of Section, $S_b = 29,301 \text{ in.}^3$

It should be noted that the properties assume full composite action between the cast-in-place concrete ($f'_c = 4 \text{ ksi}$), and the precast concrete ($f'_c = 9 \text{ ksi}$). To account for the difference in strength of the concretes, the width of the cast-in-place concrete was reduced from its true width to a width equal to the product of the modular ratio times the true width. The modular ratio was computed as follows:

$$n = \frac{E_{CIP}}{E_{PC}} = \frac{\sqrt{f'_{c,CIP}}}{\sqrt{f'_{c,PC}}} = \frac{\sqrt{4 \text{ ksi}}}{\sqrt{9 \text{ ksi}}} = 0.667$$

The total composite bent cap properties including the Stage 2 placed concrete, are as follows:

Composite (Total)

$f'_c = 9 \text{ ksi}$

Area, $A = 4,465 \text{ in.}^2$

Inertia, $I = 7,983,813 \text{ in.}^4$

Center of Gravity to Top of Section, $y_t = -89.50 \text{ in.}$

Center of Gravity about Bottom of Section, $y_b = 57.88 \text{ in.}$

Section Modulus about Top of Section, $S_t = 89,203 \text{ in.}^3$

Section Modulus about Bottom of Section, $S_b = 137,927 \text{ in.}^3$

15.6.4.5 Stage 1 Bent Cap Design

Integral bent caps are constructed in stages to facilitate superstructure construction. The Stage 1 portion of the bent cap should be designed to carry the beam reactions, which consist of the self-weight of the beams, the weight of the interior diaphragms, and the weight of the bridge deck. A summary of the beam reactions is shown in **Table 15.6.4.5-1**.

Table 15.6.4.5-1. Beam Dead Load Reactions

Component (Description)	Exterior Beam kips	Interior Beam kips
Beam	100.90	100.90
Slab	84.76	87.23
Slab Haunch	20.53	20.53
Intermediate Diaphragm	13.65	27.29
TOTAL	219.83	235.95

The Stage 1 bent cap also must carry the weight of the entire bent cap, and any associated construction loadings. The self-weight of the bent cap is 6.81 kips/ft. Construction loads are not considered for design of the bent cap.

15.6.4.5.1 Check Flexural Capacity

In addition the flexural capacity must be checked against the bent cap cracking moment. According to *LRFD Specifications* Article 5.7.3.3.2, the cracking moment is taken as:

$$M_{cr} = \text{minimum value of } (1.33M_u; 1.2f_r S) \quad (\text{LRFD Eq. 5.7.3.3.2-1})$$

where

f_r = modulus of rupture of the concrete, in.²

S = section modulus, in.³

M_u = factored moment, in-kips

Following the method outlined above, the required Stage 1 reinforcement was as follows:

Positive moment—Bottom of bent cap between columns

Demand: $M_u = 2,202$ ft-kips

Capacity: $\phi M_n = 2,477$ ft-kips [Required: 8 No. 10 bars]

Negative moment—Top of bent cap over the columns

Demand: $M_u = 1,403$ ft-kips

Capacity: $\phi M_n = 1,564$ ft-kips [Required: 5 No. 10 bars]

If a precast trapezoidal open top U-beam is used in-lieu of the cast-in-place Stage 1 section, an additional check is added to the design process. When the precast beam is erected, before the beams can be placed, the Stage 1 portion of the cast-in-place section must be constructed. This must be done before beam erection such that the cap beam can be made integral with the column reinforcement extending into the bent cap, and to increase the torsional rigidity of the section. When the concrete is placed, it will have no strength, and the precast beam must carry its own weight in addition to the weight of forms and cast-in-place concrete. Since the concrete densities have been assumed to be equal, the weight of the section equates to that of the complete cast-in-place Stage 1 section, which is 3.87 kips/ft. Using strain compatibility, the required reinforcement in the precast section was calculated to be as follows:

Positive moment—Bottom of bent cap between columnsDemand: $M_u = 983$ ft-kipsCapacity: $\phi M_n = 1,236$ ft-kips [Required: 4 No. 10 bars]Negative moment—Top of bent cap over the columnsDemand: $M_u = 664$ ft-kipsCapacity: $\phi M_n = 949$ ft-kips [Required: 4 No. 9 bars]

The composite Stage 1 bent cap section then must be designed to carry the remaining dead loads, or more specifically, the pier reactions due to the weight of the beams, the weight of the intermediate diaphragms, the weight of the deck, and the weight of the Stage 2 bent cap placement. The load demands at this stage now equate to the load demands resisted by the original cast-in-place Stage 1 section. The additional reinforcement required in the cast-in-place portion of the composite Stage 1 bent cap is as follows:

Positive moment—Bottom of bent cap between columnsDemand: $M_u = 2,202$ ft-kipsCapacity: $\phi M_n = 2,503$ ft-kips [Required: 8 No. 10 bars]Negative moment—Top of bent cap over the columns at centerline columnDemand: $M_u = 1,403$ ft-kipsCapacity: $\phi M_n = 1,578$ ft-kips [Required: 5 No. 10 bars]**15.6.4.5.2 Check Shear Capacity**

Before starting the shear design, a check has to be made to verify that the appropriate shear model is being implemented. According to requirements of Article 5.8.1 of the *LRFD Specifications*, for components in which the distance from the point of zero shear to the face of the support is greater than $2d$, or components in which a load causing more than half of the shear at a support is farther than $2d$ from the face of the support, the provisions of Article 5.8.3 for Sectional Design Model apply. Dimension d is the depth of the section, less the clear cover to the bottom of the stirrup, less half the stirrup diameter as required by WSDOT design practice. The requirement of Article 5.8.1 is satisfied for this design example, and so the remainder of this section will use the AASHTO Sectional Design Method for shear calculations.

According to Article 5.8.3 of the *LRFD Specifications*, the concrete shear resistance can be taken as:

$$\phi_v V_c = \phi_v 0.0316 \beta \sqrt{f'_c} b_v d_v \quad (\text{LRFD Eq. 5.8.3.3-3})$$

And the reinforcement shear resistance can be taken as:

$$\phi_v V_s = \frac{\phi_v A_v f_y d_v}{\tan(\theta) s} \quad (\text{LRFD Eq. 5.8.3.3-4})$$

where

A_v = area of shear reinforcement, in.²

b_v = width of the section resisting the shear, in.

d_v = critical shear depth as defined below, in.

ϕ_v = strength reduction factor for shear = 0.9

s = spacing of the transverse reinforcement, in.

The factors β and θ are associated with the section geometry and the assumed failure plane, and have been taken to equal the code-allowed 2 and 45 degrees respectively for sections with the minimum amount of shear reinforcement. The minimum required shear reinforcement by Article 5.8.3.4.1 of the *LRFD Specifications* is determined as follows:

SEISMIC DESIGN

15.6.4.5.2 Check Shear Capacity

$$A_v \geq 0.0316 \sqrt{f'_c} \frac{b_v S}{f_y} \tag{LRFD Eq. 5.8.2.5-1}$$

The critical depth, d_v , is defined as:

$$d_v = \text{maximum value of } \left(d_s - \frac{a}{2}; 0.72h; 0.9d_s \right), \text{ in.} \tag{LRFD Art. 5.8.2.9}$$

where d_s = total depth of the section as specified above, in.

Stirrups are placed in the middle section of the bent cap between the beam ends as shown in **Figure 15.6.4.5.2-1**.

Figure 15.6.4.5.2-1
Fixed Intermediate Pier Diaphragm Details

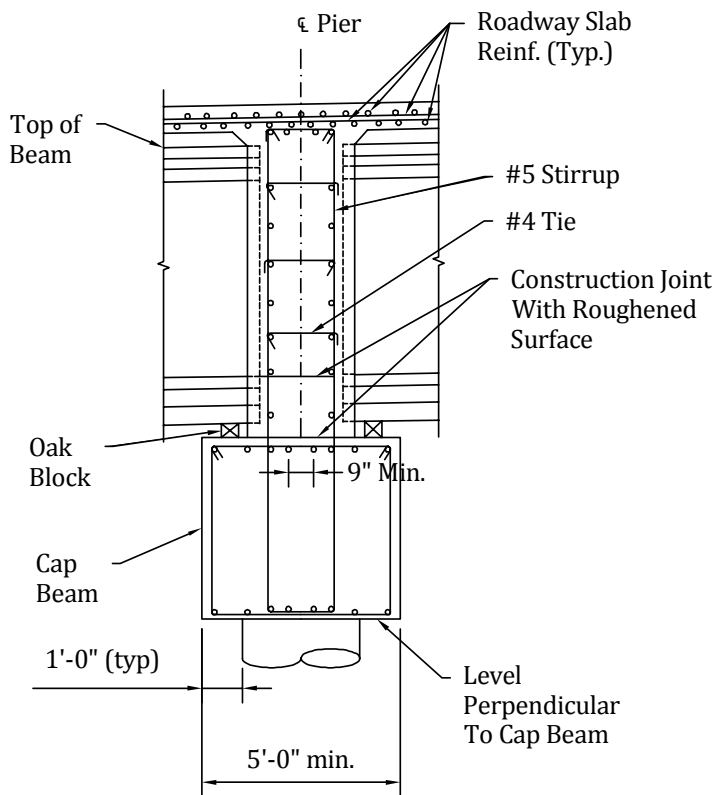
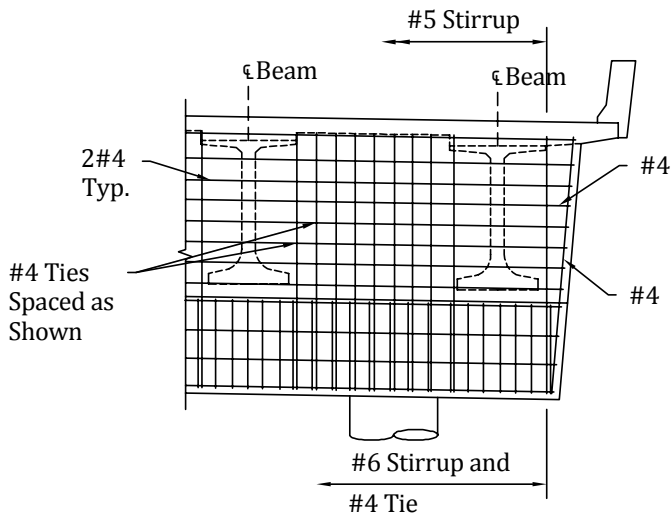


Figure 15.6.4.5.2-1
Fixed Intermediate Pier Diaphragm Details (continued)



15.6.4.5.3 Torsional Capacity

Unless specifically stated on the plans, the contractor could erect all the beams for one span before erecting the adjacent span. If this occurs, the bent cap will temporarily be subjected to a torsional demand. In addition, due to unbalanced live load conditions on the finished structure, a small torsion may exist, however, the torsional demands from the previous case should be significantly larger.

15.6.4.5.4 Shear Interface Calculation

It should be noted that in order for the cast-in-place portion to act compositely with the precast portion, adequate interface shear reinforcement must be provided.

15.6.4.6 Entire Bent Cap Design

The Stage 2 bent cap design is comprised of checking the demands from the superimposed dead loads, the live loads including impact, and the column plastic capacity demands. Example calculations of only the superimposed dead loads and the seismic demands will be shown in this example to limit the scope. The results of the live loads analysis are not discussed. These results will be compared with the extreme event loadings, and the governing case will be used for design.

15.6.4.6.1 Superimposed Dead and Live Loads

For a precast beam bridge, the superimposed dead loads are typically composed of traffic barrier loadings, utility loadings, and loadings from any deck overlays. The Susie Creek Bridge does not carry any utilities, but was designed to account for a future overlay equal to 22 psf. The traffic barrier intermediate pier reactions were 23.7 kips/beam. A summary of the superimposed dead loads are given in **Table 15.6.4.6.1-1**.

Table 15.6.4.6.1-1.
Superimposed Dead Loads

Component [Description]	Exterior Beam kips	Interior Beam kips
Barrier	23.70	23.70
Future Overlay (22 psf)	8.63	8.63
TOTAL	32.33	32.33

SEISMIC DESIGN

15.6.4.6.1 Superimposed Dead and Live Loads/15.6.4.6.2 Extreme Event Load Demands

Combining the above loadings with the results from the live loads analysis yielded the demands shown in **Table 15.6.4.6.1-2**.

Table 15.6.4.6.1-2
Combined Superimposed Dead Load and Live Load Demands

			LOAD CASES					
			(1) DL + LL M _{neg}		(2) DL + LL M _{pos}		(3) DL + LL P _{axial}	
Pier No.	Member No.	Location Along Pier	Moment ft-kips	Shear kips	Moment ft-kips	Shear kips	Moment ft-kips	Shear kips
2	1-Right Cantilever	Column 1 left	-1,969	584	-1,233	369	-1,969	584
		Column 1 right	-1,733	-708	-926	-844	-1,650	-947
	2-Between Columns	Center	472	162	2,310	317	1,751	259
		Column 2 left	1,733	708	-1,206	917	-1,368	912
3	3-Left Cantilever	Column 2 center	-1,969	-584	-1,524	-454	-1,708	-507
		Column 1 left	-1,969	584	-1,233	369	-1,969	584
	2-Between Columns	Column 1 right	-1,741	-708	-915	-844	-1,647	-948
		Center	463	162	2,321	317	1,755	259
3-Left Cantilever	Column 2 left	-1,741	708	-1,196	917	-1,356	912	
	Column 2 center	-1,969	-584	-1,524	-454	-1,708	-507	

15.6.4.6.2 Extreme Event Load Demands

The seismic analysis was done using the seismic parameters given below, and the methods outlined in Division I-A, Article 4.2 of the AASHTO *Standard Specifications*, for the Single Mode Spectral Analysis Method (Procedure 2).

Acceleration Coefficient, $A = 0.20 g$ [Division I-A, Art. 3.2]

Importance Classification, $IC = II$ [Division I-A, Art. 3.3]

The bridge was assumed classified as “other bridge”, and not essential for use following an earthquake.

Seismic Performance Category, $SPC = C$ [Division I-A, Art. 3.4]

Site Effects, $S = 1.0$ [Division I-A, Art. 3.5]

Site-dependent coefficient based on the soil profile. A “SOIL PROFILE TYPE I” was used for the design of this bridge. This is consistent with rock as the founding material.

This procedure was deemed justifiable over a multi-modal analysis due to the regularity of the bridge. The bridge is horizontally aligned within a tangent, does not have any vertical profile, the roadway width is constant, the piers are normal to the roadway, and all the spans are equal in length. In performing a modal analysis it is essential to have enough modes so that the response of each significant structural element is captured. With such a bridge, the mass is expected to primarily participate in the first mode of vibration for a respective earthquake.

The structural analysis program GTStrudl was used for the analyses. From the model, the elastic moments at the top of the pier column were as follows:

Table 15.6.4.6.2-1
Longitudinal EQ = 1.0Long + 0.3Trans

	Pier 2	Pier 3
M_x (trans) =	870 ft-kips	976 ft-kips
M_y (long) =	464 ft-kips	401 ft-kips

Table 15.6.4.6.2-2**Transverse EQ = 0.3Long + 1.0Trans**

	Pier 2	Pier 3
M_x (trans) =	2,901 ft-kips	3,088 ft-kips
M_y (long) =	261 ft-kips	216 ft-kips

The top-of-column elastic seismic demands need to be compared with the plastic capacities of the column sections. The columns for the Susie Creek Bridge had a plastic moment capacity of 3,776 ft-kips. This was calculated following the simplified method outlined in Article 4.11.4 in the *LRFD Seismic Guide Specifications* in which the shears between columns are balanced. The load is distributed linearly between columns. It is equal in magnitude, but opposite in sign at each column, and has an inflection point midway between the columns. Due to load reversal though, the bent cap should be detailed such that the moment can be applied in either direction, or in other words, such that the moment could act to induce tension on both the top and bottom of the bent cap section locally over the columns.

15.6.4.6.3 Load Summary

By inspection, the elastic seismic demands are smaller in magnitude than the plastic hinging demands. Therefore, due to the extreme event load case, the moment demands near the columns are controlled by the seismic event, with the moment demand being 3,088 ft-kips. Through comparison of this with the strength case, the superimposed dead load and live load plus impact demands, it is apparent that the extreme event load case controls both the negative and positive moment demands for sections near the columns. Near mid-span, for both the seismic and plastic hinging load cases, the moment is theoretically zero, and so the strength demand controls the design with a moment magnitude equal to 2,321 ft-kips. However, due to the short distance between columns, and the relative length that would be required to curtail reinforcement, the bottom mat bent cap reinforcement at the midspan section of the bent cap was designed for 3,088 ft-kips. The resulting reinforcement requirements are as follows:

Positive Moment—Bottom of bent cap between columns

Demand: $M_u = 3,088$ ft-kips

Capacity: $\phi M_n = 6,495$ ft-kips [Required: 8-No.10 bars]

Negative Moment—Top of bent cap over the columns

Demand: $M_u = 3,088$ ft-kips

Capacity: $\phi M_n = 4,917$ ft-kips [Required: 6-No.10 bars]

The cracking moment controlled the design of the reinforcement in the Stage 2 portion of the bent cap.

15.6.4.7 Additional Bent Cap Design Checks

Not all the bent cap design checks were made in this example. Live loads often control certain design components of the bent cap, and should be checked. In the actual bridge, the design was controlled by the live load demands.

Also, the longitudinal seismic force demands should be checked, and adequate steel should extend beyond the ends of the beams into the Stage 2 portion of the bent cap/diaphragm to handle these demands.

15.6.5 Two-Span Spliced U-Beam

15.6.5.1 Introduction

The bridge in this example represents a structure carrying a multi-lane cross street over an interstate highway in San Diego County, Calif. An integral cap is used at the pier, which is an advantage for sites with significant seismicity. A second cast-in-place splice and asymmetrical beam segments in one span represent a real-world condition where the maintenance of traffic during construction limits the placement of temporary supports. The bridge is also skewed to illustrate another condition often found in bridges of this type. The beams are spliced over the interior pier, where the segments terminate a short distance (6 in.) beyond the face of the bent cap.

An elastic design is presented to illustrate the effects of staging prestress and gravity load applications. Prestress forces and compressive strength requirements are developed from this analysis at service limit states. Safety of the structure is evaluated at strength limit states.

Shear design is presented to illustrate the effects of splicing on the shear response. Of particular interest is the interface shear capacity at the bent caps.

15.6.5.2 Description of Bridge

As shown in **Figures 15.6.5.2-1** and **15.6.5.2-2**, the location of the existing traffic lanes and orientation of the roadway improvements dictate splice beam layout, bent location, and skew of the bridge. The new structure must accommodate future widening of both the southbound and northbound lanes of Route 78 to the east, thus resulting in unsymmetrical span lengths.

Figure 15.6.5.2-1
Bridge Elevation

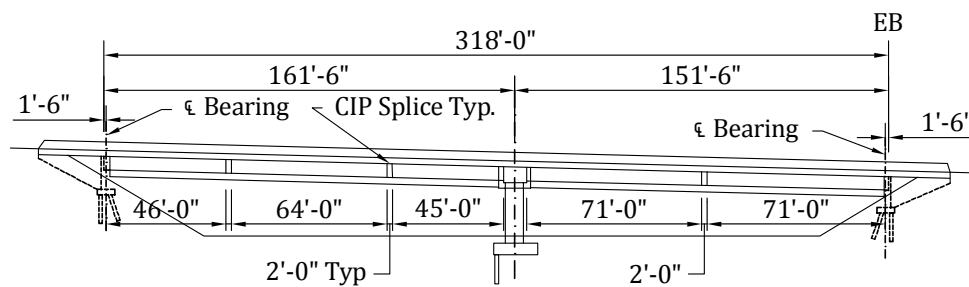
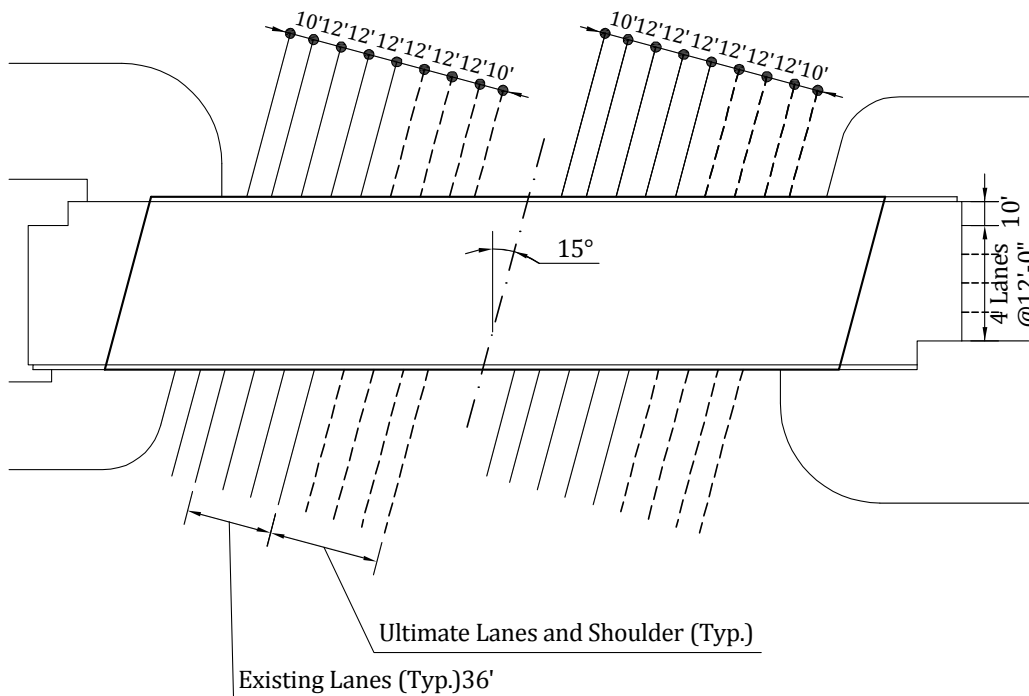


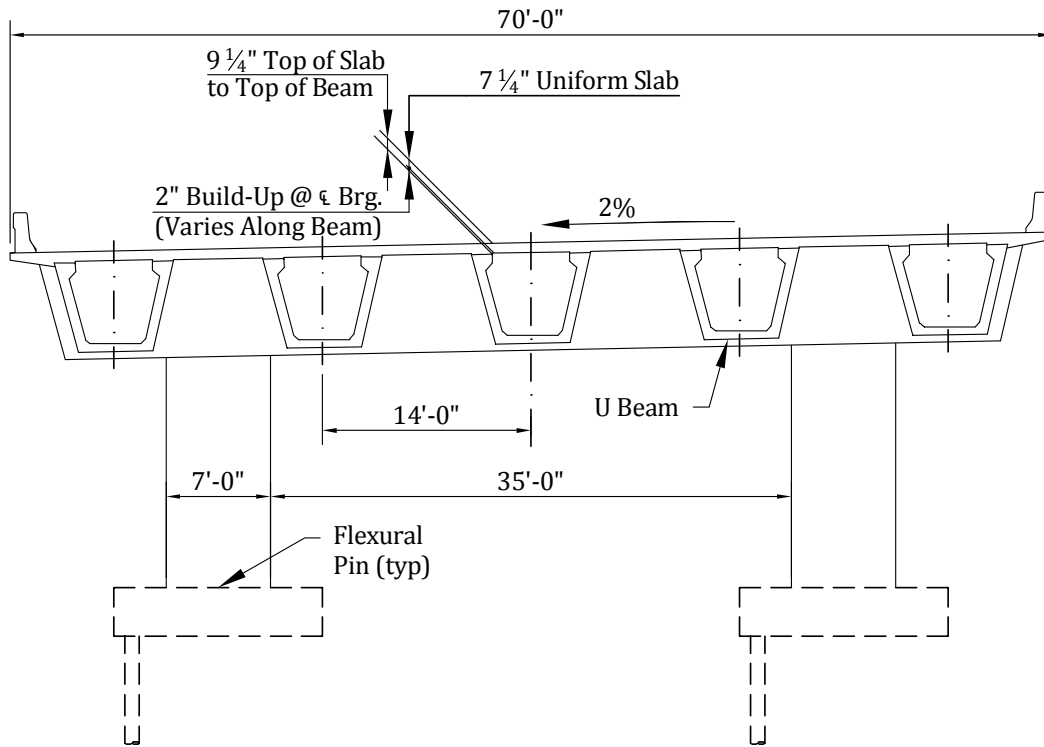
Figure 15.6.5.2-2
Plan View of Bridge



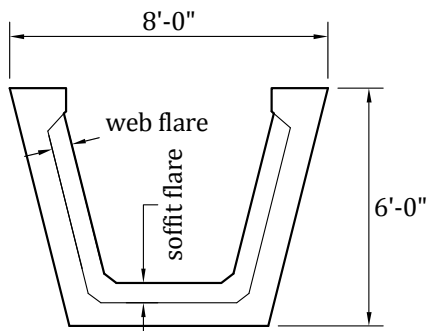
As shown in **Figure 15.6.5.2-3**, the bridge is 70.0 ft wide with a constant 2% cross slope. The beams are spaced 14.0 ft on center and are set with the soffit parallel to the deck cross-slope. This orientation allows the web widths and associated stirrups to have equal lengths, thus simplifying beam segment construction. The beam segments

terminate a short distance into the cast-in-place bent cap and at the cast-in-place end diaphragms. This termination allows the post-tensioning anchorages to be located in the cast-in-place diaphragms. Also, this termination allows level bearing surfaces to be field-constructed with greased galvanized bearing pads that allow initial prestress shortening displacements without a significant amount of temporary bracing. The bent cap is 9 in. deeper than the superstructure to improve constructability and seismic performance.

Figure 15.6.5.2-3
Bridge and Beam Sections

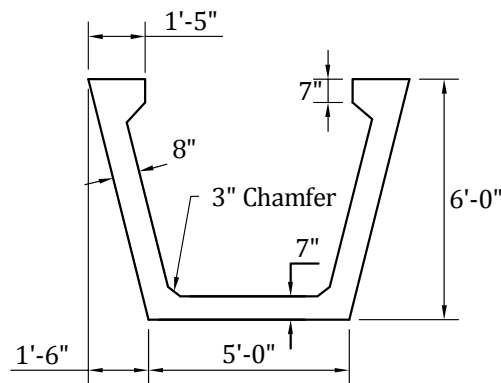


a) Typical Bridge Cross Section



Note: Web and soffit flare vary from 0" to 6" over 12'-0" from face-of-cap

b) Beam Cross Section at End



c) Typical U-Beam Cross Section

The two 7 ft circular columns supporting the bent cap are pinned at the footing in both the longitudinal and transverse directions. Ideally, this pin transfers column axial load and shear, but no moment to the footing. All

SEISMIC DESIGN

15.6.5.2 Description of Bridge/15.6.5.5 Seismic Forces

lateral resistance is provided by frame action. The primary benefit of using a flexural pin at the column base is the significantly reduced foundation size over a fixed base detail, because the footings do not need to resist the overstrength moments due to plastic hinging. However, the superstructure and bent cap must be designed to resist these plastic hinge moments.

15.6.5.3 Load Combinations

The design satisfies the following service level load combinations:

$$D + LL + PS \quad \text{Service I}$$

$$D + 0.8LL + PS \quad \text{Service III}$$

The Service I load combination is used to evaluate all components and parameters not related to the evaluation of tensile stress. The Service III load combination relates to evaluating tensile stress in design of the prestress tendons.

The following strength and extreme event limit state load combinations are evaluated as required in the *LRFD Specifications* Table 3.4.1-1:

$$\gamma_p D + 1.75LL + PS \quad \text{Strength I}$$

$$\gamma_p D + LL + PS + EQ \quad \text{Extreme Event I}$$

where γ_p is the load factor for permanent loads. ($\gamma_p = 1.25$ for self-weight of the beams and deck, and $\gamma_p = 1.50$ for future wearing surface and utilities.)

15.6.5.4 Seismic Considerations

Seismic considerations related to development of an integral column–superstructure connection under severe seismic loads are presented in this section. It is assumed the seismic forces are derived from the overstrength moment due to column plastic hinging. Components, such as the bent cap and superstructure, are designed to resist these forces with sufficient factor of safety. This section covers the seismic design and analysis in the longitudinal direction, as it relates to design of the spliced-beam superstructure. The columns are designed to resist fully reversed displacement cycles up to a structural ductility of 4 ($\mu_\Delta = 4$). As a result, significant inelastic strain of the column reinforcement will occur within the bent cap/column joint region.

In the following, a methodology for seismic design using capacity design principles is presented. Maximum plastic hinge forces are developed using overstrength material properties listed in **Table 15.6.5.4-1**. The resistance is calculated using expected material properties and no strength reduction factors are necessary.

Table 15.6.5.4-1
Material Strength for Seismic Design^a

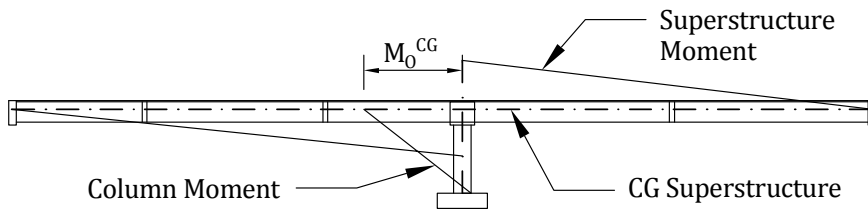
	Nominal ksi	Expected ksi	Overstrength ksi
Reinforcement			
f_{ye}	60	66	78
f_{ue}	80	88	104
Concrete			
f'_{ce}	4.0	5.2	6.8

^a Subscript “e” denotes seismic design properties.

15.6.5.5 Seismic Forces

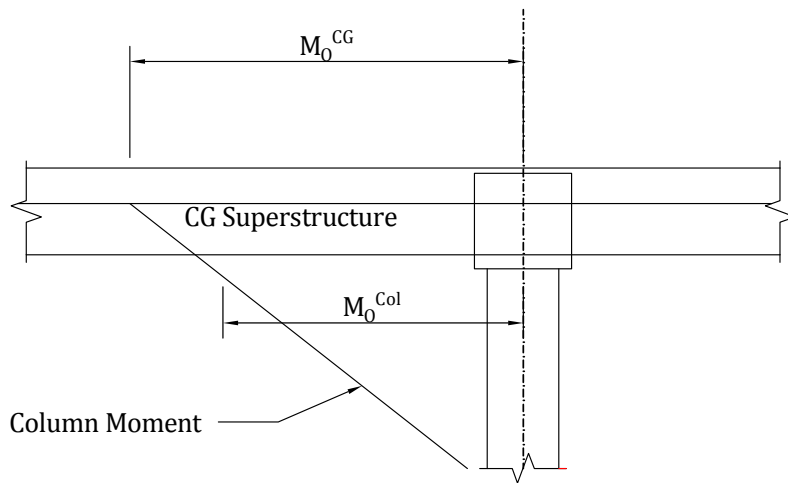
An idealized representation of the maximum seismic forces the bridge is designed to resist is shown in **Figure 15.6.5.5-1**. Seismic resistance is achieved from the ground up. First the column is designed to resist the maximum plastic moment at the top, M_o based on overstrength material properties shown in **Table 15.6.5.4-1**. The analysis to attain this moment includes strain hardening of the reinforcement, and effects of the confinement on the concrete. Based on the overstrength moment, anchorage of the column reinforcement and adequacy of the joint shear reinforcement are evaluated.

Figure 15.6.5.5-1
Seismic Moments



The column overstrength moments are extrapolated to the center of gravity of the superstructure M_o^{CG} , as shown in **Figure 15.6.5.5-2**.

Figure 15.6.5.5-2
Column Moment Detail



From column analysis:

$$M_o^{Top} = 33,000 \text{ ft-kips (top of column)}$$

$$M_o^{Base} = 5,000 \text{ ft-kips (base of column) (Although a hinge is assumed to carry no moment, the moment capacity of a hinge is significant)}$$

From the bridge geometry:

$$L_c = 20.6 \text{ ft (clear distance between top of footing and bottom face of bent cap)}$$

$$Y_{CG} = 5.08 \text{ ft (distance from top of column, i.e. bottom face of bent cap, to center of gravity of superstructure)}$$

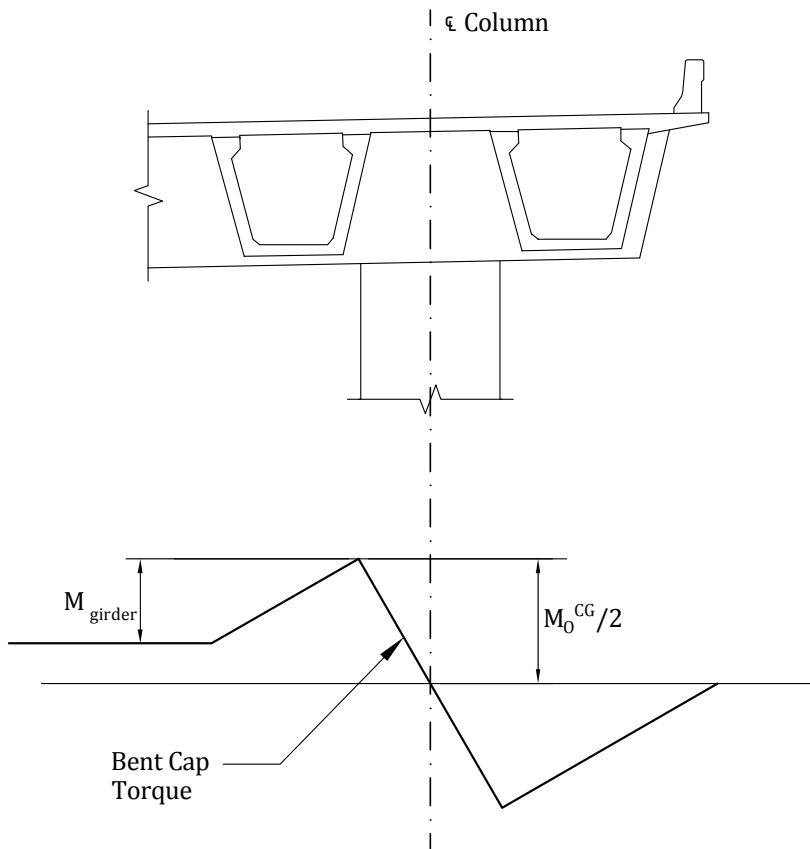
The design seismic moment at the center of gravity of the superstructure is calculated using the following:

$$\begin{aligned} M_o^{CG} &= M_o^{Top} + \frac{(M_o^{Top} + M_o^{Base})}{L_c} (Y_{CG}) \\ &= 33,000 + \frac{(33,000 + 5,000)}{20.6} (5.08) = 42,400 \text{ ft-kips} \end{aligned}$$

This moment is resisted by the bent cap through torsion. The idealized torque profile for the bent cap, shown in **Figure 15.6.5.5-3**, indicates the maximum torque occurs at the edge of the column and is equal to $M_o^{CG}/2$. The torsion in the bent cap is distributed into the superstructure based on the relative flexibility of the superstructure

and the bent cap. Hence, the superstructure does not resist column overstrength moments uniformly across the width. To account for this shear lag effect, an effective width is used to distribute the moments along the length of the bent cap according to Article 8.10 of the *LRFD Seismic Guide Specifications*.

Figure 15.6.5.5-3
Bent Cap Torque Profile



15.6.5.6 Joint Shear Design

In order for the column reinforcement to be anchored in the bent cap and to develop its overstrength capacity, the column reinforcement must extend into the bent cap as high as possible without interfering with the bent cap and deck reinforcement. For this example, the bars extend up to 9 in. below the deck (top) surface. In order to develop favorable bond strut angles this extension of the reinforcement is required even if the development length equations permit a shorter length.

The joint shear mechanism in **Figure 15.6.5.6-1** shows the column longitudinal reinforcement being clamped through struts extending from the compression zone of the column and bent cap stirrups placed on both sides of the column. Holombo et al. (2000) suggested that this clamping occurs over the top 60% of the column reinforcement extension into the bent cap with a maximum bond stress of $30\sqrt{f'_c}$ (psi) for well-confined joint regions. Based on this observation, the minimum anchorage length required is:

$$\ell_{ac} \geq \frac{0.79 d_{b\ell} f_{ye}}{\sqrt{f'_c}} \tag{Eq. 15.6.5.6-1}$$

where

- ℓ_{ac} = anchorage length, in.
- $d_{b\ell}$ = diameter of column reinforcement, in.
- f_{ye} = yield strength of reinforcement for seismic design, ksi

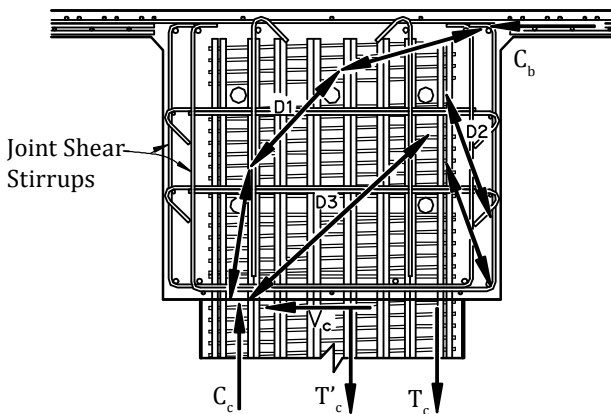
with a 1.2 multiplier for 2-bar bundles as is the case for this example. Therefore, the required development length of the No. 14 longitudinal reinforcement is:

$$\ell_{ac} = 48.72 \text{ in.}$$

$$\ell_{ac} \text{ (provided)} = 81.5 \text{ in.}$$

The joint shear force-transfer mechanism shown in **Figure 15.6.5.6-1** is based on three compression struts that provide clamping of the column longitudinal reinforcement. The first strut, D1, provides clamping of the longitudinal reinforcement making up column tension force T'_c near to the compression zone of the column, and ties into the compression zone of the superstructure. The remaining reinforcement making up T_c is clamped by the compression struts D2 and D3. The vertical and horizontal components of D2 are resisted by the vertical and horizontal legs of the joint shear stirrups, respectively, while the horizontal component D3 is resisted by the column hoops.

Figure 15.6.5.6-1
Joint Shear Force-Transfer Mechanism



- T'_c portion of column force clamped by D1
- T_c remaining column tension force clamped by D2 and D3 assumed to be 25% of the total column longitudinal reinforcement.

The *LRFD Seismic Guide Specifications*, Article 8.13.4.2, provides prescriptive amounts of reinforcement required for standard joint dimensions assuming circular columns with column reinforcement extending to the top of the joint, and there are slight differences between values prescribed. Article 8.13.4.2 recommends the following:

For joint shear reinforcement resisting the horizontal and transverse components of D2:

$$A_S^V = 0.2A_{SC} = 0.2(112.5) = 22.5 \text{ in.}^2 \tag{Eq. 15.6.5.6-2}$$

$$A_S^H = 0.1A_{SC} = 0.1(112.5) = 11.3 \text{ in.}^2 \tag{Eq. 15.6.5.6-3}$$

where

$$A_S^V = \text{total area of vertical shear reinforcement anchored in the joint, in.}^2$$

$$A_S^H = \text{total area of horizontal shear reinforcement anchored in the joint, in.}^2$$

$$A_{sc} = \text{total area of column reinforcement anchored in the joint, in.}^2$$

This reinforcement is required on each side of the bent cap and distributed over twice the width of the column.

To control cracking within the column core region, to prevent buckling, and to assist in providing bond transfer to the top of the superstructure longitudinal reinforcement, J-bars should extend at least $\frac{2}{3}$ of the height of the bent cap.

$$A_S^{J\text{-bar}} = 0.08A_{SC} = 0.08(112.5) = 9.0 \text{ in.}^2 \tag{Eq. 15.6.5.6-4}$$

The column hoop reinforcement ratio required in the joint region is calculated using the following:

$$\rho_s = 0.4 \frac{A_{SC}}{\ell_{ac}^2} = 0.4 \frac{112.5}{(81.5)^2} = 0.0067 \tag{Eq. 15.6.5.6-5}$$

However, it has been a general rule by Caltrans that the amount of transverse reinforcement in the joint region should be equal to or greater than the amount of transverse reinforcement in the column.

To prevent buckling of the reinforcement, it is suggested that:

$$\rho_s \geq 0.0002n \tag{Eq. 15.6.5.6-6}$$

where n is the number of bars. Therefore,

$$\rho_s \geq 0.0002(50) = 0.010$$

The transverse reinforcement ratio is:

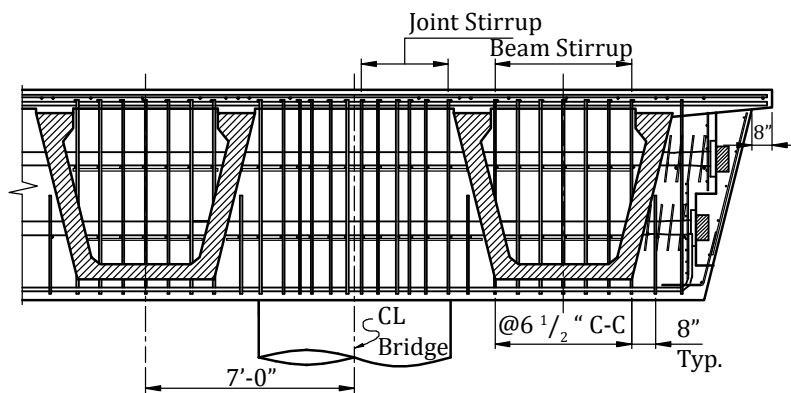
$$\rho_s = \frac{4A_h}{D_c \rho_s} \tag{Eq. 15.6.5.6-7}$$

By rearranging terms, the spacing of the column hoops within the column core region can be computed as:

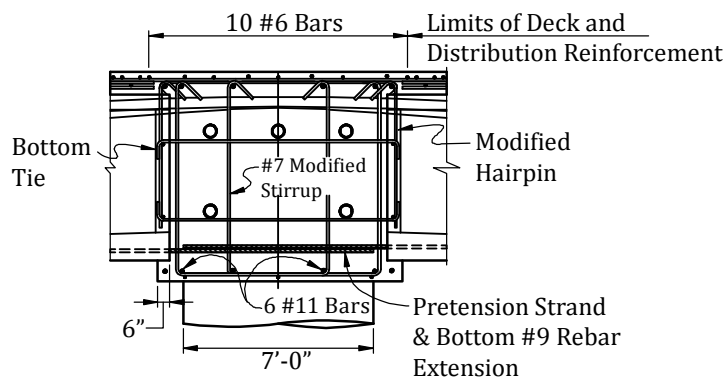
$$s \leq \frac{4A_h}{D_c \rho_s} = \frac{4(0.79)}{(79.0)(0.010)} = 4.00 \text{ in.} \tag{Eq. 15.6.5.6-8}$$

The joint shear reinforcement details are shown in **Figure 15.6.5.6-2**.

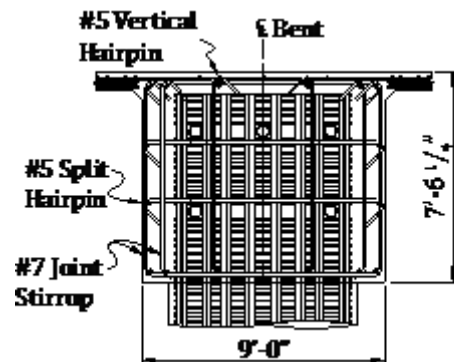
Figure 15.6.5.6-2
Bent Cap Joint Reinforcement Details



a) Bent Cap Elevation Over Column



b) Bent Cap Section Between Beams



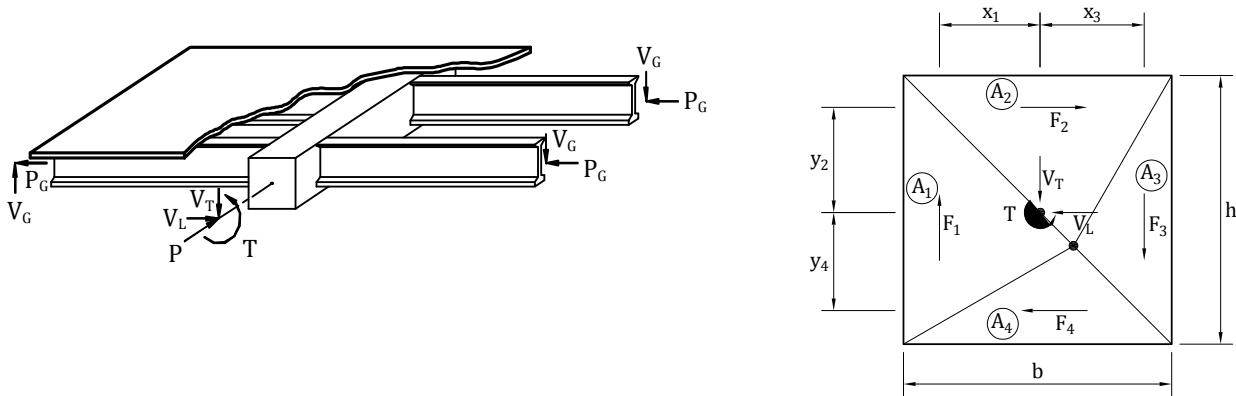
c) Bent Cap Section Over Column

15.6.5.7 Bent Cap Torsion

As mentioned previously, the bent cap resists the column plastic moment through torsional mechanisms. The peak torque, Mo^{CG} acts on a small section of bent cap between the column and side of the adjacent beam. This section is too small to form a spiral crack around the perimeter.

The mechanism shown in **Figure 15.6.5.7-1** can be described using the sand-heap analogy, where the shear stress has a constant magnitude, or slope in the analogy. However, the section resists not only torque from the plastic hinge, but also dead load shear acting vertically and the column shear acting horizontally. This requires that the apex of the triangle be offset from the center of the section. The coordinates of this apex are located through trial and error. The calculations for developing the coordinates of the apex and the associated required axial load are shown in **Tables 15.6.5.7-1** and **15.6.5.7-2**.

Figure 15.6.5.7-1
Torsion-Shear Friction Mechanism



Assumptions:

1. Shearing stress is constant over section.
2. Quadrant forces proportional to normal force P and respective area (e.g. $F_4 = A_4\mu P/A$)

Sectional Force Equilibrium:

$$T = F_1x_1 + F_2y_2 + F_3x_3 + F_4y_4$$

$$V_T = F_1 - F_3, V_L = F_2 - F_4$$

Table 15.6.5.7-1
Parameters for Torsion-Shear Friction Analysis

H	(ft)	7.52
B	(ft)	9
P	(kip)	6,000
Xo	(ft)	5.55
Yo	(ft)	2.93
μ		1.4

Table 15.6.5.7-2 Torsion-Shear Friction Analysis

Quad	Area ft ²	Force kips	x_i, y_i	Moment ft-kips
1	20.87	2,590	2.65	6,864
2	20.66	2,564	2.23	5,717
3	12.97	1,610	3.35	5,394
4	13.19	1,636	2.78	4,555
Total	67.68		$T_n =$	22,528
	$V_v =$	980		
	$V_h =$	927		

The torque demand of 21,200 ft-kips, the dead load shear of 972 kips and the column shear of 922 kips are less than their respective capacities.

The normal force, P on the friction plane consists of two components: (1) the prestress force after all losses and (2) the axial force created by the reinforcement passing through the shear plane. This force can be calculated as described by Holombo et al. (2000):

$$P = P_f + A_s(0.0005)E_s \quad \text{Eq. 15.6.5.7-1}$$

where A_s includes the prestress strand and mild reinforcement passing through the section. A total of five tendons with twenty-seven 0.6-in.-diameter strands each and twelve No. 11 bars is sufficient to develop the 6,000 kip required axial load. These five tendons are required to pass through the column core, and the column hoops must be adjusted accordingly, where each duct has an outer diameter of 4.5 in.

15.6.5.8 Superstructure Demands

The superstructure seismic moments in Span 1 differ from those in Span 2 due to the unequal span lengths and resulting differences in relative stiffness. The distribution of moments to each span can be solved by comparing the relative stiffness and computing the moments using moment distribution.

$$k_{BA} = \frac{3EI}{L_{AB}} \quad k_{BC} = \frac{3EI}{L_{BC}}$$

where

$$L_{AB} = 165 \text{ ft and } L_{BC} = 150 \text{ ft.}$$

Subscripts A , B , and C refer to piers 1, 2, and 3 respectively

$$DF_{AB} = \frac{k_{BA}}{k_{BA} + k_{BC}} = 0.476$$

$$DF_{BC} = 1 - 0.476 = 0.524$$

The superstructure seismic moment at Bent 2 in Spans 1 and 2 are:

$$M_o^{BA} = 42,400(0.476) = 20,200 \text{ ft-kips}$$

$$M_o^{BC} = 42,400(0.524) = 22,200 \text{ ft-kips}$$

It should be noted that these moments are completely reversible and therefore should be subtracted and added to the $D+PS$ moments.

As previously stated, the superstructure resistance to column plastic hinging is nonuniform along the width of the bridge. To account for this action, an effective width approximation is used, where the maximum resistance per unit of superstructure width of the actual structure is distributed over an equivalent effective width to provide an equivalent resistance. Structural testing by Holombo et al. (2000) of similar details has shown that the overstrength plastic hinge moment can be resisted equally by the two beams adjacent to the column.

$$W_s = 2S_G \quad \text{Eq. 15.6.5.8-1}$$

where S_G = spacing of the beams = 14 ft

$$W_s = 2(14.0) = 28.0 \text{ ft equivalent effective width of superstructure}$$

Based on this effective width, the moment per beam is calculated as:

$$M_{(seis)} = (M_o^{BC})S_G/W_s = 14.0/28.0 (22,200) = 11,100 \text{ ft-kips.} \quad \text{Eq. 15.6.5.8-2}$$

15.7 CITED REFERENCES

- AASHTO. 2009. *Guide Specifications for LRFD Seismic Bridge Design*, 2nd Edition. American Association of State Highway and Transportation Officials, Washington, DC. 296 pp.
https://bookstore.transportation.org/item_details.aspx?id=1915 (Fee)
- AASHTO. 2007. *LRFD Bridge Design Specifications*, 6th Edition. American Association of State Highway and Transportation Officials, Washington, DC. 1,938 pp.
https://bookstore.transportation.org/Item_details.aspx?id=1924 (Fee)
- AASHTO. 2002. *Standard Specifications for Highway Bridges*, Div. I-A. 17th Edition. American Association of State Highway and Transportation Officials, Washington, DC. 1,028 pp.
https://bookstore.transportation.org/item_details.aspx?id=51 (Fee)
- ATC. 1983. *Seismic Retrofitting Guidelines for Highway Bridges*, ATC-6-2, Applied Technology Council. Redwood City, CA. 220 pp.
<http://www.atcouncil.org/Bridge-Evaluation-and-Retrofit/Seismic-Retrofitting-Guidelines-for-Highway-Bridges/flypage.tpl.html> (Fee)
- ATC. 1996. *Improved Seismic Design Criteria for California Bridges: Provisional Recommendations*, Report No. ATC-32. Applied Technology Council, Redwood City, CA. 215 pp.
<https://www.atcouncil.org/New-Bridge-Design/Improved-Seismic-Design-Criteria-for-California-Bridges-Provisional-Recommendations/flypage.tpl.html> (Fee)
- Caltrans. 2006. *Seismic Design Criteria*, Version 1.4. California Department of Transportation, Sacramento, CA.
<http://www.dot.ca.gov/hq/esc/techpubs/manual/othermanual/other-engin-manual/seismic-design-criteria/sdc.html>
- Holombo, J., N. Priestley, and F. Seible. 1998. "Longitudinal Seismic Response of Precast Spliced Girder Bridges." Report No. SSRP-98/05, University of California at San Diego, La Jolla, CA, (April), 298 pp.
<http://structures.ucsd.edu/files/se/assets/research/SSRPList1.26.10.pdf> (Fee)
- Holombo, Jay., M. J. Nigel Priestley, and Frieder Seible. 2000. "Continuity of Precast Prestressed Spliced-Girder Bridges Under Seismic Loads." *PCI Journal*, Precast/Prestressed Concrete Institute, Chicago, IL. V. 45, No. 2, (March-April), pp. 40-63.
http://pci.org/view_file.cfm?file=JL-00-MARCH-APRIL-3.pdf
- Imbsen. 2006. *Recommended LRFD Guidelines for the Seismic Design of Highway Bridges*. NCHRP Project 20-07, Task 193. Transportation Research Board, Washington, DC.
<http://apps.trb.org/cmsfeed/TRBNetProjectDisplay.asp?ProjectID=1534>
- JRA. 2002. *Specifications for Highway Bridges*, Part V Seismic Design (in English). Japan Road Association, Tokyo, Japan.
www.road.or.jp/english/publication
- Martin, Barney T. and David H. Sanders. 2007. *Verification and Implementation of Strut-and-Tie Model in LRFD Bridge Design Specifications*. NCHRP Project Report 20-07, Task 217. Transportation Research Board, Washington, DC. 281 pp.
[http://onlinepubs.trb.org/onlinepubs/archive/NotesDocs/20-07\(217\)_FR.pdf](http://onlinepubs.trb.org/onlinepubs/archive/NotesDocs/20-07(217)_FR.pdf)
- PCI. 2011. *PCI Bridge Design Manual*, Third Edition. Precast/Prestressed Concrete Institute, Chicago, IL.
<https://pci.manuscript.com/ProductDetails.aspx?productID=117> (Fee)
- PCI. 2013. *Seismic Design of Precast Concrete Bridges State-of-the-Art Report*. SD-01-13. Precast/Prestressed Concrete Institute, Chicago, IL. 196 pp.
<https://pci.manuscript.com/ProductDetails.aspx?productID=143>
- Restrepo, Jose I., Matthew J. Tobolski, and Eric E. Matsumoto. 2011. *Development of a Precast Bent Cap System for Seismic Regions*. NCHRP Report 681. Transportation Research Board, Washington, DC. 116 pp.
http://onlinepubs.trb.org/onlinepubs/nchrp/nchrp_rpt_681.pdf

New Zealand. 2003. *Bridge Manual*, Section 5 Earthquake Resistant Design. New Zealand Transport Agency, Wellington, NZ

<http://www.nzta.govt.nz/resources/bridge-manual/index.html>

WSDOT. 2008. *Bridge Design Manual*, Section 4 Seismic Design and Retrofit. Washington State Department of Transportation

www.wsdot.gov/publications/manual/m23-50.htm

This page intentionally left blank

Additional Bridge Products

To be released at a later date.

This page intentionally left blank

RAILROAD BRIDGES

Table Of Contents

NOTATION..... 17 - 5

17.0 INTRODUCTION..... 17 - 9

17.1 TYPICAL PRODUCTS AND DETAILS 17 - 9

 17.1.1 Piles..... 17 - 9

 17.1.2 Pile Caps and Abutments 17 - 9

 17.1.3 Superstructures 17 - 9

 17.1.3.1 Slab Beams and Box Beams..... 17 - 10

 17.1.3.2 Other Products..... 17 - 10

 17.1.3.3 Connection Details 17 - 12

17.2 CONSTRUCTION CONSIDERATIONS 17 - 13

 17.2.1 Advantages..... 17 - 13

 17.2.2 Standard Designs 17 - 14

 17.2.3 Train Operations 17 - 14

 17.2.4 Construction Methods 17 - 14

 17.2.5 Substructures 17 - 14

17.3 THE AMERICAN RAILWAY ENGINEERING AND MAINTENANCE-OF-WAY ASSOCIATION LOAD PROVISIONS
..... 17 - 15

 17.3.1 AREMA Manual 17 - 15

 17.3.2 AREMA Loads 17 - 16

 17.3.2.1 Live Load..... 17 - 16

 17.3.2.2 Impact Load..... 17 - 17

 17.3.2.4 Other Loads 17 - 18

 17.3.2.5 Load Combinations 17 - 18

17.4 CURRENT DESIGN PRACTICE..... 17 - 19

 17.4.1 New Bridges 17 - 19

 17.4.2 Replacement Bridges 17 - 19

 17.4.3 Simple Span Bridges 17 - 19

 17.4.4 Skew Bridges..... 17 - 20

17.5 CASE STUDY NO. 1 - TRUSS BRIDGE REPLACEMENT 17 - 20

 17.5.1 Existing Bridge..... 17 - 20

 17.5.2 New Piles 17 - 20

 17.5.3 New Intermediate Piers..... 17 - 21

 17.5.4 New Superstructure for Approach Spans 17 - 21

 17.5.5 Truss Removal..... 17 - 21

 17.5.6 New Superstructure for Truss Spans..... 17 - 22

17.6 CASE STUDY NO. 2 - TIMBER TRESTLE REPLACEMENT 17 - 23

 17.6.1 Existing Bridge..... 17 - 23

 17.6.2 New Superstructure..... 17 - 24

 17.6.3 Substructure Construction 17 - 24

RAILROAD BRIDGES

Table Of Contents

17.6.4 Superstructure Construction..... 17 - 25

17.7 CASE STUDY NO. 3 - THROUGH PLATE GIRDER REPLACEMENT..... 17 - 25

 17.7.1 Existing Bridge..... 17 - 25

 17.7.2 Substructure Construction 17 - 25

 17.7.3 Superstructure Construction..... 17 - 27

17.8 DESIGN EXAMPLE - DOUBLE-CELL BOX BEAM, SINGLE SPAN, NONCOMPOSITE, DESIGNED IN ACCORDANCE WITH AREMA SPECIFICATIONS..... 17 - 27

 17.8.1 Background 17 - 27

 17.8.2 Introduction 17 - 27

 17.8.2.1 Geometrics..... 17 - 29

 17.8.2.2 Sign Convention..... 17 - 29

 17.8.3 Material Properties 17 - 30

 17.8.3.1 Concrete 17 - 30

 17.8.3.2 Pretensioning Strands 17 - 30

 17.8.3.3 Reinforcing Bars..... 17 - 30

 17.8.4 Cross-Section Properties for a Single Beam..... 17 - 31

 17.8.5 Shear Forces and Bending Moments..... 17 - 31

 17.8.5.1 Shear Forces and Bending Moments Due to Dead Load..... 17 - 31

 17.8.5.2 Shear Forces and Bending Moments Due to Superimposed Dead Load 17 - 32

 17.8.5.3 Shear Forces and Bending Moments Due to Live Load..... 17 - 32

 17.8.5.4 Load Combinations 17 - 33

 17.8.7 Estimate Required Prestressing Force..... 17 - 33

 17.8.8 Determine Prestress Losses..... 17 - 34

 17.8.8.1 Prestress Losses at Service Loads 17 - 34

 17.8.8.1.1 Elastic Shortening of Concrete..... 17 - 34

 17.8.8.1.2 Creep of Concrete 17 - 35

 17.8.8.1.3 Shrinkage of Concrete 17 - 35

 17.8.8.1.4 Relaxation of Prestressing Steel..... 17 - 35

 17.8.8.1.5 Total Losses at Service Loads..... 17 - 35

 17.8.8.2 Prestress Losses at Transfer..... 17 - 35

 17.8.9 Concrete Stresses..... 17 - 35

 17.8.9.1 Stresses at Transfer at Midspan 17 - 35

 17.8.9.2 Stresses at Transfer at End..... 17 - 36

 17.8.9.3 Stresses at Service Load at Midspan 17 - 36

 17.8.9.4 Stresses at Service Load at End 17 - 36

 17.8.10 Flexural Strength..... 17 - 37

 17.8.10.1 Stress in Strands at Flexural Strength 17 - 37

 17.8.10.2 Limits for Reinforcement 17 - 37

 17.8.10.3 Design Moment Strength 17 - 38

RAILROAD BRIDGES

Table Of Contents

17.8.10.4 Minimum Reinforcement.....	17 - 38
17.8.10.5 Final Strand Pattern.....	17 - 38
17.8.11 Shear Design.....	17 - 39
17.8.11.1 Required Shear Strength.....	17 - 39
17.8.11.2 Shear Strength Provided by Concrete.....	17 - 39
17.8.11.2.1 Simplified Approach	17 - 39
17.8.11.2.2 Calculate V_{ci}	17 - 40
17.8.11.2.3 Calculate V_{cw}	17 - 40
17.8.11.2.4 Calculate V_c	17 - 41
17.8.11.3 Calculate V_s and Shear Reinforcement	17 - 41
17.8.11.3.1 Calculate V_s	17 - 41
17.8.11.3.2 Determine Stirrup Spacing	17 - 41
17.8.11.3.3 Check V_s Limit.....	17 - 41
17.8.11.3.4 Check Stirrup Spacing Limits.....	17 - 42
17.8.12 Deflections.....	17 - 42
17.8.12.1 Camber Due to Prestressing at Transfer.....	17 - 42
17.8.12.2 Deflection Due to Beam Self-Weight at Transfer	17 - 42
17.8.12.3 Deflection Due to Superimposed Dead Load	17 - 42
17.8.12.4 Long-Term Deflection	17 - 42
17.8.12.5 Deflection Due to Live Load.....	17 - 43
17.9 REFERENCES	17 - 43

This page intentionally left blank

NOTATION

A	= area of cross-section of precast beam
A_{ps}	= area of one pretensioning strand or post-tensioning bar
A^*_s	= total area of strands in the tensile zone
A_v	= area of shear reinforcement
a	= depth of equivalent rectangular stress block
B	= buoyancy
b	= width of compression face of member
b_w	= width of web of a flanged member
CF	= centrifugal force
CR_c	= loss of prestress due to creep of concrete
CR_s	= loss of prestress due to relaxation of pretensioning steel
D	= dead load
DF	= live load distribution factor
d	= distance from extreme compressive fiber to centroid of the prestressing force
E	= earth pressure
E_c	= modulus of elasticity of concrete at 28 days
E_{ci}	= modulus of elasticity of concrete at transfer
EQ	= earthquake (seismic)
ES	= loss of prestress due to elastic shortening
E_s	= modulus of elasticity of pretensioning steel
E_s	= modulus of elasticity of nonpretensioned reinforcement
e_c	= eccentricity of strands at midspan
F	= longitudinal force due to friction or shear resistance at expansion bearings
f_b	= concrete stress at the bottom fiber of the beam
f'_c	= specified concrete strength at 28 days
f_{cds}	= concrete stress at the centroid of the pretensioning steel due to all dead loads except the dead load present at the time the pretensioning force is applied
f'_{ci}	= specified concrete strength at transfer
f_{cir}	= average stress in the concrete at the centroid of the pretensioning steel at transfer
f_d	= stress due to unfactored dead load at extreme fiber of section where tensile stress is caused by externally applied loads
f_{pc}	= compressive stress in concrete (after allowance for all prestress losses) at the centroid of cross section resisting externally applied loads
f_{pe}	= compressive stress in concrete due to effective pretensioning forces only (after allowance for all pretension losses) at the extreme fiber of section where tensile stress is caused by externally applied loads
f^*_{su}	= average stress in the pretensioning steel at ultimate load
f_s	= ultimate strength of pretensioning steel
f_{se}	= effective stress in pretensioning steel after losses
f_t	= concrete stress at the top fiber of the precast beam
f_y	= specified yield strength of nonprestressed reinforcement
f^*_y	= specified yield stress of pretensioning steel
h	= overall depth of precast beam
I	= moment of inertia about the centroid of the noncomposite precast beam

I	= the percentage of the live load for impact
ICE	= ice pressure
L	= span length
L	= live load
LF	= longitudinal force from live load
M_{cr}	= moment causing flexural cracking at section due to externally applied loads
M^*_{cr}	= minimum steel cracking moment
M_g	= unfactored bending moment due to precast beam self-weight
M_{LL+I}	= unfactored bending moment due to live load + impact
M_{max}	= maximum factored moment at the section due to externally applied loads
M_n	= nominal moment strength of a section
M_{SDL}	= unfactored bending moment due to superimposed dead load
M_u	= factored bending moment at the section
M_x	= bending moment at a distance x from the support
OF	= other forces (rib shortening, shrinkage, temperature, and/or settlement of supports)
P_{se}	= effective pretensioning force after allowing for all losses
P_{si}	= total pretensioning force immediately after transfer
R	= relative humidity
S_b	= noncomposite section modulus of the extreme bottom fiber of the precast beam
SF	= stream flow pressure
SH	= loss of prestress due to concrete shrinkage
S_t	= noncomposite section modulus of the extreme top fiber of the precast beam
s	= spacing of the shear reinforcement in direction parallel to the longitudinal reinforcement
V_c	= nominal shear strength provided by concrete
V_{ci}	= nominal shear strength provided by concrete when diagonal cracking results from combined shear and moment
V_{cw}	= nominal shear strength provided by concrete when diagonal cracking results from excessive principal tensile stress in web
V_D	= unfactored shear force at section due to total service dead load
V_g	= unfactored shear force due to precast beam self-weight
V_i	= factored shear force at section due to externally applied loads occurring simultaneously with M_{max}
V_{LL+I}	= unfactored shear force at section due to live load plus impact
V_p	= component of pretensioning force in the direction of the applied shear
V_s	= nominal shear strength provided by shear reinforcement
V_{SDL}	= unfactored shear force due to superimposed dead loads
V_u	= factored shear force at the section
V_x	= shear force at a distance x from the support
W	= wind load on structure
WL	= wind load on live load
w	= weight per foot
w_c	= unit weight of concrete
w_{equ}	= equivalent uniform load
x	= distance from the support
y_b	= distance from centroid to extreme bottom fiber of the noncomposite precast beam
y_{bs}	= distance from the center of gravity of strands to the bottom fiber of the beam

y_t	=	distance from centroid to extreme top fiber of the noncomposite precast beam
β_1	=	factor for the equivalent rectangular stress block
Δ	=	deflection
γ^*	=	factor for type of pretensioning steel
Φ	=	strength reduction factor
ρ^*	=	ratio of pretensioning reinforcement

This page intentionally left blank

RAILROAD BRIDGES

17.0 INTRODUCTION

Precast concrete is playing an increasingly important role in railroad bridge structures. The economy, durability, and speed of construction make precast concrete the material of choice for new and replacement railroad bridges. The focus of this chapter is on the specific requirements and guidelines for railroad bridges. Typical products and details, construction considerations, and identification of applicable AREMA (American Railway Engineering and Maintenance-of-Way Association, formerly AREA) provisions are also discussed. Two case studies and a railroad superstructure design example are presented.

17.1 TYPICAL PRODUCTS AND DETAILS

A wide variety of precast products is used for railroad bridge construction. From the ground up, these include concrete piles, pile caps, abutments, wingwalls, and superstructure beams. Over the years, many railroads have developed standards for precast concrete, including concrete mixes, member design, member detailing, and quality control.

17.1.1 Piles

Several railroads use precast, prestressed concrete piles, but their use may be limited by the capacity of track-mounted pile drivers. Concrete piles are preferred for use in marine environments. In highly corrosive locations, precast concrete pile extensions are spliced to steel pipe piles. This permits the embedment of the steel into the anaerobic soil zone and provides a more durable prestressed concrete pile in the more corrosive environment.

17.1.2 Pile Caps and Abutments

Precast concrete pile caps are widely used throughout the country. Typically, these are fabricated with an embedded plate running along the bottom of the cap. This allows welding of steel piles to the bottom of the cap. Concrete pile caps are sometimes used to support steel or timber beams, as well as concrete beams. Some railroads use precast concrete caps with precast concrete piles. The caps are cast with a socket for the pile to fit into. Grouting is used to tie the components together after installation. Prestressed concrete pile caps are often used on top of timber piles. The prestress concrete caps are fabricated with a number of sleeves for adequate connection locations between the concrete cap and timber pile.

Bridge abutments can be prefabricated and often include a backwall as part of the abutment pile cap. The bases of these abutments are similar to the pile caps and serve the same function of supporting the superstructure. Abutment backwalls and wingwalls can be precast in sections and bolted or welded together in the field.

17.1.3 Superstructures

Railroads use a wide variety of superstructure elements. Spans typically range from 12 ft to over 80 ft. Since many precast concrete spans are installed to replace timber trestles, standard span lengths for a given railroad are frequently multiples of their standard timber stringer span lengths (typically 14 to 16 ft). For spans of 12 to 20 ft, precast slab beams are frequently used. For spans in the 20- to 30-ft range, precast, prestressed concrete box beams or solid concrete slabs are the most common, although tee-beams and I-beams are occasionally used. For spans over 30 ft, box beams are dominant. Spans up to 50 ft typically use two box beams per track. Generally, these are double celled with through-voids. Through-voids allow fabricators to use removable and reusable void forms in casting the beams. This helps reduce costs. Spans over 50 ft generally use four single-void box beams per track. The shift from two beams per track on shorter spans to four on longer spans is dictated by the lifting restrictions associated with the heavier weight of the longer beams. Shear keys and transverse post-tensioned steel tie rods are frequently used to tie the box beams together with diaphragms provided at the location of the tie rods. For spans greater than 70 to 80 ft, beams with composite cast-in-place concrete decks are frequently used.

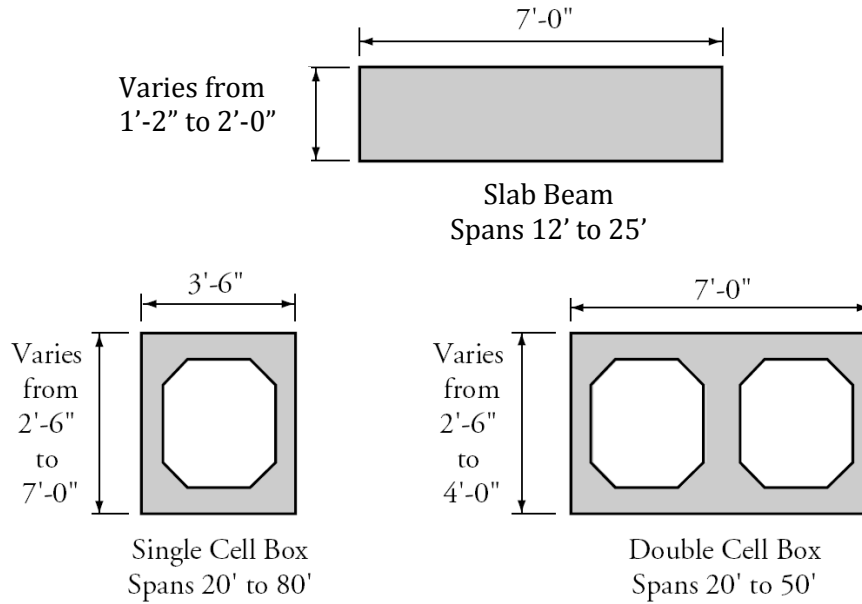
RAILROAD BRIDGES

17.1.3.1 Slab Beams and Box Beams/17.1.3.2 Other Products

17.1.3.1 Slab Beams and Box Beams

A variety of shapes with depth and width variations are available throughout the country. Designers should contact the manufacturers and the specific railroad to determine the properties and dimensions of products available for a proposed project. Typical superstructure shapes and span ranges applicable to railroad bridges are shown in **Figure 17.1.3.1-1**.

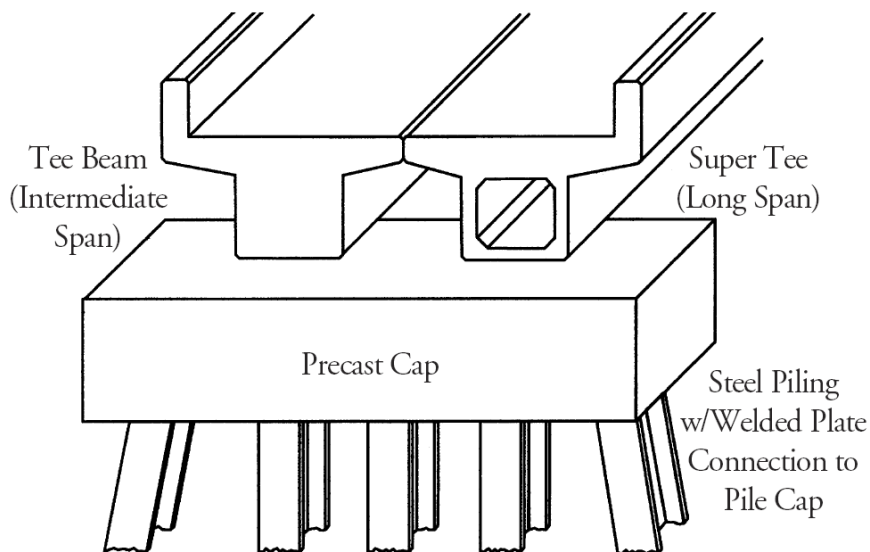
*Figure 17.1.3.1-1
Typical Precast Concrete Superstructure Shapes*



17.1.3.2 Other Products

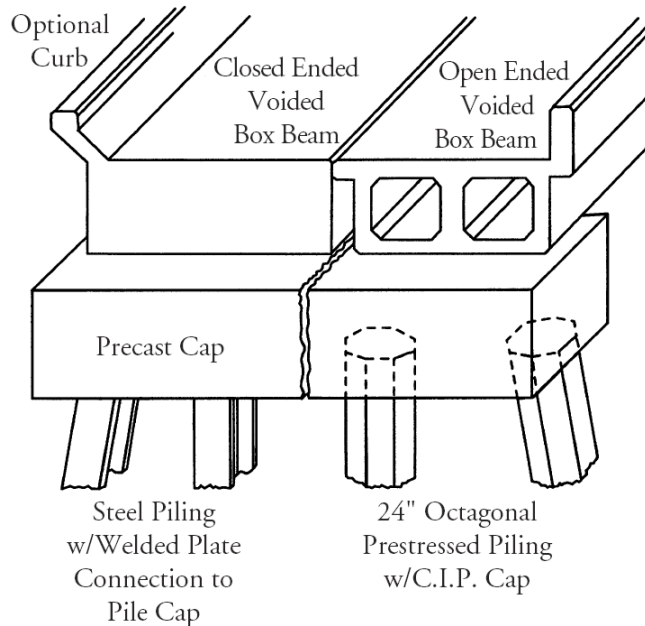
There are a few other precast products used for different span ranges. Brief descriptions of these products are given in **Figures 17.1.3.2-1** through **17.1.3.2-4**.

*Figure 17.1.3.2-1
Tee Beam
(Intermediate and Long Spans)*



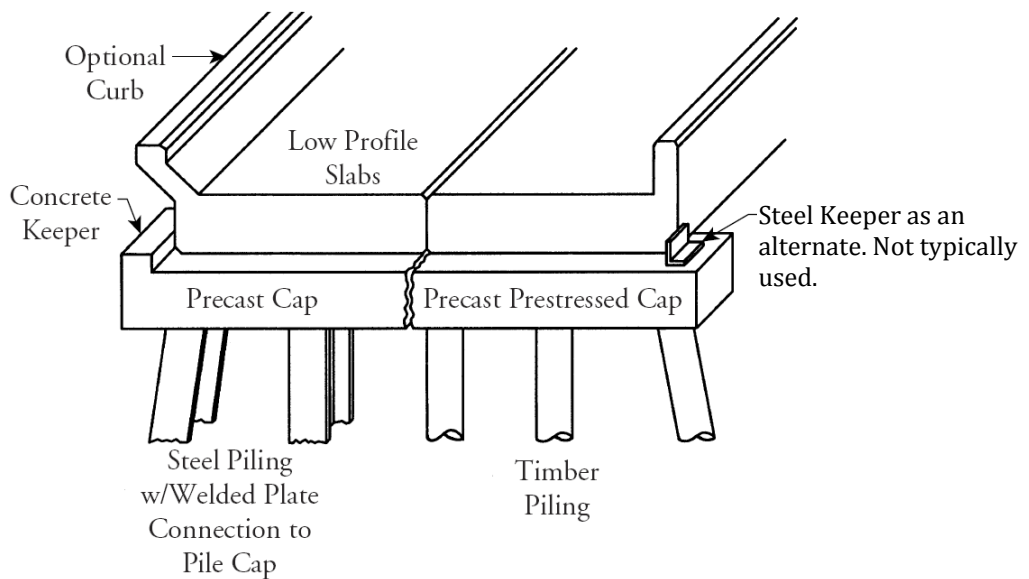
The solid single tee beam is used for spans of 20 to 34 ft, and the voided super tee for spans up to 55 ft in length. Both beams are set on a precast concrete cap that has a welded plate connection to the piles as needed.

Figure 17.1.3.2-2
Box Beam
(Intermediate Spans)



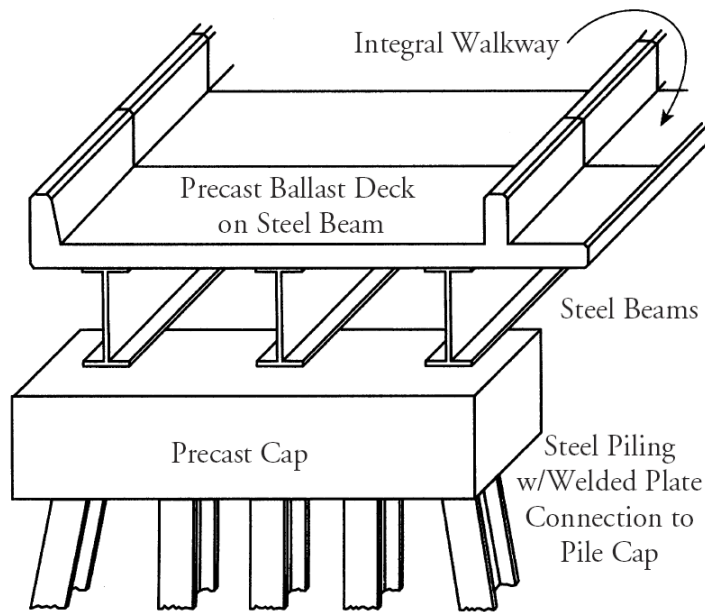
Voided box beams are used on 20- to 50-ft long spans, with optional diaphragms and curbs. Boxes may be set on precast or cast-in-place concrete caps with piling.

Figure 17.1.3.2-3
Low Profile Slab
(Short Spans)



Short span bridges up to 25 ft in length with limited headroom require the use of low profile slabs. These slabs may be set on precast caps that are either prestressed or nonprestressed.

Figure 17.1.3.2-4
Ballast Deck (With Steel Beams)



Precast, prestressed concrete deck slabs are used in a variety of lengths and widths; with new or existing steel beams. These slabs can be cast with single and double ballast curbs and with integral walkways to further speed up construction of the bridge. Some railroads prefer to cast-in-place the ballast curb and walkways.

17.1.3.3 Connection Details

Some railroads use structural steel tees or plates to cover the longitudinal joints between adjacent beams as shown in **Figure 17.1.3.3-1**. Transverse post-tensioned steel tie rods, as shown in **Figure 17.1.3.3-2**, are generally provided in multiple single-cell box beam superstructures to help the group act as a unit. Concrete or structural steel “keepers” or retainers are usually provided at the ends of the caps to limit lateral movement, as shown in **Figure 17.1.3.3-3**. Most railroads use steel tees or cover plates to cover the transverse joint between beam spans. Designers should contact the specific railroad to determine their standards and preferred connection details.

Figure 17.1.3.3-1
Steel Tee between Box Beams

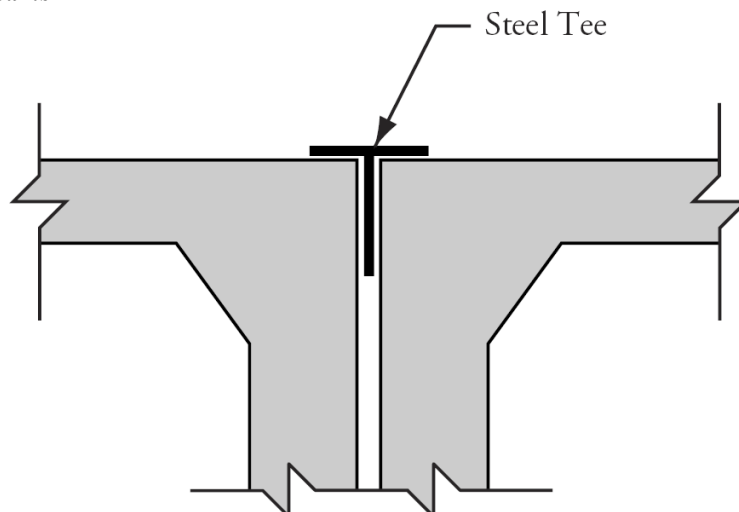


Figure 17.1.3.3-2
Post-Tensioned Steel Tie Rod

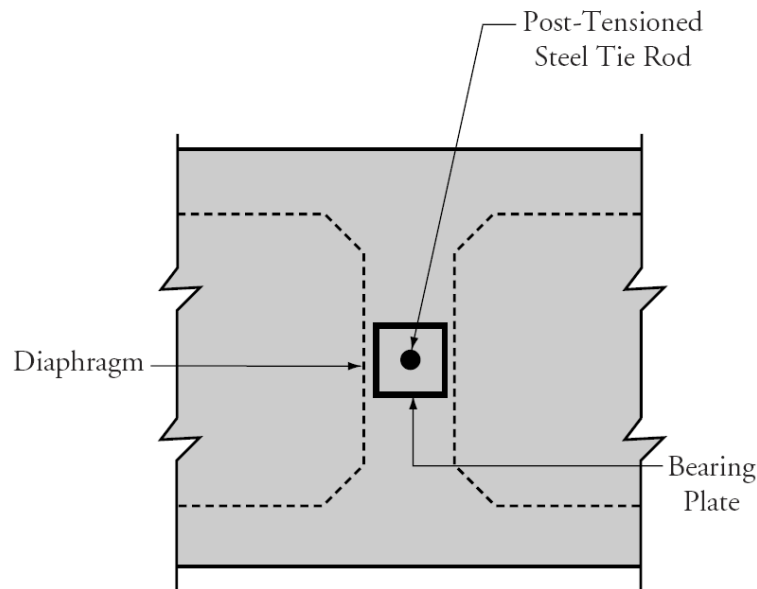
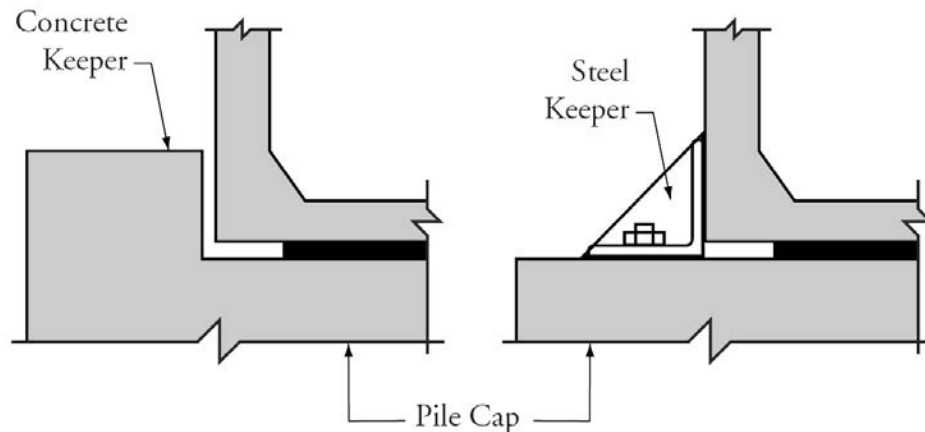


Figure 17.1.3.3-3
Concrete and Steel Keeper Details



For the steel keeper shown in **Figure 17.1.3.3-3**, a bolted connection requires greater precision to locate these embedded inserts and additional time by the designer to detail the steel keeper with a slotted connection. Often the steel keeper is field fabricated from the H-pile cut offs and is welded to an embedded plate located in the top of the abutment and pile cap.

17.2 CONSTRUCTION CONSIDERATIONS

17.2.1 Advantages

Precast concrete offers many advantages in the construction of railroad bridges. These include:

- Speed of construction—Precast concrete structures can usually be constructed faster than bridges comprised of alternative materials.
- Fabrication time—In addition to saving construction time, the lead time for fabricating elements is shorter than for competing materials such as steel.

RAILROAD BRIDGES**17.2.1 Advantages/17.2.5 Substructures**

- **Durability**—Compared with many older structures that require frequent inspections and maintenance, railroad engineers find the low maintenance requirements of precast concrete attractive. Use of concrete with low permeability and strict quality control in the casting plant help assure durable bridge components.
- **Quality**—The higher quality control of workmanship and materials available in casting plants compared to cast-in-place construction is another plus. Railroads can work with precast suppliers to ensure that members are cast to their satisfaction.
- **Site constraints**—The remote locations of many railroad bridges make the “precast” aspect of precast construction very useful. When the nearest ready-mix plant is many miles away from the site, cast-in-place construction within a railroad’s time constraints is virtually impossible.
- **Emergency response**—Precast concrete bridge elements provide components for rapid repair of bridges as a result of damage caused by derailments or timber trestle fires. Several railroads keep entire precast bridges stockpiled for rapid emergency replacement. Concrete bridges are less vulnerable to damage from fire compared to steel or timber bridges.

17.2.2 Standard Designs

Most railroads have standard precast concrete trestle bridge designs that incorporate repetition of modular precast units. These standard designs are used for replacement of existing bridges, as well as construction of new bridges. Railroads and contractors familiar with railroad bridge construction have developed low-cost methods of trestle bridge construction. These methods minimize the time that railroad operations must be suspended. In addition, precast concrete bridge components are often shipped by rail, which, in many cases, is the only way to deliver components to remote locations.

17.2.3 Train Operations

For construction of bridges, railroads normally only permit train operations to be suspended from two to eight hours at any one time depending on the day and time. If an alternate route is available, 12 to 72 hours are the normal acceptable range. Additional costs of rerouting include obtaining operating rights on another railroad and using the other railroad’s personnel. Use of either option is dependent upon the type and density of train traffic and the availability of alternate routes.

17.2.4 Construction Methods

The various methods used to construct railroad bridges to support existing trackage while minimizing disruptions to train operations include the following:

- Rolling spans on runways
- Floating spans on barges
- Pick and set
- Temporary rail line change
- Permanent rail line change
- Trestle bridge construction

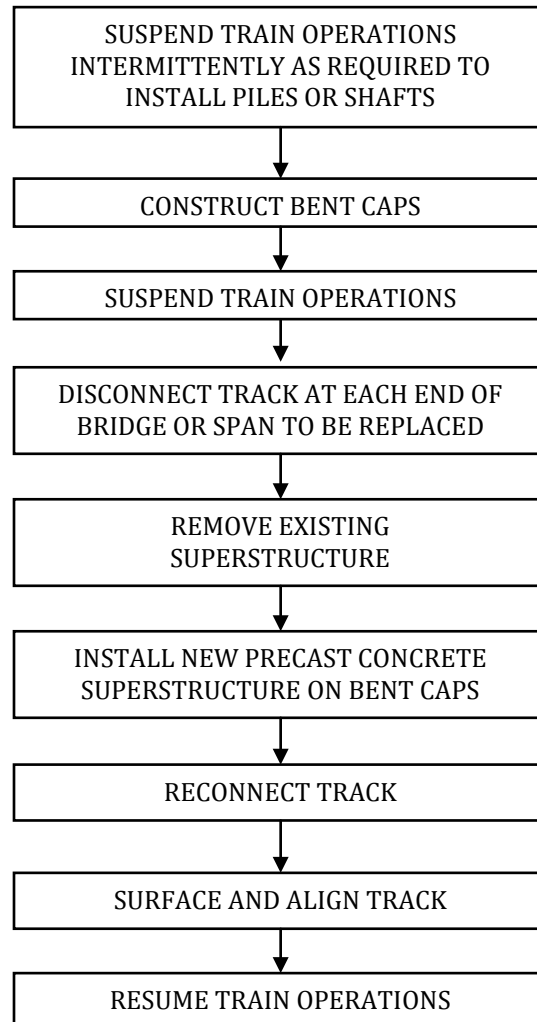
These methods are utilized because train operations cannot be suspended for the amount of time that would be required to construct the new bridge piece by piece in its permanent location.

17.2.5 Substructures

In many bridges, the existing substructure is reused and, if necessary, modified for replacement of the superstructure. Sometimes, the bridge may require new substructure elements. In both cases, the substructure work is performed beneath the existing track and superstructure so that the track is out of service for only very limited periods while driving piles or placing temporary supports. For replacement of existing bridges utilizing this method, ballast removal, as well as relocating the decks and beams of the existing bridge, may be required to allow pile driving for the new bridge. It is often necessary to reduce the speed of traffic over existing bridges during construction due to reduced load carrying capacity resulting from relocating the decks and beams.

Precast concrete beams are usually installed using pick and set methods. This method requires access to the bridge construction site for cranes that have adequate capacity to lift the beams. A typical bridge replacement procedure is illustrated in **Figure 17.2.5-1**.

Figure 17.2.5-1
*Typical Bridge Replacement
Construction Sequence*



17.3 THE AMERICAN RAILWAY ENGINEERING AND MAINTENANCE-OF-WAY ASSOCIATION LOAD PROVISIONS

This section briefly discusses the types of loads on railroad bridges. The emphasis is on those loads that are different from highway bridge loads covered in Chapter 7. Provisions of the American Railway Engineering and Maintenance-of-Way Association (AREMA) *Manual for Railway Engineering* (AREMA, 2010) are introduced relative to design loads and load combinations. In addition, applicable portions of the manual are referenced.

17.3.1 AREMA Manual

The *AREMA Manual* provides the recommended practice for railroads and others concerned with the engineering, design and construction of railroad fixed properties, allied services, and facilities. Prior to starting the design of a project, design engineers should discuss specific loadings, forces, standards, and procedures with the appropriate railroad.

RAILROAD BRIDGES

17.3.2 AREMA Loads/17.3.2.1 Live Loads

17.3.2 AREMA Loads

The *AREMA Manual* Chapter 8, Concrete Structures and Foundations, specifically addresses reinforced concrete and prestressed concrete structures. Article 2.2.3 covers the design loads and forces to be considered in the design of railroad structures supporting tracks, including bridges. Briefly, design loads include:

- | | |
|--|---|
| D = Dead Load | F = Longitudinal Force due to Friction or Shear Resistance at Expansion Bearings |
| L = Live Load | EQ = Earthquake (Seismic) |
| I = Impact | SF = Stream Flow Pressure |
| CF = Centrifugal Force | ICE = Ice Pressure |
| E = Earth Pressure | OF = Other Forces (Rib Shortening, Shrinkage, Temperature, and/or Settlement of Supports) |
| B = Buoyancy | |
| W = Wind Load on Structure | |
| WL = Wind Load on Live Load | |
| LF = Longitudinal Force from Live Load | |

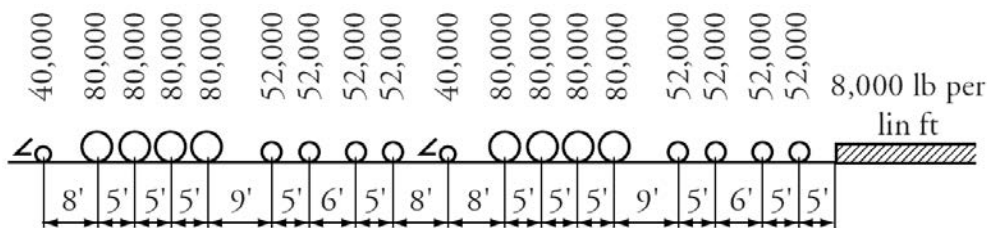
Design engineers familiar with highway bridge design will recognize the loads and forces listed above. The magnitude of the loads and forces are explained in detail in the *AREMA Manual*. Loads that are different from highway bridges are described in the following sections.

17.3.2.1 Live Load

The following description of live load is based on the *AREMA Manual*:

- (1) The recommended live load in pounds per axle and uniform trailing load for each track is the Cooper E 80 load, which is shown in **Figure 17.3.2.1-1**. **Table 17.3.2.1-1** provides a table for live load bending moments, shear forces and reactions for simple span bridges. Values for span lengths not shown are generally computed by interpolation.
- (2) The Engineer (the Railroad’s Chief Engineer) shall specify the Cooper live load to be used, and such load shall be proportional to the recommended load, with the same axle spacing.
- (3) For bridges on curves, provisions shall be made for the increased proportion carried by any truss, beam, or stringer due to the eccentricity of the load and centrifugal force.

Figure 17.3.2.1-1
Cooper E 80 Load



- (4) For members receiving load from more than one track, the design live load on the tracks shall be as follows:
 - For two tracks, full live load on two tracks
 - For three tracks, full live load on two tracks and one-half on the other track
 - For four tracks, full live load on two tracks, one-half on one track, and one quarter on the remaining track
 - For more than four tracks, as specified by the Engineer

The selection of the tracks for these loads shall be that which produces the most critical design condition in the member being designed.

RAILROAD BRIDGES

17.3.2.1 Live Loads/17.3.2.2 Impact Load

Table 17.3.2.1-1

**Maximum Bending Moments, Shear Forces, and Pier Reactions for Cooper E 80 Live Load
(Based on AREMA Manual Table 15-1-15)**

All values are for one rail (one-half track load). Maximum pier reactions are for equal span lengths.

Span Length ft	Maximum Bending Moment ft-kips	Maximum Bending Moment at Quarter Point ft-kips	Maximum Shear Forces kips			Maximum Pier Reaction kips
			End	Quarter Point	Midspan	
5	50.00	37.50	40.00	30.00	20.00	40.00
6	60.00	45.00	46.67	30.00	20.00	53.33
7	70.00	55.00	51.43	31.43	20.00	62.86
8	80.00	70.00	55.00	35.00	20.00	70.00
9	93.89	85.00	57.58	37.78	20.00	75.76
10	112.50	100.00	60.00	40.00	20.00	80.00
11	131.36	115.00	65.45	41.82	21.82	87.28
12	160.00	130.00	70.00	43.33	23.33	93.33
13	190.00	145.00	73.84	44.61	24.61	98.46
14	220.00	165.00	77.14	47.14	25.71	104.29
16	280.00	210.00	85.00	52.50	27.50	113.74
18	340.00	255.00	93.33	56.67	28.89	121.33
20	412.50	300.00	100.00	60.00	28.70	131.10
24	570.42	420.00	110.83	70.00	31.75	147.92
28	730.98	555.00	120.86	77.14	34.29	164.58
32	910.85	692.50	131.44	83.12	37.50	181.94
36	1,097.30	851.50	141.12	88.90	41.10	199.06
40	1,311.30	1,010.50	150.80	93.55	44.00	215.90
45	1,601.20	1,233.60	163.38	100.27	45.90	237.25
50	1,901.80	1,473.00	174.40	106.94	49.73	257.52
55	2,233.10	1,732.30	185.31	113.58	52.74	280.67
60	2,597.80	2,010.00	196.00	120.21	55.69	306.42
70	3,415.00	2,608.20	221.04	131.89	61.45	354.08
80	4,318.90	3,298.00	248.40	143.41	67.41	397.70
90	5,339.10	4,158.00	274.46	157.47	73.48	437.15
100	6,446.30	5,060.50	300.00	173.12	78.72	474.24

17.3.2.2 Impact Load

For both reinforced and prestressed concrete, the impact load is a percentage of the live load based on span length in ft:

$$L \leq 14 \text{ ft}, \quad I = 60 \quad \text{[AREMA Art.2.2.3d]}$$

$$14 < L \leq 127 \text{ ft}, \quad I = 225/\sqrt{L}$$

$$L > 127 \text{ ft}, \quad I = 20$$

Previously, different impact formulas were used for reinforced concrete and prestressed concrete. This discrepancy was resolved, and the resulting impact defined above is generally higher than that previously recommended for prestressed concrete, particularly for shorter spans.

RAILROAD BRIDGES

17.3.2.3 Longitudinal Force/17.3.2.5 Load Combinations

17.3.2.3 Longitudinal Force

The longitudinal force applied to the bridge is taken as the larger of:

[AREMA Art.2.2.3j]

Braking force in kips = $45 + 1.2L$, acting 8 ft above the top of the rail

Traction force in kips = $25\sqrt{L}$, acting 3 ft above the top of the rail

where L is the length in feet of the portion of the bridge under consideration. This longitudinal force is distributed to the various substructure components, taking into account their relative stiffness. The resistance of the backfill behind the abutments is utilized where applicable. The means available to transfer this longitudinal force, such as through the rail or bearings, is also to be considered. In addition, the longitudinal deflection of the superstructure due to this force must not exceed 1 in. for E 80 loading.

17.3.2.4 Other Loads

All other loads and forces are defined similarly to highway bridges although the magnitudes are different. The design engineer should refer to the *AREMA Manual* for additional information.

17.3.2.5 Load Combinations

The various combinations of loads and forces to which a structure may be subjected are grouped in a similar manner as highway bridges. Each component of the structure or foundation upon which it rests, is proportioned for the group of loads that produces the most critical design condition. The group loading combinations for service load design and load factor design are as shown in **Table 17.3.2.5-1** and **Table 17.3.2.5-2**, respectively, and are reproduced from AREMA Article 2.2.4.

Table 17.3.2.5-1
Group Loading Combinations - Service Load Design

Group	Item	Allowable Percentage of Basic Unit Stress
I	D + L + I + CF + E + B + SF	100
II	D + E + B + SF + W	125
III	Group I + 0.5W + WL + LF + F	125
IV	Group I + OF	125
V	Group II + OF	140
VI	Group III + OF	140
VII	Group I + ICE	140
VIII	Group II + ICE	150

Table 17.3.2.5-2
Group Loading Combinations - Load Factor Design

Group	Item
I	1.4 (D + 5/3(L + I) + CF + E + B + SF)
IA	1.8 (D + L + I + CF + E + B + SF)
II	1.4 (D + E + B + SF + W)
III	1.4 (D + L + I + CF + E + B + SF + 0.5W + WL + LF + F)
IV	1.4 (D + L + I + CF + E + B + SF + OF)
V	Group II + 1.4 (OF)
VI	Group III + 1.4 (OF)
VII	1.0 (D + E + B + EQ)
VIII	1.4 (D + L + I + E + B + SF + ICE)
IX	1.2 (D + E + B + SF + W + ICE)

RAILROAD BRIDGES**17.4 Current Design Practice/17.4.3 Simple Span Bridges****17.4 CURRENT DESIGN PRACTICE**

As with all engineering design practices, railroad industry practice continues to change as experience and research is incorporated into the *AREMA Manual* and individual railroad company standards and procedures. This section will discuss current railroad industry practice relative to overall railroad bridge design philosophy, skew limitations and superstructure continuity. Designers should discuss philosophies, standards, and procedures with the specific railroad as applicable to the project.

17.4.1 New Bridges

New railroad bridges are constructed to support railroad tracks over existing waterways, roadways, and other railroads. In addition, new railroad bridges are built to replace existing bridges due to the following:

- Unsatisfactory capacity to support current or future loadings
- Unsafe condition resulting from deterioration and/or poor maintenance
- Damage as a result of an accident or natural disaster
- Inadequate waterway opening
- Highway or railroad grade separation projects
- Navigation, drainage and flood control projects

17.4.2 Replacement Bridges

The large majority of railroad bridge projects usually involve existing trackage. Consequently, one of the most important considerations for the railroad bridge designer is to design the bridge such that construction will have minimal disruption to train operations. This affects design details, construction methods, and project costs. Much of today's rail traffic is under contract with the customer and the contract often includes a guarantee of service between origin and destination. Penalties and possible loss of a contract can result if unreasonable delays in the agreed upon schedule are experienced. Taking a track out of service or reducing the speed of rail traffic for an extended period of time for bridge construction can have a detrimental economic effect on the railroad. The project must be properly planned and coordinated with the operating and marketing departments of the railroad during the design and construction phases.

The use of standardized precast components speeds both the design and construction of bridges. Replacement spans can be specified by length alone, and railroad bridge workers are familiar with the sections and construction procedures. Since the vast majority of precast concrete bridges have all the superstructure below track level, vertical and horizontal clearance is not limited by these structures. This allows wide cargo or double stack containers to be shipped without clearance concerns and reduces the threat of bridge damage caused by shifted loads.

17.4.3 Simple Span Bridges

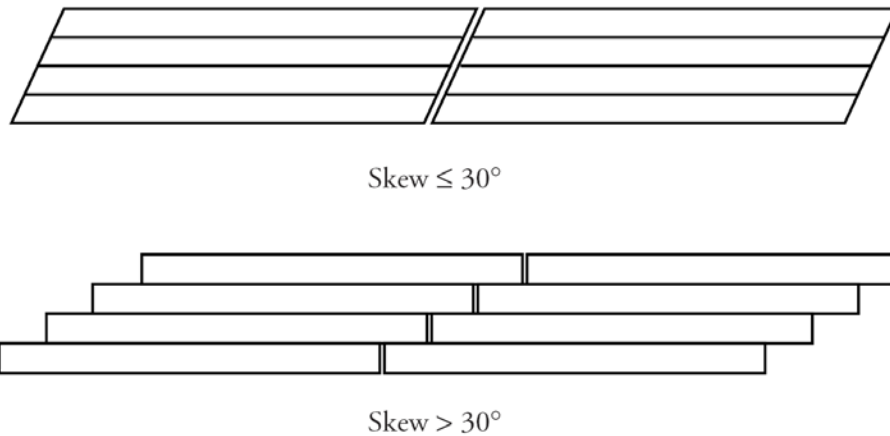
Many railroads prefer simple span bridges to continuous structures, finding them easier to install and maintain. Since they are structurally determinate, simple spans are better able to handle problems such as support settlement and thermal effects than some continuous bridges. Precast concrete elements are particularly suited to simple span construction. Additional reasons many railroads prefer simply supported bridges to continuous span bridges include the following:

- If repair or replacement of superstructure elements is necessary, less interruption to train traffic is incurred with a simple span bridge than with a continuous span bridge. Installation of simple spans can be accomplished more quickly than continuous spans.
- If a bridge experiences substructure problems such as settlement, a continuous span bridge may require immediate and more extensive work, thereby resulting in greater interruptions to train traffic.
- Simple span bridges have a proven history of performing well.

17.4.4 Skew Bridges

It is desirable to limit the end skew of railroad bridge precast beams to less than 30 degrees for constructability and placement of reinforcement in the beam (See AREMA Chapter 8 Section 2.1.7). When the bridge skew relative to the substructure exceeds 30 degrees, staggered precast elements as shown in **Figure 17.4.4-1** should be considered.

Figure 17.4.4-1
Layouts for Skewed Bridges



17.4.5 Increased Live Loading

The current Cooper E 80 loading is historically derived from two steam locomotives followed by a uniform load. This wheel spacing differs from today's diesel engine locomotives, and the load carrying capacity of rail cars has increased substantially over the years. An alternate live loading was added to *AREMA Manual* Chapter 15, Steel Structures, in 1995. This alternate loading, which uses four closely spaced axles of 100 kips each, models a typical four-axle car and provides an axle load higher than the E 80 load. This loading was included to address problems associated with fatigue on shorter span lengths. No alternate loading requirement is included for the design of structures whose primary load-carrying members are concrete.

It has been suggested that railway design criteria are overly conservative. However, it has been documented that current axle loads can be as much as 25% higher than E 80 and alternate loading requirements, such as the case of a short heavy axle car with unbalanced load effects (Unsworth 2006 and Sweeney 2010). Although loading revisions have been proposed in order to more closely model the axles of modern freight traffic, it has generally been preferred to maintain the Cooper design load but proportionately increase its magnitude. Railroad companies, such as the Canadian National Railway, have more recently required an increase in loading to E 90 or E 100.

17.5 CASE STUDY NO. 1 - TRUSS BRIDGE REPLACEMENT

17.5.1 Existing Bridge

This case study describes a Southern Pacific railroad truss bridge replacement (Marianos, 1991). This project illustrates the use of precast concrete elements to replace a structure without serious interruption to rail traffic. The existing structure consisted of a 90-ft-long timber trestle approach, two 154-ft-long through-truss spans, and a 30-ft-long plate-girder approach span.

The truss spans were nearly 90 years old and were at the end of their useful service lives due to joint wear. Since the truss spans required replacement, the railroad decided to replace the entire bridge with precast concrete.

17.5.2 New Piles

Using a track-mounted pile driver, steel H-piles were driven through the track on the timber trestle. The pile bents were spaced to give 30-ft replacement span lengths in the trestle area. After the piles were cut off at the required elevation, precast concrete bent caps were placed and the piles welded to steel plates embedded in the bottom of the caps.

RAILROAD BRIDGES**17.5.3 New Intermediate Piers/17.5.5 Truss Removal****17.5.3 New Intermediate Piers**

Since the truss spans crossed a creek subject to high flood flows, it was essential to minimize obstruction of the waterway. For this reason, new intermediate piers with four 79-ft-long precast, prestressed box beams replaced the two 154-ft-long truss spans. The 79-ft-long beams were beyond the span range of the railroad standards and required a new design.

Railroad crews built intermediate piers at midspan of each truss by driving piles through the existing truss floor systems, and the 79-ft-long box beams were ordered and fabricated.

17.5.4 New Superstructure for Approach Spans

When the substructure was completed, superstructure replacement began. The 90-ft-long timber trestle was replaced by 30-ft-long spans of precast, prestressed box beams, as shown in **Figure 17.5.4-1**. Two box beams placed side by side were used for each span. Each box beam has two through-voids and an integral ballast retaining sidewall and walkway cast on the outside edge. A shear key between the box beams helped ensure load distribution between the two beams. The box beams were placed using a track-mounted crane.

A similar 30-ft-long box beam span was used to replace the steel plate-girder span on the approach opposite the timber trestle. Precast concrete bolster blocks were used on top of the existing masonry piers to obtain the proper elevation because the new structure was shallower than the existing one.

Figure 17.5.4-1

Precast 30-ft Approach Span on Precast Bolster Blocks

**17.5.5 Truss Removal**

After the approach spans were completed, preparation began for replacing the truss spans. An area under the truss spans was filled with ballast and leveled. Railroad track panels were laid perpendicular to the bridge on the fill below the structure. Steel frames mounted on rail trucks were placed on these tracks and used to support the

RAILROAD BRIDGES**17.5.5 Truss Removal/17.5.6 New Superstructure For Truss Spans**

trusses for removal. With these preparations for truss replacement complete, a carefully orchestrated construction effort began.

First, the truss ends were jacked up to lift them off the pier. The truss was then secured to the steel frames and rolled laterally clear of the work area, as shown in **Figure 17.5.5-1**. The construction crew then finished preparations on the pier top for placing the precast, prestressed concrete box beams. This work included removing the remaining truss attachments and placing elastomeric bearing pads.

Figure 17.5.5-1

Roll-Out of Truss Span to be Replaced

**17.5.6 New Superstructure for Truss Spans**

Each 154-ft-long steel truss was replaced by two spans of precast box beams. When the pier preparation was completed, the four box beams of the first span were lifted into position using truck cranes. While workmen epoxied the longitudinal joints and shear keys between these beams, the box beams for the second span were being placed. After the joints of both spans were epoxied and handrail cables strung along the walkways, prefabricated panels of railroad track were placed on the spans. This allowed a hopper car to be moved out on the track to dump ballast on the new spans.

After the ballast was tamped and the track reconnected, the new spans were ready for rail traffic. Replacing a 154-ft-long truss span was completed in a 12-hour track closure. Several weeks later, the second truss span was replaced, completing the reconstruction.

The use of precast elements, as shown in **Figure 17.5.6-1**, allowed the speedy and economical replacement of the structure, using the railroad's own work force.

Figure 17.5.6-1
Completed Structure



17.6 CASE STUDY NO. 2 - TIMBER TRESTLE REPLACEMENT

17.6.1 Existing Bridge

This case study discusses a timber trestle bridge replacement on the Union Pacific Railroad system. Bridge 177.81 is located approximately 1.59 miles west of Marysville, Calif. on Union Pacific Railroad's Canyon Subdivision. The existing bridge, shown in **Figure 17.6.1-1**, consisted of numerous timber trestle spans and a steel plate-girder span over the Yuba River. The plate-girder was to remain in place and the timber trestle portion of the bridge was to be replaced.

Figure 17.6.1-1
Existing Plate-Girder and Timber Trestle Spans



RAILROAD BRIDGES**17.6.2 New Superstructure/17.6.3 Substructure Construction****17.6.2 New Superstructure**

Due to the volume of rail traffic and importance of on-time delivery by the Union Pacific Railroad, minimal disruption to train operations was mandatory. Substructure construction was to be performed without interference or downtime to the railroad. Superstructure change-out would be performed during “windows” approved by the railroad. A precast, prestressed concrete superstructure system was selected based on economics, speed of erection, and the ability to meet the construction constraints associated with the need for minimal disruption to train operations.

The existing timber trestle spans varied in length with an average span of slightly less than 15 ft. Based on a field survey of the timber bent locations, new bent locations were selected to minimize interference with existing timber pile bents and optimize beam spans. A span length of 44 ft was selected for the new superstructure. For this span length, 45-in.-deep double-cell, prestressed concrete box beams were determined to be the most economical structural system.

17.6.3 Substructure Construction

Based on field conditions, prevalent construction practice in the area and construction constraints governed by railroad operations, cast-in-place reinforced concrete bents were selected for the substructure. The bents consisted of 100-ft-long, 4-ft-diameter drilled shafts, 4-ft-diameter cast-in-place reinforced concrete column extensions, and cap beams. All structural components were designed in accordance with the *AREMA Manual* and Union Pacific Railroad standards and procedures.

The sequence of construction was as follows:

The existing bridge footwalk and handrail were removed as required to facilitate drilled shaft installation. The drilled shafts were spaced at 15-ft centers perpendicular to the track to allow installation of the drilled shafts without interference to railroad operations. Continuous train operations were maintained throughout the entire construction of the substructure. Due to foundation conditions, steel pipe casing was necessary for drilled shaft installation. The pipe casing was installed using a vibratory hammer. Reinforcing steel cages were set and the holes were filled with 4,000 psi compressive strength concrete. Drilled shaft column extensions, bent cap beams, and the abutment were constructed under the existing timber superstructure. Due to the depth of the new concrete beams, the bent and abutment construction were completed without interfering with the existing timber superstructure, as shown in **Figure 17.6.3-1**.

Figure 17.6.3-1
Completed Concrete Bents under Existing Timber Trestle



RAILROAD BRIDGES

17.6.4 Superstructure Construction/17.7.2 Substructure Construction

17.6.4 Superstructure Construction

Working within railroad approved construction “windows,” the timber structure was removed and precast beams were set. In a continuous, well-planned procedure, the ballast, ties and rail were placed and train operations were resumed. The use of precast concrete allowed the Union Pacific Railroad to replace a timber trestle with a stronger, more durable structural system with minimal disruption to railroad service. The completed bridge is shown in **Figure 17.6.4-1**.

*Figure 17.6.4-1
Completed Bridge Structure*

**17.7 CASE STUDY NO. 3 - THROUGH PLATE GIRDER REPLACEMENT****17.7.1 Existing Bridge**

This case study describes the replacement of a through plate girder (TPG) bridge, which carries two tracks over Bull Creek near Wellsville, Kans. The existing 70-ft 6-in. single steel span was replaced by three precast, prestressed concrete tee girder spans. Like the previous case studies described in this chapter, construction took place with minimal disruption to rail traffic, which is typical of many railroad replacement structures.

17.7.2 Substructure Construction

Sheet piling was placed between the tracks at each end of the existing bridge, and rock sockets were drilled between the existing stringers. Steel piles were centered in the sockets and the holes were filled with concrete. Precast concrete pile caps were then erected, and the embedded bottom steel plates were welded to the tops of the cut-off piles.

One unique aspect of this replacement involved the removal of the existing two-track TPG superstructure. One track structure was detached from the center TPG prior to removal, as shown in Figure 17.7.2-1. This allowed for train operations to continue on the adjacent track structure while the new superstructure was being installed.

Precast concrete wingwalls were then attached to the abutment pile caps, as shown in Figure 17.7.2-2. Both the precast pile caps and precast wingwalls are standard-type pieces preferred by this railway. The superstructure was then installed, and rail traffic was restored to this track. The process was then repeated for the adjacent track.

Figure 17.7.2-1
Removal of Existing TPG Span (Photo: Harrington & Cortelyou, Inc./BMcD)



Figure 17.7.2-2
Installation of Precast Wingwalls (Photo: Harrington & Cortelyou, Inc./BMcD)



17.7.3 Superstructure Construction

Two end spans using 27-ft 11-in.-long solid tee-girders and one center span using 33-ft 11-in.-long voided tee-girders (shown in Figure 17.7.3-1) were used in the superstructure. These tee-girders are part of the family of standard prestressed shapes used by this railway, and are 36 in. deep. Each girder supports one-half track, and includes a ballast curb, cast after prestress transfer. These tee-girders, including the super tee-girder with a 48 in. depth, can span up to 48 ft. Other prestressed members used by this railway include concrete slabs and single and double box beams. The concrete slabs are a shallow depth alternative, spanning up to 25 ft. The box beams, with depths varying from 30 to 42 in., can span up to 49 ft.

Figure 17.7.3-1

Installation of Voided T-Girder (Photo: Harrington & Cortelyou, Inc./BMcD)



17.8 DESIGN EXAMPLE - DOUBLE-CELL BOX BEAM, SINGLE SPAN, NONCOMPOSITE, DESIGNED IN ACCORDANCE WITH AREMA SPECIFICATIONS

17.8.1 Background

Prestressed concrete double-cell box beams and solid slab beams are commonly used in the railroad industry. Solid slab beams are used for spans up to 25 ft, especially when superstructure depth has to be minimized. Prestressed concrete double-cell box beams are used for spans up to 50 ft in length. Prestressed concrete single-cell box beams are more economical for spans longer than 40 ft and are used for span lengths up to 80 ft. When span lengths exceed 80 ft, prestressed concrete I-beams with a composite deck become more feasible from a design, economic, and construction point of view. This example illustrates the design of a noncomposite, prestressed concrete, double-cell box beam.

17.8.2 Introduction

In noncomposite design, the beam acts as the main structural element. Therefore, the beam has to carry all the dead loads, superimposed dead loads, and live load. The beams are assumed to be fully prestressed under service load conditions. The dead load consists of the self-weight of the beam including diaphragms. The superimposed

dead loads consist of ballast, ties, rails, concrete curbs, and handrails, as shown in **Figures 17.8.2-1** and **17.8.2-2**. The live load used for this bridge is Cooper E 80, which is described in the *AREMA Manual*, Chapter 8, Part 2, Reinforced Concrete Design, Article 2.2.3. The prestressed concrete beams are designed using the *AREMA Manual*, Chapter 8, Part 17, Prestressed Concrete Design Specifications for Design of Prestressed Concrete Members. The beams in this example are checked for both serviceability and strength requirements.

Figure 17.8.2-1
Bridge Cross-Section

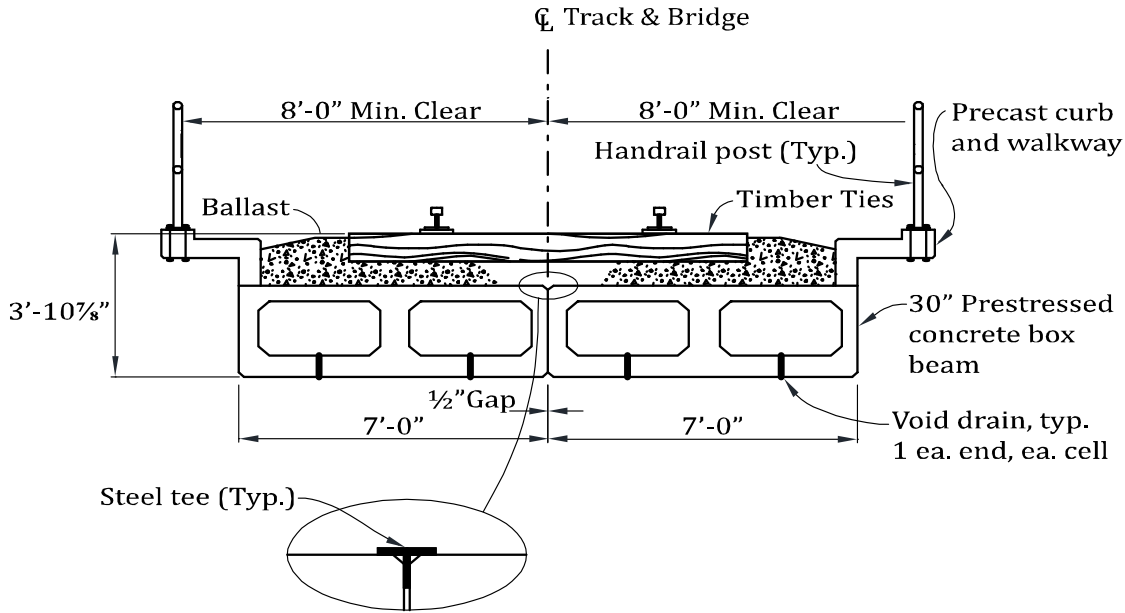
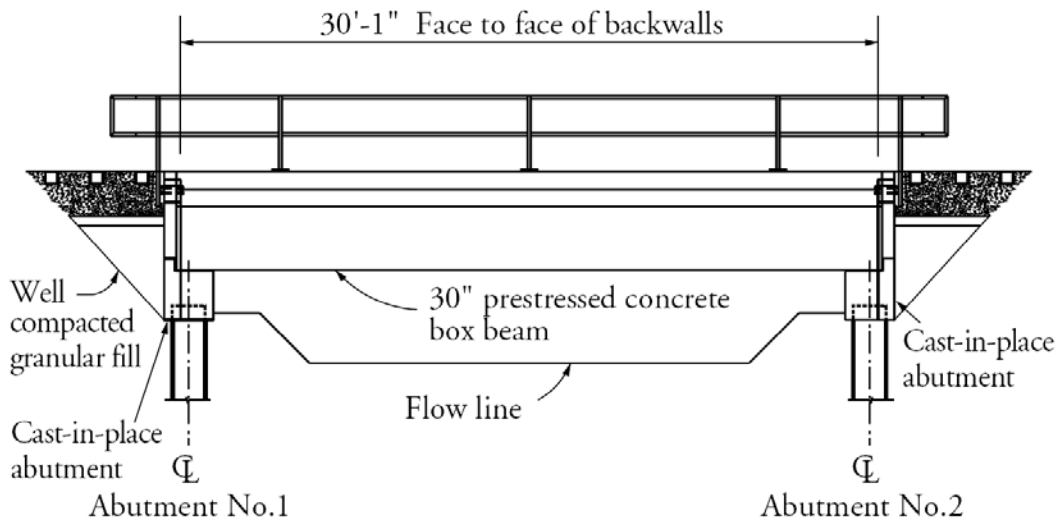


Figure 17.8.2-2
Bridge Elevation



RAILROAD BRIDGES

17.8.2 .1 Geometrics/17.8.2.3 Level Of Precision

17.8.2.1 Geometrics

For design, the bridge has the following dimensions:

Beam length = 30.0 ft

Beam width = 7.0 ft

Center-to-center distance between bearings = 29.0 ft

Bearing width (measured longitudinally) = 8 in.

Bearing length (measured transversely) = 6.67 ft

Depth of ballast = 15 in.

Timber ties: length = 9 ft; width = 9 in.; depth = 7 in.

Rail section = 132 RE (Bethlehem Steel Co.)

No. of tracks = one

17.8.2.2 Sign Convention

For concrete:

Compression positive (+ve)

Tension negative (-ve)

For steel:

Compression negative (-ve)

Tension positive (+ve)

Distance from center of gravity:

Downward positive (+ve)

Upward negative (-ve)

17.8.2.3 Level of Precision

<u>Item</u>	<u>Units</u>	<u>Precision</u>
Concrete Stress	ksi	1/1000
Steel Stress	ksi	1/10
Prestress Force	kips	1/10
Moments	ft-kips	1/10
Shears	kips	1/10
For the beam:		
Cross-Section Dimensions	in.	1/100
Section Properties	in.	1
Length	ft	1/100
Area of Prestressing Steel	in. ²	1/1000
Area of Mild Reinforcing	in. ²	1/100

Some calculations are carried out to a higher number of significant figures than common practice with hand calculation. Depending on available computation resources and designer preferences, other levels of precision may be used.

17.8.3 Material Properties

17.8.3.1 Concrete

Concrete strength at transfer, $f'_c = 4,000$ psi

Concrete strength at 28 days, $f'_c = 7,000$ psi

Concrete unit weight, $w_c = 150$ pcf

Modulus of elasticity of prestressed concrete, E_c

$$E_c = w_c^{1.5} 33 \sqrt{f'_c}, \text{ psi}$$

[AREMA Art. 2.23.4]

where

w_c = unit weight of concrete, pcf

f'_c = specified compressive strength of concrete, psi

Modulus of elasticity of concrete at transfer, using $f'_{ci} = 4,000$ psi, is:

$$E_{ci} = (150)^{1.5} (33) \sqrt{4,000} / 1,000 = 3,834 \text{ ksi}$$

Modulus of elasticity of concrete at 28 days, using $f'_c = 7,000$ psi, is:

$$E_c = (150)^{1.5} (33) \sqrt{7,000} / 1,000 = 5,072 \text{ ksi}$$

17.8.3.2 Pretensioning Strands

½-in.-diameter, seven wire, low-relaxation strands

Area of one strand, $A_{ps} = 0.153$ in.²

Ultimate tensile strength, $f_s = 270.0$ ksi

Modulus of elasticity, $E_s = 28,000$ ksi

17.8.3.3 Reinforcing Bars

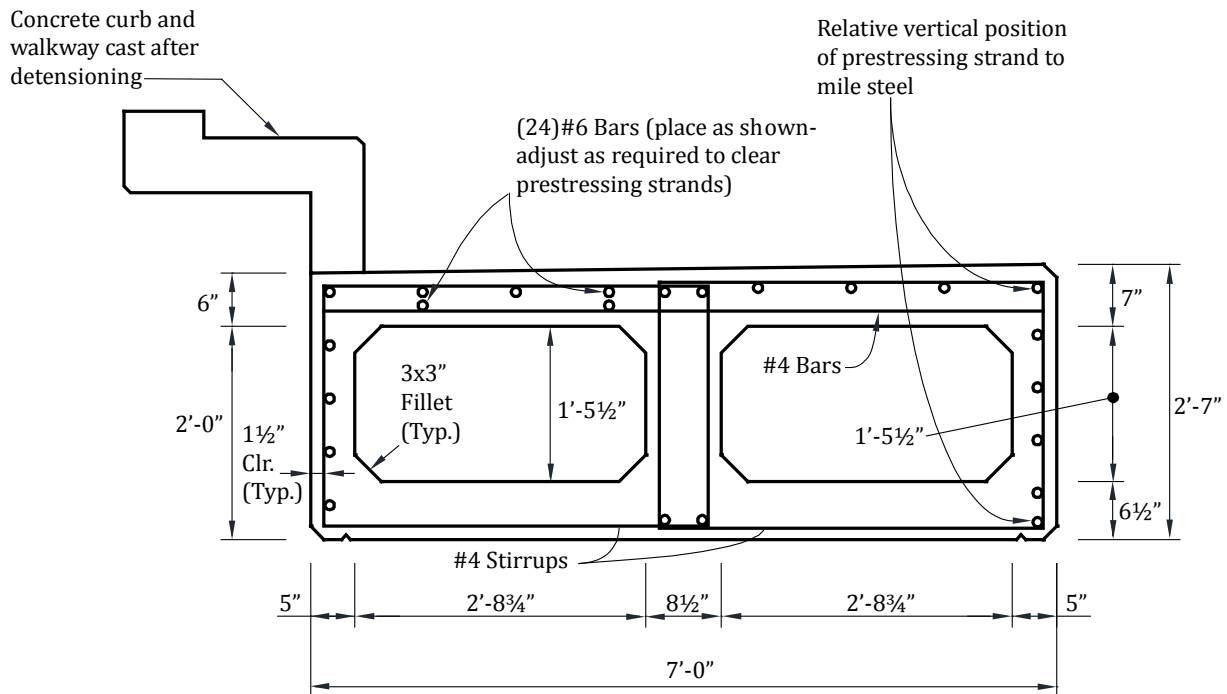
Yield strength, $f_y = 60,000$ psi

Modulus of elasticity, $E_s = 29,000$ ksi

17.8.4 Cross-Section Properties for a Single Beam

For cross-sectional dimensions of a single box beam, see **Figure 17.8.4-1**. Note that the depth varies from 30 in. to 31 in. to provide drainage.

Figure 17.8.4-1
Box Beam Cross-Section



$A =$ area of cross-section of precast beam = 1,452 in.²

$h =$ average depth of the precast beam = $(0.5)(31 + 30) = 30.5$ in.

$I =$ moment of inertia about the centroid of the precast beam = 171,535 in.⁴

$y_b =$ distance from centroid to extreme bottom fiber of the precast beam = 15.25 in.

$y_t =$ distance from centroid to extreme top fiber of the precast beam = 15.25 in.

$S_b =$ section modulus for the extreme bottom fiber of the precast beam = 11,248 in.³

$S_t =$ section modulus for the extreme top fiber of the precast beam = 11,248 in.³

NOTE: Section properties do not include precast curbs and walkway. Reinforcement in curbs and walkway not shown for clarity.

17.8.5 Shear Forces and Bending Moments

17.8.5.1 Shear Forces and Bending Moments Due to Dead Load

$$\text{Self-weight of beam} = \frac{1,452(150)}{1,000(144)} = 1.513 \text{ kips/ft}$$

Weight of end diaphragm = 1.7 kips

The equations for shear force (V_x) and moment (M_x) for uniform loads on a simple span (L) are given by:

$$V_x = w \left(\frac{L}{2} - x \right) \tag{Eq. 17.8.5.1-1}$$

$$M_x = \frac{wx}{2} (L - x) \tag{Eq. 17.8.5.1-2}$$

RAILROAD BRIDGES

17.8.5.1 Shear Forces And Bending Moments/17.8.5.3 Shear Forces And Bending Moments Due To Live Load

where

- w = weight/ft = 1.513 kips/ft
- L = span length, ft
- x = distance from the support, ft

Using the above equations, values of shear forces (V_g) and bending moments (M_g) due to dead loads are computed and given in **Table 17.8.5.1-1**.

Table 17.8.5.1-1
Shear Forces and Bending Moments per Beam

x, ft	0.0*	1.27**	4.0	6.0	7.25	10.0	14.5
V_g , kips	21.9	20.0	15.9	12.9	10.9	6.8	0.0
M_g , ft-kips	0.0	26.6	75.7	104.4	119.3	143.7	159.1
V_{SDL} , kips	19.5	17.8	14.2	11.5	9.8	6.1	0.0
M_{SDL} , ft-kips	0.0	23.7	67.4	93.0	106.3	128.1	141.7
V_{LL+I} , kips	175.0	160.3	---	---	111.5	83.4	49.8
M_{LL+I} , ft-kips	0.0	206.8	---	---	835.6	956.4	1,098.6

* At the support

** At the critical section for shear (See Section 17.8.11)

Diaphragm Load: Since distance between the centerline of the bearing and center of gravity of the diaphragm is less than the effective depth, ignore the effect of the diaphragm load in this example.

17.8.5.2 Shear Forces and Bending Moments Due to Superimposed Dead Load

Superimposed dead loads consist of ballast, ties, rails, concrete curb and walkway, and handrails.

Ballast, including track ties at 120 pcf

$$= 15/12(7.0 - 0.5 \text{ curb} + 0.04/2 \text{ gap})(0.120) = 0.978 \text{ kips/ft}$$

[AREMA Art. 2.2.3]

$$\text{Track rails, inside guardrails and fastenings at } 200 \text{ plf/track} = \frac{0.200}{2} = 0.100 \text{ kips/ft}$$

For this example, assume concrete curb and walkway area at 1.75 ft² + handrail post at 7 lb/ft = (1.75)(0.150)+7/1000 = 0.270 kips/ft

$$\text{Total superimposed dead load per beam per linear ft} = 0.978 + 0.100 + 0.270 = 1.348 \text{ kips/ft}$$

Using a uniform load of 1.348 kips/ft and **Equations 17.8.5.1-1** and **17.8.5.1-2**, values of shear forces (V_{SDL}) and bending moments (M_{SDL}) due to superimposed dead loads are computed and given in **Table 17.8.5.1-1**.

17.8.5.3 Shear Forces and Bending Moments Due to Live Load

The actions caused by the Cooper E 80 live load can be determined by using the tables in the *AREMA Manual*, Chapter 15, Section 1.15, Table 15-1-15, or by using any commercially available computer program. The values in the table are for one rail, or one half track load. In this example, a distribution factor (DF) equal to 0.5 is used, since there are two beams supporting one track.

For span lengths greater than 14 ft and less than 127 ft, the impact factor is:

$$I = \frac{225}{\sqrt{L}} = \frac{225}{\sqrt{29}} = 41.78\% \text{ of live load}$$

[AREMA Art.2.2.3d]

The values of shear forces (V_{LL+I}) and bending moments (M_{LL+I}) for live load plus impact for one beam were determined using a computer program and are given in **Table 17.8.5.1-1**.

RAILROAD BRIDGES**17.8.5.4 Load Combinations/17.8.7 Estimate Required Prestressing Force****17.8.5.4 Load Combinations**

For Group I loading:

$$\text{Service Load Design} = D + (L + I)(DF)$$

[AREMA Table 8-2-4]

$$\text{Load Factor Design} = 1.4(D + 5/3(L + I)(DF))$$

[AREMA Table 8-2-5]

Values of shear forces and bending moments for service load design and factored load design are determined from **Table 17.8.5.1-1** and given in **Table 17.8.5.4-1**.

Table 17.8.5.4-1
Shear Forces and Bending Moments for Design

	Self Wt (g)	Dead (SDL)	Live + Impact (L+I)	Total Service Load	Total Factored Load
Max. Shear Force at 1.27 ft, kips	20.0	17.8	160.3	198.1	427.0
Max. Bending Moment at Midspan, ft-kips	159.1	141.7	1098.6	1399.4	2984.5

The maximum value of shear occurs near the supports while the maximum value of bending moment occurs near midspan for a simply supported span.

17.8.6 Permissible Stresses in Concrete at Service Loads

At transfer (before time-dependent prestress losses):

[AREMA Art. 17.16.2.1]

$$\text{Compression: } 0.60 f'_{ci} = 0.60(4,000) = 2.400 \text{ ksi}$$

$$\text{Tension: } 3\sqrt{f'_{ci}} \text{ without bonded reinforcement} = 3\sqrt{4,000} = 0.190 \text{ ksi} \leq 0.200 \text{ ksi}$$

At service loads (after allowance for all prestress losses):

[AREMA Art. 17.16.2.2]

$$\text{Compression: } 0.40 f'_c = 0.40(7,000) = 2.800 \text{ ksi}$$

$$\text{Tension in precompressed tensile zone: } 0 \text{ ksi}$$

17.8.7 Estimate Required Prestressing Force

Try eccentricity of strands at midspan, $e_c = y_b - 2.5 = 12.75$ in.

Bottom tensile stress due to applied loads:

$$f_b = \frac{M_g + M_{SDL} + M_{LL+I}}{S_b}$$

Where

f_b = concrete stress at the bottom fiber of the beam, ksi

M_g = unfactored bending moment due to precast beam self-weight, ft-kips

M_{SDL} = unfactored bending moment due to superimposed dead load, ft-kips

M_{LL+I} = unfactored bending moment due to live load plus impact, ft-kips

$$f_b = \frac{12(159.1 + 141.7 + 1098.6)}{11,248} = 1.493 \text{ ksi}$$

Since allowable tensile stress in bottom fiber at service load is zero, required precompression is 1.493 ksi.

Bottom fiber stress due to prestress after all losses:

$$f_b = \frac{P_{se}}{A} + \frac{P_{se}e_c}{S_b}$$

where P_{se} = effective pretension force after allowing for all losses, kips

$$\text{Then } 1.493 = \frac{P_{se}}{1,452} + \frac{P_{se}(12.75)}{11,248}$$

and $P_{se} = 819.3$ kips

Since prestress losses are generally between 15 and 20%, assume 18% final prestress losses.

Allowable tensile stress in prestressing tendons immediately after prestress transfer is the larger of $0.82 f_y^* = (0.82)(0.9 f_s) = 0.738 f_s$ or $0.75 f_s$

$$0.75 f_s = 0.75(270) = 202.5 \text{ ksi}$$

[AREMA Art. 17.16.1.1]

$$\text{Number of strands required} = \frac{819.3}{(1 - 0.18)(202.5)(0.153)} = 32.2 \text{ strands}$$

Try 34 strands at bottom, $y_{bs} = 2.5$ in.

Plus 4 strands at mid-height, $y_{bs} = 15.25$ in.

Plus 6 strands at top, $y_{bs} = 27.50$ in.

Total No. of strands = $34 + 4 + 6 = 44$ strands

$$\text{Center of gravity of strands, } y_{bs} = \frac{34(2.5) + 4(15.25) + 6(27.50)}{44} = 7.07 \text{ in.}$$

Eccentricity of strands, $e_c = y_b - y_{bs} = 15.25 - 7.07 = 8.18$ in.

Total initial prestressing force before loss = $202.5(0.153)(44) = 1363.2$ kips

17.8.8 Determine Prestress Losses

To determine effective prestress, f_{se} , allowance for losses of prestress due to elastic shortening of concrete, ES, creep of concrete, CR_c, shrinkage of concrete, SH, and relaxation of prestressing steel, CR_s, will be calculated.

17.8.8.1 Prestress Losses at Service Loads

17.8.8.1.1 Elastic Shortening of Concrete

$$ES = \frac{E_s}{E_{ci}} f_{cir}$$

[AREMA Eq. 17-3]

where

f_{cir} = stress in concrete at centroid of prestressing reinforcement immediately after transfer, due to total prestress force and dead load acting at time of transfer, and is calculated at the section of maximum moment as follows:

$$= \frac{P_{si}}{A} + \frac{P_{si}e_c^2}{I} - \frac{M_g e_c}{I}$$

where

P_{si} = pretension force after allowing for initial losses. Taken as $0.69 f_{pu}$

$$f_{cr} = \frac{44(0.69)(0.153)(270)}{1,452} + \frac{44(0.69)(0.153)(270)(8.18)^2}{171,535} - \frac{159.1(12)(8.18)}{171,535} = 0.864 + 0.489 - 0.091 = 1.262 \text{ ksi}$$

RAILROAD BRIDGES**17.8.8.1.1 Elastic Shortening of Concrete/17.8.9.1 Stresses at Transfer at Midspan**

$$ES = \frac{28,000}{3,834} (1.262) = 9.2 \text{ ksi}$$

17.8.8.1.2 Creep of Concrete

$$CR_c = 12f_{cir} - 7f_{cds}$$

[AREMA Eq. 17-5]

where

f_{cds} = concrete stress at centroid of prestressing reinforcement, due to all dead load not included in calculation of f_{cir}

$$= \frac{M_{SDL}e_c}{I} = \frac{141.7(12)(8.18)}{171,535} = 0.081 \text{ ksi}$$

$$CR_c = 12(1.262) - 7(0.081) = 14.6 \text{ ksi}$$

17.8.8.1.3 Shrinkage of ConcreteAssume relative humidity, $R = 70\%$ (see also AREMA Fig. 8-17-1):

$$SH = 17 - 0.150R$$

[AREMA Eq. 17-6]

$$= 17 - 0.150(70) = 6.5 \text{ ksi}$$

17.8.8.1.4 Relaxation of Prestressing Steel

For pretensioning tendons with 270 ksi low-relaxation strand:

$$CR_s = 5 - 0.10ES - 0.05(SH + CR_c)$$

[AREMA Eq. 17-8b]

$$= 5 - 0.10(9.2) - 0.05(6.5 + 14.6) = 3.0 \text{ ksi}$$

17.8.8.1.5 Total Losses at Service LoadsTotal prestress losses = $9.2 + 14.6 + 6.5 + 3.0 = 33.3$ ksiFinal prestressing force, $P_{se} = (202.5 - 33.3)(0.153)(44) = 1139.1$ kips

$$\text{Percentage prestress losses} = \left(\frac{33.3}{202.5} \right) 100 = 16.4\%$$

17.8.8.2 Prestress Losses at TransferLosses due to elastic shortening, $ES = 9.2$ ksiTotal initial prestress losses = 9.2 ksiInitial prestress force after loss, $P_{si} = (202.5 - 9.2)(0.153)(44) = 1301.3$ kips

$$\text{Percentage initial prestress losses} = \left(\frac{9.2}{202.5} \right) 100 = 4.54\%$$

17.8.9 Concrete Stresses

Stresses need to be checked at several locations along the beam to ensure that the design satisfies permissible stresses at all locations at both transfer and service loads. For this design example, stresses will be checked at midspan and at the ends, which will govern straight strand designs without debonding.

17.8.9.1 Stresses at Transfer at MidspanCompute concrete stress at the top fiber of the beam, f_t :

$$f_t = \frac{P_{si}}{A} - \frac{P_{si}e_c}{S_t} + \frac{M_g}{S_t}$$

 M_g is based on overall length of 30 ft

RAILROAD BRIDGES**17.8.9.1 Stresses At Transfer At Midspan/17.8.9.4 Stresses At Service Load At End**

$$M_g = wL^2/8 = 1.513(30)^2/8 = 170.2 \text{ ft-kips}$$

$$f_t = \frac{1301.3}{1,452} - \frac{(1301.3)(8.18)}{11,248} + \frac{170.2(12)}{11,248}$$

$$= 0.896 - 0.946 + 0.182 = 0.132 \text{ ksi}$$

Compare with permissible values:

$$-0.190 \text{ ksi} < 0.132 \text{ ksi} < 2.400 \text{ ksi} \quad \text{OK}$$

Compute concrete stress at the bottom fiber of the beam, f_b :

$$f_b = \frac{P_{si}}{A} + \frac{P_{si}e_c}{S_b} - \frac{M_g}{S_b}$$

$$f_b = \frac{1301.3}{1,452} + \frac{(1301.3)(8.18)}{11,248} - \frac{170.2(12)}{11,248}$$

$$= 0.896 + 0.946 - 0.182 = 1.660 \text{ ksi}$$

Compare with permissible values:

$$-0.190 \text{ ksi} < 1.660 \text{ ksi} < 2.400 \text{ ksi} \quad \text{OK}$$

17.8.9.2 Stresses at Transfer at End

Stresses should be checked at the end of the transfer length when designing a prestressed beam (see Section 9.4.8.2 for an example of this check). However, in this design example, a standard beam design is being checked. Therefore it is conservative to check the stresses at the very end of the member, assuming the full prestress force is effective at that location. Since the strands are straight and all strands are bonded for the full length of the beam, the concrete stresses at the end are simply the stresses at midspan without the stress due to dead load moment.

$$f_t = 0.896 - 0.946 = -0.050 \text{ ksi, which is within permissible values shown above} \quad \text{OK}$$

$$f_b = 0.896 + 0.946 = 1.842 \text{ ksi, which is within permissible values shown above} \quad \text{OK}$$

17.8.9.3 Stresses at Service Load at Midspan

Compute concrete stress at the top fiber of the beam, f_t :

$$f_t = \frac{P_{se}}{A} - \frac{P_{se}e_c}{S_t} + \frac{M_g + M_{SDL} + M_{LL+I}}{S_t}$$

$$= \frac{1139.1}{1,452} - \frac{(1139.1)(8.18)}{11,248} + \frac{1399.4(12)}{11,248}$$

$$= 0.785 - 0.828 + 1.493 = 1.450 \text{ ksi} < 2.800 \text{ ksi} \quad \text{OK}$$

Compute concrete stress at the bottom fiber of the beam, f_b :

$$f_b = \frac{P_{se}}{A} + \frac{P_{se}e_c}{S_b} - \frac{M_g + M_{SDL} + M_{LL+I}}{S_b}$$

$$= \frac{1139.1}{1,452} + \frac{(1139.1)(8.18)}{11,248} - \frac{1399.4(12)}{11,248}$$

$$= 0.785 + 0.828 - 1.493 = 0.120 \text{ ksi} > 0.0 \text{ ksi} \quad \text{OK}$$

17.8.9.4 Stresses at Service Load at End

The prestress force is at its maximum value at transfer and service loads do not affect stresses at the end of the beam. Therefore, stresses at transfer will govern at the end of the beam, so there is no need to check stresses at the end at service loads.

17.8.10 Flexural Strength

17.8.10.1 Stress in Strands at Flexural Strength

In lieu of a more accurate determination of stress in pretensioning strands at nominal strength, f_{su}^* , based on strain compatibility, the following approximate value of f_{su}^* is used:

$$f_{su}^* = f'_s \left(1 - \frac{\gamma^*}{\beta_1} \rho^* \frac{f'_s}{f'_c} \right), \text{ provided } f_{se} \text{ is greater than } 0.5f'_s \quad [\text{AREMA Eq. 17-19}]$$

where

$$\begin{aligned} f_{se} &= \text{effective stress in pretensioning steel after losses} \\ &= 202.5 - 33.3 = 169.2 \text{ ksi} > 0.5(270) = 135.0 \text{ ksi} \quad \text{OK} \end{aligned}$$

$$\rho^* = \frac{A_s^*}{bd}$$

$$\gamma^* = 0.28 \text{ for low-relaxation strand}$$

$$\beta_1 = 0.85 - 0.05(f'_c - 4) \text{ and } 0.65 \leq \beta_1 \leq 0.85 \quad [\text{AREMA Art. 2.31.1}]$$

$$\beta_1 = 0.85 - 0.05(7.0 - 4) = 0.70$$

$$\begin{aligned} A_s^* &= \text{total area of pretensioning steel in tension zone} \\ &= 38(0.153) = 5.814 \text{ in.}^2 \end{aligned}$$

$$b = \text{effective flange width} = 7(12) = 84.0 \text{ in.}$$

$$\begin{aligned} d &= \text{distance from extreme compression fiber to centroid of pretensioning force} \\ &= 30.5 - \frac{34(2.5) + 4(15.25)}{38} = 26.66 \text{ in.} \end{aligned}$$

Note: In many cases, strands near or above midheight are neglected when computing d for calculating the average stress in strands at flexural strength. This is because, at the flexural strength, the strands located higher in the cross-section will not reach a strain (and stress) as high as the bottom strands. However, for this standard beam design, the strands at midheight have been included as shown above. A strain compatibility analysis (described in Sections 8.2.2.6 and 8.2.2.7) can be used to compute the strain and stress in the strands at midheight. Such an analysis for this beam indicates that the strands at midheight would reach a stress of approximately 251 ksi, which is reasonable when compared with the stress, f_{ps} , computed below. The same analysis indicates that the strands in the bottom row would reach a stress of nearly 260 ksi. Therefore, in this case, incorporating the strands at midheight has provided a reasonable result. If the strands at midheight are neglected, the strength of the section at midspan would prove to be inadequate.

$$\rho^* = \frac{A_s^*}{bd} = \frac{5.814}{84(26.66)} = 0.00260$$

$$f_{su}^* = 270 \left(1 - \left(\frac{0.28}{0.70} \right) (0.00260) \frac{270}{7.0} \right) = 259.2 \text{ ksi}$$

17.8.10.2 Limits for Reinforcement

Assuming a rectangular section, compute the reinforcement ratio as:

$$\rho^* \frac{f_{su}^*}{f'_c} = \frac{0.00260(259.2)}{7.0} = 0.0963 < 0.36\beta_1 = 0.36(0.70) = 0.25 \quad \text{OK} \quad [\text{AREMA Art. 17.5.4}]$$

17.8.10.3 Design Moment Strength

Assuming beam acts as a rectangular section:

$$\Phi M_n = \Phi \left[A_s^* f_{su}^* d \left(1 - 0.6 \rho^* \frac{f_{su}^*}{f_c'} \right) \right] \quad \text{[AREMA Eq. 17-12]}$$

where

M_n = nominal moment strength of a section

Φ = strength reduction factor for flexure = 0.95 [AREMA Art.17.15.1]

$$a = \frac{A_s^* f_{su}^*}{0.85 f_c' b} = \frac{5.814(259.2)}{0.85(7)(84)} = 3.02 \text{ in.} \quad \text{[AREMA Art.17.18.2]}$$

Average depth of top flange = 6.5 in. > 3.02 in.

Therefore, rectangular section assumption is appropriate.

Using AREMA Eq. 17-12:

$$\Phi M_n = 0.95 \left[5.814(259.2)26.66 \left(1 - 0.6 \frac{0.00260(259.2)}{7} \right) \right] \frac{1}{12} = 2996.9 \text{ ft-kips}$$

Factored moment due to dead and live loads from **Table 17.8.5.4-1** = 2984.5 ft-kips < 2996.9 ft-kips OK

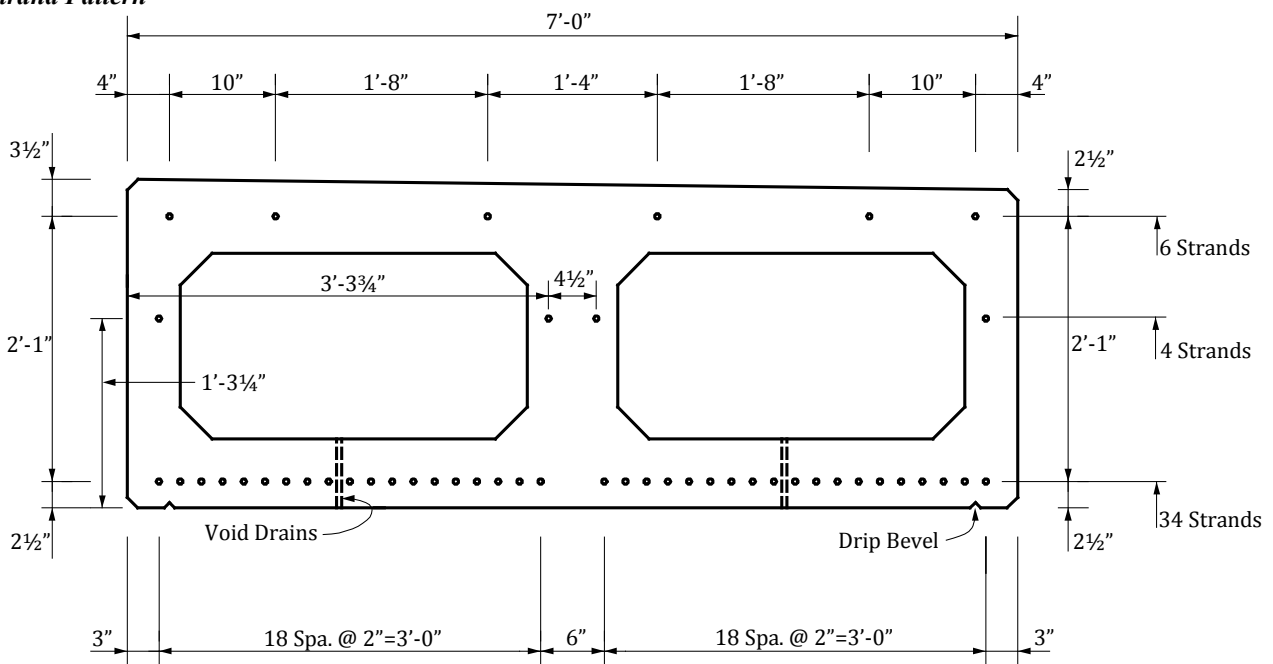
17.8.10.4 Minimum Reinforcement

The total amount of prestressed and nonprestressed reinforcement should be adequate to develop an ultimate moment at the critical section at least 1.2 times the cracking moment, M_{cr}^* : $\Phi M_n \geq 1.2 M_{cr}^*$. The calculation (not shown here but similar to the calculation in Section 9.4.10.2) yields 2996.9 ft-kips > 2519.6 ft-kips OK

17.8.10.5 Final Strand Pattern

Final strand locations are shown in **Figure 17.8.10.5-1**

Figure 17.8.10.5-1
Strand Pattern



Note: Curbs and walkways not shown.

17.8.11 Shear Design

17.8.11.1 Required Shear Strength

Prestressed concrete members subjected to shear are designed so that

$$V_u \leq \Phi (V_c + V_s) \quad [\text{AREMA Eq. 17-30}]$$

where

V_u = factored shear force at section considered

V_c = nominal shear strength provided by concrete

V_s = nominal shear strength provided by shear reinforcement

Φ = strength reduction factor for shear = 0.90 [AREMA Art. 17.15.1]

Per the *AREMA Manual*, Article 17.21.1.4, the critical section for shear is located at a distance $h/2$ from face of support. In this design example, the critical section for shear is calculated from the centerline of the bearings since the pads are not rigid and have the potential to rotate.

$$h/2 = 30.5/2 = 15.25 \text{ in.} = 1.27 \text{ ft}$$

$$V_u = 427.0 \text{ kips (from Table 17.8.5.4-1)}$$

17.8.11.2 Shear Strength Provided by Concrete

17.8.11.2.1 Simplified Approach

The shear strength provided by concrete, V_c , can be calculated by using *AREMA Manual* Eq. 17-31, provided that the effective prestress force is not less than 40% of the total tensile strength provided by the flexural reinforcement.

$$V_c = \left(0.6\sqrt{f'_c} + 700 \frac{V_u d}{M_u} \right) b_w d \quad [\text{AREMA Eq. 17-31}]$$

where

M_u = factored bending moment at the section

$$= 1.4 \left(26.6 + 23.7 + \left(\frac{5}{3} \right) (206.8) \right) = 553.0 \text{ ft-kips} \quad (\text{Table 17.8.5.1-1})$$

b_w = total web width = 5 + 8.5 + 5 = 18.5 in.

d = 26.66 in. > 0.8h = (0.8)(30.5) = 24.4 in.

Therefore, use $d = 26.66$ in.

$$\frac{V_u d}{M_u} = \frac{427.0(26.66)}{553.0(12)} = 1.72 > 1.0, \text{ use } 1.0 \quad [\text{AREMA Art. 17.21.2.1}]$$

$$V_c = \left(0.6\sqrt{7,000} + 700(1.0) \right) 18.5(26.66)/1,000 = 370.0 \text{ kips}$$

However, the maximum value of V_c is limited to:

$$5\sqrt{f'_c} b_w d = 5\sqrt{7,000}(18.5)(26.66)/1,000 = 206.3 \text{ kips} < V_c = 370.0 \text{ NG}$$

AREMA Manual Art. 17.21.2.2 allows higher values of V_c if a more detailed calculation is made. According to this method, V_c is the lesser of V_{ci} or V_{cw} .

where

V_{ci} = nominal shear strength provided by concrete when diagonal cracking results from combined shear and moment

V_{cw} = nominal shear strength provided by concrete when diagonal cracking results from excessive principal tensile stress in web

RAILROAD BRIDGES

17.8.11.2.2 Calculate V_{ci} /17.8.11.2.3 Calculate V_{cw}

17.8.11.2.2 Calculate V_{ci}

$$V_{ci} = 0.6\sqrt{f'_c}b_wd + V_D + \frac{V_iM_{cr}}{M_{max}} \quad \text{[AREMA Eq. 17-32]}$$

but not less than $\sqrt{1.7f'_c}b_wd$

where

$$\begin{aligned} V_D &= \text{shear at section due to service dead load} = V_g + V_{SDL} = 20.0 + 17.8 \\ &= 37.8 \text{ kips} \end{aligned}$$

$$\begin{aligned} M_{cr} &= \text{moment causing flexural cracking at section due to externally applied loads} \\ &= S_b(6\sqrt{f'_c} + f_{pe} - f_d) \end{aligned}$$

where

f_{pe} = compressive stress in concrete due to effective prestress force only, at the extreme fiber of section where tensile stress is caused by externally applied loads

$$\begin{aligned} f_{pe} &= \frac{P_{se}}{A} + \frac{P_{se}e_c}{S_b} \\ &= \frac{1139.1}{1,452} + \frac{1139.1(8.18)}{11,248} = 0.785 + 0.828 = 1.613 \text{ ksi} \end{aligned}$$

f_d = stress due to unfactored dead load at extreme fiber of section where tensile stress is caused by externally applied loads

$$f_d = \frac{M_g + M_{SDL}}{S_b} = \frac{(26.6 + 23.7)12}{11,248} = 0.054 \text{ ksi}$$

$$M_{cr} = \left(\frac{6\sqrt{7,000}}{1,000} + 1.613 - 0.054 \right) \frac{11,248}{12} = 1931.8 \text{ ft-kips}$$

V_i = factored shear force at section due to externally applied loads occurring simultaneously with $M_{max} = V_u - V_D = 427.0 - 37.8 = 389.2$ kips

M_{max} = maximum factored moment at the section due to externally applied loads
 $= M_u - M_g - M_{SDL} = 553.0 - 1.4(26.6) - 1.4(23.7) = 482.6$ ft-kips

$$V_{ci} = 0.6\sqrt{f'_c}b_wd + V_D + \frac{V_iM_{cr}}{M_{max}} \quad \text{[AREMA Eq. 17-10]}$$

$$= 0.6 \frac{\sqrt{7,000}}{1,000} (18.5)(26.66) + 37.8 + \frac{389.2(1931.8)}{482.6} = 1620.5 \text{ kips}$$

but not less than $1.7\sqrt{f'_c}b_wd = 1.7 \frac{\sqrt{7,000}}{1,000} (18.5)(26.66) = 70.2$ kips

Therefore,

$$V_{ci} = 1620.5 \text{ kips}$$

17.8.11.2.3 Calculate V_{cw}

$$V_{cw} = (3.5\sqrt{f'_c} + 0.3f_{pc})b_wd + V_p \quad \text{[AREMA Eq. 17-34]}$$

where

f_{pc} = compressive stress in the concrete (after allowance for all pretension losses) at the centroid of cross section resisting externally applied loads

V_p = vertical component of effective prestress force at section

= 0 for straight strands.

RAILROAD BRIDGES**17.8.11.2.3 Calculate V_{cw} /17.8.11.3.3 Check V_s Limit**

Transfer length of strands = 50 strand diameters = $50(0.5) = 25$ in. from end of beam. Since the distance $h/2 = 15.25$ in. is closer to end of member than the end of the transfer length of the prestressing strands, a reduced pretensioning force will be considered when computing V_{cw} . [AREMA Art. 17.21.2.5]

Effective prestress force at distance $h/2$ from centerline of the bearing:

$$P_{se} = \frac{(15.25 + 6.00)}{25}(1139.1) = 968.2 \text{ kips}$$

$$f_{pc} = \frac{968.2}{1,452} = 0.667 \text{ ksi}$$

Therefore,

$$V_{cw} = \left(\frac{3.5\sqrt{7,000}}{1,000} + 0.3(0.667) \right) (18.5)(26.66) + 0 = 243.1 \text{ kips}$$

17.8.11.2.4 Calculate V_c

$V_c =$ lesser of V_{ci} and V_{cw}

$$V_c = V_{cw} = 243.1 \text{ kips}$$

17.8.11.3 Calculate V_s and Shear Reinforcement**17.8.11.3.1 Calculate V_s**

$$V_s = \frac{V_u}{\phi} - V_c = \frac{427.0}{0.9} - 243.1 = 231.3 \text{ kips} \quad [\text{AREMA Eq. 17-30}]$$

17.8.11.3.2 Determine Stirrup Spacing

Required stirrup spacing is calculated as follows:

$$V_s = \frac{A_v f_y d}{s} \quad [\text{AREMA Eq. 17-35}]$$

where $A_v =$ area of shear reinforcement within a spacing, s

Try two closed stirrups, which provide (4) No. 4 bars,

$$A_v = 4(0.20) \text{ in.}^2 = 0.80 \text{ in.}^2$$

Stirrups are provided at 4 in. spacing to satisfy the minimum flexural requirements of the top slab of the box beam. Calculations for the top slab flexural reinforcement are not provided in this example.

$$\text{Spacing required, } s = \frac{A_v f_y d}{V_s} = \frac{0.80(60)(26.66)}{231.3} = 5.5 \text{ in.} > 4 \text{ in.} \quad \text{OK}$$

Use No. 4 stirrups (4 legs) at 4-in. centers.

$$A_v \text{ provided} = 4(0.20) = 0.80 \text{ in.}^2$$

Shear strength provided by stirrups,

$$V_s = \frac{0.80(60)(26.66)}{4} = 319.9 > 231.3 \text{ kips} \quad \text{OK}$$

17.8.11.3.3 Check V_s Limit

Allowable maximum shear strength provided by stirrups is:

$$\begin{aligned} 8\sqrt{f'_c} b_w d &= 8\sqrt{7,000}(18.5)(26.66)/1,000 & [\text{AREMA Art. 17.21.3.1}] \\ &= 330.1 \text{ kips} > V_s \quad \text{OK} \end{aligned}$$

17.8.11.3.4 Check Stirrup Spacing Limits

Check for maximum spacing of stirrups

$$4\sqrt{f'_c} b_w d = 4 \frac{\sqrt{7,000}}{1,000} (18.5)(26.66) = 165.1 \text{ kips} < V_s \quad [\text{AREMA Art. 17.21.3.2}]$$

Therefore, maximum spacing is lesser of $3/8h = 3/8(30.5) = 11.4$ in. or 12 in.

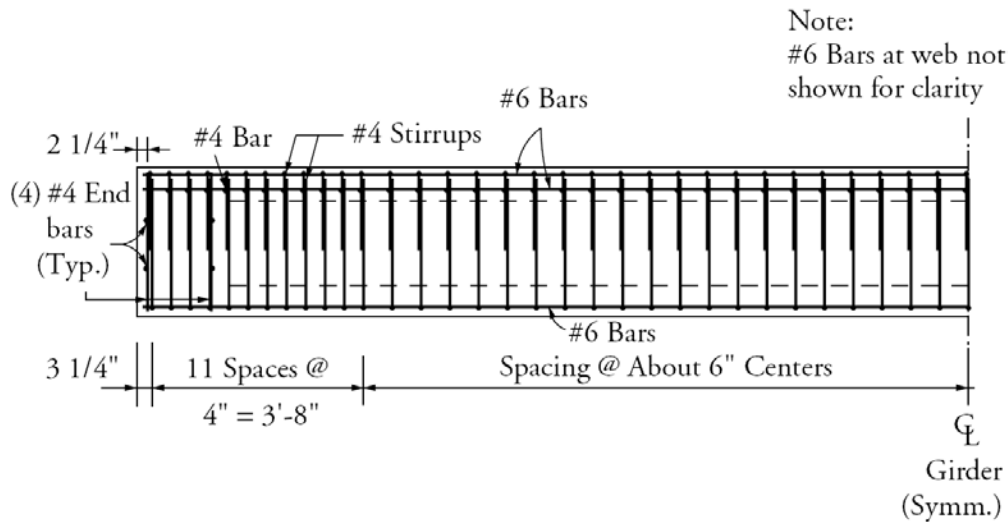
Provide No. 4 stirrups (4 legs) at 4-in. centers < 11.4 in. OK

Calculations for shear at other sections along the beam are not provided in this example.

For shear reinforcement details, see **Figures 17.8.4-1** and **17.8.11.3.4-1**

Figure 17.8.11.3.4-1

Elevation Showing Nonprestressed Reinforcement



17.8.12 Deflections

17.8.12.1 Camber Due to Prestressing at Transfer

$$\Delta = \frac{P_{si} e_c L^2}{8E_{ci} I} = - \frac{1301.3(8.18)(29(12))^2}{8(3,834)(171,535)} = -0.245 \text{ in. } \uparrow$$

17.8.12.2 Deflection Due to Beam Self-Weight at Transfer

$$\Delta = \frac{5wL^4}{384E_{ci} I} = \frac{5(1.513/12)(29(12))^4}{(384)(3,834)(171,535)} = 0.037 \text{ in. } \downarrow$$

17.8.12.3 Deflection Due to Superimposed Dead Load

$$\Delta = \frac{5wL^4}{384E_{ci} I} = \frac{5(1.348/12)(29(12))^4}{(384)(5,072)(171,535)} = 0.025 \text{ in. } \downarrow$$

17.8.12.4 Long-Term Deflection

According to *PCI Design Handbook - 7th Edition* (PCI, 2010), long-term camber and deflection of prestressed concrete members can be calculated by an approximate method using multipliers. Calculations are shown in **Table 17.8.12.4-1**.

RAILROAD BRIDGES

17.8.12.4 Long-Term Deflection/17.9 References

Table 17.8.12.4-1
Calculated Deflection, in.

	At Transfer (a)	Multiplier (b)	Erection (c) = (a)(b)	Multiplier (d)	Final (e) = (a)(d)
Prestress	-0.245 ↑	1.80	-0.441 ↑	2.45	-0.600 ↑
Self-Weight	+0.037 ↓	1.85	+0.068 ↓	2.70	+0.100 ↓
Dead Load	N/A		+0.025 ↓	3.00	+0.075* ↓
Total	-0.208 ↑		-0.348 ↑		-0.425 ↑

* This is the result of multiplying the dead load deflection at erection (c) by multiplier (d)

17.8.12.5 Deflection Due to Live Load

Live load deflection is generally calculated using influence lines. At this point, use of a computer program becomes very useful. However, for short span bridges, the designer can quickly calculate an approximate value for deflection by using the equivalent uniform load. The equivalent uniform live load, w_{equ} , for a simply supported beam can be derived from the maximum moment at midspan,

$$M_{LL+I} = \frac{w_{equ}L^2}{8}$$

$$w_{equ} = \frac{8M_{LL+I}}{L^2} = \frac{8(1098.6)(12)}{(29(12))^2} = 0.871 \text{ kips/in.}$$

$$\Delta = \frac{5(0.871)(29(12))^4}{384(5,072)(171,535)} = 0.191 \text{ in. } \downarrow$$

$$\text{Maximum allowable deflection} = \frac{L}{640} = \frac{29(12)}{640} = 0.544 \text{ in.} > 0.191 \text{ in.} \quad \text{OK}$$

[AREMA Art. 17.13]

17.9 REFERENCES

- AREMA. 2010. *AREMA Manual for Railway Engineering*, 2010 Edition, American Railway Engineering and Maintenance-of-Way Association, Landover, MD.
<http://www.arena.org/publications/mre/index.aspx>
- Marianos, W. N., Jr. 1991. "Railroad Use of Precast Concrete Bridge Structures," *Concrete International*, American Concrete Institute, Farmington Hills, MI. V. 13, No. 9, September, pp. 30-35.
http://concreteinternational.com/pages/featured_article.asp?ID=3416 (Fee)
- PCI. 2010. *PCI Design Handbook*, Seventh Edition, Precast/Prestressed Concrete Institute, Chicago, IL.
http://netforum.pci.org/eweb/dynamicpage.aspx?webcode=category&ptc_key=6ccabfe6-c4d9-4379-83b5-d257a2bde354&ptc_code=Design Guides and Standards (Fee)
- Sweeney, Robert A.P. 2006. "Railway Loadings and Reality," 7th International Conference on Short and Medium Span Bridges, CSCE, Montreal, Canada.
- Unsworth, John. 2006. "Design of Short and Medium Span Railway Bridges - Modern Practice of North American Freight Railroads", 7th International Conference on Short and Medium Span Bridges, CSCE, Montreal, Canada.

This page intentionally left blank

BRIDGE LOAD RATING

Table of Contents

NOTATION..... 18 - 5

18.1 OVERVIEW OF BRIDGE LOAD RATING 18 - 9

 18.1.1 Purpose 18 - 9

 18.1.2 Definitions 18 - 9

 18.1.3 Load Rating Procedure 18 - 9

 18.1.3.1 Collect Information on the Current Bridge Condition..... 18 - 9

 18.1.3.2 Determine Nominal Loading and Nominal Resistances 18 - 10

 18.1.3.2.1 Dead loads..... 18 - 10

 18.1.3.2.2 Live loads..... 18 - 10

 18.1.3.2.3 Impact loads..... 18 - 10

 18.1.3.2.4 Resistances 18 - 11

 18.1.3.3 Determine the Load Distribution..... 18 - 11

 18.1.3.4 Select Load and Resistance Factors 18 - 11

 18.1.3.5 Calculate the Rating Factor..... 18 - 11

18.2 LOADS AND DISTRIBUTION..... 18 - 11

 18.2.1 Dead Loads 18 - 11

 18.2.2 Live Loads 18 - 12

 18.2.2.1 AASHTO 2002 Standard Specifications..... 18 - 12

 18.2.2.2 AASHTO LRFD Specifications 18 - 13

 18.2.3 Load Distribution for Rating 18 - 14

 18.2.3.1 AASHTO 2002 Standard Specifications..... 18 - 15

 18.2.3.2 AASHTO 2010 LRFD Specifications 18 - 15

18.3 RATING METHODOLOGY..... 18 - 15

 18.3.1 Rating Equation..... 18 - 15

 18.3.2 Analysis Method..... 18 - 16

 18.3.2.1 Load Factors..... 18 - 16

 18.3.2.1.1 Design Loads 18 - 16

 18.3.2.1.2 Legal, NRL, and SHV Loads 18 - 16

 18.3.2.1.3 Permit Load..... 18 - 17

 18.3.2.2 Strength Resistance Factors..... 18 - 17

 18.3.2.3 Adjustments for Actual Conditions 18 - 17

 18.3.3 Load Rating Methods 18 - 17

 18.3.3.1 Working Stress Method..... 18 - 17

 18.3.3.2 Factored Load Method..... 18 - 18

 18.3.3.3 Load and Resistance Factor Method 18 - 19

 18.3.4 Rating Method for Prestressed Concrete Bridges..... 18 - 19

 18.3.4.1 Proper Methods for Determining the Nominal Shear Capacity..... 18 - 20

 18.3.4.2 Effects of Strand Debonding on Shear Resistance..... 18 - 24

BRIDGE LOAD RATING

Table of Contents

18.4 RATING BY LOAD TESTING..... 18 - 25

 18.4.1 Condition Assessment..... 18 - 25

 18.4.2 Test Type..... 18 - 25

 18.4.2.1 Proof Load Test..... 18 - 25

 18.4.2.2 Diagnostic Loads 18 - 26

 18.4.3 Computer Modeling and Analysis 18 - 26

 18.4.4 Required Measurements for Evaluation 18 - 26

 18.4.5 Instrumentation Plan 18 - 26

 18.4.6 Test Procedure 18 - 27

 18.4.6.1 Static Testing 18 - 27

 18.4.6.2 Dynamic Testing..... 18 - 27

 18.4.7 Analysis of Test Data..... 18 - 27

 18.4.8 Verification of Analytical Model 18 - 27

18.5 LOAD RATING REPORT 18 - 27

18.6 RATING EXAMPLE..... 18 - 28

 18.6.1 Introduction..... 18 - 28

 18.6.2 Materials and Other Information 18 - 28

 18.6.3 Section Properties..... 18 - 29

 18.6.4 Dead Load Calculations 18 - 30

 18.6.5 Stresses and Strength..... 18 - 30

 18.6.5.1 Prestress Losses 18 - 30

 18.6.5.2 Stresses and Strength 18 - 31

 18.6.6 Rating for Design Loading Based on Standard Specifications..... 18 - 32

 18.6.6.1 Live Loads 18 - 32

 18.6.6.2 Load Ratings 18 - 32

 18.6.7 Rating for Design Loading (HL-93) Based on the LRFD Specifications..... 18 - 33

 18.6.7.1 Load Calculations..... 18 - 33

 18.6.7.1.1 Dead Load 18 - 33

 18.6.7.1.2 Prestress Loss 18 - 33

 18.6.7.1.3 Live Load 18 - 33

 18.6.7.2 Strength Calculation 18 - 34

 18.6.7.3 Load Rating..... 18 - 34

 18.6.7.3.1 Strength I Load Rating..... 18 - 34

 18.6.7.3.2 Service III Load Rating 18 - 34

 18.6.7.3.2 Service I Load Rating 18 - 34

 18.6.8 Rating for Permit Loading by the LRFD Specifications 18 - 36

 18.6.8.1 Routine or Annual Type Permit 18 - 36

 18.6.8.1.1 Strength II Load Rating..... 18 - 36

BRIDGE LOAD RATING

Table of Contents

18.6.8.1.2 Service I Load Rating..... 18 - 37

18.6.8.2 Limited Crossing Escorted with No Other Traffic (Single-Trip) 18 - 37

 18.6.8.2.1 Load Rating..... 18 - 38

18.6.8.3 Limited Crossing Mixed with Traffic (Single-Trip)..... 18 - 38

 18.6.8.3.1 Load Rating..... 18 - 38

18.6.8.4 Limited Crossing Mixed with Traffic (Multiple-Trips less than 100 crossings) 18 - 38

 18.6.8.4.1 Load Rating..... 18 - 39

18.6.9 Rating by Load Testing 18 - 39

 18.6.9.1 Test Information 18 - 39

 18.6.9.2 Test Inventory Rating Factor..... 18 - 40

 18.6.9.3 Test Operating Rating Factor 18 - 40

18.6.10 Summary of Ratings 18 - 41

18.7 REFERENCES 18 - 41

This page intentionally left blank

NOTATION

A	= area of cross section of the precast beam
A_c	= area of cross section of the composite section
A_N	= area of cross section of the noncomposite section
A_{ps}	= area of prestressing strands
A_s	= area of nonprestressed reinforcement
A_v	= area of shear reinforcements
a	= depth of equivalent rectangular stress block
b	= width of top flange of a flanged member or width of rectangular section
b_e	= effective flange width
b_t	= width of top flange of I-beam
b_b	= width of bottom flange of I-beam
b_v	= effective web width taken as the minimum web width within the effective shear depth
c	= distance from the extreme compression fiber to neutral axis
C	= factored capacity
CR_c	= loss of pretension due to creep of concrete
CR_s	= loss of pretension due to relaxation of pretensioning steel
DC	= dead load effect due to structural components and attachments
DF	= LRFD distribution factor
DL	= dead load effects
DW	= dead load effect due to wearing surface and utilities
d	= distance from extreme compression fiber to centroid of the pretensioning force
d_v	= effective shear depth
E	= modulus of elasticity
E_c	= modulus of elasticity of concrete
E_{ci}	= modulus of elasticity of the beam concrete at transfer
ES	= loss of pretension due to elastic shortening
E_s	= modulus of elasticity of pretensioning reinforcement
e	= eccentricity of the strands/eccentricity of prestressing force
e_g	= distance between the centers of gravity of the beam and the deck
f_{allow}	= allowable stresses
f_{CD}	= dead load stress on composite section
f'_{cs}	= 28-day compressive strength of deck concrete
f'_{cg}	= 28-day compressive strength of girder concrete
f_{cir}	= average concrete stress at the center of gravity of the pretensioning steel due to pretensioning force and dead load of beam immediately after transfer

f_{cds}	= concrete stress at the center of gravity of the prestressing steel due to all dead loads except the dead load present at the time the prestressing force is applied
f_{CLL}	= stress from live load
f_{ct}	= dead load stress on composite section in top fiber
f_{DL}	= stresses resulting from dead loads
$f_{HS\ 20+I}$	= stresses resulting from HS-20 plus impact
f_{LL}	= live load stress
f_{LL+I}	= stresses resulting from live load plus impact acting on the composite section
f_{Nb}	= dead load stress on noncomposite section in beam bottom fiber
f_{Nt}	= dead load stress on noncomposite section in beam top fiber
f_{pe}	= compressive stress in concrete due to effective prestress forces only (after allowance for all prestress losses) at extreme fiber of section where tensile stress is caused by externally applied loads
f_{pr}	= bottom stress from prestressing force
f_{prt}	= top stress from prestressing force
f_{ps}	= average stress in prestressing steel at the time for which the nominal resistance of member is required
f_{pu}	= tensile strength of prestressing strand
f_{py}	= yield strength of prestressing strand
f_{se}	= final effective prestress after all losses
f_{SWLL}	= stress due to sidewalk live load
f_{total}	= total tensile stresses at service
f_y	= yield strength of mild steel
G	= final force effect applied to a girder
g_1	= single lane live load distribution factor
G_D	= force effect due to design loads
g_m	= multiple lane live load distribution factor
G_p	= force effect due to overload truck
I	= impact factor
I_c	= composite moment of inertia
I_N	= noncomposite moment of inertia
IM	= dynamic load allowance
K_g	= longitudinal stiffness parameter
L	= span length
LDF	= load distribution factor
LL	= live load effect
LL_{SW}	= live load effect

M_B	= barrier moment
M_D	= dead load moment
M_d	= total unfactored dead load moments
M_{FL-120}	= maximum FL-120 truck moment per lane
M_G	= unfactored bending moment due to weight of the beam/girder moment
$M_{HL-93 \text{ Design Truck}}$	= maximum LRFD design truck moment per lane
$M_{HL-93 \text{ Design Tandem}}$	= maximum LRFD design tandem moment per lane
$M_{HL-93 \text{ Design Lane Load}}$	= maximum LRFD design lane load moment per lane
$M_{WL-HS 20}$	= maximum HS 20 wheel-load moment per lane
M_L	= live load moment
M_{LL+I}	= unfactored live load plus impact moment
M_n	= nominal flexural resistance
M_S	= unfactored bending moment due to weight of the deck
M_{test}	= maximum test vehicle moment
M_u	= factored bending moment at section
M_w	= future wearing surface moment at section
$M_{WL-HS20}$	= maximum wheel-load moment, HS20 truck
N_u	= applied factored axial force taken as positive if tensile
N_w	= number of wheel loads on the tested bridge
n	= modular ratio between slab and beam materials
p	= ratio of prestressing steel
P	= permanent loads other than dead loads
P_{se}	= effective pretension force after allowing for all losses
P_{si}	= effective pretension force after allowing for the initial losses
q	= uniform load
R_n	= nominal member resistance (as inspected)
RF	= rating factor – the ratio of available live load moment or shear capacity to the moment or shear produced by the loading being investigated
RF_{OP}	= operating rating with AASHTO factored load method
RF_{IN}	= inventory rating with AASHTO factored load method
RH	= relative humidity
S	= spacing of beams
SH	= loss of pretension due to concrete shrinkage/shrinkage loss (assume $RH = 70\%$)
s	= spacing of stirrups
T	= tension tie
V_c	= shear resistance components due to concrete

V_n	= nominal shear resistance of the section considered
V_p	= shear resistance components due to inclined prestressing strand
V_r	= factored shear resistance
V_s	= shear resistance components due to shear reinforcement/shear reinforcement capacity
V_u	= factored shear force at section
WDF	= wheel load distribution factor
w_c	= unit weight of concrete
y_{bs}	= distance from the center of gravity of strands to the bottom fiber of the beam
y_{Cb}	= distance from the center of gravity of composite section to the bottom fiber of the beam
y_{Cgt}	= distance from the center of gravity of composite section to the top fiber of the girder
y_{Ct}	= distance from the center of gravity of composite section to the top fiber of the deck
y_{Nb}	= distance from centroid to the extreme bottom fiber of the non-composite beam
y_{Nt}	= distance from centroid to the extreme top fiber of the non-composite beam
Z	= a factor taken as 1.20 where the lever rule was not utilized, and 1.0 where the lever rule was used for a single lane live load distribution factor
α	= angle of inclination of transverse reinforcement to longitudinal axis
β	= factor relating effect of longitudinal strain on the shear capacity of concrete, as indicated by the ability of diagonally cracked concrete to transmit tension
β_1	= factor for concrete strength
ϵ_i	= measured strain at a cross section of the bridge
ϵ_{max}	= maximum measured strain at a cross section of the bridge
$\epsilon_{measured}$	= measured strain
γ	= load factor
γ_D	= dead load factor
γ_{DC}	= LRFD load factor for DC
γ_{DW}	= LRFD load factor for DW
γ_L	= live load factor
γ_{LL}	= evaluation live load factor
γ_p	= LRFD load factor for permanent loads other than dead loads
ϕ	= LRFD resistance factor (strength reduction)
ϕ_c	= condition factor
ϕ_s	= system factor
θ	= angle of inclination of diagonal compression stresses

Bridge Load Rating

18.1 OVERVIEW OF BRIDGE LOAD RATING

18.1.1 Purpose

Aging, environmental conditions, damage due to vehicular impact, and increased gross vehicle weights result in structural deterioration that affects the load carrying capacity of bridges. These changes impact safety and require periodic re-evaluation of bridge capacity. The capacity evaluation process is defined as load rating. The load rating of a bridge is a component of the inspection process and is used to determine both the safe load carrying capacity of a bridge and whether specific overweight vehicles can use the bridge. Load rating also determines if the bridge needs to be weight restricted, and, if so, what level of restriction (posting) is required.

Load and Resistance Factor Rating (LRFR) is performed in accordance with the procedures given in the *AASHTO Manual for Bridge Evaluation*, Second Edition, 2011. This publication addresses the use of working stress (allowable stress), load factor (factored load) ratings, and load and resistance factor ratings. It also addresses the “hierarchy” of these various analytical approaches. For consistency of presentation when this chapter refers to working stress (WS) and ultimate design, the user will need to remember if the section is addressing the *AASHTO Standard Specifications* or *LRFD Specifications*. The detailed load rating example presented later in this chapter illustrates these various specification approaches.

New bridges designed in accordance with the *LRFD Specifications* after October 1, 2010, must be rated using the Load and Resistance Factor rating method. Furthermore, for consistency in interpreting the results of bridge evaluations, it is desirable to rate all bridges designed in accordance with the *LRFD Specifications* using the Load and Resistance Factor rating method.

18.1.2 Definitions

The following are standard definitions of some of the terms used in load rating:

Inventory Rating — The load that can safely utilize the bridge for an indefinite period of time. Generally this analysis is performed in accordance with the design specifications.

Operating Rating — The absolute maximum permissible load to which the bridge can be subjected. This analysis may utilize posting avoidance techniques as specified by the jurisdiction.

Load Rating — The process of determining the live load capacity of a bridge based on its current conditions through either analysis or load testing.

Rating Factor — The ratio of available live load moment or shear capacity to the moment or shear produced by the load being investigated.

Routing Vehicle — A state defined permit truck that is used to create overload maps used in prescribing which arterial route maybe be used by a defined set of Specialize Hauling Vehicles (SHV).

18.1.3 Load Rating Procedure

Bridge load rating is dependent on a large number of variables. In order to create the analytical model, certain assumptions must be made about the individual bridge components. In addition, the engineer must decide whether the standard AASHTO equations and factors accurately model the true response of the bridge. If necessary, the equations and factors should be modified to reflect actual conditions.

To establish the load rating of a bridge, the following five steps need to be followed:

18.1.3.1 Collect Information on the Current Bridge Condition

The structural state of the bridge needs to be determined and evaluated for any criteria, which could affect performance. Variables affecting performance should be determined from an on-site-inspection so that an up-to-date condition evaluation can be made. Items, which need to be examined, include:

- Primary and secondary component condition
- Current state of existing scour
- Deck condition

BRIDGE LOAD RATING**18.1.3.1 Collect Information on the Current Bridge Condition/18.1.3.2.3 Impact Loads**

- Joint condition (expansion and contraction)
- Condition and type of bearings
- Traffic Conditions
- Any additional items required for a proper evaluation of the structure

Thorough field investigation may offer support in using less conservative values than the specified values for the optional LRFR condition factors provided in the *Manual for Bridge Evaluation*. The smoothness of the riding surface should also be examined and reported if the load rating engineer desires to specify a reduced value for dynamic load allowance in an analytical bridge evaluation, as discussed in Section 18.1.3.2.3. Generally, deck condition would not reduce ϕ_c .

Distribution of live loads and secondary dead loads in bridges with adjacent prestressed concrete units without cast-in-place (CIP) decks is influenced by the conditions of the longitudinal joints. When the joints between the prestressed units (i.e., hollow core slab, box section, double tee, etc.) are in good condition and provide adequate transverse distribution of the applied loads, secondary dead loads should be distributed equally to all units. However, cracking in the longitudinal grouted joints between adjacent beams can lead to leakage, corrosion, and, in severe cases, complete cracking of joints and loss of load transfer. When the joints between the units are cracked and the units are acting independently, engineering judgment must be used to determine load distribution, to which the S/D method of live load distribution provided in Section 4, Article 4.6.2.2 of the *AASHTO LRFD Bridge Design Specifications* (2010) could be used. NCHRP Synthesis 393 provides a good source of information on current design and construction practices of connections between adjacent box beams (Russell, 2009).

Inspection of the structure also yields information about any damage or repair since the last rating. Structural deterioration can have serious effects on the assumed analysis and rating. Damage from section loss due to impact or corrosion can affect the component strength and load distribution and could seriously reduce the true capacity of a section. Additionally, the Average Daily Truck Traffic (ADTT) volume can be evaluated and compared to the assumed or surveyed information for the bridge.

18.1.3.2 Determine Nominal Loading and Nominal Resistances**18.1.3.2.1 Dead loads**

The engineer must calculate the actual weights permanently attached to the structure and their proper configuration, i.e., point load, distributed load, etc. Recommended unit weights for various materials can be found in *LRFD Specifications*. Allowances for additional weight, which may accumulate over time, are also given. Ratings based on the *LRFD Specifications* assume worst case conditions for the component materials. While load testing may provide a better indication of the true condition, the rating engineer must recognize that properties will probably not be homogeneous throughout the structure; this variability must be considered in the analytical model.

18.1.3.2.2 Live loads

According to AASHTO requirements, the vehicle from the survey of legal vehicles that creates the maximum live load effect must be used. For example, the *LRFD Specifications* requires that all interstate highway bridge structures have a minimum design capacity equal to the HL-93 design loading. In evaluating the effects of the vehicular loading, only one such vehicle is considered to be present in each lane since the load factors, which will be applied later, were created to recognize the possibility of multiple vehicles. Vehicles with special permits may also have access to the bridge. In this case, the actual vehicle loading must also be checked prior to issuing the permit.

18.1.3.2.3 Impact loads

To account for dynamic effects, impact values are provided in both the *Standard and LRFD Specifications* as an increase in the weight of the design vehicle. These values are known to be conservative in some cases and in certain situations a reduction can be applied. For instance, in longitudinal members having spans > 40 ft with less severe surface depressions or deviations at approach slabs and/or decks, the LRFD dynamic load allowance (*IM*) may be reduced for legal vehicles and permit loads, respectively, as given in **Table 18.1.3.2.3-1**.

BRIDGE LOAD RATING

18.1.3.2.3 Impact Loads/18.2.1 Dead Loads

Table 18.1.3.2.3-1**LRFD Dynamic Load Allowance: IM [AASHTO 2011]**

Surface Roughness Rating	Description	IM
3 = Smooth	Smooth riding surface (approaches, bridge deck, and expansion joints)	10%
2 = Average	Minor surface depressions or deviations	20%
1 = Poor	Major surface depressions or deviations (approaches, bridge deck, and expansion joints)	33%

18.1.3.2.4 Resistances

According to AASHTO requirements, the nominal strength of the specified materials must be used to calculate capacity. Analytical rating of bridges will usually assume perfect boundary conditions. However, it is possible that continuous spans will not work as designed, thus providing only partial continuity. Alternatively, simple spans may actually be partially restrained at the supports. These factors can influence the calculated load carrying capacity and should be considered.

Many aspects of a bridge may be different from what was assumed in the design. Effects of composite sections acting noncompositely, and the reverse must be considered. Contributions from secondary members not originally designed as load carrying components may actually reduce the stress in the primary members. Parapets, railings, and rigid flooring may add to the structural stiffness. Accounting for the contribution of secondary members/elements to the strength of the bridge may necessitate a more complex analysis.

18.1.3.3 Determine the Load Distribution

The engineer must make certain assumptions regarding the distribution of vehicle load to the individual members across the structure. *AASHTO Standard* and *LRFD Specifications*, respectively, provide some recommendations for these distribution values. However, values measured directly from the structure or obtained analytically can be substituted. Since the assumed load distribution has a significant impact on the rating process, it is necessary to determine this distribution as accurately as possible. Later in this chapter there is an example that discusses the variation of specification-predicted versus field-obtained load distribution values. When utilizing load distribution factors for live load, the load distribution formulas from the *LRFD Specifications* should be used with the LRFR rating method, and the load distribution formulas from the *Standard Specifications* should be used with the load factor and allowable stress rating methods.

18.1.3.4 Select Load and Resistance Factors

The load and resistance factors are taken such that worst case effects are used in the rating evaluation as recommended by the *AASHTO Bridge Design Specifications* and the *Manual for Bridge Evaluation (MBE)*.

18.1.3.5 Calculate the Rating Factor

Based on the information collected in the first four steps, a rating factor can be calculated as described in Section 18.3. If the value of this rating factor is less than 1, the structure is considered deficient to carry the specific load under consideration; if it is greater than 1, the structure is satisfactory.

The items listed above will be discussed in more detail in the following sections.

18.2 LOADS AND DISTRIBUTION**18.2.1 Dead Loads**

The effects of the current condition on dead loads should be considered using material densities as provided by the *AASHTO Specifications*. Load estimates should accurately reflect any changes in cross sectional dimensions along the span. Toppings, decks, or slab components with unknown thicknesses require either a conservative estimate or several core samples so that a statistically reliable value can be obtained. In addition, load factors given in the *AASHTO Specifications* to account for variations in the material density should be used.

Application of dead load in the analysis should consider any stress changes occurring from the time of initial erection to the present such that the effects of composite sections, continuity, and any other factors, which might affect performance, are properly recognized.

BRIDGE LOAD RATING

18.2.2 Live Loads/18.2.2.1 AASHTO 2002 Standard Specifications

18.2.2 Live Loads

In the load rating process, the effect of both the basic design vehicle and all legal and special permit vehicles or applicable fatigue vehicles should be evaluated so that the critical controlling load rating value is established. Additional effects such as wind, centrifugal, thermal, or other temporary forces must be considered if applicable.

The *AASHTO Specifications* require the placement of the design or rating vehicle 1 ft away from the curb line for the design or rating of the slab, and 2 ft for the design or rating of the girders. For a concrete box girder, the slab is rated with a wheel line placed no closer than 2 ft from the curb line.

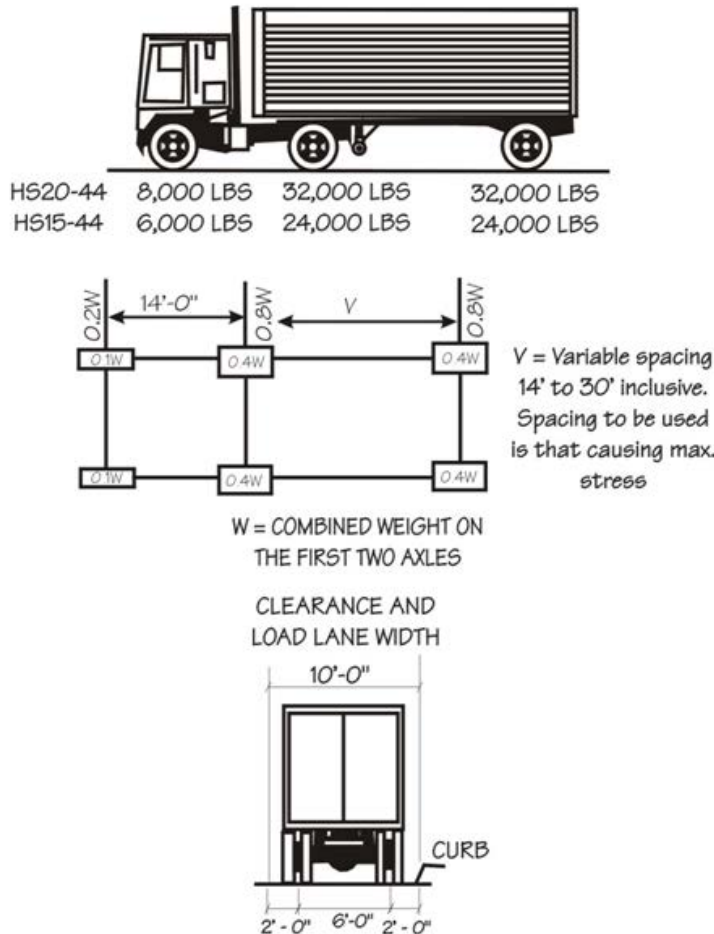
The *AASHTO Manual for Bridge Evaluation* requires vehicles to be placed in accordance with the *AASHTO Design Specifications*, but allows the engineer to use judgment in adjusting the placement according to the actual traffic patterns; however, no guidelines are provided. The following recommendations are representative examples of the cases where engineering judgment is necessary:

- Ramp structures striped for fewer lanes than the width of the structure could carry may be load rated for the actual number of lanes being carried.
- Bridges that would require posting if the full width of the structure was subject to live loads may be load rated by restricting the live load to the traveled lanes.

18.2.2.1 AASHTO 2002 Standard Specifications

For load rating per the *Standard Specifications*, there are four standard load vehicles: H15, H20, HS15, and HS20. For interstate highway structures, the minimum design vehicle is the HS20-44 or a military loading consisting of two axles, 4 ft apart with a weight of 24,000 lb each (see **Figures 18.2.2.1-1** and **18.2.2.1-2**).

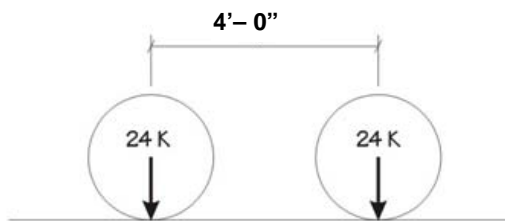
Figure 18.2.2.1-1
Standard HS Trucks



BRIDGE LOAD RATING

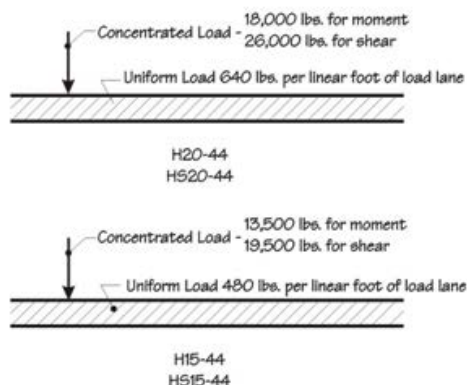
18.2.2.1 AASHTO 2002 Standard Specifications/18.2.2.2 AASHTO LRFD Specifications

Figure 18.2.2.1-2
Military Load (Standard Specifications)



The design vehicle selected should be the one that produces maximum stresses. The vehicle load is further increased for dynamic loading through application of an impact factor. In addition, a combination of uniformly distributed and concentrated loads, known as the lane load (**Figure 18.2.2.1-3**), must be compared to the design vehicle. The load creating maximum stresses should be used in the analysis. Location of the loads should be such that maximum stresses occur; in the case of continuous spans an envelope of stresses may be needed.

Figure 18.2.2.1-3
Lane Loading (Standard Specifications)



In a multiple lane bridge, it is unlikely that all lanes will be loaded simultaneously. To account for this fact, the design live load effect should be reduced depending on the number of loaded lanes as per AASHTO 3.12.1:

Number of Lanes Loaded	% of Design Load
1 or 2	100
3	90
4 or more	75

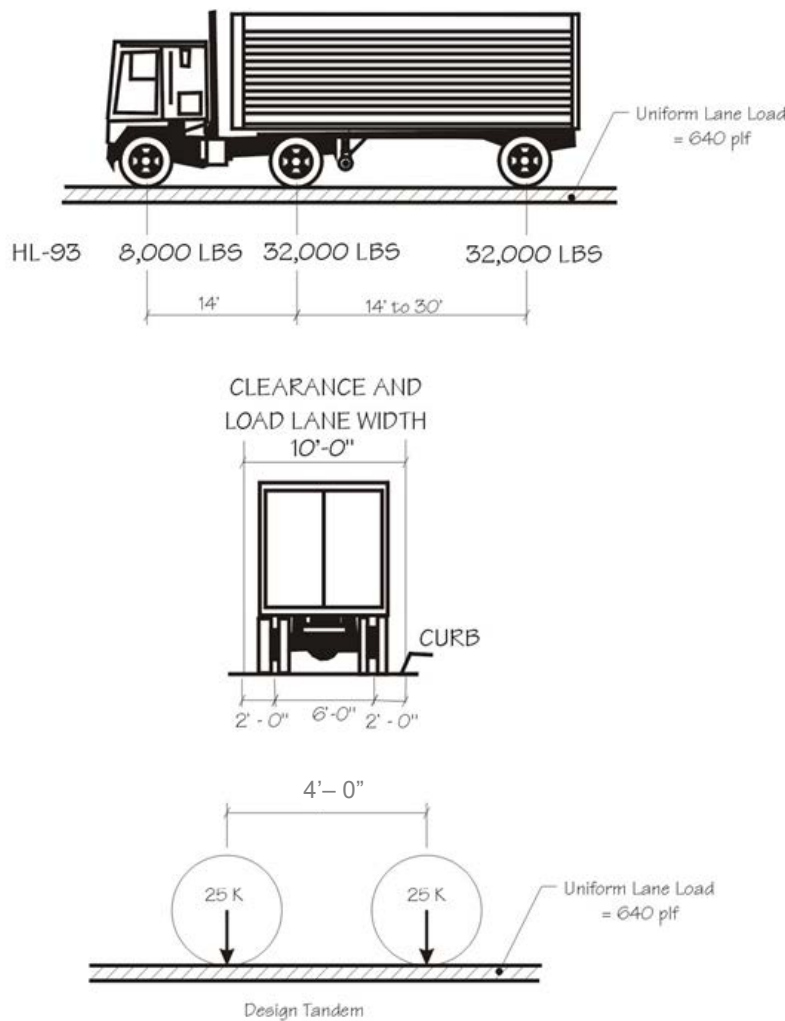
18.2.2.2 AASHTO LRFD Specifications

The standard bridge design live load used in the *LRFD Specifications* is designated HL-93 and consists of a design vehicle or tandem, combined with a uniform lane load (see **Figure 18.2.2.2-1**). For all LRFD limit states, except fatigue and fracture, the moving (vehicle) load is further increased by application of the Dynamic Load Allowance as specified in the *Manual for Bridge Evaluation*. In the analysis, the number of loaded lanes and the location of the live load should be such that maximum stresses occur.

BRIDGE LOAD RATING

18.2.2.2 AASHTO LRFD Specifications/18.2.3 Load Distribution Rating

Figure 18.2.2.2-1
LRFD Vehicular Load, HL-93



To account for the effect of multiple design vehicles on the structure simultaneously, adjustments are made to the live load as per LRFD 3.6.1.1.2:

Number of Lanes	Multiple Presence Factor, <i>m</i>
1	1.2
2	1.0
3	0.85
4 or more	0.65

18.2.3 Load Distribution for Rating

Distribution of the wheel loads for rating may utilize the simplified guidelines given in the *Standard Specifications* or the *LRFD Specifications* as applicable, unless a more detailed computer analysis is performed. For both the *Standard* and *LRFD Specifications*, the multiple presence factors, discussed above, are included in those load distribution factors given in the specifications. The provisions of the *Standard Specifications* and the *LRFD Specifications* should never be comingled when designing or load rating a structure (ie. Do not use LRFD distribution values for a working stress design with the *Standard Specifications*).

BRIDGE LOAD RATING**18.2.3.1 AASHTO 2002 Standard Specifications/18.3.1 Rating Equation****18.2.3.1 AASHTO 2002 Standard Specifications**

Longitudinal distribution of wheel loads will not be considered in the determination of end shears, reactions, and bending moment. Lateral distribution of wheel loads for shear will assume that the flooring acts as a simple span between stringers or beams. Lateral distribution of wheel loads on longitudinal elements for bending moments will follow AASHTO requirements of Articles 3.23.2.3, 3.23.4, 3.28, and Table 3.23.1.

18.2.3.2 AASHTO 2010 LRFD Specifications

Lateral distribution of wheel loads for moment and shear is given in Chapter 4 of the *LRFD Specifications*. The lever rule should be used for any structure that exceeds the range covered by the specifications. A more refined analysis procedure can be used with the appropriate multiple presence factors applied.

18.3 RATING METHODOLOGY**18.3.1 Rating Equation**

Generally, the rating of a bridge is controlled by the capacity of the member with the lowest rating. According to Section 6A.4.2 of the *Manual for Bridge Evaluation, 2nd Edition, with 2011 Interim Revisions*, the following Eq.18.3.1-1 should be used in determining the load rating of the structure:

$$RF = \frac{C - (\gamma_{DC})(DC) - (\gamma_{DW})(DW) \pm (\gamma_P)(P)}{\gamma_{LL} (LL + IM)} \quad (18.3.1-1)$$

where:

RF = rating factor

C for strength = $\phi_c \phi_s \phi R_n$

C for service = f_r

ϕ_c = condition factor

ϕ_s = system factor

ϕ = LRFD resistance factor

R_n = nominal member resistance (as inspected)

DC = dead load effect due to structural components and attachments

DW = dead load effect due to wearing surface and utilities

P = permanent loads other than dead loads

LL = live load effect

IM = dynamic load allowance

γ_{DC} = LRFD load factor for DC

γ_{DW} = LRFD load factor for DW

γ_P = LRFD load factor for permanent loads other than dead loads = 1.0

γ_{LL} = evaluation live load factor

The coefficients incorporated in Eq.18.3.1-1 may have different values depending on the type of load rating (inventory or operating), and rating method (working stress or factored load).

The condition factor ϕ_c is to provide certain reduction to account for the increased uncertainty in the resistance of deteriorated elements. System factor ϕ_s is a multiplier, which depends on the superstructure type and is utilized to reflect the level of redundancy of the superstructure system. Bridges with less redundancy level will have their factored resistance reduced. The aim of the ϕ_s term is to provide reserve capacity for traveling safety. The condition $\phi_c \phi_s \geq 0.85$ shall be applied in accordance with the *Manual for Bridge Evaluation*.

BRIDGE LOAD RATING

18.3.2 Analysis Method/18.3.2.1.2 Legal, NRL, and SHV Loads

18.3.2 Analysis Method

The load rating procedure should use approximate methods of analysis given in the *AASHTO Specification* unless a refined procedure is deemed necessary. In selection of the refined procedure, any method known to produce an accurate representation of the existing conditions may be used. These methods include, but are not limited to finite element analysis, classical numerical analysis, and bridge design programs. When a refined method is used, a table of live load distribution coefficients for extreme force effects in each span must be provided per AASHTO requirements.

18.3.2.1 Load Factors

For analysis in accordance with the *Standard Specifications*, the load factors γ and β corresponding to the respective group loading are given in Table 3.22.1A. For LRFD based analysis, the factors from the *Manual for Bridge Evaluation* and the *LRFD Specifications* are used.

18.3.2.1.1 Design Loads

The design load rating produces Inventory and Operating level rating factors for the HL-93 loading. The live load factors for the Strength I limit state shall be taken as specified in **Table 18.3.2.1.1-1**. The dynamic load allowance of 33% is applied regardless of the riding surface condition or the span length.

*Table 18.3.2.1.1-1
Load Factors for Design Load
[AASHTO, 2011]*

Evaluation Level	Load Factor
Inventory	1.75
Operating	1.35

18.3.2.1.2 Legal, NRL, and SHV Loads

The live load factors for AASHTO and State legal loads for the Strength I limit state are taken as given in **Table 18.3.2.1.2-1**, while the live load factors for the Notional Rating Load (NRL) and Specialized Hauling Vehicles (SHV) posting loads for the Strength I limit state are taken as given in **Table 18.3.2.1.2-2**. The dynamic load allowance is applied in accordance with **Table 18.1.3.2.3-1** in Section 18.1.3.2.3. It is worth mentioning that if the load rating factor is greater than 1.0 for NRL, the rating for SHV is not required. It should be noted that only one level of rating results from legal (posting level) and permit load evaluation with the Load and Resistance Factor rating method, which is considered to be an operating level that will accommodate the evaluation vehicle for an indefinite period of time.

*Table 18.3.2.1.2-1
Load Factors for Legal Loads [AASHTO, 2011]*

Traffic Volume (One direction)	Load Factor
Unknown	1.80
ADTT \geq 5000	1.80
ADTT = 1000	1.65
ADTT \leq 100	1.40

Note: Linear interpolation is permitted for other ADTT

*Table 18.3.2.1.2-2
Load Factors for NRL and SHV [AASHTO, 2011]*

Traffic Volume (One direction)	Load Factor
Unknown	1.60
ADTT \geq 5000	1.60
ADTT = 1000	1.40
ADTT \leq 100	1.15

Note: Linear interpolation is permitted for other ADTT.

BRIDGE LOAD RATING**18.3.2.1.3 Permit Load/18.3.3.1 Working Stress Method****18.3.2.1.3 Permit Load**

The live load factors for permit loads for the Strength II limit state are taken as given in **Table 18.3.2.1.3-1**, or as the factor specified in State Load Rating Policy if applicable. The dynamic load allowance is applied in accordance with **Table 18.1.3.2.3-1** in Section 18.1.3.2.3.

Table 18.3.2.1.3-1
Load Factors for Permit Load [ASHTO, 2011]

Permit Type	Frequency	Loading Condition	DF^a	ADTT (one direction)	Load Factor by Permit Weight ^b	
					Up to 100 kips	≥150 kips
Annual	Unlimited Crossings	Mix with traffic (other vehicles may be on the bridge)	Two or more lanes	> 5000	1.80	1.30
				= 1000	1.60	1.20
				< 100	1.40	1.10
					All Weights	
Special or Limited Crossing	Single-Trip	Escorted with no other vehicles on the bridge	One lane	N/A	1.15	
				Single-Trip	Mix with traffic (other vehicles may be on the bridge)	One lane
	= 1000	1.40				
	< 100	1.35				
	Multiple-Trips (less than 100 crossings)	Mix with traffic (other vehicles may be on the bridge)	One lane	> 5000	1.85	
				= 1000	1.75	
< 100				1.55		

- DF = LRFD distribution factor. When one-lane distribution factor is used, the built-in multiple presence factor should be divided out.
- For routine permits between 100 and 150 kips, interpolate the load factor by weight and $ADTT$ value. Use only axle weights on the bridge. Later in this chapter there is an example that includes the illustration of the load rating for the permit load.

18.3.2.2 Strength Resistance Factors

For analysis per the *Standard Specifications*, material strengths are reduced by the resistance factor that corresponds to the material and design group under consideration. In the *LRFD Specifications*, the resistance factors corresponding to the different limit states are used.

18.3.2.3 Adjustments for Actual Conditions

Where field inspection indicates that there is structural deterioration or a loss of section, the engineer should calculate the remaining competent structural section of concrete, reinforcement, and strands, and the resistance factor should be reduced by up to an additional 15% by LRFR to account for the uncertainty of the condition and strength. If material properties have been established by physical testing, a mean value multiplied by 0.9 along with the appropriate resistance factor can be used.

Washington and Florida adopted a slightly different methodology for the selection of resistance factors with a maximum reduction factor of up to an additional 20%. The condition factor in LRFR, systematically handles the uncertainty in condition and strength of a deteriorated member.

18.3.3 Load Rating Methods**18.3.3.1 Working Stress Method**

The general rating formula (Section 18.3.1) reduces to the following format for working stress rating in terms of *Standard Specifications*:

$$RF = \frac{f_{allow} - \Sigma f_{DL}}{f_{LL+I}} \quad (18.3.3.1-1)$$

BRIDGE LOAD RATING**18.3.3.1 Working Stress Method/18.3.3.2 Factored Load Method**

where f_{allow} , f_{DL} , and f_{LL+I} are the allowable stress, dead load stress, and live load plus impact stress, respectively. For prestressed concrete members, the allowable stresses (f_{allow}) for inventory rating should be based on the *Standard Specifications* (Article 9.15.2.2) or the *Manual for Bridge Evaluation* (Article 6B.6.3.3). Meanwhile, for the operating rating, the allowable stresses (f_{allow}) should result in moments not to exceed 75% of the ultimate moment capacity of the member (Article 9.17).

The *Manual for Bridge Evaluation* does not provide clear guidance on sidewalk live load for bridge rating. It states sidewalk loading shall not be considered coincident with traffic loading unless the engineer has reason to suspect that significant sidewalk loading will occur coincident with maximum traffic loading.

The *Standard Specifications*, Article 3.23.2.3.1.3, allows a 25% over-stress in the outside roadway stringer for the combination of dead load, sidewalk live load, vehicular live load, and impact. Therefore, the structure should be checked for the following two conditions.

- 1) $f_{DL} + f_{LL+I} + f_{SWLL} < 1.25$ (allowable stress)
- 2) $f_{DL} + f_{LL+I} < \text{allowable stress}$

where f_{SWLL} is the stress due to sidewalk live load.

The *Standard Specifications*, Article 3.24.2.2., also specifies that in designing sidewalk, slab, and supporting members, a wheel load located on the sidewalk shall be 1 ft away from the rail when there is no barrier between the sidewalk and the roadway. An element 8 in. or higher may be considered a barrier. The stress due to the combined dead, live, and impact loads shall not be greater than 150% of the allowable stresses.

A 50% overstress is allowed for this condition, therefore, the worst case of the following two load equations should be applied:

- 1) $f_{DL} + f_{LL+I} < \text{allowable stress}$ no wheel load on sidewalk.
- 2) $f_{DL} + f_{LL+I} < 1.5$ (allowable stress) wheel load on sidewalk.

18.3.3.2 Factored Load Method

The general rating formula (Section 18.3.1) reduces to the following format for factored load rating (illustrated for flexural capacity):

$$RF = \frac{\phi M_n - \gamma_D \Sigma M_D}{\gamma_L M_L (1 + I)} \quad (18.3.3.2-1)$$

where ϕ is specified in the *Standard Specifications* Article 9.14, γ_D is 1.3, and γ_L is 1.3 for operating rating and $(1.3)(1.67) = 2.17$ for inventory rating.

The *Standard Specifications*, Article 3.23.2.3.1.3, states that, when sidewalk live load is included, a load factor equal to 1.25 should be used instead of 1.67 in the ultimate strength equation. Therefore, the inventory rating should be determined from the worst case of the two following equations:

- 1) $M_u = 1.3[DL + 1.67(LL + I)]$
- 2) $M_u = 1.3[DL + 1.25(LL + I) + LL_{SW}]$

For operating rating, there is no specific guidance in the *AASHTO Specifications*. The following two equations should be checked with the worst case being used for the operating rating:

- 1) $M_u = 1.3[DL + (LL + I)]$
- 2) $M_u = 1.3[DL + 0.75(LL + I) + LL_{SW}]$

This is a reasonable approach based on the very low probability of having maximum sidewalk live load and maximum traffic live load at the same time. Where pedestrian traffic is minimal, the sidewalk live load can be considered as zero for load rating purposes.

BRIDGE LOAD RATING**18.3.3.2 Factored Load Method/18.3.4 Rating Method for Prestressed Concrete Bridges**

Similarly, when a wheel load on the sidewalk is considered, the *Standard Specifications*, Article 3.24.2.2, specifies that the inventory rating should use a beta factor of 1.0 instead of 1.67. Therefore, the worst case of the following two equations should be considered for each rating:

— Inventory Rating:

- 1) $M_u = 1.3[DL + 1.67(LL + I)]$ no wheel load on sidewalk.
- 2) $M_u = 1.3[DL + (LL + I)]$ wheel load on sidewalk.

— Operating Rating

- 1) $M_u = 1.3[DL + (LL + I)]$ no wheel load on sidewalk.
- 2) $M_u = 1.0[DL + (LL + I)]$ wheel load on sidewalk.

For other special cases, the rating formula can be derived as shown in Section 18.3.1 by equating the capacity to the load effect. In the next section the corresponding rating formulas for LRFD rating are similarly derived.

18.3.3.3 Load and Resistance Factor Method

The general rating formula (Section 18.3.1) reduces to the following format for factored load rating (illustrated for flexural capacity):

$$RF = \frac{C - (\gamma_{DC})(DC) - (\gamma_{DW})(DW)}{\gamma_{LL}(LL + IM)} \quad (18.3.3.3-1)$$

where C is the factored capacity, γ_{DC} is 1.25, γ_{DW} is 1.5 and γ_{LL} is 1.35 for operating rating and 1.75 for inventory rating.

Regarding the sidewalk live load, the corresponding rating formulas for LRFD rating can be similarly derived from Section 18.3.3.2. For the inventory rating, load effects should be determined from the worst case of the two following equations:

- 1) $M_u = 1.25 DL + 1.5 DW + 1.75(LL + I)$
- 2) $M_u = 1.25 DL + 1.5 DW + 1.3(LL + I) + LL_{SW}$

For operating ratings, the following two equations should be checked with the worst case:

- 1) $M_u = 1.25 DL + 1.5 DW + 1.35(LL + I)$
- 2) $M_u = 1.25 DL + 1.5 DW + (LL + I) + LL_{SW}$

Similarly, when a wheel load on sidewalk is considered, the worst case of the following two equations should be considered for each rating:

— Inventory Rating:

- 1) $M_u = 1.25 DL + 1.5 DW + 1.75(LL + I)$ no wheel load on sidewalk.
- 2) $M_u = 1.25 DL + 1.5 DW + 1.3(LL + I)$ wheel load on sidewalk.

— Operating Rating

- 1) $M_u = 1.25 DL + 1.5 DW + 1.35(LL + I)$ no wheel load on sidewalk.
- 2) $M_u = 1.0 DL + 1.0 DW + 1.0(LL + I)$ wheel load on sidewalk.

18.3.4 Rating Method for Prestressed Concrete Bridges

Both the working and factored load methods can be used in the load rating of bridges. However, special attention should be given to prestressed concrete members due to their unique design requirements. In a typical design of prestressed concrete members, working stress method is used in sizing the member to resist a specified

BRIDGE LOAD RATING

18.3.4 Rating Method for Prestressed Concrete Bridges/18.3.4.1 Proper Methods for Determining the Nominal Shear Capacity

allowable stress under service loads, and then the factored load method is used to check the ultimate capacity of the member. The service stress requirement, in most cases, controls the design resulting in additional prestressing strands and hence, higher ultimate capacity. Utilizing the factored load method in rating prestressed concrete elements could result in artificially high load rating that is not consistent with the original design assumptions.

To be compatible with the original design, the rating of prestressed concrete members should be conducted with both the working and factored load methods. The member load rating should be the lower value of the two methods. **Table 18.3.4-1** shows the LRFD load factors required for load rating of prestressed concrete.

Table 18.3.4-1
Limit States and Load Factors for Load Rating [AASHTO, 2008]

Bridge Type	Limit State	Dead Load γ_{DC}	Dead Load γ_{DW}	Design Load		Legal Load γ_{LL}	Permit Load γ_{LL}
				Inventory	Operating		
				γ_{LL}	γ_{LL}		
Prestressed Concrete	Strength I	1.25	1.50	1.75	1.35	Table 18.3.2.1.2-1 and 18.3.2.1.2-2	—
	Strength II	1.25	1.50	—	—	—	Table 18.3.2.1.3-1
	Service III	1.00	1.00	0.80	—	1.00	—
	Service I	1.00	1.00	—	—	—	1.00

In general, whether working stress method or factored load method is used is up to the bridge owner’s policy. Many bridge owners utilize ratings of stress and strength for purposes of load postings. Some state DOTs post for operating, some for inventory, and some post for intermediate condition. In the case of prestressed concrete, this may result in a large variation in the rating capacity for the same bridge depending on the adopted policy. Posting avoidance techniques are generally defined in a state policy. These working stress (or SLS for LRFD) policy adjustments may allow rating engineers to use an overstresses for an operating rating that may knowingly shorten the remaining service life. These approaches should always rely on strength checks (both shear and flexural) as the maximum safe load. With system preservation and extending service life to more than 100 years as a goal, bridge engineers have begun to investigate limiting working stress and the definitions and uses of inventory and operating ratings may be refined by AASHTO Subcommittee on Bridges and Structures (SCOBS) newly created Technical Committee on Preservation. In years past, using LFR approaches it was often thought more reasonable to use the working stress method to establish the inventory rating and the factored load method for operating rating. For these cases (prestressed concrete members), load posting could have been controlled by the inventory rating. In the *Manual for Bridges Evaluation* special permits for occasional over loads are based on the operating rating. Some jurisdictions have mandated the optional service checks for the operating rating computations. The rating methodology for prestressed concrete bridges is demonstrated in the example in Section 18.6.

18.3.4.1 Proper Methods for Determining the Nominal Shear Capacity

The nominal shear resistance is calculated from the *LRFD Specifications* equation 5.8.3.3-1:

$$V_n = V_c + V_s + V_p$$

Where, V_c , V_s , and V_p are the shear resistance components due to the concrete, shear reinforcement, and the inclined prestressing strand, respectively.

The V_s component is computed from AASHTO LRFD equation 5.8.3.3-4:

$$V_s = \frac{A_v f_y d_v (\cot \theta + \cot \alpha) \sin \alpha}{s}$$

When $\alpha = 90^\circ$, the above equation reduces to:

$$V_s = \frac{A_v f_y d_v \cot \theta}{s}$$

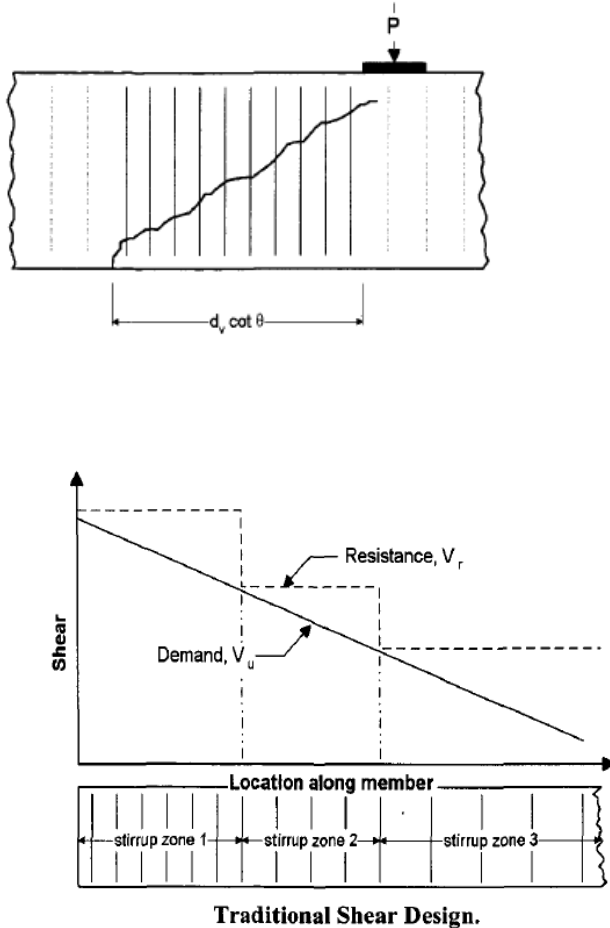
where s = spacing of stirrups, in.

BRIDGE LOAD RATING

18.3.4.1 Proper Methods for Determining the Nominal Shear Capacity

The shear reinforcement is distributed along a distance = $d_v \cot \theta$ as shown in **Figure 18.3.4.1-1** below.

Figure 18.3.4.1-1
Shear Force Diagram and Shear Reinforcements



Traditional Shear Design.

The above approach is acceptable for a design problem where the spacing along different zones is constant. This could lead to inaccuracies in an analysis problem, where various shear stirrup spacings could be present within the same zone.

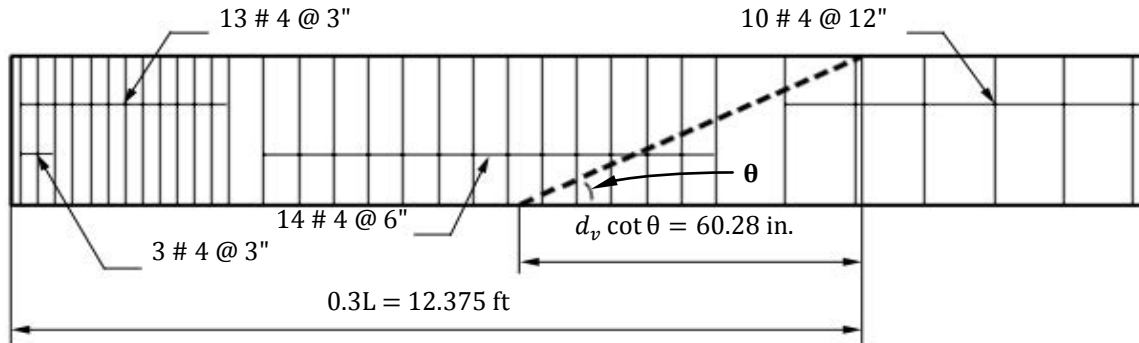
Shear failures occur over an inclined plane and a shear crack typically intersects the stirrups within the distance $d_v \cot \theta$. Each of the stirrups crossing this crack share in resisting the applied shear load and should be included in determining the nominal shear capacity at a specific section. Using the actual number of stirrups crossing the shear failure plane is the most accurate approach for determining the shear reinforcement capacity, V_s .

An illustrative example is the Type II AASHTO girder below (**Figure 18.3.4.1-2**) where routine load rating indicated shear deficiency at a section located at a distance equal to 0.3 of the span length, L .

BRIDGE LOAD RATING

18.3.4.1 Proper Methods for Determining the Nominal Shear Capacity

Figure 18.3.4.1-2
Shear Reinforcing Details and Failure Plane at 0.3L



At Section 0.3 L: $d_v = 40.6$ in. $\theta = 33^\circ$ $s = 12$ in.
 $d_v \cot \theta = 60.28$ in. Bar size: No. 4 $f_y = 60$ ksi

Counting the actual number of steel stirrups crossing the shear plane, it can be clearly seen that six stirrups with 6-in. spacing and two stirrups with 12-in. spacing will contribute to the shear resistance. The comparison between the specification approach and the exact method for calculating the concrete and steel shear contribution is shown in **Table 18.3.4.1-1**.

Table 18.3.4.1-1
Comparison between the Specification Approach and Exact Method

	Code Equation	Actual
V_c	$V_c = 0.0316 \beta \sqrt{f'_c} b_v d_v = 0.0316(2.399)\sqrt{8.5}(6.0)(40.026) = 53.07$ kips	
V_s	$V_s = \frac{A_v f_y d_v \cot \theta}{s} = \frac{0.2(60)(40.6) \cot 33.67}{12} = 60.28$ kips	Area of 8 stirrups: $A = 0.2(8) = 1.6$ in. ² $V_s = A f_y = 1.6(60) = 96$ kips

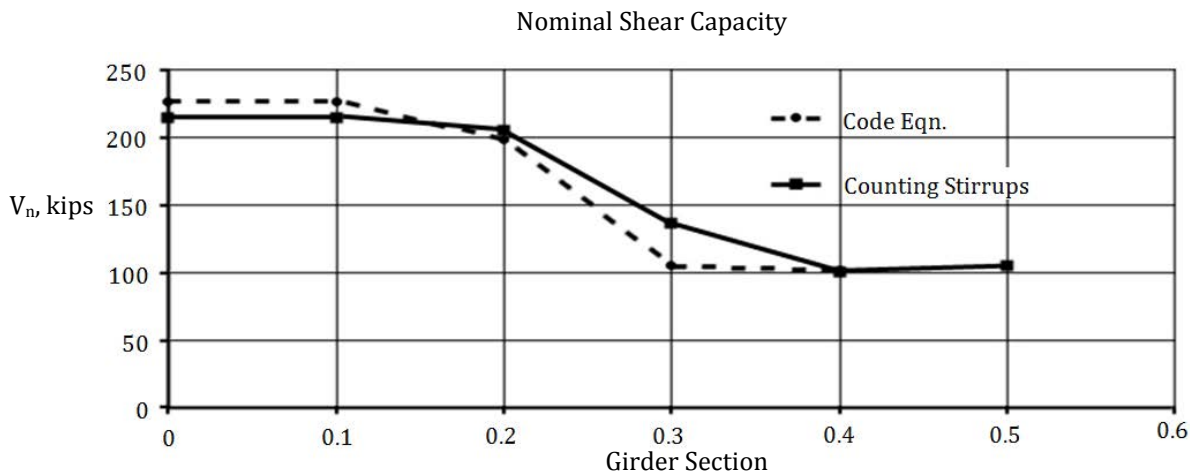
It can be seen that using the exact approach the contribution of shear reinforcement, V_s is 59% higher than that obtained using the specification approach which will result in a significant difference in the shear load rating.

It should be pointed out that the results could vary from section to section along the beam depending on the reinforcement detailing. The comparison of the two analytical approaches for the entire girder under consideration is shown in the **Figure 18.3.4.1-3**.

BRIDGE LOAD RATING

18.3.4.1 Proper Methods for Determining the Nominal Shear Capacity

Figure 18.3.4.1-3
Comparison of Two Approaches For the Entire Girder



Capacity	% L						Analysis Method
	0	0.1	0.2	0.3	0.4	0.5	
v_c	106.6	106.6	83.8	55.9	51.7	56.1	Counting the number of stirrups
v_s	132	132	144	96	60	60	
v_r	214.8	214.8	205.0	136.8	100.6	104.5	
v_c	106.6	106.6	83.8	56.0	51.7	56.1	Specification equation
v_s	145.0	145.0	137.4	60.1	59.5	61.2	
v_r	226.5	226.5	199.01	105.4	100.1	105.6	

To calculate the shear capacity of sections closer to the support than d_v , the specification does not specify which approach to use. As a matter of fact, when the section is close to the support, the shear force resistance mechanism changes and the above method may yield a lower bound answer. When the shear demand exceeds the capacity calculated at critical section, d_v the engineer should consider a refined approach like a strut-and-tie analysis. From a strut-and-tie model, it is clear that the closer the section is to the support, the higher its shear resistance capacity and for any section closer to the support than d_v , its V_s can be conservatively set to be equivalent to the capacity at the critical section, d_v .

The above approaches are strength based. If field inspections report shear cracking in the ends of girders, U-beams, or boxes, the engineer should review web principal stresses at service loads for notional legal and permitted vehicles.

BRIDGE LOAD RATING

18.3.4.1 Proper Methods for Determining the Nominal Shear Capacity/18.3.4.2 Effects of Strand Debonding on Shear Resistance

Figure 18.3.4.1-4
Forces assumed in Resistance Model Caused by Moment and Shear

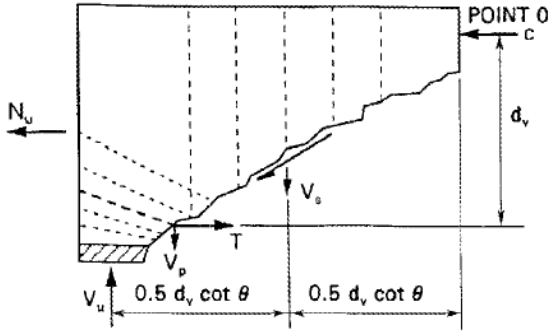


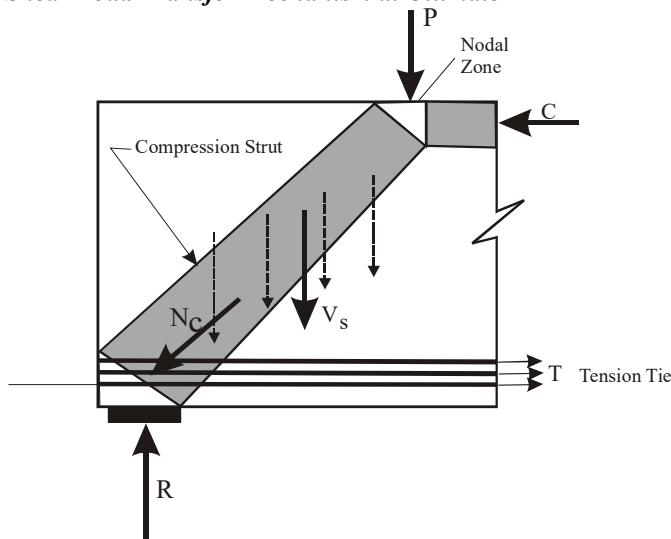
Figure C5.8.3.5-1 Forces Assumed in Resistance Model Caused by Moment and Shear.

18.3.4.2 Effects of Strand Debonding on Shear Resistance

The *Standard Specifications* does not consider the effect of strand shielding on the shear capacity of prestressed concrete girders and does not impose any limits on debonding. Therefore, the calculated shear capacity based on the *Standard Specifications* is not affected by strand debonding. Appropriate attention is needed to end zone detailing. SHA rating policies for *Standard Specification* application should address how engineers analyze end zones. The *LRFD Specifications* impose a limit of 25% on the number of debonded strands and provide clear guidance for detailing and terminating locations.

Excessive strand debonding is most often experienced in older bridges that were designed according to the *Standard Specifications*. Generally, excessive debonding of strands near the ends of the prestressed girders is an important issue in the load rating, since it impacts the tension tie capacity as shown by the load transfer mechanism in **Figure 18.3.4.2-1**.

Figure 18.3.4.2-1
Shear Load Transfer Mechanism at Ultimate



BRIDGE LOAD RATING**18.3.4.2 Effects of Strand Debonding on Shear Resistance /18.4.2.1 Proof Load Test**

The *LRFD Specifications* require a longitudinal check of the reinforcement at the face of bearing and sets a limit through LRFD Equation 5.8.3.5-2. The required anchorage force (tension tie) at the face of bearing can be calculated as:

$$A_s f_y + A_{ps} f_{py} \geq \left(\frac{V_u}{\phi} - 0.5 V_s - V_p \right) \cot \theta \quad \text{LRFD Eq. 5.8.3.5-2}$$

It can be seen in LRFD Eq. 5.8.3.5-2 that both the longitudinal steel and prestressing strands contribute to the tie strength. In cases where excessive strand debonding is encountered, special attention to the end details is important to account for any existing steel reinforcement that is developed beyond the face of the support. In cases where insufficient tie capacity exists, engineering judgment and reduction of the shear capacity will be necessary to guard against bond failure. When an older design that violates the current shielding limitation is evaluated, this LRFD approach (Eq. 5.8.3.5-2) will yield an indication to aid the evaluating engineer if there is a shear capacity deficiency.

It should be noted that while all bridges are designed for a certain design load, many states routinely allow permit loads that far exceed the design vehicle to cross their bridges.

18.4 RATING BY LOAD TESTING**18.4.1 Condition Assessment**

Before deciding to use load testing to establish a bridge's load rating, a strength evaluation should be performed as discussed above. Load testing is usually only recommended if a bridge receives an unsatisfactory rating from this evaluation. Using a load test to avoid detailed analysis is not a generally recommended practice. An engineer's recommendation to load test is also generally conditional on the underlying cause of the low rating. Typical reasons for recommending load testing may be physical damage, questionable or insufficient "as-built" plans, or any physical characteristic that affects performance but cannot be adequately accounted for in the strength evaluation. For any concrete bridge with unknown reinforcement, incremental load testing may be employed in establishing the safe load capacity.

A structure should not be load tested solely because it received an insufficient rating for a special permit vehicle. Prior to conducting a load test in these cases, the analysis method used to rate the structure must be examined. If a simplified procedure was used, a refined evaluation must be made. If this evaluation still results in a deficiency, and there are no alternative truck routes, a load test may be deemed necessary. It should be noted that a load test captures the effect of system reserve and the in-service member material strengths, which are not utilized in an analytical evaluation.

Before load testing a structure considered insufficient due to age only, a comprehensive on-site inspection must be performed. The inspection must consider the current state of the bridge components, and the basis that makes it currently obsolete. Based upon these factors, the engineer determines if the bridge requires load testing.

Prior to conducting a load test, possible ramifications must be considered. Any condition, which could cause the load testing to be a hazard to either the public or the individuals conducting the test, must be reconciled prior to the testing. Modifications such as testing at night or limiting the scope of the testing may be required.

18.4.2 Test Type

There are two types of tests: proof load and diagnostic. Proof load testing is typically recommended when the bridge exhibits signs of distress such as corrosion or damage that cannot be accurately quantified; when it is suspected that the "as-built" bridge is different from existing plans; or for any other reason that hinders determining the bridge capacity. Diagnostic loading is typically used to compare actual bridge response to analytical values, based on presumably accurate information regarding the current conditions.

18.4.2.1 Proof Load Test

During proof load testing, the bridge response is monitored while the load is applied incrementally up to a level equal to the target rating (the target ultimate live load). Testing is stopped if the measured response becomes non-linear. For example, if the target inventory rating is HS20, the bridge is loaded up to a target load of $HS20(1 + I)(2.17)$. The coefficient 2.17 is the live load factor per the *Standard Specifications*. (Note: The new

BRIDGE LOAD RATING**18.4.2.1 Proof Load Test/18.4.5 Instrumentation Plan**

Manual for Bridge Evaluation Chapter 8 uses a target live load factor (X_p) with a recommended base value of 1.40. This value may be adjusted for specific bridge conditions according to Table 8.8.3.3.1-1 of the *Manual for Bridge Evaluation* but cannot be less than 1.3 nor more than 2.2. Theoretically, this method does not rely on bridge analysis; it relies solely on field testing data to determine the load capacity of the bridge. The rating established is the lower bound of the true load capacity.

Since the bridge is loaded up to the target ultimate live load which is 2.17 times of the target standard truck loads, some precautionary measures are necessary to minimize the risk of damaging the bridge. At every load increment, the measured data is compared with predicted values before proceeding with the following load increment to ensure safety.

18.4.2.2 Diagnostic Loads

Diagnostic testing is typically conducted in two situations. The first is when information from inspection and analysis shows that the bridge cannot risk taking the target ultimate live load. The second is when based on observed behavior and experience with similar bridges, the bridge is believed capable of resisting the design loads, however, a load rating for a certain vehicle is required. In this situation, the test vehicle is placed on the bridge and the measured data is used to compare to analytical models. The load rating for a vehicle, which produces moment and shear values that are lower than the test truck, can be obtained by multiplying the test vehicle rating factor by the moment ratio. Generally, the load in diagnostic testing is lower than used in proof load testing.

Information obtained from the testing is used to validate analytical assumptions and determine whether the predicted capacity is accurate. Diagnostic testing can also be used to establish both the actual distribution of loads to the individual elements and the effects of impact.

18.4.3 Computer Modeling and Analysis

Prior to the load test, a detailed computer or hand analysis must be performed. The modeling should include all known facts about the actual conditions of the bridge to insure accurate predictions of test results. Accurate modeling includes consideration of the effects of structural continuity, composite sections, deterioration, damage levels, and transformed sections; as well as anything else which could affect the integrity of the structure.

The results of this analysis provide information on the health of the bridge and are used as a guide in the selection of the test method (whether diagnostic or proof). During the test, the results of the analysis are compared to the measured response. Any large variation in the measured response indicates a safety warning, which requires close evaluation by the test engineer.

18.4.4 Required Measurements for Evaluation

The data acquired through physical testing should provide the engineer with the information required for proper rating. Data is obtained from various instruments including strain gauges and displacement transducers. In order to select the appropriate instrumentation, the engineer must first determine what information is required. The engineer must also determine an optimal configuration of the instrumentation such that a maximum amount of information about the bridge is obtained. Strains can be measured at nearly any point below the surface of the slab. Alternatively, multiple strain gages can be configured to determine the strain distribution through an element's cross section. Placement of a line of strain gauges across the width of the bridge on the primary components will yield important data regarding the true load distribution. Additionally, strain readings can be converted to stress levels thereby checking allowable limits. Selection of the specific type of gauge is typically left to the testing engineer.

Additional data that can be obtained from load testing includes deflection and rotation. Deflection measurements can be used to determine the structure's longitudinal load distribution and to check the structure's ability to meet AASHTO criteria. Rotation measurements provide information on the structure's degree of continuity.

18.4.5 Instrumentation Plan

The rating engineer must provide an instrumentation plan, which shows instrumentation recommendation and requirements for the load test. Final approval of the plan, however, is left to the discretion of the testing engineer who must determine whether it is feasible to place instruments at the indicated locations. The testing engineer may relocate, change, or eliminate unnecessary or improperly placed instruments. Since the majority of the instrumentation is electronic, it is necessary to string (run) wires from the instrument to the data acquisition

BRIDGE LOAD RATING**18.4.5 Instrumentation Plan/18.5 Load Rating Report**

system. Currently, there are many available wired and wireless systems and the choice of a specific system may be based on price and/or the client established limitations. If wired system is used, the wires must be placed in such a manner that they will not interfere with traffic, be run over or be excessively long.

18.4.6 Test Procedure

Two test procedures are available for load testing. Proper selection of the procedure is critical for an accurate rating.

18.4.6.1 Static Testing

Static testing is conducted by incrementally placing calibrated weights on the test vehicles, then locating the vehicles at positions on the structure that create maximum stresses. Load may be applied at more than one point at the same step, especially in the case of continuous bridges, or bridges with various shear or fracture critical components. Since large structures typically require many load increments, the total time between the first and last load application may be long. Thus it may be necessary to consider temperature effects in the analysis of the test data.

Extreme caution must be used when performing static loading, in that sudden distress of the components may occur between load increments. It is the testing engineer's responsibility to stop the test at the first sign of non-linear behavior in the structure.

18.4.6.2 Dynamic Testing

Dynamic testing is primarily used to determine a more accurate value for the impact factor to use in load rating. It is also used to determine the bridge's natural frequency of vibration. Dynamic testing is performed by applying a combination of known weights to the test vehicle, then running the vehicle over the bridge at a known velocity. In order to obtain a complete envelope of the dynamic effects, runs are made using various speeds, lane locations, and weights.

18.4.7 Analysis of Test Data

During the test, the testing engineer must compare the structural response with the analytical data to ensure that the response remains in the linear-elastic range. After testing, the testing engineer will reduce the data and place it in a standard format so that the rating engineer can assess the differences between the measured and analytical results. Through data analysis, the test engineer will eliminate environmental (temperature) and electrical effects (noise) so that only pertinent results are recorded.

18.4.8 Verification of Analytical Model

It is the rating engineer's responsibility to determine the adequacy of the analytical model, identify the potential causes of differences, and make necessary adjustments. Rational reasoning must be used to explain the differences so that future analysis and rating can be performed accurately.

18.5 LOAD RATING REPORT

After the structure has been load rated, a comprehensive report includes load rating calculations and documentation (i.e. Inspection reports, testing reports, and articles referenced as part of the load rating) shall be provided with the Bridge Load Rating Summary Form as the first sheet for the load rating calculations.

The load rating should be completely documented in writing and include the following:

- All background information such as field inspection reports, material and load test data
- All supporting computations
- Clear statement of all assumptions used in performing the load rating

If refined analysis or load testing was used in a load rating, the rating report must include the live load distribution factors for all rated members.

BRIDGE LOAD RATING

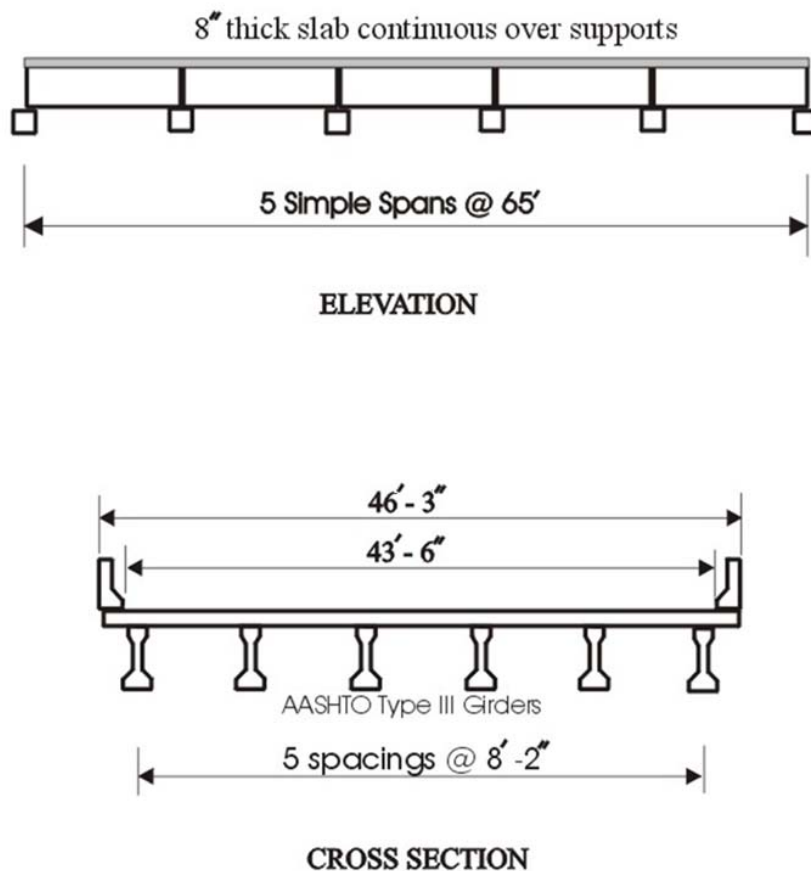
18.6 Rating Example/18.6.2 Materials and Other Information

18.6 RATING EXAMPLE

18.6.1 Introduction

This two-lane bridge, built in the 1970s, is located on State Road 30 over the Carrabelle River in Franklin County, Florida. It consists of five simple and equal spans (65 ft long). Each bridge span consists of six AASHTO Type III prestressed concrete girders spaced at 8 ft - 2 in. on centers. The total width of the bridge is 46 ft - 3 in. The bridge has an 8-in.-thick continuous concrete deck. The top ½ in. of the slab is considered to be a wearing surface. The continuity of slab is not considered in the following calculations for simplicity. **Figure 18.6.1-1** shows the bridge elevation and the typical span cross section. The following calculations demonstrate the rating process of an interior girder using non-transformed sections with the AASHTO method and the field test method. The process also illustrates the use of a state defined permit truck that is used by the overweight permitting unit as a routing vehicle.

*Figure 18.6.1-1
Bridge Details*



18.6.2 Materials and Other Information

Number of simple spans = 5

Span length = 65 ft

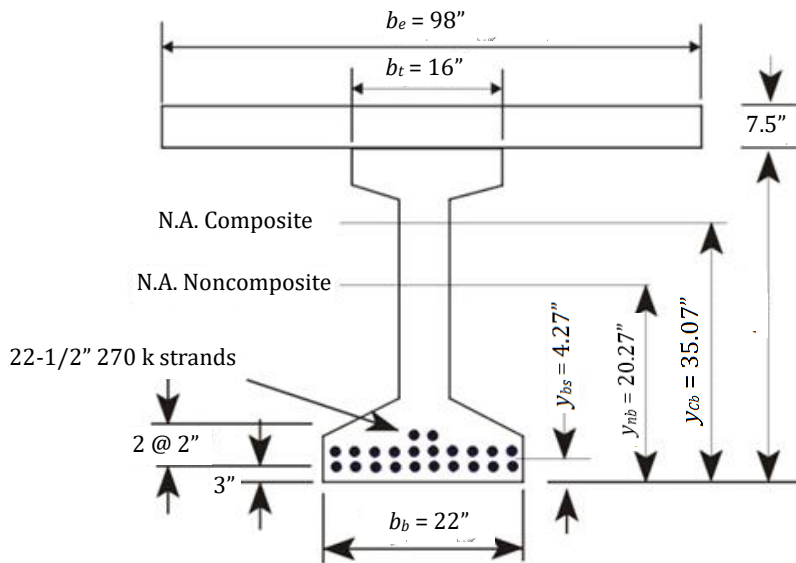
Structural slab thickness = 7.5 in.

Number of traffic lanes = 2

Bridge width = 46 ft 3 in.

Total slab thickness = 8 in.

Figure 18.6.3-1.
Cross Section at Midspan



18.6.4 Dead Load Calculations

The noncomposite section carries the girder self-weight and slab weight (8 in. thick), while the barrier and future wearing surface weights are uniformly distributed among the six girders and are carried by the composite section.

Girder moment:
$$M_G = \frac{qL^2}{8} = \frac{(560)(0.150)(65)^2}{(144)(8)} = 308.07 \text{ ft-kips}$$

Slab moment:
$$M_S = \frac{qL^2}{8} = \frac{(8.17)(8)(0.150)(65)^2}{(12)(8)} = 431.48 \text{ ft-kips}$$

Barrier moment:
$$M_B = \frac{qL^2}{8} = \frac{(0.411)(2)(65)^2}{(6)(8)} = 72.35 \text{ ft-kips}$$

Future wearing surface:
$$M_w = \frac{qL^2}{8} = \frac{(43.5)(0.025)(65)^2}{(6)(8)} = 95.72 \text{ ft-kips}$$

Total dead load moment:
$$M_d = 907.62 \text{ ft-kips}$$

18.6.5 Stresses and Strength

18.6.5.1 Prestress Losses

Initial prestressing force/strand = $(0.153)(0.69)(270.0) = 28.50 \text{ kips}$

Initial prestress force: $P_{si} = (22)(28.50) = 627.00 \text{ kips}$

Eccentricity of prestress force: $e = y_{Nb} - y_{bs} = 20.27 - 4.27 = 16.0 \text{ in.}$

BRIDGE LOAD RATING**18.6.5.1 Prestress Losses/18.6.5.2 Stresses and Strength**

$$f_{cir} = \frac{P_{si}}{A_N} + P_{si} \frac{e^2}{I_N} - M_G \frac{e}{I_N}$$

$$= \frac{627.00}{560} + (627.00) \frac{16^2}{125,390} - (308.07)(12) \frac{16}{125,390} = 1.93 \text{ ksi}$$

$$f_{c ds} = M_S \frac{e}{I_N} + \frac{(M_B + M_W)(y_{Cb} - y_{bs})}{I_c}$$

$$= (431.48)(12) \frac{16}{125,390} + \frac{(72.35 + 95.72)(12)(35.07 - 4.27)}{364,324} = 0.831 \text{ ksi}$$

Elastic shortening loss: $ES = \frac{E_s}{E_{ci}} f_{cir} = \frac{28,500}{3,834} (1.93) = 14.35 \text{ ksi}$ [Standard 9-6]

Shrinkage loss (assume RH = 70%): $SH = 17 - (0.15)RH$
 $= 17 - (0.15)(70) = 6.50 \text{ ksi}$ [Standard 9-4]

Creep loss: $CR_c = 12 f_{cir} - 7 f_{c ds}$ [Standard 9-9]
 $= (12)(1.93) - (7)(0.831) = 17.34 \text{ ksi}$

Relaxation loss: $CR_s = 5 - 0.1 ES - 0.05 (SH + CR_c)$ [Standard 9-10A]
 $= 5 - (0.1)(14.35) - (0.05)(6.5 + 17.34) = 2.37 \text{ ksi}$

Total prestress losses = $ES + SH + CR_c + CR_s = 14.35 + 6.5 + 17.34 + 2.37 = 40.56 \text{ ksi}$ [Standard 9-3]

Effective final stress, $f_{se} = 202.5 - 40.56 = 161.94 \text{ ksi}$

Effective final prestress force: $P_{se} = (22)(0.153)(161.94) = 545.09 \text{ kips}$

18.6.5.2 Stresses and Strength

In a complete design process, strength checking (bending and shear) should be conducted for all sections along the span length. While a rating process should follow the same principles as in design, the following calculation is limited to the bending strength at middle of the span and stress at the bottom of girder. Note that sign convention is that concrete compressive stresses are positive.

Dead load stress on non-composite section:

$$f_{Nb} = -\frac{(M_G + M_S) y_{Nb}}{I_N} = -\frac{(308.07 + 431.48)(12)(20.27)}{125,390} = -1.435 \text{ ksi}$$

Dead load stress on composite section:

$$f_{CD} = -\frac{(M_B + M_W) y_{Cb}}{I_c} = -\frac{(72.35 + 95.72)(12)(35.07)}{364,324} = -0.194 \text{ ksi}$$

Stress from prestress force:

$$f_{pr} = \frac{P_{se}}{A_N} + \frac{P_{se} e y_{Nb}}{I_N} = \frac{545.09}{560} + \frac{(545.09)(16)(20.27)}{125,390} = 2.383 \text{ ksi (compression)}$$

Flexural strength:

$$d = 45 + 7.5 - 4.27 = 48.23 \text{ in.}$$

BRIDGE LOAD RATING**18.6.5.2 Stresses and Strength/18.6.6.2 Load Ratings**

$$f_{ps} = f_{pu} \left[1 - \frac{\gamma}{\beta_1} \left(\frac{pf_{pu}}{f'_c} \right) \right] \quad [\text{Standard 9-17}]$$

$$= 270 \left[1 - \frac{0.28}{0.85} \left(\frac{(0.153)(22)}{(98)(48.23)} \right) \frac{270}{3.4} \right] = 264.97 \text{ ksi}$$

$$a = \frac{A_{ps} f_{ps}}{0.85 b f'_c} = \frac{(264.97)(22)(0.153)}{(0.85)(98)(3.4)} = 3.15 \text{ in.}$$

$$M_n = A_{ps} f_{ps} \left(d - \frac{a}{2} \right) = (22)(0.153)(264.97) \frac{\left(48.23 - \frac{3.15}{2} \right)}{12} = 3467.6 \text{ ft-kips}$$

18.6.6 Rating for Design Loading Based on Standard Specifications**18.6.6.1 Live Loads**

Maximum wheel-load moment: $M_{WL-HS20} = 448 \text{ ft-kips}$

$$\text{Impact factor: } I = \frac{50}{(125 + L)} = 0.26 \quad [\text{Standard 3-1}]$$

$$\text{AASHTO wheel-load distribution factor: } WDF = \frac{S}{5.5} = \frac{8.17}{5.5} = 1.49$$

$$\text{Live load moment/girder } = M_{LL+I} = (WDF)(M_{WL-HS20})(1 + I) = (1.49)(448)(1.26) = 841.1 \text{ ft-kips}$$

Live load stress (composite section): (Note: Tension is negative)

$$f_{LL+I} = -\frac{M_{LL+I} y_{Cb}}{I_c} = -\frac{(841.1)(12)(35.07)}{364,324} = -0.972 \text{ ksi}$$

Total tensile stresses at service

$$f_{total} = (f_{Nb} + f_{CD}) + f_{LL+I} + f_{pr} \\ = -(1.435 + 0.194) - 0.972 + 2.383 = -0.218 \text{ ksi below allowable stress, } f_{allow} = -0.424 \text{ ksi}$$

18.6.6.2 Load Ratings

Inventory rating with AASHTO factored load method:

$$RF_{IN} = \frac{(\phi M_n - 1.3 M_D)}{(2.17)(M_{LL+I})} = \frac{(1.0)(3,467.6) - (1.3)(907.62)}{(2.17)(841.1)} = 1.25$$

Operating rating with AASHTO factored load method:

$$RF_{OP} = \frac{(\phi M_n - 1.3 M_D)}{1.3 M_{LL+I}} = \frac{(1.0)(3,467.6) - (1.3)(907.62)}{(1.3)(841.1)} = 2.09$$

Inventory rating with AASHTO allowable stress method:

$$RF_{IN} = \frac{(f_{allow} - (f_{pe} + f_{DL}))}{f_{LL+I}} = \frac{(-0.424) - [2.383 + (-1.435 - 0.194)]}{-0.972} = 1.21$$

The inventory load rating is controlled by the service (Working Stress) requirement; therefore, the inventory rating is equal to HS24.2 truck. However, the inventory rating with the factored load method is 1.25, which shows that the use of this method may result in higher rating. The final rating factor for prestressed concrete structures should be the lesser of the values obtained by the Working Stress and Factored Load methods to ensure adherence to the original design assumptions.

BRIDGE LOAD RATING**18.6.7 Rating For Design Loading (HL-93) Based On The LRFD Specifications/18.6.7.1.3 Live Load****18.6.7 Rating for Design Loading (HL-93) Based on the LRFD Specifications**

The following rating is based on the guidelines given in the *LRFD Specifications* and is intended to illustrate the difference with *Standard Specifications*.

18.6.7.1 Load Calculations**18.6.7.1.1 Dead Load**

The dead loads are essentially the same as calculated above.

18.6.7.1.2 Prestress Loss

The procedure for calculating the prestress losses according to the *LRFD Specifications* is detailed in the design examples presented in Chapter 9. The total loss calculated per the *LRFD Specifications* is 41.58 ksi compared 40.56 ksi per the *Standard Specifications*. Therefore the effective stress is assumed the same as above, i.e., 161.94 ksi.

18.6.7.1.3 Live Load

Rating Live Load: AASHTO LRFD HL-93

Maximum truck moment per lane: $M_{HL-93 \text{ Design Truck}} = 896.0 \text{ ft-kips}$

Maximum lane moment per lane: $M_{HL-93 \text{ Design Lane Load}} = 338.0 \text{ ft-kips}$

Maximum tandem moment per lane: $M_{HL-93 \text{ Design Tandem}} = 762.5 \text{ ft-kips}$

Impact factor: $IM = 0.33$

AASHTO lane-load distribution factor for Type k cross section:

Multi-lane loading:
$$LDF = 0.075 + \left(\frac{S}{9.5}\right)^{0.6} \left(\frac{S}{L}\right)^{0.2} \left(\frac{K_g}{12.0 L t_s^3}\right)^{0.1}$$

Single-lane loading:
$$LDF = 0.06 + \left(\frac{S}{14}\right)^{0.4} \left(\frac{S}{L}\right)^{0.3} \left(\frac{K_g}{12.0 L t_s^3}\right)^{0.1}$$

where, $K_g = n(I + A e_g^2)$ [LRFD 4.6.2.2.1-1]

$$= \frac{4,287}{3,535} \left(125,390 + 560 \left(45 + 7.5 - 20.27 - \frac{7.5}{2} \right)^2 \right) = 702,913 \text{ in}^4$$

Multi-lane loading:
$$LDF = 0.075 + \left(\frac{8.17}{9.5}\right)^{0.6} \left(\frac{8.17}{65}\right)^{0.2} \left(\frac{702,913}{(12.0)(65)(7.5)^3}\right)^{0.1} = 0.726$$

Single-lane loading:
$$LDF = 0.06 + \left(\frac{8.17}{14}\right)^{0.4} \left(\frac{8.17}{65}\right)^{0.3} \left(\frac{702,913}{(12.0)(65)(7.5)^3}\right)^{0.1} = 0.527$$

As can be seen the distribution factor for multilane loading controls. The live load moment is specified as the lane load moment plus the larger of the truck or the tandem moment with the control live load distribution factor:

$$M_{LL+I} = LDF \{ M_{lane-HS 20 (Lane)} + \text{MAX}(M_{lane-HS 20 (Truck)}, M_{lane-HS 20 (Tandem)}) (1 + IM) \}$$

$$= (0.726)[338.0 + (896.0)(1.33)] = 1,110.5 \text{ ft-kips}$$

Live Load Stress:
$$f_{LL+I} = -\frac{M_{LL+I} y_{Cb}}{I_c} = -\frac{(1,110.5)(12)(35.07)}{364,324} = -1.28 \text{ ksi}$$

BRIDGE LOAD RATING**18.6.7.1.3 Live Load /18.6.7.3.2 Service I Load Rating**

It can be seen that the live load stress calculated per the LRFD Specifications is much higher than what is calculated per the Standard Specifications (1.28 ksi versus 0.972 ksi).

18.6.7.2 Strength Calculation

Since the strength calculation in the *LRFD Specifications* is similar to that in the *Standard Specifications* the detailed calculation is not presented here. To review sample calculations, see the design examples in Chapter 9.

$$M_n = A_{ps} f_{ps} \left(d - \frac{a}{2} \right)$$

$$= (22)(0.153)(264.21) \frac{\left(48.23 - \frac{3.14}{2} \right)}{12} = 3,458.0 \text{ ft-kips}$$

This is very close to using *Standard Specifications* (3,467.6 ft-kips). The minor variation in the nominal moment capacity is due to the changes in the calculations for f_{ps} and a in the *LRFD Specifications*.

18.6.7.3 Load Rating**18.6.7.3.1 Strength I Load Rating**

Inventory rating according to Strength I is:

$$RF_{IN} = \frac{(\phi M_n - 1.25(M_G + M_S + M_B) - 1.5 M_W)}{(M_{LL+I})(1.75)}$$

$$= \frac{(1.0)(3,458.0) - (1.25)(308.07 + 431.48 + 72.35) - (1.5)(95.72)}{(1,110.5)(1.75)} = 1.18$$

Although the live load moment per the LRFD analysis is 32% larger than that by the *Standard Specifications* (1110.5 ft-kips versus 841.1 ft-kips), the live load factor (Inventory) is considerably less for the LRFD analysis (1.75 versus 2.17). Thus the inventory rating for LRFD Strength I is only 5% less than that by the *Standard Specifications* (1.18 versus 1.25).

Operating rating should use the same principles that were used in the design. Therefore, the operating rating according to Strength I is:

$$RF_{OP} = \frac{(\phi M_n - 1.25(M_G + M_S + M_B) - 1.5 M_W)}{(M_{LL+I})(1.35)}$$

$$= \frac{(1.0)(3,458.0) - (1.25)(308.07 + 431.48 + 72.35) - (1.5)(95.72)}{(1,110.5)(1.35)} = 1.53$$

18.6.7.3.2 Service III Load Rating

Inventory rating with AASHTO LRFD Service III (full dead load plus 80% live load):

Allowable Tensile Stress:

$$RF_{IN} = \frac{(f_{allow} - (f_{pe} + f_{DL}))}{0.8 f_{LL+I}} = \frac{(-0.424) - [2.383 - (1.435 + 0.194)]}{(0.8)(-1.28)} = 1.15$$

Operating rating with AASHTO LRFD Service III is not required according to the *Manual for Bridge Evaluation*.

18.6.7.3.2 Service I Load Rating

The MBE does not specifically require the use of the LRFD Service I compression stress limit state. While many bridge owners are focused on asset longevity, PCI believes compression calculations are a value added check. The rating should also be done by checking compressive stress at Service I limit states.

The Service I limit state evaluation in Article 6A of the *Manual for Bridge Evaluation* is a specific permit evaluation for reinforced and prestressed concrete bridges. It is currently considered optional, but it is recommended. It is the one limit state evaluation step that is included in the *Manual for Bridge Evaluation* that is not consistent with

BRIDGE LOAD RATING

18.6.7.3.2 Service I Load Rating

the limit state combinations in design (*LFRD Specifications*). It is specifically introduced to ensure there is no yielding of nonprestressed reinforcement and prestressing strand under very heavy permit loads. It is considered acceptable to allow cracking of concrete (exceedance of the Service III limit state) for heavy permit loads. However, this check is instituted to ensure that the cracks remain acceptably small and there is no yielding of the tension steel. Illustrative Example A3 in the *Manual for Bridge Evaluation* illustrates this check, or a simpler, but more conservative check is suggested in *Manual for Bridge Evaluation* Article C6A.5.4.2.2b: "...the Engineer, may as an alternate, chose to limit unfactored moments to 75% of the nominal flexural capacity." This check is not illustrated for the FL-120 permit truck. A state may require this check as recommended by the *Manual for Bridge Evaluation*.

Four (4) cases will be checked and the final rating should be the lowest value.

Case I: The stress at the top of girder under 0.5 (permanent + transient loads)

Dead load stress on non-composite section:

$$f_{Nt} = \frac{(M_G + M_S)y_{Nt}}{I_N} = \frac{(308.07 + 431.48)(12)(24.73)}{125,390} = 1.75 \text{ ksi}$$

Dead load stress on composite section:

$$f_{Ct} = \frac{(M_B + M_w)y_{Cgt}}{I_c} = \frac{(72.35 + 95.72)(12)(45 - 35.07)}{364,324} = 0.055 \text{ ksi}$$

Stress from prestress force:

$$f_{prt} = \frac{P_{se}}{A_N} - \frac{P_{se} e y_{Nt}}{I_N} = \frac{545.09}{560} - \frac{(545.09)(16)(24.73)}{125,390} = -0.75 \text{ ksi}$$

Stress from live load:

$$f_{CLL} = \frac{(M_{LL})y_{Cgt}}{I_c} = \frac{(1110.5)(12)(45 - 35.07)}{364,324} = 0.363 \text{ ksi}$$

Allowable stress:

$$f_{allow} = 0.4 f'_{cg} = (0.4)(5.0) = 2.0 \text{ ksi}$$

Therefore, the load rating according to Service I is:

$$RF = \frac{f_{allow} - 0.5(f_{Nt} + f_{Ct} + f_{prt})}{f_{CLL}} = \frac{2.0 - (0.5)(1.75 + 0.055 - 0.75)}{0.363} = 4.06$$

Case II: The stress at the top of girder under permanent + transient loads

The calculations for f_{Nt} , f_{Ct} , f_{prt} , and f_{CLL} are identical to those calculated in Case I.

Allowable stress:

$$f_{allow} = 0.6 f'_{cg} = (0.6)(5.0) = 3.0 \text{ ksi}$$

Therefore, the load rating according to Service I is:

$$RF = \frac{f_{allow} - (f_{Nt} + f_{Ct} + f_{prt})}{f_{CLL}} = \frac{3.0 - (1.75 + 0.055 - 0.75)}{0.363} = 5.36$$

Case III: The stress at the top of slab under 0.5 (permanent + transient loads)

Dead load stress on composite section:

$$f_{Ct} = \frac{(M_B + M_w)y_{Ct}}{I_c} = \frac{(72.35 + 95.72)(12)(45 + 7.5 - 35.07)}{364,324} = 0.096 \text{ ksi}$$

BRIDGE LOAD RATING**18.6.7.3.2 Service I Load Rating/18.6.8.1.1 Service II Load Rating**

Stress from live load:

$$f_{CLL} = \frac{(M_{LL}) y_{ct}}{I_c} = \frac{(1,110.5)(12)(45 + 7.5 - 35.07)}{364,324} = 0.638 \text{ ksi}$$

Allowable stress:

$$f_{allow} = 0.4 f'_{cs} = (0.4)(3.4) = 1.36 \text{ ksi}$$

Therefore, the load rating according to Service I is:

$$RF = \frac{f_{allow} - 0.5 f_{ct}}{f_{CLL}} = \frac{1.36 - (0.5)(0.096)}{0.638} = 2.06$$

Case IV: The stress at the top of slab under permanent + transient loads

The calculations for f_{ct} and f_{CLL} are identical to that in Case III.

Allowable stress:

$$f_{allow} = 0.6 f'_{cs} = (0.6)(3.4) = 2.04 \text{ ksi}$$

Therefore, the load rating according to Service I is

$$RF = \frac{f_{allow} - f_{ct}}{f_{CLL}} = \frac{2.04 - 0.096}{0.638} = 3.05$$

The minimum of rating factor according to Service I is 2.06.

18.6.8 Rating for Permit Loading by the LRFD Specifications

Dead load and prestress loss are essentially the same as calculated above.

Live load:

Rating live load: FL-120

Maximum truck moment per lane: $M_{FL-120} = 1496.0 \text{ ft-kips}$

Impact factor: $IM = 0.33$

AASHTO single-lane load distribution factor: $LDF = 0.527$

AASHTO multi-lane load distribution factor: $LDF = 0.726$

Nominal strength: $M_n = 3,458.0 \text{ ft-kips}$

ADTT (one direction): Assumed > 5000

18.6.8.1 Routine or Annual Type Permit

For this case, the multi-lane distribution factor is used for the calculation of the live load moment as follows:

$$\begin{aligned} M_{LL+I} &= (LDF)(M_{FL-120})(1 + IM) \\ &= (0.726)(1496.0)(1 + 0.33) = 1,444.5 \text{ ft-kips} \end{aligned}$$

18.6.8.1.1 Strength II Load Rating

The rating is according to AASHTO LRFD Strength II, and the load factor as given in **Table 18.3.2.1.3-1** needs to be applied. The load factor for permit load (FL-120) is calculated by linear interpolation of the truck weight as follows.

$$1.3 + \frac{(150 - 120)}{(150 - 100)}(1.8 - 1.3) = 1.60$$

BRIDGE LOAD RATING**18.6.8.1.1 Service II Load Rating/18.6.8.2 Limited Crossing Escorted with No Other Traffic (Single Trip)**

Hence,

$$RF = \frac{(\phi M_n - 1.25(M_G + M_S + M_B) - 1.5 M_w)}{(M_{LL+I})(1.60)}$$

$$= \frac{(1.0)(3,458.0) - 1.25(308.07 + 431.48 + 72.35) - (1.5)(95.72)}{(1,444.5)(1.60)} = 1.00$$

Note that load rating for Service III limit state is not required for permit load as specified in *the Manual for Bridge Evaluation*.

18.6.8.1.2 Service I Load Rating

Case I: The stress at the top of girder under 0.5 (permanent + transient loads)

Dead load stress is same as calculated in Section 18.6.7.3.2 Case I:

Stress from live load:

$$f_{CLL} = \frac{(M_{LL}) y_{cgt}}{I_c} = \frac{(1,444.5)(12)(45 - 35.07)}{364,324} = 0.472 \text{ ksi}$$

Therefore, the load rating according to Service I is:

$$RF = \frac{f_{allow} - 0.5(f_{Nt} + f_{Ct} + f_{prt})}{f_{CLL}} = \frac{2.0 - 0.5(1.75 + 0.055 - 0.75)}{0.472} = 3.12$$

Case II: The stress at the top of girder under permanent + transient loads

Similarly to Case I, the load rating according to Service I is:

$$RF = \frac{f_{allow} - (f_{Nt} + f_{Ct} + f_{prt})}{f_{CLL}} = \frac{3.0 - (1.75 + 0.055 - 0.75)}{0.472} = 4.12$$

Case III: The stress at the top of slab under 0.5 (permanent + transient loads)

Dead load stress is same as calculated in Section 18.6.7.3.2, Case III

Stress from live load:

$$f_{CLL} = \frac{(M_{LL}) y_{ct}}{I_c} = \frac{(1,444.5)(12)(45 + 7.5 - 35.07)}{364,324} = 0.829 \text{ ksi}$$

Allowable stress:

$$f_{allow} = 0.4 f'_{cs} = (0.4)(3.4) = 1.36 \text{ ksi}$$

Therefore, the load rating according to Service I is:

$$RF = \frac{f_{allow} - 0.5 f_{Ct}}{f_{CLL}} = \frac{1.36 - 0.5(0.096)}{0.829} = 1.58$$

Case IV: The stress at the top of slab under permanent + transient loads

Similarly to Case III, the load rating according to Service I is:

$$RF = \frac{f_{allow} - f_{Ct}}{f_{CLL}} = \frac{2.04 - 0.096}{0.829} = 2.34$$

The minimum of rating factor according to Service I is 1.58

18.6.8.2 Limited Crossing Escorted with No Other Traffic (Single-Trip)

For this case, the single-lane distribution factor is used for the calculation of the live load moment, where the built-in multiple presence factor 1.2 should be divided out.

$$M_{LL+I} = (LDF/1.2)(M_{FL-120})(1 + IM)$$

$$= (0.527/1.2)(1,496.0)(1 + 0.33) = 873.8 \text{ ft-kips}$$

BRIDGE LOAD RATING**18.6.8.2.1 Load Rating/18.6.8.4 Limited Crossing with Mixed Traffic (Multiple Trips less than 100 Crossings)****18.6.8.2.1 Load Rating**

The rating is according to AASHTO LRFD Strength II with a load factor 1.15 as specified in **Table 18.3.2.1.3-1**:

$$RF = \frac{(\phi M_n - 1.25(M_G + M_S + M_B) - 1.5 M_w)}{(M_{LL+I})(1.15)}$$

$$= \frac{(1.0)(3,458.0) - 1.25(308.07 + 431.48 + 72.35) - (1.5)(95.72)}{(873.8)(1.15)} = 2.29$$

The Service I load rating is similar to that presented in Section 18.6.8.1.2, and not discussed here. Since the live load M_{LL+I} is less than that from Section 18.6.8.1(873.8 vs. 1,444.5 ft-kips), the Service I load rating will be greater than 1.58.

18.6.8.3 Limited Crossing Mixed with Traffic (Single-Trip)

This below method is being utilized by some states and is not in strict accordance with the MBE γ_L methodology. These states have an altered single trip overload procedure as specified in *LRFD Specifications* Article 4.6.2.2.5 (Special Loads with Other Traffic), the force effects resulting from heavy vehicles in one lane with routine traffic in adjacent lanes may be determined as below:

$$G = G_p \left(\frac{g_1}{Z} \right) + G_D \left(g_m - \frac{g_1}{Z} \right) \quad [\text{LRFD 4.6.2.2.4-1}]$$

where

G = final force effect applied to a girder (kips or ft-kips)

G_p = force effect due to overload truck (kips or ft-kips)

g_1 = single lane live load distribution factor

G_D = force effect due to design loads (kips or ft-kips)

g_m = multiple lane live load distribution factor

Z = a factor taken as 1.20 where the lever rule was not utilized, and 1.0 where the lever rule was used for a single lane live load distribution factor

Hence, the live load moment with impact factor is calculated as:

$$M_{LL+I} = (1,496.0)(1.33) \left(\frac{0.527}{1.2} \right) + (338.0 + (896.0)(1.33)) \left(0.726 - \frac{0.527}{1.2} \right)$$

$$= 1312.6 \text{ ft-kips}$$

18.6.8.3.1 Load Rating

The rating is according to AASHTO LRFD Strength II with load factor 1.50 as specified in **Table 18.3.2.3-1**

$$RF = \frac{(\phi M_n - 1.25(M_G + M_S + M_B) - 1.5 M_w)}{(M_{LL+I})(1.50)}$$

$$= \frac{(1.0)(3,458.0) - (1.25)(308.07 + 431.48 + 72.35) - (1.5)(95.72)}{(1,312.6)(1.50)} = 1.17$$

The service I load rating is similar to that presented in Section 18.6.8.1.2, and not discussed here. Since the live load M_{LL+I} is less than that from Section 18.6.8.1(1312.6 vs. 1444.5 ft-kips), the Service I load rating will be greater than 1.58.

18.6.8.4 Limited Crossing Mixed with Traffic (Multiple-Trips less than 100 crossings)

For this case, the live load moment is calculated the same as in Section 18.6.8.3.

BRIDGE LOAD RATING

18.6.8.4.1 Load Rating/18.6.9.1 Test Information

18.6.8.4.1 Load Rating

The rating is according to AASHTO LRFD Strength II with load factor 1.85 as specified in **Table 18.3.2.3-1**:

$$RF = \frac{(\phi M_n - 1.25(M_G + M_S + M_B) - 1.5 M_w)}{(M_{LL+I})(1.85)}$$

$$= \frac{(1.0)(3,458.0) - (1.25)(308.07 + 431.48 + 72.35) - (1.5)(95.72)}{(1,312.6)(1.85)} = 0.95$$

The Service I load rating is similar to that presented in Section 18.6.8.1.2, and not discussed here. Since the live load M_{LL+I} is less than that from Section 18.6.8.1(1312.6 vs. 1444.5 ft-kips), the Service I load rating will be greater than 1.58.

18.6.9 Rating by Load Testing

The below illustrated approach is based on a state specific practice and is not in accordance with MBE Chapter 8, it does not include all factors.

18.6.9.1 Test Information

Target inventory rating = HS20

Maximum test load = two test trucks with a gross weight of 207 kips each.

Maximum moment per test truck/lane = 1868 ft-kips

Maximum available live load stress, $f_L = f_{pe} - f_{DL} - f_{allow}$

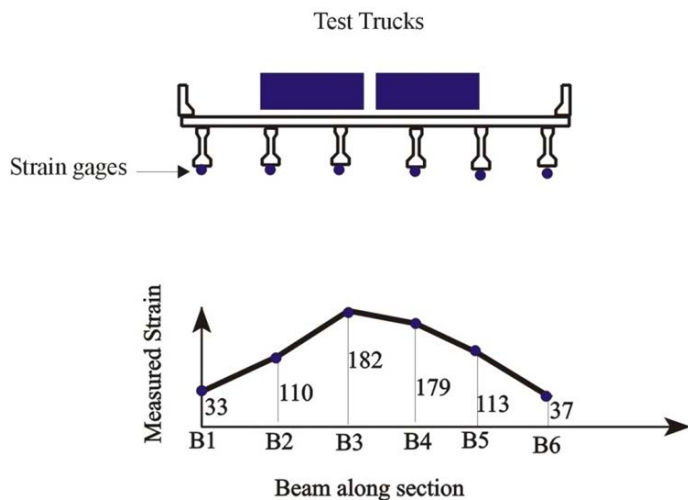
$$= 2.383 - (1.435 + 0.194) - (-0.424) = 1.178 \text{ ksi}$$

The above stress, f_L , is theoretically the maximum stress that the bridge can be subjected to without cracking. This stress corresponds to a strain value of $1.178/4,287 = 275 \times 10^{-6}$ (275 microstrains). This strain value is considered the limiting test strain to avoid any permanent damage to the bridge during testing.

In this example, the bridge was loaded incrementally using the two test trucks and the strains were monitored at all critical locations. The maximum measured strain at the bottom of the girder under the two test vehicles was 182 microstrains, which is 66% of the calculated strain limit. The bridge showed no signs of distress or cracking at any load level and stress-strain relationships were linear at all load levels.

The strain measurements across the bridge under maximum applied live loads are shown in Fig. 18.6.9.1-1.

Figure 18.6.9.1-1
Measured Strain Distribution (microstrain)



BRIDGE LOAD RATING**18.6.9.1 Test Information/18.6.9.3 Test Operating Rating Factor**

Calculate the measured wheel load distribution factor, WDF:

$$WDF = \frac{N_w \varepsilon_{max}}{\sum \varepsilon_i} = \frac{(4)(182)}{(33 + 110 + 182 + 179 + 113 + 37)} = 1.11$$

where, N_w is the number of wheel-loads on the tested bridge.

For comparison, the wheel load distribution factor from *Standard Specifications* is 1.49. The LRFD lane distribution factor needs to be multiplied by 2 for comparison, which is ($2 \times 0.726 = 1.45$) as calculated in Section 18.6.7.1.3.

Because the test vehicles are different from the HS20 truck, the stress from the test for an equivalent HS20 truck plus impact can be calculated from the ratio of test truck moment and HS20 moment as:

$$f_{HS\ 20+I} = (1 + I) \frac{M_{HS\ 20}}{M_{test}} \varepsilon_{measured} E = 1.26 \left(\frac{(2)(448)}{1,868} \right) (182)(10^{-6})(4,286) = 0.471 \text{ ksi}$$

Because the applied test load moment/lane (1,868 ft-kips / lane) is less than the ultimate design live load moment/lane [$(2.17)(896)(1.26) = 2,450$ ft-kips] the load test is considered to be diagnostic.

18.6.9.2 Test Inventory Rating Factor

The inventory load rating based on the test measurements is shown below.

$$RF_{IN} = \left[\frac{f_{pe} - f_{DL} - f_{allow}}{f_{HS\ 20+I}} \right] = \frac{2.383 - (1.435 + 0.194) - (-0.424)}{0.471} = 2.50$$

The above test inventory rating, based on test measurements, is twice the theoretical AASHTO allowable stress inventory rating obtained in Section 18.6.6. The measured low stress (0.471 ksi) compared to the theoretically calculated value (0.94 ksi) is due to many beneficial factors that are ignored in a theoretical load rating. These factors include slab continuity, diaphragms, parapet action, bearing effects, lower prestress losses, higher concrete strength, and higher concrete modulus of elasticity. In addition, the AASHTO load distribution factors are known to be very conservative resulting in the design of stronger elements than required by actual loading.

18.6.9.3 Test Operating Rating Factor

Maximum live load moment from test for equivalent HS20 plus impact:

$$M_{LL+I} = \frac{I_c}{y_{Cb}} f_{HS\ 20+I} = \left(\frac{364,324}{35.07} \right) \left(\frac{0.471}{12} \right) = 407.7 \text{ ft-kips}$$

Operating rating per the *Standard Specifications*, Factored Load Method:

$$RF_{Op} = \frac{(\phi M_n - 1.3 M_d)}{1.3 M_{LL+I}} = \frac{(1.0)(3,467.6) - (1.3)(907.62)}{(407.7)(1.3)} = 4.32$$

The inventory rating factor (2.50) and operating rating factor (4.32) are considered to be upper bounds due to the nature of diagnostic/linear analysis. Therefore, the final rating should be limited to the original design, i.e., inventory rating of HS20, or operating rating of HS33 ($1.67 \text{ HS20} = \text{HS33}$).

The above example only gives the load rating for the interior girder of the bridge. The exterior girders must be rated with the same procedure as presented above to determine the final rating, which should be the least one of all girder ratings.

BRIDGE LOAD RATING

18.6.10 Summary Ratings/18.7 References

18.6.10 Summary of Ratings

In summary, looking at the older structure that was not designed with the new reliability based *LRFD Specifications*, one arrives at the following conclusions:

Standard Specifications Rating Factors

	Inventory Rating (Notional load)	Operating Rating
LFD Strength (HS20)	1.25	2.09 (HS41.4)
LFD Service (HS20)	1.21	
LFD Proof Test (HS20)	2.50	4.32 for interior use (HS33)

LRFD Specifications Rating Factors

	Inventory Rating	Operating Rating
LRFD Strength I (HL-93)	1.18	1.53
LRFD Service III (HL-93)	1.15	
LRFD Service I (HL-93)		2.06
LRFD Strength II (HL-93) Routine Blanket Permit in mixed traffic		1.00
LRFD Service I(HL-93) Routine Blanket Permit in mixed traffic		1.58
LRFD Strength II(FL-120) Escorted single trip without others lanes loaded		2.29
LRFD Strength II(FL-120) Escorted single trip with other lanes loaded		1.17 (HS39.1)

Comparing LFD Operating $RF = (2.07)HS20 =$ capacity of HS41.4 tons.

Remember the FL-120 is the HS20 truck with an $RF = 1.67$, therefore with LRFD Strength II operating with other lanes loaded $(1.17)(HS20)(1.67) =$ capacity of HS39.1 tons. One may anticipate that LRFD would have a slightly lower permit capacity (HS 39.1) because it has a 75 year service life calibration for strength limits states and the *Standard Specifications* (HS 41.4) was published to target a 50-year service life.

18.7 REFERENCES

1. AASHTO. 2002. *Standard Specification for Highway Bridges*, 17th Edition. (HB-17). American Association of State Highway and Transportation Officials, Washington, DC.
https://bookstore.transportation.org/collection_detail.aspx?ID=15 (Fee)
2. AASHTO. 2010. *AASHTO LRFD Bridge Design Specifications*, Fifth Edition. American Association of State Highway and Transportation Officials, Washington, DC, and 2011 Interim Revisions.
https://bookstore.transportation.org/collection_detail.aspx?ID=15 (Fee)
3. AASHTO. 2010. *The Manual for Bridge Evaluation, 2nd Edition with the 2011 Interim Revision*, American Association of State Highway and Transportation Officials, Washington, DC.
https://bookstore.transportation.org/collection_detail.aspx?ID=96 (Fee)
4. Russell, H. G. 2009. *NCHRP Synthesis 393: Adjacent Precast Concrete Box Beam Bridges: Connection Details*. Transportation Research Board, Washington, DC. 75 pp.
http://onlinepubs.trb.org/onlinepubs/nchrp/nchrp_syn_393.pdf

This page intentionally left blank

REPAIR AND REHABILITATION

Table of Contents

19.1 SCOPE 19-3

19.2 REPAIR OF NEW PRODUCTS 19-3

 19.2.1 Types and Causes of Cracks..... 19-3

 19.2.1.1 Plastic Shrinkage Cracks..... 19-4

 19.2.1.2 Plastic Settlement Cracks..... 19-4

 19.2.1.3 Cracks Due to Restraint of Volume Change..... 19-4

 19.2.1.4 Differential Curing Cracks..... 19-4

 19.2.1.5 Accidental Impact Cracks..... 19-5

 19.2.1.6 Other Causes of Cracks 19-5

 19.2.2 Crack Repair 19-5

 19.2.2.1 Autogenous Healing..... 19-5

 19.2.2.2 Sealing Cracks..... 19-5

 19.2.2.3 Crack Repair by Epoxy Injection 19-6

 19.2.2.4 Crack Repair by Concrete Replacement 19-6

 19.2.3 Spalls, Voids, and Honeycombs..... 19-6

19.3 REPAIR OF PRODUCTS DAMAGED DURING CONSTRUCTION AND SERVICE LIFE 19-7

 19.3.1 Introduction 19-7

 19.3.2 Strand Splicing 19-8

 19.3.3 Repair of Spalls 19-9

 19.3.4 Preloading 19-9

 19.3.5 Corrosion Damage 19-10

 19.3.6 Bearing Rehabilitation..... 19-10

 19.3.7 Elimination of Expansion Joints 19-10

 19.3.8 Shotcrete Repair..... 19-11

19.4 STRENGTHENING TECHNIQUES..... 19-12

 19.4.1 Introduction 19-12

 19.4.2 External Post-Tensioning..... 19-12

 19.4.3 Fiber Reinforced Polymer Composites..... 19-13

19.5 SPECIFICATIONS AND MANUALS..... 19-14

 19.5.1 AASHTO Publications..... 19-14

 19.5.1.1 Guidelines for Historic Bridge Rehabilitation and Replacement, 1st Edition (AASHTO, 2008) 19-14

 19.5.1.2 Inspectors’ Guide for Shotcrete Repair of Bridges (AASHTO, 1999) 19-15

 19.5.1.3 Guide Specifications for Shotcrete Repair of Highway Bridges (AASHTO, 1998)..... 19-15

 19.5.1.4 Guide Specification for Design of Bonded FRP Systems for Repair and Strengthening of Concrete Bridge Elements (AASHTO, 2012A)..... 19-15

 19.5.2 Other Key Documents 19-15

 19.5.2.1 Manual for the Evaluation and Repair of Precast, Prestressed Concrete Bridge Products (PCI Manual 137) 19-15

REPAIR AND REHABILITATION

Table of Contents

19.5.2.2 Guide to Recommended Practices for the Repair of Impact-Damaged Prestressed Concrete Bridge Girders (Harries, et al., 2012)19-15

19.5.2.3 Concrete Repair Manual, Third Edition (ICRI, 2008)19-15

19.5.2.4 Concrete Repair Guide (ACI 546R, 2004)19-15

19.5.2.5 Guide for the Selection of Materials for the Repair of Concrete (ACI 546.3, 2006)19-15

19.5.2.6 Guide for the Design and Construction of Externally Bonded FRP Systems for Strengthening Concrete Structures (ACI 440.2R)19-15

19.6 REFERENCES19-16

Repair And Rehabilitation

19.1 SCOPE

This chapter addresses the repair and rehabilitation of precast, prestressed concrete bridge products. Repair generally involves the replacement or correction of deteriorated, damaged, or faulty materials, components, or elements of a structure (ACI 546, 2004). Bridge rehabilitation involves major work required to restore the structural integrity of a bridge as well as work necessary to correct major defects. Bridge rehabilitation projects provide general or nearly complete restoration of bridge elements or components (FHWA, 2011).

This chapter includes the following topics:

- Repair of new products prior to shipment
- Repair of deterioration or damage during construction and during service life
- Strengthening techniques
- Specifications and Manuals

The primary focus is on precast, prestressed concrete beams, although similar repair techniques can be used for other concrete products.

19.2 REPAIR OF NEW PRODUCTS

As with any manufacturing process, nonconformance can occur in precast concrete bridge products. Examples include voids or cracks in the concrete, missing or improperly located inserts or holes, and incorrect projection of reinforcement. Nonconformance falls into one of three categories:

- Those that can be accepted in spite of the nonconformance
- Those that can be repaired satisfactorily
- Those that require rejection of the member

Chapter 1 of PCI Manual 137, *Manual for the Evaluation and Repair of Precast, Prestressed Concrete Bridge Products* addresses key factors in deciding whether to accept a product as manufactured, repair it, or reject it., Manual 137 was developed by a group representing owner agencies, designers, and industry for the purpose of promoting a greater degree of uniformity with respect to the evaluation and repair procedures for precast, prestressed concrete bridge beams, deck panels, and similar precast products.

This section of the Bridge Design Manual addresses causes and repair procedures for cracks, spalls, voids, and honeycombing in new products before they are shipped. These topics are covered in greater detail in PCI Manual 137.

19.2.1 Types and Causes of Cracks

Cracks in precast, prestressed concrete products can be eliminated or minimized by constructing the members in accordance with the PCI Manual for Quality Control (PCI Manual 116, 1999). Nevertheless, cracks can occur in both the plastic concrete and the hardened concrete. Causes of cracking, crack detection, and minimizing strains and stresses that can cause cracking are discussed in Transportation Research Circular E-C107 (TRB, 2006).

Cracks in plastic concrete occur before the concrete has developed significant tensile strength. In hardened concrete, cracks develop in nonprestressed precast members when the tensile stresses exceed the tensile strength of the concrete. In prestressed concrete members, cracks in the hardened concrete occur when the tensile stresses exceed the tensile strength of the concrete combined with the internal stresses imparted by the prestressing. However, cracks in precast bridge products should not be considered the only reason to reject the member. The implication of the cracks should be evaluated in accordance with PCI Manual 137 to determine the disposition of the product.

REPAIR AND REHABILITATION**19.2.1.1 Plastic Shrinkage Cracks/19.2.1.4 Differential Curing Cracks****19.2.1.1 Plastic Shrinkage Cracks**

Plastic shrinkage occurs near the surface of freshly placed concrete when moisture evaporates from the surface faster than it is replaced by bleed water (ACI 224, 2007). Plastic shrinkage cracking is more likely to occur under conditions of high air and concrete temperature, low humidity, and high wind velocity over the concrete surface. In addition, concrete mixes with lower amounts of bleed water, such as those containing supplemental cementitious materials have a greater tendency to exhibit plastic shrinkage cracks (ACI 224, 2001). Plastic shrinkage cracks can be unsightly but do not normally affect the structural performance of the concrete member. The best solution is to prevent these cracks from occurring altogether by providing a saturated atmosphere over all exposed surfaces during the curing process. It is, therefore, important to cover the top surface of the concrete with a moisture-proof cover as soon as concrete placement and finishing are complete.

19.2.1.2 Plastic Settlement Cracks

Settlement cracks occur when concrete continues to consolidate under its own weight after initial placement, vibration, and finishing. The cracks are most likely to occur when the vertical settlement is restrained by horizontal reinforcing bars. Settlement cracking increases with larger bar sizes, higher slumps, and smaller concrete cover (Dakhil, et al., 1975). The likelihood of settlement cracking can be reduced by proper vibration of the concrete, use of the lowest possible slump, and by increasing concrete cover. As with plastic shrinkage cracks, it is best to prevent them from occurring. If necessary, they can be repaired by rubbing full of mortar.

19.2.1.3 Cracks Due to Restraint of Volume Change

Cracking in hardened concrete can occur when volume changes caused by temperature changes, elastic shortening upon release of prestress, drying shrinkage, or creep are restrained. These causes are discussed in Section 3.4.2.4.2 of this manual.

Longitudinal cracks can occur in the webs at the end of prestressed concrete beams. These cracks appear on both sides of the beam and extend various distances toward the midlength of the beam. These cracks generally appear following transfer of the prestressing force. The width of these cracks is controlled by vertical nonprestressed reinforcement provided at the ends of the beams. Nevertheless, the presence of these cracks can be a concern for owners. With this in mind, National Cooperative Highway Research Program (NCHRP) Project 18-14 was initiated to establish a user's manual for the acceptance, repair, or rejection of girders with these cracks (Tadros, et al., 2010).

Based on the research, the following proposed crack width limits were developed:

- Cracks narrower than 0.012 in. may be left unrepaired.
- Cracks ranging in width from 0.012 to 0.025 in. should be repaired by filling the cracks with approved specialty cementitious materials, and coating the end 4 ft of the girder web side faces with an approved sealant.
- Cracks ranging in width from 0.025 to 0.05 in. should be filled by epoxy injection and the end 4 ft of the girder web coated with an approved sealant.
- For girder webs exhibiting cracks wider than 0.05 in., the research team recommended that the girders be rejected unless shown by detailed analysis that the structural capacity and long-term durability are sufficient.

Although the report does not address the timing of repairs, state practices vary from repairing before shipment to repairing after girder erection and the deck has been cast. In the latter case, the crack widths are likely to be less as a result of prestress losses and the application of dead load. Consequently, a less intrusive and less expensive repair procedure may be appropriate.

19.2.1.4 Differential Curing Cracks

Differential curing temperatures can also contribute to volume change cracking. This is discussed in Section 3.4.2.4.3 of this manual.

REPAIR AND REHABILITATION**19.2.1.5 Accidental Impact Cracks/19.2.2.2 Sealing Cracks****19.2.1.5 Accidental Impact Cracks**

Another source of cracks during fabrication is from accidental impact. This type of cracking comes in all shapes and forms and must be evaluated on an individual basis.

19.2.1.6 Other Causes of Cracks

Cracks may occur from causes other than those listed in previous sections. A comprehensive description of the causes, prevention methods, engineering effects, and repair considerations for all types of cracks is provided in PCI Manual 137.

19.2.2 Crack Repair

According to ACI Committee 224 report titled *Control of Cracking in Concrete Structures* (ACI 224, 2001), tolerable crack widths are as follows:

- 0.006 in. for concrete exposed to sea water spray with wetting and drying cycles
- 0.007 in. for concrete exposed to deicing chemicals
- 0.012 in for concrete exposed to unfavorable humidity

The *PCI Manual for Evaluation and Repair of Precast, Prestressed Concrete Bridge Products* (PCI Manual 137) states that all cracks with widths of 0.006 in. or less, after transfer of the prestressing force, need not be repaired, when the condition is deemed acceptable by the owner. An exception is made for cracks in the strand transfer length.

All cracks with a width greater than 0.006 in. after transfer and in an acceptable condition should be repaired by epoxy injection. Cracks should not be repaired prior to transfer of the prestressing force.

19.2.2.1 Autogenous Healing

Autogenous healing of cracks is a hydration process in which cracks that are held tightly together heal themselves and develop a tensile strength. Autogenous healing is discussed further in Section 3.4.2.5.1 of this manual.

19.2.2.2 Sealing Cracks

Cracks can be sealed in situations where structural repair is not necessary but it is desirable to prevent water or other liquids from entering the crack. Low-viscosity monomers and resins can be used to seal cracks with surface widths of 0.001 to 0.08 in. by gravity filling (ACI 224, 2007). High molecular-weight methacrylates, urethanes, and some low viscosity epoxies have been used. The lower the viscosity, the finer the cracks that can be repaired.

A typical installation procedure consists of the following steps:

1. Clean surface and cracks by airblasting or waterblasting.
2. Allow wet surfaces to dry.
3. Pour sealant onto the surface and spread with brooms, rollers, or squeegees.
4. Work the sealant back and forth over the cracks.
5. Broom off excess material.
6. Broadcast sand over the surface before the sealant dries, if surface friction is important.

Sealants are not needed and should not be used on the top surfaces of beams that are to have a cast-in-place concrete deck over them.

Similar materials may be used on vertical faces. However, penetration of the sealers into the cracks is more difficult to achieve. In addition, the surface with the sealant may have a different appearance.

Cracks may also be treated by routing and sealing. In this technique, a walled groove is cut along the crack surface with a depth of $\frac{1}{4}$ to 1 in. A joint sealant is then placed into the dry groove and allowed to cure. The effect of this repair on structural behavior and appearance should be assessed before it is adopted.

REPAIR AND REHABILITATION**19.2.2.3 Crack Repair by Epoxy Injection/19.2.3 Spalls, Voids, and Honeycombs****19.2.2.3 Crack Repair by Epoxy Injection**

Repair of cracks by epoxy injection should be performed in accordance with the owner's specifications, PCI Manual 137, and/or the epoxy manufacturer's recommendations. Epoxy injection consists of the following steps:

1. Clean the area adjacent to the crack and blow out any debris from the crack using filtered compressed air.
2. Apply a sealer to the surface to prevent the epoxy from leaking out before it has gelled. For through-cracks, it is necessary to do this on both surfaces.
3. Install injection ports at the appropriate spacing based on width and depth of the crack but no closer than 8 in.
4. Attach equipment for epoxy injection.
5. Mix epoxy and begin injection. For horizontal cracks, injection can begin at either end. For vertical or inclined cracks, begin at the lowest point.
6. Inject epoxy until the adhesive reaches the second port. Seal off the first port and begin injection at the second port. Continue with successive ports until the crack is filled.
7. Allow the epoxy to cure for the specified length of time and in the manner specified by the manufacturer.
8. Remove the surface seal by grinding or other means.
9. Apply any other surface treatments.

All work should be performed by personnel qualified in the epoxy injection process being utilized. All work should be accomplished in the presence of the owner's representative. **Figure 19.2.2.3-1** illustrates cracks at the end of a beam that have been repaired by epoxy injection.

ACI 503.7 (2007) provides a specification for crack repair of concrete by epoxy injection.

Figure 19.2.2.3-1

Cracks Repaired by Epoxy Injection (Photo: Mohsen Shahawy, SDR Engineering Consultants Inc.)

**19.2.2.4 Crack Repair by Concrete Replacement**

Large cracks, which suggest yielding of the reinforcement, generally are not repaired by epoxy injection. If the damage is localized, an appropriate repair procedure is to remove the damaged concrete and replace it in the manner described in Section 3.4.2.3 of this manual.

19.2.3 Spalls, Voids, and Honeycombs

Surface spalls of concrete corners or edges result from handling, production procedures, and release procedures. Voids and honeycomb areas occasionally occur due to inadequate consolidation of the concrete. Repair techniques for these defects are described in Section 3.4.2 of this manual with standard repair procedures given in PCI Manual 137. Examples of concrete repair are shown in **Figures 19.2.3-1** and **19.2.3-2**.

REPAIR AND REHABILITATION

19.2.3 Spalls, Voids, and Honeycombs/19.3.1 Introduction

Figure 19.2.3-1
Repair of Concrete Corner



a) Before Repair



b) After Repair

Figure 19.2.3-2
Defective Concrete Removed Prior to Placement of Repair Material



19.3 REPAIR OF PRODUCTS DAMAGED DURING CONSTRUCTION AND SERVICE LIFE

19.3.1 Introduction

Overall guidance for the repair of concrete is provided in the following documents:

- Concrete Repair Guide (ACI 546R, 2004)
- Concrete Repair Manual, Third Edition (ICRI, 2008)
- Guide for the Selection of Materials for the Repair of Concrete (ACI 546.3, 2006)

A summary of these documents is provided in Section 19.5.2.

REPAIR AND REHABILITATION**19.3.1 Introduction/19.3.2 Strand Splicing**

This section provides an overview of various repair methods irrespective of the source of damage. Nevertheless, the selected repair method may depend on the type of damage and its cause. Damage to precast, prestressed concrete can occur during shipment, erection, and subsequent bridge construction. Damage can also occur during the service life of the bridge.

Harries, et al. (2009) identified the following sources of damage observed in prestressed concrete bridge girders:

- Impact by over-height vehicles
- Environmental distress/aging including freeze-thaw and water-induced damage
- Construction error or poor practice associated with previous repairs
- Construction errors associated with appurtenance mounting
- Poor maintenance practices
- Construction errors
- Load-related damage other than impact including the effects of natural disasters
- Extreme events such as natural disasters, fire, or explosion

According to a 2011 survey of state Departments of Transportation (DOTs) (Harries, et al., 2012), load capacity was the dominant consideration when selecting a repair method for bridge girders damaged by impact with durability of the repair and interruption of service also major considerations. Time to make the repair was a moderate consideration and cost to make the repair was not considered significant.

Several NCHRP Project reports address damage to prestressed concrete bridge girders. NCHRP Report 226 (Shanafelt and Horn, 1980) provides guidance for the assessment, inspection, and repair of damaged prestressed concrete bridge girders. NCHRP Report 280 (Shanafelt and Horn, 1985) provides guidelines for the evaluation and repair of prestressed bridge members. A more recent research project (Harries, et al., 2012) serves to update NCHRP Report 280 and provides criteria to evaluate whether to repair or to replace a prestressed concrete girder damaged by vehicular impact; identifies the gaps in the available information and practices related to repair of collision damage of prestressed girders; and includes a recommended practice for the repair of impact-damaged prestressed concrete bridge girders. Examples of repairs to concrete bridges are given in ACI SP-277 (ACI 2011).

19.3.2 Strand Splicing

Strand splicing is an efficient and simple solution to connect broken strands and allow the strands to be re-tensioned such that girder strength is restored. The strands may be tensioned using the torque wrench method, in which a specified torque is applied to a strand coupler or “turn of the nut” method to achieve a specified displacement between the ends of the strand chucks or spliced ends. Further discussion of strand splicing is provided by Harries, et al. (2012) and the Alberta Infrastructure and Transportation Department. (ABITD, 2005). The use of strand splicing to repair bridge beams damaged by vehicle impact is described by Toenjes (2005) and Turnbull, et al. (2013) as shown in **Figure 19.3.2-1**. Repair and laboratory performance of two full-size girders are described by Zobel and Jirsa (1998) and Saiidi, et al. (2000).

Strand splices are easier to install when only a few strands need splicing. The diameter of a strand chuck is such that the chucks on adjacent strands need to be staggered to avoid interference. When a large number of strands are damaged, it may be appropriate to use a combination of strand splicing and external post-tensioning. External post-tensioning is described in Section 19.4.2.

REPAIR AND REHABILITATION

19.3.2 Strand Splicing/19.3.4 Preloading

*Figure 19.3.2-1
Strand Splicing (Photo: Turnbull, et al., 2013)*



19.3.3 Repair of Spalls

Repair of spalls caused during construction and subsequent service life is similar to the repair of spalls that occur before product delivery. If the spalling has exposed reinforcing bars or prestressing strand, it is essential that all corrosion products be cleaned from the steel before the spall is repaired. Repair techniques are described in Section 3.4.2 of this manual with standard repair procedures given in PCI Manual 137. The complete repair of a concrete girder in service is shown in **Figure 19.3.3-1**.

*Figure 19.3.3-1
Repair of a Concrete Girder in Service*



19.3.4 Preloading

One technique that has been used in conjunction with both strand splicing and repair of spalls to improve durability is preloading. Preloading is the temporary application of a vertical load to the girder during its repair. When used, the preload is usually provided by loaded trucks to induce tensile stress into the bottom of the girder prior to installation of a patch. After the patch has cured, removal of the preload induces compression into the patch. It is desirable to induce sufficient precompression that the patch or the vertical interface between the patch

REPAIR AND REHABILITATION**19.3.4 Preloading/19.3.7 Elimination of Expansion Joints**

and the original concrete will not crack under full service load. However, this may require a level of preload that is impractical. Plus, it is very difficult to keep the preload force from distributing to adjacent undamaged girders. Consequently, care should be taken when preloading a structure so as to not overload the structure or cause further damage to the girder being repaired or the adjacent girders. The decision to preload, therefore, must be based on each individual situation. In a 2011 survey of state DOTs, about one half of respondents indicated that they use preloading to induce compression into concrete patches (Harries, et al., 2012).

19.3.5 Corrosion Damage

Corrosion of nonprestressed reinforcement and prestressing strand occurs as a result of water and salt penetrating the concrete to the level of the reinforcement or strand. It can also occur when the reinforcement is exposed as a result of vehicle impact or freeze-thaw damage to the concrete. The ends of simple span beams are particularly susceptible to corrosion damage because of the leakage through the expansion joints.

Guidance on the selection and application of materials for repair of corrosion damaged concrete are provided in ACI 546R (2004), ACI 546.3 (2006), and ICRI Concrete Repair Manual (2008).

19.3.6 Bearing Rehabilitation

Bridge bearings are used to support vertical loads from the superstructure as well as to allow for longitudinal movement, rotation, or transfer of longitudinal or lateral forces between the superstructure and the substructure. Early bridges used bearings consisting of multiple steel pieces, which were subject to corrosion and required constant maintenance. Today, most new construction uses reinforced elastomeric bearings. Their design is discussed in detail in Chapter 10 of this manual.

Bridge bearing rehabilitation involves some means of jacking the superstructure and substructure apart so the load is removed from the bearing and the bearing removed and repaired or replaced. In some cases, if the concrete below the bearing seat has deteriorated, the deteriorated concrete needs to be removed and replaced before the new bearing is installed. The specific details for doing this depend on the individual bridge configuration. Many state DOTs have their own bridge maintenance, repair, or rehabilitation manuals, which should be consulted.

19.3.7 Elimination of Expansion Joints

Expansion joints are provided in bridge superstructures to allow longitudinal movements and end rotations relative to the substructure. These movements and rotations are caused by application of dead and live loads, creep and shrinkage of the concrete, and temperature changes and gradients. The joints are often sealed at the deck level to prevent water, deicing salts, and debris from falling onto the beams and substructures. When joint seals are not properly maintained or replaced, water and deicing salts penetrate below the deck, which can lead to accelerated deterioration of the end of the beams and the substructure below. Therefore, elimination of expansion joints reduces maintenance costs, improves ride quality, lowers impact loads, and improves seismic resistance.

Joints can be eliminated by making the deck and beam continuous over the supports or by making only the deck continuous. The former is more easily accomplished with new bridge construction, whereas the latter can be easily accomplished when a joint or bridge deck is replaced. When only the deck is made continuous, it is often called a link slab. One important detail with the link slab is to debond a portion of the deck from the girder as illustrated in **Figure 19.3.7.-1**.

The behavior and design of link slabs have been investigated by various researchers. Caner and Zia (1998) investigated the behavior and design of link slabs connecting two adjacent simple-span girders and proposed a simple method for designing the link slab. Three design examples were developed to illustrate the method.

El-Safty and Okeil (2008) used the finite element method to investigate the response of joint-free bridge deck systems. The results were validated by comparison with experimental results. A simplified method more suitable for design purposes was presented. The study suggested that the use of debonded link slabs can be effective in extending the service lives of repaired bridges.

REPAIR AND REHABILITATION**19.3.7 Elimination of Expansion Joints/19.3.8 Shotcrete Repair**

Elimination of joints over piers and abutments involves the following steps:

- Remove expansion joint and adjacent concrete to expose deck reinforcement.
- Form area.
- Place new reinforcement to lap the existing reinforcement or use bar couplers.
- Place new deck concrete.

When cast-in-place concrete decks are totally replaced with full-depth precast, prestressed concrete slabs, it is necessary to emulate the cast-in-place connection with precast connections. These connections include small closure placements with lap-spliced reinforcement, welded connections, or mechanical couplers. (Culmo, 2011). Various connection details are given in Chapter 2 of the FHWA publication titled “Connection Details for Prefabricated Bridge Elements and Systems” (Culmo, 2009).

Figure 19.3.7-1

Joint Replacement in Progress (Photo: Virginia Department of Transportation)



19.3.8 Shotcrete Repair

Shotcreting is a process in which mortar or concrete is pneumatically projected at a high velocity onto a surface. Shotcreting is usually classified according to the process used: wet mix or dry mix. In the wet-mix process, all the constituent materials are premixed before being placed into the chamber of the delivery system. In the dry process, the cementitious materials and aggregate are premixed before being placed into the delivery equipment. Water is added at the delivery nozzle. Steel or synthetic fibers may also be included in the shotcrete material to improve flexural and shear toughness and impact resistance (ACI 506.1R, 2008). The use of shotcrete to repair a bridge pier is illustrated in **Figure 19.3.8-1**. (Anon, 2010).

According to ACI Committee 506 (ACI 506R, 2005), shotcrete was first introduced into the construction industry as a proprietary process known as Gunitite. In the early 1930s, the generic term of shotcrete was introduced by the American Railway Engineering Association to describe the process. In 1951, the American Concrete Institute adopted the term “shotcrete” to describe the dry mix process. Today, “shotcrete” is used to describe both processes.

Shotcrete is an ideal material for repair of bridges. Guide specifications for its use have been developed by a joint task force representing the American Association of State Highway and Transportation Officials, the Associated General Contractors of America, and the American Road and Transportation Builders Association (AASHTO, 1998). Another document that provides useful information is ACI 506—Guide to Shotcrete (ACI 506R, 2005). Although this document does not specifically address the use of shotcrete for repair of bridges, it contains information for the use in contract documents.

REPAIR AND REHABILITATION

19.3.8 Shotcrete Repair/19.4.2 External Post-Tensioning

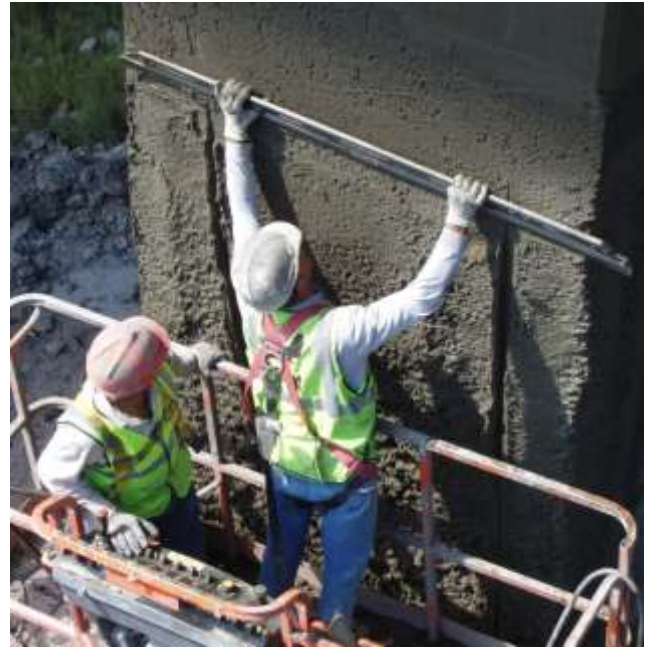
A specification for shotcrete is provided in ACI 506.2 (1995). Other information about the use of shotcrete is available from the American Shotcrete Association at www.shotcrete.org.

Figure 19.3.8-1

Shotcrete Repair of a Bridge Pier (Photos: American Shotcrete Association)



a) Preparation Before Shotcreting



b) Finishing the Shotcrete Surface

19.4 STRENGTHENING TECHNIQUES

19.4.1 Introduction

Strengthening of existing concrete bridges may be required for the following reasons:

- Offset a strength or serviceability reduction caused by a design or construction defect
- Offset a strength or serviceability reduction caused by damage while the bridge is in service
- Increase the strength or serviceability capabilities to allow a higher superimposed dead load or live load

Two techniques to enhance strength or serviceability are described in this section.

19.4.2 External Post-Tensioning

External post-tensioning is a technique that can be used to strengthen a structure as well as improve its performance at the serviceability level. In this technique, steel or carbon fiber reinforced polymer bars or strands are tensioned on the outside of the member. Special details are required to provide anchorage locations at the ends of the girders and at any deviation locations. The technique is similar to internal post-tensioning of box girder bridges except it is installed as a retrofit as illustrated in **Figure 19.4.2-1**. Determination of the amount of post-tensioning is straightforward. However, special attention is needed to the design of the anchor and deviation blocks. In some cases, these may need to be post-tensioned to the strengthened member to ensure adequate shear transfer.

External post-tensioning of bridge beams over highways is subject to damage from vehicle impact. Therefore, the girder must carry some level of load in the event that the post-tensioning is damaged. Various external post-tensioned techniques are illustrated in Harries, et al. (2012).

REPAIR AND REHABILITATION

19.4.2 External Post-Tensioning/19.4.3 Fiber Reinforced Polymer Composites

*Figure 19.4.2-1
Prestressed Concrete Bridge Girder with External Post-Tensioning*

**19.4.3 Fiber Reinforced Polymer Composites**

Fiber reinforced polymer (FRP) composites consist of a polymer matrix reinforced with a high-strength fiber. The fiber may be aramid (AFRP), carbon (CFRP), glass (GFRP), steel (SFRP), or hybrids of the materials (Harries et al., 2012). These materials may be bonded to the tension face of concrete members to increase their flexural strength or to the vertical faces to increase their shear strength. They may be made into continuous sheets or applied at discrete locations depending on the desired strengthening. They may be used to strengthen in one direction or two directions. If cracks are present, FRP may be used to control crack widths under subsequent loads. FRP materials may also be pretensioned before being bonded to the concrete member. These systems are described in more detail by Harries, et al. (2012). Several examples of repairs to bridges are described by ACI Committee 440 (2008) and Yang, et al. (2011). The use of continuous CFRP wrapping is illustrated in **Figure 19.4.3-1** (Toenjes, 2005). The use of intermittent sheets of woven CFRP to increase the shear capacity of repaired girders and to protect the girders is shown in **Figure 19.4.3-2** (Turnbull, et al., 2013). A methodology to evaluate the durability of bonded CFRP repair and strengthening systems has been developed by Dolan, et al. (2008). Recommended construction specifications and a construction process control manual for bonded FRP repair and retrofit of concrete structures using FRP composites are provided in NCHRP Report 514 (Mirmiran, et al., 2004).

The proposed specifications include eight main sections: General; Submittals; Storage, Handling, and Disposal; Substrate Repair and Surface Preparation; Installation of FRP System; Inspection and Quality Assurance; Repair of Defective Work; and Measurement and Payment. The proposed process control manual covers quality control (QC) and quality assurance (QA) prior to, during, and after completion of the repair project. It consists of planning, record keeping, inspection, and QC tests. The manual includes the following main sections: QA Policy and Program Overview; QA Guidelines for Construction Activities; and Implementing and Monitoring of the QA Program. The manual also consists of the number of QA checklists for the FRP repair projects.

REPAIR AND REHABILITATION

19.4.3 Fiber Reinforced Polymer Composites/19.5.1.1 Guidelines for Historic Bridge Rehabilitation and Replacement

Figure 19.4.3-1
Girders Repaired using Continuous CFRP Wrapping. (Photo: Toenjes, 2005)



Figure 19.4.3-2
Girders Strengthened using Intermittent Woven Sheets of CFRP (Photo: Turnbull, et al., 2013)



19.5 SPECIFICATIONS AND MANUALS

19.5.1 AASHTO Publications

19.5.1.1 Guidelines for Historic Bridge Rehabilitation and Replacement, 1st Edition (AASHTO, 2008)

This report presents a literature search, findings of a survey on the current state of historic bridge rehabilitation or replacement decision-making by state and local transportation agencies. Decision-making guidelines for historic bridges are provided. The guidelines include identification of various approaches to bringing historic bridges into conformance with current design and safety standards.

REPAIR AND REHABILITATION**19.5.1.2 Inspector's Guide for Shotcrete Repair of Bridges/****19.5.2.6 Guide for the Design and Construction of Externally Bonded FRP Systems for Strengthening Concrete Structures****19.5.1.2 Inspectors' Guide for Shotcrete Repair of Bridges (AASHTO, 1999)**

This document provides guidance to inspectors of highway bridge repair, rehabilitation, and retrofit using shotcrete. Separate parts address preconstruction preparation and construction inspection.

19.5.1.3 Guide Specifications for Shotcrete Repair of Highway Bridges (AASHTO, 1998)

These guide specifications include specifications for both dry mix shotcrete repair and wet mix shotcrete repair of bridges. A commentary addressing both dry mix and wet mix methods is provided.

19.5.1.4 Guide Specification for Design of Bonded FRP Systems for Repair and Strengthening of Concrete Bridge Elements (AASHTO, 2012A)

These guide specifications are intended for the repair and strengthening of reinforced and prestressed concrete highway bridge structures using externally bonded fiber-reinforced polymer composite systems. These guide specifications supplement the *AASHTO LRFD Bridge Design Specifications*, Sixth Edition, 2012. (AASHTO, 2012B)

19.5.2 Other Key Documents**19.5.2.1 Manual for the Evaluation and Repair of Precast, Prestressed Concrete Bridge Products (PCI Manual 137)**

This manual is a resource document to guide owners, designers, inspectors, and fabricators in reaching informed decisions regarding repair options. Engineering considerations related to individual defects are provided. Individual chapters address troubleshooting, repair procedures, methods of patching, and epoxy injection.

19.5.2.2 Guide to Recommended Practices for the Repair of Impact-Damaged Prestressed Concrete Bridge Girders (Harries, et al., 2012)

This document provides guidance for inspecting, assessing, and repairing damage to prestressed concrete bridge girders resulting from vehicular impact. This guide focuses on structural repair techniques rather than aesthetic or preventative repairs. Guidance for the latter is given by reference to other established sources. Similarly, the focus of this guide is impact damage, although the repair methods described may also be employed for similar damage from other sources. Four design examples are included.

19.5.2.3 Concrete Repair Manual, Third Edition (ICRI, 2008)

This manual includes over 70 documents from many of the associations involved in the concrete repair industry.

19.5.2.4 Concrete Repair Guide (ACI 546R, 2004)

Guidance on the selection and application of materials and methods for the repair, protection, and strengthening of concrete structures is provided. An overview of materials and methods is presented as a guide for making a selection for a particular application.

19.5.2.5 Guide for the Selection of Materials for the Repair of Concrete (ACI 546.3, 2006)

This document provides guidance on the selection of materials for the repair of concrete. An overview of the important properties of repair materials is presented as a guide for making an informed selection of repair materials that are appropriate for specific applications and service conditions.

19.5.2.6 Guide for the Design and Construction of Externally Bonded FRP Systems for Strengthening Concrete Structures (ACI 440.2R)

This document offers information on the use of FRP strengthening systems; a description of the unique material properties of FRP; and recommendations on the engineering, construction, and inspection of FRP systems used to strengthen concrete structures.

19.6 REFERENCES

AASHTO. 2008. *Guidelines for Historic Bridge Rehabilitation and Replacement*, 1st Edition. American Association of State Highway and Transportation Officials, Washington, DC. 68 pp.

https://bookstore.transportation.org/item_details.aspx?ID=1363 (Fee)

AASHTO. 2012A. *Guide Specification for Design of Bonded FRP Systems for Repair and Strengthening of Concrete Bridge Elements*, 1st Edition. American Association of State Highway and Transportation Officials, Washington, DC. 52 pp. https://bookstore.transportation.org/collection_detail.aspx?ID=118 (Fee)

AASHTO. 2012B. *AASHTO LRFD Bridge Design Specifications*, Sixth Edition, American Association of State Highway and Transportation Officials, Washington, DC. 1672 pp.

https://bookstore.transportation.org/item_details.aspx?ID=1924 (Fee)

AASHTO Task Force 37. 1998. *Guide Specifications for Shotcrete Repair of Highway Bridges*. American Association of State Highway and Transportation Officials, Washington, DC. February. 122 pp.

https://bookstore.transportation.org/item_details.aspx?ID=361 (Fee)

AASHTO Task Force 37. 1999. *Inspectors' Guide for Shotcrete Repair of Bridges*. American Association of State Highway and Transportation Officials, Washington, DC. December. 76 pp.

https://bookstore.transportation.org/item_details.aspx?ID=1359 (Fee)

ABITD. 2005. *Repair Manual for Concrete Bridge Elements*, Version 2.0. Alberta Infrastructure and Transportation Department, Alberta, Canada. 27 pp.

<http://www.transportation.alberta.ca/Content/docType30/Production/RpMConcBrEl2.pdf>

ACI. 2011. *Recent Advances in Maintenance and Repair of Concrete Bridges*, SP-277. American Concrete Institute, Farmington Hills, MI. <http://www.concrete.org/PUBS/JOURNALS/SP-HOME.ASP> (Fee)

ACI Committee 224. 2001. *Control of Cracking in Concrete Structures* (ACI 224R-01). American Concrete Institute, Farmington Hills, MI. 46 pp. <http://www.concrete.org/BookstoreNet/ProductDetail.aspx?SACode=22401> (Fee)

ACI Committee 224. 2007. *Causes, Evaluation, and Repair of Cracks in Concrete Structures* (ACI 224.1R-07). American Concrete Institute, Farmington Hills, MI. 22 pp.

<http://www.concrete.org/BookstoreNet/ProductDetail.aspx?SACode=224107> Out of print but pdf available. (Fee)

ACI Committee 440. 2008. *Guide for the Design and Construction of Externally Bonded FRP System for Strengthening Concrete Structures* (ACI 440.2-08). American Concrete Institute, Farmington Hills, MI. 76 pp.

<http://www.concrete.org/BookstoreNet/ProductDetail.aspx?itemid=440208> (Fee)

ACI Committee 503. 2007. *Specification for Crack Repair by Epoxy Injection* (ACI 503.7-09). American Concrete Institute, Farmington Hills, MI. 7 pp. <http://www.concrete.org/bookstorenet/ProductDetail.aspx?itemid=503707>

(Fee)

ACI Committee 506. 1995. *Specification for Shotcrete* (ACI 506.2-95). American Concrete Institute, Farmington Hills, MI. 8 pp. <http://www.concrete.org/bookstorenet/ProductDetail.aspx?ItemID=506295> (Fee)

ACI Committee 506. 2005. *Guide to Shotcrete* (ACI 506R-05). American Concrete Institute, Farmington Hills, MI. 40 pp. <http://www.concrete.org/BookstoreNet/ProductDetail.aspx?itemid=50605> (Fee)

ACI Committee 506. 2008. *Guide to Fiber-Reinforced Shotcrete* (ACI 506.1R-08). American Concrete Institute, Farmington Hills, MI. 12 pp. <http://www.concrete.org/BookstoreNet/ProductDetail.aspx?itemid=506108> (Fee)

ACI Committee 546. 2004. *Concrete Repair Guide*. (ACI 546R-04). American Concrete Institute, Farmington Hills, MI. 53 pp. <http://www.concrete.org/BookstoreNet/ProductDetail.aspx?itemid=54604> (Fee)

ACI Committee 546. 2006. *Guide for the Selection of Materials for the Repair of Concrete* (ACI 546.3R-06). American Concrete Institute, Farmington Hills, MI. 34 pp.

<http://www.concrete.org/BookstoreNet/ProductDetail.aspx?itemid=546306> (Fee)

REPAIR AND REHABILITATION

19.6 References

- Anon. 2010. "Abraham Lincoln Memorial Bridge." *Shotcrete*, American Shotcrete Association, Farmington Hills, MI. (Winter), pp. 34-35. http://www.shotcrete.org/pdf_files/Archive/2010Win_InfrastructureProject08.pdf
- Caner, A. and P. Zia. 1998. "Behavior and Design of Link Slabs for Jointless Bridge Decks," *PCI Journal*, Precast/Prestressed Concrete Institute, Chicago, IL. V. 43, No. 3 (May-June), pp. 68-80. http://www.pci.org/view_file.cfm?file=JL-98-MAY-JUNE-6.pdf
- Culmo, M. P. 2009. *Connection Details for Prefabricated Bridge Elements and Systems*. Report No. FHWA-IF-09-010. Federal Highway Administration, U. S. Department of Transportation, Washington, DC. 568 pp. <http://www.fhwa.dot.gov/bridge/prefab/if09010/>
- Culmo, M. P. 2011. *Accelerated Bridge Construction— Experience in Design, Fabrication and Erection of Prefabricated Bridge Elements and Systems*. Report No. FHWA-HIF-12-013. Federal Highway Administration, U. S. Department of Transportation, Washington, DC. 347 pp. <http://www.fhwa.dot.gov/bridge/abc/docs/abcmanual.pdf>
- Dakhil, F. H., P. D. Cady, and R. E. Carrier. 1975. "Cracking of Fresh Concrete as Related to Reinforcement," *ACI Journal*, Proceedings V. 72, No. 8 (August), pp. 421-428. <http://www.concrete.org/PUBS/JOURNALS/OLJDetails.asp?Home=JP&ID=11145>
- Dolan, C. W., J. Tanner, D. Mukai, et al. 2008. *Design Guidelines for Durability of Bonded CFRP Repair/Strengthening of Concrete Beams*. NCHRP Web-Only Document 155. Transportation Research Board, Washington, DC. 63 pp. http://onlinepubs.trb.org/onlinepubs/nchrp/nchrp_w155.pdf
- El-Safty, A. and A. M. Okeil. 2008. "Extending the Service Life of Bridges using Continuous Decks," *PCI Journal*, Precast/Prestressed Concrete Institute, Chicago, IL. V. 53, No. 6 (November-December), pp. 96-111. http://www.pci.org/view_file.cfm?file=JL-08-NOVEMBER-DECEMBER-10.pdf
- FHWA. 2011. *FHWA Bridge Preservation Guide*. Federal Highway Administration, Office of Infrastructure. U. S. Department of Transportation, Washington, DC. 29 pp. <http://www.fhwa.dot.gov/bridge/preservation/guide/guide.pdf>
- Harries, K. A., J. L. Kasan, and C. Aktas. 2009. *Repair Methods for Prestressed Concrete Bridges*. Report No. FHWA-PA-2009-008-PIT006. Pennsylvania Department of Transportation, Harrisburg, PA. 169 pp. <http://trid.trb.org/view.aspx?id=906269>
- Harries, K. A., J. Kasan, R. Miller, et al. 2012. *Updated Research for Collision Damage and Repair of Prestressed Concrete Beams*. NCHRP 20-07/Task 307 Final Report. Transportation Research Board, Washington, DC. May, 227 pp. <http://apps.trb.org/cmsfeed/TRBNetProjectDisplay.asp?ProjectID=3070> (Fee)
- ICRI. 2008. *Concrete Repair Manual*, Third Edition. International Concrete Repair Institute, Rosemont, IL. 2077 pp. <http://www.icri.org/bookstore/bkstr.asp> (Fee) Link to order form.
- Mirmiran, A., M. Shahawy, A. Nanni, et al. 2004. *Bonded Repair and Retrofit of Concrete Structures using FRP Composites; Recommended Construction Specifications and Process Control Manual*. NCHRP Report 514. Transportation Research Board, Washington, DC. 102 pp. http://onlinepubs.trb.org/onlinepubs/nchrp/nchrp_rpt_514.pdf
- PCI Manual 116. 1999. *Manual for Quality Control for Plants and Production of Structural Precast Concrete Products*, (MNL-116-99), Fourth Edition. Precast/Prestressed Concrete Institute, Chicago, IL. 340 pp. http://www.pci.org/view_file.cfm?file=w1728_MNL_116-99.PDF (Fee)
- PCI Manual 137. 2006. *Manual for the Evaluation and Repair of Precast, Prestressed Concrete Bridge Products*, (MNL-137-06). Precast/Prestressed Concrete Institute, Chicago, IL. 72 pp. https://netforum.pci.org/eweb/dynamicpage.aspx?webcode=category&ptc_key=5d967c30-b4c7-4993-bab8-f3cd6142e004 (Fee) *Bridge Repair Manual* is the title on the PCI website.
- Saiidi, M. S., Y. Labia, and B. Douglas. 2000. "Repair and Performance of a Full-Scale Pretensioned Concrete Girder," *PCI Journal*, Precast/Prestressed Concrete Institute, Chicago, IL. V. 45, No. 2 (March-April), pp. 96-105. http://www.pci.org/view_file.cfm?file=JL-00-MARCH-APRIL-6.pdf

REPAIR AND REHABILITATION

19.6 References

- Shanafelt, G. O. and W. B. Horn. 1980. *Damage Evaluation and Repair for Prestressed Concrete Bridge Members*. NCHRP Report 226. Transportation Research Board, Washington, DC. 66 pp.
<http://pubsindex.trb.org/view/1980/M/161040>
- Shanafelt, G. O. and W. B. Horn. 1985. *Guidelines for Evaluation and Repair of Prestressed Concrete Bridge Members*. NCHRP Report 280. Transportation Research Board, Washington, DC. 84 pp.
<http://pubsindex.trb.org/view/1985/M/271436>
- Tadros, M. K., S. S. Badie, and C. Y. Yuan. 2010. *Evaluation and Repair Procedures for Precast/Prestressed Concrete Girders with Longitudinal Cracking in the Web*. NCHRP Report 654. Transportation Research Board, Washington, DC. 75 pp. http://onlinepubs.trb.org/onlinepubs/nchrp/nchrp_rpt_654.pdf
- Toenjes, C. J. 2005. "Repair of Prestressed Concrete Girders with Carbon Fiber Reinforced Polymer Wrap." The International Bridge, Tunnel and Turnpike Association, Facilities Management Workshop, May 14-18, Toronto, Ontario. www.ibtta.org/files/PDFs/Toenjes_Chris.pdf (Accessed March 2013)
- TRB. 2006. *Control of Cracking in Concrete, State of the Art*. Transportation Research Circular E-C107. Transportation Research Board, Washington, DC. <http://onlinepubs.trb.org/onlinepubs/circulars/ec107.pdf>
- Turnbull, A. F., W. F. Young, and C. Lam. 2013. "Dingman Drive Bridge: Reinstatement of Service Strands on Prestressed Concrete Girders Damaged by Vehicle Impact." *PCI Journal*, Precast/Prestressed Concrete Institute, Chicago, IL. V. 56, No. 1 (Winter), pp. 45-54. http://www.pci.org/view_file.cfm?file=JL-13-WINTER-9.pdf
- Yang, D., B. D. Merrill, and T. E. Bradberry. 2011. "Texas' Use of CFRP Repair to Concrete Bridges." *Recent Advances in Maintenance and Repair of Concrete Bridges*, ACI SP-277. American Concrete Institute, Farmington Hills, MI. pp. 39-57.
<http://www.concrete.org/PUBS/JOURNALS/OLJDetails.asp?Home=SP&ID=51682368> (Fee)
- Zobel, R. S. and J. O. Jirsa. 1998. "Performance of Strand Splice Repairs in Prestressed Concrete Bridges," *PCI Journal*, Precast/Prestressed Concrete Institute, Chicago, IL. V. 43, No. 6 (November-December), pp. 72-84.
http://www.pci.org/view_file.cfm?file=JL-98-NOVEMBER-DECEMBER-10.pdf

Piles

To be released at a later date.

This page intentionally left blank

PEDESTRIAN BRIDGES

TABLE OF CONTENTS

21.1 INTRODUCTION 21 - 5

21.2 DESCRIPTION, GUIDELINES, AND EXAMPLES 21 - 5

 21.2.1 References Related to Pedestrian Facilities 21 - 6

 21.2.2 Pedestrian-Friendly Routes 21 - 7

 21.2.3 Considerations for Incorporating Pedestrian Bridges 21 - 8

 21.2.3.1 Planning 21 - 8

 21.2.4 Geometric Considerations and Access..... 21 - 8

 21.2.4.1 Span Capabilities 21 - 8

 21.2.4.2 Vertical Clearance..... 21 - 10

 21.2.4.3 Ramps and Approaches..... 21 - 10

 21.2.4.4 Width 21 - 12

 21.2.4.5 Grade 21 - 12

 21.2.4.6 Cross Slope..... 21 - 12

 21.2.4.7 Walkway Alignment 21 - 12

 21.2.5 Aesthetics and Amenities 21 - 14

 21.2.5.1 Architectural Finishes..... 21 - 15

 21.2.5.2 Manufacturing Capabilities 21 - 17

 21.2.5.3 Walkway Surfaces..... 21 - 17

 21.2.5.4 Aesthetic Solutions..... 21 - 18

 21.2.5.5 Thin-Set Brick Inlay Panels 21 - 19

 21.2.5.6 Formliner Mold Finishes 21 - 20

 21.2.5.7 Anti-graffiti Surfaces 21 - 21

 21.2.5.8 Public Art..... 21 - 21

 21.2.5.9 Lighting..... 21 - 21

 21.2.6 Railings and Screens 21 - 21

 21.2.6.1 Geometry 21 - 21

 21.2.6.2 Bicycle Railings 21 - 23

 21.2.6.3 ADA-Compliant Railings 21 - 23

 21.2.6.4 Design Live Loads 21 - 24

 21.2.7 Loads and Load Combinations 21 - 25

 21.2.7.1 Pedestrian Load 21 - 25

 21.2.7.2 Equestrian Load 21 - 25

 21.2.7.3 Vehicular Load 21 - 25

 21.2.7.4 Wind Load 21 - 26

 21.2.7.5 Fatigue Load..... 21 - 26

 21.2.7.6 Load Combinations 21 - 26

 21.2.8 Deflection..... 21 - 26

 21.2.9 Vibration 21 - 27

 21.2.10 Construction Details 21 - 27

PEDESTRIAN BRIDGES

TABLE OF CONTENTS

21.2.10.1 Framing and Connection Details 21 - 27

21.2.10.2 Drainage 21 - 28

21.2.10.3 Cable-Stayed Pedestrian Bridges 21 - 28

21.2.11 Vegetation and Irrigation 21 - 29

21.2.11.1 Provisions for Plantings 21 - 29

21.2.12 Case Studies 21 - 30

21.2.12.1 Canyon Park Freeway Station 21 - 30

21.2.12.1.1 Structure Description 21 - 31

21.2.12.1.2 Key Design Objectives 21 - 31

21.2.12.1.3 Features 21 - 31

21.2.12.2 Forty Foot Pedestrian Bridge 21 - 32

21.2.12.2.1 Structure Description 21 - 32

21.2.12.2.2 Key Design Objectives 21 - 33

21.2.12.2.3 Features 21 - 34

21.2.12.3 Pacific Coast Highway Pedestrian Bridge 21 - 34

21.2.12.3.1 Structure Description 21 - 35

21.2.12.3.2 Key Design Objectives 21 - 36

21.2.12.3.3 Features 21 - 37

21.2.12.4 Delta Ponds Pedestrian Bridge 21 - 37

21.2.12.4.1 Structure Description 21 - 38

21.2.12.4.2 Key Design Objectives 21 - 39

21.2.12.4.3 Features 21 - 40

21.2.12.5 David Kreitzer Lake Hodges Bicycle/Pedestrian Bridge 21 - 40

21.2.12.5.1 Structure Description 21 - 41

21.2.12.5.2 Key Design Objectives 21 - 42

21.2.12.5.3 Features 21 - 42

21.2.12.6 Glenmore Trail Legsby Road Pedestrian Bridge 21 - 42

21.2.12.6.1 Structure Description 21 - 43

21.2.12.6.2 Key Design Objectives 21 - 43

21.2.12.6.3 Features 21 - 44

21.2.12.7 DCR Access Road Bridge over Route 24 21 - 45

21.2.12.7.1 Structure Description 21 - 45

21.2.12.7.2 Key Design Objectives 21 - 46

21.2.12.7.3 Features 21 - 46

21.2.12.8 Lake Mary Pedestrian Bridges 21 - 46

21.2.12.8.1 Structure Description 21 - 47

21.2.12.8.2 Key Design Objectives 21 - 48

21.2.12.8.3 Features 21 - 48

21.2.12.9 Chambers Creek Properties North Deck Pedestrian Overpass 21 - 48

PEDESTRIAN BRIDGES

TABLE OF CONTENTS

- 21.2.12.9.1 Structure Description..... 21 - 49
- 21.2.12.9.2 Key Design Objectives..... 21 - 50
- 21.2.12.9.3 Features..... 21 - 50
- 21.3 SPECIAL USE PEDESTRIAN BRIDGES 21 - 51
- 21.3.1 Snowmobile Bridges..... 21 - 51
- 21.3.1.1 Snowmobile Bridge Case Study—Paul Bunyan Trail Bridge over Excelsior Road 21 - 52
- 21.3.1.1.1 Structure Description 21 - 53
- 21.3.1.1.2 Key Design Objectives..... 21 - 54
- 21.3.1.1.3 Features 21 - 54
- 21.3.2 Wildlife Bridges 21 - 55
- 21.3.2.1 Wildlife Bridge Case Study—Cross Florida Greenway Land Bridge Over I-75 21 - 57
- 21.3.2.1.1 Structure Description 21 - 57
- 21.3.2.1.2 Key Design Objectives..... 21 - 58
- 21.3.2.1.3 Features 21 - 58
- 21.4 CITED REFERENCES 21 - 58

This page intentionally left blank

Pedestrian Bridges

21.1 INTRODUCTION

This chapter includes pedestrian bridges and pedestrian-type bridges that may be used also for other purposes such as equestrian or wildlife crossings. These bridges may be designed under the authority of the local building official when they are used in private, commercial developments or in conjunction with public institutional building construction. In these cases, publication 343R-95 by the American Concrete Institute (ACI) titled *Analysis and Design of Reinforced Concrete Bridge Structures* (ACI Committee 343, 1995) may be used as a design guide. Pedestrian bridges are specifically included in this document. Additional information may be found in the *Building Code Requirements for Structural Concrete and Commentary* (ACI Committee 318, 2011). The requirements of these documents are not specifically discussed in this chapter.

The bridges considered in this chapter are those owned and designed by or otherwise under the authority of public entities including federal, state, or local departments of transportation. Any bridge, whether publicly or privately owned that passes over a public right-of-way, is under the authority of the public agency. For these bridges, the governing design codes are published by the American Association of State Highway and Transportation Officials (AASHTO). They are the *AASHTO LRFD Guide Specifications for the Design of Pedestrian Bridges (LRFD Pedestrian Guide Specifications, AASHTO, 2009a)* and the *AASHTO LRFD Bridge Design Specifications (LRFD Specifications, AASHTO, 2012a)*. The *LRFD Pedestrian Guide Specifications* is relevant to bridges designed for pedestrians, bicyclists, equestrian riders, and light maintenance vehicles. It adds guidance to information in the *LRFD Specifications* and deals with issues that are different, such as loadings, or require special treatment from provisions in the *LRFD Specifications*. Much of the *LRFD Pedestrian Guide Specifications* addresses issues with steel structures. Only the issues pertinent to the application and design of precast, prestressed concrete bridges are discussed in this chapter.

Additional guidance from an international perspective is provided in the publication *Bulletin 32: Guidelines for the Design of Footbridges (fib, 2005)*.

21.2 DESCRIPTION, GUIDELINES, AND EXAMPLES

These bridges are typically used in walking, bicycling, and equestrian trails. The *AASHTO LRFD Pedestrian Guide Specifications* governs their design.

The *Guide for the Development of Bicycle Facilities* (AASHTO, 2012b) defines a “shared use path” as one separated from motorized traffic and often used by pedestrians, skaters, wheelchair users, joggers, and other non-motorized users. Such trails can provide recreational opportunities or, in some instances, can serve as direct commute routes. Care must be taken when mixing pedestrian walkways with a shared use path. Bicyclists traveling at higher speeds may come into conflict with the variety of pedestrian users. It is usually not desirable to mix horse riding and bicycle traffic on the same shared use path. Horses can be startled easily and may be unpredictable if they perceive approaching bicyclists as a danger. Generally, pavement requirements for bicycle travel may not be suitable for horses.

Where there are dedicated bicycle lanes, they should be clearly marked similar to that shown in **Figure 21.2-1**.

PEDESTRIAN BRIDGES**21.2 Description, Guidelines, and Examples/21.2.1 References Related to Pedestrian Facilities****Figure 21.2-1****Markings for a Bicycle Lane and Turnouts (Northeast 36th Street Bridge, Photo: BergerABAM)****21.2.1 References Related to Pedestrian Facilities**

Several publications and laws affect the planning, design, and construction of pedestrian facilities and bridges. The following are a list and description of applicable references.

***A Policy on Geometric Design of Highways and Streets* (AASHTO Green Book, AASHTO, 2011)—**

Interactions of pedestrians with traffic are a major consideration in highway planning and design. Many communities are changing land use planning and urban design practices to both accommodate and encourage walking and bicycling. The AASHTO Green Book provides general direction on pedestrian facility design elements.

***Manual on Uniform Traffic Control Devices for Streets and Highways* (MUTCD, FHWA, 2009b)—**

Defines the nature of a pedestrian to assist designers in providing appropriate accommodations. A pedestrian is a person afoot, in a wheelchair, on skates, or a skateboard. A person afoot may use a walker or a cane, be pushing a stroller or delivery hand truck, or be assisting a youngster on a tricycle. The pedestrian may have a vision or cognitive disability, be preoccupied or lost, or be disadvantaged by weather or conditions underfoot. The concept of a “design pedestrian” should include children, older persons, and persons with disabilities for whom walking may be a primary mode chosen for independent travel. Pedestrian provisions are located in all nine parts of the manual.

***Americans with Disabilities Act* (ADA, 1990)—**A federal law that requires pedestrian facilities be accessible to and usable to people with disabilities. Title II of this act covers state and local government programs and facilities. Title II, for example, requires curb ramps along pedestrian routes. The Federal Highway Administration (FHWA) and the U. S. Department of Justice have authority to enforce provisions of the law that relate to public facilities. FHWA issued program guidance (FHWA, 2000) to aid owner agencies in the Transportation Equity Act for the 21st Century (TEA-21) legislation relating to pedestrians and bicyclists. TEA-21 mandated that walking facilities be incorporated into all transportation projects unless “exceptional circumstances” exist.

The Architectural and Transportation Barriers Compliance Board (Access Board), a federal agency committed to accessible design, has begun a rulemaking process to revise the accessibility requirements for public rights-of-way (see the Access Board website at <http://www.access-board.gov/>). They developed draft guidelines related to pedestrians and shared use paths. When finalized, the new guidelines will cover pedestrian access to sidewalks and streets, including crosswalks, curb ramps, street furnishings, pedestrian signals, parking, and other parts of the public right-of-way. The new guidelines will likely address issues such as access at street crossings for pedestrians who are blind or have low vision, wheelchair access to on-street parking, and constraints posed by space limitations, roadway design practices, slope, and terrain. Both sets of guidelines have undergone a period set aside for public comment. Comments have been received and are under consideration and final guidelines are expected.

In developing these draft guidelines, the Access Board obtained recommendations from an Advisory Committee comprising representatives from disability organizations, public works departments, transportation and traffic engineering groups, the design and civil engineering professions, government agencies, and standards-setting bodies. The Advisory Committee’s report is available on the Access Board’s website at <http://www.access-board.gov/guidelines-and-standards/streets-sidewalks/public-rights-of-way/background>. Although any ADA

PEDESTRIAN BRIDGES**21.2.1 References Related to Pedestrian Facilities/21.2.2 Pedestrian-Friendly Routes**

guidelines developed by the Access Board will not be enforceable under Title II of the ADA until the Department of Justice and the U.S. Department of Transportation issue regulations adopting them as standards, the Access Board's website provides information discussing accessibility concerns relating to curb ramps, sidewalks, pedestrian crossings, and other pedestrian routes.

The FHWA website includes the following materials related to this subject:

- "Questions and Answers About ADA/Section 504" (www.fhwa.dot.gov/civilrights/ada_qa.htm)
- A memorandum describing FHWA's oversight role on federal accessibility requirements http://www.fhwa.dot.gov/civilrights/memos/ada_memo_clarificationni.cfm
- FHWA's notice adopting the Access Board's draft accessibility guidelines for the public right-of-way as currently recommended best practices (www.fhwa.dot.gov/environment/bikeped/prwaa.htm)
- FHWA's memorandum on detectable warnings (www.fhwa.dot.gov/environment/bikeped/dwm.htm)

The process of adopting revised federal accessibility standards for public rights-of-way may be lengthy. However, it appears public agencies are attempting to follow these guidelines in advance of their becoming law. This chapter will include the standards as generally accepted.

Highway Capacity Manual (TRB, 2010)—Provides direction on calculating levels of service for pedestrians on topics such as widths of sidewalks.

21.2.2 Pedestrian-Friendly Routes

The AASHTO *Guide for the Planning, Design, and Operation of Pedestrian Facilities* (AASHTO Pedestrian Guide, AASHTO, 2004) provides guidance for designing facilities that are attractive and comfortable for pedestrians. Several factors combine to create an environment that makes walking an easy and natural choice. These include the following:

- Continuous and connected pedestrian facilities that are adequately separated from fast-moving traffic
- Safe and convenient street crossings
- Pedestrian-scale lighting
- A pleasant visual environment

The AASHTO *Pedestrian Guide* reports on common characteristics of pedestrian-friendly urban communities. These include the following factors that should be considered when planning pedestrian bridges:

- Provide safe and frequent crossing opportunities across freeways and arterials so they do not become barriers for pedestrians.
- Enhanced pedestrian access to transit stops makes taking the bus, train, or trolley more appealing.
- Furnishings such as benches, drinking fountains, and artwork create a more attractive and inviting atmosphere for walking trips.
- Street trees are an essential element in the street environment. Plantings can greatly increase the comfort level of pedestrians. Trees provide shade and shelter for pedestrians and create a sense of separation from traffic.
- Create a secure environment for pedestrians. Walking areas should have adequate pedestrian-scale lighting, open sight lines, and access to emergency services such as phones or call boxes. The best security is provided by pedestrian activity during all hours of the day.
- Frequent cleanup and repair of pedestrian facilities on a regular basis, including provisions for timely snow clearance, are essential

PEDESTRIAN BRIDGES**21.2.3 Considerations for Incorporating Pedestrian Bridges/21.2.4.1 Span Capabilities****21.2.3 Considerations for Incorporating Pedestrian Bridges**

Pedestrian connectivity should be provided across or under every vehicular bridge where there is a walking environment. Such a network can break down where a community is divided by major highways, railroads, rivers, or unique topographical features.

These barriers result in unique locations where a dedicated pedestrian bridge is desirable and may even be necessary. A properly designed and located pedestrian bridge can create these attributes and benefits:

- Improve pedestrian safety by providing a perceived advantage to crossing at grade
- Be cost effective through efficient design and effective use of materials
- Result in an attractive and durable structure through selection of materials
- Avoid crime and vandalism activity by proper location and use of lighting and other amenities
- Be inviting and convenient to pedestrians

21.2.3.1 Planning

Pedestrian bridges should be incorporated into the early stages of planning of new developments due to the need for funding. These bridges can be most beneficial under the following conditions (ITE, 1997):

- Moderate-to-high pedestrian demand
- Where a large number of children must cross, such as near a school
- Where traffic conditions encountered by pedestrians are considered unacceptable such as at wide streets or in locations with high-speed traffic or high traffic volumes
- Where one of the conditions stated above is combined with a unique pedestrian origin and destination (For example: residential neighborhood to school, parking structure to university, high-volume multi-use trail, apartment complex to shopping mall)

The effectiveness of pedestrian bridges depends on their perceived ease of use and accessibility by pedestrians. Use will generally not result from improved safety. Pedestrians tend to weigh improved safety against the extra time and effort necessary to use the facility. The degree of use tends to depend on walking distance and convenience. These facilities work only if they are on the normal path of pedestrian movements, with the least amount of vertical transition (ITE, 1997).

21.2.4 Geometric Considerations and Access**21.2.4.1 Span Capabilities**

Precast, prestressed concrete is ideally suited for the full range of span lengths normally encountered for pedestrian bridges. From short-span slab bridges to those approaching 200 ft, a wide range of applications are illustrated in this chapter. Long spans may be necessary to cross today's wide urban freeways while minimizing intermediate piers, which improves safety. One such application is the Padden Parkway Pedestrian Bridge in Vancouver, Wash., shown in **Figure 21.2.4.1-1**. The total length is 559 ft. There are two end spans of 187 ft and a center span of 185 ft. The deck width is 16 ft. The long spans were accomplished using a pair of 84-in.-deep deck bulb-tee beams in each span plus a composite cast-in-place concrete deck. This project demonstrated that the use of high-strength concrete achieved long spans to reduce exposure to traffic below and create a simple, slender solution. The project demonstrated fast construction at a very reasonable cost.

Figure 21.2.4.1-1

Padden Parkway Pedestrian Bridge, Vancouver, Wash., Crosses the Main Lanes of I-205 Plus an Exit Ramp (Photos: OBEC Consulting Engineers)



a) The Bridge is Crowned at the Right Pier to Provide Vertical Clearance Above the Ramp



b) Erecting Only Six Beams for this 559-Ft-Long Bridge Reduced Traffic Disruption



c) Only Two Piers Were Needed; Improving Safety

Practices have evolved throughout the industry to extend the span ranges of typical precast concrete products. Chapter 11, *Extending Span Ranges*, in this manual is a very good treatment of the subject. Additionally, a publication by the Transportation Research Board, *Extending Span Ranges of Precast Prestressed Concrete Girders* (Castrodale and White, 2004), is recommended for more information.

The Fifth Street Pedestrian Plaza Bridge is 256 ft 6 in. in length, with spans of 137 ft and 119 ft 6 in. These long spans are designed for vehicular traffic and also included large loads from a series of planter walls containing soil and vegetation. The bridge is supported on 74-in.-deep bulb-tee beams. The project is described in Section 21.2.4.7 and shown in **Figures 21.2.4.7-1** and **21.2.5-1**.

The Paul Bunyan Trail Bridge is a through-girder bridge, a type commonly used in Minnesota for pedestrian structures. The two, 72-in.-deep edge I-beams each have a top flange width of 30 in. and support a cast-in-place concrete deck from the webs located approximately mid-depth of the beams. The overall width of the structure is 21 ft. This three-span bridge has end spans of 110 ft 9 in. and a center span of 121 ft 6 in. The bridge is shown in **Figure 21.2.4.1-2** and in photos in Sections 21.3.1 and 21.3.1.1 where it is described in more detail.

PEDESTRIAN BRIDGES

21.2.4.1 Span Capabilities/21.2.4.3 Ramps and Approaches

Figure 21.2.4.1-2

The Paul Bunyan Trail Bridge in Baxter, Minn., is a Through-Girder Bridge with Center Span Length of 121.5 Ft (Photo: Minnesota Department of Transportation)



High-strength precast, prestressed concrete beams can take advantage of high levels of pretensioning to achieve long span lengths. These designs utilize composite precast or cast-in-place concrete decks to accommodate the large accompanying compressive stresses. Through-girder bridges have no such decks and need to be “over-reinforced” (i.e., fail to meet required flexural strength according to the *LRFD Specifications*) to achieve desired spans and satisfy deflection requirements. In order to address the ductility of the beams, the Minnesota Department of Transportation sponsored research at the University of Minnesota published in 2007, titled, “Strength and Stability of Prestressed Concrete Through-Girder Pedestrian Bridges Subjected to Vehicular Impact” (Baran et al., 2007). In addition to impact, the work looked at the response of the section, including neutral axis location, strand stress at ultimate capacity, and moment capacity, predicted by the *LRFD Specifications* and compared them with the sectional response determined from nonlinear strain compatibility analyses. Modifications were proposed to the LRFD Specifications procedure to rectify the errors in predicting sectional response.

Post-tensioning techniques are used frequently in combination with pretensioning to accomplish longer spans, continuity across multiple spans, and improved connections and durability. Chapter 11 is a good source of information about post-tensioning precast concrete beams. Also, see these publications by the Post-tensioning Institute: *Post-Tensioning Manual* (PTI, 2006), *Guide Specification for Grouted Post-Tensioning* (PTI, 2012a), and *Specification for Grouting of Post-Tensioned Structures* (PTI, 2012b). Post-tensioning was the primary reinforcement in five of the case studies in Section 21.2.12.

21.2.4.2 Vertical Clearance

The *LRFD Pedestrian Guide Specifications* requires the bottom of the superstructure to have 1.0 ft greater clearance than highway bridges to increase safety against vehicle collisions. This results in additional challenges for approaches.

21.2.4.3 Ramps and Approaches

Access to a pedestrian bridge is generally provided by stairs and ramps. Stairs may be used to supplement a ramp but cannot be the only means of access. When the slope of a ramp exceeds 5%, handrails are required on both sides. Handrails must be at a constant height of 2 ft 10 in. above the walkway. For walkways that exceed a 5% slope, the walkway should have a minimum clear distance between railings of 5 ft 0 in. In addition, there must be a level landing for every 30-in. rise in elevation. The level landings must be at least 5 ft 0 in. long, except for the bottom landing, which must be 6 ft 0 in. long. The maximum distance between level landings is:

- For grades from greater than 5.0% to 6.25%, 40 ft 0 in. maximum spacing of landings
- For grades from greater than 6.25% to the maximum permissible grade of 8.3%, 30 ft 0 in. maximum spacing

PEDESTRIAN BRIDGES

21.2.4.3 Ramps and Approaches

Approach ramps to the twin pedestrian bridges in Lake Mary, Fla., reached a grade of 8.3%. One of the ramps is shown in **Figure 21.2.4.3-1**. The ramps were framed with 30-ft-long precast concrete slabs, precast pier caps that serve as landing slabs, and precast landing walls. The project is presented in Section 21.2.12.8, Case Studies.

Figure 21.2.4.3-1

With Severe Site Constraints, These Ramps Included Slopes of 8.3% for the Lake Mary Pedestrian Bridges (Photo: Dyer, Riddle, Mills & Precourt Inc. photographed by Ben Tanner Photography)



Congested urban sites often require scissor-like ramps on a compressed footprint. The ramp shown in **Figure 21.2.4.3-2** was typical of the ramps for the San José de la Luz Pedestrian Bridge built in Guanajuato, Mexico.

Figure 21.2.4.3-2

Scissor Ramps on the San Jose de la Luz Pedestrian Bridge Were Framed with Precast Concrete Hollow-Core Slabs, Precast Columns, and Precast Landings (Rendering: Grupo Constructor Sepsa S.A. de C.V.)



Pedestrians with mobility and stamina impairments may not be able to use ramps with a vertical rise of more than 5 ft. Therefore, elevators should be considered in these cases. If an elevator is provided, an ADA-compliant ramp may be omitted.

A level transition to the bridge deck must be provided.

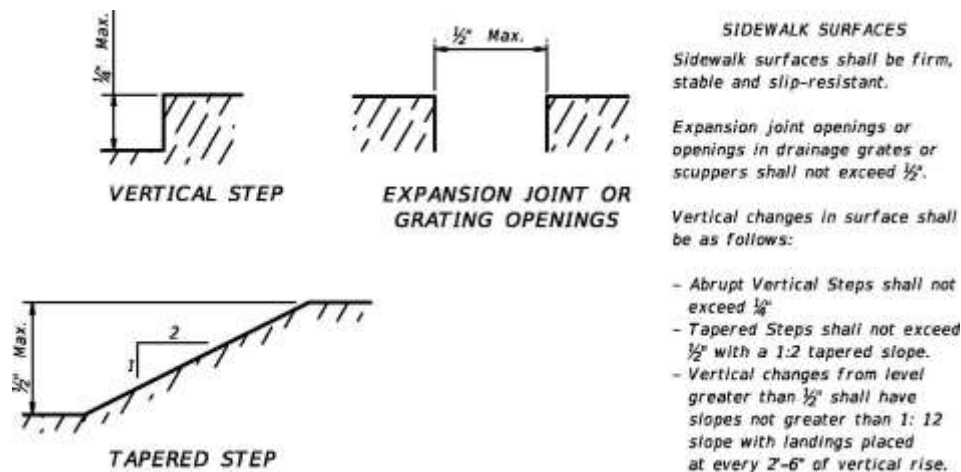
When drainage grates or expansion joint materials lie within the approach or bridge walkway, they can have openings no larger than $\frac{1}{2}$ in. in any direction. This does not apply to the cumulative travel of expansion joints but to any joints exposed to the surface travel way.

The maximum change in the elevation of horizontal surfaces is $\frac{1}{2}$ in. Between $\frac{1}{4}$ and $\frac{1}{2}$ in., the high surface must be tapered not more than 50% (1 vertical to 2 horizontal). Example details included in the Florida Department of Transportation *Structures Detailing Manual* are shown below in **Figure 21.2.4.3-3** (SDM, 2013).

PEDESTRIAN BRIDGES

21.2.4.3 Ramps and Approaches/21.2.4.7 Walkway Alignment

Figure 21.2.4.3-3
Surface Discontinuity Details Used by the Florida DOT



21.2.4.4 Width

The minimum inside clear width of a pedestrian bridge should be 8 ft. However, if approach sidewalks or trails are greater than 8 ft, the bridge should match this width. If the bridge is a shared facility with bicycles, a minimum width of 14 ft is recommended (*AASHTO Pedestrian Guide*, AASHTO, 2004). For bicycle travel, a 2-ft-wide clear area adjacent to the travel way should be provided with 3 ft being more desirable (AASHTO, 2012b). Long bridges may benefit from increased width due to the perception of tunnel narrowness when enclosed by fencing.

21.2.4.5 Grade

The vertical grade of the bridge must be no greater than 5% (1:20)

21.2.4.6 Cross Slope

The maximum slope transverse to the direction of travel is 2% (1:48).

21.2.4.7 Walkway Alignment

A straight alignment on a linear structure provides the simplest, shortest crossing. When the bridge connects areas with a high level of landscaping, such as parks and recreational settings, a meandering walkway, interspersed with plantings and amenities can be used to create a unique pedestrian experience. Comfort is a visual attribute. A meandering walkway creates a longer walking distance, but the enhanced environment is less likely to create resistance to use. Meandering walkways and plantings will require a significantly wider structure.

The next two examples are vehicular bridges that were designed as wider structures to create welcoming pedestrian experiences in their cities. While they are not exclusively pedestrian bridges, they were built specifically to enhance the pedestrian experience.

The Fifth Street Pedestrian Plaza Bridge at Georgia Tech in Atlanta, Ga., shown in **Figure 21.2.4.7-1**, was originally approximately 60 ft wide and included four 12-ft-wide traffic lanes and two 6-ft-wide sidewalks. The university constructed several attractive facilities on the opposite side of I-75/I-85 from its main campus. The football stadium is just one block away. While the replacement bridge now carries three traffic lanes, it was widened to 223 ft. It has 6-ft-wide bicycle lanes and 24-ft-wide sidewalks on each side plus landscaped areas 76 ft wide on one side and 51 ft wide on the other. The bridge carries pedestrians, bicycles, automobiles, and metro transit. The new bridge was intended to provide a wider, longer, and more attractive crossing. Just 16% of the bridge is devoted to motor vehicle traffic. Some 55% of the bridge deck is landscaped greenspace. Additional views are shown in **Figure 21.2.5-1**. More information about the planning, construction, and impact of this bridge on the university is available in articles in *ASPIRE* magazine (Aitken et al., 2008) and the *PCI Journal* (McCraven, 2008).

PEDESTRIAN BRIDGES

21.2.4.7 Walkway Alignment

Figure 21.2.4.7-1

The Pedestrian Bridge that Connects the Georgia Tech Campus Across I-75/I-85 is Essentially a Pedestrian Bridge and Park that Accommodates Vehicular Traffic (Photo: ARCADIS U.S. Inc.)



The bridge has two spans measuring 119 ft 6 in. and 137 ft. The superstructure uses AASHTO bulb-tees with a design compressive strength of 10.0 ksi. Precast concrete walls were used for planters that created boundaries for pedestrians, to hide the expressway, and to serve as sound walls. These walls ranged in height from 1 ft 6 in. to 9 ft.

Located in Redmond, Wash., the Northeast 36th Street Bridge over SR 520 (see **Fig. 21.2.4.7-2**), connects two sides of an expanding neighborhood that adjoins a recently expanded Microsoft Headquarters campus. The street crosses the freeway at a 44-degree angle and is supported on two offset landscaped lids. The length of each lid is approximately 300 ft, just shy of the length that would trigger expensive fire suppression and ventilation systems for a tunnel designation. For a structure that results in an unusually large covered area, designers should consult local and state authorities for specific requirements.

The length of the bridge along the traveled way is 414 ft. Clearly marked bicycle lanes line both sides of the vehicular travel way. The meandering pathway is separated from the 36th Street traffic by plantings and from the freeway below by berms and raised planters. The pathways connect parking and buildings on both sides of the freeway and are a vital link in a popular 5-mile-long trail system along SR 520. The project is described in an *ASPIRE* magazine article by Fernandes et al., 2011.

PEDESTRIAN BRIDGES

21.2.4.7 Walkway Alignment/21.2.5 Aesthetics and Amenities

Figure 21.2.4.7-2

The Northeast 36th Street Bridge Over SR 520 in Redmond, Wash., Provides a Park and Pedestrian Crossing Over a Busy Freeway (Photo: BergerABAM)



21.2.5 Aesthetics and Amenities

Aesthetics of structures is a unique topic and subject to personal interpretation and preferences. The individual elements of a bridge must work together to contribute to the impact of the whole structure. Chapter 5 of this manual provides information intended to help engineers incorporate the concept of aesthetics into bridge design. The following sections discuss individual features as they pertain to pedestrian structures.

Amenities include architectural features, resting areas, street furniture, benches, drinking fountains, landscaping, and public art. Examples of the creation of a welcoming environment with planters and landscaping are shown in **Figures 21.2.5-1 and 21.2.5-2**. Plantings reduce the amount of impervious surface area and help the structure blend into the surrounding environment. Park-like amenities with ample lighting create a sense of safety, comfort, and enjoyment.

All enhancements must be kept clear of the pedestrian travel way. Objects that are mounted on walls and encroach on a walkway must not protrude more than 4 in. if located between 27 in. and 6.7 ft above the walk surface. This also applies to objects mounted on a single post. If objects are mounted on multiple posts with clear spacing of 1 ft or more, the lowest edge can be no higher than 27 in. or lower than 6.7 ft. Overhead signs and plantings should be higher than 6.7 ft.

PEDESTRIAN BRIDGES

21.2.5 Aesthetics and Amenities/21.2.5.1 Architectural Finishes

Figure 21.2.5-1 Amenities Abound on the Fifth Street Pedestrian Plaza Bridge in Atlanta, Ga. (Photos: ARCADIS U.S. Inc.)



a) Precast Concrete Planter Walls Provide Interesting Relief and an Effective Sight and Sound Barrier from the Expressway Below

b) Walkway Areas are Paved with Dark Red Concrete Pavers. Amenities Include Benches and a Tubular Steel Trellis.

Figure 21.2.5-2 Pedestrian-Scale Amenities Create a Welcoming Environment



a) Northeast 36th Street Bridge Provides Dedicated Resting Areas and Ample Lighting (Photos: BergerABAM)

b) Vancouver Land Bridge Features Boardwalks that Span Wetlands Alongside the Approach Pathway and Attractive Trellises (Photo: Natural Pavement Photos)

21.2.5.1 Architectural Finishes

Attractive, durable surfaces can be created with either precast or cast-in-place concrete. Concrete can be molded into almost any imaginable shape. Many textures and patterns are manufactured in a wide range of colors. Figures 21.2.5.1-1 and 21.2.5.1-2 illustrate three examples. The PCI Architectural Precast Concrete Color and Texture Selection Guide (PCI, 2003) has a visual guide to assist designers in the initial selection of color and texture finishes for architectural precast concrete. It illustrates more than 500 colors and textures for enhancing the aesthetic quality of precast concrete panels. The guide is an extension of the information included in the architect-oriented Architectural Precast Concrete manual (PCI, 2007). Cements, pigments, coarse and fine aggregates, and texture or surface finish with various depths of exposure were considered in creating the color photographs included in the Color and Texture Selection Guide, the majority of which display two finishes on the same sample. The materials used to produce the samples are identified in the back of the guide for handy reference.

PEDESTRIAN BRIDGES

21.2.5.1 Architectural Finishes

The Westminster, Colo., Promenade Pedestrian Bridge shown in **Figure 21.2.5.1-1** connects events and activities, including facilities and eateries across the four-lane divided Westminster Boulevard. The bridge is a single span, 100 ft long and 22 ft wide. Eighteen variable-depth precast concrete arch fascia panels are used to clad three 48-in.-deep precast, prestressed concrete box beams, creating the appearance of a graceful arch. The deep blue color of the box beams and abutments cause these elements to recede in the background emphasizing the precast cladding. Reveals separating bands of textures further elongate the structure and create visual interest. Precast panels on the abutments continue the lines of the precast arch panels on the bridge. Incised and raised lettering incorporating gold leaf finish, was also utilized. The concrete paver walkway surfaces in the entertainment complex are tied together as they extend across the bridge.

Figure 21.2.5.1-1

Westminster Promenade Pedestrian Bridge in Westminster, Colo. (Photos: Martin/Martin)

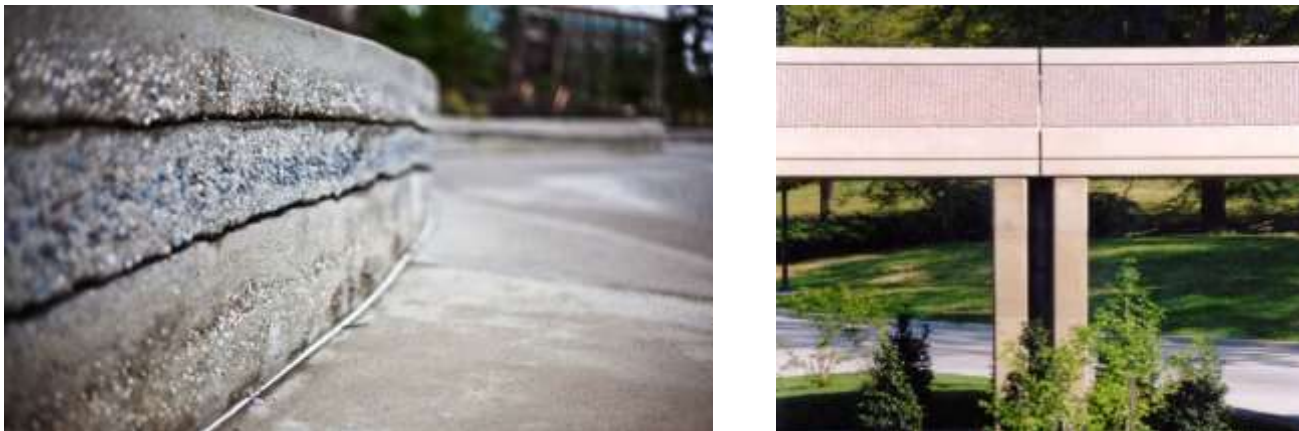


a) Precast Concrete Provides Color and Texture and Transforms a Conventional Box Beam Bridge Into an Elegant Arch

b) Alternating Bands of Texture Create Visual Interest

Figure 21.2.5.1-2

The Range of Textures and Colors in Concrete Structures is Nearly Limitless.



a) The Northeast 36th Street Bridge Features Curving Cast-In-Place Concrete Walls of Variable Height with Variable Thicknesses of Textured and Colored Concrete that Simulate the Native Sedimentary Rock. (Photo: BergerABAM) For another view, see **Figure 21.2.5.3-1a**.

b) The Fundamental Attractiveness of Precast Concrete Surfaces Combined with Texturing and the Careful Selection of Aggregates Provide a Long-Lasting, Fresh Appearance for the Life of this Structure (Photo: Carlton Abbott & Partners) See the views in **Figure 21.2.5.4-1**.

PEDESTRIAN BRIDGES**21.2.5.2 Manufacturing Capabilities/21.2.5.3 Walkway Surfaces****21.2.5.2 Manufacturing Capabilities**

Nearly all precasters have unique techniques and capabilities to produce a wide range of appealing surface finishes. Often, precasters with expertise in producing fine architectural colors, shapes, and textures will cooperate with precasters that manufacture structural precast, prestressed beams and other structural items to furnish bids as a team. Using precast manufacturers who are certified in the Precast/Prestressed Concrete Institute's (PCI's) Plant Certification Program assures designers that the work will be performed in accordance with nationally recognized quality control standards. The PCI Plant Certification Program is recognized internationally as the most reliable source for quality assurance in the design, manufacture, and installation of precast concrete products. The Program recognizes manufacturers with expertise in producing products intended for architectural versus structural applications. Plants certified in this program adhere strictly to provisions of the industry's key standards including the *Manual for Quality Control for Plants and Production of Structural Precast Concrete Products* (PCI, 1999) and the *Tolerance Manual for Precast and Prestressed Concrete Construction* (PCI, 2000) and must maintain a plant-specific quality system manual approved by PCI. Much more information about this program can be found in Appendix F of this manual and at http://www.pci.org/PCI_Certification/.

PCI certified precasters should be contacted early in schematic design to validate ideas for architectural products and finishes. Often, these experienced producers have suggestions about concepts for products and finishes used in other applications that would be appropriate for a given situation. Most producers have engineering staff that can provide data on limitations on sizes, weights, and installation details that will facilitate constructability.

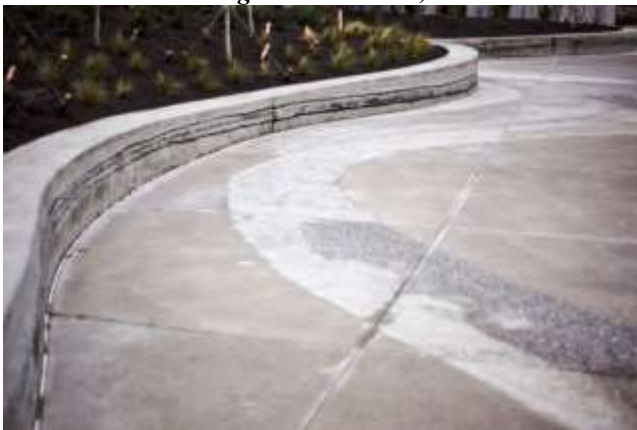
21.2.5.3 Walkway Surfaces

Walkways can be constructed with bricks and pavers but these must be installed in a manner that will prevent settling. The installation should preclude removal of individual units as an act of vandalism. Molds used to stamp the surface of cast-in-place concrete provide a wide range of patterns that emulate bricks and pavers. Sidewalk surfaces should be smooth and continuous. Limits on discontinuities are shown in **Figure 21.2.4.3-3**. Sometimes, a cast-in-place concrete surface is used for the main walkway, and incorporated with brick edging to delineate the walkway. Concrete or brick pavers are often used around and under street furniture.

Concrete pavements may be textured and/or colored. They can be effectively combined with concrete pavers or with patterns stamped into the surface. Two treatments are shown in **Figure 21.2.5.3-1**.

Figure 21.2.5.3-1

Walkway Surface Treatments are shown in the Northeast 36th Street Bridge in Redmond, Wash., and the Vancouver Land Bridge in Vancouver, Wash.



a) Sandblasted Surfaces Create Patterns and the Appearance of a Meandering Stream (Photo: BergerABAM)



b) A Pathway Leads Away From the Bridge. The Surface is Decomposed Granite with a Clear Aggregate Binder. Colored Pavers Were Laid in Symbolic Native American Patterns. (Photo: KPFF Consulting Engineers)

PEDESTRIAN BRIDGES

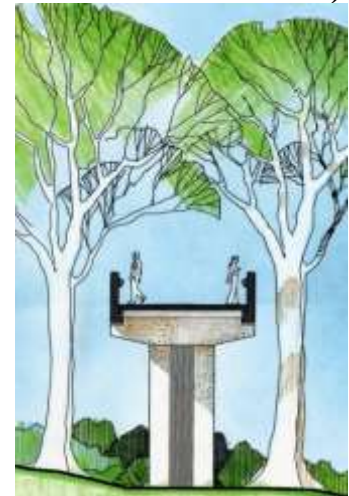
21.2.5.4 Aesthetic Solutions

21.2.5.4 Aesthetic Solutions

In addition to the many unique shapes that can be manufactured, precast and precast, prestressed concrete are well suited for long slender structures and elegant rectilinear shapes. In many environments, the simple adaptation of long thin superstructures and slender supporting elements create proportional frames that satisfy demanding sites. An example of this straightforward approach is the Colonial Williamsburg Bridge to the Past in Williamsburg, Va. **Figure 21.2.5.4-1** shows this seven-span, 464-ft-long bridge that connects Colonial Williamsburg’s visitor’s center with historic areas. By taking a direct route, the bridge reduced the perceived space between landings. Rectangular edge beams span from pier to pier and support prestressed deck panels on ledges. Textures and sandblasted finishes were also used.

Figure 21.2.5.4-1

Colonial Williamsburg’s Bridge to the Past in Williamsburg, Va. (Photo and drawing: Carlton Abbott & Partners PC)



a) The 464-Ft-Long Bridge Takes Pedestrians From the Visitor Center to Historic Areas

b) Rendering of the Bridge Cross Section

A simple pattern and texture creates a classic look that blends well with existing architecture in the Central Westchester Parkway in White Plains, N.Y. “L”-shaped beams frame the pedestrian bridge shown in **Figure 21.2.5.4-2**. It replaced a steel structure built in 1930 that was constantly being struck by vehicles. The bridge used the existing stone-faced abutments, which were raised to increase clearance to 15 ft. The span is 50 ft and the width is 8 ft 6 in. The beams are conventionally reinforced and not prestressed. Upturned legs are 4 ft 6 in. deep and 1 ft thick, providing an inside dimension of 6 ft 6 in. A 6 ft clear walkway results between handrails mounted 2 ft 10 in. above the walkway surface. The horizontal legs of the beam are 3 ft 3 in. wide and spliced together with a field closure placement. A 2-in.-thick composite concrete topping completes the deck. A 4-ft 8-in.-tall chain link fence is mounted on the vertical leg of the beam, placing the top of the fence at 8 ft 2 in. above the walkway.

PEDESTRIAN BRIDGES

21.2.5.4 Aesthetic Solutions/21.2.5.5 Thin-Set Brick Inlay Panels

Figure 21.2.5.4-2
Replacement of the Pedestrian Bridge Over Central Westchester Parkway, White Plains, N.Y. (Photos: Berger, Lehman Associates PC)



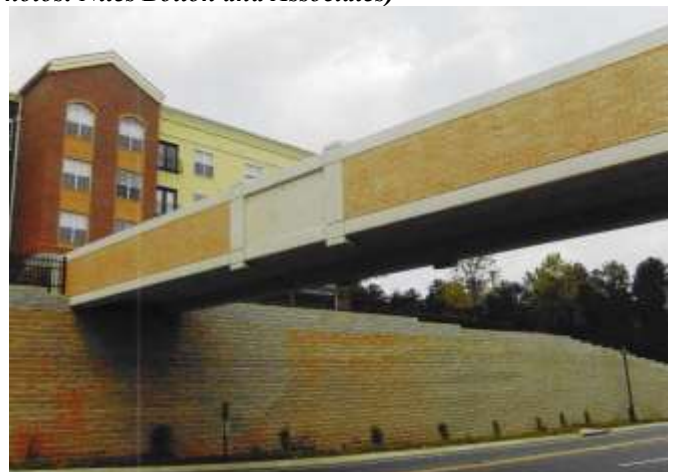
- a) The Pedestrian Bridge Over Central Westchester Parkway in White Plains, N.Y., Provides a Direct Pedestrian Route to an Elementary School
- b) Two Precast Beams were Set with only a 4-Hour Interruption of the Parkway. The Bottoms of the Beams Were Joined by a 2-Ft-Wide Cast-in-Place Closure.

21.2.5.5 Thin-Set Brick Inlay Panels

Precast concrete manufacturers regularly incorporate brick facings into their products. “Thin-set” bricks, ground to more precise dimensions than common bricks, are placed in individual pockets that are part of plastic or elastomeric liners attached to the casting forms. The extent of the liners defines the overall limits of the brick area and the brick pattern. Concrete placed against the backs of the bricks fills spaces between bricks creating the high-strength concrete “mortar joints” and permanently adhering the bricks to the panel. Thin-set bricks are available in a wide range of colors.

The Kennesaw State University Phase II Pedestrian Bridge, Kennesaw, Ga., used this technique to match brick on existing buildings and link the new structure to the campus. The bridge, 80 ft long and 12 ft wide, is shown in **Figure 21.2.5.5-1**. It is framed with two edge beams, each 5 ft 8 in. tall by 24 in. wide faced with thin-set brick. A total of four, 6-in.-thick flat slabs rest on ledges on the beams and complete the deck. All exposed concrete surfaces (including the deck) used an “antique” white concrete mixture and received a medium depth sandblast.

Figure 21.2.5.5-1
Kennesaw State University Phase II Pedestrian Bridge, Kennesaw, Ga., links New Residence Halls with Academic Buildings Across a Main Gateway Road onto Campus (Photos: Niles Bolton and Associates)



- a) Concrete Surfaces are White, Sandblasted Concrete
- b) Thin-Set Bricks Were Cast Into the Faces of the 80-Ft-Long Spandrel Beams

PEDESTRIAN BRIDGES

21.2.5.6 Formliner Mold Finishes

21.2.5.6 Formliner Mold Finishes

Formliners are typically made of elastomeric urethane. They are flexible, yet durable, and can produce outstanding detail on the surfaces of precast concrete components. Formliner finishes can be very economical because the liners may be reused a hundred times or more. These finishes are typically used on retaining walls, screens, soundwalls, or the surfaces of structural components of a bridge or ramp. **Figure 21.2.5.6-1** shows a small sample of textures and murals available.

Figure 21.2.5.6-1

Formliner Mold Finishes Can Take Many Shapes. Colors Are Generally Applied Following Casting. (Photos furnished by Scott System Inc., Denver, Colo.)



a) Sound Wall Panel, T-Rex Project, Denver, Colo. (Design Team Carter and Burgess, Steven Wilenky, Urban Design Lead, Surface Strategy LLC)



b) MSR 527 Noise Wall, Millcreek, Wash. (Washington State DOT)



c) Front Street Flyover, Castle Rock, Colo.



d) Mock-Up Panel for Pima Freeway, Scottsdale, Ariz.



e) San Tomas Aquino/Saratoga Creek Trail Corridor, Santa Clara, Calif. (Artist: Linda Patterson, Santa Clara, Calif.)



f) Cross-Town Interchange, Corpus Christi, Tex., Ashlar Stone & Custom Art, Surface (Design TxDOT)

Formliner finishes are applicable to substructure elements as well. **Figure 21.2.5.6-2** shows the use of color and relief on bridge piers that help the structure achieve its place as an important feature in this rural region.

PEDESTRIAN BRIDGES

21.2.5.6 Formliner Mold Finishes/21.2.6.1 Geometry

Figure 21.2.5.6-2

Art Relief on the Faces of the Piers in the Paul Bunyan Trail Bridge, Baxter, Minn.

(Photo: Minnesota Department of Transportation)

**21.2.5.7 Anti-graffiti Surfaces**

Proprietary anti-graffiti products are available and are often specified by owner agencies for application on accessible surfaces subject to defacement and graffiti. Individual agency specifications provide details about these products and their application.

21.2.5.8 Public Art

The use of public art can enhance the sense of place experienced by the pedestrian. Sculptures and other forms of art can make the pedestrian environment friendlier and more comfortable (*AASHTO Pedestrian Guide*). Numerous projects featured in this chapter display forms of public art.

21.2.5.9 Lighting

Pedestrian visibility, security, and comfort are enhanced with good lighting. The importance of lighting is increased when there is a concentration of dusk or nighttime pedestrian activity, such as places of worship, entertainment venues, shops, schools, and community centers. Continuous lighting is encouraged and placed to provide a relatively uniform level of ambient light. Enhanced lighting may also be installed in selected areas of pedestrian activity to create a sense of intimacy and place, and to create greater visual interest. Additional information about lighting can be found in the *Roadway Lighting Design Guide* (AASHTO, 2005). Lighting levels should conform to the latest edition of *The Lighting Handbook* of the Illuminating Engineering Society (IES, 2011).

21.2.6 Railings and Screens

Railings may be constructed of any material specified in Sections 5, 6, 7, or 8 of the *LRFD Specifications*, namely concrete, steel, aluminum, or wood. However, where exterior railings interface with habitable structures, their construction is typically governed by the building code adopted by the local code jurisdiction.

21.2.6.1 Geometry

From the top of the walkway, the minimum height of the top of the top rail is 42 in. The rail may comprise horizontal and vertical elements, or a combination of both. The lower 27 in. of the railing may not permit a 6-in.-diameter sphere to pass. The area above that may not allow an 8-in.-diameter sphere to pass. The railing should provide a safety toe rail or curb. These requirements do not apply if a chain link or metal fabric fence is used. In this case, the mesh should have openings no larger than 2 in. The openings should retain an average size beverage container.

A chain link throw screen was used on the Padden Parkway Pedestrian Bridge in Vancouver, Wash., shown in **Figure 21.2.6.1-1**. The bridge was built to comply with ADA requirements. Additional information and photos are included in Section 21.2.4.1.

Figure 21.2.6.1-1

A Pedestrian Rail is Continuous on the Bridge and is Enclosed by a Chain-Link Throw Screen Over the Travel Way (Photo: OBEC Consulting Engineers)



More elaborate railings and screens can enhance the pedestrian experience with a sense of security and improved aesthetics. The 37th Street Pedestrian Bridge in Tacoma, Wash., is shown in **Figure 21.2.6.1-2**.

Figure 21.2.6.1-2

37th Street Pedestrian Bridge in Tacoma, Wash., Features Unique Railing and Throw Screens (Photos: Washington State Department of Transportation)



a) Color on the Railings and Screen Add Appeal as do the Special Medallions

b) Rather than Terminate Abruptly, the Screen Transitions Down to the Railing at the Ramp

The railings and throw screens of the Paul Bunyan Trail Bridge in Baxter, Minn., are shown in **Figure 21.2.6.1-3**, and immediately identify the structure in both words and image. Other photos are shown in the case study in Section 21.3.1.1 including a closer view of the railing and screen. The railing is 5 ft tall on the two approach spans and varies from 6 ft to 12 ft on the center span over the roadway.

PEDESTRIAN BRIDGES

21.2.6.1 Geometry/21.2.6.3 ADA-Compliant Railings

Figure 21.2.6.1-3

The Thoughtful Use of Color Borrows From the Blue Sky, the Green Forest, and Brown Trail on this Bridge in Northern Minnesota. (All photos: Minnesota Department of Transportation)



a) The Image on the 12-Ft-Tall Screen Identifies this Bridge from Afar.



b) Colorful Railings and Screens Protect Users of the Bridge and Passersby Below While Enhancing the Structure



c) The Artistic Metal Silhouette is Attached to the 2-In.-Square Grid of the Screen with Simple Fasteners

21.2.6.2 Bicycle Railings

A bicycle railing should be considered on bridges designed to include bicyclists and where specific protection is deemed necessary. The railing should meet the same geometric requirements of the pedestrian railing. For areas that may be subject to higher speeds, or in areas where high-angle impacts are likely, a higher railing should be considered. In addition, a rub rail should be considered to prevent snagging of handlebars. The rub rail should be deep enough to protect a wide range of handlebar heights. Article C13.9.2 in the *LRFD Specifications*, includes a note that the need for rubrails is controversial among many bicyclists.

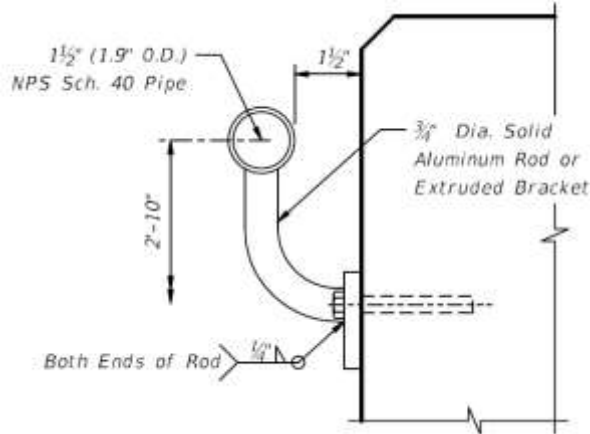
21.2.6.3 ADA-Compliant Railings

When required, handrails must be at a constant height of 2 ft 10 in. above the walkway. A sample detail of an ADA-compliant handrail is shown in **Figure 21.2.6.3-1**, taken from the Florida DOT *Structures Detailing Manual*, Figure 18.2-2 (SDM, 2013).

PEDESTRIAN BRIDGES

21.2.6.3 ADA-Compliant Railings/21.2.6.4 Design Live Loads

Figure 21.2.6.3-1
Detail of an ADA-Compliant Handrail by the Florida DOT



21.2.6.4 Design Live Loads

An ADA-compliant handrail must be designed to resist a 0.250 kip load applied either vertically or horizontally at any location along the length.

For all other pedestrian railings, the design live load is 0.050 kips/ft acting simultaneously in both vertical and horizontal directions. Each horizontal member must resist an additional concentrated load 0.20 kips acting simultaneously with the uniform load and oriented in any direction acting at the top of the member.

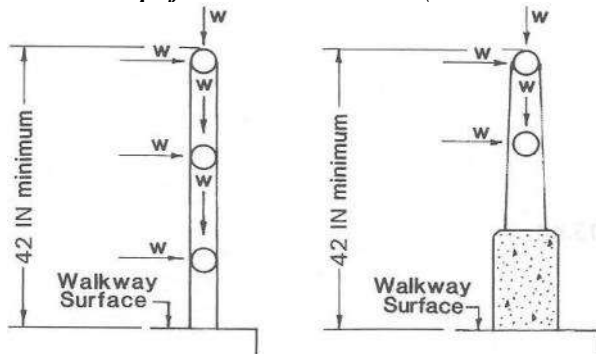
Posts must be designed for a concentrated load applied transversely at the center of gravity of the top rail. If the railing system is taller than 5 ft, the concentrated load should be placed at 5.0 ft above the top of the sidewalk surface. The magnitude of this live load on posts is:

$$P_{LL} = 0.2 + 0.050L$$

where L = post spacing, ft

The application of loads on posts and rails is illustrated in **Figure 21.2.6.4-1** taken from the *LRFD Specifications*, Figure 13.8.2-1.

Figure 21.2.6.4-1
Illustration of Application of Uniform Load
 $w = 0.050$ kips/ft on Pedestrian Rails. (Rail and Post Shapes Illustrative only)

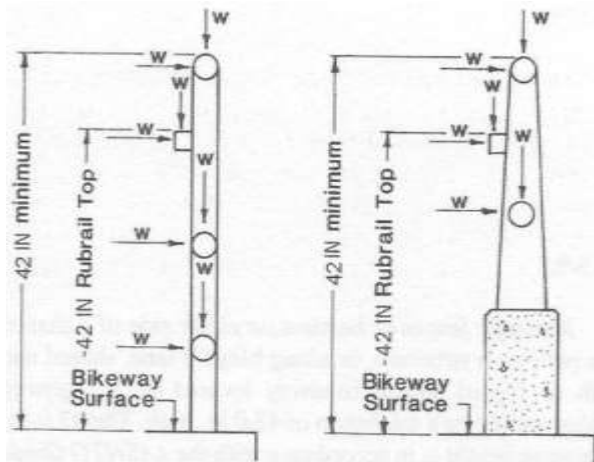


The design loads on bicycle railings are the same as those required for pedestrian railings. The exception is if the railing height is greater than 54 in., the design loads must be determined by the designer but must not be less than used for the pedestrian railing. The design load for posts must be applied at a point 54 in. above the riding surface. The application of rail loads is shown in **Figure 21.2.6.4-2** taken from the *LRFD Specifications*, Figure 13.9.3-1.

PEDESTRIAN BRIDGES

21.2.6.4 Design Live Loads/21.2.7.3 Vehicular Load

Figure 21.2.6.4-2

Illustration of Application of Uniform Load $w = 0.050$ Kips/Ft on Bicycle Rails. (Rail and Post Shapes Illustrative Only)**21.2.7 Loads and Load Combinations**

The following information on loads and loading is taken from the *LRFD Pedestrian Guide Specifications* (AASHTO, 2009a).

21.2.7.1 Pedestrian Load

All bridges in this classification are designed for a uniform pedestrian loading (PL) of 0.090 kips/ft², patterned to produce maximum load effects. Such patterning to produce maximum or minimum load effects on a given member must be on an area with the least dimension of 2.0 ft. It is not necessary to consider dynamic load allowance.

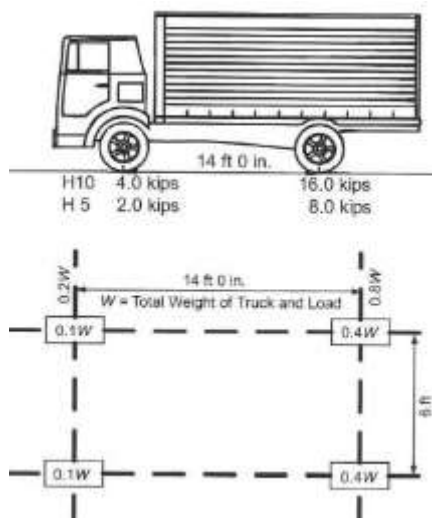
21.2.7.2 Equestrian Load

Where horses are expected, an additional equestrian loading (LL) "patch load" of 1.0 kip must be accommodated on an area 4.0 in. square. This is a requirement to assure adequate punching shear capacity of the deck.

21.2.7.3 Vehicular Load

If maintenance vehicles are allowed on the bridge or if permanent barriers are not provided to exclude vehicles, the bridge must be designed for the vehicle load (LL) shown in **Figure 21.2.7.3-1** taken from the *LRFD Pedestrian Guide Specifications*, Figure 3.2-1. The weight of the truck selected is determined by the clear width of the deck. For decks with a clear width of 7 to 10 ft, an H5 vehicle is used. A deck width over 10 ft clear requires an H10 vehicle load. The vehicle is placed to produce the maximum load effects but not in combination with the pedestrian load. The dynamic load allowance need not be considered. Usually, the pedestrian load will govern the design of the girders but the vehicle load may control the deck design.

Figure 21.2.7.3-1
Maintenance Vehicle Configuration



The unique considerations for live loads on snowmobile bridges are discussed in Section 21.3.1.

21.2.7.4 Wind Load

The structure must be designed for wind loads according to the *Standard Specifications for Structural Supports for Highway Signs, Luminaries, and Traffic Signals (Signs Specifications, AASHTO, 2013)*. The *Signs Specifications* are used rather than the *LRFD Specifications* due to the potentially flexible nature of pedestrian bridges. The Wind Importance Factor, I_r , is taken as 1.15 unless otherwise required by the owner. This loading is applied over the entire exposed elevation including enclosures and signs supported by the structure. In addition to this pressure, a vertical uplift line load [*LRFD Specifications* Article 3.8.2] determined by a pressure of 0.020 kips/ft² over the entire deck width is applied concurrently at the windward quarter point of the deck width.

Wind loads may be specified by the agency authority. For example, FDOT requires wind loads be increased by 20% in specified Florida counties considered more vulnerable. Designers should check with local agencies.

Wind pressure and effects on cable-stayed pedestrian bridges should be determined according to provisions in the *LRFD Specifications*, Articles 3.8.1.2 and 3.8.3.

21.2.7.5 Fatigue Load

A fatigue load (LL) is required to be considered in design but is not necessary for prestressed concrete. The *LRFD Pedestrian Guide Specifications* Article C3.5 exempts the pedestrian load and maintenance vehicle load from consideration as fatigue design loading due to their infrequent nature. However, wind loading as given in Section 11 of the *Signs Specifications* must be considered. The *LRFD Specifications* Article 5.5.3.1 exempts concrete deck slabs in multi-girder applications and fully prestressed concrete from the general fatigue check for reinforcement. Fatigue of concrete in compression is very unlikely in practice. See Section 8.2.1.9 in this manual.

21.2.7.6 Load Combinations

The load combinations and load factors given in the *LRFD Specifications*, Table 3.4.1-1 are applicable to these bridges with the exception of load combinations Strength II, Strength IV, and Strength V, which need not be considered. The combinations and factors for Extreme Events I & II must also be considered. In addition, where the railing system is a part of the main gravity load carrying elements of the bridge, the railing loads given in **Section 21.2.6.4** must be applied concurrently with other live loads for the strength limit states.

21.2.8 Deflection

Deflection of pedestrian bridges must be considered according to the *LRFD Pedestrian Guide Specifications*. The load combination from Service I in the *LRFD Specifications*, Table 3.4.1-1 is used. The deflection from unfactored

PEDESTRIAN BRIDGES**21.2.8 Deflection/21.2.10.1 Framing and Connection Details**

live loading on the span must not be greater than 1/360 of the span length. This amount also applies to the horizontal deflection caused by wind loading.

Agencies may limit deflections more than those in the preceding paragraph. As an example, the Florida DOT restricts the vertical and horizontal deflections to the span/500, which also includes deflection from the maintenance truck load. Any deflection from service pedestrian live load is limited to the cantilever length/300 for cantilever arms. An additional requirement is that the bridge must match the plan profile grade after application of all permanent dead loads (FDOT, 2011).

Prestressed concrete bridges with relatively high values for the product of moment of inertia and modulus of elasticity (IE) easily satisfy deflection limits. The bridges illustrated in this chapter have spans up to 187 ft. without being limited by deflections.

21.2.9 Vibration

Vibrations must be investigated as a service limit state using load combination Service I, Table 3.4.1-1, from the *LRFD Specifications*, unless waived by the owner. The concern is to ensure that the structure does not create discomfort to users. The *LRFD Pedestrian Guide Specifications* requires the vertical fundamental frequency, without live load, to be greater than 3.0 Hz (cycles per sec) and in the lateral direction, greater than 1.3 Hz.

A fundamental discussion of vibration in concrete structures is given in Section 9.7 of the *PCI Design Handbook* (PCI, 2010). It states that vibrations in a structural system are generally controlled by specifying a minimum natural frequency. The limits depend on

- permissible peak accelerations (as a fraction of gravitational acceleration),
- the mass engaged,
- degree of continuity of the system,
- environment in which the vibration occurs,
- effectiveness of interaction between connected structural components, and
- degree of damping (how quickly a vibration will decay).

The natural frequency of a floor system is important in determining how human occupants will perceive vibrations. It has been found that certain frequencies seem to set up resonance with internal organs of the human body, making these frequencies more annoying to people. The human body is most sensitive to frequencies in the range of 4 to 8 Hz. This range of natural frequencies is commonly found for typical floor systems. Floors with natural frequencies lower than 3 Hz are not recommended, because people may more readily synchronize their actions at lower frequencies.

In general, vibrations are much less likely to be a problem with stiffer, more massive concrete systems. Several projects and case studies featured in this chapter to illustrate unique features, have span lengths over 100 ft and up to 187 ft. None of these structures have experienced issues with vibration.

21.2.10 Construction Details**21.2.10.1 Framing and Connection Details**

Precast concrete used for pedestrian and special purpose bridges is not different from its use for other types of structures. This manual includes much information relevant to pedestrian bridges. Some chapters have been previously referenced. The following chapters provide information related to construction:

- Chapter 3—Fabrication and Construction
- Chapter 4—Strategies for Economy
- Chapter 10—Bearings

The *PCI Architectural Precast Concrete* manual (PCI, 2007), *PCI Design Handbook* (PCI, 2010), and the *PCI Connections Manual* (PCI, 1988) contain much information about connection details and design.

PEDESTRIAN BRIDGES

21.2.10.2 Drainage/21.2.10.3 Cable-Stayed Pedestrian Bridges

21.2.10.2 Drainage

Curbs, drains, and pipes or other means to drain the superstructure must be provided. It is never permissible to drain the pedestrian structure onto the roadway below. Drains should extend below superstructure components and be located away from substructure elements to avoid detrimental splash and wind effects.

Figure 21.2.10.2-1

The Northeast 36th Street Bridge Described in Section 21.2.4.7 has Continuous Slot Drains in the Walkway on the Structure (Photo: BergerABAM)



Drainage components such as grates over surface drains must conform to ADA and bicycle requirements.

Another example of bridge drainage is shown in **Figure 21.2.11.1-2**.

21.2.10.3 Cable-Stayed Pedestrian Bridges

Agencies should design stay systems to meet the same durability and protection standards as for post-tensioning systems including anchors, tendons, and bars. The stay system should be designed to allow removal and replacement of any one stay at one time. Wind tunnel testing and the effects of wind and the combination of wind and rain on cables should be considered. Dramatic lighting effects can be achieved with cable-stayed bridges.

Figure 21.2.10.3-1

Cable Stays Were Used in the Wichita, Kans., Riverfront Pedestrian Bridges. There are Two Bridges: 320 Ft Long Spanning the Arkansas River and 240 Ft Long Spanning the Little Arkansas River. The Superstructure Uses Match-Cast, Two-Cell, Precast Segments, 32 Ft Long and 12 Ft 4 In. Wide. (Photos: HNTB Corporation)



PEDESTRIAN BRIDGES

21.2.11 Vegetation and Irrigation/21.2.11.1 Provisions for Plantings

21.2.11 Vegetation and Irrigation**21.2.11.1 Provisions for Plantings**

Vegetation adds an attractive environment to a pedestrian bridge. The walls and plantings (see **Fig. 21.2.5-1a**) on the Fifth Street Pedestrian Plaza Bridge described in Section 21.2.4.7 are the most important aesthetic feature of the structure and define the character and nature of the space. Accommodating vegetation necessitates provisions for soil weight, providing irrigation water, and disposal of excess water. Resilient species must be selected to survive in the particular region. A minimum depth of soil should be specified to maintain the plantings selected.

Soil should be selected that minimizes the dead load on the structure. Saturated normal landscape fill has a density of approximately 110 to 120 lb/ft³. Special lightweight organic soils are available that weigh considerably less, about 90 lb/ft³, or as little as one-half the weight of natural soils. If drainage layers are required, they may use lightweight aggregates that are approximately one-half the weight of normal fills. More information is available on these applications from the Expanded Shale, Clay, and Shale Institute on their website at http://www.escsi.org/ContentPage.aspx?id=204&ekmensen=1b7c39fc_61_73_btnlink.

Concrete surfaces under and around planters must have waterproofing barriers installed that meet the specifications of the agency. Tall planter walls may require counterforts as shown in **Figure 21.2.11.1-1**.

Figure 21.2.11.1-1

Cast-In-Place Concrete Counterforts Replace Temporary Shores on the Precast Planter Walls in the Fifth Street Pedestrian Plaza Bridge (Photo: Georgia Department of Transportation)



The loads from planters can often be distributed over more beams than those directly under the planters. This may require a finite element or other analysis to define the extent of the distribution.

In addition to supplying irrigation water, drainage must also be accounted for. Planted areas reduce the square footage of impervious surface and are able to absorb some storm water that reaches the bridge before adding to the total runoff of the site. A bridge drain system that includes an inlet and pipe system (in addition to a waterproof membrane and drainage mat) may collect additional water on the bridge and dispose of it in an approved location such as a storm water system.

A unique project, the Vancouver Land Bridge, located in Vancouver, Wash., is a cast-in-place concrete structure with many features applicable to many pedestrian bridges (Shell and Whittington, 2009). A rainwater collection system uses a slight cross slope in the pavement surface that directs excess storm water into thin channels along the edges of the pathway. These channels can be seen in **Figure 21.2.5-2b**. On one side of the bridge, the channel leads to a rain garden and a dry well that allows runoff water to infiltrate slowly into the ground. On the other side, the water collects in a man-made creek and inlet, shown in **Figure 21.2.11.1-2** that leads to an underground storage pipe, which stores the water to irrigate the bridge's landscaping.

PEDESTRIAN BRIDGES

21.2.11.1 Provisions for Plantings/21.2.12.1 Canyon Park Freeway Station

Figure 21.2.11.1-2

Drop Inlet Water Runoff Storage System Used on the Vancouver Land Bridge (Photo: KPF Consulting Engineers)



21.2.12 Case Studies

This section reports on several projects constructed throughout North America. They accomplish objectives highlighted in the descriptions. Each is quite unique and together they serve to illustrate a wide range of design challenges and solutions. All projects utilized precast concrete to some extent, from a total precast solution to partial use of precast concrete for aesthetic or structural reasons. References are given to provide further information.

21.2.12.1 Canyon Park Freeway Station

Location—I-405 and SR 527, Bothell, Wash.

Purpose of Bridge—Pedestrian bridge over I-405 links a park-and-ride lot to a bus transit station

Description—Six-span pedestrian bridge and ramp, 607 ft long and 12.5 ft wide comprising a single precast, prestressed concrete trapezoidal box beam in each span and cast-in-place concrete drilled shafts, footings, columns, abutments, deck, and lower rail wall.

Owner—Sound Transit (Central Puget Sound Regional Transit Authority), Seattle, Wash.

Designer— Washington State Department of Transportation (WSDOT), Bridge & Structures Office

Precaster—Central Pre-Mix Prestress Co., Spokane, Wash.

Completion—June 2007

Reference for More Information—Canyon Park Freeway Station Bridge (Aldrich, 2009)

Figure 21.2.12.1-1

The Canyon Park Freeway Pedestrian Bridge Provides an Important Link in a Commuter Route to a Bus Transit Station near Bothell, Wash. (Photo: Washington Department of Transportation)



PEDESTRIAN BRIDGES

21.2.12.1.1 Structure Description/21.2.12.1.3 Features

21.2.12.1.1 Structure Description

The bridge over the freeway has spans of 70, 86, and 124 ft. The ramp has spans of 120, 120, and 84 ft. The usable width of the deck is 10.6 ft between pilasters. The trapezoidal box beams are 5.0 ft deep with a 5.0-ft-wide bottom flange and 6.4-ft-wide top flange. Webs are 7 in. thick. All beams were furnished with a 1-ft-thick end diaphragm. The longest girder (122.1 ft) weighed 169 kips. A free-standing steel roof system protects pedestrians from inclement weather.

21.2.12.1.2 Key Design Objectives

A context sensitive solution had been developed for this interstate corridor. This structure was the first project to implement the aesthetic features of the plan that needed to be modified for a pedestrian bridge. Trapezoidal box beams provided a shallow and attractive element for the superstructure. The roof and throw screens were a design challenge that added gravity loads and increased lateral loads from wind and earthquake. The box beams and cast-in-place deck create a torsionally rigid shape to efficiently resist external loads. Traffic interruption was a fundamental concern. The use of precast beams required only one night closure for each of the two directions of travel. Falsework was eliminated from travel ways.

Figure 21.2.12.1.2-1

Features of the Canyon Park Freeway Station Pedestrian Bridge (All photos: Washington Department of Transportation)



a) Viewed from Parking/Elevator End, Bridge's Canopy Offers Protection to Pedestrians



b) Final Span Approaches Grade at Bus Station



c) The Shape of the Trapezoidal Beam is Seen from the End of the Ramp



d) Features Include Horizontal Lines on Railing Wall and Arched Throw Screen Panels



e) Flared Columns Maintain the Context Sensitive Plan for I-405 Corridor

21.2.12.1.3 Features

The parking end of the bridge has an elevator and enclosed stair tower. Aesthetic elements include the following:

- Flared columns inspired by rhododendrons
- Horizontal lines and ridges on the lower rail walls
- Unique arched pattern for the throw screen panels
- Three attractive colors taken from the Cascade environment

PEDESTRIAN BRIDGES

21.2.12.2 Forty Foot Pedestrian Bridge/21.2.12.2.1 Structure Description

21.2.12.2 Forty Foot Pedestrian Bridge

Location—Towamencin Township, Montgomery County, Pa.

Purpose of Bridge—A context-sensitive signature bridge that creates a safe and accessible pedestrian link over five lanes of SR 63 (Forty Foot Road) that bisects the new Towamencin Town Center.

Description—Single-span pedestrian bridge 80 ft long and 40 ft wide with three spread precast, prestressed concrete box beams and two 12-ft-deep by 90-ft-long cast-in-place concrete, through fascia beams; cast-in-place planters on both sides; cast-in-place abutments; and precast, architectural concrete wingwall panels.

Owner—Towamencin Township

Funding/Construction Partner—Pennsylvania Department of Transportation, District 6

Bridge Designer—Simone Collins Inc. Landscape Architecture, Berwyn, Pa.

Structural Engineer—QBS International Inc., Pennsauken, N.J.

Precaster, Box Beams—Schuylkill Products Inc., Cressona, Pa.

Precaster, MSE Walls, Cap Finials—The Reinforced Earth Company, Vienna, Va.

Precaster, Finials and Pylon Caps—Architectural Precast Inc., Burlington, Ky.

Completion—2007

Reference for More Information—Forty Foot Pedestrian bridge (Collins, 2009)

Figure 21.2.12.2-1

Forty Foot Pedestrian Bridge in Montgomery County, Pa., Features White Concrete and Many Unique Details (All Photos: Simone Collins Landscape Architecture)

**21.2.12.2.1 Structure Description**

The uniquely-shaped cast-in-place concrete fascia beams are fully structural and have L-shaped ledges to support the deck. They are 8 ft 8 in. deep at the supports, 12 ft deep at the center, and vary in thickness from 18 to 20 in. They bear on neoprene pads on the abutments and are tied into the deck concrete with concrete buttresses hidden inside the curving, cast-in-place planters.

PEDESTRIAN BRIDGES

21.2.12.2.1 Structure Description/21.2.12.2.2 Key Design Objectives

The precast, prestressed concrete box beams are 48 in. wide with a variable depth to accommodate the forming and casting of the cambered deck. The beams are 39 in. deep at the end and taper up to 52 in. deep near midspan. The interior void in these box beams also varies in depth, maintaining a 3-in.-thick top flange and 5½-in.-thick bottom flange.

The design span between centers of bearings is 78 ft 6 in. The cambered deck serves pedestrian and bicycle traffic only, but is engineered to support an H-20 truck load for maintenance and emergency vehicles.

Figure 21.2.12.2.1-1

Architecture of the Forty Foot Bridge Acknowledges Typical Structural Features such as Corbels, Spring Points, Camber, Hinges, and Keystones



a) Fascia Beam Showing Rippled Form, Abutments, Paver-Faced Sloped Walls (Left Foreground), MSE Walls



b) Sloped Paver Walls Above MSE Retaining Walls (Upper Left) were Designed at a 1:1 Gradient Providing a Sense of Openness to Limit the Height of the Retaining Walls to 8 Ft, and Preventing a “Tunnel” Effect Under the Bridge



c) Structural Pylons Clad with Precast Architectural Wingwall Panels



d) Globe Lights were Mounted on Custom-Formed Pylon Caps

21.2.12.2.2 Key Design Objectives

Transportation improvements were planned and engineered by the Township to integrate smart land-use strategies that included parks, trails, streetscape amenities, structured parking, and incentives for private mixed-use development. When a central pedestrian bridge was selected as the preferred alternative for crossing the highway, the prominent location demanded function and aesthetics above the ordinary. The concrete fascia

PEDESTRIAN BRIDGES**21.2.12.2.2 Key Design Objectives/21.2.12.3 Pacific Coast Highway Pedestrian Bridge**

beams serve the safety function of concrete parapets, the sound-dampening function of sound walls, and the expansive surfaces for art forms.

Figure 21.2.12.2.2-1

The Cartway is Wide Enough to Serve as a “Civic” Space for Periodic Functions Within the Town Center.



a) View of Pedestrian Environment Showing the Exposed Aggregate Concrete Deck with Cast-in-Place Planters



b) Planter Wall Forms Were Designed to Echo the Parapet Line and the Wingwall Rustications

21.2.12.2.3 Features

Concrete was selected for its economy, durability, and plastic qualities that could deliver a seamless aesthetic in a single structural and artistic material. The sculptural potential of concrete inspired a collaborative process between the bridge designer and structural engineer to incorporate art considerations within the engineering decisions.

Pedestrian-scale lighting is provided with lamps on posts at the ends of the bridge and with fixtures embedded in the planter walls along the walkway.

The Art Deco motif exploits the moldability of concrete to form elegant, arch shapes in shadowed relief designed to lighten the apparent mass of the deceptively large fascia beams. Below the arches, the rippled art forms change frequency to express the fluid nature of movements below a bridge, and functionally create horizontal shadow lines designed to subtly elongate the bridge visually and “de-emphasize” the sense of its total depth. Polystyrene formliners were used to create the 4-in.-deep surface topography.

Three colors were selected for the bridge. First, bright white using white concrete made with white cement was used for many of the elements. Light green was used below the arch shape to make the rippled surface visually “recede,” creating the effect from a distance that blends with the sky and landscape beyond, making the slender white arch shape over the road appear to leap to the foreground. Finally, a light red color was used on the sand-blasted deck surface, clearly defining the promenade.

21.2.12.3 Pacific Coast Highway Pedestrian Bridge

Location—Dana Point, Calif.

Purpose of Bridge—Provides direct pedestrian access from the resort community of Dana Point to Doheny State Beach across the busy Pacific Coast Highway. It creates a structural icon and gateway for the community.

Description—Decorative, cast-in-place concrete abutments support a single span comprising two precast, prestressed concrete rectangular through beams with precast, prestressed concrete deck panels and cast-in-place concrete composite deck. The bridge is 109 ft long and 13 ft wide. The walkway is 10 ft 0 in. wide. The

PEDESTRIAN BRIDGES**21.2.12.3 Pacific Coast Highway Pedestrian Bridge/21.2.12.3.1 Structure Description**

gateway and pilaster style of the historic state park dictated the entry and boundary screen walls of the bridge. Special lighting and large mosaics were incorporated. Elevators were incorporated in the abutment towers.

Owner—City of Dana Point, Calif.

Bridge Designer—T.Y. Lin International, Riverside, Calif.

Architect—Thirtieth Street Architects, Newport Beach, Calif.

Precaster—Coreslab Structures (L.A.) Inc., Perris, Calif.

Year Built—2010

Reference for More Information—Pacific Coast Highway Pedestrian Bridge (Goedhart, 2012)

Figure 21.2.12.3-1

The Pacific Coast Highway Bridge in Dana Point, Calif., Seen at Dusk, Stands as a Gateway to the Seaside Resort Community (Photo: Rob Szajkowski, Photographer)

**21.2.12.3.1 Structure Description**

The abutment towers have a footprint approximately 49 by 13 ft and are up to 46 ft tall. One side of each abutment provides stairway access while the other side incorporates elevator access.

The superstructure comprises two 109-ft 2-in.-long precast, prestressed concrete rectangular beams, 1 ft 6 in. wide that vary from 8 ft 0 in. deep at the abutments to 6 ft 5½ in. deep at midspan. These beams feature a 2 ft tall parabolic curve in the bottom. The top rises 5½ in. to remain exactly 50 in. above the vertical curve of the deck, which also rises 5½ in. The deck has 3 in. of cast-in-place composite concrete placed on fourteen 4-in.-thick precast, prestressed concrete deck panels. These panels rest on ledge angles bolted to the inside faces of the beams. Three transverse diaphragms were used at the ends and at midspan to provide lateral stiffness.

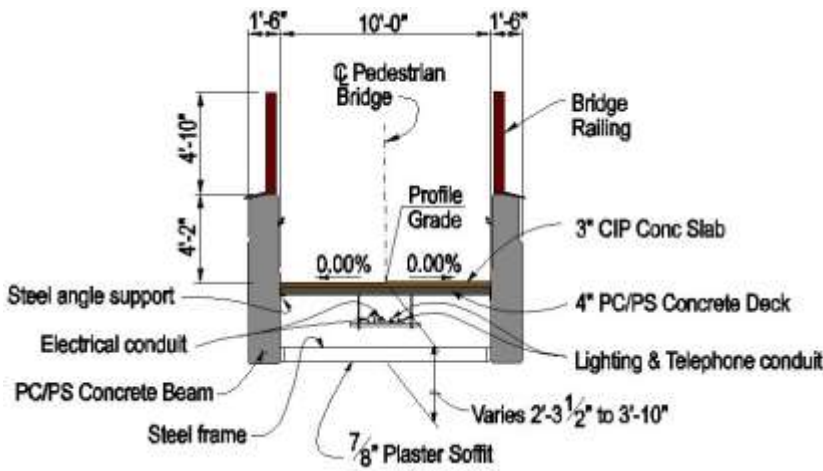
At the very bottom of the beams, a false soffit hides ducts that carry electrical, irrigation, and telephone utilities.

A 4-ft 10-in.-tall architectural metal railing is attached to steel sections welded to plates in the tops of the beams. The top of the railing is 9 ft above the walkway.

PEDESTRIAN BRIDGES

21.2.12.3.1 Structure Description/21.2.12.3.2 Key Design Objectives

*Figure 21.2.12.3.1-1
The Bridge has a Clear Walkway Width of 10 Ft*



a) Typical Section Showing the Components of the Bridge (Drawing: T.Y. Lin International)

b) The Beams also Act as the Parapet Walls along the Walkway of the Bridge. (Photo: Paul Savage, Photographer)

21.2.12.3.2 Key Design Objectives

Heavy foot traffic over this main north-south arterial caused protracted traffic delays due to long turning and through red light times required for pedestrians. In addition to enhancing traffic operations, the bridge improves pedestrian safety at a very busy intersection.

Due to the right-of-way restrictions and the city’s requirement to maintain full traffic operations on the Pacific Coast Highway, precast concrete beams were selected for the bridge span. This minimized the construction encroachment on traffic by eliminating the need for falsework in the roadway. All precast superstructure elements were erected in a single-night road closure.

*Figure 21.2.12.3.2-1
The Pacific Coast Highway Pedestrian Bridge Stands as an Iconic Addition to the Resort Community of Dana Point, Calif.*



a) Dana Point’s New Gateway includes Elevators to Provide Access for Those with Disabilities. (Photo: Coreslab Structures (L.A.) Inc.)

b) Large Murals and Other Architectural Details Can also be Observed from the Roadway. (Photo: Paul Savage, Photographer)

PEDESTRIAN BRIDGES**21.2.12.3.3 Features/21.2.12.4 Delta Ponds Pedestrian Bridge****21.2.12.3.3 Features**

Four large mosaics up to 15 ft 9 in. wide and 8 ft 6 in. tall on the street side of each abutment were created by local artists and depict the community's culture and heritage.

The superstructure beams have formed recesses on the sides along with the city name illustrated with backlit 21-in.-tall stainless steel letters at midspan. At the top of the beams, LED lights run along the full length underneath the decorative railing and pilasters. Colorful tile accents enhance the stairway and landings. Decorative metal gates located in the openings at the sidewalk level complement the railing along the span.

Due to the proximity to the ocean, corrosion protection of surfaces and steel was a concern. A ¼-in.-thick color acrylic plaster coating was applied to all exposed surfaces, which provides a smooth uniform finish and ties all of the structural elements together. The combination of the LED lighting and strategically placed spotlighting with the detailed architectural elements makes this structure eye-catching both day and night.

21.2.12.4 Delta Ponds Pedestrian Bridge

Location—Eugene, Ore.

Purpose of Bridge—Connects neighborhoods east of the Delta Highway, which runs roughly parallel to the Willamette River, and the popular riverbank path system west of the highway. The bridge skirts the south edge of the Delta Ponds city park and natural area, a backwater area hydraulically connected to the Willamette River. It provides a popular and pleasant vantage point for viewing the surrounding ponds and wildlife.

Description—A 760-ft-long, 18-ft 11-in.-wide concrete bridge featuring a 340-ft-long, asymmetric, three-span (120, 170, and 50 ft) cable-stayed section with fanned stays radiating from two legs of a "V"-shaped concrete pylon.

Owner—City of Eugene, Ore.

Designer—OBEC Consulting Engineers, Eugene, Ore.

Precaster—Knife River Prestress, Harrisburg, Ore.

Year Built—2010

Reference for More Information—Delta Ponds Pedestrian Bridge (Howe, 2012)

PEDESTRIAN BRIDGES

21.2.12.4 Delta Ponds Pedestrian Bridge/21.2.12.4.1 Structure Description

Figure 21.2.12.4-1

Delta Ponds Pedestrian Bridge in Eugene, Ore., Provided a Much Needed ADA-Compliant Link Across a Busy Highway and Sensitive Wetlands (All photos and drawings: OBEC Consulting Engineers)

**Figure 21.2.12.4-2**

In an Area of Low Buildings and Trees, the Design Team Sought to Blend the Bridge Into Its Surroundings. It Is Shown Near the End of Construction.

**21.2.12.4.1 Structure Description**

The main cable-stayed span of 170 ft uses 15 precast deck panels 10 ft long and 18 ft 11 in. wide by 1 ft 7¼ in. deep. A half-section of the precast panel is shown in **Figure 21.2.12.4.1-1a**. A thin section 14 ft 2 in. wide supports a cast-in-place composite concrete deck that is also post-tensioned together longitudinally with the

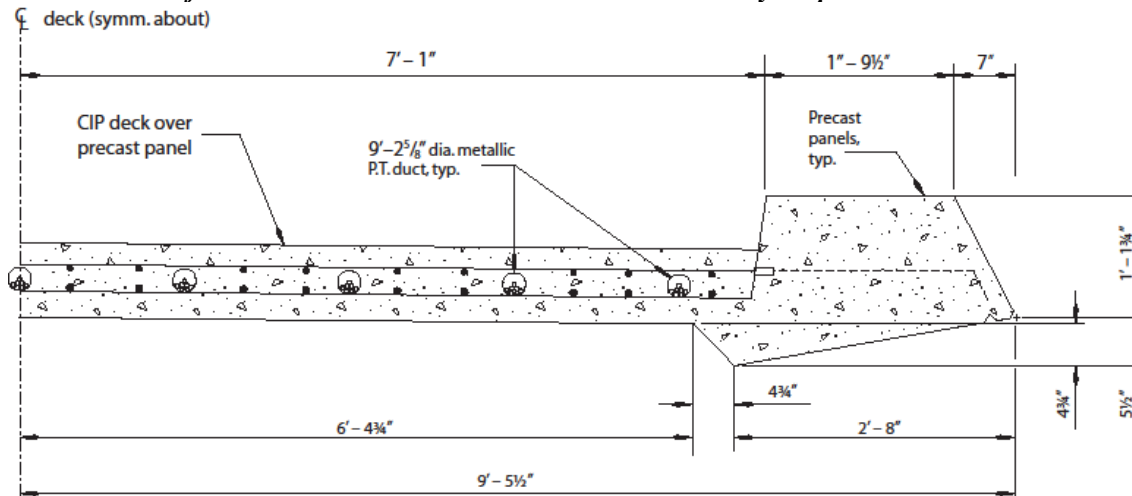
PEDESTRIAN BRIDGES

21.2.12.4.1 Structure Description/21.2.12.4.2 Key Design Objectives

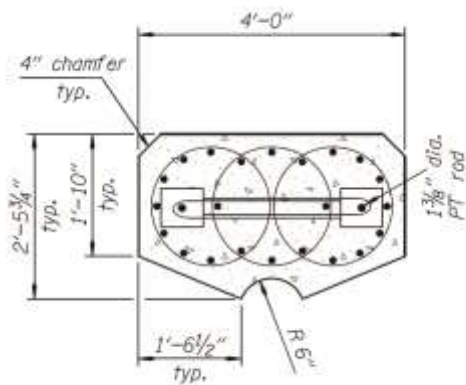
adjacent cast-in-place concrete deck spans. The combined thickness of the precast form and CIP topping is 1 ft 2¼ in. A series of thirteen 30-ft-long cast-in-place concrete spans on the west approaches and a single 30-ft-long span on the east approach comprise the bridge’s length. The pylon legs were precast. They are 88 ft long. The legs are sloped just under 8 degrees from vertical. The cross section is shown in **Figure 21.2.12.4.1-1b**. This cross section is constant except for the taper to a knife edge in the upper 3 ft. The “V” shape allows the legs to share a single 8-ft-diameter drilled shaft. This was critical since the necessary site for the foundation was restricted by an unusual concentration of utilities. The typical substructure uses 2-ft 7-in.-square columns that sit atop a single 4-ft-diameter drilled shaft at all piers. The tallest column is 33.5 ft long.

Figure 21.2.12.4.1-1

Cross Sections of the Precast Elements in the Delta Ponds Cable-Stayed Spans



a) Half Section of the Precast Deck Panel with Cast-In-Place Topping Slab and Post-Tensioning Shown. The Deck Cross-Sectional Dimensions Were Constant Throughout the Bridge.



b) Section Through the Pylon Leg Between the Bottom and the First Stay Cable

21.2.12.4.2 Key Design Objectives

The back span and 10 ft of the main span were constructed on falsework. Most of the precast panels in the main span were placed during lane closures at night. Stays were connected and adjusted during the day. This allowed little disruption to traffic during peak travel times.

The bridge provided an important safe link in an extensive network of paths in a community known for its bicycle and pedestrian friendly transportation system.

PEDESTRIAN BRIDGES**21.2.12.4.2 Key Design Objectives/21.2.12.5 David Kreitzer Lake Hodges Bicycle/Pedestrian Bridge**

The bridge also required only a very small footprint as it meandered through sensitive natural areas. It was properly proportioned to blend into the surroundings rather than overpower them.

21.2.12.4.3 Features

Late in the project, additional federal funding allowed the installation of energy-efficient light-emitting diode (LED) luminaries in lieu of planned incandescent bulbs. This funding also resulted in red LED rope lights on the deck edge and on the top stay of the main spans.

Figure 21.2.12.4.3-1

Delta Ponds Pedestrian Bridge Provides a Strong Visual Experience Both Day and Night, Pushing it Toward Landmark Status Within the Community



a) Both Pedestrian Rails and ADA-Compliant Handrails are Evident. Throw Screens are Integrated with the Stay Cables.



b) “The Lighting of the Upper Stay Preserves the Bridge’s Memorable Image at Night.” (Gottemoeller, 2012)

21.2.12.5 David Kreitzer Lake Hodges Bicycle/Pedestrian Bridge

Location—San Diego, Calif.

Purpose of Bridge—The bridge provides a regional transportation and recreational resource. It eliminated a 9-mile-long detour and became a vital link in the 55-mile-long Coast to Crest Trail within the San Dieguito River Valley Open Space Park. The bridge is now a safe crossing for bicycles that previously had to use the shoulder of the busy I-15 freeway to cross Lake Hodges.

Description—990-ft-long, three-span stress ribbon bridge, 14 ft wide and 16 in. deep

Owner—San Dieguito River Valley Open Space Park Joint Powers Authority

Designer—T.Y. Lin International, San Francisco, Calif.

Architect—Safdie Rabines Architects, San Diego, Calif.

Precaster—U.S. Concrete, San Diego, Calif.

Year Completed—2009

Reference for More Information—The David Kreitzer Lake Hodges Bicycle Pedestrian Bridge (Sanchez, 2010)

PEDESTRIAN BRIDGES

21.2.12.5 David Kreitzer Lake Hodges Bicycle/Pedestrian Bridge/21.2.12.5.1 Structure Description

Figure 21.2.12.5-1

Aerial Views of the Lake Hodges Stress Ribbon Bridge in San Diego, Calif.

(All photos and drawing: T.Y. Lin International)



a) The Lake Hodges Bridge has Three Spans of 330 ft. The I-15 Freeway can be Seen at the Lower Left Corner and is Just 1,000 Ft Away.

b) The Bridge Needed Only Two Piers in the Lake, Which is Dry Part of the Year. A Forest of Willows Flourishes in the Dry Season

21.2.12.5.1 Structure Description

It was the longest stress ribbon bridge when it was built. It has 87 precast concrete deck panels, 10 ft long, 14 ft wide, and 16 in. thick suspended from six 19-strand bearing cables (tensioned to 4,300 kips total). Six 27-strand tendons for post-tensioning were installed above the suspension cables in the troughs cast in the panels. Cast-in-place composite concrete was placed in the joints between each panel and to fill the troughs. The tendons were tensioned to 4,600 kips.

Figure 21.2.12.5.1-1

Precast Concrete Panels in the Lake Hodges Bridge

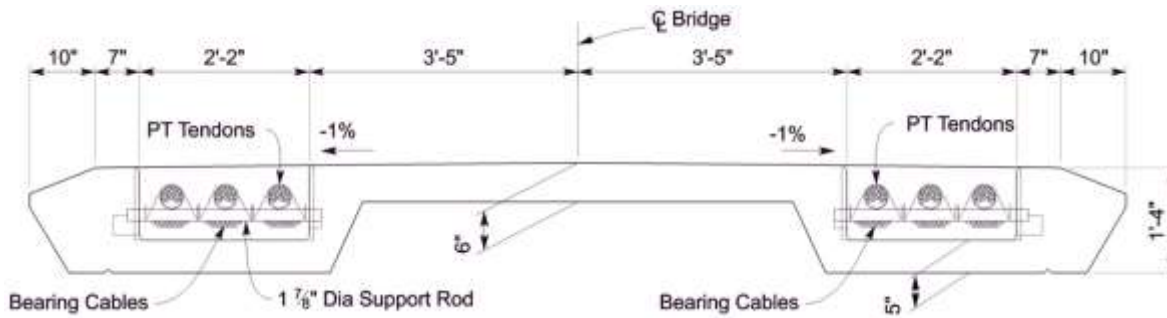


a) One of 86 Panels is Fitted Beneath the Supporting Cables

b) Following Installation of Panels, Concrete was Placed between the Panels, in the Cable and Tendon Troughs, and at the Ends of Each Span

PEDESTRIAN BRIDGES

21.2.12.5.1 Structure Description/21.2.12.6 Glenmore Trail Legsby Road Pedestrian Bridge



c) Cross Section of a Typical Precast Concrete Panel

21.2.12.5.2 Key Design Objectives

The goal was to provide a much more convenient and far safer crossing of Lake Hodges while protecting the natural waterways, sensitive lands, and threatened and endangered species. A key objective was to develop a context sensitive solution.

21.2.12.5.3 Features

The stress ribbon is the ultimate eco-friendly design. Because it can span 330 ft, only two piers were needed. Since the bridge was built by placing precast panels on bearing cables, no falsework was required. This further reduced the impact to the sensitive habitat. Additionally, the stress ribbon design makes effective use of each material: concrete in compression, steel in tension. This results in a minimal use of materials. In this sense, the bridge is a very "green" design.

Aesthetics were important in the selection of the stress ribbon. It proved to be the perfect visual complement to the site. The bridge "floats" above the water when the lake is full, and "nests" above the willow trees when the lake is dry. Visually, its slender deck has the smallest impact. From a distance the bridge almost disappears. Up close, its complementary curves fit beautifully into the rolling terrain around the lake. The long spans and thin deck result in a very light bridge that blends into the natural setting.

21.2.12.6 Glenmore Trail Legsby Road Pedestrian Bridge

Location—Calgary, Alberta, Canada

Purpose of Bridge—Connects a significant city park over an eight-lane throughway with an integral pathway system that encircles a large reservoir.

Description—A single span pedestrian bridge 212 ft long by 11.8 ft wide. It uses the largest single cast ever undertaken with ultra-high-performance fiber-reinforced concrete (UHPFRC). It incorporates unique art along and surrounding the structure. The clear span between faces of piers is 173.6 ft.

Owner—City of Calgary, Alberta

Designer—Cohos Evamy Integratedesign,™ Calgary, Alberta

Precaster—Lafarge Canada, Calgary, Alberta

Year Completed—2007

Reference for More Information—Ghoneim et al., 2010

PEDESTRIAN BRIDGES

21.2.12.6 Glenmore Trail Legsby Road Pedestrian Bridge/21.2.12.6.2 Key Design Objectives

Figure 21.2.12.6-1

The Glenmore Trail Legsby Road Pedestrian Bridge Spans 174 Ft Over Eight Lanes in Calgary, Alberta

(Photo: Tucker Photography)



21.2.12.6.1 Structure Description

The two end piers support cantilever beams, each reaching out approximately 31.7 ft to provide bearing seats for a single precast arched beam 110.2 ft long produced with UHPFRC. The drop-in beam is 3.6 ft deep at midspan, 4.6 ft at the ends, and is 11.8 ft wide. The flanges are 3.1 in. thick at the edges and 7.9 in. thick at the face of the 13.8-in.-wide stem of the single-tee shape. The cantilever beams are post-tensioned with forty-two 0.6-in.-diameter strands. The cantilever beams are 7.5 ft deep at the face of the piers. The back spans of the cantilevers are anchored to the foundation with external tension rods. Access on one side is by a straight ramp and by a scissor ramp on the other side. All walkways are 9.8 ft wide.

Figure 21.2.12.6.1-1

Ultra-High-Performance Concrete Aids in Providing a 173.6-Ft-Long Clear Span Over Eight Lanes of Traffic

(All photos: Tucker Photography)



a) Length of the Bridge Deck is 212 Ft and is Accessed by a Straight and a Scissor Ramp (Photo: Tucker Photography)



b) The Drop-In Beam Rests on the Ends of the Cantilever Beams (Photo: Tucker Photography)



c) The Soffit of the Cantilever Beam Forms the End of a Gentle Arc (Photo: Tucker Photography)

21.2.12.6.2 Key Design Objectives

The owner challenged the designers to showcase innovation. They did this through aesthetic features, innovative materials, the incorporation of public art, achieving a solution that exhibits very high durability. All cast-in-place concrete is high performance. The UHPFRC used in the center drop-in beam is impervious and exhibits no creep. The designers used a 28-day design compressive strength for the UHPFRC of 21.75 ksi.

PEDESTRIAN BRIDGES

21.2.12.6.2 Key Design Objectives/21.2.12.6.3 Features

There was no option to divert traffic around the work site on one of the busiest traffic arteries in the city. So, the road was closed from 10 p.m. Saturday night until 6 a.m. Sunday morning. During this 8-hour window, the cranes and all equipment were moved in along with the beam. After the beam was lifted into position and secured, all equipment was moved out.

21.2.12.6.3 Features

Public art was incorporated into the bridge. An artist created a series of interpretive features that highlight engineering. Themed words were cast into or inscribed on the bridge as shown in **Figure 21.2.12.6.3-1**. An interpretive panel is located near an entrance, next to a playground. The inclusion of the artwork supports the educational component of the project while adding to the user experience.

Figure 21.2.12.6.3-1

Words Appearing on the Bridge Relate to Descriptions of Components Identified on the Interpretive Panel at the Entry to the Bridge



a) “Floating” Appears on the Deck of the Drop-in Beam (Photo: Tucker Photography)

b) “Cantilevered” is Cut Into Straps on the Railing Above the Cantilevered End Beams (Photo: Cohos Evamy Integratedesign™)

c) “Anchoring Tension Rods” is Inscribed on a Concrete Wall that Partially Surrounds the Pier Shown Below (Photo: Cohos Evamy Integratedesign™)



d) The Word “Compress” is Inscribed on the Face of the Pier Column (Photo: Cohos Evamy Integratedesign™)

e) The Words “Expansion Joint” Appear on the Cover Over the Joint Between the Drop-In and Cantilevered Beams (Photo: Tucker Photography)

PEDESTRIAN BRIDGES

21.2.12.7 DCR Access Road Bridge over Route 24/21.2.12.7.1 Structure Description

21.2.12.7 DCR Access Road Bridge over Route 24

Location—Randolf, Mass.

Purpose of Bridge—Located in the Blue Hills Reservation area and surrounded by land owned by the state Department of Conservation and Recreation (DCR) in a scenic area widely used by equestrian riders

Description—Precast, post-tensioned, segmental concrete “channel” bridge that uses upturned edge beams as main structural members

Owner—Massachusetts Department of Transportation

Project Engineer—Purcell Associates, Boston, Mass.

Superstructure Engineer—International Bridge Technologies (IBT) Inc, San Diego, Calif.

Precaster—Unistress Corp., Pittsfield, Mass.

Year Completed—2010

Reference for More Information—Card and Cyran, 2010

Figure 21.2.12.7-1

The Precast, Post-Tensioned, Segmental, Access Road Bridge Eliminated Two Piers and Raised the Bottom of the Structure by 2 Ft. (Rendering: IBT)

**21.2.12.7.1 Structure Description**

The 248-ft-long bridge has two 124 ft spans. The two-span continuous precast segmental concrete superstructure is 29.7 ft wide and 5.38 ft deep. There are 31 total segments. Each edge beam is fully post-tensioned using one 12-strand tendon, one 15-strand tendon, and two 19-strand tendons. All tendons use 0.6-in.-diameter strands. Fourteen additional longitudinal tendons are provided in the deck slab, each using flat four 0.6-in.-diameter strand tendons. Transversely, the structure is fully post-tensioned before erection using flat 4-strand tendons. All non-prestressed reinforcing steel is epoxy-coated.

Typical segments were 8.2 ft long, with the two abutment segments being 5.1 ft long as shown in **Figure 21.2.12.7.1-1**.

The bridge's channel shape provides a 4-ft-high concrete parapet railing along both sides of the bridge, to which a protective screen was mounted on each of the parapets.

PEDESTRIAN BRIDGES

21.2.12.7.1 Structure Description/21.2.12.8 Lake Mary Pedestrian Bridges

Figure 21.2.12.7.1-1
The Unique “Channel” Bridge Has an Effective Depth From Top of Deck to Bottom of Structure of Just 16 In.—12 In. at the Center of the Concrete Deck Plus Up to 4 In. for an Asphalt Wearing Surface
 (Rendering and photos: IBT)



a) Shoulder Piers Were Eliminated and the Footing for the Center Pier was Reused

b) A Typical Segment was 8.2 Ft Long



c) The Usable Pathway is 19.7 Ft Wide Between Edge Beams

d) Posts For a Protective Screen Were Attached to Inserts in the Top of the Upturned Edge Beams

21.2.12.7.2 Key Design Objectives

It was necessary to raise the bridge significantly to avoid the regular truck impacts on the existing bridge. The number of piers was reduced for safety. It was necessary to avoid raising approach grades because of the scenic location, surrounding landscaping, and horse paths. Another goal was to provide a minimum service life of 75 years.

21.2.12.7.3 Features

The new bridge increased vertical clearance over Route 24 by more than 2 ft to 16 ft 5 in. without raising the approach grades. Traffic disruption was minimized by erecting all precast segments on supporting steel beams, post-tensioning them all at once, and then removing the beams. The precast segmental construction has proven highly durable for extended long-term, maintenance-free performance.

21.2.12.8 Lake Mary Pedestrian Bridges

Location—Lake Mary, Fla.

Purpose of Bridge—Provides connections for pedestrian and multi-use trails over the busy four-lane divided highway Lake Mary Boulevard in sight of city center.

Description—Two identical bridges constructed almost entirely of precast concrete. Each has a span of 153 ft with structural approach ramps totaling 480 ft. Each bridge is 758 ft long. Constrained sites were situated

PEDESTRIAN BRIDGES**21.2.12.8 Lake Mary Pedestrian Bridges/21.2.12.8.1 Structure Description**

over drainage ponds, in areas with numerous old growth oak trees, next to a city park, and all with limited rights-of-way. The sites necessitated compact, ADA-compliant ramp configurations.

Owner—Seminole County, Fla.

Designer—Dyer, Riddle, Mills & Precourt Inc., Orlando, Fla.

Precaster—Dura-Stress Inc, Leesburg, Fla.

Year Completed—2007

Figure 21.2.12.8-1

One of Two Identical Lake Mary, Fla., Precast Concrete Bridges that Cross the Busy Lake Mary Boulevard. The Dark Rectangular Reveals in All Precast Panels Were Formed With Formliners and Serve to Tie the Bridge to Its Ramps. (All photos: Dyer, Riddle, Mills & Precourt Inc., photographed by Ben Tanner Photography)

**21.2.12.8.1 Structure Description**

Each bridge has two, “L”-shaped beams, 153 ft long. The beams are 6 ft 3 in. deep. The bottom flange is 2 ft 2 in. wide, 1 ft 6 in. deep, and the width of the web is 1 ft 6 in. The bearing ledge is 8 in. wide. The bridge is 13 ft wide overall and has a clear width of 10 ft. The beams support 6-in.-thick precast, prestressed hollow-core concrete slabs, 10 ft long and 4 ft wide. The finished deck is a 3-in.-thick cast-in-place composite concrete topping.

Precast walls, 43 ft tall, 5 ft wide, and 8 in. thick frame the ends of the decorative bridge and provide an architectural transition from the main span structure to the approach ramp structures.

Precast concrete used for the ramps include tangent ramp pier caps, right- and left-turning pier caps, and 30-ft-long by 11-ft-wide by 9-in.-thick ramp slabs.

The individual pier landings are supported by precast, prestressed concrete driven piles.

PEDESTRIAN BRIDGES

21.2.12.8.1 Structure Description/21.2.12.9 Chambers Creek Properties North Deck Pedestrian Overpass

Figure 21.2.12.8.1-1

The Four Different Ramp Configurations are Seen in Both Pedestrian Bridges at Lake Mary, Fla.



a) The Bridge's Piers are Cast-In-Place Concrete Clad with Architectural Precast Concrete

b) Severe Restrictions Limited the Approach Ramps in All Directions

21.2.12.8.2 Key Design Objectives

By locating the deck near the bottom of the structural beams, the elevation required by the approach ramps was reduced. Modular components were developed to reduce the cost for these two identical bridges and modular ramp structures. A unique Mediterranean/Italian motif was created that provides a gateway to the community.

21.2.12.8.3 Features

The main beams not only carry the bridge decking but also serve as an aesthetically pleasing portion of the safety enclosure and railing system.

A high degree of architectural detail was brought to play through the use of simple formliner reveals. The versatility of formliner reveals allowed for fabrication of various precast bridge components having accents consistent with the desired style.

Construction required three road closures, each 6 hours long at night. One closure was needed to erect each beam and one closure to set all precast deck panels.

By using standardized ramp components arranged in various order alignments, the ramp structures were tailored to each site allowing the unique constraints of each site to be accommodated.

21.2.12.9 Chambers Creek Properties North Deck Pedestrian Overpass

Location—City of University Place, Wash.

Purpose of Bridge—A gateway that connects a popular public trail system at Chambers Creek Regional Park with 2½ miles of previously inaccessible beach, this pedestrian overpass provides a safe crossing over a busy BNSF Railway mainline. The bridge offers sweeping views of the public park and golf course, Puget Sound islands, and the Olympic Mountains. Future phases extend the bridge another 260 ft over Puget Sound transitioning into a viewing pier with small boat moorage.

Description—An 844-ft-long, 12-ft-wide concrete bridge featuring curved precast, prestressed concrete beams, with post-tensioning for continuity. A 30-ft-wide viewing platform is integrated into the bridge superstructure and stair units provide access from the bridge to the beach. There are 11 typical 60-ft-long spans, two 39-ft spans, and a 106-ft-long span. All spans are supported by 29-in.-deep beams. Seven of the 60-ft-long beams are curved horizontally with a 325-ft radius.

Owner—Pierce County Public Works and Utilities, Wash.

Designer—BergerABAM, Federal Way, Wash.

Precaster—Concrete Technology Corp., Tacoma, Wash.

Year Built—2010

Reference for More Information—Parrish, 2014

PEDESTRIAN BRIDGES

21.2.12.9 Chambers Creek Properties North Deck Pedestrian Overpass/21.2.12.9.1 Structure Description

Figure 21.2.12.9-1

This Pedestrian Overpass in University Place, Wash., Connects to a Public Trail System and Opens 2½ Miles of Beach to Public Use (All Photos: BergerABAM)



a) The Railroad Overpass Provides an Extension of Popular Trails and Public Access to 2½ Miles of Beach



b) An Aerial View during Construction Shows the 10 Precast, Prestressed Concrete Beams Erected In Place



c) Viewed From Under the 106-Ft-Long Span over the Railroad, the 30-Ft-Wide Viewing Platform is at the Left Edge of the Photo

21.2.12.9.1 Structure Description

All of the precast, prestressed concrete box beams are 144 in. wide and 29 in. deep. The precast beams include nine 60-ft-long spans and one 106-ft-long span. The typical cross section of the precast beams is shown in **Figure 21.2.12.9.1-1**. The asymmetric three-span (39, 106, 60 ft) main section over the BNSF tracks achieves a span-to-depth ratio of 44 for the center span, which was designed to support its weight and construction loads using pretensioning only, prior to being integrated with the adjacent spans using field post-tensioning. The apex of the walkway profile coincides with the midspan of the long span over the railroad, and the pretensioning was designed to induce camber to fit the vertical curve.

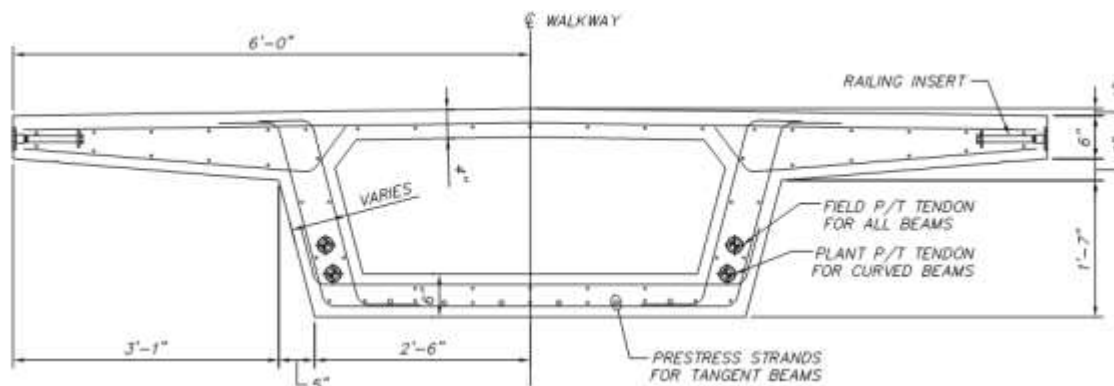
Seven of the 10 precast beams were cast with a horizontal radius of 325 ft. The cast-in-place viewing platform, with two 39-ft spans, widens to 30 ft. The stair unit with its complicated geometry consists of two cast-in-place 60-ft spans. To achieve an elegant, ribbon-like profile, the structure was detailed to maintain a consistent section with a 29-in. structural depth, including the crossbeams, railroad overpass, viewing platform, and stair units.

PEDESTRIAN BRIDGES

21.2.12.9.1 Structure Description/21.2.12.9.3 Features

Figure 21.2.12.9.1-1

Typical Precast Beam Cross Section for the Chambers Creek Pedestrian Overpass with Prestressing and Post-tensioning Shown (Drawing: BergerABAM)

**21.2.12.9.2 Key Design Objectives**

The vision for this project was to create a pedestrian- and bicycle-friendly bridge that projects an elegant, flowing ribbon with an ever-changing panoramic view of the Puget Sound, the public park, surrounding islands, and the Olympic Mountains. Integral crossbeams and closure pours allowed the superstructure to maintain a constant depth. The bridge's alignment, plan, and profile were carefully conceived to fit the natural lay of the land and provide gradual inclines, and yet allow for the repetition of elements. The design grade for the bridge was set at 4.8% to allow for construction tolerances while remaining compliant with a 5% ADA grading limit. The low-maintenance, durable concrete bridge structure was envisioned as similar in appearance to existing nearby iconic and historic gravel pit structure elements. When extended in future phases, the bridge will transition to a wide viewing pier over Puget Sound and will provide ADA accessibility to a small boat moorage facility.

21.2.12.9.3 Features

The site constraints, environmental concerns, and architectural vision for this project necessitated a complex geometry that required creative design solutions. Additional design considerations included high seismicity, poor soil conditions, a marine environment, and an active railroad line dissecting the site. The use of precast beams accommodated the tight railroad restrictions, with the erection of the span over railroad right-of-way occurring comfortably within an existing 40-minute operating window in the train schedule. The marine environment required provisions for enhanced durability that included marine specific concrete mix designs, a post-tensioning system featuring polyethylene corrugated ducts, and epoxy-coated reinforcement.

The bridge was finished with a light cable railing system that fits well with the structural aesthetics. The cable railing system was adapted to serve as throw screens over the railroad tracks. The final product is a simple, handsome structure that fits well in its surrounding aesthetic environment and has been recognized in the community as a treasured recreational asset.

PEDESTRIAN BRIDGES

21.2.12.9.3 Features/21.3.1 Snowmobile Bridges

Figure 21.2.12.9.3-1**The Chambers Creek Pedestrian Bridge Provides Unobstructed Views of the Puget Sound Islands**

- a) A Light Cable Railing Opens the Structure and Maintains the Flowing Ribbon Appearance of the Bridge
- b) Future Phases will Extend the Bridge Another 260 Ft Over Puget Sound and Transition into a Viewing Pier with a Small Boat Moorage

21.3 SPECIAL USE PEDESTRIAN BRIDGES**21.3.1 Snowmobile Bridges**

Pedestrian bridges are frequently used by more than pedestrians on a mixed use trail. Section 21.2 references the *Guide for the Development of Bicycle Facilities* (AASHTO, 2012b). It defines a “shared use path” as one separated from motorized traffic and often used by pedestrians, skaters, wheelchair users, joggers, and other non-motorized users. An exception to non-motorized use occurs in several northern states who maintain extensive networks of trails used recreationally by motorized snowmobiles. Pedestrians are not likely to be present during winter months. The trails are well marked and often maintained with snow grooming equipment to make them more convenient to users.

Bridges intended for use by snowmobiles are typically wider than 10 ft in order to permit safe passing in opposite directions. These bridges must be designed for an H10 vehicle as described in Section 21.2.7.3. This design load is considered more than adequate for the weight of snow plus snowmobiles. However, the weight of trail grooming equipment can be a concern. Some designers have the owner provide a specific anticipated groomer load and the bridge is checked accordingly to see if the H10 loading will suffice.

Another unique construction provision occurs when bridges are built as through-girder structures. On these bridges, wooden “rubrails” are added to the sides of the beams to provide a vertical wearing surface and prevent the possibility of the vehicle being snagged by a component of the beam or rail.

Figure 21.3.1-1 illustrates the use of a wooden rubrail on a through-girder bridge. This project is described in more detail in Section 21.3.1.1 and shown in **Figure 21.3.1.1-1**. The railing is mounted to the top flange of a 72-in. deep precast, prestressed concrete I-beam (painted brown in the photo). A cast-in-place concrete curb is cast on the cast-in-place deck that spans between the webs of the edge beams. The edge of the curb is flush with the edge of the top flange of the beam. Treated wooden timbers, 3 in. by 10 in., finished on four sides (S4S), are placed between the top of the curb and the bottom of the flange. They are secured by U-bolts that are anchored around a 2-in.-diameter standard pipe welded at its base to a steel plate anchored in the top of the curb. The nuts and washers on the U-bolts are recessed in the surface of the timbers. These can be seen in the photo below the angled rail braces. The butted ends of the timbers are staggered and aligned behind plates recessed into the timbers. The top rail is tapered to account for the varying grade of the deck and is snug under the top flange of the beam.

PEDESTRIAN BRIDGES

21.3.1 Snowmobile Bridges/21.3.1.1 Snowmobile Bridge Case Study—Paul Bunyan Trail Bridge over Excelsior Road

Figure 21.3.1-1
Bridge Deck, Curb, Rubrail, and Railing on a Mixed-Use Pedestrian–Snowmobile Bridge in Minnesota
(Photo: Minnesota Department of Transportation)



21.3.1.1 Snowmobile Bridge Case Study—Paul Bunyan Trail Bridge over Excelsior Road

Location—Baxter, Minn.

Purpose of Bridge—The Paul Bunyan State Trail is approximately 120 miles long and extends from Crow Wing State Park (south of Brainerd/Baxter) to Lake Bemidji State Park (north of Bemidji). It is the longest continuously paved trail in the Minnesota State Trail system, and one of the longest in the United States. Baxter is the southern terminus of the trail. Main summer uses include hiking, bicycling, and in-line skating. Snowmobiling is the primary winter use. The trail provides connections to many miles of groomed snowmobile trails in the county Grants-in-Aid trail system. The bridge provides a grade separation over a busy two-lane residential road near the trail head.

Description—This is a through-girder bridge with three spans (110-ft 9-in.-end spans and a 121-ft 6-in.-main span). The superstructure is 21 ft wide with a 16 ft inside clearance. The two end spans have a 5% grade to a crest vertical curve on the center span.

Owner—Minnesota Department of Natural Resources

Designer—Widseth Smith Nolting (WSN), Alexandria, Minn.

Precaster—Cretex Concrete Products, Maple Grove, Minn.

Year Built—2007

PEDESTRIAN BRIDGES

21.3.1.1 Snowmobile Bridge Case Study—Paul Bunyan Trail Bridge over Excelsior Road/21.3.1.1.1 Structure Description

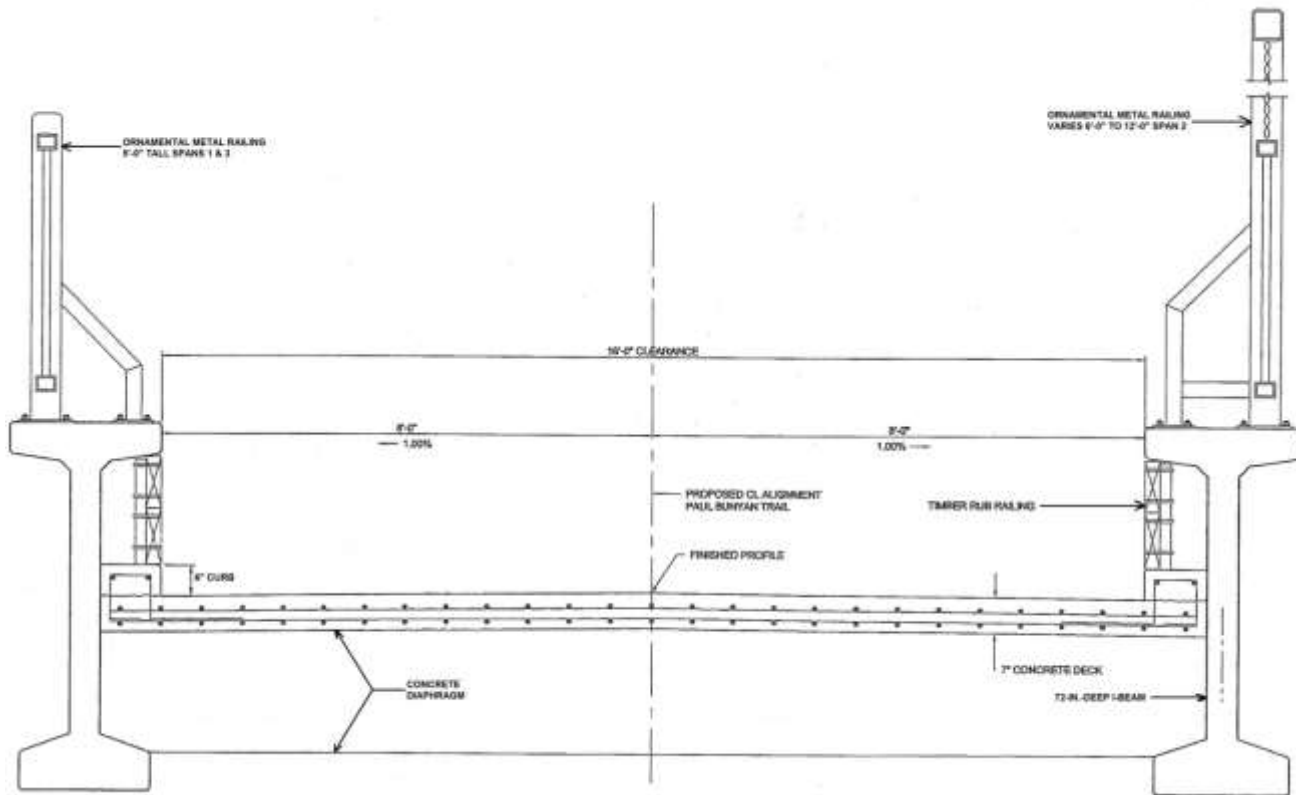
*Figure 21.3.1.1-1**This Through-Girder Bridge Features a Span of 121 Ft 6 In. with a Total Structure Depth of Only 72 In.**(Photo: Widseth Smith Nolting)***21.3.1.1.1 Structure Description**

The plan cross section of the bridge is shown in **Figure 21.3.1.1.1-1**. The edge beams are 72-in.-deep precast, prestressed concrete I-beams with 30-in.-wide top flanges, 6 in. thick at the edges, and 26-in.-wide bottom flanges, 7½ in. thick at the edges. The web is 6 in. thick. The 28-day, design compressive strength was 8 ksi. A 7-in.-thick cast-in-place concrete deck (design compressive strength of 4 ksi) is supported on cast-in-place floor beams (or diaphragms) spaced at approximately 14 ft centers. These beams are 1 ft wide and vary in depth from approximately 21 in. to 32 in. to accommodate the varying grade. They are anchored to the edge beams with threaded rods in inserts in the beam webs and sloped upper surfaces of the bottom flanges. The railings and throw screens are mounted directly to the top flanges of the I-beams. The bridge incorporates the primary design and detailing recommendations of the research conducted by the University of Minnesota on precast, prestressed concrete through-girder bridges (Baran et al., 2007).

PEDESTRIAN BRIDGES

21.3.1.1.1 Structure Description/21.3.1.1.3 Features

Figure 21.3.1.1.1-1
Cross Section of the Paul Bunyan Trail Bridge Located in Baxter, Minnesota (Drawing from project plans, edited. Used with permission of the Minnesota Department of Natural Resources)



21.3.1.1.2 Key Design Objectives

The project was conceived to provide a low-profile, aesthetically-enhanced structure that would fit easily into this rural town. Durability and ease of maintenance was an early objective.

21.3.1.1.3 Features

Special features incorporated into the bridge include the use of attractive colors for the railings and visible surfaces. Artwork was used on the recessed surfaces of the piers and on the throw screens. Durable features include high-strength concrete.

PEDESTRIAN BRIDGES

21.3.1.1.3 Features/21.3.2 Wildlife Bridges

Figure 21.3.1.1.3-1**The Multi-Use Bridge has Details that Accommodate Snowmobilers in Winter**

a) Details Provide Safe Surfaces for Pedestrians, Bicyclists, and Snowmobilers. Five Percent Grades Meet ADA Requirements. Railings and Screens Avoid a Tunnel-Like Environment. (Photo: Widseth Smith Nolting)

b) Modular Railings Mount to Top Flanges of the I-Beams. Throw Screens Use 9-Ga. Mesh with 2-In. Openings (Photo: Minnesota Department of Transportation)

21.3.2 Wildlife Bridges

An article by M. Myint Lwin, Federal Highway Administration, states, “In the design, construction, operation and maintenance of highway facilities, it is suggested to consider at least the following in the promotion of and the development of guidelines for ‘green highways and bridges:’

- Improving highway safety to motorists and wildlife by reducing collisions with wildlife
- Maintaining wildlife habitat connectivity across highway facilities
- Attention to safety, durability, mobility and economy
- Compliance with environmental and preservation laws and regulations
- Application of context sensitive solutions
- Sustainable site selection and planning
- Utilization of high performance and environmentally friendly materials, and quality workmanship
- Safeguarding air, water, soil and wetland quality
- Conservation of materials and resources
- Avoidance of negative impacts on the ecosystems

“Great global efforts are devoted to applying the concepts of ‘green highways and bridges’ to design, construction, operation, and maintenance of transportation facilities to improve livability and sustainability of the communities and wildlife habitats” (Lwin, 2009).

Each year, there are tens of thousands of accidents involving vehicles and wild animals. Numerous underpasses have been built in attempts to provide safe passage of animals under roads. These include many types of box and pipe culverts, and even short-span bridges. It appears there is more interest today in providing passage for animals over highways when the terrain is favorable. Animals appear more inclined to use such open-air passages.

One of the first wildlife overpass structures in the United States is the Cross Florida Greenway Land Bridge Over I-75 built in 2000 (Duggar and Corven, 2000). This project is especially interesting because it is designed to convey both people and wildlife and because it was Florida’s first use of their now standard concrete U-beam series. The project is described in more detail in the following case study in Section 21.3.2.1.

An organization known as ARC is dedicated to finding and implementing leading-edge solutions to human and wildlife mobility, and to long-term landscape connectivity. They are organized around three core initiatives:

PEDESTRIAN BRIDGES

21.3.2 Wildlife Bridges

communications, technology transfer, and implementation. Their website explains the organization in more detail (<http://arc-solutions.org/>).

In 2010, ARC conducted a competition to design a wildlife crossing over I-70 near Vail, Colo., which resulted in five finalist projects. A distinguished team of five international judges selected an elegant design shown in **Figure 21.3.2-1**. The judges said that the winning entry “. . . was unanimously identified as the most elegant and compelling solution. [The] proposal was at once simple and straightforward, while embodying the complexity and contradictions inherent in the competition brief. The . . . proposal makes use of known technology as well as construction techniques that are well established. These techniques are ordered in such a way as to service an overriding concern for the construction of wildlife crossings that would bear little trace of the structure below. It effectively recasts ordinary materials and methods of construction into a potentially transcendent work of design. In this regard it gives us confidence that it could be credibly imagined as a regional infrastructure across the intermountain west.” ARC is working with the Colorado Department of Transportation to site the first of possibly several such bridges.

Figure 21.3.2-1

The Winning Entry in the ARC Wildlife Bridge Competition was Submitted by a Team Comprising HNTB Engineering with Michael Van Valkenburgh & Associates and Applied Ecological Services, Inc. (HNTB + MVVA) Described in Kociolek, 2011 (Renderings: HNTB + MVVA)



- a) Two Modules are Joined at Midspan Acting as a Three-Hinged Arch, Eliminating the Need for a Center Pier. No On-Site Concrete Work is Required. Note Temporary Falsework as a Center Pier.
- b) The Bridging System Consists of Precast Modules that Serve as Abutment, Beam, and Deck—All in One. This Single Element—Created Using Straight Line, Commercially Available Formwork—is the Key to Cost-Effectiveness, Speed of Construction, and Modularity.



c) Rendering of the Wildlife Environment on the Structure

PEDESTRIAN BRIDGES**21.3.2.1 Wildlife Bridge Case Study—Cross Florida Greenway Land Bridge Over I-75/21.3.2.1.1 Structure Description****21.3.2.1 Wildlife Bridge Case Study—Cross Florida Greenway Land Bridge Over I-75**

Location—Marion County, Fla.

Purpose of Bridge—The Marjorie Harris Carr Cross Florida Greenway is a 110-mile-long corridor that extends from the Gulf of Mexico to the St. Johns River. It encompasses diverse natural habitats for observing Florida's native flora and fauna. The trail offers hiking, biking, equestrian and paddle trails, boat ramps, fishing spots, campgrounds, and picnic shelters to outdoor enthusiasts of all ages (<http://www.floridastateparks.org/crossflorida/>). Until 2000, the Cross Florida Greenway was bisected by I-75 with no bridges or underpasses. The completion of the Land Bridge connected the two major sections of the greenway for wildlife, pedestrians, bicyclists, and equestrians.

Description—The land bridge is 52 ft 6 in. wide and 204 ft 7 in. long. It is irrigated and landscaped with native vegetation in 4 ft 6 in. deep planters along both sides of the structure.

Owner—Florida Division of Recreation and Parks, Tallahassee, Fla.

Designer—DMJM, Tallahassee, Fla.

Precaster—Dura-Stress Inc, Leesburg, Fla.

Year Built—2000

Reference for More Information—Duggar and Corven, 2000; Huang et al., 2003

Figure 21.3.2.1-1

Aerial View of the Land Bridge that Connects the Cross Florida Greenway Over I-75 and Provides Safe Travel for Wildlife (Photo: Florida State Parks)

**21.3.2.1.1 Structure Description**

U-beams are appearing more frequently in bridges throughout the United States especially when aesthetic issues are deemed important. This structure is the first U-beam bridge in Florida. The bridge has two simple spans each with four precast, prestressed concrete Florida U-beams. The Florida U-beam is 5.91 ft deep, 4.59 ft wide at the bottom, and 8.73 ft wide at the top. Minimum vertical clearance over I-75 is 16.6 ft.

The beams are spaced at 12.14, 15.42, and 12.14 ft on their centerlines. Distance from edge beam centerline to edge of structure is 6.2 ft. The cast-in-place concrete deck is 7.87 in. thick. The design live load included AASHTO HS-15 to account for pedestrian loads. The 52.5 ft width is divided into an 18.1-ft-wide trail section paved with compacted shell material. The edge planting areas measure 18.1 ft wide and 4.5 ft deep bounded by retaining walls.

PEDESTRIAN BRIDGES

21.3.2.1.2 Key Design Objectives/21.4 Cited References

21.3.2.1.2 Key Design Objectives

The concept of the land bridge was to extend the greenway characteristics across the bridge and avoid the caged, tunnel effect and appearance of typical pedestrian bridges. Studies indicated the land bridge concept is utilized internationally and is conducive to wildlife usage.

21.3.2.1.3 Features

The use of a new Florida standard bridge section minimized the vertical profile. Special consideration was given to the structural aesthetics of the bridge from the I-75 motorist view as well as the aesthetic impact of the bridge on users of the greenway. The bridge's location was selected to maximize the benefit offered by the natural terrain and minimize the project footprint. The location allows the project to blend with the natural environment while causing the least possible disruption to natural vegetation both during construction and throughout the life of the project.

Figure 21.3.2.1.3-1

*Cross Florida Greenway Land Bridge
(Photo: Florida State Parks)*

**21.4 CITED REFERENCES**

AASHTO. 2004. *Guide for the Planning, Design, and Operation of Pedestrian Facilities*. 1st Edition. American Association of State Highway and Transportation Officials, Washington, DC. 142 pp.
https://bookstore.transportation.org/Item_details.aspx?id=119 (Fee)

AASHTO. 2005. *Roadway Lighting Design Guide*. American Association of State Highway and Transportation Officials, Washington, DC. 70 pp.
https://bookstore.transportation.org/Item_details.aspx?id=320 (Fee) [Appendix A, *Literature Review and References*, and Appendix B, *Lighting Basics*, updated 2010, may be downloaded without fee from this website, 50 pp.]

AASHTO. 2009a. *LRFD Guide Specifications for the Design of Pedestrian Bridges*. 2nd Edition. American Association of State Highway and Transportation Officials, Washington, DC. 864 pp.
https://bookstore.transportation.org/collection_detail.aspx?ID=6 (Fee)

AASHTO. 2009b. *Manual on Uniform Traffic Control Devices for Streets and Highways*. 2009 Edition. American Association of State Highway and Transportation Officials, Washington, DC. 36 pp.
https://bookstore.transportation.org/item_details.aspx?ID=1550 (Fee)

AASHTO. 2011. *A Policy on Geometric Design of Highways and Streets*, 6th Edition. American Association of State Highway and Transportation Officials, Washington, DC. 912 pp.
https://bookstore.transportation.org/collection_detail.aspx?ID=110&gclid=CLWA04zF4bYCFctxQgodrRMAlw (Fee)

- AASHTO. 2012a. *AASHTO LRFD Bridge Design Specifications*, 6th Edition, American Association of State Highway and Transportation Officials, Washington, DC. 1,938 pp. All references made in this chapter to the LRFD Specifications are to this document.
https://bookstore.transportation.org/collection_detail.aspx?ID=123 (Fee)
- AASHTO. 2012b. *Guide for the Development of Bicycle Facilities*. 4th Edition. American Association of State Highway and Transportation Officials, Washington, DC. 200 pp.
https://bookstore.transportation.org/collection_detail.aspx?ID=116 (Fee)
- AASHTO. 2013. *Standard Specifications for Structural Supports for Highway Signs, Luminaries, and Traffic Signals*, 6th Edition. American Association of State Highway and Transportation Officials, Washington, DC. 320 pp.
https://bookstore.transportation.org/collection_detail.aspx?ID=126 (Fee)
- ACI Committee 318. 2011. *Building Code Requirements for Structural Concrete and Commentary*. (ACI 318). American Concrete Institute, Farmington Hills, MI. 503 pp.
<http://www.concrete.org/Store/ProductDetail.aspx?ItemID=31811> (Fee)
- ACI Committee 343. 1995. *Analysis & Design of Reinforced Concrete Bridge Structures*. (ACI 343R, Reapproved 2004). American Concrete Institute, Farmington Hills, MI. 158 pp.
http://www.concrete.org/Store/ProductDetail.aspx?ItemID=34395&ReturnUrl=http%3a%2f%2fwww.concrete.org%2fStore%2fStoreResults.aspx%3fSortOrder%3dRELEVANCE%26Keyword%3d343R%23dnn_ctr5215_SearchResults34395 (Fee)
- ADA. 1990. Code of Federal Regulations, 41 CFR Part 35. Americans with Disabilities Act, Title II
http://www.ada.gov/2010_regs.htm (includes amendments effective January 1, 2009 and revisions effective March 15, 2011)
- Aitken, Jim, Mike Clements, and Tim Schmitz. 2008. "Fifth Street Pedestrian Plaza Bridge." *ASPIRE—The Concrete Bridge Magazine*, Precast/Prestressed Concrete Institute, Chicago, IL. (Winter), pp. 22–24.
http://aspirebridge.com/magazine/2008Winter/5th_street_win08.pdf
- Aldrich, Brian. 2009. "Canyon Park Freeway Station Bridge." *ASPIRE—The Concrete Bridge Magazine*, Precast/Prestressed Concrete Institute, Chicago, IL. (Winter), pp. 26–28.
http://aspirebridge.com/magazine/2009Winter/canyon_win09.pdf
- Baran, Eray, Arturo E. Schultz, and Catherine W. French. 2007. *Strength and Stability of Prestressed Concrete Through-Girder Pedestrian Bridges Subjected to Vehicular Impact*. Report No. MN/RC-2007-08. Department of Civil Engineering, University of Minnesota, Minneapolis, MN. 244 pp.
<http://www.cts.umn.edu/Publications/ResearchReports/reportdetail.html?id=1132>
- Castrodale, R. W. and Christopher D. White. 2004. Extending Span Ranges of Precast Prestressed Concrete Girders. NCHRP Report 517. Transportation Research Board, Washington, DC. 552 pp.
<http://www.trb.org/Main/Blurbs/154330.aspx>
- Collins, William. 2009. "Forty Foot Pedestrian Bridge." *ASPIRE—The Concrete Bridge Magazine*, Precast/Prestressed Concrete Institute, Chicago, IL. (Spring), pp. 22–25.
http://aspirebridge.com/magazine/2009Spring/forty_foot_spr09.pdf
- Card, Matt and Thomas Cyran. 2010. "'Channel' Bridge Improves Clearance." *ASPIRE—The Concrete Bridge Magazine*, Precast/Prestressed Concrete Institute, Chicago, IL. (Fall), pp. 32–35.
http://aspirebridge.com/magazine/2010Fall/DCR_Fall10.pdf
- Duggar Jr., Charles F. and John A. Corven. 2000. Design of the Cross Florida Greenway Land Bridge Over I-75 Using Precast Florida U-Beams. In Transportation Research Record No. 1696, Volume 2. Fifth International Bridge Engineering Conference, Transportation Research Board, Washington, DC. pp. 188-192.
<http://trid.trb.org/view/2000/C/651239> (Fee)
- FHWA. 2000. *Accommodating Bicycle and Pedestrian Travel: A Recommended Approach*. Federal Highway Administration, U. S. Department of Transportation, Washington, DC.
http://www.fhwa.dot.gov/environment/bicycle_pedestrian/guidance/design_guidance/design.cfm

PEDESTRIAN BRIDGES

21.4 Cited References

- FHWA. 2009. *Manual on Uniform Traffic Control Devices for Streets and Highways*. 2009 Edition. (with Revisions 1 and 2, May 2012). Federal Highway Administration, U. S. Department of Transportation, Washington, DC. 862 pp.
<http://mutcd.fhwa.dot.gov/pdfs/2009r1r2/mutcd2009r1r2edition.pdf>
- FDOT. 2011. *Structures Design Guidelines, Part 10—Pedestrian Bridges*. Florida Department of Transportation, Tallahassee, FL.
<http://www.dot.state.fl.us/structures/StructuresManual/2009january/DesignGuidelines/SDG10PedestrianBridges.htm>
- Fernandes, Robert L., Ross A. French, and S. Pi. C. Liu. 2011. “Creating a Level Playing Field.” *ASPIRE—The Concrete Bridge Magazine*, Precast/Prestressed Concrete Institute, Chicago, IL. (Fall), pp. 18–20.
http://aspirebridge.com/magazine/2011Fall/18-20_NE36th.pdf
- fib. 2005. *Guidelines for the Design of Footbridges*. Bulletin 32, Fédération Internationale du Béton (*fib*), Lausanne, Switzerland, 160 pp.
<http://www.fib-international.org/guidelines-for-the-design-of-footbridges> (Fee)
- Ghoneim, Gamal A. M., Vic H. Perry, and Gerald Carson. 2010. Ultra-High Performance Fibre Reinforced Concrete in Footbridges. In Proceedings of the 8th International Conference on Short and Medium Span Bridges 2010, August 3-6, Niagara Falls, Ontario, Canada. Volume 3, Paper 346, p. 2,102. Canadian Society for Civil Engineering, Montreal, Quebec, Canada
<http://www.proceedings.com/09463.html> (Fee)
- Goedhart, Pieter. 2012. “Pacific Coast Highway Pedestrian Bridge.” *ASPIRE—The Concrete Bridge Magazine*, Precast/Prestressed Concrete Institute, Chicago, IL. (Winter), pp. 22–24.
http://aspirebridge.com/magazine/2012Winter/DanaPoint_Win12_Web.pdf
- Gottmoeller, Frederick. 2012. Aesthetics Commentary in *ASPIRE—The Concrete Bridge Magazine*, Precast/Prestressed Concrete Institute, Chicago, IL. (Spring), p. 23.
http://aspirebridge.com/magazine/2012Spring/aesthetics_commentary.pdf
- Howe, Andrew. 2012. “Delta Ponds Pedestrian Bridge.” *ASPIRE—The Concrete Bridge Magazine*, Precast/Prestressed Concrete Institute, Chicago, IL. (Spring), pp. 20–23.
http://aspirebridge.com/magazine/2012Spring/DeltaPonds_Spr2012_Web.pdf
- Huang, Dongzhou, Marcus H. Ansley and Mohsen A. Shahawy. 2003. Crack Analysis of Prestressed Concrete U-Beams for Cross Florida Greenway Land Bridge. In Proceedings, 3rd International Symposium on High Performance Concrete and the National Bridge Conference, October 19-22, Orlando, Fla., published by the Precast/Prestressed Concrete Institute, Chicago, IL.
<https://www.pci.org/bookstore/storefront.aspx> (click on Bridges)
- IES. 2011. *The Lighting Handbook*. 10th Edition. Illuminating Engineering Society of North America. New York, NY. 1,328 pp.
<http://www.ies.org/handbook/> (Fee)
- ITE. 1997. *Design and Safety of Pedestrian Facilities, A Recommended Practice*. Institute of Transportation Engineers. Washington, DC. 115 pp.
<http://ecommerce.ite.org/IMIS/ItemDetail?iProductCode=RP-026A> (Fee)
- Kociolek, Angela. 2011. “‘hypar-nature’—A Precast Design for Wildlife Crossings.” *ASPIRE—The Concrete Bridge Magazine*, Precast/Prestressed Concrete Institute, Chicago, IL. (Fall), p. 12.
http://aspirebridge.com/magazine/2011Fall/12_CCCARC.pdf
- Lwin, M. Myint. 2009. “Global Efforts on Green Highways and Bridges.” *ASPIRE—The Concrete Bridge Magazine*, Precast/Prestressed Concrete Institute, Chicago, IL. (Summer), pp. 44–45.
http://aspirebridge.com/magazine/2009Summer/fhwa_news_sum09.pdf
- McCraven, Sue. 2008. “Fifth Street Pedestrian Bridge Becomes Landmark at Georgia Tech.” Parts 1 and 2. *PCI Journal*, Precast/Prestressed Concrete Institute, Chicago, IL. V. 53, No. 1 (January-February), pp. 58–82.
https://www.pci.org/Publications/PCI_Journal/2008/Jan-Feb/

PEDESTRIAN BRIDGES

21.4 Cited References

- Parrish, Myles. 2014. "Chambers Creek Bridge to the Beach." *ASPIRE—The Concrete Bridge Magazine*, Precast/Prestressed Concrete Institute, Chicago, IL. (Summer), p. 39.
<http://aspirebridge.com/magazine/2014Summer/Asp2014Summer-CCC-ChambersCreek.pdf>
- PCI. 1988. *Connections Manual*. (MNL-123-88). Precast/Prestressed Concrete Institute, Chicago, IL. 270 pp.
https://netforum.pci.org/eweb/DynamicPage.aspx?Site=PCI_NF&WebKey=9766331d-1b7d-4c4b-89cb-fc801bc30745&ListSearchFor=connections (Fee)
- PCI. 1999. *Manual for Quality Control for Plants and Production of Structural Precast Concrete Products*. MNL-116-99, Fourth Edition. Precast/Prestressed Concrete Institute, Chicago, IL.
https://netforum.pci.org/eweb/dynamicpage.aspx?webcode=category&ptc_key=a7ba327a-0cc2-48cc-bc3e-1c8f49f2168e
- PCI. 2000. *Tolerance Manual for Precast and Prestressed Concrete Construction*. (MNL-135-00). 1st Edition, Precast/Prestressed Concrete Institute, Chicago, IL. 95 pp.
https://netforum.pci.org/eweb/dynamicpage.aspx?webcode=category&ptc_key=76df87cf-beac-442d-b4fd-f15439f86d71&ptc_code=Tolerance (Fee)
- PCI. 2003. *Architectural Precast Concrete Color and Texture Selection Guide*. 2nd Edition. CTG-10. Precast/Prestressed Concrete Institute, Chicago, IL.
https://netforum.pci.org/eweb/dynamicpage.aspx?webcode=category&ptc_key=e0231fc3-3a66-4b58-8501-94e6898ded01 (Fee)
- PCI. 2007. *Architectural Precast Concrete*. 3rd Edition. MNL-122. Precast/Prestressed Concrete Institute, Chicago, IL.
https://netforum.pci.org/eweb/dynamicpage.aspx?webcode=category&ptc_key=e0231fc3-3a66-4b58-8501-94e6898ded01 (Fee)
- PCI. 2010. *Design Handbook*, 7th Edition, (MNL-120-10). Precast/Prestressed Concrete Institute, Chicago, IL.
https://netforum.pci.org/eweb/dynamicpage.aspx?webcode=category&ptc_key=6ccabfe6-c4d9-4379-83b5-d257a2bde354&ptc_code=D (Fee)
- PTI. 2006. *Post-Tensioning Manual*, 6th Edition, (PTI TAB.1-06). Post-Tensioning Institute, Farmington Hills, MI. 354 pp.
http://www.post-tensioning.org/store/PTI_TAB.1-06: Post-Tensioning Manual-sixth edition (Fee)
- PTI. 2012a. *Guide Specification for Grouted Post-Tensioning* (PTI M50.3-12) Post-Tensioning Institute, Farmington Hills, MI. 26 pp.
http://www.post-tensioning.org/store/PTI_M50.3-12: Guide Specification for Grouted PT (Fee)
- PTI. 2012b. *Specification for Grouting of Post-Tensioned Structures* (PTI M55.1-12). Post-Tensioning Institute, Farmington Hills, MI. 60 pp.
http://www.post-tensioning.org/store/PTI_M55.1-12: Specification for Grouting of PT Structures (Fee)
- Sanchez, Tony. 2010. "The David Kreitzer Lake Hodges Bicycle Pedestrian Bridge." *ASPIRE—The Concrete Bridge Magazine*, Precast/Prestressed Concrete Institute, Chicago, IL. (Summer), pp. 36–38.
http://aspirebridge.com/magazine/2010Summer/Project_Lake_Hodges.pdf
- SDM. 2013. *Structures Detailing Manual*. Florida Department of Transportation, Tallahassee, FL. 255 pp.
http://www.dot.state.fl.us/structures/StructuresManual/CurrentRelease/Vol2_SDM/SDMEx.shtm
- Shell, Tim and Stephen Whittington. 2009. "Vancouver Land Bridge." *ASPIRE—The Concrete Bridge Magazine*, Precast/Prestressed Concrete Institute, Chicago, IL. (Summer), pp. 26–29.
http://aspirebridge.com/magazine/2009Summer/vancouver_land_bridge_sum09.pdf
- TRB. 2010. *Highway Capacity Manual 2010*. Transportation Research Board, National Academy of Sciences, Washington, DC. 1,650 pp.
<http://books.trbbookstore.org/hcm10.aspx> (Fee)

This page intentionally left blank

SYMBOL	DESCRIPTION	CORRESPONDING AASHTO LRFD SPECIFICATIONS	CORRESPONDING AASHTO STANDARD SPECIFICATIONS
A	area of cross section of stringer or beam	A (4.6.2.2.1)	—
A	maximum area of the portion of the supporting surface that is similar to the loaded area and concentric with it and does not overlap similar areas for adjacent anchorage devices	A (5.10.9.7.2)	—
A	effective tension area of concrete surrounding the flexural tension reinforcement and having the same centroid as that reinforcement, divided by the number of bars or wires; when the flexural reinforcement consists of several bar sizes or wires, the number of bars or wires shall be computed as the total area of reinforcement divided by the area of the largest bar or wire used	A (5.7.3.4)	A (8.16.8.4)
A	Plan area of elastomeric Pad	—	—
A_{bs}	cross-sectional area of beam stems	—	—
A_c	area of core of spirally reinforced compression member measured to the outside diameter of the spiral	A_c (5.7.4.6)	A_c (8.18.2.2.2)
A_c	total area of the composite section	—	—
A_c	area of concrete on the flexural tension side of the member	—	—
A_{cs}	cross-sectional area of a concrete strut in strut-and-tie model	A_{cs} (5.6.3.3.1)	—
A_{cv}	area of concrete section resisting shear transfer	A_{cv} (5.8.4.1)	A_{cv} (8.16.6.4.5)
A_d	area of deck concrete (9.1a.6.3.4)		
A_g	gross area of section	A_g (5.5.4.2.1)	A_g (8.1.2)
A_g	gross area of bearing plate	A_g (5.10.9.7.2)	—
A_g	cross-sectional area of the precast beam or section		
A_h	area of shear reinforcement parallel to flexural tension reinforcement	A_h (5.13.2.4.1)	A_h (8.15.5.8, 8.16.6.8)
A_k	area of cross-section of element k		
A_o	area enclosed by centerlines of the elements of the beam	C4.6.2.2.1	—
A_{ps} , A_s	area of prestressing strand	A_{ps} (5.5.4.2.1)	A_s^* (9.17)
A_{ps}	area of Pretensioning steel	—	—
A_{PT}	area of transverse post-tensioning reinforcement	—	—
A_s	area of non-prestressed tension reinforcement	A_s (5.5.4.2.1)	A_s (9.7, 9.19)
A_s	total area of vertical reinforcement located within the distance (h/5) from the end of the beam	—	—
A_s'	area of compression reinforcement	A_s' (5.7.3.1.1)	A_s' (9.19)
A_{sf}	steel area required to develop the compressive strength of the overhanging portions of the flange	—	A_{sf} (9.17)

SYMBOL	DESCRIPTION	CORRESPONDING AASHTO LRFD SPECIFICATIONS	CORRESPONDING AASHTO STANDARD SPECIFICATIONS
A_{sk}	area of skin reinforcement per unit height in one side face	A_{sk} (5.7.3.4)	A_{sk} (8.17.2.1.3)
A_{sr}	steel area required to develop the compressive strength of the web of a flanged section	—	A_{sr} (9.17-9.19)
A_{ss}	area of reinforcement in an assumed strut of a strut-and-tie model	A_{ss} (5.6.3.3.4)	—
A_{st}	total area of longitudinal mild steel reinforcement	A_{st} (5.6.3.4.1)	A_{st} (8.16.4.1.2, 8.16.4.2.1)
A_{st}	area of longitudinal mild steel reinforcement in tie	—	—
A_t	area of one leg of closed transverse torsion reinforcement	A_t (5.8.3.6.2)	—
A_{tc}	area of transformed composite section at final time	—	—
A_{tf}	area of transformed section at final time	—	—
A_{ti}	area of transformed section at transfer	—	—
A_v	area of transverse reinforcement within a distance s	A_v (5.8.2.5)	A_v (9.20)
A_{vh}	area of web reinforcement required for horizontal shear	—	—
A_{vf}	area of shear-friction reinforcement	A_{vf} (5.8.4.1)	A_{vf} (8.15.5.4.3)
A_{vf}	area of shear reinforcement crossing the shear plane	—	—
A_{vf}	total area of reinforcement, including flexural reinforcement	A_{vf} (5.10.11.4.4)	—
A_{v-min}	minimum area of web reinforcement	—	—
a	distance from the end of beam to harp point or concentrate load	—	—
a	depth of equivalent rectangular stress block	a (5.7.2.2)	a (8.16.2.7, 9.17.2)
a	lateral dimension of the anchorage device measured	a (5.10.9.6.2)	—
a_f	distance between concentrated load and face of support	a_f (5.13.2.5.1)	—
a_v	shear span, distance between concentrated load and face of support	a_v (5.13.2.4.1)	a_v (8.15.5.8, 8.16.6.8)
B	constant	—	—
BR	vehicular braking force	BR (3.3.2)	—
b	the lateral dimension of the anchorage device measured parallel to the smaller dimension of the cross-section	b (5.10.9.6.2)	—
b	width of bottom flange of the beam	—	—
b	effective flange width	—	—
b	width of beam	b (4.6.2.2.1)	—
b	width of compression face of member	b (5.7.3.1.1)	b (8.1.2)
b	width of pier or diameter of pile	—	b (3.18.2.2.4)
b_b	width of bottom flange of beam	—	—

SYMBOL	DESCRIPTION	CORRESPONDING AASHTO LRFD SPECIFICATIONS	CORRESPONDING AASHTO STANDARD SPECIFICATIONS
b'	width of web of a flanged member	—	b' (9.1.2)
b_v, b_e	effective web width of the precast beam	b_v (5.8.2.7)	—
b_v	effective width of the shear flow path	b_v (5.8.6.3)	—
b_v	width of interface or actual contact width between the slab and the beam	b_v (5.8.4.1)	b_v (9.20)
b_w	web width	b_w (5.7.3.1.1)	b_w (8.15.5.1.1)
b_w	width of web adjusted for the presence of ducts	b_w (5.8.2.5)	—
C	centrifugal force in percent of live load	—	C (3.10.1)
C_a	creep coefficient for deflection at time of erection due to loads applied at release	—	—
C_u	ultimate creep coefficient for concrete at time of release of prestressing	—	—
C_u'	ultimate creep coefficient for concrete at time of application of the superimposed dead loads	—	—
CE	vehicular centrifugal force	CE (3.3.2)	—
CR	force effects due to creep	CR (3.3.2)	—
CT	vehicular collision force	CT (3.3.2)	—
CV	vessel collision force	CV (3.3.2)	—
$C(t, t_0)$	creep coefficient of the concrete member at a certain age	—	—
$C(t, t_j)$	creep coefficient at time t_j ($j = 0, 1, 2, \dots$)	—	—
$C_b(t, t_3)$	creep at time t for beam concrete loaded at time t_3	—	—
$C_d(t, t_3)$	creep at time t for deck concrete loaded at time t_3	—	—
c	cohesion factor	c (5.8.4.1)	—
c	vehicular braking force	—	—
c	distance from extreme compression fiber to neutral axis	c (5.7.2.2)	c (8.16.2.7)
c_1	constant related to skew factor	—	—
D	parameter used in determination of load fraction of wheel load	—	D (3.23.4.3)
D	prestressing steel elongation	—	—
D	width of distribution per lane	—	—
D	dead load	D (3.3.2)	D (3.22)
DC	dead load of structural components and nonstructural attachments	DC (5.14.2.3.2)	—
DD	downdrag	DD (3.3.2)	—
D.F.	fraction of wheel load applied to beam	—	D.F. (3.28.1)

SYMBOL	DESCRIPTION	CORRESPONDING AASHTO LRFD SPECIFICATIONS	CORRESPONDING AASHTO STANDARD SPECIFICATIONS
DFD	distribution factor for deflection	—	—
DFM	distribution factor for bending moment	—	—
DFV	distribution factor for shear force	—	—
DL	contributing dead load	—	DL (3.1)
DW	dead load of wearing surfaces and utilities	DW (3.3.2, 5.14.2.3.2)	—
d	distance from extreme compressive fiber to centroid of the pretensioning force	—	d (9.1.2)
d	depth of beam or stringer	d (4.6.2.2.1)	—
d	precast beam depth	—	—
d	distance from extreme compressive fiber to centroid of the reinforcing but not less than 0.8h . In negative moment section, the reinforcement is assumed to be located at the mid-height of the slab. For computing horizontal shear strength of composite members, d should be the distance from extreme compression fiber to centroid of tension reinforcement for entire composite section.	—	d (9.1.2)
d _b	nominal strand diameter	d _b (5.10.2.1)	d _b (8.1.2)
d _b	nominal diameter of prestressing steel	d _b (5.10.2.1)	D (9.17, 9.27)
d _c	thickness of concrete cover measured from extreme tension fiber to center of the flexural reinforcement located closest thereto	d _c (5.7.3.4)	d _c (8.16.8.4)
d _e	horizontal distance from the centerline of exterior web of the exterior beam at deck level and interior edge of curb or traffic barrier	d _e (4.6.2.2.1)	—
d _e	effective depth from extreme compression fiber to the centroid of the tensile force in the tensile reinforcement	d _e (5.7.3.3.1)	—
d _{ext}	depth of the extreme steel layer from extreme compression fiber	—	—
d _i	depth of steel layer from extreme compression fiber	—	—
d _p	distance from extreme compression fiber to the centroid of the prestressing strands	d _p (5.7.3.1.1)	—
d _s	distance from extreme compression fiber to the centroid of the non-prestressed tensile reinforcement	d _s (5.7.3.2.2)	d _t (9.7, 9.17-9.19)
d _v	effective shear depth	d _v (5.8.2.7)	—
d _v	distance between the centroid of the tension steel and the mid-thickness of the slab	—	—
d'	distance from extreme compression fiber to centroid of nonprestressed compression reinforcement	d' (5.7.3.2.2)	d' (8.1.2)

SYMBOL	DESCRIPTION	CORRESPONDING AASHTO LRFD SPECIFICATIONS	CORRESPONDING AASHTO STANDARD SPECIFICATIONS
d"	distance from centroid of gross section, neglecting the reinforcement, to centroid of tension reinforcement	—	d (8.1.2) "
E	modulus of elasticity	—	—
E	width of slab over which a wheel load is distributed	—	E (3.24.3)
E _b	the modulus of elasticity of the bearing plate material	E _b (5.10.9.7.2)	—
E _c	modulus of elasticity of concrete	E _c (5.4.2.4)	E _c (3.26.3, 8.7.1)
E _{cb}	modulus of elasticity for beam concrete		
E _{cd}	modulus of elasticity of deck concrete		
E _{ci}	modulus of elasticity of the concrete beam at transfer	E _{ci} (5.9.5.2.3a)	—
E _{eff}	effective modulus of elasticity	E _{eff} (C5.14.2.3.6)	—
E _p , E _s	modulus of elasticity of pretensioning strands	E _p (5.4.4.2)	E _s (9.16.2.1.2)
E _s	modulus of elasticity of reinforcing bars	E _s (5.4.3.2)	E _s (3.26.3, 8.7.2)
E _c *	age adjusted effective modulus of concrete for a gradually applied load at the time of release of prestressing	—	—
EH	horizontal earth pressure load	EH (3.3.2)	—
EL	miscellaneous locked-in force effects resulting from the construction process, including jacking apart of cantilevers in segmental construction	—	—
EQ	earthquake load	EQ (3.3.2)	EQ (3.22.1)
EQ	equivalent static horizontal force applied at the center of gravity of the structure	—	EQ (3.1)
ES	earth surcharge load	ES (3.3.2)	—
EV	vertical pressure from dead load of earth fill	EV (3.3.2)	—
e	eccentricity of the strands at h/2	—	—
e	eccentricity of strands at transfer length	—	—
e	correction factor	e (4.6.2.2.1)	—
e	eccentricity of a lane from the center of gravity of the pattern of beams	e (4.6.2.2.2d)	—
e	the eccentricity of the anchorage device or group of devices, with respect to the centroid of the cross-section, always taken as positive	e (5.10.9.6.3)	—
e'	difference between eccentricity of pretensioning steel at midspan and end of the beam	—	—
e _c	eccentricity of the strand at the midspan	—	—
e _d	eccentricity of deck with respect to the gross composite section	—	—

SYMBOL	DESCRIPTION	CORRESPONDING AASHTO LRFD SPECIFICATIONS	CORRESPONDING AASHTO STANDARD SPECIFICATIONS
e_e	eccentricity of prestressing force at end of beam	—	—
e_g	distance between the centers of gravity of the beam and slab	e_g (4.6.2.2.1)	—
e_g	distance between the centers of gravity of the stems and the flange of the precast beam	—	—
e_j	initial lateral eccentricity of the center of gravity with respect to the roll axis	—	—
e_m	average eccentricity at midspan	—	—
e_p	eccentricity of the prestressing strands with respect to the centroid of the section	—	—
e_{pc}	eccentricity of prestressing strands with respect to centroid of composite section	—	—
e_{tc}	eccentricity of strands with respect to transformed composite section at final time	—	—
e_{pc}	strand eccentricity at midspan with respect to centroid of girder	—	—
e_{pg}	eccentricity of strands with respect to transformed composite section at final time	—	—
e_{tf}	eccentricity of strands with respect to transformed composite section at final time	—	—
e_{ti}	eccentricity of strands with respect to transformed section at transfer	—	—
F_b	allowable tensile stress in the precompressed tensile zone at service loads	—	—
F_b	allowable bending stress	—	F_b (2.7.4.2)
F_{cj}	force in concrete for the j th component	—	—
FR	Friction force	FR (3.3.2)	—
F_{pi}	total force in strands before release	—	—
F_ϵ	reduction factor	F_ϵ (5.8.3.4.2)	—
FS_c	factor of safety against cracking	—	—
FS_f	factor of safety against failure	—	—
f	stress	—	—
f_b	concrete stress at the bottom fiber of the beam	—	—
f_b	average bearing stress in concrete on loaded area	—	f_b (8.15.2.1.3, 8.16.7.1)
f_c	extreme fiber compressive stress in concrete at service loads	—	f_c (8.15.2.1.1)

SYMBOL	DESCRIPTION	CORRESPONDING AASHTO LRFD SPECIFICATIONS	CORRESPONDING AASHTO STANDARD SPECIFICATIONS
f'_c	specified compressive strength of concrete at 28 days, unless another age is specified	f'_c (5.4.2.1)	f'_c (8.1.2)
f_{ca}	concrete compressive stress ahead of the anchorage devices	f_{ca} (5.10.9.6.2)	.
f_{cds}	average concrete compressive stress at the c.g. of the prestressing steel under full dead load	.	f_{cds} (9.16)
f_{cgp}	sum of concrete stresses at the center of gravity of pretensioning tendons, due to pretensioning force at transfer and the self-weight of the member at the section of maximum positive moment	f_{cgp} (5.9.5.2.3a)	f_{cir} (9.16)
f'_{ci}	compressive strength of concrete at time of initial prestress	f'_{ci} (5.9.1.2)	f'_{ci} (9.15)
f_{ct}	average splitting tensile strength of lightweight aggregate concrete	f_{ct} (5.8.2.2)	f_{ct} (9.1.2)
f_{cpe}	compressive stress in concrete due to effective prestress force only (after allowance for all prestress losses) at extreme fiber of section where tensile stress is caused by externally applied loads	—	—
$(f'_c)_t$	compressive strength of concrete at t days	—	—
f_{cu}	the limiting concrete compressive stress for design by strut-and-tie model	f_{cu} (5.6.3.3.1)	—
f_d	stress due to unfactored dead load, at extreme fiber of section where tensile stress is caused by externally applied loads	—	f_d (9.20)
f_f	fatigue stress range in reinforcement	f_f (5.5.3.2)	f_f (8.16.8.3)
$f_{(L+I)}$	live load plus impact bending stress	—	—
f_{min}	algebraic minimum stress level in reinforcement	f_{min} (5.5.3.2)	f_{min} (8.16.8.3)
f_n	nominal concrete bearing stress	f_n (5.10.9.7.2)	—
f_{pb}	compressive stress at bottom fiber of the beam due to prestress force	—	—
f_{pbt}	stress in the prestressing strand before transfer		
f_{pc}	compressive stress in concrete after all prestress losses have occurred either at the centroid of the cross section resisting live load or at the junction of the web and flange when the centroid lies in the flange. In a composite section, f_{pc} is the resultant compressive stress at the centroid of the composite section, or at the junction of the web and flange when the centroid lies within the flange, due to both prestress and to the bending moments resisted by the precast member acting alone.	f_{pc} (C5.6.3.5)	f_{pc} (9.20)
f_{pe}	effective stress in the prestressing stands after all losses	f_{pe} (5.6.3.4.1)	—

SYMBOL	DESCRIPTION	CORRESPONDING AASHTO LRFD SPECIFICATIONS	CORRESPONDING AASHTO STANDARD SPECIFICATIONS
f_{pe}	compressive stress in concrete due to effective prestress forces only (after allowance for all prestress losses) at extreme fiber of section where tensile stress is caused by externally applied loads	—	f_{pe} (9.20)
f_{pi}	initial stress immediately before transfer	—	—
f_{pj}	stress in the prestressing steel at jacking	f_{pj} (5.9.3)	—
f_{po}	a parameter taken as modulus of elasticity of prestressing tendons multiplied by the locked-in difference in strain between the prestressing tendons and the surrounding concrete	f_{po} (5.8.3.4.2)	—
f_{ps}	average stress in prestressing strand for which the nominal resistance of member is required	f_{ps} (C5.6.3.3.3)	—
f_{pt}	stress in prestressing steel immediately after transfer	f_{pt} (5.9.3)	—
f_{pu}, f'_s	Specified tensile strength of prestressing steel	f_{pu} (5.4.4.1)	f'_s (9.15, 9.17)
f_{py}	yield strength of prestressing strand or steel	f_{py} (5.4.4.1)	f_y^* (9.15)
f_r	the modulus of rupture of concrete	f_r (5.4.2.6)	f_r (9.18, 8.15.2.1.1)
f_s	allowable stress in steel	—	—
f_{se}	effective final pretension stress	—	—
f_{si}	effective initial pretension stress	—	—
f_{ss}	tensile stress in steel reinforcement at the service limit state	5.7.3.4	f_s (8.15.2.2)
f_{su}^*	stress in prestressing tension steel at ultimate load	—	f_{su}^*
f_t	extreme fiber tensile stress in concrete at service loads	—	f_t (8.15.2.1.1)
f_t	concrete stress at top fiber of the beam for the non-composite section	—	—
f_{tc}	concrete stress at top fiber of the slab for the composite section	—	—
f_{tg}	concrete stress at top fiber of the beam for the composite section	—	—
f_{tg}	concrete stress at top fiber of the beam for the transformed section under fatigue loading	—	—
f_y	specified yield strength of non-prestressed conventional reinforcement	f_y (5.5.4.2.1), f_y' (5.7.3.1.1)	f_y (8.1.2), f_y' (9.19)
f_y	specified yield strength of reinforcing bars	—	—
f_y	specified yield strength of compression reinforcement	—	—
f_{yh}	specified yield strength of transverse reinforcement	f_{yh} (5.7.4.6)	—
g	distribution factor	g (4.6.2.2.1)	—
H	average annual ambient mean relative humidity, percent	H (5.4.2.3.2)	RH (9.16.2.1.1)

SYMBOL	DESCRIPTION	CORRESPONDING AASHTO LRFD SPECIFICATIONS	CORRESPONDING AASHTO STANDARD SPECIFICATIONS
H	height of wall	H (A13.4.2)	—
H	overall depth of a member	—	—
H	length of a single segment	—	—
h	overall thickness or depth of a member	h (5.8.2.7)	h (9.20)
h_c	total height or depth of composite section	—	—
h_{cg}	height of center of gravity of beam above road	—	—
hd	deck thickness	—	—
h_f	compression flange thickness	h_f (5.7.3.1.1)	h_f (8.1.2)
h_r	height of roll center above road	—	—
I	live load impact	—	—
I	moment of inertia	—	—
I	moment of inertia of beam	—	—
I	moment of inertia about the centroid of the non-composite precast beam, major axis moment of inertia of beam	I_g (5.7.3.6.2)	I (9.20)
I_{bs}	moment of inertia of beam stems	—	—
I_c	moment of inertia of composite section	—	—
I_{cr}	moment of inertia of cracked section transformed to concrete	I_{cr} (5.7.3.6.2)	I_{cr} (8.13.3)
I_e	effective moment of inertia	I_e (5.7.3.6.2)	I_e (8.13.3)
I_{eff}	effective cracked section lateral (minor axis) moment of inertia	—	—
I_g	gross lateral (minor axis) moment of inertia	—	—
I_g	effective cracked section lateral (minor axis) moment of inertia	—	—
I_g	moment of inertia about the centroid of the non-composite precast beam	I_g (5.7.3.6.2)	I_g (3.23.4.3, 8.1.2, 9.20)
I_k	moment of inertia of element k	—	—
I_s	moment of inertia of reinforcement about centroidal axis of member cross section	I_s (5.7.4.3)	I_s (8.1.2)
I_{tc}	moment of inertia of the transformed composite section at final time	—	—
I_{ti}	moment of inertia of the transformed section at transfer	—	—
I_{tf}	moment of inertia of the transformed section at final time	—	—
IC	ice load	—	—
IM	vehicular dynamic load allowance	IM (3.6.1.2.5)	I (3.8.2)

SYMBOL	DESCRIPTION	CORRESPONDING AASHTO LRFD SPECIFICATIONS	CORRESPONDING AASHTO STANDARD SPECIFICATIONS
J	gross St. Venant torsional constant of the precast member	J (4.6.2.2.1)	J (3.23.4.3)
J_g	St. Venant torsional inertia	—	—
j	a factor relating lever arm to effective depth	—	—
K	a non-dimensional constant	—	—
K	factor used in calculation of average stress in pretensioning steel for strength limit state; factor related to type of strand	—	—
K	effective length factor for compression members	K (5.7.4.1)	k (8.16.5.2.3)
K	factor used for calculating time-dependent losses	—	—
K	factor used in the calculation of development length	—	—
K	wobble friction coefficient	K (5.9.5.2.2b)	K (9.16)
K_1	correction factor for source of aggregate	—	—
K_1	fraction of concrete strength available to resist interface shear	—	—
K_2	limiting interface shear resistance	—	—
K_{df}	transformed section coefficient that accounts for time-dependent interaction between concrete and bonded steel in the section being considered for time period between deck placement and final time	—	—
K_g	longitudinal stiffness parameter	K_g (4.6.2.2.1)	K (3.23.4)
K_{id}	transformed section coefficient that accounts for time-dependent interaction between concrete and bonded steel in the section being considered for time period between transfer and deck placement	—	—
K_L	factor accounting for type of steel taken as 30 for low relaxation strands and 7 for other prestressing steel, unless more accurate manufacturer's data are available	—	—
k	factor used in calculation of distribution factor for multi-beam bridges	k (4.6.2.2)	—
k	factor used in calculation of average stress in prestressing strand for Strength Limit State	—	—
k_c	a factor for the effect of the volume-to-surface ratio	k_c (5.4.2.3.2)	—
k_{cp}	correction factor for curing period	—	—
k_f	a factor for the effect of concrete strength	k_f (5.4.2.3.2)	—
k_h	correction factor for relative humidity	k_h (5.4.2.3.3)	—
k_{hc}	humidify factor for creep	—	—
k_{hs}	humidity factor for shrinkage	—	—

SYMBOL	DESCRIPTION	CORRESPONDING AASHTO LRFD SPECIFICATIONS	CORRESPONDING AASHTO STANDARD SPECIFICATIONS
k_{1a}	correction factor for loading age	—	—
k_{sh}	product of applicable correction factors = $k_{cp} (k_h) (k_s)$	—	—
k_s	correction factor for size of member	k_s (5.4.2.3.3)	—
k_{td}	time development factor	—	—
k_{tdd}	time development factor at deck placement	—	—
k_{tdf}	time development factor at final time	—	—
k_{vs}	factor for the effect of volume-to-surface ratio	—	—
L	length in feet of the span under consideration for positive moment and the average of two adjacent loaded spans for negative moment	—	L (3.8.2.1)
L	Overall beam length or design span length	—	—
LL	vehicular live load	LL (3.3.2)	L (3.22)
L_c	critical length of yield line failure pattern	L_c (A13.4.2)	—
LS	live load surcharge	LS (3.3.2)	—
L_r	intrinsic relaxation of the strand	—	—
ℓ	overall length of beam	—	—
ℓ_d	development length	—	—
ℓ_t	transfer length	—	—
ℓ_u	unsupported length of compression member	ℓ_u (5.7.4.1)	ℓ_u (8.16.5.2.1)
M_a	negative moment at the end of the span being considered	—	—
M_b	negative moment at the end of the span being considered	—	—
M_b	unfactored bending moment due to barrier weight	—	—
M_c	moment in concrete beam section	—	—
M_c	flexural resistance of barrier at its base	—	—
M_{CIP}	unfactored bending moment due to cast-in-place slab weight	—	—
M_{const}	unfactored bending moment due to construction load	—	—
M_{cr}	moment causing flexural cracking at section due to externally applied loads	M_{cr} (5.7.3.6.2)	M_{cr} (8.13.3, 9.20)
M_{cr}	cracking moment	—	M_{cr}^* (9.18)
$M_{cr}(t)$	restraint moment due to creep at time t	—	—
M_d	unfactored bending moment due to diaphragm weight per beam	—	—
M_{dnc}	noncomposite dead load moment at the section	—	$M_{d/nc}$ (9.18)
M_{el}	fictitious elastic restraint moment at the supports	—	—

SYMBOL	DESCRIPTION	CORRESPONDING AASHTO LRFD SPECIFICATIONS	CORRESPONDING AASHTO STANDARD SPECIFICATIONS
M_f	unfactored bending moment due to fatigue truck per beam	—	—
M_g	unfactored bending moment due to beam self-weight	—	—
M_g	self-weight bending moment of beam at harp point	—	—
M_{gmsp}	self-weight bending moment at midspan	—	—
M_j	unfactored bending moment due to joint concrete weight	—	—
M_k	element moment	—	—
$M_{lat=}$	lateral bending moment at cracking	—	—
M_{LL}	unfactored bending moment due to lane load per beam	—	—
M_{LL+I}	unfactored bending moment due to live load plus impact	—	—
M_{LL+LT}	unfactored bending moment due to truck load plus impact and lane load = $M_{LT} + M_{LL}$	—	—
M_{LT}	unfactored bending moment due to truck load with dynamic allowance per beam	—	—
M_{max}	maximum factored moment at section due to externally applied loads	—	M_{max} (9.20)
M_n	nominal flexural resistance	M_n (5.7.3.2.1)	M_n (9.1.2)
$M_{n/dc}$	non-composite dead load moment at the section	—	—
M_r	factored flexural resistance of a section in bending	M_r (5.7.3.2.1)	—
M_s	unfactored bending moment due to slab and haunch weights	—	—
$M_{service}$	total bending moment for service load combination	—	—
M_{sh}	shrinkage moment	—	—
$M_{sr}(t)$	restraint moment due to differential shrinkage at time t	—	—
M_{sw}	moment at section of interest due to self-weight of the member plus any permanent loads acting on the member at time of release	—	—
M_{SIP}	unfactored bending moment due to stay-in-place panel self-weight	—	—
M_u	factored moment at section $\leq \Phi M_n$	M_u (C5.6.3.1)	M_u (9.17, 9.18)
M_{ws}	unfactored bending moment due to wearing surface	—	—
M_x	bending moment at a distance (x) from the support	—	—
M_0	theoretical total moment in sections	—	—
M_{0k}	theoretical moment in section of element k	—	—
m	multiple presence factor	—	—

SYMBOL	DESCRIPTION	CORRESPONDING AASHTO LRFD SPECIFICATIONS	CORRESPONDING AASHTO STANDARD SPECIFICATIONS
m	stress ratio = $(f_y/0.85)$	—	—
N	number of segments between nodes (must be even number)	—	—
N_b	number of beams	N_b (4.6.2.2.1)	N_B (3.28.1)
N_c	internal element force in concrete	—	—
N_k	element normal force	—	—
N_L	number of loaded lanes under consideration	—	—
N_s	internal element force in steel	—	—
N_u	applied factored axial force taken as positive if tensile	—	—
N_{uc}	factored axial force normal to the cross section, occurring simultaneously with V_u to be taken as positive for tension, negative for compression; includes effects of tension due to creep and shrinkage	N_{uc} (5.13.2.4.1)	N_u (8.16.6.2.2)
N_0	theoretical total normal force in sections	—	—
N_{0k}	theoretical normal force in section of element k	—	—
n	modular ratio of elasticity - E_s/E_c	n (5.7.1)	n (8.15.3.4)
n	modular ratio between slab and beam materials	—	—
n	modular ratio between beam and deck slab concrete	—	—
n	modular ratio between prestressing strand and concrete	—	—
n_k	modular ratio of element k	—	—
n_s	modular ratio of steel element	—	—
P	concentrated wheel load	P (3.6.1.2.5)	—
P	live load intensity	P (C3.11.6.2)	—
P	live load on sidewalk	—	P (3.14.1.1)
P	load on one rear wheel of truck	—	P (3.24.3)
P	Diaphragm weight concentrated at quarter points	—	—
PPR	partial prestress ratio	—	—
P_c	permanent net compression force	P_c (5.8.4.1)	—
P_d	diaphragm weight	—	—
P_{eff}	effective post-tensioning force	—	—
P_i	total pretensioning force immediately after transfer	—	—
P_n	nominal axial load strength at given eccentricity	P_n (5.5.4.2.1)	P_n (8.1.2)
P_n	nominal axial resistance of strut or tie	P_n (5.6.3.2)	—
P_n	nominal bearing resistance	P_n (5.7.5)	—

SYMBOL	DESCRIPTION	CORRESPONDING AASHTO LRFD SPECIFICATIONS	CORRESPONDING AASHTO STANDARD SPECIFICATIONS
P_{nx}	nominal axial load strength corresponding to M_{nx} , with bending considered in the direction of the x axis only	—	P_{nx} (8.16.4.3)
P_{ny}	nominal axial load strength corresponding to M_{ny} , with bending considered in the direction of the y axis only	—	P_{ny} (8.16.4.3)
P_{nxy}	nominal axial load strength with biaxial loading	—	P_{nxy} (8.16.4.3)
P_o	nominal axial load strength of a section at 0.0 eccentricity	P_o (5.7.4.5)	P_o (8.16.4.2.1)
P_{pe}	total prestressing force after all losses	—	—
P_{pi}	total prestressing force before transfer	—	—
P_{pt}	total prestressing force immediately after transfer	—	—
P_{se}	effective pretension force after allowing for all losses	—	—
P_{si}	effective pretension force after allowing for the initial losses	—	—
P_r	factored axial resistance of strut or tie	—	—
P_u	factored tendon force	5.10.9	—
PL	pedestrian live load	PL (3.3.2)	—
PS	secondary forces from post-tensioning	—	—
p	fraction of truck traffic in a single lane	p (3.6.1.4.2)	—
p	A_s'/bd , ratio of non-prestressed tension reinforcement	—	p (9.7, 9.17-9.19)
p'	A_s'/bd , ratio of compression reinforcement	—	p' (9.19)
p*	A_s^*/bd , ratio of prestressing steel	—	p* (9.17, 9.19)
p_c	outside perimeter of the concrete section	p_c (5.8.2.1)	—
p_h	perimeter of the centerline of the closed transverse torsion reinforcement	p_h (5.8.3.6.2)	—
Q	first moment of inertia of the area above the fiber being considered	—	—
Q	statical moment of cross sectional area, above or below the level being investigated for shear, about the centroid	—	Q (9.20)
Q	total factored load	Q (3.4.1)	—
Q_i	force effects from specified loads	—	—
q_i	specified loads	q_i (3.4.1)	—
R_n	strength design factor	—	—
R_n	nominal resistance	—	—
R_u	flexural resistance factor	—	—
R_w	total transverse resistance of the railing or barrier	R_w (A13.4.2)	—
r	radius of gyration of the gross cross section	r (5.7.4.1)	r (8.16.5.2.2)
r	radius of stability	—	—

SYMBOL	DESCRIPTION	CORRESPONDING AASHTO LRFD SPECIFICATIONS	CORRESPONDING AASHTO STANDARD SPECIFICATIONS
r/h	ratio of base radius to height of rolled-on transverse deformations	r/h (5.5.3.2)	—
S	coefficient related to site conditions for use in determining seismic loads)	S (3.10.5)	—
S	surface area of concrete exposed to drying	—	—
S	span between the inside faces of the beam webs	—	—
S	effective span length of the deck slab	—	S (3.25.1.3)
S _b	section modulus for the extreme bottom fiber of the non-composite precast beam	—	—
S _{bc}	Composite section modulus for the extreme bottom fiber of the precast beam or panel	—	—
S _{btc}	section modulus for the extreme bottom fiber of the transformed composite section at final time	—	—
S _{btf}	section modulus for the extreme bottom fiber of the transformed non composite section at final time	—	—
S _c	section modulus of cast-in-place deck	—	—
S _t	section modulus for the extreme top fiber of the non-composite precast beam	—	—
S _{tc}	composite section modulus for top fiber of the structural deck slab or panel	—	—
S _{tg}	composite section modulus for top fiber of the precast beam or panel	—	—
S _{ttc}	composite section modulus for the extreme top fiber of the precast beam for transformed section at final time	—	—
S _{tff}	section modulus for the extreme top fiber of the transformed section at final time	—	—
S _{tft}	section modulus for the extreme top fiber of the transformed section at transfer	—	—
S(t,t ₀)	shrinkage strain at a concrete age of t days	—	—
SE	Force effects due to settlement	SE (3.3.2)	—
SH	Force effects due to shrinkage	SH (3.3.2, 5.14.2.3.2)	S (3.22)
SR	fatigue stress range	—	—
s	effective deck span	—	s (3.25.1.3)
s	length of a side element	s (C4.6.2.2.1)	—
s	spacing of rows of ties or stirrups	s (5.8.4.1)	—
T	collision force at deck slab level	13.4.2	—

SYMBOL	DESCRIPTION	CORRESPONDING AASHTO LRFD SPECIFICATIONS	CORRESPONDING AASHTO STANDARD SPECIFICATIONS
T_{burst}	the tensile force in the anchorage zone acting ahead of the anchorage device and transverse to the tendon axis	T_{burst} (5.10.9.6.3)	—
T_{cr}	torsional cracking resistance	T_{cr} (5.8.2.1)	—
T_n	nominal torsion resistance	T_n (5.8.2.1)	—
T_T	factored torsional resistance provided by circulatory shear flow	T_r (5.8.2.1)	—
T_u	factored torsional moment	T_u (C5.6.3.1)	—
TG	force effect due to temperature gradient	TG (3.3.2, C4.6.6)	—
TU	force effect due to uniform temperature	TU (3.3.2)	—
t	thickness of web	—	—
t	thickness of a side element	—	—
t	time, days; age of concrete at the time of determination of creep effects, days; age of concrete at time of determination of shrinkage effects, days; time after loading, days	t (5.4.2.3.2)	—
t	average thickness of the flange of a flanged member	—	t (9.17, 9.18)
t	deck thickness	—	t (3.25.1.3)
t_d	concrete age at deck placement	—	—
t_f	thickness of flange	—	—
t_f	concrete age at final stage	—	—
t_i	age of concrete at transfer	t_i (5.4.2.3.2)	—
t_{la}	loading ages in days	—	—
t_s	depth of concrete slab	t_s (4.6.2.2.1)	—
t_s	cast-in-place concrete slab thickness	—	—
t_o	age of concrete in days at the end of the initial curing period	—	—
V	design shear force at section	—	V (8.15.5.1.1)
V	distance between axles	—	—
V	variable spacing of truck axles	—	V (3.7.6)
V	volume of concrete	—	—
V_b	unfactored shear force due to barrier weight per beam	—	—
V_c	nominal shear resistance provided by tensile stresses in the concrete	V_c (5.8.2.4)	V_c (9.20, 8.16.6.1)
V_{ci}	nominal shear resistance provided by concrete when inclined cracking results from combined shear and moment	—	V_{ci} (9.20)
V_{cw}	nominal shear resistance provided by concrete when inclined cracking results from excessive principal tensions in web	—	V_{cw} (9.20)

SYMBOL	DESCRIPTION	CORRESPONDING AASHTO LRFD SPECIFICATIONS	CORRESPONDING AASHTO STANDARD SPECIFICATIONS
V_d	unfactored shear force due to barrier weight/lane	—	V_d (9.20)
V_d	shear force at section due to unfactored dead load and includes both DC and DW		
V_i	factored shear force at section due to externally applied loads occurring simultaneously with M_{max}	—	V_i (9.20)
V_{hi}	horizontal factored shear force per unit length of the beam		
V_{LL}	unfactored shear force due to lane load per beam	—	—
V_{LL+I}	unfactored shear force due to live load plus impact	—	—
V_{LL+LT}	unfactored shear force due truck load plus impact and lane load = $V_{LT} + V_{LL}$		
V_{LT}	unfactored shear force due to truck load with dynamic allowance per beam	—	—
V_{mu}	ultimate shear force occurring simultaneously with M_u	—	—
V_n	nominal shear resistance of the section considered	V_n (5.8.2.1)	V_n (8.16.6.1)
V_{ni}	nominal horizontal shear resistance		
V_{nh}	nominal horizontal shear strength	—	V_{nh} (8.16.6.5.3, 9.20)
V_p	component in the direction of the applied shear of the effective prestressing force, positive if resisting the applied shear	V_p (C5.8.2.3)	V_p (9.20)
V/S	volume-to-surface ratio of the beam	V_s (5.8.3.3)	V_s (8.16.6.1, 9.20)
V_s	shear resistance provided by shear reinforcement		
V_s	unfactored shear force due to slab and haunch weight/beam		
V_T	factored shear resistance	V_r (5.8.2.1)	—
V_u	factored shear force at section	V_u (C5.6.3.1)	V_u (8.16.6.1, 9.20)
V_u	factored shear stress on the concrete		
V_{uh}	factored horizontal shear force per unit length of the beam	—	—
V_{ws}	unfactored shear force due to wearing surface weight/beam		
V_x	shear force at a distance (x) from the support	—	—
v	factored design shear stress	v (5.8.3.4.2)	v (8.15.5.1.1)
v	permissible horizontal shear stress	—	v (9.20)
v_c	permissible shear stress carried by concrete	—	v_c (8.15.5.2)
W	edge-to-edge width of bridge	—	W (3.23.4.3)
W	total weight of beam		
WA	water load and stream pressure	WA (3.3.2)	—

SYMBOL	DESCRIPTION	CORRESPONDING AASHTO LRFD SPECIFICATIONS	CORRESPONDING AASHTO STANDARD SPECIFICATIONS
WL	wind load on live load	WL (3.3.2)	WL (3.22)
WS	wind load on structure		
w	width of clear roadway	w (3.6.1.1.1)	—
w	a uniformly distributed load	—	—
w	weight per unit length of beam		
w _b	weight of barriers per unit length	—	—
w _c	unit weight of concrete	w _c (5.4.2.4)	w _c (8.1.2)
w _g	beam self-weight per unit length	—	—
w _j	weight of joint concrete per unit length		
w _s	slab and haunch weights per unit length	—	—
w _{ws}	weight of future wearing surface per unit length	—	—
X	distance from load to point of support	—	X (3.24.5.1)
X _{ext}	horizontal distance from the center of gravity of the pattern of beams to the exterior beam	X _{ext} (C4.6.2.2.2d)	—
x	the distance from the support to the section under question	—	—
x	horizontal distance from the center of gravity of the pattern of girders to each beam	x (C4.6.2.2.2d)	—
x	length of prestressing steel element from jack end to point x	x (5.9.5.2.2b)	L (9.16)
y	height of center of gravity of beam above roll axis (beam supported from below)		
y _b	distance from centroid to the extreme bottom fiber of the non-composite precast beam	—	—
y _{bc}	distance from the centroid of the composite section to extreme bottom fiber of the precast beam	—	—
y _{bs}	distance from the center of gravity of strands to the bottom fiber of the beam	—	—
y _{btc}	distance from the centroid of the composite transformed section to the extreme bottom fiber of the beam at final time		
y _{btf}	distance from the centroid of the non-composite transformed section to the extreme bottom fiber of the beam at final time		
y _{bti}	distance from the centroid of the transformed section to the extreme bottom fiber of the beam at transfer		
y _k	distance of the centroid of element k from edge		
y _r	height of roll axis above center of gravity of beam (hanging beam)		
y _s	height above soffit of centroid of prestressing force		

SYMBOL	DESCRIPTION	CORRESPONDING AASHTO LRFD SPECIFICATIONS	CORRESPONDING AASHTO STANDARD SPECIFICATIONS
y_t	distance from centroid to the extreme top fiber of the non-composite precast beam	—	—
y_t	distance from centroidal axis of gross section, neglecting reinforcement, to extreme fiber in tension	y_t (5.7.3.6.2)	y_t (8.13.3, 9.20)
y_{tc}	distance from the centroid of the composite section to extreme top fiber of the structural deck or panel	—	—
y_{tc}	distance from centroid to the top of deck of the composite section	—	—
y_{tg}	distance from the centroid of the composite section to extreme top fiber of the precast beam or panel	—	—
Z	crack control parameter	Z (5.7.3.4)	—
Z	factor reflecting exposure conditions	—	—
z	lateral deflection of center of gravity of beam	—	—
z_{max}	distance from centerline of vehicle to center of dual tires	—	—
z_o	theoretical lateral deflection of center of gravity of beam with the full dead weight applied laterally	—	—
z'_o	theoretical lateral deflection of center of gravity of beam with the full dead weight applied laterally, computed using I_{eff} for tilt angle λ under consideration	—	—
α	angle of inclination of transverse reinforcement to longitudinal axis	α (5.8.3.3)	—
α	super-elevation angle or tilt angle of support in radians	—	—
α	factor used in calculating elastic shortening loss	—	—
α	total angular change of prestressing steel path from jacking end to a point under investigation	α (5.9.5.2.2b)	α (9.16)
α	the angle of inclination of a tendon force, with respect to the centerline of the member	α (5.10.9.6.3)	—
α_h	total horizontal angular change of prestressing steel path from jacking end to a point under investigation	α_h (5.9.5.2.2b)	—
α_s	angle between compressive strut and adjoining tension tie	α_s (5.6.3.3.3)	—
α_v	total vertical angular change of prestressing steel path from jacking end to a point under investigation	α_v (5.9.5.2.2b)	—
β	factor indicating ability of diagonally cracked concrete to transmit tension (a value indicating concrete contribution)	β (5.8.3.3)	—
β	factor relating effect of longitudinal strain on the shear capacity of concrete, as indicated by the ability of diagonally cracked concrete to transmit tension	β (5.8.3.3)	—
β_b	ratio of area of reinforcement cut off to total area of reinforcement at the section	β_b (5.11.1.2.1)	β_b (8.24.1.4.2)

SYMBOL	DESCRIPTION	CORRESPONDING AASHTO LRFD SPECIFICATIONS	CORRESPONDING AASHTO STANDARD SPECIFICATIONS
β_d	absolute value of ratio of maximum dead load moment to maximum total load moment, always positive	β_d (5.7.4.3)	β_d (8.1.2)
β_D	load combination coefficient for dead loads	—	β_D (3.22.1)
β_L	load combination coefficient for live loads	—	β_L (3.22.1)
β_1	ratio of depth of equivalent uniformly stressed compression zone assumed in the strength limit state to the depth of the actual compression zone	β_1 (5.7.2.2)	β_1 (8.16.2.7, 9.17-9.19)
Δ	deflection	—	—
Δ_{beam}	deflection due to beam self-weight	—	—
Δ_{b+ws}	deflection due to barrier and wearing surface weights	—	—
Δ_{fcdp}	change in concrete stress at center of gravity of prestressing steel due to all dead loads, except dead load acting at the time the prestressing force is applied	Δ_{fcdp} (5.9.5.4.3)	—
Δ_{fpA}	loss in prestressing steel stress due to anchorage set	Δ_{fpA} (5.9.5.1)	—
Δ_{fpCR}	loss in prestressing steel stress due to creep	Δ_{fpCR} (5.9.5.1)	CR_c (9.16)
Δ_{pES}	loss in prestressing steel stress due to elastic shortening	Δ_{pES} (5.9.5.1)	ES (9.16)
Δ_{fpF}	loss in prestressing steel stress due to friction	Δ_{fpF} (5.9.5.1)	—
Δ_{fpi}	total loss in pretensioning steel stress immediately after transfer	—	—
Δ_{fpR}	total loss in prestressing steel stress due to relaxation of steel	Δ_{fpR} (5.9.5.1)	CR_s (9.16)
Δ_{fpR1}	loss in prestressing steel stress due to relaxation of steel at transfer	Δ_{fpR1} (5.9.5.4.4b)	—
Δ_{fpR2}	loss in prestressing steel stress due to relaxation of steel after transfer	Δ_{fpR2} (5.9.5.4.4c)	—
Δ_{fpSR}	loss in prestressing steel stress due to shrinkage	Δ_{fpSR} (5.9.5.1)	SH (9.16)
Δ_{fpT}	total loss in prestressing steel stress	Δ_{fpT} (5.9.5.1)	—
Δ_f	total prestress loss, excluding friction	—	Δ_{fs} (9.16)
Δ_d	deflection due to diaphragm weight	—	—
Δ_L	deflection due to specified live load	—	—
Δ_{LL+I}	deflection due to live load and impact	—	—
Δ_{LL}	deflection due to lane load	—	—
Δ_{LT}	deflection due to design truck load and impact	—	—
Δ_{max}	maximum allowable live load deflection	—	—
Δ_p	camber due prestressing force at transfer	—	—
Δ_{SDL}	deflection due to barrier and wearing surface weights	—	—

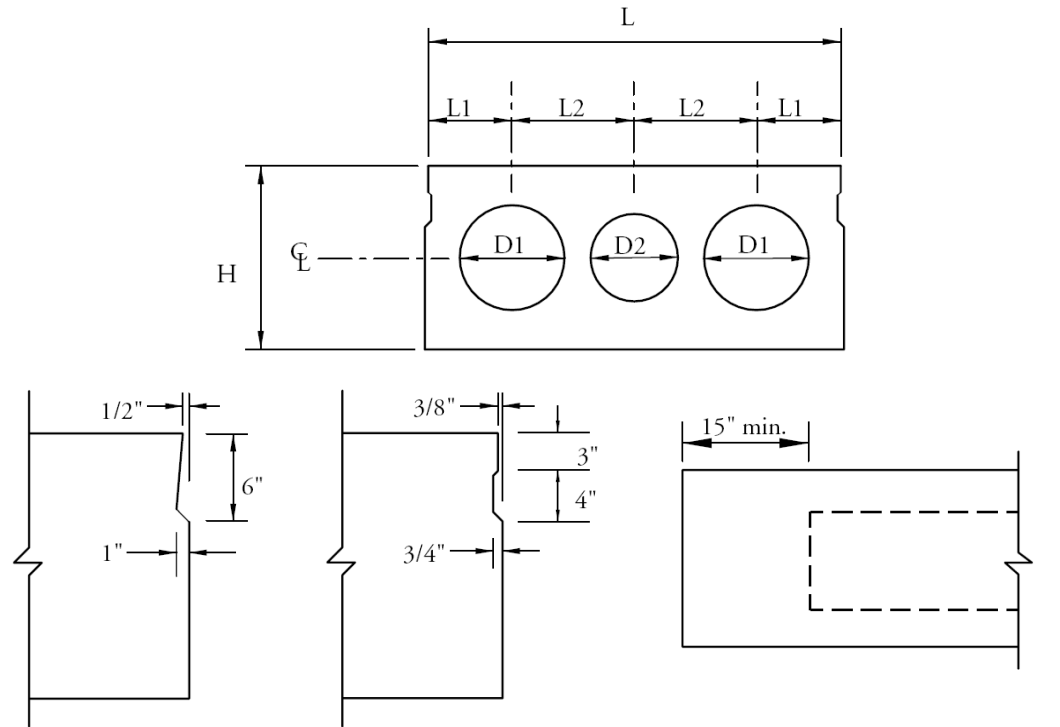
SYMBOL	DESCRIPTION	CORRESPONDING AASHTO LRFD SPECIFICATIONS	CORRESPONDING AASHTO STANDARD SPECIFICATIONS
Δ_{slab}	deflection due to the weights of slab and haunch	—	—
ϵ	strain	—	—
ϵ_{cu}	the failure strain of concrete in compression	ϵ_{cu} (5.7.3.1.2)	—
ϵ_{ps}	strain in prestressing steel	—	—
ϵ_{s}	tensile strain in cracked concrete in direction of tension tie	ϵ_{s} (5.6.3.3.3)	—
ϵ_{sh}	concrete shrinkage strain at a given time	ϵ_{sh} (5.4.2.3.3)	—
ϵ_{si}	strain in tendons corresponding to initial effective pretension stress	—	—
ϵ_{x}	longitudinal strain in the web reinforcement on the flexural tension side of the member	ϵ_{x} (5.8.3.4.2)	—
ϵ_1	principal tensile strain in cracked concrete due to factored loads	ϵ_1 (5.6.3.3.3)	—
Φ	resistance factor	Φ (5.5.4.2.1)	Φ (8.16.1.2)
Φ_{c}	curvature at midspan	—	—
Φ_0	curvature at support	—	—
γ	load factor for Fatigue I load combinations	—	γ (3.22)
γ^*	factor for type of prestressing steel = 0.28 for low-relaxation steel = 0.40 for stress-relieved steel = 0.55 for bars	—	γ^* (9.17)
γ_i	load factors	γ_i (3.4.1)	—
γ_{p}	load factor for permanent loading	γ_{p} (3.4.1)	—
η	variable load modifier which depends on ductility, redundancy and operational classification	η (3.4.1)	—
κ	a correction factor for closely spaced anchorages	κ (5.10.9.6.2)	—
λ	parameter used to determine friction coefficient and it is related to unit weight for concrete	λ (5.8.4.2)	λ (8.15.5.4, 8.16.6.4)
μ	coefficient of friction	μ (5.8.4.1)	μ (8.15.5.4.3)
μ	Poisson's ratio	—	μ (3.23.4.3)
θ	skew angle	—	—
θ	angle of inclination of diagonal compressive stresses	θ (5.8.3.3)	—
θ_{s}	angle between compression strut and longitudinal axis of the member in a shear truss model of a beam	θ_{s} (5.6.3.3.2)	—
ρ	ratio of nonprestressed reinforcement	—	ρ (8.1.2)
ρ'	compression reinforcement ratio = A_s'/b_d	—	ρ' (8.1.2)

SYMBOL	DESCRIPTION	CORRESPONDING AASHTO LRFD SPECIFICATIONS	CORRESPONDING AASHTO STANDARD SPECIFICATIONS
ρ^*	$\frac{A_s^*}{bd}$, ratio of pretensioning reinforcement	—	ρ^* (9.17, 9.19)
ρ_a	actual ratio of nonpretensioned reinforcement	—	—
ρ_b	reinforcement ratio producing balanced strain conditions	—	ρ_b (8.16.3.1.1)
ρ_{min}	minimum ratio of tension reinforcement to effective concrete area	ρ_{min} (5.7.3.3.2)	—
ρ_v	ratio of area of vertical shear reinforcement to area of gross concrete area of a horizontal section	ρ_v (5.10.11.4.2)	—
ψ	a factor that reflects the fact that the actual relaxation is less than the intrinsic relaxation	—	—
ψ	angle of harped pretensioned reinforcement	—	—
$\psi_{(t,t_i)}$	creep coefficient - the ratio of the strain which exists t days after casting to the elastic strain caused when load pi is applied ti days after casting	$\psi_{(t,t_i)}$ (5.4.2.3.2)	—
χ	aging coefficient	—	—

AASHTO Solid and Voided Slab Beams	3
AASHTO Box Beams	5
AASHTO I-Beams	7
AASHTO-PCI Bulb-Tees	9
Deck Bulb-Tees.....	11
Double Tee Beams	13
AASHTO-PCI-ASBI Standard Segment For Span-By-Span Construction.....	15
AASHTO-PCI-ASBI Standard Segment For Balanced Cantilever Construction	17

This page intentionally left blank

AASHTO Solid and Voiced Slab Beams



Typical Keyway Details

Typical Longitudinal Section

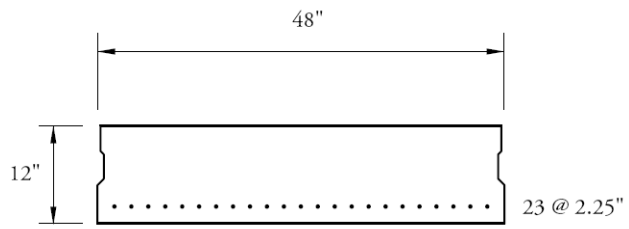
Dimension (inches)

Type	L	H	L1	L2	No. of Voids	D1	D2
SI-36	36	12	-	-	0	-	-
SII-36	36	15	10.5	7.5	2	8	-
SIII-36	36	18	10.5	7.5	2	10	-
SIV-36	36	21	10	8	2	12	-
SI-48	48	12	-	-	0	-	-
SII-48	48	15	10	14	3	8	8
SIII-48	48	18	9.5	14.5	3	10	10
SIV-48	48	21	10	14	3	12	10

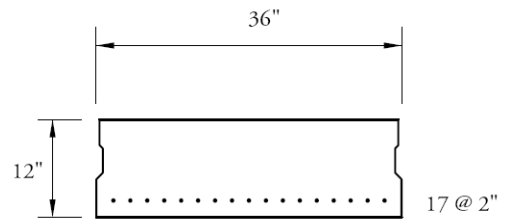
Properties

Type	Area in. ²	y _{bottom} in.	Inertia in. ⁴	Weight kip/ft
SI-36	432	6	5,184	0.45
SII-36	439	7.5	9,725	0.457
SIII-36	491	9	16,514	0.511
SIV-36	530	10.5	25,747	0.552
SI-48	576	6	6,912	0.6
SII-48	569	7.5	12,897	0.593
SIII-48	628	9	21,855	0.654
SIV-48	703	10.5	34,517	0.732

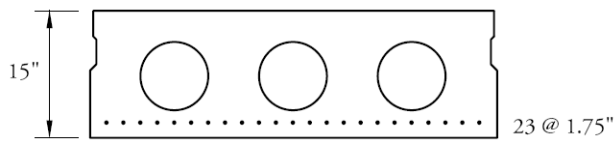
AASHTO Solid and Voided Slab Beams



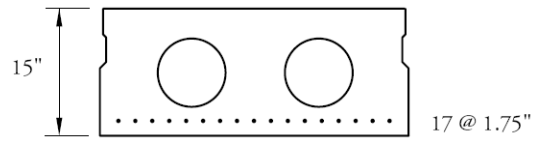
Type SI-48



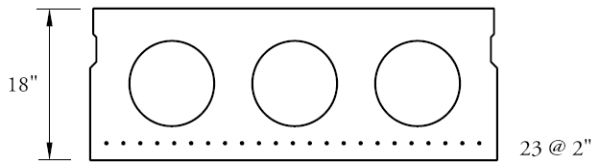
Type SI-36



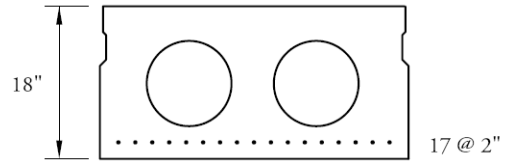
Type SII-48



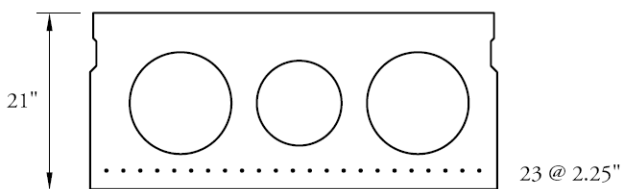
Type SII-36



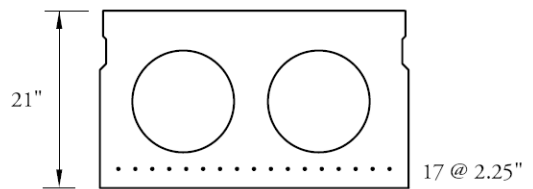
Type SIII-48



Type SIII-36

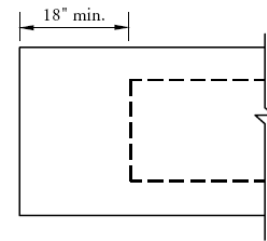
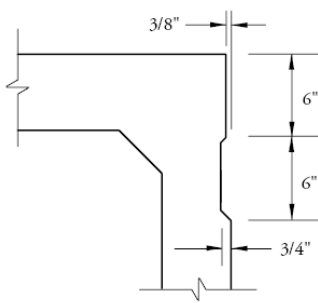
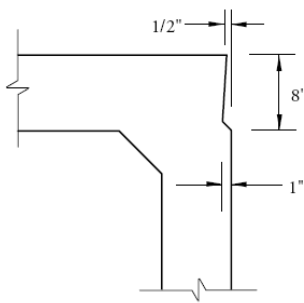
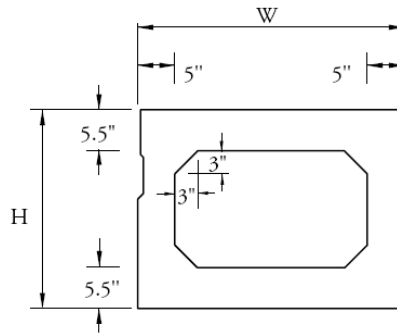


Type IV-48



Type IV-36

AASHTO Box Beams



Typical Keyway Details

Typical Longitudinal Section

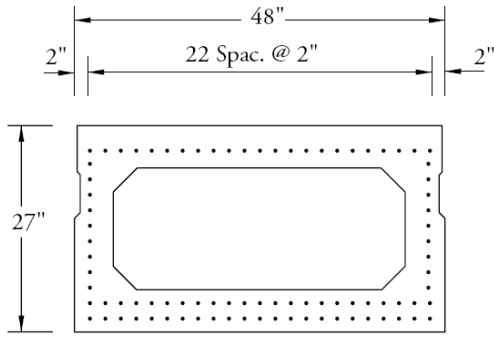
Dimensions:

Type	W	H
BI-36	36	27
BI-48	48	27
BII-36	36	33
BII-48	48	33
BIII-36	36	39
BIII-48	48	39
BIV-36	36	42
BIV-48	48	42

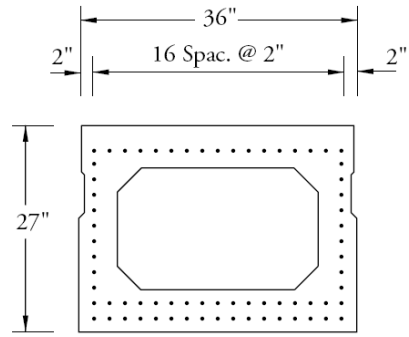
Properties:

Type	Area in. ²	y _{bottom} in.	Inertia in. ⁴	Weight kip/ft
BI-36	560.5	13.35	50,334	0.584
BI-48	692.5	13.37	65,941	0.721
BII-36	620.5	16.29	85,153	0.646
BII-48	752.5	16.33	110,499	0.784
BIII-36	680.5	19.25	131,145	0.709
BIII-48	812.5	19.29	168,367	0.846
BIV-36	710.5	20.73	158,644	0.74
BIV-48	842.5	20.78	203,088	0.878

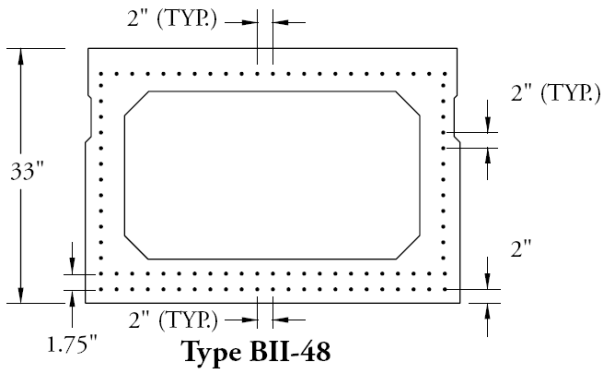
AASHTO Box Beams



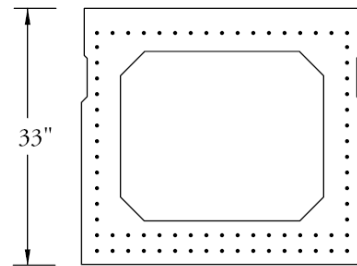
Type BI-48



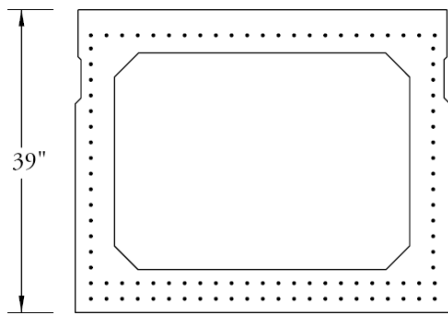
Type BI-36



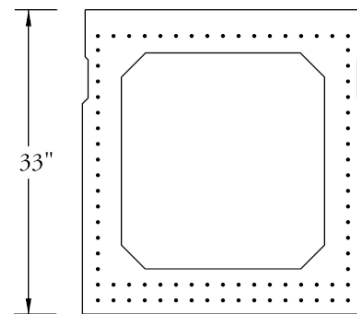
Type BII-48



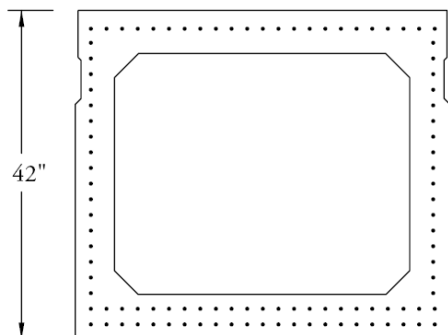
Type BII-36



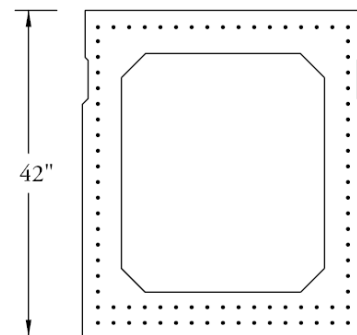
Type BIII-48



Type BIII-36

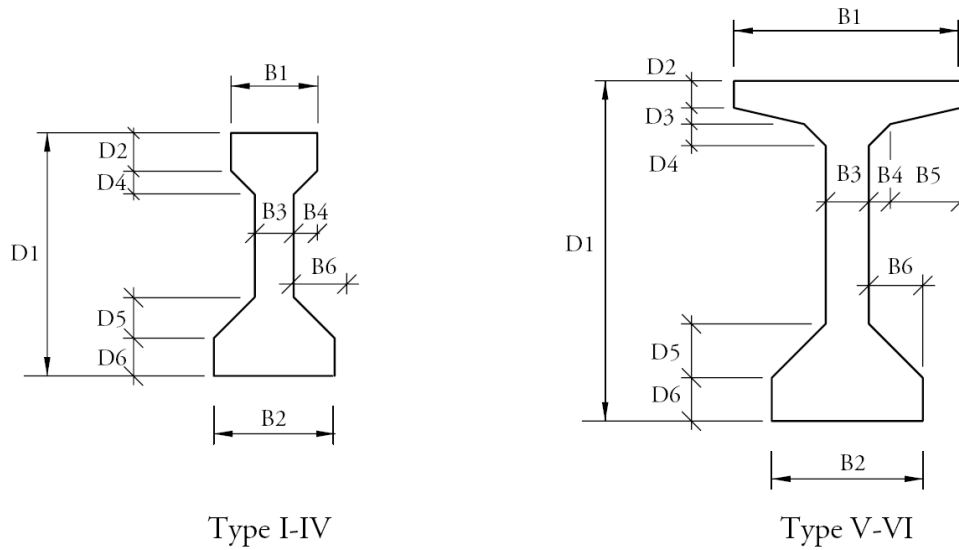


Type BIV-48



Type BIV-36

AASHTO I-Beams



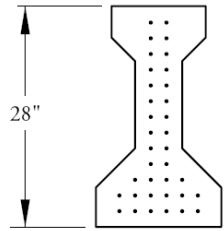
Dimensions (inches)

Type	D1	D2	D3	D4	D5	D6	B1	B2	B3	B4	B5	B6
I	28	4	0	3	5	5	12	16	6	3	0	5
II	36	6	0	3	6	6	12	18	6	3	0	6
III	45	7	0	4.5	7.5	7	16	22	7	4.5	0	7.5
IV	54	8	0	6	9	8	20	26	8	6	0	9
V	63	5	3	4	10	8	42	28	8	4	13	10
VI	72	5	3	4	10	8	42	28	8	4	13	10

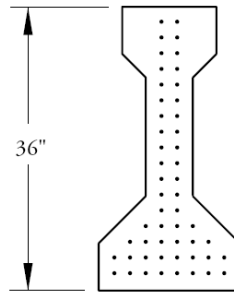
Properties:

Type	Area in. ²	y _{bottom} in.	Inertia in. ⁴	Weight kip/ft
I	276	12.59	22,750	0.287
II	369	15.83	50,980	0.384
III	560	20.27	125,390	0.583
IV	789	24.73	260,730	0.822
V	1,013	31.96	521,180	1.055
VI	1,085	36.38	733,320	1.13

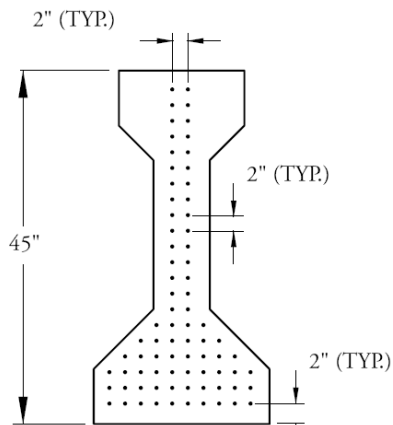
AASHTO I-Beams



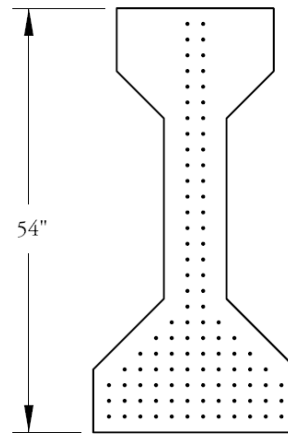
Type I



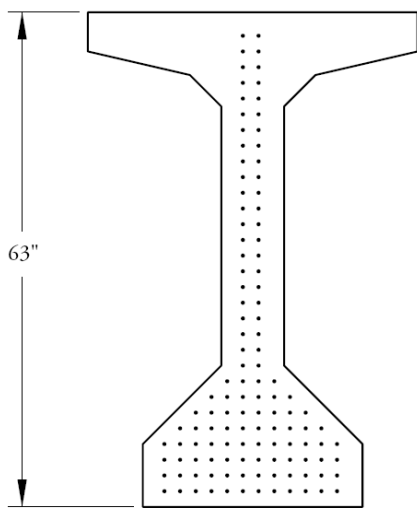
Type II



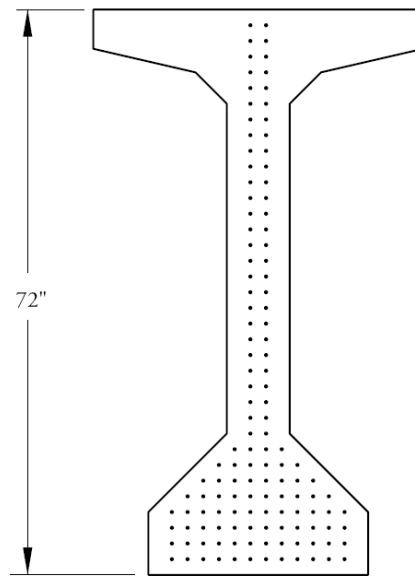
Type III



Type IV

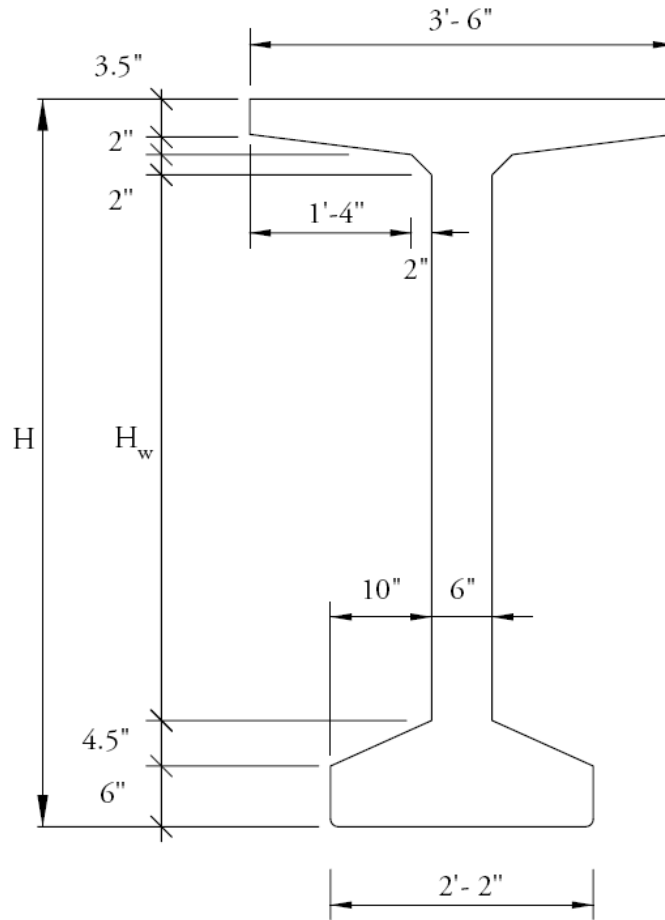


Type V



Type VI

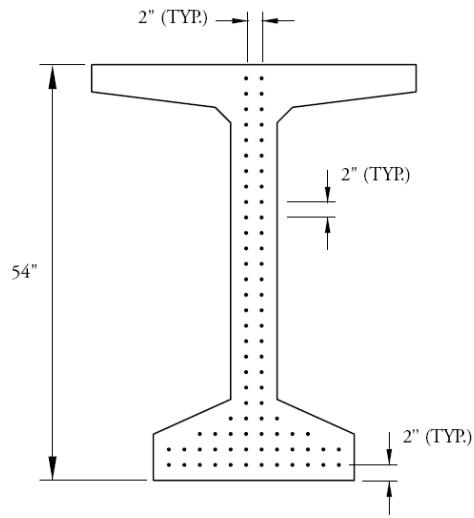
AASHTO-PCI Bulb-Tees



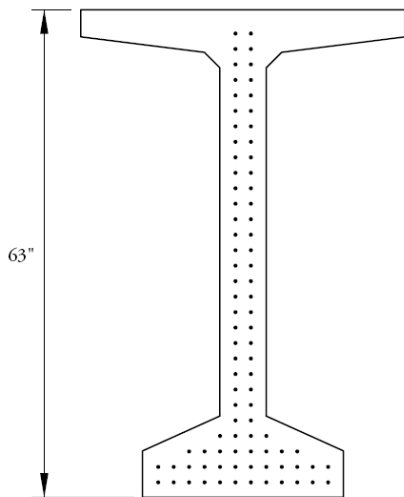
Properties

Type	H in.	H _w in.	Area in. ²	Inertia in. ⁴	y _{bottom} in.	Weight kip/ft
BT-54	54	36	659	268,077	27.63	0.686
BT-63	63	45	713	392,638	32.12	0.743
BT-72	72	54	767	545,894	36.6	0.799

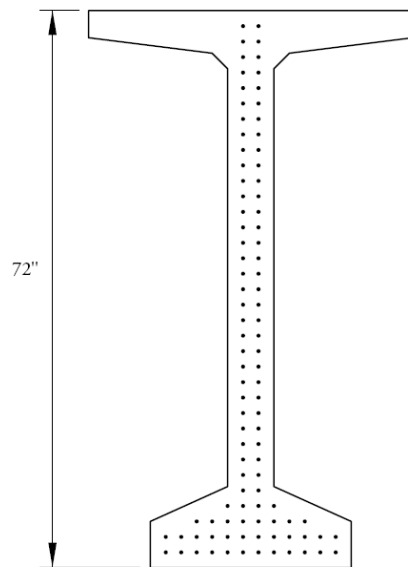
AASHTO-PCI Bulb-Tees



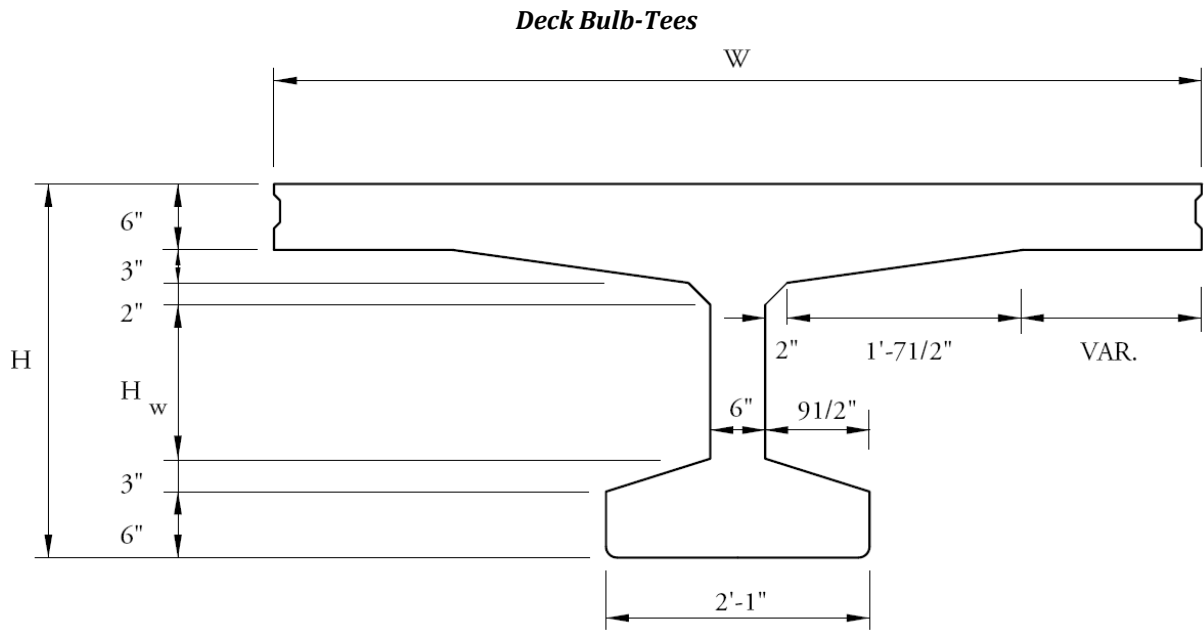
BT-54



BT-63



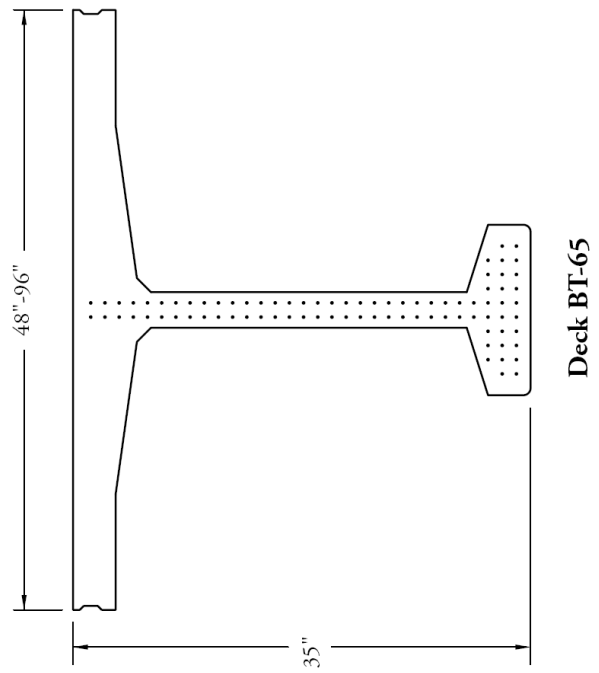
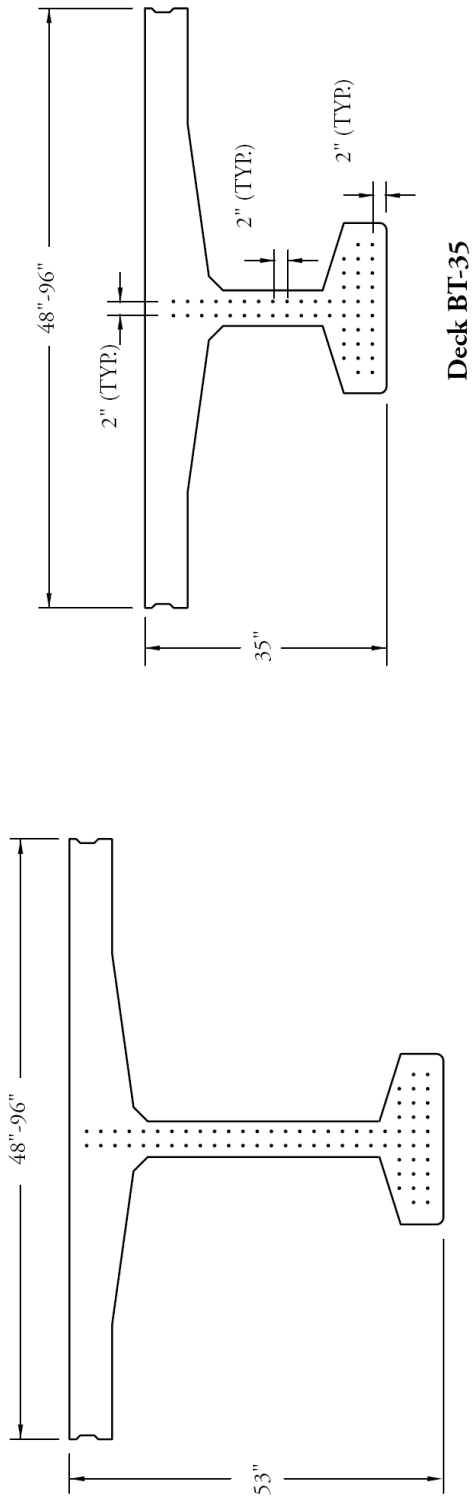
BT-72

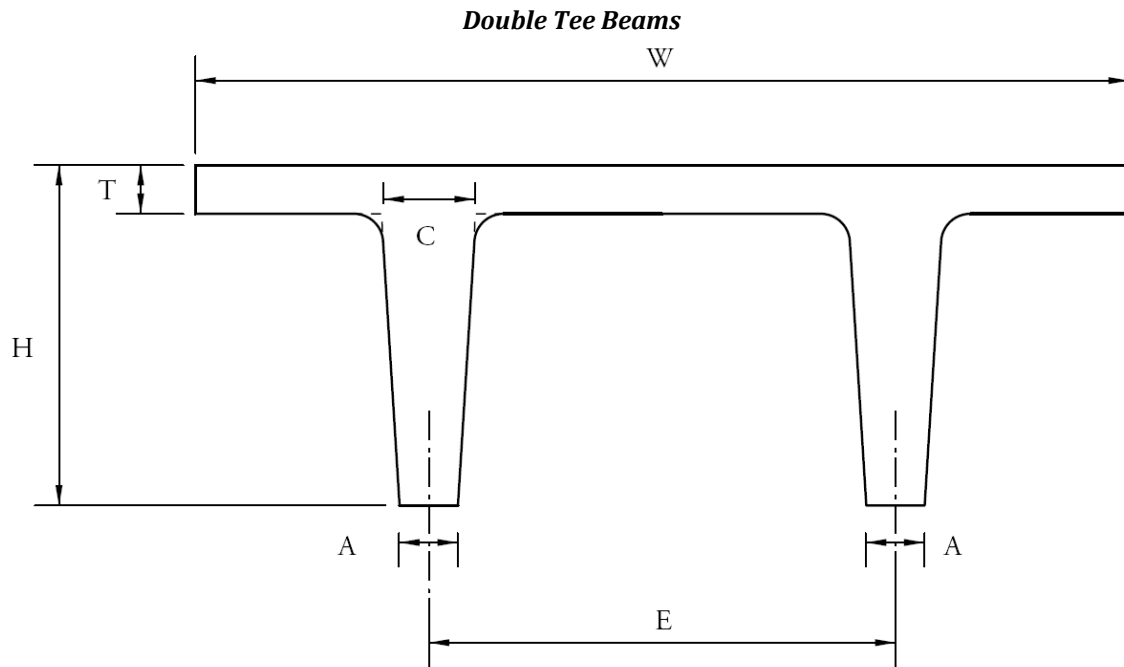


Dimensions and Properties

H in.	H _w in.	W in.	Area in. ²	Inertia in. ⁴	y _{bottom} in.	Weight kip/ft
35	15	48	677	101,540	21.12	0.75
		72	823	116,071	23.04	0.91
		96	967	126,353	24.37	1.07
53	33	48	785	294,350	31.71	0.87
		72	931	335,679	34.56	1.03
		96	1,075	365,827	36.63	1.19
65	45	48	857	490,755	38.55	0.95
		72	1,003	559,367	41.95	1.11
		96	1,147	610,435	44.46	1.27

Deck Bulb-Tees





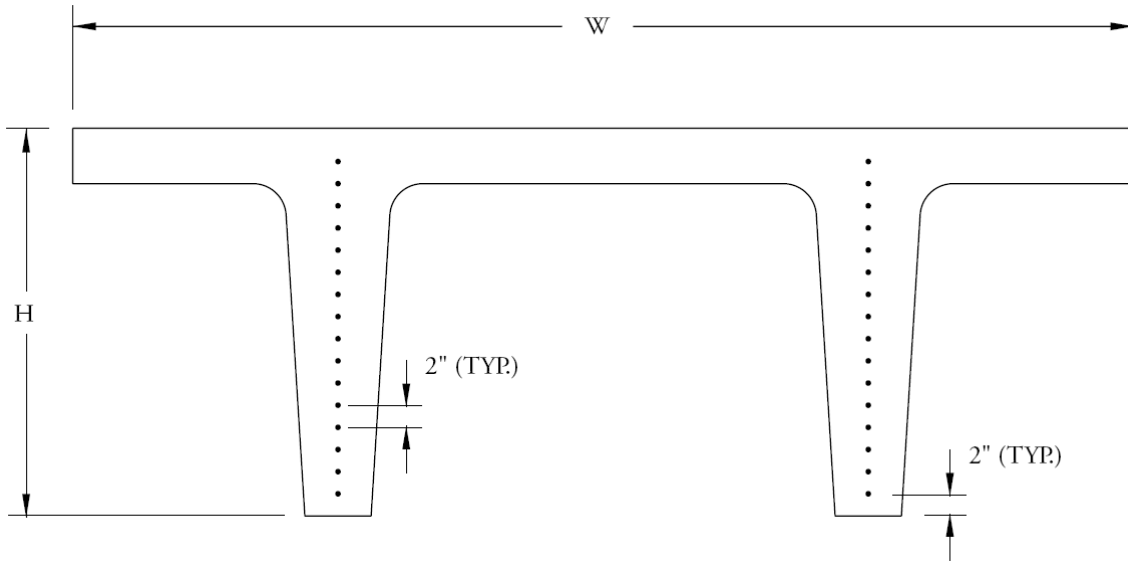
Light Sections

W ft	H in.	T in.	A in.	C in.	E in.	Area in. ²	Inertia in. ⁴	y _{bottom} in.	Weight kip/ft
5	27	5	4.5	8	36	575	33,740	18.6	0.599
6	23	5	4.5	6.5	36	558	21,366	16.61	0.582
6	27	5	4.5	8	36	635	35,758	19.15	0.662
8	27	5	3.75	5.75	48	689	32,888	20.64	0.718
8	35	5	3.75	6.5	48	787	72,421	26.2	0.82

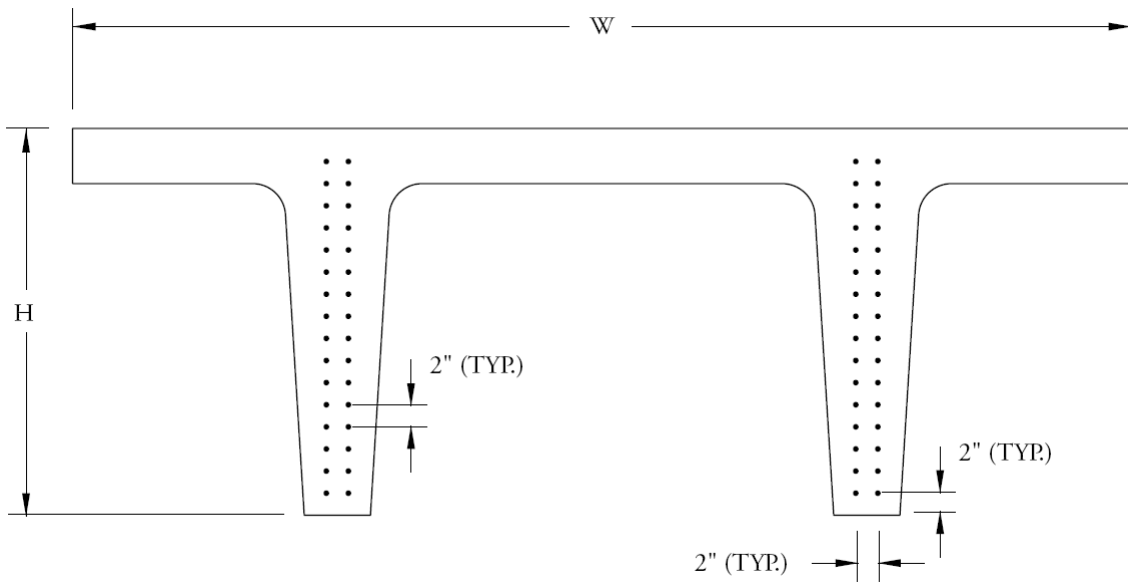
Heavy Sections

W ft	H in.	T in.	A in.	C in.	E in.	Area in. ²	Inertia in. ⁴	y _{bottom} in.	Weight kip/ft
5	36	6	6	8	30	780	90,286	23.69	0.812
6	35	5	6	9.75	48	840	90,164	23.3	0.876
7	35	5	6	9.75	48	900	95,028	23.91	0.938
8	35	5	6	9.75	48	960	99,299	24.45	1.001
6	27	5	7	9.75	48	731	45,084	18.09	0.761
7	27	5	7	9.75	48	791	47,486	18.58	0.824
8	27	5	7	9.75	48	851	49,566	19	0.886
6	21	5	7.75	9.75	48	644	22,720	14.11	0.671
7	21	5	7.75	9.75	48	704	23,903	14.48	0.733
8	21	5	7.75	9.75	48	764	24,920	14.8	0.796

Double Tee Beams

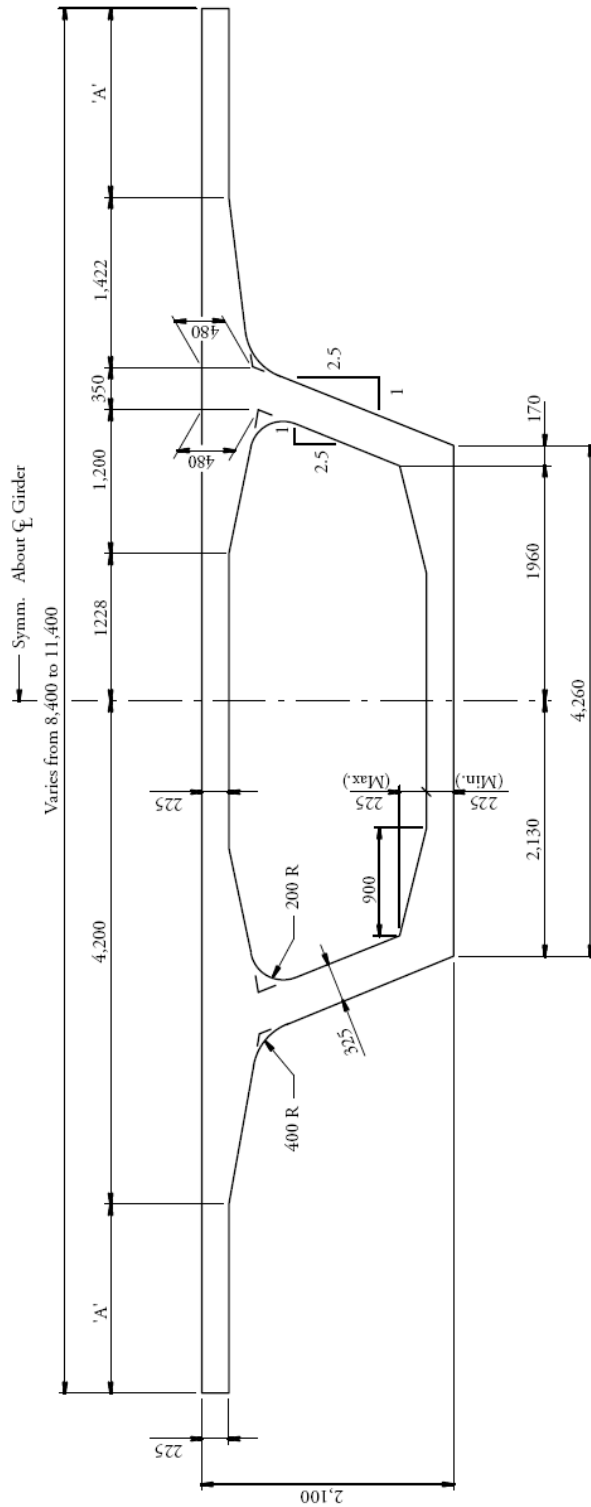


Light Sections



Heavy Sections

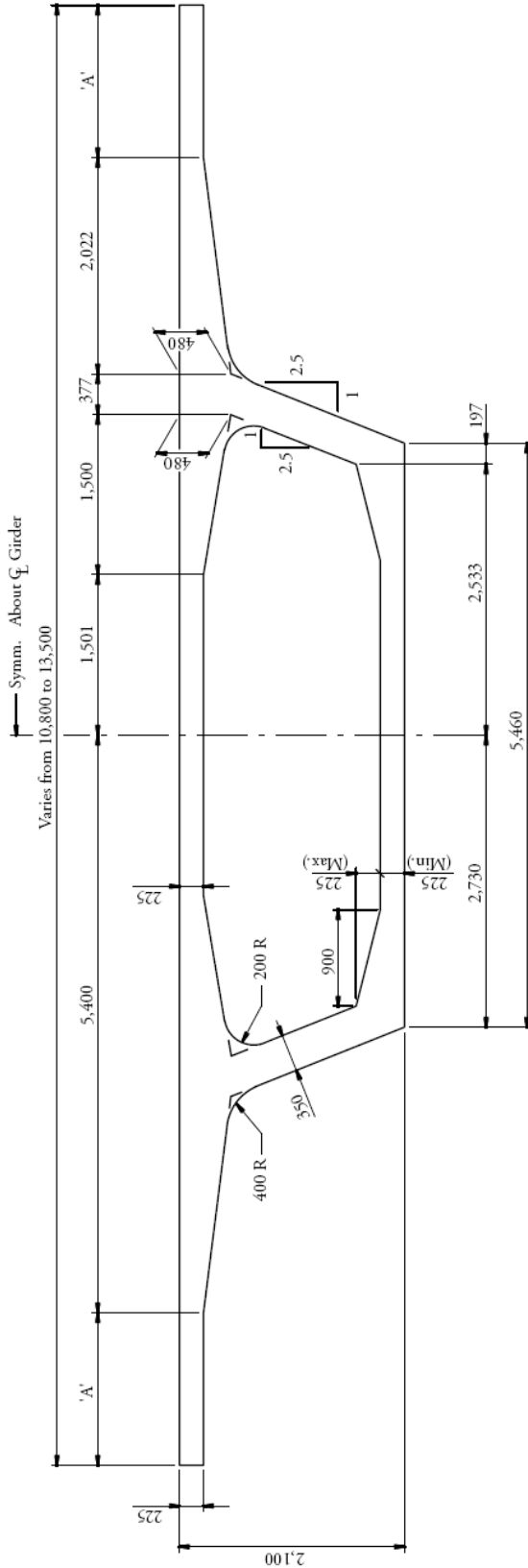
AASHTO-PCI-ASBI Standard Segment For Span-By-Span Construction



2100-1

Deck Width mm	'A' mm	Area mm ²	Wt/3,000 mm kN	I _x m ⁴	Y _t mm
8,400	0	4,916,000	360	2,967	799
8,700	150	4,984,000	365	2,999	790
9,000	300	5,051,000	370	3,030	781
9,300	450	5,119,000	375	3,060	772
9,600	600	5,186,000	380	3,089	763
9,900	750	5,254,000	385	3,118	755
10,200	900	5,321,000	390	3,145	747
10,500	1,050	5,389,000	394	3,172	739
10,800	1,200	5,456,000	399	3,199	731
11,000	1,350	5,524,000	404	3,225	723
11,400	1,500	5,591,000	409	3,250	716

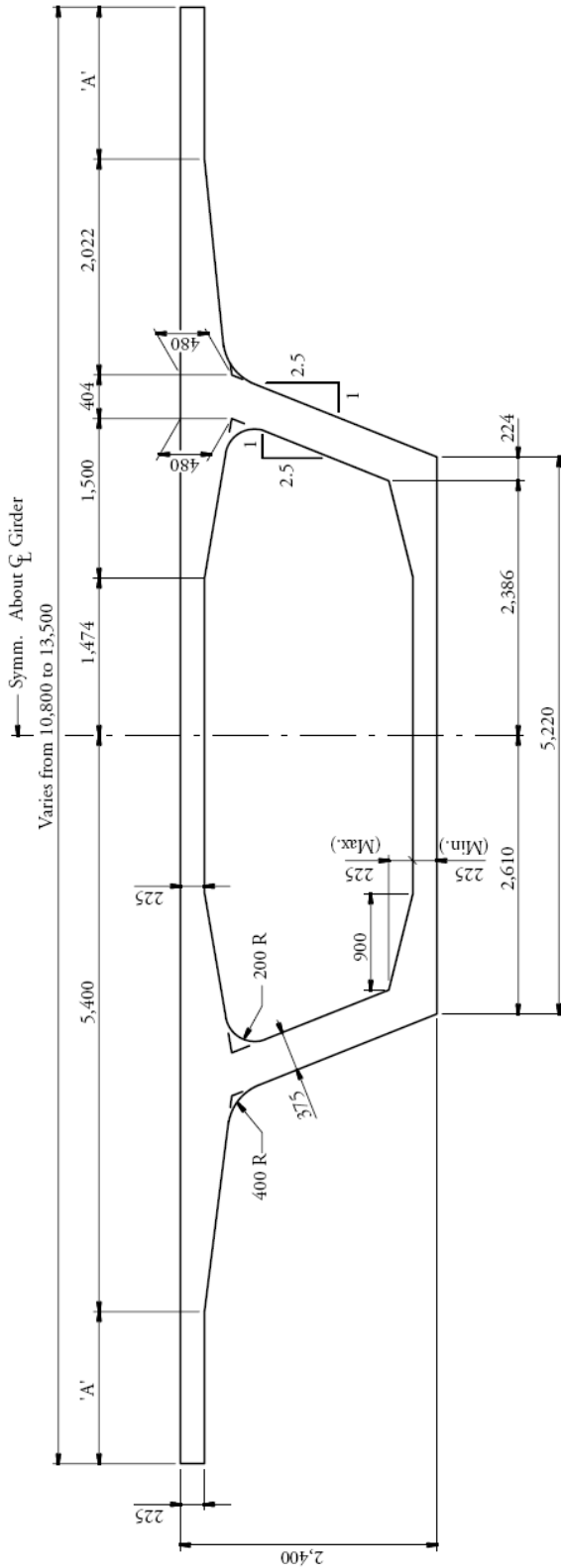
AASHTO-PCI-ASBI Standard Segment For Span-By-Span Construction



2100-2

Deck Width mm	'A' mm	Area mm ²	W _c /3,000 mm kN	I _x m ⁴	Y _t mm
11,800	0	6,050,000	443	3.685	776
11,100	150	6,117,000	448	3.715	769
11,400	300	6,185,000	453	3.744	762
11,700	450	6,252,000	458	3.772	755
12,000	600	6,320,000	463	3.800	748
12,300	750	6,387,000	468	3.827	741
12,600	900	6,455,000	472	3.854	734
12,900	1,050	6,522,000	477	3.880	728
13,200	1,200	6,590,000	482	3.906	722
13,500	1,350	6,657,000	487	3.931	715

AASHTO-PCI-ASBI Standard Segment For Balanced Cantilever Construction



2400-2

Deck Width mm	'A' mm	Area mm ²	W _t /3,000 mm kN	I _x m ⁴	Y _t mm
10,800	0	6,327,000	463	5.045	882
11,100	150	6,395,000	468	5.085	874
11,400	300	6,462,000	473	5.124	866
11,700	450	6,530,000	478	5.162	858
12,000	600	6,597,000	483	5.199	851
12,300	750	6,665,000	488	5.236	843
12,600	900	6,732,000	493	5.272	836
12,900	1,050	6,800,000	498	5.307	829
13,200	1,200	6,867,000	503	5.342	821
13,500	1,350	6,935,000	508	5.376	815

PCI REGIONAL PRODUCTS

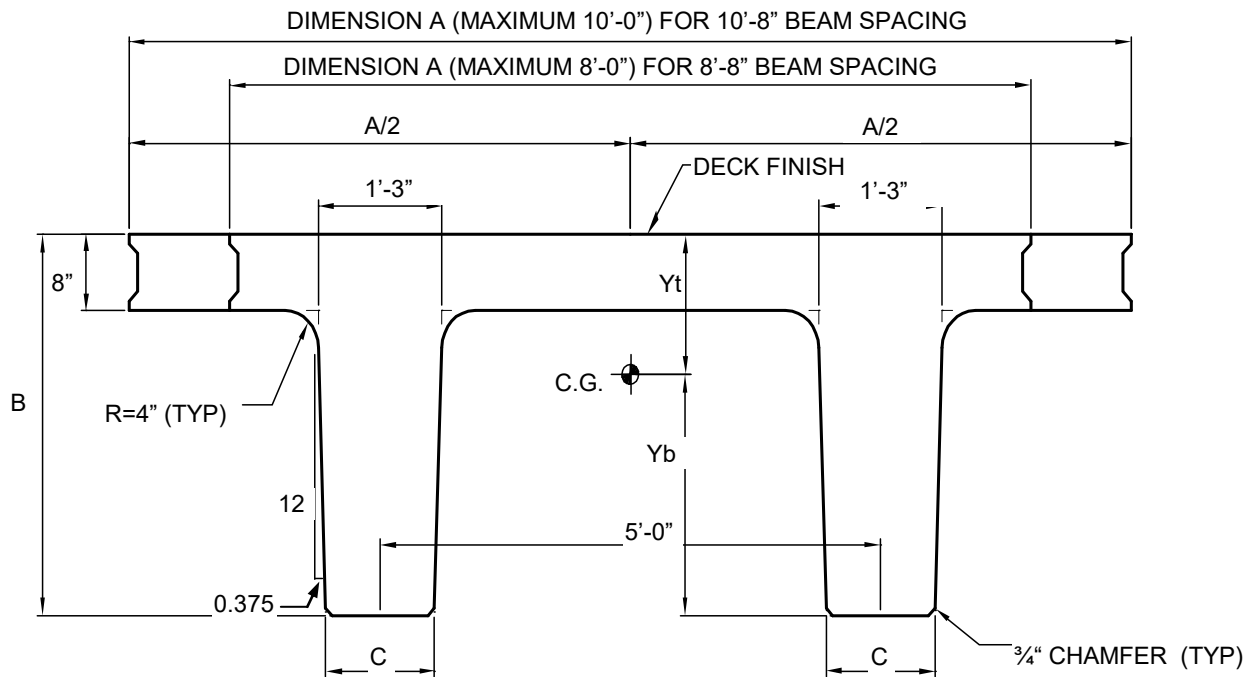
Table of Contents

NEXT D BEAMS..... Appendix C - 3
NEXT F BEAMS Appendix C - 4
PCI Zone 6 (SE Region) Spliced U-Girders Appendix C - 5

PCI REGIONAL PRODUCTS

Next D Beams

NEXT D BEAMS

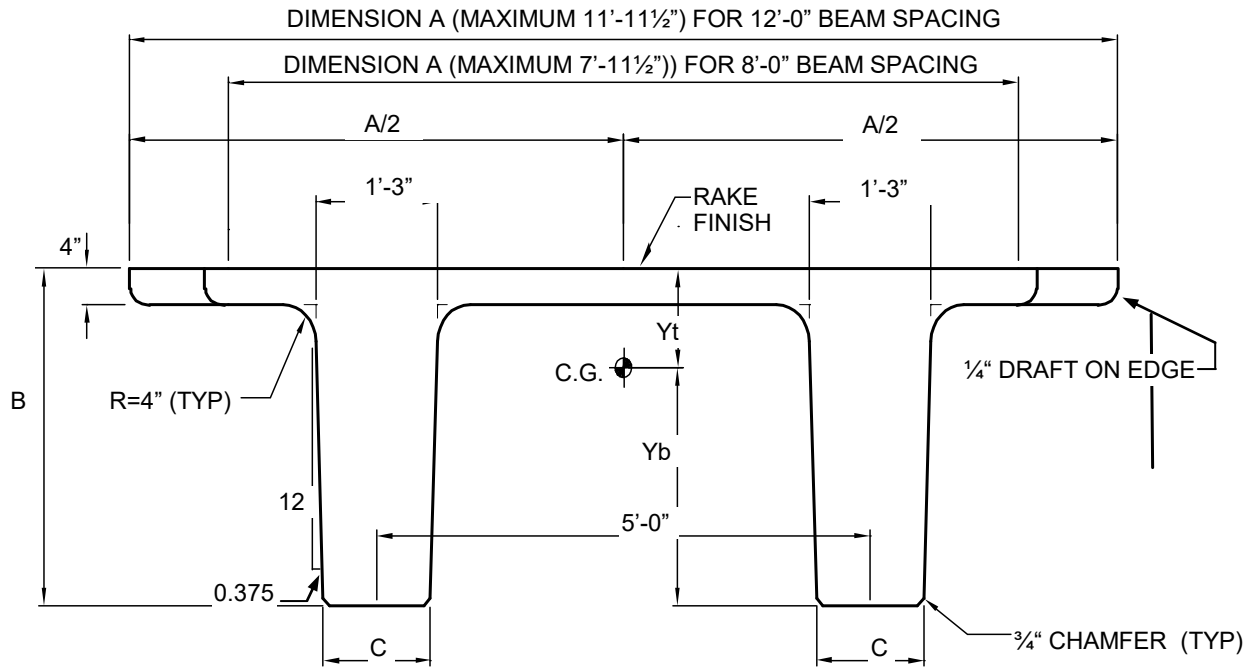


Beam Designation	Beam Width Inches	Beam Depth Inches	Base Stem Width Inches	Area IN ²	I IN ⁴	Yb Inches	Yt Inches	St IN ³	Sb IN ³	Weight PLF
	A	B	C			D	E			
Minimum Width Beams										
Next 40 D	96.00	40.00	13.00	1666	238059	25.47	14.54	16378	9348	1735
Next 36 D	96.00	36.00	13.25	1562	176674	23.03	12.97	13624	7671	1627
Next 32 D	96.00	32.00	13.50	1455	126111	20.57	11.43	11033	6131	1516
Next 28 D	96.00	28.00	13.75	1346	85651	18.06	9.94	8620	4742	1402
Maximum Width Beams										
Next 40 D	120.00	40.00	13.00	1858	258171	26.55	13.45	19201	9722	1935
Next 36 D	120.00	36.00	13.25	1754	191453	24.01	11.99	15973	7973	1827
Next 32 D	120.00	32.00	13.50	1647	136502	21.44	10.57	12920	6368	1716
Next 28 D	120.00	28.00	13.75	1538	92597	18.80	9.20	10069	4924	1602

AASHTO/PCI REGIONAL PRODUCTS

Next F Beams

NEXT F BEAMS



Beam Designation	Beam Width Inches	Beam Depth Inches	Base Stem Width Inches	Area IN ²	I IN ⁴	Yb Inches	Yt Inches	St IN ³	Sb IN ³	Weight PLF
	A	B	C			D	E			
Minimum Width Beams										
Next 36 F	95.50	36.00	13.00	1287	160240	21.77	14.23	11261	7361	1341
Next 32 F	95.50	32.00	13.25	1182	115813	19.51	12.49	9272	5936	1231
Next 28 F	95.50	28.00	13.50	1075	79901	17.24	10.76	7426	4635	1120
Next 24 F	95.50	24.00	13.75	966	51823	14.95	9.05	5726	3466	1006
Maximum Width Beams										
Next 36 F	143.50	36.00	13.00	1479	185525	23.36	12.64	14678	7942	1541
Next 32 F	143.50	32.00	13.25	1374	134258	20.98	11.02	12183	6399	1431
Next 28 F	143.50	28.00	13.50	1267	92661	18.57	9.43	9826	4990	1320
Next 24 F	143.50	24.00	13.75	1158	60045	16.12	7.88	7620	3725	1206

PCI Zone 6 (SE Region) Spliced U-Girders



PCI
Premier Provider of Concrete Solutions

NOTES TO PCI CERTIFIED PRODUCERS, OWNERS AND ENGINEERS FOR THE SPLICED U GIRDERS

PURPOSE AND INTENT OF THIS INFORMATION: PCI-CERTIFIED PLANTS IN ZONE 6 (SOUTHEAST) HAVE FORMED A TASK FORCE TO DEVELOP AND PROMOTE A SERIES OF CONCEPTS, DRAWINGS AND DETAILS THAT ILLUSTRATE THE INFORMATION NECESSARY TO THE PROPER DESIGN AND CONSTRUCTION OF THE PRECAST CONCRETE U-BEAM HAS EMERGED THE PCI-CERTIFIED PLANTS TO OFFER AN ECONOMICAL STRUCTURAL DESIGN SOLUTION FOR BOTH LONG SPAN AND CURVED TRANSPORTATION STRUCTURES TO CARRY VEHICULAR AND RAIL TRAFFIC.

BACKGROUND: THE NEED FOR COMPLEX INTERCHANGES AND LONG-SPAN GRADE SEPARATIONS HAS CREATED THE NEED FOR NEW INNOVATIVE SOLUTIONS. TRADITIONALLY, THESE STRUCTURES WERE BUILT AS CAST-IN-PLACE CONCRETE OR STRUCTURAL STEEL STRUCTURES. THE SUCCESS OF RECENT PROJECTS WHICH ARE ALL CURRENTLY IN SERVICE, CLEARLY DEMONSTRATES THE ADVANTAGES OF USING COMMERCIAL PRECAST CONCRETE COMPONENTS TO CONSTRUCT COST-EFFECTIVE, COMPLEX, LONG-SPAN STRUCTURES IN HIGH PROFILE APPLICATIONS WHERE AESTHETICS AND URBAN GEOMETRIES ARE SIGNIFICANT DESIGN CONSIDERATIONS.

ADVANCEMENTS IN THE USE OF SPLICED, POST-TENSIONED GIRDER HAVE EXTENDED THE SPAN RANGE OF PRECAST CONCRETE CONSTRUCTION. THE DEVELOPMENT OF THE U GIRDER INTRODUCED A NEW CROSS SECTION THAT HAD SUFFICIENT STRENGTH AND STABILITY TO MAKE CASTING CURVED SECTIONS FEASIBLE. COMBINING THESE TWO ADVANCEMENTS OPENED UP THE POSSIBILITY OF USING PRECAST CONCRETE FOR LONG SPAN INTERCHANGE PROJECTS.

ENHANCED DURABILITY, AND LOWER LIFE-CYCLE AND CONSTRUCTION COSTS MAKE PRECAST CONCRETE AN ATTRACTIVE DESIGN OPTION. HAVING A STRONG LOCAL MARKET HAS ENHANCED THE ECONOMICS OF USING PRECAST CONCRETE BY REDUCING LEAD TIMES FOR FABRICATION AND SHIPPING COSTS.

SPLICED GIRDER CONSTRUCTION REQUIRES ONLY VERTICAL SHORING WHICH REDUCES INTERFERENCE WITH EXISTING ROADWAYS. CONVENTIONAL CONSTRUCTION METHODS AND EQUIPMENT ARE USED TO ERECT THE GIRDERS ELIMINATING THE NEED TO INVEST IN SPECIALIZED EQUIPMENT. PCI-CERTIFIED PLANTS OFFER SHORTER LEAD TIMES FOR FABRICATION AND DELIVERY OF GIRDERS, WHICH GREATLY ENHANCES THE COST EFFECTIVENESS OF THIS TYPE OF CONSTRUCTION.

THE USE OF PRECAST CONCRETE U-GIRDERS ENABLES A PROJECT TO UNIFY THE APPEARANCE OF A PROJECT FOR ALL SPANS OF THE STRUCTURE. GIRDERS WITH SLOPED WEBS CREATE AN ATTRACTIVE STRUCTURE THAT HAS BEEN WELL RECEIVED IN HIGH VISIBILITY LOCATIONS AS A CONTEXT-SENSITIVE DESIGN.

CONSTRUCTION CHALLENGES AND SOLUTIONS: CONSTRUCTION OF THESE BRIDGES INVOLVES HANDLING AND ERECTING LARGE, HEAVY, CURVED GIRDERS IN CHALLENGING SITE CONDITIONS THAT REQUIRED TEMPORARY SUPPORT AND STABILIZATION.

SUMMARY: THE DEVELOPMENT OF THE U-GIRDERS HAS CREATED AN OPPORTUNITY TO USE PRECAST CONCRETE IN NEW APPLICATIONS FOR BRIDGE CONSTRUCTION. THE DETAILS DESCRIBED IN THIS DRAWING PACKAGE WERE DEVELOPED BASED ON CONSTRUCTED PROJECTS WITH CHALLENGING SITE CONDITIONS WHERE MAINTENANCE OF EXISTING TRAFFIC WAS ESSENTIAL. FURTHER REFINEMENT OF DESIGN DETAILS AND CONSTRUCTION METHODS ON FUTURE PROJECTS WILL CONTINUE TO ENHANCE THE ECONOMY AND EASE OF CONSTRUCTION OF THIS CONCEPT AND MAKE IT EVEN MORE ATTRACTIVE TO ENGINEERS, OWNERS AND BUILDERS. THE USE OF THESE STANDARDIZED CONSTRUCTION METHODS WILL ALLOW FOR THE CONSTRUCTION OF BRIDGES WITH SLOPED WEBS AND CURVED GIRDERS TO BE BUILT IN A COST-EFFECTIVE MANNER. THE USE OF THESE STANDARDIZED METHODS THAT THE PROBABIL FOR APPLICATION OF PRECAST CONCRETE FOR USE IN LONG-SPAN BRIDGES IS ONLY BEING BOUND BY THE ENGINEER'S CREATIVITY AND IMAGINATION. THESE BEAM SECTIONS WILL PROTECT THE PCI-CERTIFIED PLANTS FROM HAVING AN INFINITE SET OF PERMUTATIONS IN A REGION. COMPETITION IN THE BRIDGE INDUSTRY IS A GOOD DEAL FOR THE TAXPAYERS.

GENERAL NOTES

- MINIMUM 3 TENDONS TO CROSS EACH SPlice.
- WEB THICKNESS FOR 3", & 4" PLASTIC DUCTS DETERMINED PER FOOT DPT FOR BONDED TENDON CRITERIA.
- USE ASHTO AND STATE SPECIFIC CRITERIA TO PROPERLY DETAIL POST-TENSIONING.
- PRESSURE TEST ALL DUCTS PRIOR TO GROUTING.
- GRADE 60 REINFORCING STEEL IS REQUIRED.

DESIGN DATA

- ASHTO, 4TH EDITION LRFD
- DESIGN METHOD: LOAD AND RESISTANCE FACTOR DESIGN
- DEAD LOAD CURVED GIRDER: FOR GIRDER LENGTHS ALONG OUTSIDE OF CURVE.
CONCRETE UNIT WEIGHT = 155 PCF
8" STRUCTURAL + 8" SACRIFICIAL CAST-IN-PLACE DECK.
FMS ALLOWANCE 3" ASPHALT OVERLAY MAXIMUM.
147 LBS PER LIN. FT. FOR BARBER RAIL.
10 LBS PER SQ. FT. SUPERIMPOSED DEAD LOAD APPLIED TO COMPOSITE SECTION FOR CONSTRUCTION INCIDENTALS.
- LIVE LOADS: HL-93
PRECAST PRESTRESSED CONCRETE ASSUMPTIONS:
fc = 27000 PSI
fsc = 27000 PSI
LOW-LAX 0.6% STRAIN
K=0.0002, H=10.18, AL JASING MUS
ALSO SEE STRENGTH AND PROVISIONS FOR AN ADDITIONAL LONG TERM LOSS IN STRESS PER ASHTO GUIDELINES

NOTES TO DESIGNER

- THE CONCEPTS PRESENTED IN THIS SET OF DRAWINGS ARE CONCEPTUAL ONLY. ALL DESIGN PREPARED USING THE CONCEPTS PRESENTED MUST BE PREPARED BY A REGISTERED PROFESSIONAL ENGINEER AND MUST CONFORM TO ASHTO AND ALL STATE AND LOCAL DESIGN REQUIREMENTS.
- ALL DESIGNS MUST SATISFY SERVICE LOAD STRESS LIMITATIONS FOR ALL PRESTRESSED CONCRETE MEMBERS.
- ALL ULTIMATE LOAD COMBINATIONS MUST BE CHECKED FOR THE COMPOSITE SECTION.
- SERVICE AND ULTIMATE LOAD CONDITIONS MUST BE CHECKED AND CONFORM TO ASHTO AND LOCAL GUIDELINES FOR FLEXURE, SHEAR, TORSION, CRACK CONTROL AND SERVICEABILITY DURING ALL STAGES OF CASTING AND CONSTRUCTION.
- THE DESIGNER SHALL VERIFY THAT CURVED, OPEN U GIRDERS ARE CLOSED PRIOR TO PREVENT TORSIONAL CRACKING DURING CONSTRUCTION.
- DECK SLAB REINFORCING SHALL BE PROPORTIONED TO CONTROL CRACKING IN NEGATIVE MOMENT REGIONS UNDER SERVICE LOAD CONDITIONS.
- WEB THICKNESSES SHALL BE PROPORTIONED TO CONFORM TO ASHTO GUIDELINES FOR DUCT TO WEB THICKNESS RATIOS.
- PRINCIPAL TENSILE STRESSES IN GIRDER WEBS UNDER SERVICE LOADINGS WILL BE LIMITED TO CONFORM TO ASHTO GUIDELINES.

CURVED GIRDES

- GIRDERS SHALL BE ERECTED AND ALIGNED IN A MANNER TO PRODUCE A SMOOTH PROFILE IN CONTINUITY WEB TENDONS TO AVOID KINKS AND UNDESIRABLE ANGLE BREAKS.
- CONFINEMENT REINFORCING SHALL BE DESIGNED AROUND WEB TENDONS IN CURVED SECTIONS TO RESIST ALL LATERAL FORCES DUE TO CURVATURE AND INCIDENTAL MISALIGNMENTS.
- CURVED GIRDERS MAY BE ERECTED IN AN OPEN CONDITION IF TORSIONAL STRESSES ARE VERIFIED AND CONTROLLED AND STRENGTH REQUIREMENTS ARE MET DURING ALL STAGES OF CONSTRUCTION.
- SERVICE STRESSES IN ALL GIRDERS SHALL BE WITHIN ALLOWABLE LIMITS AND STRENGTH REQUIREMENTS MET FOR ALL STAGES OF CASTING, ERECTION AND CONSTRUCTION.

INDEX OF DRAWINGS

- U-1 GENERAL INFORMATION
- U-2 TYPICAL BRIDGE CROSS SECTION
- U-3 TYPICAL BRIDGE CROSS SECTION WITH PRECAST PANELS
- U-4 MAXIMUM DESIGN SPANS - SINGLE SPAN CONSTANT DEPTH GIRDERS
- U-5 MAXIMUM DESIGN SPANS - THREE SPAN HAUNCHED GIRDERS
- U-6 MAXIMUM DESIGN SPANS - THREE SPAN HAUNCHED GIRDERS
- U-7 GIRDER END AND SLICE DETAILS
- U-8 TYPICAL THREE SPAN CONSTANT DEPTH GIRDERS
- U-9 TYPICAL EXPANSION PIER
- U-10 TYPICAL INTEGRAL INTERIOR PIER
- U-11 PRECAST PANEL DETAILS
- U-12 PRECAST PANEL DETAILS
- U-13 CONSTANT DEPTH GIRDER CONSTRUCTION SEQUENCE
- U-14 HAUNCHED GIRDER CONSTRUCTION SEQUENCE
- U-15 HAUNCHED GIRDER CONSTRUCTION SEQUENCE
- U-16 ERECTION BRACING
- U-17 HAUNCHED GIRDER CONSTRUCTION SEQUENCE
- U-18 HAUNCHED GIRDER CONSTRUCTION SEQUENCE
- U-19 HAUNCHED GIRDER CONSTRUCTION SEQUENCE
- U-20 EXAMPLE ERECTION PLAN DETAILS



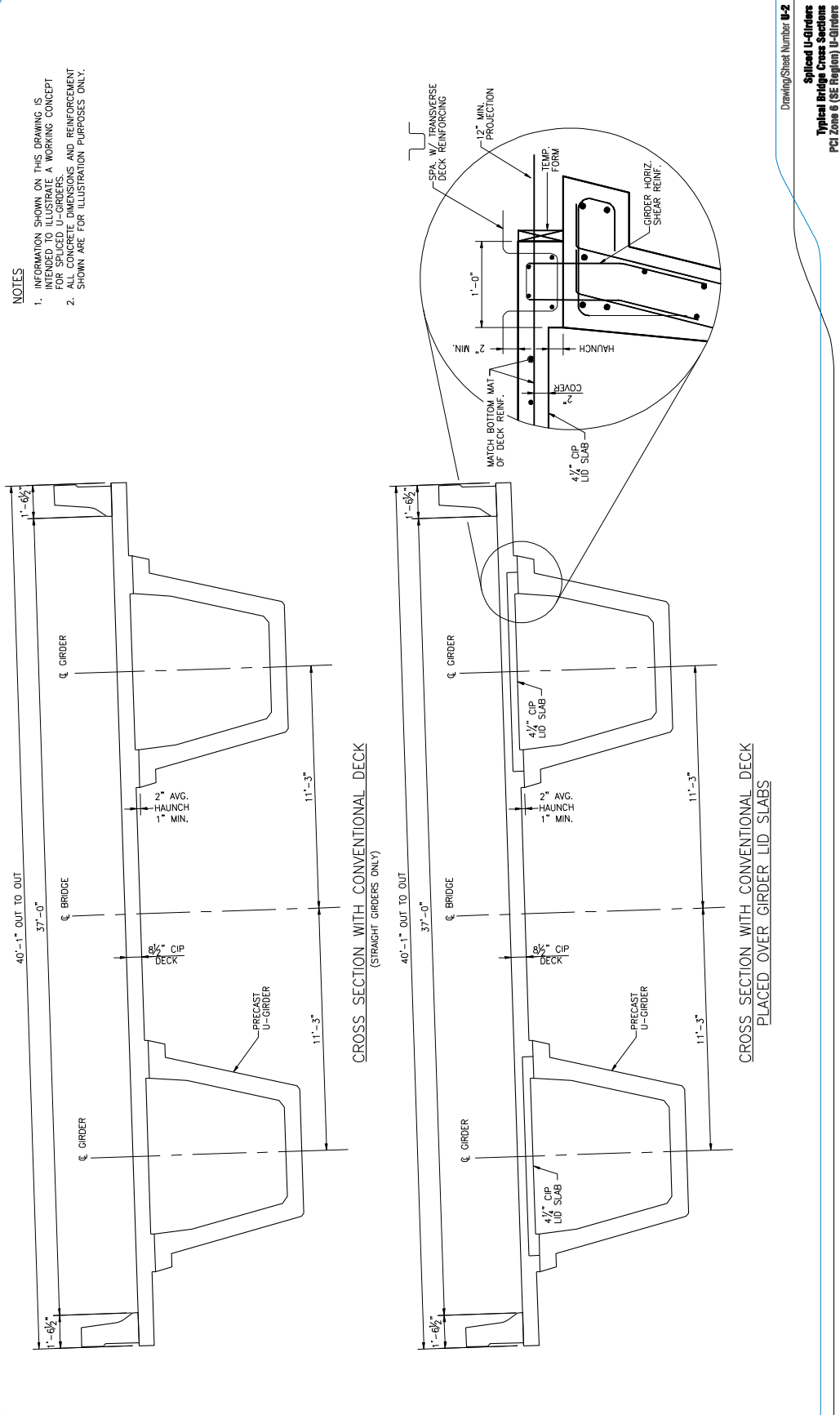
Drawing/Sheet Number U-1

General Information
PCI Zone 6 (SE Region) U-Girders

AASHTO/PCI REGIONAL PRODUCTS

PCI Zone 6 (SE Region) Spliced U-Girders

PCI Zone 6 (SE Region) Spliced U-Girders



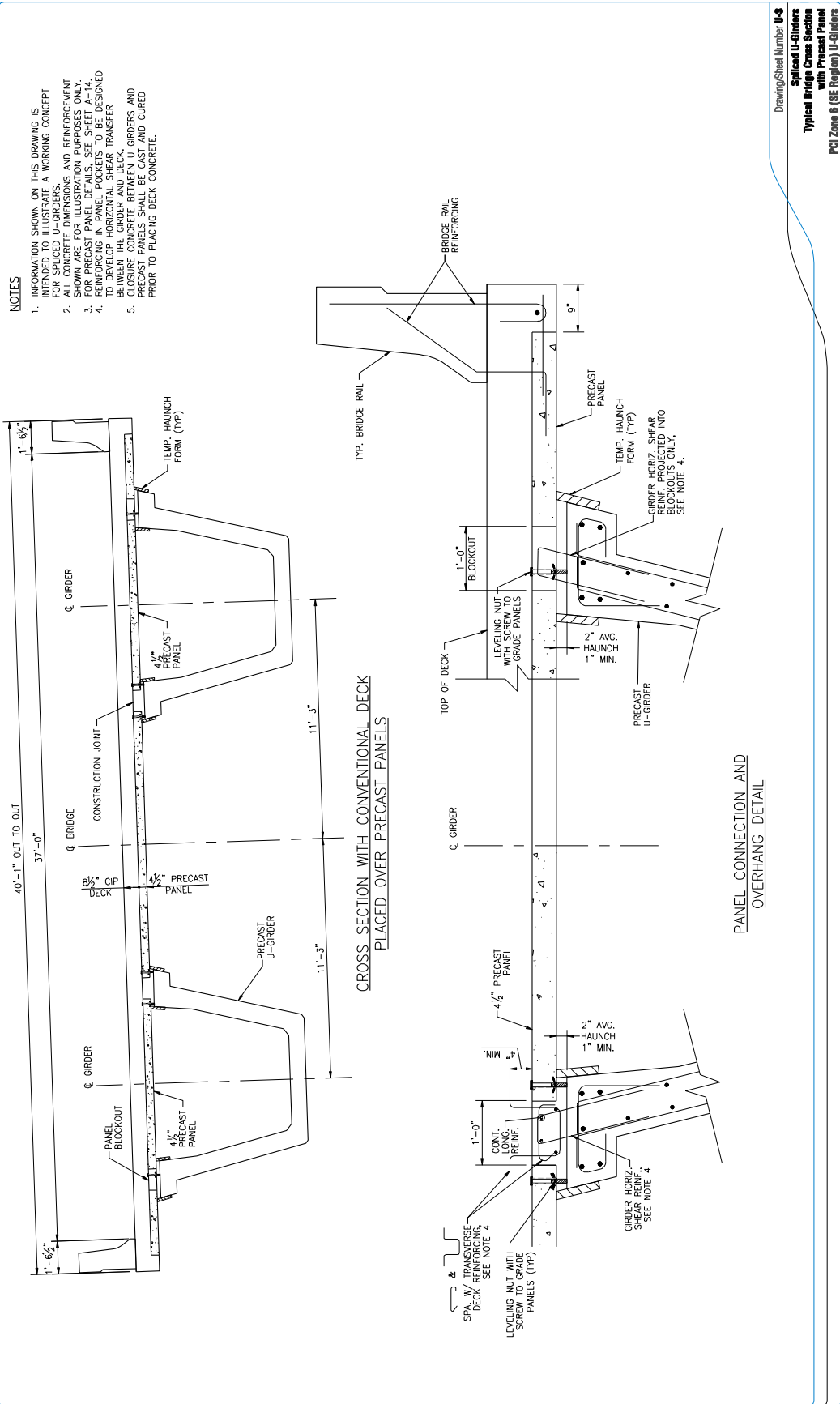
Drawing/Sheet Number **U-2**
Spliced U-Girders
Typical Bridge Cross Sections
PCI Zone 6 (SE Region) U-Girders



AASHTO/PCI REGIONAL PRODUCTS

PCI Zone 6 (SE Region) Spliced U-Girders

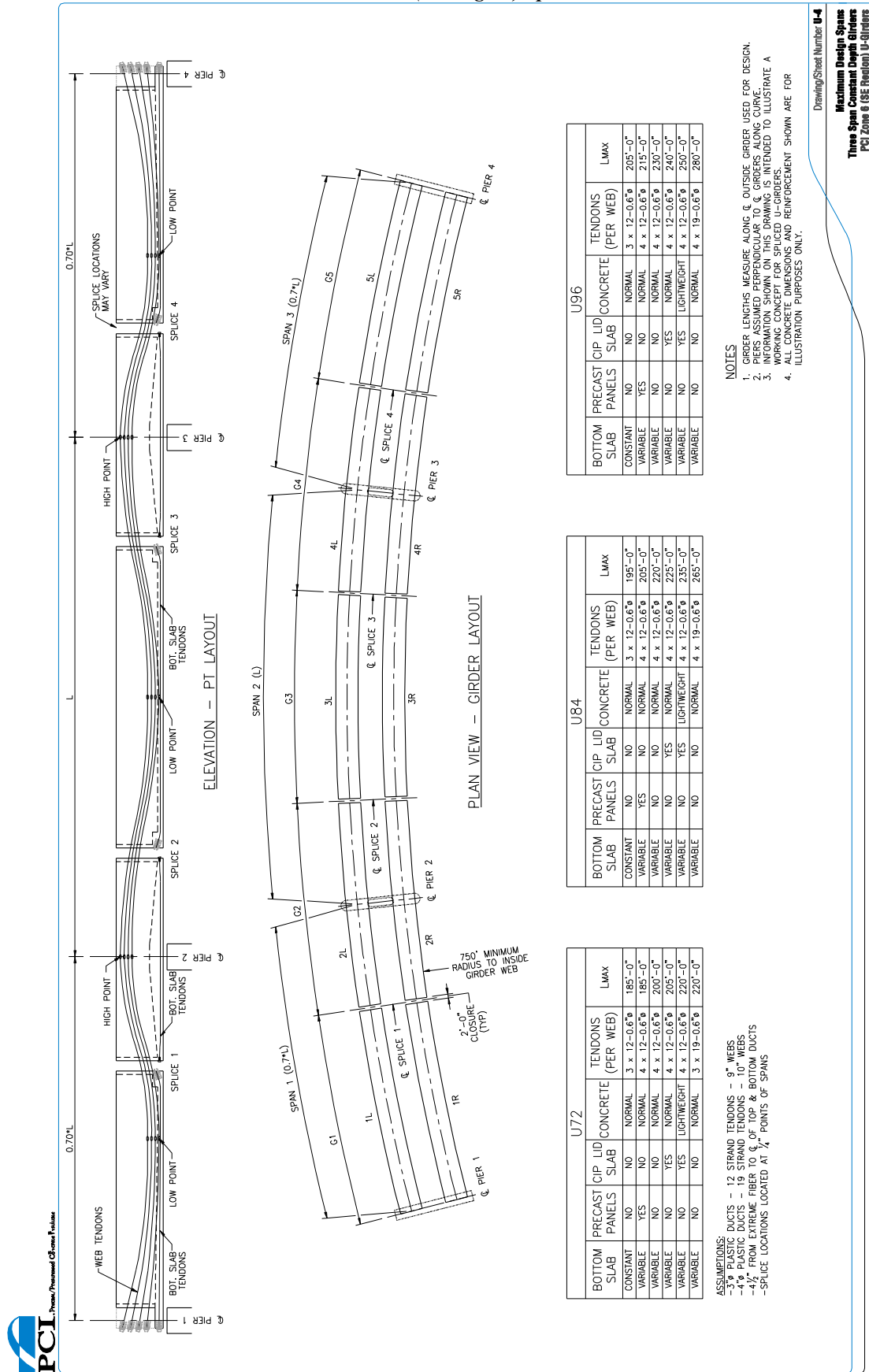
PCI Zone 6 (SE Region) Spliced U-Girders



AASHTO/PCI REGIONAL PRODUCTS

PCI Zone 6 (SE Region) Spliced U-Girders

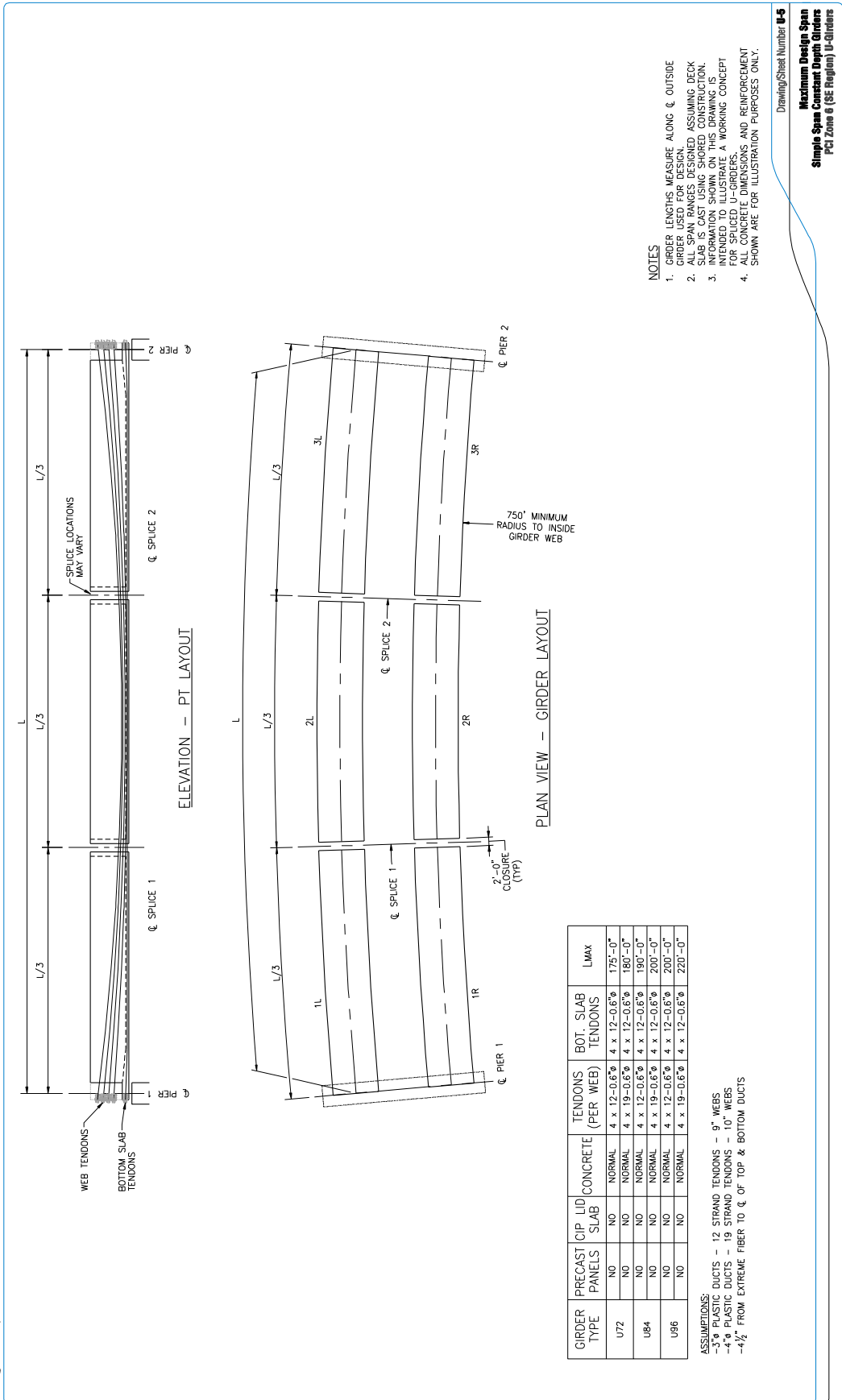
PCI Zone 6 (SE Region) Spliced U-Girders



AASHTO/PCI REGIONAL PRODUCTS

PCI Zone 6 (SE Region) Spliced U-Girders

PCI Zone 6 (SE Region) Spliced U-Girders

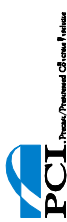


- NOTES**
1. GIRDER LENGTHS MEASURE ALONG ϕ OUTSIDE GIRDER USED FOR DESIGN.
 2. ALL SPAN RANGES DESIGNED ASSUMING DECK SLAB IS CAST USING SHORED CONSTRUCTION.
 3. INFORMATION SHOWN ON THIS DRAWING IS INTENDED TO BE USED AS A WORKING CONCEPT FOR SPliced U-GIRDERS.
 4. ALL CONCRETE DIMENSIONS AND REINFORCEMENT SHOWN ARE FOR ILLUSTRATION PURPOSES ONLY.

Drawing/Sheet Number **U-5**
Maximum Design Span
Simple Span Constant Depth Girders
PCI Zone 6 (SE Region) U-Girders

GIRDER TYPE	PRECAST PANELS	TOP LID SLAB	CONCRETE	TENDONS (PER WEB)	BOT SLAB TENDONS	L _{MAX}
U72	NO	NO	NORMAL	4 x 12-0.6"	4 x 12-0.6"	175'-0"
U84	NO	NO	NORMAL	4 x 19-0.6"	4 x 12-0.6"	180'-0"
U96	NO	NO	NORMAL	4 x 19-0.6"	4 x 12-0.6"	190'-0"
	NO	NO	NORMAL	4 x 12-0.6"	4 x 12-0.6"	200'-0"
	NO	NO	NORMAL	4 x 19-0.6"	4 x 12-0.6"	200'-0"
	NO	NO	NORMAL	4 x 19-0.6"	4 x 12-0.6"	220'-0"

ASSUMPTIONS:
 -3% PLASTIC DUCTS - 12 STRAND TENDONS - 9" WEBS
 -4% PLASTIC DUCTS - 19 STRAND TENDONS - 10" WEBS
 -4 1/2% FROM EXTREME FIBER TO ϕ OF TOP & BOTTOM DUCTS



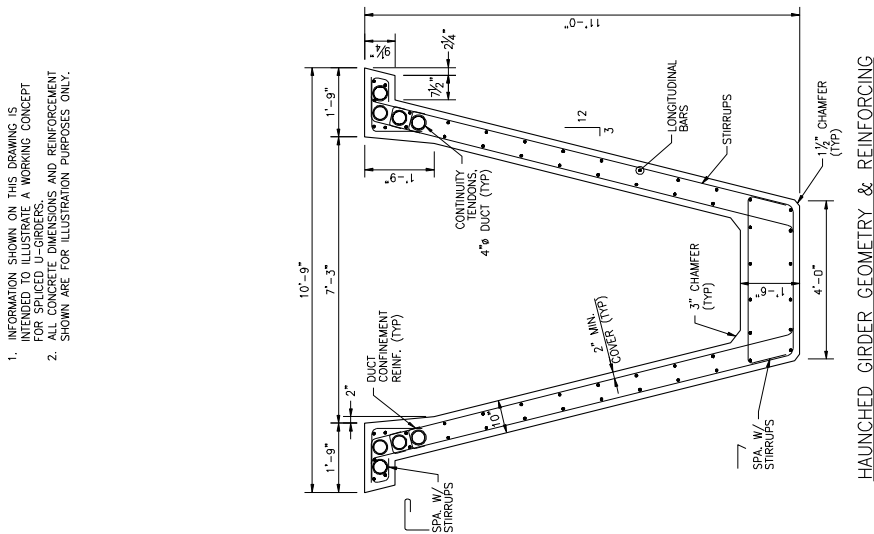
AASHTO/PCI REGIONAL PRODUCTS

PCI Zone 6 (SE Region) Spliced U-Girders

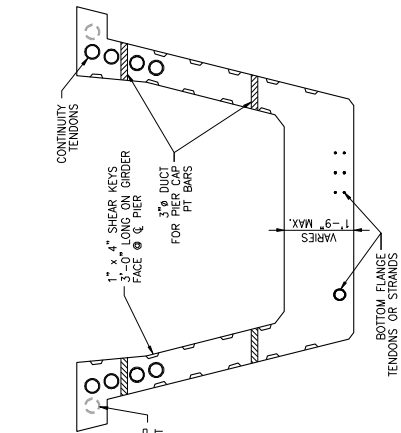
PCI Zone 6 (SE Region) Spliced U-Girders

NOTES

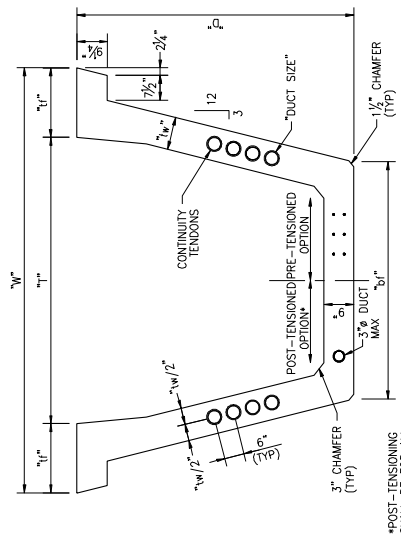
1. INFORMATION SHOWN ON THIS DRAWING IS INTENDED TO ILLUSTRATE A WORKING CONCEPT FOR SPICED U-GIRDERS.
2. ALL CONCRETE DIMENSIONS AND REINFORCEMENT SHOWN ARE FOR ILLUSTRATION PURPOSES ONLY.



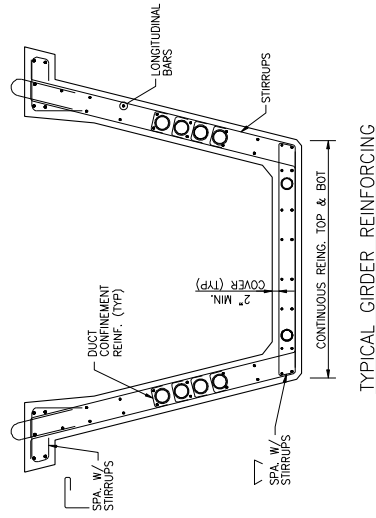
HAUNCHED GIRDER GEOMETRY & REINFORCING



GIRDER GEOMETRY OVER PIER



TYPICAL GIRDER GEOMETRY



TYPICAL GIRDER REINFORCING

GIRDER GEOMETRY									
GIRDER	D	DUCT SIZE	tw	W	T	tf	bf	WEIGHT	
U72-3	6'-0"	3"	9"	10'-1"	6'-9"	1'-8"	5'-10"	2,117 plf	
U84-3	7'-0"	3"	9"	10'-7"	7'-3"	1'-8"	5'-10"	2,349 plf	
U86-3	8'-0"	3"	9"	11'-1"	7'-9"	1'-8"	5'-10"	2,581 plf	
U72-4	6'-0"	4"	10"	10'-3"	6'-9"	1'-9"	6'-0"	2,271 plf	
U84-4	7'-0"	4"	10"	10'-9"	7'-3"	1'-9"	6'-0"	2,529 plf	
U84/132 HAUNCHED	-	4"	-	-	-	-	-	*303 kips	
U96-4	8'-0"	4"	10"	11'-3"	7'-9"	1'-9"	6'-0"	2,787 plf	

ASSUMPTIONS:
 - GIRDER UNIT WEIGHT = 150 pcf
 - GROSS GIRDER SECTION USED (DUCT VOID VOLUME NOT DEDUCTED)
 * TOTAL WEIGHT OF 98' LONG HAUNCHED PIER GIRDER

Drawing/Sheet Number **U-7**
Spliced U-Girders
Girder Dimensions and Reinforcement
PCI Zone 6 (SE Region) U-Girders



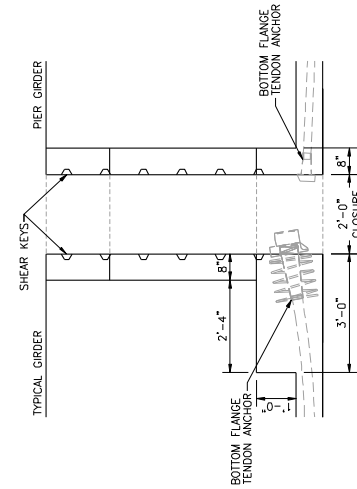
AASHTO/PCI REGIONAL PRODUCTS

PCI Zone 6 (SE Region) Spliced U-Girders

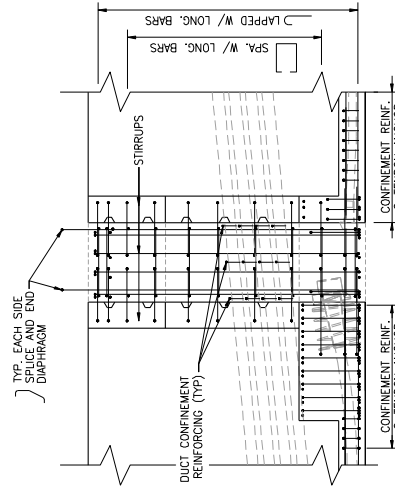
PCI Zone 6 (SE Region) Spliced U-Girders

NOTES

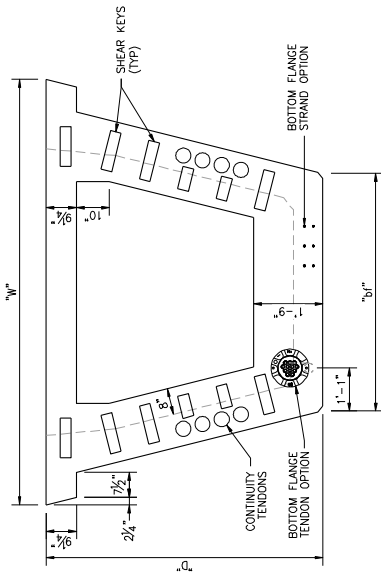
1. INFORMATION SHOWN ON THIS DRAWING IS INTENDED TO ILLUSTRATE A WORKING CONCEPT FOR SPICED U-GIRDERS.
2. ALL CONCRETE DIMENSIONS AND REINFORCEMENT SHOWN ARE FOR ILLUSTRATION PURPOSES ONLY.



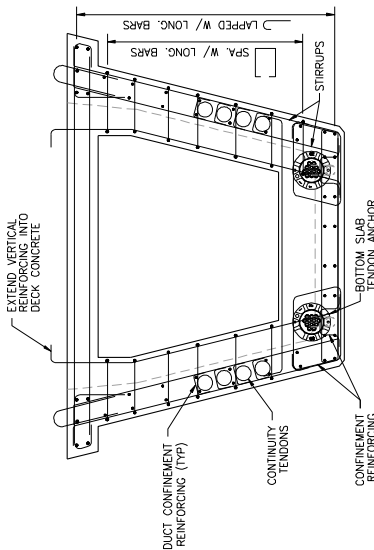
SECTION AT SPLICE



SPLICE REINFORCING SECTION



TYPICAL GIRDER END VIEW
(SEE GIRDER GEOMETRY TABLE ON SHEET A-7 FOR VARIABLE DIMENSIONS)



TYPICAL SPLICE REINFORCING

Drawing/Sheet Number **U-4**
Spliced U-Girders
Girder End and Splice Details
 PCI Zone 6 (SE Region) U-Girders

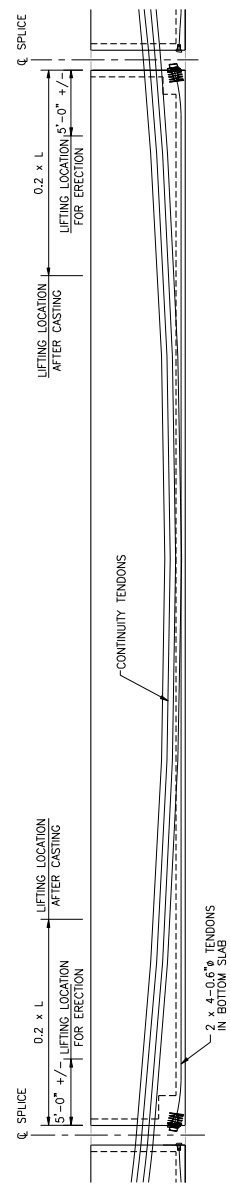
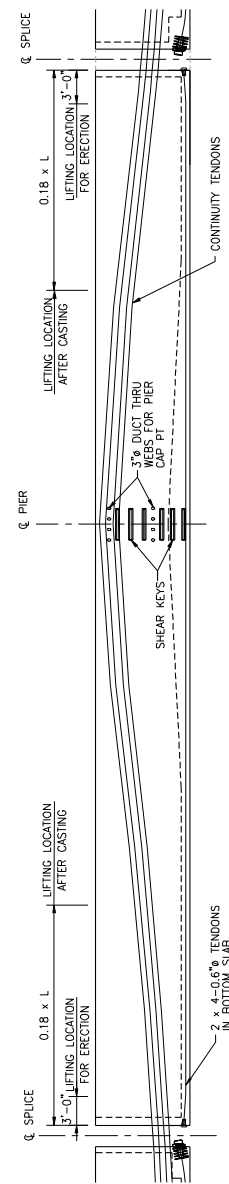
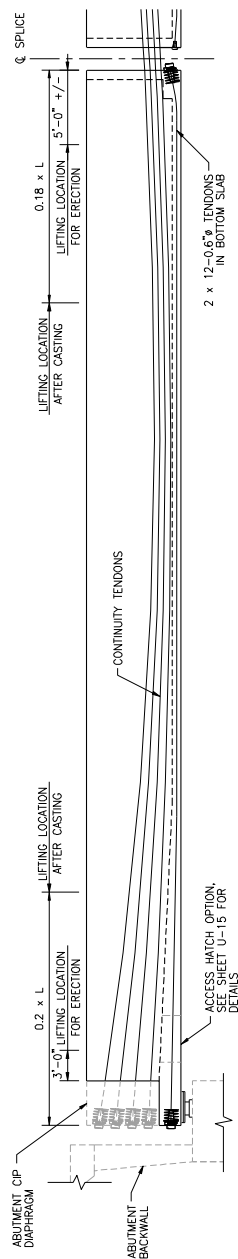


AASHTO/PCI REGIONAL PRODUCTS

PCI Zone 6 (SE Region) Spliced U-Girders

PCI Zone 6 (SE Region) Spliced U-Girders

- NOTES**
1. INFORMATION SHOWN ON THIS DRAWING IS INTENDED TO ILLUSTRATE A WORKING CONCEPT FOR SPLICED U-GIRDERS.
 2. ALL CONCRETE DIMENSIONS AND REINFORCEMENT SHOWN ARE FOR ILLUSTRATION PURPOSES ONLY.



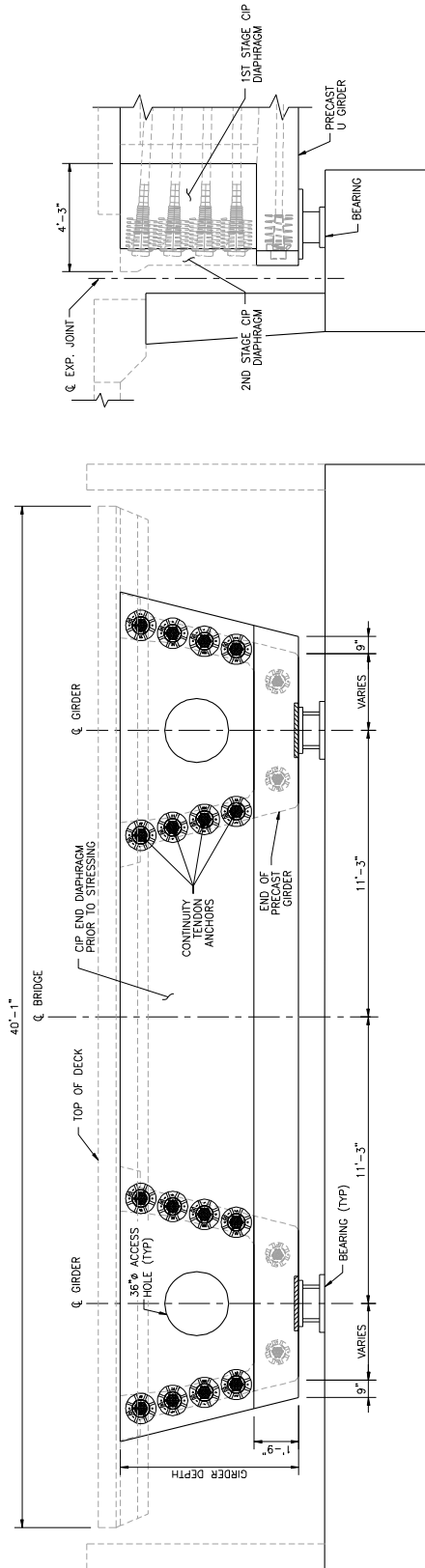
Drawing/Sheet Number **U-9**
Spliced U-Girders
Typical Three Span Constant Depth Girders
 PCI Zone 6 (SE Region) U-Girders



AASHTO/PCI REGIONAL PRODUCTS

PCI Zone 6 (SE Region) Spliced U-Girders

PCI Zone 6 (SE Region) Spliced U-Girders



SECTION AT ABUTMENT

ELEVATION AT ABUTMENT

NOTES

1. INFORMATION SHOWN ON THIS DRAWING IS INTENDED TO ILLUSTRATE A WORKING CONCEPT FOR SPICED U-GIRDERS. ALL CONCRETE DIMENSIONS AND REINFORCEMENT ARE FOR ILLUSTRATION PURPOSES ONLY.

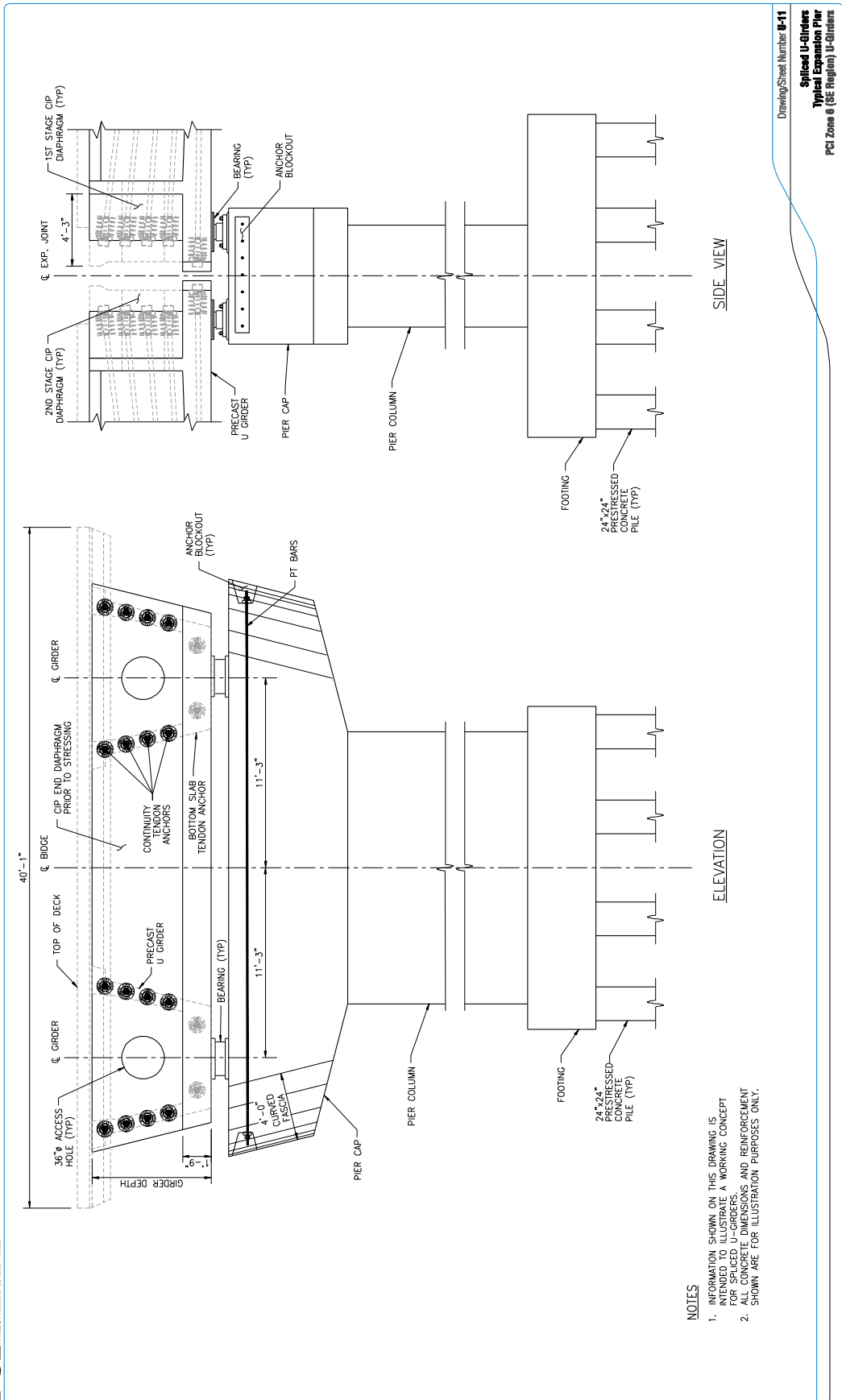
Drawing/Sheet Number B-10

Spliced U-Girders
End Diaphragm at Abutment
PCI Zone 6 (SE Region) U-Girders

AASHTO/PCI REGIONAL PRODUCTS

PCI Zone 6 (SE Region) Spliced U-Girders

PCI Zone 6 (SE Region) Spliced U-Girders



- NOTES**
1. INFORMATION SHOWN ON THIS DRAWING IS BASED ON THE ASSUMPTION OF A WORKING CONCEPT FOR SPliced U-GIRDERS.
 2. ALL CONCRETE DIMENSIONS AND REINFORCEMENT SHOWN ARE FOR ILLUSTRATION PURPOSES ONLY.

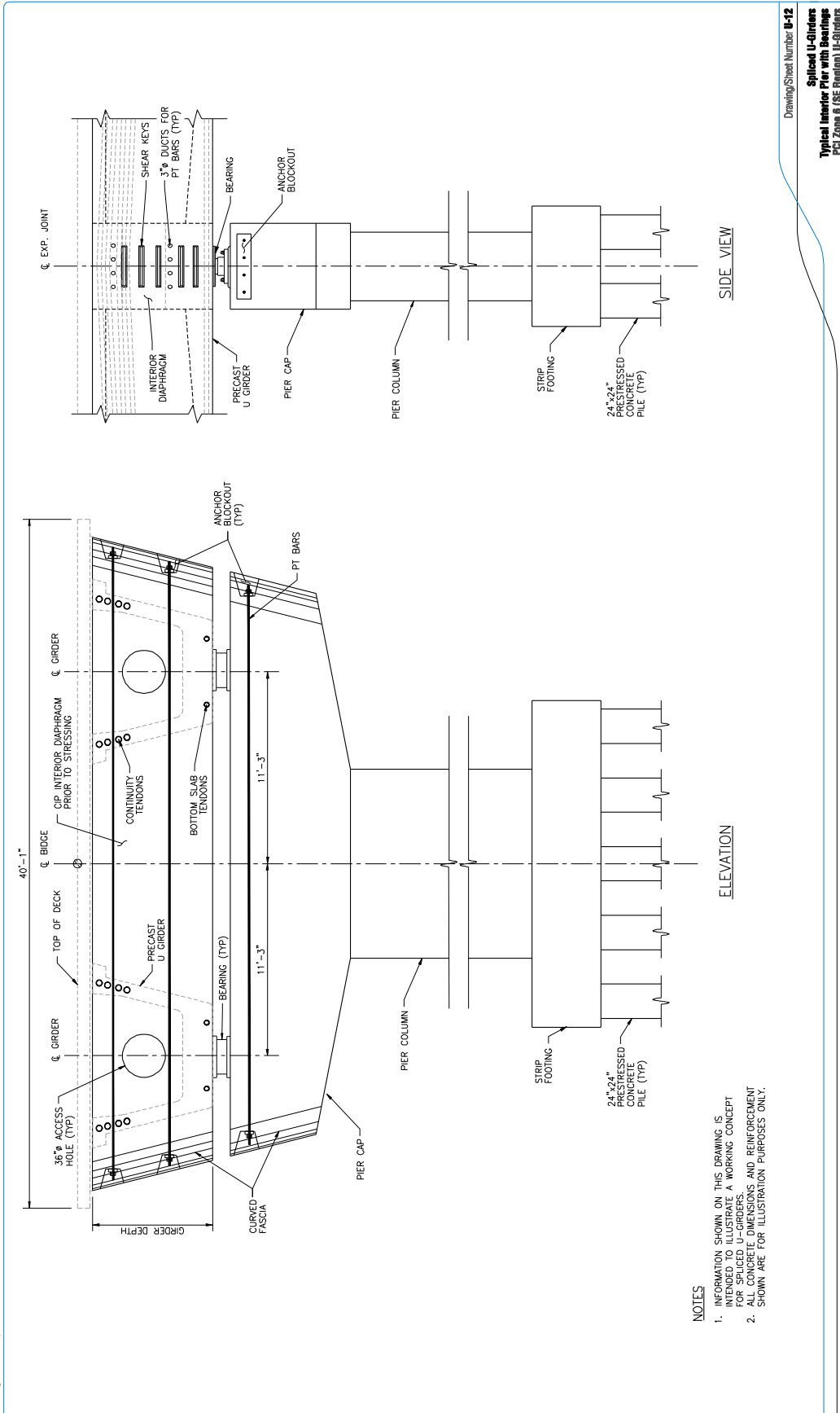
Drawing/Sheet Number **B-11**
Spliced U-Girders
Typical Expansion Pier
 PCI Zone 6 (SE Region) U-Girders



AASHTO/PCI REGIONAL PRODUCTS

PCI Zone 6 (SE Region) Spliced U-Girders

PCI Zone 6 (SE Region) Spliced U-Girders



Drawing Sheet Number **B-12**
Spliced U-Girders
Typical Interior Pier with Basins
PCI Zone 6 (SE Region) U-Girders

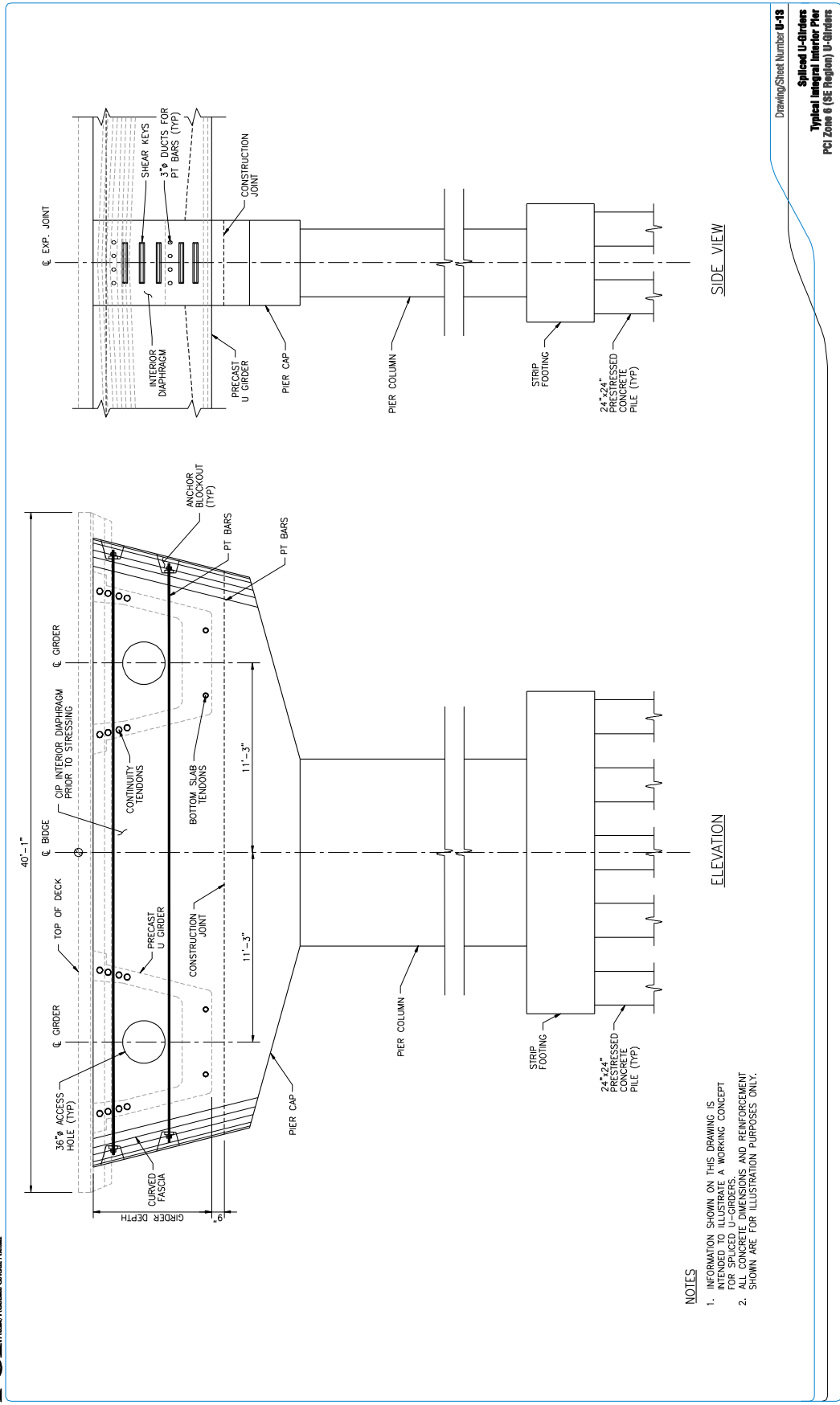
- NOTES**
1. INFORMATION SHOWN ON THIS DRAWING IS INTENDED TO ILLUSTRATE A WORKING CONCEPT FOR SPICED U-GIRDERS.
 2. ALL CONCRETE DIMENSIONS AND REINFORCEMENT SHOWN ARE FOR ILLUSTRATION PURPOSES ONLY.



AASHTO/PCI REGIONAL PRODUCTS

PCI Zone 6 (SE Region) Spliced U-Girders

PCI Zone 6 (SE Region) Spliced U-Girders



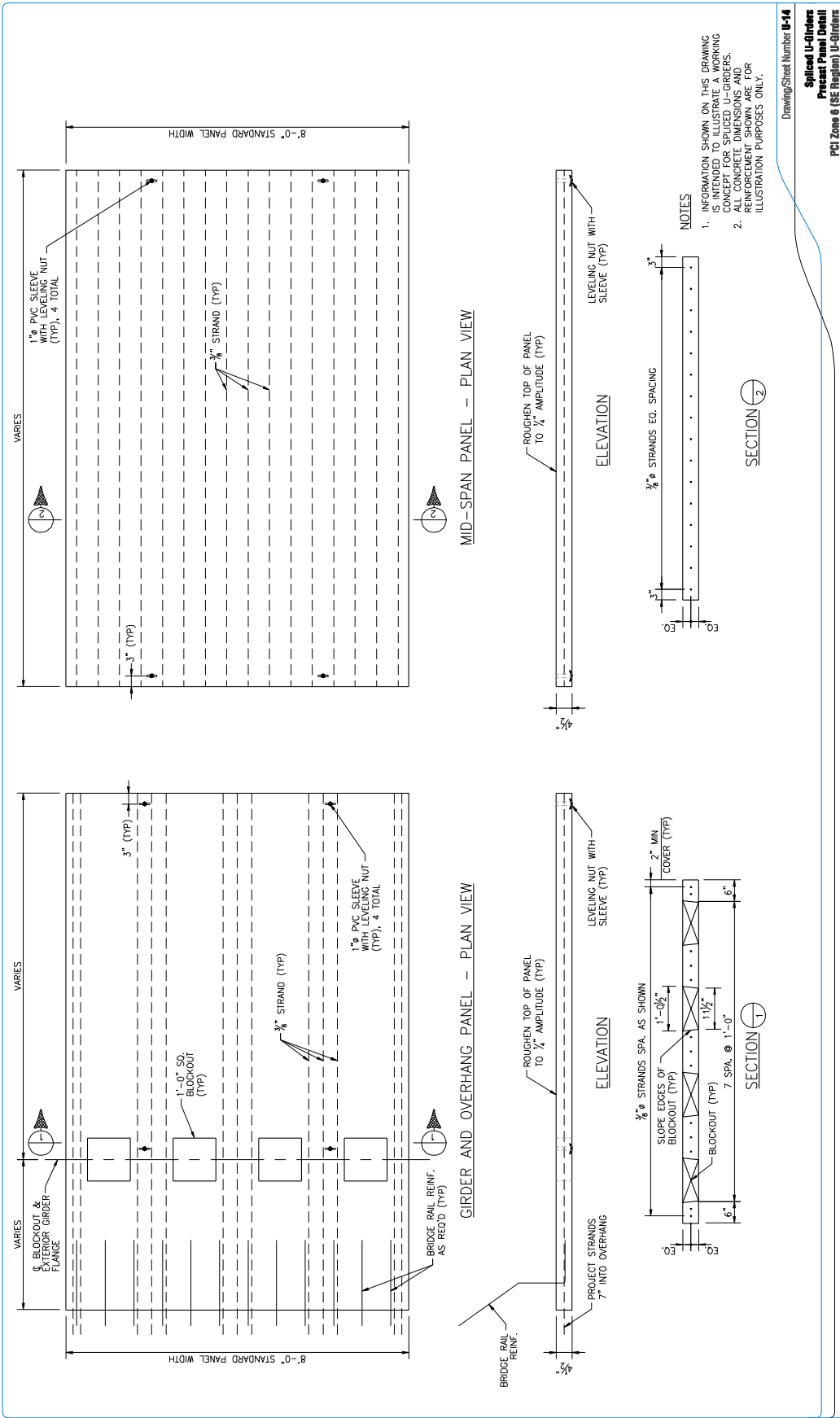
Drawing/Sheet Number **U-13**
Spliced U-Girders
Typical Integral Interior Pier
 PCI Zone 6 (SE Region) U-Girders



AASHTO/PCI REGIONAL PRODUCTS

PCI Zone 6 (SE Region) Spliced U-Girders

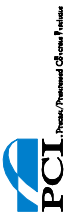
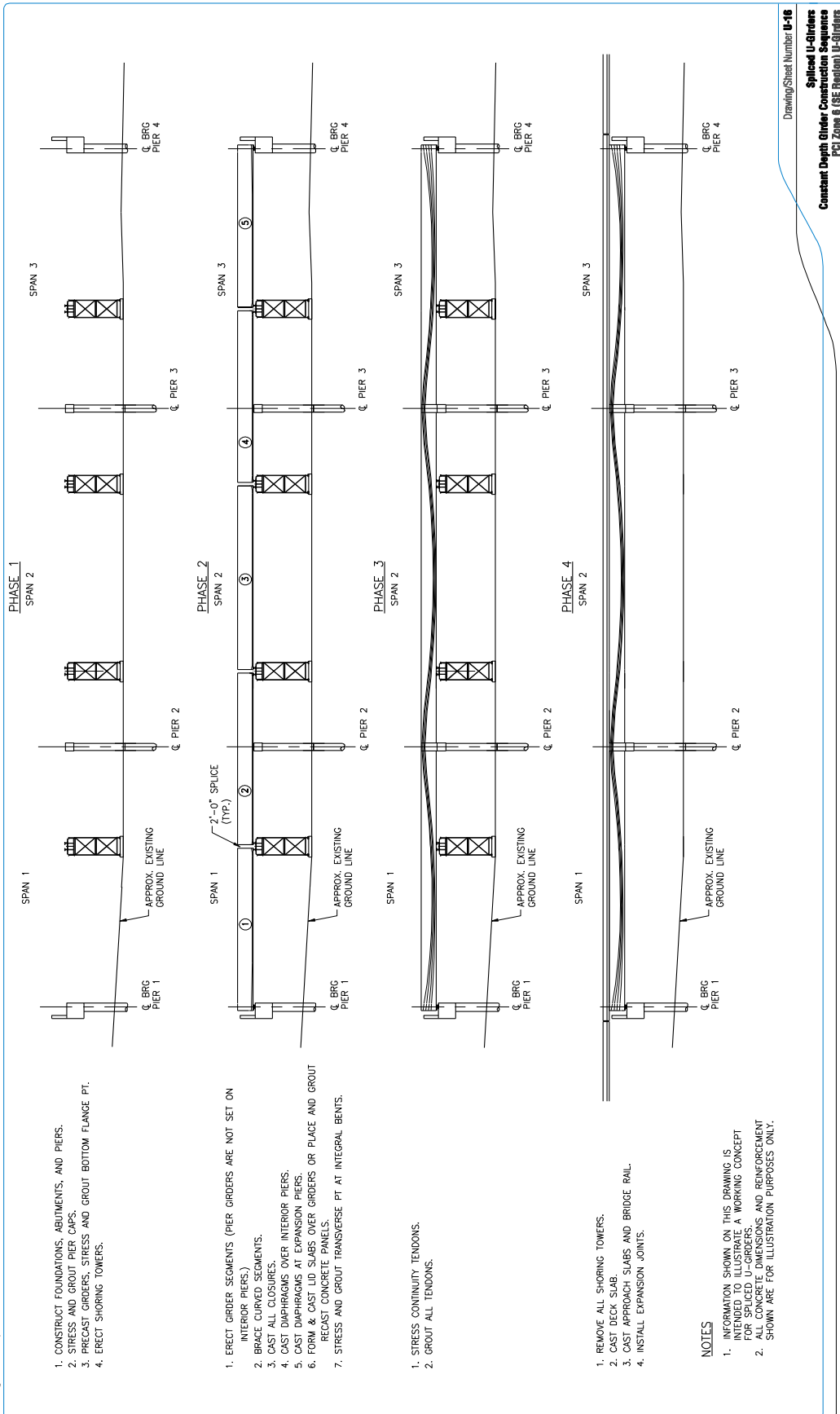
PCI Zone 6 (SE Region) Spliced U-Girders



AASHTO/PCI REGIONAL PRODUCTS

PCI Zone 6 (SE Region) Spliced U-Girders

PCI Zone 6 (SE Region) Spliced U-Girders



PCI
A Division of Paragon Construction

1. CONSTRUCT FOUNDATIONS, ABUTMENTS, AND PIERS.
2. STRESS AND GROUT PIER CAPS.
3. PRECAST GIRDERS, STRESS AND GROUT BOTTOM FLANGE PT.
4. ERECT SHORING TOWERS.

1. ERECT GIRDER SEGMENTS (PIER GIRDERS ARE NOT SET ON INTERIOR PIERS.)
2. BRACE CURVED SEGMENTS.
3. CAST ALL CLOSURES.
4. CAST DIAPHRAGMS OVER INTERIOR PIERS.
5. CAST DIAPHRAGMS AT EXPANSION PIERS.
6. FORM & CAST LID SLABS OVER GIRDERS OR PLACE AND GROUT RECAST CONCRETE PANELS.
7. STRESS AND GROUT TRANSVERSE PT AT INTEGRAL BENTS.

1. STRESS CONTINUITY TENDONS.
2. GROUT ALL TENDONS.

1. REMOVE ALL SHORING TOWERS.
2. CAST DECK SLAB.
3. CAST APPROACH SLABS AND BRIDGE RAIL.
4. INSTALL EXPANSION JOINTS.

NOTES

1. INFORMATION SHOWN ON THIS DRAWING IS BASED ON THE LATEST AVAILABLE WORKING CONCEPT FOR SPICED U-GIRDERS.
2. ALL CONCRETE DIMENSIONS AND REINFORCEMENT SHOWN ARE FOR ILLUSTRATION PURPOSES ONLY.

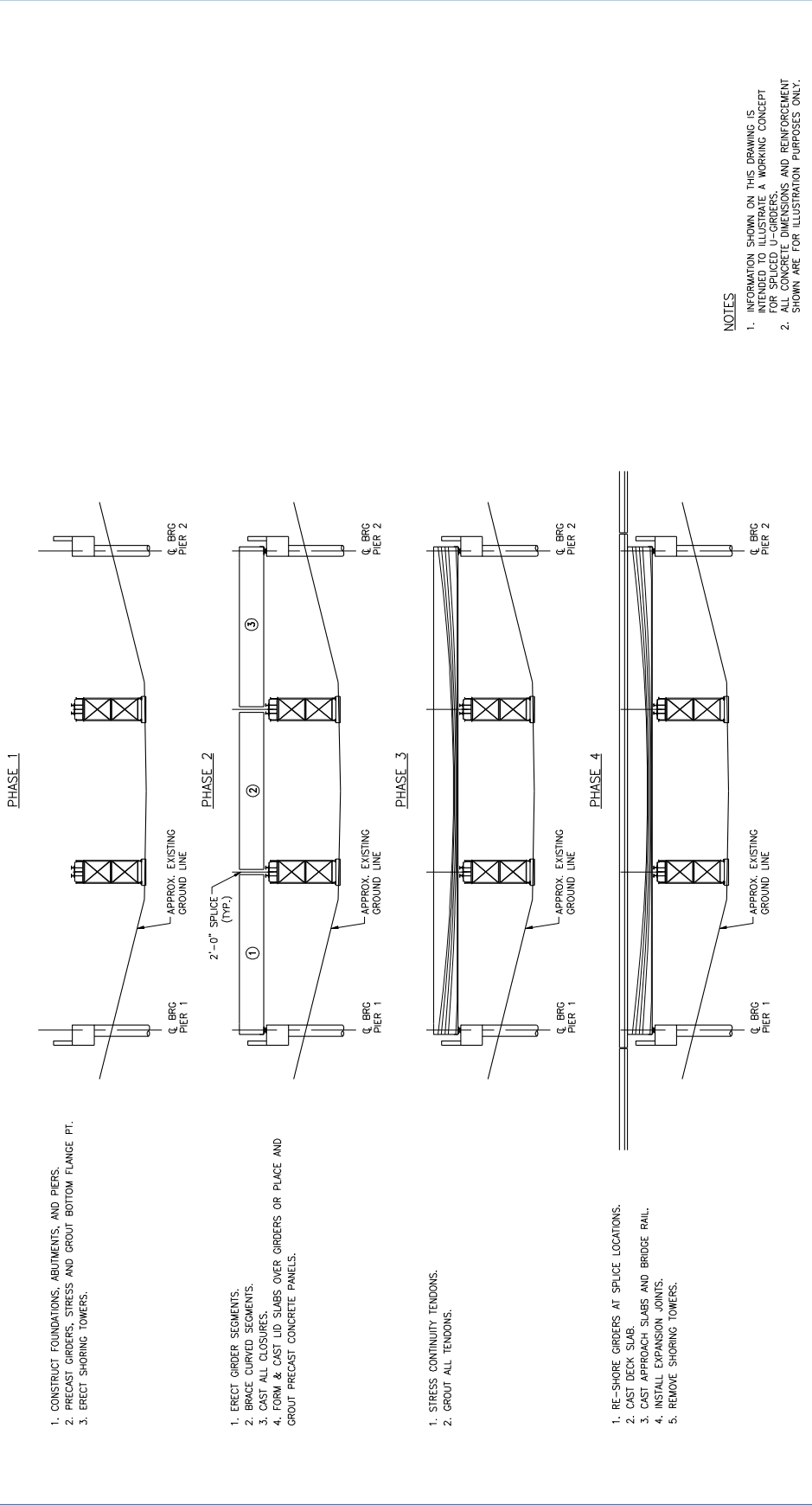
Drawing/Sheet Number U-16

Spliced U-Girders
Constant Depth Girder Construction Sequence
PCI Zone 6 (SE Region) U-Girders

AASHTO/PCI REGIONAL PRODUCTS

PCI Zone 6 (SE Region) Spliced U-Girders

PCI Zone 6 (SE Region) Spliced U-Girders



1. CONSTRUCT FOUNDATIONS, ABUTMENTS, AND PIERS.
 2. PRECAST GIRDERS, STRESS AND GROUT BOTTOM FLANGE FT.
 3. ERECT SHORING TOWERS.

1. ERECT ORDER SEGMENTS.
 2. BRACE CURVED SEGMENTS.
 3. CAST ALL CLOSURES.
 4. FORM & CAST LID SLABS OVER GIRDERS OR PLACE AND GROUT PRECAST CONCRETE PANELS.

1. STRESS CONTINUITY TENDONS.
 2. GROUT ALL TENDONS.

1. RE-SHORE GIRDERS AT SPLICE LOCATIONS.
 2. CAST DECK SLAB.
 3. CAST APPROACH SLABS AND BRIDGE RAIL.
 4. INSTALL EXPANSION JOINTS.
 5. REMOVE SHORING TOWERS.

NOTES

1. INFORMATION SHOWN ON THIS DRAWING IS FOR ILLUSTRATION PURPOSES ONLY. IT DOES NOT REPRESENT A WORKING CONCEPT FOR SPICED U-GIRDERS.
 2. ALL CONCRETE DIMENSIONS AND REINFORCEMENT SHOWN ARE FOR ILLUSTRATION PURPOSES ONLY.

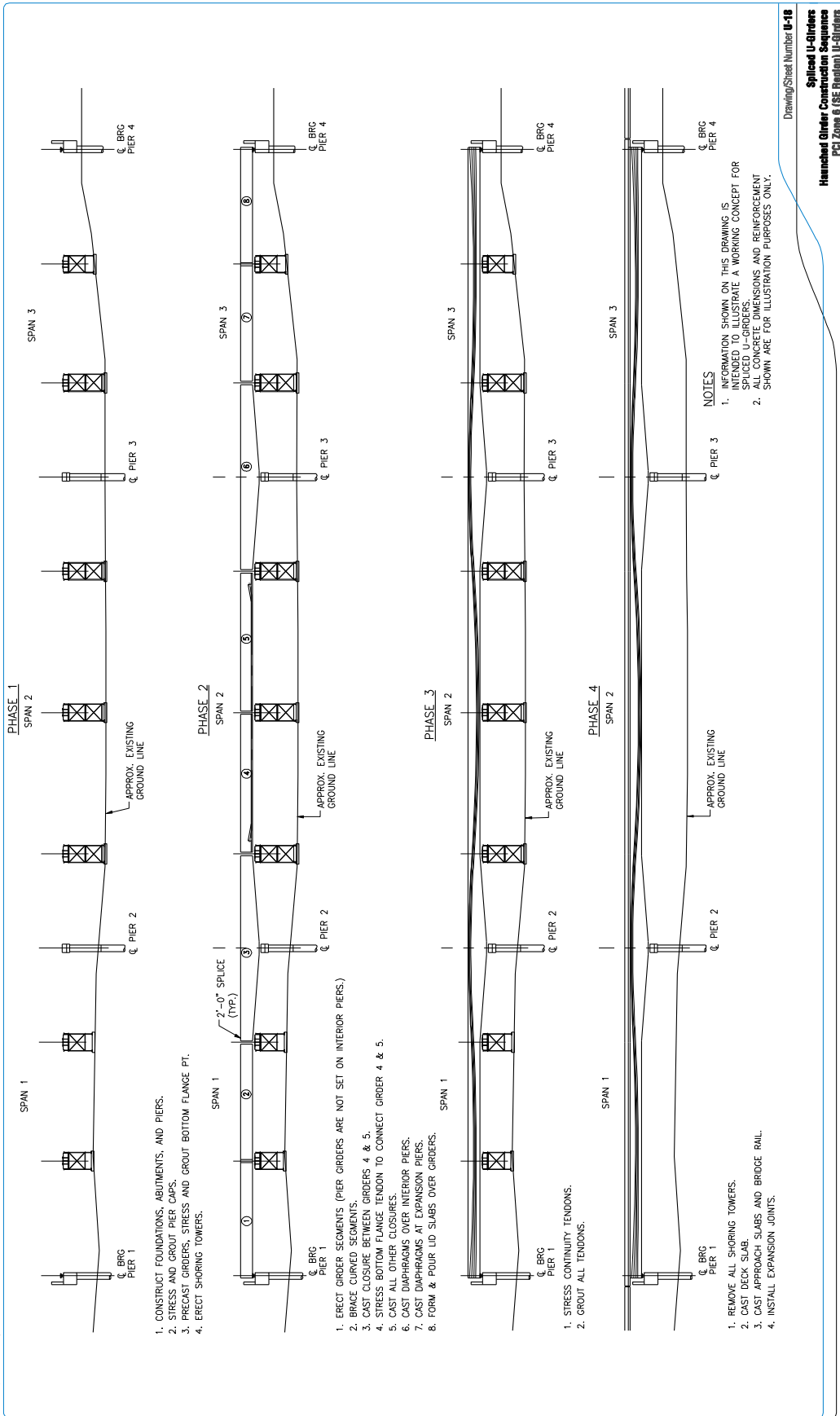
Drawing/Sheet Number U-17

Spliced U-Girders
 Simple Span Girder Construction Sequence
 PCI Zone 6 (SE Region) U-Girders

AASHTO/PCI REGIONAL PRODUCTS

PCI Zone 6 (SE Region) Spliced U-Girders

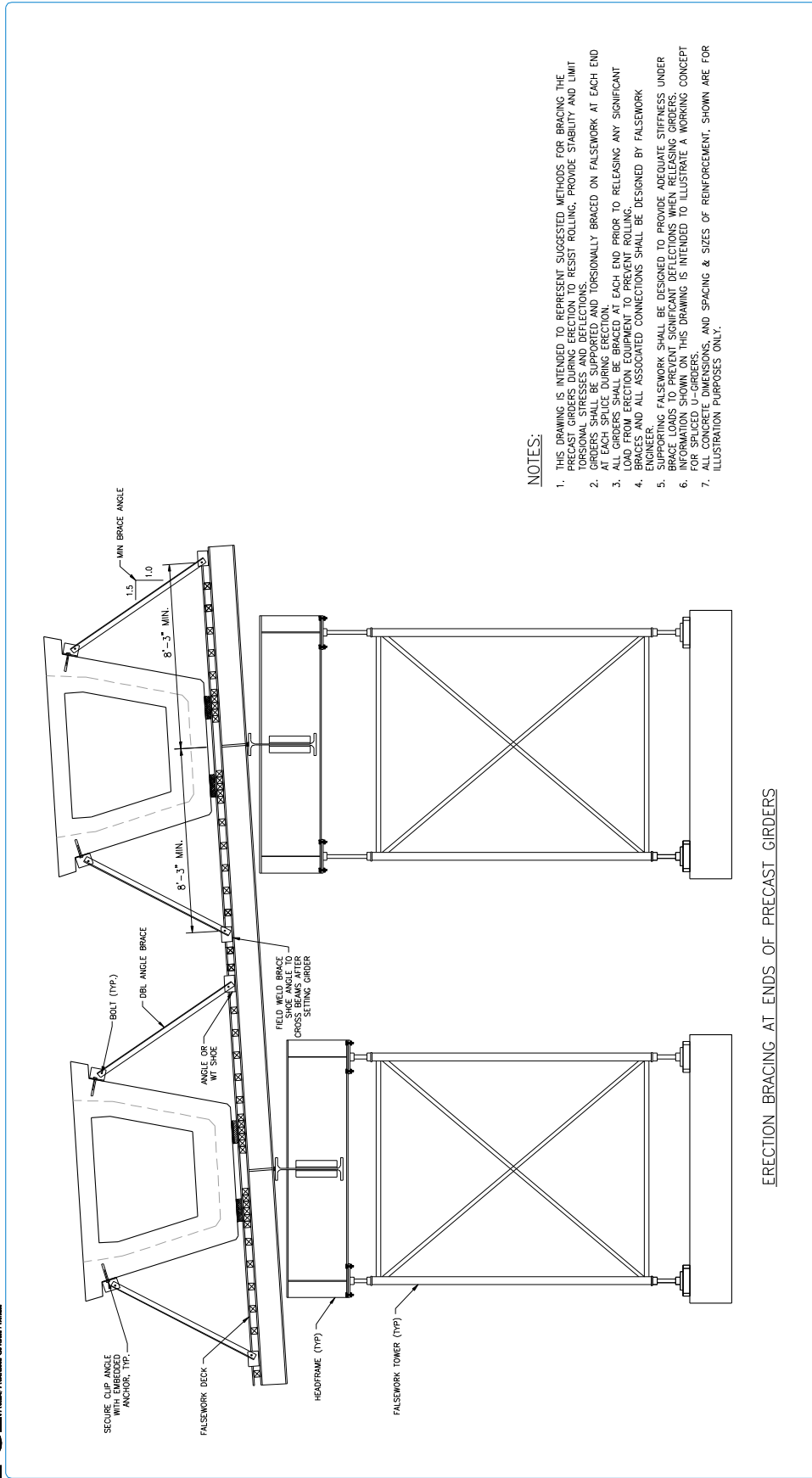
PCI Zone 6 (SE Region) Spliced U-Girders



AASHTO/PCI REGIONAL PRODUCTS

PCI Zone 6 (SE Region) Spliced U-Girders

PCI Zone 6 (SE Region) Spliced U-Girders



NOTES:

1. THIS DRAWING IS INTENDED TO REPRESENT SUGGESTED METHODS FOR BRACING THE PRECAST GIRDERS AGAINST DEFLECTIONS, RESIST ROLLING, PROVIDE STABILITY AND LIMIT TORSIONAL STRESSES AND DEFLECTIONS.
2. GIRDERS SHALL BE SUPPORTED AND TORSIONALLY BRACED ON FALSEWORK AT EACH END AT EACH SPICE DURING ERECTION.
3. ALL GIRDERS SHALL BE BRACED AT EACH END PRIOR TO RELEASING ANY SIGNIFICANT BRACE LOADS TO PREVENT SIGNIFICANT DEFLECTIONS, RESIST ROLLING.
4. BRACES AND ALL ASSOCIATED CONNECTIONS SHALL BE DESIGNED BY FALSEWORK ENGINEER.
5. SUPPORTING FALSEWORK SHALL BE DESIGNED TO PROVIDE ADEQUATE STIFFNESS UNDER BRACE LOADS TO PREVENT SIGNIFICANT DEFLECTIONS WHEN RELEASING GIRDERS.
6. INFORMATION SHOWN ON THIS DRAWING IS INTENDED TO ILLUSTRATE A WORKING CONCEPT FOR CONCRETE DIMENSIONS, AND SPACING & SIZES OF REINFORCEMENT, SHOWN ARE FOR ILLUSTRATION PURPOSES ONLY.

ERECTION BRACING AT ENDS OF PRECAST GIRDERS

Drawing/Sheet Number **U-19**

**Spliced U-Girders
Erection Bracing**
PCI Zone 6 (SE Region) U-Girders

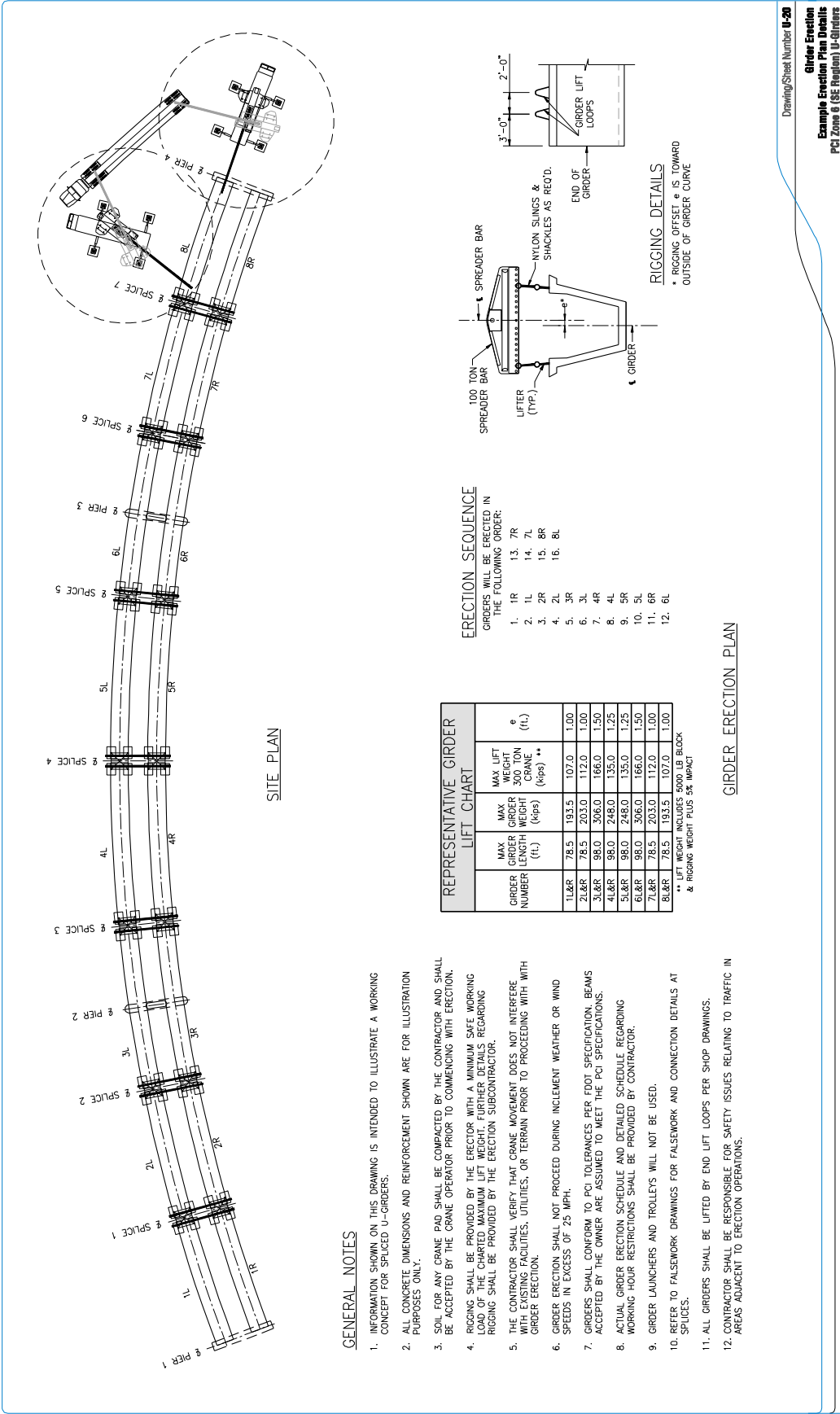
AASHTO/PCI REGIONAL PRODUCTS

PCI Zone 6 (SE Region) Spliced U-Girders

PCI Zone 6 (SE Region) Spliced U-Girders



Product/Trademark of PCI



SITE PLAN

GENERAL NOTES

1. INFORMATION SHOWN ON THIS DRAWING IS INTENDED TO ILLUSTRATE A WORKING CONCEPT FOR SPLICED U-GIRDERS.
2. ALL CONCRETE DIMENSIONS AND REINFORCEMENT SHOWN ARE FOR ILLUSTRATION PURPOSES ONLY.
3. SOIL FOR ANY CRANE PAD SHALL BE COMPACTED BY THE CONTRACTOR AND SHALL BE ACCEPTED BY THE CRANE OPERATOR PRIOR TO COMMENCING WITH ERECTION.
4. RIGGING SHALL BE PROVIDED BY THE ERECTOR WITH A MINIMUM SAFE WORKING LOAD OF THE CHARTED MAXIMUM LIFT WEIGHT. FURTHER DETAILS REGARDING RIGGING SHALL BE PROVIDED BY THE ERECTION SUBCONTRACTOR.
5. THE CONTRACTOR SHALL VERIFY THAT CRANE MOVEMENT DOES NOT INTERFERE WITH EXISTING FACILITIES, UTILITIES, OR TERRAIN PRIOR TO PROCEEDING WITH GIRDERS ERECTION.
6. GIRDER ERECTION SHALL NOT PROCEED DURING INCLEMENT WEATHER OR WIND SPEEDS IN EXCESS OF 25 MPH.
7. GIRDERS SHALL CONFORM TO PCI TOLERANCES PER FOOT SPECIFICATION. BEAMS ACCEPTED BY THE OWNER ARE ASSUMED TO MEET THE PCI SPECIFICATIONS.
8. ACTUAL GIRDER ERECTION SCHEDULE AND DETAILED SCHEDULE REGARDING WORKING HOUR RESTRICTIONS SHALL BE PROVIDED BY CONTRACTOR.
9. GIRDER LAUNCHERS AND TROLLEYS WILL NOT BE USED.
10. REFER TO FALSEWORK DRAWINGS FOR FALSEWORK AND CONNECTION DETAILS AT SPLICES.
11. ALL GIRDERS SHALL BE LIFTED BY END LIFT LOOPS PER SHOP DRAWINGS.
12. CONTRACTOR SHALL BE RESPONSIBLE FOR SAFETY ISSUES RELATING TO TRAFFIC IN AREAS ADJACENT TO ERECTION OPERATIONS.

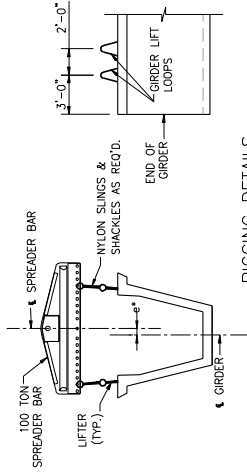
REPRESENTATIVE GIRDER LIFT CHART

GIRDER NUMBER	MAX GIRDER LENGTH (ft.)	MAX GIRDER WEIGHT (kips)	MAX LIFT WEIGHT 300 TON CRANE (kips) **	MAX LIFT WEIGHT (ft.)
1L&R	78.5	193.5	107.0	1.00
2L&R	78.5	203.0	112.0	1.00
3L&R	98.0	306.0	166.0	1.50
4L&R	98.0	248.0	135.0	1.25
5L&R	98.0	306.0	166.0	1.50
6L&R	78.5	203.0	112.0	1.00
7L&R	78.5	193.5	107.0	1.00

** LIFT WEIGHT INCLUDES 5000 LB BLOCK & RIGGING WEIGHT PLUS 5% IMPACT

ERECTION SEQUENCE

- GIRDERS WILL BE ERECTED IN THE FOLLOWING ORDER:
1. 1R
 2. 1L
 3. 2R
 4. 2L
 5. 3R
 6. 3L
 7. 4R
 8. 4L
 9. 5R
 10. 5L
 11. 6R
 12. 6L



RIGGING DETAILS

- * RIGGING OFFSET ϵ IS TOWARD OUTSIDE OF GIRDER CURVE

GIRDER ERECTION PLAN

Drawing/Sheet Number **U-20**
Girder Erection
Example Erection Plan Details
PCI Zone 6 (SE Region) U-Girders

SAMPLE SPECIFICATIONS

Table of Contents

Introduction.....Appendix D - 3

Nebraska Department of Roads Specifications.....Appendix D - 5

 705 PRECAST/PRESTRESSED CONCRETE STRUCTURAL UNITS.....Appendix D - 5

Washington Department Of Transportation Specifications..... Appendix D - 14

 6-02.3(25) PRESTRESSED CONCRETE GIRDERS Appendix D - 14

 6-02.3(26) Cast-In-Place Prestressed Concrete..... Appendix D - 22

 6-02.3(27) Concrete for Precast Units Appendix D - 22

 6-02.3(28) Precast Concrete Panels..... Appendix D - 23

SAMPLE SPECIFICATIONS

This page intentionally left blank

SAMPLE SPECIFICATIONS

Introduction

Introduction

Generic specifications for production of precast and prestressed concrete products have not been published by the Precast/Prestressed Concrete Institute (PCI). Such specifications require extensive committee involvement and a lengthy consensus approval process within the PCI structure. As a temporary substitute for generic specifications, this Appendix lists, without technical alteration, the specifications used by the states of Nebraska and Washington. Nebraska represents Midwestern conditions, while Washington represents coastal conditions. These two sets of specifications are not claimed to be model specifications, nor are they representative of conditions throughout the country as diverse geographically and economically as the United States. For example, critical evaluation of the validity of weather-related provisions for applications in hot, humid locations in the Southeast or hot, dry locations in the Southwest need to be assessed. Also, the characteristics of aggregates and other local raw materials need to be taken into account in adapting sample specifications to a particular location.

Both sets of specifications have recently been updated, and are thus reflective of most recent thinking of professionals at the Nebraska Department of Roads and the Washington State Department of Transportation. Both states are known to have leadership in the area of precast/prestressed concrete and are known to have a strong partnership with PCI and its producer members.

SAMPLE SPECIFICATIONS

Nebraska Department of Roads Specifications

This page intentionally left blank

SAMPLE SPECIFICATIONS

Nebraska Department of Roads Specifications

Nebraska Department of Roads Specifications**705 PRECAST/PRESTRESSED CONCRETE STRUCTURAL UNITS****705.01 Description**

1. This work consists of all labor, materials and equipment required in the production of precast/prestressed structural units.

705.02 Material Requirements

1. The materials used shall meet the requirements prescribed in this specification.
2. Precast/prestressed concrete structural units whose compressive strength does not achieve design strength shall be rejected.
3. The concrete class used in the manufacture of precast/prestressed structural units shall be shown in the Plans.
4. The Contractor is responsible for the concrete mix design and may use other concrete mixes which are proportioned in accordance with ACI Standard 318 and the following additional requirements:
 - a. The mix designs shall be submitted to the Engineer 30 working days before beginning any concrete work.
 - b. Concrete shall consist of Type I, Type II or Type III Portland cement, aggregate, air-entraining admixture and water. Concrete may also contain Class C or Class F fly ash, and ASTM C494 approved Type A, Type B, Type D and Type F admixtures.
 - c. The minimum cement content shall be 335 kg per cubic meter.
 - d. Coarse aggregate shall have a minimum limestone content of 30 percent of the total aggregate by mass.
 - e. Fly ash cannot exceed 15 percent of cement by mass.
 - f. Data from at least 15 individual batches shall be collected and given to the Engineer. The data collected shall include the following:
 - (1) The 28-day compressive and flexural strength test results.
 - (2) The water cement ratio.
 - (3) The air content between 2.0 percent and 6.0 percent inclusive.
 - (4) The cement and fly ash content.
 - (5) The amount of fine aggregate, coarse aggregate, and sand and gravel.
5. No change shall be made in the concrete mix design during the progress of the work without the prior written permission of the Engineer.
6. Welding reinforcing steel is prohibited unless specifically authorized by the Engineer.
7. Prestressed steel other than that specified in the Plans or Special Provisions may be furnished with the approval of the Engineer. The yield and ultimate strength and other pertinent characteristics of this steel shall be submitted to the Engineer.
8. The area of broken wires shall not exceed 2 percent of the cross-sectional area of the stressing strands when the number of strands is 14 or less.
9. The area of broken wire shall not exceed 1 percent of the cross-sectional area of the stressing strands when the number of strands exceeds 14.
10. No more than one broken wire will be allowed in a single strand.
11. Bars for post-tensioning shall be of high tensile strength steel. They shall be equipped with wedge-type end anchorages which will develop the minimum specified ultimate bar stress on the nominal bar area. The physical properties of the bar steel determined by static tensile tests shall conform to the following:

SAMPLE SPECIFICATIONS

Nebraska Department of Roads Specifications

High-Strength Steel Post-Tensioning Requirements

- Ultimate Stress 1,000.....MPa minimum
- Stress at 0.7%..... Elongation 896 MPa minimum
- Stress at 0.3%..... Elongation 517 MPa minimum
- Elongation in 20 Diameters.....4% minimum
- Modulus of Elasticity..... 172 GPa minimum
- Diameter Tolerance..... Plus or Minus 2.54 mm

12. Materials specified for testing shall be furnished 30 days before anticipated time of use. All materials required for testing shall be furnished by the Contractor to the Engineer without additional costs to the Department. The Engineer shall select a representative sample length for the various prestressed steel as follows:
 - a. Two meters for wires requiring heading.
 - b. For wires not requiring heading, sufficient length to make up one parallel-lay cable two meters long consisting of the same number of wires as the cable to be furnished.
 - c. Two meters between near ends of fittings for a strand furnished with fittings.
 - d. Two meters between threads at the ends of bars furnished with threaded ends.
13. If the anchorage assemblies are not attached to prestressing steel samples, two anchorage assemblies shall be furnished for testing, complete with distribution plates of each size or type of prestressing steel to be used.
14. Any defective material shall be rejected
15. Concrete quality control shall be the responsibility of the Contractor. Concrete shall be sampled and tested as shown in **Table 705.02**.

Table 705.02

Required Concrete Sampling and Testing		
Correlation Test	Contractor Test Samples*	Department Test Samples
Yield ASTM C138 Air meter measuring bowl.	One per day.	One per 10 Contractor tests
Air content ASTM C231 (0.8% variation allowed)	One per load	One every five production days
Concrete temperature ASTM C1064	One per load	One every five production days
Concrete Compressive Strength		
28-day strength ATM C31 Section 9.3 cure.	Two cylinders – each from a different load; and one from the last load	One set of two cylinders every five production days
56-day strength (only if 28-day strength is less than specified.) ASTM C31 Section 9.7 cure.	Two cylinders – each from a different load and from the same load as 28-day break.	NA
* At least 6 cylinders shall be made each production day and at least 2 cylinders are required from each load.		
* Cylinders shall be 150 mm by 300 mm.		

SAMPLE SPECIFICATIONS

Nebraska Department of Roads Specifications

16. Plant Approval Requirements:

- a.
 - (1) All precast/prestressed concrete structural units shall be produced in a Precast/Prestressed Concrete Institute (PCI) Certified Plant.
 - (2) The method of manufacture and quality of concrete are also subject to Department approval/inspection.
- b.
 - (1) A Contractor proposing to furnish precast/prestressed structural units shall submit the following additional details to the Department concerning the method of manufacture:
 - (i) Type, number, size and location of the prestressing elements, and the name of the manufacturer of the post-tensioning or pretensioning elements.
 - (ii) Complete information as to type, size and method of installation of devices for anchoring post-tensioning elements.
 - (iii) The proposed manufacturing methods, and the Plans and design details of proposed casting beds and forms.
- c. The use of portable pretensioning beds for the manufacture of concrete structural units or piles will not be allowed.

705.03 Construction Methods

1. The Contractor shall construct precast structures and piles as shown in the Plans.
2. The Contractor shall erect precast concrete structures and drive precast concrete piles as prescribed in the Plans.
3.
 - a. When the precast superstructure units have been erected, the Contractor shall pack the shear key openings with grout.
 - b. A pneumatic tool shall be used.
 - c. Grout to be used for constructing shear keys in the precast concrete superstructure shall be composed of either Type I or Type II Portland cement, aggregate and water.
 - (i) The aggregate shall be fine aggregate as specified for the class of concrete being furnished.
 - (ii) The Portland cement and aggregate shall be proportioned on the basis of 350 kg of dry aggregate per 100 kg of cement.
 - (iii) The water content of the grout shall be limited to that necessary for proper mixing and placement. In no case shall the total water content exceed 45 kg per 100 kg of cement.
4.
 - a. No live load shall be allowed on the superstructure units until the shear keys and tie bolts have been placed and the shear key grout cured, unless cross planking or mats not less than 190 mm in thickness and 4.2 m long are placed on the structure to distribute the load.
 - b. In no case shall the live load vehicle mass exceed:
 - (i) 23 Mg.
 - (ii) 9 Mg on any single axle
 - (iii) 18 Mg on any tandem axle.
5. Stressing Requirements
 - a.
 - (1) In all methods of tensioning, the stress induced in the prestressing elements shall be measured by the Contractor both with jacking gages and by elongation of the elements, and these results shall be the same within a five-percent tolerance.
 - (i) Means shall be provided for measuring the elongation of reinforcement to at least the nearest 3 mm.

SAMPLE SPECIFICATIONS

Nebraska Department of Roads Specifications

- (ii) All steel stressing devices, whether hydraulic jacks or screw jacks, shall be equipped with accurate reading calibrated pressure gages, rings or other devices as applicable to the jack being used.
 - (iii) All devices shall be calibrated and, if necessary, recalibrated so as to allow the stress in the prestressing steel to be computed at all times.
 - (iv) A certified calibration curve shall accompany each device.
 - (v) Safety measures must be taken by the Contractor to prevent accidents due to possible breaking of the prestressing steel or the slipping of the grips during the prestressing process.
- (2) All calibrations and tests shall be performed at no additional cost to the Department.
- (3) Pressure gages, load cells, dynamometers, and any other devices used in determination of loads and/or pressures shall be accurate in their effective range within a two-percent tolerance.
- (i) Such equipment shall be calibrated by an approved testing laboratory.
 - (ii) The laboratory shall furnish calibration curves for each device and shall certify the curves as being accurate and verifiable.
 - (iii) The calibration of tensioning devices shall be accomplished in place.
 - (iv) The configuration of jacks, gages and other components during calibration shall be exactly the same as during the actual stressing operation.
 - (v) The method of calibration shall be as approved by the Engineer.
 - (vi) Tensioning devices shall be calibrated at least once a year and anytime a system appears to be operating in an erratic or inaccurate manner, or gage pressure and elongation measurements fail to correlate.
- (4) If the strand tension indicated by the gage pressure and by elongation method fail to agree within five percent, the operation shall be carefully checked and the source of error determined before proceeding further.
- b.
- (1) The Contractor's elongation and jacking pressure measurements shall make appropriate allowance for friction and all possible slippage or relaxation of the anchorage.
 - (2) For pretensioned members, independent references shall be established adjacent to each anchorage by the Contractor to indicate any yielding or slippage that may occur between the time of initial stressing and final release of the cables.
 - (3) The Contractor may tension straight post-tensioned tendons from one end. The curved tendons shall generally be stressed by simultaneous jacking from both ends of the bar.
- c. In all stressing operations, the Contractor shall keep stressing force symmetrical about the member's vertical axis.
6. Stressing Procedure:
- a. Prestressing methods are shown in the Plans. When the Contractor elects to use a method other than that shown in the Plans, the Contractor shall submit complete shop Plans for the proposed method.

SAMPLE SPECIFICATIONS

Nebraska Department of Roads Specifications

- (1) Pretensioning method.
 - (2) Post-tensioning method.
 - (3) Combined method.
 - b. Pretensioning Method:
 - (1) The amount of stress to be given each strand by the Contractor shall be as shown in the Plans.
 - (2) All strands to be prestressed in a group shall be brought to a uniform initial tension before being given their full pretensioning. This uniform initial tension of approximately 4.5 to 9.0 kN shall be measured by a dynamometer or other approved means so that it can be used as a check against the computed and measured elongation.
 - (3) After initial tensioning, either single strand or multiple strand groups shall be stressed until the required elongation and jacking pressure are attained and reconciled within the five-percent tolerance.
 - (4) With the strand stressed in accordance with the Plan requirements and these Specifications, and with all other reinforcing in place, the Contractor shall cast the concrete to the lengths desired. Strand stress shall be maintained between anchorages until the concrete has reached the compressive strength specified in the Plans.
 - c. Post-tensioning Method: For all post-tensioned bars, the Contractor shall set the anchor plates exactly normal in all directions to the axis of the bar. Parallel wire anchorage cones shall be recessed within the beams. Tensioning shall not be done until the concrete has reached the compressive strength specified in the Plans.
 - d. Combined Method: In the event that the girders are manufactured with part of the reinforcement pretensioned and part post-tensioned, the applicable portions of the requirements listed above shall apply to each type.
7. Forms:
 - a. Forms for precast/prestressed concrete structural units shall conform to therequirements for concrete formwork as provided in Section 704.
 - b. Forms shall be accessible for the vibration and consolidation of concrete.
8. Placing Concrete:
 - a. The Contractor shall provide the Department a 4-week production schedule that is updated as necessary. Unscheduled production changes may delay fabrication when the Department elects not to reschedule inspectors.
 - b. The Engineer may observe any or all of the procedures and shall have access to all reported data anytime during fabrication. The Engineer shall report any inconsistencies to the job superintendent and note them in the plant diary.
 - c. Concrete shall not be placed before completing the forming and placing of reinforcement.
 - d.
 - (1) Concrete shall be placed continuously in each unit, take care to avoid horizontal or diagonal planes of weakness.
 - (2) However, if there is a delay in delivery of concrete, or for some other reason placement is interrupted for more than 30 minutes, then the concrete shall be rejected.
 - e.
 - (1) Special care shall be exercised to work and consolidate the concrete around the reinforcement and to avoid the formation of stone pockets, honeycombs and other defects.
 - (2) The concrete shall be consolidated by vibrating, or other means approved by the Engineer.
 - f. The forms shall be overfilled, the excess concrete screeded off, and the top surfaces finished to a uniform, even texture.

SAMPLE SPECIFICATIONS

Nebraska Department of Roads Specifications

- g. Each precast/prestressed concrete structural unit shall be stamped or marked with an identification number and its manufacture date.
 - h.
 - (1) The optimum range of concrete temperatures from the time the concrete is completely mixed until the beginning of the presteam segment of the steam curing cycle shall be 10C to 35C. Failure to operate within the optimum range shall be cause for curtailment of operations to operate consistently within the range set forth. During the preset segment of the curing cycle, the temperature of the concrete shall not exceed 38C nor fall below 10C.
 - (2) When placing concrete under cold weather conditions (ambient air temperature less than 2C), follow the cold weather Specifications in Section 1002.
 - (3) Forms and reinforcing materials shall be preheated to a minimum temperature of 5C and a maximum temperature not to exceed that of the concrete at the time of placement.
 - (4) The Contractor may preheat the drums of the mixer-trucks to the limits set for forms and reinforcing, but under no condition shall heat be applied to
9. Curing:
- a. General:
 - (1) The Contractor shall cure the concrete with wet burlap, waterproof covers, polyethylene sheets, or liquid membrane-forming compound. Liquid membrane-forming compound shall not be used on that portion of precast/prestressed concrete girders, twin tees, or bridge beams upon which concrete will be cast later.
 - (2) Water spray curing, or other moist curing methods may be used, subject to the approval of the Engineer.
 - (i) The period of curing shall be determined by the results of the compressive strength test on cylinders made during the progress of the work and cured to closely approximate the concrete strength of the product it represents.
 - (ii) Side forms may be removed 12 hours after placing the concrete, provided curing is continued with one of the approved NDOR curing procedures.
 - b. Steam or radiant heat will be allowed for accelerated curing provided the following procedure is adhered to:
 - (1) Curing chambers shall be reasonably free of leakage and shall have a minimum clearance of 75 mm between the enclosure and restricting portions of the forms in order to ensure adequate circulation of heat. The relative humidity within the curing enclosure shall be maintained between 70 and 100 percent.
 - (2) One approved continuous recording thermometer for each 35 meters of casting bed with a minimum of two continuous recording thermometers shall be located in each enclosure or curing chamber.
 - (i) Continuous temperature record charts for each casting shall be available to the Engineer for his examination and approval at anytime.
 - (ii) If the temperature records or other temperature readings taken by the Engineer indicate that hand control of heat is producing temperature changes in excess of those specified, the Engineer may direct that automatic controls which can be activated by the recording thermometers or by separate temperature switches be installed. These automatic controls are to control the rate of temperature change and maximum curing temperature according to a preset plan.
 - (3) Temperature of the curing concrete shall be 10C to 30C and shall be maintained near placement temperature until the concrete has reached initial set as determined by ASTM C403 "Time of Setting of Concrete Mixture by Penetration Resistance."
 - (i) The temperature rate of rise shall not exceed 30C per hour.

SAMPLE SPECIFICATIONS

Nebraska Department of Roads Specifications

- (ii) The concrete shall be completely covered with a waterproof curing chamber during accelerated curing periods.
 - (4) Steam jets shall not be directed at the concrete or the steel forms.
 - (5) When the heat has been applied for a minimum of 3 hours and the desired concrete temperature has been reached (not to exceed 80C), the heat source may be turned off. Should the temperature within the concrete rise above 80C, the concrete shall be rejected.
 - (6) The temperature in the concrete shall be maintained so that at any given time the difference between the highest and lowest temperature station readings will not be more than 15C.
 - (7) Eight hours after placing the concrete, individual sections may be uncovered to remove their forms. The curing may be discontinued during this operation. The section shall not be left uncovered longer than necessary and never longer than 30 minutes. Waterproofed covers shall be used to recover the product.
 - (8) After the heat source has been turned off, the curing cover shall be maintained in place during the soaking period until the release strength has been reached.
 - (9) Detensioning shall be accomplished before the temperatures of the units drop below 40C and while they are still moist.
 - (10) An automatic master slave heat curing system may be used for curing quality control cylinders.
10. Defects and Repair Procedures:
- a. After the forms are removed, stone pockets, honeycombs, or other defects may be exposed. The Engineer shall determine if these defects affect the item's structural integrity and in which case the item will be rejected.
 - b. Precast/prestressed concrete structural units which have chips, spalls, honeycomb or otherwise defective areas which are not considered detrimental to structural integrity may be used after being repaired in the following manner:
 - (1) Remove all unsound concrete.
 - (2) Coat the affected area with epoxy resin binder. Care shall be taken to prevent getting epoxy on the exposed surface.
 - (3) Fill the prepared area with Class "47B-XX" concrete mix (Aggregate larger than 10 mm is not allowed) with the type of cement used in placing the unit. Where the unit is exposed to view, white cement shall be added to give a uniform appearance with the concrete surrounding the patch.
 - (4) Place and secure formwork to ensure all required configurations.
 - (5) Cure 24 hours with wet burlap. Steam curing at 25°C will be allowed.
 - (6) The patch shall be ground smooth to remove all joints.
11. Surface Finish
- a. The exterior face of all exterior girders or beams plus the bottoms and chamfers on all lower flanges shall be given the following finish:
 - (1) All uneven form joints in excess of 3 mm shall be ground smooth.
 - (2) The surface shall be steel brushed to remove scale and laitance, and to open partially obstructed holes.
 - (3) Dampen surface.
 - (4) The grout shall consist of 1.5 parts of fine sand, 1 part of Portland cement and sufficient water to produce a consistency of thick paint. The cement used in the grout shall be a blend of regular Type I and white Portland cement to duplicate the lighter appearance of the steam-cured units.

SAMPLE SPECIFICATIONS

Nebraska Department of Roads Specifications

- (5) If necessary, an admixture which will not discolor the concrete may be used in the grout to reduce shrinkage if approved by the Engineer. Admixtures containing iron particles shall not be used.
 - (6) Apply grout to the surface.
 - (7) The surface shall be float finished with a cork or other suitable float. This operation shall completely fill all holes and depressions on the surface.
 - (8) When the grout is of such plasticity that it will not be pulled from holes or depressions, sponge rubber or burlap shall be used to remove all excess grout.
 - (9) Surface finishing during cold weather shall not be performed unless the temperature is 50C and rising. The surface shall be protected against temperature drops below 5C for a period of 12 hours after finishing.
 - (10) A uniform appearance will be required. In the event the appearance produced by the above procedure is not uniform, both in texture and coloration, other methods approved by the Engineer shall be employed.
- b. The interior face of an exterior girder or beam and all interior girders or beams shall be finished from the lower flange to the fillet of the web in accordance with subparagraphs (3), (4), (5) and (6) above.
12. Grouting for Post-Tensioned Units:
- a. The Contractor shall install steel in flexible or other approved tubes which shall be cast in the concrete and shall be pressure-grouted after the prestressing process has been completed.
 - b. Bonding grout shall be made to the consistency of thick paint and shall be mixed in the proportions as follows: Portland cement (Type I), 45 kg; Fly ash (ASTM C618), 15 kg; Water, 20 to 27 kg (adjust at site); and admixture (Interplast B), 0.5 kg.
 - c. The final grouting pressure shall be at least 550 kPa.
 - d. The Contractor shall make provisions to demonstrate to the Engineer that grouting material has completely filled all areas within the conduit.
13. The Contractor shall paint all exposed metal, except weathering grade steel.
14. Handling, Transporting and Storing:
- a.
 - (1) After precast structural units have attained a compressive strength of 20 Mpa, the Engineer shall approve the method used to remove the units from the casting beds.
 - (2) Prestressed concrete structural units shall attain the "release" strength specified in the Plans before being delivered to the site. Prestressed concrete structural units will not be incorporated in the final product until the minimum age and strength specified in the Plans is attained.
 - (3) All precast/prestressed concrete structure units shall be supported at or within 150 mm of all lifting or bearing devices. When supported at the proper positions, no part of the units shall be allowed to rest on the ground. Prestressed concrete bridge girders shall be set on a level area to prevent field bowing, and adequate supports shall be placed under their lifting or bearing devices to prevent settlement into the ground.
 - (4) The girders shall be transported in an upright position and the points of support and direction of the reactions with respect to the girder shall be approximately the same during the transportation and storage, as when the girder is in its final position. If the Contractor finds it necessary to transport or store the precast girders in some other position, the Contractor should be prepared to prove no internal damage resulted.
 - (i) Adequate padding shall be provided between tile chains and cables to prevent chipping of the concrete.
 - (ii) Live loads shall not be allowed on the superstructure units until the floor slab is placed and has attained the design strength shown in the Plans.

SAMPLE SPECIFICATIONS

Nebraska Department of Roads Specifications

15. Inspection Facilities:

- a. The Contractor shall arrange with the producer of precast/prestressed concrete structural units to provide an office laboratory, and a bathroom for the Department's inspector. The areas shall meet the following requirements:
 - (1) Thermostatically controlled heating and air conditioning shall be provided so that temperature can be maintained between 20C and 25C.
 - (2) The floors shall be tile or a similar floor covering.
 - (3) Interior and exterior walls shall be well maintained and painted.
 - (4) All exterior doors shall have cylinder locks and all keys shall be turned over to the Engineer.
 - (5) Ceiling lighting shall provide a minimum of 5,000 lx of light on all working surfaces.
 - (6) Electrical outlets shall be spaced no more than 2 m apart with no less than one outlet on any wall of the office or lab.
 - (7) A single trunk telephone shall be installed in the office and the installation charges shall be paid by the Contractor. The monthly charges shall be paid by the State.
 - (8) A fire extinguisher and first aid kit shall be provided.
 - (9) A ventilated bathroom with a toilet and sink shall be provided in the structure. A fresh water supply and drain will be required in the lab area.
 - (10) The lab, office and bathroom shall be separate rooms with interconnecting doors.
 - (11) The minimum lab area is 21 m².
 - (12) The minimum toilet area is 2 m².
 - (13) The minimum office area is 15 m².
 - (14) The Contractor shall clean and maintain the rooms and shall supply all heating fuel, electricity and water.
 - (15) The Contractor shall also supply for the sole use of the inspectors, all desks, work tables, chairs, files, lockers and sanitary supplies necessary and commensurate with the inspection of his/her plant. It is anticipated that the following minimum amount of office and lab equipment will be required: One desk with approximately 1 m x 2 m top; one upright locker or wardrobe, with shelves, approximately 1.5 m deep; two four-drawer file cabinets; one chair per inspector; one square meter of work surface per inspector in the office area; and a 1 m x 15 m lab counter with storage space beneath.

705.04 Method of Measurement and Basis of Payment

1. Precast/prestressed concrete superstructures will be measured for payment by the lump sum.
2. The cost of furnishing and maintaining the inspection facilities will not be paid for directly, but shall be considered subsidiary to the items for which the contract provides that direct payment will be made.
3. If a precast or prestressed structural item's 56-day compressive strength is less than the design strength, then the Engineer will determine if the item can be used. If the item is to be used, a payment deduction of 25 percent will be taken if the 56-day compressive strength is less than 95 percent of the design strength.
4. Payment is considered full compensation for all work prescribed in this Section including the cost of prestressing and precasting.

SAMPLE SPECIFICATIONS

Nebraska Department of Roads Specifications

Washington Department Of Transportation Specifications**6-02.3(25) PRESTRESSED CONCRETE GIRDERS**

The Contractor shall be required to perform quality control inspection. The manufacturing plant of prestressed concrete girders shall be certified by the Precast/Prestressed Concrete Institute's Plant Certification Program for the type of prestressed member to be produced and shall be approved by WSDOT as a Certified Prestress Concrete Fabricator prior to the start of production. WSDOT certification will be granted at, and renewed during, the annual prestressed plant review and approval process.

Prior to the start of production of girders, the Contractor shall advise the Engineer of the production schedule. The Contractor shall give the Inspector safe and free access to the work. If the Inspector observes any nonspecification work or unacceptable quality control practices, the Inspector will advise the plant manager. If the corrective action is not acceptable to the Engineer, the girder(s) will be rejected.

The Contracting Agency intends to perform Quality Assurance Inspection. By its inspection, the Contracting Agency intends only to facilitate the work and verify the quality of that work. This inspection shall not relieve the Contractor of any responsibility for identifying and replacing defective material and workmanship.

The various types of girders are:

- Prestressed Concrete Girder - Refers to prestressed concrete girders including Series W42G, W50G, W58G, and W74G girders, bulb-tee girders, and deck bulb-tee girders.
- Bulb-Tee Girder - Refers to a bulb-tee girder or a deck bulb-tee girder.
- Deck Bulb-Tee Girder - Refers to a bulb-tee girder with a top flange designed to support traffic loads (i.e., without a cast-in-place deck). This type of bulb-tee girder is mechanically connected to adjacent girders at the job site.

6-02.3(25)A Shop Plans

The Plans show design conditions and details for prestressed girders. Deviations will not be permitted, except as specifically allowed by these Specifications and by manufacturing processes approved by the annual plant approval process.

Shop plans shall allow the size and location of all cast-in holes for installation of deck formwork hangers and/or temporary bracing. Holes for formwork hangers shall match approved deck formwork plans designed in accordance with Section 6-02.3(16). There shall be no field-drilled holes in prestressed girders.

The Contractor shall have the option to furnish Series W74G prestressed concrete girders with minor dimensional differences from those shown in the Plans. The 2-5/8-inch top flange taper may be reduced to 1-5/8 inches and the bottom flange may be increased to 2 feet 2 inches. Other dimensions of the girder shall be adjusted as necessary to accommodate the above mentioned changes. Reinforcing steel shall be adjusted as necessary. The overall height and top flange width shall remain unchanged.

If the Contractor elects to provide a Series W74G girder with an increased web thickness, shop plans along with supporting design calculations shall be submitted to the Engineer for approval prior to girder fabrication. The girder shall be designed for at least the same load carrying capacity as the girder shown in the Plans. The load carrying capacity of the mild steel reinforcement shall be the same as that shown in the Plans.

The Contractor may alter bulb-tee girder dimensions as specified from that shown in the Plans if:

1. The girder has the same or higher load carrying capacity (using current AASHTO Design Specification);

SAMPLE SPECIFICATIONS

Nebraska Department of Roads Specifications

2. The Engineer approves, before the girder is made, complete design calculations for the girder;
3. The Contractor adjusts substructures to yield the same top of roadway elevation shown in the Plans;
4. The depth of the girder is not increased by more than 2 inches and is not decreased;
5. The web thickness is not increased by more than 1 inch and is not decreased;
6. The top flange minimum thickness of the girder is not increased by more than 2 inches, providing the top flange taper section is decreased a corresponding amount;
7. The top flange taper depth is not increased by more than 1 inch; and
8. The bottom flange width is not increased by more than 2 inches.

The Contractor shall provide four copies of the shop plans to the Engineer for approval. Only steel side forms will be approved, except plywood forms are acceptable on the end bulkheads. Approval of shop plans means only that the Engineer accepts the methods and materials. Approval does not imply correct dimensions.

6-02.3(25)B Casting

Before casting girders, the Contractor shall have possession of an approved set of shop drawings.

All concrete mixes to be used shall be pre-approved in the WSDOT plant certification process and must meet the requirements of Section 9-19.1. The temperature of the concrete when placed shall be between 50 F and 90 F. The temperature limits in Section 6-02.3(6)A do not apply to prestressed concrete girders.

Air entrainment is not required in the concrete placed into prestressed precast concrete girders unless otherwise noted. The Contractor shall use air-entrained concrete in the entire roadway deck flange of deck bulb-bee girders. Maximum and minimum air content shall be as specified in Section 6-02.3(3)A.

No welds will be permitted on steel within prestressed girders. Once the prestressing steel has been installed, no welds or grounds for welders shall be made on the forms or the steel in the girder, except as specified.

The Contractor may form circular block-outs in the girder top flanges to receive falsework hanger rods. These block-outs shall:

1. Not exceed 1 inch in diameter,
2. Be spaced no more than 72 inches apart longitudinally on the girder,
3. Be located 3 inches or more from the outside edge of the top flange on Series W42G, W50G, and W58G girders, and 6 inches or more for Series W74G girders, and
4. Be located within 1 foot 3 inches of the web centerline for bulb-tee girder.

The Contractor may form circular block-outs in the girder webs to support brackets for roadway slab falsework. These block-outs shall:

1. Not exceed 1 inch in diameter,
2. Be spaced no more than 72 inches apart longitudinally on the girder, and
3. Be positioned so as to clear the girder reinforcing and prestressing steel.

6-02.3(25)C Prestressing

Each stressing system shall have a pressure gauge or load cell that will measure jacking force. Any gauge shall display pressure accurately and readably with a dial at least 6 inches in diameter or with a digital display. Each jack and its gauge shall be calibrated as a unit and shall be accompanied by a certified calibration chart. The Contractor shall provide one copy of this chart to the Engineer. The cylinder extension during calibration shall be in approximately the position it will occupy at final jacking force.

SAMPLE SPECIFICATIONS

Nebraska Department of Roads Specifications

Jacks and gauges shall be recalibrated and recertified:

1. Annually,
2. After any repair or adjustment, and
3. Any time there are indications that the jack calibration is in error.

The Engineer may use pressure cells to check jacks, gauges and calibration charts before and during tensioning.

All load cells shall be calibrated and shall have an indicator that shows prestressing force in the strand. The range of this cell shall be broad enough that the lowest 10 percent of the manufacturer's rated capacity will not be used to measure jacking force.

From manufacture to encasement in concrete, all reinforcement used in girders shall be protected against dirt, oil, grease, damage, rust and all corrosives. If strands in the stressing bed are exposed before they are encased in concrete, the Contractor shall protect them from contamination or corrosion. The protection method requires the Engineer's approval. If steel has been damaged or if it shows rust or corrosion, it will be rejected.

6-02.3(25)D Curing

During curing, the Contractor shall keep the girder in a saturated curing atmosphere until the girder concrete has reached the required release strength. If the Engineer approves, the Contractor may shorten curing time by heating the outside of impervious forms. Heat may be radiant, convection, conducted steam or hot air. With steam, the arrangement shall envelop the entire surface with saturated steam. The Engineer will not permit hot air curing until after approving the Contractor's proposed method to envelop and maintain the girder in a saturated atmosphere. Saturated atmosphere means a relative humidity of at least 90 percent. The Contractor shall never allow dry heat to touch the girder surface at any point.

Under heat curing methods, the Contractor shall:

1. Keep all unformed girder surfaces in a saturated atmosphere throughout the curing time;
2. Embed a thermocouple (linked with a thermometer accurate to plus or minus 5° F) 6 to 8 inches from the top or bottom of the girder on its centerline and near its midpoint;
3. Monitor with a recording sensor (accurate to plus or minus 5° F) arranged and calibrated to continuously record, date and identify concrete temperature throughout the heating cycle;
4. Make this temperature record available for the Engineer to inspect;
5. Heat concrete to no more than 100° F during the first two hours after pouring the concrete, and then increase no more than 25° F per hour to a maximum of 175° F;
6. Cool concrete, after curing is complete, no more than 25° F per hour, to 100° F; and
7. Keep the temperature of the concrete above 60 F until the girder reaches release strength.

The Contractor may strip side forms once the concrete has reached a minimum compressive strength of 3,000 psi. All damage from stripping is the Contractor's responsibility.

6-02.3(25)E Contractor's Control Strength

Concrete strength shall be measured on test cylinders cast from the same concrete as that in the girder. These cylinders shall be cured under time-temperature relationships and conditions that simulate those of the girder. If the forms are heated by steam or hot air, test cylinders will remain in the coolest zone throughout curing. If forms are heated another way, the Contractor shall provide a record of the curing time-temperature relationships for the cylinders for each girder to the Engineer. When two or more girders are cast in a continuous line and in a continuous pour, a single set of test cylinders may represent all girders provided the Contractor demonstrates uniformity of casting and curing to the satisfaction of the Engineer.

SAMPLE SPECIFICATIONS

Nebraska Department of Roads Specifications

The Contractor shall mold, cure, and test enough of these cylinders to satisfy specification requirements for measuring concrete strength. The Contractor may use 4-inch by 8-inch or 6-inch by 12-inch cylinders. The required design strength shall be increased 5 percent when using 4-inch by 8-inch cylinders. This 5 percent increase will not be applied for the determination of the release strength. If heat is used to shorten curing time, the Contractor shall let cylinders cool for at least 1/2 hour before testing.

Test cylinders may be cured in a moist room or water tank in accordance with AASHTO T-23 after the girder concrete has obtained the required release strength. If, however, the Contractor intends to ship the girder prior to the standard 28-day strength test, the design strength for shipping shall be determined from cylinders placed with the girder and cured under the same conditions as the girder. These cylinders may be placed in a noninsulated, moisture-proof envelope.

To measure concrete strength in the girder, the Contractor shall randomly select two test cylinders and average their compressive strengths. The compressive strength in either cylinder shall not fall more than 5 percent below the specified strength. If these two cylinders do not pass the test, two other cylinders shall be selected and tested.

If too few cylinders were molded to carry out all required tests on the girder, the Contractor shall remove and test cores from the girder under the surveillance of the Engineer. If the Contractor casts cylinders to represent more than one girder, all girders in that line shall be cored. These cores shall measure 4 inches in diameter by web thickness high and shall be removed from just below the top flange, one approximately 3 feet to the left and the other approximately 3 feet to the right of the midpoints of the girder's length. The Engineer may accept the girder if these cores have the required compressive strength.

If the girder is cored to determine the release strength, the required patching and curing of the patch shall be done prior to shipment. If there are more than two holes or if they are not in a neutral location, they shall be patched prior to the release of prestress.

The Contractor shall coat cored holes with a Type II, Grade 2 epoxy and patch the holes using the same type concrete as that in the girder, or a mix approved during the annual plant review and approval. The girder shall not be shipped until tests show the patches have reached the required design strength of the girder.

6-02.3(25)F Prestress Release

Side and flange forms that restrain deflection shall be removed before release of the prestressing reinforcement.

All harped and straight strands shall be released in a way that will produce the least possible tension in the concrete. This release shall not occur until tests show each girder has reached the minimum compressive strength required by the Plans.

6-02.3(25)G Protection of Exposed Reinforcement

When a girder is removed from its casting bed, all bars and strands projecting from the girder shall be cleaned and painted with a minimum dry film thickness of 1 mil of paint Formula No. A-9-73. During handling and shipping, projecting reinforcement shall be protected from bending or breaking. Just before placing concrete around the painted projecting bars or strands, the Contractor shall remove from them all dirt, oil and other foreign matter.

6-02.3(25)H Finishing

The Contractor shall apply a Class 2 finish, as defined in Section 6-02.3(14), to:

1. The vertical exterior surfaces of the outside girders;
2. The bottoms, sides, and tops of the lower flanges on all girders; and
3. The bottom of the outside roadway flange of each outside bulb-tee girder section. All other girder surfaces shall receive a Class 3 finish.

SAMPLE SPECIFICATIONS

Nebraska Department of Roads Specifications

The interface on I-girders and other girders that contact the cast-in-place deck shall have a finish of dense, screeded concrete without a smooth sheen or laitance on the surface. After vibrating and screeding, and just before the concrete reaches initial set, the Contractor shall texture the interface. This texture shall be applied with a steel brooming tool that etches the surface transversely leaving grooves 1/2-inch to 1/4-inch wide, between 1/2-inch and 1/4-inch deep, and spaced 1/4-inch to 1/2-inch apart.

On the deck bulb-tee girder section, the Contractor shall test the roadway deck surface portion for flatness. This test shall occur after floating but while the concrete remains plastic. Testing shall be done with a 10-foot straightedge parallel to the girder centerline and with a flange width straightedge at right angles to the girder centerline. The Contractor shall fill depressions, cut down high spots, and refinish to correct any deviation of more than 1/4 inch within the straightedge length. This section of the roadway surface shall be finished to meet the requirements for finishing roadway slabs, as defined in Section 6-02.3(1).

The Contractor may repair rock pockets and other defects in the girder provided the repair is covered in the annual plant approval package. All other repairs and repair procedures shall be documented and approved by the Engineer prior to acceptance of the girder.

6-02.3(25)I Tolerances

The girders shall be fabricated as shown in the Plans and shall meet the dimensional tolerances listed below. Actual acceptance or rejection will depend on how the Engineer believes a defect outside these tolerances will affect the structure's strength or appearance.

1. Length (overall): $\pm 1/4$ inch per 25 feet of beam length, up to a maximum of ± 1 inch
2. Width (flanges): $+3/8$ inch, $-1/4$ inch
3. Width (narrow web section): $+3/8$ inch, $-1/4$ inch
4. Girder Depth (overall): $\pm 1/4$ inch
5. Flange Depth: $+1/4$ inch, $-1/8$ inch
6. Strand Position: $\pm 1/4$ inch from the center of gravity of a strand group and of an individual strand
7. Longitudinal Position of the Harping Point: ± 18 inches
8. Bearing Recess (center recess to beam end): $\pm 1/4$ inch
9. Beam Ends (deviation from square or designated skew): Horizontal: $\pm 1/2$ inch from web centerline to flange edge; Vertical: $\pm 1/8$ inch per foot of beam depth
10. Bearing Area Deviation from Plane (in length or width of bearing): $1/16$ inch
11. Stirrup Reinforcing Spacing: ± 1 inch
12. Stirrup Projection from Top of Beam: $\pm 3/4$ inch
13. Mild Steel Concrete Cover: $-1/8$, $+3/8$ inch
14. Offset at Form Joints (deviation from a straight line extending 5 feet on each side of joint): $\pm 1/4$ inch
15. Differential Camber Between Girders in a Span (measured in place at the job site)

For I-girders: $1/8$ inch per 10 feet of beam length (Series W42G, W50G, W58G and W74G).

For deck bulb-tee girders: Cambers shall be equalized by an approved method when the difference in cambers between adjacent girders or stages measured at mid-span exceeds $1/4$ inch.

16. Position of Inserts for Structural Connections: $\pm 1/2$ inch
17. Position of Lifting Loops: ± 3 inches longitudinal, ± 1 inch transverse
18. Weld plates for bulb-tee girders shall be placed $\pm 1/2$ inch longitudinal, and $\pm 1/8$ inch vertical

SAMPLE SPECIFICATIONS

Nebraska Department of Roads Specifications

6-02.3(25)J Horizontal Alignment

The Contractor shall check and record the horizontal alignment of both top and bottom flanges of each girder upon removal of the girder from the casting bed. The Contractor shall also check and record the horizontal alignment within a two-week period prior to shipment, but no less than three days prior to shipment. If the girder remains in storage for a period exceeding 120 days, the Contractor shall check and record the horizontal alignment at approximately 120 days. Each check shall be made by measuring the distance between each flange and a chord that extends the full length of the girder. The Contractor shall perform and record each check at a time when the alignment of the girder is not influenced by temporary differences in surface temperature. These records shall be available for the Engineer's inspection and included in the Contractor's Prestressed Concrete Certificate of Compliance.

Immediately after the girder is removed from the casting bed, neither flange shall be offset more than 1/8 inch for each 10 feet of girder length. During storage and prior to shipping, the offset (with girder ends plumb and upright and with no external force) shall not exceed 1/4 inch per 10 feet of girder length. Any girder within this tolerance may be shipped, but must be corrected at the job site to the 1/8 inch maximum offset per 10 feet of girder length before concrete is placed into the diaphragms.

The Engineer may permit the use of external force to correct girder alignment at the plant or job site if the Contractor provides stress calculations and a proposed procedure. If external force is permitted, it shall not be released until after the roadway slab has been placed and cured ten days.

6-02.3(25)K Girder Deflection

The Contractor shall check and record the vertical deflection (camber) of each girder upon removal of the girder from the casting bed. The Contractor shall also check and record the vertical deflection (camber) within a two-week period prior to shipment, but no less than three days prior to shipment. If the girder remains in storage for a period exceeding 120 days, the Contractor shall check and record the vertical deflection (camber) at approximately 120 days. The Contractor shall perform and record each check at a time when the alignment of the girder is not influenced by temporary differences in surface temperature. These records shall be available for the Engineer's inspection and included in the Contractor's Prestressed Concrete Certification of Compliance.

The "D" dimensions shown in the Plans are computed girder deflections at midspan based on a time elapse of 120 days after release of the prestressing strands. A positive (+) "D" dimension indicates upward deflection.

The Contractor shall control the deflection of prestressed concrete girders that are to receive a cast-in-place slab by scheduling fabrication or other means. The actual girder deflection at the midspan may vary from the "D" dimension at the time of slab forming by a maximum of plus 1/2 inch for girder lengths up to 80 feet and plus 1 inch for girder lengths over 80 feet. The method used by the Contractor to control the girder deflection shall not cause damage to the girders or any over stress when checked in accordance with the AASHTO Specifications. All costs, including any additional Contracting Agency engineering expenses, in connection with controlling the girder deflection shall be borne by the Contractor.

6-02.3(25)L Handling and Storage

During handling and storage, each girder shall always be kept plumb and upright. It shall be lifted only by the lifting strands at either end. Series W42G, W50G and W58G girders can be picked up at a maximum angle of 30 degrees to the vertical (measured in the longitudinal plane of the girder). All other prestressed girders shall be picked up vertical. Girders shall be braced laterally to prevent tipping or buckling as specified in the Plans.

Before moving a long girder, the Contractor shall check it for any tendency to buckling. Each girder that may buckle shall be braced on the sides to prevent buckling. This bracing shall be attached securely to the top flanges of the girder. The lateral bracing shall be in place during all lifting or handling necessary for transportation from

SAMPLE SPECIFICATIONS

Nebraska Department of Roads Specifications

the manufacturing plant to the job site and erection of the girder. The Contractor is cautioned that for some delivery routes more conservative guidelines for lateral bracing may be required. Before removing the bracing to cast diaphragms, the Contractor shall fasten all girders in place by other means.

If the Contractor wishes to deviate from these handling and bracing requirements, the vertical pickup, or the pickup location, the proposed method shall be analyzed by the Contractor’s engineer and submitted with the supporting calculations to the Engineer for approval. The Contractor’s analysis shall conform to Articles 5.2 and 5.3 of the *PCI Design Handbook, Precast and Prestressed Concrete*, Third Edition, or other approved methods. The Contractor’s calculations shall verify that the concrete stresses in the prestressed girder do not exceed those listed in Section 6-02.3(25)M.

If girders are to be stored, the Contractor shall place them on a stable foundation that will keep them in a vertical position. Stored girders shall be supported at the bearing recesses or, if there are no recesses, approximately 18 inches from the girder ends. For long-term storage of girders with initial horizontal curvature, the Contractor may wedge one side of the bottom flange, tilting the girders to control curvature. If the Contractor elects to set girders out of plumb during storage, the Contractor shall have the proposed method analyzed by the Contractor’s engineer to ensure against damaging the girder.

6-02.3(25)M Shipping

After the girder has reached its 28-day design strength, and the fabricator believes it to comply with the specification, the girder and a completed Certification of Compliance (DOT 350-151), signed by a Precast/Prestressed Concrete Institute Certified Technician or a professional engineer, acceptable to the Contracting Agency, shall be presented to the Engineer for inspection. If the Engineer finds the certification and the girder to be acceptable, the Engineer will stamp the girder “Approved for Shipment.”

No prestressed girders shall be shipped that are not stamped “Approved for Shipment.”

No bulb-tee girder shall be shipped for at least seven days after concrete placement. No other girder shall be shipped for at least ten days after concrete placement.

Girder support during shipping shall meet these requirements unless otherwise shown in the Plans:

Type of Girder	Centerline Support Within This Distance From Either End
Series W42G and W50G and all bulb-tee girders	3 feet
Series W58G	4 feet
Series W74G	5 feet

If the Contractor wishes to use other support locations, they may be proposed to the Engineer for review and approval in accordance with Section 6-02.3(25)L. The Contractor’s proposal shall include calculations showing that concrete stresses in the girders will not exceed those listed below:

Criteria for Checking Girder Stresses at the Time of Lifting or Transporting and Erecting

Stresses at both support and harping points shall be satisfied based on these criteria:

1. Allowable compression stress, $f'_c - 0.60 f'_{cm}$
 - a. f'_{cm} = compressive strength at time of lifting or transporting verified by test but shall not exceed design compressive strength (f'_c) at 28 days in psi + 1,000 psi
2. Allowable tension stress, f_t

SAMPLE SPECIFICATIONS

Nebraska Department of Roads Specifications

- a. With no bonded reinforcement = $3\sqrt{f'_{cm}}$
 - b. With bonded reinforcement to resist total tension force in the concrete computed on the basis of an uncracked section = $7.5\sqrt{f'_{cm}}$. The allowable tensile stress in reinforcement is 30 ksi (AASHTO M-31, Gr. 60)
3. Prestress Losses
 - a. 1 day to 1 month = 20,000 psi
 - b. 1 month to 1 year = 35,000 psi
 - c. 1 year or more = 45,000 psi (max.)
 4. Impact on dead load
 - a. Lifting from casting beds = 0 percent
 - b. Transporting and erecting = 20 percent

6-02.3(25)N Prestress Concrete Girder Erection

Before beginning to erect any prestressed concrete girders, the Contractor shall submit to the Engineer for review and shall have received approval for the erection plan and procedure describing the methods the Contractor intends to use. The erection plan and procedure shall provide complete details of the erection process including but not limited to:

1. Temporary falsework support, bracing, guys, deadmen and attachments to other structure components or objects;
2. Procedure and sequence of operation;
3. Girder stresses during progressive stages of erection;
4. Girder weights, lift points, and lifting devices, spreaders, angle of lifting strands in accordance with Section 6-02.3(25)L, etc.;
5. Crane(s) make and model, weight, geometry, lift capacity, outrigger size and reactions;
6. Girder launcher or trolley details and capacity (if intended for use); and
7. Locations of cranes, barges, trucks delivering girders, and the location of cranes and outriggers relative to other structures, including retaining walls and wing walls.

The erection plan shall include drawings, notes, catalog cuts, and calculations clearly showing the above listed details, assumptions, and dimensions. Material properties and specifications, structural analysis, and any other data used shall also be included. The plan shall be prepared by (or under the direct supervision of) a Professional Engineer, licensed under Title 18 RCW, State of Washington, in the branch of Civil or Structural, and shall carry the engineer's seal and signature, in accordance with Section 6-02.3(16).

The Contractor shall submit the erection plans, calculations and procedures directly to the Bridge and Structures Office, Construction Support Engineer, in accordance with Section 6-02.3(16). After the plan is approved and returned to the Contractor, all changes that the Contractor proposes shall be submitted to the Engineer for review and approval.

When prestressed girders arrive on the project, the Project Engineer will confirm that they are stamped "Approved for Shipment" and that they have not been damaged in shipment before accepting them.

The concrete in piers and crossbeams shall reach at least 80 percent of design strength before girders are placed on them. The Contractor shall hoist girders only by the lifting strands at the ends, always keeping the girders plumb and upright.

Instead of the oak block wedges shown in the Plans, the Contractor may use Douglas fir blocks if the grain is vertical.

SAMPLE SPECIFICATIONS

Nebraska Department of Roads Specifications

Before the grout pads are placed, the concrete beneath them shall be thoroughly cleaned, roughened, and wetted with water to ensure proper bonding. Pads shall be kept wet continuously until they reach a compressive strength of at least 2,000 psi. Grout pads shall reach this strength before girders are set on them. Grout compressive strength will be determined by fabricating cubes in accordance with WSDOT Test Method 813 and testing in accordance with AASHTO T-106.

The Contractor shall check the horizontal alignment of both the top and bottom flanges of each girder before placing concrete in the bridge diaphragms as described in Section 6-02.3(25)].

The Contractor shall fill all block-out holes and patch any damaged area caused by the Contractor's operation, with an approved mix, to the satisfaction of the Engineer.

6-02.3(25) Deck Bulb-Tee Girder Flange Connection

The Contractor shall submit a method of equalizing deck bulb-tee girder deflections to the Engineer for approval. This submittal shall be prepared by, or under the direction of, a professional engineer licensed under Title 18 RCW, State of Washington, and shall carry the engineer's signature and seal. This submittal shall be made a minimum of 60 days prior to field erection of the deck bulb-tee girder. Deflection equalizing methods approved for previous Contracting Agency contracts will be acceptable providing the bridge configuration is similar and the previous method was satisfactory. A listing of the previous Contracting Agency contract numbers for which the method was used shall be included with the submittal.

On the deck bulb-tee girders, girder deflection shall be equalized utilizing the approved method before girders are weld-tied and before keyways are filled. Keyways between the nonshrink grout shall have a compressive strength of 4,000 psi before the equalizing equipment is removed. Compressive strength shall be determined by fabricating cubes in accordance with WSDOT Test Method 813 and testing in accordance with AASHTO T-106.

Welding grounds shall be attached directly to the steel plates being welded when welding the weld-ties on bulb-tee girders.

No construction equipment shall be placed on the structure, other than equalizing equipment, until the girders have been weld-tied and the keyway grout has attained a compressive strength of 4,000 psi.

6-02.3(26) Cast-In-Place Prestressed Concrete

Intentionally Omitted.

6-02.3(27) Concrete for Precast Units

Concrete for precast non-prestressed units shall meet all the requirements for a Contractor-provided mix design and the following acceptance limits:

Maximum Slump	4 inches
Minimum Entrained Air	4 1/2 percent
Compressive Strength	Specified Design Strength

If the design strength of the precast concrete is 4,000 psi or less, the Contractor may use Contracting Agency provided mix design Class 4000 with air.

SAMPLE SPECIFICATIONS

Nebraska Department of Roads Specifications

Precast units shall not be removed from forms until the concrete has attained a minimum compressive strength of 70 percent of the specified design strength as verified by rebound number determined in accordance with ASTM C805.

Precast units shall not be shipped until the concrete has reached the specified design strength as determined by testing cylinders made from the same concrete as the precast units. The cylinders shall be made, handled, and stored in accordance with WSDOT Test Method 809 Method 2 and compression tested in accordance with WSDOT Test Methods 801 and 811.

6-02.3(28) Precast Concrete Panels

The Contractor shall perform quality control inspection. The manufacturing plant for precast concrete units shall be certified by the Precast/Prestressed Concrete Institute's Plant Certification Program for the type of precast member to be produced and shall be approved by WSDOT as a Certified Precast Concrete Fabricator prior to the start of production. WSDOT Certification will be granted at, and renewed during, the annual precast plant review and approval process. Products which shall conform to this requirement include noise barrier panels, wall panels, floor and roof panels, marine pier deck panels, retaining walls, pier caps and bridge deck panels.

Prior to the start of production of the precast concrete units, the Contractor shall advise the Engineer of the production schedule. The Contractor shall give the Inspector safe and free access to the work. If the Inspector observes any nonspecification work or unacceptable quality control practices, the Inspector will advise the plant manager. If the corrective action is not acceptable to the Engineer, the units(s) will be rejected.

The Contracting Agency intends to perform Quality Assurance Inspection. By its inspection, the Contracting Agency intends only to facilitate the work and verify the quality of that work. This inspection shall not relieve the Contractor of any responsibility for identifying and replacing defective material and workmanship.

If products are prestressed, all prestressing materials and methods shall be in accordance with Section 6-02.3(25).

6-02.3(28)A Shop Drawings

Before casting the structural elements, the Contractor shall submit:

1. Seven sets of shop drawings for approval by the Bridge and Structures Engineer, Department of Transportation, Transportation Building, Olympia, WA 98504; and,
2. Two sets of shop drawings to the Project Engineer.

These shop drawings shall show complete details of the methods, materials and equipment the Contractor proposes to use in prestressing/precasting work. The shop drawings shall follow the design conditions shown the Plans unless the Engineer approves equally effective variations.

The shop drawings shall contain as a minimum:

1. Unit shapes (elevations and sections) and dimensions.
2. Finishes and method of constructing the finish (i.e., forming, rolling, etc.)
3. Reinforcing, joint, and connection details.
4. Lifting, bracing, and erection inserts.
5. Locations and details of hardware attached to the structure.
6. Relationship to adjacent material.

SAMPLE SPECIFICATIONS

Nebraska Department of Roads Specifications

Approval of these shop drawings shall not relieve the Contractor of responsibility for accuracy of the drawings or conformity with the Contract. Approval will not indicate a check on dimensions.

The Contractor may deviate from the approved shop drawings only after obtaining the engineer’s approval of a written request that describes the proposed changes. Approval of a change in method, material or equipment shall not relieve the Contractor of any responsibility for completing the work successfully.

Before completion of the Contract, the Contractor shall provide the Engineer with reproducible originals of the shop drawings (and any approved changes). These shall be clear, suitable for microfilming, and on permanent sheets that conform with the size requirements of Section 6-01.9.

6-02.3(28)B Casting

Before casting precast concrete units, the Contractor and Fabrication Inspector shall have possession of an approved set of shop drawings.

All concrete mixes to be used shall be preapproved in the WSDOT plant certification process, and shall meet all the requirements for a Contractor provided mix design with the following acceptance limits:

Minimum Slump	4 inches
Maximum Slump	6 inches
Entrained Air	Per Section 6-02.3(3)A
Compressive Strength	Specified Design Strength

If the design strength of the precast concrete is 4,000 psi or less, the Contractor may use Contracting Agency-provided mix design Class 4000 with air.

Precast units shall not be removed from forms until the concrete has attained a minimum compressive strength of 70 percent of the specified design strength.

Forms may be steel or plywood faced, providing they impart the required Finish to the concrete.

6-02.3(28)C Curing

Concrete in the precast units shall be cured by either moist or accelerated curing methods. The methods to be used shall be preapproved in the WSDOT plant certification process.

1. For moist curing, the surface of the concrete shall be kept covered or moist until such time as the compressive strength of the concrete reaches the strength specified for stripping. Exposed surfaces shall be kept continually moist by fogging, spraying or covering with moist burlap or cotton mats. Moist curing shall commence as soon as possible following completion of surface finishing.
2. For accelerated curing, heat shall be applied at a controlled rate following the initial set of concrete in combination with an effective method of supplying or retaining moisture. Moisture may be applied by a cover of moist burlap, cotton matting or other effective means. Moisture may be retained by covering the unit with an impermeable sheet.

Heat may be radiant or convection or conducted stream of hot air. Heat the concrete to no more than 100°F during the first two hours after pouring the concrete, and then increase no more than 25°F per hour to a maximum of 175°F. After curing is complete, cool the concrete no more than 25°F per hour to 100°F. Maintain the concrete temperature above 60°F until the unit reaches stripping strength.

SAMPLE SPECIFICATIONS

Nebraska Department of Roads Specifications

Concrete temperature shall be monitored by means of a thermocouple embedded in the concrete (linked with a thermometer accurate to plus or minus 5 F). The recording sensor (accurate to plus or minus 5 F) shall be arranged and calibrated to continuously record, date and identify concrete temperature throughout the heating cycle. This temperature record shall be made available to the Engineer for inspection and become a part of the documentation required.

The Contractor shall never allow dry heat to directly touch exposed unit surfaces at any point.

6-02.3(28)D Contractor's Control Strength

The concrete strength at stripping and the verification of design strength shall be determined by testing cylinders made from the same concrete as that in the precast units. The cylinders shall be made, handled, and stored in accordance with WSDOT Test Method 809 Method 2 and compression tested in accordance with WSDOT test Methods 801 and 811.

For accelerated-cured units, concrete strength shall be measured on test cylinders cast from the same concrete as that in the unit. These cylinders shall be cured under time-temperature relationships and conditions that simulate those of the unit. If the forms are heated by steam or hot air, test cylinders will remain in the coolest zone throughout curing. If forms are heated another way, the Contractor shall provide a record of the curing time-temperature relationship for the cylinders for each unit to the Engineer. When two or more units are cast in a continuous line and in a continuous pour, a single set of test cylinders may represent all units provided the Contractor demonstrates uniformity of casting and curing to the satisfaction of the Engineer.

The Contractor shall mold, cure and test enough of these cylinders to satisfy specification requirements for measuring concrete strength. The Contractor may use 4-inch by 8-inch or 6-inch by 12-inch cylinders. The required design strength shall be increased 5 percent when using 4-inch by 8-inch cylinders. This 5 percent increase will not be applied for the determination of the stripping strength. The Contractor shall let cylinders cool for at least one-half hour before testing for release strength.

Test cylinders may be cured in a moist room and water tank in accordance with AASHTO T-23 after the unit concrete has obtained the required release strength. If, however, the Contractor intends to ship the unit prior to standard 28-day strength test, the design strength for shipping shall be determined from cylinders placed with the unit and cured under the same conditions as the unit. These cylinders may be placed in a noninsulated, moisture-proof envelope.

To measure concrete strength in the precast unit, the Contractor shall randomly select two test cylinders and average their compressive strengths. The compressive strength in either cylinder shall not fall more than 5 percent below the specified strength. If these two cylinders do not pass the test, two other cylinders shall be selected and tested.

6-02.3(28)E Finishing

The Contractor shall provide a finish on all relevant concrete surfaces as defined in Section 6-02.3(14), unless the Plans or Special Provisions require otherwise.

6-02.3(28)F Tolerances

The units shall be fabricated as shown in the Plans, and shall meet the dimensional tolerances listed in PCI MNL-116-85, unless otherwise required by the Plans or Special Provisions.

6-02.3(28)G Handling and Storage

The Contractor shall lift all units only by adequate devices at locations designated on the shop drawings. When these devices and locations are not shown in the Plans, Section 6-02.3(25)L shall apply.

SAMPLE SPECIFICATIONS

Nebraska Department of Roads Specifications

Precast units shall be stored off the ground on foundations suitable to prevent differential settlement or twisting of the units. Stacked units shall be separated and supported by dunnage of uniform thickness capable of supporting the units. Dunnage shall be arranged in vertical planes. The upper units of a stacked tier shall not be used as storage areas for shorter units unless substantiated by engineering analysis and approved by the Engineer.

6-02.3(28)H Shipping

Precast units shall not be shipped until the concrete has reached the specified design strength. The units shall be supported in such a manner that they will not be damaged by anticipated impact on their dead load. Sufficient padding material shall be provided between tie chains and cables to prevent chipping or spalling of the concrete.

6-02.3(28)I Erection

When the precast units arrive on the project, the Project Engineer will confirm that they are stamped "Approved for Shipment." The Project engineer will evaluate the units for damage before accepting them.

The Contractor shall lift all units by suitable devices at locations designated on the shop drawings. Temporary shoring or bracing shall be provided, if necessary. Units shall be properly aligned and leveled as required by the Plans. Variations between adjacent units shall be leveled by a method approved by the Engineer.

Bridge Design Manual Glossary

BRIDGE DESIGN MANUAL GLOSSARY

To be released at a later date.

PCI CERTIFICATION PROGRAMS

INTRODUCTION

Since 1967, the Precast/Prestressed Concrete Institute (PCI) has been a leader in the development of innovative quality programs. It was 1967 that saw the beginning of the PCI Plant Certification Program, a program that would set the pace for other construction-related certification programs that followed in later years (Duggleby, 1992). In 1985, PCI implemented its Plant Quality Personnel Certification Program and in 1999, introduced the Certified Field Auditor and Field Qualification Programs for erectors of precast concrete (Shutt, 2000).

With the ever-increasing demand for quality, the certification of manufacturers, erectors and personnel provides the customer the assurance that quality systems are being followed, personnel are qualified and control is practiced through each step of the construction process. Independent, unannounced audits help to assure process control.

PCI PLANT CERTIFICATION

The certification of a manufacturing plant by PCI ensures that the plant has developed and documented an in-depth, in-house quality system, which is based on time-tested national industry standards.

Standards

Production and quality standards are contained in the PCI publication, *Manual for Quality Control for Plants and Production of Structural Precast Concrete Products* (MNL-116). This manual has been recognized by the construction industry as the standard for the manufacture of precast and prestressed concrete since it was first printed in 1970. MNL-116 is the only such recognized national standard for the industry.

Quality System Manual

Every plant must document their specific practices in a custom Quality Systems Manual (QSM). The requirements for the QSM are contained in Division 1 and Appendix A of MNL-116. Fifteen separate sections require that all operations in the plant be addressed thoroughly by management. Each QSM must be approved by PCI prior to certification and must then be reviewed annually and updated when necessary. Plants can obtain additional assistance for compiling a QSM in the PCI publication *Preparation Guidelines for a Structural Plant Quality System Manual* (2000).

Audits and Auditors

Nearly all new plants undergo a "Precertification Evaluation" after which a plant is audited twice each year. These audits are not announced in advance. Auditors are independent, specially trained engineers. They are employed by a single consulting engineering firm under contract to PCI, which ensures consistency for every plant (Shutt, 1994).

Closing Meeting; Audit Reports

Every audit ends with a closing meeting. Auditors and key plant personnel meet to review preliminary results. If improvements are needed, they can be started right away. Later, a detailed written analysis documents observations and reasons for required improvements. The report also includes a numerical grade sheet that indicates the level of compliance with the standards.

PCI CERTIFICATION PROGRAMS**Grades**

The numerical grade sheet is organized with each section of the grade sheet corresponding to a division (chapter) of MNL-116. During an audit, each division is evaluated separately. Grades in each division must meet or exceed an established minimum value. Then, the grades for all divisions are combined into an overall grade. A minimum overall grade must also be achieved for certification. Audits are evaluated on strict pass-fail criteria. A failing grade requires a Special Immediate Audit. Failure of that audit or the subsequent Regular Audit results in loss of Certification.

Product Groups

A plant is evaluated and classified according to the type of products produced. This allows for a more product-specific inspection and analysis of a plant's specialized capabilities. It provides specifiers with more information about the production experience of precast plants.

Plants, including bridge products producers, may be certified in up to four general groups of products. The PCI manuals shown in parenthesis contain the standards for certification in that Group.

Group A

Architectural Concrete Products (MNL-117)

Group B or Group BA

Bridge Products (MNL-116) or the combination of the A and B Product Groups (MNL-116)

Group C or Group CA

Commercial (Structural) Products (MNL-116) or the combination of the A and C Product Groups (MNL-116)

Group G

Glass Fiber Reinforced Concrete Products (MNL-130)

Product Categories

The Product Groups are further divided into Categories that define a product's reinforcement or the ways in which the products are manufactured or used. Product Categories that include prestressing may incorporate pretensioning or post-tensioning or both. Bridge products producers must be certified in one of the categories within Group B or Group BA.

Group B Categories

B1 - Precast Bridge Products (no prestressed reinforcement)

Examples include pile caps, retaining wall components, three-sided boxes or arches, median barriers, parapet walls, railings, fascia panels, abutment panels, sound barriers, pier columns, pier caps, precast diaphragms and conventionally reinforced segmental units, and partial- and full-depth bridge deck panels.

B2 - Prestressed Deck and Miscellaneous Bridge Products (nonsuperstructure)

Examples include prestressed (pretensioned or plant post-tensioned) pier columns, pier beams, sound walls, fascia panels, piles, sheet piles, partial and full-depth deck panels.

B3 - Prestressed Straight-Strand Bridge Beams (superstructure)

Examples include solid-slab beams, voided slabs, box beams, I-beams, bulb tees, double tees, multiple-stemmed units, box beam segments with pretensioned or plant post-tensioned prestressing.

PCI CERTIFICATION PROGRAMS

B4 - Prestressed Deflected-Strand Bridge Beams (superstructure)

Examples include box beams, I-beams, bulb tees, double tees, multiple stemmed units and plant post-tensioned precast beams with harped tendons.

Group BA Categories

Group B Category products with an architectural finish
(see additional information that follows)

B1A - Precast Bridge Products with Architectural Finish (no prestressed reinforcement)

B2A - Prestressed Miscellaneous Bridge Products with Architectural Finish (nonsuperstructure)

B3A - Prestressed Straight-Strand Bridge Beams with Architectural Finish (superstructure)

B4A - Prestressed Deflected-Strand Bridge Beams with Architectural Finish (superstructure)

Producers may also be certified in one or more of the following Groups and Categories.

Group A Categories

AT - Miscellaneous Architectural Trim Units

A1 - Architectural Precast Concrete Products

Group C Categories

C1 - Precast Concrete Products (no prestressed reinforcement)

C2 - Prestressed Hollow-Core and Repetitively-Produced Products

C3 - Prestressed Straight-Strand Structural Members

C4 - Prestressed Deflected-Strand Structural Members

Group CA Categories

Group C Category products with an architectural finish
(see additional information that follows)

C1A - Precast Concrete Products with Architectural Finish (no prestressed reinforcement)

C2A - Prestressed Hollow-Core and Repetitively-Produced Products with Architectural Finish

C3A - Prestressed Straight-Strand Structural Members with Architectural Finish

C4A - Prestressed Deflected-Strand Structural Members with Architectural Finish

Within a Product Group, the Categories listed above are intended to be in ascending order of production complexity. A producer qualified to produce products in a given Category is automatically qualified in the preceding Categories but not in succeeding Categories. See the following Guide Qualification Specifications and accompanying notes for more details.

For more descriptive information about the types of products and projects that are represented by these Categories, contact PCI, visit the PCI website at www.pci.org, or refer to other more-detailed program literature available from PCI.

PCI CERTIFICATION PROGRAMS

Architectural Finishes—Product Groups BA and CA

Beginning with the Fourth Edition of MNL-116 (1999), an additional product distinction was made available to the specifier. The new classification defines products that have architectural finishes applied to more traditional structural products. Before now, these products were not addressed in either MNL-116 or MNL-117. The special requirements for finish, texture, color, tolerances and quality control are included at the end of each division of manual MNL-116.

Identification of BA and CA Producers

The architectural finishes designation may be applied to any “B” or “C” category. Qualified producers will be identified with the suffix “A” following their normal designation of “B1” through “B4” and “C1” through “C4.” For example, if a precaster is certified to produce precast sound barrier wall panels with conventional steel reinforcement and with an exposed aggregate surface finish, the appropriate designation will be “B1A.” A bridge-products producer that manufactures prestressed fascia panels with an architectural finish for a bridge would be required to hold “B2A” certification. Refer to the Guide Qualification Specification near the end of this appendix for information about how to specify this and other Bridge Groups and Categories.

List of Certified Plants

A current listing of all PCI Certified Plants is published quarterly in PCI’s *ASCENT* magazine. A convenient searchable list is regularly updated on the PCI website at www.pci.org, or contact Director of Quality Programs at PCI.

Endorsements

PCI Plant Certification is included in the MasterSpec of the American Institute of Architects and is required in the specifications of the following federal agencies:

- U.S. Army Corps of Engineers, Civil Works Division & Military Programs
- U.S. Naval Facilities Engineering Command (NAVFEC)
- Federal Aviation Administration
- General Services Administration
- U.S. Department of Agriculture, FSIS
- U.S. Department of Interior, Bureau of Reclamation

Plant Certification is strongly endorsed in correspondence by the Federal Highway Administration (Kane, 1996) for precast concrete bridge products and is required or accepted by more than two-thirds of the individual state departments of transportation (Merwin, 1995).

PCI PLANT QUALITY PERSONNEL CERTIFICATION

Conducting an effective quality control program requires knowledgeable and motivated testing and inspection personnel. Each must understand quality basics, the necessity for quality control, how products are manufactured, and precisely how to conduct tests and inspections. PCI has been training quality control

PCI CERTIFICATION PROGRAMS

personnel since 1974. In 1985, the first technician training manual was published by PCI and the first qualified personnel attained certification.

There are three levels of Plant Quality Personnel Certification.

PCI Plant Quality Personnel Certification, Level I

Level I requires 6 months or equivalent of approved industry experience. It requires a basic level of understanding of the many quality control issues normally encountered in a precast plant, such as:

- Quality and quality control programs, testing and measuring
- Basic concepts about concrete: water-cementitious materials ratio (w/cm), types of cements, accelerated curing concepts
- Control of purchased materials
- Precast production procedures
- Welding practices including welding of reinforcing bars and anchor studs
- Interpretation of basic shop drawings

Certification at PCI Level I requires current certification in the American Concrete Institute (ACI) Concrete Field Testing Technician Program, Grade I. The ACI certification requires a closed-book written test and precise field demonstration of seven ASTM methods to test properties of fresh concrete.

Certification at PCI Level I is accomplished by passing a closed-book written examination. Examinations may be administered locally by a PCI-approved proctor or at a PCI-conducted training school. A manual for training and self-study (TM-101) is available from PCI. Level I must be renewed by testing every 5 years unless a higher level of PCI certification has been attained.

PCI Plant Quality Personnel Certification, Level II

Level II certification requires 1 year of approved industry experience or equivalent plus PCI Level I and current ACI Level I certifications as prerequisites. Other requirements for Level II include a greater level of knowledge of most of the topics previously described for PCI Level I, as well as:

- Prestressing concepts and tensioning procedures for straight strands, including basic elongation calculations.
- Tensioning and elongation corrections that account for temperature effects, chuck seating, abutment movement and bed shortening. Calculations for elongation and corrections are required.
- Effects of accelerated curing and importance of w/cm are further emphasized. Corrections to mix proportions must be calculated to account for excess moisture in the aggregates.
- Material control tests are further explored including aggregate gradations and analysis. Calculations are required for gradation analysis.
- Plant topics include more knowledge of reading shop drawings and the procedures for welding reinforcing bars and anchor studs.

Certification through Level II is accomplished by passing a closed-book written examination. Examinations may be administered locally by a PCI-approved proctor or at a PCI-conducted training school. A manual for training and self-study for Level II (TM-101) is available from PCI. Level II must be renewed every 5 years by testing unless Level III has been attained.

PCI CERTIFICATION PROGRAMS

PCI Plant Quality Personnel Certification, Level III

Level III requires significant knowledge of concrete materials and technology. Certification at this level requires 2 years of approved industry experience (or equivalent) and attendance at a 4-day PCI school. The candidate must pass a closed-book written examination at the school. PCI Level II certification is a prerequisite. Certification at Level III is valid for life upon registration with PCI and verification of continued industry involvement every 5 years. There is a training manual (TM-103) available from PCI that covers all course topics, including:

- Properties of:
 - Basic concrete materials
 - Admixtures
 - Fresh concrete
 - Hardened Concrete
- Mix designs using normal and lightweight aggregates
- Architectural concrete
- Troubleshooting and fine-tuning concrete mixes
- Finished product evaluation
- Stud welding and welding of reinforcing steel
- Deflected prestressing strands and the calculation of deflection forces

Agency Requirement

Plant Quality Personnel Certification is required by nearly a third of the individual state departments of transportation. They require certification for plant quality personnel and for their own materials inspectors and quality assurance personnel.

SUMMARY

The precast, prestressed concrete industry, through PCI, has taken bold steps to establish industry quality standards. The standards apply to personnel, to production and operations, to quality control, and to field operations. The standards have been published and widely disseminated and are open for evaluation and written comments. All comments receive due consideration.

The PCI industry standards for quality production are demanding to achieve. Once attained and practiced regularly, adherence to these standards contributes to improved and continuing customer satisfaction. Following these standards has been shown to reduce the “cost of quality” for the owner as well as the producer.

Certification by PCI assures compliance to the published standards for quality production. Certified personnel and producers choose to demonstrate their proficiency by voluntarily undergoing examinations and audits by accredited third-party assessors.

PCI Plant and Personnel Certification are reliable means for qualifying personnel and precast concrete producers. Use the Guide Qualification Specification that follows to require PCI Certification Programs for your projects.

PCI CERTIFICATION PROGRAMS**GUIDE QUALIFICATION SPECIFICATION**

The following guide specification can be used to qualify a precast concrete manufacturer to submit a bid on your project. Generally, the easiest procedure would be to list the precast product or the various precast products included in your project. Then, determine the appropriate Product Group and Category for each product, considering the use of the product, the method of reinforcement, and special required surface finishes, if any. Show each of the products and the required Group and Category in the project specifications. Refer to the following "Notes to Specifiers" for additional discussion. Product categories that include prestressing may incorporate pretensioning or post-tensioning, or both.

Further, it is recommended that the manufacturer employ trained and certified personnel according to the Personnel Qualifications guide specification that follows.

Manufacturer Qualifications—Structural Precast Concrete

The precast concrete manufacturing plant shall be certified in the Precast/Prestressed Concrete Institute Plant Certification Program. The Manufacturer shall be certified at the time of bidding. Certification shall be in the following Product Group(s) and Category(ies):

[Select and insert one or more of the following applicable groups and categories]

Group B—Bridge-Related Products

- B1 - Precast Bridge Products (no prestressed reinforcement)
- B2 - Prestressed Miscellaneous Bridge Products (nonsuperstructure)
- B3 - Prestressed Straight-Strand Bridge Beams (superstructure)
- B4 - Prestressed Deflected-Strand Bridge Beams (superstructure)

Group BA—Bridge-Related Products that Require Architectural Finishes

- B1A - Precast Bridge Products with Architectural Finish (no prestressed reinforcement)
- B2A - Prestressed Miscellaneous Bridge Products with Architectural Finish (nonsuperstructure)
- B3A - Prestressed Straight-Strand Bridge Beams with Architectural Finish (superstructure)
- B4A - Prestressed Deflected-Strand Bridge Beams with Architectural Finish (superstructure)

Note to Specifiers:

1. Additional guide specifications, not shown here, are available from PCI for Product Groups "A," "C," and "G."
2. Categories in Product Group B are listed in ascending order of production complexity. For example, a plant certified to produce products in Category B4 is automatically certified to produce products in the preceding Categories B1, B2, and B3. However, a plant certified to produce products in Category B2, while certified for Category B1, is not certified for Categories B3 or B4.
3. Categories in Group BA are also listed in ascending order. See Notes 2 & 4.
4. Group BA supersedes Group B in the same Category. For example, a plant certified to produce products in Category B4A is automatically certified to produce products in the preceding Categories B1A, B2A, B3A, and in categories B1, B2, B3, and B4. However, a plant certified to produce products in Category B2A, while also certified for Categories B1A, B1 and B2, is not certified for Categories B3A, B4A, B3, or B4.

PCI CERTIFICATION PROGRAMS

5. A Product Group and Category should be determined and shown in the specifications for each type of precast concrete product used in a project. Separating products will enable precasters to submit bids on specific products. For example, on a project that included both prestressed piles and beams, a precaster with expertise in producing prestressed piles (with Certification B2) could submit a price on piles only. On the same project, a producer with Certification B4 could submit a price for the beams and decide to either include or exclude the piles.
6. Specify the most appropriate Product Group and Category for the project. Do not select a higher Category than necessary. Similarly, do not add "A" to a listing when not necessary to meet project requirements. Selecting an inappropriate Group or Category could result in unnecessary cost or could restrict the number of available bidders.

Personnel Qualifications

The Manufacturer shall employ a minimum of one person, regularly present in the plant, who is certified by the Precast/Prestressed Concrete Institute for Plant Quality Personnel, Level II. All other personnel regularly engaged in the measurement, testing or evaluation of products or materials shall be similarly certified, or actively pursuing certification for Plant Quality Personnel, Level I.

REFERENCES

1. AASHTO Resolution. 2009. *A Resolution of the AASHTO Highway Subcommittee on Bridges and Structures*. <http://www.pci.org> and click on the "Quality Systems" icon.
2. AISC-PCI. 2009. White paper on "Quality Systems in the Construction Industry." <http://www.pci.org> and click on the "Quality Systems" icon.
3. Duggleby, J. 1992, "Setting a Higher Standard," *ASCENT*, Precast/Prestressed Concrete Institute, Chicago, IL, Fall, pp. 28-31.
4. Miller, B. D. and Frank, D. A. 2011. "Certification Programs Creating the Right Environment for Quality and Safety." *The Construction Specifier Magazine*, 7 pp. <http://www.pci.org/> and click on the "Quality Systems" icon.
5. Nickas, W. N. and Frank, D. A. 2009. "Certification Relies on a Body of Knowledge and Continuous Improvement." *ASPIRE, The Concrete Bridge Magazine*, 4 pp. <http://www.pci.org/> and click on the "Quality Systems" icon.
6. Shutt, C. 2000, "Erector Qualification Brings Precast Quality Assurance Full Circle," *ASCENT*, Precast/Prestressed Concrete Institute, Chicago, IL, Fall, pp. 122-123. http://www.pci.org/view_file.cfm?file=AS-00FA-8.pdf
7. PCI. 2000. *Preparation Guidelines for a Structural Plant Quality System Manual*, QSM-1, Precast/Prestressed Concrete Institute, Chicago, IL, 50 pp. https://netforum.pci.org/eweb/DynamicPage.aspx?Site=PCI_NF&WebKey=636bf780-c237-4a1d-a7e4-629fbef5ca94 (Fee)
8. Shutt, C. 1994, "Ross Bryan Associates Makes the Grade," *ASCENT*, Precast/Prestressed Concrete Institute, Chicago, IL, Winter, pp. 12-16.
9. PCI. 1999. *Manual for Quality Control for Plants and Production of Structural Precast Concrete Products*, Fourth Edition, MNL-116-99, Precast/Prestressed Concrete Institute, Chicago, IL, 283 pp. https://netforum.pci.org/eweb/dynamicpage.aspx?webcode=category&ptc_key=a7ba327a-0cc2-48cc-bc3e-1c8f49f2168e&ptc_code=Quality%20Control%20&%20Quality%20Assurance (Fee)

PCI CERTIFICATION PROGRAMS

10. PCI. 1996. *Manual for Quality Control for Plants and Production of Architectural Precast Concrete Products*, Third Edition, MNL-117-96, Precast/Prestressed Concrete Institute, Chicago, IL, 236 pp.
https://netforum.pci.org/eweb/DynamicPage.aspx?Site=PCI_NF&WebKey=636bf780-c237-4a1d-a7e4-629fbef5ca94 (Fee)
11. PCI. 1991. *Manual for Quality Control for Plants and Production of Glass Fiber Reinforced Concrete Products*, MNL-130-91, Precast/Prestressed Concrete Institute, Chicago, IL, 184 pp.
https://netforum.pci.org/eweb/dynamicpage.aspx?webcode=category&ptc_key=a7ba327a-0cc2-48cc-bc3e-1c8f49f2168e&ptc_code=Quality%20Control%20&%20Quality%20Assurance (Fee)
12. Kane, A. 1996. Letter (Unpublished), Federal Highway Administration, Washington, DC.
13. Merwin, D. P. 1995, "Two States Bridge the Quality Gap," *ASCENT*, Precast/Prestressed Concrete Institute, Chicago, IL, Spring, pp. 18-21.
14. PCI. 2011. *Quality Control Technician/Inspector Level I & II Training Manual*, TM-101, Precast/Prestressed Concrete Institute, Chicago, IL, 150 pp.
https://netforum.pci.org/eweb/dynamicpage.aspx?webcode=category&ptc_key=a7ba327a-0cc2-48cc-bc3e-1c8f49f2168e&ptc_code=Quality%20Control%20&%20Quality%20Assurance
15. PCI. 1996. *Quality Control Personnel Certification Level III Training Manual*, TM-103, Precast/Prestressed Concrete Institute, Chicago, IL, 244 pp.
https://netforum.pci.org/eweb/dynamicpage.aspx?webcode=category&ptc_key=a7ba327a-0cc2-48cc-bc3e-1c8f49f2168e&ptc_code=Quality%20Control%20&%20Quality%20Assurance

This page intentionally left blank




PCI™ Precast/Prestressed Concrete Institute
200 West Adams Street | Suite 2100 | Chicago, IL 60606-5230
Phone: 312-786-0300 | Fax: 312-621-1114 | www.pci.org